

Государственное образовательное учреждение  
высшего профессионального образования  
**«Томский государственный университет  
систем управления и радиоэлектроники»**

## **ТЕМАТИЧЕСКИЙ РЕФЕРАТИВНЫЙ СБОРНИК № 20-2/1**

**“Radar Signal Processing”  
(«Обработка РЛ сигналов»)**

Публикации в трудах конференций

Источник: *Digital Library IEEEExplore*

Язык: *английский*

Глубина поиска: *2010-2011 гг.*

Дата формирования: *март 2011 г.*

Составитель: *В.И. Карнышев*

**Томск – 2011**

## ТЕМАТИЧЕСКИЙ РЕФЕРАТИВНЫЙ СБОРНИК № 20-2/1

### "Radar Signal Processing" («Обработка РЛ сигналов»)

Публикации в трудах конференций

#### "Amplitude modulation issues in Doppler radar heart signal extraction"

Medical Doppler radar research has largely been limited to obtaining respiratory and heart rates. While this information is vital for many applications, medical Doppler radar signatures carry significant other information that could lead to cardiopulmonary volume assessments, including cardiac stroke volume (SV), and cardiac output (CO). Accurate recovery of heart signal amplitude is required for these assessments. This paper presents the first analysis of amplitude modulation artifacts on heart signal recovery in Doppler radar systems. The sources of amplitude modulation artifacts are identified, including limitations of linear demodulation, and inherent affects of respiratory signal harmonics on heart signals. Experimental and simulation results demonstrate the validity of this analysis, and outline the path towards successful heart signal amplitude recovery. [C1]

#### "UWB microwave imaging system with a novel calibration approach for breast cancer detection"

A microwave imaging system prototype has been developed for early breast cancer detection. The system is based on impulse Ultra-Wideband (UWB) radar technology. A novel, practical calibration method has been applied in our system to remove the large received signals due to both skin backscattering and Tx/Rx antenna coupling, and to underline the reflection/scattering from object of interest. This calibration method is crucial to identify the malignant tissues in a low-contrast condition that the difference of dielectric properties between malignant tissues and healthy tissues is not more than 10%. The system has been used to detect the cylindrical targets from a breast model. With this novel calibration approach, our system has successfully detected and localized the targets with a diameter of 5mm in a low-contrast condition. Details of the experimental setup and experimental imaging results will be discussed in this paper. [C2]

#### "Time-of-arrival calibration for improving the microwave breast cancer imaging"

In radar based confocal microwave imaging for breast cancer detection, recorded data are synthetically focused to a confocal point within the breast. This is the basis for both data-independent and data adaptive methods to form the breast image and can be enhanced by multistatic approach. This approach inherently assumes that the propagation velocity depends only on the average dielectric property of the breast. However, in real cases, the breast tissues are inhomogeneous and therefore the propagation velocities vary for different propagation paths. Thus, use of an average propagation velocity can result in false localization. This paper proposes an auto-calibration method to compensate the time-of-arrival from confocal point to the receiving antennas. We demonstrate using simulations on FDTD numerical breast phantoms that the proposed method helps to form an enhanced image for inhomogeneous breast. [C3]

#### "Body-worn passive planar harmonic tag design for use with Doppler radar"

A body-worn passive planar harmonic tag for sensing and uniquely isolating human respiratory motion using a Doppler radar has been designed, fabricated and tested. Agilent's advanced design system 2006 provided a simulation and performance evaluation platform. This design flow is applicable for any tag design and not just dipoles which has been the design of choice for others in the past. The tag has been designed for 2.45/4.9 ghz and shown to work at distances greater than 1 meter with transmitted power levels of 10 mw. The implications of this result is that the designed tag can be used to monitor and isolate a subject's cardiopulmonary chest motion from extraneous motion, as well as enable positive identification of the subject in a suitable environment (in home or hospital). [C4]

#### "3D Multiple Maneuvering Targets Tracking in Active and Passive Radar Composite Guidance"

Active and passive radar composite guidance has been developed into a promising technology for target tracking in the electronic counter measurements (ECM) environment. Based on the technology, this paper investigates the problem of 3D multiple maneuvering targets tracking in the presence of sea clutter and jamming. We present a set of algorithms and establish a complete tracking system composed of measurement generation, data

association, track initiation, track filtering, track management, track correlation and missile guidance. The simulation results indicate that the proposed algorithms can offer significant tracking and anti-jamming performance. The ideas and methods presented will also bear important significance for developing similar tracking systems in practice. [C5]

#### "Tracking a moving target in wireless sensor networks using PDR sensors"

The Pulse-Doppler radar (PDR) is an ultrawideband radar system capable of not only detecting target location, but also measuring its radial velocity by using the Doppler Effect. However, the traditional radar signal processing techniques are mismatch with the limit computational and storage resources available on typical wireless sensor mote. In this paper, we explore the compatibility of PDRs and mote-class wireless sensor nodes by designing a new tracking system that utilizes small PDRs as sensor nodes. The system consists of several PDR sensor nodes to detect the presence and position of a moving target, a base-station node to collect the detecting data of sensor nodes, and an algorithm to estimate the location of the target from aggregated data. Our experiments which were taken place outdoor (real environment) show that the proposed system performed well to track moving objects with the average deviation error down to 0.18m. [C6]

#### "Doppler radar respiration measurement for gated lung cancer radiotherapy"

Respiration-gated radiation therapy is a promising treatment modality that precisely delivers prescribed radiation dose to the lung tumor while minimizing the incidence and severity of normal tissue complications. Conventional gating techniques either rely on implanted fiducial markers or external surrogates such as markers placed on patients' abdomen. They are either invasive to the patients or do not have sufficient accuracy. In this paper, we present a non-contact Doppler radar method to non-invasively measure the respiration signals, from which, accurate gating signals can be derived to control the linac. No marker is needed in our method, which makes it very convenient in use. We measured the respiration using a 5.8 GHz quadrature radar. Analysis of the measured signal is presented. It has been shown that the non-contact means of respiration measurement is able to supply reliable breathing motions and accurate gating signals for radiotherapy of mobile tumors. [C7]

#### "POLARSAR Image Classification Based on Polarimetric Decomposition and Generalized Discriminant Analysis"

In this paper, a new classification scheme of fully polarimetric SAR images is proposed. This is based on the joint use of the Freeman-Durden decomposition and generalized discriminant analysis, a new method for Feature extraction. After getting the powers of the three scattering mechanism components through Freeman-Durden decomposition, the Feature extraction algorithm is introduced to well exploit the information available in the full polarimetric coherency matrix. The experimental results show that using this exploited information as new features of Fisher classification, can provides fine performance and good compactness. [C8]

#### "SAR Automatic Target Recognition Based on Classifiers Fusion"

Synthetic aperture radar automatic target recognition (SAR ATR) remains a challenging problem in military and civil field. Much work has been done to improve the performance of SAR ATR systems, both in feature extraction and classifier designing. This paper designs a multiple classifier system to solve the target classification problem in the area of SAR ATR. The proposed multiple classifier system trains three classifiers on different feature sets using three leaning algorithms. The outputs of the three classifiers are combined through evidence combination rule and discounting operation of Dempster-Shafer theory of evidence. Experiments on MSTAR public data set demonstrate that the proposed multiple classifier system significantly outperforms single classifiers and also excels adaptive boosting with RBF network as base learner. [C9]

#### "On the origins of RF-based location"

This paper will provide a brief survey of the origins of RF-based location technology through the beginning of the Second World War. Direction finding (DF) was invented by John Stone Stone in 1902 and improved upon by Lee de Forest, Ettore Bellini and Alessandro Tosi. Both radar and amplitude ranging date to 1904, although these concepts were in advance of the ability of RF technology to implement. DF played a critical role in the First World War, most notably in the naval Battle of Jutland. The requirement for accurate night-time direction led classicist and cryptographer Frank Adcock to invent an improved DF system. In the 1920's, DF and related concepts came of age for civilian applications like navigation. Inventors of the period introduced a variety of other techniques were introduced including time-of-flight or transponder ranging. By the time of the Second World War, DF was a mature field and additional novel RF-based technologies were ready to be developed. [C10]

### **"A software-defined multifunctional radar sensor for linear and reciprocal displacement measurement"**

A software-defined multifunctional radar sensor is developed in this paper for linear and reciprocal displacement measurement. Experiments were performed to demonstrate the high accuracy of the two measurement methodologies. When configured in arctangent-demodulated interferometry mode with a 5.46 GHz carrier frequency, the sensor can measure the displacement with sub-millimeter error at a detection distance of 1.2 m. When configured in nonlinear vibrometer mode, the sensor can measure amplitudes of reciprocal motions with a resolution of 0.4 millimeter and less than 3% average error. [C11]

### **"Adaptive RFI Suppression Algorithm Based on CEMD for SAR Data"**

This paper proposes a novel adaptive filtering method based on complex empirical mode decomposition (CEMD) for narrowband radio frequency interference (RFI) suppression applied to SAR. This method decomposes the RFI contaminated signal into a finite and often small number of Intrinsic Mode Function (IMF). The sum of some selected IMF components is taken as reference input of adaptive filter based on the characteristics of CEMD. Experiment results show that CEMD provides an effective way to obtain reference input. The proposed method can effectively subtract RFI component from the RFI contaminated signal, which is the primary input of the adaptive interference canceller. The point-target simulation is used to show the working principle of the proposed algorithm. Experimental results based on SAR real data are also shown to verify the proposed algorithm. [C12]

### **"Considerations in measuring vital signs cross section with Doppler radar"**

This paper describes the different considerations and challenges in measuring human cardiopulmonary radar cross section (RCS). The effect of clutter on the received signal is explained as well as the importance of preserving baseband dc content for valid readings. The center estimation algorithm with dc-cancellation is presented as a solution to restore dc content in the baseband signals and to exclude clutter contribution. The far-field conditions for the target range are revisited. By modeling the human torso as a half-cylinder and assuming unity reflectivity, the ratio of the RCS of the back of the torso with respect to the front is a function of wavelength. At 2.4 GHz and for a chest breadth of 30 cm, the back is expected to have an RCS that is 10 times that of the front while the RCS of the side is expected to be 4 times smaller. [C13]

### **"A multilateral synthetic aperture wireless positioning approach to precise 3D localization of a robot tool center point"**

In this paper, a novel multilateral synthetic aperture secondary radar concept and its application for precise 3D localization of a robot tool center point (TCP) are introduced. A backscatter transponder is attached to the TCP of a robot. Spatially distributed FMCW secondary radar units pick up the backscattered phase coherent transponder signals. Based on assisting relative sensors, a synthetic aperture is created with the TCP. The developed multilateral inverse synthetic aperture reconstruction algorithm then determines a probability density function (PDF) of the spatial transponder position. By simulations and experimental results using a 5.8 GHz system with 140 MHz bandwidth it is shown, that 3D localization precision in the mm range can be achieved with the novel wireless local positioning concept even with narrowband radar systems in dense multipath environments. Heretofore, accuracies of this magnitude were only attainable with ultrawideband (UWB) systems utilizing a ten times wider bandwidth. It is shown, that the multilateral synthetic aperture locating system has the potential for a quantum leap in precise 3D wireless local positioning. [C14]

### **"Fusion of High Resolution Satellite SAR and Optical Images"**

This paper proposes a methodology for fusion of high resolution satellite SAR and Optical Panchromatic images. The main objective of fusion is to bring together complementary information contained in SAR and Optical images. The paper discusses and illustrates the issues involved in merging and choosing of suitable approaches to overcome them. The choosing of proper fusion method was explained from the point of nature of SAR and Optical wave interaction with the surface and objective of fusion. Two methods are proposed in this paper one is based on Fourier filtering and the other is based on multiresolution pyramid. The methodologies are applied on Cartosat-1 Panchromatic and TerraSAR-X images. The results and evaluation of the fusion based on entropy are presented. [C15]

### **"Robust DOA estimation of SSR signals for aircraft positioning"**

Methods to estimate Directions of Arrival (DOA) on radio signals are susceptible to hardware and signal deficiencies. In the following, the robustness of four algorithms is evaluated by numerical and experimental tests. The focus lies thereby on Secondary Surveillance Radar (SSR) signals, but the algorithms can generally be



used on any kind of radio signal. It will be shown that variants of the ESPRIT algorithm provide highly accurate DOA estimates on SSR signals even without calibration. [C16]

#### "A heterodyne 77-GHz FMCW radar with offset PLL frequency stabilization"

This contribution describes the realization of a heterodyne frequency-modulated continuous-wave (FMCW) radar system operating in the frequency band from 76 GHz to 77 GHz. To implement the heterodyne principle two voltage controlled oscillators (VCOs) are operated in order to produce frequency ramp signals with a fixed frequency offset. This allows to mitigate effects occurring in homodyne systems like, e.g., DC-offsets or low-frequency noise components. To avoid large divider values in the control loop the presented system is based on an offset phase-locked-loop configuration. In the presented implementation the same downconverter is used to implement the offset-loop for both VCOs, which has the positive effect that errors and noise influences in the downconversion process-at least partly-cancel out in the final FMCW output signal. [C17]

#### "Design and implementation of automotive 77GHz FMCW radar system based on DSP and FPGA"

In this paper, we design and implement the automotive FMCW radar based on FPGA and DSP. The proposed signal processing module and RF transceiver for 77GHz FMCW radar are integrated into an experimental vehicle and tested in a real road environment. This paper presents the designed signal processing architecture and implemented processing algorithms. [C18]

#### "High Resolution Radar Imaging Based on Compressed Sensing and Fast Bayesian Matching Pursuit"

Recently the rapid imaging based on the compressive sensing (CS) theory have attracted increasing interests, which simultaneously sampling and compressing signals or images. Radar imaging based CS is a potential way to obtain the high-resolution radar images without the constraint of Nyquist sampling rate. In this paper, we proposed a radar remote-sensing imaging approach based on compressive sensing and fast Bayesian matching pursuit (FBMP) recovery algorithm. Some experiments are taken and the results indicate that an accurate reconstruction of high-resolution radar images are obtained, with fewer measurements than most its counterparts(e.g., MP, OMP, StOMP, GPSR),but resulting in lower normalized MSE(NMSE). Although BCS obtains lower NMSE than FBMP,simultaneously with higher time complexity and sparsity. [C19]

#### "Ship Detection after Removal of Ambiguities by Using PolSAR Images"

Ambiguities in SAR image are very common phenomena. For maritime applications, as the high intensities of the ambiguities in low radar backscatter background of sea environments, they can be mistaken as targets and cause false alarms in ship detection. Thus, through the analysis of polarimetric characteristics of ships and ambiguities, we propose a ship detection method which applies the eigenvalue to differentiating the ship target and azimuth ambiguities. One set of Cband JPL AIRSAR polarimetric data covered Kojimawan Bay, Japan has been chosen to evaluate the method that can effectively remove false alarms caused by the azimuth ambiguities. [C20]

#### "A New Method of Fixed Single Observer Passive Location Based on Phase Difference Rate-of-Change"

Aimed at the disadvantages of DFRC method such as low observability and big relative error, so this paper accedes phase difference rate-of-change, put forward the DPFRC method. Combined with the extended Kalman filter (EKF) and unscented Kalman filter (UKF) algorithm, this paper proved the advantages of the UKF algorithm which applied to DPFRC method verified with the computer simulation. [C21]

#### "A New Method for Sorting Radar Signals Based on Coherency"

Radar can work on different wave bands in different period of time, which result in the Increasing-batch problem based on the existing methods of signal sorting. In order to solve this problem, Slope Discriminance was proposed in this paper. Error analysis of this proposed method shows its availability when the measurement error of frequency of receiver is below 100MHz. Simulations on same and different radiant points was given. The results show that this new method decreases the possibility of Increasing-batch and also it can be a supplement of present methods. [C22]

#### "Roof Detection in Lidar Data"

Lidar is widely used in many fields in recent years. Consequently, research of feature extraction in lidar data has

intensified. Roof of building as a stable line feature is widely used in many fields. But there is yet not a good algorithm to finish this work. In this paper, we propose a new method to extract roof of building. The roof is modeled by a symmetric exponential roof edge model and the altitude image which generated from original lidar point cloud data is smoothed by a low-pass filter ISEF which is optimal for the symmetric exponential model. And then an algorithm for roof detection and a grouping and fitting method are proposed for line feature extraction. In order to depress the effect of the noise a fusion method is used for multi-images. In the end of the paper the method is proved useful through the lidar data comes from Calgary University in the end of the paper. [C23]

#### **"A Novel Polarimetric CFAR Target Detection Method"**

A new polarimetric synthetic aperture radar (PolSAR) image CFAR target detector is proposed in this paper. By introducing the inverse Gamma distribution which is extensively used in modeling, the distribution of polarimetric matched filter (PMF) metric, denoted as  $P_{G0}$ , is derived on the product model; Furthermore, a fast and exact parameter estimation method of  $P_{G0}$  distribution is presented using the "second kind statistics" based on the Mellin transform; Finally the formula of the CFAR detection threshold is deduced, and the target detection using the proposed constant alarm rate (CFAR) detector is performed on the RADARSAT-2 PolSAR data. Experimental results demonstrate the great efficiency of the  $P_G$  distribution and the corresponding parameter estimation method in data fitting of areas with different degree of homogeneity. Moreover, the successive CFAR detector can successfully complete the automatic target detection with low false alarm rate and high detection rate in complex clutter environment where the homogeneity of terrain varies sharply. [C24]

#### **"Multitask Learning and Sparse Representation Based Super-Resolution Reconstruction of Synthetic Aperture Radar Images"**

In earth observing remote sensing fields, to recognize objects whose size approaches the limiting spatial resolution scale especially in Synthetic Aperture Radar (SAR) images, spatial resolution enhancement is usually required. In this paper, we proposed a multi-task learning and K-SVD based Superresolution image restoration method where K-SVD algorithm is employed to learn a redundant dictionary from some example image patches. In order to learn more accurate dictionary and reduce the complexity of dictionary learning, multitask learning concept is adopted to learn multiple dictionaries from the samples classified by K-means clustering. Some experiments are taken to investigate the performance of our proposed method, and the visual result and numerical guidelines both prove its superiority to some start-of-art SRIR methods. [C25]

#### **"Cooperative Synthetic Aperture Radar Image Segmentation Using Learning Sparse Representation Based Clustering Scheme"**

Based on a recent proposed and popular sparse representation based classifier (SRC), in this paper we presented a novel Learning Sparse Representation based Clustering (LSRC) scheme for Synthetic Aperture Radar (SAR) segmentation. LSRC introduces the examples-based dictionary learning technology in SRC to find a dictionary that is adaptable to sparsely representing samples, which is liable to provide more accurate approximation of samples and subsequently achieve higher classification accuracy rate. Moreover, for the intrinsic supervised nature of LSRC, we adopt an unsupervised-clustering cooperative approach to provide training samples for LSRC, in which some "good" samples with higher membership degrees are selected from the clustering result of K-means algorithm. Some experiments are taken on segmentation of both the texture images and SAR images to investigate the performance of our proposed method, and the results prove its superiority to its counterparts. [C26]

#### **"A Novel SAR Signal Reconstruction Method from Non-uniform Sampling Associated with Fractional Fourier Transform"**

A contradiction between wide swath and high spatial resolution exists in synthetic aperture radar (SAR) imaging processing. Displaced phase centers multiple azimuth beams (DPC-MAB) system can make a tradeoff between them, but it arises non-uniform sampling in the azimuth direction. In this paper, a novel reconstruction method associated with the fractional Fourier transform is proposed, which has better performance compared with the traditional one. Moreover, it can reconstruct under sampled signal successfully while the traditional method fails. Simulations verify the efficiency of the proposed method. [C27]

#### **"The Impact of High-Order Phase in Ballistic Missiles Detection"**

According to characteristic of ballistic missiles and their velocity, acceleration and jerk in radar echo, we establish the echo signal model with high-order phase echo signal characteristics, then analyze the target detection

performance by numerical simulation to get the relationship among the optimal number of pulses, signal-to-noise ratio and jerk. Finally, the simulations verify the principle of the method is correct and can provide guidance for practical applications. [C28]

### "Research on the Interference Cancelation in SFN Based Passive Radar"

It is important to get a high-quality reference signal for the cancellation and correlation detection in passive radar. The single frequency network (SFN) configuration of transmitters will cause the interference in the reference channel. The infinite impulse response filter based on the normalized least mean square rule (IIR\_NLMS) can improve the cancellation gain and signal noise ratio (SNR) of the target echo, but it has limited capability in suppressing co-channel interference. In order to solve this problem, a type of equalization filter is proposed, and then combining with the IIR\_NLMS filter, the equalization IIR\_NLMS filter is obtained. Simulation results verify the efficiency of the algorithm. [C29]

### "Determination of LIDAR Points Cloud Filtering Parameters Using Distance Image"

Filtering of LIDAR points cloud is the key of obtaining precise DEM and it has become a studying focus. Determination of the filtering parameters affects the results directly. Within this paper, it is proposed that making use of pixel position and grey information in distance image to guide determination of the filtering parameters like the block size and the threshold value. And the method is validated by a kind of filtering using the determined parameters. In experiment it is shown that this method is available. [C30]

### "The Intelligent Embedded Control Warning System for Car Reversing"

Most of the car drivers used the reverse radar or a reverse camera to detect the road situation behind the vehicle when it is engaged in reverse gear. As a matter of fact, the pedestrians can virtually know if the vehicle is backing up or not only by seeing the permanent bright reverse lamps. And as there is not much change with the reverse lamp to be seen, therefore their warning function for pedestrians seems to be still insufficient eventually. Therefore, this research tries to design a set of embedded intelligent car backup warning system so as to promote the safety of the walkers or the other drivers on the road. This embedded system uses Microsoft Win CE operating system and matches with the Mini2440 developing board. It also uses the Visual Studio 2005 for developing the intelligent touch panel operating mode. The UART interface on the Mini 2440 developing board controls the frequency converter, RC server and LED by using PIC16F877 to transform the signal of the sensors. And then, connecting to the sensors of angle, luminosity and distance so as to read the voltage value of the sensor and transferring them into actual values and followed by using 27 fuzzy logic rules to carry on the fuzzy logic deduction. And the angle of the LED reverse lamp bracket is adjusted and driven automatically according to the results of this logic deduction eventually. This research tries to do the simulated test by using a mobile frame in the same height as a real automobile. To let the test mobile frame being located 240 cm away from the obstacle and then start the driven motor and set the frequency of it to be with 60 Hz. (in other words, its speed is approximately in 2.52 Km/h.) the let the test mobile frame to stop at 40 cm in front of the obstacle. We found out that the warning lamp bracket installation angle will be changed correspondently with the distance between test mobile frame and obstacle and being declined automatically from 90 degree to 0 degree. Apparently, from the test results, it has been proven that this system can reach the goal of automatically controlled car back-up warning function truly. [C31]

### "Detection Algorithm of Laser Radar Target Based on Wavelet Transform"

Given the different transmission characteristics under the wavelet transform (WT) domain and the different distribution characteristics of frequency domain of the signal and noise, a novel approach for detecting laser radar target based on wavelet transform has been proposed. Usually, wavelet decomposition has been used to de-noise a digital signal corrupted by noise. In our approach, we applied the wavelet decomposition and modulus maximum detect the locations of laser radar echo signal. Simulations show that the proposed algorithms are more efficient than only utilizing wavelet decomposition in a big clutter background. [C32]

### "Analysis and Design of Three Loop Radar Servo System for Air Defense Missile"

In order to design a radar servo system with satisfactory response for an air defense missile, the three loop form was chosen, and the frequency domain method was used. The design approach and criteria for the three loop radar servo system was outlined in this paper. With the criteria, a servo system was designed. Then the effect of every loop was analyzed. The results shows that, with the frequency domain method and the design criteria, the designed radar servo system can obtain good response and every loop of the three loop form can't be omitted due to their essential effect. [C33]

### "New Technology and Applications on Microwave Sensors"

Presently, various microwave sensors have emerged. They have powerful performance and quite wide application domain. New technology and applications on microwave sensors are presented. A novel microwave sensor for measuring the properties of a liquid drop has been invented. A microwave based in-line sensor for steam quality is described, and test result is reported. Development a new tunable multiband UWB radar sensor and its applications to subsurface sensing is presented. Finally the technical challenges and developing prospect of microwave sensors are discussed. [C34]

### "LIDAR Depth Indicator of the Design and Research"

According to rope friction hoist in the process of ascension, because the steel wire slips or peristalsis and becomes tensile deformation by long-term usage. There will cause deviation between the display of the indicator and the actual location of lifting container. That may even cause accidents. This paper introduces a composition of new depth indicator, working principle and designing method which based on laser infrared radar technology. It can realize many functions, such as the precise indicating of the location of the lifting container and real-time monitoring, etc. Have no assistant calibration switch, without measuring transmission error, fast response and intuitive, convenient operation, etc. [C35]

### "Airport Detection in SAR Image Based on Perceptual Organization"

Being one of the key transportation targets, airport detection is of great importance in military and civil applications. In this paper we propose a new method based on perceptual organization for airport detection in large SAR image. Since the runways are the most obvious characteristic of the airport, we first design belief functions for the runway features, which include collinearity, proximity, width and texture similarity. Then we propose to use the DS-evidence theory for the fusion of all belief functions, which can serve as a criterion to decide whether the two region units can be grouped. The candidate airport can be found by grouped region growing and detected by airport knowledge. Experimental results showed the effectiveness of the proposed approach for airport detection in large complex SAR image. [C36]

### "Maximum likelihood synthetic aperture radar image formation for highly nonlinear flight tracks"

This paper develops a flexible time-domain SAR imaging algorithm that is capable of accounting for somewhat arbitrary flight track geometries and platform orientations. The proposed technique casts SAR imaging as a maximum likelihood estimation problem where the ground reflectivities are taken as the parameters to be estimated. It is shown that conventional back projection is one of two steps required to form the optimal maximum likelihood image. Simulation examples are given that compare images and impulse response functions for back projection and the maximum likelihood algorithm. [C37]

### "Forming regularized maximum likelihood strip-map synthetic aperture radar images using the block RLS algorithm"

The data matrix that is needed for forming the maximum likelihood (ML) image in strip-map synthetic aperture radar (SAR) has block structure. This structure allows for a recursive way of forming a regularized ML image using the block recursive least-squares (RLS) algorithm. The regularization serves three purposes: Properly chosen, it provides a more stable solution; it combats noise; and it allows the block RLS algorithm to be initialized. In this paper, it is shown that an optimal regularization parameter exists for this problem and that the solution to the regularized normal equations for the strip-map SAR model is solved by the block RLS algorithm. Simulated results are shown. [C38]

### "Measure of smartness"

The traditional power- and energy system is going to be smart. Smart means a set of well defined devices and techniques but nowadays smart is used as a synonym of the expression 'modern' and 'up-to-date'. Believing that the smart philosophy supports the better energy supply we should measure it. Due to the fact that today every gauge and technique is called smart, we should make distinction between different smart objectives, levels and techniques. This paper aims at introducing a quantifying technique that helps orientate in this field. We can use it if we are going to apply new smart technologies or we are going to invest into the less smart part of the network. In the following parts we summarize the elements of the smart characteristics, we measure them and we form a smartness measuring factor capable of comparing two networks or two parts of the network. Finally we show a novel visualization method, the "radar screen" of the smartness. [C39]



### "Angle-Doppler Estimation in Heavy Correlated Interference"

In this paper, a Prony estimation method on wavelet-transformed space-time signal is proposed with Adaptive Simulated Annealing (ASA) algorithm as a global optimizer. In addition to denoising property of wavelet transformation, the proposed approach appeals to its decor relating nature. Our method improves the performance of radar systems with large array antenna, such as OTH radars in STAP applications. We show that the conglomeration of Prony estimator and ASA algorithm achieve good performance in terms of detection and resolution in comparison with the classical STAP algorithm in the presence of powerful external correlated interference. Moreover, we present how to apply STAP technique to parameter estimation of target in the correlated non-Gaussian interference environments that causes Maximum Likelihood (ML) function be nonlinear with respect to the angle and Doppler. In the following, ASA algorithm is employed for global optimization of all nonlinear functions. Extensive simulations demonstrate that our proposed algorithm outperforms that previously reported estimators with extremely low computational cost. [C40]

### "Implementation of Adaptive FIR Filter for Pulse Doppler Radar"

Digital Signal Processing (DSP) systems involve a wide spectrum of DSP algorithms and their realizations are often accelerated by use of novel VLSI design techniques. Now-a-days various DSP systems are implemented on a variety of programmable signal processors or on application specific VLSI chips. This paper presents the design of Adaptive Finite Impulse Response (FIR) filter for moving target detection in various clutter conditions in Radar Receiver. The design uses pipelined COordinate Rotation Digtal Computer (CORDIC) unit and pipelined multiplier to get high system throughput and reduced latency in each of the pipelined stage. Saving area on silicon substrate is essential to the design of any pipelined CORDIC. The area reduction in proposed design can be achieved through optimization in the number of micro rotations. For better adaptation and performance of Adaptive Filters and to minimize quantization error, the numbers of iterations are also optimized. [C41]

### "A novel space cloth using resistor grid network for radar absorbers in stealth applications"

We report novel resistor grid network based space cloth for application in single and multi layer radar absorbers. The space cloth is analyzed and relations are derived for the sheet resistance in terms of the resistor in the grid network. Design curves are drawn using MATLAB and the space cloth is analyzed using HFSS™ software in a Salisbury screen for S, C and X bands. Next, prediction and simulation results for a three layer Jaumann absorber using square grid resistor network with a Radar Cross Section Reduction (RCSR) of -15 dB over C, X and Ku bands is reported. The simulation results are encouraging and have led to the fabrication of prototype broadband radar absorber and experimental work is under progress. [C42]

### "Non-contact heart rate detection using periodic variation in Doppler frequency"

Remote heart rate detection without body-attached probes is a promising technology for health care, monitoring of elderly people, emergency, and security. In this paper, we use a continuous wave (CW) microwave Doppler radar. It is important to eliminate the effect of body movement that is irrelevant to heartbeat such as respiration. In general, the displacements of them are larger than those of heartbeat. Therefore, we focus on the periodic variation of velocity of body movement due to heartbeat rather than the displacement variation of it. We detect a heart rate from a part of the wavelet frequency components with high periodicity. As a result of performance evaluation, our system enables to extract more accurate heartbeat interval than the traditional approach using the periodicity of an original Doppler signal. [C43]

### "Mathematical analysis of interpolation step of Omega-K Algorithm for GPR and its implementation"

GROUND-penetrating radar (GPR) is a mature remote sensing technique employed by engineers and scientists to obtain information from subsurface structures. These structures range from manmade objects, such as buried utilities, pavements, and unexploded ordnance, to geological formations. GPR data collection may be viewed as a mapping from the object space  $(x,y,z)$ , characterized by the object's spatial location and reflectivity, to the image space. The image space may be viewed in the space-time domain  $(x,y,t)$ , where the recorded scattered signals are displayed as a function of lateral position and time, or in the Omega-K domain  $(k_x,k_y,f)$ , where the two image sets are related by spatial-temporal Fourier transforms (FTs). Additionally, data may be recorded in the space-frequency domain  $(x,y,f)$ , as would be the case with a frequency-domain GPR. Fourier transforms allow easy conversions between the three image domains. [C44]

### "Waveform-agile mimo radar for urban terrain tracking"

We investigate the problem of tracking a moving target in urban terrain using a multiple-input and multiple-output



(MIMO) radar system. Our proposed method aims to maximize the target information using an optimal configuration of MIMO widely-separated radar sensors while exploiting multipath returns from all the sensors. Furthermore, we adaptively configure the parameters of the transmit waveforms of the MIMO system at each time step in order to minimize the overall mean-squared tracking error. We demonstrate our results using a realistic urban environment, by varying the regions of obscuration and the number of bounce path returns. An important advantage of the MIMO system is that, based on the radar configuration, it is possible to completely eliminate the obscuration regions. [C45]

#### "Heart-beat detection and ranging through a wall using ultra wide band radar"

Heart-beat detection has found many applications in military and bio-medical areas. Many of these applications focus on the use of impulse based ultra wide band (UWB) radars. This in-turn requires expensive hardware and consumes more power (for a given range) compared to stepped frequency continuous wave (SFCW) radars. However, the micro-Doppler characteristic of human body can be detected by SFCW radar at much lower sampling rates and power. It can help in distinguishing a living and a non-living target. In addition, SFCW radar can help separate Doppler signatures in down-range, thus enabling it to look for multiple human targets. UWB radars operate at a bandwidth higher than 0.5 GHz and have the benefit of high range resolution. This paper focuses on the experimentation of a technique to obtain the range and Doppler of a human body using UWB-SFCW radar and moving target indicator (MTI) filter, in the presence of an interfering wall. [C46]

#### "A Novel Image Based Multi-Channel SAR-GMTI Algorithm"

A novel three-channel SAR-GMTI algorithm based on the compressed image rather than the azimuth-uncompressed raw data is proposed, which employs the classical DPCA technique and FrFT. The chirp characteristics of DPCA signal of the moving target in the SAR image domain is investigated for the first time in this paper. The scheme introduce FrFT to detect the moving target and estimate the position, velocity and radial acceleration, which lead to a more overall description on motion parameters than that of the majority of estimation algorithms. The excellent anti-noise ability of FrFT and the ideal clutter cancellation of DPCA technique results in great GMTI performance during a clutter-rich and low SNR environment. The simulation results indicate the efficiency and availability of the novel algorithm. [C47]

#### "Advantages of Airborne Lidar Technology in Power Line Asset Management"

Airborne lidar technology is widely accepted among power utility companies as the most efficient tool for acquiring high-density and high-accuracy geo-referenced spatial data for various applications essential to power line asset management. This paper describes the typical workflow in lidar data collection. It also describes further application steps in the traditional engineering analysis required for power utilities management, including catenary modeling for thermal up-rating and vegetation encroachment analysis. It will be shown that lidar data can have exceptional precision and accuracy, enabling tight-tolerance engineering calculations for power line efficiency modeling. The paper will also briefly discuss change detection in transmission and distribution wires themselves, the underlying surface terrain and surrounding vegetation throughout the transmission corridor, and how lidar technology can help to address monitoring issues. Finally, the performance advantages of airborne laser terrain mapper (ALTM) systems are discussed in the context of applications related to power line asset management. [C48]

#### "Performance evaluation of a GPR system for mine detection using a 3D-SAR algorithm"

Within the "International Test & Evaluation Program" (ITEP) a measurement campaign (ITEP project 2.4.2.13) was held in Oberjettenberg, Germany, to evaluate novel evaluation procedures for the test and evaluation of dual sensor (DS) mine detection devices (metal detector MD and ground penetrating radar GPR). FHR contributed with a UWB GPR sensor and a novel radar data processing algorithm. The improvement of the application of a near field 3D-SAR algorithm compared to standard GPR data processing is shown in terms of the receiver operating characteristics (ROC) curve. [C49]

#### "ISAR imaging of ground moving vehicles in a curve"

The imaging of rotating objects by exploiting the change of the aspect angle is called Inverse Synthetic Aperture Radar (ISAR). The imaging of curving vehicles is done using airborne radar data and information about the vehicle's motion. This paper explains some important processing steps and shows ISAR images resulting from our experiments. [C50]

#### "Toward a network of common radar and EW sensors aboard a single or multiple cooperative

## platforms"

Up to now, combat aircrafts are fitted with Fire Control Radar (FCR), Electronic Warfare System (EWS), and radio links. Each of these systems is dedicated to a particular task and the cooperation is reduced to a minimal exchange of information between them, so far. Major system performance enhancements are to be expected from close co-operations to each other sensors. The future co-operations can be ordered in four stages. The three first ones lead progressively to a common sensor including radar and EW functions. The last one is the deployment, on a given platform, of these common multi-functions sensors on a network basis. Another focus is the cooperation between platforms. Depending on the cooperative application, low, medium or high data rates will be needed. A typical example required by such co-operations is the implementation of "ad hoc" data links using the FCR or the EWS. This kind of co-operations does not need to add specific antennas or other R.F. devices. [C51]

## "Focusing ISAR images of moving targets in real-time using time-frequency-based method"

In this paper, we present a time-frequency S-method-based approach for real-time motion compensation, image formation and image enhancement of moving targets in ISAR and SAR. This approach performs better than the Fourier transform by drastically improving images of fast, manoeuvring targets by increasing the SNR in both low and high noise environments. The method also computationally simple, requiring only slight modifications to the existing Fourier transform based algorithm. The effectiveness of this method is demonstrated through the application to simulated and experimental data sets. [C52]

## "Expedient GPR survey schemes"

Practical GPR survey schemes based on a geometrical migration algorithm are implemented and tested: (1) random GPR data collection from water surface along a tangled path and interpolation to a regular grid for bottom reconstruction; (2) double-pass B-scan with different antennas offset for estimation of the upper ground layer thickness and permittivity. [C53]

## "Digital beam forming concepts with application to spaceborne reflector SAR systems"

The trend in the conception of future spaceborne radar remote sensing is towards the use of Digital Beam Forming (DBF) techniques. These systems will comprise multiple digital channels, where the analog-to-digital converter is moved closer to the antenna. This dispenses the need for analog beam steering and by this the use of transmit/receive modules for phase and amplitude control. Digital beam forming will enable Synthetic Aperture Radar (SAR) which overcomes the coverage and resolution limitations applicable to state-of-the-art systems. Moreover, new antenna architectures, such as reflectors, already implemented in communication satellites, are being reconsidered for SAR applications. This paper is dedicated to the digital signal processing aspects of such reflector based SAR systems. After introducing the hardware concepts the beam forming algorithms are presented and demonstrated by means of numerical simulations. [C54]

## "Software for simulation of electromagnetic waves propagation through the soil with buried objects"

The software for simulation of electromagnetic waves propagation through the soil layered structure with shallow buried objects has been described in the paper. The simulation is based on the finite difference time domain (FDTD) method and allows to define ten layers of soil and four buried cuboid objects. Such virtual ground penetrating radar (GPR) system seems to be useful for test of targets detection level for different soil structure configurations as well as different transmitted radar signals and scanning methods. [C55]

## "Radar signatures of complex buried objects in ground penetrating radar"

The evaluation of radar signatures of buried objects for three experimental ground penetrating radar setups will be addressed in this paper. The contribution will present corresponding results and experiences. The performance of the imaging capabilities of the designed radar system will be assessed by reconstruction of complex shaped test objects, which have been placed within the ground. The influence of system parameters of the ground penetrating radar have been varied systematically in order to analyze their effects on the image quality. Among the modified parameters are the step size in transverse plane, height of the antenna over ground, frequency range, frequency points, antennas and varying instrument settings. A signal processing technique based on synthetic aperture radar has been applied on the measured raw data. The focus radius around a specific target has been analyzed concerning the compromise between image quality and processing time. The experiments demonstrate that the designed ground penetrating radar systems are capable for detection of buried objects with high resolution. [C56]

### "Comparison of methods of the resolution increase in GPR for the short range targets"

This paper describes different approaches for high resolution short range 3D imaging with ground penetrating radar (GPR) based on research performed at the Radar R&D (Tomsk). Radar R&D is active in the field of GPR technology and its applications more than 15 years. Ultra-wide operational bandwidth in GPR can be used to obtain high-resolution images of targets. In this paper, different approaches to high-resolution imaging with UWB radars are discussed and compared. As a rule, in existing software of the industrial radar the high-frequency filtration of signals is used that essentially limited efficiency of GPR investigation. It is described that methods of restoration for distorted signals have advantages compare filtration. Possibilities of wavelet transformation for resolution increase of short range targets are discussed. The analysis is carried out on the test images and illustrated by experimental examples. [C57]

### "Radar pulse repetitive patterns detection"

Pulse Repetition Interval (PRI) is an important parameter in the recognition of pulsed radar signals because of its distinctiveness. Pulses time of arrivals (TOA) are PRI sources. Depending on the radar function various PRI modulations are used. So PRI pattern requires the estimation of the numerous calculations to determine its values correctly. PRI complexity makes it as a distinctive parameter for electronic intelligence, under condition that the signal's parameters are estimated ambiguously and repeatedly for different series of measurements. Significant difficulty of analysis is an existence of distortions arising from the propagation properties and signals interference under measurement. In the literature much attention is paid to seeking ways to solve the problem. Proposed, are various algorithms showing good properties for certain types of modulation. They are ineffective for others PRI types. They can be successfully used in ELINT systems, while in the ESM devices, where full automation is required, their usefulness is limited. The paper presents some aspects of PRI analysis on the base of simulated and real signals. Also presented is a modification of the algorithm based on the use of autocorrelation function in the analysis of PRI. The proposed solution allows for more efficient analysis of long sequences of periodic changes in PRI (stagger, complex, dwell and switch) in terms of having a relatively short measurement sequences. [C58]

### "Scenario modeling and simulation for performance prediction of a modern radar in electronics warfare environment"

A Simulation software is presented to evaluate radar performances in EW environments. This Software includes detailed radar and Jammer Models and Scenarios including different signal losses, noise, clutter and Doppler Effect. This software simulates different passive and active jamming techniques and models coherent and no coherent effects and other factors causing losses in jamming to signal ratio (JSR). Required JSR for different techniques to be effective, is output of this simulation software for different radars. This simulation can be used for radar and jammer performance evaluation with changes in input parameters. A sample application for performance evaluation of a UAV based jammer against naval air defense radar is presented. [C59]

### "Weak signal detection using compressive receiver"

Nowadays modern radar uses more and more complex waveforms. Some waveforms are developed intentionally to make their intercept almost impossible. The main distinctive features of modern radar signal are hidden in its time-frequency structure. In the near past the problem of radar signal feature extraction was considered in time or frequency domain separately, because radar waveforms were relatively simple. Today, however, the signals should be observed simultaneously in both domains. Time-frequency distribution concept offers a new approach in radar signals classification/identification. The paper presents some results of weak, pulsed and continuous radar signals detection by the use of compressive receiver. [C60]

### "Classification of LFM radar signals based on the wavelet decomposition and the neural LVQ classifier"

The paper presents a novel approach, based on wavelet decomposition, to automatic classification of signals with the linear frequency modulation (LFM), generated by a radar emitter. The goal of radar transmitter classification is to determine the particular transmitter from which a signal originated, using only the received waveform. To categorise a current signal to the particular transmitter, the discrete wavelet decomposition of the signal is accomplished. The Learning Vector Quantisation (LVQ) algorithm is proposed as the intelligent classification algorithm. [C61]

### "Specified for air safety, monitoring atmospheric phenomena including the volcano dust"

This paper is an overview of methods and means for remote sensing of atmosphere based on backscattering of electromagnetic waves for prediction of dangerous weather phenomena zones along the route of the airplane. In addition to such traditional phenomena as turbulence, hail, icing-in-flight and thunderstorm, the approaches to distinguish areas of volcano dust is also included into consideration. [C62]

#### **"Synthesis planar array and apertures in passive HF phase array radar"**

In this paper we discuss analysis and synthesis techniques for planar arrays usage in passive HF target ranging. Three types of elements geometries are assumed and analyzed for the array. First rectangular element geometry is discussed. Then the analysis method is extended to the case of circular array in which the Fourier function is replaced by the Bessel function. As the last geometry, the non-planar array is discussed briefly. Finally the consideration in applying these arrays in HF passive radar is discussed. [C63]

#### **"Design of RF subsystem for Ku-band radar with synthesized bandwidth of 2GHz by using stepped-frequency chirp signal"**

In this paper we introduce our work on developing a Ku-band 2GHz bandwidth RF subsystem based on Stepped frequency chirp signals (SFCS) including transmitter, receiver and frequency synthesizer, as well as experimental results. Very high resolution radar image for a moving train has been obtained by using the developed RF subsystem. [C64]

#### **"Passive radar: Here comes the new generation VERA-NG"**

Abilities of passive surveillance systems open new applications for military even air traffic control purposes [C65]

#### **"The use of microwave noise from the Sun for on-line verifying azimuth alignment of surveillance radars"**

Radar system cannot operate standalone. Information about detected targets should be send to command and control system. The C2 systems often realize fusion of data coming from bigger number of radars. General problem in data fusion process is quality of received radar data. The radar data quality strongly depends on radar systems calibration and adjustment. One of the source of adjustment errors is azimuth alignment of the radar. In the paper the use of microwave noise from the Sun for on-line verifying azimuth alignment of surveillance radars will be discussed. The real results of radar alignment, advantages and disadvantages will be presented. [C66]

#### **"Incoherent addition of ISAR images from spatially distributed receivers for classification purposes"**

A popular approach for Non-Cooperative Target Identification is the use of 2D Inverse SAR images. To successfully identify a target it is necessary to compare a set of scattering centers in the ISAR image to a data base. In the conventional case of a monostatic radar, however, visibility of scattering centers varies with the target aspect angle. In this paper we show that the visibility of scattering centers can be improved by incoherent addition of images from spatially distributed radars. The main focus lies in the description and relevant results of a multistatic ISAR experiment carried out at Fraunhofer FHR. [C67]

#### **"Parameter estimation from a fraction of the period for a rotating target"**

All the techniques developed for extracting micro-Doppler features for the past decade rely primarily on the assumption that the time series of the signal contains at least one oscillation or more during the coherent integration time or imaging time. However, many applications in real-world scenarios involve short duration signals and often require the detection and the estimation of micro-Doppler characteristics. Short duration signals may contain only a fraction of an oscillation. In this paper, we develop two techniques to estimate the micro-Doppler parameters from a fraction of the period. In these scenarios, the coherent integration will cover only 1/4 and 1/2 of the oscillation. The performance of the proposed methods are evaluated using both synthetic and experimental data. [C68]

#### **"The detection performance of complex cosine CWT and entropy analysis for narrowband signals"**

The problem of detection of narrowband sinusoidal signals buried in additive noise is addressed. Detection is formulated using continuous wavelet transform (CWT) with the custom designed complex cosine wavelet and estimating the presence and frequency of useful signals in the wavelet domain. An adaptive entropy based threshold detector is proposed to detect presence and time localization of useful signal in the transform domain. A simple and pragmatic method of threshold setting as the average of minimum and maximum entropy is

proposed. Application example is focused on detection of useful signal in the harmonic radar system. Simulation results show that the proposed method also allows detection of signals with negative signal-to-noise ratio (SNR). Time-frequency characteristic of the CWT is compared with the short-time Fourier transform (STFT) for the specific mother wavelet. [C69]

#### "A comparison of 1D vertical models of biogenic gas content within a northern peatland from common mid-point and cross-borehole GPR"

Surface-based ground penetrating radar surveys are non-invasive and fast while cross-borehole methods have the potential to be more accurate and repeatable, though time consuming. In order to assess the variation between common mid-point and cross-borehole surveys as a tool for estimating free-phase gas volume in peat soils, we compared the modeled gas content results from surface-based multiple-offset data to down-hole zero-offset profiles. Accuracy of each method was also evaluated using reciprocal measurements and statistical methods. Both common mid-point and cross-borehole methods yielded repeatable measurements and resulted in a similar range of gas content estimates. Variations in gas content estimates ranged from <1%-16%, though the common mid-point measurements underestimated the gas content compared to the cross borehole measurements. [C70]

#### "Qualitative monitoring of the water content evolution in an inhomogeneous soil column"

A microwave imaging problem is considered where a soil column is surrounded by a metallic circular enclosure. This system is presently being developed to demonstrate the potentiality of non-invasive microwave imaging systems for volumetric water content monitoring. The final goal is to retrieve soil moisture information as it is an important parameter for understanding fluid flows in the soil as well as the water uptake by plant roots. Here, we address the qualitative part of the problem with the help of a rapid and rather robust sampling methods: the Linear Sampling Method (LSM) and the MUSIC method. These methods are tested for the following configuration: one water source diffuses in a heterogeneous background. We show that, to a certain extent, the evolution of the soil water content can be qualitatively monitored with the LSM. Moreover, we propose a quick way for detecting the position of the water source inside the soil column. [C71]

#### "Resolution-improved microwave tomography by means of hyperspectral analysis tools"

In microwave tomography, the underlying scattering phenomenon is often linearized to retrieve the associated induced currents maps. These maps are then summed together to provide a good estimation of the target position. This qualitative reconstruction scheme is robust with noise but has a spatial limitation linked to the bandwidth of the radiation operator. We will show that the result of this inverse source problem can be considered in a different way by storing, incidence after incidence, the reconstructed induced current maps. As in hyperspectral imaging, this hypercube can be formalized as several views of the same scene. In hyperspectral imaging, the wavelength is the varying parameter. In harmonic microwave tomography, the incidence angle is the varying parameter. By applying image processing techniques such as principal component analysis, we will show that we can improve the spatial resolution of the qualitative maps. Synthetic results in an aspect-limited configuration will be presented. [C72]

#### "4D GPR tracking of water infiltration in fractured high-porosity limestone"

Three thousand liters of water were infiltrated from a 4 m diameter pond to track flow and transport inside fractured carbonates with 20-40 % porosity. Sixteen time-lapse 3D Ground Penetrating Radar (GPR) surveys with repetition intervals between 2 hrs and 5 days monitored the spreading of the water bulb in the subsurface. Based on local travel time shifts between repeated GPR survey pairs, localized changes of volumetric water content can be related to the processes of wetting, saturation and drainage. Deformation bands consisting of thin subvertical sheets of crushed grains reduce the magnitude of water content changes but enhance flow in sheet parallel direction. This causes an earlier break through across a stratigraphic boundary compared to porous limestone without deformation bands. This experiment shows how time-lapse 3D GPR or 4D GPR can non-invasively track ongoing flow processes in rock-volumes of over 100 m<sup>3</sup>. [C73]

#### "Comparing electromagnetic induction and ground penetrating radar techniques for estimating soil moisture content"

Previous studies have demonstrated the capacity of electromagnetic geophysical methods for estimating soil moisture content. In this study, electromagnetic induction (EMI) and ground-penetrating radar (GPR) measurements were coincidentally collected along a fixed survey line to evaluate temporal changes in apparent electrical conductivity and electromagnetic direct ground wave velocity, respectively; surveys were collected at



three sites (i.e., sand, sandy loam and silt loam) during the course of a complete annual cycle of soil conditions. These two geophysical data sets correlated well during the course of the annual cycle at the silt loam site. Correlation between the two data sets was not as strong at the other two sites, with the sand site showing the lowest correlation values. Further, the geophysical data and gravimetric water content measurements obtained from the upper 0.5 metres indicate higher correlation estimates at the finer grained silt loam site relative to the sand and sandy loam sites. [C74]

### **"Communication in automotive systems: Principles, limits and new trends for vehicles, airplanes and vessels"**

This paper deals mainly with state of the art and next-decade technologies for fiber-optic data buses in automotive applications. Nowadays, fiber-optic data buses in automotive applications are exclusively used in the infotainment domain, MOST (Media Oriented System Transport). Current data rates are in the order of 150 MBit/s. Consequently, the use of LEDs and polymer optical fibers (POF) is sufficient. For higher data rates, also alternative solutions are discussed: The LED as transmitter can be replaced by a vertical surface emitting laser (VCSEL), and the plastic fiber (POF) by a polymer-cladded silica (PCS) fiber. Due to the inherent fact that, as a result, the fiber diameter is reduced, the detector area of the well-known Silicon photo diodes can also be reduced greatly. As a consequence, data rates can be extended into the Gbit/s-region. Furthermore there are different physical layers like optical wireless and radio frequency systems (Radar) to be taken into account. [C75]

### **"LIDAR-based road and road-edge detection"**

In this paper, a LIDAR-based road and road-edge detection method is proposed to identify road regions and road-edges, which is an essential component of autonomous vehicles. LIDAR range data is decomposed into signals in elevation and signals projected on the ground plane. First, the elevation-based signals are processed by filtering techniques to identify the road candidate region, and by pattern recognition techniques to determine whether the candidate region is a road segment. Then, the line representation of the projected signals on the ground plane is identified and compared to a simple road model in the top-down view to determine whether the candidate region is a road segment with its road-edges. The proposed method provides fast processing speed and reliable detection performance of road and road-edge detection. The proposed framework has been verified through the DARPA Urban Challenge to show its robustness and efficiency on the winning entry Boss vehicle. [C76]

### **"3D-segmentation of traffic environments with u/v-disparity supported by radar-given masterpoints"**

3D-segmentation of a traffic scene with two-dimensional row- and column-disparity-histograms, namely u/v-disparities, has become more and more popular for modern stereo-camera-based driver assistance systems due to its fast computation in real-time, few memory requirements and robustness against noisy or intermittent data. In this paper, we present a novel approach to support this pure vision-based method by projecting preprocessed radar-signals directly to u-disparity-space. We called the projection result "masterpoints". This data fusion on low feature-level improved the segmentation process and increased the obstacle detection rate significantly. No assumptions about obstacle-type or -size are needed. Furthermore, the algorithms can be parallelized easily and run in real-time. [C77]

### **"Reliable automotive pre-crash system with out-of-sequence measurement processing"**

In an automotive pre-crash application, it is vital to quickly and accurately estimate the position and velocity of objects in the frontal area of the vehicle. To improve such estimations, several radar sensors are fused to detect objects. Due to their different performance characteristics, their measurements can arrive at the pre-crash processing unit out-of-sequence. This work presents several techniques to integrate measurements into a tracking algorithm that arrive with such an out-of-sequence measurement (OOSM) scenario. A comprehensive complexity analysis of the algorithms is also presented. Most importantly, the algorithms are run on a test vehicle during real crash scenarios. The algorithms' performance is evaluated against reference data from a highly accurate laser scanner. It is shown that using advanced OOSM algorithms in pre-crash systems significantly increases performance and reduces computational cost compared to previous approaches. [C78]

### **"Design of an analog correlator for 22-29GHz UWB vehicular radar system using improved high gain multiplier architecture"**

An analog correlator for ultra-wideband (UWB) vehicular short-range radars (V-SRR) is presented. The correlator is designed for operation at 22-29GHz using the IBM 90nm RFCMOS process. The correlator consists of a multiplier, a Gm-C integrator, and a post amplifier. A novel four-quadrant transconductance multiplier (FQTM) is

proposed to achieve high gain, and a Gm-C integrator is designed to improve the holding time of the correlator. Simulations show that the proposed FQTM has 9.54dB gain increase, and the correlator achieves 2.3ns of holding time and uses 15 mW of power. [C79]

#### "Levy flights for improved Ladar scanning"

A new approach has been used to improve Ladar performance in real time applications based on the use of Levy statistics. This approach speeds up target detection and does not require a full scan of the field of view and the subsequent data processing. This leads to a more efficient Ladar system and opens up the possibility for more real time applications. The approach is to use "Levy flights" instead of traditional techniques, such as Raster and Lissajous scanning, to detect the target in the scene. The performances of these latter techniques and this new approach are compared for a variety of conditions. The simulation results show an enhanced performance when using Levy flights as a scanning technique. [C80]

#### "Evaluation of the influence of a scanning method on the resulting quality of the GPR images"

This paper evaluates the results of experimental 3D Ground Penetrating Radar (GPR) measurements on a physical model with a focus on reinforcement detection. It compares changes in the quality of GPR scans depending on line direction and antenna orientation. This aspect of measurement has an immense effect on the quality of results and on the ability to detect the position of reinforcement inside an investigated concrete structure. [C81]

#### "The use of high speed FIFO chips for implementation of a noise radar"

An ultra wide band spread spectrum radar (a noise radar) can be built using a system that generates two wide band spread spectrum (pseudo-random) waveforms. One waveform is transmitted by the system and one waveform is used to correlate against the received signals. Because of system dispersion, propagation channel dispersion and radar target dispersion, it is often appropriate for the receive correlation waveform to be of a different form than that of the transmitted waveform. Thus a noise radar often needs to be able to generate two different wide band waveforms with controlled differential delay time. This paper will discuss the implementation of such a system using commercially available FIFO microchips. [C82]

#### "Sea-land transitions identification for Coordinate Registration of Over The Horizon Sky-Wave Radar: Numerical model for performance analysis"

We recently proposed a correlation method for the real time Coordinate Registration (CR) of the received echo by Over The Horizon Sky Wave Radar (OTHR-SW) based on a priori knowledge of the positions of the sea-land transitions within the radar coverage area. In this paper we present a simulator that can be used for performance analysis of the proposed CR method in realistic OTHR scenarios. Some simulation result are presented and discussed assuming a single sea-land transition scenario and a geographically invariant vertical electron density profile. [C83]

#### "Detection of subsurface non-metallic objects using stepped frequency continuous wave ground penetrating radar"

In the paper, several aspects of using stepped frequency continuous wave signal in a ground penetrating radar were discussed. Radar was operating in 750-3000 MHz bandwidth, with 563 frequency steps. Test objects included non-metallic object made from wood and plastic, as well as soil with different value of permittivity, all buried at 10-15 cm. [C84]

#### "GPR resolution improvement"

Application of Kirchhoff migration allows to focus images of GPR. Often it is difficult to distinguish close objects. To improve resolution various filtrations can be applied. In this study Inverse filtration with antenna cross talk pulse is used. By this method very close objects can be distinguished. This study shows, that GPR down-range resolution is better, than cross-range resolution. [C85]

#### "A simulation tool for analysis of MTD algorithms employing STAP techniques"

The purpose of this work is development and program realization in MATLAB computational environment of a tool suitable for modeling and evaluating the performance of a pulse doppler MTD (Moving Target Detector) radar with LFM (Linear Frequency Modulated) signals employing STAP (Space Time Adaptive Processing) techniques. It supports numerical design choices with selectable system and signal processing parameters so

that different designs can be traded-off or optimized. This software tool is also able to simulate selectable target, clutter and jamming and thus particular scenarios of interest can be evaluated. The obtained results can be a good base for real time implementation. [C86]

#### "Wind turbines as distorting scattering objects for radar-clutter aspects and visibility"

Wind turbines WT are planned to be constructed often close to radar systems, e.g. air traffic control, air defense, weather radar. The WT are scatterers and may affect the radar operation in-acceptably. The WT are a clutter problem and are not false targets as sometimes treated if the WT are visible to the radar. Clutter characteristics are presented and discussed. [C87]

#### "Effects of iron pipe corrosion on GPR detection"

Many studies into the use of GPR to detect targets assume that the targets are ideal reflectors. In reality most targets have been in the ground for many years and have settled and suffered some contamination or corrosion. Iron pipe in particular can be hard to find with GPR. Some possible corrosion processes suggest that a varying conductivity and permittivity profile may be established around a pipe. The consequences of such corrosion induced profiles are that the radar return may be greatly diminished in the classic look-down GPR mode of operation. The analysis shows that the novel look through GPR mode of operation is affected far less by the corrosion induced profiles. [C88]

#### "Shaping the future of GPR soils research"

Workshops were held at the GPR08 and IWAGPR09 conferences with the intention of developing closer links between GPR users and soil spectroscopy researchers, including developing an improved understanding of the associated research needs. Both workshops were well attended and provided a useful forum that identified elements central to greater interchange of information between the two disciplines. This paper will detail the outcomes of the IWAGPR09 workshop (the GPR08 workshop having been reported on there), providing full information on the perspectives of relevant stakeholders. Included will be details of invited presentation, panel discussion and general discussion sessions. Also, full details of the outcomes of the associated questionnaire, which sought to prioritise the main concerns of stakeholders identified at the GPR08 workshop, will be provided. In conclusion, this paper will consider ways in which those concerns can be addressed, including in terms of standardisation, delivery of research needs, and data sharing. In so doing, the paper is intended to provide GPR and soil spectroscopy stakeholders with an ongoing record of their workshops in order to facilitate debate, discussion and future action. [C89]

#### "Automatic generation of a highly accurate map for driver assistance systems in road construction sites"

Road construction sites often are the reason for traffic jams and accidents due to the reduced road width. Driver assistance systems for these demanding environments highly benefit from a digital representation of the road layout. This digital map includes all important infrastructure elements, such as barriers, temporary road markings and guiding reflector posts. The paper describes the automatic generation of a detailed and highly accurate "Road Work Map" using video camera and laser scanners. [C90]

#### "State estimation of projectiles based on Doppler radar signals using EKF and UKF"

In this paper we compare two methods that lead to distance and velocity estimation of fast moving objects at very close ranges based on Doppler radar signals in real time applications. The first goal of this work has been to find an algorithm and the adjustments to get stable and precise actual state estimations using a low power Doppler radar in field applications. The claim is to reduce the measurement equipment costs. The second step will be an appraisal if this approach can be realized on a real time system. [C91]

#### "Inference of vertical soil moisture distribution using high-frequency CMP and reflection traveltime analysis"

High-frequency ground-penetrating radar (GPR) surveys were used to investigate temporal water content variations in a vertical soil column characterized by stratified clean sand deposits over multiple annual cycles. Reflection profiling and common-midpoint (CMP) soundings were coincidentally performed using 900 MHz antennas across a 2 m intensive monitoring profile. Our ability to identify fixed reflection events along a vertical soil profile permits inference of soil water flux across defined soil intervals in a non-invasive manner. Soil moisture contents were estimated from two-way traveltime measurements between seasonally coherent stratigraphic interfaces in the upper 2-3 m of soil. Interval thicknesses between stratigraphic interfaces were

estimated from normal-moveout velocity analysis of coincidentally collected CMP soundings. Interval traveltimes from reflection profiles were then converted to wave velocity using the interval thickness estimates and a volumetric water content estimate using an appropriate petrophysical relationship. The GPR effectively characterized long (e.g., seasonal trends) and short-period (e.g., distinct wetting events) variations in vertical soil moisture distribution. [C92]

### "Microwave visualization of layered dielectric half-space using range profiling of phase"

A novel method of subsurface radar data processing based on independent determination and representation of amplitude and phase profiles is described. As the phase of the reflected signal depends on dielectric properties of buried target, the proposed technique is suitable for target discrimination. The amplitude and phase information is merged in the common image by governing intensity and color of the image. The amplitude profile of the reflected signal is obtained using a standard inverse Fourier transform of the frequency domain data whereas the phase profile associated with the reflection act at the given depth is derived using a special data processing technique. Some numerical and experimental examples illustrating the method performance are presented. [C93]

### "Motion compensation for landmine detecting vehicle-borne SAR"

In this paper we consider motion compensation of vehicle-borne SAR for landmine detecting, where the motion error is one of the major challenges. Motion compensations algorithms in both azimuth and range direction are discussed. Aiming at vehicle-borne SAR, the motion compensation in range direction utilizes only one 1-axis MEMS accelerometer instead of a 6 Degrees of Freedom inertial sensor, and the motion compensation in azimuth direction can be done only by the knowledge of the vehicle's velocity. The experiment results demonstrate that the motion compensation algorithm together with a standard low-cost accelerometer can yield very useful images for vehicle-borne SAR for landmine detection. [C94]

### "Noise Waveform SAR for 2D and 3D imaging"

Generation of high resolution two-dimensional (2D) and three-dimensional (3D) images in short range applications with the help of coherent radar is the main objective of the paper. Conventional SAR generates 2D image using combination of range compression and 1D aperture synthesis via azimuth (cross-range) compression. The range resolution is limited by the signal spectrum width, while cross-range resolution is defined by the signal wavelength to synthetic aperture length ratio. We suggest applying 2D aperture synthesis that implies cross-range compression technique in both dimensions to generate 2D coherent images. Application of noise waveform with wide enough power spectrum bandwidth enables generation of 3D images of radiotransparent objects, such as trees, bushes, interior of rooms, etc. We present results of modelling of noise waveform radar with 1D and 2D aperture synthesis having various configurations of planar 2D synthetic aperture and results of experiments aimed on SAR imaging with continuous noise waveform and 2D synthetic aperture. [C95]

### "TOA association for handheld UWB radar"

Handheld ultra-wideband radars can be used with advantage during rescue, surveillance or security operations by reason that they enable to track targets moving behind walls. The radar signal processing for that purpose represents a complex process with several processing phases. In this paper, the attention is devoted to the estimation of the correct input data for the localization phase. This is done by applying a new approach that combines the time of arrival (TOA) estimation and the data-association into a single step. The performance of the proposed algorithm is illustrated by processing of real radar signals. Here, the obtained results confirm that the proposed algorithm can provide good, stable and robust TOA estimation including deghosting task solution. [C96]

### "Enhanced monopulse radar tracking using fractional Fourier filtering in the Presence of interference"

Monopulse radars are used to track a target that appears in the look direction beam width. Significant distortion is produced when manmade high power interference (jamming) is introduced to the radar processor through the radar antenna main lobe (main lobe interference) or antenna side lobe (side lobe interference). This leads to errors in the target tracking angles that may cause target mistracking. A new monopulse radar structure is presented in this paper which addresses this problem. This structure is based on the use of optimal Fractional Fourier Transform (FrFT) filtering. The improved performance of the new monopulse radar structure over the traditional monopulse processor is assessed using standard deviation angle estimation error (STDAE) for a range of simulated environments. The proposed system configurations with the optimum FrFT filters is shown to

reduce the interfered signal and to minimize the STDAE for monopulse processors. [C97]

### "Design and implementation of an integrated high resolution imaging ground penetrating radar for water pipeline rehabilitation"

Accurate and timely detection of leaks in water supply pipes is a significant environmental issue. Development of efficient non-invasive methods would lead into significant water saving and prevention of health hazards introduced by water leakage. This paper shows the ability to use a High Resolution Ground Penetrating Imaging Radar (GPIR), to be used as an instrument for water pipeline rehabilitation situations, parallel to the existing industrial equipment. In the framework of the European research initiative WATERPIPE, a Decision Support System (DSS) for the rehabilitation management of the underground water pipelines has been developed, parallel to the implementation of the GPIR. This paper briefly presents the system design, the basic principles of the algorithms' implementation and some indicative results from the initial use of the GPIR system. [C98]

### "UWB radar object recognition for SLAM"

In situations where the environment is filled with dust or smoke, like in many emergency scenarios, UWB Radar is a possible technology to still sense the surrounding and build maps, thus helping firemen and other rescue personal. In this paper, a combination of two algorithms is presented. A basic simultaneous localization and mapping (SLAM) algorithm relying on simple indoor features is used to explore the environment and build a map. This algorithm is augmented by an object-recognition (OR) algorithm that is capable of recognizing and localizing complex shapes. These shapes can be used to improve the map resolution accuracy and resolve ambiguities. First tests using an m-sequence UWB Radar indicate the feasibility of this concept. [C99]

### "Influence of turbulence onto depolarization of signal reflected from hydrometeors"

In this paper the approach to estimate reflected signal depolarization due to turbulence with a single unipolarized antenna is considered. The approach allows to make estimate by character of low frequency envelope change of reflected wave due to changing the depolarization angle of reflected wave. The frequency spectrum of low frequency envelope of reflected wave is also used as a parameter for turbulence intensity estimate. [C100]

### "Simulation of the 24GHz short range, wide band automotive radar"

In this paper we simulated 24 GHz short range, wide band automotive radar. The simulation was done using matlab. The main objective of this work is to reduce traffic accidents and potential danger that faces the driver and the vehicle as a result of the sudden collision. The model consist of six sensors distributed in different sides of the car, these devices provide exact measurement of distance and relative speed of objects in front, beside or behind. Each sensor sends signals to predict, if there is any body around the car to alarm the driver about it. These signals cover distance reach to 30 m. However, if the distance between car & object was less than 2 m the car produce sound like alarm to alert the driver of danger near and the driver can present to take the appropriate decision to avoid collision. [C101]

### "UWB radar for detection and localization of trapped people"

In this paper hardware and software aspects of detection and localization of people by their breathing are discussed. Separately, the problem of non-stationary clutter is considered. All the proposed algorithms are supported by measurement examples. [C102]

### "Quantization effect of the parameter space on the performance of hough detector"

Hough transform is proposed in literature as an effective technique for target detection in search radars. However, this detector has a disadvantage when the received SNR of radar is low. Although the distribution of noise power in the data space is often uniform and all processing cells of this space approximately receive the same power of noise, after transforming these cells to the Hough parameter space, this distribution will not remain uniform. In other words, noise power in some regions of the parameter space is greater than the others. Therefore, false alarm increases in these regions. Selecting a greater threshold to reduce the number of false detections will result a lower probability of detection in lower SNR cases. In this paper, a new quantization method is used for the parameter space which is based on the Maximum Entropy Quantization. It is verified through simulation results that by using this method, the distribution of noise power in this space will become uniform and the average probability of false alarm will be the same for all parameter cells. Also, the performance of Hough detector with a non-uniform quantized parameter space is compared to uniform quantized one through simulation scenarios and it is shown that an improvement of about 2dB results in the required SNR. A method is also introduced to solve the above mentioned problem of the Hough detector for the cases in which the



distribution of noise power in the data space is not known. [C103]

#### "Bistatic Quasi-passive noise SAR experiment"

The paper describes the concept and the preliminary results of bistatic noise SAR experiments carried out at Warsaw University of Technology (WUT). The aim of the experiment was to test the ability of simple system build of Commercial Off-The-Shelf (COTS) components to produce a focused SAR image. The demonstration system is a ground-based one. Instead of using airborne or space-borne antenna system a simple rails wagon with electronically control motor was used to generate the antenna motion. The paper presents the description of the hardware, details of the measurement campaign and the results of signal processing. [C104]

#### "Stepped delay noise radar with high dynamic range"

In the paper we propose and analyze an alternative approach to evaluation of cross correlation function in Noise Radar enabling drastically enhance dynamic range of wideband noise radar with digital signal processing. The approach is based upon digital generation of both sounding and reference signals using fast enough Arbitrary Waveform Generator (AWG) with the required delay and coherent analog reception of the radar returns. Both signals may be up converted to the required carrier frequency. Cross-correlation between the reference and radar returns is to be realized at the carrier frequency using analog mixer and low pass filter. In the paper we describe the new approach and compare it with the conventional one. [C105]

#### "Real-time signal processing in noise radar"

In Noise Radar, coherent reception of scattered signals is performed via estimation of cross-correlation between the sampled reference and radar returns. In the paper we present preliminary results of the design and implementation of FPGA-based correlator for coherent reception of noise radar returns. Parallelization of computations in FPGA gives a hope to realize an algorithm in time domain for evaluation of the cross-correlation function, comparable with the frequency-domain algorithm in efficiency. Moreover, implementation of relay-type correlator algorithm gives a hope to implement evaluation of cross-correlation algorithm which might operate much faster. We present comparison of performance and limitations of different considered designs. [C106]

#### "Analytical sensor data evaluation models for the purpose of evidential inference in electro-magnetic reconnaissance"

This paper describes what particular pieces of information about source should be taken into account to get a reasonable assessment of attribute information based on the sensor data or human originated information. It has been proven that actual sensor weights and hypotheses masses do not change randomly, but they vary in time according to tracked target motion, however not directly to the target position. It is postulated that the knowledge about target position only is insufficient and at least two dynamical coordinates target state vectors are required to reflect the target orientation, which has an influence on actual hypotheses assessment formed, on the basis of the sensor data or visual sightings. [C107]

#### "UWB radar for breath detection"

Using Breath Detection System can be detected breath rate and heart beating rate. System can be used for finding live human being behind nonmetallic obstacles. System was tested and showed good results in Test Polygon. [C108]

#### "94 GHz person scanner with circular aperture as part of a new sensor concept on airports"

In the following paper, a new concept for increasing the airport security is proposed. As a part of this innovative system, a W-band person scanner with a circular aperture for 360° scans has been built up. The usage of the Synthetic Aperture Radar (SAR) principle allows the detection of concealed objects with a resolution of 3mm in azimuth and 3 cm in range direction. [C109]

#### "Using noise modulation in practical radar systems: -Including a comparison with FMCW modulation"

This paper discusses the practical strengths and weaknesses of Noise Radar Techniques when applied to practical radar systems. It will also attempt to distinguish those features which are unique to noise modulation from those which they share with some other modulations. [C110]

### "Development of UWB microwave array radar for concealed weapon detection"

This paper describes two approaches to short-range microwave imaging by means of ultra-wideband (UWB) technology. The first approach deals with synthetic aperture radar (SAR) that employs a transmit-receive antenna pair on mechanical scanner. The second one represents a multiple input multiple output (MIMO) antenna array that scans electronically in the horizontal plane and mechanically, installed on the scanner, in the vertical plane. The mechanical scanning in only one direction reduces significantly the measurement time. Two respective prototypes have been built and compared. Both systems comprise the same 10-18 GHz antennas and multichannel video impulse electronics while the same focusing based on Kirchhoff migration is applied to acquired data for radar imaging. The study has been carried out for an application of concealed weapon detection. [C111]

### "Rank signal detection algorithms based on permutations of partial likelihood ratios"

This paper presents a new approach to design radar signal detection algorithms that are applicable when a priori information is limited. The problem is formulated as testing hypothesis on the kind of density function. A new method that uses ranks of partial likelihood ratios allows to adopt permutation test in a practical algorithm is suggested and researched. This approach gives a possibility to construct the rank detection algorithms, which are sensitive for the signal change for different situations, in the most simple and natural way. The results are useful for applications of signal detection in surveillance and remote sensing radar systems [C112]

### "Designing sparse frequency waveform using iterative algorithm"

Sparse frequency waveform with stopbands sparsely distributed over a larger spectrum band is desired in many radar and communication systems operated in a highly congested spectrum environment. In this paper, a new method for designing sparse frequency waveform with sidelobe constraint is proposed. The basic idea is to construct a penalty function based on both the Power Spectrum Density requirement and the sidelobe requirement and then minimize it through an iterative algorithm. The proposed new method is efficient in computation and can design sparse frequency waveform with large dimensions. Numerical studies with design examples illustrated the efficiency of the proposed method. [C113]

### "On the Range Precision of UWB Radar Sensors"

The precision of radar range measurements depends on certain conditions. For narrow band radar, it is well understood that signal bandwidth and random noise are essential for range resolution and accuracy. The things are more complicated for UWB radar since jitter, antenna behavior, and even the target itself will have influence. This article analyses some aspects distinguishing the UWB radar from the narrowband one with respect to resolution features. [C114]

### "Target localization by the method of joining intersections of the ellipses"

Handheld UWB radar systems used for through wall target localization are usually equipped with one transmitting and two receiving antennas. Sometimes, the radar systems of that kind are not able to localize the target with required accuracy. In order to improve the precision of the target localization, cooperative positioning based on data fusion from two independent radar systems can be used. For this purpose, the novel method of the target localization referred to as the method of joining intersections of the ellipses is introduced in this paper. This method is based on the direct calculation method extended by a decision algorithm. The performance of the proposed method will be compared with the direct calculation method by using real data obtained by measurements by the UWB radar system. [C115]

### "A concept of decentralized fusion of maritime radar targets with multisensor Kalman filter"

The paper presents a concept and an algorithm of multisensor decentralized data fusion for radar tracking of maritime targets. The fusion is performed in the space of Kalman Filter and is done by finding weighted average of single state estimates provided by each of the sensors. The article presents both algorithms-Kalman Filter for tracking objects in single sensor and combining them together to find one fused state vector. Another approach for target tracking, namely neural target tracking is also recalled in the aspect of fusion. Two approaches for data fusion-centralized and decentralized-are stated and the latter is thoroughly examined. The discussion on main problems involved in fusing process in complex radar systems is then presented. This includes coordinates transformation, track association and measurements synchronization. Future plans of including neural tracking in data fusion are presented. The article is ended with summary of the issues pointed out in it. [C116]

### "Tracking of dismounts moving in cross-range using GMTI radar"

The detection of dismounts has a variety of applications, such as tracking remotely for battlefield awareness or at check-points. In this paper we describe the sensitivity of ground moving target indication (GMTI) radar as a dismount moves in cross-range, where the radial velocity is difficult to detect but the micro-Doppler of moving dismounts makes feasible. GMTI target detections are used as a subject moves perpendicular to the beam of the radar. These measurements are compared to vehicular and animal measurements which have minimal micro-Doppler and are much more difficult to detect in their cross-range motion. Ground truth is gathered using video to validate the radar data. We find a detection probability on dismounts in excess of 85% with a low false positive rate of 2%. [C117]

#### "Broadband microwave correlation receiver for noise radar"

The idea of microwave quadrature correlation as well as the block diagram of the microwave broadband correlation receiver are presented in the paper. Measurement results for the function of noise signal correlation are shown. The application of such noise radar solution is presented for precise determination of distance changes and speed of these changes. Conclusions and future plans for the use of presented detection technique in broad-band noise radars close the paper. [C118]

#### "Stepped-frequency noise radar with short switching time and high dynamic range"

Stepped frequency technique is in wide use in radar. Narrow frequency bandwidth of the transmitted signal is an attractive feature of this technique which enables application of rather slow sampling rate. In this case, high-bit and cost effective ADCs are readily availability. However, this technique also has some drawbacks, such as: (a) Ambiguity in range measurements; (b) High level of range side lobes; (c) Low resistance against narrowband coherent interferences. To go around these drawbacks we suggest application of random waveforms with synthesized spectrum. In this case the ensemble of the probing signals realizations can be produced in different ways: (1) Stepped variation of a single frequency signal over a discrete frequency mesh according to a random law, i.e. frequency hopping with random frequency hops; (2) Step-like increase of the central frequency of a narrow band random signal over a discrete mesh of frequencies; (3) Frequency hopping of a narrow band random signal according to a random law, i.e. random frequency hopping of random signals. [C119]

#### "Robust detection in continuous-wave noise radar-experimental results"

In the paper the problem of target detection in continuous-wave noise radar in the presence of impulsive external noise is addressed. If received noise has distribution different than Gaussian, the classical correlation receiver does not provide the optimal results and the performance of the radar is seriously degraded. In order to restore the sensitivity lost due to the impulsive noise a robustification method is proposed. In the method a nonlinear function is applied to the signal in order to remove the outliers. The method is verified on real-life signals. [C120]

#### "Impact of quantization and roundoff errors on the performance of a noise radar correlator"

This paper evaluates the influence of quantization effects on the performance of correlators. The problem is decomposed into two smaller ones, each dealing with difference source of errors (quantization of input signals and finite-precision arithmetics) separately. A discussion of the first type of errors is held on a general level and applicable to any type of correlator. However, roundoff effects depend strongly on details of computations. Therefore, a case study is performed using a fixed-point FFT-based correlator, implemented using LogiCORE IP FFT v. 7.0 engine. [C121]

#### "An application of the content description language XML for modeling of information structures of electronic intelligence system"

XML language is a standard for creating rules of designed data formats. Single documents are mostly defined by XML schemas. As the basis for XML information model one can utilize UML class diagram model. This paper presents an example of application of the content description languages XML and XML Schema standards for modeling of information structures of electronic intelligence system. In particular it is related to transformation UML models to XML schema models using UML Profile and UML mapping rules. [C122]

#### "Comparison of communication signals for passive radar application"

Based on theoretical methods for synthesis of complementary signals briefly below, the authors have developed a new algorithm and software for automated synthesis of Direct sequence complementary codes. The authors propose a numerical method for analysis and comparison of this types synthesize Complementary codes with well-know code sequences like Barker and Z-complementary codes. Build on the autocorrelation and ambiguity

functions of signals, the numerical method estimates the volume of sidelobes separately for each signal. The results are obtained using the specialized software in MATLAB R2007b. [C123]

#### "Higher order statistics sensitivity to radar signal feature"

The paper 1 presents experiments on the use of higher order statistics in the procedures of identification of radar emitters. Studies aimed at testing "sensitivity" of higher order statistics of selected characteristics of the individual sources of emissions. Attention is focused on methods based on analysis of parameters of single-pulse radar emissions. [C124]

#### "Numerical analysis of MIMO radar detection performance under weibull-distributed clutter"

In this paper, the detection performance of a MIMO radar under Weibull distributed clutter is investigated. Numerical results, based on Monte-Carlo simulations, showing the detection performance are provided. The false alarm rate and the detection performance are carried out for different values of the shape parameter of the Weibull distribution and the number of transmit-receive pairs used in the MIMO radar configuration. The obtained results validate the improvements in detection performance available from a MIMO radar against a mono radar. The obtained performances are presented and discussed in this paper. [C125]

#### "Design and implementation of a highly configurable low power robust signal processor for portable ground based "multiple scan rate" surveillance radar"

FPGA based realization of a highly configurable low-power robust signal processor for a portable ground-based multiple scan rates surveillance radar is presented. Portability feature of the radar demands a compact radar system which should be able to detect low flying aerial targets against clutter/interference background. All requirements could be met in a FPGA-based design of a multi-channel signal processor to cater for low peak power large bandwidth waveforms, separate processing for special targets and an embedded softcore processor. Reliable self-test mechanisms-external as well as internal have been built into the signal processor for functional verification of entire radar system. [C126]

#### "Higher order statistics sensitivity to radar signal feature"

The paper 1 presents experiments on the use of higher order statistics in the procedures of identification of radar emitters. Studies aimed at testing "sensitivity" of higher order statistics of selected characteristics of the individual sources of emissions. Attention is focused on methods based on analysis of parameters of single-pulse radar emissions. [C127]

#### "Application of Autoregressive Model for Recognition of Meteorological Objects"

In the paper the results of development of recognition algorithm of meteorological objects by use of autoregressive model with spectrum-correlation signal processing of incoherent radar are presented. The radar hardware and experimental results on estimation of recognition efficiency are described. [C128]

#### "Applying the decision trees to radar targets recognition"

Electronic Support Measure (ESM) systems have been used to passively detect electromagnetic emission from airborne, shipborne, and landborne platforms. The paper describes a method of an automatic radar target recognition based on following principal stages: digital signal processing, feature extraction and selection and applying a combination of decision tree, minimum distance classifier and knowledge base. [C129]

#### "Use of Digital-Television terrestrial (DTV) signals for passive radars"

Purpose of this paper is the description of how to use the Digital-Television terrestrial Video (DTV) stations as a non-cooperative illuminator in bistatic radar. Based on [1] it is shown that the original DTV signal contains random and deterministic components. Analyzing the ambiguity function of the DTV signals, it is found that the deterministic components cause unwanted peaks around the desired peak pertaining to the useful echo thus the target detections is difficult to do and/or false targets can be revealed. In this paper, a new approach to improve the ambiguity function around the useful echo will be proposed. In order to study, evaluate and elaborate the DTV signal, a simulator of the complete signal was performed This paper is organized as follows: next section 1 will describe the obtained outputs of DTV simulator; section (2) will describe the complete block diagram of passive radar using DTV signal, describing the new signal processing approach to improve the ambiguity function; section (3) will describe the obtained results from a realistic scenario; section (4) will present some preliminary results about the multipath effect on the system performance. [C130]

### "Modeled gait variations in human micro-doppler"

Measurement of human motion is important for security applications. One would like to observe humans unobtrusively and without privacy issues, and using radar provides one method to detect abnormal activity without using images. In this paper we focus on modeling the characteristics of human walking parameters in order to determine signature differences that are distinguishable and to determine the variability of normal walking to be compared to armed or loaded walking. We extract micro-Doppler from motion-captured human gait models and verify the models with radar measurements. We then vary the model to determine extent of normal micro-Doppler variation in multiple dimensions of human gait. We also characterize the ability of radar to determine gender and suggest that alternative views to the frontal view may be more discriminative. [C131]

### "Cross ambiguity function analysis of the '8k-mode' DVB-T for passive radar application"

One of non-cooperative illuminators recently considered for passive radar applications is the DVB-T (Digital Video Broadcasting-Terrestrial) station. The thumbtack ambiguity function of the DVB-T signal in addition to being stationary makes such signal a good candidate for such applications. However, certain ambiguities in its ambiguity function necessitates certain issues to be carefully considered when DVB-T signals are to be utilized. In this paper, after studying the origins of these ambiguities, we propose special processing schemes to resolve them. [C132]

### "Data fusion algorithms for sea target tracking using coastal radar model"

The fusion of multiple monitoring systems data is very important, to get a full view of situation in coastal waters. Sea target tracking algorithm is modeled, coast radar system model implemented, multiple ships tracking and detection is tested. [C133]

### "Power analysis of parallel CA-CFAR FPGA design"

We provide a power analysis of a parallel implementation of the Cell Average Constant False Alarm Rate (CA-CFAR) algorithm in reconfigurable hardware, originally proposed by the authors. The design is based on a parallel processing scheme employing extensive data reuse and synchronized sliding windows over the input data sequence. A scalable parallel structure is designed and mapped on Xilinx Virtex II Pro and Altera Stratix I technology. Synthesis and post place and route results from the Xilinx ISE and Quartus II toolset suggest a linear speedup and resource utilization. More specifically, a single CFAR implementation utilizes 1.4% of the VIRTEX II Pro XC2VP30 chip and 2% for Altera EP1S25F780C5 chip, providing a throughput of 974 Mbps. The power consumption of the design is evaluated per technology. The maximum allowed frequencies are determined and compared, as well. [C134]

### "Advantages of the DVB-T signal for passive radar applications"

One of the attractive opportunistic signals for passive radar applications is the DVB-T (Digital Video Broadcasting- Terrestrial) signal. The thumbtack ambiguity function of the DVB-T signal in addition to being stationary makes such signal a good candidate for such applications. In this paper we want to consider its feasibility for this application in more details. So we first examin this signal for the main parts of the the passive radar: Resolving ambiguities before evaluating CAF and direct path intereference rejection, and then consider its processing gain in detecting targets. [C135]

### "SAR image compression based on sparse representation"

The sparse representation based on over-complete dictionary is a new image representation theory. The redundancy of over-complete dictionary can make it effectively to capture the structural characteristics of the image. In this article, we realize SAR image compression based on sparse representation. We only need to store the coefficients of sparse decomposition and the corresponding indices in order to seize the image's information. We adopt a learning method-K-SVD to construct the dictionary. Because the training examples are all from the image itself, the dictionary could be more approximative to the image's structure. The simulation indicates the proposed method is useful for SAR image compression and it outperforms the DCT based JPEG method and the wavelet based EZW and SPIHT method. [C136]

### "K band patch antenna applied in an FMCW radar"

In the paper, a project of a planar patch array antenna in K band intended for application in an FMCW alert radar sensor is shown. The structure of such an antenna consists of 24 Ч 14 patches; the results of simulation and real measurements of the antenna are presented. [C137]



### "Fully solid state radar for vessel traffic services"

A Vessel Traffic Service (VTS) is a maritime traffic monitoring system established by competent authorities. VTS systems use radars to keep track of vessel movements and to assure a safe navigation in the relevant area. For achieving their tasks, these radars must provide high spatial resolution assuring an accurate estimation of the vessel position and the discrimination of close vessels. The traditional VTS radars use magnetron for the final amplification and they are non coherent: high resolution is achieved by short-time high-peak power pulses. The last generation of VTS radars are instead pulse-Doppler and uses fully solid state technology. These new radars can meet the same high resolution with wideband long coded pulses and digital pulse compression; this solution brings to more compact, safe, reliable and flexible radars. In this paper a VTS radar based on a fully solid state architecture -LYRA 50- is presented. This radar is operative and live data can confirm the effectiveness of this solution. [C138]

### "An analysis of through- wall radar based on UWB impulse technique"

Application of through-wall radar requires the ability to detect targets through relatively high-density materials such as concrete, stone and brick. Ultra wideband (UWB) impulse technique is able to penetrate these materials. The capacity to make wall relatively transparent is due to the broad-band nature of the transmitted impulses. First of all, ultra wideband radar system block diagram is depicted. Secondly, the techniques generated UWB impulse and converted from analogue to digital are introduced in detail in the paper. Finally, some simulation results about construction materials such as concrete, stone and brick led to considerable attenuation of electromagnetic waves are analyzed, the analysis presented here can be applied to the implementation of through-wall radar. [C139]

### "Performance analysis in heterogenous environment and implementation on DSP processor of a GOWMAX CFAR detector"

In this paper we present the results of performance analysis of a GOWMAX CFAR detector in non homogenous environment. The study is made for radar targets of Swerling I type embedded in white Gaussian noise. The results are presented in terms of probability of detection and false alarm. Also we expose the algorithm considered and the results obtained for its implementation on DSK 6711 card using a DSP TM320C6711 processor. [C140]

### "One Example of classing and extracting information from GPR images for the archeology"

Ground penetrating radar (GPR) techniques are based on the possibility of sending electromagnetic pulses and registering of the signals back-scattered by the interface between propagation media of different dielectric permittivity. They had been successfully using to examine structures and materials from inside. In the studying, GPR sounding is practically used for detection and reconstruction of the fortification objects. The software for increase of efficiency of archeological researches and reduction of expenses was developed. The GPR method is practically approved for the undersurface environment monitoring for the archeology-interested zones by results of experimental and practical investigations. The estimation of GPR efficiency at monitoring researches, time and expenses on engineering-archeological works were carried out. As a result of researches, contours of fortifications sites are restored. Contours of the stone bases under dwellings are found out and restored. The investigation aims at expounding some preliminary results drawn by specific algorithms for automatically interpreting, classing and extracting explicit information from radar images. [C141]

### "Demonstrator of S band active antenna with T/R modules"

The paper presents realization, mechanical solution and measurements results of transmit and receive systems used in the Demonstrator of S-band Active Antenna. The transmit system contains T/R modules, where individual module supplies half of antenna row of planar array. The 16 antenna rows form in elevation plane cosecant squared type transmit antenna pattern and fin-beam receive antenna pattern. In azimuth plane, pencil-beam radiation pattern is formed. Five elevation positions of the receive beam is electronically set by means of digital phase shifters and attenuators applied in a receive beam forming network. The results of antenna radiation pattern measurements on a tower setup are shown. Additional information about a Control and Diagnostic System is described as well. [C142]

### "Ka-band radar sensor with selection of moving targets for airport surface monitoring"

The paper describes the peculiarities of the technical solutions, operation characteristics and results of the field tests of a prototype of the semiconductor Ka-band radar sensor with a coherent signal processing designed to

be used as a part of the surface monitoring system at airports. The prototype have been developed, fabricated and tested by IRE NASU (Kharkov, Ukraine) and OJSC SPE «Saturn» (Kiev, Ukraine). [C143]

### "Range resolution improvement for low-cost FMCW self-mixing radar"

The principals of range resolution improvement the self-mixing (autodyne) surveillance radar for object detection on distances from ones to hundred meters are considered in this paper. The description of the flow chart, main parameters and results of test bed model examination are given. Application of the self-mixing regime with internal detection allowed to make the construction easier dimensions smaller to increase reliability of the transmitter and the sensor in whole. [C144]

### "Study of double frequency method for remote sensing of liquid precipitations"

The peculiarities of double frequency method for remote sensing liquid precipitation are discussed in monodisperse approximation. The rigorous calculations of electromagnetic waves scattering by dielectric spheres and properties of radar cross section are considered. The limits of method application are discussed as well as results of experiments. [C145]

### "Autodyne system with a single antenna"

A Clapp's single tuned transistor autodyne Oscillator at 1.2 GHz with 12.25 dBm output power is designed and fabricated on a RO4003 substrate with planar capacitors and loop antenna. This small size fuse operates at 7-10 m distance from surface. [C146]

### "Utilizing Adaptive Techniques to Supress Noise In High Frequency Ground Wave Radar"

Reducing noise disturbances in the frequency segment of high frequency (HF) ground wave radar and restraining the sidelobes of strong targets that interfere with the detection of weak targets are the interesting Topic. A new method based on an adaptive techniques that solves these problems is proposed. By changing the working time of the frequency spectrum monitor (FSM), we have shown not only that radar can run in the frequency segments with lower noise disturbances, but also that the noise data produced by FSM can be exploited effectively. There is no correlation between the noise and the useful echo signal, though the correlation between noises over very short time periods is strong, . Exploiting the phenomena, we can adjust system parameters in real-time by adaptive methods to solve the two problems, namely sidelobe disturbance of strong targets and noise distrubance in the frequency segment. [C147]

### "Object recognition in ground surveillance doppler radar by using bispectrum-based time-frequency distributions"

Performance estimation and comparative study of different kinds of time-frequency distributions (TFDs), especially Wigner-Ville distribution (WVD), as well as bispectrum-based distributions: Wigner-bispecrum (WBD), parametric (PBD) and non-parametric (NPBD) obtained by real non-stationary echosignal measuring in ground surveillance Doppler radar are considered for solving moving object recognition and classification problems. Automatic target recognition (ATR) performance has been examined by using information features contained both in the TFDs and cepstral coefficients. Experimental results performed by ground surveillance radar operating in millimeter wavelength for walking human, group of walking humans, bicyclist, vehicles and vegetation clutter show that bispectrum-based approach seems to be attractive tool for ATR systems comparing to the conventional energy-based approaches. [C148]

### "Hydro-meteorological disturbaces influence on radar picture investigation"

Integration and correlation functions used in merchant ship radar nowadays increase radar detection possibility of small objects like recreation and fishery boats. These functions improve safety of maritime navigation considerably. For safety of shipping detection possibility of ship borne radars is important mainly during foggy weather, storm and heavy rain. In the article detection possibilities of FM CW and pulse radars were compared. In order to define them, there were registered, during rain and storm weather, radar video signals of two radars installed in the radar laboratory of Gdynia Maritime University located on shore line near south entrance to the port in Gdynia: pulse radar NSC 34 produced by USA Company Raytheon and CW FM radar CRM-203 produced by Telecommunication Research Institute Ltd. Gdansk Division (PIT Ltd). [C149]

### "Focused algorithms for ground penetrating radar imaging"

The paper describes the simulation results for a ground penetrating SAR radar. As a simulation model of SAR

system the pulse radar with LFM (Linear Frequency Modulation) signal has been applied. The aim of the experiment was to test ability of the SAR system to obtain fully focused image of the underground targets. Simulation results presented in the paper are the first step of realization of the project of GPR (Ground Penetrating Radar) demonstrator which is conducted by Przemysłowy Instytut Telekomunikacji S.A. in cooperation with Warsaw University of Technology. In the next step, the real data measurements are planned to be performed. During measurement campaign the GPR SAR demonstrator mounted on the rails wagon will be used to generate radar motion. [C150]

### "Refraction influence on air target elevation estimation in 3-D radars"

To estimate position of air target the three coordinates are needed: azimuth, range and elevation. The target range and azimuth coordinates errors can be estimated quite precisely. One of source of elevation estimation errors is the refraction of atmosphere (changes of altitude follow changes of refraction index). In results of refraction the false elevation coordinates are obtained. In the paper problem of target elevation estimation using different refraction profiles and usefulness of refraction profiles for medium and long range radar systems, will be also discussed [C151]

### "A novel OFDM based ground penetrating radar"

This paper proposes a novel GPR system based on the Orthogonal Frequency Division Multiplexing (OFDM) technique. The selection of the major system parameters for the OFDM based GPR are considered. An example system configuration is simulated. Target positions can be determined with high accuracy, even when in the presence of noise. Finally, the potential benefits of using OFDM for GPR are presented. [C152]

### "GPR, ERT and CPT data integration for high resolution aquifer modeling"

It is widely accepted that an integrated characterization approach is necessary to define the geometry, internal structure, material distribution and water composition of aquifers. Multiple geophysical and hydrogeological data were measured in the sub-watershed surrounding a former unlined landfill: hydrogeological data in 25 direct push full-screen wells (slug tests, water conductivity, water levels), 21 km of GPR, 5 km of 2D electrical tomography and 30 cone penetration tests (CPT) with soil moisture resistivity (SMR). The 3D data integration in gOcad facilitates data interpretation and provides the basis for a detailed numerical groundwater flow and transport models. [C153]

### "Determination of wall thickness and condition of asbestos cement pipes in sewer rising mains using Surface Penetrating Radar"

Asbestos pipes are commonly used for water and sewage pressure mains. There are very few non-destructive ways of assessing the wall thickness and condition of these Asbestos Cement (AC) pipes. Traditionally, their examination was undertaken by tapping to remove a physical specimen (a 'coupon') of the pipe. This procedure is time consuming, costly and risky. Alternatively, the mains have to be shut down to allow access by CCTV cameras. Advances in Surface Penetrating Radar (SPR) technology in recent years now means that defects in thin walled pipes can now be detected non-destructively from the outside. Selected sewage pipes of different ages, diameters and thicknesses are examined in situ using SPR. In addition, some samples of damaged pipes were examined separately. The main mechanisms for pipe deterioration are from chemical attack at the pipe obvert, and scouring at the pipe invert. The results demonstrate that SPR is an effective method for detecting areas of pipe deterioration and delamination and can detect scour depths as small as 4 mm. The SPR images clearly show a change in the shape and amplitude of the reflected signal from the inner face of the pipe walls and also an apparent increase in material thickness due to retention of water within the pipe wall material in areas affected by chemical attack. Variations are also evident in the signal reflection from the interior of the pipe wall between that at the pipe obvert and that of the side walls. These variations may be attributable to chemical attack and material changes occurring in the AC material. Variations were also observed in the shape and amplitude of reflected signal from the inner face of the pipe invert that are attributed to material loss or scouring at the invert. The SPR image also clearly recorded fluctuating levels of fluid within the pipes during the data collection. Although this makes analysis more of a challenge due to the effect on the reflected signal, this information is very important in locating areas in which pipe failures are more likely to occur through chemical attack and pipe pressure surges. Information on the size of the air pocket present within the pipe and size of the fluctuations can be determined. The signal velocities variations can be detected if the wall thickness is known. Such variations may relate to the moisture content which has been absorbed by the pipe material from the surrounding moist soil and from the pipe contents. The signal velocities determined are less accurate for very thin pipes because of the uncertainty in measuring the thickness interface in the signal. It is evident from the results of cut pipe sections that the SPR provides much better resolution of the inside surface of the pipe when

the pipes are empty. It may be possible to drain the pipes for a short duration to allow the pipes to be scanned in the empty state. This will also eliminate the problem of fluctuating water levels obscuring defects in the pipe obverts. SPR imaging is a quick and effective method which is now available for non-destructively evaluating AC pipes. [C154]

#### "A controlled experiment for water front monitoring using GPR technology"

We use a stepped frequency continuous wave (SFCW) radar and an impulse radar to monitor a water flood experiment in a sand box. The SFCW system operates in the bandwidth from 800 MHz to 2.8 GHz. The impulse radar system is bi-static and works with a central frequency of 1 GHz. The sand box is a meter-scale cylinder partially filled by sand and the water is injected gradually from the bottom of the box. We investigate the ground coupled antenna configuration for both radars. The results demonstrate that the present configuration is useful for monitoring water front movement, but that to have a field application in an oil field environment a quantitative analysis is necessary. This can be done by antenna calibration and inverse modeling. [C155]

#### "Simulation of porosity field using wavelet bayesian inversion of crosswell GPR and log data"

In this paper, we present a novel approach to simulate porosity fields constrained by borehole radar tomography images. The cornerstone of the method is the bayesian analysis of the approximation wavelet coefficients of a petro-physical analogue. The method is tested with a two-dimensional porosity field generated from a digital picture of a real sand deposit. The porosity field is translated into electrical properties and a cross-hole tomography synthetic survey is modeled using a finite-difference modeling algorithm. In parallel, an analogue deposit is created based on the geological knowledge of the area under study. The analogue porosity field is converted into electrical property fields using the same equations as previously. A synthetic GPR tomography is also computed from the latter. Wavelet decomposition of both measured and analogue tomograms and porosity analogue fields is then calculated. Based on the assumption that geophysical data carry only the large-scale information about the geological model, statistical analysis of the approximation coefficients of each variable is carried out. From the measured tomogram approximation coefficients and the cross statistics evaluated on the analogues, the approximation of the real porosity field is inferred using bayesian inference. Finally, based on the geostatistical relationships between wavelet coefficients across the different scales, all the porosity wavelet detail coefficients are simulated using a standard geostatistical simulation algorithm. The wavelet coefficients are then back transformed in the porosity space. The final simulated porosity fields contain the large wavelengths of the measured radar tomogram and the texture of the analogue porosity field. [C156]

#### "GPR of a timber structural element"

GPR of timber structural elements is not yet very common in practise but the technique has the potential for condition evaluation of timber material. In this laboratory investigation, a high frequency (2.3 GHz) radar antenna has been employed for detailed investigation of a historic timber beam from a roof structure. The GPR non-destructive diagnostic of the spruce beam was aimed at obtaining material information with a structural relevance, such as presence of knots, their position and depth, cracks, dimensional variations of geometry and extension of areas of decay. The radar scan was carried out along the beam length. The radargram obtained show very detailed information. [C157]

#### "Detection of granite landmarks in soil with GPR"

In Germany plots of land were often marked with landmarks. They are typically made from granite stones in a defined shape and have been buried closely below the surface. The suitability of GPR for the detection of landmarks has been tested. GPR laboratory experiments in a sandbox under ideal conditions as well as field trials have been carried out. The influence of the water content of soil on the GPR measurements was investigated in laboratory. In these experiments suitable characteristic parameters have been identified to distinguish granite landmarks from other reflectors. [C158]

#### "GPR characterization of rocks buried in the Martian subsoil"

This work presents theoretical and experimental analyses of GPR investigations for the detection of rocks buried in media simulating the Martian soil, in the framework of the "WISDOM" project of ExoMars mission. An experimental set-up has been built consisting in a box filled with a host material and scatterers, scannable with a GPR bistatic antenna. This set-up has also been implemented and studied through an electromagnetic CAD tool. Excellent agreement has been found between the measured and the simulated results on the scattering features, thus providing reliable information on the detectability of rocks in Martian complex subsurface scenarios. [C159]



### "GPR for large-scale estimation of groundwater recharge distribution"

The Gngangara Mound, north of Perth, Western Australia, has been investigated using Ground-Penetrating Radar (GPR). Several hundred line-kilometers of GPR of common offset data have been acquired over an area of approximately 800 km<sup>2</sup>. The acquisition of these datasets was performed at two different center frequencies (50 and 250 MHz) in order to better resolve the complexity of the hydrogeological targets of interest which are water retentive layers found above the water table. These layers impede the recharge of the surficial aquifer and may have important impact on local ecosystems but also on the management of the ground water resource. The data presented here-in demonstrate the successful imaging of the regional water table and of these water retentive layers. For the first time, these data provide insight into the spatial distribution and the continuity of these water retentive layers and provide important information to be included in the flow modeling of the ground water in this region of the world. [C160]

### "GPR reflection and dispersion analysis methods for water content: Multi-year study of GPR estimates and soil core measurements of water content"

A multi-year series of ground penetrating radar (GPR) measurements, complemented by contemporaneous soil cores, were collected at a single location in south-eastern New England, USA. The shallow subsurface is characterized by a 0.9 m thick sandy soil layer which overlies a gravelly-sand layer. Over a number of months, and different soil moisture conditions, 30 common midpoint (CMP) soundings were collected, and on each of the days, co-located soil cores were taken for analysis and comparison with the soil water content from the GPR velocities. GPR velocities were estimated using two independent methods: standard normal moveout (NMO) analysis of reflected traveltimes, and the analysis of frequency-dependent velocity dispersion of shallow GPR waveguide modes. A comparison of GPR estimated water content in the field versus gravimetrically measured water content in the lab provides a site-specific Topp-like empirical basis for predicting soil water conditions from GPR data. Although such site-specific relations may be useful, we find that for our site comparing the results of this study with the conventional Topp relation reconfirms the continuing utility of the latter. [C161]

### "Recent deformation of Quaternary sediments in the northwest Canterbury Plains, New Zealand, as inferred from GPR and seismic data"

A high-resolution seismic reflection survey in the northwest Canterbury Plains, New Zealand, has revealed a network of interconnected faults and folds underneath the seemingly undisturbed flat surface. Known rates of background seismicity in the larger area suggest ongoing deformation in the Plains, despite a lack of convincing surface expression. Ongoing deformation would be seen as disturbance of the uppermost Quaternary sediments. Unfortunately, the resolution of the seismic reflection data falls short in adequately imaging these uppermost sediments. Accordingly, we have collected > 31 kilometers of 50 MHz GPR data to provide complementary images of the uppermost Quaternary sediments. Final images show GPR-facies over the full depth range, indicative of braided river sediments. GPR images together with seismic refraction tomographic images also reveal locations where the youngest Quaternary sediments are deformed. Youngest deformation is observed only where folded Cretaceous-Tertiary and Permian-Triassic units come close to the surface. [C162]

### "Applications of GPR in mineral resource evaluations"

Since the commercialisation of ground penetrating radar (GPR) in the 1970s, radar technology has been employed for niche applications in the mining industry. Although reliant on electrically resistive environments, GPR has gained acceptance in recent years as a standard exploration method for a number of deposit types, ranging from paleochannel delineation to iron ore mapping and kimberlite imaging. Numerous case studies have been published on GPR's applications to specific mineral exploration projects. Provided herein is an overview of commercialised GPR applications for surface mineral resource evaluations, covering examples of alluvial channels, nickel and bauxitic laterites, iron ore deposits, mineral sands, coal, kimberlite and massive sulphide examples. [C163]

### "From Pseudo-3D to full-resolution GPR imaging in archaeology: A complex Roman site in Lugo, Spain"

This case study demonstrates how extra effort on data acquisition can benefit advanced interpretation of 3D GPR data over a complex Roman site situated in a semi-urban area. Two 250 MHz surveys during May 2007 and July 2008 were accomplished after Roman wall remains had been found by chance during soil remove works at Agro da Ponte (Lugo, NW Spain). First campaign covered the whole area by using a pseudo-3D strategy which was only enough for defining the areas of interest and some archaeological features. According to those results, next campaign was focused on a smaller area and based on an ultra-dense grid strategy which eventually revealed full-resolution images of walls, apses and chambers of a Roman villa. [C164]



### "Constructing hydrocarbon reservoir analogues with rapid acquisition long-range GPR"

The bounding surfaces of dunes have long been known to impart significant permeability contrasts to aeolian sequences. The resulting permeability contrasts can affect hydrocarbon flow in subsurface aeolian reservoirs, the impact of which often increases later in the life of a hydrocarbon field. In order to optimally manage petroleum reservoir development, the spatial arrangement of bounding features needs to be incorporated into subsurface models. However, adequate models cannot be obtained directly from the reservoir as no high-resolution imaging techniques exist for the inter-well area. At best, indirect inferences from an ensemble of remote data can be used to broadly constrain major features. However, many spatial parameters remain poorly constrained, particularly in 3D. GPR (Ground Penetrating Radar) has been shown to provide direct 3D imagery of near-surface deposits at a relevant scale and resolution. The resulting models may not be directly transferable to a specific subsurface scenario, but the generic spatial information can be a useful guide to reservoir engineers. Discussed herein is a case study from southern Libya employing the use of a custom long-range rapid-acquisition GPR system to develop 3D volumes over large areas. [C165]

### "Automatic classification of GPR signals"

Ground penetrating radar has been widely used in many areas. However, the processing and interpretation of acquired signals remains a challenging task since it requires experienced users to manage the whole operations. In this paper, we propose an automatic classification system to categorise GPR signals based on magnitude spectrum amplitudes and support vector machines. The system is tested on a real-world GPR data set. The experimental results show that our system can correctly distinguish ground penetrating radar signals reflected by different materials. [C166]

### "Multiscale analysis of 3D GPR data using the continuous wavelet transform"

The main goal of this paper is to extract land topographical information by analyzing the 3D GPR data by the Wavelet Transform Modulus Maxima Lines (WTMM) method. The first objective is to delimitate boundaries of each obstacle, the second is to characterize each one with a special roughness coefficient. Application on real data shows that the proposed tool can enhance the GPR data interpretation. [C167]

### "Georadar Investigation of Graves and Wall Remains in Alacahцык, Central Anatolia"

Archaeological excavations have been conducted in two distinct areas of Alacahцык, located in the northwest of Alaca in the 3orum province and one of the most important Hittite settlements. The subsurface structure of the site was investigated using Ground Penetrating Radar (GPR), which has become widespread in similar studies over the last few years. On the basis of archaeological considerations that graves of princes are thought to be situated in a defined zone (Zone A) and that the possible existence of wall remains are believed to be in another zone (Zone B), we obtained GPR data using the Ramac CU II GPR system with 100 MHz antennae in 2007. In all profiles of the study area, time slices were obtained from the data collected according to the different positions of the transmitter-receiver antennae, some of which were parallel to one another and to the profiles while others were parallel to one another and perpendicular to the profiles. This was performed after the data went through basic processing steps and were mapped to observe what types of structure extensions were involved and to what depths they occurred. The results revealed the presence of strong reflections in GPR sections, which indicated the location of wall remains and some probable princes' graves. Consequently, excavations were recommended where the presence of anomalies was observed. Archaeological finds during the following excavations corroborated the existence of remains where strong reflections were observed in the maps or radargrams. [C168]

### "Different time gain and amplitude-color arranging for ground penetrating radar data: Applied samples"

We introduced a simple time gain approximation with a functioned amplitude-color range to image all amplitudes or only selected amplitudes. First, we reduced ground wave amplitudes near to the maximum reflected / diffracted wave amplitudes of the data. Thus amplitude range of the two dimensional (2D) GPR profile section (radargram) was rescaled by maximum reflected/ diffracted wave amplitude values only for displaying the radargram. Second, we rearranged amplitude-color range with a functional approximation which was very important as well as time gain application to pick events according to the aim of the research. Third, we functioned an opaque range to obtain transparent three dimensional (3D) image of the aligned 2D radargrams. We presented 2D and 3D applications to show our approximations. [C169]

### "Mitigation of RF interference in air-launched 2 GHz GPR antennas"

Air-launched ground penetrating radar (GPR) antennas are useful for analyzing roadway, bridge, and rail-bed construction at very high speeds. The disadvantage of these antennas versus ground-coupled antennas is an increased susceptibility to radio and broadcast interference, predominantly from FM and TV broadcasting as well as cellular telephone base stations. A novel hardware/software interference removal technique has been developed that allows 2 GHz air-launched antennas to operate in the presence of most broadcast interference sources while maintaining data integrity and measurement capability of the interference-free scenario. The performance of the conventional 2 GHz air-launched antenna is compared to the new interference-rejecting system along a 182 km (113 mile) route traversing through the harshest interference-prone highways in the Greater Boston Metropolitan area. It was found that for this data collection route, the amount of unacceptable data was reduced from 18% to 7% with the new technology. It was further found that when only unpredictable interference sources are considered, namely cellular telephones, only 2% of the measurement data is impacted. Finally, a comparison of measurement results during different times of day and antenna polarizations is made, where no improvement was observed in either case. [C170]

### "Localization of buried objects"

The problem of localizing both conductive and dielectric cylinders of arbitrary known radius is dealt with in a two dimensional geometry. A reflection mode multi-frequency multi-monostatic configuration is considered. A linear inversion algorithm for objects embedded into a homogeneous medium is presented, where mutual interaction between the objects is neglected and the problem is formulated in near zone. Here, we examine, by simulated data, the application of the algorithm to subsurface prospection, involving half space geometry, lossy background medium and the presence of multiple scatterers. [C171]

### "A novel detection warning signal creation method for hand-held GPR applications"

In this paper a novel detection warning signal creation method is proposed for pulse Ground Penetrating Radar (GPR) data, especially for small non-metallic targets, in time domain. Background removal is applied to the data through a sliding window scheme and Target Energy Function (TEF) is obtained as correlation summation of consecutive A-scan signals. Then Auxiliary Detection Function (ADF) is defined and a novel automatic Detection Warning Signal (DWS) creation is applied. The proposed method has been tested specifically for a set of small sized dielectric targets which are not easily detectable. The results are promising as full detection performance and zero false alarm rate in original dataset. Moreover, it is obtained that the immunity of the proposed method against noise is very satisfactory. [C172]

### "Textile antenna for the multi-sensor (impulse GPR&EMI) subsurface detection system"

The performance of a planar elliptical dipole textile antenna for the multi-sensor (impulse GPR&EMI) subsurface detection system is investigated. This is a new application of textile antenna. The textile material of antenna does not create an EMI clutter comparing solid Cu material. The antenna characteristics of the proposed antenna in the multi-sensor head are measured and compared with the simulated ones. A buried target into soil, is successfully detected by the multi-sensor system with the usage of the textile antenna in the GPR sensor. [C173]

### "GPR research at the tomb of Zeynel Bey in Hasankeyf ancient city- Southeastern Turkey"

Hasankeyf is a town located along the Tigris River in the Batman Province in Southeastern Turkey. The tomb of Zeynel Bey ruled shortly over Hasankeyf- a rare example of its kind in Anatolia. We measured GPR data inside and around of the tomb of the Zeynel Bey to research buried archaeological remains. We imaged the results with interactive transparent 3D visualization and located archaeological remains with depth range. We determined the base structure and diffraction anomaly groups coming from a cemetery. Excavation in the tomb and around of it encouraged the new 3D image results and found a cemetery in the tomb. [C174]

### "Autonomous FMCW radar survey of Antarctic shear zone"

Radar survey of the Antarctic shear zone was conducted using an ultra-wideband (2-10 GHz) frequency modulated continuous wave (FMCW) radar. The radar was mounted on a sled and pulled by a robot that was specifically designed to operate in a harsh polar environment. Our FMCW radar had good penetration through Antarctic snow and we observed snow stratigraphy to a depth of 20 m. The radar images also revealed multiple crevasses in the shear zone. Our results demonstrate that autonomous survey using high frequency radar is feasible and safe approach for detecting hidden crevasses. [C175]

### "Diagnostic by imaging: 3D GPR investigation of brick masonry and post-tensioned concrete"

In this laboratory study, the comparison of 4 different antenna frequencies (from 1.0 to 2.6 GHz) and radar systems on the same masonry and post-tensioned concrete specimens has served to investigate the precision achievable in imaging cross sections of masonry walls with different brick layouts and of concrete slabs with metal post-tensioning ducts at varying depths. Through high-density 3D data collection and multi-phase post-processing, the work aimed at 2D and 3D data imaging for eased and enhanced diagnosis of structural elements. [C176]

### "Evaluating the practical performance of absorbing boundary conditions (ABC) in higher-order, finite-difference, time-domain (FDTD) GPR modelling"

Finite-difference, time-domain (FDTD) methods are now commonly used for the integrated forward modelling of practical GPR in a wide range of processing, inversion and analysis applications. The wide availability of high-performance computing resources has led to the development of sophisticated, higher-order, 3D models that are able to tackle real-world problems in practical time scales. However, these models are often truncated by computationally inefficient and/or poorly optimised outer absorbing boundary conditions (ABC). In this paper, we evaluate the practical performance of two of the most common techniques; (a) Perfectly Matched Layers (PML) and (b) wave matching boundaries (e.g., Higdon). We show that under certain 3D conditions, the computationally faster, wave matching boundaries can perform as well as the PML techniques and reduce the likelihood of unexpected internal reflections/errors occurring. [C177]

### "TWI in-situ experimental results"

A through-wall imaging problem is tackled by means the linear inverse scattering approach described in. In particular, here, such an approach is validated against experimental data. To this end, a CW-SF ultra-wideband radar system is used to take the measurements and an in situ scattering scenario is considered. [C178]

### "GPR investigation in different archaeological sites in Tuscany. Analysis and comparison of the obtained results"

In the last five years the collaboration between the Laboratory of Landscape Archaeology and Remote Sensing at the University of Siena and the Ground Remote Sensing Lab of the Institute of Technologies Applied to the Cultural Heritage (ITABC-CNR, Rome) produced several site prospection case histories. We focused our attention on a quite limited chronological range between late roman and the early medieval period. Chronology has a direct relationship with material culture and therefore with physical and chemical property of the archaeological stratification and of the context. We should emphasise that most of the site that has been surveyed has been also excavated or at least explored through archaeological sample excavation. The best results has been sistematically achieved through the integration with other methods as magnetic and resistivity systems. The paper will resume our experience, analyzing and comparing the different results, obtained in the sites characterised by late roman and early middle age features. [C179]

### "Mariana (Corsica). Integrating GPR in Roman urban survey"

In 2000 a new phase of archaeological field activities started on the abandoned city site of Mariana, located south of Bastia (NE-Corsica). Within the on-going international research project "Projet Collectif de Recherche: Mariana et la vall e du Golo" a joint team of the Universities of Cassino (I) and Gent (B) studies the topography of the ancient city in a diachronic framework. In this paper we will investigate the crucial role of GPR prospections integrated in a whole set of more traditional methods of non-invasive city survey and stratigraphic excavations. [C180]

### "Integrated geophysical methods for the knowledge of the urban layout of Hierapolis in Phrygia (Turkey)"

The paper concerns the various methods of geophysical prospecting (Ground Penetrating Radar, Magnetometry, Electrical Tomography) applied in Hierapolis of Phrygia, by the Italian Archaeological Mission, during the campaigns of 2007 and 2008. The integration between the different methods (in turn integrated with other exploration methods to the surface, as archaeological surveys and remote sensing from aerial platform and satellite), applied in areas of the city with different geological characteristics, allowed to retrieve important data on the urban layout in areas characterized by thick colluvial and alluvial deposits and in areas where there are extensive limestone formations that have formed recently and have incorporated the ancient remains. [C181]

### "A stepped frequency radar for use on Horizontal Directional Drills"

Horizontal Directional Drills (HDDs) are used to install utilities underground. However, the use of drills in urban environments carries the risk of striking and damaging pre-existing utilities. This paper describes the development and testing of an SFCW radar designed to be installed on the HDD head to determine the presence of obstacles in or nearby the boring path. Transmit and receive antennas are mounted on the drill shaft, behind the drill head spade, and transmit both ahead and to the side of the drill head. Data can be collected at up to 50 traces per second, and all processing and display is done in real time. Special algorithms were developed to enhance the data, and aid in obstacle detection. [C182]

### "Design and full-wave analysis of cavity-backed bow-tie antennas for low-frequency GPR applications"

In this paper, a comprehensive analysis of a novel GPR antenna featuring almost 30: 1 relative bandwidth (55 MHz->1.5GHz), with a maximum antenna size of 40 cm is performed. The antenna transient behavior, near-field radiation properties, and the impact of the ground are analyzed in details. It has been shown that the antenna exhibits reduced and short ringing, low spurious energy emission in the air region, as well as stable circuital and radiation properties over different types of soil. [C183]

### "GPR measurements and FDTD simulations for landmine detection"

Among the technologies used to improve landmine detection, Ground Penetrating Radar (GPR) techniques are being developed and tested jointly by "Sapienza" and "Roma Tre" Universities. Using three-dimensional Finite Difference Time Domain (FDTD) simulations, the electromagnetic field scattered by five different buried objects has been calculated and the solutions have been compared to the measurements obtained by a GPR system on a (1.3 Ч 3.5 Ч 0.5) m3sandbox, located in the Humanitarian Demining Laboratory at Cisterna di Latina, to assess the reliability of the simulations. A combination of pre-calculated FDTD solutions and GPR scans, may make the detection process more accurate. [C184]

### "A GPR imaging algorithm with artifacts suppression"

Based upon an image reconstruction algorithm which has been proposed in medical imaging field, an algorithm termed as Multiply Back Projection (MBP) is firstly used in GPR imaging. This algorithm is similar to the conventional Back Projection (BP) imaging algorithm except for the additional pairing multiplication procedure. In the MBP algorithm, time delays from each synthetic aperture position to a given point in the imaging area are calculated firstly. Then the backscattered signals corresponding to a certain imaging point are searched out through the time delay in each synthetic aperture position. Afterwards, the backscattered signals are multiplied in pair and the products are summed subsequently to form a result point. Experimental results present the superiority of the MBP algorithm over its original counterpart in artifacts suppression, as well as a slightly improvement in image resolution. In the end, theoretic analysis is performed to justify the validity of the MBP algorithm. [C185]

### "EM characterization of resistively loaded printed dipole antennas for GPR applications"

A resistively-loaded printed dipole antenna is modeled and the relevant circuital and radiation properties analyzed thoroughly. The optimal resistive loading is determined in order to achieve a wideband input impedance matching. Then, the electromagnetic characteristics of the individual antenna in terms of radiation efficiency and surface footprint are investigated thoroughly for different types of soil. Emphasis is put on the full-wave analysis of the antenna performance in pair configuration for different Tx-Rx separations and elevations over the ground, as well as on the analysis of the electromagnetic scattering from dielectric and metallic pipes buried at different depths and with different diameters. [C186]

### "Influence of acquisition related uncertainties on ground penetrating radar inversion results"

Ground penetrating radar non-destructive testing requirements become more demanding. In that respect, it is essential to understand how antenna transfer functions and real system dynamic range affect the amount of retrievable information from measurements. This paper examines the confidence level of linear system transfer functions, and practical aspects of noise floor influence on stepped frequency ground penetrating radar. Small inaccuracies in antenna equations directly reflect in Green's function errors. Degradation of the numerical signal resolution was imposed by limiting the data resolution to two-bytes. The capability of the field system to detect thin layering in building materials using numerical modeling studies has been investigated. This would lead to the assumption that the radar model is correct and the only errors are due to inaccuracies in the data and the finite precision determination of the system's linear transfer functions. Systematic errors characterization is partially



possible, limiting uncertainty in the data. A link seems to exist between the data precision and the possibility of information extrapolation for different settings. [C187]

### "Experimental evaluation of the antenna sub-system of the ORFEUS surface GPR"

Within ORFEUS (Optimized Radar for Finding Every Utility in the Street) project a novel antenna system for a SFCW GPR has been developed for detection and location of buried utilities. The antenna system consists of two cavity-backed resistively loaded bow ties and has been designed to cover the frequency range from 100 MHz to 1 GHz with a reasonably high radiation efficiency. The characteristics of the whole system in terms of the impedance matching to the feeding line, radiation level from the individual antenna, parasitic coupling between the transmit and receive antennas and scattering from buried objects have been experimentally investigated in realistic scenarios for different soils. [C188]

### "GPR applications in dense cities: Detection of paleochannels and infilled torrents in Barcelona GPR applications in dense cities"

Barcelona is placed in a basin delimited by the Mediterranean Sea (E), the Collserola Mountains (W) and the rivers Besos (N) and Llobregat (S). The city was built on Quaternary alluvial deposits and on the Tertiary and Palaeozoic materials of the surrounding mountains. The Quaternary materials are preponderant in the plane of the city, presenting a high lateral variability due to the paleochannels and infilled torrents existing between the Sea and the Mountains. The city was built on these heterogeneous materials. In order to prepare a detailed vulnerability map of the Barcelona city, a GPR survey provides information about the position of these geological structures. Results were compared to H/V spectral ratio measurements and soundings. [C189]

### "Monitoring of seasonal influence on spatial distribution of moisture content at a natural Kanto loam site using ground wave of GPR"

Ground penetrating radar (GPR) ground wave was used at a natural Kanto loam (i.e. Andisol) site to examine the influence of seasonal variations on surface soil-moisture content. Kanto loam is a type of volcanic ash soil found widely distributed in Japan. In order to investigate the influence of surface soil conditions on GPR based estimates, the study site was divided in two zones: with and without vegetation. Measurements were conducted at regular intervals during a three month monitoring period. Results indicated that GW was sensitive to the surface soil conditions as well as to seasonal variations. A significant increase in moisture content was observed in the vegetated zone over that of the bare zone during a period of a day after precipitation (i.e. September 1st). It shows that in the vegetated zone moisture in plants themselves, including roots, stems, and leaves, affects GPR measurements, leading to higher moisture content than in the bare zone. However, the influence of vegetation was not found to have a large impact during periods of good weather. The effectiveness of surface soil conditions with seasonal variations on GPR-based moisture content provided a clear insight to agricultural management prospectives. This research confirmed that Kanto loam can be a good GPR site for noninvasive mapping of moisture content regardless of the presence of organic matter, silt, and clay content. [C190]

### "Velocity analysis in the GPR method for loose-zones detection in the river embankments"

Determination of continuous distribution of the loose zones in the river embankment between points of geotechnical investigations is a very important matter for the embankment stability during the flooding. Presently, only non-invasive, geophysical methods can deliver such information. On the basis of numerous tests carried out by the Department of Geophysics at AGH University of Science and Technology in Cracow, the following conclusion may be drawn: zero-offset, reflection GPR profiling very seldom gives positive results at the detection of the loose-zones in the levee. Therefore, another concept of the loose-zones detection, using the GPR method, is presented in the paper. This technique is based on the modified CMP profiling, which allows to prepare a velocity map. Such a map may be used for evaluating of degree of the embankment disintegration. [C191]

### "Petroleum industry techniques yield new insights into 3D GPR data"

We have adapted petroleum industry technologies to 3D GPR datasets from a variety of geological and archaeological settings. Seismic attribute analysis designed for 3D seismic volumes of oil fields has been used to map a 19th century cemetery and to prepare a Roman archaeological site for detailed study by mapping the prior disturbances of the site. Specific seismic attributes that we have successfully applied include connectedness ("geoanomalies"), semblance (or dissimilarity), volume rendering (transparency visualization), and waveform classification. An especially powerful strategy is to use two or more attributes simultaneously via volume rendering that allows multiple visualizations. [C192]



### "Ground penetrating radar (GPR) studies in the Agios Voukolos church, Izmir, Turkey"

The Agios Voukolos church is one of the unique Orthodox constructions in Izmir. Ground penetrating radar (GPR) study was carried out to define the crypts, ossuaries and other subsurface structures under the church. Regular GPR investigations were performed by using a Ramac CU II instrument with 500 MHz center frequency shielded antennae. In addition, two small parts of the Katholikon were measured with 1000 MHz shielded antennas. Data acquired in continuous mode was processed by standard GPR processing steps. The results were given important information about deformation variations (floor cracking and the distortion of architectural elements) and subsurface relics (crypts, ossuaries etc.) inside the church. [C193]

### "Synthetic GPR modelling studies on shallow geological properties and its comparison with the real data"

The synthetic GPR modelling studies are quite important to evaluate the interpretation of shallow geological properties such as faulting, bedding, weathering etc. This study aims to simulate some shallow geological structures by GPR technique. To obtain a successful interpretation, we performed the synthetic modelling studies for paleoseismology, sedimentary and geotechnical problems using different values of electrical properties that affect the radar signals. During the modelling studies, we produced a lot of models for various subsurface conditions. Also, real GPR data was collected on some geological problems. As a result, the combined usage of the real GPR data and synthetic modelling could be contributed the joint interpretation on shallow geological structures. [C194]

### "Analysis of dispersion of pulse signals in underground tunnels using finite-difference time domain and short-time Fourier transform"

The dispersion of pulse signals of a cross borehole radar simulator for tunnel detection was analyzed using FDTD and STFT. Two simulation cases with extremely different dispersion properties were simulated by the FDTD method. In the two cases, the trace path between the transmitter and receiver penetrated an air-filled tunnel perpendicularly and obliquely, respectively. The recorded fields in the cross sectional plane during FDTD computation were decomposed into several frequency components by STFT. By analyzing the propagation behaviors of frequency components, the different dispersion characteristics according to the tunnel's oblique angle variation are visually rendered in detail. [C195]

### "Water table detection by GPR in Sardon, Salamanca, Spain"

GPR was applied in the semi-arid Sardon catchment (Salamanca, Spain) in order to analyze the distribution of the water table depth with a high spatial resolution to serve as input in the parameterization of a hydrological model. We used a pulse radar with a single 200 MHz bowtie antenna combined with a differential GPS and a survey wheel for accurate positioning. Measurements were performed following a series of transects crossing perpendicularly the bed of the Sardon streams, which were dry during that period (September 2009). We measured the depth of the water table in several observation wells to interpret and validate the GPR data. A time domain reflectometry probe was used to estimate the shallow soil dielectric permittivity and corresponding wave propagation velocity along the transects. In general, the water table was visible in the GPR data, with depths ranging from about 2 to 3 meters. [C196]

### "Experimenting with different polarization arrays in a test site"

Four GPR antenna configurations were used to illuminate the subsurface using different polarizations. We conducted field experiments in a test site where different objects were buried at a known depth. Measurements with two co-pole antenna configurations were conducted along crosswise sections. In addition, measurements in a 3D grid were carried out at the top of one of the buried objects using four different antenna configurations. We show preliminary results showing some advantages and limitations of each antenna configuration. [C197]

### "Scattering by a circular cylinder buried beneath a rough surface"

A two-dimensional scattering problem of a circular cylinder buried beneath a rough surface is analyzed through the Cylindrical Wave Approach. The fields scattered by the cylinders are sums of cylindrical waves and the concept of plane-wave spectrum is employed, to take into account reflection and transmission through the interface. The analytical expressions of the fields are derived from the small perturbation method, with a first order approximation for the reflection and transmission coefficients. Results can be obtained both in near-and far-field region, for TE and TM polarization. [C198]

### "A review of geometric issues in GPR prospecting of cylindrical structures in Cultural Heritage applications"

Cultural Heritage diagnostics often involves the application of geophysical methods like ground penetrating radar along non-planar surfaces. Sometimes, as in the investigation of columns with a small radius, the basic assumption underlying the application of conventional processing algorithms (half-space geometry) is strongly violated. Although frequently overlooked, this implies that appropriate algorithms should be developed to take into account the additional data complexity arising from the unusual acquisition setting and exceptional care should be used in interpreting the radargrams. Through numerical and real data examples an in-depth analysis of reflection/diffraction features from buried and above-surface objects is performed in this paper. [C199]

### "GPR resolution in cultural heritage applications"

The non-destructive study of historical buildings, archaeological sites and other Cultural Heritage structures requires high resolution methodologies and a good knowledge of the potential of the different methods. Laboratory measurements provide valuable information about the ability to detect different targets and to determine structural problems, but these data must be compared to the results obtained in real and complex structures. In this work, we present experimental GPR measurements made in order to determine the spatial resolution under laboratory conditions. These results were compared to the data obtained in different GPR surveys applied to Cultural Heritage. The information obtained in drillings, in visual inspections and in old documentation about the historical buildings and archaeological sites is used to determine the resolution in each case. [C200]

### "2D ground-penetrating radar AVO response to a 3D dielectric permittivity anomaly"

To evaluate the amplitude vs offset response of GPR to small distributions of hydrocarbon contamination, I acquired multi-offset 450 MHz GPR data in TE and TM modes over a buried rectangular tank filled with gasoline saturated sand. All dimensions of the tank were less than one wavelength at the characteristic antenna frequency. The permittivity ratio at the moist sand/gasoline sand boundary, estimated by fitting the Fresnel equations to the observed amplitudes and by Brewster's Angle analysis, differed from that obtained through migration velocity analysis by no more than 12%. 2D FDTD modeling reproduced amplitude characteristics for 3 of 4 target/polarization combinations and explained some deviations from the Fresnel curves. Additional deviations may be caused by out-of-plane polarization effects or heterogeneity not included in the 2D model. [C201]

### "Impact of spatial sampling and antenna polarization on 3D GPR fracture detection"

Three-dimensional Ground Penetrating Radar (3D GPR) surveys are needed to reconstruct subsurface fracture networks in terms of strike, dip and interconnectivity. This particular GPR study conducted in the Madonna della Mazza quarry (Italy) compares the impact of a dense acquisition grid versus antenna polarization on the characterization of subvertical fractures. 3D GPR data were acquired using a 250 MHz antenna over a 20 Ч 20 m area with a grid bin size of 5 Ч 5 cm. According to the quarter-wavelength criterion, profile spacing of 5 cm allows to properly sample also the high-frequency content of the signal spectrum. The results demonstrate that, rather than repeated surveys with different antenna orientation but larger profile spacing, a single survey with a regular and highly sampled grid is a preferred approach for high-resolution characterization of three-dimensional fracture networks. [C202]

### "Masonry arch bridges evaluation by means of GPR"

Some masonry arch bridges in Galicia (NW Spain) were surveyed with GPR using 250 and 500 MHz antennas. The main goal of this work was to perform an analysis of historical bridges, obtaining information about filling material homogeneity, detecting inclusions of different materials, defining structural faults -such as internal voids or cracks- and detecting ancient features -as hidden arches or previous profiles of the bridge-. Geometric 3D models of the surveyed bridges obtained with Laser Scanning methods, were used as inputs to create synthetic radargrams through FDTD simulations in order to help GPR data interpretation. [C203]

### "Determination of space behind pre-cast concrete elements in tunnels using GPR"

Many tunnels in Nordic countries are lined with prefabricated concrete elements to protect against frost and leakages. This protective lining is fixed to the rock face in a few points, but when installed renders the rock surface inaccessible, owing to the lack of predesigned inspection hatches. Safety inspections have hitherto consisted of random drilling into the concrete lining. However, such random inspection is both unreliable and expensive. Therefore Ground Penetrating Radar has been introduced in the vault walls to map the contours of

the gap more systematically. Such scanning technology provides satisfactory data, given optimal location of apertures. The scanning technique is therefore extended to the vault roof to pinpoint potential rockfalls. [C204]

#### "Singlehole borehole radar measurement using dipole array antenna fed by coaxial cable"

In this paper, we demonstrate 3-D estimation of reflectors with singlehole borehole radar. We use the dipole array antennas fed by coaxial cables as a directional antenna. Finding the phase shift among the array elements and different depths, we estimate the 3-D positions of the reflector. In the field test site, there is an interface, and we have the preliminary information on the reflector with boring core sampling. The 3-D estimation results with the directional borehole radar were reasonable. [C205]

#### "ORFEUS GPR: a very large bandwidth and high dynamic range CWSF radar"

A very large bandwidth and high dynamic range Continuous Wave Step Frequency (CWSF) Ground Penetrating Radar (GPR) has been developed with the aim to increase the detection capabilities with respect to current systems. In order to achieve this goal, an innovative electronic equipment have been designed and developed. This radar operates with ultra wide bandwidth, ultra fast scan and very high dynamic range capabilities. [C206]

#### "Influence of feed line on DOA estimation with dipole array antenna for directional borehole radar"

In this paper, we investigate the influence of the feed lines on the radar signals in the dipole array antenna fed by coaxial cables for directional borehole radar. In this investigation, we utilize a model of dipole antenna elements in circle near a conducting cylinder in a borehole. The criterion proposed in this paper is calculated, and quantifies the influence of the conducting cylinder. This criterion is tested with the data obtained in experiments in air, and we verified that the criterion represents the influence of the cylinder on the direction estimation. We made the directional borehole radar system with the dipole array antenna, which was fed by semi-rigid cables. With this system, we conducted field experiments in granite. We confirmed that we can estimate direction of arrival after processing the array signals with the band-pass filter, which was designed optimally with the criterion. [C207]

#### "Influence of HE11 mode on direct wave in singlehole borehole radar"

In this paper, we investigate influence of radar sonde eccentricity on a direct wave between a transmitting and a receiving antenna in singlehole borehole radar measurement. According to our calculation, at high frequencies above 200 MHz, guided waves play a vital role in the direct wave. We found that the most important guided wave is HE11mode, which is excited only when the antenna is eccentered in a borehole. We show that this causes artificial noise in the moving average subtraction, which is a common signal processing method used to remove the direct wave. In field experiments in granite, we conducted a special experiment, in which location and rotation of the radar sonde was controlled mechanically. We found the excitation of the HE11mode in high frequencies, when the sonde is eccentered by 1.7 cm in a borehole. These are also predicted in the theoretical analysis. [C208]

#### "Can be GPR technique useful for strength characterization of concrete?"

The possibility of material characterization through the GPR measurements, taking into account the integration with the ultrasonic technique, has been studied and possible relationships between the permittivity of materials and their bulk density are discussed. We present here two different approaches. The first one describes an attempt to correlate the mechanical strength of concrete (as well the ultrasonic velocity) with the permittivity of the material. A series of samples of concrete, characterized by different material properties, were used for georadar and ultrasonic measures, seeking correlations among experimental data. The second approach illustrates the comparison between GPR and ultrasonic techniques to detect anomalies within the concrete. A 3D tomography was performed with ultrasonic and GPR measures on a laboratory model and the data obtained are here compared. [C209]

#### "Imaging for foundation defects using GPR"

During construction of an RCC structure over the reclaimed ground following collapse of old structure, severe difficulties to piling were encountered due to obstruction by debris of previously collapsed RCC structure buried in the foundation regime. Hence GPR profiling along series of lines were carried along several lines at the twin constructions sites. GPR survey revealed presence of RCC debris scattered at a depth of 7-8m along the line of pile foundations. By identifying these scatters, the most likely trouble free locations for piling were demarcated. This facilitated quick solution to foundation obstructions and the erection of new structure was completed without further complications. [C210]

### "Mapping oil leak flow path using Step Frequency Radar: A case study"

Leakage of oil from pipelines in an oil refinery often goes unnoticed until its contamination effect is seen in the polluted ground water. In one such case study in an Indian oil refinery, the oil leak from refinery was traced only when neighbouring villagers complained of contaminated ground water. Since the source of leak was not known nor testing of leaked oil could reveal the source, this oil leak could not be arrested. In order to trace the source of oil leak, the GPR survey was done from the exit point outside the refinery and by following the flow path the survey was progressed inside the refinery campus on different benches. Finally after tracing around 700m long flow path, the particular plant was located from where leakage had originated and it was plugged. This paper describes the intricacies of GPR survey involved in this comprehensive exercise. [C211]

### "Multiple suppression in GPR image for testing back-filled grouting within shield tunnel"

In this study, Ground penetrating radar is used to detect the quality of back-filled grouting in a shield tunnel. A simulated GPR record shows that the steel bars in lining segments usually generate strong scattering and multiples, thereby obscuring the reflections from objects and making it difficult to locate the objects. Various filtering methods for multiple suppression (i.e., predictive deconvolution, f-k multiple attenuation, and Karhunen-Loeve transformation) were applied to the GPR record of a typical grouting defect model. The 'wave field prediction and removal method' is proposed, which involves predicting propagation of the GPR wave field in the lining segment. By subtracting the predicted wave field from the raw GPR record, reflections from objects are precisely abstracted. Application of the method to a synthetic GPR record revealed that the proposed method achieves better results than those obtained using existing methods. [C212]

### "Influence of pipe filling, geometry and antenna polarisation on GPR measurements"

The number of buried cables and pipes in urban areas has increased tremendously over the last decades. As the precise documentation of their layout is often missing, damage occurs frequently during construction work. Consequently there is urgent need for non-destructive methods providing reliable and fast prediction of their location. The Applied Geophysics Section of Frankfurt University takes part in the DETECTINO Project (Hildesheim, Germany) which aims at the development of an all-inclusive utility locating tool. The appraisal of GPR reflection patterns requires profound knowledge of the underlying physical processes. This is best achieved by deploying the locating tool on well defined objects, such as the Frankfurt utility detection test site providing a large variety of pipes and cables in different geotechnical settings. The exact knowledge of the geotechnical data allows the comparison of theoretical and observed data by adequate modelling. In this contribution we present modelled and measured data for pipes with varying depth, diameter and filling, for parallel and perpendicular source polarisation. [C213]

### "A 900MHz shielded bow-tie antenna system for ground penetrating radar"

A back-cavity shielded bow-tie antenna system working at 900MHz center frequency for ground-coupled GPR application is investigated numerically and experimentally in this paper. Bow-tie geometrical structure is modified for a compact design and back-cavity assembly. A layer of absorber is employed to overcome the back reflection by omni-directional radiation pattern of a bow-tie antenna in H-plane, thus increasing the SNR and improve the isolation between T and R antennas as well. The designed antenna system is applied to a prototype GPR system. Tested data shows that the back-cavity shielded antenna works satisfactorily in the 900MHz GPR system. [C214]

### "Processing stepped frequency continuous wave GPR systems to obtain maximum value from archaeological data sets"

Stepped frequency continuous wave ground penetrating radar (GPR) systems allow highly detailed data sets to be collected across a wide bandwidth using multi-element array antenna, such as the 3d-Radar GeoScope system. Although the final presentation of results is similar to time domain systems, the correct processing of the initial frequency domain data acquired in the field is essential to obtain the maximum information from the site. Consideration of the variation of bandwidth with depth, reduction of noise and background subtraction to minimise loss of data quality is required. This paper explores these themes with relation to data from archaeological sites and also considers the data processing challenges presented by high density (e.g. 0.075m Ч 0.075m) multi-hectare surveys. [C215]

### "2D and 3D GPR imaging and characterization of a carbonate hydrocarbon reservoir analogue"

We tested and adapted seismic attributes techniques on a 2-D and 3-D multi frequency GPR dataset to image



the network of stratigraphic joints and fractures, the lithological variations and to characterize the rock mass based on the response to the radar wavefield measured in an abandoned limestone quarry. We applied semi-automatic horizon mapping techniques using manually picked seeds (control points) on selected attributes and automatic extrapolation both on inline and crossline, starting from seed positions. The results were integrated and validated with direct outcrop measures and allowed to image an hydrocarbon reservoir analogue in 3-D up to a depth of over 10m below the topographic surface. [C216]

#### "Disposable stepped-frequency GPR and soil measurement devices"

Some geophysical and geotechnical scientists would wish to non-invasively measure the electromagnetic properties of soils using inexpensive, even disposable, technology. They may even wish to develop inexpensive and compact low-power GPR equipment for such uses as teaching and mitigation of construction risks during excavation. To this end, a heuristic comparison is made between a commercial Vector Network Analyser (VNA) and two very low cost VNAs sourced from the amateur radio community. The results are used to illustrate the potential for technology transfer from amateur communications to the GPR community, in order that a wider range of technologies be available for inexpensive implementation in GPR and soil spectroscopy studies. It will be shown that even very low-cost gain and phase detection semiconductor devices can be used to develop simple GPR and soil measurement systems capable of being used in the field to compliment GPR survey interpretation, as well as for standalone soil monitoring. [C217]

#### "Exploration of geological structures with GPR from helicopter and on the ground in the Letzlinger Heide (Germany)"

Geological structures and the water table were detected by GPR measurements in the sandy area of Letzlinger Heide (Germany). The glacial sediments consist of clayish lenses in sand and the water table is at a depth of more than 40 m. The strong lateral heterogeneity is known from boreholes. Different frequencies from 25 MHz to 200 MHz on the ground were used to detect these structures. The same area was used to test two helicopter-borne GPR systems operating at 30 and 100 MHz center frequency. The results of these measurements are discussed and the capabilities of the methods are shown. [C218]

#### "Sparsity enhanced fast subsurface imaging with GPR"

Sparsity of a signal starts to become very important in many applications. In subsurface imaging, generally potential targets covers a small part of the total subsurface volume to be imaged, thus the targets are spatially sparse. Under this assumption it is shown that the subsurface imaging problem can be formulated as a dictionary selection problem which can be solved quickly using basis pursuit type algorithms compared to previously published convex optimization based methods. Spatial sparsity also indicates that the number of measurements (spatial or time/frequency) that GPR collects can be reduced, decreasing the data acquisition time. Orthogonal matching pursuit algorithm is used for reconstructing sparse subsurface images. Results show that the proposed method reduces time both in data acquisition and processing compared to previous methods with similar performance. [C219]

#### "GPR-PRO: A MATLAB module for GPR data processing"

GPR-Pro, is a flexible and user friendly module developed in MATLAB for processing mainly GPR data. This module can handle the most common GPR data formats. It provides a large number of signal processing algorithms including Principal Component Analysis, FK filtering, data manipulation (matrix algebra), attributes analysis as well as toolboxes for data classification and interpretation. The user can apply different flows on the data keeping always the control of the intermediate and final results. One can easily compare sections and choose the most appropriate flow. [C220]

#### "GPR data time varying deconvolution by kurtosis maximization"

Stochastic and deterministic deconvolution methods encounter difficulties in increasing the temporal resolution of GPR data. Statistical approaches, such as predictive or spiking deconvolution are not effective when the wavelet is non-minimum phase, which is the case for GPR data. Wavelet deconvolution is not successful due to the non-stationarity of the GPR trace. Here, prior deconvolution, we apply a spectral balancing method in t-f domain which efficiently reduces the non-stationarity. The proposed methodology involves correction for phase residuals using the maximum kurtosis method. The effectiveness of this methodology is demonstrated on synthetic and real GPR data. [C221]

#### "Quantitative interpretation of RASCAN holographic radar response from inclined plane reflectors"



### **by a theoretical model"**

Holographic radar of RASCAN type provides an output signal that is amplitude-modulated by the phase variation between transmitted and received signals. In this work RASCAN radar response is compared with a model by several experiments performed in air with a 4GHz probe scanning a planar metallic reflector inclined at different angles. The radar response shows a series of dark and light stripes with spacing dependent on signal frequency and velocity, and reflector inclination angle. The model is used to interpret the amplitude variations as a function of probe position. [C222]

### **"Adaptive linear prediction based buried object detection with varying detector height"**

In the GPR underground inspection problem, received GPR signal is notably dependent on the height of the detector head. A great deal of the former research in this area assumes constant detector height, as absence of this constancy will result in undesired change in the returning signal, which will reduce the success of the detection and identification stages. In this study, we propose a buried object detection method which removes the deforming effect of the variable sensor height. In our approach, adaptive one-sided linear prediction is utilized in a specific manner. The proposed algorithm is causal, which makes it convenient for real time buried object detection applications. [C223]

### **"Modified bowtie antenna for GPR applications"**

This paper presents a novel antenna for Ground Penetrating Radar (GPR) applications. It consists of two crossed bowtie antennas loaded with an annular ring. Numerical and experimental results are reported demonstrating that the proposed antenna exhibits both a broadband impedance bandwidth and very good radiation properties. [C224]

### **"The contribution of GPR analysis to knowledge of the cultural heritage in Apulia (southern Italy)"**

The present article describes two examples of GPR studies addressed to gain a better knowledge of cultural heritage sites in Apulia, southern Italy. [C225]

### **"Freshwater ground penetrating radar the significance of seasonal temperature variation"**

Relatively high temperatures cause an increase in molecular motion as a result of weaker hydrogen bonding and a reduction in the tetrahedral geometry which in turn leads to depolarisation. Therefore a reduction in temperature aids the radar efficiency in several ways, increases the dielectric constant, reduces the velocity of the EM wave and reduces the effect of molecular vibration as a result of stronger bonds causing a reduction in depolarisation i.e. more efficient polarisation. [C226]

### **"Background removal from GPR data using Eigenvalues"**

A GPR radargram of an underground scan has reflections not only from the target but many unwanted objects known as clutters. Additionally, the signal is corrupted by the direct wave and coupling effect of the antennas and background noise. In order to successfully extract the target signature, these extra noise effects need to be eliminated. Though the clutters cannot be totally removed from the data, background removal techniques suppress their effect to quite an extent. Usually mean subtraction is used as a background removal technique but the results are just satisfactory and further improvements can be made. In this paper an Eigenvalue based background removal technique in collaboration with mean subtraction is presented. This proposed method decreases the effect of clutters and the output is much more refined. Even though this method takes slightly more time than the traditional background removal methods, the output eliminates major portion of the clutter therefore the segmentation and classification stages in an automated GPR data processing system would be much more efficient hence reducing the overall time consumption for near real time GPR data processing. The method has been implemented on a number of different data sets and the results indicate that the proposed method gives significant improvement in background removal over the existing background removal methods. [C227]

### **"Subsurface sensing at sub-terahertz and terahertz frequencies"**

Development of millimeter and sub-millimeter wavelengths technologies is of great interest lately, especially for application in terahertz imaging due to bringing high resolution. In our paper we consider a tomography approach for obtaining 3-D imaging in frequency range from 100 GHz up to 325 GHz. We applied the method which we developed earlier for low frequency sub-surface tomography, for extremely high frequencies. The considered method may be used for 3D imaging in non-destructive testing. In the paper we present a theoretical model, experimental method and the comparison of results obtained at terahertz and sub-terahertz frequencies. [C228]

### "Salt dome exploration by directional borehole radar wireline service"

3 D borehole radar, a standard logging method? This was the title of the paper, DMT contributed to the GPR conference 2000. Now this question can be answered. Since more than seven years DMT is applying directional borehole wireline services for salt dome exploration up to depths of 2000 m. The salt dome investigations can be carried out in boreholes or caverns. [C229]

### "An ultrawideband time reversal-based RADAR for microwave-range imaging in cluttered media"

This work presents a new RADAR prototype built for the purpose of imaging targets located in a cluttered environment. The system is capable of performing Phase Conjugation experiments in the ultrawideband [2-4] GHz. In addition, applying the D.O.R.T. method to the inter-element matrix allows us to selectively focus onto targets, hence reducing the clutter contribution. We aim to experimentally explore the use of this focusing wave into an inversion algorithm, in order to improve its robustness against noise. Before testing this idea, we show here the first results validating the prototype separately in the frame of selective focusing via the DORT method and of multistatic-multifrequency inversion. [C230]

### "Novel short-time MUSIC in non-linear FMCW GPR signal analysis"

A novel windowed FFT MUSIC (W-MUSIC) algorithm is presented in the context of using ground penetrating radar (GPR) to detect closely spaced targets under noisy conditions. It is seen to give a better indication of targets than stand-alone FFT and MUSIC algorithms. Distorted signals are analysed, and with the MUSIC algorithm the reported target positions suffer high degrees of error, with the FFT the main lobe broadens making it difficult to recognise closely spaced targets. The use of the Short-Time Frequency-Transform (STFT) algorithm is examined. A novel Short-Time MUSIC approach is presented, it can be used to obtain higher time-frequency resolution than STFT method. [C231]

### "GPR Signal processing in frequency domain using Artificial Neural Network for water content prediction in unsaturated subgrade"

Basing on the recent outcomes of an investigation on the water content evaluation from processing the GPR signal in the frequency domain, an accurate model for the prediction of the frequency spectrum of the reflected GPR signal as the moisture content changes is proposed. This method uses an Artificial Neural Network approach. After the training, the ANN is reasonably able to predict the frequency spectrum for a water content in a specific soil (the error in the spectrum generation computed on a validation set, after 105 training epochs, is about or less than 10% for the same soil, if the ANN is used for all kinds of soil the error increases to about 15-20%). Of course this method can be inverted generating with the trained ANN a catalogue of different spectra for different values of the soil water moisture. Using this inverse approach it is possible to predict the water content of a specific soil just comparing the real current spectrum of the reflected GPR signal with the spectra of the catalogue. This method has been successfully tested on experimental data. [C232]

### "Integrated road pavement survey using GPR and LFWD"

Ground Penetrating Radar is frequently used for inspection the road pavement. Many applications are carried out: from pavement's layer thickness estimation, to damage detection and diagnosis, from the evaluation of geotextile effectiveness to the assessment of the bridge decks. Here we propose to integrate GPR survey with the Light Falling Weight Deflectometer. LFWD is a portable instrument that is used for measuring the Young Modulus through the analysis of the propagation of elastic waves in the pavement structure. The point of strength of this approach is that it is possible to correlate geometrical and some physical characteristics, in this case dielectric constant, of pavement layers, extracted from the GPR maps, to the mechanical properties, such as young modulus, measured using LFWD. It is well known that from a GPR stand alone survey is not possible to have directly any information about the mechanical characteristics of the structure. Otherwise, following this integrated method it is possible to reach a more comprehensive description of the road pavement. This diagnostic tool for pavement damage investigations seems absolutely very promising, cost effective and efficient in its implementation. Finally two case studies are presented: the first over about 3000 m of a real pavement the second over an unpaved airport strip. [C233]

### "Wave parameter analysis of dielectric anisotropy in maritime pine timber using GPR"

The dielectric behaviour of timber in an electrical field depends on many factors, and one of the most important is the direction of the fiber. This work analyses the wave parameter variations of the dielectric response of timber according to the direction of an electrical field applied by ground penetrating radar (GPR) with a 1.6 GHz

antenna. Two types of tests were performed on samples of maritime pine timber (*Pinus pinaster* Ait.). After the acquisition process the propagation velocities, amplitudes, and spectra variations were compared for the studied fiber directions. Interesting differences were found between these parameters when the field was propagated in a parallel direction or perpendicularly to the fiber. [C234]

### "Non-destructive technique to investigate an archaeological structure: A GPR survey in the Domus Aurea (Rome, Italy)"

The discovery and touristic fruition of the Domus Aurea (Latin for "Golden House"), and the heavy rain led to the arrival of moisture, starting the slow and inevitable process of decay and collapse. Furthermore, inside the Domus Aurea, there are a lot of parts not yet excavated, attracting a continuous and archaeological interest. In order to properly plan the restoration of this building and detect buried archaeological features, a non-destructive technique, like Ground Penetrating Radar (GPR), is extensively and profitably used for its rapid data collection and its high resolution images of contrasting subsurface structural or archaeological materials. The results show not only the presence of internal lesions and detachments of the wall and vault structure, but also the existence of buried archaeological targets; these preliminary results allow future restoration plans in order to prevent the rapid degradation of this important building. [C235]

### "Real-time object detection using dynamic principal component analysis"

In this work, we contribute to the real-time detection of buried objects, with special emphasis on explosive ones, using the ground penetrating radar (GPR). When the buried objects have explosive substance, the moment of detection becomes vital. Therefore, we start the detection process right after the very first GPR signals begin to return from the buried objects. For this purpose, we adopted the studies focusing on the online process monitoring methods using principal component analysis (PCA), and adapted them to the dynamic conditions of the ground. Different objects with varying dielectric properties are buried in the test environment and used for the evaluation of the proposed method. With the observed results, it is validated that, the proposed method is employable towards the real-time object detection. [C236]

### "Electromagnetic dispersion estimated from multi-offset, ground-penetrating radar"

Exploiting the dispersion of electromagnetic surface waves as a variational indicator for various physical and hydric states of concretes requires an optimization of its extraction techniques. The validation of these techniques in homogeneous materials is fundamental before data processing of concretes at various water and chloride contents, which is the final aim of our research projects. In the first part, this paper proposes a study of one of the extraction techniques of the direct wave dispersion validated by ground penetrating radar measurements carried out in homogeneous materials such as granite and limestone. The second part is devoted to the study of a physical approach allowing to quantify the evolution of dispersion results between waveguide propagation (multiple reflexions in a slab) and dispersive wave propagation (direct wave in a slab). Finally the last part concerns the dispersion sensitivity to the different parameters related to the experimental device, in particular for the calculation uncertainties in low frequencies. The validation of this parametric study was entirely carried out by finite difference time domain simulations. [C237]

### "The effect of coupling on the determination of time zero for radar antennae"

The a priori knowledge of time zero of radar antennae is essential for an accurate GPR data processing. Indeed, an overevaluation of this parameter can induce inaccuracies in the estimation of the physical and geometrical characteristics of auscultated media from delay picking. This paper proposes experimental methodologies to obtain a stable estimation of Time Zero position through a parametric study based on picking of time signals. The experimental processing results are used to evaluate the effect of antennae coupling and the effect of variations in dielectric parameters on the calculation accuracy of the Time Zero position for various configurations of antennae. [C238]

### "On the variants of Jonscher's model for the electromagnetic characterization of concrete"

The objective of this paper is twofold. Firstly, we carry out a comparison on measurements of the dielectric permittivity of concrete among the different variants of Jonscher's model found in the literature. Each of these variants considers only a limited number of parameters (two or three) based on certain material-dependent and/or bandwidth-related simplifying assumptions. Hence, they affect the inherent "universality" of the model by imposing a tradeoff between representability and practicability. This effect becomes more pronounced for concrete mixtures with high moisture content. Secondly, we propose a computationally efficient, two-step procedure for the estimation of the four model parameters. The proposed procedure filters the linear parameters that contribute to the deviation of the model from the frequency power law by employing the Kramers-Krojnig

relations. Therefore, only two parameters need to be estimated numerically, whereas the filtered parameters are estimated in closed form as the solution of a simple linear least-squares problem. All the variants are applied to various concrete mixtures and evaluated by their goodness of fit. The obtained results show that accounting for the whole parameters of the model via the proposed procedure provides the lowest fitting error, and thus enhances the interpretation of data. [C239]

### "Evaluation of concrete water content and other durability indicators by electromagnetic measurements"

In order to use non destructive techniques (NDT) for the survey of reinforced concrete structures, it is important to show their ability to measure the cover concrete characteristics related to durability, in particular the concrete water and chloride contents. For this purpose, tests with two electromagnetic methods (GPR and capacitive probes) and impact echo method were carried out on 81 slabs of 9 different concrete mixes. Concrete porosity was ranging between 12.5 and 18%. Measurements were carried out at five different water contents. A real structure was also tested in situ. The NDT results are compared to concrete performance indicators such as porosity and water content, as well as chloride profiles. The comparisons show the complementarity of the methods to perform a pertinent diagnosis of concrete structures. [C240]

### "Complex permittivity of common minerals and one soil at low water contents"

The complex permittivity of quartz, feldspars, calcite, and non-crystalline gypsum at 4%-7% volumetric water content shows low conductivity and low-frequency dispersion. At similar water contents, montmorillonite, gypsum crystallites, and a desert soil all show unusually strong and broad low-frequency dispersion, and strong attenuation rates above 100 MHz. The desert soil contained 80% quartz, 10% feldspars, and 10% gypsum, with the gypsum appearing as crystallites and crustations on the quartz particles. Despite insignificant salt or clay mineral content, the dispersion and attenuation rates of the soil exceed those of its constituents and are similar to that of montmorillonite, with a rate exceeding 100 dB m<sup>-1</sup> by 1 GHz. We attribute this to a Maxwell-Wagner type of relaxation, likely caused by polarization resulting from surface charge and from the charge separation caused by dielectric and conductivity contrasts between the gypsum and quartz. The conductivity contrasts were likely enhanced by ions dissolved from the gypsum and feldspars into free water within, and water adsorbed on the quartz surfaces. [C241]

### "Investigation of the frequency dependent antenna transfer functions and phase center position for modeling off-ground GPR"

We compared different methods to estimate the phase center of an ultra wideband ground penetrating radar (GPR) horn antenna operating off-ground, namely, (1) extrapolation of peak-to-peak reflection values in the time domain and assuming a fixed phase center, and (2), frequency-domain full-waveform inversion assuming a frequency dependent phase center. For that purpose, we performed radar measurements at different heights above a perfect electrical conductor (PEC). A double ridged horn antenna operating in the frequency range 0.8-5.2 GHz was used. In the limits of the antenna geometry, we observed that antenna modeling results were not significantly affected by the position of the phase center, even when considering frequency dependence. This implies that the transfer function model used to model the antenna inherently accounts for the phase center position. This analysis showed that the proposed antenna model avoids the need for the frequency dependent phase center determination and is valid for any applications where the field measured by the antenna can be considered as coming from a distance larger than the antenna aperture itself, such as for off-ground GPR or telecommunications. [C242]

### "Uncertainty in ground penetrating radar models"

Uncertainty seems an ignored aspect of everyday life of a geophysicist who uses ground penetrating radar and analyses the data beyond direct interpretation methods. Several causes of uncertainty are discussed that can be classified as belonging to uncertainties in the connection of electromagnetic parameters to desired physical parameters of different application domains, or belonging to uncertainties in the input. The input is either the system transmitter, receiver combination and the antennas, or an incident field. Given the state of the community's ability to model three-dimensional data in complicated subsurface configurations and to estimate electromagnetic parameters or other desired parameters using these models in inverse modeling of measured data, it is advocated that these uncertainties are being considered in the modeling efforts to understand how they propagate through the model into the measured data, and in turn how they affect the parameter estimation results. [C243]

### "Symmetry based 3D GPR feature enhancement and extraction"



The efficient analysis of high-resolution 3D GPR data sets is of increasing importance given today's possibilities to acquire large and dense data volumes. In order to reduce data complexity and enhance the features of interest, attribute based analysis, a well-established field in reflection seismology, has received growing interest also in the GPR community. Here, we present a novel GPR attribute called phase symmetry, which is adapted from image processing. We believe that this attribute is well-suited for analyzing 3D GPR data sets. In this study, we introduce the basic concepts of phase symmetry. Using two synthetic examples and comparing phase symmetry to the well-known Canny edge detector, we illustrate that phase symmetry also provides high quality results in the presence of significant noise and smoothly varying anomalies. Using two 3D GPR field examples collected to detect buried utilities and archaeologically relevant features, respectively, demonstrates the applicability of phase symmetry to real GPR data and illustrates that this attribute is an effective tool in order to extract symmetric features embedded within a heterogeneous background. Additionally, we show that phase symmetry can be combined with the similarity attribute to jointly emphasize event symmetry and waveform similarity. [C244]

#### **"Taper-walled linearly tapered slot antenna: A low direct-coupling antenna for subsurface imaging"**

Ground penetrating radars attract attention of many researchers as a new technique to visualize antipersonnel plastic landmines. Previously we proposed a high-density and wideband array that realizes high-resolution and quick imaging. However, the high-density array sometimes suffers from direct coupling among antenna elements, which decreases the performance of the landmine detection. In this paper, we propose a new antenna element employing open slits and tapered aperture to decrease the direct coupling. [C245]

#### **"Preliminary performance of Sub-Surface Radar for the EJSM/Laplace mission"**

The Sub-Surface Radar (SSR) instrument is a core payload for the Jupiter Ganymede Orbiter (JGO) of the EJSM, which is complementary to the Ice Penetrating Radar on board the Jupiter Europa Orbiter (JEO). These instruments work at low frequency (HF/VHF band) and are designed to penetrate the surfaces of icy moons of Jupiter. The paper will present a preliminary performance model aimed to assess the penetration capability of the instrument in different operative conditions and planet's surface characteristics. [C246]

#### **"Influence of soil inhomogeneity on GPR for landmine detection"**

Landmine detection by ground-penetrating radar (GPR) becomes challenging when soil is inhomogeneous. Soil inhomogeneity causes unwanted reflections (clutter) which disturb reflections from landmines. Thorough investigations on the influence of soil inhomogeneity and clutter on GPR are important for the use in demining to assess the performance and ensure the safety of the operation. In order to observe the influence of soil inhomogeneity an irrigation test was carried out and GPR data were collected after the irrigation while soil water content distribution was changing. Correlation length and variability of soil electric properties are determined by geostatistical analysis from GPR data. The theoretical calculation of Mie scattering using the determined parameters is in good agreement with power of clutter extracted from GPR data. Therefore it is demonstrated that scattering by soil inhomogeneity is governed by Mie scattering. [C247]

#### **"Ultra wide band radar reflectometer for density profile measurement of high temperature plasmas"**

Reflectometry is considered to be one of the key diagnostics to measure density profiles or density fluctuations of fusion oriented plasmas. The electromagnetic wave launched into the plasma is reflected at the cutoff density layer of the ordinary (O) mode or the extraordinary (X) mode. The plasma density profile can be obtained by taking the phase difference between the incident wave and the reflected wave. The high resolution analysis method called signal record analysis (SRA) is utilized to calculate the phase difference. Since wide frequency band is needed for the reflectometry to measure wide density profiles, an ultrashort pulse which includes wide frequency component is utilized as a resource. Also, it is noted that the remote control system using super science information network (super-SINET) has been introduced to the present reflectometry system. [C248]

#### **"Aiding of the GPR method by other measurement techniques for liquid contamination detection"**

In the paper the selected results of measurements carried out for detection of two types of liquid contamination are presented. The authors made detection of contamination, which very often leaks to the ground, i.e. the low-conductivity hydrocarbon contamination and the high-conductivity chemical solution. Depending of the site and the type of contamination different measurement techniques were used: the GPR, the atmogeochemical measurement, the laboratory analysis, the resistivity imaging survey and the conductometry. A brief discussion about possibilities of liquid contamination detection using electrical and electromagnetic techniques is presented in the paper. [C249]



### "Using englacial radar attenuation to better diagnose the subglacial environment: A review"

The magnitude of the radar echo returned from beds underneath ice sheets has been used to identify subglacial lakes based on the prediction that wetter and flatter beds have larger reflectivities than dryer and/or rougher beds. Further quantitative diagnosis of the subglacial environment requires accurate correction for englacial dielectric attenuation, which is primarily a function of ice temperature and secondarily a function of ice chemistry. Models show that the attenuation contribution from chemistry (soluble ions) accounts for about one quarter of the attenuation averaged over the full ice thickness at Siple Dome and Vostok in Antarctica. These predictions suggest that a useful initial attenuation estimate across an ice sheet can be obtained simply with ice-temperature modeling. Methods for estimating attenuation from radar data are also reviewed, with an emphasis on the potential pitfalls of individual methods. Some discrepancies exist between attenuation estimated with ice-core data, temperature models, and radar data. We discuss strategies to improve these attenuation estimates. [C250]

### "Admittance inversion of crosshole radar data"

In this paper, a new inversion approach has been proposed using the ratio of two mutually orthogonal components of recorded electric and magnetic fields: apparent admittance. This study aims at the development of a full waveform inversion algorithm in two-dimension (2D) without the precise knowledge of source functions and without any compensations of 3D nature of radar wave propagation. To alleviate local minima problems, we developed a data weighting method based on the data misfits. The developed inversion approach was firstly demonstrated through inverting 2D FDTD simulation data of crosshole radar survey with false source signatures. Further demonstrated was that the numerical data simulated in the 3D space could be inverted by the proposed 2D algorithm with the 2D FDTD forward modeling. All numerical experiments showed that the material property distribution with remarkably high accuracy can be calculated in spite of the lack of the accurate source information and no compensations of the characteristics of radar wave propagation in 3D space. [C251]

### "Results of an experimental radar survey on the Gornergletscher glacier system (Zwillingsgletscher), Valais, Switzerland"

A 775-m 200-MHz GPR traverse was surveyed in July 2009 over a portion of the Zwillingsgletscher branch of the Gornergletscher System, Valais, Switzerland. The survey line was approximately parallel to the glacial flow direction and situated in an area of prominent wave ogive formation. The traverse shows a well-developed pattern of scattering that is strongly folded into apparent troughs and ridges with the ridges commencing at 10-20 m depth. This pattern mimics the expected ogive structure. The origin of the scattering has not yet been confirmed, but is possibly related to an onset of warmer ice or to variations in rock or sediment content. [C252]

### "Ground-Penetrating Radar reflection data sensitivity to van Genuchten parameter variations GPR reflection data sensitivity to van Genuchten parameters"

We are interested in Ground Penetrating Radar (GPR) as a geophysical tool useful for determining the depth of the ground water table (GWT) and for monitoring shallow water infiltration in sandy soils. At hydrostatic equilibrium, the water content distribution in an homogeneous ground from the vadose zone down to the water saturated zone depends on the medium water retention function. A classical way to model retention curve data is to use a van Genuchten continuous model. Using Finite Difference Time Domain simulations, we study the sensitivity of the GPR signal reflected by a van Genuchten type transition to the hydrostatic parameters. We show a power type relationship between the reflected signal amplitude and the slope of the retention curve. Furthermore, for simulating GPR reflection data acquired above a transition from unsaturated to saturated soil, geophysicists often approximate the soil water retention curve by a piece-wise linear model. We test the validity of such an approximation depending on the frequency of the radar signal and the abruptness of the retention curve. We illustrate our results with high resolution GPR data (1600 MHz) acquired above a fluctuating water table in a sand column at the laboratory scale. [C253]

### "Results of an experimental radar survey on the Gornergletscher glacier system (Zwillingsgletscher), Valais, Switzerland"

A 775-m 200-MHz GPR traverse was surveyed in July 2009 over a portion of the Zwillingsgletscher branch of the Gornergletscher System, Valais, Switzerland. The survey line was approximately parallel to the glacial flow direction and situated in an area of prominent wave ogive formation. The traverse shows a well-developed pattern of scattering that is strongly folded into apparent troughs and ridges with the ridges commencing at 10-20 m depth. This pattern mimics the expected ogive structure. The origin of the scattering has not yet been confirmed, but is possibly related to an onset of warmer ice or to variations in rock or sediment content. [C254]

### "Dynamic monitoring of fracture extension in unconsolidated sand specimen by GPR"

We conducted a GPR monitoring to observe the extension of fractures created by hydraulic fracturing. To achieve this monitoring, a measurement system with higher time accuracy and faster data acquisition rate are needed. We designed a VNA (Vector Network Analyzer) measurement system using a Vivaldi array antenna. The VNA measurement system has the time resolution of 1 ps/sample and the data acquisition rate of 0.78 sec/acquisition, where the system dynamic range is about 100 dB. The Vivaldi array antenna has a wide frequency bandwidth of 0.3 MHz~6 GHz. Comparing the actual formation of the fracture and the infiltrated region with the measurement result, we can verify the extension of the fracture indirectly. Also it may be possible to understand the relation between the pressure of the fracturing fluid and the formation of the fracture in real time. [C255]

### "Sedimentary structure of the Nazar  coastal dunes (Portugal)"

The internal structure of coastal dunes located south of Nazare was analyzed using Ground Penetrating Radar. These coastal dunes comprise stabilized dunes, located in the inner part of the dune field, and foredunes, both separated by a dry dune slack. The radargram analysis allowed the identification of five bounding surfaces that define six main aeolian sand units. The Units I, II, III and IV correspond to the progradation of foredunes seaward (NW), while Units V and VI represent the migration of a parabolic dune and a blowout, respectively, to southeast. A strong reflector separating Units I, II and III from Unit V is interpreted as a paleosol, suggesting a break in aeolian sedimentation of unknown duration, but with sufficient time for soil development. The absence of the paleosol over the Unit IV leaves some doubts in relation to its relative age, although it is indicative of the occurrence of an erosive event. Radar stratigraphic analysis provided a relative chronology of units that will be used as a framework for selecting sampling points for future absolute dating and sedimentological studies. [C256]

### "High power variable nanosecond differential pulses generator design for GPR system"

High power variable nanosecond differential pulses generators based on avalanche transistor and Marx Bank are investigated theoretically and experimentally. The circuit employs six avalanche transistors with charging and discharging circuitry for differential pulses generation and step recovery diode, Schottky diode for pulse shaping. The pulse width can be varied from 1ns to 4ns. The pulse amplitude varies from  $\pm 30V@1ns$  pulse width to  $\pm 58V@2ns$  pulse width. The repetition frequency can reach as high as 500kHz. This variable nanosecond differential pulses generator can be used in pulsed GPR system as transmitter and strobe generator in sequential sampling receiver circuit. [C257]

### "Rebars and defects detection by a GPR survey at a L'Aquila school damaged by the earthquake of April 2009"

After the earthquake of L'Aquila (Abruzzo Region, Italy) occurred on the 6th April 2009, Ground Penetrating Radar investigations of public infrastructures were performed in order to provide an early damage assessment about structural elements such as beams and pillars. In particular, here we present the results of a 1500 MHz GPR survey on a cracked beam of a public building of L'Aquila to verify the goodness of a restoration work by means of epoxy resin injections. First a classical processing routine has been performed in order to focus the rebars hyperbolas and possible reflections coming by the injections; a data volume was built and several depth-slices are here presented. The survey allowed to check the rebars geometry and the reliability of the intervention based on the epoxy resin injections. Limitations of the classical data processing approach are a great complication in imaging the scene also due to the risk of introducing subjectiveness elements in the data by the operator and to the poor resolution achieved for the deeper rebar layer. The possibility of repeating the measurements on the opposite face of the beam in order to detect the second rebar layer was here adopted as a solution of the problem; however this way of operating becomes unacceptable during an earthquake post-crisis phase. The possibility of overcoming these drawbacks was offered by the microwave-tomography (MT) technique. The MT technique was first tested by processing one of the collected profiles acquired on the joist and the result confirmed the ability of the technique to achieve good focusing also of the deeper layer of rebars. [C258]

### "Integrated prospecting in the Crypt of the Holy Spirit in Monopoli (Southern Italy)"

In this contribution we show the results obtained in relationship with GPR and ultrasonic investigations carried out in the Crypt of the Holy Spirit in Monopoli. The exploitation of integrated techniques has allowed to have a meaningful insight of the presence of interesting buried anomalies under the floor and has provided important information about the state of preservation of the columns. [C259]

### "Influence of feed line on DOA estimation with dipole array antenna for directional borehole radar"

In this paper, we investigate the influence of the feed lines on the radar signals in the dipole array antenna fed by coaxial cables for directional borehole radar. In this investigation, we utilize a model of dipole antenna elements in circle near a conducting cylinder in a borehole. The criterion proposed in this paper is calculated, and quantifies the influence of the conducting cylinder. This criterion is tested with the data obtained in experiments in air, and we verified that the criterion represents the influence of the cylinder on the direction estimation. We made the directional borehole radar system with the dipole array antenna, which was fed by semi-rigid cables. With this system, we conducted field experiments in granite. We confirmed that we can estimate direction of arrival after processing the array signals with the band-pass filter, which was designed optimally with the criterion. [C260]

### "Mapping thermal tufa deposits using GPR"

Tufa (freshwater calcareous) deposits can provide excellent targets for GPR exploration due to low clay content and low salinity. Widespread tufa deposits occur at the surface and in the shallow subsurface of Heber Valley, an alluvium-filled basin located in the Rocky Mountains of northern Utah (USA). A set of 200-MHz GPR profiles provides an unprecedented view of the internal structure of a tufa mound and its immediately surrounding platform. Our results indicate that features such as unconformities, caverns, disruptions due to voids, and "seismic" stratigraphic on-lap patterns can be mapped at high resolution. These patterns may be used to constrain interpretations of the episodic growth of a tufa system over geologic time. [C261]

### "Deployment of GPR system ALIS for humanitarian demining in Cambodia"

ALIS is a hand-held dual sensor developed by Tohoku University, Japan since 2002. Dual sensor is a general name of sensor for humanitarian demining, which are equipped with metal detector and GPR. ALIS is only one hand-held dual sensor, which can record the sensor position with sensor signals. Therefore, the data can be processed after data acquisition, and can increase the imaging capability. ALIS has been tested in some mine affected countries including Afghanistan (2004), Egypt(2005), Croatia(2006-) and Cambodia(2007-). Mine fields at each country has different conditions and soil types. Therefore tests at the real mine fields are very important. ALIS has detected more than 30 AP-Mines in evaluation test in Cambodia held in 2009. [C262]

### "GPR as an imaging device: Some problems & potential solutions"

Ground Penetrating Radar (GPR) is an invaluable tool in a wide range of applications. In each sphere of activity to which the technology is applied, however, there is a tension between gaining meaningful information and the time and resources committed to data collection, processing and interpretation. In the light of the current world economic crisis, this is not likely to ease. [C263]

### "High-resolution imaging of a vineyard in south of France using ground penetrating radar and electromagnetic induction"

GPR and EMI surveys were carried out in a vineyard in southern France in order to produce high-resolution maps of soil stratigraphy and to retrieve soil hydrogeophysical properties of the different soil layers. The preliminary results presented in this paper show large spatial variations of the vineyard soil properties, which are in accordance with the distribution of the different soil types within the study area. This is particularly observable from soil electrical conductivity data, which show strong spatial correlation with large areas of comparable values delimited by well-defined discontinuities, revealing sharp variations of soil characteristics over short distances. These discontinuities almost systematically correspond to the limits of the vineyard plots, though areas of contrasted soil electrical conductivity values are also found within some plots. Furthermore, the patterns of soil electrical conductivity are in good agreement with soil stratigraphy observed from GPR measurements. Finally, these results also highlighted compaction as a likely explanation to vine vigour problems observed locally in the vineyard. Future work will focus on the full-waveform inversion of GPR and EMI data to retrieve the properties of the different soil layers and to investigate the spatial variation of soil water availability in the study area, and provide on this basis recommendations for the vineyard management. [C264]

### "Full-waveform modeling of ground-coupled GPR antennas for wave propagation in multilayered media: The problem solved?"

We propose a full-waveform approach for modeling time and frequency domain, off-ground and on-ground radars for wave propagation in multilayered media. The radar antennas are modeled using an equivalent set of infinitesimal electric dipoles placed over the antenna aperture. The linear relations between the fields in the

transmission line, the sources, and the backscattered fields over the antenna aperture are expressed in terms of frequency dependent, global reflection and transmission coefficients, which are characteristic to the antenna. The interactions between the antenna and the layered medium are thereby accounted for. Far-field and near-field measurements are used to determine these antenna coefficients. The fields over the antenna aperture are calculated using three-dimensional Green's functions. We validated the approach using measurements with a 900 MHz centre frequency transmitting and receiving antenna situated at different heights above a copper plane. For heights larger than the antenna, a single point source and receiver was sufficient for accurately modeling the radar data. For smaller distances, using six sources and receivers provided remarkably good results. Although some simplifications were made in this paper, the proposed method shows great promise for characterizing multilayered media using full-waveform inversion, with very limited computation time compared to numerical methods. [C265]

#### **"Inversion and sensitivity analysis of GPR data with waveguide dispersion using Markov Chain Monte Carlo simulation"**

GPR data with waveguide dispersion are known to be very difficult to interpret using traditional inversion methods. Recently, an algorithm was developed that inverts dispersive GPR data using dispersion curves. Here we analyze the sensitivity of this algorithm, and determine posterior probability density functions of the inverted parameters using Markov Chain Monte Carlo simulation. This method is especially designed to work well in the presence of measurement and model error, and is applied to measured CMP data assuming a two layered subsurface. Lower frequencies determine the inverted permittivity of the lower halfspace, whereas higher frequencies contain information about the waveguide height and its permittivity. Removing the beginning or end of the dispersion curve significantly increases parameter uncertainty. [C266]

#### **"Imaging the subsurface structure of Planum Boreum with the Mars Reconnaissance Orbiter Shallow Radar"**

We review prior mapping of the subsurface structure of Planum Boreum that was conducted with 2-D sounding data from the Shallow Radar (SHARAD) instrument onboard the Mars Reconnaissance Orbiter (MRO). Widespread reflections from basal and internal interfaces of the north polar layered deposits (NPLD) occur throughout the 1,000,000-km<sup>2</sup> area. A dome-shaped zone of diffuse reflectivity up to ~1 km thick underlies two-thirds of the NPLD. This zone is associated with a basal unit identified in image data as Amazonian sand-rich layered deposits. In other areas, the NPLD base is remarkably flat-lying and co-planar with the exposed surface of the surrounding Vastitas Borealis materials. Within the NPLD, radar-layer packets that extend throughout the deposits have been mapped as five units with a total volume of 821,000 km<sup>3</sup>, exclusive of the basal unit. Application of a 3-D imaging technique commonly used in processing seismic data to the polar grid of 2-D SHARAD observations is expected to yield an improved representation of the subsurface layering geometry and greatly reduce the effects of surface clutter. [C267]

#### **"Detection and classification of landmines using AR modeling of GPR data"**

In this paper we present some results on detection and classification of low metal content anti personnel (AP) landmines using a modified version of the Auto Regressive (AR) modeling algorithm presented in. A statistical distance is computed between the AR coefficients of the measured GPR time signal and the AR coefficients of a reference database (containing the AR models of the mines of interest) and a detection is declared if this distance is below a given threshold. [C268]

#### **"Rail radar-a fast maturing tool for monitoring trackbed"**

Ground Penetrating Radar ('rail radar') technology has long been a focus for railway trackbed maintenance and renewals planning due to its non-destructive nature and its potential to offer significant efficiency savings in trackbed condition monitoring. This paper provides a brief introduction to the two main interpretation techniques (interface reflection and EM scattering) currently used to monitor railway trackbed and identify the causes of anomalous trackbed conditions. A number of survey examples and scenarios are provided and explained in detail. [C269]

#### **"Radar subsurface sounding over the putative frozen sea in Cerberus Palus, Mars"**

The area of Mars known as Cerberus Palus, suspected of harboring a frozen body of water, has been observed by the two subsurface sounding radar MARSIS and SHARAD. SHARAD data reveal subsurface interfaces at depths ranging from ~50 m to ~150 m which could be interpreted as either the bottom of an ice sheet lying over bedrock, or an interface between two lava flows. Echoes have been analyzed to estimate the dielectric



properties of the surface layer, and results favor the interpretation that no ice is present in the area. [C270]

#### "Broadband stripline to microstrip transition with constant impedance field matching section for applications in multilayer planar technologies"

This paper presents a broadband Stripline-to-Microstrip transition with constant impedance section. In the transition the structural parameters of transmission line have been used to provide smooth electromagnetic field matching together with providing unchanged characteristic impedance along transition section. This solution eliminates the necessity of impedance transformer. The transition enables easy access to stripline circuits situated on the internal layers of multilayer structures by use of typical microstrip terminals. The transition has a simple structure for the ease of fabrication with low cost. The measured performance exhibits flat frequency response over broad bandwidth. The insertion loss is less than 0.5 dB and a return loss is better than 25 dB within frequency range 1 GHz to 10 GHz [C271]

#### "AD-ESPRIT for multi-target localization in bistatic MIMO radar system"

In this paper, an ESPRIT-based approach named as AD-ESPRIT is presented to jointly estimate the directions of arrival (DOAs) and directions of departure (DODs) estimation of interesting multi-targets for bistatic MIMO radar system. The proposed method does not need two-dimensional (2-D) or multiple 1-D spectrum peak searching. Thus, the computational complexity of the proposed algorithm is reduced for the direction finding cross localization in bistatic MIMO radar system. Furthermore, the estimated DODs and DOAs is automatically determined. Simulation results are presented to verify the effectiveness of the proposed method. [C272]

#### "Radar resource management in multifunction radar"

In this paper, a multifunction radar system architecture has been introduced. Multifunction radar is a phased array radar system. A phased array radar system can adapt its parameters on a near-instantaneous basis according to the way in which it perceives its operating environments. This allows the combination of function such as tracking, surveillance, and weapon guidance, which were traditionally performed by dedicated individual radars. Multifunction radar has clear advantages of being able to instantaneously and adaptively position and control the beam, but it also brings a new set of challenges. Radar resource management is the problem of how to allocate finite available resources in an optimal way to carry out a chosen mission. [C273]

#### "X-band coupled cavity slow wave structure of the traveling wave tube for airborne application"

The paper describes the design of the conduction cooling X-band coupled cavity traveling wave tube (CC-TWT) based on the Hughes staggered slots slow wave structure (SWS) which was the first tube of this type made in the Wroclaw Division of PIT. A project of LO-700W traveling wave tube required solving various structural and technological problems e.g. effective termination based on loss ceramic buttons at the sever of RF circuits to minimize reflections and to provide proper attenuation. In this paper an approximate method for calculation of the input antenna of coaxial-line, waveguide transition and output waveguide window is also presented. [C274]

#### "Design of an electronically adaptable low-power reference cell for low-cost CMOS processes"

This paper presents the design of a voltage reference cell suitable for low-voltage and low-power applications without the usage of bipolar structures. The respective reference voltage can be trimmed within a certain range to compensate the unavoidable process variations. The chip is designed based on a 0.13  $\mu\text{m}$  CMOS technology. [C275]

#### "Broadband 444 Butler matrix in microstrip multilayer technology designed with the use of three-section directional couplers and phase correction Networks"

A two-octave 444 Butler matrix has been presented, for the first time in multilayer microstrip asymmetric coupledline technology. To achieve two-octave frequency band in terms of amplitude and phase responses a recently developed approach has been used in which multi-section coupled-line directional couplers and Schiffman C-sections are applied. A highperformance three-section coupled-line 3-dB microstrip directional coupler has been utilized as a basic element of the Butler matrix and two compensated microstripline Schiffman C-sections have been designed to provide appropriate differential phase characteristics. A very good performance has been achieved over two-octave frequency band in terms of amplitude and phase responses. The designed network can be easily applied in large microstrip networks as a surface mount element. [C276]

#### "Performance measures of wavelet families on sar images for compression hypothesis"



Synthetic Aperture Radar (SAR) techniques represent a promising alternative compared to traditional surveillance methods. The capabilities of satellite based SAR systems are confirmed and specific data exploitation methods are still to be developed to provide an efficient automatic interpretation of SAR data. The mean of this paper is to analyze and compare a set of wavelet families on ship SAR images. The outcome of this research is to bring out the important features of wavelet transform in compression of SAR images. The wavelet transform provides efficient performance especially in compression ratios, signal to noise ratio and visual quality. Wavelet Transform decomposes the SAR image into function at different resolution levels. The results provided here is a good reference for SAR application developers to choose the wavelet families. Thus the paper concludes that wavelets transform to be rapid, robust and reliable tool for SAR image compression and able to manage heterogeneous views of SAR images, where the conventional approaches may fail. [C277]

#### **"An algorithm of sorting the phased array radar signal based on RST"**

The aim of This paper is to sorting the phased array radar signal. The method is using the radar beams scanning characters of the phased array radar, then proposes an algorithm based on the rough sets theory to sort the signal of phased array radars. From researching on the characters of the phased array radar's beam scanning manners, we can use the PDW received from the receiving equipments as a set of attributes. Through using RST to reduce the attributes of phased array radar signal, we can get the rule of the attributes' nucleus. So we can sort the phased array radar signal from the electromagnet environment from using the rule. Through experiments showed that this method can get a good result and can efficiently sort the phased array radar signal. [C278]

#### **"An effective virtual ESPRIT algorithm for multi-target localization in bistatic MIMO radar system"**

In a bistatic multiple input multiple output (MIMO) radar system, the location of each interesting target can be determined by the direction finding cross localization with the direction-of-departure (DOD) and direction-of-arrival (DOA). In this paper, an effective virtual ESPRIT algorithm is proposed for jointly DOA and DOD estimation in bistatic MIMO radar system. The pairing problem is addressed as well, for jointly DOA and DOD estimation. Simulation results are presented to verify the effectiveness of the proposed method. [C279]

#### **"Fast automatic target detection of large scene SAR image based on parallel computing"**

An automatic target detection algorithm of SAR image based on parallel computing is presented in this paper. The experimental results based on constant false alarm rate detector verify that the algorithm adapts well to the parallel processing system with high performance and parallel efficiency. That means the algorithm has high real time property. [C280]

#### **"Research on availability simulation of Surface-to-Air missile weapon systems"**

A simulation method that uses discrete event simulation for availability evaluation of Surface-to-Air missile weapon systems is presented. The method uses the R&M&S data at subsystem level and the information about system topology to infer the availability information at system level by modeling the operating process of weapon system. The point and interval estimates for system availability were obtained. The example illuminated that the method is effective for availability evaluation of Surface-to-Air missile weapon systems. [C281]

#### **"Design of remote data acquisition system of passenger flow based on GPRS"**

According to acquisition data of passenger flow relay on artificial and transporting of unreal-time, this paper introduces system of acquisition data of passenger flow base on GPRS by infrared transducer and pressure transducer. Elaborate hardware scheme design of embedded microprocessor in ARM7 core, implement transporting data of passenger flow to data terminal base on GPRS in time and exact, it is provided a reliable basis for real-time scheduling in public transportation. [C282]

#### **"AD-MUSIC for jointly DOA and DOD estimation in bistatic MIMO radar system"**

In this paper, a MUSIC-based approach named as AD-MUSIC is presented to jointly estimate the directions of arrival (DOAs) and directions of departure (DODs) estimation for the direction finding cross localization of multi-targets in bistatic MIMO radar system. The MUSIC algorithm for the DOD estimation is referred to as the D-MUSIC algorithm. On the other hand, the A-MUSIC, which estimates the DOA, is introduced as well. The proposed AD-MUSIC combines two one dimensional (1-D) MUSICs along with the spatial beamforming technique to jointly estimate the DOAs and DODs. At the same time, the estimated DOAs and DODs is automatically determined. Simulation results are presented to verify the effectiveness of the proposed method. [C283]

### "Ultra wide band (UWB) transmitter with configurable design for indoor positioning"

This paper introduces a novel system design for indoor position estimation. The designed indoor positioning system is capable of detecting the coordinates of standalone ultra wide band transmitters in interior environment. An effective, but simple impulse generator has also been developed that can be used in such a positioning system. The simple impulse generator contains only three active elements. The highly configurable design methodology and the easy assembling of UWB transmitter contribute to quick evaluation of localisation algorithms. [C284]

### "Session P1: Antennas"

{no data available} [C285]

### "Session P2: CAD, modeling and passive components"

{no data available} [C286]

### "Session P3: Active networks and others"

{no data available} [C287]

### "Session C7: Antennas and microwaves for space applications I"

{no data available} [C288]

### "Session C8: Antennas and microwaves for space applications II"

{no data available} [C289]

### "Session C9: Polarimetric and Doppler Radars"

{no data available} [C290]

### "Session P4: Measurements, wireless and personal communications"

{no data available} [C291]

### "Impulse transmitting photonic antenna for ultra-wideband applications"

This paper presents a new transmitting photonic antenna based on pigtailed fiber-optic photodiode module integrated with bow-tie radiator for UWB pulse generation using a gain-switched laser diode module. [C292]

### "Realization of a transmit system using T/R modules applied in the demonstrator of S band active antenna"

The paper presents realization, mechanical solution and measurements results of a transmit system used in the Demonstrator of S-band Active Antenna. The transmit system contains T/R modules, where individual module supplies half of antenna row of planar array. The 16 antenna rows form cosecant squared radiation antenna pattern. Brief description of the whole transmit path with special attention to T/R modules is provided. The results of antenna pattern measurements on a tower setup are shown. Additional information about Power Supply System and Cooling System are described as well. [C293]

### "Red light-emitting diode degradation and low-frequency noise characteristics"

Comprehensive investigation of AlInGaP red light-emitting diodes (red LEDs) radiating at 625 nm characteristics and physical processes that take place in device structure during aging has been carried out. Analysis of noise characteristics (the emitting-light power and the LED voltage fluctuations and their cross-correlation factor) shows that investigated red LEDs degradation is caused by defects that lead to the non-radiating recombination increase in the active region or its interfaces. Our results have shown that noise characteristics are more sensitive to the formation of such defects in the red LED structure, and to its degradation. [C294]

### "Session P5: Radars"

{no data available} [C295]

## "Title page vol1"

{no data available} [C296]

## "Title page vol2"

{no data available} [C297]

## "2D DOA estimation for coherently distributed source"

In this paper, a novel two-dimensional direction of arrival (2D DOA) estimation method is proposed when coherently distributed source exists. The second-order statistics is formed to estimate the azimuth DOA with integral steering vector expressed as Schur-Hadamard product. And then the elevation DOA is estimated using advantage of the array configuration based on the eigenstructure between the steering matrix and the signal subspace of distributed sources. It has a lower computational complexity without any joint two-dimensional searching. Simulations results are included to demonstrate the performance of the proposed technique. [C298]

## "Based on embedded intelligent vehicle system"

On account of the existing vehicle for using the platform of integration is limited. Besides, computing speed is not fast enough, power-hungry, and the machine's functions are not plentiful. Many of the features which the customer need for the existing car can not be achieved on the basis of machine. With the rapid development of embedded systems applications, this paper designs a chip based on the ARM9 AT91SAM9260 new smart car system. In this design of Intelligent vehicle systems firstly introduces the main features and hardware architecture to achieve, and then analyzes the GPS, GPRS and other modules, the hardware composition and theory, and finally gives the system's software program. [C299]

## "MUSO: An M-learning & University Student Organizer platform"

Mobile devices nowadays are widespread and provide great multimedia capabilities, which make the delivery of mobile learning a more realistic approach since it can provide just in time learning on the move. Currently, students in some universities can watch live lectures or tutorials on their university website after a registration process. Some students who face difficulties in attending their lectures or tutorials due to living in remote areas would like to watch missed lecture/tutorial by downloading lecture/tutorial videos for their mobiles. This paper describes an M-learning and University Student Organizer (MUSO) application which offers solutions to these problems. MUSO is developed using Java 2 Micro Edition (J2ME) which is supported by most available mobile handsets. This application uses the internet through GPRS or WiFi connections. MUSO uses the concept of client-server architecture which gives the ability to have large data sets and decreases the computation processes on the mobile phones. This paper presents a test case for MUSO on a real university. [C300]

## "Intelligent Traffic Management system base on WSN and RFID"

With wireless communication and the speedy development of micro-electro-mechanical system (MEMS), the wireless sensor network (WSN) has aroused enthusiasm in the world. The research of intelligent transportation system base on WSN is a hotspot to solve the traffic problems in recent years. This paper first introduces intelligent transportation system base on RFID and WSN, then discusses the hardware and software design principles of the system. It has produced the wireless long-distance automatic monitor sensor network design realization plan, finally it forecasts the development of intelligent transportation system. Practice shows that the system is characterized by low cost, economic and pragmatic and high reliability. [C301]

## "Comparisons of speckle noise filtering methods on high resolution SAR image"

Numerous image processing methods to suppress the speckle noise in synthetic aperture radar (SAR) have been proposed. There is always a tradeoff between smoothing out speckle and preserving the useful spatial information (i.e. edge, texture). This paper proposed a novel index by integrating the evaluation of both speckle and edge preservation to evaluate the balance of the aforementioned two criteria. Some of the well-known adaptive speckle suppression filters are then compared and evaluated using two high resolution SAR datasets on heterogeneous areas. Experimental result shows that Kuan filter performance better in preserving image sharpness and detail while suppressing noise. [C302]

## "SAR and Landsat ETM+ image fusion using variational model"

Multispectral and synthetic aperture radar (SAR) image fusion is one of the most complex tasks to perform integration of multi-source remotely sensed imagery. Fusion of SAR and optical remote sensing image, with highly complementary characteristics, may contribute to a better understanding of the objects with the imaged scene and finally benefit to application such as precision farming/ agricultural. In this paper, we adopt a variational model to fuse SAR imagery and multispectral imagery. Experimental results on Cosmo-SkyMed SAR and Landsat-7 Enhanced Thematic Mapper Plus (ETM+) satellite images of an urban area, demonstrate accurate spectral preservation, which is indicated by high correlation between original multispectral and fused bands. [C303]

#### **"The realization of precision agriculture monitoring system based on wireless sensor network"**

Based on the analysis of the development of agricultural mechanization, the trend of agricultural service system reform, agricultural environment protection and the development of information technology, it is possible to realize the precision agriculture. This paper designs the agricultural environmental monitoring system based on the wireless sensor network (WSN). The system can real-timely monitor agriculture environmental information, such as the temperature, humidity, and light intensity. This paper introduces the theory of the monitoring system, and discusses the aspect of hardware and software design of the composed modules, network topology, network communication protocol and the present challenges. Experiments show that the node can achieve agricultural environmental information collection and transmission. The system has the feature of compact in frame, light in weight, steady in performance and facilitated in operation. It greatly improves the agricultural production efficiency and automatic level drastically. [C304]

#### **"Decision to avoid ships collision in fog and application"**

Ships officers can't look out by eyes efficiently in dense fog, and radar observing becomes only systemic and efficient aid-navigation method. This thesis analyses ships collision avoidance theory in fog according to radar plotting diagram and relative collision avoidance rules and good seamen skill custom, brings out conclusion of decision to avoid ships collision in fog, supplies reasonable support for auto Avoiding Collision. [C305]

#### **"Extraction of gap and canopy properties using LiDAR and multispectral data for forest microclimate modelling"**

The creation of gaps in forest canopies can dramatically change the microclimate and soil water balance which strongly influences the process of regeneration and biodiversity within forest ecosystems. Hence, understanding the microclimatic conditions in canopy gaps is a prerequisite in developing and improving techniques for forest management and conservation practices. However, information is scarce on how the size and shape of gaps and their spatial distribution affects the microclimate and soil water balance across forest stands. In the present study we investigated the potential for retrieving forest gap and canopy attributes from LiDAR and multispectral sensors in order to provide new opportunities for modelling forest microclimates. A spatially explicit microclimate model (FORGAP-BD) was developed which could be driven using inputs from remote sensing. The model was implemented for a study site in the broadleaved deciduous forest, Eaves Wood, UK in order to quantify the spatio-temporal dynamics of microclimates over an entire forest stand. [C306]

#### **"Characterising Reedbed habitat quality using Leaf-off LiDAR Data"**

The aim of this paper was to investigate the potential of using leaf-off LiDAR data to characterise the quality of reedbed habitats in Leighton moss, North west UK. The correlation between LiDAR derived and ground-measured heights were determined using six selected spatial buffers and the most significant selected. The results indicated that accurate estimates of canopy height were derivable from the first return data, a valuable indicator of reedbed habitat quality. However, the lack of any subsequent returns from reedbeds prevented the extraction of any further biophysical variables. This paper outlines the methodology of deriving suitable height estimates of reeds and the limitations of using leaf-off LiDAR data. [C307]

#### **"Ocean-land segmentation based on active contour model for SAR imagery"**

Ocean-land segmentation is a basis for oceanic targets detection for SAR imagery. The traditional manual segmentation method can acquire a fairly good result, while it is unable to achieve a satisfying efficiency. Thus the manual method is unsuitable for batch processing. Ocean map based land masking method requires a priori information, which restricts its application. This paper presents an automatic active contour model based ocean-land segmentation method for SAR imagery. This method forces the active contour to the real coastline by variation level set. Under the restriction of minimizing a given energy function, the method obtains the final segmentation result when the active contour is overlapped on the coastline. In addition, an optimizing method is proposed to improve its computation efficiency, which makes our segmentation method more applicable. [C308]

### "Research on the spaceborne SAR image processing and feature extraction for ocean fronts detection"

This paper discusses the interaction of short surface waves with shearing and converging current. On the basis of the spectral perturbations caused by the interaction, the influences of the interaction on the ocean surface wave spectral density and gradients are analyzed. A two-scale electromagnetic scattering model explains not only the interaction between short-wave and radar backscatter, but also the interaction between long-wave and radar backscattering. Then SAR imaging mechanism of ocean fronts is derived. In SAR images, the scale of ocean fronts is 2-3 orders larger than that of sea waves. Most of wave information is filtered out by the 2-D spatial spectrum analytics. Then the characteristic information of ocean fronts is extracted by digital image processing technology. Thus, information processing means by which characteristic information of ocean fronts can be extracted from SAR images is constructed. [C309]

### "GISTDA EOC synthetic aperture radar data processing system"

Located in Ladkrabang, Bangkok, The Earth Observation Center (EOC) of the Geo-Informatics and Space Technology Development Agency (GISTDA) is a ground station for receiving, managing, processing and archiving the Earth observation satellites data. The GISTDA EOC has two SAR data processing systems (SDPS) to support data processing from two SAR satellite constellations: RADARSAT and ALOS. This paper provides the overview of both SAR data processing systems including descriptions of the systems, data processing algorithms, architectures and functionality. The paper finally verifies the image quality characteristics of the example SAR data products generated by the two SDPS by comparing with the satellite operating agency's specifications. [C310]

### "Comparison of classical and orthogonal UWB waveforms for radar applications"

In this paper, classical UltraWideband (UWB) waveforms and orthogonal functions (Hermite and Gegenbauer) for radar applications are proposed. The use of this emergent technology in radar applications domains allows the development of compact and low-cost radars with multiple fields of application in daily life. In many classical UWB radar systems, only Gaussian and monocycle pulses are used. UWB waveforms based on orthogonal functions (Hermite and Gegenbauer) are proposed for their good resolution adapted more to radar detection function. Their multiple access capacity due to their orthogonality presents an important advantage of these waveforms. This study proposes to compare these waveforms to Gaussian and monocycle pulses with simulations for short range avoidance collision radar application. [C311]

### "A new SAR image segmentation method based on fusion"

In this paper, a new synthetic aperture radar(SAR) image segmentation approach based on fusion is proposed. The wavelet transform algorithm and morphology reconstruction algorithm fusion technique can preserve more spatial feature and more functional information content, respectively. The new fusion method are adopted 2 SAR images of the same area taken with overexposure and under exposure are used for image processing. Compared with other methods, the experimental results of the proposed method based on image fusion using real SAR images are much better in reservation of information and boundary as well as correctness of original region. [C312]

### "A novel distance-assisted localization algorithm in wireless sensor networks"

In wireless sensor networks, calculation and management of node position is a subject which has a profound theoretical basis and wide range of application. Due to the randomness of sensor network nodes and the dynamic variability of network topology, lots of algorithms can not meet the requirements of positioning accuracy. For this reason, a DV-DScale localization algorithm is proposed in this paper based on distance-assisted and hop quantization. In the algorithm, cumulative distance value is no longer directly used for maximum likelihood estimation to localization, but as scale to amend the straight-line distance between nodes and estimate the position information of nodes. Because of the low resolution of hops, the traditional localization algorithm which is based on hop can only adapt to the isotropic dense networks. The simulation results show that the proposed algorithm effectively ameliorate the positioning accuracy. Even in the case of random distribution of nodes, the algorithm can also get a higher positioning accuracy. [C313]

### "An impact point of shipboard artillery shell calculating system based on DSP and matlab-simulink simulation"

This paper introduces an impact point of shipboard artillery projectile calculating system based on DSP, and



expatiate the system model, mathematical model, working principle and matlab simulation models. Because radar having detected the trajectory of flying artillery projectile, the system calculate the whole trajectory and impact point coordinates, using DSP techniques. The simulation experiment indicate that the feasibility and practicality of the system. [C314]

#### **"Fault diagnosis expert system of artillery radar based on neural network"**

The fault of new type artillery radar is highly complex and correlative. The neural network technology was incorporated into the radar fault diagnosis after the fault features of new type artillery radar and the shortage of the expert diagnosis system were analyzed. There are many difficulties in the process of the servicing for the artillery radar, such as technology level is low, fault diagnosis is difficult. To resolve the problem, a fault diagnosis expert system was realized based on RBF(Radial Basis Function) neural network. The collectivity structure of expert system, structure and function of software were discussed. Accordingly, several key techniques such as the fault diagnosis principle of RBF neural network, knowledge database, reasoning engine were also given in detail. The application results showed that the expert system proved its feasibility and practical, the servicing efficiency and fault diagnosis ability are improved. [C315]

#### **"A despeckling algorithm combining curvelet and wavelet transforms of high resolution SAR images"**

SAR images despeckling is one of the most important research subjects in SAR images processing. Following discussion on the advantage and disadvantage of curvelet and wavelet transforms based SAR images despeckling, an algorithm which combined curvelet and wavelet transforms was proposed for despeckling of high resolution SAR images. Firstly, the curvelet and wavelet were used to denoise the original SAR image, then the related residual image between their results was acquired, which was then denoised through the curvelet transform. Finally the denoised residual image was added to the curvelet denoised image. Experimental results of TerraSAR-X high resolution images indicated that, compared with the Enhanced Lee filter, the Enhanced Frost filter, the wavelet transform based and curvelet transform based methods, the algorithm presented here had well despeckling effect, as well as fine edge-preserving ability. [C316]

#### **"Realization of position selection simulation evaluation system for artillery reconnaissance radar"**

Aiming at improving the position selection limitation of artillery reconnaissance radar by map work and field reconnaissance, Multigen Creator and Vega were adopted as the development platform of visual simulation software, the position selection simulation evaluation system of artillery reconnaissance radar was realized. The structure and function of system, three dimension scene modeling and terrain selection evaluation were discussed. Several key techniques such as improved terrain building algorithm, position evaluation algorithm were given in detail. The results show that the simulation system simulates the position selection operation process of artillery reconnaissance radar livingly and can meet the requirement of real time simulation. [C317]

#### **"A novel design of water environment monitoring system based on WSN"**

The importance of maintaining good water environment highlights the increasing need for advanced technologies. This paper proposes a novel design of water environment monitoring system based on wireless sensor networks (WSN). The system consists of three parts: sensor nodes; sink nodes and data monitoring center. The sensor nodes can be constructed with arbitrary parameter or multi-parameter sensor modules such as PH, dissolved oxygen (DO), conductivity and temperature. The measurement capacity ranges from 0 to 14 on PH value; from 0~20 mg/L on DO; from 0~2 S/cm on conductivity. The sink nodes communicate with the local or remote data monitoring center by RS232 or 3 G/GPRS. The performance shows the system can be effectively applied to some water area such as aquiculture, lake and river for distributed water environment automatic monitoring. [C318]

#### **"Simulation study of noise convolution jamming countering to SAR"**

A new active jamming technique to synthetic aperture radar (SAR) is analyzed, which is called noise convolution jamming technique, or smart noise jamming technique. This technique can receive part of the SAR's process gains, so it is superior to current noise blanketing styles. It can reduce the jamming energy and improve the utility of jamming power greatly. By selecting the noise signal's initial time and terminal time, we can control the position and width of the jamming region in order to suppress distributed targets. Theoretical analysis and computer simulation justify the validity and efficiency of the new jamming technique. [C319]

#### **"A method for specific emitter identification based on empirical mode decomposition"**

Real radio and radar signals turn out to be non-stationary and nonlinear time series, and estimating instantaneous parameters of such signals in time domain will benefit detecting and identifying specific emitters, such as civil or military radios. However, conventional methods such as Wavelet and Wigner-Ville distribution (WVD) methods are difficult to deal with these transient signals when the signal is non-stationary. To provide more efficient approach for estimating instantaneous parameters of non-stationary and identifying specific emitter with high accuracy, a new method based on empirical mode decomposition (EMD) for analyze non-stationary signal is proposed in this paper. The results show that the instantaneous frequency estimates generated by the EMD method are more accurate than those obtained by the Wavelet technique. [C320]

#### "Improved pattern synthesis method with linearly constraint minimum variance criterion"

For the pattern synthesis method of the arbitrary array antenna with the linearly constraint minimum variance criterion (LCMV-PS), the primary disadvantage is its poor adaptability, namely its performance is determined by the iterative coefficient. In order to improve its performance, the effect of the relative amplitude between synthesis pattern and its reference upon the pattern synthesis is considered adequately, via adding a proportion constant to the iterative formula, not only the pattern synthesis efficiency is improved, but also the adaptability is extended. By the novel improvement for its iterative coefficient, the application area and adaptability of the pattern synthesis method are enhanced. The last simulation attests its correctness and effectiveness. [C321]

#### "Scheduling of tasks with fuzzy dwell times in a multifunction radar"

This paper proposes an algorithm for scheduling tasks in a multifunction radar. A greedy algorithm designed for tasks with crisp dwell times is extended to situations where the dwell time is allowed to be fuzzy. The greedy scheduling algorithm attempts to schedule as many tasks as possible while maintaining temporal regularity between the task update intervals. Tasks that cannot be scheduled by the greedy algorithm are then input to the fuzzy scheduling algorithm, which adjusts the dwell time of the tasks according to their membership function until they can be scheduled. An example scheduling scenario is provided to demonstrate the behavior of the proposed algorithm. [C322]

#### "A reduced-rank STAP method based on solution of linear equations"

STAP is an effective method for clutter suppressing and Reduced-rank STAP can reduce the calculation quantity as well as memory capacity. The connection between the eigenvectors of the clutter covariance matrix and the reduced-rank subspace is analyzed. A method based on the solution of linear equations which can get the whole eigenvectors of the minimum eigenvalues is proposed. By the method, the reduced-rank STAP can be done in the noise subspace without eigen-decomposition. Analysis is made about the distribution of SINR metric in the eigen-space and the solution space. Finally, simulations via real data proved the validity and correctness of the method. [C323]

#### "Research on autocorrelation of chaotic sequence by phase space method"

Chaotic sequences have been widely used as pseudorandom sequences. But the problem of how to judge their autocorrelation function's performances are good or not, up to now, have not been solved. In the paper, by method of phase space, we studied the autocorrelation function of chaotic sequence and discovered that their performance is determined by whether its phase space trajectory is axis symmetrical. This paper deduced theorems to describe and solve these problems, and presented a simple and effective method to judge autocorrelation performance of chaotic sequences, and a method to improve their autocorrelation performance was presented, too. Many simulations were presented to verify the theorems and methods. [C324]

#### "Remove multifrequency mixture noise in processing of Wireless Communication wave/radar reflect signal by method of ICA"

The ICA technique is used to remove multifrequency mixture noise in Wireless Communication wave/radar reflects signal processing. The characteristics of Wireless Communication wave/radar reflect signals are analyzed, build up models of expectation signal and consociation mixture noise and a constituted method of the independence prognosticate machine is discussed. Use the improved algorithmic of FastICA to simulate it. From simulation results, a well effect is acquired by method of the mixture signals separate above-mentioned. Via this, it can gain source signals almost pure furthermore wider the range ratio scope of each signal channel and type of signal. The method in the text possesses very good anti-jamming ability and it is can be expand other related signal processing, so the method is widely accepted. [C325]

#### "Session C6: Radar technique"

{no data available} [C326]

### "Analysis of mode-hopping effect in fabry-perot laser diodes"

Mode-hopping effect in Fabry-Perot laser diode (LD) operation was investigated. Radiation spectra and noise characteristics (optical and electrical fluctuations and their simultaneous cross-correlation factor) are measured under stable and mode-hopping operation of the LD. At mode-hopping point LD radiation spectrum is unstable, highly correlated intensive Lorentzian-type optical and electrical fluctuations are observed. Different cross-correlation factor value and sign (positive or negative) is observed for mode-hopping noise peaks at different LD operation conditions. Origin of the intensive Lorentzian-type fluctuations during mode hopping is caused due to generation-recombination processes in defects in barrier layers. [C327]

### "Ka-band FMCW radar sensor for remote control of presence and speed of railroad-cars and trains in territory of grading belts"

The results of development of low cost radar sensors for remote control of track occupancy and railway cars speed over the territory of hump yards under heavy weather conditions are presented. The radar sensor feature is application of Ka-band FMCW autodyne (self-mixing) transmitter and digital systems for forming sounding signal and spectral processing of received signals. Sensor is equipped with the systems of remote control and transmission of radar and service information to the control point. [C328]

### "Complex radar signal source for radar receivers testing"

This paper presents a design of a Radar Signal Generator (RSG) for radar receivers testing and development (i.e. receiver dynamic measurement, pulse compression modules). RSG is a multifunction flexible radar signal source generating multichannel coherent signals with reference signal for radar station and the other auxiliary signals and noise signal. The presented design is based on digital synthesizers with high flexibility in radar signal intrapulse modulation schemes. The architecture of RSG allows complex signals generating with bandwidth up to 150MHz (the frequency range is limited with proper filters due to most used frequency ranges). Phase stability of the output signal is less 1e deviation RMS and phase noise performance of reference signals is - 134dBc/Hz@1kHz for 10MHz. [C329]

### "Opening session"

{no data available} [C330]

### "Session A1: Antenna design"

{no data available} [C331]

### "A marine testing's result of experimental radar with 64-channels digital antenna array"

In this article are analyzed a results of experimental radar with digital antenna array full-scale test against above-water targets. [C332]

### "Experimental pulse reaction estimation of the centimeter wave channel"

We solve the problem of experimental estimation of the cm wave channel pulse response. Give an estimation of the pulse response for different paths at different angular positions of the transmitting antenna. [C333]

### "Multi-radar system database integration using metrized small world technology"

The present article describes the possibility of integrating the data from several radars with shared radiolocation areas in order to acquire precise information about the targets by means of analyzing the events in neighboring spatiotemporal resolution elements. The paper suggests an algorithm for integrating the data based on creating the graph which possesses the characteristics of the "Metrized Small World". A possibility of processing the integrated data in real time is analyzed. The article describes efficient metrics for integrating multi-radar data into a single Metrized Small World graph. Examples of such algorithms are given. [C334]

### "Collapse of nonlinear spin dipole wave pulses of millimeter wave range in YIG films"

Spatiotemporal collapse of spin-dipole wave (SDW) pulses of millimeter wave range is investigated theoretically. The dispersion and diffraction coefficients of SDW have been calculated, when the retardation has been taken into account. It is demonstrated that YIG films are suitable for observing the collapse in millimeter wave range,

due to low dissipation and quite high values of dispersion and diffraction coefficients. Numerical simulations have been confirmed this result. [C335]

#### "Moving multy-scatterer target parametric identification using radar image"

The wideband coherent pulse radar provides high resolution image of the target. A model of this image is composed of the complex envelope superposition of signals diffracted by the point scatterers. The values of complex envelope are distributed over the radar image coordinate plane in accordance with the point scatterer's positions and their reflection coefficients. The radar image model is combining of the range and Doppler profiles. The parameters of the target point scatterers are processed using one dimensional data extracted from the complex discrete Fourier transform of the radar image. The Matrix Pencil algorithm is used for the parametrical target identification. [C336]

#### "Ground target position estimation in passive location"

Ground target tracking is difficult and actual problem. Because of the high target density and maneuverability, high clutter, low visibility due to terrain masking, etc., ground target tracking presents unique challenges that does not present in tracking of other targets types. But many tracking approaches have been developed for air targets and they work poorly for ground targets tracking. This article includes research work results in radar position estimation for passive range-difference location. Radio source is stationary and performs circular scan. Transmitted signal is received in three points. But beside true measurements of time difference of arrival (TDOA) there are false measurements originated by clutter. Usually clutter measurements are modeled as independent identically distributed. But real experimental data processing shows that in crosscountry its distribution may be multimodal. Therefore standard tracking algorithms are not efficient in this situation. Multimodal distribution is caused by re-reflected signal from underlying terrain. Some ground objects re-reflect signal and imitate additional (false) targets. We propose special approach to decide position estimation problem in such high clutter environment and verify it on experimental data [C337]

#### "Terahertz and sub-terahertz subsurface tomography"

Development of millimeter and sub-millimeter wavelengths technologies is of great interest lately, especially for application in so called terahertz imaging. As a rule, two main approaches are used for this purpose based on employment of active and passive methods of visualization. In our paper we consider a tomography approach for obtaining 3-D imaging in frequency range from 100 GHz up to 325 GHz. We applied the method which we developed earlier for low frequency sub-surface tomography for extremely high frequencies. The considered method may be used for nondestructive testing. In the paper we present a theoretical model, experimental method and the results obtained. [C338]

#### "Modulators of THz range based on integrated silicon P-I-N-structures in dielectric waveguides"

Modulators of terahertz (THz) range on the base of silicon integrated p-i-n-structures in the isolated silicon dielectric waveguide are investigated. For the double injection problem, the generalized boundary conditions at the injecting electrodes have been used in the case of highly doped p++, n++ regions. The silicon dielectric waveguides possess low losses in the regime without injection. The investigations of modulation properties of integrated p-i-n-structures in dielectric waveguides of THz range have demonstrated a possibility to use these structures up to the frequencies  $\ll 8$  THz. [C339]

#### "Session A3: Compatibility"

{no data available} [C340]

#### "Session B4: Filters"

{no data available} [C341]

#### "Session B1: Microwave measurements I"

{no data available} [C342]

#### "Session B2: Microwave measurements II"

{no data available} [C343]

#### "Session B5: Power amplifiers II"

{no data available} [C344]

#### "Session B6: Active microwave networks"

{no data available} [C345]

#### "Session B3: Numerical modeling I"

{no data available} [C346]

#### "Session A8: Passive components I"

{no data available} [C347]

#### "Session A4: RFID technology"

{no data available} [C348]

#### "Session A5: Antenna theory and applications"

{no data available} [C349]

#### "Session A2: Broadband and UWB antennas"

{no data available} [C350]

#### "Session A9: Passive components II"

{no data available} [C351]

#### "Session A6: Numerical modeling II"

{no data available} [C352]

#### "Session A7: Industrial applications"

{no data available} [C353]

#### "Receive system of S band active antenna demonstrator"

The paper presents realization, mechanical solution and measurements results of a receive system used in the Demonstrator of an S-band Active Antenna. The receive system employs 16 antenna rows of planar array to form fan-beam receive antenna pattern in elevation plane and pencil-beam in azimuth. Five elevation positions of a pencil receive beam is electronically set by means of digital phase shifters and attenuators applied in receive beam forming network. The receive system realizes sum and difference beam signals for both azimuth and elevation planes at beam former outputs. Brief description of the whole receive path with main blocks is presented. The results of antenna pattern measurements on a tower setup are shown. [C354]

#### "Phase drift versus temperature measurements of coaxial cables"

Radio frequency systems developed for large scientific experiments have become increasingly sensitive to phase changes in their subcomponents. Amongst the most important subassemblies there are definitely coaxial cables that provide interconnections between experiment subsystems. It is commonly known that the most important source of phase drifts in coaxial cables is their sensitivity to temperature changes. The phenomenon of phase drifts in cables is discussed in this paper. A phase drift measurement setup is described. Samples of cables of various types used in RF system installations have been measured. Measurement results are presented. [C355]

#### "X-band pulsed measurement system of transmittance changes of power amplifiers"

The paper presents a system designed for measurements of transmittance changes of amplifiers and other active N-ports. This system is especially developed for measuring the transmittance variation of X-band T/R modules used in Active Phased-Array Radars (APAR). The measurements are automatically performed with the controlled sampling period  $0.2\mu\text{s}$ – $2\mu\text{s}$  for RF pulse of  $5\mu\text{s}$ – $300\mu\text{s}$  duration and 20Hz–2kHz repetition frequency



over an 8.8GHz to 9.5GHz frequency range. The system is capable of achieving the transmittance changes with accuracy of 0.2ofor phase and 0.05dB for amplitude. [C356]

### "An integrated SiGe HBT bandpass-pulse length modulator for switch mode power amplifiers in the SHF range"

The need for efficiency improvement of conventional class-AB-amplifiers when used with non-constant envelope modulations has set up interest in introducing switch mode amplifiers in the GHz operating frequency range. In order to be suitable for the amplification of arbitrarily modulated signals, a one-bit modulator is required at the input of the switch mode amplifier. Beside bandpass delta sigma modulation (BDSM), bandpass pulse length modulation (BP-PLM) seems to be a promising approach for this task. Here, the modulator output signal switches with the cycle of the RF-carrier signal frequency itself so that no oversampling is required, thus reducing switching losses in the amplifier. The length of each pulse is varied according to the envelope signal while the phase information is contained in the position of the pulses within the carrier period. We present here the design of a bandpass pulse length modulator circuit, capable of operating at microwave carrier frequencies above 3GHz. Measurement results for a QPSK-test signal show minimum error vector magnitudes of about 1.4 %. The modulator was manufactured in a 250nm SiGe:C-BiCMOS technology at IHP GmbH, Frankfurt (Oder), Germany. [C357]

### "Analysis of helical systems containing periodical inhomogeneities"

Properties of helical systems containing periodical inhomogeneities are considered. The multiconductor line method is applied for modeling of the systems and calculations of retardation factor and input impedance. ABCD matrices are used to reveal rejection properties of lines containing periodical inhomogeneities. The method based on multiple reflection diagrams is used to determine transient responses. Possibilities to improve characteristics of helical systems containing periodical inhomogeneities are discovered. [C358]

### "Measurement of thickness and electrophysical parameters of nanometer films by means of optical and microwave methods"

The possibility to determine the thickness and electrophysical parameters of thin nanometer dielectric and metal films in sandwich-like structures using the results of measurement of reflection and transmission spectra in microwave and optical band has been shown. The results of measurement of refractive index of SnO<sub>2</sub> in the thicknesses range from 40 nm to 2.8 mkm and the results of measurement of conductivity of Cr-films applied to ceramic substrates are presented. [C359]

### "Millimeter waves controlled elements on the basis of disk dielectric resonators"

The results of experimental study of spectral, power and field characteristics of single, half-disk, spiral resonators and also coupled disk dielectric resonators (DDR) with whispering gallery modes (WGM) in millimeter wave band by means of the computerized measuring stand are presented. The possibility of design of controlled EHF elements on the basis of coupled DDRs for the probable application in terahertz and optical frequency ranges is discussed. [C360]

### "Measurement of antenna characteristics by near-and far-field techniques within time domain"

The conventional method developed over a long period in the antenna measurement technique is application of monochrome measuring signals. Measurements performed with the use of monochrome signals are named frequency-domain measurements. [C361]

### "Synthesis of microstrip multiconductor lines, operating in normal mode"

Microstrip multiconductor lines (MMCL) are broadly used in microwave areas as transmission lines, or as physical models for developing various devices: couplers, filters etc. In general case, separate waves propagate along every conductor, and interference takes place in N-conductor MMCL. Transmitted signals are not distorted if structure of propagating wave remains unchanged, i.e. normal mode wave propagates; therefore it is necessary to restrict wave propagation to normal mode in MMCL, in order to minimize signal distortion. Synthesis technique of four-conductor symmetrically coupled MMCL, operating in normal mode, is presented in this article. [C362]

### "Wavelet packet based de-noising algorithm for UWB GPR data"

For subsurface detection by UWB GPR, one of the big challenge is to eliminate background clutters. In this

paper, a wavelet packet based de-noising algorithm driven by best-tree for UWB GPR data is developed. We introduce the procedure of the de-noising algorithm, and present the experiment result of iron pipe B-scan de-noising. Later, provide the suggestion for future work. [C363]

#### "Session C5: Millimeter technology"

{no data available} [C364]

#### "Cost-effective millimeter wave-to-optical conversion with patch antenna and MMIC chipset for RoF's uplink"

A cost-effective circuitry for the RoF's base station uplink channel including millimeter-wave microstrip antenna, down-converting MMIC chipset and low-cost Fabri-Perot laser diode is proposed and simulated in detail. [C365]

#### "UWB CPW-fed monopole antenna with a band-notch function"

In this paper a CPW-fed monopole antenna with a size of (24 Ч 24 Ч 1.6 mm<sup>3</sup>) and a staircase feed line is presented. The antenna is designed for operation across the entire UWB from 3.1 to 10.6 GHz with band-notch in 5-6 GHz, by inserting a H-shape slot on the proposed CPW feeder. By changing in width and length of H-shape slot, the operation on notch-band becomes different. The proposed antenna has a reflection coefficient below -10 dB through the band frequency and reasonable gain values over the same frequency band. [C366]

#### "On the issue of the construction of wideband measuring antennae 0, 85 to 37, 5 Ghz"

Analysis of parameters of different types of measuring antennae has been conducted, the reasonability and possibility of the realization of a number of superwideband horn-lens antennae with coaxial input has been done. Presented are the results of the designing of the horn-lens antennae within the range f 0.85 to 37.5 GHz. The range is overlapped by three models of antennae: -П6-23М for 0, 85 to 17.44 GHz; -П6-65 of 2.0 to 25.95 GHz; -П6-66 of 12.05 to 37.5 GHz. Measuring antennae parameters ensure the realization of a big number of requirements of different modern devices with which these antennae work (spectrum analyzers, receivers, signal monitoring systems, etc) The wide range of frequencies, high performance and the possibility of operation under severe climatic conditions (from minus 50°C to plus 60°C) make the these antennae one of the best devices of their class. [C367]

#### "Estimation of capacity bounds of free space optical channels under strong turbulence conditions"

The last few years, the free space optical communication systems attracting research and commercial interest due to their capability of transferring data, over short distances, with high rate and security, with low cost demands and without licensing fees. The main disadvantage of these systems is that their performance depends strongly on the atmospheric conditions in the link's area. In this work, we investigate the influence of the turbulence on both the average and the outage capacity of such a system for strong turbulence channels modeled by the K-distribution. We present a novel closed-form expression for the estimation of outage capacity of the channel and we determine the practical bounds of wireless optical channels' capacity. [C368]

#### "Testing of telecom and datacom signals with a wide-bandwidth sampling oscilloscopes"

The article will discuss main procedures and best practices for testing a wide-bandwidth signals by using USB sampling oscilloscopes. The article reviews the performance parameters that are used to specify the quality of the signals and networks, and examines how they can be effectively tested and assessed. All tests for both electrical and optical signals are made with the PicoScope 9200 USB sampling oscilloscopes. [C369]

#### "Pattern matching localization in ZigBee wireless sensor networks"

This paper focuses on the results of localization based on ZigBee wireless network. Different methods of localization are discussed, and pattern matching method is selected for tests. It presents the way to adapt ZigBee network to work with localization algorithm. [C370]

#### "An optimal scheduling algorithm in spatial TDMA mobile ad hoc network"

Spatial TDMA (STDMA) is a "conflict-free" MAC protocol so that concurrent communication among the connected nodes. Therefore it can enable high spectral utilization, if optimal scheduling algorithm is achieved. As directional antenna technology developed, point to point transmission to other node could generate higher data transmission rate at the same time, lower interference with other nodes than omnidirectional antenna. Therefore

an optimal scheduling algorithm needs to design to allocate the right slot to the right node in order to achieve high efficiency spatial reuse. To achieve this aim, we propose a new optimal scheduling algorithm: Max Spatial Reuse Scheduling Algorithm (MARSA). By using of directional antenna, it allows 1-hop distance neighbor node communication with other node in same slot unless one node connect to two node. Thus this concurrent scheduling algorithm allows more node communication with other nodes in one slot. Our method based on communication graph can be achieved with low complexity. [C371]

#### **"Towards establishing traceable coaxial Type-N scattering-parameter measurements at NIT"**

We present results of our work aimed at establishing traceable coaxial type-N vector-network-analyzer scattering-parameter measurements at the National Institute of Telecommunications, Poland. To this end, we employed a set of high-grade coaxial air-dielectric transmission lines as the primary calibration standards and a calibration procedure based on the multilane through-reflect-line method. In order to verify our procedure, we compared it with the calibration procedure implemented in the vector-network-analyzer and based on an electronic calibrator. Preliminary experimental results show very good agreement between the two procedures. [C372]

#### **"High power S band T/R module"**

The paper describes S-band T/R Modules designed for use in an Active Phased Array. Brief principles of its operation are described and electrical and mechanical information are presented. Main parameters of T/R Modules are shown in the form of characteristics. Results of measurements in wide range of the ambient temperature are presented as well. Basing on the obtained results, conditions of Transmit Modules operation are defined. [C373]

#### **"Adaptive potential of spatial transmission processing techniques"**

In this paper we evaluate the adaptive potential of multi-antenna transmission systems employing precoded spacetime block codes. Based on the transmit parameters that are intended to be efficiently use, the most appropriate precoded transmission is evaluated. Several performance criteria were considered: bit error rate, capacity, spectral efficiency and link throughput. [C374]

#### **"Determination of radio refractivity using meteorological data"**

Seasonal and daily variations of radio refractivity have been analyzed in the localities of Lithuania. The method proposed in the Recommendation of International Telecommunication Union (ITU) has been used. The local meteorological data have been used in calculation of radio refractivity. The values of radio refractivity have been determined in Vilnius, Kaunas, Klaipėda, and Mažeikiai. The meteorological data collected in February, April, July and October have been used. The highest values of the radio refractivity have been observed in Klaipėda in the year 2009. In July 2009, the values of the radio refractivity were highest in all localities investigated here and over all the time of the day. [C375]

#### **"Reduced complexity schemes to greedy power allocation for multicarrier systems"**

Discrete bit loading for multicarrier systems based on the greedy power allocation (GPA) algorithm is considered in this paper. A new suboptimal scheme that independently performs GPA on groups of subcarriers and therefore can significantly reduce complexity compared to the standard GPA is proposed. These groups are formed in an initial step of a uniform power allocation (UPA) algorithm. In order to more efficiently allocate the available transmit power, two power re-distribution algorithms are further introduced by including a transfer of residual power between groups. Simulation results show that the two proposed algorithms can achieve near optimal performance in two separate and distinctive SNR regions. We demonstrate by analysis how these methods can greatly simplify the computational complexity of the GPA algorithm. [C376]

#### **"Electromagnetic study of planar pre-fractal structures using the scale changing technique"**

In this paper, the scale-changing method is used to compute the surface impedance of pre-fractal structures characterized by the coexistence of metallic patterns at multiple scale levels. The multi-scale nature of these structures is used to split them into sub-structures enclosed by appropriate boundaries. The calculation starts from the elementary substructure:  $N$  active modes excite the considered sub-structure in order to compute the corresponding surface impedance matrix useful for the transition from a scale toward another. The choice of active modes is important in order to ensure the coupling between two consecutive scales and to have a correct description of the electromagnetic state within discontinuities. Consequently, the local modal basis is divided into two parts: -Higher-order modes: localized modes essentially useful for the local electromagnetic description within

discontinuities. -Lower-order modes or active modes: travelling modes useful for the coupling between sub-structures. When localized modes are used as active, we show that the electromagnetic description within discontinuities is not correct. The surface impedance obtained by the multi-scale method is compared to the surface impedance computed by the MoM method. The error variation with the number of active modes is presented. It converges with an error less than 0.3% when a sufficient Number of active modes are used. [C377]

#### "Variable microwave time delay by utilizing optical approaches"

A new method is presented for establishing variable microwave time delay utilizing optical approaches. In many applications there is a need for a significant time delay which cannot be established by microwave methods. The optical fiber can offer a substantial time delay which can be utilized by converting the microwave signal into the optical domain and after the proper delay it is converted back to microwave. By choosing the fiber length the necessary microwave delay can be adjusted. The main contribution is the variation of the delay. That is achieved by applying a dispersive fiber and a tunable laser. When the laser wavelength is changed the delay is varied due to the fiber dispersion. That new approach is very advantageous for beam steering of phased array antennas. [C378]

#### "Using space time coding MIMO system for software-defined radio to improve BER"

The demand for mobile communication systems with global coverage, interfacing with various standards and protocols, high data rates and improved link quality for a variety of applications has dramatically increased in recent years. The Software-Defined Radio (SDR) is the recent proposal to achieve these. In SDR, new concepts and methods, which can optimally exploit the limited resources, are necessary. Multiple antenna system is one of those, which resort to transmit strategies, referred to as Space-Time Codes (STCs). It gives high quality error performance by incorporating spatial and temporal redundancy. The paper discusses the space-time block codes and highlights the trade-off between the number of transmitter and receiver antennas and the bit error rate. We simulate MIMO systems using M-ary Phase Shift Keying (PSK) and compare the results with Single Input Single Output (SISO) systems. This analysis can be helpful in choosing the desired modulation scheme depending upon the Bit error rate (BER) and Signal to noise ratio (SNR) requirements of the service. [C379]

#### "EXIT chart analysis of iteratively detected and SVD-assisted broadband MIMO-BICM schemes"

In this contribution the number of activated MIMO layers and the number of bits per symbol are jointly optimized under the constraint of a given fixed data throughput and integrity. In general, non-frequency selective MIMO links have attracted a lot of research and have reached a state of maturity. By contrast, frequency selective MIMO links require substantial further research, where spatio-temporal vector coding (STVC) introduced by Raleigh seems to be an appropriate candidate for broadband transmission channels. In analogy to bit-interleaved coded irregular modulation, a broadband MIMO-BICM scheme is introduced, where different signal constellations and mappings are used within a single codeword. Extrinsic Information Transfer (EXIT) charts are used for analyzing and optimizing the convergence behaviour of the iterative demapping and decoding. Our results show that in order to achieve the best bit-error rate, not necessarily all MIMO layers have to be activated. [C380]

#### "PER-based analysis of a mobile WiMAX system"

Among the 4G technologies that managed to impose is the IEEE 802.16e Mobile WiMAX technology. Mobile WiMAX promises to deliver high data rates over wide areas and at vehicular speeds of up to 120 km/h. The performance of such a system is greatly influenced by the type of application desired to be supported, either TCP-based (FTP, web browsing) or UDP-based (video streaming). The current paper proposes to analyze and compare the performance of a fully compliant Mobile WiMAX system operating at 2.3 GHz in a vehicular multipath fading channel (ITU M.1225 Veh.A). The results are generated on a link speed basis and are expressed in terms of the adaptive modulation and coding (AMC) switching points as well as the maximum achievable throughput and operating range. Different physical packet error rate (PER) requirements are considered, based on the quality of service (QoS) level imposed. [C381]

#### "Reference signal extraction for GSM passive coherent location"

This paper investigates two equalization methods enabling the passive coherent location (PCL) system using GSM as illuminator of opportunity to eliminate the distortion of the reference signal. The first one is the Constant Modulus Algorithm (CMA) based on a blind method. The second one using the Viterbi Algorithm to decode the transmitted bits and to regenerate the reference signal. [C382]

#### "Decoding and reconstruction of reference DVB-T signal in passive radar systems"

The paper presents a method for reception, decoding and reconstruction of DVB-T signal for the purpose of using it in passive coherent location (PCL) as a reference. The signal is received using universal COTS components not dedicated for DVB-T, contrary to common television receivers. The proposed algorithm is tested on real-life signals. [C383]

#### **"Impact of synchronization on the ambiguity function shape for PBR based on DVB-T signals"**

In this paper the use of Digital Video Broadcasting Terrestrial (DVB-T) signals is addressed for Passive Bistatic Radar (PBR). The impact of the synchronization accuracy is analyzed on the PBR Ambiguity Function (AF) shape in term of Peak to Side Lobe Ratio (PSLR), there including timing synchronization, frequency offset synchronization and frequency sampling offset synchronization. Different approaches proposed in the past are considered for the removal of the side peaks of the AF of DVB-T-based PBR. Their performance in the presence of synchronization errors are evaluated both by simulation and against a real data set collected by a PBR prototype developed and fielded at the INFOCOM Dept. of the University of Rome "La Sapienza". [C384]

#### **"SETHI flying lab: A tool for remote sensing applications"**

This paper presents the new-generation test bench SETHI, developed by ONERA, the French Aerospace Lab. SETHI is a medium range platform dedicated to environmental, scientific and security applications. This paper presents the system architecture, the development state and the future capabilities planned. Before concluding, this paper displays a set of recent significant results covering three major applications: high spatial resolution image, change detection between two acquisitions, bio mass measurement in the tropical forest. [C385]

#### **"A software defined UMTS passive radar demonstrator"**

Passive radar systems, also referred to as Passive Coherent Location systems (PCL), exploit non-cooperative illuminators of opportunity (IO) in order to detect and track targets. Some of the main advantages of such systems with respect to conventional radars include low cost architectures, low energy requirements, the capability of operating without any spectrum resource allocation and a potentially null probability of intercept. In this paper, we introduce a passive radar demonstrator based on the use of UMTS (Universal Mobile Telecommunications System) signals as a source of opportunity. An overview of the UMTS standard and some preliminary measurements are firstly presented in order to verify the suitability of the UMTS waveform for radar applications. Secondly, a low cost software defined experimental radar system is introduced together with a measurement scenario. Finally, some live data detection results are presented and discussed in order to demonstrate the capability of this passive radar system. [C386]

#### **"Signal reconstruction as an effective means of detecting targets in a DAB-based PBR"**

This paper aims to validate the method of target detection by correlating a surveillance (target) signal with a reconstructed reference signal in DAB-based Passive Bistatic Radar (PBR). Whereas most conventional PBRs condition the surveillance signal by suppressing Direct Signal Interference (DSI) and then correlate this with a similarly measured reference signal to reveal targets, the approach adopted at FHR is to correlate the surveillance signal with a perfectly reconstructed, error-free, copy to the transmitted signal. [C387]

#### **"Fusion of SAR and optical images as a method for improving target recognition on the earth surface"**

The paper presents the real-life data results of SAR and optical images data fusion. The fusion has been carried out for SAR images obtained in classical SAR, multilook SAR and multilook color mapping SAR modes. The aim of the presented images fusion was to enhance the target recognition capabilities on the Earth surface for a simple single-channel SAR receiver. [C388]

#### **"Extending range coverage with GSM passive localization by sensor fusion"**

Among the available illuminators for passive localization GSM base stations enjoy the advantage of global availability and frequency diversity. However, the low transmit power limits the achievable range. This paper studies the possibilities of range coverage extension by fusion of bistatic systems with multiple transmitters. [C389]

#### **"Deghosting in passive air surveillance systems"**

Digital Audio/Video Broadcasting (DAB/DVB-T) is already available in a large area of Europe. The advantage of using these signals for passive air surveillance is the disposability of a large range of illuminators sending an



easily decodeable digital broadcast signal. In the considered multi-static scenario, one observer provides bistatic Time Difference of Arrival (TDoA), Doppler and (with limited quality) also azimuth measurements. The main task of target tracking is to handle ghosts that arise due to problems of association between illuminators, targets and measurements. To prevent enumeration and maintaining of all association possibilities, a decision criteria needs to be found to discriminate ghosts quickly and efficiently. In this paper we try to give a general understanding of the characteristics of ghosts; we derive two different Deghosting criteria and compare their performance with respect to Monte-Carlo simulations. [C390]

### "FM based passive bistatic radar target range improvement-Part II"

The bistatic radar has been revitalized over the last few years through the rapid development of the passive bistatic radar technology. Passive bistatic radar systems have unique properties, especially is time on target high compared to traditional radar systems, as well as the freedom in choosing from the available transmitters of opportunity. This paper will focus on how to take advantage of the latter of these two special properties in order to achieve better range resolution. [C391]

### "High performance reflector-based Synthetic Aperture Radar: -A system performance analysis -"

The success of current spaceborne Synthetic Aperture Radar (SAR) is boosting the performance requirement of next generation systems. In order to cope with the evolution of SAR the design of the new systems will need to meet higher requirements for spacial and radiometric resolutions together with an increased availability. This tendency is recognized nearly independently of the application area and manifests itself through several study programs initiated by space agencies aiming at the design of future SAR systems. In this context the use of large reflectors combined with digital feed arrays for SAR has not always received adequate attention. This paper suggests an X-band spaceborne SAR system utilizing a deployable reflector together with a digital feed array, analyzes its performance and highlights its advantages compared to other systems based on direct radiating arrays. [C392]

### "Nonuniform spatial sampling in a noise SAR"

The paper presents an idea of nonuniform spatial sampling applied to a noise synthetic aperture radar. Lowering number of spatial (along-track) domain samples taken in a SAR radar may lead to spatial aliasing and incorrect reconstruction of the image. Nonuniform sampling allows to reduce the aliasing effect and reconstruct the image better. This technique may be useful when the overall number of samples or the spatial sampling frequency is limited by external constraints. The idea will be verified with an experimental noise SAR built at ISE PW. [C393]

### "Principles of the electromagnetic modelling of som microwave components, based on the circular waveguides with azimuthally magnetized ferrite"

The principles of electrodynamic analysis of the characteristics of the ferrite control components (nonreciprocal digital phase shifters, cut-off switches and isolators) which use circular waveguides, entirely filled with azimuthally magnetized ferrite or containing a coaxial disc- or ring-shaped area of the medium alluded to and a dielectric one, surrounding it or taking up its hollow, resp., and work in the normal TE<sub>01</sub> mode, are enunciated: i) employment of complex confluent hypergeometric and eventually also of real cylindrical functions; ii) indispensability of inventing of numerical methods for evaluation of some special functions of the mathematical physics: the Euler gamma function, its logarithmic derivative and the confluent functions in the complex field, as well as of the cylindrical ones in the real domain; iii) elaboration of techniques for numerical solution of complicated transcendental equations, involving complex confluent and possibly real cylindrical functions, too; iv) introduction of a new class of real numbers, called L numbers, connected with the purely imaginary roots of the equations mentioned; v) development of numerical schemes for computation of the phase curves of geometries regarded and of iterative procedures for finding the differential phase shift provided by them; vi) laying down of criteria for the operation of configurations as phase shifters, magnetically controlled cut-off switches and isolators. Each of the maxims pointed out is elucidated in detail. [C394]

### "Range Doppler SAR processing using the Fractional Fourier Transform"

The Fractional Fourier transform (FrFT), which is a generalized form of the well-known Fourier transform, has opened up the possibility of a new range of potentially promising and useful applications including radar involving the use and detection of chirp signals, pattern recognition and Synthetic Aperture Radar (SAR) image processing. In this paper the Fractional Fourier transform is applied to the Range Doppler Algorithm in order to obtain a better result in terms of resolution. The proposed technique takes advantage from the property of the FrFT to resolve with high precision chirp signals. Preliminary results are encouraging and confirms that the FrFT can be useful to perform high resolution SAR processing. [C395]

### "Fusion of data received FM-CW radar and AIS-analysis of functionality: Topic 3. Radar application"

Development of Frequency Modulated Continuous Wave (FM-CW) radars and universal shipborne Automatic Identification System (AIS) creates new questions in practical application of these technologies for purposes of ships traffic monitoring and control. Accuracy of FM-CW radar distance measurement, not achievable for pulse radars, causes questions of correctness of charted data presented by ECDIS and information about ship's position transmitted by AIS. Paper presents some questions connected with comparison of electronic chart data and FM-CW measurement accuracies and fusion of data received from AIS and radar tracking system. Described researches were conducted in the scope of research work financed by the Polish Ministry of Science and Higher Education as developmental project from the means for science in 2008-2010 years. [C396]

### "Author Index"

{no data available} [C397]

### "Blank page"

{no data available} [C398]

### "Title page vol2"

{no data available} [C399]

### "Session P2"

{no data available} [C400]

### "Short-range Ku-band hybrid-mode CW-LFM radar"

Short-range CW-LFM radar design is discussed. Hybrid mode operation consisting of pure CW and CW-LFM periods is implemented. Such algorithm allows sufficiently simplify the processing and reduce the false alarm probability. [C401]

### "Copyright page"

{no data available} [C402]

### "On the resolution performance of passive radar using DVB-T illuminations"

DVB-T signals used as illumination for passive radar offer advantageous radar signal processing properties and promise sufficiently high range resolution. Passive DVB-T radar performance assessment is based on a signal processing model including reference signal reconstruction, the influence of bit-error rates on range performance and the application of error corrections. A verification of the estimated range resolution performance is attempted using the experimental passive radar system PETRA of FHR to discriminate small civilian aircraft in close flight under realistic measurement conditions. The results encourage utilising DVB-T signals as trend-setting non-cooperative illuminations in future passive radar systems, not only in central Europe. [C403]

### "Correction of radiometric errors by multi-look processing with extended number of looks"

The application of the clutter-lock technique in case of fast and significant instabilities of the antenna orientation leads to strong geometric distortions in SAR images. In the paper we propose a radiometric correction approach which could be used with SAR processing algorithms without clutter-lock. The technique has been tested by using a Ku-band airborne SAR system, installed on a light-weight aircraft. [C404]

### "Multi-look stripmap SAR processing with built-in geometric correction"

Small airborne SAR systems suffer from trajectory deviations and instabilities of antenna orientation. These kinds of motion errors lead to significant geometric distortions in SAR images. In the paper, we describe a time-domain multi-look stripmap SAR processing algorithm with built-in geometric correction. In the algorithm, the azimuth reference functions and range migration curves are designed to produce SAR images directly on a correct rectangular grid on the ground plane. The proposed technique has been successfully tested by using a Ku-band airborne SAR system, installed on a light-weight aircraft. [C405]

### "New challenges for PCL system: 3D requirements and "Optimal" resources management for PCL air traffic survey"

For more than 15 years, the interest for PCL (Passive Coherent Location) system has been growing. It began with the analog waveforms like TV [1] and FM [2, 3], nevertheless it quickly appears that the recent digital waveforms (using COFDM modulation) could offer new interesting capabilities especially for range resolution. Despite the interesting recent progress related to these digital waveforms like the compulsory development of a specific zero-Doppler path cancellation filter [2, 4] especially for SFN mode, some new additional requirements mentioned by several potential users [5, 6] of such PCL system have appeared: • Such PCL systems are generally considered as complementary sensors for low altitude coverage. As a consequence, these systems should provide an altitude estimation and especially for these low altitude targets. • On other hand, it is also important to manage and chose the most suitable donors in a given area in order to "optimise" the system definition according to our objectives. This paper will illustrate some experimental results for site estimation using DVB-T transmitters in SFN mode. The signals are received on a 2D array. Then a brief comparison of the mutual and specific benefits expected for the main civilian broadcasters (FM, DAB, DVB-T) will be provided.

[C406]

### "Exploiting polarimetric diversity to mitigate the effect of interferences in FM-based passive radar"

In this paper the effect of interfering sources is characterized on the performance of a passive bistatic radar exploiting a FM radio broadcast transmitter. The signals emitted on same/adjacent frequency channels by other potential transmitters located in the surveillance area are shown to significantly affect the performance of the considered system in terms of both disturbance cancellation and target detection capability. To mitigate the effect of such interferences, the exploitation of different polarizations is considered for the surveillance antenna. A preliminary approach is proposed to jointly exploit the diversity of information conveyed by different polarizations. The results are shown against a real data set collected by an experimental multi-channel passive radar prototype developed and fielded at the Infocom Dept. of the University of Rome "La Sapienza" (Italy).

[C407]

### "Multiband experimental PCL system: Concept and measurement results"

Over recent years, interest in passive radar systems using non-cooperative analogue and digital broadcast transmitters as illuminators has been growing significantly. They are being considered as possible future stand-alone systems or as gap fillers for existing air surveillance systems [1]. Recently passive radar is also discussed for the deployment in border surveillance as well as for detection of land and sea targets. The technical maturity and detection performance of experimental and prototype system implementations has been steadily improving. Starting from early FM-broadcast-based systems, the evolution to DAB-based and DVB-T-based digital systems is currently ongoing. In this paper, a multiband experimental passive radar system exploiting FM, DAB and DVB-T transmitters is presented. The hybrid system concept is described and the results of various measurements with different types of aerial and sea targets are shown.

[C408]

### "Mutual coupling compensation applied to a uniform circular array"

In this paper, two approaches for compensation of mutual coupling and phase shifts in a passive radar system based on a circular array are compared. The first method is based on the measurement of the antenna scattering parameters and of further relative phase and amplitude variations between the channels introduced by the receiver analog front-end and by the analog-to-digital converter. The second method derives a total coupling matrix, which contains both the antenna and the front-end contributions, by measuring the signals transmitted from known positions. The two procedures have been applied to an FM-based passive radar that uses an 8-element circular array. It appears that for the considered geometry the antenna mutual coupling does not significantly affect the radiation pattern, while the major contribution is due to phase shifts introduced by the receiver front-end.

[C409]

### "Cargo ship RCS estimation based on HF radar measurements"

High-Frequency (HF) radars are operated in the 3-30 MHz frequency band. For oceanographic applications low transmit power HF radar systems have been developed, which use surface electromagnetic wave propagation along the salty ocean surface. The WERA HF radar system transmits a power of 30 Watts but achieves detection ranges up to 200 km. Hence the radar system can be used for many applications in coastal monitoring. The measured radar data were analyzed together with simultaneously available Automatic Identification System (AIS) information, which shows current ship position, speed, course and type. This paper presents the target reflectivity measurements as signal-to-noise ratio (SNR) to estimate the radar cross section (RCS) of cargo ships.

[C410]

### **"Reflector-based digital beam-forming radar system for space debris detection"**

The paper considers a novel radar system concept for space debris detection based on a reflector antenna and utilizing digital beam-forming techniques. The main operational principles of the system are discussed. First, a classical radar system and its performance aspects are considered. Then in terms of the considered aspects, the performance enhancements of the novel digital beam-forming radar are demonstrated. [C411]

### **"A subspace-based technique for joint DOA-DOD estimation in bistatic MIMO radar"**

In this paper, we propose a new subspace-based approach for joint DOA-DOD estimation in the bistatic MIMO radar. This method use a polynomial root findings for determining jointly the DOA-DOD directions. This algorithm allows an efficient estimation of the target DOA and DOD with automatic pairing. The simulation results of the proposed algorithms are presented and the performances are investigated and discussed. [C412]

### **"Analysis of ATR features for non-cooperative ground-based classification of ships"**

Measurements were taken at 17 GHz of a ship that was first approaching the coast-based radar and then followed a circular course between 6km and 7km distance. It is demonstrated how the high range resolution profile of the ship and consequently any ATR (automatic target recognition) classification features derived therefrom are modified by multipath as a function of range and aspect angle. For comparison, the TERPEM software is used to simulate the effect and analyse it in a more controlled way. [C413]

### **"Technological challenges of a multifunction active phased array radar for weather, air traffic control and security applications"**

By means of Active Phased Array techniques, an integrated target/weather surveillance at medium range, i.e. for Terminal Manoeuvre Area in the frame of ATC and regional weather monitoring, is possible and affordable provided that cost reduction for Transmit/Receive modules makes phased array radar affordable to civilian users. The MPAR (Multifunction Phased Array Radar) architecture allows a single equipment to satisfy different requirements for Air Traffic Control, Weather monitoring and analysis, and Security applications. The key techniques needed to achieve the required performance are (a) interleaving of functions by careful scheduling, (b) digital beam forming for target surveillance and (c) fast (electronic) scanning for the weather surveillance. The core technologies are of course those needed to implement at low cost the Transmit/Receive module (TRM), that in the proposed architecture may transmit a low peak power (order of one Watt), compatible with the low-cost requirement. [C414]

### **"Solid state C band radar for detection of hovering helicopter"**

A technical data and a project of the structure the radar detected hovering helicopters is shown in the paper. The results of research simulation and range tests of prototype are presented also. They indicate that this solution of radar was properly chosen. [C415]

### **"Energy allocation for correlated MIMO radar antennas with ricean targets"**

MIMO (multiple-input multiple-output) radar systems with widely separated transmitters and receivers have capacity to considerably improve the performance of radar systems. This is accomplished by utilizing the notion of spatial diversity as receivers can observe incoming echos originating off various aspect angles. This work attempts to alleviate the performance of MIMO systems in the existence of correlation and Ricean scattering models by proposing a power allocation scheme. The scheme adjusts weights at the antennas proportionally by taking account of any correlation and line-of-sight information present at the transmitters. Antennas who are correlated or perceive low line-of-sight reflectivity are allocated less power so that the total available energy is spread across diversity branches and strong reflectors more accordingly. Simulations are used to validate the results. [C416]

### **"An investigation of signal synthesis for radar applications"**

A method of signal synthesis is presented. After theoretical introduction an algorithm of frequency modulated (FM) signal synthesis is presented. Simulation results made in Matlab are presented in the last chapter. [C417]

### **"Classification of air targets including a rejection stage for unknown targets"**

In this paper an algorithm for Non-Cooperative Target Identification (NCTI) of airplanes is presented. The

advantage of NCTI over Identification Friend-Foe-systems (IFF-systems) is its ability to identify positively not only friendly airplanes but also neutral or hostiles ones. The approach described here uses one-dimensional radar images, so-called High Range Resolution profiles (HRR-profiles) for NCTI. However only the locations of the local maxima of the HRR-profiles were used for classification instead of using the whole HRR-profiles. Furthermore a statistical test procedure is presented that is carried out prior to the classification procedure to determine if an airplane belongs to a known or to an unknown class of airplanes without distinguishing the known classes of airplanes. [C418]

#### "Optimal sampling rate for short chirp signals"

Short broadband signals with the use of linear modulation of frequency LMF (so-called chirp signals) are widely used in locations. The aim of this paper is to study an influence of a sampling rate on single LMF signals with  $BT < 100$  compression when initial phases and shapes of the signal and IR amplitude spectra are optimized at using nonlinear operations on convolutions in the time domain. [C419]

#### "Multipath exploitation in an urban environment using a MIMO surveillance radar"

Surveillance in an urban environment under all atmospheric conditions and situations can be performed by means of radars. The multipath created by buildings and moving targets can be exploited, for example in order to increase SNR. In this paper we present the initial results of the measurements of a moving target in a roadblock scenario in non line of sight (NLOS). The results suggest that MIMO systems are suitable for urban environment surveillance. [C420]

#### "A MIMO radar for Sense and Avoid function: A fully static solution for UAV"

Up to now, UAV are employed in crisis or war times. For training purposes, some areas are especially attributed for UAV deployment in a limited space area and in a limited time slot. In the future, both for emerging civilian applications and for training purpose, these limitations will no longer be acceptable and UAV will have to be inserted in the general air traffic. Thus, "Sense and Avoid" systems will be mandatory. The radar is the most pertinent non-cooperative "all-weather" sensor because it provides, by essence, accurate ranging, direction and closing speed. In this paper, we propose a low cost radar solution based on the coherent "MIMO" principles. This design allows the implementation of the radar within the UAV airframe without any moving part. [C421]

#### "Moving target estimation using distributed MIMO radar in non-homogeneous clutter"

In this paper, we consider parameter estimation for moving target detection using a distributed MIMO radar, where the multi-static transmit-receive configuration causes non-homogeneous clutter. Specifically, the clutter power for the same resolution cell may vary significantly from one transmit-receive pair to another, due to azimuth-selective backscattering. Moreover, the clutter power may also vary across resolution cells in the neighborhood of the test cell. In this work, the non-homogeneous clutter is modeled using a subspace approach, whereby the subspace is spanned by a few Fourier bases and the non-homogeneity of the clutter is captured by coefficients that vary with different transmit-receive pairs and/or different resolution cells. The choice of the Fourier bases is based the fact that the clutter Doppler spectrum is bandlimited. We develop a maximum likelihood (ML) estimator for the parameters associated with the target and clutter. The Cramer-Rao bound (CRB) for velocity estimation is also derived. Numerical results show that the proposed estimator outperforms an alternative solution that ignores the non-homogeneous nature of the clutter. [C422]

#### "Adaptive hough detector threshold analysis in presence of randomly arriving impulse interference"

In this paper a technique of Hough detector threshold procedure for moving target detection in conditions of randomly arriving impulse interference with Poisson distributed flow and Raleigh amplitude distribution is proposed. The expressions of detection and false alarm probability are derived for a highly fluctuating Swerling II target. A comparative analysis of the performance of a Hough detector with fixed threshold and other five Hough detection structures keeping constant false alarm rates is done. These are CA CFAR (Cell Averaging Constant False Alarm Rate), EXC CFAR (Excision Constant False Alarm Rate), CFAR BI (Constant False Alarm Rate with Binary Integration), EXC CFAR BI (Excision Constant False Alarm Rate with Binary Integration) and API CFAR (Adaptive censoring Post detection Integration Constant False Alarm Rate). A method for losses estimation, which allows choosing of optimal detector parameters, is developed. Obtained are estimates of the effectiveness of Hough detector in presence of randomly arriving impulse interference and they are compared to patterns researched from other authors. The achieved results can be successfully applied for radar target detection and in the existing communication network receivers that use pulse signals. [C423]



### "Pedestrian recognition based on 24 GHz radar sensors"

Some 24GHz radar signal features are introduced in this paper for a reliable recognition of pedestrians and vehicles in an arbitrary traffic situation. It examines in particular the Doppler spectrum and the range profile.

[C424]

### "Milestones in radar and the success story of automotive radar systems"

Radio Detection and Ranging (RADAR) is a world wide well-known technique since more than 100 years, which is originally based on the invention of the German engineer Christian Hulsmeier, who applied his patent at the Kaiserliche Patentamt in Berlin on April the 30th, 1904. He called his invention Telemobiloskop in a good tradition of using Latin terms for technical subjects. The radar story started with the theoretical work of James Clerk Maxwell, followed by Heinrich Hertz, born in Hamburg, who did all the experimental work to understand the nature of electromagnetic waves. Collision avoidance between ships was the first application for this new technique. Today we come back to the collision avoidance application however now between cars. This is just the beginning of the automotive radar systems success story. [C425]

### "Ultra-wideband sensing: The road to new radar applications"

Research on ultra-wideband topics started about 50 to 60 years ago driven by needs in radar and communication technology as well as to emulate EMPs of nuclear explosions. Meanwhile, ultra-wideband sensing opens new perspectives for radar applications. Small and cost effective devices, high resolution and sensitivity, as well as low exposition by radio waves will give this radar technology access to new applications in industry, non-destructive testing, medical engineering and health care, surveillance, search and rescue, and many others more. High peak power devices will be limited to special applications and a low number of devices due to their radio interference and mostly only military interest. Therefore, this paper only deals with some aspects of high-resolution short-range sensing giving new perspectives for a wider community. [C426]

### "Increasing vehicular safety at intersections by using LFMSK modulated radar sensors"

This paper deals with environment perception for automotive application especially in intersection-related scenarios. The recognition of relevant objects within intersection-related scenarios is performed not at least with high performance 24 GHz radar sensors. These sensors are dedicated to detect objects in the surroundings of the equipped demonstrator vehicle. The modulation of the transmit signal plays an important role for precise measurements. In this paper a linear frequency modulated shift keying (LFMSK) measurement principle is proposed. [C427]

### "Angular measurement with lens based automotive radar sensors"

77 GHz automotive radar sensors based on lens antennas have a high market penetration in the field of driver assistance systems due to their compact and cost effective concept. These kinds of sensors need not only a good field of view but also the possibility to measure angles. In this paper the parameters amplitude and phase in the focal region are discussed for a diffraction dominated system. Special attention is paid to phase differences between the received signals from antennas mounted in the focal region. [C428]

### "Development milestones in 24 GHz automotive radar systems"

Driving a car means a dangerous task! There are about 5000 fatalities on German streets every year, which are absolutely too many. Drivers have strong limitations in the ability to measure precisely the distance and the speed difference between cars, which is the reason for several accidents. Therefore some assistance is needed. There is large progress in waveform and system design as well as in MMIC chip development for 24 GHz radar sensor technology [4]. [C429]

### "Passive radar from history to future"

The history of passive radar dates back to the early days of radar in 1935 when the Daventry experiment was conducted in the UK. It continues in WW II with the German Klein Heidelberg passive radar and receives new interest today, as passive covert radar (PCR) systems like Silent Sentry and Homeland Alerter 100 are ready for operation. The future of PCR will strongly depend on the availability of transmitters of opportunity such as FM-radio and digital broadcast networks. [C430]

### "A dual-use system for radar and communication with complete complementary codes"

A dual-use architecture is proposed for both radar and communication. The proposed method uses complete

complementary codes for both radar and communication signals, whose outputs almost become zero sidelobe. In this paper, the principle of the proposed method and simulation results are described. [C431]

#### "MVDR radar signal processing approach for jamming suppression in satellite navigation receivers"

The Minimum Variance Distortionless Response (MVDR) technique, which is well-known in radar signal processing, will be applied in this paper for jamming suppression in a satellite navigation receiver. Two different beamforming schemes, conventional and MVDR are applied to a satellite navigation receiver for mitigation of strong jamming before acquisition of the C/A code. The effect of beamforming on the cross-correlation performance is evaluated in terms of two quality factors: the signal-to-interference-plus-noise ratio (SINR) improvement factor estimated at the beamformer output and the post correlation signal-to-noise ratio (SNR) which will be estimated at the cross-correlator output. The simulation results demonstrate that the more effective jamming protection and as a consequence the improved performance of the C/A code acquisition are achieved using the MVDR beamformer procedure compared to the conventional one. [C432]

#### "Stabilisation of false alarm in the signal detection tasks"

The task of the known form signal detection on background of non-correlated normal interference with unknown variance is considered. The invariant to shift and scale parameters algorithm based on order statistics is suggested. The analysis of quality characteristics of the algorithm has been carried out [C433]

#### "A history of oscilloscope development in Lithuania and neighbor countries"

This article describes a history of oscilloscope development in Lithuania and neighbor countries during fifty years. Oscilloscope, general-purpose oscilloscope, digital storage oscilloscope, "traveling wave" CRT, sampling oscilloscope, service oscilloscope, oscilloscope calibrator. [C434]

#### "Fifty years of noise radar"

The talk provides a historical account of noise radar from 1959 to 2009, describe notable results from world-wide R&D activities in noise radar, and predict possible developments over the next fifty years. [C435]

#### "Radar target detection and Doppler ambiguity resolution"

A Continuous Wave (CW) radar with a linear Frequency Modulation (FM) and a very short chirp duration is considered in this paper. A single target range and Doppler frequency measurement consists of a sequence of L chirp signals with the same chirp duration. The maximum unambiguously measurable radial velocity in this case is limited by a minimum chirp duration. Therefore fast moving targets will cause ambiguous measurement results, that have to be resolved. The technique of resolving ambiguities on the basis of several subsequent measurements with different ambiguity interval lengths is well known as Chinese Remainder Theorem (CRT). It has been extensively described in literature [2]. Two different signal processing approaches to apply this technique for the resolution of ambiguities are compared in this paper. These do not differ in terms of the ambiguity resolution itself, because they are based on the same principle. The detection performance however is different. [C436]

#### "Session 9b: Electronic warfare"

{no data available} [C437]

#### "Multifrequency radar images of electrodynamics objects located behind dielectric layer in millimeter wave range"

The problem of measurements of reflectivity of different structures situated behind a dielectric slab is rather general problem, which is induced by requirements of technological radar, non-destructive testing of industrial products, building materials, underground probing. The implementation of multifrequency method for measuring microwave reflectivity in the free space allowed testing various numbers of objects with the purpose of estimating their parameters such as width, length, the form and reflecting ability. The purpose of the paper is present some results for simple objects which located behind the radiotransparent barrier. [C438]

#### "GPR signal phase structure application for estimation of distribution of soil electrical properties on depth"

The mathematical algorithms for reconstruction of the soil layers electrical characteristics using the estimated

dependency of radio waves attenuation per unit length on frequency or similar dependency on phase velocity are described in [1, 2]. To perform this reconstruction we used a well known Kramer-Kronig equation, which is then lead to a nonlinear singular integral equation for the unknown functional dependence of the soil conductivity on the frequency. Then the equation is solved by a numerical iterative method, with evaluated dependencies of conductivity and permittivity on the frequency in a range of probing signal carrier frequency as a result. The main difficulty here is an attempt to assess the functional dependence of attenuation per unit length or the phase velocity on frequency. The first method uses filtering of signal that corresponds to specific soil layer on the output of georadar receiver phase detector. Then the frequency dependence of the phase velocity of radio waves in this layer is estimated using the displacement of the object image in depth when using low-frequency and high frequency parts of the probe signal spectrum. Both the first and second algorithms do not allow obtaining highly accurately estimated electrical characteristics, so it is impossible to estimate accurately the frequency dependence of attenuation per unit length or the phase velocity of radio waves propagation in the layers of the soil. [C439]

#### "Radar identification of clouds"

In the present paper the algorithm of meteorological objects recognition is studied on the base of autoregressive (AR) model of signals reflected from the output of incoherent pulse radar, the experimental; is carried out and analysis of meteorological objects correct recognition is performed using examples of highaltitude cumulus clouds, cumulonimbus clouds and "angel-echoes" in the form of Braggs reflections from inhomogeneities in surface layer of clear atmosphere. [C440]

#### "The longitudinal slot characteristics in waveguide with dielectric layer, situated parallel to its broad walls"

Waveguide slot arrays (WSA) are widely used in ground and onboard radar-tracking, radiorelay, radionavigating systems. There is a danger of occurrence interference maxima of the higher orders in WSA on a hollow waveguides. To avoid occurrence of these maxima, distances between radiators are reduced using different ways. One of them is the use of waveguides of the  $\Pi$ -shaped form, another one consists in reduction of a waveguide width. To pull together radiators within the limits of one linear array and to reduce distances between radiators in the neighboring linear arrays it is possible to use slowing down a wave in a waveguide by insertion a dielectric layer. The purpose of the present work is to research WSA characteristics at partial overlapping along z axis of regions of the neighboring slot arrangements when the slots are cut in a wide wall of the rectangular waveguide with dielectric layer located parallel to its broad walls. [C441]

#### "Time-domain simulation of trains of oscillation pulses in a Gunn diode system with a remote resonator"

We present self-consistent time-domain simulation of trains of short oscillation pulses in a time-delay transmission-line circuit of active devices with a remote resonator for emerging radar applications. Inherent instability and essential nonlinearity of active devices makes many simulation tools inadequate for rigorous modeling of active systems with complicated dynamics of generated fields. Conventional software (e.g., SPICE) cannot easily cope with active distributed systems where the wave propagation between devices is an important part of system operation. A promising approach is the hybrid method that combines both the frequency-domain and the time-domain computations, though it suffers from various limitations (narrow-band approximation etc). For these reasons, the design of active structures is usually split in two stages dealing with either linear or nonlinear parts of the system. In this method, the attention is focused on passive components whose design is carried out in much detail. As a compromise, some assumptions have to be met in this approach such as the operation in the narrow band or in a given set of a few narrow bands, etc. In our work, we develop an alternative approach and focus attention on the nonlinear part of problem, while the linear part is chosen to be relatively simple. In this approach, the aim is the accurate self-consistent modeling of nonlinear effects through rigorous solutions of governing equations and, specifically, accurate time-domain simulations of nonlinear oscillations and non-conventional dynamics (chaos, pulses) emerging in various conditions. In addition, nonlinear power combining is investigated in a self-consistent manner. [C442]

#### "Improvement of range resolution of FMCW autodyne radar"

The principals of range resolution improvement the self-mixing FMCW radar based on analysis of the spectrum of high-order harmonics of intermediate frequency is proposed. Developed the scheme and investigated the model of Ka-band surveillance self-mixing FMCW radar with digital control and spectral processing of receiving signal. Advantages of this radar are small size, low power consumption and use of scanning antenna. [C443]

### "Measurement of intensity of liquid precipitation using double frequency radar"

The rain intensity is very important characteristic of precipitation which is useful for many fields of people activity especially for such areas as agriculture and municipal services. That is why it is of big interest now to develop new approaches to measure precipitation intensity the most popular of which is radar methods permitted to obtain data distantly and promptly for large territories. Now it is known some radar approaches for measurement of rain precipitation. But the method grounded on measurement of radar reflectance  $Z$  mm6/m3 is the most widespread. It is based on use of dependence  $Z=x^y$ , where  $x$  and  $y$  some constants, depended on climatic, geographic conditions and mechanism of precipitation formation. The main disadvantage of such approach is absence of universal correlation between radar reflectance and rain intensity. Accordingly data of different authors [1,2] the values of parameter  $x$  can be varied from 50 to 2000,  $y$  from 1 to 2,87. Such variation of parameters  $x$  and  $y$  strongly influences on accuracy of intensity measurement. [C444]

### "Diagnostics of refraction coefficient on results of meteorological parameters measurement in arbitrary points of area"

It is known the operating efficiency of radio technical systems of different function (navigation, radar, communication), to a great extent depend on condition of propagation of radio-waves is conditioned on atmosphere refraction state. It for one's turn is conditioned on spatial-temporal distribution of refraction coefficient  $n$ . And variation of mean refraction and numerous cases of so called anomalous propagation of radio-waves could lead to considerable increasing of signal level over the horizon or signal fading in the radio optical line of distance and influence on accuracy of radar and navigation measurements. At present for location the systems of global navigation is in wide application. The completely deployed GPS system of USA exists today. Russia realizes intense work on unwrapping of complete constellation of GLONAS satellites. In the Europe the development of Galileo system is finishes. To the utmost the troposphere influences on results of coordinate measurements. Ignoring of this fact leads to error of measuring of pseudo-range from 2,5 m. (in zenith) to 25 m. (while satellite elevation about 5 degrees). The possible way to decreasing of location error is taking into account troposphere influence while processing of information in the Ukrainian system of cosmic navigation provision (USCNP) [1, 2]. There are two main modes of correction: real-time and post session. For real-time processing we propose to use the data of meteorological stations are in the set of controlling-correcting stations (CCS) USCNP. At that have to be provided accuracies of coordinates determination not worth of some meters. While post session processing corrections are forming on the base of phase observations by stations of USCNP net. The obtained errors of measurement are about some centimeters. Troposphere delays in the realtime the meteorological parameters are obtained in series of points of space are used for approximation. The meteorological parameters of functions approximating dependence of temperature, pressure and humidity on latitude and longitude in the range of Ukraine are forming and giving for users on the base of these delays. Besides the parameters of functions approximating dependence of zenith troposphere delay on latitude and longitude in the range of Ukraine are forming and giving for users. Both these approaches are on the base of troposphere delays calculation using data of meteorological stations to the sea level. Truncation error of estimation is about 2.5%. The analyses is carried out [2] and shows the order of approximating model practically not influences on error of troposphere delay measurement and so we conclude about possibility of usage of zero order model, i.e. the mean data for Ukraine. We seem the bases for such conclusion is small accuracies of measurement of meteorological parameters. [C445]

### "Adaptive phase synchronization in distributed digital arrays"

Self-synchronizing distributed arrays have been investigated for a number of sensor applications such as radar. This paper discusses several methods for phase synchronizing a distributed array so that coherent processing can be performed. One of the concepts involves transmission of a beacon that is used directly as the frequency reference. After a phase synchronization process is performed sequentially across the array, measured phase differences are obtained that can be used in the digital processing to compensate for hardware and propagation channel differences. The concept was demonstrated for a two element array using commercial hardware at 2.45 GHz. Leakage cancellation techniques were employed to achieve phase accuracies of approximately 20 degrees. [C446]

### "iBoard: A highly-capable, high-performance, reconfigurable FPGA-based building block for flight instrument digital electronics"

iBoard is a highly capable, highly reusable, and modular FPGA-based common building block for instrument digital electronics. It is targeted to those space-borne instruments that require high-performance on-board processing capabilities. The paper explains the design methodology, describes requirements of flight instrument digital electronics, presents implementation of the first prototype, iBoard 2. [C447]

### "Potentialities of the Doppler spectrum of backscattered microwave signal in the problem of remote sensing of the sea surface"

Information about sea waves and the near surface wind speed is very important for meteorology. It is well-known that this information, in principle, can be obtained from a backscattered microwave signal. Evidently, the sea state determines both spectral and power characteristics of backscattered microwave signal. However, usually only a radar cross section is used for retrieval of the near surface wind speed. Considering only a radar cross section we lose the important information about the movement of sea surface that can be used for retrieval of key sea state parameters. In this paper the new description of a sea state is suggested and basic features of the microwave Doppler spectrum are discussed. We consider some features of various sea states and analyze their manifestation in the Doppler spectrum. [C448]

### "Application of double frequency radar for measurement of parameters of solid polydisperse aerosols"

In this paper the possibilities of application for double frequency remote sensing of solid aerosols are considered in the case of polydisperse medium. Use of double frequency sounding permits to evaluate effective aerosols parameters with satisfactory accuracy for "narrow"  $\Delta r \leq 0.3$  and "wide"  $\Delta r \geq 4$  distribution law. The experiments with calibrated sand particles with "narrow" distribution law (as aerosols model) confirm the possibility of satisfactory evaluation of aerosol parameters. [C449]

### "Robust DFT-based signal processing in Micro-Doppler radars"

Micro-Doppler (mD) radar is an efficient tool for surveillance systems and they are rapidly developing now. One reason for this is the potential ability of mD radars to provide additional information (features) useful for recognition of objects extracted from short-time spectral or higher-order estimates. In particular, it is known that a signal reflected from a walking human represents a set of harmonics reflected by different parts of a human body. These harmonics have amplitudes and frequencies changing in time. Joint analysis of these frequencies and their evolution in time serve as aforementioned features that are to be retrieved. [C450]

### "Doppler radar method for gas-discharge plasma research"

The aim of the paper is development and describing of remote method for low-ionized plasma characteristics research by means of homodyne two frequency Doppler radar. Gas-discharge plasma sources such as so called noise oscillators (NO) in millimeter (mm) and centimeter (cm) range (ГПП-5, ГПП-10, ГПП-11) which are widely used in microwave radio equipment for mm and cm range receiving apparatus calibration and tuning have been objects of our research. [C451]

### "Kravchenko weight functions in problems of restoration radar images at the modified synthesizing aperture"

The modified algorithms of optimum space-time signal processing (STSP) in the synthetic-aperture radar (SAR) are synthesized. They provide improvement of significant are support significant rise above the radar images (RI) resolution in comparison with classical SAR. It is earlier shown, compression system ambiguity function (AmF) on range and an azimuth is accompanied by growth of AmF sidelobe which soften contrast RI area and deform the real form of the sounded objects. The simple solution of such problems can be received by application weight processing sounding signals and amplitude-phase distribution (APD) in the antenna array aperture. As weight functions (windows, distributions) of any classical functions (Hamming, Gaus, ...) can be use. In [3-4] weight windows on the basis atomic functions Kravchenko windows. In the work are developed influence of Kravchenko windows on quality of RI formation in SAR with modified algorithms STSP are researched. In work the algorithm modified STSP in SAR is synthesized. It provides possibility of formation RI with more higher resolution, than it is possible at use of classical algorithm. The kind modified AmF depends on relation  $\sigma^\circ(F) / N_0 = 20$  (at unlimited increase of this relation the kind of AF aspires to delta-function). Thus the sizes of pixel decreases, and generated RI is characterised by bigger resolution. On such image the speckle dispersion increases also it demands the further processing. Its can be made both at a stage primary, and at a stage of secondary processing. Influence of weight windows on quality of formation RI with use classical windows, and Kravchenko new weight functions is analysed. The expediency use weight functions of Kravchenko, in specifically, window  $[h_2(x, \Delta = 0,001)]^{0,5}$ , as  $V(t)$  and  $V(r)$  is proved. [C452]

### "Optimization of statistical processing radar-tracking signals with use Kravchenko'S weight windows"



In the report on the basis of a method the peak credibility algorithms optimum processing existential signals are synthesised. The attention is converted that in these algorithms naturally arises beamforming. Necessity of introduction weight windows for these algorithms is shown. It is proved expediency of carrying out joint optimisation processing existential signals on a method of the peak credibility and weight processing signals and peak-phase allocations a field in the antenna aperture. It is shown, that use weight windows of Kravchenko allows to provide the solution tasks in view with demanded exponents quality. [C453]

#### **"Aggregated convex regularization and variational analysis technique for enhancement of mm waveband remote sensing imagery"**

In this paper, the statistical Bayesian and descriptive regularization approaches for high resolution radar image formation is detailed in many works, where such approach is adapted to the sm and mm waveband remote sensing (RS) applications considered. [C454]

#### **"Fifty years of noise radar"**

The talk provides a historical account of noise radar from 1959 to 2009, describe notable results from world-wide R&D activities in noise radar, and predict possible developments over the next years. [C455]

#### **"Sources of intense impulse microwave emission"**

Impulse electromagnetic fields of large intensity in combination with ultra-short pulse (USP) duration are widely used for modification a property of materials, creation special types of radars and test facilities at studies of electromagnetic compatibility/strength (EMC/S). Long-term experience of NSC KIPT in the area of highpower impulse radiation sources used for tests of radioand electronic equipment and components to impact of USP microwaves with narrowband (NB) and ultra-wideband (UWB) frequency ranges. [C456]

#### **"System aspects of a low-cost coherent radar system with AESA antenna for maritime applications"**

Motivated by new performance requirements and technological progress Fraunhofer FHR has initiated the development of a low-cost coherent radar system demonstrator with AESA antenna for maritime applications. The proposed system is expected to exhibit smaller operational costs and better performance than conventional shipborne navigation radar systems. In this contribution an overview of the total system was given. Emphasis was placed on the overall system design and the verification of the feasibility resorting to commercial low-cost components (COTS). The antenna front-end and the custom-designed mixed-signal integrated circuits which are the core components of the T/R-modules were presented. In the near future, a demonstrator of the antenna front-end will be completed enabling representative performance measurements. [C457]

#### **"Experiment design framework for super-high resolution imaging with the geostar configured sensor array data"**

In this work, we intend to address a novel look at the enhanced RS imaging with the mm-band array radar/SAR that employ the GeoSTAR sensor array geometry pursuing new descriptive experiment design regularization (DEDR) methodology that aggregates the concept of sensor array design with different methods for sensor system and reconstructive imaging method fusion, and report the simulation results of different DEDR-related GeoSTAR-adapted imaging techniques using the specialized elaborated software that we refer to as "Virtual Remote Sensing Laboratory" (VRSL). [C458]

#### **"Comparative analysis of regression line fitting algorithms in blind method of mixed noise variance evaluation in radar images"**

Radar images obtained by remote sensing systems as a rule are corrupted by mixed additive and multiplicative noise. To carry out high-efficiency filtering, the information about noise statistics in these images is required. However, in many practical situations such information is a priori unknown. Therefore methods able to evaluate variances simultaneously for both noise components are necessary. [C459]

#### **"Signal processing algorithms in stepped frequency continues wave ground penetrating radar"**

Broad use of underground sensing led to development of a new signal processing algorithms which can extract much more information about soil and underground objects physical characteristics. These algorithms require information about how specific attenuation is dependent upon frequency, about phase velocity of radio waves in soil or about signals phase structure in cases when underground objects are present or absent. This kind of

information can be easily obtained when using probing signal with stepped change of a carrier frequency. Radar systems with this kind of sensing signals are called Stepped Frequency Continuous Wave (SFCW) GPR.

[C460]

### "Compact millimeter-wave distance and speed measurement sensor for railway applications"

Radar sensor for use in automatic shunting system which executes remote control of track occupancy on hump yards and railroad switches and cut speed control passing along retarder position is developed. The sensors are equipped by systems of remote control and internal parameters diagnostics transmitting the radar and service information to the control point. The sensors could be applicable for use in the data nets. The main feature of the developed radar is the use of FMCW self-mixing transceiver with internal detection and digital control and spectral processing of the signal. [C461]

### "Communication of characteristics of radiation and dispersion of a lattice of flat wave guides"

As now in a radar of modern carriers the phased antenna lattice is a principal view of aerials working out of methods of the analysis and research of characteristics of dispersion of antenna lattices as the most perspective is an actual problem. Antenna lattices find wide application in quality and highly effective radar-tracking reflectors. They are applied in various areas of technics: in a radar-location, navigation, meteorology, etc. Therefore the interrelation of characteristics of radiation and dispersion is important. [C462]

### "Double frequency sounding of liquid precipitation"

Measurement of microstructure characteristics of precipitation is very important for study of process of their formation and progress. Use of the remote sensing methods is also quite interesting especially for measurement of particle size of liquid precipitation. That is why the double frequency method for measurement of particle dimensions is quite relevant. Peculiarity of liquid precipitation is dependence of their permittivity on temperature and operating wavelength. This fact essentially complicates application of double frequency method. So the goal of this paper is analysis of the method facilities in the frequency band, which is traditionally used for radio meteorology (8 mm and 3 cm). Experimental study of proposed approach was performed for single water drop by means of Doppler double frequency radar ( $\lambda_1=8$  mm and  $\lambda_2=3,2$  cm). The special measuring bench was developed for formation of drops with different sizes. The experimental data have good repeatability  $\leq 1\%$  and measurement error is about 30 %. Thereby performed experiments confirm possibility of use of double frequency method for estimation of effective drop size of liquid precipitation and their integral characteristics water content and intensity. [C463]

### "Algorithm of data processing in GPR"

Special algorithms and methods of data processing have built into the software are usually used to increase the efficiency of subsurface radar sounding with a ground penetrating radar (GPR). They are intended to improve SNR and to present results of a survey of the subsurface in a convenient for operator form. A number of different signal processing algorithms for subsurface probing are developed. Basic attention of this article is concentrated on the algorithm of automatic search for local objects using the Hough transform. Hough transform allows finding defined analytically plane curves, for example, straight lines, circles, ellipses, etc. in the monochrome image. The monochrome image is the image consisting of points of two types which are background points and points of interest. The task of Hough transform is separation the curves formed by points of interest. An example of algorithm of search for hyperbole in GPR image is discussed in the work. [C464]

### "Cooperation in distributed surveillance"

This paper discusses distributed surveillance problems, where a set of sensors, of different modalities, can sense collaboratively and continuously a certain volume of interest. Surveillance operations in complex environments, such as littoral regions, are introduced and their main features and challenges are presented. Effective cooperation among the sensors can synergistically improve the performance of these systems and can endow them with higher-level faculties, such as dynamic task allocation, communication relaying, and cooperative target search and tracking. Different forms of cooperation in distributed surveillance systems are mentioned. The paper focuses on intra-and inter-platform target cueing and handoff as augmentative forms of cooperation in distributed surveillance. [C465]

### "Session 5b: Signal processing II"

{no data available} [C466]

"Session 7a: Noise radar II"

{no data available} [C467]

"Session 6a: Noise radar I"

{no data available} [C468]

"Session 5c: UWB I"

{no data available} [C469]

"Session 4c: Radar applications"

{no data available} [C470]

"Session 6b: Tracking"

{no data available} [C471]

"Session 8a: GPR"

{no data available} [C472]

"Session P1"

{no data available} [C473]

"Session 8b: Radar systems"

{no data available} [C474]

"Title page vol1"

{no data available} [C475]

"Session 6c: UWB II"

{no data available} [C476]

"Session 9a: ISAR"

{no data available} [C477]

"Session 7b: Modelling"

{no data available} [C478]

"Session 4a: Historical session"

{no data available} [C479]

"A frequency selective magnetodielectric layer in polarimetric radar antenna track"

A periodically stratified medium consisting of alternating layers of two magnetodielectric media is considered. In the long wavelength limit such a medium might be treated as uniaxial effective substrate. For oblique incidence of TE and TM type electromagnetic waves, the reflection and transmission coefficients are found. On the basis of numerical solution of associated periodic boundary-value problem, finite scale homogenization model is discussed. Prospective applications of the slab treated for designing frequency selective structure situated in the track of polarimetric radar antenna is pointed out. [C480]

"Session 1b: SAR I"

{no data available} [C481]

## "Design of prospective spaceborne multi-aperture UWB polarimetric high performance SAR system"

Multi-aperture synthetic aperture radar (SAR) systems ensure high performance SAR imaging that is unachievable for conventional SAR. Application of modern technological capabilities in ultra-wide-band radar signals digital forming and processing (including optional modulation modes) enables realizing high performance characteristics and using operational flexibility of the SAR system. This report presents technical pattern and characteristics of the SAR, that is based on segmented polarimetric wide-band active phased array and multichannel digital subsystem for signal parameters control. The system uses technologies of 'multidimensional waveform encoding' for transmitted signal and 'digital beam forming' (DBF) for echoed signal receiving. The design main qualitative characteristics are estimated for multichannel remote sensing modes. [C482]

## "The "COMPACT" family of the small-sized airborne synthetic aperture radars (design philosophy and practical experience)"

Basic functionality and design features of the "COMPACT" family of the small-sized airborne synthetic aperture radarr(SAR) are described. Main technical characteristics of the SAR realisations in the X-, L-, P- and VHF - frequency bands are shown together with features of these application on various types of flying vehicles. Several examples of practical processing and thematic decoding of the radar data are listed that were obtained at the time of real observations in the interests of the various customers. [C483]

## "Numerical implementation of continuous-discrete IMM state estimators"

This paper deals with the problem of numerical implementation of adaptive tracking filters based on continuous-time dynamic models of target motion and on discrete-time models of radar measurement process. The particular problem considered is characterised by: non-linear and non-stationary dynamic models of target movement, uncertain parameters and relatively low data rate due to a rotating antenna. The proposed tracking filter relies basically on the continuous-discrete variant of the extended Kalman filter (EKF), the probabilistic data association (PDA) technique and the interacting multiple-model (IMM) state estimation scheme. [C484]

## "Opening session"

{no data available} [C485]

## "Session 2b: SAR II"

{no data available} [C486]

## "Session 4b: Signal processing I"

{no data available} [C487]

## "Session 3a: Passive radars III focused session"

{no data available} [C488]

## "Session 5a: MIMO"

{no data available} [C489]

## "Session 1a: Passive radars I focused session"

{no data available} [C490]

## "Session 3b: Automotive radars focused session"

{no data available} [C491]

## "Session 2a: Passive radars II focused session"

{no data available} [C492]

## "A kind of MIMO ground penetrating radar plane antenna array and corresponding imaging"

#### method"

Antenna array is widely used in real time imaging of ground penetrating radar (GPR). With circumstance restricting, the number and interval of antenna elements are difficult to fit the need of high imaging resolution. In this paper, a kind of 4-transmitter and N-receiver MIMO GPR plane antenna array is proposed. Based on phase center approximation (PCA) theory, its equivalent antenna array is a uniform square antenna array with  $4N$  T/R antenna elements, and the interval of equivalent elements is half of that of the real receiving elements. The equivalent uniform square antenna array has two synthetic apertures and can obtain the 2D information of target. So, the 2D image of the target can be derived by using narrowband transmitting signals and the 3D image can be derived by using wideband transmitting signals. Corresponding imaging method and procedure are also given in this paper. [C493]

#### "Study on Digital Management of Industrial Water System in Steel Industry"

At present, the shortage of water resources has restricted the development of steel industry. Industrial water minimization is the inevitable choice that break through the bottleneck and reduce energy consumption in enterprises. To solve problems of more extensive operating mode, lower water recycle rate and higher wastewater discharge, life cycle and digital management is very important to joint enterprises. Firstly, the accurate base data was accessed by water balance testing. Then, online monitoring, diagnosis, early warning and the use of dynamic cascade control system was established. This system can realize dosing process control and the reasonable dynamic cascade of wastewater. The model of intensive and digital management would tap maximum energy saving, water-saving potential. [C494]

#### "An improved IMM algorithm with variable structure"

In this paper, an IMM algorithm with variable structure is proposed aiming at the large amount and low efficiency of computation, which is inherent weakness of standard IMM algorithm. Based on standard IMM algorithm, the new method obtains state information of targets, and establishes rules on entrance and exit of models, with which the algorithm adjusts the model set to motion of targets. Results of simulation show that the new algorithm leads to fewer models and higher computation efficiency without lowering the tracking performance. [C495]

#### "Remote sensing retrieval of soil moisture using ENVISAT-ASAR images: A case study in suburban region of Peking, China"

Soil moisture is a highly variable component of soil, and plays an important role in materials and energy exchanges between earth and atmosphere. It is also the basic parameter of crop growing and crop yield forecast. With the features of observing large area synchronously, timely, and economically, remote sensing technique makes dynamic soil moisture monitoring possible. Soil moisture remote sensing monitoring has 30 years history and many researches have been done home and abroad in this field, including visible and infrared remote sensing based NDVI methods, hyper spectral remote sensing based algorithm, and microwave remote sensing orientated methodology and so on. Among these methods, microwave has great advantage in retrieval soil moisture because of the characteristics of all-weather, penetrability and not affected by the cloud. Through study people found that microwave is one of the most effective methods in retrieval soil moisture in various technologies. This paper summarizes the major microwave sensors and the principle of microwave remote sensing, and introduces the microwave model and soil moisture algorithm. Based on ENVISAT Radar data, with suburban farmland (wheat and corn as the main crop) of Peking as the study area, we established the microwave scattering characteristics database of local exposed surface. We used the selected model to simulate the response characteristics of backscattering coefficient influenced by a variety of parameters, such as soil moisture, surface roughness, incidence angle, polarization, etc. Then we got the updated inversion empirical model of the exposed surface, and evaluated the accuracy of model with the actually surveyed data in the field. This article makes certain contributions to the active microwave soil moisture retrieval methods study, and provide a viable model for water resources decision-making support to the Peking municipal government. [C496]

#### "Design and Practice of GPS Inspection Data Acquisition System to Telecom Pipeline Network"

Pipeline network is an important component of the telecommunications system, effective management of pipeline networks, pipeline networks and equipment to ensure safety and efficient utilization of a basic work. The network GPS inspection data collection system was designed based on unistrong expansion product in this paper. the advantages of the system was analyzed based on briefly described the overall design of the system, and principles of data acquisition and data processing methods were described, and finally system application practice was detailedly explicated, and made a detailed analysis. The actual application shows that the program can effectively meet the telecommunication resource management pipeline fast, efficient, timely, and with the original data and GIS platform for seamless docking of the job requirements. [C497]



### "The Research in New Architecture of Petroleum Drilling Instrument System"

Drilling technology in petroleum exploration and development has developed, which follows the development of sensor technologies, electronic measurement and computer network technology, more and more assistant methods are used in the course of drilling, and more information about drilling project and underground to be detected. They direct the driller to operate. At the same time they also allow the decision-makers at the base of oil field and technicians in first time to understand the progress of drilling with the schedule. And we can also receive the regional geological parameters to do other applications and decision-making. This article presents a drilling instrumentation system. It is able well site connect to the base of oil field as a whole by wireless network. They can collect and storage the state of drilling on-site and the geological data and transfer to the base quickly. This system could get the new detecting signal in drilling process, and incorporate in to our instrumentation system signal. Just because the high cost of oil professionals and the volatile political situation of oil-production region, it is the most urgent desire of many oil companies to reduce the number of technical staff in site. This paper discusses the system which could enable multiple drilling well field to share professionals and technical experts in the base, so we could achieve remote operation, remote control in this way. [C498]

### "Chinese AIS Network and Impact on the Maritime Management"

AIS (Automatic Identification System) has more and more been used on a ship to identify a target and improve the navigation safety at sea as a new type of radio navaid system. AIS network has also been constructed at the main harbor in many countries to enhance the traffic safety and the maritime management. In the paper, AIS system is briefly described. It stresses on Chinese AIS network frame. The applications and traffic management are discussed. It is analyzed that AIS network brings to the benefits and the influences on the traffic safety and the maritime management in China. Expectation of application prospect of the network is conducted. [C499]

### "Estimation of forest height, biomass and volume using support vector regression and segmentation from lidar transects and Quickbird imagery"

Lidar (light detection and ranging) remote sensing can accurately characterize forest vertical structure, such as canopy height, above-ground biomass (AGB) and timber volume; however, data acquisition is expensive. To reduce costs, one potential method is to integrate (small area) lidar transects and (large extent) optical imagery to estimate forest characteristics. Typically, multiple regression is used to link variables extracted from lidar transect data and optical imagery. Height information is then generalized from the area covered by lidar transects to other areas without lidar coverage. However, multiple regression models may not fully capture the complex relationship between variables. Fortunately, Support vector regression (SVR) provides a solution to deal with such complex nonlinear problems. Using a case study in Vancouver Island, Canada, SVR was applied to generalize canopy height from lidar transect(s) to the entire study area (2601 ha) based on a segmented Quickbird image. Results show that: (i) compared to typical multiple regression models, the SVR models provided better results for estimating canopy height; (ii) by using only one lidar transect (i.e., 8.8% cover), the SVR model generates an average canopy height estimation error of 6.2 m-which is less than a British Columbia forest inventory height class (9.0 m); and (iii) the final model estimates have relatively high correlations with field data for forest canopy height ( $R^2$ : 0.81), AGB ( $R^2$ : 0.76) and volume ( $R^2$ : 0.64), while representing dramatically reduced acquisition costs. [C500]

### "InSAR analysis over Yellow River Delta for mapping water-level changes over wetland"

Wetlands cover more than 4% of the Earth's land surface and include hydrologic and other process that are fundamental to understanding ecologic and climatic changes. It is very important for wetlands protection and re-construction to measure water level changes and consequently water-storage capacity changes in wetlands. Using VV polarization C-band and HH polarization L-band SAR data, combined with synchronous field measurement and investigation, this paper analyzes the difference of backscattering and interferometric coherence characteristics of different types of wetlands. After evaluating factors that influence interferometric coherence, the framework, for measuring water level changes using InSAR phase information, is presented in this paper. With obtained SAR data, this paper studies the InSAR-derived water level changes in Yellow-River Delta wetlands. The results show that the InSAR technology has a great potential in mapping water level changes in coastal wetlands, and InSAR-derived water level changes can supply unprecedented spatial details. [C501]

### "Multitemporal polarimetric SAR data fusion for land cover mapping"

With the development of the polarimetric Synthetic Aperture Radar (SAR), the research on the land cover classification using SAR data has developed rapidly. But the classification accuracy is serious affected by the

speckle noises on the SAR image. A new method which combines the advantages of multi temporal SAR data and quad-polarization SAR data was presented in this paper. A method of multitemporal SAR data fusion was used to eliminate the effect of the speckle noises on the SAR image. An area of 12 Ч 17 km was selected as test area. 6 multi temporal RADARSAT-2 images were used in this study to contact the land cover classification. The results show that different land cover type denote different backscattering mechanism and the backscattering coefficient value of different land cover type varies as function of time. Based on the fusion result of multi temporal polarimetric SAR data, the land cover classification was fulfilled and the results show this method can effectively distinguish the man-made buildings, forest, farm land and water. The speckle noise was obviously reduced and the visual appearance of the SAR fusion image well improved. [C502]

#### **"A study of PS-InSAR method for small area urban land subsidence"**

Persistent Scatterers for SAR Interferometry (PS-InSAR) technique allows monitoring the temporal evolution of a deformation phenomenon at millimeter level, via the generation of mean deformation velocity maps and displacement time series from a data set of acquired SAR images. However, the serious noises of multi-temporal SAR images make the selection of permanent scatters (PSs) difficult. In this paper, we propose a novel PS-InSAR method based on wavelet phase analysis to solve this problem by improving the quality of interferograms. Firstly, both the real parts and the imaginary parts of SAR interferograms are processed by wavelet decomposition. Secondly, the interferograms on every level are filtered by grads dependent adaptive filter and reconstructed. Finally, interferograms are processed to identify PSs by using two indices namely, amplitude disperse index and spatial correlation index, followed by an unwrap process to extract land subsidence information. We then use this method to process 12 ENVISAT SAR imgs covering Jiaxing city in Zhejiang province, China. The experimental results show its effectiveness in residuals and PSs identification and land subsidence extraction for plain urban area. [C503]

#### **"Estimation of wetland aboveground biomass based on SAR image: A case study of Honghe National Natural Reserve in Heilongjiang, China"**

Wetland is a significant component of the land ecosystems to discover the characteristics and ecological laws. Presently, a common method to estimate a regional wetland biomass is normally based on optical remote sensing images. The estimation of wetland biomass by Synthesize Aperture Radar (SAR) is a novel subject. As a new type sensor, SAR has advantages for wetland applications, therefore, it can be apply for generating some important information about wetland ecology and hydrology, especially with the complex ecological habitat of the transitional place between land and water, radar images can be significant tool for wetland biomass estimation. In this paper, as a case study of SAR application on Honghe National Natural Reserve (HNNR), the wet weight and dry weight field data of 28 quadrats of diverse vegetation in a growing season from the study area in 2009 were gathered, the ASAR image was acquired at the same time with field work. The backscattering coefficient of polarimetric radar and wet weight and dry weight data was taken as correlation variable, the fitting equations of regression models and water cloud model were built to estimate the wet weight and dry weight, a validation was made from 9 measured plots. The research shows the estimation of the wetland biomass by SAR image can be a supplement to optical image with a scientific significance in ecology studying. [C504]

#### **"Wetland mapping by using multi-band and multitemporal SAR images: A case study of Hong he National Natural Reserve"**

Wetland ecosystems have many important functions as the regional environment stabilization, natural species protection and ecological resources facility. Investigation and monitoring on wetland urgently need the application of remote sensing. The optional remote sensing technology is sometimes difficult to receive the data due to the bad weather, or in specific light conditions. However, radar remote sensing has a great potential for technical application in wetland mapping with its all-weather, all-time capabilities. And SAR scattering intensity is sensitive to the soil moisture of land cover and land change, therefore it is also helpful to the wetland research. In this paper, multi-band, multi-temporal SAR technique was used for wetland mapping. Unifies the SAR polarization characteristic, the backscattering characteristic of multi-temporal ENVISAT ASAR HH, HV, VV polarization data and ALOS PALSAR HH polarization data of different land use type and different vegetation type in Honghe National Natural Reserve (HNNR) were analyzed. The multi-temporal SAR data was used for vegetation classification research in decision tree classification method. And the authors use actual samples to do accuracy assessment in the way of computing confusion matrix. The result from this study shows that the improvement of water and marsh classification accuracy owes to the summer data, and the classification accuracy can be improved when we used the multitemporal data, HV polarization data in winter is more advantageous for forest map. The recognition rate of water, marsh and forest was relatively high. The classification of grass and bush had confusion. The classification accuracy of multitemporal SAR reached 79.55%. [C505]

### "Vulnerability assessment of combined impacts of sea level rise and coastal flooding for China's coastal region using remote sensing and GIS"

China's coastal region is physically and socio-economically vulnerable to accelerated sea-level rise and associated coastal flooding because of its low topography, highly developed economy and highly-dense population. In this study, we present a scenario of sea level rise and storm surge flooding along the China's coastal region over the next century and apply them to a digital elevation model (DEM) which acquired by the shuttle radar topography mission (SRTM) to illustrate the extent and spatial distribution to which coastal areas are susceptible to permanent inundation and episodic flooding due to storm events. To perform flood scenario analysis and vulnerability assessment, a method for producing several sets of data was implemented by combining remote sensing processing, the use of grid-based socio-economic data, and subsequent analysis using Geographical Information Systems (GIS). This analysis shows that inundation and coastal flooding will mainly occur in the major delta without the protection of dike systems. However, due to the concentration of population and economic activities in China's coastal region, societal and economic consequences of continued sea-level rise would be substantial. Finally, some suggestions are presented for decision-makers, and other concerned stakeholders to develop appropriate public policies and mitigation measures. [C506]

### "The Internet of Things Based on Embedded Mode Design"

This article describes a composition by the sensor and the embedded system host, and it is the internet of thing technology which collect data on the material and sent to the Internet .The system uses the ARM7 microprocessor as a core processing unit, and it will receive the temperature and humidity sensors which send real-time temperature and humidity data by TCP / IP protocol sent by the GPRS module to the GPRS public networks. Socket programming technology used to establish TCP/IP server, the host sends the data to receive the embedded information, and the data uploaded to the Internet with a rich client (Rich internet application, RIA) model for dynamic call. [C507]

### "Spatial-harmonic magnetrons with cold secondary-emission cathode: Towards unlimited lifetime"

Spatial-harmonic magnetrons with cold secondary-emission cathode are efficient high-power millimeter-wavelength oscillators. Advances in the design, realizations, and investigation of such magnetrons are reviewed. Potentials for further increasing of the lifetime of the spatial -harmonic magnetrons are considered in more details. [C508]

### "Developments in marine radar magnetrons"

Magnetrons for civil marine radar applications have been manufactured on the e2v Chelmsford site since 1947. The earliest production was of the original S band wartime designs developed by the Radiation Laboratory at MIT but it was not long before engineers at the then English Electric Valve Company began making improvements. This paper traces the development of magnetrons for marine radar from the first glass envelope "Gen 1" devices to the current state of the art in 4th generation magnetrons. Each generation of magnetrons introduced significant design innovations and the designers also took advantage of technological developments in both materials and production techniques. The key changes are described and illustrated together with some of the technological improvements that have resulted in today's highly reliable devices. These latest devices embody novel techniques for internal suppression of unwanted oscillatory modes and also use novel processing techniques to achieve unprecedented levels of performance and reliability. [C509]

### "Cavity magnetron in Russia"

The first domestic researches of the cavity magnetron in Russia were in the thirties of the XX century. In the paper it is told about destinies of the first researchers (including D. Malyarov and N. Alekseev). The Second World War not only has changed the approach to cavity magnetron development and to their practical application, but also has caused a set of transformations to the industries. There were new state decisions, enterprises, names. The further evolution of magnetron development occurred within a restriction of access to the information which has become partially excellent only in recent years. In the paper a short characteristic of history and development of the magnetron tendencies on the basis of the domestic industry is presented. [C510]

### "The study on extracting of vessels information from the SAR satellite data"

The paper introduces satellite remote sensing technology used into marine traffic investigation, to detect and analyze actual marine traffic situation on a large scale. The paper introduces characteristics of SAR image and the procedure for extracting information of vessels based on the SAR Remote Sensing image. Vessel Detection Technology is studied based on multi-source space borne SAR data, after analyzing the characteristics of

various types of vessels detection algorithm and combining with the needs of marine vessel detection and traffic investigation. According to the characteristics of SAR images, four methods of extracting ship information have been developed, including gravitational field, CFAR detection, PNN and adaptive algorithm. Taking the ERS-2 images as an example, the reliability and limitations of vessel information extracting from the satellite image is discussed. The study shows that satellite remote sensing provides a new and feasible method for marine vessel traffic investigation. At present, the technology has been developed and some tests have been carried out. However, some limitations in the system need further study, especially the impact of the sea state. [C511]

#### "Developments of radar and magnetrons in the Netherlands after 1945"

This paper covers developments and applications of radar and magnetrons in The Netherlands after 1945. The paper describes: 1. The most important participants, 2. The rapid expansion of the radar installed base, 3. A couple of magnetron-related research projects, 4. Some magnetron applications-in the M20 series radar-in (industrial) heating applications, CW magnetrons. [C512]

#### "In the labor people's name: Development of 60-kW magnetrons in the artificial famine plagued Ukraine in the early 1930's"

The emergence and formation of microwave, electronics and radar community in Ukraine had been closely tied to the invention and development of original high-power decimeter-wave split-anode magnetrons in Kharkov in the 1920-30's. Navigating their lives and research between the deadly Orwellian torrents of the early USSR, the scientists had to close their eyes on the politically motivated famine, which was devastating Ukrainian countryside. Both microwave research and development and food confiscations were done in the name of labor people. [C513]

#### "Frequency bandwidth narrowing technology for cavity magnetrons installing cavity magnetrons into commercial marine radar"

The unmodulated pulse magnetrons design and technology has advanced over the last seven years at New Japan Radio Co., Ltd. (New JRC). These developments have resulted in a dramatic reduction in the unwanted emission levels produced by magnetron devices. This was necessary to meet the increasing global demand for a more efficient use of the radio frequency spectrum, which is seen as a limited and scarce resource. These magnetrons utilise new techniques to reduce the unwanted emissions, while also improving the spectrum in the utilised frequency bandwidth. This paper explains in detail the processes and methodology used to reduce the unwanted emission levels for unmodulated pulse magnetron devices. In addition, this paper will describe Japan Radio's (JRC) commercial marine radar systems, operating in the S and X bands. [C514]

#### "Tracing systems for user&Control-Plan traffic of Packet Core of GPRS-UMTS networks"

The resources of actual tracing tools for Control-Plane and User-Plan traffic are limited and most of them are crashing under the task of tracing 100% User-Plan traffic. This paper proposes a new tracing system for UP&CP traffic of Packet Core networks, like GPRS-UMTS networks, in order to verify their functionality. [C515]

#### "Research on Improved Quality Measures for the Fuzzy Association Rules of One Airborne Radar Intelligence Database"

To address the problems of the rule redundancy and the long algorithm execution time in the process of mining one airborne radar intelligence database by the fuzzy association rules algorithm, this paper define a new QL-implicator based fuzzy support measure in order to enhance the recognition probability of the positive association rules and introduce the fuzzy conditional entropy measure (CE-measure) based on information theory to find the negative association rules, and then pruning the generated rules to shorten the run time of the algorithm. The experimental results show that the proposed method is effective, and the accuracy and efficiency for generating rules have improved significantly by comparing with the traditional fuzzy association rules algorithm. [C516]

#### "Remote Monitoring System of the Motor in GPRS Based on LabVIEW and Embedded TCP/IP"

According to the demand of actual application for motors, the software and hardware structure of remote wireless monitoring and control system for the motor based on LabVIEW and GPRS were designed. The paper presented the design principles of the motor's speed measurement system based on the singlechip, studied the communication protocol of the serial interface between singlechip and GPRS module. The remote computer monitoring platform was established with network communication technology of LabVIEW and database technology. The system was not affected by geographic location restrictions and it was suitable for the remote



monitoring and control system of the motor in different districts. [C517]

### "Early magnetron development especially in Germany"

Magnetic control was a very early form of controlling electrons. The original Braun tube was magnetically controlled, and so was the first telephone relay of Robert von Lieben. Even the first successful attempt to obtain oscillations from a (mercury cathode) tube by Frederick Vreeland in 1908 was equipped with magnetic coils. Descriptions of magnetically controlled tubes were given by several authors, e.g. in 1910 by H. Gerdien of the Siemens Co. and, two years later, a theory of electron motion in a coaxial diode, accompanied by measured results, was given by H. Greinacher. In 1918, A.W. Hull described the use of a coaxial magnetic field with a dynatron, and later he discussed the motion of electrons in a coaxial diode and gave the characteristic of plate current as a function of magnetic field strength. He also proposed an oscillator using feedback via the magnetic coil. In 1924, E. Habann published a paper on the split-anode magnetron, which can be looked at as the first 'real' magnetron oscillator. Presumably, because of the lack of application of very high frequencies at that time, the German literature of the late 1920s seems to have forgotten about the Habann generator. The (at that time) famous books, e.g. of Barkhausen or Strecker, mention for the key-word 'magnetron' the Hull tube, and for highest frequency oscillators the retarding field tube following Barkhausen-Kurz. The work on split-anode magnetrons during the later 1920s was mainly done in Japan by Okabe and in the beginning of the 1930s by Megaw in England. Starting about 1933, the interest in high frequency oscillators, and thus in magnetrons too, arose again. The main interest of application, however, lay in the field of high frequency telephone links rather than in the beginning radar developments. A special problem was the modulation of magnetrons. One method was to install a control grid for amplitude modulation. Also discussed was 'Zeitmodulation', that is pulse modulation. But the problems of modulation remained severe: e.g. the commercial telephone link coded 'Rudolf', which first appeared in 1941, was initially equipped with a magnetron, but later redesigned for a triode transmitter. Technological development led, on one hand, to high-power, water-cooled, split-anode magnetrons. On the other hand, there was the attempt to include the high frequency resonant elements into the vacuum vessel. In most cases these were Lecher type wires. The coupling to the outside was either capacitive or the Lecher wires were led through the envelope. To the author's knowledge, cavities were used only in Barkhausen type tubes called 'Resotank'. When in 1943 the magnetron type CV 64 was found in a crashed British aircraft, the political restrictions for the development of cm-wave tubes vanished in Germany. [C518]

### "Maurice Ponte and Henri Gutton, pioneers of early French studies on resonant magnetron (1932-1940)"

After a quick reminder of French scientists who pioneered the UHF domain in the 20's, emphasis is put on the decisive role of Maurice Ponte at SFR/CSF, who revived Okabe's magnetron concept in 1932 and built up a lot of high efficiency oscillating valves working within the range 3 m-70 cm. Two years later H. Gutton succeeded him and began to work on multi-segment, resonating anode design. Between 1934 to 1938 he tested a large variety of anode architectures, resulting finally in the 8-segment anode and oxide-coated cathode M-16 which in late 1939 delivered a peak power record of 1 kW at  $\lambda = 16$  cm. The M-16 found immediate applications in radio-link communications, particularly in a naval obstacle detector (a very early decimetric radar) tested on board the liner "Normandie" from mid-1935. It was improved in a dedicated laboratory established in 1936 at Le Havre. But its military adaptation had to be destroyed in June 1940 to escape the German invasion. The legacy of these works survived through the scientific exchanges established throughout this time between Dr. Ponte/Gutton at SFR and Dr. Megaw at GEC UK. They had a noticeable influence on the emergence of the British multi-cavity anode invention. In May 1940 the oxide-coated and indirectly heated cathode brought to Wembley by Ponte was the final touch. Promptly inserted in the new E-1189 GEC prototype, it proved to be an essential part of "the most valuable cargo" sent by the Tizard mission to the US a few months later. [C519]

### "From \$10,000 magetee to \$7 magetee and \$10 transmitter and receiver (T/R) on single chip"

The paper reviews the developments in microwave devices for radar applications. It starts with the development of high power magetee and magnetron to solid-state microwave devices and integrated circuits. It also covered recent development and breakthroughs in active electronically scanned arrays (AESA). [C520]

### "Integration of LIDAR data and geological maps for landslide hazard assessment in the Three Gorges Reservoir area, China"

The water storage and millions of immigrants work have a great impact on engineering geological condition which may cause slope instability in the Three Gorges Reservoir area, China. This paper presents regional assessment of landslide hazard from Zigui to Badong based on Light Detection and Ranging (LIDAR) data in combination with geological maps and landslides information of this area. Four essential parameters, including



engineering rocks, slope, slope structure and water impact, are extracted from this data. The informative model is employed to create landslide hazard map. The result shows that informative model successfully identified the stable regions as well as instable reservoir banks. Reservoir water and engineering rocks are principle control on slope stability in this area. We also divided the study area into fourteen sections according to the landslide hazard map. [C521]

### "SAR satellite image interpretation based on the multilayer level set approach"

Synthetic aperture radar, SAR, is a remote sensing way to explore the ground truth in day and night. How to interpret the given SAR images provides an import clue to study the characteristics of the imaged areas. However, the image interpretations for SAR images are difficult because of the effects of speckle signals shown in the images. In order to solve the problem, several algorithms have been proposed. The processed results show the proposed algorithms still have their own limits on reducing the effect of speckle signals. In this paper, the multilayer level set approach is employed to have the SAR images be grouped into several sub-regions such that the segmented regions are homogeneous. Based on this minimization of the energy, the multilayer level set method implicitly presents the regional boundaries as several nested level lines. By increasing iterations and preselected level values, these lines evolve close to the level boundaries based on the energy minimization. This method provides numerical stability and quick convergence. In order to implement the multilayer level set approach, several level values need to be established firstly. Those level values are determined with calculating the average values from the classified groups with applying K-means method. Based on the four-color theory, the multilayer level set method is able to generate an optimal piecewise continuous approximation for the SAR image such that each approximation sub-region is homogeneous. From the processed results, the multilayer level set approach can efficiently reduce the effect of the speckle signals, and quickly segment SAR images for further image interpretation. [C522]

### "Assessment of ASTER GDEM performance by comparing with SRTM and ICESat/GLAS data in Central China"

Recently, a new Global Digital Elevation Model (GDEM) from optical stereo data acquired by the Advanced Spaceborne Thermal Emission and Reflection Radiometer (ASTER) was released with the resolution of 1 arc sec. In this study, the performance of the new ASTER GDEM is assessed by comparing with SRTM (the Shuttle Radar Topography Mission) and point data from ICESat/GLAS (Ice, Cloud, and land Elevation Satellite/ Geoscience Laser Altimeter System). A 5°45' area (30°-35°N, 110°-115°E) with varied terrain was chosen as the study area. Standard DEM-to-DEM comparison, DEM-to-control-point comparison and visual analysis were used to evaluate the ASTER GDEM quality. The results show that the ASTER GDEM has much fewer voids than SRTM V2 (the version 2 SRTM). The ASTER GDEM has lower elevations (approximately -5m) compared with SRTM, whereas the ASTER GDEM has higher elevations (approximately 15m) compared with ICESat/GLAS points. To the vertical accuracy, the results of the ASTER GDEM compared with SRTM V4 (the version 4 SRTM), SRTM V2 and ICESat/GLAS points are 39.55m, 25.99m, 33.99m at 95% confidence respectively, exceeding 20m estimated prior to the ASTER GDEM production. The poor accuracy may be related to the high terrain relief and high ratio of lower stack number of the ASTER GDEM in the study area. The ASTER GDEM shows better performance in the flat areas than that in the mountainous areas, and the accuracy improves with the increasing stack number. The ASTER GDEM has many artifacts including inland water noises and straight lines related to the irregular stack number boundaries, which are caused by the methodology to produce the ASTER GDEM. [C523]

### "Study of the airborne LIDAR data filtering methods"

Filter of airborne LIDAR data is a primary step of data processing. This paper reviews the literature of filter algorithms from aspects of theory and performance. The methods of filtering usually are slope-based surface-based and clustering/segmentation-based. In this paper the filtering methods of Lidar data are studied and summarized especially, the advantages and shortages of the present means are discussed. In addition, prospect is also given to provide references for future research. [C524]

### "An image segmentation algorithm for SAR images based on wavelet packets frame transformation"

SAR (synthetic aperture radar) images are strongly disturbed by speckle noises, which brings difficulty to the segmentation of the SAR images. Some model-based SAR image segmentation approaches (such as the Markov random field model, fractal model) are too complex and time consuming. We propose an new method to segment the SAR images fast in this paper. First we transform the original SAR intensity image into some subimages using the wavelet packets frame transformation. Then we analyze the energy distribution in the

transformed subimages and find that the energy of the speckle noise is mainly concentrated in the high frequency subimages. So we segment the SAR image based on the gray level of the low frequency subimages using a threshold classifying method. The result shows that this method can get a satisfying segmentation result and time saving. [C525]

#### "Geodesics-based topographical feature extraction from airborne Lidar data for disaster management"

Hundreds of thousands of lives were lost in the natural disasters such as geological earthquakes, floods, landslides and mud-rock flow in every year. Nowadays, with the rapid development in airborne LiDAR techniques, extraction of the multi-scale topographical features from high-resolution topographic data acquired via airborne LiDAR would lead to fundamentally new understandings of earth essential to mapping flood, landslide and mud-rock flow hazards for decision makers. In this paper, we define topographic features in a multi-scale manner using a center-surround operator on Gaussian-weighted mean curvatures. These multi-scale topographical features would allow improved detecting, understanding and prediction of flood inundation, landslide and mud-rock flow likelihood. For example, experimental results identify that proposed method can be employed for detecting landslide. [C526]

#### "The atmosphere correction in SBAS D-InSAR land subsidence monitoring application: A case study in Jiaxing-Huzhou plain, China"

It is well known that atmospheric phase screen (APS) effect in Small Baseline Subset (SBAS) D-InSAR processing to obtain ground deformation in long time series leads to additional interferometry phase and the unreliable result. To solve the problem above, MODIS product provides a mean to stimulate atmospheric field of SAR data for reducing the APS effect in D-InSAR processing. In this paper, 12 ENVISAT ASAR images are used to process SBAS method and 6 MODIS MOD05\_L2 products are used to process atmosphere correction. A case study in the Jiaxing-Huzhou plain in Zhejiang province, China shows successfully stimulate the atmospheric field of SAR data and analysis its effect on SBAS application. [C527]

#### "Building extraction using dual-aspect high resolution SAR images"

Interpretation of SAR image in urban area is far from solved with the increase of spatial resolution, and building extraction in SAR image has remained as a tough work. Typically, the outlines of buildings are usually not complete, and the geometric distortions further complicate the appearances of buildings in high resolution SAR images. Thus, in this paper, a strategy based on dual-aspect high resolution SAR images was proposed to extract complete footprint of buildings in urban area. Experiments prove that dual-aspect SAR images, especially with high resolution, are very useful for building extraction in urban areas. [C528]

#### "Study on MIMO radar velocity resolution"

Multiple Input Multiple Output (MIMO) radar is a novel radar technique developed recently. It has many advantages over conventional phased radar in many ways such as anti-intercept of radar signal, low velocity target detection, and resolution. In this paper, the signal model and signal processing for MIMO radar is studied. And then, a simulation platform is established with Matlab. Using this platform, the advantage of velocity resolution of the MIMO radar over conventional phased array is researched. [C529]

#### "Wavelet based signal for MIMO radar"

Multiple Input Multiple Output (MIMO) radar can effectively improve radar performance by transmitting specially designed orthogonal signals. In this paper, the orthogonal wavelet division multiplexing is used because of their prominent properties such as favorable ambiguity function and high bandwidth efficiency. The signal design flow is presented in this paper. [C530]

#### "The chaotic signal design for MIMO radar"

The study of multiple-input multiple-output (MIMO) radar has received much attention from researchers in recent years. It has many advantages over conventional phased radar in many ways such as anti-intercept of radar signal, low velocity target detection, and resolution. The signal design is an important problem for radar which decides the performance of radar. In this paper, the chaotic signal is employed to the MIMO radar application. Some preprocessed method is employed to make the signal has small Crest Factor (CF), large bandwidth. Some simulation is presented to show efficiency of proposed method. [C531]

### "Multi-resolution 3D reconstruction of city statue based on laser scanning and photogrammetric concept"

In order to improve the visualization effects of some areas in cyber city, it's often required to reconstruct 3D model of city statues. In this paper, we present a pipeline to build 3D city statue model of high fidelity that fusing multi-resolution LIDAR data and high-resolution digital images. Firstly, the classic ICP algorithm is used to register multi-resolution LIDAR data. Secondly, the geometric seams between multi-resolution LIDAR data are fused by a progressive fusion strategy. Finally, a virtual camera based on basic Photogrammetry concept is proposed to do the texture mapping. Combining all kinds of automatic and semi-automatic methods, the pipeline works well for 3D reconstruction with multi-resolution laser scanning data and high-resolution digital images.

[C532]

### "Ortho-rectification of high-resolution SAR image in mountain area by DEM"

Because of the side-looking imaging characteristics, the quality of Synthetic Aperture Radar (SAR) image is badly affected by variable terrain. Such terrain can introduce large displacements in the SAR image geometry that inhibits the collocation of SAR-derived quantities with geographically referenced information acquired from other sources. So it is necessary to eliminate such inherent geometric distortions by generating a radar ortho-imagery that corresponds to a well defined map projection. In this paper, aiming at the newest high-resolution SAR data-RADARSAT-2 and TerraSAR-X, an effective ortho-rectification method was studied in detail and the result showed this method could achieve high geo-location accuracy. [C533]

### "The application of IMM in MIMO radar"

Multiple Input Multiple Output (MIMO) radar has drawn much attention from researcher. It can effectively improve radar performance by transmitting specially designed orthogonal signals. In this paper, interacting Multiple Model(IMM) estimator is applied to MIMO radar. The detection flow based on IMM is presented in this paper.

[C534]

### "Identification of inclined buildings from aerial LIDAR Data for disaster management"

Airborne laser scanning has demonstrated a strong ability to obtain the location of collapsed buildings and the dimension and characteristic of their damage. This paper focuses on the identification of inclined buildings from aerial LIDAR Data which contains amount of noise and small details. To achieve the goal, several steps were carried out in the approach: Firstly, the building's roof was classified and majority of roof types were taken into account in our research; Secondly, a chosen algorithm was used to extract the roof facets of building and also the foundation, and it was proved to be robust to eliminate the noise and give a good result; Thirdly, the geometric axis line of a building was extracted; fourthly, a method was proposed to determining whether buildings are inclined. Finally, an experimental study was made to demonstrate the feasibility of the proposed solution on disaster management. [C535]

### "A case study on co-seismic ground deformation of the Wenchuan earthquake using L-band and C-band SAR interferometry"

Synthetic aperture radar interferometry (InSAR) has been widely used for the co-seismic ground deformation monitoring. In this paper, The L-band SAR datasets acquired by ALOS PALSAR and C-band acquired by Envisat ASAR are tested respectively for monitoring the co-seismic ground deformation in the area of Dujiangyan, where the Wenchuan Ms8.0 earthquake occurred on May 12, 2008. The displacement on line of sight has been acquired with two-pass DInSAR processing. It is also found that the C-band SAR data results generally have lower coherence over high vegetated and rugged areas, while the L-band SAR with comparatively longer wavelength is more suitable for monitoring the deformation where large displacement over a small spatial extent occurs and the mountainous terrain. However, current satellite radar interferometry, because of its single-frequency signal structure, is hard to measure ground deformation with large gradients as it produce very dense fringe patterns, which cause that the ground displacement deformed in the faults cannot be measured. Although the longer wavelength of the radar signal is less susceptible to high deformation gradients, loss of correlation often still occurs in the faults caused by earthquake. So it is necessary to propose techniques which can monitor large-gradient deformation and the data fusion methods of multi-source satellite SAR images. [C536]

### "Study on accurate estimation of baseline parameters of space-borne InSAR based on GCPs"

The estimation of baseline parameters is an important step in SAR interferometry (InSAR) processing and applications, because its accuracy influences directly the quality of the final DEM generated from interferogram. In this paper, some classical methods of baseline parameters estimation, based respectively on precise orbit

data, interferogram and Ground Control Points(GCPs), are summarized and compared. For it is recognized that the baseline parameters estimation based on GCPs is the most reliable method at present, this paper concentrate on researching optimizing model of several correction algorithms based on GCPs for baseline parameters. The approach is tested with ENVISAT ASAR data over the Dujiangyan region of Sichuan Province of China. Finally, the feasibility and rationality of the proposed method is showed by comparing the quality of DEM generated from interferogram with SRTM DEM. [C537]

### "An improved filtering method for digital elevation models construction based on LiDAR"

LiDAR (Light Detection and Ranging) is a positive remote sensing technology. In this paper, with analyzed the characteristic of LiDAR data and discussed the advantages of LiDAR data, we present an improved data filtering algorithm for LiDAR data. It is basing on the last return laser pulses and tries to design an fast pre-processing LiDAR point data with the purpose of DEM Modeling from LiDAR based point cloud data. The algorithm contains two times of filtering with different aims and data process strategies. Experiments of real terrain area are presented for testing efficiency and accuracy of this filtering method. [C538]

### "Precise SAR satellite orbit parameters determination based on Ground Control Points"

Aim to solve the georeferencing problem of spaceborne SAR imagery, accounting for the orbit physics model and the impact of the earth perturbations, some description models such as four parameters model and polynomial model could be applied to determine the satellite orbit parameters. However the orbit state vectors solved by 5 satellite state vectors supplied by header file in SAR data files could hardly acquire precise orbit parameters, which would greatly effect on the accuracy of co-registration, phase unwrapping, baseline estimation and the generation of Interferogram and DEM (Digital Elevation Model). In this paper, combined with R-D (Range-Doppler) conformation equation and earth ellipsoid equation, which explicitly describe the relationship of corresponding pixel between the 2D image coordinate and the 3D cartographic coordinate of ground targets, an advanced orbit model algorithm by adding few GCPs (Ground Control Points) to improve satellite state vectors is presented. All the correlative formulas are deduced and the orbit parameters can then be iteratively determined through solving a linear equation set consisting of the error equations from all GCPs under Recursive Least Square (RLS) algorithm. The algorithm is tested on an ERS SCL (Single Complex Looked) scene with a series of simulation experiments and the improved orbit parameters and contrasted with accurate SAR orbit data supplied by DEOS institution of Delft University in Holland, which could be demonstrated of validity and stability. [C539]

### "Determination of sedimentation rate of tidal flats at the Yangtze estuary, China, using multi-temporal Landsat TM images"

Remote sensing, combined with in situ surveying, is an effective tool for monitoring the tidal flats. Airborne light detection and ranging (LIDAR) or radar interferometry can be utilized to measure precisely the surface topographic change. However, neither the satellite-borne synthetic aperture radar (SAR) nor LIDAR is an effective way to obtain appropriate data on tidal flats, mainly because of the little opportunity of finding favorable tidal conditions. Therefore, the waterline method is, so far, the only useful approach to the practical application of satellite remote sensing to monitor the tidal flat environment. The 'waterline' is defined as the boundary between a water body and an exposed land mass in a remotely sensed image. Waterline method has been applied in analyzing the horizontal evolution of tidal flat, but such approach has seldom been used for vertical development. Sedimentation rate is an important factor describing the dynamic nature of tidal flat, so waterline method to determine multi-year mean sedimentation rate was reported at Chongming Dongtan Nature Preserve in Shanghai, China in this paper. The waterlines were extracted from multi-temporal Landsat TM images by unsupervised classification method and region growing algorithm. The mean sedimentation rates were calculated at four transects according to corresponding elevation measurements and waterlines with heights assigned by hydrodynamic model. The results showed that the evolution of the bed level was changed spatially in the cross-shore profiles. The peak of accretion rate occurred at different elevations of the four profiles. Sediment surface of all profiles showed a shoreward reduction from the maximum site to the high marsh, likely due to the shoreward decrease in water energy and submergence time as well as the protective effect of marsh vegetation. The offshore decrease may be related to hydrodynamic attenuation by vegetation and settling lag. A positive relationship was demonstrated--between the mean accretion rates and surface elevation of low marsh and mudflat ( $R^2=0.8106$ ). Spatial changes in sedimentation rate were also striking at the same elevations of different profiles, which could be attributed to differences in sediment distribution and hydrodynamics. The effects of tidal marshes on hydrodynamics and sedimentation were also related to the degree of shelter from water energy. The relationship between sedimentation rate and vegetation distribution was also discussed. [C540]

### "Multi-spectral and SAR images fusion via Mallat and A trous wavelet transform"



The information which is contained in the multi-spectral and SAR images have different characteristic. Multi-spectral images contain a great deal of spectral information, whereas SAR images contain rich texture information, such as buildings and road network. SAR and TM images fusion based on the wavelet transform ensure the fusion image showing more spatial detail, not only conserving the spectral information of the multi-spectral images and reducing the distortions as well, but also highlighting the texture information of the SAR image. In this paper, the wavelet transform-based image fusion methods by using SAR and TM multi-spectral images are implemented by Mallat and a trous algorithms separately. Before the image fusion, both of the SAR and TM images have to be geographic coordinate registered in order to they having the same pixel size. In wavelet decomposition, the decomposition level is determined by statistical of entropy value. According to SAR and TM image fusion based on wavelet transform, it can be seen that the fusion image is greatly improved and both of spectral and textural information are enhanced. The value of entropy, variance, average gradient and correlation coefficients of the fusion image are analyzed for two different algorithms evaluation. By analyzing the results, It can be concluded that the image fusion by a trous wavelet transform has a good effect in experiment. [C541]

#### **"Regional aboveground forest biomass estimation using airborne and spaceborne LiDAR fusion with optical data in the Southwest of China"**

Laser altimeter systems provide an accurate measurement of canopy height, the vertical structure of vegetation and the aboveground biomass (AGB). Airborne discrete return LiDAR (Light Detection and Ranging) was used operationally in many cases and some regions; spaceborne large footprint LiDAR (ICESat GLAS) has acquired over 250 million LiDAR observations over forest regions globally. The ICESat GLAS data have been used successfully for forest height and biomass in various sites. To estimate aboveground forest biomass in the Southwest of China, products from EOS MODIS and ENVISAT MERIS were used to expand the estimation from GLAS data. Airborne LiDAR data were collected along GLAS orbit to estimate forest height and biomass for each GLAS footprint after training with 81 field measured plots. The  $R^2$  are 0.68 and 0.91 for field measured biomass and mean height estimation using airborne LiDAR data. Then the aboveground biomass was estimated from ICESat GLAS data using the equation trained by field data ( $R^2 = 0.47$ ,  $n = 185$ ). EOS MODIS Vegetation Continuous Fields (VCF) product, enhanced vegetation index (EVI) product and ENVISAT MERIS Regional Land Cover product were used to generate 175 forest classes, which included five forest canopy density classes, five vegetation index classes, and seven forest cover types. Then we combined forest aboveground biomass derived from GLAS pulses footprint with 175 forest classes to generate a continuous aboveground forest biomass map of study area. Forest aboveground biomass was minimal at 43 Mg/ha, maximal at 133 Mg/ha, averaged at 78.9 Mg/ha in the study area. The results of predicted aboveground biomass were in agreement on the amount and distribution after comparison with reference data, which showed that the predict model for GLAS successfully captured the distribution of aboveground biomass. [C542]

#### **"Large-scale, rapid detection method of surface subsidence in western mining area"**

In view of the character of mining disaster and the limitation of traditional methods of earth surface deformation monitoring in western mining area, an attempt at adopting InSAR techniques in dynamic deformation monitoring in west mining area has been developed. This paper takes Shaanxi Province Binchang mining area as study area, processes the SAR image by differential interference, obtains the deformation image of Binchang Coal Mining Area, This shows that the InSAR can rapid detect the surface subsidence areas in a large area (100 km<sup>2</sup>~100 km). InSAR technology will be widely used in mining damage dynamic monitoring in western mining area. [C543]

#### **"SAR and multi-spectral image fusion based on feature additive integration"**

Fusion of SAR image and multi-spectral (MS) image can provide complementary information about the ground observed objects. This paper presents an fusion method of SAR and multi-spectral images based on the IHS transformation and phase congruence feature extraction. The IHS transform is firstly made to MS image to separate the intensity from the hue and saturation components. Then the phase congruence is calculated from intensity component of MS image and SAR image, which can provide an absolute measure of image features that is viewing-condition-independent and is invariant to change in illumination and magnification. According to both phase congruence values, the feature of SAR image is integrated into MS image. The experiments show that the fusion method proposed has a good performance. [C544]

#### **"Production and accuracy analysis of high quality TerraSAR-X DOM"**

The production and accuracy analysis of high quality TerraSAR-X DOM are presented. The main focus is given to how to control the accuracy of ortho-rectification framework. Two SpotLight scenes of 1 meter resolution



images and two ScanSAR scenes of 3 meter resolution images in China are used as the experimental data. Based on the proposal ortho-rectification framework, the absolute accuracy of TerraSAR-X DOM can reach to less than three pixels. [C545]

#### **"A solution for the data collection in the field survey based on Mobile and Wireless GIS"**

Traditional data collection methods for geological investigation, profile measurement, and other field survey in the research community of geosciences are generally based on the manual measuring and recording by the investigators. The most popular "instruments" used in the traditional survey are pencils as well as printed hard copy charts. The methods are obviously complicated and inefficient, at the same time the collected data are always inaccurate and not compatible with the digital process in computer. For these reasons, a solution for the data collection in the field survey based on Mobile and Wireless GIS is proposed in this study. Key technologies involved in the solution are reviewed at first. Then, a prototype of mobile GIS with basic GIS functions is designed and implemented based on independent development. Important technologies of implementation some basic GIS services for data collection in mobile environment introduced and many key challenges related, which are overcome in the process of the system development, are studied in detail. [C546]

#### **"Extraction of features from airborne Lidar and onboard image data for future driver assistance systems"**

Driver assistance system is currently an active research and development field for the general goal to provide useful information to drivers in order to reduce the number of injuries and fatalities in traffic. One important component of future systems will be an accurate and reliable positioning, which can be realized by relative measurement, using onboard sensors and maps of the environment. However, a prerequisite will be that such maps can be produced fully automatically. This paper explores the use of dense laser scan data from airborne LiDAR scanning systems for the production of such 3D navigation maps, extracting features from airborne LiDAR data and onboard image data, so as to simultaneous matching and positioning based on overlapping the LiDAR data and onboard images. [C547]

#### **"Digital terrain model extraction from airborne LiDAR data in complex mining area"**

Airborne light detection and ranging (LiDAR) proved to be an adequate technique to deliver highly accurate 3D mass points of the surface. However, the surface of mining area is complex with steep slope, dense vegetation, artificial mining facilities and buildings, which is different from the flat surface of city. The main processing workflow for DTM generation from LiDAR includes points filtering and DEM interpolation. In this article, five methods for removing object points from LiDAR data in mining area were compared. These methods, including Adaptive TIN (ATIN), Elevation Threshold with Expand Window (ETEW), Maximum Local Slope (MLS), Mathematical morphology (MM), Iterative Polynomial Fitting (IPF), analyze data points based on variations of local slope, elevation and height difference between points and the interpolated surfaces. Complex mining area data set with various cliffs of quarry, trees, houses, roads and small reliefs were selected to test the filtering methods. The results show that all methods can effectively remove most object points in complex mining areas. The ATIN and MM filter generated the best result in sharp cliff area of a quarry, whereas the other algorithms tended to remove the steep edge of quarry and roads. Depending on the filtering parameters, each method experienced various omission or commission errors. Quantitative assessment shows the ATIN and IPF based on the height difference between points and surface perform better. DEM interpolation assessment experiments indicate that interpolation biases were minute. Global statistics show that Modified Shepard's method, Spline and Radial basis function interpolation methods have the lowest errors in the study area. [C548]

#### **"Elevation-map based regional hazard detection for planetary landing"**

Future planetary exploration missions will aim at landing a spacecraft in hazardous or unknown regions of a distant planet, thereby requiring an ability to autonomously detect and avoid surface hazards and land at an affirmed safe site. Descent stage is typically subdivided into several stages to detect different hazards of varying styles and sizes. This paper focuses on those large surface features that could be detected at a high altitude and we present an elevation-map based regional hazard detection algorithm using image segmentation techniques. The algorithm is tested using Martian elevation maps and testing results show that the proposed algorithm is effective at detecting typical regional hazards such as craters, ravines and ridges, and reliable in selecting a safe and cheap landing window. [C549]

#### **"A system demonstrator for the performance evaluation of a 24 GHz ISM band radar operating with OFDM waveforms"**

OFDM signals possess a high flexibility, which, besides their typical employment for wireless digital communications, makes them also suitable for radar applications. In this paper an OFDM system will be presented that offers communication and radar functions in parallel based on one joint transmit signal. A typical application area would be intelligent transportation systems, which require the ability for vehicle-to-vehicle communication as well as the need for reliable environment sensing. A system demonstrator based on commercial equipment has been set up that allows for the transmission of an OFDM signal carrying arbitrary user information. From the reflected signal radar images resolving the distances of multiple reflecting objects can be calculated. In this paper, first the employed waveform and the detailed system setup will be discussed. Then, measurement results will be shown that prove the operability of the developed system concept and its performance. [C550]

#### "Underwater FDTD ELF simulation using dedicated hardware"

The 1-core CPU, 32-core CPU and Acceleware calculations were performed for the comparison. The results show that Acceleware approach is faster than the 1-core CPU calculation and twice as fast as the 32-core CPU calculation. [C551]

#### "Substrate integrate waveguide quasi Yagi antenna using SIW-to-CPS transition for low mutual coupling"

In this paper, the substrate integrated waveguide (SIW) quasi-Yagi antenna is proposed to enhance the low mutual coupling characteristics by using the SIW-to-CPS transition. The proposed design is based on impedance and mode matching method between the antenna components, such as quasi-Yagi antenna, the CPS feed, and the SIW-to-CPS transition. Moreover, the mutual coupling between neighboring elements of a quasi-Yagi antenna array is lower than the microstrip quasi-Yagi antenna with a measured level of  $< -29$  dB for a 2element structure with  $\lambda_0/2$  (where  $\lambda_0$  is a free-space wavelength at the center frequency of 9.5 GHz) separation. The phased array system using the proposed work can be applied with low mutual coupling characteristics can be applied to various applications in modern communications and radar systems as well as millimeter wave imaging arrays. [C552]

#### "Numerical vibration analysis of a SAR antenna"

Advanced military aircrafts and modern Medium/High Altitude Long Endurance aircraft or unmanned aerial vehicles will be equipped with structurally integrated array antennas for radar applications. The inertial forces and the aerodynamic loads will cause deformations and vibrations of the total antenna. The influence of deformations and vibrations will be most significant on array antennas, which are large in terms of wavelength (high gain antennas). An example of such an antenna is an array antenna for side-looking Synthetic Aperture Radar (SAR) mounted on the aircraft. ASELN SAR applications require highly directional antennas with a narrow beam and low side-lobe levels. In order to design a light and minimally vibrating SAR antenna, modal design is applied to virtual model of the preliminary design. Then, the physical model development tests and integration verification tests will be applied on the later design steps. [C553]

#### "UWB radar target sensing and imaging for granular materials research applications"

In this paper, we investigate a first-generation prototype of a radar system that will provide a minimally invasive fully automated measurement of individual and bulk particle movement in a 3D volume. The radar system comprises inexpensive tracer particles as targets, a test signal generation and measurement unit, and a post-processing unit for imaging. The proposed target is a square retroreflector, which is made up of three orthogonal square metal plates. An array of wideband antennas surrounding the testbed is operated in monostatic mode using swept-frequency VNA measurements that are processed to mimic an ultrawideband (UWB) bandpass pulse. In our first-generation prototype, we synthesize a linear array by moving the testbed relative to a single antenna. The testbed contains one or more targets deployed in a free-space (rather than granular material) volume. We perform delay-and-sum beamforming to reconstruct an image of the testbed. Images are generated for the retroreflector at two distinct orientations (normal and oblique) relative to the array. [C554]

#### "A novel passive ultrasensitive RF temperature transducer for remote sensing and identification utilizing radar cross sections variability"

In this paper, a prototype of the novel SRR temperature sensor integrated into the passive multi-sensor identification sensing system is demonstrated as well as RCS measurements. [C555]

#### "EM techniques for the detection of breast cancer"

Radar based microwave imaging technique has great potential for breast cancer detection. It has been demonstrated by recent experiments that the data adaptive radar microwave imaging reveals good image resolution. However, purely scattered energy based image reconstruction methods can face major challenges in differentiation since the fibroconnective and glandular tissues which could have similar dielectric properties as that of malignant tissues. It has been proposed that the morphological features of the tissue can differentiate the benign from malignant tissues due to their irregular, spiculated shapes. Thus to efficiently differentiate the healthy, benign and breast tissues, this paper proposes a method that combines a novel data-independent beamformer called MWDAS method with Matrix Pencil (MP) method to first localize the suspicious region and then extract the resonant frequency and damping factor of complex natural resonance (CNR) of the malignant tissues. We employ FD-TD based computational 2D and 3D breast models for testing our method. [C556]

#### **"Design and analysis of wideband antennas for borehole and surface ground penetrating radars: Application to soil moisture content measurements"**

In this paper, we have presented original wide band antenna design associated with a crosshole and a surface GPR configuration dedicated to the dielectric characterization of the subsurface. The antenna geometries defined, usually used for UWB applications at frequencies higher than 3 GHz, have been adapted to work at lower frequencies around 500 MHz to obtain a sufficient penetration depth. Moreover, size constraints have led us to design compact geometries. The overall links in both configurations have been modeled using FDTD simulations and detailed parametric studies have been made to optimize the antenna geometries for our application. First measurements associated with the crosshole radar have allowed to validate the two types of antenna designs proposed. Concerning the surface radar the experimental validation of the antennas developed on a test site is under way. [C557]

#### **"Performance evaluation of Null-Steering Bistatic MIMO Radar"**

They propose completely opposite radar system against conventional beam-steering radars. NBMR does not need the process to form omnidirectional beam to reestimate target position when target escapes null of beam. It is shown in Fig. 2. Moreover NBMR with autocorrelation involving weighting factor never lose target because it keeps almost a same resolution for target angle from transmitter, even if target escapes null of beam. It is shown in Fig. 3. With NBMR, we can realize efficient target tracking without being detected from airplanes. [C558]

#### **"Applying non-iterative phase errors compensation method to restore radar subsurface image"**

In this paper we describe a non iterative approach to evaluate and compensate the phase errors of radar subsurface image, and implement the approach to the images based on the MARSIS (Mars Advance Radar for Subsurface and Ionosphere Sounding) data. The main idea of the approach is to build the relationship by phase error vector between the unknown perfect image and a given phase-corrupted image, use the no return area in the perfect image as the constraint condition or known condition to solve out the phase errors vector directly. [C559]

#### **"Directional coupled sectorial loops antenna for Ground Penetrating Radars applications"**

In this paper, a directional UWB antenna based on the concept of coupled sectorial loops antenna (CSLA) is presented [2] [3]. The proposed antenna uses CSLA backed by a short cylindrical cavity with a modal suppressing septum to accomplish unidirectional radiation pattern. Bandwidth enhancement is accomplished by a pair of peripheral slots and a stacked CSLA configuration. sensitivity study is carried out to optimize the geometrical parameters of the antenna in order to achieve the maximum bandwidth and uniform radiation pattern. Through this optimization, this antenna has a VSWR lower than 2.5 across a 2.7:1 frequency range without the use of absorbing foams or lossy elements. The dimension of this antenna is approximately  $0.5 \lambda_0$  at the lowest frequency of operation. [C560]

#### **"Radon transform interpretation of the Physical Optics integral and application to near and far field acoustic scattering problems"**

Radon transform(RT) interpretation of the physical optics integral and application to near and far field acoustic scattering problems are reported. Closed-form expression of the radiation integral will be found for both acoustically soft and hard surfaces, and it will be shown that as a consequence of the RT interpretation of PO integral, the surface integral reduces to a line integral over the intersection curve. The line integral will be evaluated and analytical formulae for the scattered field will be developed for the triangular patches. [C561]

### "3D imaging of passive objects using dual-sided phase conjugating sequentially switched lens"

In this paper we introduce a new concept of a dual sided phase conjugating lens operating as an imaging sensor for continuous wave or pulsed signals for passive target 3D localization. We describe the principle of operation and demonstrate the core resolution properties for single and multiple objects by the way of numerical simulation. Particularly it is shown that the characteristic resolution of a single target by the lens operating under Gaussian pulse excitation is approximately the same as that obtained using UWB synthetic aperture radar techniques. The present concept offers major advantages with respect to existing time reversal techniques which involve computationally expensive high speed digital signal processing of the scattered field. The lens only requires hardware to collect the field scattered from the target(s) and to refocus it onto these target(s). This property should be of high potential for imaging applications where refocusing has to be accomplished in a real time i.e. when high speed target acquisition is necessary. Alternatively the lens can be operated in conjunction with a conventional imaging regime, i.e. to collect the scattered field data, send it to a post processing unit for mathematical image localization. [C562]

### "Research on vibration control and structure integration of antennas in NATO/RTO/SET-131"

Integration of antennas into ground, air or water vehicles is a critical task due to the increasing number of RF and microwave systems used for communication, radar or ESM. Structural aspects such as mechanical or thermal stability, aerodynamics or outer appearance are of great importance. Methods and technology for the integration of single antennas or antenna arrays into structures of different type (e.g. glass or carbon fibre composite materials) are currently being developed at different companies and research institutes and are scope of research work in the NATO task group SET-131. The performance of a system should not be affected by the influence of the carrier platform or by electromagnetic interaction between different systems. Another important aspect are variations of the shape of a vehicle or its parts which may also degrade the overall system performance. There are different reasons for these changes, e.g. vehicle motion, moving parts such as rudders or turbines, or the impact of a projectile or collision. [C563]

### "Double-sided parallel-strip line-fed circular monopole antenna"

This work presents a double-sided parallel-strip line fed ultra-wideband circular monopole antenna. This antenna exhibits a periodic 2:1 VSWR bandwidth from 1.0-9.0 GHz and a continuous 2:1 VSWR bandwidth from 9.5-14.0 GHz. Above 14.0 GHz, the antenna exhibits a mixture of continuous and periodic 2:1 VSWR bandwidths. At 5.0 GHz the antenna radiates an omni-directional beam with a maximum gain of 5.5 dBi, and at 10.0 GHz the antenna radiates a monopulse beam in the end-fire direction with a maximum gain of 6.7 dBi. These measured results confirm the expected values from simulation. [C564]

### "Three-dimensional through wall imaging using an UWB SAR"

A 3-D UWB SAR has been designed to detect the positions of the targets behind the wall and identify them as well. The beam scanning is based on the mechanical movement of the wideband Tx/Rx Vivaldi array. The system transceiver and 3-D microwave beamforming algorithm are introduced in details. An experiment is performed to recover the 3-D images of a human mock-up. The demonstrated 3-D imaging results have indicated the capability of accurately locating, tracking and identifying human beings behind the wall. [C565]

### "Time-Reversal Processing and Autofocus of Targets Behind Complex Wall"

Through-the-wall radar imaging (TWRI) beyond a single wall is a growing area of study. A novel near-field time-reversal match filter deconvolution procedure was proposed to improve imaging behind complex periodic walls. Promising results with improved target resolution were shown. Future work will leverage such technique to tolerate errors in wall parameters leading to an autofocus approach. [C566]

### "Miniature double-ridged horn antennas composed of solid high-permittivity sintered ceramics for biomedical ultra-wideband radar applications"

Ultra-wideband (UWB) radar sensors are attracting more and more attention, e.g., for biomedical applications. In contrast to established techniques like X-ray tomography or invasive diagnostic approaches, UWB radar offers the potential for remote access and ultra-low power signal intensities. Inspired by promising studies of breast tumor imaging, we are continuing and extending our previous work on biomedical M-sequence radar and antenna techniques. We describe the development and the potential of innovative double-ridged horn antennas, based on high-permittivity sintered ceramics, which have been adapted to the envisaged biomedical applications. In this context, the miniaturization of UWB antennas, due to the restriction to small examination areas, without compromising the electromagnetic fidelity is the overall challenge. For the dielectric scaling of antennas with the



potential to operate over wide bandwidths, we focus on nearly frequency independent, high-permittivity and low-loss materials. In what follows, we describe the arduous path from the first idea to functional laboratory versions of double-ridged horn antennas based on solid sintered ceramics. In this way, the paper illustrates the successful interdependence between microwave engineering and mechanical and material engineering. [C567]

#### "Compact reflectarray antenna element using split ring resonator"

This paper presents a compact reflectarray element using split ring resonators (SRRs) for small size and high gain reflectarray design. The proposed element is constructed of dual concentric split rings and a metal line on different layers. Several design parameters of the unit cell are studied for obtaining better phase response. The proposed unit cell achieves a good phase response of 700 degrees at X-band. The unit cell size is 14 mm Ч 14 mm ( $0.36 \lambda_0 \times 0.36 \lambda_0$ ). Due to the small unit cell size, the reflectarray with the proposed element can be expected to achieve high gain. [C568]

#### "Detecting flaws in buried pipes under rough surface using the natural frequency technique"

The matrix pencil method is a MatLab friendly algorithm that generates results in real time. The technique was able to detect cracks in pipes whether they were on top of the pipe or on the bottom up to a SNR = 10dB. Also cracks in hidden and buried pipes were detected using the same technique. [C569]

#### "Radar imaging of a large building based on near-field Xpatch model"

The U.S. Army Research Laboratory's ultra-wideband (UWB) radar was used in field experiments for through-the-wall imaging of an abandoned Army barrack with an approximate 33 m by 27 m footprint. In a previous paper, we used a Physical Optics (PO) based ray tracing code simulating a far-field spotlight configuration in order to explain some scattering features observed in the experimental image (obtained via near-field strip-map configuration). In this paper, we use the same code and model for a data collection geometry that closely matches the experimental setup, and the backprojection algorithm (BPA) for image formation. The new simulated image shows an improved correlation with the measured image, further confirming the applicability of ray tracing codes for UWB imaging in a realistic environment. [C570]

#### "DFT-UTD based MoM approach for an efficient analysis of scattering from large, finite arrays in the vicinity of scattering objects"

This paper presents an efficient hybrid method for analyzing scattering/radiation from electrically large arrays in the vicinity of nearby obstacles. Electrically large arrays are widely used in several applications such as radars, remote sensing systems, and modern communication systems. In general, these arrays radiate in the presence of nearby obstacles, such as an array on a mast. The proposed approach is based on the combination of a ray-field representation of the field radiated by electrically large arrays and a DFT (Discrete Fourier Transform) representation of nonuniform array current distribution. Realistic array current distributions are nonuniform even if the array is excited uniformly due to coupling among the array elements and coupling between array and scattering objects. DFT employment for expressing nonuniform array current distribution is a robust approach, since, for practical array current distributions most of the DFT coefficients are close to zero, except for a few significant terms. [C571]

#### "Effect of primary feed polarization on phase centre location of parabolic reflector antennas"

Knowledge of the phase centre location of the antenna is of great importance in various applications, such as global positioning system (GPS), remote sensing, radars, and virtual arrays. In parabolic reflectors, the phase centre is located at the center of the aperture plane when it is illuminated by a prime-focus point source feed having an axially symmetric pattern. It is clear that if one displaces the antenna phase centre, the apparent location of the antenna will move resulting in a virtual antenna. The virtual array antenna can be thought of as an antenna having multiple identical beams, with multiple displaced phase centre locations. Such a property is desirable in remote sensing applications, to allow multiple antenna representations. Multiple phase centre reflector antennas were studied in using a dual-mode feed horn as a primary feed. In this paper, the impact of the feed polarization on the phase centre location of offset reflector antennas will be addressed. The feed is a dual mode circular waveguide antenna operating at its fundamental mode,  $TE_n$ , and the higher order mode  $TE_{21}$ . It will be shown that the phase centre displacement can be controlled by simply changing the excitation amplitude and phase of each mode, as well as employing different mode orientations. In particular, the direction of the phase centre movement will depend on the polarization of each mode. [C572]

#### "A printed extremely wideband antenna for multi-band wireless systems"



In this paper, a printed elliptical monopole antenna, which is fed by a modified, tapered microstrip feed is presented. The measurements indicate it has an extremely wide impedance bandwidth of 1.08-27.4 GHz. The antenna can support many communication and wireless other services, such as GPS, GSM1800, WLAN, UWB communication systems (3.1-10.6 GHz) and part of the UWB vehicle radar systems (22-29GHz). It is also suitable for extremely wideband spectrum monitoring, interference characterisation and similar EMC/EMI applications, as well as extremely broadband RF energy scavenging. The proposed antenna design and results are discussed. [C573]

#### "Low frequency imaging of separated objects using the ramp response technique"

In this paper, the authors have presented new results of separated objects reconstruction with the ramp response technique. With the canonical example of 2 separated spheres, we have shown that the limit of separation between these objects is given by the spatial limit of resolution, which is inversely proportional to the frequency band. Indeed, the spread in the shadow region does not impact this limit of separation, but it only affects the shape of objects; this must be compensated in the reconstruction process. [C574]

#### "Advanced through-the-wall radar imaging using spectral and wall estimation techniques"

Two techniques are introduced and combined to improve SAR imaging of TWR scenarios, namely wall estimation and spectral estimation imaging using MUSIC. It was shown that homogeneous walls can be eliminated from SAR images although a significant amount of clutter remains if the wall shows inhomogeneities. Furthermore, applying the MUSIC algorithm can significantly clear up the image and make the targets behind the wall more visible. In conclusion, both the described wall estimation technique and MUSIC imaging can enhance TWR images, allowing a clearer interpretation or building a more reliable basis for further processing like target detection. [C575]

#### "Circularly polarized supershaped dielectric resonator antennas for indoor ultra wide band applications"

A recent paper [1] has introduced a new class of dielectric resonator antennas (DRAs), the so-called supershaped DRAs (S-DRAs). This class of radiators took its name from the mathematical formula, known in literature as superformula (see [1] and references therein), that defines the geometry of the base of the dielectric prism acting as dielectric resonator (DR). S-DRAs feature wideband matching characteristics (with relative bandwidths exceeding 50%) and broadside radiation. Moreover, the radiation pattern of this family of DRAs can be varied by changing the DR shape such to become broad and rather stable over large frequency ranges. All these features, combined with the possibility of manufacturing S-DRAs in an inexpensive manner, suggest a possible application of these components in the realm of indoor communication. More specifically, such antennas could be used as access points for wireless local area networks supporting ultra wide band application. However, a closer look at the radiation properties of the S-DRAs has put in evidence the fact that some components of the radiated fields experience sharp notches along specific directions. This could cause severe fading effects in the radio channel in the case of using inexpensive receiving devices (e.g. mobile hand-held terminals). To mitigate this problem an improved version of a specific sub-set of S-DRAs is hereafter presented. The selection of DR cross-shapes having two symmetry planes allows for the excitation of two orthogonal and degenerate radiation modes that, combined, ensure circularly polarized radiated fields. A dual-point feed strategy (see [2], Ch. 7) is adopted to ensure broadband operation. Naturally, as means to ensure circularly polarized radiation, the two degenerate and orthogonal radiating modes are fed with synchronous time-harmonic signals of equal amplitude having an initial phase difference of 90°. [C576]

#### "UWB antenna array for real beam radar imaging"

The four element ultra-wideband (UWB) comb taper slot antenna array with 18 cm element spacing is used for receiving the wideband scattering signal. A double ridge wideband antenna is used as the transmitting antenna and the above developed large aperture UWB array is used as the receiving antenna. The transmitting antenna and the receiving antenna are placed close to each other for quasi monostatic radar imaging. The total linear scan length of target is 200 cm. The receiving impulse signal is achieved not only by the measurement but also by the simulation tool of GEMS. The receiving impulse signals at various positions are processed by the delay and sum algorithm. The results of real beam radar imaging from both simulation and experiment are well agreed. [C577]

#### "Application of the SHGA basing on the CFPM to hypersonic vehicle wing-body location design optimization"

The Genetic Algorithms (GA) is a kind of modern intellectual global optimization algorithm, but there are many shortcomings in some idiographic questions, and its local searching ability is worse. In this paper, aiming at the wing-body joint location of quasi-waverider hypersonic vehicle, improving on the Simple Genetic Algorithms (SGA), inducing the Constrained Flexible Polyhedron Method (CFPM), the Serial Hybrid Genetic Algorithm (SHGA) is presented. Optimizing the wing-body location with the SHGA, getting the Pareto optimal solution of the multi-objective optimization question, the best configuration is recommended. Comparing with the basic model configuration, the recommended configuration improves in the balancing, maneuverability and stability, hiding ability. The SHGA and results of this paper are valuable for hypersonic vehicle design. [C578]

#### "Simulation of UWB echoes from ground based on CPML-FDTD"

In designing some UWB-IR (ultra-wideband impulse radio) devices, the effects of ground echoes must be taken into consideration. The dispersion of soil and roughness of ground surface are significant factors in ground echoes calculation. FDTD (finite difference of time domain) algorithms applied in ground echo simulation at present have the problems of slow speed or large errors. By using multi-pole Debye model as soil dielectric coefficients, and CPML (convolutional perfectly matched layer) as absorption boundary condition, a CPML-FDTD algorithm is derived in multi-pole Debye media. Simulations are carried out under different conditions, and comparison with non-PML FDTD algorithm proves the validity and efficiency of the proposed algorithm. [C579]

#### "Feature extraction and selection for landmine detection using textures of Time-Frequency Representation"

Ground Penetrating Radar (GPR) is widely used in the probe of subsurface targets, in which the Time-Frequency Representation (TFR) approaches have been proved effective for GPR signatures. Since we can treat TFR results as 2-D images, texture analysis is an applicable way for image discrimination. In this study, we propose a target detection method based on TFR textures of GPR A-scans and then select 20 descriptors to interpret TFR image into texture features for decision. The mutual correlation and discrimination ability of the descriptors are studied based on the comparative experiment. According to the results, it is clear that the twenty descriptors are redundant and can be grouped into three weak-correlated classes: 11 descriptors of the first class and 2 of the second one are helpful and recommended to use in texture discrimination while the rest can be discarded. [C580]

#### "Radar jamming resources assignment algorithm for EW real-time decision support system of multi-platforms"

Modern naval battle forces generally include many different platforms, e.g., ships, planes, helicopters, etc. The optimal assignment of radar jamming resources distributed over these platforms is an important research aspect of EW real-time decision support system. This paper presents the mathematical model of the radar jamming resources assignment of multi-platforms and proposes the assignment algorithm based on multi-agents distributed cooperative auction. The algorithm is proved to be feasible by an example. [C581]

#### "Analysis and pattern recognition of blast furnace burden surface based on multi-radar data"

Iron making is the first stage and also an important part in steel making process, which will bring the problem of energy efficiency and economic benefits. In this process, the distribution of the blast burden impacts greatly on the production of BF (blast furnace). Therefore, the prediction of furnace burden distribution in furnace throat will play an important role in the control strategy of furnace burden. Based on the data from the multi-radar, the blast burden curve can be formed. Feature extraction and classification based on different curves (i.e. different pattern) can be made by using BP neural networks. The work proposed in this paper will be a guidance for the future research of burden surface based on the data of phased-array radar. [C582]

#### "Research on the model of Target's trail and the detection simulation of air-defense radar"

In the trace fusion system, it is the unitary way and high cost to get the data sources of air-defense radar. Aiming at those shortcomings, this paper gives a method to generate data based on the model of target's trail and the detection simulation of air radar. The emphasis is placed on the model of target's trail and the process of air-defense radar detection. First of all, the trail model is built up on the flight plane, and then converted into rectangular coordinates system. The radar detection model simulates the detection process to estimate whether the target can be found. The real-time trace data is obtained if the target is found. The experiments validated the models and algorithms. [C583]

#### "Research on modeling and simulation of cruise missile interception system based on Object-

### **Oriented Petri net"**

Petri net is a tool suited for describing system with the feature of concurrence, asynchronization, distribution and undecision. This paper studied and realized a modelling method based on Petri net which integrated Object-Oriented approach and Petri net method, calling Timed Object-Oriented Petri net. It's more powerful to describe complex system but with less complex Petri net structure. We researched how to realize this method in computer simulation and applied this theory to the confrontation simulation of cruise missile interception system, which is a very complex system. [C584]

### **"Design and realization of virtual simulation training system for certain type artillery radar"**

There are many difficulties in the process of the training for the artillery radar's position selection, such as training field is limited, the evaluation method for training is laggard. To resolve the problem, a virtual simulation and training system was designed based on Virtual Reality technology. This system developed with tools of OpenGL, Multigen-Creator, VC++6.0, and created a 3D scene with the DEM data of digital map. The system simulated virtual equipment of artillery radar, special effects of rain, snow, and fog based on collision detection technology and particle system technologies, and formed a realistic virtual battlefield environment, and composition structure, function module and key technologies of the system were discussed. Accordingly, the system implemented all the functions of scenario edit, scene display, position selection training and training evaluation. [C585]

### **"A high-performance heterogeneous embedded signal processing system based on serial RapidIO interconnection"**

The demand for high-performance embedded signal processing systems has expanded rapidly in recent years. As applications requiring faster computation capability, higher throughput bandwidth and more flexible interconnection, traditional embedded signal processing systems could not meet the demand of ever-increasing performance. The paper designs a high-performance heterogeneous embedded signal processing system based on the serial RapidIO interconnection to fulfill the next generation radar system. The system is designed based from aspects of computation capability of single processor, scale of parallelism in system, arrangement of memory architecture, interconnection topology and bandwidth. The system consists of three modules which are high-speed AD module, heterogeneous processing module including FPGA and CPU and RapidIO switch module. The system conform to Advanced Mezzanine Card (AMC) Standard and AdvancedTCA Standard and all modules aggregated by serial RapidIO. The system can perform up to 2 Gsps sampling rate, up to 550MHz processing capability on FPGA and 1.5 GHz on CPU and up to 80 Gbits/s aggregate bandwidth. And finally applications such as system dataflow and control are presented. [C586]

### **"Wide band noise interference suppression for SAR with dechirping and eigensubspace filtering"**

It is necessary to enhance the anti-jamming capability of Synthetic Aperture Radar (SAR) for ensuring its imaging performance. A new approach to suppress wide band noise interference (WBNI) based on dechirping and eigensubspace filtering was proposed in this essay, and computer simulations were performed. All results prove that this approach can effectively suppress WBNI with negligible signal distortion under the condition that the Jamming-to-Signal Ratio (JSR) is 5dB smaller than pulse compression gain. [C587]

### **"Design and realization of virtual scene explore system for artillery reconnaissance radar"**

Virtual Scene Technology is one of the important parts of VR systems. It takes charge of Vision issue in VR systems, and is the most important fact to affect the immersive of the system. There are many problems in training simulation of artillery reconnaissance radar, such as the battlefield environment isn't living, the load of assemble and disassemble is large, the training cost is high. The virtual scene explore system was developed. The general structure of VS Explore System is analyzed and demonstrated, and connection between different parts of VS explore system in system construction process is explained. Several key techniques such as the building of virtual topography based on Delaunay triangle through Delaunay arithmetic, the building of radar, virtual scene explore, etc, are also given in detail. [C588]

### **"The research of interaction management based on the IPv6 wireless mobile terminals"**

The packet switching service of the third-generation mobile communication network (3G) has provide a broader range of services, while wireless local area network (WLAN) has a faster speed in information transmission, thus making these two complementary functionally. However, with the improvement of technology and increasing of mobile users, it has a significant impact on network communication when switching the networks which result in handover latency, although the different networks allow mobile users roaming between different IP networks;

furthermore, it will lead to care-of-address of mobile users error caused by the failure of agent information return if the users move too fast. This thesis basically studies on mobile terminals in the WLAN and 3GPP, two different networks using a wireless IPv6, aiming at proposing a to reduce switching delay and position error.

[C589]

### "A target selection method for ASM based on ICP algorithm"

It's a hard task for anti-ship missile (ASM) to select the target ship from multi-objects acquired by terminal guidance radar. In this paper, a method to select the target in a ship formation is presented based on iterated closet point (ICP) algorithm. The principle of this method is described as follows: (1) a ship formation is independently detected by fire-control radar and terminal guidance radar, and the detected ships by each sensor are separately described with two point sets in a plane; (2) the target selection is realized by matching this two point sets based on ICP algorithm, i.e. finding the correspondences of points in the two point sets; (3) the correspondence of the designated ship in the point set detected by fire-control radar is the target ship to be selected. Compared with former MPR (mutual Position Relationship) method, the performance of the method in this paper is hardly influenced while the ship formation changes the course during the self-control phase of ASM. This superiority is validated by simulation results. [C590]

### "An improved particle filter based on 4D discontinuous measurements"

During the target detection of the airborne pulse Doppler (PD) radar, a 4D measurement comprised of range, azimuth, elevation and radial velocity can be obtained to track the target exactly. But the factors including the Doppler blind zone (DBZ) would result in discontinuous measurements which breaks the continuity of the target track. To be consistent with the practice, we constitute the 3D relative motion model between the airborne radar and the target based on moving platform, and deduce the character of the relative radial velocity in DBZ. According to this, an improved particle filter with relative maneuver detection is proposed. This algorithm is able to adjust the moving direction of the particles according to the type of maneuver, and maintain the tracking by predicting the possible region where the target reappear from the DBZ. The simulation results indicate the validity and feasibility of this method. [C591]

### "UWB cylindrical microwave imaging system with novel image reconstruction algorithm"

In this paper, we apply an ultra wideband radar technique to detect and locate small cylindrical objects in a dielectric cylindrical body emulating the woman's breast. We propose a new image reconstruction algorithm which exploits the monopulse radar principle involving a 2-element array antenna. Using the difference of two signals received by the elements of this array, the part of the signal due to a background being symmetric with respect to the axis of the array is removed. The remaining part is the signal which is due to a scattering object located in the off-axis position of the array. The acquired set of difference signals obtained for various locations of the probing antenna is suitably scaled and mapped to show an internal image of the scanned body. The operation of this system including the new image reconstruction algorithm is demonstrated via full EM simulations and experiment. The proposed imaging approach should be of considerable interest to researchers working in the field of microwave techniques for breast cancer detection and location. [C592]

### "Project management and data quality control"

The Building Sustainability Index (BASIX) is a government initiative at the New South Wales (NSW) Australia to assess the potential performance of new homes against a range of sustainability indices. Over the past 5 years, BASIX has grown into one of the largest environmental sustainability projects in the world and all the houses built and renovated since 2004 have to comply with the BASIX requirement. As a, a large amount of data has been collected and the data sets are grown at a daily basis. Data quality monitoring (DQM), control and the development of a standard for data quality metrics have become a business-critical issue.. In this paper, the authors, based on the BASIX development experience accumulated over the past 6 years, look into the issue of data management, data quality control and recent work carried out at the NSW Department of Planning. [C593]

### "Application of compressed sensing theory to radar signal processing"

Compressed sensing theory is a newly developed theory which unites the signal sampling and compression, based on the sparsity characteristic of signal. The union can reduce sampling rate, and then reduce computational complexity of the system without the loss of the performance of the system. The paper describes the theoretical frame and some key technical, and then illustrates the application of compressed sensing theory to radar signal processing. [C594]



### "High resolution radar imaging utilizing a portable opportunistic sensing platform"

In this paper, high resolution 3-D images generated via a portable wideband RF imaging system are presented. In contrast to traditional SAR processing, this system is able to construct high quality composite images by incorporating a handful of individual coherent radar "snapshots". In the pursuing paragraphs, system functionality and hardware integration are briefly described followed by a 3-D imaging example to display system capabilities. [C595]

### "Y-band phenomenology of indoor environment"

Characteristics of indoor environment at Y-band frequencies have been investigated. Radar measurements of hallways were carried for both vertical and horizontal polarizations. Measurement results show that horizontal polarization gives a more accurate mapping of the indoor obstacles. [C596]

### "Design of two-element probe antenna for UWB near-field imaging"

This paper has reported a microwave imaging system employing a monopulse radar technique to eliminate adverse effects of strong reflection from the air-imaged body interface. This technique is realized using a newly constructed ultra wideband twoelement probe antenna fed by a 180° hybrid. The validity of the proposed system has been verified via full-wave EM simulations. Using the signal data obtained from the outof-phase fed UWB probe and by applying a confocal image reconstruction algorithm, the presence of a 9mm-diameter cylindrical target inside the 100mm diameter container filled with vegetable oil has been detected by just visual inspection of the produced image. [C597]

### "A novel method for limiting the amplitude of SAR images with the principal axis detection"

Amplitude limiting of SAR target is one important preprocessing procedure in SAR target recognition. Traditional amplitude limiting adopted simple threshold value and is usually sensitive to noise. In this paper, a novel method for limiting amplitude is proposed, which is based on the priori knowledge that normally the strong scatter points are nearby target's principal axis. First, target's principal axis and its center is detected with the strong scatter points, then the target area is estimated and the strong scatter points' amplitude are limited by a simple smooth process. Experiments on SAR image show that the proposed method can limit the amplitude of the strong scatter points and enlarge that of the weak scattering points well. [C598]

### "On orthogonal waveform design for MIMO sonar"

MIMO sonar that transmits orthogonal waveforms via transmitter sensors is an emerging technology that has significant application potential. Compared to standard phased array sonar, orthogonal transform waveform can bring many advantages including improved angular resolution and multi-target detection ability. We derive in this paper a novel binary-phase waveform design coded by Gold sequences. This phase code is computationally efficient compared to other codes previously proposed in the literature. We provide some numerical examples to demonstrate the performances of the new code sequence. [C599]

### "A multi-sensors data fusion method based on the augmented support degree"

Due to data fusion with a large number of data on some characteristic index, an improved online data fusion method is proposed. At first, it used a fuzzy-index function to measure the mutual support degree of the observation values. Then an augmented matrix was defined as the criterion for integrated support degree of data from various sensors. According to this augmented matrix's maximum modulus eigenvectors, corresponding weight coefficients of all the observation values were allocated, hence, the final expression of data fusion and estimation was obtained. Finally, an experiment and a simulation were used to compare the proposed method with other two similar fusion methods. Simulation shows that this method is likely have higher precision and strong ability of stableness, and can be employed in uncertain environment with variable sensors. [C600]

### "Application of fuzzy pattern recognition in burden surface identification"

A kind of pattern recognition method with Fuzzy clustering is applied to identify the burden surface of blast furnace. According to the information of burden surface distribution, the target clustering analysis is used to set up a standard model database. Based on the character of distribution, each target burden surface is matched into different standard model database by using fuzzy pattern recognition method. Maximal minimal similarity method is adapted in the course of fuzzy pattern recognition. The simulation results show the effectiveness of the proposed method. [C601]



### "An adaptive modulation method based on bit preassign for HF OFDM systems"

Adaptive HF OFDM system can improve the transmission performance by bit and power loading based on the characteristic of subchannel. Greedy algorithm is the optimal method for finite granularity bit allocation, but it has high computational complexity. A new improved bit and power loading algorithm is proposed for HF OFDM systems in this paper, some bits is pre-allocated to some subchannels based on SNR, the spare bits are allocated by greedy algorithm in new method. The results of simulation reveal that the BER performance of the new method approaches to greedy algorithm when the adjustable coefficient is 0.5, and the computational complexity is lower than greedy algorithm. [C602]

### "Research on design process for complex product"

The workflow is playing a more and more important role in collaborative design due to inherent complexity of the design process. The characteristics of the development for the complex product are studied and a multi-level, modular, integrated workflow is put forward. The functions which should be provided by the workflow is discussed and based on the function the framework of workflow is set up. Then the execution pattern which takes input/output template as the drive is studied. At last, a workflow management system (WFMS) for the development of radar is illustrated. [C603]

### "Neural based optimization analysis of distributed MEMS transmission line phase shifters"

RF MEMS (Radio Frequency Micro Electro Mechanical System) technology is a key innovation for building low-loss phase shifters and other control circuits at millimeter-wave frequencies. The developments of electronic phase shifters with high insertion loss have been used in phased array radar and in wide range of systems including communications and measurement instrumentation. In this paper we propose an efficient approach based on Artificial Neural Network (ANN) for optimization of Distributed MEMS Transmission Line (DMTL) to obtain the maximum amount of phase shift with minimum insertion loss. Based on the work of Rodwell et al for analysis of loss in distributed non linear Coplanar Waveguide (CPW) line, we extend the work for optimization for best phase shift. A stand-alone model for optimization of DMTL phase shift is derived efficiently using ANN. The results from the neural models trained by Levenberg-Marquardt algorithm are in very good agreement with the theoretical results available in the literature. [C604]

### "Mitigation of radar interference with WiMAX systems"

In this paper, the effect of radar-induced electromagnetic interference (EMI) on a WiMAX base station receiver is investigated through the use of MATLAB models. The three types of radar pulses investigated include: a short, wideband, chirp pulse; a long, narrowband, chirp pulse; and a long, sinusoidal pulse. The benefits of superimposing these pulses in the guard interval and/or guard band of the WiMAX waveform are explored. [C605]

### "An MIMO-MTI approach for through-the-wall radar imaging applications"

In this paper, we apply Multiple-Input Multiple-Output (MIMO) configurations to Moving Target Identification (MTI) for urban sensing using radars. In particular, we consider MIMO-MTI formulations for detecting slow-moving personnel inside enclosed structures and behind walls. Using signal multiplexing from two transmitters and several receiver positions, it is shown that the virtual array (co-array) implementing MIMO schemes, applied to stepped-frequency radars, permit improvement in image resolution of moving targets. Laboratory experiments are conducted to validate the proposed approach with targets walking behind walls. [C606]

### "SMSE-based DSA radar waveforms"

Previous communications systems research has demonstrated that the Spectrally Modulated, Spectrally Encoded (SMSE) framework is well suited to SDR platforms and operation in both contiguous and non-contiguous spectrum given its ability to generate a wide variety of multicarrier waveforms such as OFDM, NC-OFDM, MC-CDMA, NC-MC-CDMA, CI/MC-CDMA, NCCI/MC-CDMA, and TDCS. In this paper, SMSE waveforms are extended for use in sparse frequency radar systems. Sparse frequency radar can be capable of dynamically sensing available spectrum, and tailoring the transmitted waveforms to suit the instantaneous RF environment conditions, simultaneously transmitting energy in multiple noncontiguous spectrum bands. Conventional radar performance metrics are reviewed, and a new metric is introduced which specifically addresses performance of noncontiguous spectrum waveforms through comparison to contiguous spectrum waveforms. Through simulation, various examples are shown to illustrate and characterize the impairments that are introduced in processing these classes of non-contiguous spectrum waveform returns, specifically the generation of large range sidelobes. [C607]

### "Using time reversal of multipath for intra-pulse radar-embedded communications"

This paper considers the problem of embedding a covert communication waveform into the backscatter from an illuminating radar by an RF tag/transponder within a multipath environment. We propose to exploit the multipath via time reversal, which is ideally suited for backscatter communications. Multipath time reversal induces a spatio-temporal focusing of the embedded communication waveform at the desired receiver while distorting it at all other locations thus further reducing the probability of intercept. Specifically, the paper addresses the case where the radar waveform is known to the tag/transponder thus allowing for estimation of the multipath via coherent processing (i.e. pulse compression). Within the radar-embedded communications context the use of the estimated multipath is compared with the case when no multipath knowledge is employed. [C608]

### "The impact of internal clutter motion on a sample matrix inversion space-time adaptive processing algorithm and the GMTI minimum detectable velocity"

A MATLAB simulation was constructed to better study the effects of internal clutter motion on a notional X band monostatic airborne radar employing a ground moving target indicator (GMTI) algorithm to detect slow velocity targets of low radar cross section. A sample matrix inversion (SMI) fully adapted post-Doppler space-time processor (tapered and untapered) was utilized and the internal clutter motion model of Ward [1] was applied to the overall simulation. As one would expect, the untapered version yielded slightly better results but in all cases final minimum detectable velocities of about 1.0 meter/second were obtained. By judicious choice and implementation of a reduced rank/dimension algorithm, it should be possible to obtain similar MDV results.

[C609]

### "Target RCS exploitations in compressive sensing for through wall imaging"

In this paper, target radar cross-section (RCS) is utilized to improve the performance of compressive sensing (CS) when applied to sensing through wall based on RF modality. Using step-frequency SAR imaging, it is shown that the selection of frequencies emitted at each antenna position of the SAR system can benefit from a priori knowledge of the target RCS. Frequencies with high target response allow the CS performance to be more robust to noise and are able to reveal target presence in noisy and cluttered environments. [C610]

### "Embedding information into radar emissions via waveform implementation"

In this paper an approach for the joint design of multiple receive filters is described that enables the use of different waveforms during a radar CPI while minimizing the attendant Doppler coherency degradation due to range sidelobe clutter modulation. This capability allows for a set of unique radar waveforms to serve the dual purpose of acting as communication symbols while acceptable radar performance is maintained. The receive filter design approach is based upon the well-known Least-Squares (LS) mismatch filter formulation. The novel modification is the iterative adaptation of the desired response such that all the waveform/filter pair responses are driven to be identical. [C611]

### "ISAR imaging in sea clutter via compressive sensing"

We investigate the application of compressive sensing (CS) to inverse synthetic aperture radar (ISAR) imaging of moving targets. We present our results for a simulated target immersed in different levels of sea clutter. Comparison between traditional and CS approaches to ISAR imaging reveal that our based CS algorithm offers some advantages compared to traditional ISAR imaging under certain limited operating conditions that are nevertheless of practical interest. We conclude by pointing out directions for future work in extending the results of this paper. [C612]

### "Pareto-optimal radar waveform design"

This paper deals with the problem of Pareto-optimal waveform design in the presence of colored Gaussian noise, under a similarity and an energy constraint. At the design stage, we determine the optimal radar code according to the following criterion: joint constrained maximization of the detection probability and constrained minimization of the Cramer Rao Lower Bound (CRLB) on the Doppler estimation accuracy. This is tantamount to jointly maximizing two quadratic forms under two quadratic constraints, so that the problem can be formulated in terms of a non-convex multi-objective optimization problem. In order to solve it, we resort to the scalarization technique, which reduces the vectorial problem into a scalar one using a Pareto weight defining the relative importance of the two objective functions. At the analysis stage, we assess the performance of the proposed waveform design scheme in terms of detection performance and region of achievable Doppler estimation accuracy. In particular, we analyze the role of the Pareto weight in the optimization process. [C613]

### "Waveform design for low frequency tomography"

There are multiple applications that would benefit from the ability to produce three dimensional, high resolution, imagery collected at low operating frequency; among them remote archeological survey of ruins through foliage, and searching for voids in collapsed structures and underground. High vertical resolution circular SAR requires the use of wide-to-ultra wideband waveforms, a problematic aspect in the modern RF spectral environment, particularly at lower frequencies. RF tomography offers the potential to yield high, 3-dimensional resolution using spectrally sparse, narrowband waveforms simultaneously with operation at frequencies that have demonstrated favorable penetration through intervening dielectric media. In this paper we explore this potential by evaluating minimal spatial support tomographic apertures combining diverse narrowband signals with the form (trajectory) of the monostatic collection aperture. Results are presented in terms of image quality metrics: those frequency combinations that jointly minimize peak and rms voxel sidelobe level, cardinal axis resolution length and voxel volume. It is shown that, generally, the frequency selection is a soft constraint in terms of the achievable resolution and image sidelobe levels; that the tomographic aperture with spatial sampling that is linearly continuous and substantially less than hemispherical yields high spatial resolution, and that there is interaction between the form/shape of the tomographic and the waveform set. [C614]

### "Channel probability ensemble update for multiplatform radar systems"

Cognitive radar (CR) is a recently proposed concept that depicts the radar channel in a probabilistic manner. In a multiplatform or networked radar system, some parameters or dimensions of interest are visible (i.e., resolvable) to one radar and not to others depending on the geometry of the scenario. For a radar with new measurements, Bayesian methods to update the cell ensemble probabilities in the non-visible parameters are needed. Here, we show how the overall probabilistic understanding of the channel can be updated despite the fact that some cells are non-visible or "ambiguous". Unfortunately, the number of calculations needed to accomplish a full update is exponentially related to the number of cells. As such, we also introduce a technique that reduces the calculations immensely. Finally, we apply both update techniques to a two-platform radar system trying to form a two-dimensional probability ensemble of the channel. [C615]

### "Target localization in multipath environment through the exploitation of multi-frequency array"

In this paper, we propose a multi-frequency array structure that achieves accurate target localization in a multipath environment. The use of multi-frequencies enables decorrelation in the array to operate direction-of-arrival (DOA) estimation for coherent arrival paths, whereas the spatial filtering of the signals makes the paths separable for robust range estimation. Multi-frequency radar techniques are then applied for range estimation of each path. The target position is identified by the shortest range coupled with its DOA. [C616]

### "Frequency diverse waveforms for compressive radar sensing"

High range resolution radar systems use wideband frequency modulated waveforms to estimate the spatial distribution of the scatterers in the scene. Estimation of range profiles from backscatter energy is a linear inverse problem. The emerging field of compressive sensing has provided provable performance guarantees and signal recovery algorithms for random sub-sampling of sparse or compressible signals. In this paper a novel compressive sensing strategy for radar is introduced which relies on using waveforms with frequency diversity on transmit and random aliasing on receive, that shifts the burden of the sampling operator from the receiver to the transmitter. The transmitter and receiver structure for compressive sensing is described and the sensing matrix for the proposed compressive sensing strategy is derived for use in compressive sensing recovery algorithms based on sparsity regularized inversion. A preliminary experimental demonstration of the compressive sensing strategy is given through sampling of staggered multifrequency linear FM signals through a single low rate A/D. [C617]

### "Optimal mismatched filter bank design for MIMO radar via convex optimization"

In this paper, a mismatched filter bank is designed for suppressing the autocorrelation peak sidelobe level (PSL) and the peak cross-correlation level (PCCL) of an orthogonal polyphase sequence set applied in a multiple-input multiple-output (MIMO) radar system. The mismatched filter bank is obtained by minimizing a weighted maximum of the PSL and PCCL on the basis of the convex optimization. Compared with the iteratively reweighted least squares (IRLS) method, the proposed convex method can get the optimal mismatched filter bank with the minimum PSL and PCCL, and can also control the system signal-to-noise ratio loss (SNRL). Numerical examples show that the optimal mismatched filter bank at the cost of a slight SNRL can achieve a good improvement of the PSL and a moderate improvement of the PCCL, if the filter length  $P$  and the weighting factor  $w$  between the PSL and PCCL are appropriately chosen. [C618]

### "Reduced rank detection algorithms for distributed array sensors"

Distributed sensing systems provide an inherent spatial diversity by viewing a potential target from different aspect angles. Even though the centralized fully adapted processing scheme provides optimum performance, it is impractical for reasons of computational complexity and the sample support required for weight training. This paper presents two decentralized reduced rank STAP algorithms to overcome the drawbacks of centralized fully adapted processing. [C619]

### "Compressive radar imaging using white stochastic waveforms"

In this paper, we apply the principles of compressive sampling to ultra-wideband (UWB) stochastic waveform radar. The theory of compressive sampling says that it is possible to recover a signal that is parsimonious when represented in a particular basis, by acquiring few projections on to an appropriate basis set. Drawing on literature in compressive sampling, we develop the theory behind stochastic waveform-based compressive imaging. We show that using stochastic waveforms for radar imaging, it is possible to estimate target parameters and detect targets by sampling at a rate that is considerably slower than the Nyquist rate and recovering using compressive sensing algorithms. Thus, it is theoretically possible to increase the bandwidth (and hence the spatial resolution) of an ultra-wideband radar system using stochastic waveforms, without significant additions to the data acquisition system. Further, there is virtually no degradation in the performance of a UWB stochastic waveform radar system that employs compressive sampling. We present numerical simulations to show that the performance guarantees provided by theoretical results are achieved in realistic scenarios. [C620]

### "Phase-modulated waveform design for the target detection in the presence of signal-dependent clutter"

The problem to be considered is a phase-modulated waveform design for detection of extended targets contaminated by signal-dependent clutter returns and additive channel noise in practical radar systems. We first introduce an optimal waveform design algorithm for extended target detection in a band-limited radar system by maximizing the signal-to-clutter-and-noise ratio (SCNR) at the output of the receiver, and give the analytical solution of the optimal signal energy spectral density (ESD). In order to make full use of the transmission power, a phase iterative algorithm to design the phase-modulated waveform with constant envelope is proposed, which is proven to be able to achieve a small SCNR loss by minimizing the mean-square spectral distance between the optimal waveform and the designed one. The results of extensive simulations illustrate that our approach provides less than 1 dB SCNR loss when the signal duration is greater than 1  $\mu$ s. [C621]

### "Waveform-diverse moving-target spotlight SAR"

This paper develops the theory for waveform-diverse moving-target synthetic-aperture radar. We assume that the targets are moving linearly, but we allow an arbitrary flight path and (almost) arbitrary waveforms. We consider the monostatic case, in which a single antenna phase center is used for both transmitting and receiving. We include the case of waveforms whose duration is sufficiently long that the targets and/or platform move appreciably while the data is being collected. [C622]

### "Design of an optimal radar signal waveform for a range-doppler spreading channel"

This paper deals with the optimal radar waveform design problem using the quadratically constraint quadratic programming (QCQP) in the narrowband signal echo to range-doppler extended target regime. The solution is obtained in the sense of signal to interference plus noise ratio (SINR) maximization with resolution and fixed transmit power constraints. The performance is compared with other conventional waveforms such as continuous wave (CW) pulse and linearly frequency modulated (LFM) pulse, in terms of resolution through ambiguity function. [C623]

### "The metrication of low probability of intercept waveforms"

In recent years, military radar operators have been concerned that the transmitted radar signals will beacon the presence of the radar to an enemy. If intercepted, the radar signals alert a target to an attack which could prompt evasive measures or countermeasures to be taken by the target including the possibility of a reprisal attack using an antiradiation missile. Furthermore, intercepted signals can divulge operating parameters of the radar to the enemy. In response to this low probability of intercept (LPI) requirement, waveforms have been designed to minimize the probability of intercept by an enemy receiver. These are largely based on the use of low peak powers and spread spectrum waveforms offering large processing gains. The interception of signals is a function of both the transmitted radar waveform and the intercept receiver. The aim of this work is to deduce a metric which may be used to quantify and hence compare how "discrete" many of the commonly used LPI radar



waveforms actually are. This study considers the following LPI waveforms: Linear Frequency Modulation (LFM), Sinusoidal Frequency Modulation (Sin FM), PolyPhase Shift Keying (PPSK) techniques including Frank, P1, P2, P3, and P4 codes Costas code Frequency Shift Keying (FSK), and Costas-Barker Hybrid (FSK/PSK). This work represents the first attempt to be published in the open literature to quantify the LPI properties of transmitted radar waveforms. Secure waveform coding strategies to minimize the risk of divulging radar capabilities is known as low probability of exploitation (LPE) and is not considered here. [C624]

### "Bat-inspired multi-harmonic waveforms"

Bats achieve remarkable target detection and selection performance in the most challenging environments. These activities are carried out mainly by echolocation, i.e. by transmitting pulses at ultrasound frequencies and processing the echoes from targets. Because they have relied on high level performance for survival, as a consequence of natural selection, it is believed that they have evolved in order to optimise these capabilities. Echolocation calls are very sophisticated, diverse, and commonly composed of a number of harmonic components. If evolution has resulted in multi-harmonic waveforms there might be advantages deriving by doing so. In this paper we simulate multi-harmonics waveforms and exploit advantages or disadvantages by a range analysis of their ambiguity functions. Results are discussed in relation to the radar and sonar case. [C625]

### "A multi-target detector using mutual information for noise radar systems in low SNR regimes"

Target detection is one of important roles of radar systems. In this paper, we present a detection method using total correlation based on information theory for noise radar systems which enables a system detects multiple targets at low signal to noise ratio regimes. The proposed method utilizes the largest eigenvalue of the sample covariance matrix to extract information from replica of the transmitted signal, and can perform better than the conventional total correlation detector when reflected signals have intermediate or low signal to noise ratio. In addition, in order to avoid ambiguous target detection, we find thresholds to guarantee the detection performance with the same receiving antenna elements for a given false alarm probability. The threshold is computed from the largest and smallest eigenvalue distributions based on random matrix theory. Simulations show the proposed detection method can be used for intermediate and low signal to noise ratio environments, and the thresholds provides exact target detection. [C626]

### "Time-Range Adaptive Processing for pulse agile radar"

Some radar systems utilize pulse agility to mitigate interference or synthesize bandwidth. Transmitting different waveforms on a pulse-to-pulse basis can have deleterious effects when traditional pulse-Doppler processing is employed. In this paper a recursive MMSE-based receiver design, denoted as Time-Range Adaptive Processing, is presented. The new method jointly adapts in range and Doppler, thus yielding enhanced sensitivity when compared to adaptation in each dimension separately. [C627]

### "Analysis of the performance of a multiband passive bistatic radar processing scheme"

The bistatic radar has been revitalized over the last few years through the rapid development of the passive bistatic radar technology. Passive bistatic radar systems have unique properties, especially is time on target high compared to traditional radar systems, as well as the freedom in choosing from the available transmitters of opportunity. This paper will focus on how to take advantage of the latter of these two special properties in order to achieve better range resolution while maintaining the high coherent processing interval. [C628]

### "Cognitive radar for target tracking in multipath scenarios"

In this paper, we propose a cognitive radar system for target tracking in the presence of multipath reflections. We exploit the inherent spatial diversity offered by the multipath environment by constructing a new measurement vector, which we refer to as a virtual measurement vector. We employ broadband Orthogonal Frequency Division Multiplexing (OFDM) signalling at the transmitter and implement adaptive waveform design by minimizing the posterior Cramer Rao bound (PCRB) on the target state estimates to find the optimal weights to be transmitted on each subcarrier bin of the OFDM signal. We demonstrate with numerical simulations that the mean square error in the case of a cognitive radar is significantly lower than the mean square error in the case of a standard radar. [C629]

### "An adaptive multimodal radar system with progressive resolution enhancement"

This paper describes the architecture for an adaptive multimodal RF sensor that is capable of both a wide and narrow field of view. The architecture consists of a test-bed that will enable the generation of linear frequency modulation waveforms of various bandwidths. This paper discusses the proposed architecture, multimodal



algorithm and simulation results. [C630]

### "Radar transmit waveform design for lossy propagation channels"

This paper proposes that radar transmit codes can be tailored to a specific target scene through the use of Marginal Fisher Information (MFI). Where peak sidelobe level (PSL) and Total Integrated Sidelobe Level (TISL) are metrics frequently used in determining the quality of radar transmit codes, well performing free-space waveforms with low PSL and TISL may not be optimal for lossy propagation channels. When some knowledge is available regarding the propagation characteristics of the scene, MFI can be used to develop transmit codes with significantly increased estimation accuracy over codes designed to be optimal for free-space cases. [C631]

### "Designing for spectral conformity: Issues in power amplifier design"

Spectral constraints placed upon radar systems by regulatory agencies require the design of highly linear amplifiers. Spectral spreading in power amplifiers is a result of transistors operated in the nonlinear regime to optimize efficiency. Several different methods are employed by power amplifier designers to maximize both linearity and efficiency. The methods of predistortion, feedforward, envelope tracking, Doherty, and "Linear Amplification Using Nonlinear Components" (LINC) are discussed in this paper. Tradeoffs and challenges inherent in these design approaches are surveyed. [C632]

### "Design, simulation and analysis of neural controller based Series resonant converter"

The Objective of this paper is to design Series resonant converter with 200W, 250 KHz switching frequency which is used for radar power supply and to verify the results using PSPICE. The properties of the energy feedback control, and particularly the optimal trajectory control law, are analyzed. As a result, the state space is considered to be divided into two sub-spaces that correspond to different states of the switches in the converter. An analog neural network learns to classify these two classes by means of a learning algorithm. A simple electronic implementation of this controller is proposed and applied to a series resonant converter (SRC). Results based on prototype measurements show a good improvement in the SRC response versus classical control methods based on the linearization of the state variable equations around a working point and confirm the validity of the neural approach. [C633]

### "Velocity evaluating of the moving objects"

The paper deals with methods of contactless tachometry by radar sensors. The radar sensors are characterized by a good reliability and relatively high accuracy of measurements. The goal of the paper is to propose and realize the system which would manage to measure moving objects with a pulse radar and the Matlab software. Measuring of moving objects has been realized through the radar sensor which operates in an X-frequency band. The audio output of the radar sensor has been used for the velocity measurement and for the signal processing, a PC sound card and Matlab DAQ libraries have been used. [C634]

### "Improvement of bearing-only tracking fusion strategy based on bionics with infrared sensor"

This paper\* mainly studies some improvements of bearing-only data association with a single passive sensor to overcome the existing problems in the applications of JPDA approaches for bearing-only target locating and tracking. First, some adaptive modified rules are presented by deep analysis of JPDA application. This bearing-only association approach reduces computational complexity clearly under the premise of better tracking precision. Then, an effective track management strategy is designed. This strategy helps to set up a clear tracking level and manage historical the information of the target. The application of the proposed approach in a simulation and engineering system proves its effectiveness and practicability. [C635]

### "Tracking People with a 360-Degree Lidar"

Advances in lidar technology, in particular 360-degree lidar sensors, create new opportunities to augment and improve traditional surveillance systems. This paper describes an initial challenge to use a single stationary 360-degree lidar sensor to detect and track people moving throughout a scene in real-time. The depicted approach focuses on overcoming three primary challenges inherent in any lidar tracker: classification and matching errors between multiple human targets, segmentation errors between humans and fixed objects in the scene, and segmentation errors between targets that are very close together. [C636]

### "Human Localization in a Cluttered Space Using Multiple Cameras"

The use of single and dual-camera approaches to locating a subject in a 3-D cluttered space is investigated.

Specifically, we investigate the case where the lower portion of the body may be occluded, e.g., by a chair on a bus. Experiments were conducted involving eleven subjects moving along a pre-designated route within a cluttered space. For each time instant the position of each subject was manually estimated and compared to that produced automatically. The dual camera approach was found to give significantly better performance than the single camera approach. It was found that inaccurate bounding of the lowest part of the subject, due to occlusion, led to localisation errors in range as large as 10m for the latter. Using the side bounds of the detected object, which were found to be robust, accurate azimuth estimates can be obtained for a single camera. The dual-camera approach exploits the greater degree of accuracy in azimuth to estimate the range through triangulation, giving average localisation errors of 40cm over the space of interest. [C637]

#### "Embedded control of LCC resonant converter analysis, design, simulation and experimental results"

The Objective of this paper is to design LCC resonant converter with 200W, 250 KHz switching frequency which is used for radar power supply and to verify the results using PSPICE Simulation for wide variation in loading conditions. We have used motor load (R-L-E) and embedded based triggering circuit. The embedded 'C' Program is checked in Keil Software and also triggering circuit is simulated in PSPICE Software. In this paper analysis, simulation and experimental results were presented and compared with theoretical results. [C638]

#### "Partner Selection Strategy in Cooperative Diversity Systems"

In this paper, a novel strategy for partner selection in cooperative communication system is proposed. The system model is constructed based on the user distribution in the circular area. And then the performance of the present selection method is investigated under the constraint of cooperative gain. The simulation results show that the frame error rate of the method is superior to the random selection in the cooperative area. [C639]

#### "Joint Angle Estimation for Bistatic MIMO Radar"

A new joint direction of arrivals (DOAs) and direction of departures (DODs) estimation algorithm for bistatic multiple-input multiple-output (MIMO) radar is proposed. Instead of two-dimensional nonlinear search or iterative computation, the algorithm uses a one-dimensional search to estimate the DOAs, and then the DODs can be obtained; therefore they can be paired automatically. Furthermore, the algorithm can solve the problem of joint angle estimation when angle ambiguity of DODs occurs. The performance of the proposed algorithm is validated by the simulation results. [C640]

#### "A New Improved Particle Filter Algorithm Based on UKF and GASA"

The degeneracy is the critical problem existed in particle filter (PF). In order to solve this problem, we propose a new algorithm combined PF with unscented Kalman filter algorithm (UKF) and genetic simulated annealing algorithm (GASA) in this paper. In the new algorithm, UKF is used to generate the importance proposal distribution which can match the true posterior distribution more closely, and GASA based on the survival-of-the-fitness principle is applied to enhance the diversity of samples. As a result, the simulation results indicate that the new algorithm can resolve the problem of sample degeneracy successfully and outperform other particle filter algorithms in terms of accuracy and suppression the noise. [C641]

#### "The Application of Poly-Phase Filter in Radar Signal Processing"

A multi-channel structure using half-band filter is presented as poly-phase filter to divide the wide frequency band of the Doppler radar echo into 1-1 pairs. In most of the traditional system, this filter adopts FIR (Finite Impulses Respond) structure to get linear phase and simplify the design ignoring resource consumption. Here a four-channel half-band filter based on poly-phase IIR (Infinite Impulse Respond) structure is carried out. This IIR structure can also get linear phase but need less resources. This design is simulated using Simulink in MATLAB followed by prototype C code generation and performing on the target hardware platform. The results show the correctness of this method. [C642]

#### "A New Adaptive Algorithm for Passive Multi-Sensor Maneuvering Target Tracking"

When tracking maneuvering targets, the sudden changes of target states and nonlinear problems in passive tracking cause serious decline and even divergence in the performance of some conventional algorithms. Taking this into account, a novel adaptive tracking algorithm for maneuvering targets is proposed in this paper. First, a new weighed factor could adaptively adjust the filter gain is introduced in Modified Input Estimation (MIE) algorithm to improve its tracking performance. Then, the least squares technique is combined for tracking passive multi-sensor maneuvering targets in high accuracy without any priori information of maneuver.

Simulation results show the effectiveness of the proposed algorithm. Compared with the traditional MIE and fuzzy MIE algorithm, this algorithm has a better tracking performance. [C643]

#### "A Frequency Estimation Algorithm for Pulsed Magnetron Radar Transmitter Sample Signal"

The pulsed magnetron Cloud sounding radar is one of non-coherent radar, a magnetron has a random starting phase and its frequency chirps during the transmit pulse. This paper presents a frequency estimation algorithm for pulsed magnetron radar transmitter sample signal, based on the modified Wigner-Ville time-frequency analysis. From the three groups' data of compared simulation experiment, at any condition, this paper method can get higher performance than FFT method, and can get measurement mean error less than 0.105% at low algorithm complexity. The method can be used as frequency discriminator in pulsed magnetron Cloud sounding radar AFC real-time hardware system. [C644]

#### "A Novel Spectral Parameters Estimation Approach for Weather Echoes Based on Fitting"

White noise pollution mainly reduce the precision of spectral moments estimation for weather echoes, this paper presents a novel spectral estimation method based on fitting to decrease the impact of white noise on spectral parameters estimation. Fitting polynomial is firstly formed by analyzing the spectral characteristics of weather echoes, and then calibrates the received fitted spectrum by triangle. The simulation results show that the method can successfully reduce the impact of white noise on the spectral moments estimation, and can get higher performance than FFT method with a measurement mean error less than 0.4%. So the proposed method can be applied in weather radar. [C645]

#### "Probabilistic robust hyperbola mixture model for interpreting ground penetrating radar data"

This paper proposes a probabilistic robust hyperbola mixture model based on a classification expectation maximization algorithm and applies this algorithm to Ground Penetrating Radar (GPR) spatial data interpretation. Previous work tackling this problem using the Hough transform or neural networks for identifying GPR hyperbolae are unsuitable for on-site applications owing to their computational demands and the difficulties of getting sufficient appropriate training data for neural network based approaches. By incorporating a robust hyperbola fitting algorithm based on orthogonal distance into the probabilistic mixture model, the proposed algorithm can identify the hyperbolae in GPR data in real time and also calculate the depth and the size of the buried utility pipes. The number of the hyperbolae can be determined by conducting model selection using a Bayesian information criterion. The experimental results on both the synthetic/simulated and real GPR data show the effectiveness of this algorithm. [C646]

#### "Golay waveforms and adaptive estimation"

An iterative range profile estimation process is derived for Golay waveforms. The Re-Iterative Super Resolution (RISR) algorithm is used in conjunction with Golay waveforms and processing for radar range-Doppler estimation. Various additional range-Doppler estimation methods that use RISR and Golay waveforms and processing are simulated for the sake of comparison. Range and Doppler sidelobes are seen in simulation to be mitigated to a significant extent by using RISR in conjunction with Golay waveforms and processing. [C647]

#### "Waveform diversity and advanced signaling strategies for the Hybrid MIMO Phased Array Radar"

The Hybrid MIMO Phased Array Radar, or HMPAR, is a notional concept for a multisensor radar architecture that combines elements of traditional phased-array radar with the emerging technology of Multiple-Input Multiple Output (MIMO) radar. A HMPAR comprises a large number,  $MP$ , of T/R elements, organized into  $M$  subarrays of  $P$  elements each. Within each subarray, passive element-level phase shifting is used to steer transmit and receive beams in some desired fashion. Each of the  $M$  subarrays are in turn driven by independently amplified phase-coded signals. This paper proposes new transmit signal selection strategies based on the observation that some MIMO signal sets, such as those proposed by us previously, cause a very rapid sequential or raster scan across some field of view. Exploiting this property allows one to create and process multiple beams simultaneously. Furthermore, there exists a range-angle coupling in the transmit and receive signals that may lead to high-resolution target localization. [C648]

#### "A Novel Range Detection Method for 60GHz LFM CW Radar"

The linear frequency-modulated continuous-wave (LFMCW) millimeter-wave radar has been widely used in automotive industry applications. The motivation of this paper is to propose a segmented range detection (SRD) method on the foundation of plentiful mature research on the target detection of LFM CW radar. According to the SRD method, the detection range (about 150m in the scene of vehicular collision warning) is divided into several

segments and triangular modulation waveform which consists of several different frequencies is designed. Compared with typical digital signal processing method, the SRD method can available decrease the bandwidth of the IF signal, therefore the in-band noise will be significantly reduced and the signal to noise ratio (SNR) improved. Additionally, different range resolutions can be achieved and average range resolution improved. The SRD method is also validated through multiple outdoor experiments with the use of 60 GHz LFMCW millimeter-wave radar system designed by our research group. The efficiency of the SRD method is demonstrated in terms of ranging accuracy and range resolution after the analysis of experiment results. [C649]

#### "Wireless tomography, Part I: A novel approach to remote sensing"

Wireless tomography, a novel approach to remote sensing, is proposed in Part I of this series. The methodology, literature review, related work, and system engineering are presented. Concrete algorithms and hardware platforms are implemented to demonstrate this concept. Self-cohering tomography is studied in depth. More research will be reported, following this initiative. [C650]

#### "Geometric diversity versus frequency diversity an imaging example"

In classical radar, frequency diversity offers one method of obtaining additional information about targets. With the most basic form of frequency diversity, namely increased bandwidth, high range resolution is afforded to the user. Geometric diversity can also offer the potential for increased resolution, and is the multi-static dual to frequency diversity (increased bandwidth) in classical mono-static radar. In the extreme case, 360 degrees of geometric diversity (tomography) offers sub-wavelength resolution, even under the monochromatic assumption. Operational constraints can limit the system performance. Frequency diversity and geometric diversity can be used in various combinations to obtain the best image under these constraints. For example, frequency allocation can limit the available bandwidth. Geometric diversity with a single or multiple narrowband signals can provide the required system performance. Imaging performance can be evaluated using two factors: resolution and target dynamic range. Resolution is the ability to distinguish two closely separated targets and dynamic range is the ability to determine the presence of a 'weak' target in the presence of a 'strong' target. [C651]

#### "Thinned spectrum radar waveforms"

Small phase perturbations applied to a stepped-frequency or linear-frequency-modulated radar waveform have been proposed as a means to generate frequency nulls in the spectrum of the transmitted waveform. By nulling selected frequencies (or thinning) in the spectrum of transmitted pulses, the interference between the transmitted and received signals is reduced, which facilitates the spectral cohabitation of multiple RF users. Preliminary experimental results of two methods of spectral nulling are presented with consideration to in-band and out-of-band interference. Range processing is examined to determine the effects of the phase perturbation on radar operations. [C652]

#### "Two-Step Moving Target Detection Algorithm for Automotive 77 GHz FMCW Radar"

Today, 77GHz FMCW (Frequency Modulation Continuous Wave) radar sensors are used for automotive applications. In typical automotive radar, the target of interest is a moving target. Thus, to improve the detection probability and reduce the false alarm rate, an MTD(Moving Target Detection) algorithm should be required. This paper describes the proposed two-step MTD algorithm. The 1st MTD processing consists of a clutter cancellation step and a noise cancellation step. The two steps can cancel almost all clutter including stationary targets. However, clutter still remains among the interest beat frequencies detected during the 1st MTD and CFAR (Constant False Alarm) processing. Thus, in the 2nd MTD step, we remove the rest of the clutter with zero phase variation. [C653]

#### "Thermal infrared radiosity and heat diffusion model verification and validation"

A radiosity model used for predicting effective hyperspectral emissivity spectra and radiant temperatures for rough surfaces has been developed. Here we compare the computer model results to analytic model results in order to verify that the computer model is working properly, and validate the model results by comparison to spectra measured in the field by an hyperspectral imaging spectrometer. We measured a cm-scale DEM of the test scene using a tripod-based LiDAR. The discrepancies between analytical and modeled values are less than 0.01%. Modeled emissivity spectra deviate from the measured by no more than 0.015 emissivity units. [C654]

#### "Canopy vertical structure using MODIS Bidirectional Reflectance data"

Canopy spectral invariant variables, escape probability and recollision probability, are wavelength independent and intrinsic canopy structure properties. They provide a physical interpretation of the correlation between canopy



architecture and multi-angle spectral data. The 500m Moderate resolution Imaging Spectrodiometer (MODIS) Bidirectional Reflectance Distribution Function (BRDF) product from study sites at Howland Forest, Maine are used to develop multivariate linear regression models to estimate canopy vertical structure using both escape probabilities and directional reflectance. These are compared with canopy height information which has been retrieved from the airborne Laser Vegetation Imaging Sensor (LVIS) at a finer scale spatial resolution. Both the escape probability and the directional reflectance approaches achieve similar results with correlation coefficients of 0.63-0.66. This suggests that the MODIS 500m BRDF data can be useful in extrapolating limited lidar information on canopy vertical structure to larger regional areas. [C655]

#### "A wideband variable gain amplifier with feedback DC-offset correction in 0.13 $\mu$ m CMOS technology"

A low power and area optimized wideband variable gain amplifier (VGA) has been designed in 0.13  $\mu$ m CMOS technology for an integrated Synthetic Aperture Radar (SAR) receiver. The VGA consists of three gain stages. The first stage is a resistively loaded, fixed gain source coupled pair, while the other two are variable gain degenerated differential pairs. Each stage also utilizes negative Miller capacitance to extend the bandwidth, resulting in a VGA configuration with -3 dB bandwidth of 1 GHz. The gain of the VGA can be continuously varied from 10 dB to 30 dB. The input-referred noise density is 2.8 nV/ $\sqrt{\text{Hz}}$  and the out-of-band IIP3 is -1 dBm. The circuit consumes only 5.25 mW from a 1.2 V supply (excluding the output buffer) and occupies 0.037 mm<sup>2</sup> die area. [C656]

#### "Active hyperspectral LIDAR methods for object classification"

We have studied the fusion of active hyperspectral and range (LIDAR) data to investigate the concept of an active hyperspectral LIDAR and its potential applications in the remote sensing of vegetation. We have built two prototype instruments using the newly developed supercontinuum laser technique providing a continuous spectrum, which has then been used both for combined hyperspectral and LIDAR or time-of-flight measurement. The preliminary results point out the potential of active hyperspectral methods in laser-based remote sensing applications: the combined topographic and spectral information, such as the normalized difference vegetation index (NDVI), can be used efficiently in automatic target identification and classification. [C657]

#### "Fusion of hyperspectral images and LiDAR data for civil engineering structure monitoring"

Investigation of civil engineering materials includes a wide range of applications that requires three-dimensional (3D) information. Complex structures shapes and formations within heterogeneous artificial/natural land covers under varying environmental conditions requires knowledge on the 3D status of the urban materials for better (visual) interpretation of polluted sources. Obtaining 3D information and merge them with aerial photography is not a trivial task. It is thus, strongly needed to develop new approaches for near real time analysis of the urban environment with natural 3D visualization of extensive coverage. The hyperspectral remote sensing (HRS) technology is a promising and powerful tool to assess degradation of urban materials in artificial structures by exploring possible chemical physical changes using spectral information across the VIS-NIR-SWIR spectral region (400-2500nm). This technique provides the ability for easy, rapid and accurate in situ assessment of many materials on a spatial domain within near real time condition and high temporal resolution. LiDAR technology, on the other hand, offers precise information about the geometrical properties of the surfaces within the study areas and can reflect different shapes and formations of the complex urban environment. Generating a monitoring system that is based on the integrative fusion between HRS and LiDAR data may enlarge the application envelop of each technology separately and contribute valuable information on urban runoff and planning. The aim of the presented research is to implement this direction and define set of rules for practical integration between the two datasets. A fusion process defined by integrative decision tree analysis includes spectral/spatial and 3D information is developed and presented. [C658]

#### "Vegetation management of utility corridors using high-resolution hyperspectral imaging and LiDAR"

This study examines the use of high spatial resolution hyperspectral imagery in combination with light detection and ranging (LiDAR) data and digital aerial imagery for vegetation management of utility corridors. Two different classification methods, i.e. the support vector machines (SVM) and the spectral angle mapper (SAM) were applied on the datasets to test their ability for discrimination of various vegetation species. The SVM classifier performed best with an overall accuracy of 83% applied on the hyperspectral imagery. With inclusion of the LiDAR data the accuracy could be increased to 92%. Power lines were extracted from the LiDAR data and the conductor clearance was calculated. The results were merged with the SVM classification and a species map of vegetation that could cause potential damage to the power lines was generated. The results of this study show



that an improved approach for vegetation management of utility corridors can be achieved by combining the spatial and spectral information of multi-source datasets. [C659]

#### "Mismatched filtering of chaotic codes"

Low Probability of Intercept (LPI) pulse compression waveforms find applications in secure communications. Conventional waveforms with good correlation properties fail to satisfy requirements in presence of unintentional interference. Chaotic pulse compression codes combined with mismatched sidelobe suppression filters are proposed to simultaneously improve LPI performance and meet low sidelobe level requirements of secure communications. [C660]

#### "Development of a wireless communication and localization system for VRU eSafety"

Based on the experience from two predecessor projects, a novel architecture for the detection of vulnerable road users (VRU) is developed. It combines communication and localization, following the function principles of a secondary radar. Challenges are in the accuracy, the scalability, the bandwidth availability and the limited cost and complexity of the devices. This paper describes the objective of the overall project, the architectural approach of the wireless protocol and the design flow, which has been chosen for the development, which is still in progress. [C661]

#### "Membership service specifications for safety-critical geocast in vehicular networks"

Geographic group communication is a promising technique for collaborative driving applications. While one-way, geographic broadcast (geocast) is well-studied in vehicular networks, there has been little work to address the challenging reliability problems that arise. Not only do vehicular networks experience highly variable packet loss, but communication failures are difficult to detect. The presence of vehicles in an area and thus the set of vehicles that is supposed to receive a geocast, changes continuously. Without an expectation of the vehicles that should respond to queries, communication failure cannot easily be distinguished from absence. This requires a cross-layer approach, exploiting communication, sensing and driving rules. In this paper, we propose a membership service that provides group views for geographic areas as a building block to reliable geocast. We specify the semantics of the service and discuss different ways of implementing it. Finally, we show how it can be used for safe, collaborative driving. [C662]

#### "Performance analysis of sequential detection in early warning radar applications"

In early-warning radar surveillance environment, sequential procedures are preferred to detect the targets, for they promise a reduction in the time needed to take a decision. In this paper, a sequential detection algorithm is concerned and the interplay between the parameter  $dsnr$  and the system performance is mainly discussed. Numerical results have shown that sequential detector can lead a great reduction in the average-sample-number (ASN) especially in high SNR. In order to get a proper system performance, a trade off should be made between the ASN and detection performance when choosing the parameter  $dsnr$ . [C663]

#### "The real-time gpr signals preprocessing algorithm based on LWT in high scan rate"

In this work, we use DSP mechanism for real-time Ground Penetrating Radar (GPR) data preprocessing assess in high scan-rate scenarios. The lifting wavelet transform-based algorithm takes the advantages of efficient computation and memory reduction and is a suitable solution for DSP real-time implementation. In addition, the parallel operations technique on DSP memory is applied to enhance the system efficiency. Such that we realize a 3-level pipeline data structure which can significantly release the signal preprocessing time from the data collecting and data display time etc. The experimental results demonstrate the effectiveness of the developed scheme for real-time GPR data processing. [C664]

#### "On the propagation characteristics of ultra-wideband signal in aluminum"

The UWB reflected signal at 4.7 GHz is characterized and measured for the application of short-circuited reflection material analysis with aluminum backing the sample. The sub-pulse with 120-ps pulse width is used to characterize the UWB reflected wave propagation phenomenon in some aluminum plates with different thickness. It was found the normalized amplitude of principal sub-pulse that is generated by 24th derivative of a Gaussian pulse yields a linear relation with the thickness of aluminum ranged from 1 to 10 mm. The amplitude of these high order pulses shows that there is destructive interference when combining waves reflected from front and rear interfaces of aluminum. The pulse width of these sub-pulses is insensitive to the aluminum's thickness change in the experiment. [C665]

### "A height-measuring algorithm applied to TERCOM radar altimeter"

Radar altimeter is applied to measure the height of an aircraft above the ground in terrain contour matching system (TERCOM). The total performance of the TERCOM is almost determined by the height-measuring algorithms embedded in the radar altimeter. When facing a complex terrain area with a large degree of fluctuation, the traditional radar altimetry height-measuring algorithm performance will be greatly affected, for the reason that wide-beam pulse radar altimeter illuminates widely. In order to solve the problem, this paper proposes a new algorithm named average-height algorithm, and the detailed derivation is carried out. Simulation and flying test has shown that it has good performance and can be applied to any kind of terrain. [C666]

### "An algorithm of resolving the range ambiguity using a single PRF"

A new algorithm of range ambiguity resolution is presented which is substantially different from previously proposed algorithms. The algorithm utilizes a constant pulse repetition frequency (PRF). Firstly, a merit function is designed according to the moving characteristics of the targets. Secondly, range ambiguity resolution is achieved by minimizing the merit function. Numerical simulation results indicate that the proposed algorithm can resolve the range ambiguity efficiently using a single constant PRF. [C667]

### "An inverse model for coastal acoustic tomography and its application to Chinese coastal sea"

An inverse model for coastal acoustic tomography (CAT) to reconstruct the tidal current distributions was built and applied to the Zhitouyang Bay near the Zhoushan Island, China. The range-averaged current (post-inversion result) obtained along the transmission lines by the inverse model showed a prominent semidiurnal oscillation and was in good agreement with that (pre-inversion result) obtained from the travel time difference data, producing a root-mean-square (rms) difference of 0.036 m/s. Also both the range-averaged currents agreed with the ADCP results, and their rms differences were 0.097 m/s for the post-inversion result and 0.042 m/s for the pre-inversion result. The horizontal distributions of tidal current obtained from the inverse model were in rough agreement with that of the shipboard acoustic Doppler current profiler velocity. The rms differences for the eastward and northward currents were 11.70 cm/s and 16.50 cm/s, respectively. The above results indicate that the inverse model worked well, and could be used for mapping tidal current fields in Chinese coastal region. [C668]

### "Target recognition for marine search and rescue radar"

The key point of marine search and rescue is to find out and recognize the distress objects. At present, the visual search method is usually adopted to detect the ships in distress, and this method can only be used at good sea condition and visibility. In this paper, a new target detection and recognition system is proposed. The parameters of radar transmitter and echo graphics and the invariant moments of radar images are extracted as the system's recognition features, and the system's target classifier is based on BP neural networks. The developed recognition classifier has been tested using three kinds of target images, the target's features are used as the inputs of trained BP neural networks and the outputs of networks are target classification. Sea experimental results show that the proposed method is well-clustering and with high classified accuracy. [C669]

### "A fuzzy pattern recognition method of radar signal based on neural network"

Radar signal recognition is an important step of radar countermeasure processing. The classical recognition method is called weight distance, in which the feature parameter weights are obtained by expert and then the weight distance of unknown radar signal and signal template in database is computed. For its existing subjectivity in setting of feature parameter weights with classical recognition method, and the computing method of recognition is too simple, all of which make recognition result can't reflect the true fact objectively. Considering this point, a fuzzy pattern recognition method based on neural network getting weights to radar signal recognition is studied in this paper, the feature parameter weights in this method are fixed on by neural network and then the unknown radar signal is recognized by fuzzy pattern recognition method. Simulation experiment and its result show the method in this paper is practicable and more reliable compared with classical method. [C670]

### "A novel detection scheme to mitigate the TD-LTE interference"

In this article, a novel detection scheme will be introduced into the CR system based on the Time Duplex-Long Term Evolution (TD-LTE) scheme, in which radar system is the primary user. If the CR nodes carry on the on-line energy detection to the radar signal, it will be subject to the interference originated from the TD-LTE system's Base Station (BS). We propose a new detection program employed only in the TD-LTE uplink timeslots. In this program, the interference, which is coming from the TD-LTE system's User Equipment (UE), may be weaker than it originated from BS. At the same time, the performance will be enhanced by accumulating multiple

coherent detecting results. Through theoretical analysis and simulation, the feasibility of the new program has been verified. [C671]

#### **"Coexistence studies for TD-LTE with radar system in the band 2300-2400 MHz"**

Because of the lack of dedicated frequency bands, the TD-LTE system is possibly deployed in the same band with other existed mobile systems. In this paper, the coexistence studies for the TD-LTE system with the radar system which has been widely deployed in the band 2300-2400 MHz, is presented. The dynamical system simulation methodology is utilized in the coexistence studies, and simulation results of the impacts on the system performance with different isolation distance and frequency spacing are given. The feasibility of the coexistence between TD-LTE and the radar systems is investigated and some useful conclusions are also presented. [C672]

#### **"Design and implementation of marine dumping area's monitoring system based on GPS/GPRS"**

In this paper, it advances the reasonable development programs of the waste dumping in the dumping areas and achieve the position, navigation and monitoring of the ship-borne navigation monitoring system which based on the GPS/ GPRS wireless remote monitoring technology on the embedded SPCE3200 platform. The software and the hardware which are consisted of a ship-borne information processing termination are introduced. Our work provides a low cost scheme for realizing the information-based management of the ship and the safety of the shipping and the effective management of the dumping areas. [C673]

#### **"Clutter classification in heterogeneous environments"**

In this paper, we present a preprocessing method for classification of environmental clutter surrounding in radar application. This method is developed based on Generalized Likelihood Ratio (GLR) hypotheses test, employing observed data vectors from cells surrounding each radar cell. These tests attempt to recognize the equality or inequality of clutter Covariance Matrix (CM) of radar cells. Using these tests, an algorithm is presented which classifies the clutter. Simulation results show that detectors and classifiers achieve satisfactory performance under several simulated situations of known spectral clutter models. [C674]

#### **"The fuzzy targets setting and comprehensive evaluation of the vehicle comfort"**

To vehicle development problem, setting development targets is mainly based on the benchmark test data of competitors. Usually, the target setting is subjective and ambiguous. To reform the method, fuzzy decision-making matrices were established based on Analytic Hierarchy Process (AHP), hence, the comfort targets were set quantitatively. Then, the improved radar chart was used to make comprehensive evaluation on the developing model and the competitors'. The results show that, for the fuzzy comparative problem, AHP could set the targets reasonably and quantitatively. [C675]

#### **"Experimental analysis of ground speed measuring systems for the intelligent agricultural machinery"**

Measuring machine's speed precisely is quite critical for intelligent agricultural machinery. With Advanced RISC Machines (ARM) as the speed measurement terminal, speed measurement precision was tested and studied when the sensor was served by the encoder, inductance near-switch, doppler-radar and Global Positioning System (GPS) in the Autumn-ploughed farmland. In a 40m-long testing distance, the measurement precision of the above sensors was tested when the tractor driving at 4.0km/h, 5.0km/h and 6.0km/h. After the measured speed data were contrasted to the theoretical data, the result proves that the coefficient of variation (CV) of GPS is the highest; the data from the radar is most close to the theoretical data with the error of 2.03%; the biggest error of the inductance near-switch is 2.82%; the biggest error of the encoder is 2.85%. The performance price ratio of the inductance near-switch is the highest among the four, and it can meet the requirement of intelligent agricultural machinery. [C676]

#### **"Design of target data fusion algorithm for passive radar based-on dual GSM base stations"**

The ambiguity of GSM signals transmitted by GSM base stations has a pushpin-type and low side lobe, and it's no ambiguity at distance and Doppler-axis. It's very suitable as a illuminator source of passive radar. This paper presented a mathematical model of passive radar using two GSM base stations as the illumination source, simulated with extended Kalman filter algorithm and verified the feasibility and effectiveness of the algorithm. The results shows that it can effectively overcome the defects such as low tracking accuracy and long time of target dynamic process when adopting single GSM base station to building passive radar. This system can be used as supplementary to urban low-altitude defense system so as to effectively respond to low-altitude invading enemy weapons. [C677]

### **"A new ground penetrating radar signal analysis method based on S transform"**

The paper discussed the characteristics of GPR signals of one object and two objects respectively, and studied the rule of extracting twin-peak attribute when the size of object or the distance of two objects was changing through GST. For one object, the two reflections can't be resolved in time when the diameter of object is less than or equal to  $1/3$  dominant wavelength within object medium, but the twin-peak attribute can resolve the reflections when the diameter is as small as  $1/7$  dominant wavelength, so the size can be estimated combining the attribute with time-domain waveform and the definition of a small object can be given. For two objects that each is a small object in time-frequency domain, we considered the situations where the permittivity were same or different, and it is pointed out that the attribute can improve the resolution of two objects and can estimate the distance combined with time-domain waveform. The selection rule of parameter and frequency point of twin-peak attribute was given as well so the unsystematic problem was solved. [C678]

### **"Simulation of algorithm for relief profile measurement and recognition of objects in on-board scanning pulsed laser rangefinders"**

This paper proposes the algorithm and presents the preliminary results obtained from the simulation of three-dimensional images for scanning pulsed laser rangefinders with nanosecond probe pulses. The prospects for construction of high-speed on-board devices intended for recognition of ground (above-water) objects by geometric features are demonstrated. [C679]

### **"Mining environmental data in hydrological scenarios"**

We present data mining methods which are used in a hydro-meteorological scenarios within the FP7 project ADMIRE1. The scenarios uses data mining techniques instead of more common physical models in order to predict phenomena which are not being ordinarily solved in Slovakia-water temperature, discharge wave propagation downstream of a major water reservoir and short-term rainfall prediction by analyzing radar imagery. These scenarios are one of a set of use cases, which form the Flood Forecasting Simulation Cascade-a pilot application of ADMIRE project. We describe the variables used in data mining training of these scenarios and also an introduction to the data integration methodology approach we have devised. [C680]

### **"The design and implementation of domain-specific text summarization system based on co-reference resolution algorithm"**

In order to benefit from the vast amounts of information quickly and accurately, topics on automatic abstracting have become more and more popular. Compared with the traditional automatic abstracting methods, we adopted the statistic methods and word list in domain-specific field to develop domain-specific text summarization system. Referring is a common phenomenon in the real life. In the process of text handling, referring often leads to inaccurate results. To solve the problem caused by the referring, combined with the current studies, this paper introduced co-reference resolution algorithm and the implementation of domain-specific text summarization system based on resolution algorithm. By analyzing the referring phenomenon in the original text, term frequency and sentence importance are recalculated to obtain new abstracting results. [C681]

### **"A Parallel Centralized Multi-sensor General Association Algorithm"**

This paper has researched on the problem of centralized multi-sensor multi-target tracking against a background, which has a high demand of real-time and a relative demand of tracking precision, and analyzed the advantages and disadvantages of the existent classical algorithms theoretically in this environment. Based on the research and the analysis, general association algorithm has been extended into multi-sensor system through the parallel structure and a new algorithm named parallel centralized multi-sensor general association algorithm has been proposed. In this algorithm, a lot of hypotheses are built with the measurements of each sensor and the track of each target, the score of every hypothesis could be obtained with the formula of the score function in multi-sensor general association algorithm, and the state estimation of the fusion center is gained finally. The simulation results show that this algorithm could track the targets effectively with the high density clutter and the general performance of this algorithm is better than that of sequential centralized multi-sensor joint probabilistic data association algorithm and parallel centralized multi-sensor probabilistic nearest neighbor standard function. [C682]

### **"Novel Architecture for Highly Hardware Efficient Implementation of Real Time Matrix Inversion Using Gauss Jordan Technique"**

Advent of Matrix Theory has greatly aided and simplified the analysis for variety of signal processing algorithms.



It has been proven that matrix notation is convenient for representation of signals and to perform operations on them. Many problems such as signal modeling, Wiener filtering and spectrum estimation require finding the solution or solutions to a set of linear equations. Some of the common matrix related operations include transpose, triangularization, determinant calculation, eigen value decomposition and matrix inversion. Most of these operations are computationally intensive and have been difficult to implement on real time systems and therefore are not pursued much in VLSI design. In this paper we present a highly hardware efficient and simple memory based novel architecture implementing widely established Gauss Jordan technique for finding matrix inverse. First triangularization of the matrix is done which on further processing calculates the inverse matrix.

[C683]

#### **"Blind channel estimation for MRC systems with maneuvering transmit/receive terminals"**

This paper presents a new blind channel estimation technique for maximum-ratio combining systems where the relative speed of the transmit/receive terminals may change. This changing speed is called maneuvering. The proposed blind system has a hard decision switching block which selects between different speed modes of a maneuvering terminal. The speed can be therefore tracked in a mobile data communication link. This is accomplished based on only the received data information signal, i.e., no other information (for example from a speed sensor or radar, etc.) is required. The performance of the proposed technique is evaluated by simulation and comparison is made with optimal coherent detection. The importance of introducing the switching block can be demonstrated by disabling it in the algorithm, and this results in a large degradation in performance. To assess the direct impact of the proposed blind channel estimation on the error performance, a fair comparison with a known, blind technique based on Kalman filtering is also made, with the assumption of non-maneuvering terminals. Here, improved performance is observed. [C684]

#### **"FCM-based radar target detection in medium frequency signal of radar"**

In radar target detection application fields, rich of information of targets may be included in medium frequency. Doppler shift caused by moving target is one of them. In this paper, Doppler shift and its Short Time Fourier Transform-STFT is analyzed and discussed. Since it is difficult to distinguish the Doppler shift of moving target even in frequency domain with STFF method, fuzzy C means clustering method is introduced to seek the two centers of the mixed signals in a radar scanning period. Using multiple radar scanning period, several centers can be determined by a center function using arithmetic mean filter. Finally the targets can be detected by threshold decision and calculated the detection probability. This algorithm is simple, easily to realize, with small computation burden and good target detection probability. [C685]

#### **"Hailstone detection based on time series association rules"**

Hailstone is one of main meteorological disasters and it is difficult to forecast effectively. In this paper, a new hail echo detection method based on time series association rules was proposed and a hail echo automatic detection system was built. Compared to the existing methods, the test results have shown that this method eliminated hail alert failure completely and also reduced the proportion of false alarm, raising the accuracy of hail forecast. The system was able to assist forecasters to make correct hail forecasts and provide reference to other disastrous weather forecast. [C686]

#### **"Real-time data acquisition system for pulse laser radar based on clock distribution technology"**

A high-bandwidth data acquisition system for pulse laser radar is developed. Four 250MHz of AD collecting chips are used for data acquisition under clock distribution chip, and then put together for a 1GHz Sps data sample rates. The USB protocol is used for data transmission between system and computer, the AD9520 is used for clock distribution, the FPGA is used for data acquisition, down-conversion, caching and transmission control chip, and the LVPECL and LVDS bus is used to ensure the stability of high-speed data transmission and signal process. The experimental results show that the system can satisfy the data acquisition tasks of the pulse laser radar. [C687]

#### **"Evolutionary global attitude planning for satellite signature suppression shield"**

This paper explores the global attitude planning for satellite signature suppression shields with limited attitude control abilities. Space surveillance radar and high energy laser are the main threats to on-orbit satellite. The radar detection probability and laser irradiation power are coupled with the satellite's radar cross section (RCS) and laser cross section (LCS) respectively, which are determined by the shield's attitude. This paper presents an evolutionary global attitude planning algorithm for low observable satellites, to reduce their RCS and LCS in threat directions by limited shield attitude control. A novel evolutionary strategy is developed. The strategy has problem-specific individual structure and evolutionary methods, and is able to find a near-optimal global attitude



solution with limited iterative steps. At the same time, a novel planning mathematical model and a relative evolutionary evaluation function are defined to reduce the planning's computational complexity. According to the simulation results, the algorithm is proved to be efficient. [C688]

#### **"Intrusion detection using software defined noise radar"**

The need for reliable systems for detecting intrusions into a given area has given rise to the research and use of random noise radars. This paper deals with the issues regarding the use of such systems. The advantages of the use of such radar are illustrated followed by the actual mode of implementing the system itself. The novelty in this approach is the use a software defined radio as the platform for the system as it has a number of added advantages as have been detailed Subsequently, the intrusion detection can be viewed as a classification problem and solved using any machine learning algorithm. The paper also investigates the use of support vector machines (SVM) for the above said problem and derives a suitable model for classification. The training and testing of SVM model is in progress. [C689]

#### **"A cue line based method for building modeling from LiDAR and satellite imagery"**

Building modeling in an urban environment is a challenging task yet has many applications such as urban planning, simulation of disaster scenarios, cartography, wireless network planning, line-of-sight analysis, virtual tours, and many others. This paper presents a cue line based method for residential building modeling in urban areas using airborne light detection and ranging (LiDAR) data and satellite imagery. The main contribution is the automatic isolation of building roofs and roof reconstruction based on the fusion of LiDAR data and satellite imagery. By using cue lines which are generated from satellite imagery to separate buildings from other objects (including other buildings), we are able to automatically identify individual buildings from residential clutter and re-create a virtual representation with improved accuracy and reasonable computation time. We applied the method to urban sites in the city of New Orleans and demonstrated that it identified building measurements successfully and rendered 3D models effectively. Our experiments show that our method can successfully reconstruct small buildings with relatively sparse LiDAR sampling and in the presence of noise. [C690]

#### **"Copyright page"**

The following topics are dealt with: MIMO, radar, imaging techniques, spectral cohabitation, adaptive waveforms, modulation techniques, and spectrum management. [C691]

#### **"A practical ground penetrating radar signal processing method based on wavelet transform"**

Wavelet transform is a new applied signal processing technique in recent years, its time-frequency multi-resolution and signal processing performance are analyzed in the paper. A practical ground penetrating radar signal processing method based on wavelet transform is proposed; it contrast with continuous wavelet transform, the experiments indicate that it improves the processing performance of underground target detecting. [C692]

#### **"Semi-supervised remote sensing image classification via maximum entropy"**

Remote sensing image segmentation requires multi-category classification typically with limited number of labeled training samples. While semi-supervised learning (SSL) has emerged as a sub-field of machine learning to tackle the scarcity of labeled samples, most SSL algorithms to date have had trade-offs in terms of scalability and/or applicability to multi-categorical data. In this paper, we evaluate semi-supervised logistic regression (SLR), a recent information theoretic semi-supervised algorithm, for remote sensing image classification problems. SLR is a probabilistic discriminative classifier and a specific instance of the generalized maximum entropy framework with a convex loss function. Moreover, the method is inherently multi-class and easy to implement. These characteristics make SLR a strong alternative to the widely used semi-supervised variants of SVM for the segmentation of remote sensing images. We demonstrate the competitiveness of SLR in multispectral, hyperspectral and radar image classification. [C693]

#### **"Implementation of a low cost synthetic aperture radar using Software Defined Radio"**

GNU radio is a free open-source software toolkit for building software radios, in which software defines the transmitted waveforms and demodulates the received waveforms. In this paper an attempt has been made to explore the means to use a Software Defined Radio (SDR) to implement a basic radar system and then synthetic aperture radar. An experiment where in readings at two different scenarios (free environment and metal object) are taken into account and their plots are also given. This has been attempted keeping in mind the exponential increase in chip computing power and the ability to upgrade a radio transceiver via software updates with a marginal investment, the two features which makes such a foray attractive, technology wise and cost

wise. This attempt also takes us a step closer to establishing the concept of a Cognitive radar which is software signal processing intensive. [C694]

### "Pulse Doppler radar waveforms"

Modern military airborne radars are highly sophisticated, multi-mode systems which are required to detect difficult targets in all aspects and over a large range/velocity detection space. There are particular difficulties associated with the airborne case such as the limited antenna aperture, high platform velocity and severe clutter levels which present difficult waveform design challenges. This tutorial will consider the design parameters of high pulse repetition frequency (PRF) and medium PRF waveforms commonly used in airborne pulse Doppler radar modes. The majority of this tutorial will be devoted to the issues concerning the selection of the number of PRFs and of the PRF values used in the medium PRF mode. PRF optimisation methods using evolutionary algorithms used by the author and his colleagues in a number of recent studies will be described. Examples will be given of airborne fire control radars, airborne early warning systems and active radar seekers used in anti-aircraft missiles. [C695]

### "OFDM radar waveform design for sparsity-based multi-target tracking"

We propose a sparsity-based approach to track multiple targets using an orthogonal frequency division multiplexing (OFDM) radar. The use of an OFDM signal increases the frequency diversity of our system as different scattering centers of a target resonate variably at different frequencies. We observe that in a particular pulse interval the targets lie at a few points on the delay-Doppler plane. Hence, we exploit that inherent sparsity to develop a tracking procedure. The nonzero entries of the sparse vector in our model correspond to the target scattering coefficients at different OFDM subcarriers. Therefore, the sparse vector and associated sparse measurement model exhibit block-sparsity property. We design the spectral weights of the transmitting OFDM waveform to minimize the block-coherence measure of the sparse model. In the tracking filter, we develop a block version of the compressive sampling matching pursuit (CoSaMP) algorithm. We present numerical examples to show the performance of our sparsity-based tracking approach and compare with that of a particle filter (PF). The proposed sparsity-based tracking algorithm takes significantly less computational time and provides equivalent, and sometimes better, tracking performance in comparison with the PF-based tracking. [C696]

### "Design of look-up table based architecture for wideband beamforming"

Wideband beamforming with a real-time array testbed will be studied in this paper. The algorithm and implementation architecture on wideband beamforming will be the main focus. The contribution of this paper can be summarized in the following three aspects. First, the channel imbalances among different RF chains will be taken into account. The equivalent complex baseband impulse responses of RF chains are measured from the AFRL TELA testbed. The second contribution is that the novel architecture of wideband beamforming is proposed. Look-up table (LUT) based architecture is exploited to replace the pre-steering delay component to avoid fractional delay-one implementation bottleneck. In addition, the general optimization issue for wideband beamforming is formulated as semi-definite programming (SDP), which can be efficiently solved by the convex optimization tool, e.g. CVX. [C697]

### "Adaptive design for distributed MIMO radar using sparse modeling"

Multiple Input Multiple Output (MIMO) radar systems with widely separated antennas provide spatial diversity gain by viewing the targets from different angles. In this paper, we propose an approach to accurately estimate the properties (position, velocity) of multiple targets using such systems by employing sparse modeling. We also propose a new metric to analyze the performance of the radar system. We develop an adaptive mechanism for optimal energy allocation at different transmitters. We show that this adaptive mechanism outperforms MIMO radar systems that transmit fixed equal energy across all the antennas. [C698]

### "Waveform diversity & knowledge based systems"

Summary form only given. Waveform diversity is an emerging technology that has dramatically altered the development of futuristic radar systems, as has knowledge based processing and control. With increasing numbers of radio frequency sensors and communications systems, battlefield scenarios have become more complex and continuously redefined. Our challenge will be to effectively use this technology to enhance overall performance of advanced radar systems operating within available spectrum in these battlefield environments. Technologies essential to this goal include cognition and knowledge based systems for waveform generation timing and control, and intelligent radar signal/data processing for detection, parameter estimation and track processing. Cognition is defined as the act or process of knowing, including both awareness and judgment.

Awareness of the dynamically changing spectral environment and judgment for the selection of optimal waveform parameters and sensor placement will enable dramatically improved performance for target surveillance/reconnaissance in addition to enhanced interference mitigation. A confluence of factors and technologies now makes waveform diverse knowledge based systems a logical and affordable alternative to classically designed radars. [C699]

### "Coherent MIMO radar"

Multiple-input multiple-output (MIMO) extensions to radar systems enable a number of advantages compared to traditional approaches. These advantages include improved angle estimation and target detection. In this tutorial, an overview of MIMO radar is provided, and the concept of coherent MIMO radar is defined. In addition, two topics are addressed more thoroughly: MIMO waveform/array geometry optimization for target tracking, and MIMO ground moving target indication (GMTI). [C700]

### "Wideband MIMO waveform design for transmit beampattern synthesis"

The usage of multi-input-multi-output (MIMO) systems such as a MIMO radar allows the array elements to transmit different waveforms freely. This waveform diversity can lead to flexible transmit beampattern synthesis, which is useful in many applications such as radar/sonar and biomedical imaging. In the past literature most attention was paid to receive beampattern design due to the stringent constraints on waveforms in the transmit beampattern case. Recently progress has been made on MIMO transmit beampattern synthesis but mainly only for narrowband signals. In this paper we propose a new approach that can be used to efficiently synthesize MIMO waveforms in order to match a given wideband transmit beampattern, i.e. to match a transmit energy distribution in both space and frequency. The synthesized waveforms satisfy the unit-modulus or low peak-to-average power ratio (PAR) constraints that are highly desirable in practice. Several examples are provided to investigate the performance of the proposed approach. [C701]

### "An IMM-UF algorithm for tracking highly maneuvering target"

Tracking of highly maneuvering targets with unknown behavior is a difficult problem in state estimation. This paper presents an adaptive interacting multiple model algorithm (IMM) utilizing adaptive turn rate models to track a maneuvering target. The turn rate is calculated at each step from the estimator of velocity and the radius of curvature of the trajectory of the target by using Least Square (LS) and curve fitting theory. Simulation in different scenario proves that the turn-rate estimation techniques in this adaptive framework can significantly solve the problem of tracking maneuvering targets. [C702]

### "Quantum-inspired immune clonal clustering algorithm based on watershed"

Based on the concepts and principles of quantum computing, a novel clustering algorithm, called a quantum-inspired immune clonal clustering algorithm based on watershed (QICW), is proposed to deal with the problem of image segmentation. In QICW, antibody is proliferated and divided into a set of subpopulation groups. Antibodies in a subpopulation group are represented by multi-state gene quantum bits. In the antibody's updating, the quantum mutation operator is applied to accelerate convergence. The quantum recombination realizes the information communication between the subpopulation groups so as to avoid premature convergences. In this paper, the segmentation problem is viewed as a combinatorial optimization problem, the original image is partitioned into small blocks by watershed algorithm, and the quantum-inspired immune clonal algorithm is used to search the optimal clustering centre, and make the sequence of maximum affinity function as clustering result, and finally obtain the segmentation result. Experimental results show that the proposed method is effective for texture image and SAR image segmentation, compared with the genetic clustering algorithm based on watershed (W-GAC), and the k-means algorithm based on watershed (W-KM). [C703]

### "Detecting potential human activities using coherent change detection"

This paper describes detection and interpretation of temporal changes in an area of interest using coherent change detection in repeat-pass Synthetic Aperture Radar imagery, with the main goal of detecting subtle scene changes such as potential human activities. Possibilities of introducing knowledge sources in order to improve the final result are also presented. [C704]

### "Support vector machine fusion of multisensor imagery in tropical ecosystems"

One of the major stakeholders of image fusion is being able to process the most complex images at the finest possible integration level and with the most reliable accuracy. The use of support vector machine (SVM) fusion for the classification of multisensors images representing a complex tropical ecosystem is investigated. First,

SVM are trained individually on a set of complementary sources: multispectral, synthetic aperture radar (SAR) images and a digital elevation model (DEM). Then a SVM-based decision fusion is performed on the three sources. SVM fusion outperforms all monosource classifications outputting results with the same accuracy as the majority of other comparable studies on cultural landscapes. SVM-based hybrid consensus classification does not only balance successful and misclassified results, it also uses misclassification patterns as information. Such a successful approach is partially due to the integration of DEM-extracted indices which are relevant to land cover mapping in non-cultural and topographically complex landscapes. [C705]

#### **"The lake water bloom intelligent prediction method and water quality remote monitoring system"**

According to the lagging state of water quality monitoring and problems of difficulty to predict water bloom, one water bloom prediction method based on grey-BP neural network is proposed and a system on water environmental remote monitoring and water bloom early warning based on GPRS wireless communication technology is built, which can obtain the automatic real-time monitoring information for the change of water quality and occurrence of water bloom, then provide a kind of efficient and practical system for water environment control. [C706]

#### **"The application of perceptual weighting on millimeter wave conducted speech enhancement"**

A new non-air conducted speech detecting method is developed in our laboratory by means of millimeter wave (MMW) radar. However, the resulting radar speech is of less intelligible and poor audibility since the present of the combined and colored additive noise. This paper, therefore, investigates the problem of the MMW radar speech enhancement by taking into account the frequency-domain masking properties of the human auditory system and reduces the perceptual effect of the residual noise. The results from both acoustic and listening evaluation suggest that the background noise can be reduced efficiently while the distortion of MMW radar speech remains acceptable, suggesting that the proposed algorithm achieved a better performances of noise reduction over traditional subtractive-type algorithms. [C707]

#### **"Enhancing the MIMO-OFDM Radar systems performance using GA"**

This paper proposes a new peak-to-average power ratio (PAPR) reduction method for a multiple-input multiple-output (MIMO)-orthogonal frequency division multiplexing (OFDM) systems based on a genetic algorithm (GA). It has been introduced to be compatible with Radar systems, where the GA was used to optimize the MIMO-OFDM symbols in such way that could improve the system's performance. During this work, there was a comparison that has been stated among three systems; original radar system, radar system-based MIMO-OFDM and radar system-based MIMO-OFDM uses GA. Finally, a range of simulation results are provided to demonstrate the superiority of the proposed scheme, since it is showed an enhancement in the coverage distance besides reducing the PAPR effects. [C708]

#### **"On mean revisit frequency of non-repeating satellite orbits with finite sensor range"**

The length and the frequency of the visibility times during which a fixed ground station sees a non-geosynchronous satellite is a function of the parameters of a fixed ground station and a function of the orbital parameters of the satellite. The focus, in this paper, is on the mean revisit frequency of a non-geosynchronous satellite with non-repeating ground track as seen by a fixed ground station with a finite sensor range. A mathematical analysis is provided for the calculation of the mean revisit frequency. There are several possible application areas of such visibility statistics, like optimizing a gateway's latitude to maximize the mean revisit frequency of a satellite, thus maximizing the communication possibilities. The analytical solution provides a good match with simulation results at all latitudes and the mathematical background of the analytical solution is foreseen to be useful for the analysis and design of satellite constellations. [C709]

#### **"Improvement on obstacle avoiding ability based on laser range finder"**

Mobile robot works in complicated environment have to deal with all kinds of obstacles, some obstacles may leave only a narrow way, and some obstacles moves quickly or arbitrarily, such as a child. The robot must improve its ability to quickly sensing the obstacles and tracking their state, and then avoid these obstacle and move to the original goal at the same time by motion planning. To improve the obstacle avoiding ability, a three layers obstacle avoiding policy is adopted to deal with the obstacle in different range. The dangerous obstacles are determined and the sub-goal based avoiding policy is presented. To improve the responding ability to moving object, a tracking model is set up, which takes into account the influence of moving platform. The robot may anticipate the collision possibility, collision time and position from tracking algorithm, and then three obstacle avoiding policy is presented according to the collision estimation. The experiment shows good moving object avoiding result. [C710]



### "SNR-dependent filtering for Time Of Arrival estimation in high noise"

Time of Arrival (ToA) estimation is a cornerstone of many of the remote sensing applications including radar, sonar, and reflective seismology. The conventional Matched Filter Maximum Likelihood (MFML) ToA estimator suffers from rapid deterioration in the accuracy as Signal to Noise Ratio (SNR) falls below certain threshold value. In this paper we suggest an alternative method for ToA estimation based on the fusion of measurements from biased estimators which are obtained using a pair of unmatched filters. Suboptimal but not perfectly correlated estimators are combined together to produce a robust estimator for ToA estimation in high noise. The unmatched filters pair is parameterized by a single parameter (phase shift) which is selected based on estimated SNR level. [C711]

### "The wireless extension of CAN-bus based on GPRS"

CAN-bus is applied widely in many industrial systems and vehicles. Nevertheless, in some cases, two or more distant CAN-bus segments are needed to transfer data. If the distance is too long, utilizing twisted wire pairs are impossible. In wireless method, GPRS is so far the reliable style. In this paper, a kind of CAN/GPRS gateway is designed to achieve the function of the wireless extension of CAN-bus. [C712]

### "Portable satellite backhauling solution for emergency communications"

This paper describes the portable satellite backhauling solution for emergency communications used in the e-Triage Project. The main objective of e-Triage is the efficient electronic on-site registration of the victims in Mass Casualty Incidents (MCIs) to enable a fast distribution of the information to hospitals for a better handling of victims. To achieve this, e-Triage designs the end device used to register the victims, the database where the information of the victims is saved, and the communications infrastructure necessary to transmit the data, as after a disaster event the terrestrial networks are likely to be overloaded, damaged or not operative, if they ever existed. This paper focuses on the design aspects of a hand-luggage-size suitcase that offers GSM/GPRS and WLAN to rescue teams and victims in the disaster area and connects them over satellite to the disaster-safe area. [C713]

### "Ultra-wideband transmitters based on M-sequences for high resolution radar and sensing applications"

In this paper we present a novel ultra-wideband transmitter architecture for high resolution radar and sensing applications up to 30GHz. The concept for pulse compression is based on maximal-length sequences to reduce the peak-to-average power ratio. The proposed transmitter consists of a 29-1 linear feedback shift register (LFSR) to generate the radar signal and a fully differential broadband amplifier. A variable gain control has been implemented to provide high sensitivity and decrease the dynamic range. The presented circuit architecture permits the possibility of upconversion, which drastically increases the operational flexibility of the radar system. [C714]

### "Co-construction of ontology-based knowledge base through the Web: Theory and practice"

Ontology-based knowledge base plays an increasingly important role in improving the precision and recall rate of a retrieval system. Based on Distributed Learning theory, a novel approach for the co-construction of ontology-based knowledge base is explored. Making use of the platform set up for the co-construction and sharing of domain-specific knowledge through the Web, we constructed an ontology-based knowledge base of airborne radar field. This study is expected to contribute to the effective improvement of precision and recall rate of information retrieval in the airborne radar field. Hopefully, the mode we designed and adopted for the co-construction and sharing of domain-specific knowledge base could be enlightening for other similar studies. [C715]

### "High resolution two-dimensional imaging of spinning space debris"

A high resolution two-dimensional imaging algorithm of spinning space debris is proposed in this paper. It incorporates the characteristic that the space debris rotates around its principal axis at a certain angular speed and it is applicable to various kinds of signals, such as LFM signal, random noise signal. The corresponding compensation terms are constructed by searching for matched two-dimensional parameters and the position information of scattering points is obtained by energy accumulation using FFT. CLEAN method is combined to enlarge target dynamic range. Imaging of spinning debris by noise frequency modulated continuous wave (FMCW) signal is taken as an example to be analyzed and simulated. The simulations confirm the validity of the proposed algorithm. [C716]



### "Pulse emitter identification by the use of higher order statistics"

The paper presents experiments on the use of higher order statistics in the procedures of identification of radar emitters. Studies aimed at testing "sensitivity" of higher order statistics of selected characteristics of the individual sources of emissions. Attention is focused on methods based on analysis of parameters of single-pulse radar emissions. [C717]

### "A general two-dimensional spectrum based on polynomial range model for medium-earth-orbit Synthetic Aperture Radar signal processing"

The  $k$ th-order polynomial range model (PRM) for Medium-Earth-Orbit (MEO) Synthetic Aperture Radar (SAR) signal processing is proposed, analyzed, and verified in this paper. The coefficients of the PRM are calculated according to the relative state vectors between the satellite and the given target on earth, which implies power series expansion around the beam center crossing time. In addition, the relevant two-dimensional spectrum is deduced out as well by using the principle of stationary phase (POSP) and the series reversion approximation. The accuracy of this spectrum is flexible and limited both by the order of the PRM and the order of the spectrum in an expanded form. Therefore, the PRM-based spectrum is general for MEO SAR with any azimuth resolution at any orbit height. [C718]

### "Frequency broadband signal MVDR adaptive beamforming method and application"

In this paper, frequency broadband signal beamforming methods of digital array radar (DAR) are researched and broadband signal adaptive beamforming is realized through MVDR rule. Simulation and comparison show that blocked DFT beamforming method has advantage of little calculating quantity. For non-superposition of each block destroy the relativity of signal, blocked DFT make aberrance to pulse compression and take bad influence in succedent processing. Sliding-window DFT beamforming can achieve good performance of pulse compression, but it has large calculating quantity. Improved DFT beamforming method has the same calculating quantity with blocked DFT method, and it doesn't destroy the relativity of signal so that it can achieve good performance of pulse compression and in succedent processing. Improved DFT beamforming method is fit for used in engineering. The result of its application in DAR has been given. [C719]

### "A fast range migration compensation method"

Coherent integration is usually used in matched filter radar signal processing to improve target signal to noise ratio (SNR), but the accumulation time is restrained by target's motion according to the conventional radar design principle. Keystone transform can correct range migration without the exact value of target velocity and as a result, the SNR is improved through coherently accumulating all pulses. But the usually used interpolation method has very huge calculation burden. In this paper, a fast range migration compensation method without interpolation based on keystone transform is proposed, which greatly reduce the computational cost, and is more suitable for real-time processing. The simulation results verify its effectiveness. [C720]

### "Jamming research to SAR based on frequency characteristic"

This work is concerned with developing the blanket jamming technology against SAR based on frequency characteristic. Firstly, the SAR imaging output of the shift frequency jamming style is deduced and analyzed. Then a modified shift frequency jamming to SAR, random Shift frequency jamming (RSFJ), is presented and discussed. The theoretic research and simulation show that the RSFJ is an effective blanket jamming style to SAR with the less jamming power requirement than noise jamming. [C721]

### "A novel three-dimensional data association algorithm for 2D radars and sensors"

Fast and precise data association methods are very important in heterogeneous sensor information fusion system. In order to solve the typical problem of three-dimensional data association in heterogeneous sensor system which is composed with 2D radar and IRST, a new algorithm is presented. Firstly, the precise azimuth and elevation of IRST and radial distance of 2D radar are used to obtain the possible position of target in two-dimensional coordinate, and angle statistics is constructed to eliminate most false points. Then, the two-dimensional assignment algorithm is used to achieve the optimum assignment solution. Simulation results show that the proposed method is an effective data association method, and the probability of right association is improved obviously. [C722]

### "MIMO antenna array design for airborne down-looking 3D imaging SAR"

Airborne down-looking three dimensional imaging SAR (ADL-3D-SAR) is a new radar system developed in recent years, which overcomes the shadowing effects and can gather more information compared to the conventional side looking SAR systems. However, it still has many constraints, e.g. antenna array configuration designing, cross-track resolution and vibration errors. In this paper, we focus on the designing of antenna configuration and propose several new multiple-input-multiple-output (MIMO) antenna array models which can provide more reasonable properties for 3D SAR system's stability, applicability, and vibration errors reduction. The validity of these models is discussed in the end. [C723]

#### **"System performance simulation of electronic surveillance receiver for spaceborne SAR"**

Reconnaissance equation for SAR side lobe detection is derived based on SAR movement and antenna pattern. The surveillance scene model as well as algorithm flow is also established. Requirements are given for ground electronic surveillance (ES) receiver to conduct SAR signal surveillance under given tracking time occasions. [C724]

#### **"Design and implementation of a dual-interface radar data recorder"**

This paper analyses the design and implementation of a small-scale dual-interface radar data recorder based on DSP+FPGA. It has two types of interfaces: solid-state IDE hard disk and RJ45. The recorder can save sampling data of original radar waveforms in real time for further analysis and validation. It adapts to a variety of application environments and has a high storage speed and reliable operation performance. It can be widely used in radar testing and flight experiments. [C725]

#### **"A temperature remote monitoring system of cable joint"**

In order to monitor the temperature of cable joint, this paper designed a cable joint real-time temperature monitoring system based on GPRS which is integrated of computer technology, microcomputer control technology and digital sensor technology. It described the whole structure diagram of the system, and presented the hardware circuit and software design in detail. The system takes SCM as main control chip, adopts DS18B20 to build up the temperature measurement terminals, and uses the GPRS network as a wireless transmission network to realize wireless data transmission through the TCP/IP protocol management. Experimental results show that: the system have high accuracy, it is able to identify a variety of cable faults caused from overheating effectively and can meet the needs of cable temperature monitoring. [C726]

#### **"A frequency-based inter/intra partly coherent jamming style to SAR"**

This work is concerned with developing the frequency-based jamming technology against SAR. Firstly, the shift frequency jamming to LFM radar and SAR is analyzed. Then a modified shift frequency jamming to SAR, stepped shift frequency jamming (SSFJ), is presented and discussed. The theoretic research and simulation show that the SSFJ is inter/intra partly coherent with the SAR system and has a region imaging output for protecting the distributed targets. Its jamming power is much less than other jamming styles such as noise jamming, random shift frequency jamming and etc. [C727]

#### **"A radar emitter identification method based on pulse match template sequence"**

In the dense emitter environment, the existing radar emitter identification methods can not effectively and rapidly give the class of radars with complex modulation signal. So this paper proposes a new radar emitter identification method based on pulse match template sequence and gives the structure and algorithm of this method. Through computer simulation, this method can rapidly and effectively identify the class of radar emitter. [C728]

#### **"A design of efficient transport layer protocol for wireless sensor network gateway"**

It is necessary that in the small-or-medium-size wireless sensor networks, the networking information of network and monitoring data of sensors should be sent to the remote computers through the gateway to achieve remote monitoring for the target area. Wireless sensor network data characterize strong bursts, instability of traffic and small amount of data in a single packet. Considering these features as well as the bandwidth of wireless network, the paper proposes a Transport Control Protocol (TCP) with an improved Nagle algorithm. The experiments prove that the improved algorithm obviously enhances the utilization of wireless channel and reduces system energy consumption, while it ensures transmission reliability. [C729]

#### **"Wireless video monitoring system based on image restoration technology"**

A video monitoring system based on GPRS wireless transmission technology is introduced. The system mainly consists of video monitoring modules, MCU, GPRS communication system and monitoring computer. It can use GPRS network and the Internet instead of traditional wired video system to monitor the remote targets in the environments of not suitable for cable transmission. For video degradation during the image formation and transmission process, a method of image restoration based on Hopfield neural network is introduced. Simulation results show that this method can restore the vague image effectively. [C730]

#### "High resolution radar range imaging method using bandwidth extrapolation"

The high resolution radar demands transmitting ultra wide bandwidth chirp signals, which consequently leads to increasing the system complexity and expenses. The frequency domain AR model for radar chirp signals was presented in the paper based on the bandwidth extrapolation technique together with linear prediction algorithm to broaden the effective bandwidth of the signal. The performance estimation function, namely the prediction error as a function of the linear error prediction filter length, was derived through analyzing large numbers of computer simulation experiment results. It is of considerable importance to determine the linear error prediction filter length for optimizing the bandwidth extrapolation parameters. It is demonstrated by the theoretical analysis and simulation results that the bandwidth extrapolation method is feasible and effective for increasing bandwidth of the radar signal to obtain higher range resolution. [C731]

#### "A two-stage hybrid space-time adaptive processing approach"

This paper presents a new two stage hybrid space-time adaptive processing (STAP) algorithm, which combine space-time multiple-beam (STMB) architecture and direct data domain (DDD) approach. The proposed two stage hybrid algorithm use the direct data domain approach as the first stage to suppress discrete interference in the range cell under test and use STMB method as the second stage to suppress the residue correlated interference. Therefore this approach takes advantage of the DDD and STMB method and alleviates their drawback, so it can suppress discrete interference and correlated interference simultaneously. [C732]

#### "Design of a light-weight digital beam forming antenna for future sar applications"

The CSA has been working actively during the past decade on developing various technologies for improving the capabilities of SAR antennas. Various techniques have been investigated for decreasing the mass per unit of area as well as improving the electronic capabilities of the radar. These efforts were combined to form a new concept that is presented here. The concept was defined for C-band applications but could also be applied at lower frequency. The radar antenna has a total area of 38 m<sup>2</sup>. The central aperture (~10 m<sup>2</sup>) is used on transmit and receive while the wings are receive only phased arrays spanning a total area of 28 m<sup>2</sup>. The central aperture transmits a large beam and the receive aperture captures the echo simultaneously from various directions through a digital beam synthesis. [C733]

#### "Remote control software development for a small airborne electronic support payload"

An unmanned aerial vehicle (UAV) electronic support payload (ESP) has been developed for the purpose of detecting and analyzing radar signals. The airborne payload control system (PCS) must be controlled from a ground control station (GCS) remotely through a wireless link. For the purpose, a control program, called Radar Signal Acquisition System (RSAS), has been designed, implemented and integrated with ESP. This paper introduces the ESP system, provides an overview of the general acquisition process, gives details on the RSAS and wireless link implementation using the Matlab scripting language, and finally presents some test results. [C734]

#### "Application of passive acoustic radar to automatic localization, tracking and classification of sound sources"

A concept, a practical realization and applications of a passive acoustic radar for automatic localization, tracking and classification of sound sources were presented in the paper. The device consists of a new kind of multichannel miniature sound intensity sensors and a group of digital signal processing algorithms. Contrary to active radars, it does not emit a scanning beam but after receiving surrounding sounds it provides an information about the directions of incoming acoustical signals. The acoustic sound pressure of a given event should be greater than the noise background. The practical examinations of the sensitivity and accuracy of the developed passive acoustic radar were also presented and discussed. The recognized sound events were divided into several types such as: explosion, shot, breaking glass, human scream. The information about the sound event direction can be used to the automatic and remote control of a Pan Tilt Zoom (PTZ) camera. The automatic and continuous tracking of a selected sound source movement is also possible. The proposed device can significantly improve the functionality of traditional surveillance monitoring systems. [C735]

### "An overview of range detection techniques for wireless sensor networks"

Range detection is a key problem in wireless sensor networks (WSN). In this paper, a brief overview is provided for basic techniques for this problem. The fundamental principles for range detection are inherited from RADAR systems, but careful designs need to be made to balance the expected accuracy and the device complexity, considering the limited resources of a WSN. We will introduce some basic measurement principles of range detection for WSN and some available range detection systems. We will also discuss several signal processing algorithms used for range detection. [C736]

### "Inverse synthetic aperture 3-D imaging laser radar"

Three-dimensional (3-D) Image can represent target's physical characteristic well and improve target recognition capability, however, conventional optical imaging radar which is limited by the array units or scan system cannot realize the high resolution imaging for moving targets. This paper combines the inverse synthetic aperture technology, laser signal and interferometric technique to suggest a new radar system which is called Inverse Synthetic Aperture 3-D Imaging Laser Radar, describes initial design project of this radar system, analyzes the imaging theory and implement method, and finishes the imaging simulation. The simulation shows the feasibility of this radar system and advantages of the image obtained from this radar. [C737]

### "Three-dimensional micro-doppler signature extraction in MIMO radar"

In traditional monostatic radar, only the micromotion signatures projected in line-of-sight (LOS) could be extracted from the target's echoes, which are insufficient for accurate target recognition due to the target-aspect sensitivity. In this paper, we propose an algorithm for the three-dimensional micro-Doppler signature extraction using the multi-input multi-output (MIMO) radar technique. The micro-Doppler effect in MIMO radar induced by rotation is analyzed. Profited from the multi-view of MIMO radar, the three-dimensional micro-motion features, which are not sensitive to the target's aspect anymore, are obtained by solving nonlinear multivariable equation systems. Simulations are given to validate the effectiveness of the proposed algorithm. [C738]

### "Front matter"

First Page of the Article [C739]

### "Simultaneous registration and fusion of radar and ESM by EM-EKS"

In this paper, we present an approach for radar and electronic support measure (ESM) simultaneous registration and fusion. An expectation-maximization based extended Kalman smoother (EM-EKS) is developed here to perform fusing of the system states and to simultaneously estimate the sensor biases. Computer simulations are carried out to validate the efficiencies and robustness of the proposed algorithm. [C740]

### "Radar velocity-measuring system design and computation algorithm based on ARM processor"

The real-time monitoring of vehicles velocity has become essential for traffic safety. Therefore, in order to improve the method of monitoring the velocity of vehicles on road, this paper has designed a new radar velocity-measuring system which is based on ARM processor. This system is based on Doppler principle and spectral estimation algorithm, in its hardware design part, and it takes full use of the underlying resources of ARM processor, to achieve sample, digital signal processing and peripheral control in the separate ARM core. In the software design part, it analyses the main program flow, at the same time, since the ARM processor does not support hardware floating-point operations, it puts forward the usage of fixed-point numbers to store and calculate floating-point numbers, which makes the data loading and storage minimization; And it uses ARM assembly language to write the core algorithm and takes full advantage of the 5-stage pipeline of ARM processor, to achieve the right register allocation and instruction scheduling for fine-grained control, and also to avoid the pipeline interlocks. Experimental results indicate that the accuracy of this velocity measurement system can reach  $\pm 1\text{km/h}$ . It not only can be used in traffic enforcement agencies, but also has low cost, low power consumption advantages. [C741]

### "VLSI signal processing system employing six phase codes for spread spectrum applications"

Spread Spectrum applications require a set of sequences with individually peaky auto-correlation and pair-wise cross-correlation. Obtaining such sequences is a combinatorial problem. If the auto-correlation and cross-correlation are taken in the aperiodic sense then there are hardly any theoretical aids available. Thus the problem of signal design referred to above is a challenging problem for which many global optimization algorithms like

Genetic Algorithm, Simulated Annealing and Tunneling Algorithm were reported in the literature. Recently an efficient VLSI architecture for Generation of the Six phase codes was proposed. Integrating this generation architecture with the currently proposed identification architecture provides an efficient Real-Time Hardware solution for identification and generation of the Six phase codes. The paper aims at an efficient hardware implementation of the Modified Genetic Algorithm (MGA) for the synthesis of optimal Six-Phase codes useful for Spread Spectrum applications. The VLSI System is implemented on the Field Programmable Gate Array (FPGA) as it provides the flexibility of Reconfigurability and Reprogramability. [C742]

#### "Space-time adaptive processing for sea clutter and jamming suppression in radar seekers"

When radar seeker searches and tracks moving target on sea surface, sea clutter spectra severely spread out due to the strong effect of sea conditions. Conventional methods for suppressing sea clutter have achieved poor performance. This paper mainly analyzes the sea clutter characteristics in azimuth-Doppler domain and clutter spectra with different scanning angles. Then space-time adaptive processing (STAP) technique is applied to suppress sea clutter. Research results indicate that sea clutter spectra have some special characteristics in space-time distribution, and the proposed STAP algorithm can detect slow moving targets effectively as it can suppress sea clutter and strong jamming. [C743]

#### "A new waveform for range-velocity decoupling in automotive radar"

Radar sensors for automotive applications require extremely high performance figures in terms of measurement accuracy and time. LFM CW radar sensors have the advantages of high range resolution, but it will bring out ghost targets and missed targets in multi-target detection. This paper describes a new waveform combining LFM CW with SFCW pairing is proposed and discusses in detail to demonstrate the technical differences and advantages. [C744]

#### "High-efficiency and well-integrity method for dynamic acquisition of GNSS location information"

Location-based services play an ever increasingly important role in modern society. The high efficiency and well integrity of GNSS location information is required in these services. For well integrity, a new dynamic transmission processing method named Transmission Intelligent Selecting Mechanism (TISM) is presented in this paper. Based on the detection of communication signal, different methods for information processing are selected for different signal intensity. For high efficiency, a new dynamic compression method named Time-Interval Alternated with Distance-Interval Intelligent Judging Method (TAD) is presented based on traditional compression methods Single Time-Interval method (STI) and Single Distance-Interval method (SDI). There are three different modes, high speed mode, medium speed mode and low speed mode in TAD. For different modes, different compression styles are selected. Experimental results show that TISM has made location information acquired successfully in some areas where the GPRS signal is very weak. TAD has reduced more than 75% of data and 50% of deviation comparing with STI. Thus, more than 75% of communication cost has been reserved. [C745]

#### "Compressive sensing radar imaging based on smoothed l0 norm"

Compressive sensing techniques have been shown to reduce the number of data samples beyond the Nyquist theorem, achieving perfect reconstruction of the original signal. In this paper, we propose a compressive sensing radar imaging arithmetic based on smoothed l0 norm. Simulation experiments conformed that the arithmetic has faster reconstruct speed and well reconstruct quality compare other arithmetic. [C746]

#### "A clutter suppression method based on angle-doppler compensation for airborne radar with uniform circular arrays antennas"

The clutter distribution of airborne radar with uniform circular array antennas varies with ranges and received data in different range gates are not independent identically distributed vectors, so the statistical STAP methods degrade. In this paper, based on the detailed analysis of clutter distribution for airborne radar with uniform circular array antennas, the conclusion that the non-linear relation between space angle and number of arrays results in the nonhomogeneity at range for airborne radar with circular array antennas is gained. A clutter suppression method for airborne radar with uniform circular array antennas is proposed in this paper. This method involves in a preprocessing with MADC method to align the centers of clutter spectrum in different range gates and subsequently clutter suppression in other azimuths with DBU technology. Simulation results show the validity of this method. [C747]

#### "Regularized resolution enhancement of point-based features of synthetic aperture radar image using variable quasi-norm"



Nonquadratic regularization with  $l_p$ -quasi-norm has been widely used as an efficient and powerful tool for resolution enhancement of point-based features of synthetic aperture radar (SAR) images. However, adjustment of the  $l_p$ -quasi-norm usually requires a lot of time and labor. In this paper, we propose a modified model and method for choosing regularization term. Considering the sparseness of scatterers in the scene of a SAR image, we use the generalized Gaussian distributions (GGD) as prior distributions for sampled scattering field. Our regularization model is constructed based on variable  $l_p$ -quasi-norms, and the selection of  $l_p$ -quasi-norm is achieved through estimation of the shape parameter  $p$  of the GGD by adopting a moment method. The regularization model leads to an alternating iterative algorithm. Experimental results with simulated and real data show that the method can automatically select regularization term and produce SAR images with improved spatial resolution. [C748]

#### "Ionosphere interference suppression for HF/SWR using L-shape array"

In this paper, using L-shape array for ionosphere interference suppression for high frequency surface wave radar is proposed. The linear receive array, which is used by conventional HF/SWR systems, is replaced by an L-shape array, which is effectively a combination of two linear arrays arranged perpendicular to each other. This gives the radar additional resolving power in elevation angles, which is not available in conventional HF/SWR systems with one-dimensional linear arrays, so the ionosphere interferences with high elevation angles can be better suppressed. Measured data from real HF/SWR is used in experiments to compare the ionosphere interference suppression performance of conventional linear array and the L-shape array. The result shows great performance improvement by using the L-shape array. [C749]

#### "Cover page"

The following topics are dealt with: kinematics, compressive sensing radar imaging, discrete Hilbert transform, feature extraction, nondestructive testing, dynamic programming, STAP algorithm, spread spectrum communication systems, face detection, wireless sensor networks, signal denoising, anti-jamming, information fusion, game theory, shipborne radar echo, ad hoc networks, wavelet transform, Hough transform, wind farm power, acoustic echo cancellation, speed estimation, image enhancement, curve fitting, perceptron neural nets, statistic decoding algorithm, LDPC codes, diffraction tomography, video watermarking, pulse compression technique, image analysis, cognitive OFDM, analog signal, fault diagnosis, target recognition, adaptive beamforming, nonlinearity correction imaging, computer vision, image segmentation, mobile networks, synthetic aperture radar, Kalman filtering, hidden Markov model, support vector machine, network intrusion detection, network congestion control, mobile VoIP, inertial navigation, edge detection, image resolution, image reconstruction, power control, cognitive radio, speech processing, attribute reduction, routing protocol, and incremental learning. [C750]

#### "Stepped-Frequency waveform processing for moving target based on genetic-CLEAN algorithm"

Stepped-Frequency waveform (SFW) is a very important type of high range resolution radar signal. A novel processing method for SFW based on genetic algorithm and CLEAN technique is proposed in this paper. The parameters (i.e., position, amplitude and velocity) of a point scatterer can be found by global searching with genetic algorithm. And an iterative CLEAN processing is used to eliminate the extracted point from the received data of one SFW burst. Then the high range resolution profile (HRRP) of the target can be reconstructed with the estimated parameters. Finally the effectiveness of the algorithm is verified by the simulation results. [C751]

#### "Statistical relax method for super resolution ISAR imaging"

An effective statistical method of detecting the scatterers center for super-resolution ISAR imaging is presented. By exploiting the statistics of background noise and clutters, Gaussianity test (GT) is applied to extract the scatterers center in range cells under desired constant false alarm rate (CFAR). Combined with extended Relax algorithm, super resolution ISAR image of target is generated. Theoretical analysis and experimental results of real data show that proposed method exhibit better performance with expected to conventional high resolution method. [C752]

#### "Error estimate of quadrature sampling system via discrete Hilbert transform"

Pulse Doppler radar needs accurate measurement of the quadrature sampling system error for error correction to reduce false alarm rate and improve the clutter suppressing performance and the improvement factor. This paper firstly introduces the discrete Hilbert transform to estimate the relative amplitude error and phase error of quadrature sampling system using coherent testing signal. The error function with respect to each sample is derived theoretically. Computer simulation shows that the theoretical results are effective and accurate. The results can be used to evaluate and correct the errors in the quadrature sampling system to contribute to

suppress the background moving clutter and reduce false alarm rate for the pulse Doppler radar. [C753]

#### "Shipborne radar echo signal denoising based on improved threshold and shrinkage function"

In order to denoise shipborne radar (9 GHz pulse radar) echo signal in distortion-free, smooth, and less loss, A improved threshold and shrinkage function are proposed in this paper based on the Multi-analysis wavelet threshold denoising. The denoising effects of different shrinkage function for shipborne radar echo signal were compared. The results of experiment show that better SNR and similarity and smoothness and less loss can be reached by using the proposed function to shipborne radar echo signal. [C754]

#### "Multi-cycle signal processing based on Keystone transform in LFMCW radar"

In this paper a Keystone transform based MTD processing is proposed for multi-cycle signals to solve the MTRC (migration through range cell) problem in linear frequency-modulated continuous wave (LFMCW) radar. Analysis shows that MTRC is introduced by the linear coupling of fast time and slow time in multi-cycle beat signals. Resorting to the decoupling principle of Keystone transform and under consideration of the characteristics of beat signals, a transform expression is given, which is independent of target parameters. The relation between this transform and the direct motion compensation is further discussed, and a general applicable condition is derived. Simulation results testify the conclusion and the efficiency of the method. [C755]

#### "New spatial overlap method of transmitting beam for airborne phased array radar"

A novel scanning structure of cross-circumscribed beam overlap arrangement for airborne planar phased array radar is presented, which can reduce the beam shape loss under the triangular and rectangular beam overlap arrangements. The beam shape loss and energy distribution and the probability of central detection of these structures are analyzed and compared. Simulation results show that the cross-circumscribed lattice has the lowest beam shape loss, and it can elevate the probability of central detection, and in favor of the integrality of scanning. [C756]

#### "Research on nonlinearity correction imaging algorithm of FMCW SAR"

The frequency modulated continuous wave synthetic aperture radar (FMCW SAR) is a newly proposed radar imaging system, which combines FMCW technique with synthetic aperture imaging methods and has the advantages such as small cubage, light weight, cost-efficient, highresolution, etc. In practical SAR system, the frequency and time of the frequency modulated signal can't keep linearity absolutely. The effects of nonlinear frequency modulation on range resolution and FMCW SAR imaging are analyzed. A method of polynomial fit is proposed in order to estimate the nonlinearity of the frequency modulated signal, and the nonlinearity is corrected. Nonlinear FMCW SAR imaging algorithm is researched. Then the simulation results are presented. The results show that this method is valid. [C757]

#### "An intermediary method used in direction-finding location system"

In order to deal with the NP hard in the usual direction-finding location, an intermediary techniques of data association for multiple targets tracking by multiple passive sensors are discussed. The location will be fulfilled at the assistant of a range finder. Firstly, employ one of a passive sensors equipped with the range finder in the tracking net, get an integrated measurement of the target; Secondly, translate the integrated measurement into the reference frame of the other sensors one by one, then use the translated measurement as the medium, pick up the ones associated with the translated one as a gather, Finally, let the orientation line in the gather crossed, and find the precision location though the least mean square. The simulation results show the excellent performance of the new direction-finding location method. [C758]

#### "A segmentation-based CFAR algorithm for subsurface targets detection in FLGPSAR"

Forward-Looking Ground Penetrating Synthetic Aperture Radar (FLGPSAR) has the capability of forming two-dimensional high-resolution images of subsurface objects from a standoff distance. This paper addresses the detection of subsurface targets, i.e. landmines, in FLGPSAR images. The conventional Constant False-Alarm Rate (CFAR) algorithm has been widely used in SAR image target detection, but its performance will degrade in subsurface targets detection because of the presence of interfering targets and clutter power transition. In this paper, a segmentation-based CFAR (S-CFAR) algorithm is proposed. The S-CFAR algorithm can remove the interfering targets or clutter power transition before estimating the parameters of the clutter background to achieve a better performance than the conventional CFAR algorithm. The real data processing results are given to validate the efficiency of the proposed method. [C759]

### "Transmit-receive beamforming for MIMO radar"

MIMO radar with orthogonal signal transmission is equivalent to form virtual sensors at the receiver. The virtual sensors can be used to form narrower beams with lower sidelobes. The pattern of MIMO radar can be decomposed into transmit pattern and receive pattern by mathematical analysis. In this paper, we apply conventional beamforming and MVDR beamforming algorithms to MIMO radar. At last, the comparisons of two algorithms for phased-array radar and MIMO radar are given. [C760]

### "Estimation of aircraft altitude in 2D radar intelligence networking"

An observation model of altitude estimation in 2D radar network with 2 sensors which is based on the WGS-84 ellipsoid earth is designed, and a new algorithm for target altitude estimation is presented. Through a lot of simulations and academic analysis, the performance of the algorithm is detailed analyzed. The simulation and analysis result shows that the algorithm accords to the fact of observation, makes full use of the observations, and the estimation of target altitude is improved. [C761]

### "Inverse frequency scaling algorithm (IFSA) for SAR raw data simulation"

This paper presents a SAR raw data simulation approach using the inverse frequency scaling algorithm (IFSA) based on deramp processing. It is time-saving and can take motion error into account. The limitation of the inverse chirp scaling algorithm (ICSA) on transmitted waveforms is also overcome. Simulated results show the validity of the algorithm. [C762]

### "A Gaussian particle filter for track-before-detect"

A novel track-before-detect algorithm is proposed to perform detection and tracking a weak target in radar measurements. Firstly, a Gaussian particle filter based track before detect is presented for tracking target. Secondly because of the Gaussian particle filter is only tracking algorithm and can not perform detection target, the likelihood ratio based the Gaussian particle filter is derived. Finally based on this deduction, sequential fixed size (FSS) likelihood ratio test (LRT) is used to detect target. Simulation results show that this novel algorithm can realized detection and tracking a weak target simultaneously, and the performance of detection and tracking is improved than the particle filter. [C763]

### "3-D imaging algorithm for targets with micro-motion based on HRRP sequence"

Three-dimensional (3-D) radar imaging has been widely used in target scattering diagnosis, modeling and target identification. In this paper, 3-D imaging algorithm for targets with micro-motion based on high resolution range profile (HRRP) sequence is presented. Aiming at the difficulty of getting look angle parameters of the radar directly and considering the precession feature of targets with micro-motions, a way of turning precession parameters into angle parameters indirectly is proposed. Meanwhile, for the scattering centers association, two methods are discussed and compared. Finally, performance analysis under the influence of related factors is also covered and the parameter constraints are given, and thus provide a reference for the design of 3-D radar imaging system. Simulation results are presented in the end, which prove the efficiency of the proposed method. [C764]

### "A robust space-time multiple-beam STAP algorithm"

Considering the limited sample support and computational complexity, the traditional localized STAP algorithms restrict adaptive processing in localized processing region and for the most part they have fixed system degrees of freedom (DOF). A new idea about the localized STAP algorithm which adjusting system DOFs adaptively with variable interference environment are presented, and some practical issues, such as performance metric selection, initial system DOFs selection and the recursion fast algorithm of weight are discussed. The validity of the research is proved by measurement data processing results. This algorithm is more robust in complicated interference environment, and it reduces large computational complexity and improves the performance of jammer suppression. [C765]

### "New threshold and shrinkage function for shipborne radar echo signal denoising based on wavelet transforms"

In order to denoise shipborne radar (9 GHz pulse radar) echo signal in distortion-free, smooth, and less loss, a new threshold and shrinkage function are proposed in this paper based on the Multi-analysis wavelet threshold denosing. The denoising effects of different shrinkage function for shipborne radar echo signal were compared. The results of experiment show that better SNR and similarity and smoothness and less loss can be reached by

using the proposed function to shipborne radar echo signal. [C766]

#### "Anti-jamming filtering for DRFM repeat jammer based on stretch processing"

This paper addresses issues about the rejection of false jammer targets in the presence of digital radio frequency memory (DRFM) repeat jammer. An anti-jamming filtering technique is proposed that it can eliminate this type of jamming signal. By using a stretch processing with a particular selected reference signal, the presented method can fully separate the echoes being reflected from the true targets and the signals being re-transmitted by a jammer in frequency domain. Therefore, utilizing the nonoverlapping properties of the received signals, filters or suchlike techniques can be used to reject the undesired jamming signals. Particularly, this method does not require estimation of jamming signal parameters and does not involve a great computation burden. Simulations are given to show the validity of the introduced approach. [C767]

#### "A modified track-before-detect algorithm for radar weak target"

Track-Before-Detect (TBD) is an effective method for detection weak target. In TBD a doubted target is tracked through a time sequence of frames, and then the target's energy is integrated along the tracked trajectory to lead to detection. Therefore the key of TBD methodology is how to accurate tracking target. A novel TBD algorithm is proposed based on Modified Hough Transform (MHT) and Particle Filter (PF). Firstly trajectories that are possible true target path are initiated by the MHT to obtain the region of the target, after that, this region is provided to the PF as the prior knowledge. According to this prior knowledge the false trajectories are eliminated and target is detected by the PF. Simulation results show the proposed algorithm can detect and track the weak target as low as 3 dB SNR. [C768]

#### "Tracking ground targets with road constraint using multiple hypotheses tracking"

Data association in tracking multiple targets is of vital importance for airborne surveillance radar. Multiple hypotheses tracking (MHT) is generally accepted as the preferred method for solving the data association problem in modern multiple-target tracking (MTT) systems. However, there are usually too many hypotheses to process slowly. In this paper, map information has been used to prevent unnecessary MHT track branches and improve the state estimator. The simulation results show that this new algorithm improves tracking performance in realistic environment and effectively brings down the number of track branches, while reducing largely calculating time with better accuracy. [C769]

#### "A TBD algorithm based on improved Randomized Hough Transform for dim target detection"

For the detection of dim target, the track-before-detect(TBD) methodology has been employed to integrate the target's energy through a time sequence of frames. A TBD algorithm based on improved Randomized Hough Transform for dim target detection is proposed in this paper. This algorithm uses the sequence number of frames to make sure that the point pairs are selected randomly from different frames, avoiding the unreasonable situation that initiates target's track in the same frame data. Second, it also introduces a new vote method. Based on the minimum Euclidean distance criterion, this vote method finds the optimal parameter cell to vote, making the vote result better than traditional Randomized Hough Transform (RHT). In addition, we not only increase the poll of the optimal parameter cell but also update the corresponding parameter, avoiding the large deviation between the recovered track and the real track. By simulation, we conclude that this algorithm can detect dim target more speedily and accurately than traditional RHT, especially under the background of low Signal to Noise Ratio (SNR). [C770]

#### "The research of distributed power quality on-line monitoring system based on GRPS"

In order to satisfy the requirement of power quality on-line monitoring system which is always online, cheap price and a wide coverage, the thesis puts forward to methods that GPRS(General Packet Radio Service)communications technology is applied in power quality on-line monitoring system. The main content of the system is that:the combination of DSP and MCU is used in power quality on-line monitoring system to store, display, count and analyze the collected data of voltage and current from each terminal, and communicates with supervisory computer through GPRS communication module to realize power quality monitoring in the grid. According to the need of user, it can control field device to realize the research of distributed power quality on-line monitoring System. [C771]

#### "A GPR survey on a morainic lake northerly Turin (Italy)"

A waterborne GPR survey consisting of 50 profiles with a total length of about 37 km has been executed on the morainic lake of Candia northerly Turin (Italy). The survey tested the capability of GPR in shallow low-conductive



waters to estimate bathymetry, water volume, bottom sediment type, bedding and porosity. Spotty measurements of electrical conductivity and temperature allowed for a better processing of GPR raw data. The results seem to confirm the effectiveness of GPR to give useful information providing suitable geometrical (water depth) and physical (water conductivity) conditions. [C772]

### "Advantages and restrictions of holographic subsurface radars"

Holographic subsurface radars (HSR) are not in common usage now; possibly because of the historical view amongst radar practitioners that high attenuation of electromagnetic waves in most media of interest will not allow sufficient depth of penetration. It is true that the fundamental physics of HSR prevent the possibility to change receiver amplification with time (i.e. depth) to adapt to lossy media (as is possible with impulse subsurface radar or ISR). However, use of HSR for surveying of shallow subsurface objects, defects, or inhomogeneities is an increasingly proven area of application. In this case HSR can record images with higher resolution than is possible for ISR images. This paper presents experiments with HSR imaging in media with different degrees of attenuation, and illustrates the principle of HSR through an optical analogy. [C773]

### "Full-waveform inversion of multi-offset surface GPR data"

Common ray-based techniques for analysing common midpoint (CMP) ground penetrating radar (GPR) data use only part of the measured traces and return results with limited resolution and non-quantitative values for conductivity. Due to the fact that full-waveform inversion uses all information of the measured traces, a higher resolution image of the subsurface and quantitative conductivity values can be obtained. Using an experimental dispersive CMP dataset, the results of dispersion analysis, i.e. permittivity and thickness, define the start model parameters for full-waveform inversion. After estimating an effective source wavelet, the full-waveform inversion based on a simplex search algorithm returns reliable permittivity and conductivity values of the subsurface. [C774]

### "Estimation of soil electromagnetic parameters using frequency domain techniques"

In this paper two frequency domain methods for characterization of the dielectric properties of dry sand over a broad microwave frequency range will be presented. The investigated electromagnetic parameters of the soil relevant for most GPR applications are dielectric permittivity and loss tangent. Although the majority of GPR applications concentrate on frequencies below 1 GHz, this work will investigate the constitutive parameters of soil with very low water content in three microwave bands (X, Ku and part of K) ranging from 7 to 20 GHz. In particular, this study will focus on the evaluation of the complex permittivity by means of a numerically robust evaluation rather than the well-known Nicolson-Ross-Weir (NRW) method. The proposed procedure yields the apparent real part of the permittivity and the loss tangent without the inaccuracy in the vicinity of  $\lambda_m/2$  resonances known from the NRW method. The second approach utilizes a free space measurement, in which the soil is confined by a polystyrene probe holder in a mono-static GPR setup. The measurement result of the backscattered excitation will be compared with a commercial time-domain solver based on Finite-Integration-Technique (FIT). The material parameters of the electromagnetic model are adapted iteratively in the way that measurement and simulation results coincide. The measurement results of both frequency domain methods demonstrate the validity of the estimated dielectric parameters. [C775]

### "Full-waveform inversion of crosshole ground penetrating radar data to characterize a gravel aquifer close to the Thur River, Switzerland"

Imaging results of crosshole GPR can be significantly improved by using full-waveform inversion compared to conventional ray-based inversion schemes. A recently developed 2D finite difference time domain (FDTD) vectorial full-waveform crosshole radar inversion method was made more flexible to allow using an optimized acquisition setup that reduces the measurement speed and the computational cost. This improved algorithm was used to invert crosshole GPR data acquired within a gravel aquifer in northern Switzerland. Compared to the ray-based inversion, the results from the full-waveform inversion show significantly higher resolution images in the depth range of 6m-10m. Comparison of the inversion results with borehole logs shows that porosity estimates obtained from Neutron-Neutron data correspond well with the GPR porosities derived from the permittivity distribution in the depth range 6 m-10 m and that the trends are in good qualitative agreement. Furthermore, there is a good correspondence between the conductivity tomograms and natural Gamma logs at the boundary between the gravel layer and the underlying lacustrine clay sediments. [C776]

### "Exact solution of idealized subsurface sensing problem"

Identification of subsurface objects detected by GPR requires an accurate estimate of their size and shape. In this paper, as a generalization of the migration methods based on the "exploding reflector" approximation, we



consider a model of synchronously exploding volume sources. The excited impulse radiation is registered on the earth surface. We write down a closed-form solution of the inverse problem: reconstruction of the current spatial density from the transient electric field distribution along the surface. This model solution can be used to refine practical migration algorithms. It is also interesting as a model to estimate the basic factors limiting GPR spatial resolution. [C777]

### "3-D GPR imaging of central pillar of the Mireuk stone pagoda in Korea"

Mireuk Pagoda is a very important national treasure which is known to be constructed during late Baekje kingdom about 1,500 years ago. To investigate the inner structure of central pillar of this stone pagoda, 3-D GPR and tomography imaging was applied. During this geophysical survey, we could find and define a small room in the pillar. Since full coverage was available in the radar tomography, we could obtain very accurate image of this empty room. By the disassembly of the cover stone of central pillar after this investigation, we could find great historical remaining in this room. The findings include golden jars containing relics of Buddha and written documents explaining construction history of this pagoda. [C778]

### "Integrated GPR and archaeological investigations to study the site of Aquinum (Frosinone Italy)"

To enhance the knowledge finalised to the location and conservation of the unknown buried structures below the actual studied levels, in the territory of the Ancient Aquinum (Frosinone, Italy), an integrated archaeological and ground remote sensing study has been developed during 2008-2009 and it is still in progress. Analysis of the historical and oblique aerial photographs, combined with topographical and archaeological field-walking surveys, allowed the preliminary interpretation of the main town-planning of Aquinum. To verify this preliminary interpretation an extensive geophysical surveys, employing Ground Penetrating Radar (GPR) method, has been made during 2008-2009. The obtained results indicate the good matching between the interpretation of aerial photographs and GPR images at different depths. The location, depth and size of the individuated archaeological structures were effectively estimated. Archaeological excavations made during the summer 2009, in a southern portion of the investigated area, have confirmed the results obtained with GPR method. [C779]

### "Monitoring of sequential gasoline-ethanol releases using high frequency ground penetrating radar"

Our hydrogeophysical field experiment evaluated the ability of high frequency (450 & 900 MHz) ground penetrating radar (GPR) to monitor sequential releases of gasoline followed by ethanol. The initial GPR images of the gasoline release zone reveal the development of shallow (i.e., above 10 ns) high reflectivity events and a significant velocity pull-up of an underlying stratigraphic reflection. Temporal evolution of the impacted zone reflectivity and the velocity pull-up indicate a progressive redistribution of gasoline in the impacted zone. GPR profiles obtained during frozen soil conditions clearly show that the presence of gasoline affects the freezing process. Preliminary analysis of the sequential ethanol release GPR data indicates a significant expansion of the impacted zone following this release. [C780]

### "Application of Ground penetrating Radar (GPR) exploration in Karst mountain areas"

When highway is built in Karst mountain areas of China, it is important for us to detect Karst distribution which would trigger embankment sliding, subsidence and other geological disasters. So, karst caves under different conditions, such as stochastic ground surface, random covering layer thickness, different filling styles and depth were simulated by Finite Element Method(FEM), which got the reflecting features in GPR profiles. Then, exploration of GuiZhou highway and borehole verification were introduced. [C781]

### "Practical algorithms of geometrical migration"

Practical GPR survey schemes based on a geometrical migration algorithm are implemented and experimentally tested: (1) random GPR data collection from water surface along a tangled path and interpolation to a regular grid for bottom reconstruction; (2) double-pass B-scan with different antenna offset for estimation of the upper ground layer thickness and permittivity. An analytical relation between the shape of subsurface reflecting interface with measured signal travel times is used for the reconstruction of the layer parameters. [C782]

### "Miniature multimode deep ground penetrating radar"

Deep ground penetrating radar, as its name says, is able to image the deep buried objects with high resolution. It becomes an important tool for human to know the underground world. In this paper a stepped frequency deep penetrating radar system has been developed. This miniature system is designed for three operation modes: Mode 1 is fast measurement, real-time data storage, off-line data analysis and imaging. Mode 2 is wireless real-time detection and imaging. Mode 3 is on-line real-time detection and imaging. Three modes can be switched

flexibly for different working platform, such as low altitude aircraft, planetary rover or lander, UAV (unmanned aerial vehicle), remote control vehicle and robot, vehicles or just hand holding. The miniature radar host is designed based on the embedded frame to satisfy the multi-modes operation condition including light-weight, small volume and low power consumption. [C783]

#### **"Nine steps to concrete wisdom"**

This paper presents the results of a detailed 3D investigation of 9 structural tests pits (called cells) at our offices in Australia. The data were recorded using a GSSI SIR-3000 system coupled with a 2.6 GHz antenna, with 1024 samples per trace and 500 scans per metre. A range of 5-6 ns and 16 bit data were used throughout. [C784]

#### **"Underground asset mapping with dual-frequency dual-polarized GPR massive array"**

Nowadays, GPR is one of the most effective tool for enabling the safe use of the underground; in fact, amongst the various state-of-the-art methods available, it is a noninvasive technique capable of accurately locating both metallic and non-metallic buried objects. After a multi-year development, a new system has been recently introduced on the market; due to the combined use of low and high frequency antennas (dual-frequency antennas), the use of array of sensors in different polarization and dedicated data processing techniques, the equipment enables the recreation of a 3-D volume from spatially correlated data, with clear benefit in terms of achievable performance and productivity. [C785]

#### **"EISS: An HF mono and bistatic GPR for terrestrial and planetary deep soundings"**

EISS (Electromagnetic Investigation of the SubSurface) is an HF (~2MHz) impulse Ground Penetrating Radar dedicated to deep soundings (kilometric depths) of planetary sub-surfaces. This radar has the particularity to be operated from the surface in both monostatic (transmitter and receiver at the same location) and bistatic configurations (with a small receiver separated from the transmitter that can easily be displaced on the area to be investigated). A prototype has been developed in the frame of ExoMars mission B-phase. This article mainly focuses on the bi-static mode and details the selected design, its various subsystems and its operations. Preliminary tests involving antenna impedance measurements on Earth are shown. [C786]

#### **"Automatic classification of metallic targets using pattern recognition of GPR reflection: a study in the IAG-USP Test Site, Sao Paulo (Brazil)"**

In this work, a methodology to automatically classify of metal targets using pattern recognition techniques on GPR reflection data is presented. The methodology consists of designing a multilayer perceptron (MLP) classifier based on features extracted from the targets in the subsoil, and then using it to classify hyperbolas diffraction indicating their position and depth. The classification of reflections allows a high resolution reconstruction of the subsurface with reduced computing time. The system was developed in MATLAB and applied to GPR data obtained at IAG-USP test site, located in the city of Sao Paulo, Brazil, where metallic drums were studied under controlled field conditions. This site contains different targets of variable sizes buried under different depths and it served as a model for the computational experiment. The results indicate that the automatic classification of the metallic targets in the subsoil is efficient, contributing for the reduction of the ambiguities in the geophysical data interpretation, besides having application on the subsoil mapping of utilities. [C787]

#### **"Development of a bore-head GPR for Horizontal Directional Drilling (HDD) equipment"**

ORFEUS is a Specific Targeted Research Project (STREP), partly funded by the EC, that started in November 2006. One of the objectives of the project was to design and develop a radar mounted on the drill head of Horizontal Directional Drilling (HDD) machines to provide a real-time indication, to the operator, of obstacles in the drill path. The system consists of a GPR control unit (housed in a drilling rod) and two UWB antennas. These can detect buried infrastructure that the bore-head may strike and verify a clearance zone around the drill string to ensure that new pipes may be installed with a minimum separation from adjacent plant. During the 3 year project, several key technical problems, mainly concerning electromagnetic and mechanical compatibility issues, have been solved. The system was finally tested both in experimental and operational sites. These tests confirmed the capability of the equipment to provide useful information on the obstacles in the drilling path; detection range has been evaluated to be sufficient to generate a warning message to the operator to allow corrective action to be taken, thus enabling HDD equipment to be used in greater safety. [C788]

#### **"Crosshole GPR traveltime tomography in elliptically anisotropic media"**

Owing to relatively rapid water content variations with respect to electromagnetic wavelength at GPR frequencies,

the vadose zone usually exhibits significant velocity anisotropy. Neglecting anisotropy in traveltimes tomographic reconstruction leads to artifacts that can obscure important subsurface features, the vadose zone being subject to this problem. In this paper, an algorithm for crosshole GPR geostatistical traveltimes tomography in elliptically anisotropic media is presented. The advantages of the geostatistical tomography algorithm are that the solution is regularized by the covariance of the model parameters and that stochastic simulations can be performed to appraise the variability of the solution space. The implementation relies on a fast curved raytracing scheme specifically crafted for the problem at hand. The benefits of the algorithm to image the vadose zone are illustrated through a synthetic case that is representative of typical studies in quaternary geological settings. The results show that considering anisotropy yields better fit to the data at high ray angles and reduces reconstruction artifacts. [C789]

#### "A study of GPR vertical crack responses in pavement using field data and numerical modelling"

The application of ground penetrating radar (GPR) as a non-destructive technique for characterization of pavement structure on road networks has gained considerable attention during recent years. High resolution ground coupled GPR has the potential to provide important additional information on pavement deterioration, defects and cracks, the last being the focus of this study. Crack geometry and the electrical properties of the pavement surrounding the crack can be quite variable, resulting in often complex and hard to interpret data. Therefore, FDTD numerical modelling has been employed to help understand a range of GPR vertical crack responses observed in a variety of pavements. [C790]

#### "Recent advances in RF tomography for underground imaging"

Underground imaging for tunnel detection is proposed using the principles of radio frequency (RF) tomography. In RF tomography, a set of distributed transmitters and receivers are deployed arbitrarily above the ground, or slightly buried. These transmitters radiate suitable narrowband, low-frequency waveforms into the ground. The resulting wavefront impinges upon underground objects, scattering electromagnetic energy in all directions. Receivers sample the scattered signal, mitigate direct-path leakage, retrieve the phasor of the scattered signals, and relay this information to a base station. After adaptive processing of measured data, an image of the underground facilities is achieved. [C791]

#### "A simple inversion model for the estimation of subsurface features of Mars poles"

Radar observations from Marsis have demonstrated that Martian Polar Layered Deposits (PLD's) are very transparent to radar waves. Thus, the sounder is able to detect the presence of subsurface reflections in the polar regions below the ice-rich layered deposits. The analysis of radar data makes it possible to gain information about some physical features of Mars surface. In this work an electromagnetic inversion model is used to characterize the shallower structures. This approach assumes that structure consists of layers with parallel plane interfaces and that the electromagnetic properties of the first layer are known a priori. Under these assumptions it is possible to estimate the dielectric permittivity of the subsurface structure. The inversion method has been tested in an area of South Pole and reconstruction results are shown. [C792]

#### "Tackling the non-linearity problem in GPR waveform inversion"

Crosshole radar tomography is a non-invasive tool used in diverse geological, hydrogeological and engineering investigations. Conventional tomograms provided by standard ray-based techniques have limited resolution. Higher resolution radar tomograms can be derived by using full-waveform inversion schemes. However, despite the theoretical improvement in resolution, convergence problems can arise in the application of full-waveform schemes due to the ill-posed nature of the inverse problem and the high non-linearity of the relationship between the model parameters and the scattered fields (i.e. the forward problem). We present here a new inversion scheme that starts with a low-pass filtered version of the radargrams and progressively expands the frequency bandwidth as the iterations proceed, thus reducing the likelihood of the inversion getting trapped in a local minimum. The benefits over standard full-waveform time-domain inversion are demonstrated by means of three synthetic examples. [C793]

#### "Influence of interface roughness and heterogeneities on the waveguide inversion of dispersive GPR data"

To investigate the influence of interface roughness and heterogeneous media on the inversion of dispersive GPR data, we performed 3D FDTD modeling with GPRMAX. For both the broadside and endfire source-receiver configurations the responses were calculated for models with different interface roughness and for models that include media with heterogeneities in their dielectric properties. Due to the use of multiple source-receiver offsets to calculate the phase-velocity spectrum, the signal to noise ratio was relatively good and for low interface

roughness the medium properties could be reasonably well reconstructed. Only for the largest interface roughness the data contained significant diffractions and the medium properties could not be reliably reconstructed. For variations of the relative permittivity values equal to 10% and 20%, the model parameters could still be relatively well reconstructed. [C794]

### "Attenuation of large bandwidth microwave signals in water and wet sand"

Large bandwidth microwave signals propagate in dispersive media as pulses that attenuate according to a non-exponential law. Although this is a direct consequence of wellknown theory of propagation in dispersive media, this fact is rarely acknowledged. The aim of this paper is an experimental study of this effect in fresh water and wet sand, both media of interest in Ground Penetrating Radar, which performances dramatically rely on capability of microwaves to propagate through soil. [C795]

### "Electromagnetic monitoring of concrete structures"

Non-destructive evaluation of reinforced concrete structures is an increasingly important field in the construction and civil engineering community. A large number of pathologies that affect both the concrete and the reinforced bar inside concrete are related to the presence of water and its spatial development. In this context, the quantification of both water content and bar diameter is an important phase for the diagnosis of concrete. The propagation of electromagnetic waves is controlled by its electromagnetic properties, mainly influenced by the presence of water in the case of concrete. The dielectric properties of concrete were studied as function of volumetric water content. To measure the dielectric properties of concrete as function of volumetric water content at high frequency, a HP-impedance analyser was used. More than 800 samples of concrete were analyzed and a new relationship between relative dielectric constant and volumetric water content was obtained. Furthermore the study was focused on the simulations for one centre frequency GPR applied to a range of rebar sizes common used as concrete reinforcement. This is compared with real measurements of different known rebar sizes inside concrete structures using 1GHz centre frequency antenna. Furthermore empirical relationship between rebar sizes and electromagnetic parameters was established and analytical functions were proposed. [C796]

### "Tests of sommerfeld ground wave theory using ground-penetrating radar pulses"

We have used ground-penetrating radar pulse waveforms within moveout profiles that we recorded over dielectric ground, to test the geometric amplitude attenuation rates of interfacial surface air waves predicted by classic Sommerfeld theory. The pulses allow separation of interfacial wave modes. We used horizontally polarized pulses centered from 37-390 MHz, frozen ground, and an intermediate range of tens of wavelengths over which radial polarization is predicted to exhibit anomalously low rates. As predicted, azimuthal broadside polarization at 37-45 MHz attenuated in proportion to the square of range, but the radial endfire rate was closer to the 1.6 power of range. At 360-390 MHz, both rates exhibited predicted range-squared amplitude attenuation. Not readily extractable from the theory are the rates for subsurface direct waves, for which we found, from numerical experiments, that both polarizations attenuate in proportion to the square of range. This suggests that geometric rates for all types of subsurface interfacial waves attenuate in proportion to range squared and could be subtracted from actual rates to determine material loss rates. [C797]

### "Inversion of guided waves in georadar data"

We analyze the dispersive characteristics of the electromagnetic guided waves (at georadar frequency) to infer the electrical properties of materials that constitute a layered wave guide. WARR (Wide Angle Reflection and Refraction) georadar acquisitions could be carried out in both TE (Transverse Electric) and TM (Transverse Magnetic) configuration to collect the full wavefield at different offset from the source. The dispersive curves of TE and TM modes are obtained by transforming the space-time acquisition into phase velocity-frequency domain (f-v spectrum); the relative maxima in the fv spectrum represents the different propagation modes. We adopt both global and local inversion algorithms for minimizing the misfit function between measured and theoretical curves in order to obtain a 1D model of the layered subsoil (thicknesses and electrical permittivity). [C798]

### "Nondestructive detection of delaminations in concrete bridge decks"

To detect delaminations in concrete bridge decks, nondestructive techniques (NDT) permit a frequent and large inspection of the slabs without damaging structures. This research was devoted to detect simulated defects in twelve repaired concrete slabs. These were scanned with high frequency ground penetrating radar (GPR) with the common offset (CO) and common midpoint (CMP) methods. The electromagnetic waves speed was determined from CMPs. A 3D visualization program was also created to display the CO measurements. The visibility of the inserted defects revealed to be dependent on their lateral extension, their thickness and their



constitutive material. [C799]

### "GPR as an effective tool for safety and glacier characterization: experiences and future development"

In recent times, the GPR technique has assumed an important role in glacial environment exploration. Ice thickness, bedrock description, internal water floods or underground channel, glacial structures (as snow layering and crevasses detection) form part of our experience in Antarctica and in high alpine glacier ski areas. In this paper, we present some results of these investigations exploring the possibility of combining our technical expertise on Radio Echo Sounding (RES) instrumentation to develop a system for subglacial environment exploration. [C800]

### "Multi-channel Ground Penetrating Radar based on ultra-wideband short-pulse signal: Hardware and software"

In [1, 2] recent state of our multi-channel Ground Penetrating Radar (GPR) design is reflected. In this paper we compare that former design with the new one which is free of some drawbacks. Both GPRs are suitable for diagnostics of road coatings, detection and recovery of subsurface infrastructure (pipes, cabling). GPRs include TX/RX module, antenna switch, multi-element antenna, carrier vehicle and control/processing computer with dedicated software. This software allows GUI, controls TX/RX module, accepts the data from TX/RX module, builds 3D radio image of subsurface volume. As well, dedicated software enables to estimate the geometry and electrophysical parameters of subsurface volume and objects inside of it. For this, so-called Computational diagnostics method is implemented which is based on reverse problem solution. Experimental results are presented. [C801]

### "Application of ground penetrating radar in the urban environment"

Several nondestructive testing methods have been studied to detect subsurface voids. However, few focus on deploying nondestructive methods in the congested and complex subsurface environment found in typical urban locations. This research identifies the challenges with applying Ground Penetrating Radar (GPR) techniques to locating subsurface voids and buried infrastructure in a complex urban environment. The study cataloged GPR signals representing reinforcements, concrete pipes, trolley tracks, and a large range of subsurface voids from surveys collected in downtown Louisville, Kentucky. Building upon this research, the team recreated a typical subsurface urban environment on the University of Louisville campus to develop a library of GPR images taken from known targets with defined parameters for training purposes. [C802]

### "Tapered slot antennas for ground penetrating radar"

The paper presents current results of our ground penetrating radar system design proposed for military application. It is focused especially on antennas, but includes the properties of ultrawideband generator. Several tapered slot antenna structures are presented and some of them have been fabricated. Some modifications of double ridge horn antenna are presented and their parameters are compared and discussed. [C803]

### "Accurate tools for convergence prediction of series solutions of Contrast Source Integral Equations"

Source Type Integral Equations (STIEs) provide interesting alternative formulations for the scattering from dielectric objects. In particular, the underlying operators factor into the composition product of two other linear operators, whose norms can be separately evaluated with the aid of suitable universal diagrams. Then, a specific inequality suggests that the convergence of the formal Neumann series inverting the original integral equation can be established by means of the aforementioned tools. Anyway, such an inequality sometimes provides pessimistic (i.e. stronger than actually needed) conditions in many cases of practical interest. The previous observation motivated the authors to further investigations, so leading to sharper bounds on the relevant norm of the STIEs operators. Numerical examples are reported, confirming the usefulness of the new tools. [C804]

### "Imaging of 3D magnetic targets from multiview multistatic GPR data"

Ground Penetrating Radar surveys aimed at imaging magnetic anomalies are gaining an increasing attention in several applications. In this respect, we introduce in this communication an inverse scattering strategy based on a suitable reformulation of the Linear Sampling Method (LSM). The LSM is a reliable and computationally effective imaging approach, which is exactly cast as a linear inverse problem (i.e., no approximation is required). This is made possible by restricting the processing task to the reconstruction of the shape of the anomaly and



neglecting the retrieval of the electromagnetic features. Since the LSM has been never applied to the imaging of magnetic targets from electric field data, a preliminary assessment of its reconstruction capabilities towards purely magnetic anomalies is given by means of numerical examples. [C805]

### "Effects of surface topography and wind on reflection horizons in ice sheets"

Radar horizons within the great ice sheets of Antarctica are distorted by greater snow deposition on windward than on leeward slopes. In West Antarctica, this effect can change horizon depth by tens of meters but still leave the horizons surface-conformable and continuous for hundreds of kilometers. When viewed on a scale of tens of kilometers, the additional effect of ice speed makes horizons appear falsely recumbent and suggests false historical changes in ice speed. In large regions of the high East Antarctica plateau, deposition occurs only on windward slopes to form prograding bedding sequences up to tens of kilometers long and hundreds of meters thick. Beneath the leeward slopes, long-term metamorphism transforms the bedded strata into unconformable and unstratified pseudolayers that grow with burial, merge with others, form concatenated layers more than 70 km long and over 100 m thick, and generally account for all major englacial horizons. For the largest sequences, the bed topography controls the surface topography and in large part, the way accumulation is distributed on the high plateaus. [C806]

### "An intelligent non-contact wireless monitoring system for vital signs and motion detection"

An intelligent non-contact wireless patient monitoring system is presented in this paper. The monitoring system is capable of measuring the vital signs (respiration rate and heart beat) and detecting patients' motion without physically contacting them by using a miniature Doppler radar sensor system. The system can provide all-round near-real-time 24/7 monitoring, which can be used in hospitals and homes to protect patients as a first line of defense system for wireless acute-care and wireless assisted-living. [C807]

### "Context system using pervasive Controller Area Network bus system to improve driving safety"

With more than one million people dying worldwide on the roads every year and lots of money in property losses, traffic safety remains an unsolved matter. The potentials of in-vehicle safety systems are currently investigated to improve this situation. Hence, embedded system which can collect some important context information and warn the driver in order to improve the safety of driving is needed. A Controller Area Network (CAN) bus with nodes of sensors or the node which is connected directly to the vehicle's CAN bus is very practical and powerful to collect driver's context information. This context information should not be just kept in the vehicles; it should be shared with vehicles in the same neighborhood or be sent to the information processing center. In order to have a wireless communication, communication technologies like ZigBee, GPRS are needed to be used. In this paper, we propose a context aware system for improving road safety and efficiency as well as driving comfort. The studied system is composed of the CAN bus and wireless communication system, a prototype of this system on the vehicle was also designed and tested in Citroen C4 car. A CAN bus was designed and realized by authors. Then, some context information from the vehicle existent CAN is collected and an experimental test is made. [C808]

### "GPRS-based fault monitoring for distribution grid"

The GPRS is a useful mean to solve the communication problem in the automatic system of power distribution network system. This paper designs a GPRS-based real-time system to monitor the on-off states of the switching station in the power distribution system. The system is consisting of a low-power controller of MSP430F149, the module of GR64 from WAVECOM company and detection circuits of on-off states. The IEC60870-5-101 protocol is used in the system. Therefore, it can conveniently communicate with other SCADA systems. It is reliable and stable running on site. [C809]

### "The restoration of road coats and related objects parameters based on method of computation diagnostics-Ground Penetrating Radar antennas dipole approximation"

Several approaches are considered which allow to increase the reliability of diagnostics of plane layered medium in Ground Penetrating Radar (GPR) applications. This increase is reached due to accurate account of parameters of transmit-receive antenna (via electrodynamic modeling) and radio frequency channel of GPR. [C810]

### "3D high resolution GPR survey to help the reconstruction of the archaeological stratigraphy of Lecce (Italy)"

3D high resolution Ground Penetrating Radar (GPR) survey was performed in the Crypt of the Duomo of Lecce

(South Italy), built in 1114. The GPR data revealed us a stratified subsoil in which there is a distribution, with the depth, of several "remains" referable to different epochs. Here we present and discuss the experimental evidences, comparing them with the historical-archaeological documentation. We think that they constitute a valid contribution to the knowledge of the ancient stratigraphy, as well as of the Roman history of Lecce, especially because of many suppositions have not yet found a confirmation. [C811]

#### **"Dielectric and magnetic anomaly imaging from GPR data"**

This paper deals with the reconstruction of buried targets exhibiting both dielectric and magnetic characteristics, starting from GPR data collected at the interface air/soil. The problem is tackled under a two-dimensional geometry by means of linear scalar inverse scattering and the performances of the approach will be outlined against experimental data. [C812]

#### **"How many points per scan?"**

Increasingly manufacturers are promoting equipment which claims to increase the no of sample points per scan to over 1000 points. For inexperienced GPR users, this appears to be an advantage. In reality this is misleading and giving a false promise of "improved" data. This paper demonstrates, on the basis of the Nyquist theorem that 256 sample points per radar scan is more than enough. [C813]

#### **"Detection of accelerated reinforcement corrosion in concrete by ground penetrating radar"**

This paper presents a new approach to evaluate corrosion of reinforcement in concrete by ground penetrating radar (GPR). Pulse GPRs were used to monitor the continuous corrosion process in concrete, in which the changes of amplitudes, travel times and short time fourier transform (STFT) spectrograms associated with the bar reflections were continuously measured. The yearly long corrosion process of reinforcement bar was rapidly accelerated within 10 days by impressing 2A direct current across two embedded reinforcement bars serving as anode and cathode. When corrosion started, it was found that the travel times, amplitudes and the frequency spectra from the bar reflection reached a maximum or minimum, but the trends of these parameters were then reversed when the crack became wide open. The results presented in this paper will pave the way for future corrosion characterization using GPR, both in laboratory and in field. [C814]

#### **"Use of Ground Penetrating Radar to map subsurface features at Lapa do Santo archaeological site (Brazil)"**

In this article we present some results of Ground Penetrating Radar (GPR) studies carried out at Lapa do Santo archaeological site. This cave is within Lagoa Santa karstic region, Minas Gerais State, Brazil. In the first field work, 44 GPR profiles were acquired with 100 MHz, 200 MHz, and 400 MHz shielded antennas focusing on three mains objectives: (i) to characterize stratigraphic layer; (ii) to identify geological and archaeological anomalies, and (iii) to identify potential areas aiming at assisting archaeologists in an excavation program. GPR results indicated anomalous hyperbolic reflections, and areas with high sub-horizontal reflection amplitude suggesting archaeological and geological potential targets, respectively. These results were encouraging, and then they were used to guide excavations at this site. Excavation of test units (meter by meter) allowed identifying an anthropogenic feature, e.g., a fire hearth structure, and natural features, such as speleothems and top of bedrock. Results also indicated the importance of GPR survey as a tool for orienting archaeological researches, increasing the probability of finding archaeological interest targets in an excavation program an area of environmental protection. [C815]

#### **"GPR applied to map Jabuticabeira-II coastal sambaqui archaeological site (Brazil)"**

In this work, some GPR results obtained in Jabuticabeira-II coastal sambaqui archaeological site, located in Jaguaruna region, Santa Catarina state, southern Brazil, are presented. Sambaqui is a word in Guarani (Native South American language) that means: Tamba-shells, and Qui-conic mound, or shell mound. GPR profiles present interesting anomalous reflectors most likely related to archaeological interest targets. GPR depth slices exhibit anomalies with high amplitude probably related to point reflectors. In order to give greater reliability for real result interpretations, 2D FDTD numerical modelling was accomplished, and it shows good agreement with real data obtained in the field. Then, real and synthetic results results as reference guide to archaeological excavation activities. Archaeologist from Universidade de Sao Paulo excavated Jabuticabeira-II site after GPR results analysis. Horizontal reflectors were related to sambaqui structure, and its bottom, characterized by rich archaeological layers as well as water table level. Anomaly typified by hyperbolic reflection pattern was associated with a concentration of carbonatic shells, from 3160 to 2850 cal yBP. GPR results were very important for archaeological research in development allowing adjusting excavation, and guarantee this research success. [C816]

### "Experimental investigation of different soil types for buried object imaging using impulse GPR"

Performance of electromagnetic sensors which are used to detect buried objects, is varied according to properties of soil. Most common sensor pair is EMI (Electromagnetic Induction) and GPR (Ground Penetrating Radar) for buried object detection systems. Besides the surface roughness and overlying vegetation, electrical conductivity ( $\sigma$ , (S/m)), electric permittivity ( $\epsilon$ , (F/m)), and magnetic susceptibility affects the detection performance of sensors. The electromagnetic properties of soil cause wave attenuation and change reflection coefficient of electromagnetic wave reflected from soil surface. For this reason, different soil types create various effects on sensor data, therefore performance of GPR and EMI sensors may decrease. Moreover, burial depth estimation can be performed if the soil properties are known exactly. This paper contains the effects of different soil types on impulse ground penetrating radar data, experimentally. [C817]

### "Simulation and application of GPR in Artificial Freezing Engineering"

In Artificial Freezing Engineering (AFE), the distribution of freezing soil and its defects are important to engineering safety. Based on relative permittivity measured by vector network analyzer, electromagnetic models of artificial freezing walls were made. Then Ground Penetrating Radar (GPR) exploration of AFE was simulated by Time Domain Finite Element Method (TD-FEM) coupled with freezing temperature calculation. GPR were also used in AFE exploration. The research results show that GPR exploration and numerical simulation are in good accordance with each other. [C818]

### "Design and numerical analysis of a new reconfigurable antenna for georadar applications"

We propose a new completely variable reconfigurable antenna for Ground Penetrating Radar (GPR) applications. In particular, here we present the design and the numerical analysis of the structure in total geometry morphing approach, with the aim of simulating the specific behavior of a reference bow-tie dipole. The development environment of the new device was the numerical tool HFSS (High Frequency Structure Simulator) by Ansoft which exploits the Finite Element Method (FEM). Finally, we extend the analysis of a single antenna by investigating the effect of a receiving one on the radiation properties of the transmitting antenna in dependence on the distance between them. [C819]

### "Instability analysis of Villa Arianna site in Castellammare di Stabia (Naples)"

The paper is on the use of GPR to detect features of instability affecting the structures of Villa Arianna archaeological complex. GPR data were acquired with a 250 MHz antenna on a cave excavated from an in situ deposit and inside the Villa, which lies on the top of a tuffaceous terrace. The study shows a direct correlation between the time shifts and amplitude spectra variations of the ground direct wave with the detachment surface location. [C820]

### "Experimental approach for determining the received pattern of a Rascan holographic radar antenna"

Because of the nature of image formation for holographic radar, the role and relevance of antenna radiation pattern are different than for impulse radar, and thus have not been studied. We determine theoretical Rascan radiation patterns for different dielectric media, and compare simulations to experimental data from an antenna scanned across a spherical metal target at various ranges/depths. Positions at which the received signal (phase difference between object and reference beams) are the same within a single scan, and across scans at different depths provide a 3-D approximation of the effective radiation pattern that closely agrees with the simulations. [C821]

### "Using ground penetrating radar to estimate active layer moisture conditions in the Arctic"

Polar regions, especially the Arctic, are expected to experience the largest changes in climate parameters during the coming decades, as well as increased variability. Large amounts of carbon currently stored in the arctic permafrost are expected to be released when a larger portion of the upper permafrost thaws. This will result in a deepening of the active layer, the region above the permafrost that freezes and thaws annually. Changes in this layer is thus important not only as an indicator of climate change, but also because they will alter the conditions for the vegetation and hence the ecosystem. A climate effects monitoring programme in the Zackenberg valley in the continuous permafrost zone of Northeast Greenland, has since 1995 monitored the thawing of the active layer using manual probes. Ground Penetrating Radar (GPR), a noninvasive technique that provides continuous data on the subsurface, has been widely utilized in geosciences applications and implementation of this technique in Zackenberg can greatly enhance the spatial and temporal resolution of active layer monitoring.

Hence, supplying additional knowledge of the changes in the active layer and the processes involved. This paper reports a preliminary analysis of data from a pilot project that focused on the interactions between the snow, soil and vegetation. In 2009, a GPR signal at 500 MHz was used to identify the active layer depth and to assess moisture conditions ( $\theta$ ) along a gradient of five different soil and vegetation types. The results suggest that differences in returning radar velocity can be used to estimate variations in moisture content in the active layer. [C822]

#### "The shrine of edward the confessor: A study in multi-frequency gpr investigation"

Following an earlier investigation into the 13th Century Cosmati mosaic in Westminster Abbey, Ground Penetrating Radar (GPR) investigations were commissioned in order to locate the site of a large royal tomb. Antennas of 400MHz and 4GHz frequency were used in the area of the High Altar steps and on the floor of the current Shrine Chapel. The investigation uncovered evidence of the target tomb, a number of other graves, some previously unknown, and at least one buried object. The paper briefly discusses the frequencies selected and illustrates how these have resulted in better understanding of the archaeological and historical evidence. [C823]

#### "Object dimension Vs antenna frequency"

The study deals with the performance of antenna frequency in detecting objects as a function of their dimensions. The results refer to actual data acquired with an IDS instrument, equipped with antenna frequency of 200, 600 and 2000 MHz, on an ancient wall reinforced with micro-piles, and on a concrete beam reinforced with iron bars. The micro-piles and iron bars are 0.13 m and 0.02 m in diameter respectively. The study shows that the dimensions of the objects in relation to the wavelength and the heterogeneity of the host environment, play an important role in making the interpretation of the GPR data easy in a civil engineering context. The results were validated with theoretical data. [C824]

#### "An ultra-wideband high-dynamic range GPR for detecting buried people after collapse of buildings"

An ultra wide band high dynamic range GPR radar has been tested for buried victims detection. After a building collapse, for example due to an earthquake, the priority of search and rescue teams is to localize people trapped under debris. Several tools are available to help the detection of buried humans, such as micro-cameras, high sensitivity microphones, and so on. Many of these tools present some limitations such as low penetration depth and high susceptibility to external noises. In this paper the authors test the use of an Enhanced Ultra Wide Band (UWB), Continuous Wave Stepped Frequency (CW-SF) Ground penetrating radar as rescue equipment. The radar has been experimented both in controlled environment, and in a real test site, at the Fire-fighters Station of Pisa, Italy. [C825]

#### "Half-space estimation by time gating based strategy"

In this work we deal with an estimation procedure of the Fresnel reflection coefficients for an half-space starting from GPR measurements collected under a reflection mode single view/multistatic configuration. After, the estimation of the Fresnel coefficient, the related electromagnetic parameters of the soil can be evaluated via simple algebraic relations. The problem is faced by exploiting the plane waves spectrum representation. Unfortunately when an antenna is close to the air/soil interface, interactions arise so that the actual antenna plane-wave spectrum is dependent on the searched for soil properties and consequently not known. To overcome such drawbacks, a preliminary step is introduced in the overall estimation procedure, which allows us to erase the antenna/soil interface interactions thanks to a time gating method. Numerical simulations with synthetic data are presented with the aim of assessing the effectiveness of the procedure. [C826]

#### "ALIS: GPR for humanitarian demining and its evaluation in Cambodia"

The authors developed dual sensor ALIS, which is equipped with GPR and metal detector. The image reconstruction algorithm is useful for clutter reduction and buried landmine image can be obtained. The system has been evaluated by test in minefields in Cambodia and could detect more than 30 mines. We are planning to continue this evaluation tests, and plan real deployments. [C827]

#### "Design of a pseudorandom reference codes for reduced sidelobes and spectrally clean out-of-band emissions using an extended optimal filtering approach"

In this paper we propose an extended version of the classical optimal filtering techniques to be used with binary noise codes, called m-sequences, and complementary codes. We introduce here extended optimal filters to achieve lower ACF sidelobe levels and spectrally clean waveforms with out-of-band suppression (OBS) levels



directly proportional to the filter length. [C828]

### "Multi-path EM scattering calculation for ships over time-varying sea surface"

In this paper, in order to simulate the time-varying scattering characteristics of ships over sea surface, both the reflection coefficient model for time-evolving sea surfaces and the ship motion dynamics are established and introduced into the multi-path EM scattering calculation. By combining the high-frequency asymptotic techniques for radar targets with the variations in the ship aspects and reflection coefficients of time-evolving sea surfaces, a time-varying radar signature model for ships over sea surface is developed. [C829]

### "A comprehensive system-level simulation paradigm for UWB systems"

A comprehensive simulation paradigm for UWB systems has been outlined. Its use in accurately simulating the performance of actual experimental through wall imaging radar and indoor positioning systems has been presented. The accuracy of the simulation framework has been validated experimentally using our UWB imaging radar and indoor positioning prototypes. This general framework provides a robust solution for rapid prototyping and optimizing of mixed signal UWB systems and requires accurate channel modeling. [C830]

### "Characterization of ultra-wideband wave propagation inside human body"

Ultra-wideband (UWB) has potential applications in variety of medical areas such as implant wireless sensors, microwave hyperthermia, imaging and radar. The wave propagation inside human body must be known for an efficient system design for the different applications. In this paper, UWB signal propagation inside human body is characterized for line-of-sight (LOS) scenario inside chest of a human model for the frequency range of 100-1000 MHz. The radiograph of UWB power and the spectrum of the penetrated wave into body are analyzed. The power delay profile (PDP) and the root-mean-square (RMS) delay spread of the in-body channels are obtained for the potential applications on wireless medical implant communications. [C831]

### "A practical wireless charging system based on ultra-wideband retro-reflective beamforming"

Numerous portable electronic devices (such as laptops, cell phones, digital cameras, and electric shavers) rely on rechargeable batteries and must be routinely charged by the line power. A wireless charging technique capable of delivering electromagnetic energy to these portable devices would make them tether free and "truly portable." Wireless charging is especially valuable for devices with which wired connections are intractable, e.g., unattended radio frequency identification tags and implanted sensors. In recent years, enormous research efforts have been devoted to wireless charging. In 1990s, a case study is reported to construct a point-to-point wireless electricity transmission to a small isolated village called Grand-Bassin in France. In 2007, an inductive resonance coupling scheme, which makes use of near-field coupling between two magnetic resonators, was demonstrated able to power a 60-Watt light bulb over two meters by a team of Massachusetts Institute of Technology. In addition, several companies (PowerCast, WildCharge, WiPower, etc.) have developed products targeting specific applications. Nevertheless, several technical challenges remain to be resolved in order to accomplish practical wireless charging. Specifically, (i) to achieve efficient charging over long distance, severe power loss due to electromagnetic wave propagation must be remedied; (ii) humans' exposure to electromagnetic radiation should always be kept below safety level while sufficient power is delivered to devices; and (iii) some existing systems are unsuitable for ubiquitous deployment due to high cost, large size, and/or heavy weight. In this paper, an innovative wireless charging system based on ultrawideband retro-reflective beamforming is proposed to address the above challenges. The proposed charger consists of multiple antenna elements distributed in space. According to pilot signals (which are short impulses) they receive from the target device, the antenna elements jointly-- construct a focused electromagnetic beam onto the device (i.e., beamforming). Beamforming enables spatially focused/dedicated power delivery to devices while keeping power level in all the other locations minimal. As a result, the proposed system attains high charging efficiency and leads to little hazard/interference to other objects. Performance of the proposed wireless charging system is demonstrated by some simulation results obtained by a full-wave Maxwell's equations solver. [C832]

### "Design of a tapered slot array antenna for UWB through-wall RADAR"

Ultra-wideband (UWB) RADAR based technologies have been gaining popularity recently for through-wall detection and surveillance applications. In this paper, the design and implementation of antenna for such applications is presented. An exponentially tapered slot (Vivaldi) antenna[1] is adopted. The tapered slot element being a travelling wave structure has inherently wide bandwidth with added advantages of high gain and low weight. Arrays based on Vivaldi elements have been extensively studied[2,3]. The current design is based on a segmented approach[2] with design of antenna element or array configuration based on radiation pattern requirements, followed by design of balun feed for individual elements and finally the design of feed network for



broadside radiation. In each step, the objective of good impedance match and hence low insertion loss leads to the desired bandwidth performance in the final design. [C833]

#### "Evaluation and optimization of the specific absorption rate for multi-antenna systems"

A decomposition and superposition technique is developed for the SAR analysis of a multiple antenna system. Upper and lower bounds for the total SAR can be calculated if the vector electric field from each antenna is available, while a most conservative SAR upper bound can be calculated if only SAR data from each antenna is available. A method for increasing antenna reception while decreasing peak spatial SAR was also shown. This technique combined with a beam-forming technique can be used to maximize the overall system performance and minimize the peak spatial specific absorption rate for multi-antenna wireless systems. [C834]

#### "A low cost wafer based W-band phased array"

A method to dramatically reduce the cost of W band phased antenna array system is proposed by using wafer based package concept and sub-harmonic mixing. Such phased array systems are well suited as front-ends of W-band radar and wireless communication systems and shall find many applications in defense, security and commercial sectors. [C835]

#### "Simulation of the mutual couplings among multiple antennas on large platform using multi-region multi-solver domain decomposition"

Modern aircrafts are usually equipped with multiple antennas serving for different usages, including radar, communication, etc. Many of them have highly contrasting power levels and overlapping frequency bands. The mutual couplings among antennas may cause severe electromagnetic compatibility (EMC) problem, which prevents the multiple antennas from working simultaneously. This paper proposes a multi-region multi-solver domain decomposition method (MS-DDM) to simulate the EMC problem on electrically large platform. It has been successfully applied to analyze the mutual coupling between complex antennas mounted on a real F-16 aircraft at 2GHz frequency. [C836]

#### "Analysis of transmission characteristics of a circular pipe with two open ends"

In this paper, we extend the modal formulation to characterize the transmission characteristics of a circular pipe with two open ends. Our interest in this problem stems from the possibility of using an open pipe as a transmission medium to propagate waves through an opaque wall at radar frequencies. We begin this study by developing an approximate solution for the transmitted field through a circular pipe with two open ends due to an incident plane wave. Transmission data are then collected in the laboratory using a circular metal pipe and the results are compared to simulation. It is shown that our formulation agrees well with the measurement data and therefore can be used as a good approximation to the transmission through a circular pipe with two open ends. [C837]

#### "A resistive dipole antenna excited by an impulse generator for ultra-wideband radar applications"

For UWB radar applications, a small RD and an impulse generator have been designed and fabricated. The performance of the combined RD and the impulse generator has been proved through the radar scan experiment. The results show that the combined RD and the impulse generator functions well as a UWB radar components. [C838]

#### "Investigations on a triple mode waveguide horn capable of providing scanned radiation patterns"

Feedhorn reflector antenna assemblies have been widely used for both satellite communications and Radar applications [1]. A dual mode feedhorn is presented in [2-3] where  $TE_n$  and  $TM_{0i}$  modes are excited to generate multiple phase centers when employed as a feed source for a reflector antenna. These papers [2-3] presented a technique of beam scanning in the  $\varphi = 90^\circ$  cut plane only, thereby generation of multiple phase centers in the  $\varphi = 90^\circ$  cut plane by control of the amplitude and phase of the modes. In [4] authors presented a tri-mode feedhorn design that employed  $TE_n$ ,  $TM_n$ , and  $TE_{2i}$  modes, but the effort was to reduce the cross-polarization in the far-field pattern of a linearly polarized offset parabolic reflector antenna. In this paper, we present investigation results of a triple mode ( $TE_\pi$ ,  $TM_\pi$ , and  $TE_{21}$ ) circular waveguide horn antenna with corrugated chokes which is capable of providing radiation pattern beam scanning in the range of  $\theta = \pm 24^\circ$  in both  $\varphi = 0^\circ$  and  $90^\circ$  cut planes similar to the case of a conventional phased array antenna. This is achieved by exciting all the three modes simultaneously in proper amplitude and phase. Though not discussed here, it is capable of providing multiple phase centers in both the  $\varphi = 0^\circ$  and  $90^\circ$  cut planes. The simulation design of the horn was performed using finite element method (FEM) based full wave analysis software Ansoft HFSS. The geometry

and design of the horn is discussed in section II. Simulation results of the horn are discussed in section III. Finally, section IV presents conclusion and future study. [C839]

#### "Application of a fast equivalent currents based algorithm for scattering center visualization of vehicles"

For the development of new radar sensor concepts in the automotive market comprehensive and reliable system simulation capabilities are highly desired. Since the radar channel includes both, desired and undesired contributions from the sensors environment, deterministic channel and wave propagation models are a crucial part of the whole simulation chain. Unfortunately, for some applications even asymptotic ray-based models exceed the available computational resources and further simplifications are required. Instead of brute-force ray tracing with a detailed geometrical description of the scene, one approach is based on a precomputed scattering center representation of complex objects. In this case, inverse synthetic aperture radar (ISAR) is a promising technique to estimate the required number and positions of the scattering centers. The imaging process should be fast enough to enable an investigation of a large number of bistatic configurations. In the 2D case, for range and cross-range resolution, classical Fourier processing requires twodimensional scattering data in frequency and aspect domain, which can be quite costly. Therefore, an idea presented is adapted to the existing scattering simulation code and applied to the scattering center visualization of vehicles. [C840]

#### "Synthesis of arbitrary sidelobes sum and difference patterns with common excitation weights"

The synthesis of sum and difference patterns is a canonical problem widely dealt with by researchers working on antenna array synthesis. As a matter of fact, they are used as transmitting/receiving devices for search-and-track systems (e.g., monopulse radars). Recently, the synthesis of low-sidelobe sum and difference patterns with a common aperture has been carried out by perturbing the roots of the Bayliss distribution to match as much as possible a given Taylor distribution. The discrete linear arrays have been successively obtained by sampling the resulting continuous apertures. In this work, the same array synthesis problem dealt with is addressed, and an innovative approach based on a deterministic optimization strategy is presented wherein the problem is formulated as the minimization of a linear function over a convex set. Taking advantage from the approaches for the optimal synthesis of sum and difference patterns respectively, the proposed method allows one to synthesize patterns with arbitrary sidelobes. [C841]

#### "Microstrip patch antenna array for a scalable X-band radar system"

A 32-element X-band microstrip electronic scanning array (ESA) has been developed to serve as the radiating element in a preliminary system radar testbed. An array of microstrip aperture coupled patch antennas are fed equal power through a Wilkinson power divider network and the direction of radiation is controlled by surface mount phase shifters integrated into the RF control board. While bulky physical array steering mounts greatly impact the system weight and visual signature of traditional radar systems, the electronic beam steering mechanism employed in this system minimizes each of these attributes. The details of the antenna array element in this radar ESA design will be examined in the subsequent sections. [C842]

#### "Time domain radiating model for GPR antenna"

In this paper, we suggested a method to substitute any antenna by a model based on the use of dipolar sources in the FDTD method. This approach allows to model antennas with their supports or environnement context. Thus, it makes possible to model complicated structures and oriented in any direction of space. The effectiveness of this approach is validated with Feko simulation of the original antenna. [C843]

#### "Transmit beamforming for colocated MIMO radar"

MIMO radar has seen growing interest in recent years owing to the many advantages that it offers over conventional radar, including spatial diversity and enhanced target direction resolution. Unlike standard phased array (SIMO) radar that transmits scaled versions of a single waveform from its many transmit antennas, a MIMO radar can transmit distinct waveforms from each antenna. Such an increase in the number of degrees of freedom for waveform design can potentially be used to obtain beamforming performance similar to SIMO radars with a far fewer total number of transmit and receive antennas. In recent literature, the problem of finding a signal correlation matrix that achieves a desired transmit beam pattern has been addressed, but a closed form solution for this problem has been lacking. In this paper, we first formulate a new spatial ambiguity function that simultaneously specifies the transmit beam pattern as well as the cross-correlation beam pattern. We then provide a closed form solution for the signal correlation matrix whose spatial ambiguity function is closest to a desired function (in the mean square sense), when using colocated uniform linear arrays. Further, we show how a suitable tapering window could be applied on the signal correlation matrix to tradeoff sidelobe levels for

mainlobe width in the spatial ambiguity function. [C844]

#### "MOSAICS: Multiplexed optimal signal acquisition involving compressed sensing"

It is possible to sample signals at sub-Nyquist rate and still be able to reconstruct them with reasonable accuracy provided they exhibit local Fourier sparsity. Underdetermined systems of equations, which arise out of undersampling, have been solved to yield sparse solutions using compressed sensing algorithms. In this paper, we propose a framework for real time sampling of multiple analog channels with a single A/D converter achieving higher effective sampling rate. Signal reconstruction from noisy measurements on two different synthetic signals has been presented. A scheme of implementing the algorithm in hardware has also been suggested. [C845]

#### "Analysis of the detection modes of a human presence detection millimeter-wave radiometer"

Detection of non-moving humans is important for physical security, search-and-rescue, homeland protection, and military applications, although it has proven difficult to achieve because traditional techniques have significant drawbacks. For instance, IR sensors do not detect well in warm daytime environments and radars cannot easily discriminate stationary humans. The authors have recently presented a solution by applying millimeter-wave radiometry to the detection of stationary humans in cluttered outdoor environments. MMW radiometers operate in both day and night environments and are affected only by moderate to heavy rain. Fog, smoke, or dust, which render IR sensors inoperable, are also transparent to MMW sensors. The radiometric detection system was designed to operate from a moving platform, making image recognition prohibitive due to the high computational expense of image processing in real-time with a constantly changing background. The presence-detection radiometer operates on onedimensional sensor signals, resulting in lower computation time. The system uses four detection modes: two Ka-band total power radiometers (indicated by tp1 and tp2), one Ka-band correlation radiometer (cr), and one W-band total power radiometer (tpw). The authors' previous work has demonstrated the feasibility of the detection method and introduced detection algorithms, and a future publication will present the real-time performance characteristics of the method. In this paper an analysis of the detection capabilities of the sensor system is presented by selectively removing sensor modes from the detection algorithms. In this way the dependence of the individual modes on the overall system performance is determined. The performance is analyzed using the receiver operating characteristic. [C846]

#### "ADS interleaved arrays with reconfigurable polarization"

Polarization-reconfigurable arrays play a fundamental role in radar systems in order to enhance their detection probability and cancel clutters, chaffs, and jammers. In order to reach polarization flexibility, the integration of actively controlled elements in standard array configurations is often employed, but the overall system complexity and costs significantly increase. To overcome such limitations, the use of two shared aperture arrays with independent polarizations was proposed in by exploiting an interleaving scheme based on Difference-Sets (DSs). By combining the field generated by each sub-array, arbitrary polarizations, low sidelobes, large steering angles, and narrow beamwidths can be reached with a limited complexity of the underlying feeding network. Despite its theoretical and practical advantages, only few planar array geometries can be synthesized because of the limited number of available DS sequences. [C847]

#### "Feasibility study for IED detection using forward-looking ground penetrating radar integrated with target features classification"

In this paper, we examined the natural resonance frequency and polarization features of UXO-Like IED target in forward-looking GPR configuration. Based on the simulation results, we confirm that these feature not only exist but also measurable in the case of FLGPR. It is therefore, strongly suggested that these features be included in the target classification algorithms as they are expected to improve detection, increase stand off distance and minimize false alarm rate. [C848]

#### "Quantification of the impact of the antenna non-idealities in UWB transmission systems"

In this paper the quantification of the impact of the pulse distortion of antennas on the UWB transmission is presented. As a criterion for the evaluation the fidelity is derived. For verification the system performance of a line of sight transmission, i.e. the bit error rate, for a bow-tie antenna is evaluated, based on measurements. It is shown that the fidelity significantly influences the BER, excluding interference from noise or other sources. The result is that for UWB impulse operations in communications, but also in Radar applications, besides the signal to noise ratio also the fidelity of the antennas has to be taken into account. [C849]

#### "Impulse response of Vivaldi antenna using cubic-spline and exponential taper profiles for compact

### **ground penetrating radar applications"**

The measured impulse responses of Vivaldi tapered slot antennas employing conventional exponential and cubic-spline taper profiles are presented and compared. The method used to design the tapers is based on a Chebyshev impedance transformer given in which minimizes reflection. A brief presentation is given for this design method and the profile of the tapers. Then, the experimental results and analysis of impulse response of antennas are provided. Finally, peak values of the impulse responses of the antennas are compared to the theoretical maximum achievable values and are shown to be quite close to this fundamental limit. [C850]

### **"DOA estimation of correlated sources using SMT"**

This paper uses a recently developed technique that relies on the Sparse Matrix Transform (SMT) to estimate the covariance matrix of  $D$  signals received by  $M$ -elements linear antenna array, each signal is of length  $N$  (the number of snapshots is  $N$  where  $N < M$ ). SMT based covariance estimation is particularly suited for singular covariance matrices and those with small eigenvalues. Direction of arrival (DOA) estimation using the MUSIC algorithm relies on estimating the eigenvectors associated with the noise eigenvalues which are usually minimal. Also, when the sources impinging on an array are correlated, the covariance matrix is singular, and the performance of the MUSIC algorithm degrades significantly depending on the degree of correlation among sources. This makes SMT particularly suited for DOA estimation using MUSIC for partially or fully correlated sources, and especially scenarios where it is not practical to take a large number of snapshots (such as radar applications). This paper employs SMT in the MUSIC algorithm using real radar backscatter data as the sources. Limitations and benefits of SMT based DOA estimation are discussed. [C851]

### **"Design and analysis of a 5.88GHz microstrip phased array antenna for intelligent transport systems"**

Detection of blind spot area of an intelligent mobile vehicle is presented in this paper. In order to scan the concerning area, a phased array radar is designed. The approach is of two fold. Firstly, microstrip phased array antenna with progressive phased shifter is designed and subsequently, it is optimised for improvement of performance through parametric studies and array distribution using Tchebyscheff polynomial. [C852]

### **"An amplifying reconfigurable reflectarray element"**

Reflectarray antennas are strong candidates for addressing some of the challenges faced in space communication systems, RADAR and point-to-point terrestrial links. The long distances involved demand the use of high gain antennas and furthermore these applications can benefit from adaptable radiation patterns. The large size of reflectarray antennas ensures their capability to synthesize highly directive beams. To add beam reconfigurability to reflectarray antennas, the phase shifting techniques utilized in phased array antennas can be applied, since a reflectarray can be considered as an array of reflecting elements. Electronically-controlled reflectarray elements utilize different technologies such as varactor diodes, MEMS switches and liquid crystal materials to dynamically change the phase of the scattered wave from each element. [C853]

### **"On the influence of a glass slide on the SAR distribution in Petri dishes for in vitro exposure to 2.45 GHz EM fields"**

In this paper, a numerical dosimetric analysis has been carried out through CST Microwave Studio® 2009. The homogeneity of the SAR distribution and the coupling of EM fields within the liquid in the presence of a glass slide as support for living cells, has been investigated as a function of the incident field polarization. [C854]

### **"A novel broadband Fabry-Perot resonator antenna with gradient index metamaterial superstrate"**

In this paper, a novel broadband high gain Fabry-Perot resonator antenna is proposed. This antenna is composed of a gradient index metamaterial superstrate and a U shape slot radiator backed with PEC ground plate. A single-layer FSS with the taper-sized square rings pattern is distributed on one side of planar superstrate to realize the gradient index function, which is designed to transform the spherical wave-front excited by primary source into the planar wave-front. It is demonstrated that by adding such gradient index metamaterial superstrate, the fractional 3dB gain bandwidth of this antenna can be improved to 15.4%, as compared to that of single-layer FSS with the uniform-sized square rings pattern. These results show the potential feasibility of such kind of antenna in the broadband and high directivity applications, such as the radar and communication systems. [C855]

### **"Conformal array antenna with the aspirator for the microwave mammography"**



Recently, the microwave imaging techniques attract attentions as a screening method of early breast cancer detection that takes place of an X-ray mammography. There are two categories of UWB radar and microwave tomography. A lot of basic experiments using the phantom have been reported. For such experiments, antenna array and breast are soaked in the coupling liquid in order to maximize the amount of microwave energy coupled into the breast. In addition, we must know 3D surface of the breast to remove artifact reflected by skin using averaging technique in UWB radar or to solve illposed problem in microwave tomography. In this paper, we propose a conformal array antenna for microwave mammography. When we adopt this antenna, it is not necessary to soak the breast in coupling liquid and to know 3D surface of the breast. Several antenna elements are embedded in inside of hemisphere made by silicon resin. A valve is provided on the top of the hemisphere and is connected with the aspirator. Putting the hemisphere on the breast and pulling out air by the aspirator, we made skin surface contact with inside of the hemisphere. Antenna element is designed so as to match under the condition that breast contacts with the element. Since breast surface is formed with inside of hemisphere, it is not required to measure 3D surface of the breast. [C856]

#### "Ultra wideband hemispherical microwave imaging system"

This paper has reported an automated high resolution hemispherical imaging system using ultra wideband microwave signals. At present, the system operates in the monostatic radar mode. To achieve a hemispherical scan, the imaged object is placed on the turntable (rotational axis) for a 360° scan while the elements of the array antenna are fixed and suitably spaced in vertical and azimuth directions. The operation of this system has been illustrated in an example of a simple breast phantom. [C857]

#### "Advances in waveguide-fed slot arrays"

Waveguide-fed slot arrays are employed in numerous radar, remote sensing, and communication applications in ground and space systems. Professor Elliott's significant contributions paved the way for the eventual maturity of the slot array antenna technology to the point that it is possible to design such systems in one pass without the need for any experimental data. The author worked in a research group headed by Prof. Elliott and centered at Hughes Aircraft Company, Canoga Park, CA in the early eighties. Later the author collaborated with Elliott in the study of slot arrays for a decade with funding from the University of California and the Hughes Corporate office. Subsequent work was funded by many sponsors. This paper reviews the advances made in the field of slot arrays by the author in collaboration with colleagues and students. [C858]

#### "An implementation of the impedance-boundary CFIE using linear-linear basis functions and MLFMA"

The results show that first-order LL linear basis functions may be successfully used to discretize the impedance boundary CFIE using an approach derived from that developed by Collino et al. The LL expansion yields lower errors in the calculated bistatic radar cross-section than that given by zero-order RWG basis functions with the same surface discretization mesh in all cases examined. However, LL basis functions require double the number of unknowns with the same mesh, and therefore a higher computation time. [C859]

#### "A novel directivity/beam reconfigurable M-EBG antenna"

Directivity/Beam control antennas are an interesting solution for wireless communication and radar application. To achieve a reconfigurable radiation pattern, active printed arrays are well suited thanks to an easy interconnection between printed technology and active devices. But a low performance is often obtained because of microstripline losses and coupling between elements. Moreover, in such frequency range, phase shifters and amplifiers are scarce and expensive. As an alternative to these conventional beam switching technologies, reconfigurable Electromagnetic Band-Gap (EBG) antennas can be used. [C860]

#### "Parallel FETI-EM Domain Decomposition Methods optimized for antenna arrays and metamaterials periodic structures"

Domain Decomposition Methods have demonstrated efficiency and accuracy during the resolution of Maxwell equations in the frequency domain for both RCS applications and antenna structures interactions. In the domain of finite element methods, and for the resolution of acoustic Helmholtz equations, efficient sub-domain connecting techniques have been applied and called Dual-Primal Finite Element Tearing and Interconnecting. These techniques are known under the acronym FETI-DP and have been adapted to electromagnetic (FETI-DPEM) for the calculation of antenna arrays and metamaterial periodic structures. In this paper we describe the implementation of an algebraic parallel FETI solver developed at ONERA for both acoustic and electromagnetic applications. It has been called as a library in the FEM module of the FACTOPO tool developed for both antenna



and RCS applications. [C861]

### "Optimizing narrow-wall slotted waveguide arrays using HOBIES"

The narrow-wall slotted waveguide array is widely used in many radar applications and is complicated to analyze. Previous works have been reported on how to analyze the structure. However, it is the first time that the optimization results of this waveguide array antenna are presented in this paper. Two optimization examples are given and results show that the radiation patterns are improved after optimization. [C862]

### "FDTD electromagnetic-acoustic model: A 2-D numerical coding framework"

In this work, we present a model of the electromagnetic and acoustic wave propagation using the Finite-Difference Time-Domain (FDTD) (2,2) update scheme. The model can be used to validate various algorithms used in previous numerical studies of microwave radar imaging, microwave tomography, and microwave-induced thermoacoustic imaging. Our key contribution lies in the numerical coding framework, which incorporates the simulations of the two physical processes. The advanced efficiency and organization of the computational approach, in turn, will help the development of flexible solvers. [C863]

### "Design on elliptical lens monopulse antenna"

This paper demonstrated a novel kind of two-dimensional elliptical lens antenna for monopulse applications. Simulations show that the lens antenna exhibits a very clean and symmetrical pattern on both the sum and different ports. A very deep null is achieved in the difference pattern because of the circuit symmetry. [C864]

### "Beamforming through a circular pipe with two open ends"

In this paper, beamforming through a circular pipe with two open ends has been demonstrated using the least squares approach. Through simulation it was shown that using three sources it is possible to steer the main beam of the radiation at the other end of the pipe. The simulation results were then confirmed through measurement results. This one-way beamforming concept can be extended in a straightforward way to two-way detection of a target. Thus it should be feasible to detect the bearing to a target when using a pipe as a propagation medium for through-wall radar. [C865]

### "Classification of human activities on UWB radar using a support vector machine"

In this paper, we classify seven different human activities measured by a ultra wideband (UWB) radar using a Support Vector Machine (SVM). The classification is done using the time variation of a signature of a return from a human subject. This time varying signature is unique to a particular motion because human's returns vary based on the change in the orientation of their torso and limbs. We exploit this time variation of a human's radar signature in order to classify the human activity recorded by the radar. The signature is captured by the Principle Component Analysis (PCA). The Support Vector Machine (SVM) is proposed as a classifier. The training process and the resulting classification accuracy are reported. [C866]

### "Computation of physical optics integral by Levin's algorithm on NURBS"

Non-Uniform Rational B-Splines (NURBS) are very powerful modeling tools for geometric design due to several reasons including fast and numerically stable algorithms and unified mathematical basis for representing complex objects [1]. Although target modeling is easy with NURBS, applying some numerical tools directly on NURBS is not so straightforward. Since the surface point function and derivative computation is simpler for rational Bezier surfaces (RBS), NURBS surfaces are converted to RBS by Cox-de Boor Algorithm for numerical implementations [2]. Therefore, solving a problem for RBS corresponds to solving it for NURBS surfaces. Indeed, in this paper, RBS are used for surface modeling and radar cross section (RCS) computations. The RCS computations are performed by employing Physical Optics (PO) approximation which is accurate at high frequency regions [3]. Although PO is a more efficient technique for scattering problems at high frequencies, when compared to full-wave techniques, it may be intractable due to rapid oscillations of the PO integral. In the literature, there are several methods to handle the oscillatory integrals including the stationary phase method, which is already applied to PO computations on NURBS surfaces [2, 4]. Another method proposed for highly oscillatory integrals is the Levin's method which was previously applied to PO problems, particularly RCS computation of targets modeled by quadrilaterals [5]. In this paper, the same approach is utilized on RBS. [C867]

### "Edge wall slotted waveguide antenna with low cross polarization"

A travelling wave SWGA with low cross polarization level is designed using an easy to manufacture, non-inclined

slot geometry. The modeling of the slots is done with infinite array unit cell approach. Simulation results showed promising performance in terms of side lobe and cross polarization levels. This antenna will be produced and the measurements results compared with the simulations will be presented at the conference. [C868]

### "Comparison between genetic programming and Neural Network in classification of buried unexploded ordnance (UXO) targets"

In this paper, we present the results of our next step effort in comparison of classification performances between the NN and the GP techniques based on the simulated scattering patterns of UXO-like object and non-UXO objects. For this comparative study, 2 dimensional scattering images from one UXO target and four non-UXO objects were generated by numerical simulation tool (FEKO). For non-UXO objects, the most challenging targets to discriminate from UXO, since all these objects produce resonance signal as UXO-like targets do [6], were selected. Classification performances of both techniques (NN vs. GP) in different level of noise and in the case of presence of untrained data were examined and the results and observations are discussed. [C869]

### "Performance evaluation of subsurface target recognition based on ultrawideband short-pulse excitation"

Automated Target Recognition (ATR) based on Natural Resonance Frequencies (NRFs) embedded in Ultra Wideband (UWB) transient electromagnetic signatures have been extensively studied. To our knowledge, most studies concerning ATR using the E-Pulse technique are about radar targets in free space. Recent attempts have been made to apply the E-Pulse technique for subsurface target detection. In this paper, performance evaluation of a recently proposed subsurface target recognition technique based on the E-Pulse and Baum's transform under different signal-to-noise ratios (SNR) is considered. Examples of target recognition of three different perfect electric conductor (PEC) targets sited below a frequency-dependent lossy halfspace are presented. [C870]

### "Unidirectional low profile ultra-wideband antenna for radar and communication applications"

One of the important elements in all UWB radar and communication systems are the antenna elements, which are required to be compact, light weight and to have good radiation characteristics. The most commonly used directional UWB antennas are Vivaldi antennas and ridged horn antennas. Vivaldi antennas are typically required to be a few wavelengths long to have good matching a reasonable gain which limits their use in low frequency UWB radars such as GPRs and see-through-all radars where the low operating frequency is required to penetrate moist soil or lossy walls. Ridged horns offer significantly higher gain at a smaller size but they are relatively expensive and bulky. To overcome these limitations, we present a new compact lightweight UWB antenna that has comparable gain to ridged horns but is almost 1/5th the size. [C871]

### "Mechanical scanning with a dual-layer pillbox antenna for millimeter-wave applications"

A low-profile, high performance, multi-beam, low-cost multi-layer pillbox antenna has been recently proposed by the authors [1] [2], as a possible solution for high demanding millimeter-wave applications (surveillance systems, automotive radars, telecommunication applications, etc.). In these works a passive electronic system was used for steering the antenna main beam. However, thanks to the low profile, low weight and compactness of the structure, a mechanical scanning can be an attractive solution for those applications where a continuous steering of the main beam is required for tracking moving objects or connection maintenance (satellite based telecommunication applications). This solution would be a cheaper alternative compared to expensive phased approaches or hybrid combinations of mechanical and electronic scanning. The antennas structure is shown in Fig.1. It is based on a SIW (Substrate Integrated Waveguide, [3] [4]), double layer pill-box structure where the feeding and radiating parts are located in two different substrates connected by an integrated symmetric parabolic reflector and several coupling slots (quasi-optical system). In the following the three main parts of the system (quasi-optical system, input part and radiating part) are introduced together with some numerical results at  $f_0=24.15\text{GHz}$ . [C872]

### "Terahertz reflector antenna system for a scanned and multiplexed FMCW radar"

In this contribution, the paper presents the antenna design and implementation of a mechanically scanned and multiplexed terahertz imaging radar. By using of a quasi-optical waveguide, we can multiplex our signal into two different beams and double the time acquisition of the image without increasing the number of transceivers. Only few additional optical components are needed. [C873]

### "Active phase array SAR antennas"

The paper focuses on similarities and differences between RADARSAT-2 and RADARSAT Constellation SAR antennas radio frequency (RF) architectures, both in terms of the radiating panel designs and feed networks designs. An overview of the antenna RF architecture, functional requirements and design trade-offs that led to the concept is presented. Design of key antenna units is also described. [C874]

#### "Pressure measurement from the RADAR interrogation of passive sensors"

The pressure applied to passive sensors modifies their radar echo magnitude. From the FMCW radar interrogation of such passive sensors the pressure can then be remotely measured. The first experimental results presented here demonstrate the feasibility of the wireless measurement of physical quantities from radar echo measurement of passive sensors. [C875]

#### "Planar Yagi-Uda antenna array for W-band automotive radar applications"

Complementary to an already proposed antenna concept for millimeter-wave automotive radar sensors the design of a planar Yagi-Uda antenna array has been presented. The radar antenna concept consists of end-fire antennas (or arrays) and a cylindrical parabolic reflector that can directly be integrated into the sensor's metal housing. The proposed assembly reduces the antenna substrate area while maintaining a small installation depth. The achieved gain of 16 dBi can be increased up to 22 dBi for the 4-element array by an improved power-divider network and even higher if more antenna elements are used. [C876]

#### "Enhanced detection of planar retro-reflective arrays using polarization properties"

This paper presents a design concept to aid in the detection and tracking of objects in a cluttered environment at 26 GHz. Target tracking can generally be accomplished with the use of retro-reflectors which are able to return an incident signal back in the same direction with a radar cross section (RCS) that is independent of angle of arrival for a large range of incidence angles. [C877]

#### "High-performance compact HF antenna for radar and communication applications"

Over the years there have been many systems developed in the area of HF Surface Wave Radars (HFSWR) and Over the Horizon Radars (OTHR). The increased emphasis on applications such as maritime surveillance for national security and enforcement of Economic Exclusion Zones (EEZs) continues to drive the need for efficient yet mobile and low cost HFSWR and OTHR systems. For the HFSWR systems, propagation characteristics are based on vertically polarized, high frequency (3 to 30 MHz) electromagnetic waves and this provides distinct advantages when used in medium and long range coastal surveillance type operations. The high conductivity of seawater results in relatively low attenuation of vertically polarized radio waves thus allowing for effective long range HFSWR systems. OTHR systems, on the other hand, achieve long range propagation by utilizing the refractive properties of the ionosphere. Large changes in ionospheric layers between day and night cycles cause corresponding changes in the effective radar ranges. OTHR systems cover much longer ranges than HFSWR systems while HFSWR receivers have to handle the increased noise and signal clutter during periods of increased ionospheric activity. [C878]

#### "Full polarimetric calibration of a GB-SAR system with a thin wire"

In this paper, we present the full polarimetric calibration of GB-SAR system with a thin wire whose orientation angle is 0 degree, 45 degree and 90 degree. At first we measured 0 degree, 45 degree and 90 degree inclined thin wire in order to derive calibration parameters. We also measured 30 degree and 60 degree wire in order to confirm this calibration method works well or not by using the estimated parameters. Calibration results of 30 and 60 degree wire cases are also described in this paper. [C879]

#### "A partially transparent Jaumann absorber applied to an aircraft wing profile"

We designed a partially transparent Jaumann absorber. The metallic sheet of the Jaumann was replaced by a triangular lattice Gangbuster FSS together with a polarizer. This design was applied to a wing front end. We showed that the monostatic RCS performance of the wing improves. Furthermore, the resulting screen is partially transparent around 1GHz which is assumed to be an antenna operating frequency placed inside the wing. However the resistive layers of the Jaumann absorber cause a large loss at 1 GHz for the planar case. To reduce this loss, additional work is in progress where the Jaumann absorber is replaced with a capacitive circuit absorber. [C880]

#### "Accurate evaluation of the time-domain effective height for short-pulse antennas"

A singularity-expansion-method (SEM) based approach is presented for the analysis of radiation processes in short-pulse antennas. Any time-domain electromagnetic field solver can be used to derive a minimal pole/residue spherical harmonic expansion of the equivalent currents excited on a suitable Huygens surface enclosing the radiating structure. In this way, the time-domain effective height of the antenna is evaluated in closed form as the superposition of non-uniform spherical wave contributions attenuating along with the time according to the real part of complex poles accounting for the natural resonant processes occurring in the structure under analysis. [C881]

#### **"Noninvasive breast tumor localization based on ultrawideband microwave backscatter"**

The key to surgical planning for breast conservation is tumor localization. An accurate localization of the breast tumor is essential to guide the surgeon to the lesion, and ensure its correct and adequate removal with satisfactory excision margins. Current breast tumor localization techniques are invasive and often result in a cosmetic disfigurement. In this paper, we use the ultrawide band radar-based microwave breast imaging technique to non-invasively localize (impalpable) tumors in the breast. We consider four clinically important lesion features: location, size, depth and spatial orientation within the breast. A comparison of the energy of the received signal from healthy and cancerous breasts exhibits some significant differences in some frequency bands. We, therefore, use the energy spectrum of the receiving antenna signal decomposed by wavelet transform as the input to a genetic neural network (GNN) classifier. Furthermore, for improved efficiency, we optimize the structure of the GNN for optimum initial weights and number of hidden nodes. We use CST Microwave Studio to simulate benign and malignant breast conditions, and generate a data set of 1024 cancer cases with various tumor location, size, depth and spatial orientation within the breast. Our results show that the proposed algorithm gives accurate localization of the breast lesion, and possesses a high sensitivity to small tumor sizes. Additionally, it can accurately detect and classify multiple tumors. [C882]

#### **"The pulse sequence pattern and signal processing of complex radars"**

To the EW system, the conventional radar signal description is based on radar parameters and their features, which is hard to describe the modern complex radar. A new conception of Pulse Sequence Pattern (PSP), which uses a representative pulse sequence with multi-dimension parameters as the radar signal description, is proposed in this paper firstly. And the PSP of typical radar is described in detail. At last, the fast signal processing algorithm based on the PSP is given. The experiments and computer simulations show that the description of PSP is practicable and the recognition algorithm is more effective than the conventional method. [C883]

#### **"An improved chirp scaling algorithm with capability motion compensation for SAR"**

Since a motion error is the main phase error source in the aircraft synthetic aperture (SAR), the motion errors have to properly be compensated during the SAR image reconstruction. The chirp scaling (CS) algorithm is one of the best algorithms in the practice system. An improved CS algorithm which can compensate motion error is proposed. Specially, the proposed method is based on the constant acceleration movement and the sub-aperture technique. [C884]

#### **"The effects of input signal-to-noise ratio on compressive sensing SAR imaging"**

Synthetic Aperture Radar (SAR) is an active and coherent microwave high resolution imaging system, which has the capability to image in all weather and day-or-night conditions. The high resolution required by various modes of SAR results in a huge amount of sampling data, which brings a demand for bigger storage. Recently, a novel concept based on Compressive Sensing (CS) theory asserts that an unknown sparse signal can be recovered exactly with an overwhelming probability even with highly sub-Nyquist-rate samples. In this paper, a new scheme for the test bed of CS based SAR imaging is proposed. Experimental results on some real raw SAR data reveal that there are some practical limitations on the use of CS based SAR imaging, especially for complex imaging scenes and systems with low Signal-to-Noise Ratio (SNR). [C885]

#### **"Bistatic SAR imaging with parallel flight track based on monostatic SAR processor"**

Bistatic SAR uses separated transmitter and receiver flying on different platforms, and has the ability of the exploitation of additional information contained in the bistatic reflectivity of targets. This paper provides an efficient Nonlinear-Chirp Scaling (NCLS) algorithm for bistatic SAR with parallel track configure, which is based on the bistatic-to monostatic application (BTMA). The method described is a feasible solution for the image formation of bistatic SAR with such configure. The problem of Doppler ambiguity during the NCLS Processing and the choice of reference frequency are also discussed at last. This NCLS imaging algorithm is verified with a simulation experiment. [C886]



### "A fuzzy adaptive tracking algorithm based on current statistical probabilistic data association"

In this paper, a new fuzzy adaptive maneuvering target tracking algorithm based on current statistic model is proposed. How to track a maneuvering target is a key problem of target tracking in clutter. Current statistical model needs to pre-define the value of maximum accelerations of maneuvering targets. So it may be difficult to meet all maneuvering conditions. The Fuzzy inference combined with Current statistical model is proposed to cope with this problem. Given the error and change of error in the last prediction, fuzzy system on-line determines the magnitude of maximum acceleration to adapt to different target maneuvers. Furthermore, the difficulties of the maneuvering target tracking lies in the uncertainty of state model, and the clutter make it more complex. The algorithm combines current statistical algorithm with probabilistic data association algorithm. At last, the results show this algorithm can estimate a maneuvering target in clutter efficiently. [C887]

### "A new phase unwrapping method of interferogram"

In this paper, a new two-dimensional phase unwrapping method of interferogram will be present. The method is based on the Goldstein's Branch-cut method and Region-growing method. After the unwrapping of the interferogram by using Goldstein's Branch-cut method, the amplitude image and coherence image were used to extract the error regions. And the error regions were classified into two types, which were processed by Region-growing method and Inverse Distance to a Power interpolating method respectively. The proposed method was tested with the Etna SIR-C/X-SAR interferogram, and satisfied results were achieved. [C888]

### "Low velocity small radar target detection in maritime environment"

Researches on target detection are mainly focus on the amplitude characteristics nowadays. Sometimes the only use of amplitude characteristics is not enough to describe the signal, so that the target detection performance is usually poor. In this essay a method to make use of the information "hidden" in the signal phase is put forward, the theory is based on polynomial fitting of the signal phase train structure. At last, the method is validated using actual data. [C889]

### "A new time-delay echo jamming style to SAR"

This work is concerned with developing the time-delay-based jamming technology against SAR. Traditional time-delay echo jamming can only get a point or a line false imaging when through the SAR system, which can't protect distributed targets. This paper presents a modified time-delay echo jamming style, Time-delay Inter-pulse Jitter Echo jamming (TDIJEJ). The theoretic analysis and simulation show that this interference can obtain the fast time matched processing gain of SAR thus deduce the jamming power requirement, and generate a jamming swath output for the purpose of protecting distributed targets. [C890]

### "SAR interference signal feature vector extraction and simulation based on wavelet packet analysis"

This paper studies the use of wavelet analysis method to realize the non-coherent narrow-band SAR radar signal interference suppression. Based on the full study of Irregular wavelet tree in interference detection and filtering, an adaptive filter using wavelet packet decomposition to extract the interference signal feature vector has been proposed. Simulation experiments based on this method have been carried out, by using SNR improvement, interference rejection ratio, signal distortion and other evaluation criteria to evaluate the results of interference suppression, the results show that the effect of wavelet packet filtering interference suppression is good. [C891]

### "Phase noise in RF and microwave amplifiers"

The amplifier phase noise is a critical issue in numerous fields of engineering and physics, like oscillators, frequency synthesis, telecommunications, radars, spectroscopy, in the emerging domain of microwave photonics, and in more exotic domains like radio astronomy, particle accelerators, etc. We analyze the two main types of phase noise in amplifiers, white and flicker. Using the polynomial model, the phase-noise power spectral density is  $S_{\phi}(f) = b_0 + b_{-1}/f$ . Phase noise results from adding white noise to the RF spectrum around the carrier. For a given amount of RF noise added,  $b_0$  is proportional to the inverse of the carrier power  $P_0$ . By contrast,  $b_{-1}$  is a constant parameter of the amplifier, in a wide range of carrier power. Accordingly, the flicker phase noise  $b_{-1}/f$  is independent of  $P_0$ . This fact has amazing consequences on different amplifier topologies. Connecting  $m$  equal amplifiers in parallel,  $b_{-1}$  is  $1/m$  times that of one device. Cascading  $m$  equal amplifiers,  $b_{-1}$  is  $m$  times that of one amplifier. Recirculating the signal in an amplifier so that the gain increases by a power of  $m$  (a factor of  $m$  in dB) due to positive feedback (regeneration), which for integer  $m$  is similar to the case of  $m$  amplifiers, we find that  $b_{-1}$



1 is  $m$  times that of the amplifier alone. The simplest model for the  $1/f$  phase noise is that the near-dc  $1/f$  noise phase-modulates the carrier through some parametric effect in the semiconductor. This model predicts the behavior of the (simple) amplifier and of the different amplifier topologies. Numerous measurements on amplifiers from different technologies and frequencies (HF to microwaves), also including some obsolete amplifiers, validate the theory. This model also applies to other devices, including passive components. [C892]

#### "Resolution enhancement of SAR image using the modified IBP method"

Super resolution (SR) technique can produce a high-resolution (HR) image from a set of low-resolution (LR) images with complementary information. This paper proposes a modified iterative back projection (IBP) method for SAR image resolution enhancement. In this method, a SR image is assumed and modification which contains the different high frequency information of LR images is back projected to it to get an ideal HR image. Compared with the original IBP, the modified IBP method is simpler and the modification is more accurate to speed up the iteration. Both simulated and real SAR images are used to verify the validity of the method. The results show that details and definition of the LR image processed with the method are effectively improved. [C893]

#### "The improved phase-difference algorithm of 24GHz FMCW radar for fast level tracing of bulk solid material"

For the purpose of accurately and quickly level tracing of bulk solid material, a new 24GHz FMCW radar measurement system with fast frequency Improved Phase-Differential estimation algorithm on platform of TI DSP 28335 and the low cost multiplier frequency VCO and mixer is realized, Three kinds of the fast tracing algorithm, Improved CZT algorithm, Improved ZFFT algorithm and the new Improved phased-difference algorithm (IPDA) is compared for the real time and accuracy. The results show that the IPDA is more suitable for the measurement of bulk solid material, and can be higher accuracy and faster speed. [C894]

#### "Radar echo signal detection with sparse representations"

Sparse decomposition can explore the most important or interesting features of a signal, thus it is very favorable in data compression, noise reduction, signal analysis, correction and other applications. In this paper, we propose a method of radar echo signal detection with sparse representations. In the proposed method, we first design a waveform-matched dictionary according to the a priori knowledge of the transmitted signal to sparsely represent the radar echo signal. The components in the dictionary have exactly the same waveform as the transmitted signal. With this dictionary, the echo signals of a given radar system have very sparse representation. Using the sparse representation based on the waveform-matched dictionary, the radar echo detection can be achieved. Simulation results show that the proposed method is effective and has the high anti-noise ability. [C895]

#### "Analysis of micro-doppler effect in SIMO radar"

SIMO (Single Input Multiple Output) radar system capitalizes on the receiving diversity, so it can obtain more information about the target and highly improve the target recognition capability of radar. In this paper, the micro-Doppler effect induced by rotation and vibration parts of target in SIMO radar system which transmitting single frequency signal are deduced respectively. Both the micro-Doppler effect induced by rotation and vibration are sinusoidal curves, but their amplitude vary with the selection of different receiving radar. In addition, the translation of the target's body will lead some horizontal shifts to the micro-Doppler curves with different value according to the selected receiving radar. Simulations are presented to validate the theoretic conclusions. [C896]

#### "An approach for extracting the transmitted waveforms based on compound filter for MIMO radar"

Extracting the transmitted waveforms is crucial for MIMO radar. A new extracting approach is proposed in this paper based on the compound filter. The proposed method can compress the input pulse width to a narrower one and suppress range sidelobe level lower than a matched filter. The computer simulation proves the efficiency of the method. [C897]

#### "Fast computation of cross ambiguity function for DTTB based passive radar"

A new method is proposed to calculate the cross ambiguity function (CAF) for digital television terrestrial broadcasting (DTTB) based passive radar. The Doppler frequency of the targets is much lower than sampling frequency. The cascade integrator comb (CIC) filter is utilized to realize the large change of sampling frequency. The interpolated second-order polynomials (ISOP) filter is used to compensate the passband droop caused by CIC filtering. A half-band filter is employed to get narrow transition band. And then a short point FFT is performed instead of the long point FFT. The experiment results and computation complexity are given

compared with other methods. It shows that the proposed method doesn't affect detection and estimation performance, and the computation is reduced significantly. [C898]

#### "Improved method for deinterleaving radar pulse trains with stagger PRI from dense pulse series"

Stagger PRIs detection and deinterleaving of pulse trains with stagger PRI in dense pulse series are always difficult problems in radar signal processing. In this paper, an improved detecting threshold of stagger PRIs of pulse trains and deinterleaving approach for stagger radar pulses in dense pulse series are proposed. Computer simulation experiment results of deinterleaving pulse trains with stagger PRI are used to verify the validity of the proposed method by the present method in this paper. [C899]

#### "Two-dimensional diffraction tomography algorithm of underground objects located in planar multilayer medium1"

An efficient inverse scattering algorithm is developed to reconstruct the permittivity profile of two-dimensional(2-D) dielectric objects buried in planar multilayer environment. The forward model of this inversion scheme is based upon first order Born approximation and 2-D planar multilayer scalar Green function. A planar multilayer diffraction tomography algorithm is established subsequently. Numerical results are provided to illustrate the performance of the inversion scheme. [C900]

#### "Bearing-only target tracking with improved particle filter"

In this paper, we propose an improved particle filter, and apply this new algorithm to bearing-only tracking problems. The generic particle filter (also called bootstrap filter) suffers a main drawback of not incorporating the latest observations, which is the problem we mainly focus on. An improving scheme is presented to handle this problem, and the underlying idea of the new algorithm is that, at time  $k$ , each particle is updated using Kalman filtering equations. Through this update process, the algorithm incorporates the coming observations. In the experiment, we use a bearing-only tracking model to evaluate the performance of the proposed algorithm. The experimental results show its superiority to the generic particle filter. [C901]

#### "Pulse compression technique for multi carrier phase-coded radar"

The multi-frequency complementary phase-coded signal (MCPC) has caught much attention of researchers recently as a new system radar signal. This paper provides pulse compression technique for such radar signal. Direct match filtering and synthetic filtering are proposed to compress the echo signal. After comparing their performance via amount of calculations, a wideband-synthesizing method is brought forward. It takes full usage of the multi carrier structure of MCPC signal, while keeps low calculation complexity. The two-level compression scheme is proved to be flexible in different applications. [C902]

#### "Millimeterwave radar high-resolution imaging via OFDM waveforms"

A novel combination of millimeterwave linearly frequency modulated (LFM) technology and new radar imaging techniques can provide a good high-resolution imaging sensor that can be inboard in unmanned vehicles, in which stringent limitations of size, weight and power consumption are required. This paper presents an approach of multiple transmission and multiple reception in elevation for vehicle-borne millimeterwave radar high-resolution imaging. This radar employs orthogonal frequency diversity modulated (OFDM)-LFM waveforms, so as to obtain a high-resolution imagery over a wide swath coverage. The system concepts, geometry relations and signal models are provided. Computer simulation examples are also performed. Additionally, the generation of the OFDM waveforms with parallel direct digital synthesizer (DDS)-driven phase locked loop (PLL) synthesizer is discussed, and the block diagram of the synthesizer is provided. [C903]

#### "Directional pattern modeling and simulation of triangular grid circular planar array antennas"

Based on a long range early-warning phased array radar, the directional pattern of the triangular grid circular planar array antenna is studied. The mathematical model of triangular grid circular planar array antennas pattern is established, and its computer simulation method is described. In order to form a low side-lobe pattern, the method of Taylor circular array synthesis is used to optimize the amplitude distribution of the current excitations. The practice demonstrates that the simulation method presented is very efficient and practical. [C904]

#### "A novel design of SAR scattering signal simulator based on AWG"

Synthetic Aperture Radar (SAR) raw signal simulation is crucial for SAR system design and processing algorithms. This paper proposes the simulation method of SAR RF signal via utilizing Arbitrary Waveform

Generation (AWG). At first, the SAR imaging principle is analyzed. Then, the space-borne SAR scenario model is constructed. The echoes of point target are calculated, which is impulse response of the SAR signal acquisition. At the end, based on the scattering model expressions of a random roughness surface and the electromagnetic wave shadow theory, the Radar Cross Section (RCS) simulation parameters of terrain target is calculated. 2D-FFT method is utilized to improve simulation efficiency significantly. [C905]

#### "Improved image mosaic method of ScanSAR"

For ScanSAR the mosaic of subswaths' images is very important. An improved method for scanSAR to process the mosaicking by using Range-Doppler location model is proposed in this paper. It is based on the precision of the R-D location method. This method avoids the pixel defocused and the simulation results are satisfied in practice. [C906]

#### "Phase-coded pulse compression radar carrier frequency accurate estimation"

This A new frequency estimator for Phase-coded pulse compression radar carrier frequency is proposed. First, via square nonlinear transformation, the radar signal is become one tone signal, it is possible that transformed signal is sub-nyquist sampled, and estimation value of carrier frequency will be ambiguous, a method of solving frequency ambiguity is proposed, and using FFT(Fast Fourier Transform) +FT(Fourier Transform) to improve carrier estimation precision, a method of fast peaks search is proposed. Simulation results show that the results are efficient. [C907]

#### "A novel single-channel SAR-GMTI method based on defocusing shifted difference"

A novel single channel SAR-GMTI method is proposed in this paper. When the azimuth mismatch filter performs compression, it induces shifted difference between the stationary and moving targets because of having different Doppler center. The proposed method employs this character to separate moving targets from stationary targets. It can produce two images by pulse compression which make use of two symmetrical mismatch filters in azimuth direction, and then cancel stationary and retain moving targets by subtracting one image from another. Compared with traditional methods, it is applicable to both low and high squint case and the detection capability is significantly improved. The simulation results validate the effectiveness of the proposed method. [C908]

#### "Low speed target detection with short CIT in HF surface wave radar"

High frequency surface wave radar can detect targets beyond the horizon. It needs long coherent integration time (CIT) to detect low speed targets, such as ships, in the environment with sea clutter. In order to improve the efficiency of the radar system, and avoid the Doppler broadening caused by long CIT, it is necessary to shorten coherent integration time. Modern spectrum estimation technique is adopted to extract Doppler information from HF radar echo signals. It can provide high resolution to realize ship detection in short CIT. The real data processing and analysis show that the autoregressive spectrum estimation technology is effective to detect low speed target in short CIT in high frequency surface wave radar. [C909]

#### "Enabling technology for heart health wireless assistance"

Several advances have been done in wireless body area networks for bio-monitoring, as confirmed by the fine tuning of ad-hoc standards for networking, controlling and managing a distributed sensor platform around the human body. Efficient wireless networks are becoming commercially available for several applications. In spite of that, sets of "invisible" sensors for monitoring bio-signals are still expected as enabling technology for mass-market applications. This paper aims at reviewing the current state of the art, and identifying some existing open issues and added functionalities desirable for the future in heart health wireless assistance. Some results emerging from the on-going research are presented, focusing on the implementation of an innovative contact-less miniaturized radar sensor for cardiopulmonary monitoring within a wearable textile platform. The expected future developments toward a wireless body area network are reported and discussed. [C910]

#### "Evaluation of cloud liquid absorption models at 90 and 150 GHz"

The use of microwave observations in the frequency range of 90-150 GHz holds the promise to dramatically improve the retrieval of integrated liquid water in thin clouds due to the increased sensitivity of these frequencies to the presence of liquid water. One of the largest sources of retrieval uncertainty at these frequencies is the inaccuracy of liquid water absorption models at low temperatures. The purpose of this work is to assess the performance of four liquid water absorption models by comparing model simulations with measurements collected by a microwave high-frequency radiometer (MWRHF) located at the Atmospheric Radiation Measurement (ARM) Program Climate Research Facility (ACRF) in the Southern Great Plains, OK. Measurements at 90 and 150 GHz

were collected during cloudy and cold conditions. In an attempt to isolate different sources of possible errors we give an assessment of the instrument calibration and compare clear-sky measurements with model simulations using an updated formulation for the water vapor continuum. With the help of a ceilometer and cloud radar we identified several cases of cold, thin liquid clouds and for those cases we independently retrieved liquid water path using infrared frequencies. The independently retrieved liquid water path was then used to compute brightness temperatures at 90 and 150 GHz with the four liquid absorption formulations. Simulation results were then analyzed and compared with observations. [C911]

### **"Improved high wind speed retrievals using AMSR and the next generation NASA Dual Frequency Scatterometer"**

Microwave scatterometer measurements are the standard for satellite ocean vector winds (OVW) measurements. Unfortunately, in extreme weather events, where high wind speeds are frequently associated with strong rain bands, precipitation can significantly degrade the OVW retrieval accuracy. This study addresses the feasibility of exploiting passive measurements to improve high wind speed retrievals for such extreme weather events. The Jet Propulsion Laboratory (JPL) has developed a conceptual design for a Dual Frequency Scatterometer (DFS) proposed to fly onboard the future Japan Aerospace Exploration Agency (JAXA) GCOM-W2 mission with the Advanced Microwave Scanning Radiometer (AMSR). These two instruments will provide a complimentary dataset of simultaneous and coincident active/passive measurements, which can correct for rain effects and thereby improve the OVW retrievals. End-to-end computer simulations are performed using the Weather Research and Forecasting (WRF) numerical weather model tuned to Hurricane Katrina (2005) for the 3D nature run (surface truth). Results show that the new OVW retrievals compare well to the nature run surface wind vectors and that this active/passive technique offers a robust option to extend the useful wind speed measurements range beyond the current operating scatterometers for future satellite missions. [C912]

### **"AMSR-E observations of rain and flood events over vegetated areas of LA Plata basin"**

This work analyzes AMSR-E signatures collected in two sites of La Plata basin, in South America. Within the wide Chaco forest, an area close to Las Lomitas meteorological station was selected. Here the forest is uniform, but not very dense, with biomass values in the range 70-120 t/ha. After strong rain events, appreciable variations of polarization index at C and X band were observed. As expected, the better dynamic range is obtained at C band. Also AMSR-E signatures collected during a strong flooding event in the Delta of Parana River were analyzed. Variations of polarization index are strong, as expected. Information about the water level in the river was made available by hydrometric stations. We selected specific pixels characterized by different kinds of land cover: agricultural fields, marshes, and planted forests. A significant correlation between polarization index (at various frequencies) and water level is proved. A flood monitoring algorithm based on AMSR-E brightness temperature difference is tested. Optical and radar data are used as ancillary input for calibration and validation proposes. [C913]

### **"Radio frequency interferences investigation using the airborne L-band full polarimetric radiometer CAROLS"**

In the present paper, different methods are proposed for the detection and mitigation of the undesirable effects of radio frequency interference (RFI) in microwave radiometry. The first of these makes use of kurtosis to detect the presence of non-Gaussian signals, whereas the second imposes a threshold on the standard deviation of brightness temperatures, in order to distinguish natural emission variations from RFI. Finally, the third approach is based on the use of a threshold applied to the third and fourth Stokes parameters. All of these methods have been applied and tested, with a CAROLS radiometer operating in the L-band, on data acquired during airborne campaigns made in spring 2009 over the South West of France. The performance of each, or of two combined approaches is analyzed with our database. We thus show that the kurtosis method is well adapted to pulsed RFI, whereas the method based on the second moment is well adapted to continuous-wave RFI. [C914]

### **"An improved active/passive oceanic wind vector retrieval technique"**

This paper describes the advantages of combining passive and active microwave remote sensing observations for the purpose of ocean wind vectors retrievals. Previous studies have shown that a linear combination of horizontal and vertical polarized brightness temperatures contains a robust wind direction signal. In this paper, we present results from an end-to-end simulation of ocean measurements from a Ku-band (13.4 GHz) active/passive conical scanning satellite instrument. For this simulation, realistic wind fields from the NOAA National Center for Environmental Prediction (NCEP) numerical weather model were used to produce simultaneous brightness temperatures and radar backscatter measurements. These measurements were processed using a maximum likelihood estimation technique to yield ocean wind vector retrievals that were



compared to NCEP fields. Results demonstrate significant improvements over simulated measurements for an active (radar scatterometer) sensor. [C915]

#### **"Millimeter wave interferometric radiometry for passive imaging and the detection of low-power manmade signals"**

Millimeter wave detection and imaging is becoming increasingly important with the proliferation of hostile, mobile millimeter wave threats from both weapons systems and communication links. Improved force protection, surveillance, and targeting will rely increasingly on the interception, detection, geo-sorting, and the identification of sources, such as point-to point communication systems, missile seekers, precision guided munitions, and fire control radar systems. This paper describes the Naval Research Laboratory's (NRL) demonstration broadband passive millimeter wave (mmW) interferometric imaging system. In addition to limited active signal detection, the Ka-band system will provide the potential for detecting the passive signature of non-transmitting hostile systems along with a capability for meter-precision geolocation for imaged objects. The interferometer uses a distributed array of 12 antenna elements to synthesize a large aperture. Each antenna is packaged into an individual receiver, from which a baseband signal is recorded. The correlator is software-based, utilizing signal processing techniques for visibilities, and image formation via beamforming methods. [C916]

#### **"Utilization of airborne and in situ data obtained in SGP99, SMEX02, CLASIC and SMAPVEX08 Field Campaigns for SMAP Soil Moisture Algorithm Development and Validation"**

Field experiment data sets that include coincident remote sensing measurements and in situ sampling will be valuable in the development and validation of the soil moisture algorithms of the NASA's future SMAP (Soil Moisture Active and Passive) mission. This paper presents an overview of the field experiment data collected from SGP99, SMEX02, CLASIC and SMAPVEX08 campaigns. Common in these campaigns were observations of the airborne PALS (Passive and Active L- and S-band) instrument, which was developed to acquire radar and radiometer measurements at low frequencies. The combined set of the PALS measurements and ground truth obtained from all these campaigns was under study. The investigation shows that the data set contains a range of soil moisture values collected under a limited number of conditions. The quality of both PALS and ground truth data meets the needs of the SMAP algorithm development and validation. The data set has already made significant impact on the science behind SMAP mission. The areas where complementing of the data would be most beneficial are also discussed. [C917]

#### **"An Lidar data compression method based on improved LZW and Huffman algorithm"**

Lidar raw echo data has characteristics such as huge data quantity, strong discreteness and unpredictability. According to the construction of Lidar monitoring network of atmospheric environment, the existing network can not provide enough bandwidth to transmit Lidar data in real time. In this paper, we propose a novel hybrid lossless compression algorithm to reduce the transmission amount, namely the probability statistics lossless compression algorithm base on the improved LZW(Lempel-Ziv-Welch), which combines Huffman coding. With experiment on the raw two-value atmospheric data, we verify the effectiveness of our approach that the compression ratio is close to 9.5:1 and the coding efficiency is up to 98%. [C918]

#### **"A 1V 11fJ/conversion-step 10bit 10MS/s asynchronous SAR ADC in 0.18 $\mu$ m CMOS"**

This paper presents a 10-bit SAR ADC using a variable window function to reduce the unnecessary switching in DAC network. At 10-MS/s and 1-V supply, the ADC consumes only 98  $\mu$ W and achieves an SNDR of 60.97 dB, resulting in an FOM of 11 fJ/Conversion-step. The prototype is fabricated in a 0.18 $\mu$ m CMOS technology. [C919]

#### **"Low-cost gate-oxide early-life failure detection in robust systems"**

We present a new low-cost technique for detecting gate-oxide early-life failures (ELF) to overcome reliability challenges in robust systems without requiring expensive concurrent error detection. Our approach is enabled by an on-chip clock control technique, applied during periodic on-line self-test and diagnostics, to detect delay shifts over time before functional failures occur. Using 90 nm test chips, we demonstrate the following key results: 1. A gate-oxide ELF transistor inside a combinational logic circuit results in delay shifts over time before functional failures appear. 2. The delay shifts can be successfully detected during on-line self-test and diagnostics using our on-chip clock control technique. [C920]

#### **"CAROLS campaigns 2009: First Results"**

The CAROLS, L band radiometer, is built and designed as a copy of EMIRAD II radiometer of DTU team. It is a Correlation radiometer with direct sampling and fully polarimetric (i.e 4 Stockes). It will be used in conjunction



with other airborne instruments (in particular the C-Band scatterometer (STORM) and IEEE GPS system, Infrared CIMEL radiometer and one visible camera), in coordination with in situ field campaigns for SMOS CAL/VAL. The instruments are implemented on board the French research airplane ATR42. A scientific campaign with thirteen flights is realized over south-western France, Valencia site and Bay of Biscay (Atlantic Ocean) in spring 2009. In order to qualify the radiometer data, different types of aircraft movements were realized: circle flights, wing and nose wags. Simultaneously to flights, different ground measurements were made over continental surfaces and ocean. Results show a good quality of data. For continental surfaces, important Radio-Frequency Interferences (RFI) were observed over a large part of the studied region. [C921]

#### **"Track initiation in Monostatic-Bistatic Composite High Frequency Surface Wave Radar Network based on NFE model"**

Though a Monostatic-Bistatic Composite High Frequency Surface Wave Radar Network (MBC-HFSWR Network) is established to cover the shortage of the monostatic radar, how to judge the real target update from the plausible measurements to initiate tracks quickly and accurately still remains a challenging problem. A novel method utilizing unconventional characteristics for track initiation is proposed in this paper, which uses more accurate information and avoids the problem of low detection precision of high frequency radar. A highly intelligent information fusion model which is a combination of Neural network, Fuzzy reasoning and Expert system (NFE model) is presented to solve the problem above and the validity of the provided method is demonstrated by Monte Carlo simulations. [C922]

#### **"The exposed area analysis of Barrage-type Jamming to Bistatic SAR"**

In this paper, jamming equation is established which based on working mode of Barrage-type Jamming to Bi-SAR, and the coverage region is derived under a certain J/S (Jamming-to-signal ratio) from Bi-SAR. In such circumstances, the radar receiver can detect the target area through mathematical method analysis, namely exposed area. Finally, maximal exposure area, absolute exposure area, possible exposure area and definite protected area are divided. [C923]

#### **"A three-dimensional geographic and storm surge data integration system for evacuation planning"**

The rise of offshore water caused by the high winds of a low pressure weather system, or storm surge, is a hurricane's greatest threat to human life. As weather forecasters struggle to enable coastal residents to make timely evacuation decisions, the need arises for more visually compelling and interactive storm surge visualization tools. This paper presents an interactive and three-dimensional storm surge visualization system. It integrates road, topographic, and building data to construct accurate three-dimensional models of major cities in the State of Florida. Storm surge data are then used to construct a three-dimensional ocean positioned over the terrain models. Ambient details such as wind, vegetation, ocean waves, and traffic are animated based on up-to-date wind and storm surge data. Videos of the storm surge visualizations are recorded and made available to coastal residents through a web-interface. The three-dimensional visualization of geographic and storm surge data provides a more visually compelling representation of the potential effects of storm surge than traditional two-dimensional models and is more capable to enable coastal residents to make potentially life-saving evacuation decisions. [C924]

#### **"An adapted point based tracking for vehicle speed estimation in linear spacing"**

Vehicle velocity estimation is an important aspect of intelligent transportation systems. Normally velocity is estimated using dedicated laser speed traps and Doppler radars. Recently, the use of cameras is becoming more common for the purpose of traffic surveillance and smart surveillance system. It is thus the aim of this paper to propose a method for vehicle speed estimation using these existing video cameras. In this paper, we propose a vehicle speed estimation method from video analysis. The method proposed contains several steps; image preprocessing, centroid extraction and tracking. The proposed method transforms the 2D image points into a 3D virtual world to obtain actual vehicle position in 3D space. This is to account for perspective distortion commonly seen in images. Using these 3D points and measuring the time for displacement, the vehicle speed is obtained. Experimental results have shown that the proposed method gives accurate velocity estimation. [C925]

#### **"Performance improvement of pulsed OFDM UWB systems using ATF coding"**

In this paper, we examine an enhancement of pulsed Multiband Orthogonal Frequency Division Multiplexing (pulsed MB-OFDM) systems for Synthetic Aperture Radar (SAR) Ultra-Wide Band (UWB) applications. The pulsed MB-OFDM system offers an efficient option for fulfilling the UWB high bandwidth channel requirements. This system combines the two major implementations of UWB, namely the impulse radio and the MB-OFDM, in order to capture the advantages of low hardware complexity and low power consumption in both

implementations. A modified half-rate Algebraic Time Frequency (ATF) coding will be used to achieve the proposed enhancement of the pulsed system. This enhancement will result in energy efficiency, i.e. SNR vs. SER, improvement which is particularly useful for SAR systems operating under heavy clutter. Improvements in energy efficiency are tested under different UWB channel models. Simulation results are shown to establish these improvements. [C926]

### "Research on Visualization of Radar Beam Considering Virtual Environment Effect"

In a virtual battlefield environment, the 3D visualization of the abstract information of radar beam under the environmental influence of the terrain and weather is the current development trend of the visualization of electromagnetic information. In this article, we have designed two methods by the OpenGL function to complete the drawing of the spatial beam pattern that is inserted into the virtual battlefield environment. And then we combined the stereoscopic concept with the research, and studied the information visualization methods of the radar beam that were under the influence of different environmental factors with the premise of that the radar beam parameters and the terrain elevation data and other relevant parameters were acquired. At last, the users could be able to get electromagnetic battlefield information they need vividly and intuitively, which could make them determine more promptly. [C927]

### "An application of sensor networks with data mining to patient controlled analgesia"

We designed an information integration system, iPCA, which combined wireless sensor networks with a data mining system, to help anesthesiologists provide better post-operative pain control. To reduce labor work and to collect analgesic usage information and physiological data efficiently, we connected three kinds of medical instruments with Zigbee nodes through IEEE 802.11 and Zigbee networks. We developed a positioning system that allowed the medical staff to monitor the patient's locations, so they could give immediate care when necessary. The data mining system in iPCA analyzed the patient data, and made reasonable predictions about the total analgesic dosage and the need for PCA control readjustments. We completed a prototype of iPCA, which could help the medical staff monitor the patient's health conditions and locations, and provide the anesthesiologists with useful hypotheses for better PCA control to increase patient satisfactions. [C928]

### "Car monitoring, alerting and tracking model: Enhancement with mobility and database facilities"

Statistics show that the number of cars is increasing rapidly and so is the number of car theft attempts, locally and internationally. Although there are a lot of car security systems that had been produced lately, but the result is still disappointing as the number of car theft cases still increases. The thieves are inventing cleverer and stronger stealing techniques that need more powerful security systems. This project "Car Monitoring and Tracking System" is being proposed to solve the issue. It introduces the integration between monitoring and tracking system. Both elements are very crucial in order to have a powerful security system. The system can send SMS and MMS to the owner to have fast response especially if the car is nearby. This paper focuses on using MMS and database technology, the picture of the intruder will be sent via local GSM/GPRS service provider to user (and/or) police. The Database offers the required information about car and owner, which will help the police or security authorities in their job. Moreover, in the event of theft local police and user can easily track the car using GPS system that can be link to Google Earth and other mapping software. The implementation and testing results show the success of prototype in sending MMS to owner within 40 seconds and receiving acknowledgment to the database (police or security unit) within 4 minutes. The timing and results are suitable to owner and police to take suitable action against intruder. [C929]

### "Implementation and analysis of integration GSM/GPRS modem in a TMS320VC6713 digital signal processor for vehicle location"

The rapidly evolving wireless communications environment and 3G, where the standard are constantly created and modified, has given rise to the integration of GPS (Global Positioning System) and GSM (Global System for Mobile Communication). This integration has been widely applied in many disciplines including Intelligent Transportation System (ITS) and Logistic Management to aid the users to locate their vehicles remotely. Further on, the fast growth of city transportation also has stimulated the development of VMS where it is recognized as one of the major components of ITS. However, this system is rarely being implemented on embedded system using DSP processor. Thus, this paper discusses design and implementation of GSM/GPRS integration in a TMS320VC6713 for Vehicle Location that permits users to communicate with their vehicles via a Short Message Service (SMS). This system provides an alternative solution to solve vehicle theft and hijacking problems where the system is able track the real-time moving car location by using cellular phone. The system performance analysis has been carried out where the executions of three functions have been measured in clock cycles.

[C930]

### "A Digital Pulse Drive Circuit for Continuously Modulated Semiconductor Laser"

A digital designing way of laser drive circuit for continuously modulate the frequency, pulse width and amplitude of the output of semiconductor laser has been demonstrated. Complex programmable logic device (CPLD) was utilized to generate square waves with tunable frequency, the accurate delaying chip and logic circuit which are digital controlled were used to generate electrical pulses with adjustable pulse width. The pulses were amplified by the laser diode driver. The maximum output current of the driver can be up to 600 mA. When the signal was used to drive the semiconductor laser, the shape of the pulses generated by the laser is identical with the electrical pulses. The repetition rate and pulse width of the laser pulse can be continuously adjustable from 1 to 10 kHz and 3 to 20 ns, respectively. Furthermore, the time of rising and falling edges for the laser pulse were less than 2 ns. [C931]

### "The identification test of soil texture with ground penetrating radar"

The detection of soil texture needs nondestructive methods. Ground penetrating radar (GPR) develops fast in the fields of geological and agricultural survey in the recent years. To get a quantitative recognition of soil texture, experiments were designed with GPR of 500 MHz and 250 MHz frequency. Fine sand, sieved soil and natural soil were selected and tested indoors to acquire basic soil properties, amplitude attenuation characteristics and speed of electromagnetic wave. Compared to the experimental results outdoors, soil texture in the spots can be identified and classified. The strong signal changes only happened at the surface of the medium. The study results also showed GPR could recognize silt loam and sand loam, which help us analyze the effects of soil texture on soil dielectric characteristics in the further research. [C932]

### "Research on Early-Warning Detecting Tasks Re-scheduling and Sensor Resources Allocation Strategy of Midcourse Maneuverable Ballistic Targets"

Ballistic midcourse maneuverable targets bring huge challenge to early-warning detecting tasks. The incoming threats targets could be lost in detection range of sensors and early-warning detecting tasks may be failure, which retard the response of a ballistic missile defense system and the criticality of missiles would be increased. How can the Space-based early warning system detect and track the ballistic midcourse maneuverable targets in real-time is a new issue. In this paper, a early-warning detecting tasks re-scheduling and sensor resources allocation strategy based on multi-levels is designed, sensor resources allocation rapidly come true and satisfied the dynamics and real-time tracking requirements of detecting tasks, as well as the fewer adjusting amplitude to originally resources scheme. Finally, taking the space-based early-warning detecting task of maneuverable ballistic missile for example, by which the feasibility and efficiency of the strategy are explained and proved. [C933]

### "Remote monitoring of open numerical control system"

This paper investigates hardware and software architecture of numerical control (NC) system for remote monitor, and realizes in open numerical control system on field bus. Using principles of digital dictionary and data acquisition, the remote monitoring system of open NC system is designed. After in-depth analysis of needs, the design of hardware and software is completed, and applied research on NC EDM machines is conducted. Besides, the development of prototype is completed and the functions of online data acquisition, remote monitoring and remote machining services are realized. [C934]

### "Distributed GOSCA-CFAR Detection Based on Automatic Censoring Technique"

This paper present a new distributed constant false alarm rate (CFAR) detector based on automatic censoring technique. In the scheme, every local decision of individual detector, resulting from the comparison between its sample level and the estimation of the background based on GOSCA-CFAR (generalized order statistic, cell averaging-CFAR) algorithm, takes the value zero or one. Then, the fusion center makes the final decision utilizing the total local decisions, which are transmitted from each local detector. The overall decision, which is zero or one, is obtained at the data fusion center based on "AND", "OR", and "k/N" fusion rule. The results show that for the nonhomogeneous background caused by multiple interfering targets, particularly in multiple target situation, it exhibits good robustness in distributed sensor network. Under Swerling 2 assumption, the analytic expression of detection probability and false alarm probability are derived. [C935]

### "Research on Visualization of Electromagnetic Information in Virtual Environment"

In the article we research the visualization technology of electromagnetic information. It focuses on the drawing of the signals and multi-path signals transmission in the virtual battlefield environment. Firstly, we use the

OpenGL functions to complete the drawings of the time domain signals and spatial beam patterns. Secondly, we build the propagation model which is based on the theory of geometrical optics and realize the visualization of multipath phenomenon. Finally, those drawings are inserted into the virtual battlefield environment built by Vega. Accordingly, the commanders could be able to get electromagnetic battlefield information they need vividly and intuitively, which could make them determine more promptly. [C936]

#### "Horizontal Dilution of Precision Analysis for Loran C/ Beidou Integrated Navigation System"

The positioning precision of system plays a very important role in ship navigation. As a navigation system, Loran C cannot meet the orientation precision, even not be used in some areas. Based on the principle of hyperbola location, in this paper we propose Loran C/Beidou integrated navigation system. We analyze the effect on the positioning precision of two navigation systems and the simulation of orientation precision is implemented. Additionally, we give the definition of the horizontal dilution of precision (HDOP). Theoretical analysis and extensive experimental data show that by integrating Loran C and Beidou, the orientation precision and usable area of Loran C was improved and the shortage of Beidou position system was covered simultaneity. [C937]

#### "Power-aware distributed target detection in wireless sensor networks with UWB-radar nodes"

Distributed detection of targets is one of the major applications of wireless sensor networks. Many existing results on distributed detection are either derived from analytical models or are based on simulations. In this paper, the performance of a distributed target detection system is evaluated by real measurement data obtained by UWB-radar-based sensor nodes. After local processing of the radar signal, the sensor nodes transmit their local decisions about the absence or presence of the target to a fusion center. For this purpose, a power-aware algorithm for resource allocation, which is tailored for UWB communication links is discussed. The feasibility and the effectiveness of this algorithm is evaluated by a hybrid approach based on the measurement data and simulations. [C938]

#### "The HF surface wave radar WERA. Part I: Statistical analysis of recorded data"

Surface wave (SW) over-the-horizon (OTH) radars are not only widely used for ocean remote sensing, but they can also be exploited in integrated maritime surveillance systems. This paper represents the first part of the description of the statistical and spectral analysis performed on sea backscattered signals recorded by the oceanographic WEllen RAdar (WEERA) system. Data were collected on May 13th 2008 in the Bay of Brest, France. The data statistical analysis, after beamforming, shows that for near range cells the signal amplitude fits well the Rayleigh distribution, while for far cells the data show a more pronounced heavy-tailed behavior. The causes can be traced in man-made (i.e. radio communications) and/or natural (i.e. reflections of the transmitted signal through the ionosphere layers, meteor trails) interferences. [C939]

#### "LORAMbis A bistatic VHF/UHF SAR experiment for FOPEN"

LORAMbis is the experimental part of a joint research program between Sweden and France. The objective is to evaluate the performance of low frequency bistatic SAR for clutter suppression in various applications, e.g. under-foilage target detection or mapping of urban scenes. The airborne bistatic SAR data are acquired using the VHF/UHF component of the ONERA SAR system SETHI and the VHF/UHF LORA system operated by FOI. The first data collection campaign was conducted in December 2009. Focused bistatic SAR images have been formed and indicate that the implemented synchronization method is sufficient. It is based on a GPS disciplined 10 MHz reference signal that is generated in both systems. [C940]

#### "Passive bistatic ISAR based on geostationary satellites for coastal surveillance"

The paper proposes a new passive bistatic ISAR mode for coastal surveillance based on the exploitation of the signals transmitted by telecommunication geostationary satellites. Specifically it is demonstrated that ISAR images with acceptable quality of ship targets could be obtained by using telecommunication geostationary satellites as opportunity transmitters and stationary passive devices, located near the coast, as receivers. The geostationary satellites assure a continuous and complete coverage of wide areas: moreover satellites available in the near future should also provide a bandwidth suitable for the achievement of medium slant range resolutions. Since in ISAR the target motion is exploited to obtain cross-range resolution, a network of stationary low cost receiving only devices could be therefore properly located on the coast to obtain ISAR images of ship targets of interest for the surveillance and monitoring of the maritime traffic. [C941]

#### "Slow-time SAR signal processing for UWB OFDM radar system"

Orthogonal frequency division multiplexing (OFDM) signals, commonly used for a variety of purposes in modern



communication systems, are considered from the radar perspective. An experimental system configured as ultrawideband (UWB) software-defined radar (SDR) has been assembled and tested in the synthetic aperture radar (SAR) mode at Miami University. Phase history-necessary for slow-time processing of SAR signals-was previously extracted from a single sub-carrier of OFDM pulses; in this paper we examine a more robust solution of phase history estimation using all subcarriers. The results of the estimation are compared with the ideal single-frequency phase history reconstruction. Simulation examples of cross-range recoveries in noise using both methods are provided and discussed. It is shown that the proposed novel method of slow-time OFDM SAR signal processing is, indeed, a promising technique for multicarrier UWB systems. [C942]

#### "Bayesian parametric approach for multichannel adaptive signal detection"

This paper considers the problem of space-time adaptive processing (STAP) in non-homogeneous environments, where the disturbance covariance matrices of the training and test signals are assumed random and different with each other. A Bayesian detection statistic is proposed by incorporating the randomness of the disturbance covariance matrices, utilizing a priori knowledge, and exploring the inherent Block-Toeplitz structure of the spatial-temporal covariance matrix. Specifically, the Block-Toeplitz structure of the covariance matrix allows us to model the training signals as a multichannel auto-regressive (AR) process and hence, develop the Bayesian parametric adaptive matched filter (B-PAMF) to mitigate the training requirement and alleviate the computational complexity. Simulation using both simulated multichannel AR data and the challenging KASSPER data validates the effectiveness of the B-PAMF in non-homogeneous environments. [C943]

#### "Some aspects of designing real-time digital correlators for noise radars"

Real-time operation of a noise radar correlator requires massive processing power. At present, it can be provided at a reasonable cost only by FPGA devices. However, adopting this platform makes different aspects of the design important than in the case of microprocessor-based design. In particular, our efforts are directed towards minimizing device usage, rather than number of computations. Several options are reviewed in the paper with this purpose in mind. [C944]

#### "Detection performance comparison for wideband and narrowband radar in noise"

The detection performance of wideband radars in noise is better than that of the narrowband radars under some conditions, due to higher range resolution and less target return fluctuation. The detection probabilities of wideband and narrowband radars for the wideband non-fluctuation, Rayleigh and Ricean target models in white Gaussian noise are deduced. The detection curves show that the wideband radars outperform the narrowband radars in detection performance in the case of high detection probabilities. But the detection predominance of the wideband radars is meaningless when the bandwidth of the radar is increased to a certain extent, because the integration loss of the wideband radar energy integration detector is increased with the increasing range resolution. [C945]

#### "Deriving bistatic chirp scaling algorithm based on the signal model"

This paper provides a novel view on the chirp scaling algorithm. In this new way, the chirp scaling algorithm is analyzed through its range-Doppler (RD) expression first. The RD expression can be modeled with three basic functions. The different functions can be derived by the different methods. The proposed method can reduce the approximating error of the bistatic azimuth modulation and can produce the close-form bistatic range curvature factor. Though this paper's algorithm is derived under the azimuth-invariant bistatic framework, the proposed methodology can be extended into the general case. [C946]

#### "A target alignment algorithm for through-the-wall radar imagery classification"

Sensing through the wall using radar is a valuable capability. There is considerable work in generating radar images of the interior of a room by beamforming of the radar backscatter generated in a Synthetic Aperture Radar (SAR) configuration. However, high level interpretation of the scene is a more difficult task. In previous work a minimum distance classifier was successfully used to recognize various targets placed in the scene. The approach suffered from the dependency of target features on target location. This work presents a solution to this problem by bringing the target intensity profiles into alignment with the training data prior to classification. The alignment is performed by moving the intensity profiles between locations using an Autoregressive Moving Average (ARMA) model. The classification results before and after alignment show a marked improvement. [C947]

#### "SAR imaging of forest structure at longer wavelengths"



This paper is focused on the recovery of the vertical structure of forested areas from multi-baseline and multi-polarimetric SAR surveys at P-Band and L-Band. Baseline diversity provides sensitivity to the vertical structure of the vegetation layer, resulting in the possibility to yield Tomographic reconstructions of forested areas. Yet, far more information can be inferred basing on the joint exploitation of baseline and polarization diversity, which allows the decomposition of the SAR signal into ground-only and volume-only contributions. Ground-only contributions provide an easy and viable way to phase calibrate the data stack. Volume-only contributions, if correctly identified, allow a direct imaging of the vegetation layer. Results are shown basing on both P-Band and L-Band airborne data collected in the framework of the ESA campaign BioSAR 2008. The spaceborne case is also considered, basing on simulated BioMass data. [C948]

#### "Multipath Doppler signatures from targets moving behind walls"

Detection, localization, and tracking of moving targets are highly desirable in through-the-wall sensing applications. Since the indoor environment is rich in multipath reflective sources, such as walls, floor, and ceiling, the received signal is composed of the direct path and several multipath arrivals. However, on occasions, the direct path to the target may be blocked as the target traverses behind large metallic objects such as file cabinets, etc. In such cases, multipath is the only observable return and can be exploited to detect and maintain tracking of moving targets. In this paper, we provide range-Doppler analysis of multipath arrivals for a diffuse target moving in an enclosed urban structure, which provides insight for the development of through-the-wall detection and tracking techniques based on multipath exploitation. [C949]

#### "A precise signal model for ultra high resolution SAR"

A precise signal model for ultra high resolution SAR in the two dimensional (2-D) time and frequency domain is presented. The traditional signal model is challenged because the 'stop-go' assumption can't hold any more in ultra high resolution SAR. Considering the radar's motion between transmission and reception of a pulse, the precise echo expressions in 2-D time and frequency domain are deduced. The precise signal model allows more insight into the ultra high resolution SAR imaging. [C950]

#### "An interpretation of Woodward's ambiguity function and its generalization"

We suggest a new interpretation of Woodward's ambiguity function as the expected value of an operator. The operator represents the physics of the interaction of the waveform with the object. This approach provides a new approach to understanding the return signal at the receiver and can reveal more detailed understanding of the underlying interactions within the return signal that are not usually brought out by standard signal processing techniques. [C951]

#### "Radar target detect using particle filter"

A radar target track-before-detect (TBD) algorithm using particle filter (PF) is presented in this paper. System dynamic model and measurement model are established based on a sequence of radar range-Doppler measurements using the new algorithm. Furthermore, a linear extended target model is proposed, which is more capable of describing a maneuvering target than the conventional point target model. The likelihood ratio function of the new model is also derived in this paper. Due to the accumulation of the PF-TBD over time and the effectiveness of the proposed target model, an improved probability of detection for dim target is obtained. The experimental simulations demonstrate that the proposed method is capable of detecting and tracking a target with SNR of 1 dB robustly. [C952]

#### "Passive synthetic aperture radar imaging with single frequency sources of opportunity"

In this paper we consider passive airborne receivers that use backscattered signals from sources of opportunity transmitting fixed-frequency waveforms. Due to its combined passive synthetic aperture and the fixed-frequency nature of the transmitted waveforms, we refer to the system under consideration as Doppler Synthetic Aperture Hitchhiker (DSAH). We present a novel image formation method for DSAH. Our method first correlates the windowed signal obtained from one receiver with the windowed, filtered, scaled and translated version of the received signal from another receiver. This processing removes the transmitter related variables from the phase of the Fourier integral operator that maps the radiance of the scene to the correlated signal. We next use the microlocal analysis to reconstruct the scene radiance by the weighted-backprojection of the correlated signal. This imaging algorithm can put the visible edges of the scene radiance at the correct location, and under appropriate conditions, with correct strength. Additionally, it is an analytic reconstruction technique which can be made computationally efficient. We show that the resolution of the image is directly related to the length of the support of the windowing function and the frequency of the transmitted waveform. The image reconstruction method is applicable with both cooperative and non-cooperative sources of opportunity using one or more

airborne receivers. We present numerical simulations to demonstrate the performance of the image reconstruction method and to verify the theoretical results. [C953]

#### **"Mode-Selective OTHR: A new cost-effective sensor for maritime domain awareness"**

This paper presents a new sensor concept designed to provide maritime domain awareness over large ocean areas. The Mode-Selective OTHR introduced herein achieves significant detection and tracking capability against maritime vessels relative to traditional OTHR designs because it is designed specifically to reject disturbed ionospheric propagation modes and operate only using low distortion propagation modes. The architecture of the radar is such that this rejection occurs for both the transmitter-to-surveillance-footprint and the footprint return-to-receiver propagation paths. This is achieved using recently discovered techniques for non-causal adaptive and range dependent transmit beamforming and two-dimensional apertures for both transmission and reception. It also includes new methods for using planar transmit arrays operating with extreme steer angle. [C954]

#### **"High resolution radar tomographic imaging using single-tone CW signals"**

Radar tomographic imaging is a special radar imaging technique which can achieve very high spatial resolution (up to  $j$  wavelength) but with very narrow signal bandwidth. Although the theory of radar tomography had been developed for more than 20 years, very few experimental results can be found in public literatures. In this paper, the radar tomographic imaging is investigated and some measurement results of radar tomographic imaging using single-tone CW signals are presented. The theoretical spatial resolution is achieved and good agreement is obtained between the measured and simulated results. [C955]

#### **"Performance analysis of two-step algorithm in sliding spotlight space-borne SAR"**

The focusing performances of two-step algorithm are analyzed in the paper. The convolution processing in two-step algorithm is detailed analyzed. It can be found that the operation can reduce the Doppler bandwidth effectively and overcome the alias of azimuth echo by making the residual Doppler bandwidth smaller than PRF. The formula of residual Doppler bandwidth is derived here. According to the formula, range large bandwidth signal has influence on the residual Doppler bandwidth, which is not considered in the traditional imaging algorithm. In the high resolution sliding spotlight space-borne SAR system, the residual Doppler bandwidth is affected largely by the wide range bandwidth. PRF should be larger than the residual Doppler bandwidth in two-step algorithm; else it will result in defocus of the SAR image. The computer simulation is given to verify the presented analysis. [C956]

#### **"The HF surface wave radar WERA. Part II: Spectral analysis of recorded data"**

This paper covers the second part of the analysis of data recorded by the surface wave (SW) over-the-horizon (OTH) WEllen RADar (WEA). Data were collected by two WERA systems, on May 13th 2008, during the NURC experiment in the Bay of Brest, France. The principal aim of this work is to provide an accurate characterization of the spectral components of the received signal. Secondly, this information is exploited in order to provide a simple and reliable spectral modeling tool. For this reason, auto-regressive (AR) models, also known as linear prediction (LP) models have been investigated. Our results show that at long distances, when the clutter-to-noise power ratio (CNR) is small, the main components of the spectrum can be reasonably described by an AR(12) model, with a good compromise between accuracy and simplicity. As the CNR increases higher-orders are instead to be preferred. [C957]

#### **"Delay-Doppler radar tracking using moments"**

In this paper, we propose a new blind approach for joint time delay and Doppler estimation. The delay and Doppler have been imposed onto a signal modeled as a Gaussian mixture contaminated by a non-Gaussian and non-stationary noise. The estimation is done using the moments of received signal. This procedure provides lower complexity and more accuracy relative to other rival methods such as Wigner-Ville (WV) and wavelet transform. In this method, the noise power is assumed unknown and estimated as well. Then, the proposed delay and Doppler estimation is used for radar tracking. Based on the estimated delay and Doppler, we track the position and velocity of the target. We compare the new approach against extended Kalman filter and particle filter tracker. [C958]

#### **"A probabilistic model of the radar signal-to-clutter and noise ratio for Weibull-distributed clutter"**

We consider four effects relevant to the determination of the ratio of radar signal to clutter and noise. These effects are atmospheric turbulence, target fluctuations based on the Swerling models, zero-mean Gaussian background and receiver noise, and Weibull-distributed clutter. Radar return signal levels are affected by target

fluctuations and atmospheric turbulence, characterized by target fluctuations according to the Swerling models and a lognormal distribution, respectively. Since these distributions are not independent and identically distributed (IID), they cannot be simply added, and must be treated by combining them in a manner similar to convolution. Also, clutter and noise are not IID, and must be combined in a similar way. The ratio of these two combinations comprises a probabilistic model of the ratio of radar signal to clutter and noise. This ratio is the probability that a given signal level will be achieved in the presence of atmospheric and target scintillations divided by the probability that a given clutter and noise level will be observed. To determine the ratio of the actual signal to clutter and noise, we must multiply these probabilities by the mean powers resulting from these phenomena, as will be shown later. We treat several cases of interest by varying the average radar cross section, the log intensity standard deviation of turbulence, the radar threshold-to-noise and signal-to-noise ratios, and the distribution of Weibull clutter mentioned above. [C959]

#### **"Compressed Sampling for pulse Doppler radar"**

This paper presents a study of how the Analogue to Digital Converter (ADC) sampling rate in a digital radar can be reduced-without reduction in waveform bandwidth-through the use of Compressed Sampling (CS). Real radar data is used to show that through use of chirp or Gabor dictionaries and Basis Pursuit (BP) the ADC sampling frequency can be reduced by a factor of 128, to under 1 mega sample per second, while the waveform bandwidth remains 40 MHz. The error on the reconstructed fast-time samples is small enough that accurate range-profiles and range-frequency surfaces can be produced. [C960]

#### **"Evaluation of modulus-constrained matched illumination waveforms for target identification"**

In prior work, we have applied matched illumination strategies to target identification by a closed-loop radar system. In the closed-loop system, multiple waveforms are transmitted in succession, but each is customized based on the returns from prior transmissions. In this prior work, however, the matched waveforms were not constrained to be constant modulus. This current paper evaluates the performance of closed-loop radar with constant-modulus matched illumination. We also compare the performance of non-constant-modulus illumination under a peak power constraint. Finally, we use simple target models and assume unknown orientation, rather than the deterministic or Gaussian target models used in earlier work. [C961]

#### **"Super-resolution techniques in meteorological radars: The example of wind turbines"**

The use of wind turbines to generate electricity has become a major problem in meteorological radars. Due to the low frequency resolution that these radars show, the most representative wind turbine radar signature characteristics can't be observed in operational exploration modes by using the classical Fourier spectral estimation. In this paper, we propose super-resolution techniques to improve Fourier's Doppler resolution and provide experimental results. [C962]

#### **"Human gait classification using microDoppler time-frequency signal representations"**

A time-frequency classifier is applied for human gait classification. Time-frequency (t-f) quadratic distributions are used for time-frequency signal representations. Three specific motions are considered, corresponding to three different scenarios of arm motions which describe free and confined arm swings. The microDoppler signature in the time-frequency domain of each motion style is viewed as a feature and is incorporated in a distance-based classifications measured between the test data t-f distribution and the training average t-f distributions. It is shown that the time-frequency classifier performs properly, yielding low probability of classification errors, and its performance is rather insensitive to the type of time-frequency distribution employed. Among the possible distance measures used, which include the Correlation, Bhattacharyya and Kolmogorov, the Euclidean distance provided the best results. [C963]

#### **"Adaptive strategies for discrimination between mainlobe and sidelobe signals"**

We address adaptive discrimination between the signal of interest and a sidelobe interferer. To this end, we propose a detector derived resorting to a GLRT implementation of the generalized Neyman-Pearson rule and a two-stage detection scheme. The adaptive detectors rely on secondary data, free of signal components, but sharing the statistical characterization of the noise in the cell under test, in order to guarantee the CFAR property. [C964]

#### **"Performances and limitations of Persistent Scatterers-based SAR calibration"**

The PS calibration combines external devices, like corner reflectors, transponders and the stable targets in the scene to provide continuous monitoring of the radiometric quality of a SAR instrument. The goal is to provide, on

the bases of image blocks (say 10 Ч 10 km), the precise geolocation and the radiometric calibration information. The capability of selecting such targets, their intrinsic stability and the performances achievable by a PS-aided approach are investigated in this paper. [C965]

#### "UWB radar and leaky waveguide for fall on track object identification"

This paper presents a new system for detecting and identifying objects fallen onto railway tracks. The proposed solution is based on an ultra-wideband (UWB) radar technique combined with a slotted waveguide transmission line. A rectangular section, slotted waveguide is maintained all along the railway platform and used as a succession of monostatic radars. A design procedure is described. A procedure of extraction of target's electromagnetic signatures is discussed; simulation results are produced. [C966]

#### "Robust short-range clutter suppression algorithm for forward looking airborne radar"

The short-range clutter has serious range dependence for forward looking airborne radar (FLAR). As a result, when a radar detects moving targets on far range gates, the ambiguous short-range clutter degrades the performance of ground moving target indication (GMTI) obtained by space-time adaptive processing (STAP). The elevation three dimensional adaptive processing can well mitigate the problem, but, the computational load of the method is too heavy to be applied in real scenarios. A robust elevation pre-filtering algorithm is proposed. This method does not need adaptive processing on the elevation elements in a planar-array antenna. Therefore, the computational load can be reduced greatly. This method suppresses the ambiguous short-range clutter by multi-elevation angles restriction and the cancellation weight on the clutter has a deep and wide notch. Moreover, the method is robust to the elevation angle errors. Simulation results show the validity of the method. [C967]

#### "Blind multipath separation for waveform recovery"

The separation of multipath signal components by spatial filtering in a narrowband antenna array is addressed for cases where diffuse scattering and array calibration errors may cause the spatial signatures of the received propagation modes to deviate significantly from the plane-wave array manifold. The distorted wavefronts may have complex spatial signatures that are difficult to accurately characterize and mutually resolve on the basis of array manifold models described by few parameters. Furthermore, the temporal signature of the source waveform may also be quite arbitrary, with no known deterministic or statistical properties that can be utilized for multipath separation. This problem calls for blind waveform estimation methods that rely on relatively mild assumptions. An alternative blind spatial filtering technique referred to as the Generalized Estimation of Multipath Signals algorithm, or GEMS, is introduced for this purpose and tested on experimental data provided by the high frequency (HF) radar program of the Defence Science and Technology Organization (DSTO), Australia. [C968]

#### "Efficient construction of training database for identification of aircraft HRR profiles"

High resolution range (HRR) profiles show one-dimensional radar images including the electromagnetic scattering phenomena of a target. Thus, they are not only robust to noise, but also easily obtainable in real-time. However, in order to construct a training database for successful radar target identification, a huge number of HRR profiles are needed, because they are highly dependent on the relative angle between the radar and target. In order to alleviate this difficulty, a database construction method based on the scenarios of the target's movement is proposed. The proposed method is able to provide reliable target identification performance even with a small training database. [C969]

#### "The effect of clutter on the automatic target classification accuracy in FSR"

The clutter influence on the automatic target classification (ATC) accuracy in forward scattering radar (FSR) is presented. To study the ATC at various signal-to-clutter ratios (SCR), a simulated vegetation clutter is artificially added to the real clutter-free targets recorded signals. It is shown that using conventional clutter-uncompensated ATC system can achieve high target classification accuracy at high SCR only, but the accuracy drops significantly with SCR decreasing. The employment of clutter-compensated ATC system is shown to improve significantly the classification accuracy at low SCR. [C970]

#### "SAR raw signal simulation based on sub-aperture processing"

A novel algorithm for SAR(Synthetic Aperture Radar) raw signal simulation based on sub-aperture processing is proposed. The fundamental of the algorithm is analyzed, the signal model is deduced, as well as the simulation procedures are given. Simulation results of extended scene have shown that in the condition of meeting simulation precision, the simulation speed of the algorithm is higher than that of the echo simulation algorithm based on 1D FFT(Fast Fourier Transform). [C971]



### "Parallel implementation of the wideband DOA algorithm on the IBM Cell BE processor"

The Multiple Signal Classification (MUSIC) algorithm is a powerful technique for determining the Direction of Arrival (DOA) of signals impinging on an antenna array. The algorithm is serial based, mathematically intensive, and requires substantial computing power to realize in real-time. Recently, multi-core processors are becoming more prevalent and affordable. The challenge of adapting existing serial based algorithms to parallel based algorithms suitable for today's multi-core processors is daunting. One multi-core processor will be focused on, namely the IBM Cell Broadband Engine Processor (Cell BE). The process of adapting the serial based MUSIC algorithm to the Cell BE will be analyzed in terms of parallelism and performance for DOA determination. [C972]

### "Understanding the signal structure in DVB-T signals for passive radar detection"

This paper provides a detailed overview of Digital Video Broadcasting Terrestrial (DVB-T) signal structure and the implications for passive radar systems that use these as illuminators of opportunity. In particular, we analyze the ambiguity function and make explicit its features in delay and Doppler in terms of the underlying structure of the DVB-T signal. Ambiguities will be managed via the development of a set of mismatched filter weights that will be applied to the reference signal prior to range-Doppler map formation. The development of the mismatched filter is based on previous work with an extended improvement for ambiguity peak reduction a wider variety of DVB-T signals. [C973]

### "Experimental results for OFDM WiFi-based passive bistatic radar"

In this paper the practical feasibility of a WiFi transmissions based passive bistatic radar (PBR) is analyzed. The required data processing steps are described there including the adopted techniques for: (i) the control of the signal Ambiguity Function usually yielding a high sidelobe level and (ii) the removal of the undesired signal contributions which strongly limit the useful dynamic range. The performance of the conceived system is evaluated with reference to typical signals broadcasted by a IEEE 802.11 access point exploiting an OFDM modulation. The achievable results are presented against a real data set collected by an experimental setup. This allowed us to preliminarily demonstrate the potentialities of a WiFi-based PBR for local area surveillance applications. [C974]

### "Suppression of sidelobes and noise in airborne SAR imagery using the Recursive Sidelobe Minimization technique"

The Army Research Laboratory (ARL) has recently developed the Recursive Side-lobe Minimization (RSM) technique (patent pending). The technique is integrated with a standard back-projection algorithm to form synthetic aperture radar (SAR) images with significant reduction in side-lobes and noise. We have achieved significant improvements in noise reduction by applying the RSM technique to our Ultrawideband (UWB) Synchronous Impulse Reconstruction (SIRE) forward-looking radar. This paper presents the application of the RSM technique using data from a side-looking airborne SAR system from SRI International. We describe the RSM technique, the SAR data processing, compare the baseline and RSM SAR images, and quantify the image quality in term of signal-to-noise ratio (SNR) and the statistical distribution of the image pixels to show that significant improvement achieved using the RSM technique. [C975]

### "MIMO radar sparse angle-Doppler imaging for ground moving target indication"

We present in this paper a regularized sparse signal recovery algorithm, referred to as sparse learning via iterative minimization (SLIM), to provide ground moving target indication (GMTI) through multiple-input multiple-output (MIMO) radar angle-Doppler imaging. A slow-time modulation scheme with code division multiplexing is employed to achieve transmit diversity. In this way, we avoid the high correlation properties of orthogonal waveforms and the Doppler ambiguity that is encountered with Doppler division multiplexing schemes. After removing jammer and clutter effects using semi-unitary projections, we show that SLIM, using primary data only, is able to form sparse angle-Doppler images and to provide for accurate target localization. [C976]

### "Simulation of radar signal on wind turbine"

This paper describes the radar signal features of a typical wind turbine and the simulation of the wind turbine signal based on a high resolution Doppler radar. The simulated signal is under-sampled with lower PRF to match an air traffic control (ATC) radar. The simulated signal is compared to the ATC radar data collected at two different sites. Remarkable similarities of the signal features are identified. These features may help to improve the primary radar detection and tracking performance in the future. [C977]



### "Analysis of MIMO radar ambiguity functions and implications on clear region"

Multiple input multiple output (MIMO) radar offers the potential for improved performance over more traditional single input multiple output (SIMO) radar. MIMO radar operates by transmitting separable waveforms from multiple transmitters and the resulting radar echos are received by multiple receivers. While there is a great deal of literature discussing the benefits of MIMO techniques, a handful of publications discussing the limitations of MIMO radar techniques have appeared in the literature. Of particular interest is the work addressing the reduction of the clear area in range-Doppler space. Using a particular form of the MIMO ambiguity function, it was shown for a MIMO radar transmitting  $N$  waveforms there is a reduction of the clear area by a factor of  $1/N$ . In this paper, we repeat this analysis for the ambiguity function applicable to a coherent MIMO radar. We show the MIMO ambiguity function proposed in does not fully capture some important features of coherent MIMO radar and differs from versions of the ambiguity function proposed by other authors. In the second half of this paper, we derive the MIMO ambiguity function for coded pulse train waveforms. In addition to the traditional narrowband assumption, we develop the MIMO ambiguity function using the "start-and-hop" radar signal model. [C978]

### "Range and Doppler walk in DVB-T based Passive Bistatic Radar"

This paper analyzes the effects of range and Doppler walk for a Digital Video Broadcast-Terrestrial based Passive Bistatic Radar of both simulated and experimental data. Range and Doppler walk cause energy dispersal in the correlation, thus the coherent integration time is limited by the bistatic velocity and acceleration. A method using the readily available Doppler information to compensate for the range displacement during integration due to non-zero bistatic velocity of target is described. By compensating and non-coherently adding several coherently processed intervals, the target signal to noise ratio is increased. [C979]

### "An indoor S-band radar receive array testbed"

This paper describes a multi-channel S-band radar receive system designed as a laboratory testbed system for studying wideband radar array signal processing. The receive array was designed using a combination of low-cost commercial-of-the-shelf components and a custom-designed surface-mount printed circuit board assembly. It has been tested using LFM-CW waveforms with a center frequency of 2.4 GHz and a bandwidth of 600 MHz. By using components manufactured to operate in the "Wi-Fi" wireless communications band, the cost of the system has been minimized. This paper presents the design of the system, test results, and some sample ARD surfaces from the system. [C980]

### "SKP-shrinkage estimator for SAR multi-baselines applications"

The physical properties that can be inferred from Radar data are strictly related to the kind of diversity that characterizes the data itself. Spatial (i.e.: baseline) diversity provides information about target locations, temporal diversity provides information about target displacement, whereas polarimetric diversity provides information about the target electromagnetic behavior. In all cases, covariance matrix estimation is a key issue in the framework of coherent SAR analysis of scenarios characterized by the presence of distributed targets, such as bare or rock surfaces, forested areas, or ice shelves. In this paper we consider the case where two different kinds of diversities are present within the data, such as spatial and temporal or spatial and polarimetric, and investigate the effectiveness of the shrinkage estimator for the data covariance matrix. The shrinkage estimator is obtained as an optimum convex combination between the sample covariance matrix and the structured estimator. The structured estimator is based on the hypothesis of separability of the coherence losses due to the different kinds of diversities within the data, for each target that contributes to the received signal. This hypothesis leads to expressing the data covariance matrix as a Sum of Kronecker Products (SKP), for the estimation of which fast algebraic techniques exist. [C981]

### "A quantitative method for mono- and multistatic radar coverage area prediction"

The prediction of radar coverage as a function of the position of the radar has always been a key step in radar network planning. In the past, simple geometric models backed up by the deployment of siting radars were the only options for potential site evaluation, but the development of sophisticated propagation models (e.g. AREPS [1]) has moved the technology forward to another level of prediction accuracy. Modelling takes into account atmospheric refraction, as well as terrain effects and clutter. In previous papers [2], [3] we have shown that the modelling can also cater for multistatic radar systems. In this paper we have extended our modelling to give a statistical measure of the effectiveness of a site that measures the signal to noise ratio (SNR) or (for multistatic radar) the signal to interference ratio (SIR) over regions of interest. The area is pixellated into values of SNR and SIR, and pixels meeting the required SNR and / SIR are counted. We show some results for a multistatic radar.

We conclude by indicating how we plan to include ground clutter. We mention how this method of obtaining quantitative coverage performance can be used with all forms of radar, and will be able to improve future networks of cognitive radars. [C982]

### "Conjugate gradient parametric adaptive matched filter"

The parametric adaptive matched filter (PAMF) detector for space-time adaptive processing (STAP) detection is re-examined in this paper. Originally, the PAMF detector was introduced by using a multichannel autoregressive (AR) parametric model for the disturbance signal in STAP detection. While the parametric approach brings in benefits such as significantly reduced training and computational requirements as compared with fully adaptive STAP detectors, the PAMF detector as a reduced-dimensional solution remains unclear. This paper employs the conjugate-gradient (CG) algorithm to solve the linear prediction problem arising in the PAMF detector. It is shown that CG yields not only a new computationally efficient implementation of the PAMF detector, but it also offers new perspectives of PAMF as a reduced-rank subspace detector. The CG algorithm is first introduced to provide alternative implementations for the matched filter (MF) and parametric matched filter (PMF) when the covariance matrix of the disturbance signal is known. It is then extended to the adaptive case where the covariance matrix is estimated from training data. Important issues such as unknown model order and convergence rate are discussed. Performance of the proposed CG-PAMF detector is examined by using the KASSPER and other computer generated data. [C983]

### "Software-defined radar for MIMO and adaptive waveform applications"

The development of a software-defined radar testbed is described. The testbed is to be used to explore advanced techniques such as multiple-input multiple-output radar and adaptive waveforms. The system features a fully programmable, dual-channel, arbitrary pulsed waveform generator with a quadrature downconverting receiver. The system can generate waveforms of up to 500 MHz instantaneous bandwidth at a center frequency tunable from 2-18 GHz. The RF front end features two independent transmit and receive channels that can be multiplexed between four dual-polarized transmit and four dual-polarized receive antennas. [C984]

### "Design of unimodular sequences using generalized receivers"

This paper reviews recent advances in designing unimodular sequences with good auto/cross correlation properties along with a new approach that emphasizes on independent receiver design. The general problem is to design single or multiple sequences with constant modulus in the time-domain such that their respective matched filter outputs ideally resemble delta functions and the cross-matched filter outputs are zeros. In this context CAN (cyclic-algorithm new) and WeCAN (Weighted CAN) have been proposed for designing such sequences with good auto-cross correlation properties. In this paper, the equivalence of the CAN algorithms and the classic Gerchberg-Saxton (GS) algorithm involving the sequential magnitude substitution operations in the time and frequency domain is demonstrated. The design of unimodular sequences is further generalized here by considering the receiver design to be more general than the respective matched input sequences. The receiver design is carried out by taking care of the desired output requirements and the freedom present at the input can be used to further minimize the output side-lobe level. [C985]

### "Ambiguity Function analysis of WiMAX transmissions for passive radar"

In this paper the feasibility of a WiMAX transmissions based Passive Bistatic Radar (PBR) is analysed. The Ambiguity Function (AF) of the considered waveform of opportunity is characterized with reference to different transmission modes. The signal AF is shown to yield regularly spaced undesired peaks which might strongly limit the target detection capability of a WiMAX-based PBR. These sidelobe structures have a deterministic nature mainly related to the OFDM modulation exploited by WiMAX transmissions. A proper filter, based on the knowledge of the expected value of the signal Autocorrelation Function (ACF), is implemented to cope with this limitations and its performance is evaluated against simulated data generated according to the IEEE 802.16e Standard. The proposed approach is shown to yield an effective removal of the undesired peaks in the AF thus making the considered waveform more attractive for PBR medium range surveillance. [C986]

### "Radon transform and the modified envelope correlation method for ISAR imaging of multi-target"

In multi-target ISAR imaging, if the returned signals are range non-separable and the relative radial velocity is large. We can neither resolve them in range domain nor the Doppler frequency domain. In order to solve this problem, the use of the Radon transform and a modified envelope correlation method for multi-target ISAR imaging is presented. The radon transform is used to align the range profiles coarsely. For more accuracy alignment, a modified envelope correlation method is proposed. After range alignment, phase compensation is fulfilled by Discrete chirp-Fourier transform (DCFT). The simulation results show that the method proposed in

this paper is effective. [C987]

### "Tracking maneuvering target with particle filter techniques on passive radar using FM and DVBT broadcasting signals"

In this paper, we present a Track-before-Detect algorithm for maneuvering targets, with particle filter techniques on passive radar. The particle filter uses directly the correlation output from each transmitter to give Bayesian estimation for the position and the velocity of the target. We analyze the proposed technique with analog signals (FM broadcast signal) and digital signals (DVBT broadcast signals). [C988]

### "Distributed time reversal mirror array"

An array of independent, separate, distributed time-reversal mirrors (TRMs) that can function as a large array in a coherent (collective and co-operative) manner is described. Due to the unique feature of time-reversal to compensate for the propagation delay after round-trip, the DTRMA can perform coherent integration of signals across the array through distorting media without the need for complicated array calibration and precise geo-location procedures, even after the location of a TRM has been changed. Several proof-of-concept experimental results to show both temporal and spatial focusing properties of the DTRMA are demonstrated using commercially available off-the-shelf components and instruments. [C989]

### "3 GS/s S-Band 10 Bit ADC on SiGeC Technology"

In advanced applications such as digital radar, Ultra Wide Bandwidth communications and software defined radio, the need for instantaneous bandwidth often drives system design decisions. Access to high speed data converters enabling up and down conversion directly in the L Band and S Band removes the limit imposed by bandwidth scarcity and allows the design of flexible and simplified system architectures. Broadband ADC's (Analogue to Digital Converters) are key enabling components which open up new design opportunities for digital Receiver systems. In this regard, this paper describes a new 10bit 3GS/s ADC with 5 GHz Bandwidth, based on a 200 GHz SiGeC bipolar Technology, which enables the direct digitizing of 1GHz arbitrary broadband waveforms directly in the high IF region closer to the Antenna (L-Band or S-Band). [C990]

### "Ziv-Zakai lower bound on target localization estimation in MIMO radar systems"

This paper presents the derivation of the Ziv-Zakai bound (ZZB) for the localization problem in a MIMO radar system. The target is positioned in the near-field of a network of radars of arbitrary geometry. The radars have ideal mutual time and phase synchronization. The target location is estimated by coherent processing exploiting the amplitude and phase information between pairs of radars. An analytical expression is developed for the ZZB relating the estimation mean square error (MSE) to the carrier frequency, signal bandwidth, the number of sensors, and their location. From numerical calculations of the bound, three regions of signal-to-noise ratio (SNR) can be distinguished in the performance of the location estimator: a noise-dominated region, an ambiguity region, and an ambiguity free region. In the noise-dominated region, the signals received by the radars are too weak, and thus the localization error is limited only by the a priori information about the location of the target. In the ambiguity region, the performance of the location estimator is affected by sidelobes. In the ambiguity free region, estimation errors are very small and the ZZB approaches the Cramer-Rao lower bound (CRLB). [C991]

### "Analysis of multi-sensor radar detection based on the TBD-HT approach in ECM environment"

This paper describes in details the performance of an advanced detecting algorithm for multi-sensor target Track Before Detection (TBD) through the Hough Transform (HT). The detection algorithm employs the idea of using the Hough Transform for joint detection of linear trajectory targets. The polar modification of the TBD-HT approach is applied to a multi-sensor Polar Hough detector for multi-sensor target/trajectory detection in ECM environment with a Stand-off-Jammer (SOJ). A CFAR detector is proposed for signal detection in the (r-t) space instead of fixed thresholding in order to enhance the target detectability in ECM environment. In this paper a centralized structure of a multi-sensor Polar Hough detector is considered. The expressions calculating the probability characteristics, i.e. the probability of target/trajectory detection and the false alarm probability, are analytically derived. The multi-channel TBD-HT detector probability characteristics are compared with those for the conventional signal processing. [C992]

### "A spatiotemporal model for radar HRRP sequence recognition"

A temporal factor analysis (TFA) model which can describe both the spatial structure and temporal dependency of high range resolution profiles (HRRP) has been proposed for radar HRRP sequence recognition. Variational Bayes method and Bayesian classifier are adopted for model learning and classification task, respectively. The

favorable results based on measured data show the effectiveness of this model. [C993]

#### "A novel method to detect rotor blades echo"

In this paper, the effect of the main rotor of an armed helicopter on radar return signal and its modulation condition are considered. After analyzing references and experimental data, this paper proposes a new method based on inherent modulation in main rotor echo. This method is able to enhance the probability of detection. The simulation is performed for both simulated and practical echo signal. Simulation results confirm that our proposed scheme is effective. Moreover, a new domain for distinguishing and measuring the rotation feature of a rotary target is proposed. This paper is based on practical experiments (rotation domain). [C994]

#### "Autonomic subsystems for cognition in Passive Coherent Location"

In a previous paper we mentioned that Passive Coherent Location (PCL) can be thought of as Cognitive Radar. The deployment of PCL systems (also known as Passive Bistatic Radar-PBR) is fraught with difficulty, even in the situation of a spatially static network of transmitters and receivers. It is well known that PCL systems have to take into account the strong, direct signals of cooperative and opportunistic transmitters used, and try to use terrain or antenna nulls to mitigate the receiver dynamic range requirements. Receiver position in the terrain also influences the coverage. This results in a complex planning environment requiring propagation prediction tools to assist in selection of the best site. The situation becomes worse when the network of transmitter and receivers becomes dynamic. In this paper, we discuss the cognition and networking requirements for PCL systems consisting of moving transmitters and receivers, forming a cognitive, sensor network. We show that a sensible approach would use the structure of human intelligence, which consists of a higher level integrating function, together with autonomic, lower level, subsystems. [C995]

#### "Modeling and simulation study on radar Doppler signatures of pedestrian"

This paper focuses on radar Doppler signatures of pedestrian. Firstly, an improved human walking model which describes a pedestrian as a linear-rigid target is introduced. Then radar echoes of the pedestrian under the condition of continuous wave (CW) radar signal are acquired, formulas of instantaneous Doppler are derived and movement signatures of the target are analyzed. Simulation experiments are carried out to validate the model and theoretic analysis. [C996]

#### "Characterization of UWB Radar targets: Time domain vs. frequency domain description"

In this paper a characterization of UWB Radar targets is provided, both in the frequency domain and in the time domain. This is done by firstly giving a mathematical description of the Radar target in the UWB case, then providing measurement results. The proposed characterization allows for discerning and classifying UWB targets. Moreover, in this paper a full polarimetric analysis is taken into account. [C997]

#### "Cramér-Rao bounds and TX-RX selection in a multistatic radar scenario"

Multistatic radars utilize multiple transmitter and receiver sites to provide several different monostatic and bistatic channels of observation. Multistatic passive and active systems can offer many advantages in terms of coverage and accuracy in the estimation of target signal parameters but unfortunately their performances are heavily sensitive to the position of receivers (RX) and transmitters (TX) with respect to the target trajectory. As known, geometry factors play an important role in the shape of the ambiguity function (AF) which is often used to measure the possible global resolution and large error properties of the target parameters estimates. Exploiting the relation between the ambiguity function and the Cramer-Rao lower bound (CRLB), in this work we propose an algorithm for choosing in a multistatic scenario, along the trajectory of the tracked target, the pair TX-RX with the best asymptotic performance calculated in terms of CRLB on estimation accuracy. [C998]

#### "Preliminary results of ultra-wideband through-the-wall life-detecting radar"

It is often a difficult task of knowing the location or movement of people behind barriers. To address this problem, we develop a through-the-wall life-detecting radar (TWLDR) prototype. It is a kind of ultra-wideband (UWB) radar using impulse waveform, which can penetrate non-metallic walls to detect static and moving targets behind walls. We first introduce configurations of the radar system, then describe signal processing techniques, and present experimental results in different situations at last. Results indicate that the UWB TWLDR can penetrate non-metallic walls to detect people with different locomotion states such as standing, walking along cross-range direction, walking along range direction, and the signal processing algorithm could be applied to other complex environments. [C999]



### "A robust neural network based pulse radar detection for weak signals"

In this paper we develop a neural network capable of detecting targets with weak echoes in a pulse radar. This is possible as the network is designed as a pattern classifier (in contrast to earlier work) together with a suitable but simple pre-processing of the returns. We demonstrate through simulations that such a network exhibits better range resolution and noise tolerance when compared to previous work based on neural networks. In addition, we examine the Doppler tolerance and the overall robustness of the trained network. [C1000]

### "Digital beamforming with reduced number of phase shifting and time delay elements"

A bilinear representation of polynomials is shown to result in an efficient method for digital beamforming in phased arrays, with much reduced number of phase shifting elements. The proposed structure is also shown to extend to arrays with arbitrary complex weights. The number of phase shifting elements used is of the order of the square root of the number of phases used, with no limitations on the achievable patterns. Only phase shifters and combiners are used, with no splitters. The same concept applies to reduction of the number of delay elements in wideband beamforming, and also in reduction of the number of delay elements in continuous-time FIR filters. [C1001]

### "A robust Chinese remainder theorem with its applications in moving target Doppler estimation"

The Chinese remainder theorem (CRT) is an ancient result about simultaneous congruences in number theory, which reconstructs a large integer from its remainders modulo several moduli. It is well known that the CRT has tremendous applications in many fields, such as computing and cryptography, an important one of which could be radar signal processing and radar imaging. However, it is also well-known that CRT is not robust in the sense that a small error in any remainders may cause a larger error in the reconstruction result, which will lead to a non-robust estimation. In this paper, we introduce a robust reconstruction algorithm called robust CRT. We show that, using this robust CRT algorithm, the reconstruction error is upper bounded by the maximal remainder error range named remainder error bound, if the remainder error bound is less than one quarter of the greatest common divisor (gcd) of all the moduli. Although CRT has existed for about 2500 years, this robustness is the first time in the literature. Then, we show how this robust CRT can be used into the field of radar detection and Doppler ambiguity resolution, especially for fast moving targets, and later, simulations are given to illustrate the effectiveness and validness of this robust CRT algorithm. [C1002]

### "Modified Capon and APES for spectral estimation of range migrating targets in wideband radar"

In many radar and sonar applications, the narrowband signal assumption is not respected. To preserve good performance detection and/or parameter estimation for wideband signal, it is necessary to develop appropriate signal models and processing algorithms. More specifically, the range migration of the target during the processing interval induces a coupling between range and Doppler that is not taken into account by standard algorithms such as the Capon and APES methods. In this paper, we present a modified and enhanced version of the Capon and APES algorithms for a wideband signal model. These two algorithms are adaptive filters designed for spectral estimation. Performance of the wideband-Capon and the wideband-APES algorithms are studied via numerical simulations. [C1003]

### "On the design of mismatched filters with an adjustable matched filtering loss"

We present a method for the design of mismatched filters minimizing the interference from unwanted targets (point target or clutter) under the constraint of matched filtering loss. The method seeks to find the optimum filter minimizing the interference and having a desired cross-correlation with a given transmitter waveform. The method is applied to get the minimum integrated side-lobe level filters and to optimize the receivers of the pulse diversity systems. [C1004]

### "Impulsive noise excision and performance analysis"

Interference can be a major impediment to the operational performance of radar systems. A common source of interference is impulsive noise which may appear due to regional lightning discharges or local man-made noise sources. Impulsive noise is characterized as having a large amplitude and short duration and therefore only affects a small portion of the time series. Unpredictable frequency distortion may occur during the impulsive noise period, which is partially caused by the non-perfect response of the receiver front end. In this paper we present several linear prediction methods that are used to remove the impulsive noise without introducing frequency leakage over the signal band. Theoretical performances are analyzed and compared for these methods. The effectiveness of prediction methods relative to traditional excision techniques are also demonstrated using experimental data. [C1005]



### "Frequency domain motion compensation for stepped-frequency radar under multi-target scenario"

Target motion compensation method for stepped-frequency radar was studied. Under multi-target scenario, the conventional compensation method is invalid, and a method of compensation in frequency domain was presented. The method can be used for the compensation of multi-target with different velocities. Computer simulation results are given to verify the validity of the method. [C1006]

### "Three-dimensional reconstruction of a comet nucleus by optimal control of Maxwell's equations: A contribution to the experiment CONSERT onboard space craft Rosetta"

COMet Nucleus Sounding Experiment by Radio Wave Transmission (CONSERT) is one of 20 experiments onboard the ESA mission Rosetta and aimed at the reconstruction of the unknown internal material parameter distribution of a comet nucleus. The details on the experiment setup can be found in [1], [2]. CONSERT consists of a lander module which attaches to the surface of the comet and an orbiter module which circulates the comet in space. An electromagnetic sounding of the comet nucleus will be achieved by a signal link between the lander and orbiter antenna system. We propose an optimal control approach to solve for the unknown 3D material parameter distribution of the comet nucleus. We optimize the computed electromagnetic field distribution at the receiver locations for the measured (observed) electromagnetic field distribution by controlling the material parameters. The target functional, the difference between computed and observed field for all receiver locations and time steps is minimized by means of a gradient-based quasi-Newton optimization algorithm. The optimal control problem is solved if the target functional yields its global minimum. [C1007]

### "Joint Space-Based and Ground-Based Orbit Maneuver Identification Algorithms"

With the development of the outer space enterprise, it is very crucial to manage the spatial objects, especially in the way of the non-oneself object surveillance. However, orbit maneuver has brought the major difficulty to spatial object surveillance. To solve this problem, a new orbit maneuver identification algorithm, which is based on the joint of the space-based and the ground-based supervisory systems, is proposed in this paper. The simulation results show the reliability and feasibility of the proposed method. [C1008]

### "Research for D Stability of Uncertain Discrete Time-delay Systems"

D stability of uncertain discrete-time systems with time delay was studied. When the parameters were assumed to be time-varying within a certain interval matrices, the controller guaranteed that the closed-loop system was regular, causal and D stable. The explicit formula of desired controller WSS is provided by using the solution to the linear matrix inequalities (LMI). The numerical simulation result is provided to demonstrate the effectiveness of the presented method. [C1009]

### "Routing Path Selection and Power Allocation for Distributed Detection in Wireless Sensor Networks"

The design of wireless sensor networks for signal processing applications has to consider the limited battery power of the sensor nodes. In this paper, a combined routing path selection and power allocation strategy is presented that is especially designed for distributed detection in sensor networks with a serial topology. The objective is to minimize the global probability of detection error of the serial network under a total network power constraint. The cross-layer approach for the selection of a routing path through the network is based on the local observation SNR of the sensors as well as fading conditions and is efficiently implemented by a backward greedy algorithm. After the routing path is established, a subsequently performed power allocation algorithm aims to optimally distribute a total power budget with respect to the detection performance of the sensor network. [C1010]

### "Nondestructive Detection of Standing Trees and Radar Wave Detection"

To ensure the healthy growth of trees and avoid unnecessary loss, technologies and methods of nondestructive detection appears. In this article, a method, used in standing trees' nondestructive evaluation, is coming up after compared with several technologies' advantages and disadvantages which are now widely used in home and abroad. The method, radar wave detection of standing trees, is of practical significance because of its detection without any damage. The article presents its feasibility and how to implement it. [C1011]

### "Real Aircraft Navigation Data Statistic and Rule Analysis"

To understand the actual flying rules of aircrafts in air and discriminate real and simulated aviation, the actual

statistical navigation data is calculated in this paper. These data are collected from the real flight radar track and flight plan of ATC system. By means of statistical mathematics, the acceleration, deceleration, climb and descent rate, average speed, and probability densities of varieties of aircraft types are obtained. Varieties of aircraft types show different performance and flight rules by analysis of these graphs and charts. If the aircrafts are in a similar class such as A319, B737, and B757, their flying performance would have little difference in the analysis result above. Otherwise the difference is obvious, e.g. YN12 and A319 etc. The result indicates that it is very important to consider the influence of flight condition, performance, ATC rules, regulations of airline companies, and pilots' operation habits, which are important factors to improve the fidelity of flight simulation. [C1012]

### "Technology and innovation radar-Effective instruments for the development of a sustainable innovation strategy"

This paper summarizes several years of experience in process design and methodology implementation for sustainable innovation development as carried out by the authors within several innovation projects in different industries (e.g. fixed and mobile telecommunication, high tech, logistic). The formularization of our experience has led to a research innovation approach that enables an effective innovation intelligence and technology scouting through the use of a technology and innovation radar methodology. These instruments allow the identification and evaluation of emerging business and technology trends, provide an overview of the relative maturity and assess their relevance for the company. A rating mechanism helps companies to decide when to adopt an innovation and to develop new products and services. Furthermore, the technology and innovation radars are good strategic tools for early stage identification and prioritization in order to give an approximate value judgment without detailed return on investment justifications. In later stages of the planning process, the radar tools can be used as a high-level summary of an underlying prioritization process. [C1013]

### "A Bayesian perspective on sparse regularization for STAP post-processing"

Traditional Space Time Adaptive Processing (STAP) formulations cast the problem as a detection task which results in an optimal decision statistic for a single target in colored Gaussian noise. In the present work, inspired by recent theoretical and algorithmic advances in the field known as compressed sensing, we impose a Laplacian prior on the targets themselves which encourages sparsity in the resulting reconstruction of the angle/Doppler plane. By casting the problem in a Bayesian framework, it becomes readily apparent that sparse regularization can be applied as a post-processing step after the use of a traditional STAP algorithm for clutter estimation. Simulation results demonstrate that this approach allows closely spaced targets to be more easily distinguished. [C1014]

### "Autonomous Lockout Map Construction Technique for Secondary Surveillance Radar Mode S network"

Secondary Surveillance Radar (SSR) Mode S is an air traffic control radar system with improved surveillance and datalink capability. Recently, SSR mode S network attracts attentions as a way to solve problems such as the interrogator identifier code problem or radio frequency (RF) signal environment pollution. In SSR mode S network, each site has lockout map. Lockout is a command from GS to aircraft. Aircraft stops replying to all-call if it receives lockout. Lockout map determines area where GS lockout aircraft. There are several problems in current lockout map. First, it is difficult to create optimum lockout map. Second, it becomes complex to allocate and manage lockout maps if many sites join network. As the number of sites increase, Mode S operator has to prepare many maps. To solve these problems, we propose the Autonomous Lockout Map Construction Technique for SSR Mode S network. This technique enables Mode S GS to autonomously construct optimum lockout map by exchanging aircraft and site information through network. In this paper, we describe the background and details of the proposed technique. Then we show simulation results for validating the proposed technique. [C1015]

### "ISR sensor processing and data exploitation"

Intelligence, Surveillance, and Reconnaissance, commonly abbreviated as ISR, refers to the system of sensors (data collection assets) and data analysis and dissemination resources used to provide information about strategic and tactical threats. The advances in ISR sensor technologies and the large amount of data generated from ISR systems are putting a significant demand on signal processing and data exploitation. For example, an electro-optical system can easily generate several billion bits per second while searching an area the size of a small city. Therefore, onboard front-end signal processing is needed to reduce the amount of information to a manageable size and to make the outputs compatible with existing and future communication links. Similarly, there is increasing interest in allowing data exploitation on board the platforms. This talk will address examples of front-end signal processing, demands in data exploitation, and associated high-performance embedded

computing for ISR systems. The discussion will conclude with an emphasis on graph exploitation approaches to address the conversion of sensor information into knowledge that military forces and/or strategic analysts can act on in a timely manner. [C1016]

#### "Removing autocorrelation sidelobes of phase-coded waveforms"

This paper studies autocorrelation properties of a train of identical signals overlaid with a phase coding in the case when the uncoded signal forming the train consists of several groups of identical bits. It is shown that, if the coding patterns are the rows of a mutually orthogonal complementary set matrix, the waveform's autocorrelation sidelobes around the main lobe area can be completely removed. At the same time, repetition of some bits of the uncoded signal can be used to achieve a low sidelobe level in the close vicinity of the main lobe. [C1017]

#### "Radar sensitivity, receiver calibration, and sky noise"

Sky noise is highly anisotropic and well documented with maps available on-line. This sky noise can significantly affect radar sensitivity for radars with sensitive receivers. For ALTAIR at Kwajalein, the expected effect is as much as 8 dB. Documented changes of as much as 4 dB have been observed. The anisotropy of the sky noise can be used to calibrate receiver system noise. [C1018]

#### "The instagram: A novel sounding technique for enhanced HF propagation advice"

Modern OTHR systems make extensive use of propagation support information for parameter setup advice. A novel method for increasing dimensionality and temporal resolution of this advice is demonstrated here using an instantaneously wideband waveform on a one-way path. A composite of pseudo-randomly phased, discretized, massively multi-channel signals is synthesized through a simple summing scheme. Upon reception the composite is rapidly processed in the frequency domain to produce channel scattering information simultaneously across the band. The channels may be collapsed in the Doppler domain to reduce to conventional oblique ionograms. Total integration time required to produce the full Doppler ionograms, even with low transmit powers, is reduced over conventional methods by up to three orders of magnitude leading to the term 'Instagram'. The technique is implemented on an oblique sounding system that provides the necessary direct digital arbitrary waveform generation and reception capability. A result from the initial field trial is provided. [C1019]

#### "Modified Range-Doppler imaging method for the high squint SAR"

In this paper, a modified Range-Doppler (RD) algorithm with the Keystone Transform and the rank-deficient Capon is proposed for the shorter Synthetic Aperture Radar (SAR) imaging in the high squint mode. With the decrease of the aperture time under the squint mode, the linear range-walk becomes the dominant part of the range migration. The Keystone Transform is well suitable for removal of the range walk. In order to achieve higher resolution in the azimuth domain with the shorter SAR, the rank-deficient Capon which is an efficient non-diagonal loading spectral estimation based on rank-deficient sample covariance matrix is adopted. Simulation results can obtain the finer SAR images of the proposed approaches. [C1020]

#### "X-band FMCW radar system with variable chirp duration"

For application in a short range ground based surveillance radar a combination between frequency modulated continuous wave (FMCW) transmit signals and a receive antenna array system is considered in this paper. The target echo signal is directly down converted by the instantaneous transmit frequency. The target range  $R$  will be estimated based on the measured frequency shift  $f_B$  between transmit and receive signal. Due to an extremely short chirp duration  $T_{chirp}$ , the target radial velocity  $v_r$  has only a very small influence to the measured frequency shift  $f_B$ . Therefore the radial velocity  $v_r$  will not be measured inside a single FMCW chirp but in a sequence of chirp signals and inside each individual range gate. Finally, the target azimuth angle is calculated utilizing the receive antenna array and applying a digital beamforming scheme. Furthermore, in order to unambiguously measure even high radial velocities, a variable chirp duration is proposed on a dwell to dwell basis. [C1021]

#### "Differential approach for Through-the-wall life signs detection"

A very simple and effective method for detecting life signs for Through-the-wall Imaging applications is proposed and tested on experimental data. The proposed method properly exploits a Continuous Wave Microwave Transceiver working at 10 GHz and takes advantage from the displacement of the chest due to the respiratory movement for deriving a simple differential approach for detecting the respiratory and the heartbeat activities from the measured electromagnetic field. The proposed strategy allows to detect life signs of people in furnished room under concrete walls. The measurement set-up and the applied signal processing strategies are presented. [C1022]

### "Stochastic system identification approach to radar data processing"

Space-time adaptive processing (STAP) algorithms typically consist of a data transformation step to reduce the number of degrees of freedom and a sampling step wherein radar returns from adjacent range bins are used to estimate interference statistics. The reduction in degrees of freedom, inadequate sample support, presence of target in sampled data, and range dependence of interference are some of the main reasons for STAP performance loss. In this paper, we present another approach to target detection and localization that mitigates these performance losses. The approach is based on the well-known stochastic realization algorithm from system identification theory. In this approach, we use the radar return data for a given range bin to identify a minimal stochastic state space model for the return data. The angle and Doppler for all targets in the range bin are computed from the state space matrices. All the computations involved use standard linear algebra. As interference statistics are not directly computed and since there is no sampling from adjacent range bins, the proposed approach is more robust to sample support, target in training and range dependence of clutter. A numerical comparison of the proposed approach with beam-space post-Doppler STAP using simulated data is given. [C1023]

### "Cramér-Rao lower bounds for monopulse calibration using clutter returns"

Successful geolocation of ground moving targets utilizing monopulse techniques requires accurate characterization of the array manifold (i.e. monopulse response to off-boresight targets) and antenna pointing information. Utilizing techniques similar, in spirit, to those applied in synthetic aperture radar (SAR) to estimate the Doppler centroid of an image, we develop techniques to accurately estimate azimuth monopulse slope and boresight shift of an airborne ground moving target indicator (GMTI) antenna utilizing clutter returns from normally scheduled CPIs that are also used for target detection and geolocation. A statistical signal model is developed for the clutter returns as observed through the monopulse channels. Cramer-Rao lower bounds (CRLB) are developed for monopulse slope and boresight shift and compared to CRLB developed with SAR centroiding techniques as summarized in the literature. Analytical and numerical CRLB results show potential gains of one to two orders of magnitude at moderate to high clutter to noise ratios for a sum-difference system. [C1024]

### "Advanced signaling strategies for the Hybrid MIMO Phased-Array Radar"

The Hybrid MIMO Phased Array Radar, or HMPAR, is a notional concept for a multisensor radar architecture that combines elements of traditional phased-array radar with the emerging technology of Multiple-Input Multiple Output (MIMO) radar. A HMPAR comprises a large number,  $MP$ , of T/R elements, organized into  $M$  subarrays of  $P$  elements each. Within each subarray, passive element-level phase shifting is used to steer transmit and receive beams in some desired fashion. Each of the  $M$  subarrays are in turn driven by independently amplified phase-coded signals. This paper proposes new transmit signal selection strategies based on the observation that some MIMO signal sets, such as those proposed by us previously, cause a very rapid sequential or raster scan across some field of view. Exploiting this property allows one to create and process multiple beams simultaneously. Furthermore, there exists a range-angle coupling in the transmit and receive signals that may lead to high-resolution target localization. [C1025]

### "Processing-based tuner gain correction in a wideband multi-channel receiver"

Modern radar systems often capitalize on advanced radio frequency components in the receiver front end to include wideband tuners and amplifiers, highly stable local oscillators, and high-speed analog-to-digital converters. Yet, technology demonstrators often emphasize either the hardware or the processing algorithm rather than the end-to-end system. This paper presents the hardware characterization of tuner-gain mismatch in a wideband multi-channel array and the subsequent signal processing calibration model. The gain model is empirically found to follow a T-distribution and is used to balance the amplitude across the tuners as part of the processing for time-frequency-beamforming. Phase is also shown to be the critical factor to completely correcting phase mismatch. Here, we present details of the wideband receiver front-end and the signal processing backend. [C1026]

### "Distributed energy-efficient scheduling for radar signal detection in sensor networks"

In this paper, we consider the problem of Neyman-Pearson detection of fluctuating narrowband radar signals using wireless sensor networks (WSNs), and we are interested in finding some approach which can optimize the signal detection performance jointly with the energy expenditure. Towards this goal, we propose a distributed and energy-efficient scheduling scheme to coordinate the communications between each sensor node and the fusion center. This scheduling scheme allows each sensor to make its own decision about when to send data to the



fusion center, according to its own information and without consulting any other sensors. This distributed scheduling approach greatly reduces the dependence on the fusion center, and also attains an appealing balance between the detection performance and the energy efficiency. [C1027]

#### "Range profile specific optimal waveforms for minimum mean square error estimation"

Optimal waveforms for minimum mean square error range profile estimation are investigated. An idealized measurement and waveform adaptation process is developed that yields optimal scene and range specific waveforms. This process is idealized in that during each cycle of the process, a large number of dwells are required. As part of our method, a modified version of the Adaptive Pulse Compression (APC) estimation method is used to estimate the range profile after each dwell cycle. The proposed method is analogous to the APC method in that it yields a set of range specific optimal waveforms, while the APC method yields a set of range specific optimal pulse compression filters. In certain scenarios, the measurement and waveform adaptation process yields range profile estimates that are significantly better than those derived by the APC method alone. [C1028]

#### "Detection and estimation of multi-pulse LFM CW radar signals"

The Wigner-Ville Hough transform (WVHT) has been applied to detect and estimate the parameters of linear frequency-modulated continuous-wave (LFMCW) low probability of intercept (LPI) radar waveforms. The WVHT, which is optimal for a single linear frequency modulated (LFM) signal, becomes sub-optimal when applied to LFMCW signals since the observed waveform is composed of concatenated LFM pulses. We formulate the detection and estimation problem to take into account the multiple pulses that are available in an observation interval at the intercept receiver. The new algorithm, called the periodic WVHT (PWVHT), is shown to significantly outperform the WVHT for LFMCW signals. [C1029]

#### "Detection in heterogeneous clutter by filter output prediction"

This paper introduces an innovative method for ground moving target indication with a multichannel air or spaceborne radar. It is based on comparing the power of the filtered receive signal with a predicted power level. This prediction is found using data from the range line under test only. No potentially misleading prior magnitude information is employed. Thus, the false alarm probability is stabilized and the method is especially suited for rapidly varying heterogeneous terrain. [C1030]

#### "Resolution of two point targets using sub-arrayed MIMO radar"

Recent works on MIMO radar have shown benefits in optimising the signal covariance matrix for estimation of target parameters, over the performance of conventional radar and the orthogonal waveform approach used in much of the MIMO radar literature to date. The full diversity approach requires a large amount of flexibility at the transmitter and computation prior to transmission. In this work, we study the performance of a sub-arrayed transmit beamforming approach for MIMO Radar, which greatly reduces the requirements of the transmitter, for the important case of resolving two point targets. [C1031]

#### "Multi-modal sensor system integrating COTS technology for surveillance and tracking"

The feasibility of low-cost, Commercial Off-The-Shelf (COTS) sensor nodes is studied in a distributed network, aiming at dynamic surveillance and tracking of ground targets. Data acquisition by the low-cost (<\$50 US) miniature radar is described. We demonstrate the detection, ranging and velocity estimation capabilities of the mini-radar, and compare results to simulations. Furthermore, we integrate the radar output with supplementary sensor modalities, such as acoustic and vibration transducers, and infrared sensors. The method provides innovative solutions for detecting, identifying, and tracking vehicles and dismounts over a wide area in noisy conditions. This study presents a step towards distributed intelligent decision support and demonstrates effectiveness of small cheap sensors in identifying unique but similar events. Our work supports a pervasive sensor implementation relevant to the affordable open system architecture attribute of the U.S. Air Force Layered Sensing paradigm. [C1032]

#### "Validating multipath responses of moving targets through urban environments"

This work proceeds from the paper we published in RadarCon 2009 titled "Multistatic scattering from moving targets in multipath environments", where we explored the potential to track moving ground targets with radar as they enter urban areas and become obscured by buildings. An X-band radar data collection was performed which validates the predicted multipath response, and the received multipath power in relation to the line-of-sight (LOS) response. Results from a bistatic experiment are used to examine the spatial coherency of energy



reflecting from a large, rough surface, and the power distribution in angle that illuminates a target as it traverses in front of a building. This experiment may inspire knowledge-based methods to coherently process multipath returns, beyond that of standard GMTI processing, i.e., free-space matched-filtering (FFT) and CFAR detection. [C1033]

#### "Switched array concepts for 3-D radar imaging"

A number of antenna array concepts are investigated for three-dimensional radar imaging. The concepts are based on switched arrays and wide-band signals to generate a virtual array or co-array to span a sector volume in the wave vector space to get image resolution. The proposed arrays can be used for short range imaging in penetrating radar applications. This approach is quite general and it can also be used in other system concepts. Virtual arrays have mostly been used in radio astronomy and ultrasonic imaging. The related synthetic arrays with antenna motion have been more common in radar systems. [C1034]

#### "Null placement in a circular antenna array for Passive Coherent Location systems"

Passive Coherent Radar (PCL) is heavily constrained by the level of direct signal illumination. This paper investigates null steering techniques for a circular array antenna. An 8-element circular array has been designed and a method is proposed to steer multiple nulls in different directions. We present computed performance for two nulls achieved simultaneously. An 8 element dipole array has been constructed and the VSWR results are presented. This antenna will form the basis of practical null formation measurements. [C1035]

#### "Real-time tracking of bullet trajectory based on chirp transform in a multi-sensor multi-frequency radar"

Radar-based tracking technologies enable sub-time-of-flight bullet detection and trajectory tracking before the bullet reaches its target and thus lead to effective reduction of injuries and casualties. The capability of robust detection, tracking, and trajectory prediction in a weak signal environment directly translates to the awareness time for force protection. In this paper, we develop a multi-sensor multi-frequency radar platform and proposed the use of piecewise chirp transform for effective signal enhancement when the Doppler signatures are highly time-varying. Performed upon the time-frequency representations with improved phase information, multi-sensor multi-frequency radars uniquely localize and track bullets through unambiguous range and direction-of-arrival estimations. [C1036]

#### "Dynamic direction-of-arrival estimation via spatial compressive sensing"

This work addresses a problem of dynamic spatial spectrum estimation using linear sensor array via spatial compressive sensing (SCS). Static SCS approach is generalized for scenarios with dynamic far-field sources via Kalman filter, which provides the noncoherent minimum mean squared integration of instantaneous spatial spectrum estimations. The proposed dynamic SCS approach (DSCS) is shown to be efficient in low-SNR scenarios when the spatial spectrum is nonsparse, and therefore, the static SCS-based method cannot be used. Performance of the DSCS was evaluated in bearing-only target tracking scenarios where maneuvering target was considered. [C1037]

#### "A modified range migration algorithm for airborne squint-mode spotlight SAR imaging"

Due to the reference signal based on the fixed reference range is used in the range migration (RM) algorithm, the RM algorithm is not available to process an airborne squint-mode spotlight synthetic aperture radar (SAR) data. Thus, a modified RM algorithm is developed, which can be applied on processing large scene squinted-mode spotlight SAR data without division. Based on the squint-mode spotlight SAR imaging geometry, the modified reference signal is used to dechirp the received signal. Then, using the principle of stationary phase, the presented formulation of the modified RM algorithm is analyzed. Finally, the effectiveness of the proposed method is demonstrated by some numerical simulations via a squint-mode spotlight SAR simulator. [C1038]

#### "Terminal Doppler Weather Radar enhancements"

The design of an open radar data acquisition system for the Terminal Doppler Weather Radar is presented. Adaptive signal transmission and processing techniques that take advantage of the enhanced capabilities of this new system are also discussed. Results displaying data quality improvements with respect to problems such as range-velocity ambiguity and moving clutter are shown. [C1039]

#### "Firm track loss due to M of N track initiation of a radially inbound target"

This paper examines the firm track loss incurred by a fixed frame time radar performing track initiation using search detections. Firm track loss is the additional beam energy needed to achieve a desired firm track probability on a radially inbound target compared to a stationary target at that same firm track range. Firm tracks are established using an M or more detections out of N observations criteria. The firm track loss in dB is nearly linear with the product of velocity and frame time divided by firm track range. It is also insensitive to probability of false alarm and target radar cross section fluctuation models. It can be represented by a simple quadratic equation. The loss can be included in a radar range calculation worksheet such as a Blake chart to predict firm track range. A linear relationship is found between the firm track range of a moving target and a stationary target. [C1040]

#### "Moving targets tracking for homeland protection applications: A multi-sensor approach"

The paper deals with the problem of detecting, localizing and tracking individuals through the walls by means of radio-frequency based imaging techniques. The authors presents hereinafter a new imaging method for locating and tracking the position of hidden targets (e.g. human bodies in rescue missions) thanks to the use of a multi-sensor approach. A model-based signal processor has been also developed and tested. Numerical examples confirm the effectiveness of the proposed approach and procedures. [C1041]

#### "OFDM waveforms for multistatic radars"

In this paper, the benefits of OFDM waveforms are analyzed for multistatic radar systems, where several radar stations cooperate in the same frequency band. The signal is coded over a 2D pattern, in the time and the frequency domains, using orthogonal Golay complementary sets derived from Reed-Muller codes. Binary data are also encoded in the signal. The obtained ambiguity and cross-ambiguity functions show that the OFDM signal structure is well adapted for radar applications. Transmitted waveforms have relatively low interference and sidelobe levels in the range and Doppler axis. [C1042]

#### "Phase-coded-linear-frequency-modulated waveform for low cost marine radar system"

This paper proposes a continuous waveform to realize low transmitted power in a Radar system. The proposed waveform utilizes a pulsed compression scheme based on phase-coded modulation and linear FM which combines the desirable properties of both types of modulation. This paper also verifies waveform operation under channel effects such as multipath and noise. We determine power optimization due to waveform compression gain for given system specifications and use correlation values to detect both unambiguous range and Doppler shift. With a pre-determined noise and Doppler threshold, we can distinguish targets from sea clutter. Finally, we show the improvement in accuracy of elevation measurements by simulation when auto-correlation instead of signal strength ratios are used to determine target height. [C1043]

#### "Efficient pulse-Doppler processing and ambiguity functions of nonuniform coherent pulse trains"

We propose a DFT based pulse Doppler processing receiver for staggered pulse trains. The proposed receiver is a simple extension of traditional DFT based coherent pulse train processing. We show that P DFT processors are required to process the staggered train of pulses as a coherent signal, where P is the number of available pulse positions in each pulse repetition interval (PRI). Thus the complexity of the processing hardware only increases linearly with the number of available positions. We also look at the distribution of ambiguity volume around the delay-Doppler map by varying the pulse positions and the selection of pulse shapes. [C1044]

#### "Detection of complex point targets in a MIMO radar system with distributed assets and partially correlated signals"

A complex point target is a mathematical model for a radar target that is not resolved in space, but exhibits varying complex reflectivity across different bistatic view angles. The complex reflectivity can be modeled as a complex stochastic process whose index set is the set of all bistatic view angles, and the parameters of this stochastic process follow from an analysis of a target model comprising a number of ideal point scatterers randomly located within some radius of the targets center of mass. Six different models are summarized here, with different assumed distributions on the locations of the point scatterers within the target. We develop data models for the received signals from such targets in a MIMO radar systems with distributed assets and partially correlated signals, and consider the resulting detection problem. The problem reduces to the familiar Gauss-Gauss detection problem with hypoexponential test statistic. A related problem of adapting the transmitted signals to the target model is discussed. [C1045]

#### "Radacoustic detection of projectiles by a retrodirective radar"

An X-band retrodirective radar is shown experimentally to provide two signals from a firearm deployed at moderate range: (1) the normal reflection from the airborne projectile as it approaches the radar, and (2) a secondary reflection from the muzzle-blast acoustic wave. The combination of these two signals provides projectile bearing as well as an accurate estimation of range to the shooter by a differential time-of-flight calculation. [C1046]

#### "Low angle tracking using iterative multipath cancellation in sea surface environment"

In low angle tracking, signal reflection from sea surface leads to severe errors in the target angle of arrival (AOA) estimation owing to the presence of both a target and its image in the mainlobe. In this paper, we propose a new scheme that iteratively suppresses the specular reflected signal to alleviate estimation errors. The iterative processing, which includes estimating the target angle, calculating the reflected image angle and updating the null position in beamforming, is performed to eliminate the image signal; thus, the measured target AOA including error converges to the true value. Moreover, by exploiting phase comparison method using separate aperture, there is no need to consider the distortion of the monopulse slope caused by mainbeam nulling. Design examples are presented to explicitly ascertain the accuracy of the proposed technique in estimating the true target angle. [C1047]

#### "Scaling radar measurements for advanced algorithms"

This paper describes waveform diverse signal measurements using a two channel laboratory radar system. Using a combination of a Lab-Volt™ radar training system, Tektronix™ arbitrary waveform generator (AWG), Tektronix™ digital oscilloscope (DSO), and Tektronix™ real-time spectrum analyzer (RSA), a two channel, waveform diverse, multiple-input, multiple-output (MIMO) system is configured to collect both MIMO and bistatic radar measurements. In the experiments, the radar operates at X-band and samples the echoes at radio frequency (RF) before down-conversion into in-phase and quadrature (I/Q) channels. The laboratory environment does not need any special treatment as an anechoic chamber because the system uses very short duration and low power waveforms. Measured data for the MIMO radar is presented along with discussion of the bistatic configuration. [C1048]

#### "Feature extraction and optimization of representative-slice in ambiguity function for moving radar emitter recognition"

Radar emitter recognition is an important and challenging subject in radar signal analysis and processing. In this work, an ambiguity function (AF) representative-slice based feature extraction and optimization algorithm is presented for unintentional modulation recognition of moving radar emitters. It considers near-zero slices of AF as representative feature set of radar emitters, which not only coincides with the characteristics of real radar signals, but also mitigates the computation problem and avoids undesired cross terms in existing AF based method. Direct Discriminant Ratio (DDR) criterion is further utilized to preserve the most discriminant features and boost recognition accuracy, by ranking the kernel points along the representative-slice. Experimental results validate the practical usefulness and high stability of the proposed approach on real data of moving radar emitters, as well as synthetic radar data from U.S. Naval Research Laboratory. [C1049]

#### "Exponentially embedded families for multimodal sensor processing"

The exponential embedding of two or more probability density functions (PDFs) is proposed for multimodal sensor processing. It approximates the unknown PDF by exponentially embedding the known PDFs. Such embedding is of a exponential family indexed by some parameters, and hence inherits many nice properties of the exponential family. It is shown that the approximated PDF is asymptotically the one that is the closest to the unknown PDF in Kullback-Leibler (KL) divergence. Applied to hypothesis testing, this approach shows improved performance compared to existing methods for cases of practical importance where the sensor outputs are not independent. [C1050]

#### "Proportionate-type NLMS algorithms based on maximization of the joint conditional PDF for the weight deviation vector"

In this paper, we present a proportionate-type normalized least mean square algorithm which operates by choosing adaptive gains at each time step in a manner designed to maximize the joint conditional probability that the next-step coefficient estimates reach their optimal values. We compare and show that the performance of the joint maximum conditional probability density function (PDF) one-step algorithm is superior to the proportionate normalized least mean square algorithm when operating on a sparse impulse response. We also show that the new algorithm is superior to a previously introduced algorithm which assumed that the conditional PDF could be

represented by the product of the marginal conditional PDFs, i.e., that the weight deviations are mutually conditionally independent. [C1051]

#### "Multipath exploitation with adaptive waveform design for tracking in urban terrain"

We integrate multipath exploitation with adaptive waveform design in order to increase the tracking performance of a vehicle moving in urban terrain. Mitigation of both clutter and strong multipath returns can result in increased target detection. However, exploiting multiple bounces from obstacles such as buildings can be shown to increase radar coverage and scene visibility, especially in the absence of direct line-of-sight paths. For this purpose, we formulate the multipath propagation of an arbitrary number of specular bounces in urban terrain for three-dimensional motion. We then further exploit and optimize multipath returns by dynamically selecting the parameters of the transmitted waveform to minimize the predicted mean-squared tracking error. We demonstrate our proposed approach in a realistic urban environment by varying the type of measurement to include regions of obscuration and different number of multipath bounces. [C1052]

#### "A robust detector for uniformly distributed noise"

This paper proposes a robust detector for detection of known signals in impulsive noise environments. The distribution of the noise is assumed to be a mixture of Laplacian distribution giving a sharp peak around the true value of the signal of interest and uniform distribution modeling the contributions of completely unknown noise. This type of noise appears in problems related to estimated pitch periods. In the paper we derive a robust detector for this noise model and analyze its performance. [C1053]

#### "Performance analysis of the GLRT-based array receivers for the detection of a known signal corrupted by noncircular interference"

This paper presents a performance analysis of likelihood ratio test (LRT)-based and generalized likelihood ratio test (GLRT)-based array receivers for the detection of a known signal corrupted by a potentially noncircular interference. Studying the distribution of the statistics associated with the LRT and GLRT, expressions of the probability of detection (PD) and false alarm (PFA) are given. In particular, an exact closed-form expression of PD and PFA are given for two LRT-based receivers and asymptotic (with respect to the data length) closed-form expression are given for PD and PFA for four GLRT-based receivers. Finally illustrative examples are presented in order to strengthen the obtained results. [C1054]

#### "Statistical Resolution Limit for multiple parameters of interest and for multiple signals"

The concept of Statistical Resolution Limit (SRL), which is defined as the minimal separation to resolve two closely spaced signals, is an important tool to quantify performance in parametric estimation problems. This paper generalizes the SRL based on the Cramer-Rao bound to multiple parameters of interest per signal and for multiple signals. We first provide a fresh look at the SRL in the sense of Smith's criterion by using a proper change of variable formula. Second, based on the Minkowski distances, we extend this criterion to the important case of multiple parameters of interest per signal and to multiple signals. The results presented herein can be applied to any estimation problem and are not limited to source localization problems. [C1055]

#### "A closed-form pseudolinear estimator for geolocation of scanning emitters"

A closed-form solution for scanning emitter localization has been available for the case of three sensors. For more than three sensors the traditional approach is to employ the maximum likelihood estimator, which is a nonlinear estimator with no closed-form solution. This paper develops a new closed-form pseudolinear estimator for passive localization of scanning emitters for four or more sensors. The proposed estimator achieves localization performance on par with the maximum likelihood estimator at a much reduced complexity and free from stability problems that plague iterative numerical methods for finding the maximum likelihood estimate. The new estimator is based on a modification of the pseudolinear estimator for bearings-only localization. The superior performance of the developed estimator is illustrated with numerical examples. [C1056]

#### "Distributed TDoA estimation for wireless sensor networks"

A novel distributed TDoA (Time-Difference-of-Arrival) estimation method for wireless sensor networks (WSN) is proposed in this letter. Linear frequency modulation (LFM) waves are emitted from two anchors simultaneously to create an interference field. Through the frequency measurement of local RSSI (Received Signal Strength Indication) signal, the TDoA is estimated independently at each sensor to detect range difference from the sensor to the two anchors. Furthermore, an extended method applied to mobile sensors is also presented. The proposed method only relies on radio transceivers and requires no time synchronization for sensors. Simulations

results demonstrate the effectiveness of our method. [C1057]

#### **"A sparsity-driven joint image registration and change detection technique for SAR imagery"**

This paper presents a novel Sparsity-driven joint Image REgistration and Change Detection (SIRE-CD) technique for SAR imagery. The proposed algorithm simultaneously performs two main tasks: (i) locally register the test and reference images; and (ii) perform the change detection between the two. The key innovative concept here is the sparsity-driven transformation of the signatures from the reference image to match to those of the test image at the local image patch level. In other words, we are constructing a large dictionary from the reference data and use that to find the sparsest representation that best approximates the new incoming test data. The accuracy level of the approximation determines the detected changes between the reference and the test image. We demonstrate the performance of this technique using both simulated data and real SAR imagery from the Army Research Laboratory ultra-wideband (UWB) SAR forward-looking radar. [C1058]

#### **"Single antenna time reversal detection of moving target"**

This paper is concerned with a moving target detection using time reversal in dense multipath environments. We show that the Doppler shift in the time reversal re-transmission simplifies the detector design, yet still achieves the focusing effect. Thus, the Doppler diversity is utilized to achieve high target detectability by time reversal. [C1059]

#### **"Feature extraction in Through-the-Wall radar imaging"**

This paper deals with the problem of automatic target classification or Through-the-Wall radar imaging. The proposed scheme considers stationary objects in enclosed structures and works on the SAR image rather than the raw data. It comprises segmentation, feature extraction based on superquadrics, and classification. We present a recursive splitting tree to obtain optimum parameters for feature extraction. Support vector machines and nearest neighbor classifiers are then applied to successfully classify among different indoor targets. The classification methods are tested and evaluated using real data generated from synthetic aperture Through-the-Wall radar imaging experiments. [C1060]

#### **"Distributed target detection in Through-the-Wall Radar Imaging using the bootstrap"**

The problem of distributed detection and decision fusion in Through-the-Wall Radar Imaging (TWRI) is considered. We deal with the multi-viewing case in which images corresponding to different radar locations can be collected. We present a method to adapt conventional distributed detection schemes to the scenario when no a priori knowledge about image statistics from any view is available. Further, a new scheme for estimating quality information of local detectors in a distributed detection scenario is proposed. We apply bootstrap techniques to draw inference from the radar measurements of the behind the wall scene. Simulation results as well as experimental data are used to demonstrate the performance of the proposed approach. [C1061]

#### **"Multi-target tracking using multi-modal sensing with waveform configuration"**

We investigated the joint multi-modal operation of the asymmetric character of the fields of view of radar and electro optical (EO) sensors for multi-target tracking applications. We proposed a joint multi-modal sensing mode based on using dynamic agility selection to optimize the tracking performance of multiple maneuvering targets. The proposed method jointly designs waveforms for radar sensing and resolution switching modes for EO sensing, when both sensor measurements experience high false alarm rates. Rao-Blackwellized particle filtering is used to track an unknown number of targets within an adaptive framework that yields the optimized joint sensor configuration. We demonstrated the performance of the proposed adaptive tracking system using numerical simulations. [C1062]

#### **"Multichannel SAR Autofocus using multiple low-return constraints"**

MultiChannel Autofocus (MCA) and Reversed-step MCA (RMCA) for Synthetic Aperture Radar (SAR) assume a region of low return in the focused data, and work best when the region is known accurately. In practice, the returns from within the side-lobes of the antenna footprint are highly attenuated; thus a region of highly-probable low returns is provided. However, scene-dependent features like strong reflectors in the presumed low-return region may violate the assumptions underlying MCA and RMCA, with resulting performance degradation. We consider such a scenario and propose scene-independent, random selection methods of the low-return constraints. Our simulation results show that a well-focused image can be obtained within a few trials, even when the number of anomalies is moderately large. [C1063]



### "Bandwidth-intensive FPGA architecture for multi-dimensional DFT"

Multi-dimensional (MD) Discrete Fourier Transform (DFT) is a key kernel algorithm in many signal processing algorithms, including radar data processing and medical imaging. Although there are many efficient software solutions, they are not suitable for applications that require fast response time. In this paper we focus on FPGA-based implementation of MDDFT. The proposed architecture is based on a decomposition algorithm that takes into account FPGA resources and the characteristics of off-chip memory access, namely, the burst access pattern of the Synchronous Dynamic RAM (SDRAM). The architecture can support 2D, 3D, and even higher dimensional DFT with high performance. It has been implemented on a Xilinx Virtex-5 FPGA platform and its performance for 2D and 3D DFT measured and analyzed. [C1064]

### "Step-frequency radar with compressive sampling (SFR-CS)"

This paper proposes a novel radar system, namely step-frequency with compressive sampling (SFR-CS), that achieves high target range and speed resolution using significantly smaller bandwidth than traditional step-frequency radar. This bandwidth reduction is accomplished by employing compressive sampling ideas and exploiting the sparseness of targets in the range-speed space. [C1065]

### "Radar HRRP statistical recognition with Local Factor Analysis by automatic Bayesian Ying Yang harmony learning"

Radar high-resolution range profiles (HRRPs) are typical high-dimensional non-Gaussian and inter-dimensional dependently distributed data, the statistical modelling of which is a challenging task for HRRP based target recognition. Considering the inter-dimensional dependence, a recent work applied Factor Analysis (FA) to model radar HRRP data and showed promising recognition results, which however still restricts to Gaussian distribution. This paper aims to simultaneously consider the inter-dimensional dependence and the non-Gaussian distribution, by using Local Factor Analysis (LFA) model. For not only learning parameters but also appropriately selecting the component number and local hidden dimensionalities, we adopt the automatic Bayesian Ying-Yang (BYY) harmony learning, in order to relieve the extensive computation and inaccurate evaluation encountered in the conventional two-phase implementation. Moreover, a heuristic aspect-frame partition is implemented based on the BYY harmony criterion rather than AIC or BIC in the previous work, to tackle the radar HRRP's target-aspect sensitivity. Experiments show improved recognition performances over on the same measured HRRP dataset, i.e., for both equal interval and heuristic aspect-frame partitions, LFA automatically learned by BYY always outperforms FA selected by a two-phase procedure with either AIC or BIC. [C1066]

### "Joint sparsity-driven inversion and model error correction for radar imaging"

Solution of inverse problems in imaging requires the use of a mathematical model of the observation process. However such models often involve errors and uncertainties themselves. The application of interest in this paper is synthetic aperture radar (SAR) imaging, which particularly suffers from motion-induced model errors. These types of errors result in phase errors in SAR data which cause defocusing of the reconstructed image. Mostly, phase errors vary only in cross-range direction. However, in many situations, it is possible to encounter 2D phase errors, which are both range and cross-range dependent. We propose a sparsity-driven method for joint SAR imaging and correction of 1D as well as 2D phase errors. This method performs phase error correction during the image formation process and provides focused, high-resolution images. Experimental results show the effectiveness of the approach. [C1067]

### "Synthetic Aperture Radar autofocus via Semidefinite Relaxation"

Synthetic Aperture Radar (SAR) imaging can suffer from image focus degradation due to unknown platform or target motion. Autofocus algorithms use signal processing techniques to remove the undesired phase errors. The recently proposed multichannel autofocus models formulate the problem as the solution to  $Ae^{j\phi} \approx 0$ , where  $A$  is a given matrix and  $\phi$  are the unknown phases. Previous methods approximated  $e^{j\phi}$  using the null vector of  $A$ . We propose to approximate  $e^{j\phi}$  using conic optimization and call this new autofocus algorithm Semidefinite Relaxation Autofocus (SDRA). Experimental results using a simulated SAR image shows that SDRA has promising performance advantages over existing autofocus methods. [C1068]

### "Synthesizing speech from Doppler signals"

It has long been considered a desirable goal to be able to construct an intelligible speech signal merely by observing the talker in the act of speaking. Past methods at performing this have been based on camera-based observations of the talker's face, combined with statistical methods that infer the speech signal from the facial motion captured by the camera. Other methods have included synthesis of speech from measurements taken by

electro-myelo graphs and other devices that are tethered to the talker-an undesirable setup. In this paper we present a new device for synthesizing speech from characterizations of facial motion associated with speech-a Doppler sonar. Facial movement is characterized through Doppler frequency shifts in a tone that is incident on the talker's face. These frequency shifts are used to infer the underlying speech signal. The setup is farfield and untethered, with the sonar acting from the distance of a regular desktop microphone. Preliminary experimental evaluations show that the mechanism is very promising-we are able to synthesize reasonable speech signals, comparable to those obtained from tethered devices such as EMGs. [C1069]

#### "Cramér-Rao lower bound for time reversal range estimators in N-multipath scattering environments"

As an improvement to the conventional radar range estimation based on a single forward propagation of the probing signal, the paper presents a time reversal (TR) based range estimation technique for radar tracking applications and develops the Cramer-Rao lower bounds (CRLB) for the conventional and TR range estimators in an N-multipath scattering environment, where N may assume any value. The CRLBs quantify possible improvement offered by the TR range estimator over the conventional approach. Stronger secondary multipath improves the performance of the TR range estimator as its CRLB decreases with a higher number of multipaths. [C1070]

#### "Sensitivity to basis mismatch in compressed sensing"

Compressed sensing theory suggests that successful inversion of an image of the physical world from its modal parameters can be achieved at measurement dimensions far lower than the image dimension, provided that the image is sparse in an a priori known basis. The assumed basis for sparsity typically corresponds to a gridding of the parameter space, e.g., an DFT grid in spectrum analysis. However, in reality no physical field is sparse in the DFT basis or in an a priori known basis. No matter how finely we grid the parameter space the sources may not lie in the center of the grid cells and there is always mismatch between the assumed and the actual bases for sparsity. In this paper, we study the sensitivity of compressed sensing (basis pursuit to be exact) to mismatch between the assumed and the actual sparsity bases. Our mathematical analysis and numerical examples show that the performance of basis pursuit degrades considerably in the presence of basis mismatch. [C1071]

#### "Physical Layer Techniques for Enhanced Situational Awareness"

Wireless devices are being developed that can scan spectrum to take advantage of spectrum opportunities for enhanced communication. For these devices to communicate better, it is desirable that they have an awareness of their setting. In this paper, we present a collection of techniques, which we call PLATEAU: Physical Layer Techniques for Enhanced Situational Awareness, which leverages physical layer properties from existing signals to gain an accurate picture of a device's environment as well as understanding of that device's mobility. We show through experiments using measurements from a software defined radio that, by utilizing radar and machine learning signal processing, a device can make more informed operational decisions. [C1072]

#### "Blind source extraction of cyclostationary sources with common cyclic frequencies"

A new method for blind source extraction of cyclostationary sources is presented. It is assumed that the cycle frequencies of the sources are known a priori and some of the sources have common cycle frequencies. Necessary and sufficient conditions are introduced and Jacobi method for diagonalization of complex matrices is used to find the estimations. The proposed algorithm is applied to simulated data, and effectiveness and performance of the algorithm are verified. [C1073]

#### "Constant envelope waveform design for MIMO radar"

A method for generating constant envelope (CE) waveforms to realise a given covariance matrix for a closely spaced MIMO radar system is proposed. In contrast to available algorithms, the technique provides closed form solutions for finding the required waveforms and suggests that waveforms can be chosen from finite alphabets such as binary-phase shift keying (BPSK) and quadrature-phase shift keying (QPSK). Gaussian random-variables (RV's) are mapped onto CE non-Gaussian RV's using memoryless non-linear functions. The relationship between the correlation of Gaussian RV's at the input to the nonlinear functions and non-Gaussian RV's at their output is established. Simulation results are presented to demonstrate the effectiveness of the methodology. [C1074]

#### "A ternary pulse compression code: Design and application to radar system"

In this paper, we present new developed ternary code-punctured binary sequence-pair, give its definitions and

the autocorrelation properties. We also investigate Doppler shift performance of the proposed code. The significant advantages of this ternary codes over conventional pulse compression codes, such as the widely used Barker codes, are zero autocorrelation sidelobes and the longer length of the code which can be as long as 31 so far. We apply our new ternary codes to radar system for target detection and observe that our codes outperform some other conventional pulse compression codes. [C1075]

#### "Through-the-Wall Radar Imaging using compressive sensing along temporal frequency domain"

There are increasing demands on Through-the-Wall Radar Imaging (TWRI) systems to deliver high resolution images in both range and cross range. This requires using wideband signals and large array apertures, respectively. Wideband signals are typically implemented by transmitting a series of the narrowband signals. As such, the TWRI system operation involves transmitting and receiving multiple step-frequencies at each antenna location in either a physical or a synthetic aperture radar. Compressive sensing (CS) is an effective approach for decreasing the number of samples and, subsequently, reducing the data acquisition and post-processing time. In this paper, we propose a TWRI scheme based on CS in which a sizable reduction in the number of samples along the frequency axis is achieved without significant degradation in the image. The proposed approach applies the well-known Fourier-like measurement matrix and generates radar images of almost the same desirable quality as the image employing all data samples. [C1076]

#### "MIMO radar detection under phase synchronization errors"

We consider the problem of target detection for coherent multi-input multi-output (MIMO) radar with widely separated antennas in the presence of phase synchronization mismatch between the transmitter and receiver pairs. First, we introduce a data model using von-Mises distribution to represent the phase error terms. Then we employ expectation-maximization algorithm to estimate the error distribution parameter and target returns as well as the noise variance. We develop a generalized likelihood ratio test (GLRT) target detector using these estimates and demonstrate the effect of phase uncertainties on the detection performance using Monte Carlo simulations. [C1077]

#### "Slow-time multi-frequency radar for target detection in multipath scenarios"

We propose a method to detect a target in the presence of multipath reflections, employing sequential transmission of multiple frequencies in a slow-time (pulse-to-pulse) approach. First, we develop a parametric measurement model that accounts for the multipath components at multiple frequencies as well as Doppler shifts. Then, we develop a statistical detection test and analytically evaluate its performance characteristics. Based on the performance analysis, we propose an adaptive algorithm to select the best combination from a subset of frequencies that maximizes the detection performance. Our numerical examples show that the sequential approach requires more coherent pulses to match the performance of the simultaneous usage of multiple carriers in OFDM format. We also study the extent of performance degradation due to employing a subset of available frequencies. [C1078]

#### "Design and implementation of a passive UHF RFID-based Real Time Location System"

A passive Ultra-High Frequency (UHF) Radio Frequency Identification (RFID) based Real Time Locating System (RTLS) is presented in the paper. For the validation, a reader has been developed and complemented with a tag modulator to form a complete UHF RFID-based real time locating system focused on backscattering communication. PN sequences have been used to measure the TOA and estimate the distance between reader and tag. A TX-to-RX leakage canceller has been applied in the reader RF front-end to increase the isolation and enhance the sensitivity. Measurement results indicate that the estimation accuracy in real time is about 1.6 meters and the mean estimation error of 1000 times' measurement in 1 second is less than 0.5 meter. [C1079]

#### "Cramér-Rao bound for time reversal active array direction of arrival estimators in multipath environments"

In this paper, we study the Cramer-Rao bound (CRB) for time reversal (TR) based direction of arrival (DOA) estimators operating in a rich multipath environment. Our setup is based on an array of active antennas capable of estimating the range and DOA of a passive target. We derive an analytical expression for the CRB of the TR/DOA estimator and compare it with that of the conventional DOA estimator by expressing the two CRBs in terms of the multipath parameters (multipath's attenuations and delays). Our analytical results are verified by running Ground Penetrating Radar (GPR) simulations using the electromagnetic Finite Difference Time Domain (FDTD) models. Our simulations illustrate the potential of superior performance with gains of up to 15 dB possible with the TR/DOA estimator over the conventional approach. [C1080]

### "Analytical performance assessment for multi-dimensional Tensor-ESPRIT-type parameter estimation algorithms"

Subspace-based high-resolution parameter algorithms such as ESPRIT, MUSIC, or RARE are known as efficient and versatile tools in various signal processing applications including radar, sonar, medical imaging, or the analysis of MIMO channel sounder measurements. Since these techniques are based on the singular value decomposition (SVD), their performance can be analyzed with the help of SVD-based perturbation theory. Recently we have demonstrated that in the  $R$ -dimensional case ( $R \geq 2$ ), the estimation accuracy of these schemes can be improved by replacing the measurement matrix by a measurement tensor and the SVD by the Higher-Order SVD (HOSVD). In case of ESPRIT, this gives rise to the family of Tensor-ESPRIT algorithms, e.g., standard Tensor-ESPRIT and Unitary Tensor-ESPRIT. In this paper we derive the analytical performance for Tensor-ESPRIT-type algorithms via a recently introduced perturbation theory for the HOSVD-based signal subspace estimate. All expressions are asymptotic in the SNR, but not in the sample size. We first present the explicit equations as a function of the current noise realization, where no assumption on the statistics of symbols or noise are required. Next, we show the result of performing statistical expectation over white Gaussian noise. To demonstrate the usefulness of the results we also present a compact expression for the asymptotic efficiency in the case of a single source, which is only a function of the array size. [C1081]

### "Knowledge-aided Bayesian covariance matrix estimation in compound-Gaussian clutter"

We address the problem of estimating a covariance matrix  $R$  using  $K$  samples  $z_k$  whose covariance matrices are  $\tau_k R$ , where  $\tau_k$  are random variables. This problem naturally arises in radar applications in the case of compound-Gaussian clutter. In contrast to the conventional approach which consists in considering  $R$  as a deterministic quantity, a knowledge-aided (KA) approach is advocated here, where  $R$  is assumed to be a random matrix with some prior distribution. The posterior distribution of  $R$  is derived. Since it does not lead to a closed-form expression for the minimum mean-square error (MMSE) estimate of  $R$ , both  $R$  and  $\tau_k$  are estimated using a Gibbs-sampling strategy. The maximum a posteriori (MAP) estimator of  $R$  is also derived. It is shown that it obeys an implicit equation which can be solved through an iterative procedure, similarly to the case of deterministic  $\tau_k$ s, except that KA is now introduced in the iterative scheme. The new estimators are shown to improve over conventional estimators, especially in small sample support. [C1082]

### "Energy-efficient, decision feedback equalization Using SAR-like capacitive charge summation"

A capacitive charge-sharing, decision feedback equalization (DFE) circuit is presented for use in high-speed serial link receivers. Similar to the capacitive DAC (digital-analog converters) used in successive approximation-based ADCs (analog-digital converters), the proposed one-tap DFE with half-rate quantizer demultiplexing operates at 4Gbps, consuming 0.32 mW from a 1-V supply, excluding clock power. The proposed architecture, scalable to a large number of filter taps, shows considerable advantage in regards to energy efficiency over conventional, current-switched structures. [C1083]

### "Design of intelligent node based on distributed hybrid net control system"

TMS320F2182 DSP chip is applied in the design of intelligent node hardware, and the embed system design method, Microsoft Message Bus and modularization technique are adopted in the realization of intelligent node. The paper gives the software design method of intelligent node based on CAN Bus. The data collected by intelligent node can be transmitted to computer in real time, and the distributed control system based on CAN Bus and GPRS presents the characters such as safety, real-time and economic, which is worth applying in process control field. [C1084]

### "Pulse radar altimeter terrain return model and its simulation"

A simulation model for pulse radar altimeter video echo is proposed, the calculation of all parameters in this simulation model and the correlative arithmetic of echo simulation based on this model are discussed in detail. The simulation is completed with the using of real digital elevation graphs as data source. The results shows the validity of the proposed model and simulation method. [C1085]

### "ARM9-based real-time acquisition of orchard soil information and GPRS wireless transmission control system"

This paper presents a new ARM+GPRS structure which can apply in the orchard soil information collection and transmission. It is a design of data acquisition and wireless transmission control system based on ARM9 with a microprocessor chip S3C2410, it is used for orchard soil realtime acquisition, data transmission and control



between upper and lower computers through GPRS module. It describes that how the hardware platform works and how to accomplish the design by software. The hardware platform consists of core processor, orchard soil data acquisition module and GPRS communication module. It has been proved by experiments that the system has features of small size, high performance, real-time and low-cost. [C1086]

#### **"A fast phase unwrapping algorithm based on minimum discontinuity by blocking"**

Two-dimensional phase unwrapping is one of the key problems in many signal processing applications. Flynn's minimum discontinuity phase unwrapping is one of the algorithm which can solve many different kinds of phase unwrapping problems successfully, but its computation efficiency is too low. To overcome this drawback, a blocked minimum discontinuity phase unwrapping algorithm is proposed. In the proposed algorithm, the wrapped phase image is tessellated into small blocks. Each block is unwrapped separately by minimum discontinuity phase unwrapping algorithm, and then the unwrapped blocks are merged together using minimum discontinuity approach again. The merging process has been divided into two steps. The discontinuities between the blocks are minimized firstly, and then the unwrapped image is taken as a whole to minimize the total discontinuities. This proposed algorithm is described in detail and tested on an IFSAR experimental wrapped phase image and the Etna wrapped image. Results show that the proposed algorithm works well and is more efficient than the Flynn's minimum discontinuity algorithm. [C1087]

#### **"An embedded wireless transmission system based on the extended user datagram protocol (EUDP)"**

As the application of embedded wireless communication system spreads fast in many fields, it is becoming a significant problem to obtain both high speed and reliability during the transmission of large amounts of data. This paper extends the traditional UDP protocol by adding the mechanism of package sequencing and accumulative retransmission, so as to combine the speed of UDP protocol and the reliability of the extended upper protocol and build an embedded system for transmitting large amounts of data quickly and reliably. The system is designed based on STM32 microcontroller and wireless module. Through the General Packet Radio Service (GPRS), the system can communicate both data and instructions with the remote control center via Internet. Experimental results reveal that the extended UDP protocol (EUDP) reduces the transmission delay significantly compared with the usual TCP protocol, while ensuring a considerable degree of reliability. Thus the system is ideal for transmitting large amounts of data in real time. [C1088]

#### **"The denoising method of SAR image based on Retinex"**

The traditional SAR image denoising methods are not considered a shadow of image, but the shape of shadow is used for recognition. In order to take full use of SAR image dark areas information, the method of SAR image noising based on Retinex is proposed. Firstly, SAR image is decomposed into irradiated SAR image and reflected SAR image based on Retinex model; secondly, the decomposed irradiated SAR image carries through NSCT and threshold select according to context, then NSCT inverse transform; thirdly, reflected SAR image carries through NSCT, and the dark areas information and non-dark areas information are obtained by image binarization processing to irradiated SAR image according to certain threshold value. Bilateral filtering to dark areas information and context threshold select to non-dark areas information, then NSCT inverse transform; at last, image synthesizes according to Retinex model. The method takes full use of SAR image dark areas information, and the simulation results show that the denoising effects of the method is better than other methods. [C1089]

#### **"MAP-PF wideband multitarget and colored noise tracking"**

The maximum a posteriori penalty function (MAP-PF) approach is applied to tracking the bearing and bearing rate of multiple wideband sources in unknown colored noise. The track estimation problem is formulated directly from the array data using the maximum a posteriori (MAP) estimation criterion. The penalty function (PF) method of nonlinear programming is used to obtain a tractable solution. A sequential update procedure is developed in which penalized maximum likelihood estimates of target bearings, spectra, and noise parameters are computed and then used as synthetic measurements in a set of Kalman filter trackers. The two steps are coupled via the penalty function. During parameter estimation, the penalty function prevents erroneous outlier estimates which can cause the tracker to lose track. During the tracking step, it determines the influence of the parameter estimates on the final track estimates by adaptively adjusting the measurement error variance. Performance is demonstrated on a typical sonar scenario. [C1090]

#### **"A new Fractional Fourier Transform based monopulse tracking radar processor"**

Conventional monopulse radar processors are used to track a target that appears in the look direction beam



width. The distortion produced when additional targets appear in the look direction beam width can cause severe erroneous outcomes from the monopulse processor. This leads to errors in the target tracking angles that may cause the target tracker to fail. A new signal processing algorithm is presented in this paper that is based on the use of optimal Fractional Fourier Transform (FrFT) filtering to solve this problem. The relative performance of the new filtering method over traditional based methods is assessed using standard deviation angle estimation error (STDAE) for a range of simulated environments. The proposed system configurations with the optimum FrFT filters succeeds in effectively cancelling additional target signals appearing in the look direction beam width.

[C1091]

#### "Radar-based human detection via orthogonal matching pursuit"

Many current radar-based human detection systems employ some type of Doppler or Fourier-based processing, followed by spectrogram and gait analysis to classify detected targets. However, Fourier-based techniques inherently assume a linear variation in target phase over the aperture, whereas human targets have a highly nonlinear phase history. This mismatch leads to significant loss in SNR and integration gain. In this paper, an Enhanced Optimized Non-Linear Phase (EnONLP) detector is proposed that employs a dictionary to store possible target returns generated from the human model for each combination of parameter values. An orthogonal matching pursuit algorithm is used to compute a sparse approximation to the radar return that is optimal in the least squares sense. Performance of the EnONLP algorithm is compared to that of a parameter-estimation based algorithm and conventional, fully-adaptive STAP. [C1092]

#### "Bayesian Rao and Wald test for radar adaptive detection"

This paper deals with the adaptive detection of a signal of interest in the presence of Gaussian noise with unknown covariance matrix (CM). To this end, we resort to a Bayesian approach based on a suitable model for the probability density function (PDF) of unknown CM. Under this assumption, the maximum a-posteriori (MAP) estimation of CM is derived. The MAP estimate is in turn used to yield Bayesian version of Rao and Wald test. And the importance of the a priori knowledge can be tuned through scalar variable. Remarkably the devised detectors outperform Kelly's GLRT and non Bayesian Rao and Wald test in the presence of strongly heterogeneous scenarios (where a very small number of training data is available). Meanwhile, the coincidence of Bayesian GLRT and Wald test is proved. [C1093]

#### "Multiple-frequency interferometric velocity SAR location and imaging of elevated moving target"

Locations of moving targets in synthetic aperture radar (SAR) images are determined not only by their geometric locations but also by their velocities that cause their SAR images defocused, smeared, and mis-located. With a linear antenna array, velocity synthetic aperture radar (VSAR) can detect, focus, and locate slowly moving targets well. However, it may mis-locate fast moving targets in the azimuth (cross-range) direction, and sometimes even in the ground range direction if the targets are elevated above the ground. In this paper, we propose an antenna array approach with cross-track interferometry, in which multiple wavelength signals are transmitted. It is shown that our proposed multiple-frequency interferometric velocity SAR (MFin-VSAR) can locate both slowly and fast moving elevated targets correctly. [C1094]

#### "Target detection in MIMO radar in the presence of Doppler using complementary sequences"

In this paper, we present a method for detecting a point target using multiple antennas when the relative motion between the receivers and the target induces a non-negligible Doppler shift. As a key illustrative example, we consider a 4x4 system employing a unitary matrix waveform set, e.g., formed from Golay complementary sequences. When a non-negligible Doppler shift is induced by the target motion, the wave-form matrix formed from the complementary sequences is no longer unitary, resulting in significantly degraded target range estimates. To solve this problem, we adopt a subspace based approach exploiting the observation that the receive matrix formed from matched filtering of the reflected waveforms has a (non-trivial) null-space. Through processing of the waveforms with the appropriate vector from the null-space, we can significantly improve the detection performance. We provide simulation results to confirm the theoretical analysis. [C1095]

#### "Iterative design of MIMO radar transmit waveforms and receive filter bank"

In this paper, we propose an iterative design approach to jointly optimize probing signal waveforms and a receive filter bank for a multiple-input multiple-output (MIMO) radar under a constant modulus constraint. The design goals are to approximate a desired beampattern and to minimize the auto-/cross- correlation levels of the probing signal waveforms for different time lags and between different spatial angles. Since the overall design problem is nonconvex, we propose to optimize the transmit probing signals and receive filter bank separately and alternately. The optimization of receive filter bank is a standard least squares problem, while the optimization of

the constant modulus transmit signal waveforms is a norm-constrained least squares problem which can be approximately solved using a low-rank semidefinite relaxation procedure. We demonstrate the effectiveness of our proposed approach through a simulation example. [C1096]

#### "Robust MIMO radar detection for correlated subarrays"

Previously, the well-known Optimum Gaussian Detector (OGD) has been extended to the Multiple-Input Multiple-Output (MIMO) case where all transmit-receive subarrays are considered jointly as a system such that only one detection threshold is used. In this extension, all subarrays have been assumed to be widely separated and the transmitted waveforms are assumed to be orthogonal. However, the necessary separation needed for each subarray to be uncorrelated depends on several factors and it might not be possible to ensure that this condition is always respected, especially in the case of moving platforms. Moreover, perfectly orthogonal waveforms do not exist. Hence, we consider in this paper, a new robust MIMO detector that is able to maintain the same Probability of False Alarm (Pfa) regardless of the correlation between the subarrays. [C1097]

#### "Fixed-point based autoregressive parameter estimation for space time adaptive processing"

Space time adaptive processing (STAP) is useful in radar processing to detect a target by filtering the clutter and the additive thermal noise. A derived version based on a multichannel autoregressive (M-AR) model of the clutter has the advantage of reducing the computational cost. Nevertheless, the estimation of the AR matrix parameters is a key issue because the clutter is not Gaussian in real cases. When dealing with an off-line solution, the multichannel least squares method (MLS) can be considered, but the estimation of the disturbance covariance matrix is required. In this paper, we suggest using the so-called fixed point method since it has "matrix- and texture-constant false alarm rate" property (matrix-CFAR and texture-CFAR) and it provides an unbiased and consistent estimate in a non-Gaussian case. A comparative study is then carried out between off-line M-AR based STAP methods and it points out the relevance of the solution we propose. [C1098]

#### "The role of the ambiguity function in compressed sensing radar"

As is clear from the ambiguity function (AF) uncertainty principle and the underlying matched filtering operation, pulse compression (PC) radars cannot accurately and simultaneously measure both the time delay and Doppler shift of moving targets. On the other hand, compressed sensing (CS) radar would seem to be emerging as a means to do just that, jointly to estimate the delay and Doppler shift, through convex optimization instead of matched filtering, such that PC resolution limits no longer apply. However, it turns out that the AF is closely related to the CS "dictionary coherence coefficient," which affects the optimization recoverability. In this paper we formalize this relationship. [C1099]

#### "Knowledge-aided reduced-rank STAP for MIMO radar based on joint iterative constrained optimization of adaptive filters with multiple constraints"

In this paper, a reduced-rank knowledge-aided technique for MIMO radar space-time adaptive processing (STAP) design is proposed. We focus on the advantage of MIMO radars in achieving better spatial resolution by employing the colocated antennas. The scheme is based on knowledge-aided constrained joint iterative optimization of adaptive filters (KAC-JIOAF) and takes advantage of the a priori covariance matrix by employing additional linear constraints in the design. A recursive least squares (RLS) implementation is derived to reduce the computational complexity. We evaluate the algorithm in terms of signal-to-interference-plus-noise ratio (SINR) and probability of detection PD performance and compare it with the state-of-the-art reduced-rank algorithms. Simulations show that the proposed algorithm outperforms existing reduced-rank algorithms. [C1100]

#### "Knowledge-aided STAP algorithm using convex combination of inverse covariance matrices for heterogeneous clutter"

Knowledge-aided space-time adaptive processing (KA-STAP) algorithms, which incorporate a priori knowledge into radar signal processing methods, have the potential to substantially enhance detection performance while combating heterogeneous clutter effects. In this paper, we develop a KA-STAP algorithm to estimate the inverse interference covariance matrix rather than the covariance matrix itself, by combining the inverse of the covariance known a priori,  $R_0^{-1}$ , and the inverse sample covariance matrix estimate  $R^{-1}$ . The computational load is greatly reduced due to the avoidance of the matrix inversion operation. We also develop a cost-effective algorithm based on the minimum variance (MV) criterion for computing the mixing parameter that performs a convex combination of  $R_0^{-1}$  and  $R^{-1}$ . Simulations show the potential of our proposed algorithm, which obtain substantial performance improvements over prior art. [C1101]

### "Performance analysis of a Robust Low-Rank STAP filter in low-rank Gaussian clutter"

In this paper, we consider that the disturbance of a STAP system is composed of a low-rank Gaussian clutter and a white Gaussian noise. From this model, the theoretical SNR Loss of a Robust Low-Rank STAP filter based on the Normalized Sample Covariance Matrix is derived by means of a perturbation analysis. Theoretical results are shown to be in good agreement with simulations for a realistic STAP configuration. Our analysis extends previous result on the SNR loss of Low-Rank STAP filtering based on the Sample Covariance Matrix. [C1102]

### "Angle-Doppler processing using sparse regularization"

The detection of moving objects on the ground by airborne radar is one application of space-time adaptive processing (STAP). The goal is to estimate the position and velocity of objects. This paper considers the problem as a linear inverse problem and uses  $\ell_1$ -norm regularization to promote sparsity in the solution. It is proposed that the angle-Doppler plane be explicitly segmented into the clutter ridge component and a non-clutter-ridge component. We propose that the second component be modeled as sparse-as the moving objects are assumed to be well isolated in the angle-Doppler plane. [C1103]

### "On sand ripple detection in synthetic aperture sonar imagery"

A model for the detection of sand ripples in synthetic aperture sonar (SAS) imagery is proposed. The approach is based on searching for patterns characterized by three highlight-shadow pairs-corresponding to ripple-wave crests and troughs-at different orientations and at different length-scales. The model also provides an estimate of the orientation of any ripples detected. No training data is required as the underlying physical phenomenon of ripples is modeled directly. The promise of the proposed method is demonstrated on five real, measured SAS images, for which a high probability of (ripple) detection is achieved while maintaining a very low false alarm rate. [C1104]

### "Compressive sensing-based SAR tomography"

The problem of imaging multiple scattering components in SAR tomography is addressed in this work. It is proposed to exploit the sparsity of scattering components in the elevation domain by invoking the recently-proposed compressive sensing (CS) theory to achieve the separation of multiple scattering centers with fine elevation resolution. The major advantages of the proposed CS-based method over other conventional methods are evident in single snapshot scenarios with correlated scattering components. The proposed CS-based imaging method for SAR tomography is compared to the conventional MUSIC-based imaging method and the advantages of the proposed method in a variety of imaging scenarios is shown via simulations. [C1105]

### "On the concept of MIMO radar"

Two classes of MIMO radars are briefly considered. MIMO radars with colocated antennas and coded signals represent a new and prospective concept. MIMO Radars with widely separated antennas ("Statistical MIMO radars") are a particular case of well-known Multisite (Multistatic) radar systems. Most results presented by the authors of "Statistical MIMO radars" were obtained under much more general conditions and published many years ago. Besides, ignoring some specific features of radar has led to serious errors. [C1106]

### "Clutter properties for STAP with smooth and faceted cylindrical conformal antennas"

Conformal antennas, which assume the shape of the platform, have several advantages; like reduced weight and space, aerodynamic design and increased field of view. We are interested in detection of moving ground targets with air-borne radar with faceted or smooth vertical half-cylinder or planar antennas with different subarray sizes. We simulate radar systems and study clutter properties which are important for suppressing the clutter with STAP (Space-Time Adaptive Processing), properties by which we can compare the antennas. We use old analysis tools and propose some new which are easy to interpret and draw conclusions from. We find that the faceted and smooth half-cylinder antennas have no significant differences in clutter suppression performance. The plane antenna has poorer performance. The subarray division is more important than the antenna geometry. The number of antenna channels is related to the clutter rank and the clutter fraction of the signal space. [C1107]

### "On the use of HRR data to improve target kinematics estimation: CRLB computation and comparison with simulated results"

An innovative approach to jointly estimate and compensate the radial velocity and acceleration of non-

cooperative targets in HRR (High Range Resolution) processing for a frequency stepped radar has been proposed in. The estimation is performed using different approaches mainly based on the maximization or the minimization of a proper functional (contrast, correlation-like or entropy) of the reconstructed profile. The partial improvement found for the target velocity and acceleration estimation indicates that the three analyzed "cost functions" don't reach ideal performance. Scope of this paper is to quantify the best theoretical achievable performance by means of the Cramer-Rao Lower Bounds (CRLB) and compare the obtained results in with the CRLB. [C1108]

#### **"Adaptive polarization processing for improved detection/classification of stationary targets"**

A new technique for detection of stationary or slow-moving over-resolved targets on the ground, based upon a Hotelling T-squared test/generalized inner product (GIP) approach to signal analysis is presented. This robust detector separates radar returns from interference via a coherent process. This GIP-based processing can be applied to single-receiver channel systems, multiple spatial channel systems, multiple polarization channel systems or systems with multiple spatial and polarization channels. [C1109]

#### **"Optimal block quantization for SAR data"**

A variable bit rate coding scheme designed for new generation SAR satellites is presented. This coding is based on previous schemes of Block Adaptive Quantizer (BAQ) and is intended as a possible improvement over Sentinel-1 FDBAQ. In this project, the number of quantizers is considered a design choice and the optimization is carried out looking for a set of reflectivity classes in which partition all the imaged areas on the Earth. Superior performances to those envisaged for Sentinel-1 FDBAQ are obtained in terms of SNR vs. average rate. Results come from simulations based on a 16-bit mosaic of C band reflectivity obtained by ESRIN from ENVISAT GM data and Wien University database of ENVISAT WSM radar reflectivity. [C1110]

#### **"Space-Range Adaptive Processing for waveform-diverse radar imaging"**

Waveform-diverse radar arrays have been proposed as a method to facilitate single pulse imaging as well as to potentially enable simultaneous multi-mode operation. Transmitting different waveforms on the elements of a uniform linear array consequently raises the spatial and temporal sidelobes of the receiver matched filter. In this paper a recursive minimum mean square error based receiver design denoted as Space-Range Adaptive Processing is presented. The new method is capable of mitigating space range sidelobes thereby providing enhanced sensitivity for this transmission scheme. [C1111]

#### **"The SlimSAR: A small, multi-frequency, Synthetic Aperture Radar for UAS operation"**

The SlimSAR is a small, low-cost, Synthetic Aperture Radar (SAR) and represents a new advancement in highperformance SAR. ARTEMIS employed a unique design methodology that exploits previous developments in designing the Slim-SAR to be smaller, lighter, and more flexible while consuming less power than typical SAR systems. With an L-band core, and frequency block converters, the system is very suitable for use on a number of small UAS's. Both linear-frequency-modulated continuous-wave (LFM-CW), which achieves high signal-to-noise ratio while transmitting with less power, and pulsed mode have been tested. The flexible control software allows us to change the radar parameters in flight. The system has a built-in high quality GPS/IMU motion measurement solution and can also be packaged with a small data link and a gimbal for high frequency antennas. Multi-frequency SAR provides day and night imaging through smoke, dust, rain, and clouds with the advantages of additional capabilities at different frequencies (i.e. dry ground and foliage penetration at low frequencies, and change detection at high frequencies.) [C1112]

#### **"Multistatic measurements in a controlled laboratory environment"**

In recent years, a novel mathematical framework for analyzing and designing multistatic radar systems has been proposed. It was argued through numerous simulation examples that multistatic radar system performances can be significantly improved by shaping the multistatic ambiguity function. Based on this framework, rules for waveform selection, sensor positioning and adequate weighting of different receivers have been developed. In this work, we present multistatic measurements obtained in a controlled laboratory environment to support some of these recent findings and conclusions. The experimental setup consists of a Lab-Volt™ radar system operating at X-band, Tektronix arbitrary waveform generator and Tektronix digital oscilloscope. Multistatic point target radar measurements for different system configurations are analyzed. [C1113]

#### **"Use of reference architectures to achieve low-risk, affordable radar designs"**

The availability of radar reference architectures for software and hardware can enable the development of



affordable radar systems through maximal reuse and low-risk designs. Affordability through reduced design cycle times and efficient integration and test of new radars is crucial to remain competitive and to maintain leadership in developing world-class phased-array radars. Necessary complements to these developments are reusable radar processing algorithms and functions necessary to rapidly synthesize these new radar designs. A compilation of algorithms used by common ground-based and sea-based radar reference architectures is described. Notional radar software and hardware building blocks or "widgets" are also identified. These architectural building blocks can be used to synthesize scalable radar architectures by employing software and hardware reference architectures. This synthesis approach is illustrated by providing examples using two different radar applications. This approach is applicable to all radar systems, in addition to systems-of-systems, where the building architectural blocks are the component system reference architectures. [C1114]

#### "High density FPGA based waveform generation for radars"

Various modulation techniques are usually utilized to enhance the radar performance, or to add more capabilities to the radar that otherwise would not have been possible. Digital generation methods of frequency modulated continuous wave signals include direct waveform synthesis and frequency synthesis. The implementation of waveform generation and upconversion method are described in this paper with a simplified digital implementation technique using FPGAs (Field Programmable Gate Array). The design follows a systematic approach following steps of timing generation from external encoder, baseband modulated waveform generation, upconversion of the waveform to intermediate frequency, filtering and finally frequency synthesis using external DDS (Direct Digital Synthesizer). The design is also capable of generating BITE waveform for test checking in the system. Our design is capable of generation of waveform for stationary as well as non-stationary radars. For non-stationary radars, the waveform is so generated that the doppler effect due to the movement of the radar is compensated. The paper explains more on this. This work mainly focuses on the fact that the total design has been implemented on a single FPGA and the implementation solution utilizes the efficient FPGA resources so as to meet the timings in crucial applications. Moreover, the paper enhances the features of the design with simulation and real time results used to validate the design. [C1115]

#### "A robust estimation method to coregistration error for InSAR interferometric phase"

In this paper, we propose a robust estimation method to coregistration error for synthetic aperture radar interferometry (InSAR) interferometric phase. In the method, the optimal joint data vector is determined, the true steering vector is computed according to the data vector, and then the beamforming technique with the steering vector is used to estimate the InSAR interferometric phase. The method can carry out image coregistration and interferometric phase estimation simultaneously. Theoretical analysis and computer simulation results show that the method can provide accurate estimate of the terrain interferometric phase (interferogram) even when the coregistration error reaches one pixel. [C1116]

#### "ACF-based classification of phase modulated waveforms"

Classification of radar waveform phase modulation based on a sequence of observations is a simple problem complicated by a number of nuisance parameters. Without prior knowledge of waveform carrier frequency, time offset, amplitude, initial phase, and bandwidth, application of a matched filter classifier is not achievable. One must instead rely on waveform features that are invariant to these parameters. This paper presents an invariant feature set for waveform classification. Testing of these features on simulated radar waveforms has illustrated the desired invariance properties and robustness to low signal-to-noise ratio. [C1117]

#### "Ambiguity function of SAR based on OFDM waveform"

Recently many researchers have turned their interests to Orthogonal Frequency Division Multiplexing (OFDM) signal since its promising features in radar. This paper concerns a novel Synthetic Aperture Radar (SAR) system which employs this OFDM signal. Though the OFDM will bring lots of advantages, the performance may be changed since the signal of SAR is different from conventional ones. To evaluate the change, this paper will give a theoretical analysis and the corresponding simulation results from the viewpoint of ambiguity function. This ambiguity function is equivalent to the role of Point Spread Function (PSF) which is often used in SAR for evaluating resolutions. Comparing to the conventional SAR with LFM signal, it is proved that the resolution of SAR based on OFDM is equivalent to the conventional one or even better. This ambiguity function also provides a principle for selecting various OFDM signals as the transmit signal of SAR. [C1118]

#### "Space-time array processing based on ultrawideband throb signal"

Advanced radar and radio communication systems employ space-time array processing to improve performance in terms of detection, resolution, and interference rejection. In this paper, we present the principle of space-time



array processing based on ultrawideband (UWB)-throb signal. Analogous to the well known (delay-Doppler) ambiguity function, a space-time resolution (STR) function is derived and analyzed, by computer simulations, for different signal and array parameters, i. e., pulse width, throb rate, array interelement spacing, and number of array sensors. The structure of the STR function is composed of a narrow mainlobe and low-level sidelobes located on the temporal-angular plane. Antenna energy patterns generated from the STR function clearly demonstrate the dependence of angular resolution on the various signal and array-design parameters. The trade-offs between the various design parameters for achieving high-angular resolution as well as high-temporal resolution are attractive in practice. [C1119]

#### **"Stable filters: A robust signal processing framework for heavy-tailed noise"**

The radar systems of the twenty-first century are being pushed to improve signal detection beyond current capabilities. Current systems perform poorly when the clutter departs from the Gaussian model and becomes heavy-tailed. We introduce stable filters as a general framework for signal processing in heavy-tailed scenarios. The performance gains attainable from these filters can provide significant improvements to digital systems in impulsive noise. Stable filters make use of advanced numerical optimizations to overcome the computational complexity that is common in non-linear approaches. Current performance results show superior performance of stable filters when compared with conventional linear approaches. [C1120]

#### **"Spatially-varying calibration of along-track monopulse synthetic aperture radar imagery for ground moving target indication and tracking"**

In this research, we have developed an algorithm to reduce the residual artifacts of the background clutter (that is, stationary targets) that appear in the MTI imagery that are generated by Global Signal Subspace Difference (GSSD) of the monostatic and bistatic images of an along-track monopulse synthetic aperture radar (SAR) data. We have also established the theoretical foundation for estimating the motion track and parameters of the detected moving targets. We will show the results of these algorithms on measured SAR data. [C1121]

#### **"Characterization of Doppler effects in the context of over-the-horizon radar"**

This paper addresses the problem of the characterization of Doppler effect of maneuvering targets in the context of over-the-horizon radar. The received signal has a complex Doppler structure which is composed of several arrivals, each corresponding to a particular path. In essence, it consists of several close time-frequency components with non-linear signatures in the time-frequency domain. The nonlinearities are the projections of the target's motion vectors on the propagation paths. Estimating the time-frequency contents of all paths reveals the Doppler effects characterizing the target's trajectory. Analysis of such signals in the presence of strong clutter requires effective non-stationary signal processing techniques. In this paper, we propose a new technique based on local analysis of the phase information using warped high-order ambiguity function. The results depict resolvable multipath estimates which are very close to the ground truth. [C1122]

#### **"Analysis of sea clutter distribution variation with Doppler using the compound k-distribution"**

Sea clutter is the backscattered returns received by a radar system from the sea surface. Maritime radar signal processing has the ability to partially compensate for clutter to achieve effective detection of targets on or near the sea surface. This paper investigates the fit of the compound k-distribution model to sea clutter amplitude statistics, within individual Doppler bins across the Doppler spectra. The data used was recorded with a monostatic coherent X-band radar on an airborne platform; both horizontally and vertically polarized data has been analysed. The statistics of the sea clutter distributions have been evaluated using the probabilities of false alarm (PFA), which are calculated from the sea clutter cumulative amplitude distributions. These curves are plotted as a function of detection threshold. K-distributions have been fitted to the PFA of the sea clutter across the Doppler spectrum. The variation of the fitted shape parameter with Doppler bin has been used to identify the relationship between backscattered sea clutter and Doppler. The results show a clear variation with Doppler of the shape parameter obtained from the fitted distribution. The variation is also found to change with polarisation. [C1123]

#### **"Experiments showing an improvement of angular resolution by LMMSE-based processing"**

Azimuth target resolution is of crucial importance in many applications of radar. The primary radar parameter affecting the azimuth resolution is the antenna beamwidth. However, in practice, standard signal processing techniques require the distance between targets to be more than one resolution cell. This can prove inadequate for several relevant applications. This paper describes the results obtained from experiments aimed at testing the capabilities of angular resolution between targets separated by less than the beamwidth in azimuth by means of linear minimum mean square error, LMMSE, -based processing. Results show the capabilities of this technique

of separating targets in such a scenario. The processing scheme shows a strong improvement in the resolution capability with respect to standard techniques. [C1124]

#### "Fast computations of constant envelope waveforms for MIMO radar transmit beampattern"

Designing transmit beampattern with MIMO radars generally requires the waveforms to be able to have arbitrary cross-correlation values. In contrast to the available algorithms, the proposed technique provides a closed-form solution for the synthesis of covariance matrix,  $R$ , of the waveforms to obtain desired beampattern match. To synthesis  $R$  the constraints and redundant information in  $R$  are leveraged, which convert the constrained problem into un-constrained problem. Next a novel method for generating the constant-envelope (CE) waveforms to realise the synthesised covariance matrix,  $R$ , is proposed. This method also yields a closed-form solution and choose the symbols from the binary-phase shift-keying (BPSK). Here, Gaussian random-variables (RV's) are mapped onto the CE RV's by a memoryless non-linear transformation, which converts the problem of finding the non-Gaussian RV's to realise a given covariance matrix  $R$  into finding the Gaussian RV's to realise covariance matrix  $R_g$ . Simulation results are presented to demonstrate the effectiveness of both methodologies. [C1125]

#### "Detection of runway boundary in ATC ground radar"

The radar environment is usually nonstationary and an efficient adaptation requires real-time exploitation of a priori knowledge concerning the environment surrounding the radar. In an airport contest, the radar scenario is heavily influenced by the inevitable presence of interferences, the background clutter, but other interferences (presence of vehicles and unwanted signs on the runway) contribute to make difficult the target detection. In particular, the paper addresses the detection of the runway boundary in ATC (Air Traffic Control) ground radar signal which can be not well defined due to the grass growth in different period in the islands near the runways. The grass growth can cause critical situation because the signal level of the grass zones is equal to that of the asphalt and it needs a visual analysis by a human operator to determine the presence of objects and targets in this clutter area. An active contour search algorithm (Snake algorithm) is used for detecting the runway boundary in SMR radar images. In our application a standard Snake algorithm is adapted and it is possible to obtain a reasonable approximation of the actual contour, which greatly reduces drawbacks related to the presence of the local minima. The performance of the active contour algorithm is tested on a set of radar images extracted from SMR radar images acquired in Italian airports. [C1126]

#### "A fast FRFT based detection algorithm of multiple moving targets in sea clutter"

On the basis of the detection and estimation model of multiple moving targets, a new algorithm based on wavelet packet transform (WPT) and fractional Fourier transform (FRFT) is proposed for weak moving targets detection in sea clutter. The multi-resolution property of WPT and the characteristic of good energy concentration on LFM signals in FRFT domain are combined together. At first, optimal wavelet tree is calculated using "minimum Shannon entropy" and threshold censored method is used to suppress sea clutter of different frequency bands. Then, take the absolute amplitude of signals after FRFT as test statistic and search for peaks in two dimensions with the threshold. Grading iterative method is used for parameter estimation with fast calculation speed and the shading problem between multiple targets is solved through "CLEAN" method. In the end, simulations with IPIX data indicate that the proposed algorithm has good performance of detecting low-observable moving targets in sea clutter. [C1127]

#### "STAP analysis using multi-channel airborne radar data from flight trials"

Flight trials have been performed within the NORA program in order to acquire multi-channel clutter data for different types of terrain, terrain scattered interference, and SAR data. The acquisition of clutter and terrain scattered interference has been made in order to prepare a database for future development of operational space-time adaptive processing (STAP) algorithms applicable to active electrically scanned antenna (AESA) systems employing multiple sub-aperture configurations. In this paper we show some preliminary results that illuminate the benefit of using all four dimensions of multi-channel radar data in a clutter rejection perspective. To illustrate the behavior of multi-channel clutter we employ spatial spectrum estimation methods such as Fourier and MUSIC. We also demonstrate post-Doppler STAP results for the air-to-air case. The results are very promising and indicate that multi-channel processing will indeed enhance the ability to detect targets obscured by clutter. [C1128]

#### "Signal modelling for ground moving target in complex image domain of multi-channel SAR"

For along-track multi-channel synthetic aperture radar (SAR), this paper proposes a novel ground moving target signal model in the high-resolution complex image domain. It is shown that moving targets can be divided into

three types according to the 2D motion distribution and the SPP approximation conditions. Moreover, a single target can be split into two targets in the image. All types of targets will have the same Doppler interferometric effect along multichannel images, which is decided by the target's ambiguous Doppler frequency. Furthermore, with our derived signal model, the complex image properties, i.e., amplitude reduction, azimuth shift, azimuth defocus, range blur, 2D slant, second-order phase modulation, split, interferometry and the effects of 2D accelerations are analyzed for airborne and spaceborne SAR, respectively. Finally, some experimental results are also provided to demonstrate the effectiveness of the proposed signal model and analysis. [C1129]

#### "Scan rate selection for coherent high-resolution maritime surveillance radar: An experimental study"

Scan rate selection has a crucial impact on the performance of maritime surveillance systems. In this work, a sea clutter database has been used to obtain experimental insight on the trade-off between within-scan and scan-to-scan integration. This paper extends the previous empirical studies to the case of sub-meter range resolution Ka-band coherent sea-clutter data. Results show a clear performance improvement for faster scan rates provided that the number of coherently integrated samples is high enough. [C1130]

#### "RELAX based estimation of signal and clutter echoes modeled as discrete point scatterers"

We consider the radar signal return to be originating from discrete point scatterers, and utilize this to estimate clutter echoes and calibrate a multi-channel array. The point scatterers are parameterized with a specific Doppler and spatial frequency ( $u$  and  $v$  direction). Previous work considering this formulation of clutter is the SCHISM approach. Their estimation is based on the radar version of CLEAN. For many cases where the scatterers are well separated, the CLEAN algorithm is fast and accurate. However, for closely spaced scatterers (in either Doppler or space), the CLEAN method suffers. Thus, to enhance the ability to resolve such scatterers we instead employ a new estimator (RESCUE) that uses the approach introduced in RELAX. As for SCHISM, range gates are processed individually and independently from each other and sample covariance matrices are avoided. Real world multi-channel data are used to demonstrate the proposed method. The results are very promising and indicate that this approach can indeed be used as an alternative to traditional STAP. [C1131]

#### "Maximum likelihood speed and distance estimation for OFDM radar"

A distance and speed estimation algorithm for OFDM based radar is analysed statistically. The maximum likelihood estimator is derived and compared to previous results. A connection to spectral analysis is drawn, simplifying the analysis of the estimator in question. Finally, a method to evaluate the performance of the algorithm is presented and conclusions for the structure of the OFDM signals are drawn. It is shown that the estimation algorithm works well above an SNR threshold, but rapidly degrades below. [C1132]

#### "Simplified model of dismount microDoppler and RCS"

Our goal is to be able to detect and classify dismounts, but we were lacking a quick way to estimate dismount parameters, especially with respect to angle of motion and depression angle of the radar. Micro-Doppler models have been developed which attempt to predict the human micro-Doppler response, and here we present a simplified model to quickly estimate dismount RCS and some micro-Doppler characteristics across a range of angles of motion. This model was extracted from measured radar data. We focus on modeling and measuring the characteristics of human walking parameters to determine response of dismounts to radar signals. We determine a simple closed form for RCS as a function of angle for walking dismounts as well as several rules of thumb, and we also determine a closed form for front-view micro-Doppler. [C1133]

#### "Analysis of measured radar data for Specific Emitter Identification"

Measured radar data assisted in the successful development and implementation of Specific Emitter Identification (SEI) signal processing algorithms. The aim of the algorithm is the identification of a specific emitter within a single class of emitters. The processes developed are pulse extraction, feature calculation, dimensionality reduction and classification. A pulse is detected whenever the phase changes from being random to being linear. Time domain features are then calculated from these extracted pulses to populate a feature vector. Some redundancy exists in the feature vector and a process of dimensionality reduction is followed to obtain the optimum set of features. A Fuzzy ARTMAP classifier completes the process of specific emitter identification to demonstrate the improvement in Correct Classification Decisions (CCD) using the reduced feature vector. [C1134]

#### "Waveform decorrelation for multitarget localization in bistatic MIMO radar systems"

The autocorrelation and crosscorrelation properties of transmit waveform set have great effect on the performance of MIMO radar systems. However, it is difficult to design waveform set which have ideal autocorrelation property as well as crosscorrelation one. In this paper, a decorrelation method has been proposed to cancel the effects of the autocorrelation and crosscorrelation of the transmit waveform by exploiting the given statistical properties of waveform. The correlation property of noise after decorrelation is also analyzed. Then a close form solution for localization of the multiple targets is presented via ESPRIT. Simulation results demonstrate the effectiveness of the proposed methods. [C1135]

#### **"Performance verification of symbol-based OFDM radar processing"**

In this paper a recently proposed novel processing approach for OFDM radar is verified with measurements. This processing algorithm directly calculates a radar image from the transmitted and received modulation symbols that compose the OFDM signal without the need for performing correlation operations. The implementation of a suitable system setup is described. The measurement results confirm that with this approach a very high dynamic range can be obtained. Moreover, the SNR in the measured radar images is investigated. The results prove that the proposed algorithm provides high processing gain. [C1136]

#### **"Performance prediction of Firefinder radar using high fidelity simulation"**

Thales Raytheon Systems' PC Simulation (PCS) tool allows a rapid simulated evaluation of Firefinder radar performance from a personal desktop computer. Firefinder radars are designed to track hostile rocket, artillery and mortar (RAM) projectiles in order to accurately estimate weapon ground location. The Firefinder tactical code is used within PCS. This design provides a low risk path to rapid prototyping and evaluation of candidate software changes. PCS is used to evaluate candidate software changes to the Firefinder. Candidate design changes which perform well in PCS testing require minimum system level checkout before being checked into the tactical software baseline. The PCS tool contains a simulation engine which reads program control information from input data files. The PCS tool also generates and maintains simulated targets and clutter, simulates the radar signal processing function, performs Monte-Carlo "batch" processing, produces complex target trajectories internally or from an input text file and creates simulation data recording files identical in format to those created by the actual radar. This paper summarizes the capabilities of the latest PCS. [C1137]

#### **"Automatic through the wall detection of moving targets using low-frequency ultra-wideband radar"**

This paper presents a time-domain, Moving Target Indication (MTI) processing formulation for detecting slow-moving personnel behind walls. The proposed time-domain MTI processing formulation consists of change detection and automatic target recognition algorithms. We demonstrate the effectiveness of the MTI processing formulation using data collected by an impulse-based, low-frequency, ultra-wideband radar. In this paper, we describe our radar system and algorithms used for the automatic detection of moving personnel. We also analyze the false alarm and detection rate of four operational scenarios of personnel walking inside wood and cinderblock buildings. [C1138]

#### **"A track-before-detect algorithm for statistical MIMO radar multitarget detection"**

This paper investigates the early detection problem of multiple moving targets in statistical MIMO radar systems using the track-before-detect (TBD) techniques. At first, assuming prior knowledge of the number of targets, a binary generalized likelihood ratio test (GLRT) is derived, which shows that the optimal implementation of the GLRT requires multidimensional joint search. To reduce the implementation complexity, a suboptimum multitarget TBD algorithm using successive-target-cancellation and polar Hough transform (STC-PHT) is proposed. In addition to low complexity, the new proposed algorithm doesn't need the prior information of the number of targets, and can avoid the implementation of multi-hypothesis test when the number of targets is unknown. The simulation results show that this algorithm can effectively improve the detection performance of statistical MIMO radar at low signal-to-noise ratio (SNR). [C1139]

#### **"Time-varying wideband underwater acoustic channel estimation for OFDM communications"**

We investigate two methods for estimating the matched signal transformations caused by time-varying underwater acoustic channels in orthogonal frequency division multiplexing (OFDM) communication systems. The underwater acoustic channel for this 12-20 kHz medium frequency range OFDM system is best modeled using multipath and wideband Doppler scale changes on the transmitted signal. As a result, our first channel estimation method is based on discretizing the wideband spreading function time-scale representation of the channel output using the Mellin transform. The second method is based on extracting the time-scale features of distinct ray paths in the received signal using a modified matching pursuit decomposition algorithm. We validate and discuss both methods using data from the recent Kauai Acomms MURI 2008 (KAM08) underwater acoustic



communication experiment. [C1140]

### "A study of several model selection criteria for determining the number of signals"

Addressing the problem of detecting the number of source signals as selecting the hidden dimensionality of Factor Analysis (FA) model, we investigate several model selection criteria via a new empirical analyzing tool that examines the joint effect of signal-noise ratio (SNR) and sample size  $N$  on the model selection performance. The contours of the model selection accuracies visualize a three-region partition on the space of SNR and  $N$ , and a diminishing marginal effect which trades off SNR and  $N$  on the performance. Moreover, the newly derived Variational Bayes algorithm and three variants of Bayesian Ying-Yang (BYY) algorithms are more robust against reducing SNR and  $N$ , where the BYY with priors' hyperparameters updated is the best in general. [C1141]

### "Resolution selective change detection in satellite images"

In this paper, we propose a novel method for unsupervised change detection in satellite images. A feature vector for each pixel is extracted using the multiresolution representation of the difference image which is computed from the multitemporal satellite images of the same scene acquired at different time instances. A metric for automatically estimating the number of resolution levels used in multiresolution analysis is proposed. The dimensionality of each feature vector is reduced using principal component analysis (PCA). The feature vectors are then classified into "changed" and "unchanged" classes using k-means clustering with  $k = 2$  to achieve a change detection map. Results are shown on real data and comparisons with the state-of-the-art techniques on advanced synthetic aperture radar (ASAR) images are provided. [C1142]

### "A new far field measurement method for antenna polarization characteristics based on calibrator target"

A new far-field measurement method of antenna is studied in this paper. The received signal model of antenna's beam scanning the calibrator target has been built and the measurement method is considered. The full analysis formula and practical procedure was given. The validity of research work was demonstrated by processing the observational data and simulation. This can greatly reduce the development complexity and production cost of far field test, increased the fidelity at the meanwhile. [C1143]

### "Markov model for convergence analysis of the adaptive Kronecker MIMO OTH radar beamformer"

We introduce an iterative procedure for design of adaptive KL-variate linear beamformers that are structured as the Kronecker product of  $K$ -variate (transmit) and  $L$ -variate (receive) beamformers. Focusing on MIMO radar applications for scenarios where only joint transmit and receive adaptive beamforming can efficiently mitigate multi-mode propagated backscatter interference, we introduce a Markov model for the adaptive iterative routine, specify its convergence condition, and derive final (stable) signal-to-interference-plus-noise ratio (SINR) performance characteristics. Simulation results demonstrate high accuracy of the analytical derivations. [C1144]

### "Gala Dinner/Banquet Speaker"

{no data available} [C1145]

### "Computationally efficient resampling of nonuniform oversampled SAR data"

A computationally efficient technique is developed to resample SAR data oversampled in the slow-time domain for a platform accelerating along the track. The algorithm segments the data between uniformly spaced points on the synthetic aperture, then performs a weighted average on the demodulated SAR data in each segment to adjust the effective sample position on the aperture. The weighting is derived using a first-order Taylor series approximation and used parameters from the velocity and acceleration of the platform and the radar waveform. [C1146]

### "USRP technology for multiband passive radar"

The purpose of the paper is to show how the Universal Software Radio Peripheral (USRP) technology, typically used for implementing telecommunication systems, can be used for realizing passive radars. Specifically in this paper a multiband passive radar is considered. A preliminary study on the signals of opportunity is presented where real and simulated radar ambiguity functions have been evaluated. An experimental system has been set up and live data acquired both for UMTS and DVB-T signals in order to verify the capability of the proposed passive radar demonstrator. [C1147]



### "An iterative algorithm for the construction of notched chirp signals"

This paper describes an iterative algorithm for the design of a constant-modulus finite-duration chirp-like signal having a notch in its frequency spectrum. Frequency-notched signals with good pulse compression properties are needed in wide-band radar systems that must avoid radiating into frequency bands assigned to other systems (e.g. communication and navigation systems). The algorithm is computationally efficient and provides explicit control of the notch frequency and notch order. [C1148]

### "The periodic ambiguity function-Its validity and value"

The periodic ambiguity function (PAF) relates to Woodward's ambiguity function (AF) like periodic autocorrelation relates to autocorrelation. AF is defined for a finite signal, processed by its matched filter. PAF can handle periodic signals with infinite (or large) number of periods, and a processor that is matched to fewer periods. PAF suits practical scenarios found in radar employing coherent pulse train or CW waveforms. This paper revisits the PAF and its properties, demonstrating its value and viability. [C1149]

### "Cross ambiguity function analysis of the '8k-mode' DVB-T for passive radar application"

One of non-cooperative illuminators recently considered for passive radar applications is the DVB-T (Digital Video Broadcasting- Terrestrial) station. The thumbtack ambiguity function of the DVB-T signal in addition to being stationary makes such signal a good candidate for such applications. However, certain ambiguities in its ambiguity function necessitates certain issues to be carefully considered when DVB-T signals are to be utilized in these scenarios. In this paper, after studying the origins of these ambiguities, we propose special processing schemes to resolve them. [C1150]

### "Enhanced monopulse radar tracking using filtering in fractional Fourier domain"

Monopulse radars are used to track a target that appears in the look direction beam width. The distortion produced when additional targets appear in the look direction beam width can cause severe erroneous outcomes from the monopulse tracking processor. This leads to errors in the target tracking angles that may cause target mistracking. A new monopulse radar structure is presented in this paper which offers a solution to this problem. This structure is based on the use of optimal Fractional Fourier Transform (FrFT) filtering. The improved performance of the new monopulse radar structure over the traditional monopulse processor is assessed using standard deviation angle estimation error (STDAE) for a range of simulated environments. The proposed system configurations with the optimum FrFT filters is shown to effectively cancel the additional targets' signals and to minimize the STDAE for monopulse processors even if these targets have the same Doppler frequency. [C1151]

### "The phase retrieval problem for the Radar Ambiguity Function and vice versa"

The first part of this note is based on a joint paper with A. Bonami and G. Garrigos [3] in which the phase retrieval problem for the Radar Ambiguity Function (i.e. the Radar Ambiguity Problem) has been tackled. In particular it was shown that for wide classes of signals, the radar ambiguity problem has a unique solution, up to trivial transformations. In the second part of this note, we report on ongoing work by the author where the radar ambiguity function is used as a tool to solve other phase retrieval problems. [C1152]

### "Passive bistatic WiMAX radar for marine surveillance"

In this study we investigate the feasibility of using passive bistatic radar to exploit WiMAX communication signals as transmitters of opportunity for marine surveillance. The range and Doppler characteristics of such a system are first assessed through ambiguity function analysis on a typical set of WiMAX data transmission waveforms. Theoretical simulations are then used to investigate the ability of passive WiMAX radar for detecting marine vessels within three busy shipping areas in the UK, and in the presence of noise and interference signals. The initial analysis shows a range resolution of 5.6 m is achievable. Additionally, the simulations demonstrate specific scenarios where WiMAX radar may be used as a low cost surveillance device for detecting both small and large marine vessels in port areas and open waters. [C1153]

### "Application of the CLEAN Detector to low signal to noise ratio targets"

This paper expands on the author's previous work by adapting the CLEAN algorithm to address low signal to noise (SNR) targets. The Reformulated CLEAN Detector is presented which is shown to allow the detection of low SNR targets in the presence of large targets. Performance results are presented that show how good performance can be attained by combining the correlator, CLEAN Deconvolver and Reformulated CLEAN Detector. [C1154]

### "Phased array weather / multipurpose radar"

The first phased array radar dedicated to weather observation and analysis is now instrumented with eight, simultaneous digital receivers. The addition of these additional channels will enable the use of advanced signal processing to improve signal/clutter in an adaptive mode. Elimination of strong point and ground clutter returns from the low-level, volumetrically distributed weather cell returns is a new application of adaptive processing. The NSF funded 8-channel receiver has been added to the National Weather Radar Testbed (NWRT) system in Norman, OK to enable operation as a multifunction and/or adaptive processing system. This paper will describe the system concept, system installation and early results from fielded weather data returns. [C1155]

### "Modeling terahertz heterodyne detection based on photomixing"

We present a simple model for continuous wave (CW) terahertz heterodyne detection based on photomixing. This model takes into account the antenna parameters as well as the properties of the substrate. Results from our analytical analysis can be used to obtain the appropriate values for the substrate parameters to maximize received THz signal. Focusing on the dipole antenna, we derive a simple expression for the current created by the THz field in terms of antenna length and parameters of the photomixer. [C1156]

### "False alarm control of CFAR algorithms with experimental bistatic radar data"

False alarm control performance of different constant false alarm rate (CFAR) algorithms is experimentally investigated using bistatic radar data. The CFARs under investigation include cell-averaging (CA-CFAR), smaller-of (SO-CFAR), greater-of (GO-CFAR), ordered-statistic (OS-CFAR), censored cell-averaging (CCA-CFAR), and the homogeneity detector mean-to-mean ratio (MMR) test. The experimental data was collected using an Illuminator of Opportunity (IOO) bistatic radar that is under ongoing development at DSTO. For this set of experimental data, it is observed that CFAR algorithms that have a higher CFAR loss in a homogeneous environment will have a larger theory-experiment false alarm mismatch, especially at smaller false alarm rates and larger CFAR window sizes. [C1157]

### "Establishing a common phase reference for comparing synthetic data to RF range measurements"

Discrepancies can result when creating common data sets consisting of comparable synthetic and measured range complex scattered field samples when the phase references of each do not coincide. This can be especially true when using signal processing techniques to produce one dimensional (range profiles) or two dimensional (Synthetic Aperture Radar or SAR images) representations of the target scattered field where range bins and cross-range bins are formed. Range profiles and SAR images can be misaligned or have different bin amplitudes due to target scatterers in synthetic and measured scenarios shifted with respect to one another. Obtaining equivalent data samples requires attention to the measured data calibration process and phase reference location. This paper will address the common phase reference problem by an analysis of experimental data for specific targets and rotation system. Suggestions are provided for possible solutions to current challenges. The data analysis will include synthetic and measured range data comparisons, range calibration, and target position and range alignment processes using Theodolite laser measurements. [C1158]

### "The radar information channel and system uncertainty"

The radar information channel is developed as a theoretical model for the study of uncertainty within the design, development, and research of radar signature exploitation systems. Information measures are developed which characterize sources of uncertainty and propagate the associated impacts to system performance. Sources of uncertainty are studied to form an information loss budget for trading component design options against overall system performance. [C1159]

### "A novel signal processing method for MIMO radar based on channel estimation"

Multiple Input Multiple Output (MIMO) radar is a new radar technique. It has many advantages over conventional phased radar in many ways such as anti-intercept of radar signal, low velocity target detection, and resolution. The signal transmit matrix of MIMO radar has much information such as target angle. In this paper, we analyze the signal model for MIMO radar. And then we present a new method to estimate the target angle from the matrix. At last, we show the efficiency by some simulations. [C1160]

### "Coupling optimal method of segmentation with restoration for target detection in SAR images"

High-quality segmentation is there in a need in SAR images for appropriate target detection. In this paper, the features of Wiener filter are utilized with region of interest and Boundary based segmentation technique in SAR

images. The discrete Wiener filter exhibits both linear and nonlinear characteristics. This filter compensates for the blurring due to the linear term and conserves the edges which are mainly used to distinguish the various objects with the gross representation of object of interest. The filter is defined both for edge preserving along with speckle noise cancellation in SAR images. A combination of features from two different types of multi-resolution and multi-channel filters, in general provides superior classification of SAR images. The experimental results show that the proposed boundary based and ROI technique segments the SAR image while the opted filter preserves significant features and noise removal. The fusion performance is evaluated on the basis of Mean square error, time, and signal-to-noise ratio. [C1161]

#### **"A complex SAR image compression algorithm combining set-partitioning and context prediction"**

This paper presents a new wavelet transform coding algorithm for complex Synthetic Aperture Radar (SAR) image compression. It uses a improved recursive set-partitioning procedure to compress the large blocks which are abundant in zero bits, and uses entropy coding based on adaptive context prediction model to compress the small blocks which contains non-zero bits. The experiment results showed that the new algorithm gained better compression efficiency than SPECK. We also compared with common complex SAR image compression algorithm in references using professional parameters in SAR, such as Means Phase Errors (MPE), complex spatial correlation efficient, the new algorithm gets better performances too. [C1162]

#### **"Field test implementation to evaluate a flash LIDAR as a primary sensor for safe lunar landing"**

From May 2 through May 7 of 2008, the Autonomous Landing and Hazard Avoidance Technology (ALHAT) Exploration Technology Development Program carried out a helicopter field test to assess the use of a flash LIDAR as a primary sensor during lunar landing. The field test data has been used to evaluate the performance of the LIDAR system and of algorithms for LIDAR Hazard Detection and Avoidance, Hazard Relative Navigation, and Passive Optical Terrain Relative Navigation. Reported here is a comprehensive description of the field test hardware, ground infrastructure and trajectory reconstruction methodologies. [C1163]

#### **"Analysis of flash lidar field test data for safe lunar landing"**

In May 2008, the Autonomous Landing and Hazard Avoidance Technology (ALHAT) Project conducted a helicopter field test of a commercial flash lidar to assess its applicability to safe lunar landing. The helicopter flew several flights, which covered a variety of slant ranges and viewing angles, over man-made and natural lunar-like terrains. The collected data were analyzed to assess the performance of the sensor and the performance of two algorithms: Hazard Detection (HD) and Hazard Relative Navigation (HRN). The collected flash lidar data were also used to validate a high fidelity flash lidar software model used in ALHAT Monte Carlo simulations. The field test results, combined with prior simulation results, advanced the technology readiness level of the HD algorithm to TRL 5 and the HRN algorithm to TRL 4. [C1164]

#### **"Design and Realization of an Online Power Quality Monitoring System Based on GPRS"**

In order to evaluate power quality more accurately, this paper presents a three-layer distributed online power quality monitoring system (PQMS), which uses the General Packet Radio Service (GPRS) wireless network as its communication channel. This PQMS consists of three parts: the power quality monitor (PQM), the monitoring software (MS) in upper computer and the web platform (WP). The PQM which is designed on the structure of DSP (Digital Signal Processor) + CPLD (Complex Programmable Logic Device) ensures the realtime and precise monitoring. Then the MS collects and analyzes the monitoring data. At the same time, GPRS network provides the communication channel for PQM and MS. The WP provides the monitoring data and the analysis results through internet, and supervisors can monitor and manage the power quality from a long distance. The detail design and its realization of each part are explained. Precision test of the PQM and field monitoring results with the PQMS are also discussed. [C1165]

#### **"Wavelet analysis of impulse ultra-wideband radar"**

In this paper, we have enhanced ultra-wideband (UWB) radar signal-to-noise ratio (SNR) by applying a wavelet transform (WT) based matched filter. The wavelet transform algorithm (WTA) provided enhanced reliability relative to conventional background template subtraction (BTS) approach, increasing reliability detecting targets in the nonlinear close in (<50 cm) and at the maximum distance tested (29 m.) We extrapolated the WTA can support a maximum radar range of 60 m, about twice that available with the conventional constant false alarm rate (CFAR) methods. [C1166]

#### **"Radar signal processing based on DCT compression"**

This paper has analyzed and researched the correlative characteristic of data on Synthetic Aperture Radar, adopted DCT algorithm to compress the radar video data, and verified the compression effect through simulation. The compression ratio is 1:3, so that the disadvantage should be resolved that the bandwidth of video data transmission during wireless channel is not enough. [C1167]

#### "TWR signals de-noising by using WNN"

The de-noising issue of through-the-wall radar (TWR) signal is an essential TWR's performance on detecting lives. This paper introduces TWR signal de-noising algorithm based on a wavelet neural networks (WNN). WNN owns the property of time-frequency localization of wavelet transform, as well as the excellent characteristics of artificial neural networks, self-learning and fault-tolerance, which make it a powerful tool for removing noises from noisy through-the-wall radar signals. Experimental results show that the proposed WNN based de-noising algorithm can achieve good de-noising performance and hold the useful detail of TWR signals. [C1168]

#### "Cognitive Radio under Conservative Regulatory Environments: Lessons Learned and near Term Options"

In recent regulatory decisions, spectrum regulators have been very conservative in permitting use of cognitive radio systems requiring large "safety margins". This paper describes the nature of these safety margins and the factors that lead to them. New research that might counter such concerns is suggested. Cooperative approaches involving primary user systems that actively cooperate with cognitive users are also suggested. [C1169]

#### "On the MIMO interference channel"

We propose an iterative algorithm to design optimal linear transmitters and receivers in a K-user frequency-flat MIMO Interference Channel (MIMO IFC) with full channel state information (CSI). The transmitters and receivers are optimized to maximize the Weighted Sum Rate (WSR) of the MIMO IFC. Maximization of WSR is desirable since it allows the system to cover all the rate tuples on the Pareto-optimal rate region boundary for a given MIMO IFC. The proposed algorithm is rooted in a recent result [S.S. Christensen et al., 2008] showing a correspondence between local optima of the Minimum Weighted Sum Mean Squared Error (MWSMSE) and Maximum Weighted Sum Rate (MWSR) objective functions for the MIMO Broadcast Channel (BC). This connection between the MWSR and MWSMSE is shown to hold true also in the MIMO IFC and is exploited to design an alternating minimization algorithm for MIMO IFC that maximizes the WSR. The MWSMSE-MWSR connection also allows to solve the transmit filter design subproblem in the alternating algorithm by invoking a heuristic solution first proposed in [M. Joham et al., 2002]. Another contribution of this paper is to propose an extension of [M. Stojnic et al., 2006] to MIMO problems, following the philosophy of [S.S. Christensen et al., 2008] in part. This path is shown to lead in fact to the same iterative algorithm, showing the optimality of the heuristic of [M. Joham et al., 2002] when applied in the context of the alternating transmitter-receiver optimization approach of [S.S. Christensen et al., 2008]. [C1170]

#### "3D passive source localization by a multi-array network: Noncoherent vs. coherent processing"

This paper investigates the three-dimensional passive source localization problem by a system of multiple antenna arrays. It is well-known that centralized and coherent processing of all sensor antenna outputs offers a performance benefit in comparison to decentralized processing, where the latter is easier to implement. We compare the Cramér-Rao bound on the source locations for both cases, review the decentralized direct position determination approach and outline the near-field source localization approach generalized to the three-dimensional problem. Finally, we discuss the trade-off between performance benefit and implementation complexity. [C1171]

#### "Array geometry optimization for direction-of-arrival estimation including subarrays and tapering"

This paper focuses on the estimation of the direction-of-arrival (DOA) of signals impinging on a linear sensor array. In contrast to conventional arrays, where the number of channels equals the number of sensors, we use tapered subarray structures. For this type of array, each channel consists of several sensor elements with different amplitude tapering. By this means, a pre-focussing can be achieved for angular regions, where targets are likely to appear. As a consequence, the DOA mean squared error in the corresponding regions is reduced. As the subarrays affect the statistical properties of the baseband signal model, we extend the well known definitions of the Maximum Likelihood DOA estimator and the Cramér-Rao bound (CRB). Furthermore, we present an expression for the ambiguity function for a single signal based on the Maximum Likelihood estimator. This function and the CRB are used to optimize the sensor geometry, subarray tapering and subarray configuration. As external conditions such as the range of possible DOA's, the DOA region of interest and the signal power range are also included in the optimization, the array can be adjusted to external requirements



defined by a specific application and function. By this means, optimum (single source) DOA estimation performance for a specific area of application can be achieved. An evolution strategy is used for the optimization. To show the DOA estimation performance of the optimized arrays and to confirm the validity of the extended CRB, simulation results are presented. Compared to conventional arrays, the optimized tapered subarray structures provide a significantly better DOA accuracy. [C1172]

#### "Investigation of the Tiler processor for real time hazard detection and avoidance on the Altair Lunar Lander"

The High Performance Processor (HPP) Task of the Advanced Avionics and Processor Systems (AAPS) Project, part of the Exploration Technology Development Program (ETDP), was to evaluate several high performance multicore processor architectures with respect to their ability to provide real time hazard detection and avoidance for the Constellation Program's Altair Lunar Lander. In this paper we review the Tiler Tile64 processor, the hazard detection and avoidance algorithm, strategies for parallelizing these algorithms, and preliminary performance study results. We were presented with the requirements of 30 Hz LIDAR frame processing rate and 10 second processing time for ALHAT HDA processing and were able to meet that requirement with the Tile64. We then project the performance of these algorithms on the OPERA MAESTRO Processor, a radiation tolerant version of the Tile 64 being developed by the Boeing Company. [C1173]

#### "STS-128 on-orbit demonstration of the TriDAR targetless rendezvous and docking sensor"

Neptec has developed a vision system for autonomous rendezvous and docking in space that does not require the use of cooperative markers, such as retroreflectors, on the target spacecraft. The system uses an active TriDAR 3D sensor along with embedded model based tracking algorithms to provide, out of the box, 6 degree of freedom (6DOF) relative pose information in real-time. The TriDAR (triangulation + LIDAR) sensing technology combines active triangulation and Time-of-Flight (TOF) ranging techniques within a single optical path. This design takes advantage of the complementary nature of these two technologies to provide optimal 3 dimensional data from several kilometers all the way to docking. A thermal imager is also included to provide bearing information at long range. In partnership with the Canadian Space Agency (CSA) and NASA, Neptec has space qualified the TriDAR vision system and integrated it onboard the Space Shuttle Discovery to fly as a Detailed Test Objective (DTO) on the STS-128 mission. The objective of the TriDAR DTO mission was to demonstrate the system's ability to perform acquisition and tracking of a known target in space autonomously and provide real-time relative navigation cues. Autonomous operations involve automatic acquisition of the ISS, real-time tracking as well as detection and recovery from system malfunctions and/or loss of tracking. This paper presents an overview of the TriDAR system as well as results from on-orbit testing of the TriDAR during the STS-128 Space Shuttle mission. [C1174]

#### "SMAP Observatory configuration, from concept to preliminary design"

SMAP (Soil Moisture Active and Passive) is a scientific mission to provide global mapping of Earth soil moisture and freeze/thaw state. In order to accomplish this mission the Observatory accommodates two primary Instruments L-band (1.26 GHz) Radar and L-band (1.4 GHz) Radiometer. Both Instruments use a shared 14.6 RPM spinning Antenna System with 6 m diameter deployable Reflector. The key challenges for the Observatory configuration are accommodation of the primary Instruments (Radar and Radiometer), and the supporting subsystems, all the while meeting all operations, pointing, environment requirements, and launch vehicle accommodation. This paper will describe the evolution of the SMAP Observatory configuration and major trade-offs from conceptual to preliminary design. [C1175]

#### "Statistical analysis of CloudSat data for climate model parameterization"

The development of realistic cloud parameterizations in climate models requires accurate characterizations of sub-grid distributions of thermodynamic variables. To this end, cloud liquid water content (CLWC) distributions are characterized with respect to cloud phase, cloud type, precipitation occurrence, and geo-location using CloudSat radar measurements. The probability density function (PDF) of CLWC is estimated using Maximum Likelihood Estimation. The best-estimated PDF of CLWC is found to closely follow either a gamma or a lognormal distribution depending on temperature (cloud phase), cloud type, precipitation, and geo-location. In the regions from the lower to mid-troposphere (altitudes of 1-6 km) and between the tropical and the subtropical latitudes where non-precipitating and pure-water phase clouds are dominant, the PDFs of CLWC are best described by lognormal distributions. In contrast, at altitudes above 6 km and in regions poleward of the midlatitudes, the CLWC exhibits a gamma distribution due to a high frequency of occurrence of supercooled liquid clouds, which results in the increased occurrence of low CLWC values. The data sub-sampling with respect to cloud phase and precipitation significantly affects the distribution characteristics of CLWC in some



regions. After removing the contributions of supercooled water and precipitation the CLWC PDFs transition from gamma to lognormal distributions in two types of regions: (1) the high altitude and middle-to-polar latitude regions where the contribution of mixed-phase cloud is significant; (2) the region near the surface where the contribution of precipitating cloud is considerable. [C1176]

### "Space-based passive radar enabled by the new generation of geostationary broadcast satellites"

In this paper we investigate the possibility to develop a passive radar system for mid-range air target surveillance using, as illuminator of opportunity, a high EIRP level geostationary broadcast transmitter. These satellites are being introduced recently for Satellite Mobile Digital TV broadcast purpose. Since they are designed to allow mobile users to receive satellite TV without large antennas, a sufficiently high signal power is being transmitted, making them suitable as illuminators of opportunity in a passive radar system. The possibility to resort to a quasi-stationary transmitter is shown to highly simplify the signal processing required by the passive radar system. A preliminary evaluation of the achievable SNR is conducted, showing that mid-range target detection can be achieved with reliable performance. In addition, a detailed analysis of the Doppler frequency contributions is conducted. Specifically, the Doppler frequency contribution due to the motion between target and transmitter is shown to be locally independent over the target position. The overall bistatic Doppler frequency behavior is evaluated for several possible target trajectories and some critical trajectories are identified. Finally, some remarks referred to the 2D Cross Correlation Function (2D-CCF) evaluation are reported. [C1177]

### "New detection manifolds for radar signal processing"

This paper examines direct data domain (DDD) moving target detection for multi-channel space-based radar (SBR). DDD techniques differ from data-adaptive processing methods in that they do not rely on statistically stationary and homogeneous training data in order to estimate and null out clutter or interference and thereby reveal potential targets; instead, they operate on each range-Doppler cell independently, after any necessary preprocessing to compensate for platform motion and/or array calibration. Prior work examined a maximum-likelihood angle-of-arrival (AOA) technique and the associated target power estimator to detect slow moving targets. In this paper, we extend that methodology and propose novel detection manifolds for optimally partitioning the two-dimensional statistical space. The two dimensions are formed by the passive AOA likelihood function and the estimated target power. A computer simulation of a space radar system and associated geometry is used to assess the characteristics and performance of the new concept. We show that the two-dimensional probability densities corresponding to the target absent and target present hypotheses ( $H_0$  and  $H_1$ , respectively) occupy regions in this space that are not optimally separated by independent thresholds. This immediately leads to the novel detection manifolds (or curved boundaries between detections and non-detections) that improve the detection probability while also reducing the false alarm rate. [C1178]

### "Autonomous deployment of the UAVSAR radar instrument"

The UAVSAR program was formed to provide repeat pass radar interferometry on an uninhabited aircraft platform. The UAVSAR imaging radar system is housed in an external unpressurized pod that may be attached to an Uninhabited Aerial Vehicle (UAV), although initial flight tests were performed aboard a Gulfstream-III aircraft with flight test personnel on-board. Since the radar science missions are to be eventually flown without an on-board operator, all data collection must be performed autonomously from take-off to landing. The Automatic Radar Controller (ARC) is the main instrument flight computer responsible for a myriad of tasks, including commanding the radar configuration and monitoring the aircraft flight path to search for data collection waypoints provided by an on-board flight plan. The pod environment and various hardware units are monitored during the mission to assure the radar instrument remains within an operable range. The ARC communicates with a Radar Operator Workstation (ROW) to receive updated real-time operational commands and to download up-to-date hardware status and telemetry. The ROW provides operator displays for monitoring the health of the radar system and also displays sampled radar waveforms in time and frequency domains. The aircraft location is provided by the on-board GPS/INU and downloaded by the ARC for plotting the current location onto Google maps using software developed at JPL. The UAVSAR platform has been flown throughout most of California and has recently completed successful deployments to Greenland and the Aleutian Islands. A nearly identical UAVSAR pod will be attached to a Global Hawk UAV platform in early 2010 for uninhabited operational flight tests. An additional pod containing another L-band antenna and GPS/INU unit will also be attached to the Global Hawk platform providing dual Lband data collection capability. The command and communication implementation for Global Hawk has been modified from the original GUI test U--.S. Government work not protected by U.S. copyright ? IEEEAC paper#1558, Version 1, Updated 2009:10:27 platform. During flight tests on the GUI the Radar Operator Workstation (ROW) was on-board with the test team. For the Global Hawk flight tests, the Radar Operator Workstation will be in the Global Hawk Operations Center located at the Dryden Flight Research facility. Communications to the ARC will utilize a relatively low speed Iridium satellite communications link. This

paper will describe the functionality of the UAVSAR Global Hawk radar instrument flight and ground systems. We will also discuss fault detection and recovery options provided by these systems. We will describe the capabilities of monitoring and controlling the radar instrument during flight from the Global Hawk operations facility and describe the operational timeline for a typical science mission. [C1179]

### "Improving situational awareness training for Patriot radar operators"

Situational awareness (SA) is the understanding of an environment and how one's actions affect it. We present the Cognitive Air Defense Training System (CADTS) Engagement Control System Simulator (ECS2), currently installed at Fort Bliss, Texas; which aims to increase the cognitive awareness and SA of radar operators of the MIM-104 Patriot surface-to-air missile system. The ECS2 presents multiple visualizations of environmental data on four levels: "Tactical"-the ECS operator's perspective; "Operational"-highly detailed realistic 3D representations; "Strategic"- a representational view containing the entire Earth; and "Time"- real-time game play, with pause and replay abilities. The levels vary in presentation, scope, and accuracy, so the instructor can alternate between 'available' and 'actual' information, to emphasize real world uncertainties as they may appear. Network shared objects are used to allow the differing views of the environmental data to be interchangeable during instruction and in After Action Review. The training system has an Observer Emphasis, where the observers in a classroom have access to all scenario views and a larger context, and the ECS operators in the ECS Digital Interactive Virtual Environments (DIVEs), only have access to the Tactical View as they will during actual deployment. Multiple perspectives can be presented by the instructor during instruction and in After Action Review. We will look at the Player and Observer roles, the four presentations of the environmental data within ECS2, and the technological issues involved in their creation. [C1180]

### "On the use of UWB Radio Interface for EHF satellite communications"

In this work authors investigate the use of IR (Impulse Radio) UWB (Ultra-Wide Band) technique for satellite communications at frequency bands beyond Q/V bands. In particular, the paper shows how an IR UWB communication system is sensitive to typical hardware non-idealities at those frequency bands and compares its performance with the ones of a more classical continuous wave communications system with FSK (Frequency Shift Keying) modulation. Simulation results show that BER (Bit Error Rate) performance for IR-UWB Payload (P/L) architecture operating in W band (with same data rate and bandwidth occupation) are better than a 2-FSK scheme operating at same frequencies range and considering Dirty RF (Radio Frequency) effects. [C1181]

### "LMRST-Sat: A small, high value-to-cost mission"

The Communications, Tracking, and Radar Division at NASA's Jet Propulsion Laboratory (JPL) and the Space and Systems Development Lab (SSDL) at Stanford University are collaborating to fly a nanosat-class mission for costs usually associated with small technology development tasks, a few \$100K. The mission hosts a JPLdeveloped Low Mass Radio Science Transponder (LMRST) on a university-class CubeSat bus as a satellite that occupies a total volume of two liters plus deployable antennas. In low earth orbit, the LMRST payload will provide a far-field source for calibration of Deep Space Network X-Band equipment in the form of an integer turnaround X-Band transponder with support for ranging modulation. The CubeSat bus provided by SSDL supplies power, structural support, and command and telemetry while on orbit. CubeSat development and operations are conducted as a student project. In addition to the payload functions, mission goals include space qualification of the LMRST, demonstration of nanosat capabilities and costs within NASA, and expansion of student-class projects toward eventual deep space missions. This paper describes the work completed thus far, "Phase One": development of the LMRST, satellite bus, and integrated testing; and outlines the work planned for "Phase Two": acceptance testing, launch, and operations. [C1182]

### "Performance evaluation of hazard detection and avoidance algorithms for safe Lunar landings"

Unmanned planetary landers to date have landed "blind", that is, without the benefit of onboard landing hazard detection and avoidance systems. This constrains landing site selection to very benign terrain, which in turn constrains the scientific agenda of missions. Systems for automatic surface reconstruction and for hazard detection, mapping, and assessment are becoming mature. Before they can be put to practical use, it is essential to be able to characterize their performance for the purposes of scientific evaluation and their utility to engineers planning and designing landed missions. It is also important to be able to predict performance for a variety of scenarios. The evaluation metrics need to be simple enough to be readily comprehensible but still to capture the important relevant performance parameters. In this paper we describe the process, metrics, results, and algorithm improvement recommendations from the evaluation of the performance of the hazard detection and avoidance (HDA) algorithms developed in the Autonomous Landing and Hazard Avoidance Technology (ALHAT) Project by means of Monte Carlo simulation of thousands of Lunar landings. [C1183]

### "Distributed prognostic health management with gaussian process regression"

Distributed prognostics architecture design is an enabling step for efficient implementation of health management systems. 12A major challenge encountered in such design is formulation of optimal distributed prognostics algorithms. In this paper, we present a distributed GPR based prognostics algorithm whose target platform is a wireless sensor network. In addition to challenges encountered in a distributed implementation, a wireless network poses constraints on communication patterns, thereby making the problem more challenging. The prognostics application that was used to demonstrate our new algorithms is battery prognostics. In order to present trade-offs within different prognostic approaches, we present comparison with the distributed implementation of a particle filter based prognostics for the same battery data. [C1184]

### "Differential Geometric Estimation for spacecraft formations orbits via a cooperative wireless positioning"

The estimation of relative and absolute positions of spacecraft in a formation, using a novel wireless local positioning system (WLPS), is addressed. The WLPS enables one spacecraft to measure another spacecraft's relative position vector. The Differential Geometric Filter is implemented to estimate the absolute and relative positions of the spacecraft in the formation. Two different scenarios are studied: (1) the observations include WLPS measurements only, and (2) the observations include WLPS measurements in addition to measurements for the absolute position of one spacecraft. Results show that the Differential Geometric Filter provides a fast convergence rate and stable estimation. [C1185]

### "Ground-based orbit determination for spacecraft formations"

Spacecraft formations offer interesting challenges to orbit determination, especially for ground-based tracking. In fact, the limited distances between spacecraft and the possible ambiguity of the observables gathered from the ground have an impact on the solution process. The paper aims to apply the filtering techniques on a refined dynamical model, which can include the main perturbation effects-due to the oblateness of the Earth and, at the lower altitudes, the air drag-on spacecraft trajectories, representing them in series with a remarkably limited number of terms even in eccentric case. The idea is to focus on theoretically expected behavior rather than dealing with an enriched but heavier state including parameters directly related to the perturbing effects. In such a way, it could be possible to obtain a good estimate even with limited spacecraft tracking information. This is an important asset in navigating a formation from the Earth, due to the needed partition of ground station resources among different platforms belonging to the formation, and to the possible ambiguity among the measurements, which further reduce the available data. The specific nature of the dynamic model calls for an estimator with a flexible and ?open? architecture, easily allowing for changes and additions in the model itself. Therefore, the estimator selected for testing the approach has been the Unscented Kalman Filter, versatile enough to allow for increasing model accuracy without the need for tedious computation of the Jacobian. This approach is also intended to offer a different way to investigate special perturbed configurations, via the semi-analytical and almost exact representation of the trajectories. In such a perspective, one of the first application, which is shortly outlined in the paper, will be the analysis of spacecraft formations under the J2 effect. In fact, recent studies identified a set of almost periodic relative configurations among the spacecraft. This s--et (sometimes referred as the special or magical inclination's one) has been recently identified by means of numeric search, and has also received some (partial) explanation. Due to the interest in control effort reduction, it is deemed that a better understanding of this special dynamics, possibly provided by means of a selected modeling approach, can be of some interest. [C1186]

### "Automatic Measurement of Radar Receiver Sensitivity"

This paper puts forward a method to measure the receiver sensitivity automatically. Taking an airborne radar as example, the method utilizes signal integration to improve the accuracy of the measurement. The implementation circuitry and experimental waveforms are given to demonstrate the utility of the method. [C1187]

### "The Research of Families of Odd-periodic Perfect Complementary Sequence Pairs"

The theory of families of odd-periodic perfect complementary sequence pairs(OPCSPF) is given. OPCSPF can be derived from the odd-perfect almost binary sequence and sequence pairs. Some characteristics of OPCSPF are discussed, and the necessary conditions for existence of OPCSPF is given. The methods are studied and proved which construct OPCSPF. [C1188]

### "Design of Wireless Dam Security Information System"

This paper proposed design proposal of wireless dam security information system through the GPRS technical

superiority, introduced hardware system set up based on the GPRS dam security information system in detail, proposed the functional requirements of software modules, has the actual application value. Using the GPRS technology to carry on the network data transfer, easy to use, no region limit, in the field of remote monitoring and control, especially in hydraulic engineering security information system, it has a very good application prospect. [C1189]

### "The Angle-Measuring Algorithm for the Stepped-frequency Radar Based on Dual-line Digital Phase Interferometer"

The phase interferometer is very important in the direction-finding and position of target. In this paper, the phase interferometer is employed to angle measurement of the stepped frequency radar target. By the way of dual-line digital phase interferometer, the contradiction between direction range and direction accuracy is solved. The effect of SNR and AOA on the accuracy of angle measurement is also analyzed. In order to remove the errors of amplitude and phase which is introduced by the antenna element, cable and receiver, an error correction method is presented. The algorithm of angle measurement and the method of removing errors of amplitude and phase are verified by the experiment. [C1190]

### "PMHT with Application of Road Information Based on GMTI"

Probabilistic Multi-Hypothesis Tracking (PMHT) is an algorithm for multiple target tracking when association of measurement and track is unknown. PMHT is an efficient algorithm for GMTI in cluttered environments of which the computational complexity is linear in the number of targets and measurements. An algorithm is presented in this paper to apply road information to PMHT. Road information is used to adjust estimated target state during the process of Kalman filter. Tracking performance of PMHT is increased apparently with the application of road constraint. [C1191]

### "A Wideband Beamformer Extended to MIMO Radar"

MIMO radar algorithms are the latest generation of techniques which can be applied to phased array radars. They offer the potential to improve the resolution, number of targets that can be identified, and flexibility in beam pattern design. To date, most of the work on MIMO radar has been performed assuming the signals are narrowband. However, wideband signals can also improve radar resolution, among other benefits, and are sometimes unavoidable when stringent range resolution specifications must be met. This paper presents a method for extending the MIMO narrowband model to a wideband model. This is necessary to obtain improved results from parameter estimation when the transmitted signals are wideband. The results show that the method greatly improves the results compared to those obtained when no techniques are implemented to compensate for a wideband signal. However, best performance is still obtained with a narrowband signal, and therefore the technique presented might only be of interest when a wideband signal is required. [C1192]

### "An Intelligent System on Water Quality Remote Monitor and Water Bloom Prediction"

An intelligent system on water quality GPRS remote monitor and water bloom prediction based on neural network are proposed in this paper, which can realize the automatic real-time monitor for the change of water quality and via the prediction by neural network for water bloom, thereby solve the lagging state of water quality monitor and the problem of water bloom prediction at present. [C1193]

### "Fault Diagnosis Platform For Radar Circuit Based on Virtual Instrument"

In order to improve the efficiency of the Radar circuit maintenance, in this paper, based on PXI & GPIB Hybrid Bus and virtual instrument technology, a fault diagnosis platform for Radar circuit is developed, and also a fuzzy fault tree reasoning algorithm is presented. This platform is composed of two parts: hardware and software. The hardware consists of a built-in controller and 3 kind of virtual instruments which are digital storage oscilloscope, digital multimeter and spectrum analyzer. The software is constructed by a fuzzy fault tree reasoning algorithm and an expert knowledge database which includes 198 fault tree flow charts of 20-style Radars. By experiment of this platform, the result shows that, with virtual instruments, fuzzy fault tree reasoning algorithm and expert knowledge database, the platform can locate the Radar circuit fault effectively. [C1194]

### "Time resources allocation in cognitive radar system"

This paper considers the problem of simultaneously detecting and tracking multiple targets. The main problem discussed here is the time allocation of cognitive radars in a multitarget environment. Radars are used to detect, to locate and to identify target. The radar performs three main functions: search, tracing and weapon engagement. Each of functions occupies amount of time. It is a key point that to allocate radar time resource



effectively. For cognitive radar, it should have the basic function which is learning. The radar needs to manage its resources dynamically and interactively between the setting of radar parameters to optimize the tasks the setting of radar parameters to optimize the tasks to be carried out and perceive environment highlights the role in which knowledge and intelligence will be central in cognitive radar performance. In this paper, we develop the optimization criterion based on the detection probabilities. [C1195]

#### **"Noise analysis for noncontact vital sign detectors"**

A method for analyzing the overall noise performance of vital sign detectors is introduced. For demonstration purpose, the noise analysis on a quadrature direct-conversion vital sign detector is performed. The detector is divided into three sub-systems including RF Front-end amplifiers, mixer with LO, and baseband amplifiers. The noise characteristics of the sub-systems are studied individually and combined to form the overall noise evaluation of the detector. The study on mixer sub-system results in a key design consideration of mixer. The signal-to-noise ratio at the sampler input is defined as the output SNR and is used to measure the overall noise performance of the vital sign detectors. The effect of output SNR on vital sign detection is presented. Tradeoff between output SNR and detection distance is verified by the experimental results. [C1196]

#### **"Research on Physiological Parameters Monitor Based on Multi-Functional Device"**

In accordance with the special requirements of medical devices, this paper describes the software design process of a physiological parameters monitor based on multi-functional device. The physiological parameters monitoring software achieved serial communication with physiological parameter acquisition module by adding MSComm widget. The monitoring software is designed into multi-view structure for the 5-lead ECG and 7-lead ECG drawing and it displays various parameters of patient and monitor on its dialog bar and status bar. When the monitor gets dangerous physiological signal from patient, the software drives speaker to sound in corresponding way, at the same time, it drives GSM/GPRS module to call for help by sending corresponding message to preset phone number. Test results showed that the monitoring and operational performance of the monitor reached expected requirements and both the two alarm modes could work correctly. [C1197]

#### **"A New Three-satellite High-precision RDSS/RNSS Combination Positioning Method"**

Under the guidance of the comprehensive RDSS, a new three-satellite high-precision RDSS/RNSS combination positioning method is proposed in this paper, which uses a special designed RDSS/RNSS satellite and the others RNSS satellites to determine user position. The key research focuses on its principle and intending performance and lifesaving application. [C1198]

#### **"Stochastic dynamic programming model of adaptive waveform selection"**

In cognitive radar, it is very important to select proper waveform to transmit according to different environment. The adaptivity of waveform corresponding to environment can be realized in many ways. In this paper, stochastic dynamic programming model of adaptive waveform selection is proposed. With this model, dynamic programming algorithms can be used to solve the problems of adaptive waveform selection. The necessity of adaptive waveform selection has been shown with simulations. Finally, the whole paper is summarized. [C1199]

#### **"FM jammer excision by using time-varying AR filter in spread spectrum communication systems"**

The time varying jammer signal degrades the performance of spreading spectrum communication systems. In this paper, time-varying autoregressive (TV-AR) modelling is used to represent nonstationary jammer signals. The modelling approach leads to an effective technique for jammer excision. In this work, jammer components parameterized by their instantaneous frequencies (IF) are effectively removed using the TV-AR filtering. The approach results in a minimum distortion to the desired DS/SS signals in communications. In order to reduce the computation complexity, orthogonal polynomials are used for the basis function of TV-AR model. [C1200]

#### **"Image Fusion Based on Multi-scale Kalman Filtering"**

An image fusion algorithm, based on the Multiscale Kalman Filter (MKF), has been applied to combine remotely sensed data, acquired by radars having different resolutions and can improved information carried by each input image. The considered images have been acquired during the AIRSAR Mission and SIR-C/X-SAR Mission. The data have been co-registered to refer each pixel of each image to a common regular grid. The image fusion algorithm has been tested, and the merged images have been presented at different resolutions. A lineament detection algorithm based on the Hough transform, has been applied to the full resolution input data and to the full resolution merged data. The Golden Gate bridge has been detected in both images, but the computed probability of false alarm is lower in the case of the finest scale merged image than in the finest scale input

image. This fact demonstrates that the knowledge provided by the coarser resolution data has been transferred to the merged image, improving the performance of the lineament detection algorithm. [C1201]

### "The Applications and Methods of Pedestrian Automated Detection"

Pedestrian safety is a primary traffic issue in urban environment. The use of modern sensing technologies to improve pedestrian safety has remained an active research topic for years. The applications and difficulties of pedestrian automated detection were investigated, and the existing sensing technologies such as piezoelectric sensor, infrared sensor, ultrasonic sensor, microwave radar, laser scanner and computer vision were assessed for their suitability to pedestrian automated detection, their advantages and limitations were analyzed. As any one particular type of technology may have difficulties meeting all necessary requirements in various conditions, it is pointed out that a complete and reliable sensing system for pedestrian detection can benefit from the combined use of multiple sensors. [C1202]

### "Calibration Technology of Palmer Scanning Airborne Lidar with Vector Measurements"

It is prerequisite to calibrate misalignment matrix between laser scanner and Position and Orientation System (POS) before airborne Light detection and ranging (Lidar) system being putted into survey application. A palmer scanning Lidar can present forward and backward scan intensity images of ground control areas. The pairs of biases between ground control points and central points of forward/backward scan areas are used to adjust the vector measurements of laser footprints. With a pair of non-collinear laser beam vectors and the corresponding footprint measurements of one single control area, the optimal q-method is adopted to solve the orthogonal rotation misaligning matrix. Hardware-in-loop simulation results show that algorithm satisfies the precision requirement of airborne Lidar calibration and performs robustly under various scenarios. [C1203]

### "Synthetic Aperture Radar Image Segmentation Based on Markov Random Field with Niche Genetic Algorithm"

Markov Random Field (MRF) has been found to be effective in the domains of image segmentations, since the problems can be simplified to search the optimal label fields. The challenges in MRF image segmentations arise due to the complexity of optimization. Although Genetic Algorithm (GA) has been applied into the image segmentation with MRF, yet most of algorithms defined an individual as a pixel with gray-scales coding, which is powerless to restrain the noise. On the other hand, GA emphasizes the evolution of whole label field, which could cause the over-propagation in some local areas and the convergence to partial optima. To avoid trapping into the local optima, Niche Genetic Algorithm (NGA) is introduced into the MRF image segmentation in this paper. NGA uses the sharing function to restrain the mutation between two individuals with high similarity, which could preserve the diversity of populations. Furthermore, a mechanism of fitness interaction in neighborhoods is proposed to contribute to eliminate the isolated sparkle noise in Synthetic Aperture Radar (SAR) image. The followed segmentation experiment for SAR image proved that MRF segmentation with NGA could reach a satisfied result among the noise restraint, edges preservation and computation complexity. [C1204]

### "A Modified SPECAN Algorithm for Synthetic Aperture Radar Imaging"

We present a modified SPECAN algorithm for missile-borne SAR in flat flight mode. Using the proposed technique, long azimuth sequence can be processed at memory constraint which is helpful for real time imaging. In addition, spectrum overlap can be avoided by changing kernel of chirp-z transform and data selection. Experiments on simulated data are carried out to validate the theory. [C1205]

### "Application of Butterworth Filter in Display of Radar Target Track"

The noise in the radar data results in the flutter of the flight target in display screen, which may disturb observer. A rounding method for radar target track using Butterworth filter is proposed in this paper. With the spectrum characteristics of radar target track being analyzed, the filter's parameters can be designed and figured out. Therefore, after the noise in radar signal is magnified by a transformation algorithm, it can be smoothed online. The results of MATLAB illustration show that the method has a reliable denoising performance. [C1206]

### "The Application of Long-Distance Inspecting Electric Power Parameter Based on GPRS Communications"

The system of inspecting electric power parameter based on GPRS communications was designed and the inspecting data worked by CPU was transmitted to the control center by GPRS and INTERNET net. Inspecting industrial signal in real time and long distance was realized. [C1207]

### "3D Reconstruction for Robot Navigation Based on Projection of Virtual Height Line and its Performance Evaluation"

3D reconstruction is a challenging work for the autonomous navigation of robots. This paper proposes a novel 3D reconstruction method based on projection of virtual height line (PVHL). At first partition the scene scope uniformly into grids with a certain size. Then introduce virtual height lines (VHLs) which do not exist in the scene. Each VHL is projected on left image and right image, and two projection lines are generated. Each projection line has a point of intersection with the scene, which is the only existent and visible point on the projection line. So this point has the maximum similarity metric, and the height of the point is that of the corresponding scene. Finding the height of the scene is converted to prove whether the point of intersection has the maximum similarity metric or not. The experiments to reconstruct 3D scene are performed and the results show the proposed method is feasible and effective. [C1208]

### "New Technology and Applications on Millimeter-Wave Sensors"

Some new technology and applications on millimeter-wave sensors are reviewed. A novel method of human presence detection using passive millimeter-wave (MMW) sensors is presented. The method focuses on detecting a standing human from a moving platform in a cluttered outdoor environment using MMW radiometry. Millimeter-wave stepped-frequency sensor and millimeter-wave interferometric sensor are completely realized using microwave integrated circuits (MICs) and microwave monolithic integrated circuits (MMICs). The millimeter-wave stepped-frequency sensor operates from 29.72 to 37.7GHz and has demonstrated abilities in surface and near-surface sensing, including profile mapping, liquid-level monitoring, and anti-personnel mine locating. The millimeter-wave interferometric sensor operates at 35.6GHz and has demonstrated its multi-functional capability for measurement of displacement and low velocity. A new radar sensor architecture comprising an array of transceiver modules. Target applications of the sensor are automotive driver assistance systems. Experimental results with an eight channel radar sensor in the 76-77GHz frequency band are presented, which demonstrate the feasibility of the proposed architecture and show the performance of the modulation sequence and signal processing. Finally the technical challenges of millimeter-wave sensor systems are discussed. [C1209]

### "Ground Clutter Removing for Wind Profiler Radar Signal Using Adaptive Wavelet Threshold"

Wind profiler radar signal is subject to contamination from various non-atmospheric signal. A new wind profiler radar signal processing method based on wavelet is presented for the suppression of ground clutter using adaptive threshold. By using the discrete multi-resolution analysis, we developed the adaptive wavelet domain thresholding method, which allow us to identify the coefficients relevant for clutter and to suppress them in order to obtain the reconstructed clear-air signal. The adaptive algorithm for choosing threshold that allow the processing to adjust automatically to environmental conditions. Experiments for the real radar signal show that the method presented can suppress the ground clutter from the radar signal effectively. [C1210]

### "Automated Detection in SAR Images by Using Wavelet Filtering and Hough Transform"

A novel method of automatic detection of straight lines in Synthetic Aperture Radar (SAR) images is presented in this paper. The proposed technique has been tested on a simulated SAR image, and on a real SAR image. It is based on the joint exploitation of a Wavelet Filtering Algorithm (WFA) and Hough Transform (HT) to extract geometric regular features and to detect lineaments in the considered image. The detail images produced by the proposed Wavelet Filtering Algorithm have the same resolution as the original image. The algorithm has been integrated with a moving mask method on the detected lines in order to find the beginning and the end of the segments. The experiment shows that it has a more efficient tool with respect to the traditional approach. [C1211]

### "Scattering Centers Extraction of Radar Target Using Biquaternions"

Scattering centers estimation results are significant for radar target recognition in high frequency section. This paper introduces biquaternion theory into full-polarization scattering centers extraction of radar target. Firstly, we define full-polarization scattering centers as a biquaternion model. It makes a close connection between polarization parameters. Then, we propose Bihan's BQ-MUSIC thought to extract scattering centers' position parameters. Simulations illustrate that our theory gets better estimation results compared to polarization MUSIC algorithm of complex model. [C1212]

### "Design of Solar Photovoltaic Remote Data Transmission System Based on GPRS"

Taking the Solar Sail System combined by building construction and photovoltaic generation for example, this paper designs Solar Photovoltaic Remote Data Transmission System based on GPRS which completes data

receiving, processing and evaluation indicators' calculation. The framework, composition and communication protocol of the active energy transmission were discussed in detail. The design of Data Centre including data receiving and processing based on .NET platform as well as the mathematical models of the system evaluation indicators is the focus of this paper. According to field test, the test results show that the system perfectly realized remote transmission of solar photovoltaic power and it can not only lay data foundation for calculation of system evaluation indicators, but also provide an effective and reliable basis to the model of renewable energy demonstration. [C1213]

### "Nanosecond Pulser Based on Serial Connection of Avalanche Transistors"

Generation and measure of nanosecond pulse with large amplitude are difficult problems in the field of exploration. The principle of avalanche transistor is analysed and four-stage serial connection of avalanche transistors is designed. Experimental results show that across the 50Г,В load the amplitude of the output pulse can reach 666V and half-width is 3.4 nanosecond. Repeat frequency of the pulse can reach 10KHz. Time-domain waveforms of the pulse and the measure data are shown in the paper. The pulser and the RL-loaded bowtie antenna get matched. The pulser can be fabricated easily and works well. It can be used in UWB Ground Penetrating Radar to improve its validity. [C1214]

### "Improving geometric accuracy of optical VHR satellite data using Terrasar-X data"

The very high geometric accuracy of geocoded data of the TerraSAR-X satellite has been shown in several investigations. This precision has been reached fully automatically without any human interaction and is due to good sensor calibration, high accuracy of satellite position and the low dependency on the satellites attitude solution. High resolution optical images from space don't show this high geometric precision and need further ground control information, which is mainly due to insufficient attitude knowledge. Therefore TerraSAR-X data can be used as Г,В ground control Г,В to improve the exterior orientation and thereby the geometric accuracy of orthorectified optical satellite data. The technique used is the measurement of identical points in the images, either by manual measurements or through local image matching using adapted mutual information (MI) and to estimate improvements for the exterior orientation or Rational Polynomial Coefficients (RPCs). To be able to use this intensity based method, the radar data have to be filtered before starting the matching procedure. Through adjustment calculations falsely matched points are eliminated and an optimal improvement for the attitude angles is found. The optical data are orthorectified using these improvements and the available DEM. The results are very promising and compared using conventional ground control information from maps or GPS measurements. [C1215]

### "Wearable Doppler radar with integrated antenna for patient vital sign monitoring"

A 2.45 GHz wearable Doppler radar unit with radio data link is presented for use in portable patient monitoring and emergency response. Unlike portable Electrocardiograms (ECG) or Photoplethysmography (PPG), the near-field Doppler unit enables monitoring of the person's heart rate without the need for electrical contact or optical access to the patient's skin. The Doppler unit is designed to be embedded in a clothing garment such as a shirt or vest, or used by medical emergency personal in an instrumented blanket or medical stretcher. Since the Doppler unit is placed directly on or behind the patient's torso, the extraneous signals due to relative motion artifacts is greatly reduced. Low-cost design is achieved by employing PWB microstrip elements for the integrated patch antenna, microwave oscillator, and tuning elements. Also, since the distance between the Doppler unit and the patient is fixed, it was possible to tune the detection phase to enable the use of a single mixer diode and eliminate the need for quadrature detection. Measured heart data from this technique shows clear waveform substructure similar to PQRST complex features found in captured ECG data. [C1216]

### "Hybrid array for the detection and imaging of termites"

This paper describes a 24 GHz radar receiver array, designed to detect and image termite activity, behind a wall, floor or ceiling. This hybrid array is composed of two sub-arrays. A Direction of Arrival (DOA) sub-array for wide area detection of termites, and a 3D high resolution imaging sub-array for imaging individual termites. Here, we introduce an enhanced DOA algorithm, to resolve arbitrary numbers of targets, and compare simulation results with video of actual termites. [C1217]

### "Routing and Tracking System for Mobile Vehicles in Large Area"

The paper describes a practical model for routing and tracking with mobile vehicle in a large area outdoor environment based on the Global Positioning System (GPS) and Global System for Mobile Communication (GSM). The supporting devices, GPS module-eMD3620 of AT&S company and GSM modem-GM862 of Telit company, are controlled by a 32bits microcontroller LM3S2965 implemented a new version ARM Cortex M3 core.



The system is equipped the Compass sensor-YAS529 of Yamaha company and Accelerator sensor-KXSC72050 of Koinix company to determine moving direction of a vehicle. The device will collect positions of the vehicle via GPS receiver and then sends the data of positions to supervised center by the SMS (Short Message Services) or GPRS (General Package Radio Service) service. The supervised center is composed of a development kit that supports GSM techniques-WMP100 of the Wavecom company. After processing data, the position of the mobile vehicle will be displayed on Google Map. [C1218]

#### "UHF measurement of breathing and heartbeat at a distance"

The detection of breathing and heartbeat from a distance is important for medical triage and mass casualty events as well as routine monitoring of higher-risk patients. Typical approaches include wiring up patients to devices and wearable devices, but remote detection and monitoring is both easier on the patient and easier to administer. Monitoring at low frequencies means that there is less patient risk as well as extended range and reduced power. In this paper we look at the measurement of breathing and heartbeat of human subjects at UHF frequencies. We characterize the system design and capabilities as well as the algorithmic approach to extracting the signal. We measure biometric ground truth using heartbeat sensors, respiration monitors, and accelerometers. We do accurately measure breathing, and can measure heartbeat when the subject is holding his breath, but have not yet separated the heartbeat from breathing when both are being done simultaneously. [C1219]

#### "Effects of I/Q mismatch on measurement of periodic movement using a Doppler radar sensor"

In this paper, the effect of I/Q mismatch in a 5.8 GHz direct-conversion quadrature Doppler radar sensor detecting periodic movement is studied. The measured movement amplitude under specific I/Q amplitude or phase mismatch is affected by the residual phase, which is determined by the nominal distance from the target to the antenna. It was found that there exist optimal residual phases minimizing the degradation of detection accuracy caused by amplitude and phase mismatches. Experiments were conducted to verify the theory. [C1220]

#### "A coherent low IF receiver architecture for Doppler radar motion detector used in life signs monitoring"

Continuous Wave Doppler radar has been used in human life signs monitoring from a distance. Such systems are basically motion detectors that rely on phase modulation of the radar's reflected signal due to physiological motion which is of a low frequency nature and has significant signal content close to DC. Homodyne receiver architecture is simple, but has its own limitations including DC offset and contribution of low frequency noise from mixers and baseband amplifiers. A coherent low IF architecture has been proposed for this case to improve the performance. It will be shown that SNR is improved using a simple coherent low IF configuration. This is the first reported coherent low IF transceiver architecture for Doppler radar motion sensing. [C1221]

#### "Maximizing Sum of Image Intensity Square Autofocus Algorithm"

This High quality Synthetic Aperture Radar (SAR) imaging requires that azimuth frequency modulation rate is accurately estimated. A new algorithm is proposed for autofocus in synthetic aperture radar imaging. Based on image contrast, the paper analyses the relationship between maximizing sum of image intensity square and image contrast function, and maximizing sum of image intensity square autofocus algorithm is presented. Then the bisection which substitutes for advance and retreat method reduces computation. The processing results of the measured data shows better convergence speed of bisection and the validity of the proposed algorithm. [C1222]

#### "A comparative study of nonlinear filters for target tracking in mixed coordinates"

The measurement model nonlinearity is a major challenge in target tracking. This paper presents a comparative performance study of seven nonlinear filters in handling the measurement model nonlinearity. They are: the extended Kalman filter, the unscented filter, the second order divided-differences filter, the Gauss-Hermite quadrature filter, the two-step Kalman filter, the Gaussian particle filter, and the linear minimum mean-square error tracking filter with polar measurements. Comprehensive performance evaluation and comparison of all of the above mainstream nonlinear filters over the same tracking scenarios are conducted via Monte Carlo simulation. The results can facilitate the choice and design of nonlinear tracking filters in mixed coordinates. [C1223]

#### "Turn rate estimation based on curve fitting in maneuvering target tracking"

Tracking of highly maneuvering targets with unknown behavior is a difficult problem in state estimation. This

paper presents an interacting multiple model algorithm (IMM) utilizing adaptive turn rate models to track a maneuvering target. The turn rate is calculated at each step from the estimator of velocity and the radius of curvature of the trajectory of the target by using Least Square (LS) and curve fitting theory. Simulation in different scenario proves that the turn-rate estimation techniques in this adaptive framework can significantly solve the problem of tracking maneuvering targets. [C1224]

#### "Analysis of induced surface currents on high velocity target using a relativistic approach"

Radar is an electromagnetic system used for the detection and location of objects based on reflection. It operates by radiating energy into space and detecting the echo signal reflected from an object or target. This work analyzes how currents are induced on targets by the electromagnetic waveforms radiated by an antenna when the object is moving at high velocity. It is assumed that the target is a perfect electric conductor moving at high velocity. This work analyzes how the amplitude, the frequency and the duration of these currents are affected by the target velocity. The transmitted electromagnetic waveforms can then be calculated using vector potentials and by using the Lorentz transformation, the electromagnetic waveform is transformed from the stationary reference frame to a moving reference frame. Currents induced on the object can be modeled by using the transformed waveform and the equivalence principle. The object radiates an electromagnetic waveform as a consequence of the induced currents. The radiated waveform is calculated using the vector potentials and once more the reflected waveform is transformed from the moving reference frame to the stationary reference frame using the Lorentz transformation. Finally the equivalence principle was used to calculate currents induced in the antenna by the reflected electromagnetic waveforms. The relationship of the induced current on the antenna as a function of the target velocity is analyzed. [C1225]

#### "Application of Fuzzy Logic control in automated transport systems"

This paper describes a vehicle position control strategy in relation to other vehicles and nearby obstacles with the aim of collision avoidance and improving safe driving in personal transport systems. A simplified probabilistic model together with fuzzy logic control strategy has been proposed, which considers the probability of detection of sensors to be processed by probability coverage matrix. Simulation results in Matlab (Fuzzy logic toolbox) show that the proposed method for the system can yield to more sophisticated and elaborate control strategies. Detailed probabilistic models along with a global optimisation of parameters has been found to enhance the applicability of the Fuzzy Logic scheme. The sensors are based on the radar systems. The sensor fusion to enhance the driver, vehicle, and environment are also discussed. [C1226]

#### "The comparison between the TE<sub>21</sub> mode and the four-horn monopulse technique for LEO satellite tracking"

One of the most well-known techniques, which are used in the ground stations in order to track the LEO satellites, is monopulse. Two most popular of them are four-horn and TE<sub>21</sub>mode monopulse techniques. In this paper the monopulse tracking technique using TE<sub>21</sub>mode is analyzed and compared with the four-horn monopulse tracking technique. The key parameters of TE<sub>21</sub>mode monopulse technique including the linearity and slope of the error signal are calculated. It is demonstrated that the linearity of the error signal is improved in comparison with the four-horn monopulse technique. Although the slope of the error signal decreases in the TE<sub>21</sub>mode tracking technique, the estimation of the satellite angle is more accurate in most of the cases compared to the four-horn tracking technique. [C1227]

#### "Scattering of electromagnetic radiation for a perfect electric conducting cylinder by using multiple angles of polarization"

Radar is a device which detects distant or non visible objects by means of reflected radio waves. The quality of the reflected signal depends on the shape and orientation of the target with respect to the type of polarization used. Most of the antennas currently used on radar systems employ one type of polarization at a time for target detection. This paper describes the importance of employing polarizations of multiple angles on targets, approximately at the same instant of time. To implement this idea a generalized set of equations have been derived which represent the backscatter generated by a cylindrical object. Using different angles in these equations would give the backscatters of different polarizations employed on the same target, at small time intervals. The logic behind this is that there would be at least one angle that would have the maximum signal strength in the backscatter. The backscatter for this angle would satisfy the best quality criterion as compared with the rest of the polarization angles. [C1228]

#### "Kahn-technique transmitter for L-band communication/radar"

This Kahn-technique (Envelope Elimination and Restoration) transmitter operates at 1.2 GHz and produces a PEP output of 50 W. It employs a GaN-HEMT class-F RF-power amplifier, class-S modulators, and a digital signal processor. An overall (driver + final) efficiency of 50 percent or more is maintained over the top 6 dB of the output range. The driver and final are operated to maximize overall efficiency and the predistortion corrects for amplitude and phase errors. While originally intended for pulsed radar applications, the transmitter is capable of producing a wide variety of signals with good linearity and average efficiency. [C1229]

#### **"Imaging method: A strong tool for moving target tracking by a multistatic UWB radar system"**

In this paper, imaging method for moving target tracking by a multistatic ultra-wideband radar system is described. The task of moving target tracking consists in estimation of a target trajectory based on processing of raw radar data obtained from all receiving channels of a radar system. Then, the imaging method applied for target tracking consists of such signal processing phases as raw radar data pre-processing, background subtraction, fusion of the data obtained by receiving antennas of a radar, detection, localization and tracking itself. The performance of the imaging method described in this paper is demonstrated by signal processing obtained by M-sequence UWB radar for a scenario represented by through wall tracking of a single moving target. The obtained results confirm the excellent performance of the discussed method. [C1230]

#### **"Nonparametric techniques for graphical model-based target tracking in collaborative sensor groups"**

Target tracking using collaborative sensor groups is an effective mechanism for reducing the scalability issues in distributed sensor networks. Using graphical models for such a sensor group together with appropriate class of nonparametric message passing algorithms, we explore efficient approaches to handle the related data fusion problems characterized by spatially distributed observations. Messages consisting of multiple Gaussian components have been efficiently handled with the help of nonparametric belief propagation techniques. The advantage of such an approach in a myopic radar network has been verified here using Monte Carlo simulations by comparing the tracking performance obtained with centralized and distributed fusion schemes. [C1231]

#### **"A GLRT detector in partially correlated texture based compound-Gaussian clutter"**

This paper addresses the problem of target detection in the presence of a non-Gaussian clutter modeled in compound-Gaussian form which realizes the clutter process as a product of two independent random processes 'texture' and 'speckle'. The likelihood ratio test (LRT) detector applied to this detection problem reduces the detector to a matched filter (MF) when the texture is considered as completely correlated during a coherent processing interval (CPI). However, in practical applications, the textural component exhibits a correlation which is less than unity. The conventional form of MF based detectors existing in the literature yield a significant fall in the detection performance in such clutter scenarios. In this paper, we propose a generalized likelihood ratio test (GLRT) detector which can effectively detect a fluctuating target in the presence of a compound-Gaussian clutter with partially correlated texture. The results are presented to show the performance superiority of the proposed detector over the existing MF detector in such varying texture scenarios. [C1232]

#### **"A New Detection Method for MIMO Radar Using Hidden Markov Model"**

MIMO radar is a new radar technique developed recently. It can achieve better detection performance than conventional phased radar. Based on the scattering statistic of clutter and man-made target, we propose that hidden Markov models (HMM) can be used to model the clutter and target signals, and that the HMMs can be used to detect target. Simulation results verify its efficiency. [C1233]

#### **"An Algorithm of Weak Signal's Detection on the Condition of Strong Interference"**

An algorithm which can detect weak signals on the condition of strong correlated interference is designed in the paper. The algorithm based on conventional beam forming (CBF) can put nulls on given directions. And the weights only relating to interference's direction is given in the paper. Comparing to adaptive methods, the algorithm is robust and the calculation account is smaller. Simulation results show the algorithm can put null on the strong interference's direction, getting a clear bearing track recorder while the CBF even can't get the target's track. [C1234]

#### **"RF Effect Algorithms of Terrain Environment in Signal-Level Radar System Simulation"**

In radar system simulation, the reliability of simulation results depends not only on radar and target models, but also on RF (radio frequency) environment models, including clutter, multipath and diffraction. In radar function simulation, all of these factors are treated as a single pattern-propagation factor and can only give limited

information for radar models. In signal-level simulation, radar models require that simulated echoes should include information such as delay, phase shift, doppler frequency, polarization, etc. By discussing and analyzing the principles and algorithms of RF environment effects of ground, a ground RF environment model is proposed, which can provide a reliable RF environment for signal-level simulation of radar systems. A simulation example involving clutter model is carried out and analyzed. [C1235]

#### "A Method of Weak Signal Detection Based on Duffing Oscillator"

A new signal detection and estimation method based on the intermittency transition between order and chaos is proposed. Using Melnikov function to determine the threshold of the detection system is introduced. The characteristic of Duffing oscillators with the changing of dynamics of the system is analysed. The method of detection of weak signals in strong noise based on Duffing oscillators is studied by exploiting characteristic of phase changing from chaos state to great periodic state of system nearby critical coefficient. Through analysing the intermittent chaos mechanism of Duffing oscillator, it was found that the system output is a intermittent chaotic signal when input frequency deviates the compulsory drive frequency slightly, and the deviation can be estimated by the statistic characteristic of output chaotic signal. The experiments results indicate that the signal detection method based on Duffing oscillator can detect weak sinusoidal signals with extremely low signal to noise ratio and accurately calculate to-be-detected signal frequency. [C1236]

#### "A 4.5mW digital baseband receiver for level-A evolved EDGE"

A digital baseband receiver ASIC that supports GSM/GPRS/EDGE and Evolved EDGE is implemented in 0.13  $\mu\text{m}$  CMOS technology. The design centers around two main blocks: an adaptive channel equalizer processes GMSK/8PSK/16QAM and 32 QAM modulated signals and a flexible channel decoder supports convolutional and turbo codes, as required for Evolved EDGE. The receiver occupies 2.0 mm<sup>2</sup> and the average power consumption during burst reception and processing is less than 5 mW in each of the modes. [C1237]

#### "A novel 77-GHz radar frontend with 19-GHz signal distribution on RF-PCB substrate"

A novel radar frontend for 77 GHz mid-range-radar (MRR) and short-range-radar (SRR) applications is presented. The radar sensor makes use of a Colpitts oscillator, frequency multipliers, and a transceiver (TRX) mixer. A single sensor contains up to four channels using antenna arrays for angular detection relative to the sensor. The characterization of the integrated circuit's parameters has been carried out using a two-channel sensor with waveguide (WG) transitions. A radar measurement scenario has been realized using a four-channel sensor with a differential antenna array. All sensors have been implemented on off-the-shelf printed circuit board (PCB) substrate. [C1238]

#### "MIMO radar based on reduced complexity compressive sampling"

In their previous work, the authors considered a multiple-input multiple-output (MIMO) radar implemented by a set of randomly dispersed nodes within a small scale network. Exploiting the sparseness of targets in the angle-Doppler space, compressive sampling was exploited for obtaining joint angle-Doppler information on potential targets based on a small number of observations. That approach achieves the superior resolution of MIMO radar with far fewer samples than required by conventional approaches. However, it involves a discretization of the angle-Doppler space, and as the discretization step decreases in order to achieve high resolution, complexity increases. In this paper, a scheme to reduce the complexity of the aforementioned approach for the case of slowly moving targets is considered. The complexity reduction is achieved by decoupling angle and Doppler estimation. An approach is also proposed for identifying angle estimates that correspond to jammers. [C1239]

#### "Data Transmission over GSM Adaptive Multi Rate Voice Channel Using Speech-Like Symbols"

This paper introduces a new method to transmit digital data through Global System for Mobile communications (GSM) voice channel. A novel algorithm is proposed to design a set of Speech-Like (SL) symbols which leads to design a GSM voice channel data modem to modulate and demodulate data on GSM Adaptive Multi Rate (AMR) voice codec which consist of different bit-rates. Designing a set of time-symbols is an off line procedure with the aim of minimizing symbol detection error. This modem is useful in real-time data communication with high priority. The introduced modem encodes data into SL symbols to be transmitted over GSM voice channel and the received SL symbols are decoded back to data. [C1240]

#### "Content Dependent Data Hiding on GSM Full Rate Encoded Speech"

This paper introduces a steganographic approach to embed data on compressed speech bit stream in order to hide secret data. This method may be used by any kind of encoded bit stream, but this research concentrates on



full rate (GSM 6.10) encoded bit stream. This method allows user to adjust embedded data bit-rate or speech quality. Speech quality is determined by Perceptual Evaluation of Speech Quality (PESQ) which is an objective testing. The effect of embedding data to each specific bit of GSM Full Rate coefficients, on speech quality has been investigated and the less important bits are selected to embed secret data. Meanwhile for approaching a higher speech quality, the data embedding positions are based on different speech frame types. In other words the proposed technique is modified to achieve a content dependent algorithm. [C1241]

### "The Chaotic Behavior of the Chaos-Based Phase-Coded Pulse Train Signal"

The article gives two forms of chaos sequence phase-coded radar signal, and uses ergodic criterion of chaos sequence-Lyapunov exponent as a criterion, under which the chaos-based PM radar signal having the desired autocorrelation curve, if the constraint is violated, its autocorrelation curve would be degraded. The conclusion is ensured by several simulation results. [C1242]

### "Performance analysis of range sensors for a real-time power plant coal level sensing system"

A coal-fired power plant typically has silos, bunkers or stock piles in which the fuel is placed for storage purposes. Real-time feedback sensors are utilized to sense the coal height so data can be sent to downstream systems for further processing. These systems are required to accurately sense the height of coal within the bunker or stock pile. The range information is then fed in a real-time fashion to a control system. Inaccurate measurements can result in severe environmental and safety consequences. There are many types of ranging sensors available in the marketplace. The coal-fired power plant application is especially daunting due to the particularly harsh operating conditions and reliability requirements. This research project analyzes the performance of three types of range sensors: ultrasonic, radar and laser systems. These systems are currently operational at a plant located in the North East Texas area. The ultrasonic and radar sensors were part of legacy systems and the new laser sensor was integrated as a part of this study. The feedback signals from each sensor were recorded over time and compared to measured data. The laser sensor proved to be slightly more accurate than the others, but it has some drawbacks that were listed. [C1243]

### "Determination of parameters for digital meter of doppler radars systems for the artillery systems"

Analytical choice of the digital meter parameters based on digital systems of phase synchronization (DSPS) is considered, also the simulation model design in order to perform the optimization of its parameters and to determine the temporary characteristics and the accuracy of the motion parameters of objects estimating, for the systems with autonomous navigation and ballistic training artillery systems. [C1244]

### "Optimized FPGA implementation of Multi-Rate FIR filters through Thread Decomposition"

Multirate (decimation/interpolation) filters are among the essential signal processing components in space-borne instruments where Finite Impulse Response (FIR) filters are often used to minimize nonlinear group delay and finite-precision effects. Cascaded (multi-stage) designs of Multi-Rate FIR (MRFIR) filters are further used for large rate change ratio, in order to lower the required throughput while simultaneously achieving comparable or better performance than single-stage designs. Traditional representation and implementation of MRFIR employ polyphase decomposition of the original filter structure, whose main purpose is to compute only the needed output at the lowest possible sampling rate. In this paper, an alternative representation and implementation technique, called TD-MRFIR (Thread Decomposition MRFIR), is presented. The basic idea is to decompose MRFIR into output computational threads, in contrast to a structural decomposition of the original filter as done in the polyphase decomposition. Each thread represents an instance of the finite convolution required to produce a single output of the MRFIR. The filter is thus viewed as a finite collection of concurrent threads. The technical details of TD-MRFIR will be explained, first showing its applicability to the implementation of downsampling, upsampling, and resampling FIR filters, and then describing a general strategy to optimally allocate the number of filter taps. A particular FPGA design of multi-stage TD-MRFIR for the L-band radar of NASA's SMAP (Soil Moisture Active Passive) instrument is demonstrated; and its implementation results in several targeted FPGA devices are summarized in terms of the functional (bit width, fixed-point error) and performance (time closure, resource usage, and power estimation) parameters. [C1245]

### "COTS implementation of a Sensor Planning Service GetFeasibility operation-Interim status"

This paper reports on the progress of the design and implementation of a Web-based Sensor Planning Service (SPS) that discovers sensors, formulates sensor collection tasks, and determines feasibility of collection tasks for optical and radar Earth imaging spacecraft. The design is founded on Commercial off the Shelf (COTS) mission modeling capabilities from Analytical Graphics, Inc. (AGI). An SPS providing a COTS GetFeasibility operation will make it easier for users to discover sensors that fulfill their needs. A COTS common interface will provide the

user with one well-known set of operations for the initial discovery of candidate sensors. A final selection of sensors can be carried out using the SPS operations of the individual Data Providers. The first step is a Proof of Concept Sensor-Planning Service (PoC-SPS). It includes the design and implementation of a Standard Object Catalog (SOC) and the design and prototyping of the work flow. The work flow prototyping also supports the design of an interface between system modeling language (SysML) system modeling and AGI mission modeling capabilities. The SOC is a community driven library of spacecraft, facilities and other assets with accurate and thorough descriptions of mission capabilities. The SOC is initially populated with optical and radar Earth imaging spacecraft and sensors. [C1246]

#### "Analysis of the information contained in amplitudes of the reflected signals received by space diversity radars"

In this paper cross-correlation treatment of the narrow-band signals of two different frequencies of one band of lengths of events reflected from the radar target is examined. Thus the mathematical model of reflecting characteristics of radar target is used. [C1247]

#### "Economic aspects of realization of the government programs of development of the technical systems"

In this paper the situation of information possibilities in Azov and Black Seas region is given. The search of optimal creation of complex distance monitoring system is proposed. [C1248]

#### "Input microwave devices for space surveillance radar system with identical phase-frequency characteristics"

The results of design and production of input microwave devices for space surveillance radar system with identical phase-frequency characteristics are presented in this paper. Functional design schema is suggested. [C1249]

#### "Initialization of ballistic targets tracking filters with detection probability lower than unity"

Radar tracking of a projectile flying in the Earth's atmosphere is a very complex issue to cope with, due to the need of (suboptimal) nonlinear filtering techniques. Almost all cases found in literature assume that the target trajectory is observable from the firing point to the impact point on the ground, namely the trajectory observation gets under way from the first available measurement. The radar track initiation time is actually a stochastic quantity that has to be treated by means of a statistical procedure. In this paper a preliminary analysis of the effect of a more realistic filter initialization is proposed. [C1250]

#### "Multitarget track before detect with MIMO radars"

Recent advances in Multiple-Input-Multiple-Output (MIMO) radar systems show that they have the potential to improve detection and localization performance of targets over bistatic and multistatic radars. Unlike beam forming, which presumes a high correlation between signals either transmitted or received by an array, the MIMO system exploits the independence between signals at the array elements due to transmit diversity. Previous works focus on waveform design, signal processing and target localization with MIMO radars while no attention has been given to tracking algorithms. In this work, the problem of tracking multiple targets using MIMO radars is considered. The scenario includes multiple targets in a widely-separated MIMO architecture in which Radar-Cross-Section (RCS) diversity can be utilized. Multi target version of Track-Before-Detect (TBD) algorithm is implemented for the collected  $M \times B - N$  orthogonal signals at the receiver, where  $M$  is the number of transmitters and  $N$  is the number of receivers. Besides having the advantage of integrating information over time on unthresholded measurements to yield detection and tracking simultaneously, the TBD technique enables tracking and detecting targets in low Signal-to-Noise-Ratio (SNR) environments. Also, a modified multiple sensor TBD, which weights the target observability to the sensor as a result of target RCS diversity in the likelihood calculation to best fit the centralized MIMO tracking is proposed. Finally, Monte Carlo simulations are performed to evaluate the performance of the proposed tracking algorithm. [C1251]

#### "Design of Schmidt-Kalman filter for target tracking with navigation errors"

In most target tracking formulations, the tracking sensor location is typically assumed perfectly known. Without accounting for navigation errors of the sensor platform, regular Kalman filters tend to be optimistic (i.e., the covariance matrix far below the actual mean squared errors). In this paper, the Schmidt-Kalman filter (SKF) is formulated for target tracking with navigation errors. The SKF does not estimate the navigation errors explicitly but rather takes into account (i.e., considers) the navigation error covariance provided by an on-board navigation

unit in the tracking filter formulation. Including the navigation errors leads to the so-called  $\Gamma, \tilde{B}$  consider covariance.  $\Gamma, \tilde{B}$  By exploring the structural navigation errors, the SKF is not only more consistent but also produces smaller mean squared errors than regular Kalman filters. Monte Carlo simulation results are presented in the paper to demonstrate the operation and performance of the SKF for target tracking in the presence of navigation errors. [C1252]

### "Bearings-only tracking using derived heading"

In conventional bearings-only tracking, the target states are estimated from just the bearing measurements. The accuracy of these estimates can be improved by using the heading, which can be derived from a set of measured bearings, as an additional measurement. In this paper, the target heading has been computed from a set of bearing measurements. This, along with bearings, has been used to obtain state estimates. The Cramer-Rao lower bounds for these estimates is derived and compared with that of the conventional bearings-only tracking. The use of derived headings improves the position estimates during target maneuver. This technique has been applied to multi-target tracking and is found effective particularly during target crossing. The tracking results are obtained using particle filters and compared to that of an extended Kalman filter implementation. The simulation results demonstrate the improved estimates obtained for certain target states. [C1253]

### "Kinematic separation point estimation using PMHT"

When two objects separate there is typically a period of time after the separation when the two objects are unresolved by a radar. This is due to the radar range bin resolution, which will keep two returns as one measurement until there is a clear separation. At that point, a new track will start, but where exactly did the objects separate? The actual separation point may be of interest and finding that separation point is the topic of this paper. Using the PMHT algorithm allows measurements to be  $\Gamma, \tilde{B}$  shared  $\Gamma, \tilde{B}$  between tracks, and therefore, makes an excellent algorithm for when there are closely-spaced unresolved measurements. After a separation event, while the measurements are still unresolved, there will be only one measurement for the two objects. PMHT is quite comfortable with this situation when there are fewer measurements than there are objects because the PMHT has to know a priori how many objects there are. When a new track starts, the PMHT separation point estimation algorithm will be called. Then the PMHT algorithm can add in the unresolved measurements backwards in time to determine the likely separation point. [C1254]

### "Tracking multiple unresolved targets using MIMO radars"

Multiple Input Multiple Output (MIMO) radars are a new generation of radar systems that may bring about many benefits compared to traditional phased-array and multistatic radars. Although different aspects of MIMO radars have been discussed in the literature, the application of MIMO radars in target tracking problems has not been explored in depth. Target localization using MIMO radars with co-located antennas has been discussed in the literature. The main limitation of those approaches is that the number of targets that can be uniquely localized in one cell is restricted. This paper presents a new application of MIMO radars in Multi-Target Tracking (MTT) problems. The main contribution is to show that the use of prior information about the motion of targets relaxes the limitation on the number of targets that can be uniquely detected. A general MTT problem with several targets in the same resolution cell is considered. The goal is to propose a technique to estimate targets' states and the number of targets in one cell. Because multiple targets may fall in the same cell, the measurement in a cell is associated with more than one target. Measurements are outputs of matched filters and range bins that are nonlinear functions of targets' states. Multiple hypotheses are generated based on the uncertainty in target-to-cell association. Then, the best model which gives the number of new targets whose estimates are obtained by the localization algorithm, is selected according to its likelihood. Finally, due to the nonlinearity in measurement model, a UKF based method is used to update estimates of new targets and initialize new born targets. Simulation results show the superiority of the proposed method for joint localization and tracking compared to the previous localization approach suggested in the literature for unresolved targets. [C1255]

### "A track purity approach for tracking metrics"

Proper analysis of a simulated sensor tracking problem requires the ability to correctly determine the true trajectory that underlies each track. Traditionally, kinematic assignment of tracks to truth has been used. More recently, a "track-purity" approach has been proposed to both assess the performance of kinematic truth-to-track assignment algorithms and to overcome some of the anomalies that occur when kinematic assignment is used; particularly for unresolved closely-spaced targets. The track-purity approach relies on a simulation's unique ability to identify which truth objects contribute to each measurement. Less clear are the following issues: 1) When a measurement is formed, what is the percentage contribution from each truth object in each measurement primitive, 2) How should truth contributions be combined and modified as measurement data are

passed through the various data and signal processing algorithms found in a typical monopulse phased-array radar (e.g., closely-spaced unresolved objects, direction-of-arrival estimation, measurement clustering, data assignment, filtering, and multi-sensor fusion), 3) How should truth content values be used to produce a content-based association between tracks and truth? The complete process for establishing the truth content of a track from the initial truth content of each detection to the final truth content at the output of track filtering is discussed. This discussion includes the effects of measurement clustering and centroiding, ambiguity in the measurement-to-track assignment, filter gains used to update the track's state estimate, and a truth-contribution-based method for establishing track-to-truth assignment. [C1256]

#### "Experimental radar with 64-channel digital antenna array"

In this article are analyzed a results of experimental radar with digital antenna array full-scale test against above-water targets. [C1257]

#### "Impulse radio signal processing considering the internal phase-frequency instability"

The impulse radio signal processing method is considered with taking into account their internal phase-frequency instability. [C1258]

#### "Sidelobe cancellation method at the exit of correlation processing scheme"

The criterion of sidelobe cancellation in the receiving tract of radar receiver in the case of usage binary phase-shift keying is considered. [C1259]

#### "Non-stationary EMF measurements"

Problems of accuracy improvement of non-stationary electromagnetic field (EMF) measurement is discussed. New method of calibration is proposed that allows reduction the meter's calibration error to  $\Gamma, B \pm 1$  dB. [C1260]

#### "Essence of radio signals processing in close range reconnaissance"

In this paper the approach to make a high resolution in radar is given. The structure of radar system with projector matrix filters is depicted. [C1261]

#### "Adaptive lattice filters for band-inverse covariance matrix approximations"

Theory of adaptive lattice filters, developed originally for stationary processes with Toeplitz covariance matrices, was well-established by the pioneering contributions of Burg, Kailath, Friendlander. The lattice filters are intimately related to the well-known Levinson algorithm, that requires  $O(N^2)$  operations for  $N \times N$  Toeplitz covariance matrix inversion, and exploit Burg technique for adaptive estimation of reflection coefficients that naturally preserves positive definiteness of the estimated Toeplitz covariance matrix. [C1262]

#### "Application of clustering methods for recognition of technical objects"

In this paper the clustering methods with different similarity measures were used to classifying the intercepted signals generated by electromagnetic sources to one of the previously identified  $L$  classes in  $N$ -dimensional feature space. The quality of these methods performing technical objects recognition was examined by using the computer simulated date. [C1263]

#### "Passive hindrances suppression using complex polyphase signals"

Using complex signals we get possibility of indemnification of passive hindrances in the single channel system of radio monitoring due to the use of correlation and spectral characteristics of certain class of complex signals. [C1264]

#### "Some results of radar signal detections by the use of compressive receiver"

The paper presents some results of weak, pulsed and continuous radar signals detection by the use of compressive receiver. [C1265]

#### "An analytical, imitation and experimental design of device of surveillance is after bearing frequency"

Speech goes in this lecture, about research of device of surveillance after bearing frequency, at the dynamic



change of frequency on an entrance. [C1266]

#### "Application of AR model for radar recognition of meteorological objects"

The algorithm and measuring radar for recognition of meteorological objects are described. [C1267]

#### "Measurement of parameters of solid aerosols in polydisperse medium using double frequency radar"

In this paper the double frequency method for remote sensing of solid aerosols are considered in the case of polydisperse medium, when aerosols particles are distributed by lognormal law. The results of numerical simulation for two extreme cases- $\Gamma, B_{\text{inarrow}}$  and  $\Gamma, B_{\text{wide}}$  distribution law are presented and the limits of the method applicability are estimated. [C1268]

#### "Object recognition with surveillance radar systems"

In this thesis have written description and principle of radar systems and them classification. As well as radar systems are used where and for what. The most optimal signal transmission and principles of systems in general. [C1269]

#### "Information approach to estimation of the multispectrum monitoring device efficiency"

The technique of self-descriptiveness estimation by hyperspectrum "information cube" of video spectrometers is adapted for multispectrum monitoring devices (MMD). [C1270]

#### "Multiprotocol transceiving, Formatting and Temperature monitoring FPGA based unit"

The FCT (Formatting, Communications and Temperatures) electronic unit developed at INTA's radar laboratory as part of the X-Band synthetic aperture radar project (RBX SAR, see ref) is capable of receiving up to four channels of radar pulses and echoes at 1.5 Gbps line rates, with the use of aurora protocol on top of the Virtex 5 gigabit transceivers, format these data and send them to the system's storage unit (UAD) with a parallel protocol. In addition, the FCT communicates with other units through a VME bus. It also handles the memory map of the X-band transmitting unit, as well as translates the VME parallel bus communications to this unit to a 1.5 Gbps serial aurora protocol through optical fiber. Besides, the FCT monitors and stores temperature data gathered from different units of the radar system through a serial SMBus protocol, and manages access to these data through VME bus. Finally, with a second Virtex 5, it formats, decimates and filters the received radar echoes and sends them to the real time processing unit through a serial sFPDP protocol (1.0625 Gbaud). [C1271]

#### "A stochastic-gradient method to design optimal space-time codes for MIMO radar detection"

We consider a MIMO radar system with widely-spaced transmit/receive antennas and study the problem of designing the signal waveforms transmitted by each source node so as to maximize the detection probability for a fixed false alarm rate under correlated Gaussian clutter. The proposed design procedure relies on a stochastic-gradient search and is general enough to be applied to any statistical target model. Examples are provided to compare the performance of the proposed codes with other known coding schemes. [C1272]

#### "A Hotelling T-squared GIP test for detection of over resolved targets"

A new technique for detection and discrimination of stationary or slow-moving over-resolved targets on the ground, based upon a Hotelling T-squared test/generalized inner product (GIP) approach to signal analysis is presented. This robust detector separates radar returns from interference via a coherent process. This GIP-based processing can be applied to single-receiver channel systems, multiple spatial channel systems, multiple polarization channel systems or systems with multiple spatial and polarization channels. [C1273]

#### "Microwave Doppler radar sensor with enhanced immunity against interferences"

Modern anti-armor missiles represent enormous threat for any military vehicle. Simple hand-held missiles are able to penetrate 300 mm, more sophisticated missiles up to 1000 mm of the best steel armors. Active defense methods seem to be promising ways how to face this problem. These systems are based on sensors able to detect and measure approaching threat missile and generate signals that activate a suitable counter-measure. The paper describes Doppler radar sensors designed for active defense configurations. The designed version solves one of potential problems connected with employment of these radars at military vehicles. This concerns

sufficiently high immunity against both unintentional and intentional interfering signals. [C1274]

### "System performance prediction of Firefinder radar"

Thales Raytheon Systems' PC Simulation (PCS) tool allows a rapid simulated evaluation of Firefinder radar performance from a personal desktop computer. Firefinder radars are designed to track hostile rocket, artillery and mortar (RAM) projectiles in order to accurately estimate weapon ground location. The Firefinder tactical code is used within PCS. This design provides a low risk path to rapid prototyping and evaluation of candidate software changes. PCS is used to evaluate candidate software changes to the Firefinder. Candidate design changes which perform well in PCS testing require minimum system level checkout before being checked into the tactical software baseline. The PCS tool contains a simulation engine which reads program control information from input data files. The PCS tool also generates and maintains simulated targets and clutter, simulates the radar signal processing function, performs Monte-Carlo "batch" processing, produces complex target trajectories internally or from an input text file and creates simulation data recording files identical in format to those created by the actual radar. This paper summarizes the capabilities of the latest PCS. [C1275]

### "Using an FPGA digital clock manager to generate sub-nanosecond phase shifts for lidar applications"

When using a Light Detection and Ranging (LIDAR) gun for civil engineering applications, anomalous data were observed. A laboratory system was developed to simulate ranging to moving targets in a controlled environment in order to study the anomalous data and the performance of the LIDAR gun. The laboratory system was found to require the ability to generate sub-nanosecond phase shifts which can be updated in real time. This capability is available in high-quality laboratory, but the required equipment was not available to the authors. This research examines the design and implementation of a low cost system. The final design uses an embedded processor for computation of the necessary phase shifts and possible anomalies and an FPGA system to generate the dynamic precision phase shifts. [C1276]

### "Security threats in Cognitive Radio applications"

In this paper we shall consider security aspects of Cognitive Radio (CR) and its applications. We shall cover design of a security simulation model for cognitive radio and discuss results of conducted experiments using Omnet++ simulation tool in the . Net environment. The aim of this paper is to provide an overview of various applications of CR as well as the security threats faced when applying this technology. The functions, benefits and applications of CR are analyzed, along with the challenges faced by the technology. We shall discuss in detail a several security threats faced by CR and carry out selected research on techniques used to mitigate such malicious attacks and provide examples of simulation experiments in Omnet++. [C1277]

### "A mainlobe interference suppression system based on mismatched filtering"

External interference is the major performance limiting factors of High frequency surface wave radar (HFSWR) for array signal processing. Especially when the interference falls into the main lobe, the beam pattern is distorted with conventional adaptive digital beam former for the sake of suppressing the main lobe interference. In this paper, a system for suppressing external interference is proposed. This system includes three processing modules. The first module receives the main array radar data and produces matched radar data while the second one receives the virtual auxiliary array radar data and produces mismatched radar data based on mismatch filtering. And the last one is an adaptive beam former based on the Coherent Side-lobe Cancellation (CSLC) algorithm which is connected with the former two modules. Effectiveness and practicality of this interference suppression system are confirmed by simulation data and real data processing results. [C1278]

### "SAR images segmentation using edge information"

In this paper a new segmentation method for SAR images is presented which requires applying edge detector such as Sobel, Robert, Prewitt, or canny. Then, use edge information in order to estimate the threshold values required for image segmentation. Segmenting SAR images with low contrast using the proposed method was very satisfactory and the obtained results are very promising. [C1279]

### "An improved adaptive maneuvering target tracking algorithm"

During the process of maneuvering target tracking, the difference between observation value and extrapolated value is processed as noise or maneuvering acceleration according to the range of the difference. However the maneuvering target could not be tracked while the difference is large. In this paper, a new adaptive  $\alpha$ - $\beta$  algorithm is brought out. It is that two extrapolated values are considered, while the target is being tracked. They

are normal extrapolated value and maneuvering extrapolated value. In the end of the paper, the concerning experiments are introduced. The result is that the maneuvering target can be continuous tracked. The performance of the new algorithm is also compared with that of Kalman filter. [C1280]

#### "Tomographic approaches towards focused SAR image development"

Although the similarities of synthetic aperture radar (SAR) and computer aided tomography (CAT) imaging systems have been discussed in several previously published papers, a rigorous implementation of algorithms from one modality have not fully ventured into the other modality(ies). This paper proposes image formation of synthetic aperture radar (SAR) data using techniques developed from CAT systems. The paper provides an overview of the typical signal processing involved with SAR, B-mode ultrasound, and CAT imaging systems. Simulations of SAR received echo data processed using techniques from ultrasound and CAT imaging systems are provided to showcase the possibilities. Further discussions of our proposed future work by incorporating CAT techniques to inverse SAR and real time parallel implementation using general purpose graphical processing units are presented. [C1281]

#### "Automated detection of near surface Martian ice layers in orbital radar data"

An algorithm is presented to automatically detect near surface ice layers in images from the Shallow Subsurface Radar (SHARAD) on NASA's Mars Reconnaissance Orbiter. Mars' ice-rich Northern Polar Layered Deposits (NPLD) represents an extensive geologic record of climate history. Identifying ice layers in cross-sectional images leads to understanding the three-dimensional structure of ice layers. Scientists have manually identified layers in large data volumes, but the automated algorithm will allow studying more images from over a thousand orbital crossings. A unique coordinate transformation, based upon the surface reflection, makes subsequent filtering and detection more effective on near surface layers. Results show promising capabilities for automatically detecting ice layers on Mars. [C1282]

#### "Using full motion 3D Flash LIDAR video for target detection, segmentation, and tracking"

It is now the case that well-performing flash LIDAR focal plane array devices are commercially available. Such devices give us the ability to measure and record registered 3D point cloud sequences at video frame rates. For target detection and tracking applications this allows the processes of structure from motion or multi-view stereo reconstruction to be circumvented. This allows us to construct simple and robust real-time 3D detection and tracking systems. The goal of this work is to demonstrate for the first time a proof-of-concept system using a commercial 3D Flash LIDAR camera. The system will accomplish the detection, segmentation, and tracking of human sized objects using a combination of fundamental point cloud processing algorithms. With marginal refinement efforts the result of this work is directly applicable to perimeter surveillance and site security. [C1283]

#### "Effects of signal distortion in a FMCW radar on range resolution"

Frequency Modulated Continuous Wave (FMCW) radars are used in many range measurement applications. The effects of phase errors in radar antenna, circuit dispersion and of frequency modulation nonlinearity on FMCW radar resolution have been analyzed using computer simulation and experiments with a radar prototype in the 10 GHz band. [C1284]

#### "Rough Terrain Reconstruction for Rover Motion Planning"

A two-step approach is presented to generate a 3D navigable terrain model for robots operating in natural and uneven environment. First an unstructured surface is built from a 360 degrees field of view LIDAR scan. Second the reconstructed surface is analyzed and the navigable space is extracted to keep only the safe area as a compressed irregular triangular mesh. The resulting mesh is a compact terrain representation and allows point-robot assumption for further motion planning tasks. The proposed algorithm has been validated using a large database containing 688 LIDAR scans collected on an outdoor rough terrain. The mesh simplification error was evaluated using the approximation of Hausdorff distance. In average, for a compression level of 93.5%, the error was of the order of 0.5 cm. This terrain modeler was deployed on a rover controlled from the International Space Station (ISS) during the Avatar Explore Space Mission carried out by the Canadian Space Agency in 2009. [C1285]

#### "Automated Classification of Operational SAR Sea Ice Images"

The automated classification of operational sea ice satellite imagery is important for ship navigation and environmental monitoring. Annually, thousands of large synthetic aperture radar (SAR) scenes are manually processed by the Canadian Ice Service (CIS) and pixel-level interpretation is not feasible. Trained ice analysts

divide SAR images into "polygon" areas and then identify the number and type of ice classes per polygon. Full scene unsupervised classification can be performed by first segmenting each polygon into distinct regions algorithmically. Since there is insufficient information to assign a sea ice label for each region within an individual polygon, a Markov random field formulation using joint information to label each region in a full SAR scene has been developed. This approach has been successfully applied to operational CIS data to produce pixel-level classified images and is the first known successful end-to-end process for automatically classifying operational SAR sea ice images. [C1286]

#### "Evaluation of the electric and magnetic field levels of around the medium voltage power lines in related to public health"

In this study, the electric and magnetic fields which are occurred around the medium voltage power distribution lines in the residential areas close to housing are calculated analytically. Study, different MV-LV power transmission lines (PTL) which are settlements in Antalya city center have been selected. The electric and magnetic field values which are occurred around the lines have been examined and the results were evaluated in terms of safety standards and public health. [C1287]

#### "Target localization by a multistatic UWB radar"

Moving target localization and tracking are of great interest for rescue, surveillance and security operations. The radar signal processing procedure providing the target position estimation consists of such phases of signal processing as raw radar data pre-processing, background subtraction, detection, time of arrival estimation, localization and tracking. In this paper, we will focus on the localization phase where we assume that for the target localization UWB radar equipped by one transmitting and N receiving antennas is used. Following this intention, the accuracy of the target localization provided by the least-squares method, the spherical-interpolation method and the Taylor series method applied within localization phase will be compared based on processing of radar signals obtained from real target tracking by UWB radar. The acquired results confirm that the Taylor series method can provide the best accuracy of the target positioning. [C1288]

#### "CFAR detectors for through wall tracking of moving targets by M-sequence UWB radar"

In this paper different CFAR detectors for detection of multiple targets for UWB radar system will be described. In this paper, the cell averaging CFAR (CA-CFAR) cell averaging with greatest of (CAGO-CFAR) and ordered statistics CFAR (OS-CFAR) will be represented. The detectors outputs will be illustrated and compared. The properties of all detectors will be illustrated by real radar signal processing obtained by the measurement with the M-sequence UWB radar. [C1289]

#### "Weak signal enhancement in radar signal processing"

In through wall tracking of multiple targets it is able to detect many times only a target moving closest to the radar antenna system. It results from the fact that the reflections from targets located further from the radar antennas are very weak in comparison to that target. The methods for weak signal enhancement can solve the outlined problem. In the paper, three such potential methods are described and tested on real radar signals. The achieved results confirm their ability to enhance the weak signal components with low computational complexity. [C1290]

#### "Classification of fibromyalgia syndrome by using fuzzy logic method"

Fibromyalgia syndrome (FMS), which appears frequently in females, exhibits itself the form of common pain and decreases life quality of a person significantly, is a musculoskeletal disease. Nowadays FMS diagnosis can be made according to the strict rules set by American College of Rheumatology (ACR). However, using strict rules in making diagnosis of FMS disease is not suitable, because FMS is affected from a good many systems and caused to complicated complaints. On the other hand the fuzzy logic method provides a flexible classification, because it has a rule base set by experts' personal experience alongside the ACR criteria. In this study a classification that is based on fuzzy logic is done for FMS. The measurements are taken from 30 healthy and 60 patient subjects who are also under cure at Suleyman Demirel University, Faculty of Medicine, Physiotherapy and Rehabilitation Center. Consistent results are obtained from comparing the fuzzy logic and experts' comments and experiences for the classification both classification disease and disease's degree. [C1291]

#### "Microwave FMCW Doppler radar implementation for in-house pervasive health care system"

In recent years, the research in the area of ubiquitous healthcare has intensified. There are many technological advances regarding the development of unobtrusive sensors for cardiac and respiratory activity, but the current



scenario is still far away from an everyday life fulfilled with ubiquitous healthcare systems. In this paper, it is described the usage of 24GHz microwave FMCW (frequency modulated continuous wave) Doppler radar (MDR) as one of the main components of a pervasive biomedical system that is part of an assistive environment for the people with less mobility or people with long term health condition. As parts of the present work, in this paper are mentioned the design and implementation of an assistive environment based on a MDR sensor, an experimental study concerning the microwave Doppler radar characteristics and remote sensing of heart rate and breath rate, based on acquisition and processing of the signals delivered by the used radar. [C1292]

#### **"Direction Finding via Beam Scanning and Sparse Reconstruction"**

An improved direction finding method is proposed based on unimodal characteristic of antenna pattern and sparse property of received data. Unlike the conventional methods based peak-searching and symmetric constraint, the sparse reconstruction algorithm requires less pulse and takes advantage of compressive sampling. Simulation results validate performance of the proposed method. [C1293]

#### **"Improving Performance in Neural Network Based Pulse Compression for Binary and Polyphase Codes"**

Pulse compression is important for improving range resolution, and the application of neural networks for pulse compression has been well-explored in the past. However, the practical importance of extracting rather weak echoes of targets that are either distant, or have small radar cross-section, appears to have been overlooked. Addressing this issue, neural networks with improved performance are developed in this paper for both Barker and Polyphase codes. We demonstrate that our networks perform better in such practical situations together with better noise tolerance and range resolution. [C1294]

#### **"The effects of seasonal weather differences on the bio-heat loss transferred from the human body in Antalya city"**

In this study, the effects of seasonal weather differences in Antalya city on the bio-heat losses from the human body have been investigated. For application, the monthly atmospheric temperature, relative humidity, wind speed and atmospheric pressure data, which are observed in 2006, have been used. The sensible and latent heat losses from the human body in terms of skin surface and respiration have been calculated and compared to each other. According to the obtained results, the latent and sensible heat losses from the human body have been varied considerably from season to season. Approximately ninety percent of bio-heat transferred from the human body to the surrounding is caused by the skin and the rest of 10% by respiration. [C1295]

#### **"Magnetic resonance imaging shows that muscle myofascial force transmission causes substantial sarcomere length heterogeneity in human muscles, in vivo"**

In this study, it is aimed to show, using magnetic resonance imaging (MRI), effects of epimuscular myofascial force transmission (EMFT) on sarcomere length distribution in human muscles in lower leg in vivo. The ankle angle of the subjects was fixed and 3D MR image sets were acquired for two different knee angles. Intensity based non-rigid demon algorithm was used to calculate displacement fields and Green-Lagrange strain for each voxel. To calculate the strain in local fiber direction diffusion tensor images (DTI) were acquired. It was showed that m. gastrocnemius crossing the knee has major strain distribution ( $0.125 \pm 0.010$  in proximal and  $0.073 \pm 0.014$  distal) in local fiber direction. Despite remaining isometric during the experiment, synergistic m. soleus (e.g.  $0.088 \pm 0.017$  in proximal,  $0.078 \pm 0.019$  in distal) and even antagonistic muscles ( $0.157 \pm 0.070$ ,  $0.108 \pm 0.037$ ) also show major strain distribution in the local fiber direction. [C1296]

#### **"Charged particle/cell manipulation in spiral microchannels with concentric electrodes"**

In this study, a solution has been proposed by investigating the manipulation and separation of charged particles in spiral microchannels and concentric electrodes. Proposed structure has been fabricated by using MEMS technology and characteristics of electrophoretic force has been demonstrated successfully. Negative charged particles could be manipulated at different speeds and in opposite directions depending on the amplitude and the polarity of the applied electric field. It has been planned that results of this study will be used in the differentiation of charged cells. [C1297]

#### **"The analysis of ground penetrating radar signal of small objects based on generalized S transform"**

In order to do some preliminary analyses on characteristics of ground penetrating radar (GPR) signal of objects

in time and time-frequency domain, and discuss how to roughly estimate the size of an object as well as distance between two objects, firstly the characteristics of GPR signal in time domain was studied in this paper as the size and the distance were changing respectively, secondly the characteristics in time-frequency domain was studied through generalized S transform (GST), the extraction rule of twin-peak attribute was analyzed, the determination of transformation parameter and frequency point was solved. It is pointed out that the size of an object can be estimated in combination of time domain waveform and twin-peak attribute, the definition of a small object can be given according to the size and objective, the resolution of two objects can be improved by twin-peak attribute and the distance can be roughly estimated combined with the attribute and time domain waveform. [C1298]

### "Modeling and Simulation of Adaptive Thresholding in Marine RADARs"

In order to detect targets upon sea surface or near it, marine radars should be capable of distinguishing target reflections from the sea clutter. Our proposed method in this paper relates to detection of dissimilar marine targets in an inhomogeneous environment with clutter and non-stationary noises, and is based on adaptive thresholding determination methods. Variation and mean values of the noise have been estimated in this paper, based on non-stationary, statistical methods and thresholding has been carried out using the suggested two-pole recursive filter. Fixating the rate of false alarm, the concerned threshold resolves the assumption problem of existence or absence of the signal. Performance of the mentioned algorithm has been compared with method known as CA-CFAR in terms of decreasing the losses and increasing calculation speed. The algorithm provided for detection of signal has been implemented at the end of signal-processing algorithms of sea marine radars. The results obtained from the algorithm performance in a real environment indicate appropriate workability of this method in heterogeneous environment and non-stationary interference. [C1299]

### "Intrinsic Membrane Noise in Living Cells and Its Coupling to External Fields"

The phospholipid bilayer membranes surrounding the living cells, play a crucial part in cell signaling and fundamental physiological processes responsible for sustaining life. The study reports physical rationale and some interesting experimental findings on the existence of intrinsic membrane noise (distinct from well-known  $1/f$  and Johnson noise) and coupling of living cell membranes with ambient electromagnetic fields in the Extremely Low Frequency (ELF) regime. The manifestation of these interactions is reported to be seen in the form of amplification of ambient electromagnetic fields by cell membranes and resulting currents, as detected with the help of sensitive pico-ampere and femto-ampere amplifier instrumentation. An experimental technique is introduced to measure such minuscule biological signals existent in living cells. [C1300]

### "Sensing, Triggers and Mobile (Meta)Data"

Processing spatio-temporal queries pertaining to the whereabouts of a large number of mobile entities has traditionally been the topic of the Moving Objects Databases (MOD) research. More recently, due to the advances in sensing and communication technologies, part of the Wireless Sensor Networks (WSN) applications have focused on tracking of mobile objects. These two observations are enough of to warrant a "call" for a confluence of two relatively new but established disciplines. However we observe that a research field of its own right and, historically older than both MOD and WSN-traffic/transportation management-can also capitalize on merging the existing experiences for its own information fusion desiderata. In this talk, we will overview applications from seemingly disparate domains and identify their commonalities in terms of the spatio-temporal contexts, and we will discuss how a reactive behavior with pro-active consequences can be efficiently used for large-scale management of mobile data and meta-data. [C1301]

### "Adaptive thresholding for high dual-tone signal instantaneous dynamic range in digital wideband receiver"

A primary concern in current radar receiver design involves the critical issue of setting a threshold level that is optimal for all operating conditions. A novel adaptive thresholding technique is presented to maximize both receiver sensitivity as well as dual-tone signal instantaneous dynamic range (IDR) for digital wideband receivers. The additional constraint placed for signal detection improves the false alarm rate with minimal hardware increase due to the simplicity of the proposed algorithm. Using our adaptive thresholding technique, the dual-tone IDR is very much independent from the primary signal's strength. The receiver's maximum IDR remains in a constant range, between 30 dB to 34 dB, which is below the primary signal for primary signal strengths between -4 dBm and -24 dBm. [C1302]

### "Analysis of a built-in test architecture for direct-conversion SiGe millimeter-wave receiver frontends"

This paper presents an architecture and corresponding analysis of a direct built-in test of integrated millimeter-wave radar receiver frontends. The proposed test is able to evaluate the gain of the device as well as its noise figure. Focus of this work is the prediction of the accuracy of the tested performance parameters during the design of embedded test solutions. The introduced architecture provides an advantage for cost-efficient development of next generation multigigahertz receiver frontends. The proposed test system is theoretically analyzed as well as evaluated in a simulation environment. [C1303]

#### "A New Model for Rain Clutter Cancellation in Marine Radars"

In this paper we propose a probability density function for signal contaminated by sea and rain non-stationary clutter and noise. Afterward, using the proposed pdf we estimated unknown parameters and using Hilbert transform and obtain an analytical signal to pass its imaginary part through a designed Hilbert filter. In the cell under test, we compare adaptive threshold output from the calculated real and imaginary parts of signal and make an automatic decision to whether anti rain clutter filter must be used or not. This algorithm will decrease adaptively destructive effects of rain clutter just in such cells that are contaminated with rain reflections. Our proposed algorithm is tested on real RADAR signature and implemented in a sea marine RADAR. Results show that the method has good performance in inhomogeneous clutter and different sea states. [C1304]

#### "Privacy-Aware Location-Aided Routing in Mobile Ad Hoc Networks"

Mobile Ad-hoc Networks (MANETs) enable users in physical proximity to each other to exchange data without the need for expensive communication infrastructures. Each user represents a node in the network, and executes a neighbor discovery. Typically, nodes broadcast beacon messages that are received by other participants within the sender's communication range. Routing strategies are computed on-line based on the locations of nearby nodes, and geocasting is employed to deliver data packets to their destinations. However, mobile users may be reluctant to share their exact locations with other participants, since location can disclose private details about a person's lifestyle, religious or political affiliations, etc. A common approach to protect location privacy is to replace exact coordinates with coarser-grained regions, based on the privacy profile of each user. In this paper, we investigate protocols that support MANET routing without disclosing exact positions of nodes. Each node defines its own privacy profile, and reports a cloaked location information to its neighbors. We adopt a novel strategy to advertise beacons, to prevent inference of node locations. We also propose packet forwarding heuristics that rely on cloaking regions, rather than point locations. Our extensive experimental evaluation shows that the proposed routing scheme achieves low delays and high packet delivery ratios, without incurring significant overhead compared to conventional MANET routing protocols. [C1305]

#### "Design and Development of Embedded Intelligent Public Transport Vehicular Terminal"

Intelligent public transport vehicular terminal is an important part of intelligent public transportation system. In view of the fact that the municipal transportation structure in our country and status of the public transportation-vehicular equipment, the paper presents a new type of system-design of the intelligent transportation vehicular equipment. System that is based the embedded intelligent transportation vehicular terminal and take the S3C2410A processor as the core is designed. The paper mainly makes the detailed introduction to this terminal's hardware platform design and software design based on the WINCE embedded operating system. [C1306]

#### "Portable Calibration System for Air Traffic Control Surveillance Radar"

In this article, we design a portable calibration system for air traffic control surveillance radar. This system realizes the automatic flight calibration for Secondary Surveillance Radar (SSR), and also can provide a simple flight calibration capability for any aircraft without standard equipments onboard. On the basis of high-precision GPS technology, this system is composed of a portable dual-frequency & dual-antenna GPS receiver, a portable PC and a software system by our own R&D. By analyzing the position accuracy of GPS and dual-antenna, the portable calibration system has the ability of providing automatically conversion arithmetic of coordinate system between WGS-84 and radar station center. A ground dynamic test for this system has been finished, and an actual flight data processing mission for an airport has been accomplished. [C1307]

#### "Design of Command and Dispatch System of Airport Support Vehicle"

Based on the technology of GPS/GIS/GPRS, the airport support vehicle command and dispatch system is designed in this paper. The information transmission between the vehicle mobile termination and the monitoring control center is established. The function of graphic display and phonetic warning of the airport support vehicle's working process is realized. [C1308]

### "Twin target correction for ultra-wideband radar imaging of breast tumours"

Ultra-wideband radar imaging is a promising modality of imaging for breast cancer detection, based on the dielectric contrast between healthy and pathological tissues. Its aim is to create a map of microwave scattering, and has already proven encouraging results. Unfortunately, the tumor extraction procedure used for reconstruction of the scattering volume leads to the appearance of an artifact called twin target, where a single tumor is expected. In this paper, a signal processing technique is presented to remove this twin target and enhance the contrast of the final image. The radar system and image formation algorithm are first described to explain the origin of the twin target. Experimental data are then acquired and processed by our correction algorithm, demonstrating its ability to fix the twin target issue. [C1309]

### "The vertical handoff between GSM and Zigbee networks for vehicular communication"

Wireless communication becomes important part of everyday life, and in the future, there will be new wireless technologies. Vertical handoff between networks with different wireless network interface becomes so important especially in mobile devices that move at high speed such as vehicles. The vertical handoff is required for a vehicle to connect to different wireless networks for different purpose. For example, vehicles may connect to cellular network to send short messages such as news or email, and may connect to short range networks to acquire some localized information. In this paper, we investigate the possibility and the performance of using GSM/GPRS module as an interface to cellular networks and Zigbee module as an interface to short range networks. In our experiments, we set up both soft and hard handoff scenario to measure the packet round trip time and delay. From the results, it shows that the packet round trip time (RTT) in GPRS networks on the average is around 1-2.5 seconds and in Zigbee network is less than 100 msec. In case of a hard handoff, mobile device needs to prepare for a connection to attach to networks before transferring data. From the results, the network attach time in GPRS network on the average is around 4.5-5 seconds while in Zigbee network is less than 10 msec. [C1310]

### "A neural network based optimization for wireless sensor node position estimation in industrial environments"

The sensor node position estimation is essential in wireless sensor networks. Among many localization schemes, the position estimations based on Received Signal Strength Indicator (RSSI) are mostly used in various systems and applications. However, RSSI data are highly affected from multipath propagation caused by the reflections from walls or objects. These reasons conduct the improper phenomena to radio signals. The significant variation of RSSI influences to the position estimation error especially in industrial environments. In this paper, we present a sensor node position estimation method in industrial environments and its optimization to reduce the error from multipath propagation by using neural networks. An experiment was performed in an electrical machine laboratory to evaluate the designed system in the real environment. The experimental results show that the average position error was reduced to 0.5 m. [C1311]

### "A real-time FPGA-based implementation of target detection technique in non homogenous environment"

This paper presents a high speed real-time target detection system for non homogenous environment based on FPGA Technology. The system implements a Backward Automatic Censored Ordered Statistics Detector (B-ACOSD) to maintain a Constant False Alarm Rate (CFAR) for Radar system with a time constraints in term of signal computing and target identification. The design flow and the hardware implementation of each module are introduced in detail. The proposed system can operate up to 115 MHz by using full pipeline organization and parallel computing which increase the speed up of the target detection system to satisfy the real-time constraints. The proposed architecture is designed, implemented, and tested using Stratix II EP2S60F672C3N FPGA Board. The system has the advantages of being simple, fast, and flexible with low development cost for a reference window of length 16 cells. [C1312]

### "Capability evaluation framework of multichannel ship-to-air missile weapon system against anti-ship missile saturation attack"

Anti-ship missile saturation attack is one important campaign mode in the high-tech sea battle. Aimed at the absence of capability evaluation framework of multichannel ship-to-air missile weapon system against anti-ship missile saturation attack currently, from operation control point of view, it put forward the capability evaluation simulation framework and model respectively so that it can evaluate the campaign capability under the anti-ship missile saturation attack tactics scheme, which assisted the commander decision-making effectively. [C1313]



### "Window memory accesses method in alternate row/column matrix access systems"

Many systems, such as Synthetic Aperture Radar (SAR) processing, two-dimensional image processing, 2d-FFT calculation, need access the row and column data of their matrix alternately. The DRAM memory should be used due to huge data in these systems. To improve the usage of memory bandwidth in such systems, this paper theoretically analyses the optimal window size to minimize the total number of opening/closing pages when performing in such instances by balancing the number of handling physical pages between row and column accesses. This paper presents a window-based optimal memory access method, and we implemented an FPGA-based SDRAM controller with eight simple ports, which is based on window accessing mechanism and supports commercialized SDARM. The experimental results show that the effective I/O bandwidth of external SDRAM using our window layout approach increases from 114.2MB/s of naive implementation to 730.2MB/s with over 6X speedup. In addition, we implemented two SAR processing systems with four FFT processing elements using our window-based SDRAM controller and Corner Turn method separately in FPGA chip. Results show window-based method can achieve a speedup of 2.6 compared to Corner Turn method. [C1314]

### "Remote video monitoring system based on embedded linux and GPS"

This paper presents a design and realization method for remote video monitoring system based on embedded Linux and GPRS (General Packet Radio Service) network. Monitor terminal hardware takes ARM9 S3C2410 processor for centralization, in virtue of SDRAM, USB, GPRS module, etc. Software system adopts embedded linux, the main function realized by C programming to achieve real-time camera data acquisition, image compression and network transmission through GPRS module. Monitoring center receives image data and displays after connects with the terminal. It is easier to be used in windows system. Image data can be transmitted to the monitoring center in 3-6 seconds after JPEG compression. The results showed that the monitoring system has the advantage of high reliability, high efficiency and low cost with ARM9 and GPRS network, and it provides a feasible method for remote video monitoring. [C1315]

### "Remote monitoring system for oil wells based on GPRS technology"

In order to overcome the shortcoming of traditional methods of monitoring oil wells, a design of remote monitoring system based on ARM and GPRS was presented. And then the hardware and software design methods of RTU, system networking method and the design method of background monitoring center were detailed. Using GPRS module and relying on GPRS wireless network and Internet, RTU distributed in different geographic locations can communicate with the background monitoring center. This system broke through the geographical restrictions of oil wells, provided some functions such as oil wells' data collection, remote data transmission, real-time monitor and oil wells' information release, and improved the level of automation in oil production management. The experiment showed that the system could achieve the goal of real-time monitoring of oil wells by the existing mobile communication network. [C1316]

### "Research on optimal wireless city network using mobile network"

By analyzing the various technologies, considering the network development and full use of network resources, the conclusion is gotten that the access side should combine network with 2/3G and Wi-Fi technology. Among them, 2/3G mobile network is mainly used to achieve wide-area coverage, and Wi-Fi network is used to the hot areas with high bandwidth demand for complementary coverage. Also, the core network is researched by several methods using SIM, Web and WAPI. [C1317]

### "Research on long-range and metering reading for water meter based on GPRS"

A kind of long-range and centralized automatic metering reading for water meter system is designed. The function of the GPRS network meter reading and the USB centralized meter reading are accomplished by the M23 GPRS module and the C8051F340 single chip micro-controller. The system is composed of water meter, data collector, concentrator and administer computer. The data of water consumption which will be converted into pulse signals are collected by the water meter, and these pulse signals are disposed by the data collector which can use RS-485 communication with concentrator, water user's machine can be controlled when the upper instructions are received by the way of controlling the electromotion valves. The Concentrator plays an important role in data transit and bus segregation. A USB interface is set up in the concentrator in order to avoid the failure of GPRS network, and the staff can copy the datas by computer or hand-written. The administer computer can manage the user's purchase of water and control the user's machine by sending specific instructions. [C1318]

### "Detecting and assessing the land subsidence in coal mining area using PALSAR data based on D-

### **InSAR technique"**

Land subsidence induced by mining coal is one major issue in terms of damage to infrastructures. In this paper, the potential of L-band repeat-pass differential SAR interferometry for land subsidence in coal mining area is evaluated using ALOS PALSAR data. The focus is to detect and assess the land subsidence using PALSAR data based on D-InSAR technique. Firstly it introduced the basic principle and some applications of D-InSAR. Then it introduced the information of PALSAR and test data of coal mining area. It described the procedure of data processing of two-pass D-InSAR. And it got the deformation of coal mining area. It carried out interpretation and analysis on the D-InSAR results in details. The maximum settlement of land subsidence in this coal mining area was up to 42.4cm in vertical direction in 46 days. At last, it got some valuable conclusions in monitoring the land subsidence in coal mining area using two-pass D-InSAR technique. The test proves that PALSAR data is suitable for monitoring the land subsidence in areas with vegetated land cover, such as coal mining area.

[C1319]

### **"Error analysis in phased array antenna pattern simulation"**

This paper is mainly focused on the errors leaded by improper use of approximate antenna pattern formula and common errors in phased array radar antenna pattern simulation. First, the formula of linear and planar phased array antenna pattern is derived. Then, the precise definition of argument is presented and some precise and approximate expressions of antenna pattern are listed. Finally, simulation result is shown about errors between precise and approximate antenna pattern expression. The discrepancy caused by approximate expression and common errors is also summarized and analyzed in this paper. [C1320]

### **"A novel algorithm of coherent integration for moving target detection"**

The problem of detecting moving targets which migrate between rang cells is considered. The traditional MTD method can not effectively integrate the energy of targets, because it integrates multi-pulse in the same range cell in a CPI. This paper introduces a novel algorithm of coherent integration for moving target detection (MTCI), which is calculated along the track of the moving target. A mathematical formula of MTCI algorithm is derived based on the signal model of a moving target in Chirp Radar. The integrating results of MTCI and MTD methods in the Gaussian white noise background are also compared. A Monte Carlo simulation has been performed to evaluate the detecting performance of MTCI algorithm, and the detection curves are also given. [C1321]

### **"Probability hypothesis densities for multi-sensor, multi-target tracking with application to acoustic sensors array"**

Random sets theory offers a uniform framework for the multi-source data fusion, and all problems of the data fusion could be describe, analyzed and solved in this framework. The multi-sensor multi-target tracking problem could be natural represented in the framework. It is of engineering importance to tracking low altitude moving targets with acoustic methods due to the blindness of the traditional radar detecting. In this paper, an algorithm for tracking the low altitude or ground moving targets is put forward based on the Probability Hypothesis Density (PHD) Filter. The PHD Filter based on Finite Set Statistics doesn't need consider data association for multi-target tracking, which propagates the PHD or first moment instead of the full multi-target posterior, and it could estimating the unknown and time-varying number of targets and their states under clutter environment. In the practical, we use the Sequential Monte Carlo (SMC) method to approximate the PHD. The paper presents a novel and fundamentally well-grounded framework for tracking multiple acoustic targets using PHD Filter and passive acoustic localization technique. Simulations are also presented to demonstrate the performance in tracking a randomly varying number of targets in a clutter environment. [C1322]

### **"Study on air formation to ground attack-defends decision making in duple-fuzzy condition"**

With the development of modern military technology, uncertain decision-making problems become more and more exigent to be solved in military command and control. Based on game theory, and taking air formation to ground attack-defends campaign as the background, this paper establishes an opposed dynamic decision-making model. As to the problems in military decision-making in duple-fuzzy condition in uncertainty, this paper puts forward a duple-fuzzy-influence-factor, which reflects the duple-fuzzy influence on battle units, and establishes a duple-fuzzy opposed decision-making model in anticipant value and in correlative chance way farther to get strategy equilibrium. It can be seen from the simulating results that the model disposes the duple-fuzzy status in battlefield reasonably, analyzes the fighting results objectively, and offers a powerful decision-making support for military operation. The method proposed in this paper is practically and effectively, and has a good future in its application. [C1323]

### "A novel range alignment algorithm for ISAR"

A novel technique is proposed for range alignment in inverse synthetic aperture radar (ISAR) imaging. The correlation of complex High Range Resolution Profiles of two echoes is calculated as the quality measure of range alignment, and its applicability is analyzed. The shifts introduced by the echoes are obtained in the frequency domain without interpolation, so the computation burden is greatly reduced. In addition, the shift is implemented by introducing a phase ramp in the frequency domain, which removes the integer steps in the time domain. [C1324]

### "A novel approach to synthesize the range profile via predesigned stepped-frequency waveforms"

In stepped-frequency radar systems, the phase error due to target motion in each burst makes range profiles blur. Conventional technology, such as motion compensation, requires velocity estimation to eliminate the distortion of the synthetic range profile. However, it suffers a major drawback, namely that it is difficult to achieve real-time accurate estimation of the velocity of the target. A novel technology is presented to achieve a focused target range profile via predesigned stepped-frequency waveforms. By applying a new stepped frequency waveform, HRRP of the target can be obtained by the Fourier transform without any other process. The simulation results demonstrate the effectiveness of the proposed technology. [C1325]

### "Signal and data processing for radar sensor head network"

This paper deals with basic blocks for processing and pre-processing of data acquired from radar sensor heads in developing system for the trajectory tracking. Signal processing is concentrated in acquisition unit and thus an acquisition unit and their cooperation in network are described in detail. The acquisition unit provides the capturing data from a Doppler radar head and processing a beat frequency spectrum. Collected data are transferred through a system network and controller to computer where the investigated trajectory is calculated. [C1326]

### "An Efficient Method of Pulse Repetition Interval Modulation Recognition"

A novel recognizer that automatically reports the PRI (Pulse Repetition Interval) modulation type of a radar pulse signal is developed. The proposed method utilizes the features based on the properties of PRI sequence for each PRI modulation type both in time and frequency domain. These features are defined as zeros-crossing density, harmonic amplitude ratio and sign properties of difference of the PRI sequence, which can be easily extracted from PRI sequences with small samples size. In addition, the proposed method also can be used to estimate the PRI modulation period for the periodic PRI modulation type signals. Simulation results show that the proposed approach is robust in the presence of measurement noises, missing and spurious pulses. [C1327]

### "Signal Filtering Based on Wavelet Transform and its Application in Ground Penetrating Radar"

Towards wavelet transforms part characters in time domain and frequency domain, a practical GPR signal processing method is proposed. Based on continuous wavelet transform, the main component of echo signal is extracted by energy analysis. Through scaled decomposition and frequency filtering, the disturbed component is eliminated. The SNR of reconstructed echo signal is improved. The experiments of real data indicate it improves the processing performance of underground target detecting than continuous wavelet transform. [C1328]

### "A Bayesian approach for SAR images segmentation and changes detection"

In the context of image processing and classification, an important problem is the development of accurate models for Synthetic Aperture Radar (SAR) image segmentation. In this paper we propose a highly efficient unsupervised algorithm for image segmentation and changes detection, based on the Generalized Gaussian mixture model. Our work is motivated by the fact that SAR images are highly corrupted by speckle noise, and contain non-gaussian characteristics impossible to model using rigid distributions. Generalized Gaussian mixture models are robust in the presence of noise and outliers, more flexible to adapt the shape of data, and less sensible for over-fitting the number of classes compared to Gaussian mixture. [C1329]

### "Latency-information theory"

In this paper the mathematical-physical theory of communication-observation that is part of latency-information theory (LIT) is reviewed. LIT surfaced from the confluence of classical information theory, relativity theory, quantum mechanics, statistical physics and a 1978 conjecture by the author of a structural-physical certainty-uncertainty duality for quantized control. Control, radar, physics and biochemistry applications illustrate the theory. As part of the review, LIT is revealed to communicate through latency-certainty channels and/or information-uncertainty channels for observation across latency-certainty sensors and/or information-uncertainty

sensors, a mathematical-physical efficiency perspective of the Universe in a four quadrants revolution. While the first and third quadrants are concerned with the life time of physical signal movers and the life space of physical signal retainers, respectively, the second and fourth quadrants are about the intelligence space of mathematical signal sources and the processing time of mathematical signal processors, respectively. The four quadrants of LIT are conjectured to be physically independent with their system design methodologies guided by dualities and performance bounds. Moreover, the tools of statistical physics bridge them, and inherently lead to the discovery of a novel certainty dual for thermodynamics named lingerdynamics. [C1330]

#### **"Reconfiguration-aware spectrum sharing for FPGA based software defined radio"**

This paper focuses on reconfigurable systems for software defined radio applications in which the underlying hardware is dynamically reconfigured for packet processing of multiple protocols. However, due to non-negligible reconfiguration delay overhead, the physical layer may not be able to respond to all the packets scheduled by MAC layer. In this paper, we present a reconfiguration-aware spectrum sharing and spectrum access scheduling at MAC layer. We considered four protocols similar to WiFi, WiMax, GPRS, and WCDMA on a FPGA-based system. Our results show that the optimal solution outperforms the adopted existing heuristic for time slot scheduling by 13.29%. [C1331]

#### **"Robust Novel EM-Based Direction-of-Arrival Estimation Technique for Wideband Source Signals"**

Direction-of-arrival (DOA) estimation for wideband source signals using near-field acoustic sensor networks has been drawing a lot of research interest recently. A wide variety of DOA estimation approaches are based on the predominant maximum-likelihood objective. In this paper, we would like to tackle with the DOA estimation problem based on the realistic assumption where the sources are corrupted by spatially non-white noises. We explore the respective limitations of two popular DOA methods for solving this problem, namely the SC-ML and AC-ML algorithms, and design a new expectation maximization (EM) algorithm. Through Monte Carlo simulations, it is demonstrated that our proposed EM algorithm outperforms the SC-ML and AC-ML methods in terms of the DOA accuracy. [C1332]

#### **"The Integrative Application of Anti-Jamming Technology for Radar"**

This paper analyzed some primary techniques of anti-jamming technology for radar. Simulation results show the merit of each method. And it proposed a new idea that combines some typical anti-jamming techniques together. It was a more effective way of the integrative anti-jamming technology. [C1333]

#### **"On the modelling of transient scattering under ultra wideband short-pulse electromagnetic excitation"**

Accurate modelling of electromagnetic radiation, scattering and propagation using ultra wideband (UWB) sources has been of significant interest with ongoing application in areas such as short-range communications, through-the-wall imaging, ground-penetrating radar and medical imaging etc. Numerical modelling of these applications is vital to the evaluation and enhancement of their performance. In this paper, a review of different methods for numerical modelling of the transient electromagnetic response under UWB short-pulse excitation is undertaken. The advantages, limitations and challenges of both direct and indirect time domain methods are described in detail and numerical examples of transient scattering demonstrate the use of an indirect time domain method. [C1334]

#### **"A new judging method for radar electromagnetic compatibility analysis"**

This paper proposes a new judging method of EMC based on signal detection theory. First of all, the traditional judging method of interference measure is introduced, and its disadvantage is pointed out. Then, the signal processing of radar system is analyzed, and the relationship of detection probability ( $p_d$ ) and interference to noise ratio (INR) is established. Based on the definition extension of detection probability,  $p_d$  is used to judge radar electromagnetic compatibility. Finally, simulation results indicate that the detection probability fall to 50% as the interference power exceeds the threshold 1.7 dB. This method can illuminate the interference condition between radars quantitatively and objectively. [C1335]

#### **"Computational electromagnetic modeling & simulation of ultra wideband sub-surface sensors for the detection and imaging of buried objects using spatial and spectral diversity"**

An enhanced remote sensing technique for the detection and identification of deeply buried objects is presented in this paper. A new RF Tomographic Technique is proposed for developing RF CAT Scans of buried objects using spectral and spatial diversity. This imaging technique uses an embedded ring of subsurface radiators as



the source of strong underground radiated transmissions. Distributed surface-contact sensors are used to collect the tomographic data for relay to a remote control site. Three-dimensional numerical imaging algorithms have been developed to detect, image, and characterize deeply buried objects. Distributed transmitters and receivers significantly increase unwanted mutual coupling and EM emissions that interfere with signal reception; however, by embedding the transmitters underground, reduced mutual coupling and EM emissions, and improved signal-to-noise ratios, can be achieved. Simple 2D surface SAR experiments over deep mine shafts were performed to validate and verify (V&V) the 3D processing algorithms using 2D surface SAR sensor data. The WIPL-D CEM Code was used to model and simulate (M&S) the embedded and distributed sensors and to verify the significant enhancement in the received signal-to-noise ratio obtained by burying the radiating antennas. [C1336]

#### "Some Analysis of Fuzzy CAGO/SO CFAR Detector in Non-Gaussian Background"

In order to improve radar's detection performance under non-Gaussian background clutter. We design a new distributed fuzzy CAGO/SO-CFAR detection system including two sensors. Both sensors compute the value of the membership function mapping to the false alarm space according to the samples of the reference cells, in the fusion centre two values are combined according to four kinds of fusion rule to estimate the background clutter power. The simulation results prove the detection improvement of CASO based on algebraic-sum rule under multi-target environment, and present better false-alarm-control capacity of CAGO based on MIN rule under clutter-edge environment. [C1337]

#### "Performance Analysis of OSAP-CFAR Detector in K Distribution Background"

The OSAP-CFAR employs soft rule based on fuzzy logic to give better detection probability than that of OSGO and OSSO-CFAR detectors for Weibull clutter. However, studies show that the K distribution provides a better fit for many clutter situations. The performance of the OSAP -CFAR is studied and compared with OSGO and OSSO-CFAR for the Swerling II target model in K distributed clutter. The results represent that the detection performance of OSAP-CFAR detector is superior to that of OSGO and OSSO-CFAR detectors both in the homogenous background and in multiple interfering targets situations. [C1338]

#### "Fast electric field change pulses location technique"

Using both fast and slow electric field change sensors and field mill, multi-station observations on lightning flashes in Chinese Inland Plateau was conducted during the summer of 2004. All of the stations were synchronized by GPS with a time-resolution of  $\pm 50$  ns. Using the different time of arrival (DTOA), a lightning radiation location technique, based on the fast electric field change sensor, was developed. Radiation pulses in the five intra-cloud (IC) lightning discharges which occurred on 20th August and cloud-to-ground (CG) lightning discharges which occurred on 16th July were analyzed. The results indicated that the technique developed could effectively locate the lightning radiation sources. Furthermore, the lightning discharges were compared with the Doppler radar data. Results showed that the radiation sources were well associated with the storm development. [C1339]

#### "All-optical parallelization for high sampling rate photonic ADC in fully digital radar systems"

Optical samples of RF signals are all-optically parallelized for further processing in low-speed electrical digitizers. This technique enables high-rate sampling with no additional jitter and limited SNR degradation, making this solution suitable for radar systems. [C1340]

#### "Transmit policies for MIMO radar detection and time-delay estimation"

This paper is aimed at investigating the role of Space-Time Coding (STC) for target detection and time-delay estimation through MIMO radars with widely spaced antennas. To this end we formulate the waveform optimization problem as a constrained maximization of some detection-oriented figures of merit under an accuracy constraint. Interestingly, such an additional constraint deeply modifies the optimal transmit policy. We also offer closed-form formulas of the Fisher Information in target delay estimation as a function of the singular values of the code matrix. Numerical results validating the theoretical findings are also given. [C1341]

#### "Localization performance of coherent MIMO radar systems subject to phase synchronization errors"

Localization advantages of coherent Multiple-Input Multiple-Output (MIMO) radar systems are reliant on full phase synchronization among all participating radars. Phase synchronization errors are practically inevitable, reflecting on the system localization performance. In this paper quantitative tools to assess this effect are provided. The lower bound on the mean-square error (MSE) is set by the hybrid Cramer-Rao bound (HCRB) for

the joint estimation of the target location and the phase synchronization offsets at the radars. The latter are modeled as random unknown. The HCRB of the unknown target location is shown to be equal to the CRB derived by discarding the random phase synchronization errors through marginalization, i.e., treating them as nuisance parameters. Therefore, the HCRB closed-form expression provides an asymptotically tight bound on target location estimation MSE at high signal-to-noise ratio (SNR). The bound is shown to follow the CRB in the absence of phase errors up to a threshold point, determined by the synchronization error variance, the SNR, and the number of mismatched transmitting and receiving sensors. Beyond this point, the HCRB asymptotically reaches a lower limit, proportional to the synchronization errors variance and independent of the SNR. The value of the threshold point and lower limit are determined for symmetrical radar deployments. [C1342]

#### "Diversity gain for MIMO radar employing nonorthogonal waveforms"

Initially we formulate a very general hypothesis testing problem where we attempt to distinguish between zero-mean Gaussian clutter-plus-noise only and returns which are a linear transformed version of a zero-mean Gaussian random vector plus this clutter-plus-noise. We show that the diversity gain of the optimum processing for this hypothesis testing problem must be less than or equal to the rank of the linear transform. Next we apply this result to study diversity gain for optimum MIMO radar processors for cases with  $M$  transmit antennas,  $N$  receive antennas, and a target composed of  $Q$  scatterers. If the transmitted waveforms span a lower dimension  $M'$  than  $M$ , then the largest possible diversity gain is no greater than  $\min(NM', Q)$ . We also show a diversity gain of  $\min(NM', Q)$  can be achieved under certain conditions. For a general correlated Gaussian clutter-plus-noise model and a general correlated Gaussian reflection coefficient vector, the diversity gain for noncoherent and coherent processing is discussed. Extensions of all results to cases with nonGaussian reflections and clutter-plus-noise are discussed. [C1343]

#### "Neural network-assisted reconstruction of full polarimetric SAR information"

This paper describes a novel approach to the reconstruction of synthetic aperture radar (SAR) fully polarimetric data from compact polarimetry (CP)  $\Gamma, B/\pi/4$  mode. A method is developed which utilises a multi-layer perceptron (MLP) based neural network, to perform reconstruction of scenes with various ground-cover types. In particular, the approach shows potential for the reconstruction of full polarimetry for built-up areas as a complement to existing techniques which are more suitable for natural land cover areas. Performance assessment is presented, using both L-band and C-band data, involving comparison with existing techniques using mean-squared and mean-squared-log measures. [C1344]

#### "Sparse representations for automatic target classification in SAR images"

We propose a sparse representation approach for classifying different targets in Synthetic Aperture Radar (SAR) images. Unlike the other feature based approaches, the proposed method does not require explicit pose estimation or any preprocessing. The dictionary used in this setup is the collection of the normalized training vectors itself. Computing a sparse representation for the test data using this dictionary corresponds to finding a locally linear approximation with respect to the underlying class manifold. SAR images obtained from the Moving and Stationary Target Acquisition and Recognition (MSTAR) public database were used in the classification setup. Results show that the performance of the algorithm is superior to using a support vector machines based approach with similar assumptions. Significant complexity reduction is obtained by reducing the dimensions of the data using random projections for only a small loss in performance. [C1345]

#### "Range estimation for MIMO step-frequency radar with compressive sensing"

The authors recently proposed a parameter estimation technique for multiple-input/multiple-output (MIMO) radar systems that employ compressive sensing (CS), and which applies to the case of slowly moving targets. This technique is based on the use of a step-frequency technique, and it allows angle, Doppler and range information to be estimated in a decoupled fashion. This decoupling significantly reduces the complexity of parameter estimation without a concurrent performance loss. The current paper considers the range-estimation performance of this method for the particular cases of linear and random step-frequency techniques. It is shown that the linear step-frequency technique requires less bandwidth than the random step-frequency technique in order to achieve the same performance. [C1346]

#### "MIMO radar target detection with parametric scattering correlation model"

Multiple-input multiple-output (MIMO) radars utilize various sources of diversity to improve the performance of the radar. A MIMO radar in which angular diversity is achieved by using widely distributed antennas has been proposed to reduce the impact of the fluctuations of the target radar cross-section. This type of system is also known as the statistical MIMO radar. Typically, it has been assumed that the signals received by different

antennas are either fully correlated or independent depending on the configuration. In this paper, we assume more realistically that the scattering from the target is correlated. We show that taking the correlation of the scattered signals into account can improve the probability of detecting the target. This is achieved by using a parametric model for the scattering which allows one to efficiently estimate the scattering covariance matrix. The numerical examples demonstrate that the probability of detection remains good even when parameters of the model are inaccurate. [C1347]

### "Cramer-Rao bound for joint location and velocity estimation in multi-target non-coherent MIMO radars"

In this paper, we focus on a performance bound for joint location and velocity estimation in non-coherent MIMO radars with multiple targets, which has not been studied before. Closed-form expressions for the Cramer-Rao bound are provided for a two-target case. We use numerical simulations to validate the Cramer-Rao bounds and use these bounds to study the performance of a non-coherent MIMO radar system. We analyze the influence of the distance between two targets on the estimation performance. Simulation results reveal that the spatial advantage, which was uncovered previously for a single-target case, also applies for two targets. [C1348]

### "Feasibility of range estimation using sonar LPI"

Using a detailed waveform-based simulation framework, a study on the feasibility of LPI sonar is performed for covert range estimation. A frequency selective channel filter is applied for realistic ocean simulation. The platform uses matched filtering and the target uses energy detection for processing the received signal. The objective of the platform is to estimate the range to the target while ensuring that the target still fails to detect the platform's pinging LPI waveform. A platform-target encounter scenario was designed for Monte Carlo simulation. Evaluation of system parameters was performed to assess for the feasible conditions for covert range estimation. [C1349]

### "Ordering for estimation"

A discretized version of a continuous optimization problem is considered for the case where data is obtained from a set of dispersed sensor nodes and the overall metric is a sum of individual metrics computed at each sensor. An example of such a problem is maximum likelihood estimation based on statistically independent sensor observations. By ordering transmissions from the sensor nodes, a method for achieving a saving in the average number of sensor transmissions is described. While the average number of sensor transmissions is reduced, the approach always yields the same solution as the optimum approach where all sensors transmit. The approach is described first for a general optimization problem. A maximum likelihood target location and velocity estimation example for a multiple node non-coherent MIMO radar system is later described. In particular, for cases with near ideal signals, sufficiently small surveillance region and sufficiently large signal-to-interference-plus-noise ratio, the average percentage of transmissions saved approaches 100 percent as the number of discrete grid points in the optimization problem  $Q$  becomes significantly large. In these same cases, the average percentage of transmissions saved approaches  $(Q-1)/Q \approx 100$  percent as the number of sensors  $N$  in the network becomes significantly large. Similar savings are illustrated for general optimization (or estimation) problems with well designed systems. [C1350]

### "A combined Teager-Huang and Hough Transforms for LFM signals detection"

A new method for linear FM (LFM) signals detection in the time-frequency plane using Teager-Huang Transform (THT) is proposed. Time-Frequency Representation (TFR) is viewed as an image where image processing techniques are applied to detect frequency patterns of interest. THT is used in conjunction with Hough Transform (HtT) called (THHT), where the output is a TFR free of cross-terms. THHT is applied to signals composed of LFM and the results are compared to Wigner-Ville Distribution-HtT and smoothed Wigner-Ville Distribution-HtT. Results show the good performance of the THHT in terms of detection and estimation compared to WVD based methods. [C1351]

### "Non-coherent MIMO radar in a non-Gaussian noise-plus-clutter environment"

The initial papers on MIMO radar have triggered a tremendous amount of research work recently. How the MIMO radar detector, previously designed for Gaussian noise, performs when the noise-plus-clutter is non-Gaussian is still unknown. In this paper, we evaluate the detection performance of the Gaussian detector under the non-Gaussian noise-plus-clutter in a non-coherent MIMO radar system. Using the theory of Spherically Invariant Random Vectors (SIRVs), we study three non-Gaussian noise-plus-clutter models employing the K, Laplace, and Student-T distributions, respectively. Simulations are carried out for different numbers of antennas, SNRs and false alarm probabilities. The results show that non-Gaussian noise-plus-clutter has no impact on the diversity gain of a MIMO radar system although it degrades the detection performance in some other ways. We

also verify some known results on the optimality of the Gaussian detector for SIRV noise-plus-clutter models, while showing this is not true for non-SIRV models. [C1352]

### "An Investigation on the performance of receiving Optical Beam-Forming Networks"

Next generation wideband and ultra-wideband radar antenna arrays need efficient true-time delay networks for array control. Following the great interest for optical control of antenna array beam steering, performance analysis of optical beam-formers is a must. In this paper signal to noise ratio and dynamic range of simple optical beam-forming structures with components off the shelf are investigated theoretically. Especially the effects of certain power combining components such as arrayed wave guide gratings, broadband passive optical combiners and microwave combiners inspected. It turns up that an efficient microwave combiner would surpass the optical combiners in both SNR and dynamic range. [C1353]

### "Receiver antenna array"

Our aim is to develop a microwave receiver antenna system, which can form its radiation pattern (main lobe direction, null-point direction, structure of the side lobes), measure the direction of the RF source in milliseconds. In this paper we will show the theoretical background of the antenna system, the build-up of the realized system and some measurement results. [C1354]

### "Implementation of a radar tester for air traffic control applications"

In this paper we present a method, and a fully implemented and tested hardware, for testing the operation of primary radars, may it be used in air traffic control or in military service. The realization of the radar tester was based on the theory of controlled radar cross section (CRCS), this way creating spurious targets or clutters, with known parameters, on the screen of the radar. According to the difference between the created and the measured parameters (e.g. velocity, fluctuation and distance), any minor or major degradation or failure can be detected. The tester is capable of scanning the radar system from the antenna, via microwave hardware elements, all through to the digital signal processor (DSP) unit, achieving great diagnostic properties. Emphasis was put on the realisation of the hardware. The produced equipment was tested in real life using a primary ATC radar in Hungary, with satisfying results. [C1355]

### "Modulation constellation analysis of GNSS signal using SDR receiver"

Modulation analysis is a dispensable item for the quality evaluating of GNSS signal. Tradition method based on instruments is limited to process signal with low dynamic although its accuracy is very high. This paper proposes a new method for modulation constellation analysis using GNSS software defined radio(SDR) receiver, which makes good use of the tracking module of SDR receiver to accommodate signal with great dynamic. The experiment results demonstrate the similarity between the accuracy of this method and that of instruments, as well as adaptability for signal with different dynamic. [C1356]

### "Design and implementation of real-time SAR echo simulator for natural scene"

This paper presents a real-time echo simulator for natural scene. The simulator generates SAR echo according to the radar flight trace in real time. The key technique of the echo simulator is presented first and the experiment result is shown. This simulator has been used as a general purpose verification platform for SAR real-time imaging system. [C1357]

### "Method of phase unwrapping-free DEM reconstruction of InSAS"

In this paper a kind of phase unwrapping-free digital elevation model(DEM) reconstruction method of interferometric synthetic aperture sonar(InSAS) is described. Firstly, a new method of coarse DEM generation is proposed. In the method, a pair of images are divided into small blocks and resampled to a set of reference planes. The height of each block pair is estimated by measuring the maximum coherence of the corresponding pair resampled to different reference planes. The entire heights of the blocks are interpolated to obtain the coarse DEM. After that, the resulting coarse DEM is used to flatten interferogram. The residual interferogram generally is unwrapped. Therefore phase unwrapping can be avoided. Simulation result is presented. The resulting DEM indicates that the proposed method has good potential for topographic mapping of the seafloor surface. [C1358]

### "The imaging analysis of asynchronous bistatic SAR with parallel tracks"

The imaging of bistatic SAR with asynchronous transceiver positions is studied in this paper. First of all, the geometry of the asynchronous transceiver model is constructed, and the approximation model of the echo from



the bistatic SAR is obtained based on the analysis of the instantaneous transceiver distance. Asynchronous transceiver positions will lead to non-uniform SAR data. This paper first analyzes the method for transforming the asynchronous bistatic model into a monostatic variable motion model. Then with the non-uniform FFT, it resolves the non-uniform sampling problems induced by nonconstant velocities. The simulation experiments show that the bistatic SAR images have good quality, which verifies the validity of the method presented in this paper. [C1359]

#### "Parameters extraction of crop based on PolSAR Data"

It is beneficial to extract the parameters of the objects by rich information of PolSAR (Polarimetric Synthetic Aperture Radar) data. With polSAR data of Radarsat-2, the polarimetric character of winter wheat in booting and milk stage is studied based on polarization theory. The results show that: there is a great difference between the polarimetric characters of two stages due to the change of wheat structure. Winter wheat growth can be retrieved by entropy, which changes in different way in the two stages. In booting stage, with LAI increasing, the scattering mechanism tends to be more complex. While in milk stage, with plant density increasing, the scattering mechanism tends to be simpler. The eigenvalue of  $\lambda_2$  is a valuable parameter to retrieve soil moisture with crop cover. Results show the potential advantage of polarimetric radar. [C1360]

#### "Design and implementation of embedded monitoring system for grain storage"

Meeting the requirement and development of large granaries, an embedded environmental monitoring system for grain storage based on ARM technology is designed in this paper. The overall structure of the proposed monitoring device consists of two components, one is the host computer located in control room for information processing and prediction of grain situation, the other is the lower computer terminal in the granary with grain data acquisition, signal processing and communication functions. They transmit data to each other over industrial Ethernet or GPRS networks. On this basis, the implementation methods of data monitoring terminal for grain situation based on S3C2410 microprocessor are studied in detail. The human machine interface of the terminal is developed by Qt/Embedded. Finally, the feasibility and reliability of the system has been proved by the laboratory test. [C1361]

#### "Turbines can suppress Loop Current to reduce Gulf of Mexico hurricane threat"

When the Loop Current (LC) intrudes into the Gulf of Mexico (GoM) it collects a deep pool of warm water that can energize a hurricane which passes through it. Data is presented to support the hypothesis that the LC is driven by gravity, and that its intrusion is a way of dissipating extra hydraulic drive power caused by the higher mean sea level at Grand Cayman Island compared to Grand Bahama Island. If some of this extra drive power is converted by submerged turbines into electric power for the shore grid, and the rest is dissipated by eddies shed by mooring cables and turbine structures, there will be no warm pools to energize hurricanes. Some turbine design estimates are made and a possible configuration is shown. [C1362]

#### "Mapping Geo-Pathogenic Zones and required instrumentation"

Geo-Pathogenic Zones, the areas on Earth's surface where drastic disturbances of natural electromagnetic field are detected, and their dire effects are no longer a mystery. Present human health issues cannot be resolved without considering the influence of the natural environment on human organisms. In light of recent advances in physics this important problem can no longer be ignored. The technological level of today's electrical engineering progress enables us to develop special instruments for scanning and mapping vast areas of landscapes to reveal potentially harmful factors. Geo-pathogenic zones (GPZ) are a major cause of natural impact on humans. Interaction of Earth's electromagnetic fields with local electro-physical heterogeneities are considered as a base of GPZ. Extremely low frequency electric fields, ELFEF, influencing the human brain, have been experimentally confirmed. The spinning electric field, another important phenomenon which can affect humans, has been revealed and established experimentally. The instruments depicting negative influence of GPZ can also be employed for water prospecting due to their capability to detect ELFEF and spinning fields. The results of this research are shown as electro-physical mechanisms of GPZ. [C1363]

#### "Netted sensors for higher-dimensionality performance"

Many sensors that are in service today were designed for locating objects in two dimensions. Air-traffic-control (ATC) radars, for example, are often circular-scan radars that can provide range and azimuth measurements, which can be used to locate an airliner's latitude and longitude. Radars such as these typically do not have the capability to locate an object in three dimensions, thereby providing information regarding the object's altitude. Knowledge of aircrafts' altitudes, however, is highly desirable given the demands put on ATC by the crowded skies of modern aviation. Previous work has shown how two-dimensional target-location accuracy can be

improved within the same dimensionality by combining multiple sensors. More recent work is revealing how, by netting multiple two-dimensional sensors such as circular-scan radars, three-dimensional object-location can be achieved. In this paper the concept of networking multiple two-dimensional sensors will be described. A scenario including multiple two-dimensional sensors will be presented, and analytic performance results will be provided for various sensor combinations and geometries. [C1364]

#### "Detection for signal in ELF atmospheric noise interference"

Extremely low frequency (ELF) atmospheric noise is non-Gaussian, consisting of the sum of a Gaussian background and narrow pulses caused by lightning strokes. Therefore, the conventional detection method for signal in Gaussian noise gets worse. In this paper, a new structure for signal detection in the ELF atmospheric noise is proposed. First, the ELF atmospheric noise is modeled as a symmetric  $\alpha$ -stable (S $\alpha$ S) process. Then the performance of optimum linear detector, matched filter, and locally optimum detector are examined. The FFT-based algorithm is used for calculating the probability density function (PDF). Finally, the probability of error (Pe) of each detector is compared by extensive Monte-Carlo simulation. [C1365]

#### "A velocity estimation method for Multi Carrier Phase-Coded radar"

Due to good balance among spectrum efficiency, ambiguity function and peak-to-mean envelope power ratio (PMEPR), wideband Multi-Carrier Phase-Coded (MCPC) radar has caught much attention from researchers recently. Based on separation of sub carriers from multi-frequency structure, this paper provides velocity estimation method for such radar signal. After detecting the peak Doppler spectrum of each sub carrier, the unambiguous velocity can be obtained by Least-Squared (LS) algorithm. The simulation results show that these methods can estimate the velocity of fast-moving target efficiently and guarantee the accuracy against low SNR. [C1366]

#### "Automatic target recognition of SAR images based on the fuzzy neural networks"

ATR (automatic target recognition), based on SAR (synthetic aperture radar) image, is crucial to the success of battlefield awareness and has become a very hot research topic. But many problems, which are caused by a great deal of missing, polluting, and superimposing of the signals, still generally exist in practical application, such as the low recognizing rate. How to recognize the useful signals from badly polluted images has become a difficult point in remote sensing image process. Thus, this paper will provide a way to recognize radar signal automatically by using the fuzzy neural networks. [C1367]

#### "Small target detection in SAR image using the Alpha-stable distribution model"

The Constant False Alarm Rate (CFAR) algorithm is most commonly used for small target detection in SAR images. As the goodness-of-fit of distribution model to SAR clutter has great effect on the performance of algorithm, after a comprehensive statistical analysis of background clutters of different SAR data, a modified CFAR algorithm based on the Alpha-stable distribution is proposed for detecting small targets in SAR images, especially under the extremely inhomogeneous background clutter. Considering for the complexity of Alpha-stable distribution model, the parameter estimation and threshold determining steps of the modified algorithm are introduced in detail. Performance of the algorithm is assessed by experiments on ADTS data. Compared with typical two-parameter CFAR (TP-CFAR) algorithm based on Gaussian distribution and K-CFAR algorithm based on K distribution, the proposed method is demonstrated to be most suitable for detecting small target in extremely inhomogeneous regions. [C1368]

#### "Blind separation of instantaneous linear mixtures of cyclostationary signals"

Blind separation of signals, which consists of recovering signals only from observed instantaneous linear mixtures without a priori information about the mixing matrix, is an important problem in many practical applications including radar, sonar, wireless communication and so on. For blind separation of cyclostationary signals, proposed a novel approach (PM) which dropped a pre-whitening stage usually required by many second-order statistics based methods such as AMUSE and SOBI algorithms. However, the PM algorithm has a fatal disadvantage in that it cannot fully separate all signals in the circumstance of more than two sources. To overcome this drawback, we proposed an improved PM algorithm in this paper. Several numerical simulations are also provided to illustrate the effectiveness of the proposed method. [C1369]

#### "Radar mosaic based on the explicit radar ray paths"

In radar observation, different ray paths, which influence the three-dimensional gridding process, is due to the different gradients of reflectivity. The earth's radius model, which could not describe the radar ray path in a

certain atmospheric thermodynamic condition, is the average condition of the radar ray pathway. In order to get the mosaic data of a certain thermodynamic condition, we need an arithmetic that could produce mosaic data based on the explicit radar ray paths. In this paper, we propose a method enable us to get the mosaic data based on any certain thermodynamics profiles of atmosphere. And the results are compared to the products of radar mosaic scheme based on the fixed earth's radius model in a certain atmospheric thermodynamic condition. [C1370]

#### **"Detecting and tracking of small moving target in avian radar images"**

A sequence of plane position indicator (PPI) images containing a small moving target is collected using an experimental avian radar surveillance system, which is constructed by modifying a standard marine radar. Smoothing trajectory of a small moving target is separated from the image sequence after background subtraction, clutter suppression, measurements extraction and tracking. The background image is generated by Fast Independent Component Analysis (FastICA). Low segmentation value is set in clutter suppression to improve detecting rate at the cost of introducing a great deal of clutters. Therefore, false alarm rate need to be reduced by tracking. Meanwhile, a modified Hough transform method is applied for track initiation. Monte Carlo data association is proposed for track maintenance and Kalman filtering is adopted for target state prediction and update. Finally, the trajectory is smoothed and then fused with a satellite map for further observation. [C1371]

#### **"Accurate time interval measurement method based on Vernier caliper principle"**

An accurate method by using main clock and vernier clock is introduced to measure time interval. Vernier clock is used to count the time interval. The corresponding count results are sampled by the main clock. The relationship between the sum of sampling sequence and time interval is investigated. By utilizing the sampling sequence, we can calculate the precise time difference easily. The implementation steps are listed and the resolution is analyzed. [C1372]

#### **"A new method based on the BP neural network to improve the accuracy of inversion of the vegetation height"**

The error in the estimation of the ground interferometric phase will reduce the accuracy of the inversion of the vegetation height in three-stage vegetation inversion method. Aiming at this problem, the new vegetation height inversion method based on the BP neural network is proposed. The new method directly fits the nonlinear mapping relationship between the complex correction coefficients and the vegetation height, so it reduces the height inversion error caused by the error in the estimated ground interferometric phase. The new method has better performance than the three-stage vegetation height inversion method, and the experiment results validate the superiority of the new method. [C1373]

#### **"Blind adaptive beamforming algorithm based on cyclostationary signals"**

The design of beamformer is an important aspect in array signal processing applied in several fields including radar, sonar, wireless communication and so on. The Capon beamformer, which has been used widely because of its many advantages, requires a priori knowledge of array manifold which sometimes it is difficult to obtain in some applications. Thus, the techniques of blind adaptive beamforming which don't need this information became of interest in recent years. For the cyclostationary signals encountered in numerous applications, a blind adaptive beamforming algorithm, which has a low computation complexity and fast convergence performance, is presented in this paper. [C1374]

#### **"Study on a method of compensation for the range profile of high velocity spatial targets"**

For wideband LFM signal, the paper presents a mathematical model of echo from spatial maneuvering targets and analyzes the impact of high acceleration and maneuvering on range profile quantitatively. According to invariable chirp rate, a range profile compensation algorithm based on difference is proposed. It can estimate the chirp rate accurately by FFT without acceleration and velocity estimation, so the influence of high-order coefficient is eliminated. Due to its no phase estimation, this algorithm has good anti-noise performance. In addition, the sample rate does not need to be higher than the bandwidth of LFM signal, so the processing speed is improved. The analysis is proved by simulation results. [C1375]

#### **"Study on adaptive monopulse with reduced dimension STAP technique"**

For airborne radar, the estimation performance of moving target parameters is greatly affected by the residuals of ground clutter after space-time adaptive processing (STAP). The non-homogeneity of environment, which

results in the lack of available secondary data, will make this problem worse. In this paper, a novel method, which utilizes small amount of secondary data, is proposed for getting more accurate estimation under non-homogenous environment. In this method, the spatial and temporal dimensions are reduced properly for the benefit of low secondary data support and exact clutter covariance matrix estimation; additionally, by combining a STAP processor with monopulse technique, target parameters will be obtained. The simulation results are shown this method is more accurate and adaptable than the previous adaptive monopulse with STAP method under the non-homogeneous environment. [C1376]

#### "Angle estimation of coherent multi-target for MIMO bistatic radar"

The angle estimation algorithm of coherent multi-target for MIMO bistatic radar is presented. In the algorithm, the virtual array data from multi-target in MIMO receiver is firstly decorrelated, then special matrix based on the ESPRIT method is constructed, finally the eigenvalues and the eigenvectors of the matrix are used to estimate direction of departures and direction of arrivals. In this algorithm, the parameters can be directly paired by the relationship between the eigenvalues and eigenvectors. The correctness and performance of the proposed method are verified by the computer simulation. [C1377]

#### "Contact-free measurement of heartbeat signal via a doppler radar using adaptive filtering"

It has been proven that the cardiopulmonary signs, including respiration and heartbeat signal, can be contact-free measured via a Doppler radar. However, the heartbeat signal cannot be identified when the human subject does not hold his or her breath. To resolve the problem, the adaptive noise canceller (ANC) based on recursive-least square (RLS) algorithm is presented to simultaneously measure the heartbeat and the respiration signal. Experimental results showed that not only can the heartbeat signal be well identified, but the heart rate also strongly correlated with that derived from the electrocardiogram (ECG). [C1378]

#### "Feature extraction and soft segmentation of texture images"

In this paper, we propose an efficient method for texture image segmentation. First we extract four feature channels smoothed with the total variation (TV) flow. Then we propose a soft segmentation model based on the Chan-Vese model by adding a weight in the arc length term and using a soft membership function in stead of level set function to represent the region. We derive a fast algorithm using the Additive Operator Scheme (AOS) and Chambolle's fast dual projection method. Experimental results on texture and Synthetic Aperture Radar (SAR) images show the effectiveness of our algorithm. [C1379]

#### "Parameters analysis for polarimetric SAR Based on classification accuracy"

As a multi-channel microwave remote sensing imaging radar system, polarimetric Synthetic Aperture Radar (SAR) enhances the information extraction ability for material scene in the observation area, in which the design and state monitoring for parameters play an important role in polarimetric SAR system and equipments management. This paper presents an analysis method for three typical polarimetric SAR system parameters: channel noise, polarization imbalance, and polarization isolation. We explore the polarimetric SAR image classification accuracy ratio and the relationship with three parameters above, review the statistic model of each parameter, and propose an analysis model between each parameter and the classification accuracy ratio measurement. By the polarimetric SAR image experiment, the comparative curve between each parameter and the influence on classification performance is obtained, which shows an application reference for polarimetric SAR system design and management. [C1380]

#### "Improved PGA algorithm based on adaptive range bins selection"

Phase gradient autofocus (PGA) algorithm has been proved to be a superior method for higher order phase error correction in SAR/ISAR image post processing. However, the accuracy of phase error estimation using traditional PGA algorithm is usually not guaranteed especially when there are several strong adjacent scatterers in a range bin. In this paper an improved iterative PGA approach based on adaptive range bins selection is presented. Results of real data experiments show that the improved PGA algorithm outperforms the traditional one. [C1381]

#### "SAR image despeckling using directionlet transform and Gaussian scale mixtures model"

In this paper, a novel despeckling method based on Gaussian scale mixtures (GSM) model in the directionlet domain is proposed. Before despeckling, we define a measurement of directivity of texture to calculate the directivity of texture according to the edge map. After directionlet transform, neighborhoods of coefficients at adjacent scales are modeled as GSM model. Under this model, a Bayes Least Squares (BLS) estimator is



adopted to reduce speckle noise. Quantitative and qualitative experimental results show that the proposed method is an effective despeckling tool for SAR images. The method can suppress the speckle noise and, in the meantime, preserve the scene features as much as possible. [C1382]

#### "Universal coupling curve for coupled resonators and transmission lines"

Coupled resonators and coupled transmission lines are described with the same universal curve. Resonant frequencies of coupled resonators and impedances of coupled transmission lines reveal the same dependence on coupling coefficient. This can be used to select, adjust or create the models of coupled structures. [C1383]

#### "Investigations of multilayer three-strip coplanar lines with the ferrite material"

In this paper the investigations of a multilayer coplanar line consisting of three strips located on a longitudinally magnetized ferrite are presented. In the analysis of proposed structure the coupled mode and mode matching methods are applied. Using proposed approach the ferrite coupled line junction is designed. For this junction the transmission parameters are calculated. The numerical results are verified via experiment. [C1384]

#### "Application of hybrid approach to the analysis of resonators loaded with axially symmetrical posts"

In this paper a new hybrid method is applied to the analysis of circular cavity resonators loaded with arbitrary configuration of axially-symmetrical posts. The method is based on a combination of finite difference frequency domain method and mode matching technique. In our approach each scatterer is treated as an effective circular cylinder represented by impedance matrix defined in its local coordinate system. In order to obtain the scattering parameters of an arbitrary configuration of objects in global coordinate system an analytical iterative scattering procedure (ISP) is utilized. The proposed technique is applied to determine the resonant frequencies of three different configurations of resonators. The validity of the proposed approach is verified with the analytical approach and commercial software. [C1385]

#### "Receiver Antenna Array"

Our aim is to develop a microwave receiver antenna system, which can form its radiation pattern (main lobe direction, null-point direction, structure of the side lobes), measure the direction of the RF source in milliseconds. In this paper we will show the theoretical background of the antenna system, the build-up of the realized system and some measurement results. [C1386]

#### "A new method for refractive index measurement of isotropic and anisotropic materials in millimeter and submillimeter wave range"

Based on patented by us interferometer-turning method the experimental set-up for refractive index measurement of parallel plates from isotropic and anisotropic materials in ranges millimeter-submillimeter (mm-submm) wave length have been created and described. The process of interference fringe shift measurement that based on created software has been analyzed, necessary working correlations have been given and experimental accuracy of refractive indexes measurement has been appraised. [C1387]

#### "Multi-frequency approach to the coaxial multilane through-reflect-line calibration"

We present an improved coaxial multilane through-reflect-line calibration method which allows to correct for errors in the description of calibration standards. Our approach is based on the multi-frequency formulation of the vector-network-analyzer calibration problem which accounts for the physical relationships between calibration standard S-parameters at different frequencies. We illustrate our approach with experimental results for the coaxial multilane through-reflect-line calibration with type-N airlines. We show that our calibration method significantly improves the measurement accuracy as compared with the classical multilane through-reflect-line calibration method. [C1388]

#### "Discrete shape optimization method for the non-uniform transmission line directional couplers"

In this paper a new method for a non-uniform directional couplers design is presented. It is modeled on the cascade connection of a large number of short, equal length sections of a uniform coupled transmission line. The coupling coefficient vector is optimized with the non-smooth sub-gradient algorithm. The performance of the optimization algorithm is surprisingly good. The algorithm generates many, close to optimal, solutions, with a variety of shapes. Initial profiles are almost smooth. However, at the end of optimization, shape tends to converge to a technological constraint. The optimal structure consists of a cascade connection of uniform coupled transmission line sections (of maximal coupling), separated by sections of a non-coupled transmission line.

[C1389]

#### **"Modeling of integrated microstrip bend structures on silicon substrates up to 110 GHz"**

This work describes an equivalent circuit model for microstrip bend structures on silicon substrates targeted for integrated millimeter wave circuits. The values of the lumped elements are extracted from 3D electromagnetic simulations for three different bend shapes and strip widths in the range of  $W=5-50\text{ }\mu\text{m}$  up to 110 GHz. The width dependence of the element values are derived using curve fitting algorithms and the integration of the model equations in circuit simulation environments is demonstrated. The developed model is compared with measurement results of several bend test structures fabricated in a high performance  $0.25\text{ }\mu\text{m}$  SiGe BiCMOS technology. Excellent agreement has been obtained. [C1390]

#### **"Photonic structures in the microwave band and their applications"**

The possibility to utilize microwave photonic structures for measurement parameters of nanometer films and for creating on their base functional devices of microwave electronics has been shown. A wideband waveguide matched load on the base of waveguide photonic crystal has been described. Microwave filters with transmittance controlled from -1.5 dB to -25 dB by changing the PIN-diodes bias voltage from 0 to 700 mV have been constructed. [C1391]

#### **"Analytical study and simulation of distributed phase shifter"**

This paper presents the modeling of phase shifter based on distributed CPW transmission lines combined with SMD components. It presents an analytical study of the phase shifting, the insertion loss and the return loss of proposed phase shifter. The expression of phase shifting is obtained through a global ABCD matrix of 9-sections of proposed phase shifter. [C1392]

#### **"Tuning properties of irregular posts in waveguide junctions-tunable filter application"**

In this paper the authors' hybrid method of electromagnetic wave scattering is applied to investigate the tuning properties of rectangular posts in waveguide junctions. As an example a basic waveguide filters employing several conducting cylindrical posts with rectangular cross section are considered. The size and location of the posts in a waveguide junction are optimized to obtain the required frequency response characteristic of the structures. Since, the posts are inhomogeneous, they can be used as tuning elements. In this work it is shown, that a simple rotation of rectangular posts allows one to correct any inaccuracies created during fabrication of the filter structure. A good agreement is obtained between the results of this method and own measurements of the fabricated structure. [C1393]

#### **"Design of UWB uniplanar $180^\circ$ hybrid employing ground slots and microstrip-slot transitions"**

The paper describes the design of a uniplanar  $180^\circ$  hybrid with an ultra wideband (UWB) performance. The device uses a single substrate and all its four ports are of microstripline type. Its construction is accomplished by first designing separately the out-of-phase and in-phase dividers. To merge the two devices into the hybrid, the input port of the in-phase power divider is split into two lines to overpass a ground slot in the out-of-phase divider. The proposed design strategy results in the  $180^\circ$  hybrid exhibiting a well-balanced power division between the output ports and good quality return losses of the out-of-phase (difference) and in-phase (summation) ports across the band from 3 to 11GHz. The isolation between the difference and signal ports is excellent and the differential phase shift is also close to the ideal case of  $180^\circ$  and  $0^\circ$  across this band. [C1394]

#### **"Performance and characterization of MMIC phase shifter with wire bonds interconnections"**

This paper presents some aspects of bond wire interconnections and its affect on the performance of a 6-bit phase shifter. The phase shifter operates in S-band and was connected to Rogers RO4003 substrate by the means of ball bonds. Discontinuities introduced by the interconnections were modeled as a low pass network. This non-optimal bonding worsened scattering parameters of the phase shifter by  $\sim 15\%$ . [C1395]

#### **"Line-length optimization of offset-short standards for broadband VNA calibration"**

The paper introduces a novel method for selecting optimal line lengths of multiple offset-short standards that are applied to broadband calibration of vector network analyzers (VNAs). The method is based on the design of experiments (DOE) approach and analysis of the determinant of the Fisher information matrix. To interpret results of the analysis, new terms, adopted from the filter theory, are suggested. The analysis reveals a tradeoff between solutions that provide low uncertainty and broad bandwidth of the VNA calibration. Both aspects are

vital at millimeter wavelengths, when using calibration standards based on 1.85 or 1 mm coaxial lines. The length optimization, using the DOE criterion of D-optimality, enables expanding the calibration frequency range much over that provided by the offset shorts currently available in commercial calibration kits. [C1396]

#### "Adaptive signal acquisition and wireless power transfer for an implantable prosthesis processor"

This paper describes an ADC array and wireless power transfer link for an implantable prosthetic processor which digitizes neural signals sensed by a microelectrode array. The ADC array consists of 96 variable resolution ADC base cells. The base ADC has been implemented in 0.13 $\mu$ m CMOS as a 100kS/s SAR ADC whose resolution can be varied from 3 to 8-bits with corresponding power consumption of 0.23 $\mu$ W to 0.90 $\mu$ W. The resolution of each ADC cell is adapted according to neural data content of the signal from the corresponding electrode, this reduces power consumption by a factor of 2.3 whilst maintaining an effective 7.8-bit resolution across all channels. A wireless power transfer system for implanted medical devices which uses antenna area 100 times smaller than previous designs has also been realized. Adaptive simultaneous conjugate matching and a high efficiency rectifier and regulator in 0.13 $\mu$ m CMOS together with a 4mm<sup>2</sup> antenna deliver 140 $\mu$ W at 1.2V DC from a 4cm<sup>2</sup> transmit antenna and a 0.25W 915MHz source through 15mm of tissue to power the implanted device. [C1397]

#### "Low-power low-complexity carrier-based UWB transmitter in 90nm CMOS for wireless biomedical radar sensing applications"

This paper presents a low-power low-complexity ultra-wide band (UWB) transmitter designed in 90nm CMOS technology for UWB radar sensing applications. The proposed design is carrier-based and is targeting for motion detection, biomedical imaging, and short range data communications. This non-coherent UWB transmitter, generates on-off modulated signals at different carrier frequency within the 3-10 GHz band. A voltage controlled oscillator generates a modulated pulse consisting of multiple cycles of sinusoidal waves with smaller bandwidth. The carrier frequency can be adjusted over the whole UWB frequency band by changing the capacitance of a capacitor bank. The transmitter driver controls the output power and matches the 50 $\Omega$  antenna load. The average power consumption of the transmitter is 1.85mW at a carrier frequency of 9GHz using 1V supply. [C1398]

#### "Active beamforming with interpolated FIR filterin"

The interpolated FIR (IFIR) radar was recently introduced in the context of MIMO radar theory. It was shown that this system has a signal to clutter ratio intermediate between those of the SIMO and MIMO radars. This paper considers the optimal design of the active IFIR beamformer in presence of jammers. It is shown that this beamformer can achieve beamwidths as sharp as those of colocated MIMO radars with full-length virtual arrays. At the same time, the extra complexity of MIMO radars, which arises from use of multiple transmitter waveforms and several sets of receiver matched filter banks, is not present in the IFIR realization. Design examples for IFIR radars which optimize the receiver beamforming weights in presence of jammers for fixed transmitter are also presented. [C1399]

#### "A joint block diagonalization approach to convolutive blind source separation"

This paper is concerned with blind separation of convolutive sources. The main idea is to make an explicit exploitation of block Toeplitz structure and block-inner diagonal structure in autocorrelation matrices of source signals at different time delays as well as of inherent relations among these matrices. With implementation of joint block diagonalization, a tri-quadratic cost function is introduced so that the mixture matrix can be extracted from a set of the correlation matrices of the observed vector sequence without pre-whitening. In this novel one-stage algorithm, every iteration step involves finding the closed solution to the corresponding least squares problem. Once the estimate of the mixing matrix is obtained, the source signals are retrieved by the classical least squares methods. The performance of the proposed algorithm is illustrated by simulation results. [C1400]

#### "A W-band LNA in 0.18- $\mu$ m SiGe BiCMOS"

This paper presents the design and implementation of a W-band LNA. Fabricated in a 0.18- $\mu$ m SiGe BiCMOS technology, the five-stage LNA achieves a peak power gain of 19 dB with a 3-dB bandwidth from 70-97 GHz and a minimum noise figure of 9 dB. The LNA exhibits more than 10-dB gain and input return loss  $< -12$  dB across the entire W-band (75-110 GHz). The SiGe LNA is suitable for several W-band applications including 77/79-GHz automotive radars and passive imaging in the 80-110 GHz window. [C1401]

#### "Auditory speech processing for scale-shift covariance and its evaluation in automatic speech

### recognition"

The syllables of speech contain information about the vocal tract length (VTL) of the speaker as well as the phonetic message. Ideally, the pre-processor used for automatic speech recognition (ASR) should segregate the phonetic message from the VTL information. This paper describes a method to calculate VTL-invariant auditory feature vectors from speech, using a method in which the message and the VTL are segregated. Spectra produced by an auditory filterbank are summarized by a Gaussian mixture model (GMM) to produce a low-dimensional feature vector. These features are evaluated for robustness in comparison with conventional mel-frequency cepstral coefficients (MFCCs) using a hidden-Markov-model (HMM) recognizer. A dynamic, compressive gammachirp (dcGC) auditory filterbank is also introduced. The dcGC provides a level-dependent spectral analysis, with near instantaneous compression, and two-tone suppression. [C1402]

### "Ambiguity function analysis for MCPC radar signal"

The MCPC signal using Orthogonal Frequency-Division Multiplexing structure has caught much attention of researchers recently since it has good anti-jamming capability, high spectrum efficiency and simple digital processing. This paper deduces ambiguity function expression of MCPC radar signal analyses its performance and discuss the influence of individual parameter on ambiguity function in both range and Doppler domain. Derived conclusion can provide theoretical basis for the waveform design and signal processing of the MCPC signal. [C1403]

### "A novel DOA estimation technique for coherent real-valued sources"

This paper proposes a new DOA estimation technique for coherent real-valued signal sources which is named Modified Covariance AR spectrum estimation of Modified Cross Correlation Sequence (MCCS-MC) algorithm. Firstly, we introduce the basic principle of the new technique: transform the DOA of the sources into frequency of a modified sequence, and get the arrival angles by power spectrum estimation of the sequence. Then we focus on the performance analysis of the proposed technique. Simulation results show that the algorithm not only solves the angle ambiguity problem in the DOA estimation of real-valued signals, but also precisely and stably estimates the arrival angles of coherent sine signals without spatial smoothing or matrix rebuilding. [C1404]

### "A novel method for extraction of in-pulse feature of LFM signal"

Aiming at the shortly SNR capability of wavelet-ridge in extracting in-pulse features of LFM signal, in this paper, a time-frequency associated analyzed method based on wavelet transform and time-frequency reassignment is proposed. The method is based on LFM's wavelet scalogram, and combined with time-frequency reassignment and time-frequency ridge. With the help of time-frequency reassignment in improving the time-frequency agglomeration of representations, the SNR capability of wavelet-ridge is enhanced. The result of the emulation experiments approved the feasibility of this method. [C1405]

### "Complex dielectric permittivity of composites based on dielectric matrixes with inclusions of carbon nanotubes"

Complex dielectric permittivity of composites based on two-component epoxy adhesive with different volume concentration of inclusions of multilayer carbon nanotubes and particles of fine-dispersed graphite was determined from the transmission spectra of the microwave radiation interacting with the sample under investigation. Complex dielectric permittivity of multilayer carbon nanotubes and particles of fine-dispersed graphite was determined as a result of reverse problem solving with utilization of the dependency of complex dielectric permittivity of composites on the inclusions volume fraction. It was shown that in creating composites based on dielectric matrixes with inclusions of particles of fine-dispersed graphite and carbon nanotubes the last ones provides the greater of the real part of dielectric permittivity and the lesser of the imaginary part of dielectric permittivity. [C1406]

### "Some MIMO radar advantages over phased array radar"

MIMO radar is a new radar technique developed recently. It can achieve better detection performance than conventional phased radar. In this paper, we investigate some advantages of MIMO radar on the non-ideal factor of transmitting signal such as the instability in signal phase and the spur in transmitting signal etc. And then, a simulation system was established, some simulation shows the advantage of MIMO radar over its conventional counterpart. [C1407]

### "The application of chaotic signal in MIMO radar"



Multiple Input Multiple Output (MIMO) radar is a new radar technique. It has many advantages over conventional phased radar in many ways such as anti-intercept of radar signal, low velocity target detection, and resolution. The signal design is a chief problem for radar. In this paper, we analyze the chaotic signal for MIMO radar.

[C1408]

#### "Fast Hough transform algorithm for radar detection"

In this paper, a fast algorithm for radar detection based on line Hough transform is presented. Unlike the traditional method, the idea of our proposed is that the point of data space should be mapped into the Hough parameter space of slope and intercept, where the relative position of the points in the data space is preserved. Then, only one time transformation of coordinate is employed to get the position of a batch points in parameter space. Therefore, the computation burden is significantly reduced. In addition, the detector performance is investigated. Finally, we illuminate the reduction of computation in details. [C1409]

#### "Aggregate type identification in concrete compounds using microwave transmission line and ANN"

Growing concrete market, increasing variety of concrete products and requirements for higher quality calls for a fast and accurate moisture measurement technology. A fast and accurate method for aggregate type identification in concrete compounds is presented in this paper. A transmission line and time domain sampling method for data acquisition is used. In order to find the relationship between material type and signal spectrum curve an artificial neural network classifier (ANN) is used. A total of 13 mixtures of three materials (sand, crushed granite stone and dolomite) mixed in different proportions were identified using the proposed method. Experiments have confirmed the possibility to use transmission line combined with ANN in material independent moisture measurement systems. [C1410]

#### "Dynamic mode of radiosystem with spatial structure optimization in presence of interferences"

Increase of radiosystem interference immunity is reached by application of its optimal spatial structure. In order to overcome algorithm implementation difficulties, connected with hypersensitivity to deviations from suppositions of non-stationary signal parameters and interferences parameters, the regularized algorithm of calculation robust spatial structure is offered. The solution of extreme problem, which belongs to the class of ill-conditioned problems, is searched on basis of representation of spatial structure as element of metric space. The comparative analysis of system efficiency with optimal spatial structure in static and dynamic operating modes is carried out. [C1411]

#### "Lithuanian experience of evaluation on radar antenna radiation"

A method for calculating intensity of electromagnetic fields radiated by powerful radars equipment is proposed in this paper. Taken attention that in calculations it is necessary to use average radiated power. The results of calculations show that an antenna of height 5 m radiates a power flux density at the height of a man's head less than the level permitted by Lithuanian law-20.0  $\mu\text{W}/\text{cm}^2$ . [C1412]

#### "Investigation of susceptibility of routers to high power microwave pulse radiation"

A susceptibility of different types of computer network routers to high power microwave pulse radiation was investigated. Experiments have been performed for different microwave power level, frequency band, pulse duration, and repetition rate. Experimental results were described using electronic fault models of thermal heating and parasitic charging. [C1413]

#### "Magnetic antenna for near-field UHF RFID tag"

In this paper, we propose a method of the improvement of performance of UHF RFID Tag antenna in near field. Currently, near-field UHF RFID receives a lot of attention as a possible solution for item level tagging in various applications. [C1414]

#### "RF identification and localization-recent steps towards the internet of things in metal production and processing"

This paper gives an overview on recent radio frequency local positioning and identification techniques applied in steel production and processing. It is shown that it is required to combine different radio technologies in order to track and trace the goods involved in the manufacturing processes reliably and continuously. In addition the applied components must be carefully adapted to the given application area. The presented RF technologies are key components for the future internet of things and the presented applications illustrate both, the huge potential

as well as the challenges involved with applying modern radio systems in harsh manufacturing processes.

[C1415]

### "Hybrid RFID System"

Continuous development in RFID and microcontrollers technologies gives new possibilities to create systems that are able to integrate a lot of sensors based on different technologies. This integration brings us closer to realize the Ubiquitous Network Society vision. However, many problems must be addressed before we will benefit from such systems. In this paper we describe concept of integrating RFID technology with other sensors technologies to develop a hybrid RFID system. Security issues on each level of communication are also addressed. [C1416]

### "EGSM and CDMA collocation and near field antenna estimation"

This article presents a typical collocation methods which provides an acceptable level of interference between two radio systems placed in close proximity. In particular, the importance of near field estimation was indicated as an essential element of effective isolation distance calculation for collocation purposes. [C1417]

### "Optimization parameters of dielectric in aperture-coupled stacked patch antenna on bandwidth"

The present paper described a method of analysis that can be applied to these geometries, as well as related configurations. The paper presents a model of the antenna on which the simulation was conducted on the impact parameter on bandwidth. The influence of the changes of the value of these parameters of individual layers on the bandwidth was talked over. Paper shows the analysis of multilayer microstrip antennas process is very complex and time consuming and compare between calculation and measurements. One of the most important parameters which have been calculated is the bandwidth. The paper describes a clear advantage of multilayer antennas over monolayer ones, where the bandwidth is significantly narrower. [C1418]

### "A compact double-ridged horn antenna for ground penetrating radar applications"

A compact double-ridged horn antenna for ground penetrating radar applications in the frequency range of 1-7 GHz will be presented in this work. Within this contribution the design, simulation and fabrication of such an antenna will be considered. Among the varying design parameters are linear and exponentially tapered walls as well as variations of the curvature of the dielectric waveguide between the two ridges. In addition an absorber structure and a complex shaped metallic back plate have been introduced to further improve the return loss. The primary design goal is a broad bandwidth while maintaining compact dimensions. Two modifications have been introduced in this antenna design in contrast to the standard TEM horn. By protruding the ridges from the aperture plane and filling the space between the ridges with dielectric material it is possible to lower the operating frequency without increasing the size of the original setup. The proposed design has been applied to subsurface radar application in both, field simulations by means of CST Microwave Studio and measurement in a GPR test scenario. The fabricated antenna has been verified by anechoic chamber measurements. The performance of the antenna with respect to the detection of subsurface objects will be verified by various experiments. [C1419]

### "Study of effect of corrugated edges on the radiation characteristics of GPR antenna"

This paper presents some results of studying the effect of the size of the corrugated edges of the tapered slot antenna (TSA) with elliptical taper on its radiating characteristics. Planar antennas with dimensions of 235 to 120 mm have been simulated in the free space and in the presence of dielectric medium in the near field. The modeling and near field monitoring has been performed using numerical method implemented in CST Microwave Studio software. The effect of the width of the corrugated area on the antennas edges in the range of 5 to 50 mm has been studied by computer simulations and experiments. [C1420]

### "Broadband microstrip patch antenna with reduced transversal size"

In the paper we present the proposal of broadband patch antenna with reduced transversal size. The broadband operation is obtained by means of application of thick substrate and electromagnetic coupling made of two slots. The nonresonant dimension of the antenna is reduced by using H-type slot instead of simple rectangular slot. The antenna has been designed and fabricated and 29% bandwidth for  $WFS < 1.5$  has been achieved. The broadband matching has been confirmed by the measurement of the reflection coefficient of fabricated antenna. However, the radiation pattern in E-plane shows some irregularities and needs additional research. [C1421]

### "A design and adjustment method for ultrawideband microstrip antenna design"

This paper presents a combined theoretical and experimental design and adjustment method for ultra-wideband (UWB) microstrip antennas with new geometries on the radiofrequency printed circuit board (PCB) with the permittivity  $\epsilon_r=2.3$  and the thickness  $h=1\text{mm}$ . The first theoretical design is made by using a standard 3D electromagnetic software package. The antenna specifications are measured and adjusted by the equipment Microwave Test Set IFR 6203B. The obtained antenna has the bandwidth of 600 MHz and very good impedance matching at the resonant frequency 7.2GHz ( $S_{11} = -55.7\text{dB}$ ). This method can reduce time for antenna design in the laboratory conditions. Using it with other initial antenna structures and adding other resonant strips, we can obtain other antennas with smaller dimensions on keeping their large bandwidth and small return loss. [C1422]

#### "Compact Tapered Slot Antennas for UWB microwave imaging applications"

This paper presents the design of compact Tapered Slot Antennas (TSAs) for application in an Ultra Wide Band (UWB) microwave imaging system. In the initial step, a conventional size-reduced TSA with an exponential taper for 3.1-10.6 GHz band is designed. From the radiation pattern analysis, it is found that this antenna exhibits poor directivity in the lower part of UWB. To overcome this shortfall, two modifications are investigated. One includes corrugations and the other one elliptical cuts on sides of the initial TSA. It is shown that the modified TSAs feature improved directivity while their UWB impedance characteristics are similar to the original TSA. The TSA with corrugations exhibits an almost constant directive radiation pattern across UWB. However, its gain oscillates with frequency leading to a pulse distortion. Therefore the size-reduced TSA with elliptical cuts in conducting sides looks to be the most attractive choice with respect to both directive properties and distortionless pulse transmission. [C1423]

#### "A 5.8 GHz RFID-based data transmission system as an energy efficient solution for on-board monitoring"

This paper presents a wireless data transmission system based on the RFID concept designed initially for an environment typical in aeronautics. As a response to a growing interest into wireless monitoring of various parameters onboard of modern aircraft, the author performed several experiments that were aimed at verifying to what extent a low-complexity RFID-based data transmission solution can meet basic requirements related to the expected distance between sensors, as well as the possibility to realise an efficient data link when the sensors are not installed in the line-of-sight and the transmission must rely solely on wall reflections. The paper concludes with a description of the results of the performed measurements. [C1424]

#### "Wavelets on nonuniform triangular meshes for fast basis transform"

Fast method of moment (MoM) solvers implement advanced algorithms like the fast multipole method (FMM) or wavelet transform (WLT). Applying wavelet transform yields a sparsely populated matrix and enables fast iterative solvers. However, the effort of performing the transform itself may significantly add to the overall computational complexity. Traditional methods like multiplying with a change of basis matrix are very inefficient concerning time and memory demands. In this paper, new wavelet functions are considered enabling a fast wavelet transform that uses in-place operations and has low computational complexity. [C1425]

#### "3D vector electric field distributions and dispersion characteristics of open rectangular and circular metamaterial waveguides"

Here we present the 3D vector electric field distributions of the main and the first higher modes propagating in the open metamaterial rod and hollow-core waveguides. [C1426]

#### "Advanced macromodel matrix structure cloning for FDTD"

We propose an improved macromodel-based technique for efficient analysis of the structures based on Photonic Crystals (PhC). The technique involves a new structure of the coupling matrix and advanced cloning of not only the macro-model  $\Gamma$  matrices, but also the coupling matrices SE and SH. The method allows one to shorten considerably the preprocessing time, the RAM usage and also the iterating speed of performing FDTD. With this scheme, it is possible to simulate efficiently up to several thousands of macromodels. [C1427]

#### "UWB microwave imaging system including circular array antenna"

The paper describes the design of an ultra wideband (UWB) microwave imaging system employing a 12-element circular array antenna. The array uses compact tapered slot antenna (TSA) elements operating over 3.1-10.6 GHz band. The elements of the array are activated by two coaxial SP6T switches that are connected to a vector network analyser (VNA) to achieve monostatic or multi-static radar modes of operation. In addition, the array is moved using a mechanical cylindrical scanning subsystem. This electronic/mechanical sub-system allows a fast

highresolution scan of an imaged object. The paper describes the reasons for choosing this particular imaging system configuration and provides full construction details. Also shown are the imaging results of a circular plastic container filled with a vegetable oil and small diameter circular cylindrical targets using a novel image reconstruction algorithm. [C1428]

#### "Dispersion dependencies of glass pipe waveguides filled with lossy biological liquids"

Here we present dispersion characteristic dependencies of the main mode of open cylindrical hollow-core glass waveguides filled with blood and lymph at three different internal waveguide radii and two waveguide materials when the frequency range is of 0.1 GHz to 100 GHz. The pipe waveguides were made of acrylic-glass with the permittivity 4 and glass-ceramic with the permittivity 6.9 materials. The thickness of glass was always 0.5 mm and internal radii of waveguides were 1.5, 1 and 0.5 mm. We also show here the real part of propagation constant of two empty waveguides with the internal radius equal to 0.5 mm for the four hybrid modes at the frequency range of 0.1 GHz to 300 GHz. [C1429]

#### "Millimeter wave application for non-destructive homogeneity characterization of semiconductor and dielectric wafers"

Millimeter wave technique for non-destructive material homogeneity characterization is described. The idea of this technique is the local excitation of the millimeter waves in the testing plate shape material and the measurement of the transmitted (reflected) wave amplitude and phase in different places of it, i.e. the material plate is scanned by the beam of the millimeter waves. Results of the homogeneity measurements for some semiconductor and dielectric wafers are presented. The measurement technique sensitivity is discussed. [C1430]

#### "Reduced-order models in the finite element analysis"

A novel technique of incorporating macromodels into finite element electromagnetic analysis of waveguide components is presented. Macromodels are generated by using a model order reduction algorithm (ENOR), which results in significant decrease of the number of variables, that describe the computational region. Proposed technique allows for using a few independent macromodels as well as to duplicating one macromodel in many subregions of analysed structure. Reduction of the numerical costs is obtained without sacrificing solution accuracy. Furthermore, proposed approach leads to reduction of the overall simulation time. [C1431]

#### "Verification of the mutual coupling compensation technique in small planar antenna arrays"

In this paper the quality of a technique to compensate for mutual coupling (and other phenomena) in small linear antenna arrays is investigated. This technique consists in calculation of a coupling matrix, which is then used to determine corrected antenna array excitation coefficients. Although this technique is known for more than 20 years, there is still very little information about how different phenomena existing in real antenna arrays influence their performance. In this paper the effect of mutual coupling is separated from other undesired effects, e.g. aperture edge diffraction, and its influence on coupling compensation is determined. It is shown that mutual coupling itself can be compensated very well and an ultralow sidelobe level could be achieved in practice. [C1432]

#### "A printed RFID Tag antenna for metallic objects operating in UHF band"

A design of RFID antenna for metallic object is presented. The antenna was fabricated by means of printing technique with electro conducting ink. Input impedance of designed structure was measured with network analyzer and compared to results obtained from numerical calculations. [C1433]

#### "Analysis, design and measurement of a low sidelobe level lightweight array antenna for surveillance radar applications"

This paper describes a design and a realization of a low sidelobe level lightweight array antenna in X-band. The array antenna utilizes Taylor magnitude distribution in its aperture as a sidelobe level reduction technique. The measured sidelobe level of the antenna is -22 dB in its wider dimension plane and -18 dB in its narrower dimension plane. The radiating elements of the array are cavity backed patches electromagnetically coupled to microstrip excitation stubs. The feed distribution network of the antenna is realized as a low cost microstrip corporate feed. The array antenna has been produced by means of a low cost conventional PCB technology. Measurements of a prototype unit has been presented and compared with the theoretical calculations. [C1434]

#### "Matrix analysis of antenna array for MIMO UWB systems"



The paper presents theoretical matrix analysis of antenna structure consisting of two double-element planar antennas for ultra-wideband (UWB) application in MIMO (2x2) indoor communication systems. A new approach to full electromagnetic analysis of MIMO spatial antenna array is described. Mathematical model of functional power parameters for whole MIMO UWB transmit-receive antenna structure is introduced. Results of computer simulations of different matrices describing whole antenna system and power parameters are presented. [C1435]

#### "The analysis of textile antenna array radiation pattern"

In the paper the results of investigation on the textile antenna array radiation are presented. The FDTD computer simulation method is used to simulate the radiation of textile antennas located close to the human body. The results obtained for different configurations of antenna location are presented [C1436]

#### "Multiband omnidirectional communication antenna"

In that paper design and performance of multiband omnidirectional communication antenna is presented. The antenna is fabricated in technology based on teflon laminate with metallization on both sides. It allows to implement developed solution in various commercial applications. Measured antenna covers common free of license WLAN communications frequency bands: 2.4-2.5GHz, 5.15-5.9GHz and also WiMax 3.63.8GHz band. [C1437]

#### "Enhanced direction of arrival estimation via reassigned space-time-frequency methods"

Two new space-time-frequency direction of arrival estimation algorithms are presented that decrease the estimation variance under specific conditions of narrow differential direction of arrival when multiple signals impinge upon the sensor array. The first algorithm, called Wide-Lane, provides a modest extension of existing space-time-frequency (STF) techniques by integrating a wide path along the signal's instantaneous frequency track through the time-frequency (TF) plane. The second algorithm, called Reassigned STF, utilizes the TF reassignment method to increase the signal's localization within the TF plane prior to estimating the direction of arrival with MUSIC. The performance variation of space-time MUSIC to a variety of signal structures is also presented. [C1438]

#### "Measurement and performance of digital monopulse radar array antenna"

A base band sum-difference scenario used in digital monopulse end-guidance radar system is introduced in this paper. A method used to measure the microstrip array antenna pattern at base band is presented. The result shows that the antenna pattern in this design has much better performance at null-depth of difference beam than the traditional design. The angle measurement performance based on the antenna patterns is also recommended. [C1439]

#### "Integrated Millimeter-wave passive devices based on Silicon substrate for SoP application"

In this paper, a process to fabricate BCB/Au multilayer stack on low resistivity Silicon (Si) based on the embedded package structure is developed, especially for the first time spin coating of the dielectric material on the Si substrate. Transmission lines, including micro-strip transmission lines and coplanar waveguide (CPW) lines are designed, fabricated and characterized, which performs excellently: insertion loss and return loss of the standard 50 ohm micro-strip lines are less than 0.08 dB/mm and better than 32 dB/mm respectively during the band from 20 GHz to 30 GHz. Additionally, a power divider is fabricated using the thin film micro-strip lines, which applied in the front end of a traffic flow detecting radar. This power divider has such a wonderful performance, such as insertion loss less than 0.45 dB and return loss better than 25dB with an intrinsic size of 1.6 Ч 0.84 mm<sup>2</sup>. [C1440]

#### "Minimized Ku band microstrip circulator design"

Double Y-junction is a traditional central conductor shape for microstrip circulator. In order to minimize the dimension, An improved double Y-junction microstrip circulator design in Ku band is described in this paper. In addition, a simple principle of how to select a proper kind of ferrite is introduced. The experimental model and test results are given proved the efficiency of the design. [C1441]

#### "An improved High-Frequency-Raised inversion algorithm for radar imaging"

The synthetic aperture technique can not be used to improve azimuth resolution in forward-looking mode or real aperture radar systems. In this paper, an improved High-Frequency-Raised (HFR) algorithm is introduced to enhance the azimuth resolution of radar systems. The super-resolution performance of the proposed algorithm

depends on the raise coefficient and is different for different equivalent antenna patterns. Simulation and experimental results validate the capability of the improved HFR algorithm. [C1442]

#### "Millimeter wave beam tilting array for radar system"

A new kind of millimeter wave beam tilting array is designed and validated in this paper, the array is composed of four sub arrays to acquired high gain. Beam tilting radiation pattern is realized by the quasi-traveling wave operating structure. Absorbing patch is arranged at the end of every sub array for avoiding using matching resistor to improve the radiation efficiency of the array. The beam tilting radiation pattern forming theory is researched firstly and then a model is constructed and optimized with HFSS, a 32-elements array which operates in Ka band is fabricated and measured. The performance of the array is validated by good simulation and measurement results. [C1443]

#### "A transceiver for Ku band digital monopulse radar system"

A transceiver which includes four transmitting channels, four receiving channels and four calibration channels used for Ku band digital monopulse radar system is introduced in this paper. This design may improve the performance of transmitters and receivers. The channel calibration can be carried out easily with the built-in calibration path. The amplitude and phase consistency between different channels maintains good and stable in wide frequency span as well as large power range. Relevant test results are recommended. [C1444]

#### "Design and simulation of ultra-wideband double-ridged horn antenna"

It is known to us, double-ridged horn antenna is one of common and important antenna types, it has been widely used in the EMC, measurement, radar and communication system. A 118GHz double-ridged horn antenna that possesses high performance is designed with the HFSS. VSWR, Gain and radiation pattern of the antenna can fulfill engineering demands based on the simulation of HFSS. Further, this paper shows a new comparatively method of post-cavity treatment in antenna. [C1445]

#### "Calculation of the characteristic impedance of TEM horn antenna using support vector machine"

A method based on support vector machine (SVM) is presented to calculate the characteristic impedance of transverse electromagnetic (TEM) horn antennas. The method can be used for computer aided design (CAD) of TEM horn antennas. The results obtained from the SVM model are in very good agreement with the analytical and numerical result. [C1446]

#### "Scattering characteristic of soot aggregation particles randomly distributed"

The generation multiple Mie theory (GMMT) is introduced to investigate the scattering characteristic of a soot aggregation particles randomly distributed. Computes of the Muller matrix elements are carried out at two wavelengths (0.6328 $\mu\text{m}$  and 1.06 $\mu\text{m}$ ). Some selected results are given by the equivalent medium method (EMM) and compared the results given by GMMT. The results are expected to provide useful insights into the formation mechanism and structural characteristics of randomly distributed cluster agglomerates. [C1447]

#### "A compact quasi-lumped LTCC diplexer for radar application"

An integrated quasi-lumped diplexer based on low temperature cofired ceramic (LTCC) technology is presented. The diplexer is made of L-band low pass filter (LPF) formed by lumped element and X-band band pass filter (BPF) adopting step impedance resonator (SIR). The diplexer's performance has been simulated and optimized by EM simulator. An experimental diplexer has been made and measured. The measured result of the frequency response agrees very well with the simulated one, the LPF's insertion loss is less than 1dB, and 1dB cut-off frequency is 1.46GHz; the BPF's insertion loss is less than 3.5dB, and 1dB bandwidth is about 0.6GHz at the center frequency 8.3GHz. Its good performance, small size and relatively simple structure make it a good candidate as an integrated diplexer for various LTCC systems. [C1448]

#### "Application of parallel integer coded differential evolution strategy on ultra-wide band TEM horn antenna"

With the application of global optimization algorithm, the research of parallel optimization algorithm and its realization become very important. In this paper, two kinds of parallel models of parallel integer coded differential evolution strategy, such as master-slave model, coarse-grained model, are proposed and simply evaluated. For engineering problems, the integer coding is efficient, and automatically filters unsteady solutions. They are combined with finite-difference time-domain (FDTD) method to optimize time-domain ultra-wide band (UWB)

transverse electromagnetic (TEM) horn antenna. As for the TEM horn antenna to each model, the optimization results are illustrated in order to evaluate them. [C1449]

#### **"Integrated design of wide-band wide-scan phased array antenna and couple line"**

A novel phase array antenna with integrated couple line is designed and measured in this paper. This kind of structure assures the stability of monitor system in active phased array radar system. The relative frequency band of the phased antenna array antenna is larger than 25% and it can electrical scan 60 degree both in E-plane and H-plane. The couple coefficient between the ports of different antenna elements in 8-ele structure and the couple port of couple line are in good consistence. Curve of the couple coefficient in the whole frequency band is flat. [C1450]

#### **"Edge diffraction effects on the RCS analysis of antenna array"**

Diffraction effects of the edge region within the antenna array aperture have been discussed with the numerical simulation and measurement in the antenna array monostatic Radar Cross Section (RCS) analysis. Research illustrates that the edge of array presents dominant diffraction effects on the antenna mode RCS character evaluation in a wide frequency range, and bistatic RCS character proposes Radar Absorbing Material (RAM) is an effective approach for the shielding the edge diffraction. [C1451]

#### **"The research of broadband millimeter-wave Vivaldi array antenna using SIW technique"**

A compact millimeter wave Vivaldi antenna array printed on thick substrate and fed by a substrate integrated waveguide (SIW) structure was proposed in this paper. It consists of a compact SIW binary divider, which has minimize significantly the feed structure insertion losses and achieve a broadband performance in millimeter wave range, and four-elements printed Vivaldi array. The whole antenna array was designed, fabricated, and thoroughly investigated. The whole antenna and feed net were designed, fabricated on single substrate, which takes the advantages of small size, low profile, low cost and high performance etc. The simulation results show that the design is effective and right. [C1452]

#### **"Analysis of wide-band aperture-coupled microstrip antenna array by CN-FDTD"**

The Finite Difference Time Domain (FDTD) method is widely used for radiation and scattering problems in electromagnetics due to its ability to model heterogeneous and complex geometries. And a single wideband simulation results can be provided. In this paper a three-dimensional implementation of the lumped-element by Crank-Nicolson finite-difference time-domain (CN-FDTD) algorithm has been presented to simulate a wide-band aperture-coupled microstrip antenna array with an "hour glass" shape aperture. The difference equations allow arbitrary lumped elements to be inserted into one FDTD cell, preserving the full explicit nature of the CN-FDTD scheme. As a validation of the results by the proposed method, the results by commercial software are also reported. Compared with the results of the two methods, the reasonably good agreement is found. Consequently, the accuracy of CN-FDTD application for antenna design with lumped elements in this paper is verified. [C1453]

#### **"A novel frequency scanning monopulse microstrip antenna array"**

A novel frequency scanning monopulse microstrip antenna array is proposed in this paper. The array has the frequency scanning performance in one dimension and has the monopulse performance in another dimension. The miniaturized slow-wave structure has been used to achieve the compact structure. Compared with the conventional slow-wave structure, this miniaturized slow-wave structure reduces its height to 45% of the conventional one. The 444 frequency scanning monopulse microstrip array has been designed as an example. The 444 microstrip antenna, the slow-wave structure and monopulse comparator are placed on the same layer, resulting in a very compact structure. The simulated results show that the range of the scanning angles is  $(-38^\circ, -6^\circ)$ , the gain is above 12dBi at the working bandwidth and the peak gain is 14.09dBi. [C1454]

#### **"Wide-band and low cross polarization conformal array with microstrip parasitic-dipole antenna"**

In this paper a microstrip parasitic-dipole antenna is proposed and an array is constructed by the proposed antenna on conformal conical surface. The proposed antenna has a good impedance bandwidth, lower cross-polarization. The proposed array exhibits excellent impedance bandwidth of 28.5% and can scan its patterns with lower cross-polarization compared with a conventional conformal microstrip patch array. [C1455]

#### **"Surveillance and inversion of regional atmospheric duct from multiple radar stations"**

The atmospheric duct is an anomalous refractivity structure which often occurs over large ocean surface. A surveillance and inversion method for regional atmospheric duct from multiple radar stations is introduced here. It has 1) a larger surveillance area for atmospheric ducts and 2) more accurate inversion results due to more inputted clutter information. In order to describe the M-profile for evaporation ducts more freely, an improved two-parameter M-profile is used. [C1456]

#### "Scattering characteristic from a cylindrical Salisbury screen with 1rad"

This paper presents radar cross section results from a MLFMM model of scattering from a cylindrical Salisbury screen with 1 rad. Different from some previous researches, this study is concentrated on the results at high radar frequencies such as in I and J bands (9-11 GHz). Both normal and off-normal incidence is considered. According to our calculated results by MLFMM, it exhibits better scattering performance than the same size plate. In addition, we find that in the angle range of 70-90°, a few data of the latter are smaller slightly than those of the former. However, we believe it may not affect the application in fact. Finally, in order to study the interaction between incident wave and the cylindrical Salisbury screen, the distribution of surface current and charges at 9.8 GHz are presented. [C1457]

#### "Grid-cell combination in 3D-FDTD modeling of ELF propagation of the earth"

In this paper, we have developed a model of extremely low frequency (ELF) wave propagation based on an advanced three-dimensional finite difference time-domain (3D-FDTD) method. We have studied the Schumann Resonances (SR) of the earth and three different altitude profiles of conductivity in the lossy Earth-Ionosphere Cavity. The eigen-frequencies of the model have been obtained, and the global averages of the vertical Erand tangential E $\theta$  components for these three different conductivity models have been investigated. [C1458]

#### "An efficient splitting the plane-wave FDTD method"

The paper presents a new efficient method of introduction of plane wave source into finite difference time domain (FDTD) grids: the method of splitting the plane-wave FDTD (SP-FDTD). The new equations for the 1-D propagator are based on splitted-field Maxwell's equations, and the propagator makes the 1-D and 2-D dispersion equations identical. The technique virtually eliminates numerical dispersion, filed location and polarization mismatches between propagator and main grid, for a plane wave propagating at an angle forming an integer grid cell ratio, which can represent almost any angle in theory. Through the leak test of the different incident angles of the Gauss pulse plane wave source in 2-D, it shows that, the technique can achieve a perfect total-field scattered-field separation, making leakage down to -340 dB levels. [C1459]

#### "The method of microwave power amplifier model parameter test based on the larger-signal scattering function"

Concentrating on vector network analyzer with nonlinear calibration software, this paper establishes the test systems of microwave power amplifier scattering function, introduces the essential calibration method of the test systems, and validates the correctness of calibration method. And the scattering function is acquired by testing power amplifier which has been designed, and nonlinear characteristic under practical working condition is analyzed based on the scattering function. [C1460]

#### "A Ka-band T/R front-end for phased array radar"

In this paper, a Ka-band transmitter/receiver (T/R) front-end for a phased-array radar is proposed. The transceiver includes a receiver channel and a transmitter channel. A function link shared with the receiver channel and the transmitter channel is comprised of a 5-bit phase shifter and a variable gain amplifying circuit including an attenuator and a low noise amplifier. Connection to either the final power amplifier on transmitter or the LNA on receiver is accomplished by using two single-pole double-throw switches (SPDTs). Experimental results of the front-end verify the validity of the design. A noise figure of 4.9 to 5.6 dB, a receiver gain of 24.4 to 29.4 dB and a output power from 0.74 W to 1 W are obtained within a frequency range from 34.5 GHz to 35.5 GHz. The digital phase shift provides 10.2° root-mean square(RMS) phase shift error at 35 GHz. [C1461]

#### "Illumination method for millimeter wave imaging indoors"

This paper presents an effective illumination method for millimeter wave imaging indoors based on multi-phase diversity principle. Though limited to its ability to do the image recognition accurately, it still gives a good performance for millimeter wave imaging indoors. The results from a real-time indoor millimeter wave imaging are presented, clearly showing the hidden metal objects. [C1462]



### "Acceleration of Time-Domain Finite-Element Method in electromagnetic analysis with OpenMP"

Paralleled Time-Domain Finite-Element Method (TDFEM) is developed based on OpenMP for 2-D electromagnetic scattering analysis in this paper. The matrix-vector multiplication in conjugate gradient (CG) solver is parallelized with OpenMP. As a result, the efficiency of TDFEM algorithm is accelerated dramatically with multi-processor PC. The bistatic radar cross sections (RCSs) of some typical 2-D objects are computed with paralleled TDFEM. High speedup ratio and high parallel efficiency are obtained, which provides a practical and effective acceleration method for TDFEM analysis on multi-CPU computers. [C1463]

### "Research on Si-based MEMS process in development 3D millimeter-wave multi-chip module package"

A low cost & feasible system on package solution on the basis of BCB and silicon wafer (10 Ohm-mm)-Si-Based 3D MMCM package solution is presented in this paper. What is more, a standard Si-Based MEMS process is employed to achieve package and revision of a GaAs-Based Monolithic Amplifier circuit. The measured results show that input return loss is less than 20 dB; moreover, small signal gain is more than 17 dB across 21 GHz to 26 GHz. The excellent measured results make the Si-based 3D-MMCM package solution a very attractive and feasible candidate for millimeter-wave 3D system level package applications. It is a step towards achievement of 3D system level package meeting excellent millimeter-wave performance. [C1464]

### "Design and implementation of a LTCC-based receiver front-end module"

A S-band receiver front-end module using Low Temperature Co-fired Ceramic technology is presented to be small and reliable with the main passive components such as splitter, coupler, bandpass filter, resistors and capacitors embedded in LTCC substrates. The MCM-level module with a dimension of 27mm×25mm×1.9mm, realized in interconnecting the active chips by micro-assembly technology, is shown to meet the requirements quite well in experimental test. [C1465]

### "An ultra wide band power divider/combiner based on Y-structure waveguide"

In this paper, an improved power divider/combiner based on Y-structure waveguide is proposed at ka-band (26-40 GHz). To widen the bandwidth of the divider/combiner, a stepped-impedance waveguide transformer is used, and a vertical resistive card is inserted into the divider/combiner to realize high isolation. According to EM simulations, the power divider/combiner illustrates a 42.4% effective bandwidth (ranging from 26 to 40 GHz), the return loss is better than -24 dB, and the isolation is better than -21 dB. This structure has properties of not only a wide band, low insertion loss and high output power, but also a small size, a high power combining efficiency and efficient heat sinking, and has potential for millimeter-wave broad-band high power combination. [C1466]

### "Parameter Identification Method for Ship Swaying Motion Differential Equations"

This paper introduces a solution method for ship swaying motion differential equations—maximum likelihood parameter identification method. To evaluate its data processing effects, we have taken the real-time measurement data as a research object and computed with several algorithms, at the same time compared their prediction results. The results show that parameter identification method for differential equation is reliable in calculation, whose accuracy can satisfy the demand for shipboard equipments to accurately track space targets, which is recommended to use for ship swaying measurement data processing. [C1467]

### "A Comparative Study of the DGTD Algorithm and the FVTD Algorithm in Computational Electromagnetics"

By calculating some typical electromagnetic problems, the performances of the FVTD algorithm and the DGTD algorithm for computational electromagnetics are compared systematically, including the choice of the time step, the numerical accuracy, the CPU time and the memory requirement. The FVTD algorithm is more efficient for electrically small structure and is more accuracy for the structure with curved surface, but is not suitable for large scale electromagnetic phenomenon simulating. The DGTD is more resource consuming, but it is more accurate and has the potential ability to handle electrically large structure. [C1468]

### "Design of an alpha-beta filter by combining fuzzy logic with evolutionary methods"

The  $\alpha$ - $\beta$  filter based on the Kalman-like estimation scheme has been recognized as a outstanding tool for estimating the position and velocity signals of moving objects. Nevertheless, the performance of estimation heavily depends on the parameters  $\alpha$  and  $\beta$ . In general, the choice of parameters is a trade-off optimization problem between the tracking accuracy and noise reduction capability. In order to obtain the suitable design of

$\alpha$ - $\beta$  filter for some specifications, a combined fuzzy logic and evolutionary optimization method is proposed for determining the parameter values. The simulation results are employed to illustrate the developed  $\alpha$ - $\beta$  filter which is capable of tracking the desired signals accurately and, at the same time, reducing the noise disturbance remarkably. [C1469]

#### "Notice of Violation of IEEE Publication PrinciplesExtended target tracking using an IMM based nonlinear Kalman filters"

Notice of Violation of IEEE Publication Principles"Extended Target Tracking Using an IMM Based Nonlinear Kalman Filters,"by Yucheng Zhou, Jiahe Xu, Yuanwei Jing, Georgi M. Dimirovskiin the Proceedings of the 2010 American Control Conference, July 2010, pp. 6870-6875After careful and considered review of the content and authorship of this paper by a duly constituted expert committee, this paper has been found to be in violation of IEEE's Publication Principles.This paper contains significant portions of original text from the paper cited below. The original text was copied without attribution (including appropriate references to the original author(s) and/or paper title) and without permission.Due to the nature of this violation, reasonable effort should be made to remove all past references to this paper, and future references should be made to the following article:"Extended Target Tracking Using an IMM based Rao-Blackwellised Unscented Kalman Filter,"by Zhiwen Zhong; Huadong Meng; Xiqin Wangin the Proceedings of the 9th International Conference on Signal Processing, October 2008, pp.2409-2412The unscented Kalman filter (UKF) and ensemble Kalman filter (EnKF) are developed to extended target tracking problem for high resolution sensors. The nonlinear Kalman filters are based on an ellipsoidal model, which is proposed to exploit sensor measurement of target extent. The ellipsoidal model can provide extra information to enhance tracking accuracy, data association performance, and target identification. In contrast to the most commonly used extended Kalman filter (EKF), the UKF and EnKF provide more accurate and reliable estimation performance, due to the presence of high nonlinearity of the model. Correspondingly, the EnKF has lower computational complexity than the UKF. An interacting multiple model (IMM) technique is combined with the filters to adapt the target maneuver and motion mode switching problem which is vital for nonlinear filtering. The developed IMM-UKF and IMM-EnKF algorithms on extended target tracking problem are validated and evaluated by computer simulations. [C1470]

#### "Speckle Reduction with Multiresolution Bilateral Filtering for SAR Image"

Synthetic aperture radar (SAR) images are inherently affected by multiplicative speckle noise, which requires despeckle before many other image processing and analysis applications. In this paper, a new speckle reduction method based on wavelet and bilateral filtering is proposed. Bilateral filtering is applied to the low frequency subbands of a signal obtained by wavelet transform. The new method preserves edges and protect details. Experimental results tested on real SAR images demonstrate the performance of the proposed method. [C1471]

#### "Novel Space-Time Processing Method for Airborne SAR to Detect and Image the Slowly Moving Targets"

In the paper the problem of the ground clutter rejection for airborne SAR is discussed. The features of space-time clutter filtering and clutter spectrum of airborne SAR imaging are analysed. It is pointed out that there exist some problems such as Doppler ambiguity and blind speed band expansion when STAP filtering is applied to the ground clutter cancellation. Aiming at the solving of difficulties in detecting and imaging the slowly moving target with single-channel airborne SAR, a new method suitable for multi-channel airborne SAR to detect and image the slowly moving target is proposed, which can effectively avoid the blind speed and Doppler ambiguity and keep the processed data rate lower. Computer simulation results show that this method is valid. Compared with other method for detecting and imaging the slowly moving targets, the improvement factor obtained by the proposed method is narrower than that. [C1472]

#### "Universal test bench of diesel hydraulic governor based on hardware-in-loop simulation"

The universal test bench for diesel hydraulic governor using hardware-in-loop simulation technology is established. The problems of common in use, variable-speed drive, simulation model, data acquisition and analyzing are solved. The structure of the test bench, along with the hardware and software meeting the requirement of deterministic real-time performance are introduced. Some experimental results are provided to prove the effect of the test bench, which providing a facility for a technician to conduct a general check and calibration for governor assembly. [C1473]

#### "Beamforming using passive nested arrays of sensors"

A novel approach to beamforming using a new class of sensor arrays is proposed, which can increase the

achievable degrees of freedom significantly beyond the conventional limits obtained from uniform linear arrays (ULA). This class of arrays is named as "nested arrays" since they are obtained by nesting two or more ULAs with increasing inter-sensor spacing. Using the second order statistics of the signal received by such an array in a novel way, it is possible to perform beamforming with  $O(N^2)$  degrees of freedom using only  $O(N)$  physical elements. This kind of beamforming will be shown to be essentially non linear in nature and theoretically, it is capable of nulling the effect of noise provided enough snapshots are available. [C1474]

#### "Reduced memory architecture for CORDIC-based FFT"

In this paper, a new pipelined, reduced memory CORDIC-based architecture is presented for any radix size FFT. A multi-bank memory structure and the corresponding addressing scheme are used to realize the parallel and in-place data accesses. The proposed memory-reduced CORDIC algorithm eliminates the need for storing twiddle factors and angles, resulting in significant area savings with no negative impact on performance. As a case study, the radix-2 and radix-4 FFT algorithms have been implemented on FPGA hardware. The synthesis results match the theoretical analysis and it can be observed that more than 20% reduction can be achieved in total memory logic. [C1475]

#### "Improved method for blind estimation of the variance of mixed noise using weighted LMS line fitting algorithm"

The paper addresses blind evaluation of the parameters of mixed noise in images. The conventional approach is based on line fitting in the scatter-plot of local variance estimates using LMS algorithm. This does not utilize the fact that the points in the scatter plot typically appear in clusters that depend on the image. It is shown that the use of weighted LMS algorithm that takes into account the number of points in clusters provides considerable improvement in the accuracy of line fitting and, thus, better estimation of the parameters of mixed noise. [C1476]

#### "Multi-sensor data fusion via federated adaptive filter"

The aim of this paper is to present a federated adaptive filter for use of multi-sensor data fusion systems for target tracking. The computational architecture of the filter consists of several local processors and a global processor. Each local processor incorporates a scheme of Bayesian decision theory into the multiple-model filter to develop a switching capability to react against the same target dynamics, inclusion of both maneuver and non-maneuver phases. The global processor combines the local estimates via a weighted least squares estimator for generating a global estimate. Simulation results show that proposed filter has better tracking performance than the information matrix filter. [C1477]

#### "Multi-network video streaming in a campus visit scenario"

Mobile computing devices are increasingly making use of multiple network technologies to provide seamless connectivity across changing operational contexts. Reliable delivery of video to mobile devices is particularly challenging in these dynamic and multi-network environments. This paper provides a report on our experience in applying Partially Reliable Stream Control Transmission Protocol (PR-SCTP) in a multi-network campus visit scenario. We provide a large scale evaluation of PR-SCTP along with specific site data. Our results show that PR-SCTP is a promising platform for supporting multi-network video delivery. [C1478]

#### "The design and analysis on the small-scale antenna of spread frequency radio lifesaving system"

Radio lifesaving system which is based the spread frequency system works at the MW & SW band, uses the ground wave to orientation with the characteristics of high orientation precision, short responding time and large working bound. However, as the large signal wavelength of the band, the receiver usually adopts a large whip antenna as the signal receiving equipment, which is so large that to become a technical difficulty of equipment miniaturization. To solving this problem, this paper proposes a new-designed angle reflector antenna based on the Hilbert fractal curve as the system antenna which is simulated based on the finite-difference time-domain method (FDTD). Shown as the simulation result, the antenna with the size of 30 mm Ч 30 mm can work in the band of 1.5~10 MHz has the characteristics of high gain, low VSWR, and omni-direction, meets the system requirements. [C1479]

#### "Passive RFID-based Indoor Positioning System, An Algorithmic Approach"

Radio Frequency Identification, RFID technology having been realized of its potential usages only in recent years is now widely used in multiple disciplinary industries and applications. Major of which include SCM, logistics and retail as well as manufacturing. Another key application area of RFID is its use for localisation or positioning of items and people indoors. However, signal propagation in indoor environments is error prone and make

localisation challenging. With RFID being one of the most promising technologies for indoor location awareness applications, this paper presents an algorithmic approach to locate an unknown RFID tag with the use of multiple passive RFID tags. A number of experimental results indicate a general reduction of linear positioning error mean from 3.41m to 0.61m with respect to decreasing inter-tag spacing from a maximum of 7m to a minimum of 1m, respectively. The main advantage of this technique is the reduction in number of expensive RFID readers; instead multiple inexpensive passive RFID tags placed at calculated positions provide essential data to position an unknown tag. [C1480]

#### "A thermal design methodology for power SiGe HBTs with non-uniform emitter finger spacing"

As an effective and feasible method, the technology of non-uniform emitter finger spacing has been used to alleviate the thermal effects and improve the uneven temperature profile in multi-finger power SiGe HBTs. However, for the HBT with dozens of emitter fingers, designing multiple finger spacing values becomes trivial and time-consuming. In the paper, a new thermal design methodology namely Grouping and Adjusting (GA) method is proposed to shorten design time of non-uniform spacing values. Taking a 30-finger HBT for example, the detailed design procedure of non-uniform spacing values is presented, which shows that the peak temperature is lowered by 8.3K, and the maximum temperature difference is improved by 23.5% when compared with the uniform one. Furthermore, three types of the formulas for designing the spacing values are proposed to meet the different requirement of the temperature profile. [C1481]

#### "High-repetition and -stability all-solid state pulsers based on avalanche transistor Marx circuit"

Ultra-wide spectrum (UWS) pulser, in which avalanche transistor is used as its switch, can generate high-repetition and -stability short-pulse, but its power is sharply lower than that of SOS and Tesla generators. Marx circuit is used to increase the power of this type of pulser. Different charged-capacitance and class of Marx circuit determines different waveform and peak-power of output pulse. 20-class and 30-class avalanche transistor Marx circuit pulsers are designed, and the charged-capacitance is 100 pF and 470 pF, then 4 types of waveform are get. The highest output peak-voltage is 2.9 kV, the highest repetition can reach 70 kHz, and keep a better pulse stability, jitter is less than 40 ps. [C1482]

#### "Analysis of electromagnetic scattering of cavities with nonuniform plasma coating"

The radar cross section of cavities coated with nonuniform plasma is analyzed by using the shooting and bouncing ray (SBR) method in this paper. The curvilinear triangular patches are adopted to model the surface of arbitrarily shaped cavities, so that it can meet the practical needs of engineering. The nonuniform plasma slab used to coat cavities is modeled by a series of subslabs, in which the plasma parameters are assumed to be constant. Then the reflection coefficients of the rays to coated cavity are calculated and then applied in calculating the RCS of cavities. The numerical results of the cavities coated with nonuniform plasma indicate that the parameters of the plasma slab can affect the RCS effectively. [C1483]

#### "Application of AMC on mini ultra-near radar detecting system"

To solving the isolation problem of transmitting-receiving antenna in very-near anti-missile system, this letter analyses the equivalent model of AMC, which is made of high-impedance electromagnetic surface, and shows the relationship between its reflectance and phase offset. Then a novel method is brought to improve the isolation by the AMC and the experiments show that this method is able to make the isolation reach -80 dB in a 200 M band. So it has a very huge application value because of its simple structure and low cost. [C1484]

#### "4H-SiC bipolar junction transistors for UHF and L-band long-pulse radar applications"

This paper reviews the current status of 4H-SiC RF npn bipolar junction transistors (BJT's). Process developments including precise and uniform SiC etch and low resistance p-type ohmic contact formation on a two inch SiC wafer will be presented. The high temperature operation up to 500°C and radiation hardness up to 1.6 Mrad, as well as RF performance promising for long-pulse UHF and L-band radar applications will be reported. Rationale and approaches to the further improvement to S-band will be discussed. [C1485]

#### "Classification of radar signals using time-frequency transforms and fuzzy clustering"

A method based on Smoothness Pseudo Wigner-Ville distribution and kernel principle component analysis is proposed to extract features of radar emitter signals. Then, these discriminative and low dimensional features achieved were fed to the classifier which is designed based on fuzzy Support Vector Machines (SVMs). In simulation experiments, the classification of two-class LFM signals was compared with four kernel functions. And the classifier attains over 83% overall average correct classification rate for five radar signals. Experimental



results show that the proposed methodology is efficient for complex radar signals detection and classification. [C1486]

#### **"FDTD analysis of three-dimensional target covered with inhomogeneous unmagnetized plasma"**

A normalized RC-FDTD algorithm is applied to study both the bistatic and monostatic radar scattering of perfectly conducting sphere covered with inhomogeneous unmagnetized plasma. The effects of electron density distributions and plasma collision frequencies on the radar cross section (RCS) are discussed respectively. The simulations confirm that plasma cladding can be successfully used to reduce the RCS of a conducting sphere at almost all scattering angles, although the RCS could increase at some other angles. And the back scattering results indicate that plasma cladding can reduce the RCS of the conducting sphere in a very wide frequency range. Reasonable selection of the plasma parameters can enhance the effectiveness of plasma stealth. [C1487]

#### **"Analysis of image fusion and classification for high resolution SAR data on-line"**

SAR and optical remote sensing image, with highly complementary characteristics, can enhance the integration of information utilization of remote sensing data. Adopting the new Cosmo-SkyMed SAR high-resolution image data, we inhibit speckle impact using enhanced Lee filtering. Then we fused this image with a CBERS image using local use standard deviation based on wavelet packet method. Because of fully integrating the characteristics of each image, it can retain the spectral characteristics and details of properties to the maximum extent, improve signal-to-noise ratio, and be conducive to information extraction. The experiments show that the automatic classification accuracy significantly increased and classification Kappa coefficient increased from 0.47 to 0.93 after fusion of Cosmo-SkyMed and CBERS02 data. Meanwhile, This paper employ a geospatial information processing concept model complied interoperable system framework and an implementation approach for accessing geospatial information openly by chaining individual service module to assemble complex geospatial processing and executing the processing model to deliver information. [C1488]

#### **"The innovation on the education model of the engineering management-based on the viewpoint of WSR methodology"**

Education is a system, so a well defined fostering goal is the precondition for carrying out systematically education activities for the innovation on the education model of the engineering management. Based on the WSR methodology, this paper analyzed the roots of the problems currently existed in the fostering model from three aspects, namely Renli, Shili and Wuli and proposed a new model on engineering management education. The goal is to foster forthcoming engineers with high creativity and social responsibility. [C1489]

#### **"Intelligence analysis in early warning air roster training"**

The paper introduces a new simulation system for training early warning air roster, which uses data mining technology on the massive accumulation training information for intelligence analysis. In the system, the model of association rules are established. Using this model, the system provide ability that arrange much more reasonable training plan for each early warning air roster. Furthermore, it can support an optimized decision of how to make up the team of rosters. [C1490]

#### **"EM scattering by conductor plate coated with multilayered medium having metamaterials"**

The electromagnetic scattering of conductor plate coated with multilayer medium is investigated based on the physical optics (PO) theory and the principle of equivalent impedance boundary condition (IBC). Compared with the multilayered plate coated with right-handed medium, the radar cross section (RCS) of plate composed of metamaterial and right-handed medium has a reduction of 5.76dBsm in the mirror direction. It shows that metamaterials can become a candidate of the radar absorbing material (RAM), which offers a new idea for the development of stealth technology. [C1491]

#### **"Application of VSIE method to scattering problem involving conducting and anisotropic bodies"**

Evaluation of electromagnetic scattering by anisotropic media may be of interest in many military and civil applications. This paper presents the hybrid volume and surface integral equation(VSIE) based scheme to analyze scattering from conducting and/or inhomogeneous dielectric bodies with anisotropic electromagnetic properties. The Rao-Wilton-Glisson (RWG) basis functions are used to discretize those unknowns of the matrix equations. The method of moments(MOM) technique is augmented with the fast multipole which enable large scale analysis. Finally, several numerical results are presented to demonstrate the stability and accuracy of the proposed method. [C1492]

### "Multi-target scattering analysis based on generalized higher-order finite-difference time-domain method"

A generalized higher-order finite-difference method (in which the time difference utilizes the symplectic integrator propagator and the spatial difference utilizes the discrete singular convolution) is proposed to analyze electromagnetic scattering from multiple targets. Numerical test results have demonstrated the higher stability and enhanced effectiveness of the proposed method when compared with the standard FDTD procedure. In addition, there are significant reductions in CPU time and memory space requirements when used with suitable meshes. [C1493]

### "Supporting omni-directional communications capability in variable attitude spacecraft"

This paper describes the work undertaken to provide omni-directional communications on Sapphire, a variable attitude spacecraft. Several options to solve the problem are considered and two chosen; analysis is presented to show that mission objectives can be met. [C1494]

### "Multi-objective optimization of an isoflux antenna for LEO satellite down-handling link"

A multi-objective optimization approach has been applied to the synthesis problem of the geometrical structure of antenna with complex set of requirement specification. This methodology is a promising tool for new development and application for several kind of microwave structure. [C1495]

### "Criteria for phase shifter operation of an azimuthally magnetized coaxial ferrite waveguide"

Three criteria: a physical, a mathematical and a functional one for operation of the coaxial waveguide, completely filled with azimuthally magnetized ferrite, under for normal TE<sub>01</sub> mode excitation, as a digital nonreciprocal phase shifter, are established. The first of them is deduced from the phase characteristics of configuration and determines the limits of the interval in which it provides differential phase shift for a specific value of the off-diagonal ferrite permeability tensor element. The second criterion associates the structure parameters with certain roots of its characteristic equation, expressed by complex confluent hypergeometric functions and with the related to them positive real  $L(c, \rho, n)$  numbers ( $c=3D/3$ ,  $0 < \rho < 1$ ,  $n=3D/1$ ). The third one specifies the limits of the domain of phase shifter operation. These are functions, representing in normalized form the dependence of phase shift at the cut-off frequencies and at the envelope lines, marking the end of the phase curves for negative ferrite magnetization from the side of higher frequencies, on the guide radius for a fixed central conductor thickness. [C1496]

### "Principles of the electromagnetic modelling of some microwave components, based on the circular waveguides with azimuthally magnetized ferrite"

The principles of electrodynamic analysis of the characteristics of the ferrite control components (nonreciprocal digital phase shifters, cut-off switches and isolators) which use circular waveguides, entirely filled with azimuthally magnetized ferrite or containing a coaxial disc- or ring-shaped area of the medium alluded to and a dielectric one, surrounding it or taking up its hollow, resp., and work in the normal TE<sub>01</sub> mode, are enunciated: i) employment of complex confluent hypergeometric and eventually also of real cylindrical functions; ii) indispensability of inventing of numerical methods for evaluation of some special functions of the mathematical physics: the Euler gamma function, its logarithmic derivative and the confluent functions in the complex field, as well as of the cylindrical ones in the real domain; iii) elaboration of techniques for numerical solution of complicated transcendental equations, involving complex confluent and possibly real cylindrical functions, too; iv) introduction of a new class of real numbers, called  $L$  numbers, connected with the purely imaginary roots of the equations mentioned; v) development of numerical schemes for computation of the phase curves of geometries regarded and of iterative procedures for finding the differential phase shift provided by them; vi) laying down of criteria for the operation of configurations as phase shifters, magnetically controlled cut-off switches and isolators. Each of the maxims pointed out is elucidated in detail. [C1497]

### "A design of beam forming network integrated in multilayer microstrip structure for applications in airborne SAR"

This paper presents the design, arrangement and components of multilayer microstrip beam forming network manufactured in multilayer PCB technology for application in airborne synthetic aperture radar antenna. The network has been designed for easy integration with the array of radiating elements operating in L and C bands. [C1498]

### **"Resonator techniques for reflectivity and surface resistivity at high temperature: Methodology and measurements"**

Two different methodologies based on resonator techniques are presented. The first has been realized for wide band reflectivity characterization at high temperature while the second has been developed to verify surface resistivity including roughness, surface contamination and other undesired effect. Both methods have been developed for characterization over a large temperature range. Measurement results on Ti6Al4V samples, Copper and AlBeMet ® are presented. [C1499]

### **"Control and diagnostic system for the demonstrator of S Band active antenna"**

In the paper, a Control and Diagnostic System designed for the Demonstrator of S Band Active Antenna is presented. Transmit and receive antenna radiation pattern is steered and controlled by a central computer. Diagnostic system is focused on transmit part of the demonstrator with solid state T/R modules. The key elements of diagnostic, amplitude and phase meters integrated with each transmit channel are presented. The system works in pulse condition. Real, transmit signal as reference for diagnostic system is used. Independent, built-in system of diagnostic for T/R modules are presented as well. It enables safe modules operation and failure location in service mode. The Control and Diagnostic System is based on CAN 2.0 bus what allows to operate with very high reliability and baud rate up to 1 Mb/s. [C1500]

### **"Inter-period compensation of the unambiguity range degradation in polarimetric FMCW radar with time-shifted dual-orthogonal signals"**

This paper describes a new type of sounding signals for polarimetric FMCW radar and the corresponding signal processing technique. This technique coordinates continuous transmission of two bi-cyclic LFM-signals on orthogonal polarizations and applies an advanced de-ramping processing on receive. The first signal consists of two identical LFM-signals; the second one has time shift relatively first and is composed by the same LFM-signal and its copy having negative sign. The time between the components of sounding signal prevents the frequency overlap between polarimetric components of scattered signal in the branches of every polarimetric radar channel. Thanks to this frequency gap between the signals in every time instant, a high-isolation level in polarimetric FMCW radar channels can be provided. However, the use of two LFM-signals having the same form but a relative time shift can decrease the unambiguity range, because the delayed signals scattered by far-located objects (interfering signals) can be determined as useful signals scattered by close-located objects in a cross branch in a polarimetric radar channel. The use of the proposed bi-cyclic LFM-signals and the additional summation units in the de-ramping filter allows the suppression of these interfering signals due to the phase sign change of the beat signals. As result, the developed de-ramping processing technique can be used in polarimetric FMCW radar receiver providing high-level cross-channels isolation without unambiguity range degradation for estimation of all elements of the radar target scattering matrix. [C1501]

### **"Minimizing of influence of synchronization lack between short LMF signal and filter on its compression"**

As researches show, the compression in the time domain of short single chirp (LMF) signals with low BT depends significantly on both matching the signal and matched filter (MF) impulse response (IR) parameters to a specific window and using non-linear operations on convolutions. These ways are effective only when a synchronization between those signal and MF is obtained. This work depicts as the above mentioned methods as a way of minimizing of influence of the synchronization lack. The proposed matched filtering method with the use of  $n$  parallel MFs and the other techniques allows only one sample to be obtained in the main lobe with position located in the appropriate sampling period  $T_{\text{sw}}$  with accuracy  $T_s/n$ . These approaches are expedient for use in radar and sonar array processing. [C1502]

### **"Interaction of thin conductive sheets with TE<sub>10</sub> electromagnetic wave in rectangular waveguide"**

Numerical investigation of a thin conductive layer, interacting with TE<sub>10</sub>electromagnetic field mode in rectangular waveguide, was performed. A finite-difference time-domain method with subcell technique was applied to perform the modelling. The distribution of the electric field in the layer and the reflection coefficient from it have been calculated for different length, shape and conductivity structures. These investigations can be useful for the development of high frequency microwave sensors, the operation of which is based on a non-uniform carrier heating effect in the layer. [C1503]

### **"Patch antennas setups for omnidirectional pattern to provide TTC links onboard small spacecraft"**

Advancements in patch antennas made feasible their applications in hard to sustain environments, such as

space or sea and oceans. These applications are often quite new and often represent maturing broadband communication. In many instances one of the main design objectives is to ensure omnispherical or omniazimuth coverage with patch antennas placed onboard a specific platform. With use of numerical CAD tools and with application of near-field antenna measurements, we have carry on extensive research into relevant design guidelines for ten years. In this paper we present some of our findings. [C1504]

#### **"FPGA based IF digital receiver for the PARSAX-Polarimetric agile radar"**

An FPGA-based digital receiver has been developed to perform real-time processing for the PARSAX radar. It is a fully polarimetric FMCW radar with dual-orthogonal sounding signals, which has the possibility to measure all elements of the radar targets polarization scattering matrix simultaneously, in one sweep. This paper presents the design principles including the range profile interpretation, optimal parameters selection and processing gain analysis. A novel parallel deramping processing architecture suitable for FPGA implementation is introduced; the overall digital de-ramping processing has been implemented in one chip of FPGA and verified by experimental results. [C1505]

#### **"The multiposition passive satellite system for the terrestrial radiation sources monitoring"**

We proposed an iterative algorithm for radio sources coordinates estimating by the range-difference method using the multiposition passive satellite system. We simulated the coordinates estimating algorithm. We defined requirements to the satellite orbit altitude and to the distance between the satellites for the small satellites group. We estimated time of arrival estimation accuracy, which is necessary to achieve the required coordinates estimation accuracy. [C1506]

#### **"A novel approach applied for the internal and semi-external calibration of the PARSAX dual-channel polarimetric agile radar system"**

Polarimetric agile radar is able to measure all elements of the polarization-dependent backscattering matrix (BSM) simultaneously. Polarimetric calibration is an important issue to determine the BSM accurately. This paper focuses mainly on the internal and semi-external calibration of the dual-channel polarimetric agile radar system. The paper presents a novel approach based on very up to date methods used for cross-validation between simulations and measurements. Error models of all parts of the radar system will be derived from the approach and implemented in the radar system calibration. After calibration, the good matching performance for relative measurement between two channels demonstrates the validity of the here-proposed calibration approach. [C1507]

#### **"Monopulse direction finder for harmonic radar system"**

This paper presents first results of experimental amplitude comparison monopulse direction finder for harmonic radar. Aperture coupled patch antenna arrays are used for operation in 1.5 GHz band with 10% operation bandwidth. Antennas with leaf characteristic enable 50° sector of operation in azimuth. Problems with common (circular) polarisation are discussed. [C1508]

#### **"Comparative numerical analysis of the slot antenna arrays the energy and finite element methods"**

It is described the results of numerical simulation of liner and planar antenna arrays, obtained using the program designed by the article authors. In the program are used the analytical expressions which describe the main array characteristics. The results are compared with the results obtained using HFFS. [C1509]

#### **"Simulation of direction of arrival and beamforming algorithms used in smart antenna system for software-defined radio"**

The demand for mobile communication systems with global coverage, interfacing with various standards and protocols, high data rates and improved link quality for a variety of applications has dramatically increased in recent years. The Software-Defined Radio (SDR) is the recent proposal to achieve these. In SDR, new concepts and methods, which can optimally exploit the limited resources, are necessary. Smart antenna system is one of those, which combats the co-channel interference and maximizes the user capacity of mobile communication system. The paper presents the analysis of the beamforming and direction of arrival (DOA) algorithms used in the smart antenna systems. The analysis is carried out for the MULTiple Signal Classification (MUSIC) algorithm and The Multiple Sidelobe Canceller and the Maximum SINR Beamformer algorithm using MATLAB as a simulation tool. [C1510]



### "Wideband aperture coupled microstrip array antennas for radar applications"

A new 1x2 and a 1x4 wideband aperture coupled microstrip array antennas, to work in Ku and K bands, are presented in this paper. The array antennas have VSWR < 2 from 11.4-23.8 GHz. The gain of the 1x2 array antenna is above 10 dB from 11.4-17.8 GHz and the 1x4 array has more than 12 dB gain within 11.3-17.3 GHz. Additionally, by using a 2x4 array antenna more than 16 dB gain is obtained at the frequency range of 11.5-17.2 GHz. The 1x4 array antenna was fabricated in which, good agreement is obtained between simulation and experimental results. [C1511]

### "Investigation into a folded wideband monopole antenna for use in portable devices"

This paper presents investigations into a compact antenna for use in portable devices to access almost all modern wireless services from about 800MHz to 6GHz. Initially, a microstrip-fed planar monopole of quarter-elliptical shape on FR-4 substrate is designed to generate a wide impedance bandwidth. This radiating element is augmented with a parasitic microstrip stub and a ground-plane cut to improve wideband performance. To reduce its projection area, the planar monopole is folded. The folded antenna occupies a volume of 13mm x 50mm x 5.6mm. It operates over two wide bands between 0.85 and 3.8GHz, and 4.9 and 6GHz, with reference to 6dB return loss (VSWR 3:1). Its radiation patterns are omnidirectional in the lower band and deteriorate at higher frequencies. The corresponding gain varies between 1.5 and 7dBi. [C1512]

### "Microstrip monopulse array antenna"

The new construction of microstrip monopulse array antenna is described. It consists of four radiating elements in a row. Such row is supplied by ring coupler connected at its two sides using of coaxial cable jacks. This gives possibility to get relative high radiation power that is needed in radar or radio-transmitters. Proposed array antenna construction is simple, and its measurements results show that obtained frequency band is relatively wide. [C1513]

### "On multiport antennas for MIMO-systems"

A very promising method to enlarge the radio channels capacity is the use of MIMO (Multiple Input Multiple Output) systems. The need to deploy more than one antenna leads to the problem of the restricted available space reserved for the antennas, especially on the terminals. Another fundamental problem is the evaluation of the MIMO performance in a realistic propagation environment. Only a global view will bring up a realistic picture about the improvements using multiple antenna technologies. At the beginning of the presentation basics on MIMO-technology will be given. The second part will show in a very fundamental way the realisation of a compact 4-port antenna, which provides a sufficient decoupling between the ports. Finally the system performance of this antenna is investigated. Based on the analysis of the diagram correlation coefficient and the mutual coupling of the elements a basic idea of the antenna performance is evaluated. Measured and simulated correlation coefficients of typical channel matrixes taking the antenna into account will give finally an idea of the real MIMO performance. [C1514]

### "Model order selection of the target doppler spectrum"

The information about shape and geometrical dimensions of the moving target can be extracted using Doppler spectrum. The short observation time interval corresponds to constant speeds of target scatterers as well as low resolution by Doppler frequency shift. Methods of spectral estimation are applied to identify the scatterer parameters. Two methods of a target Doppler spectrum model order selection based on information criteria are presented. [C1515]

### "Target detection in Doppler radar with PSK signals"

The aim of this article is to test the effectiveness of the known structures of radar signal processing (RSP) that employ CFAR processors in order to detect moving targets in the frequency domain, depending on the chosen width of velocity channels (the number of FFT). The Doppler radar is radar with continuous transmission of PSP (Phase Shift Keying) signals. Real records that have been produced by Doppler radar for the case of moving people or cars on the background of trees are used in the study. The results obtained lead to believe that detection of targets with CA CFAR processors provides the required effectiveness in case when the velocity channel width is correctly defined. [C1516]

### "Antenna activities in support to future candidate earth explorer core missions with a SAR"

Three candidate Earth Explorer Core Missions have been selected for Phase-A study, namely BIOMASS, CoReH2O and PREMIER. Two of the candidates are Synthetic Aperture Radar (SAR) missions: BIOMASS

operating in P-band and CoReH2O operating in Ч and Ku-band. Antenna development activities have been initiated to reduce technological risks and in support to Phase A studies. The paper describes the latest results from those activities. [C1517]

#### "Field Effect transistors for fast terahertz detection and imaging"

We present recent results on detection of terahertz radiation with nanometer size GaAs FETs and Si MOSFETs at room temperature. We demonstrate that the detection sensitivity and speed allows application of the transistors in terahertz imaging systems. At low temperatures the transistors can act as magnetic field tunable detectors. [C1518]

#### "Calibration of a 220-325 GHz vector-network-analyzer with multiple rectangular-waveguide sections"

We study the performance of the multiline through-reflect-line method in the calibration of a 220-325 GHz vector-network-analyzer with WR-03 rectangular-waveguide test-ports. The calibration method is based on multiple uniform-waveguide sections with unknown propagation constant and different lengths, a reflect standard which is assumed to be identical on both vector-network-analyzer ports but otherwise unknown, and a direct thru connection of the test ports. Experimental verification demonstrates that the multiline through-reflect-line technique yields repeatable and physically meaningful results. [C1519]

#### "PARSAX: High-resolution Doppler-polarimetric FMCW radar with dual-orthogonal signals"

The article describes the IRCTR PARSAX radar system. It is an S-band high-resolution Doppler polarimetric FMCW radar utilizing dual-orthogonal sounding signals. The signals allow for measuring in one sweep all elements of the radar targets polarization scattering matrix simultaneously. PARSAX characteristics are: modular system set-up, highly-optimised linearity and sensitivity of the RF front-end receiver, use of a flexible multi-channel arbitrary waveform generator as sounding waveforms source, high-resolution analogue to digital conversion of the received signals at sufficiently high intermediate frequency and FPGA-based programmable digital multi-channel receiver. The paper shows that PARSAX is a unique radar research platform for studying arbitrary sounding waveforms with bandwidth up to 50 MHz and processing algorithms in Doppler-polarimetric radar. [C1520]

#### "Gyrotropic waveguides analysis based on the neural networks"

The paper addresses the problem of the cylindrical gyrotropic waveguide analysis by an electrodynamical model. The technique of semi-automatic extraction of the dispersion characteristics by the use of single-layer perceptron neural network is proposed. Presented waveguide analysis algorithm is divided in four stages: initialisation of system parameters, evaluation of transcendental linear dispersion equation system, extraction of dispersion characteristics and waveguide broadband width evaluation. [C1521]

#### "Author Index"

{no data available} [C1522]

#### "Blank page"

{no data available} [C1523]

#### "Artificial neural network algorithm for automated filter tuning with improved efficiency by usage of many golden filters"

This paper shows how to improve the efficiency of the Artificial Neural Network (ANN) method for the cavity filter tuning. It was proved that the usage of many golden filters in the process of collecting the learning vectors, used in ANN training, has the significant influence in decreasing the ANN generalization error. Thus, the algorithm efficiency is increasing. The generalization error value of ANN, trained on samples from two different filters, as a norm of the filters similarity is proposed. The tuning experiment for the 6-cavities RX filters of GSM diplexer has been demonstrated. In the experiment the ANNs were trained based on the vectors collected from up to five different filters, showing the significant influence of the number of "known filters" on the ANN generalization error. [C1524]

#### "GaN class E wideband microwave power amplifier"

The simulation and experimental investigation of wideband class E power amplifier using GaN MESFET NPTB00025 was carried out. Special multi-resonant microstrip output network was used to obtain required load impedance. In addition, a single-frequency class E power amplifier was simulated and experimentally investigated for adjust values of parasitic elements of transistor's model in switching-mode power amplifiers. In the bandwidth of 500-600 MHz output power of 9.2 W with power-added efficiency of 65 % and DC supply voltage of 18 V was obtained. [C1525]

#### "Copyright page"

{no data available} [C1526]

#### "Closing session"

{no data available} [C1527]

#### "Via interconnection structures for x-band surface mount circulators"

A method for modeling and designing various via interconnection structures for surface mount circulators is presented. The circulator-via assembly and the interconnection methods are described. The microstrip-via-microstrip structure is divided into parts, each part is treated separately. The background of empirical methods and microwave network theory is shown as a basis of the design steps. Interconnections including single and double vertical via structures are compared by means of the FDTD method. Based on a previously designed X-band circulator, the effects of the via connections on the circulator performance are investigated. [C1528]

#### "Session C2: Microwave & millimeter wave oscillators"

{no data available} [C1529]

#### "Session B7: Wireless and personal communications"

{no data available} [C1530]

#### "Session B8: Microwave measurements III"

{no data available} [C1531]

#### "Session C3: Optical components and circuits"

{no data available} [C1532]

#### "Session C4: GaN | SiC technology"

{no data available} [C1533]

#### "Session C1: Power amplifiers I"

{no data available} [C1534]

#### "The Method of Designing Ultra Low Phase Noise Dielectric Resonator Oscillators"

In this paper a method of designing ultra low phase noise Dielectric Resonator Oscillators (DRO) is presented. The design procedure is described basing on an exemplary 1.3 GHz Voltage Controlled DRO realized in the negative resistance oscillator configuration. Issues of the resonator and the active circuit design important for achieving a good phase noise performance are described. Described method was used for designing a 2.85 GHz oscillator with very good results. [C1535]

#### "High temperature stability of nitride-based power HEMTs"

The temperature stability of InAlN/GaN heterostructure FETs has been tested by a stepped temperature test routine under large signal operation conditions. Devices have been successfully operated up to 900 °C for 50 hrs. Failure is thought to be contact metallization related, indicating an extremely robust InAlN/GaN heterostructure. [C1536]

#### "Metal contacts to wide bandgap semiconductor structures for RF power applications"

The increasing demand for electronic transistor with the cut-off frequency 100 GHz devices capable of function at high power and have been demonstrated this year. frequency levels, high temperatures, and harsh In order to take the full advantage of their environment is one of the most significant issue superior inherent properties several challenges of modern information society, especially in the in material processing are to be overcome. One field of RF systems for telecommunication and of the most important issue is the quality of wireless communication. Moreover, energy metal-semiconductor contacts. This is problems and environmental concerns due to especially true for both, for Schottky barriers global warming have generated the need for to be used in Schottky rectifiers and for ohmic novel semiconductor devices for active contacts being a part of any semiconductor electrical power management in areas such as device. The ohmic contacts are primarily energy generation and distribution, and important because a potential barrier of high transport where efficiency and/or high energy is inclined to form at an interface temperature operation are of the essence. Wide between metal and wide-band-gap bandgap semiconductor devices, particularly semiconductor, which consequently results in those using SiC and GaN-based materials, are low-current driving, slow switching speed, and key candidates for power-control and high- increased power dissipation. This paper speed communication devices, owing to their provides a comprehensive and critical excellent intrinsic properties, which involve assessment of fundamentals and practice of large breakdown electric field, in the 54106metal contacts to wide bandgap Vcm-1range, together with high electron semiconductors with an emphasis on high saturation drift velocity, strong hardness, and power/temperature handling capability. The good thermal conductivity. GaN is already topics covered in this paper-- are grouped in five used in high-frequency circuits and is subsections. First, deals with carrier transport attracting increasing attention as a material to mechanisms in metal-semiconductor contacts, play a leading role in the next generation of which are applicable to any metal-power electronics. On the other hand, much semiconductor system. In the next section, effort have been already put in SiC technology points specific to metal/SiC and metal/GaN and first SiC power devices have already been contacts are discussed. Then, there is a place commercialised. Moreover, SiC is the favourite for a discussion of ohmic contacts, their substrate for GaN-based high-power and high- fabrication and characterisation methods. In frequency applications. SiC also appears as particular, the issue of determining properly enabling platform for large area graphene ohmic contact resistivity is discussed in detail. electronics, while a radio-frequency graphene The main part of the paper presents most significant results concerning thermally activated reactions between metal and properties of interface and its role in formation semiconductor and formation of intermediate of Schottky barriers and ohmic contacts. For layers in metal/SiC and metal/GaN contacts. GaN-based materials experimental results on For SiC, attention focuses on the effect of an the use of MAX phases for thermally stable intermediate graphite layer on electronic metallization systems receive major interest. [C1537]

#### "Modeling of metal/insulator/GaN ultraviolet photodetector by finite element method"

A metal/insulator/GaN ultraviolet photodetector has been studied by computer simulations using finite element method. The equations of drift-diffusion model have been solved numerically in the illuminated structure taking into account electronic states at the insulator/GaN interface with a continuous U-shaped energy distribution in the GaN bandgap. The capacitance of the structure has been calculated versus the light excitation intensity and the gate voltage. The influence of the interface states on the photodetector characteristics has been discussed. [C1538]

#### "A novel multi-band frequency selective surface design and its application in a compact 60-GHz folded dipole array"

This paper describes some basic theories about the frequency selective surface (FSS). For the first time we demonstrate a novel design of a multi-band FSS to the best of our knowledge. It consists of a periodic array of concentric-square-shaped elements. Like traditional FSSs, the surface of the proposed FSS can simply be fabricated using printed circuit technology on the substrate. Simulation results show a clear dualband and possible performance variation with relevant parameters. We integrate this FSS into a compact 60-GHz folded dipole antenna array package in order to test its application. Results show that it successfully converts a single-band antenna to a multi-band one and specific resonant bands can be easily adjusted for the practical purposes. [C1539]

#### "Third harmonic generation in silicon with a 118 GHz gyrotron"

Third harmonic generation in n-type Si crystals is experimentally studied using 118 GHz gyrotron. The results are treated using new approach of the dynamical non-uniformity of the non-linear medium. [C1540]

#### "Microwave power capabilities of InAlN/GaN HEMTs"

This paper reports on microwave power results of InAlN/GaN HEMTs on silicon carbide substrate. It is shown a



power density higher than 10W/mm up to 10GHz. Investigations based on diamond substrate or heat spreaders on top of the device to improve the thermal dissipation are also described. [C1541]

#### "Microwaves reflection of centimeter wavelength range of two-dimensional square symmetry plasma photonic crystals"

In this paper, an exact approach, uniting several modern methods, to the theory of multiple scattering of wave fields in two dimensional inhomogeneous media, the so called transfer relations' method with the technique of matrix Riccati equation, is applied in a quantitative analysis with given accuracy of reflection spectra of plasma photonic crystals with square lattice symmetry. [C1542]

#### "Control system for high power solid State microwave generators 2.45 GHz band"

The paper presents development and implementation of the four high power microwave sources system used for testing phased 2.45 GHz antenna array. Each module has maximum output power of 200 watts and covers frequency band between 2.35 and 2.6 GHz. System provides possibility of independent setup of frequency, amplitude and phase of each generator (depends on mode of operation). [C1543]

#### "Design of a 54 to 63 GHz differential common collector SiGe Colpitts VCO"

The design of a 60 GHz differential common collector Colpitts VCO in SiGe HBT technology with 180 GHz ftis presented. The impact of parasitics on the negative resistance is evaluated and an extension regarding existing design equations is derived. Within a wide tuning range from 54.1 to 62.7 GHz, a phase noise performance between -98 and -90 dBc/Hz is measured at 1 MHz offset. To the knowledge of the authors this is the best phase noise performance of a 60 GHz VCO in silicon yielding such a high tuning bandwidth. At a dc voltage of 2 V and a dc current of 14 mA, the output power amounts to  $-5 \pm 1$  dBm. [C1544]

#### "Talbot effect supported millimeter wave generation"

The temporal Talbot effect enables the flexible and cost-effective generation of microwave signals. We demonstrate the generation of frequencies up to 90 GHz using an optical pulse source with a 10 GHz repetition rate. Time- and frequency domain measurements were performed. The phase noise of the generated RF tones was assessed. [C1545]

#### "Achievement and perspective of GaN technology for microwave applications"

This paper give an overview of some recent results obtained by Alcatel-Thales III-V Lab using emerging AlGaIn/GaN HEMT technology. This technology is very suitable up to Ku-Band and offer impressive power performances. The second part of the presentation will give an overview of results obtained using new InAlN/GaN heterostructures, which is expected to offer similar output power but with improved efficiencies and to cope with higher working frequencies. [C1546]

#### "InP HBT demultiplexing ICs for over 100 Gb/s optical transmission"

In this paper we present the design and optimization of decision and DEMUX circuits fabricated in a 0.7  $\mu$ m InP HBT technology. Full-rate characterization at 50 Gb/s shows CPM of 13 ps and excellent 3R capabilities. Circuits are compatible with positive and negative signal to ease high-speed interface with different types of photodiode in the photoreceiver. The decision circuit copackaged with the pin-photodetector was used as photoreceiver in 107 Gb/s optical experiment. Error-floor free demultiplexing operation with 231-1 PRBS signal was demonstrated. [C1547]

#### "Periodic FDTD modeling of 3D photonic crystals"

In this paper application of FDTD method supplemented with periodic boundary conditions to the analysis of three-dimensional photonic crystals is presented. For that purpose, a model of body-centered cubic dielectric lattice is introduced and investigated. Complex-looped FDTD algorithm is applied for the computation of a photonic bandgap diagram in the first irreducible Brillouin zone revealing dispersive properties of the lattice. [C1548]

#### "Inexpensive helical antenna for global navigation satellite systems"

In this paper theoretical and practical study of an inexpensive L-band helical antenna is presented. The geometrical parameters of the antenna were calculated using standard formulas. The frequency shift resulting

from the winding of the wire on a polyurethane (PU) core was also taken into account. Numerical analysis of the sensitivity of antenna parameters to the manufacturing process had been provided. After manufacturing the antenna an appropriate impedance matching section was designed and fabricated. Measured return loss was below -18 dB in the frequency range 1.48-1.67 GHz. Radiation patterns and axial ratio of the antenna in the direction of maximum radiation are also presented in this research. [C1549]

#### **"Tunable filters based on metal-dielectric resonators"**

A method of metal-dielectric resonator's frequency tuning is proposed. The method is suitable for electromechanical control using piezoelectric or MEMS actuator. The two-resonator and three-resonator tunable filters based on metal-dielectric structures are developed. [C1550]

#### **"A 2 W GaAs doherty amplifier for 5.5-5.6 GHz applications"**

In this paper the design of a 2 W uneven C-band Doherty power amplifier is presented. The Doherty PA is designed to achieve high efficiency for digitally modulated signals with high peak to average power ratio (PAR) used in wireless local area network (WLAN) systems around 5.6 GHz. The Doherty amplifier has been designed using two equal sized GaAs devices for the main Class- AB and peaking Class-C amplifiers. An uneven power divider is used at the input to deliver more input power to the peaking PA. The measured maximum output power of the realized uneven Doherty PA is 34 dBm with 50 % peak drain efficiency (43 % of power added efficiency). The power added (drain) efficiency is higher than 25 % (30 %) up to 6 dB of back-off. Moreover, an adjacent channel power ratio (ACPR) of -30 dBc has been measured using a digitally modulated signal of 10 MHz bandwidth. [C1551]

#### **"GaAs MMIC Doherty Power Amplifier with asymmetrical drain bias voltage"**

This paper presents a 3.4x2.3mm<sup>2</sup> MMIC Doherty Power Amplifier in pHEMT GaAs technology, designed for X-Band applications (9.6 GHz). The obtained results shown 31dBm maximum output power with a 47.6% associated drain efficiency. Moreover, in the designed 6dB of output power back-off, from 25dBm to 31dBm output power, the efficiency is higher than 30% with a related gain compression lower than 1.5dB. As will be detailed, such a performance are maintained almost constant in a frequency bandwidth greater than 10% (9.1-10.1 GHz). [C1552]

#### **"Doherty power amplifiers for handset applications"**

The efficiency and linearity are enhanced by a direct input dividing and an uneven power drive. An optimized envelope tracking (ET) operation of Doherty power amplifier (PA) is presented. The PA and the supply modulator are realized using a 2  $\mu$ m InGaP/GaAs HBT and 0.13  $\mu$ m CMOS processes, respectively. For WiMAX application, it shows a PAE of 38.6% and an EVM of 3.64% at an output power of 24.22 dBm with a gain of 24.62 dB. [C1553]

#### **"A diplexer design method using an augmented channel filter approach"**

A new method of microwave diplexer design is presented. The new technique does not require a final diplexer tuning. The method is a modification of the technique based on accurate channel filters synthesis using surrogate models of coupling coefficients in order to obtain initial structure dimensions [1]. Here the structure optimized during channel synthesis is modified to assure correct loading of the junction. By doing so, the diplexer response after channels synthesis agrees with design specification and diplexer tuning is not needed. [C1554]

#### **"Design of a dual-band GaN Doherty amplifier"**

In this paper, the design, realization and test of a dualband Doherty power amplifier (DPA) will be presented. The design has been realized in hybrid technology using a packaged GaN HEMT as active devices. A special attention will be focused on the passive structures involved in the DPA design (input power splitter, impedance transformer network, impedance inverter network and phase compensation network) showing several possible implementations and the related tricky aspects. The DPA has been designed to operate simultaneously at 2.14GHz and 3.5GHz with 6 dB of output power back off (OBO) at both frequencies. [C1555]

#### **"Design of broadband complex impedance-matching networks and their applications for broadbanding microwave amplifiers"**

In this paper design a method is presented for broadband matching of complex impedances using distributed

circuit elements. The method is a combination of the classical analytic network theory approach for lumped element matching networks and of the numerical optimization techniques. The aim is to create distributed element matching networks for Rf transistors in order to design broadband amplifiers in a systematic way. The design method is demonstrated by several realized and tested microstrip matching circuit in the 1.5...2.5GHz frequency range, which are well applicable for amplifier design. A microwave amplifier example operating in the 1...2GHz band is shown as well. [C1556]

### "Innovative maritime communications technologies"

Current maritime systems are to a large extent based on legacy analog VHF radios for ship-to-shore communications near port waters, and relatively low bandwidth digital satellite communications (SatCom) for long-range ship-to-ship/shore communications. The cost of bandwidth for SatCom networks is expected to remain high due to the cost of launching satellites into orbit and also due to the stabilizers required for presently available on-board antennas. On the other hand, the legacy VHF system comprises low bandwidth radios incapable of supporting applications requiring high data rates. Unlike the terrestrial networks, advancement in maritime communication means is severely lagging behind its land counterpart. MARINTEK is the principle investigator of the MarCom project, a joint initiative between several national and international R&D institutions, Universities and Colleges, Public Authorities and Industry, funded by the industry itself and The Norwegian Research Council's MAROFF program, which is aiming at developing a novel digital communication system platform to ensure the proliferation of innovative mobile network applications presently being widely implemented on land-based wireless systems [C1557]

### "A 27 dBm microwave amplifier with varactors-controlled matching networks"

In this paper design and development of 27dBm medium-power amplifier with varactor-based input/output matching networks is presented. The frequency tunable range of 1.3GHz to 2.6GHz was obtained for input matching  $|\Gamma| \leq 0.3$  and power gain higher than 13dBm. Adaptive impedance matching networks provide frequency adjustment and output power level optimization by means of two voltages control. The amplifier was fabricated using surface mounted technology and conventional low-cost GaAs transistor and hyperabrupt varactors. Main parameters of the implemented amplifier with nonlinear behaviour of varactors are investigated. The device can be applied to operation with constant envelope multi-standard and multi-band radio-communication systems. [C1558]

### "On BER of STBC coded MIMO systems in different indoor environments"

The spatial diversity is known to overcome the multipath propagation effects and to increase the spectral efficiency in multi antenna systems. Under IEEE 802.11n specifications channel modeling, we evaluate the error performances of WLAN employing STBC (Space Time Block Codes) with and without CSIT (Channel State Information at Transmitter) for 2x1 and 2x2 MIMO (Multiple Input Multiple Output) cases when different antenna spacing is used at transmitter and receiver. [C1559]

### "Doherty power amplifier and GaN technology"

In this paper, the features of GaN HEMT technology and Doherty Power Amplifier architecture will be investigated, as a possible answer for the stringent requirements of the next generation of wireless systems. In particular, the attention will be focused on the capabilities and the relevant drawbacks of a GaN HEMT technology when designing DPAs. The discussion of the most important DPA's design aspects will be done through the presentation of several hybrid prototypes. Experimental results will be also given to support the theoretical aspects. [C1560]

### "3 GS/s S-Band 12 bit MuxDAC on SiGeC technology"

In advanced applications such as digital radar, Ultra Wide Bandwidth communications and software defined radio, the need for instantaneous bandwidth often drives system design decisions. Access to high speed data converters enabling up and down conversion directly in the L Band and S Band removes the limit imposed by bandwidth scarcity and allows the design of flexible and simplified system architectures. Broadband DAC's (Digital to Analogue Converters) are key enabling components which open up new design opportunities for digital Synthesizer systems. In this regard, this paper describes a new 12 Bit 3GS/s DAC, based on a 200 GHz SiGeC bipolar Technology, which enables direct synthesizing of 1GHz arbitrary waveforms directly in the high IF (S\_Band) region closer to the Antenna. [C1561]

### "Asymmetric mechanisms of second-order intermodulation in downconversion mixers"

This paper addresses the issue of second-order intermodulation mechanisms with memory effects in downconversion mixers. In particular, an attempt is made to explain asymmetries in generated distortion caused by interferers situated below and above the local oscillator frequency. The analysis is carried out on a circuit level using Volterra-series techniques and provides an insight into underlying frequency-dependent mechanisms. [C1562]

#### "ADI-FDTD method for physical simulation of semiconductor devices"

This paper describes an alternating-direction implicit finite-difference time-domain method for the two-dimensional time-dependent simulation of semiconductor devices. This approach leads to the significant reduction of the semiconductor simulation time. We can reach over 80% reduction in the simulation time by using this technique while maintaining the same degree of accuracy achieved using the conventional approach. As the first step in the performance investigation, we use the electrons flow equations in the absence of holes and recombination in this paper. [C1563]

#### "Integrated cylindrical horn antenna array"

In this paper the integrated ultra wide band antenna cylindrical array consisting of eight double ridged horn antennas is presented. The mechanical and electromagnetic properties of that antenna array and their relations to its functionality in different systems are also presented. [C1564]

#### "Magnetic properties of the finemet alloys in the microwave frequency range"

In the paper measurements of the magnetic properties of powdered nanostructured alloys-Fe<sub>73,5</sub>Cu<sub>1</sub>Nb<sub>3</sub>Si<sub>13,5</sub>B<sub>9</sub>(Finemet) were presented. Measurements were realized in the coaxial line in the frequency range 0, 2-10, 2 GHz. The new technique for measuring of permittivity and permeability of powdered materials was developed. The obtained data was compared with data of powder received from milling of well known ferrite-Yttrium Garnet YIG class ferrite, named G-175. [C1565]

#### "Method of dynamic parameters measurement of high-speed D/A converters"

Developed sampling device and algorithm of digital signal processing for automated measurement of settling times of fast D/A converters is represented. The new sampling device with numerically controlled oscillators allows realizing of the different types of the time scale transformation. Using of  $\Sigma\Delta$  A/D converter and FIFO memory allows significant simplification of the device. The equations of time scale transformation ratio and sampling step are presented. A method of using of an ideal comb filter in frequency domain to filter measurement signal has been developed. It is shown that such filtering allows significant reduction of noises of measurement signal. Results of the research of developed digital signal processing algorithm are submitted. [C1566]

#### "Slotted Waveguide Antenna Arrays for Airborne Radars"

This paper presents a review of recent activities on the development of X-, Ku-, and Ka-band slotted waveguide antennas. Potential applications of the antennas include various airborne radars systems. We illustrate the implementation of the antennas into a helicopter collision avoidance and weather radar, a surveillance and tracking radar, and an airborne SAR system. The corresponding design solutions, antenna and radar characteristics are discussed as well. [C1567]

#### "A dual reflector antenna for point-to-point system applications"

In this paper design and realization of a dual reflector antenna for receiving Internet signal in the point-to-point system is presented. Three different configurations of dual reflector antenna have been considered to obtain the antenna operating in 5.2-5.8 GHz band and having small dimensions. The results of computer simulations and measurements are shown. The design was based on electromagnetic simulations using QW-V2D package (an axisymmetrical version of FDTD software). [C1568]

#### "Invited paper"

The paper provides an overview of the state of the art the area of reconfigurable antennas as the devices the most quickly developing during in recent years. This article brings together in a review manner a comprehensive summary of high quality research contributions across basic and applied sciences. As a result a broad spectrum of topics is covered reflecting the areas in which Institute of Radioelectronics's expertise is a worldwide recognized. The transdisciplinary nature of most areas aims to stress a sense of purpose in the work developed.



[C1569]

#### "FDTD modelling of plain susceptors for microwave oven applications"

A new approach for numerical modelling of microwave susceptors used as an active element in packaging of microwaveable food products were investigated. The accuracy of the method was validated in the case of estimation of reflected, absorbed, and transmitted power for the susceptor in free space, where the exact solution is known. Further, the amount of power absorbed by the susceptor was calculated for the case of the susceptor attached to the cylinder made of water. The influence of the position and size of the cylinder was considered. The amount of power absorbed by the susceptor and the cylinder were calculated. [C1570]

#### "Composite dielectric-loaded resonators for highly-stable bandstop and bandpass filters"

Use of composite-dielectric resonators, in both direct coupled and capacitively-coupled implementations, enables realization of both bandstop and bandpass filters, with similar construction, high power capability and unique, temperature-stable properties. Improving temperature stability allows for reduction in filter order by elimination of tuning guardband, while lumped element substitution for transmission line lengths provides suppression of periodic distributed element responses and thus wide stopbands for bandpass filters. [C1571]

#### "Improving the accuracy of subgridding scheme in finite differences method based on Legendre polynomials expansion"

In this article the Legendre polynomials have been used to interpolate the field at the boundary of the meshes of different densities. The numerical verification of the proposed technique has been carried out in frequency domain. It has been shown that the accuracy of the presented method is very high and stable-the error monotonically decreases as a function of the refinement factor. [C1572]

#### "On the synthesis of coupled-lossy resonator filters with unloaded quality factor control"

A technique for fast synthesis of coupling matrix low-pass prototypes of generalized Chebyshev bandpass filters with lossy resonators is presented in this paper. The coupling matrix is found by solving a nonlinear least squares problem based on zeros and poles of filter's transfer functions. Additional constraints are introduced that allow one to control the level of unloaded quality factor of resonators. [C1573]

#### "Measurements of the complex permeability of yttrium iron garnet substrates near ferromagnetic resonance"

This paper describes a simple method of measurements the complex permeability of yttrium iron garnet (YIG) substrates. The permeability of YIG is measured near a ferromagnetic resonance. The method is based on the measurements of resonant frequencies and Q-factors of YIG substrate placed into two structures: single post dielectric resonator and split post resonator. The obtained results are presented. [C1574]

#### "Krylov space iterative solvers on graphics processing units"

CUDA architecture was introduced by Nvidia three years ago and since then there have been many promising publications demonstrating a huge potential of Graphics Processing Units (GPUs) in scientific computations. In this paper, we investigate the performance of iterative methods such as cg, minres, gmres, bicg that may be used to solve large sparse real and complex systems of equations arising in computational electromagnetics. [C1575]

#### "Measurements of complex dielectric permittivity and magnetic permeability of carbon-coated Ni capsules"

With advance of multiferroic composites it becomes increasingly interesting to measure both complex dielectric permittivity and magnetic permeability simultaneously and preferably at high frequencies. In this work both of these parameters in case of carbon-coated nickel nanocapsules (Ni@C) embedded into organic matrix were measured in a waveguide set-up in 26-36 GHz frequency range. [C1576]

#### "Analysis of a new approach for tunable and reduced size balanced amplifier using thin-film BST varactors"

A new approach for tunable balanced power amplifier (PA) using barium-strontium-titanate (BST) varactors is presented and analyzed. Tunable PA utilizes the idea of reduced size tunable branch-line couplers, comprising of

BST Varactors. The simulation results indicate the feasibility of balanced amplifier from 1500 to 2500 MHz in terms of gain, reflection coefficients, and stability. The key features of the presented design are the stability of traditional balanced PA, frequency agility and 50% size reduction due to the use of reduced size branch-line couplers. [C1577]

#### "Analysis of rectangular microstrip structures by the method of moments"

Rectangular microstrip structures (RMS) are widely used in various microwave devices. Using the method of moments and principle of partial images, various techniques are created to determine charge distribution in 2D models of microstrip structures (their cross-section). In this paper, a technique for calculating surface charge distribution and total capacitance of complex 3D rectangular microstrip structures is proposed using the mentioned method and principle. To demonstrate feasibility of the proposed technique, three RMS were investigated. Obtained results are compared with the data published by other researches. Total error is typically less than 5%. [C1578]

#### "The method of improving performance of the GPU-accelerated 2D FDTD simulator"

In this paper, several methods of optimizing parallel implementation of 2D FDTD algorithm are presented. Some practical problems occurring in real simulations are taken into consideration. Moreover, the presented methods are supported with appropriate tests and practical examples. [C1579]

#### "A Comparative analysis of two wide-band rational approximations for input impedance of antennas"

Asymptotic waveform evaluation technique and the Neville-type Stoer-Bulirsch algorithm are investigated and compared as the tools for efficient performance evaluation of antennas with emphasis placed on their input impedance over a wide frequency band. Numerical results are given for a helical antenna with a truncated-cone reflector. [C1580]

#### "Design of Wilkinson power divider using stubs"

Design of Wilkinson Power Divider with open stub which has better isolation and minimal return loss is presented. The proposed device distributes the power without unbalancing its amplitude and phase, while providing constant 50 ohm impedance. Comparing with conventional Wilkinson power divider, it takes less area on substrate board. The simulated and measured results are presented and discussed. [C1581]

#### "Electromagnetic wave trapping in the split-ring-cavity system"

The single split-ring magnetic and/or electric dipole moments attaining large values at resonance ensure trapping electromagnetic wave energy in the near-field space of the ring, and in the cavity created by the ring and a reflecting wall. The self-formation of coupled resonators system manifests in sharpening the resonance. Resonance broadening to a forbidden band is proved to arise in the array of split rings ensuring bandstop filter applications. Simulation data on the field amplitude distribution and frequency domain are proved to be in reasonable agreement with experiments. [C1582]

#### "Numerical modeling in wave scattering problem for small particles"

A numerical solution to the problem of wave scattering by many small particles is studied under the assumption  $ka \ll 1$ ,  $d \gg a$ , where  $a$  is the size of the particles and  $d$  is the distance between the neighboring particles. Impedance boundary conditions are assumed on the boundaries of small particles. The results of numerical simulation show good agreement with the theory. They open a way to numerical simulation of the method for creating materials with a desired refraction coefficient. [C1583]

#### "Fresnel formulas for nondiffracting electromagnetic waves"

The generalization of Fresnel equations for non-diffracting waves are presented. The obtained equations determine refraction and reflection coefficients in case of plain interface between different media. Brewster's angle analogue and total reflection condition are obtained, as well. These equations reduces to the classical Fresnel equations in case of plane wave limit. As an application of the obtained equations, electromagnetic field distribution in a plane dielectric wave guide is examined in the new way. The obtained dispersion relations are independent of the nondiffracting wave electromagnetic field distribution. This implies, that an infinite number of electromagnetic field configurations may exist at a fixed frequency in the plain dielectric wave guide. [C1584]

### "Optimal sidelobes reduction and synthesis of circular array antennas using hybrid adaptive genetic algorithms"

In this article, a hybrid optimization method has been proposed consisting of Adaptive Genetic Algorithms (AGAs) and Constrained Nonlinear Programming (NLP) to solve the problems of performance optimization of circular array antenna consist of parallel center feeding short dipoles elements with two complex nonlinear optimization problems. In the first problem, the hybrid optimization algorithm is used to reduce the value of sidelobe level in the circular array radiation pattern by finding the optimal values of the excitation coefficients of each element in the circular array. In the second problem, a synthesis of circular array with different forms of the desired radiation pattern is considered. Several examples are considered here to verify the validity of this method. The results obtained by this method show that it is possible to obtain an array radiation pattern with low sidelobe level of -40dB in the first problem. In the second problem, it is shown that it is possible to obtain a wide flat main lobe of 60beam width, and two nulls on both sides of the main lobe with 10width for each. Comparisons were made between the results of this method and the results obtained by Standard Genetic Algorithm (SGA), and it is clearly shown that this method is more efficient and flexible in solving the problems of performance optimization of circular array antenna. [C1585]

### "Automated method of antenna factor measuring"

The antenna is an essential part of a test system. In some applications, selecting the best antenna may be very important. Unfortunately, selecting the right antenna can be a difficult task, because of variation in the way manufacturers specify and describe them. This article explains the specific method of the antenna factor (AF) as one of the main antenna parameters definition by measurement in an electromagnetic field. Automated method of antenna factor measurement (AMAFM) in anechoic chamber is described. [C1586]

### "Microwave radar for express testing of semiconductor materials"

The microwave radar for express testing of semiconductor materials consisting of pulsed magnet, transmitting and receiving antennas, HF generator, pulsed modulator and digital oscilloscope are described. In semiconductor specimen put in pulsed magnetic field a magnetoplasmic wave is excited and propagated through a specimen signal and reference signal delay is measured to find a value of concentration of free charge carriers in semiconductors. Experimental data of testing of InSb, CdHgTe specimens are presented and an acceptable correspondence of results was achieved. [C1587]

### "Efficiency of the IE-MoM approach in the analysis of dielectric bodies embedded in a cavity"

This paper presents the analysis of dielectric bodies embedded in cavities made of perfect conducting metal using numerical approaches. For a case study of resource requirements a Dielectric Resonator Filter has been designed. Different numerical approaches were presented: FEM, FDTD, FIT, MoM and they were compared due to their computational effectiveness. Two of those method FIT and MoM showed a much higher efficiency than others. Their resource requirements were compared using simulations of a case study device. This paper shows that our Method of Moment with use of Green's function for stratified media has the best performance in solving dielectric bodies embedded in metal cavity. Therefore, there is a need to develop this method. [C1588]

### "Utilization of RFID technology for fixed assets inventory process improvement"

Article describes utilization of radio frequency identification method for improvement of fixed assets inventory. It propose the solution for labor cost reduction in execution of annual company legal activities through usage of mobile RFID reader and dedicated application for handheld device and desktop computer. [C1589]

### "Vortical electromagnetic waves with a stationary power flow"

We show analytically that in source free medium vertical electromagnetic wave can be derived from electromagnetic field, described by electric and magnetic Hertz vectors. To characterize the wave's vorticity we examine moment values of the real Poynting vector versus various directions of Hertz vectors in respect of wave propagation. This enables us to distinguish pure circular polarized transverse waves, possessing constant modulus orbital angular momentum and time and space invariant Poynting vector, from those of vortical, consisting of two time invariant and two vortical time dependent components. Poynting vectors of vortical components depend on time and have opposite directions while the time unvarying components have the same direction towards the wave propagation. The result of interaction of two vortical components is time invariant orbital angular momentum and time independent power flux, which is directed perpendicular to the common power flux of unvarying components. [C1590]

### "Wideband microstrip phase shifters"

The paper presents wideband, microstrip phase shifters. Some types of the phase shifters are described. Experimental results of electrical parameters are obtained. Features of the phase shifters are discussed and showed. [C1591]

### "Planar MS-CPS bypass balun for CPS-fed textile antennas"

This paper presents the design, numerical analysis and measurements of a planar bypass balun that provides 1:4 impedance transformations between the unbalanced microstrip (MS) and balanced coplanar strip line (CPS). This type of balun is suitable for operation with small antennas fed with balanced a (parallel wire) transmission line, i.e. wire, planar dipoles and loop antennas. The balun has been applied to textile CPS-fed loop antennas, designed for operations below 1GHz. The performance of a loop antenna with the balun is described, as well as an idea of incorporating rigid circuits with flexible textile structures. [C1592]

### "Three dimensional magnetic field distributions and dispersion characteristics of rectangular and circular SiC waveguides"

Here we present the 3D vector magnetic field distributions of the main mode and the first higher modes propagating in lossy SiC rod waveguides at different temperatures and the dispersion characteristics of the SiC rectangular and circular rod waveguides. [C1593]

### "The performance of the IFM receiver in a dense signal environment"

The capabilities of multichannel IFM system for working in dense and complex signal environment have been presented in the paper. The present electromagnetic environment in microwave frequency band is filled by the complex simultaneous or overlapped signals. High performances are required from microwave receivers worked in these difficult conditions. The IFM receiver is possible to fulfill these requirements. The analysis and measurement results for simultaneous signals have been presented in the paper. The measurements for varied frequency and signal power of two simultaneous signals using multichannel IFM receiver was done and measurements results have been presented. The instantaneous frequency measurements for complex signals using dual channel IFM receiver have been done. The measurements results for LFM and FSK signals have been presented in the paper. The frequency measurement errors depend on the structure of the frequency discriminators, especially on the delay line length and microwave detectors parameters. [C1594]

### "Localization in wireless sensor networks using switched parasitic antennas"

A switched parasitic monopole antenna for 2.4 GHz ISM applications is design and investigated in this paper. One of the most promising applications for such switched-beam antennas is localization in wireless sensor networks (WSN). It is demonstrated that the use of this antenna improves accuracy of localization algorithms and allows for reduction of the number of reference nodes in localization system. [C1595]

### "Modulation-mode and power-assignment for SVD-assisted downlink multiuser MIMO systems"

Multiuser multiple-input multiple-output (MIMO) downlink (DL) transmission schemes experience both multiuser interference as well as inter-antenna interference. However, instead of treating all the users jointly as in zero-forcing (ZF) multiuser transmission techniques, the investigated singular value decomposition (SVD) assisted DL multiuser MIMO system takes the individual user's channel characteristics into account. The performed joint optimization of the number of activated MIMO layers and the number of bits per symbol along with the appropriate allocation of the transmit power shows that not necessarily all user-specific MIMO layers has to be activated in order to minimize the overall BER under the constraint of a given fixed data throughput. [C1596]

### "Optimisation of resistive sensor for ridge waveguide"

Finite-difference time-domain simulations of electromagnetic field distribution in double ridge or H-type waveguide segment with a semiconductor structure were performed. The structure serves as a resistive sensor for high power microwave pulse measurement within the working frequency range of the waveguide. As a result of the investigation, conditions for the optimal sensor with the "flattest" frequency response were determined. The best calculated sensitivity variation for the sensor was roughly  $\pm 21\%$  for WRD-250 waveguide and  $\pm 6\%$  for WRD-750 waveguide. [C1597]

### "Development strategy for GaN-based high-efficiency hybrid medium-power RF amplifiers through

### **low-cost substrate prototyping"**

Two high-efficiency power amplifiers have been designed, fabricated, and tested using a commercially available GaN HEMT transistor and a low-cost hybrid microstrip PCB. The designed hybrid modules are a "tuned load" Class B amplifier and a Class F amplifier. The simulated performances show a peak efficiency of 72 and 78 % with an output power of 5 and 4.5W respectively. The measured performance, although still satisfactory, exhibits an efficiency of 60 and 55 %, respectively, for the two stages. The paper presents a discussion on the design approach, on the intrinsic/extrinsic load to be presented to the active device, and on the cause of the efficiency drop occurring between the simulated and measurement performances. [C1598]

### **"Computer aided microstrip circulator design"**

A method for taking the advantages of electromagnetic simulation software for the design of microwave ferrite device will be presented in this paper. The design steps will be shown through the design process of a microstrip circulator working at 10 GHz. The key point of the design is using quarter-wave transformer for achieving good quality impedance matching between the 50 Ohm system and the circulator. [C1599]

### **"Design and simulation GaN based class-S PA at 900MHz"**

A Class-S Power Amplifier architecture seems to be an attractive alternative for classical PAs due to offered very high efficiency operation. Switching mode PA principle assumes combined operation based on digital, single-bit Delta-Sigma ( $\Delta\Sigma$ ) modulated signals and RF analog signals, what complicates design and analysis procedures. However the Class-S PA topology is known, there are not any universal design methods which can be unambiguous applied to considered architecture. Presented work defines and describes design method for Class-S PA based on GaN HEMT transistors. Moreover main simulation results for Class-S architecture based on Current Switching Class-D (CSCD) configuration at the carrier frequency of 900 MHz have been performed. [C1600]

### **"Compensated broadband five-section directional coupler for application in butler matrices"**

A broadband five-section symmetrical 3 dB directional coupler has been designed. In order to improve the frequency characteristic of the coupler a recently proposed compensation technique has been used. The developed coupler operates in 2-12 GHz frequency band and can be applied in a broadband 4x4 Butler matrix. [C1601]

### **"L-Band Electron Paramagnetic Resonance (EPR) spectrometer"**

The paper describes the general concept as well as potential applications of the EPR L-Band spectrometer. The latter part of the article presents the detailed construction of the L-Band microwave unit with the Loop-Gap cavity of the spectrometer. The spectrometer is mainly developed for testing irradiated food. [C1602]

### **"A 100W SiC MESFET amplifier for L-band T/R module of APAR"**

In the paper, a 100 W SiC MESFET amplifier design for especially L-band T/R module of APAR is presented. The output power higher than 100 W has been achieved by combining in a balanced configuration two single stages with Cree's 60 W CRF24060 SiC MESFETs. The amplifier design methodology is based on the small-signal model and DC characteristics of SiC MESFET. The model is extracted using the transistor S-parameters at three operating points for On-state, Off-state and normally bias. The measurements and simulations prove usefulness of the proposed method. The amplifier were excited both pulsed and cw signals for the case temperature from 60°C to 140°C. The As result of the case temperature changes the output power drop was lower than 0.5 dB on the level of 150 W. [C1603]

### **"Advanced switch-mode concepts using GaN: The class-S amplifier"**

Efficiency of power amplifiers for the wireless infrastructure is presently a hot topic. Switch-mode type amplifiers and/or more complex concepts, e.g. Doherty or envelope tracking (ET) are being explored intensively, exploiting the potential of GaN technology. This paper contributes recent results on a related approach, the class-S concept, which offers also compatibility with digital baseband processing. Its potential is evaluated based on realizations for the 450 MHz frequency band with GaN MMICs. [C1604]

### **"Path planning based on fluid mechanics for mobile robots using unstructured terrain models"**

Mobile robots using a 360° field of view LIDAR ranging sensor can generate enormous 3D point clouds. To reduce the quantity of data in memory a compression can lead to unstructured environment models such as



irregular meshes. This kind of structure can contain deformed cells and the path planning can be cumbersome. This paper presents a path planning method based on fluid mechanics able to deal with unstructured terrain models. The algorithm uses the finite element method to compute a velocity potential function free from local minima. Then, several streamlines are computed as a road map and the optimal path is selected among the candidate paths. The approach is implemented on the Canadian Space Agency (CSA) Mars Robotics Testbed (MRT) rover and tested at the CSA Mars Emulation Terrain (MET). To confirm the feasibility of the method, the path planner has been tested on 284 LIDAR scans collected in a realistic outdoor challenging terrain. [C1605]

### "Extracting general-purpose features from LIDAR data"

The detection of features from Light Detection and Ranging (LIDAR) data is a fundamental component of feature-based mapping and SLAM systems. Existing detectors tend to exploit characteristics of specific environments: corners and lines from indoor (rectilinear) environments, and trees from outdoor environments. While these detectors work well in their intended environments, their performance in different environments can be very poor. We describe a general purpose feature detector for LIDAR data that is applicable to virtually any environment. Our methods adapt classic feature detection methods from the image processing literature, specifically the multi-scale Kanade-Tomasi corner detector. Our resulting method is capable of identifying stable features at a variety of spatial scales and produces uncertainty estimates for use in a state estimation algorithm. We present results on standard datasets, including Victoria Park and Intel Research Center (both 2D), and the MIT DARPA Urban Challenge dataset (3D). [C1606]

### "Robust vehicle localization in urban environments using probabilistic maps"

Autonomous vehicle navigation in dynamic urban environments requires localization accuracy exceeding that available from GPS-based inertial guidance systems. We have shown previously that GPS, IMU, and LIDAR data can be used to generate a high-resolution infrared remittance ground map that can be subsequently used for localization. We now propose an extension to this approach that yields substantial improvements over previous work in vehicle localization, including higher precision, the ability to learn and improve maps over time, and increased robustness to environment changes and dynamic obstacles. Specifically, we model the environment, instead of as a spatial grid of fixed infrared remittance values, as a probabilistic grid whereby every cell is represented as its own gaussian distribution over remittance values. Subsequently, Bayesian inference is able to preferentially weight parts of the map most likely to be stationary and of consistent angular reflectivity, thereby reducing uncertainty and catastrophic errors. Furthermore, by using offline SLAM to align multiple passes of the same environment, possibly separated in time by days or even months, it is possible to build an increasingly robust understanding of the world that can be then exploited for localization. We validate the effectiveness of our approach by using these algorithms to localize our vehicle against probabilistic maps in various dynamic environments, achieving RMS accuracy in the 10cm-range and thus outperforming previous work. Importantly, this approach has enabled us to autonomously drive our vehicle for hundreds of miles in dense traffic on narrow urban roads which were formerly unnavigable with previous localization methods. [C1607]

### "Boundary detection based on supervised learning"

Detecting the boundaries of objects is a key step in separating foreground objects from the background, which is useful for robotics and computer vision applications, such as object detection, recognition, and tracking. We propose a new method for detecting object boundaries using planar laser scanners (LIDARs) and, optionally, co-registered imagery. We formulate boundary detection as a classification problem, in which we estimate whether a boundary exists in the gap between two consecutive range measurements. Features derived from the LIDAR and imagery are used to train a support vector machine (SVM) classifier to label pairs of range measurements as boundary or non-boundary. We compare this approach to an existing boundary detection algorithm that uses dynamically adjusted thresholds. Experiments show that the new method performs better even when only LIDAR features are used, and additional improvement occurs when image-based features are included, too. The new algorithm performs better on difficult boundary cases, such as obliquely viewed objects. [C1608]

### "Human detection and tracking via Ultra-Wideband (UWB) radar"

This paper presents an algorithm for human presence detection and tracking using an Ultra-Wideband (UWB) impulse-based mono-static radar. UWB radar can complement other human tracking technologies, as it works well in poor visibility conditions. UWB electromagnetic wave scattering from moving humans forms a complex returned signal structure which can be approximated to a specular multi-path scattering model (SMPM). The key technical challenge is to simultaneously track multiple humans (and non-humans) using the complex scattered waveform observations. We develop a multiple-hypothesis tracking (MHT) framework that solves the complicated

data association and tracking problem for an SMPM of moving objects/targets. Human presence detection utilizes SMPM signal features, which are tested in a classical likelihood ratio (LR) detector framework. The process of human detection and tracking is a combination of the MHT method and the LR human detector. We present experimental results in which a mono-static UWB radar tracks human and non-human targets, and detects human presence by discerning human from moving non-human objects. [C1609]

#### "On the global optimum of planar, range-based robot-to-robot relative pose estimation"

In this paper, we address the problem of determining the relative position and orientation (pose) of two robots navigating in 2D, based on known egomotion and noisy robot-to-robot distance measurements. We formulate this as a weighted Least Squares (WLS) estimation problem, and determine the exact global optimum by directly solving the multivariate polynomial system resulting from the first-order optimality conditions. Given the poor scalability of the original WLS problem, we propose an alternative formulation of the WLS problem in terms of squared distance measurements (squared distances WLS or SD-WLS). Using a hybrid algebraic-numeric technique, we are able to solve the corresponding first-order optimality conditions of the SD-WLS in 125 ms in Matlab. Both methods solve the minimal (3 distance measurements) as well as the overdetermined problem (more than 3 measurements) in a unified fashion. Simulation and experimental results show that the SD-WLS achieves performance virtually indistinguishable from the maximum likelihood estimator, and significantly outperforms current algebraic methods. [C1610]

#### "Global rover localization by matching lidar and orbital 3D maps"

Current rover localization techniques such as visual odometry have proven to be very effective on short to medium-length traverses (e.g., up to a few kilometres). This paper deals with the problem of long-range rover localization (e.g., 10km and up). An autonomous method to globally localize a rover is proposed by matching features detected from a 3D orbital elevation map and rover-based 3D lidar scans. The accuracy and efficiency of the algorithm is enhanced with visual odometry, and inclinometer/sun-sensor orientation measurements. The methodology was tested with real data, including 37 lidar scans of terrain from a Mars-Moon analogue site on Devon Island, Nunavut. When a scan contained a sufficient number of good topographic features, localization produced position errors of no more than 100m, and as low as a few metres in many cases. On a 10km traverse, the developed algorithm's localization estimates were shown to significantly outperform visual odometry estimates. It is believed that this architecture could be used to accurately and autonomously localize a rover on long-range traverses. [C1611]

#### "Ground plane identification using LIDAR in forested environments"

To operate autonomously in forested environments, unmanned ground vehicles (UGVs) must be able to identify the load-bearing surface of the terrain (i.e. the ground). This paper presents a novel two-stage approach for identifying ground points from 3-D point clouds sensed using LIDAR. The first stage, a local height-based filter, discards most of the non-ground points. The second stage, based on a support vector machine (SVM) classifier, operates on a set of geometrically defined features to identify which of the remaining points belong to the ground. Experimental results from two forested environments demonstrate the effectiveness of this approach. [C1612]

#### "Estimation of DOD and 2D-DOA and polarizations for bistatic MIMO radar"

Multi-parameter estimation is investigated for target discrimination and localization in multiple-input multiple-output (MIMO) radar system. With an M-element uniform linear array in the transmitter and a square array consisting of  $N_2$  pair of crossed-dipoles in the receiver, a novel method is proposed for joint estimation of direction-of-departures (DODs), two-dimensional direction-of-arrivals (2D-DOAs) and polarizations of multiple targets for bistatic MIMO radars. Its signal model is described, and the algorithm is given by exploiting rotational invariance property of ESPRIT and polarization sensitive array processing technology in transmit and receive arrays. To discriminate and localize targets in a 3-D plane, more information than those of traditional bistatic MIMO radar algorithms is provided using the proposed method. Also, by making use of polarization diversity, its resolution capability is greatly improved when two targets are closely spaced. [C1613]

#### "DOA estimation for wideband sources using cross correlation transformation"

In this paper, we consider the problem of estimating directions-of-arrival (DOAs) of wideband source signals. A new class of focusing matrices is proposed for use in the coherent signal subspace method. The new method does not require any preprocessing for initial values through using the cross correlation transformation (CCT). Numerical results show that when the DOAs fall within more than one group of one beamwidth each and there are closely spaced sources, the CCT method outperforms the methods requiring preprocessing in terms of root-

mean-square error (RMSE). [C1614]

### "All-weather perception for man-portable robots using ultra-wideband radar"

Autonomous man-portable robots have the potential to provide a wide range of new capabilities for both military and civilian applications. Previous research in autonomy for small robots has focused on vision, LIDAR, and sonar sensors. While vision and LIDAR work well in clear weather, they are seriously impaired by rain, snow, fog, and smoke. Sonar can penetrate adverse weather, but has limited range outdoors, and suffers from specular reflections indoors. For the Daredevil Project, we have investigated the use of ultra-wideband (UWB) radar to provide obstacle detection capabilities for man-portable robots. Our research shows that UWB radar can effectively penetrate adverse weather, including dense fog, and detect obstacles that would be undetectable by vision or LIDAR under the same conditions. We have developed filtering algorithms that process the raw radar returns to eliminate reflections from ground clutter and make obstacles easier to detect. We have tested this system on an iRobot PackBot equipped with both UWB radar and LIDAR, and we have demonstrated how UWB radar can be used for obstacle detection in obscured environments. [C1615]

### "On-line calibration of multiple LIDARs on a mobile vehicle platform"

In this paper, we examine the problem of extrinsic calibration of multiple LIDARs on a mobile vehicle platform. To achieve fully automated and on-line calibration, the original non-linear calibration model is reformulated as a second-order cone program (SOCP). This provides an advantage over more standard linearized approaches in that a priori information such as a default LIDAR calibration, calibration tolerances, etc., can be readily modeled. Furthermore, in contrast to general non-linear methods, the SOCP relaxation is convex, returns a global minimum, and can be solved very quickly using modern interior point methods (IPM). This enables the calibration to be estimated on-line for multiple LIDARs simultaneously. Experimental results are provided where the approach is used to successfully calibrate a pair of Sick LMS291-S14 LIDARs mounted on a mobile vehicle platform. These showed the SOCP formulation yielded a more accurate reconstruction and was 1-2 orders of magnitude faster than the traditional non-linear least-squares approach. [C1616]

### "Towards marine bloom trajectory prediction for AUV mission planning"

This paper presents an oceanographic toolchain that can be used to generate multi-vehicle robotic surveys for large-scale dynamic features in the coastal ocean. Our science application targets Harmful Algal Blooms (HABs) which have significant societal impact to coastal communities yet are poorly understood ecologically. Bloom patches can be large spatially (in kms) and unpredictable in their extent. To understand their ecology, we need to be able to bring back water samples from the 'right' places and times for lab analysis. In doing so, we target hotspots representative of intense biogeochemical activity for such sampling. Our approach uses remote sensing data to detect such hotspots using ocean color as a proxy, and advectively projects these patches spatio-temporally using surface current data from HF Radar stations. Experiments with satellite and Radar data sets are promising for large, coherent blooms. We show how these predictions can be used to select an appropriate sampling trajectory for an AUV. [C1617]

### "A hybrid SLAM representation for dynamic marine environments"

We present a hybrid SLAM system for marine environments that combines cubic splines to represent the trajectories of dynamic objects, point features to represent stationary objects and an occupancy grid to represent land masses. This hybrid representation enables SLAM to be applied in environments with moving objects, where solutions using point features alone are computationally prohibitive or where dense objects e.g. landmasses can not be represented correctly using point features. Estimation is achieved using a sliding window framework with reversible data-association and reversible model-selection. Our main contributions are: (i) a hybrid representation of the environment; (ii) occupancy grid fusion is continually refined for the duration of the sliding window; (iii) the trajectories of dynamic objects are represented using cubic splines and (iv) radar scans are re-rendered at a sub-scan resolution to compensate for the egomotion during the scan acquisition period. We show that the continual refinement of the occupancy grid greatly improves the quality of the resultant map, leading to a better estimate of the egomotion and therefore better estimates of the trajectories of dynamic objects. We also demonstrate that the use of cubic splines to represent trajectories has two major advantages: (i) the state space is compressed i.e. many vehicle poses can be represented using a single spline section and (ii) the trajectory becomes continuous and so fusing information from asynchronous sensors running at multiple frequencies becomes trivial. The efficacy of our system is demonstrated using real marine radar data, showing that it can successfully estimate the positions/velocities of objects and landmasses observed during a typical voyage on a small boat. [C1618]

### "Planar landmark detection using a specific arrangement of LIDAR scanners"

All terrestrial applications which depend on a GPS receiver for a precise position fix suffer in the urban environments. A Terrestrial Mobile Mapping System is one such application. We have been working on a Terrestrial LIDAR (Light Detection and Ranging) scanner (or Laser scanner) based Mobile Mapping System (MMS) in our laboratory. To aid the localization of our moving mapping platform (a land vehicle), we opted to use the technology similar to SLAM (Simultaneous Localization and Mapping). Our primary focus is on the urban canyons where the GPS signal perturbations are highly likely to occur. The main characteristic of an urban canyon is the planar sections of the man made buildings. In this paper, we present a specific arrangement of the LIDAR scanners tailored to extract the planar landmarks. This is the first important step in improving the localization functionality. Here we discuss about our new LIDAR system configuration and the design justifications along with the obtained results of planar landmark extraction. [C1619]

### "An obstacle-edging reflex for an autonomous lawnmower"

We developed a controller that allows our prototype lawnmower, CWRU Cutter, 1st place winner of the 2009 ION Autonomous Lawnmower Competition, to follow pre-defined paths and reflexively edge around obstacles before returning to the path. CWRU Cutter is equipped with localization sensors (GPS) and obstacle detecting sensors (LIDAR and camera). [C1620]

### "Lightweight efficient and feasible IP multimedia subsystem authentication"

In IP Multimedia Subsystem (IMS) of UMTS, IMS information is delivered through the general packet radio service (GPRS) transport network, before a user equipment (UE) can access the IMS service, it must perform both packet-switch domain and IMS authentication. It is inefficient that almost all involved steps in IMS authentication are duplicated. Hence, some one-pass IMS authentications were proposed to increase the efficiency of the IMS authentication. Unfortunately, these protocols have some problems which make them unfeasible. Therefore, we proposed a lightweight one-pass IMS authentication protocol to reduce signaling traffic. Through analysis, we found that it has minimal impact on the network functionality and will not influence the succeeding IMS re-authentication, which makes it more feasible. [C1621]

### "Relating local vision measurements to global navigation satellite systems using waypoint based maps"

Roughly 50% of all the traffic fatalities are due to lane departures [2]. There is great interest in advanced driver assistance systems that prevent unintended lane departure. Currently there are passive lane detection systems that warn the driver of unintended lane departure known as lane departure warning (LDW) systems which rely on cameras to track lane markings. LDW systems based solely on camera measurements are prone to failures due to poor environmental lighting or poor lane marking coverage. Combining the measurements from multiple sensors will create a much more robust LDW system that is not prone to failures. [C1622]

### "Lidar attitude estimation for vehicle safety systems"

This paper presents two techniques for determining vehicle pitch and roll with a 3-D lidar which will first auto-calibrate itself to the vehicle's axes. The first method presented is based on Euler angles and the second on Gaussian Processes. A 3-antenna Septentrio GPS receiver is used to assess system performance. [C1623]

### "Combine draft detector with GPS receiver to monitor barge's loadage"

In order to maintain channels and harbors at safe depths, periodic dredging is required. With increasing environmental awareness and tightening legislative control, licenses and approvals are required to dispose of dredged material. For the sake of supervision of loaded barges, this article introduces a Barge's Loadage Monitoring System (BLMS). The applications utilized in Xiamen waterway authority can display various information needed for supervising barges on electronic chart platform visually and comprehensively. The main feature of its innovation is combining draft detector with GPS and on-board transponder technologies. [C1624]

### "A spectral space-variant approach for structure indexing in Spotlight TerraSAR-X data"

Modern space missions equipped with SAR instruments provide high spatial resolution data. In such data features of urban objects, man-made structures, as well as natural targets can be identified. We propose a descriptive model based on the frequency spectra of the complex signal, that integrates the radiometric, geometric, and texture features, for scene and target indexing, to cope with the problem of large database queries and information retrieval. Considering the properties of the Spotlight imaging mode in particular, a phase



correction algorithm is applied to the data, prior to feature extraction. The assignation of a particular scene to a certain class is done using a Bayesian Support Vector Machine classifier. The method allowed for the recognition of more than thirty targets and structures in the scenes. [C1625]

#### "High-quality HRR ATR system using an improved neural recognition chain"

One of the most recent technique to design an efficient ATR system is to use high-resolution radar (HRR) imagery as input information flow. To increase the quality of such system, an interesting approach is to use powerful artificial neural networks inside of its recognition chain. Consequently, an improved neural recognition function based on modified feature extraction and selection methods and respectively, on genetic optimized RBF network architecture is described. Finally, to confirm the broached theoretical aspects, a real HRR image database was also used. [C1626]

#### "A communication waveform for radar"

This paper discusses some opportunities created by using Orthogonal Frequency Division Multiplexing signals for radar and communication at the same time. Two examples of opportunities in radar are proposed, i.e. solving the unambiguous radial speed in a single transmission and improving the signal-to-background contrast. The performance of the data link is analyzed and shown to be useful. [C1627]

#### "A potential field approach to finding minimum-exposure paths in wireless sensor networks"

A novel artificial-potential approach is presented for planning the minimum-exposure paths of multiple vehicles in a dynamic environment containing multiple mobile sensors, and multiple fixed obstacles. This approach presents several advantages over existing techniques, such as the ability of computing multiple minimum-exposure paths online, while avoiding mutual collisions, as well as collisions with obstacles sensed during the motion. Other important advantages include the ability of utilizing heterogenous sensor models, and of meeting multiple objectives, such as minimizing power required, and reaching a set of goal configurations. The approach is demonstrated through numerical simulations involving autonomous underwater vehicles (AUVs) deployed in a region of interest near the New Jersey coast, with ocean currents simulated using real coastal ocean dynamics applications radar (CODAR) data. [C1628]

#### "Self-Organizing Networks: State-of-the-art, challenges and perspectives"

In this paper, a general overview of Self-Organizing Networks (SON), and the rationale and state-of-the-art of wireless SON are first presented. The technical and business requirements are then briefly treated, and the research challenges within the field of SON are highlighted. Thereafter, the relation between SON and Cognitive Networks (CN) is covered. At last, the application of Algorithmic Information Theory (AIT) as a possible theoretical tool to support SON in addressing the growing complexity of networks is discussed. [C1629]

#### "ICA-based information extraction method for PolSAR images"

Identifying and characterizing objects in PolSAR images rely on proper backscattered signal models, correct segmentation algorithms and on exploiting the connections between the physical structure of the considered objects and their radar echos. The paper presents an ICA-based approach for characterizing physical properties of the objects on the Earth surface. Segmentation of PolSAR image is based on stochastic models. Each segment is assimilated to an object or surface type and pixels of the segment are treated like realizations of the underlying target scattering mechanism. This scattering mechanism is characterized through ICA-based approach, thus providing information about the corresponding target. The TSVM decomposition is used to analyze the mixing matrix issued from ICA and to link its values to physical properties of the target. [C1630]

#### "The generated curve in symmetrical plane for double curved antenna reflector with Cosec2 pattern beam, illuminated by a Cos4 pattern beam for primary radiator"

The paper presents a method to generate the symmetrical plan curve for a Cosec2 radiation pattern double curved antenna reflector, for the case when the primary radiation source has a Cos4 radiation pattern. There is also shown the diffraction calculus for the antenna having the reflector generated by using the calculated vertical profile. [C1631]

#### "A novel spectrum reconstruction algorithm based on FrFT for multiple azimuth beam SAR"

In this paper, we consider the problems of reconstructing the spectrum based on Fractional Fourier Transform (FrFT) from periodic non-uniformly sampled signal in multiple azimuth beams SAR system. First, based on the



theory of the paired echoes, the influence of periodic non-uniform sampling for SAR imaging has been derived. Second, signal model of non-uniformly sampling in azimuth direction has been established. Finally, detailed analysis of spectrum reconstruction algorithm in the fractional Fourier domain has been performed. In addition, the simulations are carried out to verify the correctness of the results. [C1632]

### "Meshless RPIM modeling of open-structures using PMLs"

Meshless methods are emerging as a new class of numerical techniques for modeling complex electromagnetic problems. To apply them to open structures, effective absorbing boundaries need to be developed. In this paper, the perfectly matched layer (PML) absorbing boundary condition is implemented into the meshless radial point interpolation method (RPIM) for accurate meshfree modeling of electromagnetic radiation problems in time-domain. Two benchmark radiating structures, a parallel waveguide and a conical unipole antenna, are presented to validate the effectiveness of the implementation. Comparisons are made between the numerically computed results and the measured results from previous reports and good agreements are found. In contrast to conventional FDTD technique, the RPIM modeling with the PML condition requires much less computational efforts for antenna radiation problems, thanks to its capability of conformal modeling and multi-scale solutions. [C1633]

### "High-phase-resolution 77-GHz-band radar module for near-field millimeter-wave imaging"

Near-field millimeter-wave (MMW) imaging is a unique approach for inspecting cracks in covered concrete surfaces to assess the deterioration of concrete structures. We have developed a 77-GHz-band radar module with in-phase and quadrature detection which is superior to measuring both of the amplitude and phase of MMW in a near-field range. A monostatic radar system is hybrid integrated into the module with a constant-width antipodal tapered slot antenna with an antenna gain of 14.5 dBi which is connected to a microstrip-line coupler with an isolation of higher than 26 dB using a leakage cancellation technique. In distance measurements in free space, the phase resolution is less than 8 degrees corresponding to the distance resolution of smaller than 0.01 mm, which is high enough to distinguish MMW signals scattered by the cracks from multiple reflection of the concrete surfaces and inside aggregates. [C1634]

### "Earth observation instruments with e-scan antennas state-of-the-art and outlook"

Spaceborne radars with electronically scanned antennas are in use on European satellites since the launch of Envisat in March 2002. Despite the higher complexity and consequently cost, electronically scanned antennas are more and more attractive for spaceborne radar. The return materialises either in significantly better system performance or in newly gained system feasibility. The paper will discuss firstly state-of-the-art phased array technology as used for the European Sentinel 1 C-band SAR and explore secondly the capabilities of full digital beam forming implementation for the next generation of SAR systems. Thirdly phased arrays as a feasibility prerequisite in quasi bi-static radar for future ocean altimetry, exploiting GNSS signals will be discussed. Lastly reflector based e-scan antennas will be discussed which form a good compromise between complexity and flexibility as needed for SAR systems requiring high gain antennas. A Ka-band SAR application will be presented. [C1635]

### "Commercial manufacturing practices applied to phased array radars"

Transmit/Receive Modules for Phased Array Radar are often identified as a key cost driver for the system. The cost structure of the module is driven by both the performance specifications and the choices made in design and manufacturing of the module. Seeking a path to dramatically lower the cost of T/R modules for phased array systems, commercial processes and practices have been adopted for the MMIC design, MMIC packaging and module construction. These new manufacturing approaches offer a path to cost reduction while maintaining a high level of performance. [C1636]

### "Extremely Low Frequency Electric Field Induced Mutations in Escherichia Coli K12 Strains"

Escherichia coli K12 W3110 was treated by extremely low frequency electric field (ELF EFs) 10min with the field intensity of 100, 200, 300, 400kV/m. The mutant frequency reached  $31.2 \times 10^{-6}$  at field intensity of 100kV/m, which was about 26-fold over the background ( $1.2 \times 10^{-6}$ ) and 12-fold over the controls ( $2.5 \times 10^{-6}$ ). This result indicated that the ELF EFs could act as a mutagen. The results also show that base pair (bp) substitutions were the main type of ELF EFs induced mutations. Although all types of base pair substitutions were observed, 30% of the bp substitutions were G:C → A:T transitions, 70% of the bp substitutions were A:T → T:A, G:C → T:A, A:T → C:G, G:C → C:G transversions. When the spontaneous and the ELF EFs exposure group were compared, base-pair substitutions, deletions and additions of the ELF EFs exposure group were significantly increased, and the deletion or the addition of a 5'-TGGC-3' sequence at hot spot was decreased from 82 to 26%. But the

remarkable increase in absolute Mutation Frequency (MF) of the deletion or the addition of a 5'-TGGC-3' sequence at hot spot in the ELF EFs exposure group suggested that ELF EFs did induce the mutations of this type. The spectra of our ELF EFs exposure group with increasing G:C to A:T transitions and A:T to T:A transversions indicate that ELF EFs exposure may induce SOS response. [C1637]

#### "Advanced architecture for a low cost multifunction phased array radar"

MIT Lincoln Laboratory and M/A-COM are jointly conducting a technology demonstration of affordable Multifunction Phased Array Radar (MPAR) technology for Next Generation air traffic control and national weather surveillance services. Aggressive cost and performance goals have been established for the system. The array architecture and its realization using custom Transmit and Receive Integrated Circuits and a panel-based Line Replaceable Unit (LRU) will be presented. A program plan for risk reduction and system demonstration will be outlined. [C1638]

#### "Waveguide transition to feed a fully PCB integrated dielectric rod antenna"

A microstrip line-to-circular waveguide transition is described which operates at a nominal design frequency of 77 GHz. In order to improve the transmission characteristics, an additional periodically structured shield is used. The transition is capable of exciting a dielectric rod antenna, thus enabling the realization of radar modules on a PCB substrate with a dielectric rod antenna interface. [C1639]

#### "Fast subspace decomposition null extension for two-dimensional array antenna"

A multiple null algorithm that can adjust the number, width and depth of multiple nulls in accordance with the environment requirements is proposed for the improvement of the interference cancellation capability of two-dimensional array antennas. The Fast Subspace Decomposition (FSD) and cyclic-Jacobi algorithms are employed to robustly simplify the computation of inverse interference covariance matrix and to determine the optimal weighting matrix of the multiple null digital beam former (DBF). Finally, the numerical simulations of the multiple null DBF are used to demonstrate its anti-jamming capability for the two-dimensional array antennas. The number of multipliers for computing the inverse of interference covariance matrix between FSD algorithm and Eigen value decomposition (EVD) algorithm is also compared. [C1640]

#### "Miniature radio frequency ion trap mass spectrometry"

RF ion traps are useful in chemical analysis and have added benefits when scaled to smaller dimensions. For a miniature ion trap it is ideal to be able to predict the performance of the ion trap prior to fabrication in order to save time and optimize parameters. We have developed both the simulation and fabrication of scaled ion traps. The simulation tool allows us to model miniature ion traps in order to predict how the frequency and amplitude of the RF voltage could be scaled in order to optimize the performance of the ion trap. We demonstrate the performance of a scaled ion trap array fabricated through the integration of stereolithography on circuit board and compare its performance with our ion trajectory simulator. [C1641]

#### "Piggyback modulation for UHF RFID sensors"

We introduce the technique of "piggybacking" sensor data onto existing commercial passive UHF RFID tags. Sensor data fed into a PIN diode modulator is coupled onto the tag and transmitted along with the tag ID via backscatter. The radar cross section (RCS) of the tag antenna is a function of the input impedance of the tag ASIC, coupling S-parameters, and the input impedance of the PIN diode modulator. Both analog and digital sensor signals coexisting with identification data are presented. [C1642]

#### "Novel image reconstruction algorithm for a UWB cylindrical Microwave Imaging System"

A theoretical and experimental study of a novel image reconstruction algorithm for an Ultra Wideband (UWB) Microwave Imaging System aiming at detecting and locating small targets in a homogenous circular cylindrical dielectric body is presented. The system uses a double circular scan in which the second scan is achieved after rotating by a small angle the antenna sub-system or the imaged body. The obtained two sets of data serve the purpose of subtracting the background that masks the target. Assuming that the target is asymmetric with respect to the axis of rotation, the difference data includes the original target and its negative "ghost". In order to eliminate the "ghost" only the positive valued difference data is extracted. This data is scaled and mapped to show the original target location. The validity of the proposed image reconstruction algorithm is demonstrated in an example of a cylindrical plastic container filled with a vegetable oil and small cylindrical targets. [C1643]

### "Multi-PC FDTD: Solving large scale EM problems"

After giving historical data on FDTD speed and problem sizes, the state of the art approach to fast and efficient FDTD simulations is explained for large scale structures. Future challenges include the simultaneous simulation of the RF device or antenna and its surrounding environment, increasing the modeling effort by at least an order of magnitude. An intelligent hierarchical concept exploiting the different size and speed levels of data storage (CPU-cache, RAM, hard-disc and Multi-Machine computing) is presented and analyzed to face the challenges.

[C1644]

### "A forest fire monitoring system based on GPRS and ZigBee wireless sensor network"

The significance of forest fire monitoring was determined by the importance of forest resource and the destructive of forest fire. In the paper, according to the limitation of traditional forest fire monitoring schemes, a new wireless network implementation scheme oriented to forest fire monitoring was presented based on GPRS communication technology and ZigBee technology. The related hardware schemes and software program flows were given. The forest environmental information was collected by ZigBee network and transmitted to FTP server with public network IP on the internet through GPRS network by GPRS module which was controlled by coordinator node. The monitoring center got the data, which was provided for relative experts and decision maker, from FTP server to implement the achievement of remote data from monitoring region. Through the analysis of historical data and real-time data, correct judges and decisions were made. It had strategic significance to improve the level of modernization of forest fire monitoring. [C1645]

### "A path planning achievement of car following in motion control via LiDAR sensing"

This paper presents a new car following system to track a preceding car and maintain a desired safe distance based on a laser imaging, detection, and ranging (LiDAR) sensor. The proposed system has the ability of lane change, including longitudinal and lateral control. To accomplish the car following sensing task, environment information provided by in-vehicle Lidar and monocular vision is used. A camera is an auxiliary device to map Lidar data into the output image and verify the detection ability of LiDAR. The LiDAR and camera sensors are installed on a demonstrated vehicle, and the LiDAR sensor which has one-dimensional scanning ability can measure the relative distance of the vehicle from a preceding vehicle by scanning the horizontal plane with laser beams. The relative position is processed and estimated by random sample consensus (RANSAC) method and geometry relation, and then the heading and speed of vehicle are automatically operated by an embedded processor. The speed variation tracking is implemented by fuzzy-PI algorithm, and the pure pursuit method is applied as the steering control strategy to keep up with the trajectory in lateral control. Environmental clutter becomes the main challenge in data processing when LiDAR tries to track the desired vehicle. Besides, a comfortable requirement of vehicle control is also considered and complied with the rule of ISO 2631. Thus, the proposed system integrates engine vacuum connected to throttle and active steering system with embedded ahead control algorithms into a powerful car following system in practice, which has been verified in experiments using two vehicles. The mobile hardware are built with three embedded systems using X86 processor in Linux system, and furthermore the sensing data collection is accomplished by Ethernet interface. The proposed system is carried out with theoretical application and hardware integration, and the result shows car following approach applicability. [C1646]

### "A method for determining the number of signals based on modified K-means clustering"

Determining the number of signals impinging on an array of sensors is one of the hot and important problems in array processing field. Research on estimation method which is available in colored noise field has important theoretical and practical meaning. A new method is proposed based on K-means clustering algorithm, we construct a distinguishing criteria in reason according to the difference between the signal and noise eigenvalues, and then the signal and noise eigenvalues are classified into two kinds using K-means clustering method. The method is valid in colored noise field. Computer simulation results and the available measured data confirmation prove the effective performance of the method. [C1647]

### "Resolutions of some overlap signals based on MUSIC algorithm"

In order to reduce resolution angle in direction finding system, a method based on MUSIC algorithm is proposed. According to the receiving characteristic of pulse signals in actual direction finding system, the method is proposed on the condition of some overlap signals. Because of the some overlap characteristic of signals, we can obtain a new covariance matrix by means of subtracting between two covariance matrixes which can be got from received data easily. One of the two covariance matrixes is got from the data of only one signal and the other one is from the data of two overlapped signals. It is known that we can estimate the direction of arrival from the covariance matrix of only one signal using MUSIC algorithm. Likewise, we can estimate another

direction of arrival from the new covariance matrix which is obtained by the new method. Thereupon, we get the directions of arrival of two signals. Both simulation and the test based on actual direction finding system proved that the proposed method can get smaller resolution angle with well performance. [C1648]

#### "High-dimensional Matched Subspace Detection when data are missing"

We consider the problem of deciding whether a highly incomplete signal lies within a given subspace. This problem, Matched Subspace Detection, is a classical, well-studied problem when the signal is completely observed. High-dimensional testing problems in which it may be prohibitive or impossible to obtain a complete observation motivate this work. The signal is represented as a vector in  $\mathbb{R}^n$ , but we only observe  $m$  of its elements. We show that reliable detection is possible, under mild incoherence conditions, as long as  $m$  is slightly greater than the dimension of the subspace in question. [C1649]

#### "A research on the robust digital watermark of color radar images"

Color images play a more and more important role in actual life, and the wavelet transformation technique is effective in image analyzing and processing. Thus the color-image watermark algorithm based on discrete wavelet transformation (DWT) begins to draw an increasing attention. This paper puts forward a robust watermarking algorithm based on wavelet transformation, which takes the masking of Human Visual System (HVS) in color images into full consideration, and color images are transferred from RGB space to YCbCr space. By means of the fine independence of YCbCr space, the contents and information of host images in every independent color channel can be fully excavated and then embedded in color images after being Arnold scrambled. The experimental results show that watermark embedded by this algorithm is of better robustness and invisibility. [C1650]

#### "New detection algorithm for weak target signal embedded in direct path interference using Signal Phase Matching Principle"

A detection method for weak signals embedded in direct-path interference is discussed. This method is based on FM radio signals as the illuminator of passive radar. On the basis of Signal Phase Matching Principle, a new algorithm for suppressing the direct-path interference is proposed in wave-beam domain. To improve the declining performances of the algorithm when the amplitude fluctuates, a compensatory factor is presented. The simulation results show the validity of the algorithm and the compensatory method. [C1651]

#### "Localization performance enhancement using IMM fusion in cricket sensor network"

In this paper, we propose an approach for estimating a location of moving-target over a sensor field via distributed IMM estimator with multiple pseudo measurements using trilateration positioning algorithm. Pseudo measurement which indirectly measures the position of target is defined by results of trilateration positioning coordinates. As a single node only can measure the distance to the target in Cricket sensor network, the nodes need to form groups of three to be able to perform trilateration. Also, since trilateration method ignores distance sensing error, adequate error covariance information is estimated in pseudo measurement model using self tuning method. Each distinct group can make local pseudo measurements and these data are fused with local IMM estimates. With these algorithms, localization performance enhancement of moving target is achieved.

[C1652]

#### "Robust waveform design for MIMO radars"

The problem of robust waveform design for multiple-input, multiple-output radars equipped with widely-spaced antennas is addressed here. Robust design is needed as a number of parameters are unknown, e.g., the target scattering covariance matrix and, possibly, the clutter covariance matrix. A min-max approach is proposed, so that the code matrix is designed to minimize the worst-case cost (or equivalently maximize the corresponding figure of merit) under all possible target (or target and clutter) covariance matrices. Surprisingly, the same min-max solution applies to many commonly adopted performance measures, such as the average signal-to-clutter-plus-noise ratio, the mutual information between the received signal echoes and the unknown target response, and the approximation of the detection probability in the high- and low-signal regimes. [C1653]

#### "High isolation lange-ferrite circulators with NF suppression for simultaneous transmit and receive"

This paper presents a new type of circulator that consists of three Lange couplers and two ferrite circulators for broadband, high isolation, transmit noise suppression and simultaneous transmit and receive (STAR). The operation principal of the circulator is based on quadrature phase cancellation and combination techniques. Preliminary results show that the isolation between the transmit and receive port is  $>24$  dB in frequency range of



5-12 GHz without optimization and 60 dB isolation with 800 MHz bandwidth with optimization. The NF data at the receive port show significant suppression of transmit noise for Gain-NF product that exceeds 21 dB. [C1654]

### "Research of Portable Community-Oriented Health Monitoring"

A new kind of wrist-worn health monitoring terminal is developed to realize multi-parameter measurement, wearing facilitates and reliable data transmission. The physiological parameters includes body temperature, pulse rate, breath rate and waveform, blood pressure, electrocardiograph(ECG), electroencephalogram(EEG) and the level of blood glucose real-timely. This terminal is designed by modules, which includes intelligent processing module based on MSP430, electrodes for collecting the physiological signals and electric circuit module for signal preprocessing, wireless data transmission module based on GPRS. The terminal is able to analyze the above signal. The terminals can be formed as a network based on wireless transmission. Credible and portable terminal for life indication is realized by developing micro-sensor and integrated modules for signal detecting and processing. Amounts of clinic tests have been done and the results have been approved by the doctors in hospitals and patients. [C1655]

### "A compact self-similar power combining topology"

A compact, modular 16-way combiner is presented which is based on a self-similar combiner topology. The combiner achieves a simulated passive efficiency of 38% at 77 GHz in a standard 90nm process with 1.49 $\mu$ m thick Al top metal. A 77 GHz power amplifier is built based on the combiner, combining the output power of 16 stages to achieve a Psatof 11.4dBm, small signal gain of 9.4dB, and a 3dB bandwidth of more than 11 GHz on a 0.7V supply, with the optimal MAG for the technology being approximately 5dB at 77 GHz. The power amplifier is unconditionally stable with the K factor exceeding 3.8 between 50-90 GHz. The entire architecture is based on a modular power splitting and combining network that makes the design flexible and scalable. To the best of the authors' knowledge, this is the highest Psatreported at 77 GHz in CMOS with a sub 1V quiescent Vds. [C1656]

### "Decentralized multihypothesis sequential detection"

This article is concerned with decentralized sequential testing of multiple hypotheses. In a sensor network system with limited local memory, raw observations are observed at the local sensors, and quantized into binary sensor messages that are sent to a fusion center, which makes a final decision. It is assumed that the raw sensor observations are distributed according to a set of  $M \geq 2$  specified distributions, and the fusion center has to utilize quantized sensor messages to decide which one is the true distribution. Asymptotically Bayes tests are offered for decentralized multihypothesis sequential detection by combining three existing methodologies together: tandem quantizers, unambiguous likelihood quantizers, and randomized quantizers. [C1657]

### "A new class of ternary and quaternary sequences with two-level autocorrelation"

Pseudorandom sequences with good correlation properties are widely used in communications and cryptography. The search of new sequences with two-level autocorrelation has been a very interesting problem for decades. In 2002, Gong and Golomb proposed the iterative decimation-Hadamard transform (DHT) which is an useful tool to study two-level autocorrelation sequences. They showed that for all odd  $n \leq 17$ , using the second-order decimation-Hadamard transform, and starting with a single binary m-sequence, all known two-level autocorrelation sequences of period  $2n-1$  which have no subfield factorization can be obtained. In this paper, we present a new class of ternary or quaternary sequences with two-level autocorrelation using the second-order decimation-Hadamard transform. The period of such sequences is  $2n-1$ . [C1658]

### "Nonbinary sequences with perfect and nearly perfect autocorrelations"

The design of pseudorandom sequences with optimal correlation properties forms a crucial part of communications and radar engineering. Perfect autocorrelation sequences are however exceedingly rare. We discuss a technique that yields examples of such designs over enlarged PSK (PSK+) alphabets. We also design nearly perfect autocorrelation sequences over enlarged QAM (QAM+) alphabets, compatible with contemporary wireless transmission standards. [C1659]

### "Performance analysis of an optical beam-forming network with custom microwave CAD tools"

Next generation wideband and ultra-wideband radar antenna arrays need efficient true-time delay networks for array control. Optical beam-forming networks have been considered as a promising solution in such arrays. Performance analysis of optical beam-formers is thus quiet necessary. In this paper signal to noise ratio and dynamic range of simple optical beam-forming structures are investigated with a custom microwave CAD tool. Two structures with optical and RF power combining methods are discussed. With the proposed devices'



parameters, the optical combining method shows better performance for low and moderate optical powers.

[C1660]

#### "77 GHz automotive digital beamforming radar with SiGe chipset"

In this paper, we describe the design and layout of an automotive radar sensor demonstrator for 77 GHz with a SiGe chipset and a fully parallel receiver architecture which is capable of digital beamforming and superresolution direction of arrival estimation methods in azimuth. Additionally, we show measurement results of this radar sensor mounted on a test vehicle. [C1661]

#### "Detection of weak moving targets based on 2-D range-Doppler FMCW radar Fourier processing"

This paper deals with a FMCW radar measurement scheme and a 2-D range-Doppler FMCW radar Fourier processing that is especially suited to detect very weak moving targets. A 2-D Fourier transform is applied to a larger set of consecutively measured FMCW radar beat signals. By this a phase coherent evaluation of a very long measuring time and a highly sensitive target separation in range and Doppler dimension is feasible. Applications of the proposed method are for example live sign detection of trapped or buried people, intruder detection or level measurements to organic fluids. The practical application of the described method is illustrated with a 24 GHz FMCW radar sensor system. The signal evaluation was implemented on a field programmable gate array (FPGA) to facilitate real time processing. Exemplary measurement results are presented to illustrate the capability of the applied method. [C1662]

#### "Enhanced drift in RF-power LDMOS transistors under pulsed stress conditions"

This paper presents an experimental evaluation of the reliability of LDMOS transistors with possible use in radio base station PA or for pulsed S-band Radar applications. Alternative device layouts have been investigated in a stress-test measurement system capable of generating pulses in the nanosecond range. The investigation shows that pulsed operation accelerate device drift. For the most sensitive parameter RON, pulsed operation at low supply voltage increase the drift with a factor 3 compared to constant operation. The investigation indicates that the stress is affecting the overlap or the field region but not the channel region. RESURF designed devices with decreased field in this region therefore show less RONdrift. [C1663]

#### "Considerations for future automotive radar in the frequency range above 100 GHz"

Within the last years automotive radar sensors became more and more important. Started with comfort systems like adaptive cruise control (ACC) and parking aid, the safety aspect increasingly came to the fore. In the near future not only upper class cars will be equipped with various radar applications like pre crash, collision warning and collision avoidance to increase traffic safety. Therefore many high performance radar sensors have to be integrated in the car. This paper describes the demands on future radar sensors. It is discussed how the step to higher operating frequencies could be beneficial particularly for urban situations with high traffic density. Furthermore the paper will provide and discuss design considerations for future mmW-Radar sensors in automotive safety applications. [C1664]

#### "Specification and design of a fast-tuning stepped-frequency synthesizer for a short-range-SAR-system in the K-Band"

We developed a stepped frequency synthesizer for short-range wide-beam radar applications. It is shown how a direct digital synthesizer (DDS) can be used as signal source for low-range applications. Attention was put on the tuning speed as well as on high bandwidth, frequency resolution and costs of the system. For high resolution the system was designed in the K-Band at 24 GHz. [C1665]

#### "A novel motion compensation algorithm for automotive SAR: Simulations and experiments"

In this paper a novel motion compensation algorithm for automotive SAR is presented. Aiming at automotive applications, the motion compensation algorithm utilizes only one 1-axis MEMS accelerometer instead of a 6 Degrees of Freedom inertial sensor. A complete motion compensation procedure is presented and its performance is analyzed quantitatively. The critical system parameters are designed with the help of a fully characterized simulator and Monte Carlo simulations. The experiment results demonstrate that the motion compensation algorithm together with a standard low-cost accelerometer can yield very useful images for automotive applications. [C1666]

#### "LTR analysis and signal processing for concealed explosive detection"

This paper presents the methodology for Concealed Weapon and Explosive (CWE) detection using Ultra Wideband (UWB) radar. The framework of the approach is based on the study of the Late Time Response (LTR) of the complex human-explosive object which occurs when the illuminating signal is characterised as UWB. The LTR is analysed using methods for extraction of its natural resonant frequencies which constitute a unique signature. Therefore it is investigated if the explosive or grenade resonant frequencies can be retrieved by the human-grenade LTR. [C1667]

#### **"Absolute distance measurement with asynchronous-optical-sampling terahertz impulse radar"**

We proposed a method to determine the absolute distance of a distant target using asynchronous-optical-sampling terahertz impulse radar. The determined distance was good agreement with the actual distance measured by a scale. [C1668]

#### **"Ppb standoff detection of nitric oxide in air"**

We demonstrate standoff detection of NO in air with ppb resolution. The weakly ionized plasma produced by picosecond UV laser pulses via REMPI is detected remotely by a microwave scattering technique. [C1669]

#### **"Darker than black: radiation-absorbing metamaterial"**

Taking advantage of the broadband "super-singularity" in the density of states of hyperbolic metamaterials, we develop a new approach to radiation-absorbing systems and present an experimental realization of this concept. [C1670]

#### **"Ultra wideband radar for water detection in the human body"**

In this paper an Impulse Radio Ultra Wideband (IRUWB) radar for detecting water accumulation in the human body is proposed. The method of On-body water detection is investigated both in a simulator with a bladder model and measurement system with a phantom. The Vivaldi antenna is used in the measurement system. The simulation and measurement results show the feasibility of water detection in the bladder through the reflection from the boundary of muscle and urine. The proposed concept offers also potential for continuous, wireless detecting and monitoring of the human organs ( heart, lung and bladder) and vital functions. [C1671]

#### **"Iterated simplified multiple model filters for target tracking in the presence of glint"**

The problem of target tracking in the presence of glint is investigated in the paper. Traditional interactive multiple model filters for tracking with target glint were first summarized and then simplified multiple model filters were developed in full detail according to a Gaussian assumption in the interactive multiple model structure. Novel iterated filters based on unscented Kalman filter and extended Kalman filter were put forward and then combined with simplified multiple model algorithms in order to improve tracking performance. Compared with the standard simplified multiple model filter, the proposed filters has higher estimation accuracy plus faster convergence speed. Simulation results demonstrate the conclusion above. [C1672]

#### **"Application of the combinatorial models for innovative design techniques"**

Application of the Perfect Combinatorial Sequences Theory, namely the concept of Ideal Ring Bundles (IRBs), for improving the quality indices of engineering devices or systems based on combinatorial technique is proposed in the paper. For example, resolving ability of radar is known to be of very dependent from positioning of elements in antenna array; high-performance technology of information coding and design of communication signals with favorable correlation properties demands an optimal placement of the signals in spatially and temporally distributed systems, and other examples of technological problems relating to the optimal placement of spatially or temporally distributed systems can be cited. However, a lot of well-known engineering devices, technologies or systems with non-uniform structure are very distant from perfect fulfillment of the design with respect to performance reliability, resolving ability and the other significant operating characteristics of the system. An ordinary IRB is ring-like sequence of positive integers, which form perfect partitions of a finite interval  $[1, S]$  of integers. The sum of connected subsequences of an IRB enumerate the set of integers  $[1, S]$  exactly once. This property makes IRBs useful in applications, which need to partition sets with the smallest possible number of intersections. [C1673]

#### **"77 GHz radar transceiver with dual integrated antenna elements"**

A complete radar transceiver for 77 GHz with two integrated antenna elements is presented. Based on a previously published design [1], two of the transmit and receive channels of the transceiver are supplemented

with integrated antenna elements. The antennas exhibit a well defined antenna pattern with an efficiency of better than 50%. [C1674]

#### "Particle filters for beam-space high resolution DOA estimation"

This paper addresses the application of particle filter (PF) schemes to tracking Direction-Of-Arrival (DOA) in beam-space, using a passive array of sensors with single snapshot. This proposed technique has significant ability to estimate the DOAs of multiple sources at arbitrary times throughout the observation period, and that the requirement for quasi-stationarity over a limited interval may be relaxed. According to the State-Space Model of beam-space narrowband array signals, the importance function is established. Sampling from the importance function, the algorithm estimates the bearings of sources by sequential Monte Carlo methods. Based on DOAs estimation and the observation in each snapshot, the proposed algorithm estimates the amplitudes of the sources and the variances of noise, using a maximum posteriori estimator simultaneously. Computer simulations are presented to show the performances of the algorithms. [C1675]

#### "Design of elevator audio player controlled by wireless communication"

The objective of elevator audio playing system mainly concerns the device installed in elevator to provide music, advertisement and notifications. In this paper, GPRS is utilized for mode control and wireless instruction sequence update. As the core of the whole system, STM32 Microcontroller unit can browse and manage the catalog of files in SD card. Additionally, through building-up FAT 16 File System (FS), MCU will manage sound files in player flexibly and conveniently. Thus, the device supports enables three playing modes, namely, by category, by designated order or by random order. Laboratory Experimental result proves that the designed audio playing system is of flexible and stable maneuverability. This system will bring comfortable up-and-down experience to passengers, increase efficiency of elevator management and bring gains to advertiser and elevator service provider. [C1676]

#### "Decision-making model for mobile blind compensation in jamming"

In order to solve the problem of the blind region for radar netting in jamming, based on the analysis of anti-jamming capability; this paper uses the highly mobile radar to compensate the blind region to upgrade the anti-jamming capability holistically. It defines the conception of the blind compensation gain, constructs the decision-making model and designs the genetic algorithm. The result of simulation indicates the model is effective. The model provides the decision-making evidence for mobile blind compensation and lays a foundation for reserve and application of highly mobile radars. [C1677]

#### "Research on fault monitoring for railway automatic blocking and continuous transmission lines"

The characteristics of railway automatic blocking and continuous transmission lines are studied. On this basis, a fault monitoring system is designed. Monitoring units installed on lines can detect the short fault directly (when earth fault happens, "S-injection method" is applied), and send out this information to adjacent GPRS units via Radio Frequency (RF). Then adjacent GPRS units send the data to the server. Through analyzing the gathered data, the server can locate the fault section. The test and field operation indicates that this system can identify fault section accurately and rapidly, increasing both of economic and social benefits. [C1678]

#### "Implementation of handheld remote sense image calibration system software"

This paper based on 4S(GPS, GPRS, GIS and RS technology in a integrated system) and designed a remote sense image calibration system by using a high precise GPS module which is integrated in the handheld client device. This article designed and realized a software architecture and a data storage and transfer model though the GPRS real-time network. The handheld devices based on 4S changed the poor efficiency way of the original remote sense image of the manual data acquisition, post-mapping and other operations. The efficiency of original system is also greatly enhanced by implement the digitization of external work system which is constituted on a collaborative platform within the inner work system. [C1679]

#### "An efficient nonuniform channelizer based on Adjacent Channel Merging"

An efficient nonuniform channelization method based on ACM (Adjacent Channel Merging) is proposed to extract large amount of radar signals with different band widths. The neural networks based on cosine basis functions are used to train the LP prototype filter coefficients in order to satisfy the ACM condition. Use this LP prototype filter to form windowed FFT uniform channelizer, then simply add the outputs of the adjacent channels and the nonuniform channelizer can be achieved. The proposed channelizer is simply composed of an FFT component and a few adders, so it has a smaller number of computations than DDC and TPFT channelizers. The computer

simulation results given at last shows that the proposed method also has a good channelizing performance.

[C1680]

#### "A new evidence combination method"

Considering that the Dempster rule of combination in evidence theory has disadvantages while dealing with highly conflicting evidence, a novel two-level combination method for fusing conflicting evidence is proposed in this paper. Distinguishing between highly conflicting evidence and lowly conflicting evidence, the method adopts the PCR6 rule based on DS<sub>m</sub>T in the first level of combination to solve high conflict and in the second level uses Dempster rule to keep fast convergence speed and good calculation capability, which can manage conflicting evidence with various degrees effectively and reasonably. The validity of the method proposed is demonstrated by calculation examples. [C1681]

#### "Automotive radome design-fishnet structure for 79 GHz"

Metamaterials are considered as an option for quasi-optical matching of automotive radar radomes, lowering transmission loss and minimizing reflections. This paper shows a fishnet structure design for the 79 GHz band which is suitable for this type of matching and which exhibits a negative index of refraction. The measured transmission loss is 0.9 dB at 79 GHz. A tolerance study concerning copper plating, substrate permittivity, oblique incidence, and polarization is shown. Quasi-optical measurements were done in the range of 60-90 GHz, which agree with simulated results. [C1682]

#### "Switchable power combining network for 35GHz"

Power combining networks are a key component for most radar systems. In combination with micromechanical switches the network can be used for multi-beam lens systems, filter bank etc. The main disadvantage of such a switchable power combining network are high losses. In a Doppler beam sharpening system (DBS) for 35 GHz a power combining network with Micro-Electro-Mechanical-Systems (MEMS) switches was realized. [C1683]

#### "Bistatic scattering center models for the simulation of wave propagation in automotive radar systems"

Deterministic radio channel simulations for large and complex environments at very high frequencies are a challenging task. In this paper an approach is presented in which the computational complexity is significantly reduced by using scattering center models for the most complex objects. The scattering centers are described in form of directional, bistatic scattering intensities and can be computed for the isolated complex object in advance without considering the complete environment. Thus, the simulation performance benefit is due to a significant reduction of the complexity of the geometrical representation of the scene. The parameterization of the scattering centers itself is based on an efficient high frequency asymptotic field prediction tool incorporating Geometrical Optics and other techniques. The models are designed to study deterministically the wave propagation for vehicle based radar systems operating near 80 GHz. An example for a bistatic three-dimensional parameterization is given. Furthermore, a fast Inverse Synthetic Aperture Radar (ISAR) imaging technique is applied that can be used to find the most relevant scattering center positions on the objects. [C1684]

#### "Analysis and research of proportional conflict redistribution rules in identity identification"

The research on identity identification of high conflicting evidence is a popular and difficult problem. Proportional conflict redistribution rules are a kind of effective method for dealing with high conflicting evidence. The series of proportional conflict redistribution rule (PCR1 to PCR6) are introduced and analysed in this paper. Experiments show that the six rules obtain an available conclusion which provide s reasons to the engineering application and improvement of identity identification. [C1685]

#### "Time allocation in cognitive radar for multitarget detection with dynamic programming"

The radar performs three main functions: search, tracing and weapon engagement. Each of functions occupies amount of time, energy and computation resource of the radar system. For cognitive radar, it should have the basic function which is learning. The radar needs to manage its resources dynamically and interactively between the setting of radar parameters to optimize the tasks to be carried out and perceive environment highlights the role in which knowledge and intelligence will be central in cognitive radar performance. The problem discussed here is the time allocation of cognitive radars in a multitarget environment. In this paper, we develop the optimization criterion based on the detection probabilities based on dynamic programming algorithm(DPA).

[C1686]



### **"Design and optimization of amplitude-modulated microwave backscatter transponders"**

In the current paper design rules and exemplary optimized designs for microwave backscatter transponders are presented. The overall goal of the proposed transponder design is to achieve a maximum signal to noise ratio in the radar signal of a given base-station that interrogates the transponder. To accomplish this task, it is important not only to consider the transponder modulation factor, i.e. the values of modulated/switched antenna loads, but also the resulting radar cross-section of the loaded transponder antenna. Unfortunately, both aspects are partly opposing and optimization is not straightforward. The design method presented and applied in this paper allows selecting the optimal relation between the antenna parameters and the load parameters. To prove the proposed method, exemplary designs and measurement results of 5.8 GHz backscatter transponders are shown. [C1687]

### **"Direct measurement of electron loss rate in air"**

We present direct local measurements of electron attachment and recombination rates in atmospheric air. Using a microwave scattering based resonantly enhanced multi-photon ionization scheme we monitor the electron density dynamics with nanosecond resolution. [C1688]

### **"Optimal waveform selection for software defined data acquisition system"**

This paper describes specific digital beamforming methods and prototype of the data acquisition system. Moreover, the detailed description of the beamforming and reception algorithms would explain the possible estimation criteria for given system. The modelling results and software radar prototype performance are presented. Concerning the use of spread spectrum waveforms with wideband beamforming methods, possible modes of data acquisition applications will be discussed. [C1689]

### **"Partial treatment of wind turbine blades with radar absorbing materials (RAM) for RCS reduction"**

The application of radar absorbing materials (RAM) in order to reduce the interference of wind farms with radar systems is considered as a possible mitigation solution. This paper will address the key challenges when trying to efficiently apply RAM to certain parts of the wind turbine blades to significantly reduce the scattering of radar signals. Modeling of the radar cross-section (RCS) is presented for a generic 40 meter blade wind turbine before and after applying RAM to different parts of the blade. The results of modeling possible solutions of partially RAM treated blades are compared. [C1690]

### **"Stroke detection using a broadband microwave antenna system"**

In this paper we describe a microwave based measurement setup and a signal processing algorithm for stroke detection and diagnostics. [C1691]

### **"Millimeter-wave integrated waveguide antenna arrays and beamforming networks for low-cost satellite and mobile systems"**

This paper overviews the state-of-the-art of the substrate integrated waveguide (SIW) techniques in the design and realization of innovative and low-loss millimetre-wave antenna arrays and beamforming networks for low-cost satellite and mobile systems. Novel classes of SIW-based antenna and beamforming techniques on the basis of this concept of substrate integrated circuits (SICs) are demonstrated to offer unprecedented performances and opportunities. Different structures and architectures are theoretically and experimentally studied and discussed for specific space- and ground-based applications. High-density integration and high-volume manufacturing issues are addressed. [C1692]

### **"Mutual coupling and platform effects in the synthesis of Passive Coherent Location radar array"**

Introduction and main concepts: An increasing interest in passive surveillance systems can be observed in last period. The key idea, which is also common to other non-radar applications, is to conveniently exploit opportunity signals, as analogue FM transmitters or Digital Video Broadcasters to detect and/or tracking targets [1-3]. [C1693]

### **"Vital signs monitoring with a UWB radar based on a correlation receiver"**

In the first part of this publication, vital signs detection observing small amplitude changes due to the movement of a target in front of the radar is shown. In the context of vital signs monitoring the target is the chest of human beings. This basic principle is also used in continuous wave (CW) radars, but the presented impulse-based UWB radar has moreover a range gating capability. Consequently, the target distance can be obtained and different

targets (persons) can be monitored. Several measurement results using this measurement principle for respiration and in particular for heart beat monitoring are presented and discussed. Furthermore, the shortcomings of this method are depicted. In the second part, advanced signal post-processing by deconvolution with a Wiener filter is presented, leading to an improved resolution performance for the realized UWB radar system. Promising results of this method show that small targets can be identified in a multi-target scenario. Therefore, the movement of small targets, e. g. the heart muscle within the human body, could be tracked directly. [C1694]

#### "Antenna front-end concepts of a low-cost coherent radar demonstrator for S-band application"

Some of the concepts of an AESA antenna front-end for a low-cost coherent radar system demonstrator intended for maritime applications in the S-band are presented in this contribution. Manufacturing and maintenance cost reduction with respect to present commercial systems is achieved by replacing the conventionally used magnetron RF power generation and the mechanically rotated antenna by a semiconductor transmitter and an AESA antenna with custom-developed mixed-signal integrated circuits as core components of its T/R-modules. The operation with coherent signals facilitates the application of modern signal processing techniques in order to compensate for the heavily reduced peak transmit power. [C1695]

#### "A Least-Squares Algorithm for Multipath Estimation Using an UWB-IR Link"

This paper introduces a modified complex to real amplitude least-squares (CRALS) algorithm for the estimation of dense multipath in an UWB-IR channel. The traditional CRALS is ineffective for UWB-IR signal due to its wide bandwidth and large off period. This algorithm is modified to resolve three closely spaced paths in a correlation window. One novelty of the modified algorithm is that region-based processing is used for the initial estimate in place of coordinate descent processing used in traditional algorithm, and so the long iteration due to large off period is saved. The other novelty is that the procedures are simplified because of no necessity to increase the penalty term to infinity in UWB-IR case. Its efficiency is compared to the generalized maximum-likelihood estimator (GML) by simulation in different signal to noise ratios (SNR). The reason for its efficiency improvement comes from fewer effective spectrum samples and region-based processing of correlation results. Real measurement is conducted to verify this algorithm's performance. Its estimation error of time difference of arrival (TDOA) is about 0.18ns. [C1696]

#### "Distributed Localization for Wireless Sensor Networks Using LFM Waves"

A novel distributed localization method for wireless sensor networks (WSN) is proposed in this paper. Linear frequency modulation (LFM) waves are emitted from two anchors simultaneously to create an interference field. Through the frequency measurement of local RSSI (Received Signal Strength Indication) signal, the TDoA (Time-Difference-of-Arrival) is estimated independently at each sensor to detect range difference from the sensor to the two anchors, by which the position can be determined. Furthermore, an extended method applied to mobile sensors is also presented. The proposed method only relies on radio transceivers and requires no time synchronization for sensors. Simulations results demonstrate the effectiveness of our method. [C1697]

#### "ISAR rotational motion compensation using entropy metric"

Inverse Synthetic Aperture Radar (ISAR) is an efficient tool for providing image from moving targets. When the target's maneuverability is not too serious, conventional FFT imaging algorithm is enough for providing focused image. But the target being imaged is often engaged in complicated maneuvers. So autofocusing techniques are needed. We can classify these techniques into two main categories: Parametric and nonparametric algorithms. Minimum entropy method is one of the nonparametric autofocusing methods. In this paper we present a new algorithm for autofocusing ISAR images based on entropy criterion. Simulation results show the effectiveness of the proposed algorithm. [C1698]

#### "Retrodirective array based radar (invited)"

This paper will demonstrate recent work at Queens University of Belfast as well as review the small body of literature on the new topic of Retrodirective Radar. Details are presented on the core capabilities of Retrodirective antenna arrays for near field target acquisition and pulsed far field tracking in Radar applications. [C1699]

#### "Synthetic Structural Imaging (SSI): A new ultrasound method for tracking breast cancer morphology"

A new signal interrogation concept, based on Synthetic Structural Imaging (SSI) physics, has been developed to

guide therapies. The SSI method was previously successful in radar and sonar imaging; here it is demonstrated for acoustic scattering from penetrable biological targets. Operating at ultrasonic frequencies of several hundred kilohertz, SSI trades the higher resolution of typical B-mode ultrasound imaging for a significantly stronger correlation to target shape and volume, which are among the primary tissue classifiers. Tissue phantom models were fabricated with embedded spheroidal inclusions ranging from 2.41 mm through 6.3 mm in diameter. The phantom medium was 10 wt% porcine gelatin and the inclusions were 28 wt% porcine gelatin. The inclusion dimensions were measured with calipers. The phantom was interrogated with two impulse-excited Panametrics transducers: a model V301 with a peak frequency of 0.50 MHz and a -6 dB bandwidth of 81%, and a model V314 with a peak frequency of 0.99 MHz and a -6 dB bandwidth of 77%. The backscattered RF data were digitized, recorded, and digitally bandpass-filtered. The experimental profile functions were computed. Volumes were estimated by integrating the experimental profile functions. SSI-determined volume ratios were demonstrated to be within 7% to 18% of caliper-determined volume ratios. [C1700]

### "Improving Service Availability in 3GPP Generic Access Network (GAN) by Adaptive Keep-Alive Interval (AKI)"

The Generic Access Network (GAN) developed by 3GPP extends services to unlicensed spectrum. A mobile station with multiple air interfaces can access 3GPP services through GAN and roam seamlessly between different radio access networks. However, resource management is a critical issue in GAN. To allocate GAN resources efficiently, we propose Adaptive Keep-alive Interval (AKI). By using AKI, an MS can send less signaling messages. In addition, AKI can increase system utilization by releasing unused resources. The proposed AKI is evaluated by extensive simulations. The results show that the proposed AKI can reduce signaling overhead and increase GAN utilization significantly. [C1701]

### "A Traffic Information Service-Broadcast model for mixed-equipage Aircraft Simulation"

The use of new Air Traffic Management (ATM) concepts built upon the capabilities afforded by the Automatic Dependent Surveillance-Broadcast (ADS-B) system in NextGen airspace aims to provide substantial improvements in system capacity and throughput without compromising safety relative to today's ground-directed ATM based on Secondary Surveillance Radar (SSR). These concepts rely on airborne based surveillance and include the use of airborne systems and procedures to perform traffic monitoring, self-separation, and merging and spacing. The Traffic Information Service-Broadcast (TIS-B) system is intended to provide the crucial bridge for ADS-B aircraft to employ some of these concepts during the transition phase. Although TIS-B surveillance is not expected to be of the same quality as ADS-B surveillance, it still provides aircraft state and velocity information required so that airborne systems can provide airborne separation assistance/assurance and airborne spacing capabilities (with increased separation margins). While simulation studies of these NextGen concepts in the end-state system are already underway, additional simulation models will be needed to represent the intermediate state system where not all aircraft will be equipped with ADS-B. The suitability of new ATM concepts for use in the transitional NextGen airspace with mixed equipage (Mode C, Mode S, and Mode S Extended Squitter (ES)) aircraft can be studied using simulation tools such as NASA Langley's Airspace and Traffic Operations Simulation (ATOS) enhanced with the TIS-B model described in this paper. ATOS is a distributed, Human in the Loop (HITL) simulation consisting of multiple, mid-fidelity, desktop cockpit simulators called ASTOR (Aircraft Simulation for Traffic Operations Research). This paper describes the RTCA standards-based design of the TIS-B model developed for use in ATOS. This model consists of ground and aircraft subsystems with a focus on the models of TIS-B system functional elements such as Ground Surveillance Processing (GSP), TIS-B Target Report Distribution Function (DF), Ground Link Specific Processing (GLSP), Airborne Link Specific Processing (ALSP), and Target Tracking and Report Assembly (RA). The modeling of SSR data processing functions in the GSP, including position and altitude measurement, state estimation, radar tracking, and computation of Navigation Accuracy Category (NAC) and Navigation Integrity Category (NIC) of aircraft position is discussed at length. This paper also describes how Target reports are extrapolated (to account for data latency), generated, and distributed by the DF model. A Ground Based Transceiver (GBT) model implements the GLSP functions that include generation of TIS-B messages and suppression of TIS-B messages corresponding to aircraft producing ADS-B signals being received by the GBT. Modeling of the reception of ADS-B transmissions by the GBT is included using the ADS-B reception model developed for ASTOR air-to-air reception modeling. Finally, this paper describes the modeling of the ALSP and RA functions within the ASTOR. The paper also presents and discusses the preliminary model validation test results obtained from the simulation by comparing truth and TIS-B message derived track data and provides insights into how the TIS-B model can be used to support NextGen concept studies. [C1702]

### "Angle-resolved thz time domain reflection spectroscopy of rough surfaces"

The use of a fiber-coupled terahertz TDS system offers new possibilities for angle-resolved reflection

spectroscopy. We put the focus especially on angle-resolved scattering from roughened surfaces of both dielectric and metallic surfaces. [C1703]

#### "THz fiber-based swept-source imaging radar"

We demonstrate an all-THz fiber-based swept-source imaging radar system. Our experiment shows that this radar can be used in real time to nondestructively detect and locate the concealed living objects with high stability and sensitivity. [C1704]

#### "Automatic recognition of diverse 3-D objects and analysis of large urban scenes using ground and aerial LIDAR sensors"

We describe a learning-based 3D object recognition pipeline developed under the DARPA URGENT program for analyzing a large LIDAR dataset collected by both airborne and ground platforms for an extended urban area. Our approach utilizes a novel strip-based cueing approach that incorporates the properties and context of urban objects. Strip-based cueing segments potential objects and assigns them to appropriate classification stages. Our learning-based recognition pipeline successfully recognized 17 3D object classes in LIDAR data collected in and over Ottawa, Canada with high efficiency and average accuracy of 70%. [C1705]

#### "3D optical Yagi-Uda nanoantenna array"

We fabricated three-dimensional arrays of optical Yagi-Uda nano-antennas. Due to the high directivity of the array structure the incoming light is received efficiently at the resonant wavelength in the near-infrared (around  $\lambda = 1.3 \mu\text{m}$ ). [C1706]

#### "Linearization of ultra-broadband optical chirps for precision length metrology"

We demonstrate precise active linearization of ultra-broadband ( $>5 \text{ THz}$ ) laser frequency sweeps using a self-heterodyne technique. Frequency errors less than 170 kHz relative to linearity were observed enabling very high resolution ranging over large distances. [C1707]

#### "90ps tunable true-time delay line based on photonic crystals"

A photonic crystal waveguide delay line is reported with 90ps of tunable delay over a 20GHz bandwidth. This corresponds to a maximum phase shift of  $600^\circ$ . The true-time delay characteristics are evidenced using a vector network analyzer. [C1708]

#### "High pulse-energy atmospheric aerosol lidar at 1.5-microns wavelength: Opportunities for innovation from a meteorologist's perspective"

Laser and optical engineering challenges and recent progress in the area of high pulse-energy direct-detection atmospheric lidar near 1.5 microns wavelength are described. [C1709]

#### "On Time Varying Channel Estimation Using Sparse Models"

We consider the design of sufficiently informative inputs for estimating the parameters of a time-varying linear system. Specifically, we assume the output of the system may be modeled as linear combinations of known time-varying elements whose parameters are points in an appropriately chosen grid for the parameter space, such that these parameters are sparse in comparison with the grid size. The sufficiently informative inputs we study are signals that guarantee a unique sparsest solution thereby satisfying minimum requirements for numerically solving the estimation problem. Since in practice the parameters of interest may not lie on the grid constructed for the parameter space, we discuss how our input designs can be modified to provide robustness in the presence of modeling error and noise. [C1710]

#### "SiGe BiCMOS Chip Sets for Use in an X-Band Multi-function Chip"

SiGe Radio Frequency Integrated Circuits have been designed and fabricated for use in the X-band Si-based multi-function chip, which is known as a core-chip for a Transmit/Receive module of a phased array radar systems. In this paper, six kinds of Radio Frequency Integrated Circuits will be presented such as a power amplifier, a digital serial-to-parallel converter, a Single-Pole-Double-Throw switch, an 8 dB attenuator, a 16 dB attenuator, and a 45 degree phase shifter. The power amplifier based on a cascode configuration using SiGe HBTs shows the Radio Frequency performance of the 12 dB gain and 19 dBm P1dB. The other five chips have been designed using 0.25  $\mu\text{m}$  Complementary Metal-Oxide Semiconductor technology. The digital serial-to-



parallel converter shows the perfect functional operation to 20 MHz clock. The Single-Pole-Double-Throw switch, the 8 dB and 16 dB attenuations, and the 45 degree phase shifter show good Radio Frequency performances. The most of chip sizes are very small to be lower than 1 mm<sup>2</sup>. These chip sets may make an attractive solution for a high power X-band multi-function chip for a T/R module of a phased array radar system. [C1711]

### "A Novel Homogeneous Mesh Grouping Scheme for Broadcast Cognitive Pilot Channel in Cognitive Wireless Networks"

With the irreversible trend of the convergence and cooperation among heterogeneous wireless networks, the need for network information awareness of user equipments (UEs) becomes increasingly imperative in the Cognitive Wireless Networks (CWN). As one of the candidate solutions for network information delivery for UEs, the Cognitive Pilot Channel (CPC) concept has been brought forward recently, providing UEs with the necessary network information for network selection by using the public signaling channel. Besides, both broadcast and on-demand CPC modes have been proposed for the network information delivery under the assumption that the geographical region is divided into meshes. In this paper, a novel homogeneous mesh grouping (HoMGP) scheme based broadcast CPC mode is designed to improve the efficiency of broadcast CPC mode in the CWN. The homogeneous meshes are selected and grouped based on the frequency occupancy graph, which is obtained by using the image processing techniques. By grouping the homogeneous meshes together, both the frame format and flow of the HoMGP broadcast CPC mode are designed to deliver heterogeneous network information to the UEs efficiently, which is verified by numerous simulation results. [C1712]

### "Quantum Cascade laser for elastic-backscattering LIDAR measurement"

We present an experimental demonstration for an elastic-backscattering LIDAR system measurement using a Quantum Cascade laser (QCL). The laser emits a peak power of above 13W at 80K and with a wavelength of 4.5μm. [C1713]

### "Lifetime Maximization of UWB-Based Sensor Networks for Event Detection Applications"

Ultra wideband (UWB) technology is well suited for communication in wireless sensor networks, in which low power consumption for data transmission and the availability of precise ranging information are highly desirable. In this paper, we consider the application of UWB in an event-detection sensor network, and we are interested in maximizing the network operational lifetime while satisfying requirements on the detection and false alarm probabilities. Towards the goal of lifetime maximization we (i) jointly find the optimal routes from multiple events to the sink, to avoid the bottleneck-node phenomenon which often limits lifetime, and (ii) allow adjustment of the data rate that each sensor generates to contribute to event detection, in order to balance the energy consumption among the nodes in the network. Using the UWB signal characteristics, we present a convex optimization model to solve the lifetime maximization problem. The numerical results show that the proposed framework leads to significant improvements in network operational lifetime compared to benchmark approaches. [C1714]

### "Performance of Downlink Schedulers with Superposed or Orthogonal Transmissions"

This work looks into the extension of the proportional fair (PF) scheduler to the multi-user case, where the source is transmitting several messages under the superposition coding (SC) strategy in a Gaussian Broadcast channel. Jointly with the weighted sum-rate (WSR) scheduling criterion, we derive guidelines for 2-user pairing, based both on SNR and user priority. We compare superposition coding access with frequency division multiple access, while time division is obtained naturally as a result of the user pairing. Results elucidate that the 2-user SC PF always improves the single-user PF in terms of average throughput and delay reduction, and we compare its performance with the 3-user SC PF. Finally, the WSR shows throughput gains similar to the 2-user SC PF for certain configuration of the scheduler. [C1715]

### "A target polarization recognition method for radar echoes"

This paper distinguishes ship target from chaff by their difference in depolarization characteristics using fully polarized dual-channel radar which transmits vertical and horizontal polarization wave alternately and receives co-polarization and cross-polarization components simultaneously with two channels. It recognize the target by taking advantage of the difference of the vertical and horizontal depolarization characteristic parameters of the target and chaff in radar echoes, after enlarging the difference between the cross-polarization component and co-polarization component of the radar echoes involving both target and chaff. furthermore, non-linear polarization transformation is adopted to increase the chaff and targets separability and to improve the recognition rate in result. In the end, the recognition result is proved to be more desirable by processing information in polarization domain than in time and frequency domain. [C1716]



### "A novel analytical method and error criterion of the synthetic range profile"

In this paper, a novel method to analyze the distortion of a synthetic range profile (SRP) is put forward, which is simpler and more effective, and more importantly it can be available for the present existing any synthetic wideband waveform (SWW) forms. At the same time, since the traditional error criterion of the SRP for the stepped frequency waveform (SFW) is the quadratic phase error criterion, which has some inherent faults for any synthetic wideband waveforms, a modified error criterion is proposed to overcome such shortcomings. Specific conclusions are investigated with some simulations. [C1717]

### "Research of LTCC millimeter-wave T/R module"

Low-Temperature Co-fired Ceramic (LTCC) technology is one type of Co-fired ceramic multi-chip module (MCM-C), which is a high-integration and multilayer- printed packaging technology. In this paper, a millimeter-wave T/R module was presented with a very compact module size of 55 $\times$ 13 $\times$ 10mm<sup>3</sup> and an extremely low weight of only 31 grams by this technology, its output power was greater than 30dBm. Besides, the optimum EMC design and technology of embedded passive components were used. [C1718]

### "Radar anti-jamming application of solid-state noise source"

Jamming reconnaissance receiver (JRR) is an important anti-jamming equipment of radar. In this paper, we propose a compensation method based on solid-state noise source to against the performance degradation of JRR caused by long-term aging, which can compensate all channels simultaneous and accomplish by JRR itself. First, presented the structure of JRR, analyzed the principle and structure of solid-state noise source. To reduce the influence of ambient temperature on compensation performance, then we given and compared two solutions: constant temperature mode and table lookup mode. At last, advanced a method using attenuator to simulate the influence of long-term aging, and carried on a contrast test. The test results show that, the aging process has no effect on the performance of JRR after the compensation based on solid-state noise source, the long-term stability of JRR has been improved greatly. [C1719]

### "Design of velocity radar for railway"

The main velocity-measuring methods for train are analyzed and the relative merits of these methods are given. Through the analysis, Doppler radar for train's velocity measurement stands out for its distinctive features. The design plan for velocity radar's key components was introduced, and a pre-industrial prototype was finished. Finally, the test results verified the radar's high performance. [C1720]

### "Optimum design of jamming reconnaissance receiver"

This paper presents a channelized jamming reconnaissance receiver, and analyzed false response, amplitude response and temperature drift, which influence the performance of channelized receiver. For the sake of interchangeableness, we divided the receiver into RF assembly and IF assembly, then compensated each assembly independently and estimated system error. At last, we tested the receiver under assemblies (spare parts) interchanged situations at different temperatures. The results show that both absolute and relative accuracy reach  $\pm 2$  dB. The purpose of cutting down spare parts and improving maintainability, supportability, reliability has been achieved. [C1721]

### "An approach research to segmentation of the SAR image based on the Markov random field"

Markov random field method is a very active research field in image segmentation. In this paper, a new approach to the segmentation of SAR target chip image based on the Markov random field (MRF) and Maximum a Posteriori (MAP) rule is proposed. By statistical analysis of the different regions in the SAR target chip image, the valid segmentation algorithm for choosing the iteration initial value is obtained. Compared with other segmentation algorithms such as Simulate Annealing algorithm and the Iterative Conditional Model (ICM) algorithm by the synthetic image and operational SAR image, the proposed approach in the paper can accelerate the convergence speed, reduce the iterative numbers and improve the segmentation speed. [C1722]

### "A method of over cosec square-beam shaping with sharp cut off"

Cosec square beam have receiving uniform echo performance at the same height but different distances. The level exceeds that of traditional cosec square beam. In order to restrain interfere of multipath reflect, the beam must be cut sharply on the ground. Through setting appropriate fitness functions and choosing optimal optimization algorithm, a method of over cosec square-beam shaping with sharp cut off is presented in this

paper, which can obtain result that satisfies the designed requirements of engineer. [C1723]

#### "Analysis on the refraction stealth characteristic of cylinder plasma envelopes"

The refraction stealth characteristic of two dimensional cylinder plasma envelopes is studied. Firstly, an electromagnetic (EM) problem model of EM-wave propagating through cylinder plasma envelopes is set up. Then EW-wave traces equation in cylinder plasma is derived and a novel concept of plasma refraction deviation angle is presented out. Furthermore, the relation between refraction deviation angle and incidence angle of EM-wave is yielded and the relation between refraction deviation angle and plasma density distribution is made out as well. It is shown that cylinder plasma envelopes could make distinct refraction stealth. [C1724]

#### "PMCHW-AMCBFM for analysis of electromagnetic scattering by 3-D homogenous dielectric objects"

In this article, we present a novel approach based on PMCHW integral equation formulation in conjunction with the adaptively modified characteristic basis function method (AMCBFM) to solve the scattering from homogenous dielectric bodies. In the new method, equivalent electric and magnetic currents on the surface of object are needed and expanded using RWG basis functions. AMCBFM is subsequently used into the former matrix equation. The studied object is partitioned into distinct blocks with some overlapped-domains between neighboring ones. The matrix equation is solved by direct solution instead of iterative methods. The compatibility, accuracy and efficiency of this novel approach are demonstrated by a variety of scattering problems. [C1725]

#### "Analysis of ELF attenuation rate using the geodesic FDTD algorithm"

This paper is analyzed the attenuation rate of extremely low frequency (ELF) electromagnetic waves propagating in the Earth-ionosphere system, using the geodesic FDTD model. In the simulation both the classical two-exponential model and the "Knee" model of ionosphere are used. The resulting difference among using different algorithm are also explained. [C1726]

#### "Anisotropic scattering for a magnetized cold plasma sphere"

The transformation of parameter tensors for anisotropic medium in different coordinate systems is derived. The electric field for a magnetized cold plasma sphere and the general expression of scattering field from anisotropic target are obtained. The functional relations of differential scattering cross section and the RCS for the magnetized plasma sphere are presented. Simulation results are in agree with that in the literatures, which shows the method used and results obtained are correct and the results provide a theoretical base for anisotropic target identification etc. [C1727]

#### "Performance analysis for angle measurement of monopulse radar with non-consistent amplitude-phase features"

Monopulse radar is widely used for its high angle measurement and great anti-interference performance. In this paper, a classical signal processing method of sum and difference patterns for anti-symmetrical monopulse radar using digital beam forming (DBF) technique is proposed. Effects on angle measurement performance caused by amplitude-phase non-consistency are analyzed and its corresponding simulation results are verified. These results can be used in practical engineering implementation. Furthermore, the method proposed in this paper can also be applied in other tracking radar systems which include DBF. [C1728]

#### "Engineering design of the rain mode on an ocean-dedicating radar altimeter"

Satellite radar altimeters are fundamental tools in microwave remote sensing, but traditionally they were regarded as unsuitable for rain measurement. This paper designs a rain mode on an ocean-dedicating altimeter, taking China's forthcoming HY-2 ALT as a typical example. In rain mode the altimeter receives the surface and rain echoes simultaneously, so it can estimate the rain layer structure without losing surface topography information. The variable system parameters are designed to fulfill the task with very low hardware expenses. Some key issues are discussed in detail. To achieve the compatibility of measuring both surface and rain, an adaptive digital i/q demodulator is proposed, and receiver weighting is implemented to suppress the side-lobes. Constrained by echo power, altimeter can detect rains heavier than 6 mm/hr. [C1729]

#### "GaN technology for microwave and millimeter wave applications"

After many years of development to improve the material and devices, GaN technology is now in production and poised to revolutionize many of today's Radar and Communication systems. In this paper we present an

overview of GaN development, focusing on reliability, affordability, and defense applications. [C1730]

### "Special session in honor Dr. Kiyo Tomiyasu"

This session is dedicated to the career of Dr. Kiyo Tomiyasu. His career includes technical accomplishments in microwaves, lasers, and remote sensing of the earth using satellite-borne radiometers, scatterometers, and synthetic radars. He has contributed much to MTT-S, and to IEEE, including awards and contributions to the IEEE Foundation. This special session will include invited speakers to recall activities associated with Dr. Tomiyasu, his contributions to the MTT-S AdCom and his technical accomplishments as witnessed by the speakers. Dr. Tomiyasu will receive the Thomas Alva Edison Medal at the IMS 2010 Plenary Session. This special session in honor of Dr. Kiyo Tomiyasu will be recorded and CD-ROMs made available to the session attendees. [C1731]

### "Improving estimation algorithms based on field data for a hybrid energy system"

The production of green energy is a topic of great importance nowadays and of wide interest throughout the world. The system described in this paper allows an in-depth evaluation of the energetic efficiency of the green power solution proposed to power a remote location. Our goal is to study the difference between the values proposed with the aid of theoretical algorithms for energy production estimation and the field data. By studying this differences new solutions can be proposed to optimize the algorithms. [C1732]

### "The SAR/GMTI airborne radar PAMIR: Technology and performance"

PAMIR, a multifunctional SAR/GMTI imaging radar, combines the tremendous research potential of an experimental active broadband phased array system with the wide area of imaging procedures of mono- and bistatic systems. With its two different reconfigurable antenna frontend configurations operating a very high simultaneous bandwidth of 1.8 GHz in X-band, a variety of controversial requirements can be investigated and experimentally explored. The broadband beamforming together with azimuth wide scan capabilities ( $\geq \pm 45^\circ$  @ 1.8 GHz bandwidth of the antenna aperture) requires a switchable true time delay network with time increments equivalent to a fraction of a wavelength. The subarray structure including its time delay components are described. PAMIR serves as an ideal airborne platform for broadband SAR/GMTI research activities including interferometric image formation. [C1733]

### "Development of a multi-frequency airborne radar instrumentation package for ice sheet mapping and imaging"

We have developed improved versions of three different radar systems and integrated them as an airborne instrumentation suite for sounding and imaging Polar ice sheets. The first instrument consists of a multi-channel, coherent, pulsed radar operating at VHF with up to 20 MHz bandwidth. This instrument is capable of sounding a few-kilometer thick ice while flying at altitudes up to 10 km above mean sea level. The second instrument is designed to operate at UHF using a burst of narrow-bandwidth signals to digitally synthesize a bandwidth of in excess of 300 MHz. This apparatus is used to measure internal layers of the ice sheet to a depth close to 100 m. The third component to the instrumentation package is based on a frequency-modulated continuous wave (FMCW) radar, which operates at microwave (Ku band) frequencies with up to 1 GHz of instantaneous bandwidth. This radar set is used to measure the ice sheet surface elevation profile with centimeter accuracy. We are presenting a description of each system, with emphasis on the VHF depth sounder. We also present sample field test results obtained during the 2009 austral summer season in Antarctica, as a validation of the performance of the instrument package. [C1734]

### "High-phase-resolution 77-GHz-band radar module for near-field millimeter-wave imaging"

Near-field millimeter-wave (MMW) imaging is a unique approach for inspecting cracks in covered concrete surfaces to assess the deterioration of concrete structures. We have developed a 77-GHz-band radar module with in-phase and quadrature detection which is superior to measuring both of the amplitude and phase of MMW in a near-field range. A monostatic radar system is hybrid integrated into the module with a constant-width antipodal tapered slot antenna with an antenna gain of 14.5 dBi which is connected to a microstrip-line coupler with an isolation of higher than 26 dB using a leakage cancellation technique. In distance measurements in free space, the phase resolution is less than 8 degrees corresponding to the distance resolution of smaller than 0.01 mm, which is high enough to distinguish MMW signals scattered by the cracks from multiple reflection of the concrete surfaces and inside aggregates. [C1735]

### "Laser and vision based map building techniques for mobile robot navigation"

We presents some preliminary results of the ongoing research with the final goal of building an autonomous mobile robot. To achieve this scope the mapping problem is an ineluctable one. This paper presents a visual mapping system which detects the same Speeded Up Robust Features (SURF) on the stereo pair images in order to obtain three dimensional point clouds at every robot location. The algorithm tracks the displacement of the identical features viewed from different positions to get back the robots positions. The Iterative Closest Point (ICP) algorithm is used to register the obtained landmarks in the feature based map of the entire environment. Also a mapping algorithm based on the laser system is presented which can detect the dynamic objects that are present in the robots field. The results of an indoor office environment experiments are shown. [C1736]

#### "Space Registration Algorithm Based on Constrictive Total Least Squares"

The precision of space registration is generally low with the situation of a big random error in radar network. In the case of neglecting model linearization errors, this shortcoming is due to the fact that the coefficient matrix of measurement equation exists errors. This paper presents the constrictive total least squares algorithm based on the Earth-centered Earth-fixed (ECEF) coordinates, which exploits the correlation among coefficient matrix errors. Simulation results show that the method has higher registration accuracy and faster convergence speed, compared with least squares and generalized least squares algorithm. [C1737]

#### "A Parameter Estimation Method for Moving Target in Stepped Frequency Radar"

The impact of moving target on the one-dimensional coherent imaging in stepped radar is analyzed in this paper. A cross-correlation-based estimation method of radial velocity is proposed. It is proven by analytical derivation that the cross-correlation analysis on adjacent pulses yields the quantity related to the radial acceleration and velocity of moving target, based on which the radial motion parameters of targets can be precisely estimated. The simulation results demonstrate that this approach can estimate the radial acceleration and velocity with high precision at high signal-to-noise ratio, and compensate for the raw data effectively. As a result, good high-resolution one-dimensional image could be gotten. [C1738]

#### "Adaptive Threshold for Fast Signal Detection in Multi-target Tracking"

An adaptive threshold algorithm is used for frequency-shift keying (FSK) demodulation in multi-targets and radar communication system. The special algorithm is needed because of the radar burst signal in this system. The selection of the threshold is generally a tradeoff between the goals of maximizing the probability of detection while minimizing false alarm. It replies radar pulse immediately without carrier synchronization, so the threshold is calculated by the priori knowledge of the signal amplitudes. CIC filter can save resource and is used after first down-conversion, but its performance of detection is not as good as FIR filter. Simulation results show that the adaptive threshold algorithm can reduce the probabilities of miss detection and false alarm. [C1739]

#### "Visible-infrared fusion in the frame of an obstacle recognition system"

In this article we propose different fusion schemes using information provided by visible and infrared images for road obstacle SVM-based classification. Three approaches for the fusion of VIS and IR information are presented. The early fusion yields a feature vector integrating at the feature level both visual and infrared information. The obtained bimodal feature vector is used as input to an SVM-based classification scheme. The intermediate fusion, which is performed at the kernel level combines different simple kernels of the SVM classifier in order to obtain a multiple kernel (MK). The late fusion combines matching scores of individual obstacle recognition modules in order to improve the system's final decision. In this late fusion case two methods have been considered to calculate the optimum weighting parameter: an Adaptive Fusion of Scores (AFScores) and a non-Adaptive Fusion of Scores (nAFScores). Comparative results showed that fusion-based obstacle recognition systems outperform monomodal visual and infrared obstacle recognizers. An important advantage of these fusion-based systems is their possibility to adapt to the environmental illumination conditions due to the weighting parameter which can contribute to the adjustments of the system's final decision. [C1740]

#### "Application of Kalman filtering to acoustic sound diagnostic measurement"

Application of Kalman filtering theory to data processing is a well-known. Many books and articles is devoted to radar targets tracking, as classic example we introduce, as a book more different applications can by introduced. The development theory and practice continues and we would like present one possible new application. The paper deals with problems of Kalman filter application to acoustic sound diagnostic measurement. The approaches are aimed to measurement data processing. There are results of application to the real acoustic signals of car engine are presented. [C1741]



### "The possibilities of utilization of mobile pulsed radar sensors"

The risk of collision between birds and aircrafts has been known since the time when birds and aircrafts started to occupy the same airspace. The majority of bird strikes today occur at or around airports. The paper analyses a possibility of bird and other object detection in airfields using pulsed radar sensor. The paper deals with the possibilities of utilisation of mobile pulsed radar sensor. There are analyzed possibilities of small object detection by pulsed radar sensor. The results of detection possibilities of small objects and real raw digitized radar data are presented. In the paper there are derived formulas for probability of object detection focusing on small objects. There are presented some results of radar cross section analyses. The paper presents some results achieved in the project of applied research. [C1742]

### "Design of an X-band high power solid state power amplifier based on GaN HEMT"

Based on GaN HEMT's high output power, low power loss and efficient heat dissipation, an X-band, 50W solid state power amplifier is designed. Slotted-waveguide directional coupler is designed as a 2-way power divider/combiner. At last, the output power, 165W, is combined through three power combiners by four 50W solid state power amplifiers. [C1743]

### "Design and analysis of double negative binary diffractive lens"

For a compact millimeter wave imaging system it is very important to design every component into small size, for the components in a millimeter wave system are usually much larger than those in an optical imaging system due to relatively long wave lengths. In this paper, we suggest a kind of binary diffractive lens (BDL) designed using double negative materials (DNG) as the objective lens for a millimeter wave imaging system. The DNG-BDL has not only the advantage of low profile but also small f number, which will be benefit for constructing a compact millimeter wave imaging system. Several DNG-BDL are designed and analyzed using the FDTD method. The numerical results of the focal plane field of the DNG-BDL are presented, which show that the DNG-BDL with small f number has relatively better focusing characteristic than that of a double positive BDL with same f number. [C1744]

### "Quasi-optical duplexer in 220GHz"

Recently, system designers have looked toward the higher frequency, shorter wavelength (to THz), consequently the device requires smaller and more precision. Many methods in microwave band are not feasible to THz. This paper describes a duplexer (Its main components is polarizing beam splitter and polarization converter.) works in the radar system set-up at 220GHz. After simulations, the exact model size is confirmed and the calculated data show a good result. These components have an advantage is easy to machining. At last, the main components have been fabricated and tested. And the experiment results show the feasible of this duplexer. [C1745]

### "Bistatic Synthetic Aperture Radar imagery simulation of sea surface"

A bistatic Synthetic Aperture Radar (Bis-SAR) imagery simulation of an extended sea surface is presented which is based on a facet scattering model. A semi-deterministic approach is developed to calculate high frequency bistatic raw data from the model of large sea surface. An effective method of modified nonlinear chirp scaling (NLCS) algorithm is presented to handle a general case of bistatic raw data and generate the simulation imagery of sea surface. This algorithm solves the inefficient problem for some time-domain algorithms and extends the limited number of bistatic cases to general for some frequency-domain methods. The concrete models and imagery results are illustrated. [C1746]

### "Millimeter-wave integrated waveguide power dividers for power combiner and phased array applications"

In this paper, we will propose integrated power dividing/ combining networks for power combiner and phased array applications. The design procedures for a Ka-band 4-port power combining network will be presented, together with the simulated and tested results. It has a total insertion loss lower than 0.25dB and phase difference less than  $\pm 3^\circ$  in a relative bandwidth of 4% around center frequency of 35.8GHz. The isolation between any two output ports is better than 20dB. The design and tested results for a 10-port 2-layer power combining network will also be included. Finally, we will propose a 200W Ka-band power combiner based on the integrated waveguide networks. [C1747]

### "A design of stripline-coaxial vertical transition with ultra-broadband"

A vertical transition of stripline-coaxial is presented in this paper. The discontinuousness between the stripline

and coax is decreased by increasing the diameter of the coaxial inner conductor and changing the width of the stripline at the connecting location. The simulation results indicate the vswr and insertion loss are below 1.1 and 0.1dB from 1 GHz to 18 GHz, respectively. A prototype 4 ways power divider is also developed with the proposed vertical transition, whose measured vswr is below 1.3 with 40% bandwidth. And the measured insertion loss is less than 0.5 dB. The whole performance is equivalent to the horizontal transition, even better in a certain band. The rationality and practicability of this design are confirmed. [C1748]

#### **"Intermediate frequency circuit design for a 60GHz LFM CW radar"**

This paper describes an intermediate frequency (IF) circuit design in a 60 GHz linear frequency-modulated continuous-wave (LFMCW) radar system. The IF circuit includes a preamplifier stage, an auto-gain amplifier stage and an analog-to-digital (ADC) stage. Totally the IF circuit has a gain of more than 120 dB, which helps the system to have the ability of detecting target with distance of 150 m. The details of the IF circuit design are presented and the experimental results of the whole radar prototyping system are given. [C1749]

#### **"Predesign of the wind field measuring radar for FengYun-3E meteorological satellite"**

Spaceborne microwave scatterometers have successfully provided global ocean surface wind field for two decades. Ocean wind data have become as a critical tool utilized daily by operational weather forecast and warming centers around the world. However current scatterometers still can not satisfy the requirement of achieve ocean wind vectors in nearly all weather and all wind conditions. The wind field measuring radar (WIFIR) onboard Chinese FengYun-3E meteorological satellite is being developed to attempt to overcome their shortcomings. This paper describes the predesign of the WIFIR, including the mission requirements, system design, and performance analysis. [C1750]

#### **"Fast two-dimensional imaging of scattering centers using the nonuniform FFT"**

Radar imaging of target scattering centers can be of great diagnostic utility. Conventionally, the radar image has been produced by a technique widely used in computer-aided tomography (CAT), e.g. the filtered backprojection (FBP) algorithm. FBP reconstruction produces high quality images by handling the measured data directly in polar format. However, the FBP algorithm is more computationally complex than the direct Fourier methods. This paper develops fast two-dimensional (2-D) imaging of scattering centers using a nonuniform fast Fourier transform (NUFFT) algorithm. The proposed method is first compared to the conventional FBP approach on simulated data and then applied to real data sets measured on the RCS test range. Results suggest that the NUFFT method can produce more precise images and requires much less computational time than the FBP algorithm. [C1751]

#### **"An efficient technique for extracting singularity arising in RCS computation of cylindrical antenna"**

Analysis of electromagnetic scattering characteristics from wire antennas using method of moments has been performed over the past decades. In this paper, an efficient technique is adopted to evaluate the potential and reaction integrals arising in radar cross section (RCS) computation of cylindrical antenna by method of moments. The singularity of potential and reaction integrals is extracted through the semi-analytical method. The induced current on the surface and RCS of cylindrical antenna are calculated. Numerical examples are presented to illustrate the computational accuracy and efficiency of the proposed technique. [C1752]

#### **"Scattering-based I/Q signal simulation of sea clutter returns"**

A fast Slope Summation Facet Model (SSFM) that derived from the original Bass and Fuks' two scale model (BFTSM) is proposed to describe the sea scattering including both the coherent and diffused incoherent features. This kind of facet implement can readily change the average line budget of sea return locally corresponding to the facet returns, so that it can be used to find the amplitude of each scatterer. Moreover, with the help of the approximate phase extraction procedure, the coherent radar sea clutter could be readily obtained, which easily leads to the final realization on the modeling of the radar return data of I/Q signal. [C1753]

#### **"The requirement of range sidelobe for dual-frequency precipitation radar on FengYun-3 precipitation measurement satellite"**

Pulse compression as one of the key technologies for the dual-frequency precipitation radar (DPR), which will be installed on Chinese FengYun-3 (FY3) Precipitation Measurement Satellite, is being studied. Since the backscattered echo of the sea surface is much stronger than the rain echo, the surface clutter can also contaminate the rain echo through the range sidelobe. In this paper, the model of surface clutter interference with the FY3 DPR is built, and the formulations of computing sea clutter with considering the effect of range

weighting function are deduced. Based on the analysis of sea clutter, the requirements for range sidelobe level of the FY3 DPR are proposed. [C1754]

#### "A broad-band analog phase shifter design on I-Q vector modulator"

Phase shifter is widely applied in some area, including communication and radar. In the study, the principle of broadband analog phase shifter on I-Q modulating is introduced, which is validated by the theory design using Ansoft serenade. The microwave phase shifter on I-Q modulating broadband is simulated and the corresponding entity is designed. Finally, some test are done to the phase shifter, and we sum up the design experience, all those can provide some design experience with the engineers. [C1755]

#### "Research on the one-dimensional randomly gradient index coating"

The randomly gradient index coating could create diffuse reflections in front of conducting objects, which is beneficial to suppressing their scattering main lobes. In this paper, we have made some preliminary investigations on the influence of geometry parameters and distribution mode of index gradient on the scattering characteristic and diffuse reflection performance of the randomly gradient index coating. [C1756]

#### "A novel wide beam UWB antenna design for Through-the-Wall radar"

This paper presents a novel wide beam UWB antennae design for Impulse Radio-Ultra Wide Band (IR-UWB) Through-the-Wall detection radar. The design is based on a typical bowtie slot antenna structure with an added reflector in order to achieve unidirectionality and wide beam. The effects of different parameters of the added reflector on the impedance and radiation characteristics are analyzed. The different structural parameters of antenna are optimized by numerical simulations. Simulated and measured results show that the front-to-back ratio is great than 10 dB and the beam width is approximately  $120^\circ \sim 145^\circ$  within operation band for  $|S_{11}| < -10\text{dB}$  (0.8GHz~2.3GHz). [C1757]

#### "A new hybrid-frequency radar system based on compressed sensing theory"

Inspired by compressed sensing theory, a novel radar system, called hybrid-frequency radar is proposed. It transmits multiple carrier-frequency modulated by random amplitude in each pulse, and can use much fewer pulses than that of stepped-frequency radar to achieve the same non-ambiguous range interval while the target is sparse spatially. [C1758]

#### "Angle estimation for two unresolved Swerling I targets in monopulse radar"

Most methods of angular estimation for unresolved targets are based on Swerling II targets model. These methods rely upon the use of pulse-to-pulse frequency agility. In this paper we consider the case that the fluctuation of targets observed are slow, research how the RCS fluctuation of targets affects monopulse radar system and then we address a method of resolving two unresolved targets based on the statistical feature of monopulse angular estimation for slow fluctuation targets. The result of simulation demonstrates that this method is effective. [C1759]

#### "Oblique projection polarization filtering and its performance in High Frequency Surface Wave Radar"

A novel polarization filtering method based on the oblique projection operator is proposed to improve the target detection performance for High Frequency Surface Wave Radar (HFSWR) system in this paper. The performance of the proposed oblique projection polarization filter (OPPF) is detailedly analyzed in presence of additive Gaussian white noise and the desired signal's Mean Square Error (MSE) with the estimation error of the interference polarization parameter is discussed in detail. Numerical simulation results show that the proposed OPPF can enhance the target while mitigate the interference perfectly. [C1760]

#### "Design variations of HVVFET™ transistors for high-efficiency class-AB L-band power amplifiers"

HVVFET™, with its proven RF performances, such as high power gain, high peak power density and superior ruggedness, represents a major step forward in realizing compact high-power modules for ground-based and airborne radars. In this paper, the dependence of the HVVFET's RF performances on process-related parameters-including Si epilayer thickness and top-surface gold-bump thickness (Hbump)-is examined. The packaged device with a 2mil-thick bump results in a total Cgd of 0.49pF and 0.38pF at Vds=10V and 30V respectively, from which an extrinsic component (Cgd, ext) of 0.29 pF is extracted. Independently, on a 1mil-bump sample, a Cgd, ext of 0.58 pF is obtained, doubling the value of the 2mil sample. The Cgd, ext-to-

Hump proportionality suggests that  $C_{gd}$ , which predominantly arises from the parallel-plate, air-dielectric capacitor between the gate metal trace on the package and the exposed Si bulk. When operated at 1.03GHz with  $V_{dq}=36V$  in class-AB mode, the 2mil and 1mil samples exhibit an output power of 41.2W and 42.4W at 1dB compression, with a peak power gain of 20.1dB and 19.4dB, respectively. [C1761]

### "Design of a dual-feed orthogonal polarized patch antenna array"

A dual-feed orthogonal polarized patch array with high polarized isolation has been designed in this paper. A very foundational rectangular patch is adopted to be array elements which provide desirable isolation between two feeding ports for orthogonal polarizations, and desirable axis ratio for circular-polarized array. The feed network is designed as a planar structure which can be extended to construct the larger array conveniently. Two 4 × 4 arrays are designed and fabricated to investigate the isolation performance between two feeding ports for orthogonal polarizations and the axis ratio performance for circular-polarized arrays. Simulated and measured results show that desirable performance of isolation below -40 dB and bandwidth of axis ratio less than 3 dB of 6% can be achieved. [C1762]

### "Self-adaptive frequency estimation algorithm of improving liquid level measurement precision of LFMCW radar"

Based on the Fast Fourier Transform(FFT) of sine signal sampling sequence, this article proposed a self-adaptive frequency estimation method using multi-spectral line information which is near the peak of spectral map. To solve the interpolation direction error of rectangular windows Rife ratio method, combining with triangular method, the new method self-adaptively selects different methods according to the different frequency. Experimental simulation results show that the new method has high estimation accuracy and small calculation amount, and is less affected by the signal-to-noise ratio (SNR), and is suitable for real-time signal processing in the low SNR. [C1763]

### "Detection of human targets using ultra-wide band through-the-wall radar"

In this paper, an ultra-wide band (UWB) through-the-wall radar (TWR) prototype is described, and experiments are performed on detecting human targets behind wall. An adaptive background subtraction method is applied to signal processing to reduce clutter and antenna couplings. Range-time histories of an adult male person behind wall are presented for different locomotion states such as standing, marking time, and walking along cross-range direction. [C1764]

### "FM interference suppression for PRC-CW radar based on STFT and median filtering"

The influence of FM interference on correlation detection performance of the pseudo random code continuous wave (PRC-CW) radar is analyzed. It is found that the correlation output deteriorates greatly when the FM interference power exceeds the anti-jamming limitation of the radar. According to the fact that the PRC-CW radar return signal is a wideband pseudo random signal occupying the whole TF plane, whereas the FM interference signal is well concentrated in the TF plane, a new method is proposed based on STFT and median filtering for FM interference suppression. This method implements the filtering of the received signal by substituting the median filter output for only a portion of the TF plane corrupted by the interference. The echo signals corrupted by two types of interferences including linear FM (LFM) and sinusoidal FM (SFM) forms under different signal-to-jamming ratio (SJR) situations are simulated. It is shown that the method can effectively suppress the FM interference and improve the performance of target detection significantly. [C1765]

### "Azimuth variant bistatic SAR imaging algorithm based on physical optics method"

Recently, a new bistatic point target reference spectrum, which is called extended Loffeld's bistatic formula (ELBF) is proposed. The point target simulation shows that this method can work well in the general bistatic configuration. In this paper, physical optics (PO) method is introduced to calculate the echo data from three dimensional targets for bistatic SAR. Then the original LBF and ELBF are tested for the bistatic SAR imaging by using electromagnetic simulation data. Experiment results demonstrate that compared with the conventional LBF, the ELBF has better imaging quality for azimuth variant configurations. [C1766]

### "Study on measurement model for radar electromagnetic compatibility analysis"

This paper proposes a new measurement model of electromagnetic compatibility(EMC) based on the attenuation coefficient of radar maximum range. First of all, the traditional measurement model of interference measure is introduced, and its disadvantage is pointed out. Then, the measurement model of stand-off jammer(SOJ) is analyzed, the attenuation coefficient of radar maximum range is proposed, and the relationship of the attenuation



coefficient of radar maximum range ( $\mu$ ) and several main parameters of the victim radar is established. Finally, simulation results indicate that increasing range between radars and decreasing sidelobe gain can achieve better radar EMC. This model can illuminate the interference condition between radars quantitatively and objectively.

[C1767]

#### "Optimizing polyphase signals for orthogonal netted radar"

Orthogonal netted radar systems (ONRS) can fundamentally improve radar performance by using a group of specially designed orthogonal polyphase code signals. However, the existing numerical solutions only address autocorrelation and cross-correlation properties with the result that the signals degrade severely in the presence of small Doppler shifts. In the context of these problems, a new set of polyphase sequences is presented with good correlation properties as well as resilience to Doppler shifts. These sequences are built using numerical optimization based on correlation properties as well as the Doppler effect on matched filter output, which maintains Doppler tolerance. The statistical simulated annealing algorithm and the greedy code search method are used to optimize the sequences. Correlation and Doppler results are compared with best-known sequences and shown to be superior. [C1768]

#### "Variable structure multiple model particle filter for maneuvering radar target tracking"

This paper presents two methods for maneuvering radar target tracking, one is called variable structure multiple model particle filter (VSMMPF), which combines the variable structure multiple model (VSMM) filter with a Sampling-Importance Resampling (SIR) particle filter (PF); The other one is called modified adaptive grid multiple model (AGMM), which is suitable when model parameter scope is unknown beforehand. PF is used to deal with problems with arbitrary nonlinearities and non-Gaussian noise. Thus the combination of VSMM and PF is able to deal with problems of nonlinearities, non-Gaussian and maneuvering. As one of the VSMM algorithms, Grid adaptation (GA) is unique one which can produce new model-set that are not predefined and model parameter can be any value within continuous model space. However, it only used to tracking maneuvering target in 2D coordinate turn system. Our modified AGMM could track generic planar maneuvering target. Simulation results indicate that performance of the algorithm VSMMPF outperforms interacting multiple model (IMM) PF and the AGMM PF which combines AGMM with PF runs well especially when model scope is unknown in advance.

[C1769]

#### "The design of cancellation unit against radiofrequency interference in life-detection radar"

When the life-detection radar detects the human-life existence, echoes from stationary barriers are generally so strong that make the post-amplifier saturated and submerge the useful life signal. In this paper, a method of interference suppression is discussed. To restrain strong interferences, a reference signal deriving from emission signal is used to cancel the clutters. This paper designs a cancellation system using Microcontroller Unit and the amplitude and phase modulation unit to produce the reference signal. The searching algorithm is proposed to find out the best digital values that respectively control the amplitude and phase of reference signal. To improve the efficiency of algorithm in the searching process, searching procedures of phase and amplitude are discussed. Simulation results are shown in a three-dimensional diagram. [C1770]

#### "Highly integrated 79, 94, and 120-GHz SiGe radar frontends"

This paper reflects on design aspects for multichannel frequency-continuous wave (FMCW) radar frontends from conception to application on board. In the 79-GHz domain, multi-channel applications are recapitulated, and in the 94-GHz domain, a broadband transceiver is presented along with a voltage-controlled oscillator (VCO) that covers a tuning range of 12 GHz. The functionality of the 94-GHz chipset was verified by means of a four-channel multiple-input multiple-output (MIMO) radar prototype. Finally, a highly integrated 120-GHz transceiver with on-chip signal generation is presented. [C1771]

#### "Non-Air Conducted Speech Enhancement Based on Iterative Spectral Subtraction Method"

A novel non-air conducted speech detecting method has been developed in our laboratory by using millimeter wave radar technology. Because of the special attributes of the millimeter wave, this method may considerably extend the capabilities of traditional speech detecting methods. However, radar speech is substantially degraded by additive combined noises that include radar harmonic noise, electrocircuit noise, and ambient noise. This study, therefore, proposed an iterative spectral subtraction method which can be adaptive estimate noise spectrum at every iteration time, and reduce the musical noise remained in the previous spectral subtraction process. Results from simulations as well as evaluations confirm that enhanced non-air conducted speech is more pleasant to listeners than speech produced by traditional spectral subtraction algorithms. This suggests that the proposed method satisfactorily reduces whole-frequency and musical noises and produces good speech

quality. [C1772]

### "Advanced system level simulation of UWB three-dimensional through-wall imaging radar for performance limitation prediction"

A system level framework has been developed to simulate the UWB three-dimensional through-wall radar system and accurately predict its performance limitations. Only through a novel simulation model where Agilent ADS Ptolemy simulation is used combined with its Matlab co-simulation, is it possible to accurately simulate the UWB radar system. The developed simulation model has been validated experimentally using our UWB radar prototype. The system model can be easily extended to other UWB radar systems by simply changing the input pulse shape, UWB channel environment, wall characteristics, transceiver topology, etc. Various effects such as signal quality, pulse shape, wall characteristics can be easily investigated and re-optimized for high performance 3-D imaging using our developed model. [C1773]

### "Fast response Retrodirective Radar"

This paper shows the ability of an all analogue Retrodirective Radar, the first of its type, to provide continuous surveillance and near instantaneous target acquisition while automatically beam steering in real time onto a target which is presented to it. Assessment of the phase conjugation unit shows that the Radar is capable of operating either in CW or in pulsed mode. Test results are presented which show that Retrodirective tracking of targets travelling at speeds in excess of 780 m/s is possible. To confirm tracking ability bistatic results of a small near field target are presented, and the capability is also shown to extract the position of the near field target with only very simple calculations, with no DSP circuitry required. [C1774]

### "Towards high-performance 100 GHz SiGe and CMOS circuits"

This paper presents SiGe and CMOS circuits with 100 GHz operation. The goal is to show that SiGe can be used for imaging systems due to its low  $1/f$  noise properties. A W-band SiGe imaging chip is presented with performance which is nearly as good as the best InP chips. Another goal is to show that deep-scaled CMOS can result in high performance amplifiers, detectors, and doublers at 90-110 GHz and at 180-220 GHz. The applications areas are in high data-rate communications, 100 GHz automotive radars (140 and 220 GHz) and mm-wave imaging systems. [C1775]

### "Session-WE1"

{no data available} [C1776]

### "High isolation lange-ferrite circulators with NF suppression for simultaneous transmit and receive"

This paper presents a new type of circulator that consists of three Lange couplers and two ferrite circulators for broadband, high isolation, transmit noise suppression and simultaneous transmit and receive (STAR). The operation principal of the circulator is based on quadrature phase cancellation and combination techniques. Preliminary results show that the isolation between the transmit and receive port is 24 dB in frequency range of 5-12 GHz without optimization and 60 dB isolation with 800 MHz bandwidth with optimization. The NF data at the receive port show significant suppression of transmit noise for Gain-NF product that exceeds 21 dB. [C1777]

### "Development of a multi-frequency airborne radar instrumentation package for ice sheet mapping and imaging"

We have developed improved versions of three different radar systems and integrated them as an airborne instrumentation suite for sounding and imaging Polar ice sheets. The first instrument is a multi-channel, coherent pulsed chirp radar operating at VHF with up to 30 MHz bandwidth. This radar set is capable of sounding a few-kilometer thick ice while flying at altitudes up to 10 km above mean sea level. The second instrument is designed to operate at UHF using a burst of narrow-bandwidth signals to digitally synthesize a bandwidth in excess of 300 MHz. This apparatus is used to measure internal layers of the ice sheet to a depth close to 100 m. The third component to the instrumentation package is a microwave frequency-modulated continuous wave (FMCW) radar, which is used to measure the ice sheet surface elevation profile with centimeter accuracy. We are presenting a description of each system along with field test results that validate the performance of the instrument package. [C1778]

### "System of locating and recognizing characters in complex background"

In this paper we propose a locating and recognizing character method in complex background, a system based

on this method is built. First, through color reduction to reduce the color to some main colors, then decompose the image into a series of binary images according to the representative colors. After the image decomposition, connected component analysis and combination of character area are used to locate the character area. Finally, the characters are recognized on the basis of feature extraction. The experimental results show that the method can quickly locate character area and has a high positioning accuracy; therefore, the final recognition rate is high. [C1779]

#### "A fast clutter cancellation method in quadrature doppler radar for noncontact vital signal detection"

A fast clutter cancellation technique is proposed for quadrature Doppler radar to robustly detect the vital signals when clutters enter the test environment. The dc offset at baseband varies with the change of test environment, dramatically reducing the accuracy of vital signal detection. To solve this problem, a clutter cancellation generator is employed in the radar receiver. Based on the detected dc offset values in I and Q channels, the generator produces an output signal, anti-phase to the received clutter signal, such that the clutter signal is cancelled at RF frontend. Therefore the time-varying dc offset at baseband is eliminated. The clutter cancellation method is described and the experiment was conducted to demonstrate the proposed method. [C1780]

#### "A highly integrated heterogeneous micro- and mm-wave platform"

A highly integrated platform for micro- and mm-wave frequency applications is introduced. The platform utilizes heterogeneous process modules with integrated passive and tunable devices together with silicon and GaAs MMIC technology to achieve outstanding flexibility. The different process modules are accounted for and their feasibility is proven through a number of application demonstrators from 23 GHz telecom backhauling and 77 GHz automotive radar indicating excellent performance. [C1781]

#### "Calibration of a Digital phased Array for polarimetric Radar"

When an active phased array is used for polarimetric radar applications, the system must be calibrated to reflect the fact that polarization of the transmitted and received fields is dependent on the scan angle. This paper discusses the challenges of polarimetric phased array calibration, and demonstrates these techniques using a linear array of eight S-band dual-polarized antennas connected to an active Digital Array Radar (DAR) pro-totype system. The ability to accurately measure polarimetric scattering matrices is demonstrated after using direct far-field measurements to compensate for polarization errors on receive and target reflection measurements to compensate for transmit polarization errors. [C1782]

#### "A fast clutter cancellation method in quadrature doppler radar for noncontact vital signal detection"

A fast clutter cancellation technique is proposed for quadrature Doppler radar to robustly detect the vital signals when clutters enter the test environment. The dc offset at baseband varies with the change of test environment, dramatically reducing the accuracy of vital signal detection. To solve this problem, a clutter cancellation generator is employed in the radar receiver. Based on the detected dc offset values in I and Q channels, the generator produces an output signal, anti-phase to the received clutter signal, such that the clutter signal is cancelled at RF frontend. Therefore the time-varying dc offset at baseband is eliminated. The clutter cancellation method is described and the experiment was conducted to demonstrate the proposed method. [C1783]

#### "Design and implementation of the low-power tracking system based on GPS-GPRS module"

The purpose of the research proposed in this paper is to develop a Low-Power Tracking System, which can meet the special needs of the security of a mobile device. The system contains two parts: the GPS terminal in the module receives the locating information of the tracked device, and the control center. This paper discusses both hardware and software design of the tracking system. In the end, the future research of the positioning and tracking system is discussed. [C1784]

#### "Highly integrated 79, 94, and 120-GHz SiGe radar frontends"

This paper reflects on design aspects for multi-channel frequency-continuous (FMCW) wave radar frontends from conception to application on board. In the 79-GHz domain, multi-channel applications are recapitulated, and in the 94-GHz domain, a broadband transceiver is presented along with a voltage-controlled oscillator (VCO) that covers a tuning range of 12 GHz. The functionality of the 94-GHz chipset was verified by means of a four-channel multiple-input multiple-output (MIMO) radar prototype. Finally, a highly integrated 120-GHz transceiver with on-chip signal generation is presented. [C1785]

### "Cable imaging with an active W-band millimeter-wave sensor"

A system that can detect wires and cables suspended in the air and give fair warning of such obstacles on approach is highly desirable for both commercial and military helicopter pilots alike, given the recent increase in wire strike accidents. This paper discusses the recent development of a flight capable active millimeter-wave imaging system as a candidate and potential solution for such a system. The development methodology and flight test results presented validate the functionality of this flight system as a useful development platform for advanced system concept applications even beyond cable detection and imaging. [C1786]

### "Narrowband frequency scanning array antenna at 5.8 GHz for short range imaging"

We present a frequency scanning array antenna for radar applications. A high angular range is obtained while requiring only a small frequency band. This is achieved by using a band-pass filter feed structure that increases the frequency-dependent phase difference between the individual array elements. An angular range of  $\pm 50$  degrees is obtained while using only 150 MHz bandwidth with 5.8 GHz center frequency corresponding to the ISM Band. This antenna type can be applied for detecting covered objects or for short range imaging. [C1787]

### "Cable imaging with an active W-band millimeter-wave sensor"

A system that can detect wires and cables suspended in the air and give fair warning of such obstacles on approach is highly desirable for both commercial and military helicopter pilots alike, given the recent increase in wire strike accidents. This paper discusses the recent development of a flight capable active millimeter-wave imaging system as a candidate and potential solution for such a system. The development methodology and flight test results presented validate the functionality of this flight system as a useful development platform for advanced system concept applications even beyond cable detection and imaging. [C1788]

### "THz for space: The golden age"

Over the past three decades interest in the unique spectral measurements offered by terahertz instruments operating outside the Earth's atmosphere has grown enormously. Since the historic flight of Cosmos 669 in 1974, and the first THz telescope with cryo-cooled detectors operated on board Salyut 6 in 1978, satellite instruments have performed both direct detection and heterodyne spectroscopy measurements in the interstellar medium, in external galaxies, in the atmospheres of planets and comets and in the Earth's stratosphere. Seventeen orbital instruments containing THz sensors or sources have either completed their mission objectives or are currently operational. They originate in Russia, Japan, Europe and the US and cover applications in astrophysics and cosmology; planetary and small solar system body science; and pollution, ozone and climate monitoring on the Earth. At least a dozen serious future mission proposals are under consideration, including new areas of meteorology, terrestrial planet finding and planetary radar spectroscopy. It is truly a golden age for THz space science and applications. This talk will review past, present and future space instruments carrying infrared, millimeter wave and terahertz components and their science objectives. [C1789]

### "Interferometric detection of the angular velocity of moving objects"

This paper presents a new method of detecting the angular velocity of moving objects using passive interferometry. The new technique is presented using a millimeter-wave correlation interferometer to measure the angular velocity of a moving target directly, without the need for multiple looks. As the object passes through the interferometer beam pattern the frequency of the signal output is dependent on the angular velocity of the object, and a simple time-frequency analysis visually displays the angular velocity of the target. The basic theory is presented and experimental results showing the detection of a walking person are presented. [C1790]

### "Time-domain calibration technique for ultra-wide instantaneous-bandwidth vector waveform generation using parallel I/Q channels"

An architecture for generating ultra-wide instantaneous-bandwidth vector waveforms by combining the spectra of multiple I/Q sub-channels is described. Each sub-channel consists of an I/Q modulator driven by a pair of digital-to-analog converters. A time-domain calibration technique is described that uses the measured channel response to equalize the sub-channels. The overall response of the combined system is realized by properly controlling the phases of the corrected I/Q sub-channels. Examples of wideband vector waveforms generated using the combined system will be given. [C1791]

### "A heterodyne receiver for harmonic doppler radar cardio-pulmonary monitoring with body-worn passive RF tags"



Summary form only given. Harmonic Doppler radar can be used to isolate a subject's respiratory motion from environmental clutter. In this paper, a heterodyne receiver is used to detect tag motion and human cardiopulmonary activity, with the results compared with a that using a homodyne receiver. The heterodyne system is shown to work at a greater distance from the subject (more than 160 cm) with greater sensitivity to tag motion (more than 10 dB), using the same transmitted power (10 dBm). Both homodyne and heterodyne receivers are also used to successfully detect a human heartbeat by attaching a passive harmonic tag over a subject's chest. [C1792]

### "Environmental Monitoring System Based on GIS and Wireless Communications"

To solve the problems in environmental monitoring arising from remote data acquisition, real-time transmission and analysis, this paper researched the principle of wireless communications SMS / GPRS and the technology of seamless integration with GIS. The system architecture was designed and key technical solutions were implemented. Based on the SMS / GPRS technology, the wireless real-time transmission of the remote monitoring data was achieved, and GIS visualization technology was carried out to visualize the monitoring data. Geographic affected areas were analyzed by GIS spatial analysis. The system is applicable to the environmental protection departments to realize applications such as monitor data acquisition, communication transmission, GIS management and analysis and decision-making. [C1793]

### "Session-TH3"

{no data available} [C1794]

### "Second generation transceivers for D-band radar and data communication applications"

A single chip, dual-functionality radio and FMCW radar transceiver, operating at 140 GHz is described. Doppler, loop-back and 4Gb/s NLOS radio link demos, over the air and distances exceeding one meter, are demonstrated. The second part of the paper presents novel, sub-1.8 V circuit topologies intended for a low power, high resolution 120 GHz radar transceiver with self-calibration capabilities. The measured receiver noise figure, gain and phase noise are 7.5 dB, 20 dB and -100 dBc/Hz@1MHz offset respectively. [C1795]

### "Towards high-performance > 100 GHz SiGe and CMOS circuits"

This paper presents SiGe and CMOS circuits with > 100 GHz operation. The goal is to show that SiGe can be used for imaging systems due to its low  $1/f$  noise properties. A W-band SiGe imaging chip is presented with performance which is nearly as good as the best InP chips. Another goal is to show that deep-scaled CMOS can result in high performance amplifiers, detectors, and doublers at 90-110 GHz and at 180-220 GHz. The applications areas are in high data-rate communications, > 100 GHz automotive radars (140 and 220 GHz) and mm-wave imaging systems. [C1796]

### "Analog type millimeter wave phase shifters based on MEMS tunable high-impedance surface in rectangular metal waveguide"

Possibility of compact low loss analog type millimeter wave phase shifter was demonstrated. The phase shifter is controlled by a MEMS tunable high-impedance surface placed, e.g., as a backshort or as sidewall inclusions of a rectangular metal waveguide. Reflection type phase shifter can provide differential analog phase shift from  $0^\circ$  to up to  $240^\circ$ . Reliable and tunable MEMS based high-impedance surface has been demonstrated for the first time. The insertion loss of the fabricated MEMS tunable high-impedance surface varies from 0.7 dB to a maximum of 3.5 dB (at a resonance frequency), which is a dramatic improvement over our previous non-tunable prototype. [C1797]

### "Piggyback modulation for UHF RFID sensors"

We introduce the technique of "piggybacking" sensor data onto existing commercial passive UHF RFID tags. Sensor data fed into a PIN diode modulator is coupled onto the tag and transmitted along with the tag ID via backscatter. The radar cross section (RCS) of the tag antenna is a function of the input impedance of the tag ASIC, coupling S-parameters, and the input impedance of the PIN diode modulator. Both analog and digital sensor signals coexisting with identification data are presented. [C1798]

### "THz electronics projects at DARPA: Transistors, TMICs, and amplifiers"

Revolutionary THz transmitter and receiver demonstrations are the ongoing focus of a portfolio of programs within the DARPA. Through the sponsorship of the Terahertz Electronics and related programs, a technology

base is being established to effectively generate, detect, process, and radiate sub-MMW frequencies to exploit this practically inaccessible frequency domain for imaging, radar, spectroscopy, and communications applications. Transistors, integration technologies, power amplification, and their precision metrology are the key elements under active investigation. THz InP transistors have been achieved that have enabled the world's fastest 0.48 THz monolithic integrated circuits. Compact THz high power amplifiers using micro-machined vacuum electronic devices will enable radiation sources at 1.03 THz with 15 GHz of instantaneous bandwidth. Ultimately, low-loss interconnects and integration techniques will couple TMICs with HPAs to enable THz coherent heterodyne transceivers. [C1799]

#### "Session-Wednesday-detail"

{no data available} [C1800]

#### "A light weight 8-element broadband phased array receiver on Liquid Crystal Polymer"

In this paper we present a light weight broadband phased array hybrid receiver module on a multi-layer Liquid Crystal Polymer (LCP) substrate. The phased array module has 8 channels and is designed to operate in the Ka-band, from 32-37 GHz. A broadband linear tapered slot antenna array with a corporate power combiner, chip-on-board MMICs, and all control chips necessary for beam steering are all integrated on a multi-layered near-hermetic LCP substrate. The phased array antenna has a measured bandwidth of 5 GHz with  $\pm 30^\circ$  beam steering capability from boresight, and shows less than  $6.75^\circ$  of beam squint across the full bandwidth of operation. The total size of the array is 100 mm  $\times$  100 mm with a board thickness of only 16 mils and weighs only 12.3 grams. [C1801]

#### "Spaceborne SAR Systems and technologies"

With the launch and operation of Europe's first remote sensing satellite ERS-1 in the 90's, the usefulness and need of spaceborne SAR Systems has become obvious. Meanwhile, affordable 'state of the art' technology in modern active phase array antennas has drastically improved the SAR system agility and its image performance, such that also commercial and military application is of highest interest. [C1802]

#### "A heterodyne receiver for Harmonic Doppler radar cardiopulmonary monitoring with body-worn passive RF tags"

Harmonic Doppler radar can be used to isolate a subject's respiratory motion from environmental clutter. In this paper, a heterodyne receiver is used to detect tag motion and human cardiopulmonary activity, with the results compared with a that using a homodyne receiver. The heterodyne system is shown to work at a greater distance from the subject (more than 160 cm) with greater sensitivity to tag motion (more than 10 dB), using the same transmitted power (10 dBm). Both homodyne and heterodyne receivers are also used to successfully detect a human heartbeat by attaching a passive harmonic tag over a subject's chest. [C1803]

#### "Waveguide transition to feed a fully PCB integrated dielectric rod antenna"

A microstrip line-to-circular waveguide transition is described which operates at a nominal design frequency of 77 GHz. In order to improve the transmission characteristics, an additional periodically structured shield is used. The transition is capable of exciting a dielectric rod antenna, thus enabling the realization of radar modules on a PCB substrate with a dielectric rod antenna interface. [C1804]

#### "Sidelobe level reduction in wide-angle scanning array system using pattern-reconfigurable antennas"

A technique aimed at peak sidelobe level (SLL) reduction for wide-angle scanning arrays is presented in this work, based on the use of a newly designed pattern-reconfigurable antenna (PRA). The proposed antenna consists of a monopole antenna and two parasitic strips, where each strip can be reconfigured into either a reflector or a director via PIN diode switches, leading to the beam deflection. A 2.45 GHz PRA was implemented and the measured results demonstrate three reconfigurable patterns, radiating toward two end-fire and one broadside directions, respectively. When this PRA is used in a 14 linear array, the SLL is -7.5 dB at end-fire directions and -11.8 dB at broadside. The SLL at end-fire is 7.4 dB enhancement compared to the linear array with the conventional monopole. The design principle was discussed and a Butler-matrix-fed linear array with four PRAs was implemented for demonstration. [C1805]

#### "FS-5, paper 5: Earth observation instruments with e-scan antennas state-of-the-art and outlook"

Spaceborne radars with electronically scanned antennas are in use on European satellites since the launch of Envisat in March 2002. Despite the higher complexity and consequently cost, electronically scanned antennas are more and more attractive for spaceborne radar. The return materialises either in significantly better system performance or in newly gained system feasibility. The paper will discuss firstly state-of-the-art phased array technology as used for the European Sentinel-1 C-band SAR and explore secondly the capabilities of full digital beam forming implementation for the next generation of SAR systems. Thirdly phased arrays as a feasibility prerequisite in quasi bistatic radar for future ocean altimetry, exploiting GNSS signals will be discussed. Lastly reflector based e-scan antennas will be discussed which form a good compromise between complexity and flexibility as needed for SAR systems requiring high gain antennas. A potential application in Ka-band SAR will be presented. [C1806]

#### "THz Electronics projects at DARPA: Transistors, TMICs, and amplifiers"

Revolutionary THz transmitter and receiver demonstrations are the ongoing focus of a portfolio of programs within the DARPA. Through the sponsorship of the Terahertz Electronics and related programs, a technology base is being established to effectively generate, detect, process, and radiate sub-MMW frequencies to exploit this practically inaccessible frequency domain for imaging, radar, spectroscopy, and communications applications. Transistors, integration technologies, power amplification, and their precision metrology are the key elements under active investigation. THz InP transistors have been achieved that have enabled the world's fastest 0.48 THz monolithic integrated circuits. Compact THz high power amplifiers using micro-machined vacuum electronic devices will enable radiation sources at 1.03 THz with 15 GHz of instantaneous bandwidth. Ultimately, low-loss interconnects and integration techniques will couple TMICs with HPAs to enable THz coherent heterodyne transceivers. [C1807]

#### "2D transformation optics using anisotropic transmission-line metamaterials"

In this contribution we propose a two-dimensional metamaterial unit cell which synthesizes equivalent material parameters needed for 'transformation optics', as introduced in. The proposed metamaterial consists of a grid of reactively loaded transmission-line segments and is a variation of the unit cell presented in, synthesizing also the required off-diagonal elements of the permeability tensor. The application of cloaking of the 'transformation optics' approach is taken as a test case for the novel metamaterial. The cloak we present is different from the structure presented in in that it synthesizes not only  $\mu$  and  $\epsilon$  but also  $\mu$ . [C1808]

#### "UWB array antenna utilizing novel electrical scanning system with tapped delay lines"

In this paper, we present a newly developed UWB array antenna adopting a novel electrical scanning system. This antenna was realized by introducing two new technologies. First, each antenna element is equipped with an impulse generator. Second, the phase control between the antenna elements is realized by tapped delay lines and transmitting trigger signals. An experimental UWB array antenna with 16 elements has been designed and fabricated. The measurement results showed excellent performance of the antenna. Thus, it is expected that this UWB antenna system will contribute to performance improvement, compact size and cost reduction of UWB radar systems such as obstacle detectors and anticollision sensors. Index Terms-UWB radar, array antenna, electrical scanning antenna, beam steering, phased array, delay line. [C1809]

#### "Narrowband frequency scanning array antenna at 5.8 GHz for short range imaging"

We present a frequency scanning array antenna for radar applications. A high angular range is obtained while requiring only a small frequency band. This is achieved by using a band-pass filter feed structure that increases the frequency-dependent phase difference between the individual array elements. An angular range of  $\pm 50$  degrees is obtained while using only 150 MHz bandwidth with 5.8 GHz center frequency corresponding to the ISM Band. This antenna type can be applied for detecting covered objects or for short range imaging. [C1810]

#### "Second generation transceivers for d-band radar and data communication applications"

A single chip, dual-functionality radio and FMCW radar transceiver, operating at 140 GHz is described. Doppler, loop-back, and 4Gb/s NLOS radio link demos, over the air and at distances exceeding one meter, are demonstrated. The second part of the paper presents novel, sub-1.8 V circuit topologies intended for a low power, high resolution 120 GHz radar transceiver with self-calibration capabilities. The measured receiver noise figure, gain, and phase noise are 7.5 dB, 20 dB, and -100 dBc/Hz@1MHz offset, respectively. [C1811]

#### "Calibration of a digital phased array for polarimetric radar"

When an active phased array is used for polarimetric radar applications, the system must be calibrated to reflect

the fact that polarization of the transmitted and received fields is dependent on the scan angle. This paper discusses the challenges of polarimetric phased array calibration, and demonstrates these techniques using a linear array of eight S-band dual-polarized antennas connected to an active Digital Array Radar (DAR) prototype system. The ability to accurately measure polarimetric scattering matrices is demonstrated after using direct far-field measurements to compensate for polarization errors on receive and target reflection measurements to compensate for transmit polarization errors. [C1812]

#### "Commercial manufacturing practices applied to phased array radars"

Transmit/Receive Modules for Phased Array Radar are often identified as a key cost driver for the system. The cost structure of the module is driven by both the performance specifications and the choices made in design and manufacturing of the module. Seeking a path to dramatically lower the cost of T/R modules for phased array systems, commercial processes and practices have been adopted for the MMIC design, MMIC packaging and module construction. These new manufacturing approaches offer a path to cost reduction while maintaining a high level of performance. [C1813]

#### "The SAR/GMTI airborne radar PAMIR: Technology and performance"

PAMIR, a multifunctional SAR/GMTI imaging radar, combines the tremendous research potential of an experimental active broadband phased array system with the wide area of imaging procedures of mono- and bistatic systems. With its two different reconfigurable antenna frontend configurations operating a very high simultaneous bandwidth of 1.8 GHz in X-band, a variety of controversial requirements can be investigated and experimentally explored. The broadband beamforming together with azimuth wide scan capabilities ( $\pm 45^\circ$  @ 1.8 GHz bandwidth of the antenna aperture) requires a switchable true time delay network with time increments equivalent to a fraction of a wavelength. The subarray structure including its time delay components are described. PAMIR serves as an ideal airborne platform for broadband SAR/GMTI research activities including interferometric image formation. [C1814]

#### "A highly integrated heterogeneous micro- and mm-wave platform"

A highly integrated platform for micro- and mm-wave frequency applications is introduced. The platform utilizes heterogeneous process modules with integrated passive and tunable devices together with silicon and GaAs MMIC technology to achieve outstanding flexibility. The different process modules are accounted for and their feasibility is proven through a number of application demonstrators from 23 GHz telecom backhauling and 77 GHz automotive radar indicating excellent performance. [C1815]

#### "Recent Microwave Nondestructive Measurement in Biomedical Engineering"

Recent microwave nondestructive measurement in biomedical engineering are reviewed. A novel method for non-contact monitoring of stress-induced autonomic activation through the back of a chair is developed, using a compact 24 GHz microwave radar (8 4 5 4 3 cm), without large scale equipment and placing a heavy burden on the monitored individual. This method appears to be promising for future monitoring of stress induced autonomic activation of operators and may reduce stress induced accidents. A novel in vitro test of blood analysis based on the measurement of the dielectric properties at microwave frequencies is reported. The measurements were made using rectangular cavity perturbation technique at the S-band of microwave frequency with the different samples of blood obtained from healthy donors as well as from patients. The measurements are in good agreement with clinical analysis. Novel planar type probes were developed to demonstrate the possibility of replacing the existing high cost open-ended coaxial probes. Three probes are developed. The measurement results of each probe showed excellent compatibility with those of the open-ended coaxial probe up to almost 40 GHz. The proposed planar type probes have great potentials for practical medical applications in view of low cost, disposability, and monolithic integration capability with the driving circuits. Finally the technical challenges of microwave nondestructive measurement in biomedical engineering are discussed. [C1816]

#### "Status and trends in AESA-based radar"

Radar technology, predominantly in the area of defence applications, is in a continuous process of extending its present capabilities. Especially Active Electronically Scanned Array (AESA) radars, with their unprecedented degree of operational flexibility, are currently about to revolutionise the performance of air- and spaceborne, naval and ground radars. The current status of AESA radar and the trends in system and technology advances are discussed. Trends on system level will be the use of MIMO-architectures and shared antenna apertures. [C1817]

### "Advanced system level simulation of UWB three-dimensional through-wall imaging radar for performance limitation prediction"

A system level framework has been developed to simulate the UWB three-dimensional through-wall radar system and accurately predict its performance limitations. Only through a novel simulation model where Agilent ADS Ptolemy simulation is used combined with its Matlab co-simulation, is it possible to accurately simulate the UWB radar system. The developed simulation model has been validated experimentally using our UWB radar prototype. The system model can be easily extended to other UWB radar systems by simply changing the input pulse shape, UWB channel environment, wall characteristics, transceiver topology, etc. Various effects such as signal quality, pulse shape, wall characteristics can be easily investigated and re-optimized for high performance 3-D imaging using our developed model. [C1818]

### "The new generation of European E-scan fighter radars"

Two European programmes towards an airborne E-scan radar have obtained major attention: AMSAR, a generic demonstrator for developing the technology required for an AESA radar and for proving its operational capabilities, and CAESAR that paves the way to the next generation of radar for Eurofighter. Future sub-array AESA architectures and multi-channel receivers will enable efficient jammer suppression by use of Adaptive Beam Forming. The technology basis of T/R-Modules will move to Gallium-Nitride, promising improvements in efficiency, output power and miniaturisation. [C1819]

### "Spaceborne SAR systems and technologies"

Design and development of Spaceborne Synthetic Aperture Radar Systems is one of the major activities at EADS Astrium, Friedrichshafen, Germany. Examples of recent and current developments are the TerraSAR-X and the TanDEM-X Satellites, both operating at X-band with multi-polarization capability. At C-Band, the Sentinel-1 SAR Instrument is a further example for active phased array radar currently under development in our company. In addition to the design and manufacturing of 'state of the art' active phased array SAR sensors, new techniques and technologies are under preparation. The overall objective is to upgrade significantly the image performance, to enlarge the capabilities of spaceborne SAR and to improve the performance to cost ratio. For this, digital beamforming is a key element. [C1820]

### "Fast response Retrodirective Radar"

This paper shows the ability of an all analogue Retrodirective Radar, the first of its type, to provide continuous surveillance and near instantaneous target acquisition while automatically beam steering in real time onto a target which is presented to it. Assessment of the phase conjugation unit shows that the Radar is capable of operating either in CW or in pulsed mode. Test results are presented which show that Retrodirective tracking of targets travelling at speeds in excess of 780 m/s is possible. To confirm tracking ability bistatic results of a small near field target are presented, and the capability is also shown to extract the position of the near field target with only very simple calculations, with no DSP circuitry required. [C1821]

### "GaN technology for microwave and millimeter wave applications"

After many years of development to improve the material and devices, GaN technology is now in production and poised to revolutionize many of today's Radar and Communication systems. In this paper we present an overview of GaN development, focusing on reliability, affordability, and defense applications. [C1822]

### "Advanced architecture for a low cost Multifunction Phased Array Radar"

MIT Lincoln Laboratory and M/A-COM are jointly conducting a technology demonstration of affordable Multifunction Phased Array Radar (MPAR) technology for Next Generation air traffic control and national weather surveillance services. Aggressive cost and performance goals have been established for the system. The array architecture and its realization using custom Transmit and Receive Integrated Circuits and a panel-based Line Replaceable Unit (LRU) will be presented. A program plan for risk reduction and system demonstration will be outlined. [C1823]

### "The new generation of European E-scan fighter radars"

Two European programmes towards an airborne E-scan radar have obtained major attention: AMSAR, a generic demonstrator for developing the technology required for an AESA radar and for proving its operational capabilities, and CAESAR that paves the way to the next generation of radar for Eurofighter. Future sub-array AESA architectures and multi-channel receivers will enable efficient jammer suppression by use of Adaptive



Beam Forming. The technology basis of T/R-Modules will move to Gallium- Nitride, promising improvements in efficiency, output power and miniaturisation. [C1824]

#### "UWB array antenna utilizing novel electrical scanning system with tapped delay lines"

In this paper, we present a newly developed UWB array antenna adopting a novel electrical scanning system. This antenna was realized by introducing two new technologies. First, each antenna element is equipped with an impulse generator. Second, the phase control between the antenna elements is realized by tapped lines and transmitting trigger signals. An experimental UWB array antenna with 16 elements has been designed and fabricated. The measurement results showed excellent performance of the antenna. Thus, it is expected that this UWB antenna system will contribute to performance improvement, compact size and cost reduction of UWB radar systems such as obstacle detectors and anticollision sensors. [C1825]

#### "Status and trends in AESA-based radar"

Radar technology, predominantly in the area of defence applications, is in a continuous process of extending its present capabilities. Especially Active Electronically Scanned Array (AESA) radars, with their unprecedented degree of operational flexibility, are currently about to revolutionise the performance of air- and spaceborne, naval and ground radars. The current status of AESA radar and the trends in system and technology advances are discussed. Trends on system level will be the use of MIMO-architectures and shared antenna apertures. [C1826]

#### "An Improved Peak Extraction Algorithm in PHD Based Multi-Target Tracking Algorithm Applied to Passive Radar"

To extract the target location correctly in PHD based multi-target tracking algorithm, an improved peak extraction algorithm was proposed. This new algorithm stemmed from the CLEAN technique in radar signal processing. By finding the highest peak in every iteration, the assumed target was extracted and its corresponding location information was obtained. Simulation results prove the efficiency and correctness of this new algorithm. [C1827]

#### "Ice sheet anisotropy measured with polarimetric ice sounding radar"

For polar ice sheets, valuable stress and strain information can be deduced from crystal orientation fabrics (COF) and their prevailing c-axis alignment. Polarimetric radio echo sounding is a promising technique to measure the anisotropic electromagnetic propagation and reflection properties associated with COFs. In this paper, fully polarimetric P-band data acquired with the airborne POLARIS system near the ice divide of the Greenland ice sheet are analyzed. Based on a simple electromagnetic model, these data are interpreted, and a pronounced birefringence is found. [C1828]

#### "Passive infrared localization with a Probability Hypothesis Density filter"

In passive infrared localization (PIL) humans are located based on their thermal radiation. Thus, an active tag is not required and privacy is guaranteed due to non-identifying sensors. However, in case of multi-target tracking, the non-identifying sensors result in missing associations between targets and measurements. As additionally the number of humans in the surveillance region is unknown and varying, conventional localization approaches like the JPDA or MHT filter cannot be applied since they require a fixed number of targets or are not tractable. The Probability Hypothesis Density (PHD) filter, on the other hand, that propagates only the first order moment of the multitarget probability distribution offers an efficient and elegant way to handle the aspects of missing association and varying target number. Furthermore, false measurements as well as missed detection are considered implicitly. In this paper we present an implementation of this filter for PIL that allows an accurate and reliable tracking of several humans. The accuracy and reliability are evaluated under the influence of noise. Thus, several simulations and real measurements are carried out that reveal a mean error of less than 30 cm in case of three humans. Moreover, efficiency tests show that on standard PCs update rates of more than 50 Hz are achievable. [C1829]

#### "A tracking algorithm for GNSS reflected signals on sea surface"

The observation of the ocean surface using electromagnetic sources of opportunity (GNSS signals for instance) has been a green research topic for several years. The Global Navigation Satellite System (GNSS) presents a powerful and useful technology for remote sensing, ocean surface monitoring and oceanography. Many experiments have been conducted to show the efficiency of the Global Positioning System (GPS) in applications such as ocean surface altimetry, wave height, surface current measurements, and current direction estimation

[1]. Considering the GPS link as a passive sensor for ocean monitoring, we study in this paper the possibility of tracking GPS signal reflection footprints on the sea surface to improve the acquisition and the extraction of this signal. As an analogy to the classical problem of moving targets Radar tracking, we develop a tracking algorithm based on Kalman filtering. [C1830]

#### "An integrated approach to determine parameters of a 3D volcano model by using InSAR data with metamodel technique"

In this paper, an integrated approach is presented to determine the suitable parameters of a magma-filled dyke, which causes observable deformation at the ground surface. By this approach, the finite element method (FEM) and metamodel techniques are combined. FEM is used to establish the numerical model of the dyke and to produce the data required to identify metamodel parameters. Parameter identification problems are also known as parameter estimation or inverse problems. The metamodel technique is employed to make the whole procedure efficient in the identification phase. The identification approach is carried out by a systematic routine based on particle swarm optimization (PSO) algorithm. The approach is tested with synthetic data generated by analytic models. Moreover, it has been also applied to Stromboli Volcano (Italy) as an example, and the ground deformation data is acquired by using interferometry SAR technique. With the approach, the parameters can be successfully estimated with acceptable degree of accuracy. The results also indicate that only one kind of geophysical data are not sufficient for solving such a complex problem. [C1831]

#### "A CHMT model based DE-speckling method for SAR image"

A coarse-classification based tying method for the Contourlet-domain Hidden Markov Tree model (CHMT) solution algorithm is proposed to speed up the parameters estimation; and a general SAR image filtering framework, to which any kind of shift-variant transform can be applied, is generated by applying together with the LOG Transform, mean rectification and cycle-spinning, etc. The proposed coarse classification based tying method for CHMT is applied to de-speckle the SAR image in the general framework, and the result is compared with those of some commonly-used filters. The visual effects and the statistical parameters indicate that the coarse-classification based tying method for CHMT is much faster than the other tying methods, and the CHMT based de-speckle method can achieve better result than some commonly-used filters. [C1832]

#### "Roll invariant target detection based on PolSAR clutter models"

Based on the Kennaugh-Huynen decomposition, the Target Scattering Vector Model (TSVM) allows to extract four roll-invariant parameters. Those parameters are necessary for an unambiguous description of the target scattering mechanism. The proposed method consists in applying the TSVM prior to the GLRT-LQ detector for the detection of any oriented target. [C1833]

#### "PolSAR images characterization through Blind Sources Separation techniques"

Since the backscattered signal in PolSAR images is intrinsically linked with the physical characteristics of the objects in the image, valuable information may be extracted therefrom. The paper focus is to propose a new physical characterization of the scattering target, inspired by the Blind Sources Separation techniques. [C1834]

#### "Processing of bistatic TanDEM-X data"

On June 21st, 2010, the German radar satellite TanDEM-X was launched and successfully placed in an orbit approaching the TerraSAR-X satellite until both systems will fly in close formation and will establish the only available bi-static interferometer in space. The primary TanDEM-X mission goal is to generate a global Digital Elevation Model (DEM) with a relative point-to-point height accuracy of 2 meters for moderate terrain at 12 m posting. For that purpose interferometric SAR data will be acquired over a period of 3 years in parallel to the operational running TerraSAR-X mission. Systematic processing of SAR raw data to so-called Raw-DEMs is performed by one single processing system, the Integrated TanDEM Processor (ITP). The final global DEM is then calibrated and mosaicked by a second system, the Calibration and Mosaicking Processor (MCP). The scope of this paper is to present an overview of ITP functionalities and to summarize the first processing results. [C1835]

#### "Peatland subsurface water flow monitoring using polarimetric L-band PALSAR"

The potential of L-band PALSAR for monitoring water flow beneath the peat surface is demonstrated on a bog near Lac Saint Pierre (Canada). Two polarimetric ALOS acquisitions collected at spring and fall under different water conditions are used. The Touzi decomposition, which was shown to be very promising for peatland characterization using the C-band Convair 580 SAR, is applied. Like in, the information provided by the multi-

polarization (HH, HV, and VV), the scattering type magnitude (the Cloude  $\alpha$  or the Touzi  $\alpha_s$ ), the single scattering eigenvalues and the entropy, cannot detect the presence of water underneath the peat surface. The Touzi scattering phase is shown to be the only target scattering decomposition parameter that can detect water flow variations beneath the peat surface. The fall acquisition that took place after two days rain permits demonstrating that the wave can penetrate deep into the acrotelm layer to detect the rain water that has sunk rapidly into the peat layer of high hydraulic conductivity. The spring acquisition at dry conditions permits better discrimination of poor fen from bog. The wave, which cannot detect deep water flow in the bog sublayer of low hydraulic conductivity (the catotelm), is more sensitive to the shallower fen subsurface water and this makes possible the separation of poor fen from shrub bog. The requirement for polarimetric PALSAR acquisition during summer is brought out for more effective exploitation of PALSAR unique long wavelength penetration capabilities in monitoring arctic peatland transformations related to climate change stress. [C1836]

#### "Texture estimation in sar images: The impact of scale and model order"

This paper discusses methods and parameter settings that help to estimate texture in SAR images. In general, this is a difficult task for SAR images that are characterized by speckle noise and which span a wide range of pixel magnitudes. We applied Gauss Markov Random Field (GMRF) models and Enhanced Model Based Despeckling (EMBD) to 1 meter resolution amplitude images of the German TerraSAR-X mission. The results demonstrate that one can find appropriate parameter combinations that allow robust texture estimation even for different types of target areas. [C1837]

#### "Accuracy of the engineering calibration of weather radars"

This paper provides a synopsis of the accuracy calculation for the engineering calibration of a weather radar system. The underlying meteorological radar equation is optimized in order to reduce the total uncertainty of the calibration. Special emphasis is given to the determination of the different uncertainties of the various measurements which are required for a system calibration. A spreadsheet for the calculation of the total uncertainty of the calibration is presented. [C1838]

#### "Fine structure of the upper ocean from high-resolution Terrasar-X imagery and In-Situ measurements"

We investigate small-scale features using SAR imagery, including sharp frontal interfaces, slicks of artificial and natural origin, and wakes of surface ships. Collection of the ground truth data helps in the understanding of the physical mechanisms behind the patterns visible in the image. [C1839]

#### "Polarisation and mode combinations for ship detection using RADARSAT-2"

RADARSAT-2 provides new opportunities for spaceborne monitoring of vessel traffic and fishing activities. A series of RADARSAT-2 data has been collected and analysed over Norwegian waters. ScanSAR and Standard Quad-pol images have been used in the analyses. The Norne field is used as a test site, because it is possible to image the same vessel under different conditions. The different polarisations and polarisation combinations are analysed. [C1840]

#### "Assessment of airborne lidar data for instream flow type classification"

The information of instream biotype, i.e., types, location, distribution, etc, are important for estuary environment management. Field observations carry out by ecology surveyor is the standard procedure to gather that information, which is time consuming and difficult to be applied to a large spatial extend. In this research, we propose using airborne for instream biotype classification. Texture of point clouds is the key to distinguish between flow types, and semi-variogram was employed for texture measurement of different flow types. The principle component analysis is then used for classification and data compression. The results show that the first principle components are closely related to the flow types considered in this study. [C1841]

#### "Ground topography estimation over forests considering Polarimetric SAR Interferometry"

The work detailed in this paper analyzes the topographic phase retrieval process on forested areas by means of Polarimetric Interferometric SAR data. On the basis of the Random Volume over Ground scattering model, an alternative implementation for the retrieval of the topographic phase, avoiding the bias introduced by the volumetric scattering components is presented. [C1842]

#### "SAR mapping technology and its application in difficulty terrain area"

In western China, there is a large area perennially covered by cloud, fog, ice, and snow. It is very difficult to acquire optical image for mapping in this area, so high resolution spaceborne synthetic aperture radar (SAR) images have to be used to make topographic maps. A scheme of SAR mapping technology is proposed in this paper. Digital elevation model (DEM) was extracted with stereo radargrammetry (StereoSAR), and topographic map was created with ideal SAR stereoscopic image pairs. Due to the difficult terrain, parallax edit under stereoscopic observation is used for improving matching result from stereo images. Ideal SAR stereoscopic image pairs generated with image simulation based on DEM are used for stereoscopic observation to extract topographic features. Ascending and descending image data were combined to solve the problem of lack of information caused by shadow and layover. Mapping experiment in western China shows that SAR data with resolution of 3-8 meters can be used to make topographic map at scale of 1:50,000 by the scheme of SAR mapping introduced in this paper. [C1843]

#### **"Building detection and height estimation from high-resolution insar and optical data"**

State-of-the-art satellite SAR sensors acquire data of one meter geometric ground resolution, airborne sensors achieve even higher resolutions. Nonetheless, layover and occlusion hamper interpretability of such data particularly in urban scenes. In order to overcome this drawback, we use additional information from aerial photos to detect buildings. Features are extracted from both data sets and introduced to a common feature vector followed by a classification into building sites and non-building sites with Conditional Random Fields (CRF). Furthermore, we show that the different sensor geometries of the SAR and the optical sensor may be used to estimate building heights. [C1844]

#### **"Radar observations of wave field in littoral zone"**

The dissipation of the wave energy in the littoral zone is significant for the coastal hydro- and sediment dynamics. In this presentation, a recently developed method is presented about the separate, simultaneous measurements of wave propagating field and of wave breakers' velocity, based on ground based, Doppler, X-band Radar observations. The kinetic energy of the wave field is calculated for the last 2 km of the N. Sea towards the shore, with high spatial resolution (7.5 m) and the rate of the dissipated is estimated. [C1845]

#### **"Status of the Metop ASCAT soil moisture product"**

Since December 2008 the European Organisation for the Exploitation of Meteorological Satellites (EUMETSAT) has been disseminating global 25 km ASCAT surface soil moisture data in near real-time (within 135 minutes after sensing) over its broadcast system EUMETCast. The ASCAT surface soil moisture product is thus the first truly operational satellite soil moisture product that may be used for Numerical Weather Prediction (NWP), flood forecasting and other time-critical applications. In this paper we provide information about the status of the ASCAT Level 2 soil moisture processor, review first published validation and application studies and discuss plans for further improvements. [C1846]

#### **"Spaceborne sar imaging of coastal ocean phenomena"**

Synthetic aperture radar (SAR) observes the large-scale ocean surface wind field. With SAR instruments, we can actively monitor phenomena in the coastal ocean and marine atmospheric boundary layer at very high spatial resolution (on the order of tens of meters) in all weather conditions day and night. SAR observations are particularly useful in coastal regions where clouds are usually present, causing observation problems for visible and infrared sensors. SAR sensors onboard the RADARSAT-1/2, ENVISAT, ALOS, and other satellites can provide swath coverage of about 100 to 450 km, wide enough to cover oceanic and atmospheric meso-scale features. SAR has long been used to monitor the ocean surface wind field, vessel locations, oil spills, sea state, and sea ice at NOAA. In this paper, we present several case studies. [C1847]

#### **"SAR and optical images registration using shape context"**

Image registration is the process of overlaying two or more images of the same scene taken at different times, from different view points, and /or by different sensors. A novel feature-based multi-sensor image registration system is developed. The system consists of two new points: first, edge features are extracted from images, and the features are dilated to suppress some certain kinds of noise arising from groves; second, the preprocessed features are matched using the improved shape context. The shape context has been found to be robust in hand written digit and object recognition, and now it is introduced into remote sensing image matching after some adjustments. The developed system is successfully applied to register airborne optical and C-band SAR images in our experiments, and the results demonstrate its robustness and accuracy. [C1848]



### "Filtering and segmentation of polarimetric SAR images with Binary Partition Trees"

A new multi-scale PolSAR data filtering technique, based on a Binary Partition Tree (BPT) representation of the data, is proposed. Different alternatives for the construction and the exploitation of the BPT for filtering and segmentation are presented. Results with simulated and experimental PolSAR data are presented to show the capabilities of the BPT-filtering strategy to maintain both spatial details and the polarimetric information. [C1849]

### "A novel approach for redundant integration of finite differences and phase unwrapping on a sparse multidimensional domain"

Phase unwrapping and integration of finite differences are key problems in several technical fields, among which SAR interferometry. In this paper we propose a general formulation for robust and efficient integration of finite differences and for phase unwrapping, which includes standard techniques methods as sub-cases. The proposed approach allows obtaining more reliable and accurate solutions by exploiting redundant differential estimates (not only between nearest neighboring points) and multi-dimensional information (e.g. multitemporal, multi-frequency, multi-baseline), or external data (e.g. GPS measurements). The method requires the solution of linear or quadratic programming problems, for which computationally efficient algorithms exist. The validation tests performed confirm the validity of the technique. [C1850]

### "Insar time-series analysis for management and mitigation of geological risk in urban area"

This work shows the capabilities of InSAR time series analyses to support civil protection activities in the framework of geological risk management and mitigation. We discuss the outcomes from an integrated analysis of conventional in situ investigations and observations with advanced InSAR analyses carried out for the test sites of Agrigento and Naro (Italy), affected by ground instability respectively due to landsliding and tectonic forces. The study of past ground deformations provided valuable insights into the spatial and temporal patterns and behaviors of these phenomena, helping local civil protection authorities to focus resources on the areas of maximum need and to identify the most appropriate mitigation measures to reduce the impacts on elements at risk. [C1851]

### "Radargrammetric improvements: A multi-window approach"

This paper deals with the relevance of using stereoscopic radar images in order to retrieve the relief of terrain. Firstly, the basic characteristics of the radargrammetry are described. Thus, we present the results of the radargrammetric processing using the ZNCC procedure and applied to radar images. These images are recorded by the SIR-C mission over the French Alps. The results show that the image matching can fail, especially in foreshortened areas. So, we expose two different improvement methods using several correlation windows in order to cancel the reconstruction errors. The first improvement take advantage of a multi-window approach to combine information multiplying the correlation surfaces obtained for each correlation window size. The second improvement is based on another multi-window approach that makes it possible to get correlation windows adapted to the foreshortened areas. Finally, we combine these two improvement methods to show that it's possible to make the disparity map more reliable for the first step of the pyramidal scheme. [C1852]

### "Visual tracking of multiple interacting objects through Rao-Blackwellized Data Association Particle Filtering"

A multiple object visual tracking framework is presented, which is able to manage complex object interactions, missing detections and clutter. The main contribution is the ability to deal with complex situations in which the interacting objects can change their dynamics while they are occluded. This is achieved by explicitly estimating putative locations of the occluded objects. The tracking is modeled by a Rao-Blackwellized Data Association Particle Filter (RBDAPF), which has a tractable substructure that allows to analytically compute the object positions, while the object-measurement associations are approximated by Particle Filtering. Besides improving the accuracy, this filter decomposition reduces the computational cost, since the complexity with the number of objects becomes linear instead of exponential. The Particle Filter efficiently manages the measurements from visible and occluded objects, the clutter, and missing measurements to estimate the correct data associations that lead to a robust tracking. Experimental results on surveillance videos show that the proposed RBDAPF framework is able to track multiple interacting objects in complex situations. [C1853]

### "Aspects of multivariate statistical theorywith the application to change detection"

This paper proposes a new method for change detection measurement including whole SAR imaging modes such as PolIn- SAR, partial PolInSAR and InSAR in a set of multi-temporal multidimensional SAR images. The method is based on the special case of Kullback-Leibler (KL-divergence) test, known as Mutual Information. In



order to develop an algorithm, firstly the joint distribution of PolInSAR data set, based on the second order statistics has been derived. Such a derivation accounts for the whole multi-temporal SAR images. Then the mutual information is used to measure the difference between the joint density of multi-temporal PolSAR data sets and their marginal density known as complex Wishart distribution. A comparison between the proposed and the other well-known change detection (e.g. cross correlation) technique is shown by means of real data, describing the advantages due to the fact that the proposed change detector involves almost every facet of the applied change detection. [C1854]

#### "POLSAR image classification using BP neural network based on Quantum Clonal Evolutionary Algorithm"

POLSAR image classification plays an important role in remote sensing. POLSAR data are a type of mass data and have more independent features which can represent different physical significances than optical image. Therefore, POLSAR image classification is actually a high dimensional nonlinear mapping problem. Because of the nonlinear mapping function of BP neural network, it can be used to classify POLSAR image. But BP neural network classifier is sensitive to initial weights and thresholds. Quantum Clonal Evolutionary Algorithm (QCEA) can converge to an optimal value quickly and can be used to optimize the initial weights and thresholds of BP neural network. Therefore, in this paper, BP classifier based on QCEA was used for POLSAR image classification. Firstly, optimize the initial weights and thresholds of BP neural network using QCEA. Secondly, train the optimized BP neural network classifier by gradient descent algorithm. Finally, classify the POLSAR image using the trained classifier. The validity test is demonstrated using Danish EMISAR L-band fully polarimetric data of Foulum Area (DK), Denmark. The preliminary result indicates that this method can classify most of the areas correctly. [C1855]

#### "Automatic registration of sar and optical image based on multi-features and multi-constraints"

This paper proposes a two-stage registration method for SAR and optical images based on multi-features and multi-constraints. In the first stage, closed regions are extracted automatically to achieve the coarse mapping parameters as geometrical restriction. In the second stage, Harris corner points and cross-road features are extracted, and then correlation analysis and mutual information are utilized to match the corresponding control points. After that, multi-constraints are used to delete the false matched points. The retained ones are served as ground control points for registration. The experimental results show that the method can reduce the possibility of false matching effectively and the registration error is within one pixel. [C1856]

#### "Beamwidth analysis for SAR processing of airborne depth-sounder data over ice sheets"

Information on the bedrock topography below the Greenland and Antarctic ice sheets is vital to developing models of future sea-level rise. To measure the topography, advanced data acquisition and processing techniques, including Synthetic Aperture Radar (SAR), are required. This work investigates the optimal beamwidth that would enable SAR processing to maximize the signal to noise ratio of the target. Platform height above the ice surface and bedrock roughness determine the optimal beamwidth. We found that for data collected at a "typical" altitude of 867 m, the optimal beamwidth is about 8°. In the high-altitude case, we found that beamwidth did not have a significant effect on the signal-to-noise ratio. This is probably related to scattering from the ice surface. [C1857]

#### "DSM generation from very high optical and radar sensors: Problems and potentialities along the road from the 3D geometric modeling to the Surface Model"

The availability of new high resolution optical and radar spaceborne sensors offers new interesting potentialities for the acquisition of data useful for the generation of Digital Surface Models (DSMs). The accuracy level of DSM is strictly related both to the image orientation and to the matching process. As regards the image orientation, remote sensing community usually adopts two different types of models for High Resolution Satellite Imagery (HRSI): the physical sensor models and the generalized sensor models also called rigorous and Rational Polynomial Functions (RPFs) models respectively. In a scientific software developed by the research group of Geodesy and Geomatic Area of the University of Rome "La Sapienza" both rigorous and RPFs models are implemented, with a specific tool for the terrain-independent Rational Polynomial Coefficients (RPCs) generation; the software manages the imagery acquired by several optical sensors (EROS A, Ikonos, QuickBird, Cartosat-1, WorldView-1, GeoEye-1) and by the Italian SAR constellation COSMO-SkyMed. In the same software a facility for image matching is embedded. The Area Base Matching (ABM) is used, combined with the orientation model re-parametrized in terms of RPCs. In the present work some examples of models application and DSM generation are analyzed and discussed. [C1858]

### "A new Bayesian source separation approach to blind decorrelation of SAR data"

In this paper, a novel approach for performing blind decorrelation of SAR data is proposed. A patch-wise computation of the point-spread function (PSF) is performed directly from the SAR data to account for spatial nonstationarities present in SAR. The problem of estimating the PSF is formulated as an additive source separation problem in the frequency domain, and is subsequently solved using a Bayesian least squares estimation approach based on a Fisher-Tippett log-scatter model. Experimental results using both simulated SAR data and real RADARSAT-2 SAR sea-ice data showed that the proposed decorrelation approach can successfully learn the correct PSF and significantly reduce the correlation in SAR data. [C1859]

### "Sparsity-driven focused SAR image formation"

Most imaging systems are adversely affected by the errors in the observation model. One significant example is encountered in synthetic aperture radar (SAR) imaging. Inexact measurement of the distance between the SAR sensing platform and the scene center or random delays on the transmitted signal result in model errors. These errors appear as phase errors in the SAR data and they cause defocusing of the reconstructed image. Mostly, phase errors vary only in the cross-range direction. However, in many scenarios, it is possible to encounter 2D phase errors, which are both range and cross-range dependent. In this study, a sparsity-driven method for joint SAR imaging and phase error estimation is proposed. This method is able to correct 1D as well as 2D phase errors. Experimental results show the effectiveness of the proposed method. [C1860]

### "SAR complex image analysis: A Gauss Markov and a multiple sub-aperture based target characterization"

In this paper we discuss Gauss-Markov Random Field (GMRF) based on multiple sub-aperture decomposition method for the analysis of targets in complex-valued high-resolution SAR data. Gauss-Markov Random Field (GMRF) model with a quadratic energy function as a parametric analysis parameterizes the spectrogram of the signal, whereas sub-aperture decomposition method exploits the holographic property of the spectrum at the cost of reducing resolution. This analysis helps to understand, characterize and analyze complex-valued SAR data and provides temptation to use complex-valued SAR data over detected data. [C1861]

### "Polarimetric decomposition for forest biomass retrieval"

In this paper, the decomposition of fully polarimetric SAR data into three canonical scattering mechanisms is investigated with respect to forest biomass retrieval. It is demonstrated that the dominant backscattering contribution depends strongly on the frequency, incidence angle, and stand condition. The relation between in-situ biomass measurements and the individual decomposition components is examined. [C1862]

### "Realization of the NASA Dual-Frequency Dual-Polarized Doppler Radar (D3R)"

This paper describes some of the novel technologies adopted in the realization of the NASA Dual-frequency Dual-polarized Doppler Radar (D3R) system for to be used by the GPM ground validation program. A description of the transceivers and major trades that lead to a solid-state architecture is presented. Other aspects enabling the design such as the waveform design and generation and the digital receiver is also described. Data measured from a similar power amplifier was used to estimate the expected range side lobe performance. An estimate of the expected sensitivity based on the transceiver parameters also presented. [C1863]

### "Polarimetric SAR estimation based on non-local means"

During the past few years, the non-local (NL) means have proved their efficiency for image denoising. This approach assumes there exist enough redundant patterns in images to be used for noise reduction. We suggest that the same assumption can be done for polarimetric synthetic aperture radar (PolSAR) images. In its original version, the NL means deal with additive white Gaussian noise, but several extensions have been proposed for non-Gaussian noise. This paper applies the methodology proposed in to PolSAR data. The proposed filter seems to deal well with the statistical properties of speckle noise and the multi-dimensional nature of such data. Results are given on synthetic and L-Band E-SAR data to validate the proposed method. [C1864]

### "An application of reciprocity to the numerical modeling of a GPR system"

In this paper, a technique is developed to model ground penetrating radar interactions. It combines reciprocity with the results from a full numerical model and allows one to compute a large number of scattering responses simultaneously, provided the scatterers are small. The results of an example calculation are shown and compared with a full numerical model and a possible application is demonstrated. [C1865]

### "Eigen decomposition parameter based forest mapping using Radarsat-2 PolSAR data"

In this paper, a set of polarimetric eigenvalue and eigenvector based parameters, e.g. entropy and anisotropy, are investigated for forest application. The correlation terms of the eigenvectors,  $\mu_1$  and  $\mu_2$ , are found to be better for forest mapping in both summer and winter using Radarsat-2 quad-polarimetric space borne SAR data. These are used to automatically identify forest class pixels from the volume scattering category of a Freeman-Durden Wishart unsupervised segmentation map. The algorithm scheme was developed and implemented using fully polarimetric Radarsat-2 SAR (PolSAR) data acquired in July and October and the validity was evaluated using the ground reference data created from SPOT5 K-clustering classification map. [C1866]

### "Polarimetric SAR tomography of natural environments using hybrid spectral estimators"

SAR tomography is the extension of conventional two dimensional SAR imaging principle to three dimensions. In order to improve the vertical resolution with respect to classical Fourier-based methods, high resolution approaches are used in this paper to perform SAR tomography. Both nonparametric spectral estimators, like beamforming and Capon and parametric ones, like MUSIC, maximum likelihood, are applied to real data sets and compared in terms of scatterer location accuracy and resolution. This paper addresses the discrimination of coherent scatterers presented in the natural environment and a joint approach of estimation and detection is proposed. [C1867]

### "Mean-shift and hierarchical clustering for textured polarimetric SAR image segmentation/classification"

Image segmentation and unsupervised classification are difficult problems. We propose to combine both. A clustering process is applied over segment mean values. Only large segments are considered. The clustering is composed of a mean-shift step and a hierarchical clustering step. The hierarchical grouping is based upon a powerful segmentation technique previously developed. The approach is applied on a 9-look polarimetric SAR image. Textured and non-textured image regions are considered. The K and Wishart distributions are used respectively. The unsupervised classification results can be very useful for image analysis and further supervised classification. The obtained region groups constitute an important simplification of the image. [C1868]

### "On the use of Support Vector Machines for land cover analysis with L-band SAR data"

This study investigates a new technique for land cover analysis by means of the Support Vector Machines. Intrinsic spatial variability within SAR images, beyond that caused by speckle, is of high interest for land cover characterization and classification. However, its use is still an ongoing issue due to its complex multi-scale nature. On the other hand, classification algorithms based on statistical learning methods such as the supervised Support Vector Machines (SVM) approach are implemented in a wide range of data mining applications. SVM can also be used as a technique for feature selection. In this paper, a new tool using the Recursive Feature Elimination SVM-based process (SVM-RFE) and the textural Haralick's parameters is introduced. The real contribution of textures within the land cover classification can be understood. A small set of textural parameters is determined at local scale while being optimal for the land cover discrimination. In this study, orthorectified 50m resolution data acquired by the L-band PALSAR/ALOS sensor are used. [C1869]

### "An improved CSA for one-stationary BiSAR squint mode"

The purpose of this paper is to solve the imaging problems of one-stationary bistatic synthetic aperture radar (BiSAR) squint mode. Through the analysis of the target's two-dimensional spectrum, an improved chirp scaling algorithm (CSA) is got. It can deal with the space variability of this kind of BiSAR and the simulation is done to verify the validity and feasibility of this algorithm. [C1870]

### "Coherent marine radar measurements of properties of ocean waves and currents"

Marine radars offer the capability to image ocean wave propagation by virtue of repetitive coverage of the same scene. With a typical 1.25-s rotation period, ocean wave frequencies of 0.4 Hz can be measured unambiguously. Imaged areas of the order of ten square kilometers, allow the dynamics and kinematics of ocean wave fields to be measured with higher azimuthal resolution than traditional oceanographic instruments, such as buoys or pressure sensors. Using the dispersion relation for shallow waves in coastal regions, ocean wave spectra and bathymetry can be estimated using non-coherent marine radars. The derivation of wave height or wave height spectra from marine radar imagery has had some success by relating the radar echo intensity imagery of waves to wave height using an empirically derived modulation transfer function (MTF). More recently, using a radar scattering model's dependence of the radar scattering cross section on long wave slope, good results are

reported in deep water for shipboard experiments, where winds and waves are typically in the same direction. However, in coastal waters, offshore winds blowing in a direction other than that of the incoming wave field can produce enhanced roughness on the front face of waves, resulting in a modulation of the radar wave field image that is not wave height dependent. A coherent radar can overcome these limitations using the direct measurement of the radial component of orbital wave velocity, accounting for Bragg scatter velocity. Radial orbital velocity will maximize and minimize at similar locations on long wave profiles as do radar echo intensity, so wave patterns should look very similar for the two. Thus, analysis methods similar to those used in non-coherent radar studies should be applicable to coherent radar data as well. We present recent experimental results on the retrieval of coastal ocean wave and current properties due to a storm over the Outer Banks of North Carolina in November of 2009. [C1871]

#### "Ship detection and measurement using the TerraSAR-X dual-receive antenna mode"

The detection of ships and the retrieval of parameters like vessel velocity, heading and size are important techniques for ocean and shore surveillance systems. Space borne SAR along-track interferometry (ATI) can detect ships for large areas and measure their velocity at the same time by means of interferometric phase. In this paper we report about first results of automatic ship detection using TerraSAR-X ATI. [C1872]

#### "RPC modeling for spaceborne SAR and its application in radargrammetry"

The RPC (Rational Polynomial Coefficient) model can be used as a replacement sensor model for geo-coding spaceborne SAR data. A hybrid method, combining the L-curve and the IMCCV (Iteration method by correcting characteristic value) method, for solving ill-conditioned equations in the RPC model is proposed. The hybrid method can get higher accuracy at low cost of calculation time. Based on an example in Malaysia, the application for fast RPC geocoding for stereo radargrammetry is shown. [C1873]

#### "Data acquisition of vessel ISAR data with assistance of automatic identification system"

In the past, imaging of moving vehicles using the principle of inverse synthetic aperture radar (ISAR) has typically been applied to ground moving vehicles or air and space borne objects. Nowadays, demands to image moving vessels on sea come along for both military applications and coastal surveillance. New processing algorithms have to be developed to focus ISAR data of vessels because of the complicated three-dimensional rotational motion and the sea clutter. Experimental data have to be available for the development process. To be able to acquire these data, the airborne radar sensor PAMIR of Fraunhofer FHR has been extended by integrating a receiver for automatic identification system (AIS) messages, which supports the system with position information of the vessels on sea. The paper shows the hardware integration and software implementation. Benefits of the information gained from the received AIS messages are discussed and results of first acquired data are presented. [C1874]

#### "A new SAR sensor designed for micro-satellites"

Micro Satellites ( $\mu$ SATs) are good opportunities for small countries. This paper describes a new design of a SAR for a  $\mu$ SAT. The centre frequency and the SAR processing were optimized in a way to allow the realization of a simple but capable system that provides many interesting opportunities for researchers and allows participating to international environmental monitoring and control activities. The major points of the design are a frequency that allows some penetration through vegetation and a relative small antenna in length and width. A new SAR processing concept allows a medium swath-width and an acceptable resolution. A patent is pending. [C1875]

#### "Morphological filtering of SAR interferometric images"

This paper proposes a new morphological filter for SAR interferograms. It is based on a modified version of alternate sequential filters with reconstruction (MASF), in which the structuring elements are adaptively defined according to the fringe directions. This provides a good fidelity to the fringe information while efficiently removing noise. Another feature of the proposed approach is to apply the filter on the original interferogram and on shifted version, to overcome the wrapping of the phase, and to combine the two results. The proposed filtering technique is then tested on both simulated and real data with different levels of noise. It is also compared to previous techniques according to simplicity and noise reduction. [C1876]

#### "Relations between SAR tomography and full-waveform LIDAR for structural analysis of forested areas"

Active remote sensing techniques, like SAR tomography and full-waveform LIDAR, are able to capture the 3D reflectance function at or inside objects. They are therefore of special interest for analyzing forest environments.



Research goals are the derivation and characterization of the different physical measurement aspects of data taken over forested areas, as well as establishing mutual relations in such a way that LIDAR data can be used to calibrate and correct 3D density data of SAR tomography. The paper outlines the phenomenology of forested areas in SAR tomograms and full-waveform LIDAR data and sketches a simple mathematical methodology for linking SAR and LIDAR reflection density profiles. [C1877]

#### **"Optimal algorithms for spaceborne altimeter"**

This paper is dedicated to new methods of space altimeter altitude and sea surface significant wave height (SWH) measuring. These methods are based on the fundamentals of Bayesian optimal measure method of a parameter. Optimal discriminators of the parameters are developed using the least square error of the estimate criteria, apart from others papers which mostly minimize the least square error of altimeter waveform fitting function. Potential measurement accuracy calculation results are also presented. [C1878]

#### **"Development and experiments of a passive SAR receiver system in a bistatic spaceborne/stationary configuration"**

In this paper, the development of a stationary SAR receiver system using TerraSAR-X as transmitter is described. First the bistatic geometry and expected resolution are considered. After giving an overview of the hardware setup, the expected performance of the system is evaluated. The paper ends with the processed results of a measurement campaign performed in summer and fall 2009, and a comparison with the monostatic data acquired by the TerraSAR-X satellite. [C1879]

#### **"Detection of salient features in surface current maps from dopplerized X-band radar"**

The mapping of the near surface currents and their interaction with the spatial and temporal varying bottom topography is of high significance for the experimental analysis of morphodynamic processes in coastal areas and the monitoring the effectiveness of coastal protection actions. An efficient application is also the real-time monitoring of currents in harbours to pilot large vessels [8]. The next steps of this inquiry are the application of image processing methods to extract also, together with the orientation, length scales and spatial shifts of salient current features. The correlation with salient features of the bed topography will be analyzed further together with sea state images that can also be deduced from radar data. [C1880]

#### **"Quasar SBK accurate internal calibration"**

A new compact fully polarimetric Ku band SAR system (SBK) is being developed by INTA radar Laboratory as an advanced payload for QUASAR project, which involves INTA new SAR developments for small platforms and UAV's. As an operative system, SBK shall allow precise calibration of the obtained data in order to achieve high products quality. The present paper shows SBK internal calibration concept focusing on internal calibration facility description, on ground characterization task overview and in flight calibration method. Furthermore, internal calibration accuracy estimation based on first prototypes measurements is also presented. [C1881]

#### **"Extraction of typhoon-damaged forests from multi-temporal high-resolution polarimetric SAR images"**

The purpose of this study is to extract the forests destroyed by typhoons and to quantitatively estimate the damage levels by using high-resolution polarimetric synthetic aperture radar (SAR) data. The study area is located in Tomakomai, Hokkaido, Japan. Two sets of data were acquired before and after the typhoon by the L-band airborne Pi-SAR (Polarimetric-interferometric SAR) with 3m Ч 3m resolution (4-look in azimuth direction). It was found that the values of RCS (Radar Cross Section) averaged over the whole image after the typhoon damage changed by -0.47 dB, 0.05 dB, and 0.64 dB at HH-, HV-, and VV-polarization respectively in comparison with those before the damage. To fully utilize the data, a scattering model of the linear combination of the cross- and co-polarization RCS changes was developed to estimate the damage levels. Similar analytical approaches were also applied using the three-component decomposition analysis. The changes in RCS of double-, volume- and surfacescattering mechanisms after the damage were respectively 27.5 dB, -0.20 dB and -20.3 dB. Finally, by comparing the results with the ground survey data, the accuracies of 64.1% and 77.7% were obtained for the RCS and decomposition analyses respectively. [C1882]

#### **"Rice areas mapping using ALOS PALSAR FBD data considering the Bragg scattering in L-band SAR images of rice fields"**

The objective of this paper is to assess the use of ALOS PALSAR FBD data to map rice growing areas. Image enhancement in backscattering in rice fields as a result of Bragg resonance scattering was found only at HH

polarization since double-bounce scattering is a prerequisite to Bragg resonance scattering for radar backscatter from bunches of rice plants. A rice mapping method using HV images was developed and applied to Haian test site. Validation showed that rice mapping using L-band SAR is promising when cross-polarized data are available to cope with the Bragg resonance scattering effects. [C1883]

#### **"Bistatic SAR based on Terrasar-X and ground based receivers"**

The paper presents the development of a ground based bistatic receiver using TerraSAR-X as a transmitter. The receiver subsystems like antennas, low-noise amplifiers, mixers, filters, synthesizers, etc. have been developed using low-cost monolithic devices in order to allow affordable deployment and at the same time offer final year students a challenging SAR engineering project. First raw data have been acquired on the Barcelona harbor area that has been focused producing geocoded images well matched with existing maps. A preliminary interferogram have been also produced. [C1884]

#### **"Designing an Illegal Mining Detection System based on DinSAR"**

Satellite Differential Radar Interferometry (DInSAR) has demonstrated its ability for monitoring mine-induced ground subsidence. However, it is still a challenging task to routinely identify all mining activities from the large-scale coverage interferogram, especially the illegal mines. In response to this challenge an underground mining detection system based on DInSAR is described. The system is tested over a dense mining area in Asia. With such a system it is hoped that the detection efficiency of illegal underground mining using DInSAR can be improved. [C1885]

#### **"Effect of squint imaging on beam position design of space borne SAR"**

Range migration of space borne SAR at large squint angle is much greater than the side-looking SAR, and longer echo receiving window is needed. Thus, the traditional beam position design method is invalid. In this paper, the method of drawing zebra map is improved by taking the range migration into consideration. The maximum and the minimum slant ranges during the synthetic time are derived. This paper also analyses the relation between the effective swath width and the range beam width at large squint angle. Simulation for X-SAR system proves that a given azimuth resolution limits the squint angle. STK and echo simulation are used to verify the validity of the improved beam position design method. [C1886]

#### **"Dual-polarized, coherent microwave backscatter from rough water surfaces at low grazing angles"**

We show that at low grazing angles, breaking wave effects are very important in HH polarized microwave backscatter from the ocean but less so at VV polarized backscatter. When the ocean surface is disturbed only by wind, breaking wave effects in VV backscatter are much smaller than Bragg scattering, even at low grazing angles. For HH polarization, on the other hand, breaking wave effects are very important at low grazing angles. In the presence of surface current gradients set up by internal waves, HH cross sections can exceed those at VV by as much as 10 dB near internal wave crests, indicating enhanced breaking wave effects that cannot be described as specular. Breaking effects are nearly as strong as Bragg effects in VV backscatter under these conditions. Spectral comparisons confirm these conclusions. [C1887]

#### **"Quikscat backscatter sensitivity to landscape freeze/thaw state over ALECTRA sites in Alaska from 2000 to 2007: Application to SMAP validation planning"**

The mapping of freeze/thaw state of the landscape is one of the main objectives of NASA's upcoming SMAP (Soil Moisture Active and Passive) mission. This study applies ALECTRA (Alaska Ecological Transect) biophysical network and QuikSCAT scatterometer data to evaluate some of the validation issues regarding the SMAP freeze/thaw measurements. Although the QuikSCAT data is at Ku-band frequency, rather than the L-band of the SMAP instrument, the data is utilized due to its uniquely high temporal resolution over the ALECTRA sites. The results show that multiple temperature measurements representative of individual landscape (soil, snow cover, vegetation and atmosphere) elements and spatial heterogeneity within the satellite field-of-view are important for understanding the radar backscatter process and aggregate freeze/thaw signal. The backscatter temporal dynamics and relative contribution of these landscape elements to the freeze-thaw signal varies with land cover type, seasonal weather and climate conditions. [C1888]

#### **"Road surface quality measurement using inexpensive radar"**

The near surface dielectric characteristics of pavement can indicate the overall health of roadways and bridge decks. By performing simple and fast reflectometry measurements of the near surface, it may be possible to efficiently monitor large amount of critical civil infrastructure, and provide early alerts of the initial stages of

damage. We demonstrate the variation with moisture content of surface reflected waves using a commercial-off-the-shelf 24 GHz FMCW radar. Initial experiments show that detectable amounts of water is absorbed in asphalt and concrete. The amount of absorbed water increases with micro- and macro-cracking, and this measurement will correlate with quantifiable changes in the observed return signal. [C1889]

#### "A shadow percentage estimation method for Radar look angle selection in spaceborne INSAR application"

Spaceborne INSAR (Interferometric Synthetic Aperture Radar) is an important remote sensing tool for topographic mapping, while there are inevitably shadow areas in Radar images. Shadow area has no radar echo signal or low coherence SNR (signal noise ratio). In this paper, Shadow area percentage estimation according to Radar look angle is proposed. Digital elevation model of natural terrains and ascending and descending orbits are used in simulation. This estimation method is suitable for incidence angle considerations in the phase of INSAR system design. [C1890]

#### "Doppler processing of coherent radar backscatter for ocean surface wave measurements"

The technique for extracting wave period and wave direction from a navigation radar backscattering intensity is well developed but the determination of spectral density or wave height is hindered by the complex nature of the modulation transfer function. In contrast to backscattering intensity, Doppler velocity from coherent radar is the radial velocity of the scattering objects. Its oscillatory component is contributed by ocean waves. The spectral peak component of Doppler velocity is close to the peak wave period measured by a nearby buoy and the significant wave height can be accurately calculated. With radar range coverage on the order of ten dominant wavelengths, reliable assessment of peak wave period and significant wave height is achievable with radar data as short as one second. Wave direction can also be determined with a scanning system. [C1891]

#### "Decomposition methods for the estimation of bare soil surface parameters using fully polarimetric SAR data 1"

This study wants to demonstrate that two different polarimetric target decomposition methods can improve SAR data accuracy for estimating the parameters of bare soil surface. To achieve this goal, two experiments are conducted: (1) both Freeman and Cloude decomposition methods are performed on JPL/AIRSAR L-band fully polarimetric data; and (2) Advanced Integral Equation Model (AIEM) is used to simulate backscattering coefficients. The root mean square errors (RMSEs) of  $\sigma_{0hh}$ ,  $\sigma_{0vv}$  between original data and AIEM simulated data are 1.96 and 1.25 dB. However, if Cloude method is used to decompose original data, the RMSEs will be reduced to 1.45 and 1.14dB, respectively; for Freeman method, the RMSEs are 1.64 and 1.35 dB. Therefore, polarimetric target decomposition compensation, especially Cloude method, can help to improve the accuracy of SAR data for estimating the parameters of bare soil surface. [C1892]

#### "Canopy height, crown cover, and aboveground biomass maps for the southwestern United States from MISR, 2000 and 2009"

Red band reflectance factor data from NASA's Multiangle Imaging SpectroRadiometer (MISR) were used to create maps of woody plant canopy cover, fractional height, and aboveground biomass for the southwestern United States, via inversion of a geometric-optical (GO) model provided with reflectance magnitude and anisotropy via a Li-Ross bidirectional reflectance distribution model. Crown cover, canopy height, and biomass distributions are compatible with those seen in other data sets, although there are anomalies associated with the use of the same set of background prediction coefficients over the 10-year period. [C1893]

#### "A two-pass random forests classification of airborne lidar and image data on urban scenes"

Random forests ensemble classifier showed to be suitable for classifying multisource data such as lidar and RGB image for urban scene mapping. However, two major problems remain: (1) the class boundaries are not well classified, a common issue in classification (2) the data are highly imbalanced raising another issue more specific to urban scenes. In this paper, we propose a new ensemble method based on the margin paradigm to improve the classification accuracy of minor classes. Random forests classifier is used in a two-pass methodology with an improved capability for classifying imbalanced data. [C1894]

#### "Radarsat Constellation, moving toward implementation"

The Canadian Space Agency initiated the development of a three-satellite SAR mission, known as the RADARSAT Constellation Mission (RCM), in 2005. The main objective of the mission is to assure C-band data continuity in the next decade, while allowing a greater use of data for operational applications by providing more

persistent observation over Canada and better system reliability. The Phase B contract was awarded in November 2008 for a period of 16 months. The Space and Ground Segment Requirements reviews were held at the end of February 2009. The spacecraft and Ground Segment concepts were adopted and design decisions have been taken to allow preliminary design to proceed. A Payload and Bus Preliminary Design reviews were held in Fall 2009. A Mission Preliminary Design review was held in February 2010. The CSA is currently in phase C and preparing for the Critical Design Review. Several challenges, such as the implementation of the ship detection mode or the final selection of the launcher must be resolved and important decisions must be taken to allow the progress of the program toward full implementation. The first spacecraft will be built and tested as a proto-flight and launched in 2014. The following two spacecrafts will then be built and tested in parallel and launched in 2015. [C1895]

#### "MIMO SAR processing with azimuth nonuniform sampling"

This paper analyses ambiguity suppression caused by multiple-input multiple-output (MIMO) SAR azimuth nonuniform samplings. Two methods are analyzed: azimuth spectrum reconstruction algorithm and minimum mean square error (MMSE) imaging algorithm. The azimuth spectrum reconstruction algorithm can reconstruct the scene fine resolution, while the nonideal orthogonality of multi-channel encoding waveforms causes azimuth ambiguous in SAR imaging. The MMSE imaging algorithm can perfectly reconstruct, while it requires high SNR. [C1896]

#### "Automation of object extraction from LiDAR in urban areas"

Light Detection and Ranging (LiDAR) has become a valuable data source for urban data acquisition. This paper gives an overview about current trends in the automation of object extraction from LiDAR data. These trends are caused by the technical development of LiDAR sensors that enable the acquisition of point clouds at higher resolution as well as the recording of the full waveform of the returned signal, and by the adoption of processing techniques from the Computer Vision and Pattern Recognition communities. Triggered by these developments, new applications are being found for LiDAR data. [C1897]

#### "What is the information content of TRMM precipitation radar for determining radiometer observations and vice versa?"

Both the space borne radar and the radiometer suite on the TRMM satellite observe the same column of precipitation and derive rain rates, however at different spatial resolutions. The observations from TRMM PR and TMI are fundamentally different measurements. While the radar provides a backscatter measurement resolved in the vertical direction, the radiometer is a passive instrument obtaining integrated observations over the full depth of the cloud. In addition, they respond to different physical mechanisms. Nevertheless, they observe the same precipitation medium and retrieve the same output products. Therefore, it begs the question, what type of information about radiometric observations can be directly retrieved from radar observations. This question can be further focused and stated as: To what extent can one predict the radiometric observations from radar observations? This question can be answered in several ways, and one of them is an informational theoretic approach using neural networks which is described in this paper. [C1898]

#### "Detection of land subsidence in Beijing, China, using Interferometric Point Target Analysis technique"

Land subsidence in Beijing is supposed to be caused by over-exploitation of ground water, which is leading to a rapid decline of water levels, drying out clay layers that finally result in land subsidence. The Interferometric Point Target Analysis (IPTA) is an advanced method to monitor vertical motion of the land surface over time. IPTA identifies backscattering objects, named as coherent points or points targets, at the ground surface that persistently reflect radar radiation emitted by the SAR antenna. The core component of the IPTA technique is the iterative estimation of phase differences for all measurement points over the sets of the SAR data using a linear model. In this paper, IPTA technique was used to retrieve the phase history, extract the linear deformation information from interferometry phase and weaken atmosphere phase delay in Beijing. 20 ENVISAT ASAR images acquired between June-18-2003 and March-14-2007 have been selected. The intention of this article is to demonstrate how IPTA technique could be used to extract valuable information in Beijing area. [C1899]

#### "Polarimetric and interferometric applications in a bistatic hybrid SAR mode using Terrasar-X"

A lot of bistatic experiments have recently been performed by different researchers to show the differences between monostatic and bistatic SAR. The acquired data was needed to verify the developed bistatic processing algorithms. To extend the conventional bistatic SAR experiments, we investigated whether bistatic systems can



be used in the field of bistatic interferometry and polarimetry, also shown by [3]. For this purpose we have used our stationary receiver system together with TerraSAR-X as transmitting satellite. This paper describes the experiments and shows some results we obtained using single and repeat pass SAR configurations. [C1900]

#### "A comparison on the new electronic attack techniques against pulse compression radars"

In this study, the mathematical models of Smeared and Chopping/Interleaving Spectrum techniques, which are recent electronic attack techniques against the pulse compression radars, are presented. Then, matched filter outputs are compared by means of a simulator. Moreover, the effect of the weighting filter in the radar receiver is also analyzed. [C1901]

#### "A new algorithm for wind speed at low incidence angles using TRMM Precipitation Radar data"

Large datasets from crossovers of Precipitation Radar (PR) and buoy observations clearly demonstrate that ocean PR backscatter correlates with both the near-surface wind speed and the sea surface wave slope. Multi-incidence angles PR data are used to retrieve surface wave slope parameter and normalized nadir backscatter. After that, an empirical wind speed model was developed based on those two parameters that attenuates the surface tilting effect. The inversion is defined using a multilayer perceptron neural network with radar-derived backscatter and surface wave slope parameter as inputs. Results show the root mean square errors between retrieved wind speeds and in situ buoy observations is 1.36m/s, bias is nearly zero, revealing good agreements in wind speed estimations. [C1902]

#### "Monitoring flooded area fraction in floodplains of Parana basin using passive and active microwave systems"

Over the past two decades, orbital passive microwave systems have proven to be sensitive to flood condition in large floodplains. This sensitivity is rooted in the well differentiated emission properties of calm water with respect to non-flooded land of any kind. In this paper, AMSR-E observations of an herbaceous wetland area on the Parana River sub-basin were analyzed during the 2009-10 timeframe when this region was affected by a strong and long lasting flooding. Evident effects on the difference between vertically and horizontally polarized brightness temperatures ( $\Delta T$ ) were observed at C-band. The fraction of vegetated flooded area was estimated by applying an improved algorithm which uses ENVISAT ASAR data at specific dates to calibrate AMSR-E temporal series. Also, using a theoretical emission model, the behavior of  $\Delta T$  flooded is discussed. [C1903]

#### "Iceberg size and orientation estimation using SeaWinds"

From 1999 to 2009, the SeaWinds scatterometer has been used to detect and track large Antarctic icebergs on a daily basis. Here, we develop an automated estimation algorithm to supplement iceberg position reports with estimates of the iceberg's major axis length, minor axis length, and angle of orientation. A maximum-likelihood objective function that relates measured backscatter to model-based simulated backscatter is developed. The utility of the estimation approach is analyzed in simulation and via a case study of iceberg A22a. Subsequent results agree with and supplement reports compiled by the United States National Ice Center. [C1904]

#### "The characteristics of post-seismic surface deformation of the Wenchuan MS 8.0 earthquake from InSAR"

The D-InSAR technology is used to acquire four strips of post-seismic surface deformation of Wenchuan M8 earthquake of 2008 from the ALOS/PALSAR satellite data of Japan. The result covers the Yingxiu town, Wenchuan, Shifang, Maoxian county, Beichuan, Pingwu and Qingchuan county in Sichuan Province. Some post-deformation characteristics is showed in the final result. Around Yingxiu town, the epicenter of main shock, a area of uplift is present with small amplitude 0-5cm at the northern wall of the causative fault, while relative subsidence took place with the amplitude 0-15cm on the other wall. Near Shifang county, there are slightly arranged concentric fringes, reflecting another subsidence area with amplitude 0-20cm. Around the Beichuan and Anxian county, there exists a relatively small uplift of an strip area with 0-5cm along the causative fault on its both side. A small area of dense concentric fringes(indicated by a rectangle box) appeared in 30km northeast of Qingchuan, which coincide with the locations of the aftershocks Ms6.1 of 5 Aug. 2008. On the lower wall, we can see another large uplift area of sparse concentric fringes located in more than 100km southeast of Qingchuan, because it is far from the causative fault, it's impossible so large deformation took place, and it should attribute to atmospheric component. the deformation characteristics of the whole area is complicated generally. [C1905]

#### "Characterization of volume scattering of dry sand at millimeter-wave frequencies"

Fully polarimetric measurements of volume scattering contribution from dry layer of fine sand with smooth air/sand interface were performed at millimeter-wave frequencies. The measured radar response was compared to predictions made by the numerical solution of the DMRT model. Sand particles were modeled as spherical particles. The simulated response was able to predict the angular dependence of the data but was not able to predict accurately the absolute level, especially for the cross-polarized return. Furthermore, a simpler model, which was developed earlier for asphalt surfaces and is based on 1st order solution of RT for semi-infinite medium, was tested against the measured data. The model was not able to predict the angular dependence demonstrated by the measured data. [C1906]

#### **"Validation of tie-point concepts by the DEM adjustment approach of TanDEM-X"**

The aimed accuracies for the final TanDEM-X DEM of 10m absolute and 2m relative height error will be ensured by calibration data. One crucial data set for the relative accuracy is tie-points that connect adjacent DEM acquisitions in the approximately 4km-overlap-area with each other. In this paper an improved concept for tie-point candidates is presented that is based on averaging a larger region instead of comparing single points. This concept should be more robust against noise. It is validated by applying the DEM calibration on a simulated test area, as real TanDEM-X data was not yet available. Also, the DEM calibration will be validated for the first time on a larger "real" test site by applying the TanDEM-X processing scenario. [C1907]

#### **"Forest parameter retrieval from SAR data using an estimation algorithm applied to regrowing forest stands in Queensland, Australia"**

The use of a non-linear estimation algorithm for retrieving the biomass and structure of vegetation from polarimetric Synthetic Aperture Radar (SAR) data is demonstrated for woody regrowth in Queensland, Australia dominated by *Acacia harpophylla* (Brigalow). By varying the size and density of trees and associated woody components (branches and trunks), multiple simulations of the backscattering coefficient ( $\sigma_0$ ) were performed based on the SAR simulation model of. Functions relating  $\sigma_0$  to these variables were subsequently used to generate spatial estimates from NASA JPL airborne SAR (AIRSAR) data. Above ground biomass was estimated from stem density and size measurements using available allometric relationships. The study demonstrates potential for retrieval of regrowth structure and biomass through nonlinear estimation. [C1908]

#### **"Forest biomass estimation in northeastern China using ALOS PALSAR data combined radiative transfer model"**

Forest above ground biomass (AGB) is an important variable for evaluating ecosystem function and structure across landscape, which is necessary for studying forest productivity, carbon balance and nutrient allocation in forest ecosystem. In this study, a forest biomass estimate technique based on forest backscattering database is developed, and is used to retrieve AGB of Changbai mountain area from ALOS PALSAR dual-polarization data. The forest growth model and the 3D forest radar backscattering model were combined to build a forest multi-polarization radar backscattering database. Then forest AGB was estimated based on this database using statistic regression method and look up table (LUT) method. Two types of LUT searching methods (nearest distance and distance threshold) were used to find the accurate results. The biomass retrieved from forest inventory data was taken as ground truth to evaluate the inversion methods and the precision of the AGB estimation. The inversion results derived from PALSAR FBD data shows that both the statistical regression method and nearest distance LUT method underestimate forest aboveground biomass. The distance threshold LUT method gives the better biomass estimation compared with forest inventory data, the mean absolute error (MAE) of the whole research area is less than 10 Ton/ha. [C1909]

#### **"An experiment for oil spill recognition using RADARSAT-2 image"**

In this paper, an experiment that is oriented to discriminate between different oil slicks using polarimetric SAR image was introduced. Dark patches which often appear in SAR images such as biogenic slicks, atmospheric front, and crude oil with different chemical composition were identified according to the result of Eigenvector-Eigenvalue based Incoherent Target Decomposition. The experiment demonstrated that polarimetric SAR can be of great help in classifying of oil spills. [C1910]

#### **"Characterization of forest opacity using multi-angular emission and backscatter data"**

This paper discusses the results from a series of field experiments using ground-based L-band microwave active/passive sensors. Three independent approaches are applied to the microwave data to determine vegetation opacity of coniferous trees. First, a zero-order radiative transfer model is fitted to multi-angular microwave emissivity data in a least-square sense to provide "effective" vegetation optical depth. Second, a ratio

between radar backscatter measurements with a corner reflector under trees and in an open area is calculated to obtain "measured" tree propagation characteristics. Finally, the "theoretical" propagation constant is determined by forward scattering theorem using detailed measurements of size/angle distributions and dielectric constants of the tree constituents (trunk, branches, and needles). The results indicate that "effective" values underestimate attenuation values compared to both "theoretical" and "measured" values. [C1911]

#### "A radar profiling algorithm designed for use with multiresolution radiometer measurements"

We have developed a radar profiling algorithm that can be incorporated into a larger radar+radiometer retrieval framework. The modular nature of the framework provides the opportunity to test the sensitivity of the retrieval to the inclusion of different measurements, retrieved parameters, and models for microwave scattering properties of hydrometeors. [C1912]

#### "Applicability of the iterative backward retrieval method for the GPM dual-frequency precipitation radar"

The dual-frequency precipitation radar (DPR) on the core satellite of the Global Precipitation Measurement (GPM) mission will measure the radar reflectivity factor in the Ku-band and Ka-band. A rain-rate retrieval algorithm that does not require surface reference was developed (called the MA04 method). However, MA04 cannot give the true solution in some cases of heavy rainfall. MA04 is a simplified version of the iterative backward retrieval method (IBRM) and the IBRM is equivalent to the forward retrieval method with a constraint. The purpose of this study is to clarify the essential conditions under which the IBRM and MA04 can give the true solution. [C1913]

#### "Airborne DInSAR time series at X-Band"

Differential SAR Interferometry (DInSAR) is a remote sensing technique which allows monitoring ground deformation with accuracy of the order of the transmitted wavelength by exploiting the phase difference (interferogram) of two temporally separated SAR images relevant to the same area. In addition, when more than two multi-pass acquisitions relevant to the same area are available, they can be properly combined by means of recent multitemporal DInSAR algorithms, in order to detect and follow the temporal evolution of ground deformation via the generation of spatially dense time series. Such a multitemporal DInSAR technique is nowadays developed and operative with space-borne SAR data, whereas specific problems may limit its application to airborne data. In this work, starting from the results already shown in previous works and relevant to an X-Band airborne DInSAR experiment carried out over the Perugia area (center of Italy) by using the OrbiSAR system, we carry out a DInSAR multitemporal analysis of data relevant to a 16 km (in azimuth) by 4 km (in range) region. [C1914]

#### "Potential and limitations of forward-looking bistatic SAR"

Bistatic synthetic aperture radar (SAR) operates with spatially separated transmit and receive antennas that are mounted on separated platforms. Provided that there is an overlap of both antenna footprints, the platforms can move with different velocities in arbitrary directions. A special configuration is given, when the receive antenna looks in forward direction, which is called bistatic forward-looking SAR. Besides the well known advantages of bistatic SAR like the increased information content of the data because of different RCS and scattering characteristics, such a configuration enables high resolution imaging in forward direction, which is not possible with conventional monostatic SAR systems. This paper analyzes a bistatic forward-looking configuration and demonstrates the capability and feasibility of imaging in forward or backward direction using the radar satellite TerraSAR-X as transmitter and the airborne SAR system PAMIR as receiver. [C1915]

#### "Tropical land cover change detection with polarimetric SAR data"

There is an increasing need for fast and accurate data on tropical land cover status, and a baseline for land cover monitoring. Remotely sensed SAR data are not sensitive to cloud cover and can be useful for such purpose. Polarimetric SAR data are available in orbital systems, such as RADARSAT-2, and still have to be tested for the classification of tropical land cover and the detection of land cover change, particularly forest conversion. This work presents a study of RADARSAT-2 polarimetric images, acquired in two different dates (September 2008 and October 2009), to assess their potential in classifying forest and non-forest classes in Brazilian Amazonia. SAR images were acquired following different orbit and incidence angles, which anticipated varied conditions for images interpretation and classes discrimination. The complex SAR data were classified based on the distance of Wishart, and information from field campaigns was used for the training and test samples. Classification results were compared to evaluate possibilities for change detection in the forest cover. Classification accuracy figures were around 80%. The use of RADARSAT-2 images allowed the mapping of land

cover and land cover change, considering forest and non-forest classes. [C1916]

#### **"Oil Spill statistics from SAR images in the North Eastern Baltic Sea ship route in 2007-2009"**

A large number of illegal oil pollutions impose considerable threat to marine environment especially in marginal seas like the Baltic Sea. Illegal spills are mainly detected on essential navigation routes. The monitoring of Oil Spills (OS) using remote sensing imagery (SAR data) was performed on the northeastern Baltic Sea ship route. The pre-analyzed satellite images for detecting marine pollution were provided to marine surveillance agency in Estonia. Out of 137 detected potential pollutions 76 were confirmed by aerial surveillance missions within two-year period. OS were mainly of low confidence, had small area, low contrast with surrounding water and smeared edges. The entrance to the Gulf of Finland was classified as the area where illegal spills of oil and bilge water take place, mainly. Between 30-50% of actual oil pollutions are not detected by SAR. [C1917]

#### **"High resolution optical and sar image fusion for road database updating"**

This paper addresses the issue of cartographic database creation or updating using high resolution SAR and optical images. It proposes a processing chain to create or update road databases in urban environment. The approach is composed of two steps. First, if a database is available, the presence of each database object is checked in the images. Then, we verify if road hypotheses extracted from images should be included in the database. These two steps are conducted by extracting relevant features from the images in the neighborhood of the considered object. The object removal/inclusion in the database is based on a score obtained by the fusion of features in the framework of Dempster-Shafer evidence theory. [C1918]

#### **"Extension of the Target Scattering Vector Model to the bistatic case"**

The polarimetric information has been widely used to interpret the Synthetic Aperture Radar (SAR) scene. Hence, many decompositions have been introduced to extract polarimetric parameters with a physical meaning. Nevertheless, for most of them, the reciprocity assumption is assumed. For a bistatic PolSAR sensor, the cross-polarization terms of the scattering matrix are not equal. This paper presents a generalization of the Target Scattering Vector Model (TSVM) to the bistatic case. [C1919]

#### **"Synergistic use of multi-temporal ALOS/PALSAR with SPOT multispectral satellite imagery for land cover mapping in the Ho Chi Minh city area, Vietnam"**

This paper discusses the synergistic use of multi-temporal ALOS/PALSAR and SPOT multi-spectral images for land cover classification in the Ho Chi Minh city area in Vietnam. Five PALSAR images and SPOT 2 multispectral image were used for classification. Integration of additional information such as interferometric coherence, textural data was also studied. Different combinations of multi-temporal SAR backscatter images, coherence data, SPOT multi-spectral bands, texture measures were generated and tested in order to determine the best combination, which gives the highest classification accuracy. Results indicate that the combination of SAR and optical images gives significantly higher classification accuracy than using a single type of data, and that the Support Vector Machine (SVM) classifier could outperform the Maximum Likelihood (ML) classifier in cases of classification of the combined datasets. [C1920]

#### **"The use of ALOS PALSAR imagery for Cerrado's land use and land cover mapping"**

In Brazil, land use and land cover (LULC) mappings are obtained mainly from optical images. Radar data are also promising since they are independent of solar illumination and the microwave radiation can penetrate clouds and depict differences in canopy structures. This study analyzed the potential of ALOS PALSAR data for LULC mapping of Federal District of Brazil (FD). L-band, HH-, HV- and VV-polarized amplitude images from the end of wet season were processed through the image segmentation technique by growing region. The segments were exported into a geographical information system software package as shapefile format and then visually interpreted in the computer screen. The following classes were discriminated: consolidate urban areas; urban areas in consolidation; natural grasslands; Cerrado shrubland; croplands; gallery forest; indiscriminated forests: pasturelands; reforestations; and water reservoirs. Cerrado shrubland was the most representative mapping class of the study area, followed by consolidated urban areas and natural grasslands. [C1921]

#### **"Real-time road traffic monitoring using a fast a priori knowledge based SAR-GMTI algorithm"**

Radar systems operating on high altitude platforms can provide traffic information over wide areas, independent of sunlight illumination and weather conditions. In the paper, a novel a priori knowledge based ground moving target indication (GMTI) and parameter estimation algorithm applicable on single- as well as on multi-channel synthetic aperture radar (SAR) data is presented. Only the intersection points of the moving vehicle signals with



the a priori known road axes, which are mapped into the range-compressed data domain, are evaluated. The algorithm needs low computational load and is hence well suited for real-time traffic monitoring applications.

[C1922]

### "Three-dimensional deformation field caused by the Gaize earthquake by Multi-LOS DInSAR measurement technology"

This paper firstly presents the Multi-LOS DInSAR measurement result of the coseismic deformation field caused by the Gaize Ms6.9 mainshock and Ms6.0 aftershock in Tibet, China, and then obtain the 3D deformation field based on the 3D resolving mode. The characteristic analysis of coseismic deformation field shows the rupture of mainshock is majority normal, left-lateral striking with a little rotation; and the aftershock is typical normal rupture nature. The mainshock and aftershock had induced the east and west rupture(maybe buried) successively, and produced the east and west two subsiding centers. [C1923]

### "A combined approach to detect urban features from multi-spectral and radardata"

With increase of urban population, the cities have an impact more and more important on environment. Because of artificial surface, building morphology, economical activities, traffic several natural ecosystem are modified. To analyze this impact, the land covers/land uses have to be identified exactly in an urban area. To reach this objective, remote sensing represents an important and complete source of information. Joint use of radar and optical data allows improving results of classical classification to identify the cover mode. Re-sampled to 1m resolution, the difference between the two classifications is analyzed to detect the confusion in each class corresponding to a land cover/land use. Finally, a vector process allowed to transform the geometry of the results: a polygon aggregates several pixels. Combination of results is also possible with GIS functionalities like contains, intersect, cut, and permits to propose a land cover/ land use description on the study area. [C1924]

### "Detecting depolarizing targets with satellite data: A new geometrical perturbation filter"

Target detectors using polarimetry are often focused on single (coherent) targets, since these are the ones that can be more simply characterized polarimetrically. The new proposed algorithm is aimed at the more difficult problem of partial target detection (i.e. targets with any degree of polarization). A new feature vector is defined starting from the coherency matrix, and then a perturbation method is performed. Starting from the partial target detection, a novel classification algorithm is proposed. The validation is carried out against fully polarimetric satellite data. In particular, X band TerraSAR-X and L band ALOS PALSAR are employed, providing significant agreement with the expected results and the supervised Wishart classifier. [C1925]

### "Autoregressive modeling of dechirped spotlight-mode sar rawdata in transform domain"

Raw data collected by synthetic aperture radar (SAR) is commonly assumed to be uncorrelated and with a zero-mean Gaussian distribution. In this paper, we show-both analytically and numerically-that the range-wise inverse Fourier transform of the dechirp-on-receive circular SAR data exhibits significant correlation in the azimuth direction. Moreover, we show that a block adaptive autoregressive model well represents the transformed SAR data. [C1926]

### "Investigation on moving target detection and velocity estimation with Triple-Channel MIMO-SAR"

Triple-Channel SAR system can detect moving target, and estimate its range velocity. However, the problems of blind velocity and velocity ambiguity still exit. To resolve these problems, Triple-Channel Multi-Input Multi-Output SAR (Triple-Channel MIMO-SAR) system, with a displaced phase center antenna (DPCA) and interferometry method based on matched Fourier Transform (MFT), is proposed in this paper, which could combine detection and estimation results of different working frequencies and obtain accurate Doppler frequency modulated rate estimation. Using this method, we can not only detect moving target and estimate its range velocity, but also resolve the problems of blind velocity and velocity ambiguity and get accurate azimuth velocity estimation. The effectiveness of this approach is validated by the computer simulation results. [C1927]

### "Change detection in a multitemporal series of radar images"

In the literature, several works are led around the radar images especially the detection of the cartographic objects, the 3D reconstruction and the change detection. Concerning this last application, several techniques compete to ensure the best possible result. In this paper, we aim first at developing an automatic detection procedure to compare between similarity measures. Then we propose a change detection technique based on the fusion of two similarity measures. The first one is the Contrast (C) measure [1] and the second one is the Rayleigh Distribution Ratio (RDR) measure [2]. The proposed method has been validated on simulated data and

then applied on three radar images. [C1928]

#### **"Numerical study on the statistics of the phase in backscattered signals from time-evolving sea surfaces"**

The linear and Creamer sea surface models are combined with the first-order small slope approximation (SSA1) technique and the method of ordered multiple interactions (MOMI) to study the statistics of the phase difference in backscattered signals from time-evolving sea surfaces. The impact of sea surface models and electromagnetic (EM) scattering computation methods on the backscattering signal phase is investigated. Numerical results are compared with theoretical distributions to validate the models and computational procedures proposed. Good agreements between simulated statistics and the theoretical counterparts demonstrate that the sea clutter returns are essentially joint Gaussian distributed on short time scales. [C1929]

#### **"Classification of polyphase and polytime LPI radar signals with eigenimage methods"**

LPI (Low Probability of Intercept) radars are based on an advanced architecture which makes use of coded pulses. As a synergetic byproduct, a low probability of intercept is also achieved due to the low power levels of LPI radars. In this study, some classification based methods for the uncooperative detection of LPI radar pulses are proposed. We specialized on polyphase and polytime type LPI signal pulses and developed methods for the automatic identification of these types of signals by eigenimage methods based on time-frequency transformations. [C1930]

#### **"A new bistatic doppler measurement system with reduced contamination by sidelobe echoes"**

A new bistatic Doppler measurement system with an array receiving antenna is proposed. In this system the spacing of receiving array elements is more than a wavelength (e.g. 10 wavelengths), and it leads to forming many sharp grating lobes. With these sharp lobes (beams) and some signal processing techniques like a digital beam forming, it can be expected that the effect of sidelobe contaminations, which is a serious problem of bistatic measurement, can be effectively reduced. [C1931]

#### **"Advances in the integration of ALOS PALSAR and Landsat sensor data for forest characterisation, mapping and monitoring"**

Based on case studies undertaken in tropical forests in Brazil and Indonesia and subtropical woodlands in Australia, the paper highlights how data acquired by the Advanced Land Observing Satellite (ALOS) Phased Arrayed L-band Synthetic Aperture Radar (SAR) and Landsat sensors can be integrated to better quantify the extent, biophysical characteristics and/or dynamics of undisturbed, degraded and regenerating forests. The benefits of using time-series of Landsat sensor data to support the interpretation of ALOS PALSAR data and to identify areas with greatest potential for ecosystem recovery are conveyed. [C1932]

#### **"Simulating and mitigating ionospheric effects in synthetic aperture radar"**

The ionosphere is magnetized plasma that forms above the neutral atmosphere due to solar ionization of upper atmosphere constituents. It presents an obstacle to space based synthetic aperture radar (SAR) systems since it affects the radar signals traveling through it. Its impact can be split into two groups: uniform effects (those caused by a spatially uniform non-turbulent ionosphere) and nonuniform effects (those caused by irregularities in the ionosphere). In this paper, we present a method for simulating the uniform non-turbulent effects such as dispersion, group delay, Faraday rotation, and phase shift. This method is then validated using PALSAR data of Washington, DC. We also show the coherence in this scene after ionospheric effects are added. Finally, the model is used to predict the level of ionospheric effects in future space based SAR systems such as ALOS-2. [C1933]

#### **"A specific methodology for atmospheric effect reduction on SAR interferograms"**

Interferometric Synthetic Aperture Radar (InSAR) measurements are often biased due to atmospheric effects. Especially, the tropospheric water vapor engenders a delay of SAR signal propagation. In this paper, we propose a specific methodology for atmospheric effects correction on SAR interferograms. It is based on ancillary data collected from NOAA-AVHRR sensor. The specificity of the approach consists in its applicability where no ground truth GPS measurements are available neither for calibration nor for result validation. An adaptive validation demarche is also proposed. [C1934]

#### **"Design considerations for a dual-frequency radar for sea spray measurement in hurricanes"**

Over the last few years, researchers have determined that sea spray from breaking waves can have a large effect on the magnitude and distribution of the air-sea energy flux at hurricane-force wind speeds. Characterizing the fluxes requires estimates of the height-dependent droplet size distribution (DSD). Currently, the few available measurements have been acquired with spectrometer probes, which can provide only flight-level measurements. As such, in-situ measurement of near-surface droplet fluxes in hurricanes with these instruments is, at best, extremely challenging, if at all possible. This paper describes an airborne dual-wavelength radar profiler concept to retrieve the DSD of sea spray. [C1935]

#### "Spaceborne P-band SAR for BIOMASS mission"

In the frame of the BIOMASS mission promoted by ESA for evaluating and monitoring Earth biomass, the expected performance of a P-band SAR instrument based on very large Direct Radiating Array antenna is addressed, as well as its architecture and the accommodation challenge on a platform. [C1936]

#### "Signal: SAR for ice, glacier and global dynamics"

SIGNAL is an innovative earth exploration mission proposal with the main objective to estimate accurately and repeatedly topography and topographic changes associated with mass change or other dynamic effects on glaciers, ice caps and polar ice sheets. Elevation measurements are complemented with glacier velocity measurements, providing valuable additional information for a better understanding of the hydrology of glacierized basins and of the Arctic and Antarctic water cycle. SIGNAL is capable of monitoring all critical regions with a high spatial resolution and an adequate revisit time. This paper gives an overview about the actual mission design status and provides a brief description of the topography (DEM-digital elevation map) self-calibration strategy and the estimated global interferometric performance. [C1937]

#### "Focusing general bistatic SAR data using frequency scaling"

This paper presents a method to focusing the general bistatic synthetic aperture radar (BiSAR) data. First, using the extended Taylor series, the general BiSAR data are transformed into the azimuth-invariant BiSAR one. Second, the monostatic frequency scaling algorithm is extended to the bistatic one. The numerical experiment indicates that our methodology is valid and the proposed algorithm can process the data of the general BiSAR. [C1938]

#### "Study on emitter signal recognition based on rough sets and grey association theory"

Recognition degree of unknown radar emitter signal can be describe by upper and lower approximation sets of Rough Sets. From the uncertain degree measure by multi-sensors, pessimistic and non-pessimistic distances of every object to sensors and grey association matrix can be calculated by grey association theory. According  $\alpha, \beta$  and grey association matrix, grey association degree and fusion result can gain. The simulation results show the method of combining Rough Sets and Grey Association theory is effective, and it can be applied on radar emitter signal recognition, especially in decreasing the uncertain degree introduced by multi-sensors. [C1939]

#### "Generalised decentralised fuzzy CA-CFAR detector in Pearson distributed clutter"

In this paper, we analyze the decentralized CA-CFAR detector using fuzzy fusion rules in heavy tailed clutter modeled by a Pearson distribution. We generalize our study by considering a distributed detection system with "L" detectors and using the "Maximum", "Minimum", "Algebraic sum" and "Algebraic product" fuzzy rules at the data fusion centre. We derive the membership function which maps the decision to the false alarm space and compute the threshold at the fusion centre. From the Monte-Carlo simulations conducted to assess the detection performance in homogeneous Pearson distributed clutter, we observe that the probability of detection increases with the number of detectors. However, there a maximum number of detectors ( $L = 11$ ) above which no improvement is obtained. [C1940]

#### "Feasibility of tunnel detection under rough ground surfaces using Underground Focusing Spotlight Synthetic Aperture Radar"

Detecting and imaging the presence of illicit tunnels in any given volume of soil is occasionally possible because the air that fills them is materially quite different from anything else underground. The Underground Focusing Spotlight Synthetic Aperture Radar (UF-SL-SAR) concept has been suggested for sub-surface tunnel detection due to its ability to scan large areas of terrain in a short amount of time. This paper explores the feasibility of tunnel detection under rough ground surfaces using an algorithmic implementation of the UF-SL-SAR concept. In particular, detectability is investigated as a function of tunnel depth, ground surface roughness and soil type. [C1941]

### "Currents in rivers, coastal areas, and the open ocean from TerraSAR-X along-track InSAR"

Since the first presentation of a TerraSAR-X along-track InSAR (ATI) derived current field in November 2008, considerable progress has been made with the implementation and testing of various ATI modes of the instrument, improvements of data processing techniques, and test dataset acquisitions over a variety of test sites. Furthermore, receiving and processing capabilities for TerraSAR-X data have been established at the University of Miami's Center for Southeastern Tropical Advanced Remote Sensing (CSTARS), which will permit a complete processing and analysis of TerraSAR-X ATI-derived current fields at CSTARS in the future. We give an overview of these developments and show a few results of recent experiments. [C1942]

### "The propagating speed of internal solitary waves investigated by X-band radar near Dongsha island"

Shipboard X-Band radar images acquired on June 24th, 2009 are used to study internal solitary waves (ISWs) characteristics at northeast of the South China Sea (SCS). The studied images show one ISW in a packet. A methodology based on the Radon Transform (RT) technique is introduced to calculate internal wave parameters such as direction of propagation, internal wave velocity from backscatter image. The result shows that the ISW amplitude is more than 100 meters and it approximately propagates northwestward continent shelf at a speed of 3.04 m/s. Compared with the other researches, especially only with satellite remote sensing images, the ISW propagation speed we got seems higher than other results. A new explanation is presented among different remote sensing images. The periods of most internal waves at northeast of SCS acquired from SAR images aren't regular M2 tidal period ( $T = 12.4h$ ), but less than 12.4h. This may be the reason that the ISW propagation speed we got from X-band radar images is higher than others from SAR images. [C1943]

### "Moving target refocusing algorithm for synthetic aperture radar images"

In the area of SAR imaging, it is of interest to be able to focus moving targets. In this paper, an algorithm for moving target focusing is presented. The algorithm is able to refocus a smeared moving target in a SAR image processed at one relative speed to the correct one%. The algorithm works in the frequency domain and is based on the Range Migration algorithm. The refocusing can be made on the whole SAR image or small sub images corresponding to physical areas of interest for the end user. By applying the algorithm to a small image, the computational cost is greatly reduced compared with using the full SAR image. The performance is illustrated by applying the algorithm to simulated SAR data according to the parameters for the LORA system. [C1944]

### "Automatic target recognition based on neural networks"

Several researches published about artificial neural networks are connected with military problems. This research put forward ideas connected with the processing of military information to search and identify targets-automatic target recognition (ATR). A main-purpose automatic target recognition system did not exist. The research put forward here was demonstrated on military data, however it could only be considered as a proof of principle until systems were fielded and proven "under-fire". A TR data could be in the form of non-imaging one-dimensional sensor returns, such as ultra-high range resolution radar returns for air-to-air automatic target recognition and vibration signatures from laser radar for recognition of ground targets. The ATR data could be two-dimensional images. The most common ATR images were infrared, but current systems might also deal with synthetic aperture radar images. Finally, the data could be three-dimensional, such as sequences of multiple exposures taken over time from a no stationary world. [C1945]

### "A distributed multi-agent tracking, awareness, and communication system architecture for synchronized real-time situational understanding, surveillance, decision-making, and control"

In this paper we deal with the design and analysis of an intelligent multi-agent-based architecture for synchronized real-time situational understanding, awareness, decision-making, and control in a geographically networked distributed computing environment. In particular, we focus here on the design and implementation of a middleware framework for agent intra and inter-node communication as well as computing nodes synchronization. While the proposed work finds applications in many areas including networked chemical sensors, large key infrastructures and resources such as highways and transportations, here as application of the proposed method we consider the challenging scenario case of a set of distributed collaborating radars (multi-agent) system geographically distributed over a large terrain environment with several moving targets. Here, each radar agent, taken separately, does not have the capabilities and resources to span the monitoring of the totality of a given large terrain. However, when collaborating with other radars distributed in the large terrain environment, each with similar limited capabilities, we show and illustrate the proposed distributed agents (radars) capability of not only monitoring their respective regions, but also tracking, communicating with



neighboring agents, and decision-making, to collaborating span the monitoring the totality of a given large terrain. We show how the neighboring agent radars do not necessarily have to be running on the same computing node. Similarly, as part of the scenario we also consider the case of existence of friendly and unknown forces/stressors targets that are capable of moving throughout the same distributed environment. We show how the proposed algorithms are scalable. They are implemented on the CMINDS High Performance Distributed Computing Engine (HDPC) test-bed taking full advantage of a distributed environment and multiple processing systems. [C1946]

#### **"A novel array calibration method based on spatial correlation matrix for HFSWR"**

This paper addresses a new method based on spatial correlation matrix to calibrate uniform linear array for HF Surface Wave Radar (HFSWR). Strong point echoes, such as target, clutter, transponder and so on, which are highly spatial correlated, can be used to structure spatial correlation matrix. And the matrix contains angles of echoes and phase errors information. In this paper, we use two-dimension FFT to estimate angle of strong point echo, and then obtain the corrections. Computer simulations and experimental results are conducted to show the validity of the new method. [C1947]

#### **"Space registration algorithm based on UKF using hybrid states"**

A new UKF based for radar and infrared sensor registration method is provided. A so-called "hybrid states" concept is introduced to describe target's state, which consists of the target's range, bearing and elevation and its velocity in the Cartesian coordinate system. The dynamic function and the measurement function are deduced in hybrid states. Simulation results show that the proposed method has higher accuracy and stronger robustness in the estimation of system biases. [C1948]

#### **"A comparison of experimental and modeled results of an active millimeter wave inverse synthetic aperture radar system used to perform standoff detection of person-borne improvised explosive devices"**

With the recent rise in casualties resulting from person-borne improvised explosive devices (PBIEDs) or "suicide bombers," there is an urgent need for standoff detection of such threats. An optimum system that fulfills the requirements of standoff detection must be portable, low cost, and have a high probability of detection with low probability of false alarm at a distance of at least 20 meters. Currently there are a variety of modalities being researched to perform standoff detection of PBIED's including: backscatter X-ray imaging, infrared imaging, optical detection, terahertz imaging, video analytics, and millimeter-wave (MMW) imaging. MMW imaging at 94 GHz is a very good modality for performing standoff detection of PBIEDs. MMWs can propagate through the atmosphere and clothing with very little attenuation, while at the same time do not cause damage to human skin tissue. A mono-static linear frequency modulated continuous wave (LFMCW) circular inverse synthetic aperture radar (ISAR) system has been developed and tested. A model of such a system using a two dimensional full wave analysis based on the finite difference method in the frequency domain has been developed and compared with results of the experimental system. Using a two dimensional matched filtering technique in the frequency domain, simulated images have been used as a means of performing target detection and classification. The imaging results of both simulated and experimentally obtained data is presented in this paper. Initial results using the 2D matched filtering target classification technique will also be presented. [C1949]

#### **"An improved algorithm for passive bistatic radar detection and parameters estimation"**

In passive bistatic radar system, both detection and joint estimation of time delay and Doppler shift of target are based on the cross-ambiguity function (CAF) between direct-path signals and target echoes. However, the drawback of this approach is the excessive processing load which is caused by the fast Fourier transforms (FFT) for long input samples. Since the interested frequencies of target often occupy a small portion of the whole frequency range, it only required to analyze the sub-band of the whole frequency. A decimation technique which can decrease the operation complexity was applied to solve this issue. The cascaded integrator-comb filter (CIC filter) theory was briefly introduced, followed by detailed signal processing procedures used to implement the target detection and parameters estimation. This improved algorithm needs several extra steps to decimate the signals, while greatly reduces the overall computation complexity with almost no loss of signal processing gain. Finally, the effectiveness of this proposed algorithm is verified by the real data analysis. [C1950]

#### **"Performance analysis of multiple signal detection using the ESPRIT algorithm"**

An array antenna system with an innovative signal processing algorithm "Estimation of signal parameters via rotational invariant technique" (ESPRIT) is used in this paper to estimate the direction of arrival (DOA) for multiple targets. The DOA angles are derived indirectly from the generalized eigenvalues of the auto-correlation

and cross-correlation matrices. The estimated autocorrelation and cross correlation matrices in this study are based on a combination of temporal averaging and spatial smoothing method. Two different methods of estimating the multi-signal DOA are: (1) Choice of appropriate pairs of generalized eigenvalues from the two sub-arrays according to their relative distance from the unit circle, and (2) Choice of appropriate pairs of generalized eigenvalues from the two sub-arrays according to their Euclidean distances [1]. Since the performance of the second approach provides a better estimation, it is used in this simulation study. A 19-element array antenna is used in this simulation study. Extensive computer simulations are used to demonstrate the performance of the processing algorithms. The DOA performance as a function of signal to noise ratio (SNR) and varying numbers of snapshots is presented in this paper. [C1951]

#### **"Surface current retrieval from TerraSAR-X data using Doppler measurements"**

The purpose of this paper is to investigate the estimation of surface currents directly on stripmap TerraSAR-X data, as an alternative to Along Track Interferometry. The algorithm relies on efficient baseband magnitude-based Doppler estimation, preventing the estimate from possible biases like azimuth ambiguities and strong target reflections. The validation of the algorithm is made with acquisitions over the Elbe estuary river in Germany and the Eyjafjallajökull volcano in Iceland. [C1952]

#### **"Assimilation of D-InSAR and sub-pixel image correlation displacement measurements for coseismic fault parameter estimation"**

In this paper, 2 data fusion strategies from SAR images are investigated through application to measurement of displacement field due to the Kashmir earthquake (Mw=7.6, 2005). Firstly, the 3D displacement field at the Earth's surface is retrieved by a linear inversion, using the measurements from sub-pixel image correlation and differential interferometry. In addition to the generalized least square method, a fuzzy approach is applied to represent the measurement uncertainty. Secondly, the geometry of the fault is optimized by a non linear inversion, using the same measurements. The inter-comparisons between strategies and approaches are performed in order to highlight the advantages and disadvantages of each strategy and approach. [C1953]

#### **"An innovative spaceborne radar concept for global maritime surveillance: Description and performance demonstration"**

The paper describes an alternative concept to conventional SAR instruments for ship detection over all ocean surfaces. The concept is specifically oriented for ship detection, and not for land or sea imaging. It allows wide swath coverage (as high as 1000 km). It exhibits high detection performances of small ships even in adverse sea states conditions. Its power consumption is reduced allowing a permanent operation all along the orbit. At least, it uses already developed and low cost technologies. [C1954]

#### **"X-band backscatter map generation using TerraSAR-x data"**

The goal of this work is the generation of an X-Band backscatter map by assembling images acquired by the TerraSAR-X mission. Global backscatter data is required for accurate performance estimation and instrument commanding inside the TerraSAR-X and TanDEM-X missions. Moreover, many scientific applications can be based on the analysis of backscatter behavior and evolution. The complete ground coverage will be achievable with TanDEM-X mission data. An interpolator, that allows the estimation of the backscatter for any required polarization and incidence angle from the available data, has been implemented. In this paper, the backscatter map generation algorithm will be presented, together with the first obtained results, generated using TerraSAR-X data. Moreover, the validity of the interpolation models will also be discussed, presenting the preliminary results of a statistical analysis of backscatter from TerraSAR-X data. [C1955]

#### **"Clutter detection algorithms for airborne pulse-Doppler radar"**

Clutter detection is an important stage of target detection. Clutter may not always appear around zero Doppler frequency when realistic terrain models and moving platforms are considered. Two algorithms developed for clutter detection using range-Doppler matrix elements and their performance analysis are presented in this paper. The first algorithm has higher error rates but lower computational complexity whereas the second one has lower error rates but higher computational complexity. The algorithms detect clutter position by filtering range-Doppler matrix elements via non-linear filters. [C1956]

#### **"Shallow water bathymetry with an incoherent X-band radar using small (smaller) space-time image cubes"**

The approach most commonly used in bathymetry by "depth inversion" starts by transforming a space-time cube

of ocean surface images into a wavenumber-frequency spectrum. The depth is determined by fitting the shallow water gravity wave dispersion equation to the 3D spectrum. The depth error using this method is inversely proportional to the image cube size. Very large image cubes are required for accurate bathymetry. Typical cube dimensions are on the order of 250 m  $\times$  250 m  $\times$  100 s. A new algorithm, originally developed for satellite images, can achieve the same accuracy with much smaller cubes, on the order of 100 m  $\times$  100 m  $\times$  10 s. This paper describes a test of this algorithm on low grazing angle radar data. The algorithm offers the potential for rapid near shore bathymetry surveys using marine X-band radars flown on aircraft. [C1957]

### "Combining GIS and InSAR data for 3D building reconstruction"

Today space-borne high resolution SAR sensors (e.g., TerraSAR-X, TanDEM-X, SAR-Lupe or Cosmo-SkyMed) provide SAR images up to spatial resolutions of 1-3m and even better in spotlight modes. Hence, one major issue of these missions is the development of methods to automatically derive detailed cartographic information from their data. Especially, the analysis of rural and urban areas is on demand in case of disasters (e.g., earthquakes), where active remote sensing systems are highly attractive. Here, an important issue is the development of automatic methods for damage assessment or change detection, in general. For that it is advisable to combine existing GIS data with current SAR data. In this paper an approach for 3D building reconstruction is presented, based on information fusion by utilizing GIS and InSAR data. Thereby, the GIS data are providing the 2D building footprints and the acquired InSAR data the height information. An InSAR simulation step and the subsequent assessment between the real and simulated InSAR phase data enables the extraction of the current building shape. [C1958]

### "Change detection in urban areas with high resolution SAR images using second kind statistics based G0 distribution"

This paper presents a SAR image change detection algorithm for urban areas which mainly contains three steps: (i) modeling the Synthetic Aperture Radar (SAR) image by G0 distribution; (ii) generating a change map by computing the Kullback-Leibler divergence; (iii) masking the change map to obtain the final change areas. We propose to use the second kind statistics based parameter estimation method via Mellin transform to figure out the three parameters of G0 distribution. Experiment results indicate the second kind based G0 distribution model outperforms the moment based methods and can achieve a satisfactory result. [C1959]

### "Spaceborne fully polarimetric time-series datasets for land cover analysis"

The objective of this paper is to make a review of the current status of the project entitled Evaluation of RADARSAT-2 quad-pol data for functional assessment of wetlands (Id6842), developed in the frame of the CSA-ESA SOAR-EU (Science and operational applications research for Europe) program by a consortium comprising I.E.T.R at the University of Rennes 1 and COSTEL-LETG at the University of Haute-Bretagne. The main objective of this project concerns in evaluating fully polarimetric RADARSAT-2 time-series datasets to delineate precisely effective and potential wetlands, map detailed vegetation distribution, identify agricultural practices and determine water cycle and waterlevels. [C1960]

### "Propagation of subinertial variations in the Soya Warm Current revealed by HF ocean radars"

Propagation of subinertial variations in the Soya Warm Current (SWC), which flows through the Soya Strait located between Hokkaido, Japan and Sakhalin Island, Russia, is investigated using data from HF ocean radars together with in situ observations, such as bottom-mounted acoustic Doppler current profilers (ADCPs) and coastal tide gauges. The subinertial variations with periods from 5 to 20 days were captured by the HF radars. The subinertial variations were significantly correlated with the meridional wind stress component over the region, suggesting that the sea level difference through the strait caused by wind-generated coastally-trapped waves on the east coast of Sakhalin and west coast of Hokkaido are considered to be a possible mechanism causing the subinertial variations in the SWC. Propagation of the subinertial variations was also clearly captured by the HF radars. The estimated phase velocity suggests that the subinertial variations propagate downstream along the coast as the 3rd-mode barotropic continental shelf waves. [C1961]

### "Multi-source SVM fusion for environmental monitoring in Marquesas archipelago"

Mapping plant species in montane tropical ecosystems needs the use of complementary information sources to be optimally accurate. In this paper, we study SVM fusion as a tool to classify several sources as optical, synthetic aperture radar and topographical ones. Our fusion scheme consists first in applying a single SVM on each individual data. Their outputs are then used for a SVM-based decision fusion to predict the final class membership of each sample. SVM fusion outperforms all mono-source SVM, our fusion method showing

numerous successful traits. [C1962]

### "Bistatic Radar Cross Section of a complex target on sea surface"

This paper deals with modeling interaction between Electro-Magnetic (EM) wave and the complex target. The first objective is to estimate monostatic and bistatic Radar Cross Section (RSC) of a complex target. The second objective is to present a new approach to compute the RCS of complex target (typically a boat). The target is modeled in 3D using computer aided design (CAD) to generate triangular facet meshing, as does CATIA software. From the triangular mesh, we propose to implement a parallelepiped mesh technique. This new mesh approach allow to introduce more precesely target in its environment and can be used in remote sensing domain. [C1963]

### "Analyzing tomographic SAR data of a forest with respect to frequency, polarization, and focusing technique"

In this paper, two fully-polarimetric tomographic SAR data sets of a forested area, at L-band and P-band, are analyzed with respect to the localization of scattering sources and scattering mechanisms. In particular, the 3D SAR data is examined regarding the performance of three different tomographic focusing techniques multilook standard beamforming, robust Capon beamforming, and MUSIC, as well as for both, the two frequency bands and the different polarimetric channels. [C1964]

### "Radiometric performance of the Advanced Wind Scatterometer radar ASCAT"

The Advanced Wind Scatterometer (ASCAT) instrument [1 & 2] is one of the instruments carried by the ESA / EUMETSAT METOP satellites (METOP A, B & C). The ASCAT is a six-beam radar instrument designed to measure wind fields over the oceans; the instrument also provides useful data for ice and land applications. The radiometric performance of the ASCAT carried by METOP-A is estimated and discussed. [C1965]

### "Application of aperture extrapolation beamformer in multibeam bathymetric sonar"

Limited by the cost, the size of multibeam bathymetric sonar becomes smaller. It is a significant issue to increase the beamforming capability of small aperture array. As the most commonly used method at present, virtual aperture technique together with LPAE beamforming method is discussed in detail in the paper. Compared with conventional beamforming method through theoretical analysis and computer simulation, LPAE beamforming has better performance for higher SNR, narrower receiving beams, and better resolution ability on nearly spaced goals. This method is proved to be effective, practical and superior by the processed results recorded with multibeam sonar sea trial data. [C1966]

### "The joint estimation of source number and DOA non-based on the Eigen decomposition approach"

A new concept 'propagator' for array signal processing is recently introduced, the properties of which have been proven useful for DOA (Direction of Arrival) estimation. This attractive concept is the propagator which can easily be extracted from the cross spectral matrix of the received signals for DOA estimation without Eigen-decomposition. But supplying propagator for DOA estimation has to know the number of sources received by array, which limits the application of propagator in Radar, Sonar and passive detection system. Based on multivariate analysis method, a joint estimation of the number of sources and DOA by propagator method (PM) is presented. It shows that the performance of proposed method with less complexity, effectiveness and high resolution. [C1967]

### "UWB LFM echo signal detection and time-delay estimation based on compressive sensing"

UWB linear frequency modulated (LFM) signals are widely used in radar, sonar and communication systems. In some applications, the detection of LFM signals and estimation of time-delay are very important. It needs very high sampling rate to address the problems for UWB LFM signal under Nyquist sampling theory which exceeds the current ADC capacity. In this paper, we propose a Compressive Sensing (CS) based method to solve the problem with ultra low sampling rate. We adopt an FrFt based sparse dictionary for CS because of the energy concentration property of LFM signal in the fractional Fourier domain. The performance is much better than the already existed method which used signal-matched sparse dictionary in noise condition. Experiments based on simulated data are carried out to testify the results. [C1968]

### "Altitude measurement using three circular marks"

This paper describes a system for a new altitude measurement method, using three circular marks on the



landing location for a Vertical Take-Off/Landing (VTOL) aircraft without an altimeter. This system costs less than a radar altimeter, yet it is more accurate than a pressure altimeter at low altitude and simpler than the Carrier Phase Differential Global Positioning System (CDGPS). The proposed method requires only an onboard camera, three circular marks placed on the landing site, and a control computer. The onboard camera must be facing toward the front of the aircraft and configured to detect the shape of the circular mark in image data form. The flight control computer calculates the altitude based on the known distance between the circular marks and the landing point. The accuracy of the proposed method is described in the analysis results section. [C1969]

### "Detection performance and configuration of Network Radar: A study based upon symmetry cross entropy"

Network Radar realizes the integration of the radar and radar countermeasures; it is a new trend of radar and radar countermeasures system. At first, it introduces the concept and some research results of the configuration of Network Radar. In succession, the CE (cross entropy) theory is utilized to evaluate the detection performance of Network Radar. We investigate the CE and put forward the concept of SCE (symmetry cross entropy) to compensate its inability to meet symmetry, and then prove in theory that it is a distance measure; thus the new evaluation model comes into existence which adopts the SCE as an evaluation criterion. By means of the simulations of the detection performance and configuration of Network Radar, The results prove that the method we have proposed is effective and feasible. [C1970]

### "Urban area extraction from Polarimetric SAR imagery using only positive samples"

In this paper, we present a study of extracting urban areas from Polarimetric Synthetic Aperture Radar (PolSAR) images using only positive samples. We solve this problem by learning a standard binary classifier (urban/non-urban) given an incomplete set of positive samples (urban) and a set of unlabeled samples (some of which are urban and some of which are non-urban) based on the work of Elkan and Noto. Our experiments on RADARSAT-2 fully PolSAR data show that learning with only positive samples can significantly reduces the manual work to select completed positive and negative samples that required by a traditional binary classifier, while providing satisfactory results. Meanwhile, multiple diverse features can be effectively combined for better extraction accuracy. [C1971]

### "A micro-motion feature deception jamming method to ISAR"

One of the main features of IS AR target recognition is the micro-motion feature. In order to jamming target recognition of IS AR, a micro-motion feature deception jamming method to ISAR based on digital image synthesizer is presented in this paper. In this method, the constant Doppler frequency of the scatterer in the template of false-target is replaced by the time-varying micro-Doppler frequency that produced by micro-motion scatterer, and the intercepted radar signals are modulated by the modified template of false-target in the slow time. The research results shows that this method can add the micro-motion information to the echoes of rigid body targets, and realize the micro-motion feature deception jamming to ISAR, Furthermore, the validity of the jamming method is justified by simulation experiment. [C1972]

### "Orthogonal waveform set design for netted radar"

Orthogonal netted radar system requires the transmitted waveforms with a very low autocorrelation and cross-correlation sidelobe peak level. Pseudo-random Phase Coded Modulation (PCM) waveform is suitable for orthogonal design in this sense. In this paper, the correlation properties of Gold sequences as binary phase codes are discussed. Numerical examples are presented to demonstrate the desired orthogonal properties of the coded pulse signal. The effect of Doppler shift and computation cost are also discussed. [C1973]

### "Pilot response to off-nominal conditions in merging and spacing operation"

This paper examines pilots' responses during a human-in-the-loop simulation to off-nominal conditions. During the simulation pilots used advanced flight deck tools to achieve automated spacing and merging assignments while in cruise, and prior to performing a continuous descent approach (CDA) into Louisville International Airport. The off-nominal conditions were represented by sparse and dense weather-patterned perturbations. Simulation results showed that, for the baseline nominal condition, the pilot response and the operation worked as expected. However, during off nominal conditions, qualitative analysis of traffic scenarios and quantitative data showed that pilot behavior in deviating for weather was difficult to predict, and that pilots often took aircraft-centric strategies to make decisions. These strategies lacked a system-centric perspective that could have allowed them to explore the availability of less disruptive and safer options. These responses formed emergent behaviors that may not have been anticipated by the system, and, can be attributed to the mismatches between the pilot strategies, the intended system/operation functionality, and the procedures/environment. Collectively

these mismatches created dispersion in the temporal spacing at the merge point prior to the descent, flight path stretches that are likely larger than required, higher workload, and ultimately unfavorable initial conditions for the CDA operation subsequent to the weather encounter. To further develop the interval managed CDA concept, a number of recommendations were provided for aligning these mismatches by considering the nature of the decision processes within the operational concept and incorporating them into automation designs, by developing a battery of off-nominal scenarios and by conducting simulations to model and specify what the system should and should not do. [C1974]

#### "Human-In-The-Loop simulation of area navigation visual flight procedures at atlanta international airport"

The Federal Aviation Administration (FAA) has committed to implementing Area Navigation (RNAV) procedures at airports throughout the National Airspace System (NAS). Delta Airlines (DAL) and air traffic controllers from the Atlanta Terminal Radar Approach Control (TRACON) (A80) facility have collaborated to design RNAV Visual Flight Procedures (RVFPs) at Atlanta's Hartsfield-Jackson International Airport (ATL). These procedures are comprised of a modified RNAV Standard Terminal Arrival (STAR) runway transition, a Constant Radius to Fix (RF) turn from the downwind to the final approach course, and the existing RNAV Global Positioning System (GPS) approach procedure. The RVFPs are designed to increase efficiency of properly-equipped ATL arrivals in Visual Meteorological Conditions (VMC). Implementing new RNAV procedures requires consideration of current traffic patterns to ensure a more efficient operation while maintaining high levels of operational safety. A80 requested that The MITRE Corporation's Center for Advanced Aviation System Development (CAASD) conduct a Human-In-The-Loop (HITL) simulation to evaluate the operational acceptability of implementing the proposed procedures from the pilot and controller perspectives. The HITL simulation allowed participants to identify design and procedural issues that required change. These changes were implemented during the course of the HITL simulation, yielding a procedure acceptable to both pilots and controllers. [C1975]

#### "TCAS Operational Performance Assessment in the U.S. National Airspace"

Ongoing monitoring of safety critical systems is an important means of ensuring that system performance meets requirements and facilitating proactive identification and resolution of potential problems. The Federal Aviation Administration (FAA) recently implemented one such effort, the TCAS Operational Performance Assessment (TOPA) program. This program records automatic downlinks of all TCAS Resolution Advisory (RA) events within sensor coverage and correlates the RAs with surveillance data, calculates performance parameters and permanently stores the data for future analysis. Periodic and focused reports are prepared based on these data. This paper summarizes key analyses of over 15,000 TCAS RAs collected in the period April-September 2009 at 5 major terminal areas in the U.S. National Airspace (NAS). Most RAs occurred below 5,000' in Class E airspace and involved low performance General Aviation (GA) intruders. Although no significant issues were observed with the performance of TCAS logic, the analysis showed that pilot compliance with Climb and Descend RAs did not meet system design assumptions. These results indicate that pilot training and the design of future systems must explicitly consider these factors. [C1976]

#### "A method for Ground Moving Target Indication and Velocity Estimation based on InSAR system"

For InSAR system, the increasing clutter degree of freedom (DOF) with the terrain is caused by long cross-track baseline. It degrades the performance of Ground Moving Target Indication (GMTI) greatly. In this paper a new method based on InSAR system is proposed for GMTI and Velocity Estimation. In our approach, the joint pixel technique is adopted to improve the coherence of clutter. In this way the clutter can be well cancelled. For the velocity estimation, neighboring pixel pairs is used to compensate the terrain interferometric phase. Therefore, the accuracy of velocity estimation can be improved. Stimulation experiments illustrate the effectiveness of the proposed algorithm. [C1977]

#### "System integration issues in Apollo 11"

"Houston, Tranquility Base here. The Eagle has landed." Two obscure errors almost prevented these words from being spoken. The errors were not made by the crew of Apollo 11 or by the controllers in Houston, nor were they made during the mission. Rather, they were made by engineers and managers, years before the flight. How they happened, and how they went substantially undetected and effectively ignored, is a pair of lessons in system integration that avionics engineers must never forget. The Apollo Program is justly famed as a giant leap for the techniques of management of complex system design and implementation. Nonetheless, these tools were used by human beings and so, necessarily, imperfectly. One of the most challenging tasks in any complex system is controlling and testing the interfaces between major components that are developed by different organizations. Among the management tools deployed by NASA were ICDs (Interface Control Documents). The

author has not been able to determine whether this phrase was first coined for the Apollo program or the Mercury and Gemini programs that preceded it, but it was certainly a major tool in Apollo. One of the errors under discussion here was caused by a blatant failure to update an ICD in response to an engineering change, which can be classed as a management error of omission. The other is much subtler, involving a question of how previously unsuspected vulnerabilities (to crew procedures, in this case) should be communicated when they fall outside the scope of an ICD, yet turn out to have relevance to the way the interface is used. This becomes a problem because an ICD is a top-level document limited to specifying the design parameters of one subsystem insofar as they are of concern to one other subsystem. It's not surprising that the symptoms caused by the latter problem have been totally misunderstood by almost everyone from President Nixon on down, and only partially understood even by Buzz Aldrin,--who along with Neil Armstrong had to deal with them at the time. This misunderstanding is so widespread that almost everyone with any acquaintance with the Program Alarms during the Apollo 11 landing believes that the LM's Primary Guidance Navigation System (PGNS) "failed" in some way and had to be rescued by human intervention. That is the exact opposite of the truth, which is that performance margins built into this very robust system quarantined the effects of the errors so that the landing could proceed with the designed level of human involvement, specifically dodging the "field of boulders" that the PGNS could know nothing about. This paper is largely a retelling of the higherlevel parts of a paper, Tales from the Lunar Module Guidance Computer by the author's colleague Don Eyles [1], but with the orientation changed from a historical narrative to a cautionary tale with recommendations for modern avionics development management. Results of more recent research by the author and two colleagues are also incorporated. [C1978]

### "Weber-Haykin based Automatic Censoring and detection in Weibull background"

In this paper, we study the problem of automatic target detection in Weibull clutter and multiple target situations, without any prior knowledge of neither the non-stationary clutter statistics in which the radar operates nor the number of outliers that may be present in the reference window. In doing this, we develop the Forward/Backward Order Statistic Automatic Censoring and Detection Constant False Censoring and Alarm Rates Detectors based upon the Weber-Haykin adaptive threshold (WH-based F/B-OSACD-CFCAR). These detectors select repeatedly a suitable set of ranked cells among reference cells surrounding the cell under test to estimate the unknown background level and set the adaptive threshold, accordingly. The censoring and detection performances are evaluated by means of Monte Carlo simulations. [C1979]

### "Design based on MCU for the echo simulator of the range extended target"

It is important for the high resolution radar to design the simulator for generating the echoes of the range extended target. In this paper, a simulator design which is based on Micro Controller Unit (MCU) is proposed for generating the echoes of the range extended target. Because those echoes change rapidly and the corresponding period is longer, the high speed FIFO is selected as the data cache. In the idle time of system, waveform data is transferred from MCU to FIFO, whereas in the operating time of system it is transferred from FIFO to D/A converter at a high speed in order to output the waveform. The experimental results show the design can meet the purpose of the echo simulator of range extended target. [C1980]

### "Instantaneous Frequency estimation of multicomponent signal based on complex argument distribution"

Instantaneous Frequency estimation of multicomponent signal with nonlinear frequency modulation is a challenging problem in time frequency analysis community. A new time frequency distribution named complex argument distribution is introduced to resolve this problem due to its capabilities of high concentration and low cross-term artifacts. A instantaneous frequency estimation algorithm based on this new distribution and Viterbi estimator is proposed in the paper. Experiments result show the performance of estimation algorithm with simulated data and radar data. [C1981]

### "A CKF based spatial alignment of radar and infrared sensors"

Spatial alignment is the prerequisite for the successful data fusion of multiple sensors. A CKF based spatial alignment algorithm for the estimation of bias between radar and infrared sensors on a same platform is presented. The system dynamics of this problem is established in a hybrid coordinate, i.e., the target position in the spherical coordinate while the target speed in the Cartesian one. The system bias is then estimated by the cubature Kalman filter (CKF) in an augmented system state equation. Simulation results show that the proposed algorithm is effective and efficient. [C1982]

### "Evaluating information assurance performance and the impact of data characteristics"

Research and development of new information assurance techniques and technologies is ongoing and varied.

Each new proposal and technique arrives with great promise and anticipated success as research teams struggle to develop new and innovative responses to emerging threats. Unfortunately, these techniques frequently fall short of expectation when deployed due to difficulties with false alarms, trouble operating in a non-idealized or new domain, or flexibility limiting assumptions which are only valid with specific input sets. We believe these failures are due to fundamental problems with the experimental method for evaluating the effectiveness of new ideas and techniques. This work explores the effect of a poorly understood data synthesis process on the evaluation of IA devices. The point of an evaluation is to independently determine what a detector can and cannot detect, i.e. the metric of detection. This can only be done when the data contains carefully controlled ground truth. We broadly define the term "similarity class" to facilitate discussion about the different ways data (and more specifically test data) can be similar, and use these ideas to illustrate the pre-requisites for correct evaluation of anomaly detectors. We focus on how anomaly detectors function and should be evaluated in 2 specific domains with disparate system architectures and data: a sensor and data transport network for air frame tracking and display, and a deep space mission spacecraft command link. Finally, we present empirical evidence illustrating the effectiveness of our approach in these domains, and introduce the entropy of a time series sensor as a critical measure of data similarity for test data in these domains. [C1983]

### "Challenges of remote border monitoring"

Monitoring long lengths of remote borders with ground surveillance methods, presents many challenges. This paper will discuss three in particular that must be addressed in order to build an effective remote ground surveillance system. The three issues are: (1) providing reliable and efficient power, (2) providing adequate and timely maintenance to minimize downtime, and (3) networking systems for effective data transmission. A well planned remote ground surveillance system that overcomes each of these three challenges will provide a cost-effective solution requiring minimal support infrastructure solution to meet border monitoring and protection needs. [C1984]

### "Generalized likelihood ratio test for distributed targets in heterogeneous environments"

Adaptive detection for distributed target or targets in non-homogeneous environments is studied in this paper. It is assumed that the covariance matrix of the secondary data  $M_s$  is a random matrix following inverse Wishart distribution with its conditional expectation proportional to that of the primary data, i.e.  $E(M_s | M_p) = \gamma M_p$ . Firstly, the maximum likelihood estimator (MLE) of  $M_p$ ,  $\gamma$  and target amplitudes are given and the generalized likelihood ratio test (GLRT) are proposed subsequently, which turns out to be in the form of the summed adaptive coherence estimator (ACE). The detector is coincident with the generalized adaptive subspace detector (GASD) based on deterministic unknown covariance matrix and it has CFAR property. When the target exists only in one range bin, the detector is boiled down into the ACE based on the partial homogeneous environments. [C1985]

### "A commercial approach to successful persistent radar surveillance of sea, air and land along the northern border"

The benefits of a commercial approach to the deployment of radar surveillance along the Great Lakes St. Lawrence Seaway System (GLSLSS) is discussed. Surveillance solutions must be multi-mission suitable, scalable, flexible, maintainable, upgradeable, interoperable, shareable, and affordable. This flexibility is fundamental to successfully leveraging tomorrow, investments made today in order to keep up with changing threats and technology. Not only can homeland security surveillance solutions benefit by leveraging commercial technologies, but non-sensitive target information, can drive significant human and commercial benefits. The paper presents a radar surveillance framework whose network architecture, COTS components, specially designed components and open interfaces are discussed. The modular nature of the framework includes software definable algorithms for acquisition of sea, air or land targets of interest, built-in integration of target information that fully scales in support of wide-area surveillance, and open interfaces in support of new, multi-mission situational awareness applications. [C1986]

### "High order Doppler parameter estimation of bistatic forward-looking SAR based on CPF-Radon transform"

For high quality synthetic aperture radar (SAR) processing, Doppler parameter estimation is an essential procedure. In this paper, the azimuth data of bistatic forward-looking SAR are modeled as cubic polynomial phase signals, and the CPF-Radon transform is used to estimate the high order Doppler parameter. Simulation results validate the effectiveness of this method. [C1987]

### "A study of frequency diversity MIMO radar beamforming"



Compared to traditional phased-array radar, multiple-input multiple-output (MIMO) radar can transmit multiple probing signals that are correlated or uncorrelated with each other. An interesting current research topic in MIMO radar is the frequency diversity MIMO (f-MIMO) radar. The frequency between two adjacent transmitted signals of f-MIMO radar are not identical but stepped uniformly at the same time. In this paper, a f-MIMO radar array processing model is developed. It is shown that the f-MIMO radar array processing can form a range-dimension beam, so it has the ability to distinguish targets in different ranges. The range resolution of array processing is derived, and then, the virtual array aperture of f-MIMO radar is also investigated. [C1988]

#### **"Target decomposition for fully polarimetric wideband radar system"**

For fully polarimetric wideband radar system, a novel method of radar target recognition using polarimetric feature is proposed. First, polarimetric scattering matrix is obtained from fully polarimetric high resolution range profiles (HRRPs). Then, two different kinds of polarimetric features are extracted by polarimetric target decomposition theorem. At last, K-Nearest Neighbors (KNN) classifier is applied to verify the recognition performance of these two features. The simulation experiments indicate target recognition via polarimetric features can reach a higher recognition performance in different experimental scenarios. [C1989]

#### **"Cross-correlation detection and time difference estimation in non-cooperative bistatic radar systems"**

In this paper, the basic geometrical relationship and signal energy relationship of non-cooperative bistatic radar are introduced, and the method using the cross-correlation to obtain the time difference of direct signals and target scattering echoes in noisy environment is discussed. Some experiments have been done to simulate the process of cross-correlation detection and time difference estimation. What's more, on the basis of them, some parameters affecting the performance of the algorithm, such as the signal-noise ratio, pulse width and pulse number of cross-correlation, are analyzed by Monte Carlo simulation. [C1990]

#### **"An adaptive beamforming method based on properties of cyclostationary signals"**

Blind beamforming, which consists of recovering signals only from observed instantaneous linear mixtures without a priori information about array manifold, is an important problem in many practical applications including radar, sonar, wireless communication and so on. For blind separation of cyclostationary signals encountered usually in communication, recently, reference [1] proposed a novel approach (ATH3) under the assumption that the cyclic correlation functions of signals are all real number. In this paper, we relaxed this assumption to signals with complex cyclic correlation functions, which is usually this case in practice, and proposed a method to accomplish blind adaptive beamforming. Several numerical simulations also are provided to illustrate the effectiveness of the proposed method. [C1991]

#### **"An improved passive location algorithm for maneuvering target emitter"**

With the merits as hiding receiving, far responding distance and easy-deploying, the single observation passive location has a broad application in military domain. Especially, it plays an important part in passive radar, navigation and aerospace, etc. With the information of phase-difference, phase-difference rate of change and Doppler frequency rate of change, a new algorithm based on EKF (called PFRC) is proposed. Compared with two popular passive location methods which are bearing-only (BO) and phase-difference rate of change (PRC), the PFRC has good performance in that it has higher precision and higher speed. However, the PFRC, based on the EKF, can only give a biased state estimation, which has poor robustness and precision against model mismatching and is inapplicable for maneuvering target tracking. In order to overcome the above limitations, based on the PFRC and the strong tracking filter (STF), an improved passive location algorithm is proposed. Simulation results show that the proposed algorithm has better performance. [C1992]

#### **"Zero Correlation Zone Codes and Extended Zero Correlation Zone Codes for MIMO radar signal separation"**

Pseudo random codes are easily constructed and can be used in multiple-input multiple-output (MIMO) radar to provide for signal separation. However it has the drawbacks of high aperiodic cross-correlation and auto-correlation sidelobes. Fortunately, in some applications, codes with low correlations are needed only over a narrow window. In this paper, we introduce the Zero Correlation Zone Codes (ZCZC) which have zero correlations in a narrow zone. In other applications, the targets are stationary, which allows for using a long code sequence. In this case we propose an Extended Zero Correlation Zone Codes (EZCZC) where the zero correlation zone is extended to cover the whole sidelobes area. Design examples are given. [C1993]

### "Review of Observing System Simulation Experiments to evaluate the potential impact of lidar winds on weather prediction"

Observing System Simulation Experiments (OSSEs) are an important tool for evaluating the potential impact of proposed new observing systems, as well as for evaluating trade-offs in observing system design, and in developing and assessing improved methodology for assimilating new observations. Extensive OSSEs have been conducted at NASA/GSFC and NOAA/AOML in collaboration with Simpson Weather Associates and operational data assimilation centers over the last 25 years. These OSSEs determined correctly the quantitative potential for several proposed satellite observing systems to improve weather prediction prior to their launch, and evaluated trade-offs in orbits, coverage, and accuracy for space-based wind lidars. In this paper, we summarize OSSE methodology and present results from OSSEs to assess the potential impact of lidar winds. [C1994]

### "Integrating object-oriented image analysis and decision tree algorithm for land use and land cover classification using RADARSAT-2 polarimetric SAR imagery"

Traditional pixel-based classification methods yield poor results when applied to SAR imagery because of the presence of speckle and limited information in backscatter coefficients. A novel classification method, integrating polarimetric target decomposition, object-oriented image analysis, and decision tree algorithms, is proposed for the classification of polarimetric SAR data (PolSAR). The polarimetric target decomposition is aimed at extracting physical information related to the scattering mechanism of targets for the classification of scattering data. The main purposes of the object-oriented image analysis are delineating objects and extracting various spatial and textural features. The decision tree algorithm provides an efficient way to select features and create a decision tree for the classification. A comparison between the proposed method and the Wishart supervised classification was made. The overall accuracies of these two methods were 89.34% and 79.36%, respectively. The results show that the proposed method is an effective method for the classification of PolSAR data. [C1995]

### "Maximum Likelihood texture tracking in highly heterogeneous PolSAR clutter"

This paper introduces a generalisation of the conventional Maximum Likelihood (ML) texture tracking algorithm in the context of highly heterogeneous PolSAR clutter. The statistical criterion is defined in both uncorrelated and correlated texture cases. Some results on simulated data are computed and an application on temperate glaciers velocity estimation is processed. Finally, some additional improvements are performed: an adaptative sliding windows is set and a basic Bayes inference for flow model constraint is added. [C1996]

### "Estimating rice growth parameters using X-band scatterometer data"

In this study, we constructed an X-band automatic scatterometer system and analyzed scattering characteristics of paddy rice over the whole period of rice growth from transplanting to harvesting. The backscattering coefficients were calculated from the measured data at incidence angle  $45^\circ$  and full polarization (HH, VV, HV, VH) by applying the radar equation and compared with rice growth data such as plant height, stem number, fresh and dry weight and Leaf Area Index (LAI) that were collected at the same time of each scatterometer measurement. Based on the analysis of the relation between backscattering coefficients at X-band and rice growth parameters, we predicted the rice growth parameters using the radar backscattering data. Relationship between measured and estimated grain dry weight using the X-band backscattering coefficients (VV-polarization) is highly correlated ( $R^2=0.94^{***}$ ). Results from this study show that backscattering coefficients X-band appear effective to estimate rice growth parameters. [C1997]

### "Building extraction from VHR multi-spectral images using rule-based object-oriented method: A case study"

Object-oriented classification has been demonstrated a promising method for large-scale detailed urban structure mapping using very high-resolution space-borne or airborne remote sensing images. In the paper, the object-oriented classification method for building extraction using pan-sharpened IKONOS multi-spectral images was applied to roof mapping combined with Lidar data. The scheme to produce the vector polygon database of buildings includes the following steps: (1) image pre-processing and derivation of secondary inputs to image segmentation and classification procedures; (2) segmentation of processed data layers into image objects; (3) classification of image objects; (4) export classified map objects and average building height data; and (5) polygon generalization and/or geometrical regularization. The experimental result is visually satisfactory and may suit overall investigations of building development. [C1998]

### "Retrieval of Aerosol optical thickness and size distribution from PARASOL in Pearl River Delta area"

AOTs(Aerosol optical thicknesses) and aerosol size distribution functions in Pearl River Delta area are derived from PARASOL (Polarization and Anisotropy of Reflectances for Atmospheric Science coupled with Observations from a LIDAR)multi-directional, multi-spectral polarized signals. Based on analyzing the products of AERONET(Aerosol Robotic Network), aerosol size distribution function and complex refractive index over Pearl River Delta area are received. After that, the particular aerosol model is abstracted. The land surface polarized contribution is calculated using semi empirical model as a function of surface type and NDVI, and the pure atmospheric contribution is computed with a radiative transfer code. Compared with the products of the ground-based AERONET, the derived AOTs are underestimated against AERONET measurement. The retrieved size distribution for the radii bigger than 0.2 micron is also underestimated due to that polarization is insensitive to coarse model aerosol. [C1999]

#### **"Towards fully automatic generation of land cover maps from polarimetric and metric-resolution SAR data"**

Information mining from heavy SAR images is considered from the point of view of the procedure automatization. Two schemes based on Neural Networks are evaluated, one based on the Self Organizing Map method exploiting polarimetric information and oriented to land cover classification, the other based on the Pulse-Coupled Neural Networks aiming at characterizing the imaged buildings. [C2000]

#### **"Statistics of depolarization ratio from an airborne backscatter lidar"**

An important cloud optical property derived from elastic backscatter lidars is depolarization ratio because it is used to determine cloud phase. Statistics and trends of volume depolarization ratio were analyzed for four years, 2003-2007, of Cloud Physics Lidar data during five projects of varying geographic locations and meteorological seasons. The volume depolarization ratio was computed using the parallel and perpendicular polarized 1064 nm channels. The majority of the cloud layers yielded a volume depolarization ratio between 0.3 and 0.6 with the volume depolarization ratio frequency distribution centered at 0.45 for ice clouds and 0.05 for water clouds. On average for ice clouds, volume depolarization ratio increased significantly as temperatures decreased. No trend for water clouds was observed, since all water particles are in theory spherical. [C2001]

#### **"A comparative study of polarimetric and non-polarimetric lidar in deciduous-coniferous tree classification"**

As an important active remote sensing tool in forest remote sensing, lidar is able to provide information on tree height, canopy structure, aboveground biomass, among other parameters. It has become desirable to be able to classify tree species using lidar data during recent years. Research has been performed using commercial non-polarimetric lidar in tree species classification, at either dominant species level or individual tree level. The objective of this research is to classify deciduous and coniferous trees using the newly developed polarimetric lidar system. Lidar data from five different tree species were collected in the field. These included ponderosa pine, Austrian pine, blue spruce, green ash and maple. Data were preprocessed and artificial neural network method was developed for classification. Data analysis demonstrated that the classification performance using polarimetric lidar data was far better than that using the non-polarimetric lidar data. [C2002]

#### **"National ecological observatory network (NEON) airborne remote measurements of vegetation canopy biochemistry and structure"**

The National Ecological Observatory Network (NEON) is a continental-scale research platform for discovering, understanding and forecasting the impacts of climate change, land-use change, and invasive species on ecology. Site-based flux tower and field measurements will be coordinated with high resolution, regional airborne remote sensing observations. This data combined with satellite observations, national data sets and ecosystem models will extend site-based and regional coverage to the continental scale. The NEON Airborne Observation Platform (AOP) will carry remote sensing instrumentation designed to achieve sub-meter to meter scale ground resolution to bridge scales from organism and stand scales to the scale of satellite based remote sensing. The capability of the airborne system will be well beyond existing systems in its ability to produce quantitative information about ecosystem structure and functioning covering nearly 2 million hectares each year for 30 years or more. [C2003]

#### **"QEM-based simplification of building footprints from Airborne LiDAR data"**

This paper presents a QEM-based simplification approach for extracting and delineating building footprints from Airborne LiDAR data. Our approach consists of three steps: first of all, Digital Surface Model (DSM) is generated from the raw point cloud by using the interpolation method. Secondly, the potential points on building outlines

have to be aggregated to form connected building blobs. Those blobs that exceed a certain size and have certain characteristics (e.g. consisting of planes) are supposed to be building candidates. In a third step these outlines are simplified to building footprints. The focus lies on taking the characteristics of buildings into account to produce a meaningful 2D building shape and simplifying different possibilities to generalize the building footprints. [C2004]

### "Soil dielectric and sensitivity analysis for subsurface imaging applications based on distributed Sensor Networks"

The concept of a subsurface imaging technique based on Unattended Ground Sensor Networks operating in the VHF range using ultra-wideband waveforms was recently proposed in. In this approach a forward model for realistic subsurface environment based on the Dyadic Green's function for a stratified medium and an inversion technique using an ultra-wideband near-field focusing were presented. Simulation results showed that very good lateral and depth resolution could be achieved. Before carrying out an experiment to test the proposed technique, three vital aspects of the work which are imposed by practical limitations are investigated and presented in this paper. First, the sensitivity analysis to assess the signal penetration depth in realistic subsurface environments for various frequencies is performed. Analysis of the frequency requirements of the inversion as they relate to depth resolution is also analyzed. A semi-analytic soil dielectric model originally devised for microwave frequencies is extended to VHF and validated using measurement results available in literature. [C2005]

### "The Semi-Analytic Mode Matching algorithm for GPR wave scattering from multiple complex objects buried in a dielectric half space"

The Semi-Analytic Mode Matching (SAMM) algorithm is a quick and efficient computational method that can model wave scattering from multiple objects in half spaces. This algorithm relies heavily on the appropriate choice of coordinate scattering centers (CSCs) for its modal expansions. Here, the radius of curvature method of finding CSCs is extended to "tune" the CSC loci. Because the CSC locations are essentially frequency independent and independent of the dielectric contrast between scatterer and background, it is worthwhile to analyze carefully particular scattering object shapes and store the optimal CSC locations for future use. Scattering from multiple targets buried within half spaces can be constructed from simpler simulations of the individual targets taken independently in uniform media-combining these initial simulations correctly can greatly reduce overall computational time and increase robustness in full simulations. Excellent results are found comparing SAMM and Finite Difference Frequency Domain (FDFD) for multiple 2D scattering objects 0.1-15 wavelengths in size located beneath half spaces. [C2006]

### "Generation of DEM by radargrammetric techniques"

Thanks to the signal processing applied to radar signal, radar systems can provide images with a very high resolution. With regard to these properties, one can estimate that radar images are used to get elevation terrain considering the basic characteristics of a radar image. This paper examines one way to produce DEM (Digital Elevation Models) from a mountainous area (the French Alps). So, we organize the discussion in three parts. First, we present the basic operations that the radargrammetric processing requires to be performed. So we deal with the different steps to obtain a DEM. Secondly, we expose two classical image matching improvements: the epipolar geometry and the pyramidal scheme. At the end, we present the results of DEM generation from a SIRC shuttle mission image pair and the way to improve these results. [C2007]

### "Compressive sensing for high resolution differential SAR tomography-the SL1MMER algorithm"

Differential SAR tomography extends the synthetic aperture principle into the elevation and time directions for 4-D imaging. With modern meter-resolution space-borne SAR systems like TerraSAR-X (TS-X), systematic tomographic imaging of urban infrastructure and its deformations becomes feasible. We demonstrate the potential of TS-X data for this purpose and introduce several novel concepts. Since building deformation in general is nonlinear, e.g. due to thermal dilation, we start from a tomographic system formulation that is general enough to allow for the inclusion of motion models (linear, periodic, etc.). By appropriate warping of the time axis we map the motion model function to become linear and lead to a peak in the spectral domain. For the differential tomographic inversion itself we propose a 2-D compressive sensing (CS) based approach-"SL1MMER". We demonstrate the super-resolution power and the robustness of SL1MMER both with simulated and with real data. We also show that it provides an attractive compromise between parametric and non-parametric methods. A full reconstruction of a building complex and its seasonal deformation from a stack of TS-X spotlight data is finally presented. [C2008]



### **"Processing and segmentation of COSMO-SkyMed images for flood monitoring"**

In the framework of the application of remote sensing to civil protection from floods, the problem of the detection of flooded areas in high-resolution images is addressed in this paper. Specifically, the high-resolution multitemporal observation capability offered by the current COSMO-SkyMed synthetic aperture radar (SAR) constellation is exploited. This work is framed in the context of the "OPERA-Civil protection from floods" pilot project funded by the Italian Space Agency in cooperation with the Italian Department for Civil Protection. Several SAR image processing methods are presented in order to identify flooded areas after a flood event. Both fast-ready and detailed maps are obtained from a pair of multitemporal images of the monitored area. Experiments are presented with COSMO-SkyMed images related to a flood in the areas of Alessandria (Italy). [C2009]

### **"A portable 35 GHz cross-track interferometer for topographic and surface change measurements"**

In the following, we present first results obtained from the design, construction and deployment of a 35 GHz fixed-point radar interferometer, that uses the principles of FMCW for generating a range resolving signal. Using a single transmit antenna and two receive, separated by an interferometric baseline, it is possible to determine phase differences between the two receive channels, and given the viewing geometry, to solve for the target topography. To test the system described in this short paper, it was deployed on a local mountain top, some 270m above the local terrain. With knowledge of the nominal topography (measured by the Shuttle Radar Topography Mission; SRTM), and sufficiently large interferometric height ambiguity, it is possible to solve for the topography, as seen at 35 GHz, and to monitor differences in the observed topography which may be due to differences in volume scattering, surface motion, and surface dielectric change. [C2010]

### **"Mapping earthquake damage in VHR radar images of human settlements: Preliminary results on the 6th April 2009, Italy case"**

Automated earthquake damage assessment from post-event only remotely sensed data is highly desirable, especially when new generation, Very High Resolution (VHR) spaceborne data is concerned, lacking extensive pre-event archives. Though, most damage assessment method either rely on human interpretation or on pre-post-event comparison. In this paper we illustrate some possible tracks for investigating damage assessment on post-event only data, focusing on the 6th April 2009 Abruzzi, Italy earthquake and on related COSMO/SkyMed acquisitions. [C2011]

### **"Topographic correction for biomass retrieval from P-band SAR data in boreal forests"**

The influence of the ground slope on radar backscatter has been proven to be greater for lower radar frequencies due to deeper canopy penetration. In this study, multiple heading, P-band SAR data of boreal forest in Sweden was used to find a model for topographic correction for improved biomass retrieval. Eleven models were tested and the best model was selected. The selected model was then used for biomass retrieval. Even by means of the most simplified approach, forest biomass could be established with a root-mean-square error of approximately 50 t/ha for HV and 66 t/ha for HH. [C2012]

### **"Application of Fractional Fourier Transform to finite difference time domain method"**

With the improvement in the computer speed and memory, Numerical Methods are frequently used in the solution of electromagnetic problems. Numerical Methods can be classified as the frequency domain and the time domain based methods. While the time domain methods are suitable for modeling of the transient response and wideband problems, the frequency domain methods are suitable for modeling of the steady state response and narrow band problems. A numerical method that has the advantages of both time and frequency domain approaches can be developed. Applying Fractional Fourier Transform in space and/or time can reduce the computational complexity for some cases. The Fractional Fourier Transform is a generalization of the continuous Fourier Transform. In last decades, there are several studies and applications concerning this transform. Generally, it is used in signal processing and noise filtering. In this study, Fractional Fourier Transform is applied to the Maxwell's Equations for the first time in literature. Finite difference equations are obtained by the application of finite difference approximation to the differential equations. [C2013]

### **"A new approach to modeling ice crystal aggregates and its implications for radar remote sensing"**

Backscattering cross sections of model ice crystal aggregates are computed at 35.6 GHz using the generalized multiparticle Mie (GMM) method and compared against a commonly used equivalent dielectric model (also referred to as the "soft sphere" or the "bulk" model). It is shown that the bulk model underestimates the backscattering cross sections by 7 to 20 dB over aggregate sizes from 3 to 19 mm. This raises concerns about

using bulk models for the interpretation of millimeter wave radar measurements of ice clouds and snow. [C2014]

### "Implementing a reactive semantics using OpenRTM-aist"

The expression of reactive behaviour is a significant and important requirement in robotic software engineering, since robots must cope with a wide range of unpredictable events and environments. However it is important that the semantics for reactive expression can be used across different architectures and languages. The RADAR robot programming language provides architecture- and language-independent semantics for managing the reactive parts of robot software together with the deliberative parts, allowing greater interaction between the two. We evaluate the architecture-independence of RADAR, as an example, by implementing its reactive semantics using the OpenRTM-aist component-based, distributed architecture. Our goal is to evaluate what limitations the choice of implementation environment may place on the capabilities of such an architecture-independent semantics. In our implementation, we aimed to produce a standard OpenRTM-aist system using the RADAR semantics. We have found that the architecture-independent semantics concept works well in the case of RADAR, although some specific improvements are needed for full interaction between deliberative and reactive sections of robotic software. [C2015]

### "Contribution of Cosmo/SkyMed data into PRIMI: A pilot project on marine oil pollution. results after one year of operations"

In this paper we present the Pilot Project PRIMI, designed to provide information on marine oil spills, and its validation campaign, held in august 2009, conducted with the oceanography ship Urania. During the experiment CosmoSkyMed has provided an extraordinary contribution supplying almost any day images over the area inspected by the ship and in some cases also images requested with short notice. [C2016]

### "First experiments of sector interpolated SAR tomography"

SAR Tomography (Tomo-SAR) is an experimental advanced coherent data combination mode allowing full 3-D imaging of volumetric and layover scatterers from a multibaseline (MB) synthetic aperture radar (SAR) data stack. However, the linear Fourier-based Tomo-SAR is generally affected by unsatisfactory imaging quality due to a typically low number of baselines with irregular spatial distribution. Recently, to improve the elevation focusing technique, a sector interpolation approach has been proposed by the authors, in which a set of uniform baseline data is recovered from the available non-uniform one by exploiting the a priori information about the extension of a height sector which contains the scatterers. In this work, first experiments are presented of sector interpolated Tomo-SAR carried out with real spaceborne MB SAR data acquired over the Cinecitta area of the city of Rome. [C2017]

### "The COSMO SKYMED constellation turn on the l'aquila earthquake: Dinsar results of the morfeo project"

On April 6th2009 a Mw=6.3 earthquake struck the area around the city of L'Aquila in Italy. SAR systems have been proven to be valuable sensors for analyzing the effect of earthquakes and monitoring post-seismic displacements. Due to the low deformation rate, the study of post-seismic events requires the use of a multi-temporal InSAR approach. COSMO/SKYMED is a constellation of SAR sensors of 4 X-band sensors operative also for the civilian use. Thanks to the availability of a stack of ascending acquisitions, ad hoc programmed by ASI on the area stricken by the earthquake, it was possible to provide post-seismic deformation maps by using two different multi-temporal interferometric approaches: the SPINUA and SBAS techniques. The work is carried out in the framework of the MORFEO project dedicated to the monitoring of the landslides risk by means of Earth Observation data. The displacement maps related to the post-seismic activity are presented and commented. The results clearly show the potentiality of the COSMO/SKYMED constellation use for emergency monitoring. [C2018]

### "Cognitive diversity sensing"

Radar sensing is and will continue to have great importance in both the civil and military communities. This importance will increase in proportion to the tasks that radar is able to reliably carry out. New methodologies and new technical capabilities offer the potential for new functionality and improvements in existing ones. Radar is currently going through a quiet revolution in which new methodologies are starting to be explored that highlight exiting new possibilities whilst demonstrating some of the challenges yet to be overcome. In this paper we examine the emerging topic of cognitive diversity sensing. Put simply this is the dynamic adjustment of radar parameters on both transmit and receive to maximize the extraction of desired information from the scene being surveyed. Further this brings into play the key topic of cognition exploiting the natural relationship between the

sensor and the sensed. It is this combination that provides a powerful new paradigm based on diversity sensing for future radar systems. This has huge potential enabling autonomous capabilities right across the whole spectrum of radar applications. [C2019]

#### "The analysis of surface deformation based on two-pass and three-pass D-InSAR"

The Differential Synthetic Aperture Radar Interferometry (D-InSAR) is widely used in large-scale ground deformation monitoring such as crustal deformation, seismic changes, land subsidence, landslides, volcanic deformation, glacial movement. In this paper, The deformation analysis based on two-pass differential and three-pass differential InSAR is done. We have shown that the analytic results by the three-pass differential method is better. The quality of result may be effected in phase unwrapping in two different methods. The deformation fields obtained by two different differential methods have been compared with traditional methods. With the changes in topographic factor, climatic conditions and vegetation types, the coherence effect is different, results have been given. It is not easy that the strong coherence is satisfied in three SAR images in the same time. Therefore, the optimizing methods depend on the purpose of application and the characteristics of studied area. [C2020]

#### "COSMIC-2: The future of global navigation satellite system-remote observation (GNSS-RO) sensing"

COSMIC is a joint U.S.-Taiwan 6-microsatellite demonstration mission that was launched in April 2006. It is the world's first operational GPS radio occultation (RO) mission for global Earth weather forecast; climate monitoring; atmospheric, ionospheric, and geodetic research. The GPS-RO data has been demonstrated to be valuable to the climate, meteorology, and space weather communities. COSMIC has proven to increase the accuracy of the predictions of hurricane/typhoon behavior, significantly improve long-range weather forecasts, and monitor climate change with unprecedented accuracy. COSMIC will reach the end of its design life in 2011, and the critical capability it provides will begin to degrade as satellites become no longer operational. As a result, NOAA and NSPO intend to jointly develop and launch COSMIC-2, a high-reliability next generation follow-on system. COSMIC-2 is will provide the next generation of global navigation satellite system (GNSS)-RO data to users who critically rely on it. [C2021]

#### "Hidden Markov based target detection for track-before-detect"

A tracking filter using conventional methods perform target detectios by setting a threshold at the output of the sensor's signal processor. The result of using thresholding brings out that, targets with low signal-to-noise ratio (SNR) may not be detected if the signal power is below the required threshold. Track-before-detect (TBD) techniques avoid the usage of a detection threshold and provide detecting and tracking targets with lower signal-to-noise ratios. Although TBD techniques eliminate the need for detection threshold at sensor's signal processing stage, they often use tuning thresholds at the output of the filtering stage. This paper presents a Hidden Markov Model (HMM) based target detection method for employing with TBD techniques which does not use any of the thresholding method. [C2022]

#### "New trends in SAR tomography"

In this paper a comparison between two techniques developed to recover layover solution in SAR images is presented. SAR Statistical Tomography and Compressive Sensing techniques are described and analyzed in order to provide a set of instruments for 3D SAR imaging able to tackle different scattering mechanisms in layover areas and to recover height reconstruction of an observed scene. The performances of the two techniques are compared on simulated data and some conclusions are drawn. [C2023]

#### "Overview of SMOS Level 2 Ocean Salinity processing and first results"

SMOS (Soil Moisture and Ocean Salinity), launched in November 2, 2009 is the first satellite mission addressing the salinity measurement from space through the use of MIRAS (Microwave Imaging Radiometer with Aperture Synthesis), a new two-dimensional interferometer designed by the European Space Agency (ESA) and operating at L-band. This paper presents a summary of the sea surface salinity retrieval approach implemented in SMOS, as well as first results obtained after completing the mission commissioning phase in May 2010. A large number of papers have been published about salinity remote sensing and its implementation in the SMOS mission. An extensive list of references is provided here, many authored by the SMOS ocean salinity team, with emphasis on the different physical processes that have been considered in the SMOS salinity retrieval algorithm. [C2024]

#### "Characteristic analysis of vehicle target in Quad-Pol Radarsat-2 SAR images"

Radarsat-2 satellite offers general users the Quad-Pol SAR image service with a resolution of 8 meters, which provides valuable data source for the research of traffic vehicles monitoring on Quad-Pol SAR images. According to the vehicle target in such new SAR images, this paper put forward a target characteristic analysis method, which is a combination of target RCS measurement and polarization decomposition. Moreover, it choose the large trucks as an example, give out a conclusion of characteristic analysis of vehicle targets through the on-site synchronous experimental data obtained at different incident angle. Thus provides the research foundation for further exploration of realizing the traffic monitoring with space-born Quad-Pol SAR images. [C2025]

#### **"Topographic gray level multiscale analysis and its application to histogram modification"**

This paper describes a framework for multi-scale gray level analysis of images. It defines scales based on gray levels and organizes the basic "atoms" with a topographic map. The aim of this approach is to separate a large number of pixels concentrating in a narrow range of gray values. The main advantage of the methodology is that it allows manipulating pixels according to gray levels and spatial relations simultaneously. We apply it to histogram modification of Synthetic Aperture Radar (SAR) images. The experiments on displaying and classification prove the superiority of the approach. [C2026]

#### **"A review of ionospheric effects in low-frequency SAR-Signals, correction methods, and performance requirements"**

Ionospheric signal distortions are commonplace in low-frequency space-borne SAR observations and can lead to the degradation of SAR data quality and data consistency if no signal compensation is applied. In this paper we will give an overview of the problem of ionospheric influence in SAR, PolSAR, and InSAR data. We will characterize the spatiotemporal signal properties of ionospheric signals, introduce a selection of currently available correction methods, and present a list of performance requirements to be met by ionospheric correction. [C2027]

#### **"Impact of the wave number estimation in Underground Focusing SAR images"**

This work studies the impact estimating soil wave number in Underground Focusing SAR imaging for tunnel detection applications. It is demonstrated that poor underground imaging results when wave refraction at the ground surface is neglected, but that incorporating refraction with sufficiently high estimates of soil dielectric constant produce clear target images. Using a wrong wave number for the soil incorrectly predicts the tunnel's depth, but gives positive identification of its transverse and extent. [C2028]

#### **"Rotated dihedral and volume scattering behavior in cross-polarimetric SAR"**

In this study we analyze Radarsat-2 quadruple polarization (quad-pol) mode data acquired over the Everglades wetlands in south Florida. We analyzed the phase information of each polarization mode independently, and obtained similar fringe patterns representing water level changes in all four interferograms. It is surprising, because common scattering theories indicate that cross-polarization (cross-pol) observations reflect volume scattering due to the interaction of the radar signal with upper sections of the vegetation. However, our cross-pol interferometric observations suggest that the cross-pol signal reached the water surface and scattered back to the satellite by a rotated dihedral double bounce mechanism. Based on these new observations, we developed a new scattering formulation that accounts also for double bounce component in cross-pol. [C2029]

#### **"Characterization of the scattered field by an urban area in the X-frequency band for bistatic and monostatic radar configurations"**

The application of the ray-tracing technique in combination with the asymptotic method Uniform Theory of Diffraction (UTD) for an analysis of the electromagnetic (EM) wave propagation in urban areas is presented. The frequency of the study is in the X-frequency band from 8 to 12 GHz but can be applied for Ku-band and a three-dimensional model of the geometry is proposed. The transmitter and receiver can be separated to present both bistatic and monostatic configurations. At the end of the work, we evaluate the amplitude and the phase of the far field diffracted by urban scenarios. [C2030]

#### **"Burst mode to strip-map mode SAR interferometry of ALOS PALSAR"**

A complete processing flow is proposed to implement burst mode to strip-map mode interferometry for ALOS PALSAR data. The processing flow is applied to an interferometric pair comprised of FBD (High Resolution mode [Dual polarization], belonging to strip-map mode) and WB1 (Wide observation mode, belonging to burst mode) mode of PALSAR. Interferometric products including differential interferometric phase and DEM are generated. The evaluation of these products shows satisfactory precision. [C2031]



### "Study of snowmelt impact on SST and TSM fields in the coastal zone of Barents Sea"

Spatial and temporal variations of SST and biological fields were observed in the coastal area off Novaya Zemlja, Barents Sea. Focus is on the relation between SST and biological parameters. The variations of snowmelt runoff from land (glaciers and river runoff) were estimated using SAR imagery. A relation between snowmelt input from land and ocean Chl a as well as TSM concentration was observed based on a case study. The data showed that the TSM and Chl a concentration increased significantly ~30 days after the snowmelt over land started to increase. [C2032]

### "Monitoring tree farms and coastal environments using RADARSAT-2 PolSAR data"

This paper addresses the feasibility of using RADARSAT-2 fine Quad-Pol mode to monitor coastal environment and young tree growth. It will be shown that interferometric coherence may not be high enough for the height estimation of young trees at C-band, but polarimetric sensitivity could be used for tree and crop classification. For coastal environment, we found that polarimetric signature of oyster farm reveals the effect of double bounce scattering and the orientation angle effects. [C2033]

### "Ultra-wideband radar measurements of snow thickness over sea ice"

An ultra-wideband, frequency modulated, continuous wave radar working from 2.0 to 6.5 GHz was designed, built and tested at the Center for Remote Sensing of Ice Sheets (CReSIS) at the University of Kansas to measure snow thickness over sea ice. Improvements and modifications to the existing radar, compared to previous versions, allow for snow thickness measurements from fast-moving, long-range aircraft. Over the past year, the radar has recorded snow thickness measurements over sea ice in the Arctic and Antarctic oceans as part of NASA's Operation Ice Bridge. [C2034]

### "Effects of surface roughness on sea ice freeboard retrieval with an Airborne Ku-Band SAR radar altimeter"

Results from two years of the CryoSat Validation Experiment (CryoVEx) over sea ice in the western Arctic Ocean are presented. The estimation of freeboard, the height of sea ice floating above the water level, is one of the main goals of the CryoSat-2 mission of the European Space Agency (ESA) in order to investigate sea ice volume changes on an Arctic wide scale. Freeboard retrieval requires precise radar range measurements to the ice surface, therefore we investigate the penetration of the Ku-Band radar waves into the overlying snow cover as well as the effects of sub-footprint-scale surface roughness using airborne radar and laser altimeters. We find regional variable penetration of the radar signal at late spring conditions, where the difference of the radar and the reference laser range measurement never agrees with the expected snow thickness. In addition, a rough surface can lead to biases of the airborne validation dataset, since the radar overestimates the amount of open water and thin ice as well as the freeboard of heavy ice deformation zones. [C2035]

### "A generalized logical format for inter-calibrated brightness temperatures for the global precipitation measurement mission"

An important aspect of the GPM mission is the merging of precipitation data from multiple radiometers on different satellites. This requires that each radiometer be consistently calibrated and that each be intercalibrated with a mission reference standard. For GPM the reference standard is to be the core satellite carrying a dual frequency precipitation radar and a well calibrated conically scanning radiometer. This paper describes a common format for representing these intercalibrated brightness temperatures which will be used for all radiometer products from GPM partner satellites. The use of common formats ensures that users obtain all the required information and also facilitates the rain retrieval algorithm code preparation as it can always expect to have the data that it needs for the retrieval. [C2036]

### "Scatterometer image reconstruction from aperture-filtered samples"

This paper considers sampling and reconstruction theory with application to scatterometer image reconstruction. Backscatter imaging is approached as the inversion of a noisy aperture-filtered sampling operation. A reconstruction estimator based on maximum a posteriori probability (MAP) estimation is proposed to recover the conventional samples from noisy aperture-filtered samples. Examples from the SeaWinds scatterometer and the Advanced Wind Scatterometer (ASCAT) are presented. [C2037]

### "Radargrammetry of high resolution synthetic aperture radar onboard KOMPSAT-5"

This paper reports the preliminary results on the study of radargrammetry especially for a high-resolution satellite synthetic aperture radar system. Theoretical configurations for radargrammetry in terms of coverage, orbit selection, incidence angles, height sensitivity of parallax and height resolution of DEM were calculated according to the proposed orbit characteristics and the imaging modes of KOMPSAT-5 SAR. Possible imaging strategies and mission scenarios for coverage versus rapidity are suggested for a future mission dedicated to radargrammetry. [C2038]

#### "Fusion of LiDAR data and orthoimage for automatic building reconstruction"

Recent years LiDAR data is widely used for constructing 3D terrain models which provide realistic impressions of the urban environment. This paper presents an automatic method for extracting 3D building model by the fusion of LiDAR data, 2D building outlines and orthoimage. 2D building outlines is generated by classifying the LiDAR data to terrain and off-terrain points, then detecting building edges points through step-structure detector and generalization. 2D building boundaries are added on the DSM (Digital Surface Model) from LiDAR data to generate complex buildings by using CSG with the Boolean operations of union, intersection and differences. [C2039]

#### "Extraction of frequent grouped sequential patterns from Satellite Image Time Series"

This paper presents an original data mining approach for extracting pixel evolutions and sub-evolutions from Satellite Image Time Series. These patterns, called frequent grouped sequential patterns, represent the (sub-)evolutions of pixels over time, and have to satisfy two constraints: firstly to correspond to at least a given minimum surface and secondly to be shared by pixels that are sufficiently connected. These spatial constraints are actively used to face large data volumes and to select evolutions making sense for end-users. Successful experiments on an optical and a radar SITS are presented. [C2040]

#### "Soil moisture detection using KOMPSAT-5 SAR data"

The applicability of the KOMPSAT-5 (Korea Multi-Purpose Satellite-5) SAR on soil moisture detection is addressed in this paper. At first, the penetration into and reflection from bare soil surfaces at X-band are compared with those at L-band for homogeneous and inhomogeneous moisture profiles. The sensitivities of the X-band radar backscatter on soil moisture are examined for rough bare soil surfaces. Then the sensitivities of the X-band radar backscatter on the soil moisture of vegetated surfaces are also examined for various vegetation densities and incidence angles. The applicability of an X-band radar for soil moisture detection may be as good as L-band radar for bare soil surfaces. For vegetated surfaces, the soil moisture can be detected using an X-band radar at lower incidence angles, where the upper limit of the incidence angles depends on vegetation density. [C2041]

#### "The inversion of crop height based on small-footprint waveform airborne lidar"

Due to limited vertical resolution, the waveform of vegetation whose height is relatively low will superpose on soil waveform. Therefore, lidar full-waveform data were mainly used in forestry, but no research in the crop. In this paper, in order to derive crop height, a gaussian decomposition algorithm based on transmitting waveform is adopted to distinguish the crop waveform from soil waveform, and to extract peak location and pulse width from raw waveform data, proving it is a reliable and highly accurate decomposition algorithm. Moreover, the decomposition algorithm lays the proper foundation for obtaining other crop biophysical parameters. [C2042]

#### "Extraction of building's geometric axis line from LiDAR data for disaster management"

Fast and reliable building damage analysis is crucial for survivors rescue and disaster management when a destructive natural disaster occurs which helps to limit life losses. For this purpose, a method was developed in this paper to extract building's geometric axis line from aerial LiDAR data which helps to do further building damage analysis like to identify inclined buildings. To extract building's geometric axis line, several steps were carried out such as segmentation of buildings, extraction of roof facets, fitting of mean roof plane and getting main roof. The aerial LiDAR data was captured over the area of Port-au-Prince, Haiti which contains numerous of inclined buildings. The results demonstrate the feasibility and effectiveness of the proposed approach to identify inclined building for damage management. [C2043]

#### "Glaciermonitoring: Correlation versus texture tracking"

Synthetic aperture radar (SAR) images provide scattering information which can be used under any weather conditions for glacier monitoring. Our purpose is to estimate a displacement field characterizing at each position the local speeds and orientations of the glacier displacement. Recent proposed methods build a vector field by

tracking patches between two SAR images co-registered on static areas and sensed at different times. The tracking is performed either by evaluating the correlations or the similarities from one acquisition to the other. We propose to estimate locally the displacement vectors by using either the maximum correlation or a maximum likelihood estimator. This local estimation is then refined to provide a sub-pixelic result. The efficiency of both methods are compared. [C2044]

#### "A non-local approach for SAR and interferometric SAR denoising"

Recently, non-local approaches have proved very powerful for image denoising. Unlike local filters, the non-local (NL) means introduced in decrease the noise while preserving well the resolution. In the proposed paper, we suggest the use of a non-local approach to estimate single-look SAR reflectivity images or to construct SAR interferograms. SAR interferogram construction refers to the joint estimation of the reflectivity, phase difference and coherence image from a pair of two co-registered single-look complex SAR images. The weighted-maximum likelihood is introduced as a generalization of the weighted average performed in the NL means. We propose to set the weights according to the probability of similarity which provides an extension of the Euclidean distance used in the NL means. Experiments and results are presented to show the efficiency of the proposed approach. [C2045]

#### "Data visualization and analysis tools for the Global Precipitation Measurement (GPM) Validation Network"

The Validation Network (VN) prototype for the Global Precipitation Measurement (GPM) mission compares data from the its predecessor Tropical Rainfall Measuring Mission (TRMM) satellite's Precipitation Radar (PR) to ground radar (GR) measurements from U.S. and international operational weather radars. This prototype is a major component of the GPM Ground Validation System (GVS). The VN provides a means for the precipitation measurement community to identify and resolve significant discrepancies between the GR observations and similar satellite observations. The VN prototype is based on research results and computer code Liao et al. [1]. Morris and Schwaller [3] describe the VN prototype and initial results in detail. This paper describes software tools that have been developed for visualization and statistical analysis of the original and volume matched PR and GR data. [C2046]

#### "Mapping of wind-thrown forests using satellite SAR images"

The study focuses on investigation and evaluation of wind-thrown forest mapping using satellite remotely sensed data from three synthetic aperture radar (SAR) sensors. The study is carried out at Remningstorp, a test site in the south of Sweden dominated by coniferous forest, where trees were manual felled to simulate wind-thrown forest. The satellite data consisted of time series of HH polarized SAR images acquired by the Advanced Land Observing Satellite (ALOS) Phased Array type L-band Synthetic Aperture Radar (PALSAR), Radarsat-2 (C-band) and TerraSAR-X (X-band). The results from visual interpretation of SAR images acquired before and after the simulated wind-throw together with corresponding ratio images show that ALOS PALSAR HH polarized intensity images are not able to detect wind-thrown forest, probably due to too coarse spatial resolution. In contrast, the wind-thrown forest is clearly visible in the Radarsat-2 and TerraSAR-X HH polarized images, implying that it may be possible to develop a new application using these SAR data for mapping of wind-thrown forests. [C2047]

#### "Full exploitation of the SBAS-DInSAR algorithm in active seismogenetic scenarios"

We perform a full exploitation of the Differential SAR Interferometry (DInSAR) algorithm referred to as Small Baseline Subset (SBAS) technique to investigate long term surface deformation occurring in extended, seismogenetic areas. To this aim we benefit of the SBAS technique capability to work in multi-frame and multi-sensor scenarios in order to improve the spatial and temporal coverage, as well as to employ new generation SAR sensors to increase the temporal sampling of the retrieved time series. In this work we apply the SBAS algorithm to analyze the temporal evolution of the detected displacements affecting three different seismogenetic scenarios by means of deformation time series retrieved through data acquired by European (ERS-1/2, ENVISAT) and Italian (COSMO-SkyMed) satellites. In particular, we focus on the analysis of the deformation patterns associated with the activity of the San Andreas (SAF, California, USA), the North Anatolian (NAF, Turkey) and the Paganica (PF, Abruzzo, Central Italy) Faults. The achieved results provide a clear idea of the surface deformation retrieval capability of the SBAS procedure. [C2048]

#### "Optimal parameter estimation in heterogeneous clutter for high resolution polarimetric SAR data"

This paper presents a new estimation scheme for optimally deriving clutter parameters with high resolution POLSAR data. The heterogeneous clutter in POLSAR data was described by the Spherically Invariant Random

Vectors model. Three parameters were introduced for the high resolution POLSAR data clutter: the span, the normalized texture and the speckle normalized covariance matrix. The asymptotic distribution of the novel span estimator is also investigated. The proposed method is tested with airborne POLSAR images provided by the ONERA RAMSES system. [C2049]

#### "A method to estimate Snow Water Equivalent using multi-angle X-band radar observations"

Active microwave sensors, especially high-frequency radar systems, are highly sensitive to snow pack parameters, including Snow Water Equivalent (SWE). With the availability of several X-band space-borne SAR systems, the study attempts to make use of multiple-angle SAR observations and develop relevant SWE inversion algorithms. Analysis was carried out based on parameterized scattering models for both soil surface and snowpack. It is found that the backscattering signals at two incident angles are well correlated for both soil surface and snowpack; and snow optical thickness can be well defined and estimated through snow volume scattering at two different angles. The snow and soil parameters can be estimated through two pairs of adjacent observations. The technique was tested using theoretical simulated database. Initial analysis shows that current technique needs to be further improved and a better estimation of single scattering albedo is needed. [C2050]

#### "Monitoring time-dependent volcanic dynamics at Long Valley Caldera using InSAR and GPS measurements"

Continuous monitoring Long Valley Caldera since the late 1970s, including data from seismic and geodetic networks has shown renewed episodic unrest activities with accelerated uplift separated by reduced uplift, no activity or slow deflation. We examine the time-dependent behaviors at Long Valley Caldera in 1996-2009 by integrating InSAR and continuous GPS (CGPS) measurements. The ERS-1/2 radar data between 1992 and 2008 and reprocessed three-component continuous GPS (CGPS) data from Long Valley GPS network in 1996-2009 were combined to invert for source geometry and volume change in the following deformation episodes: 97-98 uplift, 02-03 uplift, 04-07 slow subsidence, and 07-09 slow uplift. Our results show that all post-2000 events locate in the shallow depth range of ~7-9 km and have nearly identical source location, suggesting that these events are caused by the same partial melt magma source at the mid-crustal level. All three events are characterized by the low volume change, in comparison with previous 1997-1998 inflation event that has much larger volume change and steeper source geometry. If we regard post-2000 events as proxy for future eruption hazard, the inferred source dynamics (e.g., mid-crustal location and low volume change) from these post-2000 events suggest that the probability for near-term eruption is low. Our study demonstrates that CGPS, along with InSAR, are important tools in monitoring time-dependent source process at the active volcano region. [C2051]

#### "Estimation of the degree of polarization in dual-polarized SAR imagery"

Analysis of dual-polarized SAR imagery has gained new importance with the recent launches of ALOS PALSAR, RADARSAT-2, and TerraSAR-X polarimetric SAR systems. Information contained in polarimetric images, collected by these SAR systems, can be characterized by a scalar parameter called the degree of polarization. This parameter has long been recognized as one of the most important parameters characterizing a partially polarized electromagnetic wave. In this paper, we provide maximum likelihood and moment-based estimators of the degree of polarization in dual-polarized SAR imagery. We evaluate and compare the performance of these estimators on RADARSAT-2 polarimetric data, over various terrain types such as urban, vegetation, and ocean. [C2052]

#### "Individual tree species classification using structure features from high density airborne lidar data"

The paper investigated the advantage of high density airborne LiDAR data for improving species classification of individual tree. The investigation is comprised of two stages, feature extraction and classification. Several feature metrics were derived from LiDAR data, most of which were to characterize the vertical structural properties of difference species. Some other metrics were calculated statistically from intensity and return number information. A supervised decision tree algorithm was applied on the extracted features to perform both feature selection and classification. Two classification themes were carried out: classification of coniferous and deciduous trees, and classification of five species. Experiment was conducted in Canadian boreal forests dominated by mature trees. The results demonstrated LiDAR derived vertical profile metrics are capable for species classification either to separate coniferous and deciduous or to separate multiple species. The best overall classification accuracy is 81.7% validated by using the test data from the same ecosystem as the training data. [C2053]

#### "On the use of transponder measurements for high precision assessment and calibration of polarimetric Radarsat-2"



An independent assessment and calibration of polarimetric RADARSAT-2 (RS2) are conducted using transponder measurements extracted from uncalibrated data collected at various incidence angles between 20° and 40°. It is shown that RS2 antenna is highly isolated (better than -32 dB), and only crosschannel relative phase correction is required to provide calibrated data that meet comfortably the CEOS Cal-Val requirements. To take full advantage of the excellent RS2 performance in terms of low noise floor (-38 dB), transponder measurements are used for high precision assessment of RS2 calibration parameters. It is shown that the antenna cross-talks are stable with incidence angle, and only one transmitter-receiver distortion matrix is required for accurate calibration of the 20 modes of RS2 (Right looking) from 20° to 40°. A new method based on high precision transponder measurements is introduced for polarimetric RS2 calibration. Data collected at various incidence angles are used to validate the calibration. Transponder measurements using calibrated data indicate a residual cross-talk lower than -43 dB. The residual cross-channel error is lower than 0.3 dB in radiometry, and 5° in phase. [C2054]

#### "Biomass retrieval based on UAVSAR polarimetric data"

Parameters of vegetation spatial structure have important effect on the carbon cycle and biodiversity of the ecosystems. How to estimate above-ground biomass is still a problem need to be worked out. In this paper we tried to use UAVSAR datasets to discuss the relation between backscattering coefficient and local incidence angle in different forest types. By the relation, a method based on scattering mechanism for correcting radiometric distortion caused by large range of incidence angle is developed. Biomass retrieval is based on incidence angle correction. The result shows good correlation between biomass and backscattering coefficient in 1 ha scale. [C2055]

#### "Spurious signal in measurement of the third Stokes parameter from space at L-band"

Spurious spikes in the third Stokes parameter have been observed in numerical simulations of the signal expected from the L-band radiometers to be flown as part of the Aquarius instrument. These signals are present over scenes with large contrast such as land water boundaries and are due to cross polarization coupling and the relatively large footprint of the antennas. [C2056]

#### "Space-time focusing of HF skywave radar signals with application to nonlinear scattering phenomenology"

Increasing the power density incident on a target without raising the radiated power may offer a number of benefits to HF skywave radar systems. Among these is the prospect of detecting nonlinear echoes, which could greatly enhance detection in sea clutter. Other prospects include improved detection of low RCS targets and more effective use of sub-apertures for multiple simultaneous task operations. In this paper we review the physics underlying these missions and assess the potential of various approaches to concentrating energy in localized regions within the illuminated zone. [C2057]

#### "CRInSAR for landslide deformation monitoring: A case in threegorge area"

Landslide in threegorge area is a severe geohazard threatening many people. Conventional differential SAR interferometry (DInSAR) and Persistent Scatterers for SAR interferometry (PSInSAR) technique are unsuitable for landslide deformation monitoring in this area due to temporal and lack of natural phase stable point targets. The method of DInSAR using corner reflectors (CRInSAR) is a powerful tool in the vegetation area. The procedure of DInSAR using corner reflectors (CRInSAR) used by this paper is briefly introduced. Using ENVISAT ASAR time series data, the deformation of 12 corner reflectors (CR) in Shuping landslide are analyzed. As to the CR with slow creep deformation, the CRInSAR results are reliable. But as to the CR with nonlinear accelerated deformation, our CRInSAR method still needs to be enhanced. [C2058]

#### "Target detection based on granularity computing of quotient space theory using SAR image"

Target detection is a hot topic and key technique of SAR image interpretation. There are many detection methods, such as CFAR detector and Extended Fractal (EF) feature detector. In order to overcome their shortcomings and combine their merits at the same time, the combination of some different detection methods need be implemented. Granularity computing is just an approach that solves the problem at different granularity space due to different principles. Therefore, SAR image target detection based on granularity synthetic algorithm of quotient space theory is proposed in this paper. Firstly, CFAR detector and EF feature detection method are performed to generate different detection results as coarse granularity spaces. Then combine the different quotient spaces and construct the fine granularity space by using granularity synthesis algorithm. Finally, obtain the final target detection result. The experimental result of RADARSAT-I C band SAR image proves that the proposed algorithm is effective. [C2059]

### "Landslide detection by indices of LiDAR point-cloud density"

The deliverables of an airborne LiDAR survey usually include all points, ground points, digital surface models (DSM) and digital elevation models (DEM). Indices of point clouds tested in this study include density of all points, density of ground points, density of only returns, and density of multiple returns. Shallow landslides are the most common landslides triggered by torrential rainfalls and explicit fresh scars after rainfall events. Multiple returns in forest area give the possibility of differentiating landslide scars from vegetated lands. Classification results from the indices derived from these four kinds of densities are verified by the result obtained by manual interpretation of the derived nDSM images. The experiment is carried out using the dataset obtained in I-Lan County after Typhoon Kalmaegi on 17 July 2008. The results show that a proper definition of the parameters for the indices is most critical for the detection of shallow landslides. [C2060]

### "Global trends in remote sensing of human settlements"

Advances in both airborne and spaceborne remote sensing systems have provided a range of tools for monitoring and managing human settlements. In particular the availability of very high spatial resolution satellite systems has dramatically increased access to high quality two-dimensional spatial information, while laser profilers and interferometric synthetic aperture radar have allowed acquisition of the third dimension. Over the past 100 years sensor systems have changed dramatically, from early airborne cameras that imaged only small parts of an urban area on a project return basis, to very high resolution spaceborne systems, covering a wide spectral range, with regular return periods down to a few weeks or days. This paper provides a brief history of urban remote sensing, followed by an examination of the properties of current systems and their acquired data, some processing methods and urban applications. It concludes with an overview of future developments. [C2061]

### "Direct-path mitigation for underground imaging in RF Tomography"

Belowground imaging using RF Tomography is challenged by strong direct-path coupling between sensors. In this work, a direct-path mitigation procedure is introduced, consisting of two steps. First, the Tx and Rx dipoles are rotated in along particular directions that maximizes the signal with respect to the direct-path contribution. Then, the remaining contribution is removed by using a hybrid analog/digital feedback loop at the receiver side. [C2062]

### "ISAR imaging of maneuvering targets via matching pursuit"

An algorithm based on matching pursuit (MP) technique is proposed for inverse synthetic aperture radar (ISAR) imaging of maneuvering targets. The received ISAR echo is decomposed into many basis sub-signals that are generated by discretizing the target spatial domain and synthesizing the ISAR data for every discretized spatial position, and then the ISAR imaging problem is converted into the sub-signal selection problem. The basis sub-signals that indeed contribute to the ISAR echo are selected by using the MP technique, and the projection coefficients of the ISAR echo on the selected basis sub-signals represent the ISAR image. In the case of unknown rotation rate of the target, the true rotation rate is obtained by combining the MP technique with the maximum contrast search. Numerical examples show that the proposed algorithm can produce high resolution and remove sidelobe artifacts. [C2063]

### "Coherent scatterer in forest environment: Detection, properties and its applications"

In this paper, the first detection result of coherent scatterers (CSs) in forest environment is addressed. As a scatterer associated with CS, the dihedral structure consists of the tree-trunk like a vertical cylinder and the ground surface is assumed. The potential of CSs as being the phase stable scatterers as permanent scatterers will be also demonstrated with P-&L-band Pol-InSAR datasets acquired in repeat-pass InSAR mode over boreal forest test site by German Aerospace Center's E-SAR airborne system. [C2064]

### "Modeling attenuation of melting hydrometeors with a method based on volume integral equations"

The attenuation of spheroidal melting hydrometeors is simulated in C-, Ku- and Ka-band utilizing a microphysical melting layer model. The scattering properties are obtained with Mie scattering solution. In C-band the polarimetric radar parameters are computed utilizing a method based on volume integral equation. Polarization difference is detectable, but reflectivity values are regularly smaller than those calculated with Mie solution. This is dependent on the process of formatting the particle structure according to the change in liquid water mass fraction. [C2065]

### "Modification of slant range model and imaging processing in GEO SAR"

In this paper, considering the relative motion between satellite and earth during signal propagation time, the accurate analysis method for propagation slant range is presented in geosynchronous SAR. Furthermore, the difference between accurate analysis method and 'Stop-and-Go' assumption is analytically obtained. Meanwhile based on the derived accurate slant range model, it is found that the corresponding range migration correction and azimuth reference function must consider the high order term, and therefore the modified SPECAN algorithm is proposed. The simulation results verify the correctness of 'Stop-and-Go' assumption error derivation and SPECAN algorithm modification. [C2066]

### "Rotation and scale invariant template matching applied to buried object discrimination in GPR data"

In this study, a template matching approach to buried object discrimination problem is proposed over ground penetrating radar (GPR) B-scan images. The technique is scale invariant, which compensates for the change in the swinging speed of the detector. It is also rotation invariant to some extent, which reduces the number of templates to be used by compensating for the change in the scanning direction. The algorithm is tested on real GPR data and results are observed to be promising. [C2067]

### "Mapping urban subsidence with TerraSAR-X data by PSI analysis"

With a spatial resolution of up to 1 m, the German radar satellite TerraSAR-X has significantly improved the applicability of spaceborne SAR interferometry (InSAR) technique for fast ground motion monitoring due to its high spatial resolution and short time interval. In this work we present the first Permanent Scatterer Interferometry analysis with TerraSAR-X data for urban subsidence mapping in Tianjin city in China. Totally 17 scenes strip mode SAR images have been collected from Feb to Oct 2009 to perform the PSI analysis. The resulted average subsidence velocity demonstrates the ability of high resolution data for detailed monitoring of urban subsidence. Comparison between PSI result of TerraSAR-X and ENVISAT show the potential of TerraSAR-X data for urban motion as well as large scale manmade linear infrastructure monitoring. [C2068]

### "A phase screen simulator for predicting the impact of small-scale ionospheric structure on SAR image formation and interferometry"

We describe the SAR Scintillation Simulator (SAR-SS), a new phase screen model for simulating the impact of small-scale ionospheric structure on SAR image formation and interferometry. We compare simulated and observed PALSAR imagery over Brazil, and our preliminary findings show that SAR-SS can reproduce the essential features of azimuthal streaking and contrast degradation caused by small-scale structure in the ionosphere. [C2069]

### "Operational evaluation of damages in flooded areas combining Cosmo-SkyMed and multispectral optical images"

The management of a flood event requires singling out the affected area, quantifying the damages and programming an effective rescue plan. This requires rapid and easy access to all the geographical and observational information available for the target area. Optical imagery allow the identification of land uses, critical infrastructures and the extraction of important information to quantify the actual vulnerability of the area. In this case, the main advantage of satellite imagery is the much higher refresh rate with respect to classical in-situ surveys. When floods occur, the detection of flooded areas allowed by SAR observations such as those provided by Cosmo-SkyMed, helps in rapid and effective evaluation of the damage and organization of the management of the crisis. Here we present an integrated system developed by the team of the Italian Space Agency pilot project "Opera". The system allows the end user to integrate multispectral high resolution imagery and Cosmo-SkyMed products, in a 3-D environment, providing all the tools to virtually survey the observed area and extract quantitative information for many features relevant to the emergency management. The system has been tested in real time on a prolonged flooding event occurred in Januray 2010 in the Shkoder plain in Albania. [C2070]

### "Metacognition in radar"

An airborne ground looking radar sensor's performance may be enhanced by selecting algorithms adaptively as the environment changes. A short description of an airborne intelligent radar system (AIRS) is presented with a description of the knowledge based filter and detection portions. A second level of artificial intelligence (AI) processing is presented that monitors, tests, and learns how to improve and control the first level. This approach is based upon metacognition. [C2071]

### "Progressive spatial clustering of content-based satellite imagery retrieval results"

The ProgressiveDBSCAN algorithm allows for the progressive clustering of results from a geospatial information retrieval system. Results can be clustered by a combination of both their spatial and non-spatial attributes. The benefit of this clustering is that users are able to sort through the results returned from a geospatial information retrieval system in a spatial context. No longer are results from disparate locations presented to the user, but instead compact spatial clusters are displayed. There is a 98% reduction in the spatial distance between consecutive CBIR results and the spatial distance between the compact clusters; this leads to more efficient analysis of results by reducing the amount of time users spend context switching while on average only adding a few seconds to the query time. [C2072]

### "Sparsity enhanced fast subsurface imaging for stepped frequency GPRs"

A sparsity enhanced and fast data acquisition and imaging method is presented for stepped-frequency continuous-wave ground penetrating radars (SFCW GPRs). In previous work it is shown that if the target space is sparse like the point like targets, an image of the target space can be constructed with making measurements at only a small number of random frequencies by solving an  $\ell_1$  minimization problem. This greatly reduces the data acquisition time but the computational complexity for the imaging method is high. In this work, subsurface imaging is done with a suboptimal but fast method, orthogonal matching pursuit. Similar results to  $\ell_1$  minimization images are obtained within much shorter times. Also the results are sparse and less cluttered compared to standard backprojection images. [C2073]

### "A target tracking method with a single antenna using time-reversal UWB radar imaging in a multi-path environment"

UWB (Ultra Wide-Band) radar systems are promising imaging tools covering a variety of application fields including surveillance systems. UWB radar technology can provide advanced capabilities for current surveillance systems. An imaging algorithm for UWB radars, the TR (Time-Reversal) method enables high-resolution imaging in a multipath environment. Conventional TR methods have been applied to antenna array systems while our previous work proposed a TR method with a low-cost single antenna-based system. In this study, we propose a radar system with a single antenna on a vehicle in a multipath environment. This vehicle is assumed to get close to a moving target by adaptively tracking the target location. Some numerical simulation results show that the proposed low-cost system works well in a multi-path environment. [C2074]

### "Calibration system stability plans for a long-term Ecological Airborne remote sensing project"

The National Ecological Observatory Network (NEON) Airborne Observation Platform (AOP) will fly an imaging spectrometer, small footprint waveform LiDAR and high-resolution digital camera to observe both the human drivers of climate change and the biological consequences of environmental change at a continental scale. The project is planned for a 30-year period. To be meaningful as an ecological climate data record, the AOP data set must have a continuous and consistent calibration effort. This paper briefly describes plans for the development of a robust calibration and validation plan to ensure data continuity from instrument-to-instrument, flight-to-flight, and year-to-year over the lifetime of the NEON project. [C2075]

### "3D velocity model and ray tracing of antenna array GPR"

Migration is an important signal processing method that can improve signal-clutter ratio and reconstruct subsurface image. Diffraction stacking migration and Kirchhoff migration sum amplitudes along the migration trajectory, which generally is hyperbolic. But when the ground surface varies acutely, the migration trajectory is not hyperbolic. To computer the migration trajectory need the technique of ray tracing. We introduce a method of ray tracing based on 3D velocity model. Firstly, we build the 3D velocity model depending on the estimation of both ground surface topography and velocities. Then we compute the travel time between transmitter, receiver and each subsurface scattering point, and search the propagation ray depending on the Fermat's principle. The method is tested by an experiment data acquired by the stepped-frequency (SF) CMP antenna GPR system. The target is a metal ball that is buried under a sand mound. A nice result of ray tracing is shown in the case. [C2076]

### "Support vector machines regression for estimation of forest parameters from airborne laser scanning data"

Estimation of forest stand parameters from airborne laser scanning data relies on the selection of laser metrics sets and numerous field plots for model calibration. In mountainous areas, forest is highly heterogeneous and



field data collection labour-intensive hence the need for robust prediction methods. The aim of this paper is to compare stand parameters prediction accuracies of support vector machines regression and multiple regression models. Sensitivity of these techniques to the number and type of laser metrics, and use of dimension reduction techniques such as principal component and independent component analyses are also tested. Results show that support vector regression was less accurate but more stable than multiple regression for the prediction of forest parameters. [C2077]

#### "Time reversal adaptive waveform in MIMO radar"

EM multipath propagation is common in radar and wireless communications. Most radar systems are designed assuming line-of-sight (LOS), not multipath. In this paper, we extend our prior work on Multi-Input Multi-Output (MIMO) radar in the absence of interference [1], to consider MIMO radar detection in high clutter. We develop a subspace MIMO target model and a statistical model for MIMO radar clutter that accounts for the spatial and spectral properties of radar returns. We show that, using orthogonal waveform signaling, the time reversal MIMO radar yields higher detection performance than conventional statistical MIMO radar in high clutter. [C2078]

#### "Using lidar to estimate the capacity for storm water recycling and solar energy collection"

In this paper two lidar applications are addressed so that the data from large-scale airborne laser scanning of three New South Wales towns and the University of New South Wales can be used to estimate the capacity for storm water recycling and solar energy collection. The building outlines in each of these surveyed areas are extracted using the lidar point cloud to provide an accurate measurement of the total area of roofing within each region. The accurate area measurements are used with simple modelling equations to calculate the amount of rainfall runoff that could be collected and solar energy that could be produced, during an average year. The final results show the potential savings that could be produced each year if these towns and the university campus became more water and energy conscious. [C2079]

#### "Towards an improved wind and rain backscatter model for ASCAT"

The ASCAT scatterometer measures the backscatter from the ocean surface with which it infers the near-surface wind vector. When rain is present in the observation area the wind-induced backscatter is modified by the rain. This paper uses co-located observations from TRMM PR to model the effects of rain on the ASCAT observed backscatter. Two model types are considered, a phenomenological rain model and a lumped effect rain model which are comparable for most rain rates. For low rain events the ASCAT observed backscatter due to rain is not substantial, however for moderate to high rains the rain-induced backscatter from the ocean surface can be significant, and for extreme rain rates the atmospheric scattering and attenuation are dominant. [C2080]

#### "3D subsurface visualization by suppressing ground reflection and direct wave with bistatic GPR"

A ground reflection and a direct wave which propagates directly from a transmitting antenna to a receiving antenna are often arisen as issues especially for a ground penetrating radar (GPR) to monitor a near-surface region. In this paper, a 3D subsurface radar image by suppressing those components with a bistatic GPR system is presented. A relative permittivity of a ground surface is measured at the beginning, and a Brewster angle is estimated from that value. Then, the transmitting antenna is located to match an incident angle with the Brewster angle. In this case, the ground reflection does not occur, and all the energy penetrates into the ground. The direct wave is suppressed with an f-k filter which works automatically from position information of the antennas. An experimental result gives the 3D subsurface image without the ground reflection and the direct wave under a condition that a landmine model is buried at a depth of 10cm in a dry sand. [C2081]

#### "Studies of radio frequency interference at L-band using an airborne 2-D interferometric radiometer"

Potential radio frequency interference (RFI) sources at L-band include L-band radars; mobile, navigation and other satellite services; and various land services. We have collected data using our airborne L-band interferometric HUT-2D radiometer in order to support the ESA SMOS mission. We participated in April-May 2008 in ESA's rehearsal campaign for SMOS satellite validation activities in Germany and Spain. Additional data have been collected in Finland. Two basic categories of RFI have been observed: (1) Point-wise weak sources that do not saturate the HUT-2D instrument, and (2) strong sources that totally saturate the sensor over a large area. [C2082]

#### "Tidal current measurement with TerraSAR-X Along-Track Interferometry"

In this paper we describe new achievements of surface current measurements obtained by space-borne Along-

Track Interferometry (ATI). We show how tidal currents can be mapped using the TerraSAR-X satellite and adequate dual-channel SAR data processing techniques. We present results from tidal currents at the Orkney Islands that clearly demonstrate the potential and suitability of the method. [C2083]

#### "Gulf stream thermal fronts detected by synthetic aperture radar"

Our objective is to detect ocean surface features, specifically oceanic thermal fronts, through analysis of SAR (synthetic aperture radar)-derived wind stress fields. Fine-resolution measurements of near-surface wind speeds over the Gulf Stream region of the Northwest Atlantic were made using SAR images collected by RADARSAT-2. Linear statistical relationships between the wind stress curl and divergence to the crosswind and downwind components of the sea surface temperature (SST) gradient field were used to derive a new method for detecting Gulf Stream thermal fronts from Synthetic Aperture Radar (SAR) imagery. In particular, sea surface temperature front features, as suggested by corresponding AVHRR and MODIS images, are evident in both of the wind stress curl and divergence fields. [C2084]

#### "Microwave remote sensing for marine monitoring: An example of *Enteromorpha prolifera* bloom monitoring"

The bloom of algae called *Enteromorpha prolifera* posed a potential threat to the Olympic sailing competition in June 2008. Synthetic Aperture Radar (SAR) technology plays an irreplaceable role in algal blooming monitoring. Based on the analysis of various influence factors, a procedure for E.P. detection is proposed. In this paper, multi-temporal SAR images especially with short time interval, currents datum from buoys and wind products retrieved from SeaWinds scatterometer have been employed for E.P. dynamic monitoring and drift trend analysis. The result of analysis shows SAR, currents and wind datum are available for forecasting the trend of the E.P. drift. [C2085]

#### "Monostatic calibration of both TanDEM-X satellites"

The primary object of the TanDEM-X mission is to generate a highly accurate digital elevation model (DEM) with never achieved accuracy on global scale. But in addition to this bistatic TanDEM-X mission the monostatic TerraSAR-X mission have to be operated in parallel with both satellites. Consequently the second satellite TDX, successfully launched in June 2010, has to achieve the same accuracy and performance as those of the first satellite TSX, already in-flight since 2007. Thus, the monostatic calibration of the second satellite TDX is performed according to the same strategy based on effective and exact calibration techniques successfully demonstrated by the first satellite TSX. The paper discusses the calibration results of the first satellite TSX derived two years after launch by an extended re-calibration campaign executed in summer 2009, and presents first results of the second satellite TDX. But it has to be mentioned, the main calibration activities of TDX will start three weeks after launch, i.e. after uploading of this paper. [C2086]

#### "An improvement for the unsupervised Wishart Freeman classification with fully polarimetric SAR data"

In this paper, we proposed an improvement for the Wishart Freeman classification, which is based on the Wishart distance measurement and the estimation algorithm of the number of clusters for fully polarimetric SAR data. Our experimental results show the effectiveness of the proposed method. [C2087]

#### "Image partitioning with kernel mapping and graph cuts"

A novel multiregion graph cut image partitioning method combined with kernel mapping is presented. A kernel function transforms implicitly the image data into data of a higher dimension so that the piecewise constant model of the graph cut formulation becomes applicable. The method yields an effective alternative to complex modeling of the original image data while taking advantage of the rapidity of graph cuts. A variety of noise models are, thus, considered by a single model. Using a common kernel function, we minimize the objective functional by iterating (1) regions parameters update and (2) image partitioning by graph cut iterations. A comparative performance evaluation is carried out over a large set of experiments using synthetic grey level data. Besides, a set of tests with real images such as SAR and medical images is shown to demonstrate the validity of the method. [C2088]

#### "Ultra-rapid optronic processor for instantaneous ENVISAT/ASAR scene observation"

This paper introduces a real-time compact optronic SAR processor that has the capability to generate ENVISAT/ASAR image swaths of 100 km  $\times$  100 km in 10 seconds exhibiting slant plane sampling distances of 4 meters in azimuth and 1 meter in range. It may be instantaneously reconfigured to process data from any of the

7 ASAR image swath modes. In this respect, numerous SAR image sets may be produced immediately on-demand without bottleneck. A rapid SAR processor that also provides fine ground sampling distances in both azimuth and range directions could provide benefits for such applications as ship detection, landslide and flood monitoring, snow and ice coverage and glacier monitoring. [C2089]

### "Advances in the generation of deformation time series from SAR data sequences in areas affected by large dynamics"

We propose advances on the generation of deformation time series in areas affected by large deformation dynamics, where the exploitation of the differential SAR phase can be strongly limited by severe misregistration errors or by very high fringe rates. First, to overcome the former issue, we present an extension of the amplitude-based Pixel-Offset (PO) analyses by applying the Small Baseline Subset (SBAS) strategy, in order to move from the investigation of single (large) deformation events to that of dynamic phenomena. Secondly, to handle the high fringe rate interferograms, we subtract from them properly generated synthetic deformation models allowing us to reduce the fringe rate, thus helping the phase unwrapping step. The proposed approaches have been tested on ASAR-ENVISAT data acquired on Galapagos Islands and validated via continuous GPS measurements. [C2090]

### "Integration of InSAR and GIS for an estimation of ground subsidence susceptibility"

Ground subsidence susceptibility at a coal mine by integration of L-band SAR measurements and a subsidence hazard model incorporated in GIS was estimated. A subsidence hazard map was constructed using JERS-1 SAR data from the early 1990s and the subsidence hazard model. A certainty factor analysis was employed for estimating the relative weights of four control factors influencing coal mine subsidence. The relative weight of each factor was then integrated to generate a subsidence hazard index (SHI) by a fuzzy combination operator. The hazard map was validated by comparison with subsidence observed by ALOS PALSAR interferometry in 2007-2008. The results showed a good agreement between the predicted locations vulnerable to subsidence and the actual subsidence occurrences with an accuracy of about 72.5%. These results showed that the map produced by integration of InSAR and GIS can be used to predict and monitor coal mine subsidence hazards, especially in remote regions. [C2091]

### "Rain effect on polarimetric SAR observation"

The purpose of this paper is to consider the radio wave propagation of Polarimetric SAR in rain and to verify the influence of rain quantitatively. We assume the Polarimetric SAR observation model in non-spherical rain drop environments and evaluate the influence of rain at 5.405, 9.65 and 13.9GHz by calculating the rain distortion matrix with parameters of rainfall rate and the rain drop canting angle. The results show that the rain attenuation, the attenuation difference between horizontal and vertical polarization, and the cross-polarization factor increase as the frequency and rainfall rate increase, and they depend on the rain drop canting angle and the incident angle. [C2092]

### "The Soil Moisture Active Passive (SMAP) mission L-Band radar/radiometer instrument"

The Soil Moisture Active/Passive (SMAP) mission is a NASA mission identified by the NRC "decadal survey" to measure both soil moisture and freeze/thaw state from space. The mission will use both active radar and passive radiometer instruments at L-Band. In order to achieve a wide swath at sufficiently high resolution for both active and passive channels, an instrument architecture that uses a large rotating reflector is employed. The active radar will further utilize SAR processing in order to obtain the sub-footprint resolution necessary for the geophysical retrievals. The SMAP radiometer uses a more conventional real-aperture resolution, albeit with a significantly larger antenna than flown before. Both the SMAP radar and radiometer must address the effects of radiofrequency interference (RFI). [C2093]

### "Deformation in Hawaii's volcanoes obtained from a ScanSAR-to-stripmap Small Baseline Subset technique"

We investigate the displacement phenomena affecting Mauna Loa and Kilauea volcanoes at Big Island (Hawaii, USA), by applying an advanced ScanSAR-to-stripmap differential Synthetic Aperture Radar Interferometry (InSAR) approach. The implemented method, based on the application of the well-known Small Baseline Subset (SBAS) technique, allows the generation of LOS mean deformation velocity maps and corresponding time series, leading us to characterize the complex deformation of Mauna Loa and Kilauea volcanoes. The presented analysis relies on the use of a SAR dataset composed by 49 ASAR ENVISAT satellite images, relevant to both stripmap and ScanSAR operational modes, acquired on descending orbits (track 200) from January 2003 to

September 2008. Moreover, in order to assess the quality of the proposed combined ScanSAR-to-stripmap approach, we perform a comparison between the achieved DInSAR results and the LOS-projected GPS displacement measurements. [C2094]

#### **"Automated Polar ice thickness estimation from radar imagery"**

This work focuses on automating the task of estimating Polar ice thickness from airborne radar data acquired over Greenland and Antarctica. This process involves the identification and accurate selection of the ice sheet's surface location and interface between the ice sheet and the underlying bedrock for each measurement. Identifying the surface and bedrock locations in the radar imagery enables the computation of ice sheet thickness, which is important for the study of ice sheets, their volume, and how they may contribute to global climate change. The time-consuming manual approach requires sparse hand-selection of surface and bedrock interfaces by several human experts, and interpolating between the selections to save time. [C2095]

#### **"Spread E, F layer ionospheric clutter identification in range-Doppler map for HFSWR"**

Wide range covering, strong intensity, time-variant, fluctuation and irregular distribution of the spread E, F layer ionospheric clutter badly affects the system performance of High Frequency Surface Wave Radar (HFSWR). A spread E, F layer ionospheric clutter identification method is proposed based on the region segmentation results and region characteristics of the clutter. First of all, convolution template is used for locating the edge of the clutter, then the ratio of the number of the samples belonging to some segmented region and the total number of the samples in the region of interest (ROI) is used for setting the determinative threshold of the clutter region. Experiments with real data manifest that the proposed method can describe the effect of the spread ionospheric clutter to HFSWR. The quantitative analysis is consistent with the real data observation. The result can be used as a worthwhile reference for clutter mitigation, carrier frequency selection or radar system evaluation. [C2096]

#### **"Building height extraction via a deterministic approach using a TerraSAR-X data stack"**

A method for building height determination via a deterministic approach is tested using three TerraSAR-X images from Barcelona, Spain. Using this method, the height of a building wall can be determined based on the strength of the double-bounce backscattering. The approach requires knowledge of the material properties of the measured building wall and the area in near range of the building wall. For certain test buildings the approach provides good results, while for other buildings the results are erroneous. [C2097]

#### **"Analysis of the effect of radio frequency interference on interferometric phase"**

The P-band ultra wideband synthetic aperture radar shares the band with other services, as for example TV broadcast and telecommunications transmitter stations, means distortion by radio frequency interference (RFI) to the SAR. It's well known the performance of UWB-SAR is degraded due to the existence of radio frequency interference. This paper describes the problems of RFI in InSAR, and analyses the effect of RFI to interferometric phase based on simulation. [C2098]

#### **"Quantification of the topographic slope from radar satellite imagery"**

A specificity of Synthetic Aperture Radar (SAR) scenes is to display geometric distortions depending on both the system of acquisition and its relation with the topography. Establishing the geometric relationship between the radar sensor parameters and the related surface deformation should therefore provide quantitative information on the topographic surface. Here, we propose a new technique for the computation of the terrain slope, which is based on the quantification of the geometric deformation generated during the acquisition of a SAR scene. The method uses a pair of radar scenes consisting of an orthorectified image and another in slant-range geometry to compute the local topographic slope of a reference ground segment identified on both images. Computed slope values using ENVISAT-ASAR and TerraSAR-X images and compared with measurements taken in the field in the Djebel En Negueb anticline located in south-central Tunisia reach 3° with both data. [C2099]

#### **"Environmental monitoring with the imaging MIMO radars MIRA-CLE and MIRA-CLE X"**

Several applications need imaging sensors for environmental monitoring which can continuously observe an area in a 24/7 mode independently from the weather and other atmospheric obscuration like dust and smoke. Imaging MIMO radar fulfills these requirements and enables the opportunity of low-cost and robust imaging systems by synthesizing many virtual antennas out of just a few real ones. MIRA-CLE is a fully configurable and expandable experimental MIMO radar in Ka-band while MIRA-CLE X works in X-band and is intended to be a low-cost experimental system for long range applications. This paper presents both MIMO radar systems and shows and discusses first imaging results of MIRA-CLE X. [C2100]



### "Modular Radar Core for airborne and space applications"

The development of Radar Core electronics for any air and spaceborne radar units has a long space heritage at EADS in Friedrichshafen. It encompasses the spaceborne radars SIR-C/ X-SAR, SRTM, TerraSAR-X, TanDEM-X, and the oncoming PAZ mission and many airborne missions. These missions demonstrated successfully the high end radar electronics performances. EADS initiated a product development program called SmartRadar (Scalable modular aerospace radar technology) for the next generation airborne and space radars. The Radar Core development is one step in the SmartRadar development road map at EADS. To summarise the status of the development: the new hardware and related software have been flown in a demonstration flight campaign in summer 2009. For this campaign the frequency band was chosen to be at X-Band to use an available Reflector Antenna and Travelling Wave Tube Amplifier (TWTA) and Front end equipment. Synthetic Aperture Radar (SAR) image results are of very good quality and performance parameters analysed from the recorded raw data match or exceed the chosen design parameters. [C2101]

### "Shadow region imaging algorithm using array antenna based on aperture synthesis of multiple scattered waves for UWB radars"

Ultra-wide band (UWB) pulse radar has a definite advantage over optical ranging techniques, as to applicability to the harsh optical environment, such as the dark smog, or strong back-light. We have already proposed the extended Synthetic Aperture Radar (SAR) algorithm employing the multiple scattered waves, which aims at enhancing the reconstructible region of the target boundary including the shadow. However, it still suffers from the shadow region in the case of the target with a sharp inclination or deep concave boundary, because it assumes the antenna scanning whose real aperture size is too small. To resolve this difficulty, this paper proposes an extension algorithm using the array antenna model. While this extension is quite simple, the effectiveness of the proposed method is nontrivial regarding to the expansion of the imaging range. The results from numerical simulations verify that our method remarkably enhances the visible range of target surfaces without a priori knowledge of target shapes or a preliminary observation of its surroundings. [C2102]

### "Extraction of area-averaged orientation angle from POLSAR measurement"

We have shown that area-averaged structure orientation angles relative to incident angle of POLSAR in urban area can be estimated from argument of correlation coefficient of circularly-polarized observation bases. It is quite interesting that by this approach we can estimate area-averaged urban parameters even if we can not distinguish them from conventional received signal component intensity map due to lack of spatial resolution. [C2103]

### "STAP based ground moving target detectability in the airborne/spaceborne array radar"

A space-time adaptive processing (STAP) can be effective in detecting the ground moving targets from the airborne/spaceborne moving platform in the severe ground clutter and jammer environments. In this paper, the characteristics of target, ground clutter and jammer signals are analyzed and designed the adaptively weighted clutter notch filter in two dimensional spatial and temporal azimuth angle-Doppler domains. The simulation is performed for ground moving target detection by rejecting both clutter and jammer simultaneously through the STAP processing. The probability of target detection is investigated depending on the SNR and the minimum detectable velocity (MDV) in the given false alarm rate. The simulation results show that the MDV can be ideally achieved up to 2 m/s ~ 3 m/s at the 90 % of detection probability in the given false alarm rate of 10<sup>-3</sup> and 10<sup>-6</sup>. This technique may be applied for the surveillance and traffic monitoring of moving vehicle on the road. [C2104]

### "Accurate focusing of single-pass airborne InSAR data at L-band"

Long wavelength airborne single-pass InSAR systems call for very accurate SAR focusing and motion compensation algorithms. We have analyzed 3 different techniques and evaluated their performance using real data acquired with an L-band single-pass interferometer in Canada. Time domain backprojection with terrain-dependent motion compensation shows the best performance with results close to the theoretically expected values. [C2105]

### "Characterization of affected areas of the 2008 Iwate-Miyagi, Japan, earthquake using SAR intensity images"

SAR images obtained before and after a natural disaster are considered to be useful for emergency response due to its all-weather and sunlight-independent characteristics. Recently, the spatial resolutions of SAR systems have been improved significantly. In this paper, SAR intensity images acquired before and after the 2008 Iwate-

Miyagi, Japan, earthquake from ALOS/PALSAR (L-band) and TerraSAR-X (X-band) are employed to investigate the radar backscattering characteristics for various acquisition and surface conditions. The spatial resolution, radar frequency, flight path, and incidence angle were shown to affect SAR backscattering echo, depending on surface materials and roughness. It is also observed that the difference of the backscattering coefficients at the pre- and post-event times gets large and their correlation coefficient becomes small at the locations of landslides and slope failures. [C2106]

### "Contextual remote-sensing image classification by support vector machines and Markov random fields"

In the framework of remote-sensing image classification support vector machines (SVMs) have recently been receiving a very strong attention, thanks to their accurate results in many applications and good analytical properties. However, SVM classifiers are intrinsically noncontextual, which represents a severe limitation in image classification. In this paper, a novel method is proposed to integrate support vector classification with Markov random field models for the spatial context, and is validated with multichannel SAR and multispectral high-resolution images. The integration relies on an analytical reformulation of the Markovian minimum-energy rule in terms of a suitable SVM-like kernel expansion. Parameter-optimization and hierarchical clustering algorithms are also integrated in the method to automatically tune its input parameters and to minimize the execution time with large images and training sets, respectively. [C2107]

### "Pose estimation for ISAR image classification"

This paper presents aircraft target recognition (ATR) system using Inverse Synthetic Aperture Radar (ISAR) images. Knowing the pose of the target can improve the ATR performance (recognition rate and computational complexity). So, we propose in this paper a new pose estimator from ISAR images, based on the axis of symmetry and the similarity measure. The method proposed is compared with several approaches proposed recently in the literature, such as 2-D Continuous wavelet Transform and Hough transform. Once the pose of target is estimated, the classification is finally performed by K-Nearest Angle (KNA) classifier which insert the pose information into image retrieval task. [C2108]

### "RADAR and AIS sensors constellation for global maritime surveillance"

In the frame of SAMSON study (a Feasibility study of a space-based maritime surveillance system), funded by CNES, several concepts for a dual sensor RADAR + AIS (Automatic Identification System) constellation have been addressed. One of them supported by Thales Alenia Space is described in this paper. Its interest for global maritime surveillance is discussed. The constellation performance is presented in terms of revisit time and detection probability for each sensor before data fusion processing. Instruments are described as well as the proposed satellite concept. [C2109]

### "Predictive quantization of dechirped spotlight-mode SAR raw data in transform domain"

Synthetic aperture radar (SAR) systems collect large volumes of data that must be transmitted to a ground station for storage and processing. However, given the limited bandwidth of the downlink channel it is imperative that SAR data be compressed before transmission. While it is commonly believed that raw SAR data is uncorrelated, it is shown in that the inverse Fourier transform of spotlight-mode SAR exhibits non-negligible correlation that can be exploited in a predictive quantization scheme. In this paper, we propose two predictive quantization algorithms-transform-domain block predictive quantization (TD-BPQ), and transform-domain block predictive vector quantization (TD-BPVQ)-to encode dechirp-on-receive spotlight-mode SAR raw data. Experimental results indicate that, on average, TD-BPQ and TD-BPVQ outperform the well known block adaptive quantization (BAQ) by 5 and 6 dB, respectively. [C2110]

### "Z-R relation for snowfall using two small doppler radars and snow particle images"

Snowfall data was simultaneously recorded by two small Doppler radars, two high sensitive snow gages and an image processing system with high accuracy at short time interval. The snowfall rate  $R$  was measured with two gauges and radar reflectivity factor  $Z$  was measured using small bistatic X-band radar and monostatic K-band radar. The images of falling snow particles were used to obtain size distribution. Since all the measurements were located in a small area, it can be said that the obtained data corresponds well to others, and it is possible to analyze Z-R relation in detail. The relationships between two radar reflectivity factors and snowfall rate were investigated and compared to the characteristics of snow particles. [C2111]

### "Analysis of geosar dual-band InSAR data for peruvian forest"

At present there is no consensus as to which remote sensing technologies are appropriate for tropical forest biomass estimation. Cloud cover in the tropics and biomass saturation suggest that a combination of low-frequency SAR and interferometry (either PolInSAR or dual-band interferometric SAR DBInSAR) could provide a solution. Tropical forest biomass recovery using X-P DBInSAR has been demonstrated from an airborne platform using the X-P DEM height difference. This height is known to be considerably lower than the tree height as a result of penetration of microwaves into the canopy that can be significant even at X-band. We model the penetration using the RVOG model and show that in the strong attenuation approximation the interferometric coherence magnitude can be used to estimate penetration depth. We compare the model with GeoSAR DBInSAR observations of Peruvian forest, and, by comparison with LiDAR data, show that the GeoSAR Xband interferometric height can be corrected towards the upper canopy using knowledge of the coherence magnitude combined with the high-frequency "X-RVOG" model. We employ the corrected height with a biomass inversion equation derived from plot samples covered in the Peru campaign and generate a map of above ground forest biomass. [C2112]

#### "Application of KOMPSAT-5 data for emergent oil spill monitoring"

In this paper, we discussed the functionalities of KOMPSAT-5 from the emergency response perspective to oil spill detection, describing its technical abilities in terms of maneuverability, system response time, image quality, and damping ratio. The damping ratio at the X-band was higher than that at other available frequencies, which increased the probability of oil spill detection from SAR data. However, the detection of oil spills depends significantly on the wind condition and the presence of look-alikes. Oil spill detection algorithm for KOMPSAT-5 estimates wind information directly from SAR data, and is expected to enhance the detection capability. [C2113]

#### "Snow wetness retrieval inversion modeling for C-band and X-band multi-polarization SAR data"

This paper is concerning the estimation of snow wetness from multi-polarization SAR data. In this paper, microwave interaction with snow covered terrain and different scattering mechanism from snowpack and their backscattering model for developing inversion algorithm with wet snow conditions are described in order to estimate snow wetness. SAR data processing and field measurement of snow parameters are also discussed. In this study, snow wetness has been measured with a dielectric moisture meter with synchronous satellite passes over the part of snow covered Indian Himalayan region (e.g. Dhundi observatory in Himachal Pradesh, India). [C2114]

#### "Random noise SAR based on compressed sensing"

Recent theory of compressed sensing (CS) suggested that exact recovery of an unknown sparse signal can be achieved from few measurements with overwhelming probability. In this paper, we combine CS technology with a random noise SAR and proposed the concept of random noise SAR based on CS. The block diagram of the radar system and the collected data processing procedure was presented. Theoretic analysis show that the sensing matrix of the random noise SAR exhibits good restricted isometry property (RIP). When the target scene is sparse or sparse in any basis, the random noise radar based on CS can get high accuracy image by collecting far less amount of echo data than traditional noise radar does. The conclusions are all demonstrated by simulation experiments. [C2115]

#### "A real-time grid map generation and object classification for ground-based 3D LIDAR data using image analysis techniques"

A grid map generated from ground-based 3D LIDAR point clouds is a critical component for facilitating autonomous system navigation without crashing into obstacles and also to generate a road map for a large local area. This paper proposes a novel approach to generate an occupancy grid map along with object classification in real-time for autonomous ground robot applications. Based on geometric analysis of the raster-scanned LIDAR data, we formulate criteria to distinguish 3D points directly from coordinate values and generate three grid maps; occupancy, ground, and scatter maps which directly correspond to hypotheses on object type. Then 2D and 3D shape analysis are carried out to verify the object hypotheses. Our experimental results show that the new method performs well providing an autonomous system with surrounding 3D information and object classification. [C2116]

#### "Local multi-modal image matching based on self-similarity"

A fundamental problem in computer vision is the precise determination of correspondences between pairs of images. Many methods have been proposed which work very well for image data from one modality. However, with the wide availability of sensor systems with different spectral sensitivities there is growing demand to automatically fuse the information from multiple sensor types. We focus on the problem of finding point and local

region correspondences in an inter-modality imaging setup. We use a Generalized Hough Transform to determine small regions with a similar geometric relationship of local image features to robustly identify correct matches. We additionally optimize region correspondences by a fast non-linear optimization of a self-similarity distance measure. This measure outperforms standard multi-modal registration approaches like mutual information or correlation ratio in case of local image regions. The method is evaluated on Visible/Infrared (IR) and Visible/Light Detection and Ranging (LiDAR) intensity image data pairs and shows very promising results. Potential applications are numerous and include for instance multi-spectral camera calibration, multi-spectral texturing of 3D-models, multi-spectral segmentation or multi-spectral super-resolution. [C2117]

#### "SAR data collection over rain forests at VHF- and UHF-band"

Radar imaging of tropical vegetation at VHF- and UHF-band has been performed using the airborne SAR sensors CARABAS-II and LORA, respectively. The acquired data set is limited to HH-polarized registrations only. The area mapped exhibits a rough terrain with dramatic topographic variations, mostly covered by dense tropical rain forests. Multiple illumination directions spanning 360° were adopted in the data collection for both sensors to overcome the shadowing due to the high relief topography. For each heading, the SAR images generated, adjacent in azimuth and from all imaging passes, were calibrated and geocoded separately and then merged into a mosaic representing the full ground coverage. A first output from the forest backscatter analysis indicates a 12 dB lower level at VHF-band at an incidence angle of about 70°. However, this preliminary result is based on one sample point only, where the investigated forested area was located on a fairly flat ground surface. [C2118]

#### "Multi-frequency and polarimetric measurements of snow microwave reflection and emission by C- and Ku-band, combined scatterometer-radiometer systems"

In this paper the results of simultaneous and spatially coincident, dual-frequency (at C- and Ku-band), multi-polarization measurements will be represented, of bare soil and snow microwave reflective (radar backscattering coefficient) and emissive (brightness temperature) characteristics angular dependences at 5.6GHz and 15GHz. [C2119]

#### "Electromagnetic scattering from arbitrary random rough surfaces using stabilized extended boundary condition method (SEBCM) for remote sensing of soil moisture"

In this paper, the stabilized extended boundary condition method (SEBCM) is developed based on the classical EBCM to solve both 2D and 3D electromagnetic scattering from arbitrary random rough surfaces. The SEBCM gives accurate full wave solutions over large range of surface roughnesses and medium losses, which are far beyond the validity range of analytical methods, and perform with much higher efficiency than numerical methods. These properties make SEBCM a competitive forward model in the inverse problem for soil moisture retrieval from radar measurements. [C2120]

#### "Code sequence selection for SAR radiometric calibration"

It is an important significance for SAR radiometric calibration accuracy to select a proper code sequence about active coded transponder (ACT), in the process of active coding radiometric calibration using synthetic aperture radar (SAR). According to the principle of active coding radiometric calibration, a signal processing model of active coded reflected signals is proposed in this paper. And m sequences, Gold sequences and random sequences are studied. Simulation experiments with the compression of SAR azimuth signals are carried out. [C2121]

#### "2D uesprit superresolution SAR imaging algorithm"

One of the driving forces of the development of SAR image formation has been to obtain better and better image resolution. Conventional radar imaging methods based on Fourier transform provide good resolution as long as the backscattered data is available over a large bandwidth and a sufficient aspect region. The paper proposes a 2D Unitary ESPRIT superresolution SAR imaging method exploiting that the SAR image in phase history domain is a band-pass function with a main frequency support domain. Thus, the problem of superresolution SAR imaging is transformed to solve sinusoid harmonic estimation, which can be solved by 2D Unitary ESPRIT. From the experiments using simulation and measured data, we can see better resolution obtained by the method of the paper than the FFT method. [C2122]

#### "SAR focusing of P-band ice sounding data using back-projection"

SAR processing can be applied to ice sounder data to improve along-track resolution and clutter suppression.



This paper presents a time-domain back-projection technique for SAR focusing of ice sounder data. With this technique, variations in flight track and ice surface slope can be accurately accommodated at the expense of computation time. The back-projection algorithm can be easily parallelized however, and can advantageously be implemented on a graphics processing unit (GPU). Results from using the back-projection algorithm on POLARIS ice sounder data from North Greenland shows that the quality of data is improved by the processing, and the performance of the GPU implementation allows for very fast focusing. [C2123]

#### "A test statistic for high resolution polarimetric SAR data classification"

Modern SAR systems have high resolution which leads the backscattering clutter to be non-Gaussian. In order to properly classify images from these systems, a non-Gaussian noise model is considered: the SIRV model. A statistical test of equality of covariance matrices is used to classify pixels, taking into account the critical region of the test which rejects the likeliness of a covariance matrix to any of the class centers. This test is applied on experimental data obtained with the ONERA RAMSES system in X-band. The results show a good separation between natural and man-made areas of the image. [C2124]

#### "Investigating co-seismic deformation of the 2008 Wenchuan earthquake with ALOS SCANSAR interferometric observations"

On May 12th, 2008, a destructive earthquake of magnitude 8.0 struck Wenchuan. The seismic region is located at the transition zone between Qinghai-Tibet Plateau and the Sichuan Basin, which has a complex geological tectonic background. In this paper, we intend to investigate the Wenchuan earthquake using the Differential Interferometric SAR (D-InSAR) technique. Due to the large scale of the crustal deformation affected by the disastrous earthquake, SCANSAR images show more advantages than conventional strip-map mode images. And taking account the vegetation conditions, the L band images are suitable than the C band images for our study. Therefore, we choose to use ALOS SCANSAR interferometric observations to obtain a preliminary co-seismic displacement field of the Wenchuan earthquake. [C2125]

#### "Evaluation of the influence of the polarimetric calibration process on the H/A/ $\alpha$ decomposition"

The objective of this article is to evaluate the influence of the cross-talk and channel imbalance calibration on the estimation of the entropy and the alpha images. Few studies can be found in SAR literature concerning the influence of the polarimetric image calibration process on the target decomposition methods and their consequences on the characterization and discrimination of different ground targets. This influence is illustrated here by using a methodology based on an L-band fully polarimetric SAR data acquired by the SIPAM (Amazon Protection System) airborne R99-SAR over two areas of study, located in the Brazilian Amazon Forest and urban area regions. [C2126]

#### "A novel range migration algorithm of GEO SAR echo data"

The key problem of the imaging processing in geosynchronous earth orbit (GEO) SAR system is the space-variance of the Doppler parameters, which will result in the defocus of the SAR image with classical imaging algorithm. In this paper, a Modified Range Migration Algorithm (RMA) is proposed to overcome the space-variance of Doppler parameters by compensating the velocity change along the location of the target. Furthermore the simulation results fully verify the effectiveness of derived algorithm after velocity compensation. [C2127]

#### "Analysis and compensation for motion errors in FMCW SAR data"

In this paper, we present a motion error model for a Frequency-Modulated Continuous-Wave (FMCW) SAR system, and analyze the characteristics of the intrapulse motion error. Furthermore, we develop an effective compensation approach to handle motion errors based on our previous result. Finally, we validate the formulated signal model and compensation method by using simulated FMCW SAR data. [C2128]

#### "The extended SBAS technique for generating full resolution ERS/ENVISAT deformation time-series"

In this work we extend the Small Baseline Subset (SBAS) Differential SAR Interferometry approach to allow the generation of deformation time-series by processing long sequences of ERS-1, ERS-2 and ENVISAT SAR data at the full spatial resolution scale. Our idea is to avoid the generation of ERS/ENVISAT cross-interferograms, severely affected by noise phenomena, and to consider single-platform interferograms only (i.e. ERS/ERS and ENVISAT/ENVISAT interferograms), that are properly combined by applying the SVD-based SBAS approach. The presented results, achieved on two dataset relevant to the Napoli Bay area and to the Murge region (Italy),

confirm the effectiveness of the presented technique and demonstrate the relevance of deformation analysis carried out at the scale of single buildings with more than 15 years of ERS and ENVISAT acquisitions. [C2129]

### "Target localization methods for frequency-only MIMO radar"

In Multi Input-Multi Output (MIMO) radar, the target localization is possible by using only the frequencies of received signals instead of using whole data on the received signals for moving targets. As target is moving, received frequency will be shifted as doppler frequency. Received frequencies which are scattered from non-manouvering and constant speed target, can be written in two dimensional (2D) space with respect to the target coordinates. A cost function can be defined by the help of these frequencies, and than by using grid search, local minimum of this cost function can be found in (x, y) coordinates. In this work, a new target localization method is poroposed for frequency-only MIMO radar. [C2130]

### "Progressive SAR imaging technique"

A progressive SAR imaging technique is proposed as a novel SAR raw data processing scheme in this paper. Different from the classic SAR imaging algorithms which focus the SAR raw data as a whole regardless of the backscattering signal, the novel scheme discriminate the backscattering signal and choose the proper ones to be focused progressively according to some application context while the others will be discarded. The new scheme makes the SAR imaging algorithm not only focus the energy back to the scattering points but also form an image more suitable for some special applications. In this paper, a realization of the scheme present via Atomic Decomposition (AD)[1]-[3]. AD helps estimate the parameters of backscattered signal of a scattering point and detach it from the raw data. With the parameters, the backscattering-signal can be reconstructed and focused. Targets or scatter-points in the scene will be imaged progressively in a sequence of their energy due to the greedy natural of matching pursuit employed during AD. Therefore, the contents in the final SAR image can be controlled by an energy threshold. Besides the interested targets can be extracted easily from the background clutter and this may be helpful for the SAR image understanding. [C2131]

### "Evaluation of the self-consistency principle for calibration of the CASA radar network using properties of the observed medium"

The Center for Collaborative and Adaptive Sensing of the Atmosphere (CASA) has deployed a Distributive, Adaptive and Collaborative Sensing (DCAS) network of four radars in central Oklahoma. The radars operate at the X-band frequency and are capable of polarimetric and Doppler measurements. The radar network is being evaluated for Quantitative Precipitation Estimation (QPE). QPE algorithms based on radar power measurements (e.g. ZHand ZDR) require bias correction. The polarimetric self-consistency principle is applied to the CASA radar data to estimate any bias in ZH. Results show a ZHcalibration accuracy of 0.6 dBZ or less for two the analyzed events. ZHbias estimates from the self-consistency principle in rainfall are compared and validated with ZHbias estimated from the comparison of the X-band and the S-band radars' data. Comparison of the two approaches shows a difference in the ZHbias estimation of 0.61 dBZ or less and validates the use of the self-consistency principle in rainfall for the absolute radar calibration of the CASA radars. [C2132]

### "Application of the moving target detection by focusing technique in civil traffic monitoring"

This paper presents an application of the moving target detection by focusing technique (MTDF) in civil traffic monitoring. The experimental results based on simulations show that the basic civil traffic monitoring can be solved using MTDF using a single-channel airborne SAR system. With an assumption of known moving directions of vehicles, MTDF allows detecting, estimation of speed, and finally reconstructing a SAR image of the vehicles of interest. In this study, the focusing approach of MTDF is based on ultrawideband chirp scaling (UCS) algorithm. [C2133]

### "A high accuracy method for interference fringes suppression in SAR distributed targets' raw data simulation"

Interference fringes will be generated in SAR image when distributed targets' echo signal is simulated because of the uniform model of targets. The fringes can be suppressed by adding random height in space or random phase on backscatter coefficient of the distributed targets. However, the former method will introduce location error and the latter method will increase speckle noise twice in simulated image. In this paper, we develop a high accuracy method for fringes suppression based on targets' position randomizing and RCS re-sampling via bilinear interpolation. The validation of method is successfully proved by simulation results and the performance of the method is discussed on accuracy and computational complexity at the end of this paper. [C2134]

### "Calibration of a rotating multi-beam lidar"

This paper presents a technique for the calibration of multi-beam laser scanners. The technique is based on an optimization process, which gives precise estimation of calibration parameters starting from an initial estimate. The optimization process is based on the comparison of scan data with the ground truth environment. Detailed account of the optimization process and suitability analysis of optimization objective function is described, and results are provided to show the efficacy of calibration technique. [C2135]

### "Analysis of the correlation properties of digital satellite signals and their applicability in bistatic remote sensing"

This paper presents a study of relevant correlation properties of signal transmitted from commercial communication satellites in order to evaluate their potential use as "signal of opportunity" for bistatic remote sensing. The ambiguity function for the XM radio satellites was computed analytically from published information on the modulation schemes and bandwidth, under the assumption that the data modulation is random. The model was then experimentally tested by recording the received signals from these satellites. Next, a cross-correlation waveform for digital signal reflected from random rough surface was simulated. Scattering model that were originally developed for Global Navigation Satellite System (GNSS-R) signals was applied to the modified simulator to incorporate the derived ambiguity function. The simulator was then used to generate synthetic waveform with a realistic signal to noise ratio (SNR). Retrieval algorithms for ocean surface roughness and reflectivity that were derived originally for GNSS-R, were applied to these simulated signals. Non-linear least square methods were applied to invert a scattering model and estimate the slope variances of the probability density function (PDF), which best fits the measurements of the reflected XM signal waveform. The SNR for the experimental data was found to be within 0.5dB of the theoretically calculated SNR. [C2136]

### "Ship detection with RadarSat-2 Quad-Pol sar data using a notch filter based on perturbation analysis"

Target detection of marine feature is a major topic for the security and monitoring of coastlines. Synthetic Aperture Radar (SAR) has been shown to be particularly useful for this application because of its all-weather and night capability. In this paper a new ship and iceberg detection methodology is described. The algorithm proposed is based on a perturbation analysis in the target space recently developed and published by the authors, which was focused on land based target detection. The algorithm can be considered to be a negative filter focused on sea. Consequently, all the features which have a polarimetric behaviour different from the sea are detected. To demonstrate and validate the technique two RadarSat Fine Quad-Pol mode scenes were acquired off the south coast of the UK at Portsmouth harbour. An extensive ground truth campaign was also conducted that was coincident with these acquisitions. Portsmouth is one of the busiest harbours in the UK and this afforded the opportunity to capture a wide range of vessel sizes and types for analysis. [C2137]

### "A biomass estimate over the harvard forest using field measurements with radar and lidar data"

The National Research Council's decadal survey recommended DESDynI as one of the high priority missions for NASA. The mission envisions an InSAR/Lidar instrument for observing ecosystem structures on global scales with high spatial resolutions. Consistent and highly resolved global maps of biomass and carbon stocks require highly accurate observations of vegetation, in fact it is expected that such accuracies would require a combination of the high vertical precision of Lidar observations and the large spatial extent of SAR/InSAR measurements. Here we analyze radar backscatter data along with biomass estimates from a field campaign conducted in the Harvard forest in Massachusetts, USA. [C2138]

### "Earth documentation: Overpass detection using mobile Lidar"

This paper presents an application of using geo-data from Lidar and GPS/IMU to detect overpasses. Three characteristics make it a good example of processing large point sets in real-time: a stream paradigm that exploits system parallelism and memory-access coherence, a multi-level detection strategy that distributes computational burden across different operations, and a multi-resolution data structure that suits the need of detecting urban objects. Experimental results proved the excellent performance in terms of speed and accuracy. [C2139]

### "PSI analyses of land subsidence due to economic development near the city of Hangzhou, China"

In this work we mapped the spatial and temporal patterns of the land subsidence near the city of Hangzhou, China by PSI analysis with 49 scenes of ERS-1/2 SAR images acquired from 1992 to 2006 to detect and retrieve the subsidence due to economic development. The main reason of land subsidence in Hangzhou is groundwater

exploitation, which is necessary for the rapid economic development, especially in China. Xiaoshan Economic and Technological Development Zone was approved as a state-level development zone by the State Council in May, 1993. Since then the zone has been suffering land subsidence. There have been more than 300 overseas-funded enterprises with investors from 26 countries and regions by the year 2006. The development of this area can be divided into three periods according to its pace: construction period (1993-1996), stable increase period (1996-2001) and high-speed period (2001-2006). [C2140]

#### **"A nonlocal approach for SAR image denoising"**

Speckle reduction is a key step in several SAR image processing procedures. In this paper, a new despeckling technique based on the "nonlocal" denoising filter BM3D [1] is presented. The filter has been modified in order to take into account SAR image characteristics. The experimental results, conducted on both synthetic and real SAR images, confirm the potential of the proposed approach. [C2141]

#### **"Global laser pulse reflectance at 1064 nm of snow and land surfaces from the Glas satellite Lidar"**

During the development of the Geoscience Laser Altimeter System (GLAS), launched in 2003, it was understood that the values of surface pulse reflectance was an important design parameter for satellite laser altimeters and that the magnitude of observed pulse reflectance would have valuable applications. Thus a significant effort was made to obtain calibrated surface pulse reflectance from GLAS measurements. In this paper we describe the calibration and atmospheric correction procedures and present global measurement results for earth surface laser pulse reflectance. [C2142]

#### **"Investigation of forest height retrieval using SRTM-DEM and ASTER-GDEM"**

Interferometric SAR (InSAR) data have been used to measure canopy height. Polarimetric interferometric SAR (PolInSAR) data can be used to derive canopy height without using ground surface elevation data. But in most cases, only single polarization InSAR data are available and the elevation of ground surface in the forested areas is needed to get the height of the scattering phase center. On contrary, the elevation of canopy surface is relatively easy to obtain by Stereo imagery. In this study the feasibility of the estimation of forest height using SRTM-DEM and ASTER-GDEM was investigated. The ASTER-GDEM was firstly resampled to the pixel size of SRTM-DEM (3 arc-second) and then was registered to SRTM-DEM using the points selected from their aspect maps. The results showed that the registration is necessary because the geolocation error at east-west direction is about half of the pixel size. The relationship between the forest height and the elevation difference was analyzed. The results showed that the elevation difference between registered ASTER-GDEM and SRTM-DEM is positively correlated with the forest height. Although there are some problems when the terrain is rough, it provides us a way to estimate the height of mature forest in flat terrain. [C2143]

#### **"C- and Ku-band (at 5.6GHz and 13.6GHz), dual-frequency, multi-polarization, short pulse, combined scatterometer-radiometer system for low altitude platform, vessel and aircraft applications"**

In this paper C-, and Ku-band, dual frequency, multi-polarization, combined, short-pulse scatterometer-radiometer system is described, for short (from low altitude platform), middle (from vessel) and long (from aircraft) distance remote sensing applications for water surface, soil and land snow cover's microwave reflective and emissive characteristics simultaneous and spatially coincident measurements. [C2144]

#### **"Change detection for earthquake damage assessment in built-up areas using very high resolution optical and SAR imagery"**

Information on the impact of catastrophic events (e.g. earthquakes) can be derived from suitable satellite imagery by comparing data from a chosen reference before the event (pre-event) to imagery acquired shortly after the event (post-event). In this paper, we propose a novel method that detects buildings destroyed in an earthquake using pre-event very high resolution (VHR) multispectral and post-event detected VHR synthetic aperture radar (SAR) imagery. The core concept of the proposed method is the evaluation of the presence of the predicted undamaged building SAR signature in the post-event SAR scene. The decision if a building belongs to the damaged or undamaged building class is performed with a Bayesian classifier, trained either in a supervised or unsupervised manner. We show the results of the proposed method using VHR TerraSAR-X and COSMO-SkyMed, as well as VHR optical data for a subset of the town of Yingxiu, China, which was heavily damaged in the 2008 Sichuan earthquake. [C2145]

#### **"The Cloudsat Education Network: Scientifically significant collaborative research between students"**



## and scientists"

The CloudSat Education Network (CEN) is the primary education and public outreach component of the CloudSat mission. Approximately 116 schools in 16 countries around the world participate in the CEN, and are recruited from schools in the GLOBE program. Students and teachers in the CEN make atmospheric observations of temperature, precipitation, and crucially, of cloud type and cloud cover amount (including photographs of cloud observations), using a modified GLOBE Atmosphere protocol as a guide for observations. CEN observations are taken coincident with CloudSat overpasses, providing coincident spaceborne- and student surface observations. A preliminary comparison study using CEN-collected observations of cloud type during the period from 2007-2008 compared the observed cloud types to those retrieved using the CloudSat 2B-CLDCLASS product. In this preliminary study, there were 227 coincidental measurements between CEN schools and CloudSat overpasses, with an agreement rate of approximately 66% between the surface observers and satellite observations. [C2146]

## "Mapping tropical forest using ALOS PALSAR 50m resolution data with multiscale GLCM analysis"

PALSAR orthorectified HH and HV produced at 50m resolution is used for analysis. Since only two bands (HH and HV) have been limited in land cover discrimination, textures have been used as additional information for classification. This research derives second-order textures at different spatial resolutions and compares second-order textures at multiple scales to demonstrate their contributions in land cover classification. The discriminating capability of texture features is derived by the transformed divergence on several selected regions of interest. Optimum combination of backscattering and textures are used as input data into a supervised multi-resolution maximum likelihood classification. It is found that by including the texture information, the overall classification accuracy is improved by 10%. [C2147]

## "Multi-frequency and polarimetric measurements of bare and vegetated soils microwave reflection and emission by C- and Ku-band, combined scatterometer-radiometer systems"

In this paper the results of simultaneous and spatially coincident, multi-frequency, polarimetric, spatio-temporally collocated measurements of bare, dry vegetated and ash covered soils microwave reflective (radar backscattering coefficient) and emissive (brightness temperature) characteristics angular dependences at ~5.6GHz and ~15GHz are presented. During these experiments the observed area was set ablaze and multi-frequency, multi-polarization, microwave active and passive measurements at 300 incidence angle were continued for smock, fire and ash situations. For these measurements C-, and Ku-band, polarimetric, combined scatterometric-radiometric systems were used, set jointly on a mobile buggy moving along the measuring platform. Structures, operational features and the main technical characteristics of the utilized systems are presented too. The paper has an aim as well to attract attention of interested researchers and to invite them to perform their own or joint researches using available devices and facilities. [C2148]

## "Polarimetric and structural properties of forest scenarios as imaged by longer wavelength SARs"

SAR data gathered from forested areas collect contributions coming from the vegetation layer, from the ground below and from other scattering mechanisms (SMs). Multi-baseline data allow a tomographic analysis thus retrieving information about the vertical structure of the target. Multi-polarimetric acquisitions enrich the data, providing ways to identify the targets basing on their electromagnetic properties. The joint exploitation of multi-polarimetric and multi-baseline data suggests the possibility of linking the estimation of the vertical structure of different SMs with their polarimetric signature. A formal framework in which this task can be accomplished is provided by the Algebraic Synthesis (AS) technique, which extends the concepts within PolInSAR through the assumption of the Sum of Kronecker Products (SKP) structure. By assuming the presence of two SMs (for example ground and volume scattering), the SKP assumption leads to a cross dependence between the polarimetric and interferometric coherences, in that ground structure is shown to be related to volume polarimetry, and dually volume structure is shown to be related to ground polarimetry. The aim of this paper is to investigate the implications of this cross relation. Experimental results will be shown basing on a data-set of multi-polarimetric and multi-baseline SAR images at P-band acquired by DLR's E-SAR over the Krycklan catchment, in northern Sweden, in the framework of the ESA campaign BioSAR 2008. [C2149]

## "Received signal strength based localization in sensor network"

In this paper, we present the accuracy of location engine of CC2431 ZDK development kit which is widely used in sensor network localization problems. Initially, distance vs received signal strength indicator graph has been established, then accuracy of location engine and Cayley-Menger based localization algorithm have been compared. 11411 meter area test result shows that location engine is more accurate than Cayley-Menger based algorithm. [C2150]

### "Esprit-based scattering power decomposition by using modified volume scattering model"

The scattering power decomposition for POLSAR data is one of the powerful tools in the radar polarimetry. There are several model-based decomposition techniques. However, since the number of independent observables in POLSAR images is limited, these techniques require several assumptions to obtain unique solution. The authors have proposed an alternative technique with POL-InSAR dataset. By using the POL-InSAR dataset, we can increase the number of observables. However, selection of volume scattering component was still a problem. Recently, Dr. Arii et. al., proposed a generalized volume scattering model, and applied it to the POLSAR dataset with the adaptive non-negative eigenvalue decomposition technique. In this report, we apply the model to the ESPRIT-based POL-InSAR decomposition technique and verify the estimation performance experimentally. [C2151]

### "Analysis of observed information in multistatic radar network"

In this study, observed information matrix has been calculated in a multistatic radar network where an Unscented Kalman filter, that utilized bistatic range and range rate measurements, was employed as a 3D tracker. Variation of the observed information with respect to target's location in the network has been analyzed through simulations and the results are presented in contrast to tracking error. [C2152]

### "Multi-Channel RADAR Depth Sounder (MCRDS) signal processing: A distributed computing approach"

In response to problems surrounding measuring ice sheet thickness in high attenuation areas of Greenland and the Antarctic, the Center for the Remote Sensing of Ice Sheets (CReSIS) created a Multi-Channel RADAR Depth Sounder (MCRDS). The MCRDS system was used to measure ice thicknesses of up to five kilometers in depth. This system produced large datasets, which required greater processing capabilities in the field. The purpose of this project was to test processing performance on a 32-core cluster through distributed computing resources. Testing involved a six-node cluster with an attached storage array and use of the CReSIS Synthetic Aperture RADAR Processor (CSARP) through the MATLAB Distributed Server Job Manager. Performance testing was derived from average run times collected once CSARP jobs completed. The run times were then compared using an ANOVA test with a five percent significance level. [C2153]

### "Processing for airborne interferometric SAR data with high squint"

A novel approach for the highly squinted airborne InSAR data processing is presented. Using the IMU data to resolve the PRF ambiguity and moving azimuth windows according to the Doppler centroid varying in the different range, as well as combining the auto-registration imaging algorithm, such approach not only can compensate the squint effect and motion error directly at the imaging processing stage, but also can improve the coherence and restrain the interferometric phase error of the image-pair. The simulative and practical results indicate that the proposed approach is very suitable for the processing of the data with a high squint for a dual-antenna airborne InSAR system with its efficiency in improving the image quality and enhancing the interferogram and coherence. [C2154]

### "A dual-frequency SAR mosaic of the Amazon"

The development and availability of accurate landcover information is critical to the ecological science questions [Cerri, et al., 1995; Hall, et al., 1995], such as defining the rate and extent of deforestation within the Amazon. This need can only be met by techniques that are sensitive to phenomena at the scale of the landscape patch and can be efficiently applied in a consistent fashion over very large regions. For example, estimation of Amazonia's carbon budget will require a large-scale mosaic of the location and spatial extent of landcover types, forest regrowth biomass, and selective logging. Vegetation type and surface condition exert control over carbon and trace gas fluxes. Estimates of the biotic carbon pool are also important since carbon accumulation rates vary not only with vegetation types but with successional stage and management practices as well. Both the extent and carbon accumulation rates of regenerating tropical forest are poorly known. If the ages of forest disturbance can be established (i.e., from the Landsat time series), then the SAR-derived estimates of aboveground biomass can be used to estimate annual sequestering of carbon. Though these data were acquired at higher resolution, it is possible to use this data to map landcover, biomass and selective logging at a spatial scale of 100m for the Amazon basin. [C2155]

### "Comparison of crop classification capabilities of spaceborne multi-parameter SAR data"

With the arisen spaceborne multi-parameter Synthetic Aperture Radar (SAR) systems, such as Envisat ASAR,

TerraSAR-X, ALOS PALSAR, and RADARSAT-2, the interest of crop mapping has been increasing. The present study compares the capabilities of the multi-parameter SAR in discriminating the main crop types by object-based classification in Haian county of Jiangsu province, South China. Two kinds of information, SAR intensity based and SAR statistical properties based are used for Maximum Likelihood Classification (MLC) and Minimum Distance Classification (MDC) respectively. The results show that, the L-band SAR can uniquely identify mulberry from dry-land crops, such as maize and vegetable and C-band SAR has some advantages in mapping rice. Specifically, the polarimetric RADARSAT-2 data can identify the rice with accuracy about 75% ~ 80% which is similar as the result from X-band TerraSAR-X Spotlight data but higher than that from C-band dual-polarization Envisat ASAR data. Nevertheless, both of X- and C-band can hardly separate the mulberry from the other dry-land crops. [C2156]

#### "A fully polarimetric borehole radar based numerical modelling: Fully polarimetric response to synthetic fractures and "fluid substitution""

A fully polarimetric borehole radar system with four combinations of dipole and cylindrical slot antennas was developed to acquire fully polarimetric data sets in drilled boreholes. To better understand the fully polarimetric response to subsurface fractures with different roughness, in this study, synthetic fractures with different roughness are generated on a computer via fractal theory based simulation techniques. Quantitative assessment for the roughness of synthetic fractures is possible by use of three main parameters: the fractal dimension, the rms roughness at a reference length, and a length scale describing the degree of mismatch between the two fracture surfaces, allowing future detailed study of mechanical and transport properties of fractures and fully polarimetric radar response on them. Next, a 3D sub-grid FDTD numerical simulation is used to synthesize fully polarimetric data sets with synthetic fractures as primary reflectors. Based on the synthetic data sets, it is possible to evaluate the applicability of different radar polarimetry analysis approaches to physical characterization of subsurface fractures in future. [C2157]

#### "Morphological-based source extraction method for HFSW radar ship detection"

In this contribution, High Frequency Surface Wave (HFSW) radars are considered for target detection. These systems, commonly used for oceanographic purposes, are of interest in maritime surveillance because of their long range detection capabilities. Unfortunately, the received signals are strongly polluted by different noises. To improve target detection a method based on Morphological Component Analysis (MCA) is investigated. Shortly, this paper introduces HFSW radars and gives an overview of the MCA. Then, numerical results from simulated data illustrate the MCA-based target detection method. Comparisons with classical detection methods based on CFAR techniques (GOCA-CFAR and GOOS-CFAR) are proposed through Receiver Operating Characteristics (ROC) curves. [C2158]

#### "Polinsar forestry applications improved by modeling height-dependent temporal decorrelation"

We model the temporal decorrelation in volumetric media imaged by a repeat-pass SAR interferometer by using a temporal correlation function that varies with depth. An expression of this function is proposed and based on the Brownian motion of the canopy and soil elements. The spatial and temporal correlation terms are merged in a single coherence model that includes a large class of decorrelation effects, such as those induced by changes in the structure of the medium. We discuss the effects of the temporal correlation function and its implications on the parameters estimation using the POLINSAR random volume over ground model. [C2159]

#### "Contrast in speckled imagery with stochastic distances"

Synthetic aperture radar (SAR), ultrasound-B, laser, and sonar imagery are contaminated with speckle noise. The statistical modelling of such contamination is well described by the multiplicative model, which yields the G0 distribution. In particular, reliable image contrast measures are sought in order to discriminate targets. To that end, we present statistical methods based on stochastic divergences and on the Kolmogorov-Smirnov distance for G0 data. Their performance is quantified according to their test sizes and powers. A robustness analysis is also presented for several degrees of contamination. We show that the proposed tests based on triangular and arithmetic-geometric measures outperform the Kolmogorov-Smirnov distance. [C2160]

#### "Exploiting spatial domain and wavelet domain cumulants for fusion of SAR and optical images"

The aim of this paper is to introduce a novel statistical model-based image fusion method for Synthetic Aperture Radar (SAR) and optical images. The current fusion algorithms are effective only in specific areas of the scene. Hence, the fused image may not contain enough information for subsequent processing like classification and feature extraction. Our proposed method aims to keep the maximum contextual and spatial information from the source data by exploiting the relationship between spatial domain cumulants and wavelet domain cumulants. Our

contributions are in integrating the relationship between spatial and wavelet domain cumulants of source images into an image fusion process as well as in employing these wavelet cumulants for optimization of weights in a Cauchy convolution based image fusion scheme. The superior performance of the proposed algorithm is demonstrated in comparison to existing fusion algorithms using real SAR and optical images. [C2161]

#### "Comparison of alternative image representations in the context of SAR change detection"

This article compares four different alternative image representations in the context of a structure-based change detection. The framework is taken from the already published Curvelet-based change detection approach. Only the transform step is modified by inserting three additional transforms: the Laplacian pyramid, the Wavelet and the Surfacelet transform. The results of the change detection are compared to the single pixel difference image in order to find the representation that best illustrates the underlying structures. The Curvelet transform again turns out to be very powerful in describing man-made objects and landscapes. [C2162]

#### "Microphysical retrieval from dual frequency precipitation radar board GPM"

Global Precipitation Measurement (GPM) is poised to be the next generation observations from space after Tropical Rainfall Measuring Mission (TRMM). The GPM mission concept is centered on the deployment of a core observatory satellite with an active dual-frequency radar (DPR), operating at Ku and Ka bands. The DPR is expected to improve our knowledge of precipitation processes relative to single-frequency radar on microphysics retrievals. Hydrometeor classification method is a key part of any microphysical retrieval algorithm. This paper is focused on the hydrometeor classification method which might be applied to GPM DPR and maps the results to Zdr- DFR plane to cross verify with the pixel based hydrometer identification method. In addition a comparison is made between the DSD retrieval algorithm proposed by the author and other existing algorithm. [C2163]

#### "Estimation of sea ice concentration in the Sea of Okhotsk using PALSAR polarimetric data"

The objective of this research is mainly in estimating sea ice concentration from Phased-Array L-band SAR (PALSAR) polarimetric data. This paper shows the results of estimating sea ice concentration from PALSAR data acquired from 2008 to 2010. The AMSR-E sea ice concentration data are also used to verify the result of sea ice concentration derived from PALSAR data. The difference in two sea ice concentrations was found especially in AMSR-E low concentration area. The high resolution backscattering and scattering entropy images give us an idea that there is some difficulty in AMSR-E to detect thin sea ice in the Sea of Okhotsk. [C2164]

#### "Application of aspect angle normalized polsar images for urban building detection"

Variation in the building aspect angle, defined as the angle between the flight direction of a satellite (azimuth direction) and the vertical wall of a building, is a significant cause of accuracy reduction in building detection and terrain classification from Polarimetric Synthetic Aperture POLSAR (POLSAR) images. However, the existing building detection methods usually are effective for the buildings with a limited aspect angle range. Considering the relationship between the aspect angle of the building and the orientation angle shift, an aspect angle normalization method is introduced to remove the disadvantageous influences caused by the aspect angle. From a comparison between the double-bounce building detection results of the original and aspect angle normalized RadarSat-2 data acquired in Beijing, China, buildings with any aspect angle can be detected effectively from aspect angle normalized data. [C2165]

#### "Progressive change detection in time series of SAR images"

The aim of this paper is to present a general framework for change detection in a time series of radar images, for an operational purpose and in the context of environmental monitoring. The change detection procedure is turned into the framework of detecting a random signal into the noise; the detection of this signal leads to the detection of a change in the time series. This framework is based on a non-parametric detection method that assume a sparse representation of the data. When using radar images, the speckle noise invalidates the hypothesis of sparsity. Then a pre-processing technique is required to provide an appropriate sparse representation of data, whatever the initial noise characteristics. The paper focuses on the change indicator, based on recursive median filtering, yielding a piecewise regular representation of a scene obtained by spreading the statistically most reliable pixel values over the image. The recursive median filtering leads to simple change indicators that are more efficient than the Kullback-Leibler change indicator when using small analyzing sliding window. Furthermore, it induces an simple extension to perform progressive change characterization through a multi-temporal filtering approach. Results are shown with a two-date change detection from RADARSAT images and from a time series of ERS and ENVISAT images. [C2166]



### **"Investigations on the full polarimetric PALSAR data to discriminate macrophytes species in the Amazon floodplain wetland"**

The purpose of this work is to evaluate the capacity of full polarimetric L band data to discriminate macrophyte species in Amazon wetland. Fieldwork was carried out almost simultaneously to the acquisition of the full polarimetric PALSAR data. Coherent and incoherent attributes were extracted from the image, and macrophyte morphological variables were measured on the ground. The image attributes and the macrophyte variables were compared in order to evaluate their application for discriminating macrophytes species. The findings suggest that polarimetric information could be adopted to discriminate plant species based on morphology, and that estimation of plant biomass and productivity could be improved by using the polarimetric information. [C2167]

### **"On the feasibility of tsunami detection using satellite-based sea surface roughness measurements"**

Observations of tsunamis away from shore are critical for improving early warning systems and understanding of tsunami generation and propagation. Using analysis already applied to the 2004 Sumatra-Andaman tsunami, we positively identify the 2010 Chilean tsunami in satellite altimeter measurements of sea surface roughness. Use of radar backscattering strength measurements from satellite altimeters would be impractical for tsunami detection and early warning purposes due to the limited temporal and spatial resolution. On the other hand, it is likely that tsunami-induced changes in sea surface roughness are observable with other types of space- and airborne sensors that sense sea surface roughness over much wider swaths. With this in mind, we explore the feasibility of using existing instruments and technology as the basis for a tsunami detection and early warning system. [C2168]

### **"Log-polar and polar image for recognition targets"**

We describe in this paper, data processing algorithms applied on radar image in order to extract feature descriptors and then to perform recognition task. Several kinds of descriptors can be used to acquire information about target characteristics from radar images such as ISAR (Inverse Synthetic Aperture Radar) images. This paper presents two types of vector descriptors extracted via two kinds of transformed images so-called polar and log-polar images obtained respectively from the polar and log-polar mapping. In order to guarantee the invariance of some geometrical transformation, additional processing are proposed. In this paper, we present the polar and log-polar transformations and then the classification scheme adapted on correspondent polar and log-polar templates. In the classification step, log-polar and polar mapping results are compared using adapted classification scheme. [C2169]

### **"Random Forests for building detection in polarimetric SAR data"**

Building detection from Synthetic Aperture Radar (SAR) images states a particular important as well as difficult problem. The high-resolution which is necessary to distinguish single buildings as well as the geometric and dielectric properties of dense urban areas cause most assumptions to fail, that are commonly made in SAR data analysis. This paper proposes the usage of Random Forests for building detection from high-resolution Polarimetric Synthetic Aperture Radar (PolSAR) imagery. Random Forests can handle high-dimensional input and therefore a large set of different features, they are known to lead to good classification performance in terms of robustness and accuracy, and are nevertheless seldomly applied to analysis of PolSAR images in general and building detection in particular. This paper presents first results of Random Forests when applied to a building detection task and shows their successful applicability. [C2170]

### **"Deployment of the ASCAT calibration transponders"**

The METOP-A Advanced Scatterometer Radar has stringent radiometric requirements requiring regular, accurate, calibration. The specified stability of 0.2 dB or better is too demanding for targets such as rain forest or simple corner reflectors, so three highly stable return signal sources have been precisely sited to give accurate measures of the beam patterns over the satellite repeat cycle. The Scatterometer is required to provide full coverage over all the oceans, so the three calibration transponders have been installed in Turkey, as the Black Sea and Eastern Mediterranean are not used in the ASCAT programme. [C2171]

### **"Effect of the polarization on SISAR imaging and feature recognition in forward scattering radar"**

In this paper, the effect of the polarization and the multipath on shadow inverse synthetic aperture radar (SISAR) imaging is analyzed respectively in forward scattering radar (FSR). The multi-polarization and the multipath imaging results of targets, based on SISAR, are discussed respectively. In addition, the target forward scattering (FS) RCS under multi-polarization conditions are also obtained using CST simulation software to research the effect of multi-polarization on moving target feature recognition in FSR. [C2172]

### "Automatic image classification of landslides improved with terrain roughness indices in various kernel sizes"

Using spectral-only information for landslides classification is usually confusing with houses, roads, and other bare lands because these ground features have similar spectral patterns on images. The terrain roughness can be measured by significant wavelengths; some studies have linked the relationships between terrain roughness and the landslide by using numerical analyses of topography data. In this study, airborne LiDAR data of 1m grid are used to explore the possibility of improvement of landslide classification, the LiDAR-derived data include DEM slope and terrain roughness indices including diversity, dominance and relative richness with different grid size data are used to improvement classification accuracy. The improvement of accuracy when including DEM slope is 22% in producer's accuracy and 27% in user's accuracy. The accuracy of diversity, dominance and relative richness indices all are improved when kernel sizes enlarge in Maximum Likelihood and Mahalanobis Distance algorithms. [C2173]

### "Orthogonal polarimetric SAR processor based on signal and interference subspace models"

We develop a new SAR processor based on several orthogonal projections. We take into account the scattering properties of the target and the interferences by using subspace models. To detect the target without detecting the interferences, we process images from the orthogonal projection of the received signal into the target subspace and from the orthogonal projection of the received signal into a part of the interference subspace. We can combine these two images to firstly detect the target and to secondly reduce interference. This new SAR processor is applied to realistic simulated data for FoPen (Foliage Penetration) application. [C2174]

### "Electromagnetic characteristics of simple targets embedded in chiral multilayer structures"

The scattering properties of a chiral stratified multilayer structure having an printed planar electric dipole are addressed in this paper. In order to obtain the scattered fields the method of moments in spectral domain is applied. The dipole scattering is characterized by the radar cross section (RCS), the polarimetric response, the  $\alpha$ -angle from Cloude-Pottier's target decomposition theorem and the directivity function. The results point out that all parameters are sensible to variations on the chiral layer admittance. The chiral layer impinges a rotation on the polarization plane of linearly incident wave for all frequency analyzed. [C2175]

### "Recent advances in the development of the open source Toolbox for Polarimetric and Interferometric Polarimetric SAR Data Processing: The PolSARpro v4.1.5 Software"

The objective of this paper is to make a review of the current status of the PolSARpro v4.0 Software (Polarimetric SAR Data Processing and Educational Toolbox), developed under contract to ESA. The objective of this current project is to provide Educational Software that offers a tool for self-education in the field of Polarimetric SAR data analysis at University level and a comprehensive suite of functions for the scientific exploitation of fully and partially polarimetric multi-data sets and the development of applications for such data. The PolSARpro v4.0 Software establishes a foundation for the exploitation of Polarimetric techniques for scientific developments and stimulates research and applications developments using PolSAR and PolInSAR data. [C2176]

### "Characterization of ENVISAT multipolarization SAR data with bidimensional statistics"

This paper is about evaluating the interest between studying directly dual images statistical indices and the use of statistical indices build from two SAR multipolarization images. We show an original way of using this kind of images by using two dimensionned statistical calculation in a Markov random field classification. We present results of our segmentation on urban, forest and mangrove areas. Those results are computed from ENVISAT ASAR data in HH and VV polarizations in a tropical context, near Libreville. [C2177]

### "Semantic segmentation of Polarimetric SAR imagery using Conditional Random Fields"

The paper proposes a fast and accurate semantic segmentation approach for a large Polarimetric SAR (PolSAR) image using Conditional Random Fields (CRFs). It efficiently incorporates the polarimetric signatures, texture and intensity features into a unite CRFs model, and employs a fast max-margin training method for parameters learning. Experiments on RadarSat-2 PolSAR data in Flevoland test site demonstrate that our approach achieves precise segmentation results with a few well-selected training samples. [C2178]

### "Forest structure from longer wavelength SRS"

In this paper we address three topics related to SAR Tomography of forest scenarios at P-Band. In first place we discuss the role of pulse bandwidth, which is shown to play a critical role as for the capability of the Tomographic system to separate ground and canopy contributions. Accordingly, vertical resolution depends not only on baseline aperture, but also on pulse bandwidth. Another factor to be accounted for is phase calibration, as the quality of the vertical focusing carried out by SAR Tomography is strictly related to the condition that phase contributions due to platform motion or atmospheric propagation are properly compensated for. Finally, multiple scattering phenomena are likely to occur at longer wavelengths, resulting in Tomographic techniques not being suffice for the aim of discriminating ground and volume scattering. The three points above are here discussed in light of the results achieved in the framework of the ESA campaign BioSAR 2008. The analysis has been carried out by exploiting the Algebraic Synthesis technique, which provides a theoretical framework to decompose the SAR signal into ground-only and volume-only contributions. Ground-only contributions provide an easy and viable way to phase calibrate the data stack. Volume-only contributions, if correctly identified, allow a direct Tomographic imaging of the vegetation layer. The impact of pulse bandwidth is tackled by assuming a Common Band Filtering approach, which results in a vertical resolution improvement by a factor 2. [C2179]

### "Improved hurricane active/passive simulated wind vector retrievals"

Microwave scatterometers are the standard for satellite ocean vector winds (OVW) measurements, and they provide the major source of global ocean surface winds observations for scientific and operational applications. A major challenge for Ku-band scatterometry missions is to provide reliable retrievals in the presence of precipitation, particularly in extreme ocean wind events that are usually associated with intense rain. This paper explores the advantages of combining dual frequency (C- and Ku-band) scatterometer measurements and passive microwave observations to improve high wind speed retrievals. For this study, a conceptual design proposed by the Jet Propulsion Laboratory for a Dual Frequency Scatterometer (DFS) to fly onboard the future Japan Aerospace Exploration Agency (JAXA) GCOM-W2 mission with the Advanced Microwave Scanning Radiometer (AMSR) was adopted. A computer simulation that combines the DFS and AMSR measurements was used to develop an artificial neural network OVW retrieval algorithm. The Weather Research and Forecasting (WRF) numerical weather model of Hurricane Katrina (2005) was used as the nature run (surface truth), and simulated OVW retrievals demonstrate that this new technique offers a robust option to extend the useful wind speed measurements range beyond the current operating scatterometers for future satellite missions. [C2180]

### "Interferometric processing algorithms of TanDEM-X data"

The purpose of this paper is to provide an algorithmic overview of the interferometric processing embedded in the Integrated TanDEM-X Processor (ITP), settled to the generation of the raw digital elevation model (DEM). The main processing blocks are described, with a focus on the spectral matching of the azimuth spectra, the high-precision coregistration, the dual-baseline phase unwrapping and the geocoding of the products. The robustness of the algorithms is demonstrated through a dual-pass TerraSAR-X scenario. [C2181]

### "Extrapolation of LiDAR for forest structure estimation using SAR, InSAR, and optical data"

One of the most fundamental new technical challenges of a DESDynI spaceborne mission is the fusion of the several sensor modalities-LiDAR, SAR, InSAR, and Optical-in order to accurately estimate desired 3D Vegetation structures and biomass parameters at their point of intersection and to extrapolate them over continuous areas. The objective of this paper is to use both our simulation models and measured dataset to develop and validate fusion and extrapolation methods while simulating DESDynI-type missions. We use existing datasets to develop and validate our fusion and extrapolation approach, which involves using our four sensor simulators, including our fractal-based tree geometry generator, in tandem with our in-house parameter estimation software which performs fusion and retrieval functions. We then use existing field and radarlidar-VNIR data for the Boreas southern study area to validate our simulators in this region and construct a large set of boreal trees for use in our fusion and extrapolation processes. [C2182]

### "Merging multi-track PSI result for land subsidence mapping over very extended area"

The Permanent Scatterer Interferometry (PSI) technique is usually applied for surface deformation mapping at local area from 1 up to a maximum of 100 km<sup>2</sup>. Although the ability to provide deformation map of regional area exceeding 10,000 km<sup>2</sup>, the processed area of interest is mostly limited to SAR acquisitions in a single satellite track and frame. In this work we present the study of merging multi-track PSI results for land subsidence monitoring over very extended area. Apart from the description of the PSI method used for long strip SAR data processing, datum connection of multiple adjacent tracks, including conversion of a common coordinate system and the connection of the PSI derived velocity maps are demonstrated. The application of the proposed method to monitor large coverage land subsidence in the central North China Plain (NCP) is described. The presented

results obtained by merging 3 adjacent tracks of ENVISAT ASAR data acquired between Jan, 2007 and Dec, 2009, with a coverage of 2004260km<sup>2</sup> are very significant and indicate the effectiveness and potential of this technique for land subsidence mapping over very extended area. [C2183]

### "Unsupervised change detection with very high-resolution SAR images by multiscale analysis and Markov random fields"

Change detection represents an important tool in environmental monitoring and disaster management. Here, a novel unsupervised change-detection method is proposed for very high-resolution SAR images, by integrating wavelet multiscale feature extraction, Markov random fields for contextual modeling, and generalized Gaussian models. Experiments with COSMO-SkyMed data remark the effectiveness of the method as compared with previous methods. [C2184]

### "Composite scattering from electric-large target over randomly rough surface in numerical approaches"

Numerical study of radar echoes from the targets in environmental clutters has been of great interest in many applications. In this paper, the bidirectional analytic ray tracing (BART) method for composite scattering from three-dimensional (3D) electrically large complex target above a randomly rough surface is reported. Analytic tracing of polygon ray tubes in bidirectional tracing is developed to precisely calculate the illumination and shadowing of facets, which exempt large patches of the target from any finer meshing. It significantly reduces the complexity relevant to the target electric-size. Numerical examples of angularly composite scattering from a three-dimensional electrically large, e.g., a ship-like target over a randomly rough surface are presented and discussed. [C2185]

### "Towards an operational daily soil moisture index derived from combination of MODIS, ASAR and AMSR-E data"

This work aims at deriving a methodology for calculation of a soil moisture index based on the apparent thermal inertia (ATI) approach. For the processing, MODIS images have been exploited which have a higher resolution (1 km) if compared with METEOSAT images and are suitable for the ATI calculation. Furthermore, the approach considers the soil moisture estimates derived from SAR sensors and use them to calibrate the information coming from the optical data. The main advantage of this approach is to transform a soil moisture index derived from optical images in soil moisture values by using a comparison between spatial distributed data. In order to make the calibration more robust and consider the variability from different areas, three main test sites have been chosen located in Italian regions with different meteorological and landscape characteristics. In case of anomalous values due to the not appropriate acquisition time, AMSR-E soil moisture data are used as prior information in order to improve the estimates. [C2186]

### "Deriving soil moisture with the combined L-band radar and radiometer measurements"

In this study, we develop a combined active/passive technique to estimate surface soil moisture with the focus on the short vegetated surfaces. We first simulated a database for both active and passive signals under SMAP's sensor configurations using the radiative transfer model with a wide range of conditions for surface soil moisture, roughness and vegetation properties that we considered as the random orientated disks and cylinders. Using this database, we developed 1) the techniques to estimate surface backscattering and emission components and 2) the technique to estimate soil moisture with the estimated surface backscattering and emission components. We will demonstrate these techniques with the model simulated data and its validation with the airborne PALS image data from the soil moisture SGP'99 and SMEX'02 experiments. [C2187]

### "Effects of forest disturbances on forest structural parameters retrieval from lidar waveform data"

The effect of forest disturbance on the lidar waveform and the forest biomass estimation was demonstrated by model simulation. The results show that the correlation between stand biomass and the lidar waveform indices changes when the stand spatial structure changes due to disturbances rather than the natural succession. This has to be considered in developing algorithms for regional or global mapping of biomass from lidar waveform data. [C2188]

### "Development of a signal processing subsystem for a spaceborne rotating, fan-beam scatterometer"

This paper introduces an on-board signal processing subsystem of a spaceborne rotating fan-beam



scatterometer in China. The subsystem processes returned signal after downconversion to intermediate frequency. To reduce the data stream downlinked from the satellite, the final data bins are summed into 34 energy slices, each with a range resolution of 10 km. Then a simulation process is adopted to analyze the Doppler effects due to the motion of the spacecraft, and to generate the Doppler compensation table and the bin summation table. This method is also used to analyze the measurement variance  $K_{pc}$  of each detected slice. Finally, the coefficients of the expression of  $K_{pc}$  are presented. [C2189]

#### "Investigation of cirrus clouds using the calipso lidar data"

Cirrus clouds normally exist in the upper troposphere and sometimes extend into the stratosphere. Unlike low altitude clouds that have a cooling effect on solar radiation through scattering, cirrus clouds scatter only a small amount of solar radiation and prevent a large quantity of long-wave radiation from leaving the earth-atmosphere system. Cirrus clouds are globally distributed and are composed almost exclusively of non-spherical ice crystals. Tropopause cirrus tends to occur over regions of intense convective activity like equatorial Africa and South America, which are sites for vigorous continental convection, and the western Pacific, which is a site of significant oceanic convection. Few instruments can deduce the global presence of cirrus clouds. The Cloud-Aerosol Lidar and Infrared Pathfinder Satellite Observations (CALIPSO) satellite mission provides comprehensive observations of cloud vertical structure on a near-global scale. [C2190]

#### "Monitoring environmental conditions in Muuga harbor using Envisat MERIS and ASAR data"

Environmental conditions were monitored using in situ measured inherent optical properties and water sampling together with remote sensing imagery (MERIS and ASAR) in Muuga Bay, Baltic Sea. Simultaneous monitoring using different methodologies gave detailed overview of suspended matter (SPM) load into the water column during the dredging operations. MERIS FRS data enabled to receive the distribution of SPM on water surface. The measurements of inherent optical properties revealed the particle concentration on vertical scale. Backscattering from the ASAR data was in correlation with oil products determined from water samples when ballast water discharge was detected during field sampling. [C2191]

#### "Field test of KOMPSAT-5 Calibration Equipment"

Korea Aerospace Research Institute (KARI) is developing the KOMPSAT-5 (K-5, the fifth of KOREA MultiPurpose SATellite) system of which primary payload is X-band Synthetic Aperture Radar (SAR). K-5 CALVAL (Calibration & Validation) activities must be important tasks for successful operation. The field test of K-5 Calibration Equipments can support a direction of CALVAL activities during not only IOT (In-Orbit Test) phase but also normal operation phase. [C2192]

#### "High resolution D-INSAR measurement for land subsidence"

In this paper, a study area of subsidence in the city of Taiyuan has been investigated using TerraSAR-X high resolution data and D-INSAR technique. In order to determine the accurate location and shape of each subsidence center, a time series of differential interferograms has been first generated and applied to preliminary location determination and rough subsidence rate estimation for each subsidence center, then the time series analysis of persistent scatterers including single point objects and highly coherent surface pieces for each subsidence center has been used for accurate positioning of subsidence center and precise subsidence rate estimation. [C2193]

#### "Preliminary results of a low-frequency 3D-sar approach for glacier volume mapping"

First experimental results with a low-frequency, ultra wideband (UWB) radar for estimating the height of glacier beds are illustrated. We use a 3-dimensional Time-Domain Back-Projection (TDBP) algorithm which incorporates the influence of the refractivity of ice to reconstruct the glacier bed of the Aletsch Glacier in the Swiss Alps using several CARABAS data sets. As the results indicate, the proposed method underlines the ability of low-frequency Synthetic Aperture Radar (SAR) to penetrate into glacier ice and thus, to map glacier volumes on a large scale even with only few, suboptimal data acquisitions. [C2194]

#### "Radar-based human detection and characterization with non-linear phase modeling"

Many current radar-based human detection systems employ some type of Doppler or Fourier-based processing, followed by spectrogram and gait analysis to classify detected targets. However, in Fourier-based techniques the maximum output signal-to-noise ratio (SNR) is given by targets whose target phase is linear. On the contrary, the phase variation of the human target response is nonlinear. This difference causes a significant loss in SNR, and therefore detection performance. In this paper, two novel, nonlinear phase detector designs based on human

modeling are presented. In the first method, only the human torso reflections are modeled and unknown model parameters computed using Maximum Likelihood Estimation. In the second method, the entire human body is modeled as a different parametric model. The expected radar response for each combination of parameter values is stored in a database. An optimal sparse approximation to the data is found using Orthogonal Matching Pursuit. The performance of the proposed techniques and optimal space-time adaptive processing algorithm is compared and target characterization applications examined. [C2195]

#### "Monitoring of thawing process using envisat asar global mode data"

Due to the high temporal sampling rate of ASAR Global Monitoring mode, it has an application potential for analyzing seasonal changes in permafrost environment. The objective of the study is to develop a robust method for monitoring freeze/thaw cycles beyond threshold approaches. In order to use ASAR GM time-series for analyzing freeze/thaw states, a least square fitting of piecewise step function is introduced in this paper. An experiment result for Siberian permafrost area near Yakutsk illustrates that it can be a promising approach in monitoring permafrost ecosystems. [C2196]

#### "KOMPSAT-5 spotlight SAR processor using FSA with calculation of effective velocity"

In KOMPSAT-5 program, Korea Aerospace Research Institute has made SAR imaging chain analysis tool to evaluate imaging system of KOMPSAT-5. The tool consists of a simulator and a processor. The simulator simulates observation of a scene by the operational mode of KOMPSAT-5 and generates SAR raw data. The processor generates an image of the scene. This paper is about the second part of processing the simulated raw data that is acquired by the step steering sliding spotlight mode of KOMPSAT-5. For this observation mode, dechirp on receive is operated in receiving the echoes. So, extended frequency scaling algorithm is used to process the raw data in order to directly handle the dechirped data. This paper mainly contributes for the accuracy of effective velocity. The effective velocity criterions for range and azimuth processing allows that the processor uses only one scene center effective velocity in range processing and several ones in azimuth processing. In this paper, a method to increase the accuracy of calculation of effective velocity is also proposed. Simulation result shows that the proposed method is valid. [C2197]

#### "Fusion: A fully ultraportable system for imaging objects in nature"

To improve satellite-derived estimates of terrestrial plant production and exchange of CO<sub>2</sub>, water, and energy with the atmosphere, scientists need to consider ecosystem composition, structure, function, and health. This can be accomplished through the fusion of Light Detection And Ranging (LiDAR) data, which can provide 3D information about the vertical and horizontal distribution of vegetation and hyperspectral remote sensing, which can inform us about variations in biophysical variables (e.g., photosynthetic pigments) and responses to environmental stressors (e.g., heat, moisture loss). Satellite observations from upcoming Decadal Survey missions will provide NASA with the unique opportunity to fuse LiDAR data from ICESat-II, DESDynI, and LIST with hyperspectral and thermal imagery from HypSIRI and GEO-CAPE. This synergy will augment and enhance the individual science objectives of decadal survey missions, and will allow scientists the opportunity to develop 3D models of plant canopies that better describe global cycling of carbon, water and energy. Multiple NASA's Earth Science Focus Areas are served by this science, including carbon cycle and ecosystems; water and energy cycle; and climate variability and change (i.e., ecosystem responses and feedbacks to climate change). One of the major obstacles to the development of data fusion algorithms is the availability of accurately co-registered data of similar grain size. This is often the case when instruments are flown on different platforms and at different times during a field campaign. We believe that "instrument fusion" is a prerequisite to "data fusion", and we have developed a system that integrates a full-waveform LiDAR, narrow band hyperspectral imager, and broad band thermal imager in a single, compact and portable instrument package that could be readily deployed on a number of observation platforms. FUSION will provide accurate co aligned datasets that are needed for: (i) calibration and validation of satellite-derived land products; (ii) development of data fusion algorithms; and (iii) combine observations from multiple sensors to characterize ecosystem composition, structure, function, and health. [C2198]

#### "Overview of KOMPSAT-5 program, mission, and system"

Korea Aerospace Research Institute (KARI) are developing the KOMPSAT-5 system of which primary payload is X band Synthetic Aperture Radar (SAR). The program overview, mission and system characteristics of KOMPSAT-5 are described in this paper. [C2199]

#### "UWB electromagnetic borehole logging tool"

Based on a theoretical model of the geosteering borehole logging tool, which operates the broadband pulse, we

demonstrate the possibility of detecting an interface between oil- and water-saturated layers in the oil-gas formation. [C2200]

### "Temporal analysis of the magma supply system beneath the Okmok caldera by Interferometric Synthetic Aperture Radar and statistical seismology"

The temporal characteristics of the magma supply system beneath the Okmok caldera is examined using Interferometric Synthetic Aperture Radar (InSAR) and statistical seismology. Surface deformation produced by a shallow magma chamber is studied through time series analysis of InSAR imagery acquired between 1995 and 2008 by the ERS-1/2 satellites. A spherical source model (Mogi Source) is utilized to simulate the deformation pattern produced by the shallow magma chamber's fluctuating geometry. Statistical seismology provides an independent estimate of the magma chamber's depth to reduce the non-uniqueness of the Mogi source model solutions. Seismic results show that a shallow magma chamber is located approximately 4.0 km below the caldera floor. InSAR imagery indicates the chamber has expanded continuously between 1997 and 2008. Modeling results suggest that magma replenishment has occurred at an average rate of approximately  $7.0 \pm 10\text{-}3\text{km}^3/\text{year}$  and that the volume within the chamber returned to its pre-1997 eruption state by June 2008. [C2201]

### "Directional-adaptive despeckling for high-resolution SAR"

In this study, an iterative maximum a posteriori (MAP) approach using a Bayesian model of Markov random field (MRF) was proposed for despeckling images that contains speckle. Image process is assumed to combine the random fields associated with the observed intensity process and the image texture process respectively. The objective measure for determining the optimal restoration of this "double compound stochastic" image process is based on Bayes' theorem, and the MAP estimation employs the Point-Jacobian iteration to obtain the optimal solution. In the proposed algorithm, MRF is used to quantify the spatial interaction probabilistically, that is, to provide a type of prior information on the image texture and the neighbor window of any size is defined for contextual information on a local region. However, the window of a certain size would result in using wrong information for the estimation from adjacent regions with different characteristics at the pixels close to or on boundary. To overcome this problem, the new method is designed to use less information from the neighbors located in the direction to an adjacent different region and more information from the neighbors located in the inner region of same characteristics. It can reduce the possibility to involve the pixel values of adjacent region with different characteristics. [C2202]

### "Target detection above rough surfaces in microwave imaging using Compressive Sampling"

A subspace extraction approach for detection of targets embedded in the clutter is presented in this work. Subspace extraction approach that makes use of both Compressive Sampling and Principal Component Analysis (PCA) is presented in this paper. Inverse Synthetic Aperture Radar (ISAR) Imaging measurement data is used to validate the proposed approach. Experimental results of targets above rough surface with intermediate roughness are presented. Results showed the dimensionality of an intermediate scale rough surface is generally larger than the dimensionality of the finite size targets. Results showed that by compressing the dimensionality through compressive sampling and extracting the principal components, significant improvement in target subspace extraction can be achieved. [C2203]

### "Research on interferometric deformation detection for geosynchronous SAR"

The nadir track of geosynchronous satellite can be "figure-8", circular or ellipse track which could be produced with appropriate orbit parameters. In this paper, the characteristics of the interferometric deformation detection for geosynchronous SAR with circular aperture are analyzed. The connection between the interferometric phase and the deformation of repeat pass geosynchronous SAR is derived, and its potential to get three-dimensional 3D deformation measurement is interpreted. [C2204]

### "MVM based SAR image processing for ship pose estimation"

As an essential approach of SAR image interpretation, a good pose estimation calls for two conditions: an accurate extraction of the scattering centers and a thorough exploration of the structural information among them. The article focuses on these two topics successively. Firstly, the power spectrum estimation methods are recommended to improve the scattering center resolution and the Minimum Variance Method (MVM) is chosen for its sidelobe suppressing ability and signal model independence. With the segmented MVM image, the axis extraction problem is then solved by a new strategy, namely the Angle Entropy of Radon transform (AER) strategy. Data from computational electromagnetics are used for experiments. It is shown that the MVM image shows better morphologic feature than the Fourier ones (both original and Hanning-windowed), and the AER strategy achieves more accurate and robust estimation compared with the edge-based Hough transform (HT)

technique. [C2205]

### "Generic object recognition in high resolution SAR images"

This paper presents a non-parametric modeling scheme for high resolution SAR data, based on Short Time Fourier Transform which is able to integrate the radiometrical and morphological properties of the data, for object recognition, scene and target indexing, addressing the problem of large data base queries and information retrieval.. The method is assessed by using a Bayesian Support Vector Machine image search engine based on a hierarchical learning model. The method allowed for the recognition of over 30 different classes, both homogeneous and heterogeneous urban objects with high levels of details. Qualitative and quantitative measures for evaluation are presented and discussed. [C2206]

### "A ground-based Arc-scanning synthetic aperture radar (ArcSAR) system and focusing algorithms"

KIGAM and KNU are developing a ground-based Arc-scanning SAR system (ArcSAR) mounted on a truck. The system achieves the coherent integration of radar returns from ground targets by the circular motion of the antennae attached to the end of an extendable arm. Precise control of antenna position and the extended coherent-integration-length enable the formation of high-resolution, high-precision and phase-preserving SAR images. Based on the Polar Format Algorithm, two SAR-focusing algorithms were developed for the data acquired from two different scanning modes of this unique system: the scan mode and the spot mode. [C2207]

### "A filtering approach to improve deformation accuracy using large baseline, low coherence DInSAR phase images"

Phase noise in an interferogram hinders the accuracy and reliability of interferometric synthetic aperture radar (InSAR) measurements, including deformation estimation and topographic mapping. The Goldstein filter is one of the most commonly used interferogram filters to reduce the effects of phase noise. In this paper, we present a modification to the Goldstein interferogram filter such that the maximum value for the filtering parameter alpha is set to greater than 1 over less coherent areas so that aggressive filtering is implemented on incoherent areas. We also discuss the combined use of estimated coherences from linear and non-linear filters to deal with the coherence saturation due to the strong filtering, which is crucial in generating InSAR deformation products. [C2208]

### "Lidar integrated airborne imaging spectroscopy for root disease detection and measurement of foliar chemistry"

Root disease is a serious concern for the softwood timber industry. This paper reports on the development of a root disease detection procedure that applies lidar integrated with imaging spectrometer data. Chlorophyll-a was found to be significantly affected by the disease in a needle level study[I]. Chlorophyll-a was estimated from canopy reflectance through partial least squares regression and achieved an R2value of 0.82. Continuum removal metrics, which proved to be good estimators at the needle level where found to be insufficient at the canopy level. Through the union of decreased stand density and decreased foliar chlorophyll, potential disease sites were identified in the Greater Victoria Watershed District test site. [C2209]

### "Submerged dunes and breakwater embayments mapped using wave inversions of shore-mounted marine X-band radar data"

Surveying very shallow coastal areas, particularly around coastal defences, can be a logistically difficult and time consuming process. A marine-radar based bathymetry mapping technique has been used to remotely map the embayments around a series of shore-parallel breakwaters at Sea Palling on the south east coast of England during the LEACOAST2 project. The duration of the deployment spanned over 2 years, with the aim of observing any evolution of bathymetric features over that timescale while providing a clear indication of the spatial variability of wave and current patterns contributing to such evolution. The embayments generated by the shore parallel breakwaters at that site are resolved and a field of subtidal dunes with a wavelength of the order of 200m and amplitude around 1m located in approximately 6-10m of water were within the radar field of view and are evident in the remotely sensed bathymetry. Comparisons between bathymetric data obtained using conventional survey techniques and the radar based technique are presented together with measurements of tidal currents mapped using the same remote sensing method and compared with ADCP data during a storm event. [C2210]

### "Application of conventional marine radars for measuring ocean wave fields in shallow water conditions"



This work presents the estimation of wave field properties derived from X-band marine radar measurements taken close to coastal locations, where the wave fields are affected by the finite water depth conditions. The work is focused on the detection of individual waves and their related characteristics, such as the estimation of the local and instantaneous wave envelope derived from the wave elevation fields estimated from X-band marine radar time series. [C2211]

#### "Multispectral classification of remote sensing imagery for archaeological land use analysis: Prospective study"

Much of human history can be traced through the impacts of human actions upon the environment. The use of remote sensing technology offers the archeologist the opportunity to detect these impacts which are often invisible to the naked eye. The extraction of remote sensing signatures from a particular geographical region allows the generation of geophysical signature maps; this can be achieved using an accurate and recently developed multispectral image classification approach based on pixel statistics for the class description, which is referred to as the Weighted Pixel Statistics method. This paper presents the prospective study of the effectiveness that this approach provides for supervised segmentation and classification of sensed archaeological signatures for land use analysis. The results obtained with this study uses real multispectral scenes obtained with remote sensing techniques (high-resolution synthetic aperture radar) to probe the efficiency of the classification technique. [C2212]

#### "Approach for volcanic surveillance using satellite-borne microwave radiometer data"

Volcanic surveillance is one of the practical fields for remotesensing technology. Monitoring of thermal anomalies on volcanoes by infrared radiometer and detection of slight landsurface deformations around volcanoes by interferometry of synthetic aperture radar (SAR) are good examples. However, an infrared radiometer is a little nervous for clouds which cover volcanoes, and interferometry of SAR also has a weakness that the time resolution becomes low in exchange for high spatial resolution. Meanwhile, focusing on microwave radiometer, we know it is less affected by clouds than infrared radiometer. Its time resolution is also higher than interferometry of SAR. Therefore, microwave radiometer can become a promising tool for volcanic surveillance. But, a new methodology to compensate its coarse spatial resolution is essential. It was a serious problem. [C2213]

#### "A study on anomalous signal detection using HMM for ELF electromagnetic wave"

A seismic radiation emitted from the earth's crust is useful for predicting earthquakes. The electromagnetic (EM) wave in the Extremely Low Frequency (ELF) band have been observed at many places in Japan. In this paper, we propose the anomalous signal detection method based on HMM whose input vector is the amplitude density distribution of an EM wave. The amplitude density distribution is calculated from the image of an EM wave data. The optimal scale of an image to calculate an amplitude density distribution and the optimal number of states of HMM are investigated to achieve an accurate detection. [C2214]

#### "Application of TerraSAR-X data to the monitoring of urban subsidence in the city of Murcia"

This paper presents an analysis of the performance of TerraSAR-X for subsidence monitoring in urban areas. The city of Murcia has been selected as a test-site due to its high deformation rate and the set of extensometers deployed along the city that provide validation data. The obtained results have been compared with those obtained from ERS/ENVISAT data belonging to the same period and validated with the in-situ measurements. [C2215]

#### "Closed-loop pallet manipulation in unstructured environments"

This paper addresses the problem of autonomous manipulation of a priori unknown palletized cargo with a robotic lift truck (forklift). Specifically, we describe coupled perception and control algorithms that enable the vehicle to engage and place loaded pallets relative to locations on the ground or truck beds. Having little prior knowledge of the objects with which the vehicle is to interact, we present an estimation framework that utilizes a series of classifiers to infer the objects' structure and pose from individual LIDAR scans. The classifiers share a low-level shape estimation algorithm that uses linear programming to robustly segment input data into sets of weak candidate features. We present and analyze the performance of the segmentation method, and subsequently describe its role in our estimation algorithm. We then evaluate the performance of a motion controller that, given an estimate of a pallet's pose, is employed to safely engage each pallet. We conclude with a validation of our algorithms for a set of real-world pallet and truck interactions. [C2216]

### "Signal analysis and modeling of wind turbine clutter in weather radars"

Lately, the continuing expansion of wind energy industry has led to the installation of several wind farms which are often in the vicinity of the weather radars. This is a source of growing concern for the weather radar community since wind turbines interfere with the normal operation of the weather radars. The wind turbine tower can drive the receivers into saturation and the Doppler shift from the moving blades can introduce errors in the estimation of wind speed, reflectivity and rainfall rates. The radar cross-section of the wind turbines has a large temporal and spatial variation which poses additional difficulties for traditional clutter filtering algorithms. This paper presents a first-order theoretical model of the radar signature of a wind turbine that can be helpful in deducing its unique features to be incorporated in filtering out the wind turbine clutter. A comparison with the observations from an S-band radar is made later in the paper. [C2217]

### "Passive imaging exploiting multiple scattering using distributed apertures"

We develop a new passive image formation method capable of exploiting information about multiple scattering in the environment using measurements from a sparse array of receivers that rely on illumination sources of opportunity. We use a physics-based approach to model wave propagation and develop a statistical model that relates measurements at a given receiver to measurements at other receivers. We formulate the imaging problem as a spatially resolved binary hypothesis testing problem using the model between the measurements at different receivers, statistics of the objects to be imaged and statistics of the additive noise and clutter. We address the spatially resolved hypothesis testing problem by constraining the associated discriminant functional to be linear and by maximizing the signal-to-noise-ratio of the test-statistic, and use the resulting spatially resolved test-statistics to form the image. We present numerical simulations to demonstrate the performance of the passive imaging algorithm. [C2218]

### "A real time Breast Microwave Radar imaging reconstruction technique using simt based interpolation"

Breast Microwave Radar(BMR) is a novel imaging modality that is capable of producing high contrast images and can detect tumors of at least 4mm. To properly visualize the responses from the breast structures, BMR data sets must be reconstructed. In this paper, a real time BMR image formation technique is proposed. This approach is based on the use of a Single Instruction Multiple Thread(SIMT) interpolation method. By using this programming model, the proposed approach can be implemented on General Purpose Graphic Processing Unit (GPGPU) platform to speed up the reconstruction process. The proposed method yielded promising results when applied to simulated data sets obtained using anatomically accurate numeric phantoms. In average, the proposed approach yielded speed increases of one order of magnitude compared to its CPU counterpart, and two orders of magnitude with respect to current BMR reconstruction techniques. [C2219]

### "GPM Microwave Imager design, predicted performance and status"

The Global Precipitation Measurement (GPM) Microwave Imager (GMI) Instrument is being developed by Ball Aerospace and Technologies Corporation (Ball) for the GPM program at NASA Goddard. The Global Precipitation Measurement (GPM) mission is an international effort managed by the National Aeronautics and Space Administration (NASA) to improve climate, weather, and hydro-meteorological predictions through more accurate and more frequent precipitation measurements. The GPM Microwave Imager (GMI) will be used to make calibrated, radiometric measurements from space at multiple microwave frequencies and polarizations. GMI will be placed on the GPM Core Spacecraft together with the Dual-frequency Precipitation Radar (DPR). The DPR is two-frequency precipitation measurement radar, which will operate in the Ku-band and Ka-band of the microwave spectrum. The Core Spacecraft will make radiometric and radar measurements of clouds and precipitation and will be the central element of GPM's space segment. The data products from GPM will provide information concerning global precipitation on a frequent, near-global basis to meteorologists and scientists making weather forecasts and performing research on the global energy and water cycle, precipitation, hydrology, and related disciplines. In addition, radiometric measurements from GMI and radar measurements from the DPR will be used together to develop a retrieval transfer standard for the purpose of calibrating precipitation retrieval algorithms. This calibration standard will establish a reference against which other retrieval algorithms using only microwave radiometers (and without the benefit of the DPR) on other satellites in the GPM constellation will be compared. The instrument has completed the Critical Design Review phase of the program. The design of the instrument is complete. We describe the instrument and predict the performance of the GMI instrument. The instrument interfaces have been finalized and the design completed. The final mechanical and electrical interfaces are described. The mechanical interface was specifically designed to provide isolation from the spacecraft and allow accommodation on future low inclination spacecraft. An electrical interface was added coming from the spacecraft that allows the GMI integration to be blanked during Dual Precipitation Radar pulses.

The implementation of this blanking is described. The instrument is currently in the flight production phase. Status and initial test results on the flight hardware are presented. [C2220]

### "Multiresolution despeckling of VHR SAR images based on MRF segmentation"

In this work, maximum a posteriori (MAP) despeckling, implemented in the multiresolution domain defined by the undecimated discrete wavelet transform (UDWT), will be carried out on very high resolution (VHR) SAR images and compared with earlier multiresolution approaches developed by the authors. The MAP solution in UDWT domain has been specialized to SAR imagery. Every UDWT subband is segmented into statistically homogeneous segments and one generalized Gaussian (GG) PDF (variance and shape factor) is estimated for each segment. This solution allows to effectively handle scene heterogeneity as imaged by the VHR SAR system. Segmentation exploits a Tree Structured Markov Random Field (TSMRF), which is a low complexity MRF segmentation that allows the estimation of the number of segments and the segmentation itself to be carried out at the same time. Experiments performed on a single-look VHR X-band SAR images demonstrate that the segmented approach is effective whenever the classical circular Gaussian model of complex reflectivity may no longer hold. [C2221]

### "Potential of mapping soil moisture by combining radar backscatter modeling and PolSAR decomposition"

The purpose of this study is to evaluate the capability of the Oh backscattering model in combination with the Freeman Durden decomposition to estimate soil moisture over agricultural fields from fully polarimetric RADARSAT-2 C-band SAR responses. Initially, soil moisture multi-polarization retrieval was accomplished by using a look-up table (LUT) approach applied to the Oh model. Two methods were considered: the multi-polarization method and the one-unknown configuration. Of the two methods, results showed that the HH-HV inversion provided the best estimates. In the second phase, the Freeman Durden decomposition was applied to the polarimetric data. The conceptual approach for retrieving soil moisture using the surface scattering component of the total power was implemented in a LUT inversion. The algorithm attempts to minimize the difference between measured single scattering power obtained by applying the Freeman Durden decomposition and simulated total power using Oh model. When compared with the multi-polarization approach, this polarimetry-based method improves the accuracy of soil moisture estimates. [C2222]

### "Triple collocation-A new tool to determine the error structure of global soil moisture products"

Recently Triple Collocation (TC) was adopted for soil moisture application. Results from a first application indicated that the method could be useful to estimate global error patterns. Here we test the method with new data sets. The results show that the method is robust and that it allows to derive objective error estimates. [C2223]

### "Characteristics of rough surface parameters estimated from measured surface profile of finite length"

Estimation of roughness parameters of soil surface is one of the important problems in the field of radar remote sensing. In order to estimate these parameters from measured surface height-profile, data samples with sufficiently long record length are required for accurate estimation. In an actual measurement situation, however, it is difficult to get the surface height-profile in pure form because a bias and inclination of the data are unknown. In this study, we present a method for estimation of the bias and inclination from measured surface height-profile and reveal the effect of the accuracy on the parameter estimates. [C2224]

### "Target detection performance analysis for airborne passive bistatic radar"

For a ground-based/airborne passive bistatic radar, its performance is dependent on the geometrical configuration and the passive transmit signal attributes. Theoretical power budget and ambiguity function analysis using a ground-based non-cooperative transmitter of opportunity with a passive bistatic radar being airborne but stationary (airship, etc.) had shown that target detection performance is limited by the strong direct path coupling signal. In comparison, the bistatic ground clutter power is significantly lower and even more so for noise power. For the passive radar to perform satisfactorily, sufficient attenuation must be provided for the direct path and strong ground clutter signals, corresponding to increasing the height of the target peak on the ambiguity function pedestal. In addition, performance could also be improved by increasing the time-bandwidth product (assuming no target migration issues), which lowers the pedestal of the ambiguity function of the strong direct path interfering signal. [C2225]

### "Imaging algorithm and experimental demonstration of rotating scanning interferometric radiometer"

Recently, a new concept of rotation scanning synthetic aperture interferometric radiometer (RS-SAIR) has been receiving more and more attentions for its advantage of much simpler configuration with looser requirements of antenna elements. In this article, we investigate the imaging theory of RS-SAIR, and introduce the pseudo-polar FFT algorithm to deal with the polar u-v samples. It only involves 1D interpolation and 1D FFT routine that guarantee a high accuracy and computation efficiency. The sampling strategy and aliasing effect of RS-SAIR are studied with this imaging algorithm. Numerical simulations are provided to validate the associate theory. Finally we develop a 5-elements RS-SAIR instrument and carry out rotating scanning imaging experiment successfully. The first imaging results consist with the expectation. [C2226]

#### "Automatic exclusion of surface deformation in InSAR DEM generation using differential radar interferometry"

The Digital Elevation Models (DEMs) are an important source of topographical data for many scientific and engineering applications. Where topographical data are unavailable, global coverage elevation data sets, typically DEMs from remotely sensed data, are the main sources of such information. Interferometric SAR (InSAR), is a useful method for low-cost, relatively precise and wide-coverage surface DEM generation. However, ground deformation should somehow be excluded from InSAR-based DEM generation. To identify surface deformation areas, the so-called Differential InSAR (DInSAR) is a commonly used method. In this paper, the authors propose a two-step DEM generation method: the ground deformation area detection using DInSAR technique and deformation area exclusion in InSAR DEM generation by detected mask. [C2227]

#### "Evaluation of system polarization quality for polarimetric SAR imagery and target decomposition"

The quality of polarimetric synthetic aperture radar (PolSAR) imagery and its polarimetric decompositions depends on the accuracy of polarimetric observations of the SAR system and its calibration. Polarization distortions on the polarimetric measurement can be incurred due to nonideal system polarization quality and propagation factors, such as channel imbalance, cross-talk, and Faraday rotation at lower frequencies. All these distortions have varying impacts on different target types as well as different decomposition methods. In this paper, we assess the polarization quality of the PolSAR system in the context of polarimetric imagery analysis and quantify the various effects of polarization distortions on polarization target decompositions. A generic metric is defined to measure the polarization purity of the system. Considering the fact that target decomposition plays an important role in imagery analysis, we apply several widely used decomposition methods to showcase the polarimetric system requirement based on the defined metric. [C2228]

#### "Contribution of small-scale correlated fluctuations of the microstructural properties of a spatially extended geophysical target under the assessment of radar backscatter"

The study of the collective effects of radar scattering from an aggregation of discrete scatterers randomly distributed in a space is important for a better understanding of the origin of the backscatter from spatially extended geophysical targets (SEGT). We consider the microstructural irregularities of SEGТ as the essential factor that affects radar backscatter. To evaluate their contribution, this study uses the "slice" approach: particles close to the front of an incident radar wave are considered to reflect incident electromagnetic waves coherently. The radar equation for a SEGТ is derived. The equation includes contributions to the total backscatter from correlated small-scale fluctuations in the slice's reflectivity. The correlation contribution changes in accordance with an idea proposed earlier by Smith (1964) based on physical consideration. The slice approach applied allows parameterizing the features of the SEGТ's inhomogeneities. [C2229]

#### "Building detection and radar footprint reconstruction from single VHR SAR images"

The development of methods for the automatic detection and reconstruction of building radar footprints from single very high resolution (VHR) synthetic aperture radar (SAR) images is a difficult task for two main reasons: i) the very high complexity of VHR SAR images; and ii) the need to develop efficient algorithms that can be applied to large images in order to be used in real applications. In this paper we present a novel method for automatic building detection, which also reconstructs the 2D radar footprint of the detected buildings. The method is based on the extraction of a set of low-level features from the images and on their combination in more structured primitives. Then the semantic meaning of primitives is used for the definition of building candidates and for the radar footprint reconstruction. In order to process large VHR SAR images, the method has been implemented on a computer cluster. We demonstrate the effectiveness of the method using a large TerraSAR-X spotlight scene. [C2230]

#### "Unsupervised nonparametric classification of polarimetric SAR data using the K-nearest neighbor graph"



Polarimetric SAR classifications are often based on assumptions about the shape of clusters in the data space. Such a scheme will fail for nonlinear structures in the feature space, unless the classification algorithm has the capacity to describe cluster shapes in sufficient generality. Existing polarimetric SAR classification methods are faced by this exact problem: typically they initialize clusters in the Cloude-Pottier parameter space [1], further optimizing them in the coherency matrix space [2, 3]. Methods using K-means [2] or agglomeration [3] require clusters that are spherical, or compact and well separated, respectively. In the Cloude-Pottier space, these requirements are not met, so initialization in the Cloude-Pottier space cannot be consistent with optimization by K-means or agglomeration. This paper sets out to address this problem, by implementing a new data-driven clustering approach, for arbitrarily shaped clusters. It is applied to quad-polarisation data, demonstrating the new methodology's potential for forest land-cover type discrimination. [C2231]

### "Development of a three-element interferometer at 50 56 GHz for Geostationary Interferometric Microwave Sounder (GIMS)"

The Geostationary Interferometric Microwave Sounder (GIMS) is a new concept imaging radiometer proposed by CSSAR, aiming for China's next generation geostationary meteorological satellite (FY-4M). The concept of GIMS is based on aperture synthesis with a rotating circular thinned array. A three-element interferometer has been developed and tested to investigate the feasibility of the GIMS system design. A full-scale ground-based demonstrator with 27 elements is also under development, which is defined as a minimum system intended to fulfill the threshold application requirements. In this paper, the preliminary results of these activities will be reported. [C2232]

### "High-resolution mapping of fluvial landform change in arid environments using terrasars-X images"

The high resolution acquisition mode of TerraSAR-X provides a new dimension in fluvial landform change detection. Here we analyzed high resolution (5 m) coherence images with temporal baselines of up to a year from the Palpa Valley in the hyper-arid coastal desert of southern Peru. The results provide evidence that this sensor is suitable for mapping the land surface changes caused by erosion and sedimentation following rainfall and runoff events in bare desert landscape units. [C2233]

### "Implementation of a low cost, lightweight X-band antenna with integrated SiGe RF electronics"

This paper presents an organic, lightweight X-band antenna array with integrated silicon germanium (SiGe) low noise amplifiers (LNA) and 3-bit phase shifters (PS). The SiGe LNAs and PSs were successfully integrated onto an 841 lightweight antenna stack-up utilizing a multilayer liquid crystal polymer (LCP) substrate. Successful comparisons of the measured and simulated results verify a working antenna array with a return loss of around 10 dB across the frequency band of 9.25 GHz-9.75 GHz. A comparison of radiation patterns for the 841 antenna with integrated SiGe LNA and the 841 antenna with integrated SiGe LNA and PS show a 16 dB and 25 dB increase in gain, respectively. The ultimate goal is to develop an airborne X-band radar capable of a beam steering of at least  $\pm 40^\circ$  through utilization of low power highly integrated SiGe electronics on a low cost multi-layer organic platform. This paper represents the first successful demonstration of a building block prototype (i.e., a fully integrated, high gain X-band antenna with SiGe LNAs and SiGe phase shifters) that can be expanded to a complete active phased array for remote sensing applications in X-band. [C2234]

### "Improvement of ship detection accuracy by sar multi-look cross-correlation technique using adaptive CFAR"

This paper describes a novel technique to improve the accuracy of ship detection by synthetic aperture radar (SAR). The methodology is to apply the algorithm of constant false alarm rate (CFAR) to the coherence images produced by multi-look cross-correlation (MLCC) of sub-images. The experiment was carried out in the Tosa bay, Kochi, Japan using three known fishing boats and the simultaneous data acquired by the Phased Array L-band SAR (PALSAR) on board of the Japanese Land Observing Satellite (ALOS) at four different modes. The inter-look coherence images were found to fit best to Gamma distribution, and using this distribution function, CFAR was applied to the coherence image. The results showed substantial improvement in signal to noise ratio and false alarm rate as compared with the coherence image alone. In the followings, the principle of MLCC-CFAR and experimental procedure are summarized, and the results are discussed. [C2235]

### "Japanese hyper-multi spectral mission"

The hyperspectral and the multispectral (hyper-multi spectral) mission is the Japanese next generation space-borne radiometer development project. This project is a heritage from ASTER launched in December 1999. The performance of the hyperspectral radiometer is 30m ground sampling distance, 30km swath width, 10nm and

12.5nm wavelength distance for VNIR and SWIR respectively, over 450@620nm and 300@2,100nm of the signal to noise (S/N) ratio. The performance of the multispectral radiometer is 5m ground sampling distance, 90km swath width, over 200 for all bands of S/N ratio. This project will be launched on ALOS-3 of JAXA in FY2014. The panchromatic sensor with stereo viewing will also be installed on ALOS-3. [C2236]

#### **"Automatic ship detection in sar images using aegir"**

Aegir is an automatic ship detection tool developed at FFI. Now it analyses the different polarisation channels independently. The goal is to fuse the channels before the analysis starts, and to detect the ships in the fused channels. When dual-polarised data is available it is possible to look at the channels individually and combined. When fully polarised data is available, it is also possible to use the scattering matrix and decompose it in different ways. [C2237]

#### **"Bistatic SAR along track interferometry with multiple fixed receivers"**

This paper presents an along-track interferometry (ATI) study for a bistatic or multistatic SAR configuration with fixed ground receivers. This technique can be useful for sea current estimation or for any problem of Ground Motion Target Indicator (GMTI). The proximity of the ground receivers to the scene allows to be very sensitive to velocities with small baselines. This paper also proposes a multibaseline approach for ATI able to differentiate among different velocity contributions in the same resolution cell. At the end of this paper, some results over real acquired bistatic data will be presented and discussed. The data have been acquired using the C-band SAR Bistatic Receiver for Interferometric Applications (SABRINA) and ESA's ENVISAT satellite, as a transmitter of opportunity. [C2238]

#### **"Radar retrieval of subsurface parameters for layered media with nonsmooth interfaces"**

The solution to the inverse problem for a three-layer medium representing a large class of natural subsurface structures is developed in this paper using radar data. The retrieval of the layered medium parameters is accomplished as a sequential nonlinear optimization starting from the top layer and progressively characterizing the layers below. The optimization process is accomplished by an efficient iterative technique built around the solution of the forward scattering problem. The forward scattering process is formulated by using the Extended Boundary Condition Method (EBCM) and constructing reflection and transmission matrices for each interface. These matrices are then combined into the generalized scattering matrix for the entire system, from which radar scattering coefficients are then computed. To be efficiently utilized in the inverse problem, the forward scattering model is simulated over a wide range of unknowns to obtain a complete set of subspace-based equivalent closed form models that relate radar cross section coefficients to the sought-for parameters including dielectric constants of each layer and separation of the layers. The inversion algorithm is implemented as a modified conjugate-gradient-based nonlinear optimization. It is assumed that multifrequency radar measurements are available from tower-mounted or airborne platforms, for example at typical radar frequencies of L-band and P-band (UHF). It is shown that this technique results in accurate retrieval of surface and subsurface parameters, even in the presence of noise. [C2239]

#### **"Combined active and passive measurements of snow, bare and vegetated soils microwave reflective and emissive characteristics by Ka-band, combined scatterometer-radiometer system"**

In this paper the results spatio-temporally collocated measurements of bare, dry vegetated and ash covered soils microwave reflective (radar backscattering coefficient) and emissive (brightness temperature) characteristics angular dependences at ~37GHz are presented. During the experiment with dry vegetated soil the observed area was set ablaze and microwave active and passive measurements at 300 incidence angle were continued for smock, fire and ash situations. For these measurements Ka-band, polarimetric, combined scatterometric-radiometric system was used, set on a mobile buggy moving along the measuring platform. Structures, operational features and the main technical characteristics of the used system are presented too. The paper has an aim as well to attract attention of interested researchers and to invite them to perform their own or joint researches using available devices and facilities. [C2240]

#### **"A new scalloping filter algorithm for scansar images"**

Due to its specific way of scanning over multiple sub-swaths of a radar image, a ScanSAR (scanning synthetic aperture radar) cannot sample Doppler histories continuously like a regular SAR in stripmap mode. This can cause an artifact known as azimuthal scalloping, a wave-like modulation of the image intensity in azimuth direction. Although the problem is theoretically understood, many ScanSAR images of ocean scenes continue to exhibit scalloping. This hampers their use for applications such as wave and wind retrievals. We have developed an efficient descloping algorithm that can be applied to such images as a post-processing tool. We describe

how it works and show examples. [C2241]

### "Geometric refinement of road networks using network snakes and SAR images"

In this paper, a new approach for the geometric refinement of road networks using network snakes and SAR images is presented. Network snakes are based on the well-known active contour models, but in addition to the image energy and internal energy the topology is introduced into the optimization process. This graph-based active contour method enables a complete topological and shape control during the object delineation. The method is applied to the geometric refinement of road networks to improve and correct GIS-databases as a basis for traffic navigation or infrastructure planning purposes. The proposed approach is either able to deal with roads from a database as initialization in an automatic system or, alternatively, within an interactive framework to derive a geometrically optimized road network. The derived results using SAR images are evaluated with reference data to demonstrate the benefit and transferability of network snakes. [C2242]

### "Characterization of full surface roughness in agricultural soils using groundbased LiDAR"

Microwave emission and scattering models require the parametrization of surface roughness. Traditionally this has been achieved by sampling the surface in transects. In this work, roughness is characterized from 3D surface models derived from ground-based LiDAR. The dataset consist 18 surfaces with varying roughness characteristics. 2D profiles extracted from the surface model constitute the baseline to compare to traditional profiling methods. It was found that sampling using profiles produces an underestimation of the RMS<sub>h</sub> by 25-63% and an even more severe underestimation in the correlation length that can reach up to an order of magnitude difference. From the 17,178 2D extracted profiles it was determined a significant sensitivity of the roughness parameters to the detrending methods, as well as a poor fit between the experimental ACF and the exponential and Gaussian models. Finally, methodologies to detrend quasi-periodic surfaces and the decomposition of surface at different scales are proposed and illustrate the advantage of having a 3D representation. [C2243]

### "Comparing data of two airborne L-band radiometers with different spatial resolution over a heterogeneous land surface"

This paper describes a first attempt of comparing data of the two airborne L-band radiometers EMIRAD and HUT-2D over land surface. While HUT-2D is an imaging system with a high spatial resolution, EMIRAD delivers data averaged over a relatively large footprint but can be considered to be more stable. The Upper Danube catchment, located mostly in Southern Germany, is one of two major test sites in Europe for the calibration and validation activities for the Soil Moisture and Ocean Salinity (SMOS) mission launched by the European Space Agency (ESA). For the study presented in this paper, the radiometric measurements collected during the SMOS Validation Rehearsal Campaign 2008 in the Upper Danube catchment are used. The results suggest that differences between the measurements are mainly controlled by temperature effects and can be limited by implementing a temperature correction in the processing of HUT-2D data. [C2244]

### "The NASA Soil Moisture Active Passive (SMAP) mission: Overview"

The Soil Moisture Active Passive (SMAP) mission is one of the first Earth observation satellites being developed by NASA in response to the National Research Council's Decadal Survey. Its mission design consists of L-band radiometer and radar instruments sharing a rotating 6-m mesh reflector antenna to provide high-resolution and high-accuracy global maps of soil moisture and freeze/thaw state every 2-3 days. The combined active/passive microwave soil moisture product will have a spatial resolution of 10 km and a mean latency of 24 hours. In addition, the SMAP surface observations will be combined with advanced modeling and data assimilation to provide deeper root zone soil moisture and net ecosystem exchange of carbon. SMAP is expected to launch in the late 2014-early 2015 time frame. [C2245]

### "Context-dependent landmine detection with ground-penetrating radar using a Hidden Markov Context Model"

Context-dependent approaches to landmine detection have been developed in recent years to exploit the sensitivity of ground-penetrating radar (GPR) to changes in environmental conditions. Previous approaches to context-dependent fusion have only considered the special case of statistically independent observations. This work proposes the use of Hidden Markov Models, trained on the GPR background, for modeling the context of observation sequences. The performances of context-dependent fusion using two statistical context models were compared in an experiment with field data. One approach utilized a Hidden Markov Context Model (HMCM), and the other utilized a Gaussian mixture. Experimental results illustrated that the HMCM improved performance of

context-dependent fusion. These results suggest that spatial dependencies are an important source of contextual information for landmine detection that warrants further investigation. [C2246]

### "Ka-band SAR interferometry studies for the SWOT mission"

The primary objective of the National Research Council (NRC) Decadal Survey recommended SWOT (Surface Water and Ocean Topography) Mission is to measure the water elevation of the global oceans, as well as terrestrial water bodies (such as rivers, lakes, reservoirs, and wetlands), to answer key scientific questions on the kinetic energy of ocean circulation, the spatial and temporal variability of the world's surface freshwater storage and discharge, and to provide societal benefits on predicting climate change, coastal zone management, flood prediction, and water resources management. In this paper, we present the overall concept of the SWOT mission, as well as the scientific rationale, objectives and development status of the technology items currently under development. [C2247]

### "Performance analysis of atmospheric correction in InSAR data based on the Weather Research and Forecasting Model (WRF)"

The influence of the turbulent atmosphere is seen as the main performance limitation for high-quality Interferometric Synthetic Aperture Radar (InSAR) techniques in ground deformation monitoring applications. Atmospheric correction using numerical weather prediction (NWP) models is widely seen as a promising emerging technology for mitigation of atmospheric signals. First results showed promising capabilities for correction of stratified delay yet have revealed limited performance for modeling and mitigating turbulent atmospheric water vapor signals from SAR [1, 2]. This paper presents an integration of InSAR observations with predictions from the high-resolution Weather Research and Forecasting Model (WRF). Special focus is put on investigating improvements in the weather model parameterization to achieve enhanced performance in atmospheric correction. First, a statistical analysis of the quality of absolute delay predictions is presented based on a comparison of vertically integrated WRF delays with radiosonde measurements. Second, the performance of WRF for atmospheric correction of InSAR data is analyzed by comparing WRF phase delay maps to SAR interferograms and analyzing structure functions and variances of the residual atmospheric delay signal. Here, significant improvements could be achieved through modifications of the WRF model parameterization, which are highlighted in Section 3.2. From our study, we conclude that the performance of latest generation high-resolution NWP models can be significantly improved if the setup and parameterization of the model domain is optimized. [C2248]

### "Multi-baseline along track SAR interferometric systems for ground moving target indication"

In this paper we analyze the performance of ground moving target detection by means of single-baseline and dual-baseline along track interferometric synthetic aperture radar (SAR) systems, obtained using a generalized likelihood ratio test (GLRT). Detection performance are evaluated in terms of probability of detection and probability of false alarm using data simulated with TerraSAR-X parameters. [C2249]

### "Improved Variable Index constant false alarm rate radar processors"

In the cases when the statistical distribution of range return samples are not known, constant false alarm rate (CFAR) processors can be used. Cell Averaging (CA) CFAR radar processors which have the best performance in Gaussian homogeneous environments, exhibits performance degradation in the presence of an interfering target or in regions of abrupt change in the background clutter power. The Greatest of (GO) CFAR radar processors are designed to control the false alarm rate, during the clutter power transition in the reference window (non-homogeneous clutter environment). The Smallest of (SO) CFAR radar processors improve detection performance when interfering targets exist in the environment but are unable to prevent excessive false alarm in non-homogeneous environments. Variable Index (VI) CFAR processors employ a composite approach based on CA-CFAR, SO-CFAR, GO-CFAR. Enhanced VI-CFAR (EVI-CFAR) radar processors proposed in this paper, shows performance improvement in different non-homogeneous environments when compared with VI-CFAR. [C2250]

### "Advanced techniques and new high resolution SAR sensors for monitoring urban areas"

In the last years MultiDimensional (3D and 4D) Synthetic Aperture Radar (SAR) techniques, also known as SAR tomography and differential SAR tomography, are emerging in the field of coherent combination of multibaseline/multitemporal SAR data. With respect to the classical differential interferometric processing, these techniques improve the capability of detection and monitoring of the ground targets. Moreover they were proven to be effective in resolving the signal interference due to the layover effect, that may occur in areas with high density of scatterers located on vertical structures, such as urban areas. Beside the development of these advanced techniques the new generation of sensor, such as TerraSAR-X and COSMO-SKYMED with very high



spatial resolution offer new perspectives in the imaging and monitoring of urban areas. In this paper we address the application of the SAR tomography to real spaceborne data. Particularly, we show and discuss the first results of the application of this technique to high resolution TerraSAR-X data. [C2251]

#### "Monitoring grasslands with radarsat 2 quad-pol imagery"

Radarsat 2 quad polarization imagery has been used to study the effectiveness of polarimetric radar to monitor the extent and health of prairie grasslands in southern Alberta, Canada. In this report of preliminary findings, the imagery is shown to be effective in the separation of cropped lands from rangelands, and in the separation of native grasslands and improved pastures. Classification was more accurate using Freeman-Durden decomposition parameters than using Cloude-Pottier parameters. Incidence angle differences were noted and use of multiple angles in classification improved accuracy. In a second part of the study, it was shown that polarimetric imagery was capable of identifying weeds and brush growing in native rangeland, and in separating different kinds of brush and weeds. Validated sample sets were too small to allow proper accuracy assessment, but a 'performance metric' showed that accuracy would be improved by use of multiple incidence angles, and by the use of Freeman-Durden or coherency matrix parameters. [C2252]

#### "DESDynI lidar for solid earth applications"

As part of the NASA's DESDynI mission, global elevation profiles from contiguous 25 m footprint Lidar measurements will be made. Here we present results of a performance simulation of a single pass of the multi-beam Lidar instrument over uplifted marine terraces in southern Alaska. The significance of the Lidar simulations is that surface topography would be captured at sufficient resolution for mapping uplifted terraces features but it will be hard to discern 1-2m topographic change over features less than tens of meters in width. Since Lidar would penetrate most vegetation, the accurate bare Earth elevation profiles will give new elevation information beyond the standard 30-m DEM. [C2253]

#### "Studies of the influence of rainfall upon scatterometer estimates for sea surface stress: Applications to boundary layer parameterization and drag coefficient models within tropical cyclone environments"

The use of satellite scatterometers to probe the winds in and near strong tropical cyclones (TCs) is a valuable tool for both numerical weather prediction (NWP) and weather forecasters. The presence of widespread rain in these storms complicates the estimation of surface winds from the satellite. Improvements in the techniques to infer surface winds from the satellite observations, which remove the effects of rain contamination at the ocean surface, will improve the modeling efforts as they pertain to the prediction of TC intensity. This study will demonstrate the use of collated and simultaneous high-resolution rain measurements obtained from nearby Next-Generation Radar (NEXRAD) and NASA Quick Scatterometer (QuikSCAT) measurements, respectively. Through the application of the National Oceanic and Atmospheric Administration (NOAA)/Atlantic Oceanographic and Meteorological Laboratories (AOML)/Hurricane Research Division (HRD) TC wind analysis (H\*WIND; Powell and Houston [1996]), we will study the dependence of a surface normalized radar cross-section (NRCS) on the TC wind-speed and rain-rate. The objective is to better observe and understand the dependence of the drag coefficient upon the surface stress across a wide range of conditions and spatial scales within these storms. [C2254]

#### "Multi beam joined estimation for persistent scatterer interferometry"

The persistent scatterer interferometry (PSI) is a powerful technique to monitor the line of sight (LOS) deformation with millimeter accuracy in urban areas. Nowadays, this technique is well established for the sensors ERS and Envisat/ASAR. Nevertheless, the availability of high resolution SAR sensors enables new applications which require new estimation principles. Application test cases for the sensor TerraSAR-X were demonstrated already. However, the high resolution data are not really fully exploited at the moment. This paper describes a newly developed PSI estimation principle which improves the spatial resolution by the support of distributed scatterers and increases the temporal sampling by the joined estimation of different beams. The prototyped technique needs to cope with the different projections of the horizontal and vertical deformation components onto the line of sight (LOS). Basically, this allows the inversion of the beam's observation equation and finally retrieves the vertical and horizontal deformation components. [C2255]

#### "Iterative calibration of relative platform position: A new method for SAR baseline estimation"

Baseline calibration is needed in most of SAR interferometry processing. An iterative optimization of baseline with constrain of relative platform position is presented in this paper. The SAR passes which gives inaccurate

platform position is successfully detected and calibrated using this algorithm. After processing, new estimated baseline improves the quality of interferogram. Existence of reference Digital Elevation Model (DEM) error and atmospheric phase screen (APS) can also be detected from the convergence value. This method is based on a reversed concept of platform position estimation from interferometric result. Validation of method performed on multiple SAR images over Singapore. [C2256]

#### "Multibaseline gradient ambiguity resolution to support Minimum Cost Flow Phase Unwrapping"

The TanDEM-X Mission has as primary objective to generate a high resolution global Digital Elevation Model. This paper proposes a new method for multibaseline Phase Unwrapping which is the critical point of this generation. We propose to combine both Minimum Cost Flow (MCF) and Maximum a Posteriori (MAP) estimation. The latter is used to solve phase gradient ambiguities. The problem is posed as an energy minimization one and solved using Belief Propagation (BP) which is an iterative process. Nevertheless, although very good results are obtained on loopy graphs, it is not guaranteed to converge. Thus, phase unwrapping of the most accurate interferogram is finally performed with the MCF algorithm and takes as input the unwrapped gradients. [C2257]

#### "Range-Doppler ambiguity mitigation via closed-loop, adaptive PRF selection"

In this paper, we present a method of calculating and updating target probabilities in ambiguous range-Doppler cells along with an adaptive pulse repetition frequency (PRF) selection technique based on mutual information (MI). We approach the problem of updating the probability in multiple ambiguous cells by using a multiple hypothesis test for the target state. The probability ensemble is then used to determine which PRF will maximize MI on the next update. Since MI is a measure of the reduction in entropy of the ensemble, it indicates the amount of information the radar stands to learn about the channel due to the selected PRF. We compare the results of MI-based PRF selection to two other PRF selection methods and demonstrate how blind zones and clutter aliasing can be seamlessly integrated into our PRF-selection procedure. [C2258]

#### "Performance of cell averaging constant false alarm rate (CA-CFAR) processors for M-correlated sweeps in multiple target environments"

In this paper, the detection performance of CA-CFAR processor is analysed for M-correlated sweeps in Gaussian clutter environment which contains interfering targets. The performance analyses are done for different number of sweeps, M, and sweep-to-sweep correlation coefficient, R, with Swerling-I target model in homogeneous and non-homogeneous environments. [C2259]

#### "Phase retrieval in SAR interferograms using diffusion and inpainting"

A high-contrast inpainting scheme based on the Complex Ginzburg-Landau equation recently applied successfully to image restoration is applied to SAR interferograms to improve their quality and therefore final quality of Digital Elevation Models (DEMs). The new technique attempts to recover the phase values in low coherence regions through diffusion and inpainting. After phase unwrapping low coherence regions are masked and discarded and a Complex Ginzburg-Landau (CGL) inpainting scheme is applied to regions where phase values are missing. We demonstrate that the residues reduce and the proposed algorithm leads to a higher Signal-to-Noise Ratio (SNR) if compared with MCF algorithm. The restoration technique has been applied to ERS-1 and ERS-2 data sets acquired on July 1995. Results appear to be very promising: the proposed algorithm provides good performances especially in presence of strong noise level and low coherence areas with relatively small dimensions. [C2260]

#### "Successive cancellation approach for Doppler frequency estimation in pulse Doppler radar systems"

In this paper, a successive cancellation approach is proposed to estimate Doppler frequencies of targets in pulse Doppler radar systems. This technique utilizes the Doppler domain waveform structure of the received signal coming from a point target after matched filtering and pulse Doppler processing steps. The proposed technique is an iterative algorithm. In each iteration, a target that minimizes a cost function is found, and the signal coming from that target is subtracted from the total received signal. These steps are repeated until there are no more targets. The global minimum value of the cost function in each iteration is found via particle swarm optimization (PSO). Performance of this technique is compared with the optimal maximum likelihood solution for various signal-to-noise ratio (SNR) values based on Monte Carlo simulations. [C2261]

#### "The bistatic electromagnetic signature of heterogeneous sea surface: Study of the hydrodynamic

### phenomena"

In this article, we carried out a preliminary study on the hydrodynamic effect (non-linear) produced by the breaking of a coastal wave on the scattering coefficient (in horizontal and vertical polarization) in the bi-static configuration (forward propagation). We calculated in X-band (10 GHz)  $\sigma_{HH}$  and  $\sigma_{VV}$  of a series of oceanic surfaces (different phases of construction of a breaking wave ( $\theta_i = -20^\circ$ )) then we studied the different characteristics for each scattering coefficients. In this first study we considered that the maritime surface is the perfect conductor. [C2262]

### "Disaster mapping from medium spatial resolution alos palsar images"

All-day and all-weather Synthetic Aperture Radar (SAR) can measure both intensity and phase of the reflected signal. The backscattering coefficients measured by SAR reflect the backscatter characteristics of surface targets. Changes happened to a target's surface roughness, geometric and structural characteristics will result in the change of its backscattering intensity recorded in SAR image. The 2008 Wenchuan earthquake, China have caused widely distributed geological disasters, such as landslides, mudfloods and barrier lakes, which resulted in the difference between pre- and post-earthquake SAR images. Comparison between the pre- and post-earthquake SAR intensity images will reveal the damage information. In this study, PALSAR Level 1.0 data acquired for the Wenchuan earthquake were used to analyze the geological disasters. Results show that medium spatial resolution SAR data, such as 10 m resolution ALOS PALSAR data, especially when both pre- and post-earthquake images are available, are useful in revealing the distribution of landslides and barrier lakes. [C2263]

### "A modified wind vector retrieval algorithm for polarimetric scatterometer"

Experiments and theoretical analysis demonstrate that the polarimetric scatterometer has the potential in enhancing the accuracy of the wind vector retrieval. However, currently, there is no special wind vector retrieval algorithm for the polarimetric scatterometer. Based on the distribution characteristic of the objective function, a modified wind vector retrieval algorithm was designed for the conically scanning polarimetric scatterometer in this paper. Simulation experiments indicated that this algorithm could further improve the retrieval precision of the polarimetric scatterometer in comparison with the traditional algorithm, especially in the nadir- and outer-swath. By extending the wind direction range for the first and second ambiguity in the nadir- and outer-swath, the algorithm can effectively reduce the uncertainty of the wind direction solutions with error magnitude of  $0^\circ$  to  $15^\circ$ . Up to  $2^\circ$  improvement in wind direction retrieval can be achieved in the nadir track. [C2264]

### "Status, results, potentiality and evolution of COSMO-SkyMed, the Italian Earth Observation constellation for risk management and security"

COSMO-SkyMed is a Dual-Use program, devoted to produce both civilian and military applications, and as such it is required to have a fast response time, to manage conflicts and to optimize resources. In order to provide operational continuity to COSMO-SkyMed mission, the Italian Space Agency (ASI) and Italian Ministry of Defense (It-MoD) are conceiving the next generation of the system. The new system, called "COSMO-SkyMed Seconda Generazione" (CSG), starting from the well established design of the first generation, will provide the end user with outstanding characteristics consolidating its position in the frame of SAR Systems. After a description of the current COSMO-SkyMed unique in-orbit performances, functionalities and Dual-Use operations, with examples of data already acquired in the last few years, the paper will introduce the CSG mission describing the main features and capabilities that will drive the design of the new system. [C2265]

### "One-day interferometry results with the COSMO-SkyMed constellation"

COSMO-SkyMed is a Dual-Use (Civilian and Defence) End-to-End Earth Observation System aimed at establishing a global service supplying provision of data, products and services relevant to a wide range of applications, such as Risk Management, Scientific and Commercial Applications and Defence Applications. The system consists of a constellation of four LEO mid-sized satellites, each equipped with a multi-mode high-resolution SAR operating at X-band. Three out of four COSMO-SkyMed satellites have been successfully launched, while the remaining satellite will be deployed within 2010. The first two satellites have been launched in 2007 while COSMO-SkyMed-3 has been launched on October 25th 2008. Since its launch COSMO-SkyMed-3 has been put in an orbital position at  $67,5^\circ$  from COSMO-SkyMed-2, in the so-called "one-day interferometry configuration". Since then COSMO-SkyMed-2 and COSMO-SkyMed-3 are providing a interferometric pairs for a wide range of applications. [C2266]

### "Comparison of Beijing-Tianjin Intercity Railway deformation monitoring results between ASAR and

### **PALSAR data"**

First comparison experiments by different datasets were done to estimate the subsidence pattern of China Beijing-Tianjin Intercity Railway roadbed in Tianjin area in this paper. The multi-baseline differential synthetic aperture radar interferometry technique was used to give the subsidence monitoring. During the period of middle 2008 to middle 2009, the experiment results show that the roadbed is relative stable during the first year running of the Intercity Railway. And the comparison analyses show that both experiment results give the same subsidence rate pattern along the roadbed corridor, meanwhile the PALSAR results give better railway imaged but larger subsidence velocity standard deviation. [C2267]

### **"The mathematic model of multipath error in airborne interferometric SAR system"**

In airborne two-antenna interferometric SAR system, the returned pulse may be reflected by parts of the aircraft platform into the antennas, and this is called multipath effect which will cause oscillating phase errors and hence height errors. This paper presents a theoretical model to compute the multipath error. In this model the multipath phase error is a function of look angle or ideal phase, and the unknown parameters of the model can be estimated from distributed targets with known elevation. On the basis of the model, a method and processing procedure can be used to correct multipath error effectively, and this paper illustrates its successful application to interferometric SAR data collected by Institute of Electronics, Chinese Academy of Sciences. [C2268]

### **"Detection of rapid land subsidence of civil constructions with TerraSAR-X interferometry"**

The TerraSAR-X SAR system provides high spatial resolution and geometric accuracy imagery which supports well the mapping of the 3-D structure of large-scale civil infrastructure and its motions (4-D). In this work, we investigated the potential of TerraSAR-X observations for monitoring rapid land subsidence induced by reclamation activities. A case study was conducted in Hong Kong Disneyland Theme Park (DTP) at the Penny's Bay, one of the largest land reclamation projects worldwide. A total of 16 TerraSAR-X scenes were used in a small-baseline PSI method for retrieving residual reclamation settlement in the study area. The preliminary results indicate that a remarkably high density of high coherent point targets ( $>2,500$  PS point/km<sup>2</sup>) was identified in the reclamation area and a large land subsidence rate on the order of 35 cm/yr could be detected in the center of reclaimed land. The high detail level of deformation field as well as the high sensitivity regarding rapid residual settlement makes TerraSAR-X interferometry a remarkable potential Earth Observation technique to enable the detection of ground deformation related to the large-scale infrastructure development in reclaimed land. [C2269]

### **"CFAR detection based on decision fusion of order statistic CFAR and order statistic clutter map CFAR processors"**

In automatic target detection radars, adaptive constant false alarm rate (CFAR) processors, which determine the threshold, are examined. Two techniques are used for achieving the required CFAR. The first technique determines the adaptive threshold using range neighbouring cells which are located in sliding window. The second one is based on clutter map. In this technique, adaptive threshold is determined using the samples of test cell from previous scans which are assumed to contain no target. In this study, new techniques based on combining the two techniques in the data fusion system (DFS), are proposed. Analytical equations for homogeneous and nonhomogeneous environment are derived and performance analysis are carried out. [C2270]

### **"Estimation and compensation of ionospheric delay for SAR interferometry"**

For spaceborne SAR (Synthetic Aperture Radar) systems, the dispersive effects of the ionosphere on the propagation of the SAR signal can be a significant source of phase error. While at X-band frequencies the effects are small, current and future L-band systems would benefit from ionospheric compensation. We consider two ways to estimate the ionospheric delay in SAR signals and evaluate them on L-band ALOS-PALSAR acquisitions. [C2271]

### **"Two-Thresholds CFAR detection of the range-spread target based on scattering centers accumulation"**

This paper concerns the detection algorithms based on the HRR component of detecting range spread target in white Gaussian noise and designs a detector. By setting a higher false alarm probability, we can obtain the first threshold and the information of the target scattering centers. Then we accumulate the energy of the cell with a scattering center and make use of the energy accumulation as the test statistic. The proposed detector shows a better performance compared with that of the integration detector and two-threshold GLRT detector for all the matched filter input SNR for a small value of the  $N_c$  and almost equals that of the Integration detector for a large



value of the  $N_c$ . Both of the proposed detector and the Integration detector lose a little dB of the SNR comparing the BS\_CLRT detector while the SNR below -30dB for a small  $N_c$ . The proposed detector could be applicable to the target with few scattering centers and propitious to the practical radar systems because of the general targets only with several scattering centers. [C2272]

#### "ISAR imaging analysis of Bistatic FMCW radar"

This paper studies the basic issue of Bistatic ISAR imaging using FMCW radar under the model of Bistatic radar systems. Firstly, the echo signal of FMCW radar which in Bistatic system is analyzed, the coupling terms of range fast time and azimuth slow time which including uniquely in FMCW signal are extracted from the phase of echo signal; then its forms in range Doppler domain and influences to range profile are analyzed; Simultaneously the corresponding compensation algorithm is applied to compensate the coupling terms. The last simulations show that the proposed compensation algorithm in this paper improves the defocus phenomenon which caused by using FMJCW signal and can achieve good imaging of targets. [C2273]

#### "Simulation modelling the GPS signal propagation in the tropospheric ducts"

This paper presents a thorough research on the GPS (Global Positioning System) signal propagation in the tropospheric ducts with ray tracing approach and the split-step parabolic equation (SSPE) method. In recent years, radio wave propagation in the troposphere has been attended extensively by many researchers, especially for the radio wave propagation in the ducting environment and its effect on radar system and electronic system. Generally, strong gradients of humidity and temperature can be observed closely to the air-water interface leading to anomalous propagation effects such as atmospheric ducting. Radio system and radar of maritime operation are greatly influenced by the existence of atmospheric ducts, it can give a rise to over-the-horizon detection and form the radar detection shadow zone. This paper introduced the GPS signal as the initial field by the PE method to study the electromagnetic wave propagation characteristics in the tropospheric ducts, and given the results by the ray tracing approach as comparison at the same time. [C2274]

#### "A fast and robust method for target and background estimation in RCS measurements based on 'hyperaccurate' algebraic circle fit"

The sample data points, which are obtained in radar cross section (RCS) measurement, will distribute theoretically on a circle when the target moving along the direction of the illuminating plane wave. The radius of the circle represents the target signal and the center of the circle represents the background signal. Based on theoretical analysis and numerical simulation, we have implemented the fast 'hyperaccurate' algebra circle fitting algorithms to fit circles to measurement data points. At the same time, a robust least-median-of-squares method has been implemented to eliminate the outliers. According to the fitting accuracy requirement of the target and background, the sampling number and the sampling range are determined. Two different spheres are measured with this algorithm in Compact Antenna Test Range (CATR) and their target signals and background signals are well separated, which improves the measurement accuracy. [C2275]

#### "An improved PGA algorithm for ionosphere phase perturbation correction"

Ionosphere phase perturbation destroys the coherence of echo signal for sky-wave Over-The-Horizon Radar (OTHR) and broadens the spectrum of signal and clutter, which will exacerbate the property of low-speed object detection. PGA (Phase Gradient Autofocus) is an excellent perturbation correction algorithm with properties of logical, concise, robust etc for various perturbations. In particular, it will reduce computation work enormously. However, the estimate accuracy of PGA is degraded when the Bragg peak filter bandwidth is selected improperly, or the zero frequency components are not acquired exactly, then the iteration times should be increased. An improved PGA is proposed for ionosphere phase perturbation correction, which can realize adaptive selection of the first order clutter filter bandwidth. At the same time, a method of zero frequency abstraction based on Bragg frequencies symmetry is presented, which can decrease iteration times with same perturbation function estimate accuracy and higher computation efficiency. [C2276]

#### "Comparison of TEC measurements from DORIS with the NeQuick model"

Doppler Orbitography and Radio positioning Integrated by Satellite (DORIS) is a high precision satellite orbit determination and ranging system based on Doppler shift measurements from dual frequency signals propagated between ground stations and a satellite. The Doppler shift measured on the 2.036GHz signal and an additional 401.25MHz is a very potential means for scientific researches on ionosphere. In this paper, global Total Electron Content (TEC) measuring principle of the DORIS system is analyzed, and an algorithm is presented to derive the space variations of TEC from the DORIS ionospheric correction data. Finally comparison of TEC latitudinal profiles are done to with the NeQuick model. And some advices on the improvement of the DORIS system are

put forward for advantaging ionospheric sounding and tropospheric sounding. [C2277]

### "Influence of rain Doppler frequency on MMW Doppler fuze"

Guided weapon systems require a proximity fuze device to trigger the explosive warhead. Various proximity fuze types are currently employed. The millimeter wave (MMW) radio Doppler fuze is a potential advantage system, and it is required for a wide range of military application. In this paper, the MMW fuze Doppler Effect is discussed in the encounter course of fuze and target. The target Doppler frequencies (DF) caused by the target moving relative to fuze are calculated at 35 and 95GHz. The relationship of the target DF with the distance between fuze and target is obtained. The rain Doppler frequencies induced by the volumetric rain medium for the interested rain area around target moving relative to fuze are calculated at 35 and 95GHz. The relation of the rain DF with the distance between fuze and the interested rain area are given. The influences of rain DF on target DF are analyzed. It is shown that when the distance between fuze and target is less than about 30m, the difference between the rain DF and the target DF decrease gradually with the distance decreasing. The influences of rain DF clutter on target DF information become gradually bigger with the distance approach, especially, for heavier rainfall, a smaller target and a wider fuze radar beam. Therefore, when the encounter distance between fuze and target is less than about 30m, the influence of the rain Doppler clutter on the target Doppler signal is severe, and need be considered for the MMW Doppler fuze application. [C2278]

### "A novel polarimetric FM-CW radar system for laboratory remote sensing experiments"

With the advantage of compact, low cost and high resolution, the frequency-modulated continuous wave (FM-CW) radar equipped in airborne or unmanned aerial vehicles (UAVs) has been well applied to small-scale remote sensing measurements. To make laboratory experiment, our Key Laboratory of Wave Scattering and Remote Sensing Information (KLWSRSI) has developed a fully polarimetric FM-CW synthetic aperture radar (SAR) system. This system can be applied to analysis and demonstration of targets scattering mechanism and polarimetric radar imaging. [C2279]

### "Application of AWE to scattering analysis of the double-negative medium"

The PMCHWT equation of the double negative media (DNG) is obtained based on its constitutive relationship. And the surface currents and radar cross section (RCS) at a single frequency point is computed by Method of moments (MOM). The asymptotic waveform evaluation (AWE) technique for dispersive dielectric medium is deduced and applied to electromagnetic scattering analysis of double-negative medium within a given frequency band. [C2280]

### "Doppler profile estimation in VHF radar signals using wavelets"

The wind profile estimations are the fundamental objective of the Indian MST radar with the received signal ranging from nearly 3.5-25 Km height. A widely accepted narrow band model is considered, for the analysis of the signal received. Though the received signal SNR is stronger at lower altitudes, as the height progresses the strength becomes feeble and the noise dominates the received signal. The classical Time-Frequency analysis is made on the received signal from different altitudes and observed that the zero Doppler influence is significant at higher altitudes along with the noise. A Hilbert transform based DC bias removal is proposed in contrast with the existing 3 point MA technique. To handle the noise, in particular at higher altitudes a wavelet based adaptive denoising is proposed and found satisfactorily for the spectral cleaning of the Doppler spectrum. The validation of the proposed algorithm is made with the GPS data. [C2281]

### "Influence of the CNT length on complex permittivity of composite laminates and on radar absorber design in X-band"

Due to the high aspect ratio, CNT dispersed in polymer matrix composites makes large electric dipoles bringing about high dielectric constant, as well as dense percolation networks for electric conductivity. The length scale of the CNT has the definite influence on the internal structures of percolation networks, affecting the characteristics complex permittivity of the composites. In a Dajllenbach type radar absorber made of a dielectric composite, the optimal thickness of lossy layer is dependent on the characteristics of complex permittivity. In this work, radar absorbers composed of E-glass composite laminates with CNTs of different length scales were developed in X-band. The design result demonstrates the influence of the CNT length on complex permittivity of composite laminates and on microwave absorber characteristics. [C2282]

### "High resolution radar imaging based on compressed sensing using sparse stepped-frequency signal"

In the face of sparse aperture data imaging, a method for high resolution radar imaging based on compressed sensing using sparse stepped-frequency signal is proposed in this letter. In the signal stretching process, high resolution target echo can be acquired through second sample for the coarse-resolution range profile. Based on the sparsity of the signal in the spectrogram, we can construct a reasonable partial fourier sparse basis matrix to realize the sparsity of radar data. Then, the high-resolution range profile information is recovered by using the Orthogonal Matching Pursuit (OMP) algorithm, and the high resolution target imaging can be gained whose target sidelobe is suppressed efficiently. Finally, the results with simulation data validate the feasibility and superiority of the approach. [C2283]

#### **"Algorithm optimization of piecewise polynomial modeling for ionospheric perturbation correction"**

Ionosphere phase perturbation made the clutter spectrum spread and influenced the precision of parameter inverse analysis for sky wave sea state radar. Recently, an algorithm based on piecewise polynomial signal (PPS) phase model and high-order ambiguity function has been applied to resolve this problem. The determination of the order for the polynomial phase is critical in the applications of the algorithm. Two order-selecting methods based on self-adaptive polynomial model are proposed and verified by simulation. The results indicated that the new methods (frequency-domain and time-domain) based on the characteristics of high-order ambiguity function (HAF) transformation improved greatly in accuracy and that the amount of calculation is reduced. The polynomial order can be judged exactly, especially at low signal-to-noise ratio (SNR) when employing the frequency-domain method. [C2284]

#### **"Numerical simulation of GPR based on 3-D high-order FDTD"**

The high-order finite-difference time-domain (HO-FDTD) technique is used in the simulation of ground-penetrating radar modeling in three dimensions (3-D), which can improve accuracy and reduce the error caused by numerical dispersion effectively. To absorb waves reflected from edges we implement convolutional perfectly matched layer (CPML) absorbing boundaries. It can efficiently absorb the reflections and greatly increase the computation efficiency. The surface-based reflection and cross-hole GPR modeling are simulated, and numerical results show the efficiency of the method. [C2285]

#### **"Impacts of velocity deviation on spaceborne high-resolution DPCA SAR"**

Synthetic aperture radar (SAR) based on displaced phase center azimuth multi-beam (DPCA) allows for high-resolution wide-swath imaging, which can overcome the inherent limitation of conventional single-aperture SAR. However, to obtain a uniform sampling distribution in the azimuth direction, the system parameters must fulfill a stringent requirement. Velocity or pulse repetition frequency (PRF) deviation will result in a nonuniform sampling in the azimuth direction. To resolve this problem, multichannel reconstruction algorithms are often employed. In this paper, the periodic nonuniform sampling in the azimuth direction caused by velocity deviation is investigated and the impacts on imaging performance of spaceborne DPCA SAR are analyzed. Simulation examples and simulation results are also provided. [C2286]

#### **"A New Method of Bridge Target Detection on ASAR Imagery"**

The result of linear target detection is advantageous to the content analysis and interpretation of ASAR imagery and can be regarded as the imagery matching reference as well as the GIS platform input to realize the map automatic update. On the foundation of the previous studies, the method of bridge target detection based on Combined wavelet transformation and mathematical morphology analysis is proposed according to the good local characteristic, multi-resolution and effectiveness of wavelet transformation in this article, and the result is revised by combining the fine characteristics of different methods, which is applied to ASAR data of Zhaoqing and Zhuhai of China for carrying on the bridge detection as well as the comparative experiment with classical methods, such as Sobel and Canny etc detection operators. Results indicate that the combined methods can detect the target bridge perfectly on the direction and size, at the same time can restrain the target missing and false warning. [C2287]

#### **"MATLAB COM Component in Radar Signal Processing Application Development"**

There are amount of calculations come down to arithmetic when we develop programs of radar signal processing. These programs are developed under higher languages. These languages are inefficient on calculations and their arithmetic are not enough well-rounded. MATLAB is used for calculations and arithmetic, and the arithmetic in it is well-rounded and steady, so the development is efficient. But it must be under the MATLAB environment. The "All-purpose Function" method is introduced according to the existing COM-based MATLAB and Delphi mixed programming. This method not only increases programming efficiency but also enhances readability of code. [C2288]

### "An efficient approach for near-field three-dimensional imaging radar"

Linear array antennas (LAA) synthetic aperture radar (SAR) three-dimensional (3D) imaging has received a vibrant identification in recent years. This paper proposes a digital-beam forming (DBF)-based three-dimensional imaging algorithm for linear array antennas downward-looking synthetic aperture radar with single-transmitting and multiple-receiving (STMR) configuration. To establish the radar echo signal and to simplify the signal processing performance of imaging algorithm, equivalent phase centers are applied to simplify the range-history into monostatic configuration; then, parabola approximation is applied to decouple the three orthogonal variables which coupled to each other. Unlike traditional RMA 3D imaging algorithm imaging the scenario point to point, algorithm proposed by this paper processes the image in batch regardless the location of targets as 2D range-Doppler Algorithm does. Finally, we carried out the simulation and analysis on phase error to validate the feasibility of this algorithm. [C2289]

### "Texture-Based Estimation of Physical Characteristics of Sand Grains"

The common occurrence and transportability of quartz sand grains make them useful for forensic analysis, providing that grains can be accurately and consistently designated into prespecified types. Recent advances in the analysis of surface texture features found in scanning electron microscopy images of such grains have advanced this process. However, this requires expert knowledge that is not only time intensive, but also rare, meaning that automation is a highly attractive prospect if it were possible to achieve good levels of performance. Basic Image Feature Columns (BIF Columns), which use local symmetry type to produce a highly invariant yet distinctive encoding, have shown leading performance in standard texture recognition tasks used in computer vision. However, the system has not previously been tested on a real world problem. Here we demonstrate that the BIF Column system offers a simple yet effective solution to grain classification using surface texture. In a two class problem, where human level performance is expected to be perfect, the system classifies all but one grain from a sample of 88 correctly. In a harder task, where expert human performance is expected to be significantly less than perfect, our system achieves a correct classification rate of over 80%, with clear indications that performance can be improved if a larger dataset were available. Furthermore, very little tuning or adaptation has been necessary to achieve these results giving cause for optimism in the general applicability of this system to other texture classification problems in forensic analysis. [C2290]

### "Pulse Repetition Interval Modulation Recognition Using Symbolization"

Information on the pulse repetition interval (PRI) modulation of a radar signal plays an important role in detecting and identifying each radar signal in an electronic warfare support (ES) system. In this paper, we present a new method for recognizing the PRI modulation type of a radar signal using symbolization. The proposed method uses three key feature parameters extracted from symbol sequences in order to discriminate each PRI modulation type. The recognition capability of the method presented is verified through extensive simulations. [C2291]

### "Mining Heterogeneous ADS-B Data Sets for Probabilistic Models of Pilot Behavior"

The University of North Dakota is developing airspace within the state where Unmanned Aircraft Systems (UASs) can be flown without an onboard sense and avoid system or Temporary Flight Restrictions (TFRs). With funding from the U.S. Air Force, a mobile ground-based radar system capable of detecting aircraft operating in Class E airspace and the software to display such information to UAS operators is being developed. The current system uses an Automatic Dependent Surveillance-Broadcast (ADS-B) transceiver to detect any ADS-B-equipped aircraft within the vicinity, and a Ground Control Station (GCS) to detect and control the UAS. Once one or more ground-based radars are integrated into the system, it will also be capable of detecting non-cooperative aircraft (i.e. aircraft that aren't equipped with ADS-B transceivers) operating within the vicinity. The current system uses a portable, high-availability architecture. Since the system is intended to detect potential airspace conflicts from the ground, greater computational power is available to it than to onboard sense and avoid systems. The probability of a midair collision is dependent on the proximity of aircraft to each other, the performance characteristics of the aircraft, and the probabilities of pilots performing basic maneuvers with the aircraft. In this paper the authors present the results of data mining an ADS-B data set from 11 days in early 2010. Probabilistic models of pilot behavior were automatically extracted from the data using a genetic algorithm for cluster analysis. [C2292]

### "Evolutionary approach for trajectory generation of unmanned aerial vehicles (UAVs) over hostile terrain"

This research focuses on point-to-point path generation algorithms that take into account the stealthiness of



autonomous UAVs; generating stealthy paths through a region laden with enemy radars. The proposed approach assumes that the UAV has detailed information of the environment and the enemy radars in its vicinity. The evolutionary approach involves generating a preliminary cost-effective path consisting of a series of straight-line segments. The actual trajectory of the UAV is then refined using a series of cubic splines in lieu of the straight line segments, resulting in a cost-effective path traceable by the UAVs. The shape of the trajectory is approximated using cubic B-splines. Simulated results are presented, illustrating the potential benefits of such algorithms. [C2293]

#### **"Research on remote wireless monitoring system based on GPRS and MCU"**

In the remote, hazardous, distributed and external environment, such as radiation source, pollutant source and pipeline of petrol, water and gas, it is difficult to collect and send the necessary message in real-time by traditional monitoring ways. In response to this demand, this paper presents the design of wireless remote monitoring system solution that is based on the GPRS(General Packet Radio Service)and the MCU(Micro-programmed Control Unit). The reliability and real-time performance of the system have been proved through practical application in the engineering project. [C2294]

#### **"A study on optical reflectivity of laser treated aircraft surfaces"**

For UAVs on mission that involve flights into region or environment with radar detection systems, the risk of detection of the UAVs is inevitable. The situation is detrimental particularly if the flight space of the UAV is in hostile region. Various computational methods have been proposed to show positive results in mitigating the risk of radar detection. Another potential avenue to improve on the risk of radar exposure is through modification of the vehicle's surface texture to reduce the optical reflectivity. In this paper, we consider the use of laser texturing as a means to enhance the stealth of a UAV carrying mission in a hostile territory. Although the results are preliminary, they gave a clear indication of the potential of laser texturing in stealth mission planning. In general, the results show that the roughness measured in terms of depth of the grooves patterned onto the surface has a direct correlation to the surface reflectivity. [C2295]

#### **"Research and implementation of dechirp pulse compression processing algorithm"**

In the processing of digital pulse compression for wideband LFM (Linear Frequency Modulation) signal, the dechirp algorithm can effectively reduce the sampling frequency and then reduce the pressure upon following signal processing and storage. By means of theoretical simulations, this paper analyses how to choose the sampling frequency for dechirp pulse compression system, and demonstrates the factors affecting dechirp performance-sampling frequency, time delay and imbalanced SNR. Besides, we implement a dechirp algorithm on FPGA platform and provide a reference of how to choose signal bandwidth, sampling frequency and the appropriate digital pulse processing method in the design of radar system. [C2296]

#### **"An evolutionary algorithm for multiple waypoints planning with B-spline trajectory generation for Unmanned Aerial Vehicles (UAVs)"**

In this work, we focus on multiple waypoints planning that take into account the stealthiness of autonomous UAVs; generating stealthy waypoints through a region laden with enemy radars. The important goal of waypoint planning for Unmanned Aerial Vehicles (UAVs) is to generate an optimal path for UAVs to visit all of the specified waypoints. We use the Traveling Salesman Problems (TSP) optimization to solve the visitation sequence planning problem for UAVs. The aim is to find the optimal solution that minimizes the distance travelled by the UAVs with low radar risk; under the strict constraints that each waypoint is visited exactly once by the UAVs, and the flying altitude does not exceed the specified threshold so as to minimize the radar exposure. The generated solution is then refined using a series of cubic splines in lieu of the straight line segments, resulting in a cost-effective path traceable by the UAVs. The shape of the trajectory is approximated using cubic B-splines. Simulated results are presented, illustrating the potential benefits of such approach. [C2297]

#### **"Multi-objective design of monopulse antenna with Two-lbests based multi-objective particle swarm optimizer"**

Monopulse antennas form an important methodology of realizing tracking radar and they are based on the simultaneous comparison of sum and difference signals to compute the angle-error and to steer the antenna patterns in the direction of the target (i.e., the boresight direction). In this study, we consider the synthesis problem of difference patterns in monopulse antennas from the perspective of Multi-objective Optimization (MO). The synthesis problem is recast as an MO problem, where the Maximum Side-Lobe Level (MSLL) and Beam

Width (BW) of principal lobe are taken as the two objectives to be minimized simultaneously. The approached Pareto Fronts are obtained for different number of elements and subarrays using the Two-lbests based multi-objective particle swarm optimizer (2LB-MOPSO). The quality of solutions obtained is compared with the help of Pareto Fronts on the basis of the two objectives to investigate the dependence of the number of elements and the number of sub-arrays on the final solution. Then we find the best compromise solutions for 20 element array and compare the results with standard single objective Particle Swarm Optimization (PSO) that has been reported in literature so far for the synthesis problem. Our experimental results indicate the 2LB-MOPSO yields much better final results as compared to the standard single-objective approach over all considered test cases.

[C2298]

### "The design of granary environmental monitoring system based on ARM9 and ZigBee"

Grain is an important strategic resource. Due to seasonal production, there are many problems in the stored procedure. This article designs an environment monitoring system of the granary combining Embedded and ZigBee wireless sensor network technology. In the actual situation of the design, using ZigBee wireless sensor network to complete Multi-point acquisition and transmission of environment parameters, using ARM9 to achieve precise control of the barn environment as system data controller; and using GPRS to achieve the system's remote control, it greatly improves the flexibility and scalability of the warehouse management. [C2299]

### "Convex parabolic reflector antenna design with cosecant-squared radiation pattern for microwave radar systems"

In this paper, symmetric and cosecant-squared radiation patterns are obtained by using parabolic reflector antennas which have different geometrical structures. The analytical regularization method (ARM) is used to solve the problem of E-polarized wave diffraction by parabolic shaped perfectly electrical conductive (PEC) cylindrical reflector with finite thickness. The initial boundary value problem is reduced to the infinite algebraic system of the second kind, which is an equation that can in principle be solved with any predetermined accuracy by means of the truncation number. The parabolic reflector is fed by a horn antenna which is designed to illuminate the reflector aperture efficiently. In contrast to traditional parabolic reflector structure that is used to obtain pencil beam, the upper side of the reflector geometry is designed as convex to obtain cosecant-squared radiation pattern and the obtained far-field radiation patterns are investigated. [C2300]

### "A novel application for sum-difference pattern detection of signal direction using time-modulated linear arrays"

A novel application using the time-modulated linear arrays (TMLAs) in determining the direction of unknown signal with sum pattern and difference pattern for tracking radar is presented in this paper. An optimized time sequence from the differential evolution (DE) algorithm is presented to produce multiple beams simultaneously. Based on the multiple beams of the sum patterns and their corresponding difference patterns at different sidebands, the directions of incoming signals can be detected. The comparison of the performance between TMLA and conventional antenna arrays under the same parameter demonstrates that the accuracy of the direction of target in TMLA is relatively high, and the range of angle detection is several times larger than those of the conventional antenna arrays. [C2301]

### "Design of an ocean atmospheric duct signal processor"

The atmospheric refractive section plane retrieved from radar sea clutter is of importance for the enhancement of military naval radar. In this paper, an atmospheric duct signal processor with hardware of an intermediate-frequency board and a high-speed DSP board, besides the arithmetic of clutter suppression and sea clutter extraction, have been designed and implemented to get radar sea clutter power, which works synchronously together with a Doppler weather radar in the science experiment of atmospheric duct sounding. Results show that this signal processor can perfectly implement the requirement of radar sea clutter and its real-time arithmetic processing. [C2302]

### "Adaptive pulse compression via maximum signal minus interference level in clutter environments"

Standard matched filter for pulse compression causes high range sidelobes, which may mask neighboring small targets. The adaptive pulse compression (APC) based on reiterative minimum mean square error (RMMSE) can mitigate the range sidelobes in white noise. However, its performance degrades in clutter environments. In this paper, an APC algorithm based on maximum signal minus interference level criterion (MaxSMIL) is proposed, in which the result of signal power minus interference power is maximized so that interferences including range sidelobes, clutter and noise are suppressed adaptively. Simulation results show that the proposed algorithm

outperforms the APC based on RMMSE in Weibull clutter environment. [C2303]

#### "A low-complexity C-band radar for non-invasive respiration measurement"

An interferometric radar operating between 6 and 9 GHz for non-invasive measurement of the respiration rate, is presented. An adaptive RF front-end tracks slow body movements by changing the operating frequency such that the sensing system always operates in its optimum point. Experimental results have been obtained from human beings and the good correlation between the radar signals and a reference signal obtained from a conventional respiratory sensor show the validity of this approach. [C2304]

#### "Evaluation to the performance of MTI radar anti-passive jamming"

The signal processing elements and working course of MTI radar are analyzed in this paper, and theory research is also done to the element and performance of double canceller. Aiming at the Gaussian power-spectral clutter with differ velocity value and variance, this paper calculates the performance of MTI system quantitatively and the corresponding improvement factor of anti-passive jamming is achieved, the performance of MTI radar is estimated synthesized. [C2305]

#### "Subspace in signal processing and communications"

Among the most powerful and applied mathematical tools, subspace has had a wide impact in signal processing and communications, and it continuously has a magic power for solving future problems. In this talk, I will present some of the triumphant examples of subspace that I have encountered in the past 25 years. These examples range from high-resolution processing of radar signals to blind system identification for communications and to smart relays for next generation of wireless networks. [C2306]

#### "Design of SAR tomography experimental system"

In this paper, a ground-based experimental system of SAR tomography is proposed in detail. Based on the analysis for the properties of signal in the height direction of SAR tomography 3-D imaging system, the effect and relationship of parameters related to resolution in the height direction are discussed, and proper experimental system parameters are proposed. By using the general SAR tomography imaging algorithm in the experiment, the experimental system is proved feasible. [C2307]

#### "Binary orthogonal code design for MIMO radar systems"

Multiple Input Multiple Output (MIMO) radar can effectively improve radar performance by transmitting specially designed orthogonal signals. A novel algorithm is presented to design binary orthogonal code for MIMO radar system. The proposed algorithm employs the Walsh function to maintain the orthogonal property of signals. The binary orthogonal code set is obtained by executing synchronal random exchange in column and random selection from rows to coding template, with using Genetic Algorithm (GA) for optimization. The simulation results show that the algorithm is feasible. [C2308]

#### "Parameter selection of MIMO radar under the long time integration"

Long time integration is a common work mode for multiple-input multiple-output (MIMO) radar. In this mode, the accumulation effect is seriously affected by range migration. To solve this problem, we derive an expression, which describes how the accumulation output changes with the target velocity, bandwidth, and other factors, based on the MIMO radar moving target echo model. This expression quantifies the relation between the range migration and the influence factors. It can be used to determine the range of the target velocity in which the motion compensation is needed. Further, through appropriate parameter selection, such as choosing a proper transmission bandwidth etc., the influence of the range migration on accumulation output is minimized. The correctness of the theoretical results is verified by simulations. [C2309]

#### "A model of non-coherent airborne MIMO space-time adaptive processing radar"

Compared to single-input multiple-output (SIMO) radar, airborne multiple-input multiple-output (MIMO) space-time adaptive processing (STAP) radar transmits mutually orthogonal or non-coherent waveforms. The waveform diversity increases degrees of freedom (DOFs) of MIMO STAP radar and results in the variation of clutter characteristics. To make things worse, there exists many non-ideal factors in practical project that affect performance of MIMO STAP. Considering all such situations, we derive the covariance matrix of echo signals by utilizing waveform covariance matrix (WCM) and error covariance matrix tapering (CMT) to simplify the MIMO STAP in this paper. Signal to interference plus noise ratio (SINR) performance simulation results verify that

MIMO STAP radar has a better spatial resolution than SIMO radar generally and improving in orthogonality of transmitting waveforms can obtain a better SINR performance. [C2310]

#### "A novel airport surface surveillance based on multi-video fusion"

Airport surface surveillance is an important issue guaranteeing the safety. Traditionally, this depends on the SMR (Surface Movement Radar) or ASDE (Aerodrome Surface Detection Equipment). However, these equipments are very complex and expensive, which is not suitable for the simple airports. On the other hand, video is a type of common and cheaper equipment and can be mounted largely in the airports. If the video also provides the ability of motion detection while guaranteeing the precision, it can be yet regarded as a substitute for non-cooperative radar like SMR and ASDE. This paper proposed such a solution based on optical flow field detection, dynamic fuzzy clustering and multi-sensor fusion. Experiments show that the solution is not only feasible but also with high detection precision. [C2311]

#### "Analysis of anti-interception performance of MIMO radar"

As a new radar system, MIMO radar has become the hotspot in radar research. Because the key point of radar's viability in battlefield is its RF stealth ability. Though the analysis of radar transmit power and the LFM signal detect technique based on time-frequency analysis, this paper makes a discussion on the discrepancy of the anti-interception performance between MIMO radar and conventional phased array radar, and therefore draws some meaningful conclusions. [C2312]

#### "Enhanced supervised neighborhood preserving embedding for radar target recognition"

Recently, the computer vision and pattern recognition community has witnessed the rapid growth of a new kind of dimensionality reduction method, namely manifold learning. Among them, neighborhood preserving embedding (NPE) is one of the most promising techniques, which can be performed in either unsupervised or supervised mode. In this paper, a new dimensionality reduction algorithm, called enhanced supervised neighborhood preserving embedding (ESNPE), is proposed. ESNPE can enhance the local within-class relations by taking into account class label information. Moreover, neighbors are found according to a new distance metric instead of Euclidean distance, aiming for better generalization. Experimental results on radar target recognition with range profiles indicate the superior performance of the proposed method, compared with PCA, NPE and supervised NPE (SNPE). [C2313]

#### "On the edge based artifact mitigation in wavelet packet transform for enhancement of spectral estimation"

Wavelet packet transform is a recent addition to the rich arsenal of the signal processing tool box. In this article, we investigate the application of wavelet packet transform as a novel spectral analysis tool. The estimator is realized by a tree structure obtained by cascading a pair of half-band high and low pass filters. The main attraction for wavelet packets (WP) is the tradeoffs they offer in terms of satisfying various performance metrics such as frequency resolution, side lobe suppression and variance of the estimated power spectral density (PSD). Furthermore, the state of art in the application of wavelet transform for spectrum estimation is carried forward by bringing in a few optimizations which correct undesirable edge based artifacts that occur in the standard implementations. The systems are evaluated through simulation studies the results of which show that the proposed wavelet based approach offers great flexibility and adaptability apart from its performances which are significantly better than Fourier based estimates. [C2314]

#### "Evolutionary Computational Tools Aided Extended Kalman Filter for Ballistic Target Tracking"

Tracking a ballistic target in its reentry mode by considering the radar measurements is a highly complex problem in nonlinear filtering. Kalman Filter (KF) is used to estimate the position of target when the measurements are corrupted with noise. If the measurements are nonlinear (radar measurements) then Extended kalman filter (EKF) is used. For obtaining reliable estimate of the target state, filter has to be tuned before the operation which is offline. Tuning an EKF is the process of estimating the process noise covariance matrix (Q) and measurement noise covariance matrix (R). This paper presents a new method of tuning the EKF using different evolutionary algorithms. [C2315]

#### "Frequency based oscilloscope triggering scheme"

This paper presents a novel frequency based oscilloscope triggering technique for measurements involving complex waveforms that are challenging even today. Proposed technique is capable of providing stable triggering even in the case of complex periodic waveforms category where commonly used level triggering scheme fail to



perform adequately and may be used in problem of estimating many typical signal processing situations, such as Doppler estimation of radar and sonar returns, vibration measurements, geophysical data processing, and surveillance observations of the electromagnetic spectrum. For stable display of a signal in an oscilloscope, it must be triggered at its base frequency. In this technique, frequency of all harmonics present in test signal is retrieved using FFT and the base repetition rate of the signal is found by selecting the frequency of lowest harmonics present in the test signal. Numerous complex test waveforms are generated and their harmonic contents are analyzed in the virtual environment of LabVIEW™ software. To verify the efficacy of the proposed technique, it is implemented using LabVIEW™ software and PCI DAQ card. It is found that the proposed technique is equally effective in detecting the base repetition rate of complex as well as simple waveforms. Technique proposed in this paper would be of interest to instrumentation design engineers. [C2316]

#### "Quantum dash mode-locked lasers for millimeter wave signal generation and transmission"

In this paper we present the remarkable characteristics of quantum dash mode-locked lasers and how they could be used for low phase noise signal generation, for high data rate wireless transmission and radar in the millimeter wave frequency range. [C2317]

#### "Radar cross section analysis of various objects and RCS optimisation"

This work is based on the analysis and optimization of the radar cross section that is indispensable for today's defense industry. In this study, radar cross section analysis of many objects from simple geometric structures to military vehicles are made. Nowadays, when the electronic war technology is growing rapidly in, the stealth technology in radar systems became one of the indispensable factors of the defence industry and is used widely in air, land, sea and undersea platforms. Usage of these techniques that reduces the detection probability of vehicles that are very important for a country such as ship, plane, helicopter, submarine, etc. is a very important technology in defence industry. On this scope by working on stealth technology the methods for reducing radar cross section was investigated detailed. [C2318]

#### "Parallelized Physical Optics computations for Scattering Center Models in radio channel simulations"

Scattering Center Models (SCMs) are an approach to efficiently characterize electromagnetic scattering of complex shaped objects in terms of a distribution of equivalent sources. SCMs have been widely used in the area of radar target modeling, particularly for object characterization and classification. Recently, the SCM approach has been adapted to model the electromagnetic properties of vehicles embedded in a comprehensive environment for the simulation of automotive radar channels. In this paper the application of SCMs for deterministic simulations of communication channels in automotive environments is presented. The main advantage of this concept is a drastic reduction of complexity for the ray tracing simulations. Instead of using a full geometrical description of the scene, the most complex objects are replaced by an equivalent SCM and a strongly simplified surface model. The SCM of an object is determined in advance, independent from the surrounding environment. In order to achieve a precise parameterization of individual Scattering Centers (SC), the Physical Optics (PO) approximation can be applied. Unfortunately, in contrast to a parameterization based on the Geometrical Optics (GO) contribution only, this approach requires field computations for a large number of observation directions. To handle this computational challenge, a parallelization concept is presented, which is based on multi-core architectures and on the utilization of Graphics Processing Units. [C2319]

#### "Emerging Trends of Computational Grid Based Near Real Time/Real Time Flood Assessment and Forecasting Models"

From recent past, the computational Grid based flood assessment and forecasting models is getting emerged as an interdisciplinary integrated 'near real time/real time model'. Many such, Grid based flood assessment and forecasting model supports in logically integrating various components of flood related scientific simulations such as Metrological, Hydrological, Hydraulic, RADAR, LIDAR Remote Sensing, GIS, Satellite Communication and other technologies and derives the end result which can be straight away used by the disaster mitigation team member/end user. This paper mainly brings out the emerging technological trends observed in the fields of computational Grid based flood assessment and forecasting models by surveying the flood forecasting model of 'Cross Grid' as well as the operational flood model of ESA Grid. Details reflecting the technology trends and simulation methods adopted by the 'GARUDA Grid' flood assessment experimental model have been given. [C2320]

#### "Advantage of non-etching adhesion promoter on high frequency signal loss"

In the age where demands for mobile electronic devices are ever increasing, the propensity for an exponential growth of wireless data transfer is inevitable. The massive data exchange is driven by rise in the signal frequency and the trend having high frequency applications is imminent. The prolific examples of high frequency applications include the next generation 4G mobile phones, satellite communications, Wi-Fi LAN, millimeter wave radars on automobiles, CPUs and GPUs. As the frequency signals carried by electronic devices continue to elevate, there is a greater risk of compromising the signal integrity. The main contributors of high frequency signal loss are the dielectric material and conductor which signals travel on. In order to minimize signal loss, material suppliers have been developing reliable high speed dielectrics with low dissipation factors and dielectric constants. On the other hand, the conductor loss of high frequency signals is largely dependent on the surface profile and roughness of the tracks. Uneven conductor surface profile and track roughness is a product of using conventional etch-based adhesion promoter. While the conventional etch-based adhesion promoters cause no major functionality issues to the manufacturing of commodity PCBs, the impact on the signal integrity for high frequency applications can be an issue. As signal frequency escalates, a phenomenon known as the "skin effect" propagates the signals on the track surface. The coupled impact of the "skin effect" and conductor roughness is an upsurge in resistance that results in signal loss. Contrary to the etch-based adhesion promoter, non-etching adhesion promoter (NEAP) can offer a flat conductor surface and a controlled track width. This can in turn reduce the high frequency signal loss significantly. The paper makes use of a commercially available non-etching adhesion promoters and copper foils in order to investigate the influence of surface roughness on high frequency signal loss. The characterization is carried out through the use of computer simulation as well as actual sample measurement in order to determine those factors which dominate the overall loss performance. [C2321]

### "The Application of MPI-TigerSHARC in SAR Processing System"

The demand of processing speed in SAR signal processing is huge and requires more computational power than what a single processor can provide. To address these demands, an implementation of MPI (Message Passing Interface) based on link DMA for TigerSHARC DSPs is introduced in this paper. Porting MPI to the embedded system will enhance application portability and make parallel programming much easier. This paper presents a real application of range-Doppler algorithm in SAR processing system. The result shows that MPI is suitable for parallel programming, especially suitable for processing large volume of data. [C2322]

### "A Novel Application of Support Vector Machines to Detect Targets"

In this paper we develop a novel pulse radar detection scheme using Support Vector Machines (SVMs). SVMs are a powerful tool for pattern classification. Exploiting this, we design a SVM for pulse radar detection of targets embedded in noise. An adaptive pre-processing stage is included when the echoes are very weak. It is observed that the signal-to-side lobe ratio obtained is much higher compared to neural network based pulse radar detection schemes. We further examine the noise tolerance, range resolution ability and Doppler tolerance of the new algorithm for pulse compression, and compare it with the ones available in literature. [C2323]

### "FFT Simulation and Implementation in TMS 320C6713"

This paper deals with simulation and implementation of the FFT algorithm in TMS 320C6713 as a radar signal processor unit. Furthermore it has provided a new method for real-time implementation of the Fast Fourier Transform algorithm that is a very time consuming calculation, in most DSP processors. There also has been indicated a method for conducting several simultaneous operation in a guideline cycle including several accessing to the memory, producing several address using pointers and hardware multiplication. Using Ping Pong technique also didn't result in loss of any sample and so system is working as Real Time. By combining Ping Pong technique and rotating buffers this paper will reduce the speed of calculation which is very important for radar processors. Results of our innovation indicates a very good performance of the method provided in designing and making a signal processing unit of a radar system which has been tested in a real environment. [C2324]

### "Coin insertion technology for PCB thermal solution"

The thermal management of electronic products is always a headache to the high power electronics design engineer. Since all electronic components are assembled on the PCB, it's important to develop a good solution to dissipate the heat from PCB to the chassis with conduction method. There are many material and process used for PCB thermal dissipation in the industry now. Some of them like IMS (Insulated Metal Substrate), can be used only for simple circuits like LED substrate. Some like metal bonded PCB that is heavy and expensive. The standard thermal pad/via is not capable for high thermal density components like QFN. It is necessary to develop a simple PCB construction to solve the thermal problem. This paper introduces new design which embeds a small piece of metal coin inside PCB under the high power components. The attached component, like

power transistor, sits on the exposed coin surface of the new developed PCB. During operation, the heat created from the components can be effectively dissipated through the coin to another side of the PCB. The heat can then be dissipated to the chassis of equipment or another heat sink. The system thermal problem can be solved for the low thermal resistance of the heat path. Since the coin is small and light weight, it has great advantage of lower cost and very good performance. Even component with dimension as small as 3 mm long can be applied. Besides, the coin can be electrically connected to the PCB ground layer with different methods. Its electrical performance runs very well in power amplifier PCB for telecommunication industry. This paper will also simulate the thermal performance of different PCB thermal design, include four different coin insertion constructions and its comparison with thermal via PCB and IMS laminate. This technology has been used in the PCB of cell phone base station, point-to-point radio and military radar system. It is also under testing for IC substrate application now. [C2325]

#### "UWB microwave imaging via modified beamforming for early detection of breast cancer"

Ultra-wideband (UWB) microwave imaging is a promising technique for detecting early stage breast cancer, which exploits the significant contrast in dielectric properties between normal and malignant breast tissues. In this paper, we have proposed a new modified compensation method and beamforming technique for microwave imaging. We used a three dimensional (3-D) Finite Integration Technique (FIT) based breast model, with normal breast tissue, supported on a layer of chest muscle and covered by a thin layer of skin. A small sized (1 mm diameter) tumor is placed within the breast tissue layer. A pair of rounded-edge bow-tie antennas at crossed position is used for transmitting and receiving microwave signals. This antenna pair is then placed at different positions over the breast surface and the incident and backscattered signal at each position are stored. Backscatters are then processed to eliminate artifacts. Finally they are passed through the beamformer and an image is formed. The beamformer is designed with adaptive weighting to compensate both propagation attenuation and lossy medium effect. Despite using the traditional delay-and-sum approach, new delay-and-product technique is used in beamforming. This modified beamforming approach is shown to outperform its previous counterparts in terms of resolution and sensitivity. [C2326]

#### "Dynamical Weather Radar Beam Blockage Correction"

Error of quantitative rainfall estimations due to partial or total weather radar beam blockage is important in complex orographic areas. A simple method named dynamical weather radar beam blockage correction different from the operational "look-up" table method is presented. The dynamical correction method is implemented with the multiplicative factor between two antenna elevation angles. Case study of quantitative rainfall estimation shows that the dynamical beam blockage correction is effective if the beam blockage azimuths are less than 10 degrees. [C2327]

#### "Fuzzy Logic-Based Image Fusion for Multi-view Through-the-Wall Radar"

In this paper, we propose a new technique for image fusion in multi-view through-the-wall radar imaging system. As most existing image fusion methods for through-the-wall radar imaging only consider a global fusion operator, it is desirable to consider the differences between each pixel using a local operator. Here, we present a fuzzy logic-based method for pixel-wise image fusion. The performance of the proposed method is evaluated on both simulated and real data from through-the-wall radar imaging system. Experimental results show that the proposed method yields improved performance, compared to existing methods. [C2328]

#### "Low Altitude Target Tracking Algorithm with Acoustic Wireless Sensor Network"

For the problem of low altitude target tracking with acoustic wireless network, the signal propagation time delay effect must be considered. The target has been far away from its emitting position when the signal is received by sensors. This effect leads to synchronous sensors in the measurement space sample asynchronously in the state space and the sample frequency becomes unknown and time varying. In this paper, a batch type distribution fusion algorithm is proposed which consists of two steps. First, a linear search method is used for estimating the time-varying state transition time which is the parameter of least square solution for the initial state. This initial state is used again to optimize the state transition time until the iteration termination condition is satisfied. Second, a time register procedure and a distribution fusion technique are presented to obtain the global track. Simulation results verify the efficiency of the proposed method. [C2329]

#### "Compressive Sensing for Radar Sensor Networks"

Motivated by recent advances on Compressive Sensing (CS) and high data redundancy among radars in radar sensor networks, we study CS for radar sensor networks. We demonstrate that the sense-through- foliage UWB radar signals are very sparse, which means CS could be applied to radar sensor networks to tremendously

reduce the sampling rate. We propose to apply SVD-QR and maximum likelihood algorithms to CS for radar sensor networks. SVD-QR could vastly reduce the number of radar sensors, and CS is applied to the selected radar sensors for data compression. Simulations are performed and our compression ratio could be 192:1 overall. [C2330]

### "Performance Analysis of Communications & Radar Coexistence in a Covert UWB OSA System"

Far-field target detection, multi-sensor communications, and security are essential requirements of first-emergency networks. A radar-communications system is a potential opportunistic spectrum access (OSA) solution, harnessing the coexisting advantages of radio detection and ranging (RADAR), and wireless communications. A multi-functional waveform has been designed, by embedding an Orthogonal Frequency Division Multiplexing (OFDM) signal within a spectrally notched ultra-wideband (UWB) random noise waveform. Extending that development, this paper analyzes the waveform's Bit-Error-Rate (BER) and Ambiguity Function (AF) formulations to demonstrate its OSA ability, that offers reliable multi-user communications, and high range and Doppler resolution in target detection. We further conclude that up to 30% of the available UWB bandwidth can be simultaneously utilized for concealed data communications without adversely affecting radar performance or its physical layer covertness. [C2331]

### "Advances in DSP design tool flows for FPGAs"

This paper highlights recent advances in digital signal processing (DSP) design tools for Field-Programmable Gate Arrays (FPGAs), concentrating on model-based design high-level synthesis. Next generation FPGA model-based design tools provide a mechanism for abstracted design definition at the algorithmic rather than implementation level. The tools make use of FPGA structural and timing knowledge, and of mathematical and graph theory techniques to optimize and technology map the algorithm to a pipelined FPGA implementation, controlled by high level parameters and threshold settings. Such tools allow simple design space exploration and retargeting of algorithms to different device families. This design-once and retarget as required method improves productivity over manual hardware description language (HDL) coding, especially for projects which are subject to change. The simple design style, optimized generated hardware and productivity in design change and implementation exploration are highlighted with two examples; a direct radio-frequency (RF) radar design and a simple 8 by 8 beamforming design. [C2332]

### "Innovative ad-hoc wireless sensor networks to significantly reduce leakages in underground water infrastructures"

This paper presents an ICT solution to overcome the problem of water dispersion in water distribution networks. Leakage prevention and breaks identification in water distribution networks are fundamental for an adequate use of natural resources. Nowadays, all over the world, water wasting along the distribution path reaches untenable percentages (up to 80 % in some regions). Since the pipes are buried within the terrain, typically only relevant breaks are considered for restorations: excavations are very expensive and consequently the costs to identify the position of the leakage or just the position of the pipe itself are too high. To address this problem, and simplify the leakage identification process, the authors have designed a wireless network system making use of mobile wireless sensors able to detect breaks and reveal unknown tracks and monitor the pressure spectrum of the fluid flowing in the pipe. The sensors transmit the acquired data from the terrain to the surface by use of a wireless connection. On the surface ground there are stations that receive the signal, process it, and communicate with a central unit where necessary intelligent signal processing techniques are used to detect leakage sources. Compared to other leakage detection solutions already available in the market (such as: Ground penetrating radar (GPR), pure acoustic techniques and tracer gases), the proposed technique appears very efficient and much more inexpensive. [C2333]

### "Waveform Design and Optimization in Radar Sensor Network"

We investigate the use of information theory to design waveforms for the measurement of extended radar targets in radar sensor networks (RSN). The different channel gains for transmitting signals from different radar sensors are introduced to model the radar system channel. Given the transmitting signals, we optimized the estimation waveforms that maximize the mutual information between a target ensemble and the received signal within additive Gaussian noise given the transmitting signals so that characteristics of the target could be well recognized. We also study the maximum mutual information with the constraints of the number of radar sensors, waveform energy and duration, which could be taken into consideration when waveforms are designed for RSN. [C2334]

### "Extraction method of large-scale linear objects from SAR images"



Public safety concerns have been raised by potential safety problems due to deformation of infrastructures such as railways, highways and bridges. Monitoring the deformation of large-scale man-made linear objects (LMLO) by permanent scatters (PS) interferometry would be critical to prevent this kind of disasters. However, the estimation of LMLO deformation is sensitive to the influence of those random PS from nearby natural objects. Thus, extraction of LMLO from PS images is the necessary condition for an accurate monitoring of LMLO deformation. In this paper, a new procedure of extraction LMLO from SAR images is proposed based on classification, morphological operations and line recognition methods. A preliminary step, merging optical image, would be identification of man-made objects regions from background. Image of permanent scatters (PS) points from PALSAR data will then be masked to remove unrelated PS points. Then a set of morphological operations and line feature extraction methods are performed to connect PS points continuously distributed along the linear target. This method is successfully applied to a PALSAR image to extract the Lantau Link highway (LLH), Hong Kong and the experiment result demonstrates its validity on comparison with the ground truth in optical image.

[C2335]

#### "An improved BP algorithm for high-resolution MIMO imaging radar"

The back-projection (BP) algorithm is a popular imaging method. Nevertheless, there exists a difficulty that the cross-range resolution acquired by the standard BP algorithm is dependent on the bandwidth of transmitted signal when the BP algorithm is directly used to the multiple-input multiple-output (MIMO) radar for imaging a target in the cross-range direction without any variation. In this paper, an improved BP algorithm is presented for high-resolution MIMO imaging radar to avoid the difficulty associated with the standard BP algorithm.

Furthermore, the theoretical expression of the cross-range resolution associated with the improved BP algorithm is given. Different from the standard BP algorithm, the cross-range resolution acquired by the presented BP algorithm can be independent on the bandwidth of transmitted signal since the presented algorithm can straight an integration curve and make the received echoes on the integration curve be focused by phase aligning to avoid the truncation error produced by the range resolution value. Simulations based on synthetic data are provided for testing the presented method. [C2336]

#### "Design of World Expo tour sites guide system based on RFID technology"

Facing growing groups of tourists, it's obviously that the traditional manual guides can't meet the needs of each visitor. Through scientific and technological means, an electronic smart guide system based on RFID technology is establishment, Expo visitors can get more information include audio and video about comprehensive equipment, exhibits, galleries by the system. It is an important means to improve the quality of services and the degree of satisfaction for tourist. In this paper, we propose a RFID application in smart guide system that voice explanation is played automatically with no need for manual operation; describe the components of guide system, software process and a feasible plan for its upgrade. An electronic smart guide system based on RFID is designed for Shanghai World Expo. [C2337]

#### "Implementation of battlefield electromagnetic environment ontology visualization system"

The battlefield electromagnetic environment generated by the electronic equipment or system in the battlefield, has a positive or negative effect on electronic equipment. The battlefield electromagnetic environment has an important influence on modern warfare. Considering the difficulty of comprehension and operation on battlefield electromagnetic environment ontology, a visualization system of battlefield electromagnetic environment ontology is designed and implemented which can perform importing and exporting the ontology files, ontology management, ontology operation as well as ontology visualization. [C2338]

#### "Extraction of wetland combining with Radarsat and HJ data of Yellow River Delta"

Wetland types of Yellow River Delta are various and serious phenomena of 'same object with different spectrum' and 'different object with same spectrum' is one of the reasons caused low classification accuracy. Combination with multi source images is an efficient method to mitigate this influence. In the paper, principal component transform was carried out to Radarsat four polarization data and the first principal component were fused with HJ images based on HIS, Brovey, PC and Wavelet transform. A maximum likelihood classifier was applied to extract wetland information of Yellow River Delta. The experiment results demonstrated that HIS transform performed well than the others and outstood the wetland information. The results also showed that the classification accuracies of HIS merged images and the stacked images were highest, through combining two different source data to make good use of information. [C2339]

#### "A visualization method of measuring the effectiveness of early warning and detection network based on simulation"

Computer simulations are often employed by operational research analysts to evaluate the relative effectiveness of various combinations of military equipment and tactics (i.e., options) for specific tasks within a conflict scenario. In order to value the effectiveness of Early Warning and Detection (EW&D) network, this article proposing a visualization method of Measuring the Effectiveness based on simulation. This method switches the problem into the task with clear military meaning, appraises the degree of completion of these missions respectively, and represents it visually. In this paper, the process of the evaluation based on simulation is discussed, in addition evaluation indicators and representative missions are presented. At last, we verify the method by analyzing an example briefly that proves the practicality of the method. [C2340]

### "Research on imaging simulation of airborne fire control radar for simulated training"

A uniform simulation method was presented to realize ground imaging of RBM, DBS and Spotlight SAR for simulated training. The three imaging modes are widely used by modern airborne fire control radars. Considering the requirement of training real-time and the simulated images used for pilots observation, this method computed RCS images of ground based on the facet model and fused the radar image features, such as shadows, layovers and speckles, to get simulated images directly. The problem of dynamic image display in GL Studio was solved at the same time. Specially, the reality and real-time of this simulation method was evaluated qualitatively and quantitatively. Experimental and probational results show that the radar simulated images obtained by the proposed method are competent for the simulated training in army. [C2341]

### "High performance element computing architecture"

This paper will describe High Performance Element Processing Architecture as a basis for large array RADAR/Communication systems, enabling system designers to increase levels of digitization by using open standards based hardware. [C2342]

### "Subspace compressive GLRT detector for airborne MIMO Radar"

In this paper, the design of a subspace compressive GLRT (SSC-GLRT) detector has been pursued for MIMO airborne radar system when the secondary sets of data are available in addition to the primary one. It is observed that with very reduced amount of measurement data at sub-Nyquist rate that is equal to the number of virtual bi-static radar in the presence of a single target, SSC-GLRT provides the same performance as the conventional GLRT with much larger length of the data, i.e., an order of magnitude higher given by the product of the number of elements in the received antenna array and coherent pulse interval (CPI). Therefore, SSC-GLRT is much energy efficient and useful in the scenario where the computational complexity becomes a burden. Also, this paper illustrates an elegant way of mapping the angular and Doppler domain to an one dimensional discrete vector for the formulation of compressive sampling (CS) based  $\ell_1$  reconstruction of the signal subspace when it is unknown so that it can successively be used in SSC-GLRT. The simulation example further corroborates the effectiveness of the proposed SSC-GLRT detector. [C2343]

### "Using a P2P architecture for voice and radar transportation in critical command and control systems"

The Brazilian air traffic service is constituted by a civil and a military organization, which provide tracking (radar), voice and data communication (VHF, UHF and HF) services, through an integrated network. To optimize the management of its air traffic system, Brazil divides the airspace into four independent Regional Centers. In each of these regions, the existing sensors (radars and radios) send information and products to only one of the Regional Centers, forming a star topology. In case of impediment in one Regional Center (eg, electrical failure or terrorist attack), even if the service node is able to send its information, the Regional Center will collapse, since there is no means to process the information generated locally. The solution presented in this article, develops the redundancy of the system through the digitization of audio and radar signals and its subsequent transport using an peer-to-peer network. To validate this proposal, experimental flights were developed. In these flights, aircraft flying over the city of Manaus (in the center of Amazonia) were coordinated by a center installed in Brasilia, which is located about 1000 km away. After these experiments, it was concluded that using this new architecture, we can provide a performance similar to those currently in operation, enabling air traffic systems, as well as those of similar function (eg coordination of civil defense and police ) to be operated with a high degree of reliability, even when they meet a hostile environment. [C2344]

### "CELP-like compression of spotlight-mode SAR raw data in transform domain"

Transmission of synthetic aperture radar (SAR) data requires large bandwidth due to its inherently high data rate. Consequently, compression of the data is often required. In this paper, we propose a raw SAR data compression

algorithm that employs a predictive coding scheme, based on the analysis-by-synthesis encoding method. The proposed algorithm is inspired by code excited linear prediction (CELP) algorithm used in speech compression and exploits the signal correlation across azimuth of the range-wise inverse Fourier transform of the raw SAR data. Our results show that the proposed CELP-like compression algorithm is 6 dB superior to block adaptive quantization (BAQ) in signal-to-noise ratio. Also, we show that the formed SAR image after compression preserves the main features of the captured scene at low data rate contrary to that of BAQ-compressed data.

[C2345]

### "A software demonstrator for IEEE 802.21 Media Independent Handover in heterogenous networks"

In this paper we present a software demonstrator, for a system built following the directions described in the IEEE 802.21 (Media Independent Handover) standard, capable of completing an independent vertical handover. We first bring in front the field's related work, and also propose methods of implementing the components described in the standard. The architecture and the functionalities of the demonstrator application are detailed, and we also mention aspects about surpassing the difficulties that rise during the implementation process.

[C2346]

### "Design of mine detection robot for Korean mine field"

This paper presents the critical design constraints of mine detection robots for Korean minefield. As a part of a demining robot development project, the environment of Korean minefield was investigated, and the requirements for suitable robot design were determined. Most of landmines in Korean minefield were buried close to the demilitarized zone (DMZ) more than half of a century ago. The areas have not been urbanized at all since the Korea War, and the potential locations of the explosives by military tactics have been covered by vegetation. Therefore, at the initial stage of the demining robot system development, the target areas were investigated and the suitable design for Korean minefield terrain was determined. The design includes a track type main platform with a simple moving arm and a mine detection sensor (consists of a metal detector and a GPR at this stage). In addition, in order to maintain the effective distance between the landmine sensors and ground surface, a distance sensing technique for terrain adaptability was developed and briefly introduced in this paper. The overall design of this robot was determined by considering the speed of the whole mine detection process and a point of economic view to replace human in minefield. Thus, the detail of the conceptual design and the mine detection scenario is presented in this paper. [C2347]

### "Intelligent surveillance and security robot systems"

This paper presents a new security solution that integrates vision, intelligent algorithm and robot technology. The solution can be applied to guarding large facilities, critical infrastructures and national borders. While conventional security solutions rely on human operator's vigilance on the images provided by cameras, the proposed solution uses machine intelligence to compensate for human factors and robots to provide immediate counter response. The system is currently deployed at Korea National Oil Corporation's Seosan oil reserve facility. Overall structure of the system and description of each component are presented. [C2348]

### "Multipath reflectivity estimation in urban environments for Synthetic Aperture Radar images"

Synthetic Aperture Radar (SAR) images a target region reflectivity function in the multi-dimensional spatial domain of range and cross-range. SAR synthesizes a large aperture radar in order to achieve a finer azimuth resolution than the one provided by any on-board real antenna. Conventional SAR techniques assume a single reflection of transmitted waveforms from targets. Nevertheless, today's new scenes force SAR systems to work in urban environments. Consequently, multiple-bounce returns are added to direct-scatter echoes. We refer to these as ghost images, since they obscure true target image and lead to poor resolution. By analyzing the quadratic phase error (QPE), this paper demonstrates that Earth's curvature influences the defocusing degree of multipath returns. In addition to the QPE, other parameters such as integrated sidelobe ratio (ISLR), peak sidelobe ratio (PSLR), contrast (C) and entropy (E) provide us with the tools to identify direct-scatter echoes in images containing undesired returns coming from multipath. [C2349]

### "Multi-target tracking using proximity sensors"

We consider the problem of tracking multiple moving targets in a continuous field using proximity sensors, which are binary sensors that can sense target presence by performing local energy detection subject to noise. Compared with more sophisticated sensors, proximity sensors have the advantage of having lower costs and lower energy consumption, but also the disadvantage of being less accurate. In this paper, we propose a hybrid tracking scheme where a coarse-scale tracking is first performed by proximity sensors to narrow down the areas

of interest, and then a fine-scale tracking is performed by high-end sensors to estimate the exact target locations, with our focus on the former. In contrast to classic multi-target tracking which assumes 1-1 association between measurements and targets, we show that proximity measurements do not have such association and thus require a different objective. Formulating the coarse-scale tracking as a problem of tracking the histograms of targets in a cell-partitioned field, we develop both an optimal and two approximate solutions via Bayesian Filtering (BF). In particular, one of our approximate solutions decouples the tracking of different targets and thus reduces the dimensionality of BF by relaxing the likelihood function, and the other further reduces the problem into discrete space by quantizing the target mobility model and the relaxed likelihood function. Together with the optimal solution, they provide flexible tradeoffs between accuracy and complexity. Simulations show that the proposed solutions can effectively track targets to the accuracy of a cell and thus reduce uncertainty for the fine-scale tracking. [C2350]

### "Modeling the effects of wind turbines on radar returns"

Wind turbines located near radar installations can significantly interfere with a radar's ability to detect its intended targets. In order to better understand and mitigate the adverse effects of wind turbines on radar, the government and wind farm community need tools that can be used to analyze the radar returns from wind turbines. Remcom's XGtd@software is a high frequency solver capable of calculating the radar cross section of electrically large objects. In this paper, interference from wind turbines is predicted using XGtd simulations and new post-processing algorithms that calculate Doppler shift quantities based on points of interaction with the rotating turbine blades. Results of the analysis are used to calculate the bistatic radar cross section and Doppler shift from two blade orientations. In addition, the time-varying monostatic radar cross section and Doppler shift for a single wind turbine are analyzed and shown to agree well with measured data from actual wind turbines. [C2351]

### "High availability and fault management in Objective Architecture systems"

At the heart of many real-time and near real-time distributed computing systems, such as radar, navigational, missile defense, and command and control, you find mission critical requirements. This designation demands continuous system availability even in the face of system faults. Lives are at stake and mission success is at risk. Standards-based high availability and computing resource management solutions with well defined functional boundaries and interfaces are gaining traction. This is seen in such Navy examples as Aegis Modernization, Littoral Combat Ship, Common Processing System, and more recently within the PEO-IWS Objective Architecture DoD Information Technology Standards Registry (DISR). As implemented, Objective Architectures hold the promise of providing a path to meet current and future demands placed on these system designs. Examples of these demands include: increased functional density and complexity, resource consolidation, mixed criticality systems and the ever present size, weight and power concerns. The architectural approach must be both flexible and scalable to fit the broadest set of cases, minimizing or eliminating special-case solutions. There are a set of standards published by the Service Availability (SA) Forum that address these issues. SA Forum standards are currently being used in the programs mentioned above. We will also consider how SA Forum specifications can be used to support operational availability in legacy systems while laying the groundwork for evolution of the objective architecture. This paper reviews the above issues and the specific benefits brought about by a SA Forum-based solution. [C2352]

### "Power allocation schemes for target localization in widely distributed MIMO radar systems"

Widely distributed multiple-input multiple-output (MIMO) radar systems offer parameter estimation improvement for target localization, proportional to the product of the number of transmitting and receiving radars and the total transmitted power. Thus far, power allocation has been uniformly distributed between the system transmitters. For a large number of radars, the achievable localization mean-square error (MSE), with full resource allocation, may extend beyond the system predetermined performance goals, such as target localization accuracy (i.e., minimum estimation MSE) and total power radiation. In this study, power allocation schemes are developed, taking into account system constraints. The first is concerned with minimizing the total transmitted power such that a predefined estimation MSE objective is met, while keeping the transmitted power at each station within an acceptable range. The second, optimally distributes a given power budget among all transmitting radars to maximize performance, i.e., minimize the attainable localization MSE. As the Cramer-Rao bound (CRB) is known to be asymptotically tight to the maximum likelihood estimator (MLE) MSE at high SNR, it is used as a metric for the estimation MSE. The CRB is derived for a signal model that incorporates the propagation path loss, the target radar cross section (RCS), and the transmitters' powers. It is shown that uniform or equal power allocation is not in general optimal and that the proposed allocation algorithms result in a local optimum that provided either better localization MSE for the same power budget or requires less power to establish the same performance in terms of estimation MSE. A physical interpretation of these conclusions is offered. [C2353]



### "Robust target estimation in compressive sensing based colocated MIMO radar"

A colocated multiple-input multiple-output (MIMO) radar system is considered, in which the transmitters and receivers are nodes of a small scale wireless network. The sparsity of targets in the illuminated space allows target detection based on compressive sensing (CS) techniques. A receive node compresses the received signal via a linear transformation,  $\Phi$ , referred to in CS theory a measurement matrix. The compressed samples are subsequently forwarded to a fusion center, where an  $\ell_1$ -optimization problem is formulated and solved for target information. CS-based MIMO radar achieves the same localization performance as do traditional methods but with many fewer measurements. Unlike previous work, we consider the case in which the targets might be located across several range bins, and the delay of the first reflected signal is unknown and, due to the small number of compressed samples, cannot be estimated accurately. A new measurement matrix is proposed that is constructed based on the transmit signal waveforms and also accounts for all possible discretized delays of target returns within a given time window. It is shown that reduced bandwidth transmit waveforms can lead to a measurement matrix that improves signal-to-interference ratio (SIR), but on the other hand, using waveforms that are too narrowband increases the coherence of the sensing matrix, thus invalidating the conditions for the application of the CS approach. Therefore, the transmit waveforms must be chosen carefully to guarantee the desired performance. [C2354]

### "Analog auto-correlation based receiver architecture for radar systems"

Analog signal processing based radar systems enable reduction in total system power consumption, over conventional digital signal processing based radar systems. In this paper, detection performance degradation of a previously proposed system, based on analog cross-correlation, due to time synchronization is addressed and analog auto-correlation based radar architecture is proposed. By adopting the digital radio frequency memory technique, accurate and tunable delays for autocorrelation process are realized. The probability of detection performance degradation of the previously proposed system, due to mismatch, is evaluated by simulations while varying signal to noise ratios and mismatches at the matched filter. The proposed system's probability of detection performance will also be simulated versus varying signal to noise ratios, compared to the results of the previously proposed system and analysis of conditions when the proposed system is more beneficial than the previously proposed system will be made. [C2355]

### "Visual data mining analysis for information operations in complicated information environment"

The method of visual data mining analysis is important in acquiring the intelligible knowledge in massive initial data. Based on the characteristics of information operations in complicated information environment, the basic flow of requirement design and analysis for the visual data mining analysis for information operations was presented; then, take the visual data mining analysis of radar systems as the key experimental example, the spectral distribution of complicated information environment, the electromagnetic energy distribution, the ability of detection and tracking of radars as well as the assessment of the barycenter of a radar chain, etc. were discussed and analyzed in detail according to the basic content, flow and objective of the designed visual data mining analysis for information operations; finally, the outlook of the study was depicted. [C2356]

### "Studying on state prediction for radar transmitter using GM(1,1)"

Through analyzing the importance of component modules of a kind of radar transmitter, both the cathode current of multiple-beam klystron and the ripple voltage of high-voltage power supply are selected as the prediction signals. By studying on their characteristics, a improved GM (1,1) is proposed to predict the state of transmitter, where the idea of metabolism is applied to make the parameters of GM (1,1) on-line change. Particle Swarm Optimization(PSO) is used to select the best prediction dimension. The performance of the proposed method is tested, and the experiment results show that the proposed method has better prediction capability than the popularly used ARMA model, and then it provides technical support for preventive maintenance. [C2357]

### "Synthetical Generalized Discriminant Analysis for radar HRRP target recognition"

The prevalent applications of traditional statistical discriminant methods for radar High Range Resolution Profile (HRRP) target recognition are designed to obtain Common Discriminant Information (C-DI) among all classes at the expense of Individual Discriminant Information (I-DI) between them, so they may lose slight I-DI between close-set classes and result in a dissatisfied recognition performance. To overcome this weakness, we design a Distributed Generalized Discriminant Analysis (D-GDA) for I-DI extracting, and accordingly, a new variation called Synthetical Generalized Discriminant Analysis (S-GDA) is presented to deal with C-DI and I-DI equally. Experimental results for simulated data show that GDA and D-GDA are complementary in many facets and can be considered as a feature extraction method couple. Furthermore, compared with GDA and D-GDA, the

proposed S-GDA not only achieves the best recognition performance, but also is more robust to many challenges, such as noise disturbance, aspect variation and Small Sample Size (SSS) problem. All these experimental facts confirm that C-DI and I-DI are different as two aspects of Discriminant Information (DI) but both are beneficial to target recognition. [C2358]

#### "A parameter estimation method for polyphase codes using time-frequency distribution"

Due to the desirable performance, polyphase codes have been widely used in low probability of intercept radar. By analyzing the characteristic of the time-frequency distribution of polyphase codes, a new parameter estimation method based on time-frequency distribution is proposed. Simulation results show that this method have good estimate precision even in low signal-to-noise ratios. [C2359]

#### "Removing multiplicative noise by improved regularization term"

This paper focuses on the problem of multiplicative noise removal. Multiplicative noise models are central to the study of coherent imaging systems, such as synthetic aperture radar and sonar, and ultrasound and laser imaging. Classical ways to solve such problems are filtering, statistical(Bayesian) methods, variational methods, and methods that convert the multiplicative noise into additive noise, apply a variational method on the log data or shrink their coefficients in a frame and recover the result using an exponential function. We draw our inspiration from the diffusion tensor. By using a edge-directed enhancing based anisotropic diffusion as regularizer, we can derive a functional whose minimizer corresponds to the denoised image we want to recover. Both theory analysis and numerical results show that the new model has better denoising results than the known SO model with high peak signal to noise ratio. [C2360]

#### "Fast algorithm for direction of arrival based on time-frequency distributions"

Time-frequency distribution (TFD) method has received a considerable amount of attention in Direction of Arrival (DOA) estimation of multi-senor and time space processing, which lead to improved spatial resolution and source separation performances. According to the characteristic of the different time-frequency distribution of each source, a novel approach of time-frequency DOA estimation is provided based on the propagator method (PM). Compared with the conventional approaches, the presented method has lower computational complexity with insignificant performance degradation for DOA estimation. Furthermore, in the proposed method of time-frequency DOA estimation, propagator can be obtained without a priori knowledge of the number of impinging sources on array if t-f points in time-frequency domain are chosen appropriately, which widens the application of propagator to Radar, Sonar and passive detection system. The effectiveness and high resolution of the algorithms is verified via computer simulations. [C2361]

#### "Research on robust unscented regularized particle filtering"

In nonlinear and non-Gaussian systems, particle filtering is effective but it is difficult to select the importance distribution function and diverges more greatly. Aiming at this problem, the paper represents robust unscented regularized particle filtering to improve the performance of filtering. This algorithm is more suitable for filtering calculation in nonlinear system, not only because overcomes the limitations of the general particle filter and uses the equivalent weight, but also takes advantage of the high efficiency of unscented particle filtering and regularized particle filtering. In importance sampling process, the UT transformation is applied and the equivalent weight makes good use of more reasonable information, it considers the latest measured values and slows down the particle degradation. In resampling process, particles are from the continuous kernel density distribution function owned the minimum mean square error. Simulation results show that the algorithm is efficient and outperforms in terms of accuracy based on SINS/SAR integrated navigation system. [C2362]

#### "Separating respiration artifact in microwave doppler radar heart monitoring by Independent Component Analysis"

With a microwave radar, chest wall movements originating from cardiac and respiratory activity can be recorded non-contactly. A major challenge is how to separate the desired low-amplitude cardiac signal from large-amplitude artifacts, such as respiration. Commonly, the separation is performed with a narrow band-pass filter. This causes the signal edges to be rounded, which complicates the accurate timing estimation in the heart rate variability (HRV) analysis. In addition, the harmonics of the respiration signal might fall into the same frequency spectrum as the cardiac signal. In this study, we recorded data with two radars and studied signal separation using a complex-valued Independent Component Analysis (ICA). After ICA, the respiratory signal is greatly attenuated, although still present, in two of the independent components (ICs). However, respiration harmonics are reduced as well, and thus, the residual respiratory signal can be removed by filtering. [C2363]

### "Performance Characterization Parameters on Voice and Data Transmission in Mobile Terminals to Cellular Networks"

This work presents the experimental results related to performance measurements in GSM and GPRS cellular data networks. Two Mobile Terminals were used, in order to take place the scenario. Power Level, Power vs. Time, Modulation Analysis, Modulation Spectrum, (BER) Bit Error Rate and Throughput were considered in this analysis. [C2364]

### "An Efficient Frequency-Domain Velocity-Filter Implementation for Dim Target Detection"

An efficient Fourier-domain implementation of the velocity filter is presented. The Sliding Discrete Fourier Transform (SDFT) is exploited to yield a Track-Before-Detect (TBD) algorithm with a complexity that is independent of the filter integration time. As a consequence, dim targets near the noise floor of acquisition or surveillance sensors may be detected, and their states estimated, at a relatively low computational cost. The performance of the method is demonstrated using real sensor data. When processing the acquired data, the SDFT implementation is approximately 3 times faster than the equivalent Fast Fourier Transform (FFT) implementation and 16 times faster than the corresponding spatiotemporal implementation. [C2365]

### "Automatic Building Detection Using LIDAR Data and Multispectral Imagery"

An automatic building detection technique using LIDAR data and multispectral imagery has been proposed. Two masks are obtained from the LIDAR data: a 'primary building mask' and a 'secondary building mask'. The primary building mask indicates the void areas where the laser does not reach below a certain height threshold. The secondary building mask indicates the filled areas, from where the laser reflects, above the same threshold. Line segments are extracted from around the void areas in the primary building mask. Line segments around trees are removed using the normalized difference vegetation index derived from the orthorectified multispectral images. The initial building positions are obtained based on the remaining line segments. The complete buildings are detected from their initial positions using the two masks and multispectral images in the YIQ colour system. It is experimentally shown that the proposed technique can successfully detect buildings, when assessed in terms of 15 indices including completeness, correctness and quality. [C2366]

### "Chipless RFID tag with integrated sensor"

A chipless tag based on multiresonators with integrated temperature sensor is presented. The tag consists of a UWB monopole antenna loaded with multiple cascaded spiral EBGs which have a 1:1 correspondence with data bits. The data bits are encoded into the spectrum hence the tag has a unique spectral signature. The chipless tag is less sensitive to tag orientation and has smaller size than earlier generations of the tag. The temperature sensor is a NTC thermistor which changes the radar cross-section of the tag antenna. The change in radar cross-section is used to determine the temperature while the spectral signature is used to identify the tag's unique ID. A proof-of-concept tag is developed and tested which has 6-bits and operates between 2-2.6 GHz. The chipless RFID tag is designed for ultra-low cost sensing applications. [C2367]

### "Feasibility of wireless gas detection with an FMCW RADAR interrogation of passive RF gas sensor"

The feasibility of the remote measurement of gas detection from an RF gas sensor has been experimentally investigated. It consists of a Frequency-Modulated Continuous-Wave (FMCW) RADAR interrogation of an antenna loaded by the passive sensor. The frequency band of the RADAR [28.8-31GHz] allows the detection of the resonant frequencies of Whispering Gallery Modes that are sensitive to gas concentration. Reported experimental results provide the proof-of-concept of remote measurement of gas concentration fluctuation from RADAR interrogation of this new generation of passive gas sensors. [C2368]

### "Indoor location estimation system based on evolutionary matching"

The indoor Real Time Location Systems (RTLS) is attracting more and more attention while a series of challenging problem still exists such as the real-time performance, location precision, and the large amount of disturbance signal brought by complex indoor circumstances. However, existing location estimation technology cannot satisfy the requirements of indoor RTLS. In this paper, a high-precision indoor location estimation technology based on Ultra Wideband and evolutionary matching mechanism is proposed, based on which an indoor location service platform is built with intelligent alerting strategy based on Newton collision graphic engine. Experimental results show that the proposed method improves not only the location estimation accuracy but also the ability to eliminate the multipath signals with low computational cost. [C2369]

### "On the application of ethernet in a distributed radar system"

This paper firstly introduces the structure of VHF radar system and then studies the data transmission rate between the digital of VHF radar and the host computer. Through analyzing the calculating rate, the size of the data packet and the influence of UDP and TCP on the transmission rate, the author intends to find out the optimum method to meet the engineering requirements. [C2370]

### "A Multi-Objective Antenna Placement Genetic Algorithm for matched array synthesis on complex platforms"

A Multi-Objective Antenna Placement Genetic Algorithm (MO-APGA) has been proposed for the synthesis of matched antenna arrays on complex platforms. The total number of antennas required, their position on the platform, location of loads, loading circuit parameters, decoupling and matching network topology, matching network parameters and feed network parameters are optimized simultaneously. The optimization goal was to provide a given minimum gain, specific gain discrimination between the main and back lobes and broadband performance. This algorithm is developed based on the non-dominated sorting genetic algorithm (NSGA-II) and Minimum Spanning Tree (MST) technique for producing diverse solutions when the number of objectives is increased beyond two. The proposed method is validated through the design of a wideband airborne SAR. [C2371]

### "Multi-object tracking using feed-forward neural networks"

In this article we present an approach for robust multi-object tracking. Typically the task of object tracking can be divided into two subtasks: object detection and object labeling. The main focus of the work presented here is on an approach for consistently labeling objects across a series of video frames using neural networks. Due to the specialization of object detection algorithms it is necessary to divide detection and labeling to enhance their individual skills. In the evaluation we show that the developed labeling is robust against occlusions and can handle low object detection rates. [C2372]

### "Inverse filtering operation for reconstruction of distorted GPR response"

This study proposes inverse filtering operation for reconstruction of ground penetrating radar (GPR) responses in order to remove waveform distortion caused by transmitting and receiving antenna characteristics. As an example, we apply it to measured pulse response from a metallic sphere and show the effectiveness of the method. [C2373]

### "Robust adaptive coregistration of InSAR images using multisource information and joint data fusion"

This paper addresses an adaptive coregistration method of synthetic aperture radar interferometry (InSAR) phase images. The method for adaptive coregistration of InSAR images is characterized by using multisource information and joint data fusion. We propose a strategy and criteria incorporating the weighted joint data information to evaluate the accuracy of the registered method by the using the mean-squared differences. Numerical results on the simulated data demonstrate the efficiency and precision of the proposed method. [C2374]

### "Research on the 3D visualization of information operations based on STK"

Information Operation is the main style of Modern War. The visualization of Information Operations could reflect the whole operation procedure directly. At the Same time, the visualization could help the research on information Operations. This Paper analyzes the needs of the visualization of Information Operations. According to the characteristics of Information Operations, this paper focuses on to achieve the visualization of Information Operations through STK methods and techniques. [C2375]

### "Two Insar procedures for wide and noise interferograms"

In unwrapping interferograms with large size and dense residues, the path-following algorithm as a fundamental unwrapping method may produce retrieval error caused by long branch-cuts and repetitive connection of residues. In this paper, two unwrapping algorithms, i.e. the multiple patches method connecting opposite residues and the center expansion method searching opposite residues, are alternatively presented. Some examples of ENVISAT-ASAR datasets demonstrate our improvement better than conventional methods in InSAR data processing. [C2376]



### "Development of phased array systems in Japan"

This paper reviews the research and development on the phased array antennas (PAAs) for several applications in Japan. First, the author shows the historical overview of the PAA for radar, satellite and mobile communication uses. Then, the author introduces a millimeter-wave PAA as a modern application to communication systems. [C2377]

### "Multi-layer and multi-dimensional information based cooperative vehicle localization in highway scenarios"

In this paper, we propose a cooperative approach based on unscented Kalman filter (UKF) for vehicle positioning in Vehicular Ad hoc Networks (VANET). In our system, various kinematic parameters (e.g., position, speed, heading, and acceleration) of a vehicle are considered as a multi-dimensional data. Accordingly, the kinematic parameters of all the vehicles in the cluster can form a multi-layer and multi-dimensional information (MLMDI) database. Due to the motion characters, most kinematic parameters vary nonlinearly. We specially introduce the UKF to fuse the MLMDI data from different information sources, since UKF has an advantage to reckon the statistics of a random variable undergoing a non-linear transformation compared with extended Kalman filter (EKF). Simulation results show our approach can get more accurate, reliable and computationally efficient than GPS/DR system and the Extended Kalman Filter (EKF) based solution. [C2378]

### "1-D superresolution ISAR imaging algorithm"

A novel 1-D scattering centers extraction algorithm of radar target based on conjugate unitary Root-MUSIC was introduced in this paper. To improve the resolution of 1-D scattering centers, the information of conjugated data was used available by combining the observation data matrix with its conjugated data matrix. Centro-Hermitian data matrices with hermitian property was constructed by forward-backward(FB) averaging, Unitary transform was applied which convert the FB covariance matrix to a real matrix, and the computational efficiency is improved by real-valued eigendecomposition. Theory analysis and simulation result show that the new approach can improve the resolution and reduce significantly computational complexity. [C2379]

### "K-band micro-strip antenna array applied in anti-collision radar"

A K-band micro-strip array double-antenna applied in 24GHz automotive collision warning radar is presented in this paper. The double-antenna consists of two individual 14x6 elements arrays which both are placed on ROGERS RT5880 substrate with 0.254 mm thickness, one for the transmitter (TX) and one for the receiver (RX). The results of simulation show that the double-antenna has gain of 26.5dB and efficiency of 60%, the -10dB bandwidth is 1GHz from 23.6GHz to 24.6GHz, three-decibel beamwidth in azimuth is 6° and in elevation is 18°, the sub lobe suppression in azimuth is better than -20dB and in elevation is better than -15dB. The isolation between two antennas array is better than -32dB. [C2380]

### "Speckle noise reduction in SAR images using adaptive morphological filter"

Speckle noise is one of the most critical disturbances that alter the quality of Synthetic Aperture Radar (SAR) coherent images. Before using SAR images in automatic target detection and recognition, the first step is to reduce the effect of speckle noise. Several adaptive and non-adaptive filters are widely used for despeckling in SAR images. In this paper, an adaptive mathematical morphological filter is proposed to reduce the speckle noise in SAR images. The new filter performance is compared with a number of despeckling filters with different parameters. For performance measurements, several parameters were evaluated to test the filter ability to attenuate the speckle noise and keep target information. From experimental results, the new proposed morphological filter gives promising results for significantly suppressing speckle noise and preserving the potential targets. [C2381]

### "The study of Range Doppler Algorithm in focusing Bistatic SAR"

Comparing to monostatic SAR, Bistatic SAR has specific advantages, such as the reduced vulnerability in military systems, additional information about the target and characteristics of signal. Nevertheless, it brings the complication of processing algorithms because of the range history of a Bistatic target is the sum of two hyperbolic range equations, which give a double square-root term in the range equation, and the traditional RD algorithms using in monostatic SAR can not apply for processing Bistatic SAR. This paper obtained the point target signal by establishing the echo signal model, then derived the approximate two-dimensional spectrum of echo signal by using POSP, and a Range Doppler Algorithm suitable for Bistatic SAR is presented. The algorithm is validated by the simulation experiments of point targets. [C2382]

### "A method for Doppler Weather Radar raw data compression based on wavelet transform modulus maxima denoising"

A lossy data compression algorithm based on wavelet transform modulus maxima denoising (WTMM-D) has been proposed. Firstly, analysis for radar raw data is presented to identify data characteristics and correlation. Then, we transform the data format and compare the experimental results using different lossless compression algorithms to compress the transformed raw data. Finally, a method based on WTMM-D is presented, which is using a high-performance lossless compression algorithm to compress the reconstructed coefficients of WTMM-D. Experimental results show that the proposed algorithm can compress raw data efficiently under the premise of a certain distortion. [C2383]

### "Predicted radar/optical feature fusion gains for target identification"

Airborne tracking and identification (ID) of high value ground targets is a difficult task impacted by sensor, target, and environmental conditions. Layered sensing, using a combination of standoff and short-range sensors, maintains target track and identification in cluttered environments such as cities or densely vegetated areas through sensor diversity. Data, feature, decision, or information fusion is necessary for high confidence target classification to be achieved using multiple sensors and sensor modalities. Target identification performance is improved by exploiting the extra information gained from independent sensing modalities through information fusion for automatic target recognition (ATR). Increased target ID has been demonstrated using spatial-temporal multi-look sensor fusion and decision level fusion. To further enhance target ID performance and increase decision confidence, feature level fusion techniques are being investigated. A fusion performance model for feature level fusion was applied to a combination of sensor types and features to provide estimates of a fusion gain. This paper presents a fusion performance gain for Synthetic Aperture Radar (SAR), electro-optical (EO), and infrared (IR) video stationary target identification. [C2384]

### "Study of efficient broadband beamforming based on extended towed array measurement"

In this paper, extended towed array measurement and broadband beamforming in frequency domain are combined together to form a new efficient broadband beamforming based on extended towed array measurement (ETAM-FCBF). The angular resolution of this method is higher than the conventional beamforming, and the detection ability of the weak target is more excellent. Moreover, this method is fast enough for real-time processing. [C2385]

### "Analysis of an improved fixed-point loop for satellite navigation receiver"

Aim to avoid the deficiency of huge computation load and resource use in conventional fixed-point loop control method, base on the study of signal tracking method and accuracy of navigation receiver, an improved one is proposed, along with theoretical analysis and actual verification of the accuracy loss of signal tracking compared to the floating-point loop control method from the following two aspects respectively: quantization error of phase discriminator, approximation of filter coefficients, as well as the discipline when choosing appropriate filter coefficients. The results demonstrate that the accuracy loss of signal tracking in the improved method is very small with appropriate filter coefficients, which can be accepted. [C2386]

### "Radar target discrimination using neural networks"

Time domain response based neural network and frequency domain response based neural network have been proposed for radar target recognition. In this paper, we propose a natural frequency based neural network for radar target recognition. Our scheme makes advantage of an aspect angle independence of a natural frequency. In the results, we show that, for the multiple aspect angles, natural frequency based neural network is superior to time domain response based neural network. [C2387]

### "A GMTI method via comparing two consecutive phase difference maps of the same target area for small UAVs"

In this paper, we present a Ground moving target indication (GMTI) method based on the analysis of the two phase difference maps (PDM) of the same target scene obtained by one antenna phase center on a slow moving platform. For small unmanned aerial vehicles (UAVs) only one antenna is available to detect moving targets. Using a single antenna and the two PDMs method, odd numbered spatial samples are used to construct the first synthetic aperture radar (SAR) image, and the even numbered spatial samples are used to construct the second SAR image of the same target scene. The along track neighboring pixels phase difference is calculated for each image; and, thus two PDMs are generated. The phase difference values of the corresponding pixels in

the two PDMs are almost the same if there are only static objects in the target scene; while if there is a moving target with a reasonable speed in one pixel, it will generate extra phase change based on the phase change generated by the platform motion. The extra phase change generated by the moving target would be detected in comparing the two PDMs, and thus the moving target is detected. Simulations conducted confirm that the proposed method can detect ground moving targets with very low speeds. [C2388]

#### "Hyper-fuzzy modeling and control for bio-inspired radar processing"

Modern RF Radar signal processing has been receiving much attention for wide range of domains that include industrial, environmental, and military applications. Inherently, the received raw spatial-temporal signals can be 1-D, 2-D, or 3-D and are usually of uncertain nature, because of changing conditions and optical background variations. In this paper, we apply novel concepts for hyper-neural theory that allow for incorporation of variables attribute definitions and uncertainties for the purpose of effective evidential learning and subsequent key output features determination in the radar processing. Application to wide-band angle of arrival data sets at several carrier frequencies has been carried out in order to illustrate the strengths as well weakness of the approach. Using interval set-based operations together with segmentation of the data is proved useful and gave good sensitivity of detection. [C2389]

#### "Analytical studies of laser parameters for ranging and illuminating satellites from H-SLR station"

In this paper, the laser system used at the Helwan Satellite Laser Ranging Station (H-SLR) will be used in satellite's illumination as well as for satellite ranging. The estimated model which describes the energy and number of photons as well as the number of photoelectrons are investigated from the received signals of laser beam. For the ranging purposes, the equipment used at the H-SLR is described and also the method used for its calibration. The Range corrections due to the effect of the atmosphere on the laser beam is also discussed and applied for some satellites observed from Helwan. The ranging and illuminating space satellites are modeled and computed from the H-SLR parameters. The numbers of photons, of photoelectrons are then computed from the ranging data. [C2390]

#### "Comparison of pulse and FMCW based radiolocation for indoor tracking systems"

In this paper, pulse and FMCW based radiolocation techniques are compared with respect to their usability for an indoor person tracking system. The basic principles and parameters for pulse and FMCW based distance measurements are derived. To allow the calculation of the signal budget, channel models, noise limits and regulatory aspects in terms of transmit power are considered. The accuracy and the coverage range for the two approaches are estimated for ISM and UWB frequency bands. The shown advantages of FMCW with respect to coverage range, range accuracy and system requirements favour this approach for the target application, where a high path loss due to wave propagation through walls and various obstacles must be expected. [C2391]

#### "Short term DC breakdown and complex permittivity of Al<sub>2</sub>O<sub>3</sub>-and MgO-epoxy nanocomposites"

Electrical insulation based on epoxy resin is commonly used in high voltage applications. Examples are transformers, terminations, plugs or connectors. But, it is also used in high voltage applications where energy transportation or distribution is not the main purpose, e.g. in medical and industrial X-ray systems, or radar. This paper addresses the changes in the structure due to the introduction of surface functionalized nanoscale particles, namely magnesium oxide and aluminum oxide. Short term DC breakdown tests were performed alongside dielectric spectroscopy. The BD strength was measured for negative DC ramp voltages. Dielectric properties have been acquired by broadband dielectric spectroscopy. The base polymer is a commercially available bisphenol A epoxy with anhydride hardener. As filler material magnesium oxide powder was used with an average particle size of 22 nm and alumina filler with 50 nm average diameter. Both particle types were modified with a silane coupling agent, in order to achieve a uniform dispersion of particles in the host material. Neat epoxy samples were used as a reference. Both composites showed remarkable DC breakdown strength for low fillgrades. A possible explanation for this unique behavior is given and the differences between samples filled with aluminum oxide and magnesium oxide are discussed. [C2392]

#### "Antenna compensation for UWB GPR systems applied in Non-Destructive testing"

Non-Destructive testing is an enhanced technique based on applying the inverse scattering algorithms upon the received scattered Electromagnetic EM waves for computing some important parameters of the material characteristics as permittivity and reflection coefficients. Unfortunately, the Ultra Wideband (UWB) antennas can dramatically affect the received signal and result in considerable degradation of the overall performance of the UWB GPR system. The isotropic, fully matched, unity gain and frequency independent antenna assumption could never be accepted for the typical UWB antennas, where the radiation characteristics and matching

properties vary considerably with the frequency, introducing directionally asymmetric bandwidth reduction and waveform dispersion. Therefore an efficient antenna compensation technique would be introduced in this paper with the corresponding successive EM simulation results. [C2393]

#### "Measurement of pyramidal microwave absorbers using RCS methods"

In this work, a commonly used measurement techniques were used to define the reflection loss performance of pyramidal microwave absorbers mounted on a wall. The technique is namely, Radar Cross Section (RCS) measurement method. Six set of pyramidal microwave absorbers and flat square absorbers were installed at one side wall, in an RF shielded room in order to investigate the performance. Two types of cable losses measurement techniques were applied to compare its performance under different loss conditions. The reflection loss values resulting from this investigation were then analyzed and discussed. [C2394]

#### "Air traffic complexity based on dynamical systems"

This paper presents a new air traffic complexity metric based on dynamical systems. Based on a set of radar observations (position and speed) a vector field interpolating these data is constructed. Once the field has been obtained, the Lyapunov spectrum of the associated dynamical system is computed on points evenly spaced on a spatial grid. The results of the computations are summarized on complexity maps, with high values indicating areas to avoid or to carefully monitor. A first approach based on linear dynamical system enable to compute an aggregate complexity metric. In order to produce complexity maps, two extensions of the previous approach have been developed (one in space and another in space and time). Finally, an approximation is proposed in order to localize the computation of the vector field by the mean of Local Linear Models. [C2395]

#### "Continuous ant algorithm based on cooperation in radar network optimization"

From the perspective of deployment features and defense area partition, we establish the static radar network and optimal deployment model, and based on this model, we put forward the issue of high-dimensionally continuous spatial deployment. From the standpoint of ant colony optimization, and aimed at improving Continuous Multi Ant-Colony Optimization (CMACO) in which pheromone is normally distributed, we raise a Algorithm based on cooperation which faces high-dimensionally intelligent optimization. In this method, introduces queue interaction in search of ant colony, connects the mechanism of head ant guide and mass recruitment, and finally realizes cooperated search under high-dimension form. The practice of optimal design shows that this algorithm can be applied into high-dimensional, complex, and much restrained optimal problem, moreover, the optimal time takes less than that of traditional intelligent method, satisfying the warning demand of reentry stage. [C2396]

#### "Application of Newton method to natural frequency estimation"

In this paper, we propose a method for improving the accuracy of the previously extracted natural frequencies. After using the existing natural frequency extraction method, we use the extracted natural frequencies as an initial guess for the nonlinear sets of equations. The objective is to improve the accuracy of the previously extracted natural frequencies using the Newton method. The final residues and natural frequencies are obtained from the successive update of the initial residues and natural frequencies. The validity of the scheme is illustrated using the numerical results. [C2397]

#### "Atmospheric turbulence effects on radar systems"

The paper discussed the atmospheric turbulence effect such as angle-of-arrival, signal-to-clutter and noise ratio for lognormal clutter and Weibull clutter and detection probability of ultrawideband pulse in radar system. The detection probability is degraded for short pulse and for more turbulence. [C2398]

#### "NAECON 2011 Preview: "Intelligent Aerospace Sensor Integration""

The 2011 National Aerospace Electronics Conference (NAECON) will be held on July 20-22 at the Holiday Inn Conference Center in Fairborn, Ohio. The 2011 theme will be "Intelligent Aerospace Sensor Integration". This conference is a major forum for researchers, practitioners, and students interested in aerospace systems; and their impact on advanced control systems, reconfigurable computing, information processing, tomography, optics, imaging, RF devices and advanced design, radar, antennas and next-generation millimeter wave and THz applications. [C2399]

#### "Automated image segmentation for synthetic aperture radar feature extraction"



Automated segmentation routines may be used to extract scattering features in synthetic aperture radar (SAR) images. The watershed transform segments real-valued images into regions associated with a local minima. Watershed algorithms suffer from over-segmentation which, for SAR image segmentation, results in many more regions than scatterers. We consider an algorithm called Peak Region Segmentation (PRS). PRS is an inverted version of the watershed transform that seeks to group pixel regions associated with a local maxima. We implement the algorithm to segment one, two, and three-dimensional images. We extend PRS to include region merging to avoid over-segmentation. Threshold settings allow the user to strike a balance between region merging and separation of closely-spaced scatterers. Image segmentation examples are shown for 1D, 2D, and 3D SAR images. [C2400]

#### "Dantzig selector based compressive sensing for radar image enhancement"

Compressive sensing (CS) is the technique for acquiring and reconstructing a signal utilizing the apriori knowledge that it is sparse in a certain domain. This paper investigates the application of this technique to radar imaging. Present radar systems operate on high bandwidths and demands high sample rates following the Nyquist-Shannon theorem. Compressive Sensing can prove to be a good alternative to reduce data handling, complexity, weight, power demands and costs of the existing radar systems. There are two major novelties in this work. First of all we have used Dantzig selector based CS which gives better result when applied on radar images than that using the conventional  $\ell_1$ -norm based CS. Secondly, we also show that Dantzig selector based CS suppresses speckle noise in radar images. We demonstrate the results on both simulated and real radar images. [C2401]

#### "Significance of dielectrics in space technology"

The main objective of this paper is to provide a brief and necessary background of dielectrics in the field of space technology. The mobile telephone, TV, Radio, Satellite or any type of modern communication is not possible without one type of antenna or the other and no radar works without an antenna. Antenna is a sensor of electromagnetic waves. Electric and magnetic fields exist in a dielectric material and also penetrate the dielectric material freely. When an electromagnetic wave is incident normally on the surface of a dielectric, reflection and transmission takes place. In this investigation, dielectric polarization studies were made in the liquid dielectric mixtures Epichlorohydrin, p-cresol in benzene using standard methods at 308K. The values of dielectric constant, refractive index and density were measured at different concentrations. The dipolar increment value has been calculated using Huyskens method based on Onsager's theory. [C2402]

#### "Chairman's introduction for NAECON 2010"

The 2010 IEEE National Aerospace Electronics Conference (NAECON) was held July 14-16, 2010 in Fairborn, Ohio. Approximately 100 papers, tutorials and keynotes were given in various areas of aerospace electronics including: cognitive systems, UAVs, bio-sensing, novel devices, smart textiles, smart antennas, flexible displays, RF reconfigurable microelectronics, radar, photonics, wireless communications, and wearable health-monitoring systems. New this year to NAECON was the Dr. Daniel William Repperger Outstanding Paper Award, to be given in memory of the late Dr. Repperger. A few of the highlights of the conference was a very significant and historical banquet speech entitled "The Dayton NCR WWII Codebreakers", given by Deborah Anderson, daughter of Joseph Desch, who was the focus of the 2006 PBS documentary film The Dayton Codebreakers and our NAECON Grand Challenge-The Smart Vest, which had two teams competing. [C2403]

#### "Effects of polarization on wide-angle SAR classification performance"

Including polarization to circular synthetic aperture radar imagery increases the diversity of information as compared to non-polarized collections. The additional information improves classification performance in a civilian vehicle identification application. Effects of azimuth extent are also investigated. Radar imagery is represented as sets of attributed scattering centers, and vehicles are identified by a pyramid match hashing based, point pattern classifier. The experiments contrast classification performance in a variety of experiments with and without polarization. [C2404]

#### "Design of mismatched filters for oversampled signals"

Most of the prior work in the field of sidelobe suppression filtering for radar pulse compression focused on the design of mismatched filters for binary codes. However, in practice these binary codes are spectrally shaped to obtain analytic signals. The spectrally shaped binary code can be sampled at as low as the Nyquist rate, but in practice it is oversampled to avoid aliasing. The spectral shaping determines the necessary bandwidth and hence the sampling rate for the waveform. One of the spectrally efficient modulation techniques is based on quadriphase coding. As this spectrally shaped waveform is analytic, design of the mismatched filters in complex

domain is needed. In this paper, application of minimax constrained complex LMS algorithm is proposed for the design of mismatched filters for oversampled signals. [C2405]

### "Atmospheric turbulence effects on radar systems"

Atmospheric turbulence has been shown to have measurable effects on several aspects of radar performance. In this paper we discuss the perturbation of the angle-of-arrival (AOA) of radar beams caused by the atmosphere, the effects of lognormal- and Weibull-distributed clutter on detection performance, and the detection probability of ultrawideband pulses propagated through the atmosphere in the presence of turbulence and Gaussian noise. We find that AOA effects are on the order of a few microradians, which is a negligible level for most applications, but that clutter and noise, when combined with turbulent fluctuations, give some surprising results when the ratio of signal to clutter and noise is calculated. The detection of ultrawideband pulses is analogous to the "needle in a haystack" problem. In this paper, we present theories describing each of these phenomena, together with calculated results. For AOA, we have made measurements for one-way propagation that agree well with this theory, but the other phenomena have yet to be measured. [C2406]

### "Wavelet-modulated pulse for compressive sensing in SAR"

A new wavelet modulated pulse is proposed for synthetic aperture radar (SAR). Conventionally SAR image is constructed using chirp, i.e., FM in the range direction, and the Doppler effect in the azimuth direction. The proposed scheme is to physically modulate the amplitude of the radar pulse (AM) using wavelets. Such a radar pulse results in the shift of the wavelets in the temporal domain due to the range, while the Doppler effect causes variation of the scaling coefficient. In both directions, pulse compression can be achieved by taking advantage of the autocorrelation function of the compactly supported orthogonal wavelets and processing the echo signal in the two directions accordingly. Furthermore, by using wavelet modulated pulses, the echo signal is equivalent to the wavelet transform (WT) to the target area. Since WT has been proved more effective in image compression than conventional discrete cosine transform (DCT), wavelet-modulated pulse is equivalent to compression to the SAR image thus to achieve compressive sensing. Experiments have been performed using the latest embedded software defined radio (SDR) technology. Equipped with the most recent FPGA and digital signal processors along with high speed analog-to-digital and digital-to-analog converters, the SDR allows signal processing tasks commonly done by analog circuits to be performed digitally with high flexibility in algorithm design. Based on the developmental need of the user, the small form factor software defined radio (SFF SDR) can serve as a simple data collection device for waveform testing or it can be programmed into a real-time embedded radar system. [C2407]

### "WiMAX ambiguity function for PCL systems"

Passive coherent location (PCL) radar systems use signals of opportunity as the off-board source of electromagnetic illumination. The analysis of the structure, spectral, and spatial properties of emerging commercial waveforms becomes a critical component of future PCL radar systems design. This paper presents an ambiguity function analysis of the emerging IEEE 802.16 OFDM signal known as "WiMAX" for passive radar applications. The simulated WiMAX wave structure shows desirable range and Doppler resolution properties for passive radar applications. [C2408]

### "Ground-UAV platform geometries for radar imaging"

This paper provides a summary of comparative analysis pertaining to a systems trade study with platform geometries that encompass either one, two, or three distributed RF sensing platforms. The discussion is focused on analysis of a basic set of UAV trajectory parameters associated with performing sky-looking radar imaging. The baseline one-platform case corresponds to one ground-based radar transmitter/receiver. The two-platform case involves one ground-based radar transmitter/receiver and one UAV with a passive receiver and the three-platform case involves one ground-based radar transmitter and two UAV's each equipped with a passive receiver. This notional analysis is conducted with a narrow-bandwidth waveform within the L-Band region of the radar spectrum and notional parameters of the moon are adopted for the object-of-interest for radar imaging. Results indicate that the trajectories of the UAV's can be pre-selected to improve comparative radar imaging performance. [C2409]

### "Collision-avoidance radar for bicyclist and runners"

This paper provides a summary of the analysis and design process with respect to the development and prototyping of a Bicycle Radar for a Senior Capstone Project at Wright State University in collaboration with the Air Force Research Laboratory Sensors Directorate. The basic radar technology adopted for this project is a commercial integrated (miniaturized) K-band FMCW Monopulse Module that is recently designed for future

Intelligent Automotive Cruise Control Applications. The design documentation, preliminary test outputs, and discussions within the sections of this paper describe a number of novel features of this Bicycle Radar Design including the methodology for overlaying the K-band range-angle data onto streaming video on the iPhone. Additional discussions pertain to radar waveform generation, control, and processing. A section on potential follow-on activities as well as a discussion on technology options and applications of the resulting system concept is also provided. [C2410]

#### "A 2.9-30.3GHz fourth-harmonic voltage-controlled oscillator in 130nm SiGe BiCMOS technology"

Wide tuning range voltage-controlled oscillators (VCO) are envisioned for applications in radars, broadband communications, phase-locked loops and clock generation/distribution. In this paper, post-layout simulation results of a combined VCO with a ring quadrature VCO (QVCO), an exclusive-OR (XOR) and a fourth-harmonic summation block in 130nm SiGe BiCMOS technology are presented. The combined VCO can be tuned from 2.9 to 30.3GHz. At 2.9GHz, the VCO consumes 32.89mW of power and generates -56.5 dBm (2.24nW) of output power into a 50 Ohm load. At 30.3GHz, it consumes 34.2mW of power and generates -33.5 dBm (398nW) of output power. In both cases, the XOR consumes ~25mW of power and the fourth-harmonic block consumes ~5mW of power. The VCO phase noise at 10MHz offset frequency is -102.2dBc/Hz and -86.04dBc/Hz at 2.9GHz and 30.3GHz, respectively. The VCO figure of merit (FOM) is in the range of -136 to -141. The microchip area is 750µm<sup>2</sup>4500µm<sup>2</sup>. This VCO provides the widest tuning range in the 130nm ring VCOs reported till now. [C2411]

#### "A Port waterside security systemic analysis"

Most of current Port Security analyses provide a clear view of the land-side security measures (fencing, access control, area monitoring...) but the seaside security issues are not always that clearly defined (exact extent, Authority in charge, assessment of realistic threats etc.). In one hand, there is no doubt that proper seaside security measures are even more site-specific than terrestrial ones. In the other hand, providing some sort of systemic analysis can help for "setting the scene" and easing the alignment of all stakeholders for specifying the strictly compliant but most cost-effective solution lay-out. Water-side port security includes a range of activities, of preventive character, ultimately aiming at controlling who and what enters the port area from the water side. It includes crews, passengers and cargo entering on-board of large announced vessels, on-board of small un-announced surface crafts, swimmers, divers or even small submersibles. It also includes vessel under-keel appendices commonly used for smuggling and, potentially, for terrorism... Response measures are very diverse. They can range from intelligence and information management, satellite imagery, radar and VTS down to sophisticated underwater and/or above-water sensors, manned or unmanned patrolling and inspection assets etc. A number of these measures are local, but others require wide area surveillance activities and some might require controls as far as the port of departure or the last ports of call. This paper aims in providing a taxonomy of the waterside port threats and the respective means of protection / response, identifying possible gaps and technology requirements. [C2412]

#### "Evaluation of an HF-radar ship detection and tracking algorithm by comparison to AIS and SAR data"

Since several years, High Frequency (HF) Over-The-Horizon (OTH) radar is used to measure oceanographic parameters, such as currents, waves, and wind direction over large areas up to 200 km off the coast. Cost effective low power systems transmitting less than 50 Watts have been developed, e.g. the WERA (WEUen Radar), and are now commercially available. Besides their applications in oceanography within coastal monitoring systems, these systems can also be used to detect and track ships, if they are modified for this functionality. A ship detection and tracking algorithm for HF-radar has been developed at the University of Hamburg (UHH) in cooperation with the Technical University of Hamburg-Harburg (TUHH). A first evaluation of this algorithm has been done using a data set acquired at Figueira, Portugal, using an 8 MHz WERA system. In May 2009, the NATO Undersea Research Centre (NURC) initiated a measurement campaign in the Ligurian Sea off La Spezia, Italy, which involved two WERA HF-radar systems operated at 12.5 MHz, one directional waverider and a meteorological buoy. In addition AIS data were recorded and satellite borne synthetic aperture radar (SAR) images were acquired. This paper presents preliminary results which show the effectiveness of the HF-radar as a long range ( 130 km) continuous-time coverage surveillance system, despite of its low spatial resolution of 1.5 km. The performance of the HF-radar ship detection and tracking algorithms are evaluated by comparison to AIS and SAR. The detection error found for this data set is less than 1 km for 68% of the comparisons between HF-radar and (AIS) reported locations, which is comparable to previous results from the Figueira data set. [C2413]

#### "Ship detection using high resolution satellite imagery and space-based AIS"

This paper presents a trial carried out in the Malangen area close to Troms city in the north of Norway in September 2010. High resolution Synthetic Aperture Radar (SAR) images from RADARSAT-2 were used to analyse how SAR images and cooperative reporting can be combined. Data from the Automatic Identification System, both land-based and space-based, have been used to identify detected vessels in the SAR images. The paper presents results of ship detection in high resolution RADARSAT-2 Standard Quad-Pol images, and how these results together with land-based and space-based AIS can be used. [C2414]

### "Concurrent use of satellite imaging and passive acoustics for maritime domain awareness"

The research being conducted in the Center for Secure and Resilient Maritime Commerce (CSR), a DHS National Center of Excellence for Port Security examines some basic science issues and emerging technologies to improve the security of ports and inland waterways, as well as coastal and offshore operations. This research follows a layered approach utilizing above water and underwater surveillance techniques. The investigated layers include satellite-based wide area surveillance; HF Radar systems providing over-the-horizon monitoring; and nearshore and harbor passive acoustic surveillance. Integration of these systems is aimed at achieving vessel detection, classification, identification, and tracking. In this paper, we present the results of sea tests where satellite imagery was combined with concurrent passive acoustic surveillance. The wide area sensing was provided by the University of Miami CSTARS facility's electro-optical (EO) and synthetic aperture radar (SAR) satellite imaging capabilities. Satellites detected the ships using a panchromatic EO sensor FormoSat-2 and SAR from the COSMO-SkyMed constellation. The Stevens Passive Acoustic System was used for detecting sound produced by the same ships that were detected by satellites. Concurrent Satellite-Acoustic measurements provide the following advantages: 1. Increasing the probability of small vessel detection and decreasing false alarms. 2. The joint systems can provide redundant detection and classification in conditions where one of the systems fails. For example, EO satellite imaging does not work at night and in fog and cloudy conditions while acoustic detection has limits during stormy weather due to ambient noise. SAR imaging can detect vessels in all weather, but provides less detail about a specific vessel. 3. Acoustics can provide target classification and bearing and satellites can give target localization and heading. SAR data can be used to estimate vessel speed in some cases. 4. Satellite-imaging is helpful for the acoustic detection of an underwater target in cases when satellite information allows separation of surface and underwater targets. 5. Joint measurements provide more data (information) for target classification. Several tests were conducted in New York Harbor, where the satellite images and acoustic signatures of the same boats were recorded. The satellite registered a number of small boats. The small boats were acoustically detected at distances up to 4 km and the signal generated by a passenger ferry was observed at a distance up to 7 km. [C2415]

### "Maritime surveillance with integrated systems"

Securing harbors and coastlines includes the task of monitoring and detecting people or vehicles attempting to enter a confined/protected area, other than at the legitimate access points. Modern systems should provide a total solution-including sensors, software, hardware, and a "control unit" to ensure complete security. Today a standard border security system may include several platforms, providing short-range, medium-range and long-range surveillance like perimeter protection, cameras and radars on observation towers, mobile surface and subsurface observation platforms-including land vehicles as well as maritime vessels or observation aerostats and aerial vehicles carrying all kinds of sensors to give a broader view of an area of interest. The ability to integrate those different types of surveillance means is essential to get a full picture and situation awareness. The paper introduces the concept of a universal ground station as a dynamic integrator for heterogeneous sensor platforms and sensor types depending on the surveillance needs of a specific maritime area of interest. A standardized interface to outside information systems is described taking into account the future need for combined civil and military operations for maritime safety and security. [C2416]

### "Archimede: Integrated Network-Centric Harbour Protection System"

Confined/inshore waters may represent the best type of environment for the conduct of clandestine operations, especially from the sea: the features of such an environment weaken the detection and identification processes carried out by the defenders, while allowing the covert execution of illegal activities, as well as a better exploitation of surprise. The most significant illegal activities conducted in such an environment include infiltration, drugs/weapons smuggling, sabotage/disruption of infrastructures, up to terrorist acts; these activities are accomplished through the use of a variety of means of transportation, which include cigarette boats and power boats, rigid hull inflatable boats (RHIBs), Ashing vessels, sailing/leisure boats, midgets, swimmers/divers (with open/closed breathing systems), and swimmer delivery vehicles (SDV). Requirements as flexibility, rapid reaction, resilience, fast deployment, high level automation, modularity, plug & play have a key role in modern surveillance architecture definition. The paper will describe the guidelines adopted to develop a CIP (Critical Infrastructure Protection) tactical architecture in accordance with the previous requirements. The CIP system



integrates different types of sensors (e.g. radar, IR, TV, SONAR, underwater acoustic network) and classes of vehicles (Surface, Underwater, Air Unmanned Vehicles) which cooperate in a multi environmental scenario (above water, under water, sea surface, ground and air). The focus is to develop the following functionalities: fuse, classify, identify and present all the data provided by the sensors and consequently generate warnings on the Command and Control (C2) and interact automatically with the console. The integration is performed to guarantee flexibility and modularity by means of tactical gateways developed in order to decouple the C2 system from sensor systems and vehicles. In particular, these gateways are designed to translate the subsystem proprietary data in a unique format. This allows integrating every kind and numbers of systems tailoring each time the specific gateway without modifying sensors, vehicles or C2. The system shows Network-Centric features and a wide set of growth above capabilities, even vehicles/sensors swarms, due to the gateway implementing a flexible middleware oriented to publisher/subscriber philosophy. [C2417]

### "Vital Electronics, the key to the developing dynamic GIS for the Baltic or other maritime environments"

Dynamic GIS can provide geospatial information in real-time in support of first responses to natural disasters (e.g. flooding on the Baltic ecosystem), man-made disasters (e.g. oil spill in the Gulf of Mexico), and for Search and Rescue (SAR) missions. All these scenarios require the integration between the real time data acquisition and dynamic GIS. The proposed Vital Electronic System for Maritime Applications (SYSTEM) integrates: a land or sea-based Data Center; a "Mother Ship" (used for sensor deployment and local data collection); and a large number of easily deployed, disposable, intercommunicating, and intelligent "Floaters" (equipped with task-specific sensors). An embedded Vital Electronics Computer composed of a hierarchical network of a large number of wireless PSoC-based GNODEs (configurable at deployment), forms the core of SYSTEM. The Floaters include both task-specific Sensing-only GNODEs and Aggregation GNODEs dedicated to local data aggregation and global communications tasks. Sensing GNODE may be equipped with submerged sensors (e.g. water temperature, pressure, salinity, acidity, passive acoustic, SONAR), and/or above water sensors (e.g. air temperature, proximity, sound, light, thermal IR, passive RF, RADAR). Aggregation GNODEs provide absolute location (e.g. GPS or other means) and also long-range communications with the "Mother Ship", a satellite or airborne platform, and/or a land-based data center. Ultimately, the data collected by the system can be integrated with reference GIS data (such as existing terrain and sea-bottom maps, as well as other live information). The composite data should be web-accessible with the appropriate level of security to relevant agencies and other authorized users. Currently, breadboard proto-prototype Floater electronics is under development. [C2418]

### "An above-water testing's result of experimental surveillance radar with 64-channels digital antenna array"

In this article are analyzed a results of experimental radar with digital antenna array full-scale test against above-water targets, small-boat detection and tracking. [C2419]

### "Integrated visualization and analysis of threats for marine and coastal regions via a Web-based GIS"

The paper presents a Web-Based Geographic Information System for integration, visualization and analysis of data on terrorist, ecological and natural threats. The system uses Open Source solutions like the GeoServer internet map server and the OpenLayers Javascript GIS client library to provide easily accessible and up-to date information related to a region of interest. The system is composed of modules which provide the following features: (1) blast and chemical attack simulation; (2) creation of hazard distribution maps; (3) analysis of risk propagation. Apart from hazard information, which maybe obtained from the simulation modules as well as inserted manually, the system collects and integrates data from several external sensors. The latter include a satellite ground station, oil spill simulation models, a radar and Automated Identification of Ships (AIS). The open, modular structure of the system allows for easy inclusion of different data sources, such as Multibeam Sonar Systems (MBSS) and echosounder. The paper presents case studies of the system applications for analysis, visualization and mapping of threats in the coastal area of the city of Gdansk, Poland. [C2420]

### "Tracking a non-cooperative mobile target using low-power pulsed Doppler radars"

Most target tracking applications developed for wireless sensor networks thus far employ passive sensors which detect the target's emissions. Their performance is thereby dictated by the magnitude of the target's signal and the receivers' sensitivity. Instead, we propose using a network of low-power Doppler radars that actively measure the target's radial velocity. Nodes combine their measurements to solve a system of nonlinear equations that estimate the target's position and velocity. Because these equations have no closed-form solutions we solve

them using numerical methods. These methods however can lead to local minima or even diverge in the presence of even small measurement noise. For this reason we couple the proposed numerical method with an Extended Kalman filter that models the target's movement along a straight line. Clearly the target does not always follow a linear path and so we augment this simple Kalman filter with a method that detects the target's turns and updates the filter's dynamical model accordingly. The combination of the two approaches improve tracking accuracy compared to the numerical solution alone. Results from simulations and a prototype implementation suggest that the combined solution can effectively track a mobile target with average localization error as low as 25 cm in a 10x10 m outdoor field. [C2421]

### "High frequency radar for coastal marine monitoring of currents and vessels"

Use of shore-based high frequency (HF) radar systems for environmental monitoring have become widespread in many countries around the world. In the U.S. various regions, such as the west and northeast coasts, have been instrumented. In California alone, some 50 radar stations contribute to the realtime monitoring of surface currents as part of the state's Coastal Ocean Currents Monitoring Program (COCMP). As recent events in the Gulf of Mexico highlight, environmental security can often hinge upon maintaining comprehensive monitoring systems that are in place and contributing to modeling and response systems at the time of any incident. Beyond real-time surface current maps, low-cost HF radar systems have the potential to contribute to offshore vessel tracking out to ranges of 180 km from the shoreline. Instrument networks that contribute multi-use functionality, such as HF radar networks, provide for effective and efficient long-term installations. [C2422]

### "Net based waterside security applications: From small solutions to maritime security networks"

The protection of military harbours is a complex task. A force protection system integrates several sensors and databases for ashore and waterside surveillance: • passive sensors (acoustic, magnetic, CCTV, IR, FO fence) • active sensors (Radar, Diver Detection Sonar) • remote / autonomous vehicles for inspection and surveillance • chart database • information database Additionally a network-based waterside security application should integrate several additional sources and services e.g.: • WEB based Automatic Identification System (AIS) • Satellite based AIS • Access to online databases e.g. weather information, ship register data • C4I data e.g. MCCIS (NATO C4I system) or JoCIS (EADS export C4I system) Also, new technical possibilities of modern multi touch HMI approaches and aspects of user centric man machine interface design will be discussed. [C2423]

### "SCANTER 5000 and 6000 Solid State Radar: Utilisation of the SCANTER 5000 and 6000 series next generation solid state, coherent, frequency diversity and time diversity radar with software defined functionality for security applications"

Coherent, Solid State Radar technology has been available for decades, however, it did not penetrate into harbor surveillance, VTS and related applications for cost and technical reasons. Technically, the main challenge is that dynamic requirements to radar in littoral waters and build up regions are much higher than to other radar applications. Those challenges have now been met and combined with well-renowned advantages from the Terma SCANTER product range. Methods are further refined and implemented on a new technology platform. The result is a software-defined radar series, tailored to individual market segments, virtually unrestricted by dynamic constraints. The digital radar concept with software-defined functionality makes the set-up of the radar easy. Furthermore, Interference rejection against disturbance from radars on ships passing nearby the radar has also proven effective, and the dynamic range has proved to be sufficient to eliminate any artefacts from a high number of large buildings and other structures in an operational area. Operational tests have been performed with impressive results. [C2424]

### "Multiple sensor fusion for effective abnormal behaviour detection in counter-piracy operations"

We propose a two-stage method based on multiple distributed sensors for detection of piracy operations at sea. The proposed method is based on fusion of evidence from radar and optical sensors as well as AIS signals. The sensors are land based, air based and space based. In the first stage, a number of detectors perform recognition of low-level events, such as vessel speed, direction, size and identification. Their outputs act as input to the second stage, which performs fusion and disambiguation of the first-stage detections taking into account multiple sensor fusion, multi temporal fusion and distributed fusion. The result should be effective abnormal behaviour detection, by which we mean a method that is able to detect piracy operation at an early stage, i.e. close to the time, or possibly before, the attack has occurred. A numerical example with a pirate attack is presented and discussed. [C2425]

### "Multi-frequency radar systems for monitoring vital signs"

This paper presents a theoretical and experimental analysis of multi-frequency radar systems for monitoring vital signs. The main advantage of using a multi-frequency architecture is the possibility to improve the detection sensitivity of heart beats and breathing rate while cancelling the body movement with signal processing. Simulations were carried out using ADS software for three systems operating at 5.8, 24 and 35 GHz. Different parameters such as antenna gain, mixer conversion loss and LNA gain were considered in the simulations for each system in connection with their system effects. It is shown that by using adequate correlation functions of received signals, it is possible to improve the detection accuracy. Experimental results are presented to validate the analysis and proposed approach. [C2426]

#### **"Detection of SSR signals in multipath airport environments by a multichannel receiver"**

Multipath propagation is a serious problem with Secondary Surveillance Radar (SSR) systems at airport apron and taxiway areas. In this approach, effective suppression of interference (garbling) by multipath components, using a multichannel receiver is presented. Thereby the SSR header format is exploited to detect multipath components, which are then eliminated by subspace based signal suppression. Extensive tests at Frankfurt international airport show the potential of the proposed approach to significantly improve reception at problematic sites. [C2427]

#### **"An experimental study of novel scanning system suitable for UWB radar application"**

In this paper, we present a novel electrical antenna scanning system suitable for short-range UWB radars. We have developed our previously proposed UWB impulse array antenna (IAA) and experimentally verified its usefulness. This antenna scanning system features two new technologies. First, each antenna element is equipped with an impulse generator. Second, the time control between the antenna elements is realized by using tapped delay lines and by transmitting trigger signals. An experimental UWB array antenna and a trial radar have been designed and fabricated. The measurement results show excellent performance of this antenna as a scanning antenna and as a short-range radar system. Thus, it is expected that this UWB antenna scanning system will contribute to the performance improvement, size and cost reductions of short-range radar systems such as obstacle detectors, anti-collision sensors and through-wall radars. [C2428]

#### **"A 0.8-13.4GHz combined voltage-controlled oscillator with an exclusive-OR in 130nm SiGe BiCMOS"**

Wide-tuning-range voltage-controlled oscillator (VCO) design is motivated by applications in broadband communications, radars, phase-locked loops and clock generation/distribution. In this paper, post-layout simulation results of a ring quadrature VCO (QVCO) combined with an exclusive-OR (XOR) to double the frequency in 130nm SiGe BiCMOS technology are presented. The combined VCO can be tuned from 0.8 to 13.4GHz. At 0.8GHz, the VCO consumes 13.98mW of power and generates -45 dBm (32nW) of output power into 50 Ohm loads. At 13.4GHz, it consumes 15.52mW of power and generates -30 dBm (1μW) of output power. In the tuning range, the XOR consumes ~11mW of power. The VCO phase noise at 10MHz offset frequency is -100.1dBc/Hz and -91.5dBc/Hz at 0.8GHz and 13.4GHz, respectively. The VCO figure of merit (FOM) is in the range of -127 to -142. The microchip area is 450μm<sup>2</sup>. [C2429]

#### **"Azimuth estimation in periodic linear sparse array by modified amplitude comparison monopulse radar"**

Estimation of direction of arrival (DOA) of a radar backscatter signal by means of an amplitude comparison monopulse estimation scheme (ACMES) is a common high precision technique. But due to spatial undersampling in a sparse array architecture the conventional ACMES results in azimuth ambiguity. In this paper it is proposed that azimuth ambiguity due to sparse array can be mitigated by replacing the sum beam in ACMES with a flat-top beam while keeping the difference beam unchanged. This approach was adapted and simulated for a naval HF Surface Wave Radar (HF SWR) with an array sparsely distributed among 4 mobile platforms each with a dense 9 element primary array. For a single target scenario the results confirm that the proposed approach achieves a precise angular estimate using a periodic sparse linear array. [C2430]

#### **"Millimeter wave FMCW radar system simulations including a 3D ray tracing channel simulator"**

In this paper a millimeter-wave radar system simulation environment for frequency-modulated continuous-wave (FMCW) radar using a 3D ray tracing channel simulator is presented. Therefore we use Agilent's RF design environment ADS® for system simulation and calculate the channel impulse response based on the data received from a 3D ray tracer in a Matlab®-co-simulation. To reduce computing time the whole signal flow is processed in a complex baseband representation and scattering center models are used as substitute for

complex polygon targets as further improvement. Nevertheless all effects occurring at harmonic bands and at DC due to nonlinearities in the transmitter and receiver circuits are well reflected in the simulation. A typical road scenario is simulated and the results show the capabilities of the simulation technique in terms of speed and accuracy. [C2431]

### **"An improved image-based Near-Field-to-Far-Field Transformation"**

An improved approach to determination of radar cross section (RCS) of electrically large targets from the scattered field measured with a monostatic radar over a circle in the near-field of the targets is presented. The frequency- and azimuth-domain scattering data are used to calculate a reflectivity map (radar image) of the target, from which RCS of the target is determined. The characteristic features of the proposed version of Near-Field-to-Far-Field Transformation (NFFFT) are the use of the calibrated signal from the network analyzer as the input data in the transformation and an improved focusing operator for producing reflectivity maps. The combination of these features is expected to result in a practical and more accurate approach to the analysis of scattering properties of electrically large targets. [C2432]

### **"Iterative DEM retrieving from multi-baseline interferometric SAR with MIMO"**

In the recent years, there has been growing interest in exploiting multi-baseline synthetic aperture radar interferometry (MB-InSAR) to solve layover effects and phase unwrapping problem of long baseline. In this paper we propose a novel system concept for MB-InSAR based on Multiple-Input Multiple-Output (MIMO) configuration. Alamouti space-time coding scheme based on two transmitters is introduced into multi-baseline InSAR system. We investigate its performance and processing features based on our space-borne multi-baseline InSAR simulator and iterative multi-baseline data fusion algorithm. The simulation results shows that the received signal to noise ratio (SNR) and the precision of iterative multi-baseline data fusion algorithm are significantly improved under Alamouti scheme. [C2433]

### **"Fish heart motion measurements with a body-contact Doppler radar sensor"**

This paper presents preliminary results demonstrating detection of cardiac motion and monitoring of fish heart rate using a contact antenna as a less-invasive alternative to surgical electrocardiogram (ECG) measurements. Ringtail Surgeonfish were used as initial test subjects with pcb patch and spiral antennas. The frequency of operation, 2.4 GHz, was chosen as a tradeoff between antenna size and propagation. The data show the importance of antenna placement for satisfactory heart motion detection. Measured heart rates varied with time and sedation level, generally near 60 bpm. Of the antennas used, the spiral antenna-provided signal most closely matched that seen with human test subjects. [C2434]

### **"Highly-integrated multi-channel radar sensors in SiGe technology for automotive frequencies and beyond"**

Nowadays, radar based safety- and comfort features for motor vehicles are available from nearly every car maker. For the final breakthrough highly-integrated and low-cost radar sensors are required. Current developments based on silicon germanium (SiGe) heterojunction bipolar transistors show the potential to become the technology of choice for the mass market. In this contribution beside regulatory issues and radar basics, state-of-the-art concepts and semiconductor circuits for highly-integrated multi-channel radar sensors at automotive frequencies around 77 GHz and beyond at 94 GHz and 120 GHz, are summarized. Novel concepts allow, e.g., the realization of integrated multiple-input multiple-output sensors, phased array transmitters, and digital beamformers. RF signal generation, based either on fundamental frequency oscillators or on frequency multiplier techniques, is applied in monostatic or bistatic radar configurations with homodyne or heterodyne receiver concepts. Above systems were all demonstrated by using Infineon Technologies' automotive qualified B7HF200 SiGe technology. By using a modified and advanced technology applications at 120 GHz are also presented. The shown components form the basis for next generation automotive systems as well as for industrial applications, which take advantage of the commercial availability of integrated radar frontends. [C2435]

### **"Compressive sensing for high resolution radar imaging"**

In this paper we present some preliminary results on the application of Compressive Sensing (CS) to high resolution radar imaging. CS is a recently developed theory which allows reconstruction of sparse signals with a number of measurements much lower than what is required by the Shannon sampling theorem. This method has already found its way in a number of applications where the sampling rate or the acquisition time are prohibitive for real time applications, such as high resolution medical and optical imaging. Actual demonstrations of CS with experimental radar data are still very few, and therefore in this paper we apply CS to two-dimensional radar imaging with experimental data. The measurement setup contains a small number of corner reflectors which are



illuminated using a stepped sequence of frequencies, over a range of aspect angles. The CS approach uses only a random selection of frequencies and angles, to reconstruct the two-dimensional image. The results obtained with CS are compared with the one achieved with conventional focusing (Matched Filter). The results show that the corner reflectors are properly reconstructed, with a significant reduction in the amount of measurement samples. [C2436]

#### "On the polarization response using resonances for target recognition"

In most studies concerning resonance based target recognition, targets are usually excited and measured using a linear polarized basis and at the same time ignoring the cross polarization component. In this paper, the possibility of using circular polarization in this context is investigated. Numerical results of some simple wire targets demonstrate that it would be easier to fully excite all of the important resonances using a circular polarization basis with due consideration of the co- and cross-polarized directions. [C2437]

#### "Pulse reduction method for circularly polarized synthetic aperture radar"

Many types of data compression for SAR raw data have been developed during the past 30 years. Since most of them focus on reducing the number of bits required to store signal information onboard, the resulting complexity has been a great hindrance to the implementation of an efficient compression algorithm. We propose a new method of data compression that can be carried out onboard a small-sized platform. The method imposes no additional requirement on the antenna size by reducing the number of pulses needed to produce an image and compensating the missing pulses based on information provided from other pulses. The most complicated task of reconstructing the missing pulses can be performed in the ground station, not onboard the small platform. Because fewer pulses are needed, less power will be required for transmitting and receiving the pulses. This is advantageous for reducing the pulse repetition frequency (PRF), which normally becomes higher for smaller antennas. This method will be applied to our circularly polarized synthetic aperture radar (CP-SAR) system, which is currently being developed toward a mission onboard a microsatellite. [C2438]

#### "Resonant frequency optimization of coaxially fed rectangular microstrip antenna using Particle Swarm Optimization algorithm"

Coaxial probe fed rectangular microstrip antenna is a popular type of patch antenna having applications in communication and radar systems. Particle Swarm Optimization (PSO) is a popular optimization algorithm and recently it is being used for design optimization of microstrip patch antennas. In this paper PSO has been used for optimization of resonant frequency of coaxial probe fed rectangular microstrip antenna. Investigation is made at different microwave frequencies and ranging between 3 GHz and 18 GHz. The optimization problem has three variables namely, patch length, patch width and position of the feed. Results encourage the use of PSO for optimal design. [C2439]

#### "Remarks on the Cramer-Rao inequality for Doppler-based target parameter estimation"

This paper outlines the problem of multi-static Doppler-based target position and velocity estimation. The Fisher information matrix is derived given a separate target illuminator and then given a target-based isotropic signal emission. Some remarks concerning the Cramer-Rao inequality and its relationship to the estimation problem are given. Some results concerning the placement of the receivers are given and some open problems are discussed. [C2440]

#### "Electromagnetic imaging using compressive sensing"

We develop a near-field compressive sensing (CS) estimation scheme for localizing scattering objects in vacuum. The potential of CS for localizing sparse targets was demonstrated in previous work. We extend the standard far-field approach to near-field scenarios by employing the electric field integral equation to capture the mutual interference among targets. We show that the advanced modeling improves the capability to resolve closely spaced targets. We compare the performance of our algorithm with the performances of CS applied to point targets and beamforming. In this paper, we consider two-dimensional (2D) scatterers. However, the results and conclusions can be extended to three-dimensional (3D) problems. [C2441]

#### "Autonomous marine craft navigation: On the study of radar obstacle detection"

Technological advancements over the years have increased the use of Radar technology in the field of robotics, especially in marine robotics to aid obstacle detection algorithms. Obstacle detection comprises of an analytical process in which different algorithms are applied to the field of study to determine the range of objects that are within the reach of a robot. Radar signal analysis and target detection in conjunction with target tracking are

attributes required for autonomous marine navigation. The paper presents a model which converts optimal estimates of radar range values for each range spectra into multiple targets down-range and also presents an approach for power range spectra (range bins) prediction using the radar range equation with adequate information of the signal-to-noise ratio (SNR) of the radar. Obstacle detection in the presence of noise raises certain probabilities of false alarms. Target characteristics are simulated and these are fluctuating targets and non fluctuating targets. Analytical models, simulations and techniques of obstacle detection for autonomous marine craft navigation using a continuous wave radar system were points of discussion in the paper. [C2442]

#### **"Trajectory control of autonomous fixed-wing aircraft performing multiple target passive detection and tracking"**

This paper presents progress made in a previously proposed algorithm for trajectory optimization of autonomous aerial vehicles performing multiple target tracking. The base algorithm, which was described in two earlier papers, involves a variant of the model predictive control approach, built on a partially observed Markov decision process (POMDP) model of the sensor-target system. In this paper modifications and additions made to deal with fixed-wing aircraft dynamics of the controlled vehicles are described and results of simulations involving multiple fixed-wing UAVs, no-fly zones and targets are presented. [C2443]

#### **"Multifunction array lidar network for intruder detection, tracking, and identification"**

This paper describes a novel lidar sensor network based on a small, flat, optical phase array laser aperture. The network of array lidars provides collaborative automatic detection, tracking, acquisition cueing, and intruder type identification, as well as free space optics communication. The lidar consists of four optical phased arrays, each with about 1 million radiating elements in a 1-cm<sup>2</sup> aperture that enable electronic beam steering analogous to microwave array antennas. The four arrays are mounted on four sides of a stalk and have a full 360° field of view. A small number of such stalks can perform target detection over a large area. [C2444]

#### **"Maximum likelihood approach for tracking multiple mobile agents with a moving Doppler radar system"**

Tracking mobile agents with a Doppler radar system mounted on a moving vehicle is considered in this paper. Dopplers modulated from mobile agents on the single frequency continuous wave signals are analyzed in order to estimate the positions and velocities of multiple mobile agents. The measurement noise is assumed to be Gaussian and the maximum likelihood estimation is utilized to enhance the localization accuracy. [C2445]

#### **"Line-based SLAM with slow rotating range sensors: Results and evaluations"**

This paper is concerned with the Simultaneous Localization And Mapping (SLAM) application with a mobile robot moving in a structured environment using data obtained from rotating sensors such as radars or lasers. A line-based EKF-SLAM (EKF stands for Extended Kalman Filter) algorithm is presented, which is able to deal with data that cannot be considered instantaneous when compared with the dynamics of the vehicle. When the sensor motion is fast relative to the measurement time, scans become locally distorted. A mapping solution is presented, that includes sensor motion in the observation model by taking into account the dynamics of the system. Experimental results with real-world 2D-laser scanner data are presented. Moreover a performance evaluation of the results is carried out. A quantitative performance evaluation method is proposed when dealing with a 2D line map and when a ground truth is available. It is based on the bipartite graph matching and combines several criteria that are described. A comparative study is made between the output data of the proposed method and the data processed without taking into account distortion phenomena. [C2446]

#### **"Application of AIS in Marine Search and Rescue Radar"**

Nowadays marine radar detects targets by Constant False Alarm Rate (CFAR). But the search and rescue efficiency is low in poor visibility or serious interference. In this paper, we reference learning mechanism, set up the AIS information for the sample and estimate the threshold  $t$  of the search targets with Maximum Likelihood (ML). Then any ship can be distinguished and searched. Experimental results show that using this method can improve the efficiency and accuracy of marine search and rescue radar searching the targets. [C2447]

#### **"The Research of the Training Assistant Decision-Making Support System Based on Data Mining Technology"**

The key of success in the battle lies in the usual training. Training is very important to the army. The Training assistant decision-making System can sum up the training data, and provides statically result to the officers of the training department. According to the suggestion provided by the training assistant decision-making System,

the training managers can draft the training plan of the next year. Data mining, which emerged about twenty years ago, has been rapidly evolving into a widely used technique for dealing with large amount of data for army to analyze training decisions and alternative. In this paper, we show how data mining methods can be used in the training plan drafting and improve the efficiency of the Training assistant decision-making support System.

[C2448]

### "Plant Species Classification Using a 3D LIDAR Sensor and Machine Learning"

In the domain of agricultural robotics, one major application is crop scouting, e.g., for the task of weed control. For this task a key enabler is a robust detection and classification of the plant and species. Automatically distinguishing between plant species is a challenging task, because some species look very similar. It is also difficult to translate the symbolic high level description of the appearances and the differences between the plants used by humans, into a formal, computer understandable form. Also it is not possible to reliably detect structures, like leaves and branches in 3D data provided by our sensor. One approach to solve this problem is to learn how to classify the species by using a set of example plants and machine learning methods. In this paper we are introducing a method for distinguishing plant species using a 3D LIDAR sensor and supervised learning. For that we have developed a set of size and rotation invariant features and evaluated experimentally which are the most descriptive ones. Besides these features we have also compared different learning methods using the toolbox Weka. It turned out that the best methods for our application are simple logistic regression functions, support vector machines and neural networks. In our experiments we used six different plant species, typically available at common nurseries, and about 20 examples of each species. In the laboratory we were able to identify over 98% of these plants correctly. [C2449]

### "X-band radar based SLAM in Singapore's off-shore environment"

This paper presents a simultaneous localisation and mapping (SLAM) algorithm implemented on an autonomous sea kayak with a commercial off-the-shelf X-band marine radar mounted. The Autonomous Surface Craft (ASC) was driven in an off-shore test site in Singapore's southern Selat Pua marine environment. Data from the radar, GPS and an inexpensive single-axis gyro data were logged by an on-board processing unit as the ASC traversed the environment, which comprised geographical and surface vessel landmarks. An automated feature extraction routine is presented, based on a probabilistic landmark detector, followed by a clustering and centroid approximation approach. With restrictive feature modeling, and a lack of vehicle control input information, it is demonstrated that via the novel RB-PHD-SLAM Filter, useful results can be obtained, despite an actively rolling and pitching ASC on the sea surface. In addition, the merits of investigating ASC SLAM are demonstrated, particularly with respect to the map estimation, obstacle avoidance and target tracking problems. Despite the presence of GPS and gyro data, heading information on such small ASC's is greatly compromised which induces large sensing error, further accentuate by the large range of the radar sensor. This work is a step towards realising an ASC capable of performing environmental or security surveillance and reporting a real-time active awareness of the above-water scene. [C2450]

### "A lidar perception scheme for intelligent vehicle navigation"

In urban environments, detection of moving obstacles and free space determination are key issues for driving assistance systems or autonomous vehicles. This paper presents a lidar-based perception system for passenger-cars, able to do simultaneously mapping and moving obstacles detection. Nowadays, many lidars provide multi-layer and multi-echo measurements. A smart way to handle this multi-modality is to use grids projected on the road surface in both global and local frames. The global one generates the mapping and the local is used to deal with moving objects. An approach based on both positive and negative accumulation has been developed to address the remnant problem of quickly moving obstacles. This method is also well suited for multi-layer and multi-echo sensors. Experimental results carried out with an IBEO Alasca and an Applanix positioning system show the performance of such a perception strategy. [C2451]

### "ATENEA: Advanced techniques for deeply integrated GNSS/INS/LiDAR navigation"

The ATENEA (Advanced Techniques for Navigation Receivers and Applications) project aims to join deeply integrated GNSS/INS receiver architectures and LIDAR techniques to provide an advanced navigation solution. The approach is suitable for a wide range of surveying applications in difficult environments, being Urban Mapping selected as reference case. ATENEA tackles the most challenging issues of this type of applications, showing how the use of Galileo signals, integrated positioning and observable processing can in one shot solve the more severe technical issues (robustness and continuity), increase accuracy and drastically reduce the system cost. The goal of the ATENEA project is to develop an advanced technology concept for seamless navigation at the cm-level regardless of the environment. [C2452]

### "Insights about reliability of Heterojunction Bipolar Transistor under DC stress"

250GHz SiGe(C) Heterojunction Bipolar Transistor (HBT) is a high performance device with low noise figure and high transconductance particularly required in power RF circuits. Applications are various: 77GHz automotive radars, non invasive imaging in airport for example. In order to achieve such specification, aggressive design leads to use of HBT at high collector current and sometime with VCEbias higher than collector emitter breakdown voltage with open base BVCEo. This last bias condition is known to induce progressive degradation with time and must be taken into account in Design-in-Reliability model. While reverse mode has been widely investigated, reliability of direct mode biased HBT is a new research field. It has been recently investigated, the underlying damage physics is now identified, the integrity of EB and BC junctions is known to be impacted as illustrated in the simulation of Fig. 1. The present paper aims at presenting a methodology for characterizing the aging of HBT in time and translating the parameters change of its model card. [C2453]

### "Adaptive polarimetric MIMO radar detection"

This paper mainly deals with the target detecting problem using polarimetric Multiple Input and Multiple Output (MIMO) radar with unknown covariance matrix. And the GLRT-based receiver is devised by resorting to the two-step design procedure. Specifically, the GLRT is devised with known covariance, and then, a suitable estimate of covariance is obtained using secondary data to plug into the derived test. The performance is assessed by several numerical examples, and the results show that polarimetric diversity can be exploited to enhance the performance of detection. Moreover, the adaptive loss is acceptable. [C2454]

### "The KA-MLFMA hybrid algorithm for analyzing the electromagnetic scattering from a 3-D target over random rough surface"

A hybrid algorithm combining the analytic Kirchhoff approximation (KA) and the numerical multilevel fast multipole algorithm (MLFMA) is proposed to calculate the electromagnetic scattering from a composite model of three-dimensional (3-D) perfect electric conducting (PEC) object over Gaussian random rough PEC surfaces. The KA and MLFMA are used to deal with calculations of the Gaussian rough surface and the object, respectively. Meanwhile, an iterative approach is employed to analyze the coupling interactions between the object and rough surfaces. From some numerical results, it can be illustrated that this hybrid algorithm can not only give the reliable results, but also greatly reduce the computational costs comparing with conventional numerical methods. The bi-static difference field radar cross-section (RCS) of a 3-D object above random rough surfaces is also discussed in this paper. [C2455]

### "Fusion method of radar data and IFF data based on NMF"

A new fusion method of radar data and IFF data based on nonnegative matrix factorization (NMF) is proposed in this paper, due to its strong part-based representation capability. The identification data from each sensor are put into one column of the input matrix and the fusion is realized by the converging process of a cost function. The proposed fusion method does not only show better performance in the credential level, but also has the advantage of limited computational load. The proposed method is simulated to validate the effectiveness and significant improvement in comparison with the data fusion algorithm under the framework of D-S evidential theory. [C2456]

### "A frequency synchronization method for hybrid bistatic SAR using direct path signal"

We propose a frequency synchronization method for hybrid bi-static synthetic aperture radar (SAR), which denotes a SAR system with a spaceborne illuminator and an airborne receiver. Due to the high altitude difference, the method based on extracting the direct path signal is employed. The mathematical model to compute the frequency offset between the two sides' oscillators is given. Among the model, a novel method for estimating the Doppler centroid for hybrid bi-static SAR is proposed. Error analysis is carried out, and the result indicates that under normal signal to noise ratio and frequency stability level the estimation error is within the acceptable value. A simulation was performed and the result shows that the imaging result is favorable after compensation. [C2457]

### "A forward-looking 3-D SAR imaging model using unequally spaced array"

A forward-looking 3-D SAR imaging model using an unequally spaced array is proposed in this paper. Firstly, based on the problems that a real equally spaced array suffers, like heavy calculation, the couple between antenna elements, an unequally spaced array with optimized element positions, is obtained by Simulated Annealing. Compared with several different types of arrays, the unequally spaced array has obvious advantages: when the lengths of arrays are the same, it successfully avoids the presence of grating lobes in the beam



pattern, and needs much less number of array antennas than the real array does; when the number of array antennas is fixed, it has narrower main-lobe than the real array. Furthermore, the signal model of the forward-looking 3-D SAR is analyzed and using BP algorithm the simulation results are presented, validating and verifying the feasibility of this model to reconstruct a 3-D scene. [C2458]

#### "An EKF multi-baseline phase unwrapping algorithm"

This paper presents a phase unwrapping algorithm based on the extended kalman filter (EKF) for multi-baseline SAR interferometry. This algorithm achieves simultaneously noise filtering and phase unwrapping by combining an EKF with a conventional path-tracing strategy. The simulation data processing results validate the effectiveness of proposed method, and show a significant improvement with respect to some conventional algorithms in some situations. [C2459]

#### "Ionospheric phase contamination correction method using Generalized S-Transform"

This paper analyzes the instantaneous frequency (IF) estimation properties of S-Transform (ST) and proposes the reason of the poor estimation performance for ST at low frequencies. A Generalized S-Transform (GST) which has better performance than the ST at low frequencies is therefore introduced in the IF estimation. It is the first time applied in the phase contamination correction of Over-the-horizon-radar (OTHR) in this paper. The effectiveness of the GST has been studied by using the data of high frequency surface wave radar (HFSWR) with artificially added phase perturbations. Through the comparisons on the calculation complex and the effectiveness of contamination correction with the Pseudo Wigner-Ville Distribution (PWVD) method and the Modified Adaptive Short Time Fourier Transform (MASTFT) method in the referred literatures, the GST method used in this paper has much better performance. [C2460]

#### "Compressed sensing moving target detection for MIMO radar with widely spaced antennas"

The moving target detection based on compressed sensing (CS) multiple-input multiple output (MIMO) radar with widely separated antennas is studied. The centralized processing is considered. The traditional centralized MIMO radar requires an exhaustive search on every possible two dimensional target velocity, resulting in huge computational complexity. In this paper, we adopt the CS technique to drastically reduce the computational burden and evaluate the reduction of the required complexity. We derive the moving target detector for the CS MIMO radar. The performance of the proposed detector is analyzed, and the receiver operating characteristic (ROC) curves are provided. [C2461]

#### "Coexistence studies for TD-SCDMA with radar system in the band 2300-2400 MHz"

Because of the lack of sufficient frequency bands, the TD-SCDMA system is possibly deployed in the same band with other existing communication systems. In this paper, the coexistence studies for the TD-SCDMA system with the radar system, which has been widely deployed in the band 2300-2400 MHz, is presented. The dynamic system simulation methodology is utilized in the coexistence studies, and simulation results of the impacts on the system performance with different isolation distance and frequency spacing are given. The feasibility of the coexistence between TDSCDMA and the radar system is investigated and some useful conclusions are also presented. [C2462]

#### "Retrieval of oriented vegetation parameters based on experimental data of PolInSAR"

Polarimetric SAR interferometry (PolInSAR) can be used to inversion of vegetation parameters and a two-layer coherent scattering model composed of a random volume over the ground is applied usually. However, the propagation of the electromagnetic waves is anisotropic because the extinction coefficients are highly polarization dependent, the random model is inapplicable. In this paper, a new vegetation model composed of an oriented volume over the ground is employed and experimental data about the true scene can be gained through the microwave anechoic chamber. Finally, the oriented vegetation parameters are retrieved by using three-stage method. [C2463]

#### "Modeling and simulation of chaff cloud interference to SAR"

As a typical passive jamming, chaff cloud have a strong moderating effect on various radar systems. It's also one of typical interference to synthetic aperture radar (SAR). In order to study the impact of chaff cloud on the SAR, based on mathematical expression of SAR reflection deduce the formulation of single chaff reflection, obtained that there is the incoherent Gaussian white noise interference with all band in the azimuth direction. Then from single chaff reflection mathematical expression deduce the chaff cloud mathematical expression, obtained that there is the coherent interference in the radial direction. Give the calculation method of jam power.

At last show the simulation result of chaff cloud interfere. [C2464]

### "Statistical MIMO radar based on coherent signals"

Multi-Input and Multi-Output (MIMO) radar was a new radar technology in the recent years, which used spatial diversity gain of the signal instead of coherent gain in traditional phased-array radar. Using the ideal point source model, this paper made an analysis of these two kind gain's contribution to radar detection system, which was divided into two classes: the contribution to system robustness and the contribution to improve the signal-to-noise ratio. Based on this, proposed that the MIMO radar's space diversity gain could make more contribution to signal-to-noise ratio, which rationality was showed by the modification of the statistical MIMO model. The above theory was verified by simulation. [C2465]

### "Chaotic signal reconstruction with application to noise radar system"

In this paper, we present a new method that is accurate and has low computational complexity to estimate the initial condition of chaotic signal. Then the estimation method is applied to a noise radar system using noncoherent reception scheme. In the new scheme, the received signal correlates with the estimated transmitted signal by the estimation method proposed in this paper. The new scheme avoids a difficult problem that how to accomplish the transmitted signal delayed by delay lines when the signal band is large. Finally, computer simulations are performed to illustrate the effectiveness of the proposed scheme. [C2466]

### "Study of Common Simulation Platform of Pulse-Compression Radar Signal Processing: A Method of Studying Radar System"

Pulse-Compression radar signal processing simulation platform provides a new way on radar digital signal processing, which is not only low-cost, easy maintenance, as well as the characters of standardization, modularization, scalability and restructure. In this paper, we present a Pulse-Compression radar echo signal processing simulation framework and module structure based on pulse compression approach, and analyze the system's data stream through a set of simulation data in interaction, encapsulation and generalization. [C2467]

### "Passive multi target tracking with GM-PHD filter"

This paper considers the challenging problem of multitarget tracking with passive data, obtained here by geographically distributed cameras. We use a Gaussian Mixture Probability Hypothesis Density filter approach to solve this difficult problem. As we make no spatial assumptions for the birth process, we use a slightly modified filter to obtain our results. We first describe the modified filter and detail our application before we present some results obtained on a realistic test scenario. Our simulations demonstrate that the proposed Probability Hypothesis Density filter is a promising candidate for three dimensional passive multi target tracking in clutter. [C2468]

### "Active clutter reduction through fusion with passive data"

Active and passive sonar systems often provide complementary information. Active systems generally provide good localization but are subject to high rates of clutter from bottom and volumetric scatterers. Passive systems generally have good resolution only in bearing and only can detect objects that emit acoustic energy. By fusing measurements from both types of systems, the passive data can be used to reduce the clutter in the active data. The result is improved target tracking, as shown in two examples, including the injection of a single target into a recorded active clutter dataset. [C2469]

### "Gaussian Mixture initialization in passive tracking applications"

This paper describes the approximation of a nonlinear posterior density by a Gaussian Mixture (GM). The GM is used to initialize a bank of Kalman filters. For each Gaussian term, a Kalman filter is started. The basic conditions and the quality of the approximation are discussed. Examples from different tracking applications, the multistatic tracking and passive emitter localization using TDOA measurements, are investigated. The results are discussed and compared with existing approaches. The RMS error of the estimate is used as an evaluation criterion. The performance of the Gaussian Mixture approach is analyzed in Monte Carlo simulations. [C2470]

### "Simultaneous navigation and SAR auto-focusing"

Synthetic Aperture Radar (SAR) equipment is an all-weather radar imaging system that can create high resolution images by means of utilising the movement of the flying platform. Accurate knowledge of the flown trajectory is essential in order to get focused images. Recently SAR systems are becoming more used on

smaller and cheaper flying platforms like Unmanned Aerial Vehicles (UAV). Since UAVs in general have navigation systems with poorer performance than manned aircraft, the resulting images will inevitably be unfocused. At the same time, the unfocused images carry the information about the platforms trajectory that can be utilised. Here a way of using SAR images and their focus measure in a sensor fusion framework in order to simultaneously obtain both improved images and trajectory estimate is presented. The method is illustrated on a simple simulated example with promising results. Finally a discussion about the results and future work is given.

[C2471]

### "A general approach for altitude estimation and mitigation of slant range errors on target tracking using 2D radars"

When target tracking using polar (azimuth and slant range only) measurements is performed, the most usual approach is to simply ignore slant range errors and perform target position estimation on a 2D plane. In reality, slant range errors are very significant and can seriously impair tracking. 3D target tracking can mitigate the effect of slant range errors, and, in some cases, even allow altitude to be estimated. This paper analyzes previous approaches on 3D target tracking using 2D radars and their drawbacks, and proposes efficient methods (based on EKF, UKF and AMM-EKF) that can be used on realistic scenarios, without significant increase on computational cost. A robust filter initialization technique is also proposed for these methods. [C2472]

### "Parameter estimation of K distribution based on second-kind statistics"

The parameters of K distribution are estimated in this paper, and the log-cumulant estimator is proposed based on second-kind statistics. The performance of the log-cumulant estimator is tested on the Monte Carlo simulations. Parameter estimation results demonstrate that the log-cumulant estimator leads to high estimation accuracy for the small values of the shape parameter. [C2473]

### "Robust sensor fusion in real maritime surveillance scenarios"

This paper presents the design and evaluation of a sensor fusion system for maritime surveillance. The system must exploit the complementary AIS-radar sensing technologies to synthesize a reliable surveillance picture using a highly efficient implementation to operate in dense scenarios. The paper highlights the realistic effects taken into account for robust data combination and system scalability. [C2474]

### "GMTI tracking using signal strength information"

Signal strength information is a standard output of a modern radar system. Provided the amplitude of the target returns exceeds the false alarm background, the consideration of signal strength may lead to improved target estimates, depending on the scenario. In this paper a Bayesian tracking algorithm is presented which incorporates the signal strength information. In contrast to previous approaches, the knowledge on the target's signal strength is not only used for an improved calculation of the association probabilities, but it enters into the algorithm as a random variable which is sequentially estimated. By this approach it is not only possible to discriminate closely-spaced targets and improve the track continuity, but also to support possible classification and identification tasks. The signal strength fluctuations of the target returns are modeled by the Swerling-I and Swerling-III cases. As a first performance evaluation, numerical results are presented based on a multi-target simulation scenario. [C2475]

### "A simulation framework for testing GMTI trackers"

Trackers for Ground Moving Target Indicator (GMTI) radar have to be benchmarked in order to yield good results. For many benchmarking purposes, the usage of real data may become expensive and in-feasible. It may also lack of knowledge of the ground truth. Simulating GMTI situations is a less-expensive alternative to real measurements. In order to get a realistic scenario, the motion and radar cross section (RCS) of ground targets, the motion of sensor platforms and the properties of GMTI sensors have to be simulated. In this paper, considerations for a realistic motion and sensor model are presented. Then, an implementation of a framework for simulation is shown, together with first experiences in tracker benchmarking using this framework. [C2476]

### "Applying optimal search theory to inland SAR: Steve Fossett case study"

Steve Fossett, a famous adventurer, disappeared on 3 September 2007 in a remote area of Nevada during a solo pleasure flight in a small aircraft. An intense search conducted by both private parties and multiple government agencies was eventually suspended with negative results. Fossett's wreck was discovered in California's eastern Sierra Nevada mountains by a hiker almost one year later. This paper describes an independent effort to direct search efforts using probabilistic search theory and optimization techniques. Using

field data from various sources, several scenarios were constructed to establish a prior distribution of the crash site. Search efforts were assessed to generate a posterior of the crash location for future search efforts. [C2477]

### "Constrained multi-object Markov decision scheduling with application to radar resource management"

Hierarchical radar resource management uses multi object Markov decision scheduling with a constraint on the resources. In this paper we give a detailed description of constrained multi-object Markov decision scheduling in its general form and the separation that is achieved in the dynamic programming level using Lagrange multipliers. We then apply this general model to obtain a simultaneous beam and waveform scheduling method for radars based on an objective function that depends on both state and action. This method extends on a previous hierarchical method for beam scheduling with an objective function defined only on state. We further improve the objective function based on entropy reduction. This criterion makes the resource management to be more flexible in favor of measurements that carry more information. [C2478]

### "Efficient multilateration tracking with concurrent offset estimation using stochastic filtering techniques"

Multilateration systems operate by determining distances between a signal transmitter and a number of receivers. In aerial surveillance, radio signals are emitted as Secondary Surveillance Radar (SSR) by the aircraft, representing the signal transmitter. A number of base stations (sensors) receive the signals at different times. Most common approaches use time difference of arrival (TDOA) measurements, calculated by subtracting receiving times of one receiver from another. As TDOAs require intersecting hyperboloids, which is considered a hard task, this paper follows a different approach, using raw receiving times. Thus, estimating the signal's emission time is required, captured as a common offset within an augmented version of the system state. This way, the multilateration problem is reduced to intersecting cones. Estimation of the aircraft's position based on a nonlinear measurement model and an underlying linear system model is achieved using a linear regression Kalman filter [1, 2]. A decomposed computation of the filter step is introduced, allowing a more efficient calculation. [C2479]

### "Integrated GMTI radar and report tracking for ground surveillance"

The fusion of information gathered from multiple sources is essential to build a comprehensive situation picture for ground surveillance. In this paper, an approach which performs data correlation and fusion for ground moving target indicator (GMTI) radar data and SALUTE reports is described. GMTI data are simulated based on the ground truth of a military exercise and processed by a GMTI group tracker employing a Cardinalized Probability Hypothesis Density (CPHD) Filter. Multi source fusion is performed by combining the GMTI tracker and report tracker using our data fusion architecture. The scenario used in the experiment is tracking of closely spaced ground targets by GMTI, supplemented with some collected SALUTE reports. The challenges include tracking ground targets moving across foliage and tactical movement (start-stop mode). Using the designed test scenarios, this paper looks into different aspects of benefits by performing cross fusion with GMTI data and SALUTE reports. [C2480]

### "A new co-located MIMO radar system for multi-target tracking and localization"

Multiple Input Multiple Output (MIMO) radars are a new generation of radar systems that bring with them many benefits compared to traditional phased-array and multistatic radars. Target localization using MIMO radars with co-located antennas has been recently discussed in the literature. It has been shown that the maximum number of targets that can be uniquely localized in one cell is bounded. This paper presents a new application of MIMO radars in Multi-Target Tracking (MTT) problems. Firstly, the previous model for co-located MIMO radars is modified in order to guarantee the observability in received measurements. Afterwards, it is shown that using prior information about the motion of targets relaxes the limitation on the number of uniquely localized targets. For filtering part, an Un-scented Kalman Filter (UKF) algorithm is used to update states of targets. Simulation results confirm the superiority of proposed approach in estimating states of multi-targets falling in the same resolution cell. [C2481]

### "Radar cross section of the human heartbeat and respiration"

This paper describes an experimental approach for finding the radar cross section (RCS) of human heartbeats and respiratory movements. A measurement setup, a calibration routine and required processing steps are presented. Using a 2-3GHz Ultra Wideband (UWB) radar, heartbeats and respiration of a human subject were recorded from a distance of 1.14m. Combining the recorded data to measurements with a calibration sphere, the



calibrated human heartbeat and respiration RCS was detected. [C2482]

### "UWB Microwave Monopulse Radar System for breast cancer detection"

The concept of an Ultra Wideband (UWB) Monopulse Microwave Radar System for detection and location of breast cancer is described. The system uses a two-element Tapered Slot Antenna (TSA) array accompanied by a UWB 180° hybrid which scans the breast. When the breast tissue features symmetry with respect to the array axis and the hybrid enables the 180° out phase feeding operation, the array automatically eliminates background while extracting information about an off axis target. The data obtained from the scan is post-processed using a novel imaging algorithm to locate the target. The design of the required 2-element UWB array antenna and the 180° hybrid is presented. The validity of the proposed breast cancer detection method is demonstrated in an example of a simple breast phantom formed by a cylindrical plastic container filled with a vegetable oil and small cylindrical targets. [C2483]

### "A secured chaos encrypted mode-S aircraft identification friend or foe (IFF) system"

This paper introduces a new technique for aircraft identification friend or foe (IFF). The technique is based on using a proposed Chaos Advanced Encryption Standard (AES) with mode-S IFF. AES has a key size of 128 bits and a substitution-linear transformation network with 10 rounds. The sensitivity of the chaos initial condition gives the algorithm the ability to use as a second key. The first key was assigned using a soft look-up table used periodically. The second key was assigned using the date of the current day by both interrogator and the transponder. This technique gives the system more security and confidentiality which is compatible with mode-S IFF interrogation and reply messages format. It requests a new data on the reply signal. This data increase the radar performance for detection and tracking the friend targets in active and passive jamming environments. The results obtained from this technique on the simulated interrogator and transponder signals shows that this scheme can be easily implemented and provide the air defence system a secured aircraft authentication.

[C2484]

### "Search Aid System Based on Machine Vision and Its Visual Attention Model for Rescue Target Detection"

The prompt search and rescue of lifesaving target is very important in the case that a marine casualty occurs. To detect the small target in the wide views over the sea, we have proposed a machine vision system to aid search and rescue on the sea, which combines remote sensing, radar, infrared with visual light technology. One of the detection methods in this system, which is based on visual attention mechanism, is proposed in this paper to find rescue target from visual light image. The color information, image intensity and other image properties are used to generate the feature maps that form the saliency map subsequently with the weighted integrating strategy. The experimental results show that the proposed method is efficient to detect the small target in cluttered ocean scene. [C2485]

### "SAR Images Despeckling via Bayesian Shrinkage Based on Nonsubsampled Contourlet Transform"

We propose a novel and efficient SAR image despeckling via Bayesian shrinkage based on nonsubsampled contourlet transform, which has been recently introduced. Despeckling by means of contourlet transform introduce many visual artifacts due to the Gibbs-like phenomena. Nonsubsampled contour let transform is a flexible multiscale, multidirection and shift-invariant image decomposition that can be efficiently implemented via transform. A Bayesian estimator is applied to the decomposed contour let coefficients of the logarithmically transformed image to estimate the best value for the noise-free signal. Experimental results show that compared with conventional wavelet despeckling algorithm, the proposed algorithm can achieve an excellent balance between suppresses speckle effectively and preserves image details, and the significant information of original image like textures and contour details is well maintained. [C2486]

### "Path Planning for UAV in Radar Network Area"

This paper mainly introduces a path planning algorithm for the unmanned aerial vehicles (UAVs) to avoid radar network. The radar network contains several radars which have different detection ranges. In this algorithm, firstly, according to the theory of the Delaunay triangulations, a directed graph is constructed based on the locations and the detection ranges of the radars. Secondly, the Dijkstra algorithm is used to search an initial path for the UAV. Thirdly, the optimization approach is used to calculate the optimal control vector which the UAV needs when the UAV navigates to the goal position along the initial path. The simulation results showed that the paths which are planned by the algorithm not only could guide the UAV to avoid the radar network, but

also satisfy some task-required constraints, which include temporal, spatial, and UAV maneuverability constraints. [C2487]

### "Electromagnetic absorbing nanocomposites including carbon fibers, nanotubes and graphene Nanoplatelets"

Nanocomposites loaded with different types of micro/nanofillers are developed and characterized for use in electromagnetic radar absorbing materials with minimum thickness. It is demonstrated that the tailoring of the desired EM properties can be achieved by the proper choice and combination of both the filler and the matrix. In particular, graphene Nanoplatelets dispersed in a bisphenol-A based epoxy matrix feature a loss tangent lower than a few percent and tailored dielectric permittivity. The designed bilayer absorbers entirely made with nanocomposites have thicknesses of 2 mm and 1.5 mm for the X-band and Ku-band respectively. [C2488]

### "FPGA based design and implementation of an Adaptive Binary Integrator"

Binary detection integrator is characterized by its simplicity, resistance against asynchronous interference, and its good detection performance. It suffers from detection loss due to non-homogeneous background. To overcome the limitations of binary integration, the Adaptive Binary Integrator (ABI) is used. ABI achieves the advantages of automatic detection and adaptive thresholding over the binary integrator. The presented adaptive binary integrator is designed and implemented using field programmable gate arrays (FPGAs). The performance of the proposed ABI is evaluated through the Receiver Operating Characteristic (ROC). The implemented hardware is evaluated experimentally under different conditions of noise, asynchronous interference, sea clutters, and rain clutters. High probability of detection is achieved by designing the Constant False Alarm Rate (CFAR) processor which is the first stage in the proposed ABI for relatively high probability of false alarm. The final probability of false alarm is then reduced by the effect of integration. [C2489]

### "Estimating polynomial structures from radar data"

Situation awareness for vehicular safety and autonomy functions includes knowledge of the drivable area. This area is normally constrained between stationary road-side objects as guard-rails, curbs, ditches and vegetation. We consider these as extended objects modeled by polynomials along the road, and propose an algorithm to track each polynomial based on noisy range and bearing detections, typically from a radar. A straightforward Kalman filter formulation of the problem suffers from the errors-in-variables (EIV) problem in that the noise enters the system model. We propose an EIV modification of the Kalman filter and demonstrates its usefulness using radar data from public roads. [C2490]

### "Radar tracking performance when sensing and processing compressive measurements"

Radar tracking performance is improved when using waveforms at high delay-Doppler resolution with concentrated ambiguity functions. High resolution measurement acquisition and processing, however, requires high rate sampling and intensive processing. Alternatively, compressive sensing and processing can be used to significantly reduce data rates with no loss in resolution. The drawback is, however, that using compressive measurements increases ambiguity function sidelobes and thus tracking error. In this paper, compressive sensing and processing is applied to single target tracking. The effect of compressive sensing and processing on the ambiguity function sidelobes is examined. Moreover, estimation using compressively sampled and processed Bjojrck CAZAC sequences is shown to be improved over estimation using linear frequency modulated waveforms sampled at the Nyquist rate. This shows that low-rate acquisition and processing maintains reliable tracking performance at high resolution, while simplifying the receiver and reducing computational expense. [C2491]

### "Effects of high-power and transient disturbances on wireless communication systems operating inside the 2.4 GHz ISM band"

This paper deals with special HPEM sources and their effects on wireless communication systems operating inside the 2.4 GHz ISM band. Different measurements have been performed to investigate the effect of UWB and radar pulses on the receiver of a digital wireless communication system. First the coupling of UWB and radar pulses into a typical bar antenna usable for the 2.4 GHz ISM band has been measured. Based on the coupling measurements the effects in the baseband of a typical wireless receiver is being investigated for different radar and UWB pulses. Finally a worst-case analysis by using a HF switch is being investigated for a WLAN and Bluetooth system. The results show how possible interferences with different interference durations and interference repetition rates can cause effects on the performance of a wireless communication system. [C2492]

### "Parallel processing techniques for the processing of synthetic aperture radar data on FPGAs"

This paper presents a design for the parallel processing of synthetic aperture radar data using one or more Field Programmable Gate Arrays (FPGAs). Our design supports real-time computation of a two-dimensional image from a matrix of echo pulses and their corresponding response values. Components of this design include: (a) central processing pipeline to perform back projection calculations, (b) pre-fetch cache to minimize external memory access latency, (c) memory bridge that serves as the primary on-chip storage for pulse data, and (d) a pixel queue to direct image data in and out of the pipeline. Design parameters may be adjusted to achieve optimum performance, and multiple instances of this design may be replicated on-chip to achieve prespecified performance objectives. We provide a complexity analysis as a function of the input and output parameters. Simulation results based on an implementation of this design show that our design achieves 160 GFLOPs per instance on a simulated Altera Stratix III EP3SL150 FPGA, and scales well for output image size ranging from 500 × 500 pixels to 5,000 × 5,000 pixels. [C2493]

### "Real time processing of a Lattice Wave Digital matched filter"

Based on the theory of wave digital filters (WDFs), an algorithm to represent a single pulse matched filter for radar applications is described. This matched filter is obtained by calculating the coefficients of a Lattice Wave Digital Filter (LWDF) adaptors by getting the filter transfer function that results from the arbitrary amplitude transfer function method. In this paper, we are interested only in the main loop of the matched filter frequency response and its pass-band edges locations. The design methodology permits the realization of the system for real-time applications. [C2494]

### "Analysis of signal characteristic and resolution in ground forward scattering radar"

In this paper, the target magnitude signature and Doppler signature characteristics are analyzed in detail. Based on the Doppler signature, the target motion parameters can be extracted. Combining the magnitude signal and Doppler signal, the target convoy resolutions in ground forward scattering radar (FSR) are analytically obtained, which is different from the conventional shadow inverse synthetic aperture radar (SISAR) resolution. Finally the experimented results fully verify the correctness of theoretic analysis. [C2495]

### "Wide area search munition delivered by the intermediate carriers"

This article introduces a new concept of SEAD systems-wide area search munition delivered to the zone of enemy air defense by the expendable intermediate carriers. It is assumed that the expendable intermediate carriers will replace conventional aviation in SEAD missions or at least reduce the risk for conventional aircrafts. Wide area search munition agents (mini-UAVs), delivered by expendable carriers, will extend SEAD actions to the territory controlled by the enemy IADS. The proximity of the enemy radars will increase the effectiveness of the SEAD efforts and allow countering the LPI radars. [C2496]

### "Adaptive clutter map detector in nonhomogeneous environment"

The Ordered Data Variability (ODV) technique is introduced into hybrid clutter map/L-CFAR technique, which is used to process the echoes on the clutter map spatially. The new method is called as Clutter Map/ODV (CM/ODV) technique. An analytic expression of detection probability in homogeneous environment is presented, and detection performance in three different situations in nonhomogeneous environment is analyzed. The CM/ODV can censor interfering targets adaptively and prevent the masking effect, moreover, it doesn't need any priori information, so the new kind of clutter map technique performs robustly. [C2497]

### "Self-calibrated method for distributed small satellite SAR systems"

In practice, the performance of the Distributed small satellite synthetic aperture radar (DSS-SAR) systems is affected seriously by the unavoidable array errors. In this paper, the phase and position errors are considered with the gain error calibrated by the adaptive processing. The clutter echo usually has Doppler (azimuth) ambiguities which is caused by lower pulse repetition frequency (PRF) in such systems. The array error estimation method is given based on the Doppler ambiguities. By analyzing the conventional method in which the phase error and the position error are estimated by iterating between each other, we find that: the steering vector of one Doppler ambiguity associated with the zero Doppler bin is conjugate to its opposite one. So the phase error can be directly obtained though the position error exists. The proposed method is given based on this. It estimates the position error independently without iterations between them. The proposed method can perform approximately as well as the conventional method but with less computation load. Simulations can verify its effectiveness. [C2498]

### "Prominent point InSAR processing"

The statistical property of prominent points in SAR interferometry is discussed after the derivation of the probability density function of Hermitian product of two correlated Rice class SAR signals. A simple processing strategy is then provided for better phase unwrapping performance based on prominent points. The validity of the proposed method is demonstrated by ENVISAT data. Our initial results show the advantage of such algorithm over conventional ones. [C2499]

### "Point target reference spectrum of bistatic SAR with parallel flight paths"

The precise point target reference spectrum of bistatic SAR has been a difficult problem for a long time. Many of the current available algorithms have approximation during deducing. This paper deduces the precise expression in Doppler-Frequency domain with the configuration of parallel flight paths and constant velocity of each platform. At last, simulations are given to demonstrate the good focusing performance. [C2500]

### "A new method of motion estimation and imaging interval selection of ISAR system based on geometry invariance of rigid target"

In this paper, a new method of motion estimation and imaging interval selection of ISAR System is proposed. In this method, based on the 1D-to-3D reconstruction algorithm, the motion path of the rigid target can be reconstructed firstly using the 1D range data of some scatterers extracted from the high-resolution range image of ISAR. Then according to the inertia of the target, the reconstructed motion path is fitted as a smoother trace with the rotation angles estimated effectively. Finally, the Hough Transform is utilized to extract a section of linear path on the 2D plane of the two rotation angles as the selected optimum interval of the ISAR imaging. Simulation results confirm that the method we proposed is effective and can be applied flexibly in current ISAR imaging techniques. [C2501]

### "A novel algorithm for synthetic aperture radar imaging based on compressed sensing"

To achieve high-resolution images, synthetic aperture radar (SAR) faces considerable technical challenges such as huge amount of data samples and high hardware complexity. Compressed sensing (CS) theory shows that the super-resolved images can be reconstructed from an extremely smaller set of measurements than what is generally considered necessary by Nyquist/Shannon theorem. In this paper, a new algorithm of SAR imaging based on the concept of CS is presented, in which a random fractional Fourier transform (FRFT) matrix is used as the sensing matrix. By utilizing the FRFT matrix the demodulator for de-ramping the linear frequency modulation signal can be eliminated. Simulation results with both simulated and real data exhibit the validity of the proposed algorithm. [C2502]

### "Method to determine CPI for ubiquitous radar"

Ubiquitous radio: is a new radar system that provides continuous and uninterrupted multifunction capability within a coverage volume. Continuous coverage from close-in "pop-up" targets in clutter to long-range targets impacts selection of waveform parameters. The CPI (Coherent Processing Interval) must be long enough to achieve a certain signal-to-noise ratio (SNR) that insures the efficiency of detection. This paper analyzes the condition of detection in the case of low SNR, discusses three different cases that would occur during integration and presents a method to determine the CPI. The simulation results show that it is available to determine the CPI for targets detection with SNR as low as -26dB in the experimental system. [C2503]

### "Study of array collocation for MIMO radar based on beampattern synthesis"

The beampattern of MIMO (Multiple-input Multiple-output) radar is the product of transmitter and receiver beam pattern. Exploiting uniform linear array, the beampattern has no grating lobe when a certain relation between the space of transmitter element and receiver element is met. Moreover, this kind of collocation takes on maximum virtual array aperture. Exploiting non-uniform linear array, the beampattern will have better performance. Giving the restriction of array aperture and the number of element and constructing objective function based on minimum side lobe, we make use of GA (generic algorithm) to optimize the element position and then get the non-uniform linear array collocation scheme. Simulations verify the validity of the proposed method. [C2504]

### "New target detection method in strong active jamming background for polarimetric radar"

A new method of target detection for polarimetric radar in the presence of strong active jamming is proposed. Based on analysis of the polarization characterizations of the signals received by polarimetric radar, the target detection is achieved through testing on the polarization information. Comparing with the traditional method of



target detection made in time-frequency domain, the detection performance of the new method is improved because the influence of the strong active jamming is avoided. The performance of the new method is analyzed by simulation. Its validity is verified through outdoor experiment carried out by X-band polarimetric radar. [C2505]

#### "Using target radial length for data association in multiple-target tracking"

Data association plays an important role in multi-target tracking. The traditional data association algorithm uses the nearest neighbor distance method. It will make mistake in larger echo density. Feature aided data association algorithm is tend of development in multi-target tracking. Incorporating target kinematics information and feature information can increase the information dimension, and enhance the association accuracy. In this work, feature aided nearest neighbor algorithm based on radial length of target is proposed. Comparing the traditional data association algorithm, the proposed algorithm can increase the times of correct association when targets move in parallel or move crosswise, and improve the performance of data association algorithm for multi-target tracking. [C2506]

#### "A novel CFAR detector for terminal guidance coherent radar"

In different Doppler channels, the amplitude distributions of sea clutter received by terminal guidance coherent radar are different. The Rayleigh distribution and Weibull distribution can be used to describe the amplitude distribution of different Doppler channel. A novel CFAR detector is proposed. Its performance is compared with column-window CFAR detector. The simulation results confirm that the proposed CFAR detector has a better detection probability compared with column-window CFAR detector. [C2507]

#### "Analysis and suppression for nonstationary clutter in airborne conformal array radar"

The characteristics of clutter nonstationarity for airborne radar with conformal antennas array (CAA) are analyzed, and an improved angle-Doppler compensation method is proposed based on above analysis. Unlike the uniform linear antennas array (LAA), the elements of CAA distribute in three-dimension space which lead to that the clutter angle-Doppler spectrum distribution should be described in four-dimension space. According to this theory, the clutter nonstationarity for airborne radar with CAA is firstly analyzed and the nonstationary nature of it is given. Then an improved STAP method for airborne radar with CAA which compensates the mainlobe clutter in four-dimension frequency domain is proposed. Finally, the simulation shows the effectiveness of the novel method for clutter suppression in airborne radar with CAA. [C2508]

#### "A novel approach of countering centroid jamming by using INS information in terminal guidance"

During anti-ship missile (ASM) tracking ship in terminal guidance phase, echo in monopulse radar seeker receiver was generated by modeling chaff and ship as Swerling II and Swerling IV in chaff centroid jamming scenario, respectively. A generalized likelihood ratio test (GLRT) algorithm was then proposed for chaff detection in the main-beam. When the presence of the jamming was detected, one can combine target position forecast with inertial navigation system (INS) navigation solution to accomplish the homing guidance of ASM, and then when the absence of the jamming was detected, radar seeker capture and track target again, which could help achieve one's purpose of anti-jamming. Simulation showed that this method was effective and feasible due to its preferable anti-jamming performance. [C2509]

#### "Application of compressive sensing in 3D radar imaging"

By using compressive sensing technique, the data rate needed in radar imaging can be remarkably reduced. Phase reservation is the key issue for compressive sensing based radar imaging algorithm. In this paper, we propose a phase-reservation CS based pulse compression algorithm after investigation of the radar signal sparsity property, and then apply the algorithm to 3D radar imaging. Simulation results show that the phase information after CS range compression could be well preserved so as to realize 2D and 3D radar imaging. [C2510]

#### "Real-time measurement in compressive radar imaging based on AIC"

Compressive sensing techniques have been shown to reduce the number of data samples beyond the Nyquist theorem, achieving perfect reconstruction of the original signal. In this paper, we implement a real-time compressive measurement operator, based on Analog-to-Information Converter (AIC). The simulation results conform that the measurement operator works well and has as well performance as random matrix. [C2511]

#### "A TBD algorithm based on dynamic-programming for dim radar target detection"

When the received echo signal energy reflected from a target is quite small, the target cannot be detected reliably with traditional accumulation and detection method. In this paper, based on the stable factor, an improved method is proposed, which utilizes the difference of correlation characteristics between clutter and target to suppress clutter spike. Then the track-before-detect algorithm based on dynamic-programming is applied to dim radar target detection. Compared with the combination method of coherent and non-coherent integration, the predominance of the algorithm is obtained on dim radar target detection. [C2512]

#### "Multilayered diffraction tomography algorithm for ground penetrating radar"

A multilayered diffraction tomography algorithm for ground penetrating radar is derived in this paper. The algorithm considers the planar air-soil interface and uses the thought of the equivalent speed to solve the problem of multilayered medium. The first Born approximation and the dyadic Green's function are adopted to construct a linear forward model that inverted by fast Fourier transform to meet the requirement of small calculation, so we can real-time reconstruct the buried objects. Simulation results are provided to illustrate performance of this algorithm. [C2513]

#### "On separating the information of slow-mode angular motion of projectile"

The information on angular motion of projectile can be expressed by the Amplitude Modulation (AM) index of radar echo. In order to separate the information of slow-mode angular motion, a method based on Empirical Mode Decomposition (EMD) is proposed. Three issues are discussed in this article. First, the angular motion of projectile is approximated as a fast-mode circle superposing over that of the slow-mode according to the theory of exterior ballistics. Next, the characteristics of AM index that can represent the angular motion are discussed. Considering the effects of Discrete Fourier Transform (DFT) and the interference of noise, the index of AM is modeled as nonstationary time series in which the slow fluctuation corresponds to the slow-mode circular motion. Then an EMD-based separating method is suggested to obtain the index of the slow-mode motion. It includes two steps. The first step is to divide the index into a series of Intrinsic Mode Functions (IMFs) and the residual item. The second step is to reconstruct the index of the slow-mode motion with the components of the lower frequency IMFs and the residual by utilizing the prior knowledge about the difference in the periods. Compared with theoretical value and the result of stationary wavelet transform, as well as the in-flight experiment, the results show the validity and effectiveness. [C2514]

#### "Active cancellation stealth analysis of warship for LFM radar"

Active stealth of warship is an important developing direction in modern stealth technology field. Based on scattering properties of warship and characteristics of linear frequency modulated (LFM) signal and its matched filter, the cancellation signal was designed. Warship stealth was achieved through interference cancellation between cancellation signal and radar echo signal. Simulation results show that complete stealth of warship can be achieved through canceling LFM echo signal, and the scattering field of warship can be reduced by almost 10 dB even with some cancellation error. The proposed method can provide important reference for warship's active stealth in project realization. [C2515]

#### "Two methods of 3-D scattering center extraction for targets with micro-motion"

Aiming at the problem of three-dimensional scattering center extraction based on high resolution range profile (HRRP) sequence, two methods based on projection equation solving and spherical fitting were presented in this paper. Equation solving method was to solve the matrix equation based on the algebraic relations between the 1-D radial distance and 3-D position. Spherical fitting method was to extract scattering centers from the mapping graph according to the spherical distribution of 1-D projection data. In addition, a way of turning precession parameters into angle parameters indirectly was proposed for the difficulty of getting the look angle of the radar. Two methods were all verified by experiments developed with simulated and measured data. Finally, the features and performance of two methods were compared in the paper. The result indicates that the spherical fitting method is better than the equation solving method by 15dB under the same SNR. [C2516]

#### "A novel adaptive learning method for low-sidelobe step frequency waveform designing"

For a step frequency waveform, high range resolution can be achieved by inter-pulse synthesis processing and its sidelobe level can be controlled by weighting in frequency domain. However, high range sidelobe arise when the frequency steps is sparsely spaced. For this, low sidelobe can be obtained in two ways. One is by signal processing after receiving. And the other is to design the waveform with low sidelobe. In order to avoid the SNR loss, The latter is more effective. In this paper, a novel adaptive learning method is given. The method can adaptively adjust the frequencies by max sidelobe discrepancy between the matched filtering out of present and the ideal one. The result of simulation shows that it can approach the optimal frequencies for which the max

sidelobe is lowest. [C2517]

#### "A real-time algorithm for signal detection based on autocorrelation at low SNR"

In an electronic detecting system, how to capture non-cooperative signal at low SNR is always a challenging work. This paper puts forward a real-time algorithm named Shifted-N points-Correlation Algorithm for detecting LFM (Linear Frequency Modulation) pulse signal based on digital autocorrelation. Applying a gliding window of proper length to truncate infinite signal into finite length, then calculating the autocorrelation function of the signal in the window, choosing the Nth point as the current output, finally, an envelope which represents the position and intense of the signal can be obtained, while the noise can be eliminated according to its non-relativity. This is especially suitable for detecting weak signal with unknown parameters under the background of band-limited noise. Moreover, when the parameters of the receiving system have been determined, an optimum algorithm can be found for specified system based on the MSNR Criterion. Besides, it can achieve recursive operation, which is easy for hardware to apply. [C2518]

#### "Oil spill detection from polarimetric SAR image"

A new combined feature is proposed based on polarimetric features extraction. Moreover, a new oil spills detection method is developed based on the combined feature and max entropy segmentation. The application to NASA/JPL SIR-C data shows that the new combined feature and detection method are effective to oil spills detection. [C2519]

#### "Ship detection based on compound distribution with Synthetic Aperture Radar images"

Considering the variability of Synthetic Aperture Radar (SAR) imaging (different sensor, resolution) and complex condition of sea surface, the traditional single statistical model may be no longer a good choice to fit the distribution of actual sea clutter in SAR image. Based on the characteristic of Gamma distribution which is suitable to model uniform area, and G0 distribution which is adaptive to the general homogeneous and heterogeneous area, this paper established a compound distribution of G0 and Gamma model to fit the characteristics of various types of sea conditions, and use the moment estimation to improve the computational efficiency as well. Meanwhile, the algorithm combines the Constant False Alarm Rate (CFAR) detection based on dichotomy method in order to figure out the difficulties in solving the analytical expression of compound distribution. TerraSAR-X and ERS-2 images were adopted for investigating the algorithm. Experiment results illustrate that the method can achieve good performance. [C2520]

#### "New approach for improving Mutual Information in POLSAR image registration"

Aiming at the problem that information source of similarity measure is limited to image intensity usually in multi-polarization SAR registration, we propose an improved Mutual Information (MI) based on the multiple correlation information between the same polarized channels (HH, VV) in multi-polarization SAR images. In this method, by analyzing the correlation characteristics of three polarized channels in multi-polarization SAR, and using channel correlation information extracted from polarimetric covariance matrix, we compute MI in multi-polarization SAR to improve the similarity measure. Finally, the simulation results show that, in the multi-polarization SAR image registration, similarity measure information sources affect the performance of similarity measure. We compare the similarity measures with different information sources in curve sharpness and noise immunity. The results prove that the measure based on the correlation of the same polarized channels for multi-polarization SAR performs excellently. [C2521]

#### "Research on adaptive beamforming for airborne phased array radar"

PD mode is usually adopted in airborne phased array radar. However, there are two problems which severely degrade the performance of adaptive beamforming. One is the ground clutter return in the training data, the other is the target return in the training data. Therefore, in this paper, the two problems above are analyzed in detail, and then the methods suitable for engineering realization are presented. Computer simulation results are presented for illustration. [C2522]

#### "Unsupervised classification of PolInSAR image based on Shannon Entropy Characterization"

In this paper, we propose a new method for unsupervised classification of polarimetric synthetic aperture radar interferometry (PolInSAR) images based on Shannon Entropy Characterization. Firstly, we use polarimetric H (entropy) and a parameters to classify the image initially. Then, we reclassify the image according to the span of Shannon Entropy Characterization. Finally, we fuse the results of the two previous steps and merge them to the specified number of clusters. The effectiveness of this method is demonstrated on CETC38 PolInSAR data and

E-SAR PolInSAR data. [C2523]

### "Radar angular superresolution algorithm based on Bayesian approach"

Angular resolution is the key parameter of radar. Conventional means of increasing angular resolution are dependent on the size of the antenna aperture. In framework of maximum likelihood, this paper presents an iterative algorithm to restore the target location information and then to obtain angular superresolution. Theoretical analyses indicate that algorithm accelerates convergence speed and achieves angular superresolution efficiently, and computational burden is relatively small. Simulation results show that the algorithm can efficiently attenuate the effect of antenna pattern convolution and highly enhance angular resolution; test data results show an order of improvement in angular resolution over real aperture image, also confirm that the method could obtain angular superresolution. [C2524]

### "A modified anti-RGPO jamming algorithm"

An algorithm which integrated triple threshold test with nearer range selection method is presented to deal with the deficiency of RGPO jamming in this paper. The triple test has minimum probability of error decision. Nearer range selection to data association can eliminate the effect of the RGPO and clutter simultaneously. The experiment results demonstrated that the method proposed in this paper has better performance and obvious improvement on tracking precision when suffering RGPO jamming compared to the present methods. [C2525]

### "The inversion of sea state based on the micro-Doppler analysis of sea-clutter"

The real sea-clutter data are always hard to analyze due to their instinct complexity, large scale non-stationary, and lack of fundamental understanding of the natural dynamics. Measurable modeling of sea clutter is an important precondition in many research areas and practical applications, such as salvage and marine radar signal processing. However, few works have been down on the time-frequency analysis of sea clutter, especially no effective method for sea state inversion from sea clutter has been proposed. In this work, the author take into account the motion model of sea surface in typical scenarios via time-frequency and micro-Doppler effect analysis. Different contributions of the waves' velocity may provide intuitionistic ISAR images and contain certain motion parameters, from which certain sea state parameters might be inverted. Both theoretical simulation and experimental results indicate the usefulness of the model and method proposed in this work. [C2526]

### "A fast range alignment algorithm for ISAR imaging"

The envelope correlation algorithm and the minimum entropy algorithm are widely used in range alignment of inverse synthetic aperture radar (KAR) imaging. However, these types of algorithms have heavy computation burden mainly caused by the searching operation. Aiming at reducing the burden, a fast range alignment algorithm is presented in this paper. Firstly the mean location of each range profile is calculated. Then we fit the trajectory of them with linear regression model. Based on the straight line trajectory of range shift, range alignment can be accomplished. The proposed algorithm avoids the searching operation which is usually used in traditional algorithms. The computational complexity analysis shows that the computation burden of the novel algorithm is proportional to the data volume. Finally, the comparison between the proposed algorithm and the envelope correlation algorithm with real data demonstrates the validity and efficiency of the fast algorithm. [C2527]

### "A review of space target pose external measurements"

3D pose is the important parameter to express the space target motion states, which has vital meaning in application to target tracking and identification. This paper summarizes various external measurements to the 3D pose of space target, and introduces the application of the various ways, then analyzes and compares, finally, points out the trend of the 3D pose external measurements. [C2528]

### "Orthogonal waveforms design and performance analysis for MIMO sonar"

In this paper, a Multiple-Input Multiple-Output (MIMO) sonar system which can deal with multiple targets is discussed, where orthogonal waveforms are transmitted simultaneously. According to the requirement of waveform orthogonality, the orthogonal frequency division pseudo-random signal (OFD-PR), orthogonal frequency division determinant signal (OFD-LFM) and the spread-spectrum code-based signal (Gold-BPSK) are designed. The Maximum Likelihood (ML) DOA estimator and CRB for MIMO sonar is described. The performance of MIMO sonar based on different waveforms is analyzed via experiments in an anechoic water tank. Simulation and experimental results show that the waveforms which we design possess the higher resolution for multiple source DOA estimation than its phased-array and they could resolve the two targets with



a separation of 1/2 beam width at low SNR. The analysis of DOA estimates and experimental results show that the OFD-PR signal has much better performance than others. [C2529]

#### "A new method of denoising processing for synthetic aperture radar return signal"

In this paper, a denoising processing method for synthetic aperture radar raw return signal is proposed based on the DFT-DWT transform. Compared with presented transforms of DFT and DWT, the DFT-DWT transform is more efficient to extract the SAR raw return signal which is a complex 2-D signal with different properties between the two directions. After removing the out-of-band and high-frequency part of the SAR return signal's DFT-DWT transform, the noise can be eliminated efficiently. Experimental results verify that the SAR denoising processing method has a practical value for suppressing the suppression jamming and detecting the weak targets. [C2530]

#### "Interference suppression method for space-time navigation receivers based on samples selection Householder multistage wiener filter"

Due to suppression the influence of impulsive noise spikes (outliers) from desired signal direction of arrival in GPS signals. The Householder multistage wiener filter was improved, a samples selection Householder multistage wiener filter was proposed. The enhanced algorithm employed by space-time anti-jamming processing in GPS receiver, with the ability of avoiding the impulsive noise spikes influence of weights calculation, and hold the desired signal unchanged. Simulation results indicate the algorithm achieved favorable anti-jamming performance. [C2531]

#### "Overlaying orthogonal coding for sidelobe suppression in HFSW radar"

Strong sidelobes not only lead to false alarm, but also affected the target detection. By overlaying an orthogonal coding over any analog or digital signal, we can completely remove most of the ACF (auto correlation function) sidelobes without any increase to the mainlobe sidelobes. In this paper, we discuss how to choose the original signal for HFSW radar and give the affection of different overlaying matrix. [C2532]

#### "Random weighting filtering algorithm and its application in SINS/SAR Integrated Navigation System"

Strap-down Inertial Navigation System (SINS) is a typical navigation system with strong independence. To improve its performance in space, time and precision, a new Random Weighting Filtering algorithm (RWF) is proposed in this paper which adopts random weighting method. By studying its application in SINS/SAR Integrated Navigation System and comparing with other algorithms, it can be seen from the experiments that the proposed Random Weighting Filtering algorithm could significantly improve the performance of SINS/SAR Integrated Navigation System. [C2533]

#### "The combination of ACDA and FCM for Data Association in multi-target tracking"

For improving the performance of ACDA (Ant Colony Data Association) for data association in multi-target tracking, we propose the combined method of ACDA and FCM. Since FCM is a determinate algorithm, in nature based on NN (Nearest Neighbor), it could generate reasonable results in any case, which is a backup when ACDA becomes divergent. Experiments have been done in three cases-ACDA as data association method only, FCM only, and the combined method of ACDA and FCM. The results show that the performance of the combined method is superior to the other two methods. [C2534]

#### "A mover detection method based on 2-D fuzzy entropy in SAR images"

In this paper, a new technique for the moving targets detection combining incoherent and coherent information of the Synthetic Aperture Radar (SAR) images is proposed based on the measure of a two-dimensional (2-D) fuzzy entropy principle. Firstly, it extracts incoherent and coherent information from images in pixel and builds a 2-D histogram. Secondly, according to 2-D fuzzy function, image pixels are fuzzy classified into two groups: changed and unchanged then 2-D fuzzy entropy is calculated. Finally, Differential Evolution (DE) algorithm is used to maximize the entropy and the optimal parameters of the fuzzy function are obtained, which procures effective moving target detection results. [C2535]

#### "Parameter estimation of moving target for stepped-frequency radar under temporal-correlated clutter"

Proposed is a maximum likelihood (ML) estimation method to estimate the parameter of the moving target for

high range resolution stepped-frequency radar in strong clutter background. In this study the temporal correlated clutter is used. By transmitting frequency-hopping waveform and using the spectrum density of the clutter, the method may accurately estimate the moving target parameter in strong clutter. Numerical experiments illustrate the effectiveness of the proposed method. [C2536]

#### "Architecture design of spaceborne SAR imaging processing system"

The significance of on-board spaceborne SAR imaging processing is expatiated first. By analyzing the characteristics of spaceborne SAR imaging processing, a dual-layer, scalable, reconfigurable and fault-tolerant on-board spaceborne SAR real-time imaging processing system architecture, which the top layer adopts data partition parallel processing and the bottom layer adopts multi processors fine granularity close coupling, is put forward. System running efficiency is pointed out to analyze the whole system's efficiency; two system bottom realizable structures of bus sharing and bus distributing were designed. [C2537]

#### "Singularity detection of TWR echoes based on correlation"

This paper introduces a modified algorithm of singularity detection based on modulus maxima for through-wall radar (TWR) targets detection. By tracking the wavelet transform modulus maxima (WTMM) at fine scales, singularities can be detected, and the important information of human target is also selected. According to the singularities of TWR A-scan signal, it can be commendably given prominence to the targets. Finally, singularity detection based on modulus maxima was successfully realized. [C2538]

#### "Analysis of inner-pulse Doppler effect for the echoes of inverse synthetic aperture LADAR"

Inverse synthetic aperture LED AR is an active imaging system, which can achieve high resolution real time imaging for moving targets. For the traditional inverse synthetic aperture radar, the inner-pulse Doppler frequency will reduce the quality of image obviously only when the target has high speed. However, due to the ultra-high frequency and ultra-wide bandwidth of the laser signal, the influence of inner-pulse Doppler cannot be ignored even for the low speed moving targets in the ISAL. This paper analyzes the inner-pulse Doppler effect of the ISAL echoes and presents an echo model for the ISAL. Via the conventional motion compensation method, in which the accurate estimation of reference point's track is obtained after range realigning and phase focusing, the inner-pulse Doppler effect can be removed and then the image of target can be achieved. Finally, some simulation results are given in the paper. [C2539]

#### "Parameter estimation for stepped-frequency radar under temporal-spatial correlated clutter"

Proposed is a maximum likelihood (ML) estimation and minimum target error function (TEF) method to estimate the parameters of the moving target for high range resolution stepped-frequency radar in temporal-spatial correlated clutter background. The compound-Gaussian model is used for the temporal-spatial correlated clutter. Both of the velocity and range of the moving target can be accurately estimated for stepped-frequency radar. Numerical experiments illustrate the effectiveness of the proposed method. [C2540]

#### "SAR image target extraction based on 2-D leapfrog filtering"

This paper reveals that the classical R-D imaging algorithm can not remove the strong noise and extract the objects in R-D imaging image by their range and azimuth matching filters. Though 2-D DCT-DWT or 2-D DFT-DWT can be a 2-D filtering for the issue, while the algorithms need huge computation amount, they can not process SAR image real time. To solve the problem, this paper develops a new 2-D filtering algorithm based on 2-D leapfrog filter, which is good at extracting the SAR image target clearly. The 2-D recursive filter is of few multiplications for SAR image each pixel to realize fast and real-time image filtering. Practical experiments of SAR image processing have shown that the approach and algorithm are correct, effective and pragmatical. [C2541]

#### "Micro-Doppler effect analysis based on inverse synthetic aperture imaging LADAR"

Although the micro-Doppler (m-D) effect can provide additional information for target recognition, the microwave radar cannot afford enough resolution to detect the m-D effect of small targets and long distance targets. To obtain high range resolution for the extraction of the fine m-D signatures, inverse synthetic aperture imaging LADAR (ISAIL) is used here. Because of the frequency modulation continuous wave (FMCW) laser signal is used in ISAIL, the m-D effect of ISAIL is different from the microwave radar. In this paper, the m-D effect of ISAIL is analyzed and compared with that in X-band radar. The experiment results show that ISAIL can offer sufficient information of micro-motions when the feature of motions is tiny. [C2542]

### "Inverse Synthetic Aperture Radar Imaging at Low Signal-to-noise Ratio"

Inverse synthetic aperture radar (ISAR) imaging at low SNR ratio is not resolved completely. The SNR increases in time-frequency domain over the one in the time or the frequency domain alone both theoretically and numerically. This shows advantage of time-frequency analysis technique for ISAR imaging at low SNR. The reassigned Gabor spectrogram time-frequency distribution is proposed for ISAR imaging at low SNR. Finally, the real data demonstrated the validity of the method proposed. [C2543]

### "Estimation of UWB radar scattering center with GTD-based 2D state-space method"

A GTD-based 2D state-space method is presented in this paper for estimating the parameters of the scattering centers on a moving target under the ultra-wideband conditions. Firstly, this method constructs the GTD-based impulse response from the moving target in the state space equation, and then arranges the impulse response of different frequency at different time into a Hankel matrix. Next, the range and the range rate are estimated by using the Hankel matrix singular value decomposition (SVD), which effectively solves the range aliasing problem when the ranges of different scattering centers are overlapped. It occurs in the ID state space when the range is estimated only. At last, the type parameter and intensity of the scattering center are solved out by this method. The effectiveness of the method is verified by comparing the result of processing the echo data from the rotating conical target with the CRB on parameters estimation. [C2544]

### "Research on airborne chaff centroid jamming to ground radar"

In radar passive countermeasure, Chaff centroid jamming plays an important role. Whether chaff cloud is diffusing or has diffused, its RCS and position change as time goes. Chaff cloud model is constructed accordingly. The plane and centroid motion model are constructed respectively too. Based on the searching and tracking mode of the ground radar, detailed research on chaff centroid jamming is made. Simulation results show that airborne chaff centroid jamming to ground radar has a good effect. [C2545]

### "Feature evaluation and selection for polarimetric SAR image classification"

This paper presents an evaluation of different features for polarimetric SAR (PolSAR) image classification. Firstly, we select several of the polarimetric features to give a summary on them. Then we give an insight into their classification performance together with a texture feature using the support vector machine (SVM). Finally, we employ a feature combination and selection strategy that optimizes the trade-off between the feature dimension and precision. The experimental results on PolSAR data of the CETC38 demonstrate: i) the strategy works effectively in the reduction of redundant feature dimensions; ii) in comparison with the unselected feature, the classification performance and computation efficiency of the selected one are improved by this approach. [C2546]

### "General clutter modeling for airborne radar"

Clutter returns in airborne radar applications spread in Doppler frequency because of platform motion. The clutter characteristics should be analyzed in detail for designing clutter suppression algorithms. In this paper, clutter modeling method for conventional phased array airborne radar, multiple-input-multiple-output (MIMO) airborne radar, and hybrid MIMO-phased array airborne radar, all with arbitrary antenna array, is presented. Modeling of clutter intrinsic motion, sensor error, subarraying is also considered. [C2547]

### "Time delay and doppler shift estimation accuracy analyses of moving targets in non-cooperative bistatic pulse radar"

According to the characteristics of non-cooperative bistatic pulse radar systems and the issue that the doppler mismatched loss of the cross-correlation detection of moving targets is serious, two fast methods for joint time delay and doppler shift estimation of moving targets, based on segment correlation-FFT processing and modified partial segment correlation-FFT processing, are proposed, after analyzing the common methods for cross-ambiguity function processing such as direct calculation, FFT, Zoom-FFT method. The processing performance of direct calculation and partial segment correlation-FFT processing of LFM pulse-series is analyzed in theory and by simulation. And the simulation shows that the weak moving target can be detected effectively and the time delay and doppler shift can be fast estimated by the methods presented in this paper. [C2548]

### "An FPGA based semi-parallel architecture for higher order Moving Target Indication (MTI) processing"

The design and implementation of a higher order Moving Target Indication (MTI) engine is presented. This is part of a single chip radar signal processor also incorporating the subsequent algorithms. The bottleneck in use

of higher order filters for MTI is not an algorithmic one but one related to implementation. Thus the challenge is to minimize area utilization and achieve the required speed. The proposed architecture employs the use of multiple offchip memory banks for achieving the required memory bandwidth and use of dedicated FPGA resources for area minimization. The requirement of stacking a large number of radar returns in memory and then reading them all for filtering within a single return time demands a parallel memory reading and data processing approach. But this demand has to be balanced with the requirement to consume as little area as possible to leave room for the following algorithms. Considering these constraints, a semi parallel architecture employing multiple filters, each built around a DSP48 slice configured as a Multiply Accumulate (MACC) unit in a time shared manner is used. An analysis of various factors that affect speed and area is also made. The architecture is implemented on a Virtex-4SX35 FPGA using Xilinx XtremeDSP Kit. The design is tested using unprocessed baseband data from a TA-10K air traffic control radar. Results show a marked improvement in the clutter suppression capability of the radar. The design achieves the required speed using only 7% of the available FPGA slices. Thus, not only can the other algorithms be implemented on the same chip but there is room for enhancements as well. [C2549]

### "Approach for airborne radar ISAR imaging of ship target based on generalized keystone transform"

High resolution image of ship target under low SCNR condition is unable to be obtained by conventional ISAR imaging methods when long coherent integration time needed. To overcome this problem, a novel approach for imaging the ship target by airborne radar is proposed in this paper. Firstly, the generalized keystone formatting is applied to compensate the range curvature induced by long integration time. Secondly, the quadratic term of slow time in phase is eliminated by estimating the target motion parameter using Radon-Ambiguity Transform (RAT) scheme. Next, generalized keystone formatting method is used again to eliminate the residual linear range walk. Finally, the high resolution image of ship is obtained by employing the Relax algorithm. Results of both simulation and real data are presented to confirm the validity of the proposed algorithm. [C2550]

### "Research of unsupervised image change detection algorithm based on 2-D histogram"

Change detection in images of a given scene acquired at different times is one of the most interesting topics of remote image processing. In this paper, a novel image change detection algorithm is proposed based on the clustering characteristic of 2-D histogram. First, the best segmentation direction of 2-D histogram is ascertained by using Fisher criterion. Secondly, a kind of new 2-D entropy is defined to search the best threshold and segment the 2-D histogram into unchanged region and change region. Then the change area in different image is detected based on the change region of 2-D histogram. Finally, the proposed algorithm is compared to traditional algorithm. The theoretical analysis and experiment results confirm the effectiveness of the proposed means. [C2551]

### "Range Cell Migration Correction using texture mapping on GPU"

Range Cell Migration Correction (RCMC) is a key step in the imaging procedure of Synthetic Aperture Radar (SAR). The performance of RCMC affects the final SAR image quality greatly. Traditionally, RCMC is carried out via an interpolation operation on CPU, and is a time-consuming phase in the whole processing flow. In this paper, a novel RCMC technique using texture mapping is proposed. The texture mapping operation is implemented on the Graphics Processing Unit (GPU), which accelerates the operation by special hardware structure. The proposed RCMC technique can achieve a higher speed compared with the traditional methods designed for CPU. [C2552]

### "A new polarization filter based on weighted combination"

Conventional polarization filters can mitigate an interference by using the orthogonal vector of the interference polarization, but leading to distortion of the target signal in its amplitude and phase. A null phase-shifting polarization filter can reconstruct the original target signal. However, it needs some complex operations, such as a linear polarization-vector translation and compensations in amplitude and phase. In this paper, a weighted combination polarization filter is proposed, which retains the original target signal while suppressing the interference within one step. The simulation results show that the new filter is an effective means to remove the interference in the polarization domain. [C2553]

### "An improved joint subspace projection method for InSAR interferogram filtering"

In this paper, an improved joint subspace projection method for synthetic aperture radar interferometry (InSAR) interferogram filtering is proposed. Benefiting from the new formulation of joint data vector, the method does not need to calculate the noise subspace dimension before estimating the InSAR interferometric phase, thus



avoiding the effect on the estimation of the InSAR interferometric phase due to the inaccuracy of the noise subspace dimension. The method can auto-coregister the SAR images and reduce the interferometric phase noise simultaneously. [C2554]

### "Matrix transpose methods for SAR imaging system"

Matrix transpose is a very crucial procedure in the synthetic aperture radar(SAR) imaging system. This paper analyzes the existing matrix transpose methods in the signal processing of SAR imaging and proposes two new matrix transpose methods, meanwhile, the implementation steps of new methods are also introduced. Finally, an example which uses the matrix transpose methods described in this paper is given as a demonstration and the results and analysis are also presented. [C2555]

### "Spread clutter mitigation via knowledge-aided STAP in multiple-input single-output system"

In Multiple-Input Single-Output (MISO) HF surface wave radar system, the fact that bistatic operation and the movement of the receiver platform causes the nonstationarity and spreading of sea clutter, which will lead to the difficulty in detecting those immersed targets. The space-time distribution of sea clutter in different geometry is firstly investigated; and a knowledge-aided STAP scheme is proposed for mitigating the clutter. The weights of different range bins are acquired from both the clutter priori and the prefiltered training data by direct data domain (DDD) algorithm. Numerical simulation shows the proposed scheme effective. [C2556]

### "Impacts of Keystone formatting on Space-Time Adaptive Processing in airborne radar"

Keystone formatting (KF) has the capability of compensating multiple targets' (including ground clutter) range walk simultaneously without using any specific knowledge of the target motion. However, due to serious Doppler ambiguity of the fast moving targets, KF will affect the distribution of the clutter and degrade the Space-Time Adaptive Processing (STAP) performance. Based on the above reasons, the impacts of KF on the clutter distribution are analyzed firstly, and then the impacts of KF on STAP are analyzed. The conclusions obtained are helpful to figure out better methods for fast dim air moving target detection. [C2557]

### "Real-time data compression bias estimation on netted radar"

Interest in netted radar has grown tremendously in the last few years, and registration is the necessary process of radar network system. A real-time data compression Kalman filter registration algorithm is presented to correct the dynamic systematic errors based on local measurements. It is accomplished by constructing pseudomeasurements of the radar biases with additive zero-mean, white noises. Then the netted radar bias estimates are obtained dynamically by employing data compression Kalman filter algorithm. Finally, Monte Carlo simulations are employed to evaluate the performance of the proposed algorithm. Results show that the new algorithm is efficient. [C2558]

### "2-dimensional DOA estimation using ESPRIT algorithm in ARM confronting coherent decoy"

Because of the intrinsic defect of passive radar seeker (PRS) of ARM, it can't distinguish coherent decoys from far distance. Using extended-aperture confronting coherent decoys for ARM is proposed in this paper, and a new 2-dimensional DOA estimation ESPRIT algorithm is presented. This algorithm uses the characteristic of a new special array to construct a special covariance matrix. With this algorithm the DOA of coherent decoys can be estimated without spatial smoothing techniques and spectrum peak searching. Elevation and azimuth estimations can also be paired automatically. Simulations demonstrate the effectively to distinguish radar and bait from the directions of arrival and the significant performance gain realizable by this method for ARM confronting coherent decoys. [C2559]

### "The distributed passive radar 3-D imaging and analysis in wavenumber domain"

This paper studies the distributed passive radar three-dimensional (3-D) imaging under the 3-D configuration formed by the illuminators of opportunity and the distributed receivers. The echoes received by the distributed channels actually constitute the target wavenumber-domain coverage, whose characteristics such as range, uniformity and compactness greatly affect the inversion performance. Generally, the wavenumber-domain coverage of the passive radar system is small-scale, sparse and nonuniform, in which case the traditional IFFT method becomes invalid. Therefore, we propose a novel imaging method, named Spherical Coordinates Method (SCM). Furthermore, so as to get higher resolution and better imaging quality, a broader, more uniform and compact coverage in wavenumber domain is required and this can be achieved through the following three methods: increasing the number of the receivers, making use of the motion information and optimizing the disposition of the receivers. Numerical simulations verify the effectiveness of the presented method and the

rationality of the theoretical analysis. [C2560]

#### "A novel STAP method for the detection of fast dim air moving targets"

Space-time adaptive processing (STAP) is an effective method for moving target detection in airborne radar. In this paper, a novel STAP method for fast dim air moving target detection is proposed. The new method suppress clutter in the received data firstly, and then apply Keystone formatting (KF) to compensate the target's range walk. Finally, target is accumulated by the conventional space-time beamforming. Effectiveness of the new method is verified via simulation examples. [C2561]

#### "Water extraction in SAR images using GLCM and Support Vector Machine"

Traditional methods to extract water regions in SAR images usually rely on image binarization with a specified threshold. However, because of the inherent speckles in SAR images, finding an appropriate threshold is very difficult. In the paper, we propose a new method for water region extraction in SAR images using GLCM (gray-level co-occurrence matrix) based features combined with SVM (Supported vector Machine). The characteristics of water and non-water regions are distinctively depicted by GLCM based features, which are fed into the SVM classifier to extract water regions. Experiments on synthetic and real SAR images demonstrate that the proposed method achieves better results compared with two other ones. [C2562]

#### "A modified two-scale fractal sea model of the non-fully developed full-range sea spectrum"

The determination of backscattering coefficients is important to analyze echoes objective signals. To describe a rough sea surface naturally, a non-fully developed full-range sea spectrum (NDFSS) is reconstructed, and a fractal sea model based on NDFSS is presented. Based on the conventional two-scale model for backscattering coefficients, a complementary term is added for considering the skewness of sea waves. The additional part is proportional to the surface bispectrum and it is a critical part in explaining the scattering difference between upwind and downwind observations. The numerical results show this modified model is consistent with the real radar data. [C2563]

#### "A new approach to distributed passive radar imaging by 2-D NUFFT"

This paper studies distributed passive radar imaging of two-dimensional (2-D) scene. The echoes and the reflectivity of target are confirmed to be a Fourier transform pair. However, due to the space configuration based on the illuminators of opportunity, the echoes are sampled non-uniformly, which lead to the non-equispaced property of space-spectrum distribution. In this case, direct 2-D FFT reconstruction doesn't apply now. To retain the fast computing of image reconstruction like FFT, non-uniform fast Fourier transform (NUFFT) is introduced to avoid complex interpolation. We generalize NUFFT to 2-D NUFFT to tackle the problem that the space-spectrum is unequally-spaced in both directions of  $\mu$  and  $\nu$ . This new 2-D NUFFT method is compared with polar-coordinate method in efficiency and accuracy using both the analytical and numerical approaches. Simulations demonstrate that 2-D NUFFT can reduce the computational complexity while ensuring image reconstruction accuracy. So it's a promising strategy for realtime imaging of distributed passive radar. [C2564]

#### "The FAA handbook on microprocessor selection and evaluation in airborne systems"

Under the management of the Aerospace Vehicles Systems Institute (AVSI), the FAA initiated a project to study the safety concerns surrounding the use of complex commercial off-the-shelf (COTS) microprocessors and systems-on-chips (SoC) in safety-critical airborne systems. Additionally, several aerospace companies cooperated with the FAA in providing oversight, direction and technical contributions throughout the course of this project. The major product of this work is the "Handbook for the Selection and Evaluation for Microprocessors for Airborne Systems" to be published by the FAA as a set of recommendations for both regulatory personnel and systems manufacturers. This paper describes the technological trends occurring in modern COTS microprocessors and SoC that have prompted the FAA to better understand the implications of their use in airborne systems. This paper also briefly describes the purpose and structure of the Handbook and provides supplemental information regarding the evaluation platforms and analyses that were the basis for its recommendations. [C2565]

#### "Integration of a 2.5D radar simulation in a sensor simulation suite"

Recently DLR's sensor simulation toolkit F3S (flexible sensor simulation suite) has evolved from a mere proof-of-concept demonstrator to a versatile collection of sensor simulations. The main aspect of the software is to provide real-time simulation for sensors like millimeter wave radar and laser based sensors in an environment for testing enhanced vision concepts. We achieve this by making heavy use of graphics hardware acceleration

as available in recent computer hardware. The latest addition to the set of sensor simulations is a 2.5D/3D scanning radar. Other than traditional 2D radars simulating such a sensor raises some special challenges when most of the calculations should be done by the graphics hardware. We present a custom solution that extends our previous approach to 2.5D and 3D sensors while maintaining real-time in the sense that the simulation runs at least as fast as real existing sensors. [C2566]

#### "Enhancement in realism of ATC simulations by improving aircraft behaviour models"

This paper addresses the challenge to provide realistic aircraft behaviours in air traffic control simulations. Many simulation environments lack actual information on aircraft, airline or airspace-specific operational procedures: they resort to generic procedures to navigate the simulated aircraft, which may result in unsatisfying aircraft behaviours. A methodology has been developed by EURO-CONTROL to improve the aircraft behaviour model in its large-scale and real-time air traffic management simulation system, by identifying specific aircraft operation parameters from historical radar data. The simulator has been adapted to take these aircraft operation parameters into account, and the methodology was applied and tested during the last two simulations which took place at the EUROCONTROL Experimental Centre in 2010. The results of using operationally-tuned parameters during those simulations demonstrate that the analysis of flight recordings can bring valuable information about numerous flight behaviour parameters, and that the use of detailed flight behaviour models based on the parameters identified from the recordings can improve the accuracy of aircraft modeling enough that air traffic controllers liken the simulated traffic to a real traffic. [C2567]

#### "TCAS surveillance performance analysis"

The Traffic Alert and Collision Avoidance System (TCAS) Version 7 surveillance requirements were developed in the mid-1990s with the use of limited radar data. Recently, a more comprehensive radar data source has become available, enabling a thorough analysis of TCAS surveillance performance throughout the National Airspace System (NAS). This paper uses a high fidelity simulation to characterize TCAS surveillance performance in six high traffic terminal environments. Transponder utilization due to TCAS and TCAS surveillance range are compared with the interference limiting design requirements. The effect of TCAS surveillance activity on Air Traffic Control (ATC) ground radar performance is also investigated. Results indicate that the surveillance algorithms perform as intended and that TCAS has a minimal impact on ground radar. Areas of concern are noted for future investigation. [C2568]

#### "High-throughput hardware architecture of MQ arithmetic coder"

A novel byte-out architecture in MQ arithmetic coder is proposed and the new MQ-coder hardware architecture which use the novel byte-out architecture is presented, in which it can encode two CX-D pairs per cycle. The coder is described with Verilog HDL at RTL. Synthesis, fitter, assembler and timing analyzer are conducted with Quartus II 9.0. The results of timing analyzer show that the architecture can efficiently improve the throughput and clock frequency, the throughput can achieve  $117.12 \text{ MCxD} \cdot \text{s}^{-1}$  and the clock frequency can achieve 58.56 MHz. [C2569]

#### "Multiple/Distributed Target Detection for HRR"

Side lobe suppression is extremely important in precisely determining the weak echo scattering region in the presence of range side lobes. This paper addresses the signal design problem for the detection of multiple/distributed targets in high resolution radar (HRR) application with improved side lobe suppression ratio. The simulation results indicate a significant improvement in terms of noise tolerance for HRR target detection; compared to conventional binary sequences. [C2570]

#### "Correlation radar signal processing on basis of probability Kravchenko weight functions"

In this report the combined method of correlation radar signal (RS) processing based on the theory of atomic functions (AF) is examined. Examples of using of new probability Kravchenko weight functions (WF) designs are presented. Quality functional for estimate accuracy and efficiency of RS processing for concrete physical models is constructed. It is shown that the proposed approach significantly improves the quality of the coherent analysis of the RS. [C2571]

#### "The Surface Operations Data Analysis and Adaptation tool: Innovations and applications"

This paper describes the Surface Operations Data Analysis and Adaptation (SODAA) tool, which has been developed by Mosaic ATM and NASA. The SODAA tool provides database management of multiple aviation data sources including both airport surface surveillance data, flight data, flight operator-originated data and many

other aviation data sources. The paper describes the design of the SODAA system, as well as many analyses that have been conducted using SODAA. [C2572]

### "The phase statistical characteristic of InSAR image at the isolated point"

Current researches on the phase of interferometric Synthetic Aperture Radar (abbreviated as InSAR) images are restricted to the homogeneous scene with spatially constant backscatter coefficients. But in reality, there are many unknown targets or sealers with high backscatter coefficients in the ground scene, which produce several bright spots (called isolated points) in the SAR image. The phase statistical characteristic of interferogram at the isolated point is not available recently. Based on the InSAR system, the phase distribution characteristic of SAR image at the isolated point is analyzed. Furthermore, the interferometric phase probability density function at the isolated point is deduced and the phase statistical characteristic at the isolated point is analyzed in theory which is confirmed by the simulations. Finally the conclusion is obtained that the existence of isolated point can improve the interferometric phase estimation precision which establishes the theoretic foundation for calibrating the InSAR system with the interferometric phase at the sealer. [C2573]

### "An improved GVF snake model and its application to linear feature extraction from SAR images"

In this paper, an improved GVF snake model that allows controllable snakes is proposed. Two kinds of external constraint forces are exploited in the model. The first one can pin specified points on the snake and determine the basic shape of a snake. The second one avoids generating ears during curve evolution. It ensures that the curves are smooth and won't grow in a wrong direction. The improved snakes are employed to close gaps in linear feature extraction since they can fix the connection points during the deformation and provide smooth linking curves rather than straight lines. The experimental results of ridge (and ravine) extraction and road extraction from real SAR images increase the correctness and quality of extracted results. [C2574]

### "Evaluation of separation performance with ADS-B at the Philadelphia key site"

The Federal Aviation Administration's (FAA) Surveillance and Broadcast Services (SBS) Program Office has implemented one of the first enablers of the Next Generation Air Transportation System (NextGen) by installing a ground infrastructure that supports the Automatic Dependent Surveillance-Broadcast (ADS-B) data service. One of the main applications for this infrastructure is to enhance air traffic control (ATC) separation through more frequent and accurate data about aircraft. As part of the initial assessment activities, the ADS-B data was incorporated into four different automation platforms in four different key sites. One of these key sites was the Philadelphia Terminal Radar Approach Control (PHL TRACON) which uses Standard Terminal Automation Replacement System (STARS) to process and display radar data to controllers. The Philadelphia STARS was updated to accept ADS-B data in its native format. Beyond just accepting new surveillance data, however, PHL TRACON is the first location that went operational where ATC used system track positions (so called- "fused" targets) published to the ATC display to allow controllers to separate aircraft, a paradigm shift from current operations where controllers use radar "plot" positions. As part of the SBS evaluation, a working group was created that worked specifically to evaluate the end-end performance of separation services with the new data flow-ADS-B avionics, ADS-B surveillance service on the ground, and the updated STARS software. The evaluation used a comparative approach with current monopulse secondary surveillance radar (MSSR) systems as a baseline; if the new system performed as good or better than MSSR systems in separation applications, then the system was acceptable for operation. This paper describes the efforts of the SBS working group to evaluate the operational performance in Philadelphia, including the metrics used, assumptions made operational scenario development, and results from several analyses, including simulation, flight testing, and targets of opportunity operating in the TRACON airspace. [C2575]

### "Frequency modulated radar signals based on high dimensional chaotic maps"

High dimensional chaotic maps have more complicated structures and better anti-jamming performances. Frequency modulated radar signals based on high dimensional chaotic maps are proposed. The signal model is presented, characteristics are analyzed, and comparison among 1D Bernoulli map, 2D Cat map and uniform random noise with different series length is made in the paper. Simulations show well performances of the proposed signal. [C2576]

### "Toward System Oriented Runway Management"

Decisions about what airport configuration should be used and when the configuration should be changed are currently made manually by personnel in the Air Traffic Control (ATC) Tower (ATCT) or Terminal Radar Approach Control (TRACON). Over time, each airport has adapted unique local procedures related to airport configuration management, creating a challenge for both studying airport configuration management and



developing decision support technologies. At many airports, the airport configuration decision is based primarily on the weather forecast and historical experience. While configuration changes to respond to weather changes are relatively straightforward, when traffic demand motivates a configuration change, the change is often made in reaction to observing aircraft queues and delays, or not made at all, rather than proactively based on forecast traffic situations. Consequently, significant opportunity exists for automation to support airport configuration decisions that will improve airport capacity and efficiency. Moreover, NextGen technologies and procedures will cause the definition of airport configuration to expand to include how metroplex resources other than the runways are utilized. As the metroplex configuration decision space becomes more complex, the need for supporting automation will become even greater. System Oriented Runway Management (SORM) is a concept in which the configuration and use of metroplex resources are explicitly planned with a holistic perspective of the operations within the metroplex as well as the needs of the metroplex within the context of the overall National Airspace System (NAS). System Oriented Runway Management is also a significant new research initiative by the NASA Airspace Systems Program that addresses the need for automation to achieve the SORM concept. This paper introduces the SORM concept and initial research to develop automation to support airport configuration planning. [C2577]

#### **"Target detection of high-resolution radar in non-Gaussian clutter"**

The high-resolution radar echo is modeled as a range-spread target. Based on the generalized likelihood ratio test design procedure, the range-spread target detection in spherically invariant random vector clutter is addressed. And a binary integrator with constant false alarm rate property is proposed to detect the whole range-spread target, after single target scatterer detection in each range cell. Finally, the performance assessment shows that, the detection performance is improved as the number of sensors used or the clutter spike increases, while it is robust to the clutter correlation. [C2578]

#### **"The principle of synthesizing HRRP based on a new OFDM phase-coded stepped-frequency radar signal"**

Orthogonal Frequency-Division Multiplexing (OFDM) phase-coded pulse is a wideband signal, of which the range resolution is inversely proportional to the bandwidth. However, it is a challenge to synthesize large bandwidth for OFDM phase-coded pulse since wide instantaneous bandwidth and high sampling rate requirements. To solve this problem, this paper proposes a new radar signal called OFDM phase-coded stepped-frequency (OFDM-PCSF) signal, of which the pulse train is stepped frequency, and each pulse is implemented with OFDM phase-coded chips. The property of OFDM-PCSF signal is analyzed at first. And then, the mathematical expressions of the high resolution range profiles (HRRP) are derived, assuming an elementary scenario of point-scattering targets. It mainly presents the influence of velocity on HRRP and investigates the parameter design and velocity compensation, which is helpful for the realization of OFDM imaging radar. Finally, the simulation results demonstrate the validity of the conclusions. [C2579]

#### **"Target detection with distributed radar sensor networking systems (DRASENS)"**

An innovative radar sensor networking system is introduced for effective target detection. By using orthogonal coding waveforms, the number of radar echoes generated by the radar network from the same target is maximized for the best fusion processing result. Several centralized signal detection schemes are investigated for the networking system and their performances are evaluated. [C2580]

#### **"Fast one-dimensional least squares matching of InSAR images"**

Image matching is one of the key steps in Processing of InSAR. In order to improve the reliability and the rate of matching, a fast least squares matching algorithm with one-dimensional azimuth searching was proposed. The interferometric SAR images obtained by space-borne ERS-1/2 and by airborne dual-antenna system were employed to do experiments of matching. The results show that the proposed one-dimensional least squares matching algorithm was fast and effective. [C2581]

#### **"Radar track-before-detect algorithm of dim target based on track test"**

This paper proposes a track test-based track-before-detect algorithm for radar target detection. Track test is used to estimate the target motion model. The implementation of this scheme on the search tracks and the detection strategy on the energy accumulation values of tested tracks are presented. Simulation results show the proposed algorithm have better detection performance and tracking performance, compared with the dynamic programming-based track-before-detect algorithm. [C2582]

### "Parameters estimation of target with precession based on combined feature"

It is beneficial for the recognition and classification of targets to obtain geometrical and motional parameters simultaneously. This paper proposes a new method to estimate parameters of target with precession based on combined feature, which is generated by Doppler feature and high range resolution feature of target from a new radar-OFDM radar. Expanded Hough transform (EHT) is employed to establish the combined feature with range and motion information of scatterers. The paper mainly presents the principle to establish the combined feature and the estimation of precession angle, target posture and target length. Finally, the results from simulations and anechoic chamber data prove the validity of the method. [C2583]

### "Study of continuous wave radar for human motion characteristics measurement"

Human motion characteristics study based on radar is a new technique developed in recent years. This paper firstly analyzes the model of human radar returns, and then designs an X-band continuous wave radar for human motion characteristics measurement. Experiments for measuring the human motion characteristics have been performed based on the radar. The Doppler features of human motion are extracted with time-frequency analysis from actual measured data generated by the radar, which verifies the validity of the measurement data. [C2584]

### "Compressive sensing MIMO radar imaging based on inverse scattering model"

From the view of inverse scattering imaging, the paper gives basic principle of MIMO radar imaging, then applies compressive sensing (CS) to two methods. The first method is sampling and receiving echoes randomly in both frequencies and channels. The second method is sampling echoes randomly only in frequencies, and controllable space intersection is done in channels to increase the practicability. Both methods can achieve high image resolution using few echo samples. The first method has better imaging quality, but the second method is more controllable. Ulteriorly, the simulation gives detailed analysis of imaging quality and reconstruction successful probability, which is beneficial to applications of CS to MIMO radar imaging. [C2585]

### "The improvements on the enhanced WRS-88D storm identification and tracking algorithm"

SCIT is a classic algorithm in storm identification, tracking and forecasting. In this paper, we try to employ disjointed set ADT to improve the efficiency of storm identification firstly, and then try to improve the performance of SCIT tracking and forecasting strategy by optical flow methodology. [C2586]

### "A novel ISAR algorithm for the imaging of ship targets based on AM-LFM model"

Rang-Instantaneous-Doppler (RID) processing is widely used in ISAR imaging of maneuvering target and acceptable image can be achieved when the amplitude modulation effect of scatterers echoes can be neglected during intergation time, whereas, the RID method based on the assumption above does not work properly when the variant amplitude modulation of scatterers' echoes involved, such as ship target. In this paper, a multicomponent amplitude modulation and linear frequency modulation (AM-LFM) signal model developed and a fast parameter estimation technique-DechirpClean method proposed. To achieve the best quality in DechirpClean ISAR image, a new effective optimum imaging interval selection scheme addressed. The performance of proposed method is verified by comparing the result with the image produced by conventional RID method from the real data processing. [C2587]

### "Cram r-Rao bounds for estimating velocity and direction with a bistatic MIMO radar"

We derive Cramer-Rao bounds (CRB) expressions for the velocity (Doppler shift), and direction of a point target using a bistatic multiple-input multiple-output (MIMO) radar in this paper. First, we introduce the signal and noise models which satisfy the space-time separability conditions. Then, general CRB expressions are derived for a narrowband signals with the above signal and noise models. We find that the directional parameters are uncoupled with Doppler shift for the space-time separable signal and noise models. However, the directional parameters are usually coupled with each other, i.e., the direction-of-departure (DOD) with direction-of-arrival (DOA) and the azimuth angles the elevation angles are ordinarily coupled. Fortunately, the uncoupled direction estimation can be gotten by the specifical antennas placement. [C2588]

### "Detection of moving target based on fractional Fourier transform in SAR clutter"

Based on the analysis of the characteristics of SAR target echo and the time excursion of fractional Fourier transform (FRFT), the Article has put forward a time-delay balance method based on FRFT to detect the slowly moving target in SAR echo according to the characteristics of SAR ground clutter. Calculation on the FRFT of echo signal and the FRFT of echo signal after short delay time results in two complex signals, in which, the

modules of static backgrounds are just totally same, and in the range of moving target, the amplitude of module will cause an offset, therefore, when calculate the difference of the modules of two complex signals, the static background could be balanced and the moving target could be detected effectively. Simulation analysis indicates that the method in the Article shows its advantages in a background with strong clutter. [C2589]

#### "Radar imaging based on compressed sensing by random convolution"

Compressed Sensing (CS) theory provides great possibilities for resolving problems associated with traditional high resolution radar, such as high sampling rate, too many data and difficulties of real time processing. Sensing by random convolution is a universally efficient data acquisition strategy and easy to realize. This paper focuses on radar imaging technique based on CS by random convolution, researches into several different random downsampling strategies. Experiments from simulated data and real data verify the validity of the proposed imaging method, also the influences of SNR and downsampling strategy on imaging performance are analyzed and compared. Finally the problems need further research are pointed out. [C2590]

#### "Design method of parameters for pulse doppler signal to nullifying the interference of negative frequency"

This paper describes how the negative-frequency portion of the pulse doppler (PD) radar signal's spectrum extends into positive frequency and causes interference in signal processing. A novel design method of the parameters of pulse doppler signal is presented to nullifying this interference. The key idea of nullifying the interference is to place a null of the negative-frequency portion's sidelobes to the place where the interference exists. This method encounters the problem of frequency aliasing in conventional process of PD signal and it no longer works. An improved filtering process is proposed to solve this problem. Some computer simulation results are presented to illustrate the performance of the proposed parameters designing method and the improved filtering process. [C2591]

#### "Spinning targets imaging based on OMP algorithm with radial basis function"

A new radar imaging method is proposed for spinning targets in space. The rapid spin motion of the target induces multi-period sinusoidal modulation of the radar echoes in both range and doppler domain, which causes Range-Doppler (R-D) algorithm invalid in conventional radar imaging. The presented method analyzes the echo model of the target spinning around an arbitrary axis. An exponential radial basis function (RBF) is then constructed from the scatters' range profile based on a distance-weighted criterion, and the image is rebuilt by recovering the projection of the target base on orthogonal matching pursuit (OMP) algorithm with the radial basis matrix. The simulation results show that the proposed method can obtain the radar image more effectively for the target with a uniform speed spin motion. [C2592]

#### "Multi-carrier frequency MIMO HF radar using convex optimization beamforming"

In order to enhance HF radar angle resolution, and overcome target RCS scintillations, we adopt the transmitting and receiving antennas sparse deployment under bistatic pattern, the element intervals far less than range from the target to transmitters and receiver, the transmitters emit multi-carrier frequencies. In this paper, we apply CVX theory to solve the optimal weights of each element at different frequency, take advantage of multi-carrier frequency signal phase changing offset the side lobe each other. The beampattern has better angle resolution, and achieves lower side lobe. In the end, we analyze that the different frequency echo amplitude and phase impact side lobe and direction errors. [C2593]

#### "Inverse synthetic aperture ladar imaging with the Range Instantaneous Doppler algorithm"

Inverse synthetic aperture ladar (ISAL), which operates at visible or infrared wavelength, is more sensitive to maneuver than inverse synthetic aperture radar (ISAR). In this paper, we propose the Range Instantaneous Doppler (RID) algorithm for very high resolution ISAL imaging of maneuvering targets. The Wigner-Ville distribution (WVD) and the Radon transform are used for computing the time-varying Doppler spectrum of maneuvering targets. The data processing of the RID algorithm is illustrated. The simulation shows that the RID algorithm can reconstruct a clearer ISAL image of the maneuvering target than the conventional rang Doppler (RD) algorithm. This is a crucial step in developing a real ISAL system. [C2594]

#### "Deception jamming method for ISAR based on sub-Nyquist sampling technology"

Fast sampling of wideband RF signal and real time processing of vast data are great difficulties in the engineering implementation of deception jamming to ISAR. This paper proposes a sort of Sub-Nyquist Sampling-Based Method for Jamming ISAR Systems. First introduces the deception jamming technique based on false

target for ISAR. Then investigates the jamming principle of sub-Nyquist sampling modulation. Through modulating false target information on radar signals intercepted by sub-Nyquist sampling, the resulting signal can produce a train of vivid false targets. The proposed method can greatly reduce the demands on sampling rate and processing speed, its jamming performance is analyzed in detail and verified by simulation experiments. The conclusions here have certain significance to the manufacture of ISAR jammer in practical engineering. [C2595]

#### "A new cross-range scaling algorithm based on FrFT"

Inverse synthetic aperture radar (ISAR) generates two dimensional high resolution images of targets in range-Doppler domain. In order to determine the cross-range dimension of the target or implement polar formatting to reconstruct more focused ISAR images, estimation of the rotation angle is required. A new algorithm for cross-range scaling (CRS) is proposed to estimate the rotation angle, which makes use of the information hidden in the chirp rate of echoes from the scattering centers. A technique based on Fractional Fourier transform (FrFT) is used to estimate the chirp rate, simulation and real data analyses are provided to verify the effectiveness of the proposed algorithm. [C2596]

#### "A general multi-channel radar echo simulator"

A general-purpose multi-channel radar echo simulator is researched and proposed in this paper to satisfy the various needs of the radar signal processor testing. The specificity of target echo model is the main problem to achieve the generalization for a simulator. The simulator will give priority to the issue of the generalization because the generalization is always the most attractive feature for any device. Therefore, it will lose some other performance. For example, the accuracy of the target distance will be reduced since we consider the target will not move in a coherent integration frame to reduce the computation and complexity of the echo modeling. At last, implementation of a specific simulator based on FPGA and DSP is introduced, including hardware design and software processing methods. [C2597]

#### "An improved nonlinear chirp scaling algorithm with capability motion compensation for one-stationary BiSAR"

This paper deals with the imaging problem of one stationary bistatic Synthetic aperture radar (BiSAR) with motion error. Since a motion error is the main phase error source in the aircraft SAR, the motion errors have to properly be compensated during the SAR image reconstruction. The nonlinear chirp scaling (NLCS) algorithm is one of the typical algorithms in the practical radar system. An improved NLCS algorithm which can compensate motion error for One-Stationary BiSAR is proposed. Specially, the proposed method is based on the constant acceleration movement and the sub-aperture technique. [C2598]

#### "The imaging research of the ground moving targets in forward scattering radar"

The present shadow inverse synthetic aperture radar (SISAR) imaging algorithm is derived based on some assumptions for air moving objects such as long baseline, large target size and so on. For the forward scattering radar (FSR) system to detect ground moving targets, the assumption conditions are often unsatisfied because of relatively small objects size, the strong ground clutter and the short baseline length. Furthermore, the assumptions will result in distorted imaging results for the extraction of profile median line and height difference using the present imaging algorithm. To obtain the accurate imaging results of ground moving target, the more accurate signal model for ground moving target is first time presented based on Fresnel-Kirchhoff diffraction formula and high order phase approximation methods, and the modified imaging algorithm is also proposed for the accurate profile reconstruction of ground moving target. Finally, the effectiveness is verified by simulation results. [C2599]

#### "Research on Scan-GMTI technology of airborne MIMO radar based on STAP"

Through successive azimuth scanning with narrow beam steered to different angles, Scan-GMTI technology provides a significant way to implement wide-area surveillance and track a particular target simultaneously. Applying MIMO mode to Scan-GMTI, abundance channel and frequency resources provide significant advantages for STAP algorithm to implement. The space-time-frequency joint processing will provide an effective approach for improvement of detection of slowly moving targets, reduction of Doppler ambiguities and blind velocities. [C2600]

#### "An improved algorithm of velocity measurement using burst error function"

Based on modulated frequency stepped signal model, the interference phase which impacts the precision of the least burst error velocity measure method is analyzed in this paper, phase correction factor is given to improve



the accuracy of the least burst error velocity measure method for moving targets, finally the signal processing flow is given and the performance is verified by computer simulation. [C2601]

#### "The algorithm of SAR speckle noise suppressing by using generalized multi-scale CB morphology"

During forming synthetic aperture radar (SAR) image, the inherent speckle noise severely affects the application result of SAR images. To deal with this problem, based on the contour bougie morphology (CB morphology) and the generalized multiple structuring elements morphology, a novel series morphological filter was constructed to suppress the speckle noise in SAR images. Firstly, by use of the omnidirectional multiple structuring elements the generalized multi-scale morphology open-max filter was adopted to filter the noise at the cost of minimal loss of image geometrical details, and then a CB open and a CB close series filter were used to filter the remained speckle noise. Thus it can not only effectively suppress the speckle noise in images but also preserve more detailed information of the images. Lastly, the simulated SAR images and the actual SAR images are simulated, and the results prove that the algorithm presented in this paper can efficiently suppresses the speckle noise in SAR images. [C2602]

#### "Exploitation of SRTM DEM in InSAR phase unwrapping problem"

A novel approach is proposed in this paper to exploit the Shuttle Radar Topography Mission (SRTM) digital elevation model (DEM) in the interferometric synthetic aperture radar (InSAR) data processing. The proposed algorithm includes three steps: the first step is to patch the void cells in the SRTM DEM; the second step is to determine a one-to-one correspondence between the interferogram and the SRTM DEM; the third step is to eliminate the phase trend between the original and simulated interferogram. This algorithm can be applied to facilitate phase unwrapping problem. Conventional techniques approach phase unwrapping as an optimization problem, where the total branch-cuts or the gradient errors, etc. are to be minimized. Generally speaking, they consider phase unwrapping as a blind procedure, i.e., without any external guidance. The purpose of this paper is to fill this gap by introducing the SRTM DEM as guidance for phase unwrapping. Some experimental results with JESR verify the theoretical analysis and show that the method can improve the performance of the phase unwrapping to a great extent. [C2603]

#### "Relationship of target identification performance and waveform parameters"

In this paper, we established rigorous relationship between target recognition performance and the parameters of a fixed waveform via Kullback-Leibler information number of single observation (KLINs). The method we proposed takes advantage of the methodology of sequential hypothesis test. It depicts the target recognition efficiency of certain radar waveform parameter in the metric of average number of necessary signal (ANS) transmission. Compared with the traditional simulation methods in literature, it is a more efficient and valuable one to find the optimum values of a certain waveform parameter. Simulation results about the parameters of LFM signal show the validity of the method. [C2604]

#### "A quadrature Doppler radar system for sensing human respiration and heart rates"

In this paper, a Doppler radar system for cardiopulmonary detection will be described. The idea of our design is to use inexpensively commercially available motion sensor detectors. So a quadrature receiver board from AD-8347 is used. Experiment results indicate that this system can extract respiration and heartbeat rates at a short distance with digital signal processor. [C2605]

#### "Algorithm for unknown SNR estimation based on sequential Monte Carlo method in cluttered environment"

In target tracking, radar or sonar sensors provide amplitude information as well as kinematic information, e.g., range and bearing. Considering the amplitude information with kinematic information, tracker can more effectively distinguish measurement origin in cluttered environment. The tracker utilizes the amplitude information in the form of signal to noise ratio (SNR). However, a major challenge comes from the fact that the SNR is often fluctuated according to the target's aspect and effective radar cross section. So the certain level of uncertainty of SNR should be reduced. Focused on the point, we propose a novel SNR estimation algorithm based on sequential Monte Carlo method. Finally, estimated SNR is applied to the probability data association filter with amplitude information. Simulation results demonstrate the effectiveness and high accuracy of the idea of exploiting SNR estimation in heavy cluttered environments. [C2606]

#### "On performance enhancement of a following tracker using stereo vision"

A stereo vision system has a distinctive advantage capable of obtaining exact and wide range of the distance

information. The use of stereo vision system has been increased due to the advances in hardware technology. This paper deals with design of the active vision system which acquires the distance and the direction information of the target using the stereo vision system. This paper also implements the tracker that follows the main tracker, which we call a following tracker, without identifying the target. In addition, the CAMShift algorithm which tracks the target based on the color information is used to acquire the center point of the object. A following tracker algorithm generates the control input that makes the following tracker aim the same target based on the sensing results from the active vision system. A following tracker needs the exact distance information between the system and the target to track the object accurately. We first build the mathematical model of object tracking system and following tracker, design the system controllers, and then compare the tracking accuracy under the two conditions: the presence and the absence of the distant information. [C2607]

#### **"Advanced obstacles detection and tracking by fusing millimeter wave radar and image sensor data"**

Reliable object detection and recognition for Adaptive Cruise Control (ACC) by multi-sensor and multi-algorithm have attracted much attention recently. Aiming at the calibration complexity problem, a novel calibration method is proposed to calibrate the millimeter wave radar data and the CCD camera data using a homography. The proposed method does not require estimation of rotation and translation between them or intrinsic parameters of the camera. And the calibration can be done without any manual manipulation. Tracking of the detected object by radar is done in image plane as the radar is insensitive to object size and has a low object recognition rate as well. A new tracking algorithm based on Mean Shift(MS) algorithm with Unscented Kalman filter (UKF) is proposed to track the detected objects in the image plane, in which UKF is used to predict the initial position of iteration for MS algorithm. Then MS is applied to find out the accurate position of the object and positions of objects are mapped to radar plane to judge it is a new object or old one. We demonstrated the validity of the proposed methods through experiments. [C2608]

#### **"On the Signal Processing in the Life-Detection Radar Using an FMCW Waveform"**

The progresses and difficulties faced in the life-detection radar signal processing are introduced in the paper. First, the progresses in signal processing are shown, including obtaining the breathing and heartbeat frequency by using self-correlation process and composing the mode vector to discriminate a life by using time-spectrum analysis and singular value decomposition. Then, the difficulties faced now are discussed. Echoes from the obstructions in the direction of radar antenna are main interference. How to control the interferences are discussed and a combinative approach of body movement and life information detection is brought forward in the paper. [C2609]

#### **"Chirp Sub-pulse Stepped Frequency Radar Signal Processing"**

Chirp-SF signal is a new kind of high range of resolution signal. This paper firstly points out that the traditional signal processing methods will cause "ghost images" when there is more than one scatter in a distance unit. Then a new method which including interfacing each sub-pulse in the Timeline and frequency shifting to constitute a FM signal is proposed. We can solve this problem and have a high range resolution by execute the pulse compression on the synthetic signal. In the end, the simulation result is shown to prove the correction of the Algorithm. [C2610]

#### **"Future voyage data recorder based on multi-sensors and human machine interface for marine accident"**

Voyage data recorders (VDR) enable accident investigators to review procedures and instructions before an incident and help to identify the cause of any accident. The Future data recording should be capable of recording data audio and video during day and night. The recording should be of high integrity, digital as well as independent of ship supplies. Voyage data recorder, popular name black-box, is used for recording all kinds of navigation information. VDR is a data recording system designed for all vessels required to comply with the International Maritime Organization IMO's and International Convention safety of life at sea SOLAS requirements (IMO). Data from various sensors on board the vessel is collected, digitized, compressed and then stored in an externally mounted protective storage unit. The protective storage unit is a tamper-proof unit designed to withstand the extreme shock impact, pressure and heat, which could be associated with a marine incident (fire, explosion, collision, sinking, etc). This research realizes the importance of obtaining these stored data for accident analysis. This paper considers a real case accident, by downloading and replaying the data of real black box for a sunken ship in the red sea. Eventually, video recorded data of the accident will be more helpful to the investigation. [C2611]

### "Analysis of data structures used for storing and processing 3D LADAR data"

This paper compares the use of a point cloud data storage structure with a voxel based storage structure for 3D data collected with LADAR. The motivation for this work is to support the development of a classification system to model the environment of an autonomous vehicle operating in an unstructured natural setting. The classifier should be able to detect trees, bushes, and ground based on the data. Most LADAR sensors provide accurate 2-D range information in a plane, but we generate 3-D data from the sensor by articulating it using a pan-tilt mechanism. A 3-D grid of voxels is used with each voxel representing a cubic region in space with an associated value to indicate the region's occupancy. We discuss how this voxel representation compares with a point cloud representation in the process of data collection, data storage, and data processing and also look at the complexity of merging new data with old data in the same region. There are two main contributions. The first is comparing a possible voxel based data representation with one possible point cloud data representation. The second is determining reasonable parameters (voxel size, LADAR pitch angular velocity, and distance to the target) to facilitate classification of the voxel data. The scope of this paper is confined to analyzing data size, scanning time required for accurate classification, and processing efficiency. Experimental data size, density, and classification performance results are presented. [C2612]

### "Complex permittivity estimation from free space RCS measurement"

Non-destructive and non-contacting estimation of the complex permittivity of the solid materials has been proposed using the monostatic RCS measurement from the specular reflection surface. In order to isolate the surface reflection contribution from the total scattering response, time gating method is utilized. The frequency domain RCS is measured first at a certain frequency band, and the corresponding time domain result is calculated via inverse Fourier Transformation. After identifying the surface reflection contribution and selecting it with a certain time width, Fourier transformation is used to obtain the desired surface response in the frequency domain. These RCS results are then utilized to estimate the surface reflection coefficients and their permittivities. The proposed method has been tested to evaluate the permittivities of cubic granite and synthetic phantom material, and the results are compared with those obtained by a coaxial probe method. Good agreement has been found between them and the validity of our method has been confirmed. [C2613]

### "Terrain classification based on structure for autonomous navigation in complex environments"

One of the main challenges for autonomous navigation in cluttered outdoor environments is to determine which obstacles can be driven over and which need to be avoided. Especially in off-road driving, the aim is not only to recognize the lethal obstacles on the vehicle's way at all costs, but also to predict the scene category thereby giving a better decision-making framework for vehicle navigation. This paper studies terrain classification based on structure relying on sparse 3-D data from LADAR mobility sensors. While most of recent methods for LADAR processing are purely found on the local point density and spatial distribution of the 3-D point cloud directly. We, on the other hand, introduce a new approach to analyze the point cloud by considering local properties and distance variation of pixels inside edgeless areas. First of all, the edgeless areas are extracted from segmenting the 3-D point cloud into homogeneous regions by Graph-Cut technique. Secondly, the neighbor distance variation inside edgeless areas (NDVIE) features are obtained by calculating the euclidean distance of neighbor distance variation inside each region. Through extensive experiments, we demonstrate that this feature has properties complementary to the conditional local point statistics features traditionally used for point cloud analysis, and show significant improvement in classification performance for tasks relevant to outdoor navigation. [C2614]

### "MIMO radar with spatial-frequency diversity for improved detection performance"

The Multiple Input Multiple Output (MIMO) radar concept exploits the independence between signals at the array elements unlike beamforming which presumes a high correlation between signals either transmitted or received by an array. Radar Cross Section (RCS) of a complex target varies with both transmitted frequency and target geometry. By widely separating transmit and receive antennas, MIMO radar systems observe a target simultaneously from different aspects resulting in spatial diversity, thus improving the detection performance. Also by utilizing different frequencies, independent RCS of the target can be observed, thus resulting in frequency diversity. In this paper, the spatial and the frequency diversities are studied together to bring out the combined benefits. The system proposed will not only have several antennas appropriately spaced but also several operating frequencies appropriately spaced, providing a better detection performance than conventional MIMO radar systems for the same transmission power. The simulation results exhibit a better detection performance of the proposed system as compared to MIMO radar systems with only spatial diversity. [C2615]

### "Range tracking filter using measurements with uncertain delays"

In modern marine range tracking systems, both Doppler radar and range sensors are often used to enhance the detection and tracking performance against sea clutters. Due to the delays in communication links, however, the measurements of the sensors do not arrive simultaneously to the data processor where the tracking filter operates. Moreover, the magnitudes of the delays vary irregularly. To cope with this problem of uncertain time delays, in this paper, we propose a new range tracking filter algorithm by adding a ZSB (zero-scan-back) MAP (maximum a posteriori) delay estimator to conventional Kalman tracking filter. Computer simulations are carried out to demonstrate the performance of the proposed filter. [C2616]

#### "A novel method for indoor location identification"

Radio Frequency Identification (RFID) is used in different applications. RFID technologies are getting considerable attention not only from academic research but also from the applications for enterprise. One of the most important applications of RFID research is the indoor position location. Many researchers have used varied technologies to perform the action of indoor position location tracking. In our research, we will propose methods using RFID tags to perform indoor position location tracking. First, we use RFID to collect Received Signal Strength (RSS) from reference tags beforehand, and then use multiple neuron networks models to do the indoor position location learning. Finally, when the track tags are set up in indoor environments, they can find the position of neighboring reference tags by using the neuron networks and an arithmetic mean to calculate the position location values; with this method we are able to break figures down to track tag position locations. We conducted this experiment to prove that our methodology can provide better accuracy than the LANDMARC system. We conducted the experiments to test the system accuracy. [C2617]

#### "Particle Swarm Optimization aided unscented kalman filter for ballistic target tracking"

Tracking of a ballistic target in its reentry phase by considering the radar measurements is a highly complex problem in nonlinear filtering. Kalman Filter (KF) is used to estimate the positions of the target when the measurements are corrupted with noise. If the measurements (range and bearing) are nonlinear then Unscented Kalman filter (UKF) can be used. For obtaining reliable estimate of the target state, filter has to be tuned before the operation, which is offline. Tuning is the process of estimating the process noise covariance matrix (Q) and measurement noise covariance matrix (R) of the filter. This paper presents tuning of UKF using Genetic Algorithm (GA) and Particle Swarm Optimization (PSO) for ballistic target tracking. Simulation results show that the superiority of PSO tuned UKF over conventional UKF. [C2618]

#### "Study on the Signal Detection Algorithm of Weak Laser Radar Target Based on Wavelet Transform"

According to the different transmission characteristics under the wavelet transform (WT) domain and the different distribution characteristics of frequency domain of the signal and noise, a novel approach for detecting weak signal laser radar target based on wavelet transform has been proposed. In many cases, wavelet decomposition has been used to de-noise a digital signal submerged by mass noise. Differently in our approach, we applied the wavelet decomposition and the modulus maximum to detect the locations of laser radar echo signal. Simulation shows that the proposed algorithm is more efficient than only utilizing wavelet decomposition in a clutter environment. [C2619]

#### "Doppler radar vital signs monitoring using wavelet transform"

An algorithm using wavelets is used to detect heartbeat rate from a phase modulated Doppler radar signal. It is shown that the heartbeat rate can be detected up to 1.5m from the radar in a noisy environment without the need of filtering. Also the property of wavelet transform to preserve both time and frequency information is utilized to analyze the phase modulated Doppler radar signal giving information about changes in heart beat over very small intervals of time. [C2620]

#### "Key technology research of CHINA Advanced Metering Infrastructure"

This paper defines content of Advanced Metering Infrastructure (referred to as AMI), make comparative analysis of the similarities and differences between domestic and foreign AMI. This paper describes the status of China AMI related technology system and China power using information collection system architecture; proposes typical structure of China AMI; analyzes AMI related communication technologies and their applications which includes power composite optical fiber communication, power line broadband communication technology and wireless communication technology. This paper also analyzes the metering sensor networks, interoperability, digital metering, distributed generation bi-directional metering, local and remote smart control technology, demand response and other key technologies; proposes the technical requirements of smart energy meter and



smart interactive terminals, data management system. [C2621]

### "Compact microstrip antenna design for microwave imaging"

An ultra-wideband microstrip antenna design is considered with respect to applications in breast cancer detection. The underlying design concept is based on ground penetrating radar (GPR). Simulated and measured prototype performance show excellent performance in the input impedance and radiation pattern over the target range from 4 GHz to 8 GHz. The 4 GHz to 8GHz frequency band for microwave imaging perform better in comparison with other microwave frequencies. The antenna also shows a reasonable uniform radiation performance in the broadside direction which contributes to the reduction of clutter levels, thus aiding the reconstruction quality of the final image. [C2622]

### "Automatic detection of reflexion hyperbolas in gpr data with neural networks"

In order to locate cylindrical objects like pipes and cables buried underground using ground penetrating radar it is necessary to detect reflexion hyperbolas in the measured radargrams. In practice, this task is in many cases complicated due to different geological environments, incomplete or disturbed hyperbolas, and first of all the fact that nearby objects lead to hyperbolas interfering with each other. In this paper we present an automatic detection system based on a specially connected neural network using receptive fields. We show that with an adequate definition of training data the system is capable of reliably detecting reflexion hyperbolas even in those challenging situations. [C2623]

### "An environment monitoring system for valuable chinese herbal medicine growing based on wireless sensor networks"

The wireless sensor network, which refers to the combination of sensors, embedded system, MEMS, distributed information processing and wireless communication network has become a hot topic in the research field because of its wide application prospect. This paper propose the design of an environmental monitoring system for valuable medicinal herb growing based on wireless sensor network, which gives a real-time monitoring of the environment information on the target area, such as soil temperature, humidity, light intensity, soil components. This paper describes architecture of the monitoring system and gives a design of hardware platform for sensor nodes and workflow as well as the terminals of monitoring management system. [C2624]

### "Application of GPRS technology in water quality monitoring system"

The method of water quality monitoring applied by XueYe reservoir is sampling in the scene and analyzing at the laboratory at present. Based on analyzing key problem of water quality monitoring, automatic water quality monitoring system based on GPRS is provided in this paper. Considering features of water quality monitoring, the general structure and network framework of the system, and the way of access to GPRS of data monitoring center are designed based on GPRS technology. Water quality parameters collected by multi-parameter water quality probe are transmitted to data processing and monitoring center through GPRS wireless communication network of mobile. The system collects, transmits and processes water quality parameters automatically, so production efficiency and economy benefit are improved greatly. Practice has proven GPRS technology can achieve well within the complex environment of poor water quality unmonitored, and more specifically applicable to the collection point, data transmission automatically generate the field of water analysis equipment data transmission and monitoring. [C2625]

### "A new approach for classification of data transmission media in power systems"

Smart Grid denotes the integration of all elements connected to a power grid with a communication infrastructure. Recent communication systems are developed by multi layer architecture. The lowest layer in such systems is transmission media. The characteristics of the communication systems will be seriously influenced by the characteristics of its media. This paper classifies communication media of power systems as dependent or independent ones. A dependent media is part of power system which is normally owned by Independent System Operator (ISO) or distribution companies. In contrast, as an independent media, it is not normally part of power system and can be public or provided by data service providers. In this paper, first, a brief summary of popular media used in power systems is presented. Then, the two main classes of media are compared with each other. [C2626]

### "A fully integrated 77-GHz radar transmitter based on a low phase-noise 19.25-GHz fundamental VCO"

A 77-GHz automotive radar transmitter is presented. The transmitter is based on a 19.25-GHz Colpitts voltage

controlled oscillator, that feeds two cascaded frequency doubler stages. In a following medium power amplifier (MPA) the signal recovers after frequency transformation. Finally a power amplifier (PA) adds 6 dB to the power level after the MPA. In addition, an emitter follower stage connected to the oscillators output drives a switchable divide-by-16/32 stage realized in emitter-coupled-logic (ECL). [C2627]

#### "A 77-GHz down-conversion mixer architecture with built-in test capability in SiGe technology"

A 77-GHz double-balanced mixer in a 200 GHz ftsilicon-germanium technology is presented. The proposed mixer architecture is capable of simultaneous direct up- and down-conversion of two separate input signals without additional power consumption. An up-converted low-frequency test signal is coupled back into the receiver RF input path to enable a built-in functionality test of the down-conversion path of the mixer. The circuit exhibits a conversion gain of 20 dB and draws 22mA from a 3.3V supply. The fabricated chip occupies an area of 1028 Ч 1128µm<sup>2</sup>. [C2628]

#### "Weak Signal De-noising Method Based on Accumulation in Frequency Domain and Wavelet Transform"

Bioradar echoes are often very weak and submerged in noise. The SNR of radar signal is very low. Therefore, echo signal denoising is indispensable for extracting life information. In this paper, the method of weak signal denoising based on the combination of accumulation in frequency domain and wavelet transform is proposed. First, the effectiveness of frequency domain in accumulation and wavelet transform in denoising is presented respectively. Then, the combination of two methods was used to remove noise and extract useful information on the situation of Gaussian white noise. Simulation results show that the method can restrain the noise and extract useful signal effectively in low SNR. [C2629]

#### "Simulation of transient electromagnetic fields on a finite-element mesh"

This paper presents a full-wave 3D electromagnetic transient simulation method which uses an unstructured finite-element mesh. The mesh elements have a range of sizes and orientations such that, rather than forming a regular grid, they conform to the geometry of the model, respecting all its details. This paper will discuss the method and present some examples of applications. [C2630]

#### "3D simultaneous multi-beams radar processing by using planner array antennas"

In this study a planner array with beam forming and beam shaping techniques are designed in order to develop and simulate 3D simultaneous-multi-beams (3DSMB) radar. Two targets are obtained, firstly developing 3D radar with 4 simultaneous-pencil beams, secondly, developing 3D with 4 simultaneous-different beams, such as Pencil, Fan, Transmit, and Intermediate beams. The new development in this paper provides in conjunction with enhanced processing techniques superior innovative war-fighting solutions to the dramatic change in the nature of threats (i.e. Missile, Anti Radar Missile, Jammers, and heavy clutter). A new software package is developed for the 3DSMB Radar in order to obtain the lobbing pattern coverage for a complex topography, because the previous studies didn't obtain the lobbing pattern for the 3D radar. Also, the cost will be much cheaper for the new mentioned development because instead of using different radars for different tasks and different targets platforms, the new development will be one radar processing different tasks and different targets platform at the same time, in addition to minimizing size and increasing processing speed and saving processing time. [C2631]

#### "Modeling of 3D pencil beam radar (PBR) volume coverage and 3D DMC"

The actual three dimensional radar purposes are to detect the target in three dimensions range, height and azimuth angle. The objective target for this paper is to simulate and study the three dimensional 3 D radar pencil volume coverage and the evaluation of the 3 D detection map contours (DMC) in complex environment. Also, the 3D DMC and 3D volume coverage are examined for different polarizations, such as horizontal, vertical, and circular. The results show that greater DMC and volume coverage are obtained in case of using horizontal polarization than the vertical and circular polarizations, also the vertical polarization produces greater ranges and greater DMC than the circular polarization assuming that the same radar parameters and same environment for the two cases, the free space and interference conditions. Also the accuracy measurements for the elevation and azimuth angles are better when using the Pencil beam coverage. The applications of the 3D (PBR) are widely used and interested for ATC radars and the EWR for homeland defense and protection because they are offering the prediction of radar performance and radar sitting. The detection and tracking facilities are obtained simultaneously which improve the target processing time and minimizing the cost. [C2632]

#### "Optical Image and SAR Image Matching Based on Scattered Edge Feature"

In this paper, we propose a novel algorithm for matching optical image to synthetic aperture radar (SAR) image based on scattered edge feature using relaxation Hausdorff distance combined with genetic algorithm. A method is presented to extract scattered edge feature from low signal to noise ratio (SNR) SAR image via statistical and ratio model. Based on the scattered edge image from SAR and optical image, relaxation Hausdorff distance is adopted as a similarity measure because it is insensitive to noise. Genetic algorithm is used as searching strategy to achieve high computation speed for its intrinsic parallelism. Experimental results using real SAR and optical images demonstrate that the algorithm is feasible, and can achieve high matching accuracy. [C2633]

#### "The Adaptive Detector of MIMO Radar and Its Performance"

Aiming at that the echo signal lies on the target characteristic in target detection of MIMO radar, namely the RCS of target determines the echo intensity, MIMO radar adaptive detector is based on the GLRT MIMO radar. It samplings in the radar receiver, makes the test be related to the SNR and sample size, and overcomes that the amplitude of echo effect detector's performance. then The better detector is achieved. The relative entropy, which is used to test the detection performance can represent the effect of the sample size on the detection performance. It is proved by the entropy that the MIMO detector is feasible and advanced. [C2634]

#### "Nonlinear Control System Intelligent Identification Using Optimized Support Vector Machines"

Nonlinear control system identification is studied using neoteric optimized Least Squares Support Vector Machines (LS-SVM) in this paper. Firstly, a multi-layer adaptive optimizing parameters algorithm is developed for improving learning and generalization ability of least squares support vector machines. According to different learning problems, the optimization approach can obtain appropriate LS-SVM parameters adaptively. Then, a nonlinear control system is identified by improved LS-SVM. The results show that the optimization approach can acquire best-optimized parameters for LS-SVM, and optimized LS-SVM can provide excellent control system identification precision and excellent convergence. And also, the multi-layer adaptive optimizing parameters algorithm may be appropriately extended to other types of support vector machines. [C2635]

#### "A Novel Velocity Compensation Algorithm by Graph Matching Method"

A novel velocity compensation algorithm is proposed. By extracting all potential scatters of two range profiles as two point patterns, the algorithm matches the point patterns by means of graph matching method. The velocity is estimated by the distance of correspondent points. The simulation experiments on range profiles with varying SNR, false scatters, and clutter aiguilles show the robustness of the new algorithm. [C2636]

#### "Track-Before-Detect Based on Two-Stage Sampling Particle Filter"

A modified track-before-detect based on two-stage sampling particle filter is proposed for detection and tracking of a target with low signal-to-noise ratio in an image sequence. According to each component's impacting on measurement directly or not, the state vector is partitioned into two parts. Then a higher-dimensional sampling problem in TBD can be changed into two successive lower-dimensional sampling problems. This improves the efficiency of state sampling. Results on simulated data show a higher gain in performance of detection and tracking. [C2637]

#### "Design and Implementation of a 1.5Gsps Digital Channelized Receiver"

Based on the derivation of the efficient implementation structure of the frequency domain polyphase filter digital channelized receiver, a digital channelized receiver was achieved on the hardware platform with I/Q sampling, 1500Msps, 64channels. In order to ensure good performance of the system, optimization of the processor speed and processor resources was fully considered during the design process of the whole system. The actual ultra-wideband signal test results show that the digital channelized receiver is in good performance. [C2638]

#### "One Vehicular Information Service System"

This article deals with several kernel technologies applied in vehicle information service. The technology referring to GPS (Global Positioning System), GPRS (General Packet Radio Service), GIS (Geographical Information System), and Computer Network etc, as we have studied, is believed to be able to construct a Vehicle Information Service System which faces the public. Synthesizing the technologies including GPS,GPRS, GIS, image capture and compress based on ARM9 processor and embedded system to establish a intelligent vehicle service model, which emphasizes U-V-S (User-Vehicle-Server) interaction. It is a integrated application in embedded system and its application software runs on relatively real-time and multi-mission operating systems. [C2639]

### "The Eye Movement Experiment and the Usability Evaluation of the Fighter Cockpit Digital Interface"

The relationship between the eye movement experiment and the quantitative evaluation of the visibility and usability of the fighter cockpit digital interface is put forward. After analyzing the data of the eye movement experiment of simulated fighter cockpit digital interface, we can demonstrate that the four kinds of quantitative data of the eye movement which include the pilot's gaze point coordinate, the gaze point number, the pupil frequency and the event time are very sensitive to the visibility and usability evaluation of the cockpit digital interface, and that the figure of gaze point sequence can apply to the usability evaluation of the interface very well. Furthermore, we infer that the eye movement experiment can reveal the pilot's visual process and cognitive activity, which will have a great practical significance to evaluate the usability and optimize the interface. [C2640]

### "IR revolution 360 infrared panoramic camera the ultimate solution for perimeter security"

Throughout the world, security issues are becoming increasingly important due to the current political and economical situation. Formerly reserved to the Defence sector, surveillance technologies for site monitoring are now required in many sectors. To this aim, very often a multitude of sensors using different technologies are installed, i.e. radar, intensification light cameras, CCTV, infrared barriers, lasers, IR cameras. These are spread around or within the monitored area in order to secure it. [C2641]

### "Highway road traffic information and monitoring system"

Road traffic, by dimensions, weights and speeds of vehicles which is moving is a danger that requires precise deployment rules, advanced technical systems for safe movement, an appropriate infrastructure etc. Road safety is an issue of interest to all citizens, each of which can contribute to improving safety on public roads. Although the measures taken in this area have proven, road accidents remain unacceptably high. One of the main causes of serious accidents is the failure of its speed and road weather conditions. For this reason in this paper we present an electronic road traffic information and monitoring system. The system consists of a traffic information system and detection equipment and weather monitoring, video imaging to speeding vehicles and the weight permitted for movement on public roads. [C2642]

### "Direction-of-Arrival estimation for uniform sensor arrays"

The Direction-of-Arrival estimation is a ubiquitous task in array signal processing with applications in radar, sonar, acoustics, astronomy, communications, medical imaging and military applications. For this reason, several techniques were developed for estimating the arrival direction of signals. The initial methods for estimating the direction of arrival were Bartlett and Capon, but the Multiple Signal Classification (MUSIC) algorithm is one of the most popular subspace-based techniques for estimating the directions-of-arrival of multiple signal sources. This paper is making a study of techniques for estimating the signals at arrival, when at the reception a linear array of antennas is used. The presented techniques are based on the estimation of the spectrum obtained at the reception. It shows a comparison between the methods implemented: Bartlett, Capon and MUSIC. [C2643]

### "A New Range Profile Identification Method Based on Multi-Scale Entropy Feature"

In high resolution radar, one dimensional range profile supplies detailed information of targets, but it is sensitive to direction, translation and intensity. To get direction, translation and intensity invariable features, a wavelet based multi-scale entropy feature is proposed. As entropy is not dependent on the shift of range profiles and is insensitive to the direction variation, the entropy feature has a translation and direction invariable property. In the paper, the entropies of neighbor two scales were divided to eliminate the intensity sensitivity of profiles. When the proposed feature was applied into real data for target identification, good result has been obtained, which is much better than conventional methods. Therefore, the proposed multi-scale entropy feature is an effective feature for range profile identification. [C2644]

### "Study on Command Control Network Cooperation Measurement of Network Centric Artillery Combat"

Firstly, the computing method of network centric artillery combat command control network cooperation measurement is studied. Secondly, the network relationship of artillery battalion command control nodes is analyzed in detail. Thirdly, the time delay of command control system influenced by the network complexity and a combat example are also studied. The results show that the network complexity and its corresponding network cooperation affect greatly the time delay of system. This research can provide good decision-making support for artillery command control network nodes deployment and optimization. [C2645]



### "The Case Study of a Diffusion Theory Model of Adoption and Substitution for Successive Generations of Mobile Internet"

Norton model is a diffusion model to use for a substitution for successive generations of a product. There are many hypotheses on this model, one of them is that only the next generation product can substitute this generation of product, and the first several generations cannot affect the diffusion of this generation product. In fact, successive generations of a product influence each other when they diffuse in the same market, so this paper takes the factors of the influence of successive generations of a product into account Norton model, and defines the substitution influence coefficients, then constructs the extended Norton model. This paper takes the adoption and substitution for successive generations of the mobile Internet in Taiwan as an example for the application of the extended Norton model. The results is satisfied after comparing with Norton model. In the end, the paper draws a conclusion that the extended Norton model is reliable, and the fitness and the forecasting is better than that of Norton model. [C2646]

### "Research on FOA and TOA Estimation Algorithm of Galileo SAR Signal"

In order to estimate FOA and TOA accurately in Galileo Search and Rescue system by considering that the message bit width and the phase edge time are unknown, we present a new FOA and TOA estimation algorithm which combines the algorithm based on Multiple dimensions Joint Maximum Likelihood Estimation criterion and Barycenter calculation algorithm. The FOA and TOA estimation errors of this algorithm can be limited within 0.03 Hz and 12 us in the condition that carry-to-noise rate (CNR) equals to CNR treatment threshold which is 34.8 dBHz and phase edge time is 250 us for received signals. Theoretical analysis and measurement results have proved the effectiveness of this algorithm. And the algorithm has been applied to the Galileo MEOLUT station. [C2647]

### "An algorithm for detecting a maneuvering target based on TFR and Viterbi algorithm"

An algorithm for radar signal detection method based on a time-frequency representation (TFR) and Viterbi algorithm (VA) is proposed. Two TFR methods are considered, Short-time Fourier Transform (STFT) and S-method (SM). Performance and detection ability of the proposed algorithm was investigated on real radar signals of a single maneuvering target with added Gaussian noise and signal-to-noise ratio from -15 dB to -2 dB. The results show that the proposed algorithm works well even in very low SNR values. [C2648]

### "A novel multi-dimensional spectrum estimation technique"

Conventionally, to multi-dimensional spectral estimation techniques, each data snapshot in space is captured simultaneously in time. The size of the antenna array is dependent on the area of interest. In this paper, we propose a data measurement technique, which does not collect data samples within each snapshot in space simultaneously but sequentially along a predefined path, and a spectral estimation technique, which is based on the Discrete Fourier Transform (DFT), for the collected data. The key idea of these techniques is to create a large synthetic antenna aperture by displacing a small antenna array and by assuming uniform plan impinging waves. The performance is evaluated by simulation. The applications of the proposed techniques include synthetic aperture radar, radar processing and sonar systems. [C2649]

### "Performance analysis of LFM-UWB radar based on Doppler frequency"

This paper analyzes the detection probability of LFM-UWB radar based on Doppler frequency. The LFM-UWB radar system consists of a transmitted part and a received part and uses AWGN channel. The system model is verified through analysis and simulation. Frequency offset occurs in the received part caused by the mismatching between the received signal and the reference signal. Performance degradation of detection does not occur in LFM-UWB radar, with 30cm resolution when the margin of Doppler frequency is about 120Hz. [C2650]

### "Self-optimization of capacity and coverage in LTE networks using a fuzzy reinforcement learning approach"

This paper introduces a solution to enable self-optimization of coverage and capacity in LTE networks through base stations' downtilt angle adjustment. The proposed method is based on fuzzy reinforcement learning techniques and operates in a fully distributed and autonomous fashion without any need for a priori information or human interventions. The solution is shown to be capable of handling extremely noisy feedback information from mobile users as well as being responsive to the changes in the environment including self-healing properties. The simulation results confirm the convergence of the solution to the global optimal settings and that the proposed scheme provides up to 20% performance improvement when compared with an existing fuzzy logic

based reinforcement learning approach. [C2651]

### "A novel maneuvering target tracking algorithm based on moving slide window"

We propose a novel tracking algorithm called slide window tracker (SWT) suitable for maneuvering target. To efficiently estimate trajectory of moving target, we adopt a sliding piecewise linear window which includes past trace information. By adjusting the window parameters, the proposed algorithm is to reduce measurement noise and to track fast maneuvering target with little computational increment as compared to  $\alpha$ - $\beta$  tracker. Throughout the computer simulations, we verify outstanding tracking performance of the SWT algorithm in noisy linear and nonlinear trajectories. Also, we show that the SWT algorithm is not sensitive to initial model parameter selection, which gives large degree of freedom in applying the SWT algorithm to unknown time-varying measurement environments. [C2652]

### "Target detection with MSN algorithm for the bistatic radar using digital broadcasting signals"

In the bistatic radar, it is important to suppress the undesired signals such as the direct propagated signal from transmitter and its multipath components. Conventionally, the suppression method by subtracting the replicas of the undesired signals is often used. However, it requires the precise delay times of the undesired signals. In this paper we propose a new method to detect the target without any information on the undesired signals' delay times in digital terrestrial TV-based bistatic radar, the signal of which is based on orthogonal frequency division multiplexing(OFDM). This kind of the radar is called "passive bistatic radar." We adapt a scheme based on maximum signal to noise ratio(MSN) algorithm, which makes signal to interference plus noise ratio(SINR) maximum for the certain delay component. The maximum sensitivity is steered along the delay which relates to the target position, as if the search beam is steered along the direction in array signal processing. The sensitivity is steered by the weight applied to the received signal in the frequency domain. We obtain the method to estimate the weight to achieve the maximum SINR in the delay estimation which also includes the compensation for the reduction of the weight's length caused by decorrelation among the delay components. The simulation results show our proposed method without any information on the undesired signal's delays provides the sufficient performance compared to the conventional one. [C2653]

### "DOA with linear array antennas based on MoM"

Direction estimation of signal of interest has been an important issue in radar and communication system. Generally, DOA(Direction Of Arrival) methods have been researched in the field of signal processing with ideal array sensors. However, there are some problems in array antennas such as the input signal distortions in amplitude and phase, due to the mutual coupling between array elements. Therefore, the compensation techniques of mutual coupling effects in the array antenna are required for the accurate estimation of DOA. In this paper, we propose a new method of the compensation of the mutual coupling effects for the DOA estimation in the dipole array antenna by using the method of moment (MoM). Also, the proposed method is applied to the estimation of azimuth ( $\Phi$ ) and elevation ( $\theta$ ) angles using uniformly linear dipole array under noisy environments. [C2654]

### "Model-based decentralized embedded diagnosis inside vehicles: Application to Smart Distance Keeping function"

In this paper, the deployment of a fault diagnosis strategy in the Smart Distance Keeping (SDK) system with a decentralized architecture is presented. The SDK system is an advanced version of the Adaptive Cruise Control (ACC) system, implemented in a Renault-Volvo Trucks vehicle. The main goal of this work is to analyze measurements, issued from the SDK elements, in order to detect, to localize and to identify some faults that may be produced. Our main contribution is the proposition of a decentralized approach permitting to carry out an on-line diagnosis without computing the global model and to deploy it on several control units. This paper explains the model-based decentralized solution and its application to the embedded diagnosis of the SDK system inside truck with five control units connected via a CAN-bus using "Hardware In the Loop" (HIL) technique. We also discuss the constraints that must be fulfilled. [C2655]

### "Enabling roaming management in GPRS and WLAN networks based on SIP"

In the wireless networks technologies, the concept of Next Generation Networks (NGN) focuses on environments in which IP technology provides transparent connectivity. It includes the roaming and mobility management between mobile users in heterogeneous networks. We compare two roaming models in order to integrate communication and session control from GPRS to WLAN 802.11 using SIP signaling protocol. The approaches follow the classification for service composition of the SAHARA project: Cooperative Model and Brokered Model. The solutions are based on loose coupled integration and IP mobility, which provide mobile applications and

mobile services. Contributions include the selection of the better model, the design of SIP broker agent and the implementation of roaming management following the IETF specifications. [C2656]

### "Retrieval of Ground Deformation Based on TS-DInSAR Technique"

Time series interferogram analysis is an upgrade of the traditional 2/3/4-pass differential interferometry, and has been widely used to map ground deformation associated with urban subsidence, landslide, earthquake and so on. This paper analyzes some key steps in TS-DInSAR processing, including selection of high-coherent points, extraction of linear deformation, separation nonlinear deformation phase and atmospheric phase. Finally, an experiment based on TS-DInSAR technique is conducted over Taiyuan area using totally 14 ENVISAT ASAR scenes in the time span of 2003-2007, and the result of derived deformation shows good agreement with the leveling data with mean square root error of 3.1mm, demonstrating that the TS-DInSAR technique is accurate and efficient in deformation mapping over urban areas. [C2657]

### "A new parameter for FMCW radar under external interference"

Recently, ITS (Intelligent Transport System) has been studied actively which is useful for smooth traffic and safety drive of the various vehicles. Though the laser or imaging camera sensor was used for ITS, they have unstable performances and high complexity. Therefore, FMCW radar using millimeter wave has been proposed recently. Actually, 47, 60, 77, 94 and 139 GHz are assigned for the vehicle radar frequency in Europe and Japan. In this paper, FMCW radar was simulated and modeled with interference. Also, RER(Range Error Rate) was proposed to estimate the performance error due to the interference. [C2658]

### "Closure monitoring in Potash Mines using LiDAR"

Underground soft rock mines are constantly deforming-this is a normal rock response to mining excavation. Once a mine opening has been excavated or cut, the opening begins to deform into the excavation. This rock displacement, or room closure, could occur quickly or much more slowly depending on the stress changes caused by mining pattern, rock mechanical properties and in-situ rock pressure. Of particular importance to Mining Engineers and Rock Mechanics specialists is the rate of this closure and where it is occurring within the mine. Room closure is traditionally measured using simple displacement transducers; these instruments give readings only at the points where they are installed. This paper proposes the use of Laser Range Finders (LRF) in generating 3D models of the mine areas where closure needs to be monitored. With this approach, closure can be measured at many points in the room, not just at individual instrumented stations. A procedure is presented using automatic scan registration to obtain a 3D model of an area using an inexpensive 3D LRF. Test results are presented from the Allan Potash Mine. It is shown that this procedure produces results consistent with a standard closure meter in a real mine environment. The difference between the average closure measured with LRF and the closure rod ranged from 3 millimetres to 13 millimetres (4% to 14% of total displacement change). [C2659]

### "FDI(R) for satellite at Thales Alenia Space how to deal with high availability and robustness in space domain?"

European leader for satellite systems and at the forefront of orbital infrastructures, Thales Alenia Space is a joint venture between Thales (67%) and Finmeccanica (33%) and forms with Telespazio a Space Alliance. Thales Alenia Space is a worldwide reference in telecoms, radar and optical Earth observation, defense and security, navigation and science. Thales Alenia Space has 11 industrial sites in 4 European countries (France, Italy, Spain and Belgium) with over 7,200 employees worldwide. Satellite evolution and wish to design more autonomous mission imply an enhancement of satellite architecture and to pay special attention to the FDIR. Nevertheless the constraints on the FDIR technique and strategy stay still invariant: robustness, reactive detection, quick isolation / identification and validation. This paper gives first the current context of FDIR by describing the approach implemented on Telecommunication satellite and more precisely one of the most FDIR sensible subsystem: the AOCS (Attitude and Orbit Control System). Following current state of FDIR in the Space domain, some perspectives will be introduced like a centralized distributed FDIR strategy for next generation of autonomous satellites and some research tracks like active diagnosis and hybrid diagnosis. [C2660]

### "Development of farming PDA based on the zigbee wireless sensors network and GIS"

It is the basic needs for carrying out precision agriculture to acquire the farmland information in real-time. Farming PDA is developed based on wireless sensors network and GIS technology. Farming PDA integrates the Zigbee coordinator module, GPSOEM module, GPRS module, and embedded GIS module as a whole mobile intelligent farming solution. Zigbee module is used for coordinating and managing the field wireless sensors

network and for collecting the farmland information through the network. GPS module is used for collecting and managing the geographic location information of each sampling point and for collecting the boundary geographic information of the target sampling field. GPRS module is used for the remote communicating and transferring the farmland information between the farming PDA and the host PC. The farming PDA can exchange information with the host PC in real-time so that it can be used to collect the farmland information in real-time. [C2661]

### "Application of particle filter for angle measure"

In anti-ship terminal guidance radar tracking system, the target echo is always corrupted by the sea clutter. When sea clutter is large at high sea state, the signal-to-noise ratio (SNR) of the target echo is usually relatively low as a result of the effect of sea clutter. The precision of angle error extraction in radar tracking servo is low, while the fluctuating error of angle measure is large in low SNR region. The radar antenna has to adjust itself very frequently to keep tracking its target. While it leads that the radar can not always hold on tracking the target steadily. To improve the precision of angle error extraction and steady off-boresight angle measure of the target, a novel angle measure method based on particle filter is proposed, which achieves off-boresight angle estimation by approximating the posterior probability diversity with particle set, and the steps of algorithm are presented. Finally the simulation experiment confirms the valid of the proposed algorithm. [C2662]

### "Noise analysis and restrain in the fusion process of remote sensing"

Considering the noise problem of multi-spectral images and SAR, several image noise models are described in this paper. The idea of non-negative matrix factorization and rough set are used to carry out the fusion experiment. Non-negative factorization is a matrix factorization method in the restrictive condition which all elements are non-factorization. The theory of rough set is mainly about the combination between knowledge and classification, which has an effect on de-noising aspect to the image noises. On the other side, the HIS and wavelet algorithm are adopted to the multi-spectral image fusion. It can not only hold more spectral information but also improve the spatial resolution greatly. The results from the experiment on the images specified the different types of noise, and get the conclusion in the help of some evaluation methods. [C2663]

### "Adaptive network fuzzy inference system used in interference cancellation of radar seeker"

The method of adaptive network fuzzy inference system (ANFIS) applied to the interference cancellation system of radar seeker was described in this paper. When the antiaircraft missile, which adopts the pulse Doppler radar seeker, attacks the low altitude target in the down-looking mode, the seeker of missile will receive strong ground clutter. As we all know the ground clutter will seriously affect the seeker's properties of target detecting and real-time tracking. To dealing with the seeker signal, the model of clutter should be constructed firstly. But it is difficult to handle because of the uncertainties and non-completeness characteristic of the clutter model. In order to solve the problem and overcome these, the nonlinear model, which used for clutter signal processing by the ANFIS is accepted in the interference cancellation system. In some researches, it was proved that the artificial network based on ANFIS not only has the ability of nonlinear mapping but also has the function of self-learning. Especially, ANFIS has small calculating costs. In my study, to possess a desired robust model, the adaptive side lobe clutter cancellation system depended on ANFIS was introduced. Through the side lobe clutter cancellation, the signal noise ratio (SNR) of echo signal got obviously improvement. The simulation results of experiments showed that the method of ANFIS can sharply improve the detecting performance of pulse Doppler radar seeker's looking for lower altitude target. [C2664]

### "A two-stage gating algorithm for joint probability data association filter"

Gating techniques for maneuvering target tracking using a joint probability data association filter (JPDAF) are considered in this paper. A way of estimating the gate size via the performance of the data association filter has been proposed recently, by which the gate size can be estimated by looking for the optimal performance of the data association filter. Combining the elliptic tracking gate with the direction tracking gate, a modified performance estimation function was proposed. As a feasible implementation, a suboptimal two-stage gating algorithm has been proposed also. Simulation results show that the suboptimal algorithm can offer advantages of decreasing the number of the feasible association events and reducing the calculation load of JPDAF, especially in a heavy clutter and/or false alarm environment. [C2665]

### "Ballistic missile precession frequency extraction by homomorphic filtering"

In order to extract the precession frequency, which is an important feature parameter in ballistic missile target recognition, we first establish the dynamic Radar Cross Section (RCS) signal model for a conical ballistic missile warhead with precession motion. A homomorphic filter is designed to remove the scintillation effect in the RCS signal. Simulations show the practical usefulness of the proposed method in extracting an estimate of the



precession frequency. [C2666]

### "Methods and experience of using Matlab and FPGA for teaching practice in digital signal processing"

Digital Signal Processing is a curriculum closely integrated by theory, implementation and application. With the development of microelectronics technology in recent years, the emergence of variety of chips makes digital signal processing widely used in various fields. Therefore, almost all of the electronic and computer engineering departments are now offering the digital signal processing courses. The main content of this course is abstract signal processing and transforming, involving a large number of mathematical knowledge and basic theory. The Matlab software can make the signal be presented in the form of visualized graphic image. Besides, FPGA, DSP and other high-performance chips can make digital signal processing technology widely used in various fields. Leading Matlab and FPGA into the teaching of digital signal processing is useful to improve the students' mastery of the knowledge points and enhance interest in learning. In this paper, for the purpose of radar real-time processing system application, methods of using Matlab and FPGA for teaching knowledge points such as bandpass sampling, polyphase filters, FFT processing, etc. are introduced. [C2667]

### "The Applications of GPRS in the Mine Monitoring and Control System"

Remote monitoring system based on GPRS is a modern monitoring system which is composed of radio communication technology, signal collection and computer network technology. This article introduces a wireless coal mine monitoring system based on GPRS communications technology. This system proposed in this paper has achieved a good result in the test. [C2668]

### "Travel Time Forecasting Based on Phase Space Reconstruction and SVM"

Travel time forecasting is an important content of dynamic traffic navigation. Dynamic traffic data collection is the precondition of forecasting. Many traffic data collection methods have been adopted, such as loop inductive vehicle detector, radar detector, video detector, GPS floating car and so on. Due to the widely distribution, GPS floating car has become the most efficient mean to collect instantaneous traffic information. How to take use of the collected GPS floating car data to forecasting the travel time is a popular research topic. In this paper, we develop a travel time forecasting method with the combining phase space reconstruction theory and SVM. Phase space reconstruction theory is used to determine the number of forecasting variable. SVM is used to forecast the future travel time value. The efficiency of the method is illustrated through analyzing Jinan urban traffic data. [C2669]

### "Tracking Maneuvering Target on Airport Surface Based on IMM-UKF Algorithm"

Aiming at tracking maneuvering target of SMR (Surface Movement Radar), this paper establishes a constant acceleration motion model, constant turn motion model and constant velocity motion model according to the actual movement of aircraft. On the base of these models, the IMM-UKF filter tracking algorithm is designed by introducing Unscented Kalman filter (UKF) into the interacting multiple model (IMM) algorithm. And IMM-UKF is compared with IMM-EKF (extended Kalman filter) algorithms. Simulation results show that IMM-UKF algorithm has good stability, and it overcomes the divergence problem of the EKF filter. The tracking accuracy and the model of transition speed are better than IMM-EKF algorithm. [C2670]

### "Design and Implementation of an Embedded Diagnosis System for Radar Built-in Test Equipment"

This paper describes a kind of embedded diagnosis expert system for radar built-in test equipment (BITE). Based on gradation diagnosis model and fault separation tree, diagnosis knowledge is represented by integrated framework, and the direct inference, reverse inference and hybrid inference diagnosis strategy are carried out in radar system. Site test results showed that the diagnosis system could improve fault diagnosis accuracy and speed for modern radar fault diagnosis. [C2671]

### "A Novel Algorithm of Velocity Ambiguity Resolution for Wind Profiling Radar"

Wind Profiling Radar can be used to detect the distribution of atmospheric three-dimensional wind, the quality of velocity information affects its performance directly. Compared to other weather radar, wind profiling radar's velocity ambiguity is particularly prominent when used to detect signal. Multiple PRF (pulse repeat frequency) is often used in radar system in order to solve the ambiguity problem. In this way, radar system has a variety of solutions for ambiguity algorithm in signal processing. In this paper, Doppler frequency series (DFS) algorithm can recover target's true velocity from the coupling velocity estimating directly. Simulation results proved the effectiveness of the method, and show us the DFS algorithm for speed estimation performance. Finally,

optimization of one-dimensional set of algorithms-compare screening algorithm and DFS algorithm to ambiguity-resolving, given the speed estimated in the DFS algorithm superiority. [C2672]

### "Efficient parallel computation of the estimated covariance matrix"

Computation of a signal's estimated covariance matrix is an important building block in signal processing, e.g., for spectral estimation. It involves a sliding window over an input matrix, and the summation of products to construct any given output-matrix element. Any given product contributes to multiple output elements, thereby complicating parallelization. We present a novel algorithm that attains very high parallelism without repeating multiplications or requiring inter-core synchronization. Key to this is the assignment to each core of distinct diagonal segments of the output matrix, selected such that no multiplications need be repeated, and exploitation of a shared memory (including L1 cache) that obviates the need for a corresponding awkward partitioning of the memory among cores. Implementation on Plurality's shared memory many-core architecture and, in order to demonstrate additional benefits, also on the x86, reveals linear speedup and a 130-fold power-performance advantage over x86. [C2673]

### "Tunnel Construction Safety Inspection and Polymer Grouting Technology for Tunnel Quick Maintenance"

In this article, the monitoring and measuring of the Xuejiazhuang tunnel of Lingnan freeway is introduced. The fitting regression analysis for the data of curve was done. And the surrounding rock stability is studied with the regression analysis of the convergence displacement data. In order to maintain the existing void between initial lining and surrounding rock, the ground-penetrating radar nondestructive testing technology and polymer grouting technology is presented. The field test results show that the use of polymer grouting technology can repair the tunnel distress and provide an ideal manner for tunnel quick maintenance. [C2674]

### "Signal separation based on Paired-Echo Theory"

Signal separation plays a very important role in radar signal processing. The separation of radar signal and the background signals has great influence on radar signal processing. The traditional method has little efficiency when the background signal is nearly the same as the radar signal. Therefore, a more efficient method is needed. This paper is devoted to design a new type of mismatch network to modulate the transmitted signal of an active radar transponder (ART). With the help of the mismatch network, the reflected ART signal can be effectively distinguished from background signals. [C2675]

### "Research on correlation description and processing method of multi-sensor fusion"

The correlation and dependence among information from different sensors usually increase the difficulty of data fusion. Through analyzing the correlation of multi-sensor, three correlation models are deduced. They are strong-correlation, weak-correlation, and maybe-correlation. Three different methods are used corresponding to the above three correlation models. Finally, an example is enumerated to show the whole fusion process. [C2676]

### "An algorithm of signal sorting and recognition of phased array radars"

This article uses the radar beams scan characteristics of the phased array radar, and proposes an algorithm based on the rough sets theory to sort the signal of phased array radars. From the research of the character of the phased array radar's beam scanning manners, and use the PDW received from sensors as the set of attributes. So we can sort the phased array radar signal from the environment. [C2677]

### "A robust method for PRI modulation recognition"

One of the main problems of radar identification in electronic warfare support system is analysis of pulse repetition interval (PRI) modulation. In this paper a robust method of recognizing the PRI modulation type of radar signals is proposed to improve robustness of previous recognition methods as well as to reduce the complexity. Simulation results show that the proposed method achieves much better error recognition rate in case of missing and spurious pulses than other methods such as autocorrelation based techniques and the Noone method. [C2678]

### "The facilitation of SRTM DEM-derived interferogram to accurate DEM reconstruction"

A novel approach is proposed in this paper to exploit the Shuttle Radar Topography Mission (SRTM) digital elevation model (DEM) to improve the accuracy of digital elevation model (DEM) reconstruction in interferometric synthetic aperture Radar (InSAR). The proposed algorithm can be applied to facilitate the DEM reconstruction

problem, i.e, the raw and simulated interferograms can be fused by introducing a user-defined weighting factor, that is, in regions of higher coherence, the raw interferogram with the interferometry method are remained, and in regions of lower coherence, the interferogram is updated with the simulated one. Some experimental results with ERS data verify the theoretical analysis and show that the method can improve the performance of the DEM reconstruction to a great extent. [C2679]

### "Life detection based on Correntropy Spectral Density"

A life detection method based on Correntropy Spectral Density (CSD) is proposed. Because correntropy contains second and higher-order moments of the probability density function due to the nonlinearity of the kernel, it is capable of yielding higher output Signal to Noise Ratio (SNR) in non-Gaussian background when compared with traditional life detection algorithm based on the Power Spectral Density (PSD). The simulation with synthetic data and experimental results illustrate the superiority of the method. [C2680]

### "Track clustering based data association for sky-wave Over-the-horizon Radar"

The multipath propagation and low measurement precision in sky-wave Over-the-horizon Radar (OTHR) pose new challenges to data association. Aiming at the formation of ships, this paper presents a new method of data association. Firstly the plane measurement model is established, and the transformation between radar and ground coordinates is deduced according to the given ionospheres state, which leads to different propagation modes. Then measurements observed from radar are transformed to ground coordinates considering all possible propagation modes, and the transformed points in ground coordinates for each measurement are called hypothetic points. Max-min distance clustering method is adopted to divide these hypothetic points into multi-classes. The feasible classes are selected using the restriction of propagation modes, and the geometry center of clustering can be calculated by averaging the points of feasible class. Finally, the nearest neighbor method is used to associate the geometry centers of clustering among different scans and further find the correlation of measurements, propagation modes and targets. Simulation results indicate that the proposed algorithm can associate the tracks in the formation of ships effectively, and the influence of radar detection probability on the algorithm is also analyzed. [C2681]

### "Influence and compensation of target motion on monopulse estimation in PD radar"

Pulse Doppler (PD) radar system with monopulse estimation can effectively acquire the location information of weak target, since it combines the advantages of coherent integration and monopulse technique. However, as it takes some time to realize the coherent integration, target motion will result in the decline of integration efficiency, thus affects the angle measurement precision. This paper investigates the principle of monopulse estimation in PD radar and the influence of target motion on angle measurement. A modified expression for angle measured value is presented when target has tangential motion, which can be interpreted as the midpoint angle of target motion track. Moreover, the target radial motion can be compensated by envelope interpolation method in time domain with the prior information of velocity, or by Keystone transform method in frequency domain without velocity information. Finally, the availability of the modification and compensation is verified by simulation. [C2682]

### "Research on the linear frequency diverse array performance"

The application of the linear frequency diverse array (LFDA) provides the more freedom for the waveform design in time, frequency, amplitude and phase domain. The antenna pattern of the LFDA is analyzed firstly. The main-lobe width of the antenna pattern is narrower and narrower with the increasing of the frequency interval between antenna elements. The ambiguity function of both LFDA and the conventional broadband linear frequency modulation (LFM) signals is compared. The blur between range and Doppler of the LFDA ambiguity function is improved evidently. The simulation and assay indicate that the application foreground of the LFDA is comprehensive. [C2683]

### "A quick and unitary algorithm for imaging radar jamming effect evaluation"

It is complicated to effectively and quickly evaluate jamming effect on imaging radar. Based on the concept of Euclid range space, a modified jamming effect evaluation technique for imaging radar has been proposed in this paper. Difference from previous methods, the most advantage of this method is that it has quick, accurate and unitary characteristics and it resolves the problem of timeliness that anti-jamming facing urgent need. It satisfies modern warfare's high demands and real-time need and has broad application prospects. Because this method make the evaluation standard of jamming effect quantify from zero to one, according to the evaluation coefficient value size, whether the jamming mode is effective can quickly and easily be given and the jamming intensity exerted to target can be known quickly. The jamming simulation has been done with the real and raw imaging

radar data. The result demonstrates the method is effective. [C2684]

#### "Mean shift track initiation algorithm based on Hough transform"

To solve the problem of initiating tracks for multi-target in dense clutters environment, a Mean shift track initiation algorithm based on Hough transform is proposed. In the algorithm, firstly, hough transform is applied to transform observation points from input space, referred to as feature space into curves in a special parameter space; then a Mean shift clustering algorithm is executed to cluster the items gained in the parameter space, and the problem of peak seeking is also solved adaptively. Furthermore, a fuzzy influential factor, which is based on the vote number of accumulation matrix and distance between items in the parameter space and clustering center, is defined to design kernel function of Mean shift; thus clutters are removed more effectively. Experimental results show that proposed algorithm has high detection accuracy and can initiate tracks effectively. [C2685]

#### "A novel method on radar 3-D imaging"

To realize perception to local lunar surface under the condition of relative stationary before soft landing during moon discovery, a novel 3-D imaging method is proposed. The method is based on receiving digital beamforming and modulated frequency stepped radar signal processing. The outstanding feature is this method can realize 3-D imaging without relative motion between radar and target. Simulation results indicate that it can obtain coordinates of strong scattering centers accurately and reconstruct 3-D image of scene successfully. [C2686]

#### "Research on SR\_UPF ground moving target tracking algorithm using road information"

A kind of tracking algorithm using square root unscented particle filter is proposed to solve nonlinear problem caused by maneuverability of target and low measurement update rate in ground moving target tracking. Unscented transform is used to transfer state estimation and covariance matrix, where the covariance matrix has been extracted. From this, importance sampling used in particle filter can be gained. Then, the state estimation which is obtained through particle filter is projected to road according to road information if it is off road. Using one ground moving target indication sensor to track a target on road, simulation results show that the proposed algorithm can effectively solve nonlinear problem in ground moving target tracking. Compared with the conventional particle filter algorithm, the proposed algorithm not only advances the tracking precision, also reduces the needed number of particles which mean less run time will be taken. Another way, tracking performance can be further improved due to using of road information. [C2687]

#### "Three-dimensional microwave imaging with adaptive single-input-multiple-output SAR"

Three-dimensional single-input-multiple-output synthetic aperture radar (SIMO-SAR) imaging method is proposed in this paper based on Capon adaptive beam-forming technology, and we have designed the downward-looking geometry architecture and signal echo model of the imaging system. Imaging algorithm is derived from the model and simulated. The advantages of three-dimensional imaging with SIMO-SAR are shown by the simulation results that it can get the height information of the targets besides the azimuth and range information, thus the targets can be located accurately and viewed in a stereogram. Furthermore, the algorithm can give better three-dimensional resolution. [C2688]

#### "Study of Anti Jamming of Radar Signal Based on Sparse Decomposition"

In order to distill the features of radar echo-signal affected by strong jamming noise, the sparse decomposition method and BPDN (Basis Pursuit Denoising) algorithm are used to remove the noise and recover the radar echo-signal. Based on the theory analysis, the reconstruction of the radar echo-signal with different SNR and anti-jamming effect of the method is studied by the simulation. The simulation results show that the proposed method is effective for anti-jamming of radar signal. [C2689]

#### "Identifying ship echoes in CODAR HF radar data: A Kalman filtering approach"

Coastal nations have an interest in maritime domain awareness for applications in national security, coastal conservancy, fishery and stewardship of the exclusive economic zones (EEZs) along their coastlines. Maritime situational awareness involves knowing the location, speed and bearing of ships and boats in the EEZ. HF radar is a useful tool in providing ship information in real time. It is especially effective when combined with ship-borne AIS beacons. Our previously developed HF radar and AIS ship detection models estimate signal to noise ratio (SNR) as a function of range, including ducted propagation for the AIS radio signals. However, ship detection is hampered by the high variability of HF echoes from ships. This is due in part to the aspect dependence of ship



radar cross-section and to the presence of clutter bands at known Doppler shifts from both the ground and ocean waves. Tracking ships using their HF radar echoes becomes the means for effectively monitoring the presence of ships in the coastal ocean. We explore the application of Kalman filtering to the ship tracking problem, following the techniques described by J. V. Candy. This approach is described and demonstrated with a simple example. [C2690]

### "Software beam forming for ocean radar WERA features and accuracy"

The WERA system (Wave RADar) is a shore based remote sensing system to monitor ocean surface currents, waves and wind direction. This long range, high resolution monitoring system based on short radio wave radar technology. The vertical polarised electromagnetic wave is coupled to the conductive ocean surface and follows the curvature of the earth. This over the horizon oceanography radar can pick up back-scattered signals from the rough ocean surface (Bragg effect) from ranges of up to 200 km. The direction in azimuth is defined by means of the phase of the incoming electro-magnetic wave. That means the accuracy of this measured azimuth strongly depends on the quality of this phase measurements. The described Software Beam Forming method combines best accuracy with the highest temporal resolution for ocean radar applications. Compared with other beam forming methods the flexibility of this method provides more degrees of freedom for the radar site planing and makes it much easier to identify suited site locations. [C2691]

### "Characteristics of internal waves in the South China Sea Observed by a shipboard coherent radar"

In 2005 and 2007, a coherent, X-band radar was deployed in the South China Sea on two different ships. In both cases, the two parabolic antennas of the radar were fixed at grazing angles of approximately  $2^\circ$  looking toward the bow of the ship. The radar transmitted and received through a single antenna but alternated between the two antennas approximately every half second. One antenna was horizontally polarized and the other was vertically polarized. The data were analyzed by computing normalized radar cross sections and scatterer velocities as a function of ground range and time. Surface signatures of the internal waves were obvious in both types of image and at both polarizations as regions of enhanced cross sections or scatterer velocities. The collected imagery showed that at least two different types of internal waves exist in the South China Sea: small, nearly sinusoidal trains of waves and large soliton-like waves. These different types travel at very different speeds and interact with each other. The small nearly sinusoidal waves travelled at phase speeds near 1 m/s that increased as the small wave trains were overtaken by the faster solitons. Combined with other shipboard measurements, the radar measurements yielded the widths, maximum velocities, and strain rates of the solitons as well as the dependence of phase speed on amplitude. When the speeds of both the ship and the solitons were removed, the measurements showed that soliton full-widths at half-maximum ranged from about 0.5 to 4.5 km. These widths showed a dependence on the amplitude of the soliton. The phase speeds of the solitons also depended on their amplitude, reaching 3 m/s in deep water but only about 1.2 m/s in shallow water. CTD profiles were used to estimate an interface depth for a two-layer fluid model of the propagation of the solitons. The phase speeds predicted by this model agreed well with the observed dependence of the soliton phase speed on amplitude in both shallow and deep water. [C2692]

### "Surface measurement by using a fixed antenna microwave pulse Doppler radar in Sagami-bay off Hiratsuka in Japan"

A sea surface measurement system by using a microwave pulse Doppler radar has been developed. It can measure sea surface waves, sea surface currents and a sea level at one time only with the use of mathematical relations without the necessity of using any empirical relations. From September 2009 to January 2010, sea surface conditions had been measured by using a X-band microwave pulse Doppler radar at 1 km off Hiratsuka in Sagami-bay, Japan. Algorithms for obtaining of sea surface conditions from the backscattering microwaves measured by a pulse Doppler radar and some measurement results are shown in this paper. The radar measured shoaling phenomena clearly. The increasing rate of wave height became larger in proportion to the square of the wave orbital velocity. [C2693]

### "Temporal error analysis for compact cross-loop direction-finding HF radar"

Surface currents and ocean swell are measured using an HF radar with a compact cross-loop antenna design. This unique direction-finding radar has been widely used for long-term monitoring and for coastal oceanography applications over the last ten years. Numerous studies have evaluated errors associated with these devices under a host of environmental and seasonal conditions, and reliable comparisons between HF radar surface current measurements and those from other technologies indicate a range of 0.08 to 0.15 ms<sup>-1</sup>, while internal error estimates that are made using the spread of data values in a time series or spectrum from the radar systems generally lead to errors of around 0.2 ms<sup>-1</sup>. These error estimates are typically based on manufacturer-

recommended operating parameters that can include up to 25 specific parameters or assumptions made about the data. In particular, one of the dominant parameters in computing ocean surface currents from SeaSonde devices is the averaging time of both the power spectra and the computed radial components of the surface current vectors. This paper explores the relative effect of temporal averaging for two SeaSonde stations in Western Australia. By analysing 31 days of radial data, we evaluate the statistical characteristics of noise in the spectra and determine the limits to the assumption that it represents a stationary ensemble of independent samples. The improvement in accuracy as we integrate over different time intervals from 10 to 180 minutes is determined by these characteristics. These results are applied to error analysis for the radial components of surface currents and compared with the errors in the gridded values of the radial components. Finally, the effects of calibrated and uncalibrated antenna patterns on the radial components is evaluated in the context of the temporal and spatial errors. [C2694]

#### "Using a dynamic ocean surface to perform a geometric calibration of a bathymetric lidar"

A geometric calibration of an airborne lidar is an essential component to any bathymetric survey. A poorly-aligned system leads to erroneously reported depths, diminished system resolution and internally inconsistent point clouds. While most calibration procedures depend on the use of cultural features (like gabled roofs), one recently suggested methodology requires only a single broad, flat surface. Given the potential difficulty in identifying such a surface on land, this paper investigates the possibility of using the ocean surface instead. Simulations are performed to examine the anticipated influences of both surface waves and tidal variation. Finally, oceanic results are compared with the likely topographic alternative: using a narrow airport runway as the calibration surface. [C2695]

#### "Comparison of SAS processing strategies for crabbing collection geometries"

This paper presents a number of different processing strategies for generating synthetic aperture sonar (SAS) imagery when data collection suffers from significant sideways crab (where we define crab as the angle difference between track and heading). Whilst large amounts of sideways crab do not present fundamental limitations to the SAS method, the assumptions SAS processing chains are built upon are often violated under such conditions. We discuss typical assumptions and compare alternate image formation strategies. We also provide a short discussion of the fundamental limitations to crabbing systems. We found that the adjustments to our standard wavenumber-based imaging kernel increased crab-tolerance from approximately 7 degrees up to approximately 30. [C2696]

#### "The influence of rainfall upon Scatterometer estimates for sea surface stress: Applications to boundary layer parameterization and drag coefficient models within tropical cyclone environments"

The use of satellite scatterometers to probe the winds in and near strong tropical cyclones (TCs) is a valuable tool for both numerical weather prediction (NWP) and weather forecasters. The presence of widespread rain in these storms complicates the estimation of surface winds from the satellite. Improvements in the techniques to infer surface winds from the satellite observations, which remove the effects of rain contamination at the ocean surface, will improve the modeling efforts as they pertain to the prediction of TC intensity. We demonstrate the use of collated and simultaneous high-resolution rain measurements obtained from nearby Next-Generation Radar (NEXRAD) and NASA Quick Scatterometer (QuikSCAT) measurements, respectively. Through the application of the National Oceanic and Atmospheric Administration (NOAA)/Atlantic Oceanographic and Meteorological Laboratories (AOML)/Hurricane Research Division (HRD) TC wind analysis (H\*WIND; Powell and Houston [1996] ), we will study the dependence of a surface normalized radar cross-section (NRCS) on the TC wind-speed and rain-rate. The objective is to better observe and understand the dependence of the drag coefficient upon the surface stress across a wide range of conditions and spatial scales within these storms. [C2697]

#### "Worldwide internet based data acquisition from remote platforms"

A novel concept for using a low power web server integrated in a data acquisition platform for transferring data using "http" (hypertext transport protocol) has been developed by SAIV. The data is directly transferred from a field station to the end user without any intermediate links via the Global System for Mobile Communications (GSM). [C2698]

#### "Train Conformity Check System; Technology and current operation experience"

An overview is given of the technology and the performance of "Train Conformity Check System". The system provides a modular set of defect detection functions for rail vehicles, including the detection of three-dimensional profile limits violations and of overheated components. Other available defect detection systems can be

integrated to identify and arrest trains with hazardous defects, to support rolling stock maintenance planning and to increase railway lines availability. [C2699]

### "Spilled Oil Tracking Autonomous Buoy"

We are developing Spilled Oil Tracking Autonomous Buoy System (SOTABS), which is composed of a land base and several spilled oil tracking autonomous buoys (SOTAB), to detect and track spilled oil autonomously, sending real time data around them to the land base. This paper firstly deals with steady sailing performance of SOTAB-II with a sailboat shape for tracking spilled oil on the sea surface by controlling the rudder angle, and the area and direction of the sail, and then sea trials using a model of SOTAB-II with a cylindrical buoy shape to obtain its fundamental characteristics on motion. [C2700]

### "Improving target tracking performance by incorporating classification information"

This paper presents approaches for incorporating classification information into target tracking algorithms, specifically in a multistatic active sonar context. In addition, this paper describes the framework designed for simulation and classification of return time series from simulated targets and clutter in a realistic underwater environment. The simulated target and clutter returns are integrated into an existing contact-based tracking dataset (TNO Blind dataset) for which time series are unavailable. Simulations compare the integrating classification of contacts at different stages of tracking algorithms. Results show improvements in some tracking metrics with no degradation of the others. [C2701]

### "National Data Buoy Center (NDBC) support of the Integrated Ocean Observing System (IOOS)"

The National Data Buoy Center (NDBC) began implementing Integrated Ocean Observing System (IOOS) principles in 2001, when they partnered with the Gulf of Maine Ocean Observing System (GoMOOS). NDBC and GoMOOS collaborated on a project to transmit meteorological and oceanographic data from the GoMOOS buoys to NDBC in real-time. NDBC's data quality control, data format, and communications services were then used to transmit the data to the NWS Telecommunications Gateway (NWSTG), which disseminated the data to the Weather Forecast Offices (WFOs) in the region. As IOOS has matured and Regional Associations (RAs) have developed, NDBC has been a partner. NDBC shares ocean observation expertise, develops data management techniques and quality control algorithms, and keeps the RAs and IOOS informed by participating in Regional Association meetings and workshops. Using a scalable system that is able to receive increasing numbers of observations, while maintaining quality control, NDBC has increased the number of partner data providers to more than 40 and the number of partner platforms to more than 600. Many of the providers are members of RAs and Ocean Observing Systems (OOSs). The number of observations handled by NDBC will approach 10 million a year by the end of 2010. As NDBC and partner data are quality controlled at the gateway, any data that do not meet the stringent quality control algorithms are automatically assigned quality flags. The flagged data are transmitted to NDBC, where analysts reexamine the data. NDBC has also been involved in the IOOS effort to establish the technical infrastructure, standards, and protocols needed to improve delivery of ocean data through the Data Integration Format (DIF). NDBC, along with NOAA's Center for Operational Oceanographic Products and Services (CO-OPS) provide these services. Services include the NDBC Sensor Observation Service (SOS), which provides ocean temperatures, salinities, currents, waves, and winds from NDBC Coastal Buoys, IOOS Regional Coastal Ocean Observing Systems, and TAO moorings. In addition to these data, high Frequency Radar derived coastal surface currents are available through the NDBC THREDDS Data Server. A new partnership between NOAA's National Oceanographic Data Center (NODC) and NDBC will lead to the capability to preserve all of NDBC's marine datasets to meet the standards for climate observation requirements established by NOAA and the Global Climate Observation System (GCOS). Taking advantage of new techniques using Ocean Geospatial Consortium (OGC) Inc. standards and the SOS described above and funded by NOAA's IOOS Program, will enable a new degree of interoperability within and between NDBC and NODC and properly archive all NDBC Partner observations. [C2702]

### "Low resource demanding FOTA method for remote AtoN site equipment"

This paper presents a method for firmware update in memory constrained low-power controllers used in marine aids to navigation (AtoN) and telematics systems. The developed method allows carrying out firmware updates regardless of the communication channel used. This approach differs from other similar methods mainly by its low requirements to hardware and high flexibility; hence it is applicable to relatively small microcontrollers. The paper is concluded with experimental results performed on operational marine buoys. [C2703]

### "The NANOOS Visualization System (NVS): lessons learned in data aggregation, management and reuse, for a user application"

The mission of NANOOS is to coordinate and support the development, implementation, and operations of a regional coastal ocean observing system (RCOOS) for the Pacific Northwest region, as part of the U.S. IOOS. A key objective for NANOOS is to provide data and user-defined products to a diverse group of stakeholders in a timely fashion, and at spatial and temporal scales appropriate for their needs. To this end, NANOOS developed the NANOOS Visualization System (NVS), which aggregates, displays and serves meteorological and oceanographic data, derived from buoys, gliders, tide gauges, HF Radar, meteorological stations and satellites, as well as model forecast information in such a way that it presents end users with a rich, informative and user friendly experience. First released in November 2009, NVS has already undergone several significant updates. While its original focus and continued strength is on near-real-time (NRT) observations from stationary platforms (buoys, coastal stations, etc.), it has evolved to include other types of observations as well as forecast information. NVS integrates data from a wide diversity of providers across the region, ranging from county agencies, private industry and regional partnerships, to core IOOS federal programs, and state agencies and academic groups that are principal partners in NANOOS' Data Management and Communication (DMAC) efforts. Regional and national feedback confirms that NVS has been well received by ocean observing and stakeholder communities alike. This paper discusses, in detail, NVS 2.0, which was released in August 2010. In particular, we provide an in depth look at the database schema, metadata, data harvesting, and component communication. In addition, we discuss the NVS data management and communication approach in the context of the IOOS DMAC interoperability and standards-based efforts, highlighting the strengths and weaknesses of application-focused vs. strong-interoperability-focused approaches. Lessons learned both from technical and project management perspectives are also presented. Lastly, we discuss future plans for NVS. Anticipated improvements include automating asset metadata discovery and processing using IOOS standard protocols, and a NANOOS implementation of ERDDAP that will support NVS by replacing multiple, data-source-specific data harvesters with more generic and easier-to-maintain NERDDAP harvesters; and by enabling customized data subsetting and download capabilities that will be accessible through the NVS user interface. [C2704]

#### "Active position security through dynamically tunable radar"

Acquiring and securing position information is of fundamental importance in vehicular ad hoc networks and their applications. Recently, it has been shown that securing position information can be achieved by enlisting the help of on-board radar devices that have seen a phenomenal penetration of the vehicular market. However, most on-board radar devices have a static range and this can cause a number of insecurities and can add to communication delay. The main contribution of this work is a novel low-cost radar model which can dynamically tune its range by changing the signal sample size. As it turns out, the dynamically-tunable radar considerably enhances position security. [C2705]

#### "Miniature, low power, generic Doppler sonar"

The Oceanographic Systems Laboratory at Woods Hole Oceanographic Institution has developed a small, low power, single-axis, range-gated pulse-coherent Doppler sonar, that is primarily intended for boundary layer turbulence studies. This instrument is composed of a receiver-transmitter, a 24MHz analog-to-digital converter, a down converter, and a low power Digital Signal Processor (DSP). The system is capable of autonomous operation from a variety of stationary platforms, such as buoys, moorings, and bottom frames, and small mobile platforms, including gliders, profilers, towed bodies and autonomous underwater vehicles (AUVs). [C2706]

#### "Wavelet Transform and its Application to ICESat-GLAS Full Waveform Data"

Based on wavelet transform (WT), this paper proposed an approach to extract ICESat/GLAS full waveform characteristics. Through wavelet decomposition of the full waveform data, setting the threshold function and reconstructing signal, the filtered waveforms were achieved. All comparisons were performed on simulated LiDAR full waveform signals with typical back scattering noise. In the simulation and comparison, the root mean square error (RMSE) of the coefficients dropped by 0.7188 in this way, and the Signal-to-Noise Ratio (SNR) increased by 16.17 dB. The results showed that the wavelet transform method was better than the Gaussian method on de-noising and the signal by wavelet transform reserved useful information of the echo waveform. In the filtering process, the wavelet transform can effectively suppress the waveform "overlay" problem. [C2707]

#### "Research on the Optimal Disposition of Near Space Multi-sensor Platform"

In this paper, to solve the cooperative detection problem of ground observation for near space multi-sensor platform, put forward the index of multi-sensor platform optimal disposition, and the genetic algorithm is used to analyze the calculation process, finally, through an example shows the utility and value of the index and algorithms, implemented the optimal disposition of the multi-sensor platform. [C2708]



### "What can HF radar contribute to the salvage of a grounded ship?"

The area around the grounding site of the Shen Neng 1 in Great Barrier Reef waters On 3 April 2010 was monitored by an HF radar and several Acoustic Doppler Profilers. The HF radar is shown to compare well with the Profilers at the mooring sites. The radar data was used to produce a time series of surface currents at the site during the grounding and throughout the subsequent salvage and clean-up. The spatial and temporal surface current maps are ideally suited for Lagrangian tracking of notional zero buoyancy water parcels starting from the grounding site. Lagrangian 'parcels' were released at two-hour intervals after the grounding in order to identify locations of flotsam or spills. Releases at two-hour intervals through a tidal cycle followed similar tracks until, on the fifth day, a significant change in the meso-scale meteorology and oceanography occurred. It is shown that the meso-scale change had a stronger control on the destination of 'parcels' than tides. HF radar has much to offer in nudging real-time hydrodynamic models used for predictions of currents during a maritime incident like this. [C2709]

### "Comparisons of a fully coherent and coherent-on-receive marine radar for measurements of wave spectra and surface currents"

A new coherent solid state marine radar has been developed for short range coastal ocean remote sensing applications. It has been applied to the measurement of coastal ocean currents and ocean wave spectra, examples of which are reported here. The radar is based on a standard marine radar package, but using a solid state power amplifier incorporated as part of the transceiver subassembly. The solid state transceiver subassembly was developed based on a SMA-connector component prototype that was reported on at the Oceans 2019 Biloxi meeting. A series of parallel tests were run with a prototype coherent-on-receive radar, which is based on modifications to a standard Koden marine radar. For the latter, the leakage signal of the transmitted pulse is used as the reference for realigning the phase of the received echo. Due to the non-coherent nature of magnetron sources used for marine radars, the pulse-to-pulse stability of the transmitted frequency of such a system creates problems with pulse-pair phase-differencing estimates of Doppler shifts. This effect creates a rather noisy Doppler image, and mean Doppler estimates over many rotations can be in error. Data were collected with the pair of radars during the passage of 2-m waves up to 13-s period at the FRF pier in Duck NC. We report on differences in Doppler estimates for the fully coherent and coherent-on-receive marine radars for data collected during this storm, comparing with FRF measurements of wave spectra and surface currents. [C2710]

### "Frequency diversity for active sonar/radar application and optimal receiver design"

MIMO (Multiple Input Multiple Output) concept has been explored for radar/sonar application recently for improving target detection and estimation performance. The existing work in this direction mainly investigates the spatial diversity and waveform designs based on the assumption of the same carrier frequency for multiple transmitters. In this work, we investigate the frequency diversity by using multiple narrowband transmitters of different center frequencies. We prove that the ambiguity function for such signal is not an optimal receiver, and propose an optimal receiver for signals with different frequency components. [C2711]

### "On the use of time-frequency domains for the improvement of the Stochastic Matched Filter Pulse Compression scheme with a high speed computing architecture"

In several domains of engineering technologies, such as telecommunication, sonar imaging, positioning systems, radar, medical imaging ..., the main problem is to identify a transmitted useful pulse in a noise-corrupted received signal. A solution to this problem consists in using a modulated pulse for emission and a matched filter for reception. Such a concept is known as pulse-compression. Taking into account the main assumptions of the matched filter theory, the use of the bandpass transmitted pulse as matched filter's impulse response is only available if the useful signal is well known and if the noise is white, which is not the case in practice. For this reason, it has been recently proposed an alternative to the classical pulse-compression scheme taking into account the random nature of the useful signal and the coloration of the noise. This new principle is known as the SMF-PC. Although, this method allows a great improvement in terms of signal to noise ratio compared to the classical pulse-compression technique, the SMF-PC appears under optimal due to stationary assumptions. In this context, the purpose of this paper is to propose an improvement of the SMF-PC by coupling this technique with a time-frequency method. Results obtained on synthetic and real data are proposed and discussed. [C2712]

### "Microwave backscatter of ship signatures on SAR imagery"

Speckle characteristics was analyzed by computing the ENL (Equivalent Number of Looks) for sub images of 30 by 30 pixels from four RADARSAT-2 dual polarization products, two single look complex (SLC) products acquired

in wide swath single beam mode with dual polarization of HH+HV and two ScanSAR Wide (SCW) products acquired in ScanSAR Wide beam mode with dual polarization of HH+HV, which lie in the sea area around Iberian Peninsula. The speckle analysis indicates that ENL value combined with the intensity value of the SAR image should be a feasible short cut to find ship signatures out of SAR image. Based on the ENL analysis of speckle characteristics, a data set for ship signature has been derived, from which the ship signature was measured by polarimetric synthesis since the polarimetric SAR signature is an effective way of utilizing the amplitude and phase information to characterize the polarization properties of microwave backscatter. Driven by the need for a realistic microwave backscatter of ship signature model, the detailed behavior of a single ship in different polarizations and different incidence angles will be investigated by the Ray-Optical method which was developed by Burkholder et al. The purpose of this paper is to pave the way for a further improved scatter matrix model. [C2713]

### "Front matter"

The following topics are dealt with: deep ocean survey; oceanographic instruments; optical communication system; data visualization; autonomous underwater vehicles; sonar signal processing; acoustic systems; SAR imagery; water quality sensor; deepwater horizon oil spill; and marine renewable energy. [C2714]

### "Integrated Coastal Observation Network (ICON) for real-time monitoring of sea-level, sea-state, and surface-meteorological data"

National Institute of Oceanography (NIO) has established an Integrated Coastal Observation Network (ICON) of in-house designed and developed Internet-accessible real/near-real time reporting cellular based sea-level, sea-state, and surface meteorological (Met) stations at several locations on the Indian coasts & Islands (<http://inet.nio.org>). Subsurface pressure sensors and downward-looking microwave radars are incorporated in the sea-level station network. Sea-level, Met, and surface wave parameters are acquired using dedicated Linux based data loggers and uploaded to an Internet server at 5-, 10- and 30-min intervals, respectively with the use of GPRS cellular modems. The sensors and data loggers are powered from sealed lead acid batteries, which are charged through solar panels. The ICON provides graphical presentation of sea-level information (observed sea-level, predicted tide, residual sea-level); significant wave height and wave direction; and Met information (vector-averaged wind speed & direction, barometric pressure, atmospheric temperature, solar radiation, relative humidity, and rainfall). Installation of sea-level sensors free from the influence of stilling-wells and long narrow tubes renders the measurements ideal for tsunami and storm-surge studies by preventing waveform distortion and non-linearity of large-amplitude short-period signals. The network maintains accurate time-stamp of the dataset through Internet-time synchronization using network time protocol (NTP). Real-time reporting capability of ICON yields several benefits, such as (i) remote monitoring of proper working condition of individual stations; (ii) implementation of repair/maintenance in the shortest possible time, thereby minimizing break in the time-series data stream; (iii) periodic arrival of data stream from all stations at a single central server, thus yielding backup for the data from all the stations; (iv) access to the latest in-situ information; (v) allows possible-- use of data with automated real-time running numerical models for operational forecast. In contrast to the limited bandwidth provided by INSAT transmitters, coastal observations at high bandwidth at significantly low cost have become realizable using cellular GPRS network. The NIO-network allows, Internet based real/near-real time tracking and monitoring of sea-level, sea-state, and meteorological conditions along the Indian coasts and islands and from almost anywhere--an issue of considerable practical significance during natural disasters such as storm, storm-surge, and tsunami. [C2715]

### "Modeling and simulation of sea surface radar observations"

This paper describes a methodology to model and simulate the reflectivity measured by radar observing a maritime environment. The simulation principle consists of reproducing the acquisition of a Real Aperture Radar (RAR) moving along its axis. Pulse after pulse, high range resolution profiles are successively computed by summing the contribution of backscatters comprised in the radar footprint. The scatterer contributions are calculated from typical statistical distribution estimation. The simulation output, called raw data, is the concatenation of time profiles (short time) successively obtained for each radar pulse (long time). A SAR algorithm is then applied in order to form a high resolution image. The generation of the sea surface is achieved by a multi-scale model. This approach takes into account phenomena at different scales (from long wave to small objects), all in interaction in a hydrodynamic environment. It is thus possible to focus locally on contributions considered as more significant. To improve the processing time some contributions can also be retrieved from Look-Up Tables. Hence, our method performs a realistic simulation of electromagnetic interactions in a maritime environment. [C2716]

### "A network based attenuation correction system for networked dual polarization radar observations"

Electromagnetic waves backscattered from a common volume in networked radar systems are attenuated differently along the different paths. A network based attenuation correction system for a network of dual polarization radars can be developed by combining the conventional network approach and the conventional differential propagation phase based attenuation correction technique. The network based attenuation correction system proposed here has been evaluated by data from the Adaptive Sensing of the Atmosphere (CASA) Integrated Project 1 (IP1) radars, which is a radar network that can observe a weather event simultaneously by multiple radars in different locations. The preliminary results show that the network based attenuation correction algorithm retrieves reflectivity and differential reflectivity properly. [C2717]

#### "Real-time buried object detection using LMMSE estimation"

We present the application of linear minimum mean square error (LMMSE) estimation to GPR data for achieving buried object detection. Without employing any empirical assumptions, nonstationary form of Wiener-Hopf equations is applied to GPR signals to estimate the next sample in normal conditions. A large deviation from this estimation indicates the presence of a buried object. The technique is causal, which allows it to be used in real-time applications. Our approach is theoretically optimal in linear minimum mean square error sense, and it is also validated with the tests that are carried out on a comprehensive data set of GPR signals. [C2718]

#### "Sub-band phase calibration in stepped frequency GB noise SAR"

The paper describes a method of band synthesis in a stepped frequency ground-based (GB) noise synthetic aperture radar (SAR) in case the of phase offset between reference and surveillance channel changing along with the carrier frequency switching. The method is based on receive channel calibration using crosstalk signal between transmitting and receiving antenna, dominating over the scene echoes. The paper shows a method of phase offset estimation and correction and results of its application to SAR data obtained with a radar system constructed using universal commercial off-the-shelf (COTS) measurement instruments. [C2719]

#### "Performance of an ultra wideband radar for detection of water accumulation in the human bladder"

This paper presents an Impulse Radio Ultra Wideband (IR-UWB) radar for detecting water accumulation in the human bladder. The goal is to monitor the level of urine in patients who suffer from urinary incontinence. This is achieved by detecting the reflected UWB signals from the boundaries of human tissues such as muscle and urine. The reflection properties are investigated both in a simulator with a bladder model and through measurements with a phantom model. The performance of the vivaldi antenna is investigated with regards to the pulse distortion due to the near field effect and signal attenuation in the far field. The simulation and the measurement results show the potential of water detection of the human bladder by using UWB pulses. [C2720]

#### "Simulation study of relationships between Doppler-polarimetric parameters at microwave remote sensing of precipitation"

This paper studies the relationships between recently introduced differential Doppler velocity and other parameters of radar signal reflected from rain. Analytical calculation and simulation methods are used mostly. The results are checked by measurements in special cases. Some possibilities to derive information on distributed object structure are shown. [C2721]

#### "Illumination properties of multistatic planar arrays in near-field imaging applications"

The achievable illumination quality in microwave and millimeter-wave images using multistatic planar arrays is discussed. The geometrical relations between the array effective aperture and the illumination boundaries caused by the specular reflections are introduced. Afterwards, the variations in the processing gain due to diffuse and specular reflections are analyzed and verified experimentally. [C2722]

#### "Pseudo-noise waveform synthesis for SAR applications"

The paper presents the research carried out at Warsaw University of Technology on area of waveform design for Noise Synthetic Aperture Radar (SAR). The aim of the article is to present the method of creating complex pseudo-noise waveform with reduced side lobes of autocorrelation function in observation area. [C2723]

#### "Enhanced monopulse radar tracking using empirical mode decomposition"

Monopulse radar processors are used to track targets that appear in the look direction beamwidth. The target tracking information (range, azimuth angle, and elevation angle) are affected when manmade high power interference (jamming) is introduced to the radar processor through the radar antenna main lobe (main lobe

interference) or antenna side lobe (side lobe interference). This interference changes the values of the error voltage which is responsible for directing the radar antenna towards the target. A monopulse radar structure that uses filtering in the empirical mode decomposition (EMD) domain is presented in this paper. EMD is carried out for the complex radar chirp signal with subsequent denoising and thresholding processes used to decrease the noise level in the radar processed data. The performance enhancement of the monopulse radar tracking system with EMD based filtering is included using the standard deviation angle estimation error (STDAE) for different jamming scenarios and different target SNRs. [C2724]

#### "A Fit-to-Sine based processing chain to handle multiple-target scenarios"

The full coherent processing of non-equidistant sampled data has been the topic of many research activities. In this paper we propose a processing chain based on such an algorithm, the Fit-to-Sine function, which is able to handle multitarget and target/clutter radar signals. Starting from the computation of a least squares cost function in dependency of frequency, followed by a feature extraction method and the suppression of unwanted sidelobes, we conduct a simple noise/target distinction by utilizing basic fuzzy logic characteristics and operations. Finally we exemplify our processing chain and the achievable results on a real radar scenario with a target moving in strong clutter. [C2725]

#### "Submillimetric high resolution passive imaging system using synthesis aperture technique"

This paper presents a G-band [140-220 GHz] high resolution passive imaging system for personal security applications. The spatial resolution depends on the size of the antenna. Since a spatial resolution of 1 cm, at a distance of 5 m requires a very large aperture antenna equal to 1 m at 140 GHz, so it is difficult to achieve a compact system. The synthesis aperture technique allows to reduce the size of the system, while keeping a good spatial resolution. To apply this technique, the studied system is a Y-shaped radiometric interferometer. One of the advantages of such a system, is that there are no moving part, and the size of the synthesized aperture is easily expandable to meet more uses. The system design, simulated performances, and realized monolithic microwave integrated circuits results are presented. [C2726]

#### "Evaluation of a high accuracy range detection algorithm for FMCW/phase radar systems"

The FMCW radar is the most versatile radar principle used today. Depending on the system configuration, it is possible to use an FMCW radar to detect targets in the range from hundreds of kilometers down to a few centimeters. This paper describes an algorithm, which can be applied to improve the FMCW range accuracy down to a few mm. Numerical system simulations are used to evaluate the possibility of using a combination between an FMCW and a phase radar for a line based range detection at 24 GHz. [C2727]

#### "A 94-GHz receiver front end for passive millimeter-wave imaging"

We have designed and fabricated the passive millimetre-wave imaging system for receiving radiation energy from the an object and a human body. The lens and front-end of the receiver are important in the system to detect input thermal noise signal. Passive millimetre-wave imaging system required of high sensitivity and wide broadband to detect input thermal noise. The LNA module of the imaging system has gain of 65.8 dB in average linear gain and 11 GHz in bandwidth to enhance sensitivity for thermal noise and to receive it in wide-band width as well. The zero-bias Schottky diode has been used for the detector circuit to convert amplified millimeter-wave signals to DC output. [C2728]

#### "EM estimation of a generic 2D object model based on a sparse set of incomplete ISAR images"

This paper addresses the estimation of a two-dimensional model of an object, based on measurements with a network of High Range Resolution (HRR) scanning surveillance radars. While considering a dynamic radar scene, the data collected from the multiple radars at multiple scans of the antenna provide a wide, but highly sparse, coverage in 2D space. The multi-radar multi-scan data are treated as asynchronous. Inverse Synthetic Aperture Radar (ISAR) 2D imaging is independently performed within the narrow angular sector which is covered during each single radar scan. Each of the formed ISAR images is a rotated and incomplete version of the 2D profile of an extended object. The multi-look images are aligned and incoherently fused in a common 2D space. Their complementary information content is thus combined in a unique composite image. The Expectation-Maximization (EM) algorithm is further applied for parametric estimation of a low-dimensional 2D object model. This model constitutes a feature vector, useful for object classification. The local-only use of the phase in this overall sparse, but locally dense, sampling scheme accelerates significantly the de-ghosting of the formed 2D target images. Quicker convergence to an unambiguous estimate of the generic 2D object model is achieved, as compared to a purely incoherent processing of the sparse dataset. [C2729]



### "A Kalman smoothing approach for surface deformation monitoring in differential SAR interferometry"

This paper presents a Kalman smoothing approach for estimating the temporal evolution of terrain deformations, using a chronologically ordered sequence of differential synthetic aperture radar interferograms spanning a long time interval. The proposed method assumes that the interferograms are formed with respect to the same master image and that the data pairs used to generate the interferograms can have orbital separations (i.e. baselines) up to the decorrelation baseline or even larger. The algorithm presented next applies to every highly coherent pixel (known as permanent scatterers) in the image and it is independent of the interferometric processing of the SAR images; so it is essentially a post-processing step. Since it's supposed that all the SAR images are available for batch processing, the proposed algorithm is naturally a smoother. The Kalman smoother reported thereafter can be exploited successfully to estimate the line-of-sight surface deformation of a vast area. This technique has been tested on simulated deformation data and it has demonstrated an excellent capability to track the ground deformation dynamics with a high accuracy. [C2730]

### "Microwave ocean scattering at low-grazing angles with the GMoM"

The radar cross section from a rough surface becomes very small at grazing incidence, since most part of the energy travels in the forward direction. Therefore, building a model that can estimate it accurately is challenging. Here, a rigorous model is presented, based on a specific integral formalism, and tested on sea surfaces. We plan to apply this model to time-varying ocean surfaces at microwave frequencies, under a small slope assumption. The sea surfaces patches are to be tank measurements, or generated numerically. We aim at comparing the resulting Doppler spectra to first order approximate methods. [C2731]

### "HYCAM-a software-defined testbed for experimentations of new S band surface radar concepts"

In 2008, ONERA started developing a radar designed for experimental studies on new concepts for naval and surface applications. The project is called HYCAM. The aim is to be able to be representative of most of the categories of surface radars (multi-function radars, surveillance radars, target analysis systems, NCTR radars, tracking radars, weather radars,...). To achieve such a versatility, a modular and software defined architecture has been proposed thanks to modern and high performance digital technologies (FPGA, DAC, ADC). Moreover, micro-wave front-end/antennas are reconfigurable. The device is expected to be validated in 2011. In this paper, radar definition and specifications are detailed. [C2732]

### "Comparative analysis of two techniques for moving target velocity estimation"

In this paper two different algorithms for target velocity estimation are considered and compared. Traditional approaches for detecting and tracking moving targets typically rely on a multiphase strategy in which target detections are feed to a Kalman-filter-based tracker. In the present paper, two techniques for target velocity estimation in the framework of Hough Transform (HT) detection scheme are considered. The experimental results are obtained by means of numerical analysis. The quality parameter is estimated using the Monte Carlo simulation approach. A comparative analysis of the two velocity estimation techniques is done based on same parameters of the surveillance radar. The research work is performed in MATLAB computational environment. The obtained analytical results can be used in both, radar and communication receiver networks. [C2733]

### "Characterisation and cancellation of medium grazing angle sea clutter"

High grazing angle sea clutter data were collected and characterised using two different airborne radars with HH and VV polarisations. The ability to cancel sea clutter using single-channel and multi-channel coherent signal processing is investigated. [C2734]

### "Signal detection in multi-frequency Forward Scatter Radar"

The peculiarity of Forward Scatter Radar (FSR) is the absence of range resolution. As a consequence, possible low signal-to-clutter ratio is the most limiting factor in FSR detection. In this paper we will discuss non-coherent and coherent FSR Doppler signal processing and consider an alternative cross-correlation approach, which could be called 'quasi-coherent' processing. Multi-frequency radar enables correlation of Doppler output of one of the channels with another which can be considered as the matching waveform, or the reference signal, to the first signal. This leads to a compression of the FSR return by cross-correlation with enhanced processing gain, and, consequently, enhanced detection. [C2735]

### "Method of automatic target angle tracking by sum-and-difference monopulse radar invariant"

### against the polarization jamming"

Method of automatic target angle tracking by sum-and-difference monopulse radar covers radiolocation sphere and specifically monopulse direction finding systems. It can be used in order to increase guidance accuracy, for example, for anti-aircraft missiles and of unmanned aerial vehicles (UAV) to radar targets such as: radio beacons; aerial vehicles reflecting the radio signal that illuminates them; aerial vehicles and ground-based devices radiating radio signals and jamming signals. The aim of the method consists in the assurance of reliability and stability and in the enhancement of guidance accuracy of automatic target angle tracking due to elimination of automatic tracking losses and great errors arising during the influence of the signals of orthogonal polarization or polarization close to it. The proposed method provides full protection from polarization jamming for all types monopulse radars. [C2736]

### "Microwave gauging with improved angular resolution"

Angular resolution of a microwave level gauge may have positive impact on the robustness of the target detection. Therefore, an azimuthal scan can be performed with the aid of electronical or mechanical beam-steering methods. The present paper provides an overview and a comparison of signal-processing methods which improve the angular resolution of such measurements. For a given antenna, improvements can be achieved well beyond the limit of the half-power beam-width (HPBW) of that sensor. Among others, the performance of the Wiener filter and the Kalman filter for a motion-free channel is examined in greater detail since their application exhibits promising improvements on the angular resolution in both, simulations and measurements. In addition, the advantage of using a Kalman filter for a channel with statistical fluctuations is shown in simulations. [C2737]

### "Nonparametric signal detection algorithm using permutation statistics of signal partial likelihood ratios"

This paper presents a new approach to design radar signal detection algorithms that are applicable when a priori information is limited. The problem is formulated as testing the hypothesis of the kind of a density function. A new method that uses nonparametric statistics of partial likelihood ratios and allows adopting a permutation test in a practical algorithm is suggested and researched. The results can be used for signal detection and processing in different radar systems. [C2738]

### "A modular 24 GHz radar sensor for digital beamforming on transmit and receive"

A compact modular 24 GHz imaging radar sensor for digital beamforming is presented. Besides digital beamforming on receive, the advantage of multiple switched transmitters is used for increasing the angular resolution, which requires less hardware effort. The presented FMCW radar sensor provides up to eight switchable transmitters and eight receiver channels for parallel receiving, allowing digital beamforming on transmit and receive. A new switching technique via switchable amplifiers is proposed. Within the scope of this paper an overview of the whole radar sensor's architecture, design and realization is given. The performance of the sensor is successfully demonstrated and evaluated by measurements. [C2739]

### "Simulation of the PARSAX dual-channel FMCW polarimetric agile radar system"

Polarimetric agile radar can be used to estimate all elements of the polarization-dependent backscattering matrix (BSM) simultaneously. Stringent requirements, such as amplitude and phase matching between channels, cross-channel isolation and polarization isolation, for a dual-channel polarimetric agile radar system have to be investigated. The radar system simulation is a practical and effective approach to evaluate these requirements. This paper presents the modelling and simulation of the dual-channel FMCW polarimetric agile radar system by using Agilent Advanced Design System (ADS) simulation software. The paper focuses on investigating the limitations of cross-channel isolation and estimating the error of BSM components in polarimetric agile radar system simulations. [C2740]

### "2D image fuzzy deconvolution and scattering centre detection: Model and real-time FPGA implementation for automotive application"

A new non-conventional technique based on fuzzy deconvolution for scattering centre detection (F-SCD) is proposed together with its implementation in FPGA for real-time deployment in automotive collision avoidance application. F-SCD emulates the human being interpretation of radar images using fuzzy measurement of features of the radar Point Spread Function (PSF) differently from other classic detection techniques. The first stage of F-SCD detects signal from noise using image oversampling and binary integration technique. The second stage uses a fuzzy description of the radar PSF in order to discriminate among scatterers and side lobes

in the radar image. The method/IP have been implemented in FPGA and tested with a FMCW 77 GHz radar prototype in real automotive benchmarks showing high POD, low FAR and high rejection of ambiguities even with poor time-space variant PSF. [C2741]

### "Circular polarization selectivity of space-fed arrays using element rotation"

Microstrip array antennas with spatial feed can be designed to act as curved mirrors and lenses by applying appropriate phase shifts. If the array acts on circular polarization, the phase shifts can be obtained by element rotation. Arrays of this type are analyzed and it is shown that the mirror or lens effect is different for each hand of incident circular polarization. This effect is demonstrated by a prototype array lens. [C2742]

### "A wide field of view radar for Sense and Avoid on UAV using space coloring waveforms"

Up to now, UAV are employed in crisis or war times. For training purposes, some areas are especially attributed for UAV deployment in a limited space area and in a limited time slot. In the future, both for emerging civilian applications and for training purpose, these limitations will no longer be acceptable and UAV will have to be inserted in the general Air Traffic. Thus, "Sense and Avoid" systems will be mandatory. The radar is the most pertinent non-cooperative "all-weather" sensor because it provides, by essence, accurate ranging, direction and closing speed. In this paper, we propose a low cost radar solution based on space coloring waveforms. This design allows the implementation of the radar within the UAV airframe without any moving parts. [C2743]

### "2D image fuzzy deconvolution and scattering centre detection"

A new innovative technique based on fuzzy deconvolution for scattering centre detection (F-SCD) is proposed together with its implementation in FPGA for real-time deployment in UAV and automotive collision avoidance application. F-SCD emulates the human interpretation of radar images using fuzzy measurement of features of the radar Point Spread Function (PSF) differently from other classic detection techniques. The first stage of F-SCD detects signals from noise using an image oversampling and binary integration technique. The second stage uses a fuzzy description of the radar PSF in order to discriminate among scatterers and side lobes in the radar image. The method has been implemented showing high POD, low FAR and high rejection of ambiguities even with poor time-space variant PSF. [C2744]

### "New generation Doppler radar processing: Ultra-fast robust Doppler Spectrum Barycentre computation scheme in Poincaré's unit disk"

In case of short time series, we prove that we can replace classical Radar Doppler processing chain based on FFT by a new generation processing based on Lie Group Theory. We have defined a robust and ultra-fast computation of Doppler Spectrum Barycentre based on "Median Spectrum" estimation through an regularized autoregressive identification in lattice and ladder form like BURG algorithm. [C2745]

### "Passive detection and tracking of maneuvering targets with particle filter techniques using DVBT broadcasting"

We present a complete and practical particle filter-based scheme to detect, classify and track multiple maneuvering targets using DVBT-based passive radar. As in the conventional radar signal processing, the proposed technique first detects the target Doppler and bi-static range considering the outputs of long-term correlation matched filters whose level exceeds an adaptive threshold. The detections are then followed by a bank of particle based-filters. Each filter tracks a detected target and estimates its position and velocity from the analysis of short-term correlations. [C2746]

### "Antenna size versus sea clutter rejection: A new analysis of coastal radar performances and optimization"

In the field of coastal surveillance radar, and more generally in maritime environment, the overall radar performance for the detection and tracking of small target is primarily linked to the capability of the radar to reject the sea clutter. Sea clutter is the radar signal return of the sea surface illuminated by RF waves and can often be as strong as the target radar return. A conventional method to counter sea clutter is to use very large antennas providing high angular resolution trying to optimize the signal to clutter ratio in the radar processing by defining the smallest possible illuminated cell of sea surface. This paper provides an in depth analysis of the pro and cons of large slotted waveguides antennas and shows that bigger is not better: Parasitic effects, correlated to antenna dimensions, in the beam forming process of big antennas tends to degrade the antenna performance and leads to the conclusion that the optimal antenna size is often smaller than the one currently used on existing coastal surveillance radars. [C2747]

### "On wideband MIMO radar: Extended signal model and spectral beampattern design"

MIMO radar systems can increase the radar resolution, the number of targets that can be identified, and the flexibility in beampattern design in comparison with standard phased array radars. To date, most of the work on MIMO radar has been performed assuming the signals are narrowband. However, wideband signals can improve radar resolution, among other benefits, and are sometimes unavoidable when stringent range resolution specifications must be met. In this paper, we present a method for extending the MIMO narrowband model to a wideband model. Next, from the exact expression of the spatial power distribution involving the CSDM (Cross-Spectral power Density Matrix), we propose a suboptimal transmit beampattern synthesis technique, which can be used in the context of wideband signals. [C2748]

### "Multiposition bistatic radar system using radio signals of geostationary satellites for hydrometeors parameters determination"

The method using geostationary satellites to determine hydrometeors parameters and to diagnose hazardous occurrences, such as: showers, hail formations, lightnings, turbulences, etc are presented. The advantage of the multiposition bistatic radar system is a capability of detecting small objects (turbulences) owing to a sharp increase in the value of Radar cross-section of objects close to base line and its environmental safety. [C2749]

### "Strategies for sub-optimal air to air STAP in forward looking configuration"

This paper deals with the selection of adequate sub-optimal strategies for air to air STAP in a forward looking configuration. The particular scenario is characterized by: (i) need of real-time operability; (ii) strong range dependency of the clutter statistics. To overcome these two aspects, a reduction of the overall number of degrees of freedom (DOFs) has to be performed, thus sub-optimal STAP approaches must be used. In addition, the range dependency of the clutter limits the overall number of available secondary data for clutter covariance matrix estimation. Three strategies for secondary data collection are presented and the corresponding performances are compared for a sample scenario. [C2750]

### "Automatic target recognition in SAR images using multilinear analysis"

In this paper, we investigate an approach based on multilinear analysis for synthetic aperture radar automatic target recognition (SAR/ATR). High resolution SAR images are the composite consequences of multiple factors: bearing angle, grazing angle, number of views and polarisation. Linear methods like principal component analysis (PCA) require to reshape images into a high dimensional vector. This vectorisation processing breaks natural structure and correlation in the original data set. Moreover the PCA, based on a matrix singular value decomposition (SVD), allows only one factor to vary in the image database. Multilinear analysis provides a powerful mathematical framework to analyse ensembles of images resulting from the interaction of underlying factors and preserves their original shapes. In this paper, we propose a method based on multilinear principal component analysis (MPCA) to classify unlabeled targets. We form a tensor with the images of the training set and use the higher order singular value decomposition (HOSVD) to reveal interesting patterns and dependencies between images. HOSVD is also used to compress the data and remove all information belonging to the background. A multilinear projection algorithm projects the unknown target into multiple basis which characterize learned classes. Tests using real SAR images database show that the multilinear approach provides very good recognition performance with a very high compression rate. [C2751]

### "Effects of the SNR of the signal replica in LMMSE-based filtering"

A general issue in radar processing is amongst other ones to separate targets. Several advanced techniques have been developed to fulfill this objective, such as linear minimum mean square error based processing (LMMSE). Nevertheless they depend heavily on the signal replica known at the receiver, and exhibit degraded performance when this reference is not noise-free. And this is also true for the classic matched filter (MF). As such the replica used for correlation receiver can be described with a signal to noise ratio (SNR). The analysis of the effects is done for a multi-target scenario where targets are close enough for the sidelobes of a target to interfere with the main lobe of another target, and close-by weaker echos are also present. This paper shows some experimental and simulation results illustrating the effects when there is such a discrepancy between the echoing signal and the signal reference used in the processing. Also shown is the improvement when countermeasures to this problem are taken. [C2752]

### "Backscattering of wide-band HF signals from evolving ocean-like surface: 2-D direct numerical simulations and analysis"



Direct numerical simulations are used to calculate wide-band HF radar backscatter from evolving ocean-like surfaces in 2-D space. With the attainable spatial resolution of about 15 m, the large-scale wave pattern is visible in range-time plots of backscatter magnitude. The double Fourier transform of the signal magnitude or power in range and time reveals strong harmonics located along the dispersion curve of the propagating long waves. The signature is not predicted by the 1st-order Small Perturbation Method, and considering the next, 2nd order is required. It is shown that the spectral components along the expected dispersion curves in the  $\omega$ - $k$  domain can be used to retrieve the deterministic wave height of the surface. [C2753]

#### **"DC-offset compensation in a bistatic 77GHz-FMCW-radar"**

In this paper the necessity for a DC-offset compensation in a bistatic 77GHz-FMCW-radar is discussed. Measurements of DC-offset voltages of a pseudo monostatic system, with two receiver and two transceiver channels, are presented and conclusions for a bistatic application are drawn. Two reasons for DC-offset are differentiated. First, DC-offset due to the characteristics of the radar circuit itself. Second, DC-offset caused by reflections of the near environment of the radar, such as bumpers. [C2754]

#### **"Angular measurements in azimuth and elevation using 77 GHz radar sensors"**

The availability of highly integrated cost-effective 77 GHz SiGe-MMICs creates new possibilities for different applications of radar sensors in the automotive area. The ability to measure angles in azimuth and elevation will be a relevant feature for the upcoming radar generations. We present a beamforming solution for angular measurements in both directions with one single sensor, using a combination of series fed arrays and a cylindrical dielectric lens. With this solution amplitude and phase information are split up and independently used to get the azimuth respectively the elevation angle. [C2755]

#### **"W-band antenna-reflector combined in a lens"**

Automotive radars are becoming widespread for safety reasons. However their effectiveness remains doubtful since even a metal car does not have strong RCS over all angles of its body. For reduction of traffic accidents, the solution is not only surveying around car-body but also making vehicles easily visible to drivers by means of radar and other luminous sources. This paper introduces a lens antenna double as a reflector for radio and light waves as vehicle equipment. [C2756]

#### **"Through the wall detection and localization of a moving target with a bistatic UWB radar system"**

This paper presents a method for detecting and locating a moving target behind a wall with a bistatic UWB radar system. This method not only can locate a moving target, but can also be used to estimate certain parameters of a wall (dielectric constant and thickness). [C2757]

#### **"Sentinel-1 C-SAR calibration"**

The ESA Sentinels constitute the first series of operational satellites responding to the Earth Observation needs of the EU-ESA Global Monitoring for Environment and Security (GMES) programme. The GMES space component relies on existing and planned space assets as well as on new complementary developments by ESA. This paper describes the in-orbit calibration aspects for the Sentinel-1 mission. It provides an overview of the calibration requirements, and a potential technical concept for the implementation. [C2758]

#### **"Solid state pulse Doppler radars for maritime traffic surveillance-Review of architecture and trade-off analysis"**

Maritime traffic surveillance radars are in use for several decades, they are mostly based upon magnetron pulse emitters and simple non coherent signal processing. While the lack of coherent signal processing capabilities is compensated by strong pulse power, there is still a demand for improving detection and tracking performances especially in front of heavy sea clutter for detecting small and evasive targets. The solutions that address such demands are based upon the use of solid state transceivers which allow to generate and to process specifically designed waveforms incorporating for example frequency or phase codes. [C2759]

#### **"Medium-PRF detection by non-coherent integration"**

The document describes a detection and inherent ambiguity resolution scheme for Medium-PRF waveforms. Medium-PRF waveforms are characterized by ambiguous measurements of both range and doppler. Ambiguities are resolved by changing the pulse repetition frequency (PRF) from burst to burst and by combining the ambiguous results of adjacent bursts. The classical binary integration procedure applies a detection threshold on

burst level and combines detections from burst to burst including unfolding of the ambiguities. In this paper the more optimum method of non-coherent integration from burst to burst with inherent ambiguity resolution is discussed. The method provides a significantly improved detection performance. Of particular interest for non-coherent integration is the appearance of ghost targets. The paper proposes a method for deghosting. [C2760]

#### "Bio-radiolocation method at chest wall motion analysis during tidal breathing"

Influence of chest wall surface motion in bio-radar signal during tidal breathing was researched. A high-speed camera and multi-frequency radar with signal step modulation were simultaneously applied. The model of chest motion during quite breathing was used. Pairwise correlation coefficients for all the markers on the chest wall given in the model were calculated. The correlation of data from high-speed camera and bio-radar was found. Two methods were compared. [C2761]

#### "Radar polarimetry using sounding signals with dual orthogonality-PARSAX approach"

The article describes specific aspects of the radar polarimetry using sounding signals with dual-orthogonality. Such signals provide the unique opportunity to measure all elements of the polarization back-scattering matrix simultaneously, during one sweep/pulse period of radar signal. This approach has been implemented in the IRCTR PARSAX radar system, the fully polarimetric high-resolution Doppler FMCW radar. The digital architecture of the radar starts from intermediate frequency and makes the radar fully reconfigurable in terms of sounding waveforms and processing algorithms. [C2762]

#### "A radar oriented ionospheric channel model based on ray-tracing theory"

A ionospheric channel model based on raytracing theory is here proposed. Several HF ionospheric channel models based on statistical approach have been presented. The here proposed model combines the statistical method with the deterministic method, using a raytracing approach. By means of raytracing we are able to simulate any ionospheric channel condition by varying the transmission frequency in the HF band, the elevation angle, the transmitter geographical coordinates, the season, the time of day and the solar activity. The here proposed model is a useful tool to simulate a signal received by an OTH (Over-The-Horizon) radar, that uses the ionosphere as transmission channel. [C2763]

#### "Submillimeter-wave power measurements with commercial infra-red detectors"

In this paper, we present studies of the capability of commercially available infra-red detectors at submillimeter-wavelengths. The detection is based on pyro- and thermoelectric effects. These technologies have been developed to a mature level for applications in infra-red regime. The detectors are low-cost, compact, and robust-qualities that a typical submm-wave power detector does not possess. The IR detectors are not confined to be operated only in infra-red regime. The principle of power detection remains the same also at submm-wavelengths. Results of measurements at 625-814 GHz with commercial IR detectors compared to dedicated submm-wave power detectors are presented. Sensitivity and noise-equivalent power of the pyroelectric detector is estimated to be 600 V/W and 0.6  $\mu\text{W/Hz}^{1/2}$  at 784 GHz at 20-Hz chopper frequency. [C2764]

#### "A complete indoor positioning system implementing six-port interferometers"

This work presents a complete in-door microwave localization system based on six-port interferometry. Using two planar fan beam antennas and an interferometer with power detectors, the angle of arrival (AOA) from a 2.4 GHz ISM-Band transmitter is determined. With two receivers the position of the transmitter is computed from the direction angles and displayed on a PC. The manufactured prototype detects and localizes a transmitter inside a room with an accuracy of about 10 to 20 cm. It is proposed to use the system for the telemetry control of small unmanned aerial vehicles inside closed buildings where GPS systems are not available. [C2765]

#### "Radar and radio data fusion platform for future intelligent transportation system"

We present a software-defined data fusion system which integrates both radar (sensing) function and radio (communication) function within a single transceiver platform. In the proposed architecture, the radar mode and the radio mode operate in different time slots. The required modulated waveform is generated with the help of a direct digital synthesizer (DDS) that is able to control signal parameters such as amplitude, frequency and phase with very high resolution. For the radar mode, a specially arranged trapezoidal frequency modulation continuous-wave (TFMCW) modulation scheme is adopted, which combines three time intervals, namely an up-chirp, a constant-frequency period and a down-chirp. As such, range-velocity ambiguity can be resolved. Moreover, a constant-frequency period follows the radar cycle in the transmitted signal, which can be encoded with information data using different modulation schemes such as ASK, FSK, PSK, and some combinations among

them. A low-frequency prototype for the 5.9-GHz dedicated short range communication (DSRC) system was designed and prototyped. Both system simulation results and preliminary measurement results have proved the proposed concept. The presented system has demonstrated such advantages as low cost, low complexity, and versatile functionality, which promises to play an important role in the design of future intelligent transportation system. [C2766]

#### **"Monostatic scattering from an object near an ocean-like surface from an efficient fast numerical method"**

The rigorous computation of the monostatic scattering from an object near a one-dimensional sea surface (2D case) needs to solve a problem involving a high number of unknowns. By using a recently developed fast numerical method, called E-PILE+FBFA (Extended Propagation-Inside-Layer Expansion combined with Forward-Backward Spectral Acceleration), the monostatic scattering of such a complex scene can be investigated. Two canonical objects are considered in this paper: the cross and the cylinder. Results allow us to understand the physical mechanisms involved in the coupling between the object and the sea surface. [C2767]

#### **"Side-lobe suppression techniques for a uniform circular array"**

This paper provides a comparison between two different techniques for the array pattern side-lobe reduction in a passive radar system based on a circular array. The first method retrieves the phase modes pattern for the reference array and then applies a conventional tapering for the side lobe suppression of the obtained virtual uniform linear array. The second approach foresees instead an optimization algorithm in order to obtain the desired level of the side lobes. Both techniques have been adapted for being used with an 8 elements FM-based circular array for passive radar applications developed at TNO-Defence, Security and Safety in The Hague. The effect of the directional elements has been also considered for the array pattern synthesis. The different advantages of the algorithms are described and a distinction about the possible fields of application is retrieved. [C2768]

#### **"Modular RF design for QUASAR Ku-band polarimetric SAR system"**

A new compact fully polarimetric Ku band SAR system (SBK) is being developed by INTA radar Laboratory as an advanced payload for QUASAR project, which involves INTA new SAR developments for small platforms and UAV's. SBK design is based on previous developments of INTASAR program for his X-band SAR prototypes, RIX and RBX, focusing work on units miniaturization and new RF payload development. SBK RF development comprises the design of a modular KU-band RF payload mostly consisting on a highly stable Tx/Rx module, a Ku-band front-end and a planar antenna. RF design for the whole system and each of the RF related modules is shown including RF internal calibration capabilities of SBK. [C2769]

#### **"Microwave-range imagery with an ultrawideband time reversal-based RADAR"**

This work presents a new RADAR prototype built for the purpose of imaging targets located in a cluttered environment. The system is capable of performing Phase Conjugation experiments in the ultrawideband [2-4] GHz. In addition, applying the D.O.R.T. method to the inter-element matrix allows us to selectively focus onto targets, hence reducing the clutter contribution. The system has been validated by physically backpropagating the focusing wave into the medium all over the frequency band and observing the expected focusing properties. [C2770]

#### **"Calibration and characterization of a CW radar for blade tip clearance measurement"**

The calibration and characterization of a blade tip clearance sensor is proposed for gas turbine applications. This sensor is based on continuous-wave microwaves that operates at 6GHz in the version for large frame turbines. The calibration of such a sensor is a difficult problem because of the complex interaction between the microwaves and the blade tip geometry. Different geometrical parameters can influence the calibration results, which drives us towards using both the actual blade geometry and probe positioning. This study presents the calibration process of this sensor using a precision test setup. Moreover, the optimization of probe positioning is discussed in order to limit the measurement errors due to axial shift of the rotor during engine operation, which is the major source of errors for tip clearance measurement. Finally, the measurement error corresponding to an optimal probe positioning is characterized. [C2771]

#### **"MPAR: Waveform design for the weather function"**

An integrated target/weather surveillance at medium range, i.e. for the Terminal Manoeuvre Area (TMA) in the frame of Air Traffic Control (ATC) and regional weather monitoring, is made possible by MPAR (Multifunction

Phased Array Radar) techniques, allowing a single technology to satisfy different requirements. The guidelines for system design, needed for cost/benefit analysis, were described in a previous EuRAD paper. As in many other radar applications, pulse compression is a key element to achieve the required MPAR performances with low-cost solutions using relatively low-peak-power Transmit/Receive modules. This paper describes a preferred novel solution for the waveforms to be used in the weather function of the MPAR. Performance comparison with more traditional codes is also presented. [C2772]

#### "Monitoring open-pit quarries by interferometric radar for safety purposes"

A novel Ground Based Synthetic Aperture Interferometric radar was set up for slope stability monitoring in open pit quarries. It is a wide view angle system which is easily adapted to the typical geometry of a quarry, and it automatically generates interferometric DEMs of the area under investigation. The system was tested during a 40 days field survey in a stone quarry in Tuscany, Italy. [C2773]

#### "Million element ISIS array"

The DARPA ISIS Program is developing and demonstrating technologies to enable a stratospheric airship-based dual-band active-array radar system. The antenna is a UHF and X-band shared aperture with backend digital beamforming. ISIS achieves unprecedented airborne radar performance through use of a large antenna aperture instead of high transmit power. The low-power-density aperture has an areal mass density of only 2 kg/m<sup>2</sup>. A conceptual future system achieves 360° azimuth coverage using a cylindrical antenna of 36m height and 50.5m diameter. A small demonstration system scheduled for launch in 2013 has a UHF antenna cylinder 8m high and 22m in diameter. A 98m<sup>2</sup> rectangular section of this cylinder is populated with active X-band elements. The dual-band array has total receive and overhead power consumption, including off-array components, of only 5W/m<sup>2</sup>. [C2774]

#### "AMSAR-A France-UK-Germany success story in active-array radar"

DGA, BWB and D&ES initiated a radar project, called AMSAR (Airborne Multi-role Solid-state Active-array Radar) to demonstrate the enormous potential of Active Electronically Scanned Array (AESA) radar. This paper describes all the stages of the AMSAR project and the results obtained. The AMSAR demonstrator is still the only European, forward-looking multichannel active array radar with the capability of recording the outputs of more than 4 quadrants. [C2775]

#### "Copyright page"

The following topics are dealt with: phased array systems and technology; array design; radar; beamforming; calibration; measurement; testing; wideband and multifunction; communication system; MIMO array system; widefield radio astronomy arrays; overlapped subarrays and nonregular arrays; adaptive arrays; and direction finding arrays. [C2776]

#### "Gap free CONUS surveillance using dense networks of short range radars"

Dense networks of short-range radars having the potential for improved surveillance of weather and airborne targets are described. Such networks overcome the earth-curvature blockage suffered by long-range radars. This enables surveillance from the region beneath the radar coverage of today's national radar infrastructure, up through the tops of storms and flight levels. Such networks have the potential to supplement-or replace-the long range radar networks in use today. [C2777]

#### "Phased array systems and technologies in SELEX-Sistemi Integrati: State of art and new challenges"

This paper is a follow-on of [1] and [2], presented at 1996 and 2003 IEEE Intl. Symposium on Phased Array Systems and Technology, respectively. After a brief recall of 3D Long Range phased array concepts, already presented in [2], the focus is on the G-band multifunction radar systems and on the technological capabilities that SELEX-Sistemi Integrati is developing by taking advantage of its Research and Development facilities. At the end, future trends about new challenging applications and technological issues are presented and discussed. [C2778]

#### "Progress of phased array systems in Japan"

This paper reviews the research and development on the phased array antennas (PAAs) for several applications in Japan. First, the author shows the historical overview of the PAA for radar, satellite and mobile



communication uses. Then, the author introduces a millimeter-wave PAA, an optical beam forming, and an ultra wideband antenna element as modern applications of PAA systems. [C2779]

#### "Phase continuous radar test set"

A method of generating phase-continuous, coherent radar target returns is described which leverages existing Commercial Off-The-Shelf (COTS) Radio Frequency (RF) channel simulator technology. This hardware-in-the-loop system avoids the generation of unintentional spurious signals due to the discrete range steps typically utilized in traditional radar test sets. The time delay, Doppler, and amplitude variations are entirely phase continuous, replicating the true analog behavior of a real target return. Digital signal processing techniques are employed to interpolate the RF propagation and scattering effects. The interpolation smoothes the motion dynamics to ensure a pure analog signal return to the radar. The radar test set also provides physics-compliant Doppler characteristics by time domain expansion/compression of the modulation as well as the RF carrier. Often, Doppler is simply emulated with a shift in the carrier frequency only. Doppler shifts on the modulation result in degradations in radar signal processing such as pulse compression fidelity. Without properly imparting time domain expansion/compression, these degrading effects are not tested. Further, the radar test set provides correlated range/Doppler dynamic motion without discrete phase discontinuity artifacts enabling superior test performance. [C2780]

#### "Synthetic ultra-wideband radar range profile based on stepped frequency pulse trains"

In this paper, stepped frequency pulse trains are utilized to synthesize ultra-wideband radar range profile. Because of the errors of measured target velocity, the synthesized range profile still has range migration and power divergence. Therefore, a new method, called iterative dimidiating approach, is proposed. By exploiting this new technique, the range migration and range spread along range dimension can be neglected. The simulation results prove the validity of the method. [C2781]

#### "Tunable low-pass filter using fractal shaped complementary split ring resonator with ultra-wide stop-band and excellent selectivity"

This paper presents novel Hilbert fractal shaped complementary single split ring resonator (CSSRR) with a tunable transmission zero realized by negative effective permittivity of it and multi-band property attributes to Hilbert fractal geometry. Transmission characteristics of several CSSRR cells have been assessed by using full-wave electromagnetic simulation. Also miniaturization performance as well as its equivalent circuit model has been deeply investigated. Then a tunable assembled low-pass filter by periodically loading the Hilbert shaped CSSRR has been designed and simulated. Simulated results show that the designed filter has good performances such as low insertion loss (maximum 0.5dB) in passband, ultra-wide stop-band (from 2.47 up to 25GHz) as well as steep rejection with sharp transition band (2.2 to 2.47GHz) out of band. Excellent property of it has demonstrated the correctness and effectiveness of the designed concept. [C2782]

#### "Compact bandpass filter based on fractal shaped composite right/left handed transmission line with ultra-wide band, deep out-of-band suppression and enhanced passband performance"

In this paper, a novel ultra-wide band (UWB) bandpass filter (BPF) based on combined technology has been detailed researched. The proposed filter is constructed by composite right/left handed transmission line (CRLH TL) and Sierpinski carpet shaped six-staged stepped impedance lines for the first time. CRLH TL mainly consists of Koch loop shaped defected ground structure (KDGS) etched in the ground plane and series capacitive gap in the conductor strip. Equivalent circuit model is put forward and lumped parameters are also extracted for deep insight into the operation mechanism. Consistent results between electrical and EM simulation have confirmed the accuracy of the proposed equivalent circuit model. Simulated results show that the designed BPF with relatively bandwidth 129.4% owns many good performances, i.e., compact in size, relatively low insertion loss (less than 1.5dB) and comparable low return loss (better than 17.2dB) in pass band, deep suppression (better than 60dB) out of band. Thus indicate a giant application in future small size wireless communication system. [C2783]

#### "Time of arrival estimation for range-based localization in UWB sensor networks"

Accurate Localization has gained significant interest within sensor networks recently and positioning systems based on Ultra-Wideband (UWB) technology have been considered, because the UWB signals have a very good accuracy due to the high time resolution (large bandwidth). Time of Arrival (TOA) estimation of the first path is usually used for range-based localization in realistic environments within UWB sensor networks, which can be challenging in dense multipath environments. In this paper, TOA algorithms for range-based localization in UWB

sensor networks are analyzed and two new TOA estimation methods are proposed. One is the constant false alarm rate (CFAR) method, which is based on the CFAR detection theory in Radar systems. The other one is the maximum probability of detection (MPD) method, which determines the TOA estimation according to a comparison of the detection probabilities of a number of different possible TOA estimations. The performance of the proposed methods is evaluated and compared with several existing methods by computer simulation using realizations of IEEE802.15.4a channel models. [C2784]

### "Design and mutual coupling analysis on wideband wide-angle scan step-constant tapered slot antenna array"

Active reflective coefficient is a kernel design parameter in the process of ultra wideband antenna research and optimization. Mutual coupling effect, wideband and wide angle scan characters according to active reflective coefficient are analyzed in the step-constant tapered slot antenna design and fabrication for RF integrated. Measured results demonstrate that proposed antenna can achieve a bandwidth of 6-18GHz with VSWR < 2 and possesses 120° half-power beam width. [C2785]

### "Latest update of UWB regulation and standardization for medical healthcare and ITS"

A body area network (BAN) and a vehicle radar are latest applications of UWB wireless technology in microwave and millimeter wave bands, respectively. The speaker has been heavily involved in a regulatory committee on UWB and in international standardization on wireless PAN IEEE802.15.3a, 4a and BAN 802.15.6. In this keynote, background and essence of UWB regulation and standard will be introduced as well as remained problems for research, development and business. [C2786]

### "Never ending saga of phased array breakthroughs"

3, 4, 6 face "Aegis" systems developed by China, Japan, Australia, Netherlands, USA. Israel and Australia "Aegis" AESAs have an A/D at every element, a major breakthrough. GaN advancing rapidly. Will be helped by use for PCs, notebooks, cell phones, servers. Extreme MMIC: 4 X-band T/Rs on 1 SiGe chip for DARPA ISIS program; goal < \$10/TR. Raytheon funding development of low cost flat panel Xband array using COTS type PCB. MA-COM/Lincoln-Lab. development of low cost Sband flat panel array using PCB, overlapped subarrays and a T/R switch instead of a circulator. Purdue Un. developing S-band low cost Digital Array Radar; GaN PA and A/D at every element. Revolutionary 3-D Micromachining: integrated circuitry for microwave components, like 16 element Ka-band array with Butler beamformer on 13 x 2 cm<sup>2</sup> chip. Ultra low cost 77 GHz radar on 72 mm<sup>2</sup> chip together with >8 bits 1 GS/s A/D and 16 element array. Valeo-Raytheon 24 GHz phased array now available for blind spot detection in cars for just \$100's. Lincoln Lab using 2 W chip increases spurious free dynamic range of receiver plus A/D by 20 dB JPL's SweepSAR provides wide swath SAR from space with 1/6 th power required by ScanSAR. Metamaterials: 1. Can now focus 6X beyond diffraction limit at 0.38  $\mu$ m Moore's Law marches on. 2. Used in cell phones to obtain antennas 5X smaller and have 700 MHz-2.7 GHz bandwidth. 3. Provide isolation between closely spaced antennas and antenna elements. [C2787]

### "Low-profile ultra-wide band antenna array element suitable for wide scan angle and modular subarray architecture"

A planar topology of UWB wide-scan array is presented, based on the class of the aperture coupled stacked patches. Performance is aimed at achieving both wide-band and wide-scan capabilities for multifunction C-X band radar applications that require modular subarray antenna architecture. The theoretical and technological aspects that affect correct design and effective realization of the array structure are addressed. An 8x8 tile has been manufactured and a multi-element waveguide simulator has been built to validate the experimental results. The relevant results show very interesting features as concerns band and scanning characteristics. [C2788]

### "RF on Flex tile for L Band phased arrays"

Passive and active L Band phased array tiles based on RF on Flex interconnect have been successfully demonstrated. The tile is a modular building block for light weight, high performance phased arrays to be used in space based radar applications. Each tile contains 6 radiating elements with a maximum radiated power per element of ~2 W. Each tile includes two beamformers and two T/R modules per radiating element so that any transmit polarization may be formed and both V and H polarizations may be received. Each tile weighs 0.41 kg (3.9 kg/m<sup>2</sup>). In order to minimize production cost the tile is designed to be fabricated on an industry standard Printed Circuit Board assembly line and the T/R modules are packaged as Plastic Encapsulated Modules (PEMs). A thirty tile build has demonstrated high yield and a path to meeting the tile high volume production cost goal of \$50K/m<sup>2</sup>. [C2789]

### "Phase-only tapers for regular planar arrays, a heuristic nonlinear-FM approach"

We present a simple approach to constructing phase-only tapers for regular planar arrays that is analogous to the instantaneous-frequency approach classically used to construct FM-chirp waveforms with high time-bandwidth products. Design experiments for a large triangular-grid array show that the crude results yielded by this method when aperture-beamwidth products are modest can sometimes be "tweaked" into reasonableness. We conjecture that such a taper would improve upon the usual uniform-weight starting point for a nonlinear-optimization approach that seeks out a local optimum. Specific design examples presented here nominally aim to approximate a brick-wall beam and a variant of a Gaussian beam. [C2790]

### "System considerations for passive radar with GSM illuminators"

The increasing number of communication transmitters makes passive radar an attractive and simple alternative to active radar systems. GSM base stations as illuminators for passive radar enjoy the advantage of digital waveform, frequency diversity and global availability. The problems with these transmitters are the low transmit power and the more or less directive transmit patterns. These limit the achievable range. This paper studies how a useful system can be designed by fusion of bistatic systems using multiple transmitters. [C2791]

### "Electronic protection for digital shared aperture array radar"

We have developed a digital shared aperture array radar architecture which supports sub-aperture partitioning of a conformal array to improve time energy management for achieving radar search and track functions over 360 degree azimuth coverage. The digital array system consists of a plurality of digital transmit sub-arrays and digital received sub-arrays. For transmit operation, different frequencies or orthogonal waveforms can be employed for different apertures using the array control commutator. For receive operation, the sub-arrays are selected for different apertures using the receive data commutator. Essentially, the digital shared aperture supports dynamic partitioning of the aperture for multifunction applications. In this paper, we address these capabilities in the electronic protection (EP) against electronic threats, i.e. jamming and deception. Digital array radar provides digital degrees-of-freedom (DOFs) for transmit as well as for receive. These DOFs are selected by the commutators to support transmit and receive electronic protection. The receive DOFs are used for adaptive processing in jammer cancellation. These DOFs can be exploited in a number of ways through sector selection and digital beamforming to support several advanced processing architectures and algorithms. The digital array capabilities can also be exploited in monitoring jamming spectrum and estimation of the corresponding directions-of-arrival (DOAs). Digital array radar has transmit DOFs which can be used to form a transmit beam with nulls towards the deceptive jammers and separate decoy beams formed towards the deceptive jammers. [C2792]

### "Light weight digital array SAR"

A light weight SAR has been designed, suitable for short range tactical UAVs, consisting of a fully digital receive array, and a very compact active transmit antenna. The weight of the complete RF front is expected to be below 3 kg, with a power consumption below 30 W. This X-band system can provide image resolution down to 10 cm at up to 5 km range. The system makes use of FMCW technology and digital beam forming in the horizontal direction, with 24 receive channels. A switchable transmit antenna is designed, to allow wide coverage with sufficient antenna gain. RF electronics for the receive panels have been realized and tested, as well as a low phase noise transmitter. Detailed antenna design has been performed, and critical issues such as bandwidth and transmit-receive isolation have been assessed by simulation. [C2793]

### "Analog beamspace super-resolution radar processing"

Current monopulse radar does not resolve multiple sources within the main beam, a scenario that arises in a number of radar applications such as ballistic missile defense, where the incoming missile complex consists of a large number of objects; air defense, where a detection may correspond to a single plane or multiple planes; cruise missile defense for low angle target tracking in multipath; etc. This paper describes a superresolution technique designed for radar applications requiring resolving multiple targets within the main beam given a single snapshot of multiple beam data. The technique enables the practical implementation of such super-resolution algorithm by first forming multiple beams in the analog domain to provide data and degree-of-freedom (DOF) reductions without significant loss of information. Super-resolution is then achieved through the use of matrix processing techniques operating on the digitized beamspace data. The overall procedure can be considered a generalization of the monopulse processing scheme to the multi-target case. [C2794]

### "The fundamental input/output structure of a linear, time-varying array receiver"

A single-output array receiver based on static antenna elements of arbitrary geometry that drive linear, time-invariant signal processing is well known to be fully characterized by a frequency response dependent on direction-of-arrival (DOA). This paper develops the generalized characterization that results when the time-invariance requirement is removed. The special case based on periodically varying signal processing is further derived and shows such a system to be fundamentally, structurally incapable of realizing a long-sought goal in navigation engineering: a frequency shift smoothly dependent on DOA. Self-contained developments of time-varying continuous-time linear systems and of a 4D Fourier-transform view of propagating electromagnetic waves are given in the appendices. [C2795]

#### "Ultrawideband VHF/UHF dipole array antenna"

A linearly-polarized ultrawideband dipole array antenna has been developed for coverage in the VHF/UHF frequency range for communications or radar applications. The antenna design utilizes a horizontally polarized array of thick tubular dipole elements above a ground plane. Numerical electromagnetic simulations were used to analyze and optimize the antenna parameters prior to fabrication. Measurements of a 24-element ultrawideband dipole array prototype in an anechoic chamber demonstrate the antenna's return loss and gain pattern performance over a wide bandwidth. [C2796]

#### "Digital Array Radar panel development"

The Army Digital Array Radar (DAR) project's goal is to demonstrate how wide-bandgap semiconductor technology, highly-integrated transceivers, and the ever-increasing capabilities of commercial digital components can be leveraged to provide new capabilities and enhanced performance in future low-cost phased array systems. A 16-element, S-band subarray has been developed with panel-integrated, plastic-packaged gallium-nitride (GaN) amplifiers, multi-channel transceiver ICs, and digitization at the element level. In addition to full digital beamforming on transmit and receive, the DAR subarray has demonstrated efficient RF power generation exceeding 25 Watts per element, in-situ, element-level calibration monitoring and self-correction capabilities, simultaneous transmit and receive operation through subarray partitioning for an indoor target tracker, and more. An overview is given of these results and capabilities. [C2797]

#### "Parameter estimation of moving target based on linearly constrained space-time adaptive monopulse technique"

Technique of space-time adaptive processing (STAP), which is usually employed by airborne radar to reject the ground clutter and jamming and at the same time, detect the ground moving targets, can not estimate the spatial-temporal parameters of the corresponding targets. Monopulse technique, as a mature method for parameter estimation can be used on airborne radar, however, the estimation performance of this method is dramatically effected by the ground clutter and jamming components present, even when these components falls into the mainbeam interval. By combining the STAP technique with the monopulse technique, a new method for estimating the spatial-temporal parameters of moving targets is proposed and referred as to LC-STAM in this paper. Additionally, the proposed method utilizes the beam null, monopulse slope, and decoupling constraints to remove the worse influence on the beam shape from the mainbeam clutter, maintain the characteristic of the monopulse ratio, and increase the veracity of parameter estimation. Simulation results illustrated that the LC-STAM method possesses the excellent estimation performance of the spatail-temporal parameters by comparing with the other similar methods. [C2798]

#### "Adaptive cancellation of impulsive interference in phased array radar"

Performance of a pulse-Doppler radar may be severely degraded by high-power pulses emitted by other nearby radars operating in the same frequency band. Typical approaches to mitigating the resulting impulses in the received radar data may impose stressing requirements in the areas of probability of impulse detection, throughput, and estimation error. This paper proposes an adaptive nulling approach to mitigation of impulsive interference. This approach ameliorates the disadvantages associated with conventional impulse mitigation. By exploiting prior knowledge about this type of interference, the effort may be decomposed into two separate nulling stages. This provides a novel application for the Two-Step Nulling (TSN) algorithm, which has previously been used in Space-Time Adaptive Processing (STAP) applications. [C2799]

#### "Nonlinear Kalman filtering for self-calibration of airborne arrays"

The calibration of a millimeter-wave antenna array mounted on an aircraft wing is considered. The theory and implementation of nonlinear Kalman filters, which are optimal for the desired minimum mean squared error (MMSE) criterion, are considered. Numerical results are provided for a field experiment employing a 32-element Ku-band antenna array. The implementation of the algorithms is sub-optimal due to limitations in available



computational power, which reduces the model order and the accuracy of the required calculations, but the technique is effective in calibrating the array. [C2800]

#### "A carrier-based UWB transceiver in CMOS 90nm for biomedical radar sensing and sensor communications"

This paper describes a carrier-based multi-band UWB transceiver front-end in CMOS 90nm designed for full UWB band biomedical radar sensing and sensor node communications. The transceiver operates in band 3-10GHz. The transceiver consists of a transmitter and a receiver. The transmitter includes a pulse generator, a mixer, a VCO, and a driver amplifier. The receiver includes a filter bank, a ultra wideband LNAs, mixers, integrators, and decision-making circuits. The system was simulated using CMOS 90nm technology to verify functions for both the sensor communications and radar sensing. The overall power consumption is 62.75mW. [C2801]

#### "MMIC based phased array radar T/R modules"

In order to lower the cost of basic MMIC components and modules for commercial and civilian phased array applications dramatic cost reductions when compared to the present military must be realized. These cost reductions can only be achieved by employing highly integrated RFICs which are produced on high volume process lines for low cost using GaAs MMICs and Silicon based technologies where appropriate, exploiting high volume plastic packaging technologies for both low cost and high performance, and employing commercial printed circuit board and module manufacturing technologies. The viability of these approaches is already being demonstrated on a number of phased array radar projects ranging from L-Band to X-Band. Results for an ongoing S-Band Phased Array effort are the basis for this work. In this project, M/A-COM Technology Solutions' high performance pHEMT MMIC processes to produce highly integrated Tx and Rx ICs are being employed. Logic control is realized in standard low cost CMOS technology. These ICs are packaged in industry standard PQFN packages. The packaged ICs are then surface mounted to realize the T/R Module. [C2802]

#### "Optimization of multistatic passive radar geometry based on CRLB with uncertain observations"

In the present paper, we derive the Cramer-Rao Lower Bound (CRLB) with uncertain observations, namely for  $P_d < 1$ , for the 2D position measurements of a multistatic passive radar, to optimize the geometry of the system. This is an extension of the enumeration method CRLB to the multisensor case, where it is considered that the multiple receivers could detect or miss the target independently of one another. This version of the CRLB with uncertain observations is the correct measure for the realistic performance assessment of a passive radar, since typically passive radars show low values of  $P_d$  and neglecting the target miss probability, in the standard evaluation of the CRLB, provides unreliable performance assessments. The obtained CRLB is then used inside the multistatic passive radar optimization scheme derived by the authors in, to select the broadcast transmitters and the receiver locations providing the highest accuracy. The proposed approach is illustrated by means of a case study: a multistatic passive radar based on two transmitters of opportunity and a single receiver. For this case, we analyse how the Signal to Noise Ratio and the detection probability affect the measurement accuracy and the estimation accuracy and, finally, we use the theoretical CRLB to select the two transmitters among the available ones and choose the receiver location, for a target flying a specific trajectory. [C2803]

#### "S band radar target detection in an extreme advection duct event"

Mesoscale numerical weather prediction models coupled with modern parabolic equation radar performance models have allowed the resolution of four dimensional radar performance in challenging non homogeneous near surface refractivity fields at the time and location of the modeller's choice. Large scale offshore flow of warm and dry air over colder seas produces strong surface ducting. Large land-sea temperature differences can produce near shore sea breezes and surface based ducts. This paper describes modelled radar performance in such a complex ducting structure over the Persian Gulf during large scale northwest flow. The refractivity field was resolved by the Coupled Ocean Atmosphere Mesoscale Prediction System and the notional radar performance was modelled by the Advanced Refractivity Effects Prediction System. The results indicate strong spatially dependent enhancements and degradations in radar performance relative to a standard atmosphere. [C2804]

#### "Wireless indoor localization using dynamic monopulse receiver"

This paper proposes a dynamic monopulse receiver (DMR) for wireless indoor localization. By electrically steering the radiation beams to  $N$  discrete angles,  $N$  sum-difference ( $\Delta$ - $\Sigma$ ) curves can be generated in the desired field of view (FOV). The target angle can be precisely estimated using the proposed selection-and-

average algorithm. The 1-D and 2-D localization experiments were conducted, which demonstrate precise location with mean distance error as low as 0.33 m for 75% cumulative probability. [C2805]

### "Multistatic passive radar geometry optimization for target 3D positioning accuracy"

The paper presents a design procedure for a multistatic passive radar system, that aims at its performance optimization, in terms of 3D positioning accuracy. Specifically, the proposed procedure considers the main features of the considered air traffic control scenario and the main physical and geometrical features of the passive radar receivers and guides the designer to select the geometry that maximizes the three-dimensional target positioning accuracy. The procedure can be applied to any type of sources of opportunity, the final accuracy results being inversely scaled by their frequency band occupancy. The proposed procedure has been applied to two different air traffic control scenarios, namely an en-route flight and an approach path. The results show that a multistatic passive radar system with just two or three transmitters of opportunity and a single receiver is able to localize targets with positioning accuracy comparable to conventional air traffic control systems. [C2806]

### "A model-based track-before-detect strategy"

This paper addresses adaptive detection and tracking of a point-like target in thermal noise plus clutter which is assumed to be heterogeneous from one range cell to another. To this end, a track-before-detect scheme is derived and assessed; its design relies on autoregressive modeling of noise returns. A preliminary performance assessment, based upon Monte Carlo simulation, shows that it can outperform previously proposed TBD strategies. [C2807]

### "Precise radial velocity estimation using an FMCW radar"

This contribution addresses radial velocity estimation with a frequency-modulated continuous-wave (FMCW) radar system. The estimator we propose aligns the up- and downchirp information of adjacent sweeps including the phasing of the chirps. The resulting one-dimensional signal depends on the radial velocity and can therefore be used for estimation purposes. Because the phase information between nearby chirps is preserved, the accuracy is seriously increased compared to estimators that evaluate only the frequency shift due to the Doppler effect. Additionally, the range of velocities that can be estimated without ambiguity constraints is extended considerably when compared to a standard range-Doppler procedure. [C2808]

### "Fractal based detection using blind box-counting method in high resolution radars"

Sea clutter refers to the radar returns from the sea surface. Accurate modelling of sea clutter and detection of low observable targets within sea clutter are major problems in remote sensing and radar signal processing applications. Recently fractal geometry is applied to the analysis of high range resolution radar sea clutters. The box-counting method is widely used to estimate fractal dimension but it has some drawbacks rarely considered in literature. We explain the problem of box size range and present a novel method to select an appropriate range. [C2809]

### "MetaSensing compact, high resolution interferometric SAR sensor for commercial and scientific applications"

For the first time in the world airborne Frequency Modulated Continuous Wave (FMCW) Synthetic Aperture Radar (SAR) images have been acquired in interferometric mode. The paper reports on the X-band images collected by the new high resolution, compact MetaSensing interferometric SAR sensors in 2009. MetaSensing approach allows cost-effective SAR mapping by employing small, readily available Cessna 172/182 or similar in order to drastically cut the costs of current radar campaigns for scientific and commercial applications. MetaSensing X-band SAR sensor is able to transmit more than 1.4 GHz of bandwidth and its versatile two receiving channels allow along-track and cross-track interferometric acquisitions. A fully polarimetric L-band sensor is in the final test stage and is available from the third quarter of 2010. The new MetaSensing approach is an optimal solution for commercial and scientific application which requires SAR mapping on local areas. [C2810]

### "Improving SAR images: Built-in geometric and multi-look radiometric corrections"

SAR systems installed on small aircrafts and UAVs suffer from trajectory deviations and instabilities of antenna orientation. These kinds of motion errors lead to significant geometric distortions and radiometric errors in SAR images. In the paper, we describe a time-domain multi-look stripmap SAR processing algorithm with built-in geometric and multi-look radiometric corrections. Geometric correction is performed due to azimuth reference

functions and range migration curves specially designed to produce SAR images directly on a rectangular grid on the ground plane. Radiometric correction is based on multi-look processing with extended number of looks. The proposed techniques have been successfully tested with a Ku-band SAR system installed on a light-weight aircraft. [C2811]

### "Fractional Range Doppler Algorithm for SAR imaging"

Synthetic Aperture Radar systems are normally used to form high resolution images from radar backscatter. The Fractional Fourier transform (FrFT), which is a generalized form of the well-known Fourier transform, has opened up the possibility of a new range of potentially promising and useful applications that involve the use and detection of chirp signals including pattern recognition and SAR. In this paper the FrFT is applied to the well established Range Doppler Algorithm in order to obtain a superior result in terms of resolution and noise rejection. The results confirm that the FrFT can be useful to perform high resolution SAR processing and to reduce the speckle noise while enhancing the resolution and focusing accuracy. [C2812]

### "A multiple target doppler estimation algorithm for OFDM based intelligent radar systems"

In this paper an approach will be presented that allows for estimating the velocity of multiple reflecting objects with standard OFDM communication signals. The proposed technique does not require any specific coding of the transmit signal and provides high dynamic range and low sidelobe levels. This allows for an efficient acquisition of velocity information in joint communication and radar systems. The paper discusses the developed algorithm and a possible OFDM system concept for automotive applications. Measurement results are provided that prove the operability in practical scenarios. [C2813]

### "Arbitrary synthetic aperture motion compensation based on Fast Back Projection"

Back Projection imaging algorithm, whose low efficiency reduces its applications in practical projects, could work with highly nonuniform apertures. According to this reason, many scholars have presented some Fast Back Projection algorithms based on sub-aperture method. But how to compensate the motion error after sub-aperture dividing is awaited for further studying. The motion compensation method for FBP algorithm at different motion error levels is studied in this paper. Three situations denoting different motion error levels, which are only non-uniform in azimuth aperture, tracks of two-dimensional motion error and highly nonlinear even curvilinear flight tracks, are discussed here. Then it comes to a fast back projection imaging algorithm for arbitrary aperture, and this algorithm needs highly precise position information. Finally, an outside experiment is made to prove the algorithm's availability. [C2814]

### "A multi-model track-before-detect algorithm for manoeuvring target detection for Over-the-Horizon Radar"

In this paper a multi-model track-before-detect (MM-TBD) is proposed for the HF Over-The-Horizon-Radar (OTHR) manoeuvring target detection. Multiple hypotheses about target manoeuvres and echo sources are represented in the multi-model-estimation framework with each sub-filter corresponding to one hypothesis. The track output of each sub-filter is obtained based on the maximum likelihood criterion and then a generalized likelihood ratio for hypothesis test is presented to target detection. A numerical simulation is presented to show the effectiveness of the proposed algorithm. [C2815]

### "Characterisation of dismounted combatants radar signature from airborne platforms"

The radar signature of dismounted combatants as observed from a moving airborne radar platform was examined and quantified. The dismounted target presented a characteristic amplitude and frequency modulated signature which proves useful in distinguishing true targets from those due to uncanceled clutter discretely. [C2816]

### "Inter-period compensation algorithm in full-polarimetric FMCW radar"

This paper describes a new type of sounding signals for polarimetric FMCW radar and the corresponding signal processing technique. The inter-period compensation (IPC) algorithm is proposed for isolation increase in radar channels. The novelty concerns the use of orthogonal polarizations of two bi-cyclic LFM-signals having an additional phase shift every second sweep. Summation units proposed for use in the receiver channels allows for reducing the effects of interfering signals due to the specified phase of received signals over two consecutive sweep times. [C2817]

### "Exploiting the joint distribution of amplitude and monopulse ratio for chi-square fluctuating targets for target DOA estimation"

This paper deals with the Direction of Arrival (DOA) estimation for chi-square fluctuating targets. The joint Probability Density Function (PDF) of the amplitude in the sum channel and the monopulse ratio for a chi-square fluctuating targets presented in [1] is here used to derive several DOA estimators. The proposed estimators are obtained by following respectively the Maximum Likelihood criterion, the Method of Moments, and the Maximum Entropy Method. Their performance are characterized in terms of bias and standard deviation error. [C2818]

### "An implementation of step recovery diode-based UWB pulse generator"

Ultra-wideband (UWB) wireless communications and carrierless UWB radar technology use narrow nanosecond or sub-nanosecond pulse as the transmission medium. This paper presents an implementation of sub-nanosecond level pulse generator. The main principle is using the rapid step recovery characteristics of step recovery diode (SRD) to shape the driving pulse, shorten the rise time, narrow the pulse width, then gain the required UWB pulse. The final actual measured pulse width is about 600 ps, amplitude is about 5 V. It is enough for practical applications, but the ringing is a little too big, the amplitude is relatively low. The paper provides a simple method to design UWB pulse generator. Although there is some room for improvement, it has important reference value for the use of SRD in UWB pulse generating in the future. [C2819]

### "Comparison of multi-beam pillbox antennas using leaky-wave and slotted waveguide radiating parts for automotive radars at millimeter-waves"

This work deals with a comparison between multi-beam leaky-wave and slotted waveguide pillbox antennas. The antenna systems present the same pillbox architecture: feeding part, quasi-optical system and radiating part. Two different radiating parts are considered: a leaky-wave solution and an array of slotted waveguides. In particular, an array of slots etched on the uppermost metal layer of the pillbox structure and 23 waveguides with 8 radiating slots are adopted for the leaky-wave and slotted waveguide solution, respectively. The quasi-optical system and feeding part used in both antennas are the same. The quasi-optical system is made by a pin-made integrated parabola and several coupling slots, and is used to shape and focus the energy coming from the input part to the radiating part. Seven pin-made integrated horns are placed in the focal plane of the integrated parabola to radiate seven beams in the far field. The antenna performances in terms of efficiency, bandwidth and scanning capabilities are compared. Both the proposed antennas are low-cost, low profile, compact, efficient and very promising solutions for applications in the millimeter-wave range, especially for long range automotive radars. [C2820]

### "Reconfigurable digital receiver for polarimetric radar with dual-orthogonal signals"

This paper outlines the work on the design of a reconfigurable receiver for the PARSAX radar. The FPGA based digital receiver samples incoming signals at intermediate frequency (IF) and processes signals digitally instead of using more conventional analog approaches. In this way it offers more robust system stability and avoids unnecessary multi-channel calibrations of analog circuits. The processing algorithms implemented in the FPGA chips can be reconfigured adaptively regarding to different transmitted waveforms, and without changing of hardware. The successful development of reconfigurable receiver has been verified by experiment and yields maximum flexibility for the whole radar system. [C2821]

### "77 GHz FM-CW radar for FODs detection"

Foreign objects and debris (FODs) may cause accidents or disasters. The crash of a Concorde jet in France that killed 113 people in 2000 is an example of the danger created by a thin metal strip that fell from another airplane. Recently, FOD detection systems have been developed and tested on airports. Most of them are based on the association of a mm-Wave radar and an optical sensor. This paper describes the investigation, conducted together with the ENRI and LEAT on a wide band mm-Wave radar module. It is composed a 76-81 GHz front-end and a quasi-optical antenna that is a printed Fresnel reflector operating with circular polarization. The purpose of this paper is to compare the measured responses of selected. This work is conducted within a Sakura project funded by the French and Japanese Ministries of Foreign Affairs. [C2822]

### "Spatial (aperture) noise generators"

Spatial noise generators with apertures of 200 mm, 270 mm, 1500 mm were developed in OKB MEI. Spatial noise generators with apertures of 200, 270 mm are Djuar vessels filled up by boiling liquid nitrogen, with metal cylinder, fixed in liquid nitrogen's zone. One of cylinder's founding is cooled by boiling nitrogen. It is covered by radio-absorption material. Another founding, covered by heat protection radio-transparent material, is radiating



aperture of spatial noise generator. Spatial noise generators with aperture of 1500 mm is a collimating system, which consists of the parabolic reflector (part of parabolic) and radiator, which consists of aperture noise generator and additional reflector (contra-reflector). Additional reflector also provides lighting of main mirror (parabolic reflector) and forming of plane parallel collimation beam. Methodology of noise temperature unevenness measurements in the section of the collimation beam is presented. [C2823]

#### "Reconfigurable radar transmitter based on photonic microwave signal generation"

In this paper we propose a photonic technique for a reconfigurable microwave signal generation based on the beating in a photodiode of two laser modes from a regenerative Fiber Mode-Locked Laser (FMML). The excellent performance of this kind of pulsed laser guarantees high stability to the generated microwave signal even at ultra high frequencies (up to W band). Therefore, by using the proposed architecture, the performance of a reconfigurable full digital coherent radar system can be enhanced in terms of Moving Target Indicator (MTI) improvement factor. Moreover, thanks to the achievable high repetition rates and the coherence properties of the FMML, this laser scheme has also been proposed for digitizing the received signal by electro-optical sampling. Thus the advantage of using just one device for signal generation in both the transmitter and receiver chain, makes the proposed solution a cost effective architecture for microwave signal generation. Differently from the microwave synthesizers, whose performance strongly deteriorate with increasing frequencies, the photonic radio frequency generation always shows an excellent spectral purity. The results show excellent spectral purity above 5 KHz for the proposed technique compared to a state of the art Agilent synthesizer even though the timing jitter increases for integration time greater than 10 msec. In order to achieve the same stability performance at both high and low frequencies a Phase Locked Loop between the laser and a synthesizer could be used. [C2824]

#### "Using signals of the global navigation satellites for diagnostics of above land troposphere refraction"

Possibility of global navigation systems using for troposphere refraction coefficient determination is considered. Relation between measured altitude and troposphere state is determined. The method of reflecting sources number, altitude of sources location and troposphere refraction estimation on GPS and GLONASS received signal spectrums of amplitude fluctuation is proposed. [C2825]

#### "Comparison between wavefront-based shape reconstruction and beamforming for UWB near-field imaging radar"

This paper investigates the performances of a wavefront-based shape reconstruction algorithm, known as Envelope, for ultra-wideband (UWB) near-field imaging. In contrast with conventional beamforming, surface estimation is based on identification of wavefronts within the received data and direct transformation from delay time to the target shape. The algorithm is compared with conventional beamforming in terms of both imaging accuracy and speed. The influence of sparsity of data acquisition on the estimated surface image is further compared showing both advantage and problems of the methods. [C2826]

#### "Scan-to-scan sea-spikes filtering for radar"

High range resolution radars are often a solution to the problem of small target detection in the presence of sea clutter, however this solution leads to a high density of sea-spikes echoes. The number of false plots can be very high and need to be regulated in order to be able to control the tracking load and limit the number of false tracks. In this paper a solution for the Coast Watcher 10 and Coast Watcher 100 products is derived. The new patented scan-to-scan algorithm used to filter plots before tracking is presented. It uses the position and Doppler information of the plots on several scans to regulate the number of false plots at tracking level. [C2827]

#### "Detection against the background of non-Gaussian clutter from underlying surface"

The method for the operating characteristics of the radio systems estimation based on using of model of non Gaussian clutter from underlying surface (sea, land plots) is proposed. This method was done by nested semi-Markov based processes. The characteristics of parametric (Neumann-Pearson, adaptive control of threshold and filter band of moving-target indication) and non-parametric (sign and linear rank) detectors are analyzed theoretically and are compared to results of the experimental investigations. [C2828]

#### "OTHR-SW Coordinate Registration method based on sea-land transitions: Clutter model definition"

In previous works we proposed a Coordinate Registration (CR) method of the received echo by pulsed, monostatic Over The Horizon Sky Wave Radar (OTHRsw). This method takes advantage from the a priori geo-

morphological knowledge of the surveillance area (especially the coastline profile) and from the pronounced difference between the sea and land normalized backscattering coefficients. In this paper we present a model of surface clutter, its software implementation and its role in the simulation tool under development intended to recreate the complex OTHR scenario in order to analyze the performances of the proposed CR method. A brief introduction about the radar scenario is given; the main clutter model hypotheses are outlined; the adopted space-time distributions processes are motivated; the key-parameters for the model configuration are described; some examples of simulated clutter scenarios are proposed; the achieved results are finally shown. [C2829]

#### **"Comparison of accurate and simplified sub-entire-domain basis function methods in RCS computation of large-scale periodic structures"**

Accurate sub-entire-domain (ASED) and simplified sub-entire-domain (SSED) basis function methods are introduced and compared in this paper for radar cross section (RCS) computation of large-scale periodic structures. The detailed algorithms are presented and the number of unknowns, CPU time and precision of the two methods are discussed respectively. Numerical results are given to show the differences of the two methods, so that a flexible choice can be acquired for further researches and wider applications of SED method. [C2830]

#### **"Polarization diversity in Ultra-Wideband imaging systems"**

This paper presents an Ultra-Wideband (UWB) indoor imaging system with dual-orthogonal polarized antennas. Both the measurement setup and the algorithm implemented for data processing are introduced. In the presented approach, a 4Ч1 vertically oriented antenna array is used in order to perform 2D scan. For 3D imaging, single antennas are applied. Emphasis is given to the polarization diversity, through which additional properties of objects such as form, surface structure and orientation are investigated. In this way, some objects are detected, which may remain invisible for single-polarized systems. In addition, the presented approach extends UWB-Radar/Imaging with very high resolution to a high-end system with robust target detection, while providing extensive information about the environment. Such a system can be of great interest in applications such as indoor search-and-rescue operations, motion tracking and indoor navigation. [C2831]

#### **"Cost effective Wafer Level Chip Size Package technology and application to the next generation automotive radar"**

Cost effective 77GHz transmitter and receiver MMIC's, that use a three-dimensional MMIC technology optimized for flip-chip implementation, are presented. The MMIC structure incorporates inverse TFMS lines so that a ground metal can be applied to cover the whole chip surface except for interconnect pads. Four metal layers including the ground metal are formed between and the top surface of polyimide layers each of which is SiN coated for humidity proof. Hence, these MMIC chips require no package, as well as can be directly assembled on printed circuit board. The transmitter MMIC is composed of an Ч8 multiplier chain (9.5GHz/38GHz MLT, 38GHz AMP, and 38GHz/76GHz MLT), and a driver+power amplifier. A saturated output power of 14dBm has been obtained between 76 and 77GHz from this transmitter MMIC. A portion of the 38GHz amplifier output is split for the receiver mixer. The receiver MMIC is composed of multi LNA+MIX blocks and a common Ч2 multiplier block that provides a 10dBm of LO power. A receiver gain of 10dB and a noise figure of 7.8dB for a baseband frequency at 10MHz were obtained. The die size of the transmitter is 1.5mm Ч 2.0mm and the chip area of the receiver is 1.9mm Ч 1.3mm. [C2832]

#### **"Improved wide-band dual-linear polarization compact microstrip antenna array for Microwave Image system"**

This paper provides a wide-band dual-linear polarization compact antenna array for P-band Microwave Image system, where the center frequency is 400 MHz with a 200 MHz of bandwidth (50% from 300MHz to 500MHz), and the size is smaller than 1600mmЧ400mm. The array system has dual-linear polarization with a maximal gain of 14.3dB at the center frequency, a minimum gain of 10.2dB at two ends of the band and the cross-polarization level is much less than -50dB over the frequency band. In the antenna design, compactness and stability of the presented antenna array is considered firstly, which is very important in practical airborne environment. Furthermore, one of the most excellent achievements is to develop a simple wide-band match structure composed with three independent parts. [C2833]

#### **"Odd-Symmetry Template based three-step detector for IR-UWB radar"**

The detection scheme for robust detection and target location in the presence of interference is presented. The problem of detecting the slow-moving target at noisy background is addressed in this paper. A novel kind of Odd-Symmetry Template Correlation (OSTC) process is developed as the first-step of the detector. The OSTC

method has a better performance due to interference suppression than traditional ones. The Range-Extended Constraint and Threshold Feedback technique is proposed as the second-step for detecting range-extended target and controlling the false alarm rate. The Multi-Cycle Fusion method completes the third-step detection procedure, and improves the detection reliability by reducing false alarms. Experimental results are given to demonstrate the efficiency of this approach. Moreover, the effectiveness of this method allows for real-time execution. [C2834]

#### **"An improved IPCP detector of UWB radar signals based on adaptive searching window"**

The research on detection of range-extended targets has been a focus of UWB radars. The paper introduces weighted accumulation and adaptive searching to the IPCP detection, and theoretical value of detection threshold is derived in detail. Related experiment and simulation confirm that weighted accumulation increases SNR effectively and adaptive searching basically eliminates the negative effects on detection performance caused by unknown extended range of the target echoes, which guarantees the reliability and stability in practical application. [C2835]

#### **"A low-cost handheld integrated UWB radar for shallow underground detection"**

In order to fit the demands of low cost and miniaturization for ground penetrating radar (GPR), a handheld integrated high resolution UWB GPR system was developed. The design methods of the low-cost RF module with the impulse transmitter, the sequential receiver and the UWB antenna were described, and the structure of the embedded control module with the radar control unit, the data acquisition and the image process unit were also introduced. The integration improves the convenience and the stability of the system. Several experiments were carried out with the prototype. The experimental results show that the system could detect shallow underground objects effectively with high resolution. [C2836]

#### **"Power handling and temperature compensation design for passive Microwave devices"**

Summary form only given. Modern communication and radar transmitter systems require high performance RF/Microwave devices and components, to improve communication and detection range. The increase in range is accomplished by increased transmitted power and higher receiver sensitivity. The increased transmitted power requires the engineer to estimate the transmitter's power handling capability as part of the design process. In addition, the engineer has to meet several competing requirements at a specified pressure level, such as containment of transmitted bandwidth (wide or narrow, i.e., reduce adjacent channel spill over), minimize group delay variations, and reduce performance drifts with environmental condition changes (e.g., temperature, pressure, and humidity). When designing devices for these high power operations, one often has to take into account the following effects: multipactor and ionization breakdown, passive intermodulation interferences and thermal-related issues such as temperature compensation. This talk will elaborate the physics background, technical challenges and design methodologies. It will also cover the clever use of both circuit and electromagnetic modeling techniques. Numerous examples will be presented from those widely used in the industry. The method presented is general and is applicable to all device types. [C2837]

#### **"Possibilities of cloaking and invisibility at microwaves"**

Summary form only given. Recently, the topic of making objects "invisible" for electromagnetic radiation has gained much attention, following new ideas of using engineered electromagnetic materials with unusual properties for this purpose. This lecture provides a comparative review of the recent developments in this field and discusses the potentials of utilizing these ideas for various microwave and antenna applications. The lecture starts from a review of the notions of invisibility and cloaking and their relations to the classical stealth technologies of reducing radar cross section of targets. Next, we make a historical overview of earlier approaches to techniques allowing reduction of scattering from various objects. Recently proposed solutions for cloaking of objects are reviewed and compared, with the emphasis on the fundamental limitations of their performance. This topic is closely linked to the problem of creating of artificial materials with engineered electromagnetic properties. In particular, materials with equal values of relative permittivity and permeability are of interest. The lecture presents our recent developments of such materials based on mixtures of spiral inclusions and their use for cloaking applications. Furthermore, we discuss the use of electrically dense meshes of transmission lines as cloaking devices. It is shown how new cloaking techniques can be used for applications not necessarily related to cloaking of objects, for instance in new microwave lens antennas or in the design of matched absorbing layers. [C2838]

#### **"The conductivity of unidirectional and quasi isotropic carbon fiber composites"**

This paper describes a novel technique to predict the variation of the conductivity of carbon fiber reinforced

polymer versus frequency. Free space transmission/reflection and radar cross section measurements are utilised to confirm this prediction. The results indicate that the conductivity of unidirectional carbon-fiber is dependent on the polarization of the incident electric field and increases with increasing frequency for a particular polarization. [C2839]

#### **"A way to modern and cost effective packaging for RF frontends for use from microwave through millimeter wave frequencies"**

This paper describes the way from a cost intensive status of development of RF electronics to modern cost effective concepts. Military RF electronics as e.g. receivers, transmitters or complete radar frontends historically have been realized using expensive technologies to reach outstanding RF performances and reliability. Many advances in technologies, but also tradeoffs are a way to overcome expensive solutions. [C2840]

#### **"Boresight gain optimization of an UWB monopole antenna using FDTD and genetic algorithm"**

Printed planar monopoles are promising ultra wideband (UWB) antenna and can be easily integrated in communication systems by fabrication onto printed circuit boards. These planar monopoles become popular for wireless communication due to their broad bandwidth and appropriate radiation pattern. However because of the dependence of the antenna gain and the antenna aperture, as the frequency increase, the wavelength decreases, the boresight gain decreases and its variation is very large. In this paper, a new UWB elliptical monopole antenna with a printed structure fed by a microstrip line is presented. The antenna is analyzed by using the finite-difference time-domain (FDTD) method and the parameters of the shape of the antenna are determined by utilizing the genetic algorithm (GA). Through a novel ground structure of the substrate, the boresight gain equals to approximately 2.4dB in the frequency band ranges from 3GHz to 9GHz. Details of the proposed antenna design and simulated results are presented and discussed. [C2841]

#### **"Welcome to the 13th European Microwave Week 2010"**

EuMW continues its series of successful events with the 13th European Microwave Week 2010 which will be held at the CNIT la Défense, Paris, France from 26 September to 1 October 2010. This conference series has continued to grow and is now the premier event in this field in Europe. This event gathers all the international microwave community around four themed conferences:-The 40th European Microwave Conference (EuMC)-The 5th European Microwave Integrated Circuits Conference (EuMIC)-The 7th European Radar Conference (EuRAD)-The 3rd European Wireless Technology Conference (EuWiT) [C2842]

#### **"A low phase-noise SiGe Colpitts VCO with wide tuning range for UWB applications"**

An integrated differential common collector Colpitts VCO with a wide tuning range is presented in this paper. The circuit was designed and fabricated in the IHP Technologies SGB25V 250 nm SiGe:C BiCMOS process. It provides a superior low phase noise performance of -115 dBc/Hz covering the frequency range of 6.7 to 8.7 GHz for UWB pulsed frequency modulated secondary radar application. An additional common collector output buffer was implemented as well. The circuit provides an overall output power of -10 dBm single-ended with a power dissipation of 47 mW including the on-chip buffer. This paper also shows the modifications and improvements done at the mm-wave topology to reduce size and to improve the tuning range. [C2843]

#### **"Design of a passive radar network"**

This paper presents a pair of tools that can be use for design of a passive radar network (PRN). The one is called RAVLA and it is suited for searching potential sites for receivers among transmitters of opportunity as well as building up a passive radar surveillance network. The other one is called PAVA and it can be used for searching potential transmitters of opportunity for the receiver located at the certain site. Both tools presume that the properties of the transmitters and the receiver are known as well as the number of bistatic bases which are needed for the location of the target. Finally, some intermediate results of the design process of a DVB-T based passive radar network in Southern Finland are considered. [C2844]

#### **"Comparison of the time-reversal and SEABED imaging algorithms applied on ultra-wideband experimental SPR data"**

This paper presents a comparison study between a simple time-reversal algorithm (designed at LEAT) and the SEABED algorithm (designed at Kyoto University) with their application to multiple-target experiments. Data are collected with an eight element ultra-wideband antenna linear array connected to an eight port vector network analyzer, working in a frequency bandwidth starting from 1.5 GHz up to 8 GHz. Several target configurations demonstrate the advantages and disadvantages of both algorithms. [C2845]



### "UWB radar signal processing for through wall tracking of multiple moving targets"

Through wall tracking can be very helpful in the situations where the entering of a room or a building is considered hazardous and it is desired to inspect its interior from outside through the walls. In majority of such cases, the tracking of multiple moving targets is needed. The radar signal processing for this application has to deal with several supplementary tasks in comparison with a single target tracking. Their solution is included in the complex signal processing procedure introduced in this paper. The experimental results obtained by the real radar signal processing confirm good performance properties of the proposed procedure. [C2846]

### "Wind farm Gapfiller concept solution"

This paper describes a Gapfiller concept solution to mitigate the potential negative effect from a wind farm upon a military surveillance radar system. The problem is described as well as the technical solution to mitigate the problem. This paper does not describe signal processing techniques that can be applied to the main surveillance radar, but it describes some important technical requirements and a Gapfiller solution that can be used to complement a surveillance radar system. The application of a Gapfiller deployed within an offshore wind farm is described and other relevant applications are suggested. [C2847]

### "Calibration of a 2.45 GHz indoor Direction of Arrival system based on unknown antenna gain"

In this paper we discuss the calibration procedure and effectiveness for an indoor Direction of Arrival (DOA) positioning system based on a switched six-beams antenna operating at 2.45 GHz. The introduced calibration procedure consists in optimizing the radiation pattern parameters of the antenna to minimize DOA estimations error, over a limited set of known positions. The estimations are obtained by the multiple signal classification (MUSIC). We demonstrate that in a realistic indoor environment the mean errors for the DOA estimations are less than 4.9 deg for both the DOA coordinate angles  $\theta$  and  $\phi$ , with a peak error of 8 deg, while a DoA estimation accuracy less than 3 deg was observed. [C2848]

### "Quasi-Analytical method for estimating low false alarm rate"

This paper proposes a new approach for estimating low false alarm rate (FAR) using Quasi-Analytical (QA) method. The results from both theoretical analysis and simulation show that QA estimation is unbiased with obvious simulation speed improvement with respect to Monte Carlo (MC) and Conventional Importance Sampling (IS) for typical application cases. Furthermore, unlike IS approaches that rely on complex optimization procedures for optimal IS parameters or sub optimal parameters, the QA is simple to implement and computationally effective. [C2849]

### "High range resolution DVB-T Passive Radar"

Passive Radar systems, also referred to as Passive Coherent Location systems (PCL), exploit reflections from illuminators of opportunity (IO) in order to detect and track objects. Digital waveforms like DVB-T and UMTS signals offer wide bandwidth channels which allow achieving good spatial resolution. Moreover, they have spectral properties which are nearly independent of the signal content. Such waveforms exhibit an ambiguity function with a thumb-tack shape and bandwidth that is constant in time. This paper focus on the usage of multiple channels of the same IO (e.g.: DVB-T or UMTS channels) in order to improve range resolution and make target recognition and radar imaging feasible. Specifically, two different architectures based on the exploitation of multiple DVB-T channels have been considered. A DVB-T transmission system has been simulated with a Simulink® model compliant to. Simulation results are presented and discussed in order to evaluate the system performance in terms of spatial resolution. [C2850]

### "FPGA implementation of UWB radar signal processing for automotive application"

A radar signal processor of 24GHz UWB pulse radar for automotive short-range application is presented. A FPGA-based architecture for this signal processor is proposed to fulfil the real-time system requirement. The high performance of the proposed architecture was feasible since the employment of parallel hardware processing modules, like a 64-point FFT, a CFAR processor, and other extra processing modules. Also our signal processor supports the external DDR2 memory in order to speed up the data transfer between the signal processor and a memory. Also in this work, our radar system was simulated as our radar working scenarios using the variable pulse length and the phase modulation. Experimental results of the FPGA implementation are presented. [C2851]

### "Welcome to the 13th European Microwave Week 2010"

EuMW continues its series of successful events with the 13th European Microwave Week 2010 which will be held at the CNIT la Défense, Paris, France from 26 September to 1 October 2010. This conference series has continued to grow and is now the premier event in this field in Europe. This event gathers all the international microwave community around four themed conferences: -The 40th European Microwave Conference (EuMC)-The 5th European Microwave Integrated Circuits Conference (EuMIC)-The 7th European Radar Conference (EuRAD)-The 3rd European Wireless Technology Conference (EuWiT) [C2852]

### "Design and implementation of sub-GHz transmitter for ultra-wideband through-wall radar"

Ultra-wideband (UWB) transmitters for through-wall radars operating in sub-GHz frequency may enable better penetrating ability and lower attenuation than devices utilizing signals above 1 GHz frequencies. In this paper, the crucial parameter of sub-GHz unipolar pulse width is investigated by theoretical analysis and experiment. Based on these parameter data, in order to radiate the signal effectively and reduce the ringing, we design a fifth-order parallel LC high-pass filter. It shapes the unipolar pulse into the bipolar pulse which has no direct current component and slight ringing. The transmitter circuit is implemented and tested. Results indicate that it generates sub-GHz UWB pulses with 2.6 ns temporal width and 744 MHz frequency bandwidth, which appears to be suitable for the through-wall radar. [C2853]

### "UWB front-end for SAR-based imaging system"

A planarly fed UWB leaky lens antenna is presented integrated with wide band transmit and receive front-end electronics, to be used in a SAR-based imaging system. The unique non-dispersive characteristics of this antenna over a very wide bandwidth, together with the dual band front-end electronics based on 'off the shelf' components and integrated using standard PCB technology makes them very attractive as transmit-receive element for a MIMO array configuration. Design and measurement results of the leaky lens antenna characteristics are presented, and design considerations for the integrated mm-Wave electronics are discussed. [C2854]

### "A gain-enhanced semicircular disc antenna with a quasi-planar surface-mounted short TEM horn"

A constant-gain ultra-wideband semi-circular disc monopole with a quasi-planar surface-mounted short TEM horn and a semi-circular reflector is proposed. The total length of the antenna is only 70 mm i.e. nearly  $0.67 \lambda$  at 2.86 GHz. The gain of the antenna is nearly constant:  $6.5 \pm 1.1$  dBi from 2.86 GHz to 15 GHz, and  $6.5 \pm 0.7$  dBi from 3.1 GHz to 10.6 GHz. It has broad azimuth pattern and its compact integrated configuration is suitable for several ultra-wideband (UWB) wireless and radar applications. [C2855]

### "SAR-like localization of RFID tags for non-uniform trajectory"

In this paper we present a new principle for localization of backscatter RFID tags. A new algorithm comparable to synthetic aperture radar on a non-uniform trajectory is proposed. The performance is verified with measurement data acquired by a multi sensor platform which comprises radar, imaging and RFID. The identified RFID transponder positions are presented with augmented-reality visualization. The new radar approach called SAR-like is shown to have similar performance as SAR at an apparently lower computational cost. [C2856]

### "SAR-like localization of RFID tags for non-uniform trajectory"

In this paper we present a new principle for localization of backscatter RFID tags. A new algorithm comparable to synthetic aperture radar on a non-uniform trajectory is proposed. The performance is verified with measurement data acquired by a multi sensor platform which comprises radar, imaging and RFID. The identified RFID transponder positions are presented with augmented-reality visualization. The new radar approach called SAR-like is shown to have similar performance as SAR at an apparently lower computational cost. [C2857]

### "A modular 24 GHz radar sensor for digital beamforming on transmit and receive"

A compact modular 24 GHz imaging radar sensor for digital beamforming is presented. Besides digital beamforming on receive, the advantage of multiple switched transmitters is used for increasing the angular resolution, which requires less hardware effort. The presented FMCW radar sensor provides up to eight switchable transmitters and eight receiver channels for parallel receiving, allowing digital beamforming on transmit and receive. A new switching technique via switchable amplifiers is proposed. Within the scope of this paper an overview of the whole radar sensor's architecture, design and realization is given. The performance of the sensor is successfully demonstrated and evaluated by measurements. [C2858]

#### "Fidelity criterion for UWB medical diagnostic"

In this paper an Ultra Wideband (UWB) system based method is introduced, which permits to analyze and to extract information from the back reflected time domain signals originated by a UWB Radar signal impinging on the human body. The criterion is based on the fidelity parameter. In the paper the developed method is firstly mathematically introduced and then measurement results are presented. [C2859]

#### "A novel UWB Radar super-resolution object recognition approach for complex edged objects"

In this paper a novel approach for object recognition (OR) by backscattered Ultra Wideband (UWB) signals on the basis of a reference data set is presented. The aim of this robust OR is succeeded by UWB imaging, classifying and finally applying a maximum probability recognition algorithm. To provide super-resolution even under multi-scattering conditions, an advanced wavefront detection algorithm with subsequent high resolution imaging technique is performed. After postprocessing a joint moment based feature, texture feature and geometrical feature recognition algorithm is applied. The simulation-based performance evaluations show a very precise imaging and a perfect maximum probability recognition rate with additional outstanding robustness. First tests using an m-sequence UWB Radar indicate the feasibility of this concept. [C2860]

#### "A 79-GHz LTCC laminated waveguide to metallic rectangular waveguide transition using high permittivity material"

An integrated laminated waveguide (LWG) to metallic rectangular waveguide (RWG) transition based on low temperature co-fired ceramic (LTCC) technology is presented in this paper. The transition is designed for the 76-81 GHz radar frequency band using a high permittivity material ( $\epsilon_r = 7.4$ ). An additional secondary LWG structure improves both impedance matching and bandwidth. The bandwidth at -10 dB return loss is more than 5 GHz. The measurement results of the fabricated prototype agree closely with the simulation. This compact and backshort-free waveguide transition allows low-cost integration and offers the possibility of measuring E-Band radar components based on ceramic substrate. [C2861]

#### "Metamaterial matching of high-permittivity coatings for 79 GHz radar sensors"

Future automotive radar sensors in the 79 GHz regime are intended to be integrated behind painted, plastic fascia. This integration has to be carefully studied, concerning reflections coming from the bumper in line of sight of the sensor. To reduce these reflections, impedance matching of multilayer structures with high permittivities (e.g. metallic paints) is mandatory. Besides conventional matching techniques, metamaterials are a possibility to realize a matching layer. Based on an adopted parameter extraction algorithm for multilayer dielectrics, a bandwidth evaluation of a possible metamaterial design is shown. The measurement results show that for a bandwidth up to 3.8 GHz the metamaterial outperforms the benchmark. [C2862]

#### "Second order extension of power amplifiers behavioral models for accuracy improvements"

In the design process of reconfigurable radars, it is required to study the interaction between antennas and the power amplifiers in order to quantify the distortion and predict the performances of power amplifier (PA) on TX-chains. This paper presents an accurate behavioral model for PAs, based on nonlinear scattering functions, which allows taking into account large output loading impedance mismatches, i.e. Voltage Standing Wave Ratio (VSWR) up to four. First application presented is a black box modeling technique limited to Taylor first order expansion dedicated to moderate VSWR ( $VSWR \leq 3$ ). Unfortunately, the first order model is not efficient enough, so a second application is presented, showing an accurate model expanded to Taylor second order in the case of large VSWR ( $VSWR > 3$ ) which allows predicting circuit performances at system level and establishes a mixed simulation tool for a bilateral communication between amplifiers and antennas. [C2863]

#### "Session D4: Sensing and medical imaging; collision, ground-penetrating and through-wall radars"

{no data available} [C2864]

#### "Design of two flare UWB antenna dedicated to the research of alive buried victims"

This document presents the antenna design for the detection of alive victims buried under thick layers of rubble. The antenna is used with UWB Radar techniques in order to locate buried alive victims. The detection is based on the signature of alive persons by using Doppler analysis of movements and respiration. Detecting victims in this environment is very difficult due to the large dynamic range of signal levels. In fact, the reflected signal caused by the buried alive victim is very low behind other reflected or disturbing signals such as mobile phones, vegetation movements, water, rescuers... A two flares UWB antenna, light weight and easy transportable has

been specially design for the research of buried victims beneath building rubble. This paper focuses on antenna design, simulation and measurement. These measurements have been made by IETR and CEA. The experimental results show a good comparison between measurements and simulations. [C2865]

#### "Simulated and experimental wavelet-based detection of breast tumor using a UWB radar"

The objective of this work is the detection and localization of breast cancer by means of microwave imaging using Ultra Wide Band (UWB) techniques. The proposed method consists in detecting the time-of-flight signal backscattered by the tumor using continuous wavelet transform. The feasibility of this method is investigated from several simulated and experimental results using a phantom with a UWB pulsed radar. [C2866]

#### "Design of wearable communication device for body protection from EM wave using the EBG structure"

This paper presents a wearable communication device for body protection from electromagnetic wave using a electromagnetic bandgap (EBG) structure at a WCDMA band. Since wearable wireless communication devices are worked in the proximity or contact of the human body, a health risk from a electromagnetic fields generated by body worn devices is important. The EBG structures can suppress the propagation of surface current and act as a perfect magnetic conductor. Thus, it is capable of preventing a undesired electromagnetic wave from the wireless communication devices. The proposed wearable communication device has the PIFA with the EBG structure at a WCDMA band, frequency generator for the SAR testing and a dielectric case. It is a kind of watch phone worn on the human wrist. Simulation and experimental results demonstrate S-parameter, radiation pattern and the SAR value of the proposed structure. [C2867]

#### "Measurement verification of dual-orthogonal polarized UWB monopulse radar system"

In this work the practical verification of the UWB-monopulse radar is presented. Based on measurements of the antenna impulse response the look-up table is created. For radar measurements three targets are placed in vertical plane, at different angles and distances in respect to the antenna. The signals received in sum and difference beam are processed and compared with the look-up table. The presented system maintains a high range resolution delivered by UWB-technology and precise estimation of angular direction of the target. The sensing is performed with simple data processing, where no additional mechanical or electrical scanning of the antenna beam is required. [C2868]

#### "A low phase-noise SiGe Colpitts VCO with wide tuning range for UWB applications"

An integrated differential common collector Colpitts VCO with a wide tuning range is presented in this paper. The circuit was designed and fabricated in the IHP Technologies SGB25V 250nm SiGe:C BiCMOS process. It provides a superior low phase noise performance of -115 dBc/Hz covering the frequency range of 6.7 to 8.7 GHz for UWB pulsed frequency modulated secondary radar application. An additional common collector output buffer was implemented as well. The circuit provides an overall output power of -10dBm single-ended with a power dissipation of 47mW including the on-chip buffer. This paper also shows the modifications and improvements done at the mmwave topology to reduce size and to improve the tuning range. [C2869]

#### "Dual frequency & dual-linear polarization integrated Antenna array for application in Synthetic Aperture Radar"

This paper presents the design and realization of a dual frequency antenna array for application in Synthetic Aperture Radar. The array consists of 64 C-band elements interleaved with 4 L-band elements incorporated with feeding network in one integrated, multilayer, LTCC compatible structure. The Antenna has been designed to operate with dual-linear polarization in both frequency bands. The achieved bandwidths are 100 MHz in L-band and 400 MHz in C-band. Several techniques for suppressing orthogonal polarization has been implemented to achieve very low cross-polarization coefficient in both frequency bands. The beam forming network has been designed to provide modified cosec<sup>2</sup> radiation pattern suitable for radar applications. [C2870]

#### "A single bias 20W S-band HPA for radar applications"

The development of a single bias S-band MMIC HPA designed for radar T/R module applications is reported. The chip was fabricated with a low-cost 0.5 $\mu$ m GaAs PHEMT process and is composed of two stages, with a final stage of 29 mm gate-width periphery. The MMIC power amplifier is designed by using a zero gate bias configuration and therefore is attractive due to the size and cost reduction. In the frequency bandwidth 2.4-3.6GHz, the HPA biased at  $V_d=10V$  delivers an output power of 20W @ 4dB of gain compression, with an associated PAE of circa 28%. [C2871]



### "Original identification technique of passive EM sensors using loaded transmission delay lines"

This paper presents a proof of concept of an original identification technique of passive EM sensor cells. Previous works published by the authors have shown the feasibility of high sensitivity passive sensor Microsystems based on the electromagnetic transduction principle. More, other works, published by the same authors, have demonstrated the feasibility of a wireless interrogation technique of such passive measurement units. This interrogation technique is based on the measurement of the Radar Cross Section (RCS) level of the system composed of the sensor connected to an antenna. In this communication and for the identification purpose, a smart solution combining the sensor cell and a loaded transmission delay line is proposed. The length of the transmission delay line attributes unique identifier to the EM sensor cell. As it will be shown, the measured Beat signal Level spectrum, obtained by using an FMCW Radar reader, is composed of a two parts: one part related to the structural mode (which gives information about the antenna position) and a second part composed of the antenna mode (which gives us information dealing with the sensor measured value and the sensor identification in case of multiple sensor configuration). [C2872]

### "LNA and mixer for 122 GHz receiver in SiGe technology"

The paper presents 122 GHz receiver circuits including a low-noise-amplifier (LNA) and a mixer fabricated in SiGe BiCMOS technology. The design takes advantage of a novel transmission line structure with thick metal ground-shield on top of the MMIC. The LNA utilizes a two-stage cascode topology and the mixer is a Gilbert cell with additional current injection in the RF-path. Measurements of the receiver frontend show a gain of 12 dB and a noise figure below 13 dB at 121-129 GHz. The power consumption is 165 mW from a 3.5 Volt supply. The receiver frontend is intended for the use in ISM-band radar and communication systems, wide-band communication systems and in radar imaging systems. [C2873]

### "Design and development of a millimetre-wave novel passive ultrasensitive temperature transducer for remote sensing and identification"

The millimetre-wave passive temperature transducer consists of micro bimorph cantilevers (Au-Silicon) and split ring resonators, operating around 30 GHz. The temperature change causes a deflection on the bimorph cantilevers, thus results in a shift of resonant frequencies of the split ring structure. The design achieves sensitivity of 2.62 GHz/ $\mu\text{m}$  in terms of frequency shift response to cantilever deflection, corresponding to a sensitivity of 498 MHz/ $^{\circ}\text{C}$ , three order of magnitude higher than existing sensors. In terms of deflection versus temperature, the material choices for the bimorph cantilevers can be varied and adapted to different applications including those operating in harsh environments. To demonstrate proof-of-concept, a scaled prototype operating around 3 GHz is presented with Radar Cross Section measurements for remote identification. [C2874]

### "79GHz BiCMOS single-ended and differential power amplifiers"

This paper presents the performance of 79GHz power amplifiers (PAs) for automotive short range radar (SRR) application. A single-ended four stage common emitter circuit topology and a differential PA with integrated baluns are fabricated using 0.13 $\mu\text{m}$  SiGe BiCMOS process. The design and the measured results of the monolithic integrated low-voltage PAs are reported. The 79GHz differential PA, which the design is based on the single-ended PA, delivers 18dBm of maximum output power and 13.5dBm output power at 1dB compression (P1dB). The differential circuit achieves 21.5dB gain and shows 8.2% of power added efficiency (PAE) from a 1.8V supply voltage at 79 GHz. The power amplifier was fully integrated including matching elements, bias circuit and very small baluns. The chip occupies an area of 0.46mm<sup>2</sup> and 0.7mm<sup>2</sup> for the single-ended and differential configuration respectively. [C2875]

### "SAR computation in a real-sized car: Multi-exposure scenarios"

In this study, investigations have been carried out into the variation of whole-body averaged SAR values for 4 humans (one driver + three passengers) inside a realistic real-sized car. Transmitting devices used in the simulations had multiple frequencies making it a multi-exposure environment. These devices (e.g. Bluetooth, Universal Mobile Telecommunications System (UMTS) and WiMax) use differing operating frequencies and can be used in semi-echoic environments such as cars, trains, planes, etc. Results showed that the whole-body averaged SAR is below exposure limits provided by international standards and guidelines when there is 1 of each transmitter present. The results also show the whole-body averaged SAR when 2 active transmitters are simultaneously in use. Computed values are shown to be within the ICNIRP recommended limits. [C2876]

### "X-band cavity-backed slot antennas and coupled oscillator systems"

In this paper, substrate integrated waveguide (SIW) cavity-backed antennas and coupled oscillator systems are proposed. The cavity-backed structure permits to overcome potential problems such as heat dissipation and unwanted surface wave modes in large array implementations, and may provide better phase noise performances. Moreover, it provides a design parameter to control coupling among the oscillator elements. Full-wave FEM-based and harmonic balance (HB) analyses are used to design passive antennas and active antenna oscillators, whose frequency responses have been evaluated for different values of certain geometrical parameters. Based on the results obtained, different configurations of two-element coupled oscillator antenna systems have been proposed. Compact, single substrate prototypes are presented. These low cost implementations could be useful in radar and communication applications. [C2877]

#### "Information-theoretic algorithm for waveform optimization within ultra wideband cognitive radar network"

A novel information-theoretic approach for designing the excitation ultra wideband (UWB) waveforms within a cognitive radar network is developed. This method utilizes the mutual information (MI) between subsequent radar returns to extract desired information from the radar scene. With this approach, the radar system constantly learns about its surroundings and adopts its operational mode accordingly based upon the MI minimization criterion. Subsequently, the positioning algorithm makes use of this information about the radar scene to generate more accurate location estimates. Numerical results demonstrate an improvement in the probability of target detection even at low values of receive signal-to-noise ratio (SNR). The proposed algorithm also promises a better delay-Doppler resolution of the target, which can be analyzed through the radar ambiguity function (AF). Simulation data show an improvement in the target discrimination ability in the presence of noise and clutter. [C2878]

#### "50W X-Band GaN MMIC HPA: Effective power capability and transient thermal analysis"

This paper reports the performance of a two-stage X-Band MMIC GaN HPA designed for radar applications. At 20V drain voltage bias and 3dB compression point the HPA delivers more than 20W of pulsed RF power with a PAE of 35% over the 8-10.5GHz frequency range, whereas at  $V_{ds}=35V$  the MMIC provides more than 50W and 30% of PAE, with a peak power value of 58W at 9 GHz. In order to evaluate the effective HPA power capability in a real system environment and the related thermal management issues, the HPA transient thermal response for pulsed bias conditions has been investigated by means of IR thermo-camera measurements. [C2879]

#### "Integrated X-band FMCW front-end in SiGe BiCMOS"

An integrated X-band FMCW front-end is reported. The front-end unites the core functionality of an FMCW transmitter and receiver in a 0.25  $\mu m$  SiGe BiCMOS process. The chip integrates a PLL for the carrier generation, and single-side band and image-reject mixers for up- and down-conversion of the waveform. The front-end has been designed to co-operate with COTS integrated direct digital synthesizers and ADCs. The measurements show an output power of 0 dBm, P1dB at the receiver input of -11 dBm and a side band suppression of the mixer in the transmit chain of >40 dBc. The MMIC measures 1.8x1.5 mm<sup>2</sup>. This integrated front-end paves the path for future planar 2D integration of FMCW phased-array radars at X-band. [C2880]

#### "Comparative study of 2.4 GHz and 10 GHz vital signal sensing Doppler radars"

Performance and implementation complexity between 2.4 GHz radar system with homodyne and 10 GHz radar system with super-heterodyne are compared and discussed. In particular, recently proposed architectures are examined, which are implemented by identical PLL and VCO. Both the operation of two different architectures and the superior performance of these radar systems can be understood by observing what level of signal is received based on same signal conditions. 10 GHz approach yields better performance in terms of RCS and antenna gain, but at the cost of increased implementation complexity. [C2881]

#### "G-band low noise amplifier and oscillator for synthetic aperture applications"

This paper presents the results of G-Band Monolithic Microwave Integrated Circuits (MMIC) for passive imaging applications. The studied system is a Y-shaped interferometer. This kind of system provides both high resolution and a compact system. MMIC were made using a 70 nm GaAs metamorphic High Electron Mobility Transistor process from OMMIC (France). A Low-Noise Amplifier performances are presented, measurement results provide a noise figure of 5 dB with a gain of 20 dB on 10 GHz bandwidth around 140 GHz. The second circuit is an oscillator, measurement results give an oscillation frequency close to 146 GHz. [C2882]

#### "T/R-module technologies today and future trends"

After many years of development the active electronically scanned array (AESA) radar technology has reached a mature technology level. Many of today's and future radar systems will be equipped with the ASEA technology. T/R-modules are key elements in active phased array antennas for radar and electronic warfare applications. Meanwhile T/R-modules using GaAs MMICs are in mass production with high quantities. Top priority is on continuous improvement of yield figures by optimizing the spread of key performance parameters to come down with cost. To fulfill future demands on power, bandwidth, robustness, weight, multifunctional sensor capability, and overall sensor cost, new emerging semiconductor and packaging technologies have to be implemented for the next generation T/R-modules. Using GaN MMICs as HPAs and also as robust LNAs is a promising approach. Higher integration at the amplitude and phase setting section of the T/R-module is realized with GaAs core chips or even with SiGe multifunction chips. With increasing digital signal processing capability the digital beam forming will get more importance with a high impact on the T/R-modules. For lower production costs but also for sensor integration new packaging concepts are necessary. This includes the transition towards organic packages and using low cost surface-mount soldering technology. [C2883]

#### "Ramp response radar imaging: Analysis of frequency parameters"

Low frequency imaging in radar domain can have applications for stealthy or buried targets. Transient scattering response from a ramp waveform is related to the profile function of the target, namely its transverse cross-sectional area along the line-of-sight, and it thus provides information about the target size, orientation and geometrical shape. Indeed, such profile functions can be used for generating a 3-dimensional image of the target shape. However the required frequency band is very large and may involve difficulties for experiments as well as simulations. That is why, we propose to study the effect of these frequency parameters on targets profile functions and, consequently, on their reconstructed shape. [C2884]

#### "Comparison of target detection schemes in Doppler radar with PSK signals"

The aim of this article is to test the effectiveness of the known CFAR processors in order to detect moving targets in the frequency domain of real records. The purpose is to be chosen optimal CFAR detector for moving target detection. The data are obtained by portable, surveillance, Frequency Modulated Continuous Wave (FMCW) radar with Low probability of Intercept (LPI). In the paper are studied and compared CA, OS, SO, GO CFAR processors. [C2885]

#### "Digital signal processing applied to radar sensors operated in active defense systems"

The active defense (AD) is deemed a very promising way how to protect military vehicles, especially in contemporary fight against terrorism in the Third world countries. Cheap and easily accessible hand-held cumulative missiles (e.g. RPG-7) are able to penetrate up to 300 mm of the hard-hardness armour (HHA). Thus light transport military vehicles equipped typically with less than 10 mm thick armours, used frequently e.g. in Afghanistan are very vulnerable. The AD systems are based on radar sensors that detect approaching missiles and activate a suitable counter-measure able to destroy the threatening missile. The article describes the microwave curtain, which is one of the radar sensors applicable in AD systems, and signal-processing methods used for generation of ignition signals from its output signals. Practical results obtained at army shooting range are also presented. [C2886]

#### "Interferometric quadrature down-converter for 77 GHz automotive radar: Modeling and analysis"

This paper describes a millimeter wave quadrature down-converter module based on the interferometric principle. The computer model of the six-port interferometer is implemented using S-parameter measurements of a 90° hybrid coupler fabricated on thin alumina substrate. This model is validated by full two-port measurements of the six-port. Down-converter error vector modulation results are analyzed using an envelope simulation. The proposed architecture is suitable for low-cost, high-performance, reconfigurable millimeter wave automotive radar and communication front-ends. [C2887]

#### "Optimal sensor placement for multi-bistatic ISAR imaging"

Inverse Synthetic Aperture Radar (ISAR) images are typically used for target recognition and identification purposes. The target projection on the ISAR image plane depends on the target's own motions and on the relative position of target and radar. Since targets of interest are often non-cooperative, the first condition is not under the radar's control. Nevertheless, the relative radar-target position can be somehow controlled or predicted in some cases. Moreover, the use of multiple receivers enhances the likelihood that a desired radar-target position occurs during radar measurements. In this paper, the theoretical aspects of optimal sensor positioning for obtaining desired ISAR image projections are detailed. A mathematical tool will be presented that is able to predict the optimal sensor positions for maximising the probability of obtaining a desired ISAR image. Real data

will be used that demonstrate the effectiveness of the proposed tool. [C2888]

### "MIMO radars. What are they?"

Two classes of MIMO radars are briefly considered. MIMO radars with colocated antennas and coded signals represent a new and prospective concept. MIMO Radars with widely separated antennas ("Statistical MIMO radars") are a particular case of well-known Multisite (Multistatic) radar systems. Most results presented by the authors of "Statistical MIMO radars" were obtained under much more general conditions and published many years ago. Besides, ignoring some specific features of radar by the authors of "Statistical MIMO radars" has led to serious errors. [C2889]

### "Knowledge assistance for ground target tracking and resource management"

Tracking slow moving ground targets from airborne phased array radar is a challenging task. Some of the major issues are heading accuracy of slow moving target and radar resource management in clutter regions. In this paper, we propose a novel tracking framework using digital map and clutter knowledge bases to efficiently track the ground moving target using airborne phased array radar. The proposed technique uses offline processed digital map for fast retrieval of road parameters. Also, the proposed radar data processor provides feedback to populate and update the clutter knowledge-base. A fast yet robust method is employed for ground mapping of targets and to detect map features such as road junctions. Experimental results show (i) the robustness of the map knowledge assisted tracking approach when target moves along different kinds of path (i.e. on/off the road) (ii) better heading accuracies achieved by knowledge assistance and (iii) radar resource management in clutter region with knowledge-base. [C2890]

### "Study on velocity estimation of MCPC signal in wideband radar"

This paper presents a novel scheme for velocity estimation in wideband Multi-Carrier Phase-Coded (MCPC) radar, which has drawn considerable attention recently as a new generation of radar. Conventional narrowband Doppler processing preserves the phase relationship of the received pulses, thus not only increases the Signal-to-Noise Ratio (SNR), but also obtains reliable extraction of the Doppler parameters. However, the rangewalk of moving target due to the wide bandwidth makes things difficult. Additionally, it is a question of interest to researchers that is resolving velocity ambiguity within a single burst. Based on separated processing of subcarriers in MCPC echo signals, we can estimate the radial velocity of the target without ambiguity by Least Squared (LS) algorithm over the linearity curve of Doppler spectrum. The simulation results verify that this scheme can be applied to the fast-moving target efficiently. [C2891]

### "Book of abstracts"

{no data available} [C2892]

### "EuRAD 2010 abstract cards"

{no data available} [C2893]

### "Radar polarimetry for security applications"

We analyse micro-Doppler techniques and the improved performance that fully polarimetric radar techniques can add. We perform fully polarimetric measurements of the varying micro-Doppler signatures of humans as a function of elevation angle and azimuthal angle in order to try to optimize this type of system for the detection of arm motion, especially for the determination of whether someone is loaded. We determine that polarimetric measurements can isolate and highlight the arm motion for a classification as loaded or unloaded. Second, the azimuthal angle of the motion is a critical parameter to consider in ground-based systems. For choke-point observations where the direction of motion is more controlled, polarimetric radar has the potential to determine who is not loaded inappropriately and who should be checked. [C2894]

### "EuRAD 2010 detailed author index"

{no data available} [C2895]

### "Target localization methods for frequency-only MIMO radar"

When the time resolution of the signals is not so good, we can't rely on the time of arrival (TOA) information. On the other hand, if the frequency resolution of the signals is good, than frequency of arrival (FOA) informations



will be more reliable. Localization of a moving, non-maneuvering target is possible by using Doppler-shift measurements in MIMO radar systems. A new method for target localization in frequency-only MIMO radar is proposed and it is compared with previous method. These methods use only received frequencies, and all of other unknown quantities can be written by using locations of the target, the receivers and the transmitters. If the received frequencies are known only, desired area can be searched grid by grid for all possible (x, y) coordinates to find the position of the target in 2D space. [C2896]

#### "Digital antenna unit for DOA analysis in ESM systems"

In this paper, design and characterization of a novel "Direction Finding Antenna" unit (D/F DAU) are presented. The unit has been designed in order to localize electromagnetic emitters with precision direction finding capabilities. The Antenna is employed in the ELT avionics and naval modern ESM sensing system and utilizes an amplitude direction finding scheme. The main characteristic the D/F DAU is the ability to cover the signal pulses visibility in presence of simultaneous CWs emitters. An evidence of the used techniques, electromagnetic simulations, three dimensional outlines, measurements and obtained performances are explained. A paragraph of the article is focused to describe the characteristic of the Antenna to cover the signal pulses visibility in presence of simultaneous CWs emitters. [C2897]

#### "The end of indexes"

{no data available} [C2898]

#### "Millimetre wave radar imaging of mining vehicles"

This paper considers some of the complexities in regard to generating 2D and 3D radar images of mining infrastructure. It examines issues with range interpolation in multi scatterer environments and a method of modelling radar returns from vehicles. [C2899]

#### "Radar and Electronic Warfare cooperation aboard a single or multiple cooperative platforms"

Up to now, combat aircrafts are fitted with Fire Control Radar (FCR), Electronic Warfare System (EWS), and radio links. Each of these systems is dedicated to a particular task and the cooperation is reduced to a minimal exchange of information between them, so far. Major system performance enhancements are to be expected from close co-operations to each other sensors. The future co-operations can be ordered in four stages. The three first ones lead progressively to a common sensor including radar and EW functions. The last one is the deployment, on a given platform, of these common multifunctions sensors on a network basis. Another focus is the cooperation between platforms. Depending on the cooperative application, low, medium or high data rates will be needed. A typical example required by such co-operations is the implementation of "ad hoc" data links using the FCR or the EWS. This kind of co-operations does not need to add specific antennas or other R.F. devices. [C2900]

#### "Non-quasi-static modeling of the intrinsic Y22 for GaN, Si, and GaAs mm-wave FET technologies"

The extraction of accurate transistor models is essential for a reliable and efficient design of transmit/receive modules, which in turn is a keystone for the development of active electronically scanned array radars. The present paper is aimed at analysing the implementation of non-quasi-static effects for advanced millimeter-wave FET models. The non-quasi-static phenomena can be neglected at few GHz but their contributions become more and more dominant by increasing the operating frequencies. In particular, this study is focused on the investigation of the non-quasi-static effects for modeling the intrinsic short circuit output admittance for FETs based on gallium nitride, silicon, and gallium arsenide technologies. Different model solutions are carefully compared and analysed in detail. [C2901]

#### "Estimation of efficiency of a tree structured hierarchical wavelet representation of synthetic database applied to Non-Cooperative Target Recognition"

In this paper, problem of efficient representation of large database of target radar cross section is investigated in order to minimize memory requirements and recognition search time, using a tree structured hierarchical wavelet representation. Synthetic RCS of large aircrafts, in the HF-VHF bands, are used as experimental data. Hierarchical trees are built using wavelet multiresolution representation and K-means clustering algorithm. Criteria used to define these hierarchical trees are described and the obtained performances are presented. [C2902]

### "Dual frequency & dual- linear polarization integrated antenna array for application in Synthetic Aperture Radar"

This paper presents the design and realization of a dual frequency antenna array for application in Synthetic Aperture Radar. The array consists of 64 C-band elements interleaved with 4 L-band elements incorporated with feeding network in one integrated, multilayer, LTCC compatible structure. The Antenna has been designed to operate with dual-linear polarization in both frequency bands. The achieved bandwidths are 100 MHz in L-band and 400 MHz in C-band. Several techniques for suppressing orthogonal polarization has been implemented to achieve very low cross-polarization coefficient in both frequency bands. The beam forming network has been designed to provide modified cosec<sup>2</sup> radiation pattern suitable for radar applications. [C2903]

### "Foreign object debris detection using a 78 GHz sensor with cosec antenna"

This paper presents the results of FOD measurements conducted using a broadband 78 GHz radar sensor. Previous studies with a short-range setup up to 30 m showed promising results. However, to meet the requirements of the intended application, the range has to be increased significantly. As for all radar systems, the range can be extended by increasing the transmitted power and/or the antenna gain. In this work two different folded reflectarray antennas with a cosec-shaped pattern have been used to improve the system performance and range. Together with a CFAR (constant false alarm rate) algorithm and a moving target indication advances could be achieved compared to the previous setup. [C2904]

### "Design of two flare UWB antenna dedicated to the research of alive buried victims"

This document presents the antenna design for the detection of alive victims buried under thick layers of rubble. The antenna is used with UWB Radar techniques in order to locate buried alive victims. The detection is based on the signature of alive persons by using Doppler analysis of movements and respiration. Detecting victims in this environment is very difficult due to the large dynamic range of signal levels. In fact, the reflected signal caused by the buried alive victim is very low behind other reflected or disturbing signals such as mobile phones, vegetation movements, water, rescuers... A two flares UWB antenna, light weight and easy transportable has been specially design for the research of buried victims beneath building rubble. This paper focuses on antenna design, simulation and measurement. These measurements have been made by IETR and CEA. The experimental results show a good comparison between measurements and simulations. [C2905]

### "A high resolution 2D omnidirectional synthetic aperture radar scanner at K band"

In this paper a K-band 360° 2D imaging radar utilizing a synthetic aperture scanning principle is introduced. A small omnidirectional antenna is mounted on a rotating platform to create a circular synthetic aperture. Based on a broadband holographic reconstruction principle a high resolution 360° 2D image is calculated after each turn of the platform. The size of the synthetic aperture and thus the lateral resolution of the imaging system are determined by the diameter of the resulting circular antenna trajectory. In contrast to common radar scanner-concepts that utilize highly directional and thus bulky antennas, the proposed scanner concept has the advantage that it uses a small and lightweight omnidirectional antenna. This results in a much more compact radar system with notably relaxed requirements for the scanning mechanics. In addition it will be shown that the use of an omnidirectional antenna allows for very simple options to transfer energy to the radar on the rotation platform. The performance of the proposed SAR radar scanning method is illustrated with a 24 GHz FMCW radar sensor system. [C2906]

### "Loss mechanisms of folded reflectarray antennas"

Folded reflectarray antennas can provide a good solution for millimeter-wave systems requiring compact, low-cost antennas, e.g. in automotive applications. This contribution investigates different approaches of such antennas with rectangular and composite reflecting elements. Special emphasis is put on gain and antenna loss mechanisms, including increased beam-width and sidelobe level as well as metallization losses. [C2907]

### "Comparison of analog IFM and digital frequency measurement receivers for electronic warfare"

Measurement of the incoming signal's frequency is one of the most important topics of an EW receiving system. The continuous performance and reliability improvement of Analog to Digital Converters and FPGA pushed the operation frequency of these devices up to tens of GHz, thus making possible the design of quasi-full digital wideband EW receiving systems. In this paper a comparison between a traditional analog microwave IFM receiver and a modern digital frequency measurement receiver is carried out, dealing with architectural, technological and performance differences, enhancement capabilities and lifetime. [C2908]

### "Airport radar monitoring of wake vortex in all weather conditions"

To assess maturity and capability of X-band radars to monitor wake roll-ups in all weather conditions, Radar data were collected on airports, near runway at ORLY airport and just under its ILS Interception Area. Additional trials took place on Paris-CDG Airport to benchmark Lidar & Radar Technologies. Continuous Detection, characterization and profiling capabilities of wake vortices, up to a range of 2000 m, have been proved in clear air and rainy weather. Recorded data have been correlated with electromagnetic and fluid mechanical models of Wake Turbulences for better and more accurate understanding of roll-ups radar cross section (RCS) and Doppler signature. X-band Radar has been proved to be a full-fledged alternative, which can make a significant contribution to a wake vortex alert system, but to achieve as much reliability as possible, collaborative Electro-optical & electromagnetic sensors solution is envisaged encapsulated in a Wake Vortex Advisory System. These sensors could be used to permanently monitor wake turbulence on runways. [C2909]

### "A multifunctional 60-GHz system for automotive applications with communication and positioning abilities based on time reversal"

This paper reports a multi-functional 60-GHz system which performs promising performances for short-range automotive applications such as short range RADAR with communication abilities. Experimental results validate the ability of the topology to transmit high speed data in the millimetre-wave (MMW) frequency band using Pulse Position Modulation (PPM). Using the same front-end, a positioning functionality is simultaneously assumed successfully in a Time Difference Of Arrival (TDOA) configuration. Furthermore, the Time Reversal (TR) technique is introduced and its impact on the location accuracy is presented and validated by experimental results. [C2910]

### "Angle of arrival detection using Retrodirective RADAR"

In this paper, experimental results are shown for angle of arrival extraction using an analogue Retrodirective RADAR using PLL to an accuracy of  $2.5^\circ$ . Angle of arrival results from the Retrodirective RADAR were extracted from the low frequency IF phase of the PLL based phase conjugator. The target position can then be determined virtually instantaneously. Therefore the system does not require any complicated DSP post processing, so is able to operate with low power and relatively simple circuitry. This system is ideally suited to real time acquisition of fast moving projectiles. [C2911]

### "Dual-sided phase conjugating surface techniques for imaging"

We describe the principle of operation and study the imaging capabilities of a dual sided phase conjugating lens operating as an imaging sensor in free space or in an environment where significant multipath or scattering may be present. The image formation is based on the wavefront reversal properties of the phase conjugating array. By the means of numerical simulation we show that the characteristic resolution of a single dielectric target in free space is about one wavelength,  $\lambda$ , across the range and  $3-4\lambda$  along the range for CW illumination and about one centre-wavelength  $\lambda_0$  when the target is illuminated with a Gaussian packet. For multiple targets in free space resolution across and along the range is  $\sim 2\lambda_0$  when illuminated by a Gaussian packet. It is shown that a weakly scattering object can only be detected behind a lossy dielectric wall using CW or UWB phase conjugation techniques when the backscattered field from the wall is eliminated. A procedure for achieving this is proposed. Numerical simulations for through-the-wall imaging using the phase conjugating lens technique with wall backscatter elimination demonstrates the possibility for small target high-resolution imaging. [C2912]

### "Riemannian median, geometry of covariance matrices and radar target detection"

We develop a new geometric approach for radar target detection which is based on the notion of Riemannian median and the information geometry of covariance matrices. First of all, we give the definition of Riemannian median and a simple algorithm to compute it. After that, the explicit expressions of reflection coefficients parametrization of covariance matrices are obtained, with which the Riemannian metric on the manifold of covariance matrices has a very simple form. The explicit expressions of geodesics in the manifold are also obtained in order to facilitate the computation of the Riemannian median of covariance matrices. Finally, we give some simulation examples to illustrate the performance of this new method. [C2913]

### "Design challenges for millimeter wave active imaging systems"

Due to the atmospheric absorption in W-band, especially the spectrum around 94 GHz has been the frequency of choice for radar applications in reconnaissance and metrology, but more recently also for indoor security applications. However, for indoor security applications the propagation environment and scale of the application is quite different as compared to the long-range military and scientific applications. In this paper we report on the

work performed at the research group ESAT-TELEMIC on modelling and designing indoor millimeter wave imaging systems that employ coherent multi-parametric illumination in a "flash"-like configuration. We discuss trade-offs between certain system parameters and present two examples of multi-parameter imaging. We show that a 2.5D simulator is a good compromise between computational cost and ability to analyse interference effects such as speckle. We also elaborate on challenges in terms of hardware implementation, and demonstrate experimentally the potential of using printed antennas for millimeter wave security applications. [C2914]

#### "Through the wall MIMO radar detection with stepped frequency waveforms"

In this paper, we present through the wall (TTW) radar detection simulations with an emerging radar architecture which is the multiple-input multiple-output (MIMO) radar. The urban environment, especially in TTW detection, is very tough for radar detection. With the aim of improving the detection performances, we use several spaced antennas in transmission which gives a spatial diversity leading to different points of view of the scene. So as to keep diversity we choose linearly independent waveforms and more particularly we utilize the hyperbolic frequency hop codes. We first begin by introduce the problems and applications of TTW detection. Then we will present the geometric configuration of the scene and the wall attenuation and target modeling. After what, we will expose the waveforms used in transmission and the processing to perform detection. We finish with some preliminary results and conclude about this work. [C2915]

#### "New coastal radar performances: Evolution or revolution"

Based on the legacy of marine radars, historical coastal surveillance sensors were based on the cheap magnetron-slotted waveguide antenna combination and were addressing sea-lane traffic control missions. New regulations in the marine world, such as the SOLAS convention, and increasing requirements for very small objects tracking, put new requirements on radar performance. It triggered an evolution process that is transforming the coastal radar design: From a rough and simple magnetron design, it is now moving into solid state and multi-mission units. This paper addresses the key elements triggering this evolution and puts in perspective the latest developments in this fastly moving field. It addresses a key question: Are we witnessing a market driven revolution in the coastal radar domain? [C2916]

#### "Multistatic, MIMO and networked radar: The future of radar sensors?"

A review is presented of work on multistatic, MIMO and networked radar, explaining the current high degree of interest in these subjects. The enhancement of target signatures in the forward scatter geometry is explained, and some of the principles of Passive Bistatic Radar. The challenge here is to identify applications which offer a clear advantage over conventional radar approaches. Finally, some newer, longer term ideas on networked radar as an intelligent, adaptive distributed sensor system are presented and discussed. [C2917]

#### "Advanced clouds tracking for airborne weather radar & ground primary surveillance radar"

A method for modeling and tracking convective clouds within radar images is presented. An object modeling approach is used, based on the extraction of either morphological or grayscale skeletons from 2-dimensionnal cross-section of 3-dimensional radar data. Grayscale skeletons are appropriate shape descriptors for non-rigid and heterogeneous objects, in which gray-level local maxima correspond to regions of interest. The modeling scheme is enhanced by meta-data linked to some chosen points of the skeleton; this provides a good representation of the weather scene in terms of hazards for an aircraft. Skeletons are stored within a graph structure and tracked among successive pictures by means of relaxation labeling processes. The deduced advection field is used to now cast the clouds evolution. Satisfying results are obtained concerning advection forecasts. Convective activity forecasts are promising, even if they must be carefully interpreted. [C2918]

#### "Possibilities of oil slick detection on the sea surface using radar"

Possibilities of oil films detection on the sea surface and distinction them from natural marine slicks and look-alikes phenomena are discussed. [C2919]

#### "Study of different configurations of tapered-slot antenna arrays for detecting buried objects"

In this paper, results of comparative study of several designs of tapered-slot antennas for subsurface applications are presented. To this end, influence of mutual arrangement of the antennas in bi-static configuration and placed in the antenna arrays has been studied using both simulations and experiments. Major attention is paid to the behaviour of the transmitting-receiving antenna pair near the ground surface. It was found that displacement of the antennas in the array by about a half of the antenna opening suppresses unwanted lateral coupling while the resistive loading strengthens the field radiated by the antenna into the



medium. Antennas with the displacement of about 0.5 of the width of the opening exhibit weak coupling that can be fairly well subtracted. The tapered-slot antenna arrays had been fabricated and tested in a test site for the detection of low-contrasted objects like anti-personnel mines. [C2920]

#### **"MIRA-CLE X: A new imaging MIMO-radar for multi-purpose applications"**

The research field of MIMO radar offers a bunch of new opportunities for various applications. Imaging MIMO radars can be used as a significant supplement to usual SAR and phased array radars and can extend the common applications for radar. MIRA-CLE X is an X-band MIMO radar consisting of 16 transmit and 14 receive antennas. During signal processing, 224 virtual antenna elements are generated to enable 2D radar imaging. This paper presents the radar system, the signal processing approach as well as a detailed analysis of first imaging results. [C2921]

#### **"Characterization of underground objects in UWB GPR by range profiling of phase"**

In this work, a new phase-based data processing method for UWB subsurface radar is presented. The method utilizes extraction of the phase information related to the signal reflected from the particular depth inside the medium under test. This phase depends on dielectric properties of reflecting targets and thus can be used for their discrimination. Both amplitude and phase data is combined further in common GPR image where brightness is related to the amplitude of reflection and the phase profile is represented by color. The phase-extraction algorithm does not employ heavy computations and therefore is well suited for practical applications. Advantages of the method as compared to other data processing methods are shown using simulated data. The method performance is demonstrated also in several experimental examples. [C2922]

#### **"Co-array weighting in minimum-redundancy arrays for radar image enhancement"**

The pronounced lobing of minimum-redundancy arrays-a class of thinned arrays-leads to image degradation in radar applications. Co-array weighting is investigated as a possible cure. Different distributions are considered. A comparative study of pattern degradation caused by random phase errors of the individual array elements is conducted. Multiple target detection-a critical aspect of nonlinear array processing-is addressed as well in this context. The potential of the proposed approach is critically assessed by simulation. The findings are confirmed by Ka-band radar experiments performed with a synthetic array. [C2923]

#### **"Experimental characterization of channel crosstalk in interleaved array antennas for FMCW radar"**

The inter-channel isolation of an FMCW radar with interleaved transmit-receive array antennas is, for the first time, characterized by measurements on an operative system. Theoretical predictions, based on full-wave simulations, are compared to computations from the measured antenna scattering parameters. In both cases, the received signals are re-combined by using ideal equi-phase and equi-amplitude power distribution networks. Two 1 to 32 Wilkinson power dividers are then fabricated and the radar inter-channel isolation is measured directly between the input (transmit) port and the output (receive) port of the system, recording a crosstalk of -34 dB. The effects of the system non-idealities on the antenna isolation are discussed. [C2924]

#### **"Target detection and positioning in correlated scattering using widely distributed MIMO radar"**

Multiple-input multiple-output (MIMO) radars use different sources of diversity to improve the performance of the radar. A MIMO radar in which angular diversity is achieved by using widely distributed antennas has been proposed to reduce the impact of the fluctuations of the target radar cross-section. This type of system is also known as the statistical MIMO radar. Typically, it has been assumed that the scattering amplitudes of the signals received by different antennas are either fully correlated or independent depending on the configuration. However, the antennas may see similar aspects of the target in some situations leading to correlation in the scattering. In this paper, we show how the correlation of the scattering can be exploited to improve the probability of detection and positioning. This is achieved by using a parametric model for the correlation of the scattering. We also investigate how the correlation can be used for estimating the direction of arrival with an uncalibrated MIMO radar system. [C2925]

#### **"New capabilities for PCL system: 3D measurement for receiver in multidonors configuration"**

For more than 15 years, the interest for PCL (Passive Coherent Location) system has been growing. It began with the analog waveforms like TV and FM; now the interest for digital waveform has increased and especially for DVB-T (Digital Video Broadcasting-Terrestrial). Despite all these interesting progress, some new requirements mentioned by several potential users of such PCL systems have appeared like an altitude estimation and especially for low altitude targets. Some works have begun in this area especially for tracking

consideration. In order to illustrate the PCL capabilities, we'll present some elevation measurements using a 2D array with DVB transmitters in a SFN (Single Frequency Network) configuration. The corresponding 3D tracking results will also be presented. These measurements will be analysed according to the "GPS" reference plots. In a second part, after a short description of the main differences between the three main kinds of illuminators (FM, DAB, DVBT), we'll consider the complementarities of these potential donors in order to outline some elementary rules for choosing the most appropriate waveforms according to our final requirements. [C2926]

#### "Radar probing of steep gravity waves. wave tank experiment"

Results of wave tank experiment on radar probing of steep gravity waves are discussed. It was shown that Ka-radar backscatter signal from cm -dm steep surface waves is connected with gentle breaking and parasitic capillary ripples generation; backscatter signal from dm-m surface waves is connected with strong breaking and free ripples generation. [C2927]

#### "An extended NLCS algorithm for Bistatic fixed-receiver SAR imaging"

Imaging of Bistatic fixed-receiver SAR which is azimuth-dependent, is rather different from monostatic SAR, because the relative position between the transmitter and the receiver is slow-time dependent. In this paper, the Range Cell Migration (RCM) characteristics of Bistatic fixed-receiver SAR are analyzed firstly. Then the nonlinear chirp scaling (NLCS) algorithm is presented and the residual phases caused by the NLCS processing are analysed as well. An extended NLCS algorithm based on sub-aperture approach is proposed to handle the case in which the residual phases cannot be ignored for Bistatic fixed-receiver SAR. Finally, a simulation with typical parameters is performed to verify the correctness of the extended NLCS algorithm. [C2928]

#### "SAR-MTI improvement using a-priori knowledge of the road network"

This paper focuses on the SAR-MTI processor improvement by using a priori knowledge of the road networks. The proposed technique is fit for civil applications where the traffic obeys to certain rules, such as being bound to a road with a predefined direction and complying, in average, with a velocity range. This possibility is demonstrated using a mixture of simulated and real data. [C2929]

#### "Accurate time-domain modelling of MEMS antennas for wireless telemetry systems"

A singularity-expansion-method-based technique for the accurate time-domain modelling of reconfigurable MEMS antennas for wireless telemetry applications is presented. Closed-form expressions of the radiated electromagnetic field in time domain are derived in terms of the newly introduced incomplete spherical Bessel functions depending on the complex frequencies of the natural resonant processes occurring in the antenna. [C2930]

#### "3-D calibration of InISAR imaging under a condition of phase ambiguity"

Interferometric inverse synthetic aperture radar (InISAR) imaging is a recently developed powerful radar three-dimensional (3-D) imaging technique, which combines the interferometric technique and the inverse synthetic aperture radar (ISAR). The true 3-D reconstruction of target scattering centers is obtained by interferometric phase processing of different two-dimensional (2-D) ISAR images from the various image planes. However, phase ambiguity is an involved problem in the interferometric process. This paper begins with the discussion on the InISAR imaging principle, followed by the description of three-dimensional calibration technique. By linear fitting phase differences between adjacent scattering centers of the same slant-range cell, the traditional phase ambiguity can be overcome. In the end, simulation results are provided to demonstrate the behavior of the proposed algorithm. [C2931]

#### "Millimeter-wave radar for civil applications"

This contribution gives an overview of civil state-of-the-art and also some novel applications of radar sensors in the millimeter-wave frequency range, together with some general principles and a number of examples of such radar systems. [C2932]

#### "EuRAD 2010 brief author index"

{no data available} [C2933]

#### "Reviewers"

{no data available} [C2934]

## "Conference committees"

{no data available} [C2935]

## "Welcome to EuRAD 2010"

I am very pleased to welcome you on the 7th European Radar Conference which is held this year in Paris as part of the European Microwave Week (EuMW). Every year, since the beginning of this conference seven years ago, the interest in the Radar activities grown. This is due mainly to the quality of the papers, workshops and focused sessions which have been proposed during the past conferences. This level of quality has been achieved thanks to the high class research performed in advanced, either from university or from industry laboratories in the world and thanks also to the rigor of the Technical Committee which review and select the papers. The number of proposed contributions has continuously increased during the seven years and EuRAD is now established as one of the largest European and worldwide Radar events. EuRAD submission is now more than 15% of the whole EuMW which creates the necessity to increase the duration of this conference to two full days. [C2936]

## "EuMW2009 rome prizes"

{no data available} [C2937]

## "EuMA awards"

{no data available} [C2938]

## "Welcome from the president of the European Microwave Association"

It is a privilege to welcome you on behalf of the European Microwave Association (EuMA) to the 2010 European Microwave Week (EuMW) in Paris. EuMA is the organisation behind the Week, we are a non-profit international association based in Belgium, with the mission to promote microwaves in Europe and to foster networking between microwave scientists and engineers in Europe. And the European Microwave Week is the key event serving this purpose. [C2939]

## "Welcome to the 13th European Microwave Week 2010"

EuMW continues its series of successful events with the 13th European Microwave Week 2010 which will be held at the CNIT la Défense, Paris, France from 26 September to 1 October 2010. This conference series has continued to grow and is now the premier event in this field in Europe. This event gathers all the international microwave community around four themed conferences: -The 40th European Microwave Conference (EuMC)-The 5th European Microwave Integrated Circuits Conference (EuMIC)-The 7th European Radar Conference (EuRAD)-The 3rd European Wireless Technology Conference (EuWiT) [C2940]

## "Track-before-detect algorithms for bistatic sonars"

Track-before-detect (TBD) algorithms can improve track accuracy and follow low signal-to-noise ratio targets. A price paid for this increased performance is the high computational complexity of TBD implementations. In this work, we develop a new TBD approach capable of handling raw hydrophone data. In order to learn more about its performance and feasibility when applied to sonar, we use data from the sea trial PreDEMUS'06 with DEMUS sensor array of NATO Undersea Research Centre. As a first step, we introduce the sensor model for a bistatic sonar based on DEMUS receivers. Then, we formulate the TBD problem at hand as a binary hypothesis testing problem and derive a class of adaptive algorithms by using design procedures based upon the generalized likelihood ratio test. Remarkably, such detectors guarantee the constant false track acceptance rate property under the design assumptions with respect to the overall spectral properties of the noise. A preliminary performance analysis is presented. Finally, we discuss its potential to implement automatic track continuation and to prepare automatic classification for temporarily weak targets as these tasks are usually the challenges multistatic sonar systems have to overcome. [C2941]

## "Copyright page"

The following topics are dealt with: intelligent platform networks; adaptive learning algorithms; cognitive radio; spectrum sensing and management; signal estimation and tracking; Bayesian machine learning; cognitive radar

processing; waveform agile intelligent adaptive sensor signal processing; collaborative sensing techniques; learning theory and modelling; and game theoretic tools for cognitive radio. [C2942]

### "Vessel detection and classification: An integrated maritime surveillance system in the Tyrrhenian sea"

In recent years a number of organizations, both national and international, have put significant efforts in developing knowledge-based integrated maritime surveillance (IMS) systems. The final aim is to have a clear picture of the position, classification, identification and movement of cooperative and non-cooperative targets entering and leaving the 200 nautical miles limit of the Exclusive Economic Zone (EEZ). Each sensor (i.e. satellite-based, ground-based, shipborne or airborne) has its own task and, in such a context, high frequency (HF) surface wave (SW) radars are inexpensive tools for long range early warning applications in open waters. They allow maximizing the effectiveness in dealing with fisheries protection, drug interdiction, illegal immigration, terrorist threats, search and rescue tasks. This paper focuses on the possibility of combining automatic identification system (AIS) data with HFSWR data for vessel detection and classification purposes. Three algorithms for target detection in compound Gaussian HF sea clutter are presented and their performance evaluated. The combined use of AIS plots provided by cooperative targets can allow the operator to discriminate non-cooperative targets and possible threats. The concurrent exploitation of AIS and HFSWR data is presented and discussed by means of real data recorded during the NURC experiment in the northern Tyrrhenian Sea in May 2009. [C2943]

### "Metacognition in radar"

An airborne ground looking radar sensor's performance may be enhanced by selecting algorithms adaptively as the environment changes. A short description of an airborne intelligent radar system (AIRS) is presented with an in-depth description of the knowledge based filter and detection portions. A second level of artificial intelligence (AI) processing is presented that monitors, tests, and learns how to improve and control the first level. This approach is based upon metacognition. [C2944]

### "Millimeterwave radar network for foreign object detection"

Millimeterwave radar sensors are netted to cover a sufficient region of an airport and deliver as well information on position as classification of debris. To be able to miniaturize the antenna assembly, which is critical for the vicinity of a runway, the 220-GHz radar band is used. Use of this band also allows to achieve a wide signal bandwidth and consequently a high range resolution. [C2945]

### "The radar system and information flow"

The information flow through a radar system channel is studied for various component design choices including the radar measurement function, signature feature selection, and classifier decision rule. A simplified target scattering model is used to analyze the application of the information theoretical channel model. [C2946]

### "Adapting a MIMO/phased-array radar transmit beampattern to target location"

Proposed MIMO and hybrid MIMO/phased array (HMPAR) radar systems have the potential for tremendous flexibility in the choice of the transmit beampattern, through the selection of multiple transmitted signals. This paper considers how one might exploit that flexibility in light of prior information or uncertainty in target spatial location, for parameter estimation or tracking applications. We first consider an idealized problem of distributing energy across multiple target sites given a prior probability distribution on those sites. It is shown that the optimal allocation of energy would be proportional to the square root of the prior probability. Second, we propose a method to approximate this optimal distribution of energy using a MIMO radar or HMPAR radar system. The method chooses signals that realize an intrapulse beamspace scan over the region of interest, with a nonuniform distribution of scan points matched to the desired distribution of energy. [C2947]

### "Software defined RADAR a state of the art"

A software-defined radar is a versatile radar system, where most of the processing, like signal generation, filtering, up-and down conversion etc. is performed by a software. This paper presents a state of the art of software-defined radar technology. It describes the design concept of software-defined radars and the two possible implementations. A global assessment is presented, and the link with the Cognitive Radar is explained. [C2948]



### "Adaptive radar detection: A subspace identification approach"

We address adaptive detection of Swerling 2 pulse trains by an array of antennas. The disturbance is modeled in terms of a state space model and the ideas of subspace identification are used to come up with a GLRT-based detector. Such detector is compared by Monte Carlo simulation with a Kelly's detector derived assuming that returns are temporally uncorrelated (but spatially correlated) and that a proper set of secondary data is available. [C2949]

### "A unique calibration method testified by X-band polarimetric radar"

This paper explores a unique calibration method for polarimetric radar without requiring any calibration targets. The error of the polarimetric scattering matrix measurement is modeled as antenna distortion matrices and channel distortion matrices. These distortion matrices can be determined using a signal generator in anechoic chamber. The performance of the calibration method is analyzed by simulation. Its validity is verified through the experiment of an X-band polarimetric radar system. [C2950]

### "CFAR detector using GIS information"

In order to realize the constant false alarm ratio (CFAR) processing, the adaptive threshold should be used in radar signal detection. The threshold of the CFAR detector can be calculated using the clutter of range bins nearby the cell under test. In the real world, the clutter environments is always non homogeneous, which result in the performance degradation of the CFAR detector. In this paper, the CFAR detector using geographic information system (GIS) is proposed. With the knowledge of the clutter environment, the performance of the CFAR detector can be improved remarkably. The IPIX radar data are used to validate that the CFAR detector using GIS information is outperform the other conventional CFAR detectors. [C2951]

### "Radar waveform design for detection of weapons"

We present waveform design based on signature exploitation techniques for improved detection of weapons in urban sensing applications. We consider a single-antenna monostatic radar system. Under the assumption of exact knowledge of the target orientation and, hence, known impulse response, matched illumination approach is used for optimal target detection. For the case of unknown target orientation, we propose waveform design based on subspace decomposition of the target impulse response matrix corresponding to the various aspect angles. Numerical electromagnetic modeling is used to provide the impulse responses of an AK-47 assault rifle for various target aspect angles relative to the radar. Simulation results depict an improvement in the signal-to-noise-ratio (SNR) at the output of the matched filter receiver for both matched illumination and subspace waveforms as compared to a chirp waveform of the same duration and energy. [C2952]

### "Study on retrieval methods of soil water content in vegetation covering areas based on multi-source remote sensing data"

Fusion image of SAR (Radar-sat image) combined with visible spectrum remote sensing image (TM image) is used to extract soil and vegetation water content in arid oasis taking the delta oasis of Weigan and Kuqa rivers in Xinjiang as the study area. Based on the Normalized Difference Moisture Index extracted from homochromous visible spectrum remote sensing data, this thesis utilizes "water-cloud model" to wipe off vegetation influence from total backscattering coefficient of radar data and sets up the relationship between soil backscattering coefficient and soil moisture. The Result shows that in arid and semi-arid area where the main crops are cotton and corn, the combination of C- band HH polarization radar data with visible image performs well in the study of removing vegetation influence while retrieving soil water content in medium vegetated areas. [C2953]

### "Rapid waveform adaptation for nearly optimal detection in colored interference"

A cognitive radar can dynamically design its transmit waveform in response to changing environmental knowledge, which may be obtained a priori, estimated online, or both. We consider the detection of targets in wide-sense stationary additive colored Gaussian noise. Cognitive radar has been shown to provide potentially significant improvements for this problem. However, existing algorithms may be too computationally demanding for some scenarios. We present an approach that can be implemented in the most demanding scenarios. This approach trades optimality for reduced computational complexity by computing a large library of nearly optimal waveforms before operation, and retrieving them rapidly at runtime. [C2954]

### "Wind direction manifestation on HF ocean radar echoes"

A direct measure from the spectra of HF radar sea echoes is the ratio of energy in the dominant Bragg peaks. If

a single lobe is assumed for the directionality then two radar stations can be used to provide a closed solution for the direction of the lobe. In this work we examine the potential of using just one radar station to derive directional information about wind fields. It is shown that HF radar Bragg ratios are effective in providing timing and location information for features appearing on Mean Sea Level synoptic charts. [C2955]

#### **"Waves in the Southern Great Barrier Reef"**

A brief description of three different platforms (WAVEWATCH III, Acoustic Doppler Current Profiler mooring and HF ocean radar) with directional wave measurement capabilities is provided. Initial results of directional wave and wind patterns derived from observations within the southern Great Barrier Reef, Australia, show consistency with the WAVEWATCH III model. These early findings are promising for future wind-wave investigations and validation studies in this region. [C2956]

#### **"Can vertical mixing from turbulent kinetic energy mitigate coral bleaching? An application of high frequency ocean radar"**

Coral bleaching is an ecological response to stressful physical conditions observed to occur when strong insolation coupled with stratification of the water column leads to anomalous warming of the surface water. Stratification requires calm winds, the absence of waves, and an absence of currents: conditions which result in limited mixing of the water column and thus confine heat due to insolation at the ocean surface. There is a strong need to identify which of the physical parameters are more significant at any given time and, more importantly, to monitor the physical parameters in near realtime to serve as a tool for long-term planning and management for marine parks and coastal waters. This paper reviews the contribution that currents make to mixing in the water column through the dissipation of turbulent kinetic energy and takes a further step to evaluate the use of surface current data to provide an index of vertical mixing. In this work, when the surface current speed is greater than a critical value, the water column is found to be vertically mixed even in the absence of wind or waves. A phased array HF Ocean Radar deployed in the southern part of the Great Barrier Reef provides a map of surface currents with high spatial resolution (4km) every 10 minutes over the grid. These surface currents are used to predict vertical stratification and mixing which can then be used as an indication for conditions under which bleaching might occur. [C2957]

#### **"Time domain numerical simulation of microwave backscattering from sea surface for radar remote sensing"**

Time domain numerical simulation technique has been developed to understand microwave backscattering mechanisms and evaluate sea surface observation methods. Backscattering coefficients and Doppler spectra can be obtained by this simulation technique. Physical optics approximation is applied to calculate scattering electric fields. The validity of the simulation has been verified by comparing with the results of the experimental basin. The results indicate that the simulation technique is effective to calculate microwave backscattering from the water surface changing in time. As an application of the simulation, we have simulated microwave backscattering with a pulse Doppler radar to evaluate sea surface observation methods. Radar images of backscattering coefficient and Doppler velocity have been generated. The results of the simulation show that radar images of Doppler velocity are more effective than images of backscattering coefficient for sea surface observation. [C2958]

#### **"Rapid deployable HF RADAR for Norwegian emergency spill operations"**

The Norwegian company CodarNor A/S, with funding from the Norwegian Clean Seas Association for Operating Companies (NOFO) and from Innovation Norway through an industrial research and development contract, is developing a self-contained rapid deployment HF radar which can be deployed by helicopter or other means to remote and rugged locations along the Norwegian coast and operate autonomously, communicating surface current data in real time back to operators, the Norwegian Coastal Administration and drift modelers. Large-scale 2-D current maps collected from these rapid-deployable systems will be used to improve spill response efforts by blending data with drift model currents for improved drift predictions and cleanup vessel management. [C2959]

#### **"Towards the use of a team of USVs for civilian harbour protection: The problem of intercepting detected menaces"**

Protecting civilian harbours is a field which has received increasing interest after the attack of September 11th. Exploiting a team of Unmanned Surface Vehicles (USVs) for the protection of harbours is one of the areas under major investigation. Indeed the USVs could be used to perform patrolling around the crucial waterways or to investigate possible suspect vessels, increasing the effectiveness of the security system, while at the same time

decreasing the number of human beings directly exposed to threats. The coordination of such a team of USVs is the goal of an on-going joint research project, the Swarm Management Unit (SMU), between the authors' organization. This work presents the latest results of the SMU project, i.e. a menace interception system composed by the on-line selection of the best interceptor coupled with the off-line optimization of the positioning of the team of USVs. [C2960]

#### "Sea surface current mapping by Radar Doppler Current Profiler"

A Radar based method has been developed to measure surface currents directly. Applied techniques, results, capabilities and applications of this method will be discussed. [C2961]

#### "On the detection of marine mammals with ship-borne polarimetric microwave radar"

Collisions between ships and whales are not rare occurrences. Apart from constituting a major cause of death for whale species which frequent busy oceanic areas such as the North Atlantic, such collisions often result in damage to ships. Thus there is keen interest in finding reliable means of detection of whales at sufficient range to ensure successful collision avoidance. In this paper we present the results of experiments aimed at establishing the potential of polarimetric microwave radar to provide such a means. The key element in our approach is the construction of a polarimetric filter which enhances the contrast between the disturbed sea surface around the whale and the ambient sea. The results suggest that detection can be achieved under conditions where conventional uni-polar radars such as those normally found on merchant ships would fail. [C2962]

#### "X-Band radar derived sea surface elevation maps as input to ship motion forecasting"

Nautical X-Band radars used for navigation can also be used to determine spectral and individual wave properties. The sea surface reflects the incident radar beams and wave fronts become visible as stripe like pattern of high back scatter on the radar screen. When connected to a conventional nautical X-Band radar, the Wave Monitoring System WaMoS II exploits this imaging of waves to detect full directional wave spectra and to derive statistical sea state parameters as well as surface currents. WaMoS II is continuously improved with new features being developed. In particular, the sea surface elevation maps derived by WaMoS II allow to investigate and describe the spatial and temporal development of 3D ocean surface waves. The European Joint Industry Project 'On board Wave and Motion Estimator (OWME)' used this measurement technique to provide the wave information that is required to predict periods of quiescent vessel motions. A task that offers valuable support for various offshore operations like e.g. the tensioning of a tanker or the landing of a helicopter. This contribution gives an overview of the overall OWME system design showing first validation results, focusing on the method to derive wave trains using the WaMoS II system. [C2963]

#### "Waveform design with stopband and correlation constraints for cognitive radar"

One of the main objectives of cognitive radar is to adapt the spectrum of transmit waveforms to certain needs, such as avoiding reserved frequency bands or narrowband interferences. Besides spectral requirements, good correlation properties of the transmit waveforms are also desired in specific applications, such as range compression. Moreover, practical hardware constraints usually require the transmit waveforms be unimodular (i.e. only phase-modulated). In this paper, we propose a new algorithm named SCAN (stopband cyclic algorithm new) to design unimodular sequences with spectral power suppressed in arbitrary bands and with low correlation sidelobes as well. The SCAN algorithm, which starts from random initializations, can generate many sequences possessing similarly good properties. Furthermore, the SCAN algorithm is based on FFT (fast Fourier transform) operations and thus is computationally efficient, which facilitates long-sequence design and real-time waveform update. [C2964]

#### "Perimeter patrol on autonomous surface vehicles using marine radar"

Perimeter patrol enhances the utility of autonomous surface vehicles (ASVs) by enabling many security and scientific missions, including harbor protection, water sampling, and geological survey. We present a novel approach to perimeter patrol that uses only two sensors: commercial off-the-shelf available marine radar and the heading information from a GPS. Our algorithm performs computer vision morphological operations on the radar image to find a suitable path around shore and choose an appropriate next waypoint. Our method has proved robust to a variety of field conditions, allowing us to demonstrate the autonomous navigation of a 3.5 km perimeter lake. [C2965]

#### "Slocum Glider energy measurement and simulation infrastructure"

Autonomous underwater vehicles (AUVs) are indispensable tools for marine scientists to study the world's oceans. Depending on their missions, AUVs are equipped with advanced sensors (sonar, cameras, acoustic communication, bio-sensors), have on-board computers for data analysis (image analysis, data compression), and are capable of on-board decision making (resource planning, swarming). Since AUVs operate solely on battery power, power and energy management is a crucial issue. Mission-critical tradeoff decisions have to be made between energy consumption and sensing, data processing, and communication activities. Mission planning has to consider these tradeoffs when provisioning resources for expected future events, or when dealing with changing environmental conditions such as weather, water currents, and seafloor profiles. Effective power and energy management requires knowledge about the actual energy consumption of each active component within the AUV. Effective planning requires simulators that can predict energy consumptions based on expected future events and environmental conditions. In this paper, we discuss the design and implementation of a power measurement infrastructure for the Teledyne Webb research Slocum glider. This infrastructure can be used for online power/energy management or to better understand the time-dependent energy consumption profile of the active glider components during a particular mission. We also discuss the design of a new simulation environment for the Slocum glider which uses the power/energy data obtained by our measurement infrastructure, in addition to seafloor and coastal radar information. We illustrate the effectiveness of the new tools in the context of planning a glider flight across the continental shelf off the coast of New Jersey. [C2966]

#### "Doppler velocity dealiasing with millimeter wave radar RHI data"

Millimeter wave radar has a unique advantage on detecting cloud microphysical structure. However, it is easy to cause the velocity aliasing due to its short wavelength. Velocity dealiasing is an effective means of detecting wind field information with Doppler radar. This paper reviews the cause of velocity folding and proposed a human-machine interaction method aimed at millimeter wave radar in the RHI scanning. It is concluded that the algorithm is very efficient and can produce high quality velocity data. [C2967]

#### "Simultaneous estimation of AOA and polarization using differently polarized antennas"

This paper explores the simultaneous estimation method of the AOA and the polarization of the signals. Based on two differently polarized antennas, the simultaneous estimation is achieved with consideration of the cross-polar and co-polar patterns of the antennas. The performance of the method is analyzed. The validity is testified by the experiment of P-band radar system. [C2968]

#### "Estimating the parameters of a moving target in MIMO radar with widely separated antennas"

In this paper, we develop a new maximum likelihood (ML) moving target parameter estimation technique for multiple-input multiple-output (MIMO) radar. It is required for this technique that different receive antennas have the same time reference, but no synchronization of initial phases of the receive antennas is needed and, therefore, the estimation process is noncoherent. The target motion within a certain processing interval is modeled as a second-order polynomial whose coefficients are given by the initial location, velocity, and acceleration of the target. The proposed ML estimator is able to jointly process the data collected from multiple consecutive radar pulses. It is shown that the considered ML problem simplifies to the classic "overdetermined" nonlinear least-squares problem. The proposed ML estimator requires multi-dimensional search over the unknown location, velocity, and acceleration parameters. The performance of the proposed estimator is validated by simulation results. [C2969]

#### "An improved monopulse angular tracking method using adaptive digital beamforming technique"

Monopulse radar is widely used for its accurate angle measurement. However, when jamming occurs, especially in mainlobe, the performance of the monopulse technique for target estimation deteriorates greatly. In this paper, an improved method for monopulse angular tracking is proposed, which can be divided into two stages. The first one involves a digital beamforming system which is used to suppress sidelobe jamming while maintaining the mainlobe shape. The second stage is used to suppress mainlobe jamming while maintaining the monopulse ratio undistorted. The computation load of the proposed method is lower compared with that of the same category method. Simulation results are given which demonstrate that the presented approach can suppress jamming effectively, while maintaining the perfect performance with mainlobe undistorted. [C2970]

#### "Session E3: Radar techniques and applications"

{no data available} [C2971]



### "Passive radar imaging of moving targets with sparsely distributed receivers"

We develop a novel passive image formation method for moving targets using measurements from a sparse array of receivers that rely on illumination sources of opportunity. We use a physics-based approach to model the wave propagation and develop a passive measurement model that expresses the measurement at each receiver in terms of the measurement at a different receiver. This model eliminates the need for knowledge about the transmitter locations and waveforms in the proposed image formation method. We formulate the image formation problem as a Generalized Likelihood Ratio Test (GLRT) for unknown target location and velocity using the proposed passive measurement model. We form the image in spatial and velocity space using the space- and velocity-resolved test-statistics. [C2972]

### "3D Electromagnetic imaging using compressive sensing"

We develop the application of compressive sensing (CS) for solving general inverse electromagnetic problems such as three-dimensional (3D) microwave imaging. The goal is to estimate locations of unknown, but sparse targets, hidden inside dielectric bodies. The potential of CS for localizing sparse targets in vacuum or buried in ground was shown in previous work. We extend the proposed schemes by considering arbitrary embedding medium and exploiting dual-polarized measurements. We compare the performance of CS and beamforming in the breast-cancer estimation problem. [C2973]

### "MIMO GMTI radar with multipath clutter suppression"

This paper address ground-moving target indicator (GMTI) radar operation in the presence of strong multipath spread-Doppler clutter (SDC). Spacetime adaptive processing (STAP) for single-input-single-output (SIMO) radar is designed to mitigate direct-path SDC which leaks into the sidelobes of a moving radar platform. However, multipath SDC often returns via the receiver mainlobe and cannot be suppressed in a SIMO radar without also canceling the target. In this paper, we study multipath SDC mitigation using multiple-input-multiple-output (MIMO) GMTI radar. Clutter loci and adaptive array patterns for MIMO GMTI are presented in multipath SDC. By achieving range-dependent nulling on transmit, the effectiveness of MIMO GMTI radar at suppressing multipath SDC is shown. [C2974]

### "A miniaturized broadband four-port antenna based radar detection system"

A novel compact four-port antenna based receiving radar detection system is presented. Emphasis is placed on the antenna and pattern transform algorithms development. The antenna, with size of  $113 \times 113 \times 33.7\text{mm}^3$ , operated within 1.0-1.8GHz ( $S_{11} < -10\text{dB}$ ) and 5.5dBi single port gain, is designed and integrated successfully in a specific cylindrical stepped conductor. Two different pattern transform algorithms corresponding to 3 excited modes for the four-port antenna are developed and firstly compared with indoor experimental results. It shows that a indoor target can be detected successfully by the radar system with spatial resolution of 3 degrees, which is agreement well with the numerical simulations. [C2975]

### "Fast calculation of wide-band RCS for three-dimensional PEC objects based on preconditioned AWE technique"

The asymptotic waveform evaluation (AWE) technique combined with the method of moments (MOM) is often applied to accelerate the calculation of the wide-band radar cross section (RCS) of the target. However, the technique is still quite time-consuming for solving the inverse of impedance matrix when the objects are electrically large. In this paper, Krylov subspace iterative methods are applied to solve the matrix equation derived from electric field integral equation instead of matrix inverse. The dual threshold incomplete LU factorization preconditioner is adopted to improve the convergence behavior of the Krylov subspace iterative methods. The numerical computation shows that the results in this paper are in good agreement with the results obtained by the method of moments at each frequency, and the computational efficiency is improved greatly. [C2976]

### "Signal based parameter estimation for precise circular-scanning SAR imaging"

Images obtained from circular-scanning synthetic aperture radar (SAR) are mainly used for self-guidance system using the well-known scene matching techniques, where the geometry accuracy of the images is very important for high precision target location. Due to the existence of errors in parameters measurement from inertial navigation system (INS), for example, velocity and beam scanning azimuth angle especially, imaging is not optimal and geometry distortion correction also not absolute. In this paper, a new method of velocity error and scanning azimuth angle error compensation is proposed based on echo data. Doppler navigation instrument can be used to measure velocity based on Doppler shift, so Doppler measuring velocity technique is adopted in the

compensation of velocity and scanning azimuth angle error. The experimental result of a circular-scanning SAR system is given to demonstrate the validity of the proposed methodology. [C2977]

### "Target automatic recognition based on ISAR image with wavelet transform and MBLBP"

A novel feature extraction algorithm of Inverse Synthetic Aperture Radar (ISAR) image based on wavelet transform (WT) and multi-scale block local binary pattern (MB-LBP) is proposed in this paper. Firstly, the mathematical morphology method is adopted to enhance ISAR image. Secondly, 2D wavelet transform is used to get the low frequency sub-band image from the enhancement ISAR image. Then, ISAR image is divided into small regions from which block local binary pattern (BLBP) with different weight histograms are extracted and concatenated into a feature vector to be used as an efficient ISAR descriptor. At last the classification is performed by using a nearest neighbor classifier with Chi square as a dissimilarity measure in the computed feature space. The experimental results on three kinds of aircraft targets show that the method performs very well. [C2978]

### "Influence of vibration between shipboards on ship-sea integrational electromagnetic scattering in high frequency"

The vibration between shipboards on ship-sea integrational electromagnetic Scattering is presented. The numerical results of the integrational target have been obtained using MLFMM in High Frequency, computing the RCS as a function of the elevation angle and vibration angle. It has been observed that as for two different polarizations, the RCS of the integrational target have raised a dozen of dBsm as compare to non-vibration case, depending on the elevation angle and vibration angle. The RCS for each of those situations can be shown in the results section. [C2979]

### "Range Instantaneous Doppler ISAR imaging based on FRFT"

Very high resolution inverse synthetic aperture radar (ISAR) imaging of maneuvering targets is a complicated task. Due to the phase error caused by target's non-cooperative motion, we can't use conventional Fourier transform in ISAR imaging reconstruction. Therefore, the method of Range Instantaneous Doppler (RID) technique based on Fractional Fourier Transform (FRFT) is presented. First, we define a model of the ISAR received signal that is valid for maneuvering targets. In order to eliminate phase error caused by translational motion components, the strong scatter signal that backscattering from the target is used for phase compensation, which can be extracted from the echoes using FRFT. Finally, RID is proposed to reconstruct ISAR image. After time-frequency transform named SPWVD, we get the instantaneous Doppler frequency. Even without exact motion compensation, a clear image of the target, such as aircraft, is obtained, which avoids the insufficiency of conventional Fourier-based image algorithm. The theoretical analysis is validated by presenting and discussing the simulation results. [C2980]

### "Motion compensation for spaceborne/airborne hybrid bistatic SAR"

This paper concerns the compensation of known trajectory deviations in spaceborne/airborne bistatic SAR (SA-BSAR). And the motion compensation technique is effectively incorporated with the high-precision frequency domain imaging processing for SA-BSAR. Simulation results validate the proposed motion compensation method. [C2981]

### "A Migrating Target Indicator for wideband radar"

The standard way to suppress clutter in narrowband radar is to use Moving Target Indicator (MTI) cancellation techniques. High Range Resolution (HRR) radars are becoming more and more important because they can detect and track targets more accurately. As for such radars the bandwidth is increased, the resolution is decreased and leads to target range migration over the coherent pulse interval (CPI). Due to this range walk, standard low resolution MTI processing is not adapted anymore to HRR MTI radar data. We propose here to extend the principle of the MTI processing to the wideband case. We refer to this method as the Migrating Target Indicator (MiTI), since it eliminates the non-migrating targets from the received signals. [C2982]

### "Signal and image processing applications in radar ocean observations"

Signal processing is quite intensive when dealing with radar sensors. In this paper, the ability of spaceborne radars for imaging ocean surface features is explained and some of the very actual results are shown through several illustrations. The aim of such means to watch the earth is to provide useful information on a global basis regardless of the weather conditions (especially clouds) and in daylight as well as at nighttime. In this context, the main mean of observation is, without any doubt the SAR or Synthetic Aperture Radar [1]. From a signal

processing perspective, radar data and images are a very interesting domain of research. Indeed, they present non-gaussian, non-stationary and often non-linear characteristics, thus raising the challenge of their interpretation. We will first focus on the SAR signal processing and the mechanisms allowing a radar image of the ocean to be formed. Then we will detail some of the special characteristics when using SAR processing. Indeed this processing is done at the ground receiving station and present several very interesting challenges in terms of statistical behavior of the data and signal processing. The following section will deal with signal and image processing techniques aimed at achieving very high resolution spectral analysis, especially in 2D. Finally, we will present several of the main features that are detected and we will give some of the inferred parameters that can be measured and used by the oceanographic community. We will also, describe some of the environmental issues associated. [C2983]

#### "Generalization of Automatic Censored Mean Level Detector (ACMLD) for MIMO radars"

Constant False Alarm Rate (CFAR) processors are useful for detecting radar targets in background for which all parameters in the statistical distribution are not known and may be nonstationary. Many CFAR techniques have been proposed for conventional radars in nonhomogeneous background. One of the most robust CFAR detectors in multiple target situations is Automatic Censored Mean Level Detector (ACMLD) which does not require any prior knowledge about the number of interfering targets. In this paper, ACMLD algorithm is generalized for Multiple Input-Multiple Output (MIMO) radar. An exact expression for the false alarm probability of the proposed algorithm (M-ACMLD) is presented. Then, the performance analysis of M-ACMLD is studied in both homogeneous environment and multiple target situations. [C2984]

#### "CFAR detectors in presence of jammer noise"

Cell Averaging (CA)-CFAR detector is an optimum detector under the assumption of Rayleigh distributed homogenous noise background, but in presence of clipped jamming noise, it does not have the best performance. In this paper, we compare CA, GO, SO, OS, OSGO and OSSO conventional CFAR detectors to obtain superior CFAR detector in clipped jamming noise. Simulation results show that the OS-CFAR detector not only provides low loss CFAR performance in exponential background but also performs better than that of CA in clipping jammer noise situations. On other hand, by using OS detector instead of CA detector in radar, it saddles about 3dB more loss to jammer noise generator. [C2985]

#### "Front matter"

The following topics are dealt with: power electronics; digital circuits; data converters; video and image processing; wired communication; digital signal processing; analogue circuit; pipelined ADCs; RFID; RF and antenna; MEMS and sensors; biomedical circuits and systems; CMOS power regulator; GPS signal; telephone remote control system; VLSI interconnects; continuous-time delta-sigma modulator; optical transmission; FPGA; X-band polarimetric radar; wireless-LAN transceiver; nanoMOSFET; single-electron transistor hybrid circuit; and implantable medical devices. [C2986]

#### "A wireless microwave sensor for remote monitoring of heart and respiration activity"

The aim of this paper is to present a new microwave contactless sensor for heartbeat and respiration activities. The system is operating on 9 GHz. It's composed of two parts: a hardware one based on Doppler radar with a Digital Multimeter, and a software one based on the acquisition of the signals and the separation of the 2 informations of heartbeat and respiratory signals using simple filtering method with Labview. [C2987]

#### "An automatic feature extraction technique for GPR data processing in electromagnetic inverse scattering problems"

This work presents an automatic feature extraction technique for the analysis of GPR data. Despite the rapidly increasing demand for such technology, the interpretation of radargrams is still a specific task which only expert users can accomplish. As a radar probing system, in fact, the GPR is able to measure the backscattered EM waves from buried targets and the travel time of these signals, information which cannot be directly exploited, but that needs to be used in inverse scattering problems for the evaluation of the dielectric properties and spatial positions of subsurface targets. Starting from a practical example of GPR employment-the reconstruction of pavement's vertical cross section-the evaluation of the two above-mentioned features is carried out through an energy-based method, which ensures high performances and robustness to signal interference. [C2988]

#### "Model based adaptive detection algorithm with low secondary data support"

In this paper the problem of adaptive target detection in structured Gaussian clutter is considered. The clutter is

modeled as an auto-regressive process with known order but unknown parameters. To solve this problem, we have modified a well known adaptive detector (Kelly's GLRT) in four different forms. In this detector an estimation of covariance matrix is needed. In order to estimate the covariance matrix, we estimate the AR parameters based on secondary data and use the results in covariance matrix estimation. Then, we use the estimated matrix in the detector structure. In order to estimate the AR parameters using more than one set of data, we have extended four classical AR parameter estimation techniques to use more data sets. The performance of the proposed detectors have been evaluated using Monte-Carlo simulations and compared with each other. [C2989]

### "Sparse component analysis for linear mixed models"

When seeking for a sparse solution of a linear model, a common technique is the search of a solution with minimum  $\ell_1$  norm. In this paper, we present a new approach for the case of sparse linear mixed models. We combine the EM algorithm for solving the inverse problem with a decision test that guarantees sparseness by eliminating the statistically null components of the solution. We address its performance by means of simulations and illustrate its use with real radar data demonstrating its potential applications. [C2990]

### "A recursive model for partially correlated $\chi^2$ targets"

This work considers the problem of  $\chi^2$  target detection in normal (Gaussian) noise. The single pulse power, and target RCS, are  $\chi^2$  distributed with an arbitrary form factor  $k$ . The correlation between pulses is determined by target dynamics, according to a simple rule of thumb. The sequence of target pulses is constructed using a recursive model of Markov chain, and the value of the correlation coefficient is derived. An approximation of 'strict sense  $\chi^2$ ' is assumed for the probability density function (p.d.f) of the sum of the integrated pulses. The form factor  $K$  of this density is calculated in terms of the correlation coefficient, number of integrated pulses and the form factor for the single pulse p.d.f- $k$ . By determination of the normalized threshold for the given  $P_{fa}$  (probability of false alarm), the probability of detection- $P_d$  can be obtained. One way to do these calculations is using the "universal detection equation" suggested by D.K Barton (7.2005). The model can be used in radar system performance analysis and in simulations. The advantage of these methods is the elimination of the use of tables and graphs, and enabling direct computations such as in multiple situation simulations. It can be done using commercially available advanced mathematical software. [C2991]

### "Covariance-informed detection in compound-Gaussian clutter without secondary data"

We consider the problem of detecting a signal of interest in the presence of compound-Gaussian clutter, without resorting to secondary data in order to infer the clutter covariance matrix. Towards this end, we assume that both the texture  $\tau$  and the speckle covariance matrix  $R$  are random variables with some a priori distributions. Marginalizing with respect to these variables, the probability density function of the observed primary data is derived, leading to a closed-form expression for the generalized likelihood ratio test (GLRT) of the problem at hand. Accordingly, the GLRT assuming that  $\tau$  is deterministic is also derived. The two detectors are assessed through numerical simulations. [C2992]

### "Smoothing irregular data using polynomial filters"

To make provision for irregularly occurring updates a "variable-step" polynomial filter is derived which improves the smoothing-, and coasting capabilities of the 1-step predictor and the current-estimate polynomial filters. Similar to the original filters, the variable-step polynomial filter comprises an auto-initialising expanding memory filter which later switches to a fading memory filter. Results are compared by running the proposed and original filter versions in parallel. [C2993]

### "Oil spill detection in sar images using wavelets and morphology"

Oil spills at sea surface can be found at nearby vessels due to clearing tanks while sailing or by accidents. Problem of oil spill detection is considered in the paper. The basis source for the detection is radar image. The proposed method combines wavelets and morphology. Preliminary research shows that any type of morphology structural element can be used for the purpose as long as it is not too big kernel. [C2994]

### "Copyright page"

The following topics are dealt with: magnetic resonance imaging; signal processing; data processing pipeline; MIMO radar; underwater acoustic communication; covariance matrix and wireless networks. [C2995]



### **"Development of radar simulator software using AIS data for ship data"**

A radar simulator for ships is a device for effective education concerning safety in ship navigation. In existing radar simulators, it is necessary to simulate surrounding ship data, and much effort is required to input such data. Therefore, this study aims to address this problem using AIS (Automatic Identification System) data. The proposed radar simulator system simultaneously achieves the following functions: (1) the creation and display of simulated radar images based on AIS data and (2) the display and overlay of AIS information on radar screens. As a result, it is possible to train individuals in ship maneuvering using actual ship traffic of a specific ocean area as the environment in the surroundings of one's own ship. Moreover, this proposed radar simulator system works on a general PC. Thus, it is possible to have two or more people simultaneously participate in training using a network with two or more PCs. In this paper, the outline of the proposed system and simulation results are described. [C2996]

### **"High-resolution airborne SAR interferometry mapping application in Huashan mountain"**

Interferometric synthetic aperture radar (SAR) data offer the opportunity to map the western area of China, acquired from the first Chinese multi-modes airborne SAR mapping system. DEM could be obtained through airborne interferometric pairs. Furthermore, the quality of the InSAR DEM may vary significantly depending on the local topography. Aims of the approach are to smooth the noisy InSAR data, to merge the different directions DEM from the complementary interferometric pairs, to eliminate effectively spurious terrain surface points, to generate an improved 3-D visualization of the InSAR DEM scene and finally to meet DEM product accuracy requirement based on the different topography condition with a scale of 1:50,000. [C2997]

### **"Robust environment perception based on occupancy grid maps for autonomous vehicle"**

For a purposes of reduction of driving workload, traffic accidents, and so on, autonomous vehicle systems, which can drive even though no human driver rides on, have been developed all over the world. Recently, it is considered that a part of such techniques play an important roll to energy saving. To navigate the autonomous vehicle in a complex environment, it is necessary to extract static objects precisely and robustly. Moreover, about dynamic objects, it is not enough to consider its existing position, and it is considered that estimating its motion and predicting its future position are strongly demanded. In this paper, for a solution of such problems, we propose an environment perception method using a LIDAR based on Occupancy Grid Maps. [C2998]

### **"DInSAR for land subsidence monitoring using high resolution COSMO-SKYMED SAR Data: Preliminary results compared with ASAR"**

DInSAR can map ground deformation phenomena over tens-of-kilometers-wide area with centimeter-scale accuracy level, and has been considered as a powerful tool. Because of the data availability, previous DInSAR applications were mainly base on ERS, JERS, ENVISAT ASAR, and RADARSAT-1 data with resolution coarser than 10m. Nowadays, several kinds of high resolution SAR data are available for DInSAR and there are high expectations for the application of these data. In this paper, COSMO-SkyMed SAR data and grid digital elevation model ASTER GDEM (30m resolution) are used as research data. COSMO-SkyMed SAR data are preliminary processed by DInSAR technique for land subsidence mapping of Tianjin and Beijing area. Meanwhile, the DInSAR results from COSMO-SkyMed and ASAR data are preliminary compared. COSMO images are more suitable to extract high-precision ground deformation information than ASAR images in civil application given precise orbit data. While COSMO data are suitable for deformation monitoring in a relatively small and important area, ASAR data are fit for regional survey. [C2999]

### **"Privacy protection against ubiquitous marketing"**

Privacy has been recognized as an important topic in the marketing for long time. Our society is growing and adopting a more ubiquitous information-filled world with previously isolated systems evolving and being adapted to operate in completely interconnected networks. This full access to real-time public and personal data is a logical evolutionary step forward. However, the security of the individual's confidential information and our right to privacy is at stake. Many questions need to be addressed regarding the scope and volume of personal information. Seemingly, there is a tradeoff between exploiting the tremendous benefits of having shared information available to enhance the people's life and giving away one's personal privacy either directly or indirectly. The most common use of user data is in marketing, for which profiles, as collected in traditional eCommerce, are supported by data-mining the explicit self-descriptions, the behavior, and the ratings of users. For example, from credit card companies that rate based upon where you shop, to pay-per-click advertisements based upon Google searches, behavioral targeting has become an ubiquitous, if effective marketing tool. This issue has become a hot button topic for many publishers, advertisers, and privacy protection groups. Critics are concerned whether or not behavioral tracking agencies are effectively disclosing how the targeting works, and

whether or not they are offering consumers the ability to escape their radar by opting out of tracking. Despite numerous discussions on the regulation of behavioral marketing, no solution has been found that satisfies all parties. It can be said that privacy is a problem in ubiquitous marketing using consumer's situation awareness today. However, it is possible to overcome the privacy problem if careful consideration is done to the consumer. So, we should know that when does the consumer feel insecurity? How does the consumer think about the privacy problem? This-- paper examines the consumer's consideration to ubiquitous marketing. [C3000]

#### **"A method for InSAR baseline refinement and its application"**

Interferometric baseline plays a very important role in InSAR data processing, and it will directly affect the accuracy of interferometric result. In this article, three classical baseline estimation methods were described. By comparing and combining three methods, a new baseline estimation method and its flow were listed. RADARSAT-2 satellite image data and grid digital elevation model ASTER GDEM (30m resolution) in Kailuan area are used as sample data. By analyzing the differential interferometric results generated with different baseline estimation methods, it can be concluded that the new method used by this article is correct and feasible. [C3001]

#### **"Seat vibrotactile warning interface for forward vehicle collision avoidance"**

A collision warning system utilizing haptic interface is expected to be more effective than an auditory as well as visual warning types. In order to reduce the number of the traffic accidents and their injuries, this paper proposes a forward vehicle collision warning system by using seat vibrotactile interface. At first, an investigation of the frequency for using as collision warning is shown. Comparing the time response to each type of warning system, the effectiveness of seat vibrotactile warning interface is examined. Based on the examination, a forward vehicle collision warning system using seat vibrotactile is designed and installed in the experimental vehicle. Finally, the effectiveness of the proposed system is examined by test drives. [C3002]

#### **"Nondestructive measurement of diameter of reinforcing bars in concrete using an electromagnetic wave radar under the effect of cross bars"**

A method was proposed previously to measure the diameter of the deformed reinforcing bars in concrete structures nondestructively using an electromagnetic wave radar. The method estimated the periodicity of the knots of the inspected bar from the received reflections from the deformed bar and utilized the standard relationship between the knot's pitch and the diameter of the bar to measure the diameter indirectly. The effectiveness of the method was verified using test specimens where the bars were placed parallel to each other. However, in practical case, where other reinforcing bars cross the inspected bar perpendicularly, the stronger reflections from the cross bars influence the reflection from the inspected bar. The paper thus proposes a general method which eliminates such unwanted influences from the cross bars and measures the diameter accurately even in practical environment. [C3003]

#### **"Intelligent collision risk assessment based on Neural Network Ensemble"**

In this paper, we propose the collision risk assessment system. When pedestrian is detected by radar or another sensor, system could know the pedestrian's position and velocity. Using this information, system can compute the collision risk. If system does not concerned about the simulation time, Monte Carlo Simulation is simple and powerful method. But in dynamic circumstance, the position and velocity of pedestrian is changed rapidly. So I propose to apply Neural Network Ensemble in this problem. Neural Network train the network using training data, this process take a long time. But by using trained network, system can compute the collision risk quickly. However, wide range of input data can cause huge memory use, and lengthy simulation time. So we propose apply Neural Network Ensemble to this problem. Neural Network Ensemble separate the input data and training each network with different data set. This method will reduce the computation load with small error. [C3004]

#### **"Application of integrated geological prediction in expressway tunnel"**

Because of the complicated geological conditions of tunnel surrounding rocks, it is of necessity to operate geological prediction during tunnel construction. Geology analysis, seismic wave method (TSP was adopted) and GPR (ground penetrating radar) are used to make prediction in the construction of Gaojiabao Tunnel. The utilization of several prediction methods that can be seen as an integrated prediction system can avoid one-sided conclusion obtained by single method. Moreover, each conclusion can be checked and made up mutually. The application result shows that the prediction conclusions are relatively accurate, which can meet the needs of safe construction. [C3005]

### "Deformation analysis of Wenchuan earthquake based on D-InSAR with image mode"

It is considerably destructive for Wenchuan earthquake. The derived deformation field is an effective way to retrieve the geophysical parameters and study the seismic mechanism. Numerous geodetic methods can be exploited for the earthquake deformation monitoring. In spite of the high accuracy and consistent temporal scale, the results of GPS measurements are discrete. Continuous deformation field can be derived from Interferometric Synthetic Aperture Radar (InSAR). For image mode (IM) has full resolution, we will use conventional InSAR to get deformation field of Wenchuan earthquake. First, the geolocation of Longmen Mountain areas was introduced. The process of IM interferometry was analyzed in detail. At last, the deformation field was derived with the extent of 100km<sup>4</sup>100km. The results revealed that it was not the largest deformation region at the earthquake focus. The closer you get to the fault zone, the larger deformation gradient of the heading wall it become. At the same time, IM Interferometry can not reveal deformation field because IM is too narrow to obtain the entire deformation field. With the application to IM interferometry in Wenchuan earthquake, it is significant for earth science research such as earthquakes and crustal motion. [C3006]

### "SAR image target recognition based on NMF feature extraction and Bayesian decision fusion"

In this paper, a new approach of synthetic aperture radar (SAR) image target recognition based on non-negative matrix factorization (NMF) feature extraction and Bayesian decision fusion is presented for recognizing ground vehicles in MSTAR database. First, feature vectors are extracted from image chips by NMF algorithm. Support vector machine (SVM) is used to classify the feature vectors. After multiple views of the same vehicle collected at different aspects are classified by SVM, the outputs are fused by Bayesian decision fusion algorithm and then the final classification decision is generated. We evaluate NMF algorithm and the Bayesian decision fusion approach. Experimental results indicate that there are significant target recognition performance benefits in the probability of correct classification when NMF algorithm is applied and three or more views are used for Bayesian decision fusion. [C3007]

### "Precise diameter measurement of reinforcing bar and steel pipe based on bi-static model using microwave radar"

In this report, a novel signal processing method for microwave radar is considered, in order to realize precise diameter measurement of the reinforcing bars and the steel pipes in the concrete structures. Particularly, a geometric analysis which is considering the bi-static antenna configuration for the microwave propagation paths is introduced, and a diameter of the buried circular target object has been tried to measure precisely. In the proposed geometric analysis, the accurate microwave propagation length, or the accurate propagation time estimation is necessary for precise diameter measurement. Then, the improved cross-correlation envelope curve method is newly proposed, and superior propagation time estimation accuracy over the sampling interval has been accomplished. Finally, an effectiveness of the proposed methods has been confirmed experimentally, by applying them to the diameter measurement of the steel pipe in the air. Their experimental results show that the proposed methods have certain advanced performances for a precise diameter measurement. [C3008]

### "Modeling and simulation of position for the Stratospheric ISAR system"

There are many advantages to put the Inverse Synthetic Aperture Radar (ISAR) system up in the stratosphere. Compared with the Ground-based ISAR system, one problem of the Stratospheric ISAR system is the platform drifting. This paper established models for the different positions of the airship and investigated the effects of drifting on imaging. The results of simulations for Stratospheric ISAR system show effectiveness of the models. [C3009]

### "Radar Multi-Targets Real-Time Communication Based on Software Radio"

According to the modern software radio principle, a programmable general-purpose platform is designed to realize radar multi-targets real-time communication. The receiver is designed based on wideband IF sampling architecture, and cascaded with two digital attenuators. C-band signal is transformed into IF signal through twice conversions. DSP, FPGA, and ARM are used for digital signal processing. Cascaded Integrator-Comb (CIC) filter and polyphase filter are utilized to accelerate processing speed and reduce system resource consumption due to the fast signal processing. Experiment results show that the digital attenuators expand the signal dynamic range 60dB. CIC filter and channelized receiver based on polyphase filter banks can save resource consumption and improve the efficiency of signal processing. [C3010]

### "Specific Emitter Identification Based on Intrinsic Time-Scale Decomposition"

Practical signals such as communication and radar signals turn out to be non-stationary and nonlinear time

series, and estimating instantaneous parameters of such signals in time domain will benefit detecting and identifying specific emitters, such as radio stations and aerospace targets. However, conventional methods such as Wavelet and Wigner-Ville distribution (WVD) methods are difficult to deal with these transient signals when the signal is not stationary. To provide more efficient approach for estimating instantaneous parameters of non-stationary and identifying specific emitter with high accuracy, a novel method based on intrinsic time-scale decomposition (ITD) for analytic signal is proposed in this paper. The simulation results are presented to demonstrate the power and effectiveness of this novel method. [C3011]

#### "Automatic Layer-Interface Detection of Pavement Based on Matched Filter"

Ground penetrating radar (GPR) is a non-destructive and non-intrusive subsurface investigation equipment which has been widely used in the field of civil engineering. As the GPR signals are easily corrupted by noise, so it's always difficult to detect the multi-layer reflection signal of the pavement. To address the problem, In this paper we present the wavelet transform modulus maximum de-noising and Matched Filter (MF) method for clutter reduction and layer-interface automatic detection respectively. The experimental results based on simulated data using FDTD show that under the Low SNR condition, the presented algorithm outperform the MF algorithm alone. [C3012]

#### "Ultra-Thin Asphalt Pavement Layer Interface Detection and Time Delay Estimation Based on MUSIC"

Ground penetrating radar (GPR) is a non-destructive and non-intrusive subsurface investigation equipment which has been widely used in the field of civil engineering. Some challenges which GPR encountered for pavement subsurface inspection are: 1) GPR signal are easily corrupted by noise; 2) commercial GPR whose resolution is depended on system bandwidth, is not suitable for ultra-thin thickness estimation. This paper focus on using super-resolution MUSIC algorithm for ultra-thin pavement layer-interface detection and time-delay estimation compared to threshold detector and match filter. The results based on the simulation data under different conditions and measured GPR data are also presented. [C3013]

#### "Research on the Configuration of Network Radar Based on Detectable Power and Detector's SNR"

Network Radar realizes the integration of radar and radar countermeasure, thus it is a new direction for the development of radar and radar countermeasure system. This essay first introduces the existing concept and research results of the configuration of Network Radar and then it probes into how to configure the transmitters and receivers based on the method of detectable power and detector's SNR, in the end this essay provides the simulations of the configuration of Network Radar. It hopes that the research results of this essay will put the development of configuration of Network Radar forward deeply. [C3014]

#### "Theory and Measurement of Delta RCS for RFID Tag on Various Materials"

Delta radar cross section (RCS) is an important parameter for the performance of passive UHF RFID tag. It determines the bit error rate (BER) at reader side when the signal which backscattered from the tag is polluted by kinds of noises. But the measurement of delta RCS can't be obtained directly and thus, indirect method must be considered. The paper introduces our measurement methodology for tag's delta RCS, including the National Instruments (NI) RF modular and the LabVIEW based signal analysis program. This paper also has analyzed two main factors which influence delta RCS seriously, and gotten some test results when tags were attached on various material objects for different transmitted power. [C3015]

#### "Linear Combination Method for UWB Vehicular Radar Pulse Design"

Ultra wideband (UWB) vehicular radar has been studied and developed to achieve a safe driving and to promote business in an intelligent transport system. In the paper, we propose a UWB radar pulse design method that makes use of a linear multi-pulse combination of wavelet pulses which satisfy the Federal Communications Commission (FCC) regulation. Simulation results show that the UWB pulse obtained by the method have the advantages of better spectrum utility ratio and complying with the FCC spectrum mask. [C3016]

#### "A Novel Method for Recognising Radar Emitter"

A novel method for recognising radar emitter is proposed in this paper. The resemblance coefficient (CR), pulse repetition interval (PRI) mean and variance are used as the factors for recognising radar emitter which is based on the feature of these parameters. Then, the radial basis probabilistic neural networks (RBPNN) recognition is designed. Simulation experiment shows that this novel method can improve the recognition rate while it can also



improve the recognition velocity. [C3017]

### "WiTracker: An Indoor Positioning System Based on Wireless LANs"

With the rapid development of wireless local area networks, indoor positioning technology based on received signal strength in wireless networks are becoming more and more attractive. In this paper, we firstly introduced the implementation of an indoor positioning system, named WiTracker. Then three improvement mechanisms, called signal strength filter, user location filter and path tracking assistance, were proposed to improve the positioning accuracy of the WiTracker system. Thirdly, we analyzed the comprehensive performance of the WiTracker system and compared it with the Radar system. Experimental results demonstrated that the proposed WiTracker system can improve the 89% accuracy in 3 meters of Radar system to 93% in a typical office building testbed. Finally, two key influence factors to positioning accuracy were further discussed and analyzed, including number of access points, and spacing between sampling points. [C3018]

### "Diagonal Loading for STAP and Its Performance Analysis"

For the moving target detection with space-time adaptive processing (STAP), the non-homogeneity will cause the covariance matrix estimation error, which substantially results in the STAP performance degradation. Diagonal loading has long been used as a means to improve the robustness of the spatial filter against mismatches in both the desired spatial signature and the spatial correlation matrix. In this paper, we consider the application of diagonal loading to improve the detection performance for STAP, especially for the covariance matrix mismatch (statistical mismatch) in STAP, namely, there is a mismatch between the actual covariance matrix of interest and the presumed one. For the diagonal loading, the key problem is the choice of the loading level, and the method for selecting the loading level is given, and the particular performance analysis indicates that the diagonal loading can improve the detection probability and the output signal-to-noise ratio. Numerical simulations attest the validity of the analysis. [C3019]

### "An Efficient Indoor Location Algorithm Based on RFID Technology"

Virtual reference elimination algorithm is a method to investigate the location accuracy of location identification based on dynamic active RFID calibration being restricted by the number of reference tags. However, the Received Signal Strength Indicator (RSSI) values of virtual reference tags, achieved from the linear interpolation formula in VIRE, are not enough precise according to the distance-loss equation. Severe redundant calculation was induced in the case of all the tracking tags positioned intensively. The proposed location algorithm suggests a subregion selection mechanism to reduce the redundant calculation, brings forward a nonlinear interpolation algorithm to calculate the RSSI values of virtual reference tags. A trajectory revision method is used to improve the location precision as well. Simulation results demonstrate that the location accuracy of optimized algorithm is better than that of VIRE. [C3020]

### "Simulation and Analysis of the Effects of Tropospheric Scattering Channel on Signal Waveforms"

Tropospheric scattering channel is a random channel. When the signal transmitted through the troposphere, the multi-path fading could cause signal waveform distortion. In this paper, based on a valid tropospheric scattering channel model, respectively, from the time domain and frequency domain the reasons why the signal waveform was distortion were analyzed. Radar pulse as the transmit signal, and simulate the received signal waveform in different antenna beam width angle. The results show that the signal waveform is impacted in different degrees at the different antenna beam width angle. [C3021]

### "A Novel Random Sampling Method for Radar Image Compression"

In this paper, we propose a process of the radar image data by Random sampling. The sampling rate is far lower than Nyquist-Shannon sampling theorem, which shows that image data can be reconstructed from an extremely small set of measurements than what is generally considered necessary. Compressive Sampling is considered for signals and images that are sparse in a wavelet basis. A low complexity compression method for high resolution image based on block partition in wavelet region is proposed. The image is partitioned into blocks in wavelet domain and then compressed separately with CS. The bit rates for each block is allocated according to the texture complexity of the block. The proposed method eliminates the "block effect" caused by traditional block partition in pixel domain, and solves the problem caused by traditional block partition that the areas with simple texture are good in reconstruction quality while those with complicated texture are too poor to be used because of the uneven distribution of texture complexity. The experimental results show that the compression performance of the proposed method is quite similar to the results obtained by global compression. This compression method is particularly suitable for the high resolution remote sensing image which sparse in a wavelet domain. [C3022]

### "Designing of a Telematic Network to Provide Real-Time Supervision and Control for Tactical Units"

In this paper we present the design and implementation of a telematic network to provide real-time location based services for tactical units which interconnects soldiers, weapons systems, fire control units, sensors, reconnaissance and surveillance radars, as well as unmanned aerial vehicles, with company-level command and control centers to the national center at the command level and the Defense Ministry headquarters, allowing real-time transmission of voice, image and geographical data. The design is based on a telematic network in which each vehicle receives positioning information through a GPS system. It is transmitted by radio to a base station where the signal is processed. It will also be able to give orders to avoid accidents, confusion and loss of soldiers in hostile areas. A description of the proposed system is presented. Flow charts for later coding in the programming language are shown. The way of how the transmitted signal is processed and then displayed to the user is illustrated. The evaluation of the results was carried out in Venezuela with equipment purchased by the Army and the efficiency of the proposed system is verified. [C3023]

### "Data analysis of wind profiler radar(WPR) under three kinds of synoptic processes in spring on Donghai island of Zhanjiang"

Observations from the WPR located in Zhanjing are used to analysis the characteristics of wind field and virtual temperature in boundary layer under three kinds of synoptic processes during 5th-12thApril, 2010. The results show that: (1) The horizontal wind velocity first increased and then decreased with altitude in low level of spring fair weather over Zhanjing, with maxima range of 7-16 m/s, and the velocity also first increased and then decreased, with maxima less than 20 m/s in the middle level, the wind velocity was increased with altitude in high level. The horizontal wind direction was easterly in low level and southwesterly in high level, and the direction veered with altitude accompanied by warm advection. It appeared varied velocity of downdraft except for the weak updraft at the altitude of 2500-4000m. (2) During the spring fog process, the wind velocity fluctuated around 5 m/s with easterly direction in the low level and increased with altitude above 1100m which up to 19 m/s with southeasterly direction, but the velocity turned decreasing apparently around 5500m, with wind direction veering with altitude accompanied by warm advection. (3) There were two downdraft areas during precipitation, the first one was under the height of 1000m, and the second one was at the mid-level of 3000m. Updraft appeared before the onset of precipitation, and the low level was dominated by downdraft airflow after the beginning of rainfall. At the beginning of rainfall, the horizontal wind velocity shook at mid- and low-level with wider fluctuation margin of 3-9 m/s. The wind velocity increased with altitude accompanied by single warm advection and the direction was easterly below the height of 1000m, and the wind direction became more volatile with height above 1000m with alternated appeared warm and cold advection. [C3024]

### "Integrating observation systems: An example from the Great Barrier Reef"

The Australian Integrated Marine Observing System (IMOS) project has deployed a set of focused observational equipment in the southern part of the Great Barrier Reef. This represents an good case study in what it actually means to deliver an integrated set of observations, how integration can be achieved and what the real benefits of true data integration are. [C3025]

### "Sonar waveform design for optimum target detection: The impact of object burial state"

The design of transmit waveforms in sonar and radar that optimize the probability of detection of a known target is an area of active interest. Previous research has demonstrated the benefits of optimal transmit waveforms for enhanced target detection, versus the transmission of more conventional waveforms such as broadband LFM pulses. For maximum benefit, the scattering function or frequency response of the target to be detected must be known, along with the spectral or statistical properties of the environment. In this paper, we examine the impact of a mismatch between the expected frequency response of the target, for which the optimal transmit waveform was designed, and the actual frequency response of the target. In particular, we design the optimal sonar transmit waveform based on the free-field response of the target, and then examine the effects on detection performance of burial of the target in sediment. Simulations of the sonar backscatter from a steel sphere in the water column and at various stages of burial demonstrate that the impact of mismatch becomes increasingly detrimental as the target becomes increasingly buried. For fully buried targets, the impact is such that transmitting a simple broadband LFM pulse can yield improved detection relative to "optimal" waveform design wherein there is a mismatch between the expected (free-field) and actual (buried) frequency response of the target. [C3026]

### "The Integrated Marine Observing System-delivering data-streams to support marine research and

## applications"

The Integrated Marine Observing System (IMOS) is funded by the Australian Government through the National Collaborative Research Infrastructure Strategy (NCRIS) and the Education Investment Fund (EIF) to deliver data-streams from the Oceans around Australia. IMOS aims to meet the needs of the research community, address issues of national importance and contribute to international ocean observing programs. The strategic focus of IMOS is on the role of the oceans in the climate system, and the impact of major boundary currents on the continental shelf, ecosystems and biodiversity. [C3027]

## "Coherent change detection with complex logarithm transformation on SAR imagery"

A satellite-borne SAR (synthetic aperture radar) is quite promising technique for high-resolution geosurface measurement. Recently, the feature extraction method based on the CCD (coherent change detection) has been developed, which detects a small surface change on the geosurface by using the phase relationship between the plural complex SAR images of the same region in different observations. Aiming at fast and accurate detection of the surface change, the logarithm transformation method, has been proposed. This method can determine the appropriate threshold for the change detection, while enhancing the detection probability and suppressing the false alarm rate. However, it does not employ phase information of the estimated coherence function, and its detection probability deteriorates, especially in the case when target has small surface changes. To overcome this problem, a novel transformation index is proposed considering the phase difference of the coherence function. The results from the experiment modeling of geosurface measurement verify the effectiveness of the proposed method, even in the lower SNR (signal to noise ratio) situations. [C3028]

## "Comparison of ship detectors for polarimetric SAR imagery"

This paper examines the benefits of using fully polarimetric SAR imagery for ship detection. There are three related aspects to the work. First, RadarSat-2 quad-pol stripmap imagery is used to compare the performance of various ship detection algorithms/methods. The comparison is based on the use of ROC curves. Second, circular spotlight SAR imagery is used to examine how detector performance varies with the azimuth angle. Owing to the small number of available ship samples, this analysis has limitations. Third, again using the circular spotlight SAR imagery, the variation, with respect to azimuth angle, of the elements of the polarimetric covariance matrix of both the ship and the ocean are analysed. The results are as follows. Using the stripmap imagery, it is found that exploiting both polarimetry and spatial correlations greatly improves detection performance. Using the circular spotlight imagery, it is found that detection performance is variable with respect to azimuth angle and trends are hard to discern. Moreover, the performance of the Pauli double bounce detector is generally poor. It is conjectured that ship pitching motion degrades the polarimetric backscatter response in the circular spotlight imagery. Finally, the covariance matrix analysis confirms known trends for the ocean backscatter. The implication of these trends is that the polarimetric covariance matrix is sensitive to changes in azimuth angle and hence detectors based on them are also. The data indicate the extent to which this is the case. [C3029]

## "Further analysis of the modulation of high frequency radar spectra due to sea-induced antenna platform motion"

The scattering of high frequency electromagnetic waves from the ocean surface is considered for the case of the radiation source being a vertical pulsed antenna mounted on a floating platform while the receiving antenna is fixed on the shore. This represents a small extension to an earlier analysis by Walsh in which both the transmitting (TX) and receiving (RX) antennas were co-located on a floating platform and the effect of the sway was accounted for in the ocean cross section. It is known that additional features appear in the Doppler spectrum when the RX and TX antennas are permitted to sway slowly, and here a similar result is shown when only the TX antenna moves. It is seen in this case that the magnitude of the additional spectral features is reduced as compared to the case when both antennas are moving. As a motivation for continuing analytical work, a preliminary field result is depicted. [C3030]

## "An improvement to the pulse compression scheme"

The pulse-compression is a technique mainly used in sonar, radar and echography to augment the range resolution as well as the signal to noise ratio. This is achieved using a matched-filtering of the received signal with the bandpass transmitted signal. Taking into account the main assumptions of the matched filter theory, the use of the bandpass transmitted pulse as matched filter's impulse response is only available if the useful signal is well known and if the noise is white, which is not the case in practice. For this reason, we propose to improve the classical pulse-compression technique using the stochastic matched filter, which ensures a maximization of the signal to noise ratio, when the useful signal is a realization of a random process and the disturbing signal a colored noise. Results obtained on synthetic and real data are proposed and discussed. [C3031]

### "Mechanisms and system design of satellite interferometric Synthetic Aperture Radar altimeter"

Satellite radar altimeter plays an important role in microwave remote sensing, but its performance and applications on non-ocean surfaces are constrained by its poor resolution. The along-track resolution of altimeters can be improved by the synthetic aperture technology, while the cross-track resolution can be improved by the interferometric technology. Although these two technologies are well-established in side-looking radars, relevant studies on nadir-looking radar are rather inadequate. This paper reviewed the backgrounds of the synthetic aperture altimeter and interferometric altimeter. Then the mechanisms of the Interferometric Synthetic Aperture Altimeter (INSAA) are analyzed, and a set of typical INSAA system parameters are designed, especially on the phase-wrapping problem and baseline-length issue. [C3032]

### "InSAR Kalman Filter phase unwrapping algorithm based on topographic factors"

Phase unwrapping is the key step in Digital Elevation Model extraction and the measurement of surface deformation of Interferometric Synthetic Aperture Radar (InSAR). When in steep terrain or larger slope, the unwrapping result is bad and causes error transmission using the existing Kalman Filter phase unwrapping algorithm. Considering this situation, this paper presents an improved Kalman Filter phase unwrapping algorithm based on topographic factors for InSAR. It can be implemented through the introduction of the input control variable associated with topographic factors to the state-space model of Kalman Filter. Owing to the fact that the interference fringes directly reflect the change of the terrain and local fringe frequency is closely related with the local terrain slope, the local fringe frequency estimation can be used as the input control variable. In the local frequency estimation, using two-dimensional Chirp-Z transform, better estimate of the results may be quickly get. In this paper, using simulated data and real InSAR data to do the experiment, it can gain more reliable result compared with the conventional Kalman filter phase unwrapping algorithm. It is verified that the proposed algorithm can effectively deal with the situation of steep terrain and larger slope. [C3033]

### "Offshore petroleum exploration from space: A developing capability at Geoscience Australia"

Natural seepage can generate hydrocarbon slicks on the sea surface that may provide petroleum explorers with direct evidence of oil and gas below the sea bed. Remote sensing has the potential to be used as a tool for detecting such sea surface slicks, thereby identifying areas in both producing and frontier basins that are prospective for hydrocarbons. We are developing a two-pronged, remote sensing-based approach for seepage slick studies in the Australian Marine Jurisdiction: 1) building a semiautomated processing and classification system in order to scan large numbers of Synthetic Aperture Radar scenes for potential natural slick targets, and; 2) investigating the potential of optical remote sensing as a diagnostic tool for further, targeted study. Using objected-oriented classification algorithms in a bulk processing environment, large Synthetic Aperture Radar data sets were able to be efficiently screened for potential natural oil slick targets. This processing system offers a range of outputs, including classification statistics for each scene studied, as well as geo-referenced shapefiles ready for analysis in Geographic Information System software, where it can be combined with ancillary data sets for contextual analysis. Our research into the potential for optical remote sensing to enable further diagnostic study of identified, potential targets has shown that there are several commercially available, space borne sensors able to detect the types of oils found throughout the Australian Marine Jurisdiction, but that oil type is critical for this application. Further to this, we have developed an approach for performing a feasibility study of oil type versus sensor sensitivity prior to image data acquisition. [C3034]

### "The use of HF radar surface currents for computing Lagrangian trajectories: Benefits and issues"

Surface coastal currents mapped by a pair of high frequency ground-wave radars (HFR) have been used to predict Lagrangian trajectories in the proximity of Heron Island (Capricorn Bunker Group, Great Barrier Reef, Australia), and to compare with the current data measured by an Acoustic Doppler Current Profiler (ADCP) at three mooring stations. Overall the HFR and ADCP absolute current speeds showed a difference less than  $\pm 0.15$  m s<sup>-1</sup> for 68% of the observations. A good agreement between HFR (at a depth of 1.5 m) and ADCP (at a depth of 5.5 m) data were observed for the u-component (cross-shelf) which presented a stronger tidal signal, while a poor comparison was found for the v-component (north-south) more influenced by the south-easterly and northerly winds. The HFR allowed inclusion of not only the temporal, but also the spatial current variability in the tracking computation. This proved to be crucial because the Lagrangian trajectories were very sensitive to the starting position and time in the studied area, where the currents exhibit a large spatial variation imposed by tides, winds, large scale circulation and topography. One challenge in applying HFR data for Lagrangian tracking consists of estimating the missing values and including the effects of small scale fluctuations. [C3035]

### "A low power and high gain double-balanced active mixer with integrated transformer-based Baluns"



### **"dedicated to 77 GHz automotive radar applications"**

In this paper, we present a low power and high gain mixer dedicated to 77 GHz automotive radar applications. The architecture is based on a double-balanced active Gilbert cell with integrated transformer-based Baluns. These Baluns allow converting the single-ended input signals to differential with an amplitude and phase imbalance of 0.3 dB and 179°, respectively. Interconnections between devices, capacitor accesses and Tee-junctions are modeled using HFSS simulator in order to improve the simulation accuracy. The proposed mixer consumes 105 mW and achieves 16.4 dB of conversion gain and 13.2 dB of noise figure. [C3036]

### **"Forereaching motion generation of mobile robots for pedestrian face identification"**

This paper describes the generation of forereaching motion using mobile robots for pedestrian face identification. The motion generation system estimates the positions and velocity of the pedestrians and generates a path that enables the robot to forereach the target pedestrian while avoiding the other pedestrians. In this paper, the pedestrian motion estimation method, forereaching path planning method, and experiment results are described. [C3037]

### **"HF radar two-station baseline bisector comparisons of radial components"**

One simple way to evaluate errors in the radial components of surface currents is to compare the values measured from two separate radars along the baseline joining them. This is best done at the midpoint of the baseline where the areas sampled by the radars are equal. This cannot be done if the baseline is close to the coast or over land. Here we compare radial components along the perpendicular bisector of the baseline and show that the RMS difference approaches the error as the point of observation approaches the midpoint. The application of this method to SeaSonde data showed rms differences decreasing until the observations were about 25 km off shore, and then increasing. We suspect that this increase near the coast is due to a known edge effect in the processing of radials that are derived from calibrated antenna patterns. If we exclude the near-coast data points then the rms differences extrapolate to a value of about 0.10 m s<sup>-1</sup> at the midpoint of the baseline. [C3038]

### **"LFMCW SAR waveform generation with frequency nonlinearity suppression"**

Linearly frequency modulated (LFM) signals are desired in many electronic systems. For example, linearly frequency modulated continuous wave (LFMCW) radar has the good performance of lightweight, cost-effective, and high-resolution imaging. However, the presence of frequency nonlinearity in the transmitted signal will result in contrast and range-resolution degradation. In this paper, the impact of frequency nonlinearities on LFMCW synthetic aperture radar (SAR) system is addressed, and one parallel direct digital synthesizer (DDS)-driven phase locked loop (PLL) frequency synthesizer to synthesize wideband LFM signals is designed, and an adaptive system nonlinearity compensation technique is employed. In this way, an example wideband LFM synthesizer with good performance frequency linearity is designed. [C3039]

### **"Route planning for unmanned aerial vehicle based on threat probability and mission time restriction"**

In this paper, a route planning approach for unmanned aerial vehicle (UAV) with mission time restriction is investigated. According to the types and the characteristic of threats in the battlefield environment, we analyse the relation between threat extent and threat probability, build the model of threats, improve A\* algorithm through design the cost valuation function of A\* algorithm and use the variable step length strategy, it improve the search efficiency, when the route planned in safety area can't satisfy UAV mission time require, the method that suitable adding threat probability to satisfy mission time restriction was adopted. The simulation results show that the approach was feasible, effective and can plan route that satisfy the mission time requirements of UAV. [C3040]

### **"Adaptive Information Matrix Filtering fusion with nonlinear classifier"**

An adaptive filtering approach is present for fusing the tracks of multi-sensor surveillance systems. The approach is an algorithm of hierarchical estimation fusion which consists of several local nodes and a global node. A linear Kalman filter is employed by each local node to produce the track estimate of the same target. The outputs of all local nodes are transmitted to the global node. In this node, an adaptive filter, which consists of the dual-band Information Matrix Filter (IMF) and a nonlinear classifier, is utilized to combine the local estimates to generate a global estimate appropriately. The feature vectors are yielded by dual-band IMF. The classifier, which is designed by using the radial basis function network in Gaussian form, is used to divide the feature space into regions that correspond to decide the output of either high-level-band IMF or low-level-band IMF against the uncertainties of target dynamics. The proposed filter has better tracking performance than each

individual IMF. Simulation results are included to demonstrate the effectiveness of proposed filter. [C3041]

### **"Maximum likelihood estimation of target RCS in tracking"**

In this paper, a maximum likelihood (ML) approach is presented for estimating the average radar cross section (RCS), and a numerical solution to the approach is proposed based on a generalized expectation maximization (GEM) algorithm. Estimation accuracy of the approach is compared to that of a previously reported procedure. [C3042]

### **"Research on DBF SAR system in near space"**

In this paper, a SAR system with a method of Digital Beamforming (DBF) was offered, which can realize both wide swath and high resolution at the same time. This research is based on the Displaced Phase Centers Multiple system, which adopt the DBF method at the receive, and is combined with the properties and demands of near space, and through the optimization of the design and overall consideration of the antenna size, pulse repetition frequency (PRF) and the ambiguities etc, the analyzed results demonstrate that it is possible to get wide swath and high resolution, what's more, such a system combined with the advantage of the near space will create a great superiority, and is of great reference value of the near space development and applications. [C3043]

### **"Monitoring manners research on the river ice in the Yellow River"**

According to the current need of controlling ice disaster, three types automatic monitoring ice system are put forward, i.e. ice depth auto measurement system; ice depth probing system; unpiloted aircraft monitoring system. They can continuously and automatically monitor many parameters including ice thickness, water level under ice, air temperature, ice temperature, water temperature and get the ice images, drift ice velocity and the density of drift ice. The process of ice in Yellow River can be obtained by the continuous monitoring with remote images monitoring, radar detecting and unpiloted aircraft monitoring after selecting proper monitoring point. As a result, these monitoring manners provide theoretical support and technical parameters for improving ice disaster emergency monitoring techniques and conditions forecast. At the same time, the monitoring information offers more detailed support to decision maker. [C3044]

### **"Micro-doppler extraction of vibrating target based on dual-channel ATI technique in SAR"**

Aiming at extracting the time-varying micro-Doppler feature of the ground vibrating target within ground clutter environment, the method of micro-Doppler extraction based on dual-channel ATI technique is presented. The ATI technique is utilized to suppress the ground clutter, and preserve the interferometric signal of the vibrating target in the raw data domain, which is presented as a straight line along the azimuth direction. According to this feature, we can find out which range cell the signal locates at, and then by taking the time derivative of its phase, the micro-Doppler modulation can be obtained. Compared to the single-channel situation, there is no need to compensate for the Doppler shift caused by the radar's translation in advance, and we can obtain the micro-Doppler feature induced by the vibration in any direction, which will help to reduce the computation burden and improve the target detectability. Simulated results verify the validity of the proposed method. [C3045]

### **"A progressive approach for building extraction by fusing LIDAR data and co-registered bands"**

In this paper, a progressive approach is presented for building extraction from LIDAR combined with its co-registered bands. Carefully tuned Gabor wavelet filters are applied to LIDAR data for object detection on the earth, and to localize targeted objects in order to minimize hilly terrain effects. Object classification is then carried out in local areas where objects exist. The Dempster-Shafer (DS) theory of evidence is used to conduct initial classification by fusing LIDAR and its co-registered data sets; and a fuzzy Markov random field (FMRF) model takes the output from the DS theory of evidence, and is performed the further object classification to extract buildings. Finally the level set approach is employed for building boundary extraction. The testing experiments under this research have shown the potential of this approach in accurately extracting buildings from airborne LIDAR and its co-registered bands. [C3046]

### **"Simultaneous detection and tracking of multiple objects in noisy and cluttered environment using maximum likelihood estimation framework"**

We discuss a versatile framework for multiple target detection and tracking based on maximum likelihood estimation with expectation maximization and a cognitive theory called dynamic logic. In this contribution extend the framework to detection of moving objects in video sequences. The paper presents the theory and an example of detection and tracking using a real world video sequence. [C3047]

### "Target tracking in state dependent wake clutter"

Tracking methods attempt to follow the movement of a target of interest while suppressing irrelevant clutter. A particularly troublesome source of clutter is wakes that appear behind the target. This problem arises in sonar tracking of human divers, in the tracking of boats using surveillance radars, and also in radar tracking of ballistic missiles. Previous research has integrated a solution to this problem in the popular Probabilistic Data Association filter (PDAF). This paper proposes a new solution to this problem in the same framework. While previous research has used an approach described as probabilistic editing, the new solution solves the wake problem in a Bayesian framework by means of marginalization. Monte-Carlo simulations show that the new solution provides significantly increased robustness as compared to both the standard PDAF and the probabilistic editing approach. As the new solution has improved theoretical underpinnings, we hope that it can be useful for further research on tracking in the presence of wake clutter. [C3048]

### "Wind field retrieval over the ocean using X-band polarization SAR data"

An X-band wind field algorithm (XMOD) based on a linear approach is discussed in our previous work to describe the relationship between normalized radar cross section (NRCS), wind speed, wind direction and incidence angle. To apply the XMOD to TerraSAR-X data acquired in HH polarization, the two C-band polarization models are analyzed and tuned to X-band TerraSAR-X data. To demonstrate the applicability of the two models, 10m height wind speeds were computed with XMOD from several VV/HH TerraSAR-X images and validated by QuikScat and DWD model results. In addition, the wind speeds were retrieved and compared to each other from the HH and VV polarization TerraSAR-X images of the same scene at the same time. [C3049]

### "Study the feasibility of airborne LiDAR on areal earth's crust deformation surveying"

Depicting people haven't find out one efficacious method to rapidly survey the areal outburst geological disaster at present. Through analysing the characteristic and the status quo of the airborne LiDAR, the paper consider that airborne LiDAR can do it. In order to verify the feasibility of airborne LiDAR on areal earth's crust deformation surveying. First, the paper analyse the error cause and should adopte quality control measures. Then, adopte net-RTK to survey many of points three dimensions coordinate in five different terrain regions (flat, river, town, hill, mountainous region). Second, Use DEM by airborne LiDAR points cloud on 3000 m altitude to interpolate vertical coordinate on same position. Third, compute the different value between datum and processing statistics and analysis to the different values. Last, The paper draw a conclusion that airborne LiDAR on 3000 m altitude can use areal earth's crust deformation. [C3050]

### "Altitude estimation method using assumed altitude reliability based on multipath propagation model"

The problem of multipath propagation in the tracking low-altitude targets with a radar is addressed. It is well known that multipath fading causes bias errors to the target altitude over the sea. Since multipath propagation depends on the frequency of the radar waveform, the actual target altitude and range, estimation of the bias errors is difficult problem. In this paper, we propose an altitude estimation method using multipath propagation model. Our method uses the reliability of each assumed altitude hypothesis based on multipath propagation model to estimate the real altitude of targets. Through computer simulation trials, the validity of our method is confirmed. [C3051]

### "An improved CFAR detector for non-homogeneous clutter environment"

An improved CFAR detector for non-homogeneous clutter environment is proposed. At LFM CW radar receiver, after moving target detection (MTD) and linear-law envelop detector, CFAR detector is usually adopted to detect radar targets, the threshold of CFAR detector should be adaptive to the local background noise/clutter environment. Interfering targets often exist in the leading and lagging windows of the test cell which results in an increased detection threshold and a degraded probability of detection (PD). In the improved CFAR detector, an order statistic VI CFAR detector (OSVI-CFAR) is proposed to adaptively remove the interfering targets from the reference windows and increase the PD. Simulation and experiment results are given to prove the feasibility of the OSVI-CFAR detector. [C3052]

### "A SiGe-based Ku-band digital beamforming array for high speed on-the-move comm/radar system"

A digital beamforming (DBF) prototype that uses compact and low cost Balanced Antipodal Vivaldi Antenna (BAVA) array and SiGe based-receiver is presented. An example is given for a Ku-band DBF system that

demonstrates simultaneous reception of two or more full motion videos in a portable device. [C3053]

#### "Phased array digital beamforming hardware development at Applied Radar"

This paper describes technology development efforts in support of phased-array digital beamforming at Applied Radar, Inc. The development efforts are aimed at increasing the bandwidth and dynamic range and enabling real-time throughput of multi-channel array data. This digital beamforming approach enables improved calibration, increased coverage through multiple receive beams, and adaptive processing and nulling. We describe enabling component technology including multi-channel FPGA-based digital hardware and a multi-channel wideband receiver. We also discuss a multi-channel wideband receiver system that was recently developed for electronic sensing and a wideband digital receiver/exciter (DREX) for radar applications. [C3054]

#### "Calibration of panelized polarimetric phased array radar antennas: A case study"

Demand for improvements in the performance and capabilities of new polarimetric radar systems beyond those of their predominantly mechanically-rotated predecessors has led to an effort to realize large, dual-polarized phased array antennas. These arrays have changing polarization characteristics with scan angle, requiring calibration and compensation. This paper provides a qualitative discussion of the challenge in meeting polarimetric weather radar requirements, such as a low bias in differential reflectivity (ZDR) and integrated cross polarization ratio (ICPR). A case study is presented using low-cost, aperture-coupled, stacked-patch antennas, a representative example of what may be used in large polarimetric phased array applications, to predict quantitatively the performance that can be achieved through suitable calibration and size constraints. [C3055]

#### "AOA estimation of two narrowband signals using interferometry"

Conventional interferometric techniques used in electronic support (ES) systems are often limited to estimating the angle-of-arrival (AOA) of one narrowband radar signal at any given time. This paper proposes a simple, low-cost extension that enables these systems to estimate the AOA of two simultaneous narrowband radar signals using only two receivers. [C3056]

#### "Innovative aperiodic arrays for SAR spaceborne applications"

In this paper an innovative procedure for the synthesis of linear non periodic phased arrays for SAR applications is presented. The main objective consists in minimizing the number of elements while optimizing the efficiency of the amplifiers. The procedure is implemented in three steps. Preliminary results are presented demonstrating that a reduction in the number of elements in the order of 20-30% with respect to existing conventional antennas may be achieved without sacrificing the performances. [C3057]

#### "Monopulse compromise arrays-A review"

Monopulse array antennas can be synthesized through a sub-array architecture aimed at generating an optimal sum and compromise difference patterns. A strategy based on an excitation matching procedure is here reviewed. Representative numerical results are shown to assess the effectiveness of the approach. [C3058]

#### "A tray based Rotman lens array with beamforming in two dimensions for millimeter-wave radar"

A tray based Rotman lens array is presented, which consists of several low-profile Rotman lenses with beam control circuitry, miniature dual-polarized horn antenna arrays, and tray selection circuitry for elevation beamforming. The array achieves broad bandwidth from 34 to 40 GHz, and beamforming in two dimensions is realized. In azimuth, switched beamforming is implemented with the Rotman lens beam control circuitry. In elevation, adaptive beamforming using MUSIC (multiple signal classification) is implemented with the individual Rotman lens trays. A proof of concept beamforming experiment was conducted, where the locations of targets within a three dimensional space were detected with 2.5 cm range resolution. [C3059]

#### "UAVSAR Active Electronically-Scanned Array"

The Uninhabited Airborne Vehicle Synthetic Aperture Radar (UAVSAR) is an L-band (1.2-1.3 GHz) repeat pass, interferometric synthetic aperture radar (InSAR) used for Earth science applications. Using complex radar images collected during separate passes on time scales of hours to years, changes in surface topography can be measured. Due to variations in aircraft attitude between passes, antenna beam steering is required to replicate the radar look angle from pass-to-pass. This paper describes an Active Electronically Scanned Array (AESA) that provides beam steering capability in the antenna azimuth plane. The array contains 24 transmit/receive modules generating approximately 2800 W of radiated power and is capable of pulse-to-pulse



beam steering and polarization agility. Designed for high reliability as well as serviceability, all array electronics are contained in single 178cmx62cmx12cm air-cooled panel suitable for operation up to 60,000 ft altitude. [C3060]

### "Precise calibration techniques for complex SAR systems based on active phased array antennas"

In recent years, the antenna technology for spaceborne synthetic aperture radar (SAR) systems has developed from passive slotted waveguide arrays (e.g. ERS-1/2 or X-SAR) to active phased arrays (e.g. ASAR/ENVISAT or TerraSAR-X), offering electronic beam steering capabilities required for acquisitions in different swath geometries and for operation in ScanSAR and Spotlight modes. Furthermore, with an increasing number of operational applications and services, the requirements on radiometric and geometric calibration become increasingly demanding. Hence, product quality is of crucial importance and the success or failure of a mission depends essentially on the method of calibrating the SAR system in an efficient way. In example of TerraSAR-X the paper describes a precise and efficient calibration method applicable for complex spaceborne SAR systems based on an active phased array antenna. [C3061]

### "Spread Spectrum Digital Beamforming (SSDBF) radar"

Spread Spectrum Digital Beamforming (SSDBF) overcomes the CSWAP and the scalability in bandwidth-and-frequency limitations of Conventional Digital Beam Forming (CDBF) by eliminating the requirement of "one digital transceiver per element" while enabling fully capable digital beamforming with minimum hardware (and consequently minimum volume and heat dissipation) per element. SSDBF enables low-cost/low-profile/low-power digital beam forming phased arrays that scales in frequency (L through Ka and higher), bandwidth (100's MHz) and subarray size (100's elements per subarray) with a single down-converter, single digital receiver and single Nyquist-rate ADC for the entire subarray. It achieves this by replacing the MMIC T/R module at each element with much simpler bi-phase re-modulating hardware, and by re-modulating and aggregating the return signal incident at each element such that it can perfectly recover the complex baseband-equivalent of the RF signal of each element without mutual interference and with negligible noise performance degradation. The bi-phase re-modulator at each element can be extremely small and low power and amenable to implementations as simple as a single RF switch mounted directly at the antenna element with associated ON/OFF switch control logic built on the back. Thus SSDBF truly enables flat, thin, lightweight conformal phased arrays and has the potential of reducing phased array costs by, possibly, multiple orders of magnitude relative to CDBF state-of-the-art. The SSDBF parameters and waveforms are flexible, programmable and can be tailored and adapted, practically, to support any radar or communications applications. In a project for DARPA, Applied Radar is developing an X-band SSDBF-based radar prototype in which the SSDBF features and performance have been demonstrated. In this paper, we describe the SSDBF method for a radar application including simulation, indoor testbed and open-range test results. [C3062]

### "A family of G-band active electronically scanned arrays for radar applications"

The present paper describes the family of G-band Active Electronically Scanned Arrays (AESA) designed and produced by SELEX-Sistemi Integrati. The development of certain types of key components has allowed to obtain, with the same effort, AESA with different performances according to the customer needs. The overall architecture of the AESA is described. [C3063]

### "SE-IT joint M-AESA program: Overview and status"

The Multi-function Phased Array (M-AESA) program is a joint SE-IT initiative for the development of a capability driven multifunction phased array system concept. This paper will present the progress the M-AESA research and development program has made over the last three years and it follows the paper "New concepts for MRFS evolutionary trends. The M-AESA program: A joint IT-SE capability driven approach" by V. Carulli et al. presented at the Radar Conference 2008 in Rome [1]. The program, based on a number of different national initiatives, benefits from different cultural approaches and perspectives, and aims to lead an initiative in Europe for such a new family of RF systems. An overview and status of this unique R&D partnership will be discussed with a mission of evaluating new technology and system architecture for developing the next generation phased array antenna system capable of exploiting the most relevant operational functions (Radar, EW, Comm) according to the operational scenarios. However, a number of technical, operational and cost issues are still remaining to be addressed before M-AESA can become a reality. [C3064]

### "Toward common radar & EW multifunction active arrays"

Military Air platforms are fitted with Fire Control or Surveillance Radars, usually operating in X-band, Electronic Warfare Systems (EWS), and some radio links. Each of these systems is dedicated to a particular task and the cooperation is reduced to a minimal exchange of information between them mainly for avoiding mutual

disturbances. Major system performance enhancements are to be expected thanks to close co-operations of one sensor to each others and thanks to the sharing of resources, especially in the field of multifunction AESA antenna sharing. The future co-operations can be ordered in four levels. The levels one to three lead progressively to a multi-functions sensor. The last one is the deployment, on a single or multiple platforms, of compact multi-functions sensors on a network basis. Another area of co-operation is the realization of R.F. functions such as "ad-hoc" communication functions using the Radar or the EWS multifunction R.F. and antennas. [C3065]

#### "Acoustic tracking of aircraft using a circular microphone array sensor"

Runway Incursion Avoidance Systems (RIAS) are vital parts in the prevention of runway accidents at airports. Such systems depend on the accurate positioning of aircraft and ground vehicles. Today, RADAR is the predominant method, but a RADAR based system might be both impractical and too expensive for small airports. Additionally, the redundancy of several independent systems is sought after even at large airports. We investigate the application of a low-cost circular microphone array solution for acoustic detection and tracking of aircraft. The shape of the array yields 360° coverage with equal characteristics in all directions. An algorithm based on sweeps performed with the Capon adaptive beamformer followed by peak detection and thresholding is implemented for real time use. The performance of the system is tested at Evenes airport in Norway. [C3066]

#### "Adaptive space-time beamforming technique for passive radar system with ultra low signal to interference ratio"

In recent years, the passive radar, using the noncooperative illuminators of opportunity, has attracted increasing attention. We discuss beamforming technique with application to the passive radar system. For realization issue, adaptive beamforming technique can be used to detect and estimate the signal-of-interest at the output of a sensor array by means of the adaptive spatial filter to suppress interference. Specially, the adaptive beamformer based on constrained least mean squares algorithm has been derived which is capable of adjusting an array of sensors in real time to detect the signal-of-interest and eliminate interference. We will exploit the space-time processing algorithm for the passive radar system, in order to increase the degrees of freedom without limiting the system output SINR. For more efficient and practical implementation, the proposed space-time beamformer can be realized by the recursively adaptive algorithm with multiple constraints. Finally, the proposed space-time beamformer can be operated in multiple linear constraint mode to combat the angle mismatch problem. From simulation result, it is shown that the multiple constraint space-time beamformer provides better OSINR performance with resistance to strong interferences. [C3067]

#### "High precision DOA estimation of SSR transponder signals"

In this work, localization by means of DOA (Direction of Arrival) estimation is investigated. A newly developed low-cost planar linear array and improved receiver hardware is calibrated and evaluated by the use of a dedicated measurement aircraft, not based on ADS-B (Automated Dependent Surveillance-Broadcast) airborne position telegrams. It will be shown how this DOA sensor closely approaches theoretic precision limits. [C3068]

#### "MIMO radars or is it smart antennas?"

Radars were originally designed as detectors of targets. The goal was to transmit a signal with the maximum available power and then observe whether the received signal contained a portion of the transmitted signal. A matched filter was then designed using the transmitted waveform to detect the received signal and based on some statistical hypothesis testing a decision was made on whether a target is present or absent. However, when multiple targets are to be examined or one wants to search for a low observable near a large target, the conventional detection based radar processing is not adequate. A need for finding small targets in the presence of clutter and jammer evolved into an estimation theory problem rather than detection. It is illustrated that use of a phased array in a SIMO mode can perform quite well as one does not have to worry about the inhomogeneity of the clutter associated with multiple transmissions in a MIMO system as the processing becomes quite complicated. Also, the compensation of mutual coupling becomes difficult in a practical deployment on a moving platform. It is important to note that one can still exploit the advantages of super-resolution processing using estimation theory keeping the advantages of a single high power transmitting antenna in a phased array deployment. This paper illustrates such a methodology which has been in the published literature for at least a decade and compares it with the recent MIMO developments. Examples are presented related to a single snapshot based least squares methodology that can cancel interferer in the main beam using a phased array radar but performing a deterministic processing using the same number of degrees of freedom as a multisnapshot case for coherent processing. [C3069]

### "Denoising of single-look SAR images based on variance stabilization and nonlocal filters"

Synthetic-aperture radar (SAR) imaging has become an efficient tool for obtaining and retrieving useful information about surfaces of Earth and other planets. However, the formed images suffer from speckle noise, especially if single-look observation mode is used. Then, filtering is often applied to improve image quality and provide better estimation of radar cross-section and other parameters of sensed scenes. Recently, a novel class of image filters has proved to be very successful in the removal of additive white Gaussian noise from natural images; these filters are based on nonlocal image modeling, i.e. they exploit the mutual self-similarity of image patches at different locations in the image. These filters have been shown in several benchmarks to significantly outperform all previous techniques. In this paper, we evaluate the performance of nonlocal filters applied to the denoising of single-look SAR images corrupted by speckle with a Rayleigh distribution, taking advantage of exact forward and inverse variance-stabilizing transformations. Numerical simulations demonstrate the success of this approach against several known despeckling methods. [C3070]

### "On the design of integrated HF radar systems for Homeland Security applications"

In this paper, HCAC's research and development efforts on the development of integrated and low cost HF radar for coastal surveillance and other Homeland Security applications are summarized. The proposed design incorporates electrically small antenna for rapid deployment, supports operation on floating platforms by using enhanced DSP algorithms to mitigate clutter, incorporates improved propagation modeling to more accurately select optimum frequency channels based on atmospheric conditions and overcome the errors due to terrain effects, utilizes Genetic Programming for automatic target recognition and classification, and provides for passive radar operation utilizing existing broadcast transmitters to enable covert operation. [C3071]

### "Iterative focusing algorithm to estimate moving target"

In this paper, the authors have presented iterative focusing algorithm (IFA). Under the condition of the same number of bins, IFA demonstrates imaging performance superior to that obtained using DAS because of the area focusing. IFA with DAS algorithm significantly improves the amount of computation than the conventional IAA algorithm. Furthermore, by focusing the scanning area, bin size is reduced, and the estimation accuracy is improved significantly. IAF with IAA algorithm performs better than IAF with DAS algorithm. Note that IAF with IAA algorithm takes huge amount of computation. If the authors allow little ambiguity, the IFA with DAS algorithm is effective for both target imaging and computation. [C3072]

### "Adaptive filtering and target detection for ultrasonic backscattered signal"

In radar, sonar, medical ultrasound, and ultrasonic nondestructive evaluation, environmental noise makes target detection challenging. Therefore, clutter rejection and noise cancellation are necessary for the system to correctly identify targets. In this study, an adaptive filtering algorithm is used to reject clutter and detect small targets in noisy ultrasonic backscattered signals. Simulation and experimental results show that adaptive filter can efficiently reduce the clutter and improve the detection capability. [C3073]

### "High range resolution moving target indication at long stand-off ranges using minimal sampling rates in linear FMCW radar"

Combinations of high range resolution, long standoff ranges and the requirement for moving target indication in LFMW radars tend to increase the required signal sampling rate. A simple method of calculating a suitable sub-sampling rate to down-convert the signal by exactly aliasing the required information is described, providing a means of dramatically reducing the sampling rate. The technique is demonstrated in numerical simulations and with a mm-wave radar. [C3074]

### "High resolution terahertz imaging (T-ray) with a horn antenna"

We suggest a simple method overcoming the limitation of spatial resolution for wavelength by using a horn antenna. And, we verify detection limitation by THz imaging for a foreign object in flour. [C3075]

### "Combined passive and active millimeter-wave imaging system for concealed objects detection"

In this paper, a comparison between both imaging techniques is performed with the aim of integrating both in a single imaging system. It is expected that the combination of the coherent and incoherent radiation in active and passive operation will offer improved detection and identification of concealed objects. An interferometric radiometer and an active mills-cross have been studied as near field imaging systems. The main parameters have been simulated to foresee their performance as image scanning systems. Moreover, a T-shape active

imaging system has been built and measurements have been done in order to test and assess the performance of this imaging geometry. [C3076]

#### **"Measurement-based delay-and-sum signal processing for linear antenna arrays"**

The design of a delay-and-sum beamformer based on measured data is presented in this paper. Traditionally the weighting of a delay-and-sum beamformer is designed based on an idealized signal model, with specifications on the beam pattern in terms of the beam width and the sidelobe level (SLL). The goal is a trade-off between resolution and the ability to detect targets with a certain dynamic range. In this work we propose an approach to the optimization of a delay-and-sum beamformer with the same goal in mind however not based on the ideal signal model, but based on measured data. Being a measurement-based method even effects of non-idealities that are not part of the ideal signal model such as mutual coupling can be suppressed. The proposed approach is validated in simulations for a 77-GHz 36-elements non-uniform frequency-modulated continuous-wave radar array. [C3077]

#### **"Experimental validation of high-permittivity ceramic double-ridged horn antennas for biomedical ultra-wideband diagnostics"**

Low-power ultra-wideband (UWB) radar sensors are attracting more and more attention, e.g., for biomedical diagnostics. In contrast to established techniques like X-ray tomography or invasive approaches, UWB radar offers the potential for remote access and, based on suitable waveforms, ultra-low power signal intensities. This paper presents a complete characterization of a miniature ceramic double-ridged horn antenna. The input matching, radiation pattern, and impulse response reveal a performance promising for biomedical diagnostics. A further improvement and miniaturization will become accessible by optimized manufacturing processes and feed impedance, respectively. Preliminary volunteer measurements showed the suitability of the antennas for the envisaged applications and justify our approach. [C3078]

#### **"Improved range resolution for FMCW HF surface wave radar"**

A modified signal processing for FMCW waveform has been proposed that yields an improved range resolution without increasing the transmitted signal bandwidth. The chirp duration is reduced by an appropriate factor while the interval of the beat signal sequence considered for the range transform is kept constant. This modification implies a range transform over several chirp sweeps and an interleaving technique for the Doppler transform. Range resolution is improved without affecting the maximum unambiguous Doppler. This is achieved on the expense of a reduction of the maximum unambiguous range. Actually, this is not a restriction for HF SWR systems where the maximum range is limited by surface wave attenuation. However, a minimum practical range bin size is given either by the size of the targets considered or by the acceptable size of range side lobe level coming along with increasing range resolution. With this approach first and second order sea clutter is reduced which is of significant interest for ship detection. [C3079]

#### **"Low-profile dual-polarized UHF array antenna"**

A low-profile dual-polarized UHF array antenna has been developed for wide field-of-view dual sector coverage in the 250 to 450 MHz frequency range for communications or radar applications. The antenna utilizes a pair of parasitically-tuned dipole arrays for horizontal polarization and a pair of parasitically-tuned monopole arrays for vertical polarization, and both arrays are mounted on a common ground plane. The thickness of the antenna is 18.2 cm. Numerical electromagnetic simulations were used to analyze and optimize the antenna parameters prior to fabrication. Measurements of the dual-polarized prototype in an anechoic chamber demonstrate the antenna's return loss and dual-polarized radiation gain pattern performance. [C3080]

#### **"Array antenna pattern synthesis using measured active element patterns and Gram-Schmidt Orthogonalization"**

In this study, a practical and generalized method for array pattern synthesis for any given array is presented. The method is based upon measurement of active element patterns and then processing of these patterns by Gram-Schmidt Orthogonalization procedure. As the mutual coupling effects are taken fully into account by element pattern measurement, the synthesized pattern is in excellent agreement with the real behavior of the array. Usage of orthogonalization guarantees the Least Squares Error for the synthesized pattern. Combining the technique in with the proposed method, it is also possible to make Phase-Only Synthesis for a given array. The method was applied to 10 rows of X-band slotted waveguides each consisting of 44 slots. The antenna pattern was measured at a planar near field range, and practically negligible difference was observed between the predicted and measured patterns. [C3081]



### "Efficient beam scanning, energy allocation, and time allocation for search and detection"

Recently-developed unique and innovative concepts for efficient radar search and detection are reviewed. These results provide answers to the two fundamental search questions: (1) Where should the radar beam point during the next increment of search effort (energy and time)? (2) How much radar effort should be expended during the next increment of search effort? These results provide the most efficient allocation of radar search effort in both space and time which maximizes target detection performance and minimizes radar search energy and time. Typical savings of several dB of radar power-aperture product and/or expected (average) detection time are obtained. These new techniques are practical and can be used in the next generation of radars with agile beams and variable-energy search waveforms. Furthermore, the problem formulation and solution are very general, so these search and detection techniques developed for radar can also be applied to other both active (transmitting and receiving) and passive (receive only) electronic sensors: optical, IR, UV, sonar, seismic, passive RF, astronomy, etc. [C3082]

### "Bandwidth assignment for target tracking in coherent distributed aperture radar networks"

Multiple target tracking using networks of coherently integrated radar apertures is a current research topic that promises improved tracking accuracy and more efficient system implementations. The design of such tracking systems is complicated by the multiple subsystem functions involved in overall system performance. The separate isolated design of these functions results in suboptimal system performance. In this paper we consider the overall multiple radar system optimization by means of aperture waveform bandwidth allocation. In general, a greater aggregate bandwidth assigned to a target results in a more accurate target track. However, since multiple targets are simultaneously tracked, the data network transmission capacity limits the overall throughput resulting in a resource assignment problem. The assignment problem is specifically to assign available multi-radar bandwidth in a manner that maximizes the number of targets that achieve a terminal tracking error that is less than the maximum error allowed. We introduce a multistage control framework to demonstrate the performance of a proportional assignment procedure for countering a saturation attack. Conclusions for designing suitable distributed radar systems are given. [C3083]

### "The DESDynI synthetic aperture radar array-fed reflector antenna"

DESDynI is a mission being developed by NASA with radar and lidar instruments for Earth-orbit remote sensing. This paper focuses on the design of a large-aperture antenna for the radar instrument. The antenna comprises a deployable reflector antenna and an active switched array of patch elements fed by transmit / receive modules. The antenna and radar architecture facilitates a new mode of synthetic aperture radar imaging called 'SweepSAR'. A system-level description of the antenna is provided, along with predictions of antenna performance. [C3084]

### "Polarimetric phased array weather radar: Concepts for polarimetric calibration"

The National Severe Storms Laboratory (NOAA-NSSL) and the Advanced Radar Research Center at the University of Oklahoma (OU-ARRC) are presently involved in the design, development and construction of a cylindrical polarimetric phased array radar (CPPAR) to demonstrate polarimetric capabilities for weather sensing within the Multi-function Phased Array Radar (MPAR) project. The bias in radar meteorological polarimetric variables is dependent on a number of parameters like cross-to-copolar gain ratio, integrated cross-polarization level, cross-to-copolar phase, copolar beam-width mismatch and beam pointing angle mismatch [1-2]. In the first part we present a preliminary system design for CPPAR, in the second part we present a procedure for polarimetric calibration using a target of opportunity, namely rain. Polarimetric calibration such as this one is extremely important for polarimetric phased arrays, since calibration needs be done on a beam by beam basis. [C3085]

### "Analyzing SAR ambiguities in the u-v plane"

Phased array designers routinely analyze beam patterns in the u-v plane, to ensure that aliasing locations (called grating lobes) remain outside the visible beam region. A related spatial aliasing problem occurs in synthetic aperture radar (SAR) systems, where points that can fold onto other locations in an image (called ambiguities) must be kept out of the radar main beam. A well-known SAR criterion specifies the minimum area of a rectangular antenna for ambiguity-free operation. This paper employs a phased array-inspired approach to solving the SAR problem for general antennas, by overlaying SAR ambiguities onto the antenna beam pattern in the u-v plane. A theorem from Number Theory then provides the maximum beam area that does not illuminate ambiguous points, under general conditions. This maximum beam area criterion extends the classic minimum antenna area expression to non-rectangular antennas in unconventional orientations, while providing intuition and

visualization familiar from phased array design. [C3086]

#### "Analysis of a novel MIMO system for security applications"

Recent years have shown how the performances of the standard radar systems can be significantly improved by using a multiple-input multiple output (MIMO) approach. MIMO technique is an already well studied method for communications applications thanks to the benefits that it offers in multipath fading environments. This paper is aimed to present the design of a new MIMO based, short range, surveillance radar for local area security purpose. One of the main addressed features to the system under consideration is the capability to provide full 360° azimuth coverage within its working area. The following analysis will be focused on the system structure description and on the first simulated results. [C3087]

#### "Transmit/Receive Module technology and related multifunction active radars in Selex-Sistemi Integrati"

The paper deals with the SELEX-SI Transmit/Receive Module (TRM) technology and related radar applications. Since the end of '90s SELEX-SI started its activities on the active technology, establishing a 20 years Road Map including GaAs and GaN components and evolving through the increase of effective generated power and efficiency, and through the decrease of Noise Figure for sensors applications. The Road Map is comprehensive of a large frequency band interval, with specific attention to C and X band. As far as it concerns the G band radar sensor application of the active technology, this paper describes Selex-SI Active EMPAR (in the future named C-HOUND) and KRONOS radars. KRONOS and Active EMPAR are multifunctional, multi-role G-Band radars based on Active Electronically Scanned Antenna (AESA). Active EMPAR is designed as a technologic upgrade of the SELEX Sistemi Integrati well proven EMPAR Multifunctional radar system provided to the Italian and French Navies. In this paper the two radar features will be detailed in terms of implemented technical and technological solutions and related advantages in surveillance, tracking and other functionalities required for a Combat System. [C3088]

#### "Low-loss, MEMS based, broadband phase shifters"

Broadband, true time delay phase shifters based on MEMS switches provide the high instantaneous bandwidth desired for applications such as multi-frequency antenna arrays with multiple functions such as radar, communications, and ECM. MEMS based phase shifters offer significant performance advantages compared to technologies using PIN diode or MESFET switches including high linearity that does not limit the dynamic range of the receiver in a crowded signal environment. Furthermore, MEMS phase shifters offer a combination of low RF insertion loss and low switch control power consumption that is unmatched by PIN diode or MESFET technologies, giving the MEMS phase shifters a decided advantage at reducing prime power consumption in airborne or space based systems. Radant MEMS Inc., employing its high power 10 Watt MEMS switch with a demonstrated 1 trillion cycle lifetime, designed, fabricated and tested a 6-bit, 5 Watt, true time delay, 1-6 GHz, MEMS phase shifter that, with the exception of the three longest delay lines, was integrated on a single silicon die. This compact, low cost phase shifter is hermetically sealed using the same wafer capping process now employed for Radant's MEMS switches. [C3089]

#### "Development of a low-cost, man-portable, Phased Array X-Band Radar"

A compact, active scan, X-Band Phased Array Antenna has been developed and tested. This antenna is supportive of a man-portable ground surveillance Radar, and has been designed for low manufacturing cost. The design supports  $\pm 60^\circ$  azimuth scan angles, and features a "cosecant squared" elevation pattern for reduced ground clutter effects. Antenna patterns and active scanning consistent with design goals have been demonstrated. These results support the current Cobham development efforts towards a complete, low-cost, man-portable Radar system. [C3090]

#### "Antenna array diagnosis in situ: Experimental results using microwave circular holography"

This paper is presenting the experimental performance of a circular microwave holography algorithm for the troubleshooting of in-service array antennas. The experiment is conducted using an algorithm for the estimation of array element excitations from circular near field measurements. The experimental results exceed those obtained from the preliminary numerical simulations. [C3091]

#### "Phased array calibration and diagnostics utilizing a student-built planar near-field system"

A low-cost planar near-field system was designed, built, and programmed by students from the University of Rhode Island as a Capstone design project sponsored by Applied Radar, Inc. The objective of this paper is to

explore the implementation of microwave holographic metrology (MHM) for the use of calibration and diagnosis of phased array performance on this near-field system. The simplest form of MHM is to analyze the near-field data on the collected planar surface, but this is not ideal because of a loss of resolution from the spreading introduced by the measurement distance. A more attractive approach is to project a focused planar "hologram" of the radiation pattern on the surface of the aperture of the antenna under test (AUT) through manipulation of the angular spectrum. The resulting hologram allows for the observation of amplitude and phase distributions on the aperture. This paper will provide insight into the design of the back-projection algorithm and present results for faulted and calibrated phased array scenarios to verify proper functionality of the algorithm. [C3092]

#### **"Accurate antenna pattern modelling for spaceborne active phased array antennas"**

In example of measurements performed in space with TerraSAR-X, an approach for an accurate antenna characterization is described. TerraSAR-X was launched in June 2007 and is a highly flexible X-band radar satellite based on an active phased array antenna. Its primary objective is the acquisition of high quality SAR images in a multitude of possible acquisition modes. As this demand is of paramount importance, an accurate characterization of the antenna is a major task, i.e. thousands of different antenna beams being operated have to be determined precisely for compensating the impact of the antenna on SAR data products. Only then, a spaceborne SAR system based on an active phased array antenna can be successfully commissioned. This paper presents the methodology and results derived from different measurements performed for characterizing an active phased array antenna in flight. [C3093]

#### **"MIMO radar joint estimation of target location and velocity with multiple subcarrier signals"**

This paper analyzes the effect of waveform parameters on the joint target location and velocity estimation by non-coherent multiple-input multiple-output (MIMO) radar transmitting multiple subcarriers signals without energy constraint. How the number of subcarriers influence the estimation accuracy is illustrated by considering the joint Cramer-Rao bound (CRB) and the mean square error (MSE) of the maximum likelihood (ML) estimate. The non-coherent MIMO radar ambiguity function (AF) with multiple subcarriers is developed and investigated by changing the number of subcarriers, the pulse width and the frequency spacing between adjacent subcarriers. The numerical results show that more subcarriers means more accurate estimate and higher localization resolution, larger pulse width results in worse performance of target location estimation, while the frequency spacing affects target location estimation little. [C3094]

#### **"Real-time through-wall imaging using an ultrawideband multiple-input multiple-output (MIMO) phased array radar system"**

A real-time acquisition and processing architecture has been developed for an ultrawideband (UWB) S-band (2-4 GHz) multiple-input multiple-output (MIMO) phased array radar system that facilitates greater than 10 Hz imaging rates, providing a video-like radar image of what is behind a concrete wall. Video rate imaging enhances the interpretability of range vs. range through-wall and free-space radar imagery. Images are formed without a-priori information. Video framerate imaging is achieved by designing an electronically switched bi-static array using high-performance microwave components, a multi-threaded data pipeline, and efficient hardware-accelerated processing algorithms. Experiments successfully image low radar cross section (RCS) objects, fast moving objects in free-space, and a human behind a 10 cm-thick solid concrete wall. [C3095]

#### **"Scalable multifunction RF system concepts for joint operations"**

RF systems based on modular architectures have the potential of better re-use of technology, decreasing development time, and decreasing life cycle cost. Moreover, modular architectures provide scalability, allowing low cost upgrades and adaptability to different platforms. To achieve maximum benefit from modularity and scalability, the challenge is to define the front-end concept in such a way that it supports multiple functions and is applicable in multiple environments and platforms. This paper describes concepts for such modular systems that may be used for RF functions in maritime, airborne and land based systems. The first part discusses general scalability properties of various RF functions, the second part discusses example system concepts in a 'joint' scenario (land/sea/air). The focus of this paper is on X-Ku band systems: considering essential RF functions like radar and communication, and the types of platforms in maritime, land-based and airborne operations, this frequency range provides the highest potential for application in all these domains and platforms. Conceptual designs for weapon location radar, SAR/GMTI, surveillance radar and tactical data link are presented. [C3096]

#### **"A wide band low profile dual-pol "Thumbtack" array"**

A dual-pol array of 15x15 "Thumbtack" elements was built and tested for 0.5-2.0 GHz demonstration. The array

is 3 in. (7.6 cm) thick, a bout 1/8 wavelength at the low end of the band, characterized by a high impedance (~300 ohms) aperture, matching to free space's wave impedance (377 ohms) directly without a long flare as in a Vivaldi notch. The array has a square lattice of 3 in. (7.6 cm) spacing, and the "Thumbtack" element has a coincident and stationary phase center. The thin and planar structure produces very low X-pol, typically 30 dB down at bore-sight, and 15 dB at 45° of axis along the diagonal cut. The array was designed for applications that require nanosecond rise time, ultra low X-pol and non-dispersive phase response. These unique features make it possible to produce sharp images for IED detection, FOPEN SAR, see-through-the wall radars, and other EW missions. [C3097]

#### "MIMO radar for sense and avoid for UAV"

UAV are easily deployable platforms. Up to now they carry payloads (surveillance, combat) for military purposes in crisis or war time. For training, UAV are flown in special areas attributed in a limited space and a limited time slot. In the future, UAV will also be used for civilian tasks. For these reasons, UAV will have to be inserted in the general Air traffic and "Sense and Avoid" systems will be mandatory. Among the possible sensors, the radar is the most pertinent one: it is "all-weather" and provides accurate range, direction and closing speed. In this paper, a low cost solution based on the coherent "MIMO" principles is described. This solution allows the location of the radar within the UAV airframe without any moving parts, hence provides a high reliability level. The rationale of the proposed architecture is explained, then the enabling technologies and related waveforms are described. [C3098]

#### "Beampattern optimisation for sub-arrayed MIMO radar for large arrays"

The estimation of the direction of arrival (DOA) of signals in the far-field of an array has been an area of continued research. Recent advances in MIMO radar techniques have led to results whereby prior knowledge of the approximate target locations is used to generate arbitrary signals which are transmitted from an active array to improve DOA estimates. This would be a useful in a scenario such as target tracking. However, this neglects the complexities of the hardware required for larger arrays, and further, the amount of computation required on the transmit side alone. A sub-optimal method employing sub-arrays to reduce hardware requirements, and a low complexity algorithm to determine the optimal steering vectors for the arrays is presented and compared to the optimal full diversity transmit strategy. [C3099]

#### "An ultrawideband (UWB) switched-antenna-array radar imaging system"

A low-cost ultrawideband (UWB), 1.926-4.069 GHz, phased array radar system is developed that requires only one exciter and digital receiver that is time-division-multiplexed (TDM) across 8 receive elements and 13 transmit elements, synthesizing a fully populated 2.24 m long ( $\lambda/2$  element-to-element spacing) linear phased array. A 2.24 m linear phased array with a 3 GHz center frequency would require 44 antenna elements but this system requires only 21 elements and time to acquire bi-static pulses across a subset of element combinations. This radar system beamforms in the near field, where the target scene of interest is located 3-70 m down range. It utilizes digital beamforming, computed using the range migration synthetic aperture radar (SAR) algorithm. The phased array antenna is fed by transmit and receive fan-out switch matrices that are connected to a UWB LFM pulse compressed radar operating in stretch mode. The peak transmit power is 1 mW and the transmitted LFM pulses are long in time duration (2.5-10 ms), requiring the radar to transmit and receive simultaneously. It will be shown through simulation and measurement that the bi-static antenna pairs are nearly equivalent to 44 elements spaced  $\lambda/2$  across a linear array. This result is due to the fact that the phase center position errors relative to a uniform  $\lambda/2$  element spacing are negligible. This radar is capable of imaging free-space target scenes made up of objects as small as 15.24 cm tall rods and 3.2 cm tall metal nails at a 0.5 Hz rate. Applications for this radar system include short-range near-real-time imaging of unknown targets through a lossy dielectric slab and radar cross section (RCS) measurements. [C3100]

#### "Low cost Multifunction Phased Array Radar concept"

MIT Lincoln Laboratory and M/A-COM are jointly conducting a technology demonstration of affordable Multifunction Phased Array Radar (MPAR) technology for Next Generation air traffic control and national weather surveillance services. Aggressive cost and performance goals have been established for the system. The array architecture and its realization using custom Transmit and Receive Integrated Circuits and a panel-based Line Replaceable Unit (LRU) will be presented. A program plan for risk reduction and system demonstration will be outlined. [C3101]

#### "Demonstration of accurate prediction of PAVE PAWS embedded element gain"

We can now accurately theoretically predict the embedded element gain and 2-way scan loss of the PAVE



PAWS array to within 0.25 dB over 420-450 MHz band up to 60° scan and 0.4 dB up to 75° scan. When the PAVE PAWS array, which uses a bent, crossed-dipole element, was built in the 1970's tools were not available for accurate prediction. Expensive experimental trial-and-error measurements were used. The theoretical predictions were made using the Ansoft High Frequency Structure Simulator (HFSS). Accurate mutual coupling measurements made in 1977 on a 320 element PAVE PAWS test array were used for verification. [C3102]

#### "Self tapered array lattice for high efficiency transmit applications"

Applications for phased array antennas have become increasingly diverse. This is true for current state of the art radar systems (sense and avoid, imaging, weather, etc) as well as communication antennas. Many of these applications require low sidelobe performance or beam-widths tailored to a specific application. Current methods to implement amplitude taper over the array aperture involve attenuators or unequal power splitting networks. These traditional methods have negative impacts to system performance. In this paper, we present the results of the investigation of two alternate approaches for improving the EIRP and simplicity of tapered array lattices that do not make use of conventional techniques involving dissipative attenuation or unequal power dividers. These techniques are intended to improve the EIRP from a given transmit array size without compromising side-lobe suppression. A conventional approach using power dividers is presented for comparison. It is shown that the EIRP available from a transmit aperture may be increased by more than 6 dB while maintaining low side-lobe levels. [C3103]

#### "An s-band ultrawideband time reversal-based RADAR for imaging in cluttered media"

This work presents a new RADAR prototype built for the purpose of imaging targets located in a cluttered environment. The system is capable of performing Phase Conjugation experiments in the ultrawideband GHz. In addition, applying the D.O.R.T. method to the inter-element matrix allows us to selectively focus onto targets, hence reducing the clutter contribution. The system has been validated by physically backpropagating the focusing wave into the medium all over the frequency band and observing the expected focusing properties. [C3104]

#### "Concurrent multifunction transmit and receive applications with dynamic filtering"

This paper demonstrates a concept for transmitting on one set of elements of a phased array while concurrently receiving on another set at a separate frequency. Cases are analyzed using measured data from an 848 microstrip stacked patch panel array operating at 33.8GHz, and relative coupling levels from interfering elements to receive elements are characterized over various scan angles for two array configurations-side-by-side contiguous blocks and for interleaved elements at separate frequencies. It is shown that an optimum transmit frequency exists that minimizes coupled power to receiving elements in the array for a given scan angle. Additional isolation between elements is achieved with a tunable bandpass-bandstop filter cascade that, when paired with a high-linearity low-noise amplifier, reduces interference from transmitting elements to within the receiver analog-to-digital converter's (ADC) dynamic range, such that receiving elements can operate concurrently next to 25W transmitting elements. [C3105]

#### "A novel edge wall waveguide slot antenna"

In this work, a novel excitation technique for non-inclined edge wall waveguide slots is developed. The proposed method greatly facilitates the manufacturing of large edge wall slotted waveguide arrays with very low cross polarization levels at the cost of deviation from shunt slot model. Slots are characterized using the infinite array approach in two dimensions and using this characterization data, travelling wave type linear arrays are designed. A planar array is also formed using previously designed linear ones. Designed antenna arrays are simulated and the results show that the infinite array approach is suitable for the design of these types of antennas. [C3106]

#### "Detection in collision avoidance radar using active versus passive phased arrays"

This paper presents two designs for phased arrays for collision avoidance radar operating at the 76 GHz band. The two designs for the antenna use a linear waveguide horn array that is fed with a waveguide power-dividing network and is tapered to produce low side-lobe levels for low-error detection. The taper is based on a 40-dB Taylor distribution. The first design uses passive phased arrays that are stacked and bore-sighted in different directions to produce scanned beams through switching. The second design uses a single phased array with MEMS phase shifters embedded in the last stage of the waveguide power divider. The phase shifters are integrated with the help of MIC/MMIC-to-waveguide or waveguide-to-coplanar-waveguide (CPW) transitions that are housed in the waveguide sections that feed the array elements. The antenna and detection system measurement results of the passive array design are presented, along with the simulation results of the active array design. [C3107]

### "Em wave scattering by perfectly conducting disk of finite thickness"

Calculation technique for modeling of scattering characteristics for perfectly electrically conducting (PEC) disk of finite thickness is proposed. Employed algorithms are based on solving surface integral equations (IE) of the 1st and 2nd kind. The results of radar cross section (RCS) calculation for discs with various thicknesses are compared with exact results for infinitely thin disc. The backscattered radiation patterns of thin disc in E- and H-planes are presented. [C3108]

### "New Kravchenko transforms and digital UWB signal processing"

In this report the new Kravchenko transforms based on atomic distributions for digital UWB radar signal processing is proposed and proved. This approach has some advantages in comparison with Gabor transform for parameter estimation in radar. [C3109]

### "UWB noise acoustic atmospheric radar"

In this paper we discuss a new approach to create the acoustic atmospheric radar (sodar) which is based on noise sounding waveform. Such sounding waveform fits all formal requirements to UWB signals and has remarkable characteristics including extremely high range and speed resolution. It is important to remember that all these good properties exist only in the case when we have independent samples. The noise signal forms the independent samples because of its nature. The prototype of the radar is described and investigated theoretically, using computer simulation, and in natural conditions. Non-parametrical signal processing algorithm is developed based on statistical approach and digital signal processing. It has wonderful properties of invariance to the group of the noise and signal transforms and stable level of the false alarm probability can be applied for both acoustic and microwave UWB noise radars. The use of the FFT algorithm increases the speed of calculations and gives us the possibility of constructing digital random signal radars. The results of this project confirm that the random signal radar is one of the most interesting types of radar. It combines properties of UWB radar with some additional features, based on random nature of the sounding waveform. These new properties allow us to simplify signal detection algorithms and measure a distance, an azimuth and a target velocity simultaneously with high resolution and accuracy. [C3110]

### "Investigation of phase coded signals based on generalized Frank codes"

In this paper comparative analysis of spectral and correlation characteristics of phase coded signal based on Frank code is given. [C3111]

### "Copyright page"

The following topics are dealt with: GPR; radars; communication; medicine; UWB antennas; pulse generation; pulse radiation; electromagnetic compatibility; and electromagnetic metrology. [C3112]

### "Polarimetric suppression of early-time scattering for late-time target identification"

One can suppress the strong signal amplitude of the early-time scattering, relative to the late-time signal containing the natural resonances (for target identification) using various techniques. This paper discusses the use of polarization for the early-time suppression. [C3113]

### "Spectral theory analysis of UWB-oscillations in frequency synthesizers based on phase-locked loops"

In this report a general theory of phase-locked loop (PLL) for N-dimensional UWB-signals (for example radar and optical signals) is given. On the first step a discretization method for solving differential equations of the PLL systems is presented. It is shown that there are a lot of zones of synchronous in discretized PLL and a technical realization of this device (in PLL with samples). A spectral theory of analysis of oscillations in PLL with samples is given. It is shown a lot of different physical properties in PLL with samples. The effect of shape of the input signals (harmonic signals, splines and atomic functions) at the border zones of operating modes being entered into PLL with samples is examined. [C3114]

### "Scale electrodynamic modeling of ultra wideband systems"

Rules which observance is necessary at performance of scale modeling narrow-band and ultra wideband electrodynamic systems are shown. [C3115]

### "The device for remote monitoring of human's heartbeat"

This article describes creating principles of the device intended for round-the-clock human breath and heart rate monitoring. This device can be used in intensive care unit's and burns departments, maternity hospitals and also by EMERCOM employees. Heart rate detection is possible because of the Doppler effect. The Doppler frequency selection is based on the homodyne method of signal conversion. [C3116]

### "Way of an estimation trajectory instability of flight of the air targets"

In article necessity of measurement and the account for systems of construction of radar-tracking images of parameters trajectory instability flight is proved. The method of an estimation of the law of change of angular speed of turn of the air target on sequence range profiles is offered. The estimation of reliability of the received information is made at decrease in the relation a signal/noise. [C3117]

### "Estimation power and spatial characteristics of ultrawideband radar for statement of protecting handicaps"

Considered the factors that determine the conditions of radiotechnic suppress radiolines control explosive devices, an analysis of experimental studies and an estimate of parameters suppressed radiolines that allows us to determine energetically and spatial characteristics of the antenna system. On the basis of tactical considerations location ultrawideband RTS combat formations moving columns, select a maximal range of producer interference, 20 m and the spectral composition of the signal handicaps of 100 ... 3000 MHz. [C3118]

### "Sampling duration for noisy signal conversion"

A selection of the working band (sampling duration) of the sampler for optimal recording of noisy videopulse radar signals has been considered in the present work. [C3119]

### "Influence of the screen on the range properties of rarefied arrays of near-omnidirectional radiators"

The directional characteristics of arrays of isotropic radiators, Hertz dipoles and half-wave dipoles located above the screen at the arbitrary distance were theoretically investigated. To ensure minimum distortion of the form of ultra-wideband pulse signal radiated by the array, it is proposed to use the radiators of various lengths and arrange them at the different distances from the screen. [C3120]

### "The motion trajectory restoring for radar observation of living objects"

Some technologies of medical radars design are discussed in the report. Radars are intended to obtain the mechanical moving trajectory of living organism chest. Peculiarities of radar detection of targets performing seesaw motion are considered. Data obtaining and processing problems are investigated, methods of initial object motion trajectory restoring are examined by means of two quadratures use, constant component elimination and arctan-demodulation. Methods of received signal processing and computing are proposed. [C3121]

### "Design and analysis of multi-carrier multiple access systems without feedback"

In this paper we study a multiple access system without feedback supporting multiple carriers for delay critical applications with a small loss tolerance. In such a system, users transmits  $R$  times within the next  $N$  timeslots, in order to improve their success probability. In an earlier work, we considered the same problem in a single carrier system and demonstrated that the distribution of properly designed user codes significantly improved the success probability over a random selection strategy. These user codes, that determine the  $R$  slots used for transmission, corresponded to so-called  $2-(N, R, 1)$  designs. Mainly motivated by DVB-RCS satellite systems, this paper considers a system with multiple carriers with the limitation that at any time, at most one slot, and thus carrier, can be used by a single user. We introduce two static and four dynamic slot assignment schemes and under some mild assumptions provide closed form formulas for the success probability in each of these systems. For the last dynamic scheme we will show how group divisible designs are the multi-carrier equivalent of the  $2-(N, R, 1)$  designs of the single carrier system and provide a simple procedure to construct these user codes. Finally, we compare all of the proposed assignment schemes and show that the group divisible designs are superior, especially for large population sizes. Some engineering rules with respect to their usage are also provided. For two of the dynamic schemes we also compare two different strategies in case there are not enough user codes available for all users. [C3122]

### "A compact CPW resonator cell with dual-bandgap characteristics"

In this paper, a compact coplanar waveguide (CPW) resonant cell is introduced, which can exhibit dual-bandgap characteristics by only single unit. The same pattern has been adopted in the microstrip line as reported previously and here is applied to CPW. Experimental results show good agreement with numerical results. By alternating the relative position between CPW defected ground structure (DGS) and split-ring resonator (SRR), the separation between the two resonant frequencies can be controlled easily. [C3123]

### "Digital module design of a satellite rain-compatible radar altimeter"

Satellite radar altimeters play an independent role in ocean remote sensing, while the authors exploited their potential in rain measurement. This paper designs the digital system of the rain mode in an altimeter. In rain mode the altimeter receives the ocean and rain echoes simultaneously, so it can retrieve the rain layer profile without losing surface topography information. An adaptive IF-digital I/Q demodulator is designed, and all of its components are considered in turn. Afterwards the algorithm of an ocean-rain compatible processor is designed to switch the altimeter in various operate modes. [C3124]

### "Copyright page"

The following topics are dealt with: signals; systems; electronics; antenna; microwaves; millimeter-waves; circuits; radar technique; and radar application. [C3125]

### "A new method of radar target recognition based on time-frequency analysis"

In this paper, focused on three targets with simple structure, such as cone, sphere and cone, cylinder and cone, dynamic RCS echo signals is predicted with the improved Greco software. The Dynamic RCS echo signals of targets with micro-movement are preprocessed by using short time Fourier transform, and high-resolution time-frequency distribution images are obtained. A new radar target recognition method based on time-frequency distribution images is proposed. Pixel scan technique is adopted to extract the feature vector, and the nearest neighbor classifier is used for classification decision. Compared with the target recognition method based on singular value decomposition, the correction probability for recognition of the proposed method is higher. Simulation results verify the correctness and the effectiveness of the proposed method. [C3126]

### "Electromagnetic scattering by arbitrarily shaped PEC targets coated with magnetic anisotropic media using equivalent dipole-moment method"

In this article, the equivalent dipole moment (EDM) method is extended and applied to analyze the electromagnetic scattering from arbitrarily shaped three-dimensional (3D) PEC targets coated by magnetic anisotropic media. Besides the advantage of reducing the computation time, the proposed EDM method makes it unnecessary to treat the boundary condition on the surface. The numerical results indicate that the method has strong capability to calculate the RCS of three-dimensional mixed bodies consist of magnetic anisotropic media and PEC targets. [C3127]

### "A novel spiral defected ground structure and its application to the design of dual bandstop filter"

In this paper, a new type of dumbbell-shaped defected ground structure (DGS) called spiral DGS is introduced, which adopts spiral capacitance instead of direct slot capacitance. When compared with direct slot capacitance, spiral capacitance can improve coupling of capacitance, thus lower resonant frequency is obtained for the same circuit size. Simulated results show that a 3.57 GHz lower resonance is achieved, which is useful for the design of miniature devices. Based on the proposed DGS and spiral split ring resonators (SSRR), a compact dual stopband filter (DBSF) is designed and fabricated in this paper. Its dual-bandgap characteristics are verified by both simulation and measurement. [C3128]

### "Characteristics of a CPW mushroom-like resonator and its application to wideband EBG filter"

This paper proposes a novel structure called a compact coplanar waveguide (CPW) mushroom-like resonator (CCMR), which exhibits remarkable bandgap characteristics by only one single unit. The same pattern has been adopted in the compact microstrip mushroom-like resonator (CMMR) as reported previously and here is applied to CPW. When compared with CMMR, the new structure has advantages of easy fabrication and low cost due to its single-layer configuration. To investigate the CMMR deeply, the effect of structural parameters, including patch size and diameter of via, on bandgap characteristics are analyzed in detail. Also, the 1-D CCMR EBG filter is studied for various numbers of cells. Finally, the wideband CCMR EBG filter using united cells method (UCM) is designed, fabricated, and measured. The correction and validity are confirmed by the results of simulation and



experiment. [C3129]

### "Finite element analysis of three dimensional scatterers above the PEC earth"

A three-dimensional (3D) finite-element method (FEM) is introduced to study the scattering from 3D objects above the perfectly conducted earth. Numerical examples are presented to demonstrate the accuracy and efficiency of the presented method. [C3130]

### "A research of stored grain moisture detection based on RIS-K2 radar electromagnetic wave technology"

The amount of moisture in stored grain is an important factor which affects food safety. Therefore, a timely and accurate detection of the moisture content in stored grain is of great importance. Electromagnetic wave has a strong trait of penetrating, which is able to detect the moisture content of grain inside the heap in the case of non-destructive. This paper mainly takes the research of grain moisture which is based on the RIS-K2 radar electromagnetic wave technology. We carry a field test, collect and analyze the results. It shows that the RIS-K2 radar electromagnetic wave measurement of grain moisture is feasible and effective. [C3131]

### "Fused variational analysis technique for high-resolution reconstruction of remote sensing imagery"

In this study, we apply the robust error estimation theory as a basis to develop an appropriate procedure that performs the processing and enhancement of the remote sensing (RS) image contaminated by composite noise (additive and multiplicative) and degraded by the data acquisition system. The first reconstruction stage is performed using the Bayesian statistical estimators referred to as WCMAP { WCLS (Weighted Constrained Least Squares) and MAP (Maximum a Posteriori Probability) algorithms } which significantly increase the gain of image sharpness. Subsequently, we employ the isotropic diffusion and anisotropic diffusion methods for obtaining the optimal balance in reference to increasing the perceptual quality of RS images. The effectiveness of the proposed fused WCMAP method were evaluated through the comparative simulation of different RS image reconstructive. [C3132]

### "Design of high-speed digital correlator in fully polarimetric microwave radiometer"

Fully polarimetric microwave radiometer is a new type of passive microwave sensor for measuring ocean wind vector. Digital correlation technology is used in it to get all the four Stokes parameters of ocean emission in this paper. Digital correlator is the main part of fully polarimetric radiometer. In the paper, design of a novel digital correlator is presented. Two high-speed, dual A/D converters are used to sample four signals, and the sampling results are operated in FPGA-Vertex5 to make both self- and cross-correlation calculations. The test results of the correlator are given. The four channels are sampled at 360 MHz. For both 100 MHz and 150 MHz input, the correlation coefficient between the measurements and their ideal results is above 0.9999999. The whole power of digital correlator is 11.3 W. [C3133]

### "A millimeter-wave solid-state power combining circuit based on branch-waveguide directional coupler"

A new Ka-band (32-37 GHz) eight-way solid-state power combining amplifier using branch-waveguide directional coupler is proposed in this paper. By using low-loss waveguide power dividing/combining network and a monolithic microwave integrated circuit(MMIC) with a low-loss microstrip-to-waveguide transition, a high combining efficiency larger than 80% from 32 GHz to 37 GHz is achieved. With a compact structure, an easy fabrication process, and good thermal property, the power combining network could be used in millimeter-wave solid state high power combining for high efficiency in a broad-band. [C3134]

### "A new simulation model of fuse RF system"

Based on the highlight method, this paper builds up the model of the radar target especially the near field. The database of the properties of near field, which is generated by the fuse antenna, is established using FDTD method. Combining simulation of circuit with computing of near field the simulator was made for fuse system. And by means of this simulator the imitative analysis and calculation on fuse system can be more reliable and accurate. In the end the result of time-domain simulation demonstrate that the simulator can be effectively applied in the synthetic test system to the fuse of the weapon system. [C3135]

### "The usage of extremal coherent integration in the algorithms of processing of reflected signals"

The advantages of digital algorithms when processing of radar data are indicated. The directions of coherent

combining usage of returned signals in radar systems are shown. The range of new digital algorithms of the movement of air objects estimate parameters (including signals with carrier frequency tuning from impulse to impulse) is described and it is based on the list of degree of taking realizations coherence. The requirement for sound signals parameters, providing single retrieval of information, are determined. [C3136]

#### "Wireless home emergency system"

The wireless control technology, power line carrier technology, GPRS and other embedded technology are used to designs a home emergency system which receives start signal from users by wireless and uses GPRS to send help messages to specific persons, moreover starts the alarm and controls the lights to twinkle by PLC technology, so if the users are in trouble they can get help as soon as possible. The experiment result shows that this scheme can achieve the expected effect. [C3137]

#### "A wideband outdoor RCS instrumental radar with high range resolution"

Outdoor static RCS measurement is the principal means to obtain the RCS value of the full-scale targets. This paper firstly presented the imaging principles of the pulse-pulse stepped-frequency radar system. Based on the dominating characteristics of the outdoor RCS measurement, a wide-band (2-18 GHz) and two-channel RCS measurement system was designed and implemented in this paper, which could be applied to backscatter RCS measurement of the full-scale static target, and the high-resolution 2-D imaging of the scatter sources. It could provide the high-precision RCS data of target for the operational frequency range 2-18 GHz. Finally, the technical features of the instrumental radar system were also introduced in detail. This wideband RCS instrumental radar system has been successfully used in an outdoor RCS test range now. [C3138]

#### "Research on GPRS vehicle location network service system"

We can achieve vehicle location tracking on Internet by using GPRS vehicle location terminal and combining with Internet technology and GIS technology. The article gives the design structure of GPRS vehicle location network service system. The system is divided into three parts: GIS network workstations, network communications server and GPRS vehicle location terminal. Then, the article makes the brief introduction to the function of three parts of the system: GIS network workstations are responsible for sending command "Setting GPS Location Data Return Interval" to network communications server, and receiving GPS location data packet uploaded from GPRS vehicle location terminal from network communications server, making analysis of received GPS location data packet; The vehicles will be appeared as title in the specified position on the map by combining with GIS. Network communications server is responsible for receiving the command "Setting GPS Location Data Return Interval" from GIS network workstations and transmitting to the specified GPRS vehicle location terminal and receiving GPS location data packet pass backed from GPRS vehicle location terminal and distributing to the appropriate GIS network workstations simultaneously. GPRS vehicle location terminal is responsible for receiving the command "Setting GPS Location Data Return Interval" sent from network communications server and sending GPS location data collected by GPS module to network communications server. Finally, the article tests the feasibility of system design through experiment. By using the system, it will be easy and fast to make vehicle location tracking on Internet and timely access vehicle location information. [C3139]

#### "The control system for smart home based on GSM and the radio"

In order to guarantee the effective control to the appliances and ensure the safety of living environment, a control system for smart home has been designed. Based on the GSM network service and wireless communication, the system is developed with the MCU AVR mega 16 as the core. It can be divided into two working patterns: the long-distance pattern and the short- range pattern. Experiments have proved the two outstanding functions: under the long-distance pattern, the user can obtain long-distance monitoring of the living environment and get remote control to appliances through the GSM network service; under the short- range pattern, the user can observe the room environment condition through LCD and realize the short- range control to appliances using radio. [C3140]

#### "A study of automation recognition of bridge in SAR image"

According to river and bridge features in SAR (Synthetic Aperture Radar, SAR) image as well as the position relationship between bridge and river, the automatic recognition method of bridge is presented. First, the gradient of an image is calculated by gradient operator in order to get the gradient image, and river region is segmented by Fisher criterion. Then, a doubtful bridge region is extracted by morphology method, and segmented by Fisher criterion. Finally, the bridge is recognized according to the features. Experimental results show that this method can automatically and rapidly recognize bridge. [C3141]

### "A new sorting algorithm for radar emitter recognition"

The radar emitter recognition is a hotspot and difficulty for Electronic Warfare. This paper analyzed radar emitter integrated pulse data's characters and proposed a useful method for radar emitter's integrated pulse data recognition. It concluded and summarized some radar emitter recognition methods' advantages and defects, then used the characteristic values as statistic objects and calculated the weighting coefficient; at last, regarded the characters' weighting value as the sorting object and sorted the pulses. Using a train of fact data as the sample and experimented that the algorithm is effective and realizable. [C3142]

### "Rotation resistance airborne remote image real time matching algorithm"

In allusion to requirement of real time high precision matching of remote image in airborne image aided navigation system rotation resistance airborne remote image real time matching algorithm is put forward to eliminate noise and geometrical aberrance. Because of great information in remote image at first Harris corner detection algorithm is used to extract character point of remote image to increase matching speed, and modified invariant moment is done to correct image distortion caused by different time, different view angel, different sensor and so on; then robust Hausdorff distance is used to realize remote image real time matching to acquire high matching precision, then simulative experiment is done on airborne image acquired by sensor or radar and digital map stored in computer at last. Simulative experiment indicates that image matching rate of rotation resistance algorithm is better than algorithm which is not adopted modified invariant moment, and the algorithm is available and effective. [C3143]

### "Radar cross-section calculation method for antenna of P-18 radar station"

The scattered electromagnetic field calculation method for finite cylinder with resonant cross-section is considered. The method is used for calculation of radar cross-section for antenna of P-18 radar station. Also radar cross-sections for perfectly conducting antenna and antenna partially made of perfectly absorbing materials (Macdonald model) are compared. [C3144]

### "Using conformal shape, separate and dynamical apodization to improve characteristics of multibeam active phased array"

Some results of the project "Torus" are discussed. This paper is focused on 2 mutually complementary methods of improving characteristics of multibeam active phased arrays. Applications of these methods for ground based antennas, HATP and communication satellites are considered. Described methods can be also used for radars. [C3145]

### "Statistical estimation of polarimetric method potential for dangerous turbulence detection in rain"

In this paper the polarimetric approach for wind phenomena detection and study is proposed and analyzed. The polarimetric estimation of turbulence intensity is made with single unipolarized antenna radar system. The statistical estimation of proposed method is made. [C3146]

### "The study of vehicle's anti-collision early warning system based on fuzzy control"

This article mainly studies the automotive collision avoidance system based on fuzzy control. This system selects and uses millimeter-wave radar to measure the distance between two cars and the speed of a motor vehicle. First of all, create the safety distance model of the motor vehicle brake. Secondly, design the fuzzy controller for early warning. Lastly, according to the national highway safety regulation, also by analyzing the related resources theoretically, it can be testified that this system can do the trick of collision warning. [C3147]

### "Model of multi-sensor data fusion and trajectory prediction based on echo state network"

Radar receives more and more attention as an important means of access to information, and multi-sensor data fusion and track prediction become a new discipline. Compared with single radar, multi-radar system has the advantage of improving reliability of the system, enhancing the system when coverage, etc. However, this technology faces new problems when utilizing information in the complex environment. In this paper, we used the nearest data association algorithm (NNDA) to extract tracks from multifarious radar data and three spline interpolation method to make different measuring data track registration to the unity of time axis. Through the same period of fuzzy track correlation, we realized the same target track of extraction, calculated the relative radar accuracy by using the least square fitting, and applied radar tracking precision to be the integration of the weighted average method through the fusion of track-to-track reference. Finally, based on the knowledge of neural network technology, we used echo state network (ESN) to predict data, as ESN network training algorithm

is very good in effectively solving nonlinear dynamic system specifically of uncertainty model. Through simulation test, we concluded that the multi-sensor data fusion and trajectory prediction model precision accuracy is 43.18 m for uniform motion model; for a sudden turn or variable targets, precision accuracy is 122.7m; for complex moving targets, precision accuracy is 165.3m. [C3148]

#### "A study of bias error estimation method by KGBE"

Data fusion uses observations from networked multiple sensors and generates an integrated track. It achieves wide surveillance area and high accuracy, by minimizing error covariance matrix. In ideal environment, a fundamental assumption is that sensor biases are zero. However, the bias errors are not zero in real environment. As a result, the accuracy of integrated tracks deteriorate, even if the all sensors observe the same target. In this paper, we propose a new bias estimation algorithm is based on kalman filter bias estimator with grid search method. It is called the KGBE method (Kalman filter with Grid search Bias Estimator). As the result, we confirmed that the KGBE achieves higher accuracy than conventional algorithms. [C3149]

#### "Study of noise jamming based on convolution modulation to SAR"

The performance of traditional noise interference to synthetic aperture radar (SAR) is limited and to some extent it is useless. A new SAR jamming realization scheme based on convolution modulation is proposed in this essay. Theoretical analysis was presented and simulations were executed. All results prove that the proposed jamming is effective to suppress distributed targets, and much superior to traditional RF noise interference. [C3150]

#### "Detection and coordinate measurement of targets by ultra-wide band radar with antenna array"

Algorithms of digital signal processing are widely used in modern ultra-wide band (UWB) radars to solve problems of target detection and coordinate measurement. The paper deals with general algorithms of signal processing in ultra-wide band short-pulse radar with antenna array. The radar is developed for the monitoring of moving objects placed behind of radio-transparent barriers. The results of mathematical modeling are presented. [C3151]

#### "Search algorithm for local objects in GPR image"

An automatic search algorithm for local objects in GPR profile has been considered in the work. The algorithm is based on the Hough transform. The proper software tool has been developed in order to analyze the accuracy of the permittivity of ground as well as coordinates of the local object in a GPR profile. The algorithm efficiency with simulated data has been shown. The influence of the sampling-step at sounding on the algorithm accuracy has been considered. [C3152]

#### "Measurement of coordinates of the targets placed behind of radio-transparent barrier with multi-static ultra-wide band radar"

High accuracy measurement of coordinates of the targets placed behind of radio-transparent barrier (inside of closed room) using ultra-wide band (UWB) radar seems to be the perspective field of the investigation. The results of these investigations could be useful when solving problems concerned with combating terrorism, security etc. [C3153]

#### "Estimation of dielectric permittivity of medium by analysis of UWB radiolocation signals from local object"

The method of accuracy enhancement of medium permittivity estimation based on measurements of time delays of UWB signals reflected from local object and received in different points of radar scanning trace is suggested. The mathematical relations have been obtained for estimation of investigated medium permittivity and measurement errors and evaluation of algorithm accuracy gain in comparison with common methods has been made. [C3154]

#### "Practical application of UWB georadar technique for investigations of cultural heritage objects"

The UWB GPR technique is applied for investigation of covered structure of cultural heritage objects without affect their construction integrity. The obtained information is important for restorers since the most part of it is not available for conventional diagnostic methods and technical documentation is often lost. Some examples of cultural heritage objects investigations are performed. [C3155]



### "UWB Baby Monitor"

A successful case for UWB technology application to Vital Signs Monitoring Systems created by authors is presented in this paper. Baby Monitor for remote contactless monitoring of respiratory and heart rate is designed both for consumer and medical infant monitoring applications. Unlike conventional sound- and video-based baby monitors, which do not provide any useful information at infant sleep time (no sounds or static picture) the devices allow permanent parental control and effectively prevent Sudden Infant Death Syndrome (SIDS) from occurring. SIDS is reported to be leading death cause of healthy infants after one month age. [C3156]

### "Applications (GPR, radars, communication, medicine)"

{no data available} [C3157]

### "Portable system for RAC measurement based on swept frequency RCS method"

A portable device for the measurement of the reflectivity of radar absorbing coating is presented. It is based on the swept frequency RCS method. Using of this device is simple, quick and convenient than the conventional methods, as well with higher precision and more stable in performance than the other portable solutions. The design flow of this device is presented and the test results are analysed. [C3158]

### "Design of mobile robot system with remote control based on CAN-bus"

In order to realizing remote control and information collection quickly and reliably, the mobile robot with remote control is designed. In the paper, according to analysis of the overall structure, hardware circuit of the robot system is designed. Because the CAN2.0 standard only makes physical layer protocol and data link layer protocol, application layer protocol is ruled according to robot control system. In the last part of this paper, the software of master/slave computer is introduced in detail. The experiment shows that running performance of robot control system is balanced, efficient and has satisfied the practical demand. [C3159]

### "Practicability evaluation of middle atmospheric wind field based on HWM93"

Firstly, the paper describes the system model of HWM93, develops a display system of wind field in the middle atmosphere based on HWM93. The analysis and comparison was implemented between the wind field data calculated by HWM93 model, wind data observed by L-band sounding system (0-30 km) and TIDI onboard TIMED satellite (70-110 km). In the height of 0-30 km, there is a good consistency in mean zonal wind between HWM93 and L-band sounding system in December, January and February, while great difference exists below 20 km in June, July and August and good agreement is showed above 20 km in these months. The meridional wind below 30 km computed by HWM93 model is not accurate enough to reflect the actual meridional wind. In the height of 70-110 km, the mean zonal wind from HWM93 and TIDI is in good agreement above 80 km, while the mean meridional wind it has small relative difference above 80 km. The results indicate that the wind above 20 km from HWM93 model could be provided as reference and foundation for the wind information in the middle atmosphere for the regions with relatively lacking wind-measurement stations. [C3160]

### "Presentation of the field surface wave generated by an antenna at the interface of two homogeneous media"

In circumstances where the dispersion of the permittivity can be neglected, the tangential component of the surface wave is expressed through the Laplace function of two complex arguments algebraically. This reduces the computation time of the surface wave at a given point to a few milliseconds, and to determine the current in the radiating antenna, as well as the dielectric constant of the underlying surface, for the time of the order of several seconds. Obtain estimates of the surface wave field for the most typical parameters of soils. These calculations can be used to select regularizers inverse GPR for quantitative calculations of the parameters of the soil and for the qualitative interpretation of GPR data. [C3161]

### "Antenna arrays used for the cancellation of Es layer clutter"

There has Es layer clutter in the high frequency surface wave radar, and Es layer clutter have the difference arrival direction and polarized characters with the signal. Used these characters, vertically polarized antenna or horizontally polarized antenna can be added as auxiliary antenna in the high frequency surface wave radar system that uses vertically polarized antennas to suppress the Es layer clutter. The clutter-to-signal ratio in the outputs of the auxiliary antenna will affect the cancellation of the Es layer clutter in the main antennas. An antenna array consists of four vertically polarized dipoles and an antenna array consists of three horizontally polarized antennas are proposed in this paper. Used the superdirective synthetically method, the mainlobe of the

auxiliary antenna arrays are put on the direction of the Es layer clutter arrival direction, and a low sidelobe are put on the direction of the signal arrival direction. Then the auxiliary antenna arrays will have a big gain on Es layer clutter and a little gain on signal. So the cancellation of the Es layer clutter in the main antennas which use the auxiliary antenna arrays will be more effective. [C3162]

#### **"Design and implementation on wireless power meter system based on GSM network"**

This paper designs a wireless power meter system based on GSM network; the main communication way is GPRS and secondary SMS. The user can choose the different transfer modules based on different demands and can choose the Local network, dial network, ISDN, ADSL to connect into network. It accomplishes the hardware and software design in GSM network collector and the meter system software. [C3163]

#### **"Development of spaceborne radar simulator by NICT and JAXA using JMA cloud-resolving model"**

This study demonstrated preliminary results in diagnosis of the numerical model with reference to the TRMM/PR, examples of the GPM/DPR synthetic data, and application of the synthetic data to the algorithm development in the nonuniform beamfilling correction method. These were performed using a satellite radar simulation algorithm by the National Institute of Information and Communications Technology (NICT) and the Japan Aerospace Exploration Agency (JAXA) named as the Integrated Satellite Observation Simulator for Radar (ISOSIM-Radar) and a cloud-resolving model by the Japan Meteorological Agency (JMA-NHM). [C3164]

#### **"Reciprocal spectrum algorithm for radar imaging with frequency sampling waveform"**

A radar imaging algorithm named reciprocal spectrum algorithm (RSA) is proposed in this paper to get higher resolution in azimuth direction with frequency sampling waveform. Theoretical analysis and simulation results show that the algorithm can give better performance than the tradition range Doppler algorithm (RDA) at the cost of peak value reduction at the object points in radar image. [C3165]

#### **"Scientific and engineering overview of the NASA Dual-Frequency Dual-Polarized Doppler Radar (D3R) system for GPM Ground Validation"**

As an integral part of Global Precipitation Measurement (GPM) mission, Ground Validation (GV) program proposes to establish an independent global cross-validation process to characterize errors and quantify uncertainties in the precipitation measurements of the GPM program. A ground-based Dual-Frequency Dual-Polarized Doppler Radar (D3R) that will provide measurements at the two broadly separated frequencies (Ku- and Ka-band) is currently being developed to enable GPM ground validation, enhance understanding of the microphysical interpretation of precipitation and facilitate improvement of retrieval algorithms. The first generation D3R design will comprise of two separate co-aligned single-frequency antenna units mounted on a common pedestal with dual-frequency dual-polarized solid-state transmitter. This paper describes the salient features of this radar, the system concept and its engineering design challenges. [C3166]

#### **"Fetch limited sea scattering spectral model for HF-OTH skywave radar"**

Sea Normalized RCS, and Doppler spectra have been revised for HF-OTH Clutter Modelling. The Hasselmann model is firstly introduced to predict the sea directional spectrum of fetch-limited sea and results have been compared with the Pierson-Moskovitz model used for large scale ocean remote sensing. Results show that the closed fetch-limited sea has lower NRCS compared with ocean for similar wind intensity and direction. For this reasons RCS and Doppler spectra must be predicted taking into account of the fetch dimension. In future work we will generalize this interesting approach to fetch-limited wind, time-limited pulse, in order to show the waveform effect on Doppler spectrum. [C3167]

#### **"Utilization of airborne multi-aspect InSAR data for the generation of urban ortho-images"**

This paper addresses the generation of "true" RADAR ortho-images from highest resolution multi-aspect InSAR data. Due to the side-looking SAR imaging geometry, the well-known layover and shadowing effects prevent the production of truly rectified ortho-imagery from one image alone. Here, an approach for the reconstruction of Digital Surface Models of densely built inner city areas is proposed. Since in SAR interferometry each dataset pixel contains not only the interferometric phase needed for 3D reconstruction but also the corresponding amplitude or intensity value, respectively, the procedure can also be seen in the context of true ortho-rectification. [C3168]

#### **"Polarimetric sar image visualization and interpretation with covariance matrix invariants"**

In this study we give short overview of polarimetric SAR image visualization with colors. By studying the color models and polarization visualization models we propose basic principles which should be followed when presenting polarimetric information in color. We show that for different polarimetric parameters, different color models should be used, and give guidelines for color model selection. We present also two visualization schemes which are suitable for interpretation and browsing of large polarimetric SAR images. [C3169]

#### "Fully polarimetric ALOS PALSAR data applications for snow and ice studies"

In this study, the capability assessment of fully polarimetric L-band ALOS PALSAR data has been carried out for snow discrimination from other targets. Eigenvalue based polarization fraction value has been determined for assessing the capability of PALSAR data for snow discrimination. Radar snow index has been developed using polarization fraction and normalized third eigenvalue of coherency matrix. It has been found that radar snow index is more robust and simple to implement than supervised classification. [C3170]

#### "A Matchstick Model of microwave backscatter from a forest: A change of regime"

In this paper we present a forest scattering scenario consisting of solely vertical stems. Stems are the primary volume stores of forests; this model therefore simplifies the forest make-up to represent these major scatterers. This model representation is known as the "Matchstick Model" and is used as a comparison to backscatter data resulting from the combination of macro-ecology with a numerical scattering model (RT2). The "Matchstick Model" provides SAR scattering trends based on equations for the Optical and Rayleigh scattering regimes and presents forest scattering as a combination of the two. Conclusions state that saturation is a consequence of basal area and thinning limitations and ultimately that backscatter is not directly proportional to stand volume, even in the simple case of a single layer of stems. [C3171]

#### "Multichannel Coherent Radar Depth Sounder for NASA Operation Ice Bridge"

The Multichannel Coherent Radar Depth Sounder (MCoRDS) system was developed by the Center for Remote Sensing of Ice Sheets (CReSIS) to map the thickness of ice sheets. This radar system was used in Antarctica as one of the primary sensors for NASA's Operation Ice Bridge (OIB) during the fall of 2009. Compared to its predecessors, MCoRDS features several new capabilities which enabled it to successfully capture ice thickness measurements over multiple glaciers on an aerial platform. This paper will focus on the capabilities of MCoRDS and also provide a sample of the processed radar results. [C3172]

#### "Estimation of building density using Terrasar-X-Data"

This study presents an approach towards the estimation of building density by utilizing the intensity data of the German space borne very high resolution SAR system TerraSAR-X. By using reference data we segmented a SAR scene of the city of Munich, Germany, on the scale of city blocks. Then we computed first order statistics and texture measures according to Haralick on the image objects. We used a random forests regression algorithm to establish the relationship between these features and the building density taken from reference data. The result is a promising coefficient of determination of 0.63. [C3173]

#### "Oblique polarimetric SAR processor based on signal and interference subspace models"

We develop a new SAR processor based on oblique projection. We take into account the scattering properties of the target and the interferences by using subspace models. To detect the target and to reject the interferences, we process images with the oblique projection of the received signal into the target subspace along the interference one. This new SAR processor is applied to realistic simulated data for FoPen (Foliage Penetration) application. [C3174]

#### "Surface reference normalized radar cross section over land for the improvement of the TRMM PR algorithm"

The Tropical Rainfall Measuring Mission (TRMM) precipitation radar (PR) standard algorithm 2A21 produces the surface normalized radar cross section (NRCS) values under no rain conditions as functions of the incidence angle and surface physical parameters which affect surface scattering. These NRCS values are used as the reference values to calculate the path integrated attenuation (PIA) values in the surface reference technique (SRT) to perform the rain attenuation correction. This paper shows the relation between the land surface NRCS values and the three land surface physical parameters which are NDVI (Normalized Differential Vegetation Index), the surface roughness, and the soil moisture over the land for each of the incidence angles and tries to improve the methods to calculate surface reference NRCS values over the land. [C3175]

### "Applications of polarimetric decomposition technology in a dried up lake evolution"

This paper presents fundamental reason to Lop Nur "Ear" feature based on polarimetric decomposition technology. Lop Nur is located at the east Tarim Basin in China, and in history, all the major rivers running in Tarim Basin converged to this lowest place. Lop Nur belongs to arid region, and satisfies penetration conditions for SAR signals. Through comparison between decomposed volume scattering contribution and sub-surface salinity, it is found that subsurface properties (such as salinity) is the fundamental reason to "Ear" feature. And dynamic mechanism of geomorphology builds the relationship between surface and subsurface evolution processes, and indirectly unifies previous points on the reasons to formation of Lop Nur "Ear". Polarimetric technology is anticipated to be used to retrieve more information and to help extend applications in environment of arid region. [C3176]

### "Electromagnetic simulations of borehole radar for metal ore detection"

We perform finite difference time domain (FDTD) numerical simulation for metal ore detection by borehole radar. The ore-body model is adopted from a practical Ni-Cu-Pt ore body which is a magmatic deposit located in Sudbury, Canada. We design three boreholes along a cross-section perpendicular to the geological strike of the formation which is composed with overburden, ore zone, iron formation, peridotite, granite-gneiss, and sediments. We analyzed the simulated borehole radar profiles and found that some interfaces could be detected and some could not, also the ore zone is very absorptive to the wave. [C3177]

### "ESA Earth Observation educational tools contribution to the creation of awareness for World Heritage site conservation"

EO from space is a key tool to assess the effects of anthropogenic activities to our planet (e.g. deforestation, urban growth). It can provide measurements supporting the process of sustainable development, or observations allowing the detection of changes in the surface of our planet related to climate change. UNESCO and ESA have launched a call to all national and international space agencies, space research institutions and universities to make use of space technologies in order to assist developing countries in the monitoring of the World Heritage sites. ESA and UNESCO are also covering associated educational aspects by using all the results of the projects under implementation as educational material to support UNESCO's 'UN decade for education and sustainable development', within a common and joint strategy of education, targeting schools, universities and young professionals. This includes creating new tools for the creation of awareness and savoir-faire in the use of space technology for the conservation and preservation of the environment and for a sustainable development. Material derived from satellite images provided to decision makers is also being used to support teachers and school children from the surroundings of the World Heritage sites where the space partners of the 'Open Initiative' are working. In the frame of its educational activities for Earth Observation, ESA is creating particular modules oriented to UNESCO sites. All this material comes out of the different activities being implemented by partners of the ESA-UNESCO 'Open Initiative', in complete integration with the EDUSPACE programme of ESA, a platform and web-based tool for Earth Observation Education, in eight different languages, available for free to worldwide secondary schools teachers and students, aiming to provide schools with tools for teaching and learning. It offers an entry point to Earth Observation satellite data and software applications for training. The website is-- host to a multitude of didactical material inclusive high-resolution local and lower resolution global remote sensing satellite data in order to show students how to study the planet as a whole from space as well as the possibility of zooming into specific areas and natural features to investigate their behaviour over space and time. An image processing tool called LEOWorks (Learning Earth Observation), including a GIS, soon in open source, is made available for data analysis and image interpretation. New dedicated content, like case studies and projects dedicated to the monitoring of UNESCO archaeological sites and to sustainable development are presently under development. [C3178]

### "Physical optics-based method to compute the radar signature of complex objects over a sea surface"

In this paper, a model based on asymptotic methods is proposed in order to compute the scattered field from a complex maritime scene. The basic idea is to combine the geometrical optics and the physical optics technique. The sea surface is generated by using the Elfouhaily directional wave spectrum to obtain a realistic scene. Both the target and the sea surface are meshed with triangular patches in order to compute the scattered field. Simulated results are presented to validate this model through a simple configuration by comparisons with the method of moment. Then more complex scenes for different sea states and different kind of targets (PEC or inhomogeneous) are investigated. [C3179]



### "Nasa's Laser Risk Reduction Program: A risk reduction approach for technology development"

The benefits of Earth Science (ES) laser instrumentation have been proven by decades of earth-science observations. Lasers allow remote sensing of earth-system variables such as sea elevation, atmospheric composition, wind profiles, cloud cover, ice mass, and vegetation canopy. Further, orbiting platforms provide a unique vantage point that allows laser measurements on a global scale. NASA implemented the Laser Risk Reduction Program (LRRP) to identify and address capability-gap areas where new devices or processes could yield high-reliability mission-ready parts, and to develop components needed to advance the state-of-the-art of laser-based instrumentation. This paper discusses LRRP's approach and the evolution of the program's developments from inception to their planned infusion into NASA's missions. It is the first part of a three-paper presentation (Program goals and organization; 1<sup>st</sup> developments and results at the Goddard Space Flight Center (GSFC); and 2<sup>nd</sup> developments and results at Langley Research Center (LaRC)) that summarizes LRRP's goals, formulation approach, management organization, and final results. [C3180]

### "A comparison of two CA-CFAR loss calculation methods in spatially correlated K-Distributed sea clutter"

Radar target detection of targets in sea clutter modelled by compound K-distribution is examined from a statistical viewpoint by Monte Carlo simulations. The target detection is processed by Cell Averaging Constant False Alarm Rate (CA-CFAR) processor and the performance evaluations are quantified by CFAR loss. Curves for CFAR loss versus the spatial correlation and spikiness of sea clutter, number of cells of CA-CFAR processor and the number of non-coherently integrated pulses are presented. [C3181]

### "Exact discrete minimization for TV+L0 image decomposition models"

Penalized maximum likelihood denoising approaches seek a solution that fulfills a compromise between data fidelity and agreement with a prior model. Penalization terms are generally chosen to enforce smoothness of the solution and to reject noise. The design of a proper penalization term is a difficult task as it has to capture image variability. Image decomposition into two components of different nature, each given a different penalty, is a way to enrich the modeling. We consider the decomposition of an image into a component with bounded variations and a sparse component. The corresponding penalization is the sum of the total variation of the first component and the L0 pseudo-norm of the second component. The minimization problem is highly non-convex, but can still be globally minimized by a minimum s-t-cut computation on a graph. The decomposition model is applied to synthetic aperture radar image denoising. [C3182]

### "Coupling polarimetric L-Band insar and airborne lidar to characterize the geomorphological deformations in the piton de la fournaise volcano"

Until recently the coarse resolution of topographic mapping acted as a break on understanding the forces and processes that shape the Earth's surface. However, active surface deformation is an important indicator for the earth crustal dynamics since it is directly linked to earthquakes, volcanic eruptions and landslides. Both airborne laser scanning systems (LiDAR) and spaceborne interferometric synthetic aperture radars (InSAR) have provided valuable information for many case studies requiring high-resolution characterization of ground movement in relatively large areas to assess the threat and impact of natural hazards especially for volcanic eruptions. The Piton de la Fournaise volcano (Reunion Island, France) is one of the most active basaltic shield volcanoes in the world. It has reached an anomalous activity level in the past years with a major eruption occurring in April 2007. In this paper, we explore the statistical, spatial and temporal behavior of the L-Band backscattering coefficient at both HH and HV polarizations over different type of terrains in the Fournaise lava field as a function of the LiDAR intensity data. The correlation will be used in setting empirical models to correct for the L-Band phase distortion on ash and rough surfaces in volcanic terrains. [C3183]

### "Robust estimation of pasture biomass using dual-polarisation TerraSAR-X imagery"

The efficient management of pasture is a key driver of profitability for New Zealand's pastoral dairy and meat industries. In this paper, we report results from a study that tests the viability of using short-wavelength imaging radar to estimate pasture biomass. We use images from the TerraSAR-X satellite, comparing the HH & HV and VV&HV dual-polarisation combinations. Several linear models have been tested for field-measured pasture biomass. The best model is a linear regression using backscatter from the HH&HV combination, resulting in a residual standard error of 317 kg/ha. This standard error is 61% less than the standard error for the VV&HV combination (511 kg/ha), which clearly suggests adopting the HH&HV model. A model for prediction of the pasture biomass rank percentile is somewhat less convincing than the model for the pasture biomass itself. Finally, a repeated measures analysis for the HH&HV pair, suggests invariance of the regression for pasture biomass over time, except for a possible outlier date 01 September 2008. [C3184]

### "TanDEM-X commissioning phase status"

After the recent launch of the TanDEM-X satellite, the twin of TerraSAR-X, its demanding commissioning phase has started. On the one hand, it has to ensure the same monostatic operation performance as TerraSAR-X. On the other hand, the bistatic aspects have to be verified, which are essential for the acquisition of the global digital elevation model (DEM). This has to be done in a limited time period in order to keep the required nominal operation duration. This paper shows the summary of the commissioning phase activities and its running status.

[C3185]

### "Copyright"

The following topics are dealt with: SEAGRASS HABITATS; HIGH RESOLUTION DIFFERENTIAL SAR TOMOGRAPHY; FOREST COVER CHANGES; HYPERSPECTRAL IMAGERY CLASSIFICATION; REMOTE SENSING; GEOSPATIAL IMAGE ANALYSIS ALGORITHMS; SOIL MOISTURE; LAND USE CLASSIFICATION; WATER QUALITY; LAKE; RADIATIVE TRANSFER; CALIBRATION; VOLCANIC DEFORMATION; SEA SURFACE TEMPERATURE FRONT; and FLOOD MONITORING. [C3186]

### "Physical-based models of speckle for high resolution SAR images"

In this paper we present a physical model for the description of the speckle in Synthetic Aperture Radar (SAR) images. The proposed model highlights the analytical dependence of the speckle characteristics on the surface roughness and the sensor parameters. The illuminated surface is represented using the fractal geometry. In addition, a SAR raw signal simulator able to generate SAR images whose speckle characteristics are coherent with the observed surface properties is presented. [C3187]

### "Remote sensing image synthesis"

For remote sensing data, the testing analysis tools is difficult since the ground-truth data are not available in many cases. To address this issue, a novel method for image synthesis is presented for use as a evaluation test-bed. Given the scale-dependent, non-stationary nature of remotely sensed data, a new modeling approach that combines a resolution-oriented hierarchical method with a regional label-oriented binary tree structure is introduced to synthesize such complex data. In this paper, we are proposing on first synthesizing a label field, which contains the complex structural characteristics, then synthesizing the texture based on the generated label field for a more accurate modeling. Experimental results using operational RADARSAT SAR sea-ice image data show that the proposed method is capable of modeling complex, nonstationary scale structures, thus making it well-suitable to produce reliable, realistic remote sensing imagery. [C3188]

### "Synchronous retrieval of forest canopy cover by airborne LiDAR and optical remote sensing"

Forest canopy cover is retrieved Synchronous by the airborne LiDAR data and SPOT-5 HRG data, using the method of linear spectrum decomposition model combined with Li-Strahler geometric-optical model. First, the airborne LiDAR data is used to retrieve forest parameters and then the proportion of pixel not covered by crown or shadow Kgof each pixel in the sample was calculated using Li-Strahler geometric-optical model, while the linear spectrum decomposition model is used to extract the proportion of pixel not covered by crown or shadow Kgof each pixel in the whole imagery. [C3189]

### "A new global Snow Extent product based on ATSR-2 and AATSR"

The ESA project GlobSnow develops products and services for snow extent and snow water equivalent. The time series of Snow Extent (SE) products will cover the whole seasonally snow-covered Earth for the years 1995-2010 based on the optical sensors ERS-2 ATSR-2 and Envisat AATSR data. A laboratory processing chain has been developed for testing and improving algorithms in an iterative process. The final version of the laboratory processing chain will function as a reference system for the implementation of an operational system for production of the full time series of products as well as near-real-time products produced on a daily basis. The first version of the SE product set spanning 15 years of the Northern Hemisphere is expected to be ready by the end of 2010 and will be made freely available. [C3190]

### "Next generation of multi beam rotating antenna on SWIM scatterometer"

In the frame of the development of the instrument SWIM (Surface Waves Investigation and Monitoring) on the CFOSAT program (Chinese French Oceanographic Satellite) funded by CNES, Thales Alenia Space is currently developing a new multi beam rotating antenna in Ku Band. This single reflector offset antenna includes a rotating

feed comprising 6 beams. The SWIM instrument is the first ever space radar concept that is mainly dedicated to the measurement of ocean waves directional spectra and surface wind velocities through multi-azimuth and multi-incidence observations. Orbiting on a 500 km sun-synchronous orbit, its multiple Ku-band (13,575 GHz) beams illuminating from nadir to 10° incidence and scanning the whole azimuth angles (0-360°) provide with a 180 km wide swath and a quasi global coverage of the planet between the latitude of -80 and 80°. Such a wide range of observations requiring high range resolution (about 20 m on the ground) have led to design an instrument whose architecture and technology goes beyond what has been done on altimeter and scatterometer systems. At antenna subsystem level, multi-azimuth and multi-incidence observations requirements have led to design an ambitious antenna subsystem that rotates at 6 rotations per minute while transmitting RF signals towards 6 different beams in Transmit and Receive Modes. Thales Alenia Space started in January 2009 under CNES contract phase B studies on the design of this multi beam rotating antenna in order to contribute to the System Preliminary Design Review held successfully in January 2010. B Phase complementary activities are currently under progress to prepare the C/D Phase planned to start beginning of 2011. This paper aims at giving an overview of the SWIM antenna preliminary design and performances. [C3191]

#### **"Calibration accuracy enhancement in the field experiment with a ground-based scatterometer"**

An improved field-measurement technique for enhancing the calibration accuracy of a ground-based scatterometer is proposed in this paper. The automatic two-dimensional (2-D) measurement of a calibration target, so-called '2-D target scanning technique (2DTST)', gives a precise alignment between a point calibration target and an antenna bore-sight. Averaging of the calibration-target measurements increases further the accuracy and reliability of the automatic alignment. The measurement results show that the correlation among the measurements is larger than 0.95 and the error-rate is below 5% at a frequency range from 9.4 GHz to 9.9 GHz. The evaluation of the calibration accuracy using the STCT (Single Target Calibration Technique) shows that 2DTST in the field experiment can secure the precise calibration accuracy within 0.5 dB for magnitude correction and 4° for phase correction. [C3192]

#### **"Evaluation of vegetation effect on the retrieval of snow parameters from backscattering measurements: A contribution to CoReH2O mission"**

In preparation of the satellite mission CoReH2O, one of the three missions selected for scientific and technical feasibility studies within the Earth Explorer Programme of the European Space Agency, experimental and theoretical studies started in order to investigate backscatter properties of snow covered terrain and improve the methods for retrieval of snow physical properties from SAR data. The aim of this paper is to investigate the impact of vegetation in the retrieval of snow parameters from backscattering measurements. First a radiative transfer model, able to simulating scattering from a vegetated snow-covered terrain was developed and implemented. Lastly, a sensitivity analysis on snow and vegetation parameters was conducted for coniferous forest. Results confirm that with increasing biomass the sensitivity to SWE strongly decreases. Moreover when biomass is in the 0-150 m<sup>3</sup>/ha range a procedure to correct the vegetation effect in the SWE retrieval algorithm is suggested. [C3193]

#### **"Tropospheric correction for InSAR using interpolated ECMWF data and GPS Zenith Total Delay from the Southern California Integrated GPS Network"**

A tropospheric correction method for Interferometric Synthetic Aperture Radar (InSAR) was developed using profiles from the European Centre for Medium-Range Weather Forecasts (ECMWF) and Zenith Total Delay (ZTD) from the Global Positioning System (GPS). The ECMWF data were interpolated into a finer grid with the Stretched Boundary Layer Model (SBLM) using a Digital Elevation Model (DEM) with a horizontal resolution of 1 arcsecond. The output were converted into ZTD and combined with the GPS ZTD in order to achieve tropospheric correction maps utilizing both the high spatial resolution of the SBLM and the high accuracy of the GPS. These maps were evaluated for three InSAR images, with short temporal baselines (implying no surface deformation), from Envisat during 2006 on an area stretching northeast from the Los Angeles basin towards Death Valley. The RMS in the InSAR images was greatly reduced, up to 32%, when using the tropospheric corrections. Two of the residuals showed a constant gradient over the area, suggesting a remaining orbit error. This error was reduced by reprocessing the troposphere corrected InSAR images with the result of an overall RMS reduction of 15-68%. [C3194]

#### **"Spaceborne-airborne bistatic radar for UAS navigation purposes: Preliminary analysis and strawman system identification"**

The study of a novel navigation system for Unmanned Airborne System (UAS) based on bistatic Synthetic Aperture Radar (SAR) is presented. The innovative bistatic configuration builds on spaceborne radar transmitters

and airborne receivers, the latter mounted in a forward-looking geometry. Such approach, impossible or extremely demanding with a monostatic approach, allows one to achieve dual information with two different radar working modes: imaging capability can be in fact coupled with the possibility of moving target indication. The study is particularly suited on one of the most common UAS platforms: a close range, medium takeoff weight, with an endurance of roughly 7 hours and cruise speed of about 50m/s, whose requirements have been identified. The finalization of the study is achieved by the definition of a strawman system concept with different approaches. Four options are identified, with different performance and system complications/challenges. The study herein reported was carried out under ESA contract 22449/09/F/MOS. [C3195]

#### **"Improving hydrological forecasting using multi-source remote sensing data together with in situ measurements"**

This paper describes the development of information systems and techniques for improving hydrological forecasting by applying satellite observations, weather radars, and in situ measurements from automatic monitoring stations. In the methodology developed and demonstrated, the observation data are accompanied with a detailed soil and land cover information. The information system is concerned with the following physical characteristics relevant to river discharges and flooding: snow water equivalent (SWE), cumulative amount of precipitation, fraction of snow covered area during the melting period (FSC), soil moisture, and soil frost. Feasibility of the multi-source information system is demonstrated in a pilot experiment for Finnish Lapland, using the hydrological forecasting system of the Finnish Environment Institute (SYKE) as an example of a typical operational distributed model. [C3196]

#### **"Ground penetrating radar for tunnel detection"**

Ground penetrating radar (GPR) systems have important civil and military applications and can be used for surveying subsurface structures such as bunkers, tunnels and buried pipes. However, GPR systems for detecting deep tunnels still face many challenges, and their performance often depends on soil types, specific targets and subsurface geological features. This paper discusses challenges in tunnel detection and provides a useful and efficient procedure to develop system requirements and predict detection performance. [C3197]

#### **"GPR evaluation test for humanitarian demining in Cambodia"**

ALIS is a dual sensor for humanitarian demining, which is a combination of electromagnetic Induction sensor (EMI) and Ground Penetrating Radar (GPR), developed by Tohoku University, Japan. ALIS is equipped with a sensor tracking system using a CCD camera with image processing, which enables signal processing for subsurface imaging. Two sets of ALIS have been deployed in mine fields in Cambodia since 2009 and more than 50 buried landmines have been detected. We found that the Synthetic Aperture Radar processing (SAR processing) is effective not only imaging the buried objects, but also for reduction of clutter of soil. [C3198]

#### **"Nowcasting rainfall fields estimated from specific differential phase"**

This paper presents a preliminary evaluation of short-term prediction (nowcasting) of rainfall fields estimated from specific differential phase fields derived from Collaborative Adaptive Sensing of the Atmosphere X-band radar data. A Fourier-space, linear system-based nowcasting method used these rainfall fields as input to generate rainfall forecasts up to 20 min. The results show the extent to which specific differential phase-derived rainfall fields can be predicted and the utility of such predictions to be approximately 15 min. [C3199]

#### **"A novel three-step focusing algorithm for TOPSAR image formation"**

This paper conducted thorough research to the theory of space-borne TOPSAR data processing. The time-frequency characteristic of TOPSAR mode signal was analyzed and discussed in detail by mathematic derivation combined with the TOPSAR factor. Based on the analysis, an efficient and precise three-step image formation algorithm was presented for TOPSAR image formation without data division, and the operation in every step was theoretically proved effective. The de-rotation operation in the first step and deramp operation in the third step are adopted to finish the stretch in both frequency and time domains respectively, by which the azimuth folding effects in the time and frequency domains are overcome. [C3200]

#### **"IMage formation algorithm for bistatic forward-looking SAR"**

The conventional monostatic SAR shows a limitation of achieving a high azimuth (angular) resolution if a forward-looking geometry is used. Bistatic SAR offers a possibility of the forward-looking formation image, e.g. one platform operates as a separated illuminator while another works in a forward-looking mode. In this special bistatic configuration, the forward-looking beam will introduce two problems. The first one is the significant



Doppler shift, which will produce the range-azimuth coupling. The second one is that the targets located at symmetrically about the flight path of the forward-looking platform have the same antenna-to-target range which would cause the range migration ambiguity of the receiver. This paper will develop a mathematical model to describe the Doppler characteristic of bistatic forward-looking SAR (BFLSAR). Based on this model, the previous bistatic point reference spectrum (BPTRS) can be applied. Using the BPTRS, a modified range-Doppler algorithm is proposed to handle the two problems and focus BFLSAR data in the azimuth-invariant configuration. Finally, simulation experiment is used to validate the proposed model and processing approach.

[C3201]

### "Retrieval of soil moisture under vegetation using Polarimetric Scattering Cubes"

Soil moisture inversion from polarimetric SAR data has attracted significant attention for the past twenty years. Comparing with the simple case of bare surface, it is extremely complicated for vegetated terrain to invert soil moisture because of a larger number of scattering mechanisms that contributes to the observation. In this paper, we show how polarimetric decomposition technique, which decomposes SAR observations into preferred scattering mechanisms, can be used for the inversion. The result leads us to give up the use of polarimetric decomposition because of an unknown attenuation ratio caused by the canopy. Then a new inversion algorithm using Polarimetric Scattering Cubes (PSC) is introduced with simulation results to show a sensitivity to physical parameter such as vegetation distribution. Finally, we also discuss how the technique should be implemented for the real SAR data. [C3202]

### "Remote sensing atmospheric CO<sub>2</sub> column abundance using an airborne pulsed laser sounder at 13 km altitude"

Accurate global measurements of tropospheric Carbon Dioxide abundance to the "parts per million" (ppm) level is required to better quantify processes that regulate CO<sub>2</sub> exchange between atmosphere, land and ocean. To measure CO<sub>2</sub> globally NASA has planned the ASCENDS mission, Active Sensing of CO<sub>2</sub> Emissions over Nights, Days and Seasons. We report on an airborne laser-based remote sensing instrument we have developed at NASA-GSFC as a candidate for the ASCENDS mission. Preliminary analyses of data from initial flight testing to 13 km altitude indicates a CO<sub>2</sub> mixing ratio of 396 ppm from CO<sub>2</sub> column abundance where in situ sensors determine 390 ppm mixing ratio. [C3203]

### "Monitoring thickness change of the Dongkemadi Glacier on Qinghai-Tibetan Plateau using SRTM DEM and map-based topographic data"

In this paper we measured the long-term thickness change of the Dongkemadi Glacier (DG) on Tanggula Mountain, Qinghai-Tibetan Plateau, using the Shuttle Radar Topography Mission (SRTM) C-band data (2000) and a digital elevation model (DEM) generated from topographic map (1969). First we check the accuracy of SRTM DEM by comparison at 16 random independent points in surrounding non-glacier area below 5500m a.s.l., then we focus on an analysis of the glacier's surface thickness change features and a validation of the results using GPS survey data (2007) and DEM (1969) in Xiao Dongkemadi Glacier (XDG). The result shows XDG decreased by an average of 6.15m, or 0.20 m a<sup>-1</sup> between 1969 and 2000. We estimate the error of annual thickness change rate to be on the order of 5% compared to the result of field measurement while Da Dongkemadi Glacier (DDG) decreased by an average of 20.74m or 0.67m a<sup>-1</sup> (1969-2000). [C3204]

### "TropiSAR: Exploring the temporal behavior of P-Band SAR data"

The TropiSAR campaign has been conducted in August 2009 in French Guiana with the ONERA airborne system SETHI. The main objective of this campaign was to collect data to support the Phase A of the Earth Explorer candidate mission, Biomass. Several specific questions need to be addressed to answer the recommendations of the ESAC group and the data collection strategy has been constructed accordingly. The first part of the paper lists these specific questions. We then describe the selected test sites, followed by a summary on the radar instrument and the radar configuration (geometry and waveform). The data acquisition plan is provided and the temporal behaviour of the P-Band data is explored. [C3205]

### "AMSR and DFS synergy"

The Japan Aerospace Exploration Agency (JAXA), National Oceanic and Atmospheric Agency (NOAA), and Jet Propulsion Laboratory (JPL) are now proposing to launch the second satellite of the Global Change Observation Mission-W (GCOM-W2) carrying the Advanced Microwave Scanning Radiometer-3 (AMSR-3) together with Dual Frequency Scatterometer (DFS). This paper reviews sensor and science synergy of microwave scatterometers and radiometers. [C3206]

### "Logistic regression for detecting changes between databases and remote sensing images"

This paper studies database updating using optical and synthetic aperture radar images. Logistic regression is used to model the conditional probability of presence/absence of buildings given features extracted from the images. The logistic regression parameters are estimated using the maximum likelihood method. Binary hypothesis tests are then constructed from these estimates to detect changes between the optical/radar images and the existing database. The estimation and detection algorithms are evaluated using simulated and real data sets. [C3207]

### "DVB-T passive radar for vehicles detection in urban environment"

Passive radar systems exploit non-cooperative transmitter to detect targets in areas of interest. Some of the main advantages of such systems with respect to conventional radars include low cost architectures, low energy requirements and potentially null probability of intercept. In this paper a low-cost solution for vehicles detection making use of passive radar concept is presented. A Software Defined Radio (SDR) solution and commercial antennas have been used to realize a DVB-T passive radar demonstrator. An analysis of the DVB-T signal is firstly presented together with a study of its capability as radar waveform. Afterwards an experimental setup is presented and analysed and finally some results of targets detection are shown. [C3208]

### "Monitoring sea-ice and dry snow with GNSS reflections"

GPS reflected signals have become a source of opportunity for remote sensing of the Earth's surface. In this work, we present several capabilities of this technique in two different polar environments: Greenland and Antarctica. The first part is dedicated to the retrieval of sea-ice properties, giving emphasis to the study of the coherent phase for altimetric and roughness estimations, and polarimetric measurements for the determination of the ice salinity variation. The results show good agreement with a tide model and daily ice charts. On the second part, some preliminary results and analysis strategies to retrieve dry snow signatures are presented. [C3209]

### "RADARSAT-2 continuing system operations and performance"

This paper provides a status report for RADARSAT-2 system operations and performance now that two years of Routine Phase operations have been completed. Experience from the second year of operations is reviewed. System status, performance, and trends are described along with performance and achievements of the RADARSAT-2 operations functional groups. Normal operations now includes increased attention to orbital collision risk avoidance, and the RADARSAT-2 risk mitigation experience is summarized. In addition to meeting and maintaining specified performance requirements for the Routine Phase, the operations team has implemented a number of improvements to both the system and operations to provide enhanced performance. These include reduced tasking latency, enhanced beam modes, and further improved image quality. The improvements are described as part of the evolution of the mission capabilities along with some further planned enhancements. [C3210]

### "Enhanced Cloud algorithm from collocated CALIPSO, CloudSat and MODIS global boundary layer lapse rate studies"

Coincident profile information from CALIPSO's lidar and CloudSat's radar offers a unique opportunity to map the vertical structure of clouds over the globe with accuracies never before realized. At Langley NASA, both CALIPSO and CloudSat are collocated with each MODIS 1-km pixel to create a new data set named C3M (Figure 1). A year (July 2006-June 2007) of C3M data is used to derive global lapse rate maps, as an enhancement to NASA Langley's CERES Cloud Property Retrieval System (CCPRS). The lapse rates are derived for boundary layer clouds using the the cloud-top temperature from Aqua MODIS level 1 data, skin temperature over ocean and surface temperature over land from the GMAO GEOS-4, and cloud-top height from CALIPSO. The derived global lapse rate maps are used to process a month of CERES-MODIS data to calculate cloud top heights, which are compared with CALIPSO cloud top height. The comparisons shows good agreement between CERES-MODIS and CALIPSO. [C3211]

### "Investigations into high resolution mapping of precipitation features utilizing the TRMM precipitation Radar"

Precipitation measurements from the Tropical Rainfall Measuring Mission (TRMM) satellite's Precipitation Radar (PR) have been used to create high-resolution grids of precipitation features at a resolution of 0.05degrees. This grid size is on the order of a nominal PR instantaneous field of view (ifov) of 4.9km at nadir. Currently 12 years of data has been collected from the TRMM mission, resulting in sufficient sampling to begin these high-resolution

studies. Precipitation fields at this resolution show detailed, local climatological features and comparisons with topographic data sets allow for the identification of potential problem areas in the retrieval algorithms. [C3212]

### "Tree height retrieval methods using POLInSAR coherence optimization"

This paper investigates to what extent interferometric coherence optimization in radar polarimetry improves the performance of forest height inversion method using POLInSAR measured data. Based on repeat pass E-SAR data and the corresponding ground measured forest stand heights, several available forest height inversion methods are validated and compared together with coherence optimization algorithms such as the iteration for the maximization of the magnitude difference (BF-mag) coherence optimization algorithm and phase diversity (PD) coherence optimization algorithm. The results show that coherence phase optimization can improve the performance of the tree height retrieval method based on coherence phase information, but can not improve the performance of the retrieval method based on coherence amplitude information alone. Furthermore, an integrated inversion method, which combines coherence phase with coherence amplitude information and includes corresponding polarization coherence optimization and compensation of non-volume scattering decorrelation, is proposed and discussed. [C3213]

### "A comparison of estimated mixing height by multiple remote sensing instruments and its influence on air quality in urban regions"

Urban areas suffer from high pollutant loadings due to their proximity to emission sources as well as transported aerosols. Therefore it is essential to have an accurate technique for measuring the pollutants and evaluate their effect. Since the atmosphere mixing height (MH) defines the total volume available for the pollutant transport and dispersion, it is important that air-quality models can provide realistic estimates. This paper studies multiple instruments for MH determination and their potential for validating air-quality model forecasts such as WRF. In addition, use of automated PBL height retrieval using wavelet analysis is briefly described and long term statistical comparisons of MH and WRF mixing height are obtained. [C3214]

### "High-resolution 3-D radar imaging using pseudo-random noise coded waveform"

In this paper, high-resolution 3-D radar imaging using a 3-step image formation procedure based on the Huggens-Fresnel's principle is analyzed and discussed. To achieve high spatial resolution, large antenna array is required. The array can be implemented with a synthesized antenna array, or a sparse antenna array. To achieve high range resolution, pseudo-random noise (PN) coded signal waveform is used. The ability of generating high-resolution 3-D imaging is verified by computer simulation. Numerical simulation shows the reconstructed 3-D radar image of an object. PN coded signal waveforms also has the advantage of noise immunity. Applications of the high resolution 3-D radar imaging can be in ground penetration radars, microwave medical imaging, and down-looking SARs. [C3215]

### "Interpretation of buildings in high resolution sar images based on electromagnetic method"

High resolution SAR (Synthetic Aperture Radar) will provide an innovative tool for urban area applications. Nevertheless, interpretation of SAR image in urban area is far from solved by the increase of spatial resolution. It is usually difficult to establish a determined relationship between scattering centers in high resolution SAR images and the basic units of building targets. In order to thoroughly understand the backscattering behaviour of building targets in high resolution SAR images, a method of high resolution SAR imaging simulation based on electromagnetic model is proposed in this paper, which mainly includes 3-D model establishment for the building target, triangular facets partition, RCS prediction for each facet, and SAR imaging through coherent superposition of echo from each triangular facet. Through comparison of the simulated and the original SAR image, building scatter mechanisms in high resolution SAR images can be well interpreted. [C3216]

### "Observation of a boat and its wake with a Dual-Beam along-track interferometric sar"

The Dual-Beam Interferometer is an airborne instrument that combines two along-track interferometric synthetic aperture radars observing the surface below at different squints. This configuration allows retrieving vector velocities of surface flows in a single aircraft pass. The system was designed by the University of Massachusetts and saw several deployments in the early 2000s. An imagery of a boat with a rather pronounced wake system captured during one of these flights is the subject of this paper. The velocity of the vessel is estimated based on the "train off the tracks" displacement in one of the looks. This estimate, which will be affected by uncertainty in target position due to smearing, is then used to remove unknown phase biases in the interferometric channels. Retrieved velocity variations are examined along cuts traversing the wake, with the focus on its narrow "turbulent" part. We find that the reconstructed velocities 150 m behind the boat are intuitively satisfying, but we are unable to fully account for the cross-wake component of velocity at 400 m behind the vessel. [C3217]

### "Wall-to-wall mapping of forest extent and change in Tasmania using ALOS PALSAR data"

Consistent estimation of carbon stocks at national level requires the integration of wall-to-wall, time-series satellite and in situ data of forest area, type and change. In this paper we demonstrate a consistent approach to the generation of wall-to-wall time-series mosaics using ALOS PALSAR data acquired over 2007 to 2009 for Tasmania, Australia. The project is part of a series of National Demonstrators initiated by the Group on Earth Observations (GEO) Forest Carbon Tracking (FCT) task that emphasize the contribution and operational use of satellite measurements for forest monitoring and national carbon accounting. Interoperability between optical and Synthetic Aperture Radar (SAR) derived forest measurements will also be demonstrated. The project will deliver a series of forest monitoring products and technical documentation, which will be made available as a guide to GEO member countries with a desire to develop their own national carbon accounting systems. [C3218]

### "Bistatic SAR tomography: Processing and experimental results"

This paper presents across-track tomography applied to a bistatic geometry with fixed receivers. This kind of geometry can overcome some of the classical monostatic tomography limitations such as temporal decorrelation and irregular baseline distribution. The Remote Sensing Laboratory (RSLab) of the Universitat Politècnica de Catalunya (UPC) has implemented a SAR Bistatic Receiver for INTERferometric Applications, SABRINA, with 4-channels. SABRINA has been used to carry out a bistatic tomographic experiment. The acquired data has been processed with different tomographic methods and their performances compared. [C3219]

### "An improved fast Viterbi algorithm for track-before-detect"

This paper addresses the problem of moving dim target detection in radar systems using track-before-detect approaches (TBD), which are implemented by a fast Viterbi algorithm (FVA). Traditional Viterbi algorithms (VA) traverse all the resolution cells including many noise cells in every frame, whereas FVA improves the searching method by combining with a Constant False Alarm Rate (CFAR) approach to expel many noise cells, and provides the same performance with much less computational cost. What's more, it avoids target extend with no post-processing due to a novel maximization operation, and consequently reduces the complexity of the proposed algorithm. Simulation results prove the performance of the new algorithm. [C3220]

### "A novel method of SAR terrain target scattering signal simulation"

Synthetic Aperture Radar (SAR) raw signal simulation is crucial for SAR system design and processing algorithms. This paper proposes the simulation method of SAR scattering signal of big area terrain target. At first, the SAR imaging principle is analyzed. Then, the space-borne SAR scenario model is constructed. The echoes of point target are calculated, which is impulse response of the SAR signal acquisition system. In tradition, the Radar Cross Section (RCS) simulation parameters of terrain target calculation is based on the scattering model expressions of a random roughness surface and the electromagnetic wave shadow theory. The approach of this communication utilizes the practical SAR SLC (Single Look Complex) or MGD (Multi-Look Ground-range Detected) image as terrain target backscattering coefficient, instead of the traditional method aforementioned. Then, 2D-FFT method is utilized to improve simulation efficiency significantly. The results of simulation prove the validity of the approach. [C3221]

### "An EMD-based denoising method for lidar signal"

Lidar echo signal is a typical non-steady-state, non-stationary signal, and difficult to be dealt with by the traditional filtering methods. As a new signal processing theory proposed in recent years, Empirical Mode Decomposition method can adaptively divide the lidar echo signal into different intrinsic mode function (IMF) components according to different time scale, and noise mainly concentrates in the high-frequency component. However, when filtered with simply removing high frequency component, the useful signal will be possible to be reduced. In this paper, a new method which combines Empirical Mode Decomposition (EMD) with Savitzky-Golay filter is proposed. With experiments, it is indicated that our approach not only removes the noise component effectively but also maintains the useful signal, then will improve the accuracy in the next phase of data processing. [C3222]

### "MST phase unwrapping based on new weighted map"

Phase unwrapping can be cast as a minimization problem under the  $L_p$ -norm framework. In this framework, it is a critical step that derives weighted function from prior information. This letter presents a new weighted map which is calculated by local phase signal to noise ratio(SNR) based on linear phase hypothesis. The proposed weighted map can reduce slope effect of coefficient and fuse the consideration of intensity. Lastly, the tests



performed on real data confirm the validity of our method. [C3223]

### "SAR raw echo simulation of ground scene"

Synthetic Aperture Radar (SAR) raw echo simulation methods are studied in this paper. A simulation method is proposed based on fractal theory, facet model and clutter scattering characteristic model. Digital Elevation Model (DEM) of a natural terrain is used in computer simulation. The SAR raw echo simulation is realized in the frequency domain. The simulation results demonstrate that the method is effective, and the stochastic property and special geometric distortion phenomena of natural ground scene in the SAR image are reflected. [C3224]

### "Simulation of Faraday rotation on longer wavelength spaceborne polarimetric InSAR"

The effects of Faraday rotation (FR) on longer wavelength (i.e. L or P-Band) spaceborne linearly full-polarized interferometry synthetic aperture radar (Pol-InSAR) processing are addressed. A model for linearly full-polarimetric InSAR data subject to Faraday rotation is investigated. Due to Faraday rotation, the received signal in each channel will be contaminated by backscattering signals from other polarimetric channels, which consequently reduce the coherence of the two single look complex SAR images received by the same channel for PolInSAR processing. The numerical simulation results are presented, which indicates that Faraday Rotation has significant impact on the coherence of the interferograms, especially for the spaceborne longer wavelength Pol-InSAR system. [C3225]

### "Subimage fusion for high-resolution ISAR imaging"

With the improvement of resolution in the inverse synthetic aperture radar (ISAR) imaging, the effect of the rotational motion of the target is much larger than ever before. In this letter, we propose a novel subimage fusion method to compensate for the large rotational motion in high-resolution ISAR imaging. By dividing the large rotational motion into several small ones, the subimage formation can be realized easily with current ISAR imaging algorithms. At the same time, with the increasing of the number of the subimages, the change of the aspect angle during the coherent processing interval can be very large, and high resolution can be achieved. Moreover, because the whole processing is achieved with Fast Fourier Transforms and vector-multiplication operations, the proposed approach is computationally efficient and has no interpolation operation. Numerical examples are provided to demonstrate the performance of the proposed approach. [C3226]

### "Segmentation of Polarimetric SAR images using graph partitioning active contours"

In this paper, a novel segmentation method for Polarimetric Synthetic Aperture Radar (PolSAR) images is proposed. Image segmentation is formulated as a graph partitioning problem which is addressed by curve evolution. Graph partitioning active contours (GPAC) [1], which is flexible and can be classified as a region-based active contour framework, is applied to PolSAR images. In order to apply GPAC to PolSAR image segmentation, the pairwise dissimilarity between two arbitrary pixels in the image should be measured appropriately. The selection of dissimilarity measures is discussed. Synthetic and real PolSAR images are both used in the experiments to verify the proposed approach. A quantitative evaluation and comparisons of segmentation results, including iteration times of curve evolution, segmentation accuracies in term of pixel and object count, are provided. The proposed scheme has shown to be promising for PolSAR image segmentation. [C3227]

### "Prospects of new real-time radar applications for environmental remote sensing"

Remote sensing used to assess geophysical parameters on Earth is increasingly exploited and necessary for sustainable human life on Earth. A goal of using satellites to monitor changes and characteristics of Earth's surfaces is to further understanding of the planet and its systems, as well as understanding of how humans interact with and change the environment. Mostly underexploited, biomass detection via active radar remote sensing could provide a more thorough and in depth analysis of Earth. Upcoming NASA Earth monitoring satellites cover a wide range of science products and applications, but little influence is put on the possibility of harnessing data from biomass reaction to radar pulse. In addition to the benefit of radar remote sensing in observing large areas at once, an added ability of transmitting detected frequencies in nearreal-time has potential to provide countless advantages. Direct Broadcast increases possibilities and practical uses for collected data. [C3228]

### "Simulation studies on data fusion algorithms for forest structure from lidar and SAR data"

The NASA's DESDynI mission will provide global systematic lidar point-sampling data and areal coverage of L-band SAR data with polarimetric capabilities for 3-D structural studies of vegetation. The combined use of lidar's

direct sampling measurements and radar's global areal mapping capabilities creates a real opportunity to map global ecosystem structures and functions that link to carbon dynamics. However, the relationship of the lidar point-sample data and corresponding areal SAR data is yet to be established. In this study the data fusion algorithms for the estimation of parameters of forest structure from Lidar and SAR Data is investigated. The results show that SAR intensity data is sensitive to forest biomass which is less than 15kg/m<sup>2</sup>(or 150 ton/ha) and insensitive to the maximum forest height. Lidar data can be used to provide the information of forest height and the introduction of the information of forest height is helpful in the estimation of forest biomass. [C3229]

#### "Application of monopulse techniques in angle-measuring of single-beam mechanical scanning radar"

Due to large computation cost and low accuracy of traditional angel measurement in single-beam mechanical scanning radar, a new application of monopulse techniques is proposed. First of all, this paper introduces the principle of monopulse and analyzes the difference in accuracy between monopulse and the traditional methods. Based on that, engineering implementation is then discussed. Finally, experimental data obtained in detection mode for inverse synthetic aperture radar (ISAR) is processed by this method, and results demonstrate effectiveness of the proposed method. [C3230]

#### "Analysis of Faraday rotation on spaceborne CTLR compact polarimetric SAR image reconstruction"

The CTLR (circular transmit and linear receive) compact polarimetric (CP) synthetic aperture radar (SAR) system transmits only right or left circular polarized signal and receives H and V linear polarized signal. CP SAR mode has significant advantage of doubled swath width compared to the traditional full-polarimetry (FP) mode. In this paper, the effective FP data are reconstructed using Souyris' iteration algorithm from the covariance matrix of the CTLR mode CP SAR data. Then the performance of the algorithm is analyzed. Moreover, the ionospheric effect of Faraday rotation (FR) on longer wavelength (i.e. P-band) spaceborne CP SAR was introduced in the simulation. After simulating the impacts of FR on SAR image reconstruction, an information-theoretical evaluation method was proposed for analyzing the quality of SAR image reconstruction. The mutual information between the original FP data and the reconstructed FP data (namely, from the CTLR CP SAR image) as a function of FR was illustrated, for quantitatively evaluating FR on longer wavelength (e.g. P-band) spaceborne CTLR CP SAR image reconstruction. [C3231]

#### "A measurement method for Doppler frequency rate-of-change with coherent pulse train"

The information of target's acceleration is reflected in the Doppler frequency rate-of-change of the received radar signal. Limited in target's velocity, the information of Doppler frequency rate-of-change is very subtle. This information is quite difficult to measure precisely since it is very subtle and the pulse duration is very short. Therefore, a precise method is proposed to measure this information based on Morlet wavelet transform. Morlet wavelet transform has low signal-to-noise ratio (SNR) threshold. According as auto correlating the wavelet transform coefficient of radar signal, the Doppler Frequency rate-of-change is enhanced and phase ambiguity is unwrapped. By exploiting the coherent property of pulse train, the observation time is extended equivalently and so the measurement precision is improved greatly. The simulation study shows that this method has low SNR threshold and obtain the parameter measurement fast and accurately. [C3232]

#### "Compressive sensing SAR imaging with real data"

As an active and coherent microwave high resolution imaging system, Synthetic Aperture Radar (SAR) has the capability to image in all weather and day-or-night conditions. Recent advent of theory of Compressive Sensing (CS) has introduced a novel concept that an unknown sparse signal can be recovered exactly with an overwhelming probability even with highly sub-Nyquist-rate samples. In this paper, a new scheme for the test bed of CS based SAR imaging is proposed. Experimental results on some real raw SAR data reveal that there are some practical limitations on the use of CS based SAR imaging, especially for complex imaging scenes and the systems with low Signal-to-Noise Ratio (SNR). [C3233]

#### "Estimation of significant wave height from X-band marine radar images"

Radar images include abundant information about ocean waves. Sea state parameters and surface currents can be obtained by analyzing time series of radar images of the sea surface. Due to the non-linearity of the imaging mechanism of ocean waves, significant wave height ( $H_s$ ) can not be determined directly from radar images. Applying a method to infer the  $H_s$  from synthetic aperture radar (SAR) images, the  $H_s$  can be estimated from marine radar images. Comparing the  $H_s$  obtained by this method with buoy data, the results show that it is

feasible to obtain reliable data of the Hs from marine radar images. [C3234]

### "Fish-pond change detection based on short term time series of RADARSAT images and object-oriented method"

As an important type of wetlands, fish-pond provides a number of important ecosystem services. It was easily affected by human activities such as the change of cultivation structure. Tracking the fast change of fish-pond can obtain the information that the environment is impacted by human activities to what extent. In this study, we proposed a change detection procedure in order to delineate fast change fish-pond using high resolution, short term time series of SAR imagery. The procedure includes (1) SAR images preprocessing, (2) object extraction, (3) multi-temporal change characteristics analysis of fish-pond, (4) change objects classification, and (5) a final change results analysis. In this study, object-oriented method was adopted to extract and analyze the texture characteristics of fish-pond in the high spatial resolution of SAR data. Objects were generated with suitable scale parameters by means of multi-temporal segmentation approach according to the image features (including backscatter, difference and ratio of three temporal RADARSAT images, shape characters), and the changed objects were extracted through analyzing the shape index and contextual information generated by Definiens software. Six change types of fish-pond were achieved. The results indicate that high resolution SAR data can provide better information for fish-pond change detection in the study area, and the procedure proposed in this study can efficiently obtain the fast change objects with high accuracy between three short term time series SAR images, which are useful for the further classification. [C3235]

### "A 3D microwave imaging method for earth observation"

Microwave imaging techniques which can provide all-weather, day-and-night imaging capability have important applications to many fields. It is an active area to explore new microwave imaging ideas, systems and techniques. In our previous work, we proposed a new microwave imaging method for earth observation. In this method, the transmitter and receiver are located in different platforms, and only a monochromatic microwave is required to illuminate the earth surface. Numerical simulation results show that this method can produce microwave images with high spatial and radiation resolutions. In this paper, as an extension of our previous work, we study some important properties of this method, which lead to a very promising potential application in 3-dimensional (3D) imaging for earth observation. [C3236]

### "Airborne LiDAR strip adjustment based on LSM"

An airborne LiDAR system is an integration of GPS, INS, and laser scanner. Because of errors of these instruments or sub-optimalities of the GPS/INS integration, points of neighbouring laser scanner strips will usually show vertical and horizontal discrepancies. Currently the more common way for the reducing or ultimately eliminating discrepancies found in strip overlap areas is strip adjustment. Based on Microsoft Visual Studio 2008 C++ platform, a data-driven method of seven parameters conformal transformation for airborne LiDAR strip adjustment is realized in our paper, the algorithm improved Robert (2004) least squares surface matching algorithm, by introducing the Gauss-Markoff model, Acquired the unbiased minimum variance estimation for the unknown parameters. Real data sets are used to validate the method. We study the matching precision of different reference surface from two strips, the need for using Gauss-Markoff model and the matching accuracy. Experimental results show that after correction the point clouds show much better alignment and the vertical matching error is less than 0.05m. [C3237]

### "High resolution radar imaging using bandwidth extrapolation"

The resolution of a synthetic aperture radar (SAR) image, in range and azimuth, is limited by the transmitted signal bandwidth and the synthetic aperture length, respectively. Bandwidth extrapolation algorithm is one of the various superresolution techniques for improving the resolution. The frequency AR model is used in the paper to expand the effective bandwidth of the signal based on the bandwidth extrapolation together with linear prediction algorithm. The performance estimation function, namely the prediction error as a scaling power-law function of the linear error prediction filter length, is derived through analyzing large numbers of computer simulation experiments. It is of considerable importance to determine the linear error prediction filter length for optimizing the bandwidth extrapolation parameters. It is demonstrated by the theoretical analysis and simulation results that the bandwidth extrapolation method is feasible and effective for expanding the bandwidth to obtain higher resolution SAR image by applying the method to the range and azimuth directions, respectively. [C3238]

### "Analysis and modification to the method of bistatic clutter range dependence mitigation"

Clutter range dependence mitigation is very important for bistatic space-time adaptive processing (STAP) radar. The paper focuses on the technique of clutter spectrum registration-based nonuniform frequency sampling (RB-

NFS). Analysis indicates RB-NFS method brings inadequate clutter rejection and the dependence on STAP training sample number. Modifications to RB-NFS method are proposed to solve the problems. Simulations prove the correctness of analysis of RB-NFS. STAP with modified RB-NFS is hardly affected by the number of training samples and can achieve approximately optimal performance even with only two training samples. [C3239]

#### **"Power-level surveillance for an FMCW-based local positioning system"**

Local positioning systems which are based on the bistatic frequency modulated continuous wave (FMCW) radar principle generally evaluate the time of flight (TOF) of signals. However, the FMCW principle also provides the power level (PL) of the received signal, which is often neglected since various unknown parameters must be considered. In this contribution, we present a method which exploits this additional source of information by predicting its value accurately based on the knowledge of the antenna characteristics, hardware parameters, and the estimated position of the measurement transponder (MT). This information can then be used to determine the quality of each PL measurement and to discard data which are obviously corrupted. [C3240]

#### **"Wetland cover information extraction research based on the multi-polar radar images and multi-spectrum optical images fusion"**

The research takes Radarsat-2 multi-polarization radar images and ALOS multi-spectrum optical images for example, through the information filtering and extraction methods such as information quantity statistics and correlation matrix, we obtain the cognition of the spectral characteristics and detection performance of each polarization mode radar image, and select the optimal data for fusion and classification experiment. Using Brovey, PCA, HPF and Wavelet transformation methods to fuse, and adopting non-supervision, supervision and object-oriented method to carry out classification experiment, we explore the application of radar and optical remote sensing image fusion technology in the wetland area covers information extraction, which verifies the effectiveness and feasibility using radar and multi-spectral image fusion technology in the wetland cover information extraction. [C3241]

#### **"A new method of three-dimensional visualization of satellite cloud image"**

To solve the problems on 3D visualization of satellite data, such as the inaccuracy of cloud mask, ignorance of visual affect of gray, transparency and orientation, this paper brings forward a series of methods. Through radiation background to detect cloud mask and cloud top inversion etc, can obtain high precision application data, moreover, advances the revised model on aspects of gray, transparency and orientation. modeling by the methods advanced above, 3D satellite data could gain a better effect. [C3242]

#### **"SAR interference signal feature vector extraction and simulation based on wavelet packet analysis"**

This paper studies the use of wavelet analysis method to realize the non-coherent narrow-band SAR radar signal interference suppression. Based on the full study of Irregular wavelet tree in interference detection and filtering, an adaptive filter using wavelet packet decomposition to extract the interference signal feature vector has been proposed. Simulation experiments based on this method have been carried out, by using SNR improvement, interference rejection ratio, signal distortion and other evaluation criteria to evaluate the results of interference suppression, the results show that the effect of wavelet packet filtering interference suppression is good. [C3243]

#### **"Research on extracting the tree height based on LiDAR data"**

In this paper, extraction of the forest tree height based on LiDAR (Light Detection and Ranging) data was studied. A simple algorithm was proposed to compensate the result computed by the DEMs of first return and last return. The satellite image download from the GoogleEarth was used to facilitate the analysis. The algorithm was tested with these data, and had been proved to be effective. Although the data we used was not suit for extracting tree height, LiDAR has great potential in this field. [C3244]

#### **"A novel SAR fusion image segmentation method based on Markov Random Field"**

Markov Random Field (MRF) method is a popular technology in SAR image segmentation nowadays. It considers the statistical characteristics of SAR image and achieves optimal image segmentation result. In this paper, a novel SAR fusion image segmentation method based on MRF model is proposed. Firstly, the mechanism of MRF segmentation on single SAR image is studied. Secondly, the Maximum a Posterior (MAP) formula for SAR fusion image segmentation is deduced by supposing the two SAR images for fusion are statistically independent. Then the energy function of SAR fusion image segmentation is presented and the



processing steps are given. At the end, computer simulation indicates that the performance of this new approach is much better than that of single SAR image segmentation based on MRF. [C3245]

### "Synthesis of four-level Z-complementary sequences"

Sequences over the alphabet  $\{1, -1, 2, -2\}$  are called four-level sequences. Including the conventional complementary sets as special cases, the aperiodic four-level Z-complementary sets (FLZCS) with zero correlation zone (denoted by Z) are introduced, and the elementary transformations on four-level sequences and elementary operations on FLZCS are given. In particular, comparing four-level Z-complementary pairs with binary and quadriphase Z-complementary ones, the results show that the maximum zero correlation zone (denoted by  $Z_{\max}$ ) of four-level and quadriphase Z-complementary pairs is generally much longer than that of binary Z-complementary ones, and that  $Z_{\max}$  of four-level Z-complementary pairs is pretty close to that of quadriphase Z-complementary ones. It is verified that most synthesizing methods of quadriphase Z-complementary sets and their mates are also applicable to FLZCS, in addition to which, other synthesizing methods of FLZCS and their mates are provided here. [C3246]

### "A novel method of resolving velocity ambiguity in the pulse doppler radar"

In this paper, a novel method of resolving velocity ambiguity in the pulse Doppler (PD) radar is proposed. By using multi-carrier-frequency waveform and Chinese Remainder Theorem (CRT), this method is able to overcome the velocity ambiguity. Furthermore, a modified algorithm with better robustness is deduced and its performances are analyzed in detail. Specific conclusions are verified with some simulation results. [C3247]

### "In-situ broadband soil measurements: Dielectric and magnetic properties"

This paper presents an in-situ method for measuring both electric and magnetic properties of Hawaiian volcanic soil for GPR applications in a broad frequency range from 50 MHz to 1GHz. For the in-situ probe, we combined two monopole antennas with parasitic elements into one piece to achieve reflection (S11) and transmission (S21) measurements simultaneously. Finally, the in-situ probe has a shape of a multi-conductor TEM transmission line, which consists of five conducting rods, two ground plates and two coaxial feed connectors. In a typical measurement the in-situ probe is connected to a two ports vector network analyzer and system calibration is then performed to characterize the sample free device. The calibration is based on measurements of the S-parameters for sample free and sample loaded devices. A unique post processing algorithm has been developed to extract accurate constitutive parameters ( $\epsilon^*$ ,  $\mu^*$ ) from the scattering parameters (S11, S21) of the soil probe, which will be discussed in this paper. The prototype in-situ soil probe and post processing algorithm were also tested by both numerical simulation and actual soils in volcanic red soil. The simulation results showed around 1 % of error over the operational frequencies between 100 MHz and 800 MHz. Actual measurement results conducted by the in-situ probe and developed algorithms were in very good agreement with those obtained by a laboratory method. Simulation and actual measurement data will be presented in this paper. [C3248]

### "Building detection and height retrieval in urban areas in the framework of high resolution optical and SAR data fusion"

In this paper, we propose a symmetrized version of a semiautomatic processing chain, able to provide the simple 3D reconstruction of buildings in urban scenes, from high-resolution optical and SAR imagery. The new elaborated chain gives an equivalent part to the optical and SAR components, in order to fully exploit complementary information provided by proper building features in both images. First, the initial processing chain is reminded and completely illustrated on a studied scene on real data. Then, three points of improvements by process symmetrization are discussed: an augmentation of the detection rate in the footprint extraction step, an increase of the reliability attached to the estimated building heights and a joint improvement of the steps of building validation and qualification. It is shown that the appropriate combination of optical and SAR features, inside some processing steps, could give better results of reconstruction. [C3249]

### "Infrared satellite precipitation estimate using waveletbased cloud classification and radar calibration"

We have developed a methodology to enhance an infrared-based high resolution rainfall retrieval algorithm by intelligently calibrating the rainfall estimates using space-based observations. Our approach involves the following four steps: 1) segmentation of infrared cloud images into patches; 2) feature extraction using a wavelet-based method; 3) clustering and classification of cloud patches; and 4) dynamic application of brightness temperature ( $T_b$ ) and rain rate relationships, derived using satellite observations. The results show that using wavelet features along with other features increase the performance of rainfall estimate in terms of quantitative

rain/no rain area estimates. In addition, using lightning data as a feature improves the estimates as well. [C3250]

### "Potentials of a compact polarimetric SAR system"

The goal of this study is to show the potential of a compact-pol SAR system for vegetation applications. Compact-pol concept has been suggested to minimize the system design while maximize the information and is declined as the  $\pi/4$ ,  $\pi/2$  and hybrid modes. In this paper, the applications such as classification, Faraday rotation and soil moisture estimates are first reminded, then, biomass estimation from CP data is presented and a calibration procedure using external targets is proposed. Finally, the interferometry concept is added to assess the capabilities of a compact-pol system to retrieve vegetation height. [C3251]

### "Metallic objects and oil spill detection with multi-polarization SAR"

In this study, two innovative physically-based approaches have been developed to detect man-made metallic objects and oil slicks in polarimetric SAR data. They are based on the different sea surface scattering mechanisms expected with and without oil slicks and metallic objects. Experiments, accomplished over Single Look Complex (SLC) Level 1.1 quad-pol L-band ALOS PALSAR SAR data, demonstrate the effectiveness of the two approaches for oil slick and metallic target detection purposes and witness the capability of ALOS PALSAR data for such applications. [C3252]

### "Modeling lidar scene sparsity using compressive sensing"

One of the major problems associated with LIDAR sensing is that significant amounts of data must be collected to obtain detailed topographical information about a region. Current efforts to solve this problem have focused on designing compression algorithms which operate on the collected data. These, however, require the collection of large amounts of data only to discard most of it in some transformed domain. Instead, compressive sensing has demonstrated that highly accurate signal reconstructions are achievable even when sampling below the Nyquist rate. Such sensing is clearly desirable for LIDAR range data compression if it can be achieved. One notes, however, that compressive sensing requires a priori knowledge of the sparsifying basis of the signal which is a major problem for LIDAR since that basis depends not only on the underlying scene complexity but also on the laser spot size and target distance. For these reasons, the goal of this research is to take the first steps in establishing a relationship between typical LIDAR scenes of varying complexity and the sparsity of the scene compressively sampled. [C3253]

### "The snowscat ground-based polarimetric scatterometer: Calibration and initial measurements from Davos Switzerland"

The COld REgions Hydrology High-resolution Observatory (CoReH20) Mission proposes a dual frequency radar operating at 9.6 and 17 GHz utilizing VV and VH polarization [1]. By combining X and Ku-Band with both co and cross-polarization diversity it is possible to estimate the Snow Water Equivalent of dry snow. To support this proposed mission, ESA has sponsored the development of a ground-based coherent polarimetric scatterometer operating over the 9-18 GHz frequency range. ESA is supporting campaigns to acquire and process data using SnowScat for validation of Snow Water Equivalent (SWE) retrieval algorithms. [C3254]

### "Performance status of the wave scatterometer SWIM"

SWIM is a Ku-band radar designed for wave directional spectrum estimation. This radar operates at six incidence angles (from  $0^\circ$  to  $10^\circ$ ) with a complete azimuth scanning covering a swath of 180 km. The phase B (addressing preliminary design) of SWIM is currently under finalization. In, the preliminary design and associated performance analysis have been published taking into account the first results of Phase B design. This paper is focused on the last performance assessment of this phase B for all the measurements performed by the SWIM instrument. [C3255]

### "One micron laser technology advancements at GSFC"

In recent years, lasers have proven themselves to be invaluable to a variety of remote sensing applications. LIDAR techniques have been used to measure atmospheric aerosols and a variety of trace species, profile winds, and develop high resolution topographical maps. Often it would be of great advantage to make these measurements from an orbiting satellite. Unfortunately, the space environment is a challenging one for the high power lasers that would enable many LIDAR missions. Optical mounts must maintain precision alignment during and after launch. Outgassing materials in the vacuum of space lead to contamination of laser optics. Electronic components and optical materials must survive the space environment, including a vacuum atmosphere, thermal cycling, and radiation exposure. Laser designs must be lightweight, compact, and energy efficient. Many LIDAR

applications require frequency conversion systems that have never been designed or tested for use in space. For the last seven or eight years the National Aeronautical and Space Administration (NASA) has undertaken a program specifically directed at addressing the durability and long term reliability issues that face space-borne lasers (The Laser Risk Reduction Program-LRRP). [C3256]

### "On-ground tests and measurements of the Passive Advanced Unit Synthetic Aperture (PAU-SA)"

This paper presents the current state of the Passive Advanced Unit Synthetic Aperture's instrument (PAU-SA), its installation in the transportation truck, and the preliminary tests that have been performed to verify the instrument's status. [C3257]

### "3D imaging of ice sheets"

We developed and deployed, in July 2005, a wideband 8-channel synthetic aperture radar (SAR) at Summit Camp, Greenland (72.5783° N and 38.4596° W). The radar was designed to map internal layers, measure topography, and generate backscatter maps-all in a single pass. Information on ice thickness, bed topography and basal conditions is essential to the refinement of glaciological models of ice sheets, which are used to predict ice-sheet behavior (especially mass balance) and to select deep ice-core sites. This work focuses on the use of fine-resolution 3D imaging algorithms for combining all 8-channels to form cross-track image slices through the ice. As compared with traditional 2D depth sounding, these 3D images allow for the characterization of bed topography with very fine resolution. They also allow for the generation of strip-map SAR images with absolute geocoding without ground control points (these are unavailable at the bottom of the ice), and the ability to analyze the ice-sheet volume in 3D. Topography, backscattering, and 3D ice volume results are illustrated here. [C3258]

### "Atmospheric phase screen-estimation for PSInSAR applied to TerraSAR-X high resolution spotlight-data"

The PSInSAR technique, invented by Ferretti et. al. ten years ago, meanwhile has proven it's capability for very precise measurement of surface deformations. To achieve this, the influence of the atmospheric phase screen (APS) has to be removed. We investigated the APS for two series of TerraSAR-X high resolution spotlight data of a scene in Bavaria. Our approach was to consider the APS as composed of a phase ramp, a part stratified with height and a turbulent component. We estimated the turbulent component via kriging. The variograms show for short distances a regime which is not visible for lower resolutions. In this paper we discuss the choice of appropriate variogram models with respect to our data. [C3259]

### "Doppler effect and compensation in a Rotating Fanbeam Spaceborne Scatterometer"

Spaceborne Rotating Fanbeam Scatterometer, RFSCAT, has a wider continuous swath that can provide a large number of independent samples of Sigma0 for wind speed and direction retrieving. But the large swath and footprint result in a wideband Doppler frequency shift. For a low earth orbiting satellite, the maxim Doppler bandwidth between forward and backward echoes will be about 500 KHz. Even in a single echo of RFSCAT, the Doppler bandwidth is about 90 KHz, while in a pencil beam scatterometer the Doppler bandwidth is almost a single tone. A method of Doppler frequency compensation both on center frequency of transmitted pulses and signal processing section of the echoes are carried out and evaluated. [C3260]

### "Fractal based filtering of SAR images"

In this paper an innovative fractal based filtering for the analysis of SAR images of natural surfaces is presented. Its definition is based on a complete direct imaging model developed by the authors. The application of this innovative algorithm to SAR images makes it possible to obtain a complete map of the fractal dimension of the observed scene. Significant results obtained on actual SAR data are shown in the last section of the paper. [C3261]

### "Exploitation of the additive component of the polarimetric noise model for speckle filtering"

Ratio filters for speckle noise reduction in SAR imagery are recursive filters where the image structure is iteratively recovered from an initial oversmoothed image. We show that the MBPolSAR filter could be interpreted as a ratio filter applied to the off-diagonal terms of the covariance/coherency matrix. From this observation, we propose a new polarimetric ratio filter allowing us to recover the image structure from all the terms of the covariance matrix. In addition, we briefly look at how the additive noise component could also be exploited for the image structure extraction. Filtering results on both simulated and real PolSAR images are shown. [C3262]

### "SAR performance monitoring for TerraSAR-X mission"

The TerraSAR-X satellite features an advanced X-Band SAR based on the active phased array technology which allows flexible operation of Spotlight, Stripmap, and ScanSAR mode for various combinations and elevation angles. It combines the ability to acquire high resolution images for detailed analysis as well as wide swath images for overview applications. The SAR performance of the system is analysed with respect to geometric and radiometric parameters. Long-term monitoring of system parameters like instrument characteristics or SAR image quality confirms the continuous stability of the system. By launching a twin satellite TanDEM-X for global DEM acquisition, the TerraSAR-X mission is now supported by two satellites. The approach presented in the following shows how to keep the SAR performance for both satellites, TerraSAR-X and TanDEM-X. [C3263]

### "Using airborne & space lidars for large-area inventory"

NASA plans to launch two space lidar missions over the next decade, and at least one proposal for a space lidar is being considered by the European Space Agency. All designs call for single-beam or multi-beam profiling systems. These space ranging systems, like the ICESat/GLAS lidar that collected over 1.91 billion waveforms between January 2003 and October 2009, must necessarily be used as sampling tools to characterize vegetation cover and to estimate forest volume, biomass, and carbon globally. Recent investigations conducted by these authors have centered on developing, testing, and refining statistical approaches that can incorporate airborne and space lidar acquisitions to inventory large areas. [C3264]

### "Case studies of automatic change detection using AVNIR-2 onboard ALOS"

This paper suggests a new automatic change detection approach using image-object-based contextual inference. The approach first detects changed areas, and then infers what happened there. The inference process uses knowledge based on a change detection process performed by humans. It enables flexible and intuitive description of the change detection process. In this paper, we describe the results of case studies on automatic change detection using the Advanced Visible and Near Infrared Radiometer type-2 (AVNIR-2) onboard the Advanced Land Observing Satellite (ALOS, nicknamed "Daichi"). [C3265]

### "Progress in the validation of dual-wavelength aerosol retrieval models via airborne high spectral resolution lidar data"

The Constrained Ratio Aerosol Model-fit (CRAM) technique is a method for making aerosol retrievals from dual-wavelength elastic scatter lidars which attempts to constrain the retrievals so as to be consistent with a number of aerosol models thought to characterize a variety of aerosol types observed around the world. The NASA Langley Research Center Airborne HSRL is an airborne high spectral resolution lidar capable of direct measurements of aerosol extinction and backscatter at 532 nm and having the capability for elastic backscatter measurements at 1064 nm. Aerosol measurements by HSRL during the TEXas Air Quality Survey/ Gulf of Mexico Atmospheric Composition and Climate Study (TEXAQS/GoMACCS) campaign are used to validate existing aerosol models critical to the application of CRAM, in particular to data from the Cloud-Aerosol Lidar with Orthogonal Polarization (CALIOP) lidar instrument on board the Cloud-Aerosol Lidar and Infrared Pathfinder Satellite Observations (CALIPSO) satellite. [C3266]

### "Focal plane approximation for near field interferometric radiometer imaging"

Applying synthetic aperture interferometric radiometer (SAIR) in near field imaging has been receiving great interest in the recent years. Because the traditional far-field Fourier imaging theory is not valid in near-field condition, developing the proper near-field imaging techniques is the major desirable objective of near field SAIR applications. This work is devoted to establish an effective near field imaging method still with traditional far-field plane antenna array. The discrete numerical inversion method with focal plane approximation is developed. The regularization method is also introduced to deal with the ill condition and measurement errors. [C3267]

### "Oil-slick observation using single look complex TerraSAR-X dual-polarized data"

In this study single look complex (SSC) TerraSAR-X dual-polarized data are firstly exploited for sea oil slick observation purposes. An electromagnetic model which, based on the Co-polarised Phase Difference between the HH and VV channels (CPD), allows describing the X-band sea surface scattering with and without surface slicks is proposed. Following this rationale, the polarimetric approach is firstly developed and applied to X-band Synthetic Aperture Radar (SAR) data in which both certified oil slicks and look-alikes are present. Experimental results demonstrate, for the first time, that X-band dual-polarimetric SAR data are suitable for sea oil slicks observation purposes and witness the paramount importance of the TerraSAR-X dual-polarimetric mode for such application. [C3268]



### "Observational studies of atmospheric aerosols in the lower troposphere using multiple sensors"

Atmospheric aerosols play a large role in the Earth's radiation budget, but their specific radiative forcing effects vary wildly depending upon species, altitude and geographic location. A suite of instruments has been developed and deployed at Montana State University in Bozeman for the purpose of conducting altitude-resolved atmospheric aerosol studies. [C3269]

### "The preliminary temporal analysis of ground deformations in the area of Dabrowski Coal Basin (south Poland)"

In this work the preliminary temporal analysis of ground deformations in the area of Dabrowski Coal Basin was performed. In this region the intensive coal exploitation has been performed for about 200 years. The studied region covers the mining areas of seven coal mines. Moreover this area is crossed by many faults. In the described work the analysis concerned only the small, long lasting deformations that were detected using PSInSAR technique. The aim of this work was to analyze the changes in the deformations' trend between years 1992 and 2003 for each PS point. In order to perform this task the special algorithm was developed. It allows detecting maximum one (the most significant) trend change in the considered period of time. Performed analysis revealed that in the study area the changes of trend deformations occurred for about 40% of PS points. The spatial and temporal distribution of PS points with trend changes showed some regularity. This regularity may indicate the influence of coal exploitation on the values of small, long period deformations that were previously explained only by neotectonics movements. [C3270]

### "TerraSAR-X observations over the antarctic ice sheet"

An incoherent correlation approach is used to derive ice motion fields for outlet glaciers through the Transantarctic Mountains, Antarctica. High-resolution repeat-pass, left-looking-mode TerraSAR-X data from 2009 were analyzed. Detailed ice velocity patterns on the Nimrod glacier basin and Starshot glacier are presented. [C3271]

### "The BIOMASS mission-An ESA Earth Explorer candidate to measure the BIOMASS of the earth's forests"

The European Space Agency (ESA) released a Call for Proposals for the next Earth Explorer Core Mission in March 2005, with the aim to select the 7th Earth Explorer (EE-7) mission for launch in the next decade. Twenty-four proposals were received and subject to scientific and technical assessment. Six candidate missions were selected and further investigated in the preliminary feasibility studies (Phase 0). One of these missions is BIOMASS, which has recently been selected to proceed to Phase-A. BIOMASS is a response to the urgent need for greatly improved mapping of global biomass and the lack of any current space systems capable of addressing this need. [C3272]

### "Temporal snowpack density mapping using C-band multi-polarization ASAR data"

Radar remote sensing has great potential to determine the extent and properties of snow cover. Availability of spaceborne sensor dual-polarization C-band data of ENVISAT- ASAR can enhance the accuracy in measurement of snow physical parameters as compared to single polarization data measurement. This study shows the capability of C-band SAR data for estimating dry snow density over snow covered rugged terrain in Himalayan region. The snow density is an important parameter for the snow hydrology and avalanche forecasting related studies. An algorithm has been developed for estimating snow density, based on snow volume scattering and snow-ground scattering components. The radar backscattering coefficients of both HH and VV polarization and incidence angle are used as inputs in the algorithm to provide the snow dielectric constant which can be used to derive snow density using Looyenga's, semi empirical formula. Comparison was made between snow density estimated from algorithm using ENVISAT-ASAR HH and HH polarization data and the measured field value. The mean absolute error between estimated and measured snow density was found to be 24.38 kg/m<sup>3</sup>. [C3273]

### "A new polarization ratio model from C-Band RADARSAT-2 fine Quad-Pol imagery"

We propose two new analytical polarization ratio (PR) models based on the RADARSAT-2 Quad-Polarization (HH+VV+HV+VH) observations over the ocean. One is a function of incidence angle only and the other has additional dependence on wind speed. Comparisons are presented with theoretical and empirical PR models from the literature. The new PR model with wind speed and incidence angle dependence is shown to compare best with observed RADARSAT-2 data. An assessment of the PR model with only incidence angle dependence

is given using CMOD algorithms and HH-polarized images. Results suggest that this PR model can accurately convert normalized radar cross sections (NRCS) in HH polarization to VV polarization and retrieve wind speeds from RADARSAT-1 or RADARSAT-2 HH polarization images. [C3274]

### "Lidar education at Georgia Tech"

The Georgia Tech Research Institute's atmospheric laser radar (lidar) team became involved in education projects starting in 2001, when we developed an eye safe lidar with undergraduate women at Agnes Scott College in Decatur, Georgia. We have initiated several other projects since that time, including short courses, an academic course at Georgia Tech, a lidar textbook, and a lidar system designed specifically for education. The lidar education program at GTRI is reviewed here with comments about future plans and prospects. [C3275]

### "Three dimensional reconstruction of urban areas using jointly phase and amplitude multichannel images"

The aim of this paper is the three dimensional reconstruction of urban areas using Very High Resolution (VHR) images. The proposed innovative approach for the three dimensional reconstruction is based on the joint exploitation of both amplitude and interferometric phase images of a multichannel SAR system. The information provided by the amplitude data is added to the 3D reconstruction chain, considering that in urban areas edges of amplitude image are likely also present in the interferometric phase one and conversely. Differently from other works present in literature, the proposed technique exploits the amplitude image, not only to improve the phase regularization, but also to improve the phase unwrapping step. The results will show the effectiveness of the method. [C3276]

### "IMaging geodesy with TerraSAR-X"

We report on a method and experiments to achieve about 3 centimeters pixel location accuracy of TerraSAR-X SAR images. The method is based on atmospheric refraction corrections, Earth tide compensation and image correlation or the use of corner reflectors. Our method does not exploit the SAR phase and is therefore not subject to phase unwrapping problems or unknown phase offsets. [C3277]

### "Development of the LiDAR data processing system for the rapid generation of the terrestrial information"

This paper present an improved application system which can generate the 2.5D or 3D terrestrial information like DSM, DEM rapidly using LiDAR data. To process and manipulate input LiDAR data, various function modules are contained in the developed system. It allows users to display LIDAR data using TINS and even allows users to analyze the data using a profile viewer. In addition, the system also allows users to save the processed data with LAS file format, ASCII format. [C3278]

### "The Hurricane Imaging Radiometer wide swath simulation and wind speed retrievals"

The knowledge of peak winds in hurricanes is critical to classification of hurricane intensity; therefore, there is a strong interest in the operational remote sensing of ocean surface winds for monitoring tropical storms and hurricanes, especially those which threaten landfall. Presently, the airborne Stepped Frequency Microwave Radiometer (SFMR) is the state-of-the-art remote sensor for providing this information in real-time, during hurricane surveillance flights. However, for the future, NASA and NOAA are collaborating in the development of the Hurricane Imaging Radiometer (HIRAD), which is a prototype of the next-generation high-flying airborne instrument for monitoring hurricanes. This paper describes a realistic end-to-end simulation of HIRAD hurricane measurements while flying on an unmanned Global Hawk aircraft. The objective of this research is to develop baseline retrieval algorithms and provide a wind speed measurement accuracy assessment for the upcoming NASA hurricane field program, Genesis and Rapid Intensification Processes (GRIP), to be conducted in 2010. [C3279]

### "Forest change detection from L-band satellite SAR images using iterative histogram matching and thresholding together with data fusion"

In this study, we assess the efficiency of using L-band satellite SAR for forest change monitoring, by applying a combination of change detection techniques to SAR backscatter intensity images acquired over Swedish forest. We use a bi-temporal change detection approach based on image rationing. Histogram based techniques are used both for radiometric normalization and thresholding. For a final classification step, we evaluate a data fusion based change detection method that exploits the spatial and spectral information from one or multiple SAR channels. Pre-applied filters are also evaluated as alternatives to tackle low resolution and speckle. HH and HV

polarized Fine Beam Dual images, acquired 34 degrees off nadir (FBD34) by the Advanced Land Observing Satellite Phased Array type L-band Synthetic Aperture Radar (ALOS PALSAR), are used to find clear-cuts in Swedish boreal forest. Our results show that clear-cuts can be clearly extracted from L-band SAR data. [C3280]

### "Ground penetrating radar measurements: Applications to synthetic data generation and target characterization"

Ground penetrating radar (GPR) is widely studied for detection of landmines and mine-like targets; GPR is particularly useful for detecting minimum metal mines which are harder to detect using traditional metal detection devices alone. In order to expand the phenomenology for GPR, careful measurements of homogeneous and heterogeneous soils with and without targets (landmine simulants and metal objects) are performed in a controlled environment. These measurements will aid in the development of models for soil response beyond the initial air-ground interface. Such explicit models for soil will increase the effectiveness of algorithms designed to discriminate between returns from targets and from naturally occurring geologic materials and interfaces. Furthermore, careful measurement of soil characteristics will enable comparison and refinement of models of soil with embedded targets developed in electromagnetic simulations (using finite-difference time-domain codes (FDTD), e.g.). [C3281]

### "On radar sounding applications for Enceladean ice"

Due to the nature of observations taken by planetary spacecraft, many surface and atmospheric studies have been performed at the icy moons of the outer planets, which have left the many seemingly complex interior processes in these bodies left unexplored and unexplained. It is notably difficult to access the interior regions in which planetary formation and dynamics take place. This paper presents the possibility that radar measurements could contribute to the understanding of interior structure, particularly that of Enceladus, the small but notably dynamic icy moon of Saturn. The application of such radar may lead to discoveries concerning formation mechanisms and surface processes. Additionally, radar sounding will contribute measurements that aid in diagnosing the dynamics system at work in the subsurface-perhaps most notably, the source reservoir and/or dynamics of the observed water plume at the moon's south pole, in addition the moon's role as a whole in the Saturnian system. [C3282]

### "A physically-based approach to observe man-made metallic objects in dual-polarized SAR data"

An electromagnetic model to observe man-made metallic objects in dual-polarized SAR data has been developed. The model predicts that man-made metallic objects and sea surface, being characterized by completely different symmetry properties, call for a different and well-distinguishable HH-HV correlation. Following this rationale, a simple and very computer-time effective filtering technique has been developed to observe man-made metallic objects in full-resolution dual-polarized SAR data. Experiments accomplished over Single Look Complex (SLC) Fine Quad Polarization RADARSAT-2 SAR data confirm the effectiveness of the proposed approach. [C3283]

### "Quantifying the results of wind and rain on ifsar tree height estimation"

The horizontal and vertical (3D) structure of Earth's forested ecosystems are of great significance to their ecological functioning and societal uses. An IfSAR approach is one methodology whereby a forest's structure and height in particular can be successfully estimated. Critical to the successful estimation is a high correlation between multiple SAR images. Regardless of a forest's location on the Earth, wind and precipitation can significantly alter a forest's appearance to a SAR system operating in either the L or C bands and so too decrease this necessary correlation. In order to investigate and quantize the decorrelation induced by factors such as wind and rain, we have developed a model for the repeat-pass interferometric SAR response of a forest including the application of a wind field and / or a rain storm. The simulation consists of multiple interconnected parts including the generation of fractal tree geometries, a wind simulator to apply variable wind forces to the generated trees, an electromagnetic model to allow us to calculate a Single Look Complex value for the SAR return of the combined target, an image forming technique based on antenna array theory, and an image processing algorithm. Results present polarimetric coherence as a function of platform look angle, wind speed, and moisture content. An important feature of this research is the usage of a physically based realistic wind model that is based on measurements of wind effects on trees as well as realistic models of fluid flow and simple harmonic branch segment resonators. Allowing branches to bend and move out of the plane of the incident wind field enables our model to capture numerous features of a physical tree blowing in the wind. This realistic model is necessary for a realistic simulation of the effects that wind has on a given InSAR imaging system as expressed in this study by the interferometric coherence. [C3284]

### "Preliminary result of polarization property analysis using fully polarimetric GB-SAR images"

Korea Institute of Geoscience and Mineral Resources (KIGAM) and Kangwon National University (KNU) ground-based synthetic aperture radar (GB-SAR) team has been developed a fully polarimetric and interferometric GB-SAR system over past several years. The objective of this paper is to investigate an application of the obtained fully polarimetric GB-SAR images and an effective polarimetric analysis method to extract polarization properties from different terrain targets as a preliminary study. We utilized an unsupervised classification method for analyzing of a fully polarimetric GB-SAR image, in particular, Cloude and Pottier's method and a combined  $H/A/\alpha_{\perp}$  and the complex Wishart classifier method based on the  $H/A/\alpha_{\perp}$  polarimetric decomposition theorem.

[C3285]

### "AN SVM classifier with HMM-based kernel for landmine detection using ground penetrating radar"

We propose a landmine detection algorithm using ground penetrating radar data that is based on an SVM classifier. The kernel function for the SVM is constructed using discrete hidden Markov modeling (HMM). Typically, the kernel matrix could be obtained by defining an adequate similarity measure in the feature space. However, this approach is inappropriate as it is not trivial to define a meaningful distance metric for sequence comparison. Our proposed approach is based on HMM modeling and has two main steps. First, one HMM is fit to each of the  $N$  individual sequences. For each fitted model, we evaluate the log-likelihood of each sequence. This will result in an  $N \times N$  log-likelihood similarity matrix that will be adapted to serve as the kernel of the SVM classifier. In the second step, we train an SVM classifier to learn a decision boundary between the positive and negative samples. [C3286]

### "A multimodal Matching Pursuits Dissimilarity Measure applied to landmine/clutter discrimination"

The Matching Pursuits Dissimilarity Measure (MPDM) is an effective way to compare signals that are sparsely approximated using a Matching Pursuits method. The CAMP algorithm uses an MPDM distance measure in Competitive Agglomeration clustering to model and classify signals. The MPDM approach can only compare signals originating from a single source. Many landmine detection systems use multiple sensors to make simultaneous measurements of the same region of interest. In this paper we propose a Multimodal MPDM that can be used with CAMP to fuse signals from multiple sensors. We demonstrate the effectiveness of the Multimodal MPDM over the single sensor MPDM in improving discrimination of landmines from clutter objects.

[C3287]

### "The external calibration study for EarthCARE/CPR"

The Cloud Profiling Radar (CPR) is one of key sensors on EarthCARE for joint project between Europe and Japan. The CPR is developed by National Institute of Information and Communications Technology (NICT) in Japan and Japanese Aerospace Exploration Agency (JAXA). The CPR uses W-band frequency and large antenna diameter in order to obtain enough sensitivity. In other words, beam footprint becomes small but antenna scanning cannot be performed. Two external calibration methods are considered. The first method is external calibration using active radar calibrator (ARC). It is foreseen the difficulty to place exact location on sub-satellite track. The second method is external calibration using naturally distributed target, such as sea surface. We describe about test experiment for first method and statistical analysis using satellite data for second method as the feasibility study. [C3288]

### "Accelerating InSAR raw data simulation on GPU using CUDA"

This paper describes a scalable parallel method for interferometric synthetic aperture radar (InSAR) raw data simulation on graphic processing unit (GPU) with common unified device architecture (CUDA). The advantages of the new method rely on the three contributions: GPU hardware provides lots of stream processors for threads calculating, CUDA software environment runs thousands of threads working in parallel for assigned task, raw data simulation adopts the fine-grained task parallelism. Compared with OpenMP, MPI and grid computing, the method not only improves the computational efficiency greatly, but also save the resources such as hardware, electric power and room space. The results show that the method not only ensures accuracy, but also be able to obtain the speedup about 30 times. [C3289]

### "Estimation of pasture biomass and soil-moisture using dual-polarimetric X and L band SAR-accuracy assessment with field data"

This paper presents the results of a study conducted to relate X and L band polarimetric SAR backscatter to pasture soil moisture and biomass as part of an environmental monitoring program. Extensive field data was collected concurrently with satellite SAR data acquisition-including dry/wet above ground biomass, soil moisture,



surface roughness profiles and EM-38 electromagnetic sensor data. This data is used for both electromagnetically modeling the surface to work out the theoretical backscatter as well as empirical fitting regression models to the recorded SAR data and validation of existing inversion models. [C3290]

### "Diverse methods to monitoring volcanic deformation based on SAR interferometry"

In this paper, different methods for the detection of the deformation signal with SAR data based on persistent scatterer interferometry (PSI) are described. Two test sites have been selected. For experimental purposes, two corner reflectors (CRs) were installed in the Fogo volcano. The location, phase as well as intensity of corner reflectors were analyzed with 11 TerraSAR-X stripmap (TSX-SM) data. For algorithmic development and validation, four stacks of TerraSAR-X high resolution spotlight (TSX-HSL) data from the Stromboli volcano have been acquired and used for PSI processing. The PSI results of deformation and topography update are fused by using point matching method with Iterative Closest Point (ICP). This research is a part of the German volcano monitoring project Exupery, Work Package 2: 'Space based observation techniques'. [C3291]

### "Breaking wave measurements with sar depolarized returns"

The wind generates a distribution of small slope waves and sporadic steep breaking events. Such double structure of the sea surface is expected to have a strong impact on the radar scattering from the ocean surface. The signature of the double structure is in the wind speed dependence of radar returns: linear for scattering from gentle waves and cubic for breaking contribution. The composite-surface Bragg resonance (CB) theory describes the former very well. Detection of the breaking contribution remains difficult. Here we show that the depolarized (de-pol) radar return exhibits the typical double structure, its wind speed dependence increases with wind speed from linear to cubic. The increased sensitivity of the de-pol returns in high winds is ideal for hurricane wind retrieval. The strong breaking connection offers an opportunity to measure wave breaking and the associated energy dissipation and area of foam coverage from space, their quantification is important in air-sea interaction and electromagnetic and electro-optical remote sensing. [C3292]

### "Operation icebridge: Using instrumented aircraft to bridge the observational gap between icesat and icesat-2"

Operation IceBridge, a six-year NASA mission, is the largest airborne survey of Earth's polar ice ever flown. Data collected during IceBridge will help scientists bridge the gap in polar observations between NASA's Ice, Cloud and Land Elevation Satellite (ICESat), in orbit from 2003 to 2009, and ICESat-2, planned for launch in late 2015, making IceBridge critical for ensuring a continuous series of observations. Operation IceBridge is using airborne instruments to map Arctic and Antarctic areas once a year, building on two decades of repeat airborne measurements of rapidly changing areas in the Arctic. Operation IceBridge is also producing critical data that cannot be measured from space such as ice thickness measurements. The first Operation IceBridge flights were conducted in boreal spring 2009 over Greenland and the boreal fall 2009 over Antarctica. Other smaller airborne surveys around the world are also part of NASA's Operation IceBridge campaign. [C3293]

### "Surf zone surface displacement measurements using interferometric microwave radar"

Vertically polarized backscattered power, Doppler velocity, and interferometric height were measured in the nearshore ocean region using a high-resolution imaging microwave radar. The interferometric surface displacement measurements are compared with normalized radar cross sections (NRCS) and Doppler velocities, and with in situ pressure sensor estimates of wave height. The rms uncertainty in the interferometric surface displacement is computed from the data. The interferometric surface displacement measurements are intuitively satisfying in that positive displacements are generally associated with pixels that have larger NRCS values. Interferometric surface displacements compare well with heights derived from in situ pressure sensors, and we provide some possible explanations for the differences. [C3294]

### "Supporting precision agriculture with dual-polarimetric TerraSAR-X-yield prediction and identification of in-field variations to generate fertilizer prescription maps"

This paper presents studies carried out over 2 growing season in South Australia to evaluate the suitability of TerraSAR-X dual-polarimetric imagery for crop growth monitoring and yield prediction. End of season crops were observed in 2008 and significant correlation with yield was noted. Mid-season crops were observed in 2009 and due to the lower biomass no significant in field trends were observed in the SAR when compared with concurrently acquired ground NDVI sensor and multispectral optical data. Separability between different crop types is evident in both studies, but crop biomass has to be significant for any in-field variations to be apparent. [C3295]

### "Estimation of building damage ratio due to earthquakes and tsunamis using satellite SAR imagery"

In order to expand the existing C-band SAR based damage estimation model into L-band SAR, this paper introduces a likelihood function to estimate severe damage ratio by earthquakes on the basis of dataset from JERS-1/SAR (L-band SAR) images observed the 1995 Kobe earthquake and its detailed ground truth data. The model is applied to JERS-1/SAR images taken over the tsunami affected areas by the 1993 Hokkaido Nansei-oki, Japan earthquake. [C3296]

### "Topography effects on forest radar scattering, consequences on biomass retrieval"

Ground topography under vegetated area is liable to bring significant changes on radar backscattering and thereby on the associated standard retrieval algorithms dedicated to forest biomass. Within the framework of the ESA BIOMASS mission, this paper evinces the evolution of P-band polarimetric intensities with a tilted underlying ground. For that purpose, electromagnetic simulations have been achieved using our model MIPERS which theoretical specificities accounting for the topographic effects are herein described. Its originality lies mainly in the 3D characterization of the ground and the volume, as well as the coupling effects between both. This description is followed by a sensitivity analysis in order to further-on quantify the possible consequences on biomass retrieval, conducted with the two standard approaches, namely the P-HV intensity technique and the Pol-InSAR one assuming the RVoG model. This investigation have been also undertaken for a better understanding of experimental data, particularly with the BioSAR and the TropiSAR airborne campaigns over boreal and tropical forests. [C3297]

### "Use of the merged dual-frequency radar altimeter backscatter data over China land surface"

It is a special way to investigate continental surfaces using radar altimeter, besides scatterometers and Synthetic Aperture Radar among the active microwave remote sensing sensors for the altimeter works at the nadir point of satellite and at dual-frequency, which can measure the backscatters from different layers instantaneously. The aim of this paper is to merge multi-radar altimeter dual-frequency backscatter measurements over land surface to achieve better spatial and temporal resolution. The  $0.5^{\circ} \times 0.5^{\circ}$  merged altimetry backscatter maps between  $66^{\circ}$  N to  $66^{\circ}$  S over land surface every 6 days are generated in Ku, C, and S band for the period from January 2002 to June 2009. Temporal profiles of backscatters are examined for main land types (desert, forest, savanna) to validate the dataset and to analyze radar response to land surface variability through 8 years. [C3298]

### "Longtime monitoring of mine subsidence in Northern Moravia, Czech republic using different insar techniques"

In the undermined Northern Moravia region, the land is subsiding even more than a metre per year causing damages to many human-made objects. Such a fast subsidence is almost not possible to estimate using multitemporal radar interferometry techniques that were applied to ERS-2 data of 1996-2001. Classic differential radar interferometry approaches were successfully applied allowing to visually interpret the evolution of subsidence in the area using Envisat and ERS-1/2 images from years 1996-2009. Results of the radar interferometry usage have been compared with the levelling data. Because of several factors, most of the interferograms are decorrelated. These factors are depicted and several solution scenarios are pointed out. To overcome such limitations as a relatively strong vegetation cover in the area and to detect such a fast subsidence in small areas, the ALOS PALSAR images in fine resolution mode has been successfully used. [C3299]

### "Optimal sensor positioning for ISAR imaging"

ISAR imaging is a powerful signal processing that allows obtaining images of non-cooperative targets. Such images are often used as input to classification and recognition systems since they contain useful two-dimensional features. Nevertheless, the interpretation of ISAR images remains problematic since the image plane cannot be defined by the user but it depends on the target's own motions and on the relative position of it with respect to the radar. In this scenario, the only degree of freedom that is controlled by the user is the position of the sensor. In this paper, the problem of selecting an optimal position of the sensor to maximise the probability of obtaining a desired image projection plane is addressed. Moreover, mathematical tools are derived that may assist the user in deciding where to place an ISAR sensor given a priori knowledge of the scenario. [C3300]

### "KaRIn-the Ka-band radar interferometer on SWOT: Measurement principle, processing and data specificities"

The principal instrument of the SWOT (Surface Water and Ocean Topography) altimetry mission is KaRIn, a Ka-band interferometric SAR system operating on near-nadir swaths on both sides of the satellite track. This article briefly describes the measurement principle, the processing steps and the specificities of the interferometric SAR data of KaRIn as compared to conventional spaceborne SAR systems. [C3301]

### "Spatial latency reduction in GPR processing using stochastic sampling"

Ground penetrating radar (GPR) is a promising technique for buried threat detection which provides a complimentary phenomenology to electro-magnetic induction (EMI) based sensing. However, many successful GPR-based buried threat detection algorithms require data collected both before and after an object of interest is encountered to make a declaration (typically this data is used to perform background normalization, or to adequately characterize the object's shape). Samples taken past an object of interest, but before a decision is made, constitute an algorithm's "spatial latency". For vehicular mounted antennae arrays, where vehicle stopping distance is a function of vehicle dynamics, driver responsiveness, and algorithmic spatial latency, reducing an algorithm's spatial latency can increase overall system safety and help keep operators out of harm's way. In this work we propose a stochastic sampling algorithm that can help reduce spatial latency for a wide range of GPR-based buried threat detection algorithms. [C3302]

### "Use of wavelets decomposition to reduce outside transmissions during measurement of RCS"

If the RCS of a target is measured in measurement facility which is not a Faraday cage, this RCS might be corrupted by eventual outside transmissions which fill the same spectral band than measurement. In this situation, outside radiations are going to pollute the value of the measured RCS and as a consequence their level must be reduced in order to be able to get correct values of RCS. This article deals with a mathematical method which allows limiting the influence of interferences on the measured values of RCS thanks to the use of wavelets. [C3303]

### "An overview of recent advances in Polarimetric SAR information extraction: Algorithms and applications"

Recent advances in Polarimetric SAR information extractions are reviewed. Papers published in IEEE Transactions on Geoscience and Remote Sensing and IGARSS proceedings over the last five years were included. We found that PolSAR technology has reached a certain degree of maturity. The availability of high-resolution multi-frequency PolSAR data from space borne and airborne SAR systems will stimulate significant PolSAR applications. [C3304]

### "CASA dual-doppler system"

Conventional radar networks are limited at warning against low-altitude wind hazards such as tornadoes and micro-bursts due to the combined effects of their long range, far spacing, and Earth's curvature. The Collaborative Adaptive Sensing of the Atmosphere (CASA) Engineering Research Center aims to solve these limitations through dual-Doppler systems operating in densely-spaced short range radar networks. The CASA test bed radar network incorporate the Distributed Collaborative Adaptive Sensing (DCAS) model in order to optimize scanning and retrieval for fast Doppler wind field products. Under the DCAS environment, fast coordinated sector scans are made by each radar based on weather detection and competitive end-user needs. The retrieval subsystem then makes the best pair selection for dual-Doppler synthesis based on optimal beam-crossing angles for target areas. Together, they create a fast, accurate, and robust dual-Doppler system suitable for weather emergency warnings. [C3305]

### "PS-InSAR time series analysis for measuring surface deformation before the L'Aquila earthquake"

L'Aquila area has a high topography and complex geological structures, and is covered with thick vegetation and snow in areas of high topography. To monitor the characteristics of crustal deformation in this region before the 2009 L'Aquila earthquake, we apply StaMPS software to analyse 20 descending ASAR images acquired between September 2003 and March 2007 and 39 ascending ASAR images acquired between February 2003 and March 2009. In this paper, two mean LOS deformation velocity maps are acquired for this area, which reveal the same deformation pattern. Several deformation gradient in this area can be clearly identified, furthermore, we discover that most faults in this region may strike approximately NW-SE and dip  $< 90^\circ$  to SW. We also draw the conclusion that descending SAR images are superior to ascending ones in monitoring crustal deformation with InSAR in this region. [C3306]

### "A study on different PS-like methods for subsidence in Tianjin, China"

In this paper, the methods, primary PS-like method and Stanford Method for PS (StaMPS) are both studied and used to monitor the subsidence in Tianjin area. PS (Permanent Scatter) technique is possible to avoid many of the limitations of conventional DInSAR by analyzing just certain pixels which behave like point scatters and retain good correlations. Several PS-like methods have been developed and practiced by many researchers. StaMPS is a relatively new PS-like method, which uses spatial correlation of interferogram phase to find a network of stable pixels in almost all terrain without prior knowledge of temporal variations in the deformation. 17 ENVISAT SLC data for Tianjin area are used, covering from April 2003 to March 2006. The SLC scene acquired on Nov-05-2004 is chose as the master. And the results of the two methods are compared. By using the primary PS-like method and StaMPS, the subsidence field in Tianjin area has been mapped. As to PS selection, the primary PS-like method needs less input parameters and easier to understand than StaMPS. For deformation value calculation, StaMPS is good at evaluating non-linear subsidence history. [C3307]

#### "A fuzzy-logic-based approach for flood detection from Cosmo-SkyMed data"

The Cosmo-SkyMed mission offers a unique opportunity to obtain radar images useful for flood mapping, being characterized by high revisit time, thanks to the four satellites that form its constellation. In the context of a study aiming at evaluating the usefulness of Earth Observation data for managing flood events, particularly focused on Cosmo-SkyMed, an algorithm to map flooded areas from synthetic aperture radar imagery has been developed. It employs also ancillary data as a land cover map and a digital elevation model. The approach is based on the fuzzy logic because such a theory allows us to exploit the theoretical knowledge about the radar return from inundated areas and to account for simple hydraulic considerations and contextual information. [C3308]

#### "Extracting structural land cover components using small-footprint waveform lidar data"

Previous work has shown the ability of waveform LiDAR sensors to accurately describe various land cover types [1] and biomass estimates made in the field [2]. What is lacking, however, is a way to describe the different structural components that are embedded in the digitized backscattered energy from the LiDAR pulse. This study aims to extract structural components from waveform LiDAR data in terms of woody, herbaceous, and bare ground components from data collected over a savanna environment in and around Kruger National Park (KNP), South Africa. These components are comprised of metrics extracted from the waveforms and validated using biomass measurements made in field plots. Different size windows around plot centers, 3 4 3 pixels and 9 4 9 pixels (resulting in 1.5m and 4.5 m footprint, respectively), were used to examine scale effects of larger footprints. It was found that composite waveforms resembling plot sizes (9 4 9) most often are able to describe more than 80% of the woody biomass variability across the entire study site, and individually for two of the three land uses within the area. However, the herbaceous component of the waveform did not correlate well with the field measurements, while the bare ground component was verified visually in a side-by-side comparison with optical imagery. [C3309]

#### "Assessment of compact polarimetry over different tropical environment and dataset"

This paper presents different radar polarimetric modes over different study sites in Tropical environment: Full polarimetry (FP), Dual Polarimetry (DP) and Compact Polarimetry (CP). By using SVM classification, we show the capabilities of each polarimetric mode linked to the scattering model assumption of the fully polarimetric reconstruction for CP mode proposed by Souyris et al.. We are focused on 3 study sites which have different landscape: Tubuai in French Polynesia (AIRSAR data), the Fazenda Saio Nicolau in Brazil and Cayenne in French Guyana (PALSAR data). It shown that the reflection symmetry assumption may not be verified due to spatial heterogeneity or due to the definition of the study classes. Even if the choice of the DP modes is strongly dependant of the study site, the CP mode have shown equivalent or better overall accuracy than the other DP modes, particularly when the study area are very homogeneous. [C3310]

#### "Vision-based detection and tracking of aerial targets for UAV collision avoidance"

Machine vision represents a particularly attractive solution for sensing and detecting potential collision-course targets due to the relatively low cost, size, weight, and power requirements of the sensors involved (as opposed to radar). This paper describes the development and evaluation of a vision-based collision detection algorithm suitable for fixed-wing aerial robotics. The system was evaluated using highly realistic vision data of the moments leading up to a collision. Based on the collected data, our detection approaches were able to detect targets at distances ranging from 400m to about 900m. These distances (with some assumptions about closing speeds and aircraft trajectories) translate to an advanced warning of between 8-10 seconds ahead of impact, which approaches the 12.5 second response time recommended for human pilots. We make use of the enormous potential of graphic processing units to achieve processing rates of 30Hz (for images of size 1024-by-768). Currently, integration in the final platform is under way. [C3311]



### **"Assessment of tree and crown heights of a maritime pine forest at plot level using a fullwaveform UltraViolet Lidar prototype"**

This study aims to determine the potential of a new lidar prototype with an ultraviolet laser and a medium footprint for retrieving forest parameters. The lidar is embedded on an ultra-light aircraft. The choice of the Landes forest in southwestern France as study area was made regarding the flat topography of the area and the stand height consistency. We chose three plots from different stands (different height characteristics) and compared the lidar derived metrics to field measurements. To derive metrics from lidar data, we summed the lidar waveforms within a plot and calculated derived reflectance profiles to correct the lidar signal from the occlusion effect. We then retrieve plot mean total and mean crown base heights measurement from reflectance profiles. We obtain a good consistency of the lidar measurements compared to field measurements, even if we noticed the existence of a 5 to 10% bias probably linked to the lidar sampling strategy. [C3312]

### **"GNSS illuminator based high range resolution algorithm in space-surface bistatic SAR"**

Space-surface bistatic synthetic aperture radar (SS-BSAR) has gained more and more researcher's interests. In this paper, we focus on improving range resolutions of GNSS illuminator based SS-BSAR with the method of spectrum synthesis of ultra-wide-band (UWB). Narrow bandwidth signals, such as GPS P code, can be spliced into a wider signal. Simulation results show that it can effectively increase signal processing bandwidth, improve range resolution and target recognition capabilities. [C3313]

### **"Remote sensing applications for petroleum resource exploration in offshore basins of China"**

In this paper, a new approach for detecting and analyzing sea surface slicks caused by hydrocarbon seepage of offshore petroleum accumulations has been developed. This approach uses remote sensing radar technology and geophysical exploration techniques and has been developed based on hydrocarbon seepage theory. In this study, Synthetic Aperture Radar (SAR) data were used as the main data source. These data were integrated with gravity data inversed from satellite altimeter data, geophysical abnormal data from airborne magnetic data, and geological data of oil-and gas-bearing basins. Using the geographical information system, the oil and gas accumulating areas were outlined by the prospect models. This approach for the exploration and evaluation for offshore petroleum accumulations has been applied to two study areas in offshore petroleum basins in China: the Bohai Sea and Pearl River Mouth basins. By comparing the drilling outcomes and relative materials, our results show that the application of this integrated method is very effective. [C3314]

### **"Scansar signal processing and image quality enhancement with fitted-geometry doppler surface"**

In this paper, an efficient and relatively high quality ScanSAR processor is implemented based on SPECAN algorithm. The role of the accurate Doppler parameter estimation is described with regard to the processed SAR images. A method of extracting the essential Doppler parameters with high precision is introduced and its performance is verified. For this purpose, we have adopted a Doppler surface fitted-geometry method and demonstrated how it can contribute to the improved Doppler parameter estimation. [C3315]

### **"Taxi: A versatile processing chain for experimental TanDEM-X product evaluation"**

TanDEM-X is a high-resolution interferometric radar mission with the main goal of providing a global digital elevation model (DEM) of the Earth surface by means of single-pass X-band SAR interferometry. It is, moreover, the first genuinely bistatic spaceborne SAR mission, and, independently of its usual quasi-monostatic configuration, includes many of the peculiarities of bistatic SAR. An experimental, versatile, and flexible interferometric chain has been developed at DLR Microwaves and Radar Institute for the scientific exploitation of TanDEM-X data acquired in non-standard configurations. The paper describes the structure of the processing chain and focusses on some essential aspects of its bistatic part. Some experimental results performed with TerraSAR-X demonstrate the flexibility of the implemented processor. [C3316]

### **"Retrieval of raindrop shape-size relation using dual polarization radar measurements"**

Dual polarization radar measurements of rainfall parameters are based on the assumption of a mean shape-size relationship of raindrops. This paper focuses on retrieving and interpreting the mean raindrop shape-size relation from polarimetric radar observations. A procedure to retrieve the drop shape-size relation that governs the polarimetric radar observations of reflectivity ( $Z_h$ ) differential reflectivity ( $Z_{dr}$ ) and specific differential propagation phase ( $K_{dp}$ ) is presented. The mean drop shape-size relations retrieved from measurements collected by the NCAR SPOL radar during three campaigns are analyzed to explore whether the natural raindrop shape-size relation can be described by a unique model. [C3317]

### "A Ku-band rotating fan-beam scatterometer: Design and performance simulations"

This paper introduces the design and simulation results of a Ku-band rotating fan-beam radar scatterometer for ocean surface wind vector measurement. It will be flown on a small satellite dedicated to provide data for investigation of the ocean wave and ocean surface wind vector interactions, along with another payload for measurement of directional ocean wave spectra by a real-aperture radar with multiple scanned pencil beams. Key issues about the design of a Ku-band rotating fan-beam radar scatterometer, and results of performance simulations are provided as well. The performance of the system is simulated by the absolute and relative specifications. For the absolute specifications, retrieval performances for both wind speed and wind direction are evaluated, with the maximum likelihood method being employed. For the relative specifications, the figures of merit (FOM) is simulated, for comparison with other Ku-band scatterometers and optimization of system parameters. Simulation results of both the  $\sigma^\circ$  precision and wind retrieval accuracies for different wind speed from 4m/s to 24m/s will be provided, which shows that SCAT can satisfy the performance requirements within most part of the swath. [C3318]

### "A broad band lidar for precise atmospheric CO<sub>2</sub> column absorption measurement from space"

Accurate global measurement of carbon dioxide column with the aim of discovering and quantifying unknown sources and sinks has been a high priority for the last decade. In order to uncover the "missing sink" that is responsible for the large discrepancies in the budget the critical precision for a measurement from space needs to be on the order of 1ppm. To better understand the CO<sub>2</sub> budget and to evaluate its impact on global warming the National Research Council (NRC) in its recent decadal survey report (NACP) to NASA recommended a laser based total CO<sub>2</sub> mapping mission in the near future. That's the goal of Active Sensing of CO<sub>2</sub> Emissions over Nights, Days, and Seasons (ASCENDS) mission-to significantly enhance the understanding of the role of CO<sub>2</sub> in the global carbon cycle. Our current goal is to develop an ultra precise, inexpensive new lidar system for column measurements of CO<sub>2</sub> changes in the lower atmosphere that uses a Fabry-Perot interferometer based system as the detector portion of the instrument and replaces the narrow band laser commonly used in lidars with a high power broadband source. This approach reduces the number of individual lasers used in the system and considerably reduces the risk of failure. It also tremendously reduces the requirement for wavelength stability in the source putting this responsibility instead on the Fabry-Perot subsystem. [C3319]

### "Evaluation of two region based classifications in Tapajys National Forest using the ALOS/PALSAR polarimetric and interferometric coherences"

The use of phase information present in complex multi polarized images may increase the classification results. Thus, the coherence is one attribute that may be extracted from these images and used to distinguish some land cover classes. Therefore, its discriminatory capability for land use and land cover classification is analyzed. The analysis is based on the classification results of a region classifier, which needs a segmented image as one input. The influence of this kind of image input is also evaluated using of two segmentation algorithms, the SegSAR and the SPRING region growing. Two ALOS/PALSAR images acquired over Tapajos National Forest in the Brazilian Amazon were classified. The classifications were quantified by the overall accuracy, the kappa values and its variance. The classification improvement using the coherence information with intensity images was noticed for every image set. [C3320]

### "How does dew affect L-band backscatter? analysis of pals data at the Iowa validation site and implications for smap"

NASA's Soil Moisture Active Passive satellite mission will use both an L-band radiometer and radar to produce global-scale measurements of soil moisture. L-band backscatter is also sensitive to the water content of vegetation. We found that a moderate dew increased the L-band backscatter of a soybean canopy by 1 dB. Dew thus has the potential to add error to satellite observations of soil moisture. [C3321]

### "Four-component scattering power decomposition with rotation of coherency matrix"

In this presentation, a new decomposition scheme of first using a rotation of the coherency matrix followed by the four-component decomposition is presented. It is shown using airborne Pi-SAR data sets that oriented urban areas are clearly distinguished from volume scattering as double bounce objects by the rotation of coherency matrix. [C3322]

### "Integrating space-time processing into time-domain backprojection process for detection and imaging moving objects"

This paper discusses a possibility to integrate space-time processing into the time-domain backprojection process. This combination allows detection as well as imaging moving objects. Two space-time techniques, Displaced Phase Center Antenna (DPCA) and Space-Time Adaptive Processing (STAP), are considered for this integration. Simulated results based on the LORA parameters demonstrate the efficiency of detection and imaging moving objects. [C3323]

### "Use of 2D FDTD simulation and the determination of the GPR travel path angle for oblique B-scans of 2D geometries"

Scattering from a subsurface point object, such as a reinforcing steel bar embedded concrete or a tunnel buried in sand, results in a B-scan contour that is essentially hyperbolic as the Ground Penetrating Radar (GPR) passes over the object. The shape of the hyperbola can be used to determine the angle at which the GPR traveled over the point object. This information is very useful in determining the orientation and size of an object such as reinforcing steel, buried utilities, and subsurface tunnels. A 2D Finite Difference Time-Domain (FDTD) method can be used to simulate the GPR B-scan when the geometry is invariant in the third dimension and the sensors are appropriately located. The shape of the hyperbola extracted from 3D simulation, analogous to field-collected data, can be compared to a library of hyperbolas extracted from 2D simulations and used to determine the angle of the GPR travel path from the cross-sectional plane. [C3324]

### "The Slope Imaging Multi-polarization Photon-counting Lidar: Development and performance results"

The Slope Imaging Multi-polarization Photon-counting Lidar is an airborne instrument developed to demonstrate laser altimetry measurement methods that will enable more efficient observations of topography and surface properties from space. The instrument was developed through the NASA Earth Science Technology Office Instrument Incubator Program with a focus on cryosphere remote sensing. The SIMPL transmitter is an 11 KHz, 1064 nm, plane-polarized micropulse laser transmitter that is frequency doubled to 532 nm and split into four push-broom beams. The receiver employs single-photon, polarimetric ranging at 532 and 1064 nm using Single Photon Counting Modules in order to achieve simultaneous sampling of surface elevation, slope, roughness and depolarizing scattering properties, the latter used to differentiate surface types. Data acquired over ice-covered Lake Erie in February, 2009 are documenting SIMPL's measurement performance and capabilities, demonstrating differentiation of open water and several ice cover types. ICESat-2 will employ several of the technologies advanced by SIMPL, including micropulse, single photon ranging in a multi-beam, push-broom configuration operating at 532 nm. [C3325]

### "Electromagnetic infrastructure monitoring: The exploitation of GPR data and neural networks for multi-layered geometries"

In this paper, an inversion ANN-based algorithm for the estimation of geophysical properties (i.e. thickness and permittivity) of subsurface layers in stratified geometries is presented. The basic procedure for the analysis of GPR scans of single subsurface layers placed over a uniform background recently proposed by the authors has been here extended and inserted into a general framework where each stratum is recursively processed. [C3326]

### "Towards Bayesian estimator selection for QuikSCAT wind and rain estimation"

The QuikSCAT scatterometer infers wind vectors over the ocean using measurements of the surface backscatter. During rain events the QuikSCAT observations are subject to rain contamination. Three separate estimators have been developed: wind-only, simultaneous wind and rain, and rain-only, which account for rain contamination in varying degrees. This paper introduces a Bayes estimator selection technique to adaptively choose a best estimator from among the three types of estimators at each measurement location. Bayes estimator selection is introduced from a general perspective after which it is applied specifically to QuikSCAT wind and rain estimation. Bayes estimator selection is demonstrated in a case study to illustrate improvements in wind and rain estimation which can be obtained. [C3327]

### "Segmentation of lakes from the local background on the surface of Titan using Cassini SAR images"

Synthetic Aperture Radar (SAR) images of Titan, the largest satellite of Saturn, reveal quasi-circular to complex features which are interpreted to be liquid hydrocarbon lakes. One of the major problems hampering the derivation of meaningful texture information from SAR imagery is the speckle noise. It overlays real structures and causes gray value variations even in homogeneous parts of the image. A filtering technique is applied to

obtain the restored SAR images. Our method is based on probabilistic methods and regards an image as a random element drawn from a prespecified set of possible images. The TSPR (Total Sum Preserving Regularization) filter used here is based on a membrane model Markov random field approximation with a Gaussian conditional probability density function optimized by a synchronous local iterative method. The despeckle filter can be used as intermediate stage for the extraction of meaningful regions that correspond to structural units in the scene or distinguish objects of interest like lakes. [C3328]

#### "Experimental validation of the Corbella's visibility function using HUT-2D and MIRAS"

The Corbella's revision of the fundamental equation of the interferometric aperture synthesis radiometry is verified using airborne and spaceborne data. This experimental verification uses the measurements of the airborne instrument HUT-2D from the Aalto University (Helsinki), and the unique spaceborne microwave imaging radiometer by aperture synthesis (MIRAS) from the ESA's Soil Moisture and Ocean Salinity (SMOS) mission. The data acquired with those sensors support the Corbella's revision of the visibility function. The revised function predicts that visibilities depend on the contrast between the target's brightness temperature and the backward noise of the receivers emitted through the antennas. [C3329]

#### "Using airborne lidar to retrieve crop structural parameters"

Airborne LIDAR (Light Detection and Ranging) is an active remote sensing technique that measures the properties of scattered light to determine the range and intensity information of a distant target. Many studies have been reported on estimating a suite of forest characteristics such as fractional vegetation cover, leaf area index and canopy height using LIDAR data. The three characteristics of crop canopy also play key roles in vegetation radiative transfer models and yield estimation. But crops are so small and low that more than 95% pulses have ground hit, it is difficult to separate the crop and soil completely, so the methods used in forest may not be suitable for crops. In this paper, based on theoretical analysis, we propose a new method, trying to derive gap fraction of crop field using the airborne LIDAR intensity of ground hits, so we can manage to retrieve the fractional vegetation cover, LAI and the height of crop canopy. We choose corn field as study object, field validation shows that our method can accurately retrieve the three structural parameters of corn field. This study documents the great potential of LIDAR remote sensing for accurately characterizing crop canopies. [C3330]

#### "A revised geophysical model function for the advanced scatterometer (ASCAT) at NOAA/NESDIS"

The current ASCAT winds retrieval is based on the CMOD5.n geophysical model function (GMF) with the ASCAT wind data processor developed at the Royal Netherlands Meteorological Institute (KNMI). Recent validation of ASCAT wind retrieval reveals that high wind retrievals were underestimated as being compared to the operational QuikSCAT scatterometer. The goal in this paper is to improve ASCAT wind retrievals at high winds. In this paper we map the radar backscatter ( $\sigma_0$ ) as a function of extreme wind conditions as measured by an airborne scatterometer and adjusted the isotropic term in CMOD5.n to follow the aircraft GMF trend. The geophysical model QuikSCAT wind inputs are improved for  $\sigma_0$  that calculated from QuikSCAT wind inputs are improved for  $\sigma_0$  approximately  $> -15$  dB and in very good agreement with the ASCAT  $\sigma_0$  measurement. The wind retrieval validations show wind speed rms error is improved at approximately wind speed  $> 12$  m/s and example mean wind composite from two winter seasons shows significant in detection of storm-force winds. [C3331]

#### "Monitoring of collapsed built-up areas with high resolution SAR images"

A new concept for change detection algorithm for urban areas affected by earthquake is here presented. It is characterized as applicable to just one post-event amplitude Synthetic Aperture Radars (SAR) image and employs the inversion of sound scattering models already introduced in literature by the same authors. Aim of the algorithm is to try obtaining fast mapping of damaged areas and provide a first, even rough, evaluation of damage reported. In particular in this paper the overall block diagram chain and the algorithm rationale behind that framework are introduced and discussed in details. Some preliminary results are presented and the performance analyzed. New possible applications based on similar rationale are also commented. [C3332]

#### "Estimation of sea ice thickness in the Arctic Sea using polarimetric parameters of C- and X-band space-borne SAR data"

In this study, we derived the relationship between target depolarization factor and physical parameters of sea ice in order to estimate the thickness using dual-polarization C- and X-band space-borne Synthetic Aperture Radar (SAR) data. The target depolarization factor, the cross-polarized ratio of C-band SAR data, which can explain the target depolarization effect, were strongly related to changes in surface roughness of thick First-Year Ice (FYI) and Multi-Year Ice (MYI), and were almost insensitive to variations in the surface dielectric constant of thick FYI and MYI and the incidence angle of C-band SAR data. This relationship showed a high correlation



between target depolarization factor of C-band SAR data, the cross-polarized ratio, and thick FYI and MYI thickness. We validated the estimated method using RADARSAT-2 and TerraSAR-X data and ground-truth data acquired in the Arctic Sea off the northern coast of Greenland. [C3333]

### "SAR tomographic focusing by Compressive Sampling: Experiments on real data"

In this paper a 3-D SAR imaging technique based on Compressive Sampling is experimented on ERS 1-2 data. The technique is based on the sparsity property of the image to be focused along the elevation direction (i.e. only few scatterers with different elevation are present in the same range-azimuth resolution cell), exploits a reduced number of unevenly spaced acquisitions and allows an increased elevation resolution. Numerical results on real data are compared with those obtained by using Truncated Singular Value Decomposition (TSVD) techniques. [C3334]

### "Extracting trees and structure parameters via integration of LIDAR data and ground imagery"

Detailed tree information, such as tree counts, tree heights, crown base heights, diameter at breast height (DBH), and tree biomass, is critical for the effective management and quantitative analysis of trees in urban area. Automatic detection of trees, and their parameters using light detection and ranging (LiDAR) data has been widely employed. However, at the single-tree level along road in urban area, LiDAR data deposited the disadvantages such as space points, no texture information, so that the detailed tree parameters mentioned above cannot successfully be obtain at enough accuracy. This paper presented an integration of LiDAR data and ground mobile truck data. This development is driven by the fact that the information obtained from ground-mobile truck images can be substantially complemented by the data from LiDAR. [C3335]

### "Ocean wave field measurements using X-band Doppler radars at low grazing angles"

Ocean wave field observations using two types of Doppler radar systems are compared with time series measurements of the surface elevation at the USACE Field Research Facility (FRF) in Duck, NC. [C3336]

### "A polarimetric two-scale model for soil moisture retrieval"

A polarimetric two-scale surface scattering model employed to retrieve the surface parameters of bare soils from polarimetric SAR data is proposed. The scattering surface is considered as composed of slightly rough randomly tilted facets, for which the Small Perturbation Method holds. The facet random tilt causes a random variation of the local incidence angle, and a random rotation of the local incidence plane around the line of sight, which in turn causes a random rotation of the facet scattering matrix. Unlike other similar already existing approaches, our method considers both these effects. The proposed scattering model is then used to retrieve bare soil moisture and (large-scale) roughness from the co-polarized and cross-polarized ratios. The performances of the resulting retrieval algorithm is finally assessed by comparing obtained results to "in situ" measurements. To this aim, data from Little Washita campaign available in literature is employed. [C3337]

### "Microphysical retrievals of dual polarization and dual frequency ground radar for GPM ground validation"

A dual-frequency precipitation radar (DPR) will be deployed aboard GPM (Global Precipitation Measurement) core satellite in order to enhance our knowledge of precipitation microphysics. A ground based dual-frequency (Ku and Ka band) and dual-polarization radar D3R is being built to perform cross validation with GPM-DPR which helps provide insight into the physical basis of the retrieval algorithm. This paper is the follow up study of the author's previous paper where a new drop size distribution (DSD) retrieval algorithm was proposed. In this paper, the algorithm evaluation is extended to the complete region including rain, melting ice and ice based on simulation data. A possible method to classify the hydrometeor identification for dual-frequency and dual-polarization ground radar is also proposed which might be applied to D3R. [C3338]

### "Coherent MIMO radar for GMTI"

In addition to imaging, coherent MIMO radars have a strong potential for detecting moving objects and estimating their parameters. This paper investigates different MIMO schemes based on spatial, waveform, and frequency diversity for their GMTI capability. The fully configurable MIMO radar MIRACLE X is taken as the baseline design for comparing the different approaches. [C3339]

### "Trail following with omnidirectional vision"

We describe a system which follows "trails" for autonomous outdoor robot navigation. Through a combination of

visual cues provided by stereo omnidirectional color cameras and ladar-based structural information, the algorithm is able to detect and track rough paths despite widely varying tread material, border vegetation, and illumination conditions. The approaching trail region is simply modeled as a circular arc of constant width. Using an adaptive measure of color and brightness contrast between a hypothetical region and flanking areas, the tracker performs a robust randomized search for the most likely trail region and robot pose relative to it with no a priori appearance model. Stereo visual odometry improves tracker dynamics on uneven terrain and permits local obstacle map maintenance. A motion planner is also described which takes the trail shape estimate and local map to plan smooth trajectories around in-trail and near-trail hazards. Our system's performance is analyzed on several long sequences with diverse appearance and structural characteristics using ground-truth segmentations.

[C3340]

#### "Icesat lidar and global digital elevation models: applications to desdyni"

Geodetic control is extremely important in the production and quality control of topographic data sets, enabling elevation results to be referenced to an absolute vertical datum. Global topographic data with improved geodetic accuracy achieved using global Ground Control Point (GCP) databases enable more accurate characterization of land topography and its change related to solid Earth processes, natural hazards and climate change. The multiple-beam lidar instrument that will be part of the NASA Deformation, Ecosystem Structure and Dynamics of Ice (DESDynI) mission will provide a comprehensive, global data set that can be used for geodetic control purposes. Here we illustrate that potential using data acquired by NASA's Ice, Cloud and land Elevation Satellite (ICESat) that has acquired single-beam, globally distributed laser altimeter profiles ( $\pm 86^\circ$ ) since February of 2003. The profiles provide a consistently referenced elevation data set with unprecedented accuracy and quantified measurement errors that can be used to generate GCPs with sub-decimeter vertical accuracy and better than 10 m horizontal accuracy. Like the planned capability for DESDynI, ICESat records a waveform that is the elevation distribution of energy reflected within the laser footprint from vegetation, where present, and the ground where illuminated through gaps in any vegetation cover. The waveform enables assessment of Digital Elevation Models (DEMs) with respect to the highest, centroid, and lowest elevations observed by ICESat and in some cases with respect to the ground identified beneath vegetation cover. Using the ICESat altimetry data we are developing a comprehensive database of consistent, global, geodetic ground control that will enhance the quality of a variety of regional to global DEMs. Here we illustrate the accuracy assessment of the Shuttle Radar Topography Mission (SRTM) DEM produced for Australia, documenting spatially varying elevation biases of several meters in magnitude. [C3341]

#### "A distributed LiDAR processing model based on OWS and BPEL"

Traditional LiDAR post process is centralized. In centralized process model, data, process module and workflow can only be accessed within specific platform. This results in interoperability problem ranging from data sharing to functionality and workflow reuse. To tackle this problem, this paper proposes distributed process model for LiDAR post process. The distributed process model consists of interoperability solution on three aspects: data, process module and workflow. According to experiment, distributed LiDAR process model overcomes problems mentioned above. The process model and interoperability solution proposed in this paper can serve as reference to other geo-processing application. [C3342]

#### "The RADARSAT-1 imaging performance, 14 years after launch, and independent report on RADARSAT-2 image quality"

This paper summarizes the calibration monitoring activities of the Canadian Space Agency (CSA) executed under the RADARSAT Program. The performance history of the RADARSAT-1 SAR since its commissioning in 1996 is reviewed, along with the calibration systems and methodologies used, in the context of the mission's thirteen-year calibration history. Independent image quality measurements for the privately-owned RADARSAT-2, launched in 2008, are also presented. It is shown that the calibration parameters of the RADARSAT-1 SAR have consistently been maintained within the mission's design goals and specifications, mostly thanks to payload stability and timely recalibrations performed using the calibration ground equipment. For RADARSAT-2, CSA's measurements report outstanding image quality levels. [C3343]

#### "Extraction of coastal wavefield properties from X-band radar"

The dynamic wave field in a high-energy coastal environment is investigated using frequency direction wave spectra obtained by nautical X-band radar imagery. Nautical radars are generally used for navigation and ship traffic control. Under various conditions (wind speed  $> 3\text{m/s}$ , significant wave height  $> 0.5\text{m}$ ), signatures of the sea surface (sea clutter) become visible in the near range (less than 3 nautical miles) of nautical radar images. Swell and wind sea waves become visible in nautical radar images as they modulate the sea clutter signal. Since

standard X-band nautical radar systems scan the sea surface with high temporal and spatial resolution, they are able to monitor the sea surface in both time and space. The combination of the temporal and spatial wave information allows the determination of unambiguous directional wave spectra. Here, wave data collected from February-October 2005 at the US Army Corps of Engineers Field Research Facility (USACE-FRF) in Duck, North Carolina is presented. For the radar wave measurements the Wave and surface current Monitoring System WaMoS II was connected to a Furuno FR-7112 X-Band radar with a 6 feet open antenna and an update rate of 2.5s (24 rpm). The radar covers a range from 240m to 2160m from the antenna with a spatial resolution of 7.5m. The wave analysis was carried out over an area of 3.7 km<sup>2</sup> located in relative homogeneous bottom topography, off the near shore breaker bar system, in a water depth of 8m -10m. The WaMoS II wave measurements were compared to those obtained from a pressure gauge array located in the same area. Earlier WaMoS II validations provide a general indicator of the quality of the measurement performance as they were carried out for standard integral wave properties over all existing wave systems such as mean or peak wave parameters. Here the XWaves ocean wave field analysis toolbox is used to compare data sets by means of a wave spectral partitioning analysis. This approach provides a more detailed validation especially for bi- and multi modal sea states, allows for a comparison of the heights, periods and directions of individual wind sea and swell components, and tracking the evolution of specific wave systems. Such analysis methods have been successfully applied in a variety of wave model validations. The data comparison was carried out for different sea state and wind conditions. Preliminary results of the data comparison show that the WaMoS II system captures the temporal evolution of the individual wind sea and swell wave components entering the surf zone. A statistical error analysis of the isolated wind sea and swell wave systems provides a quantitative assessment of WaMoS II performance in a coastal setting. [C3344]

#### "Inferring the impact of radar incidence angle on soil moisture retrieval skill using data assimilation"

The impact of measurement incidence angle ( $\theta$ ) on the accuracy of radar-based surface soil moisture ( $\Theta_s$ ) retrievals is largely unknown due to discrepancies in theoretical backscatter models as well as limitations in the availability of sufficiently extensive ground-based  $\Theta_s$  observations for validation. Here, we apply a data assimilation-based evaluation technique for remotely-sensed  $\Theta_s$  retrievals that does not require ground-based soil moisture observations to examine the sensitivity of skill in surface  $\Theta_s$  retrievals to variations in  $\theta$ . Application of the evaluation approach to the TU-Wien European Remote Sensing (ERS) scatterometer  $\Theta_s$  data set over regional-scale (~10002 km<sup>2</sup>) domains in the Southern Great Plains (SGP) and Southeastern (SE) regions of the United States indicate a relative reduction in correlation-based skill of 23% to 30% for  $\Theta_s$  retrievals obtained from far-field ( $\theta > 50^\circ$ ) ERS observations relative to  $\Theta_s$  estimates obtained at  $\theta < 26^\circ$ . Such relatively modest sensitivity to  $\theta$  is consistent with  $\Theta_s$  retrieval noise predictions made using the TU-Wien ERS Water Retrieval Package 5 (WARP5) backscatter model. However, over moderate vegetation cover in the SE domain, the coupling of a bare soil backscatter model with a "vegetation water cloud" canopy model is shown to overestimate the impact of  $\theta$  on  $\Theta_s$  retrieval skill. [C3345]

#### "Performance and application of different image matching algorithms for investigating glacier and ice-shelf flow, permafrost creep and landslides"

This study focuses on evaluating image correlation methods for deriving surface velocity fields of glaciers, ice shelves, rock glaciers and landslides from both repeat optical and synthetic aperture radar (SAR) images. Firstly we show that low resolution MODIS images (250 m spatial resolution) can in fact be used for determining displacements on Antarctic ice shelves. In this particular case, orientation correlation operated in the frequency domain and using only the phase part of the signal performs better than normalized cross-correlation operated in the spatial domain. Secondly we demonstrate that for determining subpixel displacement when using normalized cross-correlation, image intensity interpolation before the matching process outperforms interpolation of the correlation peak after the matching. We also study methods for adaptively varying the matching template size in order to create the most reliable and accurate matches. The last part of the work shows some application studies of glacier flow from optical and SAR images, rock glacier creep and land sliding. [C3346]

#### "Mapping and change detection for boreal wetlands of North America based on JERS and PALSAR data"

We have been developing high-resolution thematic maps of wetlands throughout the North American boreal regions. We assemble a wetlands map for each region based on data collected during the late 1990s, then construct a second map based on data collected during the late 2000s. Comparison of the two maps then makes it possible to assess changes that have occurred over the course of the intervening decade.. [C3347]

#### "A scattering similarity based classification scheme for land applications of polarimetric SAR"

### **image"**

In this paper, a new classification scheme, which extracts the main scattering mechanism with target scattering similarities, is proposed. This approach not only leads to improved understanding of scattering mechanisms, but also has good performance in discriminating different scattering type of land cover. The NASA/JPL AIRSAR data is used for validating its effectiveness. [C3348]

### **"The detection performance of Neyman-Pearson detector for MIMO radar in K-distributed sea clutter"**

Use of multiple transmit and receive antennas have become a popular research area in radar community after the success of the same concept in communication. It is shown by Fishler et al. in that multi-input multi-output (MIMO) radar has considerable advantages compared to traditional radar and phased array radar systems. In this paper, detection performance of MIMO radar using Neyman-Pearson detector is investigated in K-distributed sea clutter for a practical scenario. Also, spikiness of K-distributed MIMO radar clutter is discussed with respect to the number of nodes. [C3349]

### **"Comparisons of rain rate and reflectivity between TRMM precipitation radar and Gosan S-band radar"**

As a part of GPM joint Ground Validation (GV) projects with the US and international partnership, one of the Korea Meteorological Administration (KMA) S-band radar at Gosan, Jeju Island, South Korea has been selected in the Validation Network (VN). It performs the match-up of TRMM Precipitation Radar (PR) data with ground-based radar (GR) during August 2006 to May 2008 for the rain events on criteria of at least 25 % overlap of the PR swath and 25 % or more of the points in the overlap area indicating rain certain in the PR data. 60 events with these criteria during the period have been selected to compare the reflectivity only over 18 dBZ from both radars. Overall comparisons between GR and PR reflectivity roughly 1.37 dBZ low bias over 163,586 points. The results came out good quality and recently asked the TRMM Precipitation Processing System (PPS) to add the site to the daily TRMM site overpass coincidence table (CT) product. Rain rate comparisons between GR and PR show PR over estimate the rain rate in these events. [C3350]

### **"Spatial spectrum of bistatic SAR with one fixed station"**

Bistatic synthetic aperture radar (BSAR) with one fixed station (OF-BSAR) can be used in wide area surveillance, interferometry and etc. This paper analyzed the spatial spectrum of OF-BSAR. Analytical expressions of the spatial spectrum was given. Using this result, we can determine the resolution performance of OF-BSAR. [C3351]

### **"ISAR imaging of an aircraft target USING ISDB-T digital TV based passive bistatic radar"**

Passive bistatic radars (PBRs) exploit existing transmitters such as TV broadcasts as the source of illumination. PBR is consisted of two receivers, with one antenna pointed at the source and the other at the target, and the target range is determined by correlating the signal scattered by the target with the signal directly arrived at the receiver. Since PBR does not transmit any waveform, it consumes lower power, and no frequency allocation is required. We have conducted a field experiment exploiting terrestrial digital TV broadcast to assess the feasibility of ISAR (Inverse Synthetic Aperture Radar) observation based on PBR. The wide and flat spectrum of the OFDM signal and the small gap between the channels enables us to obtain high range resolution of up to several meters by exploiting multiple physical channels. Therefore, moderate resolution ISAR imaging is expected to be possible. In this paper, PBR based ISAR algorithm is briefly explained, and the first example of observed PBR based ISAR image of an aircraft target is shown. [C3352]

### **"Full wave analysis of VHF-UHF forest bistatic scattering mechanisms an investigation on the influence of electromagnetic coupling"**

A 3D coherent scattering model simulating the interaction of electromagnetic waves with forests has been developed. It is obtained by means of a full wave approach, based on an integral representation of the electric field. A method of moments is used to solve the integral equation and compute the scattered fields related to the various scattering mechanisms as well as the contribution of tree-trunks and branches. This model is used here to evaluate the impact of electromagnetic coupling effects between a group of scatterers (which can be the branches and the trunk of a single tree, multiple tree-trunks, or multiple trees) for monostatic and/or bistatic radar configurations. To validate our model, we compare our simulation results with anechoic chamber measurements. [C3353]



### "Estimation of the degree of polarization in compact polarimetry"

The degree of polarization (DoP) has long been recognized as one of the most important parameters characterizing partially polarized electromagnetic waves. This parameter can be effectively used to describe the information content of polarimetric images collected by synthetic aperture radar (SAR) systems. Estimation of DoP is standardly performed using four measurements. In SAR compact polarimetry (CP), however, only two measurements are available. In this paper, we develop maximum likelihood estimators of the DoP, in SAR CP modes, based on only two intensity images. We evaluate and compare the performance of these estimators for different CP modes on RADARSAT-2 polarimetric data, over various terrain types such as urban, vegetation, and ocean. [C3354]

### "ALGAE: A fast algebraic estimation of interferogram phase offsets in space varying geometries"

This work deals with the estimation of terrain topography from multi-pass Synthetic Aperture Radar (SAR) interferometry (InSAR), focusing on the case where the variation of the system geometry within the imaged swath is relevant, as in airborne multi-pass interferometric campaigns. The space varying nature of the system geometry gives rise to a major issue in multi-pass InSAR analyses, in that it prevents from compensating for the presence of interferogram phase offsets by simply phase locking the data stack to a reference point, therefore hindering the retrieval of terrain topography. To cope with this issue properly we propose a novel approach that exploits the algebraic properties of the problem. Such an approach allows to cast the problem in terms of identification of a null space component for terrain topography, after which both topography and the interferogram phase offsets are quickly obtained without exploiting calibration points. [C3355]

### "Remote sensing research in undergraduate education: An international fieldwork perspective"

Institutions of higher education in the U.S. are increasing their use of project-based courses and experiential learning using projects or service in other countries. Project-based instruction provides students with an opportunity to make connections between the classroom and the world around them. Research suggests that fieldwork strongly enhances curriculum instruction and provides additional learning value to students. The goal of this grant was to increase the international content of existing curriculum by providing to students advanced skills in sampling design, geospatial statistics, and remote sensing for mapping and monitoring of crops and natural areas including semi-arid mountains, sub-tropical mountains, and tropical rain forests. This experience for the students has opened their eyes to new cultures and environments, allowed them to apply their classrooms skills in a real-world context and importantly to see how what they are learning is readily usable outside the classroom. [C3356]

### "Land cover classification based on single-polarized VHR SAR images using texture information derived via speckle analysis"

Speckle is a SAR specific noise effect caused by constructive and destructive interference from multiple scattering within the resolution cell of the imaging radar system that superposes the true radiometric and textural information of SAR images as a grainy 'salt-and-pepper' pattern. Fully developed speckle basically follows circular Gaussian image statistics. However, this assumption is not applicable for very high resolution SAR systems and for data showing sceneries with a significant amount of directional backscatter-e.g. urban areas. In those cases the multiple scattering processes within a resolution cell show-subject to the true structuring of the imaged area-rather a directional behavior than a random distribution. Consequently, the speckle is no longer fully developed. In our study we demonstrate how information on the local development of speckle can be used to differentiate between basic land cover types such as water, open land-meaning farmland, grassland and bare soil -, woodland and urban area in single-polarized, single-date VHR SAR images. The research is based on the analysis of a TerraSAR-X scene of Munich, Germany. [C3357]

### "Investigations on TOPS interferometry with TerraSAR-X"

This paper presents results on SAR interferometry with the so-called TOPSmode. The rationale to retrieve accurate interferometric products with such a mode is expounded, emphasizing the critical step of coregistering the pairs. Due to the particularities of the TOPS mode, a high Doppler-centroid is present at burst edges, demanding very high azimuth coregistration performance. A coregistration accuracy of one tenth of a pixel, as it is usually recommended with interferometric applications, will result in a large undesired azimuth phase ramp in the TOPS mode, above all at X-band. This paper presents two approaches based on the spectral diversity technique to estimate this offset with the required accuracy. Experimental results with repeat-pass TerraSAR-X data are shown to validate the proposed approach. [C3358]

### "Polarimetric scattering analysis for accurate observation of stricken man-made targets using a rotated coherency matrix"

This paper investigates polarimetric scattering features generated from man-made targets for accurately observing stricken residential area by making full use of quad. polarimetric SAR data set. First, we propose a simple improvement of the scattering power decomposition method by introducing a unitary rotation of the coherency matrix. It is found from the results of the POLSAR image analysis for a mountainous region including some stricken residential areas that by carrying out the rotation procedure, double-bounce scattering contribution can be enhanced even when the targets are oriented and/or set on small inclined ground plane. This peculiar scattering feature is utilized as a useful marker for precisely detecting man-made targets. To verify the generating and enhancing mechanism of the double-bounce scattering, we also carry out the Finite-Difference Time-Domain (FDTD) polarimetric scattering analysis for a simplified man-made target model. The dependency of the polarimetric scattering feature on the variation of squint angle is investigated. It is confirmed from the FDTD analysis for oblique squint angular range that by applying the rotation procedure before the scattering power decomposition, the double-bounce scattering contribution tends to be enhanced, and the volume scattering becomes small. [C3359]

### "Compressed sensing on ambiguity function domain for high resolution detection"

In this paper, by using compressed sensing techniques, a new approach to achieve robust high resolution detection in sparse multipath channels is presented. Currently used sparse reconstruction techniques are not immediately applicable in wireless channel modeling and radar signal processing. Here, we make use of the cross-ambiguity function (CAF) and transformed the reconstruction problem from time to delay-Doppler domain for efficient exploitation of the delay-Doppler diversity of the multi-path components. Simulation results quantify the performance gain and robustness obtained by this new CAF based compressed sensing approach. [C3360]

### "Target detection in missile warning receivers via speeded-up robust features approach"

Missile warning receivers are electronic support systems which are widely used for the protection of fixed and rotary wing aircraft against infrared guided missiles. Proposed methodology for the detection of missile threats in missile warning receivers depends upon the estimation of background from consecutive image frames. By removing the estimated background from the images, foreground objects (missile plume images) are detected. In this study, "Speeded-Up Robust Features (SURF)" methodology based on feature correspondence is used for the estimation of background motion. [C3361]

### "The microasar experiment on CASIE-09"

During the summer of 2009, the Characterization of Arctic Sea Ice Experiment 2009 (CASIE-09) operated a small, unmanned aircraft system (UAS) over the Arctic Ocean for a number of long-distance flights from Svalbard Island. In addition to other instruments, the UAS carried a small C-band synthetic aperture radar (SAR) known as MicroASAR to image sea ice roughness at 1 m resolution. This paper briefly describes the SAR, its role in CASIE-09, and presents sample SAR image results. [C3362]

### "Development of an Off-The-Grid X-band radar for weather applications"

The Student Led Test Bed (STB) is part of the NSF Engineering Research Center CASA and is currently focused in developing low-cost and low infrastructure radar networks to fill lower atmosphere gaps not covered by current technology. The first radar node, which is part of a small region radar network, will significantly improve the time and spatial resolution of the radar data measured for the lower atmosphere. This paper describes the development of an Off-The-Grid (OTG) X-band radar node that requires minimum infrastructure for its deployment and can operate using solar energy and wireless communication links. The OTG radar was developed for meteorological applications modifying a commercially available marine radar. Hardware modifications for meteorological purposes were performed as well as the design and implementation of a photovoltaic system to power the radar using solar energy. The system was moved to the Colorado State University (CSU)-CHILL National Weather Radar facility for a cross-calibration and system evaluation. Satisfactory results were obtained where it was demonstrated that the OTG radar can provide precipitation measurements with improved spatial and temporal resolution, both necessary to have better lower troposphere measurements. This OTG node is the first prototype of a low infrastructure X-band weather radar network to aid forecasts in the western region of Puerto Rico. [C3363]

### "Model level fusion of edge histogram descriptors and gabor wavelets for landmine detection with ground penetrating radar"

We propose a discriminative method for combining heterogeneous sets of features for the continuous hidden Markov model classifier. We use a model level fusion approach and apply it to the problem of landmine detection using ground penetrating radar (GPR). We hypothesize that each signature (mine or non-mine) can be characterized better by multiple synchronous sequences that can capture different and complementary features. Our work is motivated by the fact that mines and clutter objects can have different characteristics depending on the mine type, soil and weather conditions, and burial depth. Thus, different sets of specialized feature extraction mechanisms, may be needed to achieve high detection and low false alarm rates. In order to fuse the different modalities, a multi-stream continuous HMM that includes a stream relevance weighting component is developed. In particular, we modify the probability density function that characterizes the standard continuous HMM to include state and component dependent stream relevance weights. We generalize the Minimum Classification Error (MCE) objective function to include stream relevance weights and derive the necessary conditions to update all model parameters simultaneously. Results on a large collection of GPR alarms show that the proposed model level fusion outperforms the baseline HMM when each feature is used independently and when both features are combined with equal weights. [C3364]

#### "Processing of MEMPHIS millimeter wave multi-baseline InSAR data"

This paper presents a processing method for multi-baseline interferometric data acquired with the MEMPHIS airborne sensor. The processing method ingests the SAR raw data from each receiver and extends up to the generation of digital elevation models (DEMs). Critical steps include the correction of the azimuth phase undulations, the multi-baseline processing and the phase-to-DEM conversion. Methods for resolving the various hurdles were adapted to the MEMPHIS sensor and are presented here. The results obtained for a data take over a test site near Zurich, Switzerland are shown; these results are in a good agreement with comparable LIDAR products. [C3365]

#### "Monitoring slow moving landslides in the Berkeley Hills with TerraSAR-X data"

Large, slow moving landslides in the Berkeley Hills cause many damage and pose a potential threat to public safety due to the close proximity of the Hayward Fault. We have been using Differential SAR interferometry (DInSAR) and time-series analysis of SAR data to resolve the rates of the landslide motion. In this paper, we aim to interpret the new satellite TerraSAR-X data in this small landslides area. We have acquired both Stripmap data and Spotlight data. Standard InSAR method as well as Persistent Scatterer InSAR is utilized in the processing. [C3366]

#### "An improved content-adaptive mesh-generation method for image representation"

A new content-adaptive mesh-generation method for image representation, based on the greedy point-removal scheme of Demaret and Iske, is proposed. The proposed method is shown to be capable of producing meshes of higher quality than those generated by the scheme of Demaret and Iske, while requiring substantially less computation and memory. Furthermore, with the proposed method, one can easily tradeoff between mesh quality and computational/memory complexity as needed. Since a mesh-generation scheme proposed by Yang et al. is a key component of the proposed method, some factors affecting the performance of this scheme are also explored. [C3367]

#### "Theoretical and practical design considerations for a small, multi-band SAR: The SlimSAR"

The SlimSAR is a small, low-cost, Synthetic Aperture Radar (SAR) system and represents a new advancement in high-performance SAR. ARTEMIS employed a unique design methodology that exploits previous developments in designing the SlimSAR to be small, light, and flexible while consuming very little power. The system contains an L-Band core and uses block-converters to operate in a number of other bands. It also has the capability to operate in either deramp or direct-sampling mode and can collect data in two polarizations simultaneously. The flexible control software allows us to change the radar parameters in flight. Multi-frequency SAR provides day and night imaging through smoke, dust, rain, and clouds with the advantages of additional capabilities at different frequencies (i.e. dry ground and foliage penetration at low frequencies, and high-resolution change detection at high frequencies). [C3368]

#### "Advanced digital beamforming concepts for future SAR systems"

This paper reviews advanced multi-channel SAR system concepts for the imaging of wide swaths with high resolution. Several novel system architectures employing both direct radiating arrays and reflector antennas fed by a digital array are introduced and compared to each other with regard to their imaging performance. In addition, innovative SAR imaging modes are proposed which enable the mapping of ultra-wide swaths with high azimuth resolution. The new techniques and technologies have the potential to enhance the imaging performance

of future SAR systems by one order of magnitude if compared to state of the art SAR sensors like TerraSAR-X, ALOS, Radarsat-2 or Sentinel-1. [C3369]

### "Graph-based segmentation for colored 3D laser point clouds"

We present an efficient graph-theoretic algorithm for segmenting a colored laser point cloud derived from a laser scanner and camera. Segmentation of raw sensor data is a crucial first step for many high level tasks such as object recognition, obstacle avoidance and terrain classification. Our method enables combination of color information from a wide field of view camera with a 3D LIDAR point cloud from an actuated planar laser scanner. We extend previous work on robust camera-only graph-based segmentation to the case where spatial features, such as surface normals, are available. Our combined method produces segmentation results superior to those derived from either cameras or laser-scanners alone. We verify our approach on both indoor and outdoor scenes. [C3370]

### "Preliminary model for wind estimation from Cosmo/SkyMed X band SAR data"

In the paper we present a preliminary model for wind estimation from SAR data in X band. The data set we have used is composed of more than 300 Cosmo/SkyMed SAR images and the wind data obtained from the SeaWinds instrument on QuikSCAT. We have derived 18 parameters to express  $\sigma$  as function of wind intensity, direction and Radar look angle. The preliminary validation results are encouraging although our data set needs to be extended in order to increase those conditions poorly represented. [C3371]

### "Use of PALSAR polarimetric data for tropical forest stratification and comparison of simulated dual and compact polarimetric modes"

This paper presents a case study addressing the comparison between different SAR polarimetric mode for tropical forest stratification: Full polarimetry (FP), Dual Polarimetry (DP) and Compact Polarimetry (CP). These 2 latter modes are simulated using FP data acquired by the L band PALSAR sensor over 2 study sites. Cayenne in French Guyana and the Fazenda Saio Nicolau in Brazil. The classification approach used to evaluate each mode based on Support Vector Machine (SVM) algorithm shows the good capabilities of the FP mode to discriminate different kinds of vegetation. The choice of one DP mode that gives twice bigger swath than FP mode depends on the study classes. In this tropical environment the hh/hv existing mode seems to be a good choice and CP mode show a good alternative to all the actual DP modes. [C3372]

### "Development of ALOS/PALSAR data on-demand processing and providing system on GEO Grid"

GEO Grid has been proposed by AIST in order to contribute to earth science. GEO Grid mainly provides satellite and field observation data related to earth science through data search service, data processing service and data providing service. Recently, we have developed ALOS PALSAR data on-demand processing and providing system as one of GEO Grid data providing system. The system allows users to easily search and quickly receive PALSAR products without careful considerations and advanced skills. There are two important points in the system. One is seamless connection between AIST and an external archive system. The other is that the system can provided calibrated PALSAR products according to observations using Corner Reflectors. As a future plan, OGC-CSW is applied to this system for data search service. [C3373]

### "Geo-location error correction for Synthetic Aperture Radar image"

Spaceborne SAR (Synthetic Aperture Radar) image inherently contains geo-location errors which are caused by SAR image acquisition geometry, imaging mode, characteristics of reflectivity and image formation process. Since the geo-location error caused by SAR image acquisition geometry is inevitable, these errors are should be considered and corrected during the image formation process. In this paper, a geo-location error correction method is presented to analyze and correct the azimuth skew and ground range non-linearity error, and orientation error. This scheme does not require the aids of GCP and DEM, and instead directly extract the key correction parameters from the SAR raw data. Using RADARSAT-1 image, a simulation is performed to evaluate the proposed geo-location algorithm. To analyze the effect of proposed correction method, the corrected SAR images are compared with the reference image by RMSE values. [C3374]

### "Using AMSR-E land product to monitor the drought process in China"

This paper presents a method (drought index) to monitor the drought process in China. The method based on the relationship between drought and soil moisture change. Although the absolute value of soil moisture from AMSR-E land product is not accurate enough, but we can use the soil moisture change information in the temporal scale. The soil moisture product of AMSR-E from 2002 to present is used to build up the drought index.



In each EASE-GRID grid, the smallest soil moisture value and the largest soil moisture value in the 8 years are defined to dry/wet edge points and the drought index of them are 0/100. With the two edge points, we can get drought index in each grid, each day. Using the former method, we represent 4 typical drought processes in China. Result show that the drought index from AMSR-E soil moisture product can brought out the development and distribution of drought process roughly. [C3375]

#### "A system trade model for the monitoring of coastal vessels using HF surface wave radar and ship automatic identification systems (AIS)"

Coastal nations have an interest in maritime domain awareness for applications in national security, coastal conservancy, fishery and stewardship of the exclusive economic zones (EEZs) along their coastlines. Using our previously developed HF radar and AIS ship detection models we find signal to noise ratio (SNR) as a function of range, including ducted propagation for the AIS radio signals. We use these SNR estimates to find probability of detection  $P_d$  and then explore multiple systems and stations at variable spacings along the coast. Our example HF radar has significant power and aperture, similar to the Pisces radar. The AIS model is for high power (12.5 W) AIS and a significantly elevated receiver ( $\approx 250$  ft asl). A combined system of HF radar and AIS shows good capability ( $P_d > 0.9$ ) to ranges of  $\approx 125$  km for small ships and to 200 km for large ships. Considering a system of sites separated by 100 km we find that a  $P_{dof} > 0.9$  can be maintained to a distance off shore of 130 km even for small, 120 ton, ships. [C3376]

#### "Synthetic aperture radar image analysis as a tool for validation of baroclinic internal wave 3D modeling in Algeciras Bay (Strait of Gibraltar)"

This paper presents the main results obtained from the application of synthetic aperture radar (SAR) sea surface image analysis to the validation of the baroclinic internal wave 3D modeling in the Strait of Gibraltar and Algeciras Bay. Appropriate SAR images, showing the occurrence of short-wavelength oscillations in the sea surface in this area, were selected and compared with the modeled spatial fields of the M2 free-surface elevation at the corresponding tidal stages, sometimes corrected for the consideration of neap or spring episodes. A good agreement between SAR images and model fields was found. The analysis of SAR images has showed to be a powerful tool for the study of the internal wave phenomena in the Strait of Gibraltar and Algeciras Bay, providing a holistic way for the validation of 3D model experiments in that matter. [C3377]

#### "Effect of quantization on MIMO radar performance"

Multi-input multi-output (MIMO) radar systems have taken considerable attention among radar community in recent years. As stated in some publications MIMO radars have serious performance advantages compared to single-input single-output (SISO) radars. Although MIMO radars perform well theoretically, they have some practical problems. One of these problems is the data transmission rate required by MIMO radars. Quantization directly affects the amount of data to be transmitted. In this paper effects of quantization on MIMO radar performance is covered. [C3378]

#### "Adapting the sir algorithm to ASCAT"

Scatterometers have been launched primarily to measure ocean winds. The value of scatterometer data is increased by application of the SIR (Scatterometer Image Reconstruction) algorithm. The SIR algorithm enhances the effective resolution of the scatterometer data to support its use for other studies. SIR has been used successfully on several scatterometers, including QuikSCAT. In this paper, we describe how the SIR algorithm is adapted to ASCAT data. Using SZF data from ASCAT leads to the best resolution enhancement. SIR requires an estimate of the spatial extent for each measurement. We detail our method to estimate an approximate spatial response function for each ASCAT measurement. Finally, SIR parameters are tuned for use with ASCAT. [C3379]

#### "Airborne Doppler Wind Lidar investigations of western Pacific typhoon genesis and evolution"

The first ever extensive study of tropical cyclones using Doppler Wind Lidars (DWL) was conducted in 2008 within the THORPEX Pacific Asian Regional Campaign. More than 100 hours of DWL profiles were obtained with an average spacing of 3 km. These wind profiles along with dropsonde temperature, moisture and wind profiles are being used to study the genesis and evolution of tropical cyclones. Initial investigations are focused upon the impact the DWL profiles have on numerical weather prediction. [C3380]

#### "Advanced classification of UXO using fully polarimetric GPR and frequency-polarization features"

The classification of buried UXO has been a difficult task due to the large amount of false alarms resulted from

troublesome clutter objects. This paper closely examined scattering characteristics of such clutter objects by using numerical simulations. From the numerical study, we found that some clutter objects, which mainly causes the false alarms, produce multiple resonances at different frequencies and different polarizations. Based on these observations, we developed new classification algorithms which utilize the frequency-polarization dependent responses of complex targets in order to discriminate UXO-like objects from such trouble some clutters. The developed algorithms were tested by experiments in a test plot. In the test, the new classification algorithms clearly discriminated such clutters from UXO-like targets. In this paper, we present the simulation results for scattering characteristics of complex clutters and the new classification algorithm based on frequency-polarization dependent responses will be discussed. Finally, results from experimental verification will be presented. [C3381]

#### "Wide area assessment-Development and case study"

Munitions response is a high priority issue for the Department of Defense (DOD). Over 3,600 munitions response sites (MRS) are in DOD's inventory of sites with potential military munitions and explosives of concern (MEC) contamination, including unexploded ordnance (UXO) and discarded military munitions (DMM). Because many of these sites are large in size (greater than 10,000 acres), the investigation and remediation of these sites could cost billions of dollars. To address this issue, a wide area assessment (WAA) process was developed to quickly and cost effectively assess 100% of a site to reduce the footprint to only those areas with known MEC contamination (i.e. MRS). In this paper, we present a discussion of the origins of the WAA concept, a case study of its first large scale application, descriptions of the component technologies, and conclude with recommendations. [C3382]

#### "Track initiation using multiple bistatic range and range rate measurements with multidimensional assignment algorithm"

Track initiation using multiple bistatic range and range rate measurements with multidimensional assignment algorithm was investigated in this work. The assignment algorithm was tested on a problem involving three targets moving in close proximity inside a two dimensional radar network of six bistatic radar pairs. The accuracy and consistency of initiated tracks as well as measurement association performance of the assignment algorithm was demonstrated through Monte Carlo simulations. [C3383]

#### "Tandem-L: And innovative interferometric and polarimetric SAR mission to monitor earth system dynamics with high resolution"

Tandem-L is a proposal for an innovative interferometric and polarimetric radar mission that enables the systematic monitoring of dynamic processes on the Earth surface. Important mission objectives are global forest height and biomass inventories, large scale measurements of millimetric displacements due to tectonic shifts, and systematic observations of glacier movements. The innovative mission concept and the high data acquisition capacity of Tandem-L provide a unique data source to observe, analyze and quantify the dynamics of a wide range of mutually interacting processes in the bio-, litho-, hydro- and cryosphere. By this, Tandem-L will be an essential step to advance our understanding of the Earth system and its intricate dynamics. [C3384]

#### "A concept for high performance reflector-based Synthetic Aperture Radar"

The success of current spaceborne Synthetic Aperture Radar (SAR) is boosting the performance requirement of next generation systems. In order to cope with the evolution of SAR the design of the new systems will need to meet higher requirements for spatial and radiometric resolution together with an increased availability. This tendency is recognized nearly independently of the application area and manifests itself through several study programs initiated by space agencies aiming at the design of future SAR systems. In this context the use of large reflectors combined with digital feed arrays for SAR is considered a possible alternative to planar array antennas. This paper suggests an X-band spaceborne SAR system utilizing a deployable reflector together with a digital feed array, analyzes its performance and highlights its advantages compared to other systems based on direct radiating arrays. [C3385]

#### "Leaf area index (LAI) estimation based on vehicle-based laser scanning"

This paper proposes a novel approach for leaf area index (LAI) estimation based on vehicle-based laser scanning (VLS), which occurs as a state-of-the-art mapping technique. The method is advanced from the traditional terrestrial laser scanning (TLS), which has been primarily validated capable of predicting LAI. The associated schematic is to explore the correlations between VLS and TLS collections of the same trees. If positive, LAI can be retrieved with the related TLS data as reference. In this study, the consistency between the

multi-echoes per pulse received by VLS and the single-echo per pulse recorded by TLS is further tackled, and LAI, thus, can be derived more accurately. The experiments based on the real-measured VLS and TLS data have validated the applicability of VLS for estimating LAI. [C3386]

#### "Dual-polarization performance of the phase-tilt antenna array in a casa dense network radar"

In this paper the evaluation of dual-polarized scanning performance of a large planar array antenna for a solid state radar for weather is discussed. The antenna array is designed to operate at 9.36 GHz  $\pm$ 50 MHz, and the transmission and reception mode is configured to work alternatively. The antenna array architecture based on a series-fed array configuration of Dual-Polarized Aperture Coupled Patch Antennas (DP-ACPA) was designed and implemented to achieve the required radar polarimetric performance at low cost. Measured patterns of the array in the elevation and azimuth plane are used to evaluate the two principal polarimetric radar parameters (Zdr and LDR) over the scanning range in azimuth plane. It is shown that the biases in the differential reflectivity due the cross-polarization of this antenna configuration are negligible in comparison with the biases produced for the mismatch antenna patterns (H and V). [C3387]

#### "Design and Implementation of High Resolution Radar Video Transfer System"

The characteristic of radar video is analyzed in detail. The design and implementation of high resolution radar video transfer system are described. And the experiment is performed. The experimental results have revealed that the high efficient compression coding of radar video is achieved and the high resolution of echo signal is assured. The system has good practicability. [C3388]

#### "Motion Compensation for Spotlight-Mode SAR Data"

To the question that motion errors restrict improving of spotlight SAR resolution, this paper puts forward a kind of processing method that is wavenumber domain algorithm with two-step motion compensation of spotlight-mode SAR data combining phase gradient autofocus algorithm (PGA), which removes the influence of range motion error and opposite rotate error to spotlight SAR imaging and improves the quality of spotlight SAR images. Simulation results indicate this method has remarkable effect to improve the resolution of spotlight SAR. [C3389]

#### "Subsidence Monitoring by Permanent Scatterers in InSAR: A Case Study of Yancheng City in Jiangsu"

The thesis adopts time series analysis of the SAR images in 10 phases up to 4-year span of Yancheng city area in Jiangsu province, by selecting the SAR image acquired on September 3, 2005 as the main image and the rest of the SAR images as vice images, interferometric processings are carried out and 9 interferograms consisting of the terrain and the deformation information are extracted. By dealing with the 9 difference interferograms with PS technology, terrain feature spatial distribution characteristics with stable electromagnetic reflecting characteristics are successfully ascertained. After temporal and spatial analysis of the 9 unwrapping interferograms, DEM error, atmospheric delay error in the main image and the vice image are obtained, thus the PS-point nonlinear distortion of the ground is extracted. Then by integrating analysis of ground deformation direction, reference datum, floor deformation positiveness and negativeness three aspects, the surface subsidence distributed situation in time and space of Yancheng city area are discovered. [C3390]

#### "Development and Application of Mobile Water Level Monitoring Based on Multi-sensor Integration"

According to the current status of water level monitoring of inland river, this paper presents and designs a multi-sensor integrated dynamic system for mobile water level measurement, which is based on CORS(continuous operational reference system) GPS(global positioning system), GPRS(general packet radio service), PDA(personal digital assistant) technology as well as a post processing platform. The system design, signal quality control and data processing are researched in detail. This system has been used for an actual experiment. The results show that this system has high stability, reliability and flexibility. It is a very-well supplement for the present water level monitoring based on water-level stations. [C3391]

#### "The Detection of Range Extended Target Based on Adaptive Searching and Twofold Sliding Windows"

The detection of range extended target in UWB radar has been the research focus in the field of signal detection. The paper gives a detection method based on twofold sliding windows, and the theoretical value of the detection threshold using adaptive searching algorithm is derived. The simulation confirms that the detection of range extended target based on adaptive searching and twofold sliding windows shows good performance. [C3392]

### "Target Recognition Based on the Self-Correlation Function of HRRP"

The theoretical result shows that the self-correlation function not only has the time-shift invariant feature, but also largely reduces the computational work. To overcome the sensitivity of High-Resolution Range Profile(HRRP), this paper has extracted the self-correlation function of HRRP as a feature for target recognition. Templates and test data are created by using the measured data of sea targets. The results of comparison among the self-correlation function feature, the original range profiles and the amplitude spectrum feature show that the self-correlation function feature has higher recognition efficiency and better anti-noise performance.

[C3393]

### "Speckle Reduction for SAR Images Based on Adaptive Gaussian Mixture Models"

A new algorithm for suppressing speckle in synthetic aperture radar (SAR) images was proposed based on the local statistical property of wavelet coefficients. This method modeled the distribution of wavelet coefficients as an adaptive Gaussian mixture model. This model took into account geometrical structures of the coefficients within one scale and it was adaptive to the wavelet subbands corresponding to three orientations in the image. Based on this model in a Bayesian framework, a spatially adaptive Bayesian shrinkage function was obtained and each modified coefficient was decided separately. Experimental results demonstrate the proposed method improves the performance of speckle reduction and preserves the details of the image. [C3394]

### "A Study of Suppressing Strong Clutter in Radar Signal Based ICA"

It is great difficult to handle the clutter in Radar signal processing. To reduce the influence of clutter, the paper firstly attempts to use FastICA algorithm by separating the target signal and clutter to suppress the strong clutter. The pretreatment of increasing the dimension and dividing the frequency is used before Fast ICA algorithm because of the special radar complex signals. In the same matched filter conditions, Fast ICA algorithm is proved effectively through the increased peak side lobe ratio (PSLR) and signal clutter ratio (SCR). [C3395]

### "Extraction of Radar Target Length Based on High Resolution Range Profile"

In the identification of radar target based on high resolution range profile (HRRP), the target length is an important feature. It can be used not only for the rough sort to decrease the time of identification, but also for the interception of real target echo information from the raw data to reduce noise redundancy. In this paper, an adaptive difference operator for target length feature extraction from HRRP is proposed. It is used to deal with three airplane-measured data. Experimental results and analysis are provided to show that the proposed method can effectively acquire the radial projection length of the target with high precision even in case of lower Signal-to-Noise Ratio (SNR). [C3396]

### "Design of Universal Radar Signal Processor Architecture Based on Crosspoint Switch"

The traditional radar signal processor have a poor performance in scalability and universality. To solve this problem, this paper proposes a new kind of radar signal processing system architecture based on crosspoint switch. A radar signal processor is usually composed of multiple circuit boards .The crosspoint switch is able to make circuit boards connection dynamically. The connections of channels between boards can be one channel to another, one channel to several channels or several channels to one channel. A single signal processing circuit board also has the characteristics of scalability and universality. Eight general digital signal processing chips(ADSP-TS201) form a cubelike network which can be constructed a variety of parallel signal processing systems. Data transmission rate between boards can reach 18.75Gbit/s(3.125\*6). The internal processing speed of each signal processing board reaches 4.8G(600M\*8) times per second. It meets the needs of high speed real-time computing. [C3397]

### "Paddy Rice Identification Using Polarimetric SAR Data in Southern China"

Rice is one of the largest food grains in the world, providing food for more than one third of globe population. The radar remote sensing has been proved as an effective tool for rice mapping. With the emergence of spaceborne polarimetric SAR satellite, researches on polarization backscattering behavior and identification methods of paddy rice are of great significance and attract attention of remote sensing communities. Zhazuo Area located in Guizhou Province of southwest China was selected as the test site of this study. The RADARSAT-2 polarimetric data acquired at four dates were used to analyze the polarization backscattering behaviors and temporal variation characteristics of rice, and identification method for rice based on optimal polarization combination was established. This study shows that HH with HH/HV is the best polarization combination for rice identification under the adoption of linear polarization combination. [C3398]



### "DOA Estimation for Strong and Weak Signals in the Presence of Array Gain and Phase Mismatch"

A new method for estimating direction of arrival (DOA) of the strong and weak signals is proposed in the presence of array gain and phase mismatch. Firstly, the array gain and phase mismatch is estimated using the norm of the error vector between the practical steering vector and the theoretical vector of the strong signal, and then the data covariance matrix is calibrated. Secondly, the new seek vectors are obtained by the eigenbeamforming normalization with the eigenvalues and eigenvectors of the calibrated covariance matrix. Finally, the directions of arrival of all the signals are estimated according to the spatial spectrum like MUSIC with the new seek steering vector. The proposed method has the simpler computation and the more accuracy compared with RELAX and JJM. The effectiveness and the superiority are demonstrated via the simulation results. [C3399]

### "Monitoring Ground Subsidence in New Orleans with Persistent Scatterers Interferometry"

Ground subsidence and flooding are well publicized problems in the area of New Orleans, USA. Interferometric Synthetic Aperture Radar (InSAR) has been applied by various research groups to study the ground subsidence in the area as an international effort supported by the Canadian Space Agency (CSA), National Aeronautics and Space Administration (NASA) and United States Geological Survey (USGS). This paper presents some of the work carried out at the Hong Kong Polytechnic University in contribution to this effort. 23 Radarsat-1 images acquired over a 2.5-year period from December 2004 to March 2007 are used in the PS-InSAR processing. Over 23,000 PS points are identified in the area based on both the amplitude and the coherence variations in the sequence of images. A network of PS points is then formed and used in the PS solution. The LAMBDA method is used to facilitate the determination of the phase integer ambiguities. The average subsidence rate along the direction of the radar illumination determined is 2.1 mm per annum. [C3400]

### "Joint DOD and DOA Estimation Using Real Polynomial Rooting in Bistatic MIMO Radar"

An algorithm for joint direction-of-departures (DODs) and direction-of-arrivals (DOAs) estimation using real polynomial rooting in bistatic multiple-input multiple-output (MIMO) radar is presented. Compared with the conventional spectral Capon method, the proposed approach estimates the angles by the alternating maximization (AM) algorithm and one-dimensional real polynomial rooting instead of two-dimensional angle search to reduce the computational burden. The novel real root-Capon method can perform well even without the prior knowledge of the initial values of unknown parameters which is a prerequisite to AM algorithm. Furthermore, the DODs and DOAs of targets can be paired automatically. Numerical examples validate the effectiveness of the algorithm. [C3401]

### "Passive Tracking and Locating Radar Based on Double GSM Base Stations"

Passive radar is a kind of that without its own transmitter and receive the thermal emission energy of an object or its source of microwave energy reflected from the radar to detect targets. The widely distributed GSM base station signals have GMSK frequency modulation characteristics, these signals can be used as a passive radar radiation source for its ambiguity function diagram with axes at a distance and no ambiguity in Doppler shift and the high side-lobe and so on. Multi-base stations passive radar positioning system is one of the important research area. According to the urban low-altitude air defense warning system development, this paper do some researches on line and plane intersection algorithm for passive location and tracking, based on dual-GSM base stations. Meanwhile, probe into the passive tracking technics by utilizing the State-Dependent Riccati Equation Filter tracking algorithm under the dual GSM base stations. Experiments shows that the algorithms have better positioning accuracy, high efficiency and practical value. [C3402]

### "Electrical impedance tomography reconstruction using a monotonicity approach based on a priori knowledge"

Electrical Impedance Tomography (EIT) has been proposed as an alternative modality for breast imaging. Current EIT reconstruction algorithms are based in optimization procedures that aim to minimize the difference between the recorded data and a set of candidate scenarios. However, these methods produce images with diffused edges, as sharp structures are penalized by current regularization techniques. In this paper, a novel edge preserving EIT reconstruction method is proposed. This technique uses a priori information obtained from Breast Microwave Radar images to estimate the location of the dense breast regions. Then, the monotonicity of the impedance matrix of the collected data is used to reconstruct a profile of the tissue distribution in the breast region. The proposed method yielded promising results when applied to numeric phantoms generated from Magnetic Resonance Imaging datasets. [C3403]

### "Experimental demonstration of noncontact pulse wave velocity monitoring using multiple Doppler radar sensors"

In this paper, two Doppler radars are used to monitor the pulse movements at the heart and the calf in order to measure the pulse wave velocity (PWV) wirelessly. Both simulation and experiment have been performed to demonstrate the feasibility of the proposed noncontact PWV monitoring. A three-stage calibration procedure, including DC offset calibration, circuit delay calibration and antenna radiation pattern calibration, has been developed for reliable long-term PWV monitoring. The measurement results have been verified by wired contact measurement with pulse transducers. [C3404]

### "Phase unwrapping using region-based Markov Random Field model"

Phase unwrapping is a classical problem in Magnetic Resonance Imaging (MRI), Interferometric Synthetic Aperture Radar and Sonar (InSAR/InSAS), fringe pattern analysis, and spectroscopy. Although many methods have been proposed to address this problem, robust and effective phase unwrapping remains a challenge. This paper presents a novel phase unwrapping method using a region-based Markov Random Field (MRF) model. Specifically, the phase image is segmented into regions within which the phase is not wrapped. Then, the phase image is unwrapped between different regions using an improved Highest Confidence First (HCF) algorithm to optimize the MRF model. The proposed method has desirable theoretical properties as well as an efficient implementation. Simulations and experimental results on MRI images show that the proposed method provides similar or improved phase unwrapping than Phase Unwrapping MAX-flow/min-cut (PUMA) method and ZpM method. [C3405]

### "Low power and high gain double-balanced mixer dedicated to 77 GHz automotive radar applications"

In this paper, we present a mixer implemented in a 130 nm BiCMOS technology dedicated to 77 GHz automotive radar applications. The architecture is based on a double-balanced Gilbert cell with integrated transformer-based Baluns. Interconnections between devices, capacitor accesses and Tee-junctions are modeled using EM software in order to improve the simulation accuracy. The measurement results of the circuit exhibit a conversion gain and a SSB noise figure of 18.5 dB and 13.8 dB respectively over a 74 to 81 GHz band. Supplied under 2.5 V the power consumption is 80 mW and the ICP1 is -13 dBm. The transformer-based Balun allows a good input matching at the RF input port over a 16 GHz range from 72 to 88 GHz. [C3406]

### "The missile SAR echo signal simulation technology research"

SAR simulation technology is of great significance for the development of synthetic aperture radar. The paper firstly proposes the constituted principles of missile SAR echo simulation system, discusses and establishes mathematical model of the Missile SAR echo signal, and describes the target Scattering model and the geometric model on the distributed targets and described the target Scattering model and the geometric model on the distributed targets, and finally provides a theoretical basis for further study the simulation of missile-borne SAR echo system. [C3407]

### "A 45-67GHz UWB transmitter with >8dBm output power for indoor radar applications"

A transmitter IC for indoor presence and position detection based on radar is presented. The IC supports carrier frequencies between 45-67GHz, which includes the 60GHz ISM band. Wide RF bandwidth is achieved by applying low to moderate quality factor networks in the signal path. A bi-phase modulator multiplies the carrier with a pseudo-random data sequence of up to 4Gb/s for UWB signal generation. The 0.79mm<sup>2</sup>IC produces >8dBm saturated output power and >25dB small-signal gain for frequencies from 35-67GHz. At 60GHz, the saturated (differential) output power is 10.7dBm. The IC dissipates 462mW from a 3.5V supply voltage and is implemented in a 0.13μm SiGe BiCMOS IC process. [C3408]

### "A 117mW 77GHz receiver in 65nm CMOS with ladder structured tunable VCO"

A low power 77GHz receiver, suitable to be used in a FM-CW Automotive Radar has been designed using a 1P6M 65nm RFCMOS process. It has been implemented using a direct conversion architecture. The 77GHz signal generation block generates a FM-CW signal that pre-drives the external PA with a power level of -4.5dBm and also works as a Local Oscillator (LO) signal in the downconversion mixer. The ladder structured CPW differential transmission line used in the VCO core presents an inductance value of 83pH and a quality factor of 30 at 77GHz. By cutting the different ladders of the inductor, together with the implemented varactors, a tuning range of 15.8% is measured for the VCO, which is suitable to cover process variations. The front-end exhibits a

maximum voltage gain of 15 dB over the baseband and presents a LNA noise figure of 7dB at 77GHz. The VCO measured phase noise is -109dBc/Hz at 10MHz. The achieved power consumption of the complete receiver is only 117mW from a 1.5V voltage supply, 43.5mW coming from the receiver block and 73.5mW from the signal generation block. [C3409]

#### "A Novel Long-Distance Measurement Method Based on Secondary Radar"

In this paper we present a novel method for high precision long-distance measurement based on secondary radar. In this method, we employ two transceivers unit to work in an acknowledged mode as secondary radar system to achieve the round-trip time-of-flight (RTTOF), and introduce a system group delay (SGD) to estimate the time of the measurement signal through the system circuit. The real RTTOF related to the measured distance is acquired by deducting the SGD in the RTTOF. The prototype operates within the 433MHz ISM-Band. The results show the method has a good preference in long distance measurement at 1 km and the measurement principle is robust towards multi-path effect and target identification. [C3410]

#### "Multitarget Tracking Before Detection via Probability Hypothesis Density Filter"

Tracking-before-detection (TBD) is well suitable for radar detection and target tracking of low-observable objects because it makes full use of the raw sensor data without using the threshold and takes advantage of the gains of time integration. The main difficulty in the TBD is that the measurement is a highly nonlinear function of the target state and the associations of measurements are hard to be built when multiple targets are presented. Probability hypothesis density (PHD) filter is regarded as an efficient solution to multitarget tracking problems. To deal with multitarget TBD problem, a classical PHD filter, with "standard" multitarget measurement model, is proposed in this paper. The advantage of proposed filter is analyzed compared with traditional multitarget particle filter. Numerical simulations show our approach has better performance in estimated accuracy and precision of position, velocity and number of targets than multitarget particle filter. [C3411]

#### "Hybrid Method of DOA Estimation for Low-Angle Target Tracking"

In the presence of sea-surface multipath, it is difficult to estimate the direction--of--arrival (DOA) of target for the low-angle tracking problem due to the interference between the direct path and the specular path. We can apply the method of array signal processing to reduce the multipath effect. In this paper, a series of measures are adopted to eliminate the correlation, so one can distinguish the real angle of elevation from the specular, and promote the accuracy and performance of angle measuring, by using MUSIC algorithm. Stimulation results are provided to verify the feasibility of the methods in this paper. [C3412]

#### "Research on the Method of Airborne SAR Direct Geocoding Based on Correction of Systematic Error"

In this paper, a algorithm of airborne SAR Direct Geocoding based on correction of airborne SAR systematic error including slant range measurement error and time delay is put forward to improve the positioning precise, and POS/PPP technique is used to obtain radar phase center position data taking into account work efficiency. Many factors result in airborne SAR positioning accuracy, but main of them are slant range measurement error and time delay, if they couldn't be corrected precisely, the positioning accuracy won't be satisfactory. So this paper calculates the errors through some control points with P-band airborne SAR image of 2.5 meters resolution in mountain area of China (Xian, ShanXi), then we select eleven check points to make statistics. As a result, the horizontal accuracy is 12.6 meters, so the new algorithm on airborne SAR presented in this paper is efficient and practicable for airborne SAR Direct Geocoding in mountain area. [C3413]

#### "A new paradigm for telehealth implementation"

Recently, efforts have been made to treat patients at home as much as possible. In many cases, the reason for the patient staying in hospital is not that he/she actually needs active medical care. Often, the principal reason for a lengthy stay in hospital is simply continual observation. This paper explains our experience and strategy to support the treatment of patients in their own home through the remote monitoring of physiological signals. The benefits of such remote monitoring are wide-ranging; the patient can continue to live their normal life, their risk of infection is reduced, costs are significantly decreased for the hospital, and clinician time is utilised more effectively. [C3414]

#### "Clip-on wireless wearable microwave sensor for ambulatory cardiac monitoring"

We present a new type of non-contact sensor for use in ambulatory cardiac monitoring. The sensor operation is based on a microwave Doppler technique; however, instead of detecting the heart activity from a distance, the

sensor is placed on the patient's chest over the clothing. The microwave sensor directly measures heart movement rather than electrical activity, and is thus complementary to ECG. The primary advantages of the microwave sensor includes small size, light weight, low power, low-cost, and the ability to operate through clothing. We present a sample sensor design that incorporates a 2.4 GHz Doppler circuit, integrated microstrip patch antenna, and microcontroller with 12-bit ADC data sampling. The prototype sensor also includes a wireless data link for sending data to a remote PC or mobile phone. Sample data is shown for several subjects and compared to data from a commercial portable ECG device. Data collected from the microwave sensor exhibits a significant amount of features, indicating possible use as a tool for monitoring heart mechanics and detection of abnormalities such as fibrillation and akinesia. [C3415]

### "A Survey of System Platforms for Mobile Payment"

With the evolution and significant growth in wireless technology and the development of mobile commerce, businesses can achieve superior performance through the implementation of platforms for mobile payment. However, there are several platforms for mobile payment to choose from which makes the selection of an appropriate platform for specific applications a challenging task. In response to this challenge, the most common mobile payment platforms recorded in the literature have been reviewed. This paper presents the result of this review describing the advantages and disadvantages of each system and offers ranking of the technologies considered. MCDM method is used for assessing and comparing different platforms from technical and business points of view. The results indicate that SIM-based application with binary SMS offers the best solution compared to other alternatives. [C3416]

### "Design and development of autonomous driving vehicle"

In this paper, a new type of autonomous vehicle is developed. This vehicle consists of three sets of control systems to regulate the direction, brake and fuels. The sensing system is a combination of laser radar and camera. The localization system is constructed with GPS device and electronically compass. Currently, three tasks, including lane detection and following, object detection, and obstacle avoidance, has been implemented on this platform. We reported some experimental results. [C3417]

### "Research on the image mismatching points eliminating and the integrated arithmetic in the INS/SAR integrated navigation"

The error of the inertia navigation system can be modulated critically by using the real-time SAR image through image matching and positioning. The mismatching points are inevitable in the SAR aided navigation. In the integrated navigation, the measurement outliers will affect the filter seriously. In order to eliminate the effect of the mismatching points, combining the discontinuous working characteristics of the SAR image matching navigation, the paper proposes the image mismatching points eliminating arithmetic and the integrated navigation arithmetic. We found the mathematical models of the INS/SAR integrated navigation system which has the discontinuous working characteristics. And basing on the Kalman filtering information we design the arithmetic to eliminate and displace the image mismatching points. The simulation indicates the arithmetic proposed in this paper can eliminate and displace the image mismatching points availably and consequently improves the accuracy of the integrated navigation greatly. [C3418]

### "Close range coverage ship radar with distance high resolution"

Close range coverage ship radar with high (1.5 m) resolution at range was developed and implemented for navigation of boats as well as for lay-up and mooring of super-size vessels. Examples of the radar-tracking images obtained during natural tests of "River" radar manufactured as a small lot by Micran Co. (Tomsk, Russia) are given. [C3419]

### "Distribution analysis of multi-source decoying system against ARM"

Based on the theory of active decoying system against anti-radiation missile (ARM), decoying error formula was presented, decoying process of multi-source against ARM was analyzed and decoying effectiveness evaluation model was also established. In view of three-source and four-source decoying system, three simplified distributions' models (two for three-source decoying system and one for four-source decoying system) were proposed. According to given attack angle of ARM, the influence of distributions' omnidirectional change on radar and baits' protected probabilities was analyzed. Besides, illustrated by the case of four-source distribution, the effect of bait-to-radar power ratio on radar's protected probability was discussed. Simulation results have great significance in researching the operational effectiveness of multi-source decoying system against ARM. [C3420]



### "Study on strapdown decoupling technology for rolling missile using RF interferometer seeker"

Because strapdown seeker is fixed on the missile body, the guidance signal for proportion navigation law can not be directly got. And the outputs of strapdown seeker are not appropriate to be directly used in the control system of the missile, for it couples with the missile body angular motion, Aim at a strapdown seeker using RF interferometer for guidance, this article presents a decoupling method that a dynamic gyro is used to decouple from the body angular motion of the missile, The dynamic gyro is used for tracking line of sight, and at the same time line of sight rate and gimbal angle outputs are available for autopilot command application. The guidance signal for proportion navigation law is derivation from outer gimbal's precessing current of the dynamic gyro. First, the angle-measure principle of phase interferometer is analyzed in the paper; second, the decoupling principle from body angular motion is advanced in the paper. It is proved that the guidance signal, namely line of sight rate in inertial space can follow the input signals well, and the effect of body angular motion can be effectively isolated. [C3421]

### "The attitude tracking maneuvers of spaceborne spotlight SAR"

The spotlight mode of spaceborne SAR platforms often have to point its payload to immobile target on the ground which means the satellite attitude have to follow a specific trajectory in a fixed time span. In this paper, the attitude angle, angular velocities and angular accelerate are derived. A PD control law with feedforward is developed to achieve the purpose. The approach is verified using numerical simulation with external disturbance and uncertain model. [C3422]

### "An improved signal subspace decomposition method in low SNR case"

The SNR (Signal-to-Noise Ratio) of the targets in HF radar is usually not high enough and the array data length is short. Therefore, the Toeplitz construction method is applied to achieve better azimuth resolution and higher azimuth estimation accuracy than the classic covariance matrix construction method of the spatial spectrum estimation technique. However, its signal subspace and noise subspace could not be separated clearly by the conventional subspace decomposition method. In this paper, an improved signal subspace decomposition method based on the cross-correlation coefficients analysis of the eigenvectors is presented. This method uses an adaptive three sigma rule to select the eigenvectors corresponding to the smaller eigenvalues as the signal subspace. Thus, the signal subspace is divided more clearly. Then, combined with the Multiple Signal Classification (MUSIC) algorithm, the estimate performance for the coherent targets is improved. [C3423]

### "W-band pulsed radar receiver in low cost CMOS"

A CMOS heterodyne receiver integrating a phase-locked loop that includes a bulk of transmitter functions for W-band pulsed radar is realized using low leakage transistors of a low cost 65-nm bulk CMOS process with 5 thin and 1 thick metal layers used to manufacture cell phone RFIC's. The peak conversion gain of receiver is 7 dB and the minimum NF is 10.8 dB between 78 and 88 GHz in measurement. The entire receiver front-end consumes ~190 mW. [C3424]

### "A 43.5mW 77GHz receiver front-end in 65nm CMOS suitable for FM-CW Automotive Radar"

A low power mmW receiver front-end, suitable for a FM-CW Automotive Radar has been implemented using a 1P6M 65nm RFCMOS process. It has been designed using a direct conversion architecture. The input and interstage impedance matching networks have been implemented using Multi-layer Coplanar Wave guide (MCPW) based inductors. MCPW lines can realize small inductance values with high quality factor at mmW frequencies, improving gain, noise figure and power consumption performance of the receiver. It is shown that by adjusting the ground spacing and conductor width of the MCPW, an optimized 52pH inductor can achieve a quality factor of 37 at 77GHz. The fabricated front-end exhibits a maximum voltage gain of 15dB over the baseband and presents a LNA noise figure of 7dB which makes it suitable for next generation of collision avoidance systems. The achieved power consumption of the receiver front-end is only 43.5mW from a 1.5V voltage supply. [C3425]

### "A 77 GHz power amplifier using transformer-based power combiner in 90 nm CMOS"

A 77 GHz fully-integrated power amplifier (PA) with 50  $\Omega$  input and output matching has been realized in a general purpose 90 nm CMOS technology. In order to improve the output power and reduce the signal loss, a transformer and a short stub topology are employed respectively. The power amplifier achieves a saturated output power ( $P_{out,sat}$ ) of +13.2 dBm and 1dB compressed output power ( $P_{out,1dB}$ ) of +11.2 dBm with a peak power-added efficiency (PAE) of 10.4% while operated with a 1.2 V supply. [C3426]

### "Target maneuver detection using high resolution Doppler profile"

A novel maneuver detector for radar targets is described. The high resolution Doppler profile is used to detect abrupt variation in attitude as the target maneuvers, which can be extracted within the coherent processing interval. A brief introduction of the detection principle is presented, along with feasibility study results from a back propagation neural network implementation. [C3427]

### "Robust adaptive ground moving target indication technique applied to distributed spaceborne SAR system"

Through formation flying, distributed SAR satellites system can increase the number of spatial degree-of-freedom (DOFs) and provide flexible multi-baselines for SAR-GMTI (ground moving target indication), while improving the system performance. This letter proposes a robust optimum adaptive clutter suppression technique for SAR-GMTI applied to the distributed spaceborne synthetic aperture radar (SAR) systems. Some realistic problems related to the implementation of the processor are investigated, which include decorrelations from multiplicative speckle noise and moving target steering vector mismatch. Diagonal Loading (DL) techniques is resorted to improve the estimation of clutter statistics in the presence of multiplicative speckle noise. A prior information, like road network information, is integrated into the optimum adaptive processor to reduce moving target steering vector mismatch. Simulation experiments and performance analysis demonstrate the effectiveness and robustness of the proposed processor. [C3428]

### "The robust adaptive signal processing in correlated noise"

A new approach is considered for solving the problem of spatiotemporal signal processing in adaptive antenna arrays in conditions intensive correlated noise processes. The method of synthesis of robust algorithms is based on the game-theoretical principle of searching a minimum of the root-mean-square error that characterizes quality of received estimations of the existential spectra. The signal processing algorithms, constructed on this principle, relate to the class of minimax algorithms being invariant with respect to the prior uncertainty concerning noise distributions. [C3429]

### "A survey on feature extraction of SAR Images"

The feature extraction is one of the key steps for SAR ATR. It can greatly reduce the amount of information processing by SAR ATR, improve the identification efficiency, reduce the time of recognition and lower resources utilization by means of the feature extraction. In the beginning, the feature extraction methods are classified by target type and then various categories methods are summarized. Finally, some unsolved problems of feature extraction are probed. [C3430]

### "Implementation of real-time video streaming with fuzzy logic controller"

The increasing demand of video streaming recently causes a trouble on network congestion due to a huge data rate transmission. One concept to reduce such a problem is to dynamically adjust the rate of video streaming according to an available bandwidth. This paper introduces a fuzzy logic controller to control a real-time video streaming by adjusting either a frame rate or a video quality. In this paper, two experimental environments, LAN or GPRS connections, are investigated. The results show that a fuzzy logic controller is able to control a frame rate and a quality of video streaming according to an available bandwidth automatically. [C3431]

### "A Study on Removal of Radial Interference Echo with Weather Radar"

Electromagnetic disturbance (EMI) is an unpredictable event which often cause abnormal radar echo. EMI enables invariant radial interference echo (features such as sun-strobes) existing in certain directions in radar echo charts at many radar stations, the interference echo and the precipitation echo overlap in many regions. The paper key research has analyzed removal of interference echo which laps over precipitation echo, and an algorithm has been proposed. The radial interference echo could be distinguished from precipitation echo by analyzing their differences. According to the wave principle of superposition and the weather radar signal processing principle, the effective precipitation echo power was obtained by processing the echo power, thus disturbance was eliminated. The analyses results show that most of interference echo were detected and removed by the algorithm, especially in the overlap regions. It can eliminate radial interference echo and retain precipitation echo well at the same time. [C3432]

### "Eigen-Decomposition Method for RFI Suppression Applied to SAR Data"

This paper proposes a novel eigen-decomposition method for narrowband radio frequency interference

suppression for SAR. This method decomposes the eigenvectors of the RFI contaminated signal into interference subspace and signal-plus-noise subspace. The orthogonality of the two subspaces is used to suppress the RFI signals. Compared with the existing algorithms in previous literatures, the proposed method is more computationally efficient with satisfactory suppression results. Further more, this algorithm will neither estimate nor need the prior knowledge of the parameters of the interference signals. The point-target simulation is used to show the working principle of the proposed algorithm. Experimental results based on SAR real data are also shown to verify the proposed algorithm. [C3433]

#### "The Research on RIC-ISAR Image of Ship Target Based on High-Order Match-Phase Transform"

Due to the constantly changing motion of a ship target, high order phase terms which cannot be neglected and results in bad azimuth focusing are generated. In this condition the RD algorithm is not a very effective way for ISAR imaging. In fact, the azimuth position of target scattering point can also be illustrated by the instantaneous chirp rate of received signal not just by the Doppler frequency. In this paper, a new approach is proposed, which is based on Product High-Order Matched-Phase Transform (PHMT) to estimate the value of the changing rate of chirp rate, chirp rate, central frequency and amplitude, thus the high quality range-instantaneous chirp rate (RIC) ISAR image of the object can be obtained. At last, the simulation results prove the effectiveness of the method proposed. [C3434]

#### "A Methodology for Trees' Detection Using LiDAR Data in Urban Areas"

In this paper, we present an approach to detecting and locating trees using LiDAR point data. The motivation for this issue comes from urban planning and management, in which LiDAR data is used to obtain information of the cities. As for the echo characteristic of the LiDAR data is sensitive for the trees, we propose a three-step method for tree detection consisting of data- preprocessing, tree-points extraction and connectivity detection and merging, which make full use of the echo information for the LiDAR points to get the location of the trees in the urban areas. [C3435]

#### "FMCW Radar Imaging with Multi-channel Antenna Array via Sparse Recovery Technique"

A radar system composed of a single transmitter, M receiving channels is studied. Radar echo signals are acquired to estimate the angle, range and velocity in a multiple moving target scenario. The developed algorithm is based on sparse recovery technique by exploiting the sparseness of the targets in angle-range domain. It is shown in simulations for automotive scenario that the proposed algorithm yield better performance in terms of both imaging accuracy and multiple-target resolution compared with the methods of conventional beamforming and minimum variance (Capon) beamforming. [C3436]

#### "SAR Imaging of Moving Targets via Compressive Sensing"

An algorithm based on compressive sensing (CS) is proposed for synthetic aperture radar (SAR) imaging of moving targets. The received echo is decomposed into the sum of many basis sub-signals that are generated by discretizing the target spatial domain and velocity domain and synthesizing the SAR received data for every discretized spatial position and velocity candidate. In this way, the SAR imaging problem is converted into sub-signal selection problem. Thus, in the case that moving targets are sparsely distributed in the observed scene, their positions and velocities can be reconstructed by using the CS technique. It is shown that, compared with traditional algorithms, the target image produced by the proposed algorithm has higher resolution and lower side-lobe. Moreover, multiple targets with different speeds can be imaged simultaneously, so the proposed algorithm has higher efficiency. [C3437]

#### "Design of the Simulation and Assessment Software of Missile-Borne SAR Imaging System"

It is a key step to study and design the missile-borne SAR (Synthetic Aperture Radar) by the computer simulation. In this paper, we present a simulation and assessment software of the missile-borne SAR imaging system, which calculates the flight path of the missile, generates the echo data of the target, outputs the imaging result and its quality assessment. After dividing functional modules, we exhibit each function of the modules respectively. Moreover, three important problems are analyzed: the computation load of the echo data generation, the approach to generating layover and shadow of the 3D target, and the imaging algorithm and geometric correction formula. The simulation example shows the feasibility and effectiveness of the proposed software. [C3438]

#### "The Sky-Scanner System for Air Traffic Management: Test Sessions and Statistical Analysis"

Air Traffic Management (ATM) is traditionally performed by means of radar systems, but new detection and

ranging systems based on LIDAR (Ligth Detection And Ranging systems) are emerging as a critical design trend and yielding to new generation ATM paradigms. The main goal of the designers of the system under discussion was to develop a novel laser tracking technology (SKY-Scanner System) that could allow the detection and tracking of aircrafts up to at least 6 nautical miles. Moreover, the purpose was also the definition of techniques, protocols, numerical prediction tools and devices specifically designed for the analysis of the laser system performances in Air Traffic Control applications. The ultimate purpose was to define a new generation ATM paradigm that is based on radar and laser tracking data fusion, as well as on ground to air laser communications. This paper reports the test session that has been run on a prototype of the laser range finder, in order to find accuracy and possible dependence of measurement errors on temperature, humidity, distance and position of the target. The results show that high humidity and temperature can affect the accuracy of the measurements. [C3439]

#### "Research on scheme and algorithm of high-precision fault-tolerant integrated navigation for HALE UAV"

To meet the need of high-precision navigation for HALE (high-altitude long-endurance) UAV (unmanned aerial vehicle), multi-sensor fault-tolerant autonomous navigation system was researched. For the shortcoming that the GPS signal is easily interfered by electromagnetic techniques, combining sundry integrated navigation patterns such as the INS/CNS integrated navigation, the INS/SAR (Synthetic Aperture Radar) integrated navigation, and other autonomous navigation system, the fault-tolerant federated filter scheme is proposed in this paper. This scheme can effectively take advantage of multi-sensor information redundancy. When the GPS system failure occurred, the system can effectively detect and isolate the corresponding failure subsystem, and at this time the INS/CNS integrated navigation system plays a leading role in the navigation system to maintain a certain degree of navigation accuracy. By importing the SAR-aided navigation system in the terminal, the system can achieve high-precision navigation positioning. The integrated navigation system can detect failure in rapid speed, so it has a high application value in practical engineering. The simulation results by covariance analysis show that the proposed navigation scheme is feasible, and this navigation scheme has important theoretical reference value to improve accuracy and reliability of integrated navigation system for the HALE UAV. [C3440]

#### "Broad beam high-frequency bistatic cross sections of the ocean surface"

For a bistatic high-frequency radar with a broad beamwidth receiving antenna, over the range-limited clutter cell, the deviations of bistatic angle and wind direction would bring about broadened bistatic cross sections of the ocean surface in contrast to a narrow beam bistatic hf radar. Based on Eric Gill's narrow beam HF cross sections of the ocean surface, broad beam HF bistatic cross sections of the ocean surface were presented and the results were obtained by numerical simulation. The results showed that the broad beam bistatic cross sections of the ocean surface were the superposition of narrow beam and were broadened at the same time. [C3441]

#### "Surface Acoustic Wave Resonators as Passive Buried Sensors"

Acoustic wave devices are well known passive transducers for probing through a wireless link a physical quantity. Amongst the two main classes of designs-resonators and delay lines-the former have the advantage of providing informations in a narrow band signal and are hence compatible with an interrogation strategy compliant with radiofrequency (RF) emission regulations, while the latter are probed by a short RF pulse with larger instantaneous energy and shorter response time. We here demonstrate the measurement of temperature using the two configurations, and more specifically for sensors buried in soil. While we demonstrate long term stability and ruggedness of packaged resonators, and signal to noise ratio compatible with the envisioned application, the interrogation range is insufficient for most purposes and we focus towards the use of delay lines. Indeed, the interrogation method of the latter is similar to that used by Ground Penetrating RADAR (GPR) which displays interrogation ranges in the meter to tens of meters in the lower RF range, depending on soil water content, permittivity and conductivity. Thus, we demonstrate here both the temperature measurement capability of a delay buried delay line and the limit of detection of its signal. [C3442]

#### "Performance Analysis of Frequency Sweep Nonlinearities in LFM Radars"

The frequency sweep nonlinearity distortion of LFM signals is one of the most important factors that affect the performance of LFM radars. In this paper, the mathematical models for periodic frequency deviation distortion and non-periodic frequency deviation distortion of LFM signals are made. And the effects of these two types of FM nonlinearity of LFM signals on the matched-filtering pulse-compression performance of LFM radars are investigated profoundly. The computer simulation experiments are performed by using MATLAB language. Also the results are acquired and prove the correctness of preceding theoretical analyses. All the conclusions



obtained theoretically and experimentally, provide lots of indispensable theoretical basis and important experiential reference for the linearity correction of LFM signals, the design of wideband (WB) or ultra wideband (UWB) LFM radars, and the performance evaluation and performance optimization of LFM radars. [C3443]

#### "Quantifying Human Indoor Activity Using a Software Radio-Based Radar"

Human activity quantification consists of computing a numerical or qualitative metric that indicates the amount of movement a person engaged in a given time interval. Such a metric has important applications in elderly care, wellness and healthcare given the strong empirical relation between a person's health and his or her activity level. This paper proposes and evaluates methods to quantify the level of human activity in an indoor environment using a continuous wave radar. An experimental evaluation is carried out using a flexible and low-cost software defined radar platform. Results showed a good correlation between the proposed metrics and the motion sequence performed by the subject suggesting that accurate activity quantification in indoor environments can be achieved using a few simple off-body sensors. [C3444]

#### "Estimating Indoor Walking Velocity Profile Using a Software Radio-Based Radar"

Radar is an attractive technology for long term monitoring of human movement as it operates remotely, can be placed behind walls and is able to monitor a large area depending on its operating parameters. A radar signal reflected off a moving person carries rich information on his or her activity pattern in the form of a set of Doppler frequency components produced by the specific combination of limbs and torso movements. Deploying radars in indoor environments poses however challenges for the interpretation of signals reflected off a moving object due to multipath propagation. Two strategies for the estimation of human walking velocity profile in indoor environments are suggested and discussed. The accuracy of the strategies are evaluated and compared in a field experiment using a flexible and low-cost software defined radar platform. The results obtained indicate that both methods are able to estimate the velocity profile of the person's translational movement with less than 10% error. [C3445]

#### "Analysis of the quantization and saturation error for Space-borne SAR raw data compression algorithm in data domain"

The quantization and saturation error always exist in Space-borne SAR raw data compression process. The explicit formula on quantization and saturation error was not found in previous literatures, though much study has been executed. The analytical formulas of the error of quantization and saturation induced by Block Adaptive Quantization (BAQ) and Interception of High (IH) algorithms are deduced in this paper. The relationship between the standard deviation of input echo signal (SDIS) and the Signal-to-noise ratio (SNR) of these two algorithms is also given. Finally, the simulation test based on simulated SAR raw data and real data is executed to verify the work in this paper. The result of simulation test shows validity of our work which can provide a good criterion for choosing SAR raw data compression ratio parameter in engineering practice. [C3446]

#### "Research on the simplified algorithm of unobstructed areas radar calculation"

Based on the current methods of the radar's unobstructed areas calculation, this paper presents a simplified calculation, which is called the gradually reduced unobstructed areas calculation.. The projection of unobstructed areas that this method produced is intuitive, and the detection of invasive aircraft is simple, which is applicable to the calculation of a smaller range of the radar's scan. Though the verification of MATLAB, the processing speed and space using have been greatly improved. In other words, it improves not only time efficiency but also space efficiency. [C3447]

#### "The study on helicopter route planning"

Route planning is a very important part in simulation system. Under a simulated circumstance, the simulation can be improved if we can plan a reasonable flight path. This paper studies the helicopter route planning in hilly terrain. The whole route planning is divided into two levels. Firstly, the reference trajectory was planned, then replan parts of them, according to the changes in the environment (such as the emergence of new threats), and the others still in their track. Finally, on the platform of MATLAB, simulated the algorithm and the algorithm validity can be verified. [C3448]

#### "Threshold variation based analysis and implementation of an optimized AGC circuitry for digital IF receiver"

In digital receiver designs, An Automatic Gain Control (AGC) block is used to scale the power of input signal so as to meet high dynamic range requirement. This paper proposed a new method called Threshold Variation (TV)

analysis that best suits framed based Pulsed Doppler (PD) radar Step AGC design. The minimal dB control step, system threshold and the stability of Envelop Detector Filter (EDF) could be attained from TV analysis. By utilizing a Cascaded Integrator Comb (CIC) Filter and the  $\alpha|Max|+\beta|Min|$  magnitude approximation, an optimized AGC circuitry is implemented in FPGA. Our practice has proved that the circuitry has appealing performance in a digital Receiver. [C3449]

#### "Application of particle swarm optimization with stochastic inertia weight and adaptive mutation in target localization"

Target localization based on time difference of arrival (TDOA) measurements has important applications in sonar, radar and sensor networks. This paper simply introduced the target localization principle of moving emitter and the position location algorithm. Further more presented an improved particle swarm optimization with stochastic inertia weight and adaptive mutation, and adopts it to solve the target localization problem according to the batch of continuous TDOA measurements. The experimental results show that the new algorithm has higher localization accuracy, better algorithm stability and faster convergence rate. [C3450]

#### "Development of a high performance Wireless Mesh Network for video streaming"

Wireless Mesh Network (WMN) is a fast developing intelligent community network to provide multimedia services to the residents. With the latest development of technologies in broadcasting and smart mobile devices, to view videos on these handheld devices via WMN will become an essential lifestyle in the future. However, current WMN faces challenges to deliver videos to multiple users because of the constrained wireless medium. This paper addresses the challenges of video streaming in WMNs by providing a high performance design architecture to allow smooth delivery of videos. This includes the load balanced routing via multiple gateways and over multi-paths, efficient usage of the bandwidth by multicast routing, effective congestion control for video streaming and scalable video streaming to deliver videos to various devices at the same time. Practical implementation demonstrated the effectiveness of the current design and development. [C3451]

#### "A low-power wireless remote sensor node design based on GPRS"

For the limitation of transmission distance and power volume of sensor node, a low-power remote data acquisition node which implements long-distance data transmission by combining General Packet Radio Service network with wireless sensor network is designed to acquire data periodically and upload data to remote server through General Packet Radio Service network. This paper expatiates hardware design principles of the node, power management model and software protocol design of the test system. Test results show that nodes can reliably acquire and upload data, the average work current of sensor node is 34mA, the peak current of cluster-head is 260mA when cluster-head uploads data to server, and sleep mode current are both less than 35uA. Performance indicators of node can fulfill the needs of remote monitoring applications in industrial field. [C3452]

#### "The design of a GPRS-Based Intelligent Access Control System for Base Station"

This article describes the method for the design of a GPRS-Based Intelligent Access Control System for Base Station. The structure theory of the GPRS access control system is described in details in this paper. It gives topology structure between the devices in the base station, which are through up by RS485 fieldbus. In this paper, the SMS and caller identification methods and the IC card identification methods are analyzed, and it points out the advantages of the SMS and caller identification methods. Meanwhile, it gives a brief description of the function of the intelligent access control system management software. [C3453]

#### "Application research on intelligent pattern recognition methods in hail identification of weather radar"

Firstly, advantages of the learning ability of intelligent pattern recognition models, which have been used in hail identification of weather radar based on echo parameters, is discussed. Then, structures and working principles of hail identification models which based on fuzzy neural network and support vector machines (SVM) are described respectively. Finally, effect validation of hail identification has been finished by using echo samples from Chengdu and Kuitun to train the hail identification models. The experimental results show that hail identification models based on intelligent pattern recognition have the better effect than which based on the statistical pattern recognition. Besides, in the case of limited training samples, the identification model based on SVM has stronger adaptability than which based on fuzzy neural network. [C3454]

#### "Study on Defocus compensation using variable pulse repetition time stepped-frequency waveform"

In this paper, a new technology for compensating the defocus due to the velocities of multiple moving targets is

presented. By using this technology, the blur produced by defocus can be compensated when the velocities are unknown. And a method is proposed to solve the range-Doppler coupling caused by the multiple targets. The effectiveness of the algorithm is illustrated with simulation results. [C3455]

#### **"Research on intelligent monitoring and protection system of distributive multi-tower cranes"**

During construction phase of large buildings, it is of great significance to maintain safety protection on multi-tower cranes operating. Based on distributive and multi-intelligent agents design concept, and adopting ARM embedded technology, wireless network transmission, an intelligent monitor and protection system for the multi-tower cranes has been established. A multi-tower crane communication network has been set up to realize status information transmission of tower crane by adopting wireless token-ring communication. "Implication Confirm" feedback is used to speed up data transmission of communication network. Remote monitoring on working status of multi-tower cranes can be realized by using GPRS network. Field tests show the tower crane intelligent monitoring and protection system meets the requirements of monitoring construction safety of multi-tower cranes operating. [C3456]

#### **"Improved regularized particle filter algorithm for SINS/SAR integrated navigation"**

This paper presents a new improved regularized particle filter algorithm for SINS/SAR (Strap-down Inertial Navigation System / Synthetic Aperture Radar) integrated navigation system. By adopting MCMC (Markov Chain Monte Carlo) move to the regularization process, a MCMC based filtering algorithm is developed through combining local resampling with MCMC move to prevent a large number of particles from being rejected. The proposed particle filtering method prevents the degeneracy of particles and guarantees that the resultant particles have a common distribution with the practical probability function, without causing extra noises on the estimates. It also reduces the estimation variance and the computational load. By using improved regularized particle filter algorithm and extended Kalman filter algorithm, simulate for the SINS/SAR integrated navigation system. Experimental results demonstrate that the improved regularized particle filter algorithm can reduce the navigation positioning errors, and filtering performance obviously exceeds the extended Kalman filter algorithm. [C3457]

#### **"Mosaic in g the ocean/terrestrial SRTM-DEM and making t he geomorphologic relief shading map"**

Ocean and terra are the largest geomorphologic units on the earth, and there are essential differences between them. Hence, while we make the geomorphologic relief shading map, it is necessary to make the ocean/terrestrial geomorphologic relief shading map respectively. Then combining the ocean and terra map, we can get a whole geomorphologic map about the study area. However, the SRTM-DEM(Shuttle Radar Topography Mission-Digital Elevation Model) we get from USGS(United States Geological Survey) is clipped by SWBD(Shorelines and Water Bodies Database) coastline, so the coastline may be not accordance with the coastline we get about the study area. To solve this problem, we had to clip the DEM and patch the void data. Only in this way can we assure the DEM is accordance with the coastline. If the DEM is larger than the coastline, we can cut the spare parts by using the tool-extract by mask. However, if the DEM is smaller than the coastline, we have to patch the void data. This paper tries to find the best interpolating method to patch the void area according to the geomorphologic units. After that, we illustrate the processes of how to make the geomorphologic relief shading map by the software-Global Mapper. [C3458]

#### **"Compilation of DEM based on lidar data"**

Lidar has provided one new method for the digital elevation model (DEM). It has the advantage of gaining the three dimensional information, the wide measuring range, the high spatial and elevation resolution. What the lidar system gains is the cloud data, which can produce the digital surface model of the scanning area directly. However, if we want to withdraw the digit terrain model, still need to classify and process the cloud data. This article introduce how to use Lidar post-processing software such as POS software, the ALS40 post-processing software as well as the Terrasan module and the LPS module deal with the cloud data together, finally produce DEM in the ERDAS software. [C3459]

#### **"Bi-station OTH radar locating and tracking using only range and Doppler measurements"**

Azimuthal measurements of the high frequency ground wave over-the-horizon (OTH) radar are either coarse or unavailable in an actual environment. It is very hard for a single station OTH radar to performance effective tracking under that condition. A bi-station OTH radar system is proposed to triangulate target tracks using range and Doppler measurements only. Multi-sensor data association and combining positioning are key issues of this system. This paper focuses on positioning and tracking filter algorithm. The locating and tracking model is established and the extended Kalman filter (EKF) is used to solve the bi-station nonlinear tracking problem. Simulation result shows that EKF can handle this well, and the bi-station OTH radar system can meet or slightly

better than the accuracy of the conventional single station OTH radar tracking system with poor bearing resolution. [C3460]

### "Design of Tap Water Pipe's Monitoring System Based on GSM/GPRS"

This paper analyzes the whole network architecture of Tap Water Pipe's Monitoring System Based on GSM/GPRS, and then analysis the hardware design and software design of the system, through the effective design of the system reached the real-time monitoring and Leakage-Detecting of underground water-pipe system, and improve the maintenance efficiency of the system. [C3461]

### "Design and optimization of radio frequency stealth signal based on SAGA"

A good stealth performance of radio frequency (RF) signals is very important for fighters in order to have high penetration capacity, survivance capacity and combat effectiveness in an electronic warfare. Some design principles of RF stealth signals are proposed in this paper. In the light of design principles, hopping-frequency signals were proved to having the good RF stealth performance. The simulated annealing genetic algorithm (SAGA) was used to design hopping codes based on the maximal sidelobe level criterion. The performance of frequency-hopping signals was verified by experimental simulations. [C3462]

### "A design of alarm system for substation perimeter based on laser fence and wireless communication"

In recent years, with the transformer substations basically unattended, a new topic for the security of power equipments and electric power lines is presented. Many alarm systems based on ac high-voltage grid, electronic pulse fence or infrared electronic fence have been installed in substations. In this paper, we propose an intelligent anti-theft alarm system based on laser fence and wireless communication network technology. Once occlusion of the laser beams occurs, it will transmit alarm information with accurate location to the control center through ZigBee network, and then send short messages to the defender's phone by GPRS. Moreover, the on-site searchlights could be remotely controlled by SMS with GPRS network. The architecture and implementation of the system is described in detail. Practical results show that our system is high-security, low-power and low false-negative compared with the conventional anti-theft systems. [C3463]

### "Research on power spectrum estimation based on periodogram and burg algorithm"

With rapid development of modern intelligent traffic management, the measuring speed radar becomes an important device. Using Doppler principle, speed can be measured by obtaining frequency deviation signal of moving target. Traditional measuring speed method uses analog filter whose measuring accuracy is low and measuring speed is slow, so it's difficult to meet the requirements of modern intelligent traffic management. Signal processing of speed radar generally use power spectrum estimation method. This paper focuses on classical period spectral estimation and modern spectral estimation based on Burg algorithm. By comparing various algorithms in computational complexity and resolution, Burg algorithm was used to signal processing finally. Experimental and simulation results indicated that digital signal processing system would meet system requirements for measurement accuracy. [C3464]

### "A refuse-recognition method for radar HRRP target recognition based on mahalanobis distance"

In the radar automatic target recognition (RATR) system using high resolution range profile (HRRP), if a test sample has not been trained in training phase, it would lead to a full miss classification in test phase. In this paper, we design a classifier based on generalized confidence, which can efficiently refuse-recognize a new target. Firstly, principal component analysis (PCA) method is used to extract feature vector from every sample. Secondly, the classifier calculates each feature vector's generalized confidence on mahalanobis distance. Consequently, the distribution of confidence is used to define a refuse-recognition threshold for each training target. In test phase, for each trained-target in the database, we suppose that the test sample belongs to current target, calculate the generalized confidence, judge whether the test sample really belongs to the target or not via comparing the confidence with the target's refuse-recognition threshold. The final class is determined by vote. The experimental results demonstrate the effectiveness of the proposed algorithms. [C3465]

### "A bus management system based on ZigBee and GSM/GPRS"

This paper introduces a system design about bus management system based on ZigBee and GSM/GPRS, which implemented the basic functions of the intelligent public transport management system, such as monitoring the time of bus arrival, departing from the bus station and reporting stations name automatically. This system can ensure punctuality of vehicles to run, improve the automation level of reporting stations and quality of public



transport service. The management system has low cost and thus it is more feasible. [C3466]

### "A design of the Intelligent electronic control seat belt retractor based on automotive active safety technology"

Designs an Intelligent electronic control seat belt retractor, with integrated controller area network (Controller Area Network, CAN) communications, millimeter-wave radar technology, micro electro-mechanical systems (MEMS) sensor technology and embedded processing technology. The millimeter-wave radar warning signal, MEMS accelerometer information, occupants status and CAN bus data, trigger the appropriate seat belt traction control strategy, implementation of reminder, collision avoidance, thus it can protect the automotive occupants safe, and reduce or prevent occupants not to be injured during a crash. Therefore, the intelligent electronic control seat belt retractor links up active safety and passive safety technology. [C3467]

### "Simulation of radar electronic warfare range of visualization applications"

At present, applications of visualization technology are expanding, and are playing an increasingly important role in various fields. In this paper, radar visual range of electronic warfare simulation has been studied based on transcendental equation method and graphic space intersection method. This paper gives the maximum radar detection range and the detection range of two-dimensional visualization in electronic warfare simulation. In the actual simulation application, a preliminary design achieves the expected target. [C3468]

### "Coastal Radar WERA, a tool for Search and Rescue and oil spill management"

The HF-Coastal Radar "WERA" is a shore based remote sensing system to monitor ocean surface currents, waves and wind direction. This very reliable long range and high resolution monitoring system based on short radio wave radar technology. Due to the outstanding accuracy WERA can provide very valuable data to be assimilated into hydrographic models. In case of accidents in a distance of up to 200 km off the coast the real-time ocean surface current data can help Search and Rescue (SAR) operators. Presently, SAR tools are based on hydro-dynamical and atmospheric models to provide hindcast and forecast situations. Even if these oceanic numerical models are efficient to produce instantaneous maps of currents, the accuracy of derived Lagrangian trajectories often is not sufficient for search and rescue purposes. To improve these numerical models by means of realtime data it is essential that the quality of the assimilated data is very high and reliable. For this reason long term comparisons with buoy data for ground truthing and statistical analysis were carried out for more than two years. The resulting data availability (98,7 %) is outstanding and the data quality is as good as buoy data. [C3469]

### "Use of earth observation data and numerical modeling in the development of marine downstream services in Estonia"

The objective of the Global Monitoring for Environment and Security (GMES) is to provide, on a sustained basis, reliable and timely services related to environmental and security issues in support of public policy makers' needs. MyOcean is the implementation project of the GMES Marine Core Service (MCS), aiming at deploying the first concerted and integrated pan-European capacity for Ocean Monitoring and Forecasting ([www.myocean.eu.org](http://www.myocean.eu.org)). MyOcean develops upgraded European capabilities for reference marine information and provides a wide range of key ocean indicators. The MCS provides information to intermediate users who combine it with other forms of information and data to provide customized downstream services for end users. The end users range from wide public to special target groups. Downstream marine services in Estonia are built on in-situ real time and near real time measurements, satellite remote sensing imagery and numerical modeling. Two-day marine forecasts for the North-Eastern Baltic Sea are produced by 3D circulation model HIROMB-EST. The downstream service portfolio consists of following items. Real time sea level observations including history and two-day forecasts on 12 locations around the Estonian coast are available in the Internet. Sea surface temperature (SST) and salinity are complimented with near real time ferry-box observations on the cross-section between Tallinn and Helsinki. During cloud free sky SST charts are produced using MODIS (Moderate Resolution Imaging Spectroradiometer) imagery for the Gulf of Finland and Gulf of Riga. Illegal oil spills are detected from SAR imagery. The drift of the slick is simulated by Seatrack-Web and potential polluters are identified combining Seatrack Web and the Automatic Identification System (AIS). The monitoring of suspended particulate matter during harbor dredging is based on MODIS and MERIS (Medium Resolution Imaging Spectrometer) data. The laboratory analyses of water samples are used for the-- calibration and validation of satellite products. The in situ measurements of vertical profiles of absorption and attenuation coefficients are used to determine the profiles of particle origin, concentration and size distribution. Operational ice extent monitoring using SAR data is rather widespread. Optical remote sensing imagery from MODIS and MERIS sensors complement SAR imagery. Ice concentration maps are produced using the histogram analysis of MODIS

250 m reflectance data. This data is used for model evaluation with the purpose to get reliable ice forecast from the HIROMMB-EST model. Spectral optical remote sensing data from MERIS helps to identify different ice types. The determination of high spatial resolution marine and coastal wind from the Advanced Synthetic Aperture Radar (ASAR) is quite a novel application in the Estonian waters. Wind field data can be retrieved from ASAR C-band data and model results using CMOD algorithm. [C3470]

### "High-performance system design of SAR real-time signal processing"

Synthetic aperture radar is a high resolution imaging radar, SAR signal processing is an important branch of signal processing, while the performance of SAR signal processing system greatly influences the resolution of SAR image. In this paper, a high-performance signal processing system which has strong computation ability, high-width connectivity and flexible expandability is presented, meanwhile, the program design of FPGA is introduced, further more, the RD algorithm implementation result with the system proposed in this paper is provided as an illustration. [C3471]

### "Sea ice monitoring in the Baltic Sea using dual-pol C and L band SAR data"

Summary form only given. Monitoring of ice dynamics and ice type classification is an important task for understanding environmental changes as well as for safe winter navigation. SAR (Synthetic Aperture Radar) is a powerful spaceborne instrument to detect ridged ice regions as the radar backscatter is strongly influenced by geometrical properties of the ice surface. Data from polarimetric (or dual-pol) SAR sensors like Radarsat-2 and ALOS/Palsar enables to determine more precisely ice types as it contains more information about the ice surface geometry than single polarization images. Use of dual polarization SAR imagery also known as compact polarimetry has shown to be useful as it has reduced the complexity, cost and data rate of SAR image while preserving most of the capabilities of fully polarimetric image. A study for sea ice monitoring and characterization was carried out in the Baltic Sea from January to March 2009. The focus of current study was on enhanced monitoring of small scale changes/processes (ice types and dynamics) in the western Estonian archipelago sea. Secondary objective was to compare the backscatter characteristics at different frequencies (C-band and L-band) and polarizations (HH, HV, W) from various ice types (ridges, fast ice, water etc.) using data from different SAR sensors. Considering the objectives of the study high resolution SAR data from the following sensors was included: RADARSAT-2 (fine mode, HH/HV), ALOS/Palsar (fine mode, HH), ERS (image mode, W) and ASAR (wide swath, HH). Also optical remote sensing data from MODIS (Moderate Resolution Imaging Spectroradiometer) sensor was used to carry out non SAR dependent ice type classification. In addition to remote sensing imagery the meteorological data (wind measurements, air temperature, precipitation etc) from three different stations near the study area was analyzed to determine the cause of backscatter variations. A sea ice classification from C-band dual-pol Radarsat-2 imagery-- was performed. The classification on SAR image was based on entropy/alpha differences that were caused by ice type variations. Analysis showed that four ice types (level ice, fast ice, ridged ice, deformed ice and water) were identifiable from dual-pol data. Also two independent analyses that were performed on optical remote sensing imagery (MODIS) supported the classification results from Radarsat-2 data. Ice types were also determined from L-band SAR data and single polarization C-band data to characterize dependence of backscatter properties on surface type (roughness). The backscatter properties of ice types detected from RADARSAT-2 (C-band, HH/HV) were compared with single-pol data from Palsar L-band (HH), ERS (W), and ASAR (HH). Results showed that while C-band data was better for monitoring small scale ice deformations, the inclusion of L-band data improved significantly the analysis in snow covered ice regions in the coastal zone. The study provides additional information for enhanced ice monitoring in small areas (e.g. harbours, coastal zone) using high resolution data at multiple bands and polarizations. [C3472]

### "Design of a correlated Lognormal distributed sequence generator based on Virtex-IV series FPGA"

Proposed is a hardware correlated Lognormal distributed sequence generator based on the Virtex-IV XC4VFX100-10 FPGA. The random number is generated by the improved Tausworthe architecture and the non-correlated Gaussian random sequence is generated by Box-Muller algorithm. The correlated Lognormal distributed sequence is generated by zero memory non-linearity transformation with the proposed digital architecture. The complex cepstrum is used in the proposed frequency filter to generate the correlated coefficient. The logarithmic and exponential functions are calculated with CORDIC IPCore. The implementation on FPGA occupies 4210 slices, 4 block RAM and 2 DSP48s. The numeral experiment show the feasibility and accuracy of the proposed method. This proposed Lognormal distributed sequence generator can be used as a key component in a hardware radar echo and clutter simulator. [C3473]

### "SAR imagery and Seatrack Web as decision making tools for illegal oil spill combating-a case"

### study"

The number of marine pollution arising from illegal oil discharges from ship tank or bilge pumping is much greater than those spectacular ship accidents. Illegal spills are mainly detected on essential navigation routes. In every country, marine surveillance agencies are responsible for oil spill combating and on identification of illegal polluters. They rely on information that has been provided on potential oil spills by responsible institution. The first information is usually provided by satellite remote sensing. The decisions about oil combating action is taken based not only on SAR imagery, but checking confirmation from aerial surveillance and using oil spill modeling, also. SAR imagery and aerial surveillance does not provide information about the type of spilled oil, which is important input information for oil spill modeling. Different types of oil have different behavior in water and may affect the decisions about which oil combating activities should be taken. The aim of this study was to show how different type of oil behaves in water according to the Seatrack Web oil drift model, which is the main modeling tool of Estonian Border Guard who is responsible in oil combating. Current study is based on illegal oil spill accident that happened in the eastern Baltic Proper on 10 April 2010. Potential oil pollution was detected on SAR image at 9:08 UTC. Consecutive SAR image was obtained at 9:40 UTC showing no significant change of the slicks area and shape in such a short time. Oil pollution was also confirmed by aerial surveillance at 11:10 UTC. Report that was based on visual observations said that it was probably a bilge water, which started to vanish due to ship traffic. The pollution was also recorded by Side Looking Aperture Radar (SLAR). Seatrack Web model (STW) was used for the forecast of oil slick drift. The input of light and medium oil was chosen. The results showed rather different results about oil drift as well as about oil fate. In case of med--ium oil 20% of oil was expected to evaporate within a couple of hours and the rest stayed in water surface. In the case of light oil 20% was evaporated, but the rest of the oil was expected to disperse in to the water column and emerge on the surface in time to time. The light oil was simulated to drift to the NWW, while medium oil to the SW. Laboratory analyses of the sample that was taken at 14:30 UTC showed that heavy fraction of the oil (hydrocarbons C16-C36) was maintained in the water until then. In conclusion, this study shows that the information about the type of spilled oil is needed as soon as possible after the oil detection to make appropriate decision on oil combating activities. [C3474]

### "Advancing coastal upwelling observations with use of SAR data: Case study from SE Baltic"

Nowadays exploitation of satellite data, mostly infrared and visible, became a regular practice for upwelling detection and analysis. At the same time these types of satellite data strongly depend on sun illumination conditions and cloud cover, with the latter being very limiting factor specifically for the Baltic Sea. In this case SAR (Synthetic Aperture Radar) imagery not affected by clouds and with high spatial resolution can significantly contribute to upwelling observations. The aims of this study are to show how SAR complements both in situ and satellite optical data, and to examine general SAR limitations to observe sea surface temperature (SST) fronts associated with coastal upwelling. [C3475]

### "Active Traffic Management applications in Greece. The case of Attica Tollway"

Active Traffic Management (ATM) has been recently gaining a lot of attention world-wide after the successful implementation in M42 in the UK. The primary goal of ATM applications is the reduction of traffic incidents and the resulting improvement of traffic conditions. Dynamic traffic management practices can have different impacts and effectiveness in different networks. This paper discusses the opportunities and challenges related to the use of ATM in Greece and presents empirical results from the first related applications in the Attica Tollway. Furthermore, a statistical analysis of data collected from the Attica Tollway application is performed, aiming at investigating the impact of speed-limit messages on traffic flow. [C3476]

### "Visual confirmation of mobile objects tracked by a multi-layer lidar"

Integrity of the information provided by a perception system is crucial for advanced driver assistance systems intended for safety applications, like obstacle avoidance systems. A method to ensure integrity is to use different kinds of perception sources. Lidars are key sensors for multiple objects detection and tracking. Stereo vision systems (SVS) can be used to improve the tracking but, in this paper, we use also SVS to confirm the real existence of potential obstacles thanks to 3D dense reconstruction in focused regions of interest. Synchronization issues between the different sensors are addressed using predictive filtering. The proposed approach is evaluated in real conditions thanks to five use cases relevant to urban situations. Results show that this visual confirmation strategy is efficient. [C3477]

### "A new method for robust far-distance road course estimation in advanced driver assistance systems"

An advanced method for road course estimation is presented. It is based on the state-of-the-art Kalman filter

lane detection and allows for a robust sensor-based estimation of road courses in great distances. Only the parameters for the road course are estimated which results in a reduced parameter space and therewith more robustness. Instead of laterally displaced single feature points tangential structures are used as measurements in the filter model. Therefore the method is translation-invariant and applicable for all continuous differentiable road course models. As shown with video and radar input examples it is also sensor-independent and particularly suitable for sensor fusion approaches. For accuracy estimations an advanced method based on inertial navigation is used which is independent of lateral movements of the host vehicle and the road model. [C3478]

### "Ground truth evaluation of the Stixel representation using laser scanners"

Modern real-time dense stereo vision provides precise depth information for nearly every pixel of an image, indicating stereo cameras as a key sensor for future vehicle safety systems. Efficient analysis of this large amount of data by different tasks running in parallel asks for a medium level representation that decouples application specific analysis from low-level vision. Recently, the so called "Stixel World" has been proposed. It models the objects in the scene, implicitly separates them from the ground plane, encodes the freespace to maneuver and thus represents the scene in a highly compact manner that supports different recognition tasks efficiently. The potential of this new representation depends on the accuracy that can be achieved. Therefore, this paper analyzes the precision of this representation using a high performance laser scanner as reference sensor. The statistical analysis confirms the high accuracy as expected from visual inspection. [C3479]

### "Signal processing methods for non-contact cardiac detection using Doppler radar"

We investigate two signal processing methods, time and frequency-based approaches, for non-contact cardiac detection. A 5.8-GHz Doppler radar sensor was used for non-contact measurement of respiration and heart rate from stationary and semi-stationary subjects at a distance of 0.5 to 1.5 meters. We report on the accuracy of the heart rate measurements obtained using the two signal processing approaches, as compared to a reference heart rate obtained using a pulse oximeter. Simultaneous Photoplethysmograph (PPG) and non-contact sensor recordings were recorded over fifteen minute periods for five healthy subjects (4M/1F, ages 29.2±4.32 yrs) One algorithm is based on extraction of heart rate using spectral analysis and a second algorithm is based on automated detection of individual peaks associated with each cardiac cycle. Peaks were also extracted manually for comparison with the automated method. The peak-detection method was less accurate than the spectral method but suggests the possibility of acquiring beat by beat data. It was found that the signal SNR affects the ability to detect heart rates. An increase in SNR could lead to more accurate rates being obtained. The results described provide an estimate of the accuracy expected when measuring heart rate using a Doppler radar sensor. Non-contact measurement of heart rate will be useful in chronic disease monitoring for conditions such as heart failure and cardiovascular disease. [C3480]

### "Estimating surrounding vehicles' pose using computer vision"

This paper presents a computer vision-based approach to tracking surrounding vehicles and estimating their trajectories, in order to detect potentially dangerous situations. Images are acquired using a camera mounted in the egovehicle. Estimations of the distance, velocity and orientation of other vehicles on the road are obtained by detecting their lights and shadow. Because 3D information is not readily available in a mono-camera system, several sets of constraints and assumptions on the geometry of both road and vehicles are proposed and tested in this paper. Kalman filters are used to track the detected vehicles. We also study the advantages of tracking the vehicles in road space (world coordinates), or tracking the position of the lights and shadows on the image. The performance of the approaches is evaluated on video recorded in urban environment. [C3481]

### "Telecommunication systems enabling real time navigation"

Traffic is one of the most important problems in industrialized countries: roads are getting more and more crowded, especially during rush hours, with heavy consequences on people's quality of life, accidents, pollution, and fuel consumption. The transmission of up-to-date traffic information to on-board navigators would allow the redistribution of traffic flows over alternative routes, thus reducing road congestions and slowdowns. In this paper we investigate the possibility to send the information on the average-speed in any road of interest to on-board navigators by means of current broadcast and unicast communication technologies. A discussion on the most convenient transmission strategy will also be given with reference to real scenarios. [C3482]

### "AngelCare mobile system: Homecare patient monitoring using Bluetooth and GPRS."

The quick progress in technology has brought new paradigms to the computing area, bringing with them many benefits to society. The paradigm of ubiquitous computing brings innovations applying computing in people's daily life without being noticed. For this, it has used the combination of several existing technologies like wireless



communications and sensors. Several of the benefits have reached the medical area, bringing new methods of surgery, appointments and examinations. This work presents telemedicine software that adds the idea of ubiquity to the medical area, innovating the relation between doctor and patient. It also brings security and confidence to a patient being monitored in homecare. [C3483]

#### **"Clutter isolation and cardiac monitoring using harmonic doppler radar with heterodyne receiver and passive RF tags"**

A harmonic radar employing the use of harmonic passive RF tags can be successfully used to isolate the human respiration from environmental clutter. This paper describes the successful use of heterodyne receiver architecture with Doppler radar to track the heart-rate of a human being using passive body-worn harmonic tags in presence of a controlled noise generator at distances up to 120 cm. The heterodyne system results have been compared with those of a conventional Doppler radar for cardiopulmonary monitoring that fails to isolate the noise from heart-rate in presence of a noise source. [C3484]

#### **"Design radar signal interface for navigation Radar/ARPA simulator using radar display"**

Using radar/ARPA simulators for seafarers training is made mandatory by International Maritime Organization (IMO) as early as 1978. This paper presents a new radar simulator using one PC, one radar signal interface and one radar display. PC generates radar echo of any sea area and simulates all kinds of radar echo effects and features. Then the radar signal interface receives the radar echo through PC USB and outputs all kinds of signals to radar display. In the interface, lots of logical circuit is implemented by CPLD, which largely simplifies the design and improves the flexibility. Seafarers can operate the radar display in simulated environment of any sea area in Radar/ARPA Operation training. It provides more flexibility and fidelity and effectively improves the training effect. The result shows that this type of radar simulator meets with the requirements of radar simulator standard completely and has been used in our full mission ship handling simulator successfully. [C3485]

#### **"2D Beamforming for Through-the-Wall Microwave Imaging applications"**

Recently, microwave imaging has received a considerable amount of interest with respect to other imaging techniques. A large number of studies rely on microwaves, as a powerful electromagnetic tool to retrieve physical and electrical properties of penetrable and impenetrable objects. The capability of microwave signals to penetrate light opaque materials and sense distant or inaccessible objects with reasonable spatial resolution makes them attractive for different industrial, civil and medical applications. Our Through-the-Wall Microwave Imaging (TWMI) radar system facilitates us to detect and localize objects behind the wall. Measurements with mono-static radar configuration are made with various sizes of metallic materials inside the room with wooden wall (of known thickness and dielectric constant) using 2D antenna positioning assembly and scattering data is recorded in frequency domain. The simple and fast algorithm for compensation of different wave velocity inside the wall is used and the measured raw data is processed with 2D SAR Beamforming algorithm in time domain to reconstruct the image of the targets behind wall. This paper provides an overview of the basic concepts, foundation prototype system of TWMI, SAR Beamforming algorithm and Comparison of Various matched filter approaches and their effects on quality of image are elaborated in detail. [C3486]

#### **"A cascade classifier applied in pedestrian detection using laser and image-based features"**

In this paper we present a multistage method applied in pedestrian detection using information from a LIDAR and a monocular-camera mounted on an electric vehicle driving in urban scenarios. The proposed method is a cascade of classifiers trained in two subsets of features, one with laser-based features and the other with a set of image-based features. A specific training approach was developed to adjust the cascade stages in order to enhance the classification performance. The proposed method differs from the conventional cascade regarding the way the selected samples are propagated through the cascade. Thus, the subsequent stages of the proposed cascade receive both negatives and positives from previous ones, relying on a decision margin process. Experiments were conducted in off-line mode, for a set of single component classifiers and for the proposed cascade technique. The results are compared in terms of classification performance metrics and ROC curves. [C3487]

#### **"Communicating Driver Intent: A Layered Architecture for Cooperative Active Safety Applications"**

The great promise of vehicle to vehicle communications includes a reduction or even elimination of collisions and fatalities on roadways, especially of those due to driver error. A major roadblock to the effectiveness of these systems is the market penetration of cooperative Driver Assistance Systems. Many proposed and existing implementations of cooperative systems are only effective if a majority of vehicles are capable of cooperating. We propose the use of a Layered Architecture for Cooperative Active Safety Applications (LACASA) that includes

driver behavior or intent prediction as a fundamental building block for cooperative assistance systems. Simulation results show how such information could improve safety even in limited-deployment scenarios, and in wide-scale deployment, unsafe maneuvers are nearly eliminated. [C3488]

#### "Design and implementation of an OS-CFAR processor based on a new rank order filtering algorithm"

A novel rank order statistic calculation algorithm for OS CFAR is presented. OS CFAR gives improved performance in a multitarget environment as compared to CA CFAR. However, the computational requirements of sorting data arrays complicate its implementation. We present an algorithm to overcome this challenge by employing a rank order statistic finding algorithm coupled with the exploitation of parallelism offered by FPGAs. In this technique previously computed results are used to successively divide the data array in order to find the new rank order value. The design is tested on MTI processed data from a TA-10K air traffic control radar and is part of a single chip FPGA based radar signal processor. It is implemented on a Virtex-4SX35 FPGA using the Xilinx XtremeDSP kit. [C3489]

#### "A quantitative assessment of the compatibility of Ultra Wideband with radiolocation services"

In this coexistence study, the effect of an Ultra Wideband (UWB) MB-OFDM signal, as defined in the ECMA-368 standard, on an S-band radar device working in the 3.1 GHz to 3.4 GHz range is investigated. An extensive series of 6460 measurements, done with 20 different radar waveforms and for various radar and UWB signal levels is analyzed, using a laboratory test bed specifically designed for this purpose. The interfered radar signal is acquired by a spectrum analyzer and then processed on a stand-alone PC. Different post-processing techniques are applied, depending on the type of the selected radar receiver structure. [C3490]

#### "Layered Media Q Estimation for GPR signal processing using the frequency shift method"

Layered media attenuation algorithm using constant Q model for ground penetrating radar (GPR) signals processing is introduced in the paper. We can use different Q value to describe different layered media. Over the bandwidth of a GPR wavelet, the attenuation of electromagnetic waves in many geological materials is approximately linear with frequency. As a result, the change in shape of a radar pulse as it propagates through these materials can be well described using one parameter, Q, related to the slope of the linear region. Under the assumption of a frequency-independent Q model, we present a method for the estimation of layered media Q from GPR data based on a technique developed for seismic attenuation tomography using the frequency shift method, Q is computed from the downshift in the dominant frequency of the GPR signal with time. And the downshift is obtained by using the generalized S-transform. Tests on synthetic vertical radar profiling (VRP) data indicate that this method can be very effective at estimating layered media Q value of GPR signals. [C3491]

#### "Implementation of high performance signal processing system to generate spaceborne SAR imagery products"

To produce different levels of spaceborne SAR imagery product, a real-time/near real-time signal processing system is discussed. Based on analysis of optimization of SAR signal processing algorithm, especially in CS imaging and normal geometric correction for level 1-2 product, the implementation of these algorithms on specific hardware is elaborated. The structure and design of the entire system provide great flexibility and high performance. Finally, some experiments and tests have been carried out to verify the feasibility of the system in high-resolution SAR signal processing. [C3492]

#### "SAR image data compression based on contrast modulation and warped wavelet Markov modeling"

SAR image compression is very important in reducing the cost of data storage and transmission in relatively slow channels. In this paper, we propose a compression scheme driven by sharpness and contrast, rich texture information included in SAR images and speckle noise reduction within the wavelet framework. Firstly, we modulate and enhance the contrast of the original data in different scales using contrast pyramid, and then we use warped wavelet transform to capture geometric features of different scales. Finally Markov models are used to quantify how well a particular arrangement of wavelets fits our notion of edge structure. Compression performance is evaluated through subjective inspection, as well as objective performance measurements. Results clearly demonstrate the superiority of this new approach when compared to conventional SPIHT and JPEG systems. [C3493]

#### "The character inversion of the mid-course missile based on the sphere-ellipse model"

This paper is for the identification from the RCS sequence of the mid-course missile. On the base of analyzing its motion and electromagnetic scattering characteristic, a new method using RCS magnitude changes with respect to the object gesture angle for extracting the mid-course object's two-dimensional length is presented. Comparing with the traditional method, the new method overcomes the disadvantage of the necessity for the maximal and minimal RCS value of the object. The experiment results tested by the simulated and anechoic chamber data of the representative missile object show the effectiveness of the method. [C3494]

#### **"A modeling method of radar seeker in the presence of electronic warfare"**

Due to the requirements of evaluating the performance of the radar seeker in the combat conditions or in the presence of electronic warfare, this paper gives a design of A Sensitive and Generalization Modeling of The Radar Seeker simulation system, and describes its Modularization, Parameterization, Interface support, Sensitivity Analysis Support design method, a pulse Doppler radar seeker based simulation system which is designed according to the method is given in details, the working flow of the simulation system and conclusions are given at last. [C3495]

#### **"Analysis and improvement for Proportional Conflict Redistribution rules"**

The Proportional Conflict Redistribution (PCR) rules based on Dezert-Smarandache theory (DSmT) is a useful method for dealing with uncertainty problems. It is more efficient in combining conflicting evidence. Therefore, it has been successfully applied in identity identification. However, there exist shortcomings in PCR rule. So in this paper we propose a new improved rule which is based on new Proportional Conflict Redistribution. The six PCR rules (PCR1-PCR6) and improved PCR rule are analyzed and compared through numerical examples, and the results show that the improved rule is effective. [C3496]

#### **"Design and realization of a radar simulation system base on CPCI bus"**

In this paper, design and implementation of a radar signal simulation system is introduced. It is based on standard CPCI bus and follow the design principle of standardized, modular and extendable in design process. This system is made up of standard hardware and the simulated waveform can be obtained from any algorithms. This system is flexible to extend based on complexity of the algorithms. [C3497]

#### **"Doppler estimation and data detection for underwater acoustic ZF-OFDM receiver"**

A new scheme for Doppler estimation and data detection for OFDM underwater acoustic communications is derived in this paper. We design the OFDM symbol as a concatenation of two sub-blocks. The first one is shorter and carries out few data with few subcarriers whereas the second one contains both informative and pilot symbols. The first sub-block serves to estimate the Doppler scaling factor while the pilots in the second sub-block are used for estimating the equivalent channel. Both estimation approaches are based on high resolution methods for solving harmonic retrieval problems in time and frequency domains respectively. Each sub-block contains a cyclic suffix, which allows having more data to be processed. The effectiveness of the proposed scheme is evaluated by means of simulation results. [C3498]

#### **"Advances in vegetation management for power line corridor monitoring using aerial remote sensing techniques"**

This paper presents a comprehensive discussion of vegetation management approaches in power line corridors based on aerial remote sensing techniques. We address three issues 1) strategies for risk management in power line corridors, 2) selection of suitable platforms and sensor suite for data collection and 3) the progress in automated data processing techniques for vegetation management. We present initial results from a series of experiments and, challenges and lessons learnt from our project. [C3499]

#### **"Over head line real-time tracking for automatic inspection or user interface enhancement"**

Power line maintenance inspection builds around real time signal processing and mobile robotics techniques. The authors show how to take advantage of hardware and software dedicated to inspection to improve the process. Hardware solutions are first developed on the ground and later transferred to airborne systems when airworthiness compliance is verified. Over-head line tracking is based on a two stage procedure: a coarse LiDAR tracking followed by a refined video tracking. Automatic tracking allows for surveys to be carried autonomously while inspectors focus on higher level issues. Real time is essential to assist the airborne inspection crew and to improve safety. Investigation of helicopter accidents directed the research towards practical tools that minimise inspection risk. Also, real time is an effective feature to build confidence in the robotics system, improve human efficiency and reciprocally, to improve the robotics with human know-how. [C3500]

### "Micro-Doppler extraction from ballistic missile radar returns using time-frequency analysis"

The spinning motion of a ballistic missile (BM) induces periodic frequency modulations on the returned radar signal. This micro-Doppler modulation frequency is a stable and unique parameter in radar target recognition. This paper first establishes the radar signal model of the spinning missile during flight, and then extracts the micro-Doppler modulation frequency through analysis of the periodic structure of the resulting spectrogram (short time Fourier Transform (STFT))-i.e., the time-frequency distribution (TFD). In order to be used for BM target recognition we implemented a data-dependent optimal window length for the STFT. We treated the resultant TFD as an image and then used the 2-D DFT/FFT for feature extraction. Experimental results illustrate the validity of the proposed method. [C3501]

### "An inverting method of moisture constant for huge grain pile based on distribution of dielectric constant"

Aiming at the detection of moisture content of grain pile, we proposed a scheme in which Ground Penetrating Radar is applied in this paper. The method proposed is that we used a permittivity-moisture model to calculate moisture content indirectly by measuring the distribution of dielectric constant in grain pile. The precise detection is discussed in this paper under the condition of extensiveness and the calculation algorithm of dielectric constant is provided by using layer inverting method based on reflection law and refraction law. In addition, we used well logging method to obtain precise detection results to infer the accurate calibration coefficient required in layer inverting method. By this way, a higher precision can be obtained by the method. At the same time, we proposed a model named permittivity-moisture from nonlinear model of dielectric constant of mixed media. The experiment results indicate that, compared to sampling method, the calculating results of moisture content from the method has less error by combining the layer inverting algorithm and permittivity-moisture model and can meet the requires of application well. Thus can provide a convenient and practical method to the detection of huge grain pile. [C3502]

### "A research of stored grain moisture content detection based on ground penetrating radar detection technology"

The amount of moisture in stored grain is an important factor which affects food safety. Therefore, a timely and accurate detection of the moisture content in stored grain is of great importance. Electromagnetic wave has a strong trait of penetrating, which is able to detect the moisture content of grain inside the heap in the case of non-destructive. This paper mainly takes the research of grain moisture permittivity and its mathematical model which is based on the ground penetrating radar electromagnetic wave technology. It introduces the radar electromagnetic wave theory, construction of granary system's forward model, and the mathematical models of grain moisture permittivity. Through analyzing the results of the continuous section-scan measurement, we get the speed of electromagnetic waves. Then combining grain moisture-dielectric model, we calculate the dielectric constant of grain moisture. Further, we can get grain moisture content through the calculated dielectric constant. Under the guidance of the theory, we carry a field test, collect and analyze the results. It shows that the radar electromagnetic wave measurement of grain moisture is feasible and effective. [C3503]

### "Development of a test-cradle for the p-i-n diode phaseshifters"

Discrete phase-shifters are widely used in modern radars with phased-array antennas. So fast and exact measurement of phase-shifter parameters is important part of their production process. In the paper a design and parameters of the test-cradle for discrete p-i-n diode X-band phase-shifters are described. [C3504]

### "Fuzzy fusion approach for hospital illness tracking"

In multi-target hospital illness tracking, for data fusion, data with noise as input must be sent to fusion center to be filtered, associated, combined and made final decision as output. In this paper, an efficient fuzzy fusion approach for hospital illness tracking is proposed. The proposed approach is developed based on the fuzzy clustering means algorithm, which differs from many other fuzzy logic data fusion algorithms. Performance evaluation and results using simulations are reported, and a comparison with other fuzzy logic approaches based on the results described in other reference is also shown. The efficiency of the new approach has been demonstrated by the fuzzy system performance evaluation. [C3505]

### "Simulation research of microwave automatic clutter-cancellation in life-detection radar"

Clutter signal can bring interference to life-detection radar and reduce accuracy of recognition. This research attempts to resolve the problem in clutter jamming by simulation experiment. The automatic clutter-cancellation



model is established according to theories and experiments are simulated on computer. The result suggests that the variation of auto-cancellation signal is not correlative with time and precision of the cancellation but amplitude and phase of the clutter signal. The result has instructive significance for the design of digital auto-cancellation circuit in life-detection radar. [C3506]

### "Study on adopting optimum binary phase serial to enhance SNR and Penetrating of Ultrasonic Images"

This paper present adopting optimum binary phase serial to enhance signal to noise ratio and Penetrating of Ultrasonic Images. It combine the advanced theory of radar, spread spectrum communication theory and technique of pulse reflection ultrasound imaging. It completely expatiates the feasibility of coded pulse compression technique applied to medical ultrasound system. Since the signal to clutter ratio (SCR) couldn't meet the requirement of medical ultrasound imaging when adopting self-correlation decoding for optimum binary phase serial, this paper presents the CSIFIR(codes spectrum inverse filter) decoding filter and practical and efficient solutions based on the least mean square. The results show the validity of theories and the efficiency of the methods. [C3507]

### "Microwave and millimeter wave nondestructive measurement in biomedical engineering"

Recent microwave and millimeter wave nondestructive measurement in biomedical engineering are reviewed. Millimeter wave reflection from the human skin was studied in the frequency range of 37-74 GHz in steps of 1 GHz. The forearm and palm data were used to model the skin with thin and thick stratum corneum (SC), respectively. To fit the reflection data, a homogeneous unilayer and three multilayer skin models were tested. A novel in vitro test of blood analysis based on the measurement of the dielectric properties at microwave frequencies is reported. The measurements were made using rectangular cavity perturbation technique at the S-band of microwave frequency with the different samples of blood obtained from healthy donors as well as from patients. The measurements are in good agreement with clinical analysis. Noncontact measurement of heart rate variability using a compact 24 GHz microwave radar is developed, without large scale equipment and placing a heavy burden on the monitored individual. This method appears to be promising for future monitoring of stress induced autonomic activation of operators and may reduce stress induced accidents. Finally the technical challenges of microwave and millimeter wave nondestructive measurement in biomedical engineering are discussed. [C3508]

### "Deterministic propagation modeling for joint radar and communication systems"

In this paper investigations on the performances of joint radar and communication systems in realistic traffic scenarios are presented. This is achieved by combining dedicated MatLab models for transmitter and receiver with a deterministic propagation simulator based on ray-tracing. Two different approaches towards a joint implementation of radar and communications with one common transmit signal are regarded. In the simulations in particular the direction of arrival estimation with the reflected signal has been investigated for different waveforms and beam-forming algorithms. [C3509]

### "Security-related active imaging of dielectric objects attached to human bodies"

In the last years, several approaches for the detection of concealed threats at the body of a person have been developed using millimetre-waves. The utilisation of millimetre-waves allows for the detection of both metallic and non-metallic objects. Setups using active illumination mainly exploit coherence between transmitted and received signal to perform beamforming or processing along a synthetic aperture. When dielectric objects should be detected, the assumptions done in these processing steps are often no longer given. The same applies for objects that are placed in front of a reflecting background like the human skin. The effects that can occur for these conditions are discussed in this paper. [C3510]

### "Polarimetric through-the-wall imaging"

A novel full polarimetric beamforming algorithm for Through-the-wall imaging (TWI) is proposed in this paper. The far field layered medium Green's functions are incorporated in the beamformer for the quad-polarizations (VV, HV, VH and HH). Due to the incorporation of the layered medium Green's function, the imaging algorithm not only takes into account the wall reflection, bending, and delay effects but also accounts for the complex EM scattering mechanism due to the presence of the wall. By employing the Green's functions, the solving of a nonlinear equation, needed to find the wave propagation path, is avoided. Similar method can also be generalized to multilayered composite walls such as a hollow-core concrete wall. Simulation results show that the proposed method can provide high quality focused images for TWI applications. [C3511]

### **"New proposal for eliminating interferences in a radar system. Lobes at 45.5° and 24°"**

In this work we present a new proposal to initialize the weights in a Backpropagation Neuronal Network using the coefficients from a FIR Low-Pass Filter, to introduce a null in the radiation pattern in a seven- element array of antennas to eliminate interferences in a radar system. A radar system needs to eliminate the directional noise in order to obtain a cleaner signal. The method used to eliminate this kind of noise (jitter) has to be adaptive because the objective is in constant movement, therefore, the adaptation time must be as fast as possible. Our work is based on the window method to reduce the secondary lobes in fixed arrays of antennas. We modify the radiation pattern by introducing a null at 45.5° which corresponds to the secondary lobe where the interference is presented. This is achieved when we create windows from several FIR Low-Pass Filters. The coefficients of these filters are used to initialize the weight vectors of a Backpropagation Neural Network which performs the adaptive process to obtain the final parameters to achieve the noise elimination. For testing our proposal we calculate the Mean Square Error (MSE), the Signal Noise Relation (SNR) and we graphed the Radiation Pattern. In addition we calculated the Cross Correlation Index, in each iteration, between the desired signal and our results. With this method we reduced the number of iterations required by the process. [C3512]

### **"A human-automation interaction approach to the evaluation of resource allocation strategies in adaptive distributed sensor networks"**

How to design and to evaluate adaptive distributed sensor networks with respect to end user decision making is an important topic in human-automation interaction. This study evaluates four resource allocation strategies (static automation, adaptive sensing, mixed-initiative control, and control incorporating end user task analytic information) in a simulated prototype weather sensor network. Performance of each sensor network resource allocation strategy was assessed with measures of sensor coverage quality over a target geographic region of interest. Coverage measures calculated from the number of radar nodes, tilts and cycles were derived for partial (radar scan touches at least part of the analysis region) and complete coverage of the region by single and multiple (two or more) radars. Single and multi-radar coverage area scores were also derived from the cumulative fraction of the analysis regions area that was scanned. Using three weather scenarios, results show that static automation significantly outperforms the other strategies in all cases using measures of single and multi-radar complete coverage and for a uniformly distributed weather event using single and multi-radar coverage scores. Otherwise the three strategies outperform static automation. As the performance of resource allocation strategies are sensitive to the weather events themselves as well as the measures used to evaluate them, the design of next generation of algorithms should consider these performance distinctions. [C3513]

### **"Collision avoidance in a recursive nested behaviour control structure for Unmanned Aerial Vehicles"**

In this paper, the collision avoidance behaviour in a recursive nested behaviour control structure for Unmanned Aerial Vehicles will be discussed. The architecture is an extension of the behaviour-based recursive control structure, which has been applied successfully to mobile robot applications. The system structure, as an abstraction of multiple cascaded control loops with feedback mechanisms, is robust against disturbances and model uncertainties. The obstacle awareness and collision avoidance are considered to be the most important issues in the field of Unmanned Aerial Vehicles (UAV), thus more attention will be paid to this topic. The collision avoidance utilizes a potential field method tailored for UAV application domain. The formulation of a repulsion forces based on radar sensor measurement is presented. The implementation of the collision avoidance system is also described. [C3514]

### **"Research on the effect of electromagnetic radiation of 220KV power transmission and transformation project on marine radar"**

Taking cross-sea and cross-river 220 KV power transmission and transformation project as the research object, and through field observation and theoretical analysis, mathematical model of power frequency electric field of EHV (extra-high voltage) overhead transmission lines is established. This paper presents the calculation method of electric field intensity around the transmission lines, and analyzes the effect of electromagnetic radiation on radar reflection and the characteristics of radar echo. Finally, according to the research results, measures and suggestions on correct operation and use of marine radar are put forward. [C3515]

### **"A tutorial for applying DMOC to solve optimization control problems"**

This paper presents a detailed procedure to apply newly-proposed DMOC (Discrete Mechanics and Optimal Control) methodology to solve optimal control problems. DMOC is based on a direct discretization of Lagrange-d'Alembert principle for a system. First, this tutorial explains the principle of DMOC, and how to formulate the

problem in DMOC. Next the steps are shown about how to install and configure nonlinear programming solver IPOPT, and how to use the modeling language AMPL. In particular, the user-defined function is involved with AMPL to solve a more complicated problem. Furthermore, a glider example is provided in this tutorial to solve optimal control problem with the user-defined 2D time-varying B-spline ocean current model. The ocean current original data was collected by HF-Radar stations located around Monterey Bay, CA in August 2000. Practically, this tutorial is shown how to use DMOC to solve optimal control problems with IPOPT and AMPL as the components. The possible users are robotic researchers, control system engineers, operations management researchers, and so on. [C3516]

#### "Automatic monitoring and speed violation ticket system"

An automatic speed violation control system is proposed to warn the driver and using SMS communication for transmitting the speed and the unique information of the vehicle to the police station when a speed violation ticket to be issued. The system notifies a driver of certain control details in real time and prevents vehicle violation in advance via warning messages when the vehicle exceeds a safe speed zone, thus eliminating the manpower needed to use radars to check the speed of the cars or examine photographs of speeding vehicles taken by fixed cameras. [C3517]

#### "A random finite set based detection and tracking using 3D LIDAR in dynamic environments"

In this paper we describe a fully integrated system for detecting and tracking pedestrians in a dynamic urban environment. The system can reliably detect and track pedestrians to a range of 100 m in highly cluttered environments. The system uses a highly accurate 3D LIDAR from Velodyne to segment the scene into regions of interest or blobs, from which the pedestrians are determined. The pedestrians are then tracked using probability hypothesis density (PHD) filter which is based on random finite set theoretic framework. In contrast to classical approaches, this random finite set framework does not require any explicit data associations. The PHD filter is implemented using a Gaussian Mixture technique. Experimental results obtained in dynamic urban settings demonstrate the efficacy and tracking performance of the proposed approach. [C3518]

#### "Hybrid SVM-GPs learning for modeling of mitogen-activated protein kinases systems with noise"

In this paper, the hybrid support vector machines (SVM) and Gaussian process (GPs) are proposed to modeling of mitogen-activated protein kinases systems with noise. In the proposed approach, there are two-stage strategies. In stage 1, the support vector machine regression (SVMR) approach is used to filter out the some larger data set in the mitogen-activated protein kinases systems data set with noise. Because of the larger noise data in the training data set are almost removed, the large noise data's effects are reduce, so the concepts of robust statistic theory are not used to reduce the large noise data's effects. The rest of the training data set after stage 1 is directly used to training the Gaussian process for regression (GPR) in stage 2. According to the simulation results, the performance of the proposed approach is superior to the least squares support vector machines for regression, and GPR when the noise is existed in the mitogen-activated protein kinases systems. [C3519]

#### "SAR Autofocus Using Wiener Deconvolution"

This paper proposes a new approach to synthetic aperture radar (SAR) autofocus. The proposed metric-based autofocus algorithm is based on the Wiener deconvolution filter, which has the advantage of the phase error compensation as well as noise suppression. The sharpness metrics are used to measure the degree of the focus of the SAR image. To compare the performance of the metric-based SAR autofocus, we also present a detailed analysis of different sharpness metrics. Then, a guide about the optimal sharpness metric in various SAR scenes is presented. The simulation results with the real data demonstrate that the proposed algorithm has better restoration capability in comparison with conventional minimum-entropy algorithm. [C3520]

#### "Angle Estimation for Bi-static MIMO Radar Based on Tri-iterative Algorithm"

The Bi-static MIMO (multiple-input multiple-output) radar signal modal is established in this paper. And the proper coefficient of the MF (matcher filter) is chosen in order to keep the noise output has the same statistical property as the noise input. To make the computational complexity lower and the convergence speed faster, the signal subspace is used as a dimension-reducing matrix. A novel cost function is proposed based on the LS (least squares), which is solved by using the Tri-Iterative Algorithm. Afterwards, a unique closed solution in each iteration which is posed a typical least square problem is derived and the receiving and the transmitting angles are estimated for bi-static MIMO radar. It is worth mentioning that the estimated angles can be paired automatically. Finally, Simulation results are presented to verify the effectiveness of the proposed method. [C3521]

### "Study on the Time-Frequency Two Dimensional CFAR Algorithm for Moving Targets on Ground in PRC-CW Radar"

PRC-CW radar is mainly used to detect moving targets on ground. Ground clutter heaves fiercely, and its distribution is complex, which makes it difficult to detect targets correctly from time domain. The characteristics of moving targets and ground clutter differ in frequency domain. And the spectrum of targets may change with time, so, this paper designs the time-frequency two dimensional constant false alarm rate(CFAR) algorithm. Based on the analyze of pulse compression and moving targets detection(MTD) of this type radar, the two-dimensional CFAR algorithm is proved to be feasible via simulation. The results of simulation show that, the algorithm can measure the velocity and range of targets correctly. The clutter and noise are also restrained effectively. [C3522]

### "Linearly Constrained Coherent Sidelobe Canceller for Ionosphere Interference Suppression for HFSWR"

In this paper, a linearly constrained coherent sidelobe canceller for high frequency surface wave radar is presented to improve the interference cancellation performance. To overcome the target-canceling problem of traditional coherent sidelobe cancellation algorithm, a linear constrain is applied to the adaptive weight vector of auxiliary array in order to keep this adaptive weight vector within a subspace that is orthogonal to the main beam, so the target echoes in the main beam are well preserved. Measured data from real high frequency surface wave radar system is used to compare the performance of the new algorithm and the traditional one, and the results show that the new algorithm is clearly superior to the traditional algorithm. [C3523]

### "A Detector of DTTB Based Passive Radar Using FRFT and Hough Transform"

Detecting weak moving targets is an important task for digital television terrestrial broadcasting (DTTB) based passive radar. The cross ambiguity function (CAF) suffers from the range and Doppler frequency migrations caused by the velocity and acceleration of the targets. The integration gain can't increase anymore. A new detector is proposed for this problem. In this detector, the fractional Fourier transform (FRFT) is used to compensate the Doppler frequency migration, and the Hough transform is utilized to accumulate the echo of the moving targets during the long integration time. The block diagram and the procedure of this detector are given. Simulation results show that the proposed method can detect weak moving targets effectively. [C3524]

### "Two Methods for Constructing the Difference Set Pairs"

In this paper, by using the nature of Cyclotomic class, presents two new methods for constructing Different Set Pairs. The methods are based on the Cyclotomic class, and different Cyclotomic class could construct Different Set Pairs of Different parameters. New tools for using Different Set Pairs to construct Perfect discrete signal are provided. [C3525]

### "Study on the Method for Radar Signal Receiver Channel Modeling"

A modeling method for radar signal receiver channel is proposed under the situation that part of the mechanism is unknown. Firstly, the traditional identification methods including Levy least square, pulse response and frequency-domain multiply are analyzed. The experiments show that those methods are hard to get the accurate model of high order radar signal receiver channel. Then, a method of time-domain convolution numerical model using frequency response data is proposed. The simulation and experiment shows that the method is implemented easily and applied widely. It improves the efficiency and precision of system simulation and can be applied to other high order system. [C3526]

### "Information selection based on fuzzy comprehensive evaluation"

Under the modern information-based operational environment, the interface receives and processes more and more information, so organizing and selecting operational information in different combat missions are becoming more significant. Based on this background conditions, this paper sets up information selection evaluation index system, confirms the evaluation index weight by using analytic hierarchy process (AHP), and applies fuzzy comprehensive evaluation method to evaluate the importance degree of all operational information in various operational tasks. Finally, according to the importance degree of information in different operational missions, operational information is displayed on interface in reasonable way. [C3527]

### "Recent theoretical and experimental advances in electromagnetic sensing of subsurface profiles"

We present an overview of recent developments in subsurface image formation using iterative profile inversion



and focusing using concepts of tomography and SAR signal processing. Electromagnetic forward and inverse scattering techniques are presented, along with the subsequent focusing techniques. Experimental and simulation results are presented. [C3528]

#### "Large scale underwater FDTD ELF simulations using Acceleware and MPI parallel processing"

Very large FDTD simulations are being developed to determine the underwater propagation of EM signals at ELF frequencies. Two different approaches are being used to handle the large computation spaces, the use of hardware and software by Acceleware, and the use of the Message Passing Interface (MPI) for parallelization. [C3529]

#### "Characterization of layered media using full-waveform inversion of proximal GPR data"

Full-waveform inversion of proximal ground penetrating radar (GPR) data is used to determine the electromagnetic properties of layered media. The radar system consists of a vector network analyzer combined with an off-ground horn antenna operating at ultra wideband. The GPR wave propagation is modeled for a multilayered medium using a recursive Green's function computed in the frequency domain. The antenna and its interactions with the layered medium are modeled using a linear system of complex transfer functions. GPR signals were acquired in laboratory above a two-layered sand medium and two concrete slabs separated by a thin air layer (simulating a fracture). Subsequent inversions permit to retrieve the electromagnetic properties and the dimensions of these thin-layered media. For humid sand, GPR-derived dielectric permittivities showed a good agreement (RMSE = 1.65) with measured volumetric water contents. Dimensions of the three-layered concrete medium could be retrieved with a millimetric accuracy. The method is promising for the non-destructive characterization of multilayered media, including thin layers, owing to the full-waveform inversion of the radar data in a large frequency bandwidth. [C3530]

#### "SIMO-based approach for subsurface sensing"

In this paper, application of near-field digital beamforming for shallow subsurface imaging is described. The main novelty of the approach is SIMO topology of the sensing (single transmit-multiple receive antennas). Dedicated antenna systems and imaging algorithms have been developed in order to take maximal advantages from the SIMO data acquisition. Verification of the approach has been done by development of a radar system for landmine detection. Field tests have demonstrated reliable detection of antipersonnel mines by scanning velocity of 10m/s. [C3531]

#### "An evaluation method of anti-jamming performance to receiver based on sample entropy"

Aiming to make a quick and right evaluation of the anti-jamming performance to receiver, an evaluation method is put forward, in which the sample entropy (SampEn) values of input and output sequences of receiver are evaluation indexes. The analysis of simulation signals' SampEn validates the rationality of SampEn substituting for Signal to Noise Ratio (SNR), because SampEn does not change with the change of signal's amplitude, and monotonically decreases as SNR increases when SNR is in certain range. The evaluation method is able to solve the problem that the SNR gain is difficult to compute, because of the uncertain relation of signal and noise and the distortion in the receiver process. The method can also avoid the huge statistical computing, which achieves the purpose that the receiver's anti-jamming performance is evaluated only by input and output sequences, without any other conditions. Lastly, an experiment validates the feasibility and effectivity of the proposed evaluation method. [C3532]

#### "Information fusion of integrated navigation based on self-adaptive filter"

In order to realize high accuracy and excellent reliability of navigation system, information fusion technology of integrated navigation based on self-adaptive filter is researched in this paper. Inertial navigation system (INS), global navigation satellite system (GNSS), synthetic aperture radar (SAR) and barometric altimeter (BA) are taken to construct INS/GNSS/SAR/BA integrated navigation system. INS is regarded as the primary navigation equipment, and other systems are aided navigation equipments. Firstly, errors of INS, GNSS, SAR and BA are modeled and chosen as system states of integrated navigation. Based on self-adaptive filter algorithm, output information of INS and GNSS are fused in INS/GNSS integrated navigation filter, and output information of INS, SAR and BA are fused in INS/SAR/BA integrated navigation filter. Then the federated filter frame is designed, and estimations of system states from INS/GNSS and INS/SAR/BA local filters are fused once more in the master filter independently. Consequently global optimal estimations of system states are given by the master filter, which are used to correct errors of INS. Simulation results show that, position accuracy of INS/GNSS/SAR/BA integrated navigation reaches  $\pm 11.6\text{m}$ , attitude accuracy reaches  $\pm 0.52'$ , velocity accuracy reaches  $\pm 0.14\text{m/s}$ , and its reliability is very excellent when noise statistics characteristics of some navigation

equipment are variational in the navigation process. [C3533]

#### "Safety issues and damage to equipment with both Smart Grid and home network connections"

Equipment getting power from the Smart Grid often has connections to the home network, a configuration which during a lightning storm is prone to safety issues and damage. Lightning can occur as direct strikes to a service, or as nearby strikes which induce currents in a service. Protection against these events is important, and existing standards deal with these. But there is a situation that existing standards have not considered, and it can result in a shock hazard and equipment failure. This potential failure is caused by Ground Potential Rise (GPR), in a site which has two or more ground references; for example AC power grounded at the service entrance at one side of a house, and a phone line grounded via a surge protector at the opposite side. The GPR produces a voltage gradient between the two ground references. This high voltage is a potential shock hazard. It can also cause a breach of basic or enhanced insulation, with damage and potential exposure to hazardous voltages resulting. This paper discusses GPRs; how to test an equipment to see if a GPR will cause a problem; and what to do if it does. [C3534]

#### "Design of sewage flow remote monitoring system over GPRS network"

In this paper, a new sewage flow remote monitoring system over General Packet Radio Service (GPRS) is presented, which monitors the sewage flow parameter remotely in real time. In the proposed system, GPRS network is adopted as the wireless sensor network, and the data between the slave computer and the remote terminal are transmitted via the GPRS and Internet networks. Finally in the remote terminal, the Winsock control of Visual Basic 6.0 is responsible for displaying, storing and analyzing the data of the sewage flow. The system is easy to implement and has a high degree of automation, by which the acquisition, transmission and processing of the sewage flow data can be achieved in wireless, networked and intelligent manners. [C3535]

#### "Improvement of image resolution in ScanSAR simulation"

For spaceborne ScanSAR system, the wide swath is the advantage whereas it induce some problems. In this thesis the importance of accurate geometry model for ScanSAR simulation is fully analyzed. A SAR geometry model based on valid coordinate systems is proposed. It provides actual phase history and echo not only for ScanSAR but also traditional SAR system. The simulation shows that it is effective and practical. [C3536]

#### "Water objects extraction from polarimetric SAR imagery based on blind source separation and morphological reconstruction"

The SOMMR nonlinear blind source separation (BSS) method is proposed for speckle noise suppression and water objects extracting from synthetic aperture radar (SAR) imagery based on self-organizing maps (SOM) neural networks and morphological reconstruction (MR). The multiplicative speckle noise and image data are separated from multipolarimetric imagery by means of SOM neural networks. Morphological reconstruction is employed to remove the residual noise. The experimental results using ENVISAT ASAR polarimetric imagery show that the proposed method can extract water objects accurately, and the speckle noise index is better than ICA and SOM method. [C3537]

#### "Infrared object tracking based on particle filter"

A novel infrared moving object tracking method based on particle filter and mean shift algorithm is presented in this paper. Based on the framework of particle filter, the mean shift algorithm is introduced as better proposal distribution to improve the sampling efficiency. Compared to conventional particle filter, the proposed method uses much fewer particles to maintain the multi-mode distribution, and overcomes the degeneration problem effectively. Experimental results on sequential images show that our method can track steadily when the object move fast or be occluded, the overall performance of the proposed method is better than traditional particle filter algorithm. [C3538]

#### "The target detection for GPR images based on curve fitting"

Due to the complexity of the medium composition, physical characteristics and the spreading of electromagnetic waves, the extraction and automatic target detection of the Ground-penetrating Radar (GPR) is extremely complicated and has become an important issue in the practical application of GPR. In this paper, a method based on curve fitting is proposed by using the hyperbolic echo characteristics. The edge lines of GPR images firstly obtained by using image preprocessing methods and hyperbolas are fitted to approximate the edges. Finally, hyperbolic echo apex positions in the GPR images are extracted and marked on their apexes. The experimental results show that all targets are detected correctly. [C3539]

### "Target detection algorithm for spatial diversity MIMO radar with space partition"

For spatial diversity multiple input multiple output (MIMO) radar, target echo signals received by its widely separated antennas may be semi-correlated and different in SNR. According to the correlation and SNRs of received target echo signals, a space partition based target detection method is proposed, which partitions the surveillance volume into two sections, one using the coherent accumulating detector and the other using the incoherent accumulating detector. The partition method is shown to achieve an improved detection performance at a low computation cost. [C3540]

### "A model based bias field correction algorithm for SAR sea ice image"

A novel algorithm using multi-exponential model is presented in this paper for correcting the intensity bias field, produced by the variation of SAR incidence angle along SAR range direction, in SAR sea ice image. In the algorithm, the image's mean values along SAR azimuth direction are calculated firstly. Then a one-dimensional correction field is modeled by a multi-exponential model. Whereafter, the one-dimensional correction field is calculated by applying entropy minimization method. After that the original image is corrected by the two-dimensional correction field derived from the one-dimensional correction field. The experiment result indicates that the proposed algorithm is effective in correcting SAR sea ice image's incidence angle bias field. Besides, the proposed algorithm has better correction result than Karvonen's method and it does not need the incidence angle information of the image pixels. [C3541]

### "CFAR and KPCA for SAR image target detection"

A SAR target detection model based on CFAR and KPCA is presented in this paper. This Detection is divided into a pre-screening and discrimination process. Within the large-scale and low-resolution SAR imagery, pre-screening adopts classic CFAR techniques, while the discrimination process adopts kernel principal component analysis to separate the target from clutter. Experimental results show that the detection performance of our algorithm appears to be superior to the classic CFAR methodology. The combination of both pre-screening and prior knowledge of targets can effectively enhance detection rate and inhibit false alarm at the same time. [C3542]

### "Improved denoising method of SAR image"

The reduction of speckle in SAR image is necessary for processing of SAR image such as feature detection and extraction. In Contourlet transform, a drawback of Laplacian pyramid (LP) is implicit oversampling and non-orthogonal decomposition, Wavelet transform is a critically sampled scheme but it only generated three direction. Taking advantage of Wavelet and Contourlet, the proposed method is complemented by Wavelet transform in conjunction with directional filter banks. First, the proposed method derived Wavelet coefficients of entry image by Wavelet transform, then reconstruction the image only by lowpass coefficients and after processing it can derive a highpass subbands. The proposed method keeps critical sampling and it is convenient for direction filter banks partitioning the highpass subbands. The results show that the proposed method can eliminate the noise, keep edge information effectively and also avoid artifacts over Wavelet and Contourlet transform. [C3543]

### "Realization of high data rate DUC based on FPGA"

This paper discusses the issues on "how to save multiplier resource" and "how to cope with high data rate", when implementing Digital Up Converter (DUC) with Field Programmable Gate Array (FPGA). A novel implementation structure of poly-phase interpolation filter is proposed, which could reduce the consumption of multiplier by half. Parallel processing is adopted in designing Numerical Controlled Oscillator (NCO), which could generate high data rate LO required. By following these methods, a DUC module is designed for certain radar IF echo simulator, which could generate digital IF signal with data rate up to 1.2Gsps. [C3544]

### "Signal analysis of downward-looking and forward-looking array FMCW SAR"

Downward-looking and Forward-looking (DL & FL) array Synthetic Aperture Radar (SAR) can image scene beneath and in front of the platform that can not be realized by side-looking (SL) SAR. According to curve sketch of equidistance and equi-Doppler, blind zone beneath the platform and ambiguity symmetrical to the track of SL SAR are analyzed, and DL & FL array Frequency Modulated Continuous Wave (FMCW) SAR signal model is established. By virtue of signal model, expansions of range course in different forms are applied in analyzing Doppler characteristic and Range Cell Migration (RCM). Parameters affecting cross-track resolution, such as array length, target position and platform height are analyzed combining with effective array aperture. Simulation results show optimization and effectiveness of the parameters, which can provide reference for parameter design

of array SAR. [C3545]

### "Adaptive-adaptive beamforming algorithm of planar array based on one-dimensional auxiliary beam"

To avoiding two-dimensional search for the incoming angle of jamming while constructing two-dimensional auxiliary beams, an adaptive-adaptive beamforming algorithm of planar array based on one-dimensional auxiliary beam is presented in this paper. Owing to only need to estimate one-dimensional spatial angle of jamming, computational complexity of searching for the incoming angle of jamming can be reduced greatly. Thus, the approach is fit for engineering implementation. Computer simulations demonstrate the validity finally. [C3546]

### "Automated road extraction from LiDAR data based on intensity and aerial photo"

A clustering method based on intensity data is used to extract road from LiDAR data in this paper. And the result is refined by using the spectrum information of aerial images. An experiment is performed with a group of LiDAR data in BeiJing. The results presented in this paper have shown that clustering method based on intensity could extract road in some extent, but many error points exist at the same time. When fusing the spectrum information of aerial images, the experiment result is improved obviously. Large amount of error points is removed, while the point cloud of road keep down. [C3547]

### "Despeckling SAR image using nonsubsampling directionlets combining with GSM model"

As speckle noise suppression is important for Synthetic aperture radar (SAR) images processing, this paper presents an approach for SAR image despeckling based on nonsubsampling directionlets. Firstly, images are partitioned into subbands using nonsubsampling directionlets. Then, the coefficients of subbands are modeled with Gaussian scale mixtures (GSM). Besides, for reducing the speckle noise, coefficients are estimated by Bayes least square estimation. Lastly, to evaluate the performance of this despeckling method, four performance evaluation parameters are used. Experimental results show that this method performs better in comparison with the spatial filter and standard wavelet transform not only in speckle suppression, but also in detail preservation. [C3548]

### "A general radar surface target echo simulator"

A general radar echo simulator system proposed in this paper is to satisfy the various needs of the radar signal processor testing. This simulator is based on the type of echo data playback device, the surface target echo data is pre-calculated and stored in the device at first, then according to the external timing PRI signal, echo data is read out to the device processor, on which target information is modulated and interpolation operation is made. After the DA Converter, the radar echo is created. The system is simple and easy to implement general. [C3549]

### "Classifying multisensor images by support vector machine in Chongming Dongtan"

Optical remote sensing (ORS) technology has been extensively used for the investigation of the environment and resources. Considering it is heavily constrained by the weather conditions, especially in the coastal zone, the round-the-clock SAR (Synthetic Aperture Radar) data are chosen to compensate for the shortcomings of optical data. In this paper, we will use the fusion image of ASAR and TM to identify five land cover types in Chongming Dongtan. And the SVM algorithm is adopted because of its capability to take numerous and heterogeneous parameters into account. Results have been shown that the fusion data of SAR and ORS is particularly suited to account for the rainy and cloudy weather in costal zone. And the SVM algorithm has attained a high level of classification performance with the overall accuracy 90.83%. [C3550]

### "The mechanism of Pt films to suppress the electron emission of grid in TWTs"

Pulsed grid-controlled traveling-wave tubes (TWTs) are widely used in the field of space and defense for navigation and directing of radars, aircrafts, satellites, and guided missiles. In order to attain even higher frequency and power requirements, gun designs for modern microwave tubes have utilized grids, which are very close to cathode. However, during the course of the TWTs work, electron emission substances such as Ba and BaO on the cathode can be evaporated and deposited on the counter electrode. Harmful electron emission from the grid, namely, grid emission, is very likely triggered, this in turn destroys the working condition of the controlled traveling-wave tube, making it necessary to suppress the electron emission properties of the grid. Pt films as an anti-emission material have been widely used, but little is known about its electron emission suppression characteristics and surface composition at high temperature when grids works. In our investigation, Pt films were deposited onto the surface of the molybdenum grids by ion-beam-assisted deposition (IBAD). The



mechanism for electron emission suppression of the molybdenum grid coated with Pt films is discussed. [C3551]

#### "94 GHz, CW, low-voltage gyrotron"

Gyrotron are the primary high-power source of millimeter waves. Although the application of electron cyclotron heating of fusion plasmas has been primarily responsible for the gyrotron's development, many other applications exist, including millimeter-wave ceramic sintering, high-density communications, and high-resolution radar within the atmospheric windows of 35, 94, and 140 GHz. One problem with high-frequency gyrotrons is the strong magnetic fields required to satisfy the fundamental electron cyclotron resonance condition. For example, a 35-kG magnet would ordinarily be needed to generate 94 GHz at the fundamental cyclotron frequency. However, by operating the gyrotron at the sth cyclotron harmonic, the required magnetic field can be decreased by a factor of s. To develop 94-GHz oscillator that is both compact and efficient is the objective of this work. [C3552]

#### "Application of artificial fish school algorithm in UCAV path planning"

The path planning method based on artificial fish school algorithm (AFSA) was proposed to solve unmanned combat aerial vehicle (UCAV) path planning problem under the 2-D radar threats environment. According to the path planning requirements, the threat detection and artificial fish coding method were designed in detail. Besides, the method of perceiving threats was applied for advancing the feasibility of the path. A comparison of the results was made by WPSO, CFPSO and AFSA, which showed that the method we proposed in this paper was effective. AFSA was much more suitable for solving this kind of problem. [C3553]

#### "Study on aluminate of cathode emission active substances"

Microwave tubes are used at the field of radar, electron counterwork and communication widely. The cathode is the heart of the microwave tube. The impregnated aluminate Ba-W cathode is used most widely. Along with the development of microwave technology, the high performance cathode is necessary with big current density, long life. The performance of cathode is decided by aluminate of cathode emission active substances. Forming method and sintering process are very important to the emission performance of aluminate. This paper studies the emission performance of aluminate forming method and sintering process. [C3554]

#### "Design and implementation of MMS system based on GPRS modem"

Currently MMS systems, most of them existed a lot of problems, such as code confusion, large limitations on Secondary Development, bundled editing and sending. Through studying on GPRS MODEM and mechanism of MMS receiving and sending, a design project for multimedia communication system based on GPRS modem is proposed in this paper. SMIL and NowSMS platform was adopted in the design, to ensure unified coding and receiving and sending interfaces. Also, the separation of editing and receiving and sending improves the efficiency of using the system. By using this method, the MMS system can be easily embedded into other systems. [C3555]

#### "The detection of long chirp signal with small frequency rate in low SNR"

The detection of a long linear frequency-modulated signal (LFM) with small frequency rate is studied in very low signal-noise ratio (SNR). By wigner-hough transform for each subsection of the signal, the LFM signal can collect a peak in each WHT plane. Making use of the character that and the peak moves continuously in multi-frame WHT plane is same as the moving target of a image sequence, a new detection technique combined WHT with image Processing is proposed. The technique is proved out by computer simulation of keeping good performance for this signal. [C3556]

#### "The database of radar echoes from various targets with spectral analysis"

In this paper we describe a database, noted as RadEch Database, containing radar echoes from various targets. The data has been collected in controlled test environments at the premises of Military Academy-Republic of Serbia. Our goal is to provide a balanced and comprehensive database to enable reproducible research results in the field of classification of ground moving targets (pattern recognition). A time-frequency analysis of radar echoes has been performed, in order to identify the main features of the various targets. The RadEch Database is freely available for download and we hope that our database provides researchers with a valuable tool to benchmark and improve the performance of classification algorithms. [C3557]

#### "An instances sampling approach based on cellular automata for ensemble learning"

As the instances that are difficult to classify draw more attention in ensemble learning, an instances sampling

method based on cellular automata is presented. The definition of the instance cellular and the neighbor region are researched, and the instance cellular kernel is designed for describing the cellular structure and cellular dynamics rules. The dynamics transfer rules of the cellular which are suit for instances sampling are investigated by combining the dynamics transfer rule of the cellular automata with the change rule of the instances distribution. The instances distribution is modified according to the transfer rule of cellular automata. An improvable ensemble algorithm is investigated by using of the sampling method base on cellular automata. The experiment results show that our ensemble method is more accurate than those obtained through the standard method. [C3558]

#### **"A novel multi-channel SAR-GMTI algorithm based on raw data"**

This paper presents a novel SAR-GMTI algorithm based on the range-compressed raw data. FrFT is introduced to the classical three-channel DPCA system to realize the moving target detection, parameter estimation and SAR imaging, acquiring an exact GMTI image of accelerative moving targets. As a pretreatment, Keystone transform is firstly applied to process the echoes receiving from each sub-aperture respectively in order to remove the range migration. Our scheme is available even under a clutter-rich and low SNR environment. The simulation results indicate the efficiency of the method. [C3559]

#### **"Super resolution processing of SAR images by Matching Pursuit method based on Genetic Algorithm"**

This paper adopts Genetic Algorithm in reducing the complexity of the Matching Pursuit method in super resolution of SAR images. Firstly, we introduce the attributed scattering model according to the target feature of SAR images. Secondly, we introduce the sparse representation of image based on Matching Pursuit. This sparse representation evolves into a nonlinear optimization problem, which has a huge computational burden. In this part, we also introduce the structure of the Fourier dictionary, from which we search for the atoms to decompose the images. Thirdly, we introduce Genetic Algorithm to solve the nonlinear optimization problem to get a faster computational speed. Then we apply Genetic Algorithm in searching the best atom from the Fourier dictionary for each step of Matching Pursuit. The reason is given why it is possible to get the faster speed via Genetic Algorithm by analyzing the character of Genetic Algorithm itself and its relationship with the problem theoretically. Finally, we program to realize this idea. The computational results of measured MSTAR data demonstrate that Genetic Algorithm match this problem well. Thus the Matching Pursuit method based on Genetic Algorithm is really effective and fast in SAR image super resolution. [C3560]

#### **"A novel ISAR jamming method based on randomly sinusoidal phase modulation"**

In order to jamming ISAR imaging effectively, a novel jamming method based on randomly sinusoidal phase modulation is presented in this paper. This method changes randomly the frequency of the signal of sinusoidal phase modulation in the slow time. How the jamming signal affects the range alignment of ISAR is analyzed in detail. The research result shows that the jamming method can destroy severely the range alignment of ISAR and realize the unfocused image barrage jamming to ISAR. Furthermore, the validity of the jamming method is justified by simulation experiment. [C3561]

#### **"Multiple Sub-Spaces particle filtering for multi-target tracking"**

A new multiple target tracking method based on Bayesian filtering and Sequential Monte Carlo approximating method is proposed in this paper. The key principle of the proposed method is to decompose the multiple target tracking problem into multiple single target tracking problems by allocating Sub-Spaces which are sub-sets of single-target state space to targets. The computational cost of the proposed method is remarkably reduced by avoiding jointly estimating posterior probability distribution used in many conventional multi-target tracking methods. And compared with Finite Set Statistics based methods, the proposed method is more general, moreover, it could supply high level applications with trajectory of moving targets which is not available in Finite Set Statistics based method. The proposed method is tested by tracking pedestrian in video sequence captured from real-world and the tracking result shows that all targets are well tracked in real-time while the number of targets is unknown and varies with time. [C3562]

#### **"Study on pedestrian detection and tracking with monocular vision"**

Pedestrian detection is a rapidly evolving topic in many computer vision applications such as intelligent vehicle, surveillance and advanced robotics. The pedestrian collision avoidance not only requires detection of pedestrian but also requires prediction by tracking to analyze its dynamics and behaviors. The objective of this paper is to provide a method realizing pedestrian detection and tracking based on monocular vision. The first part of the paper is to detect pedestrian from the image. Both the rectangle features and edge orientation features are

calculated by integral image techniques and Adaboost is used to fulfill discriminative features selection and classifiers training. The second part contains a pedestrian tracking method based on Kalman filtering. Experiments are performed to test and verify the pedestrian detection and tracking method under normal urban environments. The experiment results show that the method can detect and track pedestrian ahead of vehicle with different sizes and postures. [C3563]

#### "Wireless communications technologies for energy networks in a non-industrialized society"

It is of great importance to the organisational strategy of the energy utility as well as to the society at large the activities involving the utility and the energy consumer's communication activities. However, we discovered that such communication activities in the poor third world countries with poor infrastructures are wholly undeveloped. This article will propose a framework to define the strategy which can leverage on the wireless technologies usage in order for the usefulness, efficiency and effective utilization of energy resources which are supplied by a particular electric utility could be further enhanced. [C3564]

#### "Application of the deconvolution method in the processing of Full-waveform Lidar data"

Full-Waveform Lidar (light detection and ranging) records the entire backscatter signals of each emitted pulse, which is benefit to know the surface features. Full-waveform Lidar has strong ability in detecting the vertical structure of vegetation and terrain. The location or height information can be extracted from the received waveform. Most common extraction techniques may be invalid sometimes, such as Gaussian decomposition will be invalid when the received signal cannot be composed of pure Gaussian function combinations. In the application of processing returned signal, the method of deconvolution has the unique advantages in extracting parameters of position, amplitude range and height. It has been widely used in spectroscopy, signal recovery, signal analysis, signal modeling and so on. In this study, deconvolution was used to remove the characteristic of the transmitted waveform from the received waveform to obtain a surface response. The simulated waveforms were used to investigate the potential of deconvolution in Full-waveform Lidar data analysis. The results showed that the Gold's method of deconvolution was suitable for solving the problem. [C3565]

#### "Detecting and Identifying Two Stationary-Human-Targets: A Technique Based on Bioradar"

Bioradar is a novel kind of radar combining the technology of radar and biomedical engineering. It can detect vital signals (such as breath, heartbeat, movement, etc.) in a certain distance through the nonmetal substances (such as brick walls, rubble, etc.) without using electrodes or sensors. However, multi-stationary-human-target identifying and locating has not been resolved yet. Based on the Ultra Wide-band (UWB) bioradar, we developed a method combining biomedical signal processing and space-frequency analysis to distinguish two stationary human subjects in different distances and to identify the location of each human subject. Experiments were done to evaluate the effectiveness of the proposed method. In 86 data sets the accuracy of distinguishing two stationary subjects reached 73%. This method may serve as a basis for further studies in developing appropriate 2-Dimension locating image reconstruction models via multi-antenna (static) UWB radar. [C3566]

#### "The correction of spaceborne satellite's yaw steering law based on the star tracker high-precision measurement"

This paper presents a successful example of how the yaw steering law used in the satellite project. Otherwise in the synthetic aperture radar satellite, the theoretic parameter of the yaw steering law can be obtained and optimized on the track, then the expected Doppler centroid will be gotten. [C3567]

#### "On exploring SVDSPM algorithm for more accurate DOA estimation of low altitude target"

There exists SVDSPM (Singular Value Decomposition based on Signal Phase Matching Principle) algorithm for direction of arrival (DOA) estimation. Our aim is to present a different SVDSPM algorithm for more accurate estimation of low altitude target. So a void reference sensor is used to explore the possibility of better performance. In the full paper, VRS-SVDSPM (SVDSPM Using a Void Reference Sensor) algorithm and pertinent experimental research are explained in much detail; here only a briefing is given. The following two topics are discussed: (1) the time delay formula and VRS-SVDSPM algorithm, with the void reference sensor located on the minus of z-axes; (2) analysis of experimental results. The results show preliminarily that: (1) VRS-SVDSPM algorithm can estimate low altitude target when CBF (Conventional Beamforming) and MUSIC (Multiple Signal Classification) can not; (2) the side lobe with VRS-SVDSPM is lower compared with that with CBF; (3) with VRS-SVDSPM algorithm, the bias of azimuth is 0.6 degree and the bias of elevation is 2.4 degree. [C3568]

#### "Performance analysis of self-calibration algorithm for concentric-UCA"

A new decoupling algorithm is proposed to estimate DOA of concentric uniform circular arrays (C-UCA). The new algorithm can calibrates mutual coupling of the inner sub-arrays, compensate for mutual coupling between sub-arrays, and then estimate DOA of signal sources. This algorithm transforms joint problem into cascade problem and gets the parameters by one dimension spectrum peak value searching, which avoids multidimensional nonlinear searching of multi-parameters joint estimation. The simulation and theoretic analysis validate the good performance of the proposed algorithm. [C3569]

#### "A new real time Range-Doppler imaging algorithm"

This paper firstly describes the processing of Range-Doppler imaging algorithm and FFT interpolation for range cell migration correction, and then forms a improved range-doppler algorithm for SAR imaging with combining the two methods, which has much less computation time. In order to eliminate computation further, the Pruning FFT technique is used. [C3570]

#### "ISAR super-resolution imaging based on sparse representation"

Super-resolution imaging technique can improve resolution of ISAR image. Traditional methods based on spectrum estimation need to know the number of scattering centers in advance, and match two-dimensional poles in two-dimensional imaging. This paper researches sparsity of ISAR frequency signal and two-dimensional signal, and make super-resolution imaging equal to signal sparse representation. By Basic Pursuit algorithm, a clearer image is obtained without the number of scattering centers estimation and match processing. [C3571]

#### "Cyclostationary spectrum sensing for Cognitive Radio and multiantenna systems"

In this paper it is shown that cyclostationary spectrum sensing for Cognitive Radio networks, applying multiple cyclic frequencies for single user detection can be interpreted in terms of optimal incoherent diversity addition for "virtual diversity branches" or SIMO radar. This approach allows proposing, by analogy to diversity combining, suboptimal algorithms which can provide near optimal characteristics for the Neyman-Pearson Test (NPT). The analysis is based on the Generalized Gaussian (Klovsky-Middleton) Channel Model, which allows obtaining the above mention NPT characteristics: probability of misdetection (PM) and probability of false alarm (Pfa) in the most general way. Some quasi-optimum algorithms such as energetic receiver and selection addition algorithm are analyzed and their comparison with the noise immunity properties (Receiver Operational Characteristics-ROC) of the optimum approach is provided as well. [C3572]

#### "Navigation Satellite Passive Radar Moving Target Detection and SAR Imaging Based on FRFT"

Conventional radars have less invisibility, but the passive radars based on TV, FM signals also have some restrictions in SAR imaging by a range of issues such as ground electromagnetic environment and signal silence. This paper presents a new method of passive SAR imaging based on navigation satellite signal with single/multiple receive-only mode in FRFT domain. The received reflection of single multiple GPS signals from target is approximately linear FM signals which can be transformed by FRFT for signal frequency and Doppler frequency detection and estimation, especially for the target SAR imaging. Simulation results shown the effectiveness of the algorithm, and help to avoid the multi-target SAR imaging interference. [C3573]

#### "Research and Design of Embedded Radar Information Processor Oriented to Pervasive Computing"

Pervasive computing has been used widely in civilian areas. In the field of aerospace, researchers also have paid more attention to pervasive computing and made scientific researches on it. According to the idea of pervasive computing, an overall program of aircraft design is introduced in this paper. Subsequently a functional schematic of radar information processor embedded in aircraft is presented. The hardware and software design and algorithms of radar information processor are introduced exhaustively. The preliminary exploration research of pervasive computing is accomplished in the aerospace electronic systems by means of this research and design. [C3574]

#### "High-Resolution RCS Measurement Inside an Anechoic Chamber"

Traditionally, continue-wave method is used in Radar Cross Section (RCS) measurement. But high-resolution information is not gained in the system. The frequency-domain data of an anechoic chamber is obtained by stepped-frequency testing. Using inverse Fast Fourier Transform (IFFT), high-resolution time-domain response is achieved. In order to meet the veracious result, unwanted signals should be eliminated. The target interference with the ground is removed by setting up isolation absorbing screen inside an anechoic chamber. It is possible to avoid antenna coupling by reasonable disposition of transmitting antenna and receiving antenna. The more



accurate measurement result is got by using time-gating function in signal processing technique. The results from simulation and experiment show that the accuracy will be improved after this method are used. [C3575]

#### "Research on imaging of SS-BISAR"

Based on the configuration and operating principle of Space-Surface Bistatic SAR (SS-BISAR), the instantaneous range course is analysed and the target's echo model is deduced in this paper. The range-Doppler algorithm fit for SS-BISAR and the effect of receiver on imaging are studied, and in the end this algorithm is validated through simulation. [C3576]

#### "A Kind of Discrete Variable Structure UCAV Guidance Law Restrict by the Entering Angle"

To solve the problem that the UCAV load data link make analog signals guidance law cannot be used directly, a kind of new discrete variable structure guidance law arithmetic is brought out, which takes the restriction of entry angle into consideration, and conquers the buffeting phenomenon when the tradition discrete variable structure control arithmetic get into sliding mode. The simulation results show that the discrete signal guidance law can meet the tactical UCAV indicator. [C3577]

#### "Multitarget tracking in clutter using two-scan data association algorithm and fixed-lag smoothing"

The performance of multitarget tracking in clutter can be improved by using higher accuracy data association algorithm and more efficient state estimation method. This paper presents a novel fixed-lag TSDA-AI smoothing algorithm, which enhances the accuracy of state estimation by using fixed-lag smoothing, and improves the probability of real "measurement-target" combination by using two-scan measurements and the associated amplitude feature in the data association method. Its efficiency has been confirmed by computer simulations. [C3578]

#### "Adaptive receivers for explorative UWB pulses"

Adjustment of receiver systems of radar stations to characteristics of reflection of complex radar-tracking targets allows considerable increasing of signal to noise ratio in the process of application of UWB pulses. Methods of signal processing based on measuring of characteristics of reflection and mathematical models of targets are offered. [C3579]

#### "Efficiency of narrow band Doppler selection of the signal in presence of the scattering from the sea"

Efficiency of narrow-band Doppler selections has been considered. Characteristics of detectors with adaptation of a threshold and rank at various polarizations of radiation and reception are estimated. [C3580]

#### "Research of an Improved Weighted Centroid Localization Algorithm and Anchor Distribution"

Localization plays an important role in Wireless Sensor Networks. This paper proposed a weighted centroid localization algorithm based on received signal strength difference (RDWCL). RDWCL utilizes RSSI difference to calculate weight so as to improve localization precision and reduce the impact of anchor density and environment changing. Anchor distribution is also introduced and analyzed in this paper. Simulation and experiment results show that compared with Centroid and Weighted Centroid, RDWCL has better performance. When anchor nodes are randomly deployed, the accuracy has been improved by 13.5%. When anchor nodes are deployed as grid, the accuracy has been improved by 25.04%. When anchor nodes are deployed as equilateral triangle, the accuracy has been improved by 27.4%. [C3581]

#### "A high resolution 2D omnidirectional synthetic aperture radar scanner at K band"

In this paper a K-band 360° 2D imaging radar utilizing a synthetic aperture scanning principle is introduced. A small omnidirectional antenna is mounted on a rotating platform to create a circular synthetic aperture. Based on a broadband holographic reconstruction principle a high resolution 360° 2D image is calculated after each turn of the platform. The size of the synthetic aperture and thus the lateral resolution of the imaging system are determined by the diameter of the resulting circular antenna trajectory. In contrast to common radar scanner-concepts that utilize highly directional and thus bulky antennas, the proposed scanner concept has the advantage that it uses a small and lightweight omnidirectional antenna. This results in a much more compact radar system with notably relaxed requirements for the scanning mechanics. In addition it will be shown that the use of an omnidirectional antenna allows for very simple options to transfer energy to the radar on the rotation platform. The performance of the proposed SAR radar scanning method is illustrated with a 24 GHz FMCW

radar sensor system. [C3582]

### "Development of wideband crosshole and surface GPR for soil characterization: FDTD modeling and experiments"

Original wide band antennas dedicated to the imaging of the subsurface by crosshole or surface radar for civil engineering application have been developed. The challenge in the developments is twofold: in the case of crosshole radar, the design of a narrow antenna less than 61 cm wide working in the frequency band [0.5;1.5] GHz, and in the case of a surface radar the design of a compact antenna less than 55 cm long working in the frequency range [0.3;1] GHz. FDTD simulations have allowed to propose optimized antenna geometries and to model both types of transmission links in the presence of a layered soil representing a moisture gradient. A first measurement campaign performed in the frequency domain in a clay sand embankment has allowed to validate the theoretical developments associated with the crosshole radar and to extract the dielectric parameters (permittivity and attenuation coefficient) as a function of the depth. The experimental validation of the surface radar will further be made and the performances of both types of radars will be compared. [C3583]

### "Method of space-time processing of non-stationary signals with application of optimal sliding windows and wavelet transforms"

This work is devoted to the development of methods of signal detection, selection and estimation of parameters of space-extended objects with high Q-factor on basis of statistical optimization of either of space-time processing of signals or dynamic scenes in the radio-technical systems. [C3584]

### "An integrated Relative Navigation system using GPS/VISNAV for ultra-close spacecraft formation flying"

To improve the accuracy and better fault-tolerant performance for ultra-close spacecraft formation flying, a Global Position System (GPS)/Vision based Navigation (VISNAV) integrated Relative Navigation and Attitude Determination (RNAD) approach was presented in this paper. Onboard GPS was used for RNAD for formation spacecraft by multi-antennas configuration. The same RNAD information was also achieved by VISNAV system separately by using multiple line-of-sight vectors observations from spacecraft to another. Optimal fusion of RNAD information from both GPS/VISNAV subsystems was achieved by a Federal Kalman Filter (FKF) architecture. Simulation results provided later indicate that the integrated system can provide a total improvement of relative navigation and attitude estimation performance in accuracy and fault-tolerant. [C3585]

### "The evaluation method of space objects collision"

With the rapid development of space technology, more and more spacecrafts have been launched into space. At the same time, the number of space debris increases dramatically and the probability of collision between space debris and spacecrafts arises accordingly. Some evaluation methods should be studied to evaluate the collision effect. According to different collision modes, this paper introduces some evaluation methods through analyzing tracking data obtained by measurement equipment and proposes relevant evaluation standards based on different collision degrees. [C3586]

### "Data association for GM-PHD with track oriented PMHT"

Gaussian Mixture probability hypothesis density (GM-PHD) filter is a closed-form solution to the probability hypothesis density filter, which could estimate states and time-varying number of targets based on theory of random finite set. Probability multiple hypotheses tracking (PMHT) is a multi-target tracking algorithm combining data association and expectation-maximization. However, GM-PHD can not give trajectories of target because of its disability of providing identity of target. Furthermore, PMHT need known number of targets and several frames trajectories of targets at first which are difficult in practical application. Firstly, we propose track oriented PMHT tracker (TO-PMHTT), then an approach of data association combining the advantage of GM-PHD with TO-PMHTT is designed in this paper. GM-PHD acts as the pre-filter of TO-PMHTT when there are no crossing targets in the scenario, while interaction between GM-PHD and TO-PMHTT is performed when targets enter crossing zone. Computer simulation results show that the method can provide association for both separated and crossing targets tracking. [C3587]

### "A novel adaptive square root recursive least squares filter algorithm of SINS/SAR integrated navigation systems"

In strapdown inertial navigation system (SINS) synthetic aperture radar (SAR) integrated navigation systems, the

time-varying parameter estimation is a challenging problem because SAR measurements are fairly few and have unequal interval. In such case, the common Kalman filter algorithm can't be convergent. Furthermore, the traditional recursive least squares (RLS) algorithm is difficult to estimate the time-varying parameter. This paper proposed a novel adaptive square root recursive least squares (ASRRLS) filter algorithm of SINS/SAR integrated navigation systems. The first characteristic of ASRRLS is introducing adaptive fading factors based on the orthogonality principle, which can effectively track the parameters' varying. The second characteristic of ASRRLS is taking covariance square root matrix instead of covariance one in the filter algorithm, which can avoid filtering divergence and improve the filter convergence speed. The ASRRLS filter algorithm is deduced and the performance is rigorously analyzed. Simulation results demonstrate the feasibility and effectiveness of the proposed approach. [C3588]

#### "Recognition method studies for radar and communication signals based on spectral correlation"

In order to address the increasing complexity of electromagnetic environments and adapt to the demanding need of the integrative electronic warfare, it is necessary to study the integrative reconnaissance technology for radar and communication signals from single-platform. At present, the systemic study of integrative reconnaissance has just begun, and the automatic recognition of modulation types is a very important research area in this field. The exploration of the method presented us the following discoveries. First, it utilizes the duty ratio to separate the two types of signals; secondly, based on the excellent features of the second order cycle spectrum it gives the spectral correlation characteristics of the conventional communication and pulse compression radar signals using the CA method; then, we refer the characteristic parameter and allow signals to be automatically identified. The simulation results verify the feasibility and correctness of this method. [C3589]

#### "Analysis of Return Signal Mechanism in Ship-Board Radar"

This paper analyzes interactions between return signals and ship-board radar. The corresponding theoretical model proves that the first-order, Bragg sea-wave spectrum's widened width in ship-board radar coincides with the theoretically spreading width analyzed in our model, creating a foundation for the research of signal resolution and clutter background statistics in ship-board radar. [C3590]

#### "Multipath Mitigation of Low Elevation for Passive Monopulse Radar Based on FRFT"

A novel algorithm for mitigating multipath effect of low elevation for passive monopulse radar based on the fractional Fourier transform (FRFT) is proposed with constructing the multipath model in this paper. Reflection LFM signal filtered and mitigated in FRFT domain. The statistical analysis is also performed which perfects the method theoretically, simulation results are provided to show the validity of our method. [C3591]

#### "Decomposition of Maneuvering Target RCS Based on Wavelet Analysis"

Considering maneuvering target RCS which changes along with the pose of target acutely, this paper brings forward a method which makes maneuvering target RCS decompose RCS of certain pose and RCS of random pose. RCS of certain pose is sensitive to the change of maneuvering target pose and it depends on the pose strongly. And RCS of random pose can be processed as noise. Basing on the characteristic, the paper uses wavelet analysis to process maneuvering target RCS sequence with De-noising. Use this method, we can obtain the RCS sequence of De-noising changed with pose( RCS sequence of certain pose). This paper also use Matlab to simulate and to validate feasibility of this method. [C3592]

#### "A Novel Crossbar Scheduling for Multi-FPGA Parallel SAR Imaging System"

In multiprocessors system, crossbar scheduling networks have been widely used for system interconnection among processors or modules in SOC (System on Chip). In this paper, a parallel SAR (Synthetic Aperture Radar) image processing system which is composed of five FPGA PE (Process Element)s is taken for the basic research platform. Then a novel compact crossbar scheduling network for multi distributed parallel PEs is proposed for communication among PEs. Different scheduling strategies are provided for different kinds of source data streams which are from external raw data and PEs. In addition, resynchronization makes data streams of all PEs synchronous when all data streams are not entirely consistent due to the efficiency of memory access and bus burst transfer. Simulation and synthesis show that only little device resource is utilized by the proposed crossbar scheduling network to meet the requirements of the system. The maximum throughput of the crossbar could be above 20Gbps when the operating frequency is 100MHz, and the minimum latency is three clock cycles. The proposed crossbar scheduling as a sub-module could be easily integrated into SAR real-time imaging system. [C3593]

### "The Application of Unsupervised Clustering in Radar Signal Preselection Based on DOA Parameters"

With the deterioration of electronic environment, using signals DOA (direction of arrival) parameters has great significance to preselect multiple radar pulses. Cluster analysis as an important means of data classification, is gradually applied to radar signal sorting. In this paper, a novel method of signal sorting flowsheet is proposed based on Fuzzy Clustering to sort emitters DOA as data objects, with dynamic clustering for reference and Gaussian distance function instead of Euclidean distance. This method avoids establishing enormous similar matrix and adapt to the change of the number of emitters. The result of simulation demonstrates that this method is effective. [C3594]

### "The Monopulse Angle Estimation Based on the Radon-Ambiguity Transform"

On the condition of amplitude-comparison monopulse radar system, for measuring the direction of multicomponent sources in the space which have same modulation format, an algorithm of Direction-of-Arrival (DOA) estimation based on Radon-Ambiguity Transform is proposed. The typical signal model is built up, and when the time-of-arrival is very approximate, it is discussed how to extract the signal amplitude of each source. And then the algorithm's results of angle measurement is given. [C3595]

### "Parameter Estimation of LFM Signal with Narrowband Jamming Based on CS"

Based on Compressive Sensing (CS), parameter estimation of Linear Frequency Modulation (LFM) signal could be done by using fewer sampling data. At the present time, there is no method that could resolve the problem that the result of parameter estimation of LFM signal with narrowband jamming is not satisfied well. As a result, this paper proposes a resolution to this problem. A Multi-component dictionary which could matching LFM signal and narrowband jamming both is constructed in this paper. And based on the Multi-component dictionary we can obtain a more effective sparse representation of signals, and then we could get a better parameter estimation of LFM signal. The experiment result shows that we could obtain more accurate parameter estimation of LFM signal with narrowband jamming by using the method this paper proposed than by others under the same condition of samples. [C3596]

### "Visualized Feature Fusion and Style Evaluation for Musical Genre Analysis"

Different kinds of features in time domain, spectral domain and cepstral domain are used for musical genre classification. In this paper, through the fusion of short-term timbral features and long-term rhythmic feature, we propose a novel method where: musical genre vector is constructed using the likelihood ratio of GMM (Gaussian Mixture Model) and radar chart is applied to provide visualized style evaluation for musical genre analysis, a promising performance is achieved over our database consisting of seven different types of music. Because of the fuzzy definition of musical genres, we also investigate the music with dual-genre based on musical genre vector and radar chart. [C3597]

### "Research on ISAR Imaging Method of Parameter Estimation Based on Optimal Imaging Period"

A clear ISAR image could not be acquired by conventional Range-Doppler (RD) method due to the non-uniformity of angular motion of ships as scatterers caused by the sea wave, thus the method for solving the problem by applying Range-Instantaneous Doppler (RID) methods are used. However, though each scatterer could be resolved from the echoes, such methods suffer from heavy calculation burden due to the searching process. An ISAR imaging method of parameter estimation based on optimal imaging period is proposed. The method chooses optimal data from all received echoes, and then achieves imaging by parameter estimation according to each range bin's Doppler data. The effects of choosing imaging period on parameter estimation is analyzed, and the steps of accomplishing the proposed method are developed. The result of estimation on real data manifests that better ISAR image can be acquired by applying the method proposed. [C3598]

### "Tri-iterative Three-Dimensional Space-Time Adaptive Processing Based on Correlation Matrix for Airborne Radar"

Because of employing elevation adaptivity, three-dimensional space-time adaptive processing (3D STAP) can achieve better performance than conventional two-dimensional (2D) STAP at the cost of higher computational load and sample support requirement. To overcome these shortcomings, a tri-iterative 3D STAP method based on correlation matrix for airborne radar is developed. In the proposed method, the quadratic cost function used in the optimum STAP is converted into three quadratic functions by using submatrices of the space-time correlation matrix, and the full dimension weight vector can be separated into three lower dimensional weight vectors. By iteratively optimizing these lower dimensional weight vectors, the proposed method can significantly decrease the



computational load and training samples requirement. Experiment results using both simulated data and measured radar data demonstrate the effectiveness of the proposed method. [C3599]

### "WLAN Indoor Tracking Method via Improved Particle Filter Algorithm"

WLAN Indoor tracking system is presented based on the comparison between the off-line pre-stored Radio-map and new recorded signal strength in the on-line phase to estimate user's motion trajectory. Furthermore, the improved particle filter tracking algorithm that consists of the particles-reference points (P-RPs) transferring for getting the likelihood function and velocity estimation from the ANN positioning results is also discussed in this paper. And also, the experiment shows that this improved particle filter tracking algorithm achieves great accuracy performance in tracking trajectory aspect without any velocity-measurement hardware. Finally, the feasibility and effectiveness of this improved WLAN indoor particle filter tracking algorithm are verified without velocity-measurement hardware. [C3600]

### "Estimation and Registration of Relative System Biases in Fire-Control Radar Network"

Fire-control radar network uses data fusion to form more accurate estimate of a target track, the prerequisite of normal data fusion is the system bias registration. In fire-control radar network, due to the existence of the approximating bias of coordinate conversion model and time synchronization bias, data fusion process brings the immitted system biases besides inherent system biases. This paper developed a system bias registration method based on Kalman filtering theory. The inherent system bias and immitted system bias are considered for modeling. The simulation results are presented and discussed. It is found that the method given in this paper is in effect. [C3601]

### "Propagation Analysis of ELF Electromagnetic Emission below the Cut-Off Frequency in Ionosphere"

The aim of this paper is to show the propagation and polarization characteristic of some types of ELF electromagnetic emission below the cutoff frequency observed by DEMETER satellite. All the analysis is based on multi-component measurement method of electric and magnetic field in ELF band. According to the wave vector and planarity and ellipticity of polarization, we can judge the property of electromagnetic emission below the cutoff frequency. Then it will help us analysis the origin of emission further. In is this paper, only three types of emission are analyzed, and their emission origins are guessed. [C3602]

## СПИСОК ЛИТЕРАТУРЫ

- C1. Boric-Lubecke O. Amplitude modulation issues in Doppler radar heart signal extraction. / Boric-Lubecke O., Lubecke V., Mostafanezhad I. // 2011 IEEE Topical Conference on Biomedical Wireless Technologies, Networks, and Sensing Systems (BioWireleSS). - Phoenix, AZ, 16-19 Jan. 2011. - P. 103-106. ↑
- C2. Yazhou Wang. UWB microwave imaging system with a novel calibration approach for breast cancer detection. / Yazhou Wang, Fathy A.E., Mahfouz M.R. // 2011 IEEE Topical Conference on Biomedical Wireless Technologies, Networks, and Sensing Systems (BioWireleSS). - Phoenix, AZ, 16-19 Jan. 2011. - P. 63-66. ↑
- C3. Fan Yang. Time-of-arrival calibration for improving the microwave breast cancer imaging. / Fan Yang, Mohan A.S. // 2011 IEEE Topical Conference on Biomedical Wireless Technologies, Networks, and Sensing Systems (BioWireleSS). - Phoenix, AZ, 16-19 Jan. 2011. - P. 67-70. ↑
- C4. Singh A. Body-worn passive planar harmonic tag design for use with Doppler radar. / Singh A., Lubecke V. // 2011 IEEE Topical Conference on Biomedical Wireless Technologies, Networks, and Sensing Systems (BioWireleSS). - Phoenix, AZ, 16-19 Jan. 2011. - P. 51-54. ↑
- C5. Fan Bo. 3D Multiple Maneuvering Targets Tracking in Active and Passive Radar Composite Guidance. / Fan Bo, Qin Yu-liang, Wang Jian-tao, Xiao Huai-tie, Huang Pu-jian. // 2011 International Workshop on Multi-Platform/Multi-Sensor Remote Sensing and Mapping (M2RSM). - Xiamen, 10-12 Jan. 2011. - P. 1-6. ↑
- C6. Young-Man Kim. Tracking a moving target in wireless sensor networks using PDR sensors. / Young-Man Kim, Anh-Duy Vu, Jea-II Han. // 2011 International Conference on Information Networking (ICOIN). - Barcelona,

26-28 Jan. 2011. - P. 394-398. ↑

C7. Changzhan Gu. Doppler radar respiration measurement for gated lung cancer radiotherapy. / Changzhan Gu, Ruijiang Li, Changzhi Li, Jiang S.B. // 2011 IEEE Topical Conference on Biomedical Wireless Technologies, Networks, and Sensing Systems (BioWireSS). - Phoenix, AZ, 16-19 Jan. 2011. - P. 91-94. ↑

C8. Zheng-rong He. POLSAR Image Classification Based on Polarimetric Decomposition and Generalized Discriminant Analysis. / Zheng-rong He, Zhi Liu, Fan Wang, Yong-chang Chen. // 2011 International Workshop on Multi-Platform/Multi-Sensor Remote Sensing and Mapping (M2RSM). - Xiamen, 10-12 Jan. 2011. - P. 1-4. ↑

C9. Xin Yu. SAR Automatic Target Recognition Based on Classifiers Fusion. / Xin Yu, Yukuan Li, Jiao L.C. // 2011 International Workshop on Multi-Platform/Multi-Sensor Remote Sensing and Mapping (M2RSM). - Xiamen, 10-12 Jan. 2011. - P. 1-5. ↑

C10. Schantz H.G. On the origins of RF-based location. 2011 IEEE Topical Conference on Wireless Sensors and Sensor Networks (WiSNet). - Phoenix, AZ, 16-19 Jan. 2011. - P. 21-24. ↑

C11. Li Lu. A software-defined multifunctional radar sensor for linear and reciprocal displacement measurement. / Li Lu, Changzhi Li, Rice J.A. // 2011 IEEE Topical Conference on Wireless Sensors and Sensor Networks (WiSNet). - Phoenix, AZ, 16-19 Jan. 2011. - P. 17-20. ↑

C12. Yu Chunrui. Adaptive RFI Suppression Algorithm Based on CEMD for SAR Data. / Yu Chunrui, Zhang Yongsheng, Dong Zhen, Liang Diannong. // 2011 International Workshop on Multi-Platform/Multi-Sensor Remote Sensing and Mapping (M2RSM). - Xiamen, 10-12 Jan. 2011. - P. 1-5. ↑

C13. Kiriazi J.E. Considerations in measuring vital signs cross section with Doppler radar. / Kiriazi J.E., Boric-Lubecke O., Lubecke V.M. // 2011 IEEE Radio and Wireless Symposium (RWS). - Phoenix, AZ, 16-19 Jan. 2011. - P. 426-429. ↑

C14. Gang Li. A multilateral synthetic aperture wireless positioning approach to precise 3D localization of a robot tool center point. / Gang Li, Vossiek M. // 2011 IEEE Topical Conference on Wireless Sensors and Sensor Networks (WiSNet). - Phoenix, AZ, 16-19 Jan. 2011. - P. 37-40. ↑

C15. Chandrakanth R. Fusion of High Resolution Satellite SAR and Optical Images. / Chandrakanth R., Saibaba J., Varadan G., Raj P.A. // 2011 International Workshop on Multi-Platform/Multi-Sensor Remote Sensing and Mapping (M2RSM). - Xiamen, 10-12 Jan. 2011. - P. 1-6. ↑

C16. Reck C. Robust DOA estimation of SSR signals for aircraft positioning. / Reck C., Berold U., Schmidt L. // 2011 IEEE Topical Conference on Wireless Sensors and Sensor Networks (WiSNet). - Phoenix, AZ, 16-19 Jan. 2011. - P. 13-16. ↑

C17. Feger R. A heterodyne 77-GHz FMCW radar with offset PLL frequency stabilization. / Feger R., Kolmhofer E., Starzer F., Wiesinger F., Scheibhofer S., Stelzer A. // 2011 IEEE Topical Conference on Wireless Sensors and Sensor Networks (WiSNet). - Phoenix, AZ, 16-19 Jan. 2011. - P. 9-12. ↑

C18. Eugen Hyun. Design and implementation of automotive 77GHz FMCW radar system based on DSP and FPGA. / Eugen Hyun, Woojin Oh, Jong-Hun Lee. // 2011 IEEE International Conference on Consumer Electronics (ICCE). - Las Vegas, NV, 9-12 Jan. 2011. - P. 517-518. ↑

C19. Min Wang. High Resolution Radar Imaging Based on Compressed Sensing and Fast Bayesian Matching Pursuit. / Min Wang, Shuyuan Yang, Yanyan Wan, Jing Wang. // 2011 International Workshop on Multi-Platform/Multi-Sensor Remote Sensing and Mapping (M2RSM). - Xiamen, 10-12 Jan. 2011. - P. 1-5. ↑

C20. Changcheng Wang. Ship Detection after Removal of Ambiguities by Using PolSAR Images. 2011 International Workshop on Multi-Platform/Multi-Sensor Remote Sensing and Mapping (M2RSM). - Xiamen, 10-12 Jan. 2011. - P. 1-4. ↑

C21. Xu Jing. A New Method of Fixed Single Observer Passive Location Based on Phase Difference Rate-of-Change. / Xu Jing, He Ming-hao, Yu Chun-lai, Chen Chang-xiao. // 2011 Third International Conference on Measuring Technology and Mechatronics Automation (ICMTMA). - Shangshai, 6-7 Jan. 2011. - Vol. 1. - P. 174-177. ↑

↑

- C22.** Zhao Bao-chang. A New Method for Sorting Radar Signals Based on Coherency. / Zhao Bao-chang, Peng Shi-rui, Yu Chun-lai, Sun Jing-jiao. // 2011 Third International Conference on Measuring Technology and Mechatronics Automation (ICMTMA). - Shangshai, 6-7 Jan. 2011. - Vol. 1. - P. 170-173. ↑
- C23.** Hanyun Wang. Roof Detection in Lidar Data. / Hanyun Wang, Cheng Wang, Shengyong Hao. // 2011 International Workshop on Multi-Platform/Multi-Sensor Remote Sensing and Mapping (M2RSM). - Xiamen, 10-12 Jan. 2011. - P. 1-5. ↑
- C24.** Wang Na. A Novel Polarimetric CFAR Target Detection Method. / Wang Na, Liu Li, Hu Canbin, Kuang Gangyao, Jiang Yongmei. // 2011 International Workshop on Multi-Platform/Multi-Sensor Remote Sensing and Mapping (M2RSM). - Xiamen, 10-12 Jan. 2011. - P. 1-6. ↑
- C25.** Shuyuan Yang. Multitask Learning and Sparse Representation Based Super-Resolution Reconstruction of Synthetic Aperture Radar Images. / Shuyuan Yang, Zhizhou Liu, Min Wang, Fenghua Sun, Licheng Jiao. // 2011 International Workshop on Multi-Platform/Multi-Sensor Remote Sensing and Mapping (M2RSM). - Xiamen, 10-12 Jan. 2011. - P. 1-5. ↑
- C26.** Shuyuan Yang. Cooperative Synthetic Aperture Radar Image Segmentation Using Learning Sparse Representation Based Clustering Scheme. / Shuyuan Yang, Junlin Zhu, Zailin Hu, Min Wang, Licheng Jiao. // 2011 International Workshop on Multi-Platform/Multi-Sensor Remote Sensing and Mapping (M2RSM). - Xiamen, 10-12 Jan. 2011. - P. 1-6. ↑
- C27.** Shi Ruofan. A Novel SAR Signal Reconstruction Method from Non-uniform Sampling Associated with Fractional Fourier Transform. / Shi Ruofan, Zhao Juan, Tao Ran. // 2011 Third International Conference on Measuring Technology and Mechatronics Automation (ICMTMA). - Shangshai, 6-7 Jan. 2011. - Vol. 1. - P. 210-213. ↑
- C28.** Hou Huiling. The Impact of High-Order Phase in Ballistic Missiles Detection. / Hou Huiling, Pang Cunsuo. // 2011 Third International Conference on Measuring Technology and Mechatronics Automation (ICMTMA). - Shangshai, 6-7 Jan. 2011. - Vol. 3. - P. 827-830. ↑
- C29.** Shan Tao. Research on the Interference Cancelation in SFN Based Passive Radar. / Shan Tao, Wu Miao, Yang Jinlu, Zhuo Zhihai. // 2011 Third International Conference on Measuring Technology and Mechatronics Automation (ICMTMA). - Shangshai, 6-7 Jan. 2011. - Vol. 3. - P. 124-127. ↑
- C30.** Hui Wang. Determination of LIDAR Points Cloud Filtering Parameters Using Distance Image. / Hui Wang, Peng-cheng Li, Jun Liu, Li-yong Wang. // 2011 International Workshop on Multi-Platform/Multi-Sensor Remote Sensing and Mapping (M2RSM). - Xiamen, 10-12 Jan. 2011. - P. 1-4. ↑
- C31.** Hsi-Chuan Huang. The Intelligent Embedded Control Warning System for Car Reversing. / Hsi-Chuan Huang, Feng-Che Tsai, Tsuo-Fei Mao. // 2011 Third International Conference on Measuring Technology and Mechatronics Automation (ICMTMA). - Shangshai, 6-7 Jan. 2011. - Vol. 3. - P. 849-852. ↑
- C32.** Jianhua Sun. Detection Algorithm of Laser Radar Target Based on Wavelet Transform. / Jianhua Sun, Pengge Ma, Ning Zheng, Jinfa Shi. // 2011 Third International Conference on Measuring Technology and Mechatronics Automation (ICMTMA). - Shangshai, 6-7 Jan. 2011. - Vol. 1. - P. 1026-1028. ↑
- C33.** Fugui Li. Analysis and Design of Three Loop Radar Servo System for Air Defense Missile. / Fugui Li, Qunli Xia, Zaikang Qi. // 2011 Third International Conference on Measuring Technology and Mechatronics Automation (ICMTMA). - Shangshai, 6-7 Jan. 2011. - Vol. 1. - P. 451-454. ↑
- C34.** Jin Li. New Technology and Applications on Microwave Sensors. / Jin Li, Qi Hui. // 2011 Third International Conference on Measuring Technology and Mechatronics Automation (ICMTMA). - Shangshai, 6-7 Jan. 2011. - Vol. 2. - P. 690-693. ↑
- C35.** Chen Ming. LIDAR Depth Indicator of the Design and Research. / Chen Ming, Wang Guangxian, Wang Xiaoming, Hong Qian. // 2011 Third International Conference on Measuring Technology and Mechatronics Automation (ICMTMA). - Shangshai, 6-7 Jan. 2011. - Vol. 2. - P. 467-469. ↑
- C36.** Wang Wei. Airport Detection in SAR Image Based on Perceptual Organization. / Wang Wei, Liu Li, Hu Canbin, Jiang Yongmei, Kuang Gangyao. // 2011 International Workshop on Multi-Platform/Multi-Sensor Remote Sensing and Mapping (M2RSM). - Xiamen, 10-12 Jan. 2011. - P. 1-5. ↑

- C37. Gunther Jake. Maximum likelihood synthetic aperture radar image formation for highly nonlinear flight tracks. / Gunther Jake, West Roger, Crookston Nate, Moon Todd. // 2011 IEEE Digital Signal Processing Workshop and IEEE Signal Processing Education Workshop (DSP/SPE). - Sedona, AZ, USA, 4-7 Jan. 2011. - P. 449-454. ↑
- C38. West Roger. Forming regularized maximum likelihood strip-map synthetic aperture radar images using the block RLS algorithm. / West Roger, Gunther Jake, Moon Todd. // 2011 IEEE Digital Signal Processing Workshop and IEEE Signal Processing Education Workshop (DSP/SPE). - Sedona, AZ, USA, 4-7 Jan. 2011. - P. 455-460. ↑
- C39. Kadar Peter. Measure of smartness. 2011 IEEE 9th International Symposium on Applied Machine Intelligence and Informatics (SAMI). - Smolenice, Slovakia, 27-29 Jan. 2011. - P. 201-205. ↑
- C40. Shahbazi Nafiseh. Angle-Doppler Estimation in Heavy Correlated Interference. / Shahbazi Nafiseh, Amindaver Hamidreza. // 2011 Second International Conference on Intelligent Systems, Modelling and Simulation (ISMS). - Phnom Penh, Cambodia, 25-27 Jan. 2011. - P. 177-182. ↑
- C41. Mandal Amritakar. Implementation of Adaptive FIR Filter for Pulse Doppler Radar. / Mandal Amritakar, Kaushik Brajesh Kumar, Kumar Brijesh, Agarwal R. P. // 2011 International Conference on Devices and Communications (ICDeCom). - Mesra, Ranchi, India, 24-25 Feb. 2011. - P. 1-5. ↑
- C42. Sudhendra Chandrika. A novel space cloth using resistor grid network for radar absorbers in stealth applications. / Sudhendra Chandrika, Mahule Vibhor, Pillai ACR, Mohanty Atanu. // 2011 International Conference on Communications and Signal Processing (ICCSP). - Kerala, India, 10-12 Feb. 2011. - P. 83-86. ↑
- C43. Sekine Masatoshi. Non-contact heart rate detection using periodic variation in Doppler frequency. / Sekine Masatoshi, Maeno Kurato. // 2011 IEEE Sensors Applications Symposium (SAS). - San Antonio, TX, USA, 22-24 Feb. 2011. - P. 318-322. ↑
- C44. Sharma Shrikant. Mathematical analysis of interpolation step of Omega-K Algorithm for GPR and its implementation. / Sharma Shrikant, Jena Paramananda, Kuloor Ramachandra. // 2011 International Conference on Communications and Signal Processing (ICCSP). - Kerala, India, 10-12 Feb. 2011. - P. 46-50. ↑
- C45. Chakraborty B. Waveform-agile mimo radar for urban terrain tracking. / Chakraborty B., Zhang J. J., Papandreou-Suppappola A., Morrell D. // 2011 IEEE Digital Signal Processing Workshop and IEEE Signal Processing Education Workshop (DSP/SPE). - Sedona, AZ, USA, 4-7 Jan. 2011. - P. 466-471. ↑
- C46. Shirodkar Shravan. Heart-beat detection and ranging through a wall using ultra wide band radar. / Shirodkar Shravan, Barua Paramita, Anuradha D, Kuloor R. // 2011 International Conference on Communications and Signal Processing (ICCSP). - Kerala, India, 10-12 Feb. 2011. - P. 579-583. ↑
- C47. Liu A. A Novel Image Based Multi-Channel SAR-GMTI Algorithm. / Liu A., Li Chen, Fei Zhao, Gangyao Kuang. // 2011 International Workshop on Multi-Platform/Multi-Sensor Remote Sensing and Mapping (M2RSM). - Xiamen, 10-12 Jan. 2011. - P. 1-4. ↑
- C48. Ussyshkin R.V. Advantages of Airborne Lidar Technology in Power Line Asset Management. / Ussyshkin R.V., Theriault L., Sitar M., Kou T. // 2011 International Workshop on Multi-Platform/Multi-Sensor Remote Sensing and Mapping (M2RSM). - Xiamen, 10-12 Jan. 2011. - P. 1-5. ↑
- C49. Uschkerat Udo. Performance evaluation of a GPR system for mine detection using a 3D-SAR algorithm. 2010 11th International Radar Symposium (IRS). - Vilnius, Lithuania, 16-18 June 2010. - P. 1-3. ↑
- C50. Gebhardt Ulrich. ISAR imaging of ground moving vehicles in a curve. / Gebhardt Ulrich, Berens Patrick, Holzner Juergen. // 2010 11th International Radar Symposium (IRS). - Vilnius, Lithuania, 16-18 June 2010. - P. 1-3. ↑
- C51. Nouvel-Fiani Myriam. Toward a network of common radar and EW sensors aboard a single or multiple cooperative platforms. / Nouvel-Fiani Myriam, Kemkemian Stephane, Chamouard Eric. // 2010 11th International Radar Symposium (IRS). - Vilnius, Lithuania, 16-18 June 2010. - P. 1-4. ↑
- C52. Thayaparan T. Focusing ISAR images of moving targets in real-time using time-frequency-based method. / Thayaparan T., Stankovic L., Suresh P., Venkataramanah K., SivaSankaraSai S., Sairam T., Shankar S.,



Nikhilesh K. // 2010 11th International Radar Symposium (IRS). - Vilnius, Lithuania, 16-18 June 2010. - P. 1-4.



C53. Popov A. V. Expedient GPR survey schemes. / Popov A. V., Morozov P. A., Edemsky D. E., Edemsky F. D., Pavlovskii B. R., Zapunidi S. A. // 2010 11th International Radar Symposium (IRS). - Vilnius, Lithuania, 16-18 June 2010. - P. 1-4.

C54. Huber Sigurd. Digital beam forming concepts with application to spaceborne reflector SAR systems. / Huber Sigurd, Younis Marwan, Patyuchenko Anton, Krieger Gerhard. // 2010 11th International Radar Symposium (IRS). - Vilnius, Lithuania, 16-18 June 2010. - P. 1-4.

C55. Pasternak Mateusz. Software for simulation of electromagnetic waves propagation through the soil with buried objects. / Pasternak Mateusz, Silko Dariusz. // 2010 11th International Radar Symposium (IRS). - Vilnius, Lithuania, 16-18 June 2010. - P. 1-4.

C56. Panzner Berthold. Radar signatures of complex buried objects in ground penetrating radar. / Panzner Berthold, Jostingmeier Andreas, Omar Abbas. // 2010 11th International Radar Symposium (IRS). - Vilnius, Lithuania, 16-18 June 2010. - P. 1-4.

C57. Lukyanov S. P. Comparison of methods of the resolution increase in GPR for the short range targets. / Lukyanov S. P., Stukach O. V., Semenchuk E. V. // 2010 11th International Radar Symposium (IRS). - Vilnius, Lithuania, 16-18 June 2010. - P. 1-3.

C58. Banasiak K. Radar pulse repetitive patterns detection. / Banasiak K., Pieniezny A. // 2010 11th International Radar Symposium (IRS). - Vilnius, 16-18 June 2010. - P. 1-4.

C59. Mofrad Reza Fatemi. Scenario modeling and simulation for performance prediction of a modern radar in electronics warfare environment. / Mofrad Reza Fatemi, Sadeghzadeh R. A. // 2010 11th International Radar Symposium (IRS). - Vilnius, Lithuania, 16-18 June 2010. - P. 1-5.

C60. Pieniezny Andrzej. Weak signal detection using compressive receiver. / Pieniezny Andrzej, Fornalik Jacek. // 2010 11th International Radar Symposium (IRS). - Vilnius, Lithuania, 16-18 June 2010. - P. 1-4.

C61. Swiercz Ewa. Classification of LFM radar signals based on the wavelet decomposition and the neural LVQ classifier. 2010 11th International Radar Symposium (IRS). - Vilnius, Lithuania, 16-18 June 2010. - P. 1-4.

C62. Yanovsky F. Specified for air safety, monitoring atmospheric phenomena including the volcano dust. 2010 11th International Radar Symposium (IRS). - Vilnius, 16-18 June 2010. - P. 1-4.

C63. Nourallahzadeh Mehdi. Synthesis planar array and apertures in passive HF phase array radar. / Nourallahzadeh Mehdi., Norouzi Yaser. // 2010 11th International Radar Symposium (IRS). - Vilnius, Lithuania, 16-18 June 2010. - P. 1-5.

C64. Zhang Yunhua. Design of RF subsystem for Ku-band radar with synthesized bandwidth of 2GHz by using stepped-frequency chirp signal. / Zhang Yunhua, Zhang Xiangkun, Zhai Wenshuai, Shi Xiaojin, Gu Xiang, Jiang Jingshan. // 2010 11th International Radar Symposium (IRS). - Vilnius, Lithuania, 16-18 June 2010. - P. 1-4.

C65. Bicik Petr. Passive radar: Here comes the new generation VERA-NG. 2010 11th International Radar Symposium (IRS). - Vilnius, Lithuania, 16-18 June 2010. - P. 1-4.

C66. Janusz M. Sc. Pietrzak. The use of microwave noise from the Sun for on-line verifying azimuth alignment of surveillance radars. / Janusz M. Sc. Pietrzak, Maciej M. Sc. Smolarczyk. // 2010 11th International Radar Symposium (IRS). - Vilnius, Lithuania, 16-18 June 2010. - P. 1-4.

C67. Briskin Stefan. Incoherent addition of ISAR images from spatially distributed receivers for classification purposes. / Briskin Stefan, Worms Josef G. // 2010 11th International Radar Symposium (IRS). - Vilnius, Lithuania, 16-18 June 2010. - P. 1-4.


















C68. Thayaparan T. Parameter estimation from a fraction of the period for a rotating target. / Thayaparan T., Stankovic L., Darkovic M., Suresh P., Venkataramaniah K., SivaSankaraSai S., Shankar S., Sairam T., Nikhilesh K. // 2010 11th International Radar Symposium (IRS). - Vilnius, Lithuania, 16-18 June 2010. - P. 1-4.

- C69.** Pavlik Radomir. The detection performance of complex cosine CWT and entropy analysis for narrowband signals. / Pavlik Radomir, Polacek Vladimir. // 2010 11th International Radar Symposium (IRS). - Vilnius, Lithuania, 16-18 June 2010. - P. 1-4. ↑
- C70.** Parsekian A. A comparison of 1D vertical models of biogenic gas content within a northern peatland from common mid-point and cross-borehole GPR. / Parsekian A., Slater L., Comas X. // 2010 13th International Conference on Ground Penetrating Radar (GPR). - Lecce, 21-25 June 2010. - P. 1-6. ↑
- C71.** Zhang X.Y. Qualitative monitoring of the water content evolution in an inhomogeneous soil column. / Zhang X.Y., Torteil H., Litman A., Ruy S. // 2010 13th International Conference on Ground Penetrating Radar (GPR). - Lecce, 21-25 June 2010. - P. 1-5. ↑
- C72.** Litman A. Resolution-improved microwave tomography by means of hyperspectral analysis tools. / Litman A., Torteil H., Guillaume M. // 2010 13th International Conference on Ground Penetrating Radar (GPR). - Lecce, 21-25 June 2010. - P. 1-5. ↑
- C73.** Grasmueck M. 4D GPR tracking of water infiltration in fractured high-porosity limestone. / Grasmueck M., Marchesini P., Eberli G.P., Zeller M., Van Dam R.L. // 2010 13th International Conference on Ground Penetrating Radar (GPR). - Lecce, 21-25 June 2010. - P. 1-6. ↑
- C74.** Toy C.W. Comparing electromagnetic induction and ground penetrating radar techniques for estimating soil moisture content. / Toy C.W., Steelman C.M., Endres A.L. // 2010 13th International Conference on Ground Penetrating Radar (GPR). - Lecce, 21-25 June 2010. - P. 1-6. ↑
- C75.** Strobel O. Communication in automotive systems: Principles, limits and new trends for vehicles, airplanes and vessels. / Strobel O., Rejeb R., Lubkoll J. // 2010 12th International Conference on Transparent Optical Networks (ICTON). - Munich, June 27 2010-July 1 2010. - P. 1-6. ↑
- C76.** Wende Zhang. LIDAR-based road and road-edge detection. 2010 IEEE Intelligent Vehicles Symposium (IV). - San Diego, CA, 21-24 June 2010. - P. 845-848. ↑
- C77.** Teutsch M. 3D-segmentation of traffic environments with u/v-disparity supported by radar-given masterpoints. / Teutsch M., Heger T., Schamm T., Zollner J.M. // 2010 IEEE Intelligent Vehicles Symposium (IV). - San Diego, CA, 21-24 June 2010. - P. 787-792. ↑
- C78.** Muntzinger M.M. Reliable automotive pre-crash system with out-of-sequence measurement processing. / Muntzinger M.M., Aeberhard M., Zuther S., Majhlisch M., Schmid M., Dickmann J., Dietmayer K. // 2010 IEEE Intelligent Vehicles Symposium (IV). - San Diego, CA, 21-24 June 2010. - P. 1022-1027. ↑
- C79.** Karandikar N. Design of an analog correlator for 22-29GHz UWB vehicular radar system using improved high gain multiplier architecture. / Karandikar N., Sungyong Jung, Sung Chul Lee, Ping Gui, Youngjoong Joo. // 2010 53rd IEEE International Midwest Symposium on Circuits and Systems (MWSCAS). - Seattle, WA, 1-4 Aug. 2010. - P. 930-933. ↑
- C80.** Al-Temeemy A.A. Levy flights for improved Ladar scanning. / Al-Temeemy A.A., Spencer J.W., Ralph J.F. // 2010 IEEE International Conference on Imaging Systems and Techniques (IST). - Thessaloniki, 1-2 July 2010. - P. 225-228. ↑
- C81.** Kordina T. Evaluation of the influence of a scanning method on the resulting quality of the GPR images. / Kordina T., Kadlecova Z., Anton O. // 2010 13th International Conference on Ground Penetrating Radar (GPR). - Lecce, 21-25 June 2010. - P. 1-6. ↑
- C82.** Walton Eric K. The use of high speed FIFO chips for implementation of a noise radar. 2010 11th International Radar Symposium (IRS). - Vilnius, Lithuania, 16-18 June 2010. - P. 1-4. ↑
- C83.** Cuccoli Fabrizio. Sea-land transitions identification for Coordinate Registration of Over The Horizon Sky-Wave Radar: Numerical model for performance analysis. / Cuccoli Fabrizio, Sermi Francesco, Facheris Luca, Giuli Dino. // 2010 11th International Radar Symposium (IRS). - Vilnius, Lithuania, 16-18 June 2010. - P. 1-4. ↑
- C84.** Kaczmarek Pawel. Detection of subsurface non-metallic objects using stepped frequency continuous wave ground penetrating radar. / Kaczmarek Pawel, Lapinski Marian, Karczewski Janusz. // 2010 11th International Radar Symposium (IRS). - Vilnius, Lithuania, 16-18 June 2010. - P. 1-4. ↑

- C85.** Dobrotin Nikita. GPR resolution improvement. / Dobrotin Nikita, Levitas Boris. // 2010 11th International Radar Symposium (IRS). - Vilnius, Lithuania, 16-18 June 2010. - P. 1-3. ↑
- C86.** Behar Vera. A simulation tool for analysis of MTD algorithms employing STAP techniques. / Behar Vera, Vassileva Boriana, Kabakchiev Christo. // 2010 11th International Radar Symposium (IRS). - Vilnius, Lithuania, 16-18 June 2010. - P. 1-4. ↑
- C87.** Greving Gerhard. Wind turbines as distorting scattering objects for radar-clutter aspects and visibility. / Greving Gerhard, Biermann Wolf-Dieter, Mundt Rolf. // 2010 11th International Radar Symposium (IRS). - Vilnius, Lithuania, 16-18 June 2010. - P. 1-4. ↑
- C88.** Pennock S.R. Effects of iron pipe corrosion on GPR detection. / Pennock S.R., Chapman D.N., Rogers C.D.F., Royal A.C.D., Naji A., Redfern M.A. // 2010 13th International Conference on Ground Penetrating Radar (GPR). - Lecce, 21-25 June 2010. - P. 1-5. ↑
- C89.** Rogers C.D.F. Shaping the future of GPR soils research. / Rogers C.D.F., Thomas A.M., Grant S.A. // 2010 13th International Conference on Ground Penetrating Radar (GPR). - Lecce, 21-25 June 2010. - P. 1-5. ↑
- C90.** Wimmer A. Automatic generation of a highly accurate map for driver assistance systems in road construction sites. / Wimmer A., Jungel T., Glujck M., Dietmayer K. // 2010 IEEE Intelligent Vehicles Symposium (IV). - San Diego, CA, 21-24 June 2010. - P. 281-286. ↑
- C91.** Podjawerschek Sonja. State estimation of projectiles based on Doppler radar signals using EKF and UKF. / Podjawerschek Sonja, Spahn Emil, Brodmann Michael, Horn Joachim. // 2010 18th Mediterranean Conference on Control & Automation (MED). - Marrakech, Morocco, 23-25 June 2010. - P. 1658-1663. ↑
- C92.** Steelman C.M. Inference of vertical soil moisture distribution using high-frequency CMP and reflection traveltime analysis. / Steelman C.M., Endres A.L. // 2010 13th International Conference on Ground Penetrating Radar (GPR). - Lecce, 21-25 June 2010. - P. 1-6. ↑
- C93.** Mikhnev V. Microwave visualization of layered dielectric half-space using range profiling of phase. / Mikhnev V., Badeev V., Vainikainen P. // 2010 11th International Radar Symposium (IRS). - Vilnius, 16-18 June 2010. - P. 1-4. ↑
- C94.** Wu Huaming. Motion compensation for landmine detecting vehicle-borne SAR. / Wu Huaming, Li Xuyang, Zwick Thomas. // 2010 11th International Radar Symposium (IRS). - Vilnius, Lithuania, 16-18 June 2010. - P. 1-4. ↑
- C95.** Lukin Konstantin A. Noise Waveform SAR for 2D and 3D imaging. / Lukin Konstantin A., Vyplavin Pavlo L., Lukin Sergei, Yarovoy Sergey. // 2010 11th International Radar Symposium (IRS). - Vilnius, Lithuania, 16-18 June 2010. - P. 1-4. ↑
- C96.** Rovnakova Jana. TOA association for handheld UWB radar. / Rovnakova Jana, Kocur Dusan. // 2010 11th International Radar Symposium (IRS). - Vilnius, Lithuania, 16-18 June 2010. - P. 1-4. ↑
- C97.** Elgamel Sherif A. Enhanced monopulse radar tracking using fractional Fourier filtering in the Presence of interference. / Elgamel Sherif A., Soraghan John J. // 2010 11th International Radar Symposium (IRS). - Vilnius, Lithuania, 16-18 June 2010. - P. 1-4. ↑
- C98.** Bimpas Matthaïos. Design and implementation of an integrated high resolution imaging ground penetrating radar for water pipeline rehabilitation. / Bimpas Matthaïos, Amditis Angelos, Uzunoglu Nikolaos. // 2010 11th International Radar Symposium (IRS). - Vilnius, Lithuania, 16-18 June 2010. - P. 1-4. ↑
- C99.** Deisler T. UWB radar object recognition for SLAM. / Deisler T., Thielecke J., Salman R., Schultze T., Willms I. // 2010 11th International Radar Symposium (IRS). - Vilnius, Lithuania, 16-18 June 2010. - P. 1-4. ↑
- C100.** Averyanova Yuliya. Influence of turbulence onto depolarization of signal reflected from hydrometeors. / Averyanova Yuliya, Aver'anov Anatoliy, Yanovsky Felix. // 2010 11th International Radar Symposium (IRS). - Vilnius, Lithuania, 16-18 June 2010. - P. 1-4. ↑
- C101.** Khraisat Y.S.H. Simulation of the 24GHz short range, wide band automotive radar. 2010 11th International Radar Symposium (IRS). - Vilnius, 16-18 June 2010. - P. 1-5. ↑

- C102.** Zaikov Egor. UWB radar for detection and localization of trapped people. 2010 11th International Radar Symposium (IRS). - Vilnius, Lithuania, 16-18 June 2010. - P. 1-4. ↑
- C103.** Hadavi M. Quantization effect of the parameter space on the performance of hough detector. / Hadavi M., Moqiseh A., Nayebe M. M. // 2010 11th International Radar Symposium (IRS). - Vilnius, Lithuania, 16-18 June 2010. - P. 1-4. ↑
- C104.** Maslikowski Lukasz. Bistatic Quasi-passive noise SAR experiment. / Maslikowski Lukasz, Kulpa Krzysztof. // 2010 11th International Radar Symposium (IRS). - Vilnius, Lithuania, 16-18 June 2010. - P. 1-3. ↑
- C105.** Lukin K. A. Stepped delay noise radar with high dynamic range. / Lukin K. A., Kononov V. M., Vyplavin P. L. // 2010 11th International Radar Symposium (IRS). - Vilnius, Lithuania, 16-18 June 2010. - P. 1-3. ↑
- C106.** Vyplavin P. Real-time signal processing in noise radar. / Vyplavin P., Melnikova E., Lukin S. // 2010 11th International Radar Symposium (IRS). - Vilnius, Lithuania, 16-18 June 2010. - P. 1-3. ↑
- C107.** Krenc Ksawery. Analytical sensor data evaluation models for the purpose of evidential inference in electro-magnetic reconnaissance. / Krenc Ksawery, Kawalec Adam, Pietkiewicz Tadeusz. // 2010 11th International Radar Symposium (IRS). - Vilnius, Lithuania, 16-18 June 2010. - P. 1-6. ↑
- C108.** Levitas Boris. UWB radar for breath detection. / Levitas Boris, Matuzas Jonas. // 2010 11th International Radar Symposium (IRS). - Vilnius, Lithuania, 16-18 June 2010. - P. 1-3. ↑
- C109.** Hantscher Sebastian. 94 GHz person scanner with circular aperture as part of a new sensor concept on airports. / Hantscher Sebastian, Lang Stefan, Hagelen Manfred, Essen Helmut. // 2010 11th International Radar Symposium (IRS). - Vilnius, Lithuania, 16-18 June 2010. - P. 1-4. ↑
- C110.** Stove A.G. Using noise modulation in practical radar systems: -Including a comparison with FMCW modulation. 2010 11th International Radar Symposium (IRS). - Vilnius, 16-18 June 2010. - P. 1-4. ↑
- C111.** Savelyev Timofey. Development of UWB microwave array radar for concealed weapon detection. / Savelyev Timofey, Zhuge Xiaodong, Yang Bill, Yarovoy Alexander, Lighthart Leo, Drozdov Michail, Levitas Boris. // 2010 11th International Radar Symposium (IRS). - Vilnius, Lithuania, 16-18 June 2010. - P. 1-4. ↑
- C112.** Bokal Zhanna. Rank signal detection algorithms based on permutations of partial likelihood ratios. / Bokal Zhanna, Sinitsyn Rustem. // 2010 11th International Radar Symposium (IRS). - Vilnius, Lithuania, 16-18 June 2010. - P. 1-4. ↑
- C113.** Wang Guohua. Designing sparse frequency waveform using iterative algorithm. / Wang Guohua, Lu Yilong. // 2010 11th International Radar Symposium (IRS). - Vilnius, Lithuania, 16-18 June 2010. - P. 1-4. ↑
- C114.** Sachs J. On the Range Precision of UWB Radar Sensors. / Sachs J., Helbig M., Herrmann R., Kmec M., Schilling K. // 2010 11th International Radar Symposium (IRS). - Vilnius, Lithuania, 16-18 June 2010. - P. 1-4. ↑
- C115.** Svecova Maria. Target localization by the method of joining intersections of the ellipses. / Svecova Maria, Kocur Dusan. // 2010 11th International Radar Symposium (IRS). - Vilnius, Lithuania, 16-18 June 2010. - P. 1-4. ↑
- C116.** Stateczny Andrzej. A concept of decentralized fusion of maritime radar targets with multisensor Kalman filter. / Stateczny Andrzej, Kazimierski Witold. // 2010 11th International Radar Symposium (IRS). - Vilnius, Lithuania, 16-18 June 2010. - P. 1-4. ↑
- C117.** Tahmoush Dave. Tracking of dismounts moving in cross-range using GMTI radar. / Tahmoush Dave, Clark John, Silvius Jerry. // 2010 11th International Radar Symposium (IRS). - Vilnius, Lithuania, 16-18 June 2010. - P. 1-6. ↑
- C118.** Susek Waldemar. Broadband microwave correlation receiver for noise radar. / Susek Waldemar, Stec Bronislaw, Recko Czeslaw. // 2010 11th International Radar Symposium (IRS). - Vilnius, Lithuania, 16-18 June 2010. - P. 1-4. ↑



- C119.** Lukin K. Stepped-frequency noise radar with short switching time and high dynamic range. / Lukin K., Mogyla A., Palamarchuk V., Cherniy V., Kravchuk A. // 2010 11th International Radar Symposium (IRS). - Vilnius, Lithuania, 16-18 June 2010. - P. 1-4. 
- C120.** Malanowski M. Robust detection in continuous-wave noise radar-experimental results. / Malanowski M., Kulpa K. // 2010 11th International Radar Symposium (IRS). - Vilnius, 16-18 June 2010. - P. 1-4. 
- C121.** Meller Michal. Impact of quantization and roundoff errors on the performance of a noise radar correlator. 2010 11th International Radar Symposium (IRS). - Vilnius, Lithuania, 16-18 June 2010. - P. 1-4. 
- C122.** Pietkiewicz Tadeusz. An application of the content description language XML for modeling of information structures of electronic intelligence system. / Pietkiewicz Tadeusz, Kawalec Adam, Krenc Ksawery. // 2010 11th International Radar Symposium (IRS). - Vilnius, Lithuania, 16-18 June 2010. - P. 1-4. 
- C123.** Kabakchiev A. Comparison of communication signals for passive radar application. / Kabakchiev A., Kyovtorov V., Kabakchiev C., Lazarov A. // 2010 11th International Radar Symposium (IRS). - Vilnius, Lithuania, 16-18 June 2010. - P. 1-4. 
- C124.** Kawalec Adam. Higher order statistics sensitivity to radar signal feature. / Kawalec Adam, Fornalik Jacek, Pieniezny Andrzej, Witczak Andrzej. // 2010 11th International Radar Symposium (IRS). - Vilnius, Lithuania, 16-18 June 2010. - P. 1-4. 
- C125.** Magaz B. Numerical analysis of MIMO radar detection performance under weibull-distributed clutter. / Magaz B., Bencheikh M. L., Wang Y., Belouchrani A. // 2010 11th International Radar Symposium (IRS). - Vilnius, Lithuania, 16-18 June 2010. - P. 1-4. 
- C126.** Jena Paramananda. Design and implementation of a highly configurable low power robust signal processor for portable ground based "multiple scan rate" surveillance radar. / Jena Paramananda, V Chandrakanth., Tripathi Bhishm, Kuloor Ramachandra, Nasir Wasim. // 2010 11th International Radar Symposium (IRS). - Vilnius, Lithuania, 16-18 June 2010. - P. 1-4. 
- C127.** Kawalec Adam. Higher order statistics sensitivity to radar signal feature. / Kawalec Adam, Fornalik Jacek, Pieniezny Andrzej, Witczak Andrzej. // 2010 11th International Radar Symposium (IRS). - Vilnius, Lithuania, 16-18 June 2010. - P. 1-4. 
- C128.** Bezruck V.M. Application of Autoregressive Model for Recognition of Meteorological Objects. / Bezruck V.M., Belov Y.N., Voitovych O.A., Netrebenko K.A., Tikhonov V.A., Rudnev G.A., Khlopov G.I., Khomenko S.I. // 2010 11th International Radar Symposium (IRS). - Vilnius, 16-18 June 2010. - P. 1-3. 
- C129.** Matuszewski Jan. Applying the decision trees to radar targets recognition. 2010 11th International Radar Symposium (IRS). - Vilnius, Lithuania, 16-18 June 2010. - P. 1-4. 
- C130.** Canini F. Use of Digital-Television terrestrial (DTV) signals for passive radars. / Canini F., Di Lallo A., Timmoneri L., Vigilante D. // 2010 11th International Radar Symposium (IRS). - Vilnius, Lithuania, 16-18 June 2010. - P. 1-4. 
- C131.** Tahmoush Dave. Modeled gait variations in human micro-doppler. / Tahmoush Dave, Silvius Jerry. // 2010 11th International Radar Symposium (IRS). - Vilnius, Lithuania, 16-18 June 2010. - P. 1-4. 
- C132.** Radmard M. Cross ambiguity function analysis of the '8k-mode' DVB-T for passive radar application. / Radmard M., Bastani M., Behnia F., Nayebi M. M. // 2010 11th International Radar Symposium (IRS). - Vilnius, Lithuania, 16-18 June 2010. - P. 1-4. 
- C133.** Vervecka Martynas. Data fusion algorithms for sea target tracking using coastal radar model. 2010 11th International Radar Symposium (IRS). - Vilnius, Lithuania, 16-18 June 2010. - P. 1-3. 
- C134.** Kyovtorov Vladimir. Power analysis of parallel CA-CFAR FPGA design. / Kyovtorov Vladimir, Kabakchiev Hristo, Kuzmanov Georgi. // 2010 11th International Radar Symposium (IRS). - Vilnius, Lithuania, 16-18 June 2010. - P. 1-4. 
- C135.** Radmard M. Advantages of the DVB-T signal for passive radar applications. / Radmard M., Bastani M., Behnia F., Nayebi M. M. // 2010 11th International Radar Symposium (IRS). - Vilnius, Lithuania, 16-18 June 2010. - P. 1-4. 

2010. - P. 1-5. ↑

**C136.** Xu Jianping. SAR image compression based on sparse representation. / Xu Jianping, Pi Yiming, Ming Rui. // 2010 11th International Radar Symposium (IRS). - Vilnius, Lithuania, 16-18 June 2010. - P. 1-4. ↑

**C137.** Brenner Tadeusz. K band patch antenna applied in an FMCW radar. / Brenner Tadeusz, Krawczyk Marek, Slarzyński Sławomir. // 2010 11th International Radar Symposium (IRS). - Vilnius, Lithuania, 16-18 June 2010. - P. 1-3. ↑

**C138.** Amato Felicia. Fully solid state radar for vessel traffic services. / Amato Felicia, Fiorini Michele, Gallone Sergio, Golino Giovanni. // 2010 11th International Radar Symposium (IRS). - Vilnius, Lithuania, 16-18 June 2010. - P. 1-5. ↑

**C139.** Jiabing Zhu. An analysis of through-wall radar based on UWB impulse technique. / Jiabing Zhu, Yi Hong. // 2010 11th International Radar Symposium (IRS). - Vilnius, 16-18 June 2010. - P. 1-5. ↑

**C140.** Houria M. Performance analysis in heterogeneous environment and implementation on DSP processor of a GOWMAX CFAR detector. / Houria M., M'hamed H., Fatiha Y.E. // 2010 11th International Radar Symposium (IRS). - Vilnius, 16-18 June 2010. - P. 1-3. ↑

**C141.** Lukyanov S. P. One Example of classing and extracting information from GPR images for the archeology. / Lukyanov S. P., Stepanov R. A., Stukach O. V. // 2010 11th International Radar Symposium (IRS). - Vilnius, Lithuania, 16-18 June 2010. - P. 1-4. ↑

**C142.** Cholewa Jacek. Demonstrator of S band active antenna with T/R modules. / Cholewa Jacek, Stachowski Bogdan, Czwartacka Anna, Szustak Konrad, Startek Dariusz, Andrzejewski Mirosław, Sender Robert, Lorens Tomasz. // 2010 11th International Radar Symposium (IRS). - Vilnius, Lithuania, 16-18 June 2010. - P. 1-4. ↑

**C143.** Melezhik P. N. Ka-band radar sensor with selection of moving targets for airport surface monitoring. / Melezhik P. N., Sidorenko Yu. B., Provalov S. A., Razskazovskiy V. B., Reznichenko N. G., Zuykov V. A., Balan M. G., Varavin A. V., Kolisnichenko M. V., Mus'kin Yu. N. // 2010 11th International Radar Symposium (IRS). - Vilnius, Lithuania, 16-18 June 2010. - P. 1-3. ↑

**C144.** Varavin A. V. Range resolution improvement for low-cost FMCW self-mixing radar. / Varavin A. V., Ermak G. P., Vasilev A. S., Evdokimov A. P., Kryzanovsky V. V. // 2010 11th International Radar Symposium (IRS). - Vilnius, Lithuania, 16-18 June 2010. - P. 1-4. ↑

**C145.** Khopov G. Study of double frequency method for remote sensing of liquid precipitations. / Khopov G., Khomenko S., Linkova A., Voitovych O. // 2010 11th International Radar Symposium (IRS). - Vilnius, 16-18 June 2010. - P. 1-3. ↑

**C146.** Alidoost S. Autodyne system with a single antenna. / Alidoost S., Sadeghzade R., Fatemi R. // 2010 11th International Radar Symposium (IRS). - Vilnius, Lithuania, 16-18 June 2010. - P. 1-5. ↑

**C147.** renzhou Gui. Utilizing Adaptive Techniques to Suppress Noise In High Frequency Ground Wave Radar. 2010 11th International Radar Symposium (IRS). - Vilnius, Lithuania, 16-18 June 2010. - P. 1-4. ↑

**C148.** Molchanov Pavel A. Object recognition in ground surveillance doppler radar by using bispectrum-based time-frequency distributions. / Molchanov Pavel A., Astola Jaakko T., Egiazarian Karen O., Khlopov Grigory I., Morozov Vladimir Ye., Pospelov Boris B., Totsky Alexander V. // 2010 11th International Radar Symposium (IRS). - Vilnius, Lithuania, 16-18 June 2010. - P. 1-4. ↑

**C149.** Tadeusz S. Hydro-meteorological disturbances influence on radar picture investigation. / Tadeusz S., Ryszard W., Sławomir P. // 2010 11th International Radar Symposium (IRS). - Vilnius, 16-18 June 2010. - P. 1-4. ↑

**C150.** Zych Mariusz. Focused algorithms for ground penetrating radar imaging. / Zych Mariusz, Gromek Damian, Gromek Artur. // 2010 11th International Radar Symposium (IRS). - Vilnius, Lithuania, 16-18 June 2010. - P. 1-5. ↑

**C151.** Jacek M.Sc. Majewski. Refraction influence on air target elevation estimation in 3-D radars. / Jacek M.Sc. Majewski, Maciej M.Sc. Smolarczyk. // 2010 11th International Radar Symposium (IRS). - Vilnius,

Lithuania, 16-18 June 2010. - P. 1-4. ↑

**C152.** Qiwei Zhang. A novel OFDM based ground penetrating radar. / Qiwei Zhang, Pennock S., Redfern M., Naji A. // 2010 13th International Conference on Ground Penetrating Radar (GPR). - Lecce, 21-25 June 2010. - P. 1-6. ↑

**C153.** Be. GPR, ERT and CPT data integration for high resolution aquifer modeling. / Be, langer C., Giroux B., Gloaguen E., Lefebvre R. // 2010 13th International Conference on Ground Penetrating Radar (GPR). - Lecce, 21-25 June 2010. - P. 1-6. ↑

**C154.** Donazzolo V. Determination of wall thickness and condition of asbestos cement pipes in sewer rising mains using Surface Penetrating Radar. / Donazzolo V., Yelf R. // 2010 13th International Conference on Ground Penetrating Radar (GPR). - Lecce, 21-25 June 2010. - P. 1-5. ↑

**C155.** Miorali M. A controlled experiment for water front monitoring using GPR technology. / Miorali M., Slob E., Arts R. // 2010 13th International Conference on Ground Penetrating Radar (GPR). - Lecce, 21-25 June 2010. - P. 1-6. ↑

**C156.** Gloaguen E. Simulation of porosity field using wavelet bayesian inversion of crosswell GPR and log data. / Gloaguen E., Dubreuil-Boisclair C., Simard P., Giroux B., Marcotte D. // 2010 13th International Conference on Ground Penetrating Radar (GPR). - Lecce, 21-25 June 2010. - P. 1-6. ↑

**C157.** Colla Camilla. GPR of a timber structural element. 2010 13th International Conference on Ground Penetrating Radar (GPR). - Lecce, Italy, 21-25 June 2010. - P. 1-5. ↑

**C158.** Martin T. Detection of granite landmarks in soil with GPR. / Martin T., Trela C., Kind T., Gil M., Wojstmann J. // 2010 13th International Conference on Ground Penetrating Radar (GPR). - Lecce, 21-25 June 2010. - P. 1-5. ↑

**C159.** Valerio G. GPR characterization of rocks buried in the Martian subsoil. / Valerio G., Galli A., Barone P.M., Lauro S.E., Mattei E., Pettinelli E. // 2010 13th International Conference on Ground Penetrating Radar (GPR). - Lecce, 21-25 June 2010. - P. 1-4. ↑

**C160.** Strobach E. GPR for large-scale estimation of groundwater recharge distribution. / Strobach E., Harris B.D., Dupuis J.C., Kepic A.W., Martin M.W. // 2010 13th International Conference on Ground Penetrating Radar (GPR). - Lecce, 21-25 June 2010. - P. 1-6. ↑

**C161.** Jacob R.W. GPR reflection and dispersion analysis methods for water content: Multi-year study of GPR estimates and soil core measurements of water content. / Jacob R.W., Hermance J.F., van der Kruk J. // 2010 13th International Conference on Ground Penetrating Radar (GPR). - Lecce, 21-25 June 2010. - P. 1-6. ↑

**C162.** Carpentier S.F.A. Recent deformation of Quaternary sediments in the northwest Canterbury Plains, New Zealand, as inferred from GPR and seismic data. / Carpentier S.F.A., Dorn C., Doetsch J.A., Campbell F.M., Horstmeyer H., Green A.G., Kaiser A.E., Campbell J., Pettinga J., Nobes D.C., Finnemore M., Jongens R. // 2010 13th International Conference on Ground Penetrating Radar (GPR). - Lecce, 21-25 June 2010. - P. 1-5. ↑

**C163.** Francke J. Applications of GPR in mineral resource evaluations. 2010 13th International Conference on Ground Penetrating Radar (GPR). - Lecce, 21-25 June 2010. - P. 1-5. ↑

**C164.** Novo Alexandre. From Pseudo-3D to full-resolution GPR imaging in archaeology: A complex Roman site in Lugo, Spain. / Novo Alexandre, Lorenzo Henrique, Rial Fernando I., Solla Mercedes. // 2010 13th International Conference on Ground Penetrating Radar (GPR). - Lecce, Italy, 21-25 June 2010. - P. 1-6. ↑

**C165.** Tatum D. Constructing hydrocarbon reservoir analogues with rapid acquisition long-range GPR. / Tatum D., Westerman R., Francke J., Hern C. // 2010 13th International Conference on Ground Penetrating Radar (GPR). - Lecce, 21-25 June 2010. - P. 1-6. ↑

**C166.** Shao W. Automatic classification of GPR signals. / Shao W., Bouzerdoum A., Phung S.L., Su L., Indraratna B., Rujikiatkamjorn C. // 2010 13th International Conference on Ground Penetrating Radar (GPR). - Lecce, 21-25 June 2010. - P. 1-6. ↑

**C167.** Ouadfeul S.-A. Multiscale analysis of 3D GPR data using the continuous wavelet transform. / Ouadfeul

S.-A., Aliouane L. // 2010 13th International Conference on Ground Penetrating Radar (GPR). - Lecce, 21-25 June 2010. - P. 1-4. ↑

C168. Aysel Seren. Georadar Investigation of Graves and Wall Remains in Alacahцуьк, Central Anatolia. / Aysel Seren, Gelisli Kenan, Acikgoz Aydanur D., Erkul Selin. // 2010 13th International Conference on Ground Penetrating Radar (GPR). - Lecce, Italy, 21-25 June 2010. - P. 1-5. ↑

C169. Kadioglu S. Different time gain and amplitude-color arranging for ground penetrating radar data: Applied samples. / Kadioglu S., Daniels J.J. // 2010 13th International Conference on Ground Penetrating Radar (GPR). - Lecce, 21-25 June 2010. - P. 1-4. ↑

C170. Roberts R. Mitigation of RF interference in air-launched 2 GHz GPR antennas. / Roberts R., Feigin J., Parrillo R. // 2010 13th International Conference on Ground Penetrating Radar (GPR). - Lecce, 21-25 June 2010. - P. 1-6. ↑

C171. Brancaccio A. Localization of buried objects. / Brancaccio A., Leone G. // 2010 13th International Conference on Ground Penetrating Radar (GPR). - Lecce, 21-25 June 2010. - P. 1-4. ↑

C172. Sezgin M. A novel detection warning signal creation method for hand-held GPR applications. 2010 13th International Conference on Ground Penetrating Radar (GPR). - Lecce, 21-25 June 2010. - P. 1-6. ↑

C173. Salman A.O. Textile antenna for the multi-sensor (impulse GPR&EMI) subsurface detection system. / Salman A.O., Bicaк E., Sezgin M. // 2010 13th International Conference on Ground Penetrating Radar (GPR). - Lecce, 21-25 June 2010. - P. 1-5. ↑

C174. Kadioglu S. GPR research at the tomb of Zeynel Bey in Hasankeyf ancient city- Southeastern Turkey. / Kadioglu S., Akyol A.A., Kadioglu Y.K., Ekinoglu E.E. // 2010 13th International Conference on Ground Penetrating Radar (GPR). - Lecce, 21-25 June 2010. - P. 1-4. ↑

C175. Koh G. Autonomous FMCW radar survey of Antarctic shear zone. / Koh G., Lever J.H., Arcone S.A., Marshall H., Ray L.E. // 2010 13th International Conference on Ground Penetrating Radar (GPR). - Lecce, 21-25 June 2010. - P. 1-5. ↑

C176. Colla Camilla. Diagnostic by imaging: 3D GPR investigation of brick masonry and post-tensioned concrete. / Colla Camilla, Juez Fernandez Ana, Garanzini Stefano, Marelli Matteo. // 2010 13th International Conference on Ground Penetrating Radar (GPR). - Lecce, Italy, 21-25 June 2010. - P. 1-7. ↑

C177. Millington T.M. Evaluating the practical performance of absorbing boundary conditions (ABC) in higher-order, finite-difference, time-domain (FDTD) GPR modelling. / Millington T.M., Cassidy N.J., Crocco L., Soldovieri F. // 2010 13th International Conference on Ground Penetrating Radar (GPR). - Lecce, 21-25 June 2010. - P. 1-5. ↑

C178. Solimene R. TWI in-situ experimental results. / Solimene R., Di Napoli R., Baratonі A., Pierri R. // 2010 13th International Conference on Ground Penetrating Radar (GPR). - Lecce, 21-25 June 2010. - P. 1-5. ↑

C179. Campana S. GPR investigation in different archaeological sites in Tuscany. Analysis and comparison of the obtained results. / Campana S., Piro S. // 2010 13th International Conference on Ground Penetrating Radar (GPR). - Lecce, Italy, 21-25 June 2010. - P. 1-6. ↑

C180. Corsi Cristina. Mariana (Corsica). Integrating GPR in Roman urban survey. / Corsi Cristina, Verdonck Lieven, Vermeulen Frank. // 2010 13th International Conference on Ground Penetrating Radar (GPR). - Lecce, Italy, 21-25 June 2010. - P. 1-6. ↑

C181. Scardozzi Giuseppe. Integrated geophysical methods for the knowledge of the urban layout of Hierapolis in Phrygia (Turkey). 2010 13th International Conference on Ground Penetrating Radar (GPR). - Lecce, Italy, 21-25 June 2010. - P. 1-6. ↑

C182. Hanson D. A stepped frequency radar for use on Horizontal Directional Drills. / Hanson D., Haddad W.S., Sjostrom K., Langman A., Ryerson K., Shafer M., Kothari K. // 2010 13th International Conference on Ground Penetrating Radar (GPR). - Lecce, 21-25 June 2010. - P. 1-6. ↑

C183. Caratelli D. Design and full-wave analysis of cavity-backed bow-tie antennas for low-frequency GPR



applications. / Caratelli D., Yarovoy A. // 2010 13th International Conference on Ground Penetrating Radar (GPR). - Lecce, 21-25 June 2010. - P. 1-10. ↑

C184. Balsi M. GPR measurements and FDTD simulations for landmine detection. / Balsi M., Esposito S., Frezza F., Nocito P., Barone P.M., Lauro S.E., Mattei E., Pettinelli E., Schettini G., Twizere C. // 2010 13th International Conference on Ground Penetrating Radar (GPR). - Lecce, 21-25 June 2010. - P. 1-5. ↑

C185. Zhou L. A GPR imaging algorithm with artifacts suppression. / Zhou L., Su Y. // 2010 13th International Conference on Ground Penetrating Radar (GPR). - Lecce, 21-25 June 2010. - P. 1-7. ↑

C186. Caratelli D. EM characterization of resistively loaded printed dipole antennas for GPR applications. / Caratelli D., Poley H., Yarovoy A. // 2010 13th International Conference on Ground Penetrating Radar (GPR). - Lecce, 21-25 June 2010. - P. 1-6. ↑

C187. Patriarca C. Influence of acquisition related uncertainties on ground penetrating radar inversion results. / Patriarca C., Mahmoudzadeh M.R., Lambot S., Slob E. // 2010 13th International Conference on Ground Penetrating Radar (GPR). - Lecce, 21-25 June 2010. - P. 1-6. ↑

C188. Caratelli D. Experimental evaluation of the antenna sub-system of the ORFEUS surface GPR. / Caratelli D., Poley H.G., Aubry P., Savelyev T., Yarovoy A., Testa C., De Pasquale G., Manacorda G. // 2010 13th International Conference on Ground Penetrating Radar (GPR). - Lecce, 21-25 June 2010. - P. 1-6. ↑

C189. Pe. GPR applications in dense cities: Detection of paleochannels and infilled torrents in Barcelona GPR applications in dense cities. / Pe, rez-Gracia V., Caselles O., Salinas V., Pujades L.G., Clape, s J. // 2010 13th International Conference on Ground Penetrating Radar (GPR). - Lecce, 21-25 June 2010. - P. 1-5. ↑

C190. Pallavi B. Monitoring of seasonal influence on spatial distribution of moisture content at a natural Kanto loam site using ground wave of GPR. / Pallavi B., Saito H., Kato M. // 2010 13th International Conference on Ground Penetrating Radar (GPR). - Lecce, 21-25 June 2010. - P. 1-5. ↑

C191. Golebiowski T. Velocity analysis in the GPR method for loose-zones detection in the river embankments. 2010 13th International Conference on Ground Penetrating Radar (GPR). - Lecce, 21-25 June 2010. - P. 1-6. ↑

C192. Keach R.W. Petroleum industry techniques yield new insights into 3D GPR data. / Keach R.W., McBride J.H., Pykles B.C. // 2010 13th International Conference on Ground Penetrating Radar (GPR). - Lecce, 21-25 June 2010. - P. 1-5. ↑

C193. Drahor Mahmut Goktug. Ground penetrating radar (GPR) studies in the Agios Voukolos church, Izmir, Turkey. / Drahor Mahmut Goktug, Ozturk Caner, Berge Meric Aziz. // 2010 13th International Conference on Ground Penetrating Radar (GPR). - Lecce, Italy, 21-25 June 2010. - P. 1-5. ↑

C194. Ojztujrk C. Synthetic GPR modelling studies on shallow geological properties and its comparison with the real data. / Ojztujrk C., Drahor M.G. // 2010 13th International Conference on Ground Penetrating Radar (GPR). - Lecce, 21-25 June 2010. - P. 1-4. ↑

C195. Sang-Wook Kim. Analysis of dispersion of pulse signals in underground tunnels using finite-difference time domain and short-time Fourier transform. / Sang-Wook Kim, Se-Yun Kim. // 2010 13th International Conference on Ground Penetrating Radar (GPR). - Lecce, 21-25 June 2010. - P. 1-5. ↑

C196. Mahmoudzadeh M.R. Water table detection by GPR in Sardon, Salamanca, Spain. / Mahmoudzadeh M.R., Lambot S., Frances A.P., Mohammed A.A., Lubczynski M. // 2010 13th International Conference on Ground Penetrating Radar (GPR). - Lecce, 21-25 June 2010. - P. 1-5. ↑

C197. Villela A. Experimenting with different polarization arrays in a test site. / Villela A., Romo J.M. // 2010 13th International Conference on Ground Penetrating Radar (GPR). - Lecce, 21-25 June 2010. - P. 1-5. ↑

C198. Fiaz M.A. Scattering by a circular cylinder buried beneath a rough surface. / Fiaz M.A., Pajewski L., Ponti C., Schettini G., Frezza F. // 2010 13th International Conference on Ground Penetrating Radar (GPR). - Lecce, 21-25 June 2010. - P. 1-5. ↑

C199. Nuzzo Luigia. A review of geometric issues in GPR prospecting of cylindrical structures in Cultural

Heritage applications. / Nuzzo Luigia, Quarta Tatiana. // 2010 13th International Conference on Ground Penetrating Radar (GPR). - Lecce, Italy, 21-25 June 2010. - P. 1-6. ↑

C200. Perez-Gracia V. GPR resolution in cultural heritage applications. / Perez-Gracia V., Di Capua D., Gonzalez-Drigo R., Caselles O., Pujades L.G., Salinas V. // 2010 13th International Conference on Ground Penetrating Radar (GPR). - Lecce, Italy, 21-25 June 2010. - P. 1-5. ↑

C201. Bradford J.H. 2D ground-penetrating radar AVO response to a 3D dielectric permittivity anomaly. 2010 13th International Conference on Ground Penetrating Radar (GPR). - Lecce, 21-25 June 2010. - P. 1-5. ↑

C202. Marchesini P. Impact of spatial sampling and antenna polarization on 3D GPR fracture detection. / Marchesini P., Grasmueck M. // 2010 13th International Conference on Ground Penetrating Radar (GPR). - Lecce, 21-25 June 2010. - P. 1-6. ↑

C203. Solla M. Masonry arch bridges evaluation by means of GPR. / Solla M., Lorenzo H., Rial F.I., Novo A., Riveiro B. // 2010 13th International Conference on Ground Penetrating Radar (GPR). - Lecce, 21-25 June 2010. - P. 1-6. ↑

C204. Lalague A. Determination of space behind pre-cast concrete elements in tunnels using GPR. / Lalague A., Hoff I. // 2010 13th International Conference on Ground Penetrating Radar (GPR). - Lecce, 21-25 June 2010. - P. 1-5. ↑

C205. Ebihara S. Singlehole borehole radar measurement using dipole array antenna fed by coaxial cable. / Ebihara S., Kawai H. // 2010 13th International Conference on Ground Penetrating Radar (GPR). - Lecce, 21-25 June 2010. - P. 1-6. ↑

C206. Parrini F. ORFEUS GPR: a very large bandwidth and high dynamic range CWSF radar. / Parrini F., Pieraccini M., Grazzini G., Spinetti A., Macaluso G., De Pasquale G., Testa C. // 2010 13th International Conference on Ground Penetrating Radar (GPR). - Lecce, 21-25 June 2010. - P. 1-5. ↑

C207. Ebihara S. Influence of feed line on DOA estimation with dipole array antenna for directional borehole radar. / Ebihara S., Hideharu H., Takashi O. // 2010 13th International Conference on Ground Penetrating Radar (GPR). - Lecce, 21-25 June 2010. - P. 1-6. ↑

C208. Ebihara S. Influence of HE11 mode on direct wave in singlehole borehole radar. / Ebihara S., Sasakura A., Takemoto T. // 2010 13th International Conference on Ground Penetrating Radar (GPR). - Lecce, 21-25 June 2010. - P. 1-7. ↑

C209. Capizzi P. Can be GPR technique useful for strength characterization of concrete?. / Capizzi P., Cosentino P., Schiavone S. // 2010 13th International Conference on Ground Penetrating Radar (GPR). - Lecce, 21-25 June 2010. - P. 1-4. ↑

C210. Balasubramaniam V.R. Imaging for foundation defects using GPR. / Balasubramaniam V.R., Jha P.C. // 2010 13th International Conference on Ground Penetrating Radar (GPR). - Lecce, 21-25 June 2010. - P. 1-5. ↑

C211. Jha P.C. Mapping oil leak flow path using Step Frequency Radar: A case study. / Jha P.C., Balasubramaniam V.R., Sandeep N., Sivaram Y.V. // 2010 13th International Conference on Ground Penetrating Radar (GPR). - Lecce, 21-25 June 2010. - P. 1-6. ↑

C212. Yonghui Zhao. Multiple suppression in GPR image for testing back-filled grouting within shield tunnel. / Yonghui Zhao, Jiansheng Wu, Xiongyao Xie, Jun Chen, Shuangcheng Ge. // 2010 13th International Conference on Ground Penetrating Radar (GPR). - Lecce, 21-25 June 2010. - P. 1-6. ↑

C213. Naser M. Influence of pipe filling, geometry and antenna polarisation on GPR measurements. / Naser M., Junge A. // 2010 13th International Conference on Ground Penetrating Radar (GPR). - Lecce, 21-25 June 2010. - P. 1-6. ↑

C214. Guo Chen. A 900MHz shielded bow-tie antenna system for ground penetrating radar. / Guo Chen, Liu R.C. // 2010 13th International Conference on Ground Penetrating Radar (GPR). - Lecce, 21-25 June 2010. - P. 1-6. ↑

C215. Sala Jacopo. Processing stepped frequency continuous wave GPR systems to obtain maximum value

from archaeological data sets. / Sala Jacopo, Linford Neil. // 2010 13th International Conference on Ground Penetrating Radar (GPR). - Lecce, Italy, 21-25 June 2010. - P. 1-6. ↑

C216. Forte E. 2D and 3D GPR imaging and characterization of a carbonate hydrocarbon reservoir analogue. / Forte E., Pipan M., Casabianca D., Di Cuia R., Riva A. // 2010 13th International Conference on Ground Penetrating Radar (GPR). - Lecce, 21-25 June 2010. - P. 1-7. ↑

C217. You Z. Disposable stepped-frequency GPR and soil measurement devices. / You Z., Cross J., Foo K.Y., Atkins P.R., Thomas A.M., Curioni G., Islas-Cital A. // 2010 13th International Conference on Ground Penetrating Radar (GPR). - Lecce, 21-25 June 2010. - P. 1-5. ↑

C218. Gundelach V. Exploration of geological structures with GPR from helicopter and on the ground in the Letzlinger Heide (Germany). / Gundelach V., Blindow N., Buschmann U., Salat C., Krellmann Y. // 2010 13th International Conference on Ground Penetrating Radar (GPR). - Lecce, 21-25 June 2010. - P. 1-6. ↑

C219. Gujrbujz A.C. Sparsity enhanced fast subsurface imaging with GPR. 2010 13th International Conference on Ground Penetrating Radar (GPR). - Lecce, 21-25 June 2010. - P. 1-5. ↑

C220. Spanoudakis S.N. GPR-PRO: A MATLAB module for GPR data processing. / Spanoudakis S.N., Vafidis A. // 2010 13th International Conference on Ground Penetrating Radar (GPR). - Lecce, 21-25 June 2010. - P. 1-5. ↑

C221. Economou N. GPR data time varying deconvolution by kurtosis maximization. / Economou N., Vafidis A. // 2010 13th International Conference on Ground Penetrating Radar (GPR). - Lecce, 21-25 June 2010. - P. 1-5. ↑

C222. Capineri L. Quantitative interpretation of RASCAN holographic radar response from inclined plane reflectors by a theoretical model. / Capineri L., Falorni P., Inagaki M., Razevig V., Bechtel T., Windsor C. // 2010 13th International Conference on Ground Penetrating Radar (GPR). - Lecce, 21-25 June 2010. - P. 1-4. ↑

C223. Yoldemir A.B. Adaptive linear prediction based buried object detection with varying detector height. / Yoldemir A.B., Sezgin M. // 2010 13th International Conference on Ground Penetrating Radar (GPR). - Lecce, 21-25 June 2010. - P. 1-4. ↑

C224. Congedo F. Modified bowtie antenna for GPR applications. / Congedo F., Monti G., Tarricone L. // 2010 13th International Conference on Ground Penetrating Radar (GPR). - Lecce, 21-25 June 2010. - P. 1-5. ↑

C225. Sammarco Mariangela. The contribution of GPR analysis to knowledge of the cultural heritage in Apulia (southern Italy). / Sammarco Mariangela, Martimucci Vincenzo, Parise Mario, Pepe Pietro. // 2010 13th International Conference on Ground Penetrating Radar (GPR). - Lecce, Italy, 21-25 June 2010. - P. 1-6. ↑

C226. Parker R. Freshwater ground penetrating radar the significance of seasonal temperature variation. 2010 13th International Conference on Ground Penetrating Radar (GPR). - Lecce, 21-25 June 2010. - P. 1-6. ↑

C227. Khan U.S. Background removal from GPR data using Eigenvalues. / Khan U.S., Al-Nuaimy W. // 2010 13th International Conference on Ground Penetrating Radar (GPR). - Lecce, 21-25 June 2010. - P. 1-5. ↑

C228. Vertiy A.A. Subsurface sensing at sub-terahertz and terahertz frequencies. / Vertiy A.A., Cetinkaya H., Tekbas M. // 2010 13th International Conference on Ground Penetrating Radar (GPR). - Lecce, 21-25 June 2010. - P. 1-4. ↑

C229. Siever K. Salt dome exploration by directional borehole radar wireline service. / Siever K., Elsen R. // 2010 13th International Conference on Ground Penetrating Radar (GPR). - Lecce, 21-25 June 2010. - P. 1-5. ↑

C230. Bellomo L. An ultrawideband time reversal-based RADAR for microwave-range imaging in cluttered media. / Bellomo L., Saillard M., Pioch S., Belkebir K., Chaumet P. // 2010 13th International Conference on Ground Penetrating Radar (GPR). - Lecce, 21-25 June 2010. - P. 1-5. ↑

C231. Wei Jiang. Novel short-time MUSIC in non-linear FMCW GPR signal analysis. / Wei Jiang, Pennock S., Shepherd P. // 2010 13th International Conference on Ground Penetrating Radar (GPR). - Lecce, 21-25 June 2010. - P. 1-6. ↑

C232. Amico F.D. GPR Signal processing in frequency domain using Artificial Neural Network for water

content prediction in unsaturated subgrade. / Amico F.D., Guattari C., Benedetto A. // 2010 13th International Conference on Ground Penetrating Radar (GPR). - Lecce, 21-25 June 2010. - P. 1-6. ↑

C233. Guattari C. Integrated road pavement survey using GPR and LFWD. / Guattari C., D'Amico F., Benedetto A. // 2010 13th International Conference on Ground Penetrating Radar (GPR). - Lecce, 21-25 June 2010. - P. 1-6. ↑

C234. Rodriguez-Abad I. Wave parameter analysis of dielectric anisotropy in maritime pine timber using GPR. / Rodriguez-Abad I., Martinez-Sala R., Garcia-Garcia F., Capuz-Lladro R. // 2010 13th International Conference on Ground Penetrating Radar (GPR). - Lecce, Italy, 21-25 June 2010. - P. 1-5. ↑

C235. Barone P.M. Non-destructive technique to investigate an archaeological structure: A GPR survey in the Domus Aurea (Rome, Italy). / Barone P.M., Mattei E., Lauro S.E., Pettinelli E. // 2010 13th International Conference on Ground Penetrating Radar (GPR). - Lecce, Italy, 21-25 June 2010. - P. 1-4. ↑

C236. Kaplan G.B. Real-time object detection using dynamic principal component analysis. / Kaplan G.B., Icoğlu O., Yoldemir A.B., Sezgin M. // 2010 13th International Conference on Ground Penetrating Radar (GPR). - Lecce, 21-25 June 2010. - P. 1-6. ↑

C237. Ihamouten A. Electromagnetic dispersion estimated from multi-offset, ground-penetrating radar. / Ihamouten A., De,robert X., Villain G. // 2010 13th International Conference on Ground Penetrating Radar (GPR). - Lecce, 21-25 June 2010. - P. 1-6. ↑

C238. Ihamouten A. The effect of coupling on the determination of time zero for radar antennae. / Ihamouten A., De,robert X., Villain G. // 2010 13th International Conference on Ground Penetrating Radar (GPR). - Lecce, 21-25 June 2010. - P. 1-6. ↑

C239. Chahine K. On the variants of Jonscher's model for the electromagnetic characterization of concrete. / Chahine K., Ihamouten A., Baltazart V., Villain G., De,robert X. // 2010 13th International Conference on Ground Penetrating Radar (GPR). - Lecce, 21-25 June 2010. - P. 1-6. ↑

C240. Villain G. Evaluation of concrete water content and other durability indicators by electromagnetic measurements. / Villain G., De,robert X., Sbartai Z.M., Balayssac J. // 2010 13th International Conference on Ground Penetrating Radar (GPR). - Lecce, 21-25 June 2010. - P. 1-6. ↑

C241. Arcone S.A. Complex permittivity of common minerals and one soil at low water contents. / Arcone S.A., Boitnott G.E. // 2010 13th International Conference on Ground Penetrating Radar (GPR). - Lecce, 21-25 June 2010. - P. 1-6. ↑

C242. Jadoon K.Z. Investigation of the frequency dependent antenna transfer functions and phase center position for modeling off-ground GPR. / Jadoon K.Z., Lambot S., Slob E., Verreken H. // 2010 13th International Conference on Ground Penetrating Radar (GPR). - Lecce, 21-25 June 2010. - P. 1-7. ↑

C243. Slob E. Uncertainty in ground penetrating radar models. 2010 13th International Conference on Ground Penetrating Radar (GPR). - Lecce, 21-25 June 2010. - P. 1-5. ↑

C244. Bojniger U. Symmetry based 3D GPR feature enhancement and extraction. / Bojniger U., Tronicke J. // 2010 13th International Conference on Ground Penetrating Radar (GPR). - Lecce, 21-25 June 2010. - P. 1-5. ↑

C245. Nakano Y. Taper-walled linearly tapered slot antenna: A low direct-coupling antenna for subsurface imaging. / Nakano Y., Hirose A. // 2010 13th International Conference on Ground Penetrating Radar (GPR). - Lecce, 21-25 June 2010. - P. 1-5. ↑

C246. Alberti G. Preliminary performance of Sub-Surface Radar for the EJSMLaplace mission. / Alberti G., Mattei S., Seu R., Bruzzone L., Ferro A., Orosei R., Olivieri A., Catallo C. // 2010 13th International Conference on Ground Penetrating Radar (GPR). - Lecce, 21-25 June 2010. - P. 1-4. ↑

C247. Takahashi K. Influence of soil inhomogeneity on GPR for landmine detection. / Takahashi K., Igel J., Preetz H. // 2010 13th International Conference on Ground Penetrating Radar (GPR). - Lecce, 21-25 June 2010. - P. 1-6. ↑

C248. Yokota Y. Ultra wide band radar reflectometer for density profile measurement of high temperature



plasmas. / Yokota Y., Mase A., Hojo H., Sato M., Tokuzawa T., Kawahata K., Nagayama Y. // 2010 13th International Conference on Ground Penetrating Radar (GPR). - Lecce, 21-25 June 2010. - P. 1-5. ↑

C249. Golebiowski T. Aiding of the GPR method by other measurement techniques for liquid contamination detection. / Golebiowski T., Tomecka-Suchon S., Marcak H., Zogala B. // 2010 13th International Conference on Ground Penetrating Radar (GPR). - Lecce, 21-25 June 2010. - P. 1-6. ↑

C250. Matsuoka K. Using englacial radar attenuation to better diagnose the subglacial environment: A review. / Matsuoka K., MacGregor J.A., Pattyn F. // 2010 13th International Conference on Ground Penetrating Radar (GPR). - Lecce, 21-25 June 2010. - P. 1-5. ↑

C251. Jung-Ho Kim. Admittance inversion of crosshole radar data. / Jung-Ho Kim, Kobayashi T., Seong Kon Lee. // 2010 13th International Conference on Ground Penetrating Radar (GPR). - Lecce, 21-25 June 2010. - P. 1-6. ↑

C252. McBride J.H. Results of an experimental radar survey on the gornergletscher glacier system (Zwillingsgletscher), Valais, Switzerland. / McBride J.H., Rupper S.B., Ritter S.M., Tingey D.G., Quick A.M., McKean A.P., Jones N.B. // 2010 13th International Conference on Ground Penetrating Radar (GPR). - Lecce, 21-25 June 2010. - P. 1-6. ↑

C253. Albane S. Ground-Penetrating Radar reflection data sensitivity to van Genuchten parameter variations GPR reflection data sensitivity to van Genuchten parameters. / Albane S., Hopmans J.W. // 2010 13th International Conference on Ground Penetrating Radar (GPR). - Lecce, 21-25 June 2010. - P. 1-5. ↑

C254. McBride John H. Results of an experimental radar survey on the Gornergletscher glacier system (Zwillingsgletscher), Valais, Switzerland. / McBride John H., Rupper Summer B., Ritter Scott M., Tingey David G., Quick Annika M., McKean Adam P., Jones Nathaniel B. // 2010 13th International Conference on Ground Penetrating Radar (GPR). - Lecce, Italy, 21-25 June 2010. - P. 1-6. ↑

C255. Dong-Hun Kim. Dynamic monitoring of fracture extension in unconsolidated sand specimen by GPR. / Dong-Hun Kim, Sato M., Ito T. // 2010 13th International Conference on Ground Penetrating Radar (GPR). - Lecce, 21-25 June 2010. - P. 1-6. ↑

C256. Ramos R. Sedimentary structure of the Nazaré coastal dunes (Portugal). / Ramos R., Freitas M.C., Andrade C., Costas S., Bristow C., Grangeia C., Hermozilha H., Senos Matias M.J. // 2010 13th International Conference on Ground Penetrating Radar (GPR). - Lecce, 21-25 June 2010. - P. 1-6. ↑

C257. Wei Ren. High power variable nanosecond differential pulses generator design for GPR system. / Wei Ren, Huaping Wang, Liu R. // 2010 13th International Conference on Ground Penetrating Radar (GPR). - Lecce, 21-25 June 2010. - P. 1-5. ↑

C258. Bavusi M. Rebars and defects detection by a GPR survey at a L'Aquila school damaged by the earthquake of April 2009. / Bavusi M., Loperte A., Lapenna V., Soldovieri F. // 2010 13th International Conference on Ground Penetrating Radar (GPR). - Lecce, 21-25 June 2010. - P. 1-5. ↑

C259. Dolce Carmen. Integrated prospecting in the Crypt of the Holy Spirit in Monopoli (Southern Italy). / Dolce Carmen, Masini Nicola, Leucci Giovanni, Persico Raffaele, Quarta Giovanni. // 2010 13th International Conference on Ground Penetrating Radar (GPR). - Lecce, Italy, 21-25 June 2010. - P. 1-4. ↑

C260. Ebihara Satoshi. Influence of feed line on DOA estimation with dipole array antenna for directional borehole radar. / Ebihara Satoshi, Hideharu Hanaoka, Takashi Okumura. // 2010 13th International Conference on Ground Penetrating Radar (GPR). - Lecce, Italy, 21-25 June 2010. - P. 1-6. ↑

C261. McBride J.H. Mapping thermal tufa deposits using GPR. / McBride J.H., Faust D.L., Guthrie W.S., Nelson S.T. // 2010 13th International Conference on Ground Penetrating Radar (GPR). - Lecce, 21-25 June 2010. - P. 1-6. ↑

C262. Sato Motoyuki. Deployment of GPR system ALIS for humanitarian demining in Cambodia. 2010 13th International Conference on Ground Penetrating Radar (GPR). - Lecce, Italy, 21-25 June 2010. - P. 1-4. ↑

C263. Utsi E. GPR as an imaging device: Some problems & potential solutions. 2010 13th International Conference on Ground Penetrating Radar (GPR). - Lecce, 21-25 June 2010. - P. 1-6. ↑

- C264.** Andre F. High-resolution imaging of a vineyard in south of France using ground penetrating radar and electromagnetic induction. / Andre F., Saussez S., Van Duraient R., van Leeuwen C., Moghadas D., Delvaux B., Vereecken H., Lambot S. // 2010 13th International Conference on Ground Penetrating Radar (GPR). - Lecce, Italy, 21-25 June 2010. - P. 1-8. ↑
- C265.** Lambot S. Full-waveform modeling of ground-coupled GPR antennas for wave propagation in multilayered media: The problem solved?. / Lambot S., Andre F., Jadoon K.Z., Slob E.C., Vereecken H. // 2010 13th International Conference on Ground Penetrating Radar (GPR). - Lecce, 21-25 June 2010. - P. 1-5. ↑
- C266.** Bikowski J. Inversion and sensitivity analysis of GPR data with waveguide dispersion using Markov Chain Monte Carlo simulation. / Bikowski J., van der Kruk J., Huisman J.A., Vereecken H., Vrugt J.A. // 2010 13th International Conference on Ground Penetrating Radar (GPR). - Lecce, 21-25 June 2010. - P. 1-5. ↑
- C267.** Putzig N.E. Imaging the subsurface structure of Planum Boreum with the Mars Reconnaissance Orbiter Shallow Radar. / Putzig N.E., Phillips R.J., Campbell B.A., Foss F.J. // 2010 13th International Conference on Ground Penetrating Radar (GPR). - Lecce, 21-25 June 2010. - P. 1-6. ↑
- C268.** Deiana D. Detection and classification of landmines using AR modeling of GPR data. / Deiana D., Anitori L. // 2010 13th International Conference on Ground Penetrating Radar (GPR). - Lecce, 21-25 June 2010. - P. 1-5. ↑
- C269.** Qing Zhang. Rail radar-a fast maturing tool for monitoring trackbed. / Qing Zhang, Eriksen A., Gascoyne J. // 2010 13th International Conference on Ground Penetrating Radar (GPR). - Lecce, 21-25 June 2010. - P. 1-5. ↑
- C270.** Orosei R. Radar subsurface sounding over the putative frozen sea in Cerberus Palus, Mars. / Orosei R., Cartacci M., Cicchetti A., Noschese R., Federico C., Frigeri A., Flamini E., Holt J.W., Marinangeli L., Pettinelli E., Phillips R.J., Picardi G., Seu R., Plaut J.J. // 2010 13th International Conference on Ground Penetrating Radar (GPR). - Lecce, 21-25 June 2010. - P. 1-4. ↑
- C271.** Maleszka Tomasz. Broadband stripline to microstrip transition with constant impedance field matching section for applications in multilayer planar technologies. / Maleszka Tomasz, Jaworski Grzegorz. // 2010 18th International Conference on Microwave Radar and Wireless Communications (MIKON). - Vilnius, Lithuania, 14-16 June 2010. - P. 1-4. ↑
- C272.** Fulai Liu. AD-ESPRIT for multi-target localization in bistatic MIMO radar system. / Fulai Liu, Jinkuan Wang. // 2010 International Conference on Computer Design and Applications (ICCD). - Qinhuaungdao, 25-27 June 2010. - Vol. 4. - P. V4-545-V4-548-545. ↑
- C273.** Lina Fan. Radar resource management in multifunction radar. / Lina Fan, Jinkuan Wang, Bin Wang. // 2010 International Conference on Computer Design and Applications (ICCD). - Qinhuaungdao, 25-27 June 2010. - Vol. 4. - P. V4-580-V4-583-580. ↑
- C274.** Wiejak Waldemar. X-band coupled cavity slow wave structure of the traveling wave tube for airborne application. 2010 18th International Conference on Microwave Radar and Wireless Communications (MIKON). - Vilnius, Lithuania, 14-16 June 2010. - P. 1-4. ↑
- C275.** Heidrich Juergen. Design of an electronically adaptable low-power reference cell for low-cost CMOS processes. / Heidrich Juergen, Brenk Daniel, Essel Jochen, Heinrich Matthias, Hofer Guenter, Holweg Gerald, Weigel Robert, Fischer Georg. // 2010 18th International Conference on Microwave Radar and Wireless Communications (MIKON). - Vilnius, Lithuania, 14-16 June 2010. - P. 1-4. ↑
- C276.** Wincza Krzysztof. Broadband 4x4 Butler matrix in microstrip multilayer technology designed with the use of three-section directional couplers and phase correction Networks. / Wincza Krzysztof, Sachse Krzysztof. // 2010 18th International Conference on Microwave Radar and Wireless Communications (MIKON). - Vilnius, Lithuania, 14-16 June 2010. - P. 1-4. ↑
- C277.** Subashini P. Performance measures of wavelet families on sar images for compression hypothesis. / Subashini P., Krishnaveni M., Thakur S.K. // 2010 International Conference on Computer Design and Applications (ICCD). - Qinhuaungdao, 25-27 June 2010. - Vol. 1. - P. V1-377-V1-381-377. ↑
- C278.** Quan Wei. An algorithm of sorting the phased array radar signal based on RST. / Quan Wei, Li Ping, Xu

Feng-kai. // 2010 International Conference on Computer Design and Applications (ICCD). - Qinhuangdao, 25-27 June 2010. - Vol. 4. - P. V4-429-V4-432-429. ↑

C279. Fulai Liu. An effective virtual ESPRIT algorithm for multi-target localization in bistatic MIMO radar system. / Fulai Liu, Jinkuan Wang. // 2010 International Conference on Computer Design and Applications (ICCD). - Qinhuangdao, 25-27 June 2010. - Vol. 4. - P. V4-412-V4-415-412. ↑

C280. Bin Zou. Fast automatic target detection of large scene SAR image based on parallel computing. / Bin Zou, Limin Li, Peng He. // 2010 International Conference on Computer Design and Applications (ICCD). - Qinhuangdao, 25-27 June 2010. - Vol. 5. - P. V5-495-V5-499-495. ↑

C281. Guo-Min Zheng. Research on availability simulation of Surface-to-Air missile weapon systems. / Guo-Min Zheng, Hui Gu. // 2010 International Conference on Computer Design and Applications (ICCD). - Qinhuangdao, 25-27 June 2010. - Vol. 5. - P. V5-99-V5-103-99. ↑

C282. Guo Zhitao. Design of remote data acquisition system of passenger flow based on GPRS. / Guo Zhitao, Wang Wenhao, Li Chan, Yuan Jinli, Gu Junhua. // 2010 International Conference on Computer Design and Applications (ICCD). - Qinhuangdao, 25-27 June 2010. - Vol. 4. - P. V4-468-V4-471-468. ↑

C283. Fulai Liu. AD-MUSIC for jointly DOA and DOD estimation in bistatic MIMO radar system. / Fulai Liu, Jinkuan Wang. // 2010 International Conference on Computer Design and Applications (ICCD). - Qinhuangdao, 25-27 June 2010. - Vol. 4. - P. V4-455-V4-458-455. ↑

C284. Feher Gabor. Ultra wide band (UWB) transmitter with configurable design for indoor positioning. 2010 18th International Conference on Microwave Radar and Wireless Communications (MIKON). - Vilnius, Lithuania, 14-16 June 2010. - P. 1-4. ↑

C285. {no data available}. Session P1: Antennas. 2010 18th International Conference on Microwave Radar and Wireless Communications (MIKON). - Vilnius, Lithuania, 14-16 June 2010. - P. 1. ↑

C286. {no data available}. Session P2: CAD, modeling and passive components. 2010 18th International Conference on Microwave Radar and Wireless Communications (MIKON). - Vilnius, Lithuania, 14-16 June 2010. - P. 1. ↑

C287. {no data available}. Session P3: Active networks and others. 2010 18th International Conference on Microwave Radar and Wireless Communications (MIKON). - Vilnius, Lithuania, 14-16 June 2010. - P. 1. ↑

C288. {no data available}. Session C7: Antennas and microwaves for space applications I. 2010 18th International Conference on Microwave Radar and Wireless Communications (MIKON). - Vilnius, Lithuania, 14-16 June 2010. - P. 1. ↑

C289. {no data available}. Session C8: Antennas and microwaves for space applications II. 2010 18th International Conference on Microwave Radar and Wireless Communications (MIKON). - Vilnius, Lithuania, 14-16 June 2010. - P. 1. ↑

C290. {no data available}. Session C9: Polarimetric and Doppler Radars. 2010 18th International Conference on Microwave Radar and Wireless Communications (MIKON). - Vilnius, Lithuania, 14-16 June 2010. - P. 1. ↑

C291. {no data available}. Session P4: Measurements, wireless and personal communications. 2010 18th International Conference on Microwave Radar and Wireless Communications (MIKON). - Vilnius, Lithuania, 14-16 June 2010. - P. 1. ↑

C292. Chizh A. Impulse transmitting photonic antenna for ultra-wideband applications. / Chizh A., Malyshev S., Jefremov S., Levitas B., Naidionova I. // 2010 18th International Conference on Microwave Radar and Wireless Communications (MIKON). - Vilnius, Lithuania, 14-16 June 2010. - P. 1-3. ↑

C293. Szustak Konrad. Realization of a transmit system using T/R modules applied in the demonstrator of S band active antenna. / Szustak Konrad, Sender Robert, Czwartacka Anna, Szymanski Piotr, Stachowski Bogdan, Cholewa Jacek, Startek Dariusz, Andrzejewski Mirosław, Lorens Tomasz. // 2010 18th International Conference on Microwave Radar and Wireless Communications (MIKON). - Vilnius, Lithuania, 14-16 June 2010. - P. 1-4. ↑

C294. Saulys Bronius. Red light-emitting diode degradation and low-frequency noise characteristics. / Saulys

Bronius, Matukas Jonas, Palenskis Vilius, Pralgauskaite Sandra. // 2010 18th International Conference on Microwave Radar and Wireless Communications (MIKON). - Vilnius, Lithuania, 14-16 June 2010. - P. 1-4. ↑

C295. {no data available}. Session P5: Radars. 2010 18th International Conference on Microwave Radar and Wireless Communications (MIKON). - Vilnius, Lithuania, 14-16 June 2010. - P. 1. ↑

C296. {no data available}. Title page vol1. 2010 18th International Conference on Microwave Radar and Wireless Communications (MIKON). - Vilnius, Lithuania, 14-16 June 2010. - P. 1. ↑

C297. {no data available}. Title page vol2. 2010 18th International Conference on Microwave Radar and Wireless Communications (MIKON). - Vilnius, Lithuania, 14-16 June 2010. - P. 1. ↑

C298. Qiang Zhao. 2D DOA estimation for coherently distributed source. / Qiang Zhao, Jinkuan Wang, Bin Wang. // 2010 International Conference on Computer Design and Applications (ICCD). - Qinhuangdao, 25-27 June 2010. - Vol. 4. - P. V4-366-V4-369-366. ↑

C299. Xu Jin. Based on embedded intelligent vehicle system. / Xu Jin, Li Yongkang, Zhou Rongyan, Liu Kai. // 2010 International Conference On Computer and Communication Technologies in Agriculture Engineering (CCTAE). - Chengdu, 12-13 June 2010. - Vol. 2. - P. 49-52. ↑

C300. Al Tunaiji A. MUSO: An M-learning & University Student Organizer platform. / Al Tunaiji A., Zemerly M.J. // 2010 3rd IEEE International Conference on Ubi-media Computing (U-Media). - Jinhua, 5-6 July 2010. - P. 155-160. ↑

C301. Lejiang Guo. Intelligent Traffic Management system base on WSN and RFID. / Lejiang Guo, Wei Fang, Guoshi Wang, Longsheng Zheng. // 2010 International Conference On Computer and Communication Technologies in Agriculture Engineering (CCTAE). - Chengdu, 12-13 June 2010. - Vol. 2. - P. 227-230. ↑

C302. Wei Zhang. Comparisons of speckle noise filtering methods on high resolution SAR image. / Wei Zhang, Jinzhong Yang, Le Yu. // 2010 International Conference On Computer and Communication Technologies in Agriculture Engineering (CCTAE). - Chengdu, 12-13 June 2010. - Vol. 3. - P. 202-204. ↑

C303. Wei Zhang. SAR and Landsat ETM+ image fusion using variational model. / Wei Zhang, Le Yu. // 2010 International Conference On Computer and Communication Technologies in Agriculture Engineering (CCTAE). - Chengdu, 12-13 June 2010. - Vol. 3. - P. 205-207. ↑

C304. Lei Xiao. The realization of precision agriculture monitoring system based on wireless sensor network. / Lei Xiao, Lejiang Guo. // 2010 International Conference On Computer and Communication Technologies in Agriculture Engineering (CCTAE). - Chengdu, 12-13 June 2010. - Vol. 3. - P. 89-92. ↑

C305. ZhiYou Cheng. Decision to avoid ships collision in fog and application. / ZhiYou Cheng, YaLing Li. // 2010 International Conference On Computer and Communication Technologies in Agriculture Engineering (CCTAE). - Chengdu, 12-13 June 2010. - Vol. 2. - P. 258-261. ↑

C306. Latif Z.A. Extraction of gap and canopy properties using LiDAR and multispectral data for forest microclimate modelling. / Latif Z.A., Blackburn G.A. // 2010 6th International Colloquium on Signal Processing and Its Applications (CSPA). - Mallaca City, 21-23 May 2010. - P. 1-5. ↑

C307. Onojeghuo A.O. Characterising Reedbed habitat quality using Leaf-off LiDAR Data. / Onojeghuo A.O., Blackburn G.A., Latif Z.A. // 2010 6th International Colloquium on Signal Processing and Its Applications (CSPA). - Mallaca City, 21-23 May 2010. - P. 1-5. ↑

C308. Zili Shan. Ocean-land segmentation based on active contour model for SAR imagery. / Zili Shan, Chao Wang, Hong Zhang, Bo Zhang. // 2010 International Conference On Computer and Communication Technologies in Agriculture Engineering (CCTAE). - Chengdu, 12-13 June 2010. - Vol. 1. - P. 215-218. ↑

C309. Zhang Bentao. Research on the spaceborne SAR image processing and feature extraction for ocean fronts detection. / Zhang Bentao, Chen Biao, Gao Guoxing. // 2010 International Conference On Computer and Communication Technologies in Agriculture Engineering (CCTAE). - Chengdu, 12-13 June 2010. - Vol. 2. - P. 473-476. ↑

C310. Nithirochananont U. GISTDA EOC synthetic aperture radar data processing system. / Nithirochananont



U., Chivapreecha S., Peanvijarnpong C., Dejhan K. // 2010 6th International Colloquium on Signal Processing and Its Applications (CSPA). - Mallaca City, 21-23 May 2010. - P. 1-6. ↑

C311. Sakkila L. Comparison of classical and orthogonal UWB waveforms for radar applications. / Sakkila L., Rivenq A., Tatkeu C., ElHillali Y., Boukour F., Rouvaen J. // 2010 6th International Colloquium on Signal Processing and Its Applications (CSPA). - Mallaca City, 21-23 May 2010. - P. 1-5. ↑

C312. Chen Wei-bin. A new SAR image segmentation method based on fusion. / Chen Wei-bin, Zhang Xin. // 2010 International Conference On Computer and Communication Technologies in Agriculture Engineering (CCTAE). - Chengdu, 12-13 June 2010. - Vol. 1. - P. 430-433. ↑

C313. Xuemai Gu. A novel distance-assisted localization algorithm in wireless sensor networks. / Xuemai Gu, Yanjun Jiang, Shuo Shi. // 2010 International Conference on Computer Design and Applications (ICCD). - Qinhuaungdao, 25-27 June 2010. - Vol. 2. - P. V2-575-V2-579-575. ↑

C314. Junqi Gu. An impact point of shipboard artillery shell calculating system based on DSP and matlab-simulink simulation. / Junqi Gu, Mingquan Shi, Shuqian Fan. // 2010 International Conference on Computer Design and Applications (ICCD). - Qinhuaungdao, 25-27 June 2010. - Vol. 3. - P. V3-565-V3-567-565. ↑

C315. Shan Xian-ming. Fault diagnosis expert system of artillery radar based on neural network. / Shan Xian-ming, Yang He-yong, Zhang Peng. // 2010 International Conference on Computer Design and Applications (ICCD). - Qinhuaungdao, 25-27 June 2010. - Vol. 2. - P. V2-426-V2-429-426. ↑

C316. Wu Junzheng. A despeckling algorithm combining curvelet and wavelet transforms of high resolution SAR images. / Wu Junzheng, Yan Weidong, Bian Hui, Ni Weiping. // 2010 International Conference on Computer Design and Applications (ICCD). - Qinhuaungdao, 25-27 June 2010. - Vol. 1. - P. V1-302-V1-305-302. ↑

C317. Shan Xian-ming. Realization of position selection simulation evaluation system for artillery reconnaissance radar. / Shan Xian-ming, Yang He-yong, Xia Hong-sen. // 2010 International Conference on Computer Design and Applications (ICCD). - Qinhuaungdao, 25-27 June 2010. - Vol. 1. - P. V1-204-V1-207-204. ↑

C318. Ning Jin. A novel design of water environment monitoring system based on WSN. / Ning Jin, Renzhi Ma, Yunfeng Lv, Xizhong Lou, Qingjian Wei. // 2010 International Conference on Computer Design and Applications (ICCD). - Qinhuaungdao, 25-27 June 2010. - Vol. 2. - P. V2-593-V2-597-593. ↑

C319. Bo Lv. Simulation study of noise convolution jamming countering to SAR. 2010 International Conference on Computer Design and Applications (ICCD). - Qinhuaungdao, 25-27 June 2010. - Vol. 4. - P. V4-130-V4-133-130. ↑

C320. Chunyun Song. A method for specific emitter identification based on empirical mode decomposition. / Chunyun Song, Jianmin Xu, Yi Zhan. // 2010 IEEE International Conference on Wireless Communications, Networking and Information Security (WCNIS). - Beijing, China, 25-27 June 2010. - P. 54-57. ↑

C321. Liu Xiaojun. Improved pattern synthesis method with linearly constraint minimum variance criterion. / Liu Xiaojun, Liu Congfeng, Guisheng Liao. // 2010 IEEE International Conference on Wireless Communications, Networking and Information Security (WCNIS). - Beijing, China, 25-27 June 2010. - P. 63-66. ↑

C322. Mir H. Scheduling of tasks with fuzzy dwell times in a multifunction radar. / Mir H., Ben Abdelaziz F. // 2010 Second International Conference on Engineering Systems Management and Its Applications (ICESMA). - Sharjah, March 30 2010-April 1 2010. - P. 1-6. ↑

C323. Huang Yao. A reduced-rank STAP method based on solution of linear equations. 2010 International Conference on Computer Design and Applications (ICCD). - Qinhuaungdao, 25-27 June 2010. - Vol. 1. - P. V1-235-V1-238-235. ↑

C324. Chen Bin. Research on autocorrelation of chaotic sequence by phase space method. / Chen Bin, Cai Peng, Zhang Yong, Huang Jian, Yun-Song Wu, Tang Jun. // 2010 IEEE International Conference on Wireless Communications, Networking and Information Security (WCNIS). - Beijing, China, 25-27 June 2010. - P. 6-12. ↑

C325. Wang Zhuo. Remove multifrequency mixture noise in processing of Wireless Communication wave/radar

reflect signal by method of ICA. / Wang Zhuo, Wang Lizhi, Yang Yong. // 2010 IEEE International Conference on Wireless Communications, Networking and Information Security (WCNIS). - Beijing, China, 25-27 June 2010. - P. 50-53. ↑

C326. {no data available}. Session C6: Radar technique. 2010 18th International Conference on Microwave Radar and Wireless Communications (MIKON). - Vilnius, Lithuania, 14-16 June 2010. - P. 1. ↑

C327. Saulys Bronius. Analysis of mode-hopping effect in fabry-perot laser diodes. / Saulys Bronius, Matukas Jonas, Palenskis Vilius, Pralgauskaite Sandra, Vysniauskas Juozas. // 2010 18th International Conference on Microwave Radar and Wireless Communications (MIKON). - Vilnius, Lithuania, 14-16 June 2010. - P. 1-4. ↑

C328. Vasilev A. S. Ka-band FMCW radar sensor for remote control of presence and speed of railroad-cars and trains in territory of grading belts. / Vasilev A. S., Varavin A. V., Ermak G. P., Popov I. V. // 2010 18th International Conference on Microwave Radar and Wireless Communications (MIKON). - Vilnius, Lithuania, 14-16 June 2010. - P. 1-3. ↑

C329. Luszczuk Mariusz. Complex radar signal source for radar receivers testing. / Luszczuk Mariusz, Szczepaniak Zenon R., Arvaniti Andrzej, Orzel-Tataczuk Emanuela. // 2010 18th International Conference on Microwave Radar and Wireless Communications (MIKON). - Vilnius, Lithuania, 14-16 June 2010. - P. 1-4. ↑

C330. {no data available}. Opening session. 2010 18th International Conference on Microwave Radar and Wireless Communications (MIKON). - Vilnius, Lithuania, 14-16 June 2010. - P. 1. ↑

C331. {no data available}. Session A1: Antenna design. 2010 18th International Conference on Microwave Radar and Wireless Communications (MIKON). - Vilnius, Lithuania, 14-16 June 2010. - P. 1. ↑

C332. Slyusar V.I. A marine testing's result of experimental radar with 64-channels digital antenna array. / Slyusar V.I., Alesyn A.M., Nikitin N.N., Shatzman L.G., Korolev N.A., Solostchev O.N., Shraev D.V., Volostchuk I.V., Bondarenko M.V., Grytzenko V.N., Malastchuk V.P. // 2010 18th International Conference on Microwave Radar and Wireless Communications (MIKON). - Vilnius, 14-16 June 2010. - P. 1-3. ↑

C333. Voroshilin E. P. Experimental pulse reaction estimation of the centimeter wave channel. / Voroshilin E. P., Mironov M. V. // 2010 18th International Conference on Microwave Radar and Wireless Communications (MIKON). - Vilnius, Lithuania, 14-16 June 2010. - P. 1-4. ↑

C334. Ponomarev Dmitry. Multi-radar system database integration using metrized small world technology. / Ponomarev Dmitry, Krylov Vladimir, Pankratov Yuri. // 2010 18th International Conference on Microwave Radar and Wireless Communications (MIKON). - Vilnius, Lithuania, 14-16 June 2010. - P. 1-3. ↑

C335. Grimalsky V. Collapse of nonlinear spin dipole wave pulses of millimeter wave range in YIG films. / Grimalsky V., Koshevaya S., Kolokoltsev O. // 2010 18th International Conference on Microwave Radar and Wireless Communications (MIKON). - Vilnius, 14-16 June 2010. - P. 1-4. ↑

C336. Konovalyuk Maxim. Moving multy-scatterer target parametric identification using radar image. / Konovalyuk Maxim, Kuznetsov Yuri, Baev Andrey. // 2010 18th International Conference on Microwave Radar and Wireless Communications (MIKON). - Vilnius, Lithuania, 14-16 June 2010. - P. 1-4. ↑

C337. Voroshilin E. P. Ground target position estimation in passive location. / Voroshilin E. P., Mironov M. V., Voroshilina E. P. // 2010 18th International Conference on Microwave Radar and Wireless Communications (MIKON). - Vilnius, Lithuania, 14-16 June 2010. - P. 1-4. ↑

C338. Vertiy A. A. Terahertz and sub-terahertz subsurface tomography. / Vertiy A. A., Cetinkaya H., Tekbas M. // 2010 18th International Conference on Microwave Radar and Wireless Communications (MIKON). - Vilnius, Lithuania, 14-16 June 2010. - P. 1-4. ↑

C339. Grimalsky V. Modulators of THz range based on integrated silicon P-I-N-structures in dielectric waveguides. / Grimalsky V., Koshevaya S., Escobedo-A J., Moroz I. // 2010 18th International Conference on Microwave Radar and Wireless Communications (MIKON). - Vilnius, Lithuania, 14-16 June 2010. - P. 1-4. ↑

C340. {no data available}. Session A3: Compatibility. 2010 18th International Conference on Microwave Radar and Wireless Communications (MIKON). - Vilnius, Lithuania, 14-16 June 2010. - P. 1. ↑

- C341.** {no data available}. Session B4: Filters. 2010 18th International Conference on Microwave Radar and Wireless Communications (MIKON). - Vilnius, Lithuania, 14-16 June 2010. - P. 1. ↑
- C342.** {no data available}. Session B1: Microwave measurements I. 2010 18th International Conference on Microwave Radar and Wireless Communications (MIKON). - Vilnius, Lithuania, 14-16 June 2010. - P. 1. ↑
- C343.** {no data available}. Session B2: Microwave measurements II. 2010 18th International Conference on Microwave Radar and Wireless Communications (MIKON). - Vilnius, Lithuania, 14-16 June 2010. - P. 1. ↑
- C344.** {no data available}. Session B5: Power amplifiers II. 2010 18th International Conference on Microwave Radar and Wireless Communications (MIKON). - Vilnius, Lithuania, 14-16 June 2010. - P. 1. ↑
- C345.** {no data available}. Session B6: Active microwave networks. 2010 18th International Conference on Microwave Radar and Wireless Communications (MIKON). - Vilnius, Lithuania, 14-16 June 2010. - P. 1. ↑
- C346.** {no data available}. Session B3: Numerical modeling I. 2010 18th International Conference on Microwave Radar and Wireless Communications (MIKON). - Vilnius, Lithuania, 14-16 June 2010. - P. 1. ↑
- C347.** {no data available}. Session A8: Passive components I. 2010 18th International Conference on Microwave Radar and Wireless Communications (MIKON). - Vilnius, Lithuania, 14-16 June 2010. - P. 1. ↑
- C348.** {no data available}. Session A4: RFID technology. 2010 18th International Conference on Microwave Radar and Wireless Communications (MIKON). - Vilnius, Lithuania, 14-16 June 2010. - P. 1. ↑
- C349.** {no data available}. Session A5: Antenna theory and applications. 2010 18th International Conference on Microwave Radar and Wireless Communications (MIKON). - Vilnius, Lithuania, 14-16 June 2010. - P. 1. ↑
- C350.** {no data available}. Session A2: Broadband and UWB antennas. 2010 18th International Conference on Microwave Radar and Wireless Communications (MIKON). - Vilnius, Lithuania, 14-16 June 2010. - P. 1. ↑
- C351.** {no data available}. Session A9: Passive components II. 2010 18th International Conference on Microwave Radar and Wireless Communications (MIKON). - Vilnius, Lithuania, 14-16 June 2010. - P. 1. ↑
- C352.** {no data available}. Session A6: Numerical modeling II. 2010 18th International Conference on Microwave Radar and Wireless Communications (MIKON). - Vilnius, Lithuania, 14-16 June 2010. - P. 1. ↑
- C353.** {no data available}. Session A7: Industrial applications. 2010 18th International Conference on Microwave Radar and Wireless Communications (MIKON). - Vilnius, Lithuania, 14-16 June 2010. - P. 1. ↑
- C354.** Cholewa Jacek. Receive system of S band active antenna demonstrator. / Cholewa Jacek, Stachowski Bogdan, Czwartacka Anna, Sender Robert, Szustak Konrad, Startek Dariusz, Andrzejewski Miroslaw, Szymanski Piotr, Lorens Tomasz. // 2010 18th International Conference on Microwave Radar and Wireless Communications (MIKON). - Vilnius, Lithuania, 14-16 June 2010. - P. 1-4. ↑
- C355.** Czuba Krzysztof. Phase drift versus temperature measurements of coaxial cables. / Czuba Krzysztof, Sikora Dominik. // 2010 18th International Conference on Microwave Radar and Wireless Communications (MIKON). - Vilnius, Lithuania, 14-16 June 2010. - P. 1-3. ↑
- C356.** Gryglewski D. X-band pulsed measurement system of transmittance changes of power amplifiers. / Gryglewski D., Wojtasiak W., Belniak M., Rosolowski D. // 2010 18th International Conference on Microwave Radar and Wireless Communications (MIKON). - Vilnius, Lithuania, 14-16 June 2010. - P. 1-4. ↑
- C357.** Hartmann Christian. An integrated SiGe HBT bandpass-pulse length modulator for switch mode power amplifiers in the SHF range. / Hartmann Christian, Haas-Zens Martin, Blau Kurt, Hein Matthias A. // 2010 18th International Conference on Microwave Radar and Wireless Communications (MIKON). - Vilnius, Lithuania, 14-16 June 2010. - P. 1-5. ↑
- C358.** Staras Stanislovas. Analysis of helical systems containing periodical inhomogeneities. / Staras Stanislovas, Katkevicius Andrius. // 2010 18th International Conference on Microwave Radar and Wireless Communications (MIKON). - Vilnius, Lithuania, 14-16 June 2010. - P. 1-4. ↑
- C359.** Usanov D. A. Measurement of thickness and electrophysical parameters of nanometer films by means of optical and microwave methods. / Usanov D. A., Skripal A.I.V., Skripal A.N.V., Abramov A. V., Bogolubov A. S.,

Bakouie A. // 2010 18th International Conference on Microwave Radar and Wireless Communications (MIKON). - Vilnius, Lithuania, 14-16 June 2010. - P. 1-4. ↑

C360. Derkach V. N. Millimeter waves controlled elements on the basis of disk dielectric resonators. / Derkach V. N., Golovashchenko R. V., Goroshko E. V., Korzh V. G. // 2010 18th International Conference on Microwave Radar and Wireless Communications (MIKON). - Vilnius, Lithuania, 14-16 June 2010. - P. 1-4. ↑

C361. Kalinin Y. N. Measurement of antenna characteristics by near-and far-field techniques within time domain. / Kalinin Y. N., Milyaev P. V., Morev V. L., Popikov M. V. // 2010 18th International Conference on Microwave Radar and Wireless Communications (MIKON). - Vilnius, Lithuania, 14-16 June 2010. - P. 1-4. ↑

C362. Mikucionis Sarunas. Synthesis of microstrip multiconductor lines, operating in normal mode. / Mikucionis Sarunas, Urbanavicius Vytautas. // 2010 18th International Conference on Microwave Radar and Wireless Communications (MIKON). - Vilnius, Lithuania, 14-16 June 2010. - P. 1-4. ↑

C363. Lu Qun. Wavelet packet based de-noising algorithm for UWB GPR data. / Lu Qun, Zhu Jin liang. // 2010 18th International Conference on Microwave Radar and Wireless Communications (MIKON). - Vilnius, Lithuania, 14-16 June 2010. - P. 1-3. ↑

C364. {no data available}. Session C5: Millimeter technology. 2010 18th International Conference on Microwave Radar and Wireless Communications (MIKON). - Vilnius, Lithuania, 14-16 June 2010. - P. 1. ↑

C365. Belkin Mikhail E. Cost-effective millimeter wave-to-optical conversion with patch antenna and MMIC chipset for RoF's uplink. / Belkin Mikhail E., Belkin Leonid. // 2010 18th International Conference on Microwave Radar and Wireless Communications (MIKON). - Vilnius, Lithuania, 14-16 June 2010. - P. 1-4. ↑

C366. Hosseini-Varkiani Mohsen. UWB CPW-fed monopole antenna with a band-notch function. / Hosseini-Varkiani Mohsen, Hojat-Kashani Farokh. // 2010 18th International Conference on Microwave Radar and Wireless Communications (MIKON). - Vilnius, Lithuania, 14-16 June 2010. - P. 1-3. ↑

C367. Kopusov V.N. On the issue of the construction of wideband measuring antennae 0, 85 to 37, 5 Ghz. / Kopusov V.N., Kasimenko V.B., Gordeev A.N. // 2010 18th International Conference on Microwave Radar and Wireless Communications (MIKON). - Vilnius, Lithuania, 14-16 June 2010. - P. 1-2. ↑

C368. Nistazakis H. E. Estimation of capacity bounds of free space optical channels under strong turbulence conditions. / Nistazakis H. E., Marinos D., Haniyas M., Aidinis C., Tsilis M., Tombras G. S., Tsigopoulos A. D., Fafalios M. E. // 2010 18th International Conference on Microwave Radar and Wireless Communications (MIKON). - Vilnius, Lithuania, 14-16 June 2010. - P. 1-3. ↑

C369. Rososkis Jakovas. Testing of telecom and datacom signals with a wide-bandwidth sampling oscilloscopes. / Rososkis Jakovas, Zaytsev Oleg. // 2010 18th International Conference on Microwave Radar and Wireless Communications (MIKON). - Vilnius, Lithuania, 14-16 June 2010. - P. 1-4. ↑

C370. Mendalka Maciej. Pattern matching localization in ZigBee wireless sensor networks. / Mendalka Maciej, Bizewski Karol, Kulas Lukasz, Nyka Krzysztof. // 2010 18th International Conference on Microwave Radar and Wireless Communications (MIKON). - Vilnius, Lithuania, 14-16 June 2010. - P. 1-4. ↑

C371. Zhong-hai Guo. An optimal scheduling algorithm in spatial TDMA mobile ad hoc network. / Zhong-hai Guo, Yong-guang Chen. // 2010 18th International Conference on Microwave Radar and Wireless Communications (MIKON). - Vilnius, Lithuania, 14-16 June 2010. - P. 1-5. ↑

C372. Kedzierski Grzegorz. Towards establishing traceable coaxial Type-N scattering-parameter measurements at NIT. / Kedzierski Grzegorz, Korszen Karol, Lewandowski Arkadiusz, Wiatr Wojciech. // 2010 18th International Conference on Microwave Radar and Wireless Communications (MIKON). - Vilnius, Lithuania, 14-16 June 2010. - P. 1-4. ↑

C373. Szustak Konrad. High power S band T/R module. / Szustak Konrad, Czwartacka Anna, Stachowski Bogdan, Lorens Tomasz, Sender Robert, Cholewa Jacek. // 2010 18th International Conference on Microwave Radar and Wireless Communications (MIKON). - Vilnius, Lithuania, 14-16 June 2010. - P. 1-4. ↑

C374. Moldovan Ancuta. Adaptive potential of spatial transmission processing techniques. / Moldovan Ancuta, Vermesan Irina, Palade Tudor, Pistea Ana-Maria, Colda Rebeca, Puschita Emanuel. // 2010 18th International



Conference on Microwave Radar and Wireless Communications (MIKON). - Vilnius, Lithuania, 14-16 June 2010. - P. 1-4. ↑

**C375.** Zilinskas Mindaugas. Determination of radio refractivity using meteorological data. / Zilinskas Mindaugas, Tamosiunas Stasys, Tamosiunaite Milda, Tamosiuniene Milda. // 2010 18th International Conference on Microwave Radar and Wireless Communications (MIKON). - Vilnius, Lithuania, 14-16 June 2010. - P. 1-4. ↑

**C376.** Al-Hanafy Waleed. Reduced complexity schemes to greedy power allocation for multicarrier systems. / Al-Hanafy Waleed, Weiss Stephan. // 2010 18th International Conference on Microwave Radar and Wireless Communications (MIKON). - Vilnius, Lithuania, 14-16 June 2010. - P. 1-4. ↑

**C377.** Mili Sonia. Electromagnetic study of planar pre-fractal structures using the scale changing technique. / Mili Sonia, Aguilu Taoufik. // 2010 18th International Conference on Microwave Radar and Wireless Communications (MIKON). - Vilnius, Lithuania, 14-16 June 2010. - P. 1-5. ↑

**C378.** Udvary Eszter. Variable microwave time delay by utilizing optical approaches. / Udvary Eszter, Jakab Laszlo, Berceli Tibor. // 2010 18th International Conference on Microwave Radar and Wireless Communications (MIKON). - Vilnius, Lithuania, 14-16 June 2010. - P. 1-4. ↑

**C379.** Naik Mehul R. Using space time coding MIMO system for software-defined radio to improve BER. / Naik Mehul R, Garg Abhishek, Aggarwal Aditya. // 2010 18th International Conference on Microwave Radar and Wireless Communications (MIKON). - Vilnius, Lithuania, 14-16 June 2010. - P. 1-4. ↑

**C380.** Benavente-Peces Cesar. EXIT chart analysis of iteratively detected and SVD-assisted broadband MIMO-BICM schemes. / Benavente-Peces Cesar, Ahrens Andreas. // 2010 18th International Conference on Microwave Radar and Wireless Communications (MIKON). - Vilnius, Lithuania, 14-16 June 2010. - P. 1-4. ↑

**C381.** Colda Rebeca. PER-based analysis of a mobile WiMAX system. / Colda Rebeca, Palade Tudor, Pucshita Emanuel, Moldovan Ancuta, Vermecan Irina. // 2010 18th International Conference on Microwave Radar and Wireless Communications (MIKON). - Vilnius, Lithuania, 14-16 June 2010. - P. 1-4. ↑

**C382.** Zemmari Reda. Reference signal extraction for GSM passive coherent location. 2010 11th International Radar Symposium (IRS). - Vilnius, Lithuania, 16-18 June 2010. - P. 1-4. ↑

**C383.** Baczyk Marcin Kamil. Decoding and reconstruction of reference DVB-T signal in passive radar systems. / Baczyk Marcin Kamil, Malanowski Mateusz. // 2010 11th International Radar Symposium (IRS). - Vilnius, Lithuania, 16-18 June 2010. - P. 1-4. ↑

**C384.** Langellotti D. Impact of synchronization on the ambiguity function shape for PBR based on DVB-T signals. / Langellotti D., Bongioanni C., Colone F., Lombardo P. // 2010 11th International Radar Symposium (IRS). - Vilnius, Lithuania, 16-18 June 2010. - P. 1-4. ↑

**C385.** Bruyant Jean-Paul. SETHI flying lab: A tool for remote sensing applications. 2010 11th International Radar Symposium (IRS). - Vilnius, Lithuania, 16-18 June 2010. - P. 1-4. ↑

**C386.** Petri D. A software defined UMTS passive radar demonstrator. / Petri D., Berizzi F., Martorella M., Mese E. Dalle, Capria A. // 2010 11th International Radar Symposium (IRS). - Vilnius, Lithuania, 16-18 June 2010. - P. 1-4. ↑

**C387.** O'Hagan D. W. Signal reconstruction as an effective means of detecting targets in a DAB-based PBR. / O'Hagan D. W., Kuschel H., Heckenbach J., Ummenhofer M., Schell J. // 2010 11th International Radar Symposium (IRS). - Vilnius, Lithuania, 16-18 June 2010. - P. 1-4. ↑

**C388.** Samczynski Piotr. Fusion of SAR and optical images as a method for improving target recognition on the earth surface. / Samczynski Piotr, Malanowski Mateusz, Kulpa Krzysztof. // 2010 11th International Radar Symposium (IRS). - Vilnius, Lithuania, 16-18 June 2010. - P. 1-4. ↑

**C389.** Nickel U.R.O. Extending range coverage with GSM passive localization by sensor fusion. 2010 11th International Radar Symposium (IRS). - Vilnius, 16-18 June 2010. - P. 1-4. ↑

**C390.** Daun Martina. Deghosting in passive air surveillance systems. 2010 11th International Radar Symposium (IRS). - Vilnius, Lithuania, 16-18 June 2010. - P. 1-8. ↑

- C391.** Olsen Karl Erik. FM based passive bistatic radar target range improvement-Part II. / Olsen Karl Erik, Woodbridge Karl, Andersen Idar A. // 2010 11th International Radar Symposium (IRS). - Vilnius, Lithuania, 16-18 June 2010. - P. 1-8. ↑
- C392.** Younis M. High performance reflector-based Synthetic Aperture Radar: -A system performance analysis -. / Younis M., Patyuchenko A., Huber S., Krieger G. // 2010 11th International Radar Symposium (IRS). - Vilnius, 16-18 June 2010. - P. 1-4. ↑
- C393.** Maslikowski Lukasz. Nonuniform spatial sampling in a noise SAR. / Maslikowski Lukasz, Misiurewicz Jacek. // 2010 11th International Radar Symposium (IRS). - Vilnius, Lithuania, 16-18 June 2010. - P. 1-6. ↑
- C394.** Georgiev G.N. Principles of the electromagnetic modelling of som microwave components, based on the circular waveguides with azimuthally magnetized ferrite. / Georgiev G.N., Georgieva-Grosse M.N. // 2010 11th International Radar Symposium (IRS). - Vilnius, 16-18 June 2010. - P. 1-6. ↑
- C395.** Clemente Carmine. Range Doppler SAR processing using the Fractional Fourier Transform. / Clemente Carmine, Soraghan John J. // 2010 11th International Radar Symposium (IRS). - Vilnius, Lithuania, 16-18 June 2010. - P. 1-4. ↑
- C396.** Tadeusz S. Fusion of data received FM-CW radar and AIS-analysis of functionality: Topic 3. Radar application. / Tadeusz S., Ryszard W., Sławomir P. // 2010 11th International Radar Symposium (IRS). - Vilnius, 16-18 June 2010. - P. 1-3. ↑
- C397.** {no data available}. Author Index. 2010 11th International Radar Symposium (IRS). - Vilnius, Lithuania, 16-18 June 2010. - P. XVII-XIX. ↑
- C398.** {no data available}. Blank page. 2010 11th International Radar Symposium (IRS). - Vilnius, Lithuania, 16-18 June 2010. - P. 1. ↑
- C399.** {no data available}. Title page vol2. 2010 11th International Radar Symposium (IRS). - Vilnius, Lithuania, 16-18 June 2010. - P. 1. ↑
- C400.** {no data available}. Session P2. 2010 11th International Radar Symposium (IRS). - Vilnius, Lithuania, 16-18 June 2010. - P. 1. ↑
- C401.** Muzhikyan Aramazd. Short-range Ku-band hybrid-mode CW-LFM radar. / Muzhikyan Aramazd, Hakhoumian Arsen, Martirosyan Stepan, Nikoghosyan Vahan, Poghosyan Nubar, Poghosyan Tigran, Rustamyan Karlen, Zakaryan Tigran. // 2010 11th International Radar Symposium (IRS). - Vilnius, Lithuania, 16-18 June 2010. - P. 1-3. ↑
- C402.** {no data available}. Copyright page. 2010 11th International Radar Symposium (IRS). - Vilnius, Lithuania, 16-18 June 2010. - P. 1. ↑
- C403.** Kuschel H. On the resolution performance of passive radar using DVB-T illuminations. / Kuschel H., Ummenhofer M., O'Hagan D., Heckenbach J. // 2010 11th International Radar Symposium (IRS). - Vilnius, Lithuania, 16-18 June 2010. - P. 1-4. ↑
- C404.** Bezvesilniy Oleksandr O. Correction of radiometric errors by multi-look processing with extended number of looks. / Bezvesilniy Oleksandr O., Gorovyi Ievgen M., Vynogradov Volodymyr V., Vavriv Dmytro M. // 2010 11th International Radar Symposium (IRS). - Vilnius, Lithuania, 16-18 June 2010. - P. 1-4. ↑
- C405.** Bezvesilniy Oleksandr O. Multi-look stripmap SAR processing with built-in geometric correction. / Bezvesilniy Oleksandr O., Gorovyi Ievgen M., Sosnytskiy Sergiy V., Vynogradov Volodymyr V., Vavriv Dmytro M. // 2010 11th International Radar Symposium (IRS). - Vilnius, Lithuania, 16-18 June 2010. - P. 1-4. ↑
- C406.** Poullin Dominique. New challenges for PCL system: 3D requirements and "Optimal" resources management for PCL air traffic survey. / Poullin Dominique, Flecheux Marc, Klein Mathieu. // 2010 11th International Radar Symposium (IRS). - Vilnius, Lithuania, 16-18 June 2010. - P. 1-3. ↑
- C407.** Bongioanni C. Exploiting polarimetric diversity to mitigate the effect of interferences in FM-based passive radar. / Bongioanni C., Colone F., Martelli T., D'Angeli R., Lombardo P. // 2010 11th International Radar Symposium (IRS). - Vilnius, Lithuania, 16-18 June 2010. - P. 1-4. ↑

- C408.** Schroder Alexander. Multiband experimental PCL system: Concept and measurement results. / Schroder Alexander, Edrich Michael, Wolschendorf Frieder. // 2010 11th International Radar Symposium (IRS). - Vilnius, Lithuania, 16-18 June 2010. - P. 1-4. ↑
- C409.** Belfiori Francesco. Mutual coupling compensation applied to a uniform circular array. / Belfiori Francesco, Monni Stefania, Van Rossum Wim, Hoozeboom Peter. // 2010 11th International Radar Symposium (IRS). - Vilnius, Lithuania, 16-18 June 2010. - P. 1-4. ↑
- C410.** Dzvonkovskaya Anna. Cargo ship RCS estimation based on HF radar measurements. / Dzvonkovskaya Anna, Rohling Hermann. // 2010 11th International Radar Symposium (IRS). - Vilnius, Lithuania, 16-18 June 2010. - P. 1-4. ↑
- C411.** Patyuchenko A. Reflector-based digital beam-forming radar system for space debris detection. / Patyuchenko A., Younis M., Krieger G. // 2010 11th International Radar Symposium (IRS). - Vilnius, 16-18 June 2010. - P. 1-4. ↑
- C412.** Bencheikh Mohamed Laid. A subspace-based technique for joint DOA-DOD estimation in bistatic MIMO radar. / Bencheikh Mohamed Laid, Wang Yide, He Hongyang. // 2010 11th International Radar Symposium (IRS). - Vilnius, Lithuania, 16-18 June 2010. - P. 1-4. ↑
- C413.** Schimpf Hartmut. Analysis of ATR features for non-cooperative ground-based classification of ships. / Schimpf Hartmut, Fuchs Hans-Hellmuth. // 2010 11th International Radar Symposium (IRS). - Vilnius, Lithuania, 16-18 June 2010. - P. 1-5. ↑
- C414.** Galati G. Technological challenges of a multifunction active phased array radar for weather, air traffic control and security applications. / Galati G., Pavan G., Scopelliti S., Infante L. // 2010 11th International Radar Symposium (IRS). - Vilnius, 16-18 June 2010. - P. 1-4. ↑
- C415.** Lesniak Wojciech. Solid state C band radar for detection of hovering helicopter. / Lesniak Wojciech, Czekala Zbigniew, Brenner Tadeusz. // 2010 11th International Radar Symposium (IRS). - Vilnius, Lithuania, 16-18 June 2010. - P. 1-4. ↑
- C416.** Akhtar Jabran. Energy allocation for correlated MIMO radar antennas with ricean targets. 2010 11th International Radar Symposium (IRS). - Vilnius, Lithuania, 16-18 June 2010. - P. 1-4. ↑
- C417.** Lesnik Czeslaw. An investigation of signal synthesis for radar applications. / Lesnik Czeslaw, Kawalec Adam, Szugajew Marcin, Solowicz Jan. // 2010 11th International Radar Symposium (IRS). - Vilnius, Lithuania, 16-18 June 2010. - P. 1-4. ↑
- C418.** Haumtratz Theresa. Classification of air targets including a rejection stage for unknown targets. / Haumtratz Theresa, Worms Josef, Schiller Joachim. // 2010 11th International Radar Symposium (IRS). - Vilnius, Lithuania, 16-18 June 2010. - P. 1-4. ↑
- C419.** Pogribny Wlodzimierz. Optimal sampling rate for short chirp signals. / Pogribny Wlodzimierz, Leszczynski Tadeusz. // 2010 11th International Radar Symposium (IRS). - Vilnius, Lithuania, 16-18 June 2010. - P. 1-4. ↑
- C420.** Deiana D. Multipath exploitation in an urban environment using a MIMO surveillance radar. / Deiana D., Kossen A. S., van Rossum W. L. // 2010 11th International Radar Symposium (IRS). - Vilnius, Lithuania, 16-18 June 2010. - P. 1-4. ↑
- C421.** Kemkemian Stephane. A MIMO radar for Sense and Avoid function: A fully static solution for UAV. / Kemkemian Stephane, Nouvel-Fiani Myriam, Cornic Pascal, Garrec Patrick. // 2010 11th International Radar Symposium (IRS). - Vilnius, Lithuania, 16-18 June 2010. - P. 1-4. ↑
- C422.** Wang Pu. Moving target estimation using distributed MIMO radar in non-homogeneous clutter. / Wang Pu, Li Hongbin, Himed Braham. // 2010 11th International Radar Symposium (IRS). - Vilnius, Lithuania, 16-18 June 2010. - P. 1-4. ↑
- C423.** Doukovska Lyubka Atanassova. Adaptive hough detector threshold analysis in presence of randomly arriving impulse interference. 2010 11th International Radar Symposium (IRS). - Vilnius, Lithuania, 16-18 June 2010. - P. 1-5. ↑

- C424.** Heuel Steffen. Pedestrian recognition based on 24 GHz radar sensors. / Heuel Steffen, Rohling Hermann. // 2010 11th International Radar Symposium (IRS). - Vilnius, Lithuania, 16-18 June 2010. - P. 1-6. ↑
- C425.** Rohling Hermann. Milestones in radar and the success story of automotive radar systems. 2010 11th International Radar Symposium (IRS). - Vilnius, Lithuania, 16-18 June 2010. - P. 1-6. ↑
- C426.** Sachs J. Ultra-wideband sensing: The road to new radar applications. 2010 11th International Radar Symposium (IRS). - Vilnius, Lithuania, 16-18 June 2010. - P. 1-4. ↑
- C427.** Meinecke Marc-Michael. Increasing vehicular safety at intersections by using LFMSK modulated radar sensors. / Meinecke Marc-Michael, Obojski Marian Andrzej, Knaup Jorn. // 2010 11th International Radar Symposium (IRS). - Vilnius, Lithuania, 16-18 June 2010. - P. 1-4. ↑
- C428.** Mayer Marcel. Angular measurement with lens based automotive radar sensors. / Mayer Marcel, Baur Klaus, Walter Thomas. // 2010 11th International Radar Symposium (IRS). - Vilnius, Lithuania, 16-18 June 2010. - P. 1-4. ↑
- C429.** Rohling Hermann. Development milestones in 24 GHz automotive radar systems. 2010 11th International Radar Symposium (IRS). - Vilnius, Lithuania, 16-18 June 2010. - P. 1-5. ↑
- C430.** Kuschel H. Passive radar from history to future. / Kuschel H., O'Hagan D. // 2010 11th International Radar Symposium (IRS). - Vilnius, Lithuania, 16-18 June 2010. - P. 1-4. ↑
- C431.** Takase Hiroshi. A dual-use system for radar and communication with complete complementary codes. / Takase Hiroshi, Shinriki Masanori. // 2010 11th International Radar Symposium (IRS). - Vilnius, Lithuania, 16-18 June 2010. - P. 1-4. ↑
- C432.** Behar Vera. MVDR radar signal processing approach for jamming suppression in satellite navigation receivers. / Behar Vera, Kabakchiev Christo, Rohling Hermann. // 2010 11th International Radar Symposium (IRS). - Vilnius, Lithuania, 16-18 June 2010. - P. 1-4. ↑
- C433.** Prokopenko I. G. Stabilisation of false alarm in the signal detection tasks. 2010 11th International Radar Symposium (IRS). - Vilnius, Lithuania, 16-18 June 2010. - P. 1-4. ↑
- C434.** Denisov Habil. Aleksandr. A history of oscilloscope development in Lithuania and neighbor countries. 2010 11th International Radar Symposium (IRS). - Vilnius, Lithuania, 16-18 June 2010. - P. 1-2. ↑
- C435.** Lukin Konstantin A. Fifty years of noise radar. / Lukin Konstantin A., Narayanan Ram M. // 2010 11th International Radar Symposium (IRS). - Vilnius, Lithuania, 16-18 June 2010. - P. 1-2. ↑
- C436.** Kronauge Matthias. Radar target detection and Doppler ambiguity resolution. / Kronauge Matthias, Schroeder Christoph, Rohling Hermann. // 2010 11th International Radar Symposium (IRS). - Vilnius, Lithuania, 16-18 June 2010. - P. 1-4. ↑
- C437.** {no data available}. Session 9b: Electronic warfare. 2010 11th International Radar Symposium (IRS). - Vilnius, Lithuania, 16-18 June 2010. - P. 1. ↑
- C438.** Drobakhin O.O. Multifrequency radar images of electrodynamics objects located behind dielectric layer in millimeter wave range. / Drobakhin O.O., Alekseev V.V., Saltykov D.Y., Saltykov A.D. // 2010 International Kharkov Symposium on Physics and Engineering of Microwaves, Millimeter and Submillimeter Waves (MSMW). - Kharkiv, 21-26 June 2010. - P. 1-3. ↑
- C439.** Sugak V.G. GPR signal phase structure application for estimation of distribution of soil electrical properties on depth. / Sugak V.G., Sugak A.V. // 2010 International Kharkov Symposium on Physics and Engineering of Microwaves, Millimeter and Submillimeter Waves (MSMW). - Kharkiv, 21-26 June 2010. - P. 1-3. ↑
- C440.** Bezruk V.M. Radar identification of clouds. / Bezruk V.M., Belov E.N., Voitovych O.A., Rudnev G.A., Khlopov G.I., Homenko S.I. // 2010 International Kharkov Symposium on Physics and Engineering of Microwaves, Millimeter and Submillimeter Waves (MSMW). - Kharkiv, 21-26 June 2010. - P. 1-3. ↑
- C441.** Lyakhovsky A.A. The longitudinal slot characteristics in waveguide with dielectric layer, situated parallel



to its broad walls. / Lyakhovsky A.A., Yatsuk L.P., Lyakhovsky A.F. // 2010 International Kharkov Symposium on Physics and Engineering of Microwaves, Millimeter and Submillimeter Waves (MSMW). - Kharkiv, 21-26 June 2010. - P. 1-3. ↑

C442. Yurchenko V.B. Time-domain simulation of trains of oscillation pulses in a Gunn diode system with a remote resonator. / Yurchenko V.B., Yurchenko L.V. // 2010 International Kharkov Symposium on Physics and Engineering of Microwaves, Millimeter and Submillimeter Waves (MSMW). - Kharkiv, 21-26 June 2010. - P. 1-3. ↑

C443. Varavin A.V. Improvement of range resolution of FMCW autodyne radar. / Varavin A.V., Ermak G.P., Vasilev A.S., Yevdokymov A.P., Kryzhanovskiy V.V. // 2010 International Kharkov Symposium on Physics and Engineering of Microwaves, Millimeter and Submillimeter Waves (MSMW). - Kharkiv, 21-26 June 2010. - P. 1-3. ↑

C444. Khlopov G. Measurement of intensity of liquid precipitation using double frequency radar. / Khlopov G., Khomenko S., Linkova A., Voitovych O. // 2010 International Kharkov Symposium on Physics and Engineering of Microwaves, Millimeter and Submillimeter Waves (MSMW). - Kharkiv, 21-26 June 2010. - P. 1-3. ↑

C445. Lutsenko V.I. Diagnostics of refraction coefficient on results of meteorological parameters measurement in arbitrary points of area. / Lutsenko V.I., Lutsenko I.V., Popov I.V., Gudkov V.N., Anh N.X. // 2010 International Kharkov Symposium on Physics and Engineering of Microwaves, Millimeter and Submillimeter Waves (MSMW). - Kharkiv, 21-26 June 2010. - P. 1-3. ↑

C446. Jenn D. C. Adaptive phase synchronization in distributed digital arrays. / Jenn D. C., Ryu Ji Heon, Yen-Chang Tsai, Broadston R. // 2010 NASA/ESA Conference on Adaptive Hardware and Systems (AHS). - Anaheim, CA, USA, 15-18 June 2010. - P. 199-204. ↑

C447. He Yutao. iBoard: A highly-capable, high-performance, reconfigurable FPGA-based building block for flight instrument digital electronics. / He Yutao, Ashtijou Mohammad. // 2010 NASA/ESA Conference on Adaptive Hardware and Systems (AHS). - Anaheim, CA, USA, 15-18 June 2010. - P. 73-74. ↑

C448. Karaev V. Potentialities of the Doppler spectrum of backscattered microwave signal in the problem of remote sensing of the sea surface. / Karaev V., Kanevsky M., Meshkov E. // 2010 International Kharkov Symposium on Physics and Engineering of Microwaves, Millimeter and Submillimeter Waves (MSMW). - Kharkiv, 21-26 June 2010. - P. 1-3. ↑

C449. Khlopov G. Application of double frequency radar for measurement of parameters of solid polydisperse aerosols. / Khlopov G., Knoechel R., Linkova A., Tepljuk A., Schuenemann K. // 2010 International Kharkov Symposium on Physics and Engineering of Microwaves, Millimeter and Submillimeter Waves (MSMW). - Kharkiv, 21-26 June 2010. - P. 1-3. ↑

C450. Lukin V.V. Robust DFT-based signal processing in Micro-Doppler radars. / Lukin V.V., Roenko A.A., Totsky A.V., Igor D. // 2010 International Kharkov Symposium on Physics and Engineering of Microwaves, Millimeter and Submillimeter Waves (MSMW). - Kharkiv, 21-26 June 2010. - P. 1-3. ↑

C451. Khomenko S.I. Doppler radar method for gas-discharge plasma research. / Khomenko S.I., Khorunzhiy M.O., Kuleshov A.N., Yefimov B.P. // 2010 International Kharkov Symposium on Physics and Engineering of Microwaves, Millimeter and Submillimeter Waves (MSMW). - Kharkiv, 21-26 June 2010. - P. 1-3. ↑

C452. Volosyuk V.K. Kravchenko weight functions in problems of restoration radar images at the modified synthesizing aperture. / Volosyuk V.K., Pavlikov V.V. // 2010 International Kharkov Symposium on Physics and Engineering of Microwaves, Millimeter and Submillimeter Waves (MSMW). - Kharkiv, 21-26 June 2010. - P. 1-3. ↑

C453. Volosyuk V.K. Optimization of statistical processing radar-tracking signals with use Kravchenko'S weight windows. / Volosyuk V.K., Pavlikov V.V. // 2010 International Kharkov Symposium on Physics and Engineering of Microwaves, Millimeter and Submillimeter Waves (MSMW). - Kharkiv, 21-26 June 2010. - P. 1-3. ↑

C454. Shkvarko Y.V. Aggregated convex regularization and variational analysis technique for enhancement of mm waveband remote sensing imagery. / Shkvarko Y.V., Tuxpan J., Santos S.R. // 2010 International Kharkov Symposium on Physics and Engineering of Microwaves, Millimeter and Submillimeter Waves (MSMW). - Kharkiv, 21-26 June 2010. - P. 1-3. ↑

- C455.** Lukin K.A. Fifty years of noise radar. / Lukin K.A., Narayanan R.M. // 2010 International Kharkov Symposium on Physics and Engineering of Microwaves, Millimeter and Submillimeter Waves (MSMW). - Kharkiv, 21-26 June 2010. - P. 1-3. ↑
- C456.** Magda I.I. Sources of intense impulse microwave emission. 2010 International Kharkov Symposium on Physics and Engineering of Microwaves, Millimeter and Submillimeter Waves (MSMW). - Kharkiv, 21-26 June 2010. - P. 1-6. ↑
- C457.** Bertuch T. System aspects of a low-cost coherent radar system with AESA antenna for maritime applications. / Bertuch T., Pamies M., Lojcker C., Knott P., Erkens H., Wunderlich R., Heinen S. // 2010 International Kharkov Symposium on Physics and Engineering of Microwaves, Millimeter and Submillimeter Waves (MSMW). - Kharkiv, 21-26 June 2010. - P. 1-6. ↑
- C458.** Shkvarko Y.V. Experiment design framework for super-high resolution imaging with the geostar configured sensor array data. / Shkvarko Y.V., Espadas V.E. // 2010 International Kharkov Symposium on Physics and Engineering of Microwaves, Millimeter and Submillimeter Waves (MSMW). - Kharkiv, 21-26 June 2010. - P. 1-3. ↑
- C459.** Zabrodina V.V. Comparative analysis of regression line fitting algorithms in blind method of mixed noise variance evaluation in radar images. / Zabrodina V.V., Abramov S.K., Abramov K.D. // 2010 International Kharkov Symposium on Physics and Engineering of Microwaves, Millimeter and Submillimeter Waves (MSMW). - Kharkiv, 21-26 June 2010. - P. 1. ↑
- C460.** Zelensky A.A. Signal processing algorithms in stepped frequency continues wave ground penetrating radar. / Zelensky A.A., Sugak A.V., Sugak V.G. // 2010 International Kharkov Symposium on Physics and Engineering of Microwaves, Millimeter and Submillimeter Waves (MSMW). - Kharkiv, 21-26 June 2010. - P. 1. ↑
- C461.** Vasilev A.S. Compact millimeter-wave distance and speed measurement sensor for railway applications. / Vasilev A.S., Varavin A.V., Ermak G.P., Popov I.V. // 2010 International Kharkov Symposium on Physics and Engineering of Microwaves, Millimeter and Submillimeter Waves (MSMW). - Kharkiv, 21-26 June 2010. - P. 1-3. ↑
- C462.** Sheverova A.V. Communication of characteristics of radiation and dispersion of a lattice of flat wave guides. 2010 International Kharkov Symposium on Physics and Engineering of Microwaves, Millimeter and Submillimeter Waves (MSMW). - Kharkiv, 21-26 June 2010. - P. 1. ↑
- C463.** Linkova A. Double frequency sounding of liquid precipitation. 2010 International Kharkov Symposium on Physics and Engineering of Microwaves, Millimeter and Submillimeter Waves (MSMW). - Kharkiv, 21-26 June 2010. - P. 1. ↑
- C464.** Shkvyrya Y. Algorithm of data processing in GPR. 2010 International Kharkov Symposium on Physics and Engineering of Microwaves, Millimeter and Submillimeter Waves (MSMW). - Kharkiv, 21-26 June 2010. - P. 1. ↑
- C465.** Benaskeur A. Cooperation in distributed surveillance. / Benaskeur A., Khamis A., Irandoust H. // 2010 International Conference on Autonomous and Intelligent Systems (AIS). - Povia de Varzim, 21-23 June 2010. - P. 1-6. ↑
- C466.** {no data available}. Session 5b: Signal processing II. 2010 11th International Radar Symposium (IRS). - Vilnius, Lithuania, 16-18 June 2010. - P. 1. ↑
- C467.** {no data available}. Session 7a: Noise radar II. 2010 11th International Radar Symposium (IRS). - Vilnius, Lithuania, 16-18 June 2010. - P. 1. ↑
- C468.** {no data available}. Session 6a: Noise radar I. 2010 11th International Radar Symposium (IRS). - Vilnius, Lithuania, 16-18 June 2010. - P. 1. ↑
- C469.** {no data available}. Session 5c: UWB I. 2010 11th International Radar Symposium (IRS). - Vilnius, Lithuania, 16-18 June 2010. - P. 1. ↑
- C470.** {no data available}. Session 4c: Radar applications. 2010 11th International Radar Symposium (IRS). - Vilnius, Lithuania, 16-18 June 2010. - P. 1. ↑

- C471. {no data available}. Session 6b: Tracking. 2010 11th International Radar Symposium (IRS). - Vilnius, Lithuania, 16-18 June 2010. - P. 1. ↑
- C472. {no data available}. Session 8a: GPR. 2010 11th International Radar Symposium (IRS). - Vilnius, Lithuania, 16-18 June 2010. - P. 1. ↑
- C473. {no data available}. Session P1. 2010 11th International Radar Symposium (IRS). - Vilnius, Lithuania, 16-18 June 2010. - P. 1. ↑
- C474. {no data available}. Session 8b: Radar systems. 2010 11th International Radar Symposium (IRS). - Vilnius, Lithuania, 16-18 June 2010. - P. 1. ↑
- C475. {no data available}. Title page vol1. 2010 11th International Radar Symposium (IRS). - Vilnius, Lithuania, 16-18 June 2010. - P. 1. ↑
- C476. {no data available}. Session 6c: UWB II. 2010 11th International Radar Symposium (IRS). - Vilnius, Lithuania, 16-18 June 2010. - P. 1. ↑
- C477. {no data available}. Session 9a: ISAR. 2010 11th International Radar Symposium (IRS). - Vilnius, Lithuania, 16-18 June 2010. - P. 1. ↑
- C478. {no data available}. Session 7b: Modelling. 2010 11th International Radar Symposium (IRS). - Vilnius, Lithuania, 16-18 June 2010. - P. 1. ↑
- C479. {no data available}. Session 4a: Historical session. 2010 11th International Radar Symposium (IRS). - Vilnius, Lithuania, 16-18 June 2010. - P. 1. ↑
- C480. Dukata Andrzej. A frequency selective magnetodielectric layer in polarimetric radar antenna track. / Dukata Andrzej, Kapelewski Jerzy, Lila Bogdan. // 2010 11th International Radar Symposium (IRS). - Vilnius, Lithuania, 16-18 June 2010. - P. 1-4. ↑
- C481. {no data available}. Session 1b: SAR I. 2010 11th International Radar Symposium (IRS). - Vilnius, Lithuania, 16-18 June 2010. - P. 1. ↑
- C482. Kovalenko A. I. Design of prospective spaceborne multi-aperture UWB polarimetric high performance SAR system. / Kovalenko A. I., Riman V. V., Shishanov A. V., Vnotchenko S. L. // 2010 11th International Radar Symposium (IRS). - Vilnius, Lithuania, 16-18 June 2010. - P. 1-3. ↑
- C483. Vnotchenko S. The "COMPACT" family of the small-sized airborne synthetic aperture radars (design philosophy and practical experience). / Vnotchenko S., Dostovalov M., Dyakov A., Dyakov I., Ermakov R., Zharovskaya E., Kovalenko A., Moussinants T., Neiman L., Riman V., Suslov V. // 2010 11th International Radar Symposium (IRS). - Vilnius, 16-18 June 2010. - P. 1-4. ↑
- C484. Sankowski Miroslaw. Numerical implementation of continuous-discrete IMM state estimators. / Sankowski Miroslaw, Buda Wojciech. // 2010 11th International Radar Symposium (IRS). - Vilnius, Lithuania, 16-18 June 2010. - P. 1-4. ↑
- C485. {no data available}. Opening session. 2010 11th International Radar Symposium (IRS). - Vilnius, Lithuania, 16-18 June 2010. - P. 1. ↑
- C486. {no data available}. Session 2b: SAR II. 2010 11th International Radar Symposium (IRS). - Vilnius, Lithuania, 16-18 June 2010. - P. 1. ↑
- C487. {no data available}. Session 4b: Signal processing I. 2010 11th International Radar Symposium (IRS). - Vilnius, Lithuania, 16-18 June 2010. - P. 1. ↑
- C488. {no data available}. Session 3a: Passive radars III focused session. 2010 11th International Radar Symposium (IRS). - Vilnius, Lithuania, 16-18 June 2010. - P. 1. ↑
- C489. {no data available}. Session 5a: MIMO. 2010 11th International Radar Symposium (IRS). - Vilnius, Lithuania, 16-18 June 2010. - P. 1. ↑
- C490. {no data available}. Session 1a: Passive radars I focused session. 2010 11th International Radar

Symposium (IRS). - Vilnius, Lithuania, 16-18 June 2010. - P. 1. ↑

C491. {no data available}. Session 3b: Automotive radars focused session. 2010 11th International Radar Symposium (IRS). - Vilnius, Lithuania, 16-18 June 2010. - P. 1. ↑

C492. {no data available}. Session 2a: Passive radars II focused session. 2010 11th International Radar Symposium (IRS). - Vilnius, Lithuania, 16-18 June 2010. - P. 1. ↑

C493. Min Lu. A kind of MIMO ground penetrating radar plane antenna array and corresponding imaging method. / Min Lu, Yutao Zhu, Yi Su, Chunlin Huang, Jian Wang. // 2010 13th International Conference on Ground Penetrating Radar (GPR). - Lecce, 21-25 June 2010. - P. 1-4. ↑

C494. Suqin Li. Study on Digital Management of Industrial Water System in Steel Industry. / Suqin Li, Jiangwei Wang. // 2010 International Conference on Internet Technology and Applications. - Wuhan, 20-22 Aug. 2010. - P. 1-6. ↑

C495. Meng Cai. An improved IMM algorithm with variable structure. / Meng Cai, Chengge Zong. // 2010 International Conference on Environmental Science and Information Application Technology (ESIAT). - Wuhan, 17-18 July 2010. - Vol. 2. - P. 507-510. ↑

C496. Xuhua Cai. Remote sensing retrieval of soil moisture using ENVISAT-ASAR images: A case study in suburban region of Peking, China. / Xuhua Cai, Huili Gong, Xiaojuan Li, Lin Zhu. // 2010 18th International Conference on Geoinformatics. - Beijing, 18-20 June 2010. - P. 1-4. ↑

C497. Xie Hong-quan. Design and Practice of GPS Inspection Data Acquisition System to Telecom Pipeline Network. / Xie Hong-quan, Guo Yuan-quan, Yu Yue-jun. // 2010 International Conference on Internet Technology and Applications. - Wuhan, 20-22 Aug. 2010. - P. 1-3. ↑

C498. BaoRong Zhong. The Research in New Architecture of Petroleum Drilling Instrument System. / BaoRong Zhong, Hong Du. // 2010 International Conference on Internet Technology and Applications. - Wuhan, 20-22 Aug. 2010. - P. 1-4. ↑

C499. Lin Changchuan. Chinese AIS Network and Impact on the Maritime Management. / Lin Changchuan, Qiu Haiqin, Qian Yaoyu, Hu Xiaorui, Da Liang. // 2010 International Conference on Internet Technology and Applications. - Wuhan, 20-22 Aug. 2010. - P. 1-4. ↑

C500. Gang Chen. Estimation of forest height, biomass and volume using support vector regression and segmentation from lidar transects and Quickbird imagery. / Gang Chen, Hay G.J., Yanlian Zhou. // 2010 18th International Conference on Geoinformatics. - Beijing, 18-20 June 2010. - P. 1-4. ↑

C501. Xie Chou. InSAR analysis over Yellow River Delta for mapping water-level changes over wetland. / Xie Chou, Shao Yun, Wan Zi. // 2010 18th International Conference on Geoinformatics. - Beijing, 18-20 June 2010. - P. 1-5. ↑

C502. Xie Chou. Multitemporal polarimetric SAR data fusion for land cover mapping. / Xie Chou, Shao Yun, Wan Zi, Zhang Fengli. // 2010 18th International Conference on Geoinformatics. - Beijing, 18-20 June 2010. - P. 1-5. ↑

C503. Fan Wang. A study of PS-InSAR method for small area urban land subsidence. / Fan Wang, Zhaoquan Huang, Le Yu, Lifan Zhou, Dengrong Zhang. // 2010 18th International Conference on Geoinformatics. - Beijing, 18-20 June 2010. - P. 1-6. ↑

C504. Yao Ye. Estimation of wetland aboveground biomass based on SAR image: A case study of Honghe National Natural Reserve in Heilongjiang, China. / Yao Ye, Chunping Zhou, Yonghua Sun, Demin Zhou. // 2010 18th International Conference on Geoinformatics. - Beijing, 18-20 June 2010. - P. 1-6. ↑

C505. Anqi Wang. Wetland mapping by using multi-band and multitemporal SAR images: A case study of Hong he National Natural Reserve. / Anqi Wang, Demin Zhou, Huili Gong. // 2010 18th International Conference on Geoinformatics. - Beijing, 18-20 June 2010. - P. 1-5. ↑

C506. Jie Yin. Vulnerability assessment of combined impacts of sea level rise and coastal flooding for China's coastal region using remote sensing and GIS. / Jie Yin, Shiyuan Xu, Jun Wang, Haidong Zhong, Yingjie Hu,



Zhane Yin, Kangfasheng Wang, Xinjian Zhang. // 2010 18th International Conference on Geoinformatics. - Beijing, 18-20 June 2010. - P. 1-4. ↑

C507. Yang Yang. The Internet of Things Based on Embedded Mode Design. / Yang Yang, Liu Yao-he, Song Ting-xin. // 2010 International Conference on Internet Technology and Applications. - Wuhan, 20-22 Aug. 2010. - P. 1-4. ↑

C508. Vavriv D. Spatial-harmonic magnetrons with cold secondary-emission cathode: Towards unlimited lifetime. 2010 International Conference on the Origins and Evolution of the Cavity Magnetron (CAVMAG). - Bournemouth, 19-20 April 2010. - P. 64-66. ↑

C509. Brady M. Developments in marine radar magnetrons. / Brady M., Edwards M. // 2010 International Conference on the Origins and Evolution of the Cavity Magnetron (CAVMAG). - Bournemouth, 19-20 April 2010. - P. 58-63. ↑

C510. Borisova N.A. Cavity magnetron in Russia. 2010 International Conference on the Origins and Evolution of the Cavity Magnetron (CAVMAG). - Bournemouth, 19-20 April 2010. - P. 23-33. ↑

C511. Yuhui Fu. The study on extracting of vessels information from the SAR satellite data. / Yuhui Fu, Hui Ma, Zhaolin Wu. // 2010 International Conference on Intelligent Control and Information Processing (ICICIP). - Dalian, 13-15 Aug. 2010. - P. 266-270. ↑

C512. de Keijzer A. Developments of radar and magnetrons in the Netherlands after 1945. 2010 International Conference on the Origins and Evolution of the Cavity Magnetron (CAVMAG). - Bournemouth, 19-20 April 2010. - P. 105-109. ↑

C513. Nosich A.I. In the labor people's name: Development of 60-kW magnetrons in the artificial famine plagued Ukraine in the early 1930's. / Nosich A.I., Kostenko A.A. // 2010 International Conference on the Origins and Evolution of the Cavity Magnetron (CAVMAG). - Bournemouth, 19-20 April 2010. - P. 82-88. ↑

C514. Obata H. Frequency bandwidth narrowing technology for cavity magnetrons installing cavity magnetrons into commercial marine radar. / Obata H., Furumoto K., Tsuji N., Hashimoto H., Kawaguchi M. // 2010 International Conference on the Origins and Evolution of the Cavity Magnetron (CAVMAG). - Bournemouth, 19-20 April 2010. - P. 34-39. ↑

C515. Mangri M. Tracing systems for user&Control-Plan traffic of Packet Core of GPRS-UMTS networks. / Mangri M., Nafornita M.M. // 2010 4th International Workshop on Soft Computing Applications (SOFA). - Arad, 15-17 July 2010. - P. 89-94. ↑

C516. Jian Cui. Research on Improved Quality Measures for the Fuzzy Association Rules of One Airborne Radar Intelligence Database. / Jian Cui, Qiang Li, Long-Po Yang, Yong Liu. // 2010 International Conference on Internet Technology and Applications. - Wuhan, 20-22 Aug. 2010. - P. 1-4. ↑


C517. Guangyou Yang. Remote Monitoring System of the Motor in GPRS Based on LabVIEW and Embedded TCP/IP. / Guangyou Yang, Jingjing Zhou, Xuwu Su, Zheng Zhang. // 2010 International Conference on Internet Technology and Applications. - Wuhan, 20-22 Aug. 2010. - P. 1-4. ↑

C518. Goerth J. Early magnetron development especially in Germany. 2010 International Conference on the Origins and Evolution of the Cavity Magnetron (CAVMAG). - Bournemouth, 19-20 April 2010. - P. 17-22. ↑

C519. Blanchard Y. Maurice Ponte and Henri Gutton, pioneers of early French studies on resonant magnetron (1932-1940). 2010 International Conference on the Origins and Evolution of the Cavity Magnetron (CAVMAG). - Bournemouth, 19-20 April 2010. - P. 5-10. ↑

C520. Brookner E. From \$10,000 magee to \$7 magee and \$10 transmitter and receiver (T/R) on single chip. 2010 International Conference on the Origins and Evolution of the Cavity Magnetron (CAVMAG). - Bournemouth, 19-20 April 2010. - P. 1-2. ↑

C521. Ye R.Q. Integration of LIDAR data and geological maps for landslide hazard assessment in the Three Gorges Reservoir area, China. / Ye R.Q., Niu R.Q., Zhao Y.N., Jiang Q.Y., Wu T., Deng Q.L. // 2010 18th International Conference on Geoinformatics. - Beijing, 18-20 June 2010. - P. 1-5. ↑

- C522.** Yishuo Huang. SAR satellite image interpretation based on the multilayer level set approach. / Yishuo Huang, Shang-Yuh Lin, Shengmin Wu. // 2010 18th International Conference on Geoinformatics. - Beijing, 18-20 June 2010. - P. 1-6. 
- C523.** Guosong Zhao. Assessment of ASTER GDEM performance by comparing with SRTM and ICESat/GLAS data in Central China. / Guosong Zhao, Huaiping Xue, Feng Ling. // 2010 18th International Conference on Geoinformatics. - Beijing, 18-20 June 2010. - P. 1-5. 
- C524.** Yangyang Zhang. Study of the airborne LIDAR data filtering methods. / Yangyang Zhang, Linjie Men. // 2010 18th International Conference on Geoinformatics. - Beijing, 18-20 June 2010. - P. 1-5. 
- C525.** Yu Zhang. An image segmentation algorithm for SAR images based on wavelet packets frame transformation. / Yu Zhang, Yongxue Liu. // 2010 18th International Conference on Geoinformatics. - Beijing, 18-20 June 2010. - P. 1-5. 
- C526.** Zhi Wang. Geodesics-based topographical feature extraction from airborne Lidar data for disaster management. / Zhi Wang, Huiying Li, Lixin Wu. // 2010 18th International Conference on Geoinformatics. - Beijing, 18-20 June 2010. - P. 1-5. 
- C527.** Fan Wang. The atmosphere correction in SBAS D-InSAR land subsidence monitoring application: A case study in Jiaxing-Huzhou plain, China. / Fan Wang, Zhaoquan Huang, Lifan Zhou, Dengrong Zhang. // 2010 18th International Conference on Geoinformatics. - Beijing, 18-20 June 2010. - P. 1-5. 
- C528.** Fengli Zhang. Building extraction using dual-aspect high resolution SAR images. / Fengli Zhang, Yun Shao, Xiao Zhang. // 2010 18th International Conference on Geoinformatics. - Beijing, 18-20 June 2010. - P. 1-5. 
- C529.** Dong Zhiming. Study on MIMO radar velocity resolution. / Dong Zhiming, Zeng Jiankui. // 2010 International Conference on Environmental Science and Information Application Technology (ESIAT). - Wuhan, 17-18 July 2010. - Vol. 2. - P. 603-606. 
- C530.** Xiang Iijuan. Wavelet based signal for MIMO radar. / Xiang Iijuan, Zeng Jiankui. // 2010 International Conference on Environmental Science and Information Application Technology (ESIAT). - Wuhan, 17-18 July 2010. - Vol. 2. - P. 607-610. 
- C531.** Xiang Lijuan. The chaotic signal design for MIMO radar. / Xiang Lijuan, Zeng Jiankui. // 2010 International Conference on Environmental Science and Information Application Technology (ESIAT). - Wuhan, 17-18 July 2010. - Vol. 2. - P. 611-614. 
- C532.** Zhichao Zhang. Multi-resolution 3D reconstruction of city statue based on laser scanning and photogrammetric concept. / Zhichao Zhang, Mingyao Ai, Zhenyu Zhang, Yixuan Zhu. // 2010 18th International Conference on Geoinformatics. - Beijing, 18-20 June 2010. - P. 1-4. 
- C533.** Zi Wan. Ortho-rectification of high-resolution SAR image in mountain area by DEM. / Zi Wan, Yun Shao, Chou Xie, Fengli Zhang. // 2010 18th International Conference on Geoinformatics. - Beijing, 18-20 June 2010. - P. 1-6. 
- C534.** Dong zhiming. The application of IMM in MIMO radar. / Dong zhiming, Zeng Jiankui. // 2010 International Conference on Environmental Science and Information Application Technology (ESIAT). - Wuhan, 17-18 July 2010. - Vol. 2. - P. 600-602. 
- C535.** Shen Yonglin. Identification of inclined buildings from aerial LIDAR Data for disaster management. / Shen Yonglin, Wu Lixin, Wang Zhi. // 2010 18th International Conference on Geoinformatics. - Beijing, 18-20 June 2010. - P. 1-5. 
- C536.** Hongyun Shi. A case study on co-seismic ground deformation of the Wenchuan earthquake using L-band and C-band SAR interferometry. / Hongyun Shi, Songlin Yang, Qulin Tan. // 2010 18th International Conference on Geoinformatics. - Beijing, 18-20 June 2010. - P. 1-4. 
- C537.** Yong Du. Study on accurate estimation of baseline parameters of space-borne InSAR based on GCPs. / Yong Du, Songlin Yang, Hongyun Shi. // 2010 18th International Conference on Geoinformatics. - Beijing, 18-20 June 2010. - P. 1-4. 

- C538.** Yongquan Li. An improved filtering method for digital elevation models construction based on LiDAR. / Yongquan Li, Xiangxi Dai, Mingxiao Wang, Zhizhou Huang. // 2010 18th International Conference on Geoinformatics. - Beijing, 18-20 June 2010. - P. 1-5. ↑
- C539.** Bin Pan. Precise SAR satellite orbit parameters determination based on Ground Control Points. / Bin Pan, Ling Liu. // 2010 18th International Conference on Geoinformatics. - Beijing, 18-20 June 2010. - P. 1-5. ↑
- C540.** Zongsheng Zheng. Determination of sedimentation rate of tidal flats at the Yangtze estuary, China, using multi-temporal Landsat TM images. / Zongsheng Zheng, Yunxuan Zhou, Xing Li, Runyuan Kuang. // 2010 18th International Conference on Geoinformatics. - Beijing, 18-20 June 2010. - P. 1-6. ↑
- C541.** Nianlong Han. Multi-spectral and SAR images fusion via Mallat and A trous wavelet transform. / Nianlong Han, Jinxing Hu, Wei Zhang. // 2010 18th International Conference on Geoinformatics. - Beijing, 18-20 June 2010. - P. 1-4. ↑
- C542.** Kebiao Huang. Regional aboveground forest biomass estimation using airborne and spaceborne LiDAR fusion with optical data in the Southwest of China. / Kebiao Huang, Yong Pang, Qingtai Shu, Tian Fu. // 2010 18th International Conference on Geoinformatics. - Beijing, 18-20 June 2010. - P. 1-6. ↑
- C543.** Yun Gong. Large-scale, rapid detection method of surface subsidence in western mining area. / Yun Gong, Caiping Meng. // 2010 18th International Conference on Geoinformatics. - Beijing, 18-20 June 2010. - P. 1-4. ↑
- C544.** Li Yan. SAR and multi-spectral image fusion based on feature additive integration. / Li Yan, Zhan Zhao, Hong Xie. // 2010 18th International Conference on Geoinformatics. - Beijing, 18-20 June 2010. - P. 1-4. ↑
- C545.** Li Yan. Production and accuracy analysis of high quality TerraSAR-X DOM. / Li Yan, Zhen Li. // 2010 18th International Conference on Geoinformatics. - Beijing, 18-20 June 2010. - P. 1-5. ↑
- C546.** Haidong Zhong. A solution for the data collection in the field survey based on Mobile and Wireless GIS. / Haidong Zhong, Ping Li, Yingjie Hu, Zhenhua Lv, Jie Yin, Bailang Yu, Jianping Wu. // 2010 18th International Conference on Geoinformatics. - Beijing, 18-20 June 2010. - P. 1-5. ↑
- C547.** Huiying Li. Extraction of features from airborne Lidar and onboard image data for future driver assistance systems. / Huiying Li, Zhi Wang, Shengbo Chen, Wenhui Li. // 2010 18th International Conference on Geoinformatics. - Beijing, 18-20 June 2010. - P. 1-4. ↑
- C548.** Haiyang Yu. Digital terrain model extraction from airborne LiDAR data in complex mining area. / Haiyang Yu, Xiaoping Lu, Xiaosan Ge, Gang Cheng. // 2010 18th International Conference on Geoinformatics. - Beijing, 18-20 June 2010. - P. 1-6. ↑
- C549.** Bei Wang. Elevation-map based regional hazard detection for planetary landing. / Bei Wang, Hutao Cui. // 2010 International Conference on Intelligent Control and Information Processing (ICICIP). - Dalian, 13-15 Aug. 2010. - P. 202-206. ↑
- C550.** Sturm C. A system demonstrator for the performance evaluation of a 24 GHz ISM band radar operating with OFDM waveforms. / Sturm C., Braun M., Zwick T., Wiesbeck W. // 2010 IEEE Antennas and Propagation Society International Symposium (APSURSI). - Toronto, ON, 11-17 July 2010. - P. 1-4. ↑
- C551.** Yang Xia. Underwater FDTD ELF simulation using dedicated hardware. / Yang Xia, Sullivan D.M. // 2010 IEEE Antennas and Propagation Society International Symposium (APSURSI). - Toronto, ON, 11-17 July 2010. - P. 1-4. ↑
- C552.** Kyungmin Kim. Substrate integrate waveguide quasi Yagi antenna using SIW-to-CPS transition for low mutual coupling. / Kyungmin Kim, Jindo Byun, Hai-Young Lee. // 2010 IEEE Antennas and Propagation Society International Symposium (APSURSI). - Toronto, ON, 11-17 July 2010. - P. 1-4. ↑
- C553.** Celik M. Numerical vibration analysis of a SAR antenna. 2010 IEEE Antennas and Propagation Society International Symposium (APSURSI). - Toronto, ON, 11-17 July 2010. - P. 1-4. ↑
- C554.** Van Niekerk C. UWB radar target sensing and imaging for granular materials research applications. / Van Niekerk C., Zastrow E., Hagness S.C., Bernhard J.T. // 2010 IEEE Antennas and Propagation Society

International Symposium (APSURSI). - Toronto, ON, 11-17 July 2010. - P. 1-4. ↑

**C555.** Thai T.T. A novel passive ultrasensitive RF temperature transducer for remote sensing and identification utilizing radar cross sections variability. / Thai T.T., Chebila F., Mehdi J.M., Pons P., Aubert H., DeJean G.R., Tentzeris M.M., Plana R. // 2010 IEEE Antennas and Propagation Society International Symposium (APSURSI). - Toronto, ON, 11-17 July 2010. - P. 1-4. ↑

**C556.** Fan Yang. EM techniques for the detection of breast cancer. / Fan Yang, Mohan A.S. // 2010 IEEE Antennas and Propagation Society International Symposium (APSURSI). - Toronto, ON, 11-17 July 2010. - P. 1-4. ↑

**C557.** Sagnard F. Design and analysis of wideband antennas for borehole and surface ground penetrating radars: Application to soil moisture content measurements. / Sagnard F., Rejiba F., Froumentin M. // 2010 IEEE Antennas and Propagation Society International Symposium (APSURSI). - Toronto, ON, 11-17 July 2010. - P. 1-4. ↑

**C558.** Sekiguchi T. Performance evaluation of Null-Steering Bistatic MIMO Radar. / Sekiguchi T., Sakaguchi K., Araki K., Arata S. // 2010 IEEE Antennas and Propagation Society International Symposium (APSURSI). - Toronto, ON, 11-17 July 2010. - P. 1-4. ↑

**C559.** Hui Zhang. Applying non-iterative phase errors compensation method to restore radar subsurface image. / Hui Zhang, Plettemeier D. // 2010 IEEE Antennas and Propagation Society International Symposium (APSURSI). - Toronto, ON, 11-17 July 2010. - P. 1-4. ↑

**C560.** Bukhari H. Directional coupled sectorial loops antenna for Ground Penetrating Radars applications. / Bukhari H., Sarabandi K. // 2010 IEEE Antennas and Propagation Society International Symposium (APSURSI). - Toronto, ON, 11-17 July 2010. - P. 1-4. ↑

**C561.** Ulku H.A. Radon transform interpretation of the Physical Optics integral and application to near and far field acoustic scattering problems. / Ulku H.A., Ergin A.A. // 2010 IEEE Antennas and Propagation Society International Symposium (APSURSI). - Toronto, ON, 11-17 July 2010. - P. 1-4. ↑

**C562.** Malyuskin O. 3D imaging of passive objects using dual-sided phase conjugating sequentially switched lens. / Malyuskin O., Fusco V. // 2010 IEEE Antennas and Propagation Society International Symposium (APSURSI). - Toronto, ON, 11-17 July 2010. - P. 1-4. ↑

**C563.** Knott P. Research on vibration control and structure integration of antennas in NATO/RTO/SET-131. / Knott P., Locker C., Algermissen S., Gruner W. // 2010 IEEE Antennas and Propagation Society International Symposium (APSURSI). - Toronto, ON, 11-17 July 2010. - P. 1-4. ↑

**C564.** Eubanks T.W. Double-sided parallel-strip line-fed circular monopole antenna. / Eubanks T.W., Kai Chang. // 2010 IEEE Antennas and Propagation Society International Symposium (APSURSI). - Toronto, ON, 11-17 July 2010. - P. 1-4. ↑

**C565.** Yazhou Wang. Three-dimensional through wall imaging using an UWB SAR. / Yazhou Wang, Fathy A.E. // 2010 IEEE Antennas and Propagation Society International Symposium (APSURSI). - Toronto, ON, 11-17 July 2010. - P. 1-4. ↑

**C566.** Chang P.C. Time-Reversal Processing and Autofocus of Targets Behind Complex Wall. / Chang P.C., Burkholder R.J., Volakis J.L. // 2010 IEEE Antennas and Propagation Society International Symposium (APSURSI). - Toronto, ON, 11-17 July 2010. - P. 1-4. ↑

**C567.** Schwarz U. Miniature double-ridged horn antennas composed of solid high-permittivity sintered ceramics for biomedical ultra-wideband radar applications. / Schwarz U., Stephan R., Hein M.A. // 2010 IEEE Antennas and Propagation Society International Symposium (APSURSI). - Toronto, ON, 11-17 July 2010. - P. 1-4. ↑

**C568.** Chi-Hyung Ahn. Compact reflectarray antenna element using split ring resonator. / Chi-Hyung Ahn, Seong-Won Oh, Kai Chang. // 2010 IEEE Antennas and Propagation Society International Symposium (APSURSI). - Toronto, ON, 11-17 July 2010. - P. 1-4. ↑

**C569.** Deek F. Detecting flaws in buried pipes under rough surface using the natural frequency technique. /



Deek F., El-Shenawee M. // 2010 IEEE Antennas and Propagation Society International Symposium (APSURSI). - Toronto, ON, 11-17 July 2010. - P. 1-4. ↑

C570. Le C. Radar imaging of a large building based on near-field Xpatch model. / Le C., Lam Nguyen, Dogaru T. // 2010 IEEE Antennas and Propagation Society International Symposium (APSURSI). - Toronto, ON, 11-17 July 2010. - P. 1-4. ↑

C571. Cetin R. DFT-UTD based MoM approach for an efficient analysis of scattering from large, finite arrays in the vicinity of scattering objects. / Cetin R., Civi O.A., Nepa P. // 2010 IEEE Antennas and Propagation Society International Symposium (APSURSI). - Toronto, ON, 11-17 July 2010. - P. 1-4. ↑

C572. Pour Z.A. Effect of primary feed polarization on phase centre location of parabolic reflector antennas. / Pour Z.A., Shafai L. // 2010 IEEE Antennas and Propagation Society International Symposium (APSURSI). - Toronto, ON, 11-17 July 2010. - P. 1-4. ↑

C573. Jianjun Liu. A printed extremely wideband antenna for multi-band wireless systems. / Jianjun Liu, Esselle K.P., Shun-Shi Zhong. // 2010 IEEE Antennas and Propagation Society International Symposium (APSURSI). - Toronto, ON, 11-17 July 2010. - P. 1-4. ↑

C574. Chauveau J. Low frequency imaging of separated objects using the ramp response technique. / Chauveau J., de Beaucoudrey N. // 2010 IEEE Antennas and Propagation Society International Symposium (APSURSI). - Toronto, ON, 11-17 July 2010. - P. 1-4. ↑

C575. Thiel M. Advanced through-the-wall radar imaging using spectral and wall estimation techniques. / Thiel M., Sarabandi K. // 2010 IEEE Antennas and Propagation Society International Symposium (APSURSI). - Toronto, ON, 11-17 July 2010. - P. 1-4. ↑

C576. Simeoni M. Circularly polarized supershaped dielectric resonator antennas for indoor ultra wide band applications. / Simeoni M., Cicchetti R., Yarovoy A., Caratelli D. // 2010 IEEE Antennas and Propagation Society International Symposium (APSURSI). - Toronto, ON, 11-17 July 2010. - P. 1-4. ↑

C577. Chao-Hsiang Liao. UWB antenna array for real beam radar imaging. / Chao-Hsiang Liao, Powen Hsu, Dau-Chyrh Chang. // 2010 IEEE Antennas and Propagation Society International Symposium (APSURSI). - Toronto, ON, 11-17 July 2010. - P. 1-4. ↑

C578. Gong Weijie. Application of the SHGA basing on the CFPM to hypersonic vehicle wing-body location design optimization. / Gong Weijie, Tang Shuo. // 2010 3rd IEEE International Conference on Computer Science and Information Technology (ICCSIT). - Chengdu, 9-11 July 2010. - Vol. 8. - P. 259-264. ↑

C579. Wang Quanmin. Simulation of UWB echoes from ground based on CPML-FDTD. / Wang Quanmin, Chen Bin, Guo Gang, Huang Kedi. // 2010 3rd IEEE International Conference on Computer Science and Information Technology (ICCSIT). - Chengdu, 9-11 July 2010. - Vol. 3. - P. 524-527. ↑

C580. Xiang Gao. Feature extraction and selection for landmine detection using textures of Time-Frequency Representation. / Xiang Gao, Guangrong Ji, Chunhe Wang, Guangyu Ji. // 2010 3rd IEEE International Conference on Computer Science and Information Technology (ICCSIT). - Chengdu, 9-11 July 2010. - Vol. 1. - P. 516-520. ↑

C581. Mingshan Lv. Radar jamming resources assignment algorithm for EW real-time decision support system of multi-platforms. / Mingshan Lv, Dongli Liu, Ning Jiang, Qi Chen. // 2010 International Conference on Intelligent Control and Information Processing (ICICIP). - Dalian, 13-15 Aug. 2010. - P. 83-86. ↑

C582. Xiang Zhou. Analysis and pattern recognition of blast furnace burden surface based on multi-radar data. / Xiang Zhou, Xiaoli Li, Dexin Liu, Yixin Yin, Xianzhong Chen, Qingwen Hou. // 2010 International Conference on Intelligent Control and Information Processing (ICICIP). - Dalian, 13-15 Aug. 2010. - P. 286-291. ↑

C583. Jun-qiang Yang. Research on the model of Target's trail and the detection simulation of air-defense radar. / Jun-qiang Yang, Zheng Mao. // 2010 3rd IEEE International Conference on Computer Science and Information Technology (ICCSIT). - Chengdu, 9-11 July 2010. - Vol. 2. - P. 55-58. ↑

C584. Yu Lei. Research on modeling and simulation of cruise missile interception system based on Object-Oriented Petri net. / Yu Lei, Tang Shuo. // 2010 3rd IEEE International Conference on Computer Science and

Information Technology (ICCSIT). - Chengdu, 9-11 July 2010. - Vol. 6. - P. 632-635. ↑

C585. Shan Xian-ming. Design and realization of virtual simulation training system for certain type artillery radar. / Shan Xian-ming, Zhao Zhi-hong, Xu Guo-xin. // 2010 3rd IEEE International Conference on Computer Science and Information Technology (ICCSIT). - Chengdu, 9-11 July 2010. - Vol. 4. - P. 280-283. ↑

C586. Wu Changrui. A high-performance heterogeneous embedded signal processing system based on serial RapidIO interconnection. / Wu Changrui, Cen Fan, Cai Huizhi. // 2010 3rd IEEE International Conference on Computer Science and Information Technology (ICCSIT). - Chengdu, 9-11 July 2010. - Vol. 2. - P. 611-614. ↑

C587. Hang Ruan. Wide band noise interference suppression for SAR with dechirping and eigensubspace filtering. / Hang Ruan, Wei Ye, Canbin Yin, Shuxian Zhang. // 2010 International Conference on Intelligent Control and Information Processing (ICICIP). - Dalian, 13-15 Aug. 2010. - P. 39-42. ↑

C588. Shan Xian-ming. Design and realization of virtual scene explore system for artillery reconnaissance radar. / Shan Xian-ming, Yang He-yong, Xiao Jun-ling. // 2010 3rd IEEE International Conference on Computer Science and Information Technology (ICCSIT). - Chengdu, 9-11 July 2010. - Vol. 4. - P. 284-287. ↑

C589. Ma Yanchun. The research of interaction management based on the IPv6 wireless mobile terminals. 2010 3rd IEEE International Conference on Computer Science and Information Technology (ICCSIT). - Chengdu, 9-11 July 2010. - Vol. 3. - P. 565-569. ↑

C590. Lu Yi. A target selection method for ASM based on ICP algorithm. / Lu Yi, Jiang Yonghua, Zhai Longjun, Li Yulong. // 2010 3rd IEEE International Conference on Computer Science and Information Technology (ICCSIT). - Chengdu, 9-11 July 2010. - Vol. 7. - P. 185-188. ↑

C591. Lan Gao. An improved particle filter based on 4D discontinuous measurements. / Lan Gao, Jing Jiang, Jiangqiao Lan, Zhenhua Xie. // 2010 International Conference on Intelligent Control and Information Processing (ICICIP). - Dalian, 13-15 Aug. 2010. - P. 25-29. ↑

C592. Bialkowski M.E. UWB cylindrical microwave imaging system with novel image reconstruction algorithm. / Bialkowski M.E., Yifan Wang, Bakar A.A., Khor W.C. // 2010 IEEE Antennas and Propagation Society International Symposium (APSURSI). - Toronto, ON, 11-17 July 2010. - P. 1-4. ↑

C593. Tien D. Project management and data quality control. 2010 IEEE International Conference on Emergency Management and Management Sciences (ICEMMS). - Beijing, 8-10 Aug. 2010. - P. 549-552. ↑

C594. Zhu Lei. Application of compressed sensing theory to radar signal processing. / Zhu Lei, Qiu Chunting. // 2010 3rd IEEE International Conference on Computer Science and Information Technology (ICCSIT). - Chengdu, 9-11 July 2010. - Vol. 6. - P. 315-318. ↑

C595. Browne K.E. High resolution radar imaging utilizing a portable opportunistic sensing platform. / Browne K.E., Burkholder R.J., Volakis J.L. // 2010 IEEE Antennas and Propagation Society International Symposium (APSURSI). - Toronto, ON, 11-17 July 2010. - P. 1-4. ↑

C596. Moallem M. Y-band phenomenology of indoor environment. / Moallem M., Sarabandi K. // 2010 IEEE Antennas and Propagation Society International Symposium (APSURSI). - Toronto, ON, 11-17 July 2010. - P. 1-4. ↑

C597. Yifan Wang. Design of two-element probe antenna for UWB near-field imaging. / Yifan Wang, Bialkowski M.E. // 2010 IEEE Antennas and Propagation Society International Symposium (APSURSI). - Toronto, ON, 11-17 July 2010. - P. 1-4. ↑

C598. Yang Yuqi. A novel method for limiting the amplitude of SAR images with the principal axis detection. / Yang Yuqi, Gao Xiaoguang, Feng Xiaoyi, Yan Kun. // 2010 3rd IEEE International Conference on Computer Science and Information Technology (ICCSIT). - Chengdu, 9-11 July 2010. - Vol. 8. - P. 200-202. ↑

C599. Long Cai. On orthogonal waveform design for MIMO sonar. / Long Cai, Xiaochuan Ma, Shasha Li. // 2010 International Conference on Intelligent Control and Information Processing (ICICIP). - Dalian, 13-15 Aug. 2010. - P. 69-72. ↑

C600. Jia Yang. A multi-sensors data fusion method based on the augmented support degree. / Jia Yang,

Fengxun Gong, Yanqiu Ma. // 2010 International Conference on Intelligent Control and Information Processing (ICICIP). - Dalian, 13-15 Aug. 2010. - P. 119-122. ↑

C601. Dexin Liu. Application of fuzzy pattern recognition in burden surface identification. / Dexin Liu, Xiaoli Li, Xiang Zhou, Yixin Yin, Xianzhong Chen, Qingwen Hou. // 2010 International Conference on Intelligent Control and Information Processing (ICICIP). - Dalian, 13-15 Aug. 2010. - P. 292-296. ↑

C602. Cheng Wei. An adaptive modulation method based on bit preassign for HF OFDM systems. / Cheng Wei, Yang Rui-juan, Fan Qi-xing, Huang Mei-rong. // 2010 3rd IEEE International Conference on Computer Science and Information Technology (ICCSIT). - Chengdu, 9-11 July 2010. - Vol. 2. - P. 606-610. ↑

C603. Yadong Sun. Research on design process for complex product. / Yadong Sun, Xu Zhang, Dehao Xu. // 2010 International Conference on Intelligent Control and Information Processing (ICICIP). - Dalian, 13-15 Aug. 2010. - P. 628-632. ↑

C604. Suganthi S. Neural based optimization analysis of distributed MEMS transmission line phase shifters. / Suganthi S., Raghavan S. // 2010 International Conference on Intelligent Control and Information Processing (ICICIP). - Dalian, 13-15 Aug. 2010. - P. 639-643. ↑

C605. Cohen L. Mitigation of radar interference with WiMAX systems. / Cohen L., Daly E., DeGraaf J., Scheff K. // 2010 International Waveform Diversity and Design Conference (WDD). - Niagara Falls, ON, 8-13 Aug. 2010. - P. 159-164. ↑

C606. Masbernat X.P. An MIMO-MTI approach for through-the-wall radar imaging applications. / Masbernat X.P., Amin M.G., Ahmad F., Ioana C. // 2010 International Waveform Diversity and Design Conference (WDD). - Niagara Falls, ON, 8-13 Aug. 2010. - P. 000188-000192. ↑

C607. Carlson J. SMSE-based DSA radar waveforms. / Carlson J., Kennedy J., Chakravarthy V. // 2010 International Waveform Diversity and Design Conference (WDD). - Niagara Falls, ON, 8-13 Aug. 2010. - P. 169-176. ↑

C608. Blunt S.D. Using time reversal of multipath for intra-pulse radar-embedded communications. / Blunt S.D., Metcalf J.G. // 2010 International Waveform Diversity and Design Conference (WDD). - Niagara Falls, ON, 8-13 Aug. 2010. - P. 000155-000158. ↑

C609. Czernik R.J. The impact of internal clutter motion on a sample matrix inversion space-time adaptive processing algorithm and the GMTI minimum detectable velocity. / Czernik R.J., SantaPietro J.J. // 2010 International Waveform Diversity and Design Conference (WDD). - Niagara Falls, ON, 8-13 Aug. 2010. - P. 000136-000141. ↑

C610. Amin M.G. Target RCS exploitations in compressive sensing for through wall imaging. / Amin M.G., Ahmad F., Wenji Zhang. // 2010 International Waveform Diversity and Design Conference (WDD). - Niagara Falls, ON, 8-13 Aug. 2010. - P. 000150-000154. ↑

C611. Blunt S.D. Embedding information into radar emissions via waveform implementation. / Blunt S.D., Cook M.R., Stiles J. // 2010 International Waveform Diversity and Design Conference (WDD). - Niagara Falls, ON, 8-13 Aug. 2010. - P. 000195-000199. ↑

C612. Raj R.G. ISAR imaging in sea clutter via compressive sensing. / Raj R.G., Farshchian M. // 2010 International Waveform Diversity and Design Conference (WDD). - Niagara Falls, ON, 8-13 Aug. 2010. - P. 200-205. ↑

C613. De Maio A. Pareto-optimal radar waveform design. / De Maio A., Piezzo M., Farina A., Wicks M. // 2010 International Waveform Diversity and Design Conference (WDD). - Niagara Falls, ON, 8-13 Aug. 2010. - P. 000224-000228. ↑

C614. Sego D.J. Waveform design for low frequency tomography. / Sego D.J., Griffiths H., Wicks M.C. // 2010 International Waveform Diversity and Design Conference (WDD). - Niagara Falls, ON, 8-13 Aug. 2010. - P. 230-237. ↑

C615. Romero R.A. Channel probability ensemble update for multiplatform radar systems. / Romero R.A., Kenyon C.M., Goodman N.A. // 2010 International Waveform Diversity and Design Conference (WDD). - Niagara

Falls, ON, 8-13 Aug. 2010. - P. 000182-000187. ↑

**C616.** Zhang Y.D. Target localization in multipath environment through the exploitation of multi-frequency array. / Zhang Y.D., Xin Li, Amin M.G. // 2010 International Waveform Diversity and Design Conference (WDD). - Niagara Falls, ON, 8-13 Aug. 2010. - P. 000206-000210. ↑

**C617.** Ertin E. Frequency diverse waveforms for compressive radar sensing. 2010 International Waveform Diversity and Design Conference (WDD). - Niagara Falls, ON, 8-13 Aug. 2010. - P. 000216-000219. ↑

**C618.** Liangbing Hu. Optimal mismatched filter bank design for MIMO radar via convex optimization. / Liangbing Hu, Hongwei Liu, Da-Zheng Feng, Bo Jiu, Xu Wang, Shunjun Wu. // 2010 International Waveform Diversity and Design Conference (WDD). - Niagara Falls, ON, 8-13 Aug. 2010. - P. 000126-000131. ↑

**C619.** Byung Wook Jung. Reduced rank detection algorithms for distributed array sensors. / Byung Wook Jung, Adve R.S., Joohwan Chun. // 2010 International Waveform Diversity and Design Conference (WDD). - Niagara Falls, ON, 8-13 Aug. 2010. - P. 000066-000070. ↑

**C620.** Shastry M.C. Compressive radar imaging using white stochastic waveforms. / Shastry M.C., Narayanan R.M., Rangaswamy M. // 2010 International Waveform Diversity and Design Conference (WDD). - Niagara Falls, ON, 8-13 Aug. 2010. - P. 000090-000094. ↑

**C621.** Tao Mao. Phase-modulated waveform design for the target detection in the presence of signal-dependent clutter. / Tao Mao, Xuhua Gong, Huadong Meng, Xiqin Wang. // 2010 International Waveform Diversity and Design Conference (WDD). - Niagara Falls, ON, 8-13 Aug. 2010. - P. 000100-000104. ↑

**C622.** Cheney M. Waveform-diverse moving-target spotlight SAR. / Cheney M., Borden B. // 2010 International Waveform Diversity and Design Conference (WDD). - Niagara Falls, ON, 8-13 Aug. 2010. - P. 000033-000034. ↑

**C623.** Lee N. Design of an optimal radar signal waveform for a range-doppler spreading channel. / Lee N., Yang H., Chun J., Jung M. // 2010 International Waveform Diversity and Design Conference (WDD). - Niagara Falls, ON, 8-13 Aug. 2010. - P. 000063-000065. ↑

**C624.** Fancey C. The metrication of low probability of intercept waveforms. / Fancey C., Alabaster C.M. // 2010 International Waveform Diversity and Design Conference (WDD). - Niagara Falls, ON, 8-13 Aug. 2010. - P. 000058-000062. ↑

**C625.** Balleri A. Bat-inspired multi-harmonic waveforms. / Balleri A., Griffiths H., Holderied M., Baker C. // 2010 International Waveform Diversity and Design Conference (WDD). - Niagara Falls, ON, 8-13 Aug. 2010. - P. 000086-000089. ↑

**C626.** Yangsoo Kwon. A multi-target detector using mutual information for noise radar systems in low SNR regimes. / Yangsoo Kwon, Narayanan R.M., Rangaswamy M. // 2010 International Waveform Diversity and Design Conference (WDD). - Niagara Falls, ON, 8-13 Aug. 2010. - P. 000105-000109. ↑

**C627.** Higgins T. Time-Range Adaptive Processing for pulse agile radar. / Higgins T., Blunt S.D., Shackelford A.K. // 2010 International Waveform Diversity and Design Conference (WDD). - Niagara Falls, ON, 8-13 Aug. 2010. - P. 115-120. ↑

**C628.** Olsen K.E. Analysis of the performance of a multiband passive bistatic radar processing scheme. / Olsen K.E., Woodbridge K. // 2010 International Waveform Diversity and Design Conference (WDD). - Niagara Falls, ON, 8-13 Aug. 2010. - P. 000142-000149. ↑

**C629.** Chavali P. Cognitive radar for target tracking in multipath scenarios. / Chavali P., Nehorai A. // 2010 International Waveform Diversity and Design Conference (WDD). - Niagara Falls, ON, 8-13 Aug. 2010. - P. 000110-000114. ↑

**C630.** Bhat S. An adaptive multimodal radar system with progressive resolution enhancement. / Bhat S., Narayanan R., Rangaswamy M. // 2010 International Waveform Diversity and Design Conference (WDD). - Niagara Falls, ON, 8-13 Aug. 2010. - P. 000095-000099. ↑

**C631.** Anglin J.P. Radar transmit waveform design for lossy propagation channels. / Anglin J.P., Stiles J.M. // 2010 International Waveform Diversity and Design Conference (WDD). - Niagara Falls, ON, 8-13 Aug. 2010. - P.



000121-000125. ↑

**C632.** Baylis C. Designing for spectral conformity: Issues in power amplifier design. / Baylis C., Wang L., Moldovan M., Martin J., Miller H., Cohen L., de Graaf J. // 2010 International Waveform Diversity and Design Conference (WDD). - Niagara Falls, ON, 8-13 Aug. 2010. - P. 000220-000223. ↑

**C633.** Muralidharan S. Design, simulation and analysis of neural controller based Series resonant converter. / Muralidharan S., Rajan C.C.A. // 2010 2nd International Conference on Mechanical and Electrical Technology (ICMET). - Singapore, 10-12 Sept. 2010. - P. 144-147. ↑

**C634.** Tkac J. Velocity evaluating of the moving objects. 2010 International Conference on Applied Electronics (AE). - Pilsen, 8-9 Sept. 2010. - P. 1-4. ↑

**C635.** Hui Chen. Improvement of bearing-only tracking fusion strategy based on bionics with infrared sensor. / Hui Chen, Zhanming Li. // 2010 9th IEEE International Conference on Cognitive Informatics (ICCI). - Beijing, 7-9 July 2010. - P. 978-982. ↑

**C636.** Shackleton J. Tracking People with a 360-Degree Lidar. / Shackleton J., VanVoorst B., Hesch J. // 2010 Seventh IEEE International Conference on Advanced Video and Signal Based Surveillance (AVSS). - Boston, MA, Aug. 29 2010-Sept. 1 2010. - P. 420-426. ↑

**C637.** Jiali Shen. Human Localization in a Cluttered Space Using Multiple Cameras. / Jiali Shen, Weiqi Yan, Miller P., Huiyu Zhou. // 2010 Seventh IEEE International Conference on Advanced Video and Signal Based Surveillance (AVSS). - Boston, MA, Aug. 29 2010-Sept. 1 2010. - P. 85-90. ↑

**C638.** Selvaperumal S. Embedded control of LCC resonant converter analysis, design, simulation and experimental results. / Selvaperumal S., Rajan C.C.A. // 2010 2nd International Conference on Mechanical and Electrical Technology (ICMET). - Singapore, 10-12 Sept. 2010. - P. 94-98. ↑

**C639.** Li Guomin. Partner Selection Strategy in Cooperative Diversity Systems. / Li Guomin, Liao Guisheng. // 2010 6th International Conference on Wireless Communications Networking and Mobile Computing (WiCOM). - Chengdu, 23-25 Sept. 2010. - P. 1-3. ↑

**C640.** Xinchao Li. Joint Angle Estimation for Bistatic MIMO Radar. / Xinchao Li, Yiduo Guo, Yongshun Zhang, Di Shen. // 2010 6th International Conference on Wireless Communications Networking and Mobile Computing (WiCOM). - Chengdu, 23-25 Sept. 2010. - P. 1-4. ↑

**C641.** Li Ming. A New Improved Particle Filter Algorithm Based on UKF and GASA. / Li Ming, Zhang Peng, Wu Yan. // 2010 6th International Conference on Wireless Communications Networking and Mobile Computing (WiCOM). - Chengdu, 23-25 Sept. 2010. - P. 1-4. ↑

**C642.** Bin-bin Cheng. The Application of Poly-Phase Filter in Rader Signal Processing. / Bin-bin Cheng, Jing Xu, Hai Zhang. // 2010 6th International Conference on Wireless Communications Networking and Mobile Computing (WiCOM). - Chengdu, 23-25 Sept. 2010. - P. 1-4. ↑

**C643.** Jinlong Yang. A New Adaptive Algorithm for Passive Multi-Sensor Maneuvering Target Tracking. / Jinlong Yang, Hongbing Ji. // 2010 6th International Conference on Wireless Communications Networking and Mobile Computing (WiCOM). - Chengdu, 23-25 Sept. 2010. - P. 1-4. ↑

**C644.** He Jian-Xin. A Frequency Estimation Algorithm for Pulsed Magnetron Radar Transmitter Sample Signal. / He Jian-Xin, Xu Zhi-Huo, Wang Yue-Xia. // 2010 6th International Conference on Wireless Communications Networking and Mobile Computing (WiCOM). - Chengdu, 23-25 Sept. 2010. - P. 1-3. ↑

**C645.** Wang Yue-Xia. A Novel Spectral Parameters Estimation Approach for Weather Echoes Based on Fitting. / Wang Yue-Xia, He Jian-Xin. // 2010 6th International Conference on Wireless Communications Networking and Mobile Computing (WiCOM). - Chengdu, 23-25 Sept. 2010. - P. 1-4. ↑

**C646.** Huanhuan Chen. Probabilistic robust hyperbola mixture model for interpreting ground penetrating radar data. / Huanhuan Chen, Cohn A.G. // The 2010 International Joint Conference on Neural Networks (IJCNN). - Barcelona, 18-23 July 2010. - P. 1-8. ↑

**C647.** Chen R.C. Golay waveforms and adaptive estimation. / Chen R.C., Higgins T. // 2010 International

Waveform Diversity and Design Conference (WDD). - Niagara Falls, ON, 8-13 Aug. 2010. - P. 257-261. ↑

C648. Fuhrmann D. Waveform diversity and advanced signaling strategies for the Hybrid MIMO Phased Array Radar. / Fuhrmann D., Browning P., Rangaswamy M. // 2010 International Waveform Diversity and Design Conference (WDD). - Niagara Falls, ON, 8-13 Aug. 2010. - P. 283. ↑

C649. Yizhong Wu. A Novel Range Detection Method for 60GHz LFM CW Radar. / Yizhong Wu, Ying Bao, Zhiguo Shi, Jiming Chen, Youxian Sun. // 2010 IEEE 72nd Vehicular Technology Conference Fall (VTC 2010-Fall). - Ottawa, ON, 6-9 Sept. 2010. - P. 1-5. ↑

C650. Qiu R.C. Wireless tomography, Part I: A novel approach to remote sensing. / Qiu R.C., Wicks M.C., Li L., Hu Z., Hou S.J., Chen P., Browning J.P. // 2010 International Waveform Diversity and Design Conference (WDD). - Niagara Falls, ON, 8-13 Aug. 2010. - P. 000244-000256. ↑

C651. Schneible J. Geometric diversity versus frequency diversity an imaging example. / Schneible J., Browning J.P., Wicks M., Yuhong Zhang. // 2010 International Waveform Diversity and Design Conference (WDD). - Niagara Falls, ON, 8-13 Aug. 2010. - P. 262-269. ↑

C652. Cook M.R. Thinned spectrum radar waveforms. / Cook M.R., Higgins T., Shackelford A.K. // 2010 International Waveform Diversity and Design Conference (WDD). - Niagara Falls, ON, 8-13 Aug. 2010. - P. 238-243. ↑

C653. Eugin Hyun. Two-Step Moving Target Detection Algorithm for Automotive 77 GHz FMCW Radar. / Eugin Hyun, Woojin Oh, Jong-Hun Lee. // 2010 IEEE 72nd Vehicular Technology Conference Fall (VTC 2010-Fall). - Ottawa, ON, 6-9 Sept. 2010. - P. 1-5. ↑

C654. Danilina I. Thermal infrared radiosity and heat diffusion model verification and validation. / Danilina I., Gillespie A.R., Smith M., Balick L., Abbott E. // 2010 2nd Workshop on Hyperspectral Image and Signal Processing: Evolution in Remote Sensing (WHISPERS). - Reykjavik, 14-16 June 2010. - P. 1-4. ↑

C655. Zhuosen Wang. Canopy vertical structure using MODIS Bidirectional Reflectance data. / Zhuosen Wang, Schaaf C.B., Philip L., Knyazikhin Y., Schull M.A., Strahler A.H., Myneni R.B., Chopping M. // 2010 2nd Workshop on Hyperspectral Image and Signal Processing: Evolution in Remote Sensing (WHISPERS). - Reykjavik, 14-16 June 2010. - P. 1-4. ↑

C656. Nehal Q. A wideband variable gain amplifier with feedback DC-offset correction in 0.13μm CMOS technology. / Nehal Q., Saari V., Halonen K. // 2010 International Conference on Signals and Electronic Systems (ICSES). - Gliwice, 7-10 Sept. 2010. - P. 221-224. ↑

C657. Kaasalainen S. Active hyperspectral LIDAR methods for object classification. / Kaasalainen S., Suomalainen J., Hakala T., Yuwei Chen, Raikkonen E., Puttonen E., Kaartinen H. // 2010 2nd Workshop on Hyperspectral Image and Signal Processing: Evolution in Remote Sensing (WHISPERS). - Reykjavik, 14-16 June 2010. - P. 1-4. ↑

C658. Brook A. Fusion of hyperspectral images and LiDAR data for civil engineering structure monitoring. / Brook A., Ben-Dor E., Richter R. // 2010 2nd Workshop on Hyperspectral Image and Signal Processing: Evolution in Remote Sensing (WHISPERS). - Reykjavik, 14-16 June 2010. - P. 1-5. ↑

C659. Frank M. Vegetation management of utility corridors using high-resolution hyperspectral imaging and LiDAR. / Frank M., Zhihong Pan, Raber B., Lenart C. // 2010 2nd Workshop on Hyperspectral Image and Signal Processing: Evolution in Remote Sensing (WHISPERS). - Reykjavik, 14-16 June 2010. - P. 1-4. ↑

C660. Nuthalapati R. Mismatched filtering of chaotic codes. 2010 International Waveform Diversity and Design Conference (WDD). - Niagara Falls, ON, 8-13 Aug. 2010. - P. 000045-000047. ↑

C661. Lill D. Development of a wireless communication and localization system for VRU eSafety. / Lill D., Schappacher M., Gutjahr A., Sikora A. // 2010 7th International Symposium on Communication Systems Networks and Digital Signal Processing (CSNDSP). - Newcastle upon Tyne, 21-23 July 2010. - P. 459-463. ↑

C662. Slot M. Membership service specifications for safety-critical geocast in vehicular networks. / Slot M., Bouroche M., Cahill V. // 2010 7th International Symposium on Communication Systems Networks and Digital Signal Processing (CSNDSP). - Newcastle upon Tyne, 21-23 July 2010. - P. 422-426. ↑

- C663.** Hui Zhang. Performance analysis of sequential detection in early warning radar applications. / Hui Zhang, Lingjiang Kong, Xiaobo Yang. // 2010 International Conference on Communications, Circuits and Systems (ICCCAS). - Chengdu, 28-30 July 2010. - P. 453-456. ↑
- C664.** Gan Lu. The real-time gpr signals preprocessing algorithm based on LWT in high scan rate. / Gan Lu, Zhou Long. // 2010 International Conference on Wavelet Analysis and Pattern Recognition (ICWAPR). - Qingdao, 11-14 July 2010. - P. 255-259. ↑
- C665.** Piscarreta D. On the propagation characteristics of ultra-wideband signal in aluminum. / Piscarreta D., Sut Kam Ho, Kam Weng Tam. // 2010 International Conference on Applications of Electromagnetism and Student Innovation Competition Awards (AEM2C). - Taipei, 11-13 Aug. 2010. - P. 197-201. ↑
- C666.** Zhang Hua. A height-measuring algorithm applied to TERCOM radar altimeter. / Zhang Hua, Hu Xiulin. // 2010 3rd International Conference on Advanced Computer Theory and Engineering (ICACTE). - Chengdu, 20-22 Aug. 2010. - Vol. 5. - P. V5-43-V5-46-43. ↑
- C667.** Wei Zhang. An algorithm of resolving the range ambiguity using a single PRF. / Wei Zhang, Lingjiang Kong, Xiaobo Yang, Xiaojing Wang. // 2010 International Conference on Communications, Circuits and Systems (ICCCAS). - Chengdu, 28-30 July 2010. - P. 444-448. ↑
- C668.** Zhu Xiao-Hua. An inverse model for coastal acoustic tomography and its application to Chinese coastal sea. / Zhu Xiao-Hua, Wu Qingsong, Zhang Chuangzheng. // 2010 Sixth International Conference on Natural Computation (ICNC). - Yantai, Shandong, 10-12 Aug. 2010. - Vol. 7. - P. 3792-3795. ↑
- C669.** Ying Shijun. Target recognition for marine search and rescue radar. / Ying Shijun, Chen Jinbiao, Shi Chaojian. // 2010 Sixth International Conference on Natural Computation (ICNC). - Yantai, Shandong, 10-12 Aug. 2010. - Vol. 2. - P. 676-679. ↑
- C670.** Ting Chen. A fuzzy pattern recognition method of radar signal based on neural network. / Ting Chen, Wei Chen. // 2010 Sixth International Conference on Natural Computation (ICNC). - Yantai, Shandong, 10-12 Aug. 2010. - Vol. 3. - P. 1178-1181. ↑
- C671.** Jian Fang. A novel detection scheme to mitigate the TD-LTE interference. / Jian Fang, Xiaopei Zhu, Biao Huang, Xingguo Zhou. // 2010 International Conference on Communications, Circuits and Systems (ICCCAS). - Chengdu, 28-30 July 2010. - P. 59-62. ↑
- C672.** Wei Liu. Coexistence studies for TD-LTE with radar system in the band 2300-2400 MHz. / Wei Liu, Jian Fang, Haifeng Tan, Biao Huang, Wenbo Wang. // 2010 International Conference on Communications, Circuits and Systems (ICCCAS). - Chengdu, 28-30 July 2010. - P. 49-53. ↑
- C673.** Guoliang Zou. Design and implementation of marine dumping area's monitoring system based on GPS/GPRS. / Guoliang Zou, Bing He, Dongmei Huang, Xianghong Kong. // 2010 Sixth International Conference on Natural Computation (ICNC). - Yantai, Shandong, 10-12 Aug. 2010. - Vol. 3. - P. 1423-1427. ↑
- C674.** Neinavaie M. Clutter classification in heterogeneous environments. / Neinavaie M., Derakhshan M., Sheikhi A., Gazor S. // 2010 23rd Canadian Conference on Electrical and Computer Engineering (CCECE). - Calgary, AB, 2-5 May 2010. - P. 1-4. ↑
- C675.** Yong Chen. The fuzzy targets setting and comprehensive evaluation of the vehicle comfort. / Yong Chen, Xiaokai Chen, Yi Lin. // 2010 Seventh International Conference on Fuzzy Systems and Knowledge Discovery (FSKD). - Yantai, Shandong, 10-12 Aug. 2010. - Vol. 3. - P. 1382-1386. ↑
- C676.** Jiangtao Qi. Experimental analysis of ground speed measuring systems for the intelligent agricultural machinery. / Jiangtao Qi, Shuhui Zhang, Yingjie Yu, Ye Li, Yan Xu. // 2010 Seventh International Conference on Fuzzy Systems and Knowledge Discovery (FSKD). - Yantai, 10-12 Aug. 2010. - Vol. 2. - P. 668-671. ↑
- C677.** Ping-chuan Zhang. Design of target data fusion algorithm for passive radar based-on dual GSM base stations. / Ping-chuan Zhang, Bu-yin Li. // 2010 Seventh International Conference on Fuzzy Systems and Knowledge Discovery (FSKD). - Yantai, Shandong, 10-12 Aug. 2010. - Vol. 4. - P. 1991-1994. ↑
- C678.** Lang Weifeng. A new ground penetrating radar signal analysis method based on S transform. / Lang Weifeng, Lin Mingxing. // 2010 International Conference on Environmental Science and Information Application

Technology (ESIAT). - Wuhan, 17-18 July 2010. - Vol. 3. - P. 683-686. ↑

C679. Legkiy V.N. Simulation of algorithm for relief profile measurement and recognition of objects in on-board scanning pulsed laser rangefinders. / Legkiy V.N., Shumeyko V.A., Balasov I.Yu. // 2010 International Conference and Seminar on Micro/Nanotechnologies and Electron Devices (EDM). - Novosibirsk, June 30 2010-July 4 2010. - P. 390-392. ↑

C680. Hluchy L. Mining environmental data in hydrological scenarios. / Hluchy L., Seleng M., Habala O., Krammer P. // 2010 Seventh International Conference on Fuzzy Systems and Knowledge Discovery (FSKD). - Yantai, Shandong, 10-12 Aug. 2010. - Vol. 6. - P. 2988-2992. ↑

C681. Shi Ziyang. The design and implementation of domain-specific text summarization system based on co-reference resolution algorithm. 2010 Seventh International Conference on Fuzzy Systems and Knowledge Discovery (FSKD). - Yantai, Shandong, 10-12 Aug. 2010. - Vol. 5. - P. 2390-2394. ↑

C682. Wang Haipeng. A Parallel Centralized Multi-sensor General Association Algorithm. / Wang Haipeng, He You, Xiong Wei. // 2010 WASE International Conference on Information Engineering (ICIE). - Beidaihe, Hebei, 14-15 Aug. 2010. - Vol. 4. - P. 118-121. ↑

C683. Chandrakanth V. Novel Architecture for Highly Hardware Efficient Implementation of Real Time Matrix Inversion Using Gauss Jordan Technique. / Chandrakanth V., Kuloor R. // 2010 IEEE Computer Society Annual Symposium on VLSI (ISVLSI). - Lixouri, Kefalonia, 5-7 July 2010. - P. 294-298. ↑

C684. Banani S.A. Blind channel estimation for MRC systems with maneuvering transmit/receive terminals. / Banani S.A., Vaughan R.G. // 2010 23rd Canadian Conference on Electrical and Computer Engineering (CCECE). - Calgary, AB, 2-5 May 2010. - P. 1-6. ↑

C685. Xiaohong Su. FCM-based radar target detection in medium frequency signal of radar. / Xiaohong Su, Jidong Suo, Xiaoming Liu, Yingchun Wang. // 2010 Seventh International Conference on Fuzzy Systems and Knowledge Discovery (FSKD). - Yantai, Shandong, 10-12 Aug. 2010. - Vol. 2. - P. 542-545. ↑

C686. Lu Zhiying. Hailstone detection based on time series association rules. / Lu Zhiying, Zhang Huan, Ma Hongmin, Jia Huizhen. // 2010 Seventh International Conference on Fuzzy Systems and Knowledge Discovery (FSKD). - Yantai, Shandong, 10-12 Aug. 2010. - Vol. 5. - P. 2143-2146. ↑

C687. Ran Xuejun. Real-time data acquisition system for pulse laser radar based on clock distribution technology. / Ran Xuejun, Wang Jianqun, Li Zhenshan, Yao Guozhong. // 2010 29th Chinese Control Conference (CCC). - Beijing, 29-31 July 2010. - P. 5701-5704. ↑

C688. Kang Su. Evolutionary global attitude planning for satellite signature suppression shield. / Kang Su, Jianjiang Zhou. // 2010 Sixth International Conference on Natural Computation (ICNC). - Yantai, Shandong, 10-12 Aug. 2010. - Vol. 5. - P. 2343-2347. ↑

C689. Chinnam D.M. Intrusion detection using software defined noise radar. / Chinnam D.M., Madhusudhan J., Nandhini C., Prathyusha S.N., Sowmiya S., Ramanathan R., Soman K.P. // 2010 International Conference on Computing Communication and Networking Technologies (ICCCNT). - Karur, 29-31 July 2010. - P. 1-6. ↑

C690. Ye Yu. A cue line based method for building modeling from LiDAR and satellite imagery. / Ye Yu, Xiaoping Liu, Buckles B.P. // 2010 International Conference on Computing Communication and Networking Technologies (ICCCNT). - Karur, 29-31 July 2010. - P. 1-8. ↑

C691. {no data available}. Copyright page. 2010 International Waveform Diversity and Design Conference (WDD). - Niagara Falls, ON, 8-13 Aug. 2010. - P. 1. ↑

C692. Lang Weifeng. A practical ground penetrating radar signal processing method based on wavelet transform. / Lang Weifeng, Lin Mingxing. // 2010 Second International Conference on Communication Systems, Networks and Applications (ICCSNA). - Hong Kong, June 29 2010-July 1 2010. - Vol. 1. - P. 452-455. ↑

C693. Erkan A.N. Semi-supervised remote sensing image classification via maximum entropy. / Erkan A.N., Camps-Valls G., Altun Y. // 2010 IEEE International Workshop on Machine Learning for Signal Processing (MLSP). - Kittila, Aug. 29 2010-Sept. 1 2010. - P. 313-318. ↑



- C694.** Chinnam D.M. Implementation of a low cost synthetic aperture radar using Software Defined Radio. / Chinnam D.M., Madhusudhan J., Nandhini C., Prathyusha S.N., Sowmiya S., Ramanathan R., Soman K.P. // 2010 International Conference on Computing Communication and Networking Technologies (ICCCNT). - Karur, 29-31 July 2010. - P. 1-7. ↑
- C695.** Alabaster C.M. Pulse Doppler radar waveforms. 2010 International Waveform Diversity and Design Conference (WDD). - Niagara Falls, ON, 8-13 Aug. 2010. - P. 1. ↑
- C696.** Sen S. OFDM radar waveform design for sparsity-based multi-target tracking. / Sen S., Nehorai A. // 2010 International Waveform Diversity and Design Conference (WDD). - Niagara Falls, ON, 8-13 Aug. 2010. - P. 000018-000022. ↑
- C697.** Zhen Hu. Design of look-up table based architecture for wideband beamforming. / Zhen Hu, Nan Guo, Qiu R., Bonior J., Lihyeh Liou, Lin D., Longbrake M., Buxa P., Dalrymple T., Seng Hong, Hary S., Tsui J. // 2010 International Waveform Diversity and Design Conference (WDD). - Niagara Falls, ON, 8-13 Aug. 2010. - P. 000001-000005. ↑
- C698.** Gogineni S. Adaptive design for distributed MIMO radar using sparse modeling. / Gogineni S., Nehorai A. // 2010 International Waveform Diversity and Design Conference (WDD). - Niagara Falls, ON, 8-13 Aug. 2010. - P. 000023-000027. ↑
- C699.** Wicks M. Waveform diversity & knowledge based systems. 2010 International Waveform Diversity and Design Conference (WDD). - Niagara Falls, ON, 8-13 Aug. 2010. - P. 1. ↑
- C700.** Bliss D.W. Coherent MIMO radar. 2010 International Waveform Diversity and Design Conference (WDD). - Niagara Falls, ON, 8-13 Aug. 2010. - P. 1. ↑
- C701.** Hao He. Wideband MIMO waveform design for transmit beam pattern synthesis. / Hao He, Stoica P., Jian Li. // 2010 International Waveform Diversity and Design Conference (WDD). - Niagara Falls, ON, 8-13 Aug. 2010. - P. 000006-000010. ↑
- C702.** Xiao Wang. An IMM-UF algorithm for tracking highly maneuvering target. / Xiao Wang, Chongzhao Han, Hui Zhang. // 2010 International Conference on Mechatronics and Automation (ICMA). - Xi'an, 4-7 Aug. 2010. - P. 1862-1867. ↑
- C703.** Yangyang Li. Quantum-inspired immune clonal clustering algorithm based on watershed. / Yangyang Li, Nana Wu, Jingjing Ma, Licheng Jiao. // 2010 IEEE Congress on Evolutionary Computation (CEC). - Barcelona, 18-23 July 2010. - P. 1-7. ↑
- C704.** Milisavljevic. Detecting potential human activities using coherent change detection. / Milisavljevic, N., Closson D., Bloch I. // 2010 2nd International Conference on Image Processing Theory Tools and Applications (IPTA). - Paris, 7-10 July 2010. - P. 482-485. ↑
- C705.** Pouteau R. Support vector machine fusion of multisensor imagery in tropical ecosystems. / Pouteau R., Stoll B., Chabrier S. // 2010 2nd International Conference on Image Processing Theory Tools and Applications (IPTA). - Paris, 7-10 July 2010. - P. 325-329. ↑
- C706.** Wang Xiaoyi. The lake water bloom intelligent prediction method and water quality remote monitoring system. / Wang Xiaoyi, Dai Jun, Liu Zaiwen, Zhao Xiaoping, Dong Suoqi, Zhao Zhiyao, Zhang Miao. // 2010 Sixth International Conference on Natural Computation (ICNC). - Yantai, Shandong, 10-12 Aug. 2010. - Vol. 7. - P. 3443-3446. ↑
- C707.** Sheng Li. The application of perceptual weighting on millimeter wave conducted speech enhancement. / Sheng Li, Jianqi Wang, Xijing Jing. // 2010 Sixth International Conference on Natural Computation (ICNC). - Yantai, Shandong, 10-12 Aug. 2010. - Vol. 6. - P. 3230-3233. ↑
- C708.** Daoud O. Enhancing the MIMO-OFDM Radar systems performance using GA. / Daoud O., Damati A., Al-Sawalmeh W. // 2010 7th International Multi-Conference on Systems Signals and Devices (SSD). - Amman, 27-30 June 2010. - P. 1-5. ↑
- C709.** Katona Z. On mean revisit frequency of non-repeating satellite orbits with finite sensor range. 2010 5th Advanced satellite multimedia systems conference (asma) and the 11th signal processing for space

communications workshop (spsc). - Cagliari, 13-15 Sept. 2010. - P. 369-374. ↑

**C710.** Fujun He. Improvement on obstacle avoiding ability based on laser range finder. / Fujun He, Xiaolei Liu, Zhijiang Du, Yueyue Ta. // 2010 International Conference on Mechatronics and Automation (ICMA). - Xi'an, 4-7 Aug. 2010. - P. 1208-1213. ↑

**C711.** Apartsin A. SNR-dependent filtering for Time Of Arrival estimation in high noise. / Apartsin A., Cooper L.N., Intrator N. // 2010 IEEE International Workshop on Machine Learning for Signal Processing (MLSP). - Kittila, Aug. 29 2010-Sept. 1 2010. - P. 427-431. ↑

**C712.** Xue Xu. The wireless extension of CAN-bus based on GPRS. / Xue Xu, Wang Changyou, Wu Huazhu, Yao Xiaofeng. // 2010 Second International Conference on Communication Systems, Networks and Applications (ICCSNA). - Hong Kong, June 29 2010-July 1 2010. - Vol. 2. - P. 281-283. ↑

**C713.** Estrem A.V. Portable satellite backhauling solution for emergency communications. / Estrem A.V., Werner M. // 2010 5th Advanced satellite multimedia systems conference (asma) and the 11th signal processing for space communications workshop (spsc). - Cagliari, 13-15 Sept. 2010. - P. 262-269. ↑

**C714.** Sewiolo B. Ultra-wideband transmitters based on M-sequences for high resolution radar and sensing applications. / Sewiolo B., Laemmle B., Weigel R. // 2010 Conference on Ph.D. Research in Microelectronics and Electronics (PRIME). - Berlin, 18-21 July 2010. - P. 1-4. ↑

**C715.** Keliang Zhang. Co-construction of ontology-based knowledge base through the Web: Theory and practice. / Keliang Zhang, Qinlong Fei. // 2010 International Conference on Natural Language Processing and Knowledge Engineering (NLP-KE). - Beijing, 21-23 Aug. 2010. - P. 1-6. ↑

**C716.** Lv Jing. High resolution two-dimensional imaging of spinning space debris. / Lv Jing, Gu Hong, Su Weimin, Zhu Mojun. // 2010 2nd International Conference on Signal Processing Systems (ICSPS). - Dalian, 5-7 July 2010. - Vol. 2. - P. V2-153-V2-157-153. ↑

**C717.** Pieniezny A. Pulse emitter identification by the use of higher order statistics. / Pieniezny A., Kawalec A., Fornalik J. // 2010 IEEE Region 8 International Conference on Computational Technologies in Electrical and Electronics Engineering (SIBIRCON). - Listvyanka, 11-15 July 2010. - P. 179-182. ↑

**C718.** Lijia Huang. A general two-dimensional spectrum based on polynomial range model for medium-earth-orbit Synthetic Aperture Radar signal processing. / Lijia Huang, Donghui Hu, Chibiao Ding, Xiaolan Qiu. // 2010 2nd International Conference on Signal Processing Systems (ICSPS). - Dalian, 5-7 July 2010. - Vol. 3. - P. V3-662-V3-665-662. ↑

**C719.** Yang Jian. Frequency broadband signal MVDR adaptive beamforming method and application. / Yang Jian, Zhang Yue, Bao Qinlong, Chen Zengping. // 2010 2nd International Conference on Signal Processing Systems (ICSPS). - Dalian, 5-7 July 2010. - Vol. 1. - P. V1-766-V1-770-766. ↑

**C720.** Lv Jing. A fast range migration compensation method. / Lv Jing, Gu Hong, Su Weimin, Zhu Mojun. // 2010 2nd International Conference on Signal Processing Systems (ICSPS). - Dalian, 5-7 July 2010. - Vol. 2. - P. V2-139-V2-143-139. ↑

**C721.** Hong-xu Huang. Jamming research to SAR based on frequency characteristic. / Hong-xu Huang, Zhi-tao Huang, Yi-yu Zhou. // 2010 2nd International Conference on Signal Processing Systems (ICSPS). - Dalian, 5-7 July 2010. - Vol. 2. - P. V2-144-V2-147-144. ↑

**C722.** Li Binbin. A novel three-dimensional data association algorithm for 2D radars and sensors. / Li Binbin, Feng Xinxi, Wang Zhaoying, Lei Yu. // 2010 2nd International Conference on Signal Processing Systems (ICSPS). - Dalian, 5-7 July 2010. - Vol. 1. - P. V1-668-V1-670-668. ↑

**C723.** Xie Wencheng. MIMO antenna array design for airborne down-looking 3D imaging SAR. / Xie Wencheng, Zhang Xiaoling, Shi Jun. // 2010 2nd International Conference on Signal Processing Systems (ICSPS). - Dalian, 5-7 July 2010. - Vol. 2. - P. V2-452-V2-456-452. ↑

**C724.** Qu Wei. System performance simulation of electronic surveillance receiver for spaceborne SAR. / Qu Wei, Yang Jinhui, Jia Xin. // 2010 2nd International Conference on Signal Processing Systems (ICSPS). - Dalian, 5-7 July 2010. - Vol. 3. - P. V3-147-V3-152-147. ↑

- C725.** Wang Jun. Design and implementation of a dual-interface radar data recorder. / Wang Jun, Jiang Hai, Zhang Yuxi, Yao Wang, Zhang Yuxian. // 2010 2nd International Conference on Signal Processing Systems (ICSPS). - Dalian, 5-7 July 2010. - Vol. 3. - P. V3-129-V3-133-129. ↑
- C726.** Wencheng Wang. A temperature remote monitoring system of cable joint. / Wencheng Wang, Lei Wang. // 2010 2nd International Conference on Signal Processing Systems (ICSPS). - Dalian, 5-7 July 2010. - Vol. 1. - P. V1-690-V1-694-690. ↑
- C727.** Huang Hong-xu. A frequency-based inter/intra partly coherent jamming style to SAR. / Huang Hong-xu, Zhou Yi-yu, Wu Jing, Huang Zhi-tao. // 2010 2nd International Conference on Signal Processing Systems (ICSPS). - Dalian, 5-7 July 2010. - Vol. 2. - P. V2-434-V2-437-434. ↑
- C728.** Gong Liangliang. A radar emitter identification method based on pulse match template sequence. / Gong Liangliang, Wu Shilong, Lv Tao. // 2010 2nd International Conference on Signal Processing Systems (ICSPS). - Dalian, 5-7 July 2010. - Vol. 3. - P. V3-153-V3-156-153. ↑
- C729.** Jin Rencheng. A design of efficient transport layer protocol for wireless sensor network gateway. / Jin Rencheng, Meng Xiao, Meng Lisha, Wang Liding. // 2010 2nd International Conference on Signal Processing Systems (ICSPS). - Dalian, 5-7 July 2010. - Vol. 1. - P. V1-775-V1-780-775. ↑
- C730.** Ping Chen. Wireless video monitoring system based on image restoration technology. / Ping Chen, Zhiqiang Wang, Qiao Wang. // 2010 8th World Congress on Intelligent Control and Automation (WCICA). - Jinan, 7-9 July 2010. - P. 4271-4275. ↑
- C731.** Lan Chen. High resolution radar range imaging method using bandwidth extrapolation. / Lan Chen, Jie Chen. // 2010 8th World Congress on Intelligent Control and Automation (WCICA). - Jinan, 7-9 July 2010. - P. 6719-6723. ↑
- C732.** Xiaoqin Wen. A two-stage hybrid space-time adaptive processing approach. / Xiaoqin Wen, Qiaoqiao Wang, Shue Bi, Linru You. // 2010 8th World Congress on Intelligent Control and Automation (WCICA). - Jinan, 7-9 July 2010. - P. 6820-6824. ↑
- C733.** Cascarano B. Design of a light-weight digital beam forming antenna for future sar applications. / Cascarano B., Colinas J., Girard R., Plourde P. // 2010 14th International Symposium on Antenna Technology and Applied Electromagnetics & the American Electromagnetics Conference (ANTEM-AMEREM). - Ottawa, ON, 5-8 July 2010. - P. 1-4. ↑
- C734.** Poliakov E. Remote control software development for a small airborne electronic support payload. / Poliakov E., Wu C., Lee J.P.Y., Antar Y.M.M. // 2010 14th International Symposium on Antenna Technology and Applied Electromagnetics & the American Electromagnetics Conference (ANTEM-AMEREM). - Ottawa, ON, 5-8 July 2010. - P. 1-4. ↑
- C735.** Kotus J. Application of passive acoustic radar to automatic localization, tracking and classification of sound sources. 2010 2nd International Conference on Information Technology (ICIT). - Gdansk, 28-30 June 2010. - P. 67-70. ↑
- C736.** Yingfei Diao. An overview of range detection techniques for wireless sensor networks. / Yingfei Diao, Minyue Fu, Huanshui Zhang. // 2010 8th World Congress on Intelligent Control and Automation (WCICA). - Jinan, 7-9 July 2010. - P. 1150-1155. ↑
- C737.** Jin He. Inverse synthetic aperture 3-D imaging laser radar. / Jin He, Xiao-you Yang, Jian-feng Wang, Qun Zhang. // 2010 2nd International Conference on Signal Processing Systems (ICSPS). - Dalian, 5-7 July 2010. - Vol. 2. - P. V2-5-V2-10-5. ↑
- C738.** Ying Luo. Three-dimensional micro-doppler signature extraction in MIMO radar. / Ying Luo, Jin He, Xian-jiao Liang, Qun Zhang. // 2010 2nd International Conference on Signal Processing Systems (ICSPS). - Dalian, 5-7 July 2010. - Vol. 2. - P. V2-1-V2-4-1. ↑
- C739.** {no data available}. Front matter. 2010 2nd International Conference on Signal Processing Systems (ICSPS). - Dalian, China, 5-7 July 2010. - Vol. 2. - P. i-xix. ↑
- C740.** Zhenhua Li. Simultaneous registration and fusion of radar and ESM by EM-EKS. / Zhenhua Li, Leung

H., Liang Tao. // 2010 8th World Congress on Intelligent Control and Automation (WCICA). - Jinan, 7-9 July 2010. - P. 1130-1134. ↑

C741. Yi Zeng. Radar velocity-measuring system design and computation algorithm based on ARM processor. / Yi Zeng, Jianmin Xu, Deng Peng. // 2010 8th World Congress on Intelligent Control and Automation (WCICA). - Jinan, 7-9 July 2010. - P. 5352-5357. ↑

C742. Balaji N. VLSI signal processing system employing six phase codes for spread spectrum applications. / Balaji N., Rao K.S. // 2010 IEEE Region 8 International Conference on Computational Technologies in Electrical and Electronics Engineering (SIBIRCON). - Listvyanka, 11-15 July 2010. - P. 257-262. ↑

C743. Zhao Lei. Space-time adaptive processing for sea clutter and jamming suppression in radar seekers. / Zhao Lei, Sun Jinping, Xu Xiaojian, Tian Jihua. // 2010 2nd International Conference on Signal Processing Systems (ICSPS). - Dalian, 5-7 July 2010. - Vol. 3. - P. V3-600-V3-604-600. ↑

C744. Bi Xin. A new waveform for range-velocity decoupling in automotive radar. / Bi Xin, Du Jinsong. // 2010 2nd International Conference on Signal Processing Systems (ICSPS). - Dalian, 5-7 July 2010. - Vol. 1. - P. V1-511-V1-514-511. ↑

C745. Jie Qin. High-efficiency and well-integrity method for dynamic acquisition of GNSS location information. / Jie Qin, Jianping Xing, Yongzhi Wang, Guojun Huang, Lingguo Meng. // 2010 2nd International Conference on Signal Processing Systems (ICSPS). - Dalian, 5-7 July 2010. - Vol. 1. - P. V1-520-V1-524-520. ↑

C746. Xie Xiao-Chun. Compressive sensing radar imaging based on smoothed l0 norm. 2010 2nd International Conference on Signal Processing Systems (ICSPS). - Dalian, 5-7 July 2010. - Vol. 1. - P. V1-6-V1-9-6. ↑

C747. Zhao Jun. A clutter suppression method based on angle-doppler compensation for airborne radar with uniform circular arrays antennas. / Zhao Jun, Zhao Jianyang, Xu Hang. // 2010 2nd International Conference on Signal Processing Systems (ICSPS). - Dalian, 5-7 July 2010. - Vol. 1. - P. V1-576-V1-579-576. ↑

C748. Guangxin Wang. Regularized resolution enhancement of point-based features of synthetic aperture radar image using variable quasi-norm. / Guangxin Wang, Hong Luo, Zhenrong Zhang. // 2010 2nd International Conference on Signal Processing Systems (ICSPS). - Dalian, 5-7 July 2010. - Vol. 1. - P. V1-500-V1-504-500. ↑

C749. Tian Wenlong. Ionosphere interference suppression for HFSWR using L-shape array. / Tian Wenlong, Li Gaopeng, Xu Rongqing. // 2010 2nd International Conference on Signal Processing Systems (ICSPS). - Dalian, 5-7 July 2010. - Vol. 1. - P. V1-484-V1-488-484. ↑

C750. {no data available}. Cover page. 2010 2nd International Conference on Signal Processing Systems (ICSPS). - Dalian, 5-7 July 2010. - Vol. 1. - P. c1. ↑

C751. Long Zhang. Stepped-Frequency waveform processing for moving target based on genetic-CLEAN algorithm. / Long Zhang, Gao Zhaozhao. // 2010 2nd International Conference on Signal Processing Systems (ICSPS). - Dalian, 5-7 July 2010. - Vol. 1. - P. V1-18-V1-21-18. ↑

C752. Long Zhang. Stistical relax method for super resolution ISAR imaging. / Long Zhang, Xiaohui He. // 2010 2nd International Conference on Signal Processing Systems (ICSPS). - Dalian, 5-7 July 2010. - Vol. 1. - P. V1-22-V1-25-22. ↑

C753. Kefei Liu. Error estimate of quadrature sampling system via discrete Hilbert transform. / Kefei Liu, Zhihua Huang, Linbing Zhao, Youyu Shen, Meizhu Liu. // 2010 2nd International Conference on Signal Processing Systems (ICSPS). - Dalian, 5-7 July 2010. - Vol. 1. - P. V1-10-V1-13-10. ↑

C754. Chen Xiaonan. Shipborne radar echo signal denoising based on improved threshold and shrinkage function. / Chen Xiaonan, Suo Jingdong, Liu Xiaoming. // 2010 2nd International Conference on Signal Processing Systems (ICSPS). - Dalian, 5-7 July 2010. - Vol. 1. - P. V1-99-V1-101-99. ↑

C755. Lu Jianbin. Multi-cycle signal processing based on Keystone transform in LFM CW radar. / Lu Jianbin, Xi Zemin, Zhang MingMin, Xiao Hui. // 2010 2nd International Conference on Signal Processing Systems (ICSPS). - Dalian, 5-7 July 2010. - Vol. 1. - P. V1-280-V1-284-280. ↑

C756. Mei Jiangtao. New spatial overlap method of transmitting beam for airborne phased array radar. / Mei



Jiangtao, Li Yong, Hu Xin. // 2010 2nd International Conference on Signal Processing Systems (ICSPS). - Dalian, 5-7 July 2010. - Vol. 1. - P. V1-268-V1-271-268. ↑

**C757.** Wang Ying. Research on nonlinearity correction imaging algorithm of FMCW SAR. / Wang Ying, Li Qingshan, Gan Deyun, Zheng Guangyong. // 2010 2nd International Conference on Signal Processing Systems (ICSPS). - Dalian, 5-7 July 2010. - Vol. 1. - P. V1-425-V1-429-425. ↑

**C758.** Huang Weiping. An intermediary method used in direction-finding location system. / Huang Weiping, Xu Yu, Wang Jie. // 2010 2nd International Conference on Signal Processing Systems (ICSPS). - Dalian, 5-7 July 2010. - Vol. 2. - P. V2-299-V2-303-299. ↑

**C759.** Yunfei Shi. A segmentation-based CFAR algorithm for subsurface targets detection in FLGPSAR. / Yunfei Shi, Tian Jin, Qian Song, Zhimin Zhou. // 2010 2nd International Conference on Signal Processing Systems (ICSPS). - Dalian, 5-7 July 2010. - Vol. 2. - P. V2-293-V2-298-293. ↑

**C760.** Yu Zhang. Transmit-receive beamforming for MIMO radar. / Yu Zhang, Jianxin Wang. // 2010 2nd International Conference on Signal Processing Systems (ICSPS). - Dalian, 5-7 July 2010. - Vol. 3. - P. V3-803-V3-806-803. ↑

**C761.** Lei Yu. Estimation of aircraft altitude in 2D radar intelligence networking. / Lei Yu, Zhu Can-bin, Feng Xin-xi, Li Bin-bin. // 2010 2nd International Conference on Signal Processing Systems (ICSPS). - Dalian, 5-7 July 2010. - Vol. 2. - P. V2-331-V2-333-331. ↑

**C762.** Bin Deng. Inverse frequency scaling algorithm (IFSA) for SAR raw data simulation. / Bin Deng, Yuliang Qin, Hongqiang Wang, Xiang Li, Yanpeng Li. // 2010 2nd International Conference on Signal Processing Systems (ICSPS). - Dalian, 5-7 July 2010. - Vol. 2. - P. V2-317-V2-320-317. ↑

**C763.** Ling Fan. A Gaussian particle filter for track-before-detect. / Ling Fan, Xiaoling Zhang. // 2010 2nd International Conference on Signal Processing Systems (ICSPS). - Dalian, 5-7 July 2010. - Vol. 2. - P. V2-309-V2-312-309. ↑

**C764.** Wang Jun. 3-D imaging algorithm for targets with micro-motion based on HRRP sequence. / Wang Jun, Yang Dong, Zhang Yuxi, Wei Shaoming. // 2010 2nd International Conference on Signal Processing Systems (ICSPS). - Dalian, 5-7 July 2010. - Vol. 2. - P. V2-283-V2-288-283. ↑

**C765.** Xi-kun Fan. A robust space-time multiple-beam STAP algorithm. / Xi-kun Fan, Fan Yang. // 2010 2nd International Conference on Signal Processing Systems (ICSPS). - Dalian, 5-7 July 2010. - Vol. 1. - P. V1-44-V1-47-44. ↑

**C766.** Chen Xiaonan. New threshold and shrinkage function for shipborne radar echo signal denoising based on wavelet transforms. / Chen Xiaonan, Suo Jingdong, Wang Xiaoqiong, Xu Zhiyuan. // 2010 2nd International Conference on Signal Processing Systems (ICSPS). - Dalian, 5-7 July 2010. - Vol. 1. - P. V1-63-V1-65-63. ↑

**C767.** Gang Lu. Anti-jamming filtering for DRFM repeat jammer based on stretch processing. / Gang Lu, Deguo Zeng, Bin Tang. // 2010 2nd International Conference on Signal Processing Systems (ICSPS). - Dalian, 5-7 July 2010. - Vol. 1. - P. V1-78-V1-82-78. ↑

**C768.** Ling Fan. A modified track-before-detect algorithm for radar weak target. / Ling Fan, Xiaoling Zhang. // 2010 2nd International Conference on Signal Processing Systems (ICSPS). - Dalian, 5-7 July 2010. - Vol. 2. - P. V2-260-V2-264-260. ↑

**C769.** Li Cuiping. Tracking ground targets with road constraint using multiple hypotheses tracking. / Li Cuiping, Sun Jinping, Mao Shiyi, Liu Desheng. // 2010 2nd International Conference on Signal Processing Systems (ICSPS). - Dalian, 5-7 July 2010. - Vol. 2. - P. V2-265-V2-269-265. ↑

**C770.** Lanling Wei. A TBD algorithm based on improved Randomized Hough Transform for dim target detection. / Lanling Wei, Xiaoling Zhang, Ling Fan. // 2010 2nd International Conference on Signal Processing Systems (ICSPS). - Dalian, 5-7 July 2010. - Vol. 2. - P. V2-241-V2-245-241. ↑

**C771.** Yong Tang. The research of distributed power quality on-line monitoring system based on GRPS. / Yong Tang, Jianye Zhang, Peng Li. // 2010 IEEE International Conference on Software Engineering and Service Sciences (ICSESS). - Beijing, 16-18 July 2010. - P. 384-387. ↑

- C772.** Sambuelli Luigi. A GPR survey on a morainic lake northerly Turin (Italy). / Sambuelli Luigi, Bava Silvia, Calzoni Corrado, Stocco Stefano. // 2010 13th International Conference on Ground Penetrating Radar (GPR). - Lecce, Italy, 21-25 June 2010. - P. 1-6. ↑
- C773.** Razevig V.V. Advantages and restrictions of holographic subsurface radars. / Razevig V.V., Ivashov S.I., Vasiliev I.A., Zhuravlev A.V., Bechtel T., Capineri L. // 2010 13th International Conference on Ground Penetrating Radar (GPR). - Lecce, 21-25 June 2010. - P. 1-6. ↑
- C774.** Busch S. Full-waveform inversion of multi-offset surface GPR data. / Busch S., van der Kruk J., Bikowski J., Vereecken H. // 2010 13th International Conference on Ground Penetrating Radar (GPR). - Lecce, 21-25 June 2010. - P. 1-4. ↑
- C775.** Panzner B. Estimation of soil electromagnetic parameters using frequency domain techniques. / Panzner B., Joistingmeier A., Abbas O. // 2010 13th International Conference on Ground Penetrating Radar (GPR). - Lecce, 21-25 June 2010. - P. 1-5. ↑
- C776.** Klotzsche A. Full-waveform inversion of crosshole ground penetrating radar data to characterize a gravel aquifer close to the Thur River, Switzerland. / Klotzsche A., van der Kruk J., Meles G.A., Doetsch J.A., Maurer H., Linde N. // 2010 13th International Conference on Ground Penetrating Radar (GPR). - Lecce, 21-25 June 2010. - P. 1-5. ↑
- C777.** Zapunidi S.A. Exact solution of idealized subsurface sensing problem. / Zapunidi S.A., Pavlovskii B.R., Edemskii F.D., Popov A.V. // 2010 13th International Conference on Ground Penetrating Radar (GPR). - Lecce, 21-25 June 2010. - P. 1-6. ↑
- C778.** Yi Myeong-Jong. 3-D GPR imaging of central pillar of the Mireuk stone pagoda in Korea. / Yi Myeong-Jong, Kim Jung-Ho, Son Jeong-Sul. // 2010 13th International Conference on Ground Penetrating Radar (GPR). - Lecce, Italy, 21-25 June 2010. - P. 1-5. ↑
- C779.** Ceraudo G. Integrated GPR and archaeological investigations to study the site of Aquinum (Frosinone Italy). / Ceraudo G., Piro S., Zamuner D. // 2010 13th International Conference on Ground Penetrating Radar (GPR). - Lecce, Italy, 21-25 June 2010. - P. 1-5. ↑
- C780.** McNaughton C.H. Monitoring of sequential gasoline-ethanol releases using high frequency ground penetrating radar. / McNaughton C.H., Mosquera J.D., Endres A.L., Freitas J.G. // 2010 13th International Conference on Ground Penetrating Radar (GPR). - Lecce, 21-25 June 2010. - P. 1-6. ↑
- C781.** Zhang Xiaojun. Application of Ground penetrating Radar (GPR) exploration in Karst mountain areas. / Zhang Xiaojun, Jiahui Huang, Lei Song, Yong Chen. // 2010 13th International Conference on Ground Penetrating Radar (GPR). - Lecce, 21-25 June 2010. - P. 1-4. ↑
- C782.** Edemsky F.D. Practical algorithms of geometrical migration. / Edemsky F.D., Morozov P.A., Edemsky D.E., Popov A.V., Pavlovskii B.R., Zapunidi S.A. // 2010 13th International Conference on Ground Penetrating Radar (GPR). - Lecce, 21-25 June 2010. - P. 1-5. ↑
- C783.** Chun-lin Huang. Miniature multimode deep ground penetrating radar. / Chun-lin Huang, Shi-ping Zhu, Ming Lu. // 2010 13th International Conference on Ground Penetrating Radar (GPR). - Lecce, 21-25 June 2010. - P. 1-5. ↑
- C784.** Yelf R. Nine steps to concrete wisdom. / Yelf R., Ward A. // 2010 13th International Conference on Ground Penetrating Radar (GPR). - Lecce, 21-25 June 2010. - P. 1-8. ↑
- C785.** Simi A. Underground asset mapping with dual-frequency dual-polarized GPR massive array. / Simi A., Manacorda G., Miniati M., Bracciali S., Buonaccorsi A. // 2010 13th International Conference on Ground Penetrating Radar (GPR). - Lecce, 21-25 June 2010. - P. 1-5. ↑
- C786.** Biancheri-Astier M. EISS: An HF mono and bistatic GPR for terrestrial and planetary deep soundings. / Biancheri-Astier M., Hassen-Khodja R., Ciarletti V., Corbel C., Simon Y., Caudoux C., Faroux J., Dolon F., Leray V., Reineix A., Plettemeier D. // 2010 13th International Conference on Ground Penetrating Radar (GPR). - Lecce, 21-25 June 2010. - P. 1-8. ↑
- C787.** dos Santos V.R.N. Automatic classification of metallic targets using pattern recognition of GPR

reflection: a study in the IAG-USP Test Site, Sao Paulo (Brazil). / dos Santos V.R.N., Porsani J.L., Hirata N.S.T. // 2010 13th International Conference on Ground Penetrating Radar (GPR). - Lecce, 21-25 June 2010. - P. 1-4.



**C788.** Manacorda G. Development of a bore-head GPR for Horizontal Directional Drilling (HDD) equipment. / Manacorda G., Miniati M., Bracciali S., Dei D., Scott H.F., Koch E., Pinchbeck D., Murgier S. // 2010 13th International Conference on Ground Penetrating Radar (GPR). - Lecce, 21-25 June 2010. - P. 1-6.

**C789.** Giroux B. Crosshole GPR traveltimes tomography in elliptically anisotropic media. / Giroux B., Gloaguen E. // 2010 13th International Conference on Ground Penetrating Radar (GPR). - Lecce, 21-25 June 2010. - P. 1-5.

**C790.** Diamanti N. A study of GPR vertical crack responses in pavement using field data and numerical modelling. / Diamanti N., Redman D., Giannopoulos A. // 2010 13th International Conference on Ground Penetrating Radar (GPR). - Lecce, 21-25 June 2010. - P. 1-6.

**C791.** Lo Monte L. Recent advances in RF tomography for underground imaging. / Lo Monte L., Erricolo D., Soldovieri F., Wicks M.C. // 2010 13th International Conference on Ground Penetrating Radar (GPR). - Lecce, 21-25 June 2010. - P. 1-6.

**C792.** Lauro S.E. A simple inversion model for the estimation of subsurface features of Mars poles. / Lauro S.E., Mattei E., Pettinelli E., Orosei R., Soldovieri F. // 2010 13th International Conference on Ground Penetrating Radar (GPR). - Lecce, 21-25 June 2010. - P. 1-4.

**C793.** Meles G.A. Tackling the non-linearity problem in GPR waveform inversion. / Meles G.A., Greenhalgh S.A., Green A.G., van der Kruk J. // 2010 13th International Conference on Ground Penetrating Radar (GPR). - Lecce, 21-25 June 2010. - P. 1-6.

**C794.** van der Kruk J. Influence of interface roughness and heterogeneities on the waveguide inversion of dispersive GPR data. / van der Kruk J., Vereecken H., Diamanti N., Giannopoulos A. // 2010 13th International Conference on Ground Penetrating Radar (GPR). - Lecce, 21-25 June 2010. - P. 1-5.

**C795.** Pieraccini M. Attenuation of large bandwidth microwave signals in water and wet sand. / Pieraccini M., Barucci A., Mecatti D., Macaluso G., Atzeni C. // 2010 13th International Conference on Ground Penetrating Radar (GPR). - Lecce, 21-25 June 2010. - P. 1-6.

**C796.** Leucci G. Electromagnetic monitoring of concrete structures. 2010 13th International Conference on Ground Penetrating Radar (GPR). - Lecce, 21-25 June 2010. - P. 1-5.

**C797.** Arcone S. Tests of sommerfeld ground wave theory using ground-penetrating radar pulses. / Arcone S., Lanbo Liu. // 2010 13th International Conference on Ground Penetrating Radar (GPR). - Lecce, 21-25 June 2010. - P. 1-5.

**C798.** Rege R.B. Inversion of guided waves in georadar data. / Rege R.B., Godio A. // 2010 13th International Conference on Ground Penetrating Radar (GPR). - Lecce, 21-25 June 2010. - P. 1-6.


**C799.** Van der Wielen A. Nondestructive detection of delaminations in concrete bridge decks. / Van der Wielen A., Courard L., Nguyen F. // 2010 13th International Conference on Ground Penetrating Radar (GPR). - Lecce, 21-25 June 2010. - P. 1-5.


**C800.** Urbini S. GPR as an effective tool for safety and glacier characterization: experiences and future development. / Urbini S., Baskaradas J.A. // 2010 13th International Conference on Ground Penetrating Radar (GPR). - Lecce, 21-25 June 2010. - P. 1-6.


**C801.** Grinev A.Y. Multi-channel Ground Penetrating Radar based on ultra-wideband short-pulse signal: Hardware and software. / Grinev A.Y., Bagno D.V., Zaikin A.E., Nikishov D.V., Andriianov A.V. // 2010 13th International Conference on Ground Penetrating Radar (GPR). - Lecce, 21-25 June 2010. - P. 1-6.


**C802.** Roackaway T. Application of ground penetrating radar in the urban environment. / Roackaway T., Rivard J.A. // 2010 13th International Conference on Ground Penetrating Radar (GPR). - Lecce, 21-25 June 2010. - P. 1-4.


**C803.** Strycek M. Tapered slot antennas for ground penetrating radar. / Strycek M., Hertl I., Pavlik R., Polacek


V. // 2010 13th International Conference on Ground Penetrating Radar (GPR). - Lecce, 21-25 June 2010. - P. 1-4. 


**C804.** Angiulli G. Accurate tools for convergence prediction of series solutions of Contrast Source Integral Equations. / Angiulli G., D'Urso M., Isernia T., Tringali S. // 2010 13th International Conference on Ground Penetrating Radar (GPR). - Lecce, 21-25 June 2010. - P. 1-4. 


**C805.** Di Donato L. Imaging of 3D magnetic targets from multiview multistatic GPR data. / Di Donato L., Catapano I., Soldovieri F., Crocco L. // 2010 13th International Conference on Ground Penetrating Radar (GPR). - Lecce, 21-25 June 2010. - P. 1-6. 


**C806.** Arcone S. Effects of surface topography and wind on reflection horizons in ice sheets. / Arcone S., Jacobel R. // 2010 13th International Conference on Ground Penetrating Radar (GPR). - Lecce, 21-25 June 2010. - P. 1-6. 


**C807.** Hu W. An intelligent non-contact wireless monitoring system for vital signs and motion detection. / Hu W., Lie D.Y.C., Kakade M.U., Ichapurapu R., Mane S., Lopez J., Li Y., Li C., Banister R.E., Dentino A., Nguyen T., Zupancic S., Griswold J. // 2010 International Conference on System Science and Engineering (ICSSE). - Taipei, 1-3 July 2010. - P. 190-194. 


**C808.** Shichao Cai. Context system using pervasive Controller Area Network bus system to improve driving safety. / Shichao Cai, Becherif M., Wack M. // 2010 IEEE/ASME International Conference on Mechatronics and Embedded Systems and Applications (MESA). - Qingdao, ShanDong, 15-17 July 2010. - P. 560-565. 


**C809.** ZhiXin Tie. GPRS-based fault monitoring for distribution grid. / ZhiXin Tie, ZhaoQing Wang. // 2010 IEEE/ASME International Conference on Mechatronics and Embedded Systems and Applications (MESA). - Qingdao, ShanDong, 15-17 July 2010. - P. 99-102. 


**C810.** Grinev A.Yu. The restoration of road coats and related objects parameters based on method of computation diagnostics-Ground Penetrating Radar antennas dipole approximation. / Grinev A.Yu., Temchenko V.S., Ilyin E.V., Bagno D.V. // 2010 13th International Conference on Ground Penetrating Radar (GPR). - Lecce, 21-25 June 2010. - P. 1-5. 


**C811.** Leucci G. 3D high resolution GPR survey to help the reconstruction of the archaeological stratigraphy of Lecce (Italy). / Leucci G., D'Agostino D., Cataldo R. // 2010 13th International Conference on Ground Penetrating Radar (GPR). - Lecce, Italy, 21-25 June 2010. - P. 1-6. 


**C812.** Persico R. Dielectric and magnetic anomaly imaging from GPR data. / Persico R., Negri S., Soldovieri F., Pettinelli E. // 2010 13th International Conference on Ground Penetrating Radar (GPR). - Lecce, 21-25 June 2010. - P. 1-5. 

**C813.** Utsi V. How many points per scan?. 2010 13th International Conference on Ground Penetrating Radar (GPR). - Lecce, 21-25 June 2010. - P. 1-4. 

**C814.** Lai W.L. Detection of accelerated reinforcement corrosion in concrete by ground penetrating radar. / Lai W.L., Kind T., Wiggenshauser H. // 2010 13th International Conference on Ground Penetrating Radar (GPR). - Lecce, 21-25 June 2010. - P. 1-5. 

**C815.** Porsani Jorge Luis. Use of Ground Penetrating Radar to map subsurface features at Lapa do Santo archaeological site (Brazil). / Porsani Jorge Luis, de Matos Guilherme Jangelme, Kipnis Renato. // 2010 13th International Conference on Ground Penetrating Radar (GPR). - Lecce, Italy, 21-25 June 2010. - P. 1-4. 

**C816.** Rodrigues Selma I. GPR applied to map Jabuticabeira-II coastal sambaqui archaeological site (Brazil). / Rodrigues Selma I., Porsani Jorge L., DeBlasis Paulo A D. // 2010 13th International Conference on Ground Penetrating Radar (GPR). - Lecce, Italy, 21-25 June 2010. - P. 1-5. 

**C817.** Nazli H. Experimental investigation of different soil types for buried object imaging using impulse GPR. / Nazli H., Bicak E., Sezgin M. // 2010 13th International Conference on Ground Penetrating Radar (GPR). - Lecce, 21-25 June 2010. - P. 1-5. 

**C818.** Song Lei. Simulation and application of GPR in Artificial Freezing Engineering. / Song Lei, Zhang Xiaojun, Li Haipeng, Zhang Houquan. // 2010 13th International Conference on Ground Penetrating Radar



(GPR). - Lecce, 21-25 June 2010. - P. 1-4. ↑

**C819.** Romano N. Design and numerical analysis of a new reconfigurable antenna for georadar applications. / Romano N., Soldovieri F., Persico R. // 2010 13th International Conference on Ground Penetrating Radar (GPR). - Lecce, 21-25 June 2010. - P. 1-5. ↑

**C820.** Orlando Luciana. Instability analysis of Villa Arianna site in Castellammare di Stabia (Naples). 2010 13th International Conference on Ground Penetrating Radar (GPR). - Lecce, Italy, 21-25 June 2010. - P. 1-4. ↑

**C821.** Inagaki M. Experimental approach for determining the received pattern of a Rascan holographic radar antenna. / Inagaki M., Bechtel T., Razevig V. // 2010 13th International Conference on Ground Penetrating Radar (GPR). - Lecce, 21-25 June 2010. - P. 1-5. ↑

**C822.** Gacitu. Using ground penetrating radar to estimate active layer moisture conditions in the Arctic. / Gacitu, a G., Tamstorf M.P., Lee S. // 2010 13th International Conference on Ground Penetrating Radar (GPR). - Lecce, 21-25 June 2010. - P. 1-5. ↑

**C823.** Utsi Erica. The shrine of edward the confessor: A study in multi-frequency gpr investigation. 2010 13th International Conference on Ground Penetrating Radar (GPR). - Lecce, Italy, 21-25 June 2010. - P. 1-7. ↑

**C824.** Orlando L. Object dimension Vs antenna frequency. 2010 13th International Conference on Ground Penetrating Radar (GPR). - Lecce, 21-25 June 2010. - P. 1-5. ↑

**C825.** Grazzini Gilberto. An ultra-wideband high-dynamic range GPR for detecting buried people after collapse of buildings. / Grazzini Gilberto, Pieraccini Massimiliano, Parrini Filippo, Spinetti Alessandro, Macaluso Giovanni, Dei Devis, Atzeni Carlo. // 2010 13th International Conference on Ground Penetrating Radar (GPR). - Lecce, Italy, 21-25 June 2010. - P. 1-6. ↑

**C826.** Solimene R. Half-space estimation by time gating based strategy. / Solimene R., D'Alterio A., Soldovieri F. // 2010 13th International Conference on Ground Penetrating Radar (GPR). - Lecce, 21-25 June 2010. - P. 1-5. ↑

**C827.** Sato M. ALIS: GPR for humanitarian demining and its evaluation in Cambodia. 2010 IEEE Antennas and Propagation Society International Symposium (APSURSI). - Toronto, ON, 11-17 July 2010. - P. 1-4. ↑

**C828.** Vazquez Alejos A. Design of a pseudorandom reference codes for reduced sidelobes and spectrally clean out-of-band emissions using an extended optimal filtering approach. / Vazquez Alejos A., Dawood M., Garcia Sanchez M. // 2010 IEEE Antennas and Propagation Society International Symposium (APSURSI). - Toronto, ON, 11-17 July 2010. - P. 1-4. ↑

**C829.** Dan Jiang. Multi-path EM scattering calculation for ships over time-varying sea surface. / Dan Jiang, Xiaojian Xu, Xiaofei Li. // 2010 IEEE Antennas and Propagation Society International Symposium (APSURSI). - Toronto, ON, 11-17 July 2010. - P. 1-4. ↑

**C830.** Yazhou Wang. A comprehensive system-level simulation paradigm for UWB systems. / Yazhou Wang, Kuhn M.J., Mahfouz M.R., Fathy A.E. // 2010 IEEE Antennas and Propagation Society International Symposium (APSURSI). - Toronto, ON, 11-17 July 2010. - P. 1-4. ↑

**C831.** Khaleghi A. Characterization of ultra-wideband wave propagation inside human body. / Khaleghi A., Balasingham I. // 2010 IEEE Antennas and Propagation Society International Symposium (APSURSI). - Toronto, ON, 11-17 July 2010. - P. 1-4. ↑

**C832.** Huiqing Zhai. A practical wireless charging system based on ultra-wideband retro-reflective beamforming. / Huiqing Zhai, Pan H.K., Mingyu Lu. // 2010 IEEE Antennas and Propagation Society International Symposium (APSURSI). - Toronto, ON, 11-17 July 2010. - P. 1-4. ↑

**C833.** Venkatarayalu N.V. Design of a tapered slot array antenna for UWB through-wall RADAR. / Venkatarayalu N.V., Yeow-Beng Gan. // 2010 IEEE Antennas and Propagation Society International Symposium (APSURSI). - Toronto, ON, 11-17 July 2010. - P. 1-4. ↑

**C834.** Minshen Wang. Evaluation and optimization of the specific absorption rate for multi-antenna systems. / Minshen Wang, Li Lin, Ji Chen, Jackson D., Kainz W., Yihong Qi, Jarmuszewski P. // 2010 IEEE Antennas and

Propagation Society International Symposium (APSURSI). - Toronto, ON, 11-17 July 2010. - P. 1-4. ↑

C835. Kuo J.W. A low cost wafer based W-band phased array. / Kuo J.W., Wang Y.E. // 2010 IEEE Antennas and Propagation Society International Symposium (APSURSI). - Toronto, ON, 11-17 July 2010. - P. 1-4. ↑

C836. Xiaochuan Wang. Simulation of the mutual couplings among multiple antennas on large platform using multi-region multi-solver domain decomposition. / Xiaochuan Wang, Zhen Peng, Jin-fa Lee. // 2010 IEEE Antennas and Propagation Society International Symposium (APSURSI). - Toronto, ON, 11-17 July 2010. - P. 1-4. ↑

C837. Whiteloni N. Analysis of transmission characteristics of a circular pipe with two open ends. / Whiteloni N., Hao Ling. // 2010 IEEE Antennas and Propagation Society International Symposium (APSURSI). - Toronto, ON, 11-17 July 2010. - P. 1-4. ↑

C838. Jihoon Kim. A resistive dipole antenna excited by an impulse generator for ultra-wideband radar applications. / Jihoon Kim, Woong Kang, Kangwook Kim. // 2010 IEEE Antennas and Propagation Society International Symposium (APSURSI). - Toronto, ON, 11-17 July 2010. - P. 1-4. ↑

C839. Sharma S.K. Investigations on a triple mode waveguide horn capable of providing scanned radiation patterns. / Sharma S.K., Tuteja A. // 2010 IEEE Antennas and Propagation Society International Symposium (APSURSI). - Toronto, ON, 11-17 July 2010. - P. 1-4. ↑

C840. Buddendick H. Application of a fast equivalent currents based algorithm for scattering center visualization of vehicles. / Buddendick H., Eibert T.F. // 2010 IEEE Antennas and Propagation Society International Symposium (APSURSI). - Toronto, ON, 11-17 July 2010. - P. 1-4. ↑

C841. Rocca P. Synthesis of arbitrary sidelobes sum and difference patterns with common excitation weights. / Rocca P., Morabito A.F., Isernia T., Massa A. // 2010 IEEE Antennas and Propagation Society International Symposium (APSURSI). - Toronto, ON, 11-17 July 2010. - P. 1-4. ↑

C842. Keller S.D. Microstrip patch antenna array for a scalable X-band radar system. / Keller S.D., Weiss S. // 2010 IEEE Antennas and Propagation Society International Symposium (APSURSI). - Toronto, ON, 11-17 July 2010. - P. 1-4. ↑

C843. Hamadi A. Time domain radiating model for GPR antenna. / Hamadi A., Guiffaut C., Reineix A., Ciarletti V., Plettemeier D. // 2010 IEEE Antennas and Propagation Society International Symposium (APSURSI). - Toronto, ON, 11-17 July 2010. - P. 1-4. ↑

C844. Srinivas A. Transmit beamforming for colocated MIMO radar. / Srinivas A., Reddy V.U. // 2010 International Conference on Signal Processing and Communications (SPCOM). - Bangalore, 18-21 July 2010. - P. 1-5. ↑

C845. Satyanarayana J.V. MOSAICS: Multiplexed optimal signal acquisition involving compressed sensing. / Satyanarayana J.V., Ramakrishnan A.G. // 2010 International Conference on Signal Processing and Communications (SPCOM). - Bangalore, 18-21 July 2010. - P. 1-5. ↑
















C846. Nanzer J.A. Analysis of the detection modes of a human presence detection millimeter-wave radiometer. / Nanzer J.A., Popova E., Rogers R.L. // 2010 IEEE Antennas and Propagation Society International Symposium (APSURSI). - Toronto, ON, 11-17 July 2010. - P. 1-4. ↑

C847. Oliveri G. ADS interleaved arrays with reconfigurable polarization. / Oliveri G., Lizzi L., Massa A. // 2010 IEEE Antennas and Propagation Society International Symposium (APSURSI). - Toronto, ON, 11-17 July 2010. - P. 1-4. ↑

C848. Hyoun-sun Youn. Feasibility study for IED detection using forward-looking ground penetrating radar integrated with target features classification. / Hyoun-sun Youn, Kobashigawa J., Evans M., Celik N., Zhengqing Yun, Baker J., Iskander M. // 2010 IEEE Antennas and Propagation Society International Symposium (APSURSI). - Toronto, ON, 11-17 July 2010. - P. 1-4. ↑

C849. Pancera E. Quantification of the impact of the antenna non-idealities in UWB transmission systems. / Pancera E., Zwirello L., Zwick T., Wiesbeck W. // 2010 IEEE Antennas and Propagation Society International Symposium (APSURSI). - Toronto, ON, 11-17 July 2010. - P. 1-4. ↑

- C850.** Ebnabbasi K. Impulse response of Vivaldi antenna using cubic-spline and exponential taper profiles for compact ground penetrating radar applications. / Ebnabbasi K., Rappaport C., Foltz H., McLean J. // 2010 IEEE Antennas and Propagation Society International Symposium (APSURSI). - Toronto, ON, 11-17 July 2010. - P. 1-4. ↑
- C851.** Jouny I. DOA estimation of correlated sources using SMT. 2010 IEEE Antennas and Propagation Society International Symposium (APSURSI). - Toronto, ON, 11-17 July 2010. - P. 1-4. ↑
- C852.** Mondal T. Design and analysis of a 5.88GHz microstrip phased array antenna for intelligent transport systems. / Mondal T., Ghatak R., Chaudhuri S.R.B. // 2010 IEEE Antennas and Propagation Society International Symposium (APSURSI). - Toronto, ON, 11-17 July 2010. - P. 1-4. ↑
- C853.** Kishor K.K. An amplifying reconfigurable reflectarray element. / Kishor K.K., Hum S.V. // 2010 IEEE Antennas and Propagation Society International Symposium (APSURSI). - Toronto, ON, 11-17 July 2010. - P. 1-4. ↑
- C854.** Fontana N. On the influence of a glass slide on the SAR distribution in Petri dishes for in vitro exposure to 2.45 GHz EM fields. / Fontana N., Pelletti C., Rogovich A., Monorchio A. // 2010 IEEE Antennas and Propagation Society International Symposium (APSURSI). - Toronto, ON, 11-17 July 2010. - P. 1-4. ↑
- C855.** Zhen-guo Liu. A novel broadband Fabry-Perot resonator antenna with gradient index metamaterial superstrate. / Zhen-guo Liu, Rui Qiang, Zhen-xin Cao. // 2010 IEEE Antennas and Propagation Society International Symposium (APSURSI). - Toronto, ON, 11-17 July 2010. - P. 1-4. ↑
- C856.** Kuwahara Y. Conformal array antenna with the aspirator for the microwave mammography. / Kuwahara Y., Suzuki K., Horie H., Hatano H. // 2010 IEEE Antennas and Propagation Society International Symposium (APSURSI). - Toronto, ON, 11-17 July 2010. - P. 1-4. ↑
- C857.** Bakar A.A. Ultra wideband hemispherical microwave imaging system. / Bakar A.A., Bialkowski M.E. // 2010 IEEE Antennas and Propagation Society International Symposium (APSURSI). - Toronto, ON, 11-17 July 2010. - P. 1-4. ↑
- C858.** Rengarajan S.R. Advances in waveguide-fed slot arrays. 2010 IEEE Antennas and Propagation Society International Symposium (APSURSI). - Toronto, ON, 11-17 July 2010. - P. 1-4. ↑
- C859.** West J.C. An implementation of the impedance-boundary CFIE using linear-linear basis functions and MLFMA. 2010 IEEE Antennas and Propagation Society International Symposium (APSURSI). - Toronto, ON, 11-17 July 2010. - P. 1-4. ↑
- C860.** Hajj M. A novel directivity/beam reconfigurable M-EBG antenna. / Hajj M., Mone, die, re T., Jecko B., Chantalat R. // 2010 IEEE Antennas and Propagation Society International Symposium (APSURSI). - Toronto, ON, 11-17 July 2010. - P. 1-4. ↑
- C861.** Barka A. Parallel FETI-EM Domain Decomposition Methods optimized for antenna arrays and metamaterials periodic structures. / Barka A., Roux F.-X. // 2010 IEEE Antennas and Propagation Society International Symposium (APSURSI). - Toronto, ON, 11-17 July 2010. - P. 1-4. ↑
- C862.** Weixin Zhao. Optimizing narrow-wall slotted waveguide arrays using HOBIES. / Weixin Zhao, Yu Zhang, Doc,oro D.G., Sarkar T.K. // 2010 IEEE Antennas and Propagation Society International Symposium (APSURSI). - Toronto, ON, 11-17 July 2010. - P. 1-4. ↑
- C863.** Zhu K.G. FDTD electromagnetic-acoustic model: A 2-D numerical coding framework. / Zhu K.G., Popovic, M. // 2010 IEEE Antennas and Propagation Society International Symposium (APSURSI). - Toronto, ON, 11-17 July 2010. - P. 1-4. ↑
- C864.** Xidong Wu. Design on elliptical lens monopulse antenna. / Xidong Wu, Huaicheng Zhao, Bo Li, Wen Wu. // 2010 IEEE Antennas and Propagation Society International Symposium (APSURSI). - Toronto, ON, 11-17 July 2010. - P. 1-3. ↑
- C865.** Whitelonis N. Beamforming through a circular pipe with two open ends. / Whitelonis N., Hao Ling. // 2010 IEEE Antennas and Propagation Society International Symposium (APSURSI). - Toronto, ON, 11-17 July 2010. - P. 1-4. ↑

- C866.** Bryan J. Classification of human activities on UWB radar using a support vector machine. / Bryan J., Youngwook Kim. // 2010 IEEE Antennas and Propagation Society International Symposium (APSURSI). - Toronto, ON, 11-17 July 2010. - P. 1-4. 
- C867.** Durgun A.C. Computation of physical optics integral by Levin's algorithm on NURBS. / Durgun A.C., Kuzuoglu M., Balanis C.A. // 2010 IEEE Antennas and Propagation Society International Symposium (APSURSI). - Toronto, ON, 11-17 July 2010. - P. 1-4. 
- C868.** Dogan D. Edge wall slotted waveguide antenna with low cross polarization. / Dogan D., Civi O.A. // 2010 IEEE Antennas and Propagation Society International Symposium (APSURSI). - Toronto, ON, 11-17 July 2010. - P. 1-4. 
- C869.** Kobashigawa J. Comparison between genetic programming and Neural Network in classification of buried unexploded ordnance (UXO) targets. / Kobashigawa J., Hyoung-sun Youn, Iskander M., Zhengqing Yun. // 2010 IEEE Antennas and Propagation Society International Symposium (APSURSI). - Toronto, ON, 11-17 July 2010. - P. 1-4. 
- C870.** Hoi-Shun Lui. Performance evaluation of subsurface target recognition based on ultrawideband short-pulse excitation. / Hoi-Shun Lui, Shuley N.V. // 2010 IEEE Antennas and Propagation Society International Symposium (APSURSI). - Toronto, ON, 11-17 July 2010. - P. 1-4. 
- C871.** Elsherbini A. Unidirectional low profile ultra-wideband antenna for radar and communication applications. / Elsherbini A., Sarabandi K. // 2010 IEEE Antennas and Propagation Society International Symposium (APSURSI). - Toronto, ON, 11-17 July 2010. - P. 1-4. 
- C872.** Ettorre M. Mechanical scanning with a dual-layer pillbox antenna for millimeter-wave applications. / Ettorre M., Gandini E., Sauleau R. // 2010 IEEE Antennas and Propagation Society International Symposium (APSURSI). - Toronto, ON, 11-17 July 2010. - P. 1-4. 
- C873.** Llombart N. Terahertz reflector antenna system for a scanned and multiplexed FMCW radar. / Llombart N., Cooper K.B., Dengler R.J., Siegel P.H. // 2010 IEEE Antennas and Propagation Society International Symposium (APSURSI). - Toronto, ON, 11-17 July 2010. - P. 1-4. 
- C874.** Fourmault A. Active phase array SAR antennas. / Fourmault A., Uher J., Allan P., Grenier C., Arsenault P. // 2010 IEEE Antennas and Propagation Society International Symposium (APSURSI). - Toronto, ON, 11-17 July 2010. - P. 1-4. 
- C875.** Chebila F. Pressure measurement from the RADAR interrogation of passive sensors. / Chebila F., Jatlouli M.M., Pons P., Aubert H. // 2010 IEEE Antennas and Propagation Society International Symposium (APSURSI). - Toronto, ON, 11-17 July 2010. - P. 1-4. 
- C876.** Beer S. Planar Yagi-Uda antenna array for W-band automotive radar applications. / Beer S., Adamiuk G., Zwick T. // 2010 IEEE Antennas and Propagation Society International Symposium (APSURSI). - Toronto, ON, 11-17 July 2010. - P. 1-4. 
- C877.** Vitaz J.A. Enhanced detection of planar retro-reflective arrays using polarization properties. / Vitaz J.A., Buerkle A., Sarabandi K. // 2010 IEEE Antennas and Propagation Society International Symposium (APSURSI). - Toronto, ON, 11-17 July 2010. - P. 1-4. 
- C878.** Baker J. High-performance compact HF antenna for radar and communication applications. / Baker J., Iskander M.F., Hyoung-Sun Youn, Celik N. // 2010 IEEE Antennas and Propagation Society International Symposium (APSURSI). - Toronto, ON, 11-17 July 2010. - P. 1-4. 
- C879.** Mastumoto M. Full polarimetric calibration of a GB-SAR system with a thin wire. / Mastumoto M., Sato M. // 2010 IEEE Antennas and Propagation Society International Symposium (APSURSI). - Toronto, ON, 11-17 July 2010. - P. 1-4. 
- C880.** Motevasselian A. A partially transparent Jaumann absorber applied to an aircraft wing profile. / Motevasselian A., Jonsson B.L.G. // 2010 IEEE Antennas and Propagation Society International Symposium (APSURSI). - Toronto, ON, 11-17 July 2010. - P. 1-4. 
- C881.** Caratelli D. Accurate evaluation of the time-domain effective height for short-pulse antennas. / Caratelli



D., Yarovoy A. // 2010 IEEE Antennas and Propagation Society International Symposium (APSURSI). - Toronto, ON, 11-17 July 2010. - P. 1-4. ↑

C882. AbdulSadda A. Noninvasive breast tumor localization based on ultrawideband microwave backscatter. / AbdulSadda A., Bouaynaya N., Iqbal K. // 2010 International Conference on Signal Processing and Communications (SPCOM). - Bangalore, 18-21 July 2010. - P. 1-4. ↑

C883. Wang Jiegui. The pulse sequence pattern and signal processing of complex radars. / Wang Jiegui, Luo Jingqing. // 2010 2nd International Conference on Signal Processing Systems (ICSPS). - Dalian, 5-7 July 2010. - Vol. 2. - P. V2-783-V2-786-783. ↑

C884. Chundong Qi. An improved chirp scaling algorithm with capability motion compensation for SAR. / Chundong Qi, Tao Zeng, Feng Li, Liang Chen. // 2010 2nd International Conference on Signal Processing Systems (ICSPS). - Dalian, 5-7 July 2010. - Vol. 3. - P. V3-234-V3-236-234. ↑

C885. Tian Jihua. The effects of input signal-to-noise ratio on compressive sensing SAR imaging. / Tian Jihua, Sun Jinping, Zhang Yuxi, Ahmad N., Su Xiaoyang. // 2010 2nd International Conference on Signal Processing Systems (ICSPS). - Dalian, 5-7 July 2010. - Vol. 3. - P. V3-533-V3-537-533. ↑

C886. Rui Li. Bistatic SAR imaging with parallel flight track based on monostatic SAR processor. / Rui Li, Zhu Zhen Bo, Yue T.Z. // 2010 2nd International Conference on Signal Processing Systems (ICSPS). - Dalian, 5-7 July 2010. - Vol. 3. - P. V3-361-V3-365-361. ↑

C887. Yu Haixia. A fuzzy adaptive tracking algorithm based on current statistical probabilistic data association. / Yu Haixia, Fu Caikui, Jiang Li. // 2010 2nd International Conference on Signal Processing Systems (ICSPS). - Dalian, 5-7 July 2010. - Vol. 2. - P. V2-757-V2-759-757. ↑

C888. Pei Wang. A new phase unwrapping method of interferogram. 2010 2nd International Conference on Signal Processing Systems (ICSPS). - Dalian, 5-7 July 2010. - Vol. 2. - P. V2-775-V2-778-775. ↑

C889. Lou Hao. Low velocity small radar target detection in maritime environment. / Lou Hao, Zhang Lefeng. // 2010 2nd International Conference on Signal Processing Systems (ICSPS). - Dalian, 5-7 July 2010. - Vol. 3. - P. V3-385-V3-388-385. ↑

C890. Huang Hong-xu. A new time-delay echo jamming style to SAR. / Huang Hong-xu, Zhou Yi-yu, Jiang Wen-li, Huang Zhi-tao. // 2010 2nd International Conference on Signal Processing Systems (ICSPS). - Dalian, 5-7 July 2010. - Vol. 3. - P. V3-14-V3-17-14. ↑

C891. Qu Wei. SAR interference signal feature vector extraction and simulation based on wavelet packet analysis. / Qu Wei, Jia Xin, Liu Shu-qian, Wu Yan-hong. // 2010 2nd International Conference on Signal Processing Systems (ICSPS). - Dalian, 5-7 July 2010. - Vol. 3. - P. V3-284-V3-287-284. ↑

C892. Rubiola E. Phase noise in RF and microwave amplifiers. / Rubiola E., Boudot R. // 2010 IEEE International Frequency Control Symposium (FCS). - Newport Beach, CA, 1-4 June 2010. - P. 109-111. ↑

C893. Huijun Su. Resolution enhancement of SAR image using the modified IBP method. / Huijun Su, Xiaoling Zhang, Shunjun Wei. // 2010 2nd International Conference on Signal Processing Systems (ICSPS). - Dalian, 5-7 July 2010. - Vol. 2. - P. V2-486-V2-489-486. ↑

C894. Chen Xianzhong. The improved phase-difference algorithm of 24GHz FMCW radar for fast level tracing of bulk solid material. / Chen Xianzhong, Miao Liangliang, Hou Qingwen. // 2010 2nd International Conference on Signal Processing Systems (ICSPS). - Dalian, 5-7 July 2010. - Vol. 3. - P. V3-181-V3-184-181. ↑

C895. Dahua Gao. Radar echo signal detection with sparse representations. / Dahua Gao, Danhua Liu, Youqian Feng, Qinli An, Fuping Yu. // 2010 2nd International Conference on Signal Processing Systems (ICSPS). - Dalian, 5-7 July 2010. - Vol. 2. - P. V2-495-V2-498-495. ↑

C896. Xian-jiao Liang. Analysis of micro-doppler effect in SIMO radar. / Xian-jiao Liang, Qun Zhang, Meng Zhu, Ying Luo. // 2010 2nd International Conference on Signal Processing Systems (ICSPS). - Dalian, 5-7 July 2010. - Vol. 2. - P. V2-343-V2-346-343. ↑

C897. Yu Zhang. An approach for extracting the transmitted waveforms based on compound filter for MIMO

radar. / Yu Zhang, Jianxin Wang. // 2010 2nd International Conference on Signal Processing Systems (ICSPS). - Dalian, 5-7 July 2010. - Vol. 1. - P. V1-665-V1-667-665. ↑

C898. Yang Jinlu. Fast computation of cross ambiguity function for DTTB based passive radar. / Yang Jinlu, Shan Tao, Tao Ran. // 2010 2nd International Conference on Signal Processing Systems (ICSPS). - Dalian, 5-7 July 2010. - Vol. 1. - P. V1-661-V1-664-661. ↑

C899. Fan Fuhua. Improved method for deinterleaving radar pulse trains with stagger PRI from dense pulse series. / Fan Fuhua, Yin Xuezhong. // 2010 2nd International Conference on Signal Processing Systems (ICSPS). - Dalian, 5-7 July 2010. - Vol. 3. - P. V3-250-V3-253-250. ↑

C900. Lei Wentai. Two-dimensional diffraction tomography algorithm of underground objects located in planar multilayer medium1. / Lei Wentai, Liu Jianxin. // 2010 2nd International Conference on Signal Processing Systems (ICSPS). - Dalian, 5-7 July 2010. - Vol. 1. - P. V1-298-V1-301-298. ↑

C901. Yuejin Lin. Bearing-only target tracking with improved particle filter. / Yuejin Lin, Fasheng Wang, Yu Han, Quan Guo. // 2010 2nd International Conference on Signal Processing Systems (ICSPS). - Dalian, 5-7 July 2010. - Vol. 1. - P. V1-333-V1-336-333. ↑

C902. Bin Deng. Pulse compression technique for multi carrier phase-coded radar. / Bin Deng, Xizhang Wei, Xiang Li. // 2010 2nd International Conference on Signal Processing Systems (ICSPS). - Dalian, 5-7 July 2010. - Vol. 1. - P. V1-329-V1-332-329. ↑

C903. Wen-Qin Wang. Millimeterwave radar high-resolution imaging via OFDM waveforms. / Wen-Qin Wang, Jingye Cai. // 2010 2nd International Conference on Signal Processing Systems (ICSPS). - Dalian, 5-7 July 2010. - Vol. 3. - P. V3-512-V3-515-512. ↑

C904. Yang Yun. Directional pattern modeling and simulation of triangular grid circular planar array antennas. / Yang Yun, Cao Jianshu, Ma Jianchun. // 2010 2nd International Conference on Signal Processing Systems (ICSPS). - Dalian, 5-7 July 2010. - Vol. 2. - P. V2-666-V2-669-666. ↑

C905. Pan Xianjun. A novel design of SAR scattering signal simulator based on AWG. / Pan Xianjun, Wu Yanhong, Jia Xin. // 2010 2nd International Conference on Signal Processing Systems (ICSPS). - Dalian, 5-7 July 2010. - Vol. 3. - P. V3-431-V3-435-431. ↑

C906. Wang Hongyan. Improved image mosaic method of ScanSAR. / Wang Hongyan, Jia Xin. // 2010 2nd International Conference on Signal Processing Systems (ICSPS). - Dalian, 5-7 July 2010. - Vol. 3. - P. V3-451-V3-453-451. ↑

C907. Donghai Li. Phase-coded pulse compression radar carrier frequency accurate estimation. / Donghai Li, Shiwen Chen, Chuang Zhao. // 2010 2nd International Conference on Signal Processing Systems (ICSPS). - Dalian, 5-7 July 2010. - Vol. 3. - P. V3-212-V3-214-212. ↑

C908. Xu Ruipeng. A novel single-channel SAR-GMTI method based on defocusing shifted difference. / Xu Ruipeng, Qiu Xiaolan, Hu Donghui, Ding Chibiao. // 2010 2nd International Conference on Signal Processing Systems (ICSPS). - Dalian, 5-7 July 2010. - Vol. 3. - P. V3-83-V3-86-83. ↑

C909. Shang Shang. Low speed target detection with short CIT in HF surface wave radar. / Shang Shang, Zhang Ning. // 2010 2nd International Conference on Signal Processing Systems (ICSPS). - Dalian, 5-7 July 2010. - Vol. 2. - P. V2-499-V2-503-499. ↑

C910. Mincica M. Enabling technology for heart health wireless assistance. / Mincica M., Pepe D., Tognetti A., Lanata, A., De Rossi D., Zito D. // 2010 12th IEEE International Conference on e-Health Networking Applications and Services (Healthcom). - Lyon, 1-3 July 2010. - P. 36-42. ↑

C911. Cadeddu M.P. Evaluation of cloud liquid absorption models at 90 and 150 GHz. / Cadeddu M.P., Turner D.D. // 2010 11th Specialist Meeting on Microwave Radiometry and Remote Sensing of the Environment (MicroRad). - Washington, DC, 1-4 March 2010. - P. 171-176. ↑

C912. Laupattarakasem P. Improved high wind speed retrievals using AMSR and the next generation NASA Dual Frequency Scatterometer. / Laupattarakasem P., Alsweiss S., El-Nimri S., Jones W.L., Veleva S., Stiles B.W., Rodriguez E., Gaston R.W. // 2010 11th Specialist Meeting on Microwave Radiometry and Remote

Sensing of the Environment (MicroRad). - Washington, DC, 1-4 March 2010. - P. 134-139. ↑

C913. Ferrazzoli P. AMSR-E observations of rain and flood events over vegetated areas of LA Plata basin. / Ferrazzoli P., Rahmoune R., Grings F., Douna V., Parmuchi G., Salvia M., Karszenbaum H. // 2010 11th Specialist Meeting on Microwave Radiometry and Remote Sensing of the Environment (MicroRad). - Washington, DC, 1-4 March 2010. - P. 63-66. ↑

C914. Parde. Radio frequency interferences investigation using the airborne L-band full polarimetric radiometer CAROLS. / Parde, M., Zribi M., Fanise P., Dechambre M., Boutin J., Reul N., Tenerelli J., Hauser D., Kerr Y. // 2010 11th Specialist Meeting on Microwave Radiometry and Remote Sensing of the Environment (MicroRad). - Washington, DC, 1-4 March 2010. - P. 300-305. ↑

C915. Alsweiss S.O. An improved active/passive oceanic wind vector retrieval technique. / Alsweiss S.O., Laupattarakasem P., Jones W.L. // 2010 11th Specialist Meeting on Microwave Radiometry and Remote Sensing of the Environment (MicroRad). - Washington, DC, 1-4 March 2010. - P. 226-229. ↑

C916. Dowgiallo D.J. Millimeter wave interferometric radiometry for passive imaging and the detection of low-power manmade signals. / Dowgiallo D.J., Twarog E.M., Rauen S., Lazio J.T., Peters W.M., McGlothlin N.R., Helmboldt J.F., Gaiser P.W. // 2010 11th Specialist Meeting on Microwave Radiometry and Remote Sensing of the Environment (MicroRad). - Washington, DC, 1-4 March 2010. - P. 211-216. ↑

C917. Colliander A. Utilization of airborne and in situ data obtained in SGP99, SMEX02, CLASIC and SMAPVEX08 Field Campaigns for SMAP Soil Moisture Algorithm Development and Validation. / Colliander A., Chan S., Yueh S., Cosh M., Bindlish R., Jackson T., Njoku E. // 2010 11th Specialist Meeting on Microwave Radiometry and Remote Sensing of the Environment (MicroRad). - Washington, DC, 1-4 March 2010. - P. 43-48. ↑

C918. YiKun Zhang. An Lidar data compression method based on improved LZW and Huffman algorithm. / YiKun Zhang, Xiao Li, DengXin Hua, Hao Chen, HaiYan Jin. // 2010 International Conference On Electronics and Information Engineering (ICEIE). - Kyoto, 1-3 Aug. 2010. - Vol. 2. - P. V2-250-V2-254-250. ↑

C919. Chun-Cheng Liu. A 1V 11fJ/conversion-step 10bit 10MS/s asynchronous SAR ADC in 0.18μm CMOS. / Chun-Cheng Liu, Soon-Jyh Chang, Guan-Ying Huang, Ying-Zu Lin, Chung-Ming Huang. // 2010 IEEE Symposium on VLSI Circuits (VLSIC). - Honolulu, HI, 16-18 June 2010. - P. 241-242. ↑

C920. Young Moon Kim. Low-cost gate-oxide early-life failure detection in robust systems. / Young Moon Kim, Kameda Y., Hyunki Kim, Mizuno M., Mitra S. // 2010 IEEE Symposium on VLSI Circuits (VLSIC). - Honolulu, HI, 16-18 June 2010. - P. 125-126. ↑

C921. Zribi M. CAROLS campaigns 2009: First Results. / Zribi M., Parde M., Hauser D., Fanise P., Boutin J., Albergel C., Calvet J.C., Crapeau M., Dechambre M., Kerr Y., Baeza E.L., Mialon A., Reverdin G., Ruis A., Saleh K., Wigneron J.P. // 2010 11th Specialist Meeting on Microwave Radiometry and Remote Sensing of the Environment (MicroRad). - Washington, DC, 1-4 March 2010. - P. 49-54. ↑

C922. Zong Hua. Track initiation in Monostatic-Bistatic Composite High Frequency Surface Wave Radar Network based on NFE model. / Zong Hua, Yu Changjun, Zhou Gongjian, Quan Taifan. // 2010 International Conference On Electronics and Information Engineering (ICEIE). - Kyoto, 1-3 Aug. 2010. - Vol. 2. - P. V2-81-V2-85-81. ↑

C923. Wei Xiang. The exposed area analysis of Barrage-type Jamming to Bistatic SAR. / Wei Xiang, Jianguo Wang, Fang Liu. // 2010 International Conference On Electronics and Information Engineering (ICEIE). - Kyoto, 1-3 Aug. 2010. - Vol. 2. - P. V2-168-V2-171-168. ↑

C924. Pava J. A three-dimensional geographic and storm surge data integration system for evacuation planning. / Pava J., Fleites F., Fang Ruan, Chatterjee K., Shu-Ching Chen, Keqi Zhang. // 2010 IEEE International Conference on Information Reuse and Integration (IRI). - Las Vegas, NV, 4-6 Aug. 2010. - P. 181-188. ↑

C925. Rahim H.A. An adapted point based tracking for vehicle speed estimation in linear spacing. / Rahim H.A., Ahmad R.B., Zain A.S.M., Sheikh U.U. // 2010 International Conference on Computer and Communication Engineering (ICCCE). - Kuala Lumpur, 11-12 May 2010. - P. 1-4. ↑

- C926.** El Sanhoury A. Performance improvement of pulsed OFDM UWB systems using ATF coding. / El Sanhoury A., Mabrouk A.H. // 2010 International Conference on Computer and Communication Engineering (ICCCE). - Kuala Lumpur, 11-12 May 2010. - P. 1-4. ↑
- C927.** Gao Ying. Research on Visualization of Radar Beam Considering Virtual Environment Effect. / Gao Ying, Liu Weiyuan, Lei Lei, Guo Shuxia. // 2010 Second International Conference on Information Technology and Computer Science (ITCS). - Kiev, 24-25 July 2010. - P. 353-356. ↑
- C928.** Yuh-Jyh Hu. An application of sensor networks with data mining to patient controlled analgesia. / Yuh-Jyh Hu, Rong-Hong Jan, Kuochen Wang, Yu-Chee Tseng, Tien-Hsiung Ku, Shu-Fen Yang, Hung-Shan Wu. // 2010 12th IEEE International Conference on e-Health Networking Applications and Services (Healthcom). - Lyon, 1-3 July 2010. - P. 353-360. ↑
- C929.** Hameed S.A. Car monitoring, alerting and tracking model: Enhancement with mobility and database facilities. / Hameed S.A., Khalifa O., Ershad M., Zahudi F., Sheyaa B., Asender W. // 2010 International Conference on Computer and Communication Engineering (ICCCE). - Kuala Lumpur, 11-12 May 2010. - P. 1-5. ↑
- C930.** Rahim H.A. Implementation and analysis of integration GSM/GPRS modem in a TMS320VC6713 digital signal processor for vehicle location. / Rahim H.A., Ahmad R.B., Zain A.S.M., Sheikh U.U. // 2010 International Conference on Computer and Communication Engineering (ICCCE). - Kuala Lumpur, 11-12 May 2010. - P. 1-5. ↑
- C931.** Song Zhi-yuan. A Digital Pulse Drive Circuit for Continuously Modulated Semiconductor Laser. / Song Zhi-yuan, Feng Li, Zhu Shao-lan, Niu Lin-quan. // 2010 Second International Conference on Information Technology and Computer Science (ITCS). - Kiev, 24-25 July 2010. - P. 244-246. ↑
- C932.** Ping Wang. The identification test of soil texture with ground penetrating radar. / Ping Wang, Zhenqi Hu, Junguo Yang, Fang Wang, Mingjie Gao. // 2010 International Conference on Advances in Energy Engineering (ICAEE). - Beijing, 19-20 June 2010. - P. 81-84. ↑
- C933.** Tang Shao-xun. Research on Early-Warning Detecting Tasks Re-scheduling and Sensor Resources Allocation Strategy of Midcourse Maneuverable Ballistic Targets. / Tang Shao-xun, Yi Xian-qing, Luo Xue-shan. // 2010 Fourth International Conference on Sensor Technologies and Applications (SENSORCOMM). - Venice, 18-25 July 2010. - P. 357-362. ↑
- C934.** Chen Shuxin. Remote monitoring of open numerical control system. / Chen Shuxin, Li PengFei. // 2010 2nd International Conference on Mechanical and Electronics Engineering (ICMEE). - Kyoto, 1-3 Aug. 2010. - Vol. 2. - P. V2-52-V2-55-52. ↑
- C935.** Panzhi Liu. Distributed GOSCA-CFAR Detection Based on Automatic Censoring Technique. / Panzhi Liu, Chendong Duan. // 2010 Second International Conference on Information Technology and Computer Science (ITCS). - Kiev, 24-25 July 2010. - P. 154-157. ↑
- C936.** Guo Shuxia. Research on Visualization of Electromagnetic Information in Virtual Environment. / Guo Shuxia, Liu Weiyuan, Zhang Jinhui, Gao Ying. // 2010 Third International Symposium on Electronic Commerce and Security (ISECS). - Guangzhou, 29-31 July 2010. - P. 185-188. ↑
- C937.** Tong Haipeng. Horizontal Dilution of Precision Analysis for Loran C/ Beidou Integrated Navigation System. / Tong Haipeng, Xu Haigang. // 2010 Third International Symposium on Electronic Commerce and Security (ISECS). - Guangzhou, 29-31 July 2010. - P. 167-170. ↑
- C938.** Bielefeld D. Power-aware distributed target detection in wireless sensor networks with UWB-radar nodes. / Bielefeld D., Mathar R., Hirsch O., Thomaj R.S. // 2010 IEEE Radar Conference. - Washington, DC, 10-14 May 2010. - P. 842-847. ↑
- C939.** Maresca S. The HF surface wave radar WERA. Part I: Statistical analysis of recorded data. / Maresca S., Greco M., Gini F., Grasso R., Coraluppi S., Thomas N. // 2010 IEEE Radar Conference. - Washington, DC, 10-14 May 2010. - P. 826-831. ↑
- C940.** Baque. LORAMBis A bistatic VHF/UHF SAR experiment for FOPEN. / Baque, R., Dreuillet P., du Plessis O.R., Cantalloube H., Ulander L., Stenstrojm G., Jonsson T., Gustavsson A. // 2010 IEEE Radar Conference. - Washington, DC, 10-14 May 2010. - P. 832-837. ↑



- C941. Pastina D. Passive bistatic ISAR based on geostationary satellites for coastal surveillance. / Pastina D., Sedehi M., Cristallini D. // 2010 IEEE Radar Conference. - Washington, DC, 10-14 May 2010. - P. 865-870. ↑
- C942. Garmatyuk D. Slow-time SAR signal processing for UWB OFDM radar system. / Garmatyuk D., Brenneman M. // 2010 IEEE Radar Conference. - Washington, DC, 10-14 May 2010. - P. 853-858. ↑
- C943. Pu Wang. Bayesian parametric approach for multichannel adaptive signal detection. / Pu Wang, Hongbin Li, Himed B. // 2010 IEEE Radar Conference. - Washington, DC, 10-14 May 2010. - P. 838-841. ↑
- C944. Meller M. Some aspects of designing real-time digital correlators for noise radars. 2010 IEEE Radar Conference. - Washington, DC, 10-14 May 2010. - P. 821-825. ↑
- C945. Fengzhou Dai. Detection performance comparison for wideband and narrowband radar in noise. / Fengzhou Dai, Penghui Wang, Hongwei Liu, Shunjun Wu. // 2010 IEEE Radar Conference. - Washington, DC, 10-14 May 2010. - P. 794-798. ↑
- C946. Feng Li. Deriving bistatic chirp scaling algorithm based on the signal model. / Feng Li, Tao Zeng, Teng Long. // 2010 IEEE Radar Conference. - Washington, DC, 10-14 May 2010. - P. 785-788. ↑
- C947. Mobasser B.G. A target alignment algorithm for through-the-wall radar imagery classification. / Mobasser B.G., Smith G.E., Estephan I. // 2010 IEEE Radar Conference. - Washington, DC, 10-14 May 2010. - P. 756-761. ↑
- C948. Tebaldini S. SAR imaging of forest structure at longer wavelengths. / Tebaldini S., d'Alessandro M.M., Rocca F. // 2010 IEEE Radar Conference. - Washington, DC, 10-14 May 2010. - P. 811-815. ↑
- C949. Setlur P. Multipath Doppler signatures from targets moving behind walls. / Setlur P., Amin M., Ahmad F. // 2010 IEEE Radar Conference. - Washington, DC, 10-14 May 2010. - P. 799-803. ↑
- C950. Zegang Ding. A precise signal model for ultra high resolution SAR. / Zegang Ding, Tao Zeng, Teng Long. // 2010 IEEE Radar Conference. - Washington, DC, 10-14 May 2010. - P. 804-806. ↑
- C951. Gray J.E. An interpretation of Woodward's ambiguity function and its generalization. 2010 IEEE Radar Conference. - Washington, DC, 10-14 May 2010. - P. 859-864. ↑
- C952. Zhaoping Wu. Radar target detect using particle filter. / Zhaoping Wu, Tao Su. // 2010 IEEE Radar Conference. - Washington, DC, 10-14 May 2010. - P. 955-958. ↑
- C953. Yarman C.E. Passive synthetic aperture radar imaging with single frequency sources of opportunity. / Yarman C.E., Ling Wang, Yazici B. // 2010 IEEE Radar Conference. - Washington, DC, 10-14 May 2010. - P. 949-954. ↑
- C954. Frazer G.J. Mode-Selective OTHR: A new cost-effective sensor for maritime domain awareness. / Frazer G.J., Meehan D.H., Abramovich Y.I., Johnson B.A. // 2010 IEEE Radar Conference. - Washington, DC, 10-14 May 2010. - P. 935-940. ↑
- C955. Hongbo Sun. High resolution radar tomographic imaging using single-tone CW signals. / Hongbo Sun, Hongchuan Feng, Yilong Lu. // 2010 IEEE Radar Conference. - Washington, DC, 10-14 May 2010. - P. 975-980. ↑
- C956. Feifeng Liu. Performance analysis of two-step algorithm in sliding spotlight space-borne SAR. / Feifeng Liu, Zegang Ding, Tao Zeng, Teng Long. // 2010 IEEE Radar Conference. - Washington, DC, 10-14 May 2010. - P. 965-968. ↑
- C957. Maresca S. The HF surface wave radar WERA. Part II: Spectral analysis of recorded data. / Maresca S., Greco M., Gini F., Grasso R., Coraluppi S., Thomas N. // 2010 IEEE Radar Conference. - Washington, DC, 10-14 May 2010. - P. 969-974. ↑
- C958. Gholizadeh M.H. Delay-Doppler radar tracking using moments. / Gholizadeh M.H., Amindavar H., Ritcey J.A. // 2010 IEEE Radar Conference. - Washington, DC, 10-14 May 2010. - P. 941-944. ↑
- C959. McMillan R.W. A probabilistic model of the radar signal-to-clutter and noise ratio for Weibull-distributed

clutter. / McMillan R.W., Kohlberg I. // 2010 IEEE Radar Conference. - Washington, DC, 10-14 May 2010. - P. 882-886. ↑

C960. Smith G.E. Compressed Sampling for pulse Doppler radar. / Smith G.E., Diethe T., Hussain Z., Shawe-Taylor J., Hardoon D.R. // 2010 IEEE Radar Conference. - Washington, DC, 10-14 May 2010. - P. 887-892. ↑

C961. Junhyeong Bae. Evaluation of modulus-constrained matched illumination waveforms for target identification. / Junhyeong Bae, Goodman N.A. // 2010 IEEE Radar Conference. - Washington, DC, 10-14 May 2010. - P. 871-876. ↑

C962. Gallardo-Hernando B. Super-resolution techniques in meteorological radars: The example of wind turbines. / Gallardo-Hernando B., Perez-Martinez F., Mucoz-Ferreras J.M., Aguado-Encabo F. // 2010 IEEE Radar Conference. - Washington, DC, 10-14 May 2010. - P. 931-934. ↑

C963. Lyonnet B. Human gait classification using microDoppler time-frequency signal representations. / Lyonnet B., Ioana C., Amin M.G. // 2010 IEEE Radar Conference. - Washington, DC, 10-14 May 2010. - P. 915-919. ↑

C964. Bandiera F. Adaptive strategies for discrimination between mainlobe and sidelobe signals. / Bandiera F., De Maio A., De Nicola S., Farina A., Orlando D., Ricci G. // 2010 IEEE Radar Conference. - Washington, DC, 10-14 May 2010. - P. 910-914. ↑

C965. Biancardi P. Performances and limitations of Persistent Scatterers-based SAR calibration. / Biancardi P., Iannini L., d'Alessandro M.M., Guarnieri A.M., Tebaldini S. // 2010 IEEE Radar Conference. - Washington, DC, 10-14 May 2010. - P. 762-766. ↑

C966. Mroue. UWB radar and leaky waveguide for fall on track object identification. / Mroue, A., Heddebaut M., Elbahhar F., Rivenq A., Rouvaen J.M. // 2010 IEEE Radar Conference. - Washington, DC, 10-14 May 2010. - P. 573-577. ↑

C967. Ming Li. Robust short-range clutter suppression algorithm for forward looking airborne radar. / Ming Li, Guisheng Liao. // 2010 IEEE Radar Conference. - Washington, DC, 10-14 May 2010. - P. 559-562. ↑

C968. Fabrizio G. Blind multipath separation for waveform recovery. / Fabrizio G., Farina A. // 2010 IEEE Radar Conference. - Washington, DC, 10-14 May 2010. - P. 563-568. ↑

C969. Park J.-I. Efficient construction of training database for identification of aircraft HRR profiles. / Park J.-I., Kim K.-T. // 2010 IEEE Radar Conference. - Washington, DC, 10-14 May 2010. - P. 590-595. ↑

C970. Rashid N.E.A. The effect of clutter on the automatic target classification accuracy in FSR. / Rashid N.E.A., Jancovic, P., Gashinova M., Cherniakov M., Sizov V. // 2010 IEEE Radar Conference. - Washington, DC, 10-14 May 2010. - P. 596-602. ↑

C971. Shunsheng Zhang. SAR raw signal simulation based on sub-aperture processing. / Shunsheng Zhang, Wei Zhang, Lingkun Kong. // 2010 IEEE Radar Conference. - Washington, DC, 10-14 May 2010. - P. 569-572. ↑


C972. Schmuland T.E. Parallel implementation of the wideband DOA algorithm on the IBM Cell BE processor. / Schmuland T.E., Jamali M.M., Longbrake M.B., Buxa P.E. // 2010 IEEE Radar Conference. - Washington, DC, 10-14 May 2010. - P. 549-552. ↑


C973. Harms H.A. Understanding the signal structure in DVB-T signals for passive radar detection. / Harms H.A., Davis L.M., Palmer J. // 2010 IEEE Radar Conference. - Washington, DC, 10-14 May 2010. - P. 532-537. ↑


C974. Falcone P. Experimental results for OFDM WiFi-based passive bistatic radar. / Falcone P., Colone F., Bongioanni C., Lombardo P. // 2010 IEEE Radar Conference. - Washington, DC, 10-14 May 2010. - P. 516-521. ↑


C975. Nguyen L. Suppression of sidelobes and noise in airborne SAR imagery using the Recursive Sidelobe Minimization technique. / Nguyen L., Innocenti R. // 2010 IEEE Radar Conference. - Washington, DC, 10-14 May 2010. - P. 522-525. ↑


- C976. Ming Xue. MIMO radar sparse angle-Doppler imaging for ground moving target indication. / Ming Xue, Roberts W., Jian Li, Xing Tan, Stoica P. // 2010 IEEE Radar Conference. - Washington, DC, 10-14 May 2010. - P. 553-558. ↑
- C977. Lok Y.F. Simulation of radar signal on wind turbine. / Lok Y.F., Jian Wang, Palevsky A. // 2010 IEEE Radar Conference. - Washington, DC, 10-14 May 2010. - P. 538-543. ↑
- C978. Sharma R. Analysis of MIMO radar ambiguity functions and implications on clear region. 2010 IEEE Radar Conference. - Washington, DC, 10-14 May 2010. - P. 544-548. ↑
- C979. Christiansen J.M. Range and Doppler walk in DVB-T based Passive Bistatic Radar. / Christiansen J.M., Olsen K.E. // 2010 IEEE Radar Conference. - Washington, DC, 10-14 May 2010. - P. 620-626. ↑
- C980. Yu J. An indoor S-band radar receive array testbed. / Yu J., Reynolds M., Krolik J. // 2010 IEEE Radar Conference. - Washington, DC, 10-14 May 2010. - P. 712-717. ↑
- C981. Rucci A. SKP-shrinkage estimator for SAR multi-baselines applications. / Rucci A., Tebaldini S., Rocca F. // 2010 IEEE Radar Conference. - Washington, DC, 10-14 May 2010. - P. 701-706. ↑
- C982. Inggs M. A quantitative method for mono- and multistatic radar coverage area prediction. / Inggs M., Lange G., Paichard Y. // 2010 IEEE Radar Conference. - Washington, DC, 10-14 May 2010. - P. 707-711. ↑
- C983. Chaoshu Jiang. Conjugate gradient parametric adaptive matched filter. / Chaoshu Jiang, Hongbin Li, Rangaswamy M. // 2010 IEEE Radar Conference. - Washington, DC, 10-14 May 2010. - P. 740-745. ↑
- C984. Frankford M.T. Software-defined radar for MIMO and adaptive waveform applications. / Frankford M.T., Majurec N., Johnson J.T. // 2010 IEEE Radar Conference. - Washington, DC, 10-14 May 2010. - P. 724-728. ↑
- C985. Pillai S.U. Design of unimodular sequences using generalized receivers. / Pillai S.U., Ke Yong Li, Richeng Zheng, Himed B. // 2010 IEEE Radar Conference. - Washington, DC, 10-14 May 2010. - P. 729-734. ↑
- C986. Colone F. Ambiguity Function analysis of WiMAX transmissions for passive radar. / Colone F., Falcone P., Lombardo P. // 2010 IEEE Radar Conference. - Washington, DC, 10-14 May 2010. - P. 689-694. ↑
- C987. LingKun Kong. Radon transform and the modified envelope correlation method for ISAR imaging of multi-target. / LingKun Kong, Wei Zhang, ShunSheng Zhang, BaoLiang Zhou. // 2010 IEEE Radar Conference. - Washington, DC, 10-14 May 2010. - P. 637-641. ↑
- C988. Jishy K. Tracking maneuvering target with particle filter techniques on passive radar using FM and DVBT broadcasting signals. / Jishy K., Lehmann F., Moruzzis M., Gosselin F., Salut G. // 2010 IEEE Radar Conference. - Washington, DC, 10-14 May 2010. - P. 642-646. ↑
- C989. Eung-Gi Paek. Distributed time reversal mirror array. / Eung-Gi Paek, Choe J.Y. // 2010 IEEE Radar Conference. - Washington, DC, 10-14 May 2010. - P. 627-630. ↑
- C990. Wingender M. 3 GS/s S-Band 10 Bit ADC on SiGeC Technology. / Wingender M., Benn A. // 2010 IEEE Radar Conference. - Washington, DC, 10-14 May 2010. - P. 695-700. ↑
- C991. Chiriac V.M. Ziv-Zakai lower bound on target localization estimation in MIMO radar systems. / Chiriac V.M., Haimovich A.M. // 2010 IEEE Radar Conference. - Washington, DC, 10-14 May 2010. - P. 678-683. ↑
- C992. Kabakchiev C. Analysis of multi-sensor radar detection based on the TBD-HT approach in ECM environment. / Kabakchiev C., Behar V., Rohling H., Garvanov I., Kyovtorov V., Kabakchieva D. // 2010 IEEE Radar Conference. - Washington, DC, 10-14 May 2010. - P. 651-656. ↑
- C993. Penghui Wang. A spatiotemporal model for radar HRRP sequence recognition. / Penghui Wang, Lan Du, Hongwei Liu. // 2010 IEEE Radar Conference. - Washington, DC, 10-14 May 2010. - P. 1005-1008. ↑
- C994. Haghshenas H. A novel method to detect rotor blades echo. / Haghshenas H., Nayebi M.M. // 2010 IEEE Radar Conference. - Washington, DC, 10-14 May 2010. - P. 1331-1334. ↑
- C995. Inggs M. Autonomic subsystems for cognition in Passive Coherent Location. / Inggs M., Lange G., ↑


Paichard Y. // 2010 IEEE Radar Conference. - Washington, DC, 10-14 May 2010. - P. 1317-1321. 


C996. Feng He. Modeling and simulation study on radar Doppler signatures of pedestrian. / Feng He, Xiaotao Huang, Chenglan Liu, Zhimin Zhou, Chongyi Fan. // 2010 IEEE Radar Conference. - Washington, DC, 10-14 May 2010. - P. 1322-1326. 


C997. Pancera E. Characterization of UWB Radar targets: Time domain vs. frequency domain description. / Pancera E., Zwick T., Wiesbeck W. // 2010 IEEE Radar Conference. - Washington, DC, 10-14 May 2010. - P. 1377-1380. 


C998. Greco M. Cramér-Rao bounds and TX-RX selection in a multistatic radar scenario. / Greco M., Stinco P., Gini F., Farina A., Rangaswamy M. // 2010 IEEE Radar Conference. - Washington, DC, 10-14 May 2010. - P. 1371-1376. 

C999. Feng He. Preliminary results of ultra-wideband through-the-wall life-detecting radar. / Feng He, Guofu Zhu, Xiaotao Huang, Miaohui Mou, Zhimin Zhou, Chongyi Fan. // 2010 IEEE Radar Conference. - Washington, DC, 10-14 May 2010. - P. 1327-1330. 


C1000. Padaki A.V. A robust neural network based pulse radar detection for weak signals. / Padaki A.V., George K. // 2010 IEEE Radar Conference. - Washington, DC, 10-14 May 2010. - P. 1305-1310. 


C1001. Fam A.T. Digital beamforming with reduced number of phase shifting and time delay elements. 2010 IEEE Radar Conference. - Washington, DC, 10-14 May 2010. - P. 1286-1288. 


C1002. Xiaowei Li. A robust Chinese remainder theorem with its applications in moving target Doppler estimation. / Xiaowei Li, Xiang-Gen Xia, Hong Liang. // 2010 IEEE Radar Conference. - Washington, DC, 10-14 May 2010. - P. 1289-1294. 


C1003. Deudon F. Modified Capon and APES for spectral estimation of range migrating targets in wideband radar. / Deudon F., Bidon S., Besson O., Tournet J.-Y., Monte, cot M., Le Chevalier F. // 2010 IEEE Radar Conference. - Washington, DC, 10-14 May 2010. - P. 1280-1285. 


C1004. Candan C. On the design of mismatched filters with an adjustable matched filtering loss. 2010 IEEE Radar Conference. - Washington, DC, 10-14 May 2010. - P. 1311-1316. 


C1005. Lu X. Impulsive noise excision and performance analysis. / Lu X., Wang J., Ponsford A.M., Kiriln R.L. // 2010 IEEE Radar Conference. - Washington, DC, 10-14 May 2010. - P. 1295-1300. 


C1006. Liu H. Frequency domain motion compensation for stepped-frequency radar under multi-target scenario. / Liu H., Guo X., Li Y., Long T. // 2010 IEEE Radar Conference. - Washington, DC, 10-14 May 2010. - P. 1301-1304. 

C1007. Landmann D. Three-dimensional reconstruction of a comet nucleus by optimal control of Maxwell's equations: A contribution to the experiment CONSERT onboard space craft Rosetta. / Landmann D., Plettemeier D., Statz C., Hoffeins F., Markwardt U., Nagel W.E., Walther A., Herique A., Kofman W. // 2010 IEEE Radar Conference. - Washington, DC, 10-14 May 2010. - P. 1392-1396. 

C1008. Sheng Qiang. Joint Space-Based and Ground-Based Orbit Maneuver Identification Algorithms. / Sheng Qiang, Zhen Shen, Dongyun Yi. // 2010 International Conference on Challenges in Environmental Science and Computer Engineering (CESCE). - Wuhan, 6-7 March 2010. - Vol. 1. - P. 121-125. 

C1009. Guo Lejiang. Research for D Stability of Uncertain Discrete Time-delay Systems. / Guo Lejiang, Chen Fangxin. // 2010 International Conference on Challenges in Environmental Science and Computer Engineering (CESCE). - Wuhan, China, 6-7 March 2010. - Vol. 2. - P. 79-81. 

C1010. Bielefeld D. Routing Path Selection and Power Allocation for Distributed Detection in Wireless Sensor Networks. / Bielefeld D., Fabeck G., Mathar R. // 2010 IEEE 71st Vehicular Technology Conference (VTC 2010-Spring). - Taipei, 16-19 May 2010. - P. 1-5. 

C1011. Lin Gao. Nondestructive Detection of Standing Trees and Radar Wave Detection. / Lin Gao, Jun Liu, Huixia Xue. // 2010 International Conference on Computing, Control and Industrial Engineering (CCIE). - Wuhan, 5-6 June 2010. - Vol. 1. - P. 304-307. 



- C1012.** Xinsheng Li. Real Aircraft Navigation Data Statistic and Rule Analysis. / Xinsheng Li, Taiyong Li. // 2010 International Conference on Computing, Control and Industrial Engineering (CCIE). - Wuhan, 5-6 June 2010. - Vol. 1. - P. 361-365. ↑
- C1013.** Golovatchev J. Technology and innovation radar-Effective instruments for the development of a sustainable innovation strategy. / Golovatchev J., Budde O. // 2010 IEEE International Conference on Management of Innovation and Technology (ICMIT). - Singapore, 2-5 June 2010. - P. 760-764. ↑
- C1014.** Parker J.T. A Bayesian perspective on sparse regularization for STAP post-processing. / Parker J.T., Potter L.C. // 2010 IEEE Radar Conference. - Washington, DC, 10-14 May 2010. - P. 1471-1475. ↑
- C1015.** Koga T. Autonomous Lockout Map Construction Technique for Secondary Surveillance Radar Mode S network. / Koga T., Mori K. // 2010 IEEE Radar Conference. - Washington, DC, 10-14 May 2010. - P. 1439-1443. ↑
- C1016.** Martinez D.R. ISR sensor processing and data exploitation. 2010 IEEE Radar Conference. - Washington, DC, 10-14 May 2010. - P. 1444-1445. ↑
- C1017.** Chebanov D. Removing autocorrelation sidelobes of phase-coded waveforms. / Chebanov D., Lu G. // 2010 IEEE Radar Conference. - Washington, DC, 10-14 May 2010. - P. 1428-1433. ↑
- C1018.** Schulz P.A. Radar sensitivity, receiver calibration, and sky noise. 2010 IEEE Radar Conference. - Washington, DC, 10-14 May 2010. - P. 1464-1466. ↑
- C1019.** Barnes R.I. The instagram: A novel sounding technique for enhanced HF propagation advice. / Barnes R.I., Earl G.F., Papazoglou M., Burchett L., Terzuoli A.J. // 2010 IEEE Radar Conference. - Washington, DC, 10-14 May 2010. - P. 1446-1449. ↑
- C1020.** Shuyan Wang. Modified Range-Doppler imaging method for the high squint SAR. / Shuyan Wang, Zhigang Su, Renbiao Wu. // 2010 IEEE Radar Conference. - Washington, DC, 10-14 May 2010. - P. 1450-1453. ↑
- C1021.** Schroeder C. X-band FMCW radar system with variable chirp duration. / Schroeder C., Rohling H. // 2010 IEEE Radar Conference. - Washington, DC, 10-14 May 2010. - P. 1255-1259. ↑
- C1022.** D'Urso M. Differential approach for Through-the-wall life signs detection. / D'Urso M., Gianota F., Lalli R., Infante L. // 2010 IEEE Radar Conference. - Washington, DC, 10-14 May 2010. - P. 1079-1082. ↑
- C1023.** Prasanth R.K. Stochastic system identification approach to radar data processing. 2010 IEEE Radar Conference. - Washington, DC, 10-14 May 2010. - P. 1064-1070. ↑
- C1024.** Prasanth R.K. Cramér-Rao lower bounds for monopulse calibration using clutter returns. / Prasanth R.K., Titi G.W. // 2010 IEEE Radar Conference. - Washington, DC, 10-14 May 2010. - P. 1071-1078. ↑
- C1025.** Fuhrmann D.R. Advanced signaling strategies for the Hybrid MIMO Phased-Array Radar. / Fuhrmann D.R., Browning J.P., Rangaswamy M. // 2010 IEEE Radar Conference. - Washington, DC, 10-14 May 2010. - P. 1128-1133. ↑
- C1026.** Saville M.A. Processing-based tuner gain correction in a wideband multi-channel receiver. / Saville M.A., Monroe K., Allen C., Martin R. // 2010 IEEE Radar Conference. - Washington, DC, 10-14 May 2010. - P. 1106-1110. ↑
- C1027.** Yang Yang. Distributed energy-efficient scheduling for radar signal detection in sensor networks. / Yang Yang, Blum R.S., Sadler B.M. // 2010 IEEE Radar Conference. - Washington, DC, 10-14 May 2010. - P. 1094-1099. ↑
- C1028.** Chen R.C. Range profile specific optimal waveforms for minimum mean square error estimation. 2010 IEEE Radar Conference. - Washington, DC, 10-14 May 2010. - P. 1042-1047. ↑
- C1029.** Geroleo F.G. Detection and estimation of multi-pulse LFM CW radar signals. / Geroleo F.G., Brandt-Pearce M. // 2010 IEEE Radar Conference. - Washington, DC, 10-14 May 2010. - P. 1009-1013. ↑
- C1030.** Kohlleppe R. Detection in heterogeneous clutter by filter output prediction. 2010 IEEE Radar

Conference. - Washington, DC, 10-14 May 2010. - P. 1014-1018. ↑

C1031. Wilcox D. Resolution of two point targets using sub-arrayed MIMO radar. / Wilcox D., Sellathurai M. // 2010 IEEE Radar Conference. - Washington, DC, 10-14 May 2010. - P. 999-1004. ↑

C1032. Kozma R. Multi-modal sensor system integrating COTS technology for surveillance and tracking. / Kozma R., Lan Wang, Iftikharuddin K., McCracken E., Khan M., Islam K., Demirel R.M. // 2010 IEEE Radar Conference. - Washington, DC, 10-14 May 2010. - P. 1030-1035. ↑

C1033. Linnehan R. Validating multipath responses of moving targets through urban environments. / Linnehan R., Schindler J. // 2010 IEEE Radar Conference. - Washington, DC, 10-14 May 2010. - P. 1036-1041. ↑

C1034. Nelander A. Switched array concepts for 3-D radar imaging. 2010 IEEE Radar Conference. - Washington, DC, 10-14 May 2010. - P. 1019-1024. ↑

C1035. Tsai P.-H.E. Null placement in a circular antenna array for Passive Coherent Location systems. / Tsai P.-H.E., Ebrahim K., Lange G., Paichard Y., Inggs M. // 2010 IEEE Radar Conference. - Washington, DC, 10-14 May 2010. - P. 1140-1143. ↑

C1036. Xin Li. Real-time tracking of bullet trajectory based on chirp transform in a multi-sensor multi-frequency radar. / Xin Li, Zhang Y.D., Amin M.G. // 2010 IEEE Radar Conference. - Washington, DC, 10-14 May 2010. - P. 1203-1207. ↑

C1037. Khomchuk P. Dynamic direction-of-arrival estimation via spatial compressive sensing. / Khomchuk P., Bilik I. // 2010 IEEE Radar Conference. - Washington, DC, 10-14 May 2010. - P. 1191-1196. ↑

C1038. An Daoxiang. A modified range migration algorithm for airborne squint-mode spotlight SAR imaging. / An Daoxiang, Huang Xiaotao, Jin Tian, Zhou Zhimin. // 2010 IEEE Radar Conference. - Washington, DC, 10-14 May 2010. - P. 1183-1186. ↑

C1039. Cho J.Y.N. Terminal Doppler Weather Radar enhancements. / Cho J.Y.N., Weber M.E. // 2010 IEEE Radar Conference. - Washington, DC, 10-14 May 2010. - P. 1245-1249. ↑

C1040. Turner E.L. Firm track loss due to M of N track initiation of a radially inbound target. 2010 IEEE Radar Conference. - Washington, DC, 10-14 May 2010. - P. 1250-1254. ↑

C1041. D'Urso M. Moving targets tracking for homeland protection applications: A multi-sensor approach. / D'Urso M., Buonanno A., Prisco G., Farina A. // 2010 IEEE Radar Conference. - Washington, DC, 10-14 May 2010. - P. 1220-1223. ↑

C1042. Paichard Y. OFDM waveforms for multistatic radars. 2010 IEEE Radar Conference. - Washington, DC, 10-14 May 2010. - P. 1187-1190. ↑

C1043. Ngwar M. Phase-coded-linear-frequency-modulated waveform for low cost marine radar system. / Ngwar M., Wight J. // 2010 IEEE Radar Conference. - Washington, DC, 10-14 May 2010. - P. 1144-1149. ↑

C1044. Rasool S.B. Efficient pulse-Doppler processing and ambiguity functions of nonuniform coherent pulse trains. / Rasool S.B., Bell M.R. // 2010 IEEE Radar Conference. - Washington, DC, 10-14 May 2010. - P. 1150-1155. ↑

C1045. Fuhrmann D.R. Detection of complex point targets in a MIMO radar system with distributed assets and partially correlated signals. / Fuhrmann D.R., VanderLaan J. // 2010 IEEE Radar Conference. - Washington, DC, 10-14 May 2010. - P. 1134-1139. ↑

C1046. Brown E.R. Radacoustic detection of projectiles by a retrodirective radar. / Brown E.R., Brown E.B. // 2010 IEEE Radar Conference. - Washington, DC, 10-14 May 2010. - P. 1180-1182. ↑

C1047. Soyeon Ahn. Low angle tracking using iterative multipath cancellation in sea surface environment. / Soyeon Ahn, Eunjung Yang, Joohwan Chun, Jungtae Kim. // 2010 IEEE Radar Conference. - Washington, DC, 10-14 May 2010. - P. 1156-1160. ↑

C1048. Brady S.H.R. Scaling radar measurements for advanced algorithms. / Brady S.H.R., Saville M.A. // ↑

2010 IEEE Radar Conference. - Washington, DC, 10-14 May 2010. - P. 1161-1166. ■

**C1049.** Lei Wang. Feature extraction and optimization of representative-slice in ambiguity function for moving radar emitter recognition. / Lei Wang, Hongbing Ji, Ya Shi. // 2010 IEEE International Conference on Acoustics Speech and Signal Processing (ICASSP). - Dallas, TX, 14-19 March 2010. - P. 2246-2249. ↑

**C1050.** Kay S. Exponentially embedded families for multimodal sensor processing. / Kay S., Quan Ding. // 2010 IEEE International Conference on Acoustics Speech and Signal Processing (ICASSP). - Dallas, TX, 14-19 March 2010. - P. 3770-3773. ↑

**C1051.** Wagner K.T. Proportionate-type NLMS algorithms based on maximization of the joint conditional PDF for the weight deviation vector. / Wagner K.T., Doroslovac, ki M.I. // 2010 IEEE International Conference on Acoustics Speech and Signal Processing (ICASSP). - Dallas, TX, 14-19 March 2010. - P. 3738-3741. ↑

**C1052.** Chakraborty B. Multipath exploitation with adaptive waveform design for tracking in urban terrain. / Chakraborty B., Li Y., Zhang J.J., Trueblood T., Papandreou-Suppappola A., Morrell D. // 2010 IEEE International Conference on Acoustics Speech and Signal Processing (ICASSP). - Dallas, TX, 14-19 March 2010. - P. 3894-3897. ↑

**C1053.** Trump T. A robust detector for uniformly distributed noise. 2010 IEEE International Conference on Acoustics Speech and Signal Processing (ICASSP). - Dallas, TX, 14-19 March 2010. - P. 3870-3873. ↑

**C1054.** Delmas J.-P. Performance analysis of the GLRT-based array receivers for the detection of a known signal corrupted by noncircular interference. / Delmas J.-P., Oukaci A., Chevalier P. // 2010 IEEE International Conference on Acoustics Speech and Signal Processing (ICASSP). - Dallas, TX, 14-19 March 2010. - P. 3878-3881. ↑

**C1055.** El Korso M.N. Statistical Resolution Limit for multiple parameters of interest and for multiple signals. / El Korso M.N., Boyer R., Renaux A., Marcos S. // 2010 IEEE International Conference on Acoustics Speech and Signal Processing (ICASSP). - Dallas, TX, 14-19 March 2010. - P. 3602-3605. ↑

**C1056.** Dog. A closed-form pseudolinear estimator for geolocation of scanning emitters. / Dog, anca y K. // 2010 IEEE International Conference on Acoustics Speech and Signal Processing (ICASSP). - Dallas, TX, 14-19 March 2010. - P. 3546-3549. ↑

**C1057.** Weile Zhang. Distributed TDoA estimation for wireless sensor networks. / Weile Zhang, Qinye Yin, Wenjie Wang. // 2010 IEEE International Conference on Acoustics Speech and Signal Processing (ICASSP). - Dallas, TX, 14-19 March 2010. - P. 2862-2865. ↑

**C1058.** Nguyen L.H. A sparsity-driven joint image registration and change detection technique for SAR imagery. / Nguyen L.H., Tran T.D. // 2010 IEEE International Conference on Acoustics Speech and Signal Processing (ICASSP). - Dallas, TX, 14-19 March 2010. - P. 2798-2801. ↑

**C1059.** Yuanwei Jin. Single antenna time reversal detection of moving target. / Yuanwei Jin, Moura J.M.F., O'Donoghue N., Harley J. // 2010 IEEE International Conference on Acoustics Speech and Signal Processing (ICASSP). - Dallas, TX, 14-19 March 2010. - P. 3558-3561. ↑

**C1060.** Debes C. Feature extraction in Through-the-Wall radar imaging. / Debes C., Hahn J., Zoubir A.M., Amin M.G. // 2010 IEEE International Conference on Acoustics Speech and Signal Processing (ICASSP). - Dallas, TX, 14-19 March 2010. - P. 3562-3565. ↑

**C1061.** Debes C. Distributed target detection in Through-the-Wall Radar Imaging using the bootstrap. / Debes C., Weiss C., Zoubir A.M., Amin M.G. // 2010 IEEE International Conference on Acoustics Speech and Signal Processing (ICASSP). - Dallas, TX, 14-19 March 2010. - P. 3530-3533. ↑

**C1062.** Zhang J.J. Multi-target tracking using multi-modal sensing with waveform configuration. / Zhang J.J., Papandreou-Suppappola A., Rangaswamy M. // 2010 IEEE International Conference on Acoustics Speech and Signal Processing (ICASSP). - Dallas, TX, 14-19 March 2010. - P. 3890-3893. ↑

**C1063.** Hyun Jeong Cho. Multichannel SAR Autofocus using multiple low-return constraints. / Hyun Jeong Cho, Munson D.C. // 2010 IEEE International Conference on Acoustics Speech and Signal Processing (ICASSP). - Dallas, TX, 14-19 March 2010. - P. 1346-1349. ↑

- C1064.** Chi-Li Yu. Bandwidth-intensive FPGA architecture for multi-dimensional DFT. / Chi-Li Yu, Chakrabarti C., Sungho Park, Narayanan V. // 2010 IEEE International Conference on Acoustics Speech and Signal Processing (ICASSP). - Dallas, TX, 14-19 March 2010. - P. 1486-1489. ↑
- C1065.** Shah S. Step-frequency radar with compressive sampling (SFR-CS). / Shah S., Yao Yu, Petropulu A. // 2010 IEEE International Conference on Acoustics Speech and Signal Processing (ICASSP). - Dallas, TX, 14-19 March 2010. - P. 1686-1689. ↑
- C1066.** Lei Shi. Radar HRRP statistical recognition with Local Factor Analysis by automatic Bayesian Ying Yang harmony learning. / Lei Shi, Penghui Wang, Hongwei Liu, Lei Xu, Zheng Bao. // 2010 IEEE International Conference on Acoustics Speech and Signal Processing (ICASSP). - Dallas, TX, 14-19 March 2010. - P. 1878-1881. ↑
- C1067.** Ojnhon N.O. Joint sparsity-driven inversion and model error correction for radar imaging. / Ojnhon N.O., C,etin M. // 2010 IEEE International Conference on Acoustics Speech and Signal Processing (ICASSP). - Dallas, TX, 14-19 March 2010. - P. 1206-1209. ↑
- C1068.** Kuang-Hung Liu. Synthetic Aperture Radar autofocus via Semidefinite Relaxation. / Kuang-Hung Liu, Wiesel A., Munson D.C. // 2010 IEEE International Conference on Acoustics Speech and Signal Processing (ICASSP). - Dallas, TX, 14-19 March 2010. - P. 1342-1345. ↑
- C1069.** Toth A.R. Synthesizing speech from Doppler signals. / Toth A.R., Kalgaonkar K., Raj B., Ezzat T. // 2010 IEEE International Conference on Acoustics Speech and Signal Processing (ICASSP). - Dallas, TX, 14-19 March 2010. - P. 4638-4641. ↑
- C1070.** Foroozan F. Cram r-Rao lower bound for time reversal range estimators in N-multipath scattering environments. / Foroozan F., Asif A. // 2010 IEEE International Conference on Acoustics Speech and Signal Processing (ICASSP). - Dallas, TX, 14-19 March 2010. - P. 3978-3981. ↑
- C1071.** Yuejie Chi. Sensitivity to basis mismatch in compressed sensing. / Yuejie Chi, Pezeshki A., Scharf L., Calderbank R. // 2010 IEEE International Conference on Acoustics Speech and Signal Processing (ICASSP). - Dallas, TX, 14-19 March 2010. - P. 3930-3933. ↑
- C1072.** Miller R. Physical Layer Techniques for Enhanced Situational Awareness. / Miller R., Trappe W. // 2010 IEEE International Conference on Acoustics Speech and Signal Processing (ICASSP). - Dallas, TX, 14-19 March 2010. - P. 2234-2237. ↑
- C1073.** Ghaderi F. Blind source extraction of cyclostationary sources with common cyclic frequencies. / Ghaderi F., Makkiabadi B., McWhirter J.G., Sanei S. // 2010 IEEE International Conference on Acoustics Speech and Signal Processing (ICASSP). - Dallas, TX, 14-19 March 2010. - P. 4146-4149. ↑
- C1074.** Ahmed S. Constant envelope waveform design for MIMO radar. / Ahmed S., Thompson J.S., Mulgrew B., Petillot Y. // 2010 IEEE International Conference on Acoustics Speech and Signal Processing (ICASSP). - Dallas, TX, 14-19 March 2010. - P. 4066-4069. ↑
- C1075.** Lei Xu. A ternary pulse compression code: Design and application to radar system. / Lei Xu, Qilian Liang, Ting Jiang. // 2010 IEEE International Conference on Acoustics Speech and Signal Processing (ICASSP). - Dallas, TX, 14-19 March 2010. - P. 4050-4053. ↑
- C1076.** Yeo-Sun Yoon. Through-the-Wall Radar Imaging using compressive sensing along temporal frequency domain. / Yeo-Sun Yoon, Amin M.G. // 2010 IEEE International Conference on Acoustics Speech and Signal Processing (ICASSP). - Dallas, TX, 14-19 March 2010. - P. 2806-2809. ↑
- C1077.** Akcakaya M. MIMO radar detection under phase synchronization errors. / Akcakaya M., Nehorai A. // 2010 IEEE International Conference on Acoustics Speech and Signal Processing (ICASSP). - Dallas, TX, 14-19 March 2010. - P. 2578-2581. ↑
- C1078.** Sen S. Slow-time multi-frequency radar for target detection in multipath scenarios. / Sen S., Nehorai A. // 2010 IEEE International Conference on Acoustics Speech and Signal Processing (ICASSP). - Dallas, TX, 14-19 March 2010. - P. 2582-2585. ↑
- C1079.** Ting-wen Xiong. Design and implementation of a passive UHF RFID-based Real Time Location



System. / Ting-wen Xiong, Jun-juan Liu, Yu-qing Yang, Xi Tan, Hao Min. // 2010 International Symposium on VLSI Design Automation and Test (VLSI-DAT). - Hsin Chu, 26-29 April 2010. - P. 95-98. ↑

**C1080.** Foroozan F. Cramér-Rao bound for time reversal active array direction of arrival estimators in multipath environments. / Foroozan F., Asif A. // 2010 IEEE International Conference on Acoustics Speech and Signal Processing (ICASSP). - Dallas, TX, 14-19 March 2010. - P. 2646-2649. ↑

**C1081.** Roemer F. Analytical performance assessment for multi-dimensional Tensor-ESPRIT-type parameter estimation algorithms. / Roemer F., Becker H., Haardt M. // 2010 IEEE International Conference on Acoustics Speech and Signal Processing (ICASSP). - Dallas, TX, 14-19 March 2010. - P. 2598-2601. ↑

**C1082.** Bandiera F. Knowledge-aided Bayesian covariance matrix estimation in compound-Gaussian clutter. / Bandiera F., Besson O., Ricci G. // 2010 IEEE International Conference on Acoustics Speech and Signal Processing (ICASSP). - Dallas, TX, 14-19 March 2010. - P. 2574-2577. ↑

**C1083.** Tao Jiang. Energy-efficient, decision feedback equalization Using SAR-like capacitive charge summation. / Tao Jiang, Chiang P. // 2010 International Symposium on VLSI Design Automation and Test (VLSI-DAT). - Hsin Chu, 26-29 April 2010. - P. 249-252. ↑

**C1084.** Yao XiaoFeng. Design of intelligent node based on distributed hybrid net control system. / Yao XiaoFeng, Xue Xu, Wu DeFeng. // 2010 2nd International Conference on Future Computer and Communication (ICFCC). - Wuhan, 21-24 May 2010. - Vol. 3. - P. V3-569-V3-572-569. ↑

**C1085.** Zhang Hua. Pulse radar altimeter terrain return model and its simulation. / Zhang Hua, Hu Xiulin. // 2010 2nd International Conference on Future Computer and Communication (ICFCC). - Wuhan, 21-24 May 2010. - Vol. 3. - P. V3-549-V3-552-549. ↑

**C1086.** Huixia Xue. ARM9-based real-time acquisition of orchard soil information and GPRS wireless transmission control system. / Huixia Xue, Lin Gao, Wenbin Li, Jun Liu, Junmei Zhang, Liu Yang. // 2010 2nd International Conference on Future Computer and Communication (ICFCC). - Wuhan, 21-24 May 2010. - Vol. 2. - P. V2-594-V2-598-594. ↑

**C1087.** Heping Zhong. A fast phase unwrapping algorithm based on minimum discontinuity by blocking. / Heping Zhong, Jinsong Tang, Dandan Liu. // 2010 2nd International Conference on Future Computer and Communication (ICFCC). - Wuhan, 21-24 May 2010. - Vol. 1. - P. V1-717-V1-721-717. ↑

**C1088.** Yuanlong Wang. An embedded wireless transmission system based on the extended user datagram protocol (EUDP). / Yuanlong Wang, Chengdong Wu, Xintong Zhang, Bingyang Li, Yunzhou Zhang. // 2010 2nd International Conference on Future Computer and Communication (ICFCC). - Wuhan, 21-24 May 2010. - Vol. 3. - P. V3-690-V3-693-690. ↑

**C1089.** Liu Dan Dan. The denoising method of SAR image based on Retinex. / Liu Dan Dan, Tang Chun Rui. // 2010 2nd International Conference on Future Computer and Communication (ICFCC). - Wuhan, 21-24 May 2010. - Vol. 3. - P. V3-625-V3-628-625. ↑

**C1090.** Bell K.L. MAP-PF wideband multitarget and colored noise tracking. / Bell K.L., Zarnich R.E., Wasyk R. // 2010 IEEE International Conference on Acoustics Speech and Signal Processing (ICASSP). - Dallas, TX, 14-19 March 2010. - P. 2710-2713. ↑

**C1091.** Elgamel S.A. A new Fractional Fourier Transform based monopulse tracking radar processor. / Elgamel S.A., Soraghan J. // 2010 IEEE International Conference on Acoustics Speech and Signal Processing (ICASSP). - Dallas, TX, 14-19 March 2010. - P. 2774-2777. ↑

**C1092.** Gujrbujz S.Z. Radar-based human detection via orthogonal matching pursuit. / Gujrbujz S.Z., Melvin W.L., Williams D.B. // 2010 IEEE International Conference on Acoustics Speech and Signal Processing (ICASSP). - Dallas, TX, 14-19 March 2010. - P. 2778-2781. ↑

**C1093.** Yu Zhou. Bayesian Rao and Wald test for radar adaptive detection. / Yu Zhou, Lin-rang Zhang. // 2010 IEEE International Conference on Acoustics Speech and Signal Processing (ICASSP). - Dallas, TX, 14-19 March 2010. - P. 2782-2785. ↑

**C1094.** Xiaowei Li. Multiple-frequency interferometric velocity SAR location and imaging of elevated moving

target. / Xiaowei Li, Xiang-Gen Xia. // 2010 IEEE International Conference on Acoustics Speech and Signal Processing (ICASSP). - Dallas, TX, 14-19 March 2010. - P. 2810-2813. ↑

**C1095.** Qureshi T.R. Target detection in MIMO radar in the presence of Doppler using complementary sequences. / Qureshi T.R., Zoltowski M.D., Calderbank R. // 2010 IEEE International Conference on Acoustics Speech and Signal Processing (ICASSP). - Dallas, TX, 14-19 March 2010. - P. 2766-2769. ↑

**C1096.** Wang Y.-C. Iterative design of MIMO radar transmit waveforms and receive filter bank. / Wang Y.-C., Hongwei Liu, Luo Z.-Q. // 2010 IEEE International Conference on Acoustics Speech and Signal Processing (ICASSP). - Dallas, TX, 14-19 March 2010. - P. 2770-2773. ↑

**C1097.** Chong C.Y. Robust MIMO radar detection for correlated subarrays. / Chong C.Y., Pascal F., Ovarlez J.-P., Lesturgie M. // 2010 IEEE International Conference on Acoustics Speech and Signal Processing (ICASSP). - Dallas, TX, 14-19 March 2010. - P. 2786-2789. ↑

**C1098.** Petitjean J. Fixed-point based autoregressive parameter estimation for space time adaptive processing. / Petitjean J., Grivel E., Roussilhe P. // 2010 IEEE International Conference on Acoustics Speech and Signal Processing (ICASSP). - Dallas, TX, 14-19 March 2010. - P. 2754-2757. ↑

**C1099.** Xiufeng Song. The role of the ambiguity function in compressed sensing radar. / Xiufeng Song, Shengli Zhou, Willett P. // 2010 IEEE International Conference on Acoustics Speech and Signal Processing (ICASSP). - Dallas, TX, 14-19 March 2010. - P. 2758-2761. ↑

**C1100.** Rui Fa. Knowledge-aided reduced-rank STAP for MIMO radar based on joint iterative constrained optimization of adaptive filters with multiple constraints. / Rui Fa, de Lamare R.C. // 2010 IEEE International Conference on Acoustics Speech and Signal Processing (ICASSP). - Dallas, TX, 14-19 March 2010. - P. 2762-2765. ↑

**C1101.** Rui Fa. Knowledge-aided STAP algorithm using convex combination of inverse covariance matrices for heterogenous clutter. / Rui Fa, de Lamare R.C., Nascimento V.H. // 2010 IEEE International Conference on Acoustics Speech and Signal Processing (ICASSP). - Dallas, TX, 14-19 March 2010. - P. 2742-2745. ↑

**C1102.** Ginolhac G. Performance analysis of a Robust Low-Rank STAP filter in low-rank Gaussian clutter. / Ginolhac G., Forster P. // 2010 IEEE International Conference on Acoustics Speech and Signal Processing (ICASSP). - Dallas, TX, 14-19 March 2010. - P. 2746-2749. ↑

**C1103.** Selesnick I.W. Angle-Doppler processing using sparse regularization. / Selesnick I.W., Pillai S.U., Ke Yong Li, Himed B. // 2010 IEEE International Conference on Acoustics Speech and Signal Processing (ICASSP). - Dallas, TX, 14-19 March 2010. - P. 2750-2753. ↑

**C1104.** Williams D.P. On sand ripple detection in synthetic aperture sonar imagery. / Williams D.P., Coiras E. // 2010 IEEE International Conference on Acoustics Speech and Signal Processing (ICASSP). - Dallas, TX, 14-19 March 2010. - P. 1074-1077. ↑

**C1105.** Khomchuk P. Compressive sensing-based SAR tomography. / Khomchuk P., Bilik I., Kasilingam D.P. // 2010 IEEE Radar Conference. - Washington, DC, 10-14 May 2010. - P. 354-358. ↑

**C1106.** Chernyak V.S. On the concept of MIMO radar. 2010 IEEE Radar Conference. - Washington, DC, 10-14 May 2010. - P. 327-332. ↑

**C1107.** Bjojrkklund S. Clutter properties for STAP with smooth and faceted cylindrical conformal antennas. / Bjojrkklund S., Boman T., Nelander A., Bjorklund S. // 2010 IEEE Radar Conference. - Washington, DC, 10-14 May 2010. - P. 315-320. ↑

**C1108.** Tilli E. On the use of HRR data to improve target kinematics estimation: CRLB computation and comparison with simulated results. / Tilli E., Ortenzi L., Prodi F. // 2010 IEEE Radar Conference. - Washington, DC, 10-14 May 2010. - P. 380-384. ↑

**C1109.** Wicks M.C. Adaptive polarization processing for improved detection/classification of stationary targets. / Wicks M.C., Yuhong Zhang, Schneible R., Bruder J. // 2010 IEEE Radar Conference. - Washington, DC, 10-14 May 2010. - P. 359-363. ↑

- C1110.** Guccione P. Optimal block quantization for SAR data. / Guccione P., Cafforio C., Guarnieri A.M. // 2010 IEEE Radar Conference. - Washington, DC, 10-14 May 2010. - P. 348-353. ↑
- C1111.** Higgins T. Space-Range Adaptive Processing for waveform-diverse radar imaging. / Higgins T., Blunt S.D., Shackelford A.K. // 2010 IEEE Radar Conference. - Washington, DC, 10-14 May 2010. - P. 321-326. ↑
- C1112.** Zaugg E. The SlimSAR: A small, multi-frequency, Synthetic Aperture Radar for UAS operation. / Zaugg E., Edwards M., Margulis A. // 2010 IEEE Radar Conference. - Washington, DC, 10-14 May 2010. - P. 277-282. ↑
- C1113.** Bradaric I. Multistatic measurements in a controlled laboratory environment. / Bradaric I., Capraro G.T., Brady S.H., Saville M.A., Wicks M.C. // 2010 IEEE Radar Conference. - Washington, DC, 10-14 May 2010. - P. 266-270. ↑
- C1114.** Jeffrey T.W. Use of reference architectures to achieve low-risk, affordable radar designs. 2010 IEEE Radar Conference. - Washington, DC, 10-14 May 2010. - P. 251-255. ↑
- C1115.** Taniza R. High density FPGA based waveform generation for radars. / Taniza R., Jadia K., Raju G.S.N., Chandramohan M. // 2010 IEEE Radar Conference. - Washington, DC, 10-14 May 2010. - P. 310-314. ↑
- C1116.** Hai Li. A robust estimation method to coregistration error for InSAR interferometric phase. / Hai Li, Renbiao Wu, Ping Han, Guisheng Liao. // 2010 IEEE Radar Conference. - Washington, DC, 10-14 May 2010. - P. 283-286. ↑
- C1117.** Rigling B.D. ACF-based classification of phase modulated waveforms. / Rigling B.D., Roush C. // 2010 IEEE Radar Conference. - Washington, DC, 10-14 May 2010. - P. 287-291. ↑
- C1118.** Fan Chongyi. Ambiguity function of SAR based on OFDM waveform. / Fan Chongyi, Huang Xiaotao, Jin Tian, Chang Wenge. // 2010 IEEE Radar Conference. - Washington, DC, 10-14 May 2010. - P. 397-401. ↑
- C1119.** Hussain M.G.M. Space-time array processing based on ultrawideband throb signal. / Hussain M.G.M., Kourah M.A.R. // 2010 IEEE Radar Conference. - Washington, DC, 10-14 May 2010. - P. 474-478. ↑
- C1120.** Nolan J.P. Stable filters: A robust signal processing framework for heavy-tailed noise. / Nolan J.P., Gonzalez J.G., Nuñez R.C. // 2010 IEEE Radar Conference. - Washington, DC, 10-14 May 2010. - P. 470-473. ↑
- C1121.** Majumder U. Spatially-varying calibration of along-track monopulse synthetic aperture radar imagery for ground moving target indication and tracking. / Majumder U., Soumekh M., Minardi M., Kirk J. // 2010 IEEE Radar Conference. - Washington, DC, 10-14 May 2010. - P. 452-457. ↑
- C1122.** Ioana C. Characterization of Doppler effects in the context of over-the-horizon radar. / Ioana C., Amin M.G., Zhang Y.D., Ahmad F. // 2010 IEEE Radar Conference. - Washington, DC, 10-14 May 2010. - P. 506-510. ↑
- C1123.** Ritchie M.A. Analysis of sea clutter distribution variation with Doppler using the compound k-distribution. / Ritchie M.A., Woodbridge K., Stove A.G. // 2010 IEEE Radar Conference. - Washington, DC, 10-14 May 2010. - P. 495-499. ↑
- C1124.** Ruggiano M. Experiments showing an improvement of angular resolution by LMMSE-based processing. / Ruggiano M., Stolp E., de Heij W., van Genderen P. // 2010 IEEE Radar Conference. - Washington, DC, 10-14 May 2010. - P. 500-505. ↑
- C1125.** Ahmed S. Fast computations of constant envelope waveforms for MIMO radar transmit beampattern. / Ahmed S., Thompson J.S., Mulgrew B., Petillot Y. // 2010 IEEE Radar Conference. - Washington, DC, 10-14 May 2010. - P. 458-463. ↑
- C1126.** Pierucci L. Detection of runway boundary in ATC ground radar. / Pierucci L., Bocchi L. // 2010 IEEE Radar Conference. - Washington, DC, 10-14 May 2010. - P. 418-421. ↑
- C1127.** Xiaolong Chen. A fast FRFT based detection algorithm of multiple moving targets in sea clutter. / Xiaolong Chen, Jian Guan. // 2010 IEEE Radar Conference. - Washington, DC, 10-14 May 2010. - P. 402-406. ↑


- C1128.** Gisseljajt M. STAP analysis using multi-channel airborne radar data from flight trials. / Gisseljajt M., Pernsta, I. T. // 2010 IEEE Radar Conference. - Washington, DC, 10-14 May 2010. - P. 407-411. ↑
- C1129.** Jia Xu. Signal modelling for ground moving target in complex image domain of multi-channel SAR. / Jia Xu, Yu Zuoi, Bing Xia, Xiang-Gen Xia, Ying-Ning Peng, Yong-Liang Wang. // 2010 IEEE Radar Conference. - Washington, DC, 10-14 May 2010. - P. 441-445. ↑
- C1130.** Carretero-Moya J. Scan rate selection for coherent high-resolution maritime surveillance radar: An experimental study. / Carretero-Moya J., Gismero-Menoyo J., Asensio-Lopez A., Blanco-del-Campo A. // 2010 IEEE Radar Conference. - Washington, DC, 10-14 May 2010. - P. 428-431. ↑
- C1131.** Pernsta. RELAX based estimation of signal and clutter echoes modeled as discrete point scatterers. / Pernsta, I. T., Jonsson R., Alenljung K. // 2010 IEEE Radar Conference. - Washington, DC, 10-14 May 2010. - P. 412-417. ↑
- C1132.** Braun M. Maximum likelihood speed and distance estimation for OFDM radar. / Braun M., Sturm C., Jondral F.K. // 2010 IEEE Radar Conference. - Washington, DC, 10-14 May 2010. - P. 256-261. ↑
- C1133.** Tahmoush D. Simplified model of dismount microDoppler and RCS. / Tahmoush D., Silvius J. // 2010 IEEE Radar Conference. - Washington, DC, 10-14 May 2010. - P. 31-34. ↑
- C1134.** Conning M. Analysis of measured radar data for Specific Emitter Identification. / Conning M., Potgieter F. // 2010 IEEE Radar Conference. - Washington, DC, 10-14 May 2010. - P. 35-38. ↑
- C1135.** Jun Li. Waveform decorrelation for multitarget localization in bistatic MIMO radar systems. / Jun Li, Guisheng Liao, Kejiang Ma, Cao Zeng. // 2010 IEEE Radar Conference. - Washington, DC, 10-14 May 2010. - P. 21-24. ↑
- C1136.** Sturm C. Performance verification of symbol-based OFDM radar processing. / Sturm C., Zwick T., Wiesbeck W., Braun M. // 2010 IEEE Radar Conference. - Washington, DC, 10-14 May 2010. - P. 60-63. ↑
- C1137.** Lam E.P. Performance prediction of Firefinder radar using high fidelity simulation. / Lam E.P., Birrell H.W., Magallon J. // 2010 IEEE Radar Conference. - Washington, DC, 10-14 May 2010. - P. 48-53. ↑
- C1138.** Martone A. Automatic through the wall detection of moving targets using low-frequency ultra-wideband radar. / Martone A., Ranney K., Innocenti R. // 2010 IEEE Radar Conference. - Washington, DC, 10-14 May 2010. - P. 39-43. ↑
- C1139.** Huang Yong. A track-before-detect algorithm for statistical MIMO radar multitarget detection. / Huang Yong, Guan Jian. // 2010 IEEE Radar Conference. - Washington, DC, 10-14 May 2010. - P. 12-16. ↑
- C1140.** Josso N.F. Time-varying wideband underwater acoustic channel estimation for OFDM communications. / Josso N.F., Zhang J.J., Fertonani D., Papandreou-Suppappola A., Duman T.M. // 2010 IEEE International Conference on Acoustics Speech and Signal Processing (ICASSP). - Dallas, TX, 14-19 March 2010. - P. 5626-5629. ↑
- C1141.** Shikui Tu. A study of several model selection criteria for determining the number of signals. / Shikui Tu, Lei Xu. // 2010 IEEE International Conference on Acoustics Speech and Signal Processing (ICASSP). - Dallas, TX, 14-19 March 2010. - P. 1966-1969. ↑
- C1142.** Celik T. Resolution selective change detection in satellite images. / Celik T., Curtis C.V. // 2010 IEEE International Conference on Acoustics Speech and Signal Processing (ICASSP). - Dallas, TX, 14-19 March 2010. - P. 970-973. ↑
- C1143.** Dai Huanyao. A new far field measurement method for antenna polarization characteristics based on calibrator target. / Dai Huanyao, Liu Yong, Li Yongzhen, Wang Xuesong, Chang Yuliang. // 2010 IEEE Radar Conference. - Washington, DC, 10-14 May 2010. - P. 17-20. ↑
- C1144.** Abramovich Y.I. Markov model for convergence analysis of the adaptive Kronecker MIMO OTH radar beamformer. / Abramovich Y.I., Frazer G.J., Johnson B.A. // 2010 IEEE Radar Conference. - Washington, DC, 10-14 May 2010. - P. 1-5. ↑





- C1145.** {no data available}. Gala Dinner/Banquet Speaker. 2010 IEEE Radar Conference. - Arlington, VA, USA, 10-14 May 2010. - P. 1. ↑
- C1146.** Goldman G.H. Computationally efficient resampling of nonuniform oversampled SAR data. 2010 IEEE Radar Conference. - Washington, DC, 10-14 May 2010. - P. 70-74. ↑
- C1147.** Berizzi F. USRP technology for multiband passive radar. / Berizzi F., Martorella M., Petri D., Conti M., Capria A. // 2010 IEEE Radar Conference. - Washington, DC, 10-14 May 2010. - P. 225-229. ↑
- C1148.** Selesnick I.W. An iterative algorithm for the construction of notched chirp signals. / Selesnick I.W., Unnikrishna Pillai S., Richeng Zheng. // 2010 IEEE Radar Conference. - Washington, DC, 10-14 May 2010. - P. 200-203. ↑
- C1149.** Levanon N. The periodic ambiguity function-Its validity and value. 2010 IEEE Radar Conference. - Washington, DC, 10-14 May 2010. - P. 204-208. ↑
- C1150.** Radmard M. Cross ambiguity function analysis of the '8k-mode' DVB-T for passive radar application. / Radmard M., Behnia F., Bastani M. // 2010 IEEE Radar Conference. - Washington, DC, 10-14 May 2010. - P. 242-246. ↑
- C1151.** Elgamel S.A. Enhanced monopulse radar tracking using filtering in fractional Fourier domain. / Elgamel S.A., Soraghan J.J. // 2010 IEEE Radar Conference. - Washington, DC, 10-14 May 2010. - P. 247-250. ↑
- C1152.** Jaming P. The phase retrieval problem for the Radar Ambiguity Function and vice versa. 2010 IEEE Radar Conference. - Washington, DC, 10-14 May 2010. - P. 230-235. ↑
- C1153.** Chetty K. Passive bistatic WiMAX radar for marine surveillance. / Chetty K., Woodbridge K., Hui Guo, Smith G.E. // 2010 IEEE Radar Conference. - Washington, DC, 10-14 May 2010. - P. 188-193. ↑
- C1154.** Foreman T.L. Application of the CLEAN Detector to low signal to noise ratio targets. 2010 IEEE Radar Conference. - Washington, DC, 10-14 May 2010. - P. 150-155. ↑
- C1155.** Yeary M. Phased array weather / multipurpose radar. / Yeary M., Crain G., Zahrai A., Kelley R., Meier J., Zhang Y., Ivic I., Curtis C., Palmer R., Yu T.-Y., Doviak R. // 2010 IEEE Radar Conference. - Washington, DC, 10-14 May 2010. - P. 140-143. ↑
- C1156.** Pahlevaninezhad H. Modeling terahertz heterodyne detection based on photomixing. / Pahlevaninezhad H., Heshmat B., Darcie T.E. // 2010 IEEE Radar Conference. - Washington, DC, 10-14 May 2010. - P. 113-116. ↑
- C1157.** Cao T.-T.V. False alarm control of CFAR algorithms with experimental bistatic radar data. / Cao T.-T.V., Palmer J., Berry P.E. // 2010 IEEE Radar Conference. - Washington, DC, 10-14 May 2010. - P. 156-161. ↑
- C1158.** Kastle M.J. Establishing a common phase reference for comparing synthetic data to RF range measurements. / Kastle M.J., Malas J.A. // 2010 IEEE Radar Conference. - Washington, DC, 10-14 May 2010. - P. 162-167. ↑
- C1159.** Malas J.A. The radar information channel and system uncertainty. / Malas J.A., Cortese J.A. // 2010 IEEE Radar Conference. - Washington, DC, 10-14 May 2010. - P. 144-149. ↑
- C1160.** Zeng Jiankui. A novel signal processing method for MIMO radar based on channel estimation. / Zeng Jiankui, Xiang Lijuan, Dong Ziming, Yuan Shangzhun. // 2010 The 2nd International Conference on Computer and Automation Engineering (ICCAE). - Singapore, 26-28 Feb. 2010. - Vol. 3. - P. 413-415. ↑
- C1161.** Subashini P. Coupling optimal method of segmentation with restoration for target detection in SAR images. / Subashini P., Krishnaveni M., Thakur S.K. // 2010 The 2nd International Conference on Computer and Automation Engineering (ICCAE). - Singapore, 26-28 Feb. 2010. - Vol. 2. - P. 761-764. ↑
- C1162.** Wen YiHong. A complex SAR image compression algorithm combining set-partitioning and context prediction. / Wen YiHong, Li Bo, Yang Kai. // 2010 The 2nd International Conference on Computer and Automation Engineering (ICCAE). - Singapore, 26-28 Feb. 2010. - Vol. 3. - P. 173-176. ↑


- C1163.** Keim J.A. Field test implementation to evaluate a flash LIDAR as a primary sensor for safe lunar landing. / Keim J.A., Mobasser S., Da Kuang, Yang Cheng, Ivanov T., Johnson A.E., Goldberg H.R., Khanoyan G., Natzic D.B. // 2010 IEEE Aerospace Conference. - Big Sky, MT, 6-13 March 2010. - P. 1-14. ↑
- C1164.** Johnson A.E. Analysis of flash lidar field test data for safe lunar landing. / Johnson A.E., Keim J.A., Ivanov T. // 2010 IEEE Aerospace Conference. - Big Sky, MT, 6-13 March 2010. - P. 1-11. ↑
- C1165.** Xie Yi. Design and Realization of an Online Power Quality Monitoring System Based on GPRS. / Xie Yi, Ouyang Sen, Chengjun Xia. // 2010 Asia-Pacific Power and Energy Engineering Conference (APPEEC). - Chengdu, 28-31 March 2010. - P. 1-4. ↑
- C1166.** Jenkins R.L. Wavelet analysis of impulse ultra-wideband radar. / Jenkins R.L., Dewberry B., Joiner L. // Proceedings of the IEEE SoutheastCon 2010 (SoutheastCon). - Concord, NC, 18-21 March 2010. - P. 155-158. ↑
- C1167.** Jiao Xin Quan. Radar signal processing based on DCT compression. / Jiao Xin Quan, Yu Jun, Wang Ge, Zhao Xin. // 2010 2nd International Asia Conference on Informatics in Control, Automation and Robotics (CAR). - Wuhan, 6-7 March 2010. - Vol. 3. - P. 270-273. ↑
- C1168.** Chen Xiaoli. TWR signals de-noising by using WNN. / Chen Xiaoli, Tian Mao, Guo Jing. // 2010 2nd International Asia Conference on Informatics in Control, Automation and Robotics (CAR). - Wuhan, 6-7 March 2010. - Vol. 1. - P. 280-283. ↑
- C1169.** Marcus M.J. Cognitive Radio under Conservative Regulatory Environments: Lessons Learned and near Term Options. 2010 IEEE Symposium on New Frontiers in Dynamic Spectrum. - Singapore, 6-9 April 2010. - P. 1-5. ↑
- C1170.** Negro F. On the MIMO interference channel. / Negro F., Shenoy S.P., Ghauri I., Slock D.T.M. // 2010 Information Theory and Applications Workshop (ITA). - San Diego, CA, Jan. 31 2010-Feb. 5 2010. - P. 1-9. ↑
- C1171.** Oispuu M. 3D passive source localization by a multi-array network: Noncoherent vs. coherent processing. / Oispuu M., Nickel U. // 2010 International ITG Workshop on Smart Antennas (WSA). - Bremen, 23-24 Feb. 2010. - P. 300-305. ↑
- C1172.** Lange O. Array geometry optimization for direction-of-arrival estimation including subarrays and tapering. / Lange O., Bin Yang. // 2010 International ITG Workshop on Smart Antennas (WSA). - Bremen, 23-24 Feb. 2010. - P. 135-142. ↑
- C1173.** Villalpando C.Y. Investigation of the Tiler processor for real time hazard detection and avoidance on the Altair Lunar Lander. / Villalpando C.Y., Johnson A.E., Some R., Oberlin J., Goldberg S. // 2010 IEEE Aerospace Conference. - Big Sky, MT, 6-13 March 2010. - P. 1-9. ↑
- C1174.** Ruel S. STS-128 on-orbit demonstration of the TriDAR targetless rendezvous and docking sensor. / Ruel S., Luu T. // 2010 IEEE Aerospace Conference. - Big Sky, MT, 6-13 March 2010. - P. 1-7. ↑
- C1175.** Eremenko A. SMAP Observatory configuration, from concept to preliminary design. / Eremenko A., Kastner J., Hoffman P. // 2010 IEEE Aerospace Conference. - Big Sky, MT, 6-13 March 2010. - P. 1-11. ↑
- C1176.** Seungwon Lee. Statistical analysis of CloudSat data for climate model parameterization. / Seungwon Lee, Kahn B.H., Teixeira J. // 2010 IEEE Aerospace Conference. - Big Sky, MT, 6-13 March 2010. - P. 1-10. ↑
- C1177.** Cristallini D. Space-based passive radar enabled by the new generation of geostationary broadcast satellites. / Cristallini D., Caruso M., Falcone P., Langellotti D., Bongioanni C., Colone F., Scafe S., Lombardo P. // 2010 IEEE Aerospace Conference. - Big Sky, MT, 6-13 March 2010. - P. 1-11. ↑
- C1178.** Ogle W.C. New detection manifolds for radar signal processing. / Ogle W.C., Goldstein J.S., Mendelson H. // 2010 IEEE Aerospace Conference. - Big Sky, MT, 6-13 March 2010. - P. 1-7. ↑
- C1179.** Vines K. Autonomous deployment of the UAVSAR radar instrument. / Vines K., Chao R. // 2010 IEEE Aerospace Conference. - Big Sky, MT, 6-13 March 2010. - P. 1-8. ↑
- C1180.** Bennett C. Improving situational awareness training for Patriot radar operators. / Bennett C., Anderson G., Brady J. // 2010 IEEE Aerospace Conference. - Big Sky, MT, 6-13 March 2010. - P. 1-7. ↑


- C1181.** Stallo C. On the use of UWB Radio Interface for EHF satellite communications. / Stallo C., Mukherjee S., Cianca E., Rossi T., De Sanctis M., Ruggieri M. // 2010 IEEE Aerospace Conference. - Big Sky, MT, 6-13 March 2010. - P. 1-11. ↑
- C1182.** Duncan C.B. LMRST-Sat: A small, high value-to-cost mission. / Duncan C.B., Dennis M.S., Kalman A.E., Stein K.A., Tesfaye Y., Lin B.I.-M., Truong-Cao E., Foster C. // 2010 IEEE Aerospace Conference. - Big Sky, MT, 6-13 March 2010. - P. 1-8. ↑
- C1183.** Huertas A. Performance evaluation of hazard detection and avoidance algorithms for safe Lunar landings. / Huertas A., Johnson A.E., Werner R.A., Maddock R.A. // 2010 IEEE Aerospace Conference. - Big Sky, MT, 6-13 March 2010. - P. 1-20. ↑
- C1184.** Saha S. Distributed prognostic health management with gaussian process regression. / Saha S., Saha B., Saxena A., Goebel K. // 2010 IEEE Aerospace Conference. - Big Sky, MT, 6-13 March 2010. - P. 1-8. ↑
- C1185.** Shu Ting Goh. Differential Geometric Estimation for spacecraft formations orbits via a cooperative wireless positioning. / Shu Ting Goh, Abdelkhalik O., Zekavat S.A. // 2010 IEEE Aerospace Conference. - Big Sky, MT, 6-13 March 2010. - P. 1-11. ↑
- C1186.** Sgubini S. Ground-based orbit determination for spacecraft formations. / Sgubini S., Palmerini G.B. // 2010 IEEE Aerospace Conference. - Big Sky, MT, 6-13 March 2010. - P. 1-7. ↑
- C1187.** Wang Yong. Automatic Measurement of Radar Receiver Sensitivity. / Wang Yong, Shao Xiaofang, Ye Lingwei. // 2010 International Conference on Measuring Technology and Mechatronics Automation (ICMTMA). - Changsha City, 13-14 March 2010. - Vol. 1. - P. 719-720. ↑
- C1188.** Jin Hui-long. The Research of Families of Odd-periodic Perfect Complementary Sequence Pairs. / Jin Hui-long, Liang Guo-dong, Xu Cheng-qian, Zhang Jin-bo. // 2010 Second International Workshop on Education Technology and Computer Science (ETCS). - Wuhan, 6-7 March 2010. - Vol. 2. - P. 315-318. ↑
- C1189.** Wu Jianyu. Design of Wireless Dam Security Information System. / Wu Jianyu, Zhang Yuntao, Liang Xi. // 2010 International Conference on Measuring Technology and Mechatronics Automation (ICMTMA). - Changsha City, 13-14 March 2010. - Vol. 1. - P. 1072-1076. ↑
- C1190.** Lou Yang. The Angle-Measuring Algorithm for the Stepped-frequency Radar Based on Dual-line Digital Phase Interferometer. / Lou Yang, Gao Meiguo, Liu Guoman, Qin Guojie. // 2010 Second International Workshop on Education Technology and Computer Science (ETCS). - Wuhan, 6-7 March 2010. - Vol. 3. - P. 23-26. ↑
- C1191.** Shang Bin. PMHT with Application of Road Information Based on GMTI. / Shang Bin, Sun Jinping, Li Shaohong. // 2010 International Conference on Measuring Technology and Mechatronics Automation (ICMTMA). - Changsha City, 13-14 March 2010. - Vol. 2. - P. 903-906. ↑
- C1192.** Middleton S. A Wideband Beamformer Extended to MIMO Radar. / Middleton S., van Wyk A., Jardin P., Nadal F., Cilliers J. // 2010 International Conference on Measuring Technology and Mechatronics Automation (ICMTMA). - Changsha City, 13-14 March 2010. - Vol. 1. - P. 381-385. ↑
- C1193.** Wang Xiao-yi. An Intelligent System on Water Quality Remote Monitor and Water Bloom Prediction. / Wang Xiao-yi, Xu Ji-ping, Liu Zai-wen, Dai Jun, Zhu Shi-ping. // 2010 International Conference on Measuring Technology and Mechatronics Automation (ICMTMA). - Changsha City, 13-14 March 2010. - Vol. 1. - P. 521-524. ↑
- C1194.** Xie Guang-jun. Fault Diagnosis Platform For Radar Circuit Based on Virtual Instrument. / Xie Guang-jun, Yan Shi-qiang, Tang Zi-yue, Rui Li. // 2010 International Conference on Measuring Technology and Mechatronics Automation (ICMTMA). - Changsha City, 13-14 March 2010. - Vol. 2. - P. 245-248. ↑
- C1195.** Lina Fan. Time resources allocation in cognitive radar system. / Lina Fan, Jinkuan Wang, Bin Wang, Dongmei Shu. // 2010 International Conference on Networking, Sensing and Control (ICNSC). - Chicago, IL, 10-12 April 2010. - P. 727-730. ↑
- C1196.** Xiaogang Yu. Noise analysis for noncontact vital sign detectors. / Xiaogang Yu, Changzhi Li, Jianshan Lin. // 2010 IEEE 11th Annual Wireless and Microwave Technology Conference (WAMICON). - Melbourne, FL, ↑


12-13 April 2010. - P. 1-4. 


**C1197.** ZhiHong Tian. Research on Physiological Parameters Monitor Based on Multi-Functional Device. / ZhiHong Tian, FengZhi Qiu. // 2010 International Conference on Biomedical Engineering and Computer Science (ICBECS). - Wuhan, 23-25 April 2010. - P. 1-4. 


**C1198.** Chang-jiang Dou. A New Three-satellite High-precision RDSS/RNSS Combination Positioning Method. / Chang-jiang Dou, Bin-qi Zhang, Shu-sen Tan, Teng Long. // 2010 Second International Workshop on Education Technology and Computer Science (ETCS). - Wuhan, 6-7 March 2010. - Vol. 2. - P. 288-290. 


**C1199.** Bin Wang. Stochastic dynamic programming model of adaptive waveform selection. / Bin Wang, Jinkuan Wang, Xin Song, Ling Cai. // 2010 International Conference on Networking, Sensing and Control (ICNSC). - Chicago, IL, 10-12 April 2010. - P. 267-272. 


**C1200.** Lichuan Liu. FM jammer excision by using time-varying AR filter in spread spectrum communication systems. 2010 International Conference on Networking, Sensing and Control (ICNSC). - Chicago, IL, 10-12 April 2010. - P. 117-121. 


**C1201.** Zhao Tongzhou. Image Fusion Based on Multi-scale Kalman Filtering. / Zhao Tongzhou, Wang Yanli, Wang Haihui. // 2010 Second International Workshop on Education Technology and Computer Science (ETCS). - Wuhan, 6-7 March 2010. - Vol. 3. - P. 207-215. 


**C1202.** Qian Hong-bo. The Applications and Methods of Pedestrian Automated Detection. / Qian Hong-bo, Han Hao. // 2010 International Conference on Measuring Technology and Mechatronics Automation (ICMTMA). - Changsha City, 13-14 March 2010. - Vol. 3. - P. 806-809. 


**C1203.** Dayong Zhang. Calibration Technology of Palmer Scanning Airborne Lidar with Vector Measurements. / Dayong Zhang, Wenqi Wu, Liangqing Lu, Meiping Wu. // 2010 International Conference on Measuring Technology and Mechatronics Automation (ICMTMA). - Changsha City, 13-14 March 2010. - Vol. 1. - P. 775-778. 


**C1204.** Lu Xiaodong. Synthetic Aperture Radar Image Segmentation Based on Markov Random Field with Niche Genetic Algorithm. / Lu Xiaodong, Zhou Jun, He Yuanjun. // 2010 International Conference on Measuring Technology and Mechatronics Automation (ICMTMA). - Changsha City, 13-14 March 2010. - Vol. 3. - P. 718-721. 


**C1205.** Fang Lili. A Modified SPECAN Algorithm for Synthetic Aperture Radar Imaging. / Fang Lili, Wang Xuetian, Wang Yifeng. // 2010 International Conference on Measuring Technology and Mechatronics Automation (ICMTMA). - Changsha City, 13-14 March 2010. - Vol. 1. - P. 153-156. 

**C1206.** Wu Xiao-chao. Application of Butterworth Filter in Display of Radar Target Track. / Wu Xiao-chao, Wang Guo-liang, Fang Li-xin, Yan Liao-liao. // 2010 International Conference on Measuring Technology and Mechatronics Automation (ICMTMA). - Changsha City, 13-14 March 2010. - Vol. 1. - P. 605-607. 

**C1207.** Jiang Jian-ming. The Application of Long-Distance Inspecting Electric Power Parameter Based on GPRS Communications. 2010 International Conference on Measuring Technology and Mechatronics Automation (ICMTMA). - Changsha City, 13-14 March 2010. - Vol. 3. - P. 779-781. 

**C1208.** Huahua Chen. 3D Reconstruction for Robot Navigation Based on Projection of Virtual Height Line and its Performance Evaluation. / Huahua Chen, Yifei Jiang, Jianwu Zhang. // 2010 International Conference on Measuring Technology and Mechatronics Automation (ICMTMA). - Changsha City, 13-14 March 2010. - Vol. 1. - P. 3-6. 

**C1209.** Jin Li. New Technology and Applications on Millimeter-Wave Sensors. / Jin Li, Zhang Ning, Zhao Qingling. // 2010 International Conference on Measuring Technology and Mechatronics Automation (ICMTMA). - Changsha City, 13-14 March 2010. - Vol. 2. - P. 764-767. 

**C1210.** Wei-hua Ai. Ground Clutter Removing for Wind Profiler Radar Signal Using Adaptive Wavelet Threshold. / Wei-hua Ai, Yun-xian Huang, Ming-bao Hu, Chao-ling Shen. // 2010 International Conference on Measuring Technology and Mechatronics Automation (ICMTMA). - Changsha City, 13-14 March 2010. - Vol. 2. - P. 370-373. 





- C1211.** Wang Haihui. Automated Detection in SAR Images by Using Wavelet Filtering and Hough Transform. / Wang Haihui, Wang Yanli, Zhao Tongzhou. // 2010 Second International Workshop on Education Technology and Computer Science (ETCS). - Wuhan, 6-7 March 2010. - Vol. 3. - P. 202-206. ↑
- C1212.** Fei Wang. Scattering Centers Extraction of Radar Target Using Biquaternions. / Fei Wang, Qi Ge, Jianjiang Zhou, Huawei Chen. // 2010 International Conference on Measuring Technology and Mechatronics Automation (ICMTMA). - Changsha City, 13-14 March 2010. - Vol. 3. - P. 307-310. ↑
- C1213.** Hao Ai-hong. Design of Solar Photovoltaic Remote Data Transmission System Based on GPRS. / Hao Ai-hong, Zhang Xiao-li, Xuwei, Lian Xiao-qin. // 2010 International Conference on Measuring Technology and Mechatronics Automation (ICMTMA). - Changsha City, 13-14 March 2010. - Vol. 1. - P. 1038-1042. ↑
- C1214.** Zou Ai-min. Nanosecond Pulser Based on Serial Connection of Avalanche Transistors. / Zou Ai-min, Wang Hui-bo, Wang Yan-zhang, Cheng De-fu. // 2010 International Conference on Measuring Technology and Mechatronics Automation (ICMTMA). - Changsha City, 13-14 March 2010. - Vol. 2. - P. 752-755. ↑
- C1215.** Reinartz P. Improving geometric accuracy of optical VHR satellite data using Terrasar-X data. / Reinartz P., Muller R., Suri S., Schwind P. // 2010 IEEE Aerospace Conference. - Big Sky, MT, 6-13 March 2010. - P. 1-10. ↑
- C1216.** Fletcher R.R. Wearable Doppler radar with integrated antenna for patient vital sign monitoring. / Fletcher R.R., Kulkarni S. // 2010 IEEE Radio and Wireless Symposium (RWS). - New Orleans, LA, 10-14 Jan. 2010. - P. 276-279. ↑
- C1217.** Le Marshall N. Hybrid array for the detection and imaging of termites. / Le Marshall N., Rankin G., Tirkel A. // 2010 IEEE Radio and Wireless Symposium (RWS). - New Orleans, LA, 10-14 Jan. 2010. - P. 288-291. ↑
- C1218.** Thuong Le-Tien. Routing and Tracking System for Mobile Vehicles in Large Area. / Thuong Le-Tien, Vu Phung-The. // 2010. DELTA '10. Fifth IEEE International Symposium on Electronic Design, Test and Application. - Ho Chi Minh City, 13-15 Jan. 2010. - P. 297-300. ↑
- C1219.** Silvius J. UHF measurement of breathing and heartbeat at a distance. / Silvius J., Tahmouh D. // 2010 IEEE Radio and Wireless Symposium (RWS). - New Orleans, LA, 10-14 Jan. 2010. - P. 567-570. ↑
- C1220.** Yan Yan. Effects of I/Q mismatch on measurement of periodic movement using a Doppler radar sensor. / Yan Yan, Changzhi Li, Jianshan Lin. // 2010 IEEE Radio and Wireless Symposium (RWS). - New Orleans, LA, 10-14 Jan. 2010. - P. 196-199. ↑
- C1221.** Mostafanezhad I. A coherent low IF receiver architecture for Doppler radar motion detector used in life signs monitoring. / Mostafanezhad I., Boric-Lubecke O., Lubecke V. // 2010 IEEE Radio and Wireless Symposium (RWS). - New Orleans, LA, 10-14 Jan. 2010. - P. 571-574. ↑
- C1222.** Gao Xugang. Maximizing Sum of Image Intensity Square Autofocus Algorithm. / Gao Xugang, Su Weimin, Gu Hong. // 2010 Asia-Pacific Conf on (CICC-ITOE) Innovative Computing & Communication, 2010 Intl Conf on and Information Technology & Ocean Engineering. - Macao, 30-31 Jan. 2010. - P. 170-172. ↑
- C1223.** Katkuri J.R. A comparative study of nonlinear filters for target tracking in mixed coordinates. / Katkuri J.R., Jilkov V.P., Li X.R. // 2010 42nd Southeastern Symposium on System Theory (SSST). - Tyler, TX, 7-9 March 2010. - P. 202-207. ↑
- C1224.** Xiao Wang. Turn rate estimation based on curve fitting in maneuvering target tracking. / Xiao Wang, Chongzhao Han. // 2010 42nd Southeastern Symposium on System Theory (SSST). - Tyler, TX, 7-9 March 2010. - P. 194-196. ↑
- C1225.** Ochoa H.A. Analysis of induced surface currents on high velocity target using a relativistic approach. / Ochoa H.A., Nakka R.K. // 2010 42nd Southeastern Symposium on System Theory (SSST). - Tyler, TX, 7-9 March 2010. - P. 217-221. ↑
- C1226.** AlGhamdi A.S. Application of Fuzzy Logic control in automated transport systems. / AlGhamdi A.S., Eren H., Mansour A. // 2010 IEEE Sensors Applications Symposium (SAS). - Limerick, 23-25 Feb. 2010. - P. 216-219. ↑

- C1227.** Nateghi J. The comparison between the TE21 mode and the four-horn monopulse technique for LEO satellite tracking. / Nateghi J., Mohammadi L. // 2010 The 12th International Conference on Advanced Communication Technology (ICACT). - Phoenix Park, 7-10 Feb. 2010. - Vol. 1. - P. 403-406. ↑
- C1228.** Narkimelli S. Scattering of electromagnetic radiation for a perfect electric conducting cylinder by using multiple angles of polarization. / Narkimelli S., Ochoa H.A. // 2010 42nd Southeastern Symposium on System Theory (SSST). - Tyler, TX, 7-9 March 2010. - P. 60-65. ↑
- C1229.** Raab F.H. Kahn-technique transmitter for L-band communication/radar. / Raab F.H., Poppe M.C. // 2010 IEEE Radio and Wireless Symposium (RWS). - New Orleans, LA, 10-14 Jan. 2010. - P. 100-103. ↑
- C1230.** Kocur D. Imaging method: A strong tool for moving target tracking by a multistatic UWB radar system. / Kocur D., Gamec J., Svecova M., Gamcova M., Rovnakova J. // 2010 IEEE 8th International Symposium on Applied Machine Intelligence and Informatics (SAMI). - Herlany, 28-30 Jan. 2010. - P. 11-19. ↑
- C1231.** Paul P.V. Nonparametric techniques for graphical model-based target tracking in collaborative sensor groups. / Paul P.V., Rajbabu V. // 2010 National Conference on Communications (NCC). - Chennai, 29-31 Jan. 2010. - P. 1-5. ↑
- C1232.** Roy L.P. A GLRT detector in partially correlated texture based compound-Gaussian clutter. / Roy L.P., Kumar R.V.R. // 2010 National Conference on Communications (NCC). - Chennai, 29-31 Jan. 2010. - P. 1-5. ↑
- C1233.** Zeng Jiankui. A New Detection Method for MIMO Radar Using Hidden Markov Model. / Zeng Jiankui, Xiang Lijuan, Dong Zhiming, Yuan Shangzun. // 2010. ICCMS '10. Second International Conference on Computer Modeling and Simulation. - Sanya, Hainan, 22-24 Jan. 2010. - Vol. 2. - P. 341-343. ↑
- C1234.** Zhou Wei. An Algorithm of Weak Signal's Detection on the Condition of Strong Interference. / Zhou Wei, Hui Jun-ying, Mei Ji-dan, Sheng Xue-li. // 2010. ICCMS '10. Second International Conference on Computer Modeling and Simulation. - Sanya, Hainan, 22-24 Jan. 2010. - Vol. 3. - P. 230-232. ↑
- C1235.** Wang Quanmin. RF Effect Algorithms of Terrain Environment in Signal-Level Radar System Simulation. / Wang Quanmin, Wang Chuncai, Guo Gang, Huang Kedi. // 2010. ICCMS '10. Second International Conference on Computer Modeling and Simulation. - Sanya, Hainan, 22-24 Jan. 2010. - Vol. 4. - P. 178-181. ↑
- C1236.** Jian-xiong Wang. A Method of Weak Signal Detection Based on Duffing Oscillator. / Jian-xiong Wang, Chulin Hou. // 2010. IC4E '10. International Conference on e-Education, e-Business, e-Management, and e-Learning. - Sanya, 22-24 Jan. 2010. - P. 387-390. ↑
- C1237.** Benkeser C. A 4.5mW digital baseband receiver for level-A evolved EDGE. / Benkeser C., Bubenhofer A., Qiuting Huang. // 2010 IEEE International Solid-State Circuits Conference Digest of Technical Papers (ISSCC). - San Francisco, CA, 7-11 Feb. 2010. - P. 276-277. ↑
- C1238.** Starzer F. A novel 77-GHz radar frontend with 19-GHz signal distribution on RF-PCB substrate. / Starzer F., Forstner H.P., Wagner C., Feger R., Scheibhofer S., Fischer A., Jager H., Stelzer A. // 2010 IEEE Radio and Wireless Symposium (RWS). - New Orleans, LA, 10-14 Jan. 2010. - P. 360-363. ↑
- C1239.** Yao Yu. MIMO radar based on reduced complexity compressive sampling. / Yao Yu, Petropulu A.P., Poor H.V. // 2010 IEEE Radio and Wireless Symposium (RWS). - New Orleans, LA, 10-14 Jan. 2010. - P. 21-24. ↑
- C1240.** Shahbazi A. Data Transmission over GSM Adaptive Multi Rate Voice Channel Using Speech-Like Symbols. / Shahbazi A., Rezaei A.H., Sayadiyan A., Mosayyebpour S. // 2010. ICSAP '10. International Conference on Signal Acquisition and Processing. - Bangalore, 9-10 Feb. 2010. - P. 63-67. ↑
- C1241.** Shahbazi A. Content Dependent Data Hiding on GSM Full Rate Encoded Speech. / Shahbazi A., Soltanmohammadi E., Rezaei A.H., Sayadiyan A., Mosayyebpour S. // 2010. ICSAP '10. International Conference on Signal Acquisition and Processing. - Bangalore, 9-10 Feb. 2010. - P. 68-72. ↑
- C1242.** Shao Chao. The Chaotic Behavior of the Chaos-Based Phase-Coded Pulse Train Signal. / Shao Chao, Lu Peng-Fei, Ma Jian, Guan Yin-Ying. // 2010. ICSAP '10. International Conference on Signal Acquisition and Processing. - Bangalore, 9-10 Feb. 2010. - P. 263-267. ↑

- C1243.** Taylor R. Performance analysis of range sensors for a real-time power plant coal level sensing system. / Taylor R., Shirvaikar M. // 2010 42nd Southeastern Symposium on System Theory (SSST). - Tyler, TX, 7-9 March 2010. - P. 188-193. ↑
- C1244.** Kaninskiy V. Determination of parameters for digital meter of doppler radars systems for the artillery systems. / Kaninskiy V., Budaretskiy Y., Grabchak V., Prokopenko V. // 2010 International Conference on Modern Problems of Radio Engineering, Telecommunications and Computer Science (TCSET). - Lviv-Slavske, 23-27 Feb. 2010. - P. 101. ↑
- C1245.** Zheng J.X. Optimized FPGA implementation of Multi-Rate FIR filters through Thread Decomposition. / Zheng J.X., Nguyen K., Yutao He. // 2010 IEEE Aerospace Conference. - Big Sky, MT, 6-13 March 2010. - P. 1-10. ↑
- C1246.** Kaslow D. COTS implementation of a Sensor Planning Service GetFeasibility operation-Interim status. 2010 IEEE Aerospace Conference. - Big Sky, MT, 6-13 March 2010. - P. 1-19. ↑
- C1247.** Vasiliev D. Analysis of the information contained in amplitudes of the reflected signals received by space diversity radars. 2010 International Conference on Modern Problems of Radio Engineering, Telecommunications and Computer Science (TCSET). - Lviv-Slavske, 23-27 Feb. 2010. - P. 113. ↑
- C1248.** Petlyuk I. Economic aspects of realization of the government programs of development of the technical systems. / Petlyuk I., Tymchuk O. // 2010 International Conference on Modern Problems of Radio Engineering, Telecommunications and Computer Science (TCSET). - Lviv-Slavske, 23-27 Feb. 2010. - P. 114. ↑
- C1249.** Semenyuk A. Input microwave devices for space surveillance radar system with identical phase-frequency characteristics. / Semenyuk A., Oblakevych V., Panasyuk M. // 2010 International Conference on Modern Problems of Radio Engineering, Telecommunications and Computer Science (TCSET). - Lviv-Slavske, 23-27 Feb. 2010. - P. 105. ↑
- C1250.** Reali F. Initialization of ballistic targets tracking filters with detection probability lower than unity. / Reali F., Palmerini G., Farina A., Graziano A., Giompapa S., Parisi B. // 2010 IEEE Aerospace Conference. - Big Sky, MT, 6-13 March 2010. - P. 1-11. ↑
- C1251.** Habtemariam B.K. Multitarget track before detect with MIMO radars. / Habtemariam B.K., Tharmarasa R., Kirubarajan T. // 2010 IEEE Aerospace Conference. - Big Sky, MT, 6-13 March 2010. - P. 1-9. ↑
- C1252.** Chun Yang. Design of Schmidt-Kalman filter for target tracking with navigation errors. / Chun Yang, Blasch E., Douville P. // 2010 IEEE Aerospace Conference. - Big Sky, MT, 6-13 March 2010. - P. 1-12. ↑
- C1253.** Panakkal V.P. Bearings-only tracking using derived heading. / Panakkal V.P., Velmurugan R. // 2010 IEEE Aerospace Conference. - Big Sky, MT, 6-13 March 2010. - P. 1-11. ↑
- C1254.** Dunham D.T. Kinematic separation point estimation using PMHT. / Dunham D.T., August S.E. // 2010 IEEE Aerospace Conference. - Big Sky, MT, 6-13 March 2010. - P. 1-6. ↑
- C1255.** Gorji A.A. Tracking multiple unresolved targets using MIMO radars. / Gorji A.A., Tharmarasa R., Kirubarajan T. // 2010 IEEE Aerospace Conference. - Big Sky, MT, 6-13 March 2010. - P. 1-14. ↑
- C1256.** Smith L.D. A track purity approach for tracking metrics. / Smith L.D., Register A., Dale Blair W., Levedahl M. // 2010 IEEE Aerospace Conference. - Big Sky, MT, 6-13 March 2010. - P. 1-11. ↑
- C1257.** Slyusar V.I. Experimental radar with 64-channel digital antenna array. / Slyusar V.I., Nikitin N.N., Shatzman L.G., Korolev N.A., Solostchev O.N., Shraev D.V., Volostchuk I.V., Alesyn A.M., Bondarenko M.V., Grytzenko V.N., Malastchuk V.P. // 2010 International Conference on Modern Problems of Radio Engineering, Telecommunications and Computer Science (TCSET). - Lviv-Slavske, 23-27 Feb. 2010. - P. 95. ↑
- C1258.** Shynkaruk O. Impulse radio signal processing considering the internal phase-frequency instability. / Shynkaruk O., Chesanovskiy I. // 2010 International Conference on Modern Problems of Radio Engineering, Telecommunications and Computer Science (TCSET). - Lviv-Slavske, 23-27 Feb. 2010. - P. 47. ↑
- C1259.** Pravda V.I. Sidelobe cancellation method at the exit of correlation processing scheme. / Pravda V.I., Bychkov V.E. // 2010 International Conference on Modern Problems of Radio Engineering, Telecommunications

and Computer Science (TCSET). - Lviv-Slavske, 23-27 Feb. 2010. - P. 52. ↑

**C1260.** Bienkowski P. Non-stationary EMF measurements. / Bienkowski P., Trzaska H. // 2010 International Conference on Modern Problems of Radio Engineering, Telecommunications and Computer Science (TCSET). - Lviv-Slavske, 23-27 Feb. 2010. - P. 61-62. ↑

**C1261.** Tymchuk V. Essence of radio signals processing in close range reconnaissance. 2010 International Conference on Modern Problems of Radio Engineering, Telecommunications and Computer Science (TCSET). - Lviv-Slavske, 23-27 Feb. 2010. - P. 276. ↑

**C1262.** Lekhovyt'skiy D. Adaptive lattice filters for band-inverse covariance matrix approximations. / Lekhovyt'skiy D., Ryabykha V., Zaryt'skiy V., Zhuga G., Rachkov D., Semenyaka A. // 2010 International Conference on Modern Problems of Radio Engineering, Telecommunications and Computer Science (TCSET). - Lviv-Slavske, 23-27 Feb. 2010. - P. 338. ↑

**C1263.** Matuszewski J. Application of clustering methods for recognition of technical objects. 2010 International Conference on Modern Problems of Radio Engineering, Telecommunications and Computer Science (TCSET). - Lviv-Slavske, 23-27 Feb. 2010. - P. 39-40. ↑

**C1264.** Sumyk M. Passive hindrances suppression using complex polyphase signals. / Sumyk M., Yankevych R. // 2010 International Conference on Modern Problems of Radio Engineering, Telecommunications and Computer Science (TCSET). - Lviv-Slavske, 23-27 Feb. 2010. - P. 64. ↑

**C1265.** Kawalec A. Some results of radar signal detections by the use of compressive receiver. / Kawalec A., Pieniezny A. // 2010 International Conference on Modern Problems of Radio Engineering, Telecommunications and Computer Science (TCSET). - Lviv-Slavske, 23-27 Feb. 2010. - P. 87-88. ↑

**C1266.** Bondarev A. An analytical, imitation and experimental design of device of surveillance is after bearing frequency. / Bondarev A., Borsuk O. // 2010 International Conference on Modern Problems of Radio Engineering, Telecommunications and Computer Science (TCSET). - Lviv-Slavske, 23-27 Feb. 2010. - P. 91. ↑

**C1267.** Bezruk V. Application of AR model for radar recognition of meteorological objects. / Bezruk V., Belov E., Voitovych O., Netrebenko K., Tikhonov V., Rudnev G., Khlopov G., Khomenko S. // 2010 International Conference on Modern Problems of Radio Engineering, Telecommunications and Computer Science (TCSET). - Lviv-Slavske, 23-27 Feb. 2010. - P. 93. ↑

**C1268.** Linkova A. Measurement of parameters of solid aerosols in polydisperse medium using double frequency radar. 2010 International Conference on Modern Problems of Radio Engineering, Telecommunications and Computer Science (TCSET). - Lviv-Slavske, 23-27 Feb. 2010. - P. 77. ↑

**C1269.** Sergiy G. Object recognition with surveillance radar systems. 2010 International Conference on Modern Problems of Radio Engineering, Telecommunications and Computer Science (TCSET). - Lviv-Slavske, 23-27 Feb. 2010. - P. 78. ↑

**C1270.** Dyakov A. Information approach to estimation of the multispectrum monitoring device efficiency. 2010 International Conference on Modern Problems of Radio Engineering, Telecommunications and Computer Science (TCSET). - Lviv-Slavske, 23-27 Feb. 2010. - P. 86. ↑

**C1271.** de Porras Bernacer R. Multiprotocol transceiving, Formatting and Temperature monitoring FPGA based unit. 2010 VI Southern Programmable Logic Conference (SPL). - Ipojuca, 24-26 March 2010. - P. 147-150. ↑

**C1272.** Venturino L. A stochastic-gradient method to design optimal space-time codes for MIMO radar detection. / Venturino L., Ke Dong, Xiaodong Wang, Lops M. // 2010 European Wireless Conference (EW). - Lucca, 12-15 April 2010. - P. 752-757. ↑

**C1273.** Wicks M.C. A Hotelling T-squared GIP test for detection of over resolved targets. / Wicks M.C., Yuhong Zhang, Schneible R., Browning J.P. // 2010 European Wireless Conference (EW). - Lucca, 12-15 April 2010. - P. 766-773. ↑

**C1274.** Jenik V. Microwave Doppler radar sensor with enhanced immunity against interferences. / Jenik V., Hudec P. // 2010 15th International Conference on Microwave Techniques (COMITE). - Brno, 19-21 April 2010. - P. 117-120. ↑



- C1275.** Lam E.P. System performance prediction of Firefinder radar. / Lam E.P., Walker Birrell H., Magallon J. // 2010 4th Annual IEEE Systems Conference. - San Diego, CA, 5-8 April 2010. - P. 500-504. ↑
- C1276.** Gaughan W. Using an FPGA digital clock manager to generate sub-nanosecond phase shifts for lidar applications. / Gaughan W., Butka B. // 2010 VI Southern Programmable Logic Conference (SPL). - Ipojuca, 24-26 March 2010. - P. 163-166. ↑
- C1277.** Chaczko Zenon. Security threats in Cognitive Radio applications. / Chaczko Zenon, Wickramasooriya Ruckshan, Klempous Ryszard, Nikodem Jan. // 2010 14th International Conference on Intelligent Engineering Systems (INES). - Las Palmas, Spain, 5-7 May 2010. - P. 209-214. ↑
- C1278.** Gaopeng Li. A mainlobe interference suppression system based on mismatched filtering. / Gaopeng Li, Dan Song, Rongqing Xu. // 2010 2nd International Conference on Computer Engineering and Technology (ICCET). - Chengdu, 16-18 April 2010. - Vol. 7. - P. V7-233-V7-238-233. ↑
- C1279.** Al-Zahrani R.A. SAR images segmentation using edge information. / Al-Zahrani R.A., El-Zaar A. // 2010 2nd International Conference on Computer Engineering and Technology (ICCET). - Chengdu, 16-18 April 2010. - Vol. 4. - P. V4-496-V4-499-496. ↑
- C1280.** Jiagen Jin. An improved adaptive maneuvering target tracking algorithm. / Jiagen Jin, Wenfeng Li, Xiaohong Xue, Junrong Bao. // 2010 2nd International Conference on Computer Engineering and Technology (ICCET). - Chengdu, 16-18 April 2010. - Vol. 7. - P. V7-366-V7-369-366. ↑
- C1281.** Tay P. C. Tomographic approaches towards focused SAR image development. / Tay P. C., Yearly M. B., Huck R. C., Cheng S., Sluss J. J., Taylor J. L., Phillips J. // 2010 IEEE Southwest Symposium on Image Analysis & Interpretation (SSIAI). - Austin, TX, USA, 23-25 May 2010. - P. 113-116. ↑
- C1282.** Freeman Greg J. Automated detection of near surface Martian ice layers in orbital radar data. / Freeman Greg J., Bovik Alan C., Holt John W. // 2010 IEEE Southwest Symposium on Image Analysis & Interpretation (SSIAI). - Austin, TX, USA, 23-25 May 2010. - P. 117-120. ↑
- C1283.** Natale D.J. Using full motion 3D Flash LIDAR video for target detection, segmentation, and tracking. / Natale D.J., Tutwiler R.L., Baran M.S., Durkin J.R. // 2010 IEEE Southwest Symposium on Image Analysis & Interpretation (SSIAI). - Austin, TX, 23-25 May 2010. - P. 21-24. ↑
- C1284.** Bezousek P. Effects of signal distortion in a FMCW radar on range resolution. / Bezousek P., Hajek M., Pola M. // 2010 15th International Conference on Microwave Techniques (COMITE). - Brno, 19-21 April 2010. - P. 113-116. ↑
- C1285.** Gingras D. Rough Terrain Reconstruction for Rover Motion Planning. / Gingras D., Lamarche T., Bedwani J.-L., Dupuis E. // 2010 Canadian Conference on Computer and Robot Vision (CRV). - Ottawa, ON, May 31 2010-June 2 2010. - P. 191-198. ↑
- C1286.** Ochilov S. Automated Classification of Operational SAR Sea Ice Images. / Ochilov S., Clausi D.A. // 2010 Canadian Conference on Computer and Robot Vision (CRV). - Ottawa, ON, May 31 2010-June 2 2010. - P. 40-46. ↑
- C1287.** Ojgel E.G. Evaluation of the electric and magnetic field levels of around the medium voltage power lines in related to public health. / Ojgel E.G., Ojzen S., Helhel S. // 2010 15th National Biomedical Engineering Meeting (BIYOMUT). - Antalya, 21-24 April 2010. - P. 1-5. ↑
- C1288.** S. Target localization by a multistatic UWB radar. / S,vecova, M., Kocur D., Zetik R., Rovn,a,kova, J. // 2010 20th International Conference Radioelektronika (RADIOELEKTRONIKA). - Brno, 19-21 April 2010. - P. 1-4. ↑
- C1289.** Urdzi. CFAR detectors for through wall tracking of moving targets by M-sequence UWB radar. / Urdzi,k D., Kocur D. // 2010 20th International Conference Radioelektronika (RADIOELEKTRONIKA). - Brno, 19-21 April 2010. - P. 1-4. ↑
- C1290.** Rovn. Weak signal enhancement in radar signal processing. / Rovn,akova, J., Kocur D. // 2010 20th International Conference Radioelektronika (RADIOELEKTRONIKA). - Brno, 19-21 April 2010. - P. 1-4. ↑

- C1291.** Arslan E. Classification of fibromyalgia syndrome by using fuzzy logic method. / Arslan E., Yııldız S., Kojlukaya E., Albayrak Y. // 2010 15th National Biomedical Engineering Meeting (BIYOMUT). - Antalya, 21-24 April 2010. - P. 1-5. ↑
- C1292.** Postolache O. Microwave FMCW Doppler radar implementation for in-house pervasive health care system. / Postolache O., Madeira R.N., Giraio P.S., Postolache G. // 2010 IEEE International Workshop on Medical Measurements and Applications Proceedings (MeMeA). - Ottawa, ON, April 30 2010-May 1 2010. - P. 47-52. ↑
- C1293.** Ruiming Yang. Direction Finding via Beam Scanning and Sparse Reconstruction. / Ruiming Yang, Yipeng Liu, Qun Wan, Wanlin Yang. // 2010 Second International Conference on Networks Security Wireless Communications and Trusted Computing (NSWCTC). - Wuhan, Hubei, 24-25 April 2010. - Vol. 2. - P. 7-9. ↑
- C1294.** Padaki A.V. Improving Performance in Neural Network Based Pulse Compression for Binary and Polyphase Codes. / Padaki A.V., George K. // 2010 12th International Conference on Computer Modelling and Simulation (UKSim). - Cambridge, 24-26 March 2010. - P. 278-283. ↑
- C1295.** Bilgili M. The effects of seasonal weather differences on the bio-heat loss transferred from the human body in Antalya city. / Bilgili M., Sahin B., Simsek E., Yasar A. // 2010 15th National Biomedical Engineering Meeting (BIYOMUT). - Antalya, 21-24 April 2010. - P. 1-5. ↑
- C1296.** Yaman A. Magnetic resonance imaging shows that muscle myofascial force transmission causes substantial sarcomere length heterogeneity in human muscles, in vivo. / Yaman A., Baan G.C., Huijing P.A., Ojzturk C., Yujcesoy C.A. // 2010 15th National Biomedical Engineering Meeting (BIYOMUT). - Antalya, 21-24 April 2010. - P. 1-3. ↑
- C1297.** Yilmaz G. Charged particle/cell manipulation in spiral microchannels with concentric electrodes. / Yilmaz G., Bayraktar E., Kujlah H. // 2010 15th National Biomedical Engineering Meeting (BIYOMUT). - Antalya, 21-24 April 2010. - P. 1-4. ↑
- C1298.** Huang Jilin. The analysis of ground penetrating radar signal of small objects based on generalized S transform. / Huang Jilin, Huang Zhonglai, Zhang Jianzhong. // 2010 2nd International Conference on Computer Engineering and Technology (ICCET). - Chengdu, 16-18 April 2010. - Vol. 7. - P. V7-555-V7-559-555. ↑
- C1299.** Alae Mohammad. Modeling and Simulation of Adaptive Thresholding in Marine RADARs. / Alae Mohammad, Amiri Reza, Firoozmand Mohsen, Sepahvand Morteza. // 2010 Fourth Asia International Conference on Mathematical/Analytical Modelling and Computer Simulation (AMS). - Kota Kinabalu, Malaysia, 26-28 May 2010. - P. 276-281. ↑
- C1300.** Bukhari M.H.S. Intrinsic Membrane Noise in Living Cells and Its Coupling to External Fields. / Bukhari M.H.S., Miller J.H., Shah Z.H. // 2010 Second International Conference on Computer Research and Development. - Kuala Lumpur, 7-10 May 2010. - P. 540-544. ↑
- C1301.** Trajcevski Goce. Sensing, Triggers and Mobile (Meta)Data. / Trajcevski Goce, Choudhary Alok, Scheuermann Peter. // 2010 Eleventh International Conference on Mobile Data Management (MDM). - Kansas City, MO, USA, 23-26 May 2010. - P. 331-335. ↑
- C1302.** Benson S. Adaptive thresholding for high dual-tone signal instantaneous dynamic range in digital wideband receiver. / Benson S., Chen C.-I.H. // 2010 IEEE Instrumentation and Measurement Technology Conference (I2MTC). - Austin, TX, 3-6 May 2010. - P. 616-619. ↑
- C1303.** Kissinger D. Analysis of a built-in test architecture for direct-conversion SiGe millimeter-wave receiver frontends. / Kissinger D., Agethen R., Weigel R. // 2010 IEEE Instrumentation and Measurement Technology Conference (I2MTC). - Austin, TX, 3-6 May 2010. - P. 944-948. ↑
- C1304.** Alae Mohammad. A New Model for Rain Clutter Cancellation in Marine Radars. / Alae Mohammad, Amiri Reza, Moghadam Amir Sheykhiha, Sepahvand Morteza. // 2010 Fourth Asia International Conference on Mathematical/Analytical Modelling and Computer Simulation (AMS). - Kota Kinabalu, Malaysia, 26-28 May 2010. - P. 296-301. ↑
- C1305.** Ghinita Gabriel. Privacy-Aware Location-Aided Routing in Mobile Ad Hoc Networks. / Ghinita Gabriel, Azarmi Mehdi, Bertino Elisa. // 2010 Eleventh International Conference on Mobile Data Management (MDM). -

Kansas City, MO, USA, 23-26 May 2010. - P. 65-74. ↑

**C1306.** Changsheng Zhu. Design and Development of Embedded Intelligent Public Transport Vehicular Terminal. / Changsheng Zhu, Jianbo Liang, Xugang Miao, Wenyi Feng. // 2010 International Conference on Computing, Control and Industrial Engineering (CCIE). - Wuhan, 5-6 June 2010. - Vol. 2. - P. 236-239. ↑

**C1307.** Chen Zhu. Portable Calibration System for Air Traffic Control Surveillance Radar. / Chen Zhu, Xiaofeng Shi. // 2010 International Conference on Computing, Control and Industrial Engineering (CCIE). - Wuhan, 5-6 June 2010. - Vol. 2. - P. 76-80. ↑

**C1308.** Li-wen Wang. Design of Command and Dispatch System of Airport Support Vehicle. / Li-wen Wang, Jiang-long Wei, Xiao-lin Liu, Sheng-fei Liu, Xu-dong Shi. // 2010 International Conference on Computing, Control and Industrial Engineering (CCIE). - Wuhan, 5-6 June 2010. - Vol. 1. - P. 290-293. ↑

**C1309.** Deprez J.-F. Twin target correction for ultra-wideband radar imaging of breast tumours. / Deprez J.-F., Klemm M., Smith P.P., Craddock I. // 2010 IEEE International Symposium on Biomedical Imaging: From Nano to Macro. - Rotterdam, 14-17 April 2010. - P. 213-216. ↑

**C1310.** Chumkamon S. The vertical handoff between GSM and Zigbee networks for vehicular communication. / Chumkamon S., Tuvaphanthaphiphat P., Keeratiwintakorn P. // 2010 International Conference on Electrical Engineering/Electronics Computer Telecommunications and Information Technology (ECTI-CON). - Chaing Mai, 19-21 May 2010. - P. 603-606. ↑

**C1311.** Thongpul K. A neural network based optimization for wireless sensor node position estimation in industrial environments. / Thongpul K., Jindapetch N., Teerapakajornet W. // 2010 International Conference on Electrical Engineering/Electronics Computer Telecommunications and Information Technology (ECTI-CON). - Chaing Mai, 19-21 May 2010. - P. 249-253. ↑

**C1312.** Djemal R. A real-time FPGA-based implementation of target detection technique in non homogenous environment. 2010 5th International Conference on Design and Technology of Integrated Systems in Nanoscale Era (DTIS). - Hammamet, 23-25 March 2010. - P. 1-6. ↑

**C1313.** Jihua Dou. Capability evaluation framework of multichannel ship-to-air missile weapon system against anti-ship missile saturation attack. / Jihua Dou, Jing Zhou, Zhitong Zhong. // 2010 2nd International Conference on Computer Engineering and Technology (ICCET). - Chengdu, 16-18 April 2010. - Vol. 3. - P. V3-522-V3-525-522. ↑

**C1314.** Jie Zhou. Window memory accesses method in alternate row/column matrix access systems. / Jie Zhou, Yong Dou, Yuanwu Lei, Yazhuo Dong. // 2010 2nd International Conference on Computer Engineering and Technology (ICCET). - Chengdu, 16-18 April 2010. - Vol. 3. - P. V3-201-V3-205-201. ↑

**C1315.** Li Bing. Remote video monitoring system based on embedded linux and GPS. / Li Bing, Sun JianPing. // 2010 2nd International Conference on Computer Engineering and Technology (ICCET). - Chengdu, 16-18 April 2010. - Vol. 3. - P. V3-218-V3-221-218. ↑

**C1316.** Wang Yin-wen. Remote monitoring system for oil wells based on GPRS technology. / Wang Yin-wen, Hou Min-xian. // 2010 2nd International Conference on Computer Engineering and Technology (ICCET). - Chengdu, 16-18 April 2010. - Vol. 7. - P. V7-607-V7-611-607. ↑

**C1317.** Lixia Liu. Research on optimal wireless city network using mobile network. 2010 2nd International Conference on Computer Engineering and Technology (ICCET). - Chengdu, 16-18 April 2010. - Vol. 2. - P. V2-653-V2-656-653. ↑

**C1318.** Wenhong Wu. Research on long-range and metering reading for water meter based on GPRS. / Wenhong Wu, Wenjun Wu, Xinping Wu. // 2010 2nd International Conference on Computer Engineering and Technology (ICCET). - Chengdu, 16-18 April 2010. - Vol. 7. - P. V7-725-V7-727-725. ↑

**C1319.** Zhiyong Wang. Detecting and assessing the land subsidence in coal mining area using PALSAR data based on D-InSAR technique. / Zhiyong Wang, Guolin Liu, Tian'en Chen, Jixian Zhang, Guoman Huang. // 2010 2nd International Conference on Computer Engineering and Technology (ICCET). - Chengdu, 16-18 April 2010. - Vol. 3. - P. V3-222-V3-226-222. ↑

- C1320.** Liang Wen. Error analysis in phased array antenna pattern simulation. / Liang Wen, Tao Zeng, XiaoLiang Li. // 2010 2nd International Conference on Computer Engineering and Technology (ICCET). - Chengdu, 16-18 April 2010. - Vol. 6. - P. V6-287-V6-290-287. ↑
- C1321.** Wang Yao. A novel algorithm of coherent integration for moving target detection. / Wang Yao, Wang Shan. // 2010 2nd International Conference on Advanced Computer Control (ICACC). - Shenyang, 27-29 March 2010. - Vol. 4. - P. 235-239. ↑
- C1322.** Lin Xiaodong. Probability hypothesis densities for multi-sensor, multi-target tracking with application to acoustic sensors array. / Lin Xiaodong, Zhu Linhu, Li Zhengxin. // 2010 2nd International Conference on Advanced Computer Control (ICACC). - Shenyang, 27-29 March 2010. - Vol. 5. - P. 218-222. ↑
- C1323.** Li Zhang. Study on air formation to ground attack-defends decision making in duple-fuzzy condition. / Li Zhang, Pengfei Li. // 2010 2nd International Conference on Computer Engineering and Technology (ICCET). - Chengdu, 16-18 April 2010. - Vol. 6. - P. V6-698-V6-702-698. ↑
- C1324.** Jiemin Hu. A novel range alignment algorithm for ISAR. / Jiemin Hu, Weidong Jiang, Yaowen Fu, Xiang Li. // 2010 2nd International Conference on Computer Engineering and Technology (ICCET). - Chengdu, 16-18 April 2010. - Vol. 5. - P. V5-358-V5-362-358. ↑
- C1325.** Jiemin Hu. A novel approach to synthesize the range profile via predesigned stepped-frequency waveforms. / Jiemin Hu, Weidong Jiang, Yaowen Fu, Jing Ning. // 2010 2nd International Conference on Computer Engineering and Technology (ICCET). - Chengdu, 16-18 April 2010. - Vol. 5. - P. V5-363-V5-366-363. ↑
- C1326.** Fuchs M. Signal and data processing for radar sensor head network. / Fuchs M., Sebesta J. // 2010 20th International Conference Radioelektronika (RADIOELEKTRONIKA). - Brno, 19-21 April 2010. - P. 1-4. ↑
- C1327.** Guobing Hu. An Efficient Method of Pulse Repetition Interval Modulation Recognition. / Guobing Hu, Yu Liu. // 2010 International Conference on Communications and Mobile Computing (CMC). - Shenzhen, 12-14 April 2010. - Vol. 2. - P. 287-291. ↑
- C1328.** Wei Xu. Signal Filtering Based on Wavelet Transform and its Application in Ground Penetrating Radar. / Wei Xu, Chaoyang Xu. // 2010 International Conference on Communications and Mobile Computing (CMC). - Shenzhen, 12-14 April 2010. - Vol. 3. - P. 77-81. ↑
- C1329.** Elguebaly T. A Bayesian approach for SAR images segmentation and changes detection. / Elguebaly T., Bouguila N. // 2010 25th Biennial Symposium on Communications (QBSC). - Kingston, ON, 12-14 May 2010. - P. 24-27. ↑
- C1330.** Fera E.H. Latency-information theory. 2010 IEEE Sarnoff Symposium. - Princeton, NJ, 12-14 April 2010. - P. 1-8. ↑
- C1331.** Kooti H. Reconfiguration-aware spectrum sharing for FPGA based software defined radio. / Kooti H., Bozorgzadeh E., Shenghui Liao, Lichun Bao. // 2010 IEEE International Symposium on Parallel & Distributed Processing, Workshops and Phd Forum (IPDPSW). - Atlanta, GA, 19-23 April 2010. - P. 1-4. ↑
- C1332.** Lu Lu. Robust Novel EM-Based Direction-of-Arrival Estimation Technique for Wideband Source Signals. / Lu Lu, Hsiao-Chun Wu, Huang S.C.-H. // 2010 International Conference on Communications and Mobile Computing (CMC). - Shenzhen, 12-14 April 2010. - Vol. 3. - P. 72-76. ↑
- C1333.** Mingjiu Lv. The Integrative Application of Anti-Jamming Technology for Radar. / Mingjiu Lv, Ming Zhou, Qinglei Du. // 2010 2nd International Workshop on Intelligent Systems and Applications (ISA). - Wuhan, 22-23 May 2010. - P. 1-4. ↑
- C1334.** Hoi-Shun Lui. On the modelling of transient scattering under ultra wideband short-pulse electromagnetic excitation. / Hoi-Shun Lui, Shuley N.V. // 2010 Asia-Pacific Symposium on Electromagnetic Compatibility (APEMC). - Beijing, 12-16 April 2010. - P. 854-857. ↑
- C1335.** Guiyuan Li. A new judging method for radar electromagnetic compatibility analysis. / Guiyuan Li, Hou Zhang, Haiyang Xu. // 2010 Asia-Pacific Symposium on Electromagnetic Compatibility (APEMC). - Beijing, 12-16 April 2010. - P. 653-656. ↑



- C1336.** Norgard J. Computational electromagnetic modeling & simulation of ultra wideband sub-surface sensors for the detection and imaging of buried objects using spatial and spectral diversity. / Norgard J., Musellman R., Drozd A. // 2010 Asia-Pacific Symposium on Electromagnetic Compatibility (APEMC). - Beijing, 12-16 April 2010. - P. 544-547. ↑
- C1337.** Long Cai. Some Analysis of Fuzzy CAGO/SO CFAR Detector in Non-Gaussian Background. / Long Cai, Xiaochuan Ma, Shefeng Yan, Chengpeng Hao, Rongbo Wang. // 2010 2nd International Workshop on Intelligent Systems and Applications (ISA). - Wuhan, 22-23 May 2010. - P. 1-4. ↑
- C1338.** Chengpeng Hao. Performance Analysis of OSAP-CFAR Detector in K Distribution Background. / Chengpeng Hao, Long Cai. // 2010 2nd International Workshop on Intelligent Systems and Applications (ISA). - Wuhan, 22-23 May 2010. - P. 1-4. ↑
- C1339.** Wang Dongfang. Fast electric field change pulses location technique. / Wang Dongfang, Yuan Tie, Zhang Guangshu, Zhang Tong. // 2010 Asia-Pacific Symposium on Electromagnetic Compatibility (APEMC). - Beijing, 12-16 April 2010. - P. 1158-1161. ↑
- C1340.** Ghelfi P. All-optical parallelization for high sampling rate photonic ADC in fully digital radar systems. / Ghelfi P., Lingmei Ma, Xiaoxia Wu, Minyu Yao, Willner A.E., Bogoni A. // 2010 Conference on (OFC/NFOEC) Optical Fiber Communication (OFC), collocated National Fiber Optic Engineers Conference. - San Diego, CA, 21-25 March 2010. - P. 1-3. ↑
- C1341.** Jajamovich G.H. Transmit policies for MIMO radar detection and time-delay estimation. / Jajamovich G.H., Lops M., Xiaodong Wang. // 2010 4th International Symposium on Communications, Control and Signal Processing (ISCCSP). - Limassol, 3-5 March 2010. - P. 1-4. ↑
- C1342.** Godrich H. Localization performance of coherent MIMO radar systems subject to phase synchronization errors. / Godrich H., Haimovich A.M. // 2010 4th International Symposium on Communications, Control and Signal Processing (ISCCSP). - Limassol, 3-5 March 2010. - P. 1-5. ↑
- C1343.** Qian He. Diversity gain for MIMO radar employing nonorthogonal waveforms. / Qian He, Blum R.S. // 2010 4th International Symposium on Communications, Control and Signal Processing (ISCCSP). - Limassol, 3-5 March 2010. - P. 1-6. ↑
- C1344.** Thanh-Hai Le. Neural network-assisted reconstruction of full polarimetric SAR information. / Thanh-Hai Le, McLoughlin I., Ken Yoong Lee, Bretschneider T. // 2010 4th International Symposium on Communications, Control and Signal Processing (ISCCSP). - Limassol, 3-5 March 2010. - P. 1-5. ↑
- C1345.** Thiagarajan J.J. Sparse representations for automatic target classification in SAR images. / Thiagarajan J.J., Ramamurthy K.N., Knee P., Spanias A., Berisha V. // 2010 4th International Symposium on Communications, Control and Signal Processing (ISCCSP). - Limassol, 3-5 March 2010. - P. 1-4. ↑
- C1346.** Yao Yu. Range estimation for MIMO step-frequency radar with compressive sensing. / Yao Yu, Petropulu A.P., Poor H.V. // 2010 4th International Symposium on Communications, Control and Signal Processing (ISCCSP). - Limassol, 3-5 March 2010. - P. 1-5. ↑
- C1347.** Aittomaki T. MIMO radar target detection with parametric scattering correlation model. / Aittomaki T., Koivunen V. // 2010 4th International Symposium on Communications, Control and Signal Processing (ISCCSP). - Limassol, 3-5 March 2010. - P. 1-5. ↑
- C1348.** Chuanming Wei. Cramer-Rao bound for joint location and velocity estimation in multi-target non-coherent MIMO radars. / Chuanming Wei, Qian He, Blum R.S. // 2010 44th Annual Conference on Information Sciences and Systems (CISS). - Princeton, NJ, 17-19 March 2010. - P. 1-6. ↑
- C1349.** Park J.D. Feasibility of range estimation using sonar LPI. / Park J.D., Miller D.J., Doherty J.F., Thompson S.C. // 2010 44th Annual Conference on Information Sciences and Systems (CISS). - Princeton, NJ, 17-19 March 2010. - P. 1-6. ↑
- C1350.** Blum R.S. Ordering for estimation. 2010 44th Annual Conference on Information Sciences and Systems (CISS). - Princeton, NJ, 17-19 March 2010. - P. 1-6. ↑
- C1351.** Cexus J.C. A combined Teager-Huang and Hough Transforms for LFM signals detection. / Cexus J.C.,

Boudraa A.O., Bouchikhi A. // 2010 4th International Symposium on Communications, Control and Signal Processing (ISCCSP). - Limassol, 3-5 March 2010. - P. 1-5. ↑

C1352. Xun Chen. Non-coherent MIMO radar in a non-Gaussian noise-plus-clutter environment. / Xun Chen, Blum R. // 2010 44th Annual Conference on Information Sciences and Systems (CISS). - Princeton, NJ, 17-19 March 2010. - P. 1-6. ↑

C1353. Shabani M. An Investigation on the performance of receiving Optical Beam-Forming Networks. / Shabani M., Akbari M. // 2010 International Workshop on Antenna Technology (iWAT). - Lisbon, 1-3 March 2010. - P. 1-4. ↑

C1354. Dudas L. Receiver antenna array. / Dudas L., Rosner V., Seller R., Kazi K., Nguyen Thi Ngoc Minh. // MELECON 2010-2010 15th IEEE Mediterranean Electrotechnical Conference. - Valletta, 26-28 April 2010. - P. 1283-1286. ↑

C1355. Micskei T. Implementation of a radar tester for air traffic control applications. / Micskei T., Dudas L., Seller R., Orban J. // MELECON 2010-2010 15th IEEE Mediterranean Electrotechnical Conference. - Valletta, 26-28 April 2010. - P. 274-279. ↑

C1356. Tian Yonghua. Modulation constellation analysis of GNSS signal using SDR receiver. / Tian Yonghua, Zeng Dazhi, Song Yuanyuan. // 2010 The 2nd IEEE International Conference on Information Management and Engineering (ICIME). - Chengdu, 16-18 April 2010. - P. 244-247. ↑

C1357. Liang Wen. Design and implementation of real-time SAR echo simulator for natural scene. / Liang Wen, Tao Zeng. // 2010 The 2nd IEEE International Conference on Information Management and Engineering (ICIME). - Chengdu, 16-18 April 2010. - P. 201-204. ↑

C1358. Shengxiang Bai. Method of phase unwrapping-free DEM reconstruction of InSAR. / Shengxiang Bai, Jinsong Tang, Ming Chen, Sen Zhang. // 2010 International Conference on Image Analysis and Signal Processing (IASP). - Zhejiang, 9-11 April 2010. - P. 60-63. ↑

C1359. Peng Suiyang. The imaging analysis of asynchronous bistatic SAR with parallel tracks. / Peng Suiyang, Zhang Jun, Ou Qiong, Lu Dawei, Shen Zhenkang. // 2010 International Conference on Image Analysis and Signal Processing (IASP). - Zhejiang, 9-11 April 2010. - P. 16-21. ↑

C1360. Aimin Cai. Parameters extraction of crop based on PolSAR Data. / Aimin Cai, Yun Shao, Huaze Gong. // 2010 International Conference on Image Analysis and Signal Processing (IASP). - Zhejiang, 9-11 April 2010. - P. 12-15. ↑

C1361. Xiaodong Zhang. Design and implementation of embedded monitoring system for grain storage. / Xiaodong Zhang, Xiujuan Li, Jie Zhang. // 2010 The 2nd IEEE International Conference on Information Management and Engineering (ICIME). - Chengdu, 16-18 April 2010. - P. 197-200. ↑

C1362. LaRosa R. Turbines can suppress Loop Current to reduce Gulf of Mexico hurricane threat. 2010 Long Island Systems Applications and Technology Conference (LISAT). - Farmingdale, NY, 7-7 May 2010. - P. 1-6. ↑

C1363. Krinker M. Mapping Geo-Pathogenic Zones and required instrumentation. / Krinker M., Goykadosh A. // 2010 Long Island Systems Applications and Technology Conference (LISAT). - Farmingdale, NY, 7-7 May 2010. - P. 1-4. ↑

C1364. Mesecher D.K. Netted sensors for higher-dimensionality performance. 2010 Long Island Systems Applications and Technology Conference (LISAT). - Farmingdale, NY, 7-7 May 2010. - P. 1-5. ↑

C1365. Tianhui Fu. Detection for signal in ELF atmospheric noise interference. / Tianhui Fu, Suihua Zhou, Xiaobing Zhang. // 2010 The 2nd IEEE International Conference on Information Management and Engineering (ICIME). - Chengdu, 16-18 April 2010. - P. 409-412. ↑

C1366. Bin Deng. A velocity estimation method for Multi Carrier Phase-Coded radar. / Bin Deng, Bin Sun, Xizhang Wei, Xiang Li. // 2010 The 2nd IEEE International Conference on Information Management and Engineering (ICIME). - Chengdu, 16-18 April 2010. - P. 227-230. ↑

C1367. Han Ping. Automatic target recognition of SAR images based on the fuzzy neural networks. / Han Ping,

Gao Shan. // 2010 The 2nd IEEE International Conference on Information Management and Engineering (ICIME). - Chengdu, 16-18 April 2010. - P. 102-104. ↑

**C1368.** Jia Xu. Small target detection in SAR image using the Alpha-stable distribution model. / Jia Xu, Wei Han, Xiu-feng He, Ren-xi Chen. // 2010 International Conference on Image Analysis and Signal Processing (IASP). - Zhejiang, 9-11 April 2010. - P. 64-68. ↑

**C1369.** Rongbo Wang. Blind separation of instantaneous linear mixtures of cyclostationary signals. / Rongbo Wang, Chaohuan Hou, Dong Chen. // 2010 International Conference on Image Analysis and Signal Processing (IASP). - Zhejiang, 9-11 April 2010. - P. 492-495. ↑

**C1370.** He Jian-Xin. Radar mosaic based on the explicit radar ray paths. / He Jian-Xin, Deng Yong, Li Zheng, Wu Rong. // 2010 International Conference on Image Analysis and Signal Processing (IASP). - Zhejiang, 9-11 April 2010. - P. 477-483. ↑

**C1371.** Chen Weishi. Detecting and tracking of small moving target in avian radar images. / Chen Weishi, Ning Huansheng, Li Jing. // 2010 International Conference on Image Analysis and Signal Processing (IASP). - Zhejiang, 9-11 April 2010. - P. 473-476. ↑

**C1372.** Yuanyuan Song. Accurate time interval measurement method based on Vernier caliper principle. / Yuanyuan Song, Dazhi Zeng, Yonghua Tian. // 2010 International Conference on Image Analysis and Signal Processing (IASP). - Zhejiang, 9-11 April 2010. - P. 553-555. ↑

**C1373.** Li Tingwei. A new method based on the BP neural network to improve the accuracy of inversion of the vegetation height. / Li Tingwei, Liang Diannong, Huang HaiFeng, Zhu Jubo. // 2010 International Conference on Image Analysis and Signal Processing (IASP). - Zhejiang, 9-11 April 2010. - P. 544-547. ↑

**C1374.** Rongbo Wang. Blind adaptive beamforming algorithm based on cyclostationary signals. / Rongbo Wang, Chaohuan Hou, Jun Yang. // 2010 International Conference on Image Analysis and Signal Processing (IASP). - Zhejiang, 9-11 April 2010. - P. 488-491. ↑

**C1375.** Zhang Kun-fan. Study on a method of compensation for the range profile of high velocity spatial targets. / Zhang Kun-fan, Feng Zhi-hong, Ma De-bao. // 2010 International Conference on Image Analysis and Signal Processing (IASP). - Zhejiang, 9-11 April 2010. - P. 450-453. ↑

**C1376.** Renbiao Wu. Study on adaptive monopulse with reduced dimension STAP technique. / Renbiao Wu, Lu Wang, Zhigang Su. // 2010 International Conference on Image Analysis and Signal Processing (IASP). - Zhejiang, 9-11 April 2010. - P. 159-163. ↑

**C1377.** Yongshun Zhang. Angle estimation of coherent multi-target for MIMO bistatic radar. / Yongshun Zhang, Yiduo Guo, Xinliang Niu, Guoqing Zhao. // 2010 International Conference on Image Analysis and Signal Processing (IASP). - Zhejiang, 9-11 April 2010. - P. 146-149. ↑

**C1378.** Guohua Lu. Contact-free measurement of heartbeat signal via a doppler radar using adaptive filtering. / Guohua Lu, Fang Yang, Xijing Jing, Jianqi Wang. // 2010 International Conference on Image Analysis and Signal Processing (IASP). - Zhejiang, 9-11 April 2010. - P. 89-92. ↑

**C1379.** Fang Li. Feature extraction and soft segmentation of texture images. / Fang Li, Ruihua Liu, Chaomin Shen. // 2010 International Conference on Image Analysis and Signal Processing (IASP). - Zhejiang, 9-11 April 2010. - P. 367-370. ↑

**C1380.** Wang Xiaojun. Parameters analysis for polarimetric SAR Based on classification accuracy. / Wang Xiaojun, Li Hao, Wu Yonghui, Yan Shusheng, Li Lianhua. // 2010 International Conference on Image Analysis and Signal Processing (IASP). - Zhejiang, 9-11 April 2010. - P. 268-271. ↑

**C1381.** Yuan Deng. Improved PGA algorithm based on adaptive range bins selection. / Yuan Deng, Yunhua Zhang. // 2010 International Conference on Image Analysis and Signal Processing (IASP). - Zhejiang, 9-11 April 2010. - P. 232-235. ↑

**C1382.** Ning Ma. SAR image despeckling using directionlet transform and Gaussian scale mixtures model. / Ning Ma, Zeming Zhou, Peng Zhang, Chun He. // 2010 2nd International Conference on Future Computer and Communication (ICFCC). - Wuhan, 21-24 May 2010. - Vol. 2. - P. V2-636-V2-640-636. ↑

- C1383.** Abramowicz Adam. Universal coupling curve for coupled resonators and transmission lines. 2010 18th International Conference on Microwave Radar and Wireless Communications (MIKON). - Vilnius, Lithuania, 14-16 June 2010. - P. 1-4. ↑
- C1384.** Marynowski Wojciech. Investigations of multilayer three-strip coplanar lines with the ferrite material. / Marynowski Wojciech, Mazur Jerzy. // 2010 18th International Conference on Microwave Radar and Wireless Communications (MIKON). - Vilnius, Lithuania, 14-16 June 2010. - P. 1-3. ↑
- C1385.** Kusiek Adam. Application of hybrid approach to the analysis of resonators loaded with axially symmetrical posts. / Kusiek Adam, Lech Rafal, Mazur Jerzy. // 2010 18th International Conference on Microwave Radar and Wireless Communications (MIKON). - Vilnius, Lithuania, 14-16 June 2010. - P. 1-3. ↑
- C1386.** Dudas Levente. Receiver Antenna Array. / Dudas Levente, Rosner Vilmos, Seller Rudolf, Kazi Karoly, Minh Nguyen Thi Ngoc. // 2010 18th International Conference on Microwave Radar and Wireless Communications (MIKON). - Vilnius, Lithuania, 14-16 June 2010. - P. 1-4. ↑
- C1387.** Andrushchak N. A. A new method for refractive index measurement of isotropic and anisotropic materials in millimeter and submillimeter wave range. / Andrushchak N. A., Bobitskii Ya. V., Maksymyuk T. V., Syrotynsky O. I., Andrushchak A. S., Karbovnyk I. D. // 2010 18th International Conference on Microwave Radar and Wireless Communications (MIKON). - Vilnius, Lithuania, 14-16 June 2010. - P. 1-3. ↑
- C1388.** Lewandowski Arkadiusz. Multi-frequency approach to the coaxial multiline through-reflect-line calibration. / Lewandowski Arkadiusz, Wiatr Wojciech, Dobrowolski Janusz. // 2010 18th International Conference on Microwave Radar and Wireless Communications (MIKON). - Vilnius, Lithuania, 14-16 June 2010. - P. 1-4. ↑
- C1389.** Miazga Przemyslaw. Discrete shape optimization method for the non-uniform transmission line directional couplers. 2010 18th International Conference on Microwave Radar and Wireless Communications (MIKON). - Vilnius, Lithuania, 14-16 June 2010. - P. 1-3. ↑
- C1390.** Zhang Zihui. Modeling of integrated microstrip bend structures on silicon substrates up to 110 GHz. / Zhang Zihui, Gruner Daniel, Boeck Georg. // 2010 18th International Conference on Microwave Radar and Wireless Communications (MIKON). - Vilnius, Lithuania, 14-16 June 2010. - P. 1-4. ↑
- C1391.** Usanov D.A. Photonic structures in the microwave band and their applications. / Usanov D.A., Skripal A.V., Abramov A.V., Bogolubov A.S., Kulikov M.Y., Ponomarev D.V. // 2010 18th International Conference on Microwave Radar and Wireless Communications (MIKON). - Vilnius, 14-16 June 2010. - P. 1-9. ↑
- C1392.** Ould-Elhassen M. Analytical study and simulation of distributed phase shifter. / Ould-Elhassen M., Mabrouk M., Ghazel A., Benech P. // 2010 18th International Conference on Microwave Radar and Wireless Communications (MIKON). - Vilnius, 14-16 June 2010. - P. 1-2. ↑
- C1393.** Lech Rafal. Tuning properties of irregular posts in waveguide junctions-tunable filter application. / Lech Rafal, Kusiek Adam, Mazur Jerzy. // 2010 18th International Conference on Microwave Radar and Wireless Communications (MIKON). - Vilnius, Lithuania, 14-16 June 2010. - P. 1-4. ↑
- C1394.** Bialkowski Marek E. Design of UWB uniplanar 180° hybrid employing ground slots and microstrip-slot transitions. / Bialkowski Marek E., Wang Yifan. // 2010 18th International Conference on Microwave Radar and Wireless Communications (MIKON). - Vilnius, Lithuania, 14-16 June 2010. - P. 1-4. ↑
- C1395.** Szymanski Piotr. Performance and characterization of MMIC phase shifter with wire bonds interconnections. 2010 18th International Conference on Microwave Radar and Wireless Communications (MIKON). - Vilnius, Lithuania, 14-16 June 2010. - P. 1-4. ↑
- C1396.** Wiatr Wojciech. Line-length optimization of offset-short standards for broadband VNA calibration. 2010 18th International Conference on Microwave Radar and Wireless Communications (MIKON). - Vilnius, Lithuania, 14-16 June 2010. - P. 1-4. ↑
- C1397.** O'Driscoll S. Adaptive signal acquisition and wireless power transfer for an implantable prosthesis processor. / O'Driscoll S., Meng T.H. // Proceedings of 2010 IEEE International Symposium on Circuits and Systems (ISCAS). - Paris, May 30 2010-June 2 2010. - P. 3589-3592. ↑
- C1398.** Xubo Wang. Low-power low-complexity carrier-based UWB transmitter in 90nm CMOS for wireless



biomedical radar sensing applications. / Xubo Wang, Dinh A., Teng D. // Proceedings of 2010 IEEE International Symposium on Circuits and Systems (ISCAS). - Paris, May 30 2010-June 2 2010. - P. 3477-3480. ↑

**C1399.** Vaidyanathan P.P. Active beamforming with interpolated FIR filterin. / Vaidyanathan P.P., Ching-Chih Weng. // Proceedings of 2010 IEEE International Symposium on Circuits and Systems (ISCAS). - Paris, May 30 2010-June 2 2010. - P. 173-176. ↑

**C1400.** Xianfeng Xu. A joint block diagonalization approach to convolutive blind source separation. / Xianfeng Xu, Da-Zheng Feng, Wei Xing Zheng. // Proceedings of 2010 IEEE International Symposium on Circuits and Systems (ISCAS). - Paris, May 30 2010-June 2 2010. - P. 805-808. ↑

**C1401.** Gilreath L. A W-band LNA in 0.18- $\mu\text{m}$  SiGe BiCMOS. / Gilreath L., Jam V., Heydan P. // Proceedings of 2010 IEEE International Symposium on Circuits and Systems (ISCAS). - Paris, May 30 2010-June 2 2010. - P. 753-756. ↑

**C1402.** Patterson R.D. Auditory speech processing for scale-shift covariance and its evaluation in automatic speech recognition. / Patterson R.D., Walters T.C., Monaghan J., Feldbauer C., Irino T. // Proceedings of 2010 IEEE International Symposium on Circuits and Systems (ISCAS). - Paris, May 30 2010-June 2 2010. - P. 3813-3816. ↑

**C1403.** Bin Deng. Ambiguity function analysis for MCPC radar signal. / Bin Deng, Bin Sun, Xizhang Wei, Xiang Li. // 2010 2nd International Conference on Industrial Mechatronics and Automation (ICIMA). - Wuhan, China, 30-31 May 2010. - Vol. 2. - P. 650-653. ↑

**C1404.** Liu Jian-wei. A novel DOA estimation technique for coherent real-valued sources. / Liu Jian-wei, Chen Hui. // 2010 2nd International Conference on Industrial Mechatronics and Automation (ICIMA). - Wuhan, China, 30-31 May 2010. - Vol. 2. - P. 135-138. ↑

**C1405.** Chen Chang-xiao. A novel method for extraction of in-pulse feature of LFM signal. / Chen Chang-xiao, He Ming-hao, Yu Chunlai. // 2010 2nd International Conference on Industrial Mechatronics and Automation (ICIMA). - Wuhan, China, 30-31 May 2010. - Vol. 2. - P. 692-697. ↑

**C1406.** Usanov D.A. Complex dielectric permittivity of composites based on dielectric matrixes with inclusions of carbon nanotubes. / Usanov D.A., Skripal A.V., Romanov A.V. // 2010 18th International Conference on Microwave Radar and Wireless Communications (MIKON). - Vilnius, 14-16 June 2010. - P. 1-4. ↑

**C1407.** Zeng Jiankui. Some MIMO radar advantages over phased array radar. / Zeng Jiankui, Dong Ziming. // 2010 2nd International Conference on Industrial Mechatronics and Automation (ICIMA). - Wuhan, China, 30-31 May 2010. - Vol. 2. - P. 211-213. ↑

**C1408.** Zeng Jiankui. The application of chaotic signal in MIMO radar. 2010 2nd International Conference on Industrial Mechatronics and Automation (ICIMA). - Wuhan, China, 30-31 May 2010. - Vol. 2. - P. 214-216. ↑

**C1409.** Jiankui Zeng. Fast Hough transform algorithm for radar detection. / Jiankui Zeng, Xiang Lijuan. // 2010 2nd International Conference on Industrial Mechatronics and Automation (ICIMA). - Wuhan, China, 30-31 May 2010. - Vol. 2. - P. 207-210. ↑

**C1410.** Lengvinas Gintautas. Aggregate type identification in concrete compounds using microwave transmission line and ANN. / Lengvinas Gintautas, Deksnys Vytutas. // 2010 18th International Conference on Microwave Radar and Wireless Communications (MIKON). - Vilnius, Lithuania, 14-16 June 2010. - P. 1-4. ↑

**C1411.** Parshin Yu. N. Dynamic mode of radiosystem with spatial structure optimization in presence of interferences. / Parshin Yu. N., Gusev S. I. // 2010 18th International Conference on Microwave Radar and Wireless Communications (MIKON). - Vilnius, Lithuania, 14-16 June 2010. - P. 1-4. ↑

**C1412.** Maceika Kazimieras. Lithuanian experience of evaluation on radar antenna radiation. 2010 18th International Conference on Microwave Radar and Wireless Communications (MIKON). - Vilnius, Lithuania, 14-16 June 2010. - P. 1-4. ↑

**C1413.** Dagys Mindaugas. Investigation of susceptibility of routers to high power microwave pulse radiation. / Dagys Mindaugas, Kancleris Zilvinas, Ragulis Paulius, Simniskis Rimantas, Tamosiunas Vincas. // 2010 18th International Conference on Microwave Radar and Wireless Communications (MIKON). - Vilnius, Lithuania, 14-

16 June 2010. - P. 1-3. ↑

**C1414.** Dhaouadi M. Magnetic antenna for near-field UHF RFID tag. / Dhaouadi M., Mabrouk M., Ghazel A. // 2010 18th International Conference on Microwave Radar and Wireless Communications (MIKON). - Vilnius, Lithuania, 14-16 June 2010. - P. 1-2. ↑

**C1415.** Vossiek Martin. RF identification and localization-recent steps towards the internet of things in metal production and processing. / Vossiek Martin, Miesen Robert, Wittwer Joachim. // 2010 18th International Conference on Microwave Radar and Wireless Communications (MIKON). - Vilnius, Lithuania, 14-16 June 2010. - P. 1-8. ↑

**C1416.** Kozlowski Kamil. Hybrid RFID System. / Kozlowski Kamil, Bizewski Karol, Michalek Maciej, Kulas Lukasz, Nyka Krzysztof. // 2010 18th International Conference on Microwave Radar and Wireless Communications (MIKON). - Vilnius, Lithuania, 14-16 June 2010. - P. 1-4. ↑

**C1417.** Juchniewicz Jakub. EGSM and CDMA collocation and near field antenna estimation. / Juchniewicz Jakub, Bandurski Wojciech. // 2010 18th International Conference on Microwave Radar and Wireless Communications (MIKON). - Vilnius, Lithuania, 14-16 June 2010. - P. 1-4. ↑

**C1418.** Bugaj Marek. Optimization parameters of dielectric in aperture-coupled stacked patch antenna on bandwidth. / Bugaj Marek, Wnuk Marian. // 2010 18th International Conference on Microwave Radar and Wireless Communications (MIKON). - Vilnius, Lithuania, 14-16 June 2010. - P. 1-4. ↑

**C1419.** Panzner Berthold. A compact double-ridged horn antenna for ground penetrating radar applications. / Panzner Berthold, Jostingmeier Andreas, Omar Abbas. // 2010 18th International Conference on Microwave Radar and Wireless Communications (MIKON). - Vilnius, Lithuania, 14-16 June 2010. - P. 1-4. ↑

**C1420.** Maksimovitch Yelena. Study of effect of corrugated edges on the radiation characteristics of GPR antenna. / Maksimovitch Yelena, Mikhnev Valeri, Vainikainen Pertti. // 2010 18th International Conference on Microwave Radar and Wireless Communications (MIKON). - Vilnius, Lithuania, 14-16 June 2010. - P. 1-4. ↑

**C1421.** Pergol Mariusz. Broadband microstrip patch antenna with reduced transversal size. / Pergol Mariusz, Zieniutycz Włodzimierz, Mazur Mateusz. // 2010 18th International Conference on Microwave Radar and Wireless Communications (MIKON). - Vilnius, Lithuania, 14-16 June 2010. - P. 1-3. ↑

**C1422.** Phan Hong Phuong. A design and adjustment method for ultrawideband microstrip antenna design. / Phan Hong Phuong, Nguyen Dat Son. // 2010 18th International Conference on Microwave Radar and Wireless Communications (MIKON). - Vilnius, Lithuania, 14-16 June 2010. - P. 1-4. ↑

**C1423.** Wang Yifan. Compact Tapered Slot Antennas for UWB microwave imaging applications. / Wang Yifan, Bakar Aslina Abu, Bialkowski Marek E. // 2010 18th International Conference on Microwave Radar and Wireless Communications (MIKON). - Vilnius, Lithuania, 14-16 June 2010. - P. 1-4. ↑

**C1424.** Kopyt Pawel. A 5.8 GHz RFID-based data transmission system as an energy efficient solution for on-board monitoring. 2010 18th International Conference on Microwave Radar and Wireless Communications (MIKON). - Vilnius, Lithuania, 14-16 June 2010. - P. 1-4. ↑

**C1425.** Ambrozkiwicz Mikolaj. Wavelets on nonuniform triangular meshes for fast basis transform. / Ambrozkiwicz Mikolaj, Jacob Arne F. // 2010 18th International Conference on Microwave Radar and Wireless Communications (MIKON). - Vilnius, Lithuania, 14-16 June 2010. - P. 1-4. ↑

**C1426.** Gric Tatjana. 3D vector electric field distributions and dispersion characteristics of open rectangular and circular metamaterial waveguides. / Gric Tatjana, Asmontas Steponas, Nickelson Liudmila. // 2010 18th International Conference on Microwave Radar and Wireless Communications (MIKON). - Vilnius, Lithuania, 14-16 June 2010. - P. 1-4. ↑

**C1427.** Podwalski Jakub. Advanced macromodel matrix structure cloning for FDTD. / Podwalski Jakub, Kulas Lukasz, Mrozowski Michal. // 2010 18th International Conference on Microwave Radar and Wireless Communications (MIKON). - Vilnius, Lithuania, 14-16 June 2010. - P. 1-2. ↑

**C1428.** Bialkowski Marek E. UWB microwave imaging system including circular array antenna. / Bialkowski Marek E., Wang Yifan, Bakar Aslina Abu, Khor Wee Chang. // 2010 18th International Conference on Microwave

Radar and Wireless Communications (MIKON). - Vilnius, Lithuania, 14-16 June 2010. - P. 1-4. ↑

C1429. Zylkov D. Dispersion dependencies of glass pipe waveguides filled with lossy biological liquids. / Zylkov D., Nickelson L., Asmontas S., Martavicius R. // 2010 18th International Conference on Microwave Radar and Wireless Communications (MIKON). - Vilnius, 14-16 June 2010. - P. 1-4. ↑

C1430. Laurinavic. Millimeter wave application for non-destructive homogeneity characterization of semiconductor and dielectric wafers. / Laurinavicius A., Anbinderis T. // 2010 18th International Conference on Microwave Radar and Wireless Communications (MIKON). - Vilnius, 14-16 June 2010. - P. 1-4. ↑

C1431. Fotyga Grzegorz. Reduced-order models in the finite element analysis. / Fotyga Grzegorz, Nyka Krzysztof, Kulas Lukasz. // 2010 18th International Conference on Microwave Radar and Wireless Communications (MIKON). - Vilnius, Lithuania, 14-16 June 2010. - P. 1-2. ↑

C1432. Zamlynski Mariusz. Verification of the mutual coupling compensation technique in small planar antenna arrays. / Zamlynski Mariusz, Slobodzian Piotr. // 2010 18th International Conference on Microwave Radar and Wireless Communications (MIKON). - Vilnius, Lithuania, 14-16 June 2010. - P. 1-4. ↑

C1433. Borowiec Robert. A printed RFID Tag antenna for metallic objects operating in UHF band. 2010 18th International Conference on Microwave Radar and Wireless Communications (MIKON). - Vilnius, Lithuania, 14-16 June 2010. - P. 1-4. ↑

C1434. Toshev Alexander G. Analysis, design and measurement of a low sidelobe level lightweight array antenna for surveillance radar applications. 2010 18th International Conference on Microwave Radar and Wireless Communications (MIKON). - Vilnius, Lithuania, 14-16 June 2010. - P. 1-4. ↑

C1435. Czawka Giennadij. Matrix analysis of antenna array for MIMO UWB systems. / Czawka Giennadij, Garbaruk Marek, Nowakowski Marek. // 2010 18th International Conference on Microwave Radar and Wireless Communications (MIKON). - Vilnius, Lithuania, 14-16 June 2010. - P. 1-4. ↑

C1436. Januszkiewicz Lukasz. The analysis of textile antenna array radiation pattern. 2010 18th International Conference on Microwave Radar and Wireless Communications (MIKON). - Vilnius, Lithuania, 14-16 June 2010. - P. 1-4. ↑

C1437. Mazur Mateusz. Multiband omnidirectional communication antenna. 2010 18th International Conference on Microwave Radar and Wireless Communications (MIKON). - Vilnius, Lithuania, 14-16 June 2010. - P. 1-4. ↑

C1438. Miller S.R. Enhanced direction of arrival estimation via reassigned space-time-frequency methods. / Miller S.R., Spanias A.S., Papandreou-Suppappola A., Santucci R. // Proceedings of 2010 IEEE International Symposium on Circuits and Systems (ISCAS). - Paris, May 30 2010-June 2 2010. - P. 2538-2541. ↑

C1439. Zhuo Zhang. Measurement and performance of digital monopulse radar array antenna. / Zhuo Zhang, Guoqiang Zhao, Xingyao Zeng, Houjun Sun, Xin Lv. // 2010 International Conference on Microwave and Millimeter Wave Technology (ICMMT). - Chengdu, 8-11 May 2010. - P. 983-986. ↑

C1440. Huajiang Wang. Integrated Millimeter-wave passive devices based on Silicon substrate for SoP application. / Huajiang Wang, Liang Wu, Jiajie Tang, Rong Qian, Yang Hou, Wei Wang, Lingyun Li, Xiaowei Sun, Le Luo. // 2010 International Conference on Microwave and Millimeter Wave Technology (ICMMT). - Chengdu, 8-11 May 2010. - P. 1963-1966. ↑

C1441. Keyan Tian. Minimized Ku band microstrip circulator design. / Keyan Tian, Li Zhi You, Hua Liu. // 2010 International Conference on Microwave and Millimeter Wave Technology (ICMMT). - Chengdu, 8-11 May 2010. - P. 1967-1968. ↑

C1442. Linfeng He. An improved High-Frequency-Raised inversion algorithm for radar imaging. / Linfeng He, Qingxia Li, Yi Leng, Jian Dong, Guoping Hu. // 2010 International Conference on Microwave and Millimeter Wave Technology (ICMMT). - Chengdu, 8-11 May 2010. - P. 987-990. ↑

C1443. Boren Zheng. Millimeter wave beam tilting array for radar system. / Boren Zheng, Zhiqin Zhao, Dakui Wu. // 2010 International Conference on Microwave and Millimeter Wave Technology (ICMMT). - Chengdu, 8-11 May 2010. - P. 991-993. ↑

- C1444.** Zhuo Zhang. A transceiver for Ku band digital monopulse radar system. / Zhuo Zhang, Guoqiang Zhao, Xingyao Zeng, Houjun Sun, Xin Lv. // 2010 International Conference on Microwave and Millimeter Wave Technology (ICMMT). - Chengdu, 8-11 May 2010. - P. 979-982. ↑
- C1445.** Hengfei Xu. Design and simulation of ultra-wideband double-ridged horn antenna. / Hengfei Xu, Yang Zhou, En Li, Hongxiu Liu, Qing Wang, Ziming Zhong. // 2010 International Conference on Microwave and Millimeter Wave Technology (ICMMT). - Chengdu, 8-11 May 2010. - P. 950-952. ↑
- C1446.** Gu Min. Calculation of the characteristic impedance of TEM horn antenna using support vector machine. / Gu Min, Yang Feng. // 2010 International Conference on Microwave and Millimeter Wave Technology (ICMMT). - Chengdu, 8-11 May 2010. - P. 895-897. ↑
- C1447.** Li Zheng-jun. Scattering characteristic of soot aggregation particles randomly distributed. / Li Zheng-jun, Wu Zhen-sen, Li Huan, Yuan Qiong-kun. // 2010 International Conference on Microwave and Millimeter Wave Technology (ICMMT). - Chengdu, 8-11 May 2010. - P. 2007-2010. ↑
- C1448.** Zhengwei Wang. A compact quasi-lumped LTCC diplexer for radar application. / Zhengwei Wang, Jinming Lai, Shirong Bu, Zhengxiang Luo. // 2010 International Conference on Microwave and Millimeter Wave Technology (ICMMT). - Chengdu, 8-11 May 2010. - P. 860-863. ↑
- C1449.** Chang Lei. Application of parallel integer coded differential evolution strategy on ultra-wide band TEM horn antenna. / Chang Lei, Liao Cheng, Zheng Xuan, Chen Ling-Lu, Su Gang. // 2010 International Conference on Microwave and Millimeter Wave Technology (ICMMT). - Chengdu, 8-11 May 2010. - P. 937-939. ↑
- C1450.** Changning Wan. Integrated design of wide-band wide-scan phased array antenna and couple line. / Changning Wan, Hongchao Wu, Chenhai Xia. // 2010 International Conference on Microwave and Millimeter Wave Technology (ICMMT). - Chengdu, 8-11 May 2010. - P. 940-943. ↑
- C1451.** Zhi Xu. Edge diffraction effects on the RCS analysis of antenna array. / Zhi Xu, Xuequan Yan, Zhenghe Feng, Shuxi Gong, Qizhong Liu. // 2010 International Conference on Microwave and Millimeter Wave Technology (ICMMT). - Chengdu, 8-11 May 2010. - P. 1995-1998. ↑
- C1452.** Li Bin. The research of broadband millimeter-wave Vivaldi array antenna using SIW technique. / Li Bin, Dong Liang, Zhao Jiao-cheng. // 2010 International Conference on Microwave and Millimeter Wave Technology (ICMMT). - Chengdu, 8-11 May 2010. - P. 997-1000. ↑
- C1453.** Yu Nai. Analysis of wide-band aperture-coupled microstrip antenna array by CN-FDTD. / Yu Nai, RuiNa Xing, Dan Sun. // 2010 International Conference on Microwave and Millimeter Wave Technology (ICMMT). - Chengdu, 8-11 May 2010. - P. 823-826. ↑
- C1454.** Wang H. A novel frequency scanning monopulse microstrip antenna array. / Wang H., Ni J., Sun W.Z., Ma X.F., Sheng W.X. // 2010 International Conference on Microwave and Millimeter Wave Technology (ICMMT). - Chengdu, 8-11 May 2010. - P. 1118-1121. ↑
- C1455.** Yan-Ying Bai. Wide-band and low cross polarization conformal array with microstrip parasitic-dipole antenna. / Yan-Ying Bai, Shaoqiu Xiao, Zhuo-Fu Ding, Bing-Zhong Wang. // 2010 International Conference on Microwave and Millimeter Wave Technology (ICMMT). - Chengdu, 8-11 May 2010. - P. 1114-1117. ↑
- C1456.** Zhang Jin-Peng. Surveillance and inversion of regional atmospheric duct from multiple radar stations. / Zhang Jin-Peng, Wu Zhen-Sen, Hu Rong-Xu, Dong Cui. // 2010 International Conference on Microwave and Millimeter Wave Technology (ICMMT). - Chengdu, 8-11 May 2010. - P. 1177-1180. ↑
- C1457.** ChongHua Fang. Scattering characteristic from a cylindrical Salisbury screen with 1rad. / ChongHua Fang, Hui Tan, Qi Zhang, DaGang Xie. // 2010 International Conference on Microwave and Millimeter Wave Technology (ICMMT). - Chengdu, 8-11 May 2010. - P. 1153-1155. ↑
- C1458.** Hangang Xia. Grid-cell combination in 3D-FDTD modeling of ELF propagation of the earth. / Hangang Xia, Yi Wang, Qunsheng Cao. // 2010 International Conference on Microwave and Millimeter Wave Technology (ICMMT). - Chengdu, 8-11 May 2010. - P. 782-785. ↑
- C1459.** Wang Hui. An efficient splitting the plane-wave FDTD method. / Wang Hui, Huang Zhi-xiang, Wu Xian-liang, Liu Xiao-yong. // 2010 International Conference on Microwave and Millimeter Wave Technology (ICMMT).



- Chengdu, 8-11 May 2010. - P. 842-844. ↑

**C1460.** Zhang Chao. The method of microwave power amplifier model parameter test based on the larger-signal scattering function. / Zhang Chao, Nian Fushun, Liang Shengli, Cao Zhiying. // 2010 International Conference on Microwave and Millimeter Wave Technology (ICMMT). - Chengdu, 8-11 May 2010. - P. 1090-1093. ↑

**C1461.** Li Guiping. A Ka-band T/R front-end for phased array radar. / Li Guiping, Xu Jun, Luo Shendu, Wang Maoyan. // 2010 International Conference on Microwave and Millimeter Wave Technology (ICMMT). - Chengdu, 8-11 May 2010. - P. 1001-1004. ↑

**C1462.** Shi X. Illumination method for millimeter wave imaging indoors. / Shi X., Yang M.H., Guan F.H., Sun X.W. // 2010 International Conference on Microwave and Millimeter Wave Technology (ICMMT). - Chengdu, 8-11 May 2010. - P. 1005-1007. ↑

**C1463.** Ben Sun. Acceleration of Time-Domain Finite-Element Method in electromagnetic analysis with OpenMP. / Ben Sun, Lanlan Ping, Xiaoxiang He. // 2010 International Conference on Microwave and Millimeter Wave Technology (ICMMT). - Chengdu, 8-11 May 2010. - P. 845-848. ↑

**C1464.** Liang Wu. Research on Si-based MEMS process in development 3D millimeter-wave multi-chip module package. / Liang Wu, Huajiang Wang, Jiajie Tang, Rong Qian, Yang Hou, Wei Wang, Sun Hao, Lingyun Li, Xiaowei Sun, Le Luo. // 2010 International Conference on Microwave and Millimeter Wave Technology (ICMMT). - Chengdu, 8-11 May 2010. - P. 1049-1052. ↑

**C1465.** Li Zhong-yun. Design and implementation of a LTCC-based receiver front-end module. / Li Zhong-yun, Zeng Geng-hua, Chen Peng, Yang Jian-yu. // 2010 International Conference on Microwave and Millimeter Wave Technology (ICMMT). - Chengdu, 8-11 May 2010. - P. 1053-1056. ↑

**C1466.** Huilin Chen. An ultra wide band power divider/combiner based on Y-structure waveguide. / Huilin Chen, Xiaoqiang Xie, Ruimin Xu. // 2010 International Conference on Microwave and Millimeter Wave Technology (ICMMT). - Chengdu, 8-11 May 2010. - P. 853-855. ↑

**C1467.** Zhang Zhonghua. Parameter Identification Method for Ship Swaying Motion Differential Equations. / Zhang Zhonghua, Li Xiaoyong, Yang Lei, Chen Guiming, Wu Yi. // 2010 Third International Joint Conference on Computational Science and Optimization (CSO). - Huangshan, Anhui, China, 28-31 May 2010. - Vol. 1. - P. 205-208. ↑

**C1468.** Cong Deng. A Comparative Study of the DGTD Algorithm and the FDTD Algorithm in Computational Electromagnetics. / Cong Deng, Wenlu Yin, Shunlian Chai, Junjie Mao. // 2010 Third International Joint Conference on Computational Science and Optimization (CSO). - Huangshan, Anhui, 28-31 May 2010. - Vol. 1. - P. 56-59. ↑

**C1469.** Ting-En Lee. Design of an alpha-beta filter by combining fuzzy logic with evolutionary methods. / Ting-En Lee, Juhng-Peng Su, Ker-Wei Yu, Kuo-Hsien Hsia, Chun-Chieh Wang. // 2010 International Symposium on Computer Communication Control and Automation (3CA). - Tainan, 5-7 May 2010. - Vol. 2. - P. 270-273. ↑

**C1470.** Yucheng Zhou. Notice of Violation of IEEE Publication PrinciplesExtended target tracking using an IMM based nonlinear Kalman filters. / Yucheng Zhou, Jiahe Xu, Yuanwei Jing, Dimirovski G.M. // 2010 American Control Conference (ACC). - Baltimore, MD, June 30 2010-July 2 2010. - P. 6876-6881. ↑

**C1471.** Lu Bibo. Speckle Reduction with Multiresolution Bilateral Filtering for SAR Image. / Lu Bibo, Ku Yongxia. // 2010 International Conference on Machine Vision and Human-Machine Interface (MVHI). - Kaifeng, China, 24-25 April 2010. - P. 700-703. ↑

**C1472.** Ling Wang. Novel Space-Time Processing Method for Airborne SAR to Detect and Image the Slowly Moving Targets. / Ling Wang, Lugu Zhen, Yalin Guan. // 2010 Third International Joint Conference on Computational Science and Optimization (CSO). - Huangshan, Anhui, 28-31 May 2010. - Vol. 2. - P. 435-439. ↑

**C1473.** Weidong Zhang. Universal test bench of diesel hydraulic governor based on hardware-in-loop simulation. / Weidong Zhang, Yourong Zhang, Shihua Liu, Guangyao Ouyang, Zhenming Liu. // 2010 International Symposium on Computer Communication Control and Automation (3CA). - Tainan, 5-7 May 2010. - Vol. 1. - P. 350-353. ↑

- C1474.** Pal P. Beamforming using passive nested arrays of sensors. / Pal P., Vaidyanathan P.P. // Proceedings of 2010 IEEE International Symposium on Circuits and Systems (ISCAS). - Paris, May 30 2010-June 2 2010. - P. 2840-2843. ↑
- C1475.** Xin Xiao. Reduced memory architecture for CORDIC-based FFT. / Xin Xiao, Oruklu E., Saniie J. // Proceedings of 2010 IEEE International Symposium on Circuits and Systems (ISCAS). - Paris, May 30 2010-June 2 2010. - P. 2690-2693. ↑
- C1476.** Abramov S. Improved method for blind estimation of the variance of mixed noise using weighted LMS line fitting algorithm. / Abramov S., Zabrodina V., Lukin V., Vozel B., Chehdi K., Astola J. // Proceedings of 2010 IEEE International Symposium on Circuits and Systems (ISCAS). - Paris, May 30 2010-June 2 2010. - P. 2642-2645. ↑
- C1477.** Li-Wei Fong. Multi-sensor data fusion via federated adaptive filter. 2010 International Symposium on Computer Communication Control and Automation (3CA). - Tainan, 5-7 May 2010. - Vol. 1. - P. 209-212. ↑
- C1478.** Xu Buyun. Multi-network video streaming in a campus visit scenario. / Xu Buyun, Hughes Danny, Man Ka Lok. // 2010 3rd International Conference on Information Sciences and Interaction Sciences (ICIS). - Chengdu, China, 23-25 June 2010. - P. 699-703. ↑
- C1479.** Lin Zhao. The design and analysis on the small-scale antenna of spread frequency radio lifesaving system. / Lin Zhao, Yang Liu, Yang Chen. // 2010 International Conference on Mechanic Automation and Control Engineering (MACE). - Wuhan, 26-28 June 2010. - P. 2938-2942. ↑
- C1480.** Manzoor Farhan. Passive RFID-based Indoor Positioning System, An Algorithmic Approach. / Manzoor Farhan, Huang Yi, Menzel Karsten. // 2010 IEEE International Conference on RFID-Technology and Applications (RFID-TA). - Guangzhou, China, 17-19 June 2010. - P. 112-117. ↑
- C1481.** Jin D.Y. A thermal design methodology for power SiGe HBTs with non-uniform emitter finger spacing. / Jin D.Y., Zhang W.R., Guan B.L., Chen L., Hu N., Xiao Y., Wang R.Q. // 2010 International Conference on Microwave and Millimeter Wave Technology (ICMMT). - Chengdu, 8-11 May 2010. - P. 510-513. ↑
- C1482.** Yuan Xuelin. High-repetition and -stability all-solid state pulsed based on avalanche transistor Marx circuit. / Yuan Xuelin, Ding Zhenjie, Hao Qingsong, Yu Jianguo, Zeng Bo, Hu Long. // 2010 International Conference on Microwave and Millimeter Wave Technology (ICMMT). - Chengdu, 8-11 May 2010. - P. 454-455. ↑
- C1483.** Jianjun Ding. Analysis of electromagnetic scattering of cavities with nonuniform plasma coating. / Jianjun Ding, Shang S., Rushan Chen, Fan Z.H. // 2010 International Conference on Microwave and Millimeter Wave Technology (ICMMT). - Chengdu, 8-11 May 2010. - P. 148-151. ↑
- C1484.** Tan Yuan. Application of AMC on mini ultra-near radar detecting system. / Tan Yuan, Yang Yong, Liang Ruihai, Yuan Naichang. // 2010 International Conference on Microwave and Millimeter Wave Technology (ICMMT). - Chengdu, 8-11 May 2010. - P. 2037-2039. ↑
- C1485.** Feng Zhao. 4H-SiC bipolar junction transistors for UHF and L-band long-pulse radar applications. / Feng Zhao, Sudarshan T.S., Tiefeng Shi. // 2010 International Conference on Microwave and Millimeter Wave Technology (ICMMT). - Chengdu, 8-11 May 2010. - P. 2055-2058. ↑
- C1486.** Ren Mingqiu. Classification of radar signals using time-frequency transforms and fuzzy clustering. / Ren Mingqiu, Cai Jinyan, Zhu Yuanqing. // 2010 International Conference on Microwave and Millimeter Wave Technology (ICMMT). - Chengdu, 8-11 May 2010. - P. 2067-2070. ↑
- C1487.** Zhengli Han. FDTD analysis of three-dimensional target covered with inhomogeneous unmagnetized plasma. / Zhengli Han, Jun Ding, Peilin Chen, Zhaocheng Zhang, Chenjiang Guo. // 2010 International Conference on Microwave and Millimeter Wave Technology (ICMMT). - Chengdu, 8-11 May 2010. - P. 125-128. ↑
- C1488.** Zhang Deng-hui. Analysis of image fusion and classification for high resolution SAR data on-line. / Zhang Deng-hui, Zhang Han-kui, Xie Bin, Huang Zhao-quan, Yu Le, Cao Yun-yun. // 2010 2nd International Conference on Education Technology and Computer (ICETC). - Shanghai, 22-24 June 2010. - Vol. 1. - P. V1-267-V1-271-267. ↑

- C1489.** Dezhi Jin. The innovation on the education model of the engineering management-based on the viewpoint of WSR methodology. / Dezhi Jin, Zhaotong Zhang, Meigui Han, Jianming Yang. // 2010 2nd International Conference on Education Technology and Computer (ICETC). - Shanghai, 22-24 June 2010. - Vol. 3. - P. V3-408-V3-412-408. ↑
- C1490.** Yang Yuhai. Intelligence analysis in early warning air roster training. / Yang Yuhai, Xiong Jiajun, Jiang Surong, Bin Xuelian. // 2010 2nd International Conference on Education Technology and Computer (ICETC). - Shanghai, 22-24 June 2010. - Vol. 4. - P. V4-427-V4-429-427. ↑
- C1491.** He-lin Yang. EM scattering by conductor plate coated with multilayered medium having metamaterials. / He-lin Yang, Ting Xiao, Yong-zhi Cheng, Min-hua Li, Bo-xun Xiao, Guo-ping Zhang. // 2010 International Conference on Microwave and Millimeter Wave Technology (ICMMT). - Chengdu, 8-11 May 2010. - P. 129-131. ↑
- C1492.** Lu Tian. Application of VSIE method to scattering problem involving conducting and anisotropic bodies. / Lu Tian, Zhao Yanwen, Yang Yingyi. // 2010 International Conference on Microwave and Millimeter Wave Technology (ICMMT). - Chengdu, 8-11 May 2010. - P. 102-106. ↑
- C1493.** Hai Li. Multi-target scattering analysis based on generalized higher-order finite-difference time-domain method. / Hai Li, ZhenHai Shao, Swee Ping Yeo, Meng Hiot Lim, Yew Kong Leong. // 2010 International Conference on Microwave and Millimeter Wave Technology (ICMMT). - Chengdu, 8-11 May 2010. - P. 88-90. ↑
- C1494.** Brenchley Mark. Supporting omni-directional communications capability in variable attitude spacecraft. / Brenchley Mark, Garner Peter, Maynard Kevin, Butlin Tim, Krabel Eckhard. // 2010 18th International Conference on Microwave Radar and Wireless Communications (MIKON). - Vilnius, Lithuania, 14-16 June 2010. - P. 1-6. ↑
- C1495.** Ravanelli R. Multi-objective optimization of an isoflux antenna for LEO satellite down-handling link. / Ravanelli R., Iannicelli C., Baldecchi N., Franchini F. // 2010 18th International Conference on Microwave Radar and Wireless Communications (MIKON). - Vilnius, Lithuania, 14-16 June 2010. - P. 1-4. ↑
- C1496.** Georgieva-Grosse Mariana Nikolova. Criteria for phase shifter operation of an azimuthally magnetized coaxial ferrite waveguide. / Georgieva-Grosse Mariana Nikolova, Georgiev Georgi Nikolov. // 2010 18th International Conference on Microwave Radar and Wireless Communications (MIKON). - Vilnius, Lithuania, 14-16 June 2010. - P. 1-4. ↑
- C1497.** Georgiev Georgi Nikolov. Principles of the electromagnetic modelling of some microwave components, based on the circular waveguides with azimuthally magnetized ferrite. / Georgiev Georgi Nikolov, Georgieva-Grosse Mariana Nikolova. // 2010 18th International Conference on Microwave Radar and Wireless Communications (MIKON). - Vilnius, Lithuania, 14-16 June 2010. - P. 1-6. ↑
- C1498.** Jaworski Grzegorz. A design of beam forming network integrated in multilayer microstrip structure for applications in airborne SAR. / Jaworski Grzegorz, Maleszka Tomasz. // 2010 18th International Conference on Microwave Radar and Wireless Communications (MIKON). - Vilnius, Lithuania, 14-16 June 2010. - P. 1-4. ↑
- C1499.** Parshin Vladimir. Resonator techniques for reflectivity and surface resistivity at high temperature: Methodology and measurements. / Parshin Vladimir, Serov Eugenie, Ravanelli Rodolfo, van't Klooster C. G. M. // 2010 18th International Conference on Microwave Radar and Wireless Communications (MIKON). - Vilnius, Lithuania, 14-16 June 2010. - P. 1-5. ↑
- C1500.** Startek Dariusz. Control and diagnostic system for the demonstrator of S Band active antenna. / Startek Dariusz, Andrzejewski Mirosław, Czwartacka Anna, Cholewa Jacek, Szustak Konrad, Stachowski Bogdan, Szymanski Piotr. // 2010 18th International Conference on Microwave Radar and Wireless Communications (MIKON). - Vilnius, Lithuania, 14-16 June 2010. - P. 1-4. ↑
- C1501.** Babur Galina. Inter-period compensation of the unambiguity range degradation in polarimetric FMCW radar with time-shifted dual-orthogonal signals. / Babur Galina, Krasnov Oleg A., Ligthart Leo P. // 2010 18th International Conference on Microwave Radar and Wireless Communications (MIKON). - Vilnius, Lithuania, 14-16 June 2010. - P. 1-4. ↑
- C1502.** Pogribny Włodzimierz. Minimizing of influence of synchronization lack between short LMF signal and filter on its compression. / Pogribny Włodzimierz, Leszczynski Tadeusz. // 2010 18th International Conference on Microwave Radar and Wireless Communications (MIKON). - Vilnius, Lithuania, 14-16 June 2010. - P. 1-4. ↑

- C1503.** Kancleris Z. Interaction of thin conductive sheets with TE<sub>10</sub> electromagnetic wave in rectangular waveguide. / Kancleris Z., Silekas G., Čiegis R. // 2010 18th International Conference on Microwave Radar and Wireless Communications (MIKON). - Vilnius, 14-16 June 2010. - P. 1-4. ↑
- C1504.** Kabacik Pawel. Patch antennas setups for omnidirectional pattern to provide TTC links onboard small spacecraft. / Kabacik Pawel, Byndas Arkadiusz, Maleszka Tomasz, Hornik Monika, Gorski Przemyslaw. // 2010 18th International Conference on Microwave Radar and Wireless Communications (MIKON). - Vilnius, Lithuania, 14-16 June 2010. - P. 1-5. ↑
- C1505.** Zongbo Wang. FPGA based IF digital receiver for the PARSAX-Polarimetric agile radar. / Zongbo Wang, Krasnov O.A., Ligthart L.P., van der Zwan F. // 2010 18th International Conference on Microwave Radar and Wireless Communications (MIKON). - Vilnius, 14-16 June 2010. - P. 1-4. ↑
- C1506.** Mironov M. V. The multiposition passive satellite system for the terrestrial radiation sources monitoring. / Mironov M. V., Voroshilin E. P., Sharygin G. S. // 2010 18th International Conference on Microwave Radar and Wireless Communications (MIKON). - Vilnius, Lithuania, 14-16 June 2010. - P. 1-4. ↑
- C1507.** Li Zhijian. A novel approach applied for the internal and semi-external calibration of the PARSAX dual-channel polarimetric agile radar system. / Li Zhijian, Ligthart L. P., Huang Peikang, Lu Weining, van der Zwan W. F., Krasnov O. A. // 2010 18th International Conference on Microwave Radar and Wireless Communications (MIKON). - Vilnius, Lithuania, 14-16 June 2010. - P. 1-4. ↑
- C1508.** Hertl Ivo. Monopulse direction finder for harmonic radar system. / Hertl Ivo, Strycek Michal, Polacek Vladimir, Brno VTUo. // 2010 18th International Conference on Microwave Radar and Wireless Communications (MIKON). - Vilnius, Lithuania, 14-16 June 2010. - P. 1-3. ↑
- C1509.** Naumovich N. Comparative numerical analysis of the slot antenna arrays the energy and finite element methods. / Naumovich N., Yurtsev O., Kizimenko V., Moskaliov D., Joubko A. // 2010 18th International Conference on Microwave Radar and Wireless Communications (MIKON). - Vilnius, Lithuania, 14-16 June 2010. - P. 1-3. ↑
- C1510.** Naik Mehul R. Simulation of direction of arrival and beamforming algorithms used in smart antenna system for software-defined radio. / Naik Mehul R., Suri Gaurav, Shetty Pavan. // 2010 18th International Conference on Microwave Radar and Wireless Communications (MIKON). - Vilnius, Lithuania, 14-16 June 2010. - P. 1-4. ↑
- C1511.** Mohanna Shahram. Wideband aperture coupled microstrip array antennas for radar applications. / Mohanna Shahram, Ghassemi Nasser. // 2010 18th International Conference on Microwave Radar and Wireless Communications (MIKON). - Vilnius, Lithuania, 14-16 June 2010. - P. 1-2. ↑
- C1512.** Bialkowski Marek. E. Investigation into a folded wideband monopole antenna for use in portable devices. / Bialkowski Marek. E., Razali Ahmad Rashidy, Boldaji Ashkan. // 2010 18th International Conference on Microwave Radar and Wireless Communications (MIKON). - Vilnius, Lithuania, 14-16 June 2010. - P. 1-4. ↑
- C1513.** Kolosowski Authors W. Microstrip monopulse array antenna. / Kolosowski Authors W., Sedek E., Gajewski Authors P., Jeziorski A. // 2010 18th International Conference on Microwave Radar and Wireless Communications (MIKON). - Vilnius, Lithuania, 14-16 June 2010. - P. 1-3. ↑
- C1514.** Heberling D. On multiport antennas for MIMO-systems. / Heberling D., Oikonomopoulos-Zachos Ch. // 2010 18th International Conference on Microwave Radar and Wireless Communications (MIKON). - Vilnius, Lithuania, 14-16 June 2010. - P. 1-3. ↑
- C1515.** Gorbunova Anastasia. Model order selection of the target doppler spectrum. / Gorbunova Anastasia, Kuznetsov Yuri. // 2010 18th International Conference on Microwave Radar and Wireless Communications (MIKON). - Vilnius, Lithuania, 14-16 June 2010. - P. 1-4. ↑
- C1516.** Kabakchiev Christo. Target detection in Doppler radar with PSK signals. / Kabakchiev Christo, Garvanov Ivan, Daskalov Panayot. // 2010 18th International Conference on Microwave Radar and Wireless Communications (MIKON). - Vilnius, Lithuania, 14-16 June 2010. - P. 1-4. ↑
- C1517.** Klooster K. v. t. Antenna activities in support to future candidate earth explorer core missions with a SAR. / Klooster K. v. t., Heliere Florence, Lin Chung-Chi. // 2010 18th International Conference on Microwave



Radar and Wireless Communications (MIKON). - Vilnius, Lithuania, 14-16 June 2010. - P. 1-4. ↑

**C1518.** Knap W. Field Effect transistors for fast terahertz detection and imaging. / Knap W., Nadar S., Videlier H., Boubanga-Tombet S., Coquillat D., Dyakonova N., Teppe F., Karpierz K., Lusakowski J., Sakowicz M., Seliuta D., Kasalynas I., Valusis G., Monfray S., Skotnicki T. // 2010 18th International Conference on Microwave Radar and Wireless Communications (MIKON). - Vilnius, Lithuania, 14-16 June 2010. - P. 1-3. ↑

**C1519.** Lewandowski A. Calibration of a 220-325 GHz vector-network-analyzer with multiple rectangular-waveguide sections. / Lewandowski A., Wiatr W. // 2010 18th International Conference on Microwave Radar and Wireless Communications (MIKON). - Vilnius, 14-16 June 2010. - P. 1-4. ↑

**C1520.** Krasnov Oleg A. PARSAX: High-resolution Doppler-polarimetric FMCW radar with dual-orthogonal signals. / Krasnov Oleg A., Ligthart Leo P., Li Zhijian, Babur Galina, Wang Zongbo, van der Zwan Fred. // 2010 18th International Conference on Microwave Radar and Wireless Communications (MIKON). - Vilnius, Lithuania, 14-16 June 2010. - P. 1-5. ↑

**C1521.** Plonis Darius. Gyrotropic waveguides analysis based on the neural networks. / Plonis Darius, Malisauskas Vacius, Serackis Arturas. // 2010 18th International Conference on Microwave Radar and Wireless Communications (MIKON). - Vilnius, Lithuania, 14-16 June 2010. - P. 1-4. ↑

**C1522.** {no data available}. Author Index. 2010 18th International Conference on Microwave Radar and Wireless Communications (MIKON). - Vilnius, Lithuania, 14-16 June 2010. - P. xxi-xxv. ↑

**C1523.** {no data available}. Blank page. 2010 18th International Conference on Microwave Radar and Wireless Communications (MIKON). - Vilnius, Lithuania, 14-16 June 2010. - P. 1. ↑

**C1524.** Michalski Jerzy Julian. Artificial neural network algorithm for automated filter tuning with improved efficiency by usage of many golden filters. 2010 18th International Conference on Microwave Radar and Wireless Communications (MIKON). - Vilnius, Lithuania, 14-16 June 2010. - P. 1-3. ↑

**C1525.** Makarov Denis G. GaN class E wideband microwave power amplifier. / Makarov Denis G., Krizhanovski Vladimir G., Kistchinsky Andrew A. // 2010 18th International Conference on Microwave Radar and Wireless Communications (MIKON). - Vilnius, Lithuania, 14-16 June 2010. - P. 1-3. ↑

**C1526.** {no data available}. Copyright page. 2010 18th International Conference on Microwave Radar and Wireless Communications (MIKON). - Vilnius, Lithuania, 14-16 June 2010. - P. 1. ↑

**C1527.** {no data available}. Closing session. 2010 18th International Conference on Microwave Radar and Wireless Communications (MIKON). - Vilnius, Lithuania, 14-16 June 2010. - P. 1. ↑

**C1528.** Jakab Laszlo. Via interconnection structures for x-band surface mount circulators. / Jakab Laszlo, Hosszu Sandor, Berceli Tibor. // 2010 18th International Conference on Microwave Radar and Wireless Communications (MIKON). - Vilnius, Lithuania, 14-16 June 2010. - P. 1-4. ↑

**C1529.** {no data available}. Session C2: Microwave & millimeter wave oscillators. 2010 18th International Conference on Microwave Radar and Wireless Communications (MIKON). - Vilnius, Lithuania, 14-16 June 2010. - P. 1. ↑

**C1530.** {no data available}. Session B7: Wireless and personal communications. 2010 18th International Conference on Microwave Radar and Wireless Communications (MIKON). - Vilnius, Lithuania, 14-16 June 2010. - P. 1. ↑

**C1531.** {no data available}. Session B8: Microwave measurements III. 2010 18th International Conference on Microwave Radar and Wireless Communications (MIKON). - Vilnius, Lithuania, 14-16 June 2010. - P. 1. ↑

**C1532.** {no data available}. Session C3: Optical components and circuits. 2010 18th International Conference on Microwave Radar and Wireless Communications (MIKON). - Vilnius, Lithuania, 14-16 June 2010. - P. 1. ↑

**C1533.** {no data available}. Session C4: GaN | SiC technology. 2010 18th International Conference on Microwave Radar and Wireless Communications (MIKON). - Vilnius, Lithuania, 14-16 June 2010. - P. 1. ↑

**C1534.** {no data available}. Session C1: Power amplifiers I. 2010 18th International Conference on Microwave

Radar and Wireless Communications (MIKON). - Vilnius, Lithuania, 14-16 June 2010. - P. 1. ↑

**C1535.** Piekarski Jan. The Method of Designing Ultra Low Phase Noise Dielectric Resonator Oscillators. / Piekarski Jan, Czuba Krzysztof. // 2010 18th International Conference on Microwave Radar and Wireless Communications (MIKON). - Vilnius, Lithuania, 14-16 June 2010. - P. 1-4. ↑

**C1536.** Maier D. High temperature stability of nitride-based power HEMTs. / Maier D., Alomari M., Kohn E., Diforte-Poisson M.-A., Dua C., Delage S. L., Grandjean N., Carlin J.-F., Chuvilin A., Kaiser U., Troadec David, Gaquiere Christophe. // 2010 18th International Conference on Microwave Radar and Wireless Communications (MIKON). - Vilnius, Lithuania, 14-16 June 2010. - P. 1-4. ↑

**C1537.** Piotrowska A. Metal contacts to wide bandgap semiconductor structures for RF power applications. / Piotrowska A., Kaminska E., Borysiewicz M., Adamus Z., di Forte Poisson M.-A., Barcz A., Dynowska E., Pec B., Toth L. // 2010 18th International Conference on Microwave Radar and Wireless Communications (MIKON). - Vilnius, Lithuania, 14-16 June 2010. - P. 1-2. ↑

**C1538.** Adamowicz Boguslawa. Modeling of metal/insulator/GaN ultraviolet photodetector by finite element method. / Adamowicz Boguslawa, Miczek Marcin, Bidzinski Piotr, Hashizume Tamotsu. // 2010 18th International Conference on Microwave Radar and Wireless Communications (MIKON). - Vilnius, Lithuania, 14-16 June 2010. - P. 1-3. ↑

**C1539.** Chang W. L. A novel multi-band frequency selective surface design and its application in a compact 60-GHz folded dipole array. / Chang W. L., Luo J. Y. // 2010 18th International Conference on Microwave Radar and Wireless Communications (MIKON). - Vilnius, Lithuania, 14-16 June 2010. - P. 1-4. ↑

**C1540.** Narkowicz R. Third harmonic generation in silicon with a 118 GHz gyrotron. / Narkowicz R., Siegrist M. R., Moreau Ph., Hogge J. P., Raguotis R., Brazis R. // 2010 18th International Conference on Microwave Radar and Wireless Communications (MIKON). - Vilnius, Lithuania, 14-16 June 2010. - P. 1-4. ↑

**C1541.** De Jaeger J. C. Microwave power capabilities of InAlN/GaN HEMTs. / De Jaeger J. C., Gaquiere C., Douvry Y., Defrance N., Hoel V., Delage S., Sarazin N., Morvan E., Alomari M., Kohn E., Dussaigne A., Carlin J. F., Kusmik J., Ostermaier C., Pogany D. // 2010 18th International Conference on Microwave Radar and Wireless Communications (MIKON). - Vilnius, Lithuania, 14-16 June 2010. - P. 1-4. ↑

**C1542.** Barabanenkov Mikhail Yu. Microwaves reflection of centimeter wavelength range of two-dimensional square symmetry plasma photonic crystals. 2010 18th International Conference on Microwave Radar and Wireless Communications (MIKON). - Vilnius, Lithuania, 14-16 June 2010. - P. 1-3. ↑

**C1543.** Korpas Przemyslaw. Control system for high power solid State microwave generators 2.45 GHz band. / Korpas Przemyslaw, Gryglewski Daniel, Wojtasiak Wojciech, Gwarek Wojciech. // 2010 18th International Conference on Microwave Radar and Wireless Communications (MIKON). - Vilnius, Lithuania, 14-16 June 2010. - P. 1-3. ↑

**C1544.** Barghouthi Atheer. Design of a 54 to 63 GHz differential common collector SiGe Colpitts VCO. / Barghouthi Atheer, Ellinger Frank. // 2010 18th International Conference on Microwave Radar and Wireless Communications (MIKON). - Vilnius, Lithuania, 14-16 June 2010. - P. 1-4. ↑

**C1545.** Neumann Niels. Talbot effect supported millimeter wave generation. / Neumann Niels, Haas Michael, Plettemeier Dirk, Dresden TU, Schaeffer Christian. // 2010 18th International Conference on Microwave Radar and Wireless Communications (MIKON). - Vilnius, Lithuania, 14-16 June 2010. - P. 1-3. ↑

**C1546.** Delage Sylvain L. Achievement and perspective of GaN technology for microwave applications. / Delage Sylvain L., Morvan Erwan, Sarazin Nicolas, Aubry Raphael, Chartier Eric, Jardel Olivier, diForte-Poisson Marie-Antoinette, Dua Christian, Jacquet Jean-Claude, Piotrowicz Stephane, Piotrowska Anna., Kaminska Eliana., De Jaeger Jean-Claude, Gaquiere Christophe, Heinlen Ulrich, Kohn Ehrard, Alomari Mohammed, Maier David, Kuzmik Jan, Pogany Dionyz. // 2010 18th International Conference on Microwave Radar and Wireless Communications (MIKON). - Vilnius, Lithuania, 14-16 June 2010. - P. 1-5. ↑

**C1547.** Konczykowska A. InP HBT demultiplexing ICs for over 100 Gb/s optical transmission. / Konczykowska A., Jorge F., Dupuy J.-Y., Riet M., Godin J., Scavennec A., Bach H.-G., Mekonnen G. G., Pech D., Schubert C. // 2010 18th International Conference on Microwave Radar and Wireless Communications (MIKON). - Vilnius, Lithuania, 14-16 June 2010. - P. 1-4. ↑

- C1548.** Salski Bartlomiej. Periodic FDTD modeling of 3D photonic crystals. / Salski Bartlomiej, Gwarek Wojciech. // 2010 18th International Conference on Microwave Radar and Wireless Communications (MIKON). - Vilnius, Lithuania, 14-16 June 2010. - P. 1-3. ↑
- C1549.** Sorokosz Lukasz. Inexpensive helical antenna for global navigation satellite systems. / Sorokosz Lukasz, Zieniutycz Wlodzimierz. // 2010 18th International Conference on Microwave Radar and Wireless Communications (MIKON). - Vilnius, Lithuania, 14-16 June 2010. - P. 1-4. ↑
- C1550.** Pratsiuk Borys. Tunable filters based on metal-dielectric resonators. / Pratsiuk Borys, Prokopenko Yuriy, Poplavko Yuriy. // 2010 18th International Conference on Microwave Radar and Wireless Communications (MIKON). - Vilnius, Lithuania, 14-16 June 2010. - P. 1-3. ↑
- C1551.** Markos A.Z. A 2 W GaAs doherty amplifier for 5.5-5.6 GHz applications. / Markos A.Z., Gruner D., Bathich K., Boeck G. // 2010 18th International Conference on Microwave Radar and Wireless Communications (MIKON). - Vilnius, 14-16 June 2010. - P. 1-4. ↑
- C1552.** Colantonio Paolo. GaAs MMIC Doherty Power Amplifier with asymmetrical drain bias voltage. / Colantonio Paolo, Giannini Franco, Giofre Rocco, Piacentini Marco, Piazzon Luca. // 2010 18th International Conference on Microwave Radar and Wireless Communications (MIKON). - Vilnius, Lithuania, 14-16 June 2010. - P. 1-4. ↑
- C1553.** Kim Bumman. Doherty power amplifiers for handset applications. / Kim Bumman, Kang Daehyun, Choi Jinsung, Kim Dongsu. // 2010 18th International Conference on Microwave Radar and Wireless Communications (MIKON). - Vilnius, Lithuania, 14-16 June 2010. - P. 1-3. ↑
- C1554.** Balewski Lukasz. A diplexer design method using an augmented channel filter approach. / Balewski Lukasz, Mrozowski Michal. // 2010 18th International Conference on Microwave Radar and Wireless Communications (MIKON). - Vilnius, Lithuania, 14-16 June 2010. - P. 1-4. ↑
- C1555.** Colantonio Paolo. Design of a dual-band GaN Doherty amplifier. / Colantonio Paolo, Feudo Fabio, Giannini Franco, Giofre Rocco, Piazzon Luca. // 2010 18th International Conference on Microwave Radar and Wireless Communications (MIKON). - Vilnius, Lithuania, 14-16 June 2010. - P. 1-4. ↑
- C1556.** Fuzy Csaba. Design of broadband complex impedance-matching networks and their applications for broadbanding microwave amplifiers. / Fuzy Csaba, Zolomy Attila. // 2010 18th International Conference on Microwave Radar and Wireless Communications (MIKON). - Vilnius, Lithuania, 14-16 June 2010. - P. 1-4. ↑
- C1557.** Bekkadal Fritz. Innovative maritime communications technologies. 2010 18th International Conference on Microwave Radar and Wireless Communications (MIKON). - Vilnius, Lithuania, 14-16 June 2010. - P. 1-4. ↑
- C1558.** Rosolowski Dawid W. A 27 dBm microwave amplifier with varactors-controlled matching networks. / Rosolowski Dawid W., Wojtasiak Wojciech, Gryglewski Daniel. // 2010 18th International Conference on Microwave Radar and Wireless Communications (MIKON). - Vilnius, Lithuania, 14-16 June 2010. - P. 1-4. ↑
- C1559.** Vermesan Irina. On BER of STBC coded MIMO systems in different indoor environments. / Vermesan Irina, Moldovan Ancuta, Palade Tudor, Colda Rebeca. // 2010 18th International Conference on Microwave Radar and Wireless Communications (MIKON). - Vilnius, Lithuania, 14-16 June 2010. - P. 1-4. ↑
- C1560.** Colantonio P. Doherty power amplifier and GaN technology. / Colantonio P., Giannini F., Giofre R., Piazzon L. // 2010 18th International Conference on Microwave Radar and Wireless Communications (MIKON). - Vilnius, Lithuania, 14-16 June 2010. - P. 1-4. ↑
- C1561.** Bore Francois. 3 GS/s S-Band 12 bit MuxDAC on SiGeC technology. / Bore Francois, Chantier Nicolas. // 2010 18th International Conference on Microwave Radar and Wireless Communications (MIKON). - Vilnius, Lithuania, 14-16 June 2010. - P. 1-4. ↑
- C1562.** Dufrene Krzysztof. Asymmetric mechanisms of second-order intermodulation in downconversion mixers. / Dufrene Krzysztof, Weigel Robert. // 2010 18th International Conference on Microwave Radar and Wireless Communications (MIKON). - Vilnius, Lithuania, 14-16 June 2010. - P. 1-4. ↑
- C1563.** Mirzavand R. ADI-FDTD method for physical simulation of semiconductor devices. / Mirzavand R., Abdipour A., Moradi G., Movahhedi M. // 2010 18th International Conference on Microwave Radar and Wireless

Communications (MIKON). - Vilnius, Lithuania, 14-16 June 2010. - P. 1-4. ↑

**C1564.** Mazur Mateusz. Integrated cylindrical horn antenna array. / Mazur Mateusz, Kostka Stanislaw. // 2010 18th International Conference on Microwave Radar and Wireless Communications (MIKON). - Vilnius, Lithuania, 14-16 June 2010. - P. 1-4. ↑

**C1565.** Kubacki R. Magnetic properties of the finemet alloys in the microwave frequency range. / Kubacki R., Nowosielski L., Przesmycki R., Ferenc J., Frender R. // 2010 18th International Conference on Microwave Radar and Wireless Communications (MIKON). - Vilnius, 14-16 June 2010. - P. 1-4. ↑

**C1566.** Kvedaras Vygaudas. Method of dynamic parameters measurement of high-speed D/A converters. / Kvedaras Vygaudas, Kvedaras Rokas, Ustinavicius Tomas. // 2010 18th International Conference on Microwave Radar and Wireless Communications (MIKON). - Vilnius, Lithuania, 14-16 June 2010. - P. 1-4. ↑

**C1567.** Sekretarov S. S. Slotted Waveguide Antenna Arrays for Airborne Radars. / Sekretarov S. S., Vavriv D. M., Shevtsova L. V. // 2010 18th International Conference on Microwave Radar and Wireless Communications (MIKON). - Vilnius, Lithuania, 14-16 June 2010. - P. 1-4. ↑

**C1568.** Olszewska Marzena. A dual reflector antenna for point-to-point system applications. / Olszewska Marzena, Gwarek Wojciech. // 2010 18th International Conference on Microwave Radar and Wireless Communications (MIKON). - Vilnius, Lithuania, 14-16 June 2010. - P. 1-4. ↑

**C1569.** Yashchyshyn Y. M. Invited paper. 2010 18th International Conference on Microwave Radar and Wireless Communications (MIKON). - Vilnius, Lithuania, 14-16 June 2010. - P. 1-9. ↑

**C1570.** Soltysiak Michal. FDTD modelling of plain susceptors for microwave oven applications. / Soltysiak Michal, Gwarek Wojciech, Celuch Malgorzata, Erle Ulrich. // 2010 18th International Conference on Microwave Radar and Wireless Communications (MIKON). - Vilnius, Lithuania, 14-16 June 2010. - P. 1-4. ↑

**C1571.** Snyder Richard V. Composite dielectric-loaded resonators for highly-stable bandstop and bandpass filters. 2010 18th International Conference on Microwave Radar and Wireless Communications (MIKON). - Vilnius, Lithuania, 14-16 June 2010. - P. 1-5. ↑

**C1572.** Kowalczyk Piotr. Improving the accuracy of subgridding scheme in finite differences method based on Legendre polynomials expansion. / Kowalczyk Piotr, Kulas Lukasz, Mrozowski Michal. // 2010 18th International Conference on Microwave Radar and Wireless Communications (MIKON). - Vilnius, Lithuania, 14-16 June 2010. - P. 1-3. ↑

**C1573.** Szydlowski Lukasz. On the synthesis of coupled-lossy resonator filters with unloaded quality factor control. / Szydlowski Lukasz, Lamecki Adam, Mrozowski Michal. // 2010 18th International Conference on Microwave Radar and Wireless Communications (MIKON). - Vilnius, Lithuania, 14-16 June 2010. - P. 1-3. ↑

**C1574.** Derzakowski K. Measurements of the complex permeability of yttrium iron garnet substrates near ferromagnetic resonance. / Derzakowski K., Krupka J. // 2010 18th International Conference on Microwave Radar and Wireless Communications (MIKON). - Vilnius, 14-16 June 2010. - P. 1-3. ↑

**C1575.** Dziekonski Adam. Krylov space iterative solvers on graphics processing units. / Dziekonski Adam, Mrozowski Michal. // 2010 18th International Conference on Microwave Radar and Wireless Communications (MIKON). - Vilnius, Lithuania, 14-16 June 2010. - P. 1-4. ↑

**C1576.** Ivanov M. Measurements of complex dielectric permittivity and magnetic permeability of carbon-coated Ni capsules. / Ivanov M., Rudys S., Lapinskas S., Banyas J., Macutkevicius J., Yermakov A.Y., Uimin M.A., Mysik A.A., Shenderova O. // 2010 18th International Conference on Microwave Radar and Wireless Communications (MIKON). - Vilnius, 14-16 June 2010. - P. 1-4. ↑

**C1577.** Ali Faraz. Analysis of a new approach for tunable and reduced size balanced amplifier using thin-film BST varactors. / Ali Faraz, Lourandakis Errikos, Gloeckler Roman, Fischer Georg, Weigel Robert. // 2010 18th International Conference on Microwave Radar and Wireless Communications (MIKON). - Vilnius, Lithuania, 14-16 June 2010. - P. 1-4. ↑

**C1578.** Metlevskis Edvardas. Analysis of rectangular microstrip structures by the method of moments. / Metlevskis Edvardas, Urbanavicius Vytautas. // 2010 18th International Conference on Microwave Radar and Wireless Communications (MIKON). - Vilnius, Lithuania, 14-16 June 2010. - P. 1-4. ↑



Wireless Communications (MIKON). - Vilnius, Lithuania, 14-16 June 2010. - P. 1-4. ↑

**C1579.** Konczak P. The method of improving performance of the GPU-accelerated 2D FDTD simulator. / Konczak P., Sypniewski M. // 2010 18th International Conference on Microwave Radar and Wireless Communications (MIKON). - Vilnius, 14-16 June 2010. - P. 1-4. ↑

**C1580.** Karwowski Andrzej. A Comparative analysis of two wide-band rational approximations for input impedance of antennas. / Karwowski Andrzej, Noga Artur, Surma Maciej. // 2010 18th International Conference on Microwave Radar and Wireless Communications (MIKON). - Vilnius, Lithuania, 14-16 June 2010. - P. 1-2. ↑

**C1581.** Sanadhya Ankit. Design of Wilkinson power divider using stubs. / Sanadhya Ankit, Mathur Anirudh, Chouhan Mahendra Singh, Singh Kiran. // 2010 18th International Conference on Microwave Radar and Wireless Communications (MIKON). - Vilnius, Lithuania, 14-16 June 2010. - P. 1-4. ↑

**C1582.** Kazakevicius Vladimiras. Electromagnetic wave trapping in the split-ring-cavity system. / Kazakevicius Vladimiras, Narkowicz Ryszard, Brazis Romuald. // 2010 18th International Conference on Microwave Radar and Wireless Communications (MIKON). - Vilnius, Lithuania, 14-16 June 2010. - P. 1-4. ↑

**C1583.** Andriychuk M. I. Numerical modeling in wave scattering problem for small particles. / Andriychuk M. I., Ramm A. G. // 2010 18th International Conference on Microwave Radar and Wireless Communications (MIKON). - Vilnius, Lithuania, 14-16 June 2010. - P. 1-4. ↑

**C1584.** Ivaska V. Fresnel formulas for nondiffracting electromagnetic waves. / Ivaska V., Jonkus V. // 2010 18th International Conference on Microwave Radar and Wireless Communications (MIKON). - Vilnius, Lithuania, 14-16 June 2010. - P. 1-4. ↑

**C1585.** Noaman Ali Abdulhadi. Optimal sidelobes reduction and synthesis of circular array antennas using hybrid adaptive genetic algorithms. / Noaman Ali Abdulhadi, Abdallah Abdul Kareem S., Ali Ramzy S. // 2010 18th International Conference on Microwave Radar and Wireless Communications (MIKON). - Vilnius, Lithuania, 14-16 June 2010. - P. 1-4. ↑

**C1586.** Matousek Zdenek. Automated method of antenna factor measuring. / Matousek Zdenek, Sostronek Mikulas, Ochodnický Jan. // 2010 18th International Conference on Microwave Radar and Wireless Communications (MIKON). - Vilnius, Lithuania, 14-16 June 2010. - P. 1-3. ↑

**C1587.** Novickij Jurij. Microwave radar for express testing of semiconductor materials. 2010 18th International Conference on Microwave Radar and Wireless Communications (MIKON). - Vilnius, Lithuania, 14-16 June 2010. - P. 1-2. ↑

**C1588.** Bieda Bartosz. Efficiency of the IE-MoM approach in the analysis of dielectric bodies embedded in a cavity. / Bieda Bartosz, Slobodzian Piotr. // 2010 18th International Conference on Microwave Radar and Wireless Communications (MIKON). - Vilnius, Lithuania, 14-16 June 2010. - P. 1-4. ↑

**C1589.** Cudo Marcin. Utilization of RFID technology for fixed assets inventory process improvement. 2010 18th International Conference on Microwave Radar and Wireless Communications (MIKON). - Vilnius, Lithuania, 14-16 June 2010. - P. 1-3. ↑

**C1590.** Ivaska Vladislavas. Vortical electromagnetic waves with a stationary power flow. / Ivaska Vladislavas, Kalesinskas Vidas. // 2010 18th International Conference on Microwave Radar and Wireless Communications (MIKON). - Vilnius, Lithuania, 14-16 June 2010. - P. 1-4. ↑

**C1591.** Slaba Mirosław. Wideband microstrip phase shifters. 2010 18th International Conference on Microwave Radar and Wireless Communications (MIKON). - Vilnius, Lithuania, 14-16 June 2010. - P. 1-4. ↑

**C1592.** Maleszka Tomasz. Planar MS-CPS bypass balun for CPS-fed textile antennas. 2010 18th International Conference on Microwave Radar and Wireless Communications (MIKON). - Vilnius, Lithuania, 14-16 June 2010. - P. 1-4. ↑

**C1593.** Gric Tatjana. Three dimensional magnetic field distributions and dispersion characteristics of rectangular and circular SiC waveguides. / Gric Tatjana, Nickelson Liudmila, Asmontas Steponas. // 2010 18th International Conference on Microwave Radar and Wireless Communications (MIKON). - Vilnius, Lithuania, 14-16 June 2010. - P. 1-4. ↑

- C1594.** Gruchaila-Wesierski Henryk. The performance of the IFM receiver in a dense signal environment. / Gruchaila-Wesierski Henryk, Czyzewski Miroslaw, Slowik Adam. // 2010 18th International Conference on Microwave Radar and Wireless Communications (MIKON). - Vilnius, Lithuania, 14-16 June 2010. - P. 1-4. ↑
- C1595.** Sulkowska Monika. Localization in wireless sensor networks using switched parasitic antennas. / Sulkowska Monika, Nyka Krzysztof, Kulas Lukasz. // 2010 18th International Conference on Microwave Radar and Wireless Communications (MIKON). - Vilnius, Lithuania, 14-16 June 2010. - P. 1-4. ↑
- C1596.** Ahrens Andreas. Modulation-mode and power-assignment for SVD-assisted downlink multiuser MIMO systems. / Ahrens Andreas, Benavente-Peces Cesar. // 2010 18th International Conference on Microwave Radar and Wireless Communications (MIKON). - Vilnius, Lithuania, 14-16 June 2010. - P. 1-4. ↑
- C1597.** Ragulis Paulius. Optimisation of resistive sensor for ridge waveguide. / Ragulis Paulius, Tamosiunas Vincas, Kancleris Zilvinas, Simniskis Rimantas, Tamosiuniene Milda. // 2010 18th International Conference on Microwave Radar and Wireless Communications (MIKON). - Vilnius, Lithuania, 14-16 June 2010. - P. 1-4. ↑
- C1598.** Fang Jie. Development strategy for GaN-based high-efficiency hybrid medium-power RF amplifiers through low-cost substrate prototyping. / Fang Jie, Moreno J., Quaglia R., Tinivella R., Camarchia V., Pirola M., Ghione G. // 2010 18th International Conference on Microwave Radar and Wireless Communications (MIKON). - Vilnius, Lithuania, 14-16 June 2010. - P. 1-4. ↑
- C1599.** Hosszu Sandor. Computer aided microstrip circulator design. / Hosszu Sandor, Jakab Laszlo, Berceli Tibor. // 2010 18th International Conference on Microwave Radar and Wireless Communications (MIKON). - Vilnius, Lithuania, 14-16 June 2010. - P. 1-4. ↑
- C1600.** Samulak Andrzej. Design and simulation GaN based class-S PA at 900MHz. / Samulak Andrzej, Fischer Georg, Weigel Robert. // 2010 18th International Conference on Microwave Radar and Wireless Communications (MIKON). - Vilnius, Lithuania, 14-16 June 2010. - P. 1-4. ↑
- C1601.** Gruszczynski Slawomir. Compensated broadband five-section directional coupler for application in butler matrices. / Gruszczynski Slawomir, Sachse Krzysztof. // 2010 18th International Conference on Microwave Radar and Wireless Communications (MIKON). - Vilnius, Lithuania, 14-16 June 2010. - P. 1-4. ↑
- C1602.** Idzkowski B. L-Band Electron Paramagnetic Resonance (EPR) spectrometer. / Idzkowski B., Duchiewicz J., Dobrucki A., Duchiewicz T., Francik A., Sadowski S., Walesiak S., Kutynia A., Blaszczyk J. // 2010 18th International Conference on Microwave Radar and Wireless Communications (MIKON). - Vilnius, Lithuania, 14-16 June 2010. - P. 1-4. ↑
- C1603.** Wojtasiak W. A 100W SiC MESFET amplifier for L-band T/R module of APAR. / Wojtasiak W., Gryglewski D. // 2010 18th International Conference on Microwave Radar and Wireless Communications (MIKON). - Vilnius, 14-16 June 2010. - P. 1-4. ↑
- C1604.** Heinrich Wolfgang. Advanced switch-mode concepts using GaN: The class-S amplifier. / Heinrich Wolfgang, Wentzel Andreas, Meliani Chafik. // 2010 18th International Conference on Microwave Radar and Wireless Communications (MIKON). - Vilnius, Lithuania, 14-16 June 2010. - P. 1-6. ↑
- C1605.** Gingras D. Path planning based on fluid mechanics for mobile robots using unstructured terrain models. / Gingras D., Dupuis E., Payre G., de Lafontaine J. // 2010 IEEE International Conference on Robotics and Automation (ICRA). - Anchorage, AK, 3-7 May 2010. - P. 1978-1984. ↑
- C1606.** Yangming Li. Extracting general-purpose features from LIDAR data. / Yangming Li, Olson E.B. // 2010 IEEE International Conference on Robotics and Automation (ICRA). - Anchorage, AK, 3-7 May 2010. - P. 1388-1393. ↑
- C1607.** Levinson J. Robust vehicle localization in urban environments using probabilistic maps. / Levinson J., Thrun S. // 2010 IEEE International Conference on Robotics and Automation (ICRA). - Anchorage, AK, 3-7 May 2010. - P. 4372-4378. ↑
- C1608.** Kiho Kwak. Boundary detection based on supervised learning. / Kiho Kwak, Huber D.F., Jeongsook Chae, Kanade T. // 2010 IEEE International Conference on Robotics and Automation (ICRA). - Anchorage, AK, 3-7 May 2010. - P. 3939-3945. ↑

- C1609.** SangHyun Chang. Human detection and tracking via Ultra-Wideband (UWB) radar. / SangHyun Chang, Wolf M., Burdick J.W. // 2010 IEEE International Conference on Robotics and Automation (ICRA). - Anchorage, AK, 3-7 May 2010. - P. 452-457. ↑
- C1610.** Trawny N. On the global optimum of planar, range-based robot-to-robot relative pose estimation. / Trawny N., Roumeliotis S.I. // 2010 IEEE International Conference on Robotics and Automation (ICRA). - Anchorage, AK, 3-7 May 2010. - P. 3200-3206. ↑
- C1611.** Carle P.J.F. Global rover localization by matching lidar and orbital 3D maps. / Carle P.J.F., Barfoot T.D. // 2010 IEEE International Conference on Robotics and Automation (ICRA). - Anchorage, AK, 3-7 May 2010. - P. 881-886. ↑
- C1612.** McDaniel M.W. Ground plane identification using LIDAR in forested environments. / McDaniel M.W., Nishihata T., Brooks C.A., Iagnemma K. // 2010 IEEE International Conference on Robotics and Automation (ICRA). - Anchorage, AK, 3-7 May 2010. - P. 3831-3836. ↑
- C1613.** Hong Jiang. Estimation of DOD and 2D-DOA and polarizations for bistatic MIMO radar. / Hong Jiang, De-Fa Wang, Chang Liu. // 2010 19th Annual Wireless and Optical Communications Conference (WOCC). - Shanghai, 14-15 May 2010. - P. 1-5. ↑
- C1614.** Jinliang Cao. DOA estimation for wideband sources using cross correlation transformation. / Jinliang Cao, Zhiwen Liu, Yougen Xu. // 2010 19th Annual Wireless and Optical Communications Conference (WOCC). - Shanghai, 14-15 May 2010. - P. 1-4. ↑
- C1615.** Yamauchi B. All-weather perception for man-portable robots using ultra-wideband radar. 2010 IEEE International Conference on Robotics and Automation (ICRA). - Anchorage, AK, 3-7 May 2010. - P. 3610-3615. ↑
- C1616.** Chao Gao. On-line calibration of multiple LIDARs on a mobile vehicle platform. / Chao Gao, Spletzer J.R. // 2010 IEEE International Conference on Robotics and Automation (ICRA). - Anchorage, AK, 3-7 May 2010. - P. 279-284. ↑
- C1617.** Das J. Towards marine bloom trajectory prediction for AUV mission planning. / Das J., Rajany K., Frolov S., Pyy F., Ryany J., Caron D.A., Sukhatme G.S. // 2010 IEEE International Conference on Robotics and Automation (ICRA). - Anchorage, AK, 3-7 May 2010. - P. 4784-4790. ↑
- C1618.** Bibby C. A hybrid SLAM representation for dynamic marine environments. / Bibby C., Reid I. // 2010 IEEE International Conference on Robotics and Automation (ICRA). - Anchorage, AK, 3-7 May 2010. - P. 257-264. ↑
- C1619.** Narayana Keerthi. Planar landmark detection using a specific arrangement of LIDAR scanners. / Narayana Keerthi, Goulette Francois, Steux Bruno. // 2010 IEEE/ION Position Location and Navigation Symposium (PLANS). - Indian Wells, CA, USA, 4-6 May 2010. - P. 1057-1069. ↑
- C1620.** Daltorio Kathryn A. An obstacle-edging reflex for an autonomous lawnmower. / Daltorio Kathryn A., Rolin Amaury D., Beno Jonathan A., Hughes Bradley E., Schepelmann Alexander, Branicky Michael S., Quinn Roger D., Green James M. // 2010 IEEE/ION Position Location and Navigation Symposium (PLANS). - Indian Wells, CA, USA, 4-6 May 2010. - P. 1079-1092. ↑
- C1621.** Jianqing Fu. Lightweight efficient and feasible IP multimedia subsystem authentication. / Jianqing Fu, Chunming Wu, Jian Chen, Rong Fan, Lingdi Ping. // 2010 International Conference on Networking and Information Technology (ICNIT). - Manila, 11-12 June 2010. - P. 139-144. ↑
- C1622.** Allen John W. Relating local vision measurements to global navigation satellite systems using waypoint based maps. / Allen John W., Bevy David M. // 2010 IEEE/ION Position Location and Navigation Symposium (PLANS). - Indian Wells, CA, USA, 4-6 May 2010. - P. 1204-1211. ↑
- C1623.** Britt Jordan. Lidar attitude estimation for vehicle safety systems. / Britt Jordan, Broderick David J., Bevy David, Hung John. // 2010 IEEE/ION Position Location and Navigation Symposium (PLANS). - Indian Wells, CA, USA, 4-6 May 2010. - P. 1226-1231. ↑
- C1624.** Weng Yuezhong. Combine draft detector with GPS receiver to monitor barge's loadage. / Weng Yuezhong, Chen Jinhai, Peng Guojun, Zhang Xinggu. // 2010 IEEE/ION Position Location and Navigation

Symposium (PLANS). - Indian Wells, CA, USA, 4-6 May 2010. - P. 127-131. ↑

**C1625.** Popescu A. A spectral space-variant approach for structure indexing in Spotlight TerraSAR-X data. / Popescu A., Patrascu C., Singh J., Datcu M. // 2010 8th International Conference on Communications (COMM). - Bucharest, 10-12 June 2010. - P. 169-172. ↑

**C1626.** Vizitiu I.-C. High-quality HRR ATR system using an improved neural recognition chain. / Vizitiu I.-C., Popescu F., Stoica A. // 2010 8th International Conference on Communications (COMM). - Bucharest, 10-12 June 2010. - P. 217-220. ↑

**C1627.** van Genderen P. A communication waveform for radar. 2010 8th International Conference on Communications (COMM). - Bucharest, 10-12 June 2010. - P. 289-292. ↑

**C1628.** Ferrari S. A potential field approach to finding minimum-exposure paths in wireless sensor networks. / Ferrari S., Foderaro G. // 2010 IEEE International Conference on Robotics and Automation (ICRA). - Anchorage, AK, 3-7 May 2010. - P. 335-341. ↑

**C1629.** Marchetti N. Self-Organizing Networks: State-of-the-art, challenges and perspectives. / Marchetti N., Prasad N.R., Johansson J., Tao Cai. // 2010 8th International Conference on Communications (COMM). - Bucharest, 10-12 June 2010. - P. 503-508. ↑

**C1630.** Totir F. ICA-based information extraction method for PolSAR images. / Totir F., Vasile G., Gay M., Anton L., Ilie G. // 2010 8th International Conference on Communications (COMM). - Bucharest, 10-12 June 2010. - P. 149-152. ↑

**C1631.** Maza. The generated curve in symmetrical plane for double curved antenna reflector with Cos<sup>2</sup> pattern beam, illuminated by a Cos<sup>4</sup> pattern beam for primary radiator. / Maza, re P., Szilagyi A., Stoica D.-S., Ca, za, naru D., Stoica A., Maza, re C., Nicolaescu I. // 2010 8th International Conference on Communications (COMM). - Bucharest, 10-12 June 2010. - P. 251-254. ↑

**C1632.** Baoliang Zhou. A novel spectrum reconstruction algorithm based on FrFT for multiple azimuth beam SAR. / Baoliang Zhou, Shunsheng Zhang, Wei Zhang, Chunyang Dai, Lingkun Kong. // 2010 IEEE International Conference on Information and Automation (ICIA). - Harbin, 20-23 June 2010. - P. 1218-1222. ↑

**C1633.** Yiqiang Yu. Meshless RPIM modeling of open-structures using PMLs. / Yiqiang Yu, Zhizhang Chen. // 2010 IEEE MTT-S International Microwave Symposium Digest (MTT). - Anaheim, CA, 23-28 May 2010. - P. 97-100. ↑

**C1634.** Mochizuki S. High-phase-resolution 77-GHz-band radar module for near-field millimeter-wave imaging. / Mochizuki S., Oka S., Togo H., Kukutsu N. // 2010 IEEE MTT-S International Microwave Symposium Digest (MTT). - Anaheim, CA, USA, 23-28 May 2010. - P. 1. ↑

**C1635.** Ludwig M. Earth observation instruments with e-scan antennas state-of-the-art and outlook. / Ludwig M., Buck C. H., D'Addio S., Torres R., Rostan F., Schaefer C., Croci R. // 2010 IEEE MTT-S International Microwave Symposium Digest (MTT). - Anaheim, CA, USA, 23-28 May 2010. - P. 1. ↑

**C1636.** Carlson D. J. Commercial manufacturing practices applied to phased array radars. / Carlson D. J., Weigand C., Curcio D., Boles T. // 2010 IEEE MTT-S International Microwave Symposium Digest (MTT). - Anaheim, CA, USA, 23-28 May 2010. - P. 1. ↑

**C1637.** Zhiqing Song. Extremely Low Frequency Electric Field Induced Mutations in Escherichia Coli K12 Strains. / Zhiqing Song, Yunzhang Liang. // 2010 4th International Conference on Bioinformatics and Biomedical Engineering (iCBBE). - Chengdu, 18-20 June 2010. - P. 1-4. ↑

**C1638.** Herd J. Advanced architecture for a low cost multifunction phased array radar. / Herd J., Duffy S., Weber M., Brigham G., Weigand C., Curcio D. // 2010 IEEE MTT-S International Microwave Symposium Digest (MTT). - Anaheim, CA, USA, 23-28 May 2010. - P. 1. ↑

**C1639.** Poprawa F. Waveguide transition to feed a fully PCB integrated dielectric rod antenna. / Poprawa F., Zanati A., Zirotf A., Ellinger F. // 2010 IEEE MTT-S International Microwave Symposium Digest (MTT). - Anaheim, CA, USA, 23-28 May 2010. - P. 1. ↑



- C1640.** Jeich Mar. Fast subspace decomposition null extension for two-dimensional array antenna. / Jeich Mar, Shin-Ru Wu. // 2010 the 5th IEEE Conference on Industrial Electronics and Applications (ICIEA). - Taichung, 15-17 June 2010. - P. 1863-1867. ↑
- C1641.** Maas J. D. Miniature radio frequency ion trap mass spectrometry. / Maas J. D., Xu W., Hendricks P. I., Chappell W. J. // 2010 IEEE MTT-S International Microwave Symposium Digest (MTT). - Anaheim, CA, USA, 23-28 May 2010. - P. 1. ↑
- C1642.** Chen H. Piggyback modulation for UHF RFID sensors. / Chen H., Bhadkamkar A., van der Weide D. W. // 2010 IEEE MTT-S International Microwave Symposium Digest (MTT). - Anaheim, CA, USA, 23-28 May 2010. - P. 1. ↑
- C1643.** Bialkowski M.E. Novel image reconstruction algorithm for a UWB cylindrical Microwave Imaging System. / Bialkowski M.E., Yifan Wang, Abu Bakar A., Wee Chang Khor. // 2010 IEEE MTT-S International Microwave Symposium Digest (MTT). - Anaheim, CA, 23-28 May 2010. - P. 477-480. ↑
- C1644.** Wien A. Multi-PC FDTD: Solving large scale EM problems. / Wien A., Lauer A., Wolff I. // 2010 IEEE MTT-S International Microwave Symposium Digest (MTT). - Anaheim, CA, 23-28 May 2010. - P. 972-975. ↑
- C1645.** Guozhu Wang. A forest fire monitoring system based on GPRS and ZigBee wireless sensor network. / Guozhu Wang, Junguo Zhang, Wenbin Li, Dongxu Cui, Ye Jing. // 2010 the 5th IEEE Conference on Industrial Electronics and Applications (ICIEA). - Taichung, 15-17 June 2010. - P. 1859-1862. ↑
- C1646.** Chan Wei Hsu. A path planning achievement of car following in motion control via LiDAR sensing. / Chan Wei Hsu, Tsung Hua Hsu, Chun Hsiung Chen, Yung Yuan Kuo. // 2010 the 5th IEEE Conference on Industrial Electronics and Applications (ICIEA). - Taichung, 15-17 June 2010. - P. 1411-1416. ↑
- C1647.** Chunjie Zhang. A method for determining the number of signals based on modified K-means clustering. / Chunjie Zhang, Xicai Si, Jiling Xie. // 2010 IEEE International Conference on Information and Automation (ICIA). - Harbin, 20-23 June 2010. - P. 451-454. ↑
- C1648.** Ping Chu. Resolutions of some overlap signals based on MUSIC algorithm. / Ping Chu, Weijian Si, Shenghe Sun. // 2010 IEEE International Conference on Information and Automation (ICIA). - Harbin, 20-23 June 2010. - P. 466-469. ↑
- C1649.** Balzano L. High-dimensional Matched Subspace Detection when data are missing. / Balzano L., Recht B., Nowak R. // 2010 IEEE International Symposium on Information Theory Proceedings (ISIT). - Austin, TX, 13-18 June 2010. - P. 1638-1642. ↑
- C1650.** Li Yushen. A research on the robust digital watermark of color radar images. / Li Yushen, Hao Yanling, Wang Chenye. // 2010 IEEE International Conference on Information and Automation (ICIA). - Harbin, 20-23 June 2010. - P. 1091-1096. ↑
- C1651.** Dong-ze Lv. New detection algorithm for weak target signal embedded in direct path interference using Signal Phase Matching Principle. / Dong-ze Lv, Feng Shen. // 2010 IEEE International Conference on Information and Automation (ICIA). - Harbin, 20-23 June 2010. - P. 1182-1187. ↑
- C1652.** Ha-ryong Song. Localization performance enhancement using IMM fusion in cricket sensor network. / Ha-ryong Song, Seok-hyoung Lee, Ju-hong Yoon, Shin V. // 2010 IEEE International Conference on Information and Automation (ICIA). - Harbin, 20-23 June 2010. - P. 1526-1531. ↑
- C1653.** Grossi E. Robust waveform design for MIMO radars. / Grossi E., Lops M., Venturino L., Tulino A.M. // 2010 IEEE International Symposium on Information Theory Proceedings (ISIT). - Austin, TX, 13-18 June 2010. - P. 1633-1637. ↑
- C1654.** Cheung S.K. High isolation large-ferrite circulators with NF suppression for simultaneous transmit and receive. / Cheung S.K., Weedon W.H., Caldwell C.P. // 2010 IEEE MTT-S International Microwave Symposium Digest (MTT). - Anaheim, CA, 23-28 May 2010. - P. 1352-1355. ↑
- C1655.** Genghuang Yang. Research of Portable Community-Oriented Health Monitoring. / Genghuang Yang, Shuyan Ren, Yan Bian, Li Zhao, Shigang Cui. // 2010 4th International Conference on Bioinformatics and Biomedical Engineering (iCBBE). - Chengdu, 18-20 June 2010. - P. 1-4. ↑

- C1656.** Sengupta Kaushik. A compact self-similar power combining topology. / Sengupta Kaushik, Hajimiri Ali. // 2010 IEEE MTT-S International Microwave Symposium Digest (MTT). - Anaheim, CA, USA, 23-28 May 2010. - P. 244-247. ↑
- C1657.** Yan Wang. Decentralized multihypothesis sequential detection. / Yan Wang, Yajun Mei. // 2010 IEEE International Symposium on Information Theory Proceedings (ISIT). - Austin, TX, 13-18 June 2010. - P. 1393-1397. ↑
- C1658.** Honggang Hu. A new class of ternary and quaternary sequences with two-level autocorrelation. / Honggang Hu, Guang Gong. // 2010 IEEE International Symposium on Information Theory Proceedings (ISIT). - Austin, TX, 13-18 June 2010. - P. 1292-1296. ↑
- C1659.** Boztas S. Nonbinary sequences with perfect and nearly perfect autocorrelations. / Boztas S., Parampalli U. // 2010 IEEE International Symposium on Information Theory Proceedings (ISIT). - Austin, TX, 13-18 June 2010. - P. 1300-1304. ↑
- C1660.** Shabani Mostafa. Performance analysis of an optical beam-forming network with custom microwave CAD tools. / Shabani Mostafa, Akbari Mahmood. // 2010 18th Iranian Conference on Electrical Engineering (ICEE). - Isfahan, Iran, 11-13 May 2010. - P. 100-104. ↑
- C1661.** Richter M.D. 77 GHz automotive digital beamforming radar with SiGe chipset. / Richter M.D., Schneider M., Wenig P., Weigel R. // 2010 German Microwave Conference. - Berlin, 15-17 March 2010. - P. 210-213. ↑
- C1662.** Ali F. Detection of weak moving targets based on 2-D range-Doppler FMCW radar Fourier processing. / Ali F., Vossiek M. // 2010 German Microwave Conference. - Berlin, 15-17 March 2010. - P. 214-217. ↑
- C1663.** Vestling L. Enhanced drift in RF-power LDMOS transistors under pulsed stress conditions. / Vestling L., Bengtsson O., Olsson J. // 2010 German Microwave Conference. - Berlin, 15-17 March 2010. - P. 182-185. ↑
- C1664.** Kojhler M. Considerations for future automotive radar in the frequency range above 100 GHz. / Kojhler M., Gumbmann F., Schujr J., Schmidt L.-P., Blojcher H.-L. // 2010 German Microwave Conference. - Berlin, 15-17 March 2010. - P. 284-287. ↑
- C1665.** Reichthalhammer T. Specification and design of a fast-tuning stepped-frequency synthesizer for a short-range-SAR-system in the K-Band. / Reichthalhammer T., Biebl E.M. // 2010 German Microwave Conference. - Berlin, 15-17 March 2010. - P. 218-221. ↑
- C1666.** Huaming Wu. A novel motion compensation algorithm for automotive SAR: Simulations and experiments. / Huaming Wu, Zwick T. // 2010 German Microwave Conference. - Berlin, 15-17 March 2010. - P. 222-226. ↑
- C1667.** Vasalos A. LTR analysis and signal processing for concealed explosive detection. / Vasalos A., Vasalos I., Heung-Gyoon Ryu, Fotinea S.-E. // 2010 German Microwave Conference. - Berlin, 15-17 March 2010. - P. 166-169. ↑
- C1668.** Yasui T. Absolute distance measurement with asynchronous-optical-sampling terahertz impulse radar. / Yasui T., Ohgi Y., Kabetani Y., Yokoyama S., Araki T. // 2010 Conference on Lasers and Electro-Optics (CLEO) and Quantum Electronics and Laser Science Conference (QELS). - San Jose, CA, 16-21 May 2010. - P. 1-2. ↑
- C1669.** Dogariu A. Ppb standoff detection of nitric oxide in air. / Dogariu A., Miles R.B. // 2010 Conference on Lasers and Electro-Optics (CLEO) and Quantum Electronics and Laser Science Conference (QELS). - San Jose, CA, 16-21 May 2010. - P. 1-2. ↑
- C1670.** Narimanov E.E. Darker than black: radiation-absorbing metamaterial. / Narimanov E.E., Li H., Barnakov Yu.A., Noginov M.A. // 2010 Conference on Lasers and Electro-Optics (CLEO) and Quantum Electronics and Laser Science Conference (QELS). - San Jose, CA, 16-21 May 2010. - P. 1-2. ↑
- C1671.** Xuyang Li. Ultra wideband radar for water detection in the human body. / Xuyang Li, Pancera E., Zwirello L., Huaming Wu, Zwick T. // 2010 German Microwave Conference. - Berlin, 15-17 March 2010. - P. 150-153. ↑

- C1672.** Yuzhe Wang. Iterated simplified multiple model filters for target tracking in the presence of glint. / Yuzhe Wang, Xiaoping Shi, Yin Zhu. // 2010 Chinese Control and Decision Conference (CCDC). - Xuzhou, 26-28 May 2010. - P. 1673-1677. ↑
- C1673.** Riznyk V. Application of the combinatorial models for innovative design techniques. / Riznyk V., Bandyrska O., Yurchak I. // 2010 Proceedings of VIth International Conference on Perspective Technologies and Methods in MEMS Design (MEMSTECH). - Lviv, 20-23 April 2010. - P. 53-55. ↑
- C1674.** Hasch J. 77 GHz radar transceiver with dual integrated antenna elements. / Hasch J., Wostradowski U., Gaier S., Hansen T. // 2010 German Microwave Conference. - Berlin, 15-17 March 2010. - P. 280-283. ↑
- C1675.** Shanbin Zhang. Particle filters for beam-space high resolution DOA estimation. / Shanbin Zhang, Wentao Fan, Xinhua Zhang. // 2010 2nd International Conference on Future Computer and Communication (ICFCC). - Wuhan, 21-24 May 2010. - Vol. 2. - P. V2-722-V2-725-722. ↑
- C1676.** Xintong Zhang. Design of elevator audio player controlled by wireless communication. / Xintong Zhang, Chengdong Wu, Yuanlong Wang, Bingyang Li, Yunzhou Zhang. // 2010 2nd International Conference on Future Computer and Communication (ICFCC). - Wuhan, 21-24 May 2010. - Vol. 2. - P. V2-801-V2-804-801. ↑
- C1677.** Yang Longpo. Decision-making model for mobile blind compensation in jamming. / Yang Longpo, Xiong Jiajun. // 2010 2nd International Conference on Future Computer and Communication (ICFCC). - Wuhan, 21-24 May 2010. - Vol. 1. - P. V1-548-V1-551-548. ↑
- C1678.** Yan Suyun. Research on fault monitoring for railway automatic blocking and continuous transmission lines. / Yan Suyun, Wang Yi, Shu Hong. // 2010 2nd International Conference on Future Computer and Communication (ICFCC). - Wuhan, 21-24 May 2010. - Vol. 3. - P. V3-432-V3-435-432. ↑
- C1679.** Kaihua Xu. Implementation of handheld remote sense image calibration system software. / Kaihua Xu, Jian Chen, Rui Wang, Yuhua Liu. // 2010 2nd International Conference on Future Computer and Communication (ICFCC). - Wuhan, 21-24 May 2010. - Vol. 2. - P. V2-664-V2-668-664. ↑
- C1680.** Yang Jun. An efficient nonuniform channelizer based on Adjacent Channel Merging. / Yang Jun, Yuan Sijie. // 2010 2nd International Conference on Future Computer and Communication (ICFCC). - Wuhan, 21-24 May 2010. - Vol. 3. - P. V3-408-V3-411-408. ↑
- C1681.** Jin Hongbin. A new evidence combination method. / Jin Hongbin, Lan Jiangqiao, Li Hongfei. // 2010 2nd International Conference on Future Computer and Communication (ICFCC). - Wuhan, 21-24 May 2010. - Vol. 1. - P. V1-382-V1-385-382. ↑
- C1682.** Fitzek F. Automotive radome design-fishnet structure for 79 GHz. / Fitzek F., Abou-Chahine Z., Rasshofer R.H., Biebl E.M. // 2010 German Microwave Conference. - Berlin, 15-17 March 2010. - P. 146-149. ↑
- C1683.** Shoykhetbrod O. Switchable power combining network for 35GHz. / Shoykhetbrod O., Nujalier D. // 2010 German Microwave Conference. - Berlin, 15-17 March 2010. - P. 94-97. ↑
- C1684.** Buddendick H. Bistatic scattering center models for the simulation of wave propagation in automotive radar systems. / Buddendick H., Eibert T., Hasch J. // 2010 German Microwave Conference. - Berlin, 15-17 March 2010. - P. 288-291. ↑
- C1685.** Tian Kangsheng. Analysis and research of proportional conflict redistribution rules in identity identification. / Tian Kangsheng, Li Hongfei, Jin Hongbin. // 2010 2nd International Conference on Future Computer and Communication (ICFCC). - Wuhan, 21-24 May 2010. - Vol. 1. - P. V1-254-V1-257-254. ↑
- C1686.** Lina Fan. Time allocation in cognitive radar for multitarget detection with dynamic programming. / Lina Fan, Jinkuan Wang, Dongmei Shu, Bin Wang. // 2010 Chinese Control and Decision Conference (CCDC). - Xuzhou, 26-28 May 2010. - P. 839-842. ↑
- C1687.** Aleksieieva A. Design and optimization of amplitude-modulated microwave backscatter transponders. / Aleksieieva A., Vossiek M. // 2010 German Microwave Conference. - Berlin, 15-17 March 2010. - P. 134-137. ↑
- C1688.** Dogariu A. Direct measurement of electron loss rate in air. / Dogariu A., Shneider M.N., Miles R.B. // 2010 Conference on Lasers and Electro-Optics (CLEO) and Quantum Electronics and Laser Science Conference

(QELS). - San Jose, CA, 16-21 May 2010. - P. 1-2. ↑

**C1689.** Ruuben Toomas. Optimal waveform selection for software defined data acquisition system. / Ruuben Toomas, Berdnikova Julia, Muursepp Ivo, Madar Urve. // 2010 Proceedings of the Fourth European Conference on Antennas and Propagation (EuCAP). - Barcelona, Spain, 12-16 April 2010. - P. 1-5. ↑

**C1690.** Rashid Laith. Partial treatment of wind turbine blades with radar absorbing materials (RAM) for RCS reduction. / Rashid Laith, Brown Anthony. // 2010 Proceedings of the Fourth European Conference on Antennas and Propagation (EuCAP). - Barcelona, Spain, 12-16 April 2010. - P. 1-5. ↑

**C1691.** Fhager Andreas. Stroke detection using a broadband microwave antenna system. / Fhager Andreas, McKelvey Tomas, Persson Mikael. // 2010 Proceedings of the Fourth European Conference on Antennas and Propagation (EuCAP). - Barcelona, Spain, 12-16 April 2010. - P. 1-3. ↑

**C1692.** Wu Ke. Millimeter-wave integrated waveguide antenna arrays and beamforming networks for low-cost satellite and mobile systems. / Wu Ke, Cheng Yu Jian, Djerafi Tarek, Chen Xiao Ping, Fonseca Nelson, Hong Wei. // 2010 Proceedings of the Fourth European Conference on Antennas and Propagation (EuCAP). - Barcelona, Spain, 12-16 April 2010. - P. 1-5. ↑

**C1693.** Bernardi G. Mutual coupling and platform effects in the synthesis of Passive Coherent Location radar array. / Bernardi G., D'Urso M., Farina A., Felaco M., Meliado E. F. // 2010 Proceedings of the Fourth European Conference on Antennas and Propagation (EuCAP). - Barcelona, Spain, 12-16 April 2010. - P. 1-2. ↑

**C1694.** Leib Mario. Vital signs monitoring with a UWB radar based on a correlation receiver. / Leib Mario, Menzel Wolfgang, Schleicher Bernd, Schumacher Hermann. // 2010 Proceedings of the Fourth European Conference on Antennas and Propagation (EuCAP). - Barcelona, Spain, 12-16 April 2010. - P. 1-5. ↑

**C1695.** Locker C. Antenna front-end concepts of a low-cost coherent radar demonstrator for S-band application. / Locker C., Pamies M., Bertuch T., Knott P., Erkens H., Wunderlich R., Heinen S. // 2010 Proceedings of the Fourth European Conference on Antennas and Propagation (EuCAP). - Barcelona, Spain, 12-16 April 2010. - P. 1-5. ↑

**C1696.** Luo Yanjia. A Least-Squares Algorithm for Multipath Estimation Using an UWB-IR Link. / Luo Yanjia, Law Choi Look. // 2010 IEEE Wireless Communications and Networking Conference (WCNC). - Sydney, Australia, 18-21 April 2010. - P. 1-6. ↑

**C1697.** Weile Zhang. Distributed Localization for Wireless Sensor Networks Using LFM Waves. / Weile Zhang, Qinye Yin, Wenjie Wang. // 2010 IEEE Wireless Communications and Networking Conference (WCNC). - Sydney, NSW, 18-21 April 2010. - P. 1-5. ↑

**C1698.** Sedighin F. ISAR rotational motion compensation using entropy metric. / Sedighin F., Modarres Hashemi M. // 2010 18th Iranian Conference on Electrical Engineering (ICEE). - Isfahan, Iran, 11-13 May 2010. - P. 288-293. ↑

**C1699.** Fusco V. Retrodirective array based radar (invited). / Fusco V., Buchanan N. B. // 2010 Proceedings of the Fourth European Conference on Antennas and Propagation (EuCAP). - Barcelona, Spain, 12-16 April 2010. - P. 1-4. ↑

**C1700.** Winder A.A. Synthetic Structural Imaging (SSI): A new ultrasound method for tracking breast cancer morphology. / Winder A.A., Jadidian B., Muratore R. // 2010 39th Annual Ultrasonic Industry Association Symposium (UIA). - Cambridge, MA, 12-14 April 2010. - P. 1-4. ↑

**C1701.** Chen Kai-Hsiu. Improving Service Availability in 3GPP Generic Access Network (GAN) by Adaptive Keep-Alive Interval (AKI). / Chen Kai-Hsiu, Chen Jyh-Cheng. // 2010 IEEE Wireless Communications and Networking Conference (WCNC). - Sydney, Australia, 18-21 April 2010. - P. 1-6. ↑

**C1702.** Satapathy G. A Traffic Information Service-Broadcast model for mixed-equipage Aircraft Simulation. / Satapathy G., Chen J., Tolani D., Sturdy J.L., Henion J.T., Kubat G. // 2010 Integrated Communications Navigation and Surveillance Conference (ICNS). - Herndon, VA, 11-13 May 2010. - P. E3-1-E3-15-1. ↑

**C1703.** Robine. Angle-resolved thz time domain reflection spectroscopy of rough surfaces. / Robine, C., Wiegand C., Rujhle K., Ellrich F., Weinland T., Beigang R. // 2010 Conference on Lasers and Electro-Optics



(CLEO) and Quantum Electronics and Laser Science Conference (QELS). - San Jose, CA, 16-21 May 2010. - P. 1-2. ↑

**C1704.** Tseng Tzu-Fang. THz fiber-based swept-source imaging radar. / Tseng Tzu-Fang, Huang Yu-Wei, Kuo Chung-Chiu, Huang Yu-Jing, Sun Chi-Kuang. // 2010 Conference on Lasers and Electro-Optics (CLEO) and Quantum Electronics and Laser Science Conference (QELS). - San Jose, CA, USA, 16-21 May 2010. - P. 1-2. ↑

**C1705.** Owechko Yuri. Automatic recognition of diverse 3-D objects and analysis of large urban scenes using ground and aerial LIDAR sensors. / Owechko Yuri, Medasani Swarup, Korah Thommen. // 2010 Conference on Lasers and Electro-Optics (CLEO) and Quantum Electronics and Laser Science Conference (QELS). - San Jose, CA, USA, 16-21 May 2010. - P. 1-2. ↑

**C1706.** Dregely D. 3D optical Yagi-Uda nanoantenna array. / Dregely D., Taubert R., Giessen H. // 2010 Conference on Lasers and Electro-Optics (CLEO) and Quantum Electronics and Laser Science Conference (QELS). - San Jose, CA, 16-21 May 2010. - P. 1-2. ↑

**C1707.** Barber Z.W. Linearization of ultra-broadband optical chirps for precision length metrology. / Barber Z.W., Renner C.J., Babbitt W.R., Reibel R.R., Roos P.A., Berg T., Kaylor B., Greenfield N. // 2010 Conference on Lasers and Electro-Optics (CLEO) and Quantum Electronics and Laser Science Conference (QELS). - San Jose, CA, 16-21 May 2010. - P. 1-2. ↑

**C1708.** Combrie S. 90ps tunable true-time delay line based on photonic crystals. / Combrie S., Bourderionnet J., Colman P., Dolfi D., De Rossi A. // 2010 Conference on Lasers and Electro-Optics (CLEO) and Quantum Electronics and Laser Science Conference (QELS). - San Jose, CA, USA, 16-21 May 2010. - P. 1-2. ↑

**C1709.** Mayor Shane D. High pulse-energy atmospheric aerosol lidar at 1.5-microns wavelength: Opportunities for innovation from a meteorologist's perspective. 2010 Conference on Lasers and Electro-Optics (CLEO) and Quantum Electronics and Laser Science Conference (QELS). - San Jose, CA, USA, 16-21 May 2010. - P. 1-2. ↑

**C1710.** Sharp M. On Time Varying Channel Estimation Using Sparse Models. / Sharp M., Scaglione A. // 2010 IEEE International Conference on Communications (ICC). - Cape Town, 23-27 May 2010. - P. 1-6. ↑

**C1711.** Jin-Cheol Jeong. SiGe BiCMOS Chip Sets for Use in an X-Band Multi-function Chip. / Jin-Cheol Jeong, In-Bok Yom. // 2010 Second International Conference on Advances in Satellite and Space Communications (SPACOMM). - Athens, 13-19 June 2010. - P. 25-30. ↑

**C1712.** Qixun Zhang. A Novel Homogeneous Mesh Grouping Scheme for Broadcast Cognitive Pilot Channel in Cognitive Wireless Networks. / Qixun Zhang, Zhiyong Feng, Guoyi Zhang. // 2010 IEEE International Conference on Communications (ICC). - Cape Town, 23-27 May 2010. - P. 1-6. ↑

**C1713.** Paschke Katrin. Quantum Cascade laser for elastic-backscattering LIDAR measurement. / Paschke Katrin, Liu Peter Q., Michel Anna P. M., Smith James, Moshary Fred, Gmachl Claire. // 2010 Conference on Lasers and Electro-Optics (CLEO) and Quantum Electronics and Laser Science Conference (QELS). - San Jose, CA, USA, 16-21 May 2010. - P. 1-2. ↑

**C1714.** Shirazi G.N. Lifetime Maximization of UWB-Based Sensor Networks for Event Detection Applications. / Shirazi G.N., Lampe L. // 2010 IEEE International Conference on Communications (ICC). - Cape Town, 23-27 May 2010. - P. 1-6. ↑

**C1715.** Agustin A. Performance of Downlink Schedulers with Superposed or Orthogonal Transmissions. / Agustin A., Vidal J., Muc,oz O. // 2010 IEEE International Conference on Communications (ICC). - Cape Town, 23-27 May 2010. - P. 1-5. ↑

**C1716.** Xi Li. A target polarization recognition method for radar echoes. / Xi Li, Lianshan Lin, Xianhe Shao. // 2010 International Conference on Microwave and Millimeter Wave Technology (ICMMT). - Chengdu, 8-11 May 2010. - P. 1644-1647. ↑

**C1717.** Wei Peng. A novel analytical method and error criterion of the synthetic range profile. / Wei Peng, Xuegang Wang, Bin Tang, Hongang Wu. // 2010 International Conference on Microwave and Millimeter Wave Technology (ICMMT). - Chengdu, 8-11 May 2010. - P. 1648-1651. ↑

- C1718.** Qian Kewei. Research of LTCC millimeter-wave T/R module. 2010 International Conference on Microwave and Millimeter Wave Technology (ICMMT). - Chengdu, 8-11 May 2010. - P. 1444-1446. ↑
- C1719.** Ruihai Liang. Radar anti-jamming application of solid-state noise source. / Ruihai Liang, Yong Yang, Xiaofa Zhang, Naichang Yuan. // 2010 International Conference on Microwave and Millimeter Wave Technology (ICMMT). - Chengdu, 8-11 May 2010. - P. 1629-1632. ↑
- C1720.** Bo Lv. Design of velocity radar for railway. 2010 International Conference on Microwave and Millimeter Wave Technology (ICMMT). - Chengdu, 8-11 May 2010. - P. 1637-1639. ↑
- C1721.** Ruihai Liang. Optimum design of jamming reconnaissance receiver. / Ruihai Liang, Yuan Tan, Xiaofa Zhang, Naichang Yuan. // 2010 International Conference on Microwave and Millimeter Wave Technology (ICMMT). - Chengdu, 8-11 May 2010. - P. 1640-1643. ↑
- C1722.** Wang Ling. An approach research to segmentation of the SAR image based on the Markov random field. / Wang Ling, Lu Gui Zhen, Guan Ya Lin. // 2010 International Conference on Microwave and Millimeter Wave Technology (ICMMT). - Chengdu, 8-11 May 2010. - P. 1420-1423. ↑
- C1723.** Yao Xu. A method of over cosec square-beam shaping with sharp cut off. / Yao Xu, Cao Xiang-yu, Xu Xiao-fei, Yang Qun. // 2010 International Conference on Microwave and Millimeter Wave Technology (ICMMT). - Chengdu, 8-11 May 2010. - P. 1368-1371. ↑
- C1724.** Lai-xuan Ma. Analysis on the refraction stealth characteristic of cylinder plasma envelopes. / Lai-xuan Ma, Hou Zhang, Li Zhu, Xiang-jun Gao. // 2010 International Conference on Microwave and Millimeter Wave Technology (ICMMT). - Chengdu, 8-11 May 2010. - P. 1695-1698. ↑
- C1725.** Guodong Han. PMCHW-AMCBFM for analysis of electromagnetic scattering by 3-D homogenous dielectric objects. / Guodong Han, Yun Xu, Jiade Yuan, Changqing Gu. // 2010 International Conference on Microwave and Millimeter Wave Technology (ICMMT). - Chengdu, 8-11 May 2010. - P. 1329-1332. ↑
- C1726.** Yi Wang. Analysis of ELF attenuation rate using the geodesic FDTD algorithm. / Yi Wang, Hangang Xia, Qunsheng Cao. // 2010 International Conference on Microwave and Millimeter Wave Technology (ICMMT). - Chengdu, 8-11 May 2010. - P. 1413-1415. ↑
- C1727.** Li Ying-le. Anisotropic scattering for a magnetized cold plasma sphere. / Li Ying-le, Li Jin, Wang Ming-jun, Dong Qun-feng, Tang Gao-feng. // 2010 International Conference on Microwave and Millimeter Wave Technology (ICMMT). - Chengdu, 8-11 May 2010. - P. 1398-1404. ↑
- C1728.** Liang Chen. Performance analysis for angle measurement of monopulse radar with non-consistent amplitude-phase features. / Liang Chen, Weixing Sheng. // 2010 International Conference on Microwave and Millimeter Wave Technology (ICMMT). - Chengdu, 8-11 May 2010. - P. 1382-1385. ↑
- C1729.** Xu Xi-Yu. Engineering design of the rain mode on an ocean-dedicating radar altimeter. / Xu Xi-Yu, Liu He-Guang, Liu Peng. // 2010 International Conference on Microwave and Millimeter Wave Technology (ICMMT). - Chengdu, 8-11 May 2010. - P. 1719-1722. ↑
- C1730.** Kolias N. J. GaN technology for microwave and millimeter wave applications. / Kolias N. J., Whelan C. S., Kazior T. E., Smith K. V. // 2010 IEEE MTT-S International Microwave Symposium Digest (MTT). - Anaheim, CA, USA, 23-28 May 2010. - P. 1. ↑
- C1731.** Horton J. B. Special session in honor Dr. Kiyo Tomiyasu. 2010 IEEE MTT-S International Microwave Symposium Digest (MTT). - Anaheim, CA, USA, 23-28 May 2010. - P. 1. ↑
- C1732.** Vigu C. Improving estimation algorithms based on field data for a hybrid energy system. / Vigu C., Gota D.I., Capatana D. // 2010 IEEE International Conference on Automation Quality and Testing Robotics (AQTR). - Cluj-Napoca, 28-30 May 2010. - Vol. 3. - P. 1-4. ↑
- C1733.** Wilden H. The SAR/GMTI airborne radar PAMIR: Technology and performance. / Wilden H., Brenner A.R. // 2010 IEEE MTT-S International Microwave Symposium Digest (MTT). - Anaheim, CA, 23-28 May 2010. - P. 534-537. ↑
- C1734.** Rodriguez-Morales F. Development of a multi-frequency airborne radar instrumentation package for ice

sheet mapping and imaging. / Rodriguez-Morales F., Gogineni P., Leuschen C., Allen C., Lewis C., Patel A., Byers K., Smith L., Shi L., Panzer B., Blake W., Crowe R., Gifford C. // 2010 IEEE MTT-S International Microwave Symposium Digest (MTT). - Anaheim, CA, 23-28 May 2010. - P. 157-160. ↑

**C1735.** Mochizuki S. High-phase-resolution 77-GHz-band radar module for near-field millimeter-wave imaging. / Mochizuki S., Oka S., Togo H., Kukutsu N. // 2010 IEEE MTT-S International Microwave Symposium Digest (MTT). - Anaheim, CA, 23-28 May 2010. - P. 636-639. ↑

**C1736.** Majdik A.L. Laser and vision based map building techniques for mobile robot navigation. / Majdik A.L., Szoke I., Tamas L., Popa M., Lazea G. // 2010 IEEE International Conference on Automation Quality and Testing Robotics (AQTR). - Cluj-Napoca, 28-30 May 2010. - Vol. 1. - P. 1-6. ↑

**C1737.** Lei Hu. Space Registration Algorithm Based on Constrictive Total Least Squares. / Lei Hu, Yue-song Lin, Yun-fei Guo. // 2010 International Conference on Intelligent Computation Technology and Automation (ICICTA). - Changsha, 11-12 May 2010. - Vol. 3. - P. 359-362. ↑

**C1738.** Liu Lin. A Parameter Estimation Method for Moving Target in Stepped Frequency Radar. / Liu Lin, Tian Jin-jun, Liu Zhao-hui. // 2010 International Conference on Intelligent Computation Technology and Automation (ICICTA). - Changsha, 11-12 May 2010. - Vol. 1. - P. 289-292. ↑

**C1739.** Shang Haiying. Adaptive Threshold for Fast Signal Detection in Multi-target Tracking. / Shang Haiying, An Jianping, An Weiyu, Han Hangcheng. // 2010 International Conference on Intelligent Computation Technology and Automation (ICICTA). - Changsha, China, 11-12 May 2010. - Vol. 1. - P. 429-432. ↑

**C1740.** Apatean A. Visible-infrared fusion in the frame of an obstacle recognition system. / Apatean A., Rusu C., Rogozan A., Benshrir A. // 2010 IEEE International Conference on Automation Quality and Testing Robotics (AQTR). - Cluj-Napoca, 28-30 May 2010. - Vol. 1. - P. 1-6. ↑

**C1741.** Macalak J. Application of Kalman filtering to acoustic sound diagnostic measurement. 2010 13th International Symposium MECHATRONIKA. - Trencianske Teplice, 2-4 June 2010. - P. 84-86. ↑

**C1742.** Tkac J. The possibilities of utilization of mobile pulsed radar sensors. 2010 13th International Symposium MECHATRONIKA. - Trencianske Teplice, 2-4 June 2010. - P. 10-13. ↑

**C1743.** Ni Feng. Design of an X-band high power solid state power amplifier based on GaN HEMT. / Ni Feng, Fang Jianhong, Feng Hao, Wang Chaoyang, Liu Jianwei. // 2010 International Conference on Microwave and Millimeter Wave Technology (ICMMT). - Chengdu, 8-11 May 2010. - P. 1916-1918. ↑

**C1744.** Wang Z.X. Design and analysis of double negative binary diffractive lens. / Wang Z.X., You L.Z. // 2010 International Conference on Microwave and Millimeter Wave Technology (ICMMT). - Chengdu, 8-11 May 2010. - P. 1502-1505. ↑

**C1745.** Jiechen Chen. Quasi-optical duplexer in 220GHz. / Jiechen Chen, Xuettian Wang, Yingqiao Li. // 2010 International Conference on Microwave and Millimeter Wave Technology (ICMMT). - Chengdu, 8-11 May 2010. - P. 1282-1285. ↑

**C1746.** Yan-Wei Zhao. Bistatic Synthetic Aperture Radar imagery simulation of sea surface. / Yan-Wei Zhao, Min Zhang, Hui Chen, Ping Zhou. // 2010 International Conference on Microwave and Millimeter Wave Technology (ICMMT). - Chengdu, 8-11 May 2010. - P. 1231-1234. ↑

**C1747.** Xianrong Zhang. Millimeter-wave integrated waveguide power dividers for power combiner and phased array applications. / Xianrong Zhang, Qingyuan Wang, Ao Liao, Yuanbin Xiang. // 2010 International Conference on Microwave and Millimeter Wave Technology (ICMMT). - Chengdu, 8-11 May 2010. - P. 233-235. ↑

**C1748.** Rong Shen. A design of stripline-coaxial vertical transition with ultra-broadband. / Rong Shen, Dewu Kong, Dan Sun. // 2010 International Conference on Microwave and Millimeter Wave Technology (ICMMT). - Chengdu, 8-11 May 2010. - P. 1514-1517. ↑

**C1749.** Ying Bao. Intermediate frequency circuit design for a 60GHz LFM CW radar. / Ying Bao, Zhiguo Shi, Kangsheng Chen. // 2010 International Conference on Microwave and Millimeter Wave Technology (ICMMT). - Chengdu, 8-11 May 2010. - P. 270-273. ↑

- C1750.** Yin Honggang. Predesign of the wind field measuring radar for FengYun-3E meteorological satellite. / Yin Honggang, Dong Xiaolong. // 2010 International Conference on Microwave and Millimeter Wave Technology (ICMMT). - Chengdu, 8-11 May 2010. - P. 1228-1230. ↑
- C1751.** Shiyong Li. Fast two-dimensional imaging of scattering centers using the nonuniform FFT. / Shiyong Li, Chong Li, Bocheng Zhu. // 2010 International Conference on Microwave and Millimeter Wave Technology (ICMMT). - Chengdu, 8-11 May 2010. - P. 1204-1207. ↑
- C1752.** Jing Li. An efficient technique for extracting singularity arising in RCS computation of cylindrical antenna. / Jing Li, Yufa Sun. // 2010 International Conference on Microwave and Millimeter Wave Technology (ICMMT). - Chengdu, 8-11 May 2010. - P. 1201-1203. ↑
- C1753.** Hui Chen. Scattering-based I/Q signal simulation of sea clutter returns. / Hui Chen, Min Zhang, Hong-Cheng Yin. // 2010 International Conference on Microwave and Millimeter Wave Technology (ICMMT). - Chengdu, 8-11 May 2010. - P. 1197-1200. ↑
- C1754.** Yin Honggang. The requirement of range sidelobe for dual-frequency precipitation radar on FengYun-3 precipitation measurement satellite. / Yin Honggang, Dong Xiaolong. // 2010 International Conference on Microwave and Millimeter Wave Technology (ICMMT). - Chengdu, 8-11 May 2010. - P. 1224-1227. ↑
- C1755.** Jun Yin. A broad-band analog phase shifter design on I-Q vector modulator. / Jun Yin, Wanshun Jiang, Zhigang Zhang. // 2010 International Conference on Microwave and Millimeter Wave Technology (ICMMT). - Chengdu, 8-11 May 2010. - P. 632-635. ↑
- C1756.** Xin Mi Yang. Research on the one-dimensional randomly gradient index coating. / Xin Mi Yang, Qiang Cheng, Tie Jun Cui. // 2010 International Conference on Microwave and Millimeter Wave Technology (ICMMT). - Chengdu, 8-11 May 2010. - P. 1208-1211. ↑
- C1757.** Qinlong Lu. A novel wide beam UWB antenna design for Through-the-Wall radar. / Qinlong Lu, Lingyun Zhou, Chaoman Tan, Lu Guanghua. // 2010 International Conference on Microwave and Millimeter Wave Technology (ICMMT). - Chengdu, 8-11 May 2010. - P. 1912-1915. ↑
- C1758.** Yin Zhiping. A new hybrid-frequency radar system based on compressed sensing theory. / Yin Zhiping, Xu Hao, Chen Weidong. // 2010 International Conference on Microwave and Millimeter Wave Technology (ICMMT). - Chengdu, 8-11 May 2010. - P. 1731-1734. ↑
- C1759.** Zhou LanFeng. Angle estimation for two unresolved Swerling I targets in monopulse radar. / Zhou LanFeng, Zhang Min, Zhao YiNan. // 2010 International Conference on Microwave and Millimeter Wave Technology (ICMMT). - Chengdu, 8-11 May 2010. - P. 1622-1625. ↑
- C1760.** Ai-Jun Liu. Oblique projection polarization filtering and its performance in High Frequency Surface Wave Radar. / Ai-Jun Liu, Xing-Peng Mao, Wei-Bo Deng. // 2010 International Conference on Microwave and Millimeter Wave Technology (ICMMT). - Chengdu, 8-11 May 2010. - P. 1618-1621. ↑
- C1761.** Cai W.Z. Design variations of HVVFET™ transistors for high-efficiency class-AB L-band power amplifiers. / Cai W.Z., Rice D., Gogoi B.P., Le P., Davies R.B., Lutz D., Sucro M. // 2010 International Conference on Microwave and Millimeter Wave Technology (ICMMT). - Chengdu, 8-11 May 2010. - P. 1925-1928. ↑
- C1762.** Qian Ye. Design of a dual-feed orthogonal polarized patch antenna array. / Qian Ye, Danping Wang, Min Wang, Wen Wu, Jianzhong Zhao. // 2010 International Conference on Microwave and Millimeter Wave Technology (ICMMT). - Chengdu, 8-11 May 2010. - P. 1031-1034. ↑
- C1763.** Lei Zhu. Self-adaptive frequency estimation algorithm of improving liquid level measurement precision of LFM CW radar. / Lei Zhu, Liang Dong, Shu-dong Liu, Dao-li Sun. // 2010 International Conference on Microwave and Millimeter Wave Technology (ICMMT). - Chengdu, 8-11 May 2010. - P. 1626-1628. ↑
- C1764.** He Feng. Detection of human targets using ultra-wide band through-the-wall radar. / He Feng, Zhu Guofu, Huang Xiaotao, Zhou Zhimin. // 2010 International Conference on Microwave and Millimeter Wave Technology (ICMMT). - Chengdu, 8-11 May 2010. - P. 1750-1753. ↑
- C1765.** Cai Zhengyu. FM interference suppression for PRC-CW radar based on STFT and median filtering. /



Cai Zhengyu, Chen Wenwu, Chen Rushan. // 2010 International Conference on Microwave and Millimeter Wave Technology (ICMMT). - Chengdu, 8-11 May 2010. - P. 1610-1613. ↑

C1766. Yang Z.W. Azimuth variant bistatic SAR imaging algorithm based on physical optics method. / Yang Z.W., Shang S., Chen J.Q., Liu Z.W., Chen R.S. // 2010 International Conference on Microwave and Millimeter Wave Technology (ICMMT). - Chengdu, 8-11 May 2010. - P. 1762-1765. ↑

C1767. Guiyuan Li. Study on measurement model for radar electromagnetic compatibility analysis. / Guiyuan Li, Hou Zhang, Xiong Yin, Hailin Tian. // 2010 International Conference on Microwave and Millimeter Wave Technology (ICMMT). - Chengdu, 8-11 May 2010. - P. 1559-1562. ↑

C1768. Chen Wenwu. Optimizing polyphase signals for orthogonal netted radar. / Chen Wenwu, Cai Zhengyu, Chen Rushan, Zhao Zhao. // 2010 International Conference on Microwave and Millimeter Wave Technology (ICMMT). - Chengdu, 8-11 May 2010. - P. 1614-1617. ↑

C1769. Min Zhang. Variable structure multiple model particle filter for maneuvering radar target tracking. / Min Zhang, Weidong Chen. // 2010 International Conference on Microwave and Millimeter Wave Technology (ICMMT). - Chengdu, 8-11 May 2010. - P. 1754-1757. ↑

C1770. Wei Chongyu. The design of cancellation unit against radiofrequency interference in life-detection radar. / Wei Chongyu, Liu Chen, Yang Yang. // 2010 International Conference on Microwave and Millimeter Wave Technology (ICMMT). - Chengdu, 8-11 May 2010. - P. 1758-1761. ↑

C1771. Jahn M. Highly integrated 79, 94, and 120-GHz SiGe radar frontends. / Jahn M., Stelzer A., Hamidipour A. // 2010 IEEE MTT-S International Microwave Symposium Digest (MTT). - Anaheim, CA, 23-28 May 2010. - P. 1324-1327. ↑

C1772. Sheng Li. Non-Air Conducted Speech Enhancement Based on Iterative Spectral Subtraction Method. / Sheng Li, JianQi Wang, XiJing Jing. // 2010 4th International Conference on Bioinformatics and Biomedical Engineering (iCBBE). - Chengdu, 18-20 June 2010. - P. 1-4. ↑

C1773. Wang Y. Advanced system level simulation of UWB three-dimensional through-wall imaging radar for performance limitation prediction. / Wang Y., Kuhn M. J., Fathy A. E. // 2010 IEEE MTT-S International Microwave Symposium Digest (MTT). - Anaheim, CA, USA, 23-28 May 2010. - P. 1. ↑

C1774. Buchanan N. B. Fast response Retrodirective Radar. / Buchanan N. B., Fusco V., Sundaralingam P. // 2010 IEEE MTT-S International Microwave Symposium Digest (MTT). - Anaheim, CA, USA, 23-28 May 2010. - P. 1. ↑

C1775. Rebeiz G.M. Towards high-performance 100 GHz SiGe and CMOS circuits. / Rebeiz G.M., May J.W., Uzunkol M., Shin W., Inac O., Chang M. // 2010 IEEE MTT-S International Microwave Symposium Digest (MTT). - Anaheim, CA, 23-28 May 2010. - P. 1. ↑

C1776. {no data available}. Session-WE1. 2010 IEEE MTT-S International Microwave Symposium Digest (MTT). - Anaheim, CA, USA, 23-28 May 2010. - P. 1-5. ↑

C1777. Cheung S. K. High isolation lange-ferite circulators with NF suppression for simultaneous transmit and receive. / Cheung S. K., Weedon W. H., Caldwell C. P. // 2010 IEEE MTT-S International Microwave Symposium Digest (MTT). - Anaheim, CA, USA, 23-28 May 2010. - P. 1. ↑

C1778. Rodriguez-Morales F. Development of a multi-frequency airborne radar instrumentation package for ice sheet mapping and imaging. / Rodriguez-Morales F., Gogineni P., Leuschen C., Allen C. T., Lewis C., Patel A., Byers K., Smith L., Blake W., Panzer B., Shi L., Crowe R., Gifford C. // 2010 IEEE MTT-S International Microwave Symposium Digest (MTT). - Anaheim, CA, USA, 23-28 May 2010. - P. 1. ↑

C1779. Tian Liyan. System of locating and recognizing characters in complex background. / Tian Liyan, Xiao Jin, Hu Xiaoguang. // 2010 the 5th IEEE Conference on Industrial Electronics and Applications (ICIEA). - Taichung, 15-17 June 2010. - P. 202-206. ↑

C1780. Ting-Yueh Chin. A fast clutter cancellation method in quadrature doppler radar for noncontact vital signal detection. / Ting-Yueh Chin, Kun-Ying Lin, Sheng-Fuh Chang, Chia-Chan Chang. // 2010 IEEE MTT-S International Microwave Symposium Digest (MTT). - Anaheim, CA, 23-28 May 2010. - P. 764-767. ↑

**C1781.** Alleaume P.-F. A highly integrated heterogeneous micro- and mm-wave platform. / Alleaume P.-F., Aspemyr L., Gevorgian S., Houdbert J.-C., Jacobsson H., Pettersson L., Platt D., Salter M., Vorobiev A. // 2010 IEEE MTT-S International Microwave Symposium Digest (MTT). - Anaheim, CA, 23-28 May 2010. - P. 461-464.



**C1782.** Fulton C. J. Calibration of a Digital phased Array for polarimetric Radar. / Fulton C. J., Chappell W. J. // 2010 IEEE MTT-S International Microwave Symposium Digest (MTT). - Anaheim, CA, USA, 23-28 May 2010. - P. 1.



**C1783.** Chin T. A fast clutter cancellation method in quadrature doppler radar for noncontact vital signal detection. / Chin T., Lin K., Chang S., Chang C. // 2010 IEEE MTT-S International Microwave Symposium Digest (MTT). - Anaheim, CA, USA, 23-28 May 2010. - P. 1.



**C1784.** Peng Wang. Design and implementation of the low-power tracking system based on GPS-GPRS module. / Peng Wang, Zhiwen Zhao, Chongbin Xu, Zushun Wu, Yi Luo. // 2010 the 5th IEEE Conference on Industrial Electronics and Applications (ICIEA). - Taichung, 15-17 June 2010. - P. 207-210.



**C1785.** Jahn M. Highly integrated 79, 94, and 120-GHz SiGe radar frontends. / Jahn M., Stelzer A., Hamidipour A. // 2010 IEEE MTT-S International Microwave Symposium Digest (MTT). - Anaheim, CA, USA, 23-28 May 2010. - P. 1.



**C1786.** Goshi D.S. Cable imaging with an active W-band millimeter-wave sensor. / Goshi D.S., Liu Y., Mai K., Bui L., Shih Y. // 2010 IEEE MTT-S International Microwave Symposium Digest (MTT). - Anaheim, CA, 23-28 May 2010. - P. 1620-1623.



**C1787.** Fackelmeier A. Narrowband frequency scanning array antenna at 5.8 GHz for short range imaging. / Fackelmeier A., Biebl E.M. // 2010 IEEE MTT-S International Microwave Symposium Digest (MTT). - Anaheim, CA, 23-28 May 2010. - P. 1266-1269.



**C1788.** Goshi D. Cable imaging with an active W-band millimeter-wave sensor. / Goshi D., Liu Y., Mai K., Bui L., Shih Y. // 2010 IEEE MTT-S International Microwave Symposium Digest (MTT). - Anaheim, CA, USA, 23-28 May 2010. - P. 1.



**C1789.** Siegel P.H. THz for space: The golden age. 2010 IEEE MTT-S International Microwave Symposium Digest (MTT). - Anaheim, CA, 23-28 May 2010. - P. 816-819.



**C1790.** Nanzer J. A. Interferometric detection of the angular velocity of moving objects. 2010 IEEE MTT-S International Microwave Symposium Digest (MTT). - Anaheim, CA, USA, 23-28 May 2010. - P. 1.



**C1791.** Qiu J.X. Time-domain calibration technique for ultra-wide instantaneous-bandwidth vector waveform generation using parallel I/Q channels. 2010 IEEE MTT-S International Microwave Symposium Digest (MTT). - Anaheim, CA, 23-28 May 2010. - P. 1.



**C1792.** Singh A. A heterodyne receiver for harmonic doppler radar cardio-pulmonary monitoring with body-worn passive RF tags. / Singh A., Lubecke V.M. // 2010 IEEE MTT-S International Microwave Symposium Digest (MTT). - Anaheim, CA, 23-28 May 2010. - P. 1.



**C1793.** Ming Huang. Environmental Monitoring System Based on GIS and Wireless Communications. / Ming Huang, Yinbin Wu. // 2010 4th International Conference on Bioinformatics and Biomedical Engineering (iCBBE). - Chengdu, 18-20 June 2010. - P. 1-4.



**C1794.** {no data available}. Session-TH3. 2010 IEEE MTT-S International Microwave Symposium Digest (MTT). - Anaheim, CA, USA, 23-28 May 2010. - P. 1-4.



















**C1795.** Sarkas I. Second generation transceivers for D-band radar and data communication applications. / Sarkas I., Laskin E., Hasch J., Chevalier P., Voinigescu S. P. // 2010 IEEE MTT-S International Microwave Symposium Digest (MTT). - Anaheim, CA, USA, 23-28 May 2010. - P. 1.



**C1796.** Rebeiz G.M. Towards high-performance > 100 GHz SiGe and CMOS circuits. / Rebeiz G.M., May J., Uzunkol M., Shin W., Inac O., Chang M. // 2010 IEEE MTT-S International Microwave Symposium Digest (MTT). - Anaheim, CA, 23-28 May 2010. - P. 1320-1323.



- C1797.** Chicherin D. Analog type millimeter wave phase shifters based on MEMS tunable high-impedance surface in rectangular metal waveguide. / Chicherin D., Sterner M., Oberhammer J., Dudorov S., Aberg J., Raisanen A.V. // 2010 IEEE MTT-S International Microwave Symposium Digest (MTT). - Anaheim, CA, 23-28 May 2010. - P. 61-64. 
- C1798.** Huan-Yang Chen. Piggyback modulation for UHF RFID sensors. / Huan-Yang Chen, Bhadkamkar A., van der Weide D.W. // 2010 IEEE MTT-S International Microwave Symposium Digest (MTT). - Anaheim, CA, 23-28 May 2010. - P. 1776-1779. 
- C1799.** Albrecht J.D. THz electronics projects at DARPA: Transistors, TMICs, and amplifiers. / Albrecht J.D., Rosker M.J., Wallace H.B., Tsu-Hsi Chang. // 2010 IEEE MTT-S International Microwave Symposium Digest (MTT). - Anaheim, CA, 23-28 May 2010. - P. 1118-1121. 
- C1800.** {no data available}. Session-Wednesday-detail. 2010 IEEE MTT-S International Microwave Symposium Digest (MTT). - Anaheim, CA, USA, 23-28 May 2010. - P. 1-20. 
- C1801.** Chieh J.-C.S. A light weight 8-element broadband phased array receiver on Liquid Crystal Polymer. / Chieh J.-C.S., Anh-Vu Pham, Dalrymple T.W., Kuhl D.G., Garber B.B., Aihara K. // 2010 IEEE MTT-S International Microwave Symposium Digest (MTT). - Anaheim, CA, 23-28 May 2010. - P. 1024-1027. 
- C1802.** Heer C. Spaceborne SAR Systems and technologies. / Heer C., Fischer C., Schaefer C. // 2010 IEEE MTT-S International Microwave Symposium Digest (MTT). - Anaheim, CA, 23-28 May 2010. - P. 538-541. 
- C1803.** Singh A. A heterodyne receiver for Harmonic Doppler radar cardiopulmonary monitoring with body-worn passive RF tags. / Singh A., Lubecke V. // 2010 IEEE MTT-S International Microwave Symposium Digest (MTT). - Anaheim, CA, 23-28 May 2010. - P. 1600-1603. 
- C1804.** Poprawa F. Waveguide transition to feed a fully PCB integrated dielectric rod antenna. / Poprawa F., Zanati A., Zirotti A., Ellinger F. // 2010 IEEE MTT-S International Microwave Symposium Digest (MTT). - Anaheim, CA, 23-28 May 2010. - P. 640-643. 
- C1805.** Jen-Chieh Wu. Sidelobe level reduction in wide-angle scanning array system using pattern-reconfigurable antennas. / Jen-Chieh Wu, Chia-Chan Chang, Ting-Yueh Chin, Shao-Yu Huang, Sheng-Fuh Chang. // 2010 IEEE MTT-S International Microwave Symposium Digest (MTT). - Anaheim, CA, 23-28 May 2010. - P. 1274-1277. 
- C1806.** Ludwig M. FS-5, paper 5: Earth observation instruments with e-scan antennas state-of-the-art and outlook. / Ludwig M., Buck C.H., D'Addio S., Torres R., Rostan F., Schaefer C., Croci R. // 2010 IEEE MTT-S International Microwave Symposium Digest (MTT). - Anaheim, CA, 23-28 May 2010. - P. 544-547. 
- C1807.** Albrecht J. D. THz Electronics projects at DARPA: Transistors, TMICs, and amplifiers. / Albrecht J. D., Rosker M. J., Wallace H. B., Chang T. // 2010 IEEE MTT-S International Microwave Symposium Digest (MTT). - Anaheim, CA, USA, 23-28 May 2010. - P. 1. 
- C1808.** Zedler M. 2D transformation optics using anisotropic transmission-line metamaterials. / Zedler M., Eleftheriades G.V. // 2010 IEEE MTT-S International Microwave Symposium Digest (MTT). - Anaheim, CA, 23-28 May 2010. - P. 33-36. 
- C1809.** Sakai F. UWB array antenna utilizing novel electrical scanning system with tapped delay lines. / Sakai F., Ohta K. // 2010 IEEE MTT-S International Microwave Symposium Digest (MTT). - Anaheim, CA, USA, 23-28 May 2010. - P. 1. 
- C1810.** Fackelmeier A. Narrowband frequency scanning array antenna at 5.8 GHz for short range imaging. / Fackelmeier A., Biebl E. // 2010 IEEE MTT-S International Microwave Symposium Digest (MTT). - Anaheim, CA, USA, 23-28 May 2010. - P. 1. 
- C1811.** Sarkas I. Second generation transceivers for d-band radar and data communication applications. / Sarkas I., Laskin E., Hasch J., Chevalier P., Voinigescu S.P. // 2010 IEEE MTT-S International Microwave Symposium Digest (MTT). - Anaheim, CA, 23-28 May 2010. - P. 1328-1331. 
- C1812.** Fulton C. Calibration of a digital phased array for polarimetric radar. / Fulton C., Chappell W.J. // 2010 IEEE MTT-S International Microwave Symposium Digest (MTT). - Anaheim, CA, 23-28 May 2010. - P. 161-164. 



- C1813.** Carlson D.J. Commercial manufacturing practices applied to phased array radars. / Carlson D.J., Weigand C., Curcio D., Boles T. // 2010 IEEE MTT-S International Microwave Symposium Digest (MTT). - Anaheim, CA, 23-28 May 2010. - P. 676-679.
- C1814.** Wilden A. Brenner. The SAR/GMTI airborne radar PAMIR: Technology and performance. 2010 IEEE MTT-S International Microwave Symposium Digest (MTT). - Anaheim, CA, USA, 23-28 May 2010. - P. 1.
- C1815.** Alleaume P. A highly integrated heterogeneous micro- and mm-wave platform. / Alleaume P., Aspemyr L., Gevorgian S., Houdbert J., Jacobsson H., Pettersson L., Platt D., Salter M., Vorobiev A. // 2010 IEEE MTT-S International Microwave Symposium Digest (MTT). - Anaheim, CA, USA, 23-28 May 2010. - P. 1.
- C1816.** Zhang Xuehui. Recent Microwave Nondestructive Measurement in Biomedical Engineering. / Zhang Xuehui, Yu Zhining. // 2010 4th International Conference on Bioinformatics and Biomedical Engineering (iCBBE). - Chengdu, 18-20 June 2010. - P. 1-4.
- C1817.** Holpp W. Status and trends in AESA-based radar. 2010 IEEE MTT-S International Microwave Symposium Digest (MTT). - Anaheim, CA, USA, 23-28 May 2010. - P. 1.
- C1818.** Yazhou Wang. Advanced system level simulation of UWB three-dimensional through-wall imaging radar for performance limitation prediction. / Yazhou Wang, Kuhn M.J., Fathy A.E. // 2010 IEEE MTT-S International Microwave Symposium Digest (MTT). - Anaheim, CA, 23-28 May 2010. - P. 165-168.
- C1819.** Holpp W. The new generation of European E-scan fighter radars. 2010 IEEE MTT-S International Microwave Symposium Digest (MTT). - Anaheim, CA, USA, 23-28 May 2010. - P. 1.
- C1820.** Heer C. Spaceborne SAR systems and technologies. / Heer C., Fischer C., Schaefer C. // 2010 IEEE MTT-S International Microwave Symposium Digest (MTT). - Anaheim, CA, USA, 23-28 May 2010. - P. 1.
- C1821.** Buchanan N.B. Fast response Retrodirective Radar. / Buchanan N.B., Fusco V.F., Sundaralingam P. // 2010 IEEE MTT-S International Microwave Symposium Digest (MTT). - Anaheim, CA, 23-28 May 2010. - P. 153-156.
- C1822.** Kolias N.J. GaN technology for microwave and millimeter wave applications. / Kolias N.J., Whelan C.S., Kazior T.E., Smith K.V. // 2010 IEEE MTT-S International Microwave Symposium Digest (MTT). - Anaheim, CA, 23-28 May 2010. - P. 1222-1225.
- C1823.** Herd J. Advanced architecture for a low cost Multifunction Phased Array Radar. / Herd J., Duffy S., Weber M., Brigham G., Weigand C., Curcio D. // 2010 IEEE MTT-S International Microwave Symposium Digest (MTT). - Anaheim, CA, 23-28 May 2010. - P. 676-679.
- C1824.** Holpp W. The new generation of European E-scan fighter radars. 2010 IEEE MTT-S International Microwave Symposium Digest (MTT). - Anaheim, CA, 23-28 May 2010. - P. 530-533.
- C1825.** Sakai F. UWB array antenna utilizing novel electrical scanning system with tapped delay lines. / Sakai F., Ohta K. // 2010 IEEE MTT-S International Microwave Symposium Digest (MTT). - Anaheim, CA, 23-28 May 2010. - P. 1262-1265.
- C1826.** van Bezouwen H. Status and trends in AESA-based radar. / van Bezouwen H., Feldle H.-P., Holpp W. // 2010 IEEE MTT-S International Microwave Symposium Digest (MTT). - Anaheim, CA, 23-28 May 2010. - P. 526-529.
- C1827.** Zhao Li-quan. An Improved Peak Extraction Algorithm in PHD Based Multi-Target Tracking Algorithm Applied to Passive Radar. / Zhao Li-quan, Zhao Dan-feng, Xu Cong. // 2010 6th International Conference on Wireless Communications Networking and Mobile Computing (WiCOM). - Chengdu, 23-25 Sept. 2010. - P. 1-3.
- C1828.** Dall J. Ice sheet anisotropy measured with polarimetric ice sounding radar. 2010 IEEE International Geoscience and Remote Sensing Symposium (IGARSS). - Honolulu, HI, 25-30 July 2010. - P. 2507-2510.
- C1829.** Kemper J. Passive infrared localization with a Probability Hypothesis Density filter. / Kemper J., Hauschildt D. // 2010 7th Workshop on Positioning Navigation and Communication (WPNC). - Dresden, 11-12



March 2010. - P. 68-76. ↑

**C1830.** Tay S. A tracking algorithm for GNSS reflected signals on sea surface. / Tay S., Coatanhay A., Maussang F., Garelo R. // 2010 IEEE International Geoscience and Remote Sensing Symposium (IGARSS). - Honolulu, HI, 25-30 July 2010. - P. 3821-3824. ↑

**C1831.** Hao Zhang. An integrated approach to determine parameters of a 3D volcano model by using InSAR data with metamodel technique. / Hao Zhang, Xiaoying Cong, Eineder M., Bletzinger K.-U. // 2010 IEEE International Geoscience and Remote Sensing Symposium (IGARSS). - Honolulu, HI, 25-30 July 2010. - P. 1648-1651. ↑

**C1832.** Deng Lei. A CHMT model based DE-speckling method for SAR image. / Deng Lei, Zhao Wenji, Hu Deyong, Hu Zhuowei, Cao Gaoming. // 2010 IEEE International Geoscience and Remote Sensing Symposium (IGARSS). - Honolulu, HI, 25-30 July 2010. - P. 1569-1572. ↑

**C1833.** Bombrun L. Roll invariant target detection based on PolSAR clutter models. / Bombrun L., Vasile G., Gay M., Ovarlez J., Pascal F. // 2010 IEEE International Geoscience and Remote Sensing Symposium (IGARSS). - Honolulu, HI, 25-30 July 2010. - P. 2511-2514. ↑

**C1834.** Totir F. PolSAR images characterization through Blind Sources Separation techniques. / Totir F., Vasile G., Bombrun L., Gay M. // 2010 IEEE International Geoscience and Remote Sensing Symposium (IGARSS). - Honolulu, HI, 25-30 July 2010. - P. 4039-4042. ↑

**C1835.** Breit H. Processing of bistatic TanDEM-X data. / Breit H., Fritz T., Balss U., Niedermeier A., Eineder M., Yague-Martinez N., Rossi C. // 2010 IEEE International Geoscience and Remote Sensing Symposium (IGARSS). - Honolulu, HI, 25-30 July 2010. - P. 2640-2643. ↑

**C1836.** Touzi R. Peatland subsurface water flow monitoring using polarimetric L-band PALSAR. / Touzi R., Gosselin G. // 2010 IEEE International Geoscience and Remote Sensing Symposium (IGARSS). - Honolulu, HI, 25-30 July 2010. - P. 750-753. ↑

**C1837.** Datcu M. Texture estimation in sar images: The impact of scale and model order. / Datcu M., Espinoza-Molina D., de Miguel A., Schwarz G. // 2010 IEEE International Geoscience and Remote Sensing Symposium (IGARSS). - Honolulu, HI, 25-30 July 2010. - P. 2844-2847. ↑

**C1838.** Gekat F. Accuracy of the engineering calibration of weather radars. / Gekat F., Hille M., Niese H., Pool M. // 2010 IEEE International Geoscience and Remote Sensing Symposium (IGARSS). - Honolulu, HI, 25-30 July 2010. - P. 1096-1099. ↑

**C1839.** Soloviev A. Fine structure of the upper ocean from high-resolution Terrasar-X imagery and In-Situ measurements. / Soloviev A., Maingot C., Fujimura A., Fenton J., Gilman M., Matt S., Lehner S., Velotto D., Brusch S. // 2010 IEEE International Geoscience and Remote Sensing Symposium (IGARSS). - Honolulu, HI, 25-30 July 2010. - P. 1944-1947. ↑

**C1840.** Hannevik T.N. Polarisation and mode combinations for ship detection using RADARSAT-2. 2010 IEEE International Geoscience and Remote Sensing Symposium (IGARSS). - Honolulu, HI, 25-30 July 2010. - P. 3676-3679. ↑

**C1841.** Yu-Li Lin. Assessment of airborne lidar data for instream flow type classification. / Yu-Li Lin, Chi-Kuei Wang. // 2010 IEEE International Geoscience and Remote Sensing Symposium (IGARSS). - Honolulu, HI, 25-30 July 2010. - P. 930-933. ↑

**C1842.** Lo. Ground topography estimation over forests considering Polarimetric SAR Interferometry. / Lo,pez-Martinez C., Alonso A., Fa,bregas X., Papathannassiou K.P. // 2010 IEEE International Geoscience and Remote Sensing Symposium (IGARSS). - Honolulu, HI, 25-30 July 2010. - P. 3612-3615. ↑

**C1843.** Jixian Zhang. SAR mapping technology and its application in difficulty terrain area. / Jixian Zhang, Shucheng Yang, Zheng Zhao, Guoman Huang. // 2010 IEEE International Geoscience and Remote Sensing Symposium (IGARSS). - Honolulu, HI, 25-30 July 2010. - P. 3608-3611. ↑

**C1844.** Wegner J.D. Building detection and height estimation from high-resolution insar and optical data. / Wegner J.D., Ziehn J.R., Soergel U. // 2010 IEEE International Geoscience and Remote Sensing Symposium

(IGARSS). - Honolulu, HI, 25-30 July 2010. - P. 1928-1931. ↑

**C1845.** Flampouris S. Radar observations of wave field in littoral zone. / Flampouris S., Seemann J., Ziemer F. // 2010 IEEE International Geoscience and Remote Sensing Symposium (IGARSS). - Honolulu, HI, 25-30 July 2010. - P. 948-951. ↑

**C1846.** Wagner W. Status of the Metop ASCAT soil moisture product. / Wagner W., Bartalis Z., Naeimi V., Park S., Figa-Saldana J., Bonekamp H. // 2010 IEEE International Geoscience and Remote Sensing Symposium (IGARSS). - Honolulu, HI, 25-30 July 2010. - P. 276-279. ↑

**C1847.** Xiaofeng Li. Spaceborne sar imaging of coastal ocean phenomena. / Xiaofeng Li, Pichel W., Xiaofeng Yang. // 2010 IEEE International Geoscience and Remote Sensing Symposium (IGARSS). - Honolulu, HI, 25-30 July 2010. - P. 1956-1959. ↑

**C1848.** Lei Huang. SAR and optical images registration using shape context. / Lei Huang, Zhen Li, Rui Zhang. // 2010 IEEE International Geoscience and Remote Sensing Symposium (IGARSS). - Honolulu, HI, 25-30 July 2010. - P. 1007-1010. ↑

**C1849.** Alonso-Gonzalez A. Filtering and segmentation of polarimetric SAR images with Binary Partition Trees. / Alonso-Gonzalez A., Lopez-Martinez C., Salembier P. // 2010 IEEE International Geoscience and Remote Sensing Symposium (IGARSS). - Honolulu, HI, 25-30 July 2010. - P. 4043-4046. ↑

**C1850.** Costantini M. A novel approach for redundant integration of finite differences and phase unwrapping on a sparse multidimensional domain. / Costantini M., Malvarosa F., Minati F. // 2010 IEEE International Geoscience and Remote Sensing Symposium (IGARSS). - Honolulu, HI, 25-30 July 2010. - P. 1565-1568. ↑

**C1851.** Cigna F. Insar time-series analysis for management and mitigation of geological risk in urban area. / Cigna F., Del Ventisette C., Liguori V., Casagli N. // 2010 IEEE International Geoscience and Remote Sensing Symposium (IGARSS). - Honolulu, HI, 25-30 July 2010. - P. 1924-1927. ↑

**C1852.** Fayard F. Radargrammetric improvements: A multi-window approach. / Fayard F., Meric S., Pottier E. // 2010 IEEE International Geoscience and Remote Sensing Symposium (IGARSS). - Honolulu, HI, 25-30 July 2010. - P. 3604-3607. ↑

**C1853.** del Blanco C.R. Visual tracking of multiple interacting objects through Rao-Blackwellized Data Association Particle Filtering. / del Blanco C.R., Jaureguizar F., Garcia N. // 2010 17th IEEE International Conference on Image Processing (ICIP). - Hong Kong, 26-29 Sept. 2010. - P. 821-824. ↑

**C1854.** Erten E. Aspects of multivariate statistical theory with the application to change detection. / Erten E., Reigber A., Hellwich O. // 2010 IEEE International Geoscience and Remote Sensing Symposium (IGARSS). - Honolulu, HI, 25-30 July 2010. - P. 1960-1963. ↑

**C1855.** Bin Zou. POLSAR image classification using BP neural network based on Quantum Clonal Evolutionary Algorithm. / Bin Zou, Huijun Li, Lamei Zhang. // 2010 IEEE International Geoscience and Remote Sensing Symposium (IGARSS). - Honolulu, HI, 25-30 July 2010. - P. 1573-1576. ↑

**C1856.** Zhenhua Wang. Automatic registration of sar and optical image based on multi-features and multi-constraints. / Zhenhua Wang, Junping Zhang, Ye Zhang, Bin Zou. // 2010 IEEE International Geoscience and Remote Sensing Symposium (IGARSS). - Honolulu, HI, 25-30 July 2010. - P. 1019-1022. ↑

**C1857.** Smith L. Beamwidth analysis for SAR processing of airborne depth-sounder data over ice sheets. / Smith L., Paden J., Leuschen C., Gogineni S. // 2010 IEEE International Geoscience and Remote Sensing Symposium (IGARSS). - Honolulu, HI, 25-30 July 2010. - P. 4596-4599. ↑

**C1858.** Crespi M. DSM generation from very high optical and radar sensors: Problems and potentialities along the road from the 3D geometric modeling to the Surface Model. / Crespi M., Capaldo P., Fratarcangeli F., Nascetti A., Pieralice F. // 2010 IEEE International Geoscience and Remote Sensing Symposium (IGARSS). - Honolulu, HI, 25-30 July 2010. - P. 3596-3599. ↑

**C1859.** Wong A. A new Bayesian source separation approach to blind decorrelation of SAR data. / Wong A., Fieguth P. // 2010 IEEE International Geoscience and Remote Sensing Symposium (IGARSS). - Honolulu, HI, 25-30 July 2010. - P. 4035-4038. ↑

- C1860.** Onhon N.O. Sparsity-driven focused SAR image formation. / Onhon N.O., Cetin M. // 2010 IEEE 18th Signal Processing and Communications Applications Conference (SIU). - Diyarbakir, 22-24 April 2010. - P. 352-355. ↑
- C1861.** Singh J. SAR complex image analysis: A Gauss Markov and a multiple sub-aperture based target characterization. / Singh J., Soccorsi M., Datcu M. // 2010 IEEE International Geoscience and Remote Sensing Symposium (IGARSS). - Honolulu, HI, 25-30 July 2010. - P. 1585-1588. ↑
- C1862.** Sauer S. Polarimetric decomposition for forest biomass retrieval. / Sauer S., Kugler F., Seung-Kuk Lee, Papathanassiou K. // 2010 IEEE International Geoscience and Remote Sensing Symposium (IGARSS). - Honolulu, HI, 25-30 July 2010. - P. 4780-4783. ↑
- C1863.** Vega M. Realization of the NASA Dual-Frequency Dual-Polarized Doppler Radar (D3R). / Vega M., Carswell J., Chandrasekar V., Schwaller M., Mishra K.V. // 2010 IEEE International Geoscience and Remote Sensing Symposium (IGARSS). - Honolulu, HI, 25-30 July 2010. - P. 4815-4818. ↑
- C1864.** Deledalle C.-A. Polarimetric SAR estimation based on non-local means. / Deledalle C.-A., Tupin F., Denis L. // 2010 IEEE International Geoscience and Remote Sensing Symposium (IGARSS). - Honolulu, HI, 25-30 July 2010. - P. 2515-2518. ↑
- C1865.** McFadden M. An application of reciprocity to the numerical modeling of a GPR system. / McFadden M., Scott W.R. // 2010 IEEE International Geoscience and Remote Sensing Symposium (IGARSS). - Honolulu, HI, 25-30 July 2010. - P. 4709-4712. ↑
- C1866.** Yang Li. Eigen decomposition parameter based forest mapping using Radarsat-2 PolSAR data. / Yang Li, Wen Hong, Fang Cao, Erxue Chen, Goodenough D.G., Hao Chen, Peng Wang, Richardson A. // 2010 IEEE International Geoscience and Remote Sensing Symposium (IGARSS). - Honolulu, HI, 25-30 July 2010. - P. 4784-4787. ↑
- C1867.** Yue Huang. Polarimetric SAR tomography of natural environments using hybrid spectral estimators. / Yue Huang, Ferro-Famil L., Reigber A. // 2010 IEEE International Geoscience and Remote Sensing Symposium (IGARSS). - Honolulu, HI, 25-30 July 2010. - P. 146-149. ↑
- C1868.** Beaulieu J. Mean-shift and hierarchical clustering for textured polarimetric SAR image segmentation/classification. / Beaulieu J., Touzi R. // 2010 IEEE International Geoscience and Remote Sensing Symposium (IGARSS). - Honolulu, HI, 25-30 July 2010. - P. 2519-2522. ↑
- C1869.** Longepe N. On the use of Support Vector Machines for land cover analysis with L-band SAR data. / Longepe N., Rakwatin P., Isoguchi O., Shimada M., Uryu Y. // 2010 IEEE International Geoscience and Remote Sensing Symposium (IGARSS). - Honolulu, HI, 25-30 July 2010. - P. 3263-3266. ↑
- C1870.** Zeng Dazhi. An improved CSA for one-stationary BiSAR squint mode. / Zeng Dazhi, Wang Rui, Long Teng, Zeng Tao. // 2010 IEEE International Geoscience and Remote Sensing Symposium (IGARSS). - Honolulu, HI, 25-30 July 2010. - P. 1577-1580. ↑
- C1871.** Trizna D. Coherent marine radar measurements of properties of ocean waves and currents. 2010 IEEE International Geoscience and Remote Sensing Symposium (IGARSS). - Honolulu, HI, 25-30 July 2010. - P. 4737-4740. ↑
- C1872.** Suchandt S. Ship detection and measurement using the TerraSAR-X dual-receive antenna mode. / Suchandt S., Runge H., Steinbrecher U. // 2010 IEEE International Geoscience and Remote Sensing Symposium (IGARSS). - Honolulu, HI, 25-30 July 2010. - P. 2860-2863. ↑
- C1873.** Xueyan He. RPC modeling for spaceborne SAR and its application in radargrammetry. / Xueyan He, Xiaohong Wei, Lu Zhang, Balz T., Mingsheng Liao. // 2010 IEEE International Geoscience and Remote Sensing Symposium (IGARSS). - Honolulu, HI, 25-30 July 2010. - P. 3600-3603. ↑
- C1874.** Berens P. Data acquisition of vessel ISAR data with assistance of automatic identification system. 2010 IEEE International Geoscience and Remote Sensing Symposium (IGARSS). - Honolulu, HI, 25-30 July 2010. - P. 122-125. ↑
- C1875.** Braun H.M. A new SAR sensor designed for micro-satellites. 2010 IEEE International Geoscience and Remote Sensing Symposium (IGARSS). - Honolulu, HI, 25-30 July 2010. - P. 122-125. ↑

Remote Sensing Symposium (IGARSS). - Honolulu, HI, 25-30 July 2010. - P. 213-215. ↑

**C1876.** Re. Morphological filtering of SAR interferometric images. / Rejichi S., Chaabane F., Tupin F., Bloch I. // 2010 IEEE International Geoscience and Remote Sensing Symposium (IGARSS). - Honolulu, HI, 25-30 July 2010. - P. 1581-1584. ↑

**C1877.** Jutzi B. Relations between SAR tomography and full-waveform LIDAR for structural analysis of forested areas. / Jutzi B., Thiele A., Meyer F., Hinz S. // 2010 IEEE International Geoscience and Remote Sensing Symposium (IGARSS). - Honolulu, HI, 25-30 July 2010. - P. 3267-3270. ↑

**C1878.** Grishechkin B.Y. Optimal algorithms for spaceborne altimeter. / Grishechkin B.Y., Baskakov A.I. // 2010 IEEE International Geoscience and Remote Sensing Symposium (IGARSS). - Honolulu, HI, 25-30 July 2010. - P. 640-642. ↑

**C1879.** Reuter S. Development and experiments of a passive SAR receiver system in a bistatic spaceborne/stationary configuration. / Reuter S., Behner F., Nies H., Loffeld O., Matthes D., Schiller J. // 2010 IEEE International Geoscience and Remote Sensing Symposium (IGARSS). - Honolulu, HI, 25-30 July 2010. - P. 118-121. ↑

**C1880.** Seemann J. Detection of salient features in surface current maps from dopplerized X-band radar. / Seemann J., Cysewski M., Ziemer F., Heineke M., Riethmujller R. // 2010 IEEE International Geoscience and Remote Sensing Symposium (IGARSS). - Honolulu, HI, 25-30 July 2010. - P. 4741-4744. ↑

**C1881.** Castillo Mena J. Quasar SBK accurate internal calibration. / Castillo Mena J., Cuerda Munoz J.M., Larranaga Sodupe J.R. // 2010 IEEE International Geoscience and Remote Sensing Symposium (IGARSS). - Honolulu, HI, 25-30 July 2010. - P. 2864-2867. ↑

**C1882.** Haipeng Wang. Extraction of typhoon-damaged forests from multi-temporal high-resolution polarimetric SAR images. / Haipeng Wang, Ouchi K., Ya-Qiu Jin. // 2010 IEEE International Geoscience and Remote Sensing Symposium (IGARSS). - Honolulu, HI, 25-30 July 2010. - P. 3271-3274. ↑

**C1883.** Feilong Ling. Rice areas mapping using ALOS PALSAR FBD data considering the Bragg scattering in L-band SAR images of rice fields. / Feilong Ling, Zengyuan Li, Erxue Chen, Xin Tian, Lina Bai, Fengyu Wang. // 2010 IEEE International Geoscience and Remote Sensing Symposium (IGARSS). - Honolulu, HI, 25-30 July 2010. - P. 1461-1464. ↑

**C1884.** Broquetas A. Bistatic SAR based on Terrasar-X and ground based receivers. / Broquetas A., Fortes M., Siddique M.A., Duque S., Merlano J.C., Lopez-Dekker P., Mallorqui J.J., Aguasca A. // 2010 IEEE International Geoscience and Remote Sensing Symposium (IGARSS). - Honolulu, HI, 25-30 July 2010. - P. 114-117. ↑

**C1885.** Zhe Hu. Designing an Illegal Mining Detection System based on DinSAR. / Zhe Hu, Linlin Ge, Xiaojing Li, Rizos C. // 2010 IEEE International Geoscience and Remote Sensing Symposium (IGARSS). - Honolulu, HI, 25-30 July 2010. - P. 3952-3955. ↑

**C1886.** Wang Zhiqian. Effect of squint imaging on beam position design of space borne SAR. / Wang Zhiqian, Li Chunsheng, Yu Ze, Zhang Yongqiang, Yang Wei. // 2010 IEEE International Geoscience and Remote Sensing Symposium (IGARSS). - Honolulu, HI, 25-30 July 2010. - P. 4648-4651. ↑

**C1887.** Plant W.J. Dual-polarized, coherent microwave backscatter from rough water surfaces at low grazing angles. 2010 IEEE International Geoscience and Remote Sensing Symposium (IGARSS). - Honolulu, HI, 25-30 July 2010. - P. 4729-4732. ↑

**C1888.** Colliander A. Quikscat backscatter sensitivity to landscape freeze/thaw state over ALECTRA sites in Alaska from 2000 to 2007: Application to SMAP validation planning. / Colliander A., McDonald K., Zimmermann R., Linke T., Schroeder R., Kimball J., Njoku E. // 2010 IEEE International Geoscience and Remote Sensing Symposium (IGARSS). - Honolulu, HI, 25-30 July 2010. - P. 1269-1272. ↑

**C1889.** Rappaport C. Road surface quality measurement using inexpensive radar. / Rappaport C., Holbrook D., Adams C., Busuioc D., Doughty J. // 2010 IEEE International Geoscience and Remote Sensing Symposium (IGARSS). - Honolulu, HI, 25-30 July 2010. - P. 4318-4321. ↑



- C1890.** Yu Wang. A shadow percentage estimation method for Radar look angle selection in spaceborne INSAR application. / Yu Wang, Xing-dong Liang. // 2010 IEEE International Geoscience and Remote Sensing Symposium (IGARSS). - Honolulu, HI, 25-30 July 2010. - P. 1481-1484. ↑
- C1891.** Hwang P.A. Doppler processing of coherent radar backscatter for ocean surface wave measurements. / Hwang P.A., Sletten M.A., Toporkov J.V., Trizna D.B. // 2010 IEEE International Geoscience and Remote Sensing Symposium (IGARSS). - Honolulu, HI, 25-30 July 2010. - P. 4733-4736. ↑
- C1892.** Weilin Yuan. Decomposition methods for the estimation of bare soil surface parameters using fully polarimetric SAR data 1. / Weilin Yuan, Qiming Qin, Shihong Du, Xinyi Shen, Hongbo Jiang, Yan Ma, Shixiong Liu. // 2010 IEEE International Geoscience and Remote Sensing Symposium (IGARSS). - Honolulu, HI, 25-30 July 2010. - P. 1273-1276. ↑
- C1893.** Chopping M. Canopy height, crown cover, and aboveground biomass maps for the southwestern United States from MISR, 2000 and 2009. / Chopping M., Shimada S., Bull M., Martonchik J. // 2010 IEEE International Geoscience and Remote Sensing Symposium (IGARSS). - Honolulu, HI, 25-30 July 2010. - P. 56-59. ↑
- C1894.** Li Guo. A two-pass random forests classification of airborne lidar and image data on urban scenes. / Li Guo, Chehata N., Boukir S. // 2010 17th IEEE International Conference on Image Processing (ICIP). - Hong Kong, 26-29 Sept. 2010. - P. 1369-1372. ↑
- C1895.** Colinas J. Radarsat Constellation, moving toward implementation. / Colinas J., Se,guin G., Plourde P. // 2010 IEEE International Geoscience and Remote Sensing Symposium (IGARSS). - Honolulu, HI, 25-30 July 2010. - P. 3232-3235. ↑
- C1896.** Yueguan Lin. MIMO SAR processing with azimuth nonuniform sampling. / Yueguan Lin, Bingchen Zhang, Wen Hong, Yirong Wu, Yang Li. // 2010 IEEE International Geoscience and Remote Sensing Symposium (IGARSS). - Honolulu, HI, 25-30 July 2010. - P. 4652-4655. ↑
- C1897.** Rottensteiner F. Automation of object extraction from LiDAR in urban areas. 2010 IEEE International Geoscience and Remote Sensing Symposium (IGARSS). - Honolulu, HI, 25-30 July 2010. - P. 1343-1346. ↑
- C1898.** Balaji C. What is the information content of TRMM precipitation radar for determining radiometer observations and vice versa?. / Balaji C., Chaturvedi M., Srinivasa Ramanujam K., Chandrasekar V., Cuong Nguyen, Martinez M. // 2010 IEEE International Geoscience and Remote Sensing Symposium (IGARSS). - Honolulu, HI, 25-30 July 2010. - P. 1899-1902. ↑
- C1899.** Hongli Zhao. Detection of land subsidence in Beijing, China, using Interferometric Point Target Analysis technique. / Hongli Zhao, Jinghui Fan, Xiaofang Guo, Jianping Chen, Ye Xia, Daqing Ge, Lu Zhang, Yubao Qiu, Chang Zhong. // 2010 IEEE International Geoscience and Remote Sensing Symposium (IGARSS). - Honolulu, HI, 25-30 July 2010. - P. 1553-1556. ↑
- C1900.** Nies H. Polarimetric and interferometric applications in a bistatic hybrid SAR mode using Terrasar-X. / Nies H., Behner F., Reuter S., Loffeld O., Wang R. // 2010 IEEE International Geoscience and Remote Sensing Symposium (IGARSS). - Honolulu, HI, 25-30 July 2010. - P. 110-113. ↑
- C1901.** Seri. A comparison on the new electronic attack techniques against pulse compression radars. / Seri,n M., Yilmaz A.E., Navruz I. // 2010 IEEE 18th Signal Processing and Communications Applications Conference (SIU). - Diyarbakir, 22-24 April 2010. - P. 447-450. ↑
- C1902.** Xiaoqing Chu. A new algorithm for wind speed at low incidence angles using TRMM Precipitation Radar data. / Xiaoqing Chu, Yijun He, Gengxin Chen. // 2010 IEEE International Geoscience and Remote Sensing Symposium (IGARSS). - Honolulu, HI, 25-30 July 2010. - P. 4162-4165. ↑
- C1903.** Salvia M. Monitoring flooded area fraction in floodplains of Paran6 basin using passive and active microwave systems. / Salvia M., Grings F., Perna P., Ferrazzoli P., Rahmoune R., Barber M., Douna V., Karszenbaum H. // 2010 IEEE International Geoscience and Remote Sensing Symposium (IGARSS). - Honolulu, HI, 25-30 July 2010. - P. 142-145. ↑
- C1904.** Stuart K.M. Iceberg size and orientation estimation using SeaWinds. / Stuart K.M., Long D.G. // 2010 IEEE International Geoscience and Remote Sensing Symposium (IGARSS). - Honolulu, HI, 25-30 July 2010. - P. ↑

2394-2397. ↑

**C1905.** Xiaogang Song. The characteristics of post-seismic surface deformation of the Wenchuan MS 8.0 earthquake from InSAR. / Xiaogang Song, Xinjian Shan, Chunyan Qu, Yufei Han, Guifang Zhang, Limin Guo, Guohong Zhang. // 2010 IEEE International Geoscience and Remote Sensing Symposium (IGARSS). - Honolulu, HI, 25-30 July 2010. - P. 1210-1213. ↑

**C1906.** Nashashibi A.Y. Characterization of volume scattering of dry sand at millimeter-wave frequencies. / Nashashibi A.Y., Sarabandi K., Al-Zaid F., Alhumaidi S. // 2010 IEEE International Geoscience and Remote Sensing Symposium (IGARSS). - Honolulu, HI, 25-30 July 2010. - P. 3067-3069. ↑

**C1907.** Huber M. Validation of tie-point concepts by the DEM adjustment approach of TanDEM-X. / Huber M., Gruber A., Wessel B., Breunig M., Wendleder A. // 2010 IEEE International Geoscience and Remote Sensing Symposium (IGARSS). - Honolulu, HI, 25-30 July 2010. - P. 2644-2647. ↑

**C1908.** Clewley D. Forest parameter retrieval from SAR data using an estimation algorithm applied to regrowing forest stands in Queensland, Australia. / Clewley D., Lucas R.M., Moghaddam M., Bunting P., Dwyer J., Carreiras J. // 2010 IEEE International Geoscience and Remote Sensing Symposium (IGARSS). - Honolulu, HI, 25-30 July 2010. - P. 1238-1241. ↑

**C1909.** Zhifeng Guo. Forest biomass estimation in northeastern China using ALOS PALSAR data combined radiative transfer model. / Zhifeng Guo, Wenjian Ni, Guoqing Sun. // 2010 IEEE International Geoscience and Remote Sensing Symposium (IGARSS). - Honolulu, HI, 25-30 July 2010. - P. 1497-1500. ↑

**C1910.** Wei Tian. An experiment for oil spill recognition using RADARSAT-2 image. / Wei Tian, Yun Shao, Junna Yuan, Shiang Wang, Yang Liu. // 2010 IEEE International Geoscience and Remote Sensing Symposium (IGARSS). - Honolulu, HI, 25-30 July 2010. - P. 2761-2764. ↑

**C1911.** Kurum M. Chracterization of forest opacity using multi-angular emssion and backscatter data. / Kurum M., O'Neill P.E., Lang R.H., Joseph A.T., Cosh M.H., Jackson T.J. // 2010 IEEE International Geoscience and Remote Sensing Symposium (IGARSS). - Honolulu, HI, 25-30 July 2010. - P. 2051-2054. ↑

**C1912.** Munchak S.J. A radar profiling algorithm designed for use with multiresolution radiometer measurements. / Munchak S.J., Kummerow C. // 2010 IEEE International Geoscience and Remote Sensing Symposium (IGARSS). - Honolulu, HI, 25-30 July 2010. - P. 102-105. ↑

**C1913.** Seto S. Applicability of the iterative backward retrieval method for the GPM dual-frequency precipitation radar. / Seto S., Iguchi T. // 2010 IEEE International Geoscience and Remote Sensing Symposium (IGARSS). - Honolulu, HI, 25-30 July 2010. - P. 106-109. ↑

**C1914.** Perna S. Airborne DInSAR time series at X-Band. / Perna S., Wimmer C., Moreira J., Fornaro G. // 2010 IEEE International Geoscience and Remote Sensing Symposium (IGARSS). - Honolulu, HI, 25-30 July 2010. - P. 2868-2871. ↑

**C1915.** Walterscheid I. Potential and limitations of forward-looking bistatic SAR. / Walterscheid I., Espeter T., Klare J., Brenner A.R., Ender J.H.G. // 2010 IEEE International Geoscience and Remote Sensing Symposium (IGARSS). - Honolulu, HI, 25-30 July 2010. - P. 216-219. ↑

**C1916.** Servello E.L. Tropical land cover change detection with polarimetric SAR data. / Servello E.L., Kuplich T.M., Shimabukuro Y.E. // 2010 IEEE International Geoscience and Remote Sensing Symposium (IGARSS). - Honolulu, HI, 25-30 July 2010. - P. 1477-1480. ↑

**C1917.** Anderson S. Oil Spill statistics from SAR images in the North Eastern Baltic Sea ship route in 2007-2009. / Anderson S., Raudsepp U., Uiboupin R. // 2010 IEEE International Geoscience and Remote Sensing Symposium (IGARSS). - Honolulu, HI, 25-30 July 2010. - P. 1883-1886. ↑

**C1918.** Poulain V. High resolution optical and sar image fusion for road database updating. / Poulain V., Inglada J., Spigai M., Tournet J., Marthon P. // 2010 IEEE International Geoscience and Remote Sensing Symposium (IGARSS). - Honolulu, HI, 25-30 July 2010. - P. 2747-2750. ↑

**C1919.** Bombrun L. Extension of the Target Scattering Vector Model to the bistatic case. 2010 IEEE International Geoscience and Remote Sensing Symposium (IGARSS). - Honolulu, HI, 25-30 July 2010. - P. ↑

4047-4050. ↑

**C1920.** Hai Tung Chu. Synergistic use of multi-temporal ALOS/PALSAR with SPOT multispectral satellite imagery for land cover mapping in the Ho Chi Minh city area, Vietnam. / Hai Tung Chu, Linlin Ge. // 2010 IEEE International Geoscience and Remote Sensing Symposium (IGARSS). - Honolulu, HI, 25-30 July 2010. - P. 1465-1468. ↑

**C1921.** Sano E.E.S. The use of ALOS PALSAR imagery for Cerrado's land use and land cover mapping. / Sano E.E.S., Santos E.M., Meneses P.R. // 2010 IEEE International Geoscience and Remote Sensing Symposium (IGARSS). - Honolulu, HI, 25-30 July 2010. - P. 1458-1460. ↑

**C1922.** Baumgartner S.V. Real-time road traffic monitoring using a fast a priori knowledge based SAR-GMTI algorithm. / Baumgartner S.V., Krieger G. // 2010 IEEE International Geoscience and Remote Sensing Symposium (IGARSS). - Honolulu, HI, 25-30 July 2010. - P. 1843-1846. ↑

**C1923.** Shunying Hong. Three-dimensional deformation field caused by the Gaize earthquake by Multi-LOS DInSAR measurement technology. / Shunying Hong, Xuhui Shen, Xiaogang Song, Xinjian Shan, Zhirong Liu, Yaqiong Dai, Chunli Kang, Feng Jing. // 2010 IEEE International Geoscience and Remote Sensing Symposium (IGARSS). - Honolulu, HI, 25-30 July 2010. - P. 765-768. ↑

**C1924.** Long N. A combined approach to detect urban features from multi-spectral and radardata. / Long N., Simonetto E., Bocher E. // 2010 IEEE International Geoscience and Remote Sensing Symposium (IGARSS). - Honolulu, HI, 25-30 July 2010. - P. 1469-1472. ↑

**C1925.** Marino A. Detecting depolarizing targets with satellite data: A new geometrical perturbation filter. / Marino A., Cloude S., Woodhouse I. // 2010 IEEE International Geoscience and Remote Sensing Symposium (IGARSS). - Honolulu, HI, 25-30 July 2010. - P. 1847-1850. ↑

**C1926.** Ikuma T. Autoregressive modeling of dechirped spotlight-mode sar rawdata in transform domain. / Ikuma T., Naraghi-Pour M., Lewis T. // 2010 IEEE International Geoscience and Remote Sensing Symposium (IGARSS). - Honolulu, HI, 25-30 July 2010. - P. 4640-4643. ↑

**C1927.** Gao Han. Investigation on moving target detection and velocity estimation with Triple-Channel MIMO-SAR. / Gao Han, Li Jingwen, Yang Wei. // 2010 IEEE International Geoscience and Remote Sensing Symposium (IGARSS). - Honolulu, HI, 25-30 July 2010. - P. 4636-4639. ↑

**C1928.** Benzid S. Change detection in a multitemporal series of radar images. / Benzid S., Deledalles C., Abdelfattah R., Chaabane F., Tupin F. // 2010 IEEE International Geoscience and Remote Sensing Symposium (IGARSS). - Honolulu, HI, 25-30 July 2010. - P. 1473-1476. ↑

**C1929.** Xiaofei Li. Numerical study on the statistics of the phase in backscattered signals from time-evolving sea surfaces. / Xiaofei Li, Xiaoqian Xu. // 2010 International Conference on Electromagnetics in Advanced Applications (ICEAA). - Sydney, NSW, 20-24 Sept. 2010. - P. 855-858. ↑

**C1930.** Kocaadam E. Classification of polyphase and polytime LPI radar signals with eigenimage methods. / Kocaadam E., Ozkazanc Y. // 2010 IEEE 18th Signal Processing and Communications Applications Conference (SIU). - Diyarbakir, 22-24 April 2010. - P. 173-176. ↑

**C1931.** Kawamura S. A new bistatic doppler measurement system with reduced contamination by sidelobe echoes. / Kawamura S., Hanado H., Sugitani S., Nakagawa K. // 2010 IEEE International Geoscience and Remote Sensing Symposium (IGARSS). - Honolulu, HI, 25-30 July 2010. - P. 4150-4153. ↑

**C1932.** Lucas R.M. Advances in the integration of ALOS PALSAR and Landsat sensor data for forest characterisation, mapping and monitoring. / Lucas R.M., Armston J., Carreiras J., Nugroho N., Clewley D., de Grandi F. // 2010 IEEE International Geoscience and Remote Sensing Symposium (IGARSS). - Honolulu, HI, 25-30 July 2010. - P. 1851-1854. ↑

**C1933.** Roth A.P. Simulating and mitigating ionospheric effects in synthetic aperture radar. / Roth A.P., Huxtable B.D., Chotoo K., Chotoo S.D. // 2010 IEEE International Geoscience and Remote Sensing Symposium (IGARSS). - Honolulu, HI, 25-30 July 2010. - P. 2892-2895. ↑

**C1934.** Abdelfattah R. A specific methodology for atmospheric effect reduction on SAR interferograms. /

Abdelfattah R., Chokmani K., Chaabane N. // 2010 IEEE International Geoscience and Remote Sensing Symposium (IGARSS). - Honolulu, HI, 25-30 July 2010. - P. 1637-1640. ↑

C1935. Esteban-Fernandez D. Design considerations for a dual-frequency radar for sea spray measurement in hurricanes. / Esteban-Fernandez D., Durden S.L., Chaubell J., Cooper K.B. // 2010 IEEE International Geoscience and Remote Sensing Symposium (IGARSS). - Honolulu, HI, 25-30 July 2010. - P. 2896-2899. ↑

C1936. Ramongassie S. Spaceborne P-band SAR for BIOMASS mission. / Ramongassie S., Castiglioni S.K., Lorenzo J., Labiole E., Baudasse Y., Svara C., Luigi C., Heliere F., Mangelot C., Klooster K.V., Fonseca N., Diez H., Belot D. // 2010 IEEE International Geoscience and Remote Sensing Symposium (IGARSS). - Honolulu, HI, 25-30 July 2010. - P. 2880-2883. ↑

C1937. Borner T. Signal: SAR for ice, glacier and global dynamics. / Borner T., De Zan F., Lopez-Dekker P., Krieger G., Hajnsek I., Papathanassiou K., Villano M., Younis M., Danklmayer A., Dierking W., Nagler T., Rott H., Lehner S., Fugen T., Moreira A. // 2010 IEEE International Geoscience and Remote Sensing Symposium (IGARSS). - Honolulu, HI, 25-30 July 2010. - P. 2884-2887. ↑

C1938. Feng Li. Focusing general bistatic SAR data using frequency scaling. / Feng Li, Tao Zeng, Teng Long. // 2010 IEEE International Geoscience and Remote Sensing Symposium (IGARSS). - Honolulu, HI, 25-30 July 2010. - P. 1589-1592. ↑

C1939. Guo Qiang. Study on emitter signal recognition based on rough sets and grey association theory. / Guo Qiang, Guan Xin, Zhang Zheng-chao, Zhao Jing. // 2010 IEEE 10th International Conference on Signal Processing (ICSP). - Beijing, 24-28 Oct. 2010. - P. 2336-2340. ↑

C1940. Meziani H.A. Generalised decentralised fuzzy CA-CFAR detector in Pearson distributed clutter. / Meziani H.A., Soltani F. // 2010 IEEE 10th International Conference on Signal Processing (ICSP). - Beijing, 24-28 Oct. 2010. - P. 1915-1918. ↑

C1941. Quivira F. Feasibility of tunnel detection under rough ground surfaces using Underground Focusing Spotlight Synthetic Aperture Radar. / Quivira F., Fassbender K., Martinez-Lorenzo J.A., Rappaport C.M. // 2010 IEEE International Conference on Technologies for Homeland Security (HST). - Waltham, MA, 8-10 Nov. 2010. - P. 357-362. ↑

C1942. Romeiser R. Currents in rivers, coastal areas, and the open ocean from TerraSAR-X along-track InSAR. / Romeiser R., Suchandt S., Runge H., Graber H. // 2010 IEEE International Geoscience and Remote Sensing Symposium (IGARSS). - Honolulu, HI, 25-30 July 2010. - P. 3059-3062. ↑

C1943. Haibin Lv. The propagating speed of internal solitary waves investigated by X-band radar near Dongsha island. / Haibin Lv, Yijun He, Hui Shen, Limin Cui, Chang-e Dou. // 2010 IEEE International Geoscience and Remote Sensing Symposium (IGARSS). - Honolulu, HI, 25-30 July 2010. - P. 4705-4708. ↑

C1944. Sjojgren T.K. Moving target refocusing algorithm for synthetic aperture radar images. / Sjojgren T.K., Vu V.T., Pettersson M.I. // 2010 IEEE International Geoscience and Remote Sensing Symposium (IGARSS). - Honolulu, HI, 25-30 July 2010. - P. 4110-4113. ↑

C1945. Sheng-Zhong Huang. Automatic target recognition based on neural networks. 2010 International Conference on Intelligent Computing and Integrated Systems (ICISS). - Guilin, 22-24 Oct. 2010. - P. 516-519. ↑

C1946. Megherbi D.B. A distributed multi-agent tracking, awareness, and communication system architecture for synchronized real-time situational understanding, surveillance, decision-making, and control. / Megherbi D.B., Levesque P. // 2010 IEEE International Conference on Technologies for Homeland Security (HST). - Waltham, MA, 8-10 Nov. 2010. - P. 549-555. ↑

C1947. Song Xiaoguo. A novel array calibration method based on spatial correlation matrix for HFSWR. / Song Xiaoguo, Wei Yinheng, Cui Yan, Xu Rongqing. // 2010 IEEE 10th International Conference on Signal Processing (ICSP). - Beijing, 24-28 Oct. 2010. - P. 344-347. ↑

C1948. Li Dong-wei. Space registration algorithm based on UKF using hybrid states. / Li Dong-wei, Xie Wei-xin, Huang Jian-jun, Huang Jing-xiong, Jin Kai-chun. // 2010 IEEE 10th International Conference on Signal Processing (ICSP). - Beijing, 24-28 Oct. 2010. - P. 340-343. ↑



- C1949.** Fernandes J.L. A comparison of experimental and modeled results of an active millimeter wave inverse synthetic aperture radar system used to perform standoff detection of person-borne improvised explosive devices. / Fernandes J.L., Obermeier R., Hagelen M., Martinez-Lorenzo J.A., Rappaport C.M. // 2010 IEEE International Conference on Technologies for Homeland Security (HST). - Waltham, MA, 8-10 Nov. 2010. - P. 428-434. ↑
- C1950.** Cai-sheng Zhang. An improved algorithm for passive bistatic radar detection and parameters estimation. / Cai-sheng Zhang, Guo-jun Li, Xiao-ming Tang, You He. // 2010 IEEE 10th International Conference on Signal Processing (ICSP). - Beijing, 24-28 Oct. 2010. - P. 2303-2306. ↑
- C1951.** Lok A.T.Y. Performance analysis of multiple signal detection using the ESPRIT algorithm. / Lok A.T.Y., Aliyazicioglu Z., Hwang H.K. // 2010 IEEE 10th International Conference on Signal Processing (ICSP). - Beijing, 24-28 Oct. 2010. - P. 1910-1914. ↑
- C1952.** Rossi C. Surface current retrieval from TerraSAR-X data using Doppler measurements. / Rossi C., Runge H., Breit H., Fritz T. // 2010 IEEE International Geoscience and Remote Sensing Symposium (IGARSS). - Honolulu, HI, 25-30 July 2010. - P. 3055-3058. ↑
- C1953.** Yan Y. Assimilation of D-InSAR and sub-pixel image correlation displacement measurements for coseismic fault parameter estimation. / Yan Y., Trouve, E., Bissierier A., Mauris G., Galichet S., Pinel V., Pathier E. // 2010 IEEE International Geoscience and Remote Sensing Symposium (IGARSS). - Honolulu, HI, 25-30 July 2010. - P. 3664-3667. ↑
- C1954.** Richard J. An innovative spaceborne radar concept for global maritime surveillance: Description and performance demonstration. / Richard J., Enjolras V., Schoeser C., Angelliaume S., Durand P. // 2010 IEEE International Geoscience and Remote Sensing Symposium (IGARSS). - Honolulu, HI, 25-30 July 2010. - P. 257-259. ↑
- C1955.** Rizzoli P. X-band backscatter map generation using TerraSAR-x data. / Rizzoli P., Brautigam B., Wollstadt S., Mittermayer J. // 2010 IEEE International Geoscience and Remote Sensing Symposium (IGARSS). - Honolulu, HI, 25-30 July 2010. - P. 3450-3453. ↑
- C1956.** Gujingojr A. Clutter detection algorithms for airborne pulse-Doppler radar. / Gujingojr A., Gezici S. // 2010 IEEE 18th Signal Processing and Communications Applications Conference (SIU). - Diyarbakir, 22-24 April 2010. - P. 724-727. ↑
- C1957.** Abileah R. Shallow water bathymetry with an incoherent X-band radar using small (smaller) space-time image cubes. / Abileah R., Trizna D.B. // 2010 IEEE International Geoscience and Remote Sensing Symposium (IGARSS). - Honolulu, HI, 25-30 July 2010. - P. 4330-4333. ↑
- C1958.** Thiele A. Combining GIS and InSAR data for 3D building reconstruction. / Thiele A., Hinz S., Cadario E. // 2010 IEEE International Geoscience and Remote Sensing Symposium (IGARSS). - Honolulu, HI, 25-30 July 2010. - P. 2418-2421. ↑
- C1959.** Zili Shan. Change detection in urban areas with high resolution SAR images using second kind statistics based G0 distribution. / Zili Shan, Chao Wang, Hong Zhang, Fan Wu. // 2010 IEEE International Geoscience and Remote Sensing Symposium (IGARSS). - Honolulu, HI, 25-30 July 2010. - P. 4600-4603. ↑
- C1960.** Marechal C. Spaceborne fully polarimetric time-series datasets for land cover analysis. / Marechal C., Pottier E., Hubert-Moy L., Corgne S., Allain-Bailhache S., Meric S. // 2010 IEEE International Geoscience and Remote Sensing Symposium (IGARSS). - Honolulu, HI, 25-30 July 2010. - P. 859-862. ↑
- C1961.** Ebuchi N. Propagation of subinertial variations in the Soya Warm Current revealed by HF ocean radars. / Ebuchi N., Fukamachi Y., Ohshima K.I. // 2010 IEEE International Geoscience and Remote Sensing Symposium (IGARSS). - Honolulu, HI, 25-30 July 2010. - P. 3051-3054. ↑
- C1962.** Pouteau R. Multi-source SVM fusion for environmental monitoring in Marquesas archipelago. / Pouteau R., Stoll B., Chabrier S. // 2010 IEEE International Geoscience and Remote Sensing Symposium (IGARSS). - Honolulu, HI, 25-30 July 2010. - P. 2719-2722. ↑
- C1963.** Bennani Y. Bistatic Radar Cross Section of an complex target on sea surface. / Bennani Y., Khenchaf A., Comblet F., Ali-Yahia A. // 2010 IEEE International Geoscience and Remote Sensing Symposium (IGARSS).

- Honolulu, HI, 25-30 July 2010. - P. 2543-2546. ↑

**C1964.** Frey O. Analyzing tomographic SAR data of a forest with respect to frequency, polarization, and focusing technique. / Frey O., Meier E. // 2010 IEEE International Geoscience and Remote Sensing Symposium (IGARSS). - Honolulu, HI, 25-30 July 2010. - P. 150-153. ↑

**C1965.** Wilson J.J.W. Radiometric performance of the Advanced Wind Scatterometer radar ASCAT. / Wilson J.J.W., Anderson C., Figa Saldana J., Bonekamp H. // 2010 IEEE International Geoscience and Remote Sensing Symposium (IGARSS). - Honolulu, HI, 25-30 July 2010. - P. 1092-1095. ↑

**C1966.** Tian Zhou. Application of aperture extrapolation beamformer in multibeam bathymetric sonar. / Tian Zhou, Shan Li, Haisen Li, Lu Yin. // 2010 IEEE 10th International Conference on Signal Processing (ICSP). - Beijing, 24-28 Oct. 2010. - P. 2349-2352. ↑

**C1967.** Liu Lutao. The joint estimation of source number and DOA non-based on the Eigen decomposition approach. / Liu Lutao, Si Xicai, Wang Ligu. // 2010 IEEE 10th International Conference on Signal Processing (ICSP). - Beijing, 24-28 Oct. 2010. - P. 376-380. ↑

**C1968.** Jianping Xu. UWB LFM echo signal detection and time-delay estimation based on compressive sensing. / Jianping Xu, Yiming Pi, Zongjie Cao. // 2010 IEEE 10th International Conference on Signal Processing (ICSP). - Beijing, 24-28 Oct. 2010. - P. 2435-2438. ↑

**C1969.** Hyeon-Cheol Lee. Altitude measurement using three circular marks. 2010 IEEE/AIAA 29th Digital Avionics Systems Conference (DASC). - Salt Lake City, UT, 3-7 Oct. 2010. - P. 5.D.1-1-5.D.1-8-1. ↑

**C1970.** Liu Yueping. Detection performance and configuration of Network Radar: A study based upon symmetry cross entropy. / Liu Yueping, Jiang Qiuxi, Guo Hangxing. // 2010 IEEE 10th International Conference on Signal Processing (ICSP). - Beijing, 24-28 Oct. 2010. - P. 2266-2269. ↑

**C1971.** Ying Liu. Urban area extraction from Polarimetric SAR imagery using only positive samples. / Ying Liu, Wen Yang, Xin Xu, Hong Sun. // 2010 IEEE 10th International Conference on Signal Processing (ICSP). - Beijing, 24-28 Oct. 2010. - P. 2332-2335. ↑

**C1972.** Zhu Ben-yu. A micro-motion feature deception jamming method to ISAR. / Zhu Ben-yu, Xue Lei, Bi Da-ping. // 2010 IEEE 10th International Conference on Signal Processing (ICSP). - Beijing, 24-28 Oct. 2010. - P. 2287-2290. ↑

**C1973.** Long Cai. Orthogonal waveform set design for netted radar. / Long Cai, Xiaochuan Ma, Sheng Yan, Qi Xu. // 2010 IEEE 10th International Conference on Signal Processing (ICSP). - Beijing, 24-28 Oct. 2010. - P. 1228-1231. ↑

**C1974.** Nhut Tan Ho. Pilot response to off-nominal conditions in merging and spacing operation. / Nhut Tan Ho, Johnson W., Martin P., Lachter J., Dao A., Brandt S., Battiste V. // 2010 IEEE/AIAA 29th Digital Avionics Systems Conference (DASC). - Salt Lake City, UT, 3-7 Oct. 2010. - P. 4.D.3-1-4.D.3-13-1. ↑

**C1975.** Ferrante J. Human-In-The-Loop simulation of area navigation visual flight procedures at atlanta international airport. / Ferrante J., Zondervan D. // 2010 IEEE/AIAA 29th Digital Avionics Systems Conference (DASC). - Salt Lake City, UT, 3-7 Oct. 2010. - P. 4.B.3-1-4.B.3-10-1. ↑

**C1976.** Olson W.A. TCAS Operational Performance Assessment in the U.S. National Airspace. / Olson W.A., Olszta J.E. // 2010 IEEE/AIAA 29th Digital Avionics Systems Conference (DASC). - Salt Lake City, UT, 3-7 Oct. 2010. - P. 4.A.2-1-4.A.2-11-1. ↑

**C1977.** Jun Wen. A method for Ground Moving Target Indication and Velocity Estimation based on InSAR system. / Jun Wen, Guisheng Liao, Shengqi Zhu. // 2010 IEEE 10th International Conference on Signal Processing (ICSP). - Beijing, 24-28 Oct. 2010. - P. 2299-2302. ↑

**C1978.** Blair-Smith H. System integration issues in Apollo 11. 2010 IEEE/AIAA 29th Digital Avionics Systems Conference (DASC). - Salt Lake City, UT, 3-7 Oct. 2010. - P. 4.E.1-1-4.E.1-11-1. ↑

**C1979.** Chabbi S. Weber-Haykin based Automatic Censoring and detection in Weibull background. / Chabbi S., Laroussi T., Barkat M. // 2010 IEEE 10th International Conference on Signal Processing (ICSP). - Beijing, 24-

28 Oct. 2010. - P. 1919-1922. ↑

**C1980.** Zhigang Su. Design based on MCU for the echo simulator of the range extended target. / Zhigang Su, Lianghai Yu, Renbiao Wu. // 2010 IEEE 10th International Conference on Signal Processing (ICSP). - Beijing, 24-28 Oct. 2010. - P. 514-517. ↑

**C1981.** Yong-xiang Liu. Instantaneous Frequency estimation of multicomponent signal based on complex argument distribution. / Yong-xiang Liu, Peng Kou, Xiang Li, Zhao-wen Zhuang. // 2010 IEEE 10th International Conference on Signal Processing (ICSP). - Beijing, 24-28 Oct. 2010. - P. 207-210. ↑

**C1982.** Huang Jianjun. A CKF based spatial alignment of radar and infrared sensors. / Huang Jianjun, Zhong Jiali, Jiang Feng. // 2010 IEEE 10th International Conference on Signal Processing (ICSP). - Beijing, 24-28 Oct. 2010. - P. 2386-2390. ↑

**C1983.** DeVale J.P. Evaluating information assurance performance and the impact of data characteristics. / DeVale J.P., Tan K.M.C. // 2010 IEEE International Conference on Technologies for Homeland Security (HST). - Waltham, MA, 8-10 Nov. 2010. - P. 15-21. ↑

**C1984.** Pratap P. Challenges of remote border monitoring. / Pratap P., Kallberg J.M., Thomas L.A. // 2010 IEEE International Conference on Technologies for Homeland Security (HST). - Waltham, MA, 8-10 Nov. 2010. - P. 303-307. ↑

**C1985.** Xiuqin Shang. Generalized likelihood ratio test for distributed targets in heterogeneous environments. / Xiuqin Shang, Hongjun Song. // 2010 IEEE 10th International Conference on Signal Processing (ICSP). - Beijing, 24-28 Oct. 2010. - P. 2242-2245. ↑

**C1986.** Nohara T.J. A commercial approach to successful persistent radar surveillance of sea, air and land along the northern border. 2010 IEEE International Conference on Technologies for Homeland Security (HST). - Waltham, MA, 8-10 Nov. 2010. - P. 276-282. ↑

**C1987.** Wenchao Li. High order Doppler parameter estimation of bistatic forward-looking SAR based on CPF-Radon transform. / Wenchao Li, Jianyu Yang, Yulin Huang, Junjie Wu. // 2010 IEEE 10th International Conference on Signal Processing (ICSP). - Beijing, 24-28 Oct. 2010. - P. 2239-2241. ↑

**C1988.** Xiang-Ru Li. A study of frequency diversity MIMO radar beamforming. / Xiang-Ru Li, Zhao Zhang, Wu-Xing Mao, Xiao-Mo Wang, Jun Lu, Wen-Sheng Wang. // 2010 IEEE 10th International Conference on Signal Processing (ICSP). - Beijing, 24-28 Oct. 2010. - P. 352-356. ↑

**C1989.** Qiu Wei. Target decomposition for fully polarimetric wideband radar system. / Qiu Wei, Chen Jian-jun, Zhao Hong-zhong, Zhao Feng. // 2010 IEEE 10th International Conference on Signal Processing (ICSP). - Beijing, 24-28 Oct. 2010. - P. 2246-2249. ↑

**C1990.** Ge Xianjun. Cross-correlation detection and time difference estimation in non-cooperative bistatic radar systems. / Ge Xianjun, He You, Song Jie. // 2010 IEEE 10th International Conference on Signal Processing (ICSP). - Beijing, 24-28 Oct. 2010. - P. 2261-2265. ↑

**C1991.** Rongbo Wang. An adaptive beamforming method based on properties of cyclostationary signals. / Rongbo Wang, Chaohuan Hou. // 2010 IEEE 10th International Conference on Signal Processing (ICSP). - Beijing, 24-28 Oct. 2010. - P. 319-322. ↑

**C1992.** Lu Fang. An improved passive location algorithm for maneuvering target emitter. / Lu Fang, Li Xian Yu, Yang Xiaojun. // 2010 IEEE 10th International Conference on Signal Processing (ICSP). - Beijing, 24-28 Oct. 2010. - P. 2341-2344. ↑

**C1993.** Changzheng Ma. Zero Correlation Zone Codes and Extended Zero Correlation Zone Codes for MIMO radar signal separation. / Changzheng Ma, Tat Soon Yeo, Qiang Guo, Chee Seng Tan, Pingjun Wei, Guoxiong Xu. // 2010 IEEE 10th International Conference on Signal Processing (ICSP). - Beijing, 24-28 Oct. 2010. - P. 2345-2348. ↑

**C1994.** Atlas R. Review of Observing System Simulation Experiments to evaluate the potential impact of lidar winds on weather prediction. 2010 IEEE International Geoscience and Remote Sensing Symposium (IGARSS). - Honolulu, HI, 25-30 July 2010. - P. 2587-2590. ↑

- C1995.** Zhixin Qi. Integrating object-oriented image analysis and decision tree algorithm for land use and land cover classification using RADARSAT-2 polarimetric SAR imagery. / Zhixin Qi, Yeh A.G.-O., Xia Li, Zheng Lin. // 2010 IEEE International Geoscience and Remote Sensing Symposium (IGARSS). - Honolulu, HI, 25-30 July 2010. - P. 3098-3101. ↑
- C1996.** Harant O. Maximum Likelihood texture tracking in highly heterogeneous PolSAR clutter. / Harant O., Bombrun L., Vasile G., Ferro-Famil L., Gay M. // 2010 IEEE International Geoscience and Remote Sensing Symposium (IGARSS). - Honolulu, HI, 25-30 July 2010. - P. 4031-4034. ↑
- C1997.** YiHyun Kim. Estimating rice growth parameters using X-band scatterometer data. / YiHyun Kim, SukYoung Hong, Eunyoung Choe, Hoonyol Lee. // 2010 IEEE International Geoscience and Remote Sensing Symposium (IGARSS). - Honolulu, HI, 25-30 July 2010. - P. 1258-1260. ↑
- C1998.** Qulin Tan. Building extraction from VHR multi-spectral images using rule-based object-oriented method: A case study. / Qulin Tan, Qingchao Wei, Fei Liang. // 2010 IEEE International Geoscience and Remote Sensing Symposium (IGARSS). - Honolulu, HI, 25-30 July 2010. - P. 2754-2756. ↑
- C1999.** Zhe Jiang. Retrieval of Aerosol optical thickness and size distribution from PARASOL in Pearl River Delta area. / Zhe Jiang, Liangfu Chen, Minghui Tao, Lin Su. // 2010 IEEE International Geoscience and Remote Sensing Symposium (IGARSS). - Honolulu, HI, 25-30 July 2010. - P. 1145-1148. ↑
- C2000.** Pratola C. Towards fully automatic generation of land cover maps from polarimetric and metric-resolution SAR data. / Pratola C., Del Greco M., Del Frate F., Schiavon G., Solimini D. // 2010 IEEE International Geoscience and Remote Sensing Symposium (IGARSS). - Honolulu, HI, 25-30 July 2010. - P. 3102-3105. ↑
- C2001.** Yorks J.E. Statistics of depolarization ratio from an airborne backscatter lidar. / Yorks J.E., McGill M.J., Hlavka D.L., Hart W.D. // 2010 IEEE International Geoscience and Remote Sensing Symposium (IGARSS). - Honolulu, HI, 25-30 July 2010. - P. 2579-2582. ↑
- C2002.** Songxin Tan. A comparative study of polarimetric and non-polarimetric lidar in deciduous-coniferous tree classification. / Songxin Tan, Haider A. // 2010 IEEE International Geoscience and Remote Sensing Symposium (IGARSS). - Honolulu, HI, 25-30 July 2010. - P. 1178-1181. ↑
- C2003.** Johnson B.R. National ecological observatory network (NEON) airborne remote measurements of vegetation canopy biochemistry and structure. / Johnson B.R., Kuester M.A., Kampe T.U., Keller M. // 2010 IEEE International Geoscience and Remote Sensing Symposium (IGARSS). - Honolulu, HI, 25-30 July 2010. - P. 2079-2082. ↑
- C2004.** Zhi Wang. QEM-based simplification of building footprints from Airborne LiDAR data. / Zhi Wang, Hui-Ying Li, Li-Xin Wu. // 2010 IEEE International Geoscience and Remote Sensing Symposium (IGARSS). - Honolulu, HI, 25-30 July 2010. - P. 1186-1189. ↑
- C2005.** Dagefu F.T. Soil dielectric and sensitivity analysis for subsurface imaging applications based on distributed Sensor Networks. / Dagefu F.T., Sarabandi K. // 2010 IEEE International Geoscience and Remote Sensing Symposium (IGARSS). - Honolulu, HI, 25-30 July 2010. - P. 1839-1842. ↑
- C2006.** Morgenthaler A.W. The Semi-Analytic Mode Matching algorithm for GPR wave scattering from multiple complex objects buried in a dielectric half space. / Morgenthaler A.W., Rappaport C.M. // 2010 IEEE International Geoscience and Remote Sensing Symposium (IGARSS). - Honolulu, HI, 25-30 July 2010. - P. 4713-4716. ↑
- C2007.** Fayard F. Generation of DEM by radargrammetric techniques. / Fayard F., Meric S., Pottier E. // 2010 IEEE International Geoscience and Remote Sensing Symposium (IGARSS). - Honolulu, HI, 25-30 July 2010. - P. 4342-4345. ↑
- C2008.** Xiao Xiang Zhu. Compressive sensing for high resolution differential SAR tomography-the SL1MMER algorithm. / Xiao Xiang Zhu, Bamler R. // 2010 IEEE International Geoscience and Remote Sensing Symposium (IGARSS). - Honolulu, HI, 25-30 July 2010. - P. 17-20. ↑
- C2009.** Dellepiane S. Processing and segmentation of COSMO-SkyMed images for flood monitoring. / Dellepiane S., Angiati E., Vernazza G. // 2010 IEEE International Geoscience and Remote Sensing Symposium (IGARSS). - Honolulu, HI, 25-30 July 2010. - P. 4807-4810. ↑



- C2010.** Siqueira P. A portable 35 GHz cross-track interferometer for topographic and surface change measurements. / Siqueira P., Vedantham H., Swochak T. // 2010 IEEE International Geoscience and Remote Sensing Symposium (IGARSS). - Honolulu, HI, 25-30 July 2010. - P. 4811-4814. ↑
- C2011.** Dell'Acqua F. Mapping earthquake damage in VHR radar images of human settlements: Preliminary results on the 6th April 2009, Italy case. / Dell'Acqua F., Gamba P., Polli D. // 2010 IEEE International Geoscience and Remote Sensing Symposium (IGARSS). - Honolulu, HI, 25-30 July 2010. - P. 1347-1350. ↑
- C2012.** Soja M.J. Topographic correction for biomass retrieval from P-band SAR data in boreal forests. / Soja M.J., Sandberg G., Ulander L.M.H. // 2010 IEEE International Geoscience and Remote Sensing Symposium (IGARSS). - Honolulu, HI, 25-30 July 2010. - P. 4776-4779. ↑
- C2013.** Sayin I. Application of Fractional Fourier Transform to finite difference time domain method. / Sayin I., Arikan F., Arikan O. // 2010 IEEE 18th Signal Processing and Communications Applications Conference (SIU). - Diyarbakir, 22-24 April 2010. - P. 728-731. ↑
- C2014.** Botta G. A new approach to modeling ice crystal aggregates and its implications for radar remote sensing. / Botta G., Aydin K., Verlinde J. // 2010 IEEE International Geoscience and Remote Sensing Symposium (IGARSS). - Honolulu, HI, 25-30 July 2010. - P. 2353-2354. ↑
- C2015.** Biggs G. Implementing a reactive semantics using OpenRTM-aist. / Biggs G., MacDonald B.A. // 2010 IEEE/RSJ International Conference on Intelligent Robots and Systems (IROS). - Taipei, 18-22 Oct. 2010. - P. 994-999. ↑
- C2016.** Nirchio F. Contribution of Cosmo/SkyMed data into PRIMI: A pilot project on marine oil pollution. results after one year of operations. / Nirchio F., Pandiscia G., Ruggieri G., Santoleri R., Pinardi N., Trivero P., Castellani C., Tataranni F., Masini A., Adamo M., Archetti R., Biamino W., Bignami F., Bohm E., Borasi M., Nardelli B.B., Cavagnero M., Colao F., Colella S., Coppini G., Debetto V., De Carolis G., De Dominicis M., Forneris V., Fontebasso F., Griffo A., Iacono R., Lombardi E., Marullo S., Manzella G., Mercatini A., Napolitano E., Pisano A., Reseghetti F., Sorgente R., Sprovieri M., Terranova G., Volpe G., Zambianchi E. // 2010 IEEE International Geoscience and Remote Sensing Symposium (IGARSS). - Honolulu, HI, 25-30 July 2010. - P. 4799-4802. ↑
- C2017.** Lombardini F. First experiments of sector interpolated SAR tomography. / Lombardini F., Pardini M. // 2010 IEEE International Geoscience and Remote Sensing Symposium (IGARSS). - Honolulu, HI, 25-30 July 2010. - P. 21-24. ↑
- C2018.** Bovenga F. The COSMO SKYMED constellation turn on the l'aquila earthquake: Dinsar results of the morfeo project. / Bovenga F., Candela L., Casu F., Fornaro G., Guzzetti F., Lanari R., Nitti D.O., Nutricato R., Reale D. // 2010 IEEE International Geoscience and Remote Sensing Symposium (IGARSS). - Honolulu, HI, 25-30 July 2010. - P. 4803-4806. ↑
- C2019.** Baker C.J. Cognitive diversity sensing. 2010 International Conference on Electromagnetics in Advanced Applications (ICEAA). - Sydney, NSW, 20-24 Sept. 2010. - P. 875-878. ↑
- C2020.** Qu Ning-ning. The analysis of surface deformation based on two-pass and three-pass D-InSAR. / Qu Ning-ning, Zhu Guang, Zhao Xi-an, Jing Chang-feng, Lv Jing-guo. // 2010 IEEE International Geoscience and Remote Sensing Symposium (IGARSS). - Honolulu, HI, 25-30 July 2010. - P. 4561-4563. ↑
- C2021.** Cook K. COSMIC-2: The future of global navigation satellite system-remote observation (GNSS-RO) sensing. / Cook K., Wilczynski P. // 2010 IEEE International Geoscience and Remote Sensing Symposium (IGARSS). - Honolulu, HI, 25-30 July 2010. - P. 3825-3828. ↑
- C2022.** Tug. Hidden Markov based target detection for track-before-detect. / Tug,ac, S., Efe M. // 2010 IEEE 18th Signal Processing and Communications Applications Conference (SIU). - Diyarbakir, 22-24 April 2010. - P. 554-557. ↑
- C2023.** Baselice F. New trends in SAR tomography. / Baselice F., Budillon A., Ferraioli G., Pascazio V., Schirinzi G., Evangelista A. // 2010 IEEE International Geoscience and Remote Sensing Symposium (IGARSS). - Honolulu, HI, 25-30 July 2010. - P. 25-28. ↑
- C2024.** Font J. Overview of SMOS Level 2 Ocean Salinity processing and first results. / Font J., Boutin J.,

Reul N., Spurgeon P., Ballabrera J., Chuprin A., Gabarro, C., Gourrion J., He, nocq C., Lavender S., Martin N., Martinez J., McCulloch M., Meirold-Mautner I., Petitcolin F., Portabella M., Sabia R., Talone M., Tenerelli J., Turiel A., Vergely J.L., Waldteufel P., Yin X., Zine S. // 2010 IEEE International Geoscience and Remote Sensing Symposium (IGARSS). - Honolulu, HI, 25-30 July 2010. - P. 3146-3149. ↑

**C2025.** Bo Zhang. Characteristic analysis of vehicle target in Quad-Pol Radarsat-2 SAR images. / Bo Zhang, Hong Zhang, Chao Wang, Fan Wu, Yi-xian Tang. // 2010 IEEE International Geoscience and Remote Sensing Symposium (IGARSS). - Honolulu, HI, 25-30 July 2010. - P. 3142-3145. ↑

**C2026.** Chu He. Topographic gray level multiscale analysis and its application to histogram modification. / Chu He, Xin-Ping Deng, Gui-Song Xia, Wen Yang, Hong Sun. // 2010 17th IEEE International Conference on Image Processing (ICIP). - Hong Kong, 26-29 Sept. 2010. - P. 369-372. ↑

**C2027.** Meyer F. A review of ionospheric effects in low-frequency SAR-Signals, correction methods, and performance requirements. 2010 IEEE International Geoscience and Remote Sensing Symposium (IGARSS). - Honolulu, HI, 25-30 July 2010. - P. 29-32. ↑

**C2028.** Quivira F. Impact of the wave number estimation in Underground Focusing SAR images. / Quivira F., Martinez-Lorenzo J.A., Rappaport C.M. // 2010 IEEE International Geoscience and Remote Sensing Symposium (IGARSS). - Honolulu, HI, 25-30 July 2010. - P. 4310-4313. ↑

**C2029.** Sang-Hoon Hong. Rotated dihedral and volume scattering behavior in cross-polarimetric SAR. / Sang-Hoon Hong, Wdowinski S. // 2010 IEEE International Geoscience and Remote Sensing Symposium (IGARSS). - Honolulu, HI, 25-30 July 2010. - P. 3138-3141. ↑

**C2030.** Ngoc Truong Minh Nguyen. Characterization of the scattered field by an urban area in the X-frequency band for bistatic and monostatic radar configurations. / Ngoc Truong Minh Nguyen, Lautru D., Roussel H. // 2010 IEEE International Geoscience and Remote Sensing Symposium (IGARSS). - Honolulu, HI, 25-30 July 2010. - P. 2999-3002. ↑

**C2031.** Cunren Liang. Burst mode to strip-map mode SAR interferometry of ALOS PALSAR. / Cunren Liang, Qiming Zeng, Xiaai Cui, Jian Jiao. // 2010 IEEE International Geoscience and Remote Sensing Symposium (IGARSS). - Honolulu, HI, 25-30 July 2010. - P. 4023-4026. ↑

**C2032.** Uiboupin R. Study of snowmelt impact on SST and TSM fields in the coastal zone of Barents Sea. / Uiboupin R., Arino O. // 2010 IEEE International Geoscience and Remote Sensing Symposium (IGARSS). - Honolulu, HI, 25-30 July 2010. - P. 4212-4215. ↑

**C2033.** Jong-Sen Lee. Monitoring tree farms and coastal environments using RADARSAT-2 PolSAR data. / Jong-Sen Lee, Ainsworth T.L., Yanting Wang, Kun-Shan Chen, Chih-Tien Wang. // 2010 IEEE International Geoscience and Remote Sensing Symposium (IGARSS). - Honolulu, HI, 25-30 July 2010. - P. 3134-3137. ↑

**C2034.** Panzer B. Ultra-wideband radar measurements of snow thickness over sea ice. / Panzer B., Leuschen C., Patel A., Markus T., Gogineni S. // 2010 IEEE International Geoscience and Remote Sensing Symposium (IGARSS). - Honolulu, HI, 25-30 July 2010. - P. 3130-3133. ↑

**C2035.** Hendricks S. Effects of surface roughness on sea ice freeboard retrieval with an Airborne Ku-Band SAR radar altimeter. / Hendricks S., Stenseng L., Helm V., Haas C. // 2010 IEEE International Geoscience and Remote Sensing Symposium (IGARSS). - Honolulu, HI, 25-30 July 2010. - P. 3126-3129. ↑

**C2036.** Stocker E.F. A generalized logical format for inter-calibrated brightness temperatures for the global precipitation measurement mission. / Stocker E.F., Stout J., Kummerow C., Berg W. // 2010 IEEE International Geoscience and Remote Sensing Symposium (IGARSS). - Honolulu, HI, 25-30 July 2010. - P. 844-846. ↑

**C2037.** Williams B.A. Scatterometer image reconstruction from aperture-filtered samples. / Williams B.A., Long D.G. // 2010 IEEE International Geoscience and Remote Sensing Symposium (IGARSS). - Honolulu, HI, 25-30 July 2010. - P. 1835-1838. ↑

**C2038.** Hoonyol Lee. Radargrammetry of high resolution synthetic aperture radar onboard KOMPSAT-5. 2010 IEEE International Geoscience and Remote Sensing Symposium (IGARSS). - Honolulu, HI, 25-30 July 2010. - P. 1246-1249. ↑

- C2039.** Hui-Ying Li. Fusion of LiDAR data and orthoimage for automatic building reconstruction. / Hui-Ying Li, Sheng-Bo Chen, Zhi Wang, Wen-Hui Li. // 2010 IEEE International Geoscience and Remote Sensing Symposium (IGARSS). - Honolulu, HI, 25-30 July 2010. - P. 1194-1197. ↑
- C2040.** Julea A. Extraction of frequent grouped sequential patterns from Satellite Image Time Series. / Julea A., Me,ger N., Rigotti C., Doin M.-P., Lasserre C., Trouve, E., Bolon P., La,za,rescu V. // 2010 IEEE International Geoscience and Remote Sensing Symposium (IGARSS). - Honolulu, HI, 25-30 July 2010. - P. 3434-3437. ↑
- C2041.** Yisok Oh. Soil moisture detection using KOMPSAT-5 SAR data. / Yisok Oh, Soon-Gu Kwon, Ji-Hwan Hwang. // 2010 IEEE International Geoscience and Remote Sensing Symposium (IGARSS). - Honolulu, HI, 25-30 July 2010. - P. 1250-1253. ↑
- C2042.** Mengwei Zhou. The inversion of crop height based on small-footprint waveform airborne lidar. / Mengwei Zhou, Qinhua Liu, Qiang Liu, Qing Xiao, Bo Zhong. // 2010 IEEE International Geoscience and Remote Sensing Symposium (IGARSS). - Honolulu, HI, 25-30 July 2010. - P. 1190-1193. ↑
- C2043.** Yonglin Shen. Extraction of building's geometric axis line from LiDAR data for disaster management. / Yonglin Shen, Zhi Wang, Lixin Wu. // 2010 IEEE International Geoscience and Remote Sensing Symposium (IGARSS). - Honolulu, HI, 25-30 July 2010. - P. 1198-1201. ↑
- C2044.** Deledalle C.-A. Glaciermonitoring: Correlation versus texture tracking. / Deledalle C.-A., Nicolas J.-M., Tupin F., Denis L., Fallourd R., Trouve, E. // 2010 IEEE International Geoscience and Remote Sensing Symposium (IGARSS). - Honolulu, HI, 25-30 July 2010. - P. 513-516. ↑
- C2045.** Deledalle C. A non-local approach for SAR and interferometric SAR denoising. / Deledalle C., Tupin F., Denis L. // 2010 IEEE International Geoscience and Remote Sensing Symposium (IGARSS). - Honolulu, HI, 25-30 July 2010. - P. 714-717. ↑
- C2046.** Morris K.R. Data visualization and analysis tools for the Global Precipitation Measurement (GPM) Validation Network. / Morris K.R., Schwaller M.R. // 2010 IEEE International Geoscience and Remote Sensing Symposium (IGARSS). - Honolulu, HI, 25-30 July 2010. - P. 847-850. ↑
- C2047.** Fransson J.E.S. Mapping of wind-thrown forests using satellite SAR images. / Fransson J.E.S., Pantze A., Eriksson L.E.B., Soja M.J., Santoro M. // 2010 IEEE International Geoscience and Remote Sensing Symposium (IGARSS). - Honolulu, HI, 25-30 July 2010. - P. 1242-1245. ↑
- C2048.** Manzo M. Full exploitation of the SBAS-DInSAR algorithm in active seismogenetic scenarios. / Manzo M., Berardino P., Bonano M., Casu F., Lanari R., Manconi A., Manunta M., Pepe A., Pepe S., Sansosti E., Solaro G., Tizzani P., Zeni G. // 2010 IEEE International Geoscience and Remote Sensing Symposium (IGARSS). - Honolulu, HI, 25-30 July 2010. - P. 1206-1209. ↑
- C2049.** Vasile G. Optimal parameter estimation in heterogeneous clutter for high resolution polarimetric SAR data. / Vasile G., Pascal F., Ovarlez J., Zozor S., Gay M. // 2010 IEEE International Geoscience and Remote Sensing Symposium (IGARSS). - Honolulu, HI, 25-30 July 2010. - P. 855-858. ↑
- C2050.** Jinyang Du. A method to estimate Snow Water Equivalent using multi-angle X-band radar observations. / Jinyang Du, Jiancheng Shi, Chuan Xiong. // 2010 IEEE International Geoscience and Remote Sensing Symposium (IGARSS). - Honolulu, HI, 25-30 July 2010. - P. 3774-3776. ↑
- C2051.** Zhen Liu. Monitoring time-dependent volcanic dynamics at Long Valley Caldera using InSAR and GPS measurements. / Zhen Liu, Danan Dong, Lundgren P. // 2010 IEEE International Geoscience and Remote Sensing Symposium (IGARSS). - Honolulu, HI, 25-30 July 2010. - P. 665-668. ↑
- C2052.** Shirvany R. Estimation of the degree of polarization in dual-polarized SAR imagery. / Shirvany R., Chabert M., Tournet J.-Y. // 2010 17th IEEE International Conference on Image Processing (ICIP). - Hong Kong, 26-29 Sept. 2010. - P. 1401-1404. ↑
- C2053.** Jili Li. Individual tree species classification using structure features from high density airborne lidar data. / Jili Li, Baoxin Hu, Gunho Sohn, Linhai Jing. // 2010 IEEE International Geoscience and Remote Sensing Symposium (IGARSS). - Honolulu, HI, 25-30 July 2010. - P. 2099-2102. ↑
- C2054.** Touzi R. On the use of transponder measurements for high precision assessment and calibration of

polarimetric Radarsat-2. / Touzi R., Hawkins R.K., Co,te, S. // 2010 IEEE International Geoscience and Remote Sensing Symposium (IGARSS). - Honolulu, HI, 25-30 July 2010. - P. 4847-4850. ↑

C2055. Zhiyu Zhang. Biomass retrieval based on UAVSAR polarimetric data. / Zhiyu Zhang, Guoqing Sun, Lixin Zhang, Zhifeng Guo, Wenli Huang. // 2010 IEEE International Geoscience and Remote Sensing Symposium (IGARSS). - Honolulu, HI, 25-30 July 2010. - P. 604-607. ↑

C2056. Le Vine D.M. Spurious signal in measurement of the third Stokes parameter from space at L-band. / Le Vine D.M., Dinnat E.D., Jacob S.D., Abraham S., de Mattheaieis P. // 2010 IEEE International Geoscience and Remote Sensing Symposium (IGARSS). - Honolulu, HI, 25-30 July 2010. - P. 3772-3773. ↑

C2057. Anderson S.J. Space-time focusing of HF skywave radar signals with application to nonlinear scattering phenomenology. 2010 International Conference on Electromagnetics in Advanced Applications (ICEAA). - Sydney, NSW, 20-24 Sept. 2010. - P. 16-19. ↑

C2058. Jinghui Fan. CRInSAR for landslide deformation monitoring: A case in threegorge area. / Jinghui Fan, Hongli Zhao, Pengfei Tu, Yi Wang, Xiaofang Guo, Daqing Ge, Guang Liu. // 2010 IEEE International Geoscience and Remote Sensing Symposium (IGARSS). - Honolulu, HI, 25-30 July 2010. - P. 3956-3959. ↑

C2059. Bin Zou. Target detection based on granularity computing of quotient space theory using SAR image. / Bin Zou, Qingchao Jia, Lamei Zhang, Ye Zhang. // 2010 17th IEEE International Conference on Image Processing (ICIP). - Hong Kong, 26-29 Sept. 2010. - P. 4601-4604. ↑

C2060. Jin-King Liu. Landslide detection by indices of LiDAR point-cloud density. / Jin-King Liu, Wei-Chen Hsu, Mon-Shieh Yang, Yu-Chung Shieh, Tian-Yuan Shih. // 2010 IEEE International Geoscience and Remote Sensing Symposium (IGARSS). - Honolulu, HI, 25-30 July 2010. - P. 3960-3963. ↑

C2061. Forster B. Global trends in remote sensing of human settlements. 2010 IEEE International Geoscience and Remote Sensing Symposium (IGARSS). - Honolulu, HI, 25-30 July 2010. - P. 1339-1342. ↑

C2062. Monte L.L. Direct-path mitigation for underground imaging in RF Tomography. / Monte L.L., Patton L.K., Wicks M.C. // 2010 International Conference on Electromagnetics in Advanced Applications (ICEAA). - Sydney, NSW, 20-24 Sept. 2010. - P. 27-30. ↑

C2063. Gang Li. ISAR imaging of maneuvering targets via matching pursuit. / Gang Li, Hao Zhang, Xiqin Wang, Xiang-Gen Xia. // 2010 IEEE International Geoscience and Remote Sensing Symposium (IGARSS). - Honolulu, HI, 25-30 July 2010. - P. 1625-1628. ↑

C2064. Iribe K. Coherent scatterer in forest environment: Detection, properties and its applications. / Iribe K., Papathanassiou K., Hajnsek I., Sato M., Yokota Y. // 2010 IEEE International Geoscience and Remote Sensing Symposium (IGARSS). - Honolulu, HI, 25-30 July 2010. - P. 3247-3250. ↑

C2065. von Lerber A. Modeling attenuation of melting hydrometeors with a method based on volume integral equations. / von Lerber A., Piepponen T., Koskinen J., Moiseev D., Kestilaj A., Tyynelaj J., Nousiainen T., Koistinen J., Sihvola A., Ylaj-Oijala P., Praks J., Hallikainen M., Pulliainen J. // 2010 IEEE International Geoscience and Remote Sensing Symposium (IGARSS). - Honolulu, HI, 25-30 July 2010. - P. 2355-2358. ↑

C2066. Cheng Hu. Modification of slant range model and imaging processing in GEO SAR. / Cheng Hu, Feifeng Liu, Wenfu Yang, Tao Zeng, Teng Long. // 2010 IEEE International Geoscience and Remote Sensing Symposium (IGARSS). - Honolulu, HI, 25-30 July 2010. - P. 4679-4682. ↑

C2067. Yoldemir A.B. Rotation and scale invariant template matching applied to buried object discrimination in GPR data. / Yoldemir A.B., Sezgin M. // 2010 IEEE International Geoscience and Remote Sensing Symposium (IGARSS). - Honolulu, HI, 25-30 July 2010. - P. 3366-3369. ↑

C2068. Daqing Ge. Mapping urban subsidence with TerraSAR-X data by PSI analysis. / Daqing Ge, Yan Wang, Ling Zhang, Xiaofang Guo, Ye Xia. // 2010 IEEE International Geoscience and Remote Sensing Symposium (IGARSS). - Honolulu, HI, 25-30 July 2010. - P. 3323-3326. ↑

C2069. Carrano C.S. A phase screen simulator for predicting the impact of small-scale ionospheric structure on SAR image formation and interferometry. / Carrano C.S., Groves K.M., Caton R.G. // 2010 IEEE International Geoscience and Remote Sensing Symposium (IGARSS). - Honolulu, HI, 25-30 July 2010. - P. 162-165. ↑



- C2070.** Angiati E. Operational evaluation of damages in flooded areas combining Cosmo-SkyMed and multispectral optical images. / Angiati E., Boni G., Candela L., Castelli F., Dellepiane S., Delogu F., Pintus F., Rudari R., Serpico S.B., Traverso S., Versace C. // 2010 IEEE International Geoscience and Remote Sensing Symposium (IGARSS). - Honolulu, HI, 25-30 July 2010. - P. 2414-2417. ↑
- C2071.** Capraro G.T. Metacognition in radar. / Capraro G.T., Wicks M.C. // 2010 International Conference on Electromagnetics in Advanced Applications (ICEAA). - Sydney, NSW, 20-24 Sept. 2010. - P. 693-696. ↑
- C2072.** Klaric M. Progressive spatial clustering of content-based satellite imagery retrieval results. / Klaric M., Scott G., Shyu C. // 2010 IEEE International Geoscience and Remote Sensing Symposium (IGARSS). - Honolulu, HI, 25-30 July 2010. - P. 36-39. ↑
- C2073.** Tuncer M.A.C. Sparsity enhanced fast subsurface imaging for stepped frequency GPRs. / Tuncer M.A.C., Gujbuz A.C. // 2010 IEEE 18th Signal Processing and Communications Applications Conference (SIU). - Diyarbakir, 22-24 April 2010. - P. 443-446. ↑
- C2074.** Sakamoto T. A target tracking method with a single antenna using time-reversal UWB radar imaging in a multi-path environment. / Sakamoto T., Sato T. // 2010 IEEE International Geoscience and Remote Sensing Symposium (IGARSS). - Honolulu, HI, 25-30 July 2010. - P. 3319-3322. ↑
- C2075.** Kuester M.A. Calibration system stability plans for a long-term Ecological Airborne remote sensing project. / Kuester M.A., Johnson B.R., Kampe T.U., McCorkel J. // 2010 IEEE International Geoscience and Remote Sensing Symposium (IGARSS). - Honolulu, HI, 25-30 July 2010. - P. 593-595. ↑
- C2076.** Xuan Feng. 3D velocity model and ray tracing of antenna array GPR. / Xuan Feng, Wenjin Liang, Qi Lu, Cai Liu, Lili Li, Lilong Zou, Sato M. // 2010 IEEE International Geoscience and Remote Sensing Symposium (IGARSS). - Honolulu, HI, 25-30 July 2010. - P. 4204-4207. ↑
- C2077.** Monnet J.-M. Support vector machines regression for estimation of forest parameters from airborne laser scanning data. / Monnet J.-M., Berger F., Chanussot J. // 2010 IEEE International Geoscience and Remote Sensing Symposium (IGARSS). - Honolulu, HI, 25-30 July 2010. - P. 2711-2714. ↑
- C2078.** Yuanwei Jin. Time reversal adaptive waveform in MIMO radar. / Yuanwei Jin, OrDonoughue N., Moura J.M.F. // 2010 International Conference on Electromagnetics in Advanced Applications (ICEAA). - Sydney, NSW, 20-24 Sept. 2010. - P. 741-744. ↑
- C2079.** Conway D. Using lidar to estimate the capacity for storm water recycling and solar energy collection. / Conway D., Samsung Lim. // 2010 IEEE International Geoscience and Remote Sensing Symposium (IGARSS). - Honolulu, HI, 25-30 July 2010. - P. 4545-4548. ↑
- C2080.** Owen M.P. Towards an improved wind and rain backscatter model for ASCAT. / Owen M.P., Long D.G. // 2010 IEEE International Geoscience and Remote Sensing Symposium (IGARSS). - Honolulu, HI, 25-30 July 2010. - P. 2531-2534. ↑
- C2081.** Hayashi N. 3D subsurface visualization by suppressing ground reflection and direct wave with bistatic GPR. / Hayashi N., Sato M. // 2010 IEEE International Geoscience and Remote Sensing Symposium (IGARSS). - Honolulu, HI, 25-30 July 2010. - P. 4592-4595. ↑
- C2082.** Hallikainen M. Studies of radio frequency interference at L-band using an airborne 2-D interferometric radiometer. / Hallikainen M., Kainulainen J., Seppänen J., Hakkarainen A., Rautiainen K. // 2010 IEEE International Geoscience and Remote Sensing Symposium (IGARSS). - Honolulu, HI, 25-30 July 2010. - P. 2490-2491. ↑
- C2083.** Suchandt S. Tidal current measurement with TerraSAR-X Along-Track Interferometry. / Suchandt S., Runge H., Romeiser R., Tous-Ramon N., Steinbrecher U. // 2010 IEEE International Geoscience and Remote Sensing Symposium (IGARSS). - Honolulu, HI, 25-30 July 2010. - P. 2432-2435. ↑
- C2084.** Perrie W. Gulf stream thermal fronts detected by synthetic aperture radar. / Perrie W., Tao Xie. // 2010 IEEE International Geoscience and Remote Sensing Symposium (IGARSS). - Honolulu, HI, 25-30 July 2010. - P. 2426-2427. ↑
- C2085.** Shiang Wang. Microwave remote sensing for marine monitoring: An example of *Enteromorpha prolifera*

bloom monitoring. / Shiang Wang, Fengli Zhang, Yun Shao, Wei Tian, Huaze Gong. // 2010 IEEE International Geoscience and Remote Sensing Symposium (IGARSS). - Honolulu, HI, 25-30 July 2010. - P. 4530-4533. ↑

**C2086.** Schwerdt M. Monostatic calibration of both TanDEM-X satellites. / Schwerdt M., Gonzalez J.H., Bachmann M., Schrank D., Schulz C., Dojring B. // 2010 IEEE International Geoscience and Remote Sensing Symposium (IGARSS). - Honolulu, HI, 25-30 July 2010. - P. 2636-2639. ↑

**C2087.** Fang Cao. An improvement for the unsupervised Wishart Freeman classification with fully polarimetric SAR data. / Fang Cao, Wen Hong, Pottier E. // 2010 IEEE International Geoscience and Remote Sensing Symposium (IGARSS). - Honolulu, HI, 25-30 July 2010. - P. 320-322. ↑

**C2088.** Ben Salah M. Image partitioning with kernel mapping and graph cuts. / Ben Salah M., Mitiche A., Ben Ayed I. // 2010 17th IEEE International Conference on Image Processing (ICIP). - Hong Kong, 26-29 Sept. 2010. - P. 245-248. ↑

**C2089.** Marchese L. Ultra-rapid optronic processor for instantaneous ENVISAT/ASAR scene observation. / Marchese L., Doucet M., Harnisch B., Suess M., Bourqui P., Legros M., Desnoyers N., Guillot L., Mercier L., Savard M., Martel A., Chateauneuf F., Bergeron A. // 2010 IEEE International Geoscience and Remote Sensing Symposium (IGARSS). - Honolulu, HI, 25-30 July 2010. - P. 685-687. ↑

**C2090.** Casu F. Advances in the generation of deformation time series from SAR data sequences in areas affected by large dynamics. / Casu F., Manconi A., Pepe A., Manzo M., Lanari R. // 2010 IEEE International Geoscience and Remote Sensing Symposium (IGARSS). - Honolulu, HI, 25-30 July 2010. - P. 2618-2621. ↑

**C2091.** Jong-Kuk Choi. Integration of InSAR and GIS for an estimation of ground subsidence susceptibility. / Jong-Kuk Choi, Joong-Sun Won, Sang-Wan Kim, Ki-Dong Kim, Joo-Hyung Ryu, Hong-Rhyong Yoo. // 2010 IEEE International Geoscience and Remote Sensing Symposium (IGARSS). - Honolulu, HI, 25-30 July 2010. - P. 4588-4591. ↑

**C2092.** Yasuma H. Rain effect on polarimetric SAR observation. / Yasuma H., Fukuchi H. // 2010 IEEE International Geoscience and Remote Sensing Symposium (IGARSS). - Honolulu, HI, 25-30 July 2010. - P. 2047-2050. ↑

**C2093.** Spencer M. The Soil Moisture Active Passive (SMAP) mission L-Band radar/radiometer instrument. / Spencer M., Wheeler K., White C., West R., Piepmeier J., Hudson D., Medeiros J. // 2010 IEEE International Geoscience and Remote Sensing Symposium (IGARSS). - Honolulu, HI, 25-30 July 2010. - P. 3240-3243. ↑

**C2094.** Pepe A. Deformation in Hawaii's volcanoes obtained from a ScanSAR-to-stripmap Small Baseline Subset technique. / Pepe A., Ortiz A.B., Bonano M., Lanari R., Lundgren P., Rosen P.A. // 2010 IEEE International Geoscience and Remote Sensing Symposium (IGARSS). - Honolulu, HI, 25-30 July 2010. - P. 769-772. ↑

**C2095.** Reid M.A. Automated Polar ice thickness estimation from radar imagery. / Reid M.A., Gifford C.M., Jefferson M., Akers E.L., Finyom G., Agah A. // 2010 IEEE International Geoscience and Remote Sensing Symposium (IGARSS). - Honolulu, HI, 25-30 July 2010. - P. 2406-2409. ↑

**C2096.** Yang Li. Spread E, F layer ionospheric clutter identification in range-Doppler map for HFSWR. / Yang Li, Ning Zhang, Qiang Yang. // 2010 17th IEEE International Conference on Image Processing (ICIP). - Hong Kong, 26-29 Sept. 2010. - P. 1397-1400. ↑

**C2097.** Kang Liu. Building height extraction via a deterministic approach using a TerraSAR-X data stack. / Kang Liu, Balz T., Mingsheng Liao. // 2010 IEEE International Geoscience and Remote Sensing Symposium (IGARSS). - Honolulu, HI, 25-30 July 2010. - P. 2920-2923. ↑

**C2098.** Bin Ding. Analysis of the effect of radio frequency interference on interferometric phase. / Bin Ding, Mao Sheng Xiang, Xing Dong Liang. // 2010 IEEE International Geoscience and Remote Sensing Symposium (IGARSS). - Honolulu, HI, 25-30 July 2010. - P. 4628-4631. ↑

**C2099.** Dhont D. Quantification of the topographic slope from radar satellite imagery. / Dhont D., Pajot E., Rudant J. // 2010 IEEE International Geoscience and Remote Sensing Symposium (IGARSS). - Honolulu, HI, 25-30 July 2010. - P. 4584-4587. ↑

- C2100.** Klare J. Environmental monitoring with the imaging MIMO radars MIRA-CLE and MIRA-CLE X. / Klare J., Saalman O., Wilden H., Brenner A.R. // 2010 IEEE International Geoscience and Remote Sensing Symposium (IGARSS). - Honolulu, HI, 25-30 July 2010. - P. 3781-3784. ↑
- C2101.** Zahn R. Modular Radar Core for airborne and space applications. / Zahn R., Kirscht M., Weidmann K. // 2010 IEEE International Geoscience and Remote Sensing Symposium (IGARSS). - Honolulu, HI, 25-30 July 2010. - P. 677-680. ↑
- C2102.** Kidera S. Shadow region imaging algorithm using array antenna based on aperture synthesis of multiple scattered waves for UWB radars. 2010 IEEE International Geoscience and Remote Sensing Symposium (IGARSS). - Honolulu, HI, 25-30 July 2010. - P. 4055-4058. ↑
- C2103.** Komatsu Y. Extraction of area-averaged orientation angle from POLSAR measurement. / Komatsu Y., Aso Y., Fukuchi H. // 2010 IEEE International Geoscience and Remote Sensing Symposium (IGARSS). - Honolulu, HI, 25-30 July 2010. - P. 4051-4054. ↑
- C2104.** Jung J.S. Stap based ground moving target detectability in the airborne/spaceborne array radar. / Jung J.S., Jung Kim, Kwag Y.K. // 2010 IEEE International Geoscience and Remote Sensing Symposium (IGARSS). - Honolulu, HI, 25-30 July 2010. - P. 4632-4635. ↑
- C2105.** Schwajbisch M. Accurate focusing of single-pass airborne InSAR data at L-band. / Schwajbisch M., Mercer B., Qiaoping Zhang, Wei Huang. // 2010 IEEE International Geoscience and Remote Sensing Symposium (IGARSS). - Honolulu, HI, 25-30 July 2010. - P. 2625-2628. ↑
- C2106.** Yamazaki F. Characterization of affected areas of the 2008 Iwate-Miyagi, Japan, earthquake using SAR intensity images. / Yamazaki F., Inoue H., Wen Liu. // 2010 IEEE International Geoscience and Remote Sensing Symposium (IGARSS). - Honolulu, HI, 25-30 July 2010. - P. 4660-4663. ↑
- C2107.** Moser G. Contextual remote-sensing image classification by support vector machines and Markov random fields. / Moser G., Serpico S.B. // 2010 IEEE International Geoscience and Remote Sensing Symposium (IGARSS). - Honolulu, HI, 25-30 July 2010. - P. 3728-3731. ↑
- C2108.** Saidi M.N. Pose estimation for ISAR image classification. / Saidi M.N., Toumi A., Khenchaf A., Hoeltzener B., Aboutajdine D. // 2010 IEEE International Geoscience and Remote Sensing Symposium (IGARSS). - Honolulu, HI, 25-30 July 2010. - P. 4620-4623. ↑
- C2109.** Ramongassie S. RADAR and AIS sensors constellation for global maritime surveillance. / Ramongassie S., Taveneau N., Calmettes T., Richard J., Challamel R., Autran O., Foix V., Durand P. // 2010 IEEE International Geoscience and Remote Sensing Symposium (IGARSS). - Honolulu, HI, 25-30 July 2010. - P. 3793-3796. ↑
- C2110.** Ikuma T. Predictive quantization of dechirped spotlight-mode SAR raw data in transform domain. / Ikuma T., Naraghi-Pour M., Lewis T. // 2010 IEEE International Geoscience and Remote Sensing Symposium (IGARSS). - Honolulu, HI, 25-30 July 2010. - P. 3789-3792. ↑
- C2111.** Shiina T. Z-R relation for snowfall using two small doppler radars and snow particle images. / Shiina T., Kubo M., Muramoto K. // 2010 IEEE International Geoscience and Remote Sensing Symposium (IGARSS). - Honolulu, HI, 25-30 July 2010. - P. 4122-4125. ↑
- C2112.** Williams M.L. Analysis of geosar dual-band InSAR data for peruvian forest. / Williams M.L., Silman M., Saatchi S., Hensley S., Sanford M., Yohannan A., Kofman B., Reis J., Kampes B. // 2010 IEEE International Geoscience and Remote Sensing Symposium (IGARSS). - Honolulu, HI, 25-30 July 2010. - P. 1398-1401. ↑
- C2113.** Duk-jin Kim. Application of KOMPSAT-5 data for emergent oil spill monitoring. / Duk-jin Kim, Moon W.M., Ji-Hwan Hwang, Youn-soo Kim. // 2010 IEEE International Geoscience and Remote Sensing Symposium (IGARSS). - Honolulu, HI, 25-30 July 2010. - P. 1254-1257. ↑
- C2114.** Singh G. Snow wetness retrieval inversion modeling for C-band and X-band multi-polarization SAR data. / Singh G., Venkataraman G. // 2010 IEEE International Geoscience and Remote Sensing Symposium (IGARSS). - Honolulu, HI, 25-30 July 2010. - P. 4664-4667. ↑
- C2115.** Hai Jiang. Random noise SAR based on compressed sensing. / Hai Jiang, Bingchen Zhang, Yueguan

Lin, Wen Hong, Yirong Wu, Jin Zhan. // 2010 IEEE International Geoscience and Remote Sensing Symposium (IGARSS). - Honolulu, HI, 25-30 July 2010. - P. 4624-4627. ↑

C2116. Sang-Mook Lee. A real-time grid map generation and object classification for ground-based 3D LIDAR data using image analysis techniques. / Sang-Mook Lee, Jeong Joon Im, Bo-Hee Lee, Leonessa A., Kurdila A. // 2010 17th IEEE International Conference on Image Processing (ICIP). - Hong Kong, 26-29 Sept. 2010. - P. 2253-2256. ↑

C2117. Bodensteiner C. Local multi-modal image matching based on self-similarity. / Bodensteiner C., Huebner W., Juengling K., Mueller J., Arens M. // 2010 17th IEEE International Conference on Image Processing (ICIP). - Hong Kong, 26-29 Sept. 2010. - P. 937-940. ↑

C2118. Flood B. SAR data collection over rain forests at VHF- and UHF-band. / Flood B., Frojllind P.-O., Gustavsson A., Jonsson T., Larsson B., Lundberg M., Murdin D., Stenstrojm G., Ulander L.M.H. // 2010 IEEE International Geoscience and Remote Sensing Symposium (IGARSS). - Honolulu, HI, 25-30 July 2010. - P. 1394-1397. ↑

C2119. Hambaryan A.K. Multi-frequency and polarimetric measurements of snow microwave reflection and emission by C- and Ku-band, combined scatterometer-radiometer systems. / Hambaryan A.K., Arakelyan A.K., Hambaryan V.K., Karyan V.V., Manukyan M.R., Grigoryan M.L., Hovhannisyan G.G., Arakelyan A.A., Darbinyan S.A. // 2010 IEEE International Geoscience and Remote Sensing Symposium (IGARSS). - Honolulu, HI, 25-30 July 2010. - P. 1733-1736. ↑

C2120. Xueyang Duan. Electromagnetic scattering from arbitrary random rough surfaces using stabilized extended boundary condition method (SEBCM) for remote sensing of soil moisture. / Xueyang Duan, Moghaddam M. // 2010 IEEE International Geoscience and Remote Sensing Symposium (IGARSS). - Honolulu, HI, 25-30 July 2010. - P. 1386-1389. ↑

C2121. Yiding Wang. Code sequence selection for SAR radiometric calibration. / Yiding Wang, Yuanshu Li, Zhulei Wang. // 2010 IEEE International Geoscience and Remote Sensing Symposium (IGARSS). - Honolulu, HI, 25-30 July 2010. - P. 209-212. ↑

C2122. Ping Zhang. 2D uesprit superresolution SAR imaging algorithm. / Ping Zhang, Zhen Li, Quan Chen. // 2010 IEEE International Geoscience and Remote Sensing Symposium (IGARSS). - Honolulu, HI, 25-30 July 2010. - P. 4067-4070. ↑

C2123. Kusk A. SAR focusing of P-band ice sounding data using back-projection. / Kusk A., Dall J. // 2010 IEEE International Geoscience and Remote Sensing Symposium (IGARSS). - Honolulu, HI, 25-30 July 2010. - P. 4071-4074. ↑

C2124. Formont P. A test statistic for high resolution polarimetric SAR data classification. / Formont P., Ovarlez J.-P., Pascal F., Vasile G., Ferro-Famil L. // 2010 IEEE International Geoscience and Remote Sensing Symposium (IGARSS). - Honolulu, HI, 25-30 July 2010. - P. 1871-1874. ↑

C2125. Xi'ai Cui. Investigating co-seismic deformation of the 2008 Wenchuan earthquake with ALOS SCANSAR interferometric observations. / Xi'ai Cui, Qiming Zeng, Cunren Liang, Jian Jiao. // 2010 IEEE International Geoscience and Remote Sensing Symposium (IGARSS). - Honolulu, HI, 25-30 July 2010. - P. 4612-4615. ↑

C2126. Correia A.H. Evaluation of the influence of the polarimetric calibration process on the H/A/alpha decomposition. / Correia A.H., da Costa Freitas C., Mura J.C. // 2010 IEEE International Geoscience and Remote Sensing Symposium (IGARSS). - Honolulu, HI, 25-30 July 2010. - P. 2039-2042. ↑

C2127. Feifeng Liu. A novel range migration algorithm of GEO SAR echo data. / Feifeng Liu, Cheng Hu, Tao Zeng, Teng Long, Lihua Jin. // 2010 IEEE International Geoscience and Remote Sensing Symposium (IGARSS). - Honolulu, HI, 25-30 July 2010. - P. 4656-4659. ↑

C2128. Wang R. Analysis and compensation for motion errors in FMCW SAR data. / Wang R., Loffeld O., Nies H., Peters V., Hajgelen M., Essen H. // 2010 IEEE International Geoscience and Remote Sensing Symposium (IGARSS). - Honolulu, HI, 25-30 July 2010. - P. 4075-4078. ↑

C2129. Bonano M. The extended SBAS technique for generating full resolution ERS/ENVISAT deformation



time-series. / Bonano M., Manunta M., Marsella M., Lanari R. // 2010 IEEE International Geoscience and Remote Sensing Symposium (IGARSS). - Honolulu, HI, 25-30 July 2010. - P. 4616-4619. ↑

C2130. Kalkan Y. Target localization methods for frequency-only MIMO radar. / Kalkan Y., Baykal B. // 2010 IEEE 18th Signal Processing and Communications Applications Conference (SIU). - Diyarbakir, 22-24 April 2010. - P. 439-442. ↑

C2131. Kaizhi Wang. Progressive SAR imaging technique. / Kaizhi Wang, Xingzhao Liu, Wenxian Yu, Junli Chen, Guozhong Chen. // 2010 IEEE International Geoscience and Remote Sensing Symposium (IGARSS). - Honolulu, HI, 25-30 July 2010. - P. 4083-4086. ↑

C2132. Trabal J.M. Evaluation of the self-consistency principle for calibration of the CASA radar network using properties of the observed medium. / Trabal J.M., Chandrasekar V., Gorgucci E., McLaughlin D.J. // 2010 IEEE International Geoscience and Remote Sensing Symposium (IGARSS). - Honolulu, HI, 25-30 July 2010. - P. 4126-4129. ↑

C2133. Vu V.T. Application of the moving target detection by focusing technique in civil traffic monitoring. / Vu V.T., Sjojgren T.K., Pettersson M.I., Marques P.A.C. // 2010 IEEE International Geoscience and Remote Sensing Symposium (IGARSS). - Honolulu, HI, 25-30 July 2010. - P. 4118-4121. ↑

C2134. Dazhi Zeng. A high accuracy method for interference fringes suppression in SAR distributed targets' raw data simulation. / Dazhi Zeng, Hanwei Sun, Tao Zeng, Teng Long. // 2010 IEEE International Geoscience and Remote Sensing Symposium (IGARSS). - Honolulu, HI, 25-30 July 2010. - P. 4675-4678. ↑

C2135. Muhammad N. Calibration of a rotating multi-beam lidar. / Muhammad N., Lacroix S. // 2010 IEEE/RSJ International Conference on Intelligent Robots and Systems (IROS). - Taipei, 18-22 Oct. 2010. - P. 5648-5653. ↑

C2136. Shah R. Analysis of the correlation properties of digital satellite signals and their applicability in bistatic remote sensing. / Shah R., Garrison J.L., Grant M.S., Katzberg S.J., Geng Tian. // 2010 IEEE International Geoscience and Remote Sensing Symposium (IGARSS). - Honolulu, HI, 25-30 July 2010. - P. 4114-4117. ↑

C2137. Marino A. Ship detection with RadarSat-2 Quad-Pol sar data using a notch filter based on perturbation analysis. / Marino A., Walker N., Woodhouse I. // 2010 IEEE International Geoscience and Remote Sensing Symposium (IGARSS). - Honolulu, HI, 25-30 July 2010. - P. 3704-3707. ↑

C2138. Ahmed R. A biomass estimate over the harvard forest using field measurements with radar and lidar data. / Ahmed R., Siqueira P., Bergen K., Chapman B., Hensley S. // 2010 IEEE International Geoscience and Remote Sensing Symposium (IGARSS). - Honolulu, HI, 25-30 July 2010. - P. 4768-4771. ↑

C2139. Cheng Qian. Earth documentation: Overpass detection using mobile Lidar. / Cheng Qian, Gale B., Bach J. // 2010 17th IEEE International Conference on Image Processing (ICIP). - Hong Kong, 26-29 Sept. 2010. - P. 3901-3904. ↑

C2140. Dapeng Yan. PSI analyses of land subsidence due to economic development near the city of Hangzhou, China. / Dapeng Yan, Daqing Ge, Jin Yang, Ling Zhang, Yan Wang, Xiaofang Guo. // 2010 IEEE International Geoscience and Remote Sensing Symposium (IGARSS). - Honolulu, HI, 25-30 July 2010. - P. 2410-2413. ↑

C2141. Parrilli S. A nonlocal approach for SAR image denoising. / Parrilli S., Poderico M., Angelino C.V., Scarpa G., Verdoliva L. // 2010 IEEE International Geoscience and Remote Sensing Symposium (IGARSS). - Honolulu, HI, 25-30 July 2010. - P. 726-729. ↑

C2142. Spinhirne J.D. Global laser pulse reflectance at 1064 nm of snow and land surfaces from the Glas satellite Lidar. / Spinhirne J.D., Palm S.P. // 2010 IEEE International Geoscience and Remote Sensing Symposium (IGARSS). - Honolulu, HI, 25-30 July 2010. - P. 646-648. ↑

C2143. Wenjian Ni. Investigation of forest height retrieval using SRTM-DEM and ASTER-GDEM. / Wenjian Ni, Zhifeng Guo, Guoqing Sun, Hong Chi. // 2010 IEEE International Geoscience and Remote Sensing Symposium (IGARSS). - Honolulu, HI, 25-30 July 2010. - P. 2111-2114. ↑

C2144. Arakelyan A. C- and Ku-band (at 5.6GHz and 13.6GHz), dual-frequency, multi-polarization, short pulse, combined scatterometer-radiometer system for low altitude platform, vessel and aircraft applications. /

Arakelyan A., Hambaryan A., Karyan V., Hovhannisyan G., Grigoryan M., Arakelyan A., Simonyan M., Poghosyan T., Poghosyan N. // 2010 IEEE International Geoscience and Remote Sensing Symposium (IGARSS). - Honolulu, HI, 25-30 July 2010. - P. 4470-4473. ↑

C2145. Brunner D. Change detection for earthquake damage assessment in built-up areas using very high resolution optical and SAR imagery. / Brunner D., Bruzzone L., Lemoine G. // 2010 IEEE International Geoscience and Remote Sensing Symposium (IGARSS). - Honolulu, HI, 25-30 July 2010. - P. 3210-3213. ↑

C2146. Rogers M. The Cloudsat Education Network: Scientifically significant collaborative research between students and scientists. / Rogers M., Vane D. // 2010 IEEE International Geoscience and Remote Sensing Symposium (IGARSS). - Honolulu, HI, 25-30 July 2010. - P. 84-86. ↑

C2147. Rakwatin P. Mapping tropical forest using ALOS PALSAR 50m resolution data with multiscale GLCM analysis. / Rakwatin P., Longepe N., Isoguchi O., Shimada M., Uryu Y. // 2010 IEEE International Geoscience and Remote Sensing Symposium (IGARSS). - Honolulu, HI, 25-30 July 2010. - P. 1234-1237. ↑

C2148. Hambaryan A. Multi-frequency and polarimetric measurements of bare and vegetated soils microwave reflection and emission by C- and Ku-band, combined scatterometer-radiometer systems. / Hambaryan A., Arakelyan A., Hambaryan V., Karyan V., Manukyan M., Grigoryan M., Hovhannisyan G., Arakelyan A., Darbinyan S. // 2010 IEEE International Geoscience and Remote Sensing Symposium (IGARSS). - Honolulu, HI, 25-30 July 2010. - P. 4466-4469. ↑

C2149. Tebaldini S. Polarimetric and structural properties of forest scenarios as imaged by longer wavelength SRS. / Tebaldini S., D'Alessandro M.M., Monti Guarnieri A., Rocca F. // 2010 IEEE International Geoscience and Remote Sensing Symposium (IGARSS). - Honolulu, HI, 25-30 July 2010. - P. 3251-3254. ↑

C2150. Taraktas. Received signal strength based localization in sensor network. / Taraktas, K.F., Ceylan O., Yagci, B. // 2010 IEEE 18th Signal Processing and Communications Applications Conference (SIU). - Diyarbakir, 22-24 April 2010. - P. 804-807. ↑

C2151. Yamada H. Esprit-based scattering power decomposition by using modified volume scattering model. / Yamada H., Komaya R., Yamaguchi Y., Sato R. // 2010 IEEE International Geoscience and Remote Sensing Symposium (IGARSS). - Honolulu, HI, 25-30 July 2010. - P. 3255-3258. ↑

C2152. Soysal G. Analysis of observed information in multistatic radar network. / Soysal G., Efe M. // 2010 IEEE 18th Signal Processing and Communications Applications Conference (SIU). - Diyarbakir, 22-24 April 2010. - P. 808-811. ↑

C2153. Powell J. Multi-Channel RADAR Depth Sounder (MCRDS) signal processing: A distributed computing approach. / Powell J., Hayden L. // 2010 IEEE International Geoscience and Remote Sensing Symposium (IGARSS). - Honolulu, HI, 25-30 July 2010. - P. 3358-3361. ↑

C2154. Lideng Wei. Processing for airborne interferometric SAR data with high squint. / Lideng Wei, Songtao Han, Maosheng Xiang. // 2010 IEEE International Geoscience and Remote Sensing Symposium (IGARSS). - Honolulu, HI, 25-30 July 2010. - P. 4668-4670. ↑

C2155. Pierce L. A dual-frequency SAR mosaic of the Amazon. / Pierce L., Barros O. // 2010 IEEE International Geoscience and Remote Sensing Symposium (IGARSS). - Honolulu, HI, 25-30 July 2010. - P. 4671-4674. ↑

C2156. Xin Tian. Comparison of crop classification capabilities of spaceborne multi-parameter SAR data. / Xin Tian, Erxue Chen, Zengyuan Li, Su Z.B., Feilong Ling, Lina Bai, Fengyu Wang. // 2010 IEEE International Geoscience and Remote Sensing Symposium (IGARSS). - Honolulu, HI, 25-30 July 2010. - P. 359-362. ↑

C2157. Zhao J.G. A fully polarimetric borehole radar based numerical modelling: Fully polarimetric response to synthetic fractures and "fluid substitution". / Zhao J.G., Sato M. // 2010 IEEE International Geoscience and Remote Sensing Symposium (IGARSS). - Honolulu, HI, 25-30 July 2010. - P. 3929-3932. ↑

C2158. Grosdidier S. Morphological-based source extraction method for HFSW radar ship detection. / Grosdidier S., Baussard A., Khenchaf A. // 2010 IEEE International Geoscience and Remote Sensing Symposium (IGARSS). - Honolulu, HI, 25-30 July 2010. - P. 3708-3711. ↑

- C2159.** Lavalley M. Polinsar forestry applications improved by modeling height-dependent temporal decorrelation. / Lavalley M., Simard M., Pottier E., Solimini D. // 2010 IEEE International Geoscience and Remote Sensing Symposium (IGARSS). - Honolulu, HI, 25-30 July 2010. - P. 4772-4775. ↑
- C2160.** Frery A.C. Contrast in speckled imagery with stochastic distances. / Frery A.C., Nascimento A.D.C., Cintra R.J. // 2010 17th IEEE International Conference on Image Processing (ICIP). - Hong Kong, 26-29 Sept. 2010. - P. 69-72. ↑
- C2161.** Gormus E.T. Exploiting spatial domain and wavelet domain cumulants for fusion of SAR and optical images. / Gormus E.T., Canagarajah C.N., Achim A.M. // 2010 17th IEEE International Conference on Image Processing (ICIP). - Hong Kong, 26-29 Sept. 2010. - P. 1209-1212. ↑
- C2162.** Schmitt A. Comparison of alternative image representations in the context of SAR change detection. / Schmitt A., Wendleder A., Wessel B., Roth A. // 2010 IEEE International Geoscience and Remote Sensing Symposium (IGARSS). - Honolulu, HI, 25-30 July 2010. - P. 284-287. ↑
- C2163.** Le M. Microphysical retrieval from dual frequency precipitation radar board GPM. / Le M., Chandrasekar V., Lim S. // 2010 IEEE International Geoscience and Remote Sensing Symposium (IGARSS). - Honolulu, HI, 25-30 July 2010. - P. 3482-3485. ↑
- C2164.** Wakabayashi H. Estimation of sea ice concentration in the Sea of Okhotsk using PALSAR polarimetric data. / Wakabayashi H., Sakai S. // 2010 IEEE International Geoscience and Remote Sensing Symposium (IGARSS). - Honolulu, HI, 25-30 July 2010. - P. 2398-2401. ↑
- C2165.** Lu Zhang. Application of aspect angle normalized polsar images for urban building detection. / Lu Zhang, Huadong Guo, Xinwu Li, Wenxue Fu. // 2010 IEEE International Geoscience and Remote Sensing Symposium (IGARSS). - Honolulu, HI, 25-30 July 2010. - P. 2735-2738. ↑
- C2166.** Mercier G. Progressive change detection in time series of SAR images. 2010 IEEE International Geoscience and Remote Sensing Symposium (IGARSS). - Honolulu, HI, 25-30 July 2010. - P. 3086-3089. ↑
- C2167.** Sartori L.R. Investigations on the full polarimetric PALSAR data to discriminate macrophytes species in the Amazon floodplain wetland. / Sartori L.R., Imai N.N., Mura J.C., de Moraes Novo E.M.L., Silva T.S.F. // 2010 IEEE International Geoscience and Remote Sensing Symposium (IGARSS). - Honolulu, HI, 25-30 July 2010. - P. 413-416. ↑
- C2168.** Hamlington B.D. On the feasibility of tsunami detection using satellite-based sea surface roughness measurements. / Hamlington B.D., Leben R.R., Godin O.A., Irisov V.G. // 2010 IEEE International Geoscience and Remote Sensing Symposium (IGARSS). - Honolulu, HI, 25-30 July 2010. - P. 3035-3038. ↑
- C2169.** Toumi A. Log-polar and polar image for recognition targets. / Toumi A., Khenchaf A. // 2010 IEEE International Geoscience and Remote Sensing Symposium (IGARSS). - Honolulu, HI, 25-30 July 2010. - P. 1609-1612. ↑
- C2170.** Hansch R. Random Forests for building detection in polarimetric SAR data. / Hansch R., Hellwich O. // 2010 IEEE International Geoscience and Remote Sensing Symposium (IGARSS). - Honolulu, HI, 25-30 July 2010. - P. 460-463. ↑
- C2171.** Fromberg A.F. Deployment of the ASCAT calibration transponders. / Fromberg A.F., Pritchard E.W., Wright N.G., Wilson J.J., Kayal G. // 2010 IEEE International Geoscience and Remote Sensing Symposium (IGARSS). - Honolulu, HI, 25-30 July 2010. - P. 3486-3489. ↑
- C2172.** Dazhi Zeng. Effect of the polarization on SISAR imaging and feature recognition in forward scattering radar. / Dazhi Zeng, Xiaoliang Li, Cheng Hu, Teng Long. // 2010 IEEE International Geoscience and Remote Sensing Symposium (IGARSS). - Honolulu, HI, 25-30 July 2010. - P. 1613-1616. ↑
- C2173.** Mon-Shieh Yang. Automatic image classification of landslides improved with terrain roughness indices in various kernel sizes. / Mon-Shieh Yang, Ming-Chang Lin, Jin-King Liu, Ming-Chee Wu. // 2010 IEEE International Geoscience and Remote Sensing Symposium (IGARSS). - Honolulu, HI, 25-30 July 2010. - P. 527-529. ↑
- C2174.** Brigui F. Orthogonal polarimetric SAR processor based on signal and interference subspace models. /

Brigui F., Thiron-Lefevre L., Ginolhac G., Forster P. // 2010 IEEE International Geoscience and Remote Sensing Symposium (IGARSS). - Honolulu, HI, 25-30 July 2010. - P. 2523-2526. ↑

C2175. Sant'Anna S.J.S. Electromagnetic characteristics of simple targets embedded in chiral multilayer structures. / Sant'Anna S.J.S., da S Lacava J.C., Fernandes D. // 2010 IEEE International Geoscience and Remote Sensing Symposium (IGARSS). - Honolulu, HI, 25-30 July 2010. - P. 3031-3034. ↑

C2176. Pottier E. Recent advances in the development of the open source Toolbox for Polarimetric and Interferometric Polarimetric SAR Data Processing: The PolSARpro v4.1.5 Software. 2010 IEEE International Geoscience and Remote Sensing Symposium (IGARSS). - Honolulu, HI, 25-30 July 2010. - P. 2527-2530. ↑

C2177. Gouinaud C. Characterization of ENVISAT multipolarization SAR data with bidimensional statistics. / Gouinaud C., Gouinaud P. // 2010 IEEE International Geoscience and Remote Sensing Symposium (IGARSS). - Honolulu, HI, 25-30 July 2010. - P. 1597-1600. ↑

C2178. Wen Yang. Semantic segmentation of Polarimetric SAR imagery using Conditional Random Fields. / Wen Yang, Xun Zhang, Lijun Chen, Hong Sun. // 2010 IEEE International Geoscience and Remote Sensing Symposium (IGARSS). - Honolulu, HI, 25-30 July 2010. - P. 1593-1596. ↑

C2179. Tebaldini S. Forest structure from longer wavelength SRS. / Tebaldini S., Rocca F. // 2010 IEEE International Geoscience and Remote Sensing Symposium (IGARSS). - Honolulu, HI, 25-30 July 2010. - P. 158-161. ↑

C2180. Alsweiss S. Improved hurricane active/passive simulated wind vector retrievals. / Alsweiss S., Laupattarakasem P., El-Nimri S., Jones W.L., Hristova-Veleva S. // 2010 IEEE International Geoscience and Remote Sensing Symposium (IGARSS). - Honolulu, HI, 25-30 July 2010. - P. 2535-2538. ↑

C2181. Yague-Martinez N. Interferometric processing algorithms of TanDEM-X data. / Yague-Martinez N., Rossi C., Lachaise M., Rodriguez-Gonzalez F., Fritz T., Breit H. // 2010 IEEE International Geoscience and Remote Sensing Symposium (IGARSS). - Honolulu, HI, 25-30 July 2010. - P. 3518-3521. ↑

C2182. Benson M.L. Extrapolation of LiDAR for forest structure estimation using SAR, InSAR, and optical data. / Benson M.L., Pierce L.E., Bergen K.M., Sarabandi K., Kailai Zhang, Ryan C.E. // 2010 IEEE International Geoscience and Remote Sensing Symposium (IGARSS). - Honolulu, HI, 25-30 July 2010. - P. 1633-1636. ↑

C2183. Daqing Ge. Merging multi-track PSI result for land subsidence mapping over very extended area. / Daqing Ge, Ling Zhang, Yan Wang, Xiaofang Guo, Ye Xia. // 2010 IEEE International Geoscience and Remote Sensing Symposium (IGARSS). - Honolulu, HI, 25-30 July 2010. - P. 3522-3525. ↑

C2184. Moser G. Unsupervised change detection with very high-resolution SAR images by multiscale analysis and Markov random fields. / Moser G., Serpico S.B. // 2010 IEEE International Geoscience and Remote Sensing Symposium (IGARSS). - Honolulu, HI, 25-30 July 2010. - P. 3082-3085. ↑

C2185. Ya-Qiu Jin. Composite scattering from electric-large target over randomly rough surface in numerical approaches. / Ya-Qiu Jin, Feng Xu. // 2010 IEEE International Geoscience and Remote Sensing Symposium (IGARSS). - Honolulu, HI, 25-30 July 2010. - P. 3545-3548. ↑

C2186. Notarnicola C. Towards an operational daily soil moisture index derived from combination of MODIS, ASAR and AMSR-E data. / Notarnicola C., Ventura B., Pasoli L., Di Giuseppe F., Zebisch M. // 2010 IEEE International Geoscience and Remote Sensing Symposium (IGARSS). - Honolulu, HI, 25-30 July 2010. - P. 816-819. ↑

C2187. Jiancheng Shi. Deriving soil moisture with the combined L-band radar and radiometer measurements. / Jiancheng Shi, Chen K.S., Tsang L., Jackson T., Njoku E., Van Zyl J., O'Neill P., Entekhabi D., Johnson J., Moghaddam M. // 2010 IEEE International Geoscience and Remote Sensing Symposium (IGARSS). - Honolulu, HI, 25-30 July 2010. - P. 812-815. ↑

C2188. Ranson K.J. Effects of forest disturbances on forest structural parameters retrieval from lidar waveform data. / Ranson K.J., Sun G. // 2010 IEEE International Geoscience and Remote Sensing Symposium (IGARSS). - Honolulu, HI, 25-30 July 2010. - P. 4370-4373. ↑

C2189. Wenming Lin. Development of a signal processing subsystem for a spaceborne rotating, fan-beam



scatterometer. / Wenming Lin, Xiaolong Dong, Di Zhu. // 2010 IEEE International Geoscience and Remote Sensing Symposium (IGARSS). - Honolulu, HI, 25-30 July 2010. - P. 4166-4169. ↑

C2190. Paul S.D. Investigation of cirrus clouds using the calipso lidar data. 2010 IEEE International Geoscience and Remote Sensing Symposium (IGARSS). - Honolulu, HI, 25-30 July 2010. - P. 4142-4145. ↑

C2191. Sipelgas L. Monitoring environmental conditions in Muuga harbor using Envisat MERIS and ASAR data. / Sipelgas L., Uiboupin R., Raudsepp U. // 2010 IEEE International Geoscience and Remote Sensing Symposium (IGARSS). - Honolulu, HI, 25-30 July 2010. - P. 409-412. ↑

C2192. Shin JaeMin. Field test of KOMPSAT-5 Calibration Equipment. / Shin JaeMin, Lee KwangJae, Kim JinHee. // 2010 IEEE International Geoscience and Remote Sensing Symposium (IGARSS). - Honolulu, HI, 25-30 July 2010. - P. 805-807. ↑

C2193. Xia Ye. High resolution D-INSAR measurement for land subsidence. / Xia Ye, Kaufmann H. // 2010 IEEE International Geoscience and Remote Sensing Symposium (IGARSS). - Honolulu, HI, 25-30 July 2010. - P. 1541-1544. ↑

C2194. Henke D. Preliminary results of a low-frequency 3D-sar approach for glacier volume mapping. / Henke D., Meier E. // 2010 IEEE International Geoscience and Remote Sensing Symposium (IGARSS). - Honolulu, HI, 25-30 July 2010. - P. 2027-2030. ↑

C2195. Gujrbujz S.Z. Radar-based human detection and characterization with non-linear phase modeling. / Gujrbujz S.Z., Melvin W.L., Williams D.B. // 2010 IEEE 18th Signal Processing and Communications Applications Conference (SIU). - Diyarbakir, 22-24 April 2010. - P. 586-589. ↑

C2196. Sang-Eun Park. Monitoring of thawing process using envisat asar global mode data. / Sang-Eun Park, Bartsch A., Sabel D., Wagner W. // 2010 IEEE International Geoscience and Remote Sensing Symposium (IGARSS). - Honolulu, HI, 25-30 July 2010. - P. 2031-2034. ↑

C2197. Dong-Hyun Kim. KOMPSAT-5 spotlight SAR processor using FSA with calculation of effective velocity. / Dong-Hyun Kim, Jae-Cheol Yoon, Jae-Min Shin, Moon-Gyu Kim. // 2010 IEEE International Geoscience and Remote Sensing Symposium (IGARSS). - Honolulu, HI, 25-30 July 2010. - P. 801-804. ↑

C2198. Corp L.A. Fusion: A fully ultraportable system for imaging objects in nature. / Corp L.A., Cook B.D., Middleton E.M., Cheng Y., Huemmmrich K.F., Campbell P.K.E. // 2010 IEEE International Geoscience and Remote Sensing Symposium (IGARSS). - Honolulu, HI, 25-30 July 2010. - P. 1671-1674. ↑

C2199. Sang-Ryool Lee. Overview of KOMPSAT-5 program, mission, and system. 2010 IEEE International Geoscience and Remote Sensing Symposium (IGARSS). - Honolulu, HI, 25-30 July 2010. - P. 797-800. ↑

C2200. Epov M.I. UWB electromagnetic borehole logging tool. / Epov M.I., Mironov V.L., Muzalevskiy K.V., Yeltsov I.N. // 2010 IEEE International Geoscience and Remote Sensing Symposium (IGARSS). - Honolulu, HI, 25-30 July 2010. - P. 3565-3567. ↑

C2201. JuneK W.N. Temporal analysis of the magma supply system beneath the Okmok caldera by Interferometric Synthetic Aperture Radar and statistical seismology. / JuneK W.N., Jones W.L., Woods M.T. // 2010 IEEE International Geoscience and Remote Sensing Symposium (IGARSS). - Honolulu, HI, 25-30 July 2010. - P. 1545-1548. ↑

C2202. Sang-Hoon Lee. Directional-adaptive despeckling for high-resolution SAR. 2010 IEEE International Geoscience and Remote Sensing Symposium (IGARSS). - Honolulu, HI, 25-30 July 2010. - P. 808-811. ↑

C2203. Gunnala S.K. Target detection above rough surfaces in microwave imaging using Compressive Sampling. / Gunnala S.K., Camacho L.M., Tjuatja S. // 2010 IEEE International Geoscience and Remote Sensing Symposium (IGARSS). - Honolulu, HI, 25-30 July 2010. - P. 3498-3501. ↑

C2204. Leilei Kou. Research on interferometric deformation detection for geosynchronous SAR. / Leilei Kou, Xiaoqing Wang, Jinsong Chong, Maosheng Xiang. // 2010 IEEE International Geoscience and Remote Sensing Symposium (IGARSS). - Honolulu, HI, 25-30 July 2010. - P. 3502-3505. ↑

C2205. Chong-wen Duan. MVM based SAR image processing for ship pose estimation. / Chong-wen Duan,

Wei-dong Hu, Xiao-yong Du. // 2010 IEEE International Geoscience and Remote Sensing Symposium (IGARSS). - Honolulu, HI, 25-30 July 2010. - P. 1605-1608. ↑

C2206. Popescu A. Generic object recognition in high resolution SAR images. / Popescu A., Costache M., Singh J., Datcu M., Schwarz G. // 2010 IEEE International Geoscience and Remote Sensing Symposium (IGARSS). - Honolulu, HI, 25-30 July 2010. - P. 1629-1632. ↑

C2207. Hoonyol Lee. A ground-based Arc-scanning synthetic aperture radar (ArcSAR) system and focusing algorithms. / Hoonyol Lee, Seong-Jun Cho, Kwang-Eun Kim. // 2010 IEEE International Geoscience and Remote Sensing Symposium (IGARSS). - Honolulu, HI, 25-30 July 2010. - P. 3490-3493. ↑

C2208. Ghulam A. A filtering approach to improve deformation accuracy using large baseline, low coherence DInSAR phase images. / Ghulam A., Amer R., Ripperdan R. // 2010 IEEE International Geoscience and Remote Sensing Symposium (IGARSS). - Honolulu, HI, 25-30 July 2010. - P. 3494-3497. ↑

C2209. Quinn G.S. Lidar integrated airborne imaging spectroscopy for root disease detection and measurement of foliar chemistry. / Quinn G.S., Niemann K.O., Goodenough D.G. // 2010 IEEE International Geoscience and Remote Sensing Symposium (IGARSS). - Honolulu, HI, 25-30 July 2010. - P. 4385-4388. ↑

C2210. Bell P.S. Submerged dunes and breakwater embayments mapped using wave inversions of shore-mounted marine X-band radar data. 2010 IEEE International Geoscience and Remote Sensing Symposium (IGARSS). - Honolulu, HI, 25-30 July 2010. - P. 4334-4337. ↑

C2211. Nieto-Borge J.C. Application of conventional marine radars for measuring ocean wave fields in shallow water conditions. / Nieto-Borge J.C., Mata-Moya D., Jarabo-Amores P., Reichert K., Hessner K. // 2010 IEEE International Geoscience and Remote Sensing Symposium (IGARSS). - Honolulu, HI, 25-30 July 2010. - P. 4338-4341. ↑

C2212. Villalon-Turrubiates I.E. Multispectral classification of remote sensing imagery for archaeological land use analysis: Prospective study. / Villalon-Turrubiates I.E., Llovera-Torres M.J. // 2010 IEEE International Geoscience and Remote Sensing Symposium (IGARSS). - Honolulu, HI, 25-30 July 2010. - P. 323-326. ↑

C2213. Maeda T. Approach for volcanic surveillance using satellite-borne microwave radiometer data. / Maeda T., Takano T. // 2010 IEEE International Geoscience and Remote Sensing Symposium (IGARSS). - Honolulu, HI, 25-30 July 2010. - P. 520-522. ↑

C2214. Ito Y. A study on anomalous signal detection using HMM for ELF electromagnetic wave. / Ito Y., Itai A., Yasukawa H., Takumi I., Hata M. // 2010 IEEE International Geoscience and Remote Sensing Symposium (IGARSS). - Honolulu, HI, 25-30 July 2010. - P. 1601-1604. ↑

C2215. Monells D. Application of TerraSAR-X data to the monitoring of urban subsidence in the city of Murcia. / Monells D., Centolanza G., Mallorqui J.J., Duque S., Lopez-Dekker P., Tomas R., Herrera G., Lopez-Sanchez J.M., Vicente F., Navarro-Sanchez V.D., Mulas J. // 2010 IEEE International Geoscience and Remote Sensing Symposium (IGARSS). - Honolulu, HI, 25-30 July 2010. - P. 3506-3509. ↑

C2216. Walter M.R. Closed-loop pallet manipulation in unstructured environments. / Walter M.R., Karaman S., Frazzoli E., Teller S. // 2010 IEEE/RSJ International Conference on Intelligent Robots and Systems (IROS). - Taipei, 18-22 Oct. 2010. - P. 5119-5126. ↑

C2217. Mishra K.V. Signal analysis and modeling of wind turbine clutter in weather radars. / Mishra K.V., Chandrasekar V. // 2010 IEEE International Geoscience and Remote Sensing Symposium (IGARSS). - Honolulu, HI, 25-30 July 2010. - P. 3561-3564. ↑

C2218. Ling Wang. Passive imaging exploiting multiple scattering using distributed apertures. / Ling Wang, Il-Young Son, Yazici B. // 2010 17th IEEE International Conference on Image Processing (ICIP). - Hong Kong, 26-29 Sept. 2010. - P. 1385-1388. ↑

C2219. Flores-Tapia D. A real time Breast Microwave Radar imaging reconstruction technique using simt based interpolation. / Flores-Tapia D., Pistorius S. // 2010 17th IEEE International Conference on Image Processing (ICIP). - Hong Kong, 26-29 Sept. 2010. - P. 1389-1392. ↑

C2220. Newell D.A. GPM Microwave Imager design, predicted performance and status. / Newell D.A., Rait G.,

Ta T., Berdanier B., Draper D., Kubitschek M., Krimchansky S. // 2010 IEEE International Geoscience and Remote Sensing Symposium (IGARSS). - Honolulu, HI, 25-30 July 2010. - P. 546-549. ↑

C2221. Alparone L. Multiresolution despeckling of VHR SAR images based on MRF segmentation. / Alparone L., Argenti F., Bianchi T., Abbate M., D'Elia C., Mariano P., Meta A. // 2010 IEEE International Geoscience and Remote Sensing Symposium (IGARSS). - Honolulu, HI, 25-30 July 2010. - P. 288-291. ↑

C2222. Merzouki A. Potential of mapping soil moisture by combining radar backscatter modeling and PolSAR decomposition. / Merzouki A., McNairn H., Pacheco A. // 2010 IEEE International Geoscience and Remote Sensing Symposium (IGARSS). - Honolulu, HI, 25-30 July 2010. - P. 4419-4422. ↑

C2223. Scipal K. Triple collocation-A new tool to determine the error structure of global soil moisture products. / Scipal K., Dorigo W., de Jeu R. // 2010 IEEE International Geoscience and Remote Sensing Symposium (IGARSS). - Honolulu, HI, 25-30 July 2010. - P. 4426-4429. ↑

C2224. Nishimoto M. Characteristics of rough surface parameters estimated from measured surface profile of finite length. 2010 IEEE International Geoscience and Remote Sensing Symposium (IGARSS). - Honolulu, HI, 25-30 July 2010. - P. 4436-4439. ↑

C2225. Tan D.K.P. Target detection performance analysis for airborne passive bistatic radar. / Tan D.K.P., Lesturgie M., Hongbo Sun, Yilong Lu. // 2010 IEEE International Geoscience and Remote Sensing Symposium (IGARSS). - Honolulu, HI, 25-30 July 2010. - P. 3553-3556. ↑

C2226. Zhang C. Imaging algorithm and experimental demonstration of rotating scanning interferometric radiometer. / Zhang C., Liu H., Yan J.Y., Sun W.Y., Zhang S.W., Liu H.G., Wu J. // 2010 IEEE International Geoscience and Remote Sensing Symposium (IGARSS). - Honolulu, HI, 25-30 July 2010. - P. 534-537. ↑

C2227. Jung Hum Yu. Automatic exclusion of surface deformation in InSAR DEM generation using differential radar interferometry. / Jung Hum Yu, Linlin Ge. // 2010 IEEE International Geoscience and Remote Sensing Symposium (IGARSS). - Honolulu, HI, 25-30 July 2010. - P. 2916-2919. ↑

C2228. Yanting Wang. Evaluation of system polarization quality for polarimetric SAR imagery and target decomposition. / Yanting Wang, Ainsworth T.L., Jong-Sen Lee. // 2010 IEEE International Geoscience and Remote Sensing Symposium (IGARSS). - Honolulu, HI, 25-30 July 2010. - P. 2043-2046. ↑

C2229. Yurchak B.S. Contribution of small-scale correlated fluctuations of the microstructural properties of a spatially extended geophysical target under the assessment of radar backscatter. 2010 IEEE International Geoscience and Remote Sensing Symposium (IGARSS). - Honolulu, HI, 25-30 July 2010. - P. 3557-3560. ↑

C2230. Ferro A. Building detection and radar footprint reconstruction from single VHR SAR images. / Ferro A., Brunner D., Bruzzone L. // 2010 IEEE International Geoscience and Remote Sensing Symposium (IGARSS). - Honolulu, HI, 25-30 July 2010. - P. 292-295. ↑

C2231. Richardson A. Unsupervised nonparametric classification of polarimetric SAR data using the K-nearest neighbor graph. / Richardson A., Goodenough D.G., Chen H., Moa B., Hobart G., Myrvold W. // 2010 IEEE International Geoscience and Remote Sensing Symposium (IGARSS). - Honolulu, HI, 25-30 July 2010. - P. 1867-1870. ↑

C2232. Hao Liu. Development of a three-element interferometer at 50 56 GHz for Geostationary Interferometric Microwave Sounder (GIMS). / Hao Liu, Ji Wu, Shengwei Zhang, Jingye Yan, Lijie Niu, Cheng Zhang, Bin Li. // 2010 IEEE International Geoscience and Remote Sensing Symposium (IGARSS). - Honolulu, HI, 25-30 July 2010. - P. 554-557. ↑

C2233. Baade J. High-resolution mapping of fluvial landform change in arid environments using terrasars-X images. / Baade J., Schmullius C. // 2010 IEEE International Geoscience and Remote Sensing Symposium (IGARSS). - Honolulu, HI, 25-30 July 2010. - P. 2159-2162. ↑

C2234. Patterson C.E. Implementation of a low cost, lightweight X-band antenna with integrated SiGe RF electronics. / Patterson C.E., Thirvikraman T.K., Yepes A.M., Bhattacharya S.K., Cressler J.D., Papapolymerou J. // 2010 IEEE International Geoscience and Remote Sensing Symposium (IGARSS). - Honolulu, HI, 25-30 July 2010. - P. 681-684. ↑


- C2235.** Ouchi K. Improvement of ship detection accuracy by sar multi-look cross-correlation technique using adaptive CFAR. / Ouchi K., Seong-In Hwang. // 2010 IEEE International Geoscience and Remote Sensing Symposium (IGARSS). - Honolulu, HI, 25-30 July 2010. - P. 3716-3719. ↑
- C2236.** Ohgi N. Japanese hyper-multi spectral mission. / Ohgi N., Iwasaki A., Kawashima T., Inada H. // 2010 IEEE International Geoscience and Remote Sensing Symposium (IGARSS). - Honolulu, HI, 25-30 July 2010. - P. 3756-3759. ↑
- C2237.** Hannevik T.N. Automatic ship detection in sar images using aegir. 2010 IEEE International Geoscience and Remote Sensing Symposium (IGARSS). - Honolulu, HI, 25-30 July 2010. - P. 3712-3715. ↑
- C2238.** Duque S. Bistatic SAR along track interferometry with multiple fixed receivers. / Duque S., Lopez-Dekker P., Merlano J.C., Mallorqui J.J. // 2010 IEEE International Geoscience and Remote Sensing Symposium (IGARSS). - Honolulu, HI, 25-30 July 2010. - P. 4099-4102. ↑
- C2239.** Goykhman Y. Radar retrieval of subsurface parameters for layered media with nonsmooth interfaces. / Goykhman Y., Moghaddam M. // 2010 IEEE International Geoscience and Remote Sensing Symposium (IGARSS). - Honolulu, HI, 25-30 July 2010. - P. 4458-4461. ↑
- C2240.** Arakelyan A. Combined active and passive measurements of snow, bare and vegetated soils microwave reflective and emissive characteristics by Ka-band, combined scatterometer-radiometer system. / Arakelyan A., Grigoryan M., Hambaryan A., Arakelyan A. // 2010 IEEE International Geoscience and Remote Sensing Symposium (IGARSS). - Honolulu, HI, 25-30 July 2010. - P. 4462-4465. ↑
- C2241.** Romeiser R. A new scalloping filter algorithm for scansar images. / Romeiser R., Horstmann J., Graber H. // 2010 IEEE International Geoscience and Remote Sensing Symposium (IGARSS). - Honolulu, HI, 25-30 July 2010. - P. 4079-4082. ↑
- C2242.** Butenuth M. Geometric refinement of road networks using network snakes and SAR images. 2010 IEEE International Geoscience and Remote Sensing Symposium (IGARSS). - Honolulu, HI, 25-30 July 2010. - P. 449-452. ↑
- C2243.** Fernandez Diaz J.C. Characterization of full surface roughness in agricultural soils using groundbased LiDAR. / Fernandez Diaz J.C., Judge J., Slatton K.C., Shrestha R., Carter W.E., Bloomquist D. // 2010 IEEE International Geoscience and Remote Sensing Symposium (IGARSS). - Honolulu, HI, 25-30 July 2010. - P. 4442-4445. ↑
- C2244.** Dall'Amico J.T. Comparing data of two airborne L-band radiometers with different spatial resolution over a heterogeneous land surface. / Dall'Amico J.T., Kainulainen J., Loew A., Mauser W. // 2010 IEEE International Geoscience and Remote Sensing Symposium (IGARSS). - Honolulu, HI, 25-30 July 2010. - P. 538-541. ↑
- C2245.** O'Neill P. The NASA Soil Moisture Active Passive (SMAP) mission: Overview. / O'Neill P., Entekhabi D., Njoku E., Kellogg K. // 2010 IEEE International Geoscience and Remote Sensing Symposium (IGARSS). - Honolulu, HI, 25-30 July 2010. - P. 3236-3239. ↑
- C2246.** Ratto C. Context-dependent landmine detection with ground-penetrating radar using a Hidden Markov Context Model. / Ratto C., Torrione P., Morton K., Collins L. // 2010 IEEE International Geoscience and Remote Sensing Symposium (IGARSS). - Honolulu, HI, 25-30 July 2010. - P. 4192-4195. ↑
- C2247.** Esteban-Fernandez D. Ka-band SAR interferometry studies for the SWOT mission. / Esteban-Fernandez D., Lee-Lueng Fu, Rodriguez E., Brown S., Hodges R. // 2010 IEEE International Geoscience and Remote Sensing Symposium (IGARSS). - Honolulu, HI, 25-30 July 2010. - P. 4401-4402. ↑
- C2248.** Gong W. Performance analysis of atmospheric correction in InSAR data based on the Weather Research and Forecasting Model (WRF). / Gong W., Meyer F., Webley P.W., Morton D., Liu S. // 2010 IEEE International Geoscience and Remote Sensing Symposium (IGARSS). - Honolulu, HI, 25-30 July 2010. - P. 2900-2903. ↑
- C2249.** Budillon A. Multi-baseline along track SAR interferometric systems for ground moving target indication. / Budillon A., Evangelista A., Pascasio V., Schirinzi G. // 2010 IEEE International Geoscience and Remote Sensing Symposium (IGARSS). - Honolulu, HI, 25-30 July 2010. - P. 2924-2927. ↑





- C2250.** Ujn Y.C. Improved Variable Index constant false alarm rate radar processors. / Ujn Y.C., Ujner K.M. // 2010 IEEE 18th Signal Processing and Communications Applications Conference (SIU). - Diyarbakir, 22-24 April 2010. - P. 740-743. ↑
- C2251.** Reale D. Advanced techniques and new high resolution SAR sensors for monitoring urban areas. / Reale D., Fornaro G., Paucillo A., Zhu X., Adam N., Bamler R. // 2010 IEEE International Geoscience and Remote Sensing Symposium (IGARSS). - Honolulu, HI, 25-30 July 2010. - P. 1800-1803. ↑
- C2252.** Buckley J.R. Monitoring grasslands with radarsat 2 quad-pol imagery. / Buckley J.R., Smith A.M. // 2010 IEEE International Geoscience and Remote Sensing Symposium (IGARSS). - Honolulu, HI, 25-30 July 2010. - P. 3090-3093. ↑
- C2253.** Sauber J. DESDynI lidar for solid earth applications. / Sauber J., Hofton M., Bruhn R., Luthcke S., Blair B. // 2010 IEEE International Geoscience and Remote Sensing Symposium (IGARSS). - Honolulu, HI, 25-30 July 2010. - P. 1903-1906. ↑
- C2254.** Weissman D.E. Studies of the influence of rainfall upon scatterometer estimates for sea surface stress: Applications to boundary layer parameterization and drag coefficient models within tropical cyclone environments. / Weissman D.E., Winterbottom H.R., Bourassa M.A. // 2010 IEEE International Geoscience and Remote Sensing Symposium (IGARSS). - Honolulu, HI, 25-30 July 2010. - P. 4154-4157. ↑
- C2255.** Adam N. Multi beam joined estimation for persistent scatterer interferometry. / Adam N., Gernhardt S., Eineder M., Bamler R. // 2010 IEEE International Geoscience and Remote Sensing Symposium (IGARSS). - Honolulu, HI, 25-30 July 2010. - P. 4403-4406. ↑
- C2256.** Tiangang Yin. Iterative calibration of relative platform position: A new method for SAR baseline estimation. / Tiangang Yin, Christophe E., Soo Chin Liew, Sim Heng Ong. // 2010 IEEE International Geoscience and Remote Sensing Symposium (IGARSS). - Honolulu, HI, 25-30 July 2010. - P. 4407-4410. ↑
- C2257.** Lachaise M. Multibaseline gradient ambiguity resolution to support Minimum Cost Flow Phase Unwrapping. / Lachaise M., Bamler R., Gonzalez F.R. // 2010 IEEE International Geoscience and Remote Sensing Symposium (IGARSS). - Honolulu, HI, 25-30 July 2010. - P. 4411-4414. ↑
- C2258.** Kenyon C.M. Range-Doppler ambiguity mitigation via closed-loop, adaptive PRF selection. / Kenyon C.M., Goodman N.A. // 2010 International Conference on Electromagnetics in Advanced Applications (ICEAA). - Sydney, NSW, 20-24 Sept. 2010. - P. 608-611. ↑
- C2259.** Sahin E. Performance of cell averaging constant false alarm rate (CA-CFAR) processors for M-correlated sweeps in multiple target environments. / Sahin E., Uner M. // 2010 IEEE 18th Signal Processing and Communications Applications Conference (SIU). - Diyarbakir, 22-24 April 2010. - P. 479-482. ↑
- C2260.** Borzi. Phase retrieval in SAR interferograms using diffusion and inpainting. / Borzi, A., Di Bisceglie M., Galdi C., Pallotta L., Uilo S.L. // 2010 IEEE International Geoscience and Remote Sensing Symposium (IGARSS). - Honolulu, HI, 25-30 July 2010. - P. 2912-2915. ↑
- C2261.** Sog. Successive cancelation approach for Doppler frequency estimation in pulse Doppler radar systems. / Sog,anci, H., Gezici S. // 2010 IEEE 18th Signal Processing and Communications Applications Conference (SIU). - Diyarbakir, 22-24 April 2010. - P. 348-351. ↑
- C2262.** Ben Khadra S. The bistatic electromagnetic signature of heterogeneous sea surface: Study of the hydrodynamic phenomena. / Ben Khadra S., Khenchaf A. // 2010 IEEE International Geoscience and Remote Sensing Symposium (IGARSS). - Honolulu, HI, 25-30 July 2010. - P. 3549-3552. ↑
- C2263.** Yanfang Dong. Disaster mapping from medium spatial resolution alos palsar images. / Yanfang Dong, Qi Li, Aixia Dou, Xiaoqing Wang. // 2010 IEEE International Geoscience and Remote Sensing Symposium (IGARSS). - Honolulu, HI, 25-30 July 2010. - P. 2167-2170. ↑
- C2264.** Xuetong Xie. A modified wind vector retrieval algorithm for polarimetric scatterometer. / Xuetong Xie, Mingsen Lin, Zhou Huang, Juhong Zou, Dongxuan Tian, Lixia Liu, Xiaoning Wang, Shiwei Dong. // 2010 IEEE International Geoscience and Remote Sensing Symposium (IGARSS). - Honolulu, HI, 25-30 July 2010. - P. 4184-4187. ↑


- C2265.** Caltagirone F. Status, results, potentiality and evolution of COSMO-SkyMed, the Italian Earth Observation constellation for risk management and security. / Caltagirone F., De Luca G., Covello F., Marano G., Angino G., Piemontese M. // 2010 IEEE International Geoscience and Remote Sensing Symposium (IGARSS). - Honolulu, HI, 25-30 July 2010. - P. 4393-4396. ↑
- C2266.** Covello F. One-day interferometry results with the COSMO-SkyMed constellation. / Covello F., Battazza F., Coletta A., Battagliere M.L., Bellifemine V., Candela L. // 2010 IEEE International Geoscience and Remote Sensing Symposium (IGARSS). - Honolulu, HI, 25-30 July 2010. - P. 4397-4400. ↑
- C2267.** Tao Li. Comparison of Beijing-Tianjin Intercity Railway deformation monitoring results between ASAR and PALSAR data. / Tao Li, Zhang Hong, Wang Chao, Tang Yixian. // 2010 IEEE International Geoscience and Remote Sensing Symposium (IGARSS). - Honolulu, HI, 25-30 July 2010. - P. 3514-3517. ↑
- C2268.** Yongfei Mao. The mathematic model of multipath error in airborne interferometric SAR system. / Yongfei Mao, Maosheng Xiang, Lideng Wei, Songtao Han. // 2010 IEEE International Geoscience and Remote Sensing Symposium (IGARSS). - Honolulu, HI, 25-30 July 2010. - P. 2904-2907. ↑
- C2269.** Liming Jiang. Detection of rapid land subsidence of civil constructions with TerraSAR-X interferometry. / Liming Jiang, Hui Lin, Baoqiang Xiang. // 2010 IEEE International Geoscience and Remote Sensing Symposium (IGARSS). - Honolulu, HI, 25-30 July 2010. - P. 3510-3513. ↑
- C2270.** Can M.M. CFAR detection based on decision fusion of order statistic CFAR and order statistic clutter map CFAR processors. / Can M.M., Ujner M. // 2010 IEEE 18th Signal Processing and Communications Applications Conference (SIU). - Diyarbakir, 22-24 April 2010. - P. 558-561. ↑
- C2271.** Brcic R. Estimation and compensation of ionospheric delay for SAR interferometry. / Brcic R., Parizzi A., Eineder M., Bamler R., Meyer F. // 2010 IEEE International Geoscience and Remote Sensing Symposium (IGARSS). - Honolulu, HI, 25-30 July 2010. - P. 2908-2911. ↑
- C2272.** Cao Jinkun. Two-Thresholds CFAR detection of the range-spread target based on scattering centers accumulation. / Cao Jinkun, Yan Hang, Chen Gang. // 2010 IEEE 10th International Conference on Signal Processing (ICSP). - Beijing, 24-28 Oct. 2010. - P. 2307-2311. ↑
- C2273.** Xiao-peng Zhu. ISAR imaging analysis of Bistatic FMCW radar. / Xiao-peng Zhu, Qun Zhang, Hongwei Li. // 2010 9th International Symposium on Antennas Propagation and EM Theory (ISAPE). - Guangzhou, Nov. 29 2010-Dec. 2 2010. - P. 540-543. ↑
- C2274.** Guang-cheng Li. Simulation modelling the GPS signal propagation in the tropospheric ducts. / Guang-cheng Li, Li-xin Guo, Yu Liang. // 2010 9th International Symposium on Antennas Propagation and EM Theory (ISAPE). - Guangzhou, Nov. 29 2010-Dec. 2 2010. - P. 592-595. ↑
- C2275.** Xiaolin Yang. A fast and robust method for target and background estimation in RCS measurements based on 'hyperaccurate' algebraic circle fit. / Xiaolin Yang, Shaohui Quan, Qinghui Liu. // 2010 9th International Symposium on Antennas Propagation and EM Theory (ISAPE). - Guangzhou, Nov. 29 2010-Dec. 2 2010. - P. 622-625. ↑
- C2276.** Xue Li. An improved PGA algorithm for ionosphere phase perturbation correction. / Xue Li, Wei-bo Deng, Pei-nan Jiao, Yong-Li Ji. // 2010 9th International Symposium on Antennas Propagation and EM Theory (ISAPE). - Guangzhou, Nov. 29 2010-Dec. 2 2010. - P. 426-429. ↑
- C2277.** Hong-Bo Zhang. Comparison of TEC measurements from DORIS with the NeQuick model. / Hong-Bo Zhang, Ming Ou, Wei-Min Zhen. // 2010 9th International Symposium on Antennas Propagation and EM Theory (ISAPE). - Guangzhou, Nov. 29 2010-Dec. 2 2010. - P. 469-472. ↑
- C2278.** Yang Ruike. Influence of rain Doppler frequency on MMW Doppler fuze. / Yang Ruike, Li Lei, Zhong Pu, Liu Kexiang. // 2010 9th International Symposium on Antennas Propagation and EM Theory (ISAPE). - Guangzhou, Nov. 29 2010-Dec. 2 2010. - P. 521-524. ↑
- C2279.** Haipeng Wang. A novel polarimetric FM-CW radar system for laboratory remote sensing experiments. / Haipeng Wang, Ya-Qiu Jin. // 2010 9th International Symposium on Antennas Propagation and EM Theory (ISAPE). - Guangzhou, Nov. 29 2010-Dec. 2 2010. - P. 662-665. ↑


- C2280.** Yu-Xin Sun. Application of AWE to scattering analysis of the double-negative medium. / Yu-Xin Sun, Ming-Sheng Chen, Xian-liang Wu, Mei Yang, Hui Wang. // 2010 9th International Symposium on Antennas Propagation and EM Theory (ISAPE). - Guangzhou, Nov. 29 2010-Dec. 2 2010. - P. 913-916. ↑
- C2281.** Lakshmi S.L. Doppler profile estimation in VHF radar signals using wavelets. / Lakshmi S.L., Kanth V.R., Rajan S.V., Reddy A.S.R. // 2010 International Conference on Signal and Image Processing (ICSIP). - Chennai, 15-17 Dec. 2010. - P. 243-249. ↑
- C2282.** Jin Bong Kim. Influence of the CNT length on complex permittivity of composite laminates and on radar absorber design in X-band. / Jin Bong Kim, Jun Hyung Byun. // 2010 10th IEEE Conference on Nanotechnology (IEEE-NANO). - Seoul, 17-20 Aug. 2010. - P. 635-638. ↑
- C2283.** Qiang Lei. High resolution radar imaging based on compressed sensing using sparse stepped-frequency signal. / Qiang Lei, Hongwei Li, Qun Zhang, Feng Zhu, Xi Wen. // 2010 9th International Symposium on Antennas Propagation and EM Theory (ISAPE). - Guangzhou, Nov. 29 2010-Dec. 2 2010. - P. 670-674. ↑
- C2284.** Xue Li. Algorithm optimization of piecewise polynomial modeling for ionospheric perturbation correction. / Xue Li, Wei-bo Deng, Pei-nan Jiao, Yong-Li Ji. // 2010 9th International Symposium on Antennas Propagation and EM Theory (ISAPE). - Guangzhou, Nov. 29 2010-Dec. 2 2010. - P. 802-805. ↑
- C2285.** Yi-cai Mei. Numerical simulation of GPR based on 3-D high-order FDTD. / Yi-cai Mei, Zhi-xiang Huang, Xian-liang Wu, Xin-gang Ren, Hong-mei Du. // 2010 9th International Symposium on Antennas Propagation and EM Theory (ISAPE). - Guangzhou, Nov. 29 2010-Dec. 2 2010. - P. 872-875. ↑
- C2286.** Yue-Feng Tan. Impacts of velocity deviation on spaceborne high-resolution DPCA SAR. / Yue-Feng Tan, Zhu Xueyong, Wen-Qin Wang. // 2010 International Conference on Computational Problem-Solving (ICCP). - Lijiang, 3-5 Dec. 2010. - P. 442-445. ↑
- C2287.** Hui He. A New Method of Bridge Target Detection on ASAR Imagery. / Hui He, Kun Liu. // 2010 International Conference on Multimedia Communications (Mediacom). - Hong Kong, 7-8 Aug. 2010. - P. 35-38. ↑
- C2288.** Bian Xiaolin. MATLAB COM Component in Radar Signal Processing Application Development. / Bian Xiaolin, Wang Jinbo. // 2010 International Conference on Information Management, Innovation Management and Industrial Engineering (ICIII). - Kunming, 26-28 Nov. 2010. - Vol. 4. - P. 397-399. ↑
- C2289.** Wei Zhao. An efficient approach for near-field three-dimensional imaging radar. / Wei Zhao, Jingye Cai, Wen-Qin Wang. // 2010 International Conference on Computational Problem-Solving (ICCP). - Lijiang, 3-5 Dec. 2010. - P. 43-46. ↑
- C2290.** Newell A.J. Texture-Based Estimation of Physical Characteristics of Sand Grains. / Newell A.J., Griffin L.D., Morgan R.M., Bull P.A. // 2010 International Conference on Digital Image Computing: Techniques and Applications (DICTA). - Sydney, NSW, 1-3 Dec. 2010. - P. 504-509. ↑
- C2291.** Kyu-Ha Song. Pulse Repetition Interval Modulation Recognition Using Symbolization. / Kyu-Ha Song, Dong-Weon Lee, Jin-Woo Han, Byung-Koo Park. // 2010 International Conference on Digital Image Computing: Techniques and Applications (DICTA). - Sydney, NSW, 1-3 Dec. 2010. - P. 540-545. ↑
- C2292.** Marsh R. Mining Heterogeneous ADS-B Data Sets for Probabilistic Models of Pilot Behavior. / Marsh R., Ogaard K. // 2010 IEEE International Conference on Data Mining Workshops (ICDMW). - Sydney, NSW, 13-13 Dec. 2010. - P. 606-612. ↑
- C2293.** Kan Ee May. Evolutionary approach for trajectory generation of unmanned aerial vehicles (UAVs) over hostile terrain. / Kan Ee May, Ho Jiun Sien, Yeo Swee Ping, Shao Zhen Hai. // 2010 International Conference on Computational Problem-Solving (ICCP). - Lijiang, 3-5 Dec. 2010. - P. 51-54. ↑
- C2294.** Liu Zhong-xuan. Research on remote wireless monitoring system based on GPRS and MCU. / Liu Zhong-xuan, Jiang Xiao-yu, Han Zhao-fu, Zong Yan-tao, Du Meng. // 2010 International Conference on Computational Problem-Solving (ICCP). - Lijiang, 3-5 Dec. 2010. - P. 392-394. ↑
- C2295.** Wang Z.K. A study on optical reflectivity of laser treated aircraft surfaces. / Wang Z.K., Lim M.H., Zheng H.Y. // 2010 International Conference on Computational Problem-Solving (ICCP). - Lijiang, 3-5 Dec. 2010. ↑


- P. 275-278. 


**C2296.** Wang Jun. Research and implementation of dechirp pulse compression processing algorithm. / Wang Jun, Jiang Hai, Zhang Yuxi, Yao Wang. // 2010 International Conference on Computational Problem-Solving (ICCP). - Lijiang, 3-5 Dec. 2010. - P. 428-431. 


**C2297.** Kan Ee May. An evolutionary algorithm for multiple waypoints planning with B-spline trajectory generation for Unmanned Aerial Vehicles (UAVs). / Kan Ee May, Ho Jiun Sien, Yeo Swee Ping, Shao Zhen Hai. // 2010 International Conference on Computational Problem-Solving (ICCP). - Lijiang, 3-5 Dec. 2010. - P. 77-81. 


**C2298.** Shi-Zheng Zhao. Multi-objective design of monopulse antenna with Two-lbests based multi-objective particle swarm optimizer. / Shi-Zheng Zhao, Suganthan P.N., Pal S., Basak A., Das S. // 2010 International Conference on Computational Problem-Solving (ICCP). - Lijiang, 3-5 Dec. 2010. - P. 209-214. 


**C2299.** Li Xinchun. The design of granary environmental monitoring system based on ARM9 and ZigBee. / Li Xinchun, Wang Na. // 2010 International Conference on Computational Problem-Solving (ICCP). - Lijiang, 3-5 Dec. 2010. - P. 395-398. 


**C2300.** Yurduseven O. Convex parabolic reflector antenna design with cosecant-squared radiation pattern for microwave radar systems. / Yurduseven O., Tujrk A.S. // 2010 National Conference on Electrical, Electronics and Computer Engineering (ELECO). - Bursa, 2-5 Dec. 2010. - P. 469-473. 


**C2301.** Xinyin Huang. A novel application for sum-difference pattern detection of signal direction using time-modulated linear arrays. / Xinyin Huang, Shiwen Yang, Gang Li, Zaiping Nie. // 2010 International Symposium on Intelligent Signal Processing and Communication Systems (ISPACS). - Chengdu, 6-8 Dec. 2010. - P. 1-4. 


**C2302.** Li XueHua. Design of an ocean atmospheric duct signal processor. / Li XueHua, He ZiShu, He JianXin, Duan ShouYuan. // 2010 International Symposium on Intelligent Signal Processing and Communication Systems (ISPACS). - Chengdu, 6-8 Dec. 2010. - P. 1-4. 


**C2303.** Meifang Luo. Adaptive pulse compression via maximum signal minus interference level in clutter environments. / Meifang Luo, Lingjiang Kong. // 2010 International Symposium on Intelligent Signal Processing and Communication Systems (ISPACS). - Chengdu, 6-8 Dec. 2010. - P. 1-4. 


**C2304.** Gerrits J.F.M. A low-complexity C-band radar for non-invasive respiration measurement. / Gerrits J.F.M., Vetter R., Farserotu J.R., Hennemann C., Hubner M., Decotignie J. // 2010 3rd International Symposium on Applied Sciences in Biomedical and Communication Technologies (ISABEL). - Rome, 7-10 Nov. 2010. - P. 1-5. 


**C2305.** Sun Qing. Evaluation to the performance of MTI radar anti-passive jamming. / Sun Qing, Zhang Qi-liang, Sun Yong. // IET 3rd International Conference on Wireless, Mobile and Multimedia Networks (ICWMNN 2010). - Beijing, China, 26-29 Sept. 2010. - P. 282-284. 

**C2306.** Yingbo Hua. Subspace in signal processing and communications. 2010 International Symposium on Intelligent Signal Processing and Communication Systems (ISPACS). - Chengdu, 6-8 Dec. 2010. - P. 1. 

**C2307.** Rui Min. Design of SAR tomography experimental system. / Rui Min, Honglin Long, Jinfeng Wang. // 2010 International Symposium on Intelligent Signal Processing and Communication Systems (ISPACS). - Chengdu, 6-8 Dec. 2010. - P. 1-4. 

**C2308.** Sun Ying. Binary orthogonal code design for MIMO radar systems. / Sun Ying, Zishu He, Hongming Liu, Li Jun, Shangwei Gao. // 2010 International Symposium on Intelligent Signal Processing and Communication Systems (ISPACS). - Chengdu, 6-8 Dec. 2010. - P. 1-4. 

**C2309.** Chao Li. Parameter selection of MIMO radar under the long time integration. / Chao Li, Hongming Liu, Jun Li, Huiyong Li, Bin Wu. // 2010 International Symposium on Intelligent Signal Processing and Communication Systems (ISPACS). - Chengdu, 6-8 Dec. 2010. - P. 1-4. 

**C2310.** Yongzhe Li. A model of non-coherent airborne MIMO space-time adaptive processing radar. / Yongzhe Li, Zishu He, Jun Li, Huiyong Li, Hongming Liu. // 2010 International Symposium on Intelligent Signal Processing and Communication Systems (ISPACS). - Chengdu, 6-8 Dec. 2010. - P. 1-4. 



- C2311.** Yu Lu. A novel airport surface surveillance based on multi-video fusion. / Yu Lu, Changzhong Liu, Zhengning Wang, Honggang Wu. // 2010 International Symposium on Intelligent Signal Processing and Communication Systems (ISPACS). - Chengdu, 6-8 Dec. 2010. - P. 1-4. ↑
- C2312.** Qi yang. Analysis of anti-interception performance of MIMO radar. / Qi yang, Li jun, Liu hongming, Li huiyong. // 2010 International Symposium on Intelligent Signal Processing and Communication Systems (ISPACS). - Chengdu, 6-8 Dec. 2010. - P. 1-3. ↑
- C2313.** Yun Zhou. Enhanced supervised neighborhood preserving embedding for radar target recognition. / Yun Zhou, Xuelian Yu, Minglei Cui, Xuegang Wang. // 2010 International Symposium on Intelligent Signal Processing and Communication Systems (ISPACS). - Chengdu, 6-8 Dec. 2010. - P. 1-4. ↑
- C2314.** Lakshmanan M.K. On the edge based artifact mitigation in wavelet packet transform for enhancement of spectral estimation. / Lakshmanan M.K., Ariananda D.D., Nikookar H. // 2010 3rd International Symposium on Applied Sciences in Biomedical and Communication Technologies (ISABEL). - Rome, 7-10 Nov. 2010. - P. 1-5. ↑
- C2315.** Kumar K.S. Evolutionary Computational Tools Aided Extended Kalman Filter for Ballistic Target Tracking. / Kumar K.S., Dustakar N.R., Jatoth R.K. // 2010 3rd International Conference on Emerging Trends in Engineering and Technology (ICETET). - Goa, 19-21 Nov. 2010. - P. 588-593. ↑
- C2316.** Khan S.A. Frequency based oscilloscope triggering scheme. / Khan S.A., Nigam A., Agarwala A.K., Thomas M.S. // 2010 International Conference on Power, Control and Embedded Systems (ICPCES). - Allahabad, Nov. 29 2010-Dec. 1 2010. - P. 1-5. ↑
- C2317.** van Dijk F. Quantum dash mode-locked lasers for millimeter wave signal generation and transmission. / van Dijk F., Charbonnier B., Constant S., Enard A., Fedderwitz S., Formont S., Lealman I.F., Lecoche F., Lelarge F., Moodie D., Ponnampalam L., Renaud C., Robertson M.J., Seeds A.J., Stojhr A., Weiss M. // 2010 23rd Annual Meeting of the IEEE Photonics Society. - Denver, CO, 7-11 Nov. 2010. - P. 187-188. ↑
- C2318.** Yurduseven O. Radar cross section analysis of various objects and RCS optimisation. / Yurduseven O., Yurduseven O., Turk A.S. // 2010 National Conference on Electrical, Electronics and Computer Engineering (ELECO). - Bursa, 2-5 Dec. 2010. - P. 474-478. ↑
- C2319.** Buddendick H. Parallelized Physical Optics computations for Scattering Center Models in radio channel simulations. / Buddendick H., Eibert T.F. // 2010 IEEE Vehicular Networking Conference (VNC). - Jersey City, NJ, 13-15 Dec. 2010. - P. 64-71. ↑
- C2320.** Manavalan M. Emerging Trends of Computational Grid Based Near Real Time/Real Time Flood Assessment and Forecasting Models. / Manavalan M., Chattopadhyay S., Mangala M., Rao Y.S. // 2010 3rd International Conference on Emerging Trends in Engineering and Technology (ICETET). - Goa, 19-21 Nov. 2010. - P. 471-475. ↑
- C2321.** Zee A. Advantage of non-etching adhesion promoter on high frequency signal loss. / Zee A., Massey R. // 2010 5th International Microsystems Packaging Assembly and Circuits Technology Conference (IMPACT). - Taipei, 20-22 Oct. 2010. - P. 1-4. ↑
- C2322.** Zheng Zhe. The Application of MPI-TigerSHARC in SAR Processing System. / Zheng Zhe, Yuan Li, Li Hai. // 2010 International Conference on Digital Manufacturing and Automation (ICDMA). - ChangSha, 18-20 Dec. 2010. - Vol. 2. - P. 625-628. ↑
- C2323.** Padaki A.V. A Novel Application of Support Vector Machines to Detect Targets. / Padaki A.V., George K. // 2010 Second International Conference on Computational Intelligence, Modelling and Simulation (CIMSIM). - Bali, 28-30 Sept. 2010. - P. 3-8. ↑
- C2324.** Amiri R. FFT Simulation and Implementation in TMS 320C6713. / Amiri R., Gholamian M., Alaee M. // 2010 Second International Conference on Computational Intelligence, Modelling and Simulation (CIMSIM). - Bali, 28-30 Sept. 2010. - P. 321-325. ↑
- C2325.** Chien-Cheng Lee. Coin insertion technology for PCB thermal solution. / Chien-Cheng Lee, Wu-Yung Chen. // 2010 5th International Microsystems Packaging Assembly and Circuits Technology Conference (IMPACT). - Taipei, 20-22 Oct. 2010. - P. 1-4. ↑

- C2326.** Paul M.K. UWB microwave imaging via modified beamforming for early detection of breast cancer. / Paul M.K., Sagar M.A.K., Hussain S.U., Rashid A.B.M.H. // 2010 International Conference on Electrical and Computer Engineering (ICECE). - Dhaka, 18-20 Dec. 2010. - P. 642-645. ↑
- C2327.** Zhang Yaping. Dynamical Weather Radar Beam Blockage Correction. / Zhang Yaping, Cheng Minghu. // 2010 International Conference on Digital Manufacturing and Automation (ICDMA). - ChangSha, 18-20 Dec. 2010. - Vol. 1. - P. 593-596. ↑
- C2328.** Seng C.H. Fuzzy Logic-Based Image Fusion for Multi-view Through-the-Wall Radar. / Seng C.H., Bouzerdoum A., Tivive F.H.C., Amin M.G. // 2010 International Conference on Digital Image Computing: Techniques and Applications (DICTA). - Sydney, NSW, 1-3 Dec. 2010. - P. 423-428. ↑
- C2329.** Yunfei Guo. Low Altitude Target Tracking Algorithm with Acoustic Wireless Sensor Network. / Yunfei Guo, Anke Xue, Hongyang Chen, Huajie Chen, Sezaki K. // 2010 IEEE Global Telecommunications Conference GLOBECOM 2010. - Miami, FL, 6-10 Dec. 2010. - P. 1-5. ↑
- C2330.** Qilian Liang. Compressive Sensing for Radar Sensor Networks. 2010 IEEE Global Telecommunications Conference GLOBECOM 2010. - Miami, FL, 6-10 Dec. 2010. - P. 1-5. ↑
- C2331.** Surender S.C. Performance Analysis of Communications & Radar Coexistence in a Covert UWB OSA System. / Surender S.C., Narayanan R.M., Das C.R. // 2010 IEEE Global Telecommunications Conference GLOBECOM 2010. - Miami, FL, 6-10 Dec. 2010. - P. 1-5. ↑
- C2332.** Jervis M. Advances in DSP design tool flows for FPGAs. 2010-MILCOM 2010 MILITARY COMMUNICATIONS CONFERENCE. - San Jose, CA, Oct. 31 2010-Nov. 3 2010. - P. 2041-2046. ↑
- C2333.** Trincherо D. Innovative ad-hoc wireless sensor networks to significantly reduce leakages in underground water infrastructures. / Trincherо D., Stefanelli R., Cisoni L., Kadri A., Abu-Dayya A., Hasna M., Khattab T. // 2010 ITU-T Kaleidoscope: Beyond the Internet?-Innovations for Future Networks and Services. - Pune, 13-15 Dec. 2010. - P. 1-4. ↑
- C2334.** Lei Xu. Waveform Design and Optimization in Radar Sensor Network. / Lei Xu, Qilian Liang. // 2010 IEEE Global Telecommunications Conference GLOBECOM 2010. - Miami, FL, 6-10 Dec. 2010. - P. 1-5. ↑
- C2335.** Zhi-Qiang Wei. Extraction method of large-scale linear objects from SAR images. / Zhi-Qiang Wei, Lin Hui, Shi Chaojian, Peng Jing, Chen Fulong. // 2010 International Conference on Audio Language and Image Processing (ICALIP). - Shanghai, 23-25 Nov. 2010. - P. 1552-1556. ↑
- C2336.** A-lei Chen. An improved BP algorithm for high-resolution MIMO imaging radar. / A-lei Chen, Dang-wei Wang, Xiao-yan Ma. // 2010 International Conference on Audio Language and Image Processing (ICALIP). - Shanghai, 23-25 Nov. 2010. - P. 1663-1667. ↑
- C2337.** Yin Ye. Design of World Expo tour sites guide system based on RFID technology. / Yin Ye, Zhou Jun, Yin Jian. // 2010 International Conference on Audio Language and Image Processing (ICALIP). - Shanghai, 23-25 Nov. 2010. - P. 1026-1030. ↑
- C2338.** Zeng Liang. Implementation of battlefield electromagnetic environment ontology visualization system. / Zeng Liang, Meng Fan-feng. // 2010 International Conference on Audio Language and Image Processing (ICALIP). - Shanghai, 23-25 Nov. 2010. - P. 1002-1006. ↑
- C2339.** Chen Liang. Extraction of wetland combining with Radarsat and HJ data of Yellow River Delta. / Chen Liang, Liu Xuegong, He Houjun, Han Lin. // 2010 International Conference on Audio Language and Image Processing (ICALIP). - Shanghai, 23-25 Nov. 2010. - P. 1614-1618. ↑
- C2340.** Fei Wang. A visualization method of measuring the effectiveness of early warning and detection network based on simulation. / Fei Wang, Guang-ya Si, Zhen-bao Dong, Zheng Wang, Meng Shang. // 2010 International Conference on Audio Language and Image Processing (ICALIP). - Shanghai, 23-25 Nov. 2010. - P. 1366-1371. ↑
- C2341.** Chen Yang. Research on imaging simulation of airborne fire control radar for simulated training. / Chen Yang, Ji Gang, Sun Wen-zhu, Sun Zhong-yun, Liu Yun-xiang. // 2010 International Conference on Audio Language and Image Processing (ICALIP). - Shanghai, 23-25 Nov. 2010. - P. 1356-1360. ↑

- C2342.** Pilaud W. High performance element computing architecture. 2010-MILCOM 2010 MILITARY COMMUNICATIONS CONFERENCE. - San Jose, CA, Oct. 31 2010-Nov. 3 2010. - P. 2035-2040. ↑
- C2343.** Ahmed K. Subspace compressive GLRT detector for airborne MIMO Radar. / Ahmed K., Kothuri S., Patwary M., Abdel-Maguid M. // 2010 16th Asia-Pacific Conference on Communications (APCC). - Auckland, Oct. 31 2010-Nov. 3 2010. - P. 302-306. ↑
- C2344.** de Barros Barrete A. Using a P2P architecture for voice and radar transportation in critical command and control systems. / de Barros Barrete A., Yano E.T. // 2010-MILCOM 2010 MILITARY COMMUNICATIONS CONFERENCE. - San Jose, CA, Oct. 31 2010-Nov. 3 2010. - P. 1169-1174. ↑
- C2345.** Naraghi-Pour M. CELP-like compression of spotlight-mode SAR raw data in transform domain. / Naraghi-Pour M., Cortez R., Ikuma T., Lewis T. // 2010-MILCOM 2010 MILITARY COMMUNICATIONS CONFERENCE. - San Jose, CA, Oct. 31 2010-Nov. 3 2010. - P. 870-874. ↑
- C2346.** Andrei V. A software demonstrator for IEEE 802.21 Media Independent Handover in heterogenous networks. / Andrei V., Popovici E.C., Fratu O., Halunga S. // 2010 9th International Symposium on Electronics and Telecommunications (ISETC). - Timisoara, 11-12 Nov. 2010. - P. 199-204. ↑
- C2347.** Seong Pal Kang. Design of mine detection robot for Korean mine field. / Seong Pal Kang, Junho Choi, Seung-Beum Suh, Sungchul Kang. // 2010 IEEE Workshop on Advanced Robotics and its Social Impacts (ARSO). - Seoul, 26-28 Oct. 2010. - P. 53-56. ↑
- C2348.** Kyunghoon Kim. Intelligent surveillance and security robot systems. / Kyunghoon Kim, Soonil Bae, Kwanghak Huh. // 2010 IEEE Workshop on Advanced Robotics and its Social Impacts (ARSO). - Seoul, 26-28 Oct. 2010. - P. 70-73. ↑
- C2349.** de Arriba-Ruiz I. Multipath reflectivity estimation in urban environments for Synthetic Aperture Radar images. / de Arriba-Ruiz I., Perez-Martinez F., Munioz-Ferreras J.M. // 2010-MILCOM 2010 MILITARY COMMUNICATIONS CONFERENCE. - San Jose, CA, Oct. 31 2010-Nov. 3 2010. - P. 864-869. ↑
- C2350.** Ting He. Multi-target tracking using proximity sensors. / Ting He, Bisdikian C., Kaplan L., Wei Wei, Towsley D. // 2010-MILCOM 2010 MILITARY COMMUNICATIONS CONFERENCE. - San Jose, CA, Oct. 31 2010-Nov. 3 2010. - P. 1777-1782. ↑
- C2351.** Ohs R.R. Modeling the effects of wind turbines on radar returns. / Ohs R.R., Skidmore G.J., Bedrosian G. // 2010-MILCOM 2010 MILITARY COMMUNICATIONS CONFERENCE. - San Jose, CA, Oct. 31 2010-Nov. 3 2010. - P. 272-276. ↑
- C2352.** Mills S. High availability and fault management in Objective Architecture systems. 2010-MILCOM 2010 MILITARY COMMUNICATIONS CONFERENCE. - San Jose, CA, Oct. 31 2010-Nov. 3 2010. - P. 2304-2309. ↑
- C2353.** Godrich H. Power allocation schemes for target localization in widely distributed MIMO radar systems. / Godrich H., Petropulu A., Poor H.V. // 2010-MILCOM 2010 MILITARY COMMUNICATIONS CONFERENCE. - San Jose, CA, Oct. 31 2010-Nov. 3 2010. - P. 846-851. ↑
- C2354.** Yao Yu. Robust target estimation in compressive sensing based colocated MIMO radar. / Yao Yu, Athina P.P., Poor H.V. // 2010-MILCOM 2010 MILITARY COMMUNICATIONS CONFERENCE. - San Jose, CA, Oct. 31 2010-Nov. 3 2010. - P. 852-857. ↑
- C2355.** Lee M. Analog auto-correlation based receiver architecture for radar systems. / Lee M., Beck S., Kyutae Lim, Laskar J. // 2010-MILCOM 2010 MILITARY COMMUNICATIONS CONFERENCE. - San Jose, CA, Oct. 31 2010-Nov. 3 2010. - P. 842-845. ↑
- C2356.** Zhiqiang Li. Visual data mining analysis for information operations in complicated information environment. / Zhiqiang Li, Guanya Si, Tuohuang Guo, Xi Wu, Jingyu Yang, Runtao Hu, Fei Wang. // 2010 International Conference on Audio Language and Image Processing (ICALIP). - Shanghai, 23-25 Nov. 2010. - P. 969-974. ↑
- C2357.** Xu Lijia. Studying on state prediction for radar transmitter using GM(1,1). / Xu Lijia, Kang ZhiLiang. // 2010 2nd International Conference on Information Science and Engineering (ICISE). - Hangzhou, China, 4-6 Dec. 2010. - P. 5462-5465. ↑

- C2358.** Jiansheng Fu. Synthetical Generalized Discriminant Analysis for radar HRRP target recognition. / Jiansheng Fu, Kuo Liao, Wanlin Yang. // 2010 2nd International Conference on Information Science and Engineering (ICISE). - Hangzhou, China, 4-6 Dec. 2010. - P. 4106-4109. ↑
- C2359.** Xu Wei. A parameter estimation method for polyphase codes using time-frequency distribution. / Xu Wei, Chen Mao, Zhang Guan Jie. // 2010 2nd International Conference on Information Science and Engineering (ICISE). - Hangzhou, China, 4-6 Dec. 2010. - P. 4870-4874. ↑
- C2360.** Zhilong Zhao. Removing multiplicative noise by improved regularization term. / Zhilong Zhao, Xiaoqing Shang. // 2010 2nd International Conference on Information Science and Engineering (ICISE). - Hangzhou, China, 4-6 Dec. 2010. - P. 1405-1408. ↑
- C2361.** Lutao Liu. Fast algorithm for direction of arrival based on time-frequency distributions. / Lutao Liu, Ligu Wang. // 2010 IEEE International Conference on Information Theory and Information Security (ICITIS). - Beijing, 17-19 Dec. 2010. - P. 772-775. ↑
- C2362.** Li Xue. Research on robust unscented regularized particle filtering. / Li Xue, Shesheng Gao, Jianchao Wang. // 2010 IEEE International Conference on Information Theory and Information Security (ICITIS). - Beijing, 17-19 Dec. 2010. - P. 790-793. ↑
- C2363.** Zakrzewski M. Separating respiration artifact in microwave doppler radar heart monitoring by Independent Component Analysis. / Zakrzewski M., Vanhala J. // 2010 IEEE Sensors. - Kona, HI, 1-4 Nov. 2010. - P. 1368-1371. ↑
- C2364.** Jime. Performance Characterization Parameters on Voice and Data Transmission in Mobile Terminals to Cellular Networks. / Jime, nez-Licea M., Vidal-Beltra, n S., Lopez-Bonilla J.L. // 2010 Electronics, Robotics and Automotive Mechanics Conference (CERMA). - Morelos, Sept. 28 2010-Oct. 1 2010. - P. 220-224. ↑
- C2365.** Kennedy H.L. An Efficient Frequency-Domain Velocity-Filter Implementation for Dim Target Detection. 2010 International Conference on Digital Image Computing: Techniques and Applications (DICTA). - Sydney, NSW, 1-3 Dec. 2010. - P. 39-44. ↑
- C2366.** Awrangjeb M. Automatic Building Detection Using LIDAR Data and Multispectral Imagery. / Awrangjeb M., Ravanbakhsh M., Fraser C.S. // 2010 International Conference on Digital Image Computing: Techniques and Applications (DICTA). - Sydney, NSW, 1-3 Dec. 2010. - P. 45-51. ↑
- C2367.** Preradovic S. Chipless RFID tag with integrated sensor. / Preradovic S., Karmakar N. // 2010 IEEE Sensors. - Kona, HI, 1-4 Nov. 2010. - P. 1277-1281. ↑
- C2368.** Hallil H. Feasibility of wireless gas detection with an FMCW RADAR interrogation of passive RF gas sensor. / Hallil H., Chebila F., Menini P., Pons P., Aubert H. // 2010 IEEE Sensors. - Kona, HI, 1-4 Nov. 2010. - P. 759-762. ↑
- C2369.** Wei Zhang. Indoor location estimation system based on evolutionary matching. / Wei Zhang, Congfeng Jiang, Xindong You, Yunfa Li, Peijun Liu. // 2010 2nd International Conference on Information Science and Engineering (ICISE). - Hangzhou, China, 4-6 Dec. 2010. - P. 4570-4573. ↑
- C2370.** Zhoujie Yan. On the application of ethernet in a distributed radar system. / Zhoujie Yan, Qiongzhi Wu, Fang Nan. // 2010 IEEE International Conference on Information Theory and Information Security (ICITIS). - Beijing, 17-19 Dec. 2010. - P. 678-681. ↑
- C2371.** Mythili P. A Multi-Objective Antenna Placement Genetic Algorithm for matched array synthesis on complex platforms. / Mythili P., Osoba P.E., Michielssen E. // 2010 IEEE International Conference on Communication Systems (ICCS). - Singapor, 17-19 Nov. 2010. - P. 109-112. ↑
- C2372.** Jainen U. Multi-object tracking using feed-forward neural networks. / Jainen U., Paul C., Wittke M., Hahner J. // 2010 International Conference of Soft Computing and Pattern Recognition (SoCPaR). - Paris, 7-10 Dec. 2010. - P. 176-181. ↑
- C2373.** Nishimoto M. Inverse filtering operation for reconstruction of distorted GPR response. / Nishimoto M., Tomura K. // TENCON 2010-2010 IEEE Region 10 Conference. - Fukuoka, 21-24 Nov. 2010. - P. 2036-2039. ↑



- C2374.** Zhijie Mao. Robust adaptive coregistration of InSAR images using multisource information and joint data fusion. / Zhijie Mao, Zhiwei Yang, Xin Wu, Jin Meng, Ran Li, Yu Song, Changfu Dong, Zhijun Yan. // 2010 International Conference on Audio Language and Image Processing (ICALIP). - Shanghai, 23-25 Nov. 2010. - P. 1700-1704. ↑
- C2375.** Xi Wu Guangya. Research on the 3D visualization of information operations based on STK. / Xi Wu Guangya, Si Zhiqiang, Li Xiaofeng, Hu Jingyu Yang. // 2010 International Conference on Audio Language and Image Processing (ICALIP). - Shanghai, 23-25 Nov. 2010. - P. 921-925. ↑
- C2376.** Zhi-Qiang Wei. Two Insar procedures for wide and noise interferograms. / Zhi-Qiang Wei, Hui Lin, Shi Chaojian, Peng Jing. // 2010 International Conference on Audio Language and Image Processing (ICALIP). - Shanghai, 23-25 Nov. 2010. - P. 1719-1723. ↑
- C2377.** Chiba I. Development of phased array systems in Japan. / Chiba I., Konishi Y., Nishino T. // TENCON 2010-2010 IEEE Region 10 Conference. - Fukuoka, 21-24 Nov. 2010. - P. 410-415. ↑
- C2378.** Zhenhong Shao. Multi-layer and multi-dimensional information based cooperative vehicle localization in highway scenarios. / Zhenhong Shao, Wenfeng Li, Yi Wu, Lianfeng Shen. // 2010 12th IEEE International Conference on Communication Technology (ICCT). - Nanjing, 11-14 Nov. 2010. - P. 567-571. ↑
- C2379.** Cao Peng. 1-D superresolution ISAR imaging algorithm. / Cao Peng, Liang Hua-qiang, He Wei-chao. // 2010 12th IEEE International Conference on Communication Technology (ICCT). - Nanjing, 11-14 Nov. 2010. - P. 659-661. ↑
- C2380.** Xu Feng. K-band micro-strip antenna array applied in anti-collision radar. / Xu Feng, Chen Xu, Wang Xin'an. // 2010 12th IEEE International Conference on Communication Technology (ICCT). - Nanjing, 11-14 Nov. 2010. - P. 1240-1243. ↑
- C2381.** Mashaly A.S. Speckle noise reduction in SAR images using adaptive morphological filter. / Mashaly A.S., AbdElkawy E.E.F., Mahmoud T.A. // 2010 10th International Conference on Intelligent Systems Design and Applications (ISDA). - Cairo, Nov. 29 2010-Dec. 1 2010. - P. 260-265. ↑
- C2382.** Wang linyu. The study of Range Doppler Algorithm in focusing Bistatic SAR. / Wang linyu, Zhao hongfang. // 2010 2nd International Conference on Information Science and Engineering (ICISE). - Hangzhou, China, 4-6 Dec. 2010. - P. 7077-7080. ↑
- C2383.** Xiao Li. A method for Doppler Weather Radar raw data compression based on wavelet transform modulus maxima denoising. / Xiao Li, Xuehong Cao, Chen Li, Yue Zhang. // 2010 12th IEEE International Conference on Communication Technology (ICCT). - Nanjing, 11-14 Nov. 2010. - P. 424-427. ↑
- C2384.** Kahler B. Predicted radar/optical feature fusion gains for target identification. / Kahler B., Blasch E. // Proceedings of the IEEE 2010 National Aerospace and Electronics Conference (NAECON). - Fairborn, OH, 14-16 July 2010. - P. 405-412. ↑
- C2385.** Li Zheng. Study of efficient broadband beamforming based on extended towed array measurement. / Li Zheng, Huang Yong, Li Yu, Huang Hai Ning. // 2010 IEEE Youth Conference on Information Computing and Telecommunications (YC-ICT). - Beijing, 28-30 Nov. 2010. - P. 323-326. ↑
- C2386.** Liu Feng. Analysis of an improved fixed-point loop for satellite navigation receiver. / Liu Feng, Li Xin, Zhang Bing-qi. // 2010 IEEE Youth Conference on Information Computing and Telecommunications (YC-ICT). - Beijing, 28-30 Nov. 2010. - P. 427-431. ↑
- C2387.** Joon-Ho Lee. Radar target discrimination using neural networks. / Joon-Ho Lee, Hyo-Tae Kim. // Proceedings of the IEEE 2010 National Aerospace and Electronics Conference (NAECON). - Fairborn, OH, 14-16 July 2010. - P. 358-360. ↑
- C2388.** Zhonghai Wang. A GMTI method via comparing two consecutive phase difference maps of the same target area for small UAVs. / Zhonghai Wang, Blasch E.P., Khanh Pham, Genshe Chen. // Proceedings of the IEEE 2010 National Aerospace and Electronics Conference (NAECON). - Fairborn, OH, 14-16 July 2010. - P. 369-373. ↑
- C2389.** Salim O.M. Hyper-fuzzy modeling and control for bio-inspired radar processing. / Salim O.M., Abdel-

Aty-Zohdy H.S., Zohdy M.A. // Proceedings of the IEEE 2010 National Aerospace and Electronics Conference (NAECON). - Fairborn, OH, 14-16 July 2010. - P. 392-395. ↑

C2390. Ibrahim M. Analytical studies of laser parameters for ranging and illuminating satellites from H-SLR station. / Ibrahim M., El-Hameed A.M.A., Attia G.F. // 2010 High-Capacity Optical Networks and Enabling Technologies (HONET). - Cairo, 19-21 Dec. 2010. - P. 133-137. ↑

C2391. Strobel A. Comparison of pulse and FMCW based radiolocation for indoor tracking systems. / Strobel A., Eickhoff R., Ziroff A., Ellinger F. // 2010 Future Network and Mobile Summit. - Florence, 16-18 June 2010. - P. 1-8. ↑

C2392. Andritsch T. Short term DC breakdown and complex permittivity of Al<sub>2</sub>O<sub>3</sub>-and MgO-epoxy nanocomposites. / Andritsch T., Kochetov R., Morshuis P.H.F., Smit J.J. // 2010 Annual Report Conference on Electrical Insulation and Dielectric Phenomena (CEIDP). - West Lafayette, IN, 17-20 Oct. 2010. - P. 1-4. ↑

C2393. Kenzy A. Antenna compensation for UWB GPR systems applied in Non-Destructive testing. / Kenzy A., Soliman A., El-Hadidy M. // 2010 IEEE Middle East Conference on Antennas and Propagation (MECAP). - Cairo, 20-22 Oct. 2010. - P. 1-4. ↑

C2394. Hassan N. Measurement of pyramidal microwave absorbers using RCS methods. / Hassan N., Idris H.A., Malek M.F.A., Taib M.N., Wan Ali W.K., Soh P.J., Abdullah al-Hadi A., Wee Fwen Hoon. // 2010 International Conference on Intelligent and Advanced Systems (ICIAS). - Manila, 15-17 June 2010. - P. 1-5. ↑

C2395. Delahaye D. Air traffic complexity based on dynamical systems. / Delahaye D., Puechmorel S. // 2010 49th IEEE Conference on Decision and Control (CDC). - Atlanta, GA, 15-17 Dec. 2010. - P. 2069-2074. ↑

C2396. Hu Chong-hai. Continuous ant algorithm based on cooperation in radar network optimization. / Hu Chong-hai, Jiang Wei, Wang Tie-jun. // 2010 International Conference on Management Science and Engineering (ICMSE). - Melbourne, VIC, 24-26 Nov. 2010. - P. 224-233. ↑

C2397. Joon-Ho Lee. Application of Newton method to natural frequency estimation. / Joon-Ho Lee, Hyo-Tae Kim. // Proceedings of the IEEE 2010 National Aerospace and Electronics Conference (NAECON). - Fairborn, OH, 14-16 July 2010. - P. 212-214. ↑

C2398. McMillan R.W. Atmospheric turbulence effects on radar systems. Proceedings of the IEEE 2010 National Aerospace and Electronics Conference (NAECON). - Fairborn, OH, 14-16 July 2010. - P. 1-153. ↑

C2399. {no data available}. NAECON 2011 Preview: "Intelligent Aerospace Sensor Integration". Proceedings of the IEEE 2010 National Aerospace and Electronics Conference (NAECON). - Dayton, OH, USA, 14-16 July 2010. - P. 1. ↑

C2400. Jackson J.A. Automated image segmentation for synthetic aperture radar feature extraction. Proceedings of the IEEE 2010 National Aerospace and Electronics Conference (NAECON). - Fairborn, OH, 14-16 July 2010. - P. 45-49. ↑

C2401. Mann S. Dantzig selector based compressive sensing for radar image enhancement. / Mann S., Phogat R., Mishra A.K. // 2010 Annual IEEE India Conference (INDICON). - Kolkata, 17-19 Dec. 2010. - P. 1-4. ↑

C2402. Indira T. Significance of dielectrics in space technology. / Indira T., Thenappan T. // 2010 Recent Advances in Space Technology Services and Climate Change (RSTSCC). - Chennai, 13-15 Nov. 2010. - P. 333-335. ↑

C2403. Ewing Robert L. Chairman's introduction for NAECON 2010. / Ewing Robert L., Abdel-Aty-Zohdy Hoda S., Frantom Barbara L. // Proceedings of the IEEE 2010 National Aerospace and Electronics Conference (NAECON). - Dayton, OH, USA, 14-16 July 2010. - P. 1-21. ↑

C2404. Dungan K.E. Effects of polarization on wide-angle SAR classification performance. / Dungan K.E., Potter L.C. // Proceedings of the IEEE 2010 National Aerospace and Electronics Conference (NAECON). - Fairborn, OH, 14-16 July 2010. - P. 50-53. ↑

C2405. Nuthalapati R. Design of mismatched filters for oversampled signals. Proceedings of the IEEE 2010 National Aerospace and Electronics Conference (NAECON). - Fairborn, OH, 14-16 July 2010. - P. 173-176. ↑

- C2406.** McMillan R.W. Atmospheric turbulence effects on radar systems. Proceedings of the IEEE 2010 National Aerospace and Electronics Conference (NAECON). - Fairborn, OH, 14-16 July 2010. - P. 181-196. ↑
- C2407.** Da Xu. Wavelet-modulated pulse for compressive sensing in SAR. / Da Xu, Tongret R., Zheng Y.F., Ewing R.L. // Proceedings of the IEEE 2010 National Aerospace and Electronics Conference (NAECON). - Fairborn, OH, 14-16 July 2010. - P. 197-202. ↑
- C2408.** del Arroyo J.R.G. WiMAX ambiguity function for PCL systems. / del Arroyo J.R.G., Jackson J., Temple M. // Proceedings of the IEEE 2010 National Aerospace and Electronics Conference (NAECON). - Fairborn, OH, 14-16 July 2010. - P. 54-59. ↑
- C2409.** Mitra A.K. Ground-UAV platform geometries for radar imaging. Proceedings of the IEEE 2010 National Aerospace and Electronics Conference (NAECON). - Fairborn, OH, 14-16 July 2010. - P. 76-83. ↑
- C2410.** Johnson A. Collision-avoidance radar for bicyclist and runners. / Johnson A., Rupp C., Wolf B., Lang Hong, Mitra A. // Proceedings of the IEEE 2010 National Aerospace and Electronics Conference (NAECON). - Fairborn, OH, 14-16 July 2010. - P. 84-91. ↑
- C2411.** Yang Lin. A 2.9-30.3GHz fourth-harmonic voltage-controlled oscillator in 130nm SiGe BiCMOS technology. / Yang Lin, Kotecki D.E. // 2010 17th IEEE International Conference on Electronics, Circuits, and Systems (ICECS). - Athens, 12-15 Dec. 2010. - P. 396-399. ↑
- C2412.** Garnier B. A Port waterside security systemic analysis. / Garnier B., Andritsos F. // 2010 International Waterside Security Conference (WSS). - Carrara, Italy, 3-5 Nov. 2010. - P. 1-6. ↑
- C2413.** Gurgel Klaus-Werner. Evaluation of an HF-radar ship detection and tracking algorithm by comparison to AIS and SAR data. / Gurgel Klaus-Werner, Schlick Thomas, Horstmann Jochen, Maresca Salvatore. // 2010 International Waterside Security Conference (WSS). - Carrara, Italy, 3-5 Nov. 2010. - P. 1-6. ↑
- C2414.** Hannevik Tonje N. Ship detection using high resolution satellite imagery and space-based AIS. / Hannevik Tonje N., Olsen Oystein, Skauen Andreas N., Olsen Richard. // 2010 International Waterside Security Conference (WSS). - Carrara, Italy, 3-5 Nov. 2010. - P. 1-6. ↑
- C2415.** Bruno Michael. Concurrent use of satellite imaging and passive acoustics for maritime domain awareness. / Bruno Michael, Chung Kil Woo, Salloum Hady, Sedunov Alexander, Sedunov Nikolay, Sutin Alexander, Graber Hans, Mallas Paul. // 2010 International Waterside Security Conference (WSS). - Carrara, Italy, 3-5 Nov. 2010. - P. 1-8. ↑
- C2416.** Burkle Axel. Maritime surveillance with integrated systems. / Burkle Axel, Essendorfer Barbara. // 2010 International Waterside Security Conference (WSS). - Carrara, Italy, 3-5 Nov. 2010. - P. 1-8. ↑
- C2417.** Cresta Matteo. Archimede: Integrated Network-Centric Harbour Protection System. / Cresta Matteo, Storti Enrico, Simetti Enrico, Casalino Giuseppe. // 2010 International Waterside Security Conference (WSS). - Carrara, Italy, 3-5 Nov. 2010. - P. 1-4. ↑
- C2418.** Kochanski Ted. Vital Electronics, the key to the developing dynamic GIS for the Baltic or other maritime environments. / Kochanski Ted, Rucinski Andrzej, Stepnowski Andrzej, Waraksa Marcin, Zurek Jerzy. // 2010 International Waterside Security Conference (WSS). - Carrara, Italy, 3-5 Nov. 2010. - P. 1-8. ↑
- C2419.** Slyusar V. I. An above-water testing's result of experimental surveillance radar with 64-channels digital antenna array. / Slyusar V. I., Nikitin N. N., Shatzman L. G., Korolev N. A., Solostehev O. N., Shraev D. V., Volostchuk I. V., Alesyn A. M., Bondarenko M. V., Grytzenko V. N., Malastchuk V. P. // 2010 International Waterside Security Conference (WSS). - Carrara, Italy, 3-5 Nov. 2010. - P. 1-4. ↑
- C2420.** Stepnowski A. Integrated visualization and analysis of threats for marine and coastal regions via a Web-based GIS. / Stepnowski A., Kulawiak M., Chybicki A., Rucinski A. // 2010 International Waterside Security Conference (WSS). - Carrara, 3-5 Nov. 2010. - P. 1-6. ↑
- C2421.** Lim Jong Hyun. Tracking a non-cooperative mobile target using low-power pulsed Doppler radars. / Lim Jong Hyun, Terzis Andreas, Wang I-Jeng. // 2010 IEEE 35th Conference on Local Computer Networks (LCN). - Denver, CO, USA, 10-14 Oct. 2010. - P. 913-920. ↑

- C2422.** Laws Kenneth. High frequency radar for coastal marine monitoring of currents and vessels. / Laws Kenneth, Vesecky John, Paduan Jeffrey D. // 2010 International Waterside Security Conference (WSS). - Carrara, Italy, 3-5 Nov. 2010. - P. 1-5. ↑
- C2423.** Muller Rolf. Net based waterside security applications: From small solutions to maritime security networks. / Muller Rolf, Brook Chris. // 2010 International Waterside Security Conference (WSS). - Carrara, Italy, 3-5 Nov. 2010. - P. 1-6. ↑
- C2424.** Pedersen Jens Christian. SCANTER 5000 and 6000 Solid State Radar: Utilisation of the SCANTER 5000 and 6000 series next generation solid state, coherent, frequency diversity and time diversity radar with software defined functionality for security applications. 2010 International Waterside Security Conference (WSS). - Carrara, Italy, 3-5 Nov. 2010. - P. 1-8. ↑
- C2425.** Andersson Maria. Multiple sensor fusion for effective abnormal behaviour detection in counter-piracy operations. / Andersson Maria, Johansson Ronnie. // 2010 International Waterside Security Conference (WSS). - Carrara, Italy, 3-5 Nov. 2010. - P. 1-7. ↑
- C2426.** Chioukh L. Multi-frequency radar systems for monitoring vital signs. / Chioukh L., Boutayeb H., Deslandes D., Ke Wu. // 2010 Asia-Pacific Microwave Conference Proceedings (APMC). - Yokohama, 7-10 Dec. 2010. - P. 1669-1672. ↑
- C2427.** Reck C. Detection of SSR signals in multipath airport environments by a multichannel receiver. / Reck C., Berold U., Schmidt L.-P. // 2010 Asia-Pacific Microwave Conference Proceedings (APMC). - Yokohama, 7-10 Dec. 2010. - P. 1685-1688. ↑
- C2428.** Sakai F. An experimental study of novel scanning system suitable for UWB radar application. / Sakai F., Ohta K. // 2010 Asia-Pacific Microwave Conference Proceedings (APMC). - Yokohama, 7-10 Dec. 2010. - P. 1689-1692. ↑
- C2429.** Yang Lin. A 0.8-13.4GHz combined voltage-controlled oscillator with an exclusive-OR in 130nm SiGe BiCMOS. / Yang Lin, Kotecki D.E. // 2010 17th IEEE International Conference on Electronics, Circuits, and Systems (ICECS). - Athens, 12-15 Dec. 2010. - P. 426-429. ↑
- C2430.** Gupta A. Azimuth estimation in periodic linear sparse array by modified amplitude comparison monopulse radar. / Gupta A., Fickenscher T., Herschel R., Holters M., Hinz J. // 2010 Asia-Pacific Microwave Conference Proceedings (APMC). - Yokohama, 7-10 Dec. 2010. - P. 2083-2086. ↑
- C2431.** Dudek M. Millimeter wave FMCW radar system simulations including a 3D ray tracing channel simulator. / Dudek M., Wahl R., Kissinger D., Weigel R., Fischer G. // 2010 Asia-Pacific Microwave Conference Proceedings (APMC). - Yokohama, 7-10 Dec. 2010. - P. 1665-1668. ↑
- C2432.** Osipov A. An improved image-based Near-Field-to-Far-Field Transformation. / Osipov A., Kobayashi H., Suzuki H. // 2010 Asia-Pacific Microwave Conference Proceedings (APMC). - Yokohama, 7-10 Dec. 2010. - P. 1693-1696. ↑
- C2433.** Xiaojin Shi. Iterative DEM retrieving from multi-baseline interferometric SAR with MIMO. / Xiaojin Shi, Yunhua Zhang. // 2010 Asia-Pacific Microwave Conference Proceedings (APMC). - Yokohama, 7-10 Dec. 2010. - P. 1388-1391. ↑
- C2434.** Hafner N. Fish heart motion measurements with a body-contact Doppler radar sensor. / Hafner N., Lubecke V. // 2010 Asia-Pacific Microwave Conference Proceedings (APMC). - Yokohama, 7-10 Dec. 2010. - P. 1416-1419. ↑
- C2435.** Stelzer Andreas. Highly-integrated multi-channel radar sensors in SiGe technology for automotive frequencies and beyond. / Stelzer Andreas, Feger Reinhard, Jahn Martin. // 2010 Conference Proceedings ICECom. - Dubrovnik, Croatia, 20-23 Sept. 2010. - P. 1-11. ↑
- C2436.** Anitori L. Compressive sensing for high resolution radar imaging. / Anitori L., Otten M., Hoogeboom P. // 2010 Asia-Pacific Microwave Conference Proceedings (APMC). - Yokohama, 7-10 Dec. 2010. - P. 1809-1812. ↑
- C2437.** Hoi-Shun Lui. On the polarization response using resonances for target recognition. / Hoi-Shun Lui, Shuley N.V. // 2010 Asia-Pacific Microwave Conference Proceedings (APMC). - Yokohama, 7-10 Dec. 2010. - P.



1813-1816. ↑

C2438. Wissan V. Pulse reduction method for circularly polarized synthetic aperture radar. / Wissan V., Setiadi B., Bayuaji L., Sumantyo J. T. Sri, Kuze H. // 2010 Asia-Pacific Microwave Conference Proceedings (APMC). - Yokohama, Japan, 7-10 Dec. 2010. - P. 1324-1327. ↑

C2439. Gangopadhyaya M. Resonant frequency optimization of coaxially fed rectangular microstrip antenna using Particle Swarm Optimization algorithm. / Gangopadhyaya M., Mukherjee P., Gupta B. // 2010 Annual IEEE India Conference (INDICON). - Kolkata, 17-19 Dec. 2010. - P. 1-3. ↑

C2440. Bishop A.N. Remarks on the Cramer-Rao inequality for Doppler-based target parameter estimation. / Bishop A.N., Smith M. // ---. - Brisbane, QLD, 7-10 Dec. 2010. - P. 199-204. ↑

C2441. Nikolic. Electromagnetic imaging using compressive sensing. / Nikolic, M.M., Gongguo Tang, Djordjevic, A., Nehorai A. // 2010 48th Annual Allerton Conference on Communication, Control, and Computing (Allerton). - Allerton, IL, Sept. 29 2010-Oct. 1 2010. - P. 1737-1741. ↑

C2442. Onunka C. Autonomous marine craft navigation: On the study of radar obstacle detection. / Onunka C., Bright G. // 2010 11th International Conference on Control Automation Robotics & Vision (ICARCV). - Singapore, 7-10 Dec. 2010. - P. 567-572. ↑

C2443. Sarunic P.W. Trajectory control of autonomous fixed-wing aircraft performing multiple target passive detection and tracking. / Sarunic P.W., Evans R.J. // ---. - Brisbane, QLD, 7-10 Dec. 2010. - P. 169-174. ↑

C2444. Krill J.A. Multifunction array lidar network for intruder detection, tracking, and identification. / Krill J.A., O'Driscoll M.J., Gross M.C., Papadakis S.J., Ricciardi G.F., Peri J.S., Bankman I.N. // ---. - Brisbane, QLD, 7-10 Dec. 2010. - P. 43-48. ↑

C2445. Herath S.C.K. Maximum likelihood approach for tracking multiple mobile agents with a moving Doppler radar system. / Herath S.C.K., Pathirana P.N. // ---. - Brisbane, QLD, 7-10 Dec. 2010. - P. 193-198. ↑

C2446. Vivet D. Line-based SLAM with slow rotating range sensors: Results and evaluations. / Vivet D., Checchin P., Chapuis R. // 2010 11th International Conference on Control Automation Robotics & Vision (ICARCV). - Singapore, 7-10 Dec. 2010. - P. 423-430. ↑

C2447. Ying Shijun. Application of AIS in Marine Search and Rescue Radar. / Ying Shijun, Lu Ying, Xia Peng. // 2010 Second WRI Global Congress on Intelligent Systems (GCIS). - Wuhan, 16-17 Dec. 2010. - Vol. 2. - P. 65-68. ↑

C2448. Shi Ziyang. The Research of the Training Assistant Decision-Making Support System Based on Data Mining Technology. 2010 Second WRI Global Congress on Intelligent Systems (GCIS). - Wuhan, 16-17 Dec. 2010. - Vol. 1. - P. 180-184. ↑

C2449. Weiss U. Plant Species Classification Using a 3D LIDAR Sensor and Machine Learning. / Weiss U., Biber P., Laible S., Bohlmann K., Zell A. // 2010 Ninth International Conference on Machine Learning and Applications (ICMLA). - Washington, DC, 12-14 Dec. 2010. - P. 339-345. ↑

C2450. Mullane J. X-band radar based SLAM in Singapore's off-shore environment. / Mullane J., Keller S., Rao A., Adams M., Yeo A., Hover F.S., Patrikalakis N.M. // 2010 11th International Conference on Control Automation Robotics & Vision (ICARCV). - Singapore, 7-10 Dec. 2010. - P. 398-403. ↑

C2451. Moras J. A lidar perception scheme for intelligent vehicle navigation. / Moras J., Cherfaoui V., Bonnifant P. // 2010 11th International Conference on Control Automation Robotics & Vision (ICARCV). - Singapore, 7-10 Dec. 2010. - P. 1809-1814. ↑

C2452. Ferna. ATENEA: Advanced techniques for deeply integrated GNSS/INS/LiDAR navigation. / Ferna,ndez A., Diez J., de Castro D., Dovic F., Silva P.F., Friess P., Wis M., Colomina I., Lindenberger J., Ferna,ndez I. // 2010 5th ESA Workshop on Satellite Navigation Technologies and European Workshop on GNSS Signals and Signal Processing (NAVITEC). - Noordwijk, 8-10 Dec. 2010. - P. 1-8. ↑

C2453. Cacho F. Insights about reliability of Heterojunction Bipolar Transistor under DC stress. / Cacho F., Ighilahriz S., Diop M., Roy D., Huard V. // 2010 IEEE International Integrated Reliability Workshop Final Report

(IRW). - Fallen Leaf, CA, 17-21 Oct. 2010. - P. 139-141. ↑

C2454. Guolong Cui. Adaptive polarimetric MIMO radar detection. / Guolong Cui, Lingjiang Kong, Xiaobo Yang, Jianyu Yang. // 2010 International Symposium on Intelligent Signal Processing and Communication Systems (ISPACS). - Chengdu, 6-8 Dec. 2010. - P. 1-4. ↑

C2455. Wei Liu. The KA-MLFMA hybrid algorithm for analyzing the electromagnetic scattering from a 3-D target over random rough surface. / Wei Liu, Zhiqin Zhao, Wei Yang, Zaiping Nie. // 2010 International Symposium on Intelligent Signal Processing and Communication Systems (ISPACS). - Chengdu, 6-8 Dec. 2010. - P. 1-4. ↑

C2456. Yu-qian Li. Fusion method of radar data and IFF data based on NMF. / Yu-qian Li, Yi-ming Pi, Zongjie Cao, Bing Liu. // 2010 International Symposium on Intelligent Signal Processing and Communication Systems (ISPACS). - Chengdu, 6-8 Dec. 2010. - P. 1-4. ↑

C2457. Zhou Peng. A frequency synchronization method for hybrid bistatic SAR using direct path signal. / Zhou Peng, Pi Yiming, Dai Yongshou. // 2010 International Symposium on Intelligent Signal Processing and Communication Systems (ISPACS). - Chengdu, 6-8 Dec. 2010. - P. 1-4. ↑

C2458. Lan Lv. A forward-looking 3-D SAR imaging model using unequally spaced array. / Lan Lv, Xiaoling Zhang, Zongjie Cao. // 2010 International Symposium on Intelligent Signal Processing and Communication Systems (ISPACS). - Chengdu, 6-8 Dec. 2010. - P. 1-4. ↑

C2459. Xianming Xie. An EKF multi-baseline phase unwrapping algorithm. / Xianming Xie, Yiming Pi, Rui Min. // 2010 International Symposium on Intelligent Signal Processing and Communication Systems (ISPACS). - Chengdu, 6-8 Dec. 2010. - P. 1-4. ↑

C2460. Rong Sun. Ionospheric phase contamination correction method using Generalized S-Transform. / Rong Sun, Zhiqin Zhao, Zaiping Nie. // 2010 International Symposium on Intelligent Signal Processing and Communication Systems (ISPACS). - Chengdu, 6-8 Dec. 2010. - P. 1-4. ↑

C2461. Shuangling Wang. Compressed sensing moving target detection for MIMO radar with widely spaced antennas. / Shuangling Wang, Qian He, Zishu He. // 2010 International Symposium on Intelligent Signal Processing and Communication Systems (ISPACS). - Chengdu, 6-8 Dec. 2010. - P. 1-4. ↑

C2462. Haifeng Tan. Coexistence studies for TD-SCDMA with radar system in the band 2300-2400 MHz. / Haifeng Tan, Wei Liu, Deliang Meng, Biao Huang, Wenbo Wang. // 2010 3rd IEEE International Conference on Broadband Network and Multimedia Technology (IC-BNMT). - Beijing, 26-28 Oct. 2010. - P. 451-456. ↑

C2463. Xingzhao Liu. Retrieval of oriented vegetation parameters based on experimental data of PolInSAR. / Xingzhao Liu, Jie Ren, Linxi Zhang, Chufeng Hu. // 2010 3rd IEEE International Conference on Broadband Network and Multimedia Technology (IC-BNMT). - Beijing, 26-28 Oct. 2010. - P. 1150-1153. ↑

C2464. Leng Chuanhang. Modeling and simulation of chaff cloud interference to SAR. / Leng Chuanhang, He Qiang, Pi Yiming. // 2010 International Symposium on Intelligent Signal Processing and Communication Systems (ISPACS). - Chengdu, 6-8 Dec. 2010. - P. 1-3. ↑

C2465. Yuyu Liao. Statistical MIMO radar based on coherent signals. / Yuyu Liao, Zishu He. // 2010 International Symposium on Intelligent Signal Processing and Communication Systems (ISPACS). - Chengdu, 6-8 Dec. 2010. - P. 1-4. ↑

C2466. Lidong Liu. Chaotic signal reconstruction with application to noise radar system. / Lidong Liu, Jinfeng Hu, Zishu He, Chunlin Han, Chi Lu. // 2010 International Symposium on Intelligent Signal Processing and Communication Systems (ISPACS). - Chengdu, 6-8 Dec. 2010. - P. 1-4. ↑

C2467. Zilu Tang. Study of Common Simulation Platform of Pulse-Compression Radar Signal Processing: A Method of Studying Radar System. / Zilu Tang, Xinyu Yao. // 2010 International Conference on Computational and Information Sciences (ICCIS). - Chengdu, 17-19 Dec. 2010. - P. 424-427. ↑

C2468. Laneuville D. Passive multi target tracking with GM-PHD filter. / Laneuville D., Houssineau J. // 2010 13th Conference on Information Fusion (FUSION). - Edinburgh, 26-29 July 2010. - P. 1-7. ↑

- C2469.** Aughenbaugh J.M. Active clutter reduction through fusion with passive data. / Aughenbaugh J.M., Yocom B.A., La Cour B.R. // 2010 13th Conference on Information Fusion (FUSION). - Edinburgh, 26-29 July 2010. - P. 1-8. ↑
- C2470.** Daun M. Gaussian Mixture initialization in passive tracking applications. / Daun M., Kaune R. // 2010 13th Conference on Information Fusion (FUSION). - Edinburgh, 26-29 July 2010. - P. 1-8. ↑
- C2471.** Sjanic Z. Simultaneous navigation and SAR auto-focusing. / Sjanic Z., Gustafsson F. // 2010 13th Conference on Information Fusion (FUSION). - Edinburgh, 26-29 July 2010. - P. 1-7. ↑
- C2472.** Aoki E.H. A general approach for altitude estimation and mitigation of slant range errors on target tracking using 2D radars. 2010 13th Conference on Information Fusion (FUSION). - Edinburgh, 26-29 July 2010. - P. 1-8. ↑
- C2473.** Zengguo Sun. Parameter estimation of K distribution based on second-kind statistics. / Zengguo Sun, Chongzhao Han, Xianghui Yuan. // 2010 13th Conference on Information Fusion (FUSION). - Edinburgh, 26-29 July 2010. - P. 1-6. ↑
- C2474.** Garci. Robust sensor fusion in real maritime surveillance scenarios. / Garci, J., Guerrero J.L., Luis A., Molina J.M. // 2010 13th Conference on Information Fusion (FUSION). - Edinburgh, 26-29 July 2010. - P. 1-8. ↑
- C2475.** Mertens M. GMTI tracking using signal strength information. / Mertens M., Ulmke M. // 2010 13th Conference on Information Fusion (FUSION). - Edinburgh, 26-29 July 2010. - P. 1-8. ↑
- C2476.** Schujller G. A simulation framework for testing GMTI trackers. / Schujller G., Mertens M. // 2010 13th Conference on Information Fusion (FUSION). - Edinburgh, 26-29 July 2010. - P. 1-8. ↑
- C2477.** Keller C.M. Applying optimal search theory to inland SAR: Steve Fossett case study. 2010 13th Conference on Information Fusion (FUSION). - Edinburgh, 26-29 July 2010. - P. 1-8. ↑
- C2478.** Rezaeian M. Constrained multi-object Markov decision scheduling with application to radar resource management. / Rezaeian M., Moran B. // 2010 13th Conference on Information Fusion (FUSION). - Edinburgh, 26-29 July 2010. - P. 1-8. ↑
- C2479.** Dunau P. Efficient multilateration tracking with concurrent offset estimation using stochastic filtering techniques. / Dunau P., Packi F., Beutler F., Hanebeck U.D. // 2010 13th Conference on Information Fusion (FUSION). - Edinburgh, 26-29 July 2010. - P. 1-8. ↑
- C2480.** Ho Keong Chan. Integrated GMTI radar and report tracking for ground surveillance. / Ho Keong Chan, Hian Beng Lee, Xuhong Xiao, Ulmke M. // 2010 13th Conference on Information Fusion (FUSION). - Edinburgh, 26-29 July 2010. - P. 1-7. ↑
- C2481.** Gorji A.A. A new co-located MIMO radar system for multi-target tracking and localization. / Gorji A.A., Tharmarasa R., Kirubarajan T. // 2010 13th Conference on Information Fusion (FUSION). - Edinburgh, 26-29 July 2010. - P. 1-8. ↑
- C2482.** Aardal O. Radar cross section of the human heartbeat and respiration. / Aardal O., Hamran S., Berger T., Hammerstad J., Lande T.S. // 2010 IEEE Biomedical Circuits and Systems Conference (BioCAS). - Paphos, 3-5 Nov. 2010. - P. 53-57. ↑
- C2483.** Bialkowski M.E. UWB Microwave Monopulse Radar System for breast cancer detection. / Bialkowski M.E., Yifan Wang, Abbosh A. // 2010 4th International Conference on Signal Processing and Communication Systems (ICSPCS). - Gold Coast, QLD, 13-15 Dec. 2010. - P. 1-4. ↑
- C2484.** El-Badawy E.A. A secured chaos encrypted mode-S aircraft identification friend or foe (IFF) system. / El-Badawy E.A., El-Masry W.A., Mokhtar M.A., Hafez A.S. // 2010 4th International Conference on Signal Processing and Communication Systems (ICSPCS). - Gold Coast, QLD, 13-15 Dec. 2010. - P. 1-6. ↑
- C2485.** Ran Xin. Search Aid System Based on Machine Vision and Its Visual Attention Model for Rescue Target Detection. / Ran Xin, Ren Lei. // 2010 Second WRI Global Congress on Intelligent Systems (GCIS). - Wuhan, 16-17 Dec. 2010. - Vol. 2. - P. 149-152. ↑

- C2486.** Zhang De-xiang. SAR Images Despeckling via Bayesian Shrinkage Based on Nonsubsampled Contourlet Transform. / Zhang De-xiang, Gao Qing-wei, Wu Xiao-pei. // 2010 International Conference on Computational and Information Sciences (ICCIS). - Chengdu, 17-19 Dec. 2010. - P. 885-888. ↑
- C2487.** Fu Xiao-wei. Path Planning for UAV in Radar Network Area. / Fu Xiao-wei, Liu Zhong, Gao Xiao-guang. // 2010 Second WRI Global Congress on Intelligent Systems (GCIS). - Wuhan, 16-17 Dec. 2010. - Vol. 3. - P. 260-263. ↑
- C2488.** De Bellis G. Electromagnetic absorbing nanocomposites including carbon fibers, nanotubes and graphene Nanoplatelets. / De Bellis G., De Rosa I.M., Dinescu A., Sarto M.S., Tamburrano A. // 2010 IEEE International Symposium on Electromagnetic Compatibility (EMC). - Fort Lauderdale, FL, 25-30 July 2010. - P. 202-207. ↑
- C2489.** Ahmed F.M. FPGA based design and implementation of an Adaptive Binary Integrator. / Ahmed F.M., Moustafa K.H., Fouad A., Fahmy A. // 2010 IEEE International Symposium on Signal Processing and Information Technology (ISSPIT). - Luxor, 15-18 Dec. 2010. - P. 409-413. ↑
- C2490.** Lundquist C. Estimating polynomial structures from radar data. / Lundquist C., Orguner U., Gustafsson F. // 2010 13th Conference on Information Fusion (FUSION). - Edinburgh, 26-29 July 2010. - P. 1-7. ↑
- C2491.** Kyriakides I. Radar tracking performance when sensing and processing compressive measurements. 2010 13th Conference on Information Fusion (FUSION). - Edinburgh, 26-29 July 2010. - P. 1-8. ↑
- C2492.** Klujnder C. Effects of high-power and transient disturbances on wireless communication systems operating inside the 2.4 GHz ISM band. / Klujnder C., ter Haseborg J.L. // 2010 IEEE International Symposium on Electromagnetic Compatibility (EMC). - Fort Lauderdale, FL, 25-30 July 2010. - P. 359-363. ↑
- C2493.** Chapman W. Parallel processing techniques for the processing of synthetic aperture radar data on FPGAs. / Chapman W., Ranka S., Sahni S., Schmalz M., Majumder U.K. // 2010 IEEE International Symposium on Signal Processing and Information Technology (ISSPIT). - Luxor, 15-18 Dec. 2010. - P. 17-22. ↑
- C2494.** Moustafa K.H. Real time processing of a Lattice Wave Digital matched filter. / Moustafa K.H., Ahmed F.M., Romeh M., Fahmy A. // 2010 IEEE International Symposium on Signal Processing and Information Technology (ISSPIT). - Luxor, 15-18 Dec. 2010. - P. 404-408. ↑
- C2495.** Cheng Hu. Analysis of signal characteristic and resolution in ground forward scattering radar. / Cheng Hu, XiaoLiang Li, Mike C., Teng Long. // 2010 IEEE 10th International Conference on Signal Processing (ICSP). - Beijing, 24-28 Oct. 2010. - P. 1969-1972. ↑
- C2496.** Zotov V. Wide area search munition delivered by the intermediate carriers. / Zotov V., Xiaoguang Gao. // 2010 IEEE 10th International Conference on Signal Processing (ICSP). - Beijing, 24-28 Oct. 2010. - P. 1964-1968. ↑
- C2497.** Meng Xiangwei. Adaptive clutter map detector in nonhomogeneous environment. / Meng Xiangwei, Qu Fuyong. // 2010 IEEE 10th International Conference on Signal Processing (ICSP). - Beijing, 24-28 Oct. 2010. - P. 2231-2234. ↑
- C2498.** Xu Qing. Self-calibrated method for distributed small satellite SAR systems. / Xu Qing, Liao Guisheng, Liu Aifei, Zhang Juan. // 2010 IEEE 10th International Conference on Signal Processing (ICSP). - Beijing, 24-28 Oct. 2010. - P. 2083-2086. ↑
- C2499.** HaiJun Wei. Prominent point InSAR processing. / HaiJun Wei, Haifeng Huang, Zhen Dong, Jubo Zhu. // 2010 IEEE 10th International Conference on Signal Processing (ICSP). - Beijing, 24-28 Oct. 2010. - P. 2079-2082. ↑
- C2500.** Li Ning. Point target reference spectrum of bistatic SAR with parallel flight paths. / Li Ning, Wang Luping. // 2010 IEEE 10th International Conference on Signal Processing (ICSP). - Beijing, 24-28 Oct. 2010. - P. 2075-2078. ↑
- C2501.** YingKang Zhang. A new method of motion estimation and imaging interval selection of ISAR system based on geometry invariance of rigid target. / YingKang Zhang, ShaoHai Hu, Yang Xiao. // 2010 IEEE 10th International Conference on Signal Processing (ICSP). - Beijing, 24-28 Oct. 2010. - P. 1955-1958. ↑



- C2502.** Hongxia Bu. A novel algorithm for synthetic aperture radar imaging based on compressed sensing. / Hongxia Bu, Xia Bai, Ran Tao. // 2010 IEEE 10th International Conference on Signal Processing (ICSP). - Beijing, 24-28 Oct. 2010. - P. 2210-2213. ↑
- C2503.** Bao Qing-long. Method to determine CPI for ubiquitous radar. / Bao Qing-long, Zhang Yue, Yang Man, Chen Zeng-ping. // 2010 IEEE 10th International Conference on Signal Processing (ICSP). - Beijing, 24-28 Oct. 2010. - P. 1927-1930. ↑
- C2504.** Niu Zhaoyang. Study of array collocation for MIMO radar based on beampattern synthesis. / Niu Zhaoyang, Zhang Jianyun, Mao Yunxiang, Wang Wei. // 2010 IEEE 10th International Conference on Signal Processing (ICSP). - Beijing, 24-28 Oct. 2010. - P. 1931-1934. ↑
- C2505.** Chang Yuliang. New target detection method in strong active jamming background for polarimetric radar. / Chang Yuliang, Li Yongzhen, Wang Xuesong, Xiao Shunping. // 2010 IEEE 10th International Conference on Signal Processing (ICSP). - Beijing, 24-28 Oct. 2010. - P. 1947-1950. ↑
- C2506.** Zhao Feng. Using target radial length for data association in multiple-target tracking. / Zhao Feng, Zhao Hong-zhong, Huang Meng-jun, Qiu Wei. // 2010 IEEE 10th International Conference on Signal Processing (ICSP). - Beijing, 24-28 Oct. 2010. - P. 2257-2260. ↑
- C2507.** Chen Jianjun. A novel CFAR detector for terminal guidance coherent radar. / Chen Jianjun, Qiu Wei, Huang Mengjun, Fu Qiang. // 2010 IEEE 10th International Conference on Signal Processing (ICSP). - Beijing, 24-28 Oct. 2010. - P. 2253-2256. ↑
- C2508.** Duan Ke-qing. Analysis and suppression for nonstationary clutter in airborne conformal array radar. / Duan Ke-qing, Xie Wen-chong, Wang Yong-liang. // 2010 IEEE 10th International Conference on Signal Processing (ICSP). - Beijing, 24-28 Oct. 2010. - P. 2087-2091. ↑
- C2509.** Lai Qingfu. A novel approach of countering centroid jamming by using INS information in terminal guidance. / Lai Qingfu, Dai Huanyao, Zhao Jing, Feng Dejun, Wang Xuesong. // 2010 IEEE 10th International Conference on Signal Processing (ICSP). - Beijing, 24-28 Oct. 2010. - P. 2121-2124. ↑
- C2510.** Xie Xiao-Chun. Application of compressive sensing in 3D radar imaging. 2010 IEEE 10th International Conference on Signal Processing (ICSP). - Beijing, 24-28 Oct. 2010. - P. 2117-2120. ↑
- C2511.** Xie Xiao-Chun. Real-time measurement in compressive radar imaging based on AIC. 2010 IEEE 10th International Conference on Signal Processing (ICSP). - Beijing, 24-28 Oct. 2010. - P. 2113-2116. ↑
- C2512.** Xue Wang. A TBD algorithm based on dynamic-programming for dim radar target detection. / Xue Wang, Wanjie Song, Zijiang Zhang, Hanmei Zhu. // 2010 IEEE 10th International Conference on Signal Processing (ICSP). - Beijing, 24-28 Oct. 2010. - P. 2133-2136. ↑
- C2513.** Wu Renbiao. Multilayered diffraction tomography algorithm for ground penetrating radar. / Wu Renbiao, Cao Yunqian, Liu Jiaxue. // 2010 IEEE 10th International Conference on Signal Processing (ICSP). - Beijing, 24-28 Oct. 2010. - P. 2129-2132. ↑
- C2514.** Yuanqin Wang. On separating the information of slow-mode angular motion of projectile. / Yuanqin Wang, Ruoyu Zhang, Jing Sun. // 2010 IEEE 10th International Conference on Signal Processing (ICSP). - Beijing, 24-28 Oct. 2010. - P. 2125-2128. ↑
- C2515.** Ying-chun Xiang. Active cancellation stealth analysis of warship for LFM radar. / Ying-chun Xiang, Chang-wen Qu, Feng Su, Ming-jun Yang. // 2010 IEEE 10th International Conference on Signal Processing (ICSP). - Beijing, 24-28 Oct. 2010. - P. 2109-2112. ↑
- C2516.** Wang Jun. Two methods of 3-D scattering center extraction for targets with micro-motion. / Wang Jun, Yang Dong, Zhang Yuxi. // 2010 IEEE 10th International Conference on Signal Processing (ICSP). - Beijing, 24-28 Oct. 2010. - P. 2100-2104. ↑
- C2517.** Wei Yinsheng. A novel adaptive learning method for low-sidelobe step frequency waveform designing. / Wei Yinsheng, Yang Siliang. // 2010 IEEE 10th International Conference on Signal Processing (ICSP). - Beijing, 24-28 Oct. 2010. - P. 2096-2099. ↑

- C2518.** Shaocheng Liu. A real-time algorithm for signal detection based on autocorrelation at low SNR. / Shaocheng Liu, Biao Jin, Hujun Yang, Tao Su. // 2010 IEEE 10th International Conference on Signal Processing (ICSP). - Beijing, 24-28 Oct. 2010. - P. 2092-2095. ↑
- C2519.** Wang Wenguang. Oil spill detection from polarimetric SAR image. / Wang Wenguang, Lu Fei, Wu Peng, Wang Jun. // 2010 IEEE 10th International Conference on Signal Processing (ICSP). - Beijing, 24-28 Oct. 2010. - P. 832-835. ↑
- C2520.** Fan Wu. Ship detection based on compound distribution with Synthetic Aperture Radar images. / Fan Wu, Congshan Gao, Chao Wang, Hong Zhang, Bo Zhang. // 2010 IEEE 10th International Conference on Signal Processing (ICSP). - Beijing, 24-28 Oct. 2010. - P. 1841-1844. ↑
- C2521.** Xuan Yanyan. New approach for improving Mutual Information in POLSAR image registration. / Xuan Yanyan, Huang Yulin, Yang Jianyu. // 2010 IEEE 10th International Conference on Signal Processing (ICSP). - Beijing, 24-28 Oct. 2010. - P. 853-856. ↑
- C2522.** Rongfeng Li. Research on adaptive beamforming for airborne phased array radar. / Rongfeng Li, Lei Ren, Lingyan Dai. // 2010 IEEE 10th International Conference on Signal Processing (ICSP). - Beijing, 24-28 Oct. 2010. - P. 1935-1938. ↑
- C2523.** Wei Yan. Unsupervised classification of PolInSAR image based on Shannon Entropy Characterization. / Wei Yan, Wen Yang, Ying Liu, Hong Sun. // 2010 IEEE 10th International Conference on Signal Processing (ICSP). - Beijing, 24-28 Oct. 2010. - P. 2192-2195. ↑
- C2524.** Zhou Daolin. Radar angular superresolution algorithm based on Bayesian approach. / Zhou Daolin, Huang Yulin, Yang Jianyu. // 2010 IEEE 10th International Conference on Signal Processing (ICSP). - Beijing, 24-28 Oct. 2010. - P. 1894-1897. ↑
- C2525.** Hai-quan Xu. A modified anti-RGPO jamming algorithm. / Hai-quan Xu, Guo-hong Wang, Jing Bai. // 2010 IEEE 10th International Conference on Signal Processing (ICSP). - Beijing, 24-28 Oct. 2010. - P. 2555-2559. ↑
- C2526.** Nie Lei. The inversion of sea state based on the micro-Doppler analysis of sea-clutter. / Nie Lei, Yang Jin, Li Kang-Le, Jiang Wei-dong, Zhuang Zhao-wen. // 2010 IEEE 10th International Conference on Signal Processing (ICSP). - Beijing, 24-28 Oct. 2010. - P. 2206-2209. ↑
- C2527.** Zhijiao Wang. A fast range alignment algorithm for ISAR imaging. / Zhijiao Wang, Xia Bai, Ran Tao. // 2010 IEEE 10th International Conference on Signal Processing (ICSP). - Beijing, 24-28 Oct. 2010. - P. 2214-2217. ↑
- C2528.** Chen Hai. A review of space target pose external measurements. / Chen Hai, Shan Gan-lin, Zhao Jun. // 2010 IEEE 10th International Conference on Signal Processing (ICSP). - Beijing, 24-28 Oct. 2010. - P. 2518-2522. ↑
- C2529.** Shi Wentao. Orthogonal waveforms design and performance analysis for MIMO sonar. / Shi Wentao, Huang Jianguo, Cui Xiaodong, Hou Yunshan. // 2010 IEEE 10th International Conference on Signal Processing (ICSP). - Beijing, 24-28 Oct. 2010. - P. 2382-2385. ↑
- C2530.** Qiu Chaoyang. A new method of denoising processing for synthetic aperture radar return signal. / Qiu Chaoyang, Hu Shaohai. // 2010 IEEE 10th International Conference on Signal Processing (ICSP). - Beijing, 24-28 Oct. 2010. - P. 283-286. ↑
- C2531.** QingDong Huang. Interference suppression method for space-time navigation receivers based on samples selection Householder multistage wiener filter. / QingDong Huang, LinRang Zhang, GuangYue Lu, Chun Wang. // 2010 IEEE 10th International Conference on Signal Processing (ICSP). - Beijing, 24-28 Oct. 2010. - P. 143-146. ↑
- C2532.** Li Chao. Overlaying orthogonal coding for sidelobe suppression in HFSW radar. / Li Chao, Zhang Ning. // 2010 IEEE 10th International Conference on Signal Processing (ICSP). - Beijing, 24-28 Oct. 2010. - P. 1890-1893. ↑
- C2533.** Gu Yu. Random weighting filtering algorithm and its application in SINS/SAR Integrated Navigation

System. / Gu Yu, Mei Mi, Gu Jian-hua. // 2010 IEEE 10th International Conference on Signal Processing (ICSP). - Beijing, 24-28 Oct. 2010. - P. 2531-2534. ↑

C2534. Kang Li. The combination of ACDA and FCM for Data Association in multi-target tracking. / Kang Li, Xie Wei-xin, Huang Jian-jun. // 2010 IEEE 10th International Conference on Signal Processing (ICSP). - Beijing, 24-28 Oct. 2010. - P. 1429-1432. ↑

C2535. Gao Fei. A mover detection method based on 2-D fuzzy entropy in SAR images. / Gao Fei, Zhou Rui, Sun Jinping, Yu Zhenming. // 2010 IEEE 10th International Conference on Signal Processing (ICSP). - Beijing, 24-28 Oct. 2010. - P. 2218-2221. ↑

C2536. Huang D. Parameter estimation of moving target for stepped-frequency radar under temporal-correlated clutter. / Huang D., Zeng D.Z., Long T., Yu J.Y. // 2010 IEEE 10th International Conference on Signal Processing (ICSP). - Beijing, 24-28 Oct. 2010. - P. 2514-2517. ↑

C2537. Xie Yizhuang. Architecture design of spaceborne SAR imaging processing system. / Xie Yizhuang, Zhu Bocheng. // 2010 IEEE 10th International Conference on Signal Processing (ICSP). - Beijing, 24-28 Oct. 2010. - P. 2283-2286. ↑

C2538. Chen Xiaoli. Singularity detection of TWR echoes based on correlation. / Chen Xiaoli, Tian Mao, Guo Jing. // 2010 IEEE 10th International Conference on Signal Processing (ICSP). - Beijing, 24-28 Oct. 2010. - P. 2279-2282. ↑

C2539. Yang Xiaoyou. Analysis of inner-pulse Doppler effect for the echoes of inverse synthetic aperture LADAR. / Yang Xiaoyou, Chi Long, Zhang Qun, Wang Chong, Zhou Liang. // 2010 IEEE 10th International Conference on Signal Processing (ICSP). - Beijing, 24-28 Oct. 2010. - P. 2295-2298. ↑

C2540. Huang D. Parameter estimation for stepped-frequency radar under temporal-spatial correlated clutter. / Huang D., Zeng D.Z., Long T., Yu J.Y. // 2010 IEEE 10th International Conference on Signal Processing (ICSP). - Beijing, 24-28 Oct. 2010. - P. 1939-1942. ↑

C2541. Zhixing Liu. SAR image target extraction based on 2-D leapfrog filtering. / Zhixing Liu, Shaohai Hu, Yang Xiao, Guangzhi Qu, Kiseon Kim. // 2010 IEEE 10th International Conference on Signal Processing (ICSP). - Beijing, 24-28 Oct. 2010. - P. 1943-1946. ↑

C2542. Jin He. Micro-Doppler effect analysis based on inverse synthetic aperture imaging LADAR. / Jin He, Qun Zhang, Ying Luo, Xiaoyou Yang, Xi Wen. // 2010 IEEE 10th International Conference on Signal Processing (ICSP). - Beijing, 24-28 Oct. 2010. - P. 2071-2074. ↑

C2543. Yanwei Ju. Inverse Synthetic Aperture Radar Imaging at Low Signal-to-noise Ratio. / Yanwei Ju, Li Yu, Yang Wang, Xiaobin Chu. // 2010 International Conference on Artificial Intelligence and Computational Intelligence (AICI). - Sanya, 23-24 Oct. 2010. - Vol. 2. - P. 106-110. ↑

C2544. Wei Shaoming. Estimation of UWB radar scattering center with GTD-based 2D state-space method. / Wei Shaoming, Wang Jun, Sun Jinping, Guo Peng. // 2010 IEEE 10th International Conference on Signal Processing (ICSP). - Beijing, 24-28 Oct. 2010. - P. 2270-2273. ↑

C2545. Changwen Qu. Research on airborne chaff centroid jamming to ground radar. / Changwen Qu, Yanan Li. // 2010 IEEE 10th International Conference on Signal Processing (ICSP). - Beijing, 24-28 Oct. 2010. - P. 2250-2252. ↑

C2546. Lijun Chen. Feature evaluation and selection for polarimetric SAR image classification. / Lijun Chen, Wen Yang, Ying Liu, Hong Sun. // 2010 IEEE 10th International Conference on Signal Processing (ICSP). - Beijing, 24-28 Oct. 2010. - P. 2202-2205. ↑

C2547. Wang Yong-liang. General clutter modeling for airborne radar. / Wang Yong-liang, Xie Wen-chong, Duan Ke-qing, Zhang Xi-chuan. // 2010 IEEE 10th International Conference on Signal Processing (ICSP). - Beijing, 24-28 Oct. 2010. - P. 2274-2278. ↑

C2548. Ge Xianjun. Time delay and doppler shift estimation accuracy analyses of moving targets in non-cooperative bistatic pulse radar. / Ge Xianjun, Song Jie, He You. // 2010 IEEE 10th International Conference on Signal Processing (ICSP). - Beijing, 24-28 Oct. 2010. - P. 2291-2294. ↑

- C2549.** Ali Z. An FPGA based semi-parallel architecture for higher order Moving Target Indication (MTI) processing. / Ali Z., Arshad A., Razzaq U. // 2010 21st IEEE International Symposium on Rapid System Prototyping (RSP). - Fairfax, VA, 8-11 June 2010. - P. 1-7. ↑
- C2550.** Zhang Long. Approach for airborne radar ISAR imaging of ship target based on generalized keystone transform. / Zhang Long, He Xiao hui. // 2010 IEEE 10th International Conference on Signal Processing (ICSP). - Beijing, 24-28 Oct. 2010. - P. 2137-2141. ↑
- C2551.** Wenbang Sun. Research of unsupervised image change detection algorithm based on 2-D histogram. / Wenbang Sun, Haiyan Tang, Hexin Chen, Guang Yu. // 2010 IEEE 10th International Conference on Signal Processing (ICSP). - Beijing, 24-28 Oct. 2010. - P. 686-689. ↑
- C2552.** Bin Liu. Range Cell Migration Correction using texture mapping on GPU. / Bin Liu, Kaizhi Wang, Xingzhao Liu, Wenxian Yu. // 2010 IEEE 10th International Conference on Signal Processing (ICSP). - Beijing, 24-28 Oct. 2010. - P. 2172-2175. ↑
- C2553.** Jun Liu. A new polarization filter based on weighted combination. / Jun Liu, Zijing Zhang. // 2010 IEEE 10th International Conference on Signal Processing (ICSP). - Beijing, 24-28 Oct. 2010. - P. 2168-2171. ↑
- C2554.** Hai Li. An improved joint subspace projection method for InSAR interferogram filtering. / Hai Li, Renbiao Wu. // 2010 IEEE 10th International Conference on Signal Processing (ICSP). - Beijing, 24-28 Oct. 2010. - P. 2188-2191. ↑
- C2555.** Mingming Bian. Matrix transpose methods for SAR imaging system. / Mingming Bian, Fukun Bi, Feng Liu. // 2010 IEEE 10th International Conference on Signal Processing (ICSP). - Beijing, 24-28 Oct. 2010. - P. 2176-2179. ↑
- C2556.** Chunbo Liu. Spread clutter mitigation via knowledge-aided STAP in multiple-input single-output system. / Chunbo Liu, Shuyu Shen, Baixiao Chen. // 2010 IEEE 10th International Conference on Signal Processing (ICSP). - Beijing, 24-28 Oct. 2010. - P. 2180-2183. ↑
- C2557.** Qiongqiong Jia. Impacts of Keystone formatting on Space-Time Adaptive Processing in airborne radar. / Qiongqiong Jia, Renbiao Wu, Hai Li. // 2010 IEEE 10th International Conference on Signal Processing (ICSP). - Beijing, 24-28 Oct. 2010. - P. 2164-2167. ↑
- C2558.** Li Da. Real-time data compression bias estimation on netted radar. / Li Da, Zhang Fan. // 2010 IEEE 10th International Conference on Signal Processing (ICSP). - Beijing, 24-28 Oct. 2010. - P. 2152-2155. ↑
- C2559.** Jianbin Zou. 2-dimensional DOA estimation using ESPRIT algorithm in ARM confronting coherent decoy. / Jianbin Zou, Kai Gao, Eryang Zhang. // 2010 International Conference on Future Information Technology and Management Engineering (FITME). - Changzhou, 9-10 Oct. 2010. - Vol. 2. - P. 238-241. ↑
- C2560.** Liu Changchang. The distributed passive radar 3-D imaging and analysis in wavenumber domain. / Liu Changchang, Xu Hao, He Xuezhi, Chen Weidong. // 2010 IEEE 10th International Conference on Signal Processing (ICSP). - Beijing, 24-28 Oct. 2010. - P. 2051-2054. ↑
- C2561.** Renbiao Wu. A novel STAP method for the detection of fast dim air moving targets. / Renbiao Wu, Qiongqiong Jia, Hai Li. // 2010 IEEE 10th International Conference on Signal Processing (ICSP). - Beijing, 24-28 Oct. 2010. - P. 2160-2163. ↑
- C2562.** Wentao Lv. Water extraction in SAR images using GLCM and Support Vector Machine. / Wentao Lv, Qiuzhe Yu, Wenxian Yu. // 2010 IEEE 10th International Conference on Signal Processing (ICSP). - Beijing, 24-28 Oct. 2010. - P. 740-743. ↑
- C2563.** Zhan Xu. A modified two-scale fractal sea model of the non-fully developed full-range sea spectrum. / Zhan Xu, Fang Su, Jianwei Wan, Lizhi Cheng. // 2010 IEEE 10th International Conference on Signal Processing (ICSP). - Beijing, 24-28 Oct. 2010. - P. 2156-2159. ↑
- C2564.** He Xuezhi. A new approach to distributed passive radar imaging by 2-D NUFFT. / He Xuezhi, Xu Hao, Liu Changchang, Wang Dongjin, Chen Weidong. // 2010 IEEE 10th International Conference on Signal Processing (ICSP). - Beijing, 24-28 Oct. 2010. - P. 2067-2070. ↑



- C2565.** Lee J.D. The FAA handbook on microprocessor selection and evaluation in airborne systems. / Lee J.D., Gupta N., Mahapatra R.N., Manners B.E. // 2010 IEEE/AIAA 29th Digital Avionics Systems Conference (DASC). - Salt Lake City, UT, 3-7 Oct. 2010. - P. 5.E.4-1-5.E.4-9-1. ↑
- C2566.** Peinecke N. Integration of a 2.5D radar simulation in a sensor simulation suite. / Peinecke N., Groll E. // 2010 IEEE/AIAA 29th Digital Avionics Systems Conference (DASC). - Salt Lake City, UT, 3-7 Oct. 2010. - P. 3.A.6-1-3.A.6-9-1. ↑
- C2567.** Gillet S. Enhancement in realism of ATC simulations by improving aircraft behaviour models. / Gillet S., Nuic A., Mouillet V. // 2010 IEEE/AIAA 29th Digital Avionics Systems Conference (DASC). - Salt Lake City, UT, 3-7 Oct. 2010. - P. 2.D.4-1-2.D.4-13-1. ↑
- C2568.** Rose C.E. TCAS surveillance performance analysis. / Rose C.E., Panken A.D., Harman W.H., Wood L. // 2010 IEEE/AIAA 29th Digital Avionics Systems Conference (DASC). - Salt Lake City, UT, 3-7 Oct. 2010. - P. 3.B.4-1-3.B.4-13-1. ↑
- C2569.** Peng Zhou. High-throughout hardware architecture of MQ arithmetic coder. / Peng Zhou, Zhao Bao-jun. // 2010 IEEE 10th International Conference on Signal Processing (ICSP). - Beijing, 24-28 Oct. 2010. - P. 430-433. ↑
- C2570.** Moinuddin M.M. Multiple/Distributed Target Detection for HRR. / Moinuddin M.M., Reddy Y.M., Pasha I.A., Kishore K.L. // 2010 International Conference on Advances in Recent Technologies in Communication and Computing (ARTCom). - Kottayam, 16-17 Oct. 2010. - P. 446-450. ↑
- C2571.** Kravchenko V.F. Correlation radar signal processing on basis of probability Kravchenko weight functions. / Kravchenko V.F., Churikov D.V. // 2010 IEEE 10th International Conference on Signal Processing (ICSP). - Beijing, 24-28 Oct. 2010. - P. 1906-1909. ↑
- C2572.** Brinton C. The Surface Operations Data Analysis and Adaptation tool: Innovations and applications. / Brinton C., Lindsey J., Graham M. // 2010 IEEE/AIAA 29th Digital Avionics Systems Conference (DASC). - Salt Lake City, UT, 3-7 Oct. 2010. - P. 1.B.5-1-1.B.5-11-1. ↑
- C2573.** Zhu Lingfeng. The phase statistical characteristic of InSAR image at the isolated point. / Zhu Lingfeng, Xu Huaping. // 2010 IEEE 10th International Conference on Signal Processing (ICSP). - Beijing, 24-28 Oct. 2010. - P. 2059-2062. ↑
- C2574.** Xin-ping Deng. An improved GVF snake model and its application to linear feature extraction from SAR images. / Xin-ping Deng, Chu He, Hong Sun. // 2010 IEEE 10th International Conference on Signal Processing (ICSP). - Beijing, 24-28 Oct. 2010. - P. 2063-2066. ↑
- C2575.** Castle M.W. Evaluation of separation performance with ADS-B at the Philadelphia key site. / Castle M.W., Trinh T., Mayer C., Parry C. // 2010 IEEE/AIAA 29th Digital Avionics Systems Conference (DASC). - Salt Lake City, UT, 3-7 Oct. 2010. - P. 2.C.2-1-2.C.2-15-1. ↑
- C2576.** Yang Jin. Frequency modulated radar signals based on high dimensional chaotic maps. / Yang Jin, Qiu Zhao-kun, Nie Lei, Zhuang Zhao-wen. // 2010 IEEE 10th International Conference on Signal Processing (ICSP). - Beijing, 24-28 Oct. 2010. - P. 1923-1926. ↑
- C2577.** Atkins S. Toward System Oriented Runway Management. 2010 IEEE/AIAA 29th Digital Avionics Systems Conference (DASC). - Salt Lake City, UT, 3-7 Oct. 2010. - P. 2.A.2-1-2.A.2-12-1. ↑
- C2578.** Jian Tao. Target detection of high-resolution radar in non-Gaussian clutter. / Jian Tao, Su Feng, He You, Gu Xuefeng, Shen Jian. // 2010 IEEE 10th International Conference on Signal Processing (ICSP). - Beijing, 24-28 Oct. 2010. - P. 2047-2050. ↑
- C2579.** Kai Huo. The principle of synthesizing HRRP based on a new OFDM phase-coded stepped-frequency radar signal. / Kai Huo, Bin Deng, Yongxiang Liu, Weidong Jiang, Junjie Mao. // 2010 IEEE 10th International Conference on Signal Processing (ICSP). - Beijing, 24-28 Oct. 2010. - P. 1994-1998. ↑
- C2580.** Hai Deng. Target detection with distributed radar sensor networking systems (DRASENS). 2010 IEEE 10th International Conference on Signal Processing (ICSP). - Beijing, 24-28 Oct. 2010. - P. 1951-1954. ↑

- C2581.** Jin Guowang. Fast one-dimensional least squares matching of InSAR images. / Jin Guowang, Zhang Hongmin, Xu Qing. // 2010 IEEE 10th International Conference on Signal Processing (ICSP). - Beijing, 24-28 Oct. 2010. - P. 1060-1063. ↑
- C2582.** Shu Lin Liu. Radar track-before-detect algorithm of dim target based on track test. / Shu Lin Liu, Hai Bo Liu. // 2010 IEEE 10th International Conference on Signal Processing (ICSP). - Beijing, 24-28 Oct. 2010. - P. 1985-1988. ↑
- C2583.** Kai Huo. Parameters estimation of target with precession based on combined feature. / Kai Huo, Yongxiang Liu, Weidong Jiang, Xiang Li. // 2010 IEEE 10th International Conference on Signal Processing (ICSP). - Beijing, 24-28 Oct. 2010. - P. 1989-1993. ↑
- C2584.** Zhao-kun Qiu. Study of continuous wave radar for human motion characteristics measurement. / Zhao-kun Qiu, Dong-ze Li, Wei-dong Jiang. // 2010 IEEE 10th International Conference on Signal Processing (ICSP). - Beijing, 24-28 Oct. 2010. - P. 1078-1081. ↑
- C2585.** Xu Hao. Compressive sensing MIMO radar imaging based on inverse scattering model. / Xu Hao, He Xuezhi, Yin Zhiping, Wang Dongjin, Chen Weidong. // 2010 IEEE 10th International Conference on Signal Processing (ICSP). - Beijing, 24-28 Oct. 2010. - P. 1999-2002. ↑
- C2586.** Yu Luo. The improvements on the enhanced WRS-88D storm identification and tracking algorithm. / Yu Luo, Zaihua Guo, Linyan Luo, Liangfu Li. // 2010 IEEE 10th International Conference on Signal Processing (ICSP). - Beijing, 24-28 Oct. 2010. - P. 2018-2021. ↑
- C2587.** Zhang Long. A novel ISAR algorithm for the imaging of ship targets based on AM-LFM model. / Zhang Long, Si Dong Sen. // 2010 IEEE 10th International Conference on Signal Processing (ICSP). - Beijing, 24-28 Oct. 2010. - P. 2147-2151. ↑
- C2588.** Hao-wen Chen. Cramér-Rao bounds for estimating velocity and direction with a bistatic MIMO radar. / Hao-wen Chen, Wei Zhou, Xiang Li, Zhao-wen Zhuang. // 2010 IEEE 10th International Conference on Signal Processing (ICSP). - Beijing, 24-28 Oct. 2010. - P. 2142-2146. ↑
- C2589.** Guo H.Y. Detection of moving target based on fractional Fourier transform in SAR clutter. / Guo H.Y., Guan J. // 2010 IEEE 10th International Conference on Signal Processing (ICSP). - Beijing, 24-28 Oct. 2010. - P. 2003-2006. ↑
- C2590.** Liu Jihong. Radar imaging based on compressed sensing by random convolution. / Liu Jihong, Xu Shaokun, Gao Xunzhang, Li Xiang. // 2010 IEEE 10th International Conference on Signal Processing (ICSP). - Beijing, 24-28 Oct. 2010. - P. 2007-2010. ↑
- C2591.** ChaoJie Liang. Design method of parameters for pulse doppler signal to nullifying the interference of negative frequency. / ChaoJie Liang, Wei Liu. // 2010 IEEE 10th International Conference on Signal Processing (ICSP). - Beijing, 24-28 Oct. 2010. - P. 2011-2014. ↑
- C2592.** Yang Yuhao. Spinning targets imaging based on OMP algorithm with radial basis function. / Yang Yuhao, Ma Yuanpeng, Yin Zhiping, Wang Dongjin, Chen Weidong. // 2010 IEEE 10th International Conference on Signal Processing (ICSP). - Beijing, 24-28 Oct. 2010. - P. 1981-1984. ↑
- C2593.** Qiang Yang. Multi-carrier frequency MIMO HF radar using convex optimization beamforming. / Qiang Yang, Shenghui Zhou, Weibo Deng. // 2010 IEEE 10th International Conference on Signal Processing (ICSP). - Beijing, 24-28 Oct. 2010. - P. 2031-2034. ↑
- C2594.** Hong Chen. Inverse synthetic aperture radar imaging with the Range Instantaneous Doppler algorithm. / Hong Chen, Yanhong Wu, Can-bin Yin, Yuntao Li. // 2010 IEEE 10th International Conference on Signal Processing (ICSP). - Beijing, 24-28 Oct. 2010. - P. 2027-2030. ↑
- C2595.** Xu Shaokun. Deception jamming method for ISAR based on sub-Nyquist sampling technology. / Xu Shaokun, Liu Jihong, Fu Yaowen, Li Xiang. // 2010 IEEE 10th International Conference on Signal Processing (ICSP). - Beijing, 24-28 Oct. 2010. - P. 2023-2026. ↑
- C2596.** Jianjun Gao. A new cross-range scaling algorithm based on FrFT. / Jianjun Gao, Fulin Su. // 2010 IEEE 10th International Conference on Signal Processing (ICSP). - Beijing, 24-28 Oct. 2010. - P. 2043-2046. ↑

- C2597.** Chengfa Xu. A general multi-channel radar echo simulator. / Chengfa Xu, Yongbin Hong, Junling Wang, Lizhi Zhao. // 2010 IEEE 10th International Conference on Signal Processing (ICSP). - Beijing, 24-28 Oct. 2010. - P. 2039-2042. ↑
- C2598.** Chundong Qi. An improved nonlinear chirp scaling algorithm with capability motion compensation for one-stationary BiSAR. / Chundong Qi, Tao Zeng, Feng Li. // 2010 IEEE 10th International Conference on Signal Processing (ICSP). - Beijing, 24-28 Oct. 2010. - P. 2035-2038. ↑
- C2599.** Li Xiao Liang. The imaging research of the ground moving targets in forward scattering radar. / Li Xiao Liang, Hu Cheng, Zhu Yu, Long Teng, Mao Cong. // 2010 IEEE 10th International Conference on Signal Processing (ICSP). - Beijing, 24-28 Oct. 2010. - P. 2019-2022. ↑
- C2600.** Bo Zou. Research on Scan-GMTI technology of airborne MIMO radar based on STAP. / Bo Zou, Zhen Dong, Dian-nong Liang. // 2010 IEEE 10th International Conference on Signal Processing (ICSP). - Beijing, 24-28 Oct. 2010. - P. 1973-1976. ↑
- C2601.** Haibo Liu. An improved algorithm of velocity measurement using burst error function. / Haibo Liu, Yongxin Wang, Teng Long. // 2010 IEEE 10th International Conference on Signal Processing (ICSP). - Beijing, 24-28 Oct. 2010. - P. 1977-1980. ↑
- C2602.** Jie Kang. The algorithm of SAR speckle noise suppressing by using generalized multi-scale CB morphology. / Jie Kang, Gang Yang. // 2010 IEEE 10th International Conference on Signal Processing (ICSP). - Beijing, 24-28 Oct. 2010. - P. 1106-1109. ↑
- C2603.** Hou Jianguo. Exploitation of SRTM DEM in InSAR phase unwrapping problem. / Hou Jianguo, Chu Yu, Yang Chengsheng. // 2010 IEEE 10th International Conference on Signal Processing (ICSP). - Beijing, 24-28 Oct. 2010. - P. 2222-2226. ↑
- C2604.** Fan Meimei. Relationship of target identification performance and waveform parameters. / Fan Meimei, Liao Dongping, Ding Xiaofeng, Li Xiang. // 2010 IEEE 10th International Conference on Signal Processing (ICSP). - Beijing, 24-28 Oct. 2010. - P. 2227-2230. ↑
- C2605.** Po Li. A quadrature Doppler radar system for sensing human respiration and heart rates. / Po Li, De-chun Wang. // 2010 IEEE 10th International Conference on Signal Processing (ICSP). - Beijing, 24-28 Oct. 2010. - P. 2235-2238. ↑
- C2606.** Seung Hwan Bae. Algorithm for unknown SNR estimation based on sequential Monte Carlo method in cluttered environment. / Seung Hwan Bae, Yong Hoon Kim, Seok Jae Lee, Joo Hong Yoon, Shin V. // 2010 International Conference on Control Automation and Systems (ICCAS). - Gyeonggi-do, 27-30 Oct. 2010. - P. 1004-1009. ↑
- C2607.** Nam-Gyu Oh. On performance enhancement of a following tracker using stereo vision. / Nam-Gyu Oh, Jae-II Cho, Kiheon Park. // 2010 International Conference on Control Automation and Systems (ICCAS). - Gyeonggi-do, 27-30 Oct. 2010. - P. 1259-1262. ↑
- C2608.** Xianru Liu. Advanced obstacles detection and tracking by fusing millimeter wave radar and image sensor data. / Xianru Liu, Zixing Cai. // 2010 International Conference on Control Automation and Systems (ICCAS). - Gyeonggi-do, 27-30 Oct. 2010. - P. 1115-1120. ↑
- C2609.** Wei Chong Yu. On the Signal Processing in the Life-Detection Radar Using an FMCW Waveform. / Wei Chong Yu, Wang Da Quan. // 2010 Third International Symposium on Information Processing (ISIP). - Qingdao, 15-17 Oct. 2010. - P. 213-216. ↑
- C2610.** Wei Chongyu. Chirp Sub-pulse Stepped Frequency Radar Signal Processing. / Wei Chongyu, Yang Yang, Cheng Junxian. // 2010 Third International Symposium on Information Processing (ISIP). - Qingdao, 15-17 Oct. 2010. - P. 251-254. ↑
- C2611.** Morsi I. Future voyage data recorder based on multi-sensors and human machine interface for marine accident. / Morsi I., Zaghloul M.S., Essam N. // 2010 International Conference on Control Automation and Systems (ICCAS). - Gyeonggi-do, 27-30 Oct. 2010. - P. 1635-1638. ↑
- C2612.** Chilton R. Analysis of data structures used for storing and processing 3D LADAR data. / Chilton R.,

Crane C., Kuk Cho. // 2010 International Conference on Control Automation and Systems (ICCAS). - Gyeonggi-do, 27-30 Oct. 2010. - P. 1496-1501. ↑

C2613. Shirai H. Complex permittivity estimation from free space RCS measurement. / Shirai H., Ishikawa M. // 2010 Third International Conference on Communications and Electronics (ICCE). - Nha Trang, 11-13 Aug. 2010. - P. 290-293. ↑

C2614. Nguyen D.V. Terrain classification based on structure for autonomous navigation in complex environments. / Nguyen D.V., Kuhnert L., Schlemper J., Kuhnert K.-D. // 2010 Third International Conference on Communications and Electronics (ICCE). - Nha Trang, 11-13 Aug. 2010. - P. 163-168. ↑

C2615. Shanbhag K.V. MIMO radar with spatial-frequency diversity for improved detection performance. / Shanbhag K.V., Deb D., Kulkarni M. // 2010 IEEE International Conference on Communication Control and Computing Technologies (ICCCCT). - Ramanathapuram, 7-9 Oct. 2010. - P. 66-70. ↑

C2616. Ick-Ho Whang. Range tracking filter using measurements with uncertain delays. / Ick-Ho Whang, Sung-Jin Cho, Dong-Gyun Choe. // 2010 International Conference on Control Automation and Systems (ICCAS). - Gyeonggi-do, 27-30 Oct. 2010. - P. 2133-2137. ↑

C2617. Rung-Ching Chen. A novel method for indoor location identification. / Rung-Ching Chen, Yu-Cheng Lin. // 2010 2nd International Symposium on Aware Computing (ISAC). - Tainan, 1-4 Nov. 2010. - P. 257-262. ↑

C2618. Jatoth R.K. Particle Swarm Optimization aided unscented kalman filter for ballistic target tracking. / Jatoth R.K., Rao D.N., Kumar K.S. // 2010 IEEE International Conference on Communication Control and Computing Technologies (ICCCCT). - Ramanathapuram, 7-9 Oct. 2010. - P. 455-460. ↑

C2619. Jianhua Sun. Study on the Signal Detection Algorithm of Weak Laser Radar Target Based on Wavelet Transform. / Jianhua Sun, Pengge Ma, Ning Zheng, Jinfa Shi. // 2010 Third International Symposium on Information Processing (ISIP). - Qingdao, 15-17 Oct. 2010. - P. 225-227. ↑

C2620. Tariq A. Doppler radar vital signs monitoring using wavelet transform. / Tariq A., Shiraz H.G. // 2010 Loughborough Antennas and Propagation Conference (LAPC). - Loughborough, 8-9 Nov. 2010. - P. 293-296. ↑

C2621. Shiming Tian. Key technology research of CHINA Advanced Metering Infrastructure. / Shiming Tian, Xu RenWu. // 2010 International Conference on Power System Technology (POWERCON). - Hangzhou, 24-28 Oct. 2010. - P. 1-7. ↑

C2622. Adnan S. Compact microstrip antenna design for microwave imaging. / Adnan S., Abd-Alhameed R.A., Hragha H.I., Elfegani I.T.E., Child M.B. // 2010 Loughborough Antennas and Propagation Conference (LAPC). - Loughborough, 8-9 Nov. 2010. - P. 389-392. ↑

C2623. Birkenfeld S. Automatic detection of reflexion hyperbolas in gpr data with neural networks. 2010 World Automation Congress (WAC). - Kobe, 19-23 Sept. 2010. - P. 1-6. ↑

C2624. Xiaomiao Zuo. An environment monitoring system for valuable chinese herbal medicine growing based on wireless sensor networks. / Xiaomiao Zuo, Wanlin Gao, Qing Wang, Lina Yu, Zhen Li, Jianing Zhao, Jin Wang. // 2010 World Automation Congress (WAC). - Kobe, 19-23 Sept. 2010. - P. 71-75. ↑

C2625. Qiulan Wu. Application of GPRS technology in water quality monitoring system. / Qiulan Wu, Yong Liang, Yongxiang Sun, Chengming Zhang, Pengzeng Liu. // 2010 World Automation Congress (WAC). - Kobe, 19-23 Sept. 2010. - P. 7-11. ↑

C2626. Shahraeini M. A new approach for classification of data transmission media in power systems. / Shahraeini M., Javidi M.H., Ghazizadeh M.S. // 2010 International Conference on Power System Technology (POWERCON). - Hangzhou, 24-28 Oct. 2010. - P. 1-7. ↑

C2627. Starzer F. A fully integrated 77-GHz radar transmitter based on a low phase-noise 19.25-GHz fundamental VCO. / Starzer F., Fischer A., Forstner H.P., Knapp H., Wiesinger F., Stelzer A. // 2010 IEEE Bipolar/BiCMOS Circuits and Technology Meeting (BCTM). - Austin, TX, 4-6 Oct. 2010. - P. 65-68. ↑

C2628. Kissinger D. A 77-GHz down-conversion mixer architecture with built-in test capability in SiGe technology. / Kissinger D., Knapp H., Maurer L., Weigel R. // 2010 IEEE Bipolar/BiCMOS Circuits and



Technology Meeting (BCTM). - Austin, TX, 4-6 Oct. 2010. - P. 200-203. ↑

C2629. Wei Chong Yu. Weak Signal De-noising Method Based on Accumulation in Frequency Domain and Wavelet Transform. / Wei Chong Yu, Zhu Wei Juan. // 2010 Third International Symposium on Information Processing (ISIP). - Qingdao, 15-17 Oct. 2010. - P. 130-133. ↑

C2630. Vogel M.H. Simulation of transient electromagnetic fields on a finite-element mesh. / Vogel M.H., Songoro H. // 2010 Loughborough Antennas and Propagation Conference (LAPC). - Loughborough, 8-9 Nov. 2010. - P. 97-100. ↑

C2631. Mahdi Q.S. 3D simultaneous multi-beams radar processing by using planner array antennas. 2010 Loughborough Antennas and Propagation Conference (LAPC). - Loughborough, 8-9 Nov. 2010. - P. 625-628. ↑

C2632. Mahdi Q.S. Modeling of 3D pencil beam radar (PBR) volume coverage and 3D DMC. 2010 Loughborough Antennas and Propagation Conference (LAPC). - Loughborough, 8-9 Nov. 2010. - P. 621-624. ↑

C2633. Hui Cheng. Optical Image and SAR Image Matching Based on Scattered Edge Feature. 2010 International Conference on Multimedia Information Networking and Security (MINES). - Nanjing, Jiangsu, 4-6 Nov. 2010. - P. 1-4. ↑

C2634. Xuhua Huang. The Adaptive Detector of MIMO Radar and Its Performance. / Xuhua Huang, Jinmang Liu, Xiangjun Li. // 2010 2nd International Conference on Information Engineering and Computer Science (ICIECS). - Wuhan, 25-26 Dec. 2010. - P. 1-4. ↑

C2635. Jia-yuan Zhu. Nonlinear Control System Intelligent Identification Using Optimized Support Vector Machines. / Jia-yuan Zhu, Hong Zhou, Xian-cong Huang, Mao-hui Li. // 2010 2nd International Conference on Information Engineering and Computer Science (ICIECS). - Wuhan, 25-26 Dec. 2010. - P. 1-3. ↑

C2636. Liu Guiming. A Novel Velocity Compensation Algorithm by Graph Matching Method. / Liu Guiming, Qin Xiaoming, Tan Zhiguo. // 2010 2nd International Conference on Information Engineering and Computer Science (ICIECS). - Wuhan, 25-26 Dec. 2010. - P. 1-4. ↑

C2637. Xinhua Liang. Track-Before-Detect Based on Two-Stage Sampling Particle Filter. / Xinhua Liang, Quan Pan, Feng Yang, Yanjun Chen. // 2010 2nd International Conference on Information Engineering and Computer Science (ICIECS). - Wuhan, 25-26 Dec. 2010. - P. 1-4. ↑

C2638. Xu Shichao. Design and Implementation of a 1.5Gbps Digital Channelized Receiver. / Xu Shichao, Liu Guoman, Gao Meiguo, Qin Guo Jie. // 2010 2nd International Conference on Information Engineering and Computer Science (ICIECS). - Wuhan, 25-26 Dec. 2010. - P. 1-4. ↑

C2639. Zhiwei Tang. One Vehicular Information Service System. / Zhiwei Tang, Wancai Li. // 2010 2nd International Conference on Information Engineering and Computer Science (ICIECS). - Wuhan, 25-26 Dec. 2010. - P. 1-4. ↑

C2640. Wang Haibo. The Eye Movement Experiment and the Usability Evaluation of the Fighter Cockpit Digital Interface. / Wang Haibo, Xue Chengqi, Liu Qing. // 2010 2nd International Conference on Information Engineering and Computer Science (ICIECS). - Wuhan, 25-26 Dec. 2010. - P. 1-4. ↑

C2641. Leboucher V. IR revolution 360 infrared panoramic camera the ultimate solution for perimeter security. 2010 IEEE International Carnahan Conference on Security Technology (ICCST). - San Jose, CA, 5-8 Oct. 2010. - P. 425-428. ↑

C2642. Cadariu M. Highway road traffic information and monitoring system. / Cadariu M., Crainic M.S. // 2010 9th International Symposium on Electronics and Telecommunications (ISETC). - Timisoara, 11-12 Nov. 2010. - P. 61-64. ↑

C2643. Vesa A. Direction-of-Arrival estimation for uniform sensor arrays. / Vesa A., Iozsa A. // 2010 9th International Symposium on Electronics and Telecommunications (ISETC). - Timisoara, 11-12 Nov. 2010. - P. 249-252. ↑

C2644. Cheng Ping. A New Range Profile Identification Method Based on Multi-Scale Entropy Feature. / Cheng Ping, Liu Hai-tian, Zhao Jia-qun. // 2010 2nd International Conference on Information Engineering and

Computer Science (ICIECS). - Wuhan, 25-26 Dec. 2010. - P. 1-4. ↑

**C2645.** Li Xiaoquan. Study on Command Control Network Cooperation Measurement of Network Centric Artillery Combat. / Li Xiaoquan, Lan Pengfei, Zhang Xuejie, Cheng Yi. // 2010 2nd International Conference on Information Engineering and Computer Science (ICIECS). - Wuhan, 25-26 Dec. 2010. - P. 1-4. ↑

**C2646.** Jinghui Yang. The Case Study of a Diffusion Theory Model of Adoption and Substitution for Successive Generations of Mobile Internet. / Jinghui Yang, Shoucheng Luo. // 2010 2nd International Conference on Information Engineering and Computer Science (ICIECS). - Wuhan, 25-26 Dec. 2010. - P. 1-4. ↑

**C2647.** Wang Kun. Research on FOA and TOA Estimation Algorithm of Galileo SAR Signal. / Wang Kun, Dong Zhi-hong, Wu Si-liang. // 2010 2nd International Conference on Information Engineering and Computer Science (ICIECS). - Wuhan, 25-26 Dec. 2010. - P. 1-5. ↑

**C2648.** Rakovic. An algorithm for detecting a maneuvering target based on TFR and Viterbi algorithm. / Rakovic, P., Dakovic, M., Stankovic, L., Thayananthan T. // 2010 XIth International Workshop on Symbolic and Numerical Methods, Modeling and Applications to Circuit Design (SM2ACD). - Gammath, 4-6 Oct. 2010. - P. 1-4. ↑

**C2649.** Viet-Ha Pham. A novel multi-dimensional spectrum estimation technique. / Viet-Ha Pham, Grenier D., Chouinard J.-Y. // 2010 International Conference on Advanced Technologies for Communications (ATC). - Ho Chi Minh City, 20-22 Oct. 2010. - P. 50-55. ↑

**C2650.** Sang-Dong Kim. Performance analysis of LFM-UWB radar based on Doppler frequency. / Sang-Dong Kim, Jong-Hun Lee. // 2010 International Conference on Information and Communication Technology Convergence (ICTC). - Jeju, 17-19 Nov. 2010. - P. 297-298. ↑

**C2651.** Razavi R. Self-optimization of capacity and coverage in LTE networks using a fuzzy reinforcement learning approach. / Razavi R., Klein S., Claussen H. // 2010 IEEE 21st International Symposium on Personal Indoor and Mobile Radio Communications (PIMRC). - Istanbul, 26-30 Sept. 2010. - P. 1865-1870. ↑

**C2652.** Jinho Bae. A novel maneuvering target tracking algorithm based on moving slide window. / Jinho Bae, Chong Hyun Lee, Hyoung-Goo Jeon. // 2010 IEEE 21st International Symposium on Personal Indoor and Mobile Radio Communications (PIMRC). - Istanbul, 26-30 Sept. 2010. - P. 1701-1706. ↑

**C2653.** Asada J. Target detection with MSN algorithm for the bistatic radar using digital broadcasting signals. / Asada J., Sasase I. // 2010 IEEE 21st International Symposium on Personal Indoor and Mobile Radio Communications (PIMRC). - Istanbul, 26-30 Sept. 2010. - P. 1060-1065. ↑

**C2654.** Sang Kon Moon. DOA with linear array antennas based on MoM. / Sang Kon Moon, Junho Kim, Hoon-Gee Yang, Kyung Bin Bae, Won Woo Lee, Young-Seek Chung. // 2010 International Conference on Information and Communication Technology Convergence (ICTC). - Jeju, 17-19 Nov. 2010. - P. 535-536. ↑

**C2655.** Nasri O. Model-based decentralized embedded diagnosis inside vehicles: Application to Smart Distance Keeping function. / Nasri O., Shraim H., Dague P., Heron O., Cartron M. // 2010 Conference on Control and Fault-Tolerant Systems (SysTol). - Nice, 6-8 Oct. 2010. - P. 17-23. ↑

**C2656.** Rosas Mendieta D.S. Enabling roaming management in GPRS and WLAN networks based on SIP. / Rosas Mendieta D.S., Ramirez Rojas O. // 2010 International Congress on Ultra Modern Telecommunications and Control Systems and Workshops (ICUMT). - Moscow, 18-20 Oct. 2010. - P. 769-776. ↑

**C2657.** Guangtong Sun. Retrieval of Ground Deformation Based on TS-DInSAR Technique. / Guangtong Sun, Yonghong Zhang, Hongan Wu. // 2010 2nd International Conference on Information Engineering and Computer Science (ICIECS). - Wuhan, 25-26 Dec. 2010. - P. 1-4. ↑

**C2658.** Sang Kon Moon. A new parameter for FMCW radar under external interference. / Sang Kon Moon, Junho Kim, Hoon-Gee Yang, Kyung Bin Bae, Won Woo Lee, Young-Seek Chung. // 2010 International Conference on Information and Communication Technology Convergence (ICTC). - Jeju, 17-19 Nov. 2010. - P. 411-412. ↑

**C2659.** Errington A.F.C. Closure monitoring in Potash Mines using LiDAR. / Errington A.F.C., Daku B.L.F., Prugger A. // IECON 2010-36th Annual Conference on IEEE Industrial Electronics Society. - Glendale, AZ, 7-10

Nov. 2010. - P. 2823-2827. ↑

**C2660.** Olive X. FDI(R) for satellite at Thales Alenia Space how to deal with high availability and robustness in space domain?. 2010 Conference on Control and Fault-Tolerant Systems (SysTol). - Nice, 6-8 Oct. 2010. - P. 837-842. ↑

**C2661.** Che Yanshuang. Development of farming PDA based on the zigbee wireless sensors network and GIS. / Che Yanshuang, Li Minzan, Zheng Lihua, Deng Xiaolei. // 2010 World Automation Congress (WAC). - Kobe, 19-23 Sept. 2010. - P. 459-462. ↑

**C2662.** Chen Jianjun. Application of particle filter for angle measure. / Chen Jianjun, Feng Guoyu, Huang Mengjun, Fu Qiang. // 2010 IEEE International Conference on Intelligent Computing and Intelligent Systems (ICIS). - Xiamen, 29-31 Oct. 2010. - Vol. 1. - P. 598-601. ↑

**C2663.** Cui Ni. Noise analysis and restrain in the fusion process of remote sensing. / Cui Ni, Zequn Guan. // 2010 IEEE International Conference on Intelligent Computing and Intelligent Systems (ICIS). - Xiamen, 29-31 Oct. 2010. - Vol. 3. - P. 490-495. ↑

**C2664.** Xiang Li. Adaptive network fuzzy inference system used in interference cancellation of radar seeker. 2010 IEEE International Conference on Intelligent Computing and Intelligent Systems (ICIS). - Xiamen, 29-31 Oct. 2010. - Vol. 2. - P. 93-97. ↑

**C2665.** Xiangyang Liu. A two-stage gating algorithm for joint probability data association filter. / Xiangyang Liu, Keke Wang, Delong Li, Jia Xu, Jin Pan. // 2010 IEEE 10th International Conference on Signal Processing (ICSP). - Beijing, 24-28 Oct. 2010. - P. 381-384. ↑

**C2666.** Lihua Liu. Ballistic missile precession frequency extraction by homomorphic filtering. / Lihua Liu, McLernon D., Ghogho M., Weidong Hu. // 2010 IEEE 10th International Conference on Signal Processing (ICSP). - Beijing, 24-28 Oct. 2010. - P. 259-262. ↑

**C2667.** Zhang Yuxi. Methods and experience of using Matlab and FPGA for teaching practice in digital signal processing. / Zhang Yuxi, Kang Li, Wang Jun, Sun Jinping, Wang Zulin. // 2010 International Conference on Education and Management Technology (ICEMT). - Cairo, 2-4 Nov. 2010. - P. 414-417. ↑

**C2668.** An Ji-yu. The Applications of GPRS in the Mine Monitoring and Control System. / An Ji-yu, Ma Song-bo. // 2010 International Conference on E-Product E-Service and E-Entertainment (ICEEE). - Henan, 7-9 Nov. 2010. - P. 1-4. ↑

**C2669.** Sun Zhanquan. Travel Time Forecasting Based on Phase Space Reconstruction and SVM. / Sun Zhanquan, Feng Jinqiao, Liu Wei. // 2010 International Conference on Optoelectronics and Image Processing (ICOIP). - Haiko, 11-12 Nov. 2010. - Vol. 2. - P. 692-695. ↑

**C2670.** Gong Shuli. Tracking Maneuvering Target on Airport Surface Based on IMM-UKF Algorithm. / Gong Shuli, Wu Honglan, Tao Cheng, Huang Shengguo. // 2010 International Conference on Optoelectronics and Image Processing (ICOIP). - Haiko, 11-12 Nov. 2010. - Vol. 2. - P. 671-675. ↑

**C2671.** Zhang Xianzhi. Design and Implementation of an Embedded Diagnosis System for Radar Built-in Test Equipment. / Zhang Xianzhi, Sheng Wen. // 2010 International Symposium on Intelligence Information Processing and Trusted Computing (IPTC). - Huanggang, 28-29 Oct. 2010. - P. 173-176. ↑










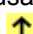
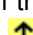

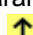




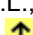
**C2672.** Zhang Fu-gui. A Novel Algorithm of Velocity Ambiguity Resolution for Wind Profiling Radar. / Zhang Fu-gui, Du Yu-ming. // 2010 International Conference on E-Product E-Service and E-Entertainment (ICEEE). - Henan, 7-9 Nov. 2010. - P. 1-3. ↑

**C2673.** David L. Efficient parallel computation of the estimated covariance matrix. / David L., Galperin A., Green O., Birk Y. // 2010 IEEE 26th Convention of Electrical and Electronics Engineers in Israel (IEEEI). - Eliat, 17-20 Nov. 2010. - P. 000977-000981. ↑

**C2674.** Xu Jianguo. Tunnel Construction Safety Inspection and Polymer Grouting Technology for Tunnel Quick Maintenance. / Xu Jianguo, Hou Yujie, Huang Liang. // 2010 International Conference on Optoelectronics and Image Processing (ICOIP). - Haiko, 11-12 Nov. 2010. - Vol. 2. - P. 706-709. ↑

- C2675.** Yiding Wang. Signal separation based on Paired-Echo Theory. / Yiding Wang, Yuanshu Li. // 2010 IEEE 10th International Conference on Signal Processing (ICSP). - Beijing, 24-28 Oct. 2010. - P. 1898-1901. ↑
- C2676.** Zou Jiangwei. Research on correlation description and processing method of multi-sensor fusion. / Zou Jiangwei, Xin Yulin, Xu Shiyong, Chen Zengping. // 2010 IEEE 10th International Conference on Signal Processing (ICSP). - Beijing, 24-28 Oct. 2010. - P. 2439-2442. ↑
- C2677.** Quan Wei. An algorithm of signal sorting and recognition of phased array radars. / Quan Wei, Li Ping, Xu Fengkai. // 2010 IEEE 10th International Conference on Signal Processing (ICSP). - Beijing, 24-28 Oct. 2010. - P. 1877-1880. ↑
- C2678.** Mahdavi A. A robust method for PRI modulation recognition. / Mahdavi A., Pezeshk A.M. // 2010 IEEE 10th International Conference on Signal Processing (ICSP). - Beijing, 24-28 Oct. 2010. - P. 1873-1876. ↑
- C2679.** Zhenlin Wang. The facilitation of SRTM DEM-derived interferogram to accurate DEM reconstruction. / Zhenlin Wang, Zheng Xiang, Kaizhi Wang, Xingzhao Liu, Wenxian Yu. // 2010 IEEE 10th International Conference on Signal Processing (ICSP). - Beijing, 24-28 Oct. 2010. - P. 1886-1889. ↑
- C2680.** Lingjiang Kong. Life detection based on Correntropy Spectral Density. / Lingjiang Kong, Principe J.C. // 2010 IEEE 10th International Conference on Signal Processing (ICSP). - Beijing, 24-28 Oct. 2010. - P. 168-171. ↑
- C2681.** Xia Chen. Track clustering based data association for sky-wave Over-the-horizon Radar. / Xia Chen, Hongwen Yang, Weidong Hu. // 2010 IEEE 10th International Conference on Signal Processing (ICSP). - Beijing, 24-28 Oct. 2010. - P. 1881-1885. ↑
- C2682.** Jun Wang. Influence and compensation of target motion on monopulse estimation in PD radar. / Jun Wang, Peng Guo, Peng Lei, Shaoming Wei. // 2010 IEEE 10th International Conference on Signal Processing (ICSP). - Beijing, 24-28 Oct. 2010. - P. 2312-2315. ↑
- C2683.** Chen Yong-guang. Research on the linear frequency diverse array performance. / Chen Yong-guang, Li Yun-tao, Wu Yan-hong, Chen Hong. // 2010 IEEE 10th International Conference on Signal Processing (ICSP). - Beijing, 24-28 Oct. 2010. - P. 2324-2327. ↑
- C2684.** Li Yuan. A quick and unitary algorithm for imaging radar jamming effect evaluation. / Li Yuan, Li Dashe. // 2010 IEEE 10th International Conference on Signal Processing (ICSP). - Beijing, 24-28 Oct. 2010. - P. 2328-2331. ↑
- C2685.** Lijun Zhou. Mean shift track initiation algorithm based on Hough transform. / Lijun Zhou, Weixin Xie, Liangqun Li. // 2010 IEEE 10th International Conference on Signal Processing (ICSP). - Beijing, 24-28 Oct. 2010. - P. 1263-1266. ↑
- C2686.** Honghua Yan. A novel method on radar 3-D imaging. / Honghua Yan, Xiongjun Fu, Ping Li, Meiguo Gao. // 2010 IEEE 10th International Conference on Signal Processing (ICSP). - Beijing, 24-28 Oct. 2010. - P. 2316-2319. ↑
- C2687.** Gao Caicai. Research on SR\_UPF ground moving target tracking algorithm using road information. / Gao Caicai, Chen Wei. // 2010 IEEE 10th International Conference on Signal Processing (ICSP). - Beijing, 24-28 Oct. 2010. - P. 1259-1262. ↑
- C2688.** Li Yuan. Three-dimensional microwave imaging with adaptive single-input-multiple-output SAR. / Li Yuan, Chen Huilian, Fan Hui, Yuan Da, Xie Qingsong, Liu Peiqiang. // 2010 IEEE 10th International Conference on Signal Processing (ICSP). - Beijing, 24-28 Oct. 2010. - P. 2320-2323. ↑
- C2689.** Fuping Yu. Study of Anti Jamming of Radar Signal Based on Sparse Decomposition. / Fuping Yu, Youqian Feng, Dahua Gao, Qinli An. // 2010 International Symposium on Intelligence Information Processing and Trusted Computing (IPTC). - Huanggang, 28-29 Oct. 2010. - P. 569-572. ↑
- C2690.** Vesecky J.F. Identifying ship echoes in CODAR HF radar data: A Kalman filtering approach. / Vesecky J.F., Laws K.E. // OCEANS 2010. - Seattle, WA, 20-23 Sept. 2010. - P. 1-8. ↑
- C2691.** Helzel T. Software beam forming for ocean radar WERA features and accuracy. / Helzel T., Kniephoff M. // OCEANS 2010. - Seattle, WA, 20-23 Sept. 2010. - P. 1-3. ↑



- C2692.** Plant W.J. Characteristics of internal waves in the South China Sea Observed by a shipboard coherent radar. / Plant W.J., Keller W.C., Hayes K., Chatham G. // OCEANS 2010. - Seattle, WA, 20-23 Sept. 2010. - P. 1-7. 
- C2693.** Rheem C. Surface measurement by using a fixed antenna microwave pulse Doppler radar in Sagami-bay off Hiratsuka in Japan. / Rheem C., Katsura Y. // OCEANS 2010. - Seattle, WA, 20-23 Sept. 2010. - P. 1-4. 
- C2694.** Atwater D.P. Temporal error analysis for compact cross-loop direction-finding HF radar. / Atwater D.P., Heron M.L. // OCEANS 2010. - Seattle, WA, 20-23 Sept. 2010. - P. 1-6. 
- C2695.** Gonsalves M.O. Using a dynamic ocean surface to perform a geometric calibration of a bathymetric lidar. OCEANS 2010. - Seattle, WA, 20-23 Sept. 2010. - P. 1-9. 
- C2696.** Callow H.J. Comparison of SAS processing strategies for crabbing collection geometries. OCEANS 2010. - Seattle, WA, 20-23 Sept. 2010. - P. 1-9. 
- C2697.** Weissman D.E. The influence of rainfall upon Scatterometer estimates for sea surface stress: Applications to boundary layer parameterization and drag coefficient models within tropical cyclone environments. / Weissman D.E., Winterbottom H.R., Bourassa M.A. // OCEANS 2010. - Seattle, WA, 20-23 Sept. 2010. - P. 1-7. 
- C2698.** Sagstad B. Worldwide internet based data acquisition from remote platforms. / Sagstad B., Gytre T. // OCEANS 2010. - Seattle, WA, 20-23 Sept. 2010. - P. 1-6. 
- C2699.** Favo F. Train Conformity Check System; Technology and current operation experience. / Favo F., Bocchetti G., Mazzino N., Lancia A. // 2010 Electrical Systems for Aircraft, Railway and Ship Propulsion (ESARS). - Bologna, 19-21 Oct. 2010. - P. 1-4. 
- C2700.** Kato N. Spilled Oil Tracking Autonomous Buoy. / Kato N., Hiratsuka M., Senga H., Suzuki H., Yoshie M., Fujita I., Tanaka T. // OCEANS 2010. - Seattle, WA, 20-23 Sept. 2010. - P. 1-9. 
- C2701.** Hanusa E. Improving target tracking performance by incorporating classification information. / Hanusa E., Mortensen W.H., Krout D.W., McLaughlin J. // OCEANS 2010. - Seattle, WA, 20-23 Sept. 2010. - P. 1-7. 
- C2702.** Crout R.L. National Data Buoy Center (NDBC) support of the Integrated Ocean Observing System (IOOS). OCEANS 2010. - Seattle, WA, 20-23 Sept. 2010. - P. 1-5. 
- C2703.** Moorits E. Low resource demanding FOTA method for remote AtoN site equipment. / Moorits E., Jervan G. // OCEANS 2010. - Seattle, WA, 20-23 Sept. 2010. - P. 1-5. 
- C2704.** Mayorga E. The NANOOS Visualization System (NVS): lessons learned in data aggregation, management and reuse, for a user application. / Mayorga E., Tanner T., Blair R., Jaramillo A.V., Lederer N., Risien C.M., Seaton C. // OCEANS 2010. - Seattle, WA, 20-23 Sept. 2010. - P. 1-9. 
- C2705.** Gongjun Yan. Active position security through dynamically tunable radar. / Gongjun Yan, Weiming Yang, Jingli Li, Ashok V.G. // 2010 IEEE 7th International Conference on Mobile Adhoc and Sensor Systems (MASS). - San Francisco, CA, 8-12 Nov. 2010. - P. 733-738. 
- C2706.** Jaffre F.M. Miniature, low power, generic Doppler sonar. / Jaffre F.M., Austin T.C., Terray G. // OCEANS 2010. - Seattle, WA, 20-23 Sept. 2010. - P. 1-4. 
- C2707.** Hongbo Wu. Wavelet Transform and its Application to ICESat-GLAS Full Waveform Data. / Hongbo Wu, Yanqiu Xing. // 2010 International Symposium on Intelligence Information Processing and Trusted Computing (IPTC). - Huanggang, 28-29 Oct. 2010. - P. 373-377. 
- C2708.** Dongyang Zhang. Research on the Optimal Disposition of Near Space Multi-sensor Platform. / Dongyang Zhang, Yanyan Zhou, Shucai Huang, Daozhi Wei. // 2010 International Symposium on Intelligence Information Processing and Trusted Computing (IPTC). - Huanggang, 28-29 Oct. 2010. - P. 475-478. 
- C2709.** Heron M.L. What can HF radar contribute to the salvage of a grounded ship?. / Heron M.L., Mantovanelli A., Steinberg C., King B. // OCEANS 2010. - Seattle, WA, 20-23 Sept. 2010. - P. 1-4. 

- C2710.** Trizna D.B. Comparisons of a fully coherent and coherent-on-receive marine radar for measurements of wave spectra and surface currents. OCEANS 2010. - Seattle, WA, 20-23 Sept. 2010. - P. 1-5. ↑
- C2711.** Ning Ma. Frequency diversity for active sonar/radar application and optimal receiver design. OCEANS 2010. - Seattle, WA, 20-23 Sept. 2010. - P. 1-4. ↑
- C2712.** Courmontagne P. On the use of time-frequency domains for the improvement of the Stochastic Matched Filter Pulse Compression scheme with a high speed computing architecture. / Courmontagne P., Julien G., Bouhier M.E. // OCEANS 2010. - Seattle, WA, 20-23 Sept. 2010. - P. 1-10. ↑
- C2713.** Bo Wang. Microwave backscatter of ship signatures on SAR imagery. / Bo Wang, Chapron B., Mercier G., Garello R. // OCEANS 2010. - Seattle, WA, 20-23 Sept. 2010. - P. 1-5. ↑
- C2714.** {no data available}. Front matter. OCEANS 2010. - Seattle, WA, 20-23 Sept. 2010. - P. 1-151. ↑
- C2715.** Prabhudesai R.G. Integrated Coastal Observation Network (ICON) for real-time monitoring of sea-level, sea-state, and surface-meteorological data. / Prabhudesai R.G., Joseph A., Agarwadekar Y., Mehra P., Kumar K.V., Luis R. // OCEANS 2010. - Seattle, WA, 20-23 Sept. 2010. - P. 1-9. ↑
- C2716.** Ghaleb A. Modeling and simulation of sea surface radar observations. / Ghaleb A., Even S., Garello R., Chapron B., Pinel N., de Beaucoudrey N., Comblet F., Parenthoen M., Pottier E. // OCEANS 2010. - Seattle, WA, 20-23 Sept. 2010. - P. 1-7. ↑
- C2717.** Lim S. A network based attenuation correction system for networked dual polarization radar observations. / Lim S., Chandrasekar V., Wang Y. // 2010 IEEE International Geoscience and Remote Sensing Symposium (IGARSS). - Honolulu, HI, 25-30 July 2010. - P. 2333-2336. ↑
- C2718.** Yoldemir A.B. Real-time buried object detection using LMMSE estimation. / Yoldemir A.B., Sezgin M. // 2010 European Radar Conference (EuRAD). - Paris, Sept. 30 2010-Oct. 1 2010. - P. 364-367. ↑
- C2719.** Mas. Sub-band phase calibration in stepped frequency GB noise SAR. / Mas,likowski L., Malanowski M. // 2010 European Radar Conference (EuRAD). - Paris, Sept. 30 2010-Oct. 1 2010. - P. 200-203. ↑
- C2720.** Xuyang Li. Performance of an ultra wideband radar for detection of water accumulation in the human bladder. / Xuyang Li, Pancera E., Niestoruk L., Stork W., Zwick T. // 2010 European Radar Conference (EuRAD). - Paris, Sept. 30 2010-Oct. 1 2010. - P. 212-215. ↑
- C2721.** Yanovsky F.J. Simulation study of relationships between Doppler-polarimetric parameters at microwave remote sensing of precipitation. / Yanovsky F.J., Glushko D. // 2010 European Radar Conference (EuRAD). - Paris, Sept. 30 2010-Oct. 1 2010. - P. 148-151. ↑
- C2722.** Ahmed S.S. Illumination properties of multistatic planar arrays in near-field imaging applications. / Ahmed S.S., Schiessl A., Schmidt L.-P. // 2010 European Radar Conference (EuRAD). - Paris, Sept. 30 2010-Oct. 1 2010. - P. 29-32. ↑
- C2723.** Kulpa J. Pseudo-noise waveform synthesis for SAR applications. / Kulpa J., Mas,likowski Ł., Kulpa K. // 2010 European Radar Conference (EuRAD). - Paris, Sept. 30 2010-Oct. 1 2010. - P. 25-28. ↑
- C2724.** Elgamel S.A. Enhanced monopulse radar tracking using empirical mode decomposition. / Elgamel S.A., Soraghan J.J. // 2010 European Radar Conference (EuRAD). - Paris, Sept. 30 2010-Oct. 1 2010. - P. 57-60. ↑
- C2725.** Weiss A. A Fit-to-Sine based processing chain to handle multiple-target scenarios. / Weiss A., Onic A. // 2010 European Radar Conference (EuRAD). - Paris, Sept. 30 2010-Oct. 1 2010. - P. 53-56. ↑
- C2726.** Desruelles G. Submillimetric high resolution passive imaging system using synthesis aperture technique. / Desruelles G., Rolland N., Rolland P. // 2010 European Radar Conference (EuRAD). - Paris, Sept. 30 2010-Oct. 1 2010. - P. 280-283. ↑
- C2727.** Pahl P. Evaluation of a high accuracy range detection algorithm for FMCW/phase radar systems. / Pahl P., Kayser T., Pauli M., Zwick T. // 2010 European Radar Conference (EuRAD). - Paris, Sept. 30 2010-Oct. 1 2010. - P. 160-163. ↑

- C2728.** Tae-Jong Baek. A 94-GHz receiver front end for passive millimeter-wave imaging. / Tae-Jong Baek, Sang-Jin Lee, Yong-Hyun Baek, Dong-Sik Ko, Min Han, Seok-Gyu Choi, Hyun-Jun Lim, Yeon-Sik Chae, Jin-Koo Rhee. // 2010 European Radar Conference (EuRAD). - Paris, Sept. 30 2010-Oct. 1 2010. - P. 348-351. ↑
- C2729.** Fasoula A. EM estimation of a generic 2D object model based on a sparse set of incomplete ISAR images. / Fasoula A., Driessen H., van Genderen P. // 2010 European Radar Conference (EuRAD). - Paris, Sept. 30 2010-Oct. 1 2010. - P. 240-243. ↑
- C2730.** Chirico D. A Kalman smoothing approach for surface deformation monitoring in differential SAR interferometry. / Chirico D., Schirinzi G. // 2010 European Radar Conference (EuRAD). - Paris, Sept. 30 2010-Oct. 1 2010. - P. 491-494. ↑
- C2731.** Soriano G. Microwave ocean scattering at low-grazing angles with the GMoM. / Soriano G., Guerin C., Saillard M. // 2010 European Radar Conference (EuRAD). - Paris, Sept. 30 2010-Oct. 1 2010. - P. 5-8. ↑
- C2732.** Constancias L. HYCAM-a software-defined testbed for experimentations of new S band surface radar concepts. / Constancias L., Brouard P., Chaumette E., Brun A., Attia S. // 2010 European Radar Conference (EuRAD). - Paris, Sept. 30 2010-Oct. 1 2010. - P. 324-327. ↑
- C2733.** Doukovska L. Comparative analysis of two techniques for moving target velocity estimation. / Doukovska L., Angelova D. // 2010 European Radar Conference (EuRAD). - Paris, Sept. 30 2010-Oct. 1 2010. - P. 431-434. ↑
- C2734.** McDonald M. Characterisation and cancellation of medium grazing angle sea clutter. / McDonald M., Cerutti-Maori D., Damini A. // 2010 European Radar Conference (EuRAD). - Paris, Sept. 30 2010-Oct. 1 2010. - P. 172-175. ↑
- C2735.** Gashinova M. Signal detection in multi-frequency Forward Scatter Radar. / Gashinova M., Sizov V., Zakaria N.A., Cherniakov M. // 2010 European Radar Conference (EuRAD). - Paris, Sept. 30 2010-Oct. 1 2010. - P. 276-279. ↑
- C2736.** Markin E. Method of automatic target angle tracking by sum-and-difference monopulse radar invariant against the polarization jamming. 2010 European Radar Conference (EuRAD). - Paris, Sept. 30 2010-Oct. 1 2010. - P. 499-502. ↑
- C2737.** Kolb S. Microwave gauging with improved angular resolution. / Kolb S., Stolle R., Strobel R. // 2010 European Radar Conference (EuRAD). - Paris, Sept. 30 2010-Oct. 1 2010. - P. 192-195. ↑
- C2738.** Sinitsyn R.B. Nonparametric signal detection algorithm using permutation statistics of signal partial likelihood ratios. / Sinitsyn R.B., Bokal Z.M., Kolchenko L.V. // 2010 European Radar Conference (EuRAD). - Paris, Sept. 30 2010-Oct. 1 2010. - P. 260-263. ↑
- C2739.** Harter M. A modular 24 GHz radar sensor for digital beamforming on transmit and receive. / Harter M., Kornbichler A., Zwick T. // 2010 European Radar Conference (EuRAD). - Paris, Sept. 30 2010-Oct. 1 2010. - P. 507-510. ↑
- C2740.** Zhijian Li. Simulation of the PARSAX dual-channel FMCW polarimetric agile radar system. / Zhijian Li, Lighthart L.P., Peikang Huang, Weining Lu, van der Zwan W.F., Krasnov O.A. // 2010 European Radar Conference (EuRAD). - Paris, Sept. 30 2010-Oct. 1 2010. - P. 168-171. ↑
- C2741.** Bodereau F. 2D image fuzzy deconvolution and scattering centre detection: Model and real-time FPGA implementation for automotive application. / Bodereau F., Giubolini L., Mallejac P., Pizzardi A. // 2010 European Radar Conference (EuRAD). - Paris, Sept. 30 2010-Oct. 1 2010. - P. 427-430. ↑
- C2742.** Phillion R.H. Circular polarization selectivity of space-fed arrays using element rotation. / Phillion R.H., Okoniewski M. // 2010 European Radar Conference (EuRAD). - Paris, Sept. 30 2010-Oct. 1 2010. - P. 527-530. ↑
- C2743.** Kemkemian S. A wide field of view radar for Sense and Avoid on UAV using space coloring waveforms. / Kemkemian S., Nouvel-Fiani M., Cornic P., Garrec P. // 2010 European Radar Conference (EuRAD). - Paris, Sept. 30 2010-Oct. 1 2010. - P. 220-223. ↑
- C2744.** Giubolini L. 2D image fuzzy deconvolution and scattering centre detection. / Giubolini L., Pazandak

P. // 2010 European Radar Conference (EuRAD). - Paris, Sept. 30 2010-Oct. 1 2010. - P. 423-426. ↑

C2745. Chaire C. New generation Doppler radar processing: Ultra-fast robust Doppler Spectrum Barycentre computation scheme in Poincaré's unit disk. / Chaire C., Barbaresco F. // 2010 European Radar Conference (EuRAD). - Paris, Sept. 30 2010-Oct. 1 2010. - P. 196-199. ↑

C2746. Jishy K. Passive detection and tracking of maneuvering targets with particle filter techniques using DVBT broadcasting. / Jishy K., Lehmann F., Gosselin F., Moruzzis M., Salut G. // 2010 European Radar Conference (EuRAD). - Paris, Sept. 30 2010-Oct. 1 2010. - P. 419-422. ↑

C2747. Marquis E. Antenna size versus sea clutter rejection: A new analysis of coastal radar performances and optimization. 2010 European Radar Conference (EuRAD). - Paris, Sept. 30 2010-Oct. 1 2010. - P. 97-100. ↑

C2748. Jardin P. On wideband MIMO radar: Extended signal model and spectral beampattern design. / Jardin P., Nadal F., Middleton S. // 2010 European Radar Conference (EuRAD). - Paris, Sept. 30 2010-Oct. 1 2010. - P. 392-395. ↑

C2749. Mytsenko I. Multiposition bistatic radar system using radio signals of geostationary satellites for hydrometeors parameters determination. / Mytsenko I., Khrameyda D. // 2010 European Radar Conference (EuRAD). - Paris, Sept. 30 2010-Oct. 1 2010. - P. 145-147. ↑

C2750. Cristallini D. Strategies for sub-optimal air to air STAP in forward looking configuration. / Cristallini D., Burger W. // 2010 European Radar Conference (EuRAD). - Paris, Sept. 30 2010-Oct. 1 2010. - P. 308-311. ↑

C2751. Porge. Automatic target recognition in SAR images using multilinear analysis. / Porge, s T., Favier G. // 2010 European Radar Conference (EuRAD). - Paris, Sept. 30 2010-Oct. 1 2010. - P. 41-44. ↑

C2752. Ruggiano M. Effects of the SNR of the signal replica in LMMSE-based filtering. / Ruggiano M., van Genderen P. // 2010 European Radar Conference (EuRAD). - Paris, Sept. 30 2010-Oct. 1 2010. - P. 188-191. ↑

C2753. Toporkov J.V. Backscattering of wide-band HF signals from evolving ocean-like surface: 2-D direct numerical simulations and analysis. / Toporkov J.V., Sletten M.A. // 2010 European Radar Conference (EuRAD). - Paris, Sept. 30 2010-Oct. 1 2010. - P. 9-12. ↑

C2754. Mittelstrass D. DC-offset compensation in a bistatic 77GHz-FMCW-radar. / Mittelstrass D., Steinbuch D., Walter T., Waldschmidt C., Weigel R. // 2010 European Radar Conference (EuRAD). - Paris, Sept. 30 2010-Oct. 1 2010. - P. 447-450. ↑

C2755. Baur K. Angular measurements in azimuth and elevation using 77 GHz radar sensors. / Baur K., Mayer M., Rack V., Vogel D., Walter T. // 2010 European Radar Conference (EuRAD). - Paris, Sept. 30 2010-Oct. 1 2010. - P. 184-187. ↑

C2756. Kohmura A. W-band antenna-reflector combined in a lens. / Kohmura A., Futatsumori S., Yonemoto N., Matsuzaki M. // 2010 European Radar Conference (EuRAD). - Paris, Sept. 30 2010-Oct. 1 2010. - P. 356-359. ↑

C2757. Xiao-wei Zhao. Through the wall detection and localization of a moving target with a bistatic UWB radar system. / Xiao-wei Zhao, Gague A., Lie,be C., Khamlichi J., Me,nard M. // 2010 European Radar Conference (EuRAD). - Paris, Sept. 30 2010-Oct. 1 2010. - P. 204-207. ↑

C2758. Snoeij P. Sentinel-1 C-SAR calibration. / Snoeij P., Attema E., Traver I.N., Torres R. // 2010 European Radar Conference (EuRAD). - Paris, Sept. 30 2010-Oct. 1 2010. - P. 352-355. ↑

C2759. Mangini G. Solid state pulse Doppler radars for maritime traffic surveillance-Review of architecture and trade-off analysis. / Mangini G., Kassab R., Bourret N., Potet P., Nouvel P., Penarier A., Boulant C., Gasquet D. // 2010 European Radar Conference (EuRAD). - Paris, Sept. 30 2010-Oct. 1 2010. - P. 93-96. ↑

C2760. Schikorr M. Medium-PRF detection by non-coherent integration. 2010 European Radar Conference (EuRAD). - Paris, Sept. 30 2010-Oct. 1 2010. - P. 224-227. ↑

C2761. Korchagina D.A. Bio-radiolocation method at chest wall motion analysis during tidal breathing. / Korchagina D.A., Alekhin M.D., Anishchenko L.N. // 2010 European Radar Conference (EuRAD). - Paris, Sept.



30 2010-Oct. 1 2010. - P. 475-478. ↑

**C2762.** Krasnov O.A. Radar polarimetry using sounding signals with dual orthogonality-PARSAX approach. / Krasnov O.A., Ligthart L.P. // 2010 European Radar Conference (EuRAD). - Paris, Sept. 30 2010-Oct. 1 2010. - P. 121-124. ↑

**C2763.** Olivadese D. A radar oriented ionospheric channel model based on ray-tracing theory. / Olivadese D., Berizzi F., Cacciamano A., Capria A. // 2010 European Radar Conference (EuRAD). - Paris, Sept. 30 2010-Oct. 1 2010. - P. 105-108. ↑

**C2764.** Tamminen A. Submillimeter-wave power measurements with commercial infra-red detectors. / Tamminen A., Ala-Laurinaho J., Rissanen A.V. // 2010 European Radar Conference (EuRAD). - Paris, Sept. 30 2010-Oct. 1 2010. - P. 288-291. ↑

**C2765.** Peik S.F. A complete indoor positioning system implementing six-port interferometers. / Peik S.F., Monsees F., Meyer C., Szczuka R., Pojtsch T. // 2010 European Radar Conference (EuRAD). - Paris, Sept. 30 2010-Oct. 1 2010. - P. 515-518. ↑

**C2766.** Liang Han. Radar and radio data fusion platform for future intelligent transportation system. / Liang Han, Ke Wu. // 2010 European Radar Conference (EuRAD). - Paris, Sept. 30 2010-Oct. 1 2010. - P. 65-68. ↑

**C2767.** Kubicke G. Monostatic scattering from an object near an ocean-like surface from an efficient fast numerical method. / Kubicke G., Bourlier C. // 2010 European Radar Conference (EuRAD). - Paris, Sept. 30 2010-Oct. 1 2010. - P. 1-4. ↑

**C2768.** Belfiori F. Side-lobe suppression techniques for a uniform circular array. / Belfiori F., Monni S., Van Rossum W., Hoogeboom P. // 2010 European Radar Conference (EuRAD). - Paris, Sept. 30 2010-Oct. 1 2010. - P. 113-116. ↑

**C2769.** del Castillo Mena J. Modular RF design for QUASAR Ku-band polarimetric SAR system. / del Castillo Mena J., Sevilleja S.S., Sodupe J.R.L. // 2010 European Radar Conference (EuRAD). - Paris, Sept. 30 2010-Oct. 1 2010. - P. 459-462. ↑

**C2770.** Bellomo L. Microwave-range imagery with an ultrawideband time reversal-based RADAR. / Bellomo L., Pioch S., Saillard M. // 2010 European Radar Conference (EuRAD). - Paris, Sept. 30 2010-Oct. 1 2010. - P. 216-219. ↑

**C2771.** Kwapisz D. Calibration and characterization of a CW radar for blade tip clearance measurement. / Kwapisz D., Hafner M., Queloz S. // 2010 European Radar Conference (EuRAD). - Paris, Sept. 30 2010-Oct. 1 2010. - P. 320-323. ↑

**C2772.** Galati G. MPAR: Waveform design for the weather function. / Galati G., Pavan G., Scopelliti S. // 2010 European Radar Conference (EuRAD). - Paris, Sept. 30 2010-Oct. 1 2010. - P. 152-155. ↑

**C2773.** Mecatti D. Monitoring open-pit quarries by interferometric radar for safety purposes. / Mecatti D., Macaluso G., Barucci A., Noferini L., Pieraccini M., Atzeni C. // 2010 European Radar Conference (EuRAD). - Paris, Sept. 30 2010-Oct. 1 2010. - P. 37-40. ↑

**C2774.** Clark T. Million element ISIS array. / Clark T., Jaska E. // 2010 IEEE International Symposium on Phased Array Systems and Technology (ARRAY). - Waltham, MA, 12-15 Oct. 2010. - P. 29-36. ↑

**C2775.** Milin J. AMSAR-A France-UK-Germany success story in active-array radar. / Milin J., Moore S., Burger W., Tribouloy P., Royden M., Gerster J. // 2010 IEEE International Symposium on Phased Array Systems and Technology (ARRAY). - Waltham, MA, 12-15 Oct. 2010. - P. 11-18. ↑

**C2776.** {no data available}. Copyright page. 2010 IEEE International Symposium on Phased Array Systems and Technology (ARRAY). - Waltham, MA, 12-15 Oct. 2010. - P. 1. ↑

**C2777.** McLaughlin D.J. Gap free CONUS surveillance using dense networks of short range radars. 2010 IEEE International Symposium on Phased Array Systems and Technology (ARRAY). - Waltham, MA, 12-15 Oct. 2010. - P. 37-43. ↑

- C2778.** Cetronio A. Phased array systems and technologies in SELEX-Sistemi Integrati: State of art and new challenges. / Cetronio A., D'Urso M., Farina A., Lanzieri C., Timmoneri L., Teglia M. // 2010 IEEE International Symposium on Phased Array Systems and Technology (ARRAY). - Waltham, MA, 12-15 Oct. 2010. - P. 44-49. ↑
- C2779.** Chiba I. Progress of phased array systems in Japan. / Chiba I., Konishi Y., Nishino T. // 2010 IEEE International Symposium on Phased Array Systems and Technology (ARRAY). - Waltham, MA, 12-15 Oct. 2010. - P. 19-28. ↑
- C2780.** Sward W.S. Phase continuous radar test set. / Sward W.S., Reed D.E. // 2010 IEEE AUTOTESTCON. - Orlando, FL, 13-16 Sept. 2010. - P. 1-5. ↑
- C2781.** Li-min Yang. Synthetic ultra-wideband radar range profile based on stepped frequency pulse trains. / Li-min Yang, Wei-min Su, Hong Gu. // 2010 IEEE International Conference on Ultra-Wideband (ICUWB). - Nanjing, 20-23 Sept. 2010. - Vol. 2. - P. 1-4. ↑
- C2782.** He-xiu Xu. Tunable low-pass filter using fractal shaped complementary split ring resonator with ultra-wide stop-band and excellent selectivity. / He-xiu Xu, Guang-ming Wang, Lu K. // 2010 IEEE International Conference on Ultra-Wideband (ICUWB). - Nanjing, 20-23 Sept. 2010. - Vol. 2. - P. 1-3. ↑
- C2783.** He-xiu Xu. Compact bandpass filter based on fractal shaped composite right/left handed transmission line with ultra-wide band, deep out-of-band suppression and enhanced passband performance. / He-xiu Xu, Guang-ming Wang, Chen-xin Zhang, Jian-gang Liang. // 2010 IEEE International Conference on Ultra-Wideband (ICUWB). - Nanjing, 20-23 Sept. 2010. - Vol. 2. - P. 1-3. ↑
- C2784.** Guowei Shen. Time of arrival estimation for range-based localization in UWB sensor networks. / Guowei Shen, Zetik R., Honghui Yan, Hirsch O., Thoma R.S. // 2010 IEEE International Conference on Ultra-Wideband (ICUWB). - Nanjing, 20-23 Sept. 2010. - Vol. 2. - P. 1-4. ↑
- C2785.** Jing Shen. Design and mutual coupling analysis on wideband wide-angle scan step-constant tapered slot antenna array. / Jing Shen, Zhi Xu, Ting Zheng. // 2010 IEEE International Conference on Ultra-Wideband (ICUWB). - Nanjing, 20-23 Sept. 2010. - Vol. 2. - P. 1-4. ↑
- C2786.** Kohno Ryuji. Latest update of UWB regulation and standardization for medical healthcare and ITS. 2010 IEEE International Conference on Ultra-Wideband (ICUWB). - Nanjing, China, 20-23 Sept. 2010. - Vol. 1. - P. 7-11. ↑
- C2787.** Brookner E. Never ending saga of phased array breakthroughs. 2010 IEEE International Symposium on Phased Array Systems and Technology (ARRAY). - Waltham, MA, 12-15 Oct. 2010. - P. 61-73. ↑
- C2788.** Infante L. Low-profile ultra-wide band antenna array element suitable for wide scan angle and modular subarray architecture. / Infante L., De Luca A., Teglia M. // 2010 IEEE International Symposium on Phased Array Systems and Technology (ARRAY). - Waltham, MA, 12-15 Oct. 2010. - P. 157-163. ↑
- C2789.** Jacomb-Hood A. RF on Flex tile for L Band phased arrays. / Jacomb-Hood A., Lier E., Martin B., Teixeira J., Papula P., Destefano T., Nelson S., Anderson S., Walker M., Jones C., Anderson R., Channabasappa E. // 2010 IEEE International Symposium on Phased Array Systems and Technology (ARRAY). - Waltham, MA, 12-15 Oct. 2010. - P. 144-151. ↑
- C2790.** Coleman J.O. Phase-only tapers for regular planar arrays, a heuristic nonlinear-FM approach. / Coleman J.O., Scholnik D.P., McPhail K.R. // 2010 IEEE International Symposium on Phased Array Systems and Technology (ARRAY). - Waltham, MA, 12-15 Oct. 2010. - P. 113-120. ↑
- C2791.** Nickel U.R.O. System considerations for passive radar with GSM illuminators. 2010 IEEE International Symposium on Phased Array Systems and Technology (ARRAY). - Waltham, MA, 12-15 Oct. 2010. - P. 189-195. ↑
- C2792.** Kai-Bor Yu. Electronic protection for digital shared aperture array radar. / Kai-Bor Yu, Turner E.L. // 2010 IEEE International Symposium on Phased Array Systems and Technology (ARRAY). - Waltham, MA, 12-15 Oct. 2010. - P. 170-176. ↑
- C2793.** Otten M. Light weight digital array SAR. / Otten M., Maas N., Bolt R., Anitori L. // 2010 IEEE International Symposium on Phased Array Systems and Technology (ARRAY). - Waltham, MA, 12-15 Oct. 2010.

- P. 177-182. ↑

**C2794.** Kai-Bor Yu. Analog beamspace super-resolution radar processing. / Kai-Bor Yu, Fernandez M.F. // 2010 IEEE International Symposium on Phased Array Systems and Technology (ARRAY). - Waltham, MA, 12-15 Oct. 2010. - P. 102-106. ↑

**C2795.** Coleman J.O. The fundamental input/output structure of a linear, time-varying array receiver. 2010 IEEE International Symposium on Phased Array Systems and Technology (ARRAY). - Waltham, MA, 12-15 Oct. 2010. - P. 74-78. ↑

**C2796.** Fenn A.J. Ultrawideband VHF/UHF dipole array antenna. / Fenn A.J., Hurst P.T., Krieger J.D., Sandora J.S., Parad L.I. // 2010 IEEE International Symposium on Phased Array Systems and Technology (ARRAY). - Waltham, MA, 12-15 Oct. 2010. - P. 79-82. ↑

**C2797.** Chappell W. Digital Array Radar panel development. / Chappell W., Fulton C. // 2010 IEEE International Symposium on Phased Array Systems and Technology (ARRAY). - Waltham, MA, 12-15 Oct. 2010. - P. 50-60. ↑

**C2798.** Renbiao Wu. Parameter estimation of moving target based on linearly constrained space-time adaptive monopulse technique. / Renbiao Wu, Lu Wang, Zhigang Su, Jingxiong Huang. // 2010 IEEE International Symposium on Phased Array Systems and Technology (ARRAY). - Waltham, MA, 12-15 Oct. 2010. - P. 107-112. ↑

**C2799.** Marshall D.F. Adaptive cancellation of impulsive interference in phased array radar. 2010 IEEE International Symposium on Phased Array Systems and Technology (ARRAY). - Waltham, MA, 12-15 Oct. 2010. - P. 83-88. ↑

**C2800.** Renjian Zhao. Nonlinear Kalman filtering for self-calibration of airborne arrays. / Renjian Zhao, Goeckel D.L., Mead J.B. // 2010 IEEE International Symposium on Phased Array Systems and Technology (ARRAY). - Waltham, MA, 12-15 Oct. 2010. - P. 89-101. ↑

**C2801.** Xubo Wang. A carrier-based UWB transceiver in CMOS 90nm for biomedical radar sensing and sensor communications. / Xubo Wang, Anh Dinh, Teng D. // 2010 IEEE International Conference on Ultra-Wideband (ICUWB). - Nanjing, 20-23 Sept. 2010. - Vol. 2. - P. 1-4. ↑

**C2802.** Carlson D.J. MMIC based phased array radar T/R modules. / Carlson D.J., Weigand C., Boles T. // 2010 European Radar Conference (EuRAD). - Paris, Sept. 30 2010-Oct. 1 2010. - P. 455-458. ↑

**C2803.** Anastasio V. Optimization of multistatic passive radar geometry based on CRLB with uncertain observations. / Anastasio V., Colone F., Di Lallo A., Farina A., Gumiero F., Lombardo P. // 2010 European Radar Conference (EuRAD). - Paris, Sept. 30 2010-Oct. 1 2010. - P. 340-343. ↑

**C2804.** Marshall R.E. S band radar target detection in an extreme advection duct event. / Marshall R.E., Horgan K.H. // 2010 European Radar Conference (EuRAD). - Paris, Sept. 30 2010-Oct. 1 2010. - P. 176-179. ↑

**C2805.** Jen-Chieh Wu. Wireless indoor localization using dynamic monopulse receiver. / Jen-Chieh Wu, Chia-Chan Chang, Ting-Yueh Chin, Sheng-Fuh Chang, Mao-Ching Chiu, Chia-Yang Hsu, Ruey-Hsuan Lee. // 2010 European Radar Conference (EuRAD). - Paris, Sept. 30 2010-Oct. 1 2010. - P. 69-72. ↑

**C2806.** Gumiero F. Multistatic passive radar geometry optimization for target 3D positioning accuracy. / Gumiero F., Nucciarone C., Anastasio V., Lombardo P., Colone F. // 2010 European Radar Conference (EuRAD). - Paris, Sept. 30 2010-Oct. 1 2010. - P. 467-470. ↑

**C2807.** Lops M. A model-based track-before-detect strategy. / Lops M., Mancino M., Orlando D., Ricci G., Venturino L. // 2010 European Radar Conference (EuRAD). - Paris, Sept. 30 2010-Oct. 1 2010. - P. 300-303. ↑

**C2808.** Haderer A. Precise radial velocity estimation using an FMCW radar. / Haderer A., Scherz P., Stelzer A. // 2010 European Radar Conference (EuRAD). - Paris, Sept. 30 2010-Oct. 1 2010. - P. 164-167. ↑

**C2809.** PourNejatian N.M. Fractal based detection using blind box-counting method in high resolution radars. / PourNejatian N.M., Nayebi M.M. // 2010 European Radar Conference (EuRAD). - Paris, Sept. 30 2010-Oct. 1 2010. - P. 407-410. ↑

- C2810.** Meta A. MetaSensing compact, high resolution interferometric SAR sensor for commercial and scientific applications. / Meta A., Trampuz C. // 2010 European Radar Conference (EuRAD). - Paris, Sept. 30 2010-Oct. 1 2010. - P. 21-24. ↑
- C2811.** Bezvesilniy O.O. Improving SAR images: Built-in geometric and multi-look radiometric corrections. / Bezvesilniy O.O., Gorovyi I.M., Sosnytskiy S.V., Vynogradov V.V., Vavriv D.M. // 2010 European Radar Conference (EuRAD). - Paris, Sept. 30 2010-Oct. 1 2010. - P. 256-259. ↑
- C2812.** Clemente C. Fractional Range Doppler Algorithm for SAR imaging. / Clemente C., Soraghan J.J. // 2010 European Radar Conference (EuRAD). - Paris, Sept. 30 2010-Oct. 1 2010. - P. 248-251. ↑
- C2813.** Sturm C. A multiple target doppler estimation algorithm for OFDM based intelligent radar systems. / Sturm C., Braun M., Zwick T., Wiesbeck W. // 2010 European Radar Conference (EuRAD). - Paris, Sept. 30 2010-Oct. 1 2010. - P. 73-76. ↑
- C2814.** Yanghuan Li. Arbitrary synthetic aperture motion compensation based on Fast Back Projection. / Yanghuan Li, Qian Song, Tian Jin, Zhimin Zhou. // 2010 European Radar Conference (EuRAD). - Paris, Sept. 30 2010-Oct. 1 2010. - P. 487-490. ↑
- C2815.** Wang Zeng-fu. A multi-model track-before-detect algorithm for manoeuvring target detection for Over-the-Horizon Radar. / Wang Zeng-fu, Zhang Mei, Liang Yan, Pan Quan. // 2010 European Radar Conference (EuRAD). - Paris, Sept. 30 2010-Oct. 1 2010. - P. 463-466. ↑
- C2816.** McDonald M. Characterisation of dismounted combatants radar signature from airborne platforms. / McDonald M., Damini A. // 2010 European Radar Conference (EuRAD). - Paris, Sept. 30 2010-Oct. 1 2010. - P. 45-48. ↑
- C2817.** Babur G.P. Inter-period compensation algorithm in full-polarimetric FMCW radar. / Babur G.P., Krasnov O.A., Ligthart L.P. // 2010 European Radar Conference (EuRAD). - Paris, Sept. 30 2010-Oct. 1 2010. - P. 156-159. ↑
- C2818.** Sedehi M. Exploiting the joint distribution of amplitude and monopulse ratio for chi-square fluctuating targets for target DOA estimation. / Sedehi M., Colone F., Lombardo P. // 2010 European Radar Conference (EuRAD). - Paris, Sept. 30 2010-Oct. 1 2010. - P. 304-307. ↑
- C2819.** Anfu Zhu. An implementation of step recovery diode-based UWB pulse generator. / Anfu Zhu, Fu Sheng, Anxue Zhang. // 2010 IEEE International Conference on Ultra-Wideband (ICUWB). - Nanjing, 20-23 Sept. 2010. - Vol. 2. - P. 1-4. ↑
- C2820.** Ettorre M. Comparison of multi-beam pillbox antennas using leaky-wave and slotted waveguide radiating parts for automotive radars at millimeter-waves. / Ettorre M., Gandini E., Sauleau R. // 2010 European Radar Conference (EuRAD). - Paris, Sept. 30 2010-Oct. 1 2010. - P. 292-295. ↑
- C2821.** Zongbo Wang. Reconfigurable digital receiver for polarimetric radar with dual-orthogonal signals. / Zongbo Wang, Krasnov O.A., Babur G.P., Ligthart L.P., van der Zwan F. // 2010 European Radar Conference (EuRAD). - Paris, Sept. 30 2010-Oct. 1 2010. - P. 332-335. ↑
- C2822.** Mazouni K. 77 GHz FM-CW radar for FODs detection. / Mazouni K., Kohmura A., Futatsumori S., Yonemoto N., Dauvignac J., Pichot C., Migliaccio C. // 2010 European Radar Conference (EuRAD). - Paris, Sept. 30 2010-Oct. 1 2010. - P. 451-454. ↑
- C2823.** Bragin I.V. Spatial (aperture) noise generators. / Bragin I.V., Sgibnev V.P., Istukov I.V., Savin B.N., Elizavetova E.L. // 2010 European Radar Conference (EuRAD). - Paris, Sept. 30 2010-Oct. 1 2010. - P. 511-514. ↑
- C2824.** Laghezza F. Reconfigurable radar transmitter based on photonic microwave signal generation. / Laghezza F., Berizzi F., Capria A., Cacciamano A., Ghelfi P., Serafino G., Bogoni A. // 2010 European Radar Conference (EuRAD). - Paris, Sept. 30 2010-Oct. 1 2010. - P. 336-339. ↑
- C2825.** Gudkov V.N. Using signals of the global navigation satellites for diagnostics of above land troposphere refraction. / Gudkov V.N., Lutsenko V.I., Lutsenko I.V., Anh N.X., Popov I.V., Sinitskiy V.B. // 2010 European Radar Conference (EuRAD). - Paris, Sept. 30 2010-Oct. 1 2010. - P. 495-498. ↑



- C2826.** Xiaodong Zhuge. Comparison between wavefront-based shape reconstruction and beamforming for UWB near-field imaging radar. / Xiaodong Zhuge, Yarovoy A. // 2010 European Radar Conference (EuRAD). - Paris, Sept. 30 2010-Oct. 1 2010. - P. 208-211. ↑
- C2827.** Reuillon P. Scan-to-scan sea-spikes filtering for radar. / Reuillon P., Parenty F., Perret F. // 2010 European Radar Conference (EuRAD). - Paris, Sept. 30 2010-Oct. 1 2010. - P. 272-275. ↑
- C2828.** Lutsenko V.I. Detection against the background of non-Gaussian clutter from underlying surface. / Lutsenko V.I., Lutsenko I.V., Popov I.V. // 2010 European Radar Conference (EuRAD). - Paris, France, Sept. 30 2010-Oct. 1 2010. - P. 411-414. ↑
- C2829.** Cuccoli F. OTHR-SW Coordinate Registration method based on sea-land transitions: Clutter model definition. / Cuccoli F., Facheris L., Giuli D., Sermi F. // 2010 European Radar Conference (EuRAD). - Paris, Sept. 30 2010-Oct. 1 2010. - P. 101-104. ↑
- C2830.** Wei Xu. Comparison of accurate and simplified sub-entire-domain basis function methods in RCS computation of large-scale periodic structures. / Wei Xu, Zhichun Zhang, Sun B., Xiaoxiang He. // 2010 IEEE International Conference on Ultra-Wideband (ICUWB). - Nanjing, 20-23 Sept. 2010. - Vol. 1. - P. 1-4. ↑
- C2831.** Xuyang Li. Polarization diversity in Ultra-Wideband imaging systems. / Xuyang Li, Adamiuk G., Janson M., Zwick T. // 2010 IEEE International Conference on Ultra-Wideband (ICUWB). - Nanjing, 20-23 Sept. 2010. - Vol. 1. - P. 1-4. ↑
- C2832.** Tsukashima K. Cost effective Wafer Level Chip Size Package technology and application to the next generation automotive radar. / Tsukashima K., Kubota M., Baba O., Tango H., Yonamine A., Tokumitsu T., Hasegawa Y. // 2010 European Microwave Conference (EuMC). - Paris, 28-30 Sept. 2010. - P. 280-283. ↑
- C2833.** Yuan Yuan. Improved wide-band dual-linear polarization compact microstrip antenna array for Microwave Image system. / Yuan Yuan, Zhi Xu, Xuequan Yan. // 2010 IEEE International Conference on Ultra-Wideband (ICUWB). - Nanjing, 20-23 Sept. 2010. - Vol. 2. - P. 1-4. ↑
- C2834.** Liu Kaikai. Odd-Symmetry Template based three-step detector for IR-UWB radar. / Liu Kaikai, Xu Hao, Ren Jingjing, Chen Weidong. // 2010 IEEE International Conference on Ultra-Wideband (ICUWB). - Nanjing, 20-23 Sept. 2010. - Vol. 2. - P. 1-4. ↑
- C2835.** Xu Hao. An improved IPCP detector of UWB radar signals based on adaptive searching window. / Xu Hao, Liu Kaikai, Ma Yunfei, Wang Dongjin, Chen Weidong. // 2010 IEEE International Conference on Ultra-Wideband (ICUWB). - Nanjing, 20-23 Sept. 2010. - Vol. 2. - P. 1-4. ↑
- C2836.** Shun Dai. A low-cost handheld integrated UWB radar for shallow underground detection. / Shun Dai, Lihua Liu, Guangyou Fang. // 2010 IEEE International Conference on Ultra-Wideband (ICUWB). - Nanjing, 20-23 Sept. 2010. - Vol. 2. - P. 1-4. ↑
- C2837.** Ming Yu. Power handling and temperature compensation design for passive Microwave devices. 2010 European Microwave Conference (EuMC). - Paris, 28-30 Sept. 2010. - P. 351. ↑
- C2838.** Tretyakov S. Possibilities of cloaking and invisibility at microwaves. 2010 European Microwave Conference (EuMC). - Paris, 28-30 Sept. 2010. - P. 350. ↑
- C2839.** Galehdar A. The conductivity of unidirectional and quasi isotropic carbon fiber composites. / Galehdar A., Nicholson K.J., Rowe W.S.T., Ghorbani K. // 2010 European Microwave Conference (EuMC). - Paris, 28-30 Sept. 2010. - P. 882-885. ↑
- C2840.** Brokmeier A. A way to modern and cost effective packaging for RF frontends for use from microwave through millimeter wave frequencies. / Brokmeier A., Geist T., Puchinger J. // 2010 European Microwave Conference (EuMC). - Paris, 28-30 Sept. 2010. - P. 609-611. ↑
- C2841.** Bo Tian. Boresight gain optimization of an UWB monopole antenna using FDTD and genetic algorithm. / Bo Tian, Zhengjie Li, Chunyang Wang. // 2010 IEEE International Conference on Ultra-Wideband (ICUWB). - Nanjing, 20-23 Sept. 2010. - Vol. 1. - P. 1-4. ↑
- C2842.** Dambrine Gilles. Welcome to the 13th European Microwave Week 2010. 2010 European Microwave

Conference (EuMC). - Paris, France, 28-30 Sept. 2010. - P. 1. ↑

C2843. Esswein A. A low phase-noise SiGe Colpitts VCO with wide tuning range for UWB applications. / Esswein A., Dehm-Andone G., Weigel R., Aleksieieva A., Vossiek M. // 2010 European Wireless Technology Conference (EuWIT). - Paris, 27-28 Sept. 2010. - P. 229-232. ↑

C2844. Isohookana M. Design of a passive radar network. / Isohookana M., Pyykonen J. // 2010 European Radar Conference (EuRAD). - Paris, Sept. 30 2010-Oct. 1 2010. - P. 443-446. ↑

C2845. Cresp A. Comparison of the time-reversal and SEABED imaging algorithms applied on ultra-wideband experimental SPR data. / Cresp A., Yedlin M.J., Sakamoto T., Aliferis I., Sato T., Dauvignac J.-Y., Pichot C. // 2010 European Radar Conference (EuRAD). - Paris, Sept. 30 2010-Oct. 1 2010. - P. 360-363. ↑

C2846. Rovn. UWB radar signal processing for through wall tracking of multiple moving targets. / Rovn,a,kova, J., Kocur D. // 2010 European Radar Conference (EuRAD). - Paris, Sept. 30 2010-Oct. 1 2010. - P. 372-375. ↑

C2847. Aarholt E. Wind farm Gapfiller concept solution. / Aarholt E., Jackson C.A. // 2010 European Radar Conference (EuRAD). - Paris, Sept. 30 2010-Oct. 1 2010. - P. 236-239. ↑

C2848. Maddio S. Calibration of a 2.45 GHz indoor Direction of Arrival system based on unknown antenna gain. / Maddio S., Cidronali A., Giorgetti G., Manes G. // 2010 European Radar Conference (EuRAD). - Paris, Sept. 30 2010-Oct. 1 2010. - P. 77-80. ↑

C2849. Dingqing Lu. Quasi-Analytical method for estimating low false alarm rate. 2010 European Radar Conference (EuRAD). - Paris, Sept. 30 2010-Oct. 1 2010. - P. 264-267. ↑

C2850. Conti M. High range resolution DVB-T Passive Radar. / Conti M., Berizzi F., Petri D., Capria A., Martorella M. // 2010 European Radar Conference (EuRAD). - Paris, Sept. 30 2010-Oct. 1 2010. - P. 109-112. ↑

C2851. Haengseon Son. FPGA implementation of UWB radar signal processing for automotive application. / Haengseon Son, Seonyoung Lee, Kyungwon Min. // 2010 European Wireless Technology Conference (EuWIT). - Paris, 27-28 Sept. 2010. - P. 49-52. ↑

C2852. Dambrine Gilles. Welcome to the 13th European Microwave Week 2010. 2010 European Wireless Technology Conference (EuWIT). - Paris, France, 27-28 Sept. 2010. - P. 1. ↑

C2853. Wu Qing. Design and implementation of sub-GHz transmitter for ultra-wideband through-wall radar. / Wu Qing, Zheng Kuangyu, Li Qiao, Xiong Huagang. // 2010 IEEE International Conference on Ultra-Wideband (ICUWB). - Nanjing, 20-23 Sept. 2010. - Vol. 1. - P. 1-4. ↑

C2854. Monni S. UWB front-end for SAR-based imaging system. / Monni S., Grooters R., Neto A., Nennie F.A. // 2010 European Wireless Technology Conference (EuWIT). - Paris, 27-28 Sept. 2010. - P. 149-152. ↑

C2855. Ranga Y. A gain-enhanced semicircular disc antenna with a quasi-planar surface-mounted short TEM horn. / Ranga Y., Verma A.K., Esselle K.P., Weily A.R. // 2010 European Wireless Technology Conference (EuWIT). - Paris, 27-28 Sept. 2010. - P. 177-180. ↑

C2856. Kunkel S. SAR-like localization of RFID tags for non-uniform trajectory. / Kunkel S., Ming-Shih Huang, Bieber R., Vossiek M. // 2010 European Wireless Technology Conference (EuWIT). - Paris, 27-28 Sept. 2010. - P. 281-284. ↑

C2857. Kunkel S. SAR-like localization of RFID tags for non-uniform trajectory. / Kunkel S., Ming-Shih Huang, Bieber R., Vossiek M. // 2010 European Microwave Conference (EuMC). - Paris, 28-30 Sept. 2010. - P. 1758-1761. ↑

C2858. Harter M. A modular 24 GHz radar sensor for digital beamforming on transmit and receive. / Harter M., Kornbichler A., Zwick T. // 2010 European Microwave Conference (EuMC). - Paris, 28-30 Sept. 2010. - P. 1698-1701. ↑

C2859. Pancera E. Fidelity criterion for UWB medical diagnostic. / Pancera E., Li X., Zwick T., Wiesbeck W. // 2010 IEEE International Conference on Ultra-Wideband (ICUWB). - Nanjing, 20-23 Sept. 2010. - Vol. 2. - P. 1-4. ↑

- C2860.** Salman R. A novel UWB Radar super-resolution object recognition approach for complex edged objects. / Salman R., Willms I. // 2010 IEEE International Conference on Ultra-Wideband (ICUWB). - Nanjing, 20-23 Sept. 2010. - Vol. 2. - P. 1-4. ↑
- C2861.** Xin Wang. A 79-GHz LTCC laminated waveguide to metallic rectangular waveguide transition using high permittivity material. / Xin Wang, Stelzer A. // 2010 European Microwave Conference (EuMC). - Paris, 28-30 Sept. 2010. - P. 664-667. ↑
- C2862.** Fitzek F. Metamaterial matching of high-permittivity coatings for 79 GHz radar sensors. / Fitzek F., Rasshofer R.H., Biebl E.M. // 2010 European Microwave Conference (EuMC). - Paris, 28-30 Sept. 2010. - P. 1401-1404. ↑
- C2863.** El Nashef G.Z. Second order extension of power amplifiers behavioral models for accuracy improvements. / El Nashef G.Z., Torres F., Mons S., Reveyrand T., Mone, die, re T., N'Goya E., Que, re, R. // 2010 European Microwave Conference (EuMC). - Paris, 28-30 Sept. 2010. - P. 1030-1033. ↑
- C2864.** {no data available}. Session D4: Sensing and medical imaging; collision, ground-penetrating and through-wall radars. 2010 IEEE International Conference on Ultra-Wideband (ICUWB). - Nanjing, China, 20-23 Sept. 2010. - Vol. 2. - P. 1-3. ↑
- C2865.** Denoual J.M. Design of two flare UWB antenna dedicated to the research of alive buried victims. / Denoual J.M., Floc'h J.M., Mutzig J.P., Massaloux P., Ducasse F., Minvielle P., Labarthe C. // 2010 European Microwave Conference (EuMC). - Paris, 28-30 Sept. 2010. - P. 1710-1713. ↑
- C2866.** Lazaro A. Simulated and experimental wavelet-based detection of breast tumor using a UWB radar. / Lazaro A., Girbau D., Villarino R. // 2010 European Microwave Conference (EuMC). - Paris, 28-30 Sept. 2010. - P. 373-376. ↑
- C2867.** Sang-il Kwak. Design of wearable communication device for body protection from EM wave using the EBG structure. / Sang-il Kwak, Dong-Uk Sim, Jong Hwa Kwon, Hyung Do Choi. // 2010 European Microwave Conference (EuMC). - Paris, 28-30 Sept. 2010. - P. 1433-1436. ↑
- C2868.** Zwirello L. Measurement verification of dual-orthogonal polarized UWB monopulse radar system. / Zwirello L., Adamiuk G., Wiesbeck W., Zwick T. // 2010 IEEE International Conference on Ultra-Wideband (ICUWB). - Nanjing, 20-23 Sept. 2010. - Vol. 2. - P. 1-4. ↑
- C2869.** Esswein A. A low phase-noise SiGe Colpitts VCO with wide tuning range for UWB applications. / Esswein A., Dehm-Andone G., Weigel R., Aleksieieva A., Vossiek M. // 2010 European Microwave Conference (EuMC). - Paris, 28-30 Sept. 2010. - P. 1599-1602. ↑
- C2870.** Jaworski G. Dual frequency & dual-linear polarization integrated Antenna array for application in Synthetic Aperture Radar. / Jaworski G., Maleszka T., Gruszczynski S., Wincza K. // 2010 European Microwave Conference (EuMC). - Paris, 28-30 Sept. 2010. - P. 1714-1717. ↑
- C2871.** Bettidi A. A single bias 20W S-band HPA for radar applications. / Bettidi A., Cetronio A., Lavanga S., Nanni A. // 2010 European Microwave Conference (EuMC). - Paris, 28-30 Sept. 2010. - P. 1639-1642. ↑
- C2872.** Jatlaoui M.M. Original identification technique of passive EM sensors using loaded transmission delay lines. / Jatlaoui M.M., Chebila F., Bouaziz S., Pons P., Aubert H. // 2010 European Microwave Conference (EuMC). - Paris, 28-30 Sept. 2010. - P. 1106-1109. ↑
- C2873.** Winkler W. LNA and mixer for 122 GHz receiver in SiGe technology. / Winkler W., Debski W., Schmalz K., Borngrajber J., Scheytt C. // 2010 European Microwave Conference (EuMC). - Paris, 28-30 Sept. 2010. - P. 529-532. ↑
- C2874.** Thai T.T. Design and development of a millimetre-wave novel passive ultrasensitive temperature transducer for remote sensing and identification. / Thai T.T., Chebila F., Mehdi J.M., Pons P., Aubert H., DeJean G.R., Tentzeris M.M., Plana R. // 2010 European Microwave Conference (EuMC). - Paris, 28-30 Sept. 2010. - P. 45-48. ↑
- C2875.** Demirel N. 79GHz BiCMOS single-ended and differential power amplifiers. / Demirel N., Kerherve, E., Plana R., Pache D. // 2010 European Microwave Conference (EuMC). - Paris, 28-30 Sept. 2010. - P. 1690-

1693. ↑

**C2876.** Harris L.-R. SAR computation in a real-sized car: Multi-exposure scenarios. / Harris L.-R., Zhadobov M., Sauleau R. // 2010 European Microwave Conference (EuMC). - Paris, 28-30 Sept. 2010. - P. 224-227. ↑

**C2877.** Giuppi F. X-band cavity-backed slot antennas and coupled oscillator systems. / Giuppi F., Collado A., Bozzi M., Georgiadis A., Via S., Perregrini L. // 2010 European Microwave Conference (EuMC). - Paris, 28-30 Sept. 2010. - P. 340-343. ↑

**C2878.** Nijssure Y. Information-theoretic algorithm for waveform optimization within ultra wideband cognitive radar network. / Nijssure Y., Chen Y., Rapajic P., Yuen C., Chew Y.H., Qin T.F. // 2010 IEEE International Conference on Ultra-Wideband (ICUWB). - Nanjing, 20-23 Sept. 2010. - Vol. 2. - P. 1-4. ↑

**C2879.** Costrini C. 50W X-Band GaN MMIC HPA: Effective power capability and transient thermal analysis. / Costrini C., Cetronio A., Romanini P., Breglio G., Irace A., Riccio M. // 2010 European Microwave Conference (EuMC). - Paris, 28-30 Sept. 2010. - P. 1650-1653. ↑

**C2880.** Suijker E. Integrated X-band FMCW front-end in SiGe BiCMOS. / Suijker E., de Boer L., Visser G., van Dijk R., Poschmann M., van Vliet F. // 2010 European Microwave Conference (EuMC). - Paris, 28-30 Sept. 2010. - P. 1082-1085. ↑

**C2881.** Yong-Jun An. Comparative study of 2.4 GHz and 10 GHz vital signal sensing Doppler radars. / Yong-Jun An, Young-Pyo Hong, Byung-Jun Jang, Jong-Gwan Yook. // 2010 European Microwave Conference (EuMC). - Paris, 28-30 Sept. 2010. - P. 501-504. ↑

**C2882.** Desruelles G. G-band low noise amplifier and oscillator for synthetic aperture applications. / Desruelles G., Rolland N., Rolland P. // 2010 European Microwave Conference (EuMC). - Paris, 28-30 Sept. 2010. - P. 525-528. ↑

**C2883.** Schuh P. T/R-module technologies today and future trends. / Schuh P., Sledzik H., Reber R., Widmer K., Fleckenstein A., Schweizer B., Oppermann M. // 2010 European Microwave Conference (EuMC). - Paris, 28-30 Sept. 2010. - P. 1540-1543. ↑

**C2884.** Chauveau J. Ramp response radar imaging: Analysis of frequency parameters. / Chauveau J., de Beaucoudrey N. // 2010 European Microwave Conference (EuMC). - Paris, 28-30 Sept. 2010. - P. 569-572. ↑

**C2885.** Kabakchiev C. Comparison of target detection schemes in Doppler radar with PSK signals. / Kabakchiev C., Garvanov I., Daskalov P., Donkov P., Kabakchieva D. // 2010 European Radar Conference (EuRAD). - Paris, Sept. 30 2010-Oct. 1 2010. - P. 268-271. ↑

**C2886.** Hudec P. Digital signal processing applied to radar sensors operated in active defense systems. / Hudec P., Plasil J., Dohnal P. // 2010 European Radar Conference (EuRAD). - Paris, Sept. 30 2010-Oct. 1 2010. - P. 483-486. ↑

**C2887.** Tatu S.O. Interferometric quadrature down-converter for 77 GHz automotive radar: Modeling and analysis. / Tatu S.O., Cojocaru R.I., Moldovan E. // 2010 European Radar Conference (EuRAD). - Paris, Sept. 30 2010-Oct. 1 2010. - P. 125-128. ↑

**C2888.** Martorella M. Optimal sensor placement for multi-bistatic ISAR imaging. / Martorella M., Haywood B., Nel W., Gaffar Y., Palmer J., Bates B., Giusti E., Berizzi F. // 2010 European Radar Conference (EuRAD). - Paris, Sept. 30 2010-Oct. 1 2010. - P. 228-231. ↑

**C2889.** Chernyak V.S. MIMO radars. What are they?. 2010 European Radar Conference (EuRAD). - Paris, Sept. 30 2010-Oct. 1 2010. - P. 137-140. ↑

**C2890.** Nigam C. Knowledge assistance for ground target tracking and resource management. / Nigam C., Rathi A., Vardhani J.P. // 2010 European Radar Conference (EuRAD). - Paris, Sept. 30 2010-Oct. 1 2010. - P. 388-391. ↑

**C2891.** Bin Sun. Study on velocity estimation of MCPC signal in wideband radar. / Bin Sun, Xi-zhang Wei, Xiang Li. // 2010 European Radar Conference (EuRAD). - Paris, Sept. 30 2010-Oct. 1 2010. - P. 376-379. ↑

↑



- C2892.** {no data available}. Book of abstracts. 2010 European Radar Conference (EuRAD). - Paris, France, Sept. 30 2010-Oct. 1 2010. - P. 1-23. ↑
- C2893.** {no data available}. EuRAD 2010 abstract cards. 2010 European Radar Conference (EuRAD). - Paris, France, Sept. 30 2010-Oct. 1 2010. - P. 1-134. ↑
- C2894.** Tahmoush D. Radar polarimetry for security applications. / Tahmoush D., Silvius J. // 2010 European Radar Conference (EuRAD). - Paris, Sept. 30 2010-Oct. 1 2010. - P. 471-474. ↑
- C2895.** {no data available}. EuRAD 2010 detailed author index. 2010 European Radar Conference (EuRAD). - Paris, France, Sept. 30 2010-Oct. 1 2010. - P. 1-58. ↑
- C2896.** Kalkan Y. Target localization methods for frequency-only MIMO radar. / Kalkan Y., Baykal B. // 2010 European Radar Conference (EuRAD). - Paris, Sept. 30 2010-Oct. 1 2010. - P. 396-399. ↑
- C2897.** Alleva V. Digital antenna unit for DOA analysis in ESM systems. / Alleva V., Baccello D., Bartocci M., Orobello B. // 2010 European Radar Conference (EuRAD). - Paris, Sept. 30 2010-Oct. 1 2010. - P. 479-482. ↑
- C2898.** {no data available}. The end of indexes. 2010 European Radar Conference (EuRAD). - Paris, France, Sept. 30 2010-Oct. 1 2010. - P. 1. ↑
- C2899.** Brooker G. Millimetre wave radar imaging of mining vehicles. / Brooker G., Martinez J., Hennessey R. // 2010 European Radar Conference (EuRAD). - Paris, Sept. 30 2010-Oct. 1 2010. - P. 284-287. ↑
- C2900.** Kemkemian S. Radar and Electronic Warfare cooperation aboard a single or multiple cooperative platforms. / Kemkemian S., Nouvel-Fiani M., Chamouard E. // 2010 European Radar Conference (EuRAD). - Paris, Sept. 30 2010-Oct. 1 2010. - P. 328-331. ↑
- C2901.** Crupi G. Non-quasi-static modeling of the intrinsic Y22 for GaN, Si, and GaAs mm-wave FET technologies. / Crupi G., Caddemi A., Schreurs D.M.M., Raffo A., Avolio G., Homayouni S.M., Vannini G. // 2010 European Radar Conference (EuRAD). - Paris, Sept. 30 2010-Oct. 1 2010. - P. 316-319. ↑
- C2902.** Brousseau C. Estimation of efficiency of a tree structured hierarchical wavelet representation of synthetic database applied to Non-Cooperative Target Recognition. 2010 European Radar Conference (EuRAD). - Paris, Sept. 30 2010-Oct. 1 2010. - P. 49-52. ↑
- C2903.** Jaworski G. Dual frequency & dual- linear polarization integrated antenna array for application in Synthetic Aperture Radar. / Jaworski G., Maleszka T., Gruszczynski S., Wincza K. // 2010 European Radar Conference (EuRAD). - Paris, Sept. 30 2010-Oct. 1 2010. - P. 523-526. ↑
- C2904.** Feil P. Foreign object debris detection using a 78 GHz sensor with cosec antenna. / Feil P., Zeitler A., Nguyen T.P., Pichot C., Migliaccio C., Menzel W. // 2010 European Radar Conference (EuRAD). - Paris, Sept. 30 2010-Oct. 1 2010. - P. 33-36. ↑
- C2905.** Denoual J.M. Design of two flare UWB antenna dedicated to the research of alive buried victims. / Denoual J.M., Floc'h J.M., Mutzig J.P., Massaloux P., Ducasse F., Minvielle P., Labarthe C. // 2010 European Radar Conference (EuRAD). - Paris, Sept. 30 2010-Oct. 1 2010. - P. 519-522. ↑
- C2906.** Ali F. A high resolution 2D omnidirectional synthetic aperture radar scanner at K band. / Ali F., Urban A., Vossiek M. // 2010 European Radar Conference (EuRAD). - Paris, Sept. 30 2010-Oct. 1 2010. - P. 503-506. ↑
- C2907.** Menzel W. Loss mechanisms of folded reflectarray antennas. / Menzel W., Keyrouz S., Jiang Li, Dieter S. // 2010 European Radar Conference (EuRAD). - Paris, Sept. 30 2010-Oct. 1 2010. - P. 180-183. ↑
- C2908.** Pandolfi C. Comparison of analog IFM and digital frequency measurement receivers for electronic warfare. / Pandolfi C., Fitini E., Gabrielli G., Megna E., Zaccaron A. // 2010 European Radar Conference (EuRAD). - Paris, Sept. 30 2010-Oct. 1 2010. - P. 232-235. ↑
- C2909.** Barbaresco F. Airport radar monitoring of wake vortex in all weather conditions. 2010 European Radar Conference (EuRAD). - Paris, Sept. 30 2010-Oct. 1 2010. - P. 85-88. ↑
- C2910.** Bocquet M. A multifunctional 60-GHz system for automotive applications with communication and

positioning abilities based on time reversal. / Bocquet M., Loyez C., Lethien C., Deparis N., Heddebaut M., Rivenq A., Rolland N. // 2010 European Radar Conference (EuRAD). - Paris, Sept. 30 2010-Oct. 1 2010. - P. 61-64. ↑

C2911. Buchanan N.B. Angle of arrival detection using Retrodirective RADAR. / Buchanan N.B., Fusco V. // 2010 European Radar Conference (EuRAD). - Paris, Sept. 30 2010-Oct. 1 2010. - P. 133-136. ↑

C2912. Fusco V. Dual-sided phase conjugating surface techniques for imaging. / Fusco V., Malyuskin O. // 2010 European Radar Conference (EuRAD). - Paris, Sept. 30 2010-Oct. 1 2010. - P. 296-299. ↑

C2913. Le Yang. Riemannian median, geometry of covariance matrices and radar target detection. / Le Yang, Arnaudon M., Barbaresco F. // 2010 European Radar Conference (EuRAD). - Paris, Sept. 30 2010-Oct. 1 2010. - P. 415-418. ↑

C2914. Ocket I. Design challenges for millimeter wave active imaging systems. / Ocket I., Schreurs D., Tavakoli V., Qi F., Nauwelaers B., Stiens J. // 2010 European Radar Conference (EuRAD). - Paris, Sept. 30 2010-Oct. 1 2010. - P. 312-315. ↑

C2915. Boudamouz B. Through the wall MIMO radar detection with stepped frequency waveforms. / Boudamouz B., Millot P., Pichot C. // 2010 European Radar Conference (EuRAD). - Paris, Sept. 30 2010-Oct. 1 2010. - P. 400-402. ↑

C2916. Marquis E. New coastal radar performances: Evolution or revolution. 2010 European Radar Conference (EuRAD). - Paris, Sept. 30 2010-Oct. 1 2010. - P. 380-383. ↑

C2917. Griffiths H. Multistatic, MIMO and networked radar: The future of radar sensors?. 2010 European Radar Conference (EuRAD). - Paris, Sept. 30 2010-Oct. 1 2010. - P. 81-84. ↑

C2918. Costes C. Advanced clouds tracking for airborne weather radar & ground primary surveillance radar. / Costes C., Artis J., Barbaresco F. // 2010 European Radar Conference (EuRAD). - Paris, Sept. 30 2010-Oct. 1 2010. - P. 141-144. ↑

C2919. Ermakov S. Possibilities of oil slick detection on the sea surface using radar. / Ermakov S., da Silva J.C.B., Magalhaes J.M., Sergievskaya I. // 2010 European Radar Conference (EuRAD). - Paris, Sept. 30 2010-Oct. 1 2010. - P. 13-16. ↑

C2920. Maksimovitch Y. Study of different configurations of tapered-slot antenna arrays for detecting buried objects. / Maksimovitch Y., Mikhnev V., Vainikainen P. // 2010 European Radar Conference (EuRAD). - Paris, Sept. 30 2010-Oct. 1 2010. - P. 384-387. ↑

C2921. Klare J. MIRA-CLE X: A new imaging MIMO-radar for multi-purpose applications. / Klare J., Saalman O. // 2010 European Radar Conference (EuRAD). - Paris, Sept. 30 2010-Oct. 1 2010. - P. 129-132. ↑

C2922. Mikhnev V. Characterization of underground objects in UWB GPR by range profiling of phase. / Mikhnev V., Vainikainen P. // 2010 European Radar Conference (EuRAD). - Paris, Sept. 30 2010-Oct. 1 2010. - P. 368-371. ↑

C2923. Rezer K. Co-array weighting in minimum-redundancy arrays for radar image enhancement. / Rezer K., Jacob A.F. // 2010 European Radar Conference (EuRAD). - Paris, Sept. 30 2010-Oct. 1 2010. - P. 117-120. ↑

C2924. Trampuz C. Experimental characterization of channel crosstalk in interleaved array antennas for FMCW radar. / Trampuz C., Lager I.E., Simeoni M., Ligthart L.P. // 2010 European Radar Conference (EuRAD). - Paris, Sept. 30 2010-Oct. 1 2010. - P. 439-442. ↑

C2925. Aittomaki T. Target detection and positioning in correlated scattering using widely distributed MIMO radar. / Aittomaki T., Koivunen V. // 2010 European Radar Conference (EuRAD). - Paris, Sept. 30 2010-Oct. 1 2010. - P. 403-406. ↑

C2926. Poullin D. New capabilities for PCL system: 3D measurement for receiver in multidonors configuration. / Poullin D., Flecheux M., Klein M. // 2010 European Radar Conference (EuRAD). - Paris, Sept. 30 2010-Oct. 1 2010. - P. 344-347. ↑

- C2927.** Sergievskaya I. Radar probing of steep gravity waves. wave tank experiment. / Sergievskaya I., Ermakov S., Kapustin I. // 2010 European Radar Conference (EuRAD). - Paris, Sept. 30 2010-Oct. 1 2010. - P. 17-20. ↑
- C2928.** Qilei Zhang. An extended NLCS algorithm for Bistatic fixed-receiver SAR imaging. / Qilei Zhang, Wenge Chang, Xiangyang Li. // 2010 European Radar Conference (EuRAD). - Paris, Sept. 30 2010-Oct. 1 2010. - P. 252-255. ↑
- C2929.** Marques P. SAR-MTI improvement using a-priori knowledge of the road network. 2010 European Radar Conference (EuRAD). - Paris, Sept. 30 2010-Oct. 1 2010. - P. 244-247. ↑
- C2930.** Caratelli D. Accurate time-domain modelling of MEMS antennas for wireless telemetry systems. / Caratelli D., Massaro A., Yarovsky A., Cingolani R. // 2010 European Radar Conference (EuRAD). - Paris, Sept. 30 2010-Oct. 1 2010. - P. 531-534. ↑
- C2931.** Cheng-lan Liu. 3-D calibration of InSAR imaging under a condition of phase ambiguity. / Cheng-lan Liu, Feng He, Xun-zhang Gao. // 2010 European Radar Conference (EuRAD). - Paris, Sept. 30 2010-Oct. 1 2010. - P. 435-438. ↑
- C2932.** Menzel W. Millimeter-wave radar for civil applications. 2010 European Radar Conference (EuRAD). - Paris, Sept. 30 2010-Oct. 1 2010. - P. 89-92. ↑
- C2933.** {no data available}. EuRAD 2010 brief author index. 2010 European Radar Conference (EuRAD). - Paris, France, Sept. 30 2010-Oct. 1 2010. - P. 1-10. ↑
- C2934.** {no data available}. Reviewers. 2010 European Radar Conference (EuRAD). - Paris, France, Sept. 30 2010-Oct. 1 2010. - P. 1-2. ↑
- C2935.** {no data available}. Conference committees. 2010 European Radar Conference (EuRAD). - Paris, France, Sept. 30 2010-Oct. 1 2010. - P. 1. ↑
- C2936.** Eudeline Philippe. Welcome to EuRAD 2010. / Eudeline Philippe, Migliaccio Claire, Dauvignac Jean Yves. // 2010 European Radar Conference (EuRAD). - Paris, France, Sept. 30 2010-Oct. 1 2010. - P. 1. ↑
- C2937.** {no data available}. EuMW2009 rome prizes. 2010 European Radar Conference (EuRAD). - Paris, France, Sept. 30 2010-Oct. 1 2010. - P. 1. ↑
- C2938.** {no data available}. EuMA awards. 2010 European Radar Conference (EuRAD). - Paris, France, Sept. 30 2010-Oct. 1 2010. - P. 1-2. ↑
- C2939.** Heinrich Wolfgang. Welcome from the president of the European Microwave Association. 2010 European Radar Conference (EuRAD). - Paris, France, Sept. 30 2010-Oct. 1 2010. - P. 1. ↑
- C2940.** Dambrine Gilles. Welcome to the 13th European Microwave Week 2010. 2010 European Radar Conference (EuRAD). - Paris, France, Sept. 30 2010-Oct. 1 2010. - P. 1. ↑
- C2941.** Orlando D. Track-before-detect algorithms for bistatic sonars. / Orlando D., Ehlers F., Ricci G. // 2010 2nd International Workshop on Cognitive Information Processing (CIP). - Elba, 14-16 June 2010. - P. 180-185. ↑
- C2942.** {no data available}. Copyright page. 2010 2nd International Workshop on Cognitive Information Processing (CIP). - Elba, 14-16 June 2010. - P. 1. ↑
- C2943.** Maresca S. Vessel detection and classification: An integrated maritime surveillance system in the Tyrrhenian sea. / Maresca S., Greco M., Gini F., Grasso R., Coraluppi S., Horstmann J. // 2010 2nd International Workshop on Cognitive Information Processing (CIP). - Elba, 14-16 June 2010. - P. 40-45. ↑
- C2944.** Capraro G.T. Metacognition in radar. / Capraro G.T., Wicks M.C., Schneible R. // 2010 2nd International Workshop on Cognitive Information Processing (CIP). - Elba, 14-16 June 2010. - P. 1-6. ↑
- C2945.** Essen H. Millimeterwave radar network for foreign object detection. / Essen H., Luedtke G., Warok P., Koch W., Schikora M., Wild K. // 2010 2nd International Workshop on Cognitive Information Processing (CIP). - Elba, 14-16 June 2010. - P. 7-10. ↑

- C2946.** Malas J.A. The radar system and information flow. / Malas J.A., Cortese J.A. // 2010 2nd International Workshop on Cognitive Information Processing (CIP). - Elba, 14-16 June 2010. - P. 17-22. ↑
- C2947.** Fuhrmann D.R. Adapting a MIMO/phased-array radar transmit beampattern to target location. / Fuhrmann D.R., Browning J.P., Rangaswamy M. // 2010 2nd International Workshop on Cognitive Information Processing (CIP). - Elba, 14-16 June 2010. - P. 354-359. ↑
- C2948.** Debatty T. Software defined RADAR a state of the art. 2010 2nd International Workshop on Cognitive Information Processing (CIP). - Elba, 14-16 June 2010. - P. 253-257. ↑
- C2949.** Bandiera F. Adaptive radar detection: A subspace identification approach. / Bandiera F., Orlando D., Ricci G., Scharf L.L. // 2010 2nd International Workshop on Cognitive Information Processing (CIP). - Elba, 14-16 June 2010. - P. 243-246. ↑
- C2950.** Chang Yuliang. A unique calibration method testified by X-band polarimetric radar. / Chang Yuliang, Li Yongzhen, Wang Xuesong, Xiao Shunping. // 2010 Asia Pacific Conference on Postgraduate Research in Microelectronics and Electronics (PrimeAsia). - Shanghai, 22-24 Sept. 2010. - P. 279-282. ↑
- C2951.** Xie Hongsen. CFAR detector using GIS information. / Xie Hongsen, Zou Kun. // 2010 Second IITA International Conference on Geoscience and Remote Sensing (IITA-GRS). - Qingdao, 28-31 Aug. 2010. - Vol. 2. - P. 272-274. ↑
- C2952.** Ahmad F. Radar waveform design for detection of weapons. / Ahmad F., Amin M.G. // 2010 2nd International Workshop on Cognitive Information Processing (CIP). - Elba, 14-16 June 2010. - P. 258-262. ↑
- C2953.** Zhang Ying. Study on retrieval methods of soil water content in vegetation covering areas based on multi-source remote sensing data. 2010 Second IITA International Conference on Geoscience and Remote Sensing (IITA-GRS). - Qingdao, 28-31 Aug. 2010. - Vol. 2. - P. 369-372. ↑
- C2954.** Rossler C.W. Rapid waveform adaptation for nearly optimal detection in colored interference. / Rossler C.W., Patton L.K. // 2010 2nd International Workshop on Cognitive Information Processing (CIP). - Elba, 14-16 June 2010. - P. 232-236. ↑
- C2955.** Heron M.L. Wind direction manifestation on HF ocean radar echoes. / Heron M.L., Marrone P. // OCEANS 2010 IEEE-Sydney. - Sydney, NSW, 24-27 May 2010. - P. 1-6. ↑
- C2956.** Jaffre. Waves in the Southern Great Barrier Reef. / Jaffre, s J.B.D., Heron M.L., Middleditch A., Steinberg C.R., Durrant T.H. // OCEANS 2010 IEEE-Sydney. - Sydney, NSW, 24-27 May 2010. - P. 1-4. ↑
- C2957.** DiMassa D.D. Can vertical mixing from turbulent kinetic energy mitigate coral bleaching? An application of high frequency ocean radar. / DiMassa D.D., Heron M.L., Mantovanelli A., Heron S.F., Steinberg C. // OCEANS 2010 IEEE-Sydney. - Sydney, NSW, 24-27 May 2010. - P. 1-5. ↑
- C2958.** Yoshida T. Time domain numerical simulation of microwave backscattering from sea surface for radar remote sensing. / Yoshida T., Chang-Kyu Rheem. // OCEANS 2010 IEEE-Sydney. - Sydney, NSW, 24-27 May 2010. - P. 1-6. ↑
- C2959.** Whelan C.W. Rapid deployable HF RADAR for Norwegian emergency spill operations. / Whelan C.W., Barrick D.E., Lilleboe P.M., Breivik W., Kjelaas A., Fernandez V., Alonso-Martirena A. // OCEANS 2010 IEEE-Sydney. - Sydney, NSW, 24-27 May 2010. - P. 1-3. ↑
- C2960.** Simetti E. Towards the use of a team of USVs for civilian harbour protection: The problem of intercepting detected menaces. / Simetti E., Turetta A., Casalino G., Cresta M. // OCEANS 2010 IEEE-Sydney. - Sydney, NSW, 24-27 May 2010. - P. 1-7. ↑
- C2961.** Cysewski M. Sea surface current mapping by Radar Doppler Current Profiler. / Cysewski M., Seemann J., Ziemer F. // OCEANS 2010 IEEE-Sydney. - Sydney, NSW, 24-27 May 2010. - P. 1-7. ↑
- C2962.** Anderson S.J. On the detection of marine mammals with ship-borne polarimetric microwave radar. / Anderson S.J., Morris J.T. // OCEANS 2010 IEEE-Sydney. - Sydney, NSW, 24-27 May 2010. - P. 1-6. ↑
- C2963.** Reichert K. X-Band radar derived sea surface elevation maps as input to ship motion forecasting. /



Reichert K., Dannenberg J., van den Boom H. // OCEANS 2010 IEEE-Sydney. - Sydney, NSW, 24-27 May 2010. - P. 1-7. ↑

C2964. Hao He. Waveform design with stopband and correlation constraints for cognitive radar. / Hao He, Stoica P., Jian Li. // 2010 2nd International Workshop on Cognitive Information Processing (CIP). - Elba, 14-16 June 2010. - P. 344-349. ↑

C2965. Oleynikova E. Perimeter patrol on autonomous surface vehicles using marine radar. / Oleynikova E., Lee N.B., Barry A.J., Holler J., Barrett D. // OCEANS 2010 IEEE-Sydney. - Sydney, NSW, 24-27 May 2010. - P. 1-5. ↑

C2966. Woithe H.C. Slocum Glider energy measurement and simulation infrastructure. / Woithe H.C., Chigirev I., Aragon D., Iqbal M., Shames Y., Glenn S., Schofield O., Seskar I., Kremer U. // OCEANS 2010 IEEE-Sydney. - Sydney, NSW, 24-27 May 2010. - P. 1-8. ↑

C2967. Lixue Song. Doppler velocity dealiasing with millimeter wave radar RHI data. / Lixue Song, Ming Wei. // 2010 Second IITA International Conference on Geoscience and Remote Sensing (IITA-GRS). - Qingdao, 28-31 Aug. 2010. - Vol. 2. - P. 216-218. ↑

C2968. Chang Yuliang. Simultaneous estimation of AOA and polarization using differently polarized antennas. / Chang Yuliang, Li Yongzhen, Wang Xuesong, Xiao Shunping. // 2010 Asia Pacific Conference on Postgraduate Research in Microelectronics and Electronics (PrimeAsia). - Shanghai, 22-24 Sept. 2010. - P. 283-286. ↑

C2969. Hassanein A. Estimating the parameters of a moving target in MIMO radar with widely separated antennas. / Hassanein A., Vorobyov S.A., Gershman A.B., Rubsamen M. // 2010 IEEE Sensor Array and Multichannel Signal Processing Workshop (SAM). - Jerusalem, 4-7 Oct. 2010. - P. 57-60. ↑

C2970. Liang Chen. An improved monopulse angular tracking method using adaptive digital beamforming technique. / Liang Chen, Weixing Sheng, Xiaofeng Ma, Hao Wang. // 2010 International Symposium on Signals Systems and Electronics (ISSSE). - Nanjing, 17-20 Sept. 2010. - Vol. 2. - P. 1-4. ↑

C2971. {no data available}. Session E3: Radar techniques and applications. 2010 International Symposium on Signals Systems and Electronics (ISSSE). - Nanjing, 17-20 Sept. 2010. - Vol. 2. - P. 1. ↑

C2972. Ling Wang. Passive radar imaging of moving targets with sparsely distributed receivers. / Ling Wang, Yazici, B. // 2010 IEEE Sensor Array and Multichannel Signal Processing Workshop (SAM). - Jerusalem, 4-7 Oct. 2010. - P. 257-260. ↑

C2973. Nikolic M. 3D Electromagnetic imaging using compressive sensing. / Nikolic M., Gongguo Tang, Nehorai A. // 2010 IEEE Sensor Array and Multichannel Signal Processing Workshop (SAM). - Jerusalem, 4-7 Oct. 2010. - P. 37-40. ↑

C2974. Hickman G. MIMO GMTI radar with multipath clutter suppression. / Hickman G., Krolik J.L. // 2010 IEEE Sensor Array and Multichannel Signal Processing Workshop (SAM). - Jerusalem, 4-7 Oct. 2010. - P. 65-68. ↑

C2975. Hong-Li Peng. A miniaturized broadband four-port antenna based radar detection system. / Hong-Li Peng, Wen-Yan Yin, Jun-fa Mao, Yadong Zhang, Liang Zhou. // 2010 International Symposium on Signals Systems and Electronics (ISSSE). - Nanjing, 17-20 Sept. 2010. - Vol. 2. - P. 1-4. ↑

C2976. Zhao Ke-ming. Fast calculation of wide-band RCS for three-dimensional PEC objects based on preconditioned AWE technique. / Zhao Ke-ming, Sun Yu-fa. // 2010 International Symposium on Signals Systems and Electronics (ISSSE). - Nanjing, 17-20 Sept. 2010. - Vol. 2. - P. 1-4. ↑

C2977. Manyi Tao. Signal based parameter estimation for precise circular-scanning SAR imaging. / Manyi Tao, Yong Li, Daiyin Zhu, Qiyu Chai. // 2010 International Symposium on Signals Systems and Electronics (ISSSE). - Nanjing, 17-20 Sept. 2010. - Vol. 2. - P. 1-4. ↑

C2978. Fang Wang. Target automatic recognition based on ISAR image with wavelet transform and MBLBP. / Fang Wang, Weixing Sheng, Xiaofeng Ma, Hao Wang. // 2010 International Symposium on Signals Systems and Electronics (ISSSE). - Nanjing, 17-20 Sept. 2010. - Vol. 2. - P. 1-4. ↑

- C2979.** ChongHua Fang. Influence of vibration between shipboards on ship-sea integrational electromagnetic scattering in high frequency. / ChongHua Fang, Qi Zhang, XinYang Shi. // 2010 International Symposium on Signals Systems and Electronics (ISSSE). - Nanjing, 17-20 Sept. 2010. - Vol. 2. - P. 1-4. ↑
- C2980.** Huang Jianjia. Range Instantaneous Doppler ISAR imaging based on FRFT. / Huang Jianjia, Yali Qin, Hongliang Ren, Wen Hao. // 2010 International Symposium on Signals Systems and Electronics (ISSSE). - Nanjing, 17-20 Sept. 2010. - Vol. 2. - P. 1-4. ↑
- C2981.** Liu Zhe. Motion compensation for spaceborne/airborne hybrid bistatic SAR. / Liu Zhe, Yang Jianyu, Zhang Xiaoling. // 2010 International Symposium on Signals Systems and Electronics (ISSSE). - Nanjing, 17-20 Sept. 2010. - Vol. 2. - P. 1-4. ↑
- C2982.** Deudon F. A Migrating Target Indicator for wideband radar. / Deudon F., Le Chevalier F., Bidon S., Besson O., Savy L. // 2010 IEEE Sensor Array and Multichannel Signal Processing Workshop (SAM). - Jerusalem, 4-7 Oct. 2010. - P. 249-252. ↑
- C2983.** Garelo R. Signal and image processing applications in radar ocean observations. 2010 10th International Conference on Information Sciences Signal Processing and their Applications (ISSPA). - Kuala Lumpur, 10-13 May 2010. - P. 810-818. ↑
- C2984.** Janatian N. Generalization of Automatic Censored Mean Level Detector (ACMLD) for MIMO radars. / Janatian N., Modarres-Hashemi M., Sheikhi A. // 2010 10th International Conference on Information Sciences Signal Processing and their Applications (ISSPA). - Kuala Lumpur, 10-13 May 2010. - P. 430-433. ↑
- C2985.** Zaimbashi A. CFAR detectors in presence of jammer noise. / Zaimbashi A., Sheikhi A. // 2010 10th International Conference on Information Sciences Signal Processing and their Applications (ISSPA). - Kuala Lumpur, 10-13 May 2010. - P. 426-429. ↑
- C2986.** {no data available}. Front matter. 2010 Asia Pacific Conference on Postgraduate Research in Microelectronics and Electronics (PrimeAsia). - Shanghai, 22-24 Sept. 2010. - P. i-xiv. ↑
- C2987.** Sadek S. A wireless microwave sensor for remote monitoring of heart and respiration activity. / Sadek S., Ghattas L., Fawaz L. // 2010 Mediterranean Microwave Symposium (MMS). - Guzelyurt, 25-27 Aug. 2010. - P. 374-376. ↑
- C2988.** Caorsi S. An automatic feature extraction technique for GPR data processing in electromagnetic inverse scattering problems. / Caorsi S., Stasolla M. // 2010 Mediterranean Microwave Symposium (MMS). - Guzelyurt, 25-27 Aug. 2010. - P. 184-187. ↑
- C2989.** Sheikhi A. Model based adaptive detection algorithm with low secondary data support. / Sheikhi A., Zamani A., Hatam M., Karimi M. // 2010 10th International Conference on Information Sciences Signal Processing and their Applications (ISSPA). - Kuala Lumpur, 10-13 May 2010. - P. 177-180. ↑
- C2990.** Hurtado M. Sparse component analysis for linear mixed models. / Hurtado M., von Ellenreider N., Muravchik C., Nehorai A. // 2010 IEEE Sensor Array and Multichannel Signal Processing Workshop (SAM). - Jerusalem, 4-7 Oct. 2010. - P. 137-140. ↑
- C2991.** Ephrath A. A recursive model for partially correlated  $\chi^2$  targets. 2010 IEEE Sensor Array and Multichannel Signal Processing Workshop (SAM). - Jerusalem, 4-7 Oct. 2010. - P. 229-232. ↑
- C2992.** Bandiera F. Covariance-informed detection in compound-Gaussian clutter without secondary data. / Bandiera F., Besson O., Ricci G. // 2010 IEEE Sensor Array and Multichannel Signal Processing Workshop (SAM). - Jerusalem, 4-7 Oct. 2010. - P. 241-244. ↑
- C2993.** Reyneke P. Smoothing irregular data using polynomial filters. / Reyneke P., Morrison N., Kourie D., de Ridder C. // 2010 PROCEEDINGS ELMAR. - Zadar, 15-17 Sept. 2010. - P. 393-397. ↑
- C2994.** Kuzmanic. Oil spill detection in sar images using wavelets and morphology. / Kuzmanic, I., Vujovic, I. // 2010 PROCEEDINGS ELMAR. - Zadar, 15-17 Sept. 2010. - P. 337-340. ↑
- C2995.** {no data available}. Copyright page. 2010 IEEE Sensor Array and Multichannel Signal Processing Workshop (SAM). - Jerusalem, 4-7 Oct. 2010. - P. 1. ↑

- C2996.** Wakabayashi N. Development of radar simulator software using AIS data for ship data. / Wakabayashi N., Makino H., Mori K., Shiotani S. // OCEANS 2010 IEEE-Sydney. - Sydney, NSW, 24-27 May 2010. - P. 1-5. ↑
- C2997.** Zheng Zhao. High-resolution airborne SAR interferometry mapping application in Huashan mountain. / Zheng Zhao, Jixian Zhang, Guoman Huang, Fenfen Hua, Shucheng Yang, Shaoping Deng. // 2010 Second IITA International Conference on Geoscience and Remote Sensing (IITA-GRS). - Qingdao, 28-31 Aug. 2010. - Vol. 2. - P. 571-574. ↑
- C2998.** Suganuma N. Robust environment perception based on occupancy grid maps for autonomous vehicle. / Suganuma N., Matsui T. // Proceedings of SICE Annual Conference 2010. - Taipei, 18-21 Aug. 2010. - P. 2354-2357. ↑
- C2999.** JingHui Fan. DInSAR for land subsidence monitoring using high resolution COSMO-SKYMED SAR Data: Preliminary results compared with ASAR. / JingHui Fan, HongLi Zhao, Xiaofang Guo. // 2010 Second IITA International Conference on Geoscience and Remote Sensing (IITA-GRS). - Qingdao, 28-31 Aug. 2010. - Vol. 2. - P. 157-160. ↑
- C3000.** Asahi Y. Privacy protection against ubiquitous marketing. Proceedings of SICE Annual Conference 2010. - Taipei, 18-21 Aug. 2010. - P. 1434-1436. ↑
- C3001.** Hong-Li Zhao. A method for InSAR baseline refinement and its application. / Hong-Li Zhao, Jing-Hui Fan, Xiao-Fang Guo. // 2010 Second IITA International Conference on Geoscience and Remote Sensing (IITA-GRS). - Qingdao, 28-31 Aug. 2010. - Vol. 2. - P. 161-164. ↑
- C3002.** Higuchi M. Seat vibrotactile warning interface for forward vehicle collision avoidance. / Higuchi M., Raksincharoensak P. // Proceedings of SICE Annual Conference 2010. - Taipei, 18-21 Aug. 2010. - P. 1370-1373. ↑
- C3003.** Tanaka S. Nondestructive measurement of diameter of reinforcing bars in concrete using an electromagnetic wave radar under the effect of cross bars. / Tanaka S., Begum H. // Proceedings of SICE Annual Conference 2010. - Taipei, 18-21 Aug. 2010. - P. 2731-2736. ↑
- C3004.** Bumsung Kim. Intelligent collision risk assessment based on Neural Network Ensemble. / Bumsung Kim, Baehoon Choi, Seongkeun Park, Euntai Kim. // Proceedings of SICE Annual Conference 2010. - Taipei, 18-21 Aug. 2010. - P. 2893-2895. ↑
- C3005.** Sheng Chen. Application of integrated geological prediction in expressway tunnel. / Sheng Chen, Jiahua Shu, Qiaosen Luj, Guichun Zhu. // 2010 Second IITA International Conference on Geoscience and Remote Sensing (IITA-GRS). - Qingdao, 28-31 Aug. 2010. - Vol. 1. - P. 540-543. ↑
- C3006.** Jiang Ting-Chen. Deformation analysis of Wenchuan earthquake based on D-InSAR with image mode. / Jiang Ting-Chen, Wang Xiu-Ping. // 2010 Second IITA International Conference on Geoscience and Remote Sensing (IITA-GRS). - Qingdao, 28-31 Aug. 2010. - Vol. 1. - P. 189-192. ↑
- C3007.** Huan Ruohong. SAR image target recognition based on NMF feature extraction and Bayesian decision fusion. / Huan Ruohong, Pan Yun, Mao Keji. // 2010 Second IITA International Conference on Geoscience and Remote Sensing (IITA-GRS). - Qingdao, 28-31 Aug. 2010. - Vol. 1. - P. 496-499. ↑
- C3008.** Takayama J.-y. Precise diameter measurement of reinforcing bar and steel pipe based on bi-static model using microwave radar. / Takayama J.-y., Yoshinaga T., Ohyama S., Ohtake Y. // Proceedings of SICE Annual Conference 2010. - Taipei, 18-21 Aug. 2010. - P. 1218-1223. ↑
- C3009.** Lu Ye. Modeling and simulation of position for the Stratospheric ISAR system. / Lu Ye, Jing Xiaojun, You Siqing, Qi Zhaoqun, Sun Songlin. // 2010 Second IITA International Conference on Geoscience and Remote Sensing (IITA-GRS). - Qingdao, 28-31 Aug. 2010. - Vol. 1. - P. 525-528. ↑
- C3010.** Hangcheng Han. Radar Multi-Targets Real-Time Communication Based on Software Radio. / Hangcheng Han, Jianping An, Weiyu An. // 2010 6th International Conference on Wireless Communications Networking and Mobile Computing (WiCOM). - Chengdu, 23-25 Sept. 2010. - P. 1-4. ↑
- C3011.** Chunyun Song. Specific Emitter Identification Based on Intrinsic Time-Scale Decomposition. / Chunyun Song, Yi Zhan, Lin Guo. // 2010 6th International Conference on Wireless Communications Networking and

Mobile Computing (WiCOM). - Chengdu, 23-25 Sept. 2010. - P. 1-4. ↑

**C3012.** Huilin Zhou. Automatic Layer-Interface Detection of Pavement Based on Matched Filter. / Huilin Zhou, Shaoyi Li, Jian Zhu. // 2010 6th International Conference on Wireless Communications Networking and Mobile Computing (WiCOM). - Chengdu, 23-25 Sept. 2010. - P. 1-3. ↑

**C3013.** Huilin Zhou. Ultra-Thin Asphalt Pavement Layer Interface Detection and Time Delay Estimation Based on MUSIC. / Huilin Zhou, Qiang Zhang, Jian Zhu. // 2010 6th International Conference on Wireless Communications Networking and Mobile Computing (WiCOM). - Chengdu, 23-25 Sept. 2010. - P. 1-4. ↑

**C3014.** Liu Yueping. Research on the Configuration of Network Radar Based on Detectable Power and Detector's SNR. / Liu Yueping, Jiang Qiuxi, Guo Hangxing. // 2010 6th International Conference on Wireless Communications Networking and Mobile Computing (WiCOM). - Chengdu, 23-25 Sept. 2010. - P. 1-4. ↑

**C3015.** She Kai. Theory and Measurement of Delta RCS for RFID Tag on Various Materials. / She Kai, He Yigang, Li Bing, Hou Zhouguo, Zhu Yanqing, Zuo Lei. // 2010 6th International Conference on Wireless Communications Networking and Mobile Computing (WiCOM). - Chengdu, 23-25 Sept. 2010. - P. 1-4. ↑

**C3016.** Bin Xia. Linear Combination Method for UWB Vehicular Radar Pulse Design. / Bin Xia, Hong Xie, Qian Liu, Nan Xie. // 2010 6th International Conference on Wireless Communications Networking and Mobile Computing (WiCOM). - Chengdu, 23-25 Sept. 2010. - P. 1-3. ↑

**C3017.** Jiaming Zhang. A Novel Method for Recognising Radar Emitter. / Jiaming Zhang, Yi He. // 2010 6th International Conference on Wireless Communications Networking and Mobile Computing (WiCOM). - Chengdu, 23-25 Sept. 2010. - P. 1-3. ↑

**C3018.** Yongxiang Zhao. WiTracker: An Indoor Positioning System Based on Wireless LANs. / Yongxiang Zhao, Huaibei Zhou, Meifang Li. // 2010 6th International Conference on Wireless Communications Networking and Mobile Computing (WiCOM). - Chengdu, 23-25 Sept. 2010. - P. 1-4. ↑

**C3019.** Liu Xiaojun. Diagonal Loading for STAP and Its Performance Analysis. / Liu Xiaojun, Liu Congfeng, Liao Guisheng. // 2010 6th International Conference on Wireless Communications Networking and Mobile Computing (WiCOM). - Chengdu, 23-25 Sept. 2010. - P. 1-4. ↑

**C3020.** Weiguang Shi. An Efficient Indoor Location Algorithm Based on RFID Technology. / Weiguang Shi, Kaihua Liu, Ying Ju, Ge Yan. // 2010 6th International Conference on Wireless Communications Networking and Mobile Computing (WiCOM). - Chengdu, 23-25 Sept. 2010. - P. 1-5. ↑

**C3021.** Yang Ming. Simulation and Analysis of the Effects of Tropospheric Scattering Channel on Signal Waveforms. / Yang Ming, Liu Chengguo, Jin Rui, Zhang Ertao. // 2010 6th International Conference on Wireless Communications Networking and Mobile Computing (WiCOM). - Chengdu, 23-25 Sept. 2010. - P. 1-4. ↑

**C3022.** Liang Zhang. A Novel Random Sampling Method for Radar Image Compression. / Liang Zhang, Ming-Sheng Chen, Lei Xu, Xian-Liang Wu. // 2010 6th International Conference on Wireless Communications Networking and Mobile Computing (WiCOM). - Chengdu, 23-25 Sept. 2010. - P. 1-4. ↑

**C3023.** Bolivar J. Designing of a Telematic Network to Provide Real-Time Supervision and Control for Tactical Units. / Bolivar J., Kai Liu, Hernandez E. // 2010 6th International Conference on Wireless Communications Networking and Mobile Computing (WiCOM). - Chengdu, 23-25 Sept. 2010. - P. 1-5. ↑

**C3024.** Xu Feng. Data analysis of wind profiler radar(WPR) under three kinds of synoptic processes in spring on Donghai island of Zhanjiang. / Xu Feng, Niu Shengjie, Wang Jing, Zhang Yu, Yue Yan-yu, Zhao Li-juan, Xu Dan. // 2010 Second IITA International Conference on Geoscience and Remote Sensing (IITA-GRS). - Qingdao, 28-31 Aug. 2010. - Vol. 1. - P. 287-290. ↑

**C3025.** Bainbridge S.J. Integrating observation systems: An example from the Great Barrier Reef. / Bainbridge S.J., Steinberg C.R., Heron M.L., Furnas M.J. // OCEANS 2010 IEEE-Sydney. - Sydney, NSW, 24-27 May 2010. - P. 1-4. ↑

**C3026.** Hamschin B. Sonar waveform design for optimum target detection: The impact of object burial state. / Hamschin B., Loughlin P. // OCEANS 2010 IEEE-Sydney. - Sydney, NSW, 24-27 May 2010. - P. 1-6. ↑



- C3027.** Moltmann T. The Integrated Marine Observing System-delivering data-streams to support marine research and applications. / Moltmann T., Proctor R., Hill K., McGowen M. // OCEANS 2010 IEEE-Sydney. - Sydney, NSW, 24-27 May 2010. - P. 1-8. ↑
- C3028.** Hoshino T. Coherent change detection with complex logarithm transformation on SAR imagery. / Hoshino T., Kidera S., Kirimoto T. // Proceedings of SICE Annual Conference 2010. - Taipei, 18-21 Aug. 2010. - P. 286-290. ↑
- C3029.** Crisp D.J. Comparison of ship detectors for polarimetric SAR imagery. / Crisp D.J., Keevers T. // OCEANS 2010 IEEE-Sydney. - Sydney, NSW, 24-27 May 2010. - P. 1-8. ↑
- C3030.** Walsh J. Further analysis of the modulation of high frequency radar spectra due to sea-induced antenna platform motion. / Walsh J., Ryan B., Gill E., El Khoury J. // OCEANS 2010 IEEE-Sydney. - Sydney, NSW, 24-27 May 2010. - P. 1-4. ↑
- C3031.** Courmontagne P. An improvement to the pulse compression scheme. / Courmontagne P., Julien G., Bouhier M.E. // OCEANS 2010 IEEE-Sydney. - Sydney, NSW, 24-27 May 2010. - P. 1-10. ↑
- C3032.** Xu Xi-Yu. Mechanisms and system design of satellite interferometric Synthetic Aperture Radar altimeter. / Xu Xi-Yu, Liu He-Guang, Yang Shuang-Bao. // 2010 Second IITA International Conference on Geoscience and Remote Sensing (IITA-GRS). - Qingdao, 28-31 Aug. 2010. - Vol. 2. - P. 209-211. ↑
- C3033.** Guolin Liu. InSAR Kalman Filter phase unwrapping algorithm based on topographic factors. / Guolin Liu, Huadong Hao, Fanlin Yang, Man Yan, Zhixing Du, Yamin Dang. // OCEANS 2010 IEEE-Sydney. - Sydney, NSW, 24-27 May 2010. - P. 1-6. ↑
- C3034.** Wettle M. Offshore petroleum exploration from space: A developing capability at Geoscience Australia. / Wettle M., Daniel P.J., Logan G.A., Thankappan M. // OCEANS 2010 IEEE-Sydney. - Sydney, NSW, 24-27 May 2010. - P. 1-7. ↑
- C3035.** Mantovanelli A. The use of HF radar surface currents for computing Lagrangian trajectories: Benefits and issues. / Mantovanelli A., Heron M.L., Prytz A. // OCEANS 2010 IEEE-Sydney. - Sydney, NSW, 24-27 May 2010. - P. 1-6. ↑
- C3036.** Mariano A. A low power and high gain double-balanced active mixer with integrated transformer-based Baluns dedicated to 77 GHz automotive radar applications. / Mariano A., Leite B., Majek C., Taris T., Deval Y., Be,gueret J.-B., Belot D. // 2010 8th IEEE International NEWCAS Conference (NEWCAS). - Montreal, QC, 20-23 June 2010. - P. 81-84. ↑
- C3037.** Tanaka K. Forereaching motion generation of mobile robots for pedestrian face identification. / Tanaka K., Takeuchi E., Ohno K., Tadokoro S., Yonezawa T. // Proceedings of SICE Annual Conference 2010. - Taipei, 18-21 Aug. 2010. - P. 859-862. ↑
- C3038.** Atwater D.P. HF radar two-station baseline bisector comparisons of radial components. / Atwater D.P., Heron M.L. // OCEANS 2010 IEEE-Sydney. - Sydney, NSW, 24-27 May 2010. - P. 1-4. ↑
- C3039.** Wen-Qin Wang. LFM CW SAR waveform generation with frequency nonlinearity suppression. 2010 Second IITA International Conference on Geoscience and Remote Sensing (IITA-GRS). - Qingdao, 28-31 Aug. 2010. - Vol. 1. - P. 380-383. ↑
- C3040.** Wang Xinzeng. Route planning for unmanned aerial vehicle based on threat probability and mission time restriction. / Wang Xinzeng, Ci Linlin, Li Junshan, Yu Ning. // 2010 Second IITA International Conference on Geoscience and Remote Sensing (IITA-GRS). - Qingdao, 28-31 Aug. 2010. - Vol. 1. - P. 27-30. ↑
- C3041.** Li-Wei Fong. Adaptive Information Matrix Filtering fusion with nonlinear classifier. Proceedings of SICE Annual Conference 2010. - Taipei, 18-21 Aug. 2010. - P. 2214-2219. ↑
- C3042.** Young-Hun Jung. Maximum likelihood estimation of target RCS in tracking. / Young-Hun Jung, Sun-Mog Hong, Sang-Hong Seo. // Proceedings of SICE Annual Conference 2010. - Taipei, 18-21 Aug. 2010. - P. 3344-3346. ↑
- C3043.** Zeng Yejuan. Research on DBF SAR system in near space. / Zeng Yejuan, Dai Yuehua. // 2010

Second IITA International Conference on Geoscience and Remote Sensing (IITA-GRS). - Qingdao, 28-31 Aug. 2010. - Vol. 1. - P. 129-132. ↑

C3044. Deng Yu. Monitoring manners research on the river ice in the Yellow River. / Deng Yu, Zhang Baosen. // 2010 Second IITA International Conference on Geoscience and Remote Sensing (IITA-GRS). - Qingdao, 28-31 Aug. 2010. - Vol. 1. - P. 111-113. ↑

C3045. Wei Zhang. Micro-doppler extraction of vibrating target based on dual-channel ATI technique in SAR. / Wei Zhang, Chuangming Tong, Qun Zhang, Xiao Zhang. // 2010 Second IITA International Conference on Geoscience and Remote Sensing (IITA-GRS). - Qingdao, 28-31 Aug. 2010. - Vol. 1. - P. 422-425. ↑

C3046. Hong Wei. A progressive approach for building extraction by fusing LIDAR data and co-registered bands. / Hong Wei, Wei Xu. // Proceedings of SICE Annual Conference 2010. - Taipei, 18-21 Aug. 2010. - P. 756-762. ↑

C3047. Ilin R. Simultaneous detection and tracking of multiple objects in noisy and cluttered environment using maximum likelihood estimation framework. / Ilin R., Deming R.W. // OCEANS 2010 IEEE-Sydney. - Sydney, NSW, 24-27 May 2010. - P. 1-7. ↑

C3048. Brekke E. Target tracking in state dependent wake clutter. / Brekke E., Hallingstad O., Glattetre J. // OCEANS 2010 IEEE-Sydney. - Sydney, NSW, 24-27 May 2010. - P. 1-10. ↑

C3049. Yongzheng Ren. Wind field retrieval over the ocean using X-band polarization SAR data. / Yongzheng Ren, Mingxia He, Lehner S. // 2010 Second IITA International Conference on Geoscience and Remote Sensing (IITA-GRS). - Qingdao, 28-31 Aug. 2010. - Vol. 1. - P. 43-46. ↑

C3050. Shi Jian-qing. Study the feasibility of airborne LiDAR on areal earth's crust deformation surveying. / Shi Jian-qing, Jiang Ting-chen. // 2010 Second IITA International Conference on Geoscience and Remote Sensing (IITA-GRS). - Qingdao, 28-31 Aug. 2010. - Vol. 1. - P. 193-197. ↑

C3051. Takabayashi Y. Altitude estimation method using assumed altitude reliability based on multipath propagation model. / Takabayashi Y., Matsuzaki T., Kameda H. // Proceedings of SICE Annual Conference 2010. - Taipei, 18-21 Aug. 2010. - P. 2196-2201. ↑

C3052. Renli Zhang. An improved CFAR detector for non-homogeneous clutter environment. / Renli Zhang, Yiwei Zou, Weixing Sheng, Xiaofeng Ma, Hao Wang. // 2010 International Symposium on Signals Systems and Electronics (ISSSE). - Nanjing, 17-20 Sept. 2010. - Vol. 2. - P. 1-4. ↑

C3053. Elsallal W. A SiGe-based Ku-band digital beamforming array for high speed on-the-move comm/radar system. / Elsallal W., Jensen D., Palandech R., Timmerman J., West J., Atesal Y., Cetinoneri B., Rebeiz G. // 2010 IEEE International Symposium on Phased Array Systems and Technology (ARRAY). - Waltham, MA, 12-15 Oct. 2010. - P. 868-875. ↑

C3054. Weedon W.H. Phased array digital beamforming hardware development at Applied Radar. 2010 IEEE International Symposium on Phased Array Systems and Technology (ARRAY). - Waltham, MA, 12-15 Oct. 2010. - P. 854-859. ↑




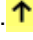











C3055. Fulton C. Calibration of panelized polarimetric phased array radar antennas: A case study. / Fulton C., Chappell W. // 2010 IEEE International Symposium on Phased Array Systems and Technology (ARRAY). - Waltham, MA, 12-15 Oct. 2010. - P. 860-867. ↑

C3056. Ly P.Q.C. AOA estimation of two narrowband signals using interferometry. / Ly P.Q.C., Elton S.D., Gray D.A. // 2010 IEEE International Symposium on Phased Array Systems and Technology (ARRAY). - Waltham, MA, 12-15 Oct. 2010. - P. 1004-1009. ↑

C3057. Luison C. Innovative aperiodic arrays for SAR spaceborne applications. / Luison C., Landini A., Angeletti P., Toso G., Valle P., Capece P., Selleri S., Pelosi G. // 2010 IEEE International Symposium on Phased Array Systems and Technology (ARRAY). - Waltham, MA, 12-15 Oct. 2010. - P. 959-964. ↑

C3058. Manica L. Monopulse compromise arrays-A review. / Manica L., Rocca P., Massa A. // 2010 IEEE International Symposium on Phased Array Systems and Technology (ARRAY). - Waltham, MA, 12-15 Oct. 2010. - P. 879-882. ↑

- C3059.** Schulwitz L. A tray based Rotman lens array with beamforming in two dimensions for millimeter-wave radar. / Schulwitz L., Mortazawi A. // 2010 IEEE International Symposium on Phased Array Systems and Technology (ARRAY). - Waltham, MA, 12-15 Oct. 2010. - P. 850-853. ↑
- C3060.** Sadowy G. UAVSAR Active Electronically-Scanned Array. / Sadowy G., Brown K., Chamberlain N., Figueroa H., Fisher C., Grando M., Hamilton G., Vorperian V., Zawadzki M. // 2010 IEEE International Symposium on Phased Array Systems and Technology (ARRAY). - Waltham, MA, 12-15 Oct. 2010. - P. 763-770. ↑
- C3061.** Schwerdt M. Precise calibration techniques for complex SAR systems based on active phased array antennas. / Schwerdt M., Bachmann M., Schrank D., During B., Brautigam B., Gonzalez J.H., Schulz C. // 2010 IEEE International Symposium on Phased Array Systems and Technology (ARRAY). - Waltham, MA, 12-15 Oct. 2010. - P. 695-699. ↑
- C3062.** Bergamo M.A. Spread Spectrum Digital Beamforming (SSDBF) radar. 2010 IEEE International Symposium on Phased Array Systems and Technology (ARRAY). - Waltham, MA, 12-15 Oct. 2010. - P. 665-672. ↑
- C3063.** Mosca S. A family of G-band active electronically scanned arrays for radar applications. 2010 IEEE International Symposium on Phased Array Systems and Technology (ARRAY). - Waltham, MA, 12-15 Oct. 2010. - P. 785-788. ↑
- C3064.** Ouacha A. SE-IT joint M-AESA program: Overview and status. / Ouacha A., Fredlund A., Andersson J., Hindsefelt H., Rinaldi V., Scattoni C. // 2010 IEEE International Symposium on Phased Array Systems and Technology (ARRAY). - Waltham, MA, 12-15 Oct. 2010. - P. 771-776. ↑
- C3065.** Kemkemian S. Toward common radar & EW multifunction active arrays. / Kemkemian S., Nouvel-Fiani M. // 2010 IEEE International Symposium on Phased Array Systems and Technology (ARRAY). - Waltham, MA, 12-15 Oct. 2010. - P. 777-784. ↑
- C3066.** Hafizovic I. Acoustic tracking of aircraft using a circular microphone array sensor. / Hafizovic I., Nilsen C.C., Kjolerbakken M. // 2010 IEEE International Symposium on Phased Array Systems and Technology (ARRAY). - Waltham, MA, 12-15 Oct. 2010. - P. 1025-1032. ↑
- C3067.** Juinn-Horng Deng. Adaptive space-time beamforming technique for passive radar system with ultra low signal to interference ratio. / Juinn-Horng Deng, Jeng-Kuang Hwang, Chih-Yang Lin, Shu-Min Liao. // 2010 IEEE International Conference on Wireless Information Technology and Systems (ICWITS). - Honolulu, HI, Aug. 28 2010-Sept. 3 2010. - P. 1-4. ↑
- C3068.** Reck C. High precision DOA estimation of SSR transponder signals. / Reck C., Berold U., Schmidt L.-P. // 2010 IEEE International Conference on Wireless Information Technology and Systems (ICWITS). - Honolulu, HI, Aug. 28 2010-Sept. 3 2010. - P. 1-4. ↑
- C3069.** Sarkar T.K. MIMO radars or is it smart antennas?. / Sarkar T.K., Palma M.S. // 2010 IEEE International Conference on Wireless Information Technology and Systems (ICWITS). - Honolulu, HI, Aug. 28 2010-Sept. 3 2010. - P. 1-4. ↑
- C3070.** Majkitalo M. Denoising of single-look SAR images based on variance stabilization and nonlocal filters. / Majkitalo M., Foi A., Fevrale D., Lukin V. // 2010 International Conference on Mathematical Methods in Electromagnetic Theory (MMET). - Kyiv, 6-8 Sept. 2010. - P. 1-4. ↑
- C3071.** Baker J. On the design of integrated HF radar systems for Homeland Security applications. / Baker J., Celik N., Omaki N., Kobashigawa J., Hyoung-Sun Youn, Iskander M.F. // 2010 IEEE International Conference on Wireless Information Technology and Systems (ICWITS). - Honolulu, HI, Aug. 28 2010-Sept. 3 2010. - P. 1-4. ↑
- C3072.** Okamoto Y. Iterative focusing algorithm to estimate moving target. / Okamoto Y., Ohtsuki T. // 2010 IEEE International Conference on Wireless Information Technology and Systems (ICWITS). - Honolulu, HI, Aug. 28 2010-Sept. 3 2010. - P. 1-4. ↑
- C3073.** Monroe D. Adaptive filtering and target detection for ultrasonic backscattered signal. / Monroe D., In Soo Ahn, Yufeng Lu. // 2010 IEEE International Conference on Electro/Information Technology (EIT). - Normal, IL, 20-22 May 2010. - P. 1-6. ↑

- C3074.** Middleton R.J.C. High range resolution moving target indication at long stand-off ranges using minimal sampling rates in linear FMCW radar. / Middleton R.J.C., Macfarlane D.G., Robertson D.A. // 2010 35th International Conference on Infrared Millimeter and Terahertz Waves (IRMMW-THz). - Rome, 5-10 Sept. 2010. - P. 1-3. 
- C3075.** Geun-Ju Kim. High resolution terahertz imaging (T-ray) with a horn antenna. / Geun-Ju Kim, Woo-Kyung Han, Jung-Il Kim, Seok-Gy Jeon. // 2010 35th International Conference on Infrared Millimeter and Terahertz Waves (IRMMW-THz). - Rome, 5-10 Sept. 2010. - P. 1-2. 
- C3076.** Abril J. Combined passive and active millimeter-wave imaging system for concealed objects detection. / Abril J., Nova E., Broquetas A., Torres F., Romeu J., Jofre L. // 2010 35th International Conference on Infrared Millimeter and Terahertz Waves (IRMMW-THz). - Rome, 5-10 Sept. 2010. - P. 1-2. 
- C3077.** Schmid C.M. Measurement-based delay-and-sum signal processing for linear antenna arrays. / Schmid C.M., Feger R., Scheiblhofer S., Stelzer A. // 2010 IEEE International Conference on Wireless Information Technology and Systems (ICWITS). - Honolulu, HI, Aug. 28 2010-Sept. 3 2010. - P. 1-4. 
- C3078.** Schwarz U. Experimental validation of high-permittivity ceramic double-ridged horn antennas for biomedical ultra-wideband diagnostics. / Schwarz U., Stephan R., Hein M.A. // 2010 IEEE International Conference on Wireless Information Technology and Systems (ICWITS). - Honolulu, HI, Aug. 28 2010-Sept. 3 2010. - P. 1-4. 
- C3079.** Fickenscher T. Improved range resolution for FMCW HF surface wave radar. / Fickenscher T., Herschel R., Holters M., Gupta A., Hinz J. // 2010 IEEE International Conference on Wireless Information Technology and Systems (ICWITS). - Honolulu, HI, Aug. 28 2010-Sept. 3 2010. - P. 1-4. 
- C3080.** Fenn A.J. Low-profile dual-polarized UHF array antenna. / Fenn A.J., Hurst P.T., Sandora J.S., Krieger J.D., Parad L.I. // 2010 IEEE International Symposium on Phased Array Systems and Technology (ARRAY). - Waltham, MA, 12-15 Oct. 2010. - P. 599-602. 
- C3081.** Ercil E. Array antenna pattern synthesis using measured active element patterns and Gram-Schmidt Orthogonalization. / Ercil E., Yildirim E., Inal M.E. // 2010 IEEE International Symposium on Phased Array Systems and Technology (ARRAY). - Waltham, MA, 12-15 Oct. 2010. - P. 357-360. 
- C3082.** Matthiesen D.J. Efficient beam scanning, energy allocation, and time allocation for search and detection. 2010 IEEE International Symposium on Phased Array Systems and Technology (ARRAY). - Waltham, MA, 12-15 Oct. 2010. - P. 361-368. 
- C3083.** Deaett M.A. Bandwidth assignment for target tracking in coherent distributed aperture radar networks. / Deaett M.A., Naimark L. // 2010 IEEE International Symposium on Phased Array Systems and Technology (ARRAY). - Waltham, MA, 12-15 Oct. 2010. - P. 344-347. 
- C3084.** Chamberlain N. The DESDynI synthetic aperture radar array-fed reflector antenna. / Chamberlain N., Ghaemi H., Giersch L., Harcke L., Hodges R., Hoffman J., Johnson W., Jordan R., Khayatian B., Rosen P., Sadowy G., Shaffer S., Shen Y., Veilleux L., Wu P. // 2010 IEEE International Symposium on Phased Array Systems and Technology (ARRAY). - Waltham, MA, 12-15 Oct. 2010. - P. 381-386. 
- C3085.** Galletti M. Polarimetric phased array weather radar: Concepts for polarimetric calibration. / Galletti M., Zrnic D., Doviak D., Guifu Zhang, Crain J. // 2010 IEEE International Symposium on Phased Array Systems and Technology (ARRAY). - Waltham, MA, 12-15 Oct. 2010. - P. 387-393. 
- C3086.** Leifer M.C. Analyzing SAR ambiguities in the u-v plane. 2010 IEEE International Symposium on Phased Array Systems and Technology (ARRAY). - Waltham, MA, 12-15 Oct. 2010. - P. 369-375. 
- C3087.** Belfiori F. Analysis of a novel MIMO system for security applications. / Belfiori F., Hoogeboom P. // 2010 IEEE International Symposium on Phased Array Systems and Technology (ARRAY). - Waltham, MA, 12-15 Oct. 2010. - P. 338-343. 
- C3088.** Marescialli L. Transmit/Receive Module technology and related multifunction active radars in Selex-Sistemi Integrati. / Marescialli L., Perillo M., Tarantino M. // 2010 IEEE International Symposium on Phased Array Systems and Technology (ARRAY). - Waltham, MA, 12-15 Oct. 2010. - P. 238-244. 



- C3089.** Lampen J. Low-loss, MEMS based, broadband phase shifters. / Lampen J., Majumder S., Chilyoung Ji, Maciel J. // 2010 IEEE International Symposium on Phased Array Systems and Technology (ARRAY). - Waltham, MA, 12-15 Oct. 2010. - P. 219-224. ↑
- C3090.** Bajgot D.A. Development of a low-cost, man-portable, Phased Array X-Band Radar. 2010 IEEE International Symposium on Phased Array Systems and Technology (ARRAY). - Waltham, MA, 12-15 Oct. 2010. - P. 183-188. ↑
- C3091.** Nicolas J.-J. Antenna array diagnosis in situ: Experimental results using microwave circular holography. 2010 IEEE International Symposium on Phased Array Systems and Technology (ARRAY). - Waltham, MA, 12-15 Oct. 2010. - P. 306-310. ↑
- C3092.** Logan J.T. Phased array calibration and diagnostics utilizing a student-built planar near-field system. / Logan J.T., Reinhard D.S., Hauck K.E. // 2010 IEEE International Symposium on Phased Array Systems and Technology (ARRAY). - Waltham, MA, 12-15 Oct. 2010. - P. 279-286. ↑
- C3093.** Bachmann M. Accurate antenna pattern modelling for spaceborne active phased array antennas. / Bachmann M., Schwerdt M., Dojring B., Schulz C. // 2010 IEEE International Symposium on Phased Array Systems and Technology (ARRAY). - Waltham, MA, 12-15 Oct. 2010. - P. 267-270. ↑
- C3094.** Min Jiang. MIMO radar joint estimation of target location and velocity with multiple subcarrier signals. / Min Jiang, Jianguo Huang, Yunshan Hou. // 2010 IEEE International Symposium on Phased Array Systems and Technology (ARRAY). - Waltham, MA, 12-15 Oct. 2010. - P. 398-402. ↑
- C3095.** Ralston T.S. Real-time through-wall imaging using an ultrawideband multiple-input multiple-output (MIMO) phased array radar system. / Ralston T.S., Charvat G.L., Peabody J.E. // 2010 IEEE International Symposium on Phased Array Systems and Technology (ARRAY). - Waltham, MA, 12-15 Oct. 2010. - P. 551-558. ↑
- C3096.** Otten M. Scalable multifunction RF system concepts for joint operations. / Otten M., de Wit J., Smits F., van Rossum W., Huizing A. // 2010 IEEE International Symposium on Phased Array Systems and Technology (ARRAY). - Waltham, MA, 12-15 Oct. 2010. - P. 492-497. ↑
- C3097.** Livingston S. A wide band low profile dual-pol "Thumbtack" array. / Livingston S., Lee J.J. // 2010 IEEE International Symposium on Phased Array Systems and Technology (ARRAY). - Waltham, MA, 12-15 Oct. 2010. - P. 477-483. ↑
- C3098.** Kemkemian S. MIMO radar for sense and avoid for UAV. / Kemkemian S., Nouvel-Fiani M., Cornic P., Garrec P. // 2010 IEEE International Symposium on Phased Array Systems and Technology (ARRAY). - Waltham, MA, 12-15 Oct. 2010. - P. 573-580. ↑
- C3099.** Wilcox D. Beampattern optimisation for sub-arrayed MIMO radar for large arrays. / Wilcox D., Sellathurai M. // 2010 IEEE International Symposium on Phased Array Systems and Technology (ARRAY). - Waltham, MA, 12-15 Oct. 2010. - P. 567-572. ↑
- C3100.** Charvat G.L. An ultrawideband (UWB) switched-antenna-array radar imaging system. / Charvat G.L., Kempel L.C., Rothwell E.J., Coleman C.M., Mokole E.L. // 2010 IEEE International Symposium on Phased Array Systems and Technology (ARRAY). - Waltham, MA, 12-15 Oct. 2010. - P. 543-550. ↑
- C3101.** Herd J. Low cost Multifunction Phased Array Radar concept. / Herd J., Duffy S., Carlson D., Weber M., Brigham G., Weigand C., Cursio D. // 2010 IEEE International Symposium on Phased Array Systems and Technology (ARRAY). - Waltham, MA, 12-15 Oct. 2010. - P. 457-460. ↑
- C3102.** Brookner E. Demonstration of accurate prediction of PAVE PAWS embedded element gain. / Brookner E., Porter B., Kaichiang Chang, Yueh-Chi Chang, Zwillinger D., Considine B., Sikina T. // 2010 IEEE International Symposium on Phased Array Systems and Technology (ARRAY). - Waltham, MA, 12-15 Oct. 2010. - P. 417-422. ↑
- C3103.** Shroyer A. Self tapered array lattice for high efficiency transmit applications. / Shroyer A., Darnel E. // 2010 IEEE International Symposium on Phased Array Systems and Technology (ARRAY). - Waltham, MA, 12-15 Oct. 2010. - P. 410-416. ↑

- C3104.** Bellomo L. An s-band ultrawideband time reversal-based RADAR for imaging in cluttered media. / Bellomo L., Pioch S., Saillard M., Spano E. // 2010 IEEE International Symposium on Phased Array Systems and Technology (ARRAY). - Waltham, MA, 12-15 Oct. 2010. - P. 394-397. ↑
- C3105.** Snow T. Concurrent multifunction transmit and receive applications with dynamic filtering. / Snow T., Naglich E.J., Chappell W.J. // 2010 IEEE International Symposium on Phased Array Systems and Technology (ARRAY). - Waltham, MA, 12-15 Oct. 2010. - P. 461-466. ↑
- C3106.** Dogan D. A novel edge wall waveguide slot antenna. / Dogan D., Civi O.A. // 2010 IEEE International Symposium on Phased Array Systems and Technology (ARRAY). - Waltham, MA, 12-15 Oct. 2010. - P. 453-456. ↑
- C3107.** Zaghloul A.I. Detection in collision avoidance radar using active versus passive phased arrays. / Zaghloul A.I., Wellman R., Anthony T.K. // 2010 IEEE International Symposium on Phased Array Systems and Technology (ARRAY). - Waltham, MA, 12-15 Oct. 2010. - P. 432-439. ↑
- C3108.** Zalevsky G.S. Em wave scattering by perfectly conducting disk of finite thickness. / Zalevsky G.S., Nechitaylo S.V., Sukharevsky O.I., Sukharevsky I.O. // 2010 International Conference on Mathematical Methods in Electromagnetic Theory (MMET). - Kyiv, 6-8 Sept. 2010. - P. 1-4. ↑
- C3109.** Kravchenko V.F. New Kravchenko transforms and digital UWB signal processing. / Kravchenko V.F., Churikov D.V. // 2010 5th International Conference on Ultrawideband and Ultrashort Impulse Signals (UWBUSIS). - Sevastopol, 6-10 Sept. 2010. - P. 54-58. ↑
- C3110.** Sinitsyn R.B. UWB noise acoustic atmospheric radar. / Sinitsyn R.B., Yanovsky F.J. // 2010 5th International Conference on Ultrawideband and Ultrashort Impulse Signals (UWBUSIS). - Sevastopol, 6-10 Sept. 2010. - P. 48. ↑
- C3111.** Prudyus I.N. Investigation of phase coded signals based on generalized Frank codes. / Prudyus I.N., Sumyk M.M., Yankevych R.V. // 2010 5th International Conference on Ultrawideband and Ultrashort Impulse Signals (UWBUSIS). - Sevastopol, 6-10 Sept. 2010. - P. 88-89. ↑
- C3112.** {no data available}. Copyright page. 2010 5th International Conference on Ultrawideband and Ultrashort Impulse Signals (UWBUSIS). - Sevastopol, 6-10 Sept. 2010. - P. 2. ↑
- C3113.** Baum C.E. Polarimetric suppression of early-time scattering for late-time target identification. 2010 5th International Conference on Ultrawideband and Ultrashort Impulse Signals (UWBUSIS). - Sevastopol, 6-10 Sept. 2010. - P. 12-15. ↑
- C3114.** Kravchenko V.F. Spectral theory analysis of UWB-oscillations in frequency synthesizers based on phase-locked loops. / Kravchenko V.F., Kravchenko O.V., Safin A.R. // 2010 5th International Conference on Ultrawideband and Ultrashort Impulse Signals (UWBUSIS). - Sevastopol, 6-10 Sept. 2010. - P. 22-29. ↑
- C3115.** Titov A.N. Scale electrodynamic modeling of ultra wideband systems. / Titov A.N., Gribanov A.N. // 2010 5th International Conference on Ultrawideband and Ultrashort Impulse Signals (UWBUSIS). - Sevastopol, 6-10 Sept. 2010. - P. 273-274. ↑
- C3116.** Shirokov I.B. The device for remote monitoring of human's heartbeat. / Shirokov I.B., Slesareva A.V., Korepanov A.L. // 2010 5th International Conference on Ultrawideband and Ultrashort Impulse Signals (UWBUSIS). - Sevastopol, 6-10 Sept. 2010. - P. 195-196. ↑
- C3117.** Prohorkin A.G. Way of an estimation trajectory instability of flight of the air targets. 2010 5th International Conference on Ultrawideband and Ultrashort Impulse Signals (UWBUSIS). - Sevastopol, 6-10 Sept. 2010. - P. 189-191. ↑
- C3118.** Vlasik S.N. Estimation power and spatial characteristics of ultrawideband radar for statement of protecting handicaps. / Vlasik S.N., Yermakov G.V., Zima I.I. // 2010 5th International Conference on Ultrawideband and Ultrashort Impulse Signals (UWBUSIS). - Sevastopol, 6-10 Sept. 2010. - P. 180-182. ↑
- C3119.** Ruban V.P. Sampling duration for noisy signal conversion. / Ruban V.P., Pochanin G.P. // 2010 5th International Conference on Ultrawideband and Ultrashort Impulse Signals (UWBUSIS). - Sevastopol, 6-10 Sept. 2010. - P. 275-277. ↑

- C3120.** Gorobets N.N. Influence of the screen on the range properties of rarefied arrays of near-omnidirectional radiators. / Gorobets N.N., Bulgakova A.A. // 2010 5th International Conference on Ultrawideband and Ultrashort Impulse Signals (UWBUSIS). - Sevastopol, 6-10 Sept. 2010. - P. 223-225. ↑
- C3121.** Ochotnikov D.A. The motion trajectory restoring for radar observation of living objects. 2010 5th International Conference on Ultrawideband and Ultrashort Impulse Signals (UWBUSIS). - Sevastopol, 6-10 Sept. 2010. - P. 201-203. ↑
- C3122.** Peeters G.T. Design and analysis of multi-carrier multiple access systems without feedback. / Peeters G.T., Van Houdt B. // 2010 22nd International Teletraffic Congress (ITC). - Amsterdam, 7-9 Sept. 2010. - P. 1-8. ↑
- C3123.** Shu-hong Fu. A compact CPW resonator cell with dual-bandgap characteristics. / Shu-hong Fu, Chuang-ming Tong, Ming Zhou, Li-nan Wu, Xi-min Li. // 2010 International Symposium on Signals Systems and Electronics (ISSSE). - Nanjing, 17-20 Sept. 2010. - Vol. 2. - P. 1-3. ↑
- C3124.** Xu Xi-Yu. Digital module design of a satellite rain-compatible radar altimeter. / Xu Xi-Yu, Liu He-Guang, Liu Peng. // 2010 International Symposium on Signals Systems and Electronics (ISSSE). - Nanjing, 17-20 Sept. 2010. - Vol. 2. - P. 1-3. ↑
- C3125.** {no data available}. Copyright page. 2010 International Symposium on Signals Systems and Electronics (ISSSE). - Nanjing, 17-20 Sept. 2010. - Vol. 1. - P. 1. ↑
- C3126.** Weixing Sheng. A new method of radar target recognition based on time-frequency analysis. / Weixing Sheng, Kang Pan, Fang Wang, Xiaofeng Ma, Hao Wang. // 2010 International Symposium on Signals Systems and Electronics (ISSSE). - Nanjing, 17-20 Sept. 2010. - Vol. 2. - P. 1-4. ↑
- C3127.** Xiaoqiao Deng. Electromagnetic scattering by arbitrarily shaped PEC targets coated with magnetic anisotropic media using equivalent dipole-moment method. / Xiaoqiao Deng, Changqing Gu, Jiade Yuan, Zhuo Li, Yonggang Zhou. // 2010 International Symposium on Signals Systems and Electronics (ISSSE). - Nanjing, 17-20 Sept. 2010. - Vol. 2. - P. 1-4. ↑
- C3128.** Ming Zhou. A novel spiral defected ground structure and its application to the design of dual bandstop filter. / Ming Zhou, Chuang-ming Tong, Shu-hong Fu, Li-nan Wu, Xi-min Li. // 2010 International Symposium on Signals Systems and Electronics (ISSSE). - Nanjing, 17-20 Sept. 2010. - Vol. 2. - P. 1-3. ↑
- C3129.** Shuhong Fu. Characteristics of a CPW mushroom-like resonator and its application to wideband EBG filter. / Shuhong Fu, Chuangming Tong, Ximin Li. // 2010 International Symposium on Signals Systems and Electronics (ISSSE). - Nanjing, 17-20 Sept. 2010. - Vol. 1. - P. 1-4. ↑
- C3130.** Xuewei Ping. Finite element analysis of three dimensional scatterers above the PEC earth. / Xuewei Ping, Tie Jun Cui. // 2010 International Symposium on Signals Systems and Electronics (ISSSE). - Nanjing, 17-20 Sept. 2010. - Vol. 1. - P. 1-3. ↑
- C3131.** Zhangming Yu. A research of stored grain moisture detection based on RIS-K2 radar electromagnetic wave technology. / Zhangming Yu, Yuan Zhang, Feiyu Lian, Maixia Fu. // 2010 International Conference on Educational and Information Technology (ICEIT). - Chongqing, 17-19 Sept. 2010. - Vol. 3. - P. V3-265-V3-267-265. ↑
- C3132.** Tuxpan-Vargas J. Fused variational analysis technique for high-resolution reconstruction of remote sensing imagery. / Tuxpan-Vargas J., Santos-Arce S. // 2010 7th International Conference on Electrical Engineering Computing Science and Automatic Control (CCE). - Tuxtla Gutierrez, 8-10 Sept. 2010. - P. 351-356. ↑
- C3133.** Lu Hao. Design of high-speed digital correlator in fully polarimetric microwave radiometer. / Lu Hao, Wang Zhen-Zhan, Liu Jing-Yi, Jiang Jing-Shan. // 2010 International Symposium on Signals Systems and Electronics (ISSSE). - Nanjing, 17-20 Sept. 2010. - Vol. 1. - P. 1-4. ↑
- C3134.** Lei Wang. A millimeter-wave solid-state power combining circuit based on branch-waveguide directional coupler. / Lei Wang, Jun Xu, Li Zhao, Dong Ran, Mao-Yan Wang. // 2010 International Symposium on Signals Systems and Electronics (ISSSE). - Nanjing, 17-20 Sept. 2010. - Vol. 1. - P. 1-3. ↑
- C3135.** Junpeng Wang. A new simulation model of fuse RF system. / Junpeng Wang, Qianli Yang, Zhenya Lei,

Fei Wang, Ke Li, Xiuxiang Liu. // 2010 International Symposium on Signals Systems and Electronics (ISSSE). - Nanjing, 17-20 Sept. 2010. - Vol. 1. - P. 1-4. ↑

C3136. Mitrofanov D.G. The usage of extremal coherent integration in the algorithms of processing of reflected signals. 2010 5th International Conference on Ultrawideband and Ultrashort Impulse Signals (UWBUSIS). - Sevastopol, 6-10 Sept. 2010. - P. 183-185. ↑

C3137. Wu Dengfeng. Wireless home emergency system. / Wu Dengfeng, Zhao Hongwei, Wang Peng, Chen Peng. // 2010 International Conference on Computer, Mechatronics, Control and Electronic Engineering (CMCE). - Changchun, 24-26 Aug. 2010. - Vol. 5. - P. 312-315. ↑

C3138. Xinhao Zhang. A wideband outdoor RCS instrumental radar with high range resolution. / Xinhao Zhang, Gang Peng, Zhenrong Wang, Zhaohui Liu, Xia Chen. // 2010 International Conference on Computer, Mechatronics, Control and Electronic Engineering (CMCE). - Changchun, 24-26 Aug. 2010. - Vol. 5. - P. 265-268. ↑

C3139. Yougui Liu. Research on GPRS vehicle location network service system. / Yougui Liu, Baoxing Bai. // 2010 International Conference on Computer, Mechatronics, Control and Electronic Engineering (CMCE). - Changchun, 24-26 Aug. 2010. - Vol. 4. - P. 401-404. ↑

C3140. Xu Yang. The control system for smart home based on GSM and the radio. / Xu Yang, Lei Zhang, Jiasheng Sun. // 2010 International Conference on Computer, Mechatronics, Control and Electronic Engineering (CMCE). - Changchun, 24-26 Aug. 2010. - Vol. 6. - P. 134-137. ↑

C3141. Zhang Li-ping. A study of automation recognition of bridge in SAR image. / Zhang Li-ping, He Jin-qi, Dai Hongliang, Wan Chun-ming. // 2010 International Conference on Computer, Mechatronics, Control and Electronic Engineering (CMCE). - Changchun, 24-26 Aug. 2010. - Vol. 5. - P. 391-394. ↑

C3142. Quan Wei. A new sorting algorithm for radar emitter recognition. / Quan Wei, Li Ping, Wu Di, Xu Feng-kai. // 2010 International Conference on Computer, Mechatronics, Control and Electronic Engineering (CMCE). - Changchun, 24-26 Aug. 2010. - Vol. 5. - P. 407-410. ↑

C3143. Yang Li-mei. Rotation resistance airborne remote image real time matching algorithm. 2010 International Conference on Computer, Mechatronics, Control and Electronic Engineering (CMCE). - Changchun, 24-26 Aug. 2010. - Vol. 2. - P. 502-505. ↑

C3144. Sukharevsky O. Radar cross-section calculation method for antenna of P-18 radar station. / Sukharevsky O., Belevshchuk Y., Vasilets V., Nechitaylo S. // 2010 International Conference on Mathematical Methods in Electromagnetic Theory (MMET). - Kyiv, 6-8 Sept. 2010. - P. 1-4. ↑

C3145. Sergeev I. Using conformal shape, separate and dynamical apodization to improve characteristics of multibeam active phased array. / Sergeev I., Ushakov Yu., Demidenko E. // 2010 International Conference on Mathematical Methods in Electromagnetic Theory (MMET). - Kyiv, 6-8 Sept. 2010. - P. 1-4. ↑

C3146. Averyanova Y. Statistical estimation of polarimetric method potential for dangerous turbulence detection in rain. / Averyanova Y., Averyanov A., Yanovsky F. // 2010 International Conference on Mathematical Methods in Electromagnetic Theory (MMET). - Kyiv, 6-8 Sept. 2010. - P. 1-4. ↑

C3147. Fangxiao Cheng. The study of vehicle's anti-collision early warning system based on fuzzy control. / Fangxiao Cheng, Danyang Zhu, Zhijun Xu. // 2010 International Conference on Computer, Mechatronics, Control and Electronic Engineering (CMCE). - Changchun, 24-26 Aug. 2010. - Vol. 3. - P. 275-277. ↑

C3148. Meng Li. Model of multi-sensor data fusion and trajectory prediction based on echo state network. / Meng Li, Bo Lv, Wei Dong, Dawei Wang. // 2010 International Conference on Computer, Mechatronics, Control and Electronic Engineering (CMCE). - Changchun, 24-26 Aug. 2010. - Vol. 1. - P. 338-341. ↑

C3149. Matsuzaki T. A study of bias error estimation method by KGBE. / Matsuzaki T., Kameda H., Uchida J., Hiroshima F. // 2010 IEEE International Conference on Control Applications (CCA). - Yokohama, 8-10 Sept. 2010. - P. 452-457. ↑

C3150. Wei Ye. Study of noise jamming based on convolution modulation to SAR. / Wei Ye, Hang Ruan, Shu-xian Zhang, Li Yan. // 2010 International Conference on Computer, Mechatronics, Control and Electronic



Engineering (CMCE). - Changchun, 24-26 Aug. 2010. - Vol. 6. - P. 169-172. ↑

**C3151.** Myakinkov A.V. Detection and coordinate measurement of targets by ultra-wide band radar with antenna array. / Myakinkov A.V., Smirnova D.M. // 2010 5th International Conference on Ultrawideband and Ultrashort Impulse Signals (UWBUSIS). - Sevastopol, 6-10 Sept. 2010. - P. 150-152. ↑

**C3152.** Shkvrya Y. Search algorithm for local objects in GPR image. 2010 5th International Conference on Ultrawideband and Ultrashort Impulse Signals (UWBUSIS). - Sevastopol, 6-10 Sept. 2010. - P. 153-155. ↑

**C3153.** Myakinkov A.V. Measurement of coordinates of the targets placed behind of radio-transparent barrier with multi-static ultra-wide band radar. / Myakinkov A.V., Smirnova D.M. // 2010 5th International Conference on Ultrawideband and Ultrashort Impulse Signals (UWBUSIS). - Sevastopol, 6-10 Sept. 2010. - P. 147-149. ↑

**C3154.** Yastrebov Yu.V. Estimation of dielectric permittivity of medium by analysis of UWB radiolocation signals from local object. / Yastrebov Yu.V., Kostyleva V.V., Nikolaev V.A. // 2010 5th International Conference on Ultrawideband and Ultrashort Impulse Signals (UWBUSIS). - Sevastopol, 6-10 Sept. 2010. - P. 174-176. ↑

**C3155.** Yastrebov Yu.V. Practical application of UWB georadar technique for investigations of cultural heritage objects. / Yastrebov Yu.V., Kostyleva V.V., Nikolaev V.A., Barilko M.S. // 2010 5th International Conference on Ultrawideband and Ultrashort Impulse Signals (UWBUSIS). - Sevastopol, 6-10 Sept. 2010. - P. 171-173. ↑

**C3156.** Ziganshin E.G. UWB Baby Monitor. / Ziganshin E.G., Numerov M.A., Vygodov S.A. // 2010 5th International Conference on Ultrawideband and Ultrashort Impulse Signals (UWBUSIS). - Sevastopol, 6-10 Sept. 2010. - P. 159-161. ↑

**C3157.** {no data available}. Applications (GPR, radars, communication, medicine). 2010 5th International Conference on Ultrawideband and Ultrashort Impulse Signals (UWBUSIS). - Sevastopol, Ukraine, 6-10 Sept. 2010. - P. 136-137. ↑

**C3158.** Wang Liang. Portable system for RAC measurement based on swept frequency RCS method. / Wang Liang, Xue Ming Hua, Hong Tao. // 2010 International Conference on Computer, Mechatronics, Control and Electronic Engineering (CMCE). - Changchun, 24-26 Aug. 2010. - Vol. 2. - P. 1-4. ↑

**C3159.** Chenggang Zhao. Design of mobile robot system with remote control based on CAN-bus. / Chenggang Zhao, Xiangke Han. // 2010 International Conference on Computer, Mechatronics, Control and Electronic Engineering (CMCE). - Changchun, 24-26 Aug. 2010. - Vol. 2. - P. 103-105. ↑

**C3160.** She Yong. Practicability evaluation of middle atmospheric wind field based on HWM93. / She Yong, Qiao He. // 2010 International Conference on Computer, Mechatronics, Control and Electronic Engineering (CMCE). - Changchun, 24-26 Aug. 2010. - Vol. 6. - P. 373-377. ↑

**C3161.** Rudenchik A.E. Presentation of the field surface wave generated by an antenna at the interface of two homogeneous media. / Rudenchik A.E., Volkovskaya L.B., Reznikov A.E., Bezrukova E.G. // 2010 5th International Conference on Ultrawideband and Ultrashort Impulse Signals (UWBUSIS). - Sevastopol, 6-10 Sept. 2010. - P. 132-133. ↑

**C3162.** Long Zhao. Antenna arrays used for the cancellation of Es layer clutter. / Long Zhao, Xingwei Wang. // 2010 2nd IEEE International Conference on Information and Financial Engineering (ICIFE). - Chongqing, 17-19 Sept. 2010. - P. 512-516. ↑

**C3163.** Zheng Wenzheng. Design and implementation on wireless power meter system based on GSM network. 2010 International Conference on Computer, Mechatronics, Control and Electronic Engineering (CMCE). - Changchun, 24-26 Aug. 2010. - Vol. 2. - P. 76-79. ↑

**C3164.** Kubota T. Development of spaceborne radar simulator by NICT and JAXA using JMA cloud-resolving model. / Kubota T., Eito H., Aonashi K., Hashimoto A., Iguchi T., Hanado H., Shimizu S., Yoshida N., Oki R. // 2010 IEEE International Geoscience and Remote Sensing Symposium (IGARSS). - Honolulu, HI, 25-30 July 2010. - P. 1304-1307. ↑

**C3165.** Gaohuan Lv. Reciprocal spectrum algorithm for radar imaging with frequency sampling waveform. / Gaohuan Lv, Kaizhi Wang, Xingzhao Liu, Wenxian Yu, Guozhong Chen, Junli Chen. // 2010 IEEE International Geoscience and Remote Sensing Symposium (IGARSS). - Honolulu, HI, 25-30 July 2010. - P. 4683-4685. ↑

- C3166.** Chandrasekar V. Scientific and engineering overview of the NASA Dual-Frequency Dual-Polarized Doppler Radar (D3R) system for GPM Ground Validation. / Chandrasekar V., Schwaller M., Vega M., Carswell J., Mishra K.V., Meneghini R., Cuong Nguyen. // 2010 IEEE International Geoscience and Remote Sensing Symposium (IGARSS). - Honolulu, HI, 25-30 July 2010. - P. 1308-1311. ↑
- C3167.** Paladini R. Fetch limited sea scattering spectral model for HF-OTH skywave radar. / Paladini R., Dalle Mese E., Berizzi F., Garzelli A., Martorella M., Capria A. // 2010 IEEE International Geoscience and Remote Sensing Symposium (IGARSS). - Honolulu, HI, 25-30 July 2010. - P. 4177-4180. ↑
- C3168.** Schmitt M. Utilization of airborne multi-aspect InSAR data for the generation of urban ortho-images. / Schmitt M., Stilla U. // 2010 IEEE International Geoscience and Remote Sensing Symposium (IGARSS). - Honolulu, HI, 25-30 July 2010. - P. 3937-3940. ↑
- C3169.** Praks J. Polarimetric sar image visualization and interpretation with covariance matrix invariants. / Praks J., Hallikainen M., Koeniguer E.C. // 2010 IEEE International Geoscience and Remote Sensing Symposium (IGARSS). - Honolulu, HI, 25-30 July 2010. - P. 2035-2038. ↑
- C3170.** Venkataraman G. Fully polarimetric ALOS PALSAR data applications for snow and ice studies. / Venkataraman G., Singh G., Yamaguchi Y. // 2010 IEEE International Geoscience and Remote Sensing Symposium (IGARSS). - Honolulu, HI, 25-30 July 2010. - P. 1776-1779. ↑
- C3171.** Brolly M. A Matchstick Model of microwave backscatter from a forest: A change of regime. / Brolly M., Woodhouse I.H. // 2010 IEEE International Geoscience and Remote Sensing Symposium (IGARSS). - Honolulu, HI, 25-30 July 2010. - P. 3295-3298. ↑
- C3172.** Lei Shi. Multichannel Coherent Radar Depth Sounder for NASA Operation Ice Bridge. / Lei Shi, Allen C.T., Ledford J.R., Rodriguez-Morales F., Blake W.A., Panzer B.G., Prokopiack S.C., Leuschen C.J., Gogineni S. // 2010 IEEE International Geoscience and Remote Sensing Symposium (IGARSS). - Honolulu, HI, 25-30 July 2010. - P. 1729-1732. ↑
- C3173.** Schmidt M. Estimation of building density using Terrasar-X-Data. / Schmidt M., Esch T., Klein D., Thiel M., Dech S. // 2010 IEEE International Geoscience and Remote Sensing Symposium (IGARSS). - Honolulu, HI, 25-30 July 2010. - P. 1936-1939. ↑
- C3174.** Brigui F. Oblique polarimetric SAR processor based on signal and interference subspace models. / Brigui F., Thiron-Lefevre L., Ginolhac G., Forster P. // 2010 IEEE International Geoscience and Remote Sensing Symposium (IGARSS). - Honolulu, HI, 25-30 July 2010. - P. 4027-4030. ↑
- C3175.** Okamoto K. Surface reference normalized radar cross section over land for the improvement of the TRMM PR algorithm. / Okamoto K., Komukai J., Shige S., Manabe T. // 2010 IEEE International Geoscience and Remote Sensing Symposium (IGARSS). - Honolulu, HI, 25-30 July 2010. - P. 1316-1318. ↑
- C3176.** Yun Shao. Applications of polarimetric decomposition technology in a dried up lake evolution. / Yun Shao, Huaze Gong, Guojun Wang, Aimin Cai. // 2010 IEEE International Geoscience and Remote Sensing Symposium (IGARSS). - Honolulu, HI, 25-30 July 2010. - P. 4499-4502. ↑
- C3177.** Sixin Liu. Electromagnetic simulations of borehole radar for metal ore detection. / Sixin Liu, Junfeng Zhou, Junjun Wu, Zhaofa Zeng. // 2010 IEEE International Geoscience and Remote Sensing Symposium (IGARSS). - Honolulu, HI, 25-30 July 2010. - P. 2992-2994. ↑
- C3178.** Sarti F. ESA Earth Observation educational tools contribution to the creation of awareness for World Heritage site conservation. / Sarti F., Hernandez M., Bigot J.C., Dransfeld S., Orient A.R. // 2010 IEEE International Geoscience and Remote Sensing Symposium (IGARSS). - Honolulu, HI, 25-30 July 2010. - P. 90-93. ↑
- C3179.** Rochdi M. Physical optics-based method to compute the radar signature of complex objects over a sea surface. / Rochdi M., Baussard A., Khenchaf A. // 2010 IEEE International Geoscience and Remote Sensing Symposium (IGARSS). - Honolulu, HI, 25-30 July 2010. - P. 2976-2979. ↑
- C3180.** Torres-Martinez E. Nasa's Laser Risk Reduction Program: A risk reduction approach for technology development. / Torres-Martinez E., Heaps W.S., Singh U.N. // 2010 IEEE International Geoscience and Remote Sensing Symposium (IGARSS). - Honolulu, HI, 25-30 July 2010. - P. 3106-3109. ↑

- C3181.** Hamurcu A.C. A comparison of two CA-CFAR loss calculation methods in spatially correlated K-Distributed sea clutter. / Hamurcu A.C., Hizal A. // 2010 IEEE 18th Signal Processing and Communications Applications Conference (SIU). - Diyarbakir, 22-24 April 2010. - P. 772-775. ↑
- C3182.** Denis L. Exact discrete minimization for TV+L0 image decomposition models. / Denis L., Tupin F., Rondeau X. // 2010 17th IEEE International Conference on Image Processing (ICIP). - Hong Kong, 26-29 Sept. 2010. - P. 2525-2528. ↑
- C3183.** Heggy E. Coupling polarimetric L-Band insar and airborne lidar to characterize the geomorphological deformations in the piton de la fournaise volcano. / Heggy E., Sedze M., Bretar F., Jacquemoud S., Rosen P.A., Wada K., Staudacher T. // 2010 IEEE International Geoscience and Remote Sensing Symposium (IGARSS). - Honolulu, HI, 25-30 July 2010. - P. 1911-1913. ↑
- C3184.** McNeill S.J. Robust estimation of pasture biomass using dual-polarisation TerrASAR-X imagery. / McNeill S.J., Pairman D., Belliss S.E., Dalley D., Dynes R. // 2010 IEEE International Geoscience and Remote Sensing Symposium (IGARSS). - Honolulu, HI, 25-30 July 2010. - P. 3094-3097. ↑
- C3185.** Gonzalez J.H. TanDEM-X commissioning phase status. / Gonzalez J.H., Bachmann M., Hofmann H. // 2010 IEEE International Geoscience and Remote Sensing Symposium (IGARSS). - Honolulu, HI, 25-30 July 2010. - P. 2633-2635. ↑
- C3186.** {no data available}. Copyright. 2010 IEEE International Geoscience and Remote Sensing Symposium (IGARSS). - Honolulu, HI, 25-30 July 2010. - P. ii. ↑
- C3187.** Di Martino G. Physical-based models of speckle for high resolution SAR images. / Di Martino G., Iodice A., Riccio D., Ruello G. // 2010 IEEE International Geoscience and Remote Sensing Symposium (IGARSS). - Honolulu, HI, 25-30 July 2010. - P. 2980-2983. ↑
- C3188.** Ying Liu. Remote sensing image synthesis. / Ying Liu, Wong A., Fieguth P. // 2010 IEEE International Geoscience and Remote Sensing Symposium (IGARSS). - Honolulu, HI, 25-30 July 2010. - P. 2467-2470. ↑
- C3189.** Chunxiang Cao. Synchronous retrieval of forest canopy cover by airborne LiDAR and optical remote sensing. / Chunxiang Cao, Min Xu, Yunfei Bao, Hao Zhang. // 2010 IEEE International Geoscience and Remote Sensing Symposium (IGARSS). - Honolulu, HI, 25-30 July 2010. - P. 2660-2663. ↑
- C3190.** Solberg R. A new global Snow Extent product based on ATSR-2 and AATSR. / Solberg R., Wangenstein B., Amlien J., Koren H., Metsajmaki S., Nagler T., Luoju K., Pulliainen J. // 2010 IEEE International Geoscience and Remote Sensing Symposium (IGARSS). - Honolulu, HI, 25-30 July 2010. - P. 1780-1783. ↑
- C3191.** Lorenzo J. Next generation of multi beam rotating antenna on SWIM scatterometer. / Lorenzo J., Demeestere F., Brossier J., Pouyez S., Enjolras V., Rey L., Amiot T., Tison C., Castellan P. // 2010 IEEE International Geoscience and Remote Sensing Symposium (IGARSS). - Honolulu, HI, 25-30 July 2010. - P. 3478-3481. ↑
- C3192.** Ji-Hwan Hwang. Calibration accuracy enhancement in the field experiment with a ground-based scatterometer. / Ji-Hwan Hwang, Seong-Min Park, Yisok Oh. // 2010 IEEE International Geoscience and Remote Sensing Symposium (IGARSS). - Honolulu, HI, 25-30 July 2010. - P. 1100-1103. ↑
- C3193.** Macelloni G. Evaluation of vegetation effect on the retrieval of snow parameters from backscattering measurements: A contribution to CoReH2O mission. / Macelloni G., Brogioni M., Montomoli F., Fontanelli G., Kern M., Rott H. // 2010 IEEE International Geoscience and Remote Sensing Symposium (IGARSS). - Honolulu, HI, 25-30 July 2010. - P. 1772-1775. ↑
- C3194.** Lofgren J.S. Tropospheric correction for InSAR using interpolated ECMWF data and GPS Zenith Total Delay from the Southern California Integrated GPS Network. / Lofgren J.S., Bjojndahl F., Moore A.W., Webb F.H., Fielding E.J., Fishbein E.F. // 2010 IEEE International Geoscience and Remote Sensing Symposium (IGARSS). - Honolulu, HI, 25-30 July 2010. - P. 4503-4506. ↑
- C3195.** Renga A. Spaceborne-airborne bistatic radar for UAS navigation purposes: Preliminary analysis and strawman system identification. / Renga A., Graziano M.D., D'Errico M., Moccia A., Menichino F., Vetrella S., Accardo D., Corrado F., Cuciniello G., Nebula F., Del Monte L. // 2010 IEEE International Geoscience and

Remote Sensing Symposium (IGARSS). - Honolulu, HI, 25-30 July 2010. - P. 3474-3477. ↑

**C3196.** Kajrnaj J. Improving hydrological forecasting using multi-source remote sensing data together with in situ measurements. / Kajrnaj J., Huttunen M., Metsajmäki S., Vehviläinen B., Podsechin V., Pulliainen J., Lemmetyinen J., Kuitunen T., Rauste Y., Berglund R. // 2010 IEEE International Geoscience and Remote Sensing Symposium (IGARSS). - Honolulu, HI, 25-30 July 2010. - P. 1749-1752. ↑

**C3197.** Kuloglu M. Ground penetrating radar for tunnel detection. / Kuloglu M., Chen C. // 2010 IEEE International Geoscience and Remote Sensing Symposium (IGARSS). - Honolulu, HI, 25-30 July 2010. - P. 4314-4317. ↑

**C3198.** Sato M. GPR evaluation test for humanitarian demining in Cambodia. 2010 IEEE International Geoscience and Remote Sensing Symposium (IGARSS). - Honolulu, HI, 25-30 July 2010. - P. 4322-4325. ↑

**C3199.** Ruzanski E. Nowcasting rainfall fields estimated from specific differential phase. / Ruzanski E., Chandrasekar V. // 2010 IEEE International Geoscience and Remote Sensing Symposium (IGARSS). - Honolulu, HI, 25-30 July 2010. - P. 4694-4697. ↑

**C3200.** Yang Wei. A novel three-step focusing algorithm for TOPSAR image formation. / Yang Wei, Li Chunsheng, Chen Jie, Wang Pengbo. // 2010 IEEE International Geoscience and Remote Sensing Symposium (IGARSS). - Honolulu, HI, 25-30 July 2010. - P. 4087-4090. ↑

**C3201.** Wang R. Image formation algorithm for bistatic forward-looking SAR. / Wang R., Loffeld O., Nies H., Peters V. // 2010 IEEE International Geoscience and Remote Sensing Symposium (IGARSS). - Honolulu, HI, 25-30 July 2010. - P. 4091-4094. ↑

**C3202.** Aari M. Retrieval of soil moisture under vegetation using Polarimetric Scattering Cubes. / Aari M., van Zyl J.J., Kim Y. // 2010 IEEE International Geoscience and Remote Sensing Symposium (IGARSS). - Honolulu, HI, 25-30 July 2010. - P. 1323-1326. ↑

**C3203.** Allan G.R. Remote sensing atmospheric CO<sub>2</sub> column abundance using an airborne pulsed laser sounder at 13 km altitude. / Allan G.R., Hasselbrack W., Riris H., Abshire J.B., Weaver C., Jianping Mao, Xiaoli Sun, Andrews A.E. // 2010 IEEE International Geoscience and Remote Sensing Symposium (IGARSS). - Honolulu, HI, 25-30 July 2010. - P. 2595-2598. ↑

**C3204.** Qiang Xing. Monitoring thickness change of the Dongkemadi Glacier on Qinghai-Tibetan Plateau using SRTM DEM and map-based topographic data. / Qiang Xing, Zhen Li, Jianmin Zhou. // 2010 IEEE International Geoscience and Remote Sensing Symposium (IGARSS). - Honolulu, HI, 25-30 July 2010. - P. 1769-1771. ↑

**C3205.** Dubois-Fernandez P. TropiSAR: Exploring the temporal behavior of P-Band SAR data. / Dubois-Fernandez P., Oriot H., Coulombeix C., Cantalloube H., Ruault du Plessis O., Le Toan T., Daniel S., Chave J., Blanc L., Davidson M., Petit M. // 2010 IEEE International Geoscience and Remote Sensing Symposium (IGARSS). - Honolulu, HI, 25-30 July 2010. - P. 1319-1322. ↑

**C3206.** Ebuchi N. AMSR and DFS synergy. / Ebuchi N., Liu W.T. // 2010 IEEE International Geoscience and Remote Sensing Symposium (IGARSS). - Honolulu, HI, 25-30 July 2010. - P. 1812-1814. ↑

**C3207.** Chabert M. Logistic regression for detecting changes between databases and remote sensing images. / Chabert M., Tournet J.-Y., Poulain V., Inglada J. // 2010 IEEE International Geoscience and Remote Sensing Symposium (IGARSS). - Honolulu, HI, 25-30 July 2010. - P. 3198-3201. ↑

**C3208.** Capria A. DVB-T passive radar for vehicles detection in urban environment. / Capria A., Petri D., Martorella M., Conti M., Dalle Mese E., Berizzi F. // 2010 IEEE International Geoscience and Remote Sensing Symposium (IGARSS). - Honolulu, HI, 25-30 July 2010. - P. 3917-3920. ↑

**C3209.** Fabra F. Monitoring sea-ice and dry snow with GNSS reflections. / Fabra F., Cardellach E., Nogues-Correig O., Oliveras S., Ribo S., Rius A., Belmonte-Rivas M., Semmling M., Macelloni G., Pettinato S., Zasso R., D'Addio S. // 2010 IEEE International Geoscience and Remote Sensing Symposium (IGARSS). - Honolulu, HI, 25-30 July 2010. - P. 3837-3840. ↑

**C3210.** Hillman A. RADARSAT-2 continuing system operations and performance. / Hillman A., Rolland P., Periard R., Luscombe A., Chabot M., Chen C., Martens N. // 2010 IEEE International Geoscience and Remote Sensing Symposium (IGARSS). - Honolulu, HI, 25-30 July 2010. - P. 3841-3844. ↑



Sensing Symposium (IGARSS). - Honolulu, HI, 25-30 July 2010. - P. 3228-3231. ↑

**C3211.** Sun-Mack S. Enhanced Cloud algorithm from collocated CALIPSO, CloudSat and MODIS global boundary layer lapse rate studies. / Sun-Mack S., Minnis P., Kato S., Yan Chen, Yuhong Yi, Gibson S., Heck P., Winker D., Ayers K. // 2010 IEEE International Geoscience and Remote Sensing Symposium (IGARSS). - Honolulu, HI, 25-30 July 2010. - P. 201-204. ↑

**C3212.** Kidd C. Investigations into high resolution mapping of precipitation features utilizing the TRMM precipitation Radar. / Kidd C., Kwiatkowski J., Nesbitt S. // 2010 IEEE International Geoscience and Remote Sensing Symposium (IGARSS). - Honolulu, HI, 25-30 July 2010. - P. 2337-2340. ↑

**C3213.** Huanmin Luo. Tree height retrieval methods using POLInSAR coherence optimization. / Huanmin Luo, Erxue Chen, Jian Cheng, Xiaowen Li. // 2010 IEEE International Geoscience and Remote Sensing Symposium (IGARSS). - Honolulu, HI, 25-30 July 2010. - P. 3259-3262. ↑

**C3214.** Chuen-Meei Gan. A comparison of estimated mixing height by multiple remote sensing instruments and its influence on air quality in urban regions. / Chuen-Meei Gan, Wu Y.H., Gross B.M., Arend M., Moshary F., Ahmed S. // 2010 IEEE International Geoscience and Remote Sensing Symposium (IGARSS). - Honolulu, HI, 25-30 July 2010. - P. 730-733. ↑

**C3215.** Chen V.C. High-resolution 3-D radar imaging using pseudo-random noise coded waveform. 2010 IEEE International Geoscience and Remote Sensing Symposium (IGARSS). - Honolulu, HI, 25-30 July 2010. - P. 718-721. ↑

**C3216.** Fengli Zhang. Interpretation of buildings in high resolution sar images based on electromagnetic method. / Fengli Zhang, Yun Shao, Zi Wan, Xiao Zhang. // 2010 IEEE International Geoscience and Remote Sensing Symposium (IGARSS). - Honolulu, HI, 25-30 July 2010. - P. 2727-2730. ↑

**C3217.** Toporkov J.V. Observation of a boat and its wake with a Dual-Beam along-track interferometric sar. / Toporkov J.V., Hwang P.A., Sletten M.A., Frasier S.J., Farquharson G., Perkovic D. // 2010 IEEE International Geoscience and Remote Sensing Symposium (IGARSS). - Honolulu, HI, 25-30 July 2010. - P. 1940-1943. ↑

**C3218.** Mitchell A.L. Wall-to-wall mapping of forest extent and change in Tasmania using ALOS PALSAR data. / Mitchell A.L., Milne A., Tapley I., Lowell K., Caccetta P., Lehmann E., Zheng-Shu Zhou. // 2010 IEEE International Geoscience and Remote Sensing Symposium (IGARSS). - Honolulu, HI, 25-30 July 2010. - P. 1230-1233. ↑

**C3219.** Duque S. Bistatic SAR tomography: Processing and experimental results. / Duque S., Lopez-Dekker P., Merlano J.C., Mallorqui J.J. // 2010 IEEE International Geoscience and Remote Sensing Symposium (IGARSS). - Honolulu, HI, 25-30 July 2010. - P. 154-157. ↑

**C3220.** Ning Zhang. An improved fast Viterbi algorithm for track-before-detect. / Ning Zhang, Song Hao, Yang Li. // 2010 3rd International Congress on Image and Signal Processing (CISP). - Yantai, 16-18 Oct. 2010. - Vol. 7. - P. 3125-3128. ↑

**C3221.** Xianjun Pan. A novel method of SAR terrain target scattering signal simulation. / Xianjun Pan, Yanhong Wu, Xin Jia. // 2010 3rd International Congress on Image and Signal Processing (CISP). - Yantai, 16-18 Oct. 2010. - Vol. 6. - P. 2961-2965. ↑

**C3222.** YiKun Zhang. An EMD-based denoising method for lidar signal. / YiKun Zhang, XiaoChang Ma, DengXin Hua, YingAn Cui, LianSheng Sui. // 2010 3rd International Congress on Image and Signal Processing (CISP). - Yantai, 16-18 Oct. 2010. - Vol. 8. - P. 4016-4019. ↑

**C3223.** Chen Xin. MST phase unwrapping based on new weighted map. / Chen Xin, Tang Jing-Song. // 2010 3rd International Congress on Image and Signal Processing (CISP). - Yantai, 16-18 Oct. 2010. - Vol. 9. - P. 4408-4412. ↑

**C3224.** Yan Shen. SAR raw echo simulation of ground scene. / Yan Shen, Xinmin Wang, Houjin Chen, Xiaoli Hao. // 2010 3rd International Congress on Image and Signal Processing (CISP). - Yantai, 16-18 Oct. 2010. - Vol. 5. - P. 2251-2254. ↑

**C3225.** Haizhong Ma. Simulation of Faraday rotation on longer wavelength spaceborne polarimetric InSAR. /

Haizhong Ma, Jie Chen, Xunjun Yin. // 2010 3rd International Congress on Image and Signal Processing (CISP). - Yantai, 16-18 Oct. 2010. - Vol. 5. - P. 2255-2259. ↑

C3226. Hongxian Wang. Subimage fusion for high-resolution ISAR imaging. / Hongxian Wang, Yi Liang, Mengdao Xing, Shouhong Zhang. // 2010 3rd International Congress on Image and Signal Processing (CISP). - Yantai, 16-18 Oct. 2010. - Vol. 5. - P. 2260-2264. ↑

C3227. Bin Liu. Segmentation of Polarimetric SAR images using graph partitioning active contours. / Bin Liu, Huanyu Wang, Kaizhi Wang, Xingzhao Liu, Wenxian Yu. // 2010 3rd International Congress on Image and Signal Processing (CISP). - Yantai, 16-18 Oct. 2010. - Vol. 3. - P. 1454-1459. ↑

C3228. Franklin A.G. Prospects of new real-time radar applications for environmental remote sensing. / Franklin A.G., Coronado P.L. // 2010 IEEE International Geoscience and Remote Sensing Symposium (IGARSS). - Honolulu, HI, 25-30 July 2010. - P. 1914-1917. ↑

C3229. Sun G. Simulation studies on data fusion algorithms for forest structure from lidar and SAR data. / Sun G., Ni W., Ranson K.J. // 2010 IEEE International Geoscience and Remote Sensing Symposium (IGARSS). - Honolulu, HI, 25-30 July 2010. - P. 3287-3290. ↑

C3230. Junhao Xie. Application of monopulse techniques in angle-measuring of single-beam mechanical scanning radar. / Junhao Xie, Xiaodong Feng, Yesu Yuan, Shaobin Li. // 2010 3rd International Congress on Image and Signal Processing (CISP). - Yantai, 16-18 Oct. 2010. - Vol. 6. - P. 2971-2974. ↑

C3231. Yu Li. Analysis of Faraday rotation on spaceborne CTRLR compact polarimetric SAR image reconstruction. / Yu Li, Jie Chen, Xunjun Yin. // 2010 3rd International Congress on Image and Signal Processing (CISP). - Yantai, 16-18 Oct. 2010. - Vol. 4. - P. 2017-2021. ↑

C3232. Chunlai Yu. A measurement method for Doppler frequency rate-of-change with coherent pulse train. / Chunlai Yu, Minghao He, Fang Wan, Changxiao Chen. // 2010 3rd International Congress on Image and Signal Processing (CISP). - Yantai, 16-18 Oct. 2010. - Vol. 8. - P. 3729-3732. ↑

C3233. Yuxi Zhang. Compressive sensing SAR imaging with real data. / Yuxi Zhang, Jinping Sun, Jihua Tian, Ahmad N., Xiaoyang Su. // 2010 3rd International Congress on Image and Signal Processing (CISP). - Yantai, 16-18 Oct. 2010. - Vol. 4. - P. 2026-2029. ↑

C3234. Feng Wang. Estimation of significant wave height from X-band marine radar images. / Feng Wang, Jian Wang, Shujuan Wang. // 2010 3rd International Congress on Image and Signal Processing (CISP). - Yantai, 16-18 Oct. 2010. - Vol. 5. - P. 2172-2174. ↑

C3235. Kai Liu. Fish-pond change detection based on short term time series of RADARSAT images and object-oriented method. / Kai Liu, Bin Ai, Shugong Wang. // 2010 3rd International Congress on Image and Signal Processing (CISP). - Yantai, 16-18 Oct. 2010. - Vol. 5. - P. 2175-2179. ↑

C3236. Xiwen Zhao. A 3D microwave imaging method for earth observation. 2010 3rd International Congress on Image and Signal Processing (CISP). - Yantai, 16-18 Oct. 2010. - Vol. 2. - P. 507-510. ↑

C3237. Liying Wang. Airborne LiDAR strip adjustment based on LSM. / Liying Wang, Zhengjun Liu, Weidong Song, Haitao Li. // 2010 3rd International Congress on Image and Signal Processing (CISP). - Yantai, 16-18 Oct. 2010. - Vol. 6. - P. 2727-2731. ↑

C3238. Lan Chen. High resolution radar imaging using bandwidth extrapolation. / Lan Chen, Jie Chen. // 2010 3rd International Congress on Image and Signal Processing (CISP). - Yantai, 16-18 Oct. 2010. - Vol. 8. - P. 3591-3595. ↑

C3239. Yingchun Li. Analysis and modification to the method of bistatic clutter range dependence mitigation. / Yingchun Li, Jingwen Li. // 2010 3rd International Congress on Image and Signal Processing (CISP). - Yantai, 16-18 Oct. 2010. - Vol. 7. - P. 3308-3312. ↑

C3240. Pfeil R. Power-level surveillance for an FMCW-based local positioning system. / Pfeil R., Pichler M., Scherz P., Stelzer A., Stelzhammer G. // 2010 International Conference on Indoor Positioning and Indoor Navigation (IPIN). - Zurich, 15-17 Sept. 2010. - P. 1-10. ↑

- C3241.** Jianmin Wang. Wetland cover information extraction research based on the multi-polar radar images and multi-spectrum optical images fusion. / Jianmin Wang, Fanshuai Meng, Huan Yu. // 2010 3rd International Congress on Image and Signal Processing (CISP). - Yantai, 16-18 Oct. 2010. - Vol. 5. - P. 2298-2301. ↑
- C3242.** Ji-Ping Guan. A new method of three-dimensional visualization of satellite cloud image. / Ji-Ping Guan, Zhi-Quan Yin, Zhu-Hui Jiang. // 2010 3rd International Congress on Image and Signal Processing (CISP). - Yantai, 16-18 Oct. 2010. - Vol. 5. - P. 2465-2468. ↑
- C3243.** Wei Qu. SAR interference signal feature vector extraction and simulation based on wavelet packet analysis. / Wei Qu, Xin Jia, Shuqian Liu, Yanhong Wu. // 2010 3rd International Congress on Image and Signal Processing (CISP). - Yantai, 16-18 Oct. 2010. - Vol. 7. - P. 3234-3238. ↑
- C3244.** Pei Wang. Research on extracting the tree height based on LiDAR data. 2010 3rd International Congress on Image and Signal Processing (CISP). - Yantai, 16-18 Oct. 2010. - Vol. 5. - P. 2236-2239. ↑
- C3245.** Huaping Xu. A novel SAR fusion image segmentation method based on Markov Random Field. / Huaping Xu, Wei Wang, Xianghua Liu. // 2010 3rd International Congress on Image and Signal Processing (CISP). - Yantai, 16-18 Oct. 2010. - Vol. 3. - P. 1297-1300. ↑
- C3246.** Xudong Li. Synthesis of four-level Z-complementary sequences. / Xudong Li, Li Hao. // 2010 3rd International Congress on Image and Signal Processing (CISP). - Yantai, 16-18 Oct. 2010. - Vol. 9. - P. 4463-4466. ↑
- C3247.** Yue-bin Chen. A novel method of resolving velocity ambiguity in the pulse doppler radar. / Yue-bin Chen, Wei Peng, Qing-chang Wu, Wu-bang Hao, Chang Liu. // 2010 3rd International Congress on Image and Signal Processing (CISP). - Yantai, 16-18 Oct. 2010. - Vol. 9. - P. 4321-4323. ↑
- C3248.** Hyoung-sun Youn. In-situ broadband soil measurements: Dielectric and magnetic properties. / Hyoung-sun Youn, Loon Yip Lee, Iskander M. // 2010 IEEE International Geoscience and Remote Sensing Symposium (IGARSS). - Honolulu, HI, 25-30 July 2010. - P. 4483-4486. ↑
- C3249.** Sportouche H. Building detection and height retrieval in urban areas in the framework of high resolution optical and SAR data fusion. / Sportouche H., Tupin F., Denise L. // 2010 IEEE International Geoscience and Remote Sensing Symposium (IGARSS). - Honolulu, HI, 25-30 July 2010. - P. 3660-3663. ↑
- C3250.** Mahrooghy M. Infrared satellite precipitation estimate using waveletbased cloud classification and radar calibration. / Mahrooghy M., Anantharaj V.G., Younan N.H., Petersen W.A., Turk F.J., Aanstoots J. // 2010 IEEE International Geoscience and Remote Sensing Symposium (IGARSS). - Honolulu, HI, 25-30 July 2010. - P. 2345-2348. ↑
- C3251.** My-Linh Truong-Loi. Potentials of a compact polarimetric SAR system. / My-Linh Truong-Loi, Dubois-Fernandez P., Pottier E., Freeman A., Souyris J.-C. // 2010 IEEE International Geoscience and Remote Sensing Symposium (IGARSS). - Honolulu, HI, 25-30 July 2010. - P. 742-745. ↑
- C3252.** Nunziata F. Metallic objects and oil spill detection with multi-polarization SAR. / Nunziata F., Li X., Migliaccio M., Montuori A., Pichel W. // 2010 IEEE International Geoscience and Remote Sensing Symposium (IGARSS). - Honolulu, HI, 25-30 July 2010. - P. 2765-2768. ↑
- C3253.** Castorena J. Modeling lidar scene sparsity using compressive sensing. / Castorena J., Creusere C.D., Voelz D. // 2010 IEEE International Geoscience and Remote Sensing Symposium (IGARSS). - Honolulu, HI, 25-30 July 2010. - P. 2186-2189. ↑
- C3254.** Werner C. The snowscat ground-based polarimetric scatterometer: Calibration and initial measurements from Davos Switzerland. / Werner C., Wiesmann A., Strozzi T., Schneebeli M., Majtzer C. // 2010 IEEE International Geoscience and Remote Sensing Symposium (IGARSS). - Honolulu, HI, 25-30 July 2010. - P. 2363-2366. ↑
- C3255.** Tison C. Performance status of the wave scatterometer SWIM. / Tison C., Amiot T., Enjolras V., Hauser D., Rey L., Souyris J.C., Castellan P. // 2010 IEEE International Geoscience and Remote Sensing Symposium (IGARSS). - Honolulu, HI, 25-30 July 2010. - P. 4170-4173. ↑
- C3256.** Heaps W.S. One micron laser technology advancements at GSFC. 2010 IEEE International

Geoscience and Remote Sensing Symposium (IGARSS). - Honolulu, HI, 25-30 July 2010. - P. 3110-3113. ↑

**C3257.** Ramos-Perez I. On-ground tests and measurements of the Passive Advanced Unit Synthetic Aperture (PAU-SA). / Ramos-Perez I., Bosch-Lluis X., Camps A., Valencia E., Rodriguez-Alvarez N., Vall-Ilossera M., Forte G. // 2010 IEEE International Geoscience and Remote Sensing Symposium (IGARSS). - Honolulu, HI, 25-30 July 2010. - P. 3114-3117. ↑

**C3258.** Paden J. 3D imaging of ice sheets. / Paden J., Allen C., Gogineni P. // 2010 IEEE International Geoscience and Remote Sensing Symposium (IGARSS). - Honolulu, HI, 25-30 July 2010. - P. 2611-2613. ↑

**C3259.** Even M. Atmospheric phase screen-estimation for PSInSAR applied to TerraSAR-X high resolution spotlight-data. / Even M., Schunert A., Schulz K., Soergel U. // 2010 IEEE International Geoscience and Remote Sensing Symposium (IGARSS). - Honolulu, HI, 25-30 July 2010. - P. 2928-2931. ↑

**C3260.** Di Zhu. Doppler effect and compensation in a Rotating Fanbeam Spaceborne Scatterometer. / Di Zhu, Xiaolong Dong, Wenming Lin, Yun R. // 2010 IEEE International Geoscience and Remote Sensing Symposium (IGARSS). - Honolulu, HI, 25-30 July 2010. - P. 1089-1091. ↑

**C3261.** Di Martino G. Fractal based filtering of SAR images. / Di Martino G., Iodice A., Riccio D., Ruello G., Zinno I. // 2010 IEEE International Geoscience and Remote Sensing Symposium (IGARSS). - Honolulu, HI, 25-30 July 2010. - P. 2984-2987. ↑

**C3262.** Foucher S. Exploitation of the additive component of the polarimetric noise model for speckle filtering. / Foucher S., Farage G., Lopez-Martinez C. // 2010 IEEE International Geoscience and Remote Sensing Symposium (IGARSS). - Honolulu, HI, 25-30 July 2010. - P. 312-315. ↑

**C3263.** Brajutigam B. SAR performance monitoring for TerraSAR-X mission. / Brajutigam B., Rizzoli P., Gonzalez C., Weigt M., Schrank D., Schulze D., Schwerdt M. // 2010 IEEE International Geoscience and Remote Sensing Symposium (IGARSS). - Honolulu, HI, 25-30 July 2010. - P. 3454-3457. ↑

**C3264.** Nelson R. Using airborne & space lidars for large-area inventory. / Nelson R., Stehl G., Holm S., Gregoire T., Naesset E., Gobakken T. // 2010 IEEE International Geoscience and Remote Sensing Symposium (IGARSS). - Honolulu, HI, 25-30 July 2010. - P. 2463-2466. ↑

**C3265.** Hashimoto S. Case studies of automatic change detection using AVNIR-2 onboard ALOS. / Hashimoto S., Onosato M., Tadono T., Hori M., Moriyama T. // 2010 IEEE International Geoscience and Remote Sensing Symposium (IGARSS). - Honolulu, HI, 25-30 July 2010. - P. 3644-3647. ↑

**C3266.** McPherson C. Progress in the validation of dual-wavelength aerosol retrieval models via airborne high spectral resolution lidar data. / McPherson C., Reagan J., Hostetler C., Hair J., Ferrare R. // 2010 IEEE International Geoscience and Remote Sensing Symposium (IGARSS). - Honolulu, HI, 25-30 July 2010. - P. 1714-1717. ↑

**C3267.** Zhang C. Focal plane approximation for near field interferometric radiometer imaging. / Zhang C., Wu J., Liu H., Yan J.Y. // 2010 IEEE International Geoscience and Remote Sensing Symposium (IGARSS). - Honolulu, HI, 25-30 July 2010. - P. 3118-3121. ↑

**C3268.** Velotto D. Oil-slick observation using single look complex TerraSAR-X dual-polarized data. / Velotto D., Migliaccio M., Nunziata F., Lehner S. // 2010 IEEE International Geoscience and Remote Sensing Symposium (IGARSS). - Honolulu, HI, 25-30 July 2010. - P. 3684-3687. ↑

**C3269.** Repasky K.S. Observational studies of atmospheric aerosols in the lower troposphere using multiple sensors. / Repasky K.S., Nehrir A.R., Hoffman D.S., Thomas M., Carlsten J.L., Shaw J.A. // 2010 IEEE International Geoscience and Remote Sensing Symposium (IGARSS). - Honolulu, HI, 25-30 July 2010. - P. 2583-2586. ↑

**C3270.** Porzycka S. The preliminary temporal analysis of ground deformations in the area of Dabrowski Coal Basin (south Poland). / Porzycka S., Lesniak A. // 2010 IEEE International Geoscience and Remote Sensing Symposium (IGARSS). - Honolulu, HI, 25-30 July 2010. - P. 903-905. ↑

**C3271.** Floricioiu D. TerraSAR-X observations over the antarctic ice sheet. / Floricioiu D., Jezek K., Eineder M., Farness K., Abdel Jaber W., Yague-Martinez N. // 2010 IEEE International Geoscience and Remote Sensing Symposium (IGARSS). - Honolulu, HI, 25-30 July 2010. - P. 3110-3113. ↑



Symposium (IGARSS). - Honolulu, HI, 25-30 July 2010. - P. 2614-2617. ↑

**C3272.** Scipal K. The BIOMASS mission-An ESA Earth Explorer candidate to measure the BIOMASS of the earth's forests. / Scipal K., Arcioni M., Chave J., Dall J., Fois F., LeToan T., Lin C., Papathanassiou K., Quesgan S., Rocca F., Saatchi S., Shugart H., Ulander L., Williams M. // 2010 IEEE International Geoscience and Remote Sensing Symposium (IGARSS). - Honolulu, HI, 25-30 July 2010. - P. 52-55. ↑

**C3273.** Singh G. Temporal snowpack density mapping using C-band multi-polarization ASAR data. / Singh G., Venkataraman G., Yamaguchi Y., Park S.E. // 2010 IEEE International Geoscience and Remote Sensing Symposium (IGARSS). - Honolulu, HI, 25-30 July 2010. - P. 1784-1787. ↑

**C3274.** Biao Zhang. A new polarization ratio model from C-Band RADARSAT-2 fine Quad-Pol imagery. / Biao Zhang, Perrie W., Hwang P.A., Yijun He. // 2010 IEEE International Geoscience and Remote Sensing Symposium (IGARSS). - Honolulu, HI, 25-30 July 2010. - P. 1948-1951. ↑

**C3275.** Gimmetstad G. Lidar education at Georgia Tech. / Gimmetstad G., West L. // 2010 IEEE International Geoscience and Remote Sensing Symposium (IGARSS). - Honolulu, HI, 25-30 July 2010. - P. 87-89. ↑

**C3276.** Shabou A. Three dimensional reconstruction of urban areas using jointly phase and amplitude multichannel images. / Shabou A., Tupin F., Ferraioli G., Pascasio V. // 2010 IEEE International Geoscience and Remote Sensing Symposium (IGARSS). - Honolulu, HI, 25-30 July 2010. - P. 4831-4834. ↑

**C3277.** Eineder M. IMaging geodesy with TerraSAR-X. / Eineder M., Xiaoying Cong, Minet C., Steigenberger P., Fritz T., Jaber W.A. // 2010 IEEE International Geoscience and Remote Sensing Symposium (IGARSS). - Honolulu, HI, 25-30 July 2010. - P. 4827-4830. ↑

**C3278.** SeungJoon Kwon. Development of the LiDAR data processing system for the rapid generation of the terrestrial information. / SeungJoon Kwon, SungWoong Shin. // 2010 IEEE International Geoscience and Remote Sensing Symposium (IGARSS). - Honolulu, HI, 25-30 July 2010. - P. 3902-3904. ↑

**C3279.** Amarin R.A. The Hurricane Imaging Radiometer wide swath simulation and wind speed retrievals. / Amarin R.A., Jones L., Johnson J., Ruf C., Miller T.L., Uhlhorn E. // 2010 IEEE International Geoscience and Remote Sensing Symposium (IGARSS). - Honolulu, HI, 25-30 July 2010. - P. 4290-4293. ↑

**C3280.** Pantze A. Forest change detection from L-band satellite SAR images using iterative histogram matching and thresholding together with data fusion. / Pantze A., Fransson J.E.S., Santoro M. // 2010 IEEE International Geoscience and Remote Sensing Symposium (IGARSS). - Honolulu, HI, 25-30 July 2010. - P. 1226-1229. ↑

**C3281.** Schwartz N.R. Ground penetrating radar measurements: Applications to synthetic data generation and target characterization. / Schwartz N.R., Zaghloul A.I. // 2010 IEEE International Geoscience and Remote Sensing Symposium (IGARSS). - Honolulu, HI, 25-30 July 2010. - P. 3362-3365. ↑

**C3282.** Walker C.C. On radar sounding applications for Enceladean ice. / Walker C.C., Liemohn M.W., Parkinson C.D. // 2010 IEEE International Geoscience and Remote Sensing Symposium (IGARSS). - Honolulu, HI, 25-30 July 2010. - P. 4522-4525. ↑

**C3283.** Nunziata F. A physically-based approach to observe man-made metallic objects in dual-polarized SAR data. / Nunziata F., Migliaccio M., Brown C.E. // 2010 IEEE International Geoscience and Remote Sensing Symposium (IGARSS). - Honolulu, HI, 25-30 July 2010. - P. 3007-3010. ↑

**C3284.** Benson M. Quantifying the results of wind and rain on ifsar tree height estimation. / Benson M., Pierce L., Sarabandi K. // 2010 IEEE International Geoscience and Remote Sensing Symposium (IGARSS). - Honolulu, HI, 25-30 July 2010. - P. 3275-3278. ↑

**C3285.** Moon-Kyung Kang. Preliminary result of polarization property analysis using fully polarimetric GB-SAR images. / Moon-Kyung Kang, Kwang-Eun Kim, Hoonyol Lee, Seong-Jun Cho, Jae-Hee Lee. // 2010 IEEE International Geoscience and Remote Sensing Symposium (IGARSS). - Honolulu, HI, 25-30 July 2010. - P. 4019-4022. ↑

**C3286.** Hamdi A. AN SVM classifier with HMM-based kernel for landmine detection using ground penetrating radar. / Hamdi A., Missaoui O., Frigui H. // 2010 IEEE International Geoscience and Remote Sensing Symposium

(IGARSS). - Honolulu, HI, 25-30 July 2010. - P. 4196-4199. ↑

**C3287.** Glenn T.C. A multimodal Matching Pursuits Dissimilarity Measure applied to landmine/clutter discrimination. / Glenn T.C., Wilson J.N., Ho K.C. // 2010 IEEE International Geoscience and Remote Sensing Symposium (IGARSS). - Honolulu, HI, 25-30 July 2010. - P. 4200-4203. ↑

**C3288.** Horie H. The external calibration study for EarthCARE/CPR. / Horie H., Ohno Y., Takahashi N. // 2010 IEEE International Geoscience and Remote Sensing Symposium (IGARSS). - Honolulu, HI, 25-30 July 2010. - P. 1895-1898. ↑

**C3289.** Zhang Fan. Accelerating InSAR raw data simulation on GPU using CUDA. / Zhang Fan, Wang Bingnan, Xiang Mao-sheng. // 2010 IEEE International Geoscience and Remote Sensing Symposium (IGARSS). - Honolulu, HI, 25-30 July 2010. - P. 2932-2935. ↑

**C3290.** Dhar T. Estimation of pasture biomass and soil-moisture using dual-polarimetric X and L band SAR-accuracy assessment with field data. / Dhar T., Menges C., Douglas J., Schmidt M., Armston J. // 2010 IEEE International Geoscience and Remote Sensing Symposium (IGARSS). - Honolulu, HI, 25-30 July 2010. - P. 1450-1453. ↑

**C3291.** Xiaoying Cong. Diverse methods to monitoring volcanic deformation based on SAR interferometry. / Xiaoying Cong, Eineder M., Gernhardt S., Minet C. // 2010 IEEE International Geoscience and Remote Sensing Symposium (IGARSS). - Honolulu, HI, 25-30 July 2010. - P. 661-664. ↑

**C3292.** Hwang P.A. Breaking wave measurements with sar depolarized returns. / Hwang P.A., Biao Zhang, Perrie W. // 2010 IEEE International Geoscience and Remote Sensing Symposium (IGARSS). - Honolulu, HI, 25-30 July 2010. - P. 1952-1955. ↑

**C3293.** Studinger M. Operation icebridge: Using instrumented aircraft to bridge the observational gap between icesat and icesat-2. / Studinger M., Koenig L., Martin S., Sonntag J. // 2010 IEEE International Geoscience and Remote Sensing Symposium (IGARSS). - Honolulu, HI, 25-30 July 2010. - P. 1918-1919. ↑

**C3294.** Farquharson G. Surf zone surface displacement measurements using interferometric microwave radar. / Farquharson G., Frasier S.J., Raubenheimer B., Elgar S. // 2010 IEEE International Geoscience and Remote Sensing Symposium (IGARSS). - Honolulu, HI, 25-30 July 2010. - P. 2428-2431. ↑

**C3295.** Dhar T. Supporting precision agriculture with dual-polarimetric TerraSAR-X-yield prediction and identification of in-field variations to generate fertilizer prescription maps. / Dhar T., Menges C., Gray D., Douglas J., Wilksch L. // 2010 IEEE International Geoscience and Remote Sensing Symposium (IGARSS). - Honolulu, HI, 25-30 July 2010. - P. 1446-1449. ↑

**C3296.** Matsuoka M. Estimation of building damage ratio due to earthquakes and tsunamis using satellite SAR imagery. / Matsuoka M., Koshimura S., Nojima N. // 2010 IEEE International Geoscience and Remote Sensing Symposium (IGARSS). - Honolulu, HI, 25-30 July 2010. - P. 3347-3349. ↑

**C3297.** Villard L. Topography effects on forest radar scattering, consequences on biomass retrieval. / Villard L., Borderies P., Le Toan T., Koleček T., Albinet C. // 2010 IEEE International Geoscience and Remote Sensing Symposium (IGARSS). - Honolulu, HI, 25-30 July 2010. - P. 60-63. ↑

**C3298.** Le Yang. Use of the merged dual-frequency radar altimeter backscatter data over China land surface. / Le Yang, Hejuan Du, Hongzhang Ma, Qinhua Liu. // 2010 IEEE International Geoscience and Remote Sensing Symposium (IGARSS). - Honolulu, HI, 25-30 July 2010. - P. 1454-1457. ↑

**C3299.** Milan L. Longtime monitoring of mine subsidence in Northern Moravia, Czech republic using different insar techniques. / Milan L., Eva J. // 2010 IEEE International Geoscience and Remote Sensing Symposium (IGARSS). - Honolulu, HI, 25-30 July 2010. - P. 3331-3334. ↑

**C3300.** Martorella M. Optimal sensor positioning for ISAR imaging. 2010 IEEE International Geoscience and Remote Sensing Symposium (IGARSS). - Honolulu, HI, 25-30 July 2010. - P. 4819-4822. ↑

**C3301.** Fjш. KaRIn-the Ka-band radar interferometer on SWOT: Measurement principle, processing and data specificities. / Fjш,rtoft R., Gaudin J.-M., Pourthie N., Lion C., Mallet A., Souyris J.-C., Ruiz C., Koudogbo F., Duro J., Ordoqui P., Arnaud A. // 2010 IEEE International Geoscience and Remote Sensing Symposium

(IGARSS). - Honolulu, HI, 25-30 July 2010. - P. 4823-4826. ↑

**C3302.** Torrione P. Spatial latency reduction in GPR processing using stochastic sampling. / Torrione P., Collins L. // 2010 IEEE International Geoscience and Remote Sensing Symposium (IGARSS). - Honolulu, HI, 25-30 July 2010. - P. 3354-3357. ↑

**C3303.** Cariou R. Use of wavelets decomposition to reduce outside transmissions during measurement of RCS. 2010 International Conference on Electromagnetics in Advanced Applications (ICEAA). - Sydney, NSW, 20-24 Sept. 2010. - P. 791-794. ↑

**C3304.** Jong-Sen Lee. An overview of recent advances in Polarimetric SAR information extraction: Algorithms and applications. / Jong-Sen Lee, Ainsworth T.L. // 2010 IEEE International Geoscience and Remote Sensing Symposium (IGARSS). - Honolulu, HI, 25-30 July 2010. - P. 851-854. ↑

**C3305.** Chandrasekar V. CASA dual-doppler system. / Chandrasekar V., Martinez M., Sean Zhang. // 2010 IEEE International Geoscience and Remote Sensing Symposium (IGARSS). - Honolulu, HI, 25-30 July 2010. - P. 4138-4141. ↑

**C3306.** Bin Liu. PS-InSAR time series analysis for measuring surface deformation before the L'Aquila earthquake. / Bin Liu, Yi Luo, Jingfa Zhang, Lixia Gong, Wenliang Jiang, Liyan Ren. // 2010 IEEE International Geoscience and Remote Sensing Symposium (IGARSS). - Honolulu, HI, 25-30 July 2010. - P. 4604-4607. ↑

**C3307.** Hongli Zhao. A study on different PS-like methods for subsidence in Tianjin, China. / Hongli Zhao, Huanhuan Liu, Jinghui Fan, Liu Guang, Jianping Chen, Xiaofang Guo, Peidong Jin, Lu Zhang, Yubao Qiu. // 2010 IEEE International Geoscience and Remote Sensing Symposium (IGARSS). - Honolulu, HI, 25-30 July 2010. - P. 3925-3928. ↑

**C3308.** Pierdicca N. A fuzzy-logic-based approach for flood detection from Cosmo-SkyMed data. / Pierdicca N., Pulvirenti L., Chini M., Guerriero L., Ferrazzoli P. // 2010 IEEE International Geoscience and Remote Sensing Symposium (IGARSS). - Honolulu, HI, 25-30 July 2010. - P. 4796-4798. ↑

**C3309.** McGlinchy J. Extracting structural land cover components using small-footprint waveform lidar data. / McGlinchy J., Van Aardt J., Rhody H., Kerekes J., Ientiluci E., Asner G.P., Knapp D., Mathieu R., Kennedy-Bowdoin T., Erasmus B.F.N., Wessels K., Smit I.P.J., Wu J., Sarrazin D. // 2010 IEEE International Geoscience and Remote Sensing Symposium (IGARSS). - Honolulu, HI, 25-30 July 2010. - P. 1976-1979. ↑

**C3310.** Lardeux C. Assessment of compact polarimetry over different tropical environment and dataset. / Lardeux C., Niamen D., Routier J.B., Giraud A., Frison P.L., Pottier E., Rudant J.P. // 2010 IEEE International Geoscience and Remote Sensing Symposium (IGARSS). - Honolulu, HI, 25-30 July 2010. - P. 3279-3282. ↑

**C3311.** Mejias L. Vision-based detection and tracking of aerial targets for UAV collision avoidance. / Mejias L., McNamara S., Lai J., Ford J. // 2010 IEEE/RSJ International Conference on Intelligent Robots and Systems (IROS). - Taipei, 18-22 Oct. 2010. - P. 87-92. ↑

**C3312.** Allouis T. Assessment of tree and crown heights of a maritime pine forest at plot level using a fullwaveform UltraViolet Lidar prototype. / Allouis T., Durrieu S., Cuesta J., Chazette P., Flamant P.H., Coueron P. // 2010 IEEE International Geoscience and Remote Sensing Symposium (IGARSS). - Honolulu, HI, 25-30 July 2010. - P. 1382-1385. ↑

**C3313.** Jie Zhen. GNSS illuminator based high range resolution algorithm in space-surface bistatic SAR. / Jie Zhen, Zhenhua Zhang, Shunjun Wu, Guoman Huang. // 2010 IEEE International Geoscience and Remote Sensing Symposium (IGARSS). - Honolulu, HI, 25-30 July 2010. - P. 4608-4611. ↑

**C3314.** Xiaoxia Huang. Remote sensing applications for petroleum resource exploration in offshore basins of China. / Xiaoxia Huang, Zhenhai Zhu, Hongga Li. // 2010 IEEE International Geoscience and Remote Sensing Symposium (IGARSS). - Honolulu, HI, 25-30 July 2010. - P. 4511-4513. ↑

**C3315.** Woo-Kyung Lee. Scansar signal processing and image quality enhancement with fitted-geometry doppler surface. / Woo-Kyung Lee, Jung-Hwan Song. // 2010 IEEE International Geoscience and Remote Sensing Symposium (IGARSS). - Honolulu, HI, 25-30 July 2010. - P. 4063-4066. ↑

**C3316.** Prats P. Taxi: A versatile processing chain for experimental TanDEM-X product evaluation. / Prats P.,

Rodriguez-Cassola M., Marotti L., Naninni M., Wollstadt S., Schulze D., Tous-Ramon N., Younis M., Krieger G., Reigber A. // 2010 IEEE International Geoscience and Remote Sensing Symposium (IGARSS). - Honolulu, HI, 25-30 July 2010. - P. 4059-4062. ↑

**C3317.** Gorgucci E. Retrieval of raindrop shape-size relation using dual polarization radar measurements. / Gorgucci E., Baldini L., Chandrasekar V. // 2010 IEEE International Geoscience and Remote Sensing Symposium (IGARSS). - Honolulu, HI, 25-30 July 2010. - P. 4134-4137. ↑

**C3318.** Xiaolong Dong. A Ku-band rotating fan-beam scatterometer: Design and performance simulations. / Xiaolong Dong, Di Zhu, Wenming Lin, Heugang Liu, Jingshan Jiang. // 2010 IEEE International Geoscience and Remote Sensing Symposium (IGARSS). - Honolulu, HI, 25-30 July 2010. - P. 1081-1084. ↑

**C3319.** Georgieva E.M. A broad band lidar for precise atmospheric CO<sub>2</sub> column absorption measurement from space. / Georgieva E.M., Heaps W.S., Huang W. // 2010 IEEE International Geoscience and Remote Sensing Symposium (IGARSS). - Honolulu, HI, 25-30 July 2010. - P. 649-652. ↑

**C3320.** Scofield G.B. Evaluation of two region based classifications in Tapajys National Forest using the ALOS/PALSAR polarimetric and interferometric coherences. / Scofield G.B., Dutra L.V., da Costa Freitas C., Siqueira S.J., Anna S., Silva D.L.A. // 2010 IEEE International Geoscience and Remote Sensing Symposium (IGARSS). - Honolulu, HI, 25-30 July 2010. - P. 3426-3429. ↑

**C3321.** Hornbuckle B.K. Howdoes dew affect L-band backscatter? analysis of pals data at the Iowa validation site and implications for smap. / Hornbuckle B.K., Rowlandson T.L., Russell E., Kaleita A., Logsdon S., Kruger A., Simon Yueh, De Roo R.D. // 2010 IEEE International Geoscience and Remote Sensing Symposium (IGARSS). - Honolulu, HI, 25-30 July 2010. - P. 4835-4838. ↑

**C3322.** Yamaguchi Y. Four-component scattering power decomposition with rotation of coherency matrix. / Yamaguchi Y., Sato A., Sato R., Yamada H., Boerner W.-M. // 2010 IEEE International Geoscience and Remote Sensing Symposium (IGARSS). - Honolulu, HI, 25-30 July 2010. - P. 1327-1330. ↑

**C3323.** Vu V.T. Integrating space-time processing into time-domain backprojection process for detection and imaging moving objects. / Vu V.T., Sjojgren T.K., Pettersson M.I. // 2010 IEEE International Geoscience and Remote Sensing Symposium (IGARSS). - Honolulu, HI, 25-30 July 2010. - P. 4106-4109. ↑

**C3324.** Belli K. Use of 2D FDTD simulation and the determination of the GPR travel path angle for oblique B-scans of 2D geometries. / Belli K., Rappaport C., Udall C., Hines M., Wadia-Fascetti S. // 2010 IEEE International Geoscience and Remote Sensing Symposium (IGARSS). - Honolulu, HI, 25-30 July 2010. - P. 4721-4724. ↑

**C3325.** Dabney P. The Slope Imaging Multi-polarization Photon-counting Lidar: Development and performance results. / Dabney P., Harding D., Abshire J., Huss T., Jodor G., Machan R., Marzouk J., Rush K., Seas A., Shuman C., Xiaoli Sun, Valett S., Vasilyev A., Yu A., Yunhui Zheng. // 2010 IEEE International Geoscience and Remote Sensing Symposium (IGARSS). - Honolulu, HI, 25-30 July 2010. - P. 653-656. ↑

**C3326.** Caorsi S. Electromagnetic infrastructure monitoring: The exploitation of GPR data and neural networks for multi-layered geometries. / Caorsi S., Stasolla M. // 2010 IEEE International Geoscience and Remote Sensing Symposium (IGARSS). - Honolulu, HI, 25-30 July 2010. - P. 4717-4720. ↑

**C3327.** Owen M.P. Towards Bayesian estimator selection for QuikSCAT wind and rain estimation. / Owen M.P., Long D.G. // 2010 IEEE International Geoscience and Remote Sensing Symposium (IGARSS). - Honolulu, HI, 25-30 July 2010. - P. 1331-1334. ↑

**C3328.** Bratsolis E. Segmentation of lakes from the local background on the surface of Titan using Cassini SAR images. 2010 IEEE International Geoscience and Remote Sensing Symposium (IGARSS). - Honolulu, HI, 25-30 July 2010. - P. 906-909. ↑

**C3329.** Martin-Porqueras F. Experimental validation of the Corbella's visibility function using HUT-2D and MIRAS. / Martin-Porqueras F., Kainulainen J., Martin-Neira M., Corbella I., Oliva R., Castro R., Barbosa J., Gutierrez A. // 2010 IEEE International Geoscience and Remote Sensing Symposium (IGARSS). - Honolulu, HI, 25-30 July 2010. - P. 4286-4289. ↑

**C3330.** Yaokui Cui. Using airborne lidar to retrieve crop structural parameters. / Yaokui Cui, Kaiguang Zhao,



Wenjie Fan, Xiru Xu. // 2010 IEEE International Geoscience and Remote Sensing Symposium (IGARSS). - Honolulu, HI, 25-30 July 2010. - P. 2107-2110. ↑

C3331. Soisuvarn S. A revised geophysical model function for the advanced scatterometer (ASCAT) at NOAA/NESDIS. / Soisuvarn S., Jelenak Z., Chang P.S., Qi Zhu. // 2010 IEEE International Geoscience and Remote Sensing Symposium (IGARSS). - Honolulu, HI, 25-30 July 2010. - P. 1335-1338. ↑

C3332. Guida R. Monitoring of collapsed built-up areas with high resolution SAR images. / Guida R., Iodice A., Riccio D. // 2010 IEEE International Geoscience and Remote Sensing Symposium (IGARSS). - Honolulu, HI, 25-30 July 2010. - P. 2422-2425. ↑

C3333. Jin-Woo Kim. Estimation of sea ice thickness in the Arctic Sea using polarimetric parameters of C- and X-band space-borne SAR data. / Jin-Woo Kim, Duk-jin Kim, Byong Jun Hwang. // 2010 IEEE International Geoscience and Remote Sensing Symposium (IGARSS). - Honolulu, HI, 25-30 July 2010. - P. 2402-2405. ↑

C3334. Budillon A. SAR tomographic focusing by Compressive Sampling: Experiments on real data. / Budillon A., Evangelista A., Schirizzi G. // 2010 IEEE International Geoscience and Remote Sensing Symposium (IGARSS). - Honolulu, HI, 25-30 July 2010. - P. 3785-3788. ↑

C3335. Xuemei Gong. Extracting trees and structure parameters via integration of LIDAR data and ground imagery. / Xuemei Gong, Daiyong Wei, Guoqing Zhou. // 2010 IEEE International Geoscience and Remote Sensing Symposium (IGARSS). - Honolulu, HI, 25-30 July 2010. - P. 2703-2706. ↑

C3336. Lyzenga D. Ocean wave field measurements using X-band Doppler radars at low grazing angles. / Lyzenga D., Nwogu O., Trizna D., Hathaway K. // 2010 IEEE International Geoscience and Remote Sensing Symposium (IGARSS). - Honolulu, HI, 25-30 July 2010. - P. 4725-4728. ↑

C3337. Iodice A. A polarimetric two-scale model for soil moisture retrieval. / Iodice A., Natale A., Riccio D. // 2010 IEEE International Geoscience and Remote Sensing Symposium (IGARSS). - Honolulu, HI, 25-30 July 2010. - P. 1265-1268. ↑

C3338. Le M. Microphysical retrievals of dual polarization and dual frequency ground radar for GPM ground validation. / Le M., Chandrasekar V., Lim S. // 2010 IEEE International Geoscience and Remote Sensing Symposium (IGARSS). - Honolulu, HI, 25-30 July 2010. - P. 2349-2352. ↑

C3339. Cerutti-Maori D. Coherent MIMO radar for GMTI. / Cerutti-Maori D., Klare J. // 2010 IEEE International Geoscience and Remote Sensing Symposium (IGARSS). - Honolulu, HI, 25-30 July 2010. - P. 1085-1088. ↑

C3340. Rasmussen C. Trail following with omnidirectional vision. / Rasmussen C., Yan Lu, Kocamaz M. // 2010 IEEE/RSJ International Conference on Intelligent Robots and Systems (IROS). - Taipei, 18-22 Oct. 2010. - P. 829-836. ↑

C3341. Carabajal C.C. Icesat lidar and global digital elevation models: applications to desdyni. / Carabajal C.C., Harding D.J., Suchdeo V.P. // 2010 IEEE International Geoscience and Remote Sensing Symposium (IGARSS). - Honolulu, HI, 25-30 July 2010. - P. 1907-1910. ↑

C3342. Lingjun Kang. A distributed LiDAR processing model based on OWS and BPEL. / Lingjun Kang, Qunying Wu, Ying Yuan. // 2010 IEEE International Geoscience and Remote Sensing Symposium (IGARSS). - Honolulu, HI, 25-30 July 2010. - P. 3628-3631. ↑

C3343. Srivastava S. The RADARSAT-1 imaging performance, 14 years after launch, and independent report on RADARSAT-2 image quality. / Srivastava S., Cote S., Muir S., Hawkins R. // 2010 IEEE International Geoscience and Remote Sensing Symposium (IGARSS). - Honolulu, HI, 25-30 July 2010. - P. 3458-3461. ↑

C3344. Hessner K. Extraction of coastal wavefield properties from X-band radar. / Hessner K., Hanson J.L. // 2010 IEEE International Geoscience and Remote Sensing Symposium (IGARSS). - Honolulu, HI, 25-30 July 2010. - P. 4326-4329. ↑

C3345. Crow W.T. Inferring the impact of radar incidence angle on soil moisture retrieval skill using data assimilation. / Crow W.T., Wagner W., Naeimi V. // 2010 IEEE International Geoscience and Remote Sensing Symposium (IGARSS). - Honolulu, HI, 25-30 July 2010. - P. 1261-1264. ↑

- C3346.** Haug T. Performance and application of different image matching algorithms for investigating glacier and ice-shelf flow, permafrost creep and landslides. / Haug T., Debella-Gilo M., Karstensen J., Kajajb A. // 2010 IEEE International Geoscience and Remote Sensing Symposium (IGARSS). - Honolulu, HI, 25-30 July 2010. - P. 3636-3639. ↑
- C3347.** Whitcomb J. Mapping and change detection for boreal wetlands of North America based on JERS and PALSAR data. / Whitcomb J., Moghaddam M., McDonald K., Podest E., Chapman B. // 2010 IEEE International Geoscience and Remote Sensing Symposium (IGARSS). - Honolulu, HI, 25-30 July 2010. - P. 1371-1373. ↑
- C3348.** Qiang Chen. A scattering similarity based classification scheme for land applications of polarimetric SAR image. / Qiang Chen, Yong-Mei Jiang, Ling-Jun Zhao, Jun Lu, Ding Hong. // 2010 17th IEEE International Conference on Image Processing (ICIP). - Hong Kong, 26-29 Sept. 2010. - P. 1361-1364. ↑
- C3349.** Yazı. The detection performance of Neyman-Pearson detector for MIMO radar in K-distributed sea clutter. / Yazı, A., Hamurcu A.C., Baykal B. // 2010 IEEE 18th Signal Processing and Communications Applications Conference (SIU). - Diyarbakir, 22-24 April 2010. - P. 165-168. ↑
- C3350.** Jun-Dong Park. Comparisons of rain rate and reflectivity between TRMM precipitation radar and Gosan S-band radar. / Jun-Dong Park, Mi-Lim Ou, Morris K.R., Schwaller M.R. // 2010 IEEE International Geoscience and Remote Sensing Symposium (IGARSS). - Honolulu, HI, 25-30 July 2010. - P. 4698-4700. ↑
- C3351.** Junjie Wu. Spatial spectrum of bistatic SAR with one fixed station. / Junjie Wu, Jianyu Yang, Yulin Huang, Haiguang Yang. // 2010 IEEE International Geoscience and Remote Sensing Symposium (IGARSS). - Honolulu, HI, 25-30 July 2010. - P. 4095-4098. ↑
- C3352.** Suwa K. ISAR imaging of an aircraft target USING ISDB-T digital TV based passive bistatic radar. / Suwa K., Nakamura S., Morita S., Wakayama T., Maniwa H., Oshima T., Maekawa R., Matsuda S., Tachihara T. // 2010 IEEE International Geoscience and Remote Sensing Symposium (IGARSS). - Honolulu, HI, 25-30 July 2010. - P. 4103-4105. ↑
- C3353.** Bellez S. Full wave analysis of VHF-UHF forest bistatic scattering mechanisms an investigation on the influence of electromagnetic coupling. / Bellez S., Roussel H., Dahon C. // 2010 IEEE International Geoscience and Remote Sensing Symposium (IGARSS). - Honolulu, HI, 25-30 July 2010. - P. 2547-2550. ↑
- C3354.** Shirvany R. Estimation of the degree of polarization in compact polarimetry. / Shirvany R., Chabert M., Tourneret J.-Y. // 2010 IEEE International Geoscience and Remote Sensing Symposium (IGARSS). - Honolulu, HI, 25-30 July 2010. - P. 722-725. ↑
- C3355.** Tebaldini S. ALGAE: A fast algebraic estimation of interferogram phase offsets in space varying geometries. / Tebaldini S., Gatti G., Mariotti d'Alessandro M., Rocca F. // 2010 IEEE International Geoscience and Remote Sensing Symposium (IGARSS). - Honolulu, HI, 25-30 July 2010. - P. 2622-2624. ↑
- C3356.** Storie C.D. Remote sensing research in undergraduate education: An international fieldwork perspective. / Storie C.D., Bugden-Storie J. // 2010 IEEE International Geoscience and Remote Sensing Symposium (IGARSS). - Honolulu, HI, 25-30 July 2010. - P. 1114-1117. ↑
- C3357.** Esch T. Land cover classification based on single-polarized VHR SAR images using texture information derived via speckle analysis. / Esch T., Schenk A., Thiel M., Ullmann T., Schmidt M., Dech S. // 2010 IEEE International Geoscience and Remote Sensing Symposium (IGARSS). - Honolulu, HI, 25-30 July 2010. - P. 1875-1878. ↑
- C3358.** Prats P. Investigations on TOPS interferometry with TerraSAR-X. / Prats P., Marotti L., Wollstadt S., Scheiber R. // 2010 IEEE International Geoscience and Remote Sensing Symposium (IGARSS). - Honolulu, HI, 25-30 July 2010. - P. 2629-2632. ↑
- C3359.** Sato R. Polarimetric scattering analysis for accurate observation of stricken man-made targets using a rotated coherency matrix. / Sato R., Yamaguchi Y., Yamada H. // 2010 IEEE International Geoscience and Remote Sensing Symposium (IGARSS). - Honolulu, HI, 25-30 July 2010. - P. 746-749. ↑
- C3360.** Gujldog. Compressed sensing on ambiguity function domain for high resolution detection. / Gujldog,an M.B., Pilancı, M., Arıkan O. // 2010 IEEE 18th Signal Processing and Communications Applications Conference (SIU). - Diyarbakir, 22-24 April 2010. - P. 65-68. ↑

- C3361.** Salman M. Target detection in missile warning receivers via speeded-up robust features approach. / Salman M., Ojzkazan, Y. // 2010 IEEE 18th Signal Processing and Communications Applications Conference (SIU). - Diyarbakir, 22-24 April 2010. - P. 57-60. ↑
- C3362.** Long D.G. The microasar experiment on CASIE-09. / Long D.G., Zaugg E., Edwards M., Maslanik J. // 2010 IEEE International Geoscience and Remote Sensing Symposium (IGARSS). - Honolulu, HI, 25-30 July 2010. - P. 3466-3469. ↑
- C3363.** Pablos-Vega G.A. Development of an Off-The-Grid X-band radar for weather applications. / Pablos-Vega G.A., Colom-Usta, riz J.G., Cruz-Pol S., Trabal J.M., Chandrasekar V., George J., Junyent F. // 2010 IEEE International Geoscience and Remote Sensing Symposium (IGARSS). - Honolulu, HI, 25-30 July 2010. - P. 1077-1080. ↑
- C3364.** Missaoui O. Model level fusion of edge histogram descriptors and gabor wavelets for landmine detection with ground penetrating radar. / Missaoui O., Frigui H., Gader P. // 2010 IEEE International Geoscience and Remote Sensing Symposium (IGARSS). - Honolulu, HI, 25-30 July 2010. - P. 3378-3381. ↑
- C3365.** Magnard C. Processing of MEMPHIS millimeter wave multi-baseline InSAR data. / Magnard C., Meier E., Small D., Essen H., Brehm T. // 2010 IEEE International Geoscience and Remote Sensing Symposium (IGARSS). - Honolulu, HI, 25-30 July 2010. - P. 4302-4305. ↑
- C3366.** Ling Lei. Monitoring slow moving landslides in the Berkeley Hills with TerraSAR-X data. / Ling Lei, Yingqing Zhou, Jingwen Li, Burgmann R. // 2010 IEEE International Geoscience and Remote Sensing Symposium (IGARSS). - Honolulu, HI, 25-30 July 2010. - P. 230-232. ↑
- C3367.** Adams M.D. An improved content-adaptive mesh-generation method for image representation. 2010 17th IEEE International Conference on Image Processing (ICIP). - Hong Kong, 26-29 Sept. 2010. - P. 873-876. ↑
- C3368.** Zaugg E.C. Theoretical and practical design considerations for a small, multi-band SAR: The SlimSAR. / Zaugg E.C., Edwards M.C., Margulis A. // 2010 IEEE International Geoscience and Remote Sensing Symposium (IGARSS). - Honolulu, HI, 25-30 July 2010. - P. 126-129. ↑
- C3369.** Krieger G. Advanced digital beamforming concepts for future SAR systems. / Krieger G., Younis M., Gebert N., Huber S., Bordonni F., Patyuchenko A., Moreira A. // 2010 IEEE International Geoscience and Remote Sensing Symposium (IGARSS). - Honolulu, HI, 25-30 July 2010. - P. 245-248. ↑
- C3370.** Strom J. Graph-based segmentation for colored 3D laser point clouds. / Strom J., Richardson A., Olson E. // 2010 IEEE/RSJ International Conference on Intelligent Robots and Systems (IROS). - Taipei, 18-22 Oct. 2010. - P. 2131-2136. ↑
- C3371.** Nirchio F. Preliminary model for wind estimation from Cosmo/SkyMed X band SAR data. / Nirchio F., Venafrà S. // 2010 IEEE International Geoscience and Remote Sensing Symposium (IGARSS). - Honolulu, HI, 25-30 July 2010. - P. 3462-3465. ↑
- C3372.** Lardeux C. Use of PALSAR polarimetric data for tropical forest stratification and comparison of simulated dual and compact polarimetric modes. / Lardeux C., Niemen D., Routier J.B., Giraud A., Frison P.L., Pottier E., Rudant J.P. // 2010 IEEE International Geoscience and Remote Sensing Symposium (IGARSS). - Honolulu, HI, 25-30 July 2010. - P. 1855-1858. ↑
- C3373.** Takeyama Y. Development of ALOS/PALSAR data on-demand processing and providing system on GEO Grid. / Takeyama Y., Kodama S., Nakamura K., Matsuoka M., Yamamoto N. // 2010 IEEE International Geoscience and Remote Sensing Symposium (IGARSS). - Honolulu, HI, 25-30 July 2010. - P. 2315-2317. ↑
- C3374.** Song S.H. Geo-location error correction for Synthetic Aperture Radar image. / Song S.H., Rho S.H., Jung C.H., Kwag Y.K. // 2010 IEEE International Geoscience and Remote Sensing Symposium (IGARSS). - Honolulu, HI, 25-30 July 2010. - P. 3406-3409. ↑
- C3375.** Wu Shengli. Using AMSR-E land product to monitor the drought process in China. / Wu Shengli, Zhu Xiaoxiang. // 2010 IEEE International Geoscience and Remote Sensing Symposium (IGARSS). - Honolulu, HI, 25-30 July 2010. - P. 3894-3897. ↑

- C3376.** Vesecky J.F. A system trade model for the monitoring of coastal vessels using HF surface wave radar and ship automatic identification systems (AIS). / Vesecky J.F., Laws K.E., Paduan J.D. // 2010 IEEE International Geoscience and Remote Sensing Symposium (IGARSS). - Honolulu, HI, 25-30 July 2010. - P. 3414-3417. ↑
- C3377.** Gonza. Synthetic aperture radar image analysis as a tool for validation of baroclinic internal wave 3D modeling in Algeciras Bay (Strait of Gibraltar). / Gonza, Iez C.J., Lopez L., Gomez-Enri J., Gomiz J.J., Alvarez O., Bruno M., Macanes R., Villares P. // 2010 IEEE International Geoscience and Remote Sensing Symposium (IGARSS). - Honolulu, HI, 25-30 July 2010. - P. 952-954. ↑
- C3378.** Yazici A. Effect of quantization on MIMO radar performance. / Yazici A., Baykal B. // 2010 IEEE 18th Signal Processing and Communications Applications Conference (SIU). - Diyarbakir, 22-24 April 2010. - P. 546-549. ↑
- C3379.** Lindsley R.D. Adapting the sir algorithm to ASCAT. / Lindsley R.D., Long D.G. // 2010 IEEE International Geoscience and Remote Sensing Symposium (IGARSS). - Honolulu, HI, 25-30 July 2010. - P. 3402-3405. ↑
- C3380.** Emmitt G.D. Airborne Doppler Wind Lidar investigations of western Pacific typhoon genesis and evolution. 2010 IEEE International Geoscience and Remote Sensing Symposium (IGARSS). - Honolulu, HI, 25-30 July 2010. - P. 2591-2594. ↑
- C3381.** Hyoung-sun Youn. Advanced classification of UXO using fully polarimetric GPR and frequency-polarization features. / Hyoung-sun Youn, Evans M., Kobashigawa J., Iskander M. // 2010 IEEE International Geoscience and Remote Sensing Symposium (IGARSS). - Honolulu, HI, 25-30 July 2010. - P. 3374-3377. ↑
- C3382.** Foley J. Wide area assessment-Development and case study. / Foley J., Hodgson J. // 2010 IEEE International Geoscience and Remote Sensing Symposium (IGARSS). - Honolulu, HI, 25-30 July 2010. - P. 3370-3373. ↑
- C3383.** Bozdog. Track initiation using multiple bistatic range and range rate measurements with multidimensional assignment algorithm. / Bozdog, an A.O., Efe M. // 2010 IEEE 18th Signal Processing and Communications Applications Conference (SIU). - Diyarbakir, 22-24 April 2010. - P. 435-438. ↑
- C3384.** Krieger G. Tandem-L: And innovative interferometric and polarimetric SAR mission to monitor earth system dynamics with high resolution. / Krieger G., Hajnsek I., Papathanassiou K., Eineder M., Younis M., De Zan F., Huber S., Lopez-Dekker P., Prats P., Werner M., Shen Y., Freeman A., Rosen P., Hensley S., Johnson W., Veilleux L., Grafmueller B., Werninghaus R., Bamler R., Moreira A. // 2010 IEEE International Geoscience and Remote Sensing Symposium (IGARSS). - Honolulu, HI, 25-30 July 2010. - P. 253-256. ↑
- C3385.** Younis M. A concept for high performance reflector-based Synthetic Aperture Radar. / Younis M., Patyuchenko A., Huber S., Krieger G., Moreira A. // 2010 IEEE International Geoscience and Remote Sensing Symposium (IGARSS). - Honolulu, HI, 25-30 July 2010. - P. 249-252. ↑
- C3386.** Yi Lin. Leaf area index (LAI) estimation based on vehicle-based laser scanning. / Yi Lin, Hyypa J. // 2010 IEEE International Geoscience and Remote Sensing Symposium (IGARSS). - Honolulu, HI, 25-30 July 2010. - P. 3422-3425. ↑
- C3387.** Salazar J.L. Dual-polarization performance of the phase-tilt antenna array in a casa dense network radar. / Salazar J.L., Knapp E.J., McLaughlin D.J. // 2010 IEEE International Geoscience and Remote Sensing Symposium (IGARSS). - Honolulu, HI, 25-30 July 2010. - P. 3470-3473. ↑
- C3388.** Chaowei Zhang. Design and Implementation of High Resolution Radar Video Transfer System. / Chaowei Zhang, Pengshu Dong, Guoning Ding, Qibin Deng, Chengda Yu, Yongfeng Wang. // 2010 International Conference on Electrical and Control Engineering (ICECE). - Wuhan, 25-27 June 2010. - P. 3540-3542. ↑
- C3389.** Tan Ge-wei. Motion Compensation for Spotlight-Mode SAR Data. 2010 International Conference on Multimedia Technology (ICMT). - Ningbo, 29-31 Oct. 2010. - P. 1-4. ↑
- C3390.** Bo Wang. Subsidence Monitoring by Permanent Scatterers in InSAR: A Case Study of Yancheng City in Jiangsu. / Bo Wang, Suozhong Chen, Hongyan Yi, Lei Mao. // 2010 International Conference on Multimedia Technology (ICMT). - Ningbo, 29-31 Oct. 2010. - P. 1-6. ↑



- C3391.** Hongmei Zhang. Development and Application of Mobile Water Level Monitoring Based on Multi-sensor Integration. / Hongmei Zhang, Weiliang Tao, Ming Cao. // 2010 International Conference on Electrical and Control Engineering (ICECE). - Wuhan, 25-27 June 2010. - P. 803-806. ↑
- C3392.** Xu Hao. The Detection of Range Extended Target Based on Adaptive Searching and Twofold Sliding Windows. / Xu Hao, Ma Yunfei, Jiang Tao, Wang Dongjin, Chen Weidong. // 2010 International Conference on Electrical and Control Engineering (ICECE). - Wuhan, 25-27 June 2010. - P. 4803-4806. ↑
- C3393.** Chen Nan. Target Recognition Based on the Self-Correlation Function of HRRP. / Chen Nan, Xue Minghua. // 2010 International Conference on Electrical and Control Engineering (ICECE). - Wuhan, 25-27 June 2010. - P. 4787-4789. ↑
- C3394.** Yanqiu Cui. Speckle Reduction for SAR Images Based on Adaptive Gaussian Mixture Models. / Yanqiu Cui, Tao Zhang, Shuang Xu, Houjie Li. // 2010 International Conference on Electrical and Control Engineering (ICECE). - Wuhan, 25-27 June 2010. - P. 1985-1988. ↑
- C3395.** Sijia Chen. A Study of Suppressing Strong Clutter in Radar Signal Based ICA. / Sijia Chen, Jianguo Wang. // 2010 International Conference on Multimedia Technology (ICMT). - Ningbo, 29-31 Oct. 2010. - P. 1-5. ↑
- C3396.** Liao Kuo. Extraction of Radar Target Length Based on High Resolution Range Profile. / Liao Kuo, Yang Wanlin. // 2010 International Conference on Electrical and Control Engineering (ICECE). - Wuhan, 25-27 June 2010. - P. 956-959. ↑
- C3397.** Fudong Wen. Design of Universal Radar Signal Processor Architecture Based on Crosspoint Switch. / Fudong Wen, Wei Zhu, Baixiao Chen. // 2010 International Conference on Multimedia Technology (ICMT). - Ningbo, 29-31 Oct. 2010. - P. 1-4. ↑
- C3398.** Kun Li. Paddy Rice Identification Using Polarimetric SAR Data in Southern China. / Kun Li, Yun Shao, Fengli Zhang. // 2010 International Conference on Multimedia Technology (ICMT). - Ningbo, 29-31 Oct. 2010. - P. 1-4. ↑
- C3399.** Liang Xu. DOA Estimation for Strong and Weak Signals in the Presence of Array Gain and Phase Mismatch. / Liang Xu, Cao Zeng, Gui-sheng Liao, Jun Li. // 2010 International Conference on Multimedia Technology (ICMT). - Ningbo, 29-31 Oct. 2010. - P. 1-4. ↑
- C3400.** Jiangping Long. Monitoring Ground Subsidence in New Orleans with Persistent Scatterers Interferometry. / Jiangping Long, Xiaoli Ding. // 2010 International Conference on Multimedia Technology (ICMT). - Ningbo, 29-31 Oct. 2010. - P. 1-5. ↑
- C3401.** Xiaoli Liu. Joint DOD and DOA Estimation Using Real Polynomial Rooting in Bistatic MIMO Radar. / Xiaoli Liu, Guisheng Liao. // 2010 International Conference on Multimedia Technology (ICMT). - Ningbo, 29-31 Oct. 2010. - P. 1-4. ↑
- C3402.** Zhang Ping-chuan. Passive Tracking and Locating Radar Based on Double GSM Base Stations. / Zhang Ping-chuan, Li Bu-yin. // 2010 International Conference on Electrical and Control Engineering (ICECE). - Wuhan, 25-27 June 2010. - P. 1466-1469. ↑
- C3403.** Flores-Tapia D. Electrical impedance tomography reconstruction using a monotonicity approach based on a priori knowledge. / Flores-Tapia D., Pistorius S. // 2010 Annual International Conference of the IEEE Engineering in Medicine and Biology Society (EMBC). - Buenos Aires, Aug. 31 2010-Sept. 4 2010. - P. 4996-4999. ↑
- C3404.** Li Lu. Experimental demonstration of noncontact pulse wave velocity monitoring using multiple Doppler radar sensors. / Li Lu, Changzhi Li, Lie D.Y.C. // 2010 Annual International Conference of the IEEE Engineering in Medicine and Biology Society (EMBC). - Buenos Aires, Aug. 31 2010-Sept. 4 2010. - P. 5010-5013. ↑
- C3405.** Ying Dong. Phase unwrapping using region-based Markov Random Field model. / Ying Dong, Jim Ji. // 2010 Annual International Conference of the IEEE Engineering in Medicine and Biology Society (EMBC). - Buenos Aires, Aug. 31 2010-Sept. 4 2010. - P. 3309-3312. ↑
- C3406.** Mariano A. Low power and high gain double-balanced mixer dedicated to 77 GHz automotive radar

applications. / Mariano A., Taris T., Leite B., Majek C., Deval Y., Kerherve, E., Be,gueret J.-B., Belot D. // 2010 Proceedings of the ESSCIRC. - Seville, 14-16 Sept. 2010. - P. 490-493. ↑

C3407. Jinsheng Li. The missile SAR echo signal simulation technology research. 2010 International Conference on Computer Application and System Modeling (ICCASM). - Taiyuan, 22-24 Oct. 2010. - Vol. 5. - P. V5-469-V5-471-469. ↑

C3408. Veenstra H. A 45-67GHz UWB transmitter with >8dBm output power for indoor radar applications. / Veenstra H., Notten M., Zhao D., Long J.R. // 2010 Proceedings of the ESSCIRC. - Seville, 14-16 Sept. 2010. - P. 190-193. ↑

C3409. Berenguer R. A 117mW 77GHz receiver in 65nm CMOS with ladder structured tunable VCO. / Berenguer R., Gui Liu, Akhiyat A., Kamtikar K., Yang Xu. // 2010 Proceedings of the ESSCIRC. - Seville, 14-16 Sept. 2010. - P. 494-497. ↑

C3410. Boren Zheng. A Novel Long-Distance Measurement Method Based on Secondary Radar. / Boren Zheng, Beniu Zhang, Zaixian Qing, Xiaolong Liu. // 2010 International Conference on Electrical and Control Engineering (ICECE). - Wuhan, 25-27 June 2010. - P. 198-200. ↑

C3411. Huisi Tong. Multitarget Tracking Before Detection via Probability Hypothesis Density Filter. / Huisi Tong, Hao Zhang, Huadong Meng, Xiqin Wang. // 2010 International Conference on Electrical and Control Engineering (ICECE). - Wuhan, 25-27 June 2010. - P. 1332-1335. ↑

C3412. Xuebing Han. Hybrid Method of DOA Estimation for Low-Angle Target Tracking. / Xuebing Han, Hao Zhang, Huadong Meng, Xiqin Wang. // 2010 International Conference on Electrical and Control Engineering (ICECE). - Wuhan, 25-27 June 2010. - P. 4687-4690. ↑

C3413. Zhanjun Song. Research on the Method of Airborne SAR Direct Geocoding Based on Correction of Systematic Error. / Zhanjun Song, Jixian Zhang, Guoman Huang, Zheng Zhao, Jujie Wei. // 2010 International Conference on Multimedia Technology (ICMT). - Ningbo, 29-31 Oct. 2010. - P. 1-4. ↑

C3414. Dilmaghani R. A new paradigm for telehealth implementation. / Dilmaghani R., Ghavami M., Bobarshad H. // 2010 Annual International Conference of the IEEE Engineering in Medicine and Biology Society (EMBC). - Buenos Aires, Aug. 31 2010-Sept. 4 2010. - P. 3915-3918. ↑

C3415. Fletcher R.R. Clip-on wireless wearable microwave sensor for ambulatory cardiac monitoring. / Fletcher R.R., Kulkarni S. // 2010 Annual International Conference of the IEEE Engineering in Medicine and Biology Society (EMBC). - Buenos Aires, Aug. 31 2010-Sept. 4 2010. - P. 365-369. ↑

C3416. Tehrani M.A. A Survey of System Platforms for Mobile Payment. / Tehrani M.A., Amidian A.A., Muhammadi J., Rabiee H.R. // 2010 Fourth International Conference on Management of e-Commerce and e-Government (ICMeCG). - Chengdu, 23-24 Oct. 2010. - P. 376-381. ↑

C3417. Meng Gao. Design and development of autonomous driving vehicle. / Meng Gao, Kezhong He, Huaping Liu, Fuchun Sun. // 2010 3rd International Symposium on Systems and Control in Aeronautics and Astronautics (ISSCAA). - Harbin, 8-10 June 2010. - P. 798-802. ↑

C3418. Wang Dan. Research on the image mismatching points eliminating and the integrated arithmetic in the INS/SAR integrated navigation. / Wang Dan, Xiong Zhi, Chen Fang, Liu Jian-ye. // 2010 3rd International Symposium on Systems and Control in Aeronautics and Astronautics (ISSCAA). - Harbin, 8-10 June 2010. - P. 1485-1490. ↑

C3419. Dotsenko V.V. Close range coverage ship radar with distance high resolution. / Dotsenko V.V., Nosov D.M., Osipov M.V., Rovkin M.E., Surkov A.S., Khlusov V.A. // 2010 20th International Crimean Conference Microwave and Telecommunication Technology (CriMiCo). - Sevastopol, 13-17 Sept. 2010. - P. 1253-1254. ↑

C3420. Juanjuan Zhao. Distribution analysis of multi-source decoying system against ARM. / Juanjuan Zhao, Dongli Ma. // 2010 3rd International Symposium on Systems and Control in Aeronautics and Astronautics (ISSCAA). - Harbin, 8-10 June 2010. - P. 167-171. ↑

C3421. Tao Guo. Study on strapdown decoupling technology for rolling missile using RF interferometer seeker. / Tao Guo, Qunli Xia, Zaikang Qi. // 2010 3rd International Symposium on Systems and Control in Aeronautics

and Astronautics (ISSCAA). - Harbin, 8-10 June 2010. - P. 823-828. ↑

C3422. Liqiang Xu. The attitude tracking maneuvers of spaceborne spotlight SAR. / Liqiang Xu, Junli Chen, Guozhong Chen, Xiaowei Shao, Dengping Duan. // 2010 3rd International Symposium on Systems and Control in Aeronautics and Astronautics (ISSCAA). - Harbin, 8-10 June 2010. - P. 29-33. ↑

C3423. Yuguan Hou. An improved signal subspace decomposition method in low SNR case. / Yuguan Hou, Yiyi Shen. // 2010 3rd International Symposium on Systems and Control in Aeronautics and Astronautics (ISSCAA). - Harbin, 8-10 June 2010. - P. 143-146. ↑

C3424. Ning Zhang. W-band pulsed radar receiver in low cost CMOS. / Ning Zhang, Kenneth K.O. // 2010 IEEE Custom Integrated Circuits Conference (CICC). - San Jose, CA, 19-22 Sept. 2010. - P. 1-4. ↑

C3425. Berenguer R. A 43.5mW 77GHz receiver front-end in 65nm CMOS suitable for FM-CW Automotive Radar. / Berenguer R., Gui Liu, Akhiyat A., Kamtikar K., Yang Xu. // 2010 IEEE Custom Integrated Circuits Conference (CICC). - San Jose, CA, 19-22 Sept. 2010. - P. 1-4. ↑

C3426. Tao-Yao Chang. A 77 GHz power amplifier using transformer-based power combiner in 90 nm CMOS. / Tao-Yao Chang, Chao-Shiun Wang, Chong-Kuang Wang. // 2010 IEEE Custom Integrated Circuits Conference (CICC). - San Jose, CA, 19-22 Sept. 2010. - P. 1-4. ↑

C3427. Yilong Zhu. Target maneuver detection using high resolution Doppler profile. / Yilong Zhu, Hongqi Fan, Zaiqi Lu. // 2010 International Conference on Computer Application and System Modeling (ICCAS). - Taiyuan, 22-24 Oct. 2010. - Vol. 4. - P. V4-133-V4-135-133. ↑

C3428. Wei Pan. Robust adaptive ground moving target indication technique applied to distributed spaceborne SAR system. / Wei Pan, Bin Cai. // 2010 International Conference on Computer Application and System Modeling (ICCAS). - Taiyuan, 22-24 Oct. 2010. - Vol. 5. - P. V5-289-V5-293-289. ↑

C3429. Sytnik O.V. The robust adaptive signal processing in correlated noise. / Sytnik O.V., Kartashov V.M., Suprun A.A. // 2010 20th International Crimean Conference Microwave and Telecommunication Technology (CriMiCo). - Sevastopol, 13-17 Sept. 2010. - P. 1233-1234. ↑

C3430. Li Yi-Bo. A survey on feature extraction of SAR Images. / Li Yi-Bo, Zhou Chang, Wang Ning. // 2010 International Conference on Computer Application and System Modeling (ICCAS). - Taiyuan, 22-24 Oct. 2010. - Vol. 1. - P. V1-312-V1-317-312. ↑

C3431. Duangmanee P. Implementation of real-time video streaming with fuzzy logic controller. / Duangmanee P., Uthansakul P. // 2010 International Conference on Wireless Communications and Signal Processing (WCSP). - Suzhou, 21-23 Oct. 2010. - P. 1-6. ↑

C3432. Zhou Jiao. A Study on Removal of Radial Interference Echo with Weather Radar. / Zhou Jiao, Gao Yuchun. // 2010 International Conference on Multimedia Technology (ICMT). - Ningbo, 29-31 Oct. 2010. - P. 1-5. ↑

C3433. Yu Chunrui. Eigen-Decomposition Method for RFI Suppression Applied to SAR Data. / Yu Chunrui, Zhang Yongsheng, Dong Zhen, Liang Diannong. // 2010 International Conference on Multimedia Technology (ICMT). - Ningbo, 29-31 Oct. 2010. - P. 1-4. ↑

C3434. Xu Yi. The Research on RIC-ISAR Image of Ship Target Based on High-Order Match-Phase Transform. / Xu Yi, Li Ya-chao, Xing Meng-dao. // 2010 International Conference on Multimedia Technology (ICMT). - Ningbo, 29-31 Oct. 2010. - P. 1-4. ↑

C3435. Hongchao Ma. A Methodology for Trees' Detection Using LiDAR Data in Urban Areas. / Hongchao Ma, Chunjing Yao. // 2010 International Conference on Multimedia Technology (ICMT). - Ningbo, 29-31 Oct. 2010. - P. 1-4. ↑

C3436. Peng Wang. FMCW Radar Imaging with Multi-channel Antenna Array via Sparse Recovery Technique. / Peng Wang, Huadong Meng, Yimin Wei. // 2010 International Conference on Electrical and Control Engineering (ICECE). - Wuhan, 25-27 June 2010. - P. 1018-1021. ↑

C3437. Jun Wang. SAR Imaging of Moving Targets via Compressive Sensing. / Jun Wang, Gang Li, Yimin Liu, Xiqin Wang. // 2010 International Conference on Electrical and Control Engineering (ICECE). - Wuhan, 25-27

June 2010. - P. 1855-1858. ↑

C3438. Zhou Peng. Design of the Simulation and Assessment Software of Missile-Borne SAR Imaging System. / Zhou Peng, Xu Yi, Li Yachao, Xing Mengdao. // 2010 International Conference on Multimedia Technology (ICMT). - Ningbo, 29-31 Oct. 2010. - P. 1-4. ↑

C3439. Salerno M. The Sky-Scanner System for Air Traffic Management: Test Sessions and Statistical Analysis. / Salerno M., Costantini G., Carota M., Casali D., Todisco M., Pomarico G. // 2010 First International Conference on Sensor Device Technologies and Applications (SENSORDEVICES). - Venice, 18-25 July 2010. - P. 162-166. ↑

C3440. Chen Hai-ming. Research on scheme and algorithm of high-precision fault-tolerant integrated navigation for HALE UAV. / Chen Hai-ming, Xiong Zhi, Wang Rong, Liu Jian-ye. // 2010 3rd International Symposium on Systems and Control in Aeronautics and Astronautics (ISSCAA). - Harbin, 8-10 June 2010. - P. 768-773. ↑

C3441. Chou Yong-bin. Broad beam high-frequency bistatic cross sections of the ocean surface. / Chou Yong-bin, Zhang Ning, Xie Jun-hao. // 2010 3rd International Symposium on Systems and Control in Aeronautics and Astronautics (ISSCAA). - Harbin, 8-10 June 2010. - P. 1407-1410. ↑

C3442. Friedt J.-M. Surface Acoustic Wave Resonators as Passive Buried Sensors. / Friedt J.-M., Re, tornaz T., Martin G., Laroche T., Alzuaga S., Baron T., Carry E., Ballandras S., Simonnet J.-P. // 2010 First International Conference on Sensor Device Technologies and Applications (SENSORDEVICES). - Venice, 18-25 July 2010. - P. 183-189. ↑

C3443. Shibing Hu. Performance Analysis of Frequency Sweep Nonlinearities in LFM Radars. 2010 International Conference on Electrical and Control Engineering (ICECE). - Wuhan, 25-27 June 2010. - P. 3977-3980. ↑

C3444. Godana B. Quantifying Human Indoor Activity Using a Software Radio-Based Radar. / Godana B., Leus G., Barroso A. // 2010 First International Conference on Sensor Device Technologies and Applications (SENSORDEVICES). - Venice, 18-25 July 2010. - P. 38-43. ↑

C3445. Godana B. Estimating Indoor Walking Velocity Profile Using a Software Radio-Based Radar. / Godana B., Leus G., Barroso A. // 2010 First International Conference on Sensor Device Technologies and Applications (SENSORDEVICES). - Venice, 18-25 July 2010. - P. 44-51. ↑

C3446. Yuan Xin-Zhe. Analysis of the quantization and saturation error for Space-borne SAR raw data compression algorithm in data domain. / Yuan Xin-Zhe, Hua Bin. // 2010 International Conference on Computer Application and System Modeling (ICCSM). - Taiyuan, 22-24 Oct. 2010. - Vol. 5. - P. V5-577-V5-580-577. ↑

C3447. Pan Guangzhen. Research on the simplified algorithm of unobstructed areas radar calculation. / Pan Guangzhen, Yin Yixin. // 2010 International Conference on Computer Application and System Modeling (ICCSM). - Taiyuan, 22-24 Oct. 2010. - Vol. 13. - P. V13-464-V13-466-464. ↑

C3448. Shi Qiong. The study on helicopter route planning. 2010 International Conference on Computer Application and System Modeling (ICCSM). - Taiyuan, 22-24 Oct. 2010. - Vol. 13. - P. V13-507-V13-510-507. ↑

C3449. Jianpeng Fan. Threshold variation based analysis and implementation of an optimized AGC circuitry for digital IF receiver. / Jianpeng Fan, Benyuan Liu, Zaiqi Lu. // 2010 International Conference on Computer Application and System Modeling (ICCSM). - Taiyuan, 22-24 Oct. 2010. - Vol. 10. - P. V10-64-V10-68-64. ↑

C3450. Jinjie Yao. Application of particle swarm optimization with stochastic inertia weight and adaptive mutation in target localization. / Jinjie Yao, Jinxiao Pan, Yan Han, Liming Wang. // 2010 International Conference on Computer Application and System Modeling (ICCSM). - Taiyuan, 22-24 Oct. 2010. - Vol. 13. - P. V13-251-V13-254-251. ↑

C3451. Xu Zhou. Development of a high performance Wireless Mesh Network for video streaming. / Xu Zhou, Shancang Li, Xinheng Wang. // 2010 International Conference on Computer Application and System Modeling (ICCSM). - Taiyuan, 22-24 Oct. 2010. - Vol. 12. - P. V12-324-V12-328-324. ↑

C3452. Duan Shihong. A low-power wireless remote sensor node design based on GPRS. / Duan Shihong, Yu



Yanwei, Wan Yadong, Wang Qin. // 2010 International Conference on Computer Application and System Modeling (ICCASM). - Taiyuan, 22-24 Oct. 2010. - Vol. 12. - P. V12-483-V12-488-483. ↑

**C3453.** Shi Chunfang. The design of a GPRS-Based Intelligent Access Control System for Base Station. 2010 International Conference on Computer Application and System Modeling (ICCASM). - Taiyuan, 22-24 Oct. 2010. - Vol. 13. - P. V13-608-V13-611-608. ↑

**C3454.** She Yong. Application research on intelligent pattern recognition methods in hail identification of weather radar. / She Yong, Yu Lei, Wei Yi. // 2010 International Conference on Computer Application and System Modeling (ICCASM). - Taiyuan, 22-24 Oct. 2010. - Vol. 11. - P. V11-554-V11-558-554. ↑

**C3455.** Hu Guang. Study on Defocus compensation using variable pulse repetition time stepped-frequency waveform. / Hu Guang, Zeng Dazhi, Long Teng. // 2010 International Conference on Computer Application and System Modeling (ICCASM). - Taiyuan, 22-24 Oct. 2010. - Vol. 11. - P. V11-559-V11-562-559. ↑

**C3456.** Gu Liang-yao. Research on intelligent monitoring and protection system of distributive multi-tower cranes. / Gu Liang-yao, Yang yue, Chen Feng. // 2010 International Conference on Computer Application and System Modeling (ICCASM). - Taiyuan, 22-24 Oct. 2010. - Vol. 11. - P. V11-540-V11-543-540. ↑

**C3457.** Yi Gao. Improved regularized particle filter algorithm for SINS/SAR integrated navigation. / Yi Gao, Shesheng Gao, Yu Gu. // 2010 International Conference on Computer Application and System Modeling (ICCASM). - Taiyuan, 22-24 Oct. 2010. - Vol. 9. - P. V9-70-V9-74-70. ↑

**C3458.** Zhou Zengpo. Mosaic in g the ocean/terrestrial SRTM-DEM and making t he geomorphologic relief shading map. / Zhou Zengpo, Cheng Weiming. // 2010 International Conference on Computer Application and System Modeling (ICCASM). - Taiyuan, 22-24 Oct. 2010. - Vol. 9. - P. V9-653-V9-657-653. ↑

**C3459.** Jiang Ruibo. Compilation of DEM based on lidar data. / Jiang Ruibo, Wang Dongmei, Yang Mingdong, Yang Fuqin, Pan Jiechen, Xu Liang. // 2010 International Conference on Computer Application and System Modeling (ICCASM). - Taiyuan, 22-24 Oct. 2010. - Vol. 9. - P. V9-650-V9-652-650. ↑

**C3460.** Zhou Gong-jian. Bi-station OTH radar locating and tracking using only range and Doppler measurements. / Zhou Gong-jian, Fu Tian-jiao, Yu Chang-jun, Quan Tai-fan, Cui Nai-gang. // 2010 International Conference on Computer Application and System Modeling (ICCASM). - Taiyuan, 22-24 Oct. 2010. - Vol. 9. - P. V9-88-V9-92-88. ↑

**C3461.** Min-Song Li. Design of Tap Water Pipe's Monitoring System Based on GSM/GPRS. / Min-Song Li, Fen-Fen Zhang. // 2010 International Conference on Computer Application and System Modeling (ICCASM). - Taiyuan, 22-24 Oct. 2010. - Vol. 14. - P. V14-549-V14-552-549. ↑

**C3462.** Yongsheng Xiao. Design and optimization of radio frequency stealth signal based on SAGA. / Yongsheng Xiao, Jianjiang Zhou, Fei Wang, Weiqiang Liu, Zhengwei Zhu. // 2010 International Conference on Computer Application and System Modeling (ICCASM). - Taiyuan, 22-24 Oct. 2010. - Vol. 2. - P. V2-580-V2-584-580. ↑

**C3463.** Chunjuan Wei. A design of alarm system for substation perimeter based on laser fence and wireless communication. / Chunjuan Wei, Junjie Yang, Wu Zhu, Jian Lv. // 2010 International Conference on Computer Application and System Modeling (ICCASM). - Taiyuan, 22-24 Oct. 2010. - Vol. 3. - P. V3-543-V3-546-543. ↑

**C3464.** Li Li. Research on power spectrum estimation based on periodogram and burg algorithm. / Li Li, Hong He. // 2010 International Conference on Computer Application and System Modeling (ICCASM). - Taiyuan, 22-24 Oct. 2010. - Vol. 3. - P. V3-695-V3-698-695. ↑

**C3465.** Liao Kuo. A refuse-recognition method for radar HRRP target recognition based on mahalanobis distance. / Liao Kuo, Jiansheng Fu, Yang wanlin. // 2010 International Conference on Computer Application and System Modeling (ICCASM). - Taiyuan, 22-24 Oct. 2010. - Vol. 4. - P. V4-503-V4-506-503. ↑

**C3466.** Lv Zhian. A bus management system based on ZigBee and GSM/GPRS. / Lv Zhian, Hu Han. // 2010 International Conference on Computer Application and System Modeling (ICCASM). - Taiyuan, 22-24 Oct. 2010. - Vol. 7. - P. V7-210-V7-213-210. ↑

**C3467.** Bai Zhanyuan. A design of the Intelligent electronic control seat belt retractor based on automotive

active safety technology. / Bai Zhanyuan, Xu Aidong, Jin Ni. // 2010 International Conference on Computer Application and System Modeling (ICCASM). - Taiyuan, 22-24 Oct. 2010. - Vol. 3. - P. V3-403-V3-406-403. ↑

C3468. Zhiqiang Shi. Simulation of radar electronic warfare range of visualization applications. / Zhiqiang Shi, Shiqing Tang, Xiaochao Zhang. // 2010 International Conference on Computer Application and System Modeling (ICCASM). - Taiyuan, 22-24 Oct. 2010. - Vol. 7. - P. V7-93-V7-96-93. ↑

C3469. Valentin M. Coastal Radar WERA, a tool for Search and Rescue and oil spill management. / Valentin M., Helzel T., Mariette V., Thomas N. // 2010 IEEE/OES US/EU Baltic International Symposium (BALTIC). - Riga, 24-27 Aug. 2010. - P. 1-4. ↑

C3470. Raudsepp U. Use of earth observation data and numerical modeling in the development of marine downstream services in Estonia. / Raudsepp U., Uiboupin R., Sipelgas L., Lagemaa P., Kouts T., Lips U. // 2010 IEEE/OES US/EU Baltic International Symposium (BALTIC). - Riga, 24-27 Aug. 2010. - P. 1-11. ↑

C3471. Bian Ming-ming. High-performance system design of SAR real-time signal processing. / Bian Ming-ming, Gao Li-ning, Xie Yi-Zhuang, Tan Xu-Bin. // 2010 International Conference on Computer Application and System Modeling (ICCASM). - Taiyuan, 22-24 Oct. 2010. - Vol. 12. - P. V12-126-V12-129-126. ↑

C3472. Uiboupin R. Sea ice monitoring in the Baltic Sea using dual-pol C and L band SAR data. / Uiboupin R., Sipelgas L. // 2010 IEEE/OES US/EU Baltic International Symposium (BALTIC). - Riga, 24-27 Aug. 2010. - P. 1-2. ↑

C3473. Huang D. Design of a correlated Lognormal distributed sequence generator based on Virtex-IV series FPGA. / Huang D., Zeng D.Z., Long T., Yu J.Y. // 2010 International Conference on Computer Application and System Modeling (ICCASM). - Taiyuan, 22-24 Oct. 2010. - Vol. 2. - P. V2-340-V2-343-340. ↑

C3474. Anderson S. SAR imagery and Seatrack Web as decision making tools for illegal oil spill combating-a case study. / Anderson S., Uiboupin R., Verjovkina S., Raudsepp U. // 2010 IEEE/OES US/EU Baltic International Symposium (BALTIC). - Riga, 24-27 Aug. 2010. - P. 1-6. ↑

C3475. Kozlov I. Advancing coastal upwelling observations with use of SAR data: Case study from SE Baltic. / Kozlov I., Dailidienė I., Kudryavtsev V. // 2010 IEEE/OES US/EU Baltic International Symposium (BALTIC). - Riga, 24-27 Aug. 2010. - P. 1-2. ↑

C3476. Antoniou C. Active Traffic Management applications in Greece. The case of Attica Tollway. / Antoniou C., Kopelias P., Papadimitriou F. // 2010 13th International IEEE Conference on Intelligent Transportation Systems (ITSC). - Funchal, 19-22 Sept. 2010. - P. 237-242. ↑

C3477. Rodri. Visual confirmation of mobile objects tracked by a multi-layer lidar. / Rodri, guez F S.A., Fre,mont V., Bonnifait P., Cherfaoui V. // 2010 13th International IEEE Conference on Intelligent Transportation Systems (ITSC). - Funchal, 19-22 Sept. 2010. - P. 849-854. ↑

C3478. Meis U. A new method for robust far-distance road course estimation in advanced driver assistance systems. / Meis U., Klein W., Wiedemann C. // 2010 13th International IEEE Conference on Intelligent Transportation Systems (ITSC). - Funchal, 19-22 Sept. 2010. - P. 1357-1362. ↑

C3479. Pfeiffer D. Ground truth evaluation of the Stixel representation using laser scanners. / Pfeiffer D., Morales S., Barth A., Franke U. // 2010 13th International IEEE Conference on Intelligent Transportation Systems (ITSC). - Funchal, 19-22 Sept. 2010. - P. 1091-1097. ↑

C3480. Vasu V. Signal processing methods for non-contact cardiac detection using Doppler radar. / Vasu V., Heneghan C., Arumugam T., Sezer S. // 2010 IEEE Workshop on Signal Processing Systems (SIPS). - San Francisco, CA, 6-8 Oct. 2010. - P. 368-373. ↑

C3481. Nuevo J. Estimating surrounding vehicles' pose using computer vision. / Nuevo J., Parra I., Sjojberg J., Bergasa L.M. // 2010 13th International IEEE Conference on Intelligent Transportation Systems (ITSC). - Funchal, 19-22 Sept. 2010. - P. 1863-1868. ↑

C3482. Bazzi A. Telecommunication systems enabling real time navigation. / Bazzi A., Masini B.M., Pasolini G., Torreggiani P. // 2010 13th International IEEE Conference on Intelligent Transportation Systems (ITSC). - Funchal, 19-22 Sept. 2010. - P. 1057-1064. ↑

- C3483.** Ribeiro A.G.C.D. AngelCare mobile system: Homecare patient monitoring using Bluetooth and GPRS. / Ribeiro A.G.C.D., Maitelli A.L., Valentim R.A.M., Brandaio G.B., Guerreiro A.M.G. // 2010 Annual International Conference of the IEEE Engineering in Medicine and Biology Society (EMBC). - Buenos Aires, Aug. 31 2010-Sept. 4 2010. - P. 2200-2203. ↑
- C3484.** Singh A. Clutter isolation and cardiac monitoring using harmonic doppler radar with heterodyne receiver and passive RF tags. / Singh A., Lubecke V. // 2010 Annual International Conference of the IEEE Engineering in Medicine and Biology Society (EMBC). - Buenos Aires, Aug. 31 2010-Sept. 4 2010. - P. 1445-1448. ↑
- C3485.** Liu Xiuwen. Design radar signal interface for navigation Radar/ARPA simulator using radar display. / Liu Xiuwen, Yin Yong, Jin Yicheng, Zhang Xinyu. // 2010 Second Pacific-Asia Conference on Circuits, Communications and System (PACCS). - Beijing, 1-2 Aug. 2010. - Vol. 1. - P. 442-445. ↑
- C3486.** Aamna M. 2D Beamforming for Through-the-Wall Microwave Imaging applications. / Aamna M., Ammar S., Rameez T., Shabeeb S., Rao N.I., Safwat I. // 2010 International Conference on Information and Emerging Technologies (ICIET). - Karachi, 14-16 June 2010. - P. 1-6. ↑
- C3487.** Premebida C. A cascade classifier applied in pedestrian detection using laser and image-based features. / Premebida C., Ludwig O., Silva M., Nunes U. // 2010 13th International IEEE Conference on Intelligent Transportation Systems (ITSC). - Funchal, 19-22 Sept. 2010. - P. 1153-1159. ↑
- C3488.** Doshi A. Communicating Driver Intent: A Layered Architecture for Cooperative Active Safety Applications. / Doshi A., Trivedi M.M. // 2010 13th International IEEE Conference on Intelligent Transportation Systems (ITSC). - Funchal, 19-22 Sept. 2010. - P. 373-378. ↑
- C3489.** Ali Z. Design and implementation of an OS-CFAR processor based on a new rank order filtering algorithm. / Ali Z., Arshad A., Razzaq U., Sana S., Ahmed A.H., Harris A.M. // 2010 International Symposium on System on Chip (SoC). - Tampere, 29-30 Sept. 2010. - P. 158-162. ↑
- C3490.** Fortuny J. A quantitative assessment of the compatibility of Ultra Wideband with radiolocation services. / Fortuny J., Rabbachin A., Cano-Pons E., Fuehrer D., Almorox P. // 2010 7th International Symposium on Wireless Communication Systems (ISWCS). - York, 19-22 Sept. 2010. - P. 16-20. ↑
- C3491.** Lili Zhang. Layered Media Q Estimation for GPR signal processing using the frequency shift method. / Lili Zhang, Sixin Liu, Junjun Wu. // 2010 International Conference on Computer Application and System Modeling (ICCSM). - Taiyuan, 22-24 Oct. 2010. - Vol. 11. - P. V11-324-V11-327-324. ↑
- C3492.** Ge Shiqi. Implementation of high performance signal processing system to generate spaceborne SAR imagery products. / Ge Shiqi, Chen Liang, Long Teng. // 2010 International Conference on Computer Application and System Modeling (ICCSM). - Taiyuan, 22-24 Oct. 2010. - Vol. 11. - P. V11-282-V11-286-282. ↑
- C3493.** Haiyan Jin. SAR image data compression based on contrast modulation and warped wavelet Markov modeling. / Haiyan Jin, Xueming Sun. // 2010 International Conference on Computer Application and System Modeling (ICCSM). - Taiyuan, 22-24 Oct. 2010. - Vol. 11. - P. V11-262-V11-266-262. ↑
- C3494.** Ding Xiao-Feng. The character inversion of the mid-course missile based on the sphere-ellipse model. / Ding Xiao-Feng, Zhang Yue-Hui, Wei Xi-Zhang, Li Yong. // 2010 International Conference on Computer Application and System Modeling (ICCSM). - Taiyuan, 22-24 Oct. 2010. - Vol. 11. - P. V11-333-V11-336-333. ↑
- C3495.** Cao Yuan. A modeling method of radar seeker in the presence of electronic warfare. / Cao Yuan, Li Yunjie, Hu Guangli, Liu Yong, Ma Xiao. // 2010 International Conference on Computer Application and System Modeling (ICCSM). - Taiyuan, 22-24 Oct. 2010. - Vol. 11. - P. V11-456-V11-460-456. ↑
- C3496.** Li Hongfei. Analysis and improvement for Proportional Conflict Redistribution rules. / Li Hongfei, Jin Hongbin, Tian Kangsheng, Fei Xiaoyan. // 2010 International Conference on Computer Application and System Modeling (ICCSM). - Taiyuan, 22-24 Oct. 2010. - Vol. 11. - P. V11-401-V11-404-401. ↑
- C3497.** Liu Haibo. Design and realization of a radar simulation system base on CPCI bus. / Liu Haibo, Zeng Dazhi. // 2010 International Conference on Computer Application and System Modeling (ICCSM). - Taiyuan, 22-24 Oct. 2010. - Vol. 11. - P. V11-366-V11-369-366. ↑

- C3498.** Kibangou A.Y. Doppler estimation and data detection for underwater acoustic ZF-OFDM receiver. / Kibangou A.Y., Ros L., Siclet C. // 2010 7th International Symposium on Wireless Communication Systems (ISWCS). - York, 19-22 Sept. 2010. - P. 591-595. ↑
- C3499.** Zhengrong Li. Advances in vegetation management for power line corridor monitoring using aerial remote sensing techniques. / Zhengrong Li, Walker R., Hayward R., Mejias L. // 2010 1st International Conference on Applied Robotics for the Power Industry (CARPI). - Montreal, QC, 5-7 Oct. 2010. - P. 1-6. ↑
- C3500.** Gomes-Mota J. Over head line real-time tracking for automatic inspection or user interface enhancement. / Gomes-Mota J., Gusmao T. // 2010 1st International Conference on Applied Robotics for the Power Industry (CARPI). - Montreal, QC, 5-7 Oct. 2010. - P. 1-6. ↑
- C3501.** Lihua Liu. Micro-Doppler extraction from ballistic missile radar returns using time-frequency analysis. / Lihua Liu, McLernon D., Ghogho M., Weidong Hu. // 2010 7th International Symposium on Wireless Communication Systems (ISWCS). - York, 19-22 Sept. 2010. - P. 780-784. ↑
- C3502.** Bai Hao. An inverting method of moisture constant for huge grain pile based on distribution of dielectric constant. / Bai Hao, Zhang Ji-Xin. // 2010 International Conference on Computer Application and System Modeling (ICCSM). - Taiyuan, 22-24 Oct. 2010. - Vol. 11. - P. V11-110-V11-115-110. ↑
- C3503.** Bai Hao. A research of stored grain moisture content detection based on ground penetrating radar detection technology. / Bai Hao, Lian Fei-yu. // 2010 International Conference on Computer Application and System Modeling (ICCSM). - Taiyuan, 22-24 Oct. 2010. - Vol. 11. - P. V11-100-V11-105-100. ↑
- C3504.** Grigoryev A.D. Development of a test-cradle for the p-i-n diode phaseshifters. / Grigoryev A.D., Rebrov A.N., Ulanova T.A. // 2010 International Conference on Actual Problems of Electron Devices Engineering (APEDE). - Saratov, 22-23 Sept. 2010. - P. 123-128. ↑
- C3505.** Xue-mei Lei. Fuzzy fusion approach for hospital illness tracking. / Xue-mei Lei, Xue-feng Zheng. // 2010 3rd International Conference on Biomedical Engineering and Informatics (BMEI). - Yantai, 16-18 Oct. 2010. - Vol. 6. - P. 2645-2649. ↑
- C3506.** Yang Zhang. Simulation research of microwave automatic clutter-cancellation in life-detection radar. / Yang Zhang, Zhao Li, Teng Jiao, Hao Lv, Jianqi Wang. // 2010 3rd International Conference on Biomedical Engineering and Informatics (BMEI). - Yantai, 16-18 Oct. 2010. - Vol. 5. - P. 2098-2100. ↑
- C3507.** Yalin Miao. Study on adopting optimum binary phase serial to enhance SNR and Penetrating of Ultrasonic Images. / Yalin Miao, Lan Hu, Yan Yang, Hongfei Hao. // 2010 3rd International Conference on Biomedical Engineering and Informatics (BMEI). - Yantai, 16-18 Oct. 2010. - Vol. 2. - P. 583-588. ↑
- C3508.** Li Jin. Microwave and millimeter wave nondestructive measurement in biomedical engineering. / Li Jin, Zhao Qingling. // 2010 3rd International Conference on Biomedical Engineering and Informatics (BMEI). - Yantai, 16-18 Oct. 2010. - Vol. 4. - P. 1523-1527. ↑
- C3509.** Sturm C. Deterministic propagation modeling for joint radar and communication systems. / Sturm C., Braun M., Wiesbeck W. // 2010 URSI International Symposium on Electromagnetic Theory (EMTS). - Berlin, 16-19 Aug. 2010. - P. 942-945. ↑
- C3510.** Bertl S. Security-related active imaging of dielectric objects attached to human bodies. / Bertl S., Detlefsen J. // 2010 URSI International Symposium on Electromagnetic Theory (EMTS). - Berlin, 16-19 Aug. 2010. - P. 950-953. ↑
- C3511.** Wenji Zhang. Polarimetric through-the-wall imaging. / Wenji Zhang, Thajudeen C., Hoorfar A. // 2010 URSI International Symposium on Electromagnetic Theory (EMTS). - Berlin, 16-19 Aug. 2010. - P. 471-474. ↑
- C3512.** Campa Arvizu C.F. New proposal for eliminating interferences in a radar system. Lobes at 45.5° and 24°. / Campa Arvizu C.F., Acevedo Mosqueda M.A. // 2010 IEEE Latin-American Conference on Communications (LATINCOM). - Bogota, 15-17 Sept. 2010. - P. 1-6. ↑
- C3513.** Hogan B. A human-automation interaction approach to the evaluation of resource allocation strategies in adaptive distributed sensor networks. / Hogan B., Bass E.J., Westbrook D. // 2010 IEEE International Conference on Systems Man and Cybernetics (SMC). - Istanbul, 10-13 Oct. 2010. - P. 1755-1762. ↑



- C3514.** Kandil A.A. Collision avoidance in a recursive nested behaviour control structure for Unmanned Aerial Vehicles. / Kandil A.A., Wagner A., Gotta A., Badreddin E. // 2010 IEEE International Conference on Systems Man and Cybernetics (SMC). - Istanbul, 10-13 Oct. 2010. - P. 4276-4281. ↑
- C3515.** Mingjun Ye. Research on the effect of electromagnetic radiation of 220KV power transmission and transformation project on marine radar. / Mingjun Ye, Shijun Ying, Ying Lu, Peng Xia. // 2010 IEEE International Conference on Systems Man and Cybernetics (SMC). - Istanbul, 10-13 Oct. 2010. - P. 3439-3443. ↑
- C3516.** Weizhong Zhang. A tutorial for applying DMOC to solve optimization control problems. / Weizhong Zhang, Inanc T. // 2010 IEEE International Conference on Systems Man and Cybernetics (SMC). - Istanbul, 10-13 Oct. 2010. - P. 1857-1862. ↑
- C3517.** Saif A.A. Automatic monitoring and speed violation ticket system. / Saif A.A., Sammak H., Matar D., Al-Midani O. // 2010 IEEE International Conference on Systems Man and Cybernetics (SMC). - Istanbul, 10-13 Oct. 2010. - P. 1068-1075. ↑
- C3518.** Kalyan B. A random finite set based detection and tracking using 3D LIDAR in dynamic environments. / Kalyan B., Lee K.W., Wijesoma S., Moratuwage D., Patrikalakis N.M. // 2010 IEEE International Conference on Systems Man and Cybernetics (SMC). - Istanbul, 10-13 Oct. 2010. - P. 2288-2292. ↑
- C3519.** Jin-Tsong Jeng. Hybrid SVM-GPs learning for modeling of mitogen-activated protein kinases systems with noise. / Jin-Tsong Jeng, Sheng-Lun Jheng, Chen-Chia Chuang. // 2010 IEEE International Conference on Systems Man and Cybernetics (SMC). - Istanbul, 10-13 Oct. 2010. - P. 2293-2298. ↑
- C3520.** Lijuan Liu. SAR Autofocus Using Wiener Deconvolution. / Lijuan Liu, Xia Bai, Juan Zhao, Ran Tao. // 2010 First International Conference on Pervasive Computing Signal Processing and Applications (PCSPA). - Harbin, 17-19 Sept. 2010. - P. 1256-1259. ↑
- C3521.** Niu Zhaoyang. Angle Estimation for Bi-static MIMO Radar Based on Tri-iterative Algorithm. / Niu Zhaoyang, Zhang Jianyun, Zheng Zhidong. // 2010 First International Conference on Pervasive Computing Signal Processing and Applications (PCSPA). - Harbin, 17-19 Sept. 2010. - P. 1264-1267. ↑
- C3522.** Han Ning. Study on the Time-Frequency Two Dimensional CFAR Algorithm for Moving Targets on Ground in PRC-CW Radar. / Han Ning, Liu Limin, Han Zhuangzhi, Shang Chaoxuan. // 2010 First International Conference on Pervasive Computing Signal Processing and Applications (PCSPA). - Harbin, 17-19 Sept. 2010. - P. 1277-1280. ↑
- C3523.** Tian Wen-long. Linearly Constrained Coherent Sidelobe Canceller for Ionosphere Interference Suppression for HFSWR. / Tian Wen-long, Li Gao-peng, Xu Rong-qing. // 2010 First International Conference on Pervasive Computing Signal Processing and Applications (PCSPA). - Harbin, 17-19 Sept. 2010. - P. 618-623. ↑
- C3524.** Jin-lu Yang. A Detector of DTTB Based Passive Radar Using FRFT and Hough Transform. / Jin-lu Yang, Tao Shan, Ran Tao. // 2010 First International Conference on Pervasive Computing Signal Processing and Applications (PCSPA). - Harbin, 17-19 Sept. 2010. - P. 212-215. ↑
- C3525.** Jia Yan-guo. Two Methods for Constructing the Difference Set Pairs. / Jia Yan-guo, Ren Fu-zheng, Ji Yong-feng, Liu Yong-shan, Ren Jun. // 2010 First International Conference on Pervasive Computing Signal Processing and Applications (PCSPA). - Harbin, 17-19 Sept. 2010. - P. 675-678. ↑
- C3526.** Wu Fufu. Study on the Method for Radar Signal Receiver Channel Modeling. / Wu Fufu, Han Zhuangzhi, He Qiang, Wang Zhiyun. // 2010 First International Conference on Pervasive Computing Signal Processing and Applications (PCSPA). - Harbin, 17-19 Sept. 2010. - P. 1232-1235. ↑
- C3527.** Feng Liying. Information selection based on fuzzy comprehensive evaluation. / Feng Liying, Jiao Li, Xue Qing, Zhang Shi, Chen Jiayi, Xu Yiliu. // 2010 International Conference on Information Networking and Automation (ICINA). - Kunming, 18-19 Oct. 2010. - Vol. 1. - P. V1-158-V1-162-158. ↑
- C3528.** Moghaddam M. Recent theoretical and experimental advances in electromagnetic sensing of subsurface profiles. / Moghaddam M., Albahkali M., Xueyang Duan, Goykhman Y., Tabatabaeenejad A. // 2010 URSI International Symposium on Electromagnetic Theory (EMTS). - Berlin, 16-19 Aug. 2010. - P. 145-147. ↑

- C3529.** Sullivan D.M. Large scale underwater FDTD ELF simulations using Acceleware and MPI parallel processing. / Sullivan D.M., Yang Xia, Mansoori A. // 2010 URSI International Symposium on Electromagnetic Theory (EMTS). - Berlin, 16-19 Aug. 2010. - P. 104-106. ↑
- C3530.** Minet J. Characterization of layered media using full-waveform inversion of proximal GPR data. / Minet J., Patriarca C., Slob E.C., Vanclooster M., Lambot S. // 2010 URSI International Symposium on Electromagnetic Theory (EMTS). - Berlin, 16-19 Aug. 2010. - P. 1004-1007. ↑
- C3531.** Yarovoy A. SIMO-based approach for subsurface sensing. / Yarovoy A., Xiaodong Zhuge. // 2010 URSI International Symposium on Electromagnetic Theory (EMTS). - Berlin, 16-19 Aug. 2010. - P. 245-248. ↑
- C3532.** Tao Zhang. An evaluation method of anti-jamming performance to receiver based on sample entropy. / Tao Zhang, Zhiliang Ren, Changcun Sun, Yaobo Li. // 2010 International Conference on Information Networking and Automation (ICINA). - Kunming, 18-19 Oct. 2010. - Vol. 1. - P. V1-516-V1-519-516. ↑
- C3533.** Yang Bo. Information fusion of integrated navigation based on self-adaptive filter. / Yang Bo, Peng Huihuang, Zhang Youhong, Shan Bin. // 2010 International Conference on Information Networking and Automation (ICINA). - Kunming, China, 18-19 Oct. 2010. - Vol. 2. - P. V2-1-V2-5-1. ↑
- C3534.** Martin A.R. Safety issues and damage to equipment with both Smart Grid and home network connections. 2010 IEEE Symposium on Product Compliance Engineering (ISPC). - Boston, MA, 18-20 Oct. 2010. - P. 1-5. ↑
- C3535.** Yanmin Ning. Design of sewage flow remote monitoring system over GPRS network. / Yanmin Ning, Dean Zhao, Jiajun Guan, Shichang Gong. // 2010 Second International Conference on Computational Intelligence and Natural Computing Proceedings (CINC). - Wuhan, 13-14 Sept. 2010. - Vol. 2. - P. 296-299. ↑
- C3536.** Hongyan Wang. Improvement of image resolution in ScanSAR simulation. / Hongyan Wang, Xin Jia. // 2010 3rd International Congress on Image and Signal Processing (CISP). - Yantai, 16-18 Oct. 2010. - Vol. 5. - P. 2048-2051. ↑
- C3537.** Dong Wang. Water objects extraction from polarimetric SAR imagery based on blind source separation and morphological reconstruction. / Dong Wang, Weifeng Zhou, Wei Fan, Xingwei Jiang, Ping Qin. // 2010 3rd International Congress on Image and Signal Processing (CISP). - Yantai, 16-18 Oct. 2010. - Vol. 3. - P. 1028-1032. ↑
- C3538.** Yong Yu. Infrared object tracking based on particle filter. / Yong Yu, Yan-fang Che. // 2010 3rd International Congress on Image and Signal Processing (CISP). - Yantai, 16-18 Oct. 2010. - Vol. 3. - P. 1508-1511. ↑
- C3539.** Yayu Liu. The target detection for GPR images based on curve fitting. / Yayu Liu, Meiqing Wang, Qiurong Cai. // 2010 3rd International Congress on Image and Signal Processing (CISP). - Yantai, 16-18 Oct. 2010. - Vol. 6. - P. 2876-2879. ↑
- C3540.** Shenghua Zhou. Target detection algorithm for spatial diversity MIMO radar with space partition. / Shenghua Zhou, Kuiying Yin, Tao Luo, Hongwei Liu. // 2010 3rd International Congress on Image and Signal Processing (CISP). - Yantai, 16-18 Oct. 2010. - Vol. 9. - P. 4152-4155. ↑
- C3541.** Jianshe Wang. A model based bias field correction algorithm for SAR sea ice image. / Jianshe Wang, Wenhui Lang, Xuezhi Yang, Gengzhong Wang. // 2010 3rd International Congress on Image and Signal Processing (CISP). - Yantai, 16-18 Oct. 2010. - Vol. 5. - P. 2075-2079. ↑
- C3542.** WanJing Meng. CFAR and KPCA for SAR image target detection. / WanJing Meng, Tao Ju, HongYun Yu. // 2010 3rd International Congress on Image and Signal Processing (CISP). - Yantai, 16-18 Oct. 2010. - Vol. 4. - P. 1832-1835. ↑
- C3543.** Can Ding. Improved denoising method of SAR image. / Can Ding, Changwen Qu, Feng Su. // 2010 3rd International Congress on Image and Signal Processing (CISP). - Yantai, 16-18 Oct. 2010. - Vol. 2. - P. 712-715. ↑
- C3544.** Guoying Sun. Realization of high data rate DUC based on FPGA. / Guoying Sun, Yunjie Li, Meiguo Gao, Guangli Hu. // 2010 3rd International Congress on Image and Signal Processing (CISP). - Yantai, 16-18

Oct. 2010. - Vol. 6. - P. 3013-3016. ↑

**C3545.** Haiping Hou. Signal analysis of downward-looking and forward-looking array FMCW SAR. / Haiping Hou, Changwen Qu, Qiang Zhou, Feng Su. // 2010 3rd International Congress on Image and Signal Processing (CISP). - Yantai, 16-18 Oct. 2010. - Vol. 9. - P. 4267-4270. ↑

**C3546.** Rongfeng Li. Adaptive-adaptive beamforming algorithm of planar array based on one-dimensional auxiliary beam. / Rongfeng Li, Can Rao, Lingyan Dai, Shifeng Zhao. // 2010 3rd International Congress on Image and Signal Processing (CISP). - Yantai, 16-18 Oct. 2010. - Vol. 7. - P. 3300-3303. ↑

**C3547.** Liang Gong. Automated road extraction from LiDAR data based on intensity and aerial photo. / Liang Gong, Yongsheng Zhang, Zhengguo Li, Quanfu Bao. // 2010 3rd International Congress on Image and Signal Processing (CISP). - Yantai, 16-18 Oct. 2010. - Vol. 5. - P. 2130-2133. ↑

**C3548.** Qingwei Gao. Despeckling SAR image using nonsubsampling directionlets combining with GSM model. / Qingwei Gao, Chi Zhang, Yixiang Lu. // 2010 3rd International Congress on Image and Signal Processing (CISP). - Yantai, 16-18 Oct. 2010. - Vol. 2. - P. 664-667. ↑

**C3549.** Chengfa Xu. A general radar surface target echo simulator. / Chengfa Xu, Jingliang Bai, Ronggang Wu, Yongbin Hong. // 2010 3rd International Congress on Image and Signal Processing (CISP). - Yantai, 16-18 Oct. 2010. - Vol. 8. - P. 3677-3680. ↑

**C3550.** Li-hua Wang. Classifying multisensor images by support vector machine in Chongming Dongtan. / Li-hua Wang, Yun-xuan Zhou, Xing Li. // 2010 3rd International Congress on Image and Signal Processing (CISP). - Yantai, 16-18 Oct. 2010. - Vol. 5. - P. 2134-2138. ↑

**C3551.** TianJun Li. The mechanism of Pt films to suppress the electron emission of grid in TWTs. / TianJun Li, Tao Feng, BingYao Jiang, XiangHuai Liu, YiWei Chen, Zhuo Sun. // 2010 8th International Vacuum Electron Sources Conference and Nanocarbon (IVESC). - Nanjing, 14-16 Oct. 2010. - P. 303-304. ↑

**C3552.** Xin-Jian Niu. 94 GHz, CW, low-voltage gyrotron. / Xin-Jian Niu, Ling Gu, Hong-Fu Li. // 2010 8th International Vacuum Electron Sources Conference and Nanocarbon (IVESC). - Nanjing, 14-16 Oct. 2010. - P. 341-342. ↑

**C3553.** Qianzhi Ma. Application of artificial fish school algorithm in UCAV path planning. / Qianzhi Ma, Xiujuan Lei. // 2010 IEEE Fifth International Conference on Bio-Inspired Computing: Theories and Applications (BIC-TA). - Changsha, 23-26 Sept. 2010. - P. 555-559. ↑

**C3554.** Li Zhishun. Study on aluminate of cathode emission active substances. / Li Zhishun, Wang Yuchun. // 2010 8th International Vacuum Electron Sources Conference and Nanocarbon (IVESC). - Nanjing, 14-16 Oct. 2010. - P. 532-533. ↑

**C3555.** Jingping Yi. Design and implementation of MMS system based on GPRS modem. / Jingping Yi, Wanlin Gao, Shuliang Zhang, Ganghong Zhang, Jinyu Zang. // 2010 Second International Conference on Computational Intelligence and Natural Computing Proceedings (CINC). - Wuhan, 13-14 Sept. 2010. - Vol. 2. - P. 201-204. ↑

**C3556.** Wei Yu. The detection of long chirp signal with small frequency rate in low SNR. / Wei Yu, Liu Ying. // 2010 Second International Conference on Computational Intelligence and Natural Computing Proceedings (CINC). - Wuhan, 13-14 Sept. 2010. - Vol. 1. - P. 337-339. ↑

**C3557.** Andric. The database of radar echoes from various targets with spectral analysis. / Andric, M.S., Bondz,ulic, B.P., Zrnica, B.M. // 2010 10th Symposium on Neural Network Applications in Electrical Engineering (NEUREL). - Belgrade, 23-25 Sept. 2010. - P. 187-190. ↑

**C3558.** Min Fang. An instances sampling approach based on cellular automata for ensemble learning. / Min Fang, Zhang Xiao Song. // 2010 IEEE Fifth International Conference on Bio-Inspired Computing: Theories and Applications (BIC-TA). - Changsha, 23-26 Sept. 2010. - P. 560-564. ↑

**C3559.** Liu A. A novel multi-channel SAR-GMTI algorithm based on raw data. / Liu A., Li Chen, Fei Zhao, Gangyao Kuang. // 2010 3rd International Congress on Image and Signal Processing (CISP). - Yantai, 16-18 Oct. 2010. - Vol. 3. - P. 1489-1493. ↑

- C3560.** Rubing Xi. Super resolution processing of SAR images by Matching Pursuit method based on Genetic Algorithm. 2010 3rd International Congress on Image and Signal Processing (CISP). - Yantai, 16-18 Oct. 2010. - Vol. 5. - P. 2066-2070. ↑
- C3561.** Zhu Ben-yu. A novel ISAR jamming method based on randomly sinusoidal phase modulation. / Zhu Ben-yu, Xue Lei, Liu Yue-ping. // 2010 3rd International Congress on Image and Signal Processing (CISP). - Yantai, 16-18 Oct. 2010. - Vol. 9. - P. 4166-4169. ↑
- C3562.** Weicun Xu. Multiple Sub-Spaces particle filtering for multi-target tracking. / Weicun Xu, Qingjie Zhao, Guanqun Yu, Jun Zheng. // 2010 3rd International Congress on Image and Signal Processing (CISP). - Yantai, 16-18 Oct. 2010. - Vol. 1. - P. 340-344. ↑
- C3563.** Lie Guo. Study on pedestrian detection and tracking with monocular vision. / Lie Guo, Linhui Li, Yibing Zhao, Mingheng Zhang. // 2010 2nd International Conference on Computer Technology and Development (ICCTD). - Cairo, 2-4 Nov. 2010. - P. 466-470. ↑
- C3564.** Parhizkar B. Wireless communications technologies for energy networks in a non-industrialized society. / Parhizkar B., Navaratnam S., Gachagua S.R., Alizadeh S. // 2010 2nd International Conference on Computer Technology and Development (ICCTD). - Cairo, 2-4 Nov. 2010. - P. 105-109. ↑
- C3565.** Rong Zhu. Application of the deconvolution method in the processing of Full-waveform Lidar data. / Rong Zhu, Yong Pang, Zhongjun Zhang, Guangcai Xu. // 2010 3rd International Congress on Image and Signal Processing (CISP). - Yantai, 16-18 Oct. 2010. - Vol. 6. - P. 2975-2979. ↑
- C3566.** Zhang Yang. Detecting and Identifying Two Stationary-Human-Targets: A Technique Based on Bioradar. / Zhang Yang, Jing Xijing, Jiao Teng, Zhang Zhu, Lv Hao, Wang Jianqi. // 2010 First International Conference on Pervasive Computing Signal Processing and Applications (PCSPA). - Harbin, 17-19 Sept. 2010. - P. 981-985. ↑
- C3567.** Sun Yingmei. The correction of spaceborne satellite's yaw steering law based on the star tracker high-precision measurement. / Sun Yingmei, Chen Junli, Wan Xiangcheng, Zhang Jiu Ling, Wang Yun. // 2010 3rd International Symposium on Systems and Control in Aeronautics and Astronautics (ISSCAA). - Harbin, 8-10 June 2010. - P. 178-180. ↑
- C3568.** Hui Xiao. On exploring SVDSPM algorithm for more accurate DOA estimation of low altitude target. / Hui Xiao, Jun Yuan. // 2010 International Conference on Wireless Communications and Signal Processing (WCSP). - Suzhou, 21-23 Oct. 2010. - P. 1-4. ↑
- C3569.** Chen Hui. Performance analysis of self-calibration algorithm for concentric-UCA. / Chen Hui, Bao Zheng. // 2010 International Conference on Wireless Communications and Signal Processing (WCSP). - Suzhou, 21-23 Oct. 2010. - P. 1-5. ↑
- C3570.** Zhang Fenghui. A new real time Range-Doppler imaging algorithm. / Zhang Fenghui, Wang Yanfei, Song Hongmei. // 2010 3rd International Symposium on Systems and Control in Aeronautics and Astronautics (ISSCAA). - Harbin, 8-10 June 2010. - P. 119-122. ↑
- C3571.** Fan Ye. ISAR super-resolution imaging based on sparse representation. / Fan Ye, Fan Zhang, Jubo Zhu. // 2010 International Conference on Wireless Communications and Signal Processing (WCSP). - Suzhou, 21-23 Oct. 2010. - P. 1-6. ↑
- C3572.** Kontorovich V. Cyclostationary spectrum sensing for Cognitive Radio and multiantenna systems. / Kontorovich V., Ramos-Alarco, n F., Filio R.O., Primak S. // 2010 International Conference on Wireless Communications and Signal Processing (WCSP). - Suzhou, 21-23 Oct. 2010. - P. 1-6. ↑
- C3573.** Pengge Ma. Navigation Satellite Passive Radar Moving Target Detection and SAR Imaging Based on FRFT. / Pengge Ma, Lin Qi, Enqing Chen, Ning Zheng. // 2010 First International Conference on Pervasive Computing Signal Processing and Applications (PCSPA). - Harbin, 17-19 Sept. 2010. - P. 767-770. ↑
- C3574.** Zhang Chunxia. Research and Design of Embedded Radar Information Processor Oriented to Pervasive Computing. / Zhang Chunxia, Dong Wenjie, Tian Xiyang, Zhang Jun, Zhou Chunmei, Lin Jinyong. // 2010 First International Conference on Pervasive Computing Signal Processing and Applications (PCSPA). - Harbin, 17-19 Sept. 2010. - P. 427-431. ↑



- C3575.** Linxi Zhang. High-Resolution RCS Measurement Inside an Anechoic Chamber. / Linxi Zhang, Kai Ding, Nanjing Li, Jie Ren. // 2010 International Forum on Information Technology and Applications (IFITA). - Kunming, 16-18 July 2010. - Vol. 3. - P. 252-255. ↑
- C3576.** Zhang Gui-ping. Research on imaging of SS-BISAR. / Zhang Gui-ping, Jia Xin, Wang Xiao-mei, Fu Yun. // 2010 International Conference on Wireless Communications and Signal Processing (WCSP). - Suzhou, 21-23 Oct. 2010. - P. 1-4. ↑
- C3577.** Li Zhaoqiang. A Kind of Discrete Variable Structure UCAV Guidance Law Restrict by the Entering Angle. / Li Zhaoqiang, Zhou Deyun, Xu Jiadong. // 2010 International Forum on Information Technology and Applications (IFITA). - Kunming, 16-18 July 2010. - Vol. 3. - P. 237-240. ↑
- C3578.** Wu Wei. Multitarget tracking in clutter using two-scan data association algorithm and fixed-lag smoothing. 2010 3rd International Symposium on Systems and Control in Aeronautics and Astronautics (ISSCAA). - Harbin, 8-10 June 2010. - P. 196-201. ↑
- C3579.** Lagovsky B.A. Adaptive receivers for explorative UWB pulses. 2010 20th International Crimean Conference Microwave and Telecommunication Technology (CriMiCo). - Sevastopol, 13-17 Sept. 2010. - P. 1235-1236. ↑
- C3580.** Lutsenko V.I. Efficiency of narrow band Doppler selection of the signal in presence of the scattering from the sea. / Lutsenko V.I., Lutsenko I.V., Popov I.V. // 2010 20th International Crimean Conference Microwave and Telecommunication Technology (CriMiCo). - Sevastopol, 13-17 Sept. 2010. - P. 1231-1232. ↑
- C3581.** Qingru Kong. Research of an Improved Weighted Centroid Localization Algorithm and Anchor Distribution. / Qingru Kong, Xinyu Yang, Xiangjun Dai. // 2010 International Conference on Cyber-Enabled Distributed Computing and Knowledge Discovery (CyberC). - Huangshan, 10-12 Oct. 2010. - P. 400-405. ↑
- C3582.** Ali F. A high resolution 2D omnidirectional synthetic aperture radar scanner at K band. / Ali F., Urban A., Vossiek M. // 2010 European Microwave Conference (EuMC). - Paris, 28-30 Sept. 2010. - P. 1694-1697. ↑
- C3583.** Sagnard F. Development of wideband crosshole and surface GPR for soil characterization: FDTD modeling and experiments. / Sagnard F., Rejiba F., Froumentin M. // 2010 European Microwave Conference (EuMC). - Paris, 28-30 Sept. 2010. - P. 332-335. ↑
- C3584.** Zherybyatyev D.P. Method of space-time processing of non-stationary signals with application of optimal sliding windows and wavelet transforms. / Zherybyatyev D.P., Volosyuk V.K., Gorbunenko O.A. // 2010 20th International Crimean Conference Microwave and Telecommunication Technology (CriMiCo). - Sevastopol, 13-17 Sept. 2010. - P. 1227-1228. ↑
- C3585.** Junli Chen. An integrated Relative Navigation system using GPS/VISNAV for ultra-close spacecraft formation flying. / Junli Chen, Xiaoliang Wang, Xiaowei Shao, Dengping Duan. // 2010 3rd International Symposium on Systems and Control in Aeronautics and Astronautics (ISSCAA). - Harbin, 8-10 June 2010. - P. 803-808. ↑
- C3586.** Xinfeng Wang. The evaluation method of space objects collision. / Xinfeng Wang, Yanjun Li, Gongyou Wu, Rongzhi Zhang. // 2010 3rd International Symposium on Systems and Control in Aeronautics and Astronautics (ISSCAA). - Harbin, 8-10 June 2010. - P. 849-852. ↑
- C3587.** Shicang Zhang. Data association for GM-PHD with track oriented PMHT. / Shicang Zhang, Jianxun Li, Binyi Fan, Liangbin Wu. // 2010 3rd International Symposium on Systems and Control in Aeronautics and Astronautics (ISSCAA). - Harbin, 8-10 June 2010. - P. 386-391. ↑
- C3588.** Yunjie Qu. A novel adaptive square root recursive least squares filter algorithm of SINS/SAR integrated navigation systems. / Yunjie Qu, Wenhui Wang, Lu Zhang, Bangqing Li, Kai Yu. // 2010 3rd International Symposium on Systems and Control in Aeronautics and Astronautics (ISSCAA). - Harbin, 8-10 June 2010. - P. 1142-1145. ↑
- C3589.** Xiao-lin Zhang. Recognition method studies for radar and communication signals based on spectral correlation. / Xiao-lin Zhang, Wen-ting You, Qiang Guo, He-yang Cao. // 2010 3rd International Symposium on Systems and Control in Aeronautics and Astronautics (ISSCAA). - Harbin, 8-10 June 2010. - P. 363-366. ↑

- C3590.** Zhang Zhong. Analysis of Return Signal Mechanism in Ship-Board Radar. / Zhang Zhong, Dingqun Maqinglin. // 2010 First International Conference on Pervasive Computing Signal Processing and Applications (PCSPA). - Harbin, 17-19 Sept. 2010. - P. 703-706. ↑
- C3591.** Qian Wei-qiang. Multipath Mitigation of Low Elevation for Passive Monopulse Radar Based on FRFT. / Qian Wei-qiang, Qiao Xiao-lin, Zhu Xiang-peng, Wei Yu-mei. // 2010 First International Conference on Pervasive Computing Signal Processing and Applications (PCSPA). - Harbin, 17-19 Sept. 2010. - P. 948-951. ↑
- C3592.** Tong Jun. Decomposition of Maneuvering Target RCS Based on Wavelet Analysis. / Tong Jun, Shan Ganlin. // 2010 First International Conference on Pervasive Computing Signal Processing and Applications (PCSPA). - Harbin, 17-19 Sept. 2010. - P. 972-976. ↑
- C3593.** Huanghui Shen. A Novel Crossbar Scheduling for Multi-FPGA Parallel SAR Imaging System. / Huanghui Shen, Jing Wang, Chenyu Yuan, Zhensong Wang, Weimin Zheng. // 2010 First International Conference on Pervasive Computing Signal Processing and Applications (PCSPA). - Harbin, 17-19 Sept. 2010. - P. 394-397. ↑
- C3594.** Xiang-Peng Zhu. The Application of Unsupervised Clustering in Radar Signal Preselection Based on DOA Parameters. / Xiang-Peng Zhu, Ming Jin, Wei-Qiang Qian, Shuai Liu, Yu-Mei Wei. // 2010 First International Conference on Pervasive Computing Signal Processing and Applications (PCSPA). - Harbin, 17-19 Sept. 2010. - P. 956-959. ↑
- C3595.** Yu Nan. The Monopulse Angle Estimation Based on the Radon-Ambiguity Transform. / Yu Nan, Jin Ming, Qiao Xiao-lin. // 2010 First International Conference on Pervasive Computing Signal Processing and Applications (PCSPA). - Harbin, 17-19 Sept. 2010. - P. 824-828. ↑
- C3596.** Bing Liu. Parameter Estimation of LFM Signal with Narrowband Jamming Based on CS. / Bing Liu, Ping Fu. // 2010 First International Conference on Pervasive Computing Signal Processing and Applications (PCSPA). - Harbin, 17-19 Sept. 2010. - P. 487-490. ↑
- C3597.** Qingjun Yao. Visualized Feature Fusion and Style Evaluation for Musical Genre Analysis. / Qingjun Yao, Haifeng Li, Jiayin Sun, Lin Ma. // 2010 First International Conference on Pervasive Computing Signal Processing and Applications (PCSPA). - Harbin, 17-19 Sept. 2010. - P. 883-886. ↑
- C3598.** Jiang Yicheng. Research on ISAR Imaging Method of Parameter Estimation Based on Optimal Imaging Period. / Jiang Yicheng, Yin Songqiao. // 2010 First International Conference on Pervasive Computing Signal Processing and Applications (PCSPA). - Harbin, 17-19 Sept. 2010. - P. 513-516. ↑
- C3599.** Jie He. Tri-iterative Three-Dimensional Space-Time Adaptive Processing Based on Correlation Matrix for Airborne Radar. / Jie He, Da-zheng Feng, Xiang Cong, Hui Lv. // 2010 First International Conference on Pervasive Computing Signal Processing and Applications (PCSPA). - Harbin, 17-19 Sept. 2010. - P. 715-718. ↑
- C3600.** Yubin Xu. WLAN Indoor Tracking Method via Improved Particle Filter Algorithm. / Yubin Xu, Jingyu Liu, Lin Ma, Lang Peng. // 2010 First International Conference on Pervasive Computing Signal Processing and Applications (PCSPA). - Harbin, 17-19 Sept. 2010. - P. 1078-1082. ↑
- C3601.** Hong Xu. Estimation and Registration of Relative System Biases in Fire-Control Radar Network. / Hong Xu, Zhuangzhi Han, Qiang He, Chaoxuan Shang. // 2010 First International Conference on Pervasive Computing Signal Processing and Applications (PCSPA). - Harbin, 17-19 Sept. 2010. - P. 5-8. ↑
- C3602.** Haiyan Yu. Propagation Analysis of ELF Electromagnetic Emission below the Cut-Off Frequency in Ionosphere. / Haiyan Yu, Hongjuan Zhou, Bingxia Cao, Xiaolin Qiao. // 2010 First International Conference on Pervasive Computing Signal Processing and Applications (PCSPA). - Harbin, 17-19 Sept. 2010. - P. 799-802. ↑